TRANSACTIONS

OF THE

AMERICAN SOCIETY

OF

CIVIL ENGINEERS

(INSTITUTED 1852)

VOLUME 125, PART I

1960

Edited by the Executive Secretary, under the direction of the Committee on Publications.

Reprints from this publication, which is copyrighted, may be made on condition that the full title of paper, name of author, and page reference (or paper number) are given.

NEW YORK
PUBLISHED BY THE SOCIETY
1960

Trans
TA
1
A526
V.125
pt.1

Copyright 1960 by the AMERICAN SOCIETY OF CIVIL ENGINEERS

NOTE—The Society is not responsible for any statement made or opinion expressed in its publications.

CONTENTS

No.		Page
3011	DIGITAL COMPUTATION FOR STIFFNESS MATRIX ANALYSIS	
	By John S. Archer	1
3012	CELLULAR COFFERDAMS AND DOCKS	
	By Edward M. Cummings	13
	Discussion:	
	By Samuel Heyman	34
	Cevdet Z. Erzen	37
	Edward M. Cummings	43
3013	ANALYTICAL AND EXPERIMENTAL STUDY OF HELICOIDAL GIRDERS	
	By Yee F. Young and Alexander C. Scordelis	46
3014	DESIGN AND PERFORMANCE OF VERMILION DAM	
	By Karl Terzaghi and Thomas M. Leps	63
	Discussion:	
	By Maurice L. Dickinson	86
	John R. Kiely	88
	Ralph W. Spencer	89
	Philip J. West	90
	Joseph H. Birman	93
	Bruce R. Laverty	94
	Karl Terzaghi and Thomas M. Leps	99
3015	WATER—A LIMITING RESOURCE	
	By Robert O. Thomas	101
	Discussion:	
	By Douglas R. Woodward	112
	Donald McCord Baker	114
	Alfred R. Golze	117
	Robert O. Thomas	119
3016	TRENDS IN PIPELINE CONSTRUCTION	
	By James W. Hall	123
3017	USE OF MODELS TO STUDY GROUND-WATER PROBLEMS	
	By Kenneth R. Wright	133
3018	CLAY STRENGTH INCREASE CAUSED BY REPEATED LOADING	
	By H. Bolton Seed, Robert L. McNeill, and Jacques De Gueinin	141
	Discussion:	
	By Richard G. Ahlvin	161
	D. Hugh Trollope	163
	H. Bolton Seed, Robert L. McNeill, and Jacques De Guenin	164

No.		Page
3019	DISTRIBUTION OF SEDIMENT IN LARGE RESERVOIRS	
	By Whitney M. Borland and Carl R. Miller	166
3020	CONSTRUCTION OF THE VARIABLE-ANGLE LAUNCHER	
	By Arthur C. Bravo	181
3021	AMPLIFIED STRESS AND DISPLACEMENT IN GUYED TOWERS	
	By Robert S. Rowe	199
	Discussion:	
	By Vitelmo Bertero	215
	Robert S. Rowe	225
3022	GARRISON DAM TEST TUNNEL: A SYMPOSIUM	
	FOREWORD	229
	INVESTIGATION AND CONSTRUCTION	
	By Harris H. Burke	230
	EVALUATION OF TEST RESULTS	
	By Kenneth S. Lane	268
	Discussion:	
	By A. A. Eremin	307
3023	INELASTIC BUCKLING IN STEEL	
	By Geerhard Haaijer and Bruno Thurlimann	308
	Discussion:	
	By Paul P. Bijlaard	338
	Geerhard Haaijer and Bruno Thurlimann	343
3024	HYDRAULIC DESIGN OF COLUMBIA RIVER NAVIGATION LOCKS	
	By George C. Richardson and Marvin J. Webster	345
3025	NUMERICAL SOLUTIONS FOR INTERCONNECTED BRIDGE GIRDERS	
	By Henry Malter	365
	Discussion:	
	By Dronnadula V. Reddy	383
	Henry Malter	386
3026	SELECTION OF DESIGN WAVE FOR OFFSHORE STRUCTURES	
	By Charles L. Bretschneider	388
	Discussion:	
	By J. E. Chappelear	414
	Charles L. Bretschneider	415
3027	PIPELINE FIELD WELDING AND QUALITY CONTROL METHODS	
	By Armand G. Barkow	417
3028	MOMENTS IN BEAMS BY THE METHOD OF PARTIAL MOMENTS	
	By Harry Posner	430
	Discussion:	
	By William S. Walker and Joseph T. Kolibal	451
	A. A. Eremin	452
	Lembit Kald	453
	Harry Posner	454

No.		Page
3029	SELF-AERATED FLOW IN OPEN CHANNELS	
	By Lorenz G. Straub and Alvin G. Anderson	456
	Discussion:	
	By Michele Viparelli	482
	Lorenz G. Straub and Alvin G. Anderson	485
3030	LOWER-COST CANAL LINING PRACTICE	
	By Richard J. Willson	487
	Discussion:	
	By Frederick L. Hotes	500
	Richard J. Willson	501
3031	EARTHQUAKE RESPONSE OF ELEVATED TANKS AND VESSELS	
	By Donald F. Moran and James A. Cheney	503
	Discussion:	
	By A. A. Eremin	515
	Donald F. Moran and James A. Cheney	515
3032	HYDRAULIC PROBLEM SOLUTION ON ELECTRONIC COMPUTERS	
	By Edward A. Lawler and Frank V. Druml	517
3033	CONTAINMENT SPHERE FOR DRESDEN STATION	
	By Leonard P. Zick, James T. Dunn, and James B. Maher	536
3034	WELDED PIPELINE BRANCH CONNECTIONS	
	By Everett C. Rodabaugh and Henry H. George	554
3035	THE COLUMBIA RIVER CONTROLLED	
	By Louis H. Foote	583
	Discussion:	
	By Roy T. Bessey	597
	Louis H. Foote	601
3036	STRENGTH OF REINFORCED CONCRETE BEAMS	
	By Sidney A. Guralnick	603
	Discussion:	
	By Henry J. Cowan	633
	Robert F. Warner	634
	Bela Goschy and George Balazs	635
	Kuang-Han Chu	636
	Sidney A. Guralnick	637
3037	ELECTRIC PIPELINE FOR HIGH-VISCOSITY FUEL	
	By Albert G. Purdue	644
3038	WATER FORCES ON ACCELERATED CYLINDERS	
	By Alan D. K. Laird, Charles A. Johnson, and Robert W. Walker	652
3039	BLAST PHENOMENA FROM A NUCLEAR BURST	
	By Ferd E. Anderson, Jr.	667
3040	FLOW TESTING BY AMMONIA DISPLACEMENT	
	By Jack N. White and Thomas Thawley	673

No.		Page
3041	COMPACTED CLAY: A SYMPOSIUM	
	STRUCTURE	
	By T. William Lambe	682
	Discussion:	
	By D. Hugh Trollope	706
	Benno P. Warkentin and Raymond N. Y. Yong	707
	Gerald A. Leonards	709
	D. P. Krynine	712
	Dean R. Freitag	714
	T. William Lambe	716
	ENGINEERING BEHAVIOR	
	By T. William Lambe	718
	Discussion:	
	By Alfred C. Scheer	741
	Rayond N. Y. Yong and Benno P. Warhentin	742
	J. MacNeil Turnbull	743
	Jose A. Jimenez Salas	746
	D. Hugh Trollope	753
	T. William Lambe	754
3042	NUMERICAL SOLUTIONS FOR BEAMS ON ELASTIC FOUNDATIONS	
	By Henry Malter	757
	Discussion:	
	By Norman J. Ryker, Jr.	770
	Alexander Dodge	774
	Lymon C. Reese	786
	Victor R. Bergman	789
	Henry Malter	790
3043	UNDERSEEPAGE CONTROL AT FORT RANDALL DAM	
	By Stanley T. Thorfinnson	792
3044	LATERAL BRACING OF COLUMNS AND BEAMS	
	By George Winter	807
	Discussion:	
	By Anthony A. Chibaro	826
	Giles G. Green	827
	Bruce G. Johnston	830
	Marvin A. Larson	830
	William Zuk	838
	George Winter	840
3045	TORQUE-LOADED CONTINUOUS BEAMS OF PROFILE SECTION	
	By Donovan H. Young and John F. Brahtz	846
3046	FORCES INDUCED ON A LARGE VESSEL BY SURGE	
	By John T. O'Brien lnd David I. Kuchenreuther	855
	Discussion:	
	By Basil W. Wilson	877
	J. T. O'Brien and D. I. Kuchenreuther	883

No.		Page
3047	CONCRETE BEAMS AND COLUMNS WITH BUNDLED REINFORCEMENT	
	By Norman W. Hanson and Hans Reiffenstuhl	889
	Discussion:	
	By Homer M. Hadley	905
3048	ARCH DAMS: A SYMPOSIUM	
	FOREWORD	910
	DESIGN AND OBSERVATION IN PORTUGAL	
	By M. Rocha, J. Laginha Serafim, and Antonio F. Da Silveira	911
	Discussion:	
	By Robert E. Glover	949
	Fred A. Houck	950
	By Manuel Rocha, J. Laginha Serafim, and Antonio F. da Silveira	952
	DEVELOPMENT IN ITALY	
	By Carlo Semenza	954
	OBSERVED BEHAVIOR IN ITALY	
	By Dino Tonini	974
3049	GEOTECHNICAL PROPERTIES OF GLACIAL LAKE CLAYS	
	By Tien H. Wu	994
	Discussion:	
	By T. Cameron Kenney	1012
	Tien H. Wu	1021
3050	DESIGN FEATURES OF THE GEORGE WASHINGTON BRIDGE LOWER DECK	
	By Irvine P. Gould	1022
3051	FACTOR OF SAFETY IN DESIGN OF TIMBER SCRUCTURES	
	By Lyman W. Wood	1033
	Discussion:	
	By E. George Stern	1045
	Richard G. Kimbell	1045
	Emilio Rosenblueth	1046
	Ludvik Cizek	1048
	Milos Vorlicek	1049
	Lyman W. Wood	1051
3052	SLEUTHING THE BEHAVIOR OF A RIVER	
	By Edward J. Cleary	1053
	Discussion:	
	By Bernd H. Dieterich	1066
	George E. Walker	1070
	Edward J. Cleary	1071
3053	FREEWAYS IN URBAN PLANNING	
	By Harold M. Lewis	1072
	Discussion:	
	By Richard A. Haber and William J. Miller, Jr.	1081
	George H. Herrold	1083
	Harold M. Lewis	1085

No.		Page
3054	STRUCTURAL DYNAMICS IN EARTHQUAKE-RESISTANT DESIGN	
	By John A. Blume	1088
	Discussion:	
	By Lydik S. Jasobsen	1122
	A. A. Eremin	1124
	Emilio Rosenblueth	1124
	Michael J. Murphy, R. Ivan Skinner, and Keith M. Adams	1126
	Reuben W. Binder	1128
	John A. Blume	1129
3055	RESISTANCE PROPERTIES OF SEDIMENT-LADEN STREAMS	
	By Vito A. Vanoni and George N. Nomicos	1140
	Discussion:	
	By Emmett M. Laursen	1167
	Tsung-Lien Chou	1168
	Daryl B. Simons and Everett V. Richardson	1170
	Vito A. Vanoni and George N. Nomicos	1172
3056	ELASTI-PLASTIC ANALYSIS OF CONTINUOUS FRAMES AND BEAMS	
	By Lawrence P. Johnson, Jr. and Herbert A. Sawyer, Jr.	1176
	Discussion:	
	By Giuliano Augusti	1192
	Tullio Renzulli	1194
	Emilio Rosenblueth	1198
	A. A. Eremin	1202
	Lawrence P. Johnson, Jr. and Herbert A. Sawyer, Jr.	1203
3057	AMBUKLAO ROCK-FILL DAM, DESIGN AND CONSTRUCTION	
	By E. Montford Fucik and Robert F. Edbrooke	1207
	Discussion:	
	By Frederic L. Lawton	1222
	Jose O. Lahoz	1223
	E. Montford Fucik and Robert F. Edbrooke	1226
3058	STABILITY OF COASTAL INLETS	
	By Per Brunn and Frans Gerritsen	1228
	Discussion:	
	By Robert E. Hickson	1259
	Per Bruun and Frans Gerritsen	1264
3059	DELTA PROJECT: A SYMPOSIUM	
	GENERALITIES ON COASTAL PROCESSES AND PROTECTION	
	By Johannes B. Schijf	1268
	Discussion:	
	By Richard Silvester	1278
	Johannes B. Schijf	1279
	TIDAL COMPUTATIONS IN COASTAL AREAS	
	By J. J. Dronkers	1281
	HYDRAULIC INVESTIGATIONS FOR THE DELTA PROJECT	
	By H. A. Ferguson	1290

No.		Page
3060	METEORIC VERSUS NOMETEORIC GROUND WATER By Harold E. Thomas and Donald E. White	1304
3061	HYDROLOGY OF URBAN RUNOFF By A. L. Tholin and Clint J. Keifer	1308
	Discussion:	
	By Peter O. Wolf	1355
	M. B. McPherson and Joseph Willis	1357
	Paul Bock	1361
	Carl F. Izzard and Charles L. Armentrout	1365
	A. L. Tholin	1370
	Clint J. Keifer	1373
3062	PROGRESS IN ASCE ANNUAL ADDRESS AT THE CONVENTION, RENO, NEVADA, JUNE 22, 1960 By Frank A. Marston, President	1380
	MEMOIRS OF DECEASED MEMBERS: ABSTRACTS	1393
	SUBJECT INDEX	1447
	AUTHOR INDEX	1466

ERRATA

Transactions, Vol. 124, 1959

Pages 709 and 738, footnotes 1 and 23 to read: Prof. of Civ. Engrg., Univ. of Florida, Gainesville, Fla.

Page 737, Fig. 15 (a), (b), and (c) omitted in the paper appear as Plates 1, 2, and 3, respectively, in the May 1958 Journal of the Soil Mechanics and Foundations Division, *Proceedings Paper* 1657, pp. 1657-17 to 1657-19.

Page 838, in Fig. 8, the Legend should be

Dashed line—chlorination

Solid line—no chlorination

FOREWORD

The Transactions of the American Society of Civil Engineers, Volume 125, 1960, consists of two parts, of which this is Part I. Volume 125, Part II (which is available only in cloth binding) is a Symposium on Rockfill Dams, the "core" of which is a series of papers presented before the Power Division of ASCE in June 1958 at Portland, Oregon. The decision to issue the second part to Volume 125 was made by the ASCE Committee on Publications in June 1960, in Reno, Nevada, when it became apparent that the interest in this subject warranted the publication of a volume of Transactions devoted exclusively to the science of rockfill dams.

AMERICAN SOCIETY OF CIVIL ENGINEERS

Founded November 5, 1852

TRANSACTIONS

Paper No. 3011

DIGITAL COMPUTATION FOR STIFFNESS MATRIX ANALYSIS

By John S. Archer,[1] M. ASCE

SYNOPSIS

An energy development of the basic theory for the stiffness matrix method of structural analysis is contained herein. The method is particularly adaptable to a systematic analysis of any structure which may be described as a composition of simple structural elements, such as beams and plates.

Application of the technique to the analysis of structures is presented, with an example to show how the procedure works in a typical case. The present application of the technique to the analysis of aircraft structures is also described. Some suggestions are given for a practical method of developing a similar procedure for individual needs.

INTRODUCTION

History.—The stiffness matrix type of structural analysis was described in 1944 by Gabriel Kron.[2] The first practical application of the technique using digital computers was reported by H. U. Schuerch[3] in December 1951. Samuel Levy[4] investigated the stiffness matrix procedure which was published in July and September 1953. Gilbert Best and M. Phillip Keating[5] described the technique based on their experience with the IBM 701. D. Williams[6] prepared a

Note.—Published essentially as printed here, in October, 1958, in the Journal of the Structural Division, as Proceedings Paper 1814. Positions and titles given are those in effect when the paper was approved for publication in Transactions.

1 Project Structures Engr., Convair, General Dynamics Corp., Fort Worth, Tex.

2 "Tensorial Analysis and Equivalent Circuits of Elastic Structures," by G. Kron, Journal, Franklin Inst., Vol. 238, No. 6, 1944.

3 "Vibration Mode Analysis For Delta Wing Structure," by H. U. Schuerch, Convair Memo DG-G-100, San Diego, December 18, 1951.

4 "Structural Analysis and Influence Coefficients for Delta Wings," by S. Levy, Journal of the Aeronautical Sciences, Vol. 20, No. 7, July, 1953.

5 "A Stiffness Matrix Method of Delta Wing Stress Analysis," by G. Best and M. P. Keating, Convair SRG-16, Fort Worth, Tex., September 8, 1953.

6 "Recent Developments In the Structural Approach to Aeroelastic Problems," by D. Williams, Journal of the Royal Aeronautical Society, London, Eng., June, 1954.

comprehensive paper on the subject. The following year the technique of using matrix algebra for the analysis of aircraft structures was published by Raymond L. Bisplinghoff.[7]

Theory.—Let U represent the strain energy stored within a structure that is loaded by the forces $P_1, P_2, \ldots, P_i, \ldots, P_n$. The temperature of the material remains constant and the supports are rigid. Applying Castigliano's theorem of structure equilibrium (Theorem I):

$$P_i = \frac{\partial U}{\partial \delta_i} \quad \ldots\ldots\ldots\ldots\ldots\ldots \quad (1)$$

in which δ_i is the deflection of the point of application of the load P_i in the direction of P_i.

If the strain energy is evaluated in terms of the loads P_i acting upon the structure we may expand Eq. 1 as follows:

$$P_i = \frac{\partial U}{\partial \delta_i} = \sum_j \left(\frac{\partial U}{\partial P_j}\right)\left(\frac{\partial P_j}{\partial \delta_i}\right) \quad \ldots\ldots\ldots\ldots\ldots \quad (2)$$

If the structure is assumed to be elastic, then Castigliano's theorem for linear structures (Theorem II) may be applied:

$$\delta_j = \frac{\partial U}{\partial P_j} \quad \ldots\ldots\ldots\ldots\ldots\ldots \quad (3)$$

Substituting Eq. 3 into Eq. 2,

$$P_i = \sum_j \delta_j \left(\frac{\partial P_j}{\partial \delta_i}\right) \quad \ldots\ldots\ldots\ldots\ldots\ldots \quad (4)$$

The partial derivative $\frac{\partial P_j}{\partial \delta_i}$ represents the force developed at point j due to a deflection of point i, all other points remaining fixed. This force is represented by the symbol s_{ji}, the subscript j representing the point at which the force acts, and the subscript i representing the point at which the unit deflection is imposed. With this substitution, Eq. 4 becomes:

$$P_i = \sum_j \delta_j s_{ji} \quad \ldots\ldots\ldots\ldots\ldots\ldots \quad (5)$$

From Betti's Law or the generalized Maxwells' law of reciprocal deflections we obtain the relation

$$s_{ji} = s_{ij} \quad \ldots\ldots\ldots\ldots\ldots\ldots \quad (6)$$

and, hence,

$$P_i = \sum_j \delta_j s_{ij} \quad \ldots\ldots\ldots\ldots\ldots\ldots \quad (7)$$

Writing Eq. 7 in its expanded form,

$$P_i = s_{i1}\delta_1 + s_{i2}\delta_2 + \ldots + s_{ij}\delta_j + \ldots + s_{in}\delta_n \quad \ldots\ldots \quad (8)$$

---

[7] "Aeroelasticity," by R. L. Bisplinghoff, H. Ashley and R. L. Halfmann, Addison-Wesley Publishing Co. Inc., Cambridge, Mass., 1955.

It is evident from the expanded form that Eq. 7 is a superposition equation expressing the total load at point i as the sum of the loads developed by each deflection component δ_j acting by itself. Each part of Eq. 7 describes an independent component of the structural behavior. The components may represent translation or rotation. The total number of components is the number of degrees of freedom that the idealized structure possesses.

Using matrix algebra notation, Eq. 7 may be rewritten as

$$P = S\,\delta \qquad (9)$$

in which P is a vector or column matrix made up of load components $P_1, P_2, \ldots, P_i, \ldots, P_n$; and δ is a vector made up of the deflection components $\delta_1, \delta_2, \ldots, \delta_i, \ldots \delta_n$, and S is a square matrix consisting of an ordered array of the stiffness influence coefficients s_{ij} of Eq. 7. Matrix S is called the stiffness matrix of the structure. In the expanded form, Eq. 9 appears as follows:

$$\begin{Bmatrix} P_1 \\ P_2 \\ \vdots \\ P_i \\ \vdots \\ P_n \end{Bmatrix} = \begin{bmatrix} s_{11} & s_{12} & \cdots & s_{1j} & \cdots & s_{1n} \\ s_{21} & s_{22} & & s_{2j} & & s_{2n} \\ \vdots & \vdots & & \vdots & & \vdots \\ s_{i1} & s_{i2} & & s_{ij} & & s_{in} \\ \vdots & \vdots & & \vdots & & \vdots \\ s_{n1} & s_{n2} & \cdots & s_{nj} & \cdots & s_{nn} \end{bmatrix} \begin{Bmatrix} \delta_1 \\ \delta_2 \\ \vdots \\ \delta_j \\ \vdots \\ \delta_n \end{Bmatrix} \qquad \ldots\ldots (10)$$

Eq. 9 may be manipulated similar to an ordinary algebraic equation. For instance, it may be solved for the deflections by premultiplying both sides of the equation by the inverse of the stiffness matrix S.

$$\delta = S^{-1}\,P = F\,P \qquad (11)$$

The symbol F represents the inverse of the stiffness matrix which in turn represents the flexibility influence coefficient matrix. It is composed of an ordered array of the flexibility influence coefficients $f_{i\,j}$. In the expanded form it appears as follows:

$$\begin{Bmatrix} \delta_1 \\ \delta_2 \\ \cdot \\ \cdot \\ \cdot \\ \delta_i \\ \cdot \\ \cdot \\ \cdot \\ \delta_n \end{Bmatrix} = \begin{bmatrix} f_{11} & f_{12} \cdots f_{1j} \cdots f_{1n} \\ f_{21} & f_{22} \cdots f_{2j} \cdots f_{2n} \\ \cdot & \cdot \quad \cdot \quad \cdot \\ \cdot & \cdot \quad \cdot \quad \cdot \\ \cdot & \cdot \quad \cdot \quad \cdot \\ f_{i1} & f_{i2} \cdots f_{ij} \cdots f_{in} \\ \cdot & \cdot \quad \cdot \quad \cdot \\ \cdot & \cdot \quad \cdot \quad \cdot \\ \cdot & \cdot \quad \cdot \quad \cdot \\ f_{n1} & f_{n2} \cdots f_{nj} \cdots f_{nn} \end{bmatrix} \begin{Bmatrix} P_1 \\ P_2 \\ \cdot \\ \cdot \\ \cdot \\ P_j \\ \cdot \\ \cdot \\ \cdot \\ P_n \end{Bmatrix} \quad \ldots (12)$$

In a typical problem, Eq. 11 must be constructed and solved for the deflections in terms of the loads. The direct determination of the coefficients f_{ij} of Eq. 11 is difficult and impractical for a large indeterminate structure. However, the coefficients s_{ij} of Eq. 9 are readily calculated. The usual procedure is to compute the stiffness matrix coefficients directly from the known properties of the individual elements of the idealized structure. The coefficients of the flexibility matrix are obtained through the mathematical operation of inverting the stiffness matrix.

After the deflections of the structure are found, the stresses developed in the structure may be determined. This is accomplished by using the stiffness matrix of the individual elements of the structure. Using computed deflections and equations of the same type as Eq. 9, the internal loads on individual parts of the structure are obtained readily. After the internal forces on the individual elements have been obtained, the stresses in the structure can be readily computed.

PRESENT APPLICATIONS

Structure analyses have been performed on the IBM 701 for structures having up to 106 independent coordinates. The structures analyzed were idealized as a group of interconnected structural elements. These elements consisted of beams, torque tubes, torque boxes, and concentrated springs (Fig. 1). The procedure followed for a typical stress analysis was as follows:

1. Compute the stiffness matrices for the individual structural elements (Fig. 2(a)). Store the results on magnetic tape.
2. Assemble the stiffness matrix for the complete structure by bringing together the coefficients for all structural elements and adding corresponding coefficients (Fig. 2(b)). Individual coordinate identification numbers are indispensible for keeping the coefficients in order.
3. Invert the stiffness matrix to obtain the flexibility matrix for the structure ($F = S^{-1}$).
4. Compute the deflections by determining the matrix product of the applied load vector and the flexibility matrix ($\delta = F\,P$).

5. Compute the internal forces on the individual structural elements by computing the product of the appropriate deflections with the stiffness matrices for the individual structural elements.

$$\begin{Bmatrix} P_{2A} \\ P_{3A} \end{Bmatrix} = [A] \begin{Bmatrix} \delta_2 \\ \delta_3 \end{Bmatrix} \quad \ldots\ldots\ldots (13a)$$

$$\begin{Bmatrix} P_{3B} \\ P_{4B} \end{Bmatrix} = [B] \begin{Bmatrix} \delta_3 \\ \delta_4 \end{Bmatrix} \quad \ldots\ldots\ldots (13b)$$

$$\begin{Bmatrix} P_{1C} \\ P_{2C} \\ P_{5C} \\ P_{6C} \end{Bmatrix} = [C] \begin{Bmatrix} \delta_1 \\ \delta_2 \\ \delta_5 \\ \delta_6 \end{Bmatrix} \quad \ldots\ldots\ldots (13c)$$

and

$$\begin{Bmatrix} P_{6D} \\ P_{7D} \end{Bmatrix} = [D] \begin{Bmatrix} \delta_6 \\ \delta_7 \end{Bmatrix} \quad \ldots\ldots\ldots (13d)$$

The largest problems, of the order of 106 independent coordinates, required a total of 4 hr to assemble the stiffness matrix and 8 hr to invert in order to obtain the flexibility matrix. Double precision arithmetic was used in this operation. Each stress calculation for a given load condition was obtained in an additional $1\frac{1}{2}$ hr of computing time. Smaller problems were solved in considerably less time.

The analysis of beam elements was performed considering bending deformation only. A linear variation in moment of inertia from one end of a beam to the other was assumed. In addition to the stress analyses, normal mode analyses were successfully performed. In such an analysis, the natural frequencies and normal mode shapes were computed by an iteration technique.

The IBM 704 is much faster and has a larger speed storage capacity than the 701 computer. Therefore, a substantial savings in time can be realized by its use. Experience indicates that a matrix representing 100 independent coordinates can be assembled in 1 hr and inverted in 3 hr.

The 704 computer program has incorporated the following additions and refinements to the aforementioned 701 computer program:

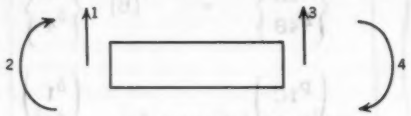
1. Shear deformation is included in the analysis of beams.
2. Effect of tapering flanges is computed.
3. Rectangular structural plates may be analyzed using a lattice analogy representation.
4. Beam moments of inertia are automatically computed if desired.
5. Length and direction of beams are determined by the computer from basic geometric input.

The stiffness matrix structural analysis has been coded on the Remington Rand 1103, a computer comparable to the IBM 701. The sizes of the problems

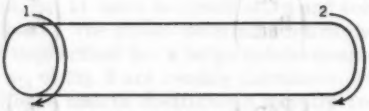
worked by the 1103 computer were generally smaller than those worked by the 701 computer. However, the speed with which a given problem could be worked was greater for the 1103.

APPLICATION TO STRUCTURES

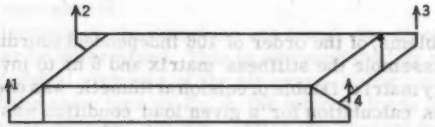
Indeterminate Trusses.—A bridge truss could be analyzed easily by the stiffness matrix technique, but because the analysis of a determinate truss problem is simple, it would not be worthwhile to analyze it on a high-speed



(*a*) BEAM SEGMENT



(*b*) TORQUE TUBE



(*c*) TORQUE BOX



(*d*) CONCENTRATED SPRING

FIG. 1.—INDIVIDUAL ELEMENT STIFFNESS MATRIX

digital computer. This is not always the case in the design of an indeterminate truss.

Consider the truss in Fig. 3(a). The distortion and loads on this structure can be described by two orthogonal displacements at each joint. Hence, the analysis of the structure requires a matrix of order 17 for its solution. If a secondary stress analysis is required, it may be obtained simultaneously with the primary analysis. However, a rotation displacement at each joint must be represented, requiring a matrix of order 27 for its solution (Fig. 3(b)). The stress analysis of the truss gives the forces in all members and the deflections of all joints. For a structure of this type the order of the matrix is generally much greater than the degree to which the structure is indeterminate.

Building Frames.—For the simple building bent (Fig. 4(a)) the distortion is completely defined by five coordinates: One rotation at each joint, and one displacement at the roof level. Even in the case of a more complicated broken story bent (Fig. 4(b)) only twelve coordinates are necessary.

It is evident from these examples that the analysis of building frames could be accomplished by using the stiffness matrix technique of analysis. If three-

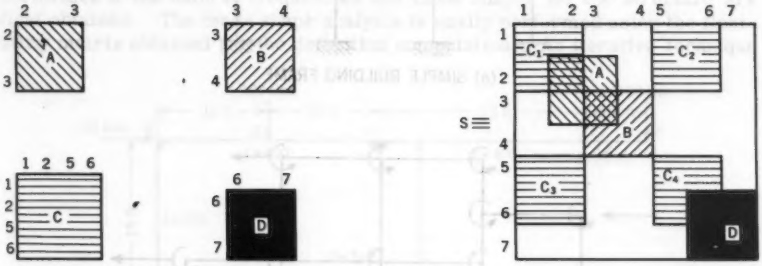
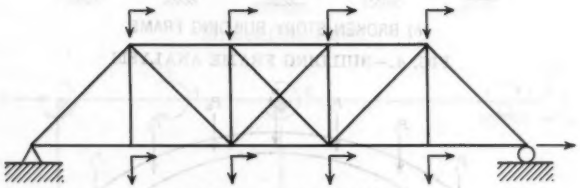
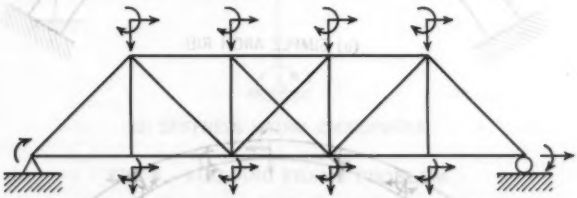


FIG. 2.—STIFFNESS MATRIX PROCEDURE



(a) PRIMARY STRESS ANALYSIS

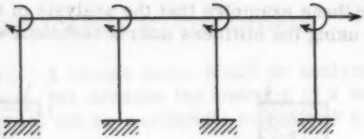


(b) PRIMARY AND SECONDARY STRESS ANALYSIS

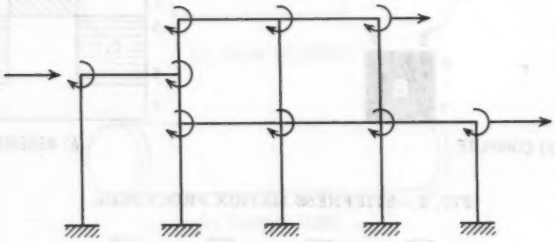
FIG. 3.—INDETERMINATE TRUSS ANALYSIS

dimensional frames are to be analyzed, the torsion of the building, as well as axial deformation of the columns may be included. The computed answer in this type of problem gives the rotation and translation of each end of the columns and beams, and the moments in the members.

Miscellaneous Structures.—The arch rib structure, Fig. 5(a), may be represented by a series of straight beam segments between the load points. The distortion and loading of the structure can then be represented by a system of coordinates (Fig. 5(b)). Twenty-one coordinates are required for a stiffness

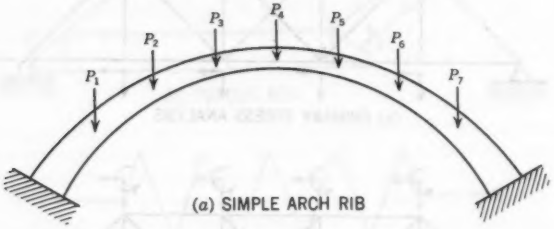


(*a*) SIMPLE BUILDING FRAME

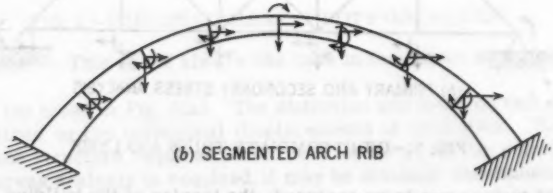


(*b*) BROKEN STORY BUILDING FRAME

FIG. 4.—BUILDING FRAME ANALYSIS



(*a*) SIMPLE ARCH RIB



(*b*) SEGMENTED ARCH RIB

FIG. 5.—ARCH RIB ANALYSIS

matrix analysis. Moments, shears, and axial thrusts are computed at each end of each segment. The stiffness matrix technique can also be used in the analysis of arch dams, suspension bridges, towers, and shell-type structures. A

stiffness matrix analysis on high-speed computers makes it practical to analyze shells subjected to complex asymmetrical air load distributions.

Natural Mode Analysis.—Most structures are not analyzed to determine their response to dynamic forces with two possible exceptions: (1) The structure analyzed to determine the effect of earthquakes upon it, and (2) the structure designed to resist the effect of a bomb blast. In either case, the computation of the dynamic response of the structure to a transient load is easily performed if the natural frequencies and mode shapes for the structure are first obtained. The mode shape analysis is easily performed using the flexibility matrix obtained for the deflection computation. An iterative technique

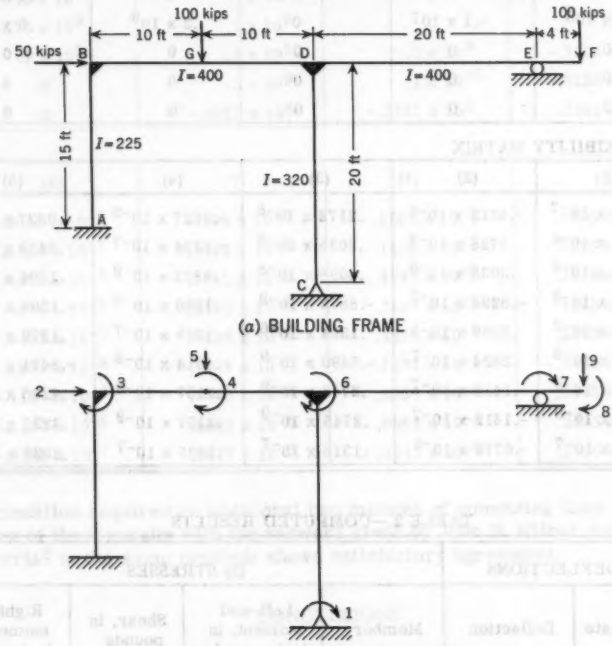


FIG. 6.—BUILDING FRAME PROBLEM

converging on the lowest mode has given the best results.

Example.—The building frame (Fig. 6(a)) has been analyzed on the 704 computer for the load condition shown. Five punched data cards contained the input geometry, stiffness, and load data. The load and deflection coordinates used for the stiffness matrix are shown in Fig. 6(b).

The stiffness matrix (Table 1(a)) and the flexibility matrix (Table 1(b)) were computed, assembled, and printed in four minutes on the 704 computer. The deflections in Table 2(a) and the stresses in Table 2(b) obtained for the given

TABLE 1.—COMPUTED

(a) STIFFNESS MATRIX

(1)	(2)	(3)	(4)	(5)
$.16 \times 10^9$	$-.1 \times 10^7$	0	0	0
$-.1 \times 10^7$	$.22 \times 10^5$	$-.125 \times 10^7$	0	0
0	$-.125 \times 10^7$	$.55 \times 10^9$	$.2 \times 10^9$	$-.5 \times 10^7$
0	0	$.2 \times 10^9$	$.8 \times 10^9$	0
0	0	$-.5 \times 10^7$	0	$.16 \times 10^4$
$.8 \times 10^8$	$-.1 \times 10^7$	0	$.2 \times 10^9$	$.5 \times 10^7$
0	0	0	0	0
0	0	0	0	0
0	0	0	0	0

(b) FLEXIBILITY MATRIX

(1)	(2)	(3)	(4)	(5)
$.1005 \times 10^{-7}$	$.5312 \times 10^{-6}$	$.2172 \times 10^{-8}$	$-.3027 \times 10^{-9}$	$.9397 \times 10^{-7}$
$.5312 \times 10^{-6}$	$.8725 \times 10^{-4}$	$.3035 \times 10^{-6}$	$-.8294 \times 10^{-7}$	$.8259 \times 10^{-5}$
$.2172 \times 10^{-8}$	$.3035 \times 10^{-6}$	$.4098 \times 10^{-8}$	$.8873 \times 10^{-9}$	$.1394 \times 10^{-6}$
$-.3027 \times 10^{-9}$	$-.8294 \times 10^{-7}$	$-.8873 \times 10^{-9}$	$.1580 \times 10^{-8}$	$-.1368 \times 10^{-7}$
$.9397 \times 10^{-7}$	$.8259 \times 10^{-5}$	$.1394 \times 10^{-6}$	$-.1368 \times 10^{-7}$	$.1272 \times 10^{-4}$
$-.9608 \times 10^{-9}$	$.2824 \times 10^{-7}$	$-.5490 \times 10^{-9}$	$-.4314 \times 10^{-9}$	$-.8471 \times 10^{-7}$
$.4804 \times 10^{-9}$	$-.1412 \times 10^{-7}$	$.2745 \times 10^{-9}$	$.2157 \times 10^{-9}$	$.4235 \times 10^{-7}$
$.4804 \times 10^{-9}$	$-.1412 \times 10^{-7}$	$.2745 \times 10^{-9}$	$.2157 \times 10^{-9}$	$.4235 \times 10^{-7}$
$.2306 \times 10^{-7}$	$-.6776 \times 10^{-6}$	$.1318 \times 10^{-7}$	$.1035 \times 10^{-7}$	$.2033 \times 10^{-5}$

TABLE 2.—COMPUTED RESULTS

(a) DEFLECTIONS		(b) STRESSES			
Coordinate (1)	Deflection (2)	Member (3)	Left-end moment, in inch=pounds (4)	Shear, in pounds (5)	Right-end moment, in inch=pounds (6)
1	0.0383[a]	AB	$.4118 \times 10^7$	-33,074	$-.1835 \times 10^7$
2	5.1200[b]	BG	$-.1835 \times 10^7$	-27,603	$-.5148 \times 10^7$
3	0.0304[a]	GD	$-.5148 \times 10^7$	72,397	$.3540 \times 10^7$
4	-0.00448[a]	DE	$-.5224 \times 10^6$	22,176	$.4800 \times 10^7$
5	1.8890[b]	EF	$.4880 \times 10^7$	-100,000	0
6	-0.0125[a]	CD	....	-16,126	$-.4062 \times 10^7$
7	0.0303[a]	..	....	....	....
8	0.0399[a]	..	....	....	....
9	1.7600[b]	..	....	....	....

[a] In radians. [b] In inches.

MATRIX COEFFICIENTS

(6)	(7)	(8)	(9)
$.8 \times 10^8$	0	0	0
$-.1 \times 10^7$	0	0	0
0	0	0	0
$.2 \times 10^9$	0	0	0
$.5 \times 10^7$	0	0	0
$.76 \times 10^9$	$.1 \times 10^9$	0	0
$.1 \times 10^9$	$.12 \times 10^{10}$	$.5 \times 10^9$	$-.3125 \times 10^8$
0	$.5 \times 10^9$	$.1 \times 10^{10}$	$-.3125 \times 10^8$
0	$-.3125 \times 10^8$	$-.3125 \times 10^8$	$.1302 \times 10^7$

(6)	(7)	(8)	(9)
$-.9608 \times 10^{-9}$	$.4804 \times 10^{-9}$	$.4804 \times 10^{-9}$	$.2306 \times 10^{-7}$
$.2824 \times 10^{-7}$	$-.1412 \times 10^{-7}$	$-.1412 \times 10^{-7}$	$-.6776 \times 10^{-6}$
$-.5490 \times 10^{-9}$	$.2745 \times 10^{-9}$	$.2745 \times 10^{-9}$	$.1318 \times 10^{-7}$
$-.4314 \times 10^{-9}$	$.2157 \times 10^{-9}$	$.2157 \times 10^{-9}$	$.1035 \times 10^{-7}$
$-.8471 \times 10^{-7}$	$.4235 \times 10^{-7}$	$.4235 \times 10^{-7}$	$.2033 \times 10^{-5}$
$.2275 \times 10^{-8}$	$-.1137 \times 10^{-8}$	$-.1137 \times 10^{-8}$	$-.5459 \times 10^{-7}$
$-.1137 \times 10^{-8}$	$.5569 \times 10^{-8}$	$.5569 \times 10^{-8}$	$.2673 \times 10^{-6}$
$-.1137 \times 10^{-8}$	$.5569 \times 10^{-8}$	$.9569 \times 10^{-8}$	$.3633 \times 10^{-6}$
$-.5459 \times 10^{-7}$	$.2673 \times 10^{-6}$	$.3633 \times 10^{-6}$	$.1590 \times 10^{-4}$

load condition required an additional two minutes of computing time. A comparison of these results with the answers given by John B. Wilbur and Charles H. Norris[8] to the same problem shows satisfactory agreement.

CONCLUSIONS

A major drawback to the application of high-speed digital computers is the initial difficulty of having a given type of problem set up and coded. This operation is expensive because it requires trained coding personnel and, generally, an expert in the field in which the problem will be used. If the problem is large, it requires a considerable effort for checkout to the point where the program is operational. Therefore, the use of a digital computer can be justified only if several problems are to be solved, or if the problem can be solved only by using the computer.

Several alternatives are available to surmount this difficulty. One such alternative is to join other interested parties to develop the required programs on a joint basis. If an accessible university has adequate computing facilities, the required coding may be obtained economically through monetary support

[8] "Elementary Structural Analysis," by J. B. Wilbur and C. H. Norris, McGraw-Hill Book Co., Inc., New York, 1958.

of a graduate thesis topic. Finally, there is the possibility of developing the required program by modification of an existing program obtained from other users of similar computers.

Structural analysis problems of all types can be solved on high-speed computers using the stiffness matrix technique. This procedure appears particularly adaptable to the use of high-speed digital computers. The application of the technique to the solution of structural problems presents no greater difficulties than those already surmounted for the analysis of aircraft structures.

AMERICAN SOCIETY OF CIVIL ENGINEERS

Founded November 5, 1852

TRANSACTIONS

Paper No. 3012

CELLULAR COFFERDAMS AND DOCKS

By Edward M. Cummings,[1] F. ASCE

With Discussion by Messrs. Samuel Heyman, Cevdet Z. Erzen, and Edward M. Cummings.

SYNOPSIS

A theory is presented for the design against failure by tilting of cellular cofferdams. This theory is substantiated by model tests and gives results that are consistent with those obtained in the field. Several previously published theories are examined and important inconsistencies are noted. The proposed theory is then used to investigate the design of a cofferdam on rock and a dock in sand.

INTRODUCTION

The first cellular cofferdam was constructed at Black Rock Harbor, near Buffalo, N. Y. in 1908. This was followed by the construction, in 1910, of a cofferdam around the sunken battleship Maine in Havana Harbor, Cuba. Since that time cellular cofferdams have become quite common in the construction of dams, locks, sewage-disposal plants, and other structures that cover comparatively large areas. Cellular-type structures have also been used for permanent installations such as docks, retaining walls, breakwaters, piers, drydocks, wet berths for floating drydocks, lock walls, and mooring dolphins.

TYPES OF CELLULAR COFFERDAMS

Three types of cellular cofferdams are shown in Fig. 1. For the circular-cell type, Fig. 1(a), the quantity of steel sheet piling is practically constant for

Note.—Published, essentially as printed here, in September, 1957, in the Journal of the Waterways and Harbors Division, as Proceedings Paper 1366. Positions and titles given are those in effect when the paper or discussion was approved for publication in Transactions.

[1] Sales Mgr., Bethlehem Steel Co., Bethlehem, Pa.

a cofferdam of a given depth regardless of the diameter of the cells. Because of this, for structures of more than average depth, less steel is usually required than for the diaphragm type, Fig. 1(b). Designers can therefore increase the safety factor without additional cost except for the need for additional fill. For structures such as docks, however, even the quantity of fill is a constant. Another advantage of the circular-cell type is that each cell may be filled individually. This is of importance in rough water where storms are apt to demolish empty cells. Also, in swiftly flowing or rough water, it is possible to erect successive cells by moving the pile-driving equipment onto the previously filled cell. Therefore, the circular-cell type is usually selected for the deepest and most difficult jobs.

The diaphragm-type cofferdam, Fig. 1(b), usually requires less sheet piling for cofferdams of average or less than average height, and is considered by most contractors to be somewhat easier and more economical to construct in quiet water than the circular-cell type. The cells should be filled in stages in order not to dislocate the crosswalls. It is usual practice during filling not to permit the level of fill in one cell to vary by more than 5 ft from that in the adjacent cells. For very deep cofferdams, close spacing of the crosswalls is necessary to keep the interlock tension within permissible limits. However, this reduced spacing increases the quantity of sheet piling beyond that needed for circular-cell cofferdams.

The modified circular-cell cofferdam, Fig. 1(c), has been used infrequently. Its advantage is that it is simpler to construct than the circular-cell type, and each cell can be filled separately. The stresses in the special piles at the junctures of the arcs must be investigated with special care. This type is not recommended for cofferdams of extreme depth.

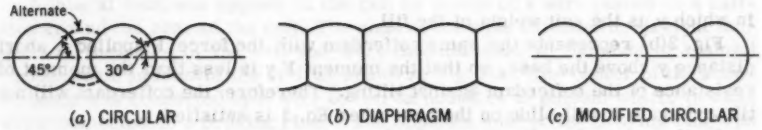
Notation.—The letter symbols adopted for use in this paper are defined where they first appear, in the illustrations or in the text, and are arranged alphabetically for convenience of reference in the Appendix.

CELLULAR COFFERDAMS ON ROCK

In designing cellular cofferdams on rock, the possible methods of failure that must be investigated are (a) sliding on the rock, (b) bursting of the cells due to tension failure of the sheet-pile interlocks, and (c) excessive leaning or tilting of the cells due to shear failure of the fill inside the cells.

Interior-Sliding Theory.—The material contained herein is based on the premise that the stability of a cellular cofferdam against failure by tilting depends largely on the horizontal shear resistance of the soil in the cells, with interlock friction assisting to a lesser extent.

Fig. 2(a) represents a cofferdam of height H and average width b filled with sand having an angle of internal friction ϕ. It is further assumed for this case that interlock friction is zero, and that the cofferdam depends entirely on the fill for its stability. Also, the angle of friction between the base of the cofferdam and the rock is assumed to be ϕ. If a force, F, per unit of length of the



(a) CIRCULAR (b) DIAPHRAGM (c) MODIFIED CIRCULAR

FIG. 1.—TYPES OF CELLULAR COFFERDAMS

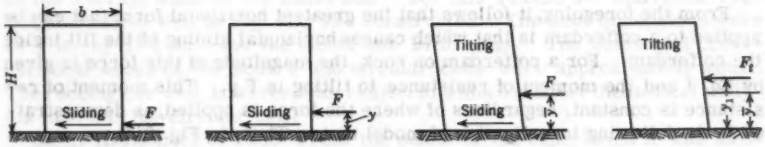


FIG. 2.—COFFERDAM ON ROCK



FIG. 3.—MODEL OF CIRCULAR COFFERDAM

cofferdam is applied very close to the base, the cofferdam will begin to slide on the base when

$$F = \gamma H b \tan \phi \quad \ldots\ldots\ldots\ldots\ldots\ldots \quad (1)$$

in which γ is the unit weight of the fill.

Fig. 2(b) represents the same cofferdam with the force F applied a short distance y above the base, so that the moment F y is less than the moment of resistance of the cofferdam against tilting. Therefore, the cofferdam will not tilt and again it will slide on the base when Eq. 1 is satisfied.

As the point of application of the force is raised, a point will be reached where the cofferdam continues to slide and also starts to tilt, as shown in Fig. 2(c). Because it is known that the force necessary to make the cofferdam slide is given by Eq. 1, one can conclude that this is also the force that makes the cofferdam tilt when applied at the distance $\bar{y}$ above the base. The moment of resistance against tilting is therefore $F \bar{y}$.

When a force F_t sufficient to make the cofferdam tilt is applied at a distance y_1 (which is greater than $\bar{y}$) above the base, as shown in Fig. 2(d), the cofferdam will not slide because $F_t < F$.

From the foregoing, it follows that the greatest horizontal force that can be applied to a cofferdam is that which causes horizontal sliding of the fill inside the cofferdam. For a cofferdam on rock, the magnitude of this force is given by Eq. 1 and the moment of resistance to tilting is $F \bar{y}$. This moment of resistance is constant, regardless of where the force is applied, as demonstrated in the following investigation of model tests. Thus, in Fig. 2(d),

$$F_t y_1 = F \bar{y} \quad \ldots\ldots\ldots\ldots\ldots\ldots \quad (2)$$

From Eq. 2 it follows that the moment of resistance against tilting remains constant for distributed loads, such as water pressure or earth pressure.

Model Tests.—In the subsequent description of the model tests, a theory is developed that determines the magnitude of the moment of resistance against tilting. The load measurements demonstrate very close agreement with the theory, and the theory indicates reasonable safety factors for the large number of successful cofferdams that have been constructed.

Model Cells.—In 1947 the writer began experimenting with model cells in an effort to develop the foregoing theory, and the model shown in Fig. 3 was constructed. The diameter and height of this model were both 24 in. Wood staves $\frac{5}{16}$ in. by $1\frac{1}{2}$ in. by 2 ft were selected to simulate sheet piles. A screw-eye was placed in the outside of each stave at $\frac{1}{2}$ in., 8 in., and 1 ft $11\frac{1}{2}$ in. from the bottom, and light wire was threaded through the screw-eyes to retain the staves in a circular shape. The cell rested on a platform and preliminary tests showed that the friction between a wooden platform and the fill was not great enough to develop the shear of the fill inside the cell. Consequently, a concrete base with a rough surface was placed on the wooden platform.

The staves comprising the shell of the cell were placed loosely with spaces between them of approximately $\frac{1}{8}$ in. Because they were not in contact, no interlock friction could be developed as in the steel sheet-pile prototype, and it was possible to study the action of the fill separately.

The fill selected for the cell was fine crushed stone of graded sizes, the largest particle being approximately $\frac{1}{2}$ in. in its greatest dimension. The fill weighed 91.9 lb per cu ft. Stone was selected rather than sand because it did

not flow between the cracks of the staves and because it was completely non-cohesive. It was thought that even slight cohesion or arching in the sand might confuse the results in a model test, whereas they would not be important in the full-scale prototype.

A lateral load was applied to the cell by means of a wire placed in a half-loop around the rear of the cell. The ends of the wire extended in straight tangents at the sides of the cell and were then fastened to the ends of a small wooden beam in front of the cell, as shown in Fig. 3(a). The center of the wooden beam was connected by a wire to two turnbuckles in tandem which, in turn, were connected to a proving ring. The opposite side of the proving ring was connected to a wooden beam that reacted against a knee-braced frame. The sills of the frame extended under and were fastened to the platform on which the cell rested resulting in a closed system.

This arrangement permitted the testing of the cell with a lateral load applied at any elevation from the bottom of the cell to the top. Fig. 3(b) shows the model circular cell loaded to failure with the load applied 8 in. from the bottom.

The computations of stability of cellular cofferdams are customarily based on the average width of the cofferdam. For this reason the equivalent rectangular model cell in Fig. 4(a) was constructed. The plan dimensions were 24 $\frac{1}{2}$ in. by 19 $\frac{1}{8}$ in., and the model was 24 in. high. The horizontal cross-sectional areas of the square and circular cells were approximately equal. The rectangular cell, however, was subject to a much simpler theoretical analysis than was the circular cell.

Shear Resistance of Fill.—From the outset of the experiment it was theorized that the fill inside a cell does not remain in an active-pressure state when the cell is subjected to lateral pressure, and that the vertical shear of the fill is increased by the lateral pressure. It was decided that a logical approach would be to compare the vertical shear of the fill when the cell was first loaded laterally and then not loaded. To accomplish this, three wooden test blocks of rectangular cross section were placed in the fill as shown in Fig. 5(a) for the circular cell and Fig. 6(a) for the rectangular cell. The test blocks were all cut from a smooth white-pine plank, their dimensions being $\frac{3}{4}$ in. by 2 $\frac{1}{2}$ in. by 2 ft 2 in. The width of each block was placed normal to the direction of lateral load, as shown in Fig. 4(b). The blocks were carefully placed in the empty cell and held in position as the fill was placed loosely around them, in order not to develop any unusual pressure conditions in the fill surrounding the blocks.

Using the gallows frame shown in Fig. 4(b), and by means of a turnbuckle and spring balance, the force required to pull each wooden block was determined. Fig. 5(b) shows the pull required with no lateral load for each block for the circular cell, and Fig. 6(b) shows the pull for the rectangular cell.

It was found that for consistent results a cell could be used for only one experiment. Therefore, after the pull tests were completed, the cell in each case was dismantled and rebuilt. The circular cell was then laterally loaded with a 250-lb force applied 8 in. from the base, and with this load held constant, each wooden block was pulled. The same procedure was followed for the rectangular cell, except that the lateral load was 200 lb. The results of these pull tests are shown in Fig. 5(c) for the circular cell and 6(c) for the rectangular cell. Each value for the circular cell is the result of three tests—for the rectangular cell, one test.

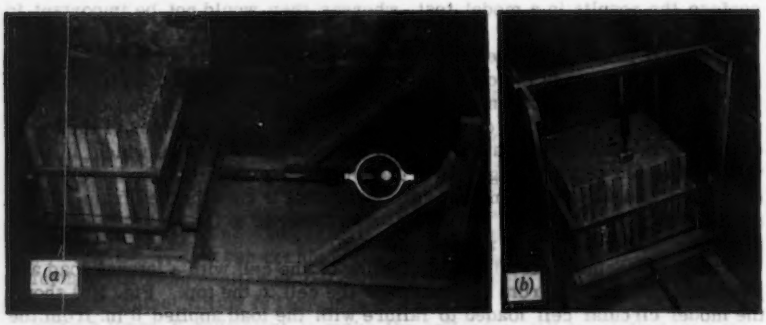
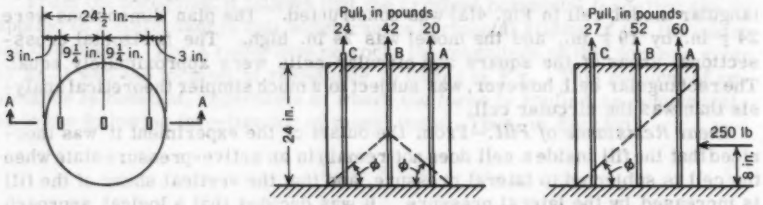
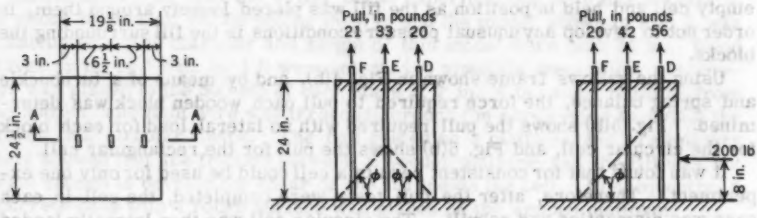


FIG. 4.—EQUIVALENT RECTANGULAR CELL



(a) PLAN (b) SECTION A–A WITH NO LATERAL LOAD (c) SECTION A–A WITH LATERAL LOAD OF 250 LB

FIG. 5.—PULL TESTS FOR CIRCULAR CELL



(a) PLAN (b) SECTION A–A WITH NO LATERAL LOAD (c) SECTION A–A WITH LATERAL LOAD OF 200 LB

FIG. 6.—PULL TESTS FOR RECTANGULAR CELL

The following inferences may be drawn from a comparison of the forces required to pull the wooden blocks when the cells were not laterally loaded as shown in Figs. 5(b) and 6(b) and then laterally loaded, as shown in Figs. 5(c) and 6(c):

1. The force required to pull the blocks is an indication of the magnitude of the vertical shear in the fill.

2. The pull required for the blocks in the center of each cell before lateral load is applied is considerably greater than for the blocks near the outside of the cell. This led to the conclusion that the fill under the ϕ-lines shown in Figs. 5(b) and 6(b) is in a different shear condition than the balance of the fill. The material beneath the ϕ-cone may be said to be at rest, and the balance of the material is in an active-pressure state.

3. It should be noted that block A, for the circular cell, Fig. 5, required only a 20-lb pull for the cell not loaded, but the pull increased to 60 lb when a lateral load of 250 lb was applied to the cell. Similarly, for the rectangular cell, Fig. 6, block D required only 20 lb for the cell not laterally loaded, and 56 lb when a lateral load of 200 lb was applied.

4. Of equal importance is the fact that block C for the unloaded circular cell required a 24-lb pull, while for the loaded cell there was hardly any increase, the pull being 27 lb. Likewise, for the rectangular cell, block F required a 21-lb pull for the unloaded cell, whereas only 20 lb was required for the loaded cell.

5. Blocks B and E, both in the middle of the respective cells, experienced increase in shear resistance over the condition described in item 2.

The conclusion is drawn from the foregoing that the shear condition of the fill was completely transformed by the lateral pressure applied to the cell. Furthermore, increase in shear was not transmitted horizontally across the full width of the cell, as the effect of lateral pressure on one side was lost on the other side of the cell. This observation led to the conclusion that the fill above the ϕ-lines of Figs. 5(c) and 6(c) remained substantially in an active-pressure state, whereas the part of the fill below the ϕ-lines changed to a passive-pressure state as a result of the application of the lateral load.

The foregoing experiments led to the following conclusions concerning the action of the fill in a cellular cofferdam:

Fig. 7(a) represents the cross section of a sand-filled cellular cofferdam on a horizontal rock base, the cofferdam having tilted due to lateral pressure, as indicated by the dotted lines. The line A-B represents a plane at the angle ϕ to the base. The shear resistance of the fill on plane AB is exactly equal to the tendency of the fill above to slide on the plane AB, because ϕ is the angle of internal friction. As the cofferdam tilts, A moves to A', and the new plane A'B makes an angle with the base greater than ϕ. The shear resistance on plane A'B is less than the tendency to slide on that plane. Therefore, as the cofferdam tilts, the fill above plane A'B slides down the steepened slope within the limitations imposed by the sheet piling. The fill that lies below plane AB is transformed into a passive-pressure state by the lateral pressure, and is surcharged by the fill above that plane.

Theory of Resistance to Failure by Tilting.—Fig. 7(b) represents the tilting failure of a cellular cofferdam by sliding on planes parallel to the rock base, which is assumed horizontal. The plane AB is plotted at the angle ϕ.

In Fig. 7(c) the line AB again represents a plane at the angle ϕ to the horizontal base. As previously noted, the fill above plane AB slides on AB when

the cofferdam tilts. Therefore, in developing the maximum resistance of the cofferdam to tilting, no internal lateral resistance is accumulated between the top of the cofferdam at point F, and point A. The sheet-pile envelope, stiffened by the fill above point A, serves to transmit forces applied to the exterior of the cofferdam above point A, to the completely confined material within the prism ABG.

In Fig. 7(c) the force F_y which develops the ultimate lateral shear resistance accumulated at any depth y below A is equivalent to the resistance to sliding

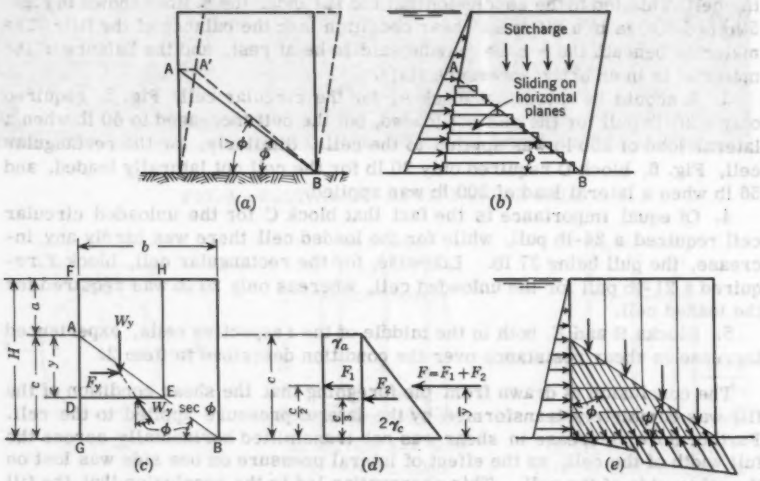


FIG. 7.—SAND-FILLED CELLULAR COFFERDAM ON A HORIZONTAL ROCK BASE

of the prism FHED on plane DE, which in turn, is equal to the weight W_y of the prism times the tangent of the angle of internal friction, ϕ. Thus,

$$F_y = W_y \tan \phi \quad \ldots\ldots\ldots\ldots\ldots\ldots \quad (3)$$

and

$$W_y = \gamma\ (a + y)\ y \cot \phi \quad \ldots\ldots\ldots\ldots\ldots \quad (4)$$

Substituting Eq. 4 into Eq. 3 results in

$$F_y = \gamma\ (a\ y + y^2) \quad \ldots\ldots\ldots\ldots\ldots\ldots \quad (5)$$

The force, F, which develops the ultimate lateral shear resistance of the entire cell is obtained by substituting y = c in Eq. 5 to result in

$$F = \gamma\ (a\ c + c^2) \quad \ldots\ldots\ldots\ldots\ldots\ldots \quad (6)$$

in which

$$c = b \tan \phi \quad \ldots\ldots\ldots\ldots\ldots\ldots \quad (7a)$$

and

$$a = H - c \quad \ldots\ldots\ldots\ldots\ldots\ldots \quad (7b)$$

It will be noted from this derivation that the lateral force, F, which develops the maximum lateral resistance is equal to the weight of the fill in the cell times the tangent of the angle of internal friction. Thus,

$$F = \gamma\ b\ h \tan \phi \quad \ldots\ldots\ldots\ldots\ldots\ldots \quad (8)$$

Eq. 6 is represented graphically by Fig. 7(d). The area of this diagram is equal to F. The moment of resistance M_r of F about the base of the cofferdam is therefore

$$M_r = \left(F_1 \frac{c}{2}\right) + \left(F_2 \frac{c}{3}\right) \quad \ldots\ldots\ldots\ldots\ldots\ldots \quad (9)$$

which can be changed to

$$M_r = \left(\gamma\ a\ c \frac{c}{2}\right) + \left(\gamma\ c^2 \frac{c}{3}\right) \quad \ldots\ldots\ldots\ldots\ldots\ldots \quad (10a)$$

or

$$M_r = \gamma \left(\frac{a\ c^2}{2} + \frac{c^3}{3}\right) \quad \ldots\ldots\ldots\ldots\ldots\ldots \quad (10b)$$

The height, $\bar{y}$, of the resultant F above the base, may be found from

$$\bar{y} = \frac{M_r}{F} = \frac{M_r}{\gamma\ b\ h \tan \phi} \quad \ldots\ldots\ldots\ldots\ldots\ldots \quad (11)$$

Testing of Model Cells.—As previously noted, lateral-load tests were conducted on the circular and rectangular cells shown in Figs. 3 and 4(a).

The first tests were performed on the circular cell shown in Fig. 3. The lateral load was first applied close to the bottom and gradually increased until the cell slid on the rough concrete base. It was noted that the resistance to sliding was considerably increased by the shear set up by the wooden-stave shell of the model cell gripping the rough surface of the concrete. This gripping effect was eliminated by permitting the low spots in the concrete to become filled with rock dust and particles of the stone fill used in the cells. This procedure had the further advantage in that the angle of friction for sliding on the base became the same as the angle of internal friction of the fill in the cell. Because of this it was possible to obtain very satisfactory values of the angle of internal friction of the fill by determining the resistance to sliding of the cell, the weight of fill in the cell being known.

In addition to determining the lateral force necessary to develop the resistance to sliding, loads were also applied 6 in., 8 in., 12 in., 18 in., and 23 in. above the base. It was found that approximately $1\frac{1}{2}$ in. of tilting of the top was required to develop the ultimate resisting moment. In every case, the heel of the cell raised off the base approximately $\frac{1}{2}$ in. by the time the ultimate load

was reached. This raising applied, of course, only to the wooden staves, the fill remaining on the concrete base.

As the cell tilted, there was a very noticeable subsidence (approximately 1 in.) of the fill on the toe side of the cell, and a piling up of the fill on the heel side. On the heel side, despite the fact that the shell raised $\frac{1}{2}$ in., the surface of the fill remained as high as the top of the shell of the cell.

An individual cell could be used for only one measurement of lateral load, because pulling the cell back to a vertical position after tilting involved so much manipulation of the fill that it increased in density. This resulted, in turn, in an increase in the angle of internal friction. The angle of internal friction increased from approximately 37° 40' to 42° 0' in one cell which was tested five times, the cell being straightened up between tests.

The angle of internal friction of the fill was 38° 56', and was determined as previously described. This result was in good agreement with the angle of the slope of repose, which was 36° 42'.

TABLE 1.—LATERAL LOAD TESTS OF RECTANGULAR MODEL CELLS
COMPARISON OF TEST RESULTS WITH THEORY

Cell No.	Height, y, in inches		Load at Failure, F_y, in pounds		Resisting Moment at Failure, M_r, in foot-pounds		Percentage of error
	Initial	Final	Actual	M_r/y	Actual	per Eq. 10(b)	
(1)	(2)	(3)	(4)	(5)	(6)	(7)	(8)
7	6	6 5/8	431	442	238	244	-2.5
3	8	8 1/2	331	345	234	244	-4.1
1	12	12 1/2	233	234	243	244	-0.4
6	18	18 3/8	153	159	234	244	-4.1
5	23	23 5/16	133	126	258	244	5.7
							-1.1[a]

[a] Average error.

Table 1 gives the magnitude of the lateral load required for tilting the rectangular cell for various heights of the point of application of the load. The height y above the base is given both for the start and the conclusion of each test, the difference between the two being the distance that the heel of the cell raised during the test. The final height was used in the computations of the theoretical F_y and theoretical M_r, given in Cols. 5 and 7 respectively, of Table 1. The cell was dismantled and rebuilt for each test. It should be noted that in Cols. 4 and 5 there is close agreement between the actual load measured and the theoretical load computed using Eq. 10b. One should also note that the resisting moment remained virtually constant for all of the points of application of the load, and that the variation from the theoretical load computed from Eq. 10b was 0.4% to 5.7%, with an average error of only 1.1%.

Fig. 8 shows the theoretical lateral load plotted against the height of the point of application of the load. The actual measurements of loads (Table 1) for the various cells are indicated. It should be noted that the measured points are in close proximity to the theoretical curve.

For the left-hand part of the curve in Fig. 8 the theoretical resistance is constant and is equal to F in Eq. 8. The highest point at which the force can

be applied is the distance $\bar{y}$ given by Eq. 11. At any point higher than $\bar{y}$ the cell tilts from a force less than F.

Because the base under the model cells was prepared so that the angle of friction for sliding on the base was the same as the angle of internal friction of the fill in the cells, the value of F was also the resistance to sliding on the base. The values for sliding for cells 7 and 1 are shown near the left-hand end of the curve. The angle of internal friction, ϕ, was determined from these two values, as previously explained.

Resistance to Tilting Due to Interlock Friction.—An important factor adding to the resistance of a cellular cofferdam against failure by tilting is interlock friction. As an aid to estimating the magnitude of this resistance, it is convenient to assume a cofferdam composed of rectangular cells with straight crosswalls uniformly spaced at any distance, s.

It is customary to assume that the active-pressure condition of the fill is represented by

$$P = \frac{1}{2} \gamma H^2 \tan^2 \left(45^\circ - \frac{\phi}{2}\right) \quad \ldots\ldots\ldots\ldots\ldots\ldots (12)$$

in which P is the total pressure per running foot of cofferdam for the total depth, H. The interlock tension in the crosswall is then P s. Assuming a coefficient of friction, f, in the interlocks, the friction in the interlocks is p s f. If b_1 is the width of one pile, then the couple P s f b_1 is the moment of resistance of one pile of the crosswall against tilting. If there are n piles in the crosswall, the total resistance of the crosswall to tilting becomes P s f n b_1. However n b_1 equals the average width b of the cofferdam and, therefore, the total moment of resistance to tilting of the crosswall is P s f b. Because the crosswalls are uniformly spaced at a distance s, the resisting moment due to interlock friction (M_p), per foot of cofferdam, is

$$M_f = P f b \quad \ldots\ldots\ldots\ldots\ldots\ldots\ldots\ldots (13)$$

Combining Eqs. 10b and 13 yields the total moment of resistance of a cellular cofferdam filled with sand, gravel, sand and gravel, or crushed rock, and resting on a horizontal rock base—

$$M_t = \gamma \left(\frac{a\, c^2}{2} + \frac{c^3}{3}\right) + P f b \quad \ldots\ldots\ldots\ldots\ldots\ldots (14)$$

Many precedents have established the practice of designing cellular cofferdams on rock so that the average width is not less than 0.85 of the height, or b/H = 0.85. The average width b of a diaphragm-type cofferdam (Fig. 1(b)) is computed by dividing the area enclosed by the cell by the distance between crosswalls. For the circular-cell type (Fig. 1(a)) the area of one cell is added to the area between cells and the sum is divided by the center-to-center distance of the cells.

The pressure of fresh water per linear foot of cofferdam is

$$\frac{1}{2}\ 62.5\ H^2 = 31.25\ H^2$$

The active moment of water pressure is then

$$M_w = 31.25\ H^2 \times \frac{H}{3} = 10.42\ H^3$$

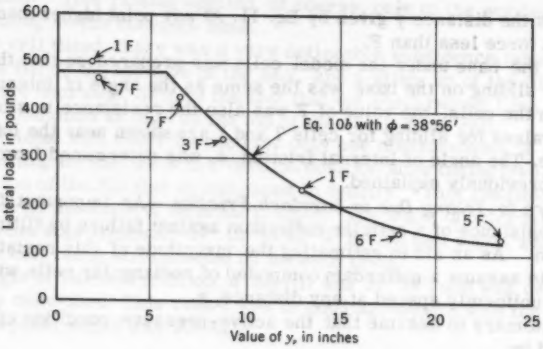


FIG. 8.—COMPARISON OF THEORETICAL WITH ACTUAL RESISTANCE

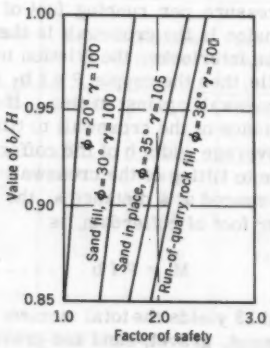


FIG. 9.—FACTOR OF SAFETY AGAINST TILTING

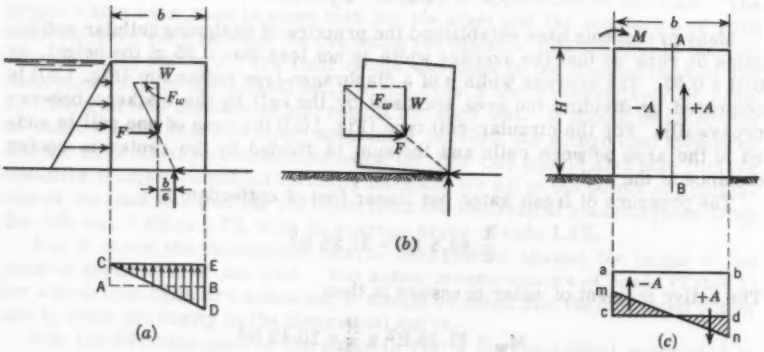


FIG. 10.—DESIGN THEORIES

The factor of safety against tilting due to water pressure, N_{tw}, is obtained by dividing the moment of resistance from Eq. 14 by the active moment of the water pressure—

$$N_{tw} = \frac{M_t}{M_w} \quad \ldots\ldots\ldots\ldots\ldots\ldots (15)$$

If the angle of internal friction of the fill or of the soil in place at the site is not determined by laboratory methods, the following values are suggested:

	ϕ, in degrees	γ, in pounds per cubic foot
Sand fill	30	100
Sand in Place	35	105
Rock fill (run of quarry)	38	100

Fig. 9 shows the factor of safety against tilting due to the pressure of fresh water, for each of the foregoing, for values of the ratio b/H from 0.85 to 1.00.

Previously Published Methods of Design.—The designers of cellular cofferdams in the period from 1908 to 1923, investigated the possibility of overturning in a manner similar to that used for mass retaining walls. In fact, this method is still used by many designers (1959). In Fig. 10(a) the resultant F_w of the weight W of the fill and the horizontal thrust F was required to intersect the base within the middle third. When this precaution was taken, the assumption was that the factor of safety against overturning was at least 3.0. When the resultant is at the edge of the middle third as shown in Fig. 10(a), the base pressure, according to this theory, would be represented by the triangle CED, the rectangle ACEB representing the uniformly distributed base pressure before the application of the lateral load. For the condition shown, the heel of the cofferdam, including the fill, is beginning to lift off the rock base. The compression on the base to the left of the centerline is less than the previously uniformly distributed base pressure, and is zero at the heel. This decrease in base pressure can be accomplished only by tension in the fill to the left of the centerline. Because sand, which is commonly used for fill in cellular cofferdams, is essentially noncohesive, and can develop tension in only small amounts, if at all, it follows that this assumption of the base pressure is incorrect.

Carrying the reasoning one step further, the cofferdam would still have a factor of safety of 1.0 and not be on the verge of failure until it is loaded as shown in Fig. 10(b). The heel of the cofferdam is shown raised slightly off the rock base, and the base pressure is now represented by a single vertical force and a horizontal force both applied at the very toe of the cofferdam. There is, of course, no possibility that this could happen.

The overturning theory, although based on a fallacy, produces satisfactory results where sand, or gravel and sand fill is used on a rock base. However, the factor of safety is not 3 when this procedure is followed. The model cells previously described failed under a lateral load only 1.40 times the load that caused the resultant to intersect the base at the edge of the middle third.

The weakness of the overturning theory is that it does not take into account the shear resistance of the fill. There have been several notable failures and near failures that have occurred because of the use of clay fill, or because of the existence of soft clay at the site, where failure resulted from deficient shear resistance of the soil. The middle third requirement in these cases did not prevent failure.

Another theory[2] is based on the assumption that the maximum internal shear occurs along the centerline AB, Fig. 10(c), and that the cofferdam will fail when this shear becomes excessive. The shaded triangles in the lower sketch of Fig. 10(c) represent the stress produced on the base by the overturning moment, M. If A is the area of one of the triangles, then

$$M = \frac{2}{3} b A \quad \ldots\ldots\ldots\ldots\ldots\ldots \quad (16a)$$

or

$$A = \frac{3 M}{2 b} \quad \ldots\ldots\ldots\ldots\ldots\ldots \quad (16b)$$

The shearing force on plane AB is A, and is equal to the product of the earth pressure and the coefficient of internal friction, tan ϕ. The shear on plane AB is thus

$$V_{ab} = \frac{1}{2} \gamma H^2 C_p \tan \phi \quad \ldots\ldots\ldots\ldots\ldots\ldots \quad (17)$$

in which C_p is the coefficient of pressure. If the Rankine coefficient $\tan^2 (45 - \phi/2)$ is substituted for C_p, Eq. 17 becomes

$$V_{ab} = \frac{1}{2} \gamma H^2 \tan^2 \left(45 - \frac{\phi}{2}\right) \tan \phi \quad \ldots\ldots\ldots\ldots\ldots\ldots \quad (18)$$

which can be simplified to

$$V_{ab} = \frac{1}{2} \gamma H^2 k_\phi \quad \ldots\ldots\ldots\ldots\ldots\ldots \quad (19)$$

by the substitution

$$k_\phi = \tan^2 \left(45 - \frac{\phi}{2}\right) \tan \phi \quad \ldots\ldots\ldots\ldots\ldots\ldots \quad (20)$$

For any given cofferdam, $1/2 \gamma H^2$ is a constant. In Fig. 11(a) the values of k_ϕ are plotted against values of ϕ. The curve indicates that the maximum shear on plane AB occurs when $\phi = 30^\circ$. Selected stone, with $\phi = 45^\circ$ (point M) would be no better than poor material with $\phi = 17^\circ$ (point N). For material with $\phi = 90^\circ$ (an imaginary soil with infinite shear resistance as tan ϕ is infinity), the shear, and thus the resisting moment against tilting, would be zero, as though the cells were left filled with water.

Fig. 11(b) illustrates the factors of safety based on this theory for a cofferdam with the ratio of average width to height of 0.85, a proportion that has been used successfully. The curve is plotted for values of ϕ from 0° to 90°. The maximum factor of safety is only 0.9, for $\phi = 15^\circ$. As the quality of the fill improves, the factor of safety decreases, becoming zero for $\phi = 90^\circ$.

D. P. Krynine, F. ASCE, in discussing[3] the foregoing theory, suggested a value for C_p of

$$C_p = \frac{\cos^2 \phi}{2 - \cos^2 \phi} \quad \ldots\ldots\ldots\ldots\ldots\ldots \quad (21)$$

---

2 "Stability and Stiffness of Cellular Cofferdams," by Karl Terzaghi, Transactions, ASCE, Vol. 110, 1945, p. 1083.

3 Discussion by D. P. Krynine of "Stability and Stiffness of Cellular Cofferdams," by Karl Terzaghi, Transactions, ASCE, Vol. 110, 1945, p. 1175.

This value of C_p gives a maximum factor of safety for the problem of Fig. 11(b) of 1.43 when $\phi = 30°$, and the same factor when $\phi = 20°$. As the quality of the fill improves, the factor decreases, again becoming zero when $\phi = 90°$.

When $\phi = 30°$ is substituted into Eq. 21, the value of C_p is 0.60, almost double the Rankine coefficient of pressure. Interlock tension is generally computed using the Rankine coefficient. Doubling the pressure by using Eq. 21 is not in accord with usual practice.

Application of Theory.—Actual field conditions vary somewhat from the theoretical concept of a cofferdam. For example, the surface of the fill in the cells is sometimes several feet below the top of the cofferdam. Another factor is that for a cofferdam on rock the fill is saturated for some distance above the rock, the depth of saturation depending on the porosity of the fill, the roughness of the rock, and the provisions for drainage of the fill.

The cellular cofferdam for the Pickwick Landing Lock near Pickwick, Tenn., on the Tennessee River affords a good opportunity to test the theory presented herein, taking into account several of the variables that occurred during the life of the cofferdam. The cofferdam was of the type shown in Fig. 1(a), the main cells being 59.89 ft in diameter, on 61.66-ft centers with an average width of 47.3 ft. Fig. 12(a) indicates a cross section of the cofferdam. Assuming

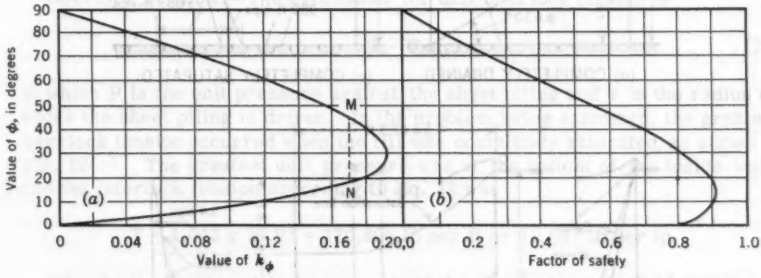


FIG. 11.—RELATIONSHIP BETWEEN ϕ AND k_ϕ AND BETWEEN ϕ AND THE FACTOR OF SAFETY FOR A COFFERDAM WITH b/H = 0.85

(a) complete drainage of the fill; (b) $\phi = 30°$ for dry sand fill; and (c) $\gamma = 100$ lb per cu ft, the moment of resistance against tilting is given from Eq. 14 as 2,054 ft-kips. Fig. 12(a) shows the river near flood stage, close to the top of the cofferdam. The moment of the water pressure about the base was then 1,464 ft-kips. The factor of safety is therefore 2,054/1,464 = 1.40.

Robert T. Colburn, F. ASCE, has presented[4] complete information on this cofferdam, including curves showing the saturation level inside the cells for various stages of the river. Fig. 12(b) shows, approximately, one curve obtained when the river began to fall after reaching flood stage. A part of the fill is submerged, and a direct application of Eq. 14 is not feasible. The resisting moment of the fill is therefore computed on the basis of increments using the theory on which Eq. 10b is based. For example, to obtain the increment between A and B, one must determine the difference between the weights of the prisms OACE and OBDF. The increment, then, is this difference multiplied

[4] Discussion by R. T. Colburn of "Stability and Stiffness of Cellular Cofferdams," by Karl Terzaghi, Transactions, ASCE, Vol. 110, 1945, p. 1136.

by tan ϕ. The other increments are computed in a similar manner. The total resisting moment of the fill is the sum of the products of the increments and their respective distances above the rock base. The weight of the submerged fill is taken as 60 lb per cu ft, and of the dry fill as 100 lb per cu ft.

Another important source of resisting moment results from the differential water level inside the cofferdams. The pressure against the inside of the wall on the river side is equal to the active pressure of submerged earth plus the full head of water. The pressure against the inside of the wall on the dewatered side is the earth pressure plus the pressure due to a considerably reduced head of water. These pressures are shown in Fig. 12(b). It is readily seen that these unbalanced pressures inside the cofferdam add to the stability against tilting.

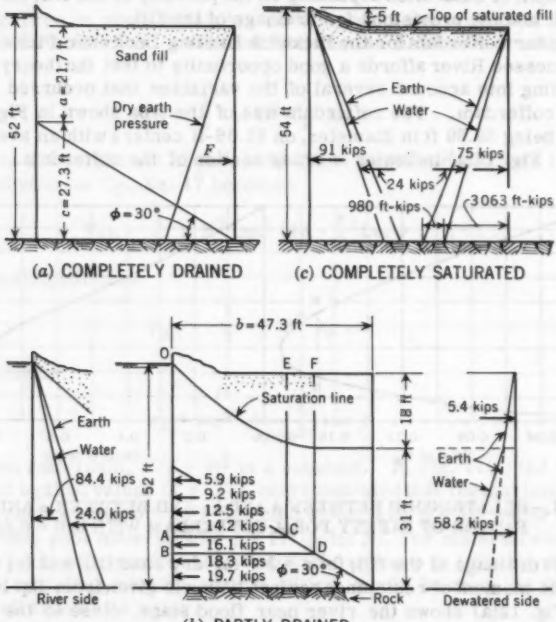


FIG. 12.—PICKWICK LANDING COFFERDAM

Another source of resisting moment under this partly saturated condition is the increased interlock tension due to the water pressure which is added to the earth pressure against the inner wall of the cofferdam. This pressure is shown in Fig. 12(b) and produced a resisting moment of 903 ft-kips.

Taking into account all of the foregoing factors, the total resisting moment against tilting becomes 2,987 ft-kips. At this stage the water pressure due to 52 ft of water was 84.4 kips, with a moment of 1,464 ft-kips. The factor of safety, therefore, is 2,987/1,464 = 2.04. The foregoing indicates a factor of safety due to the differential water level greater than that for the cells assumed completely drained.

Mr. Colburn also stated[4] that the cofferdam withstood a head of the full height of the cofferdam without any visible signs of weakening and that at this point the fill was completely saturated, as there was discharge from weep holes near the top. This condition is shown in Fig. 12(c). Because the fill was saturated, its resisting moment against tilting was 0.6 of that for the dry condition of Fig. 12(a). The resisting moment then becomes:

Source of moment	Moment, in foot-kips
From fill in cells, 1,486 x 0.6	892
From water against outer wall	1,640
From water against inner wall	-1,226
From interlock friction, 99.0 x 0.3 x 47.3	1,404
Total	2,710

The water pressure for a 54-ft head was 91,125 lb, with a moment of 1,640 ft-kips and the factor of safety was then 2,710/1,640 = 1.65.

Again, the factor against tilting is adequate, confirming Mr. Colburn's observation concerning no visible signs of weakening. In this case, however, the stability is obtained at the expense of rather high interlock stress.

Interlock Tension.—The expression for unit interlock tension is

$$T = P\,r \qquad (22)$$

in which P is the unit pressure against the sheet piling and r is the radius on which the sheet piling is driven. In the problem being examined, the greatest interlock tension occurred when the fill was completely saturated, as shown in Fig. 12(c). The greatest unit pressure was at the bottom of the inside wall, and the interlock tension according to Eq. 22 was

$$T = 4{,}043 \times 29.95 = 120{,}800 \text{ lb per ft or } 10{,}067 \text{ lb per in.}$$

The sheet piling used had a guaranteed interlock strength of 16,000 lb per in. The factor of safety was therefore 1.60. It is advisable, if possible, to hold interlock stress down to a factor of safety of approximately 2.0, as there is always the possibility that stresses will be set up in the interlocks during driving, particularly where there is a considerable depth of hard overburden. Adequate provision for drainage of the cells is desirable in order to lower the saturation level in the cells, and thereby reduce the interlock tension.

Sliding.—There is no evidence available of the failure by sliding of a cellular cofferdam on a rock foundation. Perhaps the best explanation of this is the grip that the steel sheet piling has on the rock surface. If the surface of the rock is soft, the steel will penetrate a few inches and this will add to the resistance against sliding. Even where the rock surface is hard, natural irregularities in the rock surface provide adequate resistance against sliding. In so far as the sliding resistance of the fill on the rock surface is concerned, the coefficient of friction cannot exceed tan ϕ of the sand, for if it were greater, a lesser resistance to sliding would exist in the sand immediately above the rock. For the Pickwick Landing cofferdam the least resistance to sliding occurred for the condition of Fig. 12(c), in which the fill was completely saturated. Using the unit values previously assumed, the resistance to sliding of the fill on the rock was 80,300 lb and water pressure against the cofferdam

was 91,125 lb, for a 54-ft head. These values indicate that the water pressure against the cofferdam exceeded the sliding resistance of the fill, and that the grip of the steel on the rock was the determining factor preventing sliding. The importance of drainage of the fill is again emphasized, because if the fill had been completely drained as in Fig. 12(a), or partly as in Fig. 12(b), the resistance to sliding would have been increased due to the increased weight of the fill.

COFFERDAMS ON FOUNDATIONS OTHER THAN ROCK

While most cellular cofferdams in recent years have been constructed on rock foundations, there have been many cofferdams constructed on sand foundations, notably for the locks and dams on the Mississippi River. The chief problem encountered was seepage under the cofferdam through the sand. To correct this condition a sand berm is placed against the inner face of the cofferdam for two purposes, first to force the flow net of the seepage water away from the toe of the cofferdam in order to prevent upward flowing water from making the sand foundation quick adjacent to the toe of the cofferdam, and, second, to add to the stability against tilting.

This type of cofferdam has been examined elsewhere[5] and illustrations of cofferdams of this type have been presented.[6]

Cellular cofferdams on clay foundations are rare. A large structure built in the 1920's began to fail by tilting and by excessive base pressure at the toe, when the water had been pumped down only part of the way. It was stabilized by a heavy sand berm against the inner face. In this case, the soil enclosed by the cells was original clay of deficient shear value.

Cellular cofferdams have been constructed successfully in very soft clay where resistance against tilting has been provided by other means. For example, in 1932 an extremely large cofferdam was constructed in the Hudson River, New York, N. Y., between 48th St. and 52nd St. Here, the river bottom is very soft clay for great depths, underlain by hardpan over rock. Stability against tilting was obtained with a heavy rock-fill berm against the inner face of the cofferdam.

In general, it may be stated that the consistency of clay at a site must be of the stiff or hard categories unless some such precaution is taken.

CELLULAR DOCKS AND PIERS

Cellular construction, besides being used for cofferdams, is also used for such structures as docks, piers, breakwaters, mooring dolphins, and retaining walls. Where soil conditions are appropriate, permanent structures of this type possess a high degree of stability. In addition to its ability to resist static forces, cellular construction can absorb such forces as wave action, ice, and the normal impact of ships.

Cellular construction is considered for docks where the depth of water required exceeds the range of depth for which a sheet-pile bulkhead is feasible, or where bedrock occurs at an elevation that does not permit sufficient penetration for a sheet-pile bulkhead. Conditions are suitable where the cells rest

---

5 "Cofferdams," by Lazarus White and Edmund A. Prentis, Columbis Univ. Press, New York, N. Y., 1950.

6 "Typical Installations of Steel Sheet Piling," Bethlehem Steel Co., Bethlehem, Pa., 1954.

on bare rock; or on rock with an overburden of firm soil such as sand, sand and gravel, or stiff clay; or where the cells are driven into such firm soils. If the rock or firm soil is overlain by mud or soft clay, the poor soil must be removed either by predredging the site or by excavating inside the cells before filling. It is of the greatest importance that the cells rest on a base of hard or firm material that possesses the bearing capacity to sustain the weight of the filled cells, and that the original soil and the fill in the cells have adequate shear value to resist the lateral pressure against the cells. Several failures of cellular construction occurred where the cells were driven into soft

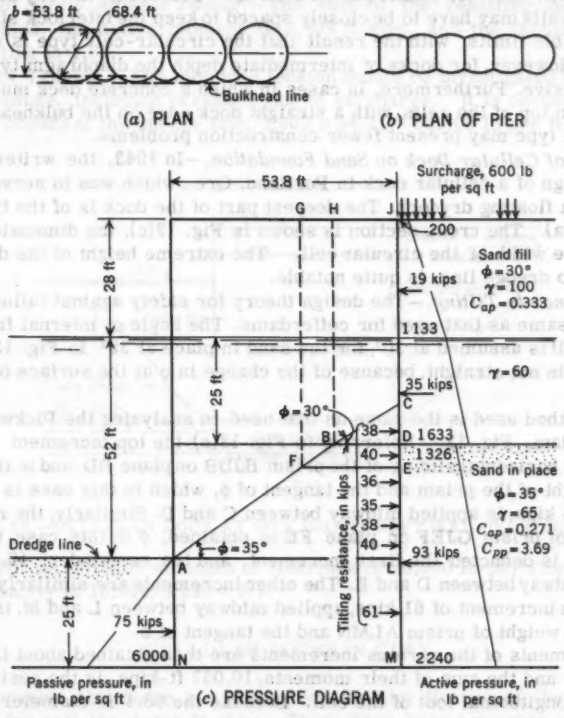


FIG. 13.—SWAN ISLAND CELLULAR DOCK

soil. In such cases, placing good fill on top of mud or very soft clay does not result in material of good shear resistance. Usually, the heavy sand fill will sink into the soft material and lose its separate identity, the result being a mixture of the sand and soft material which has no better shear resistance than the original soft soil.

Fig. 13(a) illustrates a plan of a circular-cell type of cellular dock. Only one connecting arc is required where there is earth fill on one side. For piers and breakwaters where there is water on both sides, the second connecting arc is necessary. One important precaution should be taken in designing the connecting arc for a dock when a deck with a straight edge is required. It should

not be designed so that it is tangent to the dock line, but approximately 2 ft back from the dock line. The reason for this is that the main circular cells increase their diameter approximately 1½% when the pressure of the fill takes up the slack in the sheet-pile interlocks. The result is that the chord distance of the connecting arc is appreciably shortened. Because the middle ordinate of the arc is very sensitive to shortening of the chord distance, the arc will bulge beyond the bulkhead line appreciably. This makes construction of the deck and fender system difficult and expensive unless the foregoing precaution is taken.

The diaphragm type shown in Fig. 1(b) is also suitable for docks and piers, and has been used for numerous structures. For docks in very deep water, the crosswalls may have to be closely spaced to keep the interlock stress within reasonable limits, with the result that the circular-cell type is more economical. However, for docks of intermediate depth the diaphragm type may be less expensive. Furthermore, in cases in which a concrete deck must be constructed on top of the cells, with a straight dock edge on the bulkhead line, the diaphragm type may present fewer construction problems.

Design of Cellular Dock on Sand Foundation.—In 1943, the writer assisted in the design of a cellular dock in Portland, Ore., which was to serve as a wet berth for a floating drydock. The deepest part of the dock is of the type shown in Fig. 13(a). The cross section is shown in Fig. 13(c), the dimension b being the average width of the circular cell. The extreme height of the dock, 80 ft from top to dredge line, is quite notable.

Resistance to Tilting.—The design theory for safety against failure by tilting is the same as that used for cofferdams. The angle of internal friction for the sand fill is assumed at 30°, for the sand in place at 35°. In Fig. 13(c), ABC, the ϕ-line is not straight, because of the change in ϕ at the surface of the sand in place.

The method used is the same as that used in analyzing the Pickwick Landing cofferdam, Fig. 12. Referring to Fig. 13(c) the top increment is the resistance to horizontal sliding of the prism HJDB on plane BD, and is the product of the weight of the prism and the tangent of ϕ, which in this case is 30°. The product, 38 kips, is applied midway between C and D. Similarly, the resistance to sliding of prism GJEF on plane FE is obtained, ϕ in this case being 35°. From this is deducted the first increment, and the remainder, 40.4 kips, is applied midway between D and E. The other increments are similarly obtained. The bottom increment of 61 kips, applied midway between L and M, is the product of the weight of prism ALMN and the tangent of ϕ.

The moments of the various increments are then obtained about the bottom of the cell, and the sum of their moments, 10,057 ft-kips, is the resisting moment per longitudinal foot of the cell. Because the 68.4-ft-diameter cells are on 73.1-ft centers, the resisting moment per foot of dock is proportionately reduced to 9,400 ft-kips per foot of dock. No value is given to the soil between cells, because there was only one sheet-pile connecting arc.

Resistance Due to Interlock Friction.—As in the case of cofferdams, interlock friction adds to the resistance to tilting. In this case, the active pressure without surcharge is taken only down to the dredge line, because the passive pressure of the fill below that elevation will prevent tension in the interlocks. The active pressure is readily determined from Fig. 13(c) by deducting the pressure due to surcharge. The resulting pressure, P, is 81 kips per foot of dock. The resisting moment is 1,306 ft-kips per foot of dock.

Passive-Pressure Moment.—Tilting is further resisted by the passive pressure of the soil against the outboard face of the cell. For $\phi = 35°$, the coefficient

of passive pressure C_{pp} is 3.69. The intensity of passive pressure at El. -77.0 is, therefore, 25 x 65 x 3.69 = 6,000 lb per sq ft. The total passive pressure is 75 kips applied at the centroid of the diagram and the resisting moment about El. -77.0 is therefore 623 ft-kips.

Active-Pressure Moment.—The active-pressure diagram of Fig. 13(c) is obtained by using a coefficient of pressure C_{ap} for sand fill of 0.333, corresponding to an angle of internal friction $\phi = 30^0$. For sand in place the coefficient is 0.271. The total pressure applied at the centroid is shown in Fig. 13(c) for each part of the pressure diagram. The moment of the active pressure about the bottom of the cell at El. -77.0 is 6,098 ft-kips.

Factor of Safety Against Tilting.—The sum of the resisting moments is 11,329 ft-kips, the active moment is 6,098 ft-kips, and the factor of safety against tilting is 1.86.

Interlock Tension.—The interlock tension should be investigated for the full active pressure, including pressure due to surcharge. It is obvious that the maximum occurs at the dredge line: 1,803 x 34.21 = 61,800 lb per ft = 5,150 lb

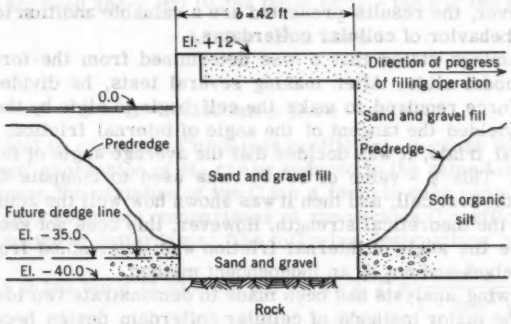


FIG. 14.—CELLULAR DOCK AT SITE WHERE SOFT SOIL OVERLIES ROCK

per in. For an ultimate strength of interlock of 16,000 lb per linear in., the factor of safety is 16,000/5,150 = 3.1.

CELLULAR DOCKS IN CLAY

It is apparent that there is a great need for clarification of the principles of design for cellular docks in clay. There have been a number of failures, and in practically every case the cause was due to not recognizing that adequate horizontal shearing strength of the clay in the cells is the most important prerequisite for stability against failure by tilting. Cellular docks have been designed in very soft clay, sometimes overlain by mud, with the expectation that the cellular construction, of itself, would provide the necessary stability. In most such cases stability was investigated by the overturning method, with the resultant passing through the middle third, as previously noted.

In assessing the suitability of a particular site for a cellular design, a simple rule for preliminary investigation is to compare the total active pressure with the sum of the horizontal shear value of the clay in the cells and the passive pressure on the outboard side, if any. The dock shown in Fig. 14 is an

example of this. Consideration was first given to a cellular dock without predredging. Laboratory analysis indicated a unit shear for the very soft silt of only 250 lb per sq ft. The total horizontal shear resistance of the silt in the cells would have been only a fraction of the active pressure, as the surcharge of the fill on the silt would have resulted in excessive lateral pressure. As indicated in Fig. 14 the silt was predredged and the cells were filled with sand and gravel. Sand and gravel fill was placed immediately behind the cells with progress shoreward, in order to eliminate the possibility of a mud wave against the cells.

DISCUSSION

SAMUEL HEYMAN,[7] A.M. ASCE.—Additional tests on cellular cofferdams are required for determining where in the fill the actual plane of failure occurs. However, the results presented are a valuable addition to the available data on the behavior of cellular cofferdams.

Mr. Cummings stated that ϕ was determined from the force required to make the model slide. After making several tests, he divided the average horizontal force required to make the cell begin to slide by the weight of the cell. This yielded the tangent of the angle of internal friction, ϕ, of the soil. After several trials, it was decided that the average angle of internal friction was 38° 56'. This ϕ - value of 38° 56' was used to compute the theoretical strength of the test cell, and then it was shown how well the actual test results agreed with the theoretical strength. However, this does not seem to be justified, because the angle of internal friction was determined from the test results themselves and not by an independent method.

The following analysis has been made to demonstrate two ideas. The first is that all the major methods of cellular cofferdam design become invalid at extreme, unrealistic values of ϕ. The second is a comparison of the various design methods in the range of practical values.

To demonstrate the first idea, the resisting moment of the cohesionless fill as determined by the author has been compared with the resisting moment of cohesionless fill as determined by Terzaghi.[2] Terzaghi states that the unit shearing resistance along a vertical plane of the cohesionless fill is equal to $\frac{1}{2} \gamma H^2 C \tan \phi$ in which C is the horizontal earth pressure coefficient. Terzaghi analyzed this force, and from the dimensions of cells that have worked satisfactorily decided that C "must be considerably greater than the active Rankine pressure" coefficient, and that "for the middle part of the fill in the cells (C) ranges between 0.4 and 0.5." The author, however, in the examination of Terzaghi's method considers it as using the active Rankine pressure along the vertical plane. In the published discussions of Terzaghi's paper,[2] Mr. Krynine demonstrated[3] (and Terzaghi approved[8]) by a Mohr's circle analysis that this coefficient, C should be equal to

$$C = \frac{\cos^2 \phi}{2 - \cos^2 \phi} \quad \ldots\ldots\ldots\ldots\ldots\ldots\ldots (23)$$

[7] Consulting Engineer, New York, N. Y.

[8] "Stability and Stiffness of Cellular Cofferdams," by Karl Terzaghi, Transactions, ASCE, Vol. 110, 1945, p. 1187.

Terzaghi's formula for the moment of resistance of the cohesionless earth fill in the cofferdam against vertical shear is

$$M_s = \frac{\gamma b H^2}{3} C \tan \phi \quad \ldots\ldots\ldots\ldots\ldots\ldots (24)$$

When the relationship of b = 0.85 H is assumed,

$$M_s = 0.283 \gamma H^3 C \tan \phi \quad \ldots\ldots\ldots\ldots\ldots\ldots (25)$$

For any given cell $0.283 \gamma H^3$ is a constant. Thus, C tan ϕ, and, therefore, M_s vary solely with ϕ.

The moment of resistance of the sand as expressed by Cummings in Eq. 10 (b) is equal to

$$M_s = \gamma \left(\frac{a c^2}{2} + \frac{c^3}{3} \right) \quad \ldots\ldots\ldots\ldots\ldots\ldots (26)$$

Substituting c = b tan ϕ, a = H - b tan ϕ, and Terzaghi's relationship, b = 0.85 H, Eq. 26 reduces to:

$$M_s = \left(0.283 \gamma H^3\right) [0.362 \tan \phi (3.53 - \tan \phi)] \tan \phi$$

$$= 0.283 \gamma H^3 B \tan \phi \quad \ldots\ldots\ldots\ldots\ldots\ldots (27)$$

in which:

$$C = B = 0.362 \tan \phi (3.53 - \tan \phi) \quad \ldots\ldots\ldots\ldots\ldots\ldots (28)$$

The term B will be called the Cummings coefficient. Because both Terzaghi's and Cummings' expression of M_s can be reduced to the same form, it is sufficient to compare the variation of the C tan ϕ term in each case.

Fig. 15 and Fig. 16 are comparisons of the various C coefficients that are used in the design of cofferdams. The following designations are used: For curve 1, C = 0.362 tan ϕ (3.53 - tan ϕ); curve 2, $C = \frac{\cos^2 \phi}{2 - \cos^2 \phi}$; curve 3, C = 0.4; curve 4, C = 0.5; and curve 5, $C = \tan^2\left(45 - \frac{\phi}{2}\right) \tan \phi$. The term C tan ϕ rather than C alone has been plotted against ϕ because C tan ϕ is the entire parameter that varies with ϕ, and it is consistent with the author's C tan ϕ presentation. As determined from Fig. 15 when $\phi = 90°$, the Cummings' coefficient, B, times tan ϕ approaches minus infinity (curve 1). When describing Terzaghi's method and believing that Terzaghi's method utilizes active Rankine pressure for failure along a vertical plane through the fill, the author points out under the heading "Previously Published Methods of Design," that when ϕ becomes 90° "... the shear, and thus the resisting moment against tilting, would be zero, as though the cells were left filled with water." Using the Cummings method, when $\phi = 90°$ the shearing resistance of the material within the cell would be infinitely worse than plain water.

As stated previously, the original formulas were not established for such extreme values of ϕ. In the case of Cummings' formulas the value of a and c can never be greater than H, which would limit the value of ϕ to approximately 47°, using the b = 0.85 H relationship. This demonstrates that all theories give impossible results for impossible ϕ values.

The values of C tan ϕ in the range of practical values of ϕ for a cohesionless soil are shown in Fig. 16. As can be seen, in curve 1, Cummings' design method is the least conservative for ϕ values greater than 30°, and that using

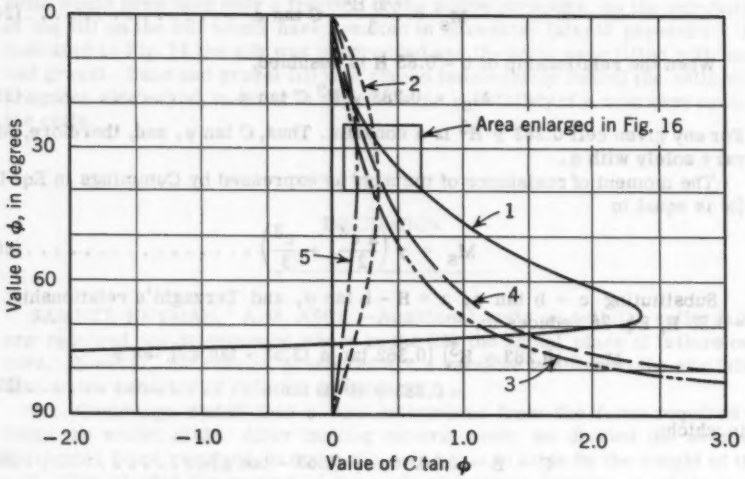

0
30
60
90
Value of φ, in degrees
−2.0
−1.0
0
1.0
2.0
3.0
Value of C tan φ
Area enlarged in Fig. 16
1
2
3
4
5

FIG. 15

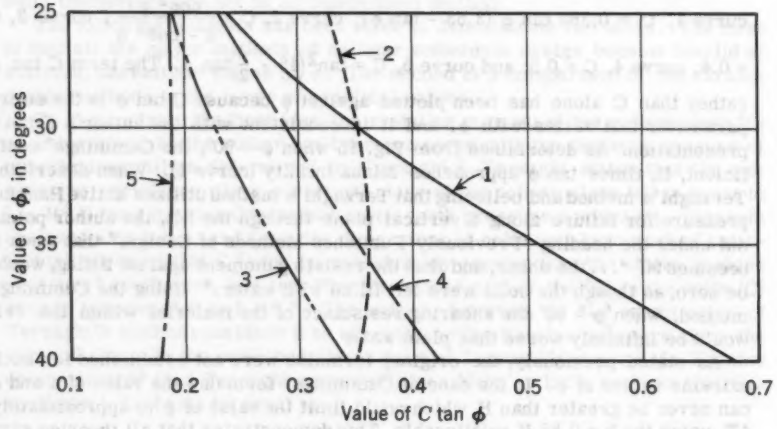

25
30
35
40
Value of φ, in degrees
0.1
0.2
0.3
0.4
0.5
0.6
0.7
Value of C tan φ
1
2
3
4
5

FIG. 16

the coefficient of active pressure times the tangent of ϕ for shear along a vertical plane (curve 5) is the most conservative design method by a wide margin. For ϕ less than 30° Krynine's method (curve 2) is less conservative than the Cummings' method, and at $\phi = 30°$ the maximum of Terzaghi's range is with 20% of both Cummings' and Krynine's values. Because the differences in design coefficients, especially near $\phi = 30°$, are smaller than the normal factor of safety used in design, cellular cofferdams have been successfully designed by the various methods discussed herein.

CEVDET Z. ERZEN[9].—Mr. Cummings considers horizontal planes in a cellular cofferdam as the planes of failure due to shear in soil, and introduces a theory based on this assumption. This concept seems justifiable when a model with 3/4 in.-thick vertical planks that correspond to very stiff piles in the prototype is observed. Inasmuch as the back of the model remains straight, thus producing deflection varying linearly, and considering the theories of Rankine and Coulomb, there is no reason why the planes of failure in the cell must be horizontal.

The use of 3/4-in. planks in 19 1/8-in.-by-24-in. cells that corresponds to very stiff piles in the prototype creates doubts as to the exact duplication of the behavior of cells with flexible sheet piles.

Dimensional analysis of such a system renders

$$v = \frac{F}{E\,L}\, f\left(\frac{F}{E\,L^2}\,,\ \frac{F}{E\,L^4}\right) \ldots\ldots\ldots (29)$$

in which u is the deflection of sheet piling; F represents the applied external load; G is the flexural rigidity of pile; L is equal to the length of pile; and E is the modulus of elasticity of material.

Denoting the scale factor of the model by k, the following result:

$$k_u = \frac{k_F}{k_E\ \ k_L}\,,\quad k_F = k_E\,k_L^{\,2} \quad \text{and} \quad k_G = k_E\,k_L^{\,4}.$$

Taking the modulus of elasticity of white pine at 1,250,000 psi, the following are found:

$$k_E = \frac{30{,}000}{1{,}250} = 24;\ k_F = 24\,k_L^{\,2};\ k_G = 24\,k_L^{\,4};\ \text{and}\ k_u = k_L.$$

Assuming that the cofferdam is ten times the size of the model, $k_F = 2{,}400$; $k_G = 240{,}000$; and $k_u = 10$.

Thus, the line load applied on the cofferdam is

$$F = \frac{200}{2}\ (2{,}400) = 240 \text{ kips per ft.}$$

The flexural rigidity of the sheet pile is found to be

$$E_p\,I_p = (240{,}000)\ \frac{1}{12}\ (12)\ (.75)^3\ E_m$$

[9] Frederic R. Harris, Inc., New York, N. Y.

in which E_p is the modulus of elasticity of the sheet pile material. The subscripts p and m denote prototype and model respectively. Solving for the moment of inertia of the sheet pile yields

$$I_p = \frac{10}{\frac{100}{24}} = 4{,}220 \text{ in.}^4 \text{ per ft}$$

This is equivalent to using 24WF160 instead of the MP 101 of MP 102 sections that possess an almost negligible moment of inertia.

Because the bending of such a heavy section is insignificant, deflection varies linearly from zero at the bottom to a maximum at top. If it were assumed that this would produce slip planes due to shear on horizontal planes, the theory introduced in the paper would be correct. However, according to the Rankine or Coulomb theory, the planes of failure are different from the horizontal planes.

It is further attempted to show the existence of two zones, namely, active and passive, by means of pull-out tests on rods embedded in sand. In the opinion of the writer, the proximity of the outer rods to the boundary must be considered in evaluating the results, especially in tests indicated in Figs. 5(b) and 6(t) in which no external force is applied. Neither the plastic nor the elastic concept of stress in circular disks seems to justify the substantial difference in loads in Fig. 5(b). Therefore it seems logical to consider the effect of the boundary on the stresses acting on the rods.

In the paper, the resisting moment of the cell against overturning forces is considered to be the sum of the resistance due to interlock friction and that due to shearing strength of the soil. Clearly, the moment of resistance of each pile is $P \times s \times f \times b$, is no stress on the cross-sectional area of the diaphragm exists or if this stress is constant. However, bending stresses exist on the cross sections of the piles even when the cells are not embedded (as in the case of cells on rock), by virtue of the bending stresses in the soil that are transferred to the diaphragm through shear acting between the piles and the soil inside the cell. Therefore, the moment of resistance is not due to interlock friction acting at the ends of the diaphragm, but is due to the vertical shear at center which is some part of the cell. Thus, this moment is

$$M_f = \frac{2}{3} P \times f \times b \quad \ldots\ldots\ldots\ldots\ldots\ldots (30)$$

The difference between the external moment and the value of Eq. 30 must be resisted by shear in the soil acting on a vertical plane.

The writer has used the concept of the existence of plastic and elastic zones within a cell in the design of cofferdams. Such an analysis should be consistent with the laws of statics and Coulomb's theory. An elastic zone may exist irrespective of the dimensions of a cell. The forces in the plastic zone are given according to Rankine's or Coulomb's theory. Once these forces and the two zones are determined, the stresses in the elastic zone may be computed by treating this section separately with all the known loads from the plastic zone acting on it.

The failure of the cell is possible if the maximum shearing strength of the soil in the cell is exceeded unless the overturning moment is less than the momoment given by Eq. 30 and also if the sliding along its base is prevented. These principles may be explained by considering a cell resting on rock and holding back a fill.

Fig. 17(a) shows such a cell. The ratio of depth of point J from top to height of the cell is denoted by α_E; α_H is the ratio of depth of point H from top to height of the cell; P_{a1} represents the active pressure due to soil behind the cell acting on the cell; P_{a2} denotes the active pressure due to soil inside the cell; and P_p is the passive pressure. The area ABCDA is in a state of plastic equilibrium in which the shear in the vertical and horizontal planes is zero. The active pressure on plane AB is

$$P_a = 1/2\ \gamma_2\ H^2\ k_a \quad \ldots\ldots\ldots\ldots\ldots\ldots (31)$$

in which γ_2 is the unit weight of soil inside the cell. Subscript 2 refers to the plastic zone, and, similarly, subscript 1 will refer to the fill outside the cell.

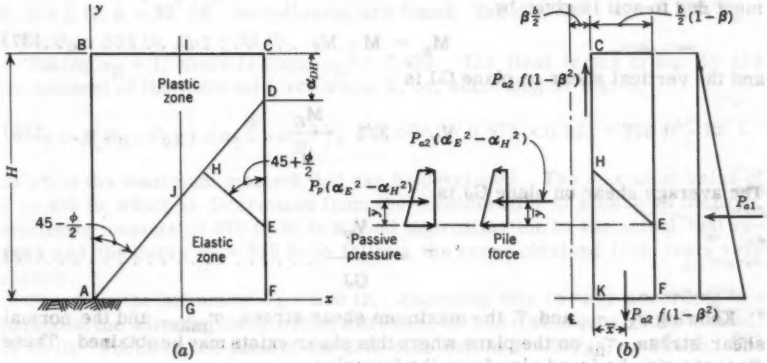


FIG. 17.—CELL RESTING ON ROCK

This pressure is transmitted through the diaphragms to the back piles of the cell and is resisted by the elastic zone. If the elastic zone is ADFA, the total force acting on DF is

$$F_T = 1/2\ \gamma_1\ H^2\ k_a + 1/2\ \gamma_2\ H^2\ k_a\ (1 - \alpha_D{}^2) \ldots\ldots\ldots (32)$$

in which γ_1 is the unit weight of soil outside the cell. The coefficient of active pressure is k_a, and α_D is the ratio of depth of point D from top to height of the cell, and the shear on the base AF is

$$V_{AF} = 1/2\ \gamma_1\ H^2\ k_a \quad \ldots\ldots\ldots\ldots\ldots (33)$$

If G is the midpoint between A and F, and assuming the shear is equally distributed between AG and GF, the total normal force on plane GJ is found from a free body diagram of forces acting on ICFGI or IGABI. Summing up forces in the x-direction results in

$$F_x = 1/2\ \gamma_1\ H^2\ k_a + 1/2\ \gamma_2\ H^2\ k_a\ (1 - \alpha_J{}^2) - \frac{V_{AF}}{2} \ldots\ldots (34)$$

in which α_J is the ratio of depth of point J from top to height of the cell, and the second term is the force due to the pull in the diaphragm between G and J. The

maximum shearing stress in the soil may be found from Mohr's circle of stress. For this purpose, normal stress on GJ is

$$\sigma_x = \frac{F_x}{GJ} \quad \ldots\ldots\ldots\ldots\ldots\ldots (35)$$

and the normal stress on a horizontal plane is

$$\sigma_y = \gamma_2 \left(\frac{H + \alpha_J H}{2} \right) \quad \ldots\ldots\ldots\ldots\ldots\ldots (36)$$

The shear on plane GJ is found from the moment of the fill about the base. Because the external moment is resisted by the soil and the sheet piling, the moment due to soil is given by

$$M_s = M - M_f \quad \ldots\ldots\ldots\ldots\ldots\ldots (37)$$

and the vertical shear on plane GJ is

$$V_v = 3/2 \quad \frac{M_s}{b} \quad \ldots\ldots\ldots\ldots\ldots\ldots (38)$$

The average shear on plane GJ is

$$\tau = \frac{V_v}{GJ} \quad \ldots\ldots\ldots\ldots\ldots\ldots (39)$$

Knowing σ_x, σ_y, and τ, the maximum shear stress, τ_{max}, and the normal shear stress, τ_n, on the plane where this shear exists may be obtained. These stresses may be found also from the formulas

$$\tau_{max} = \sqrt{\frac{(\sigma_x - \sigma_y)^2}{2} + \tau^2} \quad \ldots\ldots\ldots\ldots (40)$$

and

$$\sigma_n = \frac{\sigma_x + \sigma_y}{2} \quad \ldots\ldots\ldots\ldots\ldots\ldots (41)$$

in which σ_n is the normal unit stress on a plane where shearing unit stress is maximum. If $\tau_{max} > \sigma_n \tan \phi$, then failure occurs internally and M_s becomes zero. In this case, in order that the external forces of the fill may be still resisted, the moment of the interlock friction must be greater than the external moment.

The boundaries of the elastic zone are determined from a consideration of the laws of statics. The elastic zone is not necessarily a triangle ADFA as shown in Fig. 17(a), but it may have the boundary AHEFA. To find this zone a free body diagram is drawn of a vertical section through H as in Fig. 17(b) in which the volume of soil HEFKH is considered separated from the sheet piles. Therefore, only the forces acting on the soil above HE and those acting on the sheet piles are considered.

Summing up the forces in the x-direction there is found as the first condition.

$$F_x = P_{a1}\,\alpha_E^2 + P_{a2}\left(\alpha_E^2 - \alpha_H^2\right) > P_\rho\left(\alpha_E^2 - \alpha_H^2\right) \quad \ldots\ldots(42)$$

and the second condition is that due to overturning. Taking a moment about E,

$$P_{a1}\,\alpha_E^2\,\frac{\alpha_E H}{3} + P_{A2}\left(\alpha_E^2 - \alpha_H^2\right)\bar{y} > P_\rho\left(\alpha_E^2 - \alpha_H^2\right)\bar{y} + P_{A2}\,f\left(1 - \beta^2\right)\bar{X} \quad \ldots\ldots(43)$$

in which the last term is the friction force in the interlock. These are the two equations that determine the elastic zone.

As an example, consider the cell shown in Fig. 6. With γ = 91.9 lb per cu ft, H = 2 ft, $\phi = 38^\circ 56'$, the following are found: Tan ϕ = 0.81, k_a = 0.228, K_p = 4.39, P_p = 803 lb, P_{a2} = 42 lb.

Taking α_E = 1, there is found $\alpha_H^2 = 0.428$. The first terms in Eq. 42 are the moment of the external force about E, or, according to Fig. 6,

$$F_y > 2\left(P_p - P_{a2}\right)\left(\alpha_E^2 - \alpha_H^2\right)\bar{y} = 2 \times 761 \times 0.572 \times 0.321 = 279 \text{ ft - lb}$$

which is the maximum moment that can be developed. The maximum value of F is 485 lb, which is determined from the consideration of sliding on the base. Maximum moment of 279 ft-lb is a good approximation to the actual test results and the curve F_y = 279 ft-lb follows the curve obtained from tests very closely.

Shear on the bottom is V_b = 200 lb. Assuming this to vary according to a parabola, the shearing force within a distance of 3 in (where the rod is located) is 13 lb. Force on the back of the 2-ft-wide cell is F + 2 P_{a2}, or 284 lb. The normal force at three positions of the rod are

$$F_{N1} = 284 - 13 = 271 \text{ lb}$$

$$F_{N2} = 284 - 100 = 184 \text{ lb}$$

$$F_{N3} = R + P_{a2}\left(1 - 0.75^2\right) - 187 = 50 \text{ lb}$$

from which the force necessary to pull each rod becomes

$$F_1 = \frac{271}{24.5}\ 2.5 \times 2 \times 0.81 = 45 \text{ lb}$$

$$F_2 = 30 \text{ lb}$$

and

$$F_3 = 10 \text{ lb}$$

The example given in Fig. 13 is treated here for demonstration. The elastic zone begins at A and makes an angle of 27.5° with the vertical and changes to 30° as shown in Fig. 18. First, Eq. 42 is used to determine if there is any possibility of failure plane through L. Here, L corresponds to point E, and E to H of Fig. 17. In Eq. 42, $P_{a1}\,\alpha_E^2$ = 96, $P_{a2}\left(\alpha_E^2 - \alpha_H^2\right)$ = 31, and $P_p\left(\alpha_E^2 - \alpha_H^2\right)$ = 426. Because $P_{a1}\,\alpha_E^2 + P_{a2}\left(\alpha_E^2 - \alpha_H^2\right) \not> P_p\left(\alpha_E^2 - \alpha_H^2\right)$ fail-

ure does not occur along BL. Similarly, Eqs. 42 and 43 are not satisfied for failure among ME. Therefore, the elastic zone is bounded by line ABC.

The total shear along NM is $V_V = 147 - 75 = 72$ kips and the normal force on KG with $\alpha_A^2 - \alpha_G^2 = 0.85$ and $\underline{F} = 147 + 87 \times .85 - 72/2 = 185$ kips.

Therefore, $\alpha_x = \frac{185}{74} = 2.5$ kips per ft.

The vertical pressure midway between K and G is $\alpha_y = 5.2$ kips per sq ft and

$$M_S = 6{,}098 - (623) - (2/3 \quad 1{,}306) = 4{,}605$$

$$V = 3/2 \frac{M_S}{b} = 128 \text{ kips}$$

giving $$\tau = \frac{128}{74} = 1.74 \text{ kips per sq ft}$$

Using these values the maximum shear is found to be

$$\tau_{max} = 2.21 \text{ kips per sq ft}$$

and

$$\tau_n = 3.8 \text{ kips per sq ft}$$

$$\tau_{all} = 3.85 \times 0.70 = 2.70 \text{ kips per sq ft}$$

Because the maximum allowable unit shearing stress, τ_{all}, $> \tau_{max}$, the soil is in a state of elastic equilibrium. However, in other cases the maximum shearing stress in the lower zone may exceed the maximum allowable shear in which case a state of plastic equilibrium through the cell exists.

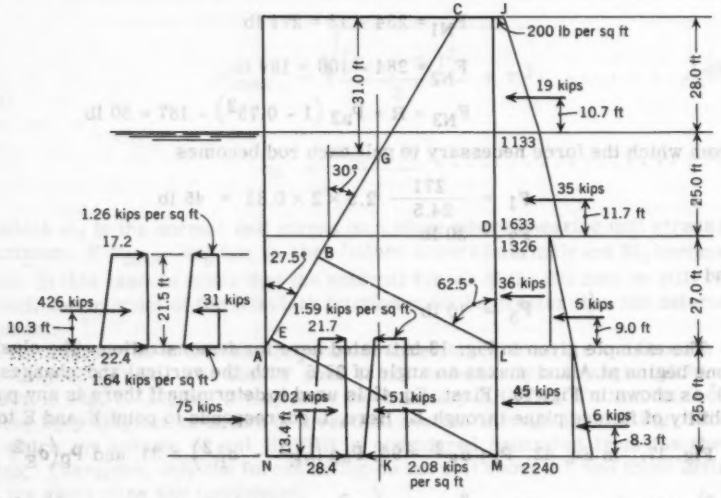


FIG. 18.—EXAMPLE GIVEN IN FIG. 13

The theory given by the writer determines these zones through the use of Eqs. 42 and 43 and also establishes the state of equilibrium of the lower zone--whether elastic or plastic. If the lower zone is in a plastic state, as a first condition, the external moment must be resisted by the moment of the interlock friction. The second condition of equilibrium is that due to sliding. For equilibrium the sliding forces must be less than the sum of the resisting forces and the shear on the bottom due to overburden. Finally, the equilibrium of the overturning moment of the external forces must be satisfield.

EDWARD M. CUMMINGS,[10] F. ASCE.--Mr. Heyman suggests additional tests on cellular cofferdams to determine where in the fill the actual plane of failure occurs. In connection with the model studies on which the paper was based, a preliminary model was constructed to determine whether there is any definite plane of failure. This model was 12 in. by 12 in. and 1 ft high. It was filled with white sand, except that horizontal thin layers of black sand were placed at approximately 1 $\frac{1}{2}$-in. intervals. Thin transparent plastic strips 3/4 in. wide were used to simulate sheet piles, and were retained by two light exterior wood frames. When this model was tilted by a lateral force, the black streaks of sand showed clearly that there was no definite plane of rupture. The flow of the material was similar to that of a plastic mass, and the black sand layers remained approximately horizontal, although there was a tendency of the sand to pile up on the side on which the force was applied, and to subside on the opposite side of the cell. This was also observed in the larger models described in the paper.

Mr. Heyman notes that the angle of internal friction of the fill material was determined by making the cell slide on a base comprised of the same material. He states that this procedure was unjustified, because the angle of internal friction was determined from the test results themselves, and not by an independent method. However, it is pointed out that the angle of internal friction was checked by measuring the natural slope of repose, the latter being only approximately 2° less than the angle determined by making the cell slide. It is generally accepted that for noncohesive soil, the natural slope of repose defines the lower boundary of the angle of internal friction.

It is considered significant that the force that caused the model cell to slide also caused it to tilt when the force was applied at the critical height, $\bar{y}$, above the base. This fact demonstrated that the tilting of a cell is identified with horizontal sliding of the fill in the cell. This is the basis of the theory presented.

Mr. Heyman notes that the writer examined the Terzaghi[2] theory of failure on a vertical neutral plane, on the basis of the Rankine coefficient of pressure, although Terzaghi later accepted Krynine's coefficient. The reason that the Rankine coefficient was examined is that there are at least three texts[11,12,13]

---

10 Sales Mgr., Bethlehem, Steel Co., Bethlehem, Pa.

11 "Foundations of Structures," by Clarence W. Dunham, McGraw-Hill Book Co., Inc., New York, N. Y., 1950, p. 450.

12 "Substructure Analysis and Design," by Paul Anderson, The Ronald Press Co., New York, N. Y., 1947, p. 177.

13 "Shore Protection Planning and Design," Beach Erosion Board, Corps of Engrs., U. S. Dept. of the Army, Washington, D. C., 1954.

that use only the Rankine coefficient in their presentation of the Terzaghi theory. This, combined with the fact that engineers are using the Rankine coefficient with the Terzaghi theory in designing, indicated that this basis was pertinent.

Assuming a proportion of b = 0.85 H, Heyman puts Eq. 10(b) for the moment of resistance of the sand fill in the same form as Terzaghi's equation, and thus derives a coefficient of pressure, B. He then examines this coefficient for values of ϕ from 0° to 90°, thereby subjecting it to the same rigorous treatment that the writer used in investigating the Terzaghi coefficient. In principle, there can be no objection to this, but in doing so Mr. Heyman assumed conditions beyond those for which Eq. 10(b) was derived. The equation was derived from the condition shown in Fig. 7(c). Fig. 19 shows the condition for $\phi = 60°$, and it is obvious that Eq. 10(b) could not be derived from it.

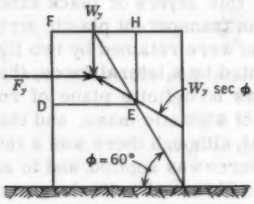


FIG. 19.—CONDITIONS FOR $\phi = 60°$

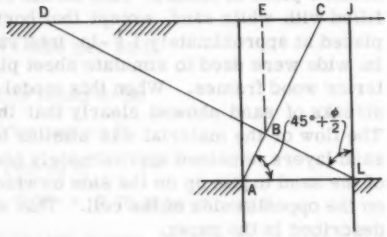


FIG. 20.—MODIFIED FIG. 18

Fig. 15 and Fig. 16 showing ϕ versus C tan ϕ is not correct for the coefficient, B (curve 1) for values of ϕ greater than 45°. The theory presented in the paper is based on resistance to horizontal shear that is proportional to tan ϕ, which, in turn, increases as ϕ increases. Thus, there is no reversal in the theoretical resistance for higher values of ϕ as indicated in Mr. Heyman's graph for coefficient B. From a practical standpoint, of course, there can hardly be any fill material with ϕ greater than 45°.

Mr. Erzen discusses the use of 3/4-in-thick vertical planks used to simulate sheet piles in the model cells. The model cells were made with wood staves 5/16 in. by 1 $\frac{1}{2}$ in. by 2 ft, and not with 3/4-in. planks. He introduces consideration of the bending strength of the model sheet piles in his analysis. If bending had been a factor, it would have resulted in higher total resistance than the horizontal shear value of the fill, which was the greatest resistance developed by the model cells. Undoubtedly, Mr. Erzen was influenced by Fig. 3(b), in which extreme tilting and distortion had taken place, far beyond the point at which the cell developed its maximum resistance. This occurred after approximately 1 $\frac{1}{2}$ in. of movement of the top. Fig. 3(b) shows approximately 6 $\frac{1}{2}$ in. of movement.

Mr. Erzen presents a new theory for lateral resistance to tilting as shown in Fig. 18. He assumes that sliding will occur on a plane that makes an angle of 45° + ϕ/2 with the vertical. Fig. 20 is a reproduction of a section of Fig. 18 with modifications. He assumes that the lateral resistance against sliding on plane LB is equal to the Rankine passive wall pressure JL minus the wall pressure EB. However, the Rankine theory proves that the plane of least resistance is 45° + ϕ/2 only when the surface of the ground is horizontal for an indefinite

distance, in which case the plane LBD of Fig. 20 is the plane of least resistance. For any other condition the plane of rupture is not inclined at $45^0 + \phi/2$ to the vertical.

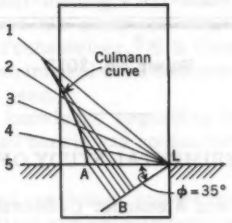


FIG. 21.—PLANE OF LEAST RESISTANCE

Fig. 21 determines the plane of least resistance by the Culmann method. Plane LB is plotted at the angle ϕ below the horizontal, and planes L1 to L5 are trial planes of rupture. Line AB is the smallest intercept between LB and the Culmann curve, and its length gives the resistance to sliding on the horizontal plane L5. The least resistance to sliding is therefore on a horizontal plane, and not the plane at $45^0 + \phi/2$ as Mr. Erzen assumes.

AMERICAN SOCIETY OF CIVIL ENGINEERS

Founded November 5, 1852

TRANSACTIONS

Paper No. 3013

ANALYTICAL AND EXPERIMENTAL STUDY OF HELICOIDAL GIRDERS

By Yee F. Young,[1] and Alexander C. Scordelis,[2] A. M. ASCE

SYNOPSIS

A study is presented of a helicoidal girder, fixed at the ends, subtending a horizontal angle of 180°, and having a slope of 30°. Four girders, each having a different uniform rectangular cross section throughout its length, are investigated. The determination of the influence lines for the reactions due to vertical load is illustrated, using analytical and experimental methods. Final results are presented in tabulated and graphical form. End reactions under uniform load over half span and full span are also given, and the effect of the width-to-depth ratio of the cross section on end reactions and internal forces is examined.

INTRODUCTION

Since 1950, a number of helicoidal staircases, supported only at the ends, have been designed and built.[3,4] This architecturally fascinating structure may be visualized as being a circular bow girder with one end displaced vertically out of the plane of the other.

A problem that immediately confronts the designer of such a structure is the elementary one of determining end reactions. Victor R. Bergman, M. ASCE, has suggested[5] that for design purposes it may be adequate to determine the

Note.—Published, essentially as printed here, in September, 1958, in the Journal of the Structural Division, as Proceedings Paper 1756. Positions and titles given are those in effect when the paper was approved for publication in Transactions.

1 Engr.-Structures, North American Aviation, Inc., Fresno, Calif.

2 Assoc. Prof. of Civ. Engrg., Univ. of California, Berkeley, Calif.

3 "Revolutionary Staircase Built of Prestressed Concrete," by G. Magnel, Civil Engineering, Vol. 21, No. 9, 1951, pp. 25-27.

4 "Rapid Concrete Construction in Spain," by N. B. Bourne, Concrete and Construction Engineering, Vol. 45, No. 10, London, 1950, pp. 357-362.

5 "Helicoidal Staircases of Reinforced Concrete," by V. R. Bergman, Journal, A.C.I., Vol. 28, No. 4, October, 1956, pp. 403-412.

end reactions by reducing the girder to its horizontal projection, and thus analyze it as a bow girder. This simplification neglects the inherent strength of the three-dimensional structure. In the case of a helicoidal staircase built for a showroom in Antwerp, Belgium, Gustav Magnel[3] obtained experimental data, as a basis for design, by test-loading a full-scale model. However, the test results failed to substantiate his computed values. Analytical studies have been presented by Wilhelm Fuchssteiner,[6] H. S. Gedizli,[7] and Jacques S. Cohen,[8] but thus far, very little experimental work has been done to verify the applicability of the theories being used.

Because of the lack of knowledge regarding the behavior of this type of structure, the study reported herein was conducted with the purpose of investigating the following items:

1. The nature of the end reactions, and the method by which they may be evaluated using both analytical and experimental approaches;
2. A comparison between the end reactions obtained for the structure by analyzing its horizontal projection as a bow girder and by analyzing it as a true helicoid;
3. The effect of the width-to-depth ratio of the cross section on the end reactions; and
4. The applicability of the analytical solution to structures with large transverse dimensions, because the analysis does not take into account the additional resistance provided by slab action.

The geometry of a helicoidal girder may be defined physically (Fig. 1) in terms of its radius, r; horizontal angle, ϕ; helix angle, α; width, b; and depth, h. Four girders were analyzed in this study, all having the same horizontal angle ($\phi = 180^0$) and the same helix angle ($\alpha = 30^0$) but each having a different width-to-depth ratio, b/h. The nominal width-to-depth ratios of the girders investigated were 1 to 1, 4 to 1, 8 to 1, and 16 to 1.

Notation.—The letter symbols adapted for use in this paper are defined where they first appear, in the illustrations or in the text, and are arranged alphabetically for convenience of reference in the Appendix.

ANALYTICAL SOLUTION

The helicoidal girder fixed at the ends, under vertical load, is a structure that is statically indeterminate to the sixth degree. It may be analyzed by considering the six reactions at one end (Fig. 2) as redundants. Then, using the principle of superposition, the following equations (known as the Maxwell-Mohr equations), may be written:

$$\delta_{xo} + X_x \delta_{xx} + X_y \delta_{xy} + X_z \delta_{xz} + X_t \delta_{xt} + X_p \delta_{xp} + X_r \delta_{xr} = 0 \quad . . \quad (1)$$

$$\delta_{yo} + X_x \delta_{yx} + X_y \delta_{yy} + X_z \delta_{yz} + X_t \delta_{yt} + X_p \delta_{yp} + X_r \delta_{yr} = 0 \quad . . \quad (2)$$

---

6 "Die freitragende Wendeltreppe (Spannungsberechnung und Bewehrung)," by W. Fuchssteiner, Beton-und Stahlbetonbau, Vol. 49, No. 11, Berlin, 1954, pp. 256-258.

7 Discussion by H. S. Gedizli of "Die freitragende Wendeltreppe," by W. Fuchssteiner, Beton-und Stahlbetonbau, Vol. 50, No. 9, Berlin, 1955, p. 297.

8 "Design of Helical Staircases," by J. S. Cohen, Concrete and Construction Engineering, Vol. 50, No. 5, London, 1955, pp. 181-194.

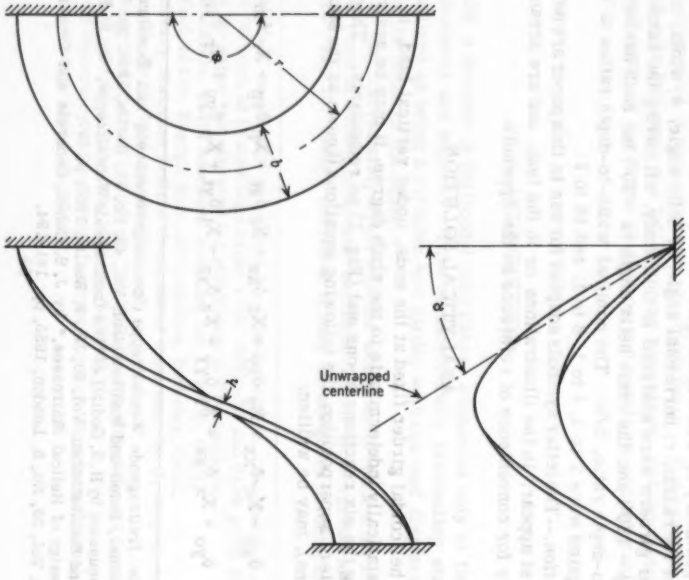


FIG. 1.—LEFT-HAND HELICOIDAL GIRDER

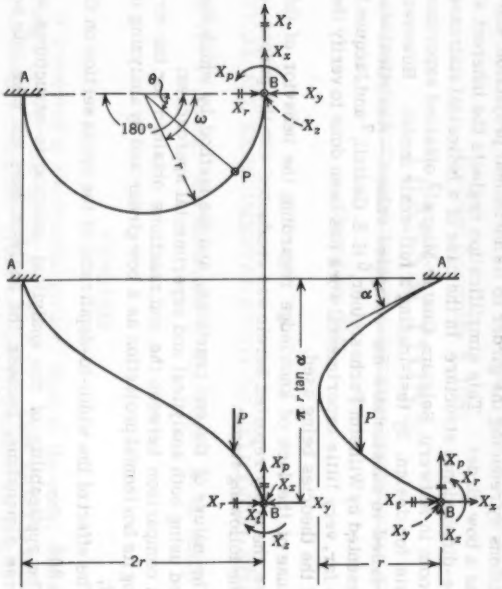


FIG. 2.—POSITIVE DIRECTION OF REDUNDANTS IN HELICOIDAL GIRDER

$$\delta_{zo} + X_x \delta_{zx} + X_y \delta_{zy} + X_z \delta_{zz} + X_t \delta_{zt} + X_p \delta_{zp} + X_r \delta_{zr} = 0 \quad . . \quad (3)$$

$$\delta_{to} + X_x \delta_{tx} + X_y \delta_{ty} + X_z \delta_{tz} + X_t \delta_{tt} + X_p \delta_{tp} + X_r \delta_{tr} = 0 \quad . . . \quad (4)$$

$$\delta_{po} + X_x \delta_{px} + X_y \delta_{py} + X_z \delta_{pz} + X_t \delta_{pt} + X_p \delta_{pp} + X_r \delta_{pr} = 0 \quad . . \quad (5)$$

and

$$\delta_{ro} + X_x \delta_{rx} + X_y \delta_{ry} + X_z \delta_{rz} + X_t \delta_{rt} + X_p \delta_{rp} + X_r \delta_{rr} = 0 \quad . . \quad (6)$$

In Eqs. 1 through 6, X_x, X_y, and X_z represent the redundant forces in the direction of the x, y, and z axes, respectively; X_t, X_r, and X_p are the redundant moments acting about the x, y, and z axes, respectively; and δ_{xo}, δ_{yo}, . . ., δ_{ro} denote displacements due to load, P, with redundants equal to zero. The terms δ_{xx}, δ_{yx}, . . ., δ_{rx}, are displacements due to $X_x = 1$; δ_{xy}, δ_{yy}, . . ., δ_{ry}, represent displacements due to $X_y = 1$; δ_{xz}, δ_{yz}, . . ., δ_{rz}, are displacements due to $X_z = 0$; δ_{xt}, δ_{yt}, . . ., δ_{rt} denote displacements due to $X_t = 1$; δ_{xp}, δ_{yp}, . . ., δ_{rp}, are displacements due to $X_p = 1$; and δ_{xr}, δ_{yr}, . . ., δ_{rr}, represent displacements due to $X_r = 1$. The term displacement is understood to mean angular as well as linear displacement.

In order to obtain a solution for the redundants the displacements must be evaluated. There are forty-two displacements in Eqs. 1 through 6, but using Maxwell's law of reciprocal displacements ($\delta_{xy} = \delta_{yx}$, . . .) this number reduces to twenty-seven. These displacements may be determined using the method of virtual work:

$$\delta_{xy} = \delta_{yx} = \int \frac{M_{rx}\, M_{ry} ds}{EI_r} + \int \frac{M_{sx}\, M_{sy} ds}{EI_s} + \int \frac{T_x\, T_y ds}{GJ_e} \quad . . . . . \quad (7)$$

in which M_{rx}, M_{sx}, and T_x represent bending and torsional moments in the girder due to $X_x = 1$; M_{ry}, M_{xy}, and T_y denote bending and torsional moments in the girder due to $X_y = 1$; EI_r, and EI_s represent bending stiffnesses about the r-axis and s-axis, respectively (Fig. 3); E is the modulus of elasticity; I represents the moment of inertia; GJ_e is the torsional stiffness about the e-axis; G denotes the modulus of elasticity in shear; and J is the torsional stiffness constant.

After the displacement coefficients have been evaluated they may be substituted into Eqs. 1 through 6 and the redundants may be found by solving these simultaneous equations.

Formulas for each of the necessary twenty-seven displacements have been derived and are given in the Appendix. The equations given are for a girder having a horizontal angle $\phi = 180^0$. These equations are expressed in terms of the load position, θ; the helix angle; the radius; and the bending and torsional stiffnesses. An inspection of these equations will reveal that they are quite complex and care must be exercised in evaluating them numerically for a specific case.

In order to compare the results of an analytical solution with an experimental solution, the four girders used in the model analysis (described subsequently) were analyzed using the equations shown in the Appendix together with Eqs. 1 through 6.

All girders had the same helix angle of 30^0 and were of rectangular cross section. The cross-sectional dimensions of these girders, with the bending

and torsional stiffnesses, are given in Table 1. The models were made of plexiglass which had a modulus of elasticity, E, of 462 kips per sq in. and a modulus of elasticity in shear, G, of 162 kips per sq in. These physical constants of the material were obtained experimentally. The torsional stiffness constants, J_e, of the cross sections were obtained from the expression

$$J_e = k_1 \, b \, h^3 \quad \ldots\ldots\ldots\ldots\ldots\ldots \quad (8)$$

in which k_1 is a constant depending on the width-to-depth ratio. The values of k_1 were obtained from the work[9] of Stephen Timoshenko and James N. Goodier.

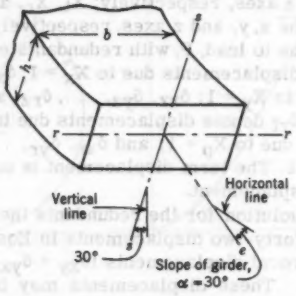


FIG. 3.—BENDING AND TORSIONAL AXIS INDICATED ON SECTION CUT NORMAL TO LONGITUDINAL AXIS OF GIRDER

TABLE 1.—SECTIONAL PROPERTIES OF THE HELICOIDAL GIRDERS

Nominal b-to-h ratio	Actual b, in inches	Actual h, in inches	Actual value of b/h	I_r, in inches^4 x 10^{-4}	I_s, in inches^4 x 10^{-4}	Value of k_1	J_e, in inches^4 x 10^{-4}	E I_r, in kip-inches^2	E I_s, in kip-inches^2	G J_e, in kip-inches^2
(1)	(2)	(3)	(4)	(5)	(6)	(7)	(8)	(9)	(10)	(11)
1:1	0.256	0.245	1.04	3.15	3.43	0.146	5.50	0.146	0.158	0.089
4:1	1.033	0.244	4.22	12.6	224	0.283	42.8	0.582	10.3	0.693
8:1	1.987	0.244	8.14	24.1	1,590	0.304	87.8	1.11	73.5	1.42
16:1	4.000	0.249	16.04	51.7	13,300	0.333	207	2.39	614	3.35

End reactions for each girder were obtained analytically for a concentrated vertical load placed successively at five locations along the girder. Thus, a total of twenty solutions were involved in obtaining the influence ordinates shown in Table 2. Influence lines for end reaction are shown graphically in Fig. 4.

[9] "Theory of Elasticity," by S. Timoshenko and J. N. Goodier, 2d Ed., McGraw-Hill Book Co., Inc., New York, 1951, p. 277.

The signs given in Table 2 correspond to the positive direction of redundants as shown in Fig. 2. For convenience in the plotting of Figs. 4(a), (b), and (e), the positive direction of the redundants has been reversed.

In order to compare the foregoing results with those found by analyzing the horizontal projection of the structure as a bow girder, the influence lines for X_z, X_t, and X_r obtained from a bow-girder analysis are shown in Figs. 4(c), (d), and (e). These three reactions are the only ones that exist in the case of a planar bow girder. Tabulated ordinates for these influence lines may be found in a number of publications.[10,11,12,13]

TABLE 2.—INFLUENCE-LINE ORDINATES FOR REACTIONS AT BOTTOM OF HELICOIDAL GIRDER PRODUCED BY A CONCENTRATED VERTICAL LOAD

Nominal b-to-h ratio	Value of θ	Value of X_x	Value of X_y	Value of X_z	Value of $X_{t/R}$	Value of $X_{r/R}$	Value of $X_{p/R}$
(1)	(2)	(3)	(4)	(5)	(6)	(7)	(8)
1:1	30°	-0.0446	-0.0665	0.9046	0.0873	-0.3599	0.0869
	60°	-0.1276	-0.0917	0.7103	0.1937	-0.4388	0.1860
	90°	-0.1674	0.0000	0.5000	0.1938	-0.3482	0.1674
	120°	-0.1276	0.0917	0.2898	0.1068	-0.1959	0.0691
	150°	-0.0446	0.0665	0.0955	0.0234	-0.0593	0.0021
4:1	30°	-0.1448	-0.3387	0.7526	0.2179	-0.1874	0.3605
	60°	-0.4072	-0.4645	0.5022	0.4240	-0.0736	0.7029
	90°	-0.5314	0.0000	0.5000	0.3247	-0.0181	0.5314
	120°	-0.4072	0.4645	0.4978	0.0770	-0.0538	0.1115
	150°	-0.1448	0.3393	0.2477	-0.0359	-0.0501	-0.0712
8:1	30°	-0.1649	-0.4586	0.6867	0.2684	-0.1347	0.4570
	60°	-0.4630	-0.6286	0.4118	0.5041	0.0243	0.8632
	90°	-0.6041	0.0000	0.5000	0.3528	0.0479	0.6042
	120°	-0.4630	0.6286	0.5882	0.0403	-0.0504	0.0629
	150°	-0.1649	0.4593	0.3138	-0.0709	-0.0665	-0.1276
16:1	30°	-0.1716	-0.5091	0.6592	0.2893	-0.1141	0.4964
	60°	-0.4813	-0.6973	0.3740	0.5356	0.0606	0.9252
	90°	-0.6277	0.0000	0.5000	0.3621	0.0693	0.6279
	120°	-0.4813	0.6973	0.6260	0.0229	-0.0536	0.0375
	150°	-0.1716	0.5099	0.3417	-0.0863	-0.0750	-0.1531

It is interesting to note that in the case of the bow-girder analysis that the results obtained for the four girder cross sections differ by such a small amount that for practical purposes the same influence line may be used for all four.

10 "Numerical Analysis of Frames with Curved Girders," by J. P. Michalos, Transactions, ASCE, Vol. 121, 1956, pp. 521-543.

11 "The Solution of Closed Circular Rings by the Conjugate Ring Method," by M. B. Hogan, Bulletin, Univ. of Utah, Vol. 38, No. 14, 1948.

12 "Influence Lines for Horizontally Curved Fixed-End Beams of Circular Arc Plan," by R. B. B. Moorman and M. B. Tate, Bulletin, Univ. of Missouri, Vol. 48, No. 26, October, 1947.

13 "A Study of the Circular Arch Bow Girder," by A. H. Gibson and E. G. Richie, D. Van Nostrand and Co., New York, 1915.

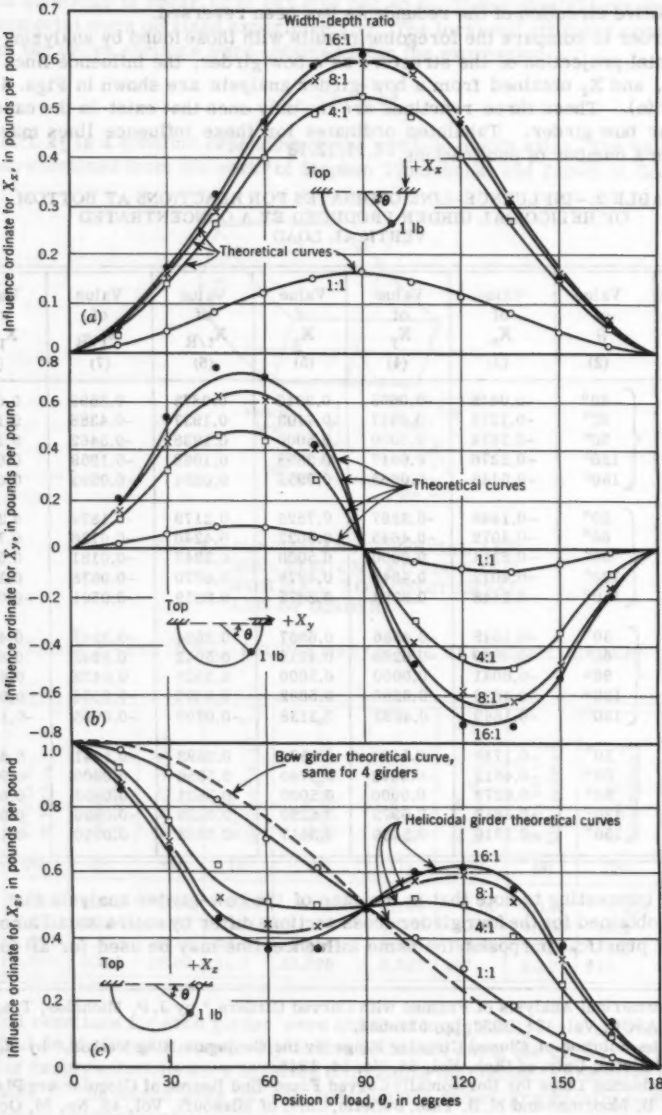


FIG. 4.—INFLUENCE LINES

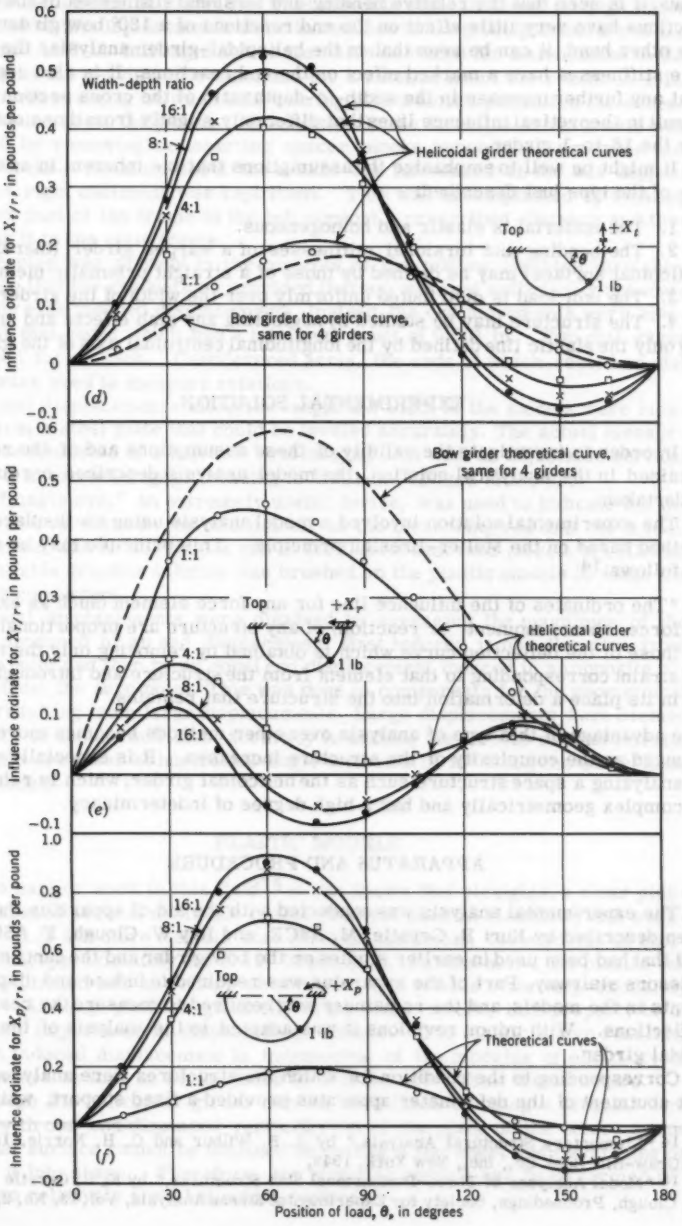


FIG. 4.—CONTINUED

Thus, it is seen that the relative bending and torsional stiffnesses of the cross sections have very little effect on the end reactions of a 180° bow girder. On the other hand, it can be seen that in the helicoidal-girder analysis, the relative stiffnesses have a marked effect on the end reactions. It is also apparent that any further increase in the width-to-depth ratio of the cross section would result in theoretical influence lines that differ only slightly from those obtained for the 16-to-1 girder.

It might be well to emphasize the assumptions that are inherent in an analysis of the type just described:

1. The material is elastic and homogeneous.
2. The bending and torsional stiffnesses of a warped girder (therefore a helicoidal surface) may be defined by those of a straight prismatic member.
3. The unit load is distributed uniformly over the width of the girder.
4. The structure may be studied by neglecting any slab effects and analyzing only the elastic line defined by the longitudinal centroidal axis of the girder.

EXPERIMENTAL SOLUTION

In order to investigate the validity of these assumptions and of the results obtained in the analytical solution, the model analysis described herein was undertaken.

The experimental solution involved a model analysis using the displacement method based on the Muller-Breslau principle. This principle may be stated as follows:[14]

> "The ordinates of the influence line for any force element (such as axial force, shear, moment, or reaction) of any structure are proportional to those of the deflection curve which is obtained by removing only the restraint corresponding to that element from the structure and introducing in its place a deformation into the structure that remains."

The advantage of this type of analysis over other methods becomes more pronounced as the complexity of the structure increases. It is especially useful in analyzing a space structure such as the helicoidal girder, which is relatively complex geometrically and has a high degree of indeterminacy.

APPARATUS AND PROCEDURE

The experimental analysis was conducted with the aid of apparatus that has been described by Kurt H. Gerstle, M. ASCE, and Ray W. Clough, F. ASCE,[15] and that had been used in earlier studies on the bow girder and the cantilevered scissors stairway. Part of the apparatus was required to induce end displacements in the models, and the remainder was required to measure the resulting deflections. With minor revisions it was adapted to the analysis of the helicoidal girder.

Corresponding to the condition for which the structures were analyzed, the left abutment of the deformeter apparatus provided a fixed support, while the

---

14 "Elementary Structural Analysis," by J. B. Wilbur and C. H. Norris, 1st Ed., McGraw-Hill Book Co., Inc., New York, 1948.

15 "Model Analyses of Three-Dimensional Slab Structures," by K. H. Gerstle and R. W. Clough, Proceedings, Society for Experimental Stress Analysis, Vol. 13, No. 2, 1955.

right abutment remained movable. This movable right abutment through which all but one of the displacements were introduced is the principal feature of the apparatus. An 8-in. milling machine turntable provided for translations in the direction of the y-axis and z-axis, and for a rotation about the x-axis. A 4-in. channel arm swinging between ball-bearing pillow blocks permitted the necessary rotation about the y-axis. Translation in the direction of the x-axis was achieved by removing or inserting spacer blocks between the turntable and pillow blocks. Rotation about the z-axis was introduced at the left support while the right abutment was kept fixed. This was accomplished by rotating the upper part of the frame at the left support a prescribed distance and then rebolting it to the main frame.

Some play was present in the controls of the milling machine turntable, enough so that the graduations provided thereon were not sufficiently accurate to measure the induced displacements. Instead, the end movements were measured by dial gages which had a minimum count of 0.001 in. Two dial gages were used for a check. Cantilevered arms, the ends of which rested on dial gages, were used to measure rotations.

Vertical displacements along the length and width of the models were measured from a steel plate that could be leveled accurately. The actual measuring device consisted of a movable overhanging arm with an adjustable vertical rod and a micrometer gage, reading to 0.001 in., affixed to the end.

The "magic eye," an extremely useful device, was used to indicate the instant of contact between the micrometer on the measuring rod and the model. When contact was established, a gap in the fluorescent tube closed. A colloidal water-soluble graphite solution was brushed on the plastic models to make the surfaces conductive.

Vertical displacements were obtained by averaging the magnitude of the volume produced by an end displacement first induced in one direction from the zero point and then by an equal end displacement induced in an opposite direction from the zero point. This was done to compensate for the geometrical errors resulting from large displacements. Large displacements were deemed necessary to assure sufficient accuracy in making the various measurements. Readings were taken at horizontal-angle intervals of 15° along the centerlines of the models.

PLASTIC MODELS

From earlier work in this field[15] it was known that plexiglas, a clear plastic, possessed several desirable model qualities such as flexibility and workability. It is far more flexible than steel or aluminum, the modulus of elasticity being approximately 0.5×10^6 lb per sq in. Furthermore, the plastic can be easily formed into any shape when heated to a pliable state (approximately 300° F). Although plastics generally creep under stress, this property is of secondary importance in displacement models. The elastic curve resulting from an induced displacement is independent of the modulus of elasticity of the structure as long as the modulus is constant throughout the structure.

Although the helicoidal girder may be visualized as being a circular bow girder with one end displaced vertically out of the plane of the other, a true helicoidal surface cannot be obtained by cutting a flat sheet and then lifting or bending it into shape. Therefore, the plexiglas models had to be formed between two relatively rigid helicoidal surfaces.

These two surfaces were obtained by first constructing a pattern of the 4-in.-wide model, having a centerline radius of 12 in., using gypsum cement reinforced with expanded metal. This pattern in turn was used to cast an aluminum model of the helicoidal girder. Two rigid surfaces were now available to form the plastic models. This was achieved by heating a $\frac{1}{4}$-in. flat sheet of plastic to the proper temperature and forming it to the desired shape by clamping it between the gypsum-cement pattern and the aluminum casting. The first model so constructed was the 4-in.-wide model, and very little difficulty was experienced in displacing it in the apparatus. Subsequently, three more models of smaller widths (2 in., 1 in., and $\frac{1}{4}$ in.) were made by performing the same operation as for the 4-in. model and then trimming the edges from both sides toward the centerline. All models had a 12-in. centerline radius.

RESULTS OF THE MODEL ANALYSIS

The results of the model analyses are plotted in Fig. 4. Agreement between the experimental values and the influence lines obtained from the theoretical analyses is generally good and seems to justify the assumptions made in the theoretical analysis. No systematic order of deviations is apparent, the deviations varying in nature from curve to curve for a particular model.

Influence lines for reactions resulting from concentrated vertical loads acting along the centerline of the girder have been shown in Fig. 4. In slab-like structures these influence lines should extend across the width of the structure as well as through the length of the structure so that influence surfaces can be plotted. In the case of the 4-in.-wide model, experimental influence ordinates were obtained at the inner and outer edges of the girder as well as along the centerline. These values are not recorded herein, but it is important to note that a linear relationship existed for the influence ordinates across the width of the structure, the ordinate at the centerline being the average ordinate at any radial section. Inasmuch as these structures are normally designed for a load per unit of horizontal projected area it is apparent that a centerline analysis is sufficient for design purposes.

END REACTIONS UNDER DISTRIBUTED LOAD

Having obtained influence lines for end reactions, it is now a relatively simple task to obtain end reactions under any distributed loading condition by determining the area under the influence line between the two limits of the distributed load. In design, the three cases of a uniformly distributed load over the whole span, the bottom half, and the top half are perhaps of greatest importance. For this reason the curves for reactions at the bottom end versus the width-to-depth ratio of girder cross section are given in Fig. 5 for these three cases. The sign convention is as illustrated in Fig. 2. A study of these curves reveals, in almost all cases, a rapid initial change of end reactions with increasing width-to-depth ratios between 1 and 4, but a relatively small change between 8 and 16. Table 1, which gives the section properties of the girders, shows that between the 8 to 1 and 16 to 1 ratios the (EI_r/EI_s)-ratio changes considerably while there is only a small change in the (EI_r/GJ_e)-ratio. Apparently, the controlling factor in the behavior of the girder, after I_s has reached a sufficiently large value, is the ratio of (EI_r/GJ_e).

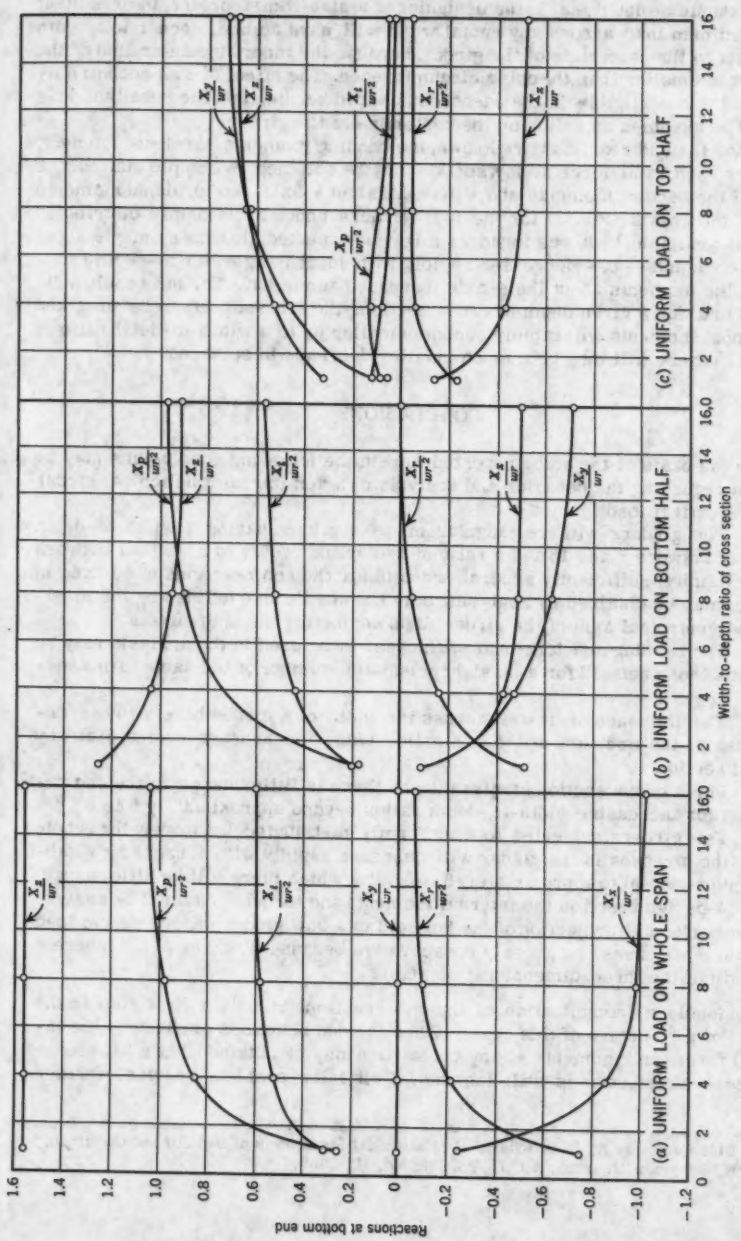


FIG. 5.—END REACTIONS AT BOTTOM OF HELICOIDAL GIRDER

It should be noted that in the designing of a slab-like structure, the resultant of a uniform load across any radial width will have a small eccentricity with respect to the centerline of the girder, because the inner circumference of the girder is smaller than the outer circumference. The effect of this eccentricity of load was negligible in the cases considered herein, and the resultant load could be assumed as acting on the centerline of the girder.

Once the end reactions are known, the bending moments, torsional moment, shears, and axial force at any section may be obtained by simple statics. A plot of the bending moments about the r-axis and s-axis, and torsional moments about the e-axis (Fig. 3) for the four girders under a uniformly distributed load is available.[16] It was found, as might be expected, that the moments about the r-axis and e-axis decreased rapidly with increasing width-to-depth ratio, while the moments about the s-axis increased somewhat. The net result indicates that for a given depth of cross section, the stresses due to bending and torsional moments will rapidly become smaller up to a width-to-depth ratio of 8 to 1. There will then be a much smaller decrease in stresses.

CONCLUSIONS

On the basis of the study reported herein the following conclusions may be drawn regarding the behavior and analysis of a semicircular helicoidal girder under vertical load:

1. For girders with rectangular cross sections having a width-to-depth ratio of between 1 and 16 and a ratio of centerline radius to a width of between 3 and infinity, sufficiently accurate results for the end reactions to be used in design may be obtained by analyzing only the elastic line defined by the longitudinal centroidal axis of the girder, thus neglecting the slab effects.
2. The bending and torsional stiffnesses to be used in the analysis may be taken as those defined for a straight prismatic member of the same cross section.
3. The influence ordinates across the width of a girder have a linear relationship, the ordinate at the centerline being the average ordinate at any radial section.
4. For a cross section of given depth there is little change in the end reactions for increasing width-to-depth ratios beyond approximately 6 to 8.
5. For girders subjected to a uniformly distributed load over the whole span, the stresses in the girder will decrease rapidly with increasing width-to-depth ratios up to approximately 6 to 8, after which there will be little change.
6. A design based on the internal moments and torques obtained by analyzing the horizontal projection of the helicoid as a bow girder under uniform load will, in most cases, be grossly conservative because it neglects the inherent strength of the three-dimensional structure.

Obviously a determination of the end reactions is only a first step in the design of a structure of this type. When the end reactions are known, the internal forces and moments at any cut section may be obtained, but a knowledge of stress distribution is still lacking. This later problem requires further

16 Discussion by A. C. Scordelis of "Helicoidal Staircases of Reinforced Concrete," by V. R. Bergman, Journal, A.C.I., Vol. 28, No. 12, 1957.

study. However, in reinforced concrete structures the proportioning of sections and reinforcement must, in all probability, be based on approximate methods rather than "exact" stress formulas.

APPENDIX

The following equations express the displacements at the bottom end of a helicoidal girder subtending a horizontal angle, ϕ, equal to 180° due to a vertical concentrated load P.

$$\delta_{xx} = \frac{r^3}{EI_r}\left[\frac{\tan^2\alpha}{\cos\alpha}\right]\left[\frac{\pi^3}{6} + \frac{\pi}{4}\right] + \frac{r^3}{EI_s}\left[\frac{1}{\cos\alpha}\right](\cos^2\alpha)\left(\frac{3\pi}{2}\right) + (\sin^2\alpha)\left(\frac{5\pi}{2}\right)$$

$$+ (\sin\alpha\tan\alpha)^2\left(\frac{\pi^3}{6} - \frac{\pi}{4}\right) + \frac{r^3}{GJ_e}\left[\frac{1}{\cos\alpha}\right](\sin^2\alpha)\left(\frac{\pi^3}{6} - \frac{5\pi}{4}\right) \quad \ldots\ldots (9)$$

$$\delta_{xy} = \delta_{yx} = \frac{r^3}{EI_r}\left[\frac{\tan^2\alpha}{\cos\alpha}\right]\left[\frac{\pi^2}{4}\right] + \frac{r^3}{EI_s}\left[\frac{1}{\cos\alpha}\right]\left[2\cos^2\alpha - 2\sin^2\alpha\right.$$

$$\left. - (\sin\alpha\tan\alpha)^2\left(\frac{\pi^2}{4}\right)\right] + \frac{r^3}{GJ_e}\left[\frac{\sin^2\alpha}{\cos\alpha}\right]\left[4 - \frac{\pi^2}{4}\right] \quad \ldots\ldots (10)$$

$$\delta_{xz} = \delta_{zx} = \frac{r^3}{EI_r}\left[-\frac{\tan\alpha}{\cos\alpha}\right]\left[\frac{\pi}{4}\right] + \frac{r^3}{EI_s}[\sin\alpha]\left[\frac{3\pi}{2} + (\tan^2\alpha)\left(\frac{5\pi}{4}\right)\right]$$

$$+ \frac{r^3}{GJ_e}[-\sin\alpha]\left[\frac{\pi}{4}\right] \quad \ldots\ldots (11)$$

$$\delta_{xp} = \delta_{px} = \frac{r^2}{EI_s}[\cos\alpha]\left[\pi + (\tan^2\alpha)\ (\pi)\right] \quad \ldots\ldots (12)$$

$$\delta_{xr} = \delta_{rx} = \frac{r^2}{EI_r}\left[\frac{\tan\alpha}{\cos\alpha}\right]\left[\frac{\pi^2}{4}\right] + \frac{r^2}{EI_s}[\sin\alpha](\tan^2\alpha)\left(\frac{\pi^2}{4}\right) + 2\Big]$$

$$+ \frac{r^2}{GJ_e}[\sin\alpha]\left[\frac{\pi^2}{4} - 2\right] \quad \ldots\ldots (13)$$

$$\delta_{xt} = \delta_{tx} = \frac{r^2}{EI_r}\left[\frac{\tan\alpha}{\cos\alpha}\right]\left[\frac{\pi}{4}\right] + \frac{r^2}{EI_s}[-\sin\alpha]\left[\frac{\pi}{2} + (\tan^2\alpha)\left(\frac{\pi}{4}\right)\right]$$

$$+ \frac{r^2}{GJ_e}[\sin\alpha]\left[\frac{\pi}{4}\right] \quad \ldots\ldots (14)$$

$$\delta_{yy} = \frac{r^3}{EI_r}\left[\frac{\tan^2\alpha}{\cos\alpha}\right]\left[\frac{\pi^3}{6} - \frac{\pi}{4}\right] + \frac{r^3}{EI_s}\left[\frac{1}{\cos\alpha}\right]\left[(\cos^2\alpha)\left(\frac{\pi}{2}\right) - (\sin^2\alpha)\left(\frac{\pi}{2}\right)\right.$$

$$\left. + (\sin\alpha\tan\alpha)^2\left(\frac{\pi^3}{6} + \frac{\pi}{4}\right)\right] + \frac{r^3}{GJ_e}\left[\frac{\sin^2\alpha}{\cos\alpha}\right]\left[\frac{\pi^3}{6} + \frac{5\pi}{4}\right] \quad \ldots\ldots (15)$$

$$\delta_{yz} = \delta_{zy} = \frac{r^3}{EI_r}\left[-\frac{\tan\alpha}{\cos\alpha}\right]\left[\frac{\pi^2}{4}\right] + \frac{r^3}{EI_s}[\sin\alpha]\left[2 - 2\tan^2\alpha - (\tan^2\alpha)\left(\frac{\pi^2}{4}\right)\right] + \frac{r^3}{GJ_e}[-\sin\alpha]\left[4 + \frac{\pi^2}{4}\right] \quad \ldots\ldots (16)$$

$$\delta_{yp} = \delta_{py} = \frac{r^2}{EI_s}[2(\cos\alpha - \sin\alpha\tan\alpha)] + \frac{r^2}{GJ_e}\left[\frac{4\sin^2\alpha}{\cos\alpha}\right] \quad \ldots\ldots (17)$$

$$\delta_{yr} = \delta_{ry} = \frac{r^2}{EI_r}\left[\frac{\tan\alpha}{\cos\alpha}\right]\left[\frac{\pi}{4}\right] + \frac{r^2}{EI_s}[\sin\alpha]\left[\frac{\pi}{2} - (\tan^2\alpha)\left(\frac{\pi}{4}\right)\right] + \frac{r^2}{GJ_e}[-\sin\alpha]\left[\frac{3\pi}{4}\right] \quad \ldots\ldots (18)$$

$$\delta_{yt} = \delta_{ty} = \frac{r^2}{EI_r}\left[\frac{\tan\alpha}{\cos\alpha}\right]\left[\frac{\pi^2}{4}\right] + \frac{r^2}{EI_s}\left[(\sin\alpha\tan^2\alpha)\left(\frac{\pi^2}{4}\right)\right] + \frac{r^2}{GJ_e}\left[(\sin\alpha)\left(\frac{\pi^2}{4}\right)\right] \quad \ldots\ldots (19)$$

$$\delta_{zz} = \frac{r^3}{EI_r}\left[\left(\frac{1}{\cos\alpha}\right)\left(\frac{\pi}{2}\right)\right] + \frac{r^3}{EI_s}\left[\frac{\sin^2\alpha}{\cos\alpha}\right]\left[\frac{3\pi}{2}\right] + \frac{r^3}{GJ_e}\left[(\cos\alpha)\left(\frac{3\pi}{2}\right)\right] \quad \ldots\ldots (20)$$

$$\delta_{zp} = \delta_{pz} = \frac{r^2}{EI_s}[(\sin\alpha)(\pi)] + \frac{r^2}{GJ_e}[(-\sin\alpha)(\pi)] \quad \ldots\ldots (21)$$

$$\delta_{zr} = \delta_{rz} = \frac{r^2}{EI_s}\left[\frac{2\sin^2\alpha}{\cos\alpha}\right] + \frac{r^2}{GJ_e}[2\cos\alpha] \quad \ldots\ldots (22)$$

$$\delta_{zt} = \delta_{tz} = \frac{r^2}{EI_r}\left[\left(-\frac{1}{\cos\alpha}\right)\left(\frac{\pi}{2}\right)\right] + \frac{r^2}{EI_s}\left[\left(-\frac{\sin^2\alpha}{\cos\alpha}\right)\left(\frac{\pi}{2}\right)\right] + \frac{r^2}{GJ_e}\left[(-\cos\alpha)\left(\frac{\pi}{2}\right)\right] \quad \ldots\ldots (23)$$

$$\delta_{pp} = \frac{r}{EI_s}[(\cos\alpha)(\pi)] + \frac{r}{GJ_e}\left[\left(\frac{\sin^2\alpha}{\cos\alpha}\right)(\pi)\right] \quad \ldots\ldots (24)$$

$$\delta_{pr} = \delta_{rp} = \frac{r}{EI_s}[2\sin\alpha] + \frac{r}{GJ_e}[-2\sin\alpha] \quad \ldots\ldots (25)$$

$$\delta_{pt} = \delta_{tp} = 0 \quad \ldots\ldots (26)$$

$$\delta_{rr} = \frac{r}{EI_r}\left[\left(\frac{1}{\cos\alpha}\right)\left(\frac{\pi}{2}\right)\right] + \frac{r}{EI_s}\left[\left(\frac{\sin^2\alpha}{\cos\alpha}\right)\left(\frac{\pi}{2}\right)\right] + \frac{r}{GJ_e}\left[(\cos\alpha)\left(\frac{\pi}{2}\right)\right] \quad \ldots\ldots (27)$$

$$\delta_{rt} = \delta_{tr} = 0 \quad \ldots\ldots (28)$$

$$\delta_{tt} = \frac{r}{EI_r}\left[\left(\frac{1}{\cos\alpha}\right)\left(\frac{\pi}{2}\right)\right] + \frac{r}{EI_s}\left[\left(\frac{\sin^2\alpha}{\cos\alpha}\right)\left(\frac{\pi}{2}\right)\right] + \frac{r}{GJ_e}\left[(\cos\alpha)\left(\frac{\pi}{2}\right)\right] \quad \ldots\ldots (29)$$

$$\delta_{xo} = \frac{P\,r^3}{EI_r}\left[-\frac{\tan\alpha}{\cos\alpha}\right]\left[\left(\frac{\cos\theta}{4}\right)\left(\theta\cos 2\theta - \frac{1}{2}\sin 2\theta - \pi\right) - \left(\frac{\sin\theta}{4}\right)\left(\frac{1}{2}\right.\right.$$

$$\left. + \pi^2 - \theta^2 - \theta\sin 2\theta - \frac{\cos 2\theta}{2}\right)\Bigg] + \frac{P\,r^3}{EI_s}\left[-\sin\alpha\right]\Big[(\pi - \theta)$$

$$+ \left(\tan^2\alpha\right)(\pi - \sin\theta + \theta\cos\theta) + (\cos\theta)\left(\frac{\pi}{2} - \frac{\theta}{2} - \frac{\sin 2\theta}{4}\right)$$

$$+ \left(\frac{\sin\theta}{4}\right)(\cos 2\theta - 1) - \left(\frac{\tan^2\alpha}{4}\right)(\cos\theta)\left(\theta\cos 2\theta - \frac{1}{2}\sin 2\theta - \pi\right)$$

$$- \left(\frac{\tan^2\alpha}{4}\right)(\sin\theta)\left(\pi^2 - \frac{1}{2} - \theta^2 + \theta\sin 2\theta + \frac{\cos 2\theta}{2}\right)\Big]$$

$$+ \frac{P\,r^3}{GJ_e}\left[-\sin\alpha\right]\Big[\theta - \frac{5}{8}\sin\theta + \frac{1}{4}\left(\theta^2 - \pi^2\right)\sin\theta + \frac{3}{2}\theta\cos\theta$$

$$- \frac{\pi}{4}\cos\theta + \frac{3}{8}\cos\theta\sin 2\theta - \frac{3}{8}\sin\theta\cos 2\theta - \frac{\theta}{4}\sin\theta\sin 2\theta$$

$$- \frac{\theta}{4}\cos\theta\cos 2\theta\Big] \quad \ldots\ldots (30)$$

$$\delta_{yo} = \frac{P\,r^3}{EI_r}\left[\frac{\tan\alpha}{\cos\alpha}\right]\left[\left(\frac{\cos\theta}{4}\right)\left(\pi^2 - \frac{1}{2} - \theta^2 + \theta\sin 2\theta + \frac{\cos 2\theta}{2}\right)\right.$$

$$\left. - \frac{\sin\theta}{4}\left(\theta\cos 2\theta - \frac{1}{2}\sin 2\theta - \pi\right)\right] + \frac{P\,r^3}{EI_s}\left[-\sin\alpha\right]\Big[1 + \cos\theta$$

$$- \left(\tan^2\alpha\right)(1 + \cos\theta + \theta\sin\theta) - \left(\frac{\cos\theta}{4}\right)(\cos 2\theta - 1) - \left(\frac{\sin\theta}{2}\right)$$

$$\left(\pi - \theta + \frac{\sin 2\theta}{2}\right) - \left(\frac{\tan^2\alpha}{4}\right)(\cos\theta)\left(\frac{1}{2} + \pi^2 - \theta^2 - \theta\sin 2\theta\right.$$

$$\left. - \frac{\cos 2\theta}{2}\right) - \left(\frac{\tan^2\alpha}{4}\right)(\sin\theta)\left(\theta\cos 2\theta - \frac{1}{2}\sin 2\theta - \pi\right)\Big]$$

$$+ \frac{P\,r^3}{GJ_e}\left[-\sin\alpha\right]\Big[-(1 + \cos\theta + \theta\sin\theta) - (1 + \cos\theta) - \left(\frac{\cos\theta}{4}\right)$$

$$\left(\frac{3}{2} + \pi^2 - \theta^2 - \theta\sin 2\theta - \frac{3}{2}\cos 2\theta\right) - \left(\frac{\sin\theta}{4}\right)\left(\theta\cos 2\theta\right.$$

$$\left. - \frac{3}{2}\sin 2\theta - 3\pi + 2\theta\right)\Big] \quad \ldots\ldots (31)$$

$$\delta_{zo} = \frac{P\,r^3}{EI_r}\left[-\frac{1}{\cos\alpha}\right]\left[\left(\frac{\cos\theta}{2}\right)\left(\pi - \theta + \frac{\sin 2\theta}{2}\right) - \left(\frac{\sin\theta}{4}\right)(\cos 2\theta - 1)\right]$$
$$+ \frac{P\,r^3}{EI_s}\left[-\frac{\sin^2\alpha}{\cos\alpha}\right]\left[\pi - \theta + \left(\frac{\cos\theta}{2}\right)\left(\pi - \theta - \frac{\sin 2\theta}{2}\right) + \left(\frac{\sin\theta}{4}\right)\right.$$
$$\left.(\cos 2\theta - 1)\right] + \frac{P\,r^3}{GJ_e}\left[-\cos\alpha\right]\left[\pi - \theta + \left(\frac{\cos\theta}{2}\right)\left(\pi - \theta - \frac{\sin 2\theta}{2}\right)\right.$$
$$\left. + \left(\frac{\sin\theta}{4}\right)(\cos 2\theta - 1)\right] \quad \ldots\ldots\ldots\ldots\ldots\ldots\ldots\ldots\ldots (32)$$

$$\delta_{po} = \frac{P\,r^2}{EI_s}\left[-\sin\alpha\right]\left[(\pi - \theta) - \sin\theta\right] + \frac{P\,r^2}{GJ_e}\left[\sin\alpha\right]\left[(\pi - \theta) - \sin\theta\right] \quad \ldots (33)$$

$$\delta_{ro} = \frac{P\,r^2}{EI_r}\left[-\frac{1}{\cos\alpha}\right]\left[\left(\frac{\cos\theta}{4}\right)(\cos 2\theta - 1) - \left(\frac{\sin\theta}{2}\right)\left(\pi - \theta - \frac{\sin\theta}{2}\right)\right]$$
$$+ \frac{P\,r^2}{EI_s}\left[-\frac{\sin^2\alpha}{\cos\alpha}\right]\left[1 + \cos\theta - \left(\frac{\cos\theta}{4}\right)(\cos 2\theta - 1) - \left(\frac{\sin\theta}{2}\right)\right.$$
$$\left.\left(\pi - \theta + \frac{\sin 2\theta}{2}\right)\right] + \frac{P\,r^2}{GJ_e}\left[-\cos\alpha\right]\left[1 + \cos\theta - \left(\frac{\cos\theta}{4}\right)(\cos 2\theta - 1)\right.$$
$$\left. - \left(\frac{\sin\theta}{2}\right)\left(\pi - \theta + \frac{\sin 2\theta}{2}\right)\right] \quad \ldots\ldots\ldots\ldots\ldots\ldots\ldots\ldots (34)$$

and

$$\delta_{to} = \frac{P\,r^2}{EI_r}\left[\frac{1}{\cos\alpha}\right]\left[\left(\frac{\cos\theta}{2}\right)\left(\pi - \theta + \frac{\sin 2\theta}{2}\right) - \left(\frac{\sin\theta}{4}\right)(\cos 2\theta - 1)\right]$$
$$+ \frac{P\,r^2}{EI_s}\left[-\frac{\sin^2\alpha}{\cos\alpha}\right]\left[-\sin\theta - \left(\frac{\cos\theta}{2}\right)\left(\pi - \theta - \frac{\sin 2\theta}{2}\right) - \left(\frac{\sin\theta}{4}\right)\right.$$
$$\left.(\cos 2\theta - 1)\right] + \frac{P\,r^2}{GJ_e}\left[-\cos\alpha\right]\left[-\sin\theta - \left(\frac{\cos\theta}{2}\right)\left(\pi - \theta - \frac{\sin 2\theta}{2}\right)\right.$$
$$\left. - \left(\frac{\sin\theta}{4}\right)(\cos 2\theta - 1)\right] \quad \ldots\ldots\ldots\ldots\ldots\ldots\ldots\ldots\ldots (35)$$

AMERICAN SOCIETY OF CIVIL ENGINEERS

Founded November 5, 1852

TRANSACTIONS

Paper No. 3014

DESIGN AND PERFORMANCE OF VERMILION DAM

By Karl Terzaghi,[1] Hon. M. ASCE and Thomas M. Leps,[2] F. ASCE

With Discussion by Messrs. Maurice L. Dickinson; John R. Kiely; Ralph W. Spencer; Philip J. West; Joseph H. Birman; Bruce R. Laverty; and Karl Terzaghi and Thomas M. Leps.

SYNOPSIS

This paper describes the design and performance of a zoned earth dam in the Sierra Nevada, California, on marginal glacial deposits. The pattern of stratification is so intricate that it was impracticable to determine all the essential geological features of the subsoil in advance of construction. Therefore, it was necessary to check on the design assumption during construction and to modify some details of the original design in accordance with the findings. As a result, the finished structure is as safe and satisfactory as if all the essential properties of the site had been known in advance of construction.

INTRODUCTION

The dam site is located at an elevation of approximately 7,500 ft above sea level, in the valley of Mono Creek, a northern tributary of the South Fork of the San Joaquin River in central California. The site was investigated for the first time in 1918 to determine the watershed and capacity of the reservoir. Exploratory drilling in 1924 revealed unfavorable foundation conditions for the concrete dam then being considered, and the project was temporarily abandoned. It was reconsidered in 1940 on the basis that an earthfill dam could be shown to be feasible. The earthfill dam, as built, has a maximum height of 160

Note.—Published, essentially as printed here, in August, 1958, in the Journal of the Soil Mechanics and Foundations Division, as Proceedings Paper 1728. Position and titles given are those in effect when the paper or discussion was approved for publication in Transactions.

[1] Prof. Emeritus, Harvard Univ., Cambridge, Mass.

[2] Mgr. of Organization and Procedures, Southern Calif. Edison Co., Los Angeles, Calif.

ft above the original ground surface, and a 4,300 ft crest length. Construction was begun in May, 1953, and the dam was completed at the end of 1954. The reservoir formed by the dam adds 125,000 acre-ft to the total storage capacity of the reservoirs previously built in the San Joaquin basin. A description of the entire hydroelectric power development utilizing the water resources of the basin, and a brief account of the construction of the Vermilion Dam has been presented elsewhere.[3]

GEOLOGY OF THE DAM SITE

Before the Pleistocene ice age, the present location of Mono Creek Valley was occupied by an erosion valley carved out of granite. Locally, the surface of the granite was covered by the remnants of a flow of pre-Pleistocene basaltic lava. At the dam site, the bottom of the old riverbed is situated at a depth of approximately 250 ft below the deepest point of the present valley. An outcrop of the basaltic lava is situated a short distance upstream from the dam site, west of the old course of Mono Creek.

During the Pleistocene ice age, the valleys descending from the summit region of the Sierra Nevada were invaded repeatedly by valley glaciers descending to an altitude of a few hundred feet below that of the dam site. The glaciers deposited subglacial, marginal and fluvio-glacial materials in the valleys. At the dam site, the youngest member of the glacial deposits consists of a set of low, terminal moraines resting on impervious glacial till. At the west end of the dam site, the remnants of a kame terrace were encountered.

The upper part of the fluvio-glacial sediments beneath the youngest till sheet contains one large lens and several smaller lenses of silt with a variable thickness. The continuity of at least the youngest fluvio-glacial and glacial lake deposits was disrupted by small erosion valleys carved out by streamlets emerging from the glaciers and subsequently backfilled with silty to clean sand and sand-gravel mixtures. Therefore, the pattern of stratification of the subsoil at the dam site is so erratic that it was impracticable to determine its average coefficient of permeability on the basis of the results of laboratory tests.

Upstream from the dam site, the subsoil consists of coarse-grained, somewhat silty, fluvio-glacial and post-glacial river deposits with an almost horizontal surface, underlying an area of the valley floor with a length of several miles and a width of several thousand feet. Formerly, Mono Creek meandered on this floor. In recent geological times, the meandering creek began to erode, forming incised meanders with steep side slopes. At the dam site, the creek has cut to a depth of 40 ft below the old valley floor.

The details of the glacial geology of the dam site were investigated during the summers of 1950 and 1951. The location of the terminal moraines and the kame terrace at the west abutment are shown in Fig. 1. Fig. 2 is an idealized geological profile of the subsoil along the centerline of the dam. The results of the geological survey furnished the basis for a tentative interpretation of the

---

[3] "Earth-Fill Dam Adds Large Capacity to San Joaquin Storage," by R. W. Spencer, Civil Engineering, Vol. 25, No. 3, 1955.

boring records and for making reasonably realistic assumptions concerning the subsoil conditions for design purposes.

SUBSOIL EXPLORATIONS

In 1924, 18 boreholes were made at the site and in the proximity of the present dam. On the basis of the results, the project was temporarily abandoned. In 1946, the site exploration was resumed. The exploratory work included 14 borings with an average depth of 100 ft and a maximum depth of 269 ft. The exploration also included the digging of 2 test pits with a depth of approximately 30 ft each, 3 open cuts across terminal moraines and several bulldozer trenches on the steep slopes of the present erosion valley of Mono Creek. Eight of the 14 drill holes were located along the centerline of the dam and spaced approximately 600 ft apart. The other holes were drilled in the proximity of the toe of the dam.

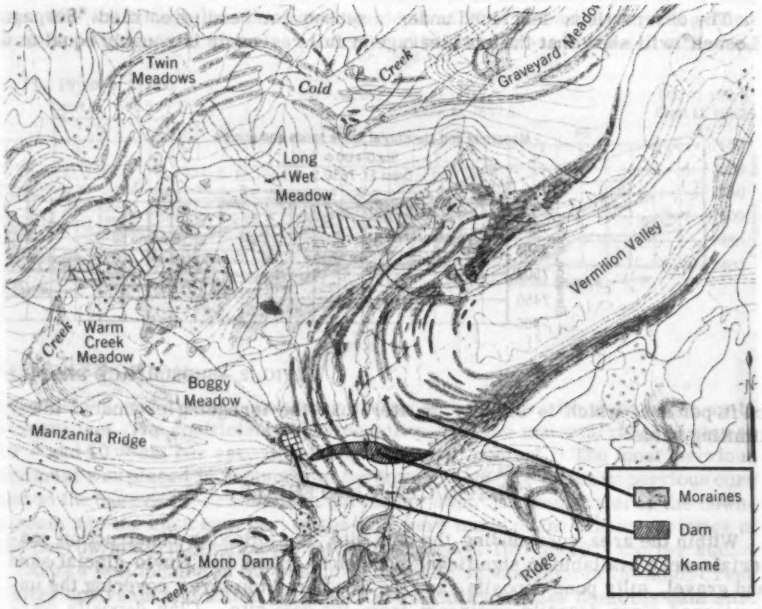


FIG. 1.—GLACIAL GEOLOGY OF VERMILION VALLEY

The crest of the dam is approximately 4,300 ft long and the base has a maximum width of 800 ft. If the drill holes had been spaced 20 ft both ways, subsoil exploration would have required several thousand drill holes and a prohibitive amount of testing. However, judging from the pattern of stratification visible on the sides of open cuts, for instance on the exposure shown in Fig. 3, the results would still have left a wide margin for interpretation. Therefore, at a site such as that of Vermilion Dam, the exploratory drill holes merely serve the purpose of supplementing the results of the geological survey. At Vermilion Dam, 14 borings sufficed to obtain all of the required information.

Any additional exploratory work would have increased the cost of exploration without furnishing any significant contribution to the knowledge of the site.

The tests on the samples recovered from drill holes and test pits included grain size determination and permeability tests. Even within the fluvio-glacial deposits the value of the coefficient of permeability, k, was extremely variable. It ranged between 10^{-1} and 10^{-6} cm per sec. Owing to the silt content of the sediments, the average was rather low, and the coefficient of permeability in a vertical direction, k_v, was consistently smaller than the corresponding value, k_h, for horizontal directions.

The results of the permeability tests made it possible to obtain at least an upper and lower limiting value for the loss of water, Q, due to seepage out of the reservoir, by using the flow net method. Assuming that

1. $k_h = 9 \times 10^{-3}$ cm per sec, $k_v = 10^{-3}$ cm per sec, Q = 29 cu ft per sec; and
2. $k_h = k_v \times 10^{-3}$ cm per sec, and Q = 4 cu ft per sec.

The observations described under a subsequent heading entitled "Seepage Losses" will show that the total leakage at full reservoir is roughly equal to 6

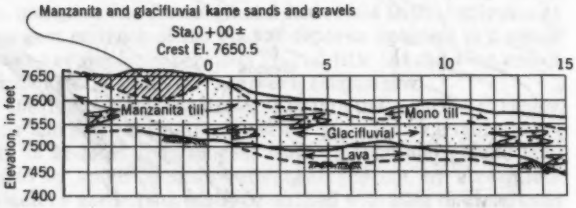


FIG. 2.—SUBSURFACE PROFILE

cu ft per sec, which is slightly greater than the foregoing estimated lower limiting value.

CONSTRUCTION MATERIALS

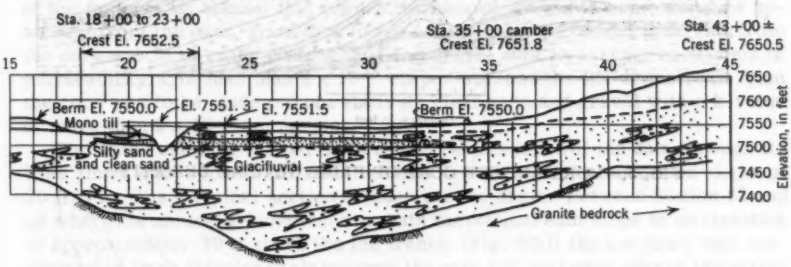
Within the area surrounding the dam site, the following construction materials were available in significant quantities: Stony till, fluvio-glacial sand and gravel, silty pond deposits, and the weathered top layer covering the unweathered river deposits upstream from the dam site. Clay deposits were conspicuously absent. Even the pond or lake deposits contained no more than a trace of clay.

Because of the absence of clay in the earlier stages of the exploratory work, all efforts were concentrated on locating suitable materials for the relatively impervious section of the proposed earth dam and for the construction of a relatively impervious blanket to be placed upstream from the dam. After the borrow pits were opened, it was found to be equally difficult to find very pervious material, because the bulk of the glacial outwash contained at least traces of silt or rock flour.

On the basis of the results of the geological survey, four general areas were selected as potential sources for suitable construction materials. The location

of these areas with reference to the dam site is shown in Fig. 4. Area 1, at a distance of approximately one mile west of the dam, consisted of a marshy meadow covering the surface of a stratified, locally varved deposit of fine silty sand and silt that was laid down in a pond. In order to estimate the available quantity, auger borings with an average depth of 20 ft and a maximum depth of 90 ft, spaced approximately 400 ft both ways were made. It was found that the laboratory coefficient of permeability of the material ranged between 10^{-6} and 10^{-2} cm per sec, and averaged 10^{-5} cm per sec. The natural water content of the material was above optimum. Therefore, it was decided to lower the water table beneath the meadow by approximately 5 ft by means of 10 ft deep drainage trenches (Fig. 4). Because the deposit contained more or less continuous layers of fine, clean sand, drainage was effective. Most of the material derived from Area 1 was classified as impervious and was used for constructing the blanket and core.

Borrow Areas 2 and 3 were close to and north of the eastern part of the dam site. The water table was at an average depth of 20 ft below the original ground surface. Most of the material encountered in these areas consisted of fluvio-



ALONG AXIS OF DAM

glacial sand and gravel, containing scattered boulders with a diameter up to several feet. The coefficient of permeability, k, of the material ranged between 10^{-2} and 10^{-5} cm per sec, depending on the silt content. The most pervious material was placed in contact with the downstream face of the impervious core and on the base of the downstream part of the dam. The remainder of the downstream and the upstream part of the dam were made of the siltier varieties of the borrow material, with a permeability range of 10^{-3} to 10^{-4} cm per sec.

Area 4 was located on the wide and almost horizontal floor of the Mono Creek Valley upstream and within a distance of two to four miles from the dam site. The deposit was explored by means of auger holes, 10 ft deep, spaced 700 ft in the direction of the valley and 500 ft at right angles to it. The borings showed that the area was underlain by pervious and semi-pervious fluvio-glacial deposits and river sand and gravel. The uppermost 3 ft of the deposit were slightly weathered and relatively impervious. The water table was located at an average depth of 9 ft below the valley floor. By excavating the uppermost section of the deposit to an average depth of 5 ft and by mixing the pervious and impervious materials present within this layer, 1.3×10^6 cu yd of compacted fill material with an average permeability of 10^{-5} cm per sec was obtained. Such a blend of the top 5 ft of Area 4 furnished the bulk of the impervious core of the dam. The mixing was satisfactorily performed by excavating

the material along a 5 ft high vertical face, using elevating graders. A portable sprinkler system was used to add moisture to the surface materials. The output averaged 20 cu yd per minute for each loader.

The material beneath the 5 ft thick excavated layer was relatively pervious sand and gravel having an average coefficient of permeability of 10^{-3} cm per



FIG. 3.—MORAINE WITH CORE OF FLUID GLACIAL DEPOSITS

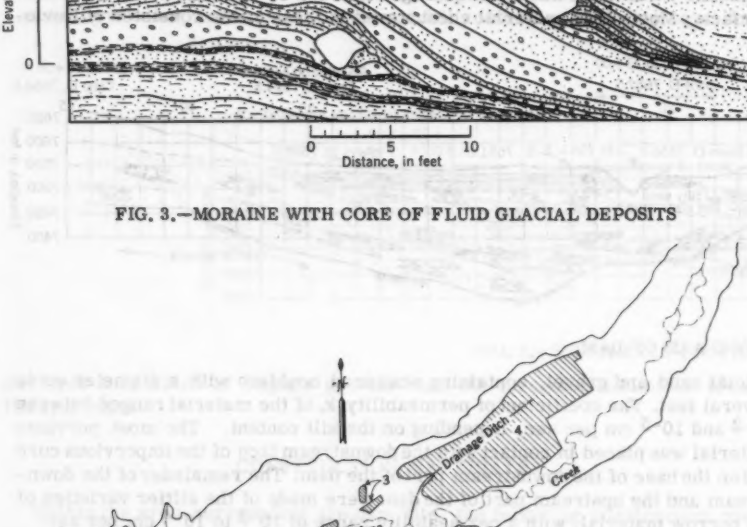


FIG. 4.—LOCATION OF BORROW AREAS AND DRAINAGE DITCHES

sec. Some 1.5×10^6 cu yd of this material was excavated and built into the upstream and downstream parts of the dam. Some of the borrow pit excavation for such material extended well below groundwater table, necessitating the excavation of the drainage ditch shown on Fig. 4. The pervious materials were

loaded by carrying scrapers pulled by a rubber-tired tractor and assisted in loading by two crawler tractors.

DESIGN OF THE DAM

The design of the dam was governed by the following considerations:

1. Owing to the scarcity of impervious materials, the construction of a zoned earth dam was indicated.
2. The average permeability of the substrata is high, and
3. The cost of a cutoff of over 200 ft to bedrock would be prohibitive.

Therefore, it was necessary to cover the ground surface upstream from the dam with an impervious blanket, and to provide adequate drainage facilities along the downstream toe to eliminate the possibility of a failure due to piping.

Fig. 5 is a plan of the dam, Fig. 6(a) shows a vertical section through the highest part of the dam at Station 21 + 00, and Fig. 6(b), a section at Station 28 + 00. The impervious core of the dam rises above the downstream fringe of the impervious blanket that covers the natural ground to some distance upstream from the dam. According to the original design, the fill upstream from the core was to be made of silty sand and gravel with an average coefficient of permeability, k, of less than 2×10^{-3} cm per sec, and the fill downstream from the core was to be made out of relatively clean sand and gravel with a k-value of more than 2×10^{-3} cm per sec.

The water entering the pervious downstream section of the dam through its base flows into a toe drain installed in a trench having a maximum depth of 20 ft. Fig. 7 is a typical section through the toe drain. Between Station 22 and 28 where the natural ground rises beneath the downstream slope to an elevation of approximately 70 ft above the toe trench (Fig. 6(b)) the toe drain was supplemented by an interior drain between the core and the upper edge of the buried north slope of Mono Creek (Fig. 5).

Because of the predominantly horizontal stratification of the subsoil and the presence in the subsoil of lenses and layers of silt with unknown horizontal dimensions underlain by very pervious sediments, it was conceivable that the hydrostatic pressure acting on the base of silty layers might lift the floor of the valley downstream from the dam. Therefore, it was decided to supplement the toe drain with relief wells as shown in Figs. 7 and 10. At the maximum section of the dam, where the danger of heave was greatest, the wells were drilled to an average depth of 70 ft and the spacing ranged between 50 ft and 100 ft. Beyond the maximum section of the dam and the outer boundaries of the Mono Creek stream bed, the wells were drilled to a depth of approximately 50 ft and the spacing was increased to 200 ft (Fig. 10).

The stability computation for the dam was made by the Swedish Circle method. In any investigated section, a large part of the critical circle was in the natural ground, beneath the base of the fill. The factor of safety with respect to sliding along the potential surface of sliding depends to a large extent on the average intensity of the pore water pressures along the surface. Because of the relatively high permeability and low compressibility of the core material, it was justified to assume that the construction pore water pressures would be negligible. The pore water pressures due to leakage out of the reservoir are determined by the pattern of seepage through the subsoil. This pattern was unknown until the reservoir was filled for the first time. Therefore, the stability computations were made on the basis of what appeared to be the

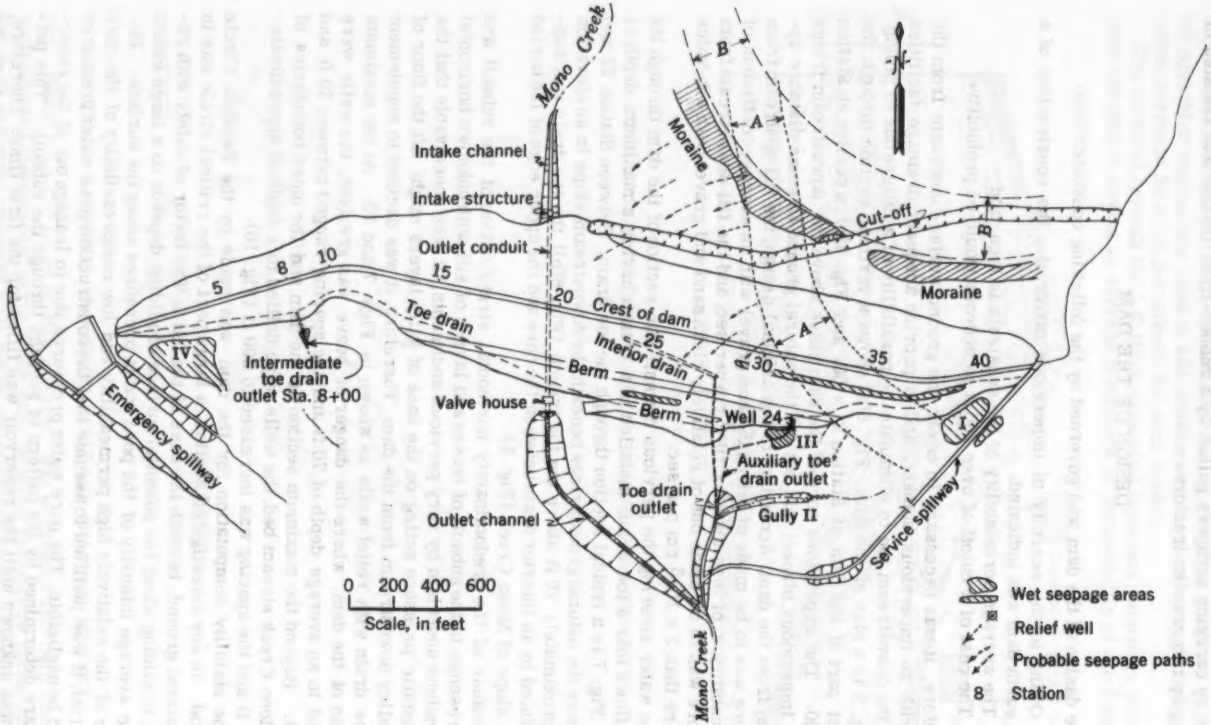
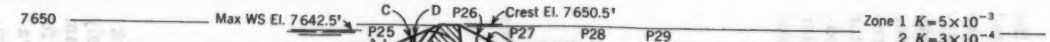


FIG. 5.—GENERAL PLAN SHOWING WET AREAS AND PROBABLE SUBSURFACE SEEPAGE PATHS



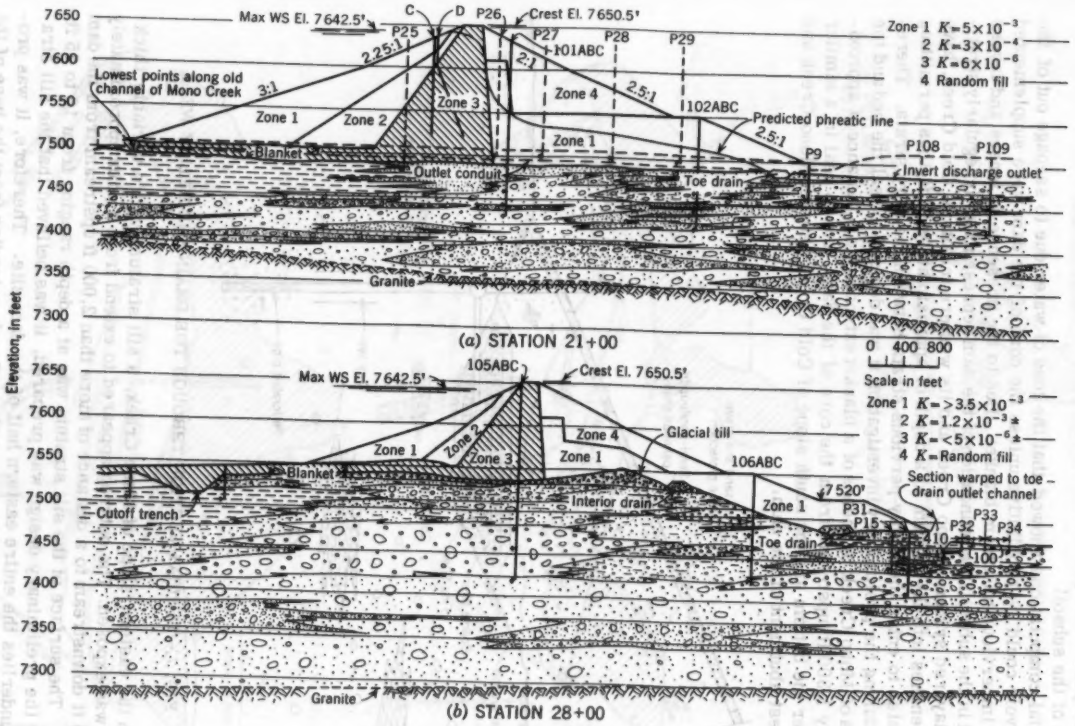


FIG. 6.—CROSS SECTIONS OF THE DAM

highest pore water pressures compatible with general geological characteristics of the subsoil.

Trial computations showed that the loss of water due to seepage out of the reservoir could be prohibitive unless the core of the dam were supplemented by an impervious upstream blanket. Due to the presence of lenses and layers of silt in the subsoil, the foundation of the dam represents an irregularly stratified, layered system. Mono Creek and its western tributary, Cold Creek, have cut trenches into the system to a depth of approximately 40 ft, thus permitting the water to enter the highly pervious strata between the silty strata. Therefore, during the preliminary investigation it was decided to seal the bed and the slopes of Mono Creek by means of a blanket extending to a distance of approximately 1,300 ft upstream from the core of the dam, and to seal in a similar manner the bottom and the south slope of Cold Creek between Mono Creek and the west abutment of the dam.

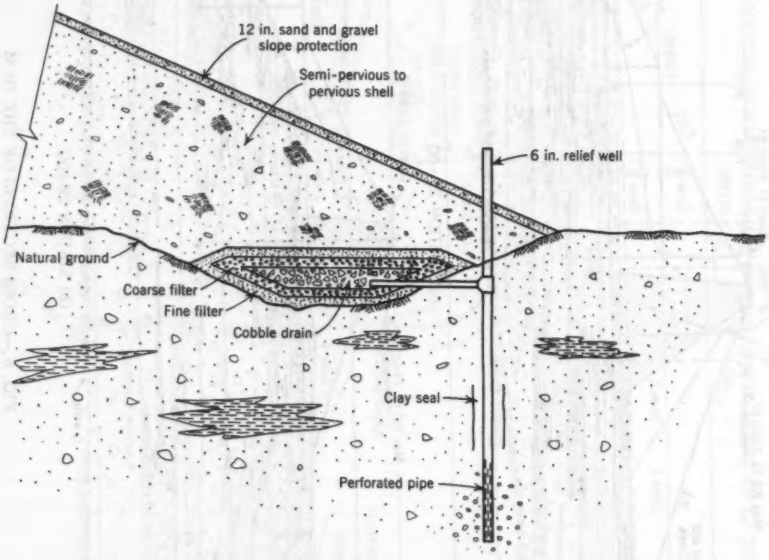


FIG. 7.—TYPICAL SECTION THROUGH TOE DRAIN AND RELIEF WELL

On the eastern slope of Mono Creek, a silt stratum with a variable thickness was exposed. The outcrop appeared to extend from a point approximately 1,000 ft downstream to a distance of more than 2,000 ft upstream from the dam site. The surface of the silt stratum was at a depth ranging from 10 to 25 ft. When the preliminary design was prepared, it was believed that the silt stratum underlies the entire eastern half of the dam site. Therefore, it was proposed to construct a cutoff east of Mono Creek, extending from the base of the core into the silt stratum as shown in Fig. 8(a). Subsequently, the modification shown in Fig. 8(b) was proposed to offset expected seepage through the east abutment area. However, before the construction drawings were prepared, exploration disclosed that the dam was above a narrow but deep pervious gap in the silt stratum. Therefore, the location for the cutoff was shifted into the position shown in Fig. 8(c). The core and the cutoff are connected to each

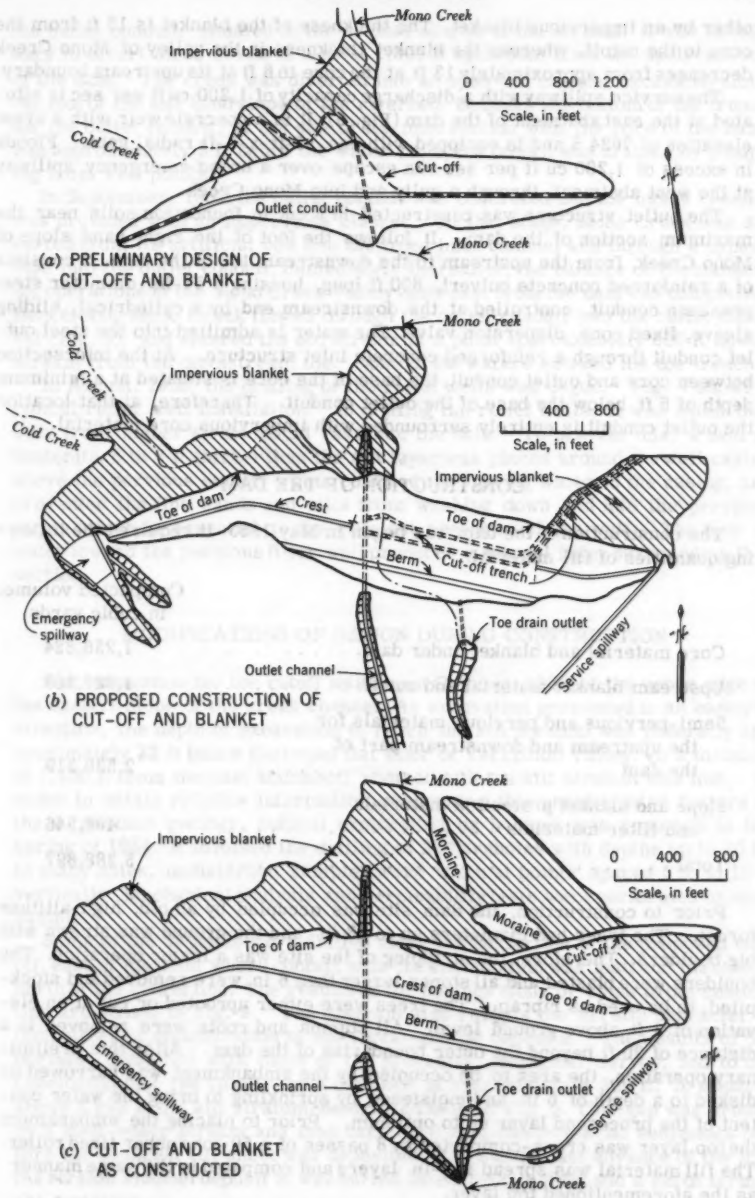


FIG. 8.—THREE STAGES IN DESIGN OF THE CUTOFF AND BLANKET

other by an impervious blanket. The thickness of the blanket is 13 ft from the core to the cutoff, whereas the blanket thickness in the valley of Mono Creek decreases from approximately 13 ft at the core to 6 ft at its upstream boundary.

The service spillway with a discharge capacity of 1,200 cu ft per sec is situated at the east abutment of the dam (Fig. 5). It is a concrete weir with a crest elevation of 7634.5 and is equipped with one 15-ft-x-8-ft radial gate. Floods in excess of 1,200 cu ft per sec can escape over a broad emergency spillway at the west abutment, through a gully and into Mono Creek.

The outlet structure was constructed in a cut in foundation soils near the maximum section of the dam. It follows the foot of the right-hand slope of Mono Creek, from the upstream to the downstream toe of the dam. It consists of a reinforced concrete culvert, 800 ft long, housing a 54-in. diameter steel pressure conduit, controlled at the downstream end by a cylindrical, sliding sleeve, fixed cone, dispersion valve. The water is admitted into the steel outlet conduit through a reinforced concrete inlet structure. At the intersection between core and outlet conduit, the base of the core is situated at a minimum depth of 5 ft below the base of the outlet conduit. Therefore, at that location the outlet conduit is entirely surrounded with impervious core material.

CONSTRUCTION OF THE DAM

The construction of the dam was begun in May 1953. It required the following quantities of fill material:

	Compacted volume, in cubic yards
Core material and blanket under dam	1,236,824
Upstream blanket material and cutoff	1,027,208
Semi-pervious and pervious materials for the upstream and downstream part of the dam	2,538,319
Slope and blanket protection materials and filter materials	486,546
Total	5,288,897

Prior to construction, the dam site was occupied by an old, high-altitude forest. The trees had diameters up to 48 in. and the ground was strewn with big boulders. Therefore, the stripping of the site was a major operation. The boulders were blasted and all stones larger than 6 in. were removed and stockpiled, to be used as riprap. The trees were either uprooted or cut at an elevation of 1 ft above ground level. All stumps and roots were removed to a distance of 20 ft beyond the outer boundaries of the dam. After this preliminary operation, the area to be occupied by the embankment was harrowed or disked to a depth of 6 in. and moistened by sprinkling to bring the water content of the processed layer up to optimum. Prior to placing the embankment the top layer was cross-compacted by 8 passes of a 50-ton rubber tired roller. The fill material was spread in 8-in. layers and compated in the same manner as the aforementioned top layer.

Construction was begun in June, 1953, by making the excavations for the toe drain, the outlet conduit, and for the outlet channel. In order to excavate for

the outlet conduit, situated in the normal course of the stream, it was necessary to divert Mono Creek at a point 1,200 ft upstream from the upstream toe of the dam. The creek was diverted into an open-cut channel excavated along the foot of the left hand slope of the riverbed. Because the bottom of the trench for the outlet conduit, at the site of its intersection with the core of the dam, was approximately 5 ft below the water table, the trench was drained by pumping from well points.

In September, 1953, the outlet conduit was concreted and the intake channel was provided with an impervious blanket. At that stage, Mono Creek was diverted from its artificial bed into the lined inlet channel and through a bypass pipe into the outlet conduit; immediately thereafter, the balance of the blanketing operations in the Mono Creek Valley upstream from the dam was completed. Henceforth, Mono Creek flowed through the outlet conduit into the outlet channel (Fig. 5), and entered the old stream at a point approximately 800 ft downstream from the downstream toe. None of its waters entered the toe trench.

In August, 1953, the drilling of the relief wells was begun. Fig. 7 shows a typical relief well installation. In drilling the relief wells, it was noted that silts from higher strata would cave into the hole. To prevent this, a seal of bentonite, 6 to 8 ft thicker than the silt layer was placed around the well casing above the pervious strata. This confined the flowing water to the casing, and prevented the fine sands and silts from washing down and into the pervious strata which is essential to the efficient operation of the well. The flow of water toward the pervious filter well produces a natural filter surrounding this section.

MODIFICATIONS OF DESIGN DURING CONSTRUCTION

The excavation for the cutoff was begun October, 1953, at the upper edge of the eastern slope of the creek channel. As excavation proceeded in an easterly direction, the depth of excavation to reach the silt stratum was generally approximately 22 ft below the broad flat floor of Vermilion Valley. At a distance of 1,400 ft from the east abutment, contact with the silt stratum was lost. In order to obtain reliable information concerning this unanticipated feature of the subsurface geology, subsoil exploration by borings was resumed in the spring of 1954. It involved the drilling of 28 boreholes with depths up to 90 ft. In many holes, undisturbed samples were taken at points spaced 5 ft to 10 ft vertically. Mechanical analysis and permeability tests were performed on each sample.

Some of the 28 holes were drilled along the centerline of the proposed cutoff, east of the point where contact with the silt stratum was lost, and the others north of the centerline. The results of the borings along or close to the centerline are shown in Fig. 9. The diagram also reveals the erratic character of the pattern of stratification of the fluvio-glacial deposits. The results of the borings, combined with those of the preceding geological survey, led to the conclusion that the cutoff, for a distance of approximately 300 ft, is situated above a gap in the silt stratum, designated as A in Fig. 5. This gap was eroded by a melt-water stream and then backfilled with fluvio-glacial sediments before the youngest till sheet was deposited. During the last advance of the ice, the stream channel deposit A was buried beneath a till sheet and a set of terminal moraines.

After the ice retreated from the terminal moraine designated as M in Fig. 5, a stream channel B was eroded along the inner or northern edge of the moraine

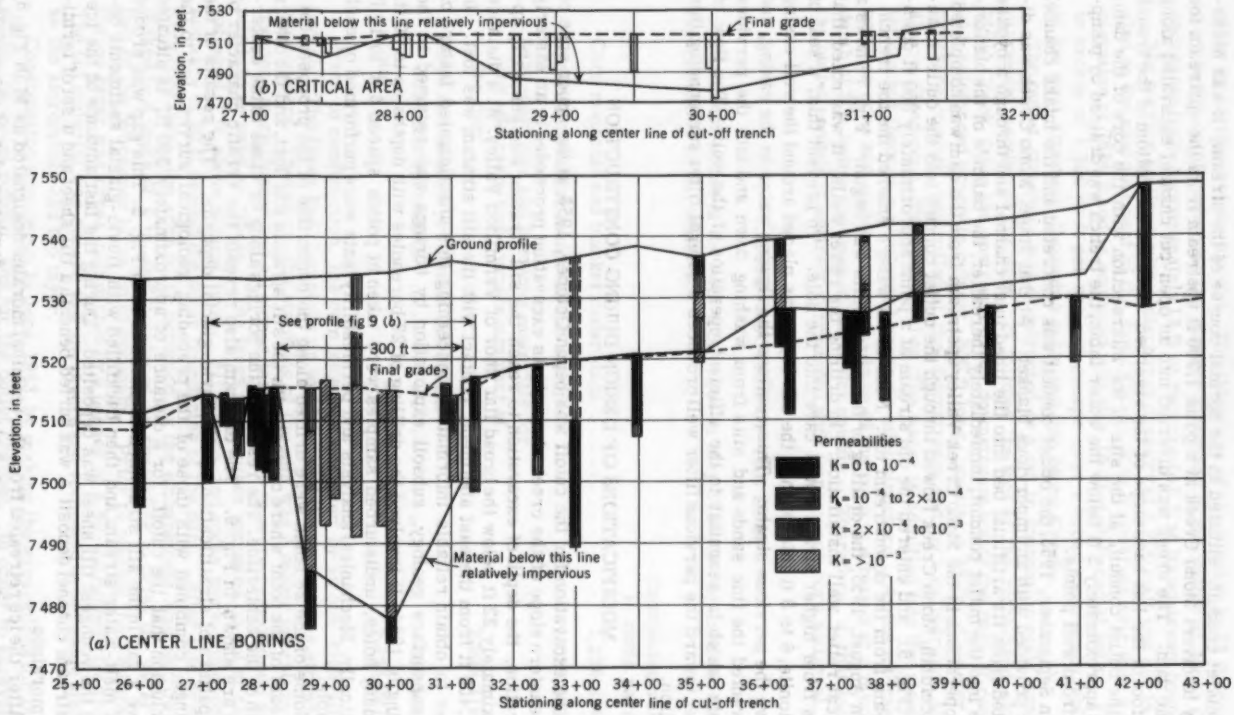


FIG. 9.—EXPLORATORY BORINGS FOR CUTOFF TRENCH EAST OF MONO CREEK

and backfilled with fluvio-glacial sediments. At a distance of about 600 ft north of the cutoff, the bottom of the younger stream channel deposit B intersects the top surface of the older one, A. Hence, at that point water can flow out of the reservoir through the deposit B into and through the deposit A under the dam towards the left hand slope of Mono Creek downstream from the dam.

For economic reasons, it was decided to excavate the cutoff trench to a depth not in excess of 25 ft along the entire line indicated on Fig. 5 notwithstanding the fact that over a length of 300 ft the base of the cutoff is on fluvio-glacial sediments and not on silt. However, in order to reduce the quantity of water that will escape out of the reservoir into the stream channel deposit A, the section of the cutoff above the gap was supplemented by a blanket extending from the cutoff in an upstream direction along B in Fig. 5, to a point beyond the area where the stream channel deposits A, and B intersect. The resulting layout for cutoff and blanket is shown in Fig. 8(c).

Another modification of the original project became necessary when it was realized that the available quantity of highly pervious sand and gravel was smaller than anticipated. The cost of screening the silty embankment material would have been prohibitive. Therefore, it was decided to subdivide the downstream section of the dam into a very pervious and a less pervious section. The very pervious material was placed on the base of the dam and against the lower part of the downstream face of the core of the dam as shown in Figs. 6(a) and 6(b) Zone I. Because the estimated line of seepage is entirely within the very pervious material, this modification of the design had no effect on the stability conditions.

Finally, the necessity of some minor modifications of the original design was realized when the observations during the first filling of the reservoir began to reveal the pattern of subsurface drainage. These modifications involved chiefly the installation of drains in the natural ground downstream from the dam.

MEANS FOR OBSERVATION

The performance of the dam has been observed by means of piezometers, discharge gages, and settlement reference points. The pattern of subsurface drainage and the performance of the relief wells was disclosed by the piezometer readings. The relationship between the water level in the reservoir and the amount of leakage out of the reservoir was determined by correlating the measured discharge at the outlets of the drains with the corresponding water level in the reservoir. The settlement of the different parts of the dam was measured by repeating from time to time the survey of the settlement reference points.

The design of the piezometers had to be adapted to the permeability of the soil surrounding the perforated tip and the location of the upper end of the piezometer with reference to that of the tip. Therefore, three different types of piezometers, A to C, have been used.

Type A.—Observation wells, for measuring the pore water pressures in pervious material, that consist of 1-in.-diameter tubes terminating in well points, installed in 8-in. drill holes. Above the well points, the space between tubes and natural ground was filled with compacted clay.

Type B.—Casagrande piezometers, for measuring pore pressures at multiple elevations in one well within the body of the dam and in the foundation soils.

Type C.—Bourdon gages, attached to the outlet ends of tubes extending through the side walls of the outlet conduit into the surrounding fill material.

The initial piezometer installation consisted of 24 piezometers of Type A placed midway between the relief wells; 7 triple piezometers of Type B with tips located below the base of the dam; 5 piezometers of Type B in the subsoil downstream from the dam between the outlet channel and the abandoned channel of Mono Creek; 4 piezometers of Type B with tips in the core; 8 Type A piezometers with tips in the downstream section of the dam; and 5 Type C piezometers in the side walls of the outlet conduit. A total of 53 piezometers were used. Their locations are shown on Fig. 10.

Each of the 7 triple piezometers of Type B consists of three 1/2-in.(outside diameter)plastic tubes installed in one 4-in. drill hole. The tips are approximately at elevation 7,420, 7,450, and 7,480. Between tips, the space between tubes and natural ground was sealed with clay. The uppermost tips at elevation 7,480, were approximately 15 ft below the level of the original bottom of the valley of Mono Creek at its intersection with the centerline of the dam. During the first filling of the reservoir supplementary piezometers were installed at those few points where additional information concerning the pore pressure conditions was called for.

When the filling of the reservoir was begun, the loss of water due to seepage was measured at two points. One of them was in the short section of abandoned stream bed of Mono Creek, 310 ft downstream from the lowest point of the toe drain at Station 28. The second one was at Station 8 at the bottom of a gentle sag in the toe drain between the west abutment of the dam and Station 10. The Station 8 toe drain outlet consists of a 90° V-notch weir equipped with a staff gage. The outlet at Station 28 consists of an 18-in. rectangular weir plate and is equipped with an automatic recorder.

During the first filling of the reservoir, water seeped out of the ground at three points downstream from the dam. At these points the seepage was collected in drains and gaging devices were installed at the outlets of the drains.

In addition to the piezometers and gaging stations, settlement reference points were established. These are spaced at intervals of 300 ft and consist of brass markers inserted into the tops of cylindrical concrete blocks with a diameter of 12 in. The base of each block is 4 ft below the fill surface. Ten such points are on the crest of the dam and five are on the downstream berm. Provisions have also been made for measuring the settlement of the invert of the outlet conduit.

PATTERN OF SEEPAGE

As was expected on the basis of the geological history of the glacial substrata of the dam site, the piezometer readings disclosed an intricate, three-dimensional pattern of seepage. In some sections, the flow lines rise and in others they descend in the direction of the flow. Therefore, at different elevations the curves of equal piezometric pressure have a different shape. This is shown in Fig. 10 which represents the curves of equal piezometric heads at elevations 7,420 and 7,480 respectively for full reservoir. If the relief wells had not been drilled, the piezometric levels at elevations 7,420, downstream from the highest part of the dam, could have been higher than those shown in Fig. 10, thus involving the possibility of the formation of boils on the valley floor, or even of a heave of the floor. Therefore, the installation of the relief wells was an essential precaution.

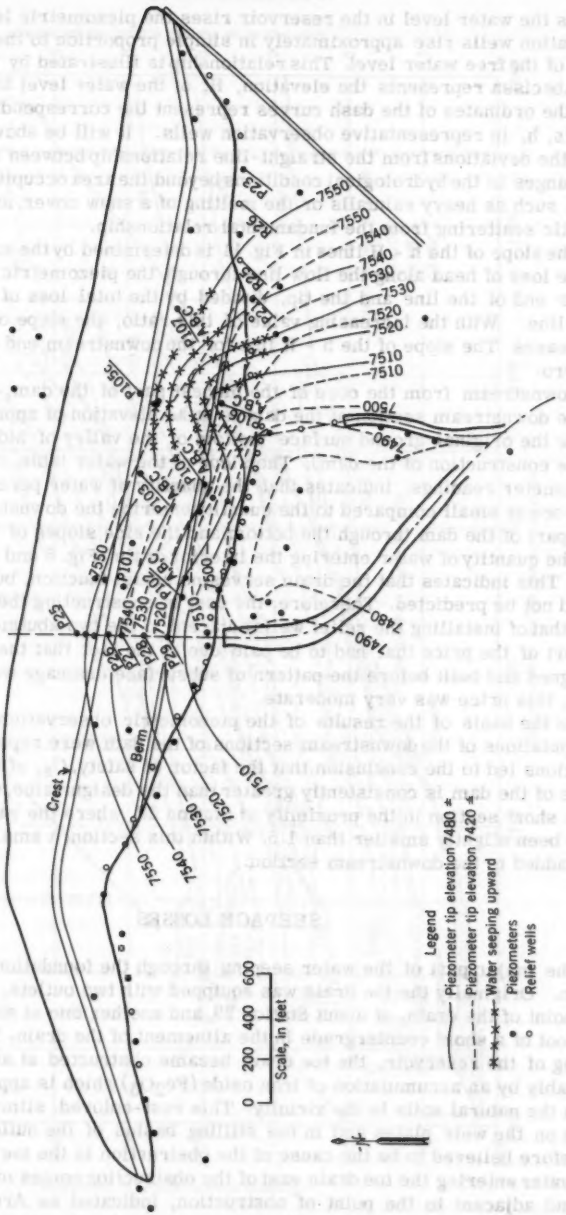


FIG. 10.—CURVES OF EQUAL PIEZOMETRIC LEVEL AT FULL RESERVOIR

As the water level in the reservoir rises the piezometric levels in the observation wells rise approximately in simple proportion to the corresponding rise of the free water level. This relationship is illustrated by Fig. 11 in which the abscissa represents the elevation, H, of the water level in the reservoir, and the ordinates of the dash curves represent the corresponding piezometric levels, h, in representative observation wells. It will be shown subsequently that the deviations from the straight-line relationship between h and H are due to changes in the hydrological conditions beyond the area occupied by the reservoir, such as heavy rainfalls or the melting of a snow cover, and not due to an erratic scattering from the fundamental relationship.

The slope of the h - H lines in Fig. 11 is determined by the value of the ratio of the loss of head along the flow line through the piezometric tip between the upper end of the line and the tip, divided by the total loss of head along the flow line. With the increasing value of this ratio, the slope of the h - H line decreases. The slope of the h - H line for the downstream end of any flow line is zero.

Downstream from the core of the highest part of the dam, the water table in the downstream section of the dam is at an elevation of approximately 45 ft above the original ground surface (bottom of the valley of Mono Creek prior to the construction of the dam). The slope of the water table, disclosed by the piezometer readings, indicates that the quantity of water percolating through the core is small compared to the quantity entering the downstream section of this part of the dam through the bottom and the side slopes of Mono Creek.

The quantity of water entering the interior drain (Fig. 5 and 6(b)) is negligible. This indicates that the drain serves no useful function, but this however, could not be predicted. Therefore, the cost of constructing the interior drain, like that of installing the relief wells adjacent to the two abutments of the dam, is part of the price that had to be paid due to the fact that the dam had to be designed and built before the pattern of subsurface drainage was known. However, this price was very moderate.

On the basis of the results of the piezometric observations, the stability computations of the downstream sections of the dam were repeated. The computations led to the conclusion that the factor of safety, G_S, of the downstream slope of the dam is consistently greater than the design value, $G_S = 1.5$, except for a short section in the proximity of Station 28, where the value of G_S might have been slightly smaller than 1.5. Within this section, a small amount of fill was added to the downstream section.

SEEPAGE LOSSES

The major part of the water seeping through the foundation enters the toe drain. Originally the toe drain was equipped with two outlets, one at the lowest point of the drain, at about Station 28, and another one at about Station 8 at the foot of a short countergrade in the alinement of the drain. During the first filling of the reservoir, the toe drain became obstructed at about Station 32, probably by an accumulation of iron oxide (Fe_2O_3) which is apparently leached from the natural soils in the vicinity. This rust-colored, slimy sediment collects on the weir plates and in the stilling basins of the outlet weirs and is therefore believed to be the cause of the obstruction in the toe drain. Most of the water entering the toe drain east of the obstruction comes out of the natural ground adjacent to the point of obstruction, indicated as Area III in Fig. 5. There the seepage water is collected in a drain leading to a gaging device.

7570

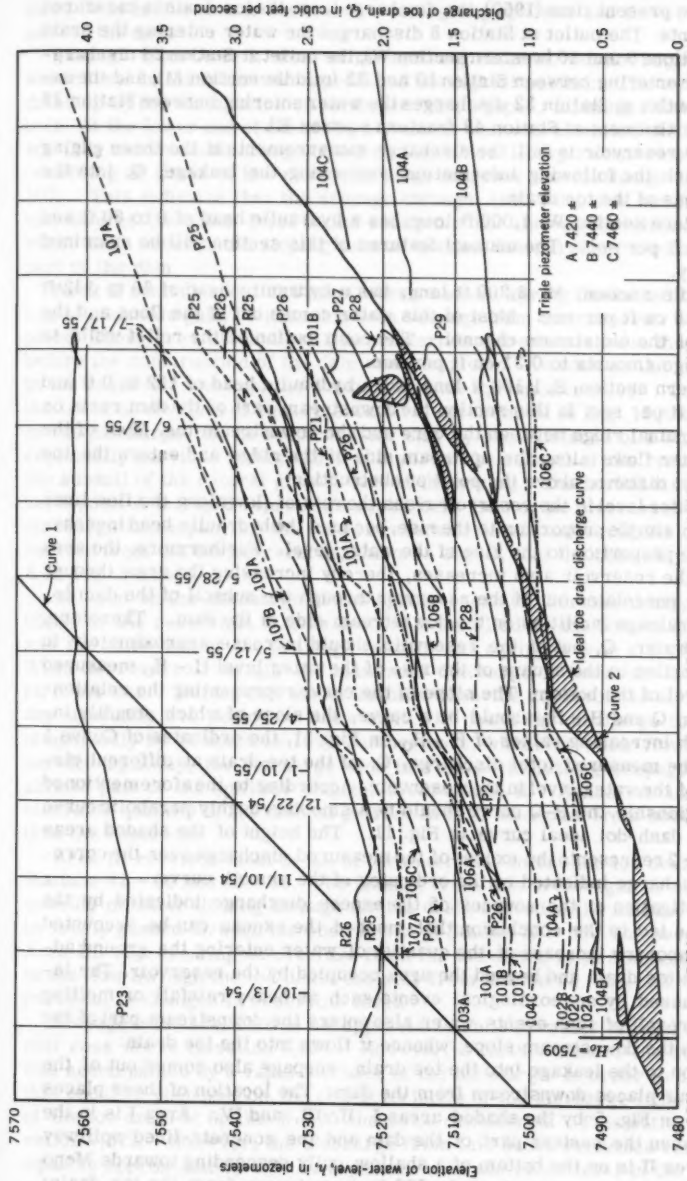


FIG. 11.—RELATIONSHIP OF TOE DRAIN DISCHARGES AND PIEZOMETRIC LEVEL VERSUS RESERVOIR WATER SURFACE ELEVATION

Hence, at the present time (1960), the discharge from the toe drain is measured at three points. The outlet at Station 8 discharges the water entering the drain between Stations 0 and 10 (western section W), the outlet at Station 28 discharges the water entering between Station 10 and 32 (middle section M), and the unintentional outlet at Station 32 discharges the water entering between Station 32 and the east abutment at Station 43 (eastern section E).

When the reservoir is full, the discharge measurements at the three gaging points furnish the following information concerning the leakage, Q, into the three sections of the toe drain.

The western section, W, 1,000 ft long, has a hydraulic head of 0 to 60 ft and Q_w = 0.5 cu ft per sec. The unusual features of this section will be examined subsequently.

The middle section, M, 2,200 ft long, has a hydraulic head of 60 to 142 ft and Q_m = 3.8 cu ft per sec. Most of this water comes out of the floor and the side slope of the old stream channel. The contribution of the relief wells to this discharge amounts to 0.3± cu ft per sec.

The eastern section, E, 1,100 ft long, has a hydraulic head of 112 to 0 ft and Q_e = 0.7 cu ft per sec. In this section the downstream part of the dam rests on a gentle morainal ridge between the core and the downstream toe. Most of the seepage water flows along the upstream side of the ridge and enters the toe drain a short distance above the point of obstruction.

As the water level in the reservoir rises the rate of flow along the flow lines increases in simple proportion to the rise, because the hydraulic head increases in simple proportion to the rise of the water level. Furthermore, the area flooded by the reservoir also increases, thereby increasing the area through which water percolates out of the reservoir through the subsoil of the dam towards the drainage facilities on the downstream side of the dam. Therefore, the loss of water, Q, out of the reservoir should increase approximately in direct proportion to the square of the rise of the water level $H - H_o$ measured from the level of the bottom. The slope of the curve representing the relationship between Q and $H - H_o$ should be a curve, the slope of which steadily increases with increasing values of $H - H_o$. In Fig. 11, the ordinates of Curve 1 represent the measured total discharge, Q, of the toe drain at different elevations, H, of the water level in the reservoir. According to the aforementioned simple relationship, the H-Q curve should be a smooth, roughly parabolic curve such as the dash-dot ideal curve in Fig. 11. The height of the shaded areas above Curve 2 represents the excess of the measured discharge over the corresponding discharge indicated by the ordinates of the smooth curve.

An investigation of the sources of the excess discharge indicated by the shaded areas led to the conclusion that most of the excess can be accounted for by a temporary increase of the quantity of water entering the ground adjacent to the toe drain and beyond the area occupied by the reservoir. The increase is caused by meteorological events such as heavy rainfall or melting snow. As a result of such events, water also enters the downstream part of the dam through the downstream slope, whence it flows into the toe drain.

In addition to the leakage into the toe drain, seepage also comes out of the ground at four places downstream from the dam. The location of these places is indicated in Fig. 5 by the shaded areas I, II, III, and IV. Area I is in the corner between the eastern part of the dam and the concrete-lined spillway channel; Area II is on the bottom of a shallow gully descending towards Mono Creek from the east, approximately 500 ft downstream from the toe drain; Area III is at the downstream toe near the obstruction in the toe drain; and

Area IV is in the corner between the emergency spillway and the westernmost part of the dam.

Seepage from Area I, west of the spillway channel, did not begin until the water level in the reservoir approached its highest position. The wet area was dried up by the installation of perforated drain pipes, forming a fishbone pattern. At the lower end of the drain, a V-notch weir was installed. At full reservoir, the maximum discharge is 0.2 cu ft per sec. Heavy rainstorms and thaws occurring at times of low reservoir stage increase the discharge as much as 50%. This indicates that the seepage through Area I depends not only on the elevation of the water level in the reservoir but also on the elevation of the water table beneath the sloping natural ground downstream from the eastern part of the dam.

Area II centers about the point where a small spring flowed out of the bottom of a shallow gully. Within this area seepage from the reservoir was anticipated. Therefore a stockpile of filter materials was established in the proximity before the construction of the dam was completed. As soon as the water level in the reservoir went up, the discharge of the spring increased. Considering the trend of the lines of equal piezometric level shown in Fig. 10, the increase of the discharge can be accounted for only by the existence of a layer of exceptionally pervious sediments leading from the subsoil of the reservoir into the subsoil of the natural ground east of the spring. The buried stream channel deposit A in Fig. 5 represents such a belt. Hence, the increase of the spring discharge accompanying the rise of reservoir level confirmed the conclusion derived from the boring records, shown in Fig. 9, that the belt-shaped deposit A in Fig. 5 exists.

As soon as the discharge of the spring began to increase during the first filling of the reservoir, a deep drain was installed on the bottom of the gully and the outlet end of the drainage conduit was equipped with a V-notch weir. When the reservoir is full, the maximum discharge of the drain is 0.5 to 0.7 cu ft per sec. During the winter months when the reservoir is at low stage, any unusually wet period or snow melt will cause the discharge to increase temporarily by as much as 10%. Furthermore, whenever water flows over the service spillway, the discharge also increases, indicating seepage from the unlined part of the spillway channel toward Area II. Hence, at times a considerable quantity of the discharge from Area II can come from sources other than the reservoir.

Area III receives most or all of the water that enters the toe drain between Stations 32 + 00 and 43 + 00. The leakage from this area began as soon as the quantity of water flowing through the toe drain exceeded the amount that could be freely passed through the obstruction at Station 32 + 00. The seepage from Area III, representing an overflow from the toe drain, is in simple proportion to the flow through the toe drain easterly from Station 32 + 00, and hence proportional to changes in reservoir level.

Seepage from Area IV was not appreciable until the water level in the reservoir rose above elevation 7,634. However, a further rise of the water level was accompanied by a rapid increase of the discharge. In order to understand this peculiar phenomenon, the characteristics of the discharge from the outlet of the toe drain at Station 8 + 00 should be considered. This outlet is at elevation 7,572. However, the discharge from this outlet remained constant and equal to approximately 0.04 cu ft per sec until the water level in the reservoir arrived at approximately elevation 7,610, which is the elevation of the base of the kame deposit underlying the west end of the dam (Figs. 1 and 2). Further

rise of the water level was associated with rapid increase of the discharge at Station 8 + 00. This is shown by Curve C_2 in Fig. 12, representing the relationship between the water level in the reservoir and the discharge at Station 8 + 00. As soon as the reservoir water level rose to elevation 7,634, an appreciable amount of water also began to emerge from Area IV, and the discharge from this area increased rapidly with increasing elevation of the reservoir level. The relationship between the water level in the reservoir and the discharge from Area IV is shown by Curve C_3. The discharge from Area IV is represented by the shaded area between curves C_2 and $C_2 + C_3$.

Both the seepage from Area IV and the abnormal characteristics of the discharge of the toe drain at Station 8 + 00 can adequately be explained by assuming that the permeability of the kame deposit is much higher than that of the fluvio-glacial deposits underlying the eastern part of the dam, including the

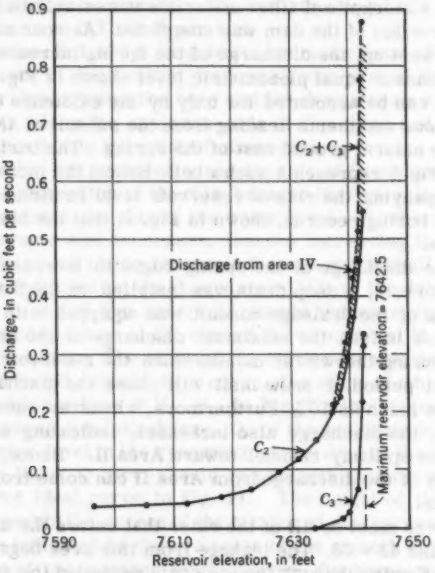


FIG. 12.—RESERVOIR WATER SURFACE ELEVATION VERSUS DISCHARGE FROM AREA IV

section between Stations 32 and 43. Once the water level in the reservoir rises above elevation 7,634, the toe drain no longer suffices to unwater the kame deposit and, as a consequence, part of the water comes out of the adjacent ground downstream from the toe drain. While the water level in the reservoir rose from 7,634 to its maximum level, 7,642, during the first filling of the reservoir, the discharge increased from 0 to 0.33 cu ft per sec.

The seepage from Area IV was brought under control by the installation of an inverted filter covering the area and by perforated drain pipes. The discharge is measured at the downstream end of the collector drain.

The following is a summary of the results of the discharge measurements made during the second filling of the reservoir prior to which time discharge

from all seepage areas had been intercepted by collector drains and permanent gaging stations installed.

	Discharge at full reservoir, Q, in cubic feet per second
Toe drain, section W, Station 0 to 10	0.55
Toe drain, section M, Station 10 to 32	3.17
Toe drain, section E, Station 32 to 43	0.70
Seepage Area I (east abutment)	0.17
Seepage Area II (gully drain)	0.53
Seepage Area III (in section E above)	
Seepage Area IV (west abutment)	0.39
Total	5.51

Before the water level reached its highest elevation for the first time, the fill material exposed on the downstream slope of the dam became moist along several horizontal lines between the highest part of the dam and the east abutment, and at a few points in these lines minor sloughing over areas of 2 to 3 sq ft occurred. However, the quantity of seepage responsible for the sloughing was imperceptible. The bands were in the random material and were generally above the upper boundary of the highly pervious Zone 1 part of the downstream section of the dam (Fig. 6). Subsequent investigations showed that each one of the moist bands was above an exceptionally silty layer of fill material. On account of the variable silt content of the borrow pit material, the formation of such layers was inevitable. The situation was easily brought under control by drilling vertical holes through the layers down to the pervious Zone 1 fill material and filling the holes with clean gravel. Thereupon sloughing stopped.

SETTLEMENT

Settlements are very slight because the site was glacially preloaded, and the fill well compacted. Also, the well-graded materials of the subsoil and the dam contained little or no clay.

The maximum settlement of the invert of the outlet conduit is 0.27 ft. Since the time when the dam was completed, the crest has settled a maximum of 0.12 ft.

CONCLUSIONS

If the pattern of stratification of the subsoil of an earth dam is as erratic as that of the subsoil of the Vermilion Dam, information concerning the essential features of the subsoil conditions can be obtained only by a thorough geological survey supplemented by borings at points to be chosen on the basis of geological considerations and by soil tests on representative samples. The few borings that were made at the site of the Vermilion Dam fully served their purpose. Exploratory work in excess of what has been performed at that site would not have furnished any vital additional information to the knowledge of the site prior to construction.

The most complete information that can be obtained at a reasonable cost concerning significant features of a dam site on a subsoil with an erratic pattern of stratification still leaves a wide margin for interpretation. Therefore,

the construction drawings accompanying the invitation for tenders are inevitably based on more or less arbitrary assumptions concerning the character of the subsoil. While these assumptions are being made, the engineer in charge of design should consider, on the basis of the results of the geological survey, all the uncertainties involved, and make all the provisions necessary for detecting the errors in these assumptions before it is too late to modify the design during construction.

The Vermilion Dam is as safe and almost as economical as it would have been if all the significant features of the subsoil, including the pattern of seepage, had been known in advance of construction. The cost of the installation of those parts of the dam, such as the interior drain, which were afterwards found to be superfluous, were nominal. After the reservoir was filled for the first time, there was no gap in knowledge of the performance of the dam, and every phase of its performance is clearly understood. This gives the owners and the state engineer the assurance that the dam is satisfactory in every respect.

ACKNOWLEDGMENTS

The writers wish to thank Wallace L. Chadwick, F. ASCE, and Ralph W. Spencer, F. ASCE of the Southern California Edison Company. Credit is also given to Philip J. West, Joseph H. Birman, Oscar N. Kulberg, Harold A. Barber, Donald W. Taylor, Ian Campbell, and Julian Hinds, F. ASCE. Final engineering, construction drawings and construction management were provided by Bechtel Corporation under the direction of John R. Kiely, F. ASCE.

DISCUSSION

MAURICE L. DICKINSON,[4] F. ASCE.—The writer had the pleasure of being associated with this interesting project throughout its design and construction, and commends the thorough treatment presented by the authors.

By way of emphasizing the complex heterogeneous and variable nature of the foundation and the materials available for construction, it seems worth pointing out that construction of a dam of this size at this site would not have been considered feasible relatively few years ago. The advances in knowledge of soil mechanics engineering and its application to the interpretation of geology were major factors in making this dam possible.

The authors include only a brief description of the low level outlet extending through the dam foundation. The writer believes that this structure is worthy of additional comment concerning the somewhat unusual problems of soil mechanics and foundation engineering. The outlet works as seen in Fig. 13 consist of:

1. A submerged intake structure with trashracks and an oil-pressure operated shutoff gate; 2. An 8 ft inside diameter modified horseshoe section reinforced concrete culvert, housing a free-standing 54-in. diameter steel pipe

[4] Chf. Hydr. Engr., Bechtel Corp. Los Angeles, Calif.

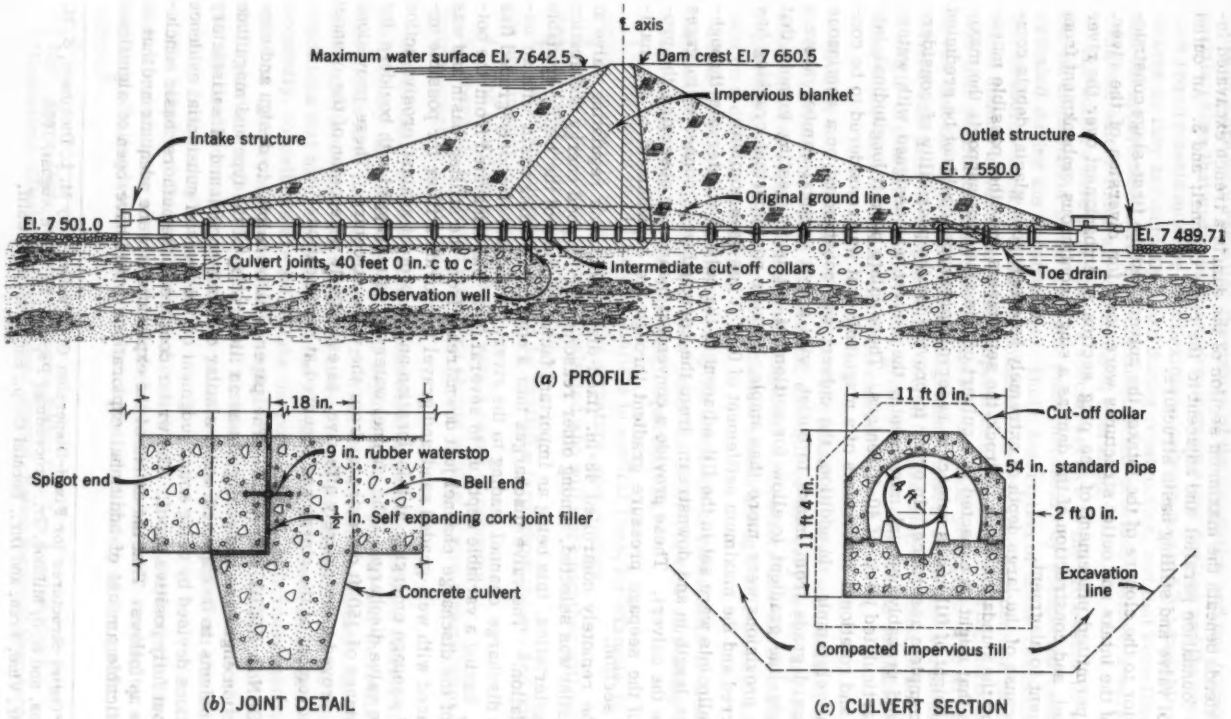


FIG. 13.—OUTLET WORKS

that extends beneath the maximum section of the dam in a trench excavated into the foundation parallel and adjacent to the river channel; and 3. An outlet control valve and stilling basin structure.

Prior to the closure of the intake, the culvert and the first-stage construction of the intake and outlet structures were used for diversion of the river. This permitted placement of the plug section of embankment over the river channel, and construction of the dam as a single continuous embankment from abutment to abutment.

Because of the large depth of extremely heterogeneous glacial debris comprising the foundation above bedrock, the settlements and other possible movements that might be expected in a culvert of this size (that supports the maximum height of fill and is subject to reservoir pressure) could not be predicted with complete assurance. In order to provide for the possibility of considerable and probably unequal movements, the culvert was designed with watertight articulated joints of 40-ft centers. These joints permit longitudinal, lateral, and rotational movements of a magnitude that was considered to be conservatively ample. In addition, the culvert was constructed on a continuous downward grade from intake to outlet, with a 3-ft vertical camber above a straight-line gradient to allow for settlement. It is interesting to note that these provisions were more than ample, because no important cracking has occurred and the maximum settlement of 0.27 ft has been nominal.

Wellpoints were set in the fill adjacent to the culvert at intervals throughout its length in and downstream from the core and were connected to gages inside the culvert. These provide a convenient means for observing the profile of the seepage pressure gradient through the embankment at its maximum section.

The remotely controlled 48-in. fixed-dispersion cone regulating valve at the outlet was selected, among other reasons, for its good energy dissapation characteristics, this being an important factor because of the highly erodable foundation.[5] The valve discharges into a concrete stilling basin with an unlined discharge channel leading to the river. A deposit of poorly-graded fine sand, having a variable depth up to several feet, was excavated from the bottom of the discharge channel just downstream from the stilling basin and was replaced with well-graded sand and gravel to provide a filter for possible upward seepage emerging at this location and to protect against erosive action of the valve discharge. The channel waterway is riprapped with boulders for a distance of 150 ft downstream from the valve structure. These provisions have proved to be entirely effective, as essentially no erosion of the channel or movement of the riprap has occurred at this location.

JOHN R. KIELY,[6] F. ASCE.—The paper will be helpful to design and construction engineers and geologists as an illustration of the type and magnitude of problems to be expected under similar circumstances, and of satisfactory solutions devised by using sound judgment on the basis of substantial evidence without fully positive proof. The writer concurs in the authors' basic conclusions as follows: That the extent of the explorations were adequate and that no practicable amount of additional explorations would have been of significant

[5] "Outlet Structures for Fixed-Dispersion Cone Valves," by M. L. Dickinson, S. M. Barnes, and R. S. Milmoe, Jr., Proceedings Paper 1725, ASCE, August, 1958.

[6] Sr. Vice. Pres. and Dir., Bechtel Corp., San Francisco, Calif.

value in more fully revealing the nature of the foundation and the borrow materials. Also, that under similar circumstances, the designs and the construction requirements must be kept flexible in order to be readily adaptable to conditions as they are actually found during construction, and that Vermilion Dam and its appurtenant structures as constructed provides positive assurance of complete safety under all conditions of operation.

The authors have performed a special service to the profession by including an examination of the changes made necessary by unexpected conditions revealed during the construction. Their description of these conditions and the measures adopted to best accomplish the intended purposes in an economical manner reveals the close cooperation between engineering and construction that permitted desirable changes to be made promptly. The writer believes that the organizational arrangements under which the work was performed with the full responsibility for all engineering and construction under a single organization contributed greatly to the expeditious handling of the many unforeseeable conditions encountered.

RALPH W. SPENCER,[7] F. ASCE.—The construction and successful operation of the Vermilion Dam is an excellent example of the very necessary cooperation between expert consultants, engineer-contractors and the owner's own engineering staff in solving the problem of constructing a safe and economical dam on a difficult foundation.

This discussion will consider only the functions of consultants or a consultant board. For the owner's view point the selection of a consulting board should be influenced by the following requirements:

1. The board should have specialists in several lines; for example, in foundations, materials to be used in the structure, and geology.
2. Board members should be selected who will work together without submerging their individual judgments.
3. The board members should be available throughout the job and not only for preliminary consultation.
4. The board members should have a sense of economy.
5. Above all, the board members should be able to give mature judgment in their respective specialties.

Occasionally, owners retain a consultant or consulting board merely to give preliminary advice or to lend their reputation to a project and thereafter the consultants have little or no contact. When this occurs consultants have found from experience that the failure of others to adjust designs to fit the varying conditions that nature provides on the job may result in serious errors. Consequently, consultants are apt to take the position that their recommendations must be ultra-conservative in order that even a careless designer or builder will achieve a safe structure. Such a structure is rarely economical and if the site conditions and construction practices are far enough from the original assumptions, it may not be safe.

The subject of the relationship of consultants, clients, and contractors has been covered in an article published elsewhere and merits reading by every engineer dealing with important structures when safety of the public is involved.[8]

---

[7] Mgr., Engrg. Dept., Southern California Edison Co., Los Angeles, Calif.

[8] "Consultants, Clients and Contractors," Journal, Boston Society of Engineers.

In the case of the Vermilion Dam, the consultants, the engineer-contractor, and the owner's staff worked diligently throughout the job to fit the structure to the highly varying conditions provided by nature. Many of these conditions could not be determined in advance by any reasonable amount of exploration. The excellent performance of the Vermilion Dam is convincing evidence that such a problem has been well solved.

PHILIP J. WEST.[9]—The conclusions reached in this informative paper may well serve as practical guides to engineers and geologists charged with the design of major earthfill dams to be located on thick, erratic, alpine glacial deposits where (1) complete and accurate interpretations of subsurface information based on preconstruction investigations are virtually impossible to make, and (2) when behavior of underseepage pattern and flow cannot be either fully ascertained or understood until after careful observation of the performance of the dam during the filling of the reservoir.

These items are of special interest to the writer because of association with the development of the local subsurface glacial geology both before and during construction of the dam, and with later attempts to account for occurrences of unusual underseepage phenomena. Accordingly, it is believed that a brief presentation of events and studies that led to significant conclusions regarding the causes of certain underseepage abnormalities observed during the initial partial filling of the reservoir will be of additional interest.

Under the heading "Seepage Losses," the author pointed out that toe drain discharge, Q, in excess of the amount that could normally be anticipated from reservoir underseepage alone, could be accounted for by a temporary increase of the quantity of water entering the ground adjacent to the toe drain and beyond the area occupied by the reservoir, from heavy rainfall, or snow melt. However, prior to the concept that underseepage discharge irregularities that developed during the initial filling of the reservoir could be accounted for by meteorological events, it was considered likely that such irregularities in underseepage were attributable to changes in the average mass permeability of the subsoil, that resulted from internal subsurface erosion, deposition, and the subsequent flushing of water veins. Such an irregularity in the reservoir head-toe drain discharge curve is represented in Fig. 14 by the shaded area above the smooth and roughly parabolic ideal H-Q curve. The simple relationship between the loss of water, Q, that seeps through the foundation from the reservoir and the reservoir water level, H, during the initial partial filling of the reservoir is shown in Fig. 14.

A noticeable variation in toe drain discharge versus time occurred during the spring of 1954. Before the intake gates were closed on November 12, 1954, the physical conditions that caused this variation were evaluated. It became evident that ground water flowing into the toe drain during the snow melt and runoff season could increase the toe drain discharge as much as 0.20 cu ft per sec above a so-called base underseepage flow caused by normal underground movement of water downstream through the valley fill.

Because the initial major departure from the ideal H-Q curve (during the period from January 11 to May 30, 1955) covered the observed local snow melt and runoff season in the Vermilion Dam area, it became apparent that the increase in toe drain discharge could have been created by increased flows of ground water from sources other than the reservoir into the toe drain. It was

[9] Sr. Engrg. Geologist, Southern California Edison Co., Los Angeles, Calif.

believed, therefore, that in addition to seepage of reservoir water, incremental flows entering the toe drain could possibly be derived from the following other sources: (1) Percolation of meltwater from snow accumulated on the downstream face of the dam between Station 9 + 00 and 42 + 00, and (2) surface and near-surface ground water contributed from the abutment areas.

In analyzing the variations of toe drain discharge that occurred during the time in which the reservoir rose from elevation 7,515 in October, 1954 (the month prior to the closing of the gates) to a peak elevation of approximately 7,600 in July, 1955, reference was made to a number of charts and graphs that were prepared from available weather and hydrologic data. The attempt was made to determine whether a relationship existed between factors such as temperature, precipitation, reservoir water-surface elevation, runoff, and toe drain discharge.

A diagram was then prepared to show the periods of precipitation (in form of rain or snow water content), together with the approximate dates of snow

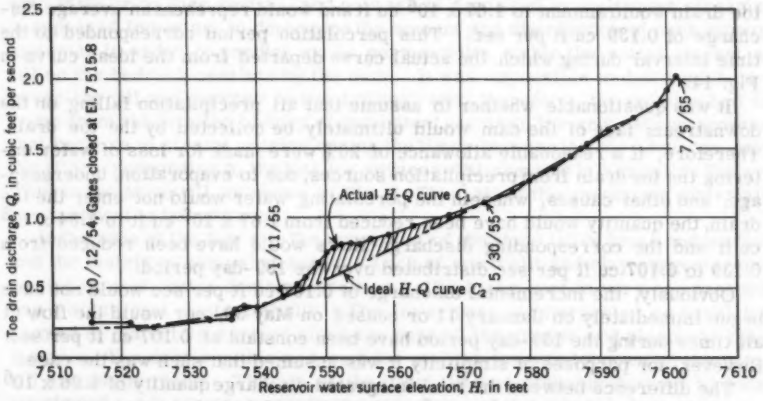


FIG. 14.—RELATIONSHIP OF TOE DRAIN DISCHARGE TO RESERVOIR WATER SURFACE ELEVATION

melt, local runoff, and ground water rise. The construction of this diagram was based principally on the interpretive and correlative information derived from the basic weather data recorded at the damsite and at other local weather stations. A chronological series of construction progress aerial photographs showing the extent of snow cover was also referred to in establishing the limiting dates of snowfall and melt.

By integration of the area bounded by the limiting curves (actual and ideal H-Q curves) in Fig. 14, and plotted against time, it was possible to determine the total volumetric quantity of increased discharge above the expected amount. This incremental quantity was computed to be 1.69×10^6 cu ft. Such a quantity, distributed evenly over the 139-day period from January 11 to May 30, 1955, would have been represented by an average flow of 0.141 cu ft per sec.

It was believed that water from precipitation that fell on the downstream face of the dam could percolate eventually into the toe drain and be discharged.

Also, the flow would follow a somewhat inclined path downstream, generally concentrated above the random fill material, within the highly permeable 2-ft-thick protective facing.

During the 1954-55 precipitation period a total of 1.93 ft of water in the form of snow and rain fell in the damsite area. From November 12, 1954, to January 11, 1955, 8.39 in. of water in the form of snow accumulated on the downstream face of the dam. During the second week of January, 1955, the snow began to melt in the damsite area and the percolation of meltwater caused ground water to rise. By April 28, all the snow that had accumulated on the downstream face during the winter had melted, and also by that time approximately 13 in. of additional precipitation had fallen. By May 30 (termination date of local snow melt and significant precipitation), a total of 1.93 ft of water had fallen in the damsite area during the 1954-1955 precipitation season.

If all of the precipitation (1.93 ft of water) that fell on the entire surface area of the downstream face of the dam between Station 9 + 00 and 42 + 00 during the period from November 12, 1954, to May 30, 1955, percolated into the toe drain during the snow melt period, the total amount of water entering the toe drain would amount to 1.67×10^6 cu ft and would represent an average discharge of 0.139 cu ft per sec. This percolation period corresponded to the time interval during which the actual curve departed from the ideal curve in Fig. 14.

It was questionable whether to assume that all precipitation falling on the downstream face of the dam would ultimately be collected by the toe drain. Therefore, if a reasonable allowance of 20% were made for loss of water entering the toe drain from precipitation sources, due to evaporation, underseepage, and other causes, wherein the percolating water would not enter the toe drain, the quantity would have been reduced from 1.67×10^6 cu ft to 1.34×10^6 cu ft and the corresponding discharge flows would have been reduced from 0.139 to 0.107 cu ft per sec distributed over the 139-day period.

Obviously, the incremental discharge of 0.107 cu ft per sec would not have begun immediately on January 11 or ceased on May 30, nor would the flow at all times during the 139-day period have been constant at 0.107 cu ft per sec. However, for purposes of simplicity it was assumed that such was the case.

The difference between the total integrated discharge quantity of 1.96×10^6 cu ft and the quantity of 1.34×10^6 cu ft that could have been reasonably expected from precipitation seepage water was 0.35×10^6 cu ft. This quantity corresponded to a discharge deficiency of approximately 0.03 cu ft per sec distributed over the 139-day period. Thus, this small flow deficiency must have been accounted for by seepage entering the toe drain from sources other than from rainfall and snow melt seepage under the downstream face.

During the spring and summer of 1954 it was seen that a rise in ground water could increase the toe drain discharge an average of 0.10 cu ft per sec for over a period of at least 2½ to 3 months (April 10 to July 10, 1954). Accordingly, at some period during the January 11 to May 30, 1955, interval, seepage of groundwater into the toe drain from the abutment areas, could have supplemented the discharge rate at least 0.10 cu ft per sec for a similar 75-day period to provide an incremental flow amounting to a total discharge volume of 0.65×10^6 cu ft. On this basis the toe drain discharge flow from the ground water source prorated over the 139-day period (January 11 to May 30, 1955) could have amounted to 0.06 cu ft per sec. Thus, the discharge deficiency of 0.03 cu ft per sec could have been more than accounted for by abutment ground water discharge.

It appears that a correlation existed between the anomalous toe drain discharge that occurred during the period from January 11 to May 30, 1955, and the percolation into the toe drain of water originating from rainfall and snow melt on the downstream face of the dam, and also with seasonal fluctuations of the abutment area ground water table. Therefore, from this study it was concluded that the irregularity in the actual H-Q curve in Fig. 14 could be entirely accounted for by a seasonal incremental flow of water into the toe drain entirely separate from flow caused by the reservoir.

JOSEPH H. BIRMAN.[10]—In view of the success of the Vermilion Dam, there are several aspects of the local geology that need further examination. These features may be significant in regard to planning for other dams on thick fill in glaciated canyons.

As there had been at least four separate ice advances through Vermilion Valley, four layers of glacial till might have been expected—each till layer associated with glacifluvial outwash. Because till is directly deposited by ice with little or no size sorting, and outwash is deposited by meltwater streams, it appeared important to determine the amount and distribution of each type of material in order to predict gross permeability within the entire blanket of fill on the bedrock overlain by the dam. It was impossible to distinguish between the till and outwash in the drilling, and, therefore, the solution had to come from the detailed history of geological events in the area. It now appears that because of stream erosion during the times between the ice advances, only the till corresponding to the last ice advance still remains in Vermilion Valley. This is the Mono till, as shown in Fig. 6. Thus, all of the underlying materials are believed to be outwash.

In the area of the dam site the upper part of the Mono till is loose and earthy, and the matrix is somewhat sandy. Lack of much silt and clay suggests winnowing by melt water during deposition. The lower part is very compact and has a significant content of silt. The lower part is interpreted as basal till formed of materials carried along the base of the glacier and plastered over the area. The debris within and upon the melting ice was let down on the basal till already in place. The silt of the basal till was probably derived by local gouging of a silt stratrum within the upper part of the outwash deposited as a down-valley derivative of the advancing glacier and later overridden by it.

The silt stratum clearly indicates that a pond or small lake existed for a time in the area where the dam has been built. The deposit is outstandingly laminated, and although silt is predominant, there is some clay and locally fine sand. The silt layers are gray, minutely cross-bedded internally, and ripple-marked. Most of the layers are 0.5 cm to 1.5 cm thick, and there is some lateral variation in thickness. Gray color is due to content of heavy, ferromagnesian minerals such as horneblende and magnetite. The clay layers are white to pale yellowish-green, 1 mm to 2 mm thick. They are neither cross-bedded nor ripplemarked, and are remarkably constant in thickness. The darker, coarser-grained layers are believed to represent the summer deposits, and the light clay layers the winter deposits of annual varve pairs. If the varve interpretation is correct, the lake existed for approximately 1,000 yr in the time interval between the two latest ice advances in Vermilion Valley. The position of the silt stratum and lack of visible organic detritus suggests that the advancing Mono-age glacier (the latest) was not far up-valley while the lake was

[10] Chmn., Dept. of Geology, Occidental College, Los Angeles, Calif.

in existence. The lake deposits and associated deposits are interpreted as proglacial outwash subsequently overridden by the glacier itself.

The question occurs as to what dammed the lake that seems to have existed so long at the present dam site and that was developed on almost identical materials. Moraine damming or bedrock damming are eliminated easily by the abundance of geological evidence. Only outwash was (and still is) available in a topographic position to impound a body of water at the elevation of the silt stratum. This outwash was deposited from small glaciers on the south wall of the valley, downstream from the dam site, and from the San Joaquin trunk glacier that thrust a lobe into the Mono Creek re-entrant (Fig. 1). It is stressed that the moraines of these glaciers were not formed until after the deposition of the outwash within which the silt stratum occurs. The outwash was formed while the glaciers were advancing and before they reached their maximum extent. Thus, it seems that an ancient geological experiment indicated that a lake of some duration could successfully be impounded in Vermilion Valley. This seemed especially obvious in that during the geological experiment the more impervious Mono till, that now underlies the dam site area of the present lake had not yet been formed.

BRUCE R. LAVERTY,[11] A. M. ASCE.—In view of the writer's association with the project both during and after the construction period, it is believed that a discussion of the observed performance of the dam during several seasons of satisfactory operation would be of interest.

To properly monitor the performance of the dam, a comprehensive observation program has been maintained. It consists primarily of performing frequent piezometer measurements, seepage measurements, and settlement and alinement surveys. These measurements were begun before the dam was completed. Aerial photographs have also been utilized to define seepage patterns in the natural ground downstream from the dam.

During the first partial filling of the reservoir in 1955 and again during its first filling to capacity in 1956, resident observers at the damsite measured all piezometers and seepage weirs weekly. During the periods of high reservoir level, key piezometers and weirs were read daily. The performance of each well was plotted and analyzed daily to maintain a current evaluation of the pattern and amount of seepage developing within the embankment and through the complex foundation materials.

Because the dam has performed satisfactorily for five seasons, the frequency of the observations has been somewhat reduced and the period between measurements is now contingent on the operation of the reservoir. During the spring and summer when the reservoir is filling rapidly, the piezometers and the leakage weirs are read biweekly. During the winter months when the level of the water in the reservoir is low, the frequency of observations is reduced to bimonthly measurements of the piezometers and monthly readings of the weirs. The magnitude of the observation program may be inferred from Table 1, which indicates the number of individual observations made at each well and weir from 1955 to 1959.

During 1956 the more important piezometers were read nearly every working day. The less significant piezometers were read with approximately one-fourth the frequency of the key wells.

---

[11] Asst. Chief, Civil Engr., Souther California Edison Co., Los Angeles, Calif.

Fifty-three piezometers were installed during construction of the dam. However, in areas where more complete information was subsequently found desirable, additional piezometers were installed following the construction period. At present (1960), there are 100 piezometers maintained and read regularly.

The level of the water in the piezometers is sounded by using a water level indicator. The 3/4-in.-diameter piezometers used in the shell and along the toe of the dam have proven adequate in size. The deep foundation piezometers that are 3/8-in. plastic tubing have proved less successful because of their small size.

During 1955, the first season of operation, the reservoir was partly filled. The maximum pore water pressure anticipated at each piezometer at full reservoir level was predicted by extrapolating the curves plotted from the piezometric data obtained under these conditions. The stability analyses of the critical sections of the dam were repeated utilizing the values of the predicted maximum pore water pressures. The analyses indicated that, as finally constructed, the dam would be safe under the seepage regimen developed by full hydrostatic loading.

After each observation made during the reservoir filling period, the measured piezometric head in each of the wells was compared with trend lines

TABLE 1.—NUMBER OF OBSERVATIONS MADE AT PIEZOMETERS AND WEIRS

Measuring Stations	Year				
	1955	1956	1957	1958	1959
	Number of Observations				
Piezometers	42	204	11	7	8
Weirs	42	208	20	22	19

terminating at the maximum predicted values developed for the final stability studies. When steady-state seepage was developed under full reservoir conditions, it was found that the predicted maxima were conservative and that the actual piezometric heads developed were, with minor exceptions, less than anticipated. Table 2 shows the predicted pressures and the maximum measured pressures at full reservoir level in representative key piezometer wells. During 1955 the reservoir reached a maximum elevation of 7,603. The pressures are expressed in terms of the elevation of the piezometric surface.

As shown in Table 2, the highest observed piezometric levels occurred during the first filling of the reservoir in 1956. Slightly decreased pressures were measured in succeeding years. This decrease is attributed to the development of natural drainage patterns and seepage paths through and beneath the dam. The high piezometric levels indicated in 1956 are also attributed, in part, to the exceptional precipitation that occurred during this season. Studies have shown that heavy precipitation or rapid snow melt significantly influence the performance measurements.

The data obtained from the observation wells are tabulated and plotted to provide a continuous record of the performance of each well. The analysis of these plotted data is done promptly to insure the early detection of any deviation from previous patterns.

As a supplement to the extensive investigations regarding anticipated seepage through the heterogeneous glacial deposits comprising the foundations of the dam, an electrical analogy model of the embankment and foundation was

TABLE 2.—PREDICTED AND MAXIMUM MEASURED PRESSURES

Well[a] (1)	Final design, Predicted maximum water surface elevation, in feet (2)	Date				
		1955 (3)	1956 (4)	1957 (5)	1958 (6)	1959 (7)
		Maximum actual water surface elevation, in feet				
P-25	7,564	7,545.1	7,553.1	7,548.1	7,547.1	7,541.1
P-26	7,553	7,534.3	7,543.0	536.0	7,534.0	7,528.2
P-29	7,526	7,514.5	7,520.0	7,516.0	7,515.0	7,511.4
P-9	7,500	7,491.7	7,495.0	7,495.2	7,494.6	7,493.4
P-101A	7,553	7,536.8	7,545.0	7,539.0	7,537.9	7,533.0
P-101B	7,545	7,532.3	7,541.0	7,535.0	7,534.0	7,529.5
P-102A	7,514	7,507.5	7,512.0	7,509.0	7,505.7	7,505.1
P-102B	7,517	7,512.7	7,518.0	7,517.0	7,512.5	7,509.9

[a] Well locations are shown in Fig. 6(a).

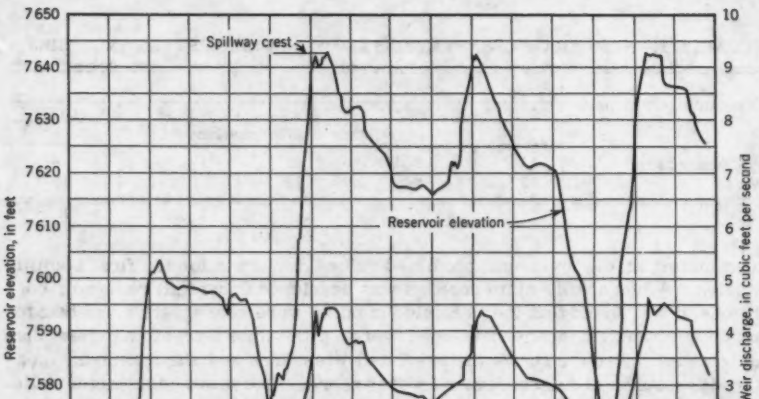


FIG. 15.—RESERVOIR OPERATION AND MEASURED SEEPAGE

constructed during the design period. From the results of this study the total amount of seepage at full reservoir level was estimated to be on the order of 4 cu ft per sec. This estimate compares remarkably well with the measured

maximum seepage of 4 $\frac{1}{2}$ cu ft per sec which is the maximum measured discharge through the toe drain. In a manner similar to that for the piezometer records, individual continuous plots are also kept of the measured discharges through the seepage weirs.

Fig. 15 illustrates the relationship of measured seepage to reservoir elevation. The quantities of seepage collected from the toe drain discharge lines and the seepage collected downstream from the dam are indicated.

Of interest, and demonstrated in Fig. 15, is the remarkable sensitivity of seepage discharge to reservoir elevation. The nearly immediate response of seepage to a change of reservoir elevation indicates the development of mature seepage paths through the embankment and foundation. This immediate response together with the stable piezometer performance indicates that no latent high seepage pressures are developing that could cause piping or otherwise reduce the stability of the embankment.

Because heavy precipitation and rapid snow melt influence performance measurements, it is necessary to evaluate the significance of erratic peaks or anomalies in otherwise consistent curves. Therefore, continuous records are maintained of precipitation and temperature at the damsite. An example of the value of such weather data was the investigation to explain the reason for the toe drain discharge increase in April, 1958, during a lowering reservoir elevation as shown in Fig. 15. This was found by examination of the daytime temperature and the precipitation records for the month.

In April, 1958, both the area immediately downstream from the dam and the downstream slope of the embankment were covered by several feet of snow. As the daytime temperature rose above freezing, the local snow melted rapidly, causing a general increase in ground-water elevation. Some of this water undoubtedly entered the toe drain, and additional water also seeped through the embankment into the drain. This same rise in temperature marked the beginning of the spring runoff period at higher elevations in the watershed. Consequently, shortly thereafter the gates were closed and the reservoir began to fill.

Settlement and alinement surveys are conducted periodically to measure any embankment movement. These data are plotted in Fig. 16. To date (1960), the total maximum post-construction settlement of the crest has been slightly over 0.10 ft and the maximum downstream movement at the crest has been 0.27 ft. The remarkably low magnitude of the post-construction movement of the dam results from the high placement density of the earth embankment as well as from the settlement-resistant qualities of the glacially preloaded foundations. Also shown on Fig. 16(e) are the settlement measurements at the concrete discharge conduit. This figure, which demonstrates the settlement from the constructed grades, shows the maximum settlement of the conduit to be 0.27 ft. In addition, the conduit is checked periodically for cracks and leaks, and the distance across each articulated expansion joint is measured. No significant movement has been recorded in the conduit joints. An aerial view of the dam soon after completion is shown in Fig. 17.

The cost of the present observation program averages $6,000 per yr. Included in this expenditure are the procurement and analysis of data and the costs of transporting observers to the comparatively remote damsite by helicopter or snow-cat during the winter months when the access roads are impassible. The expenditure also provides for an annual review of the results of the observation program by an outside engineering firm.

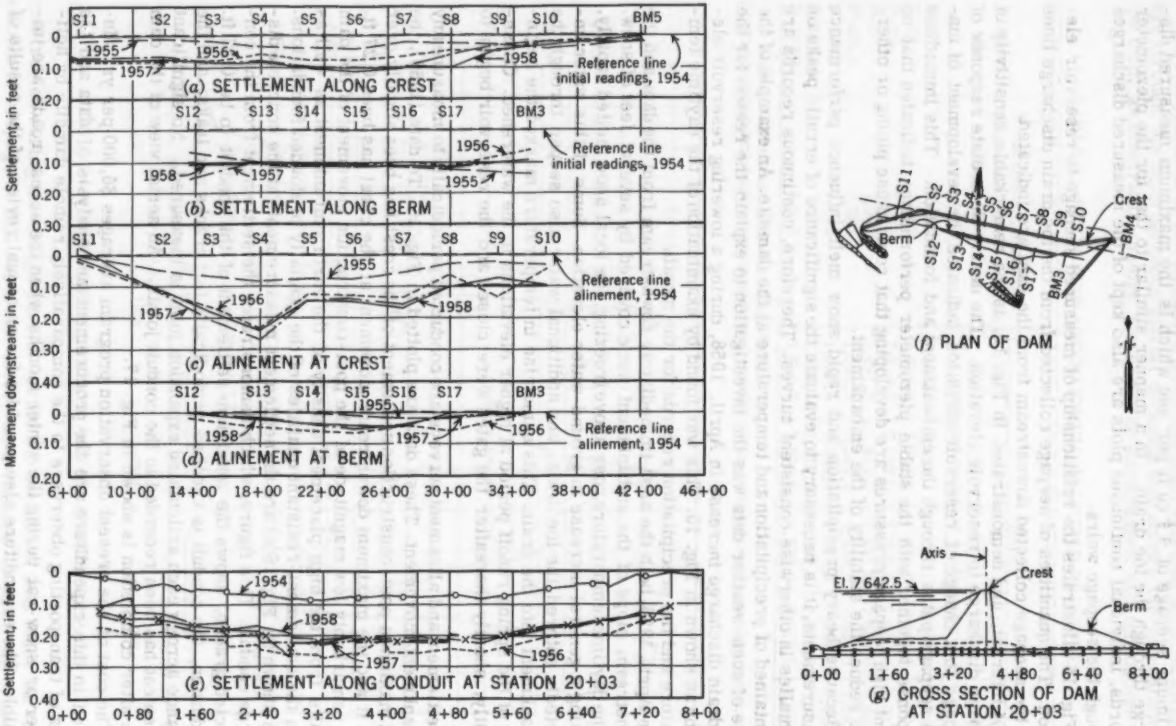


FIG. 16.—SETTLEMENT AND DEFLECTION MEASUREMENTS

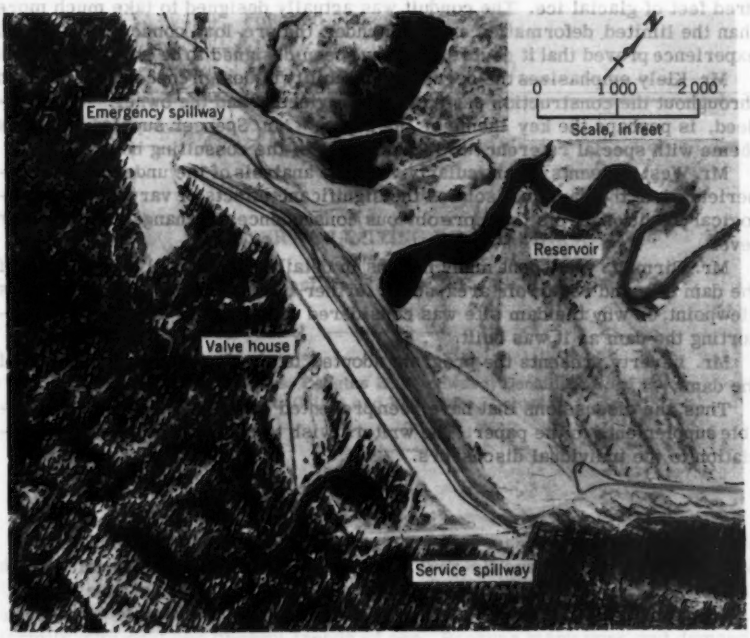


FIG. 17.—VERMILION DAM SOON AFTER COMPLETION

This observation program has thus enabled the owner and the State of California Department of Water Resources, the public agency accountable for the safety of the dam, to evaluate adequately the performance of the dam.

KARL TERZAGHI,[12] HON. M. ASCE, and T. M. LEPS,[13] F. ASCE.—The writers were particularly pleased to note that the paper stimulated six engineers who were associated closely with the design and measurement of performance of Vermilion Dam to draw upon their personal experiences with the project in the preparation of discussions of the paper. Each discussion supplements the paper with valuable thoughts and experiences.

Mr. Dickinson outlines the design and successful performance of the outlet conduit through the dam. This reinforced concrete, articulated joint conduit was founded on heterogeneous glacial debris having a depth of over 200 ft. Mr. Dickinson mentions that a maximum settlement of 0.27 ft has been measured in the conduit. This occurred under a maximum fill height of 145 ft. The reason that settlement was so minor undoubtedly lies in the finding of engineering

---

[12] Prof. Emeritus, Harvard Univ., Cambridge, Mass.
[13] Mgr. of Organization & Procedures, Southern Calif. Edison Co., Los Angeles, Calif.

geologists that the site had been glacially pre-loaded by at least several hundred feet of glacial ice. The conduit was actually designed to take much more than the limited deformation expected under the pre-load concept, and actual experience proved that it could safely have been designed to be less articulated.

Mr. Kiely emphasizes the degree of flexibility in design concepts maintained throughout the construction period by the engineers and the owner. This, indeed, is perhaps the key theme of the paper. Mr. Spencer supplements this theme with special reference to the functions of the consulting board.

Mr. West presents a particularly valuable analysis of the underseepage experienced at the dam and isolates the significant effects of varying meteorological conditions from the more obvious consequences of changes in reservoir level.

Mr. Birman, who spent many months in detailed geological examination of the dam site and reservoir area, sheds further light from a glacial geologist's viewpoint, on why the dam site was considered and why it is adequate for supporting the dam as it was built.

Mr. Laverty presents the program adopted to check on the performance of the dam.

Thus, the discussions that have been presented can be viewed as most valuable supplements to the paper. The writers wish to express their great appreciation to the individual discussers.

AMERICAN SOCIETY OF CIVIL ENGINEERS

Founded November 5, 1852

TRANSACTIONS

Paper No. 3015

WATER—A LIMITING RESOURCE

By Robert O. Thomas,[1] F. ASCE

With Discussion by Messrs. Douglas R. Woodward; Donald McCord Baker; Alfred R. Golze; and Robert O. Thomas

SYNOPSIS

This paper emphasizes the probable degree of magnitude of the anticipated demand for water in the United States. The over-all availability of water in the United States is compared with the major domestic, agricultural, and industrial demands made on the supply. It ventures to predict future demands in conformity with past and present trends of use. Because many uses and demands are neglected, the paper is not designed to be comprehensive in scope. It is designed to evoke discussion of the implications inherent in the apparent adverse balance between supply and probable demand, and to engender recommendations for present and future action to prevent exhaustion of the supply.

INTRODUCTION

The availability and use of water is vital to the maintenance of present-day civilization. The use and frequently the consumption of water is necessary in the production of food and fiber, the generation of fuel-electric energy, the manufacture of industrial products, and the maintenance of the domestic environment of the individual.

The available water supplies of the United States are apparently insufficient to support a growing population, accompanied by a modest increase in the standard of living, for more than a comparatively short period in the future. It is

Note.—Published, essentially as printed here, in September, 1958, in the Journal of the Irrigation and Drainage Division, as Proceedings Paper 1754. Positions and titles given are those in effect when the paper or discussion was approved for publication in Transactions.

[1] Superv. Hydr. Engr., State Dept. of Water Resources, Sacramento, Calif.

of vital importance that immediate action be taken to accelerate pure and applied research and the design of necessary facilities, directed to the accomplishment of the demineralization of sea water efficiently and economically. This must be accomplished by the turn of the century and will require that a sizeable part of domestic, municipal, and industrial uses be supplied from such a source.

The paper is limited to an examination of the major uses of the available water supply. Other uses of importance not discussed herein are evaporation from water surfaces, utilization of water for maintenance of stream flow, the support of fish and wildlife, transportation, dilution of poor quality waters and effluents, and hydroelectric energy generation. These uses of the common water supply must be kept in mind, however, because they exert considerable influence on the quality of water available for all uses. Neither is consideration given to the re-use of water supplies or to possibilities of the repeated utilization of the same quantity of water. Many of the uses considered are contemporary in time and the demands are cumulative. Additionally, the majority of the uses considered occur in the valley sections of stream basins, in which opportunities for regulatory storage between consecutive uses are rarely found. This is not to decry the existence of groundwater storage nor the possibilities inherent for long-term regulation of water supplies through its proper use. The characteristics of groundwater storage, however, are not such as to facilitate month-to-month regulatory storage.

This paper does not evaluate the effect of varying monthly flow in the streams of the country, but presumes that sufficient storage, either above or below the surface of the ground, will be provided to regulate that part of the available supply which is determined to be usable, with consideration to all competing demands. Nor does it give consideration to the geographical availability of water in various parts of the country, because it presumes that the necessary diversion and transmission of water supplies will be accomplished to the maximum extent practicable.

An additional source of water supply which has not been considered is artificial nucleation. It is felt that this method of generating precipitation will be of principal value in the amelioration of drought in dry-farmed areas, but that because of the limited availability of natural storage sites for additional water supplies, it cannot be considered a dependable resource. Therefore, it is believed that weather modification would be of little assistance to irrigated agriculture, or to domestic and industrial uses of water. In certain limited areas, however, in which spring and summer stream flow is supplied largely by melting snowpack, current applied research in snowpack augmentation gives indication of favorable results.

WATER SUPPLY

The national water supply is assumed to be the quantity of water currently available for development in the streams and rivers of the country. The quantity considered is that which remains after the evapotranspiration requirements of nature have been satisfied from precipitation. Much of the water evaporated or transpired is used to support the growth of food and fiber crops on more than 300,000,000 acres of farmland and to maintain pasturage on almost 800,000,000 acres devoted to the production of animal products. In addition, large quantities are required to provide for the growth of natural forests and

the maintenance of nearly 31,000,000 acres of water surface in the lakes and reservoirs of the country. Therefore, it is assumed that the upper limit of presently available supply is represented by the average annual runoff to the stream system. The quantity of runoff is shown in Table 1.

TABLE 1.—ANNUAL RUNOFF IN THE UNITED STATES, 1921-45[a]

Basin (1)	Area, in square miles (2)	Average annual runoff, in acre-feet (3)
North Atlantic slope	148,000	152,000,000
South Atlantic Slope and Eastern Gulf of Mexico	284,000	235,000,000
Mississippi River	1,250,000	449,000,000
Hudson Bay	48,000	3,600,000
St. Lawrence River	130,000	101,000,000
Western Gulf of Mexico	320,000	39,800,000
Colorado River	246,000	16,700,000
Great Basin	215,000	12,500,000[b]
Pacific Slope in California	117,000	57,900,000
Columbia River and coastal streams in Oregon and Washington	262,000	250,000,000
Totals	3,020,000	1,317,500,000

[a] "Annual Runoff in the United States," by W. B. Langbein, Circular No. 52, Geol. Survey, U.S. Dept. of the Interior, Washington, D.C., 1949.
[b] Estimated by the author.

The average runoff of 1,317,500,000 acre-ft, as given in Table 1, amounts to approximately 8.1 in. in depth on the total area. Studies by the United States Weather Bureau indicate that, for the 1921-45 period, the annual precipitation amounted to approximately 30 in. in depth. Thus, the indicated evapotranspiration use of water amounted to approximately 21.8 in. annually.

WATER USE

Public water supply systems, serving areas containing populations in excess of 25,000 people, provided water supplies amounting to 13,174,000 acre-ft to 79,596,000 persons in 1953.[2] This is equivalent to approximately 148 gal per day per person. Using this computed daily use, annual quantities of municipal water use as reported by the Geological Survey, United States Department of the Interior (U.S.G.S.) have been expressed in terms of the population served. Table 2 presents water-use data for 1950 and 1955. Saline water used by industry, according to U.S.G.S. data, is not included in the quantities of water given in Table 2.

Assuming that the rural daily per capita use, amounting to approximately 60 gal, represents personal requirements for domestic uses, it appears that

[2] "Statistical Abstract of the United States, 1956," U. S. Dept. of Commerce, Washington, D.C., 1956.

approximately 88 gal per day per capita are used for public and industrial purposes in areas served by municipal systems. Public uses for parks, flushing, and washing streets are believed to be a minor component of this use.

Therefore, it is assumed that 75 gal per day per capita are used in industrial activities other than fuel-electric energy generation, resulting in the industrial use, from municipal supplies, of 7,900,000 acre-ft in 1950 and 9,700,000 acre-ft in 1955. The total industrial use of water supply, other than for power generation, is estimated to be 29,600,000 acre-ft in 1950 and 45,500,000 acre-ft in 1955.

Water used for irrigation represented an application of 3.37 ft in depth on the irrigated area in 1950, and 3.14 ft in depth in 1955. This compares with the over-all national average of 1.82 ft in depth used in evapo-transpiration

TABLE 2.—USE OF FRESH WATER IN THE UNITED STATES[a]

Class of use	1950			1955		
	Quantity, in acre-feet	Daily use, in gallons per capita	Population served	Quantity, in acre-feet	Daily use, in gallons per capita	Population served
(1)	(2)	(3)	(4)	(5)	(6)	(7)
(a) Individual and incidental industrial						
Rural	4,030,000	64	56,100,000	2,800,000	56	50,300,000
Municipal	15,700,000	148	94,600,000	19,000,000	148	114,900,000
(b) Industrial, from private sources						
Fuel-electric power generation	43,000,000	...	...	67,200,000	...	...
Other industry	21,700,000	...	...	35,800,000	...	...
Irrigation	88,500,000	...	...	90,700,000	...	...
Totals	172,930,000	...	150,700,000	215,500,000	...	165,200,000

[a] "Estimated Use of Water in the United States," by K. A MacKichan, Circular No. 115, 1950, Circular No. 398, 1955, Geological Survey, U.S. Dept. of the Interior, Washington, D.C.

processes. Because the volume and value of crop growth is, to a certain point, related closely to the quantity of water consumed in the growth process, it is assumed that a similar relationship could be obtained in comparing crop values from irrigated and dry-farmed areas. Table 3 presents available data bearing on this relationship.

The irrigated acreage in the entire United States (Table 6) has increased from 6.6% of the total cropped acreage in 1939, to 7.6% in 1949. However, the proportion is small and it is not believed to affect greatly the general conclusion, drawn from the data in Table 3, that the irrigated acreage will produce

twice the value and volume of the dry-farmed acreage. A comparison of the quantity of water available to promote crop growth, as given previously, leads to a similar general conclusion.

GROSS NATIONAL PRODUCT

The gross national product (GNP) represents the total national output of goods and services at market prices. It measures this output in terms of the expenditures by which these goods are acquired. The goods and services included in GNP are, for the most part, those actually brought for final use. The GNP also measures the product attributable to the factors of production supplied by the population. The GNP is thus representative of total production and of the current standard of living.

TABLE 3.—CROP VALUES IN THE UNITED STATES[a]

Year	U.S. Bureau of Reclamation Projects			Total United States		
	Irrigated acreage	Value of crops, in millions of dollars	Value per acre, in dollars	Harvested crop acreage	Value of crops, in millions of dollars	Value per acre, in dollars
(1)	(2)	(3)	(4)	(5)	(6)	(7)
1939	3,140,000	114.1	37	324,000,000	5,700	18
1944	4,164,000	411.2	99	353,000,000	14,440	41
1949	4,821,000	351.7	73	352,000,000	16,300	46
	Average		70			35

[a] "Statistical Abstract of the United States, 1956," U.S. Dept. of Commerce, Washington, D.C., 1956.

TABLE 4.—GROSS NATIONAL PRODUCT IN THE UNITED STATES

Year	GNP, in Millions of Dollars[a]			Population, in Thousands			GNP, in Dollars per Capita	
	Farm	Other	Total	Farm	Other	Total	Farm	Total
(1)	(2)	(3)	(4)	(5)	(6)	(7)	(8)	(9)
1910	15,950	...	...	32,100	59,872	91,972	173	...
1920	16,790	...	...	31,820	73,890	105,710	159	...
1930	17,070	132,230	149,300	30,570	92,205	122,775	139	1,216
1940	19,530	152,070	171,600	30,550	101,119	131,669	148	1,303
1950	23,130	241,570	264,700	25,015	125,682	150,697	153	1,757
1955	25,200	293,600	318,800	22,310	142,940	165,250	153	1,929

[a] In 1947 dollars.

The gross national product,[2] both total and farm, is given in Table 4, together with per capita values, for the period since 1910. The values given, based on standard values in terms of 1947 dollars, are comparable among themselves. It appears that the GNP attributable to farm production has remained fairly stable since 1930. On the other hand, the nonfarm GNP, representing all other goods and services provided to the nation, has increased almost 160%

in the 25-yr period from 1930 to 1955. This value integrates the effects of increases in the standard of living and the production of many goods and services unknown, or in the experimental stage, a quarter of a century ago.

Water is an essential factor in the manufacture of many of the products which, collectively, constitute our material standard of living. Therefore, it is believed that there should be some relationship between the use of water and the GNP attributable to sources other than agriculture. Such a relationship is shown in Table 5 for the years 1950 and 1955. Data on industrial use of water are readily available for these years. It appears that the per capita use of water in support of production is increasing at a very rapid rate. The per capita value of the GNP is also increasing, although at a lesser rate.

A projection of the trend of increase in the non-agricultural GNP indicates an estimated value of approximately $3,450 per capita with a population of 300,000,000, and $4,500 per capita with a population of 450,000,000, an increase of 194% and 253% as compared to the 1955 per capita value, respectively. For the purpose of this paper, it is assumed conservatively that the use of water to support the total product will increase approximately 50% to a value of 0.40 acre-ft per capita, with a population of 300,000,000, and will continue to increase at the same rate with future increases in population. The effect on the use of water will be examined subsequently.

TABLE 5.—INDUSTRIAL FRESH WATER USE IN THE UNITED STATES

Year	Population, in thousands	Industrial Water Use				Nonagricultural GNP	
		In thousand acre-feet		In acre-feet per capita		In millions of dollars	In dollars per capita
		Fuel-electric	Other	Fuel-electric	Other		
(1)	(2)	(3)	(4)	(5)	(6)	(7)	(8)
1950	150,697	43,000	29,600	0.285	0.196	241,570	1,603
1955	165,250	67,200	45,500	0.407	0.275	293,600	1,777

Water used in agriculture provides for the growth of food and fiber products for consumption and for the production of feed for livestock. Of the approximately 1,904,000,000 acres comprising the continental United States, agricultural operations make use of approximately 1,158,000,000 acres. Croplands amount to 394,000,000 acres and pasturage and grazing occupy approximately 764,000,000 acres. This general relationship has remained essentially stabilized since 1910, increased farm productivity having apparently compensated for increases in population. Inasmuch as the production of animal products is as essential a part of the standard of living as foods and fibers, it is believed that the available cropland will remain at the present level in the future. Of the remaining lands in the United States, 555,000,000 acres are forest and woodland acres, and 191,000,000 acres are devoted to miscellaneous uses, or are otherwise unavailable for agricultural operations.

The harvested cropland in the United States, both dry-farmed and irrigated, for the period since 1910, is shown in Table 6. In a preceding section, it has been estimated that an irrigated acre will, on the average, produce twice the crop volume of the dry-farmed acre. On this basis, an equivalent harvested

acreage has been computed (Table 6), consisting of dry-farmed acreage plus twice the irrigated acreage.

The equivalent dry-farmed acreage per capita has exhibited a consistent downward trend from 3.66 acres per capita in 1910 to 2.19 acres in 1955. At the same time the farm GNP, in terms of 1947 dollars, has increased from approximately $47 per acre in 1910 to approximately $70 per acre in 1955. Inasmuch as it has been indicated that the farm GNP per capita has apparently stabilized at approximately $155, it is felt that the farming industry has, at this time, essentially reached a position of agricultural and economic balance. In the immediate future, increases in population should, therefore, be accompanied by generally equivalent increases in over-all productivity. With a stabilized cropland area, this will require increases in the irrigated acreage.

TABLE 6.—CROPPED ACREAGE IN THE UNITED STATES

Year	Population, in millions	Cropped Acreage, in Millions of Acres				Equivalent cropped acreage, per capita
		Dry-farmed	Irrigated	Total	Equivalent acreage[a]	
(1)	(2)	(3)	(4)	(5)	(6)	(7)
1910	91.97	307.57	14.43	322.0	336.4	3.66
1920	105.71	342.81	19.19	362.0	381.2	3.61
1930	122.78	339.45	19.55	359.0	379.5	3.08
1940	131.67	299.86	21.14	321.0	342.1	2.60
1950	150.70	318.77	26.23	245.0	371.2	2.46
1955	165.25	304.10	28.90	333.0	361.9	2.19
. . .	180.0	318.0	30.0	348.0	378.0	2.1
. . .	200.0	326.0	37.0	363.0	400.0	2.0
. . .	250.0	256.0	122.0	378.0	500.0	2.0
. . .	300.0	188.0	206.0	394.0	600.0	2.0
. . .	350.0	158.0	236.0	394.0	630.0	1.8
. . .	400.0	148.0	246.0	394.0	640.0	1.6
. . .	450.0	148.0	246.0	394.0	640.0	1.4+

[a] Dry-farmed acreage plus twice the irrigated acreage.

Further major reduction in the acreage cropped per capita will probably occur when the GNP attributable to farm production increases in per capita value. Such increases will create conditions conductive to intensification of efforts to improve cropping practices. These efforts will be directed toward land management, soil conservation, proper use of water and fertilizers, and similar advanced practices. It is not contemplated, however, that the cropped acreage will expand at the expense of that devoted to production of animal products. The management of the latter acreage will be forced, by economic pressure, to improve productivity in a manner paralleling that of the cropped acreage. It is felt that the requirement of continually increased productivity is in itself a sufficient challenge without the added incubus of a reduction in available acreage.

The prediction of future trends in agricultural water utilization is based on assumptions which, in turn, result in predictions valid only for the indicated circumstances. The assumptions made herein are:

1. The present degree of utilization of agricultural land is 67% in a scale of 100. In other words, a 50% increase in present per acre volume of production can be made.

2. The present trend of improvement in productivity of cropped acreage will continue and result in a value of 2.0 equivalent acres per capita with a population of 200,000,000.

3. The value of 2.0 equivalent acres per capita will be maintained until a population of 300,000,000 has been reached, after which time it will decrease to 1.4 acres, representing 100% utilization, with a population of 450,000,000.

TABLE 7.—ESTIMATED AGRICULTURAL WATER REQUIREMENTS IN THE UNITED STATES

Year	Population, in millions	Irrigated Acreage, in Millions of Acres		Water Requirements, in Millions of Acre-feet		
		Semi-arid region	Humid region	Semi-arid region	Humid region	Total
(1)	(2)	(3)	(4)	(5)	(6)	(7)
1950	150.7	26.23	. . .	88.5	. . .	88.5
1955	165.25	27.90	1.0	89.4	1.3	90.7
. . .	180.0	28.5	1.5	92.6	1.9	94.5
. . .	200.0	32.0	5.0	104.0	6.0	110.0
. . .	250.0	79.0	43.0	257.0	54.0	311.0
. . .	300.0	125.0	81.0	406.0	101.0	507.0
. . .	350.0	141.0	95.0	458.0	119.0	577.0
. . .	400.0	147.0	99.0	478.0	124.0	602.0
. . .	450.0	147.0	99.0	478.0	124.0	602.0

Total croplands: Semi-arid region—235,000,000 acres; Humid region—159,000,000 acres.

4. Harvested cropland will expand to include the total available 394,000,000 acres at a population of 300,000,000. Other required expansion will take place through increases in irrigated acreage.

5. Of the present (1955) irrigated acreage, 1,000,000 acres is assumed to exist in other than the principal irrigation states. It is assumed that two-thirds of the total cropland acreage will ultimately be irrigated in both present irrigation (semi-arid) and dry-farmed (humid) areas. It is further assumed that increases in irrigated lands in both areas will occur in a parallel manner.

6. The annual applied water requirement of irrigated land in the semi-arid regions will be 3.25 acre-ft per acre. In the humid regions the supplemental requirement will be 1.25 acre-ft per acre. Tables 6 and 7 show the application of the previous assumptions. It will be noted that future projections in these

and succeeding tables are based on population. The year in which this population is attained is not shown, because it depends on the specific projection favored by the reader.

INDUSTRIAL USE OF WATER

It has been shown previously that the industrial use of water has undergone a tremendous percentage increase in the period from 1950 to 1955. It is probable that the increase in the standard of living, as represented by the nonfarm GNP, from approximately $1,600 to approximately $1,775 per capita (Table 5), has contributed to the increase in the industrial use of water. It is assumed that the 1955 use of water, in general industrial activities, amounting to approximately 0.28 acre-ft per capita, will undergo an increase of approximately 50% to 0.40 acre-ft per capita when the population has reached 300,000,000 and maintain the same rate of increase thereafter. This increase is assumed to occur in conformity with increases in the standards of living, although at a lesser rate due to the necessity for increased productivity per acre-ft of water.

TABLE 8.—ESTIMATED WATER REQUIREMENTS FOR STEAM POWER GENERATION

Year	Population, in millions	Energy, in billions of kilowatt-hours	Percentage of Total Energy Production		Kilowatt-Hours per Capita		Water Use	
			Steam	Hydro	Total	Steam	In acre-feet per capita	In millions of acre-feet
(1)	(2)	(3)	(4)	(5)	(6)	(7)	(8)	(9)
1930	122.8	90.4	66	34	736	...	...	...
1940	131.7	140.3	67	33	1,065	...	...	...
1950	150.7	325.4	71	29	2,160	1,530	0.285	43
1955	165.3	546.4	79	21	3,305	2,610	0.407	67
...	180.0	675.0	81	19	3,750	3,040	0.46	83
...	200.0	820.0	83	17	4,100	3,400	0.50	100
...	250.0	1,190.0	85	15	4,750	4,040	0.58	145
...	300.0	1,550.0	87	13	5,150	4,480	0.63	189
...	350.0	1,925.0	88	12	5,500	4,840	0.67	235
...	400.0	2,325.0	89	11	5,800	5,160	0.71	284
...	450.0	2,700.0	90	10	6,000	5,400	0.73	329

It is also assumed that the use of electrical energy and of water used in generating steam energy will, based on projection of present trends, increase in the future to the extent shown in Table 8. The estimated general industrial increase in water use is set forth in Table 9(a).

DOMESTIC AND MUNICIPAL USES OF WATER

It was previously estimated that the domestic use of water by individuals averaged 60 gal per day per capita and that municipal and miscellaneous uses, except industrial, averaged 13 gal per day per capita. It is assumed that domestic and municipal uses, due to increased use in parks and recreational areas, as well as other uses, will, in the future, increase approximately 67%

to an overall figure of 125 gal per day per capita with a doubled population of approximately 350,000,000 and remain constant thereafter. Water requirements computed in accordance with such assumptions are given in Table 9(b).

CONCLUSIONS

The foregoing presentation has emphasized the probable degree of magnitude of the anticipated demand for water in the United States. Exception may readily be taken to many of the assumptions made in order to predict total requirements. However, although analyses of the various separate uses of water may be challenged, it is believed that the general indications of tremendous increases in demand during the next few decades are significant in their implications.

The assumptions and projections made in the course of this analysis were, it is believed, conservative in relation to present trends of use. Therefore, it is felt that the predicted use of water, as stated herein, can be expected to occur as a result of growth in population and increased standards of living. In this connection, estimates prepared by others are of interest. W. S. Paley[3] estimated that the requirement for the use of water by 1980 would amount to 392,000,000 acre-ft annually. The equivalent estimate by the writer amounts to 368,000,000 acre-ft. Douglas R. Woodward,[4] F. ASCE, has estimated the water use by 1980 to amount to 669,000,000 acre-ft, with a population of approximately 275,000,000. His estimate agrees closely, in terms of quality versus population, with that used in this paper. The writer, however, has used the United States Census Bureau conservative estimate, involving a return to the prewar birth rate by 1975, and hence does not reach that population until shortly after the year 2000.

TABLE 9.—ESTIMATED INDUSTRIAL, DOMESTIC AND MUNICIPAL WATER REQUIREMENTS

Year	Population, in millions	(a) General Industrial Water Requirements		(b) Domestic and Municipal Water Requirements	
		Water use, in acre-feet per capita	Water use in millions of acre-feet	Water use, in gallons per day per capita	Total water use, in millions of acre-feet
(1)	(2)	(3)	(4)	(5)	(6)
1950	150.70	0.196	29.6	70	11.8
1955	165.25	0.275	45.5	65	12.1
. . .	180.0	0.31	55.0	77	16.0
. . .	200.0	0.34	68.0	89	20.0
. . .	250.0	0.37	92.0	101	28.0
. . .	300.0	0.40	120.0	113	38.0
. . .	350.0	0.43	151.0	125	49.0
. . .	400.0	0.46	184.0	125	56.0
. . .	450.0	0.49	221.0	125	63.0

With more than 15% of the available water supply presently utilized, and with the prospect of doubling the present population by the first decade of the next century, only approximately 50 years remain to establish, and to a large

[3] "Subsurface Facilities of Water Management and Patterns of Supply," Interior and Insular Affairs Committee, House of Representatives, 83rd Cong., 1956, p. 6.

[4] "Availability of Water in the United States, with Special Reference to Industrial Needs by 1980," by D. R. Woodward, Industrial College of the Armed Forces Student Thesis, 1957.

extent implement, the substitution of alternative sources of water for much of the existing and future demand. The regulatory storage requirements needed to make 40% to 50% of the total national water supply available for use are large, although that quantity of water will apparently be required solely for use by irrigated agriculture before the end of the century.

The total estimated future demands on water supply in the United States are given in Table 10. The anticipated date by which such a demand may be expected, based upon the most conservative of the Census Bureau estimates of population growth, is given in column 1. It should be pointed out, however, that estimates of water demand that have been made in this paper are related to population and not to time. The purpose of the time scale (column 1) in Table 10 is solely to emphasize the immediacy of the problems presented.

Little information is available on total investment in water service facilities. That which is most readily available[2] pertains to irrigation water supply

TABLE 10.—ESTIMATED FUTURE WATER USE IN THE UNITED STATES

Year	Population, in millions	Water Use, in Millions of Acre-Feet					Percentage of total supply
		Irrigation	Domestic and municipal	Electric power	General industry	Total	
(1)	(2)	(3)	(4)	(5)	(6)	(7)	(8)
1950	150.7	88.5	11.8	43.0	29.6	172.9	13.1
1955	165.25	90.7	12.1	67.0	45.5	215.3	16.3
1965[a]	180.0	94.5	16.0	83.0	55.0	248.5	18.8
1975[a]	200.0	110.0	20.0	100.0	68.0	298.0	22.6
1995[a]	250.0	311.0	28.0	145.0	92.0	576.0	43.7
2015[a]	300.0	507.0	38.0	189.0	120.0	854.0	64.8
2035[a]	350.0	577.0	49.0	235.0	151.0	1,012.0	76.8
2055[a]	400.0	602.0	56.0	384.0	184.0	1,126.0	85.4
2070[a]	450.0	602.0	63.0	329.0	221.0	1,215.0	92.2

[a] Estimated year in which attained.

investment during the period from 1940 to 1950. During that period, more than 800 million dollars on a rapidly rising cost scale, was expended to bring irrigation water to approximately 5,000,000 acres previously unirrigated. On that basis, the prospective cost of providing a water supply by the year 2000 for almost 160,000,000 acres not now irrigated, but required to feed a population of 275,000,000, would be an estimated 26 billion dollars, or 13 times the 1950 historical capital investment for all irrigation enterprises. Based on the U. S. Bureau of Reclamation composite price index, the cost would be 34 billion dollars, or approximately $310 per unit increase in population. This does not take future increases in construction cost into account.

The foregoing cost pertains only to water supplies for irrigated agriculture. Additionally, there will be correspondingly large sums involved in providing water supplies for domestic, municipal, and industrial uses. From the financial point of view, when contemplating the investment of funds in such amounts during either the next quarter or half century, the questions of source of funds and ability to amortize appear to be paramount. Therefore, it is felt that the immediate initiation of positive action is imperative.

A preliminary analysis suggests several courses of action that may tend to counteract or offset the adverse water supply situation presented by this analysis. It is believed that the following list will serve to indicate the widespread implications and the basic nature of the approach to national water conservation policy:

1. Continuing and intensified public education in water conservation practices;
2. Re-use by the steam-electric industry (after heat removal) of most of the water required for cooling generating equipment and the production of steam;
3. Redesign of some industrial equipment to utilize saline or waste waters;
4. Strict economy in the use of agricultural water and further development of methods of accelerating food and fiber production in relation to evapotranspiration;
5. Reclamation, local storage, and re-use of industrial process water;
6. Accelerated research in the processes of demineralization of saline or brackish water;
7. Construction and operation of sea water conversion plants along the coast, and the use of demineralized sea water for all domestic and industrial purposes on all possible lands;
8. Establishment of nuclear-electric energy generating plants near the seacoast, utilizing sea water for operation, and transmission of the output considerable distances inland, even at the sacrifice of generated power;
9. Integration of the economies of the United States and Canada, utilizing the combined land and water resources for the best interests of both; and
10. Relocation of industry to the seacoast, reserving the interior for agriculture to the maximum extent. This, of course, requires that national defense industrial dispersion requirements be subordinated.

Eventually, in spite of the possible measures taken to conserve and supplement the available water supply, the burgeoning population of the world will, in the future, present the engineering profession with problems that can scarcely be imagined today. However, the present-day engineer must assume the responsibility of instituting all of the conservation measures available within the limits of our existing technology. This is the present challenge that is facing the engineering profession.

DISCUSSION

DOUGLAS R. WOODWARD,[5] F. ASCE.—The author has presented a paper of concern to engineers and laymen alike. Whereas one may differ in degree with his conclusions, he has ably demonstrated that the future problems of supplying water to the many needs of the United States will be both serious and challenging. The author also presents convincing evidence to show that water must be considered as a national resource as well as a local or regional resource.

[5] Staff Engr., Dir.'s Office, U. S. G. S., Washington, D. C.

Although Mr. Thomas does not set up a demand-supply analysis, such an analysis is implied in Table 2. The table might have been more helpful if he had included an estimate of consumptive losses (evapo-transpiration), which are more important than the amount of water withdrawn for use. Another way in which our water resources are depleted is through excessive degradation in quality, which restricts re-use. It seems important, therefore, to include in a water supply study of this nature some estimate of the net effects resulting from the use of water.

The evidence showing that water resources must be managed more intelligently is overwhelming, yet very little has been done to view the problem in broad perspective. A proposal for a continuing national inventory of water[6] has not yet been put into practice, although the concept is sound and the need pressing.

Estimation of future water requirements is very problematic. The author has attempted to estimate these requirements for the time our population has reached 450,000,000 but this seems to have been done largely on the basis of extrapolation. The writer would like to point out some of the problems of such long-range speculation.

The statement that water is an essential factor in all aspects of the economy is commonly accepted, and as a corollary, it is assumed that the current unit usage of water is necessary to our way of life. This acceptance of unit requirements as a mandatory requirement is not completely realistic. Except for use of water to sustain both animal and plant life, substitutes can and will be made for many of the current usages of water. Unit uses can also be greatly reduced for many purposes, such as for irrigation. Current irrigation practices do not derive high efficiencies in the use of water, and in the future, present irrigation practices may be considered primitive and profligate.

Use of water in large quantities for most industrial purposes is, in part, a convenience. The opportunities for reducing the use of water in industry are many. Water for cooling purposes, although currently a common practice, is by no means necessary. Air cooling and recirculation of water provide alternatives that are used already to some degree.[7]

An analysis of current uses of water for industrial purposes reveals a wide range in practice. For example, use of water in steel production ranges from near minimal quantities used at a plant on the west coast to large uses in the more humid east. Unit usage ranges in a ratio of roughly 1 to 50. However, in the case of limited usage, practically 100% of the water is evaporated. Similar ranges in practice occur in the use of water in other industries.

The author's analysis of future use of water for agriculture, mainly irrigation, requires careful study. There is evidence[8] that the author's estimate of 1.25 acre-ft per acre required for irrigation in the humid portions of the United States is excessive. Furthermore, the total moisture deficiency, shown elsewhere,[8] need not be met for successful crop production. Thus, Mr. Thomas' estimate of 124,000,000 acre-ft per year for future water requirements for the humid part of the United States appears to be too high.

---

[6] "A Program to Strengthen the Scientific Foundation in Natural Resources," House Document 706, 81st Cong., 2d Session, 1954.

[7] "Low Temperature Cooling Using Combination of Minimum Water and Maximum Air," Oil and Gas Journal, Vol. 56, No. 25, Hudson Engineering Corp., 1958, pp. 128–129.

[8] "Potential Use of Water by Irrigation in the Humid Area," by Keith H. Beauchamp, Proceedings Paper 1750, ASCE, September, 1958.

The author seems to imply that irrigation agriculture in the semi-arid zone of the United States is inherently preferable to growing of crops elsewhere. This is derived from the data in Table 3, from which he concludes that arid-zone irrigation is inherently more productive because it produces crops of approximately double the value per acre as compared with other types of agriculture. However, irrigation agriculture is intensive regardless of its location, whereas much of general agriculture is extensive in character.

In projecting irrigation requirements for semi-arid parts of the United States, Mr. Thomas concludes that an ultimate water requirement of 3.25 acre-ft per acre for 147,000,000 acres, or a total requirement of 478,000,000 acre-ft is necessary. Two factors require further scrutiny. The assumed requirement of 3.25 acre-ft per acre seems too high. Much of the semi-arid zone not now irrigated is currently growing dry-land crops, especially grains, and has an annual precipitation, concentrated during the growing season, of 12 in. to 20 in. For example, in the Missouri Basin, average water deficiency ranges from 3 in. to 20 in. according to Charles Thornthwaite.[9]

The other factor requiring scrutiny is the source of supply for the computed requirement of 478,000,000 acre-ft of water. The only area of any substantial water surplus, in the order of magnitude required to satisfy the estimated demand, is the narrow strip on the Pacific northwest coast. This area of surplus is hundreds of miles from the points of possible use. Furthermore, other demands for that water will be competitive with its use for irrigation.

One further feature of the agricultural requirement analysis is the author's assumption that the amount of land available for agriculture is fixed. Millions of acres of agricultural land in humid parts of the United States can be developed from swamp lands and from lands now used for forests or other low value uses.[10] Furthermore, such lands can even now be developed for costs far less than the cost of land in many proposed irrigation developments.

Whereas Mr. Thomas does mention increasing productivity per acre, he discounts it as a major factor in future food production. He seems, also, to not consider the many other possible ways in which food might be produced, such as greater use of the sea environment. In the future, much of the extensive farming in the humid areas will be replaced with intensive farming, increasing productivity per acre through this means alone.[11]

Mr. Thomas has done a service in pointing out the nature and scope of the national water problem, and the suggestions of methods by which the problem can be resolved are timely and constructive. Many things must be done and much capital invested to insure a future supply of water.

DONALD McCORD BAKER,[12] F. ASCE.—In Table 1, the author gives the average annual runoff for the eleven drainage basins of the United States as 1,317,500,000 acre-ft, or 436.3 acre-ft per square mile for the 3,020,000 square miles of this country.

---

9 "The Water Balance," by C. W. Thornthwaite and J. R. Mather, Publications in Climatology, Drexel Inst. of Tech., Climatology Lab., Vol. VIII, No. 1, Centerton, N. J., 1955.

10 "Our Wealth of Land Resources," by C. P. Barnes and F. J. Marschner, Land, U. S. Dept. of Agric. Yearbook, U. S. Govt. Printing Office, Washington, D. C., 1958, pp. 10-18.

11 "Balanced Development of Resources," by Carl P. Heisig, Hugh H. Wooten, and Raymond P. Christensen, ibid., pp. 584-592.

12 Cons. Engr., Los Angeles, Calif.

Table 11 expands Table 1 to show the average annual runoff per square mile for each of the eleven basins. This quantity ranged from a maximum of 1027.0 acre-ft per square mile for the North Atlantic Basin, or 235.3% of the average, to 58.1 acre-ft per square mile for the Great Basin, or 13.3% of the average. The average annual runoff from the North Atlantic Basin is 17.7 times that of the Great Basin. No data is given by the author as to maximum or minimum annual runoff from these basins, nor as to cyclic variations in runoff.

The heaviest average annual runoff per square mile naturally occurs in those basins having the heaviest precipitation. Average slope of these basins, soil cover, and evaporation and transpiration losses also affect the average annual runoff.

TABLE 11.—RUNOFF IN THE UNITED STATES—1921-1945

Basin (1)	Area, in square miles (2)	Average annual runoff, in acre-feet (3)	Acre-feet per square mile (4)
North Atlantic Slope	148,000	152,000,000	1,027.0
South Atlantic Slope and Eastern Gulf of Mexico	284,000	235,000,000	827.5
Mississippi River	1,250,000	449,000,000	359.2
Hudson Bay	48,000	3,600,000	75.0
St. Lawrence River	130,000	101,000,000	776.9
Western Gulf of Mexico	320,000	39,800,000	124.4
Colorado River	246,000	16,700,000	67.9
Great Basin	215,000	12,500,000	58.1
Pacific Slope in California	117,000	57,900,000	494.9
Columbia River and Coastal Streams in Oregon and Washington	262,000	250,000,000	954.2
Totals	3,020,000	1,317,500,000	436.3

Not all of this runoff, however, can be made available for use, even in those basins in which average annual fluctuations in runoff are small, and low cost storage is ample and adequate.

In many sections of the country, runoff is required to supply water for navigation. Were the water not available for this use, large and costly railroads and highways, in addition to those now constructed, would be required as a substitute means of transportation for moving goods and people.

In suburban and rural areas, the daily per capita use of water for domestic purposes is probably approximately 50 to 60 gal. Use for stock in certain rural areas may double this amount.

The author arrives at the conclusion that the value of crops from irrigated acreage in this country is twice that of crops from unirrigated harvested acreage. This conclusion is based on records of value of crops per acre in the

years 1939 to 1944 and 1949, from approximately 3 to 5,000,000 acres irrigated on projects of the United States Bureau of Reclamation (USBR), and some 324 to 352 hundred million acres in cropped acreage in the entire United States during the same period. Mr. Thomas also states that by the time national population has reached 450,000,000 persons (Table 10 estimates that this will occur in the year 2070), there will be 602,000,000 acre-ft of water used annually for irrigation.

In reaching this conclusion, general amounts are used. It must be borne in mind that most of the irrigable but unirrigated acreage exists in the arid sections of the country, west of the 100th meridian, and that the land included in USBR projects is of a better type than cropped land in general. In addition, there is probably not sufficient water in the drainage basins located west of the 100th meridian to irrigate all unirrigated land in the area, and water would have to be imported to the area from a humid region, provided that such importation was feasible. This large topic is not examined by the author.

Two of the most important questions that arise in connection with the topic are: (1) How much land exists, in acres, in the arid section of the country where it is located, and how much water would such land require for irrigation; and (2) would the cost of bringing such land under irrigation be within the limits of feasibility.

In reviewing the various data presented by the author, it appears that the quantities referred to are those of water used, not of water consumed. If this is the case, a certain part of the water used will ultimately return to stream flow through ground water basins, sewage treatment plants, or other sources; and much of it will probably be available for re-use. No data are presented from which net consumptive use of water used may be estimated.

The author presents figures of water consumed in producing steam electric power, and assumes (Table 10) that when the national population has reached 450,000,000, 90% of the power produced will be from steam, and 10% from hydroelectric sources. No data are given to support these figures, but it seems to the writer that with all of the domestic, irrigation, and navigation development that will be necessary, new hydroelectric power sources will be brought into being to increase this hydroelectric source percentage.

In Table 10 the author estimates that by the year 2070, approximately 110 years from now, the national population will have reached 450,000,000, and the population and use of water by that date will be the following, multiplied by the 1955 use:

Population	2.72
Domestic and industrial	5.2
Irrigation	6.6
Electric power generation	4.9
General industry	5.0

The author also states (Table 10) that this population of 450,000,000 will be using 1,215,000,000 acre-ft per yr, or 92.2% of the total annual supply.

The last statement assumes that actual streamflow, as it occurs in a state of nature, can be modified through storage and brought to places of use in a feasible manner. It also assumes that much of the water existing in surplus areas of the humid sections of the country can be developed and transported vast distances to the arid sections, at feasible costs.

It should be noted that by the year 2070, practically one-half of the water used by this estimated population of 450,000,000 will be for irrigation, and almost one-quarter of it for electric power development. In general, power can be transmitted from place of generation to place of use at feasible cost, whereas in many instances irrigation water cannot be.

The author presents ten courses of action that he believes will tend to counteract or offset the adverse water supply situation described in his paper. The most striking of these is the relocation of industry to the sea coast, reserving the interior sections of the country for agriculture to the maximum extent possible.

Such a policy, if evolved, would completely change the character of our national economy. It would mean the location of the bulk of our population on the seacoast, a complete change in our transportation system to carry agricultural and mineral products to industrial areas for processing, and return many of them inland to points of consumption. However, some of his conclusions pertaining to conservation are well founded.

The author does not examine the manner in which the estimate of 450,000,000 national population by the year 2070 is reached. Generally, improvement in living standards of a people reduces both birth and death rates, and the writer questions the author's estimate of the national population in the year 2070.

Mr. Thomas' conclusions seem to be based almost solely on generalities and averages. Economic feasibility will enter into many of his recommendations, such as bringing surplus water from basins of high yield to areas of low yield for irrigation use therein, the use of treatment of saline water located at sea level, and transportation of such water inland, in many cases over mountain ranges.

The idea of a more widespread policy of water conservation in this country is sound, but with it must be performed a detailed study of the feasibility of many of the ideas suggested. There is little question that as time goes on, the United States will have to give some thought to developing such a policy. It is hoped that the paper will start people thinking along this line.

ALFRED R. GOLZE,[13] F. ASCE.—The paper is a conservative argument for civil engineers and public works administrators to appreciate the seriousness of water conservation requirements throughout the United States and the need for appraisal of those requirements on a long-range basis.

The introduction states:

> "This paper does not evaluate the effect of varying monthly flow in the streams of the country, but presumes that sufficient storage, either above or below the surface of the ground, will be provided to regulate that part of the available supply which is determined to be usable, with consideration to all competing demands."

This is a strong assumption in that conservation storage of the major rivers in the East, such as the Connecticut, the Hudson, and the Susquehanna, to mention only a few, is unlikely to occur in the degree necessary to meet requirements. Unless the engineers of the future devise some other way to secure the conservation benefit of river flows without storage, fresh water will flow unused to the ocean indefinitely.

---

[13] Asst. Commr., Bur. of Reclam., U. S. Dept. of the Interior, Washington, D. C.

Mr. Thomas assumes also that necessary diversion and transmission of water supplies will be accomplished to the "maximum extent practicable." Apparently, the author means to the maximum "economic" extent practicable. Then, this too is a strong assumption, unless the country could afford to pay the price for a gallon of water delivered at point of consumption that it now pays per gallon for crude petroleum delivered at the refinery, which seems unlikely.

Table 7 indicates the estimated agricultural water requirements in the United States. This table shows irrigated acreages in millions of acres for certain populations. For a 200,000,000 population, it indicates that the semi-arid region is estimated to have 32,000,000 irrigated acres, which is not an unreasonable prediction. However, for a 250,000,000 population, which in point of time would occur not long after the 200,000,000 population, and which is an increase of 25%, Table 7 shows 79,000,000 irrigated acres, an increase of 147%. It would be practically impossible to increase our irrigated acreage in the semi-arid region by the amount indicated in this table, from the view-point of both available water and land, to say nothing of cost. The final numbers in Column 3, showing 147,000,000 irrigated acres in the semi-arid region for a population of 450,000,000, is in excess of published amounts on the ultimate development of the western states. It would be helpful to see the 120,000,000 new acres plotted on a map with a name source of water for each one. As far as the work of the USBR is concerned, its long-range water studies do not, as yet, show any proposals leading to acreage of that magnitude under the most ideal economic conditions.

As stated previously, the writer has agreed with the premise at hand. There is much concern over the growing seriousness of fresh water shortages now spreading throughout the United States. The paper, as is indicated in the introduction, omits an examination of a number of factors that have some bearing on the conservation of water. For example, Mr. Thomas could have mentioned that inventions presently unknown but that are likely to be developed in the next century will have a large impact on the consumption of fresh water, just as air conditioning has had in the past two decades. Also, with more research in such fields as evaporation control, some counterbalance to consumptive use may be expected.

Of the ten items listed in the Conclusions of the paper, there is no question about the first five items, but the second five justify additional comment in the interest of clarifying what the author has in mind.

No. 6 is identified as "accelerated research in the processes of demineralization of saline or brackish water." The Department of Interior, since 1950, has conducted an extensive program of research into the various processes for economic conversion of saline or brackish waters into fresh water. The construction of five pilot plants has been authorized. It is to be expected that within the next 10-yr period this phase of fresh water development may be an important step forward to the point that use of saline or brackish water resource for industrial or municipal use may be a reality in areas in which underground or precipitation flows are currently dwindling or high development costs prevail.

No. 7 calls for construction and operation of sea-water conversion plants along the coasts. It could be supplemented by pointing out that the Department of the Interior's saline water program also provides for conversion of brackish waters at inland sources and that important bodies of inland waters that are too saline for industrial, municipal, or irrigation uses are being studied for possible treatment and conversion to fresh waters.

No. 8 suggests that nuclear electrical generating power should be located near the seacoast with the output transmitted considerable distances inland. The apparent great economic value of nuclear generating plants is their freedom from fuel source, making it possible to place them close to load centers without reference to source of fuel. Locating nuclear plants along the seacoast to secure the benefit of sea water for operation would place a greater economic value on water than on the cost of output transmission. With the large deposits of coal still to be used and petroleum available at reasonable cost, seaside nuclear power plants do not appear to be part of the water conservation picture.

No. 9 refers to integrating the economies of the United States and Canada to utilize the combined land and water resources to the best interest of all. This work has been going on for some time through the International Boundary Commission, not only for Canada but also for Mexico. The adjustment of the water flows of international streams entering or leaving Canada and Mexico involves complicated international legal and administrative as well as engineering, matters. As they are brought to a conclusion, the full use and development of the international stream flows may be expected.

In No. 10, Mr. Thomas suggests that all industry in the United States be relocated to the seacoast, with agriculture situated in the interior of the country. He recognizes that an ideal world-wide peace would have to exist to make this possible. Until that situation occurs, No. 10 will have to be deferred. It might be noted that in California, industry seems to be moving toward the seacoast, and California water problems undoubtedly stem in large measure from that fact. An interesting matter for economists to debate is whether under ideal peace conditions it would be practical to have all industry located along the coastlines, with costly housing and traffic problems, and the interior of the country devoted to agriculture. It is probable that an unbalanced geographical economy would not be favored at this time, and a long period of educational preparation would be necessary.

Water is still about the cheapest commodity for services rendered, and today most of the country has enough fresh water for its miscellaneous needs, reflecting the foresight of previous planning. In California the state is proceeding with the State Water Plan, but is undecided as to the best way it should be developed. A unified effort will eventually be developed as the pressure of public opinion grows. Texas, which alternately suffers from drought and floods, is an ideal region for water conservation. It also has a State Water Plan, based on assistance from several federal agencies, which is being readied for Congressional authorization. Other states in the west are working to meet these problems as they arise.

In the east, where the states are smaller and urban development is well established, it is more difficult to develop a coordinated plan, but cities such as New York have worked out a solution and are keeping abreast of their requirements. Washington, D. C., which is furnished its water supply by the Army's Corps of Engineers, is agitating for storage on the Potomac River or its tributaries to provide a long-range supply for the years ahead.

Mr. Thomas has called attention to a growing problem that engineers in the irrigation and water conservation field of activity cannot afford to ignore.

ROBERT O. THOMAS,[14] F. ASCE.—It was stated that the paper was written to "evoke discussion of the implications inherent in the apparent adverse balance between supply and probable demand, and to engender recommendations

[14] Superv. Hydr. Engr., State Dept. of Water Resources, Sacramento, Calif.

for present and future action." The paper concluded with a prediction of a demand approximately 93% of the average annual supply when a population of 450,000,000 was attained in the United States. The basic purpose of a "view-with-alarm" essay is, of course, to emphasize the implications of the problem posed, on a consciously generalized basis, in order to reinforce the claim of immediacy in ascertaining the solution. It was felt that thereby the door was left open for discussers to point out:

1. The population of the country is increasing at a rapid rate.
2. The increase may exhaust our water supplies if past trends of excessive and improvident use continue into the future.
3. The actual year of exhaustion, whether it be 2070 or 2170, or 2270, matters little. The important point that must be faced is the prospect of exhaustion.
4. Nevertheless, the population must be provided with a place to live, with shelter, food, and clothing, and with employment, which implies basic, as well as processing, industry and services.
5. The maximum amount of natural fresh water which can be made available may be only approximately one-half the predicted demand.
6. Therefore, engineers must start now to study and plan so that the solution may be available when needed.

Additionally, it was felt that the implications were sufficiently serious and immediate to require conscious and intensive effort in arriving at the solution. It is suggested that a program such as the following may be appropriate:

1. Comprehensive planning, by the states or by the federal government in cooperation with the states, should begin immediately for each river basin. This would determine, with full consideration to topography, availability of surface and underground storage capacity, quantity and variation of water supply, and requirements of all competing uses, the maximum quantity of water which can be conserved in the individual basins. This quantity will probably vary in the range of 40% to 75% of the average annual supply. The sum of this quantity would be the maximum quantity that the nation can plan on using. The actual quantity which can be put to use may be somewhat less, due to difficulties that might be encountered in effecting distribution.
2. The availability and capability of the land and other resources of each river basin, together with their ability to support a population and effect beneficial use of the basin water supplies, must also be determined. This will enable determination either of the availability of excess supplies, permitting export of the surplus, or of deficiencies, requiring import to meet demand.
3. The physical and economic considerations affecting possible exports and imports will then be studied. This will result in the master plan for utilization of our natural, or meteoric, water resources.
4. Finally, it will be possible to predict, with a fair degree of certainty, the quantity of water that must be secured from other sources, such as the oceans, and the location and nature of the uses which will be made of such supplies.

It is felt that an appreciable length of time is necessary to make these detailed studies and that the extension of present use trends into the foreseeable future (40 to 50 yr) is such that the time may have already passed when this work should have been initiated.

Mr. Woodward takes exception to the estimate of 1.25 acre-ft per acre required in the humid areas, and to the prediction of a demand for 124,000,000

acre-ft per year. It is pointed out that the 1.25 acre-ft per acre includes the return water allowance (irrigation efficiency) and that the estimated total is really of little moment at this time. What is important is the realization that the requirement will be huge, even if only one-half or two-thirds of the estimated quantity, and plans should now be started to meet the requirement when it occurs.

Mr. Woodward has misinterpreted the statement relative to the value of irrigated and dry-farmed crops. The conclusion, as given in the paper under the heading "Water Use," is "irrigated acreage will produce twice the value and volume of dry-farmed acreage." The fact that available data on irrigation pertains principally to the semi-arid zone does not impute "semi-arid" to the conclusions drawn.

Mr. Woodward has justly pointed out that some types of land use may be subject to critical review and analysis. This view is certainly concurred in, and may be an appropriate aspect of study in connection with point 9 which suggests "integration of the economies of the United States and Canada." Whereas full agreement cannot be given to the implication that forestation might be a low-value use, it may well be that many lands now devoted to production of forest products might better be used for food production while forestry is practiced in more barren or less easily accessible areas.

Mr. Golze's initial points are covered in the introductory material to this closure, in which the scope of studies required to provide the basis for intelligent and competent planning is briefly presented. On the subject of demineralization of saline waters, it is respectfully submitted that opinion as to the sufficiency of present activities of the Office of Saline Water is entirely subjective. The writer definitely feels that they should be augmented considerably. So far as authorization of pilot plants by Congress is concerned, an unduly long time often elapses between authorization and appropriation.

The suggestion for integration of the economies of the United States and Canada encompasses objectives far beyond the scope of boundary commissions or treaties dividing the waters of international streams. The vast expanse of Canada contains tremendous mineral, land, and water resources which, when combined with the population and other resources of the United States, could result in appreciable benefits to both nations. Therefore, the words "integration" and "economies" in reference to the United States and Canada were meant to imply the maximum of cooperative effort in each and every aspect of human endeavor.

With regard to Mr. Golze's final point, it has been officially stated[15] that the annual overdraft on developed water resources of California amounted, in 1955, to approximately 4,000,000 acre-ft. Assuming that if the Feather River and Delta Diversion projects were given major impetus and financing this year (1960), that the water provided could be delivered by 1970, a ten-year construction period; that the annual overdraft by that date would only approximate 6,000,000 acre-ft; and that the cumulative overdraft in 1955 (although figures are not readily available) amounted to only 15,000,000 acre-ft, then the cumulative overdraft by the time delivery of project water occurred would be 90,000,000 acre-ft. This is no small quantity of water. Yet, the water made available by the presently authorized project is only of the order of 4,000,000 acre-ft per year, approximately equal to the 1955 overdraft. It is felt that

15 "The California Water Plan," Calif. Dept. of Water Resources, Bulletin No. 3, May, 1957, p. 16.

similar situations, in principle although not in magnitude, are occurring in other sections of the country. It is believed that the 10-yr comprehensive, detailed study which resulted in the California Water Plan, and from which the foregoing conclusions are derived, is both singular and unique in this country. It is suggested that many other regions might be surprised at the answers which might be derived from similar studies.

It is felt that most of Mr. Baker's comments have already been answered, at least in part. However, with regard to the magnitude of hydroelectric generation, two aspects seem worthy of mention. First, the estimate of hydroelectric power increased from 115 billion kilowatt hours to 270 billion kilowatt hours, an appreciable gain in itself. Second, the fluctuation of demand for hydro power, unless ample reregulation facilities are provided, is alternatively competitive to timing of demand accruing from many other uses of water. Because power may be produced by substitute facilities, it was assumed the power considerations would be secondary to other demands for use of water supplies.

AMERICAN SOCIETY OF CIVIL ENGINEERS

Founded November 5, 1852

TRANSACTIONS

Paper No. 3016

TRENDS IN PIPELINE CONSTRUCTION

By James W. Hall,[1] M. ASCE

SYNOPSIS

Improvements in the art of constructing large-diameter pipelines and long-distance oil and gas lines are presented herein. Unit costs have remained approximately the same due to rapid developments in methods and equipment for pipeline construction. Future developments are outlined briefly.

INTRODUCTION

In early civilizations the efficacy of the pipeline was recognized and utilized. The Chinese are believed to have piped water through bamboo lines in 5000 B.C., and by 900 B.C. they were piping natural gas to brine evaporators. By 200 B.C., Rome had a water system that handled 332,000,000 gal of water per day, in which most of the small-diameter pipe was of lead. Bronze piping with silver faucets was found in the ruins of the famed baths at Caracalla. From the standpoint of size and of engineering design, this piping system was not excelled for 2,000 yr. The first underground system of iron pipe constructed in Paris in 1685 contained pipes that were 1 m long and coupled by bolted flanges. Part of this system is still in use today.

The importance of the numerous pipelines carrying water and other products is obvious, but, as considered here, pipelines are limited to the oil and gas pipelines forming the vast underground network that interlaces the nation from coast to coast.

The year 1959 marked the 100th anniversary of the oil and gas industry in America, and this coincides closely with the birth of oil and gas pipelining. In 1862 the world's first crude line using centrifugal pumps was constructed in the booming oil fields of Pennsylvania by J. L. Hutchings, inventor of the rotary pump. This line was constructed of 2-in. cast iron pipe with leaded sealed

Note.—Published, essentially as printed here, in January, 1959, in the Journal of the Pipeline Division, as Proceedings Paper 1906. Positions and titles given are those in effect when the paper was approved for publication in Transactions.

[1] Pres., Hallmac Construction Co., Houston, Tex.

joints. In 1879 "The Big Benson Pipeline" was constructed over the Alleghenies from Bradford, Pa., to Williamsport, Pa. This line was 6 in. in diameter, 125 miles long, and was constructed of cast iron screw pipe. In 1887 this line was extend across the Ox-Bow Range, Pa., to New York—and aside from crossing mountains, Benson laid 21,000 ft of line in New York Harbor.

The discovery of oil in the southwest early in this century put pipelining into high gear, and many of the high-speed, cross-country construction methods used today can be traced back to this time when the only mobile pieces of equipment on jobs were horse-drawn. In 1911 welding made its appearance and in 1924 the first long distance all-welded natural gas pipeline was constructed. It was 14 in., 16 in., and 18 in. in diameter and ran 214 miles from Webster Parish, La., to Beaumont, Tex.

In the late 1920's, pipelines received the great impetus that will seemingly continue for years to come. The large gas fields discovered in the southwest coupled with the heavy increase in demand for crude oil, created a situation which brought to fruition the dreams of the pipeliner. Large-diameter, long-distance lines became a necessity. Up until this time, pipelines had been designed by the hip-pocket method. This held true from design through construction to operation. When companies lacked precedent and criteria for design, they simply developed individual formulas and principles. Many of these were based on insufficient information and erroneous logic. However, constant trial and error evolved satisfactory practices, even though a statement of the principles on which these practices were based continued to be vague. Many construction practices, both good and bad, retained their acceptance because of the prejudices of those in authority, rather than because of any analytical evaluation from the engineering viewpoint.

During the past 30 yr a myriad of improvements have come to pipeline construction—from the field, from engineering departments, and from manufacturers of equipment. Virtually all of these improvements had their origin in the competition which is an outgrowth of our system of free enterprise. Pipeline engineers have worked constantly to improve design and techniques to obtain pipelines of highest quality and insure service to the customers of their company. Manufacturers have consistently improved construction equipment to increase sales and profits, and contractors have found more satisfactory ways of constructing lines at lower prices for their clients. These combined efforts have produced the results that made pipelines competitive with other forms of energy transportation. In the past 30 yr pipeline expansion has closely approached the rate of growth of our gross national product, as indicated by Fig. 1.

As long as pipelines were of comparatively short length and small diameter the construction man was able to fit makeshift construction methods to his needs. The advent of longer lines and larger diameters presented new problems and a new challenge. The enormous investments required by the longer, larger lines required more speed in construction, for the slow and tedious manual methods used in the past were no longer adequate. Equipment was needed, equipment capable of handling the great weights of pipe involved—equipment capable of covering vaster distances at high speed. Manufacturers responded to the call of the times and through the years have never ceased improving equipment. Each year mobile pieces of equipment have improved in efficiency at a rate of approximately 2% per year.

The methods and equipment for pipeline construction developed so rapidly that it is difficult to know whether development of equipment followed demand or whether demand followed availability of equipment and methods. In any

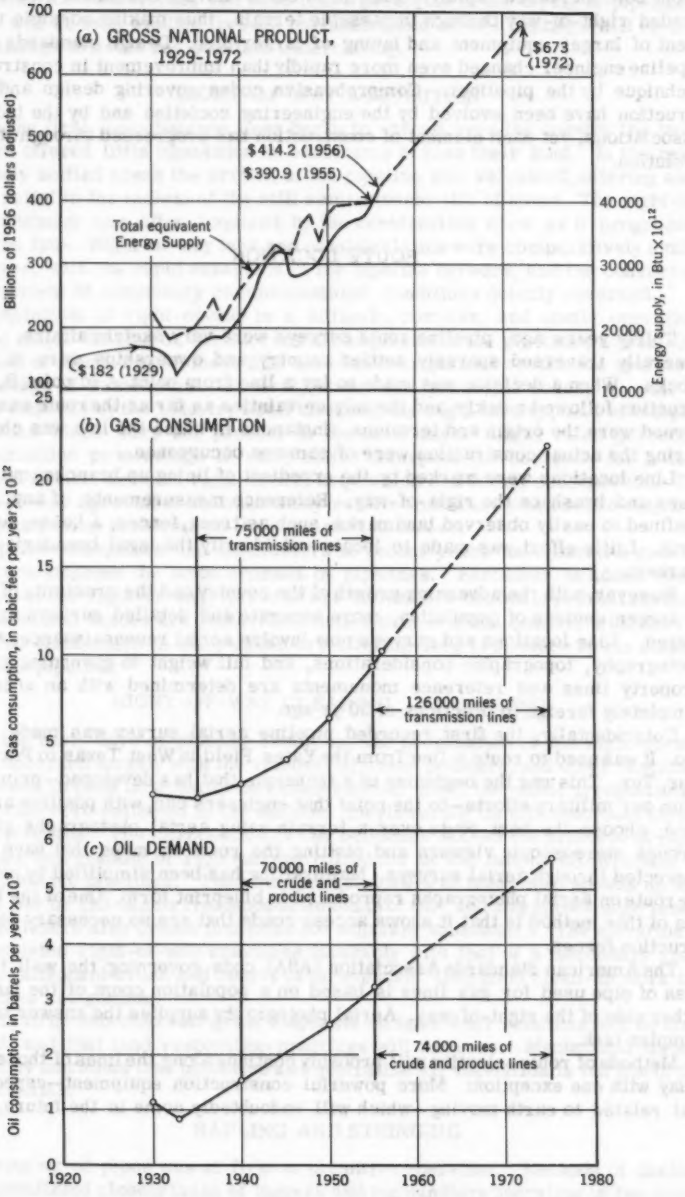

(a) GROSS NATIONAL PRODUCT, 1929-1972
$673 (1972)
$414.2 (1956)
$390.9 (1955)
Total equivalent Energy Supply
$182 (1929)
Billions of 1956 dollars (adjusted)
Energy supply, in Btu X 10^12
(b) GAS CONSUMPTION
75000 miles of transmission lines
126000 miles of transmission lines
Gas consumption, in cubic feet per year X 10^12
(c) OIL DEMAND
70000 miles of crude and product lines
74000 miles of crude and product lines
Oil consumption, in barrels per year X 10^9
1920
1930
1940
1950
1960
1970
1980

FIG. 1

event both increased rapidly. Enormous earth-moving equipment cleared and graded right-of-way through impassable terrain, thus making possible movement of larger equipment and laying of larger pipe. Design standards of the pipeline engineer changed even more rapidly than improvement in construction technique by the pipeliner. Comprehensive codes covering design and construction have been evolved by the engineering societies and by the industry associations, yet each element of construction has progressed through its own evolution.

ROUTE LOCATION

Thirty years ago, pipeline route surveys were very sketchy affairs. Lines generally traversed sparsely settled country and ownerships were in large blocks. When a decision was made to lay a line from point A to point B, construction followed quickly, and the only certainties as far as the route was concerned were the origin and terminus. Instances in which the line was changed during the actual construction were of common occurrence.

Line locations were marked by the expedient of lining up branches cut from trees and brush on the right-of-way. Reference measurements, if any, were confined to easily observed landmarks, such as trees, fences, a house, and so forth. Little effort was made to locate and identify the legal boundaries with markers.

However, with the advancing growth of the country and the proximity of lines to larger centers of population, more accurate and detailed surveys are required. Line locations and surveys now involve aerial reconnaissance, aerial photography, topographic considerations, and full weight to governing codes. Property lines and reference monuments are determined with an accuracy completely foreign to practices of 30 yr ago.

Coincidentally, the first recorded pipeline aerial survey was made 30 yr ago. It was used to route a line from the Yates Field in West Texas to Port Arthur, Tex. This was the beginning of a technique that has developed—primarily from our military efforts—to the point that engineers can, with positive assurance, choose the best route over a terrain using aerial photographs viewed through stereoscopic viewers and plotting the route on maps that have been corrected through aerial surveys. Map drafting has been simplified by plotting the route on aerial photographs reproduced in blueprint form. One of the benefits of this method is that it shows access roads that are so necessary to construction forces.

The American Standards Association (ASA) code governing the wall thickness of pipe used for gas lines is based on a population count of the land on either side of the right-of-way. Aerial photography supplies the answer to this complex task.

Methods of route selection will probably continue along the lines of those used today with one exception: More powerful construction equipment—especially that related to earth moving—which will undoubtedly come in the future, will

mean that difficult terrain will pose fewer problems in the laying of pipelines. There will be less winding through mountains, and river crossings will be laid deep enough to avoid any possible undercutting.

RIGHT-OF-WAY ACQUISITION

As the first long-distance lines began to spread over the country the landowners offered little opposition to easements across their land. In the more sparsely settled areas the arrival of the pipeline was welcomed, offering as it did a relief to the tedium of the still semi-pioneer life of some. The right-of-way easement was often acquired by the construction crew as it progressed with the line. Right-of-way fees and damage claims were comparatively small. However, with the rapid expansion of the pipeline network, and the concurrent development of community communications, conditions quickly reversed.

Acquisition of right-of-way is a difficult, complex, and costly operation, having major bearing on the successful completion of the pipeline project. Opposition of competing forms of fuel have led to organized resistance by a large percentage of landowners. Federal, state, and municipal codes, as well as codes imposed by the industry itself affecting the right-of-way, lead to complex questions which were not present in the early days. Legal rules governing condemnation proceedings in many states interpose the necessity for a long interval of time between right-of-way acquisition and actual construction. The right-of-way agreement contains many restrictions and construction requirements imposing problems on the construction forces.

Pipeline companies and contractors in recent years have exerted greater efforts to improve the lands crossed by pipelines. Fertilizer is added to the top soil of the right-of-way, terraces are built where needed to prevent erosion, and gates and fences are restored to better than original quality, with the result that landowners in many areas are offering less resistance to the coming of a new pipeline.

RIGHT-OF-WAY CLEARING AND GRADING

In the early days of pipeline evolution, the preparation of the right-of-way was concerned largely with the removal of trees, boulders, and other obstacles that would impede or actually halt construction. Even the minor irregularities of terrain were reflected in the finished line, lowering its efficiency and structural strength. The introduction of the bulldozer solved the problem of rapid clearing and grading of right-of-way called for by the rate of construction on long-distance pipelines. The powerful bulldozers of today with speeds up to 8 miles per hr can handle tremendous amounts of dirt and can uproot huge trees.

Bulldozers also create problems for adjacent landowners. The elevation of a completed right-of-way compares favorably with that of a secondary road, but the attendant brush and debris is an eyesore. Only good clean-up work can minimize antagonism.

It is to be expected that great emphasis on landowner relations will be continued, and that land restoration practices will improve. Mechanical mastication by machines that pulverize and neutralize all vegetation is but one of the possibilities.

HAULING AND STRINGING

Stringing of pipes was at first a primitive operation. Methods of hauling pipe paralleled closely those of loggers and rig handlers operating in the areas

where the lines were first constructed. Pipe was usually of small diameter and the properties of the metal did not call for extreme care in handling.

With the advent of the long lines in the late 1920's, more efficient means of stringing were called for. Small trucks were at first utilized, and although the pipe was laboriously loaded by hand, little regard was given to its care in handling during shipment and subsequent unloading.

The stringing operation is now a highly specialized one, and the industry is served by firms that operate fleets of large high-speed trucks and heavy handling equipment designed especially for pipeline work. Properties of pipe used in present construction coupled with the high operating pressures require great care in handling. Gouges, dents, and abrasions of the surface considered unimportant 30 yr ago are of great concern today as sources of possible line failures. Pipe is guarded carefully from the mill to the ditch. It is loaded on rail cars or trucks by handling machinery equipped with specially designed tongs to protect the pipe ends. The bolsters that clamp and support the pipe during its journey toward the line are designed to give proper support and prevent scratches on the pipe surfaces. The pipe is inspected as it is unloaded onto stringing trucks and again after it has been deposited on the right-of-way.

As new steels are developed, pipe will be handled with even greater care, and acceptable tolerances for out-of-roundness and depth of surface scratches will become smaller and smaller.

DITCHING

In the early days of pipelining, the pipe was laid on top of the ground and was buried only where it crossed roads and similar places. By 1928 extensive ditching requirements were becoming more common. However, the objective of the ditch for the most part was to protect the line from vandalism rather than for specific benefit of design and operation. Increased diameters, changes in products handled, and expansion of agricultural operations resulted in definite ditch specifications. Through the years, depth of cover was increased to provide protection from physical damage from construction and farming equipment.

At first, ditching was a manual operation, accomplished by spreading hundreds of "hands" along the line—each digging a "joint" of ditch. While unbelievable amounts of ditch were dug in this manner, mechanization was inevitable. The laborer's pick and shovel were replaced by the digging wheel, and the jack drill and sledge replaced by air drills.

Ditch specifications are now considered carefully. In addition to the problems of the past, bigger ditch for larger-diameter pipe creates problems of stress and strain imposed on the pipe by increased back-fill load, restraint, and bedding. Mammoth high horsepower ditching machines make ditching across difficult terrain a high-speed operation.

The handling of surface and subsurface rock presents a more difficult problem, but with the efficiency of present rock-drilling equipment and explosives, ditch is made through granite, malipi and other hard igneous formations at unbelievable speed. The actual techniques currently employed in ditching through rock will vary with the kind of rock, the terrain, the weather, the depth, and the length of line. Techniques used vary with the number of contractors operating in the same areas.

New drills have been developed which will reduce one of the greatest expenses in rock ditching. Flame drilling is a present possibility, and sonic

drills will probably take the place of many present ditching techniques. A portable rock crusher of high efficiency will undoubtedly make its appearance soon to simplify the task of disposing of the blasted rock.

PIPE BENDING

As recently as the late 1920's bending problems were solved on an individual basis. In some cases no bends were made at all. Flexure of the pipe was used to navigate changes in directions or to follow the contours of the surface. In choppy terrain, or in areas requiring sharp bends, field men would improvise to meet the situation. Smaller diameter pipe of soft steel could be "cold sprung" by suspending it between points and having as many men as could be accommodated on the section jump up and down until a "set" of desired magnitude was achieved. This method of bending left a large margin of error, and lack of fit was compensated by digging the ditch deeper or wider, or by filling in as might be required. Introduction of larger diameters of pipe eliminated the "stomp" method of bending and other means were utilized. Joint couplings allowed a certain amount of flexure in order that long sweeping curves equivalent to pipe flexure could be achieved. The first efforts to solve the problem of field bending of large diameter pipe resulted in "wrinkle bends," which were a deformity of the pipe wall on the inside of the curve. These wrinkle bends were of a radius small enough to serve requirements, but the wrinkle created points of stress in the pipe that were considered hazardous, both during construction and operation.

Field bending machines for large diameter pipe were developed as a solution. These machines, which were first introduced in the early 1940's, and are now manufactured in all sizes up to 36 in. can cold smooth bend pipe in the field to a radius of up to 1° - 3° deflection for each pipe diameter. The completed bends are free of detectable tied-in stress or deformity of section, and cold stretch bending is generally accepted as a standard by the industry.

WELDING

It was only natural that welding processes should supplant mechanical means of joining pipe. Early welding utilized oxygen and acetylene, and in 1928 electric arc-welding was introduced on the pipeline. It was considered so newsworthy that a 45-mile high-pressure pipeline welded entirely with electric arc-welds was reported[2] in 1928. The welds produced by the bare electrodes of this early procedure left so much to be desired that welding with bare rods was restricted to "roll" welding, with tie-in welds made by oxygen-acetylene welds. The coated rod with reversed polarity appeared in 1930, and was rapidly improved along with the skill of the operator so that now "welding" on pipelines has come to mean electric arc-welding.

Many ingenious attempts have been made to weld pipe joints automatically in the field. These include pressure-welding techniques, submerged arc procedures, and numerous others. Some success has been achieved by adopting the submerged arc process to double-jointing operations, but welding continues to be primarily a manual operation. Because welding depends to a great extent on the approach of the individual operator, extensive inspection procedures

[2] The Welding Engineer, Vol. 13, No. 4, 1928, p. 39.

have developed in the industry. Earlier, however, inspection consisted only of being certain that a certain amount of rod was deposited on the welds.

Inspection techniques have progressed with the welding arts so that at present the field weld on a pipeline is subject to quality controls equal to many high precision plant operations. Spacing, alinement, arc heat and length, rate of rod deposit, as well as weather conditions, are all of concern to the contractor and engineer. In field control, X-ray, ultra-sonic, and magnaflux techniques, as well as dye penetration are all now used, so that field welds are consistently stronger than the parent metal.

New rods of great promise are being developed, and greater knowledge of metallurgy is providing answers to past difficulties. Weldable steels with tensile strengths ranging well over 100,000 lb per sq in. have been developed, and it is expected that this new pipe will be utilized in pipeline construction shortly.

COATING AND WRAPPING

The first pipelines were laid bare but it was observed that different soil conditions created serious corrosion effects on pipe, and that some method of protection was indicated. Various materials were tried but the choice was soon narrowed to asphalt and coal-tar base products. At first this type of material was heated in pots over wood or oil fires and ladled into buckets for manual application to the pipe. As the speed of pipeline construction increased, it was necessary to make the coating operation more mobile and efficient. Heating pots were placed on wheels with oil burners to furnish heat, the pipe was rolled in sections on dollies, and hot material was poured on by hand. Such methods left "holidays" or discontinuity in the surface and extensive repairs to the original coating was required. In 1938 the traveling-type combination coating and wrapping machine was developed.

Present-day machines, traveling along the pipelines, can clean the metal of the pipe, apply primer, draw the hot material for application directly to the pipe from automatically-heated and agitated pots traveling along the right-of-way, and, finally, can wrap the coated pipe with reinforcements of glass fibers, felt, paper, or other material.

With such methods the coatings are of high quality with a discontinuity being the exception rather than the rule. Tests applied with electronic devices called "jeeps" reveal any defects in the coating in order that they can be repaired before the pipe is put in the ditch.

Although the larger part of pipe is coated with asphalt or coal-tar base materials, plastic materials have been tried, tested, and accepted for use on some pipelines. Coatings of asphalt and inert aggregates applied in thick coatings are used for special applications.

Many research laboratories are at work on developing a coating that will reduce the cost of pipeline protection. Aside from the dry plastic coatings, there are several spray-on coatings that require no complex equipment for application to the pipe or for subsequent protection of the pipe. This material and material similar to it is still in the developmental stage, but it will greatly simplify pipeline construction, because even minor disturbances can shut down the coating operation, thus adding to the cost of the project. Pipe clad with

corrosion-resistant metals is also being considered. Rubber, nylon, and other plastic materials have been successfully combined with steels, and steel is being glass-coated with bonds of fantastic strengths.

LOWERING-IN

As the speed of pipeline construction increased during the years, changes in lowering procedures have been rapid. Early procedures for lowering pipe was based on the use of "mope poles" providing leverage to move the pipe over the ditch and to lower it. Steel tripods equipped with hand winches displaced the mope pole on many jobs, and this development was followed by the sideboom tractor.

The sideboom tractor has become the symbol of the pipeline spread and is the standard method of lowering-in pipe. It remains essentially the same piece of equipment as originally conceived. Refinements in control, speed, size, and weight have given it a high degree of utility. Sidebooms travel along the right-of-way and pick up completed sections of pipe, moving them over into the ditch in one smooth operation.

Earlier, slack loops were left in pipelines to allow for contraction in cold weather. The amount of slack required and the method of handling slack provided one of the unending controversies of pipeline construction. Through the years, less and less slack has been required, and today some companies make no provision for slack at all.

Lowering-in practices in the future will, without doubt, vary in accordance with other operating units on the pipeline spreads. As pipeline technology continues to advance, all operations may one day take place over the ditch. There has been at least one attempt to develop a portable extruding machine that could manufacture pipe over the ditch.

CLEAN-UP

In the late 1920's and early 1930's, clean-up of the right-of-way consisted largely of backfilling the ditch. Little thought was given to dressing or cleaning the right-of-way. Spoil was heaped over the pipe and often interfered with natural or previous drainage. Little was done to prevent erosion, which often happened when water followed the construction path.

Under present-day requirements, clean-up of right-of-way becomes a highly important factor in the pipeline constructor's operations. All debris, brush, and timber is disposed of to prevent scouring of the soil or conditions contributing to rapid erosion. Loose dirt graded from the right-of-way is generally restored in a manner that prevents or delays erosion of the loose soil. Terraces are carefully graded to divert heavy runoff across the right-of-way to more stable areas. Grass and other vegetation is sown on the right-of-way to aid in the stabilization of the soil. All of the work done to stabilize the surface of the right-of-way contributes to minimizing damage to the land, and thus reduces in some degree the damage incurred by the landowner. Perhaps the most important aspect of clean-up in recent years has been the improvement in community relations between pipeliners and landowners.

CONCLUSIONS

A review of the development of the trends in pipeline construction over the years serves to illuminate an important point. That is, regardless of the rate

of development there is always room for improvement. As long as pipelines continue to provide the most efficient means of moving their contents to market and as long as the market continues to expand, pipeline construction will continue at a proportionate rate. However, when other means of energy transportation become more efficient, pipeline construction will wane. The pipeline engineer's problem and duty, therefore, is to strive for improvement of materials and methods, and to oppose inefficient practices within the industry or unwarranted restrictive regulation from outside.

Through combined efforts of the design and construction engineers, the unit costs of pipeline construction work remain at, or very close to, prices of 20 yr ago. Despite inflation, increased cost of labor, equipment and materials, pipeline construction costs represent one of the comparative bargains of the economy. Part of the explanation is the increased efficiency of the pipeline spread, which has progressed from a makeshift mule-team operation to a compact, mobile unit.

As the most efficient form of energy transportation, the continued growth of the pipeline industry seems assured. Between 1960 and 1970 it is estimated that pipeline companies will spend more than $45,000,000,000 for new facilities.

If, with the acceptance of other forms of energy, the use of pipelines should decline as a medium of transmission, other uses offer unlimited opportunity. Present possibilities are transportation of pulp for paper mills and of slurry for cement plants, as well as conduction of multiple channels of microwaves. High-speed pneumatic freight and personnel carriers are also possibilities that engineering will achieve.

AMERICAN SOCIETY OF CIVIL ENGINEERS

Founded November 5, 1852

TRANSACTIONS

Paper No. 3017

USE OF MODELS TO STUDY GROUND-WATER PROBLEMS

By Kenneth R. Wright,[1] M. ASCE

SYNOPSIS

When adverse field conditions preclude a direct field investigation of a ground-water problem, models can often be utilized to advantage in the determination of directions of flow, velocities, location of hydraulic divides, and in forecasting conditions that may occur in the future. Two types of models, electric analog plotter and hydraulic, were found satisfactory for the investigation of a ground-water problem located in an unconfined aquifer.

The electric analog plotter was somewhat limited by the necessity of assuming a system of a single density, but otherwise it offered valuable detailed information on the flow patterns. The hydraulic model, while operating satisfactorily with different density liquids, also allowed the study of non-equilibrium conditions. This enabled the introduction of a time scale that made it possible to forecast future events that would be difficult to obtain by mathematical analysis. The two models checked each other in their field of mutual results. This demonstrates their usefulness in the investigation of ground-water problems.

INTRODUCTION

A method of approach is presented toward solving ground-water problems when field conditions preclude a more direct field investigation because of physical or economic reasons. This study was initiated to determine whether model studies, both hydraulic and electric analog plotter types, could be set up based on several known field conditions to determine the unknown field conditions. The unknowns include location of hydraulic divides, directions of flow, and projection of events into the future.

Note.—Published, essentially as printed here, in December, 1958, in the Journal of the Irrigation and Drainage Division, as Proceedings Paper 1862. Positions and titles given are those in effect when the paper was approved for publication in Transactions.

[1] Partner, Wheeler and Wright, Cons. Engrs., Denver, Colo.

The actual problem to which the model tests were applied was the disposition of papermill wastes, sometimes called "lignin" (lignosulfonate), by ponding on the surface of the ground and allowing subsequent infiltration into the ground water. The field location of the waste disposal problem is 5 mi south of Wausau, Wis., in the Wisconsin River Valley. The infiltration ponds were situated 350 ft from the west bank of the Wisconsin River. Directly across the river, 600 ft from the east bank, was an industrial water well pumping approximately 500 gpm.

The waste liquid, on reaching the ground-water, traveled along with the ground-water and discharged into the river.[2] Some waste, however, found its way into the zone of influence of the well and subsequently contaminated the well water.[3]

GEO-HYDRAULIC CONDITIONS

The Wisconsin River has produced a terrace and flood plain system approximately a half-mile wide at the ponding area. Hills of Precambrian rock to the east and west outline the old river valley. The present river channel, 400 ft wide, is approximately 60 ft below the highest terrace of the valley and 30 ft below the ground surface elevation bordering the river. A crystalline rock basement of Precambrian age is 125 ft below the ground surface in the ponding area.

The aquifer is unconfined and composed of sand and gravel. It ranges in thickness from 100 ft to 130 ft in the lower terrace that contains the pond sites. The water table in this terrace ranges from 5 ft below the surface near the ponds to approximately 25 ft below at the well. From a pumping test it was determined that the transmissibility coefficient was approximately 100,000 gpd per ft and the coefficient of storage was 0.10.

On the west side of the river the movement of ground water is normal to and toward the river. On the east side of the river the ground-water movement is much more complicated because of the cone of depression of the well interacting with a constantly changing river elevation. It is also affected by a negative boundary condition to the east. The movement of the ground water on the east side of the river is toward the well in the area of influence of the cone of depression. Outside this cone, the general movement is toward the river. The cone of depression of the well intersects the river at all times except briefly during periods of river stage recession.[5]

The average gradient of the piezometric surface to the west of the river is 0.006 ft per ft. The normal nonpumping gradient on the east side of the river

---

2 "The Theory of Ground Water Motion," by M. K. Hubbert, The Journal of Geology, Volume XLVIII, No. 8, November-December, 1940.

3 "Water," by G. G. Parker, The Yearbook of Agriculture, U. S. Dept. of Agriculture, Washington, D. C., 1955, pp. 615–620.

4 "Ground Water in Wisconsin," by W. J. Drescher, Information Circular No. 3, Wisconsin Geological Survey, Univ. of Wisconsin, 1956.

5 "Some Effects of Precipitation on Ground Water in Wisconsin," by W. J. Drescher, Information Circular No. 1, Wisconsin Geological Survey, Univ. of Wisconsin, 1955.

could not be determined because of the nearly continuous pumping of the well. From a detailed study of the negative boundaries and recharge zone, however, it was estimated at 0.003 ft per ft.

MODEL STUDIES

The two models used in this study were the electric plotter (Fig. 1), similar to the analog field plotter, and the hydraulic model (Fig. 2).

Electric plotter.—The advantages of the electric plotter are the ease with which it can be set up to fit almost any situation and the speed and accuracy with which the equipotential lines can be plotted. The electrical solution, whether it be quantitative or qualitative, accomplishes in minutes what otherwise might require hours of tedious numerical analysis.[6] It is limited, however, to two-dimensional operation and cannot be used to investigate the flow patterns of liquids of different densities.

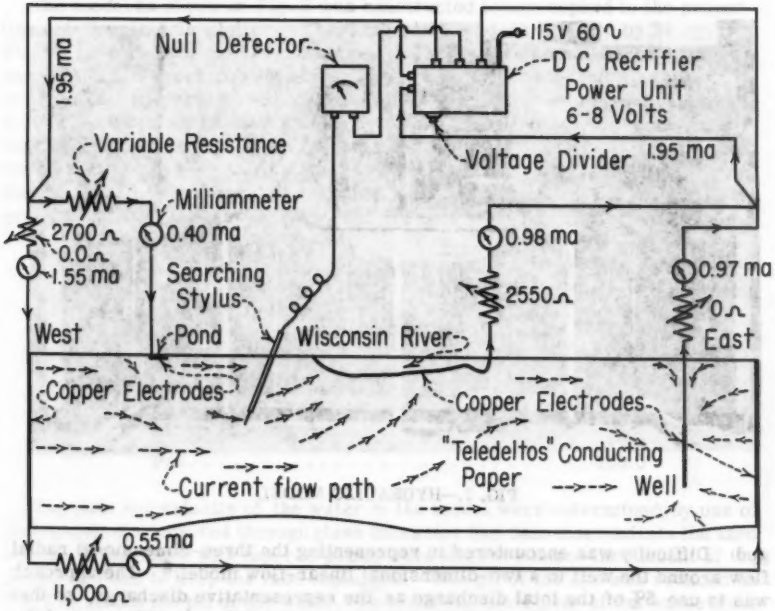


FIG. 1.—ELECTRIC ANALOG PLOTTER MODEL ELECTRIC CIRCUIT

In applying the model to the problem at hand, carbon-impregnated conducting paper was cut to represent a cross section of the aquifer normal to the river and passing through the pond and the supply well on either side of the river (Fig. 1). The representative width, 60 ft was chosen to coincide with the scale and dimensions of the hydraulic model.

To obtain a quantitative determination of the current flow within the conducting paper, it was necessary to control the current input at each of the

[6] "Theoretical Groundwater Movement Based on Electrical Analogs," by R. H. Brown and H. E. Skibitzke, Analysis of Basic Data Concerning Groundwater in the Yuma Area, Arizona, USGS Report, 1956.

several sources and output at each of the sinks. This was done by using variable resistances and adjusting them, until, with the aid of milliammeters, the parallel circuit was balanced as desired—the current in the sources and sinks being proportional to those in the field. The sources were the west ground-water increment, the east ground-water increment, and the pond. The sinks consisted of the river and the water well.

The operation of the electric plotter is based on the fact that Ohm's law ($E = RI$) is similar to Darcy's law for two-dimensional laminar flow ($H = KQ$), in which E corresponds to head H, R to hydraulic resistance K, and I corresponds to rate of flow Q. The ground-water sources, represented by the electrodes at either end of the conducting paper, supply approximately 37,200 gpd from the west and 20,500 gpd from the east in a 60-ft-thick section. Thus, the current supplied to the electrodes was 1.00 ma and 0.55 ma, respectively. The pond electrode was supplied with 0.40 ma representing approximately 14,900

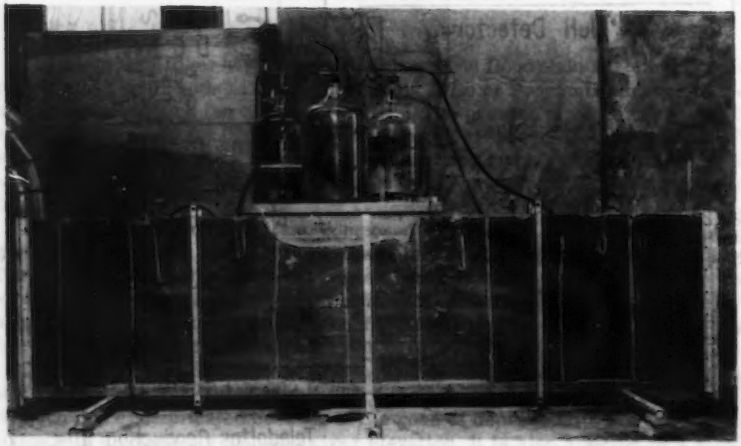


FIG. 2.—HYDRAULIC MODEL

gpd. Difficulty was encountered in representing the three-dimensional radial flow around the well in a two-dimensional linear-flow model.[6] The approach was to use 5% of the total discharge as the representative discharge, so that 0.97 ma was taken out at this sink, representing 36,000 gpd. The rest of the current in the circuit had to leave by the river electrode and amounted to 0.98 ma, equivalent to 36,600 gpd. The total current put into the circuit amounted to 1.95 ma representing 72,600 gpd. Thus 1.00 ma was equivalent to 37,200 gpd.

The results of the electric plotter are given in Fig. 3. Note that the path of the waste from the pond to the river shows very little downward movement, traveling only through the extreme upper part of the aquifer. This is due to the fact that the waste had to be considered as having the same specific gravity as the water and because it was impossible to show the mixing of the two miscible fluids. The ground water from the west divided at el 1,070, and above

that elevation discharged into the river. The ground water below traveled to the well. The river also contributed water to the well. The boundary of this discharge began at station 10 + 11 and leveled out at el 1,121 in its travel to the east.

Hydraulic model.—The conditions set up on the electric plotter were also set upon a hydraulic model. In this way fluids of any density can be used, nonequilibrium conditions can be studied, and future events can be forecast.[7] The model, as constructed for this study, has an infinite variety of applications and is limited in use only by the ingenuity of the investigator. Its purpose was three fold: First, to check the flow results of the electric plotter with one liquid of constant density; second, to determine the effect of adding another liquid of greater density to the system; and third, to study nonequilibrium conditions such as those produced by creating a flood stage in the river, stoppage of ponding, or changing the discharge of the well.

The model as shown in Fig. 2 was constructed to correspond to the proportions of the electric plotter. The dimensions chosen were 96 by 24 by 3 in. The sides were made of 3/8-in. lucite held together by small structural steel angles. An 80-mesh copper screen used to construct the well was also used at either end of the model to obtain a constant vertical potential at those points. A 20-mesh screen was used for the river and pond lining. The Precambrian basement domes were made of glazing putty, as were the vertical 1/4-in.-deep strips placed every 10 in. to insure against short-circuiting the liquids along the sand-lucite interface. The aquifer, consisting of silica sand from a local gravel pit, had a porosity of 32%. The size analysis of the sand is as follows:

Sieve Size	Percentage as Large or Larger
20	11.3
40	47.5
60	81.6
80	96.4
100	98.4
200	99.9
Pan	100.0

The path and velocity of the water in the model were determined by use of fluorescein dye injected through glass tubes that had been inserted into the sand aquifer.[8] The tubes with tapered points were used to control the amount of injected dye and to keep the tube unplugged. The pH of the dye was reduced to 7 1/2 to match the pH of the water. To trace the movement of the waste from the pond, dye was added directly to the pond. The piezometric surface was determined from manometer tubes placed at various points along the length of the model. Rubber tube siphons and constant head bottles were used to add liquids to the model. All liquid movements in the model were due to gravity, all movement being laminar flow with Reynold's number controlling the hydraulic similitude obtained.

---

7 "Recent Groundwater Investigations in the Netherlands," by W. F. J. M. Krul and F. A. Liefrinck, Elsevier Publishing Co., New York, N. Y., 1946.

8 "Dispersion of a Moving Salt Water Boundary," by Paul R. Day, Transactions, Am. Geophysical Union, Vol. 37, No. 5, October, 1956.

A calcium chloride solution was used to represent the waste fluid when applying this model to the Wisconsin River Valley problem. The specific gravity of the solution and the waste fluid were equalized at 1.03. The quantities introduced into the model were limited by the permeability of the sand aquifer. All quantities were proportional to and approximately 0.0006 of the field quantities. To simplify the measurements, convenient reductions were made as follows: 37,200 gpd would be represented by 37.2 ml per 40 sec, and 14,900 gpd by 14.9 ml per 40 sec. The dye markers were placed at critical points to locate hydraulic divides and to determine typical velocities.

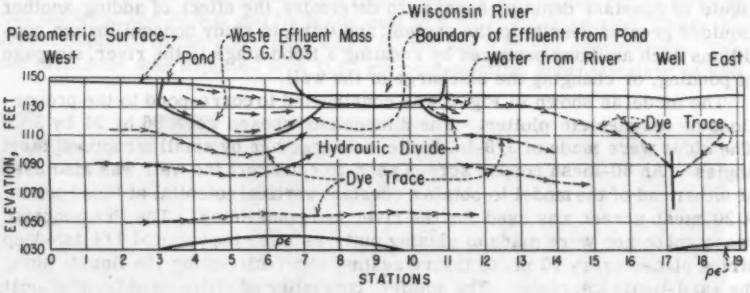


FIG. 3.—ELECTRIC ANALOG PLOTTER MODEL STUDY

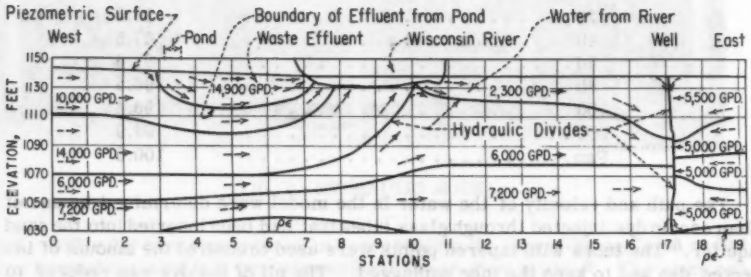


FIG. 4.—HYDRAULIC MODEL STUDY

The results of the hydraulic model test are shown in Fig. 4. The ponded waste interface reached a minimum elevation of 1,106 ft, while in the field it could be expected to be much lower than this.[9] Because the depth to which the waste sank in the aquifer is determined partly by time, the 135-day travel time in the field can be expected to result in deeper penetration than the 2-hr travel time in the model. However, this discrepancy could be minimized by using smaller model quantities and thus lower velocities.[10] This would, of course, extend the length of time of the test.

9 "The Quantitative Approach to Ground-Water Investigations," by J. G. Ferris and A. N. Sayre, Economic Geology, 50th Anniversary Volume, 1955.

10 "Field Measurements of the Rate of Movement of Underground Waters," by C. S. Slichter, U. S. Dept. of the Interior, Washington, D. C., 1904, pp. 29-49.

The discharge from the river to the well was easily defined because the river water had been heavily colored by the dye coming from the pond. The discharge zone began at station 10 + 30 and, in traveling to the well, leveled off at el 1,121.

The nonequilibrium conditions caused complete reversals of flow in some instances and only minor changes in velocities or direction in others. Effects of stoppage of ponding or well discharge were simulated simply by cutting off the respective model source or sink. The condition of river flood stage was simulated by adding water directly to the river so that the elevation of the river surface rose to the appropriate level.

Forecasts of future conditions were made by relating model velocities of waste and water movement to the field velocities by using a determined velocity ratio. A velocity ratio of 1 in. per min in the model equal to 10 ft per day in the field was arrived at by equating model velocities with known field velocities. The field velocities were determined by actual field tests and confirmed by analytical methods.

COMPARISON OF RESULTS

To compare the results of the hydraulic model with those of the electric plotter, ordinary water was used in the hydraulic model to represent the pond-

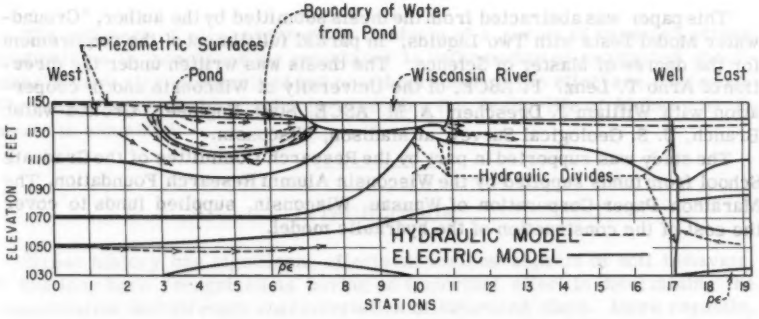


FIG. 5.—COMPARISON OF HYDRAULIC AND ELECTRIC ANALOG PLOTTER MODELS RESULTS

ed waste. In this way identical conditions were created in both models. The results of the tests of the two models are shown in Fig. 5. The ponded waste boundary in the hydraulic model reached a minimum elevation of 1,113 ft, while that in the electric plotter model reached only el. 1,116 ft. The interface between the discharge from the river and from the west ground-water source to the well was somewhat above and to the east of the interface as determined by the electric plotter. The hydraulic divide between the west ground water going to the river and to the well as determined by the electric plotter model is within a few feet of the divide determined by the hydraulic model. The results of the two types of models are close enough that either model can be considered reliable and capable of producing satisfactory results when movements of liquid of one density are being investigated.

The model results check with known field conditions, except that the sinking of the waste in the models is minimized. The contribution of water by the river to the cone of depression of the well has been verified by mathematical analysis and field observations. The movement of water under the river from west to east has also been verified by waste-liquid contamination tests performed in the field. Several fluid velocity measurements made in the field have substantiated the comparable velocities as determined in the model.

CONCLUSIONS

From the model tests described and the results obtained, it can be stated that quantitative ground-water analyses can be made on either the electric plotter model or the hydraulic model. Directions of flow are easily determined by the path of the dye streaks in the hydraulic model and by the indicated potential drops in the electric plotter model. In the same manner, hydraulic divides can be fairly accurately located. Even such unknowns as unmeasurable ground-water discharges can usually be determined. Finally, the forecast of conditions that may occur in the future can be made because of the possibility of incorporating a time scale into the hydraulic model tests.

ACKNOWLEDGMENTS

This paper was abstracted from the thesis submitted by the author, "Ground-water Model Tests with Two Liquids," in partial fulfillment of the requirement for the degree of Master of Science. The thesis was written under the direction of Arno T. Lenz, F. ASCE, of the University of Wisconsin and in cooperation with William J. Drescher, A. M. ASCE, Staff Engineer, Ground-water Branch, U. S. Geological Survey, at Madison, Wisconsin.

The study was supported in part by the Research Committee of the Graduate School from funds supplied by the Wisconsin Alumni Research Foundation. The Marathon Paper Corporation of Wausau, Wisconsin, supplied funds to cover the cost of the construction of the hydraulic model.

AMERICAN SOCIETY OF CIVIL ENGINEERS

Founded November 5, 1852

TRANSACTIONS

Paper No. 3018

CLAY STRENGTH INCREASE CAUSED BY REPEATED LOADING

By H. Bolton Seed,[1] M. ASCE, Robert L. McNeill,[2] A. M. ASCE, and Jacques de Guenin[3]

With Discussion by Messrs. Richard G. Ahlvin; D. Hugh Trollope; and H. Bolton Seed, Robert L. McNeill, and Jacques de Guenin

SYNOPSIS

The influence of stress history in the form of a series of repeated stress applications in increasing the resistance to deformation of compacted specimens of silty clay is described and possible causes of the effect are presented. The significance of the results in assessing the design life of highway pavements is examined.

INTRODUCTION

Stress history has significant effects on various aspects of soil behavior. It has long been recognized as having an important effect in determining the consolidation and strength characteristics of saturated clays. More recently, changes in the sequence of pressure application have also been shown to affect the swelling characteristics of clays. Therefore, it is perhaps not surprising to find that stress history, in the form of a series of applications of a constant stress, affects the deformation characteristics of partially saturated clays. Nevertheless, it might not have been anticipated that repeated loading would increase rather than decrease the resistance to deformation of soils having an initially high degree of saturation.

Note.—Published, essentially as printed here, in May, 1958, in the Journal of the Soil Mechanics and Foundations Division, as Proceedings Paper 1645. Positions and titles given are those in effect when the paper or discussion was approved for publication in Transactions.

1 Assoc. Prof. of Civ. Engrg., Univ. of California, Berkeley, Calif.

2 Staff Engr., Woodward, Clyde and Assocs., Oakland, Calif.

3 At present, in French Armed Services; formerly Graduate Research Engr., Inst. of Transp. and Traffic Engrg., Univ. of California, Berkeley, Calif.

A study of soil deformation under repeated loading has been conducted, wherein soil specimens in triaxial compression cells were subjected to a series of applications of a constant axial stress.[4] The primary purpose of these investigations was to determine the deformation occurring during the period of application of repeated loads, many of which were too light to cause failure. However, when the necessary information on this aspect of soil behavior had been obtained, the specimens were usually loaded to failure as in the normal type of strength test. It was observed on a number of occasions that specimens loaded to failure in this way appeared to be appreciably stronger than comparable specimens not subjected previously to repeated loading, and, generally, greater strength increases resulted from increased intensities of the repeated stress applications.

A typical example of this behavior is shown in Fig. 1, which presents the results of tests on 4 specimens trimmed from the same compacted sample of silty clay soil. The specimens, having a water content of 14% and a dry density of 109.3 lb per cu ft, were first subjected to a confining pressure of 1 kg per sq cm in triaxial compression cells. Two of these specimens were then

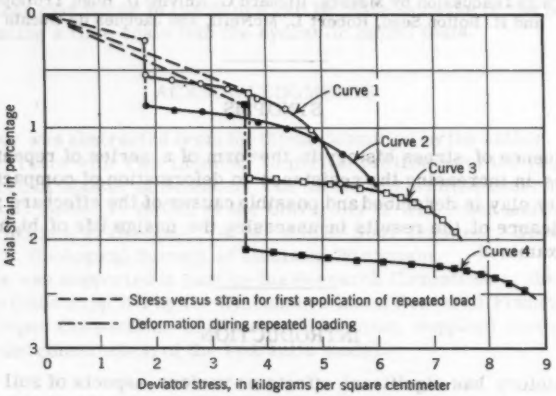


FIG. 1.—EFFECT OF REPEATED LOADING ON THE STRENGTH OF PARTLY SATURATED SILTY CLAY

subjected to 12,000 and 60,000 repetitions of a deviator stress of 1.8 kg per sq cm, causing axial strains of 0.55% and 0.8% respectively. The other 2 specimens were subjected to 10,000 and 65,000 repetitions of a deviator stress of 3.6 kg per sq cm, causing axial strains of 1.45% and 2.12% respectively. The 4 specimens were then loaded to failure. The specimen with the least deformation during repeated loading had a strength of 5.4 kg per sq cm (curve 1) and the specimen with the highest deformation during repeated loading had a strength of 8.75 kg per sq cm (curve 4). The specimens with 0.8% and 1.45% strains during repeated loading had strengths of 5.9 (curve 2) and 7.5 kg per sq cm (curve 3), respectively. Thus, in this case the repeated application of a constant stress caused an increase in strength of more than 50% for the strongest specimen.

[4] "Effects of Repeated Loading on the Strength and Deformation of Compacted Clay," by H. B. Seed, C. K. Chan, and C. L. Monismith, Proceedings, Highway Research Board, Washington, D. C., Vol. 34, 1955.

Because the foregoing tests were conducted on partly saturated specimens, the increase in strength due to repeated load applications may be attributed partly to an increase in density of the specimens during the tests. A part of the measured strength increase may be due also to an increase in thixotropic strength with time.[5] However, the magnitude of the strength increase is surprising in view of the relatively small deformation occurring during repeated loading and the short time interval of several days between the various specimens being loaded to failure.

It is also interesting that an increase in density could have occurred in these tests. The test results in Fig. 1 were obtained on samples compacted by 125 tamps, using a tamping pressure of 225 lb per sq in., to a relative density of 90%, based on the modified American Association of State Highway Officials (AASHO) compaction test. If, as the strength data imply, a series of applications of the 1.8 kg per sq cm deviator stress (corresponding to a total axial stress of 40 lb per sq in.) may cause a further increase in density, the beneficial effects of traffic loads in increasing the density of partly saturated subgrades can have significant effects in the performance of highway pavements.

In view of this possible significance, it was thought desirable to investigate further the magnitude of the strength increase that might result from repeated stress applications, and the influence of densification on this effect.

EFFECT OF REPEATED LOADING ON SOIL STRENGTH

To study the effect of repeated loading on the strength of soil specimens, a comprehensive series of tests were conducted on a silty clay soil from Vicksburg, Miss. This soil had a liquid limit of 37 and a plastic limit of 23.

Tests were performed on samples of various water contents having degrees of compaction varying from 90% to 95%, based on the modified AASHO compaction test. The soil was mixed to the desired water content 1 day before compaction and stored for 24 hr in an airtight container. Samples were then compacted in 6-in.-diameter molds, using the Triaxial Institute kneading compactor[6] to form specimens 4½ in. high. All specimens were compacted in five layers using 15 or 25 tamps per layer and a tamping pressure of between 75 and 350 lb per sq in., depending on the density desired.

From each compacted sample 4 identical specimens having a diameter of 1.4 in. and a height of 4 in. were trimmed. Each specimen was placed between a lucite cap and base and surrounded by two thin rubber membranes with a layer of grease between the membranes. The membranes were sealed against the lucite cap and base by means of neoprene O-rings and the entire specimen was stored under water. After approximately 10 days, 2 of the specimens trimmed from any one compacted sample were placed in triaxial compression cells, subjected to a confining pressure of 1 kg per sq cm and then to between 80,000 and 180,000 applications of a constant deviator stress sufficiently large to cause between 1% and 2% strain of the specimens over a period of approximately 4 days. On the 14th day after the specimens had been prepared, the repeated loading was stopped and the 2 specimens were removed from the triaxial

---

5 "Thixotropic Characteristics of Compacted Clays," by H. B. Seed and C. K. Chan, Transactions, ASCE, Vol. 124, 1959, pp. 894-925.

6 "Some Relationships Between Density and Stability of Subgrade Soils," by H. B. Seed and C. L. Monismith, Bulletin No. 93, Highway Research Board, Washington, D. C., 1954.

compression cells. They were then placed in another cell with provisions for drainage in the cap and base, the confining pressure of 1 kg per sq cm was reapplied, and the specimens were loaded to failure in a normal type of strength test. At the same time the 2 specimens trimmed from the same sample but not subjected to repeated loading were loaded to failure using the same test procedure. The results of three tests of this kind, which are typical of those obtained in a number of other tests, are shown in Figs. 2, 3, and 4. Each curve shown in these figures is the average for two tests performed on similar specimens.

Figs. 2(a), 3(a), and 4(a) indicate the stress vs strain relationships of specimens of silty clay in normal strength tests before and after repeated loading. The solid curves represent the relationships obtained during a normal loading procedure with a rate of deformation equal to 0.04 in. per min. The broken curves represent the deformations during repeated loading with the duration

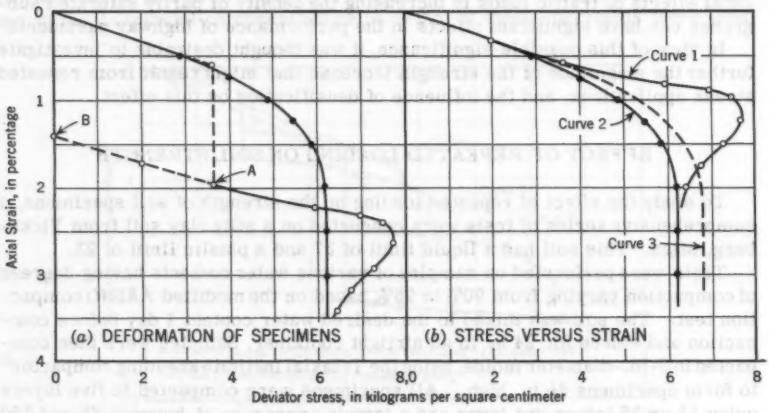


FIG. 2.—TEST 1

of stress application equal to 0.2 sec and the frequency of stress application equal to 20 cycles per min. Figs. 2(b), 3(b), and 4(b) show a comparison of the stress versus strain curves of specimens in the normal strength tests.

Fig. 2(a) shows test data for specimens having a water content of 13.5%, a dry density of 105.7 lb per cu ft, and a degree of saturation of 60%. In normal triaxial compression tests of the unconsolidated-undrained type but with the ends of the specimens open to the atmosphere, and using a lateral pressure of 1 kg per sq cm, these specimens had a strength of 6.2 kg per sq cm. Specimens subjected to the same confining pressure showed an axial strain of 0.62% when subjected to a deviator stress of 3.65 kg per sq cm for a period of 0.2 sec, and continued to deform when this same stress was repeatedly applied and removed. During the 90,000th application of the stress the specimens showed an axial strain of 1.95% (point A) and after the stress was removed, a residual strain of 1.4%. On being loaded to failure under the same conditions as the previously unloaded specimens, these specimens had a strength of 7.75 kg per sq cm.

As seen from Fig. 2(b), the specimens subjected to repeated loading (curve 1) had a different form of stress versus strain curve from the specimens not subjected to repeated loading (curve 2) in addition to having a higher strength. In this figure the stress versus strain characteristics of the specimens during the normal strength tests are plotted from the same origin. The specimens previously subjected to repeated loading were initially stiffer, developed their maximum strength at a lower strain, exhibited a reduced resistance to deformation when deformed beyond the point of maximum strength, and had a residual strength approximately equal to that of the previously unloaded specimens. Curve 3 represents the stress versus strain relationship for the specimen assuming maximum possible densification during repeated loading.

Similar effects of repeated loading are shown in Figs. 3(a) and 3(b) for specimens having a water content of 15.3%, an initial dry density of 108.1 lb per cu ft, and an initial degree of saturation of 74%. Point A indicates the residual deformation after 140,000 repeated stress applications. Curve 1 is the

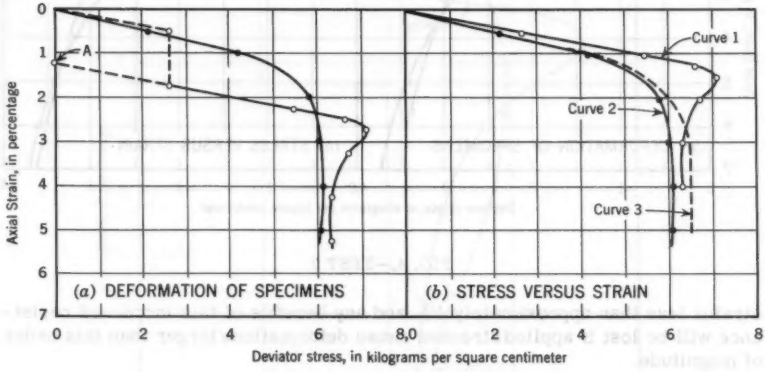


FIG. 3.—TEST 2

stress versus strain relationship for a specimen previously subjected to 140,000 repeated stress applications, curve 2 is for a specimen not previously loaded, and curve 3 shows the stress versus strain relationship for a specimen assuming the maximum possible densification during repeated loading.

For specimens having a water content of 18.3%, an initial dry density equal to 107.6 lb per cu ft, and a higher degree of saturation of 86%, a different effect was indicated, as seen in Figs. 4(a) and 4(b). In this case (Fig. 4(a)) specimens having a strength of approximately 3.5 kg per sq cm under normal loading conditions exhibited a residual deformation of 0.65% after being subjected to 150,000 applications of a deviator stress of 1.0 kg per sq cm (point A). On being loaded to failure these specimens were appreciably stiffer than previously unloaded specimens but did not consistently have higher strengths. In Fig. 4(b), curve 1 is the stress versus strain relationship for a specimen previously subjected to 150,000 repeated stress applications and curve 2 is for a specimen not previously loaded.

It would appear that the effect of repeated loading on the stress versus deformation characteristics of the soil depends on the initial degree of saturation of the specimen on which the tests are conducted. In all cases, specimens previously subjected to repeated loading were appreciably stiffer or more resistant to deformation and had higher strengths for specimens with low degrees of saturation. However, when the deformation exceeded approximately 3% or 4% strain they exhibited resistances to deformation essentially the same as those of similar specimens not subjected to repeated loading. This would seem to indicate that the increase in resistance to deformation is apparent only at

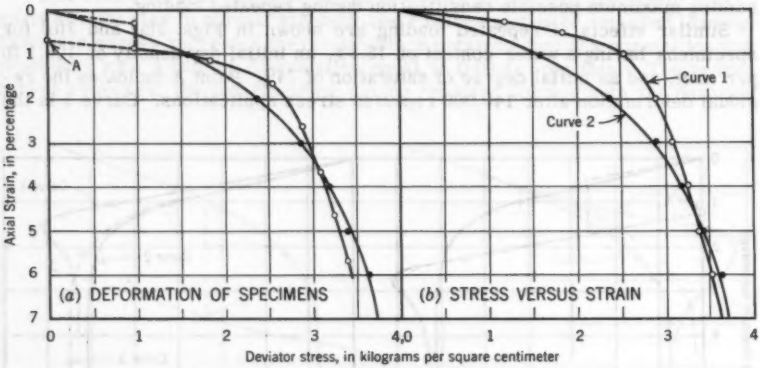


FIG. 4.—TEST 3

strains less than approximately 4%, and any benefits of this increased resistance will be lost if applied stresses cause deformations larger than this order of magnitude.

INFLUENCE OF INCREASED RESISTANCE TO DEFORMATION IN DETERMINING SOIL BEHAVIOR UNDER REPEATED LOADING

Because the repeated application of stress to a soil specimen causes an increase in stiffness or resistance to deformation of the soil in a normal type of strength test, it might also be expected that the soil would become more resistant to deformation under repeated loads of increased magnitude. That such an effect does occur is shown by the test data in Figs. 6 and 7.

Figs. 5 and 6 show the results of a series of unconfined compression tests on silty clay specimens compacted on the dry side of optimum at a water content of 16.3% to a dry density of 108.8 lb per cu ft and a degree of saturation of 80%. Each curve in these figures is the average for at least two tests on apparently identical specimens. Fig. 5 shows a comparison between the stress versus strain relationship of these specimens in a normal strength test (rate of deformation equal to 0.15 in. per min) with the stress versus strain curves obtained after the specimens had been subjected to 100,000 applications of a deviator stress of 1.5 kg per sq cm at a rate of 20 per min. Each stress application was for 0.25 sec. Curve 1 and curve 2 represent the stress versus

strain relationships for specimens tested after repeated stress application and for those with no previous stress application, respectively. Curve 3 indicates the deformation during repeated stress application. On completion of the repeated stress applications the specimens had a residual strain of 0.95% (point A), and when loaded to failure showed a higher strength and were considerably stiffer than the specimens tested with no previous stress application. These results are similar to those presented in Figs. 2, 3, and 4.

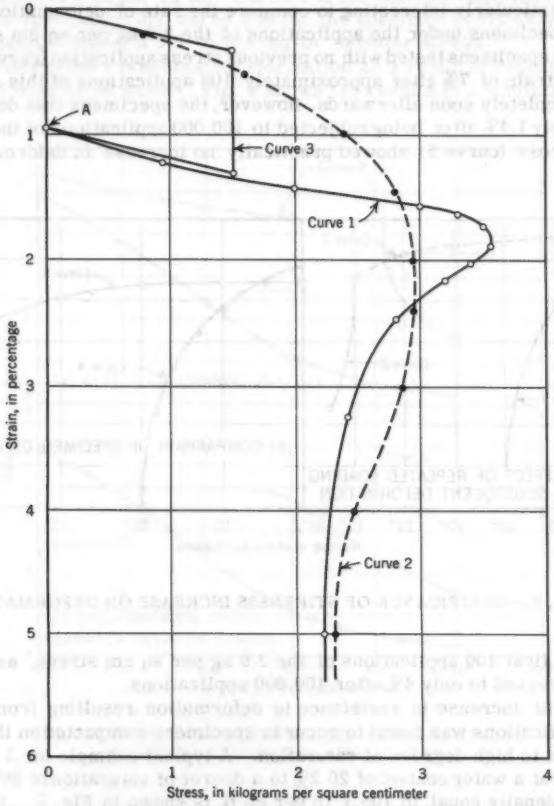


FIG. 5.—EFFECT OF REPEATED LOADING ON THE STRESS VERSUS STRAIN RELATIONSHIP

The significance of this increase in stiffness on the deformation occurring during repeated stress application is shown by the test data for similar specimens in Fig. 6(a). Specimens subjected directly to a repeated stress of 2.9 kg per sq cm at a rate of 20 applications per min (each application having a duration of 0.25 sec) deformed slightly more than 1% during the first application,

continued to deform with each subsequent application, and failed completely after approximately 100 stress applications (curve 1). However, the specimens previously subjected to 100,000 applications of a 1.5 kg per sq cm stress (curve 2) were subsequently able to withstand a further 200,000 applications of the 2.9 kg per sq cm stress without deforming more than 4.6% (curve 3). Under the first 100,000 applications of the 1.5 kg per sq cm stress these specimens deformed 1.4% and the deformation increased to 4.6% after an additional 200,000 applications of the 2.9 kg per sq cm stress.

It is particularly interesting to compare the rate of deformation of the two sets of specimens under the applications of the 2.9 kg per sq cm stress (Fig. 6(b)). The specimens tested with no previous stress application (curve 4) showed an axial strain of 7% after approximately 100 applications of this stress, and failed completely soon afterwards. However, the specimens that deformed approximately 1.4% after being subjected to 100,000 applications of the 1.5 kg per sq cm stress (curve 5) showed practically no increase in deformation at all

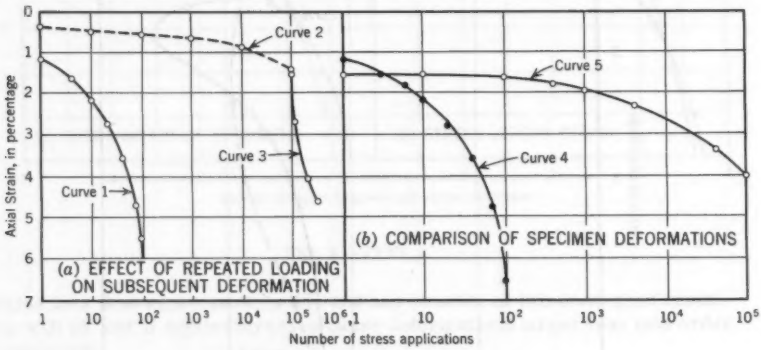


FIG. 6.—SIGNIFICANCE OF STIFFNESS INCREASE ON DEFORMATION

during the first 100 applications of the 2.9 kg per sq cm stress, and the axial strain increased to only 4% after 100,000 applications.

A similar increase in resistance to deformation resulting from repeated stress applications was found to occur in specimens compacted on the wet side of optimum to high degrees of saturation. A typical example for 2 specimens compacted at a water content of 20.2% to a degree of saturation of 89% and having a dry density equal to 105.1 lb per cu ft is shown in Fig. 7. Both specimens were tested in triaxial compression using a confining pressure of 14.1 lb per sq in. In Fig. 7(a), one of the specimens was subjected directly to repeated applications of a 7-lb-per-sq-in. deviator stress (curve 1), each stress application having a duration of 0.25 sec, at a rate of 10 applications per min. The second specimen was subjected first to 12,000 applications of a 5.6-lb-per-sq-in. deviator stress of the same duration and frequency (curve 2) and then the repeated deviator stress was increased to 7 lb per sq in. as for the first specimen (curve 3). It will be seen that the specimen subjected to 12,000 applications of the lighter stress before being subjected to an increased stress

deformed only 2.25% after 100,000 applications, as compared with a deformation of 2.9% after this number of applications to the previously unloaded specimen. In this case also, the specimen subjected to 12,000 applications of the lighter load showed very little increase in deformation after 500 applications of the 7-lb-per-sq-in. stress, though subsequent stress applications caused a substantial increase in deformation.

Fig. 7(b) is a comparison of the specimen deformations under the repeated deviator stress of 7 lb per sq in. Curve 4 is for the specimen having no previous stress application, and curve 5 is for the specimen previously subjected to 12,000 applications of a 5.6-lb-per-sq-in. deviator stress.

No such increased resistance to deformation as a result of repeated loading is observed in tests on sands. Fig. 8 shows the results of a similar series of

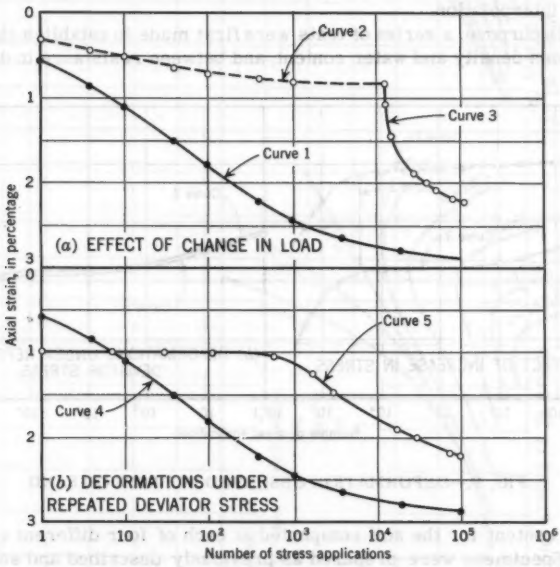


FIG. 7.—INCREASED DEFORMATION RESISTANCE DUE TO REPEATED STRESS APPLICATION

tests performed on specimens of a medium fine sand having a void ratio of 0.676 ± 0.002. The duration of stress applications was 0.33 sec, with the frequency of stress applications equal to 20 per min; the lateral pressure of 14.3 lb per sq in. Fig. 8(a) shows the effect of increase in stress on the fine sand during repeated loading. Curve 1 is for a specimen loaded with a repeated deviator stress equal to 22.7 lb per sq in. and curves 2 and 3 are for specimens subjected to a repeated deviator stress of 34.1 lb per sq in. Fig. 8(b) is a comparison of the deformations of the specimens under the repeated deviator stress of 34.1 lb per sq in. Curve 4 is for the specimen with no previous stress application, and curve 5 is for the specimen previously subjected to

23,000 applications of a 22.7-lb-per-sq-in. deviator stress. The deformations in curve 4 are almost identical with those of curve 5, with no evidence of any stiffening effect due to the previous stress applications.

INFLUENCE OF DENSIFICATION ON RESISTANCE TO DEFORMATION

The nature of the effect of repeated loading on soil behavior in the preceding tests suggests that a primary cause of the increase in stiffness of the specimens is the increase in density which would be expected to occur during the repeated application of loads. To determine the significance of an increase in density on the deformation characteristics of the soil, a series of tests were conducted on specimens at various water contents and densities in order that the behavior of a specimen at any water content and density might be determined by interpolation.

For this purpose, a series of tests were first made to establish the relationship between density and water content, and between resistance to deformation

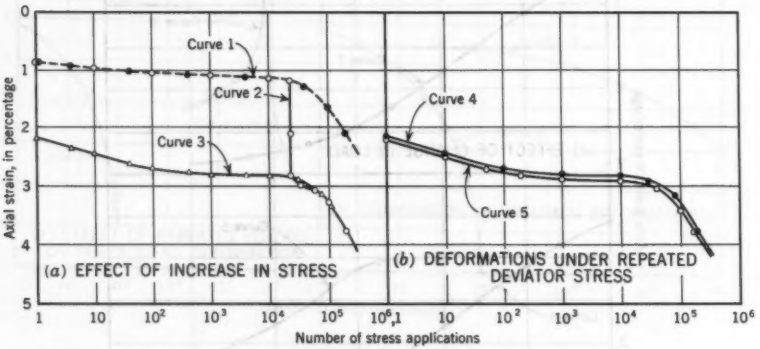


FIG. 8.—DEFORMATION OBSERVED IN TESTS ON SAND

and water content for the soil compacted at each of four different compactive efforts. Specimens were prepared as previously described and subjected to triaxial compression tests of the unconsolidated-undrained type 14 days after preparation. From the results of these tests the stresses required to cause various amounts of strain of the specimens were determined. Fig. 9(a) shows the density versus water content relationship for each compactive effort and Fig. 9(b) the corresponding stress required to cause 2% strain versus water content relationship for the same specimens. For specimens prepared at each compactive effort the stress required to cause 2% strain is low on the wet side of optimum. However, it begins to increase as the optimum water content is approached, continues to increase with decreasing water content on the dry side of optimum even though the density of the samples is decreasing, and finally begins to decrease slightly at still lower water contents.

From such data it is possible to determine by interpolation the relationship between stress required to cause 2% strain and dry density for various constant values of water content w. For example, at a water content of 14% a specimen

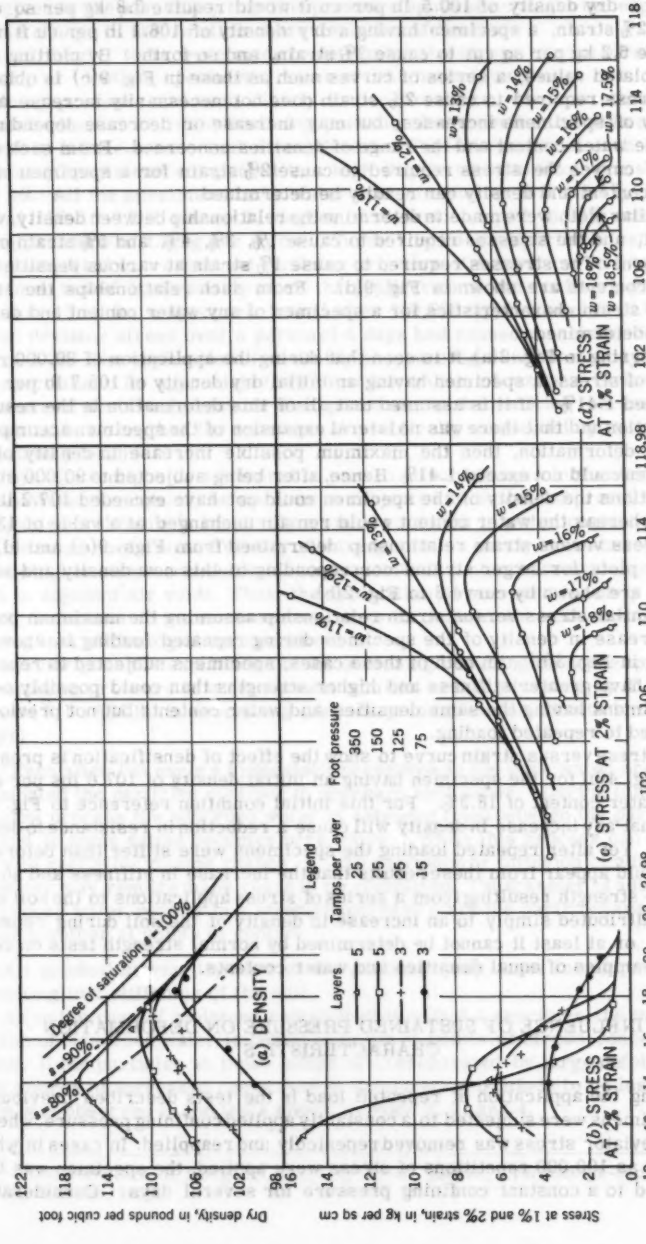


FIG. 9.—STRESS VERSUS STRAIN CHARACTERISTICS AT VARIOUS DENSITIES

having a dry density of 100.5 lb per cu ft would require 3.8 kg per sq cm to cause 2% strain, a specimen having a dry density of 106.1 lb per cu ft would require 6.2 kg per sq cm to cause 2% strain, and so forth. By plotting these interpolated values, a series of curves such as those in Fig. 9(c) is obtained. The stress required to cause 2% strain does not necessarily increase as the density of specimens increases, but may increase or decrease depending on both the water content and the range of densities concerned. From such a series of curves the stress required to cause 2% strain for a specimen of any water content and density can readily be determined.

Similar plots were made to determine the relationship between density, water content, and the stresses required to cause 1%, 3%, 4%, and 5% strain of the specimens. The stresses required to cause 1% strain at various densities and water contents are shown in Fig. 9(d). From such relationships the stress versus strain characteristics for a specimen of any water content and density can be determined.

Referring to Fig. 2(a), it is seen that during the application of 90,000 repetitions of stress, a specimen having an initial dry density of 105.7 lb per cu ft deformed 1.41%. If it is assumed that all of this deformation is the result of compaction and that there was no lateral expansion of the specimen accompanying the deformation, then the maximum possible increase in density of the specimen could not exceed 1.41%. Hence, after being subjected to 90,000 stress applications the density of the specimen could not have exceeded 107.2 lb per cu ft, whereas the water content would remain unchanged at a value of 13.5%. The stress versus strain relationship determined from Figs. 9(c) and (d) and similar plots for larger strains corresponding to this new density and water content are shown by curve 3 in Fig. 2(b).

A similar stress versus strain relationship assuming the maximum possible increase in density of the specimen during repeated loading is shown by curve 3 in Fig. 3(b). In both of these cases, specimens subjected to repeated loading have greater stiffness and higher strengths than could possibly occur in specimens having the same densities and water contents but not previously subjected to repeated loading.

No stress versus strain curve to show the effect of densification is presented in Fig. 4(b) for the specimen having an initial density of 107.6 lbs per cu ft and a water content of 18.3%. For this initial condition reference to Fig. 9(d) shows that any increase in density will cause a reduction in resistance to deformation. Yet after repeated loading the specimens were stiffer than before.

It would appear from these results that the increase in stiffness and sometimes in strength resulting from a series of stress applications to the soil cannot be attributed simply to an increase in density of the soil during repeated loading, or at least it cannot be determined by normal strength tests on compacted samples of equal densities and water contents.

INFLUENCE OF SUSTAINED PRESSURE ON DEFORMATION CHARACTERISTICS

During the application of repeated load in the tests described previously, the specimens were subjected to a constantly applied confining pressure, whereas the deviator stress was removed repeatedly and reapplied. In cases in which as many as 100,000 repetitions of stress were applied, the specimen was thus subjected to a constant confining pressure for several days. Consideration

was given to the possibility that this pressure application might be responsible for the change in deformation characteristics of the soil.

Accordingly, tests were made to determine the stress versus strain relationship of identical specimens, some of which were subjected to a constant confining pressure and immediately loaded to failure, whereas others were maintained under constant confining pressure for a number of days and then loaded to failure in a normal strength test. Typical results of such tests on silty clay specimens compacted to a high degree of saturation are shown in Fig. 10. All the specimens had a water content equal to 18.5 ± 0.1%, dry density of 110.3 ± 0.2 lb per cu ft, degree of saturation equal to 94%, and a confining pressure of 1.0 kg per sq cm. Curve 1 is for the specimen tested after being subjected to a sustained confining pressure of 4 days, curve 2 is for the specimen tested immediately after the application of the confining pressure, and curve 3 is for a specimen tested after 110,000 applications of 0.6 kg per sq cm deviator stress over a period of 4 days had caused a residual deformation of 1.3%. The application of confining pressure for a number of days causes the specimen to be appreciably stiffer at low values of strain. However, the influence of sustained pressure disappears as the deformation increases, and the ultimate strength of the specimen is practically unaffected by the period of sustained pressure.

This effect might be attributed in part to minor changes in the distribution of moisture throughout the specimens subjected to sustained pressure. In a compacted soil there is inevitably a small variation in water content throughout the mass due to nonuniformity of mixing, and in a partly saturated soil there will be higher stress concentrations near points of contact between larger grains than in adjacent air voids. Thus, the application of pressure is likely to cause small decreases in water content at points throughout the soil structure, resulting in a stiffening of the specimen.

Another possible explanation of the stiffening resulting from the application of confining pressure is a mechanism similar to that advanced by T. William Lambe,[7] F. ASCE, in describing secondary compression effects in saturated clays:

> "Even after the excess hydrostatic pressures in the pore water are dissipated the particles continue to approach each other. During this very slow process the adsorbed water is extruded from between the particles and to some extent becomes pore water. While this process can occur with negligible volume change . . . the extrusion or diffusion of adsorbed water may require many years to be completed. The transfer of adsorbed to pore water results in a strength increase since the particles are closer together at points of contact."

Such a gradual moving together of the particles may occur in compacted clay resulting in a stiffening of the soil.

As in the case of moisture redistribution within a specimen, the major diffusion of adsorbed water is likely to occur at points of stress concentration. Thus, if the particles at these points are reseparated by large deformations, this source of increased resistance to deformation is likely to be lost. Such a loss was observed in the tests shown in Figs. 2, 3, and 4.

---

[7] "The Structure of Inorganic Soil," by T. W. Lambe, Proceedings-Separate 315, ASCE, October, 1953.

Whereas the stiffening of the specimens due to application of a sustained confining pressure is undoubtedly partly responsible for the observed increase in stiffness of the specimens in the triaxial compression tests under repeated load, it cannot alone be responsible for the increased stiffness observed in these tests. This is seen in Fig. 10, in which specimens subjected to repeated stress applications are considerably stiffer and stronger than those subjected to sustained confining pressure for an equal period of time. Furthermore, as shown in Fig. 5, there is a considerable increase in stiffness and strength of

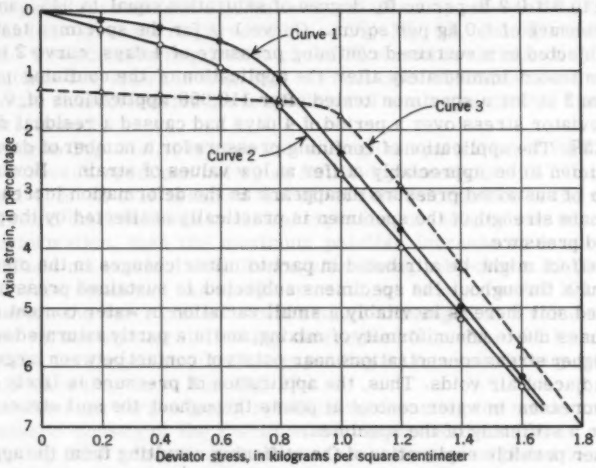


FIG. 10.—EFFECT OF SUSTAINED CONFINING PRESSURE

specimens subjected to repeated axial stress even when no confining pressure is applied.

CAUSES OF INCREASED RESISTANCE TO DEFORMATION

Because the observed increase in stiffness of soil specimens during repeated loading tests cannot be attributed entirely to the influence of densification or of the confining pressure, other possible changes in the characteristics of the specimens must be considered.

Examination of the test data seems to indicate that specimens subjected to greater deformations during repeated loading subsequently possess the greater resistance to deformation. However, the larger deformations are necessarily associated with greater magnitudes and numbers of applications of the repeated stress, and it is believed that these two factors rather than the resulting strain are primarily responsible for the increased stiffness of a specimen.

The significance of the number of stress applications is shown by the test data in Fig. 11. The silty clay specimens tested had a water content of 17.0 ± 0.1, a dry density equal to 108.5 lb per cu ft, a degree of saturation of 84%, and

a confining pressure equal to 1.0 kg per sq cm. In this series of tests, 3 specimens trimmed from the same compacted sample were subjected to repeated loads of different magnitudes until each of the specimens had an axial strain of 3.55%. When this strain was reached the specimens were loaded to failure as in a normal strength test.

For the specimens subjected to the highest repeated stress, 8,000 applications were required to produce this deformation. For the specimens subjected to lighter loads, 30,000 and 350,000 applications were required respectively. The progress of deformation during repeated loading is shown in Fig. 11(a). Curves 1, 2, and 3 are for repeated deviator stresses of 0.98, 1.10, and 1.28 kg per sq cm respectively.

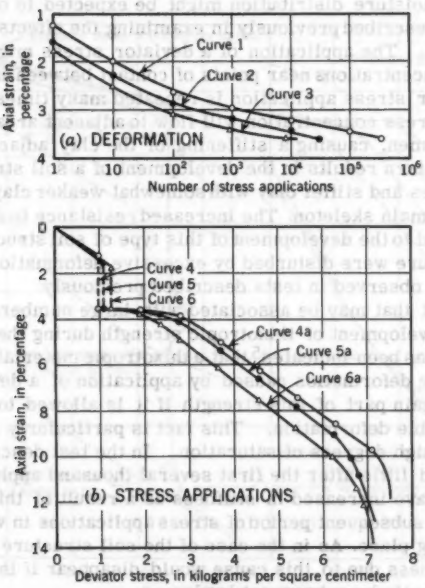


FIG. 11.—EFFECT OF NUMBER AND MAGNITUDE OF STRESS APPLICATIONS

The stress versus strain curves of the specimens during the normal loading procedure are shown in Fig. 11(b). Lines 4, 5, and 6 show the deformations occurring during 350,000, 30,000, and 8,000 repeated stress applications, and curves 4a, 5a, and 6a indicate the stress versus strain curves of the specimens after the repeated stress applications. It will be seen that although the 3 specimens had equal initial deformations after repeated loading, the specimens subjected to the greater number of stress applications had the highest stiffness and strength, whereas the specimens subjected to the least number of stress applications had the least resistance to further deformation.

Thus, a large number of lighter stress applications appears to have a greater effect on the subsequent behavior of a soil than a smaller number of applications of a higher stress. However, Fig. 1 shows that for specimens having the same number of repeated stress applications, the larger the magnitude of the repeated stress, the greater is the increase in strength. Therefore, the observed increase in stiffness appears to be associated primarily with the number and magnitude of the repeated stress applications.

Because the effect is not due to densification, it would seem that the change in deformation characteristics must be attributed to other changes occurring within the specimen as a result of repeated loading, and is associated possibly with changes in moisture distribution or structural arrangement of the soil grains, or with an increase in resistance to deformation caused by thixotropy.

Changes in moisture distribution might be expected to occur in a fashion similar to that described previously in examining the effects of sustained confining pressures. The application of a deviator stress might be expected to cause stress concentrations near points of contact between larger grains, and, when the deviator stress application is repeated many times, the moisture in these zones of stress concentration will flow to adjacent areas of lower stress within the specimen, causing a stiffening of the clay adjacent to the larger grains. This in turn results in the development of a soil structure consisting of larger particles and stiffer clay with somewhat weaker clay forming the matrix between the main skeleton. The increased resistance to deformation would then be attributed to the development of this type of soil structure and would be lost if the structure were disturbed by excessive deformation. Such a loss at high strains was observed in tests described previously.

Another effect that may be associated with large numbers of stress applications is the development of thixotropic strength during the period of stress applications. It has been indicated[5] that a thixotropic material may lose strength as a result of the deformation caused by application of a deviator stress and subsequently regain part of this strength if it is allowed to rest without any further appreciable deformation. This fact is particularly important in clay samples having high degrees of saturation. In the test described previously, the soil deformed little after the first several thousand applications, and thus might possibly have increased in stiffness as a result of thixotropic strength regain during the subsequent period of stress applications in which little deformation was taking place. As in the case of the soil structure deformation, any increase in stiffness due to this cause would disappear if the specimen were deformed sufficiently by subsequent loads.

Finally, there is the possibility that a series of repeated stress applications might cause changes in the structural arrangement of grains in the compacted specimens. The increased resistance to deformation seems to be developed by a large number of applications of stress over a period during which the soil deforms little. The repeated pressure application may cause particles to move slightly closer together by extrusion of adsorbed water with a resulting increase in strength. A discussion of the influence of pressure and time on the structure and strength of compacted clays has been presented by T. W. Lambe.[8]

It is important to recognize that the increased resistance to deformation appears to be lost if the soil is deformed appreciably after the increased resistance has been developed. This is apparent in Figs. 2 and 3, which show

[8] "Compacted Clay: Engineering Behavior," by T. W. Lambe, ASCE, Transactions, 1960.

that the residual strength of the specimens previously subjected to repeated loading is approximately the same as that of previously unloaded specimens and is reached at axial strains of 2% to 3%. Again, in Fig. 4 the increased resistance to deformation of specimens previously subjected to repeated loading is apparently lost when they subsequently reach a deformation of approximately 4%.

The loss of the increased resistance developed during repeated loading when the soil is subsequently deformed appreciably is well demonstrated by the data in Fig. 12. These data were obtained in unconfined compression tests on silty clay specimens having a water content of 18.2%, a dry density equal to 110.3 lb per cu ft, and a degree of saturation of 93%. The repeated stress applica-

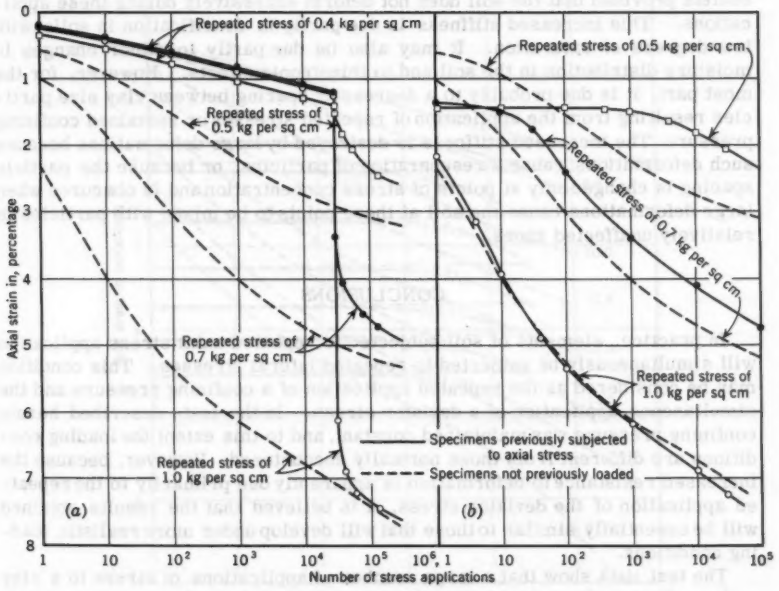


FIG. 12.—EFFECT OF STRESS CHANGE ON DEFORMATION

tions had a frequency of 20 per min, and a duration of 0.2 sec. In these tests specimens were first subjected to 30,000 applications of an axial stress of 0.4 kg per sq cm causing the deformations indicated by the solid lines in Fig. 12. On some specimens the repeated axial stress was then increased to 0.5 kg per sq cm, and on others to 0.7 kg per sq cm, and 1.0 kg per sq cm.

The deformations of the specimens under further repeated stress applications were then compared with those of specimens subjected to the higher stresses without previous load application; the latter deformations are shown by the dashed lines in Fig. 12. It is apparent from a comparison of the deformations occurring under repeated applications of the 0.5-kg-per-sq-cm axial stress that the 30,000 applications of the 0.4-kg-per-sq-cm axial stress caused

some stiffening of the soil. Even after 30,000 applications of this stress the previously loaded specimens had deformed considerably less than previously unloaded specimens.

However, for those specimens on which the repeated axial stress was changed to 0.7 kg per sq cm, the effect of the previous stiffening is less apparent, and as seen from Fig. 12, when the repeated stress was increased to 1.0 kg per sq cm, the stiffening effects of the previous stress application disappeared completely. In addition to indicating the nature of the effect, these data also show the necessity of avoiding large stress changes if the increased resistance is to be used to practical advantage.

In general, then, it appears that a large number of stress applications can cause an increased resistance to deformation in a soil having a constant water content provided that the soil does not deform excessively during these applications. This increased stiffness is due partly to densification in soils with low degrees of saturation. It may also be due partly to minor changes in moisture distribution in the soil and to thixotropic effects. However, for the most part, it is due probably to a decreased spacing between clay size particles resulting from the application of repeated stresses or sustained confining pressure. The increased stiffness is destroyed by large deformations because such deformations cause a reseparation of particles, or because the particle spacing is changed only at points of stress concentration and is obscured when large deformations cause the soil at these points to be mixed with particles in relatively unaffected zones.

CONCLUSIONS

In practice, elements of soil subjected to repeated axial stress application will simultaneously be subjected to repeated lateral stresses. This condition may be considered as the repeated application of a confining pressure and the simultaneous application of a deviator stress. In the tests described herein confining pressure was maintained constant, and to this extent the loading conditions are different from those normally encountered. However, because the increased resistance to deformation is apparently due primarily to the repeated application of the deviator stress, it is believed that the results obtained will be essentially similar to those that will develop under more realistic loading conditions.

The test data show that a large number of applications of stress to a clay soil can cause an increase in resistance to deformation. The number of applications required to produce this effect was not determined but there were some indications that it is more than 1,000. Furthermore, in all of the tests conducted, the deformation during the repeated stress applications was relatively small. These facts are worthy of emphasis because under other conditions a series of applications of stress may result in a decreased resistance to deformation. If the magnitude of the repeated stress is sufficiently large to cause an increase in density and the soil is gradually compacted by repeated application of the stress to a high degree of saturation, a decrease in strength occurs.[6,9] This condition appears to be associated with somewhat larger deformations of the soil during loading and smaller numbers of stress applications.

9 "Reduction in Soil Strength with Increase in Density," by C. R. Foster, Transactions, ASCE, Vol. 120, 1955.

Whether there is an increase in resistance to deformation is likely to depend, therefore, on the magnitude and number of the repeated stress applications.

The tests described were all performed on specimens maintained at constant water content throughout the period of repeated loading, whereas in actual practice a soil will often be able to gain or lose water by drainage during the period of repeated stress applications. Although the effects of stress history are evidenced in specimens having a high degree of saturation and, therefore, little tendency to absorb water by swelling, the influence of this additional factor requires further study before the validity of the observed effect can be considered established for practical conditions.

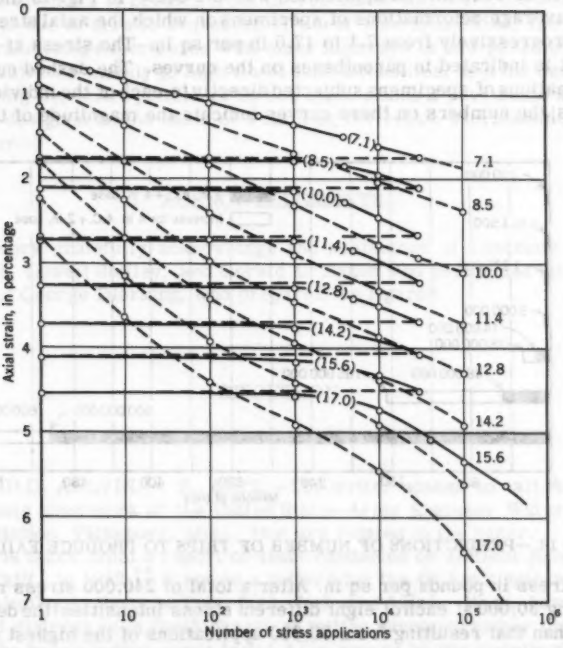


FIG. 13.—DEFORMATIONS UNDER PROGRESSIVELY INCREASED REPEATED STRESS

However, it appears from the results that the increased resistance to deformation resulting from a series of applications of stress might be an important factor affecting the performance of highway pavements. If a clay soil is subjected to a series of applications of light traffic loads, then apparently it may subsequently be more resistant to deformation under heavier traffic loads and may not deform excessively under loads that might otherwise cause pavement failure. The extent to which this will occur probably depends on the relative magnitudes of the number of applications of different stresses, on the magnitude of stress changes, and on the possible influence of water content changes.

It seems likely, however, that the effect might be a significant factor in determining the number of repetitions of stress which can be applied to a pavement before failure occurs. Furthermore, it may greatly complicate the problem of determining the destructive effects on highway pavements resulting from a series of repeated stress applications of different intensities.

This is well illustrated by the test data presented in Fig. 13 which shows the deformations of specimens of silty clay subjected to a repeated stress that was under progressively increased in magnitude every 30,000 applications. No confining pressure was used in the tests. All the specimens had a water content of 17.4 ± 0.15%, a dry density of 112.0 ± 0.2 lb per cu ft and a degree of saturation of 93%; the frequency of stress application was 20 per min, and the duration of each stress application was 0.2 sec. In Fig. 13 the solid line indicates average deformations of specimens on which the axial stress was increased progressively from 7.1 to 17.0 lb per sq in. The stress at each stage of the test is indicated in parentheses on the curves. The dashed curves show the deformations of specimens subjected directly to each of the individual stress intensities; the numbers on these curves indicate the magnitude of the repeat-

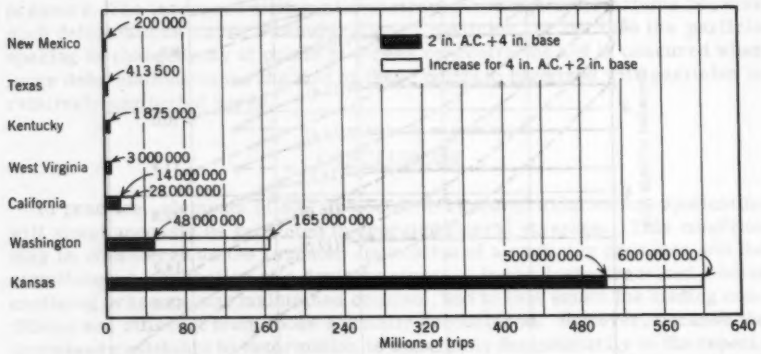


FIG. 14.—PREDICTIONS OF NUMBER OF TRIPS TO PRODUCE FAILURE

ed axial stress in pounds per sq in. After a total of 240,000 stress repetitions (comprising 30,000 at each of eight different stress intensities) the deformation was less than that resulting from 30,000 applications of the highest stress intensity alone, and was equal to that produced by only 1,500 applications of this stress intensity. It appears from these data that there is no simple method of assessing the cumulative effects of a series of wheel loads of different intensities on clay soils from data concerning their individual effects.

The practical difficulty of determining the service life of a highway pavement is shown by the wide variation in the predictions of the various state highway departments of the number of load repetitions which would cause failure in the WASHO test road at Malad, Idaho.[10] After being provided with samples of the soil, each state highway department was asked to predict the number of repetitions of a given axle load that would cause failure. The collected results of these predictions are shown in Fig. 14. There is clearly a wide variation in experiences of the life of a highway pavement in different parts of the country.

10 "Flexible Pavement Design Correlation Study," Bulletin No. 183, Highway Research Board, Washington, D. C., 1956.

There are many factors to be included in such a prediction, and it is not the intent of this paper to infer that the variations in the predictions in Fig. 12(b) are due simply to variations in the stress history of pavements used as a basis for the predictions. However, it seems that experience with older highways on which the magnitude of the wheel loads has been increased gradually over a number of years are likely to be widely different from those on which heavy wheel loads have been imposed soon after construction, and that the latter are likely to fail at a much smaller number of stress applications. This fact alone might be responsible for a substantial difference between the service lives of otherwise similar pavements.

Finally, the test data indicate also the extreme difficulties likely to be encountered in attempts to predict, from the results of soil tests, the deformation of pavements due to erratic sequences of wheel load intensities, the care required in translating experiences with older highways to new pavements which are to be subjected mainly to high wheel load intensities, and the desirability of considering the entire pattern of stress applications if pavements are eventually to be designed on the basis of a limiting deflection with maximum safety and economy.

ACKNOWLEDGMENTS

The authors gratefully acknowledge the assistance of Clarence K. Chan, A. M. ASCE, Lowell Shifley, and Gerald L. Baker who performed some of the tests, and of George Dierking, who prepared the figures.

DISCUSSION

RICHARD G. AHLVIN,[11] F. ASCE.—The writer wishes to call attention to several items from work of the United States Army Engineer Waterways Experiment Station, Vicksburg, Miss., that are related to the paper.

Fig. 15 is taken from a report of tests conducted on airfield pavements at Stockton, Calif., in 1942.[12] It shows a pattern for the 40-kip single-wheel load (curve 1) similar to those in Figs. 6(a), 7(a), and 12(a). Here, however, the measure of distress is in the thickness of failing pavement rather than in axial strain. The break in this curve (point A) is caused by the distribution of test traffic over three adjacent wheel paths, whereas prior traffic (1,600-load repetitions) was in a single wheel path. Curve 2 apparently would have resulted if all load repetitions had been applied in three adjacent wheel paths. The pattern for the 25-kip single-wheel load (curve 3), which is for test traffic in three adjacent wheel paths throughout, indicates that the break in curve 1 would not have occurred if the early traffic had been distributed.

This leads to the question of the build-up of residual stresses in a pavement construction or triaxial specimen. The residual stresses that can be built up

---

11 Engr., Chf., Special Proj. Sect., Flexible Pavement Branch, Soils Div., U. S. Army Engr. Waterways Experiment Sta., Corps of Engrs., Vicksburg, Miss.

12 "Report on Stockton Runway Test Section," Calif. Dept. of Public Works, Div. of Highways, September, 1942.

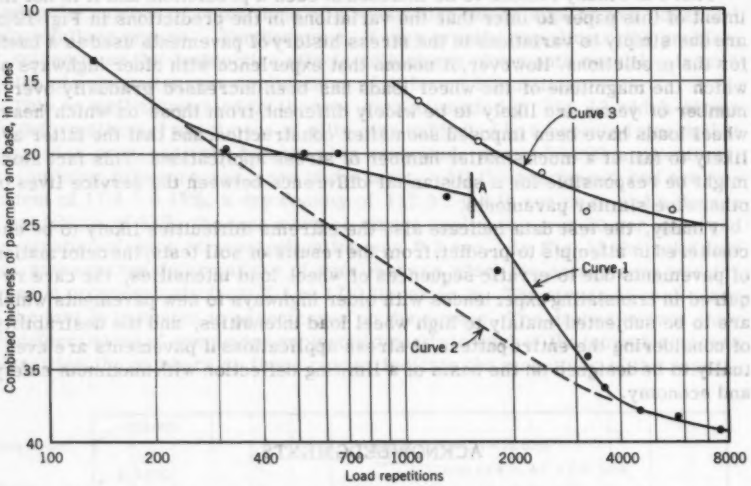


FIG. 15.—DEVELOPMENT OF FAILURE IN AN ACCELERATED TRAFFIC TEST SECTION

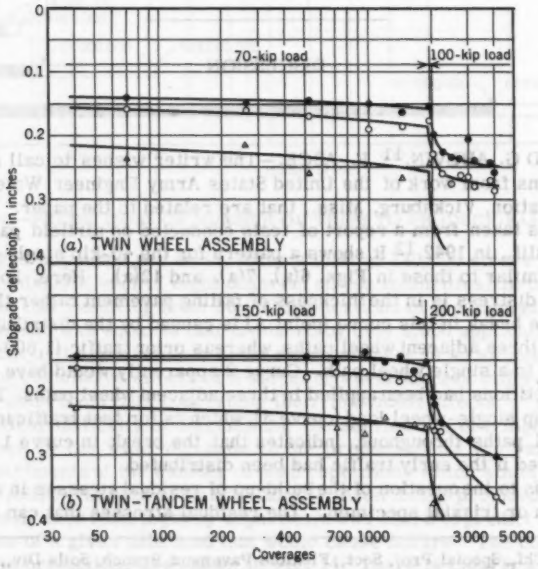


FIG. 16.—SUBGRADE DEFLECTION IN AN ACCELERATED TRAFFIC TEST SECTION

by repeated application of a single stress pattern and that lend strength to the construction or specimen can be destroyed by a reversal of stresses. This phenomenon should be considered in studies of this nature.

Fig. 16 shows field data comparable to the test data presented in the paper. These data are from a report of tests conducted in 1949 and 1950.[13] A test section consisting of three items of various strengths, all on medium-strength clay-silt subgrade, was subjected to loading by twin wheels in one lane and tandem wheels in another. In each case, 2,000 coverages of one loading were applied, followed by 2,000 coverages of a significantly heavier loading. A coverage consists of wheel passes in immediately adjacent paths, sufficient to cover the lane being trafficked. Unfortunately, no comparable data are available for a test in which the larger loading might have been applied with no prior lighter load traffic. However, failures experienced in these test items under the heavier loadings, rather than showing more strength than expected, indicated that projections made from the pattern of previously proved design criteria were somewhat unconservative.

Lastly, the writer wishes to refer to some triaxial testing conducted on a fine, uniform, dry sand in which the specimen was loaded repeatedly. Cycles of loading were 50 or less, rather than the thousands of load repetitions reported by the authors. However, just as the work reported for sands, the results show that successive applications of loading increased the stiffness of the specimen but had no significant effect on its ultimate strength.

D. HUGH TROLLOPE,[14] M. ASCE.—In the present study two factors in particular emerge. First, repeated load applications can, under appropriate conditions, affect considerably the stress-strain properties of the soil, and, second, that intensive research is necessary to evaluate the resulting behavior. It is interesting to note that for the tests described, the induced structural effects diminish with an increasing initial degree of saturation. It is likely that a significant factor in this behavior is the reduction of effective compressibility of the pore fluid with increasing water content. At high degrees of saturation at least a part of the applied deviator stress would be absorbed in a build-up of pore pressures, thus limiting the effectiveness of the contribution of the repeated loading to structural change.

In eliminating the possibility of the observed changes being due to over-all densification of the specimens the authors have drawn attention to the influence of the microstructure on this behavior. It has occurred to the writer that if the observed stiffening could be attributed to physical changes in a relatively small zone of potential failure within the specimens, then this would influence the interpretation of the results to highway performance.

Consider the case of a load applied repeatedly to highway subgrade through a wheel of tire width b. The inference that could be drawn from these tests is that the zone of failure corresponding to this tire width would be reinforced by repeated load application (Fig. 17). The maximum depth of increased soil strength due to loaded area b is represented by y. If now a tire of width b_1 ($> b$) but of the same contact pressure is passed over the subgrade, this load

---

13 "Design of Flexible Airfield Pavements for Multiple-Wheel Landing Gear Assemblies: Test Section with Lean Clay Subgrade," Technical Memorandum No. 3-349, Report No. 1, U. S. Army Engr. Waterways Experiment Sta., Corps of Engrs., Vicksburg, Miss., September, 1952.

14 Reader in Civ. Engrg., Univ. of Melbourne, Victoria, Australia.

would create shear stresses in a zone not previously improved by the passing of tire with width b. This does not invalidate the authors' conclusions concerning the importance of both magnitude and number of repetitions in assessing the effect of repeated loading, but rather indicates that under certain conditions the width of the loaded area (tire width) may be an important additional variable.

Despite objections by D. P. Krynine,[15] it is clear that carefully controlled laboratory investigations of this type are by far the most important tool in the

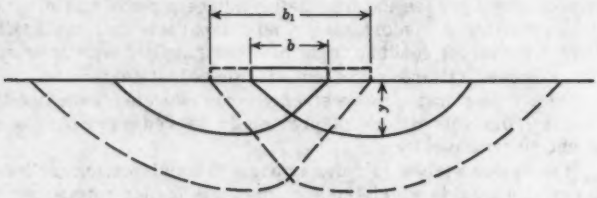


FIG. 17.—LOAD REPEATEDLY APPLIED TO A HIGHWAY SUBGRADE

task of rationalizing the art of pavement design. Systematic field observation can be expected only after the relative influence of the principal variables has been accomplished, and this has certainly not been done in many aspects of soil engineering, particularly in pavement engineering. Experience should surely have taught us that skilled laboratory investigation is the most economical way of handling such problems.

In conclusion the writer thanks the authors for a most interesting and valuable contribution.

H. BOLTON SEED,[16] M. ASCE, ROBERT L. McNEILL,[17] A. M. ASCE, and JACQUES DeGUENIN.[18]—The data reported by Mr. Ahlvin in Fig. 15 indicate clearly that stress repetitions on a single wheel path induced a stiffening of the soil similar to that reported in the paper. However, stress repetitions on adjacent wheel paths apparently destroyed the cause of the stiffening. The writers agree that this effect requires careful consideration in extrapolating the results of laboratory triaxial compression tests to actual field conditions. They are inclined to believe that the permanence of the stiffening effect under these conditions may well depend largely on the magnitude of the deformations induced by the wheel loads. When the deformations are large, the stiffening effect will be destroyed (in manner similar to that shown in Fig. 12(a)), but if the deformations resulting from wheel load applications in adjacent paths are small, the stiffening effect may remain.

Similar considerations apply to the test data reported by Mr. Ahlvin in Fig. 16. Here again the increases in stress (between 30% and 50%) may have been

---

[15] Discussion by D. P. Krynine of "Thixotropic Characteristics of Compacted Clays," by H. B. Seed and C. K. Chan, Transactions, ASCE, Vol., 124, 1959, pp. 917-923.

[16] Assoc. Prof. of Civ. Engrg., Univ. of California, Berkeley, Calif.

[17] Engr., Woodward, Clyde and Assocs., Oakland, Calif.

[18] At present, in the French Armed Services; formerly Graduate Research Engr., Inst. of Transp. and Traffic Engrg., Univ. of California, Berkeley, Calif.

great enough that any stiffening effect induced by the initial stress repetitions was destroyed (Fig. 12(a)). However, it is also doubtful whether the 2,000 repetitions of the lower wheel loads would induce any appreciable stiffening of the soil in these tests. The writers' experiences show that 10,000 or more stress repetitions are usually required before any appreciable stiffening effect is produced.

Mr. Trollope's observations on the influence of the tire width on the depth of soil in which an increased resistance to deformation might be developed show another factor requiring careful consideration in assessing the influence of laboratory test results in actual pavement performance.

The great complexity of any analysis of pavement behavior is no doubt responsible for the largely empirical methods of design currently in use. However, even if suitable analytical procedures cannot be developed in the foreseeable future, it is the authors belief that clarification and examination of all of the factors involved will undoubtedly lead to better understanding and to improvements in design methods.

AMERICAN SOCIETY OF CIVIL ENGINEERS

Founded November 5, 1852

TRANSACTIONS

Paper No. 3019

DISTRIBUTION OF SEDIMENT IN LARGE RESERVOIRS

By Whitney M. Borland,[1] M. ASCE and Carl R. Miller,[2] M. ASCE

SYNOPSIS

In planning and developing multipurpose reservoirs it is necessary to make an allocation of storage space for sediment accumulation. This sediment accumulation, in turn, influences the design of the dam because of its effect on active storage capacity requirements, outlet sill elevations, recreational facilities, and backwater conditions. Therefore, it is necessary to predict the probable distribution of the sediment in the reservoir with time.

Two methods of predicting the probable sediment distribution are given and an example shown. One method is basically mathematical (area-increment method), whereas the other is a mathematical procedure developed on the basis of actual experiences (empirical area-reduction method). The area in which additional study is needed to evolve procedures that will give consistently reliable predictions of sediment distribution under varying conditions is described.

INTRODUCTION

When a dam is constructed to store water for useful purposes, sediment being transported by the water is unfortunately also stored. Unlike water, the sediment cannot be effectively released through the reservoir or put to useful purposes. In most cases, it is inevitable that the useful storage capacity behind a dam will be reduced in time by sediment accumulation until replacement storage is necessary. In many countries reservoirs constructed years ago have become completely filled with sediment deposits rendering them practically useless. Because most large reservoirs in this country are relatively new, only a small number have yet been substantially reduced in capacity.

Note.—Published, essentially as printed here, in April, 1958, in the Journal of the Hydraulics Division, as Proceedings Paper 1587. Positions and titles given are those in effect when the paper was approved for publication in Transactions.

[1] Head, Sedimentation Sect., U. S. Bur. of Reclam., Denver, Colo.

[2] Hydr. Engr., Leader, Channel Stability Investigation, Watershed Tech. Research Branch, Agric. Research Sta., Beltsville, Md.

However, future generations will be faced with replacing storage capacity lost to sediment in our major reservoirs. Replacement of many reservoirs may not be easy because the most economical reservoir sites are currently being used. Removal of sediment from a reservoir by mechanical means is not economically feasible at present, but increases in the value of an acre-foot of water may change this. Various methods have been suggested and tried for removing, reducing, or bypassing sediments. Although none has yet supplied us with a solution, particularly in large reservoirs, perhaps some day when the need becomes acute a method will be evolved. Of course, the economic value of a reservoir may become less with new methods of power production and water supply.

THE PROBLEM

In present day analysis planners seldom look beyond one or two generations in determining the water supply to be provided by a structure. Often the structure size is dictated by available water supply and economical considerations. Indeed, the pay-out period on all projects built by agencies such as the United States Bureau of Reclamation (USBR) is usually less than 100 yr. However, in planning the storage allocations it is the Bureau's policy to provide for 100 yr of sedimentation unless it can be demonstrated by economic analysis that a lesser allotment is justified.

At one time it was believed that sediment always deposited in the bottom elevations of a reservoir rather than depositing throughout the full range of reservoir depth. It is now fully realized that sediment deposits will spread throughout the reservoir, reducing the incremental capacity at all elevations. Factors that influence the mode of deposition include:

1. Reservoir shape
2. Sediment characteristics
3. Reservoir operation
4. Sediment-reservoir volume ratio
5. Inflow-capacity relationship

Fig. 1 shows reservoirs under various sedimentation conditions. In Fig. 1(a) the reservoir is under initial conditions with no sediment deposited. Fig. 1(b) shows the reservoir partially filled with sediment of dominantly coarse particle sizes and normally full of water. The reservoir in Fig. 1(c) is partially filled with sediment of dominantly silt and fine sand particle sizes and normally moderate reservoir drawdown. In Fig. 1(d) the reservoir is partially filled with sediment of dominantly silt and clay particle sizes and there is considerable reservoir drawdown. Fig. 1(e) shows the reservoir filled with sediment, and at this stage, trap efficiency becomes zero and remaining available storage is maintained by sluicing at outlets. There are other factors, of course, such as salt cedar infestation and amount and location of tributary inflow within the reservoir, but these factors, when existing, require special considerations.

Of immediate concern in planning and designing a dam and reservoir is the effect of sediment accumulation on design considerations. Major design considerations include:

1. Elevation to which sediment will accumulate at the dam in a given period of time. This information will affect the design elevation of the river outlet

and power penstock sills. Sometimes an adjustable stoplog-type trashrack arrangement is used that provides flexibility in the outlet elevation to allow complete use of the water storage at all times. Stoplogs are added as the sediment accumulates.

2. Reduction of active storage capacity. If this loss can be predicted the structure height can be set to provide the required water supply storage. Often, the effect of sediment accumulation on the water supply is evaluated through the operation studies.

3. Deposits of sediment in the upper reaches of the reservoir.[3] These deposits can result in a significant increase in the water surface elevations upstream. This will, in turn, endanger upstream installations and developments, particularly during periods of high water inflow. The dangerous condition results because the reservoir water surface is usually high when the inflowing stream is at flood stage. This condition must be considered in the designs.

4. Effect on recreational developments around the reservoir. The sediment deposits could influence the location of such facilities, especially when

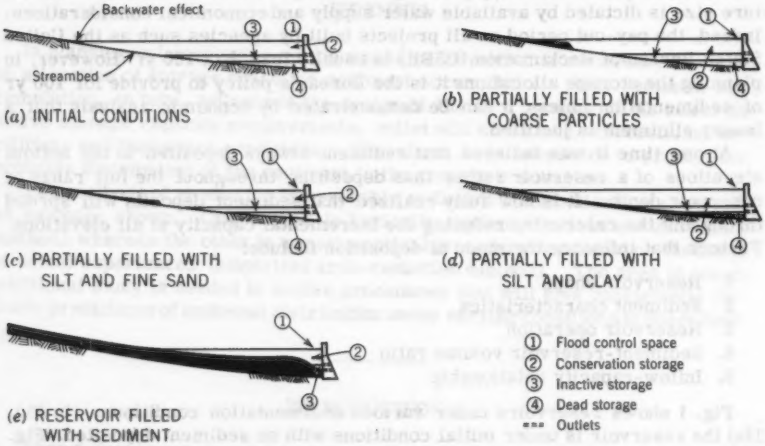


FIG. 1.—RESERVOIRS UNDER VARIOUS SEDIMENTATION CONDITIONS

the reservoir is one that will have considerable drawdown exposing sediment deposits.

5. Reservoir planned solely for sediment accumulation. In this case the probable sediment accumulation is of primary importance. A considerable portion of the total sediment stored may be above crest elevation of the reservoir.

---

[3] "Report on Reservoir Delta Reconnaissance," by Donald C. Bondurant, Sediment Series No. 6, Missouri River Basin Div., Corps of Engrs., U. S. Army, Omaha, Nebr., June, 1955.

Therefore, it is evident that estimating only the amount of sediment inflow to a reservoir is not sufficient. How and where this sediment will deposit must be predicted.

METHODS FOR PREDICTING SEDIMENT DISTRIBUTION

Two methods that can be used in predicting the manner in which sediment will be distributed will now be presented. The first method, which is strictly mathematical, is known as the area-increment method, and was developed by Eugene A. Cristofano.[4] The second method, a mathematical procedure developed on the basis of actual occurrences in large reservoirs, is identified herein as the empirical area-reduction method.[5] Both procedures involve the adjustment of the original surface areas to reflect the decrease in area with

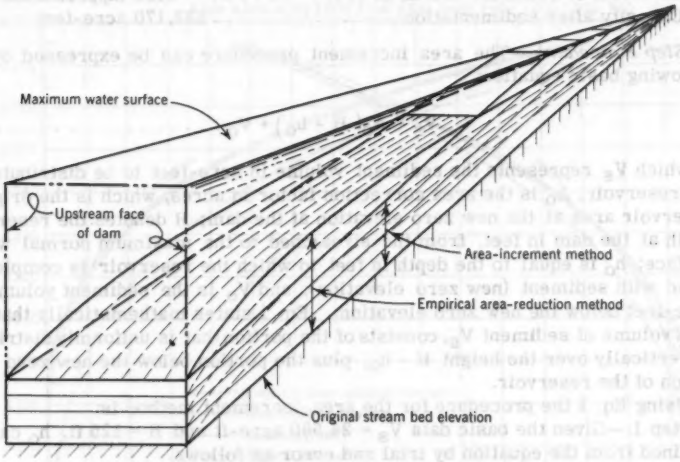


FIG. 2.—COMPARISON OF THE EMPIRICAL AREA-REDUCTION AND THE AREA-INCREMENT METHODS.

sedimentation. Fig. 2 shows a comparison of the empirical area-reduction and the area-increment methods of predicting distribution of sediment in a reservoir.

AREA INCREMENT METHOD

The area increment procedure is based on the assumption that the sediment deposition in a reservoir can be approximated by reducing the reservoir area at each reservoir elevation by a fixed amount. This involves a series of approximations. By using the average end area or prismoidal formulas, the reservoir capacities are computed on the basis of reduced surface areas until the total reservoir capacity below maximum normal water surface is essentially the same as the predetermined capacity obtained by subtracting the sediment accumulation with time from the original capacity. Using Alamogordo

4 "Area Increment Method for Distributing Sediment in a Reservoir," by Eugene A. Cristofano, Area Planning Off., U. S. Bur. of Reclam., Albuquerque, N. Mex., Sept., 1953.

5 "Interim Report Distribution of Sediment in Reservoirs," by Div. of Proj. Investigations, Hydrology Branch, U. S. Bur. of Reclam., Denver, Colo., June, 1954.

Reservoir on the Pecos River in New Mexico[6] as an example, the step procedure for the area-increment method is as follows. The procedure shown is an adaptation developed by W. T. Moody.[7] The basic information for Alamogordo Reservoir as obtained in the 1944 resurvey is:

Stream-bed elevation at dam	4150
Maximum water surface elevation	4275
Spillway crest elevation	4275
Original reservoir depth at dam	125 feet
Original capacity at elevation 4275	156,750 acre-feet
Annual sediment inflow	3600 acre-feet
Period of sedimentation	6.8 years
Sediment accumulation	24,580 acre-feet
Elevation of sediment at dam in 1944	4190 (approximately)
Capacity after sedimentation	132,170 acre-feet

Step Procedure.—The area increment procedure can be expressed by the following basic equation:

$$V_S = A_O(H - h_O) + V_O \quad \ldots\ldots\ldots\ldots\ldots\ldots \quad (1)$$

in which V_S represents the sediment volume in acre-feet to be distributed in the reservoir; A_O is the area correction factor in acres, which is the original reservoir area at the new zero elevation at the dam; H denotes the reservoir depth at the dam in feet, from the streambed to the maximum normal water surface; h_O is equal to the depth in feet to which the reservoir is completely filled with sediment (new zero elevation); and V_O is the sediment volume in acre-feet below the new zero elevation. Eq. 1 states mathematically that the total volume of sediment V_S, consists of the portion that is uniformly distributed vertically over the height $H - h_O$, plus the portion below the new zero elevation of the reservoir.

Using Eq. 1 the procedure for the area-increment method is:

Step 1.—Given the basic data V_S = 24,580 acre-ft and H = 125 ft, h_O can be obtained from the equation by trial and error as follows.

The terms V_O, h_O, and A_O are obtained by assuming h_O and reading V_O and A_O from the original area-capacity curves in Fig. 3 at that indicated elevation.

First trial: Assuming h_O = 25 ft, then A_O = 150 acres, V_O = 1,600 acre-ft, and

$$24{,}580 = 150\ (125 - 25) + 1{,}600 \neq 16{,}600.$$

Second trial: Assuming h_O = 34 ft then A_O = 235 acres, V_O = 3,300 acre-ft, and

$$24{,}580 = [235\ (125 - 34) + 3{,}300] \approx 24{,}680.$$

The new zero elevation at the dam is 4150 + 34 = 4184, and the area correction factor is equal to 235 acres.

---

[6] "Resurvey of Alamogordo Reservoir," U. S. Corps of Engrs., Albuquerque Office, Albuquerque, N. Mex., April, 1944.

[7] "Review of Area Increment Method for Distributing Sediment in a Reservoir," by William T. Moody, Exp. Design Analysis Sec., U. S. Bur. of Reclam., Denver, Colo., June, 1954.

Step 2.—Compute the accumulative sediment volume by the average end-area formula (Table 1, Column 5) by applying the area correction factor at each depth increment (Column 4). The computed volume should check the predetermined sediment volume within 1%.

Step 3.—Reduce the original areas at each increment by the area correction factor of 235 acres to give the revised area in Table 1 (Column 6 = Column 2 - Column 4).

Step 4.—Determine the revised capacity in Table 1, Column 7 by reducing the original capacity at each increment by the sediment accumulation (Column 7 = Column 3 - Column 5).

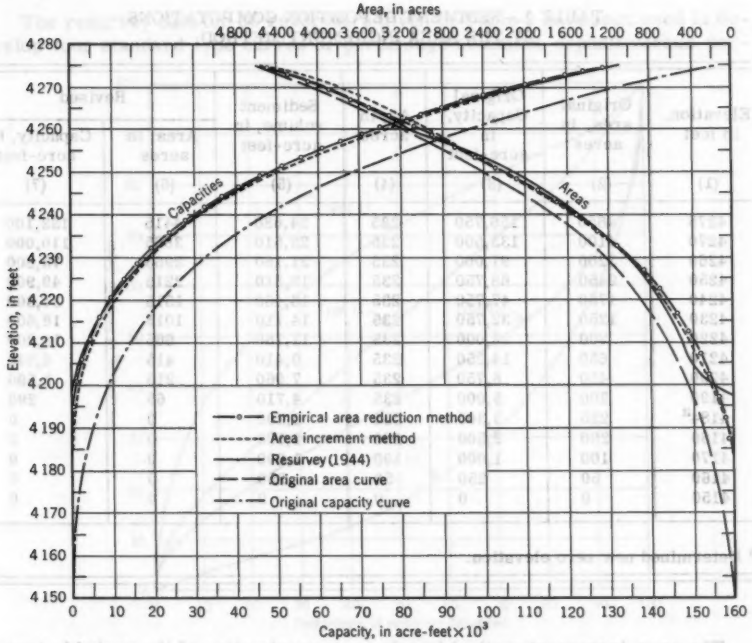


FIG. 3.—AREA-CAPACITY CURVES.

The results obtained are compared with the actual resurvey curves in Fig. 3.

The basic equation for this method is useful in making a quick estimate of the depth of sediment at a dam over a given time period. By referring to the original area-capacity curves and by knowing the amount of sediment that will accumulate in x years, with a few approximations the equation can be balanced, and thereby the height to which sediment will accumulate at the dam may be derived. Once this is established, the area reduction can readily be applied at each interval of depth up to maximum normal water surface, and the probable area-capacity curves after sedimentation can be determined.

It should be noted that there is no smooth reduction in area from the original to the revised condition between maximum normal water surface and the next increment above it in the flood control pool. This can be corrected, if desired, by allowing some sediment to deposit above maximum normal water surface and by making the area correction factor progressively smaller, starting a few intervals below the maximum normal water surface elevation and extending a few intervals above. The surface area for the before and after condition should be the same at the uppermost elevation. Some additional trial and error will be necessary to get the computed sediment volume to equal the predetermined volume.

TABLE 1.—SEDIMENT DEPOSITION COMPUTATIONS BY THE AREA INCREMENT METHOD

Elevation, in feet	Original area, in acres	Original Capacity, in acre-feet	A_o, in acres	Sediment volume, in acre-feet	Revised	
					Area, in acres	Capacity, in acre-feet
(1)	(2)	(3)	(4)	(5)	(6)	(7)
4275	4650	156,750	235	24,680	4415	132,100
4270	4100	133,500	235	23,510	3865	110,000
4260	3200	97,000	235	21,160	2965	75,800
4250	2450	68,750	235	18,810	2215	49,900
4240	1750	47,750	235	16,460	1515	31,300
4230	1250	32,750	235	14,110	1015	18,600
4220	900	22,000	235	11,760	665	10,200
4210	650	14,250	235	9,410	415	4,840
4200	450	8,750	235	7,060	215	1,690
4190	300	5,000	235	4,710	65	290
4184[a]	235	3,300	235	3,300	0	0
4180	200	2,500	200	2,500	0	0
4170	100	1,000	100	1,000	0	0
4160	50	250	50	250	0	0
4150	0	0	0	0	0	0

[a] Determined new zero elevation.

The area-increment method is only an approximation of the probable location of the sediment deposits. It is known that sediment does not generally reduce the surface areas by the same amount at every elevation. However, comparisons have been made between the results obtained by this method and the actual resurvey results, and good agreement has been obtained in most cases. It should be noted that the applicability of the method decreases with an increase in the ratio of volume of sediment to capacity. Also, the accuracy decreases with any deviation of the reservoir in question from a more or less standard type. Usually the arbitrary stipulation is that if the 100-yr sediment accumulation exceeds 15% of the original capacity, a more exacting method of dis-

tributing the sediment should be applied. In any case, the area-increment method is a good first-check procedure for determining the probable sediment distribution.

EMPIRICAL AREA-REDUCTION METHOD

The empirical area-reduction method for determining the probable sediment distribution is accomplished through two main steps:

1. Classify the reservoir using four basic, standard-type curves that were developed from actual resurvey data.
2. Make a trial and error type computation using the average end area or prismoidal formulas until the capacity computed equals the predetermined capacity.

The resurvey data for 30 reservoirs given in Table 2 have been used to develop four standard type curves of percentage sediment deposit versus percentage reservoir depth shown in Fig. 4. The reservoirs included in establishing the four standard types vary widely in location, type operation, and sediment characteristics. Capacities range from 40,000 to 30,000,000 acre-ft, with a few exceptions. The depth is based on the difference between streambed elevation at the dam (zero capacity) and elevation at maximum normal water surface. The general classification resulting from the analysis of the data from the 30 reservoirs is as follows:

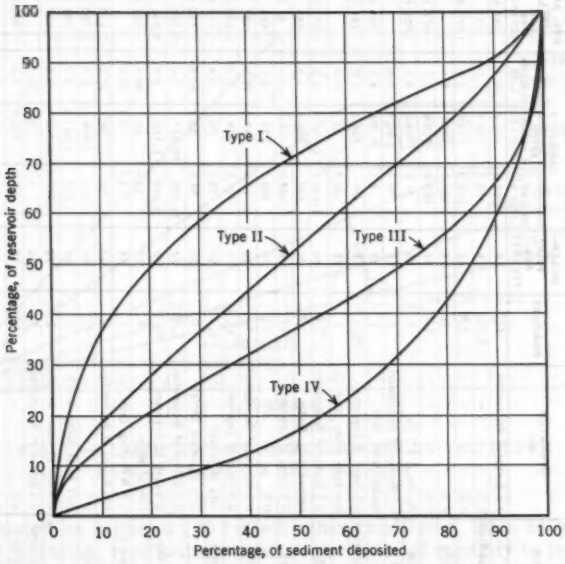


FIG. 4.—TYPE CURVES

Value of M	Reservoir type	Standard classification
1.0-1.5	Gorge	IV
1.5-2.5	Hill	III
2.5-3.5	Flood plain-foothill	II
3.5-4.5	Lake	I

TABLE 2.—RESERVOIRS USED IN ESTABLISHING STANDARD TYPE CURVES.

RESERVOIR	TYPE	LOCATION	STREAM	OPERATED BY	** PURPOSE	RESERVOIR AGE (YEARS)	CAPACITY			AVG. ANNUAL INFLOW		CAPACITY INFLOW	DAM HEIGHT (SPILLWAY CREST) (FT.)	RESERVOIR AREA (ACRES)	DRAINAGE AREA (SQ. MI.)
							ORIGINAL (1000 AF)	AFTER X YEARS (1000 AF)	PERCENT LOSS	LONG TIME (1000 AF)	PD OF SED. (YRS.)				
Alamogordo	II	New Mexico	Pecos	U.S Bureau of Reclamation	FC,I	20	156.8	132.2	15.7	196.4	7	0.803	132	4,650	4,393
Altus	II	Oklahoma	No. Fork Red River	U.S. " " "	D,FC,I	14	156.7	148.6	5.1	127	7	1.234	85	6,793	2,560
Arrowrock	III	Idaho	Boise	U.S. " " "	I,FC	42	279.2	271.6	2.8	1,572.5	32	0.178	255	3,089	2,170
Belle Fourche	II	South Dakota	Belle Fourche	U.S. " " "	I	54	208.8	192	8.1				78	8,040	4,480
Buffalo Bill	I	Wyoming	Shoshone	U.S. " " "	I,P	47	455.8	439.8	3.5	979.5	31	0.466	233	6,711	1,470
Bullards Bar	III	California	North Yuba	Pacific G.& E. Co.	P	38	31.5	28.9	8.3	1,058.6	20	0.0295	175	500	400
Cold Springs	II	Oregon	Fee Canal	U.S.Bureau of Reclamation	I	49	55.3	50.3	9.1				85	1,550	
Combie	I	California	Bear	Nevada Irrig. Dist.	I	29	8.6	7.8	8.3	204.6	7	0.0418	69	338	130
Conchas	I	New Mexico	Conchas Canadian	U.S. Corps of Engineers	FC,I,P	18	601	566.2	5.8	266.5	10	2.253	178	13,552	7,350
Cucharas	I	Colorado	Cucharas	Huerfano Valley Ditch Co.	I	45	38.3	23	39.8		27			1,349	608
Elephant Butte	I	New Mexico	Rio Grande	U.S.Bureau of Reclamation	I,P	40	2,634.8	2,197.6	16.6	1,077.6	32	2.445	193	37,848	25,923
Exchequer	III	California	Merced	Merced Irrig. Dist.	I,P	31	289	285.6	1.2	989	20	0.292	302	2,939	1,027
Fort Supply	III	Oklahoma	Wolf Creek	U.S.Corps of Engineers	FC	16	107.3	106.1	1.1	61.5	8	1.745	48	7,282	1,735
Great Salt Plains	I	Oklahoma	Salt Fork	U.S. " " "	FC	16	308	292	5.1	424	8	0.726	38	38,600	3,200
Guernsey	I	Wyoming	North Platte	U.S.Bureau of Reclamation	I,P	30	73.8	49.2	33.4	1195	20	0.068	91	2,329	16,200
John Martin	IV	Colorado	Arkansas	U.S.Corps of Engineers	FC,I	15	701.2	675.1	3.73	453.2	6	1.546	110	30,252	18,933
Lake Cheesman	I	Colorado	South Platte	City of Denver	D,FC	56	79.1	78	1.4	140.8	31	0.562	212	874	1,766
Lake Corpus Christi	I	Texas	Nueces	City of Corpus Christi	D	23	54.4	39.4	27.6	730.4	14	0.0745	46	5,493	16,800
Lake Mead	II	Arizona, Nevada	Colorado	U.S.Bureau of Reclamation	I,P,FC	22	31,250	29,827	4.6	13,200	12	2.368	571	158,000	167,800
Lake Texoma	II	Oklahoma	Washita, Red	U.S.Corp of Engineers	FC,P	15	5,659	5,720	2.4	4,531	6	1.176	130	286,524	38,291
Lake Waco	III	Texas	Bosque	City of Waco	D	27	39.4	22	44.1	407.2	17	0.0967	44	2,801	1,666
Little Rock	II	California	Little Rock Cr.	L.R.& P. Irrig. Dist. 1/	I	33	4.2	3.4	20.5		22		101	94	68
Mc Millan	II	New Mexico	Pecos	U.S.Bureau of Reclamation	I	63	91	38.7	57.5	273.5	46	0.333	32	5,400	16,985
Pathfinder	III	Wyoming	North Platte	U.S. " " "	P,I	48	1,056	1,016	3.8	1,350.5	41	0.782	184	22,600	10,700
Roosevelt	II	Arizona	Salt	Salt River Valley W.U.A.	D	50	1,522	1,381.6	9.2	793.7	39	1.918	235	17,280	5,670
San Carlos	III	Arizona	Gila	U.S.Bur. of Indian Affairs	I	29	1,267.4	1,210	4.5	255.1	19	4.97	215	19,581	12,900
Santa Anita	II	Montana	High Line Canal	U.S.Bureau of Reclamation	I	20	1.1	0.8	30				30		
Seminoe	I	Wyoming	North Platte	U.S. " " "	P,I	18	722.0	712.9	1.0	906.8	11	1.131	195	15,280	7,348
Stony Gorge	II	California	Stony Creek	U.S. " " "	I	29	48.9	48.2	1.4	176.9	17	0.285	114	1,275	199
Tongue River	II	Montana, Wyoming	Tongue	Montana State W.C. Board	FC,I	18	72.5	69.4	4.2	310	9	0.234	72	3,497	1,740

** D = Domestic water FC = Flood Control I = Irrigation P = Power

1/ Little Rock and Palmdale Irrigation District

The term M is the reciprocal of the slope n of the line obtained by plotting reservoir depth as ordinate, against reservoir capacity as abscissa, on log-log paper, as indicated in Fig. 5. It should be noted that a lake type does not necessarily have to be out on the plains nor does a gorge type have to be in the mountains. The gorge type (IV) is the poorest defined of the four classifications.

In applying the standard type curves to a proposed reservoir, it is first necessary to determine the type that fits the reservoir involved. First selection of type is obtained by plotting depth versus initial reservoir capacity on log-log paper (Fig. 5). This usually gives a straight line relationship or in some cases two straight lines.[8] The slope of the line, or lines, gives an indication of the type. Generally a curve showing rapid increase in capacity with depth indicates a large basin-type reservoir, whereas a small increase in capacity with depth indicates a gorge-type reservoir. This information classifies the reservoir according to shape. The standard-type curve can then be select-

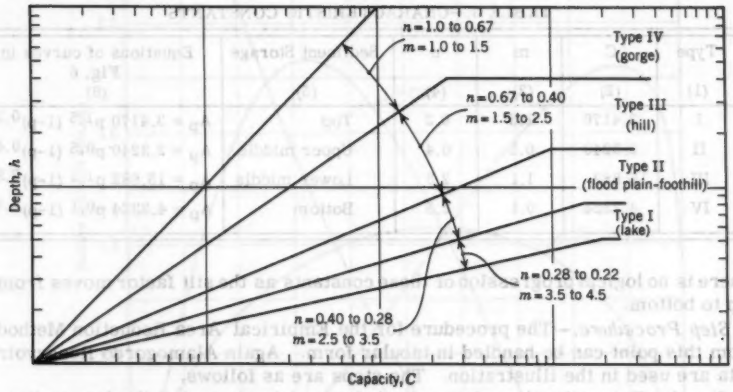


FIG. 5.—CLASSIFICATION OF RESERVOIRS BY THE DEPTH VERSUS CAPACITY RELATIONSHIP

ed and adjusted as necessary to reflect other conditions, such as anticipated reservoir operation, type sediment inflow, or ratio of capacity to inflow. The type curve of percentage depth versus percentage sediment deposit finally adopted may be a combination of two types or could fall in between two of the four basin types, but generally one of the four basic types will fit the conditions involved. It can be seen that considerable judgment is sometimes involved in making this selection.

Having selected a type sediment deposit curve the remainder of the procedure is mathematical. The four standard type sediment-versus-depth curves have been converted to area design curves in Fig. 6 for use in the computations. The area design curves have relative sediment storage as the ordinate, and

[8] "Functional Design of Flood Control Reservoirs," by C. J. Posey and Fu-Te I, Transactions, ASCE, Vol. 105, 1940, pp. 1638-1647.

relative depth as the abscissa. The area under the curve in each case equals unity. Other curves can be produced as long as the area under the curve is unity. The conversion from the standard type sediment deposit curves to the area design curves has been made by Moody by applying Eq. 2.

$$A_p = C\, p^m (1-p)^n \quad \ldots\ldots\ldots\ldots\ldots\ldots \quad (2)$$

in which A_p represents a dimensionless relative area at a relative distance p above the streambed and C, m, and n are dimensionless constants determined by the type of reservoir. Numerical values of m, and n, were computed by trial and error using a least square procedure to make the analytical curve the best possible fit to the field survey data. With m and n determined, C is fixed by the consideration that the total area under the A_p curve must be unity. The characteristic constants C, m, and n determined for the four types of reservoirs are given in Table 3.

TABLE 3.—CHARACTERISTIC CONSTANTS

Type	C	m	n	Sediment Storage	Equations of curves in Fig. 6
(1)	(2)	(3)	(4)	(5)	(6)
I	3.4170	1.5	0.2	Top	$A_p = 3.4170\, p^{1.5} (1-p)^{0.2}$
II	2.3240	0.5	0.4	Upper middle	$A_p = 2.3240\, p^{0.5} (1-p)^{0.4}$
III	15.882	1.1	2.3	Lower middle	$A_p = 15.882\, p^{1.1} (1-p)^{2.3}$
IV	4.2324	0.1	2.5	Bottom	$A_p = 4.2324\, p^{0.1} (1-p)^{2.5}$

There is no logical progression of these constants as the silt factor moves from top to bottom.

Step Procedure.—The procedure for the Empirical Area Reduction Method from this point can be handled in tabular form. Again Alamogordo Reservoir data are used in the illustration. The steps are as follows.

Step 1.—Determine the relative depth for each increment at the dam as listed in Table 4, Column 4. This is merely the ratio of the incremental depth to the total depth (maximum normal water surface to streambed—El. 4275 to 4150). This is determined from values in Table 4, Column 1.

Step 2.—Determine values of relative sediment area A_p from Fig. 6 after the standard type curve has been selected from Fig. 4. For Alamogordo a type II has been determined. Enter the curve in Fig. 6 with relative depth for each increment and read corresponding A_p values. These have been listed in Table 4, Column 5.

Step 3.—Select a first approximation of the probable sediment elevation at the dam after sedimentation. Areas at and below this elevation will equal areas in Column 2. Sediment areas for each depth increment above the estimated new zero elevation are obtained by dividing the original area at zero elevation (Column 2) by the corresponding A_p value (Column 5) and multiplying this ratio (K) by the A_p values at each succeeding increment. For example, referring to Table 4: Assuming zero elevation of 4190, the surface area A_s = 300 acres, and A_p at El. 4190 = 1.125, therefore

$$K = \frac{300}{1.125} = 266.7$$

The new area at each succeeding elevation is the A_p at that elevation multiplied by 266.7.

Step 4.—With the sediment areas established (Column 6) the incremental sediment volumes can be computed by the average end-area formula and entered in Column 7. Columns 6 and 7 represent the first approximation. If the sediment volume summation in Column 7 exceeds or is less than that desired

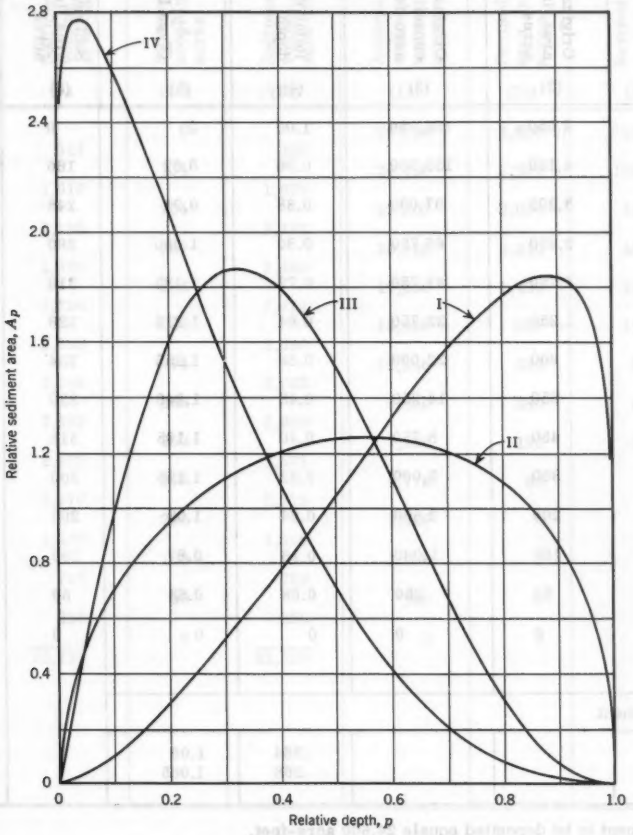


FIG. 6.—AREA DESIGN CURVES.

a second approximation is made. Second and third approximations are shown in Columns 8 through 11. Note that the new zero elevation may not occur at an even contour interval. In the example shown, the new zero elevation is 4183.5. When making the evaluation at odd increments the original area capacity curves (Fig. 3) and Fig. 6 are referred to.

TABLE 4.—SEDIMENT DEPOSITION BY THE

Elevation, in feet	Original area, in acres	Original capacity, in acre-feet	Relative depth	A_p (Type II)	First Trial	
					Sediment area, in acres	Sediment volume, in acre-feet
(1)	(2)	(3)	(4)	(5)	(6)	(7)
4275	4,650	156,750	1.00	0	0	
						415
4270	4,100	133,500	0.96	0.62	166	
						2,070
4260	3,200	97,000	0.88	0.93	248	
						2,690
4250	2,450	68,750	0.80	1.090	290	
						3,030
4240	1,750	47,750	0.72	1.185	316	
						3,220
4230	1,250	32,750	0.64	1.235	328	
						3,310
4220	900	22,000	0.56	1.255	334	
						3,320
4210	650	14,250	0.48	1.240	330	
						3,240
4200	450	8,750	0.40	1.195	318	
						3,090
4190	300	5,000	0.32	1.125	300	
						2,500
4180	200	2,500	0.24	1.02	200	
						1,500
4170	100	1,000	0.16	0.87	100	
						750
4160	50	250	0.08	0.63	50	
						250
4150	0	0	0	0	0	
						29,385
Supplement						
4183			.264	1.06		
4183.5			.268	1.065		

[a] Sediment to be deposited equals 24,600 acre-feet.

Step 5.—Accumulate the sediment volumes shown in Column 11 and enter them in Column 12.

Step 6.—Determine the revised areas for after sedimentation (Column 13 = Column 2 - Column 10).

Step 7.—Determine the revised capacities (Column 14 = Column 3 - Column 12).

EMPIRICAL AREA REDUCTION METHOD[a]

Second Trial		Third Trial				
Sediment area, in acres	Sediment volume, in acre-feet	Sediment area, in acres	Sediment volume, in acre-feet	Accumulated sediment volume, in acre-feet	Revised area, in acres	Revised capacity, in acre-feet
(8)	(9)	(10)	(11)	(12)	(13)	(14)
0		0		24,515	4,650	132,200
	322		335			
129		134		24,180	3,970	109,300
	1,615		1,675			
194		201		22,505	3,000	74,500
	2,105		2,190			
227		237		20,315	2,210	48,440
	2,370		2,465			
247		256		17,850	1,490	29,900
	2,520		2,615			
257		267		15,235	980	17,520
	2,590		2,690			
261		271		12,545	630	9,460
	2,595		2,695			
258		268		9,850	380	4,400
	2,535		2,630			
249		258		7,220	190	1,530
	2,415		2,505			
234		243		4,715	60	285
	2,170		2,215			
200		200		2,500	0	0
	1,500		1,500			
100		100		1,000	0	0
	750		750			
50		50		250	0	0
	250		250			
0		0		0	0	0
	23,737		24,515			

Usually two or three trials are all that are necessary to obtain the desired balance. If the summed volume is within 1% of the predetermined volume, sufficient accuracy has been attained.

There are several advantages to the empirical area-reduction method. It permits the classification of a proposed reservoir into a standard type that

immediately gives an indication of the manner in which the sediment will distribute. A portion of the sediment can readily be deposited above maximum normal water surface (flood control space) in the computations by selecting a top elevation above maximum normal water surface in determining relative depths. In a large reservoir the sediment deposits above maximum normal water surface will seldom exceed 10% of the total in a 50-yr to 100-yr period, except in those dams that are for sediment retention only. The method gives a good approximation of the height of sediment at the dam at various time intervals.

CONCLUSIONS

A comparison of the area-increment method, the empirical area-reduction method, and actual reservoir resurvey area and capacity curves demonstrates the adequacy of the methods (Fig. 3). However, in the two methods demonstrated it is evident that a procedure in which all the major factors affecting sediment disposition are considered is still needed. Also, several major factors affecting reservoir sediment distribution such as density currents, delta development, and density of deposits with time, not discussed herein, need additional study and evaluation to develop procedures for predicting the effect of these items on conditions in and upstream from the reservoir.

AMERICAN SOCIETY OF CIVIL ENGINEERS

Founded November 5, 1852

TRANSACTIONS

Paper No. 3020

CONSTRUCTION OF THE VARIABLE-ANGLE LAUNCHER

By Arthur C. Bravo,[1] F. ASCE

SYNOPSIS

The construction of the unique ordnance testing device termed the variable-angle launcher, including some unusual solutions to the construction problems are described herein.

INTRODUCTION

The U. S. Naval Ordnance Test Station's variable-angle launcher, a $2,000,000 test facility, is located at the Station's Morris Dam Torpedo Range near Azuza, Calif. Designed to launch various types of projectiles into the water under controlled conditions at high velocities and variable entry angles, the variable-angle launcher permits the detailed study of projectile water-entry performance. It has served as a valuable tool in developing improved air-launched torpedoes that can be released by aircraft at high altitudes and at high release speeds.

The launcher consists of a 22 1/2-in. torpedo-launching tube, 300 ft long, mounted on a movable 300-ft, all-welded steel bridge. The upper end of the bridge is supported by a welded structural steel carriage that rides on rails up and down the 45° slope of a peninsula jutting into Morris Dam Reservoir. The lower end of the launcher bridge is supported by a second, transverse bridge 95 ft long that rests on two steel barges floating in the water. The weight of the launcher and carriage is balanced by a 600-ton counterweight car that rides on rails up and down the back slope of the peninsula. The elevation angle can be varied between 10° and 40° by moving the upper end up or down the tracks on the 45° slope. The launcher can also be rotated in azimuth by adjusting the position of the barges and transverse bridge.

Note.—Published, essentially as printed here, in August, 1957, in the Journal of the Construction Division, as Proceedings Paper 1343. Positions and titles given are those in effect when the paper was approved for publication in Transactions.

[1] Project Mgr., Holmes & Narver, Los Angeles, Calif.

Projectiles are launched at velocities up to 800 fps by means of a compressed air system. The compressed air, at 1,000 psi is contained in a 500 cu ft, all-welded air flask, and is released into the launcher tube by means of a quick-acting 22½-in. sleeve that opens in 0.10 sec. A complex electronic system controls the launching process. Elaborate instrumentation, photographic, acoustic, and electronic, provides information on the position, attitude, velocities, and accelerations of projectiles during launching and water entry.

The planning of the structure, the functions, and characteristics of the structural elements,[2] a description of the steel structures,[3] and the mechanical and electrical features of the launcher[4] have been presented elsewhere. This includes the projectile launching equipment, handling and transport, equipment, operating equipment used to change the launcher angle and test instrumentation.

ORGANIZATION

The construction project was divided into a number of phases and subcontracted on a bid basis according to the type of work involved. Careful organization of the work was necessary to permit the simultaneous operation of several contractors in the limited working areas. Factors involved were the coordination of work accomplished in one location by more than one contractor, movement and storage of heavy equipment and material, means to avoid disrupting research programs in progress, required sequence and timing of operation, and contract time limits.

CONCRETE STRUCTURE

The natural condition of the foundation for the concrete structure and the methods employed to stabilize the foundation were described elsewhere.[5]

The concrete structures described in this article include the 30° counterweight slab on the back slope of the hill, the main cellular structure at the crest of the hill, and the 45° launcher slab on the front slope.

Counterweight Slab.—The counterweight slab distributed the wheel loads of the counterweight car to the foundation. The slab design permitted the use of reinforced concrete or reinforced gunite. Gunite was chosen because it was less expensive. It was used on the part of the slope below the cellular structure.

In construction of the slab, the overburden was first removed from the slope by hand methods. Plywood forms were placed for sides and steps. After the form work was completed, the reinforcement was placed. The mixer, compressor, compression chamber, and materials were on the edge of the bank just west of the slope. Here, sand and cement were mixed in two-sack batches and transported to the compression chamber by means of a chute. The required water was obtained from a storage tank at the site and was applied to

---

2 "The Variable-Angle Launcher: A Naval Ordnance Testing Facility," by John L. Cox, Proceedings Paper 1339, ASCE, August, 1957.

3 "Variable-Angle Launcher: Steel Construction," by N. D. Whitman, Jr., Proceedings Paper 1341, ASCE, August, 1957.

4 "Variable-Angle Launcher: Mechanical and Electrical Features," by F. L. Carlisle, Proceedings Paper 1342, ASCE, August, 1957.

5 "Variable-Angle Launcher: Concrete Structures and Foundation Treatment," by J. H. Jennison, Proceedings Paper 1340, ASCE, August, 1957.

the nozzle with a pressure that varied from 45 psi to 74 psi. The mix used consisted of one part of cement to 4½ parts of sand.

In an effort to keep the working surface free of rebound, the contractor chose to start guniting from the top of the slope. However, rebound still accumulated on the slope. Placing the gunite was especially difficult because of the heavy mat of reinforcing steel and wood templates used for spacing the rail anchor bolts. Fig. 1 shows the counterweight slope with the steel reinforcement and forms in place prior to guniting. A total of 210 cu yd of gunite was placed with a minimum thickness of 18 in. Curing was maintained for six days by spraying water on the slope.



FIG. 1.—THE COUNTERWEIGHT SLOPE.

It was expected that the slab gunite would meet the specified strength of 3,000 psi in 28 days inasmuch as the gunite test cylinders made during the placing of the slab tested satisfactorily. The test cylinders, 6 in. in diam and 12 in. in length, were shot into a ¼-in. mesh hardware cloth cylinder. The cylinders indicated an average 28-day strength of 3,840 psi.

Cores of 4 in. diam taken from the cured slab showed an average strength of 2,100 psi at an age in excess of 28 days and a density of 137 pcf. The cores also showed a deficient bond between layers of gunite and between gunite and reinforcing bars, as well as frequent occurrence of sand pockets. A view of the cores is shown in Fig. 2. Cores that contained obvious surface deficiencies were not tested.

The foundation is sufficiently strong that uniform pressure under the slab is not required. Despite the deficiencies of the gunite, it was thought that the strength of the slab was sufficient to serve its purpose, and the type of failure that might occur would be progressive cracking or disintegration which could be observed. Such failure of the slab would not endanger the structure, and repairs could be made at a later date if necessary. During replacement, a test program could be maintained with nominal limitations of launching angle. In the light of the government's urgent need for the completed project, the slab was accepted as constructed.

The rails chosen for the counterweight track were 90 lb per yd and the track was made standard gage. The rails are anchored by pairs of 1-in. bolts spaced on 3-ft centers. After the curing of the gunite, the rails were alined and grouted into place.



FIG. 2.—CORES TAKEN FROM THE COUNTERWEIGHT SLOPE.

Main Structure.—The main concrete structure is a cellular continuation of the slopes of the launcher ramp and the counterweight ramp. It also forms the structural support for the main drive machinery, houses various electrical machinery and instruments, and furnishes laboratory space. Cantilever balconies provide access to the launcher ramp from the main structure at several points. The walls of the cells were 12 in., 18 in., and 24 in. in thickness, depending on the loading. The continuous footing for each side is 10 ft wide having a maximum depth of 7½ ft. Considerable quantities of steel conduit for electrical and instrumentation wiring are incorporated in the various walls and slabs.

The excavation for the structure was accomplished by a 3/4-yd shovel and dump trucks. Benches for footings were hand-excavated using pneumatic tools. Approximately 19,000 cu yd of excavated material was hauled 1/8 of a mile and deposited in a ravine.

Form work was started from both ends of the structure. The pouring of concrete alternated between the launcher slope side and the counterweight side. Floor slabs and walls were built before the launcher and counterweight slab sections of the main structure were poured. The steps and curbs on the counterweight slope of the cellular structure were constructed with movable steel forms that cast eight steps each.



FIG. 3.—PARTIALLY COMPLETED CELLULAR STRUCTURE ON COUNTERWEIGHT SIDE OF MAIN STRUCTURE.

All concrete placed in the main structure was mixed on the site in a self-propelled 1 cu yd mixer. Sand and aggregate mixed at the batching plant in Azuza, Calif., was hauled approximately 7 miles to the mixer by trucks. Sacked cement was added to the mixer, and water was measured automatically and added.

In general, the concrete was poured in sections of approximately 50 cu yd. The concrete was placed in the forms with a bottom dump, 1-yd bucket, and a crane. Approximately 2,140 cu yd of concrete were poured in this manner. A view of the form work for the cellular structure and partly-completed counterweight slope is shown in Fig. 3.

Launcher Slab.—The launcher slab below the main structure serves the primary purpose of supporting and anchoring the rails for the carriage. This slab was poured directly on the rough surface of the rock foundation. Poured concrete was specified for the launcher slab because the gunite on the counterweight slab proved inferior and because the launcher slab required heavier reinforcement and presented difficult working conditions on the 45° slope. Another factor considered was the importance of obtaining bond between the concrete and the main rail anchor bolts that must resist heavy uplift forces.

The initial excavation for the slab was done using a 2-yd dragline from a bench cut near the top of the slope. Benches and steps were cut into the 45° slope using pneumatic tools. Approximately 5,000 cu yd of excavated material was deposited in the lake at the toe of the slope. Final surface cleaning was done by hand labor and sluicing before pouring the slab.

The principal reinforcement consisted of 1¼-in. square bars on 6-in. centers in the top and 1-in. round bars on 6-in. centers on the bottom placed transversely to the slab. Longitudinal reinforcement in both top and bottom was supplied by 1-in. round bars on 16-in. centers.

The lower mat of reinforcing steel was fitted to the shape of the slope and the upper mat set to specified grade. Both mats were supported by reinforced steel legs welded to the mat with the lower ends set in crevices in the rock. Where possible, the mats were tied to steel dowels previously grouted into the slope.

The launcher slab was formed with a movable steel form built by the contractor for this purpose. The structural steel form consisted of a channel-shaped steel face plate backed by steel beams and channel reinforcement with wheels at the four corners. A view of the movable form is shown in Fig. 4. The assembly was rolled up the slope on rails set on heavy timber falsework just beyond the side limits of the slab. Holes were drilled in the face plate for the accurate placement of the launcher rail anchor bolts. To move from one pour to the next, it was necessary to lift the form off the anchor bolts. This was done with hydraulic jacks mounted near the four wheels. The jacks were also used to set the form to accurate grade before anchoring it to the steel mat.

To insure exact spacing of the bolts, the lower line of bolt holes on the form were placed over the upper line of bolts in the previous pour. This overlapping served as a good grade control for the bottom of the form. The form was set to line with a transit before each pour and was pulled up the slope by the tagline of a crane. Steps, curbs and launcher rail indents were also cast by the movable form. The form, which poured a 25-ft section of slab, was moved, set, and the concrete placed, in a period of two days.

A 1-cu yd concrete mixer was set on a bench at the top of the slope. A steel car of 1-cu yd capacity was set on rails that were attached to the upper mat of slab reinforcement and the car was moved up and down the track by a winch anchored to the top of the main structure at elevation 1,387. Concrete was mixed and poured into a 1-cu yd bottom dump bucket. The bucket was swung by a crane over to the ramp car into which the concrete was dumped for transport to the pour. The car discharged into sheet metal troughs for lateral distribution at the pour site. Approximately 1,640 cu yd of concrete were poured by this method. The slab had a minimum thickness of 4 ft. The contractor chose to use calcium chloride as an admixture to the concrete on the launcher slope in order to accelerate setting. The average mix used was in a 1:2-4:3.3 proportion by weight with 8 lb of calcium chloride added per batch.

Special rails for the carriage were anchored to the launcher slab by the previously placed 2-in. anchor bolts and grouted in place. These rails were heavy weldments designed to provide running surfaces for the dual wheels of the carriage and 7-in. pin holes for the locking pins of the carriage. The rails and a crane were loaded on a barge and then moved to the bottom of the launcher slope. The two bottom rails were set on the anchor bolts by the crane, and the



FIG. 4.—LAUNCHER SLAB DURING CONSTRUCTION.

remaining rails were placed one at a time by a pneumatic-tired car that straddled the anchor bolts for one rail. The car was equipped with chain hoists for raising and lowering the rails and was moved up and down the launcher ramp by a winch.

With survey control by the survey crew, the contractor juggled the rails up and down the slope with jacks, come-alongs, and shims until they were properly

set. After final alinement, the contractor placed stiff grout under the rail base edge and wet grout under the center of the base plates, which embedded shear lugs welded to the underside of the rail base.

STEEL STRUCTURES

The steel structures include the barges, connecting bridge, launcher bridge, counterweight car, and the carriage.

Barges.—The two barges supporting the connecting bridge were fabricated at the contractor's shops using all-welded construction. The barges were 60 ft long, 35 ft wide, and 12 ft deep and weighed 67 tons. Longitudinal and transverse bulkheads divided the interior into 12 compartments.

The sides, ends, and deck of the hull as well as the bulkheads were constructed of $\frac{1}{4}$-in. plate and the bottom was constructed of 5/16-in. plate. The bottom and end plates were stiffened with ST 9WF23.5 on 2-ft-9-in. centers, the side plates with 6-x-4-x-3/8 angle on 2-ft-9-in. centers, and the deck with 5-x-3$\frac{1}{2}$-x-5/16 angle on 2-ft-9-in. centers. A $\frac{1}{2}$-in. plate was fabricated into part of the deck to receive the connecting bridge anchor seats.

Steel plate was cut with a torch to the predetermined sizes that would be fitted together and welded to form the bottom, sides, and ends of the hull. The pieces were tack-welded together on the shop floor prior to completing the welds with automatic welding machines. Stiffeners were then welded to the built-up sheets.

After the bottom of the hull had been shored up in the yard, the bulkheads forming the compartment were welded into place. The sides and ends were then welded to the bottom and to the bulkheads. The deck, previously assembled, was then lowered into place and welded. Hand arc-welding was used during assembly, and sequence-welding was used to reduce distortion.

The exteriors of the barges were painted with hot-applied bitumastic enamel which provided a long lasting protective coating that would minimize maintenance. The interiors of the barges were painted with one coat of red lead primer and two coats of cold-applied bitumastic paint. The interior of each compartment can be inspected periodically using man holes in the deck that provide access to each compartment.

The load limitations of a highway bridge and the restrictions imposed by narrow canyon walls made it necessary to cut the barges in half before transporting them by truck. The 30-x-35-ft half-sections were transported to an erection area located on the reservoir approximately a mile upstream from the variable-angle launcher site. A view of a half-section of the barge during transportation is shown in Fig. 5. The halves of the barges were then installed on ways that had been built by the contractor for launching the barges. A field-weld transverse to the bridge amidship was used to connect the two halves. The field-welding area was retouched with paint prior to the launching and the deck work was completed after launching.

Connecting Bridge.—The connecting bridge is a 95-ft span, all-welded structure connecting the two barges and supporting the outer end of the launcher bridge. The connecting bridge contains approximately 38.5 tons of structural steel. The centerline distance between the 95-ft-long bottom chords is 20 ft 9 1/8 in., and the distance between the 22-ft-long top chords is 4 ft.

The lower chord and upper chord members consisted of 14-in. WF-sections while the diagonals were 10-in. WF-sections. Lower chord transverse diagonal members were constructed from 12-in. WF-sections and the upper chord bracing was fabricated from $\frac{1}{2}$-in. steel plate with 3/8-x-3 3/4-in. plate stiffeners on 2-ft-3-in. centers.

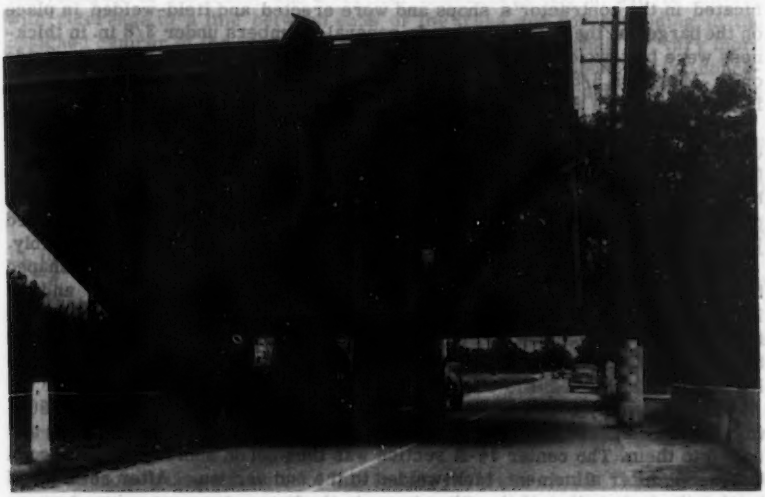


FIG. 5.—A HALF-SECTION OF THE BARGE ON A TRAILER.



FIG. 6.—CONNECTING BRIDGE BEING ASSEMBLED ON THE BARGES AT THE ERECTION SITE.

The trusses, a 34-ft center section, and two 30½-ft. end sections, were fabricated in the contractor's shops and were erected and field-welded in place on the barges at the erection area. In general, members under 3/8 in. in thickness were butt-welded together with the members beveled at 60° on one side only. Members 3/8 in. and over were beveled at 60° on both sides. All beveling was done with a cutting torch.

The centerline of the truss members was scribed on the steel floor in the contractor's shop. Wide flange sections were cut to size and the flange cut off for joint flaring. The sections were then tack-welded to the floor. Plates that had been cut previously and rolled to the correct curvature were tacked into place. The sections were then welded together except at the predetermined joints in the chords and diagonals which were left for field-welding at assembly.

Wide flange sections were cut to size and welded together forming X-shaped bracing for the lower diagonal system, the vertical diagonal system, and the inclined portal system. At the intersection of the wide flange members, curved filler plates were welded to the flanges of the members. After welding had been completed, the sections were wire-brushed and given a shop coat of red lead primer.

Field assembly began at the site by alining the two barges. The first 30½-ft truss section was set by a crane in the two supports on the one barge and bolted to them. The center 34-ft section was then set on shoring on the second barge and, after alinement, tack-welded to the end section. After setting and bolting the end section of the other truss to the barge, temporary bracing was welded to both trusses to maintain alinement. The lower chord horizontal diagonal bracing and the vertical diagonal bracing were then set in place and tack-welded to the one truss. The center section of the other truss was set in place and, after alinement, tack-welded onto the structure. After checking alinement in all directions, the members were completely welded together. A view of the connecting bridge during field fabrication is shown in Fig. 6.

After completion of the welding, the barges were moved apart and the two remaining end sections of the trusses set on shoring and welded to the center sections. The end bracing section and the remainder of the lower chord bracing was then welded to the structure. The barges were pulled apart to the required spacing and the end section bolted down to their supports. The welds were wire-brushed and primed with a coat of red lead primer and the entire structure was sprayed with a coat of aluminum paint.

Launcher Bridge.—The launcher bridge is an all-welded structure 22 ft wide, 35 ft deep, and having a 300-ft span length. The main trusses are 12-panel Pratt type and the transverse frames at each panel are three-story, two-bay, rigid frames. Conventional cross-bracing was used in the horizontal planes of the upper and lower chords. The centerline vertical members as well as the web members of the trusses were stabilized at the third points by longitudinal stringers.

Members were mostly 14-in. WF-sections or equivalent sections made by welding three plates together. These welded sections were supplied at the contractor's option because of the long unavailability of rolled shapes. Steel-work was fabricated in the contractor's shop and transported to the erection area on the shore of the reservoir. Approximately 251 tons of structural steel were fabricated into the launcher bridge exclusive of deck grating and railings.

Tolerances for erection of the launcher as given in the specifications were as follows:

"a. In the total length of either truss, a horizontal tolerance of one inch will be allowed with reference to a vertical plane connecting the centerlines of the

end verticals of the truss, and a vertical tolerance of one in. will be allowed with reference to a line between ends of the truss and corresponding to the designed camber of the truss. However, local alignment shall not vary more than 3/8 in. from a longitudinal line, to specified camber, connecting two corresponding points 50 ft apart, or from a vertical plane through corresponding points 50 ft apart.

"b. The completed truss shall be within one in. of the length shown on the drawings.

"c. Any point on one truss shall be within $\frac{1}{2}$ in. of a line perpendicular to the plane of the other truss at a corresponding point.

"d. Distance between top and bottom chords of each truss shall be within $\frac{1}{2}$ in. of the dimensions shown on the drawings.

"e. The horizontal distance between truss chords shall be within $\frac{1}{4}$ in. of the dimensions shown on the drawings."

The first phase of shop work consisted of the fabrication of the frames. The 14-in. WF-sections were torch-cut to length and assembled on the floor of the contractor's shop. The lower transverse member of the frame was not welded into the assembly, but was welded into the lower chord or deck assembly. During welding the members were held in alinement by tack-welding to the floor.

The second phase consisted of fabricating the lower chord. The lower chord or deck structure was assembled on a timber falsework built to include the required camber. The deck structure consisted of the lower chord of the trusses, the lower transverse frame member, the cross-bracing, and the girders for the decking. Fabrication consisted of tack-welding together the 14-in. WF-sections of the truss chord. The lower member of the frame was then tack-welded to the chord section and the cross-bracing tack-welded in. After checking alinement and camber, final welding was started. During welding, careful check of alinement was made to keep the fabrication within the allowable tolerances.

During the welding of the lower chord structure, radiographing of welds was begun. A number of welds were found to be unsatisfactory because they contained slag deposits or hairline cracks, or because full penetration of weld was not accomplished. All deficient welds were chipped out and rewelded. A cross section of one of the unsatisfactory welds is shown in Fig. 7. The weld was not back chipped and poor penetration resulted.

To improve the welding, a record was kept of the work done by each welder. Also, the inspector approved the back chipping of each weld before the welder could continue. Radiographs of welds made after this system was put into effect indicated no poor welds. After the full 300 ft of lower chord structure had been welded, it was cut into approximately 50-ft sections for transportation to the erection area.

The third phase of shop work consisted of cutting to size the WF-sections that comprise the upper chord, vertical diagonals, and upper cross-bracing members. All fabricated members were given one coat of red lead primer before they were transported to the erection area by truck and trailer. At the erection area the lower chord sections were set again on a timber falsework with built-in camber and tack-welded together. The transverse panels were lifted into place individually by a crane and held until side diagonal members and other braces were tack-welded sufficiently to hold the panels rigid.

Succeeding panels, diagonals, and top chord were set in place and tack-welded together. After checking alinement and fabrication tolerances, the various members were welded together. During the welding process, 12 gasoline-driven electric arc-welding machines were being used. Fig. 8 shows how the various members were assembled into the bridge.

After the main structure was welded, the deck grating and movable stairway were installed. As the welders progressed, painters followed with a field coat of red lead. When the steel erection and red lead painting were completed, the entire structure was sprayed with the final coat of aluminum paint.

The launching tube and the air tank were then installed in the bridge. The 45-ton tank was lifted from the trailer bed by a 60-ton speedcrane and a truck



FIG. 7.—CROSS SECTION OF A WELD CUT OUT OF A LAUNCHER BRIDGE MEMBER.

crane and set on the ground at the breech end of the launcher bridge. Two longitudinal erection beams and several bracing members were welded between panels P-0 and P-1 of the bridge as supports for the tank. Three cranes lifted the tank to the entrance section of panel P-0, and a bulldozer with a line reeved through a snatch block at P-1 and tied to the tank pulled the tank part way into the bridge. The cranes then swung the tank to the required position.

The transportation of the completed bridge to the launcher site was accomplished by floating the bridge down the lake on barges. The timber falsework was removed by jacking up the bridge and lowering it onto two sets of rollers. The forward set was laid at a skew angle so that the bridge could be turned through an angle of 20° in order to bring the lower end panel P-12 over the

connecting bridge pillow blocks. When the bridge had been rolled into the required position, ballast water in the barges was pumped out to bring the pillow blocks up to the lower pivot pins. After the launcher bridge had been seated on the connecting bridge, the shore end of the launcher bridge was rolled toward the lake to pick up the load at the panel points P-3 and P-4. A barge of 156 pontoons was moved under the launcher bridge between the connecting bridge and the shore. Timber cribbing had been built up in the center of the barge to a height of approximately 25 ft.

When the bridge had been rolled out so that panels P-3 and P-4 were over the cribbing, the lake level was raised approximately 2 ft by discharging water from San Gabriel Canyon Dam No. 1 into Morris Dam lake to lift the shore end

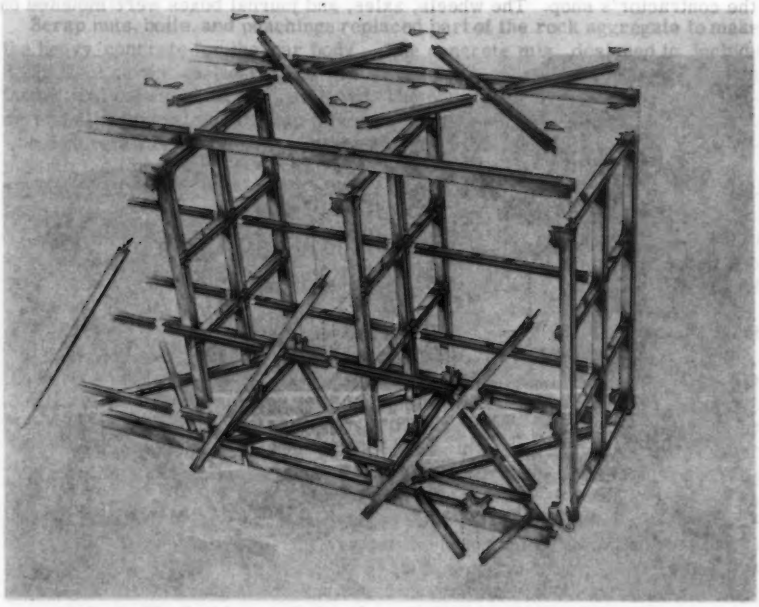


FIG. 8.—METHOD OF FIELD ASSEMBLY OF THE LAUNCHER BRIDGE.

of the bridge off the rollers. The bridge was then floated down the lake to the launcher slope, a distance of approximately 1 mi. Fig. 9 is a view of the launcher bridge during transportation.

It was then necessary to raise the lake level approximately 17 ft to bring the horizontal pivot casting to the elevation of the pivot platform of the support carriage. The support carriage had previously been set on the launcher slope, as described subsequently.

When the bridge reached the launcher slope, it was slowly jockeyed into place on the support carriage. The heavy weldment that transmits the longitudinal and transverse loads to the carriage had been suspended below the launcher bridge at panel point P-0 during transportation. After the bridge was

in the correct position, the weldment was lowered onto the carriage and welded to it.

During the welding of the weldment to the carriage, windstay cables were reeved, giving an outboard anchor against lateral movement of the bridge. The pontoons of the temporary barge were filled with water to lower it enough to float from under the bridge.

Counterweight Car.—The car operates on a 30° slope and acts as a counterbalance for the launcher bridge. It consists of a steel frame or chassis mounted on 20 railway-car wheels and a concrete body. The counterweight car is attached to sixteen 2 $\frac{1}{8}$-in. steel cables that reeve through the main drive equipment and terminate at connections to the bridge support carriage.

The 50-ft-x-10-ft all-welded counterweight car chassis was fabricated in the contractor's shop. The wheels, axles, and journal boxes were mounted on

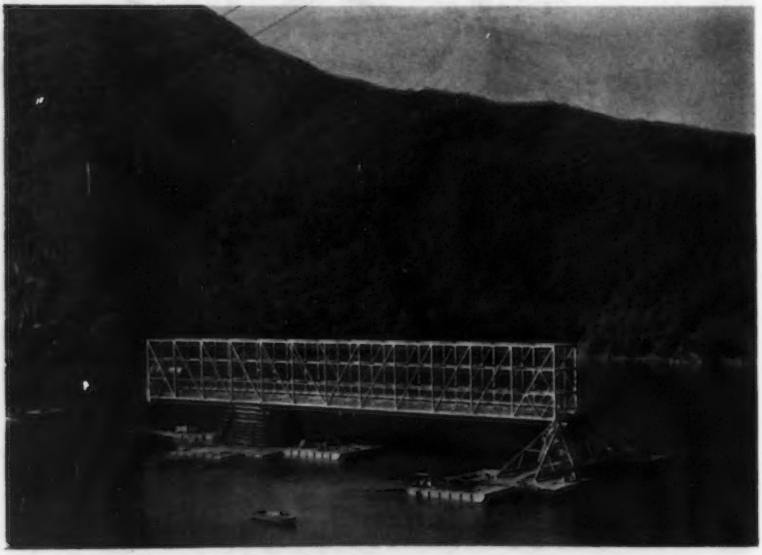


FIG. 9.—LAUNCHER BRIDGE BEING TRANSPORTED FROM THE ERECTION SITE TO THE LAUNCHER SLOPE.

the chassis in the shop. This assembly was transported to the launcher site by truck and unloaded by a 60-ton speedcrane located on the west side of the structure. While setting the car chassis on the rails, the crane upset and dropped the car to the ground on the east side of the slope. The car broke loose, rolled down a ravine and plunged into the lake. Navy divers later located the car in 105 ft of water and it was almost completely buried in mud.

With the aid of blocks and tackle attached to the connecting bridge mounted on two barges, the chassis was retrieved from the mud and towed to the erection area. It was then cut in half with an acetylene torch and hauled back to the contractor's plant for clean-up and minor repairs.

Later, the car was returned to the counterweight ramp where it was installed on the rails in two pieces. The two sections were then welded together. The car was held in position on the rails by a steel bumper anchored to the concrete structure.

The drawbar assembly, a heavy weldment, was welded to the forward end of the chassis. The reinforcing steel mat for the concrete body that had been fabricated in the contractor's shop was welded to the drawbar assembly. This reinforcing mat consisted of seventeen 1-in. sq bars running longitudinally and 5/8-in. round bars welded at right angles to the 1-in. bars.

Plywood forms prefabricated into panels, were secured to the car chassis and filled with concrete to form the car body and the interior compartment for the ballast block. The steel chassis served as the bottom form in the pouring of the concrete.

Scrap nuts, bolts, and punchings replaced part of the rock aggregate to make the heavy concrete for the car body. The concrete mix, designed to include 3,200 lb of scrap steel per cu yd with seven sacks of cement, thus produced a theoretical density of 225 lb per cu yd. The concrete was mixed in a ½-yd mixer, and all aggregate and scrap was weighed before being placed in the mixer. The concrete was transferred from the mixer to bottom drop buckets for pouring into the forms.

Blocks of heavy concrete poured in wooden forms provided additional ballast for the counterweight car. Two sizes, 1 ft x 1 ft 6 in. x 3 ft 6 in. and 8 in. x 1 ft x 2 ft 6 in. were poured. The concrete mix was designed to include 5,400 lb of scrap steel per cu yd with 5.5 sacks of cement per cu yd, and a maximum of 6 3/4 gal of water per sack of cement thus produced a theoretical density of 270 lb per cu yd.

Carriage.—The carriage is a complex welded structure supporting the breech end of the launcher bridge. It can be moved up or down the slope and locked to the rails with hydraulically actuated pins. The carriage consists of a heavy structural-steel space framework, mounted with a launcher bridge support deck, compressor platform, revolving platform, fixed upper platform, and four wheel assemblies. Each wheel assembly contains four standard railway-car wheels complete with roller bearing journal boxes and 7-in. locking pins. The pins are located 33 ft 8 3/4 in. apart along the longitudinal axis of the carriage.

The launcher bridge support deck, compressor platform, revolving platform, fixed upper platform, and wheel assemblies were fabricated as units in the contractor's shop. Extreme care in alinement and welding sequence was required in the fabrication of the wheel assemblies and the launcher bridge support deck. The locking pin holes through the two plates of the wheel assemblies were line-bored to maintain the center of the holes directly opposite each other.

After the units were fabricated in the shop, they were cleaned and sprayed with one coat of red lead primer and then transported to the erection site.

The carriage was assembled at the erection area. Close inspection and precise workmanship were needed to keep within the tolerances allowed. The relationship between pin holes in the wheel assemblies was one of the most critical factors to control. The pin holes had to be spaced correctly because longitudinal adjustment of the rear pins was not provided. Any appreciable error in pin-spacing would make it impossible to insert the pins into the holes in the track.

At the erection site the contractor poured four concrete footings on which were bolted two rails similar to the rails on the slope. These rails contained

the pin holes that spaced the wheel assemblies. The four wheel assemblies were set on the rails and the pins put through the holes to provide a lock for the assemblies. The remainder of the carriage was then assembled. Fig. 10 is a view of the carriage during the field assembly at the erection site. After the launcher bridge support deck, the compressor platform, and the connecting members had been erected on the wheel assemblies, the completed structure was sprayed with one coat of red lead and a final coat of aluminum paint.

Transportation to the launcher slope was accomplished by mounting two rails, similar to those on which the carriage was erected, on a pontoon barge with ends extending beyond one end. Two 7½-ton gasoline winches were welded to the barges outside the gage of the rails. Pins were used to secure the overhanging ends of the barge rails to the lake-end of the erection rails and



FIG. 10.—THE CARRIAGE DURING ERECTION.

the assembled carriage was pulled aboard the barge. The carriage was transported down the lake to the foot of the launcher slope.

The overhanging ends of the barge rails were pinned to steel anchor blocks set previously on concrete bases at the bottom of the main launcher rails. A 50-ton block was anchored up the slope to each rail and one block to each upper wheel assembly. A single cable was reeved from one winch through the four blocks and to another winch, thus providing adequate drum capacity. The pull of the two winches was used to draw the carriage onto the launcher rails, where it was anchored with the locking pins.

The contractor completed the fabrication of the carriage on the slope: Attaching the shop-fabricated upper fixed platform, the bridge shoe arc rails, the framework for the overhead crane, and the hydraulic and lubricating systems. The two arc rails supporting the launcher bridge required accurate setting so that the top of the two rails would be in the same horizontal plane. After considering a number of methods, it was decided to bring the rails to grade by means of adjusting screws through the track base and then filling up any space between the rail base and the top of the carriage platform with an alloy of low melting point.

Rigging.—A separate contractor was retained for the rigging of the various items of the variable-angle launcher. Rigging items were numerous, and only those of primary importance are described in this paper.

In order to place the main drive hoist unit on the top platform of the concrete structure of the variable-angle launcher, at El. 1,387, the contractor erected a 90-ft gin pole on the west area at El. 1,340. The load line fed into a heavy skid-mounted, gasoline-driven hoist set that was anchored at the east entrance to the arch at El. 1,340. The gin pole was guyed to both slopes of the structure and to heavy concrete blocks set on trailers.

The main hoist frame, weighing approximately 40 tons, was lifted over the top of the concrete structure and set on rollers. The frame was rolled into place, lowered onto the anchor bolts, and set to line and grade. The forward drum was raised and set in place on the frame. Then the sixteen $2\frac{1}{8}$-in. cables were draped across the drum and frame and down the two slopes. The aft drum was raised and set in place on the frame and the cables from the counterweight end wrapped over this drum. Finally, the top drum was raised and mounted and the counterweight ends of the cables brought over and dropped down the counterweight ramp into position for assembly to the counterweight car.

The base of the frame was grouted into place with a nonshrink cement. The gear reducer, magnetic brake, and motor were then raised into place, coupled, alined, and grouted.

For photographic purposes, the launching range was equipped with an overhead cable system. The main 3/4-in. cable on which the camera car rides was attached to a tower located on top of the concrete structure. It extended 1,800 ft down-range to a Y-connection supported by two 3/4-in. cables 1,100 ft long and was anchored to winches tied to the canyon walls by concrete and steel dead-men. Materials for the anchorage were carried up the steep slopes on the backs of laborers. After setting the dead-man anchors, the winch frames were lined and tied to the anchors. The cables were attached to the towers and anchor winches, the free ends pulled to a barge on the lake, the Y-joint attached, and the system pulled to line and grade by use of the anchorage winches.

The variable-angle launcher was dedicated on May 7, 1948. Since that time it has served as an important testing device in the field of underwater research for the United States Department of Navy.

ACKNOWLEDGMENTS

The construction was under the jurisdiction of the Bureau of Yards and Docks of the United States Department of the Navy, with Captain H. L. Mathews acting as Officer in Charge of Construction, and Commander C. E. Langlois as Resident Officer in Charge of Construction. The design was the responsibility of the Development Engineering Section of the Underwater Ordnance Division of

the U. S. Naval Ordnance Test Section, China Lake, Calif., (Pasadena Area). William H. Saylor, head of Underwater Ordnance Division, and James H. Jennison, F. ASCE, chief engineer, were in charge of design. Consultants employed on the project were: Coast Marine Engineering Company; Frederick J. Converse, F. ASCE, consulting foundation engineer; Frank G. Denison, Jr., naval architect; Vladimir P. Pentegoff, consulting geologist; Quinton Engineers, Ltd.; and Nathan D. Whitman, Jr., F. ASCE, consulting structural engineer. The General Tire and Rubber Company, Calif., was prime contractor. Major subcontracts were awarded to United Concrete Pipe Corporation for steel structures and to Norman I. Fadel for concrete structures.

AMERICAN SOCIETY OF CIVIL ENGINEERS

Founded November 5, 1852

TRANSACTIONS

Paper No. 3021

AMPLIFIED STRESS AND DISPLACEMENT IN GUYED TOWERS

By Robert S. Rowe,[1] M. ASCE

With Discussion by Vitelmo Bertero, and Robert S. Rowe

SYNOPSIS

A simplified method for the determination of the slack stress in the guys of a tower subjected to wind load is presented. Equations for the determination of displacements at guy levels are developed in terms of the wind load, initial guy tension, and slack stress.

A useful method for solving problems pertaining to the buckling or amplification of stress and displacement in guyed towers has also been developed. Only fundamental concepts are used and those are extended to include the displacement of the tower axis due to external loads and internal distortions. The increase, or amplification, of the computed stress, and displacement or bending moment at the center of a loaded section of the tower (when the displacements of the axis are included in the analysis) are developed and presented in graphic form.

INTRODUCTION

The guyed tower is a structural form that has become increasingly important because of the need for high television and radio towers. The typical television tower (Fig. 1) is 1,000 ft high. The term s, representing the triangular cross-section distance, is usually 10 ft. It has 5-in. round legs of T = 1 steel, girts and diagonals of A-7 steel, and a total weight of 440 kips. A wind load of 200 lb per ft of tower is acting. The total vertical component of the tower reaction, V, is 800 kips and the horizontal component of the reaction, H, at the base is 23.8 kips. The properties of the guys are shown in Table 1.

Note.—Published, essentially as printed here, in October, 1958, as Proceedings Paper 1821. Positions and titles given are those in effect when the paper or discussion was approved for publication in Transactions.

[1] Prof. and Chmn., Dept. of Civ. Engrg., Duke Univ., Durham, N. C.

Considerable time is spent on the preliminary design and analysis of tall steel towers because of the lack of a simplified method for performing those operations.[2] The ordinary methods of structural mechanics for flexible steel towers should not be used, because the displacements (which are normally neglected) may increase or amplify the stresses, which, in turn, continue to increase the displacements. Any refinements that are introduced into an analysis are included for reasons of safety rather than of economy.

To determine the stresses in a guyed tower, it is necessary first to assume a preliminary design. Generally, the effect of variations can be determined

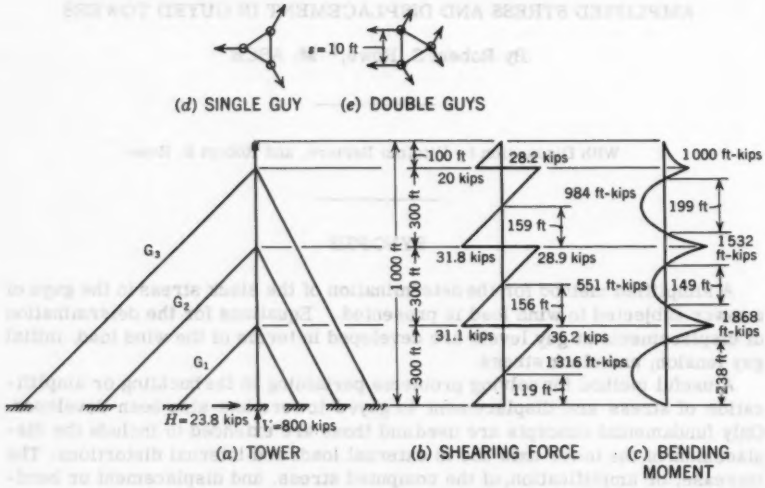


FIG. 1.—TYPICAL GUYED TOWER

TABLE 1.—PROPERTIES OF THE GUYS

Guy (1)	Single guys, Fig. 1(d)		Double guys, Fig. 1(e)	
	Bridge strand diameter, in inches (2)	Initial tension per guy, in Kips (3)	Bridge strand diameter, in inches (4)	Initial tension per guy, in Kips (5)
G 1	1 5/8	63.4	1 3/8	31.7
G 2	1 9/16	56.4	1 1/8	28.7
G 3	1 3/8	45.6	1	22.8

only by analyzing several designs. Because this process requires a great amount of time and labor, elaborate analysis is seldom practical. A device useful in determining the influence of displacements on the preliminary design is termed an "amplification chart," by which the structural action, as well as

[2] "Design of Multi-Level Guyed Towers: Structural Analysis," by E. Cohen and H. Perrin, Proceedings Paper 1356, ASCE, September, 1951.

the effects of varying the tower proportions, can be visualized easily. This amplification chart may be modified for conditions other than those specified originally. Thus, one chart developed from simple structural concepts, can serve for the various tower types, proportions, materials, loading, and computed stresses. The results obtained are extended by successive correction to include the displacement of the tower axis. These results agree closely with the results obtained by the formal methods of structural mechanics.

HORIZONTAL DISPLACEMENTS

Notation.—The letter symbols adapted for use in this paper are defined where they first appear, in the illustrations or in the text, and are arranged alphabetically, for convenience of reference, in the Appendix.

Horizontal Displacements Due to Wind.[3]—The horizontal displacements of a tower depend on the wind direction, slack stress, and initial tension in the guys. For the wind direction in Fig. 2 (Wind I), the horizontal displacements of the tower axis at a guy level may be computed approximately by Eq. 1.

$$\Delta H_1 = \frac{(P_w + P_s - P_i)}{\sin \alpha} \frac{L_g}{A_g E_g} \quad \ldots\ldots\ldots\ldots \quad (1)$$

in which P_w, P_s, and P_i are the wind, slack, and initial forces in a guy, respectively; α represents the angle between the guy and the vertical; L_g is the guy length; A_g denotes the cross-sectional area of an individual guy; and E_g is the modulus of elasticity of the guy.

The wind force in a guy is defined as

$$P_w = \frac{H}{\sin \alpha} \quad \ldots\ldots\ldots\ldots\ldots\ldots \quad (2)$$

in which H is the component of total horizontal wind reaction to a guy.

Thus, before it is possible to determine horizontal displacements, it is necessary to determine the slack force, P_s. The slack force depends on the wind reaction, H, the initial force, P_i, in the guy and changes in the guy geometry. The relationship between the various forces may be obtained from statics. For convenience, changes in guy geometry are not included in the following development.

Considering the sum of the vertical forces, V = 0, then

$$(P_w + 3\,P_s - 3\,P_i) \cos \alpha = 0 \quad \ldots\ldots\ldots\ldots \quad (3)$$

But $\cos \alpha \neq 0$, therefore

$$(P_w + 3\,P_s - 3\,P_i) = 0 \quad \ldots\ldots\ldots\ldots \quad (4)$$

and for a selected factor of safety, F. S. = 2.5, the design load, P_d, may be computed as follows:

$$P_d = P_w = P_s = \frac{\text{B. S.}}{\text{F. S.}} = 0.4\ \text{B. S.} \quad \ldots\ldots\ldots\ldots \quad (5)$$

---

3 "Design of Multi-Level Guyed Towers: Wind Loading," by E. Cohen and H. Perrin, Proceedings Paper 1355, ASCE, September, 1957.

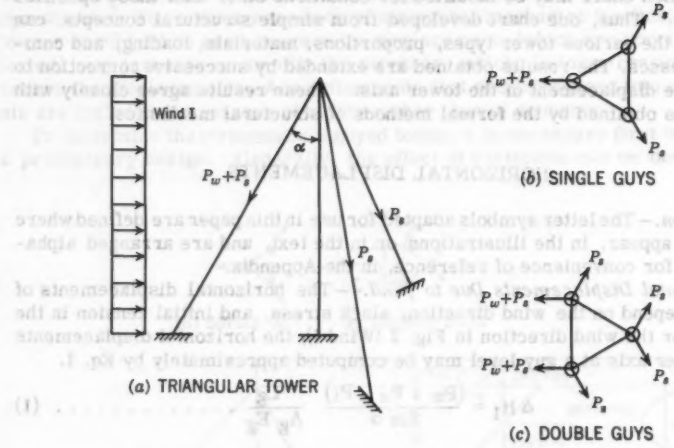


FIG. 2.—FORCES DUE TO WIND I

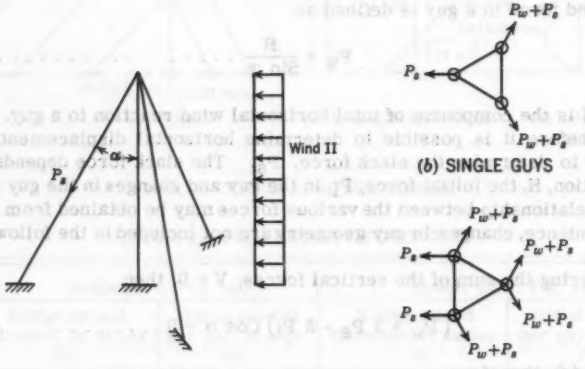


FIG. 3.—FORCES DUE TO WIND II

in which B. S. is the breaking strength of the cable. The approximated slack force would be

$$P_{s1} = 1.5\ P_i - 0.2\ B.\ S. = P_i - 1/3\ P_w \quad \ldots\ldots\ldots\ldots (6)$$

Similarly, for the wind direction in Fig. 3 (Wind II) the horizontal displacement may be computed as follows:

$$\Delta H_2 = \frac{2\left(P_w + P_s - P_i\right)}{\sin \alpha} \frac{L_g}{A_g E_g} \quad \ldots\ldots\ldots\ldots (7)$$

For the same design load, or total change in guy stress, the displacement for Wind II is double that of Wind I. For example, consider an arbitrarily chosen value for the initial tension:

$$P_i = 0.2\ B.\ S. \quad \ldots\ldots\ldots\ldots\ldots\ldots (8)$$

The corresponding value of the slack force for Wind I would then be

$$P_{si} = 0.1\ B.\ S. \quad \ldots\ldots\ldots\ldots\ldots\ldots (9)$$

and the allowable value of the wind load would be

$$P_w = 0.3\ B.\ S. \quad \ldots\ldots\ldots\ldots\ldots\ldots (10)$$

The corresponding magnitude of the horizontal displacement, ΔH, for Wind I, computed by Eq. 1 is

$$\Delta H = \frac{0.2\ B.\ S.}{\sin \alpha} \frac{L_g}{A_g E_g} = \frac{2}{3} \frac{P_w}{\sin \alpha} \frac{L_g}{A_g E_g} \quad \ldots\ldots\ldots (11)$$

Substituting Eq. 2 in Eq. 11 the horizontal displacement becomes

$$\Delta H_1 = \frac{2}{3} \frac{H}{\sin^2 \alpha} \frac{L_g}{A_g E_g} \quad \ldots\ldots\ldots\ldots\ldots (12)$$

Horizontal Displacements Due to Guy Lengthening or Shortening.—Because guyed towers are sensitive to changes in guy tension, extreme caution must be used to insure simultaneous lengthening or shortening of all guys that meet at a particular tower level. Small changes in the tension of a single guy will alter the geometry of the tower axis and may cause buckling, because the small horizontal displacements are amplified by the large axial forces.

Consider a typical guyed tower (Fig. 1). The horizontal displacement, ΔH, may be determined from fundamental relations between statics and geometry, and from the way in which they are related through the properties of the materials. Eq. 13 is derived for guy lengthening or guy shortening, Δe, at a given guy level.

The cross-sectional area of the tower is assumed constant for convenience. Therefore

$$\Delta H = \Delta e \frac{2}{\sin \alpha} \left(1 + 3\ \cos^3 \alpha \frac{A_g E_g}{A_T E_T}\right) \quad \ldots\ldots\ldots (13)$$

in which A_T and E_T are the cross-sectional area and the modulus of elasticity of the tower, respectively.

However, Eq. 13, based on the original geometry, is only approximate, because changes in tower geometry must be included in the analysis. A convenient technique, useful to include changes in geometry, is to multiply computed values by the amplification factor. Thus, the computed transverse displacement, ΔH, may be corrected for changes in geometry by multiplying it by the amplification factor, ϕ. The total horizontal displacement, ΔH_t, may then be computed:

$$\Delta H_t = \Delta e \frac{2}{\text{Sin } \alpha}\left(1 + 3 \text{ Cos}^3 \alpha \frac{A_g E_g}{A_T E_T}\right)\phi \quad \ldots\ldots\ldots\ldots (14)$$

The value of ϕ for displacement is obtained easily from Fig. 4(a).

AMPLIFICATION CHART

The amplification chart (Fig. 4(a)) shows the increase, or amplification, of displacements due to combined axial compression, plus the transverse bending when the displacements of the axis are included in the analysis. The axial stress is denoted by f_a and the bending stress by f_b. The amplification factor ϕ is equal to f_{bt}/f_b or $\Delta H_t/\Delta H$, and f_{bt} is the total amplified bending stress. Fig. 4(a) is based on a computed total stress

$$f = f_a + f_b \quad \ldots\ldots\ldots\ldots\ldots\ldots\ldots (15)$$

of 20 kips per sq in. at the center of a tower section between points of inflection. A uniformly distributed wind load is assumed to be supported throughout the tower height. This selected wind loading is used even though it does not produce the maximum bending unit stress, because it is easy to analyze and almost correct. For a computed stress (Eq. 15), at the center of the tower section between points of inflection, that is not equal to 20 kips per sq in., (that is, for the higher working stresses associated with the higher-strength steels), the value of L/r should be multiplied by $\sqrt{f/20}$.

Transverse loads on a guyed tower cause the elastic curve to move away from the tower axis. The displacements resulting from transverse bending are the moment arms for the dead load and the live load axial forces. Although the displacements are small, the additional bending moments may be large, because the live load plus the dead-load axial forces are large. In flexible members the bending stresses and displacements are increased, or amplified, by the additional bending moment resulting from the product of the large axial forces and the transverse bending displacements. The total horizontal displacement, ΔH_t, with changes in geometry included, is:

$$\Delta H_t = \Delta H \phi \quad \ldots\ldots\ldots\ldots\ldots\ldots\ldots (16)$$

The amplified total combined stress is

$$f_t = f_a + f_b \phi \quad \ldots\ldots\ldots\ldots\ldots\ldots\ldots (17)$$

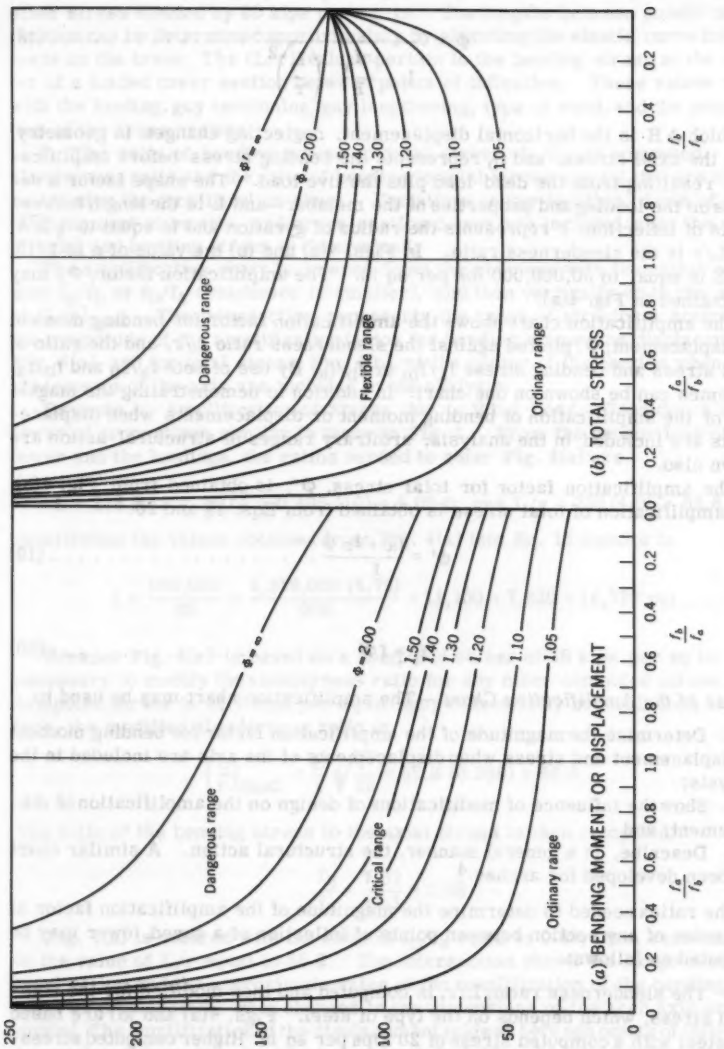


FIG. 4.—AMPLIFICATION CHART

and

$$\Phi = \frac{1}{1 - \frac{nf_a}{E}\left(\frac{L}{r}\right)^2} \quad \ldots\ldots\ldots\ldots\ldots (18)$$

in which ΔH is the horizontal displacement, neglecting changes in geometry, f_a is the axial stress, and f_b represents the bending stress before amplification, resulting from the dead load plus the live load. The shape factor n depends on the loading and properties of the member—and L is the length between points of inflection; r represents the radius of gyration and is equal to $\sqrt{I/A}$; and L/r is the slenderness ratio. In Figs. 4(a) and (b) the value of n is 1/10, and E is equal to 30,000,000 lbs per sq in. The amplification factor, Φ, may be obtained in Fig. 4(a).

The amplification chart shows the amplification factor for bending moment or displacement, Φ, plotted against the slenderness ratio L/r, and the ratio of axial stress and bending stress f_a/f_b, or f_b/f_a. By use of both f_a/f_b and f_b/f_a, extremes can be shown on one chart. In addition to demonstrating the magnitude of the amplification of bending moment or displacements when displacements are included in the analysis, arbitrary ranges of structural action are shown also.

The amplification factor for total stress, Φ', is obtained from Fig. 4(b). The amplification of total stress is obtained from Eqs. 19 and 20.

$$\Phi' = \frac{f_a + f_b \Phi}{f} \quad \ldots\ldots\ldots\ldots\ldots\ldots (19)$$

and

$$f_t = f\Phi' \quad \ldots\ldots\ldots\ldots\ldots\ldots (20)$$

Use of the Amplification Chart.—The amplification chart may be used to

1. Determine the magnitude of the amplification factor for bending moment or displacement and stress when displacements of the axis are included in the analysis;
2. Show the influence of modifications of design on the amplification of displacement; and
3. Describe, in a general manner, the structural action. A similar chart has been developed for arches.[4]

The ratios needed to determine the magnitude of the amplification factor at the center of any section between points of inflection of a guyed tower may be computed as follows:

1. The slenderness ratio, L/r, is computed and then modified for the computed stress, which depends on the type of steel. Figs. 4(a) and (b) are based on a steel with a computed stress of 20 kips per sq in. Higher computed stresses may be allowed for the higher strength steels. If the computed stress is other than 20 kips per sq in., the modified slenderness ratio needed to enter the chart, $(L/r)_{mod}$, is determined by multiplying the slenderness ratio for the

4 "Amplification of Stress in Flexible Steel Arches," by R. S. Rowe, Transactions, ASCE, Vol. 119, 1954, p. 910-926.

stress other than 20 kips per sq. in. by the square root of the quotient of the other stress divided by 20 kips per sq. in. The lengths between points of inflection can be determined approximately by sketching the elastic curve for the loads on the tower. The (L/r)-values pertain to the bending stress at the center of a loaded tower section between points of inflection. These values vary with the loading, guy tensioning, guy lengthening, type of steel, and the properties of the cross section.

2. The ratio of bending stress to axial stress, f_b/f_a, is computed. The slenderness ratio and the ratio of bending to axial stress are all that are needed to enter the amplification chart. Variations in guy location, depth of section, moment of inertia, and cross-sectional area are included when the ratio of axial and bending stress is determined.

The amplification chart is entered from the abscissa with the ratios of either f_a/f_b or f_b/f_a (whichever is smaller), and then vertically up to the value of $(L/r)_{mod}$. The intersection represents the range of structural action and the magnitude of the amplification factor for bending moment or displacement, Fig. 4(a), and for total stress, Fig. 4(b), at the center of the section when displacements of the axis are included in the analysis.

Example 1: Amplification of Stress due to Wind Load.—Consider a steel tower of proportions similar to those in Fig. 1. From the proportions of the tower and the loadings, the ratios needed to enter Fig. 4(a) are

$$L = 238 \text{ ft}, \; r = \sqrt{I/A} = 0.405\,(10) = 4.05 \text{ ft}, \text{ and } L/r = 238/4.05 = 58.8.$$

Substituting the values obtained from Fig. 4(a) into Eq. 15 results in

$$f = \frac{668{,}000}{60} + \frac{1{,}316{,}000\,(5.75)}{900} = 11{,}100 + 7{,}620 = 18{,}720 \text{ psi}$$

Because Fig. 4(a) is based on a computed stress of 20 kips per sq in. it is necessary to modify the slenderness ratio for any other computed stress. The computed stress is 21.9 kips per sq in. (guy eccentricity not included), therefore, the modified slenderness ratio is

$$\left(\frac{L}{r}\right)_{mod.} = \frac{L}{r}\sqrt{\frac{f}{20}} = 58.8\,(0.966) = 56.8$$

The ratio of the bending stress to the axial stress is then computed:

$$\frac{f_b}{f_a} = \frac{7.62}{11.1} = 0.68$$

Fig. 4(a) is entered with the ratio of f_b/f_a equal to 0.68, then, vertically up to the value of L/r equal to 56.8. The intersection shows the range of structural action and the approximate value of the amplification of the bending moment or displacement when changes in the dimensions of the arch axis are included. The amplification of the displacement midway between points of inflection interpolated from the chart is approximately 1.16 and is the flexible range of structural action. Thus, the actual stress obtained from Eq. 17 is:

$$f_t = 11{,}100 + 7{,}620\,(1.16) = 20{,}050 \text{ psi}$$

Similarly, the total stress can be obtained from Fig. 4(b), in which the amplification factor for total stress ϕ', interpolated from the chart, is 1.07. The total stress computed by Eq. 20 is

$$f_t = 18{,}720\ (1.07) = 20{,}050 \text{ psi}$$

Example 2: Amplification of Stress due to Guy Lengthening or Guy Shortening.—To show the dangers of guy lengthening or shortening, suppose that after the tower has been erected it is discovered that the tension in the lower set of guys needs to be increased or decreased by 15% of the guy breaking strength. For the typical tower (Fig. 1), with a set of single guys 1 5/8 in. in diameter at the first guy level, 9% of the breaking strength of 324,000 lb corresponds to a change in tension of 29,160 lb. This change corresponds to the guy lengthening or shortening, Δe (changes due to sag are of a secondary nature and negligible):

$$\Delta e = \frac{P\,L}{A\,E} \qquad \ldots\ldots\ldots\ldots\ldots\ldots\ldots\ldots (21)$$

in which P is a force due to the change in tension; L represents the length of the guy, in in.; A is the cross-sectional area of the guy; and E is the modulus of elasticity of the guy. Substituting into Eq. 21,

$$\Delta e = \frac{29{,}160 \times 424 \times 12}{1.59 \times 25{,}000{,}000} = 3.73 \text{ in.}$$

The corresponding horizontal displacement, ΔH, of the tower at the first guy level is computed from Eq. 13:

$$\Delta H = 3.73 \times \frac{2}{0.707}\,(1 + 0.02) = 10.6 \text{ in.}$$

If only one guy is lengthened or shortened instead of all three guys meeting at the same level simultaneously, the axis of the tower will change in accordance with the geometry in Fig. 5 for the lengthening of G_1. Secondary effects are small and not included herein. The length between points of inflection has increased greatly from the original length of 238 ft (Fig. 1) to 480 ft (Fig. 5), corresponding to a slenderness ratio of $\frac{L}{r} = \frac{480}{4.05} = 120$.

The critical buckling stress, f_x, for a steel tower with the slenderness ratio of 120 was computed as 20,600 lb per sq in. from Eq. 22.

$$f_x = \frac{\pi^2\,E}{(L/r)^2} \qquad \ldots\ldots\ldots\ldots\ldots\ldots\ldots\ldots (22)$$

The critical stress, f_x, is an ultimate stress with no factor of safety included.

Using Eq. 23, the part of the bending moment due to a horizontal displacement is equal to 1,030 ft-kips.

$$M_b = c\,\frac{6\,E\,I\,\Delta H}{L^2} \qquad \ldots\ldots\ldots\ldots\ldots\ldots\ldots\ldots (23)$$

in which c is a factor that depends on the end fixity at the supports. For the problem under consideration, c = 0.6.

Additional bending moments, M_a, result from the axial forces multiplied by the relative horizontal tower displacements. The axial force above the section under consideration is composed of the tower weight, W = 264 kips, and initial guy tension, P_i = 218 kips. Substituting in Eq. 24,

$$M_a = (W + P_i)\,\Delta H \quad \ldots\ldots\ldots\ldots\ldots\ldots (24)$$

$$M_a = (264 + 218)\,(10.6/12) = 425 \text{ ft-kips.}$$

The computed bending moment, M, is the sum of the moments due to tower displacement plus the moment resulting from the axial force multiplied by displacement.

$$M = M_b + M_a \quad \ldots\ldots\ldots\ldots\ldots\ldots (25)$$

Therefore

$$M = 1{,}030 + 425 = 1{,}455 \text{ ft-kip.}$$

The corresponding computed stress with changes in geometry due to loads not included, is obtained from Eq. 15:

$$f = \frac{480{,}000}{59} + \left(\frac{1455{,}000}{990}\right)(5.75)$$

$$f = 8{,}140 + 8{,}450 = 16{,}590 \text{ psi}$$

Thus, the stress computed in the usual manner is not the total stress in the tower, because changes in geometry must be included.

The actual total stress, amplification included, may be obtained by use of Eq. 17. From Fig. 4(a) for L/r = 120 and $f_a/f_b = 0.96$, $\Phi = 1.7$. Thus, f_t = 8,140 + 8,450 (1.7) = 22,510 psi.

Similarly, the total stress computation by use of Fig. 4(b) is

$$f_t = f\Phi = 16{,}590\ (1.36) = 22{,}560 \text{ psi}$$

The tower of this example will probably collapse, because the computed total stress of 22,500 psi exceeds the critical stress of 20,600 psi.

The corresponding amplified horizontal displacement as computed by Eq. 16 is

$$\Delta H_t = 10.6 \text{ X } 1.7 = 18.0 \text{ in.}$$

Possible solutions include simultaneous lengthening or shortening of all the guys that meet at a given level and by increasing the number of guy levels from three to four or five.

Influence of Modifications on the Amplification of Stress.—The amplification of stress in guyed towers subjected to combined axial compression and transverse bending is influenced by the slenderness ratio L/r, the type of steel or computed stress, and the ratio f_a/f_b. The amplification of stress can be reduced by decreasing the slenderness ratio. For a given length between inflection points, l, the amplification of stress decreases for increasing values of the radius of gyration.

A higher allowable computed stress is permitted for certain types of steel and for wind load. The relative amplification of stress is influenced by variations in the allowable or computed stress (Eq. 18). An increase in the computed stress results in a disproportionate increase in amplification, particularly for larger values of the slenderness ratio.

Use of the Amplification Chart to Describe Structural Action.—The amplification chart (Fig. 4) may be useful in describing the range of the structural action of guyed towers. The chart has been divided into three arbitrary ranges: (a) The ordinary range, (b) the flexible range, and (c) the dangerous range.

The ordinary range shows that the analysis, by customary methods of structural mechanics, gives sufficiently accurate results. In the ordinary range, changes in the dimensions of the tower cross section and changes in the displacement of the tower axis have little influence on the amplification of stress. Therefore (to that degree), superposition of effects is applicable. In the ordinary range, for a given slenderness ratio of less than 70 and for values of f_a/f_b from 0.5 to 2.0, the amplification of stress remains constant, regardless of the loading and proportions of the tower. For decreasing values of f_a/f_b and

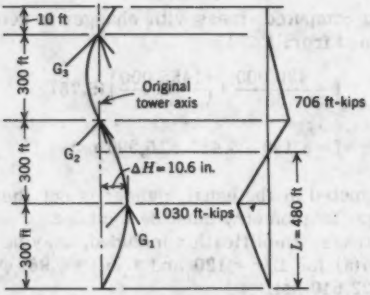


FIG. 5.—DISPLACED TOWER AXIS

f_b/f_a less than 0.5, the amplification of stress decreases for constant values of L/r. Fig. 4(b) has been drawn for a total stress before amplification of 20 kips psi. If the computed stress is greater than 20 kips per sq in., it is necessary to consider the corresponding disproportionate increase in the amplification. The amplification of displacements (Fig. 4(a)), for constant L/r, increases with increasing values of f_a/f_b. In the ordinary range, elastic buckling is highly improbable except for relatively small values of f_b/f_a, at which values the amplification of displacements is relatively large.

In the flexible range, the ordinary methods of structural mechanics must be modified and extended to include the effects of displacements. Superposition of effects is not applicable, and it is not permissible to separate live load and dead load. The amplification of stress in this range has been arbitrarily limited to from 10% to 50%. The area of constant amplification of stress for a given (L/r)=ratio is less pronounced in the flexible range. The amplification of stress increases for increasing values of f_a/f_b up to a certain value and then decreases. The amplification of displacements continues to increase for increasing values of f_a/f_b.

Variations in loading and in properties of the tower have more influence on the amplification of stress in the flexible range than in the ordinary range. Amplification of stress is more pronounced for small changes in the slenderness ratio. Attention is given to variations in the computed stress, because increases in this stress result in disproportionate increases in the amplification. Elastic buckling may be possible at relatively larger values of L/r and for values of f_a/f_b greater than unity.

In the dangerous range, the amplification of stress is greater than 50%. In this range the amplification of stress and displacement is so large that there is danger of elastic or plastic buckling. The line separating elastic and plastic buckling depends, to some extent, on the type of steel used. The higher allowable stresses associated with silicon, nickel, and T-1 steel result in disproportionate increases in amplification.

For an assumed tower design, the amplification chart shows immediately if danger exists, and what modifications are indicated to avoid this danger without elaborate computations.

AMPLIFICATION OF STRESS AND DISPLACEMENTS

The bending moment obtained from only the wind live load is not the actual bending moment in the structure. The moments resulting from guy eccentricity have not been included herein. The bending moment resulting from the transverse loads is increased, or amplified, by additional bending caused by the axial forces. Usually a guyed tower is designed so that the live load deflections are small. The bending moment due to the axial force is computed by multiplying the axial force by the distance from the elastic curve to the original tower axis.

If the displacements of the tower are neglected, the same bending moment will be determined for the wind load only as for the wind load plus axial forces. Thus, by the usual theory, it is permissible to separate the wind load from the guy tensioning and to add the partial effects to obtain the total effect.

In a guyed tower the displacements of the tower axis, although small, may form a large part of the dead-load plus the wind-load bending moment, as shown in Fig. 6. If the displacements of the tower axis are included, larger bending moments will be determined for the wind load plus the dead load than for the wind load only. The transverse displacements are moment arms for the combined wind-load plus the dead-load axial forces. When the displacements of the axis are included, it is not permissible to separate the live load from the dead load. Not only are the bending moments and the displacements increased or amplified by the live load plus dead-load axial forces, but the sums of the partial effects of the live load and the dead load are not equal to the total effect. However, it is often convenient to permit an arbitrary allowable increase to the results obtained by assuming that the structure does not deform, and still be safe.

The stages of additional bending continue, and may be represented by a mathematical series that may or may not converge. If the bending continues to increase (nonconvergent series), the structure will collapse. Fig. 6 shows a straight member subjected to both axial and transverse loads. The equation for the displacement at the center of the beam is:

$$\Delta = \frac{n\, M_o\, L^2}{E\, I} \qquad \ldots\ldots\ldots\ldots\ldots\ldots\ldots\ldots (26)$$

in which M_o is the ordinate of the bending moment diagram at the center of the beam; I is the moment of inertia of the beam; and the shape factor $n = \frac{1}{9.6}$ for a simply supported beam with uniformly distributed wind live load. A more complete development of the amplification factor is presented elsewhere.[2]

The bending moment for the transverse loads is increased by additional bending caused by the axial forces. The shape factor for the transverse loads, n_b, is not the same as the shape factor for the axial loads, n_a. For ordinary

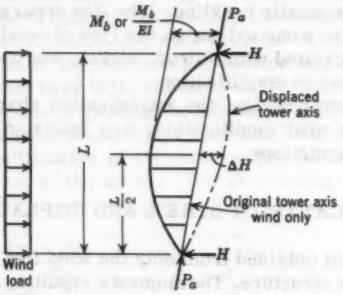


FIG. 6.—AXIAL FORCES AND TRANSVERSE WIND LOAD

guyed towers, the error resulting from setting n_a equal to n_b is small, approximately 3%.

The additional bending moment (Fig. 6) is

$$M_a = P_a \Delta_b \quad \ldots\ldots\ldots\ldots\ldots\ldots (27)$$

in which P_a is the axial force and Δ_b represents the transverse displacement due to M_b. The additional bending moment causes a further displacement,

$$\Delta_a = \frac{n_a P_a \Delta_b L^2}{E I} \quad \ldots\ldots\ldots\ldots\ldots\ldots (28)$$

and an increased bending moment

$$M_a' = P_a \frac{n_a P_a \Delta_b L^2}{E I} \quad \ldots\ldots\ldots\ldots\ldots\ldots (29)$$

This process is continued, and the total bending moment is represented by

$$M_t = M_b + P_a \Delta_b + P_a \Delta_b n_a \left(\frac{P_a L^2}{E I}\right) + P_a \Delta_b n'_a n_a \left(\frac{P_a L^2}{E I}\right)^2 \cdots \quad \ldots\ldots\ldots\ldots\ldots\ldots (30)$$

in which n'_a is the new shape factor.

If $n_a P_a L^2/(E I) < 1$, and letting successive values of n equal n_a

$$M_t = M_b + \frac{P_a \Delta_b}{1 - \frac{n_a P_a L^2}{E I}} \quad \ldots\ldots\ldots\ldots\ldots\ldots (31)$$

Eq. 31 can also be written as

$$M_t = M_b \frac{1 - \frac{n_a P_a L^2}{E I} + \frac{n_b P_a L^2}{E I}}{1 - \frac{n_a P_a L^2}{E I}} \quad \ldots\ldots\ldots\ldots (32)$$

By setting n_a equal to n_b, an approximate expression for the amplification of displacements and bending moments is obtained.

$$M_t = \frac{M_b}{1 - \frac{n_a P_a L^2}{E I}} = M_b \Phi \quad \ldots\ldots\ldots\ldots\ldots\ldots (33)$$

and

$$\Delta = \Delta_b \Phi \quad \ldots\ldots\ldots\ldots\ldots\ldots\ldots\ldots (34)$$

The quantity

$$\frac{1}{1 - \frac{n_a P_a L^2}{E I}}$$

is the amplification factor, Φ.

The total stress for a straight member of tower section, subjected to both axial and transverse loads, can be computed from Eq. 17. However, this equation does not include the effects of temperature change, plastic flow, and movement of the tower base.

This investigation and the amplification formula for a horizontal, straight member are applicable also to a curved member with supports on the same elevation.[4]

CONCLUSIONS

Simplified equations for the determination of displacements of guy levels in a tower have been developed in terms of the wind load, initial guy tension, and slack stress. Amplification charts for stress and displacement that have been found useful in the predesign of guyed towers have also been presented. These charts show the increase or amplification of stress and displacement at the center of a section between points of inflection of a guyed tower, when displacements of the axis are included in the analysis. In the development of the chart only familiar concepts were used.

The value of the chart is that it shows immediately when elaborate methods of analysis are necessary in the design of flexible towers. The chart indicates also what modifications may be made, so that the ordinary methods of structural mechanics may give adequate results.

APPENDIX.—NOTATION

The following symbols, adapted for use in the paper and for the guidance of discussers, conform essentially with "American Standard Letter Symbols for

Structural Analysis" (ASA Z10.8-1949), prepared by a committee of the American Standards Association with Society representation, and approved by the Association in 1949:

- A = area:
  - A_g = cross-sectional area of a guy;
  - A_t = cross-sectional area of the tower;
- B. S. = breaking strength of the cable;
- b = transverse displacement due to M_b;
- c = factor depending on the end fixity at the supports;
- E = modulus of elasticity:
  - E_g = modulus of elasticity of a guy;
  - E_t = modulus of elasticity of the tower;
- e = guy lengthening or shortening;
- F. S. = factor of safety;
- f = total stress:
  - f_a = axial stress;
  - f_b = bending stress;
  - f_{bt} = total amplified bending stress;
  - f_t = amplified total combined stress (total stress);
  - f_x = critical buckling stress;
- G_1, G_2, G_3 = guys;
- H = total horizontal wind reaction at guy junction;
- ΔH_1 = horizontal displacement for Wind I;
- ΔH_2 = horizontal displacement for Wind II;
- ΔH = horizontal displacement;
- ΔH_t = total horizontal displacement;
- I = moment of inertia;
- L = length between points of inflection;
- L_g = guy length, as in Eq. 1;
- M = computed bending moment:
  - M_a = additional bending moment;
  - M_b = bending moment due to horizontal displacement;
  - M_o = ordinate of the bending moment diagram at the center of the beam;
  - M_t = total bending moment;
  - M'_a = increased bending moment;

n = shape factor:
n_a = shape factor for the axial loads;
n_b = shape factor for the transverse loads;
n'_a = new shape factor;
P = force:
P_a = axial force;
P_d = design load;
P_{d1} = design load for wind load I;
P_{d2} = design load for wind load II;
P_i = initial force in a guy (tension);
P_s = slack force in a guy;
P_{s1} = slack force for wind load I;
P_{s2} = slack force for wind load II;
P_w = wind force in a guy;
r = radius of gyration;
s = cross-sectional distance;
V = vertical force;
W = tower height;
α = angle between the guy and the vertical;
Δ = displacement at the center of the beam;
Δ_a = further displacement;
ϕ = amplification factor;
ϕ' = amplification factor for total stress.

DISCUSSION

VITELMO BERTERO,[5] A. M. ASCE.—The writer agrees that the method developed by the author for determining the slack in the guy and the horizontal displacements due to wind load is simple and easy to perform. However, it is felt that this method is based on a set of working formulas that do not offer accuracy satisfactory for tall towers.

The relationship between the live load force, the initial tension, and the slack stress in the guys was obtained from simplified equations, where the effect of the sag of the cable and the effect of wind pressure along the length of

[5] Lecturer, Civ. Engrg., Univ. of California, Berkeley, Calif.

the guy were neglected. The writer believes that these effects should be included and, in order to show the relative importance of each one, they will be considered separately.

In a study made by Myle J. Holley, Jr., M. ASCE, and the writer,[6] it was found that if the effect of the wind along the guy is neglected, the following expression relating upper end displacement to the change in guy tension of an individual guy is useful in the study of the behavior of a guy group (Fig. 7).

$$\Delta d = \frac{d}{E} \sec^2 \gamma \Delta f_m + \frac{\rho^2 d^3 \sec^2 \gamma}{24 f_m^2} \left[1 - \frac{1}{\left(\frac{1 + \Delta f_m}{f_m} \right)^2} \right] \quad \ldots . \quad (35)$$

in which Δd is the horizontal displacement of the upper end of the guy; d denotes the initial horizontal projection of the guy; γ represents the inclination

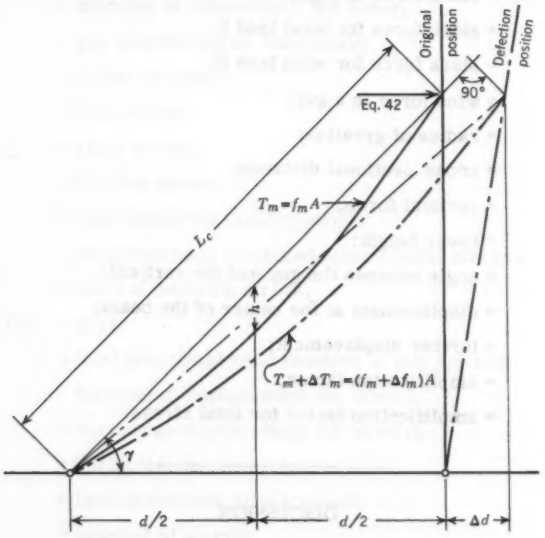


FIG. 7.—DISPLACEMENT OF THE UPPER AND OF A SINGLE GUY

of the chord; f_m is the mid-length unit stress of the guy; Δf_m is equal to the change in the mid-length unit stress f_m of the guy; and ρ denotes the density of the guy and is equal to $\frac{\text{weight per foot}}{\text{metallic area}}$.

The first term of Eq. 35 represents the horizontal displacement that would result if the cable were considered as a tie rod, that is, a straight two-force

6 "Investigation of Large Multi-Guyed Towers," by M. V. Holley and V. Bertero, Massachusetts Inst. of Technology, Dept. of Civ. and San. Engrg., June, 1955.

member. The second term of this equation may be considered as a correction to the tie rod displacement, to account for the effect of sag. This correction is approximated, but it is believed to be of satisfactory accuracy for application to the range of sag ratios (h/d) encountered in properly designed guyed towers. h is the sag and d is defined above (see Fig. 7).

By consideration of the compatibility of displacement of windward and leeward guys and the required conditions of equilibrium, the displacement versus change in tension of the individual guys can be combined to obtain curves which define the resistance function of a group of guys, that is, the relationship between displacement of the group and net force that the group exerts on the tower.

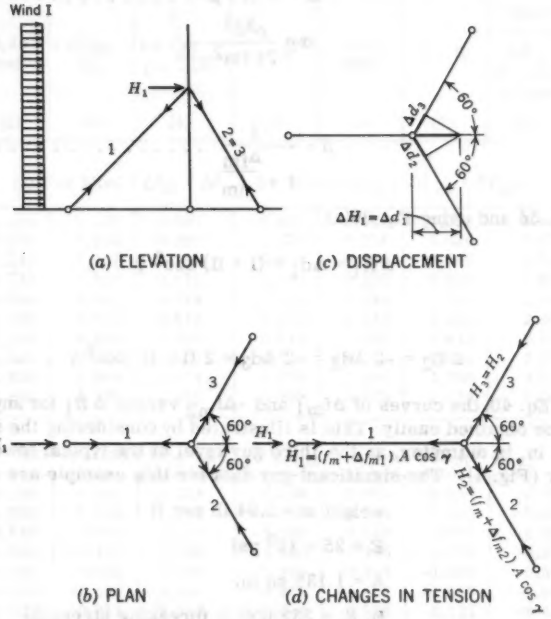


FIG. 8.—DISPLACEMENT AND CHANGES IN TENSION DUE TO WIND I

Considering the case classified by the author as Wind I and if ΔH is the horizontal displacement of the tower at the guy connection in Fig. 8, then,

$$\Delta d_1 = \Delta H_1 \quad \ldots\ldots\ldots\ldots\ldots\ldots (36)$$

$$\Delta d_2 = \Delta d_3 = 0.5\, \Delta H_1 \quad \ldots\ldots\ldots\ldots\ldots\ldots (37)$$

and

$$H_1 = (\Delta f_{m1} - \Delta f_{m2})\, A \times \cos \gamma \quad \ldots\ldots\ldots\ldots\ldots\ldots (38)$$

Eq. 35 can be written as

$$\Delta d = (I + II) \sec^2 \gamma \quad \ldots\ldots\ldots\ldots\ldots\ldots (39a)$$

in which

$$I = m\, \Delta f_m \quad \ldots\ldots\ldots\ldots\ldots\ldots (39b)$$

$$m = \frac{d}{E} \quad \ldots\ldots\ldots\ldots\ldots\ldots (39c)$$

$$II = \alpha\,(1 - \beta^2) \quad \ldots\ldots\ldots\ldots\ldots\ldots (39d)$$

$$\alpha = \frac{\rho^2 d^3}{24\, fm^2} \quad \ldots\ldots\ldots\ldots\ldots\ldots (39e)$$

and

$$\beta = \frac{1}{1 + \frac{\Delta_{fm}}{f_m}} \quad \ldots\ldots\ldots\ldots\ldots\ldots (39f)$$

From Eq. 36 and using Eq. 39(a)

$$\Delta H_1 = \Delta d_1 = (I + II) \sec^2 \gamma \quad \ldots\ldots\ldots\ldots\ldots\ldots (40)$$

and

$$\Delta H_2 = -2\, \Delta d_2 = -2\, \Delta d_3 = 2\,(I + II) \sec^2 \gamma \quad \ldots\ldots\ldots (41)$$

Using Eq. 40, the curves of Δf_{m1} and $-\Delta f_{m2}$ versus ΔH_1 for any particular case can be obtained easily. This is illustrated by considering the set of single guys, $1\frac{1}{8}$ in. in diameter, at the third guy level of the typical tower shown by the author (Fig. 1). The significant guy data for this example are as follows.[7]

weight w = 3.94 lb per ft

$E = 25 \times 10^6$ psi

A = 1.135 sq in.

B. S. = 232,000 lb (breaking strength)

$\rho = \frac{w}{A} = 3.46$ lb per ft per sq in.

$\rho^2 = 12$ lb per ft per sq in., squared.

For cable 1,

d = +900 ft

For cables 2, and 3,

d = -900 ft

[7] "Wire Rope Engineering Handbook," United States Steel, Cleveland, Ohio, 1946.

Considering for the initial mid-length tension, the value selected by the author, P_i = 0.2 B. S. = 46.400 lb, the corresponding initial unit tension is

$$f_m = \frac{46,400}{1,135} = 40,900 \text{ psi}$$

For this value of f_m, the variation of ΔH with changes Δf_{m1} and $-\Delta f_{m2}$ and $-\Delta f_{m3}$ can be computed as indicated in Table 3.

TABLE 3.—COMPUTATION OF ΔH

Δf_m, in pounds per square inch	I, in feet[a]	$\frac{\Delta f_m}{f_m}$	$\beta = \frac{1}{1+\frac{\Delta f_m}{f_m}}$	$1-\beta^2$	II, in feet[b]	I + II	Wind I: $\Delta H_1 = (I + II)2$, in feet	Wind II: $\Delta H_2 = (I+II)4$, in feet
(1)	(2)	(3)	(4)	(5)	(6)	(7)	(8)	(9)
(a) For Wind I $\Delta f_m = \Delta f_{m1}$, for Wind II $\Delta f_m = \Delta f_{m2} = \Delta f_{m3}$								
5,000	0.180	0.122	0.890	0.210	0.046	0.226	0.452	0.904
10,000	0.360	0.244	0.803	0.357	0.078	0.438	0.876	1.752
15,000	0.540	0.367	0.731	0.468	0.102	0.642	1.284	2.568
20,000	0.720	0.489	0.671	0.550	0.120	0.840	1.680	3.360
25,000	0.900	0.611	0.620	0.615	0.134	1.034	2.068	4.136
30,000	1.080	0.733	0.576	0.669	0.146	1.226	2.452	4.904
35,000	1.260	0.855	0.539	0.710	0.155	1.415	2.830	5.660
40,000	1.440	0.978	0.505	0.745	0.162	1.602	3.204	6.408
45,000	1.620	1.100	0.476	0.774	0.168	1.788	3.576	7.152
50,000	1.800	1.222	0.450	0.798	0.174	1.974	3.948	7.896
(b) For Wind I $\Delta f_m = \Delta f_{m2} = \Delta f_{m3}$, for Wind II $\Delta f_m = \Delta f_{m1}$								
-5,000	-0.180	-0.122	1.138	-0.295	-0.064	-0.244	-0.976	-0.488
-10,000	-0.360	-0.244	1.321	-0.745	-0.161	-0.521	-2.084	-1.042
-15,000	-0.540	-0.367	1.578	-1.485	-0.325	-0.865	-3.460	-1.730
-17,500	-0.630	-0.428	1.746	-2.050	-0.448	-1.078	-4.312	-2.156
-20,000	-0.720	-0.489	1.955	-2.830	-0.616	-1.336	-5.344	-2.672
-22,500	-0.810	-0.550	2.220	-3.930	-0.857	-1.667	-6.668	-3.334
-25,000	-0.900	-0.611	2.565	-5.600	-1.221	-2.121	-8.484	-4.242
-26,000	-0.936	-0.635	2.740	-6.500	-1.435	-2.371	-9.484	-4.742
-27,000	-0.972	-0.660	2.940	-7.650	-1.670	-2.642	-10.564	-5.282
-28,000	-1.008	-0.684	3.160	-9.000	-1.960	-2.970	-11.880	-5.940
-29,000	-1.044	-0.709	3.460	-10.800	-2.360	-3.404	-13.616	-6.808

[a] $I = 3.6 \times 10^{-5} \Delta f_m$. [b] $II = 0.218 (1 - \beta^2)$.

The values of Δf_{m1}, and $-\Delta f_{m2} = -\Delta f_{m3}$ were plotted versus the obtained values of ΔH_1 (Fig. 9). The curves in the right quadrant are drawn for Wind I. Selecting a factor of safety, F. S. = 2.5, as the author suggested, the maximum allowable tension in the cable is

$$T_{allowable} = \frac{B.\ S.}{F.\ S.} = \frac{232,000 \text{ lb}}{2.5} = 92,800 \text{ lb.}$$

For initial mid-length tension of $T_m = P_i = 46{,}400$ lb, the maximum initial tension in the cable, which occurs at the upper end, may be computed from:

$$T_{i\ max.} = \sqrt{\left(T_m \sin\gamma + \frac{w^d/\cos\gamma}{2}\right)^2 + (T_m \cos\gamma)^2} \quad \ldots\ldots (42)$$

Therefore

$$T_{i\ max} = \sqrt{\left(46{,}400 \times 0.707 + \frac{3.94 \times 900}{2 \times 0.707}\right)^2 + (46{,}400 \times 0.707)^2} = 48{,}500 \text{ lb}$$

Thus, the allowable value of the wind load, H_1, is that producing a horizontal displacement of ΔH_1 at the third guy level consistent with a change in the tension of guy 1, $\Delta T_1 = 92{,}800 - 48{,}500 = 44{,}300$ lb. This corresponds to $\Delta f_{m1} = \frac{44{,}300}{1.135} = 39{,}000$ psi. For this value of Δf_{m1} the magnitude ΔH_1 can be computed using Eq. 40 and is $\Delta H_1 = 3.12$ ft. This value may also be read directly

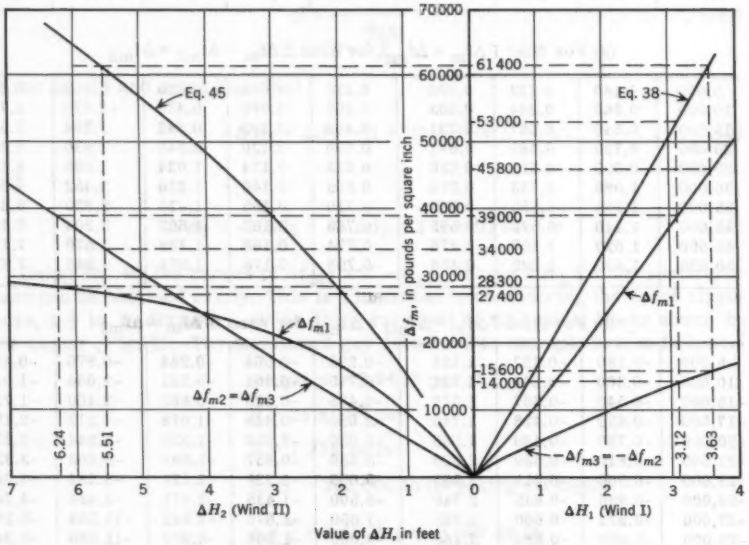


FIG. 9.—DISPLACEMENT VERSUS CHANGE IN TENSION

from the curve of Fig. 9. From the same figure, it can be seen that for $\Delta H_1 = 3.12$ ft, cables 2 and 3 undergo a change in tension, $\Delta f_{m2} = \Delta f_{m3} = -14{,}000$ psi. Consequently, the allowable wind load, H_1, can be obtained using Eq. 38.

$$H_1 = \left[39{,}000 - (14{,}000)\right] 1.135 \times 0.707 = 42{,}600 \text{ psi}$$

which in terms of the breaking strength of the cable becomes

$$H_1 = \frac{42{,}600}{232{,}000} \text{ B. S.} = 0.184 \text{ B. S.}$$

The mid-length tension in the guys 2 and 3 would be

$$T_{m2} = T_{m3} = (40{,}900 - 14{,}000)\ 1.135 = 30{,}600 \text{ lb} = 0.132 \text{ B. S.}$$

This value corresponds to what the author designated as slack force, P_{s1}.

The increase in the vertical force on the mast would be

$$\Delta V = (39{,}000 - 2 \times 14{,}000) \times 1.135 \times 0.707 = 8.850 \text{ lb}$$

or

$$\Delta V = 0.0835\ V$$

in which V is the initial vertical force on the mast, and is equal to

$$V = 3\left(40{,}900 \times 1.135 \times 0.707 + \frac{1}{2} \times 3.94 \times \frac{900}{0.707}\right) = 106{,}000 \text{ lb.}$$

If the case classified by the author in Wind II is considered, it is evident that because the wind direction is reversed from that shown in Fig. 8, the following equations result:

$$\Delta d_1 = -\Delta H_2 \quad \ldots\ldots\ldots\ldots\ldots\ldots (43)$$

$$\Delta d_2 = \Delta d_3 = 0.5\ \Delta H_2 \quad \ldots\ldots\ldots\ldots\ldots\ldots (44)$$

and

$$H_2 = (\Delta f_{m2} - \Delta f_{m1})\ A \cos \gamma \quad \ldots\ldots\ldots\ldots\ldots\ldots (45)$$

using Eq. 39,

$$\Delta H_2 = -\Delta d_1 = (I + II) \sec^2 \gamma \quad \ldots\ldots\ldots\ldots\ldots\ldots (46)$$

and

$$\Delta H_2 = 2\ \Delta d_2 = 2\ \Delta d_3 = 2(I + II) \sec^2 \gamma \quad \ldots\ldots\ldots\ldots\ldots\ldots (47)$$

Taking advantage of the values already computed in Table 2 for Wind I, the curves shown on the left quadrant of Fig. 9 can be plotted. Using these curves, it can be shown that the allowable wind load, H_2, is

$$H_2 = (39{,}000 + 28{,}300)\ 1.135 \times 0.707 = 54{,}000 \text{ lb}$$

and the required horizontal displacement to produce this net force is

$$\Delta H_2 = 6.24 \text{ ft}$$

When comparing H_1 and H_2 it is clear, that Wind I controls. Consequently, the maximum allowable wind load would be $H_1 = 0.184$ B. S., instead of 0.30 B. S. sin $\alpha = 0.212$ B. S. as found by the author.

If the value of $H_1 = 0.30$ B. S. sin α is considered, according to the author's Eq. 11 the magnitude of the corresponding horizontal displacement is

$$\Delta H = \frac{0.2 \text{ B. S.}}{\sin \alpha} \frac{L_g}{A_g E_g} = \frac{0.2 \times 232{,}000 \times 900/0.707}{0.707 \times 1.135 \times 25 \times 10^6} = 2.94 \text{ ft.}$$

This value is the same for both Wind I and Wind II. However, when the sag effect is considered, using the Eq. 35, the following more accurate values result:

Wind I.—According to Eq. 38, the total change in unit stress required by $H_1 = 0.3$ B. S. sin α is

$$\Delta f_{m1} - \Delta f_{m2} = \frac{0.3 \times 232{,}000 \times 0.707}{1.135 \times 0.707} = 61{,}400 \text{ psi}$$

Considering this value and using the curves of Fig. 9 (right quadrant), $\Delta H_1 = 3.63$ ft and

$$\Delta f_{m1} = 45{,}800 \text{ psi}$$

$$\Delta f_{m2} = \Delta f_{m3} = -15{,}600 \text{ psi}$$

These changes in the unit stress of the guys originate an increase in the vertical force on the mast, which can be computed as follows:

$$\Delta V = (45{,}800 - 2 \times 15{,}600)\ 1.135 \times 0.707 = 11.700 \text{ lb}$$

or

$$\Delta V = \frac{11{,}700}{106{,}000} V = 0.11\ V$$

The forces in cables 2 and 3, that correspond to what the author termed slack force P_{s1}, would be equal to $\frac{(40{,}900 - 15{,}600)}{40{,}900}$ 0.2 B. S. = 0.124 B. S.

Wind II.—Substituting Eq. 45 for $H_2 = 0.30$ B. S. sin α, the total change in unit stress is $\Delta f_{m2} - \Delta f_{m1} = 61{,}400$ psi. The following values can be obtained using the curves on the left quadrant of Fig. 9, $\Delta H_2 = 5.51$ ft; $\Delta f_{m1} = -27{,}400$ lb psi; and $\Delta f_{m2} = \Delta f_{m3} = 34{,}000$ psi.

Therefore, $\Delta V = (2 \times 34{,}000 - 27{,}400) \times 1.135 \times 0.707 = 32.700$ lb or $\Delta V = 0.308\ V$ and the force in guy 1, which corresponds to the author's designation P_{s2} would equal $\frac{(40{,}900 - 27{,}400) \times 0.2 \text{ B. S.}}{40{,}900} = 0.066$ B. S.

Table 4 summarizes the result obtained by applying the simplified method presented by the author and those obtained by including the sag effect according to the method suggested by the writer.

The considerable discrepancies between the results given in Table 4 indicate clearly the importance of the sag effect. The simplified equations developed by the author neglecting this effect yield not only a larger value for the allowable wind load but also displacements that are considerably smaller than those to be expected, especially when Wind II is considered. Although the author assumes that there is no change in the vertical force on the mast, the consideration of the sag effect shows an increase of more than 30% of the initial vertical force.

Regarding the influence of the wind pressure acting on a guy, there are two effects or modifications that must be considered. First, the force that the guy exerts on the undisplaced tower is modified. Second, the relationships between guy tension and upper-end displacement are modified. To account for both of these effects in a rigorous way complicates the analysis. Practical approximation to these effects were suggested in various forms.[6,8,9]

Because of the lack of information about the exact wind pressure used by the author in computing the 200 lb per ft of tower, the writer could not evaluate with accuracy the effect that the consideration of the wind on the guys would have in the example discussed. However, to illustrate the importance of this effect, a new analysis of the behavior of the third guy level group was performed, including the effect of wind pressure of 50 lb per sq ft acting on the guys. This

TABLE 4.—RESULTS FOR THE THIRD SET OF GUYS[a]

Method	(a) Wind load I				(b) Wind load II = 0.30 B.S. sine α		
	H_1	P_{s1}	ΔH or ΔH_1	ΔV, in % of V	P_{s2}	ΔH or ΔH_2	ΔV, in % of V
(1)	(2)	(3)	(4)	(5)	(6)	(7)	(8)
Author's method	0.30 B.S. sine α	0.10 B.S.	2.94	0.00	0.00	2.94	0.00
Method including sag effect	0.26 B.S. sine α	0.13 B.S.	3.12	8.35			
	Using 0.30 B.S. sin α	0.12 B.S.	3.63	11.10	0.066 B.S.	5.51	30.80

[a] Assuming P_1 = 0.20 B.S.

analysis was done according to a suggested method,[4] and the following results were obtained:

Wind I.—The allowable wind load on the tower, H_1, is reduced to 0.15 B. S. sin α, and the corresponding horizontal displacement ΔH_1 = 2.82 ft. The initial vertical force, V, on the mast experiences an increase ΔV of 35.4% of V.

When an allowable wind load H_1 = 0.30 B. S. sin α as obtained by the author was considered, the maximum tension force in the windward guy became equal to 0.53 B. S., and the corresponding horizontal displacement equal to 4.85 ft. The increase in vertical load ΔV becomes 48% of the initial V.

Wind II.—For H_2 = 0.30 B. S. sin α, ΔH_2 became equal to 3.75 ft and the initial vertical force on the mast, V, underwent an increase of 40% of V.

If the above results are compared with those obtained by the writer (Table 4), the importance of the effect of wind pressure along the guy becomes evident. Therefore, it is clear that neither the sag effect nor the effect of wind on guys

8 "Design of Multi-Level Guyed Towers," by E. Cohen and H. Perrin, Proceedings Paper 1356, ASCE, September, 1957.

9 "The Analysis of the Structural Behavior of Guyed Antenna Masts Under Wind and Ice Loading," by G. T. Schott, F. R. Thurston, and P. T. Pocock, National Research Labs., Ottawa, Canada, November, 1954.

can be neglected without introducing considerable inaccuracy. Because in all cases the author's method yields values that are nonconservative, it is evident that this method should be used cautiously.

With the presentation of the amplification charts for stress and displacement, the author has made a practical contribution to the engineers interested in the design of guyed towers. Frequently the tower geometry and anticipated leg stress associated with tower axial load are such as to render the use of beam column theory unnecessary.[6,10]

The author's charts of Fig. 4 can be used to determine whether beam column theory needs to be applied. The trend toward high-strength alloy steel with accompanying high values, f_a, would seem to imply that the amplification of stress will be increasingly important, particularly for large towers. Moreover, if design is based on ultimate load basis (and the writer believes that is desirable), the larger values of the unit stress associated with axial force occurring at ultimate load may require the application of beam-column theory.

According to the arbitrary limitations for the different ranges of the structural action that were suggested, the results obtained for the amplification of displacement and stress in the case of example 1 seem to indicate that the tower is in the ordinary range and not in the flexible range as stated by the author.

The writer investigated[6] the effect of guy tension maladjustments (due either to improper installation or to service conditions) and agrees with the author concerning the danger of guy lengthening and shortening. However, it is felt that concerning the formulas developed and used by the author, the following facts should be mentioned for clarification.

The author's statement under the heading, "Horizontal Displacements," that "Eq. 13 is derived for guy lengthening or guy shortening, Δe, at a given guy level," is not clear. It seems that even if the sag effect is neglected (as suggested by the author) and a set of three single guy is assumed, Eq. 13 determines the horizontal displacement, ΔH, that the upper end connection undergoes when the initial tension in only one guy is increased or decreased by $\Delta e \times \frac{A_g E_g}{L_g}$. Using the relationships given in Fig. 8(c) and (d), it can be shown that in order to produce this change in tension it would be necessary to shorten or to lengthen the guy in $3\,\Delta e$.

Eq. 13 was derived neglecting the sag effect but including the effect of the vertical displacement that the upper end connection of the guy undergoes as a consequence of the variation in the compression force on the tower. As it was stated previously, the writer believes that the sag effect cannot be neglected. On the other hand, the author felt that the effect of vertical displacement of the tower is usually small and it may be neglected as will be illustrated in the following discussion of the results obtained by the author in his example 2. Assuming a change in tension of 29,160 lb the author obtained a Δe equal to 3.73 in. and a $\Delta H = 10.60$ in., where the effect of the vertical displacement of the tower is only 2% and consequently may be neglected. The importance of the sag effect can be shown by comparing the results obtained by using the author's Eq. 13 with those determined by the application of Eq. 35 suggested by the writer. Although Eq. 13 will yield identical values for a certain change in tension whether this change is an increase or decrease, and regardless of the

---

[10] Discussion by Myle T. Holley and Vitelmo Bertero of "Design of Multi-Level Guyed Towers: Structural Analysis," Proceedings Paper 1576, ASCE, March, 1958.

magnitude of the identical tension, the use of Eq. 35 will show considerable difference. For example, assuming that the initial tension in the lower set of guys considered by the author was 31.700 lb as it is indicated in Table 1, and if the tension in one guy is increased by 29.160 lb, the upper connection would undergo a $\Delta H = 11.75$ in. On the other hand, if the tension is decreased by 29.160 lb, the ΔH becomes equal to 264.0 in.

Referring to the displaced position of the tower axis indicated in Fig. 5, it is not clear to the writer how this could be obtained. If this was the result of lengthening only one guy of G_1, as suggested by the author, it seems that the guy group G_2 had to move to the right from the original position and not to the left. Moreover, the horizontal displacement, ΔH, of the tower at the first guy level, G_1 was computed from Eq. 13 under the assumption that the tower could move freely. This is not the case in Fig. 5, because the guy groups, G_2 and G_3, will restrain the movement of the tower and, consequently, the actual ΔH at G_1 would be somewhat less. The writer is not certain how the value of $P_i = 218$ kips used in Eq. 24 was obtained. It would be helpful if the author stated what initial tension was used for each guy level in this example.

In determining the actual total stress and horizontal displacement at guy level G_1, an amplification factor of $\Phi = 1.7$ was used. This value was obtained directly from the chart of Fig. 4(a), using $L/r = 120$. The validity of the procedure for the case under consideration seems to be doubtful because of the following reasons. As stated by the author, under the heading "Amplification Chart" "the amplification chart is based on a computed total stress of 20 kips per sq in. at the center of a tower section between points of inflection. A uniformly distributed wind load is assumed to be supported throughout the tower height." In example 2, not only does the tower not support any uniformly distributed load, and the bending stress is computed not at the center, but what is more important, between the points of inflection, guy group G_1 exists, which will restrain the amplification of the horizontal displacement ΔH at guy level G_1.

The effectiveness of guy group G_1 in restraining the amplification of ΔH will depend on the tension that exists in each guy. However, it is evident that not only the amplification factor, Φ, would be smaller than 1.7, but also that the critical buckling stress would be larger than the value of 20,600 lb psi determined by the author, using Eq. 22. A more accurate approach to the problem is to consider the part of the tower between the inflection points as a continuous bar on three supports that are not on a straight line, the middle one of which is elastic.

ROBERT S. ROWE,[11] M. ASCE.—Mr. Bertero is correct in questioning the use of simplified equations for analysis of tall towers. The writer regrets that the paper did not make clear that the simplified techniques presented were for the preliminary design of guyed towers and that a more exact procedure should be used for analysis. The writer agrees with Mr. Bertero that changes in geometry of the guys do have an important effect and must be included for tall towers as far as the final analysis is concerned.

Fig. 10 shows the percentage error in horizontal distance by neglecting sag effects, as a function of the height of the tower, h, with initial tension, P_i, as

[11] Prof. and Chmn., Dept. of Civ. Engrg., Duke Univ., Durham, N. C.

the parameter. The percentage error was determined as follows:

$$\% = 100 \left\{ \frac{\frac{\delta^2 h^3 \sec^2 \alpha}{24\, P_i} \left[1 - \frac{1}{\left(1 + \Delta P_i / P_i\right)^2} \right]}{\frac{h}{E} \Delta P_i \sec^2 \alpha} \right\} \quad \ldots\ldots (48)$$

in which δ is 3.46 lb per ft; the galvanized bridge strands were considered to have a breaking strength of 204,500 psi; and α represents the angle between guy and vertical. For towers less than 500 ft in height the error is less than 4% but as the height increases the error increases significantly.

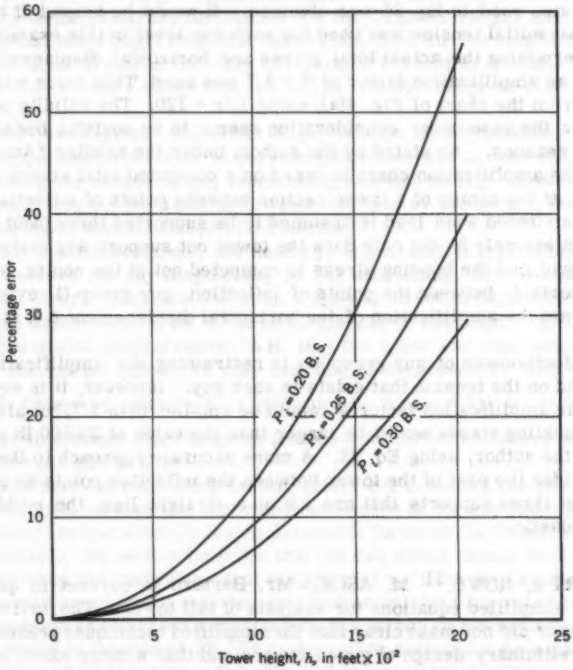


FIG. 10.—PERCENTAGE ERROR VERSUS TOWER HEIGHT

When sag effects are included, a change in the vertical force on the tower due to guyed tensioning will occur. The change in vertical force resulting from sag effects is a part of the total vertical force due to guy tensioning, wind load, and the dead load of the tower and antenna. Even though a change in vertical force might be a significant part of the initial guy tension, it is a much smaller

part of the total vertical force. A more important factor which must be included is the eccentric guy moment resulting from the fact that the guy connection is on the tower leg and not at the centroid of the tower cross section.

The writer appreciates Mr. Bertero's detailed evaluation of the factors pertaining to tall guyed towers.

AMERICAN SOCIETY OF CIVIL ENGINEERS
Founded November 5, 1852
TRANSACTIONS

Paper No. 3022

GARRISON DAM TEST TUNNEL
A SYMPOSIUM

Page

Foreword 229

Investigation and Construction
by Harris H. Burke, F. ASCE 230

Evaluation of Test Results
by Kenneth S. Lane, F. ASCE 268
With Discussion by A. A. Eremin 307

FOREWORD

This symposium describes an extensive 6-yr study of tunnel loading in a 36-ft-diameter tunnel test section at Garrison Dam on the Missouri River, near Bismarck, N. Dak. The tunnel investigation includes the application of the results to the 8 prototype tunnels, construction of these tunnels through clay shale, and examination of their initial performance. The evaluation of these results includes the development of new theoretical concepts.

INVESTIGATION AND CONSTRUCTION

By Harris H. Burke,[1] F. ASCE

SYNOPSIS

One of the major design problems encountered on the Garrison Dam Project on the Missouri River near Bismarck, N. Dak. was the determination of the magnitude and distribution of earth pressure on the eight nearly parallel tunnels that form part of the outlet works. Originally, it was planned to utilize cut-and-cover conduits located on the flood plain west of the Missouri River for the outlet works, but difficult foundation conditions led to the use of multiple tunnels. In order to check the basic assumptions used in the design of the tunnels, a program of measurements and observations on a full-scale section of one of the tunnels was undertaken.

This paper describes the test section investigation, and the design and construction of the main tunnel. The results of observations, both in the test section and at selected observation stations throughout six of the eight tunnels, are examined. Only the more significant studies are given herein. The complete investigation[2] by the Corps of Engineers is filed in the Engineering Societies Library and in the library of the United States Army Engineers Waterways Experiment Station, United States Department of the Army, Corps of Engineers, Vicksburg, Miss.

INTRODUCTION

Garrison Dam is one of the major units of the comprehensive program for the control of the Missouri River system, known as the Pick-Sloan Plan. It is located 75 miles north of Bismarck, N. Dak., and has a rolled fill embankment with a maximum height of more than 200 ft and a length greater than 2 miles. A description of this project, which was constructed by the Corps of Engineers, has been given by John S. Seybold,[3] F. ASCE.

The outlet works shown in Fig. 1 are located on the west abutment and consist of an intake structure, eight 1,200-ft-long circular tunnels, power facilities, and a stilling basin. Five of the tunnels are for power use and were excavated to a bore of 35 ft and lined with 3 ft of concrete. Two of the regulating tunnels have diameters of 22 ft with 2½ ft of concrete lining. The last regulating tunnel has a diameter of 26 ft with 2 ft 9 in. of concrete lining. The tunnels were constructed with temporary steel rib support which was encased by the permanent lining of reinforced concrete.

Note.—Published, essentially as printed here, in November, 1957, in the Journal of the Soil Mechanics and Foundations Division, as Proceedings Paper No. 1438. Positions and titles given are those in effect when the paper was approved for publication in Transactions.

[1] Superv. Engr., Hydro Power Branch, Bechtel Corp., San Francisco, Calif.

[2] "Report of Test Tunnel, Garrison Dam," Garrison Dist.; Corps of Engrs., U. S. Dept. of the Army, Part 1, August, 1949, and Part II, July, 1953.

[3] "Constructors Roll Nearly One Million Yards a Week Into Garrison Dam," by J. S. Seybold, Civil Engineering, Vol. 19, No. 10, 1949.

The tunnels were mined through the Fort Union formation,[4] a compact clay shale of Tertiary age consisting of continentally-deposited, gently dipping beds ranging from clays to sands. The beds are often cross-bedded, and range from thin partings to a thickness of 15 ft or more with the clayey phases predominating. Beds of lignite ranging from a few inches to several feet thick are found within the formation. Two major lignite beds were encountered within

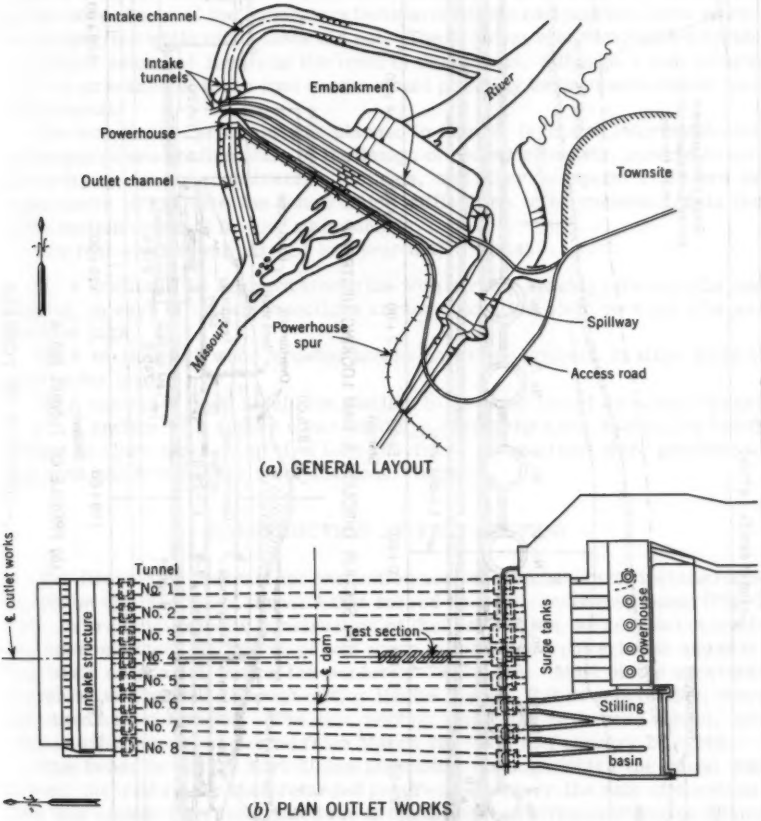
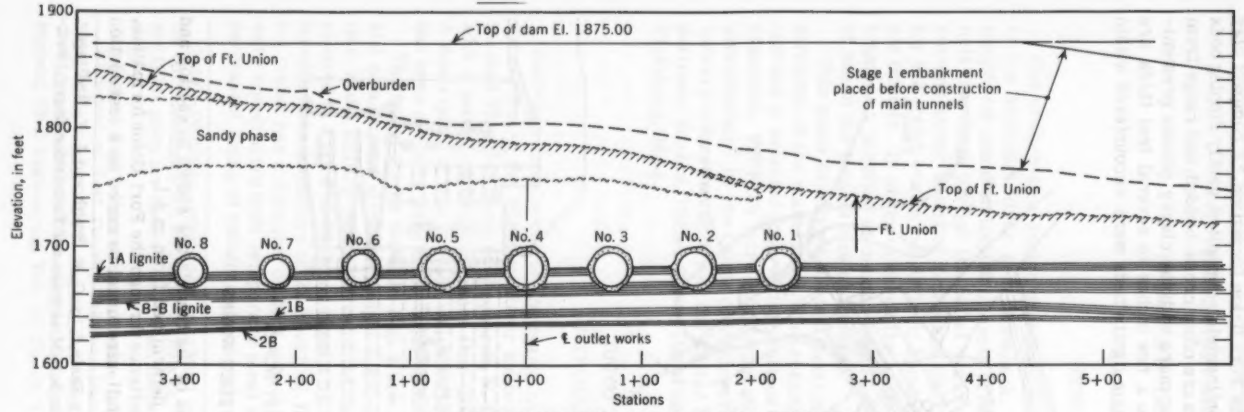


FIG. 1.—OUTLET WORKS

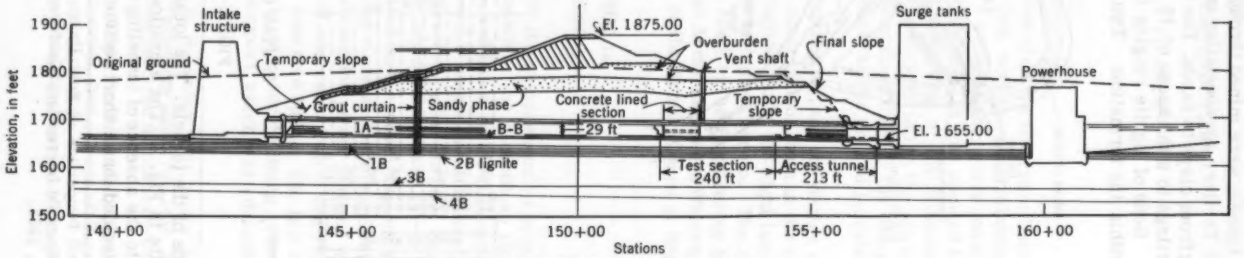
the plane of the tunnels. The locations of the tunnels are shown in section and in profile in Fig. 2. The elevation is determined from m.s.l.

Due to the absence of tunneling experience through the Fort Union formation, it was decided that a short section of full-size tunnel be mined as a test section

[4] "Soil Properties of Fort Union Clay Shale," by C. K. Smith and J. F. Redlinger, Proceedings, 3d International Conference on Soil Mechanics and Foundation Engrg., Switzerland, 1953.



(*a*) SECTION THROUGH ℄ DAM LOOKING UPSTREAM



(*b*) PROFILE OF TUNNEL NO. 4

FIG. 2.—LOCATION OF TUNNELS

and that a comprehensive program of measurements be instituted in order to develop design and construction data. In the tunnel design studies, it was found that very little was known about mining through formations similar to the Fort Union one and of the magnitude and distribution of pressures that would be developed in such a material. It was thought that the Fort Union formation might become an energetically swelling material when the preconsolidation due to 1,000 ft of overburden (since removed by erosion) was released by mining the tunnel bore. Some of the laboratory tests on drill hole samples indicated swelling properties while other tests did not. The problem was complicated by the two major seams of lignite at the level of the tunnels, although it was thought that the presence of these coal seams would probably be favorable rather than detrimental.

The test section program was planned to furnish technical information for development and confirmation of the design of the main tunnels, provide an opportunity to develop construction methods, and allow prospective bidders an opportunity to evaluate the construction difficulties to be encountered in the construction contract for the main tunnels.

The test section was divided into four major parts:

(1) A section of 12 segment steel ribs with varying spacing between ribs and lagging, in each of three subsections arranged to allow yield between ribs and between lags;

(2) A section with wood crusher blocks between segments to allow yield of ribs under load;

(3) A section of fixed steel ribs similar to the main tunnel construction; and

(4) A section with slotted concrete lining having the slots spanned by heavy beams to allow measurement of load reactions. Transitions were provided at the ends and between the steel and concrete parts.

CONSTRUCTION OF TEST SECTION

The first major contract for excavation and main embankment included construction of a section of tunnel 4 that served as a full-scale test tunnel (Fig. 2 (b)). In order to expedite construction of the test section, an access cut totaling approximately 890,000 cu yd was made in the Stage I powerhouse and stilling basin excavation during the winter of 1947-1948. Most of the excavated material was wasted although major lignite layers, 3 ft or more thick, were salvaged and stockpiled. The test section, including an access tunnel, was constructed during the period from March 29, 1948, to February 26, 1949.

The behavior of the Fort Union formation, through which the tunnel was mined, favored rather than retarded progress. However, the rate of construction was slower than anticipated due to operational and organizational problems of the contractor. This slower rate of progress allowed sufficient time to make more comprehensive measurements than had been planned on most of the test installations, causing little or no conflict with construction operations.

To reach the full bore test section, situated far enough back from the temporary excavation slope to take a substantial load, an access tunnel 9 ft wide and 11 ft high was mined by hand methods into the formation 213 ft from the portal. The face was drilled in a varying pattern to a depth of 6 ft using six-point, side-hole jackhammer bits and later, 2 in. coal auger bits turned by electric drills. Electrically detonated permissible dynamite was used to break out the face. The blasted material was hand loaded into dump cars traveling

on 36-in. gage track and hauled in and out of the tunnel by a cable and air powered winch. Approximately 2 ft of lignite coal, left in place above the crown of the access tunnel, formed a satisfactory roof that allowed timbering to lag behind the face as much as 60 ft.

The access tunnel excavation was continued into the test section proper for a distance of 6 ft. From this extension a 6-ft-by-7-ft shaft was raised to the crown of the test section. The shaft was enlarged laterally at the top of the upper, 1-A, lignite to approximately full tunnel size and the crown above the lignite was supported temporarily by a timber arch framework. The lateral enlargement was continued downward to form a short section of full circle tunnel and the first two steel ribs were erected. The top part of the full bore enlargement was then lengthened both forward and backward. During this enlargement the crown was supported on temporary timber ribs with tight timber lagging. Water seeping into the tunnel from the 1-A lignite greatly hindered operations in making the raise and enlargement. Although the quantity of water was small, it complicated construction by causing swelling and sloughing of the clay, and especially by causing slippery footing in the restricted working space. To eliminate this undesirable condition, mining was suspended and the lignite was grouted from horizontal drill holes. Subsequent grouting was used at necessary intervals during the construction of the test tunnel and was generally effective in minimizing seepage. After the initial grouting, the slot enlargement was extended to a length of approximately 20 ft and the initial "jumbo" was erected. Mining then proceeded with a full face operation.

The heading was drilled with hand-held electric drills that rotated coal augers. The operators worked both from the jumbo platforms and on the tunnel invert. Both lignite and clay were drilled to a depth of approximately 6 ft in order that two ribs could be erected each round, without an excessive amount of hand excavation. Ten delays were used for blasting. The lower part of the face was blasted out into the excavated tunnel first in order that the balance of the face could drop down in successive sections according to the delays used. An electrically-powered mucker was utilized for loading muck cars which were pulled in and out of the tunnel by a cable operated from a hoist outside the portal. Final cleanup from each round was accomplished by hand loading into the mucker bucket. During the mucking operation the crown was supported by 6 in. I-beams 12 ft long, supported by the rib steel and cantilevered out from the supported section. These beams were moved ahead after each blast. After mucking was completed two 12-segment steel ribs were erected and initial blocking was placed. In general, only enough blocking was placed to hold the ribs in proper shape and position through the next blast, after which blocking was finished while the blasted material from the next round was being excavated.

In August, 1948, after the test tunnel had been under construction for four months, a major change in supervision and work methods was made. A more powerful mucker was used in combination with larger muck cars and a battery-powered electric locomotive, all operating on 24-in. gage track. The jumbo was modified to provide a wider working area for the mucker by placing the supporting wheels on rails near the springline of the tunnel. Excavation and rib erection proceeded essentially as before except that mucking was speeded up considerably by allowing empty and full cars to pass. The test tunnel was mined and ribs set in the six-month period from May 3 to November 3, 1948. Mining of the initial slot, enlargement of the bore to allow the jumbo erection,

and erection of the jumbo required until July 23. Thereafter, progress was rather slow but at an increasing rate until August 26 when the construction was reorganized. At that time, approximately one-fourth of the tunnel had been excavated. In the following two months, mining was completed.

The ends of the test section were benched at the levels of the two major lignites and supported by partial circle ribs. The vertical clay faces between the lignites and above the upper lignite had a tendency to slough. Therefore, transverse bulkheads, backfilled with gravel, were provided to support the vertical faces. During excavation no significant swelling or squeezing of the formation was noted—it stood in a vertical face permitting full face excavation. The Fort Union formation behaved as a weak rock breaking out in block-like fragments up to a cu yd or more in size. The block-like structure resulted in a varying overbreak of up to 3 ft in some cases. The average overbreak in the crown half of the test section was 1.8 ft and 0.7 ft for the entire circular section.

Section 4-D, at one end of the test section, was concreted during the period from November 12, 1948, to January 17, 1949. After placing the invert, which comprised the bottom 60°, both sidewalls were placed simultaneously to the springline followed by a separate pour from the springline to the crown. Concrete was mixed in a 1/2 cu yd mixer, using natural sand and crushed granite coarse aggregate. The mixer discharged directly into the hopper of a gasoline-powered pumpcrete machine that pumped the concrete through a 8-in. line into the invert forms or to an electrically-powered pumpcrete machine inside the tunnel that relayed the concrete into the side and arch forms. During placing, the level in both sides of the arch and side pours was maintained at nearly the same elevation by alternately moving the discharge line from one side to the other. The concrete was vibrated internally by men working inside the forms. End bulkheads were used for the invert and the concrete was screeded to grade. For the side and arch pours, steel forms, supplemented by timber end bulkheads, were mounted on a form carriage which was rebuilt after having served as the drill and erection jumbo. A small gallery was excavated above the ribs at the crown to accommodate the concrete pipeline. This gallery was left open after concreting and was not filled until after the completion of the observation program. After concreting, voids between the concrete and the Fort Union formation above the springline were grouted with neat cement grout under a low (10 lb per sq in.) pressure.

During construction of the test section, water seeping from the upper lignite was generally stopped effectively by grouting the lignite and cracks in the adjacent clay. However, continued ground movement after completion of the tunnel caused some of the cracks to reopen and allowed water to seep out of the lignites and over the clay. Continued exposure to this slight seepage caused the clay to soften and slough out, leaving the lignite intermittently unsupported. The size of the sloughed areas varied considerably, with the largest slough approximately 6 ft deep and 10 ft long. It was recognized earlier that this sloughing would be detrimental when tunnel 5 was mined alongside, but repair of the sloughed areas was delayed until December, 1949, when the main tunnel contractor was well established on the project and had men available to accomplish the repair. Then all loose and softened clay was removed and bank-run gravel was tamped into the cavities behind steel lagging which was welded to the tunnel ribs. Where water was actively emerging from the lignite, corrugated sheet metal drains were inserted below the lignite to catch the drainage. In all other areas, minor amounts of seepage emerging from the lignite were

Reinforced concrete linings 3 ft thick were provided in tunnels 1 through 5 which had 29 ft inside diameters (after placing lining). In tunnel 6, having an inside diameter of 26 ft, the concrete lining placed was 2 ft 9 in. thick and in tunnels 7 and 8, with inside diameters of 22 ft, 2 ft 6 in. of concrete lining was provided. Transverse reinforcing bars, $1\frac{1}{4}$ in. square, were placed on 12-in. centers near the inside face. The temporary support ribs served as the outer transverse reinforcement. Longitudinal reinforcing was provided for stresses caused by temperature, bending due to rebound near the portals and settlement under the embankment. It was also used for the probable tension in the tunnel barrel due to other factors such as shear stresses from the embankment load, longitudinal rebound near the portals, and consideration of slope stability. A typical cross section of the concrete lining is shown in Fig. 3. In the regulating tunnels where a particularly dense concrete surface was required, the surface of the invert pour was subjected to a vacuum process, and absorptive form lining was required for the section of the side pours below the springline.

TABLE 1.—SUMMARY OF RIB STEEL SIZES

Tunnel number	Diameter of tunnel, in feet	Load Conditions		Steel Rib Size for 3-foot Spacing	
		Maximum overburden and surcharge,[a] in feet	Percentage of maximum overburden[b]	500 to 600 feet of tunnel length[c]	300 to 350 feet of tunnel length[d]
(1)	(2)	(3)	(4)	(5)	(6)
1	29	145	50	10 WF 72	8 WF 48
2	29	145	50	10 WF 72	8 WF 48
3	29	145	50	10 WF 72	8 WF 48
4	29	145	50	10 WF 72	8 WF 48
5	29	145	50	10 WF 72	8 WF 48
6	26	150	40	10 WF 54	8 WF 40
7	22	160	40	10 WF 49	8 WF 35
8	22	160	40	10 WF 49	8 WF 35

[a] At centerline of dam. [b] Assumed for design of the temporary support. [c] Near centerline of dam where load is maximum. [d] At each end where load is less than maximum.

Pipes placed at regular spacing and at points of high overbreak were provided for grouting voids in the crown.

Mining.—As in the test section the Fort Union formation behaved as a soft rock during mining. Thus, it was possible to complete mining of each tunnel before starting to concrete. Mining was successfully carried forward by blasting and excavating for the full height of the face in rounds of 6 to 8 ft depending on the rib spacing.

Special jumbos of novel arrangement considerably increased progress.[6] The jumbos, mounted on rails just below the springline, cleared the entire bottom section of the tunnel, thus allowing mucking, setting steel, and drilling to be carried on simultaneously. Two jumbos were provided for the 29-ft-diameter

[6] "Garrison Tunnels Are Moving Fast," Engineering News-Record, January, 1951.

allowed to drain down through the gravel and out between the laggings. This gravel filter repair effectively stopped further sloughing and re-established support of the clay as continued movement tended to tighten the gravel.

Prior to mining tunnel 5, analysis of observations indicated that crushing of redwood blocks between rib segments in one of two yielding rib sections had not progressed far enough to allow the ribs to develop the strength necessary to prevent excessively high strains in the soil pillar between tunnels 4 and 5 as it took additional load due to mining tunnel 5. The crusher blocks were stressed in their plastic range so that a relatively small increase in load would have resulted in a considerable diameter shortening. The ultimate possible diameter shortening was computed to be approximately 5 in. in addition to the 2 to 3 in. which had already occurred.

Because this appeared to approach the strain limit of the soil, and in order to provide more favorable support for this section under the extreme loading condition expected when mining the adjacent tunnel, the section was strengthened by a concrete lining in January and in February of 1950. The adjacent smaller yield section, 4-B_2, had already yielded enough that the ultimate possible yield would not overstrain the soil pillar. Accordingly, that section was not reinforced.

CONSTRUCTION OF OUTLET TUNNELS

Description of Design.—To achieve over-all economy the tunnels were constructed closely together, with a spacing of approximately one diameter between tunnels. This minimized the size of the costly intake and outlet structures and the powerhouse, and decreased the amount of excavation. In addition, the tunnels were shortened considerably by cutting steep temporary excavation slopes, generally 1 on 1. Berms were placed in the slopes at lignite layers to catch seepage and the slopes were flattened slightly through a sand stratum near the ground surface. The temporary slopes were flattened later into permanent slopes by backfill around the portals, as seen in Fig. 2(b). The over-all stability of the steep temporary slopes was reduced by mining the tunnels and this required the portal structures to be designed in order to reinforce the slope.[5]

Temporary support of the Fort Union formation during mining was provided by circular steel ribs designed for a maximum working stress of 24,000 lb per sq in. All ribs were initially designed for spacing of 3 ft to permit use of only one length spacer and lagging. The original design of rib steel sizes, given in Table 1, was developed in November, 1948, when only limited data from the test tunnel were available. Later data from the test section and observations in the main tunnels allowed the spacing to be increased to 4 ft and made possible a reduction in weight of rib steel.

A limited initial supply of steel ribs included ribs fabricated with both four and eight segments per rib to permit flexibility of operation and thus allow optional mining methods. Later orders were limited to the four segment ribs after experience showed these to be best suited to the adopted erection method. Bolted segment joints were provided with splice plates. They were welded to provide tensile strength in the joints equal to a stress of 18,000 lb per sq in. on a cross section of steel equal to two-thirds of the rib section.

[5] "Special Portals for Outlet Tunnels Maintain Stability at Garrison Dam," by K. S. Lane, Civil Engineering, Vol. 22, No. 9, 1952.

power tunnels, and one each was provided for the 22-ft and 26-ft regulating tunnels (Fig. 4). Due largely to the careful design and operation of the jumbos, the eight tunnels were constructed with an excellent safety record, and there were no fatal accidents during the main tunnel contract.

After each blast the jumbo was moved up to the face, and the crown and upper section of the face were supported by jacks mounted on the jumbo. Erection of the steel ribs was begun with the crown segment and progressed down the sides toward the invert. Mucking and drilling for the next round were carried on simultaneously. Drilling began at the crown and progressed toward the invert. By the time the invert was completely mucked and the invert segment of the rib was set, the entire face was drilled and ready for loading for the next blast. Drilling was accomplished with 1½-in.-diameter coal augers turned by hand-held air drills. To provide for variations in material the drilling pattern was varied. A typical loading pattern consisted of 60 to 90 holes

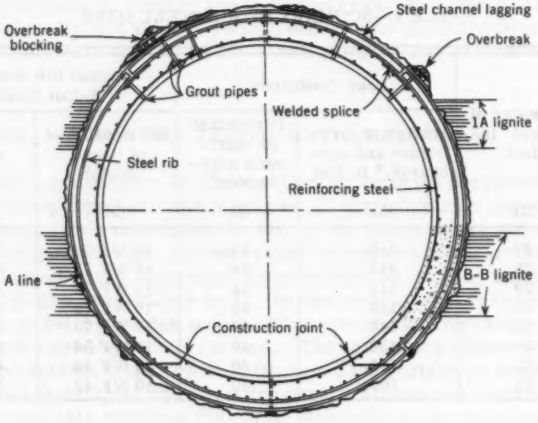


FIG. 3.—CROSS SECTION OF CONCRETE LINING

loaded with approximately five hundred 1/3-lb sticks of permissible dynamite using a primer of 40% dynamite for every three sticks of 20% dynamite and standard delays from number 0 to number 11. Approximately 0.6 lb of powder was used for each cubic yard of excavation.

A major factor in the rapid excavation was the electric mucking machines which were modified by the addition of a hopper and an air-operated double chute that discharged alternately into cars on a double track behind the mucker.[6] Two air hoists mounted on the rear of the mucker pulled empty cars onto either of two tracks behind the mucker and held the car to the mucker during loading. A similar hoist at the side of the tunnel was used to pull loaded cars back from the mucker. The double discharge chute on the mucker allowed discharge into a car on either track, thus permitting the mucker to operate practically continuously with no time lost for changing cars. Behind the rear limit of travel of the mucker, full and empty cars were switched onto the proper

track by means of a diamond switch. Battery-powered locomotives were used for haulage.

Erection of steel ribs proceeded concurrently with the mucking operation, beginning with the top segment. This segment was held in place and supported from the jumbo by means of hydraulic and screw jacks. The side segments were raised into position and bolted to the crown segment. The invert segment was placed into position and bolted to the side segments, as the last operation after mucking the invert.

Wood blocking was used as needed between the bore and the ribs. The specifications required a minimum of 16 blocking points per rib evenly spaced to prevent excessive concentrations of load. Open lagging was used around the springline, except near the portals for a length of 15 to 20 ribs where solid lagging was used in the top 120° of the crown. Open lagging was spaced with a



FIG. 4.—DOWNSTREAM PORTALS

maximum distance of 3½ ft center to center of lags. Where additional support was considered necessary, the lags were placed closer together. In the top half of the tunnel, 2-in.-by-4-in. wire mesh was specified to catch local falls from the crown. In general, the opening lagging served only to support this mesh and ordinarily did not bear against the bore. The load on the ribs was carried entirely through the blocking.

Except for some slaking and local falls, the Fort Union formation held up extremely well. Due to horizontal bedding planes and vertical joints, the clay had a blocky structure which caused the bore to break in the shape of an inverted stair composed of a series of near vertical and horizontal surfaces. Overbreak was greatest at the crown and was reasonably small throughout the tunnels, averaging 0.6 ft outside the outer flanges of the ribs. The largest overbreak encountered during the excavation occurred in tunnel 2 where the formation broke back approximately 11 ft above the ribs over an area 12 ft by 15 ft.

Because the lignites which cut through the tunnels had been exposed in both the intake and powerhouse excavations in early 1948, drainage in the tunnel area had been thorough. This reduced considerably the amount of water seepage to be handled during the main tunnel contract and little water was encountered during mining. However, small amounts of seepage were encountered occasionally in low pockets in the upper, or 1-A lignite near the springline and in limestone concretions found occasionally near the crown. Where seepage spots were encountered, the bore was lagged tight and the space between the lagging and the formation was packed with pit-run gravel.

Concreting.—Because aggregates suitable for concrete were not available at the site, all aggregates were transported by rail. Sand was obtained from a source near Detroit Lakes, Minn., a haul of 330 miles, and coarse aggregates were shipped 205 miles from a source near Greene-Grano, N. Dak. Aggregates were not shipped during the winter months, but were stockpiled during the summer to allow continuous operation through the winter. Aggregates were transported from the stockpiles to bins at the batching plant on a conveyor belt. Cement was shipped to the site in bottom-dump hopper cars and stored in a 7,300 barrel capacity silo to be transported by an air-activated cement conveyor from the storage silo to the batching plant.

The batching-mixing plant located in the powerhouse excavation near the downstream portals had a bin capacity for 500 barrels of cement and sufficient aggregates to produce 100 cu yd of concrete. All batching and weighing for the pair of 2-cu-yd tilting mixers was done automatically with tapes recording the weight of each ingredient. Concrete was placed at a maximum temperature of 60° and a minimum temperature of 40°. This narrow range of placing temperatures required cooling the mixing water and aggregates during the summer and the heating of aggregates during cold weather. The 3-in. maximum size aggregate concrete for the portals was transported from the mixing plant to the forms in buckets hauled by trucks. These buckets were handled into the forms by crawler-type cranes.

Concrete for the tunnel lining was placed in 24-ft monoliths using 1 1/2-in. maximum size aggregate. Pumpcrete machines were used to transport concrete from the mixing plant into the tunnels. When the pumping distance was greater than could be handled by one pump, booster pumps were provided at intervals of approximately 800 ft. Concrete for the inverts was pumped directly into place.

Where not placed against a previous monolith, bulkhead forms were provided at the ends and a formed construction joint (Fig. 3) was used at the sides of the invert pours. The form for the construction joint served as a track for a screed. Invert pours for the regulating tunnels were vacuum-treated to remove excess water and were then finished by light troweling to remove fins left by the vacuum process. Prior to positioning the collapsible steel arch forms, any of the fallen Fort Union clay shale caught by the protective wire mesh in the crown was removed, together with any loose blocking. Wherever necessary, lagging was also removed to allow free movement of concrete.

Two overhead concrete lines, or slick pipes, were used for the arch and side pours. Men working inside the forms distributed and vibrated the concrete except in the extreme top of the arch where the slick pipes were buried in the concrete and withdrawn slowly as placing progressed. As an aid to placing the 6-in. slump concrete, air was injected at intervals into the discharge line. This air slugging was held to a minimum in order not to distort the steel

forms or blow out the wooden bulkheads at the end of each pour. In the regulating tunnels absorptive form lining of 10-oz duck was used below the springline, whereas the concrete above the springline was placed directly against the forms. Forms were generally stripped 24 hr after placing was completed and the concrete was cured for 14 days by water sprays.

The upper 120° section of the crown was grouted with mortar grout through grout pipes placed during construction (Fig. 3) to fit the overbreak pattern. In general, only a small quantity of grout was required, indicating that the overbreak voids in the uppermost part of the crown had been adequately filled with concrete. It was originally planned to grout in two stages with the second stage being a neat cement grout. However, when early results of the second-stage grouting proved the grout take to be minor, the second-stage grouting was discontinued except for approximately 100 ft at the main grout curtain. A decrease in grout take when the interval between the first and second-stage grouting was increased indicated that swelling of the Fort Union formation may have filled voids left after the first-stage grouting.

Construction Order and Progress.—Tunnel 7 was mined first, primarily because its portal was completed first. Tunnel 5 was mined next in order to measure the effect of mining an adjacent tunnel past the test section part of tunnel 4. Tunnels 2, 8, 6, 4, 1, and 3 were mined in that order, with mining generally being underway in two tunnels simultaneously. As a result of the order of mining, widely different loading conditions occurred on the concrete linings. Tunnels 2, 5, and 7 were subjected to mining of an adjacent tunnel on both sides after being lined. This was termed the multiple tunnel case. Except for the test section part, tunnel 4 was mined alongside the already lined tunnel 5 and after being concreted was subjected to the adjacent mining of tunnel 3. Tunnels 3 and 6 were mined between two previously concreted tunnels, and the two end tunnels, 1 and 8, were mined adjacent to a previously concreted tunnel.

Construction of the eight tunnels, together with the downstream portals and connecting retaining walls, was performed at a cost of $14,275,216. Notice to proceed was issued on March 29, 1949, and the entire work was completed by June 1, 1951. During the summer of 1949, the contractor assembled his plant, constructed his shops, yard, and aggregate storage facilities, and began actual construction on August 15 with the initial excavation for portal 7. Mining was started in tunnel 7 on December 10 and the tunnel was holed through on February 28, 1950. Together with portal construction and tunnel lining, mining continued on two or more tunnels concurrently and all mining was completed in January, 1951.

After the preliminary operations of opening the portal and erecting the jumbo were completed, mining progress averaged 20 ft per day for three 8-hr shifts for the five 35-ft bore tunnels, 22 ft per day for the 31.5-ft bore tunnel 6, and 26 ft per day for the 27-ft bore tunnels 7 and 8. Fig. 4 shows the downstream portals in July, 1950 at the midpoint of construction.

INSTRUMENTATION

The main objective of the tunnel test section program was to provide design data for the main tunnels. It was planned as a method of approaching such problems as the magnitude and distribution of external pressures, rate of pressure development, possibility of pressure relief by allowing yield during construction, and load transfer due to mining adjacent tunnels. To develop these

design data, the test section and main tunnel observation programs were planned to include the following types of measurements:

1. Determination of stress in the steel tunnel ribs by means of strain measurements with mechanical strain gages.
2. Measurements of changes in shape of the tunnel ribs and concrete lining by means of a precise tape extensometer.
3. Measurements of earth movements and pore water pressures around the bore of the test section.
4. Measurement of earth pressures on the slotted concrete section of the test section and strains in the concrete reinforcing steel, and steel ribs.
5. Miscellaneous measurements such as compression of crusher blocks at rib joints, movement of moisture around the bore of the tunnel, and movements of the tunnel and surrounding soil.

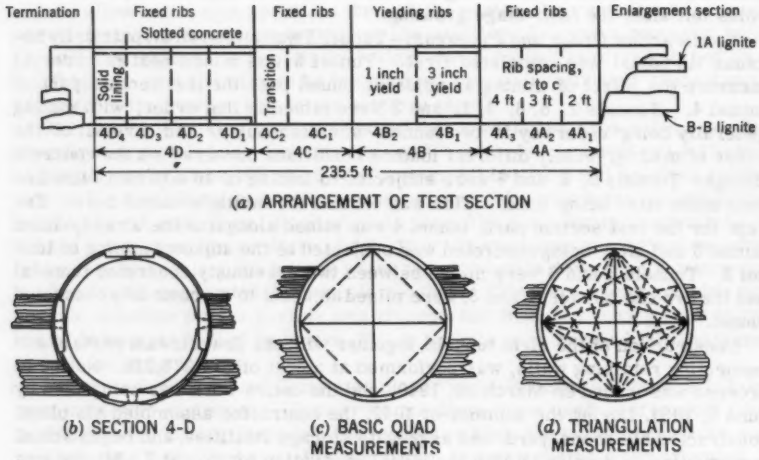


FIG. 5.—LAYOUT OF TEST SECTION

Arrangement of Test Section.—As shown in Fig. 5(a), the test section part of tunnel 4 was arranged in four main sections.

Section 4-A was supported by fixed steel ribs with bolted joints and was designed to allow yield of the Fort Union formation through square open spaces between lags arranged so the space between lags was approximately equal to the space between ribs. This section was divided into three subsections with the ribs spaced 2, 3, and 4 ft on centers.

Section 4-B was a yielding rib section with redwood blocks placed between the rib segments at each joint so that crushing of the blocks would allow the rib to yield. The 4-B section was divided into two subsections arranged to allow different amounts of yield. Section $4\text{-}B_1$ has thick crusher blocks between rib segments to allow approximately 3 in. of radial yield, and section $4\text{-}B_2$ had thinner crusher blocks to provide radial yield of approximately 1 in. It was anticipated that the blocks would crush approximately one-half of their thickness under the design loads.

Section 4-C was designed as a fixed rib section similar to section 4-A but with lagging spaced so that openings between lags were approximately equal to the width of a lag. Section 4-C had two subsections, one planned to be the major measuring station most comparable to the main tunnel construction, and a transition section into the concrete lined section.

The concrete lined section, 4-D, was constructed with slots in the lining at the crown, invert, and springlines. These slots were spanned with 30 WF210 steel beams which approximated the thrust resistance of the concrete lining. Measurement of stress in the steel spanning the slots allowed the vertical and horizontal reactions on the tunnel to be weighed. Section 4-D was divided into

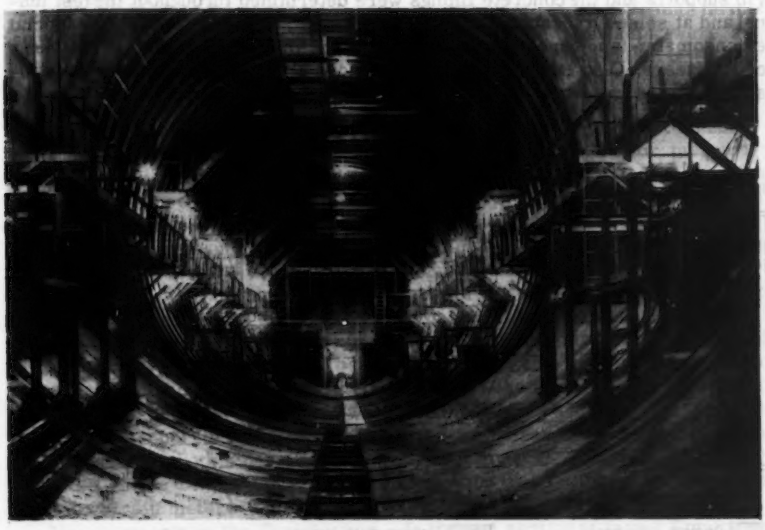


FIG. 6.—CATWALKS FOR ACCESS TO MEASUREMENT POINTS

four subsections: (a) A transition from the steel rib section, (b) the main measuring section, (c) a transition section at the end of the main measuring section, and (d) a nonslotted terminal section provided to eliminate end effects in the main measuring section.

Prior to mining the test section, a shaft was sunk from the ground surface above section $4\text{-}C_2$. This shaft was used later to measure ground movements and served for ventilation of the test tunnel. A system of catwalks and stairways at selected ribs in each section provided access to observation stations throughout the test tunnel (Fig. 6).

Types of Measurements.—As indicated in Fig. 7, mechanical measurements were made at selected locations in six of the tunnels and extensively in the test section of tunnel 4. In addition electrical measurements were made in section 4-D of the test tunnel. In general, the mechanical measurements were strain readings used to determine both strain and stress in a variety of locations. These ranged from measurement of the stretch of the main tunnels to stress

determinations in the steel ribs and reinforcing steel by means of mechanical strain gages. Electrical readings were taken to determine strain in concrete and steel members, and pressure for the Fort Union formation against the tunnel bore.

Mechanical Measurements.—Throughout the test section investigation, the most useful mechanical measurements were strain readings with 2-in. and 10-in. Whittemore strain gages. From these strain measurements, stresses in the steel ribs were determined throughout the test tunnel as well as at selected locations in tunnels 2, 5, and 7. In addition, stresses were determined in the reinforcing steel at selected locations in the concrete linings of several of the tunnels. Horizontal and vertical diameter changes of both the temporary rib supports and the concrete linings were determined throughout the test tunnel and at selected locations in the main tunnels. This was done with a special extensometer tape especially manufactured for this investigation by the Corps of Engineers, Ohio River Division Laboratory at Mariemont, Ohio. This instrument was patterned after a measuring device used in 1934 and 1935 by the

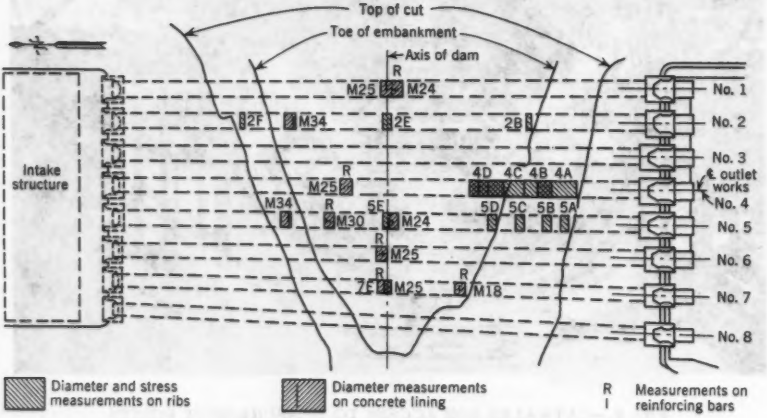


FIG. 7.—LOCATION OF MEASUREMENTS

Metropolitan Water District of Southern California for precise chord measurements on the Fan Hill conduit of the Colorado River Aqueduct.[7]

The extensometer tape was essentially a nickle-steel tape to which was attached a dial gage reading to 0.001 in. with an extension range of 2 in. The tape was punched with holes at intervals of 2.000 in. This allowed the tape to be secured to a frame or head containing the dial gage with a pin and clamp arrangement in precise increments of 2 in. Hooks were provided on both ends of the instrument and corresponding hooks were installed at ends of diameters or chords to be measured. Constant tension was applied to the tape by means of a calibrated adjustable spring device contained in the measuring head. Hooks on the ribs were precisely formed to the same radius as the radius of the hooks

[7] "An Invar-Tape Extensometer," by C. H. Heilbron, Jr., and W. H. Saylor, Civil Engineering, Vol. 6, No. 2, 1936.

on the ends of the extensometer and were chrome plated to minimize error due to corrosion and wear.

At one or two ribs in the center of each major section within the test tunnel intensive stress and shape measurements were made. Other mechanical measurements included readings of the amount of crushing of the wood blocks between rib segments in the yielding section of the test tunnel, strain gage measurement of the slippage at the rib segment joints, determination of the ground surface settlement over the test tunnel, and heave of the test tunnel due to release of vertical load on the invert. The twist of the test tunnel was determined, as adjacent tunnels were mined past, as well as the movement of the ventilation shaft as the test tunnel was mined. The measurement of the movement of the ground toward the tunnel bore by means of reference points termed spearheads driven into the soil around the bore and in the heading were also measured. As well, the pore pressure in the clay, and elongation of the tunnels due to yield toward the excavations were measured.

Electrical Measurements.—Two types of electrical instruments were included in the test tunnel instrumentation—pressure cells for direct measurement of stress against the concrete lining, and strain meters for measuring strain in the concrete lining and in the reinforcing steel and steel ribs. Two types of pressure cells were used, the Waterways Experiment Station type[8] which utilizes SR-4 strain gages to measure the deflection of an internal diaphragm under pressure of a liquid held within a contained chamber, and the Carlson stress meter,[9] which utilizes an elastic wire strain meter to measure deflection of a similar diaphragm. Both types of cells used a Wheatstone bridge for making observations and require load calibration prior to installation.

The earth pressure cells were mounted on the west side of test section 4-D and were fairly well distributed between the crown and the invert in an effort to measure directly the stress distribution and the effect of mining adjacent tunnel 5. Carlson strain meters were used to measure strains and temperatures in the concrete lining and were placed in the concrete at various depths in the lining on both sides of the tunnel. Strain gages of the SR-4 type were mounted on the reinforcing steel and steel ribs in positions adjacent to the Carlson strain meters.

Measurements in the Test Section.—In the test section of tunnel 4 major dependence was placed on the mechanical types of measuring instruments, primarily the extensometer and Whittemore strain gage readings. Measurements were referenced on each rib to positions corresponding to a clock face when looking into the tunnel. Thus, 12 o'clock denoted the crown location, 3 o'clock the right springline, 6 o'clock the invert position, and 9 o'clock the left springline. Throughout the test section horizontal diameter measurements were made on each of the 80 ribs together with a basic pattern of 10-in. gage line measurements at the 3 o'clock and 9 o'clock positions. On every other rib through the steel rib sections, additional vertical diameter and diagonal chord measurements, and basic pattern strain gage readings were made at the crown and invert.

At selected ribs, further strain gage readings were taken around the entire circumference of the rib, and subsequent chord determinations were made in a 12-point triangulation pattern (Fig. 5(d)).

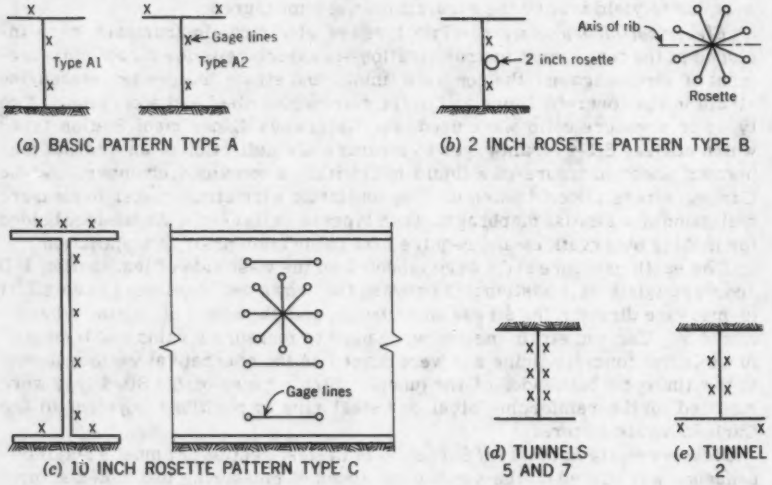
---

[8] "Soil Pressure Cell Investigation, Interim Report," Technical Memorandum No. 210-1, U. S. Waterways Experiment Station, Vicksburg, Miss., July, 1944.

[9] "Five Years Improvement of the Elastic Wire Strain Meters," by R. W. Carlson, Engineering News-Record, Vol. 114, No. 20, May, 1935, pp. 696-697.

Strain Gage Measurements.—Stress readings in the steel were derived by Whittemore strain gages based on zero stress condition determined by initial observations on the rib segments prior to erection. In tunnel 4 the Whittemore strain gage readings were made in three general patterns as shown in Fig. 8(a), 8(b), and 8(c). The basic pattern, type A group, Fig. 8(a), consisted of two 10-in. gage lines on the web and one or two 10-in. gage lines on the inside flange. The gage lines were positioned at the midpoint of the rib segment at the 3 o'clock and 9 o'clock position of all ribs, and at the 6 o'clock and 12 o'clock position of all evenly numbered ribs throughout the length of the steel rib section.

At the 3 o'clock, 9 o'clock, and 12 o'clock positions the flange gage line (type A1 pattern) was offset from the axis of the rib in order to allow the Whittemore strain gage to clear the extensometer hooks. At the 6 o'clock position,



(*a*) BASIC PATTERN TYPE A

(*b*) 2 INCH ROSETTE PATTERN TYPE B

(*c*) 10 INCH ROSETTE PATTERN TYPE C

(*d*) TUNNELS 5 AND 7

(*e*) TUNNEL 2

FIG. 8.—PATTERNS OF STRAIN GAGE LINES

two flange lines were provided on either side of the extensometer hook (type A2 pattern). The type B pattern (Fig. 8(b)) consisted of three 10-in. gage lines arranged in the same pattern as the type A group with four 2-in. gage lines forming a strain rosette on the web of the segment. These were located two to a segment on each rib segment of the six 12-point triangulation ribs in the steel rib sections. The type C pattern (Fig. 8(c)) consisted of nine 10-in. gage lines parallel with the axis of the rib and three additional 10-in. gage lines arranged to form a rosette on the web. These groups were located on each of the heavy ribs spanning the four slots in the concrete lined section.

Early in the measurement program, it became apparent that bending of the steel ribs probably was not in the plane of the rib section. To investigate this possibility, special groups of closely spaced 10-in. gage lines were installed on five ribs. Spacing and number of gage lines of these special measurement

stations varied, but gage lines were approximately 1 in. apart in a parallel pattern around the rib. From these measurements it was clearly established that bending occurred at an angle to the rib which varied from rib to rib.

In order to establish the probable observation error, eight strain gage lines, one on each of the triangulation ribs, were measured daily for 5 months, in exactly the same manner as routine observations. Based on these measurements, the probable order of accuracy of strain gage observations was found to be in the order of ± 600 lb per sq in. unit stress in the steel, including errors due to different instruments and various observers but excluding very infrequent erratic observations.

Extensometer Measurements.—Horizontal diameters were measured on each rib to determine the trend of the rings to deform under load. Basic quad measurements were made on every other rib throughout the test section. As shown in Fig. 5(c), the basic quad consisted of horizontal and vertical diameters together with the four chords connecting the ends of the diameters. After the measurement program was underway, it became apparent that the high order of accuracy of the extensometer tape permitted the use of the horizontal and vertical diameters without resorting to the diagonal chord measurements. As a result, the diagonal chord measurements were discontinued.

At the center of each of the main observation sections, readings were made on 22 chords arranged in the 12-point triangulation measurement pattern shown in Fig. 5(d) to determine deformation of the complete ring relative to the invert. Twist or rotation of the tunnel was determined by direct measurement between a plumb line dropped from the 12 o'clock position and the 6 o'clock position. From a series of daily observations over a 5-month check period at six of the horizontal diameters, it was determined that individual measurements could be checked by different observers with different instruments within an accuracy of approximately 0.002 in. However, the total probable error from all causes over the entire period was in the magnitude of ± 0.010 in.

Miscellaneous Mechanical Measurements.—Although the bulk of the mechanical measurements in the test program consisted of extensometer tape and Whittemore strain gage observations, many other types of mechanical readings were made to measure, as fully as practicable, the movements and deflections of the tunnel and the surrounding ground. Based on the experience in the Chicago subway tunnel tests,[10] it was considered desirable to include measurements of soil movements around the test section in the observation program. The original program of measurements included observations to determine settlement of the ground surface above the tunnel and movement of soil toward the heading as well as radially toward the open bore. Construction of the ventilation shaft provided an additional opportunity to measure ground movements and pore pressure changes as the tunnel approached and passed the shaft location.

Twenty-two settlement points were installed in three lines on the ground surface above the test section. Standard survey equipment was used for level observations to 0.001 ft and levels were referenced to a permanent bench mark approximately one mile away. Ground surface settlements ranging from 0.02 ft to 0.08 ft were observed above the test section before the reference points were obliterated by construction of the embankment. The steel casing of the

[10] "Earth Pressure and Shearing Resistance of Plastic Clay," A Symposium by Karl Terzaghi, Ralph B. Peck, and W. S. Housel, Transactions, ASCE, Vol. 108, 1943, pp. 964-1109.

ventilation shaft was stepped down in 2-in.-diameter increments from 48 in. at the top to 40 in. at the crown of the tunnel. At each slip joint between casings of different diameters the vertical movement of the casing sections was measured by a steel tape from the settlement point on top of the casing.

Movement in the shaft continued throughout the entire observation period showing a slow, steady, downward movement of the ground ranging from 0.14 ft near the surface to 0.28 ft near the crown of the tunnel when measurements were stopped in July, 1950. The deformation took the form of an elongation, or stretch, of the ground, practically all of which occurred as the tunnel was mined. After mining, each subsequent loading event caused additional settlement but only a small additional elongation in the ground.

Measurements were made throughout the course of the investigation to detect heave, elongation, and twist or rotation of the tunnel. Heave was measured by a survey of the tunnel invert referenced to bench marks set in the powerhouse excavation area and in the access tunnel. The heave ranged from 0.5 ft. at the portal to 0.15 ft at the north end of section 4-D measured from a point zero established subsequent to excavation. In the center of the powerhouse excavation, 1.5 ft of rebound due to excavation unloading was measured on gages established prior to the start of the excavation.[11]

Elongation was measured by survey observations on horizontal control points which were established and measured at the time of tunnel construction. A slight stretch of the tunnel was revealed as the slope yielded toward the excavation. Twist was determined by plumb line observations on the basic quad and 12-point triangulation measurement ribs, disclosing a slight roll of the top of the test section away from the adjacent tunnels as they were mined. The tendency of the soil around the test tunnel to move into the bore was observed by measurements on spearheads, or reference points driven or drilled into the soil surrounding the tunnel bore.

Originally, it was planned to install both temporary and permanent spearheads. The temporary spearheads were those that could be driven into the soil ahead of the heading and observed for a short period of time until they were removed by excavation as the tunnel advanced. When relatively small movements were seen on a few temporary spearheads installed in the access tunnel and in the early part of the test section, further installation of temporary spearheads was discontinued. Permanent spearheads for observations over long periods of time were installed in the ventilation shaft and in a radial pattern at two ribs in section 4-A.

The initial installation was supplemented by permanent spearheads at the end sections and later by additional radial spearheads in sections 4-B and 4-C just prior to mining tunnel 5. The spearheads indicated a continued slow plastic movement of the Fort Union formation toward the tunnel throughout the single tunnel case. The rate of movement was very small, but during a 1-yr period sizeable total movements were observed. As much as 0.2 ft of movement of the soil relative to the ribs was noticed in section 4-A although measurements in section 4-B and 4-C reported smaller movements. End spearheads moved inward 0.04 ft at the south end and from 0.07 to 0.18 ft at the north end.

As an aid in interpreting the load distribution on the ribs, the detailed pattern of blocking and overbreak was obtained by photographing the excavated

11 "Rebound Gages Check Movement Analysis at Garrison Dam," by K. S. Lane and S. J. Occhipinti, Proceedings, 3d International Conference on Soil Mechanics and Foundation Engineering, Switzerland, August, 1953.

surface of the entire test section after blocking. Overbreak was measured in reference to the rib, generally at the rib segment joints, and at segment midpoints, with additional measurements at quarter points wherever necessary. Lignite beds were referenced to each rib. Measurement of crusher block compression between the rib segments in the yielding rib section 4-B were made with a vernier caliper or a micrometer both measuring to 0.001 in. Lateral movement, or slippage, of the rib segment joint plates was measured on a 10-in. strain gage line installed with one gage hole on each joint plate at every joint on each 12-point triangulation rib in sections 4-A, 4-B, and 4-C. Slippage of joints was negligible.

Nine double-tube closed system piezometers,[12] modified by the addition of a brass driving point, were installed in the formation surrounding the test tunnel and the vent shaft. Six piezometers were placed in the soil between tunnels 4 and 5, and three were installed above the test tunnel from the vent shaft. Prior to mining tunnel 5 adjacent to the installation of the test section, the addition of six piezometers in the soil pillar between the two tunnels, and eight radial piezometers with the tips approximately 5 ft from the bore, was completed. Piezometers installed from the vent shaft showed some pressure increase as the heading approached and passed the shaft. Two of the three piezometers in the shaft appeared to be located near drainage layers that affected the observations. However, one piezometer indicated a pressure of approximately 30 ft of water above the tip throughout the single tunnel case.

The piezometers installed in the clay from inside the tunnel showed, in general, steady pressure decreases as would be expected in a consolidating material. In an effort to measure moisture movement, a system of moisture sampling was set up at selected stations to take periodic samples of soil at various depths from the tunnel bore. Due to variations in soil, this program was relatively unproductive and was discontinued.

Electrical Measurements.—A comprehensive electrical instrumentation program was accomplished in section 4-D where four types of electrical instruments were installed in the center part of the slotted concrete section.

Earth pressure cells were installed around the west side of the tunnel from crown to invert. The first pressure cells were rigidly mounted and early observations indicated high and rapidly increasing pressures. It became apparent that these cells were acting as blocking points, attracting load that arched onto the stiff cells from adjacent unsupported zones. As pressure on the cells approached their design limit, the more heavily loaded cells were relieved by releasing their supports or by adding blocking adjacent to the cells. Because this type of relief was temporary, subsequent cells were installed with loose bolted mounts or flexible mounts.

Load increase from doming back of the heading was greater when cells were installed close to the heading and was less when they were placed further back. This indicated that doming occurred within approximately 60 ft back of the heading. Generally, in the first month after the concrete lining was placed, there was a reduction in pressure that was considerable for the rigidly mounted cells and that was significantly less for the loosely mounted cells. This indicated that the high stress concentrations at the blocking points tended to dissipate

---

12 "Ten Years of Pore Pressure Measurements," by F. C. Walker and W. W. Daehn, Proceedings, 2d International Conference on Soil Mechanics and Foundation Eng., Rotterdam, June, 1948.

when full support was provided by the concrete lining. The cells quickly indicated changes in pressure due to temperature changes and loading such as the addition of the embankment and the load increase caused by the mining of tunnel 5.

Qualitatively, the pressure cells consistently registered changes in load and often furnished the first indication of load change. From a quantitative standpoint, the results were not dependable, due primarily to eccentricities of loading for which the cells were not designed or particularly adaptable. The mortality rate of earth pressure cells was high. Two out of 16 Carlson cells and 19 out of 22 Waterways Experiment Station cells failed, although several of the failed Waterways Experiment Station type cells subsequently gave responses which seemed qualitatively reasonable. Because eccentric loading conditions are inherent in tunnels where loading is apt to be irregular and with tangential components, it was concluded that earth pressure cells used in this investigation were not suited to pressure measurements in such installations.

Duplicate installations of Carlson elastic wire strain meters were placed in groups of three at different depths through the concrete lining at locations slightly less than 45° above and below the horizontal axis on both sides of section 4-D. Strains were converted to stress on the basis of modulus of elasticity determined on small cast and cored specimens of the concrete lining. Baldwin-Southward SR-4 strain gages were installed on the reinforcing steel and steel ribs at locations near the Carlson strain meters. The Carlson strain meters operated quite satisfactorily over the entire test period. Unfortunately, no "zero load" control meters were used and the temperature corrections, as approximated from theoretical considerations, were so great that the actual stresses were masked by the corrections.

Although the SR-4 gages were carefully bonded to the steel with bakelite cement and carefully waterproofed with sealed metal enclosures for gages and leads, only 7 out of the 16 SR-4 gage installations remained operative after concreting was completed. None of the gages survived the entire observation period and those gages which did operate for part of the time showed extremely inconsistent results. The high mortality rate and the inconsistent results indicate that the installation technique must be further developed before SR-4 gages are satisfactory for long-term field installations of this nature.

Main Tunnels.—Because the extensometer tape and Whittemore strain gage observations were the most reliable and satisfactory observation methods used in the test section program, measurements in the main tunnels were confined generally to these two types. However, other special measurements were made as the occasion required. To obtain data on the inter-effects of tunnels 4 and 5 as tunnel 5 was mined alongside the test section, measurements similar to those in the test section, but limited considerably in scope, were made. As shown in Fig. 7, these measurements were made at four sections opposite corresponding sections 4-A, 4-B, 4-C, and 4-D.

Additional measurements were made at the centerline of the dam in section 5-E and on ribs in tunnels 2, 5, and 7 (Table 2). In tunnels 5 and 7, 10-in. Whittemore strain gage observations were made on three lines equally spaced on both sides of the web, as shown on Fig. 8(d). In tunnel 2, where smaller rib steel was used, only two gage lines were used on the web supplemented by two additional gage lines on the inside flange as seen in Fig. 8(e). Chord and diameter measurements were made with the extensometer tape in the same manner as in the test section.

Measurements were made on the concrete linings of all the finished tunnels except 3 and 8. These measurements consisted of horizontal and vertical diameters at the locations shown in Fig. 7. As the diameter measuring stations

TABLE 2.—NUMBER OF RIBS OBSERVED IN EACH SECTION

(a) Tunnel								
2			5					7
(b) Section								
2-B (1)	2-E (2)	2-F (3)	5-A (4)	5-B (5)	5-C (6)	5-D (7)	5-E (8)	7-E (9)
(c) Tape measurements								
Horizontal Diameter								
2	5	2	5	4	4	5	5	5
Vertical Diameter								
2	5	2	5	...	...	5	5	5
8 Point Chords								
...	...	...	1	...	...	1	...	...
(d) Strain gage measurements								
Horizontal at 3 and 9 o'clock								
2	5	2	5	4	4	5	5	5
Vertical at 6 and 12 o'clock								
2	5	2	5	...	...	5	5	5
12 points								
...	...	...	1	...	...	1	...	...
(e) Spear Heads								
...	...	...	Radial	...	Radial	Radial	...	...
(f) Rib Size								
8 WF 48	10 WF 72	8 WF 48	10 WF 72	10 WF 72	10 WF 72	10 WF 72	10 WF 72	10 WF 49
(g) Rib spacing center to center, in feet								
4	3.5	4	3	3	...	3	3	4

were established during construction, the vertical diameter was rotated slightly to avoid interference with construction operations at the invert. Extensometer hooks were installed from a light jumbo. Most of the horizontal diameter stations were installed immediately after construction but installation of

some of the vertical diameters was postponed until the crown was more readily accessible. Horizontal diameter measurements were made from a light magnesium ladder. The vertical diameter was measured by inserting the end of the extensometer tape into the crown hook by use of a bamboo pole with the extensometer head being read at the invert.

Measurements of stress were made on several of the transverse bars in the inner ring of reinforcing at the invert in five of the tunnels as shown in Fig. 7. For these measurements, the concrete was chipped from around the bars and two 10-in. Whittemore strain gage lines were installed on each bar. Generally, two bars 10-ft apart were observed at each measurement location. The gage lines were established at various times after concreting. Some were installed after only the invert had been placed when the bars were considered to be under zero stress, whereas others were established after the full lining had been placed and the bars were already under stress. Where gage lines were established on stressed bars the true zero stress condition was determined by cutting the bars upon completion of the observations.

The elongation of tunnel 5 due to yield toward the portals was observed by measurements between a series of cadmium-plated expansion bolts originally set 100 ft apart near the invert construction joint. Observations were made with a tape under a constant pull of 25 lb and fully supported throughout its length by the concrete lining.

OBSERVATION RESULTS

Test Section: Single Tunnel Case, Steel Rib Sections.—For the single tunnel case, during the period from mining the test section until just prior to mining adjacent tunnel 5, the only change in the external load was the addition of the embankment. In general, slow increases of stresses and deformations were observed throughout the period with a definite increase in rate as the embankment was being built.

Diameter Changes.—Throughout the test section, the vertical diameter decreases and the horizontal diameter increases continued over the entire measurement period and developed rapidly in each steel rib after it was set in place. The greatest deformation in each rib occurred as the heading was advanced, and the soil load arched onto the rib slowed down after the heading had progressed sufficiently to allow the full effect of arching to be felt. The average diameter changes in each section of the test tunnel are shown in Fig. 9(a), 9(b), 9(c), and 9(d). In the yielding rib section, 4-B, the rate of crushing of the redwood blocks between rib segments exceeded the rate of diameter change from external load. The circumferential shortening due to crushing of the blocks increased the amount of vertical diameter shortening and decreased the amount of horizontal diameter lengthening. Thus, large vertical diameter decreases and relatively small horizontal diameter decreases were observed. In all other sections the vertical diameter shortening was only slightly greater in magnitude than the horizontal diameter lengthening.

Stresses.—In general, stresses in the steel ribs were quite low throughout the test section and especially low in the crusher block section, as shown in Fig. 9(e), 9(f), 9(g), and 9(h). The average unit stress on rib cross sections in compression are indicated. Stresses increased most rapidly immediately after the ribs were erected. A noticeable increase in stress was observed in the

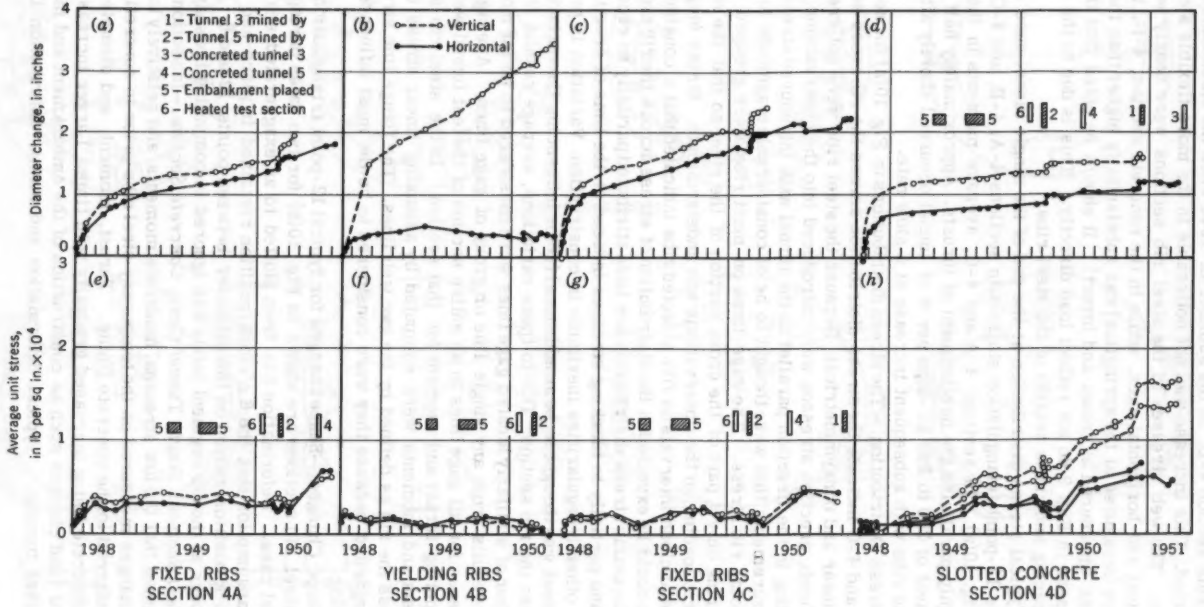


FIG. 9.—DIAMETER CHANGES AND WEB STRESSES

concrete section 4-D, in the summer of 1949 when the embankment was constructed. This increase was not noticeable in the more flexible steel rib sections. The web stresses in the steel rib sections were nearly equal on the vertical and horizontal axes, while in the concrete section, 4-D, the vertical stress (measured at the springline) was substantially higher than the horizontal stress (measured at crown and invert). It should be noted that the unit web stresses in Fig. 9 do not reflect load directly. This is due to the differences in spacing and cross section of the steel ribs.

Typical stress distribution at the end of the single tunnel case determined at the 12-point triangulation stations in sections 4-A, 4-B, and 4-C are shown in Fig. 10(a). In sections 4-A and 4-C, average moments in the steel ribs roughly paralleled the development of thrusts. Approximately half of the total moment of 200 to 250 in.-kips per ft of tunnel occurred shortly after erection of the ribs with subsequent increase at a slow rate.

Stress Distribution.—The stress distributions in Fig. 10(a) for sections 4-A, 4-B and 4-C indicate the stress distribution across the rib cross section to be nonlinear and nonsymmetrical. Because the steel ribs were not erected exactly plumb, erection stresses were introduced into the observations. Tipping or bending in the direction parallel to the tunnel axis introduced stresses into the measurements that were thought to be of considerable magnitude in relation to the total rib stress. The gage lines on most ribs were grouped in patterns covering only a part of the cross section of the steel so that the effect of eccentric loading on the observations was indeterminate. Stress measurements made at close intervals on five selected ribs indicated that a considerable variation could be expected in the distribution of stress across the rib cross section.

Eccentric stress distribution has been attributed partially to eccentric loading and partially to blocking stresses induced at the time of erection together with other irregularities inevitable in construction. Variation in properties of the steel was thought to be an additional factor influencing the variation in stress across the rib section. Due to these variations, average results from a large number of similarly located gage lines were considered to be far more reliable than results from any single line or group of gage lines. Average gage line stresses for all gage lines in an entire section of the test tunnel were used for computing thrust and moment for that section. In the steel rib sections the thrusts and moments were computed by assuming linear stress distribution across the rib as defined by the two web lines. The flange line stresses were disregarded because they were considered to be the most influenced by cross bending.

Shape Changes.—Shape changes for typical 12-point triangulation ribs within the steel rib sections are shown in Fig. 10(b) for two dates during the single tunnel case. Deformation has been plotted to an exaggerated scale based on the assumption that the 6 o'clock position remained in place and that the 12 o'clock position moved on the diameter between points 12 and 6. The minor slippage at the rib segment joints was ignored in computing the shape changes.

Test Section: Single Tunnel Case, Concrete Section.—In section 4-D, it was assumed that the low stresses, moderate moments, and relatively large diameter changes measured on the temporary steel ribs prior to concreting were not transferred to the concrete lining. Thrust, moment, and diameter change of the concrete lining increased gradually with time. Larger increases followed major load changes such as construction of the embankment and mining of the adjacent tunnels. Typical deformation and stress distribution in the steel

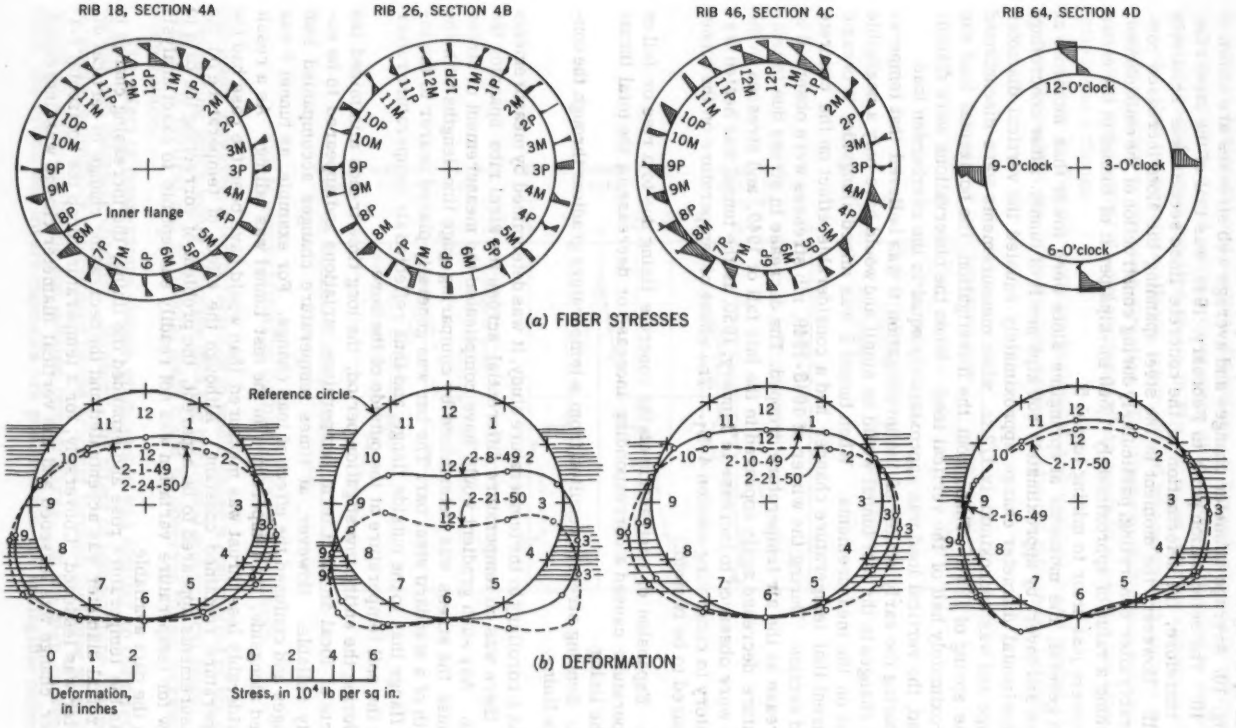


FIG. 10.—TYPICAL STRESSES AND DEFORMATIONS

beams spanning the slots in the concrete just prior to mining tunnel 5 are shown in Fig. 10. Average diameter changes and average web stresses are shown in Fig. 10. The deformation prior to February, 1949, was that of the steel ribs, and, therefore, the deformation of the concrete lined section was relatively small. However, the moment in the steel spanning the slots increased considerably after concreting, particularly during construction of the embankment, reaching a value of approximately 1,500 in.-kips per ft of tunnel in the crown and invert just prior to mining tunnel 5.

In general, the moments at springline slots were lower than moments at crown and invert by approximately 500 kips per ft of tunnel. After concreting, the horizontal diameter change approximately equaled the vertical diameter change and was approximately 1/2 in. when measurements were discontinued in the spring of 1951. Throughout the investigation, the horizontal load was approximately half of the vertical load. When the observations were discontinued, the vertical load was approximately equal to the overburden load.

During the early stages of the investigation it was believed that temperature changes in the test tunnel would be small and would have only a negligible effect on the measurements. When tunnel 5 was mined alongside, it became apparent that temperature changes had a considerable effect on the concrete lined section. During the winter of 1948-1949, rib stresses were observed to decrease as the air temperature dropped. The decrease in stress due to temperature decrease again appeared in the late fall of 1949, and stresses in the ribs were observed to increase in January, 1950, as the tunnel was heated preparatory to concreting section 4-B_1. The effect of temperature on the tunnel appeared to be twofold:

1. Expansion or contraction of the concrete lining due to a rise or fall of temperature caused a corresponding increase or decrease in the total thrust on the lining.
2. Bending stresses resulted from a temperature gradient through the concrete lining.

As a corollary to the temperature study, it was determined by measurements that there was no temperature differential across the steel ribs spanning the slots. Any such gradient would have complicated the measurement of stress because the stress was determined by comparing gage line lengths with the length of a standard steel bar. The bar was generally placed nearer to the inside flange than to the outside flange, and thus reflected air temperature rather than the soil temperature at the outside of the bore.

During the entire investigation period, the long time trends minimized the effects of local or short term temperature variations and appeared to be entirely reliable. However, at times temperature changes accompanied load changes and confused the effect of load change. For example, as tunnel 5 was mined alongside, the temperature in the test tunnel was falling. As a result considerably less thrust was measured than would have been the case had the temperature remained constant. Although the effect of temperature on the measurements appeared to be apparent, the problem of correcting the data to allow for temperature variation was not readily susceptible to exact analysis with the data available.

As the temperature rose and expanded the lining, the increasing change in horizontal diameter was accentuated and the decreasing change in vertical diameter was lessened. Conversely, for a temperature drop the horizontal diameter change was lessened and the vertical diameter change was increased.

In plots of horizontal and vertical diameters, it became especially noticeable that temperature drops cause a divergence of the plots. This led to development of the difference function shown in Fig. 11, using correct algebraic signs in order that temperature effects are indicated whenever both curves move, roughly parallel, in the same direction. The algebraic difference between the horizontal and vertical diameter change plots tends to eliminate the effect of temperature change.

As shown in Fig. 11, both the horizontal and vertical loads tended to increase throughout the investigation period as did the difference between the

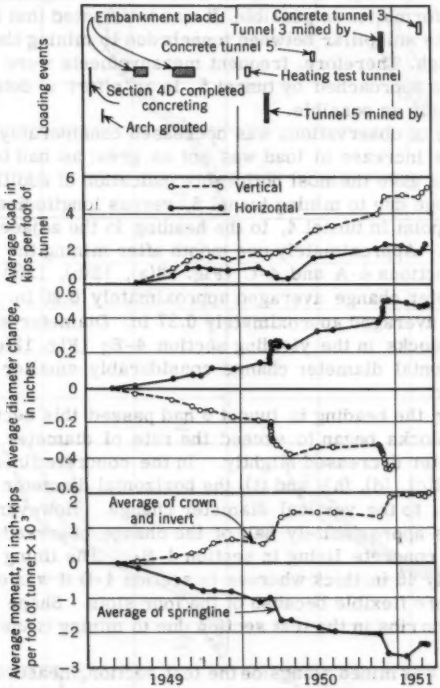


FIG. 11.—DEVELOPMENT OF DIFFERENCE FUNCTIONS

two loads. However, a temperature drop would cause a contraction of the concrete lining which would decrease both the horizontal and vertical loads. Increases in vertical and horizontal loads could be observed for an increase of temperature.

The effect of temperature change on moments was similar to the effect on thrusts and diameter changes. However, the effect of temperature change on moments is probably complicated by the gradient through the lining when subjected to different inside and outside temperatures. In the sign convention used, the crown and invert moments are positive and the springline moments

are negative. Thus, the moment difference function is equal to the numerical difference between the two curves (Fig. 11). As with the thrust and diameter difference, the moment difference function appeared to be a better indicator of the effect of load change than the moments at individual slots.

The readily apparent similarity of the differences between the two curves of each plot on Fig. 11 seemed to offer a simple direct approach to the problem of temperature effects and is examined further by K. S. Lane.[13]

Test Tunnel: Multiple Tunnel Case.—As tunnel 5 was mined alongside tunnel 4 in early March, 1950, and followed by the mining of tunnel 3 in late November, the multiple tunnel case was developed. Extensive observations were taken in the test section in tunnel 4, as well as in the adjacent tunnels, to develop as much information as possible. It was anticipated that the load increase on tunnel 4 and the soil pillar between tunnels due to mining the adjacent tunnel might be quite high. Therefore, frequent measurements were made in the test section as it was approached by tunnel 5, in an effort to detect any signs of overstress as early as possible.

The frequency of observations was decreased considerably when it became apparent that the increase in load was not as great as had been anticipated. Diameter changes gave the most noticeable indication of additional load. Plots of diameter change due to mining tunnel 5, versus longitudinal distance from the observation point in tunnel 4, to the heading in the adjacent tunnel 5, are shown in Fig. 12. Approximately one month after mining the adjacent tunnels past steel rib sections 4-A and 4-C (Fig. 12(a), 12(b), 12(f), and 12(g)), the horizontal diameter change averaged approximately 0.20 in. and the vertical diameter change averaged approximately 0.27 in. Diameter shortening due to crushing of the blocks in the yielding section 4-B_2 (Fig. 12(e) and 12(f)) resulted in a horizontal diameter change considerably smaller than that of the vertical diameter.

Ten days after the heading in tunnel 5 had passed this section, the rate of crushing of the blocks began to exceed the rate of diameter change and the horizontal diameter decreased slightly. In the concrete lined sections 4-B_1 and 4-D, (Fig. 12(c), (d), (h), and (i)) the horizontal diameter change was approximately equal to the vertical diameter change. However, the change in section 4-B_1 was approximately half of the change observed in section 4-D, due to the stiffer concrete lining in section 4-B_1. The lining in section 4-B_1 was approximately 48 in. thick whereas in section 4-D it was only 36 in. thick, and somewhat more flexible because of the four slots. Shape changes at each of the triangulation ribs in the test section due to mining tunnel 5 are shown in Fig. 13.

When tunnel 3 was mined alongside the test section, measurements had been discontinued except in section 4-D. However, some horizontal diameter measurements in section 4-C and horizontal and vertical diameter measurements in section 4-B_1, before and after tunnel 3 was mined past, were in the same range as the diameter changes due to mining tunnel 5. Thus, it was indicated that the load was thrown onto the test section by mining each of the adjacent tunnels was in the same range.

Stresses in the beams across the springline slots of section 4-D increased approximately 4,000 lb per sq in. due to mining tunnel 5. The increase was approximately two-thirds of the total unit stress from the single case including addition of embankment load. The corresponding increase in horizontal

---

13 "Evaluation of Test Results," by K. S. Lane, Transactions, ASCE, Vol. 125, 1960.

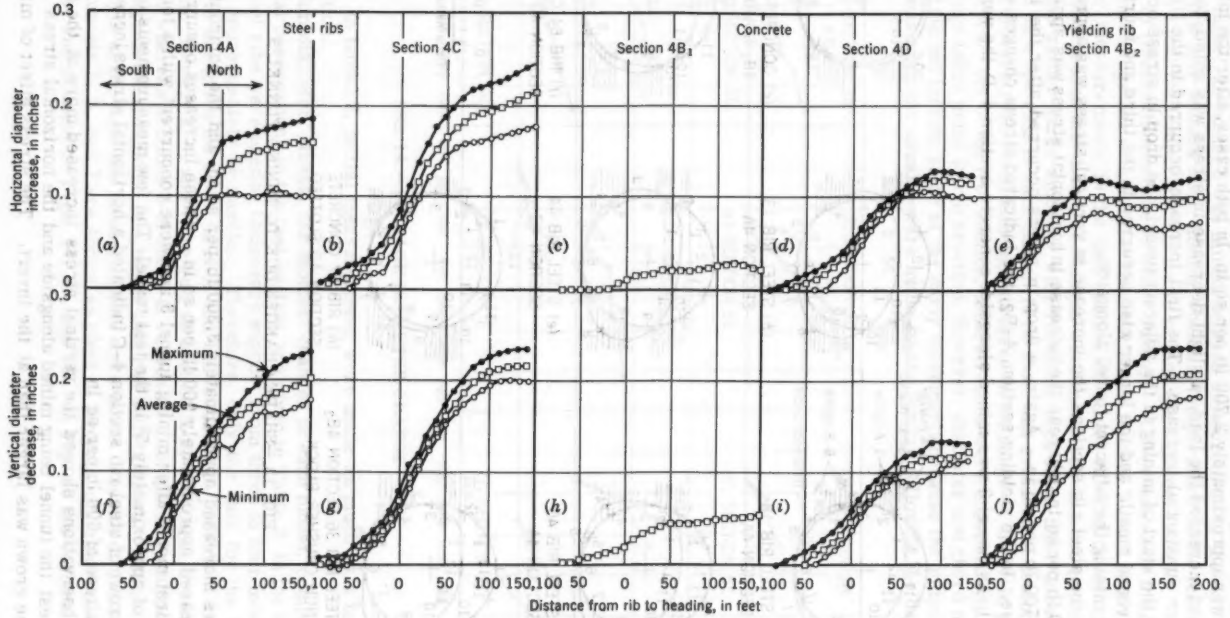


FIG. 12.—DIAMETER CHANGES IN TEST SECTION DUE TO MINING TUNNEL 5

load was approximately 2,700 lb per sq in. In both cases, after the initial mining had increased the load, a slight decrease in stress was noted, followed by a later substantial increase. The first increase occurred in the first month after the start of mining in the adjacent tunnel, the drop in stress occurred in the second month, and the larger rise occurred in the third and fourth months after mining the adjacent tunnel alongside.

In the steel rib sections, the increase in vertical stress was approximately 3,000 lb per sq in. whereas the increase in horizontal stress was approximately 2,700 lb per sq in. Again, a drop in stress occurred after the initial increase. In the yielding section, 4-B_2, the indicated stress changes were very small. As tunnel 3 was mined alongside concrete section 4-D, the vertical unit

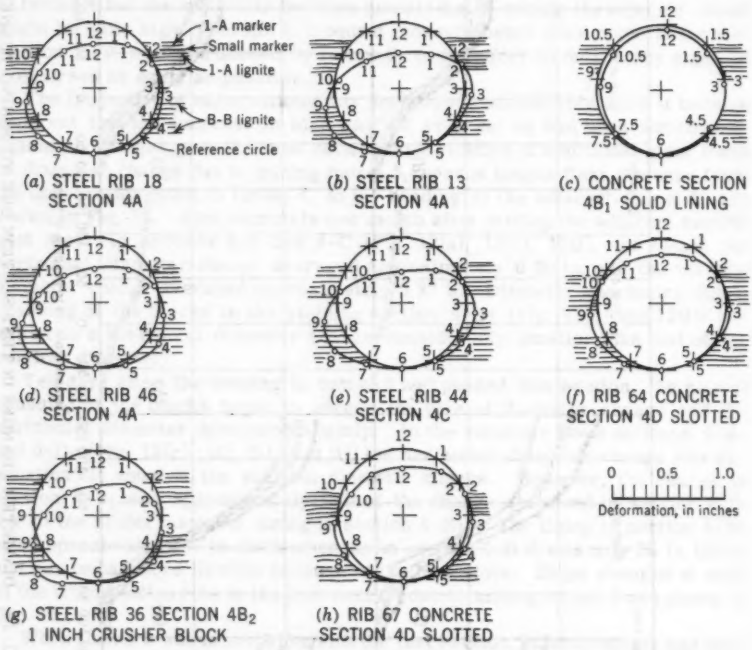


FIG. 13.—SHAPE CHANGES DUE TO MINING TUNNEL 5

stress increased approximately 3,200 lb per sq in. and the horizontal stress increased approximately 900 lb per sq in. These increases occurred during the first month after mining tunnel 3 and were concurrent with a temperature rise of approximately 5° in the test tunnel. The few measurements obtained in the crown of steel rib section 4-C indicated a horizontal stress increase in the magnitude of 600 lb per sq in.

Observations showed the vertical stress increased more at the springline nearest the tunnel being mined alongside and the horizontal stress measured at the crown was larger than at the invert. The stress effect of mining each

adjacent tunnel was approximately the same. However, the falling temperature in the test tunnel, as tunnel 5 was mined, delayed measurement of the full load increase until four months after mining when the temperature in the test tunnel rose to equal the temperature prior to mining the adjacent tunnel.

Results of Observation on Ribs in Other Tunnels.—Observations on the steel ribs of tunnel 5 together with similar observations in tunnels 7 and 2 confirmed the earlier measurements in the test section of tunnel 4. Relatively small average web stresses and diameter changes were measured in most cases, although some rather large amounts with resulting high outer fiber stresses were found on a few ribs in each tunnel. In no case was evidence of crumpling or actual rib overstress noted although stresses in the range of the yield point were observed. As in the test section, total stresses were observed with the zero readings taken prior to rib erection. However, diameter and chord measurements did not include some of the early movements because the initial diameter measurements usually were made on the Sunday following the day of

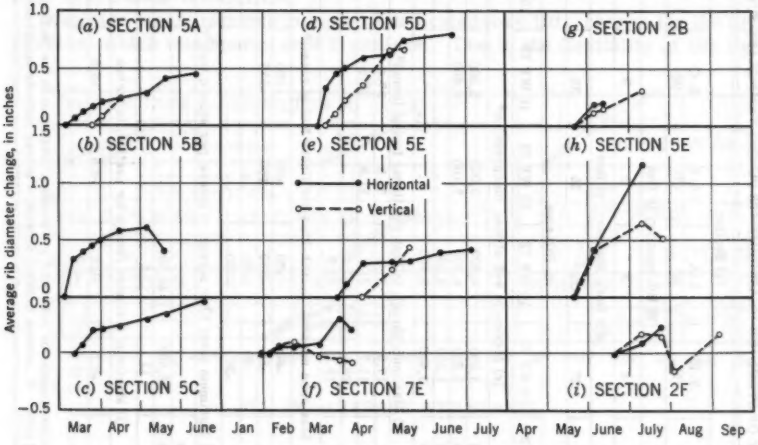


FIG. 14.—AVERAGE DIAMETER CHANGE

erection. In tunnel 2, initial measurements were made as much as a month after erection.

Maximum diameter, stress, and moment changes in each tunnel, compared with similar observations in the test section, are given in Table 3. In the main tunnels steel ribs were used as temporary support from three to four months, averaging approximately 3½ months. Therefore, only the data for the first four months are given for sections 4-A and 4-C in order to provide a usable comparison. Tunnels 2, 4, and 7, as well as section 5-E, represent the single tunnel case whereas sections 5-A and 5-C represent a temporarily supported tunnel alongside the completed test tunnel that had both temporary and permanent supports at the time the measurements were made. Results of measurements in tunnels 2, 5, and 7 are shown as plots of average diameter change, web stress, and moment on Figs. 14, 15, and 16. In Fig. 15 the vertical plot

TABLE 3.—SUMMARY OF STEEL RIB MEASUREMENTS DURING TEMPORARY SUPPORT PERIOD

Clock position (1)	(a) Section										
	2-B (2)	2-F (3)	2-E (4)	7-E (5)	5-A (6)	5-B (7)	5-C (8)	5-D (9)	5-E (10)	4-A (11)	4-C (12)
	(b) Rib spacing, in feet										
	4	4	3½	4	3	3	3	3	3	3	3
	(c) Bore diameter, in feet										
	35	35	35	27	35	35	35	35	35	36	36
	(d) Rib size										
	8 WF 48	8 WF 48	10 WF 72	10 WF 72	10 WF 72	10 WF 72	10 WF 72	10 WF 72	10 WF 72	12 WF 99	12 WF 99
	(e) Maximum web stress, compression[a]										
3	6,600	6,000	10,400	3,300	4,400	5,000	5,300	5,800	8,300	4,070	2,160
6	7,200	4,600	10,400	2,200	4,400	3,100	4,600	4,800	9,700	3,820	2,250
9	12,400	5,900	16,100	5,300	5,300	...	...	8,300	8,600	3,300	2,160
12	6,800	9,000	12,500	3,600	5,700	...	...	5,800	8,300	3,980	2,160
	(f) Maximum thrust, in kips per linear foot of tunnel[a]										
3	23.3	21.2	62.9	17.5	31.1	35.3	37.4	41.0	58.6	39.5	21.0
6	25.4	16.2	62.9	11.7	31.1	21.9	32.5	33.9	68.5	37.1	21.8
9	43.8	20.8	97.4	28.1	37.4	...	...	58.6	60.7	32.0	21.0
12	24.0	31.8	75.6	19.1	40.2	...	...	41.0	58.6	38.6	21.0
	(g) Maximum moment, in inch-kips per linear foot of tunnel[a,c]										
3	-60	-110	-100	+80	+60	+80	-150	+90	-70	-191	+153
6	-170	-50	-90	+80	+230	-160	+130	-40	+180	-175	-197
9	-120	+280	+780	-60	+280	...	...	+360	-320	+155	+225
12	+190	+260	+360	+200	+280	...	...	+270	+300	+292	+350
	(h) Maximum outer fiber stress, in pounds per square inch[b,d]										
Measured	40,000	+2,600	+39,100	...	...	...	...	...	...	+8,700	+20,000
Computed	28,600	+40,000	+40,000	+26,500	-30,000	...	...	-40,000	-35,000	-14,000	-14,000
Clock position	6	6	6	12	6	...	...	6	6	6	3
	(i) Maximum diameter change for section, in inches										
Horizontal	+0.3	+0.2	+0.7	+0.1	+0.5	+0.6	+0.5	+0.8	+0.4	+0.9	+1.1
Vertical	-0.2	-0.2	-1.1	-0.3	-0.2	...	...	-0.7	-0.4	-1.1	-1.4

[a] Average of all measured ribs in the section. [b] Approximate for individual rib showing maximum in the section. [c] + moments indicate couple increases radius of rib; - moments indicate couple decreases radius of ribs. [d] + stress indicate tension; - stress indicate compression.

is the average of the 3 o'clock and 9 o'clock positions, and the horizontal plot is the average of the 6 o'clock and 12 o'clock positions.

Diameter changes in tunnel 5 averaged approximately 0.5 in., which was less than the average of approximately 1.0 in. (Fig. 9) in the test section at comparable periods after erection, although lighter steel was used in tunnel 5. The difference was probably due to early rapid movement which was not included in the observations in the main tunnels. The average thrusts, expressed as average unit web stresses, were low, varying between 4,000 and 8,000 lb per sq in. Moments were generally low, ranging from 0 to 1,000 in.-kips. However, on two ribs near the axis of the dam, stresses in the range of 30,000 lb per sq in. were found on the inside flanges (extrapolated to the flange on the assumption of linear stress distribution across the rib). Radial spearheads in section 5-A, 5-C, and 5-D indicated slight movements toward the bore ranging generally from 0.02 ft to 0.04 ft with a maximum of 0.08 ft measured relative to the ribs. Movement usually occurred at a rather uniform rate within the first month after installation.

Diameter measurements in tunnel 7 indicated very little change for the light rib steel which was spaced on 4 ft centers. Due to the flexibility of the light

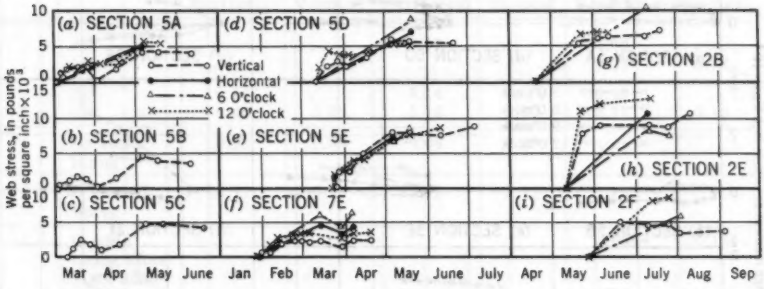


FIG. 15.—AVERAGE WEB STRESS

rib support, stresses in the ribs were relatively low, ranging from 2,000 to a maximum average of less than 6,000 lb per sq in. The horizontal and vertical thrusts were approximately equal with corresponding low moments. Outer fiber stresses extrapolated from the web stresses ranged from 16,000 to 29,000 lb per sq in. in compression and 3,700 to 4,900 lb per sq in. in tension.

Average diameter changes in tunnel 2 were small except in section 2-E. The maximum horizontal diameter changes at individual ribs were 0.35 in. in section 2-B, 1.0 in. in section 2-E, and 0.35 in. in section 2-F. The corresponding maximum vertical diameter changes were 0.25 in. in sections 2-B and 2-F and 1.35 in. in section 2-E. Average unit web stresses and moments were relatively small although outer fiber stresses at or over the yield point of 39,000 lb per sq in. were measured in the invert of each measuring station, and stresses ranging from 21,000 to 37,000 lb per sq in. in compression and up to 24,000 lb per sq in. in tension were measured at the crown. The largest stresses, moments, and diameter changes occurred in section 2-E where seepage caused loosening of blocking and resulted in unsupported spans of 15 ft or more between blocking points on the west side of the tunnel.

The extreme fiber stresses shown in Table 3 are the maximums for individual ribs within each observation section. Because the main tunnel observation sections contained from two to five ribs, the average results of observations are less reliable than observations in the test section of tunnel 4 where measurements were made on nine or ten ribs in each individual section.

Results of Observations on Concrete Lining of Other Tunnels.—Limited measurements of horizontal and vertical diameter changes were made on the concrete linings of tunnels 1, 2, 4, 5, 6, and 7. Settlement profiles were observed in tunnels 1 and 5, and measurements were made in tunnel 5 to determine elongation. Stresses and stress changes were observed in reinforcing bars exposed at the inverts of tunnels 2, 4, 5, and 7.

Diameter changes ranged from 0.1 to 0.35 in. with the vertical diameter decrease approximately the same magnitude as the horizontal diameter increase during the period up to the spring of 1953 when measurements were discontinued just prior to diversion of the river through the tunnels. The results of measurements on the different tunnels are not directly comparable, because

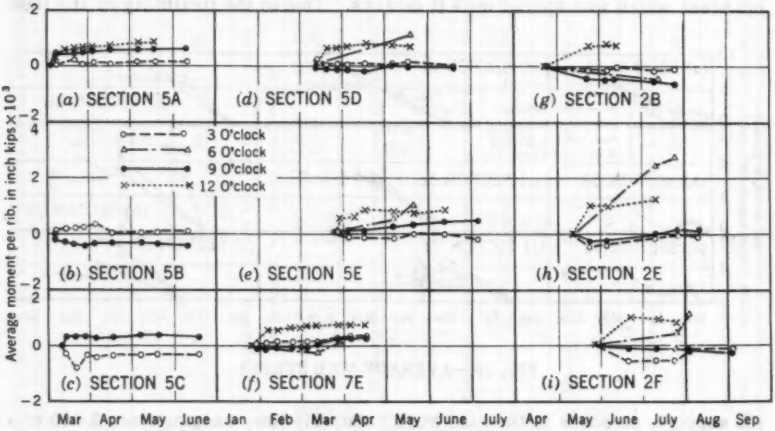


FIG. 16.—AVERAGE MOMENTS

the measurements were begun at somewhat different times after concreting and thus reflect only the effects of events subsequent to initial observations. Undoubtedly, the largest contribution to diameter change was caused by mining adjacent tunnels. These changes are compared in Table 4. With the exception of section 4-B_1 where the change was distinctly less, presumably due to the thicker concrete lining, the changes were generally of the same magnitude.

The effect of contact grouting at a maximum pressure of 50 lb per sq in. was so minor that it was masked by the effect of temperature changes. The temperature effect was the same as that found in the slotted concrete section, 4-D. A drop in temperature would increase the shortening of the vertical diameter and decrease the lengthening of the horizontal diameter.

A reinforcing bar in monolith 18 of tunnel 7 was found to be under a tension stress of 7,000 lb per sq in., which represented the combined effect of mining

both adjacent tunnels. In tunnel 5 an increase in bar stress of approximately 12,000 lb per sq in. and in tunnel 4 an increase of about 15,000 lb per sq in. were noted upon mining one adjacent tunnel. Total unit stress in the bars ranged up to 36,000 lb per sq in. and was affected significantly by temperature changes. Part of the observed stress due to temperature change was caused by the method of observation in which the exposed section of the bar acted partly as if held by fixed supports at each end. The effect of temperature change was probably much greater in the exposed test bars than in normal embedded bars. The technique of measuring stresses on exposed bars is considered applicable only in cases in which temperatures can be maintained constant.

TABLE 4.—DIAMETER CHANGES OF CONCRETE LININGS[a]

Location (1)		First adjacent tunnel[b] (2)		Second adjacent tunnel[b] (3)		Subsequent change (4)	
Tunnel	Monolith	Diameter					
		Horizontal	Vertical	Horizontal	Vertical	Horizontal	Vertical
7	25[c]	....	....	0.07	....	0.09	....
	18	....	....	....	....	0.13	0.18
5	24[c]	0.14	....	0.14	....	0.10	....
	34	0.05	0.09	0.10	0.07	0.11	0.10
4	B1 solid lining	0.03	0.06	0.06	0.03	....	....
4	D slotted lining	0.11	0.13	0.12	0.11	....	....
4	D solid lining after slots concreted	....	....	....	....	0.054+	0.13+
2	34	0.07	....	0.10	....	0.05	....

[a] In inches. [b] Changes due to mining adjacent tunnel approximately one month after adjacent tunnel mined by. [c] Centerline of dam.

Results of elongation measurements in tunnel 5 shown in Fig. 17 are based on the assumption of zero movement at the dam centerline and yielding toward each end. Chaining point No. 7 was assumed to be fixed. By April, 1953, over 2 in. of elongation had been observed with practically no additional elongation after that date. Measurements showed the monolith joint openings were wider in the winter with distinctly less opening near the ends of the tunnel where longitudinal reinforcement was heavier. In the early winter of 1951, the total elongation between portals was 0.09 ft whereas the sum of the joint opening measurements was approximately 0.33 ft. This indicates that the joint open-

ings were not primarily due to over-all elongation but were attributable mainly to shrinkage and contraction of the concrete due to temperature variation.

CONCLUSIONS

Economy.—The test section investigation allowed a considerable reduction in the steel rib support for the main tunnels. A major but undetermined saving in construction costs was made possible by having a full size section of tunnel available for inspection and observation by bidders on the main tunnel contract. The construction experience gained in mining allowed the main tunnel contractor to plan operations with considerably more knowledge of actual mining conditions than would have been possible with a smaller pilot tunnel.

Construction.—Several innovations in construction, notably the use of jumbos mounted on rails well above the invert, and the modification of the mucker to allow continuous loading of muck cars resulted in considerable economy of construction and allowed the project to proceed at a rapid rate. The Fort Union material was much more favorable for mining than was originally anticipated,

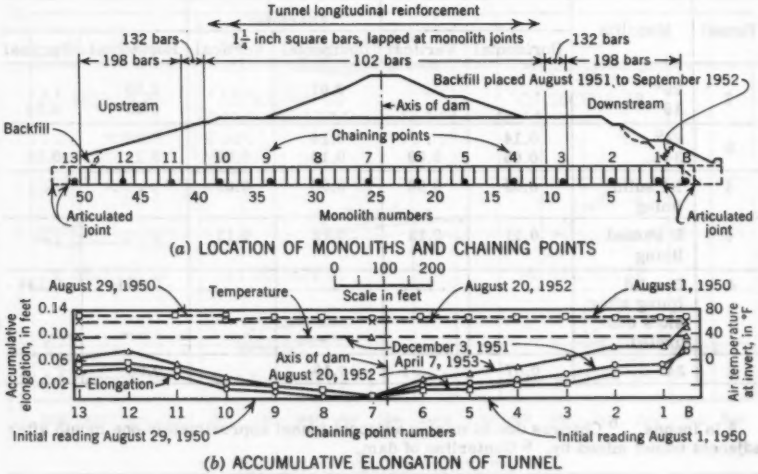


FIG. 17.—ELONGATION OF TUNNEL 5

allowing a mining sequence of two ribs per blast. Little difficulty was encountered with seepage and the blocky Fort Union formation did not exhibit significant swelling nor squeezing properties. Full length mining was feasible before concreting was started in each tunnel, thus simplifying greatly the construction procedure. The yielding rib section indicated that a sizeable decrease in pressure could be obtained but the pressures on the steel rib sections were sufficiently low that such special precautions were not considered necessary for the main tunnels. The excavated bore was well-filled by the concrete lining so that only a minimum of grouting was required in the crown.

Instrumentation.—The mechanical instrumentation performed far better than the electrical instruments. The Whittemore strain gages performed very well and the extensometer tapes were quite successful. While the trends established by the pressure cells apparently reflect the load changes rather well,

the pressure cells were not satisfactory for quantitative measurements. Tangential components complicate the loading to such an extent that, with the present state of pressure cell design, they are not considered suitable for use in installations similar to the test tunnel. Carlson strain meters operated satisfactorily throughout the observation period, but an established base from which to determine quantitative results is necessary. The SR-4 gage installation was unsatisfactory.

Measurement of stress in the reinforcing steel after chipping out the surrounding concrete was satisfactory, but effects of temperature changes complicate the stress relationships to such an extent that similar observations are recommended only in cases in which the temperature is fairly constant. The temperature changes throughout the investigation program were greater than were originally anticipated. Most of the early measurements were made at relatively constant temperatures, but during later phases of the investigation temperature changes masked load effects to a considerable extent. Should such an investigation be undertaken again, it would be well to make provision for regulation of temperature throughout the entire observation period.

EVALUATION OF TEST RESULTS

By Kenneth S. Lane,[1] F. ASCE

With Discussion by A. A. Eremin

SYNOPSIS

The principal methods used in evaluating observations of the tunnel test section at Garrison Dam are presented herein. Principal results were loading on the temporary support ribs, magnitude and distribution of load on the permanent concrete lining, and a better understanding of the inherent safety of a circular lining provided by ring action. Certain new analytical methods are presented, with their possible application to other tunnels.

INTRODUCTION

The problem of loads reaching a tunnel in soil or weak rock is sufficiently complex that a fully rational solution should not be expected. This solution depends not only on ground conditions but also on the stiffness of the tunnel section, because the stiffer the tunnel, the more load it is likely to attract. Hence experience with other tunnels plays a major role in tunnel design, but is applicable only in so far as the similarity both of tunnel sections and ground conditions can be evaluated for adequate comparison. When available experience may seem inadequate, a cautious and investigative procedure is advisable.

This was the case at Garrison Dam because there was no prior experience with tunnels in the Fort Union formation of clay-shale where the tunnelling was to take place. This shale formation, which contains beds of lignite coal, can be described either as a heavily preconsolidated hard clay or as a soft rock. Because the record of experience had frequently shown difficulties with tunneling in stiff clays,[2,3] and because early laboratory tests gave some indication of similarity between the Fort Union formation and the energetically swelling clays of Paris and Belgium, it was decided in the early stages to construct a full-size, 240-ft length of one of the main tunnels to serve as a test tunnel. The more significant results are examined from the standpoint of their evaluation and application in relation to the Garrison tunnels and for future use.

Note.—Published, essentially as printed here in November, 1957, in the Journal of the Soil Mechanics and Foundations Division, as Proceedings Paper 1439. Positions and titles given are those in effect when the paper or discussion was approved for publication in Transactions.

[1] Chf., Foundations and Materials Branch, Kansas City Dist., Corps of Engrs., Kansas City, Mo.; formerly Chf., Soils and Geology Branch, Garrison Dist., Riverdale, N. Dak.

[2] "Tunneling," by H. S. Drinker, John Wiley & Sons, Inc., New York, N. Y., 1888.

[3] "Practical Tunneling," by F. W Simms, 4th Ed., London, 1896.

Notation.—The letter symbols adapted for use in this paper are defined where they first appear, in the illustrations or in the text, and are arranged alphabetically for convenience of reference in the Appendix.

TUNNEL LOADS

Loading Cases.—Fig. 1 shows contours of total overburden load after placing the embankment of the dam. The numbers are in units of tons per square feet at the crown of the tunnels. It also shows the tunnel layout including the location of test tunnel 4, and the sections in other tunnels where stresses were measured on steel ribs of the temporary support. These load contours were determined by dividing the embankment loading and the excavation unloadings into a series of strip loads and then computing the net stress at the crown of the tunnels for the Boussinesq[4] case of stress distribution. The test tunnel was constructed prior to placing the embankment in a region where the initial overburden load was approximately 6.6 tons per sq ft. Before mining the main tunnels, the embankment was added in order to avoid a load change after tunneling. This resulted in increasing the load on the test tunnel to 6.8 tons per sq ft in section 4-A and 8.3 tons per sq ft in section 4-D. The main tunnels were then constructed in the order shown progressively by stages in Fig. 2(a) to 2(d), for the reach opposite the test tunnel. This created the following general load cases:

Single Tunnel Case.—A single tunnel is mined, temporarily supported by steel ribs and then converted to the permanent concrete lining. This applied to the test tunnel and tunnels 2, 5, and 7 for the period prior to mining the adjacent tunnels on each side.

Surface Loading Case.—A load is added at the ground surface after the tunnel is mined. In this case the embankment served as the additional load. The surface loading case applied only to the test tunnel because the embankment was placed prior to mining the other tunnels.

Multiple Tunnel Case.—The load is shared between three tunnels and the intervening ground pillars due to adjacent mining on each side of a previously built tunnel. This applied to the test tunnel and tunnels 2, 5, and 7.

Other Cases.—Although several other conditions are indicated, such as mining between two previously concreted tunnels or beside one of them, the observations did not cover such cases except to show them as less severe than the aforementioned three cases.

Measured Loads.—Typical loads measured on the steel ribs are shown by Fig. 3, and Fig. 4 shows the loads measured on the slotted concrete test section 4-D. Except in the test tunnel, the data cover the single tunnel case for the 2½ to 4 months period when the ribs served as temporary support prior to concreting.

For this single tunnel case, the vertical load on the ribs of the 35-ft to 36-ft bore tunnels was in the range of 10% to 15% of the overburden load, as indicated in Table 1. The vertical load on section 7-E was significantly lower which was probably caused by a greater percentage of the load being arched over this smaller diameter tunnel. The low load on section 4-B was due to the much greater yielding resulting from crushing of the wooden blocks that were placed at each rib joint in this test section. The smaller load on section 4-C,

[4] "Application des potentiels a l'etude de l'equilibre et du mourement des solids elastiques," Paris, Gauthier-Villars, 1885.

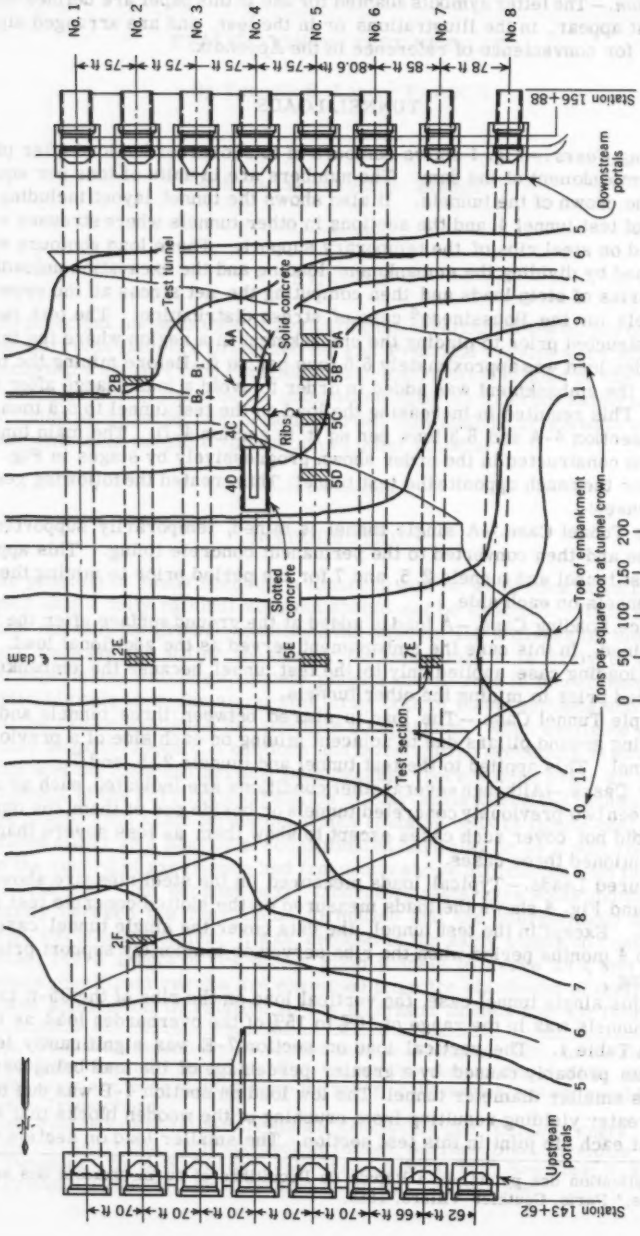


FIG. 1.—TOTAL OVERBURDEN LOAD

as contrasted with 4-A, was considered to be due partly to the slightly more flexible ribs and different mining methods in 4-C and partly to the arching of some load over to adjacent concrete section 4-D. This latter point has been independently studied by Aly A. A. Sabry.[5] It is significant that the rib load increased with overburden load. This is seen by comparing sections 5-A and 5-B outside the toe of the dam with section 5-E at the center of the dam. The loading conditions for tunnel 5 were similar to those for tunnel 4.

For the surface loading case of adding the embankment, the contribution from this load change increased the vertical load on rib section 4-C by approximately 0.1 to 0.2 tons per sq ft, or less than the 0.5 tons per sq ft increase in overburden load computed for the embankment effect. In contrast, the stiffer concrete section 4-D attracted load, the vertical tunnel load increase of approximately 2 tons per sq ft being greater than the 1.3 tons per sq ft computed increase in overburden. Because of this tendency for the stiffer concrete lining to attract more than its share of an added load, the bulk of the embankment load was placed before constructing the main tunnels.

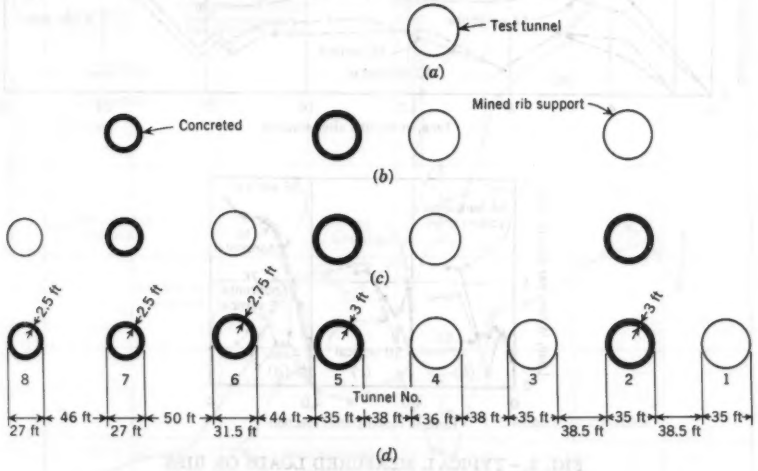


FIG. 2.—ORDER OF CONSTRUCTION

Although measurements were taken on the concrete lining in tunnels 2, 5, and 7, sufficient data for analysis of the multiple tunnel case were obtained only in the test tunnel. As shown by Figs. 3 and 4, the mining of an adjacent tunnel resulted in a definite load increase on the previously constructed tunnel. This increase was much greater on the stiff concrete section 4-D than on the more flexible rib sections 4-A and 4-C. At the end of the measurements, concrete section 4-D was carrying essentially 100% of the overburden load.

Extent of Doming and Arching.—A recently mined tunnel acts as a yielding hole in the ground. A part of the load above is arched over the tunnel to the ground at each side, with the balance carried by the temporary support of the

[5] "Analysis of Field Observations on the Test Tunnel at Garrison Dam," by Aly A. A. Sabry, thesis presented to the University of Illinois, at Urbana, 1952.

tunnel. At the heading, the load is transferred in four directions (to each side, forward to the ground in front of the heading, and backward to the tunnel support) as a doming action. This action is of interest in considering the possible transfer of load between adjacent tunnel sections of different rigidity. Doming is also significant from a construction standpoint as being indicative of the maximum distance that can be mined ahead before erecting support. As used herein, the term doming is applied to the load transfer at the heading, and the term arching is applied to the load transfer to each side of the tunnel behind the region of doming, which advances with progress of the heading.

For the single tunnel case some evidence of the lateral extent of doming was furnished by piezometers installed from the vent shaft. When the test tun-

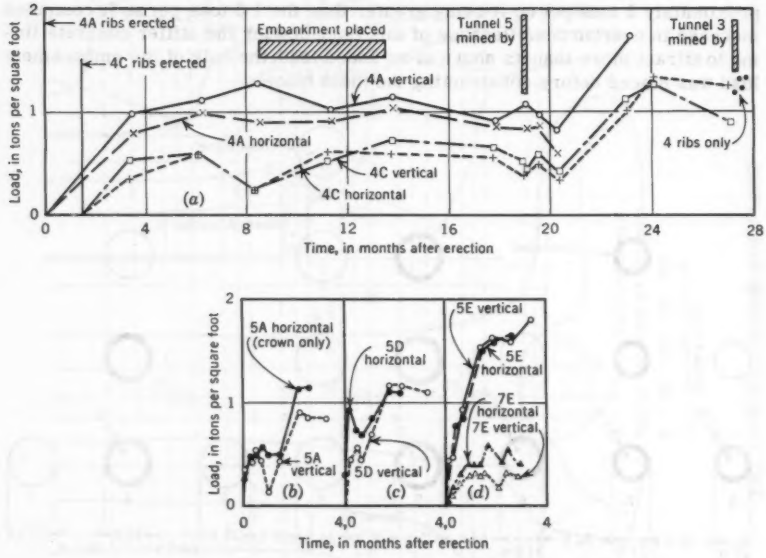


FIG. 3.—TYPICAL MEASURED LOADS ON RIBS

nel heading approached to within a distance of approximately 30 ft, these piezometers showed a definite increase in the pore water pressure that continued as the heading passed. This indicated that the area of stress increase extended at least 30 ft forward of the heading. Further evidence was obtained from plots of diameter change versus distance from the measuring rib to the heading, which generally showed a high rate of diameter change while the heading was advancing to a certain distance beyond the rib, and then a decrease in rate as the heading progressed further. This distance to the heading was considered a measure of the extent of doming of the load to the ribs back of the heading, and most frequently ranged from 30 ft to 45 ft with an average of approximately 38 ft, as shown by data obtained during mining of the test tunnel.

For the multiple tunnel case, a more positive measure of the extent of doming was obtained from the diameter changes in the test tunnel that occurred

during the mining of tunnel 5 alongside (see Fig. 12 of the accompanying paper by Mr. Burke). When the heading of tunnel 5 approached to approximately 60 ft to 80 ft from any rib measured in tunnel 4, its diameter change began to accelerate, indicating that the effect of doming extended approximately this distance forward of the heading of tunnel 5. As the heading passed the measuring rib, the rate of diameter change became a maximum and then decreased gradually as tunnel 5 advanced and changed the load transfer condition from that of

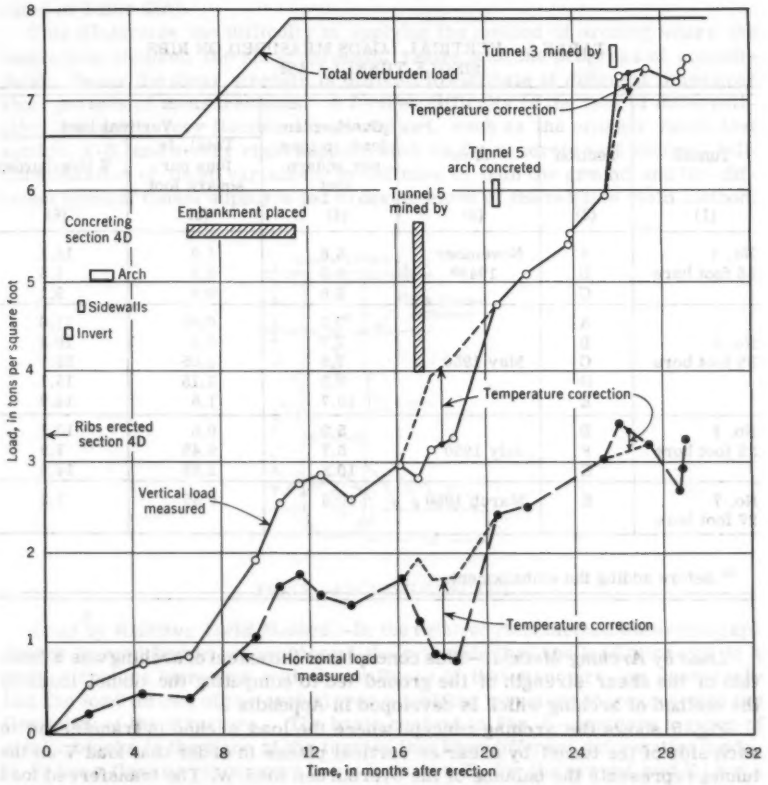


FIG. 4.—MEASURED LOADS FOR SLOTTED CONCRETE SECTION 4-D

doming to that of arching. Because the continued yield of the ribs of tunnel 5 was accompanied by a comparable yield in the opposite sections of tunnel 4, the arching across tunnel 5 extended at least the 70-ft distance over to tunnel 4, or two bore diameters.

These observations indicate that the extent of doming was approximately one diameter, or 35 ft, in the single tunnel case and at least twice this in the multiple tunnel case. The evidence shows also that the extent of arching was

of the same general magnitude. Although the rate of mining tunnel 5 opposite the test tunnel (approximately 15 ft per day) was considerably faster than the mining of the test tunnel (approximately 3 ft per day), it is likely that the increase in extent of arching in the multiple tunnel case was caused mainly by an increase in shear strength of the ground. In the period of 1½ yr between mining the test tunnel and then mining tunnel 5, such a strength increase would be expected from consolidation of the ground around the test tunnel under its loading from the single tunnel case and from the added embankment load.

TABLE 1.—VERTICAL LOADS MEASURED ON RIBS
SINGLE TUNNEL CASE

Tunnel	Section	Time	Overburden load, in tons per square foot	Vertical load	
				Total, in tons per square foot	% Overburden
(1)	(2)	(3)	(4)	(5)	(6)
No. 4	A	November	6.6	1.0	15.1
36 foot bore	B	1948[a]	6.6	0.3	4.5
	C		6.6	0.6	9.1
	A		7.3	0.85	11.6
No. 5	B		7.7	0.8	10.3
35 foot bore	C	May 1950	7.8	1.05	13.7
	D		8.3	1.15	15.1
	E		10.7	1.6	14.9
No. 2	B		5.9	0.6	10.1
35 foot bore	F	July 1950	5.7	0.45	7.9
	E		10.8	1.55	14.6
No. 7	E	March 1950	10.9	0.35	3.2
27 foot bore					

[a] Before adding the embankment.

Load by Arching Method.—This concept that the extent of arching was a function of the shear strength of the ground led to computing the tunnel loads by the method of arching which is developed in Appendix I.

Fig. 5 shows the arching concept where the load arched is transferred to each side of the tunnel by shear on vertical planes in order that load V on the tunnel represents the balance of the overburden load, W. The transferred load V_s, depends on the unit shear strength, s, being a function of the effective or intergranular stress, σ, for which the following three conditions were recognized:

$s_1 = f(\sigma_1)$, the initial condition with effective soil weight buoyant below the original water table and saturated above; $s_2 = f(\sigma_2)$, the condition after lowering the water table by excavation, which exposed lignite beds at the plane of the tunnels, at the downstream portals. The soil would then be at saturated weight because the open-jointed lignites acted as horizontal drains directing the seepage forces downward; and $s_3 = f(\sigma_3)$, the condition after adding the embankment load. Early loads on the test tunnel in the single tunnel case were

checked by comparing them with the loads computed from the arching method, based on the initial shear strength, s_1, as indicated in Table 2, column 3. However, as tunnel 7 and tunnel 5 were mined, the loads measured on the ribs were much smaller than those computed with the same shear strength, s_1. Attempts were made to estimate the extent of consolidation in increasing the effective stress from σ_1 toward σ_2 and even toward σ_3, which resulted in a value of s near s_2. Although the computed loads were reduced by using this higher shear strength, they were still considerably higher than the measured values, as indicated in Table 2(A).

This illustrates the difficulty in applying the method of arching where the controlling element, the shear strength, varies with the progress of consolidation. Hence the shear strength is difficult to estimate at different times over short periods of measurements. A further difficulty is the lack of differentiation between a very flexible tunnel support, such as the crusher block test section, 4-B, and a very rigid support, such as the concrete test section, 4-D. Consideration of these variations in stiffness of both the ground and the different types of tunnel supports led to development of the relative yield method.

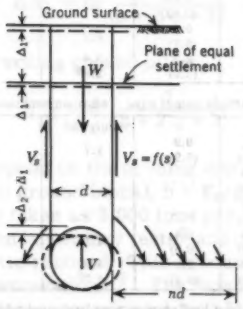


FIG. 5.—ARCHING CONCEPT

Load by Relative Yield Method.—In the relative yield method the arching approach is modified in recognition of the principle that the load attracted to a rigid structure increases with the stiffness of that structure, or conversely that the load thrown off or arched over a yielding structure increases with the flexibility of the structure. The basic concept in Fig. 6 considers a group of elastic blocks in the plane of the tunnels that have different deformation moduli, E_t for a flexible rib support being less than E_s for the ground, and E_c for a stiff concrete lining being greater than E_s. The ground above the tunnels is considered as a series of blocks with the loads transferred between adjacent blocks by shears on their boundaries. The lower boundary at the invert is assumed either to be rigid or to settle uniformly in order that the significant deflections occur in the height, d, of the elastic blocks. With these assumptions, the relations for the vertical tunnel loads are derived in Appendix II, the final equations for the three principal load cases being as follows:

Single Tunnel Case.—Load on flexible rib support:

$$V = W\left(1 - \frac{n}{b+n}\right) \quad \ldots\ldots\ldots\ldots\ldots\ldots \quad (1)$$

TABLE 2.—INITIAL AND RETROSPECT LOAD COMPUTATION

Section	(A) Initial Load Computation[a,b]					(B) Retrospect Load Computation[a,b]		
	Overburden load	Computed load: Arching $f(s_1)$	Arching $f(s_2)$	Relative yield	Measured load	Overburden load	Computed by relative yield	Measured load
(1)	(2)	(3)	(4)	(5)	(6)	(7)	(8)	(9)
(a) Single tunnel case - before embankment								
					Nov. '48			Nov. '48
4A	6.6	0.9	...	0.9	1.0	6.6	1.1	1.0
$4B_1$	6.7	1.0	...	0.05	0.4	...	...	...
$4B_2$	6.7	1.0	...	0.05	0.3	...	...	...
4C	6.6	0.9	...	0.4	0.6	6.6	0.55	0.6
4D	6.6	0.9	Ribs Alone	0.7	0.55	6.6	0.7 Ribs Alone	0.55
(b) Surface loading case - embankment added								
					Sept. '49			Sept. '49
4A	6.8	1.1	...	0.9 (0.5)	1.1	6.8	(1.15)	1.1
$4B_1$	7.0	1.3	...	0.05 (0.03)	0.4	...	...	...
$4B_2$	7.0	1.3	...	0.05 (0.03)	0.4	...	...	...
4C	7.1	1.4	...	0.4 (0.3)	0.7	7.1	(0.6)	0.7
4D	7.9	2.2	...	2.8 (3.0)	3.4 2.8[d]	7.9	(3.2)	3.4 2.8[d]
(c) Multiple tunnel case - after embankment								
					July '50			July '50
4A	6.8	1.1 (1.9)	1.1 (2.1)	0.9 (0.9)	1.7	6.8	(1.55)	1.7
$4B_1$	7.0	1.3 (2.1)	1.3 (2.3)	...	...	...	...	...
$4B_2$	7.0	1.3 (2.1)	1.3 (2.3)	...	...	...	...	...
4C	7.1	1.4 (2.2)	1.4 (2.4)	0.4 (0.5)	1.1	7.1	(0.8)	1.1
4D	7.9	2.2 (3.0)	2.2 (3.2)	2.8 (6.3)	5.5 4.7[d]	7.9	(6.0)	5.5 4.7[d]
(d) Surface loading case - embankment added								
5A	7.3	(8.0)	...	(8.0)[c]	...	7.3	(7.3)[c]	
5B	7.7	(8.4)	...	(8.4)[c]	...	...	...	
5C	7.8	(8.5)	...	(8.7)[c]	...	7.8	(7.9)[c]	
5D	8.3	(9.0)	...	(9.2)[c]	...	8.3	(8.2)[c]	
(e) Single tunnel case - after embankment								
2E	...	...	...	...	...	10.8	1.4	1.55
2B	...	...	...	...	...	5.9	0.5	0.6
2F	...	...	...	...	...	5.7	0.5	0.45
5E	10.7	3.7	2.5	0.35 (0.15)	1.6	10.7	1.8	1.6
7E	10.9	2.6	0.6	0.4 (0.1)	0.35	10.9	1.4	0.35
(f) Multiple tunnel case - after embankment								
					June '50			June '50
5A	7.3	1.1 (1.8)	0 (0)	0.2 (0.1)	0.85	7.3	(0.55)	0.85
5B	7.7	1.5 (1.8)	0 (0.2)	0.3 (0.1)	0.80	...	...	...
5C	7.8	1.6 (2.3)	0 (0.3)	0.3 (0.1)	1.05	7.8	(0.6)	1.05
5D	8.3	2.1 (2.8)	0.7 (0.8)	0.3 (0.1)	1.15	8.3	(0.5)	1.15

[a] All loads are vertical, in tons per square foot. [b] Values in parenthesis are for n = 2, all others are for n = 1. [c] On soil block before mining tunnel 5. [d] Determined from web and flange stresses, all others from web stresses only.

Surface Loading Case.—Load increase from adding a unit load, p, at the surface;
On stiff concrete lining:

$$\Delta V_c = p\,d\left[1 + \frac{n(c-1)}{c+n}\right] \quad \ldots\ldots\ldots\ldots\ldots \quad (2)$$

On flexible rib support:

$$\Delta V_r = p\,d\left[1 - \frac{n\,(1-b)}{b+n}\right] \quad \ldots\ldots\ldots\ldots\ldots \quad (3)$$

Multiple Tunnel Case.—Load increase from mining adjacent to a previously concreted tunnel:
Load on rib support of the tunnel being mined,

$$V = W\,\frac{b}{(b+2\,c+3)} \quad \ldots\ldots\ldots\ldots\ldots \quad (4)$$

Load increase on the concreted tunnel,

$$\Delta V_c = W\,\frac{c}{(b+2\,c+3)} \quad \ldots\ldots\ldots\ldots\ldots \quad (5)$$

Load increase on the intervening ground pillar,

$$V_{p1} = W\,\frac{1}{(b+2\,c+3)} \quad \ldots\ldots\ldots\ldots\ldots \quad (6)$$

These load equations depend on the arching distance, n d, and on the stiffness ratios (tunnel block to ground block), $b = E_t/E_s$ and $c = E_c/E_s$.

For the ground, E_s was taken as 2,000 tons per sq ft. This value had been reasonably established from laboratory tests[6] and confirmed by field measurements of the rapid or elastic rebound. This rebound ranged from 1 to 2 ft due to unloading by the large excavations.[7] The tunnel moduli, E_t and E_c, were obtained from plots of the measured vertical load V, versus the vertical diameter change, D_y, similar to Fig. 7 where the values of E_c, E_s, and E_t are in tons per square feet. In early computations when preliminary data were available only from the test tunnel, E_t for various locations in the main tunnels was estimated from the following relationship derived in Appendix III:

$$E_t = \frac{12\,E\,I}{r^3\,\delta\left(1 - V_H/V_V\right)} \quad \ldots\ldots\ldots\ldots\ldots \quad (7)$$

in which V_H/V_V is the horizontal-vertical load ratio and the quantities E, r, δ, and I are the modulus of elasticity, radius, spacing, and cross-sectional moment of inertia, respectively, of the steel ribs. Although Eq. 7 might have been applied directly as a first approximation, it proved more useful as an indication of how E_t varied with its pertinent elements—that is, directly with I,

---

6 "Soil Properties of Fort Union Clay Shale," by C. K. Smith and J. F. Redlinger, Proceedings, 3rd International Conference on Soil Mechanics and Foundations Engrg., Switzerland, 1953.

7 "Designing for Foundation Movements at Garrison Dam," by K. S. Lane, Proceedings, 5th Congress on Large Dams, Paris, 1955.

inversely with r^3, and inversely with δ. Hence for initial computations, moduli for the main tunnels were assumed to vary according to these relationships from the value of E_t determined for test section 4-C.

Results of these computations with preliminary data are presented in Table 2(A). In the test tunnel the check with measured loads (Column 6) was good with the load arched 1 diameter (n = 1) for the (a) single tunnel and surface loading

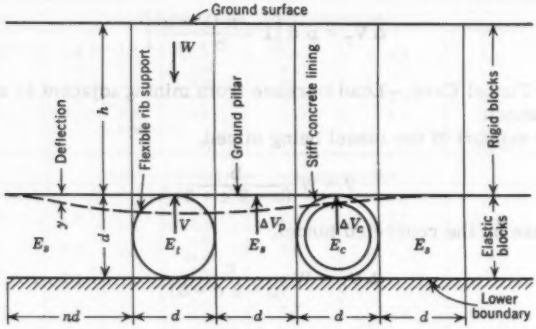


FIG. 6.—RELATIVE YIELD CONCEPT

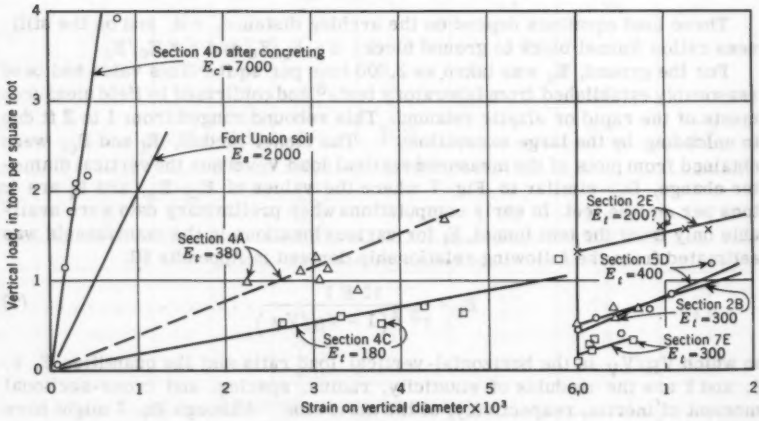


FIG. 7.—TYPICAL DEFORMATION MODULI

cases (b), while for the multiple tunnel case (c), it was better with the load arched 2 diameters (n = 2). In tunnels 5 and 7 the computed load was consistently lower than the measured load, but the check was adequate for practical use in estimating the vertical load for selecting rib sizes, because, as described later, this was controlled more by bending moment than by direct thrust.

On completion of the investigation, the computations were repeated, using final data from tunnels 2, 5, and 7, and further data from the test tunnel. Values of E_t were determined from plots of vertical load versus vertical diameter change. Where the vertical diameter was not measured, the horizontal diameter change was used and assumed equal to the vertical. Table 2(B) shows the results of this retrospect computation, based on the load arched 1 diameter in the single tunnel case and arched 2 diameters thereafter, considering the shear strength of the adjacent ground pillars increased by consolidation under the loading arched over by mining of the single tunnel. In the test tunnel the check of the measured loads (column 9) was good for all three cases, considering that the load measured in section 4-D was so complicated by a temperature change during the mining of tunnel 5 that it was difficult to estimate the proper value of the measured load. In the other tunnels the check was likewise successful, except for tunnel 7, which had the smallest diameter of the tunnels measured.

Closer checks could doubtless be obtained by further refinements. One such refinement would be an allowance for further yield of the ground pillar due to consolidation, which would gradually increase the load on the tunnel. However, the relative yield method proved adequate for practical usage and checked the measured loads considerably closer than the arching method. The relative yield method, of course, involves uncertainties in choosing values of E_s, n, and E_t, a usual problem in choosing soils and materials constants. However, in this application the pertinent ratios of these factors did not vary widely, because n was certainly not less than 1 nor more than 3; $b = E_T/E_S$ for the sizes of ribs used appeared to vary in the range of from 0.1 to 0.2 (except for the unusually flexible crusher block test section); and $c = E_c/E_S$ was used in the range of from 3 to 4 for the slotted concrete test section, and probably was somewhat greater for the full circle concrete lining of the main tunnels.

A major advantage of the relative yield method was its ability to picture the load transfer between tunnels and ground, away from yielding points and toward stiff points. For example, comparing Eqs. 2 and 3, these expressions show how an added surface load is attracted by a stiff concrete tunnel and thrown off by a tunnel with yielding support. From the test tunnel data the small stiffness of the rib support was apparent and of the order of 10% to 20% that of the ground. The great stiffness of the concrete lining was $3\frac{1}{2}$ or more times that of the ground. The stiffness of the tunnel lining determined not only the amount of vertical load reaching the tunnel, but was also the principal factor controlling the amount of horizontal load.

Horizontal-Vertical Load Ratio.—At nearly all of the measuring sections the vertical load was consistently greater than the horizontal load. The vertical diameter shortened, and the horizontal diameter increased. This indicated the vertical as the activating load causing the vertical diameter to decrease and the horizontal diameter to lengthen, forcing out the support at the spring lines to build up the horizontal as the passive load. This performance is shown by the data on Fig. 3, and by Fig. 10 of the paper by Mr. Burke.

The only significant exceptions were sections 2-F and 7-E where the horizontal load was found to be slightly greater than the vertical load and the diameter changes behaved erratically. Because tunnels 2 and 7 were outside tunnels at the time of mining, it is conjectured that residual horizontal stress in the Fort Union formation could have been responsible for the horizontal load being slightly greater than the vertical load.

The geologic history of the site is compatible with the presence of such residual horizontal stresses, because at one time the area was loaded by 1,000 ft

of additional overburden which would have caused comparatively high horizontal stresses. Subsequently this overburden was eroded, followed by cutting of the river valley, which allowed a lateral yield to reduce the horizontal stress. Some evidence of residual stresses was observed at the base of the powerhouse excavation where vertical slots tended to close a few hours after cutting by a coal saw. However, this occurred near the bottom of the pre-glacial river valley and was not observed at the higher elevation of the tunnels.

In the single tunnel case the horizontal load on the flexible rib support was approximately equal to the vertical load and the horizontal-vertical load ratio ranged from 0.8 to 1.1. In the stiff slotted concrete section the ratio was much lower, ranging from 0.4 to 0.6 and averaging 0.5, as shown by Fig. 8. This (V_H/V_V)-ratio was temporarily reduced by the adjacent mining of tunnel 5 when in rib section 4-A it dropped from 0.9 to 0.8 and in section 4-C from 0.85

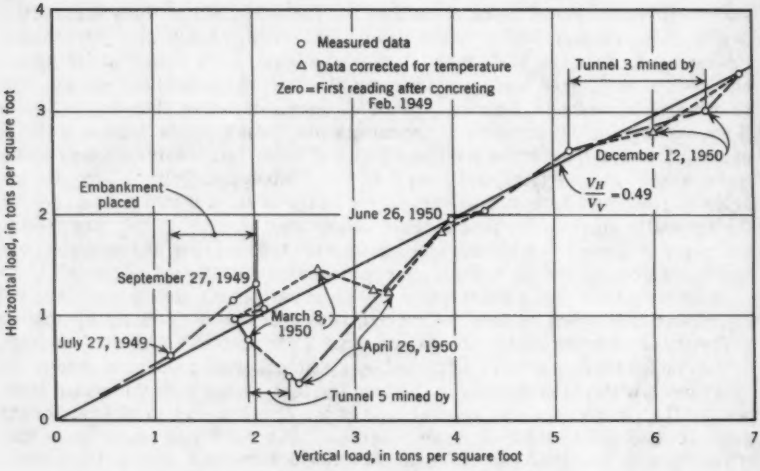


FIG. 8.—HORIZONTAL LOAD VERSUS VERTICAL LOAD FOR SLOTTED CONCRETE SECTION

to 0.7, followed in both cases by recovery to its earlier value. In the stiff concrete section 4-D this temporary reduction was much greater with the (V_H/V_V)-ratio falling as low as 0.25, although the true picture was considerably obscured by the effect of a concurrent temperature drop. It is likely that the horizontal load was reduced temporarily as a result of a small yield laterally toward the open bore of tunnel 5. This was definitely indicated by a temporary drop registered by the pressure cells at the spring line as the heading of tunnel 5 passed by section 4-D.

Effect of Temperature Changes.—In the early stages of excavating, the temperature inside the test tunnel approached the narrow range of ground temperature (approximately 50° F to 55° F). This was true also during the mining of each of the main tunnels. Thereafter the temperature varied considerably in the range of 0° F to 70° F as wind blew through the open tunnels or as they

were heated when concreting was performed in the winter. During the measuring period the inside temperature in concrete test section 4-D varied from 45° F to 75° F, which considerably influenced the measured results. This is apparent from Fig. 9, in which the data are plotted as changes since concreting, based on the concept that stress in the concrete is derived solely from subsequent load changes. As tunnel 5 was mined adjacent to it, the expected increase in thrust in section 4-D was masked by the effects of a concurrent temperature drop, with the effect on the moment and diameter changes being similar but of less magnitude.

With the lining exterior at essentially constant ground temperature, the effect of an inside temperature change on the concrete lining is complex. A temperature increase expands the lining, increasing both the vertical and horizontal loads. However, with a temperature decrease, the lining contracts away from the soil and the shear stress in the ground above increases. This causes more of the load to be arched over, which reduces the tunnel load, at least until the soil yields sufficiently under the increased stress to follow the contraction of the lining. By drastically simplifying the conditions to the case of a homogeneous ring tightly fitted in a hole within an elastic medium, Carneal K. Smith, F. ASCE obtained a theoretical solution for the effect of a temperature change on the thrust. By selecting two relatively short periods with approximately the same temperature at the beginning and end of the period, the measured loads were corrected to the basis of a constant temperature within the chosen short period. However, this would not necessarily correct the loads to their absolute value which would be affected by the prior temperature history. The results are shown on Fig. 4, and thus with the temperature influence removed, the effects from mining tunnel 5 were more nearly equal to those caused by mining tunnel 3.

As a more direct approach to the temperature effect in terms of observed data, a type of difference function plot devised by Harris H. Burke, F. ASCE, proved the most useful of the many plots tried. This utilized the load difference, $V_V - V_H$, the diameter change difference, $D_x - D_y$, and the difference between the crown and spring line moments, $M_C - M_S$. The significance of these difference functions can be understood by examining the diameter change difference as an example. The normal condition was for the horizontal change, D_x, to increase, and the vertical change, D_y, to decrease. A rise in temperature would expand the lining, thus accentuating the increase in D_x and reducing the decrease in D_y, with the converse holding true for a temperature drop. In the diameter change plot on Fig. 9(d) this divergence from the normal trend is apparent during September, 1949, December, 1949, and April, 1950; and is shown by Fig. 11 of the paper by Mr. Burke. Assuming the entire ring to be affected by a uniform temperature change, the vertical and horizontal diameter changes would be approximately the same numerically. Hence, if the horizontal and vertical diameter changes due to a particular load event were a plus and a minus 0.63 in. respectively, and if the diameter change due to a temperature rise during the same period were a +0.2 in. expansion, then the next measured change of horizontal diameter would be +0.83 in., and that of the vertical diameter -0.43 in. The algebraic difference between the diameter changes due to the load event would be $D_x - D_y$, or 0.63 - (-0.63), or +1.26 in., and the difference in the measured changes would be +0.83 - (-0.43) or +1.26 in., or equal to twice the numerical average of the two diameter changes.

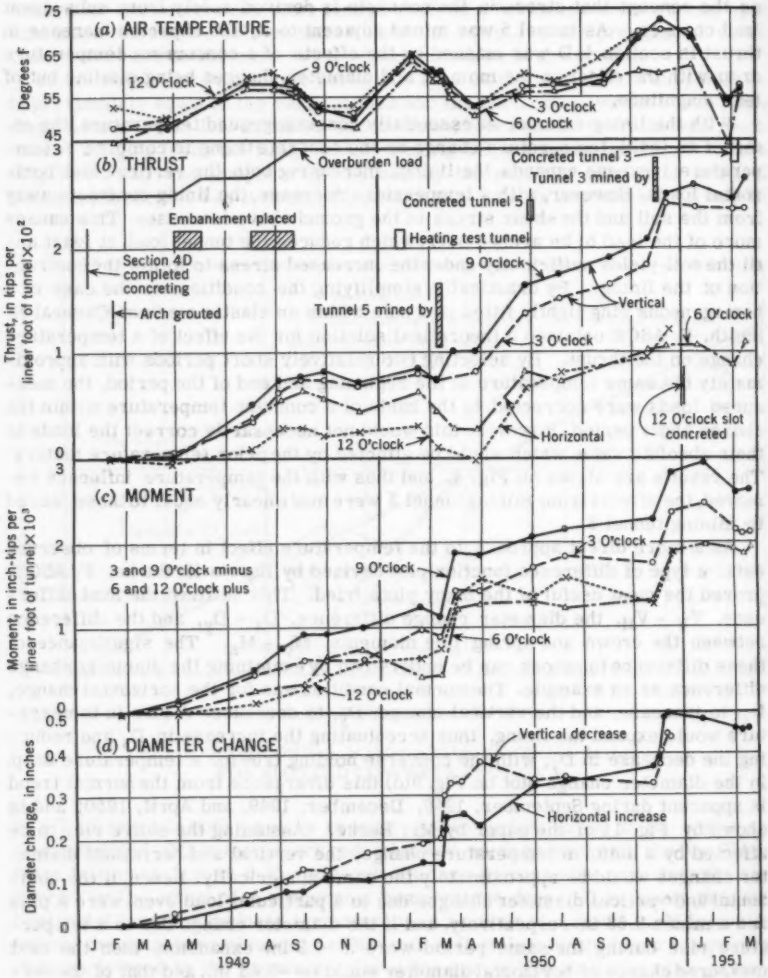


FIG. 9.—CHANGES SINCE CONCRETING SECTION 4-D

Because this algebraic difference between the two diameter changes tended to eliminate the effect of the temperature change, plots of the difference functions were utilized as shown by Fig. 10. This type of plot indicated that the principal loading events were accompanied by major changes with a gradual change occurring during the intervening periods. In the sign convention used, D_y and M_s are negative so that algebraically, $D_x - D_y$ is twice the average diameter change, and $M_c - M_s$ is twice the average of the four moments at the crown, invert, and both spring lines. The fact that these three difference functions could be matched by adjusting the scales in Fig. 10 indicates that they

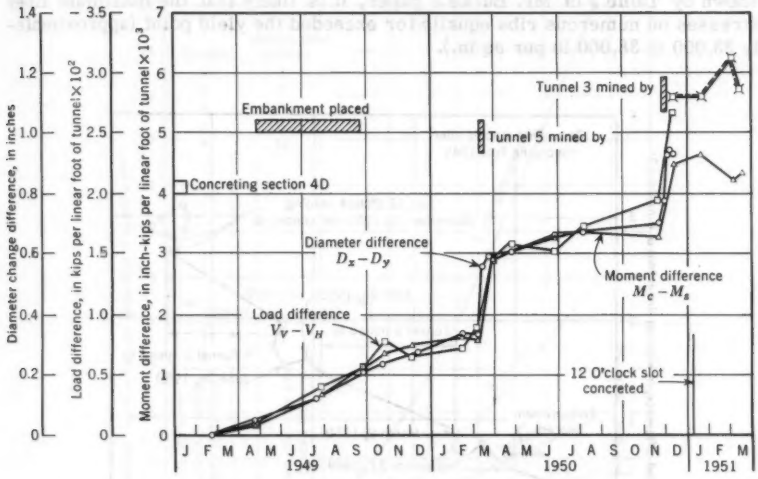


FIG. 10.—DIFFERENCE FUNCTIONS FOR SLOTTED CONCRETE SECTION

were interrelated. As an example, Fig. 11 shows that the moment difference, $M_c - M_s$, was a linear function of the load difference $V_V - V_H$.

BENDING MOMENTS

Moments in Steel Ribs.—Results of rib measurements for the period the ribs served as temporary support prior to their encasement in the concrete lining are summarized in Table 3 of the paper by Mr. Burke. All sections represent a single tunnel case except sections 5-A, B, C, and D, which were mined beside the correspondingly lettered sections of the test tunnel. Some of the moments at the invert and spring line were opposite in sign from those moments that would be obtained with the vertical load as the activating load. These moments were sometimes reversed in sign at different times. The crown moment was most consistent in sign and nearly always the largest of the four clock positions. Comparing section 5-A at the toe of the dam with section 5-E at the centerline, there was no apparent increase in moment as the overburden load increased. Of greater significance was the increase in moment with the stiffness of the supporting ring, as illustrated by the curves of Fig. 12.

The stress due to flexure was about 75 per cent of the total rib stress, or approximately three times the 25% contribution from thrust. Outer fiber stresses of 30,000 to 40,000 lb per sq in. were observed at all measuring sections except 4-A and 4-C where the rib section was unusually heavy for testing purposes. These stresses were either measured directly at the inner flange or computed on the basis of linear distribution using two or three measurements on the web. On a few ribs in the test tunnel, stresses were investigated at some 20 to 80 points closely spaced around the cross section, which showed considerable bending in both directions. Considering that this crossbending would result in significantly higher fiber stress at the flange ends than that shown by Table 3 of Mr. Burke's paper, it is likely that the maximum fiber stresses on numerous ribs equalled or exceeded the yield point (approximately 33,000 to 38,000 lb per sq in.).

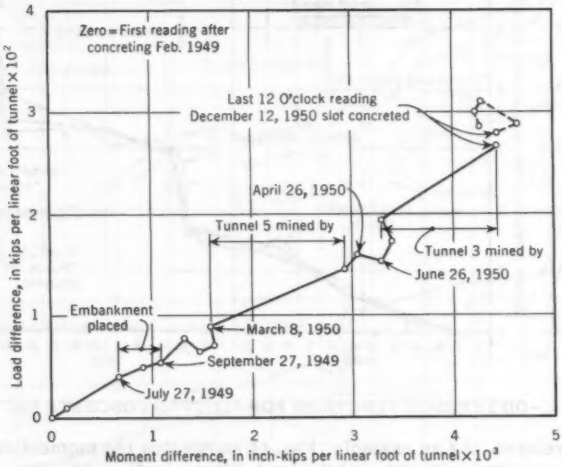


FIG. 11.—LOAD DIFFERENCE VERSUS MOMENT DIFFERENCE FOR SLOTTED CONCRETE SECTION

Causes of Moment in Ribs.—The most obvious cause of moment in a ring is the difference between the vertical and horizontal loads, $V_V - V_H$. However, on most of the steel ribs the vertical and horizontal loads were so nearly equal that only a small part of the observed moment could be attributed to the small load difference actually measured. Hence, the major causes of the rib moment were considered as irregularities from the blocking loadings, erection stresses, and similar factors inevitable in practical tunnel construction. Perhaps a sizeable part of the erection stress was contributed by the jumbo weight (carried by brackets supporting rails at the spring line) and from the temporary loads from crown and breast jacks reacting against the jumbo. However, it is likely that the inevitable irregularity in blocking loads was a more important factor, resulting from variations in the size and spacing of the blocks and in the concentrated load created at each blocking point by the initial wedging or the subsequent wedging or a combination of both.

R. V. Proctor[8] has suggested that in rock tunneling the rib moment increases with the spacing between blocks because the rise of arc between blocking points increases. In general, the range of blocking spacing in the Garrison tunnels was not sufficiently great to afford a check of this concept. In the test tunnel, where the ribs were used as elastic measuring rings, substantially continuous blocking was placed between the lags. This resulted in a reasonably uniform blocking pattern covering perhaps 75% of the rib area available for support. In the main tunnels the ribs were required to be blocked at a mini-

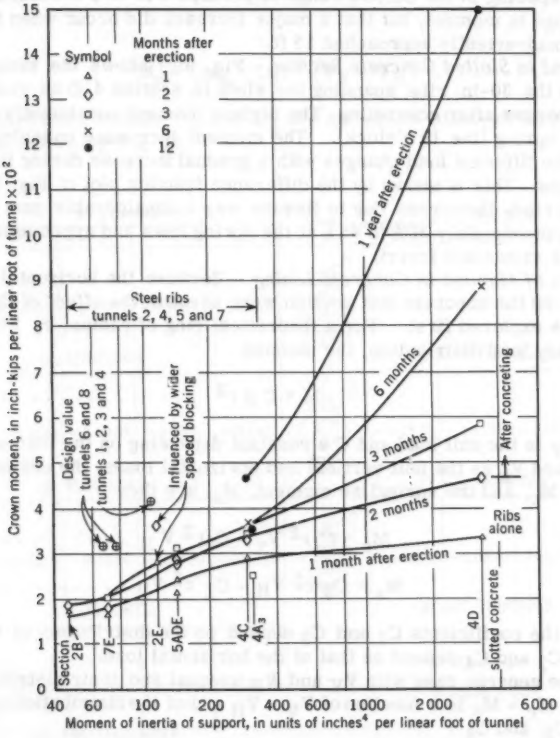


FIG. 12.—CROWN MOMENT VERSUS STIFFNESS OF SUPPORT

mum of 16 points, including each of the 4 joints, but actual blocking usually exceeded this, particularly in the crown. In general, the spacing was 2 ft to 3 ft in the crown and approximately 4 ft in the invert, considering both the soil contacts and the intermediate blocks as points of support. At the spring lines there was some tendency for wider and more irregular blocking spacing, which

8 "Rock Tunneling with Steel Supports," by R. V. Proctor and T. L. White, Commercial Shearing and Stamping Co., Youngstown, Ohio, 1946, p. 207.

probably contributed to the varying signs of moments observed here. Comparing the moments of the close-spaced blocking in the test tunnel with those for the slightly wider blocking in the other tunnels, there was no significant difference when the effect of stiffness was considered, as shown by Fig. 12.

Occasionally, blocking was lost and loosened when the ground softened from seepage. One of these instances occurred at measuring section 2-E where the effective blocking spacing was thus increased up to approximately 15 ft. With this spacing, the moments were very high and the maximum fiber stress reached the yield point. Hence, it appears for the Garrison tunnels that varying the blocking spacing in the narrow range of perhaps 1 ft to 3 ft caused no significant change in moment, but that a major increase did occur when the blocking spacing inadvertently approached 15 ft.

Moment in Slotted Concrete Section.—Fig. 9(c) shows the moments measured on the 30-in. ribs spanning the slots in section 4-D as resulting from stress changes after concreting. The highest moment consistently occurred at the west spring line (9 o'clock). The moment increased considerably at the time of the different load changes with a gradual increase during the intervening periods. This is shown by the difference function plot of Fig. 19. As with the steel ribs, the stress due to flexure was a considerable part of the total stress, approximately 30% to 45% at the spring lines and approximately 60% to 75% at the crown and invert.

Causes of Moment in Concrete Lining.—Because the horizontal and vertical loads on the concrete test section were unequal, the effect of this load difference is explored first. For a theoretical ring of radius, r, Fig. 13 shows that for any load distribution, the moment

$$M = C\,p\,r^2 \quad \ldots\ldots\ldots\ldots\ldots\ldots \quad (8)$$

in which p is the unit load and C a constant depending on the load distribution. With V_v and V_h as the unit vertical and horizontal loads, the crown and invert moment, M_c, and the springline moment, M_s, are then

$$M_c = C_1 r^2 V_v - C_4 r^2 V_H \quad \ldots\ldots\ldots\ldots\ldots \quad (9a)$$

$$M_s = C_3 r^2 V_H - C_2 r^2 V_V \quad \ldots\ldots\ldots\ldots\ldots \quad (9b)$$

in which the coefficients C_1 and C_2 depend on the distribution of the vertical load and C_3 and C_4 depend on that of the horizontal load.

For the general case with V_V and V_H unequal and their distributions also different, $M_c - M_s$ is a function of $V_V - V_H$ and of the distribution coefficients, C_1, C_2, C_3, and C_4

$$M_c - M_s = r^2 [(C_1 + C_2)V_V - (C_3 + C_4)V_H] \quad \ldots\ldots\ldots \quad (10)$$

For a more specific case, if V_V is unequal to V_H but both have the same type of distribution curve, $C_1 = C_3$ and $C_2 = C_4$, so that $C_1 + C_2 = C_3 + C_4$ and $M_c - M_s$ is then a linear function of $V_V - V_H$:

$$M_c - M_s = r^2 (C_3 + C_4)(V_V - V_H) \quad \ldots\ldots\ldots\ldots \quad (11)$$

and, by similar derivation, the diameter change difference, $D_x - D_y$, is also a linear function of $V_V - V_H$:

$$(D_x - D_y) = \frac{r^4}{EI}(C' + C'')(V_V - V_H) \quad \ldots\ldots\ldots\ldots (12)$$

in which the constants C' and C" depend on the load distribution.

Only for the simple distribution of a uniform load does $C_3 = C_4$ so that

$$M_c - M_s = 2\,C'_3\,(V_V - V_H) \quad \ldots\ldots\ldots\ldots (13)$$

and

$$M_c = -M_s = C_3 r^2\,(V_V - V_H) \quad \ldots\ldots\ldots\ldots (14)$$

For other load distributions C_3 and C_4 are not equal, although they are often nearly so as shown by Fig. 13.

Load	Ring coefficients M_c	M_s	D_x	D_y
(a) UNIFORM	+0.2500	−0.2500	+0.1667	−0.1667
(b) PARABOLIC	+0.2188	−0.1979	+0.137	−0.142
(c) DRUCKER	+0.2075	−0.1816	+0.1277	−0.1310
(d) 180° TRIANGLE	+0.1793	−0.1541	+0.1086	−0.1118
(e) 120° TRIANGLE	+0.1684	−0.1396	+0.0996	−0.1033
(f) 90° TRIANGLE	+0.1512	−0.1189	+0.0862	−0.0904
(g) 60° TRIANGLE	+0.1208	−0.0875	+0.0646	−0.0688

$M = \text{Coeff.} \times pr^2$

$D = \text{Coeff.} \times \frac{pr^4}{EI}$

FIG. 13.—RING COEFFICIENTS

For any combination of load distributions, Eq. 10 gives $V_V - V_H$ as the principal factor responsible for the moment. For the specific case in which V_V and V_H have the same shaped distribution curve, Eqs. 11 and 12 show that $M_c - M_s$ and $D_x - D_y$ vary linearly with $V_V - V_H$. Evidence that this specific case applied to section 4-D throughout most of its loading history is shown by the linearity of the plot of observed $M_c - M_s$ versus $V_V - V_H$ in Fig. 11 and by that of a similar plot of $D_x - D_y$ versus $V_V - V_H$. It is remarkable that the

slotted concrete ring performed in a manner that created the same type of distribution for the horizontal as for the vertical load, particularly in view of the differences between the theoretical and actual rings.

Comparison of Slotted Concrete and Theoretical Ring.—The actual conditions at sections 4-D necessarily included many departures from a theoretical ring, any one of which would tend to contribute further to the moment. Local variations in stiffness of the supporting ground were undoubtedly present. One such variation was the possibility of the lignite layers acting as hard spots because both geologic evidence and laboratory tests on unfissured specimens showed the lignite stiffer than the surrounding hard clay. However, there was at least an equal possibility that the open joints initially present in the lignites and their subsequent enlargement by yielding toward the open bore, would make the horizontal deformation characteristics of the lignite in situ comparable to that of the adjacent ground. Although not fully conclusive, the weight of evidence from the ground yield measured by the spearheads and the generally smooth shape changes, both of the steel ribs and of the concrete rings, suggests that the lignites approached the latter case of acting as one with the surrounding ground. Because grouting would tend to make the lignites stiffer, it was minimized except where it could not be avoided at crossings of the grout curtains.

The four slots acted as major discontinuities. The original intension was to span the slots with a steel section having a load resistance comparable to that of the concrete lining. This objective was not realized in regard to bending resistance, although it was reasonably met with respect to thrust. Restudy showed the as-built moment of inertia (in units of inches^4 per linear foot of tunnel) varied from a low of 26,000 at the slots to a maximum of 180,000 at regions of greater overbreak near the crown, with 96,000 being the average around the concreted tunnel. This much lower stiffness at the slots tended to make them act as hinges.

The loads arched over to section 4-D during adjacent mining would be expected to be inclined. Some evidence of this was afforded by the tendency of the crown to roll away from the side where adjacent mining was underway. Because the thrusts and moments in section 4-D were measured only on horizontal and vertical axes, they would not represent the maximum values created by an inclined load, at least in respect to finding any of the theoretical moment coefficients applicable.

LOAD ON SLOTTED CONCRETE SECTION

Limitations of Ring Theory.—The usual theoretical equations for moments and deflections of rings (see Fig. 13) are derived for idealized cases and consider a relatively thin ring of homogeneous, isotropic, elastic material with a constant cross-sectional moment of inertia. The deflections are those resulting from moment alone, with the additional deflections from thrust being neglected. Many of the stress equations for reinforced concrete are to a considerable degree empirical from experimental studies with beams, so it is questionable if these equations are adequate for concrete rings. Although other factors could be listed, these are sufficient to indicate the considerable limitations of available ring theory.

Even more significant were the complicated conditions of the actual case. These conditions included the ring having a variable moment of inertia, the part-elastic, part-plastic behavior of the actual materials and the horizontal

load apparently dependent on ring flexure and vertical load to a greater degree than foreseen from the theoretical solutions. Hence, in seeking a load distribution compatible with the performance of the slotted test section, close agreement between theory and measurement was not expected or obtained.

Load Distribution.—The general procedure was to determine by trial the type of load distribution best fitting the measured data. Theoretical ring coefficients for several basic load diagrams are shown in Fig. 13 and were determined from solutions based on the theory of elasticity.[9,10,11] More complex distributions were obtained by combining these basic diagrams. Although several procedures were tried, final studies were concentrated on the following two procedures.

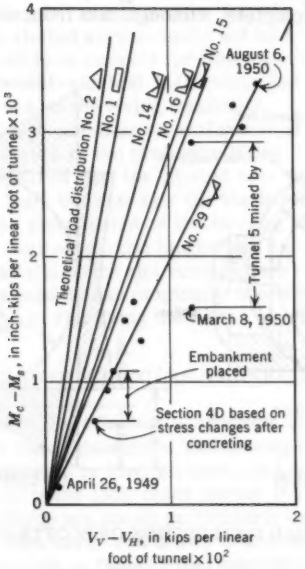


FIG. 14.—MOMENT DIFFERENCE VERSUS THRUST DIFFERENCE

The first procedure utilized the linear relationship found between the moment difference $M_C - M_S$, and the thrust difference $V_V - V_H$. Fig. 14 shows the result of a horn-shaped loading (distribution No. 29) that gave a reasonable fit with the measured data for nearly the entire loading period to August, 1950.

---

9 "The Structural Design of Flexible Pipe Culverts," by M. G. Spangler, Public Roads, Vol. 18, No. 12, February, 1938.

10 "Elastic Energy Theory," by J. A. Van Den Brock, John Wiley & Sons, Inc., New York, N. Y. 2d Ed., 1946, p. 283.

11 "Determination of Lateral Passive Soil Pressure and Its Effect on Tunnel Stresses," by M. A. Drucker, Journal, Franklin Inst., May, 1943.

At this time adjacent mining began in tunnel 3 and there was a change in the load distribution as shown by the offset in the curve of Fig. 11.

The second procedure involved assuming a type of load distribution, computing its moment and diameter changes, and then comparing these with the measured data. To handle a number of load distributions, the study was conducted in terms of dimensionless ratios: V_H/V_V, M_c/M_s, and D_x/D_y. Effect of a variable, I, was investigated for a few cases and found to be considerable. However, the solution was too complex for general application. This second procedure also indicated a horn load, with a very reasonable fit for the moment data and a poorer but fair fit for the diameter change data.

The conclusion from both procedures was a horn load combined with a small uniform load as illustrated in Fig. 15. The load data shown on Fig. 15(b) was obtained on September 1, 1949, when $V_H/V_V = 0.6$ and placement of the embankment was nearly complete. Although data from subsequent dates involving

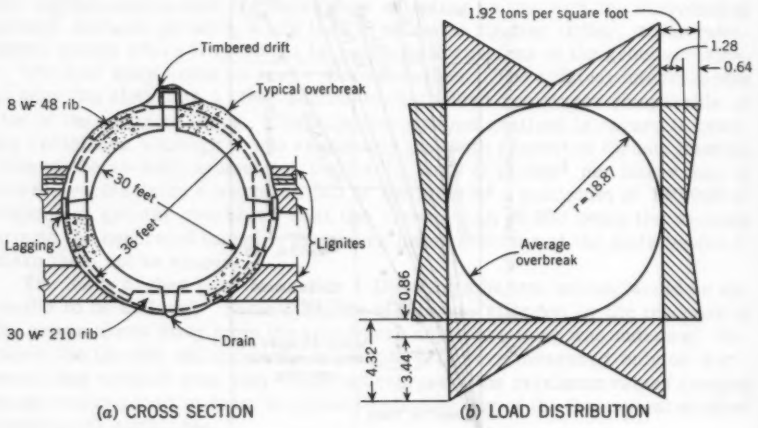


FIG. 15.—LOAD DISTRIBUTION ON SLOTTED CONCRETE

heavier loading did not fit as well, the agreement was sufficient to indicate that a horn type of load distribution prevailed for most of the loading history of section 4-D.

Effect of Slots.—Although it was certainly not anticipated that the slots would affect the load distribution to the degree indicated by Fig. 15, reconsideration in the light of the arching and relative yield concepts showed that the details of the slot construction could permit significant yield, thus causing the slots to shed load. For convenience in later concreting of the top slot, the contractor was allowed to place a 3-ft-by-3-ft drift at the crown. The increased width from overbreak and the relatively light timbering of this drift acted to permit more yield at the crown than at the other slots (see Fig. 15). At the invert, a section of half-round corrugated metal pipe was placed as a drain, while at both spring lines 10-in. channel lagging was placed on its side to span between the rib flanges and was back-packed with sand.

All of these slot details would permit some yield relative to the adjacent concrete lining that would result in the load arching over to either side of the slot—a maximum at the crown and probably a minimum at the spring lines. This yielding ability of the slots offered a confirmation of the horn load as a plausible load distribution and created doubt as to whether the slotted concrete section was an acceptable model of the prototype tunnels.

Slotted Section as a Model of the Prototype.—As there were no slots in the concrete lining of the main tunnels, a horn load distribution would not be applicable there. Also, the full circle prototype lining would be stiffer and, hence, would undergo less deflection than the test section with the slots acting as hinges. Table 4 of Mr. Burke's paper, indicates the deflection varied with the flexibility of the concrete lining. Slotted test section 4-D was the most flexible of the sections measured. Section 4-B_1 was the least flexible due to its approximately 4-ft lining thickness, and prototype tunnels 2 and 5 represented an intermediate case. The slotted section could not be a true model of the prototype unless it were possible to correct for this difference in flexibility, as the vertical load, the horizontal-vertical load ratio, and the bending moment all depend in varying degrees on the lining flexibility.

The data did not permit quantitative evaluation of such correction for the moderately greater stiffness of the prototype lining. However, from a qualitative standpoint it appeared that the slotted test section was an acceptable model for the vertical load, but only fair for the horizontal load, and no model at all for either the load distribution or the bending moment. Although the unintended action of the slots as partial hinges and the unforeseen yielding permitted by the as-built details of the slot construction resulted in slotted section 4-D being far less of a model than originally hoped for, its performance was nevertheless a great aid in clarifying the action of circular tunnel lining.

ACTION OF CIRCULAR TUNNEL LINING

Performance of Slotted Test Section.—As shown in Fig. 10, the various loading events (addition of the embankment and mining of adjacent tunnels) each caused a pronounced increase in load, moment, and diameter change at section 4-D, while a gradual increase took place during the intervals between these load changes. These effects are shown particularly well by the plot of $V_V - V_H$ in Fig. 16. The trend lines have been drawn to average the data, and show that the effect of adjacent mining in tunnel 3 was approximately the same as that in tunnel 5. They also show that the rate of gradual increase in $V_V - V_H$ was essentially constant over the period of measurement, although this rate would be expected to decrease as the vertical load approached its ultimate value. This increase between loading events was probably due to consolidation of the adjacent ground pillars under the loading of the single tunnel case from mining section 4-D. Fig. 16 can also be considered a curve of $V_V/2$, because in Fig. 8, $V_H = \frac{1}{2} V_V$. Thus, $V_V - V_H = \frac{1}{2} V_V = V_H$, and Fig. 16 is also a curve of V_H.

The linear relation of the plot of $V_V - V_H$ versus $M_C - M_S$ in Fig. 11 and of $V_V - V_H$ versus $D_X - D_Y$ is strong evidence that both V_V and V_H had the same type of load distribution curve, which was one of the unexpected results of the measurements.

Effect of Stiffness.—Perhaps the most consistent results from the various types of data were shown in the tendency for the flexible rib support to shed

load and for the stiff concrete lining to attract it. The values of moment were higher than anticipated and increased decidedly with stiffness as shown in Fig. 12. For the flexible ribs, V_H/V_V was approximately equal to one, and the moment was moderate but still controlling in the selection of the rib section. For the slotted concrete section, V_H/V_V was approximately one-half and the moment was high. The stiffness of the tunnel appeared to be the principal factor controlling the vertical and the horizontal loads as well as the moment. From Eq. 7 stiffness seems to vary inversely with the diametric strain and, thus, to be a function of EI/r^3.

Ring Action.—From the over-all investigation, it seems that a circular tunnel ring can be visualized as carrying its activating load, V_a, as one increment of V_V, which is balanced by the horizontal load, V_H, and as a second increment which is supplied by the bending resistance of the ring, B_r. Where V_V

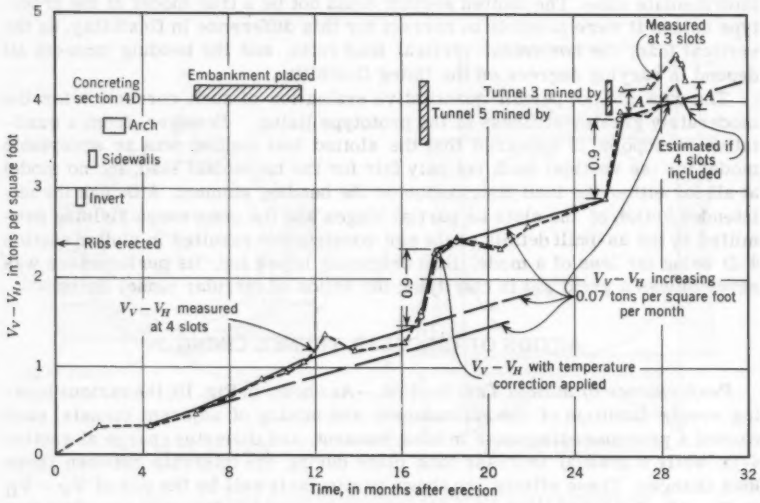


FIG. 16.—LOAD DIFFERENCE VERSUS TIME FOR SLOTTED CONCRETE SECTION

and V_H have the same type of distribution, as was indicated for the Garrison tunnels, Eq. 11 can be written as

$$(V_V - V_H) = f(M) \quad \ldots\ldots\ldots\ldots\ldots\ldots \quad (15a)$$

or

$$(V_V = V_H + f(M) \quad \ldots\ldots\ldots\ldots\ldots\ldots \quad (15b)$$

in which the moment function may approach the bending resistance of the ring.

If the ring is very flexible, having only a negligible bending resistance it readily deforms, creating a passive horizontal load $V_H = V_V$. Thus V - H = 0, and $M = 0 = B_r$.

If the ring is very stiff with a large bending resistance, then the deformation is small, V_H is small, $V_V - V_H$ is large, and M is high. As a limiting case with V_H negligible, $V_H = 0$, $V_V - V_H = V_V$, and $M = B_r$. Thus, with some oversimplification, this concept can be represented by writing Eq. 15 in the form

$$V_V = V_H + B_r \quad \ldots\ldots\ldots\ldots\ldots\ldots (16)$$

This illustrates the automatic safety inherent in a circular tunnel ring which is capable of self-adjustment to accommodate its load conditions. If the vertical load approaches or exceeds B_r, the ring deforms further, building up the passive load, V_H which then permits the ring to carry an even greater load. Should the combined stress from moment and thrust reach the yield point, the bending resistance may be reduced but the ring is then more flexible so that its deflection increases, further increasing V_H, with any reduction in B_r being offset by the increase in V_H. Thus, a circular ring is capable of adjusting itself to carry the activating load, V_a by a combination of stresses and deformations that very likely follow the principles of least work.

If the concrete lining is so stiff that its high bending resistance initially carries most of the vertical load with resulting high fiber stress, cracking of the lining will then make the ring more flexible so that it reaches equilibrium in carrying further increments of the vertical load by building up the passive load, V_H. As a limiting case in a considerably cracked condition, the lining might approach a segmented arch as a series of hinged blocks, able to take high thrust but low moment and possessing considerable flexibility. This would be somewhat like the English practice of using precast concrete segments in lieu of cast iron segments, with a thin sheet of compressible material in each circumferential joint to introduce some flexibility.[12] Such a segmented ring is entirely safe and is actually able to carry a considerably higher load without overstress than the stiffer ring could before cracking, provided the deformations are small and the ring maintains its integrity without buckling.

Performance of Prototype Lining.—Some cracking in the concrete lining of the main tunnels has appeared, generally as fine hair cracks in a fairly consistent pattern of longitudinal cracks at the crown and invert, and of transverse cracks which seldom extend below the arch. Cracking is normal for reinforced concrete under significant loading. When the stress in the reinforcing steel reaches even a moderate tension, the outer fiber of the few inches of concrete cover over the reinforcement is stressed beyond the tensile strength of the concrete. The longitudinal cracks are considered due to moment and the transverse cracks due to a combination of shrinkage, temperature, flexure from settlement and rebound, plus a direct tension from the spreading effect of the triangular load of the dam. Some evidence showed that the cracking was accentuated by sharp temperature drops when winter winds blew through the tunnels. This exposure was more severe than it would be under operating conditions and could be minimized on future projects by use of temporary bulkheads. The cracks were mapped during final inspection in the spring of 1951. It is significant that nearly all of the cracking was found in tunnels 2, 5, and 7, which were subjected to adjacent mining, and that practically no cracking was evident in tunnels 3 and 6, which were constructed between previously concreted

12 "Tunnel Lining, With Special Reference to a New Form of Reinforced Concrete Lining," by G. L. Groves, Journal, Inst. of C. E., London, March, 1943.

tunnels. This confirms the relative yield method in indicating the multiple tunnel case as that responsible for the most severe loading.

There is no question that the prototype tunnels are heavily loaded, particularly those subjected to adjacent mining. For such tunnels, load estimates have been made on the assumptions that (1) V_V reached 100% overburden, (2) V_H and V_V had the same type of distribution, and (3) cracking during the multiple tunnel loading decreased the stiffness of the prototype to that of the slotted test section, thus resulting in $V_H/V_V = \frac{1}{2}$. This study resulted in a curve similar to Fig. 16, somewhat modified to fit the actual time of loading events and to reflect the increased overburden load at the center of the dam. A study was based on $V_H/V_V = \frac{1}{2}$, and another study on V_H/V_V equal to less than $\frac{1}{2}$ prior to cracking. For either study, available theory indicated large diameter changes of several inches although the actual diameter changes were only a small fraction of an inch. This illustrates the inadequacy of the ring theory. A more realistic appraisal is afforded by the smooth shape changes and the small diameter changes actually measured in the prototype tunnels (approximately $\frac{1}{4}$ to 1/3 in.). This showed that the tunnels are performing quite satisfactorily, fully preserving their integrity and utilizing the automatic safety of ring action in adjusting themselves to the loading conditions.

Diameter measurements were continued at some locations on the concrete lining until the tunnels were flooded by diversion in the spring of 1953. These measurements gave some evidence that the tunnels mined between previously concreted tunnels had begun to share the load. When the tunnels were successively unwatered in the spring of 1954, more limited measurements showed only minor diameter changes during the elapsed year, thus indicating that the tunnels are approaching equilibrium. From spot checks the cracking did not appear to have increased in the five power tunnels but had done so in smaller tunnels 6, 7, and 8. This might be explained by the greater ring stiffness of the smaller diameter tunnels because stiffness probably varies inversely with the cube of the diameter.

APPLICATION TO RIB DESIGN

Original Design.—For contract advertising purposes an initial rib design was developed in the fall of 1948 when sections 4-A and 4-C of the test tunnel had been supported by ribs for approximately three months. These test sections were then carrying approximately 15% of the overburden load which was reasonably checked by the arching method based on the initial shear strength, s_1 (Table 2(A)). Computation by this same method indicated rib loading in the range of 30% to 60% overburden for tunnels 1 and 5, and 20% to 35% for the smaller tunnels 6, 7, and 8. It is interesting to note that this analysis by the arching method indicated the heaviest loading on those tunnels mined into an area already stressed by the load arched over during mining of the two adjacent tunnels. The actual condition was quite different as those tunnels mined between previously concreted tunnels experienced only a moderate initial load, which was more correctly evaluated by the relative yield method.

From these findings, the ribs were designed principally for carrying thrust caused by 50% overburden for tunnels 1 to 5, and 40% for tunnels 6, 7, and 8. This resulted in a 3-ft spacing of 10 in., 49-lb-to-72-lb ribs beneath the center of the dam and 8-in., 35-lb-to-48-lb ribs at the end sections near the toes of the dam, as the ribs were proportioned for the variations in overburden load

(Fig. 1). The contract was awarded on a unit price per pound with provision to vary the rib spacing up to 4 ft, a distance that was shown by the test tunnel experience as roughly the safe maximum for supporting loose blocks.

Evolution of As-Built Design.—Early results, first in tunnel 7 and then in tunnel 5, showed the measured thrust to be considerably smaller than was estimated from the arching method. This led to development of the relative yield method as a more realistic approach. However, the bending moment was much higher than anticipated, or than could be accounted for by the small difference between the measured vertical and horizontal thrusts. As previously shown, the moment was responsible for a very high percentage of the total combined rib stress. With the moment thus apparently dependent of other than the overall loading, the empirical relationship of Fig. 12 between moment and rib stiffness was developed as rapidly as data became available from the various rib measuring sections. For revising the rib design, the moment criterion was taken from this job experience curve as twice the average moment measured in the pertinent section, but not less than the maximum measured on any individual rib. The reason for considering an individual maximum was to guard against the crippling of one rib which could have started a progressive failure in the period of temporary support when the ribs act individually prior to their encasement in concrete. Fig. 12 shows these moment design values which were combined with thrust estimated by the relative yield method, and used for redesigning the ribs.

The as-built design evolved in several stages as further data became available and generally resulted in a 4-ft rib spacing, except in approximately the first half of tunnels 5 and 7, and in local regions where blocky ground required closer support from a safety standpoint. It was sometimes necessary to use ribs that were on hand or that were being fabricated so that the final construction was occasionally heavier than needed. However, numerous measurements, plus considerations of cross-bending previously mentioned, indicated that the outer fiber stress probably approached the yield point on many ribs, so that the as-built design came close to the practical limit of economy. The saving in rib steel amounted to over 4,500,000 lb, or approximately $750,000 below the original design.

Suggested Future Procedure.—In light of the foregoing experience, the following procedure deserves consideration in similar work.

1. Estimate the maximum permissible rib spacing from the safety standpoint of preventing falls of loose blocks, as judged from the character of the formation, experience with a test drift, and other pertinent factors.
2. Plan so that the ribs are used to furnish support only for the single tunnel case for a moderate period before being encased in concrete.
3. Estimate the vertical load by the relative yield method and estimate the horizontal load from the principle that the more flexible the rib ring, the more nearly will the horizontal load approach the vertical load.
4. Estimate the maximum bending moment, considering that it increases with the rib stiffness and with wider blocking spacing.
5. Design the ribs for a working stress below the yield point and provide for an opportunity to vary the rib spacing (and under some conditions possibly also the cross section).

6. Install occasional groups of adjacent ribs with strain gage lines and measure the actual stresses. As job experience and the pattern of thrust and moment become established, modify the rib design for the balance of the work.

CONCLUSIONS

Some of the results of the investigation were reasonably definite, some inconclusive, and some unanticipated. The stress pattern in the steel ribs was adequately established, the major contribution being due somewhat unexpectedly to bending moment. The use of this information in redesigning the ribs resulted in a considerable saving in steel amounting to approximately $750,000. A less tangible but much larger saving is believed to have accrued from the lower bids resulting from the opportunity the test tunnel afforded bidders to appraise the work with much less uncertainty than is usual in tunneling.

Comparison of the concrete lining with the slotted test section was handicapped by the tendency of the slots to act as partial hinges. Thus, the adequacy of the prototype full-circle lining was more realistically shown by its demonstrated ability to adjust itself automatically to the load conditions according to the principles of ring action. However, the slotted test section was helpful in clarifying the action of tunnel lining, which may aid in reducing some of the present inadequacies of the ring theory. The over-all results of the investigation indicated that with some over-simplification a circular tunnel lining can be considered as carrying part of the vertical load by its bending resistance, and carrying the balance by yielding to build up the horizontal or passive load.

The effect of tunnel stiffness was marked, both on the vertical load attracted and on the resulting horizontal load and bending moment. Where the tunnel was stiffer than the adjacent ground it attracted load, where less stiff it shed load, thus confirming the comparison of rigid and flexible tunnels offered by Karl Terzaghi, Hon. M. ASCE.[13] For a single tunnel case (either one tunnel or a series of tunnels spread sufficiently to avoid inter-effects), increased application of this principle should result in significant savings by utilizing more flexible linings and relying on the ground to carry the major part of the overburden load.

The problem is more complex for the multiple tunnel case in which the tunnels are close enough to affect each other. Under some conditions it should be possible to mine all tunnels and then allow the ground pillars to consolidate fully under their increased load before placing the permanent lining. Thus, with no further deformation of the ground pillars, there would be no increase in load on the tunnel, which would permit a relatively light lining. This procedure was investigated but rejected for the Garrison tunnels, because it would overload the ground pillars unless the construction schedule were prolonged unduly to allow time for the pillars to gain strength by consolidation before permitting any adjacent mining.

Thus, for the relatively closely spaced Garrison tunnels, it was considered necessary to design the concrete lining for a thrust of 100% overburden. The data showed that this load was essentially reached, at least on those tunnels subjected to adjacent mining. Although reinforced concrete has many advantages, the nature of the material is such that proportioning to carry such a high thrust leads inevitably to a relatively thick section of considerable stiffness with its accompanying disadvantage of a tendency to carry much of the load by

---

13 "Liner Plate Tunnels on the Chicago (Ill.) Subway," by K. Terzaghi, Transactions, ASCE, Vol. 108, 1943, p. 970.

its bending resistance. Some study was given to a scheme of carrying the permanent loads by a more flexible section utilizing heavier rib steel and lighter concrete. However, this seemed to offer no cost advantage and appeared likely to increase the construction problems. For tunnels required to carry high thrust, it seems likely that the ideal tunnel lining has yet to be developed.

ACKNOWLEDGMENTS

During the course of this tunnel investigation Brig. Generals William W. Wanamaker, F. ASCE, and John S. Seybold, F. ASCE, served in turn as District Engineer of the Garrison District, Corps of Engineers, with Robert H. Hayes, F. ASCE, as Chief, Engineering Division; Richard D. Field, F. ASCE, as Chief, Design Branch; and Hilbert F. Michel, F. ASCE, as Head, Structural and Civil Section. The investigation was conducted under the direction of Kenneth S. Lane, F. ASCE, with the work divided between Harris H. Burke, F. ASCE, as Head, Field Test Section, handling the measurements, particularly assisted by Kenneth T. Lord; and Carneal K. Smith, M. ASCE, as Head, Soils Design Section handling analysis of the results, particularly assisted by Robert E. Torp-Smith, M. ASCE. Advice in planning the test tunnel and interpretation of the results was obtained from a Board of Advisors consisting of George E. Bertram, F. ASCE, Ralph B. Peck, F. ASCE, Robert R. Philippe, Willard J. Turnbull, F. ASCE, and the late Donald W. Taylor, M. ASCE.

APPENDIX I. VERTICAL LOAD BY ARCHING THEORY

The idea of ground arching around a yielding support has been developed by William Cain,[14] Anson Marston,[15] Karl Terzaghi,[16] and others. Fig. 5 shows this concept applied to a tunnel beneath a considerable depth of overburden where part of the overburden load, W, is transferred by shears, V_S, on vertical planes at each side of the tunnel. These vertical planes have been taken 1 diam apart in view of evidence from lignite mines in the Fort Union formations where collapse of a drift usually produces a depression at the surface that is not much wider than the drift. For judging the probable distribution of the load, V_S, the theoretical solution for stress around a yielding hole in a uniform stress field appeared reasonably applicable. This solution is plotted in Fig. 17(a) from the theory of elasticity for V = 0 and verified by photoelastic experiments.[17] The stress is a maximum at the crown, decreasing to a comparatively small value approximately 2 diam above the crown. In Fig. 17(a), W represents the total overburden load on the tunnel, or dw where w is the unit overburden load at crown of the tunnel.

Assuming a constant shear modulus, making the deformation directly proportional to the shear stress, the deformation diagram then would be of the

14 "Earth Pressure, Walls & Bins," by W. Cain, John Wiley & Sons, Inc., 1916, p. 208.

15 "The Theory of Loads on Pipes in Ditches and Tests of Cement and Clay Drain Tile and Sewer Pipe," by A. Marston and A. O. Anderson, Proceedings, A.S.T.M. 1913, p. 13, 303–312.

16 "Theoretical Soil Mechanics," by K. Terzaghi, John Wiley & Sons, Inc., 1943, p. 69.

17 "Photoelasticity," by M. Frocht, John Wiley & Sons, Inc., 1941, Vol. I, p. 225.

same shape as the shear stress diagram. Fig. 17(c) shows the ground movements measured as settlement of telescopic sections of the vent shaft located above section 4-C of the test tunnel. The similarity between the diagram of measured movements and that of the theoretical shear stress distribution is good evidence of the applicability of the latter, although it was derived for a case of uniform initial stress in a vertical direction only. Because the objective is a workable means of estimating the vertical tunnel load, this analysis neglects any initial horizontal stress field. The variation of the properties of the ground and the dependence of the horizontal load on the magnitude of the vertical load are so complex that such refinement seems unjustified.

For computing purposes the theoretical distribution curves are simplified to triangles as shown in Fig. 17(b). The area of the triangle DEF represents

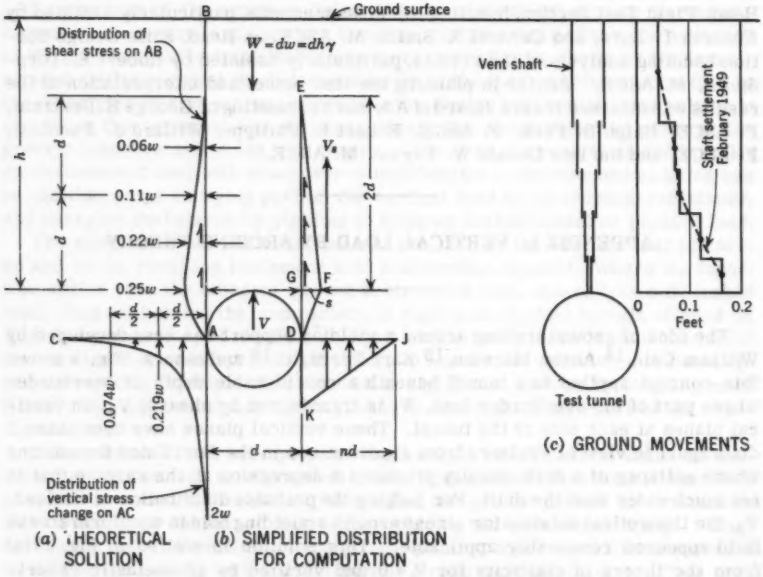


FIG. 17.—ARCHING THEORY

the total shear on the plane DE and is equal to the vertical stress increase on the plane DJ, represented by the area of the triangle DJK. It is assumed that the shear stress FG at the crown reaches the available shear strength, s, which is represented by the Coulomb equation:

$$s = c + K\sigma \tan \phi \quad \ldots\ldots\ldots\ldots\ldots\ldots (17)$$

in which the no-load shear strength c is taken as 0.7 tons per sq ft and the friction angle ϕ is 20°. These are the usual design values for the Fort Union

formation and were derived principally from studying the shear strength required to maintain existing slopes as described by Smith and Redlinger. The stress, σ, is the vertical effective or intergranular stress and K is the ratio of horizontal to vertical stress. The value of K is uncertain and is herein assumed equal to one. It could be greater in the event of high horizontal stress remaining from the load of past overburden, as mentioned previously in the examination of the ratio of horizontal to vertical load.

From Fig. 17(b) the tunnel load is then

$$V = W - 2\,V_s = dw - 2.5\,ds \quad \ldots\ldots\ldots\ldots (18)$$

where

$$W = dw = d\,h\gamma \quad \ldots\ldots\ldots\ldots\ldots\ldots (19)$$

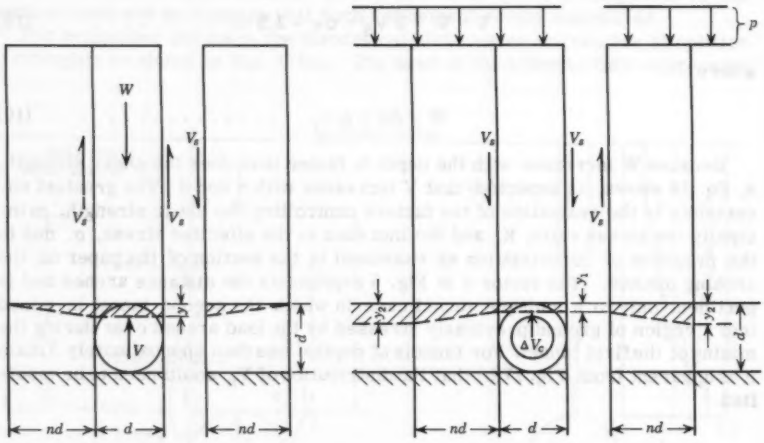
Because W increases with the depth, h, faster than does the shear strength, s, Eq. 18 shows, as expected, that V increases with h and d. The greatest uncertainty is the evaluation of the factors controlling the shear strength, principally the stress ratio, K, and the increase in the effective stress, σ, due to the progress of consolidation as examined in the section of the paper on the arching method. The factor n in Fig. 5 represents the distance arched and is pertinent only to a multiple tunnel case in which the second tunnel is mined into a region of ground previously stressed by the load arched over during the mining of the first tunnel. For tunnels at depths less than approximately 3 diam it is apparent from Fig. 17(b) that the distribution of V_s would need to be modified.

APPENDIX II. VERTICAL LOAD BY RELATIVE YIELD THEORY

The vertical load by relative yield theory was initially developed by Carneal K. Smith, by modifying the method of arching to allow for the effect of varying degrees of rigidity supplied by the tunnel supports. Fig. 6 shows the basic concept with a series of elastic blocks at the plane of the tunnels somewhat like the blocks considered by W. Cain[18] in studies of culvert loading. These blocks deform according to Hooke's law in direct proportion to their loading but have different deformation moduli: E_t for the rib supported tunnel, E_s for the ground, and E_c for the concrete lined tunnel, so that $E_t < E_s < E_c$. The lower boundary at the invert is considered a plane of no movement or at least of uniform settlement. Ground above the tunnels is considered as a series of blocks the depth of which, h, is so much greater than their width, d (Fig. 6), that each block is rigid within itself. Loads are transferred between the blocks by shear on their boundaries, as in the arching concept, although in this case the distribution of this shear stress is not pertinent.

[18] "Earth Pressure Experiments on Culvert Pipe," by W. Cain, G. M. Braune, and H. F. Janda, Public Roads, November, 1929, Appendix I.

With these simplifying assumptions the relations for the tunnel loads can be obtained by simple statics. The mathematics of the derivation have been intentionally kept simple, using large finite blocks instead of infinitesimals, because the numerous uncertainties in properties of both ground and tunnel supports do not warrant refinements. The basic symbols are defined by Fig. 6 in which y is the deflection, ΔV_p represents load increase on the ground pillar, and ΔV_c denotes the load increase on the concreted tunnel.



(a) SINGLE TUNNEL CASE (b) SURFACE LOADING CASE

FIG. 18.—SINGLE TUNNEL AND SURFACE LOADING CASES

Single Tunnel Case.—Consider a single tunnel, Fig. 18(a), mined with rib support sufficiently flexible that the modulus of the tunnel block E_t is less than that of the ground E_s, so that $E_t = bE_s$. In the tunnel block,

$$\text{Strain} = \frac{\text{Stress}}{E_t} = \frac{y}{d} = \frac{\frac{W - 2V_s}{d}}{bE_s} \quad \ldots\ldots\ldots\ldots \text{(20a)}$$

or

$$y = \frac{W - 2V_s}{bE_s} \quad \ldots\ldots\ldots\ldots\ldots\ldots \text{(20b)}$$

In the adjacent soil block, the transferred load V_s causes an average deflection y/2:

$$\frac{\frac{y}{2}}{d} = \frac{\frac{V_s}{nd}}{E_s} \quad \ldots\ldots\ldots\ldots\ldots\ldots \text{(21a)}$$

or

$$y = \frac{2\,V_s}{nE_s} \quad \ldots\ldots\ldots\ldots\ldots\ldots \text{(21b)}$$

Because the deflection must be the same at the boundary between blocks, combining Eq. 20b and Eq. 21b results in

$$V_s = \frac{n\,W}{2\,(b+n)} \quad \ldots\ldots\ldots\ldots\ldots\ldots (22)$$

Thus the tunnel load is

$$V = W - 2V_s = W\left(1 - \frac{n}{b+n}\right) \quad \ldots\ldots\ldots\ldots\ldots (23)$$

Surface Loading Case.—Consider a unit load, p, added at the surface which produces a general deflection, y_2, (Fig. 18(b)):

$$\frac{y_2}{d} = \frac{p}{E_s} \quad \ldots\ldots\ldots\ldots\ldots\ldots (24a)$$

or

$$y_2 = \frac{pd}{E_s} \quad \ldots\ldots\ldots\ldots\ldots\ldots (24b)$$

Consider the tunnel to be stiffer than the soil, in order that $y_1 < y_2$ and $E_c = cE_s$. Then, in the tunnel block

$$\frac{y_1}{d} = \frac{pd + 2V_s}{cE_s} \quad \ldots\ldots\ldots\ldots\ldots\ldots (25a)$$

or

$$y_1 = \frac{pd + 2V_s}{cE_s} \quad \ldots\ldots\ldots\ldots\ldots\ldots (25b)$$

and in the block adjacent to the tunnel where V_s causes the difference in deflection $(y_2 - y_1)$ or an average of half this:

$$\frac{\frac{y_2 - y_1}{2}}{d} = \frac{V_s}{\frac{nd}{E_s}} \quad \ldots\ldots\ldots\ldots\ldots\ldots (26a)$$

or

$$y_2 - y_1 = \frac{2\,V_s}{nE_s} \quad \ldots\ldots\ldots\ldots\ldots\ldots (26b)$$

Substituting Eq. 24b and Eq. 25b for y_2 and y_1 in Eq. 26b results in

$$2V_s = pd\,\frac{n\,(c-1)}{c+n} \quad \ldots\ldots\ldots\ldots\ldots\ldots (27)$$

Therefore, the load increase on the concreted tunnel is

$$\Delta V_c = pd + 2V_s = pd\left[1 + \frac{n(c-1)}{c+n}\right] \quad \ldots\ldots\ldots\ldots (28)$$

By substituting b for c, Eq. 28 then covers the load increase on a tunnel with flexible rib support. However, as $b < 1$, $(b - 1)$ is negative, thus the rib support equation can be written in the following more usable form, the shears V_s being reversed from those in Fig. 18(b):

$$\Delta V_r = pd - 2V_s = p\,d\left[1 - \frac{n(1-b)}{b+n}\right] \quad \ldots\ldots\ldots\ldots (29)$$

Multiple Tunnel Case.—Consider an arrangement of 3 tunnels, as in Fig. 19. The relatively stiff concrete lining has been placed in tunnels 2 and 4. Tunnel 3 is now mined with its more flexible rib support, which causes a load increase ΔV_{p1} on the two adjacent pillars and a load increase, ΔV_c, on tunnels 2 and 4. As shown in Fig. 19, ΔV_{p2} represents the lesser increase on the ground pillars on other side of the concreted tunnels. To keep the problem within the realm

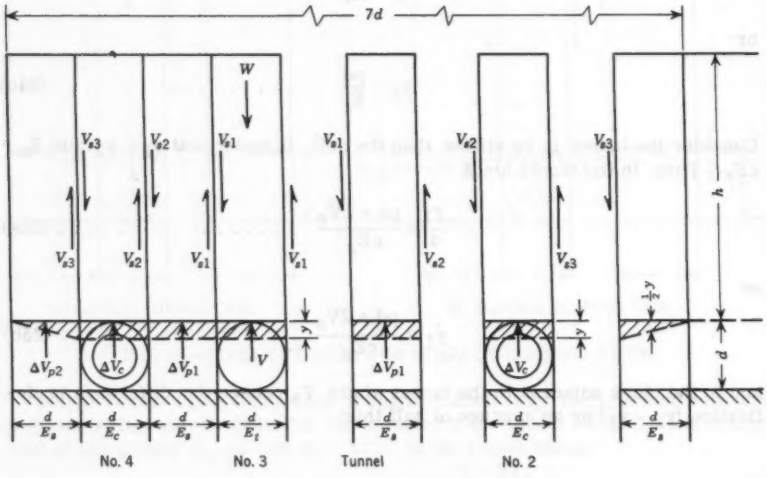


FIG. 19.—MULTIPLE TUNNEL CASE

of simple statics, the depth, h, is assumed to be sufficient for the ground above the tunnels to act as a rigid beam resulting in a constant deflection, y, over the 3 tunnels. A part of the overburden load, W, above tunnel 3 is then transferred to each side by the shears V_{s1}, V_{s2}, and V_{s3} (Fig. 19). Relations between the deformation moduli of pillar and tunnel blocks are $E_c > E_s > E_t$, so that $E_c = cE_s$ and $E_t = bE_s$. The deflection equations in the 4 different types of blocks are then

$$\frac{y}{d} = \frac{\dfrac{W - 2V_{s1}}{d}}{bE_s} \quad \ldots\ldots\ldots\ldots\ldots\ldots (30a)$$

or

$$y = \frac{W - 2V_{s1}}{bE_s} \quad \ldots\ldots\ldots\ldots\ldots\ldots (30b)$$

and

$$\frac{y}{d} = \frac{\frac{V_{s1} - V_{s2}}{d}}{E_s} \quad \ldots\ldots\ldots\ldots\ldots\ldots (31a)$$

or

$$y = \frac{V_{s1} - V_{s2}}{E_s} \quad \ldots\ldots\ldots\ldots\ldots\ldots (31b)$$

and

$$\frac{y}{d} = \frac{\frac{V_{s2} - V_{s3}}{d}}{cE_s} \quad \ldots\ldots\ldots\ldots\ldots\ldots (32a)$$

or

$$y = \frac{V_{s2} - V_{s3}}{cE_s} \quad \ldots\ldots\ldots\ldots\ldots\ldots (32b)$$

and

$$\frac{\frac{y}{2}}{d} = \frac{\frac{V_{s3}}{d}}{E_s} \quad \ldots\ldots\ldots\ldots\ldots\ldots (33a)$$

or

$$y = \frac{V_{s3}}{E_s} \quad \ldots\ldots\ldots\ldots\ldots\ldots (33b)$$

Combining Eq. 30b and Eq. 31b,

$$V_{s1} = \frac{W + b\,V_{s2}}{b + 2} \quad \ldots\ldots\ldots\ldots\ldots\ldots (34)$$

Combining Eq. 32b and Eq. 33b,

$$V_{s3} = \frac{V_{s2}}{(2c + 1)} \quad \ldots\ldots\ldots\ldots\ldots\ldots (35)$$

Substituting Eq. 34 in Eq. 31 b and Eq. 35 in Eq. 32b and then equating, results in

$$V_{s2} = \frac{W}{2}\left[\frac{(2c + 1)}{(b + 2c + 3)}\right] \quad \ldots\ldots\ldots\ldots\ldots\ldots (36)$$

Substituting Eq. 36 in Eq. 34,

$$V_{s1} = \frac{W}{2}\left[\frac{(2c+3)}{(b+2c+3)}\right] \quad \ldots\ldots\ldots\ldots\ldots\ldots (37)$$

and substituting Eq. 36 in Eq. 35

$$V_{s3} = \frac{W}{2}\left[\frac{1}{(b+2c+3)}\right] \quad \ldots\ldots\ldots\ldots\ldots\ldots (38)$$

Thus, the tunnels and pillar loads are:
Load on the temporary supports of tunnel 3:

$$V = W - 2\,V_{s1} = W\,\frac{b}{(b+2c+3)} \quad \ldots\ldots\ldots\ldots\ldots\ldots (39)$$

Load increase on the pillars adjacent to tunnel 3:

$$\Delta V_{p1} = V_{s1} - V_{s2} = W\,\frac{1}{(b+2c+3)} \quad \ldots\ldots\ldots\ldots\ldots\ldots (40)$$

Load increase on the concrete lining of tunnels 2 and 4:

$$\Delta V_c = V_{s2} - V_{s3} = W\,\frac{c}{(b+2c+3)} \quad \ldots\ldots\ldots\ldots\ldots\ldots (41)$$

Numerous other assumptions are possible. For example, the average deflection of the concreted tunnel could be assumed as y/2, which would make the length of the soil beam 5 d. This would be somewhat more compatible with the observed deflection of the concreted tunnel as less than the deflection of the adjacent tunnel being mined, plus the tendency for the top of the concreted tunnel to roll away from the side where adjacent mining was underway. This change would increase V and decrease ΔV_c, which again would be in slightly better agreement with the observed data.

Where the tunnels are located at a shallow depth so that the soil beam above cannot be assumed rigid, then it has appeared practical to derive equations considering the bending of this beam. Similarly, the lower boundary or plane of zero movement could be taken at some depth below the tunnels. The work of Hetenyi[19] could be used for solutions in which it is necessary to consider the behavior of a flexible beam on an elastic foundation. These refinements would result in more complex equations and did not appear justified for use in the Garrison tunnels, because the above simpler solutions gave results entirely adequate for practical usage.

APPENDIX III. THEORETICAL MODULUS OF RIB SUPPORT

If actual measurements are lacking, the deformation modulus, E_t, for a rib-supported tunnel can be estimated from the following equations for use as a

[19] "Beams on Elastic Foundations," by Hetenyi, Scientific Series XVI, Univ. of Michigan Studies, Ann Arbor, Mich., p. 97.

first approximation in the relative yield method. For a case with a uniformly distributed load, p, the vertical diameter change (decrease) D_y, (also the horizontal diameter change (increase), D_x) of a circular ring is as follows from Fig. 13:

$$D_y = \frac{pr^4}{6\,EI} \quad \ldots\ldots\ldots\ldots\ldots\ldots (42)$$

The effects of a vertical load, V_V, and a horizontal load, V_H are:

$$D_y = \frac{V_V}{2r}\,\frac{r^4}{6\,EI} - \frac{V_H}{2r}\,\frac{r^4}{6\,EI} = \frac{r^3\,(V_V - V_H)}{12\,E\,I} \quad \ldots\ldots\ldots (43)$$

By definition, the tunnel modulus $E_t = \frac{\text{stress}}{\text{strain}}$, in which the stress is $\frac{V_V}{2r\delta}$ and the strain is $\frac{D_y}{2r}$, δ being the distance between ribs. Therefore,

$$E_t = \frac{\dfrac{V_V}{2r\delta}}{\dfrac{r^3}{12\,EI}\,\dfrac{(V_V - V_H)}{2r}} \quad \ldots\ldots\ldots\ldots\ldots (44)$$

which reduces to

$$E_t = \frac{12\,EI}{r^3\,\delta\left(1 - \dfrac{V_H}{V_V}\right)} \quad \ldots\ldots\ldots\ldots\ldots\ldots (45)$$

All of the values of Eq. 45 are either known or can be computed except for the (V_H/V_V)-ratio which must be estimated. Furthermore, consideration should be given to the effect of bolted joints causing the actual rib to be somewhat more flexible, and, therefore, to have a lower value of E_t than might be obtained with a welded ring. In this connection an advance test was conducted on one ring, loading it with several cables at various diametric locations, with the general result that the more irregular the loading, the greater did the bolted ring depart from the theoretical ring, while with a more uniform loading, it tended to approach but not equal the performance of a theoretical ring.

APPENDIX IV. NOTATION

The following symbols, adapted for use in the paper and for the guidance of discussers, conform essentially with "Glossary of Terms and Definitions in Soil Mechanics," prepared by the Committee on Glossary of Terms and Definitions in Soil Mechanics of the Soil Mechanics and Foundations Division, Proceedings Paper 1826, October 1958:

B_r = bending resistance of the ring;

b and c = stiffness ratios (tunnel to ground), in Eq. 1 to 6;
C, C' = coefficients depending on load distribution, in Fig. 13;
D_x = horizontal diameter change (increase);
D_y = vertical diameter change (decrease);
d = tunnel bore diameter;
E = modulus of elasticity of steel;
E_c = deformation moduli of the stiff concrete lining;
E_s = deformation moduli of the ground;
E_t = deformation moduli of the tunnel with flexible rib support;
h = depth;
I = cross-sectional moment of inertia of the steel ribs;
K = ratio of horizontal to vertical stress;
M = moment:
  M_c = crown and invert moments;
  M_s = spring line moments;
n = arching factor;
p = unit load;
r = radius of the steel ribs;
s = shear strength:
  c = no-load shear strength;
s_1, s_2, s_3 = shear strengths at various conditions;
V = load:
  V_a = activating load;
  V_H = horizontal load;
  V_V = vertical load;
V_s = transferred load or shear;
ΔV_c = load increase on concreted tunnel;
ΔV_p = load increase on the ground pillar;
ΔV_r = load increase on a tunnel with flexible rib support;
W = total overburden load;
w = unit overburden load;
y = deflection;
δ = distance between ribs;
σ = effective or intergranular stress;
ϕ = angle of internal friction; and
γ = unit weight of overburden.

DISCUSSION

A. A. EREMIN,[20] M. ASCE.—The test tunnel method of investigation opens the ground and gives an unobstructed access for exploring purposes. Disadvantages of this method are that it is costly and time-consuming. It has been used where the test tunnel could be used as a part of the final tunneling as the case of the Garrison tunnels. With similar intention, many railroad tunnels are bored with timber supports, which were replaced with permanent concrete lining after an extensive study of the ground in the bore was performed. This method of ground exploring has also been used when the exploring tunnel could be used for the utilities as in the case of the Moffat railroad tunnel in Colorado, where the exploring pilot tunnel was later used for conveying water in the waterwork project.

Mr. Lane has stated, under the heading "Conclusions,"

> "* * *a considerable saving in steel amounting to approximately $740,000. A much larger saving is believed to have accrued from the lower bids, resulting from the opportunity the test tunnel afforded bidders to appraise the work with much less uncertainty than is usual in tunneling."

The well-known methods of ground exploring with the drill test bores have recently given satisfactory information for the contractors in estimating the cost of many tunnel projects.

The Pali tunnels for a two-lane highway bored through the Koolau mountain ridge near Honolulu, Hawaii, constructed in 1957, were designed after a careful study of the ground by the drill bores tests. Construction of the Pali tunnels was performed according to design plans, based on the bore-test information without any major changes. The construction was completed ahead of the scheduled time of project completion. Furthermore, with minor changes, the same tunnel design details were adopted for construction of the new parallel tunnels, which are under construction at the present time (1959).

The lowest bidder on the new tunnels has shown almost the same unit prices for the tunnel excavation and tunnel concrete lining items (with the usual corrections) as given in accordance with the cost index factors[21] shown in Engineering News-Record.

The lining of the Pali tunnels consists of the reinforced concrete arch with the embedded steel ribs similar to those used in the Garrison tunnels, except that the Pali tunnels have a "horseshoe" section. The Pali tunnels have been described by the writer elsewhere.[22]

---

[20] Assoc. Bridge Engrg. Dept., Div. of Highways, State Dept. of Public Works, Sacramento, Calif.

[21] Engineering News-Record, Vol. 158, February 21, 1957, p. 55.

[22] "Tunnels, Underground Structures, and Air Raid Shelters," by A. A. Eremin, Civil Engineering, Vol. 28, March, 1958, p. 114.

AMERICAN SOCIETY OF CIVIL ENGINEERS

Founded November 5, 1852

TRANSACTIONS

Paper No. 3023

INELASTIC BUCKLING IN STEEL

By Geerhard Haaijer,[1] and Bruno Thürlimann,[2] Members, ASCE

With Discussion by Messrs. P. P. Bijlaard; and Geerhard Haaijer and Bruno Thürlimann

SYNOPSIS

Plastic design methods assume that local buckling of flanges and webs of WF-beams will not occur during the formation of plastic hinges. Such severe conditions made the re-examination of the problem of plate buckling in the inelastic range necessary. In contradiction to accepted opinions, it was found that steel columns and plates can be compressed beyond the yield point and even into the strain hardening range without buckling. Theoretical results for the required geometric proportions are presented and comparison is made to experimental results obtained from tests on model columns, angles, and WF-beams. Furthermore, consideration is given to the problem of buckling between the elastic limit and the yield stress.

INTRODUCTION

Statement of Problem.—The elastic design of steel structures is based on the concept of a specified safety factor against nominal yielding of the most stressed fibers. For the detail design of flanges and webs of WF-beams and other plate elements, it is therefore sufficient if the yield stress is reached without premature local buckling. However, newer methods such as plastic design propose to base the design on the actual load-carrying capacity of the

Note.—Published, essentially as printed here, in April, 1958, in the Journal of the Engineering Mechanics Division, as Proceedings Paper 1581. Positions and titles given are those in effect when the paper or discussion was approved for publication in Transactions.

[1] Research Engr., Applied Research Lab., U. S. Steel Corp., Monroeville, Pa.

[2] Prof. of Structural Engrg., Swiss Federal Inst. of Technology, Zurich, Switzerland.

structure. The working loads are determined as a specified percentage of the ultimate load, which will be realized only if the members undergo plastic deformations at a number of sections without local or lateral buckling, producing a consequent fall-off in bending moment resistance. This process is generally referred to as the formation of plastic hinges and redistribution of moments. It is therefore evident that plastic design imposes more severe conditions on the local buckling characteristics of the plate element of structural members and requires a reappraisal of the problem of inelastic buckling.

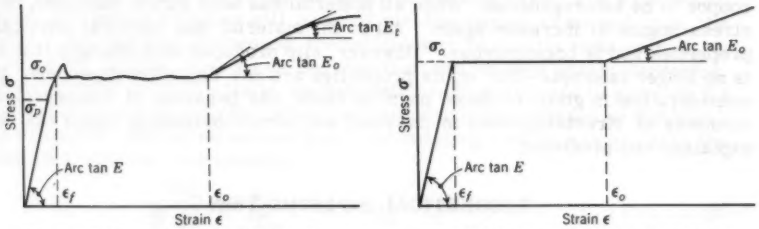
In the existing literature pertaining to the buckling of columns and plates compressed beyond the elastic limit of the material, it is generally accepted that elements made of structural steel will invariably buckle once the yield stress is reached. Stephen Timoshenko stated:[3]

> "To obtain a compressive load on a bar larger than the load producing the yield-point stress, it is necessary to prevent the bar from lateral buckling at the yield point by applying some lateral constraint."

and:

> "Experiments show that, when the compressive stress reaches the yield point of the material * * * the plate buckles for any value of the ratio b/h."

Essentially the same conclusions may be drawn from the equations for inelastic buckling presented by Friedrich Bleich.[4] Both the column and plate



(*a*) TYPICAL STRESS-STRAIN CURVE OF MILD STEEL

(*b*) SIMPLIFIED STRESS-STRAIN CURVE

FIG. 1.—STRESS-STRAIN CURVES

buckling equations contain the factor E_t/E. When the yield stress is reached, the tangent modulus E_t reduces to zero and buckling seems unavoidable. It thus appears impossible to compress structural steel elements beyond the initial yield strain, ϵ_f, without buckling (Fig. 1(a)). This situation would invalidate one of the basic assumptions of plastic analysis and make it inapplicable to structural design if the reasoning involved were not in error. Although the aforementioned theories give a fair account of buckling in the elastic range and

---

[3] "Theory of Elastic Stability," by S. Timoshenko, McGraw-Hill Book Co., Inc., New York, 1936, pp. 159, 385.

[4] "Buckling Strength of Metal Structures," by F. Bleich, McGraw-Hill Book Co., Inc., New York, 1952, Eqs. 21, 653.

in the inelastic range between the proportional limit and the initial yield point strain, ϵ_f, they are not applicable to cases beyond this range.

This paper constitutes a continuation and extension, including pertinent test data, of a previous study of the stability of plates stressed into the strain-hardening range.[5]

Notation.—The letter symbols adapted for use in this paper are defined where they first appear and are arranged alphabetically, for convenience of reference, in the Appendix.

Inelastic Behavior of Structural Steel.—For an understanding of the new approach presented herein, an explanation of the inelastic behavior of structural steel is necessary. Fig. 1(a) shows the stress-strain diagram of a coupon in tension or compression. In the elastic range, the material exhibits homogeneous and isotropic behavior. Yielding commences rather abruptly without any significant indication of a proportional limit. At the yield stress, σ_o, considerable straining takes place without an increase in stress so that the tangent modulus, E_t, seems to reduce to zero. However, ϵ is an average strain, derived from the measurement of an elongation or shortening over a certain gage length. There is no material within this gage length between the yield strain, ϵ_f, and the strain at the beginning of strain-hardening, ϵ_o. The mechanism of yielding is discontinuous, taking place in small slip bands by a sudden jump of strain from ϵ_f to ϵ_o. The slip bands form successively, starting at a weak point, such as an inclusion or a point of stress concentration, and then spread out into the rest of the specimen.[6]

During yielding, some of the material is still elastic while the yielded zones have reached the point of strain-hardening, ϵ_o, causing the material within the coupon to be heterogeneous. When all material has been strain-hardened, the stress begins to increase again. All of the material has identical physical properties and is homogeneous. However, slip produces such changes that it is no longer isotropic—that is, its properties are now direction-dependent. If consideration is given to these physical facts, the behavior of compression elements of structural steel in the yield and strain-hardening range can be explained and predicted.

THEORETICAL INVESTIGATION

Inelastic Column Buckling.—Before treating the problem of plate buckling, it is advantageous to summarize the behavior of columns. The elastic buckling stress of a slender column is given by:

$$\sigma_e = \frac{\pi^2 E}{\left(\frac{l}{r}\right)^2} \quad \ldots\ldots\ldots\ldots\ldots\ldots \quad (1)$$

in which E is the modulus of elasticity; l represents the effective column length; and r is equal to the radius of gyration.

---

[5] "Plate Buckling in the Strain-Hardening Range," by G. Haaijer, Transactions, ASCE, Vol. 124, 1959, pp. 117–148.

[6] "Theory of Flow and Fracture of Solids," by A. Nadai, McGraw-Hill Book Co., Inc., New York, 1950, p. 297.

In the inelastic range, the theoretical stress at which bifurcation of equilibrium occurs (bending commences) is characterized by the tangent modulus stress,[4]

$$\sigma_t = \frac{\pi^2 E_t}{\left(\frac{l}{r}\right)^2} \quad \ldots\ldots\ldots\ldots\ldots\ldots \quad (2)$$

The maximum stress lies between σ_t and the reduced modulus stress,

$$\sigma_r = \frac{\pi^2 E_r}{\left(\frac{l}{r}\right)^2} \quad \ldots\ldots\ldots\ldots\ldots\ldots \quad (3)$$

For a rectangular section the reduced modulus is given by[3]

$$E_r = \frac{4 E E_t}{\left(\sqrt{E} + \sqrt{E_t}\right)^2} \quad \ldots\ldots\ldots\ldots\ldots\ldots \quad (4)$$

For design purposes, the possible increase of the maximum stress beyond the tangent modulus stress is generally neglected. If the tangent modulus E_t is given, the behavior of a column can be predicted.

On the basis of the simplified stress-strain diagram (Fig. 1(b)), buckling would be elastic up to the yield point stress, σ_o. The slenderness ratio (l/r) corresponding to initiation of yielding is obtained by inserting into Eq. 1 the values $\sigma_e = \sigma_o$ and E. For smaller values of l/r, buckling will not occur immediately once the yield strain ϵ_f is reached, but yielding will commence, with the formation of slip bands along the length of the specimen. For a pin-ended column, the worst situation will occur if yielding begins to spread from the center. The bending stiffness of the middle part is greatly reduced to $E_o I$, E_o being the tangent modulus of the zone that has reached strain-hardening. The end-pieces are still elastic, so that their bending stiffness is given by E I (Fig. 2(a)). Assuming that the column is continuously compressed so that buckling will occur without strain reversal, the buckling condition is given by the following transcendental equation:[7]

$$\sqrt{\frac{E_o}{E}} \tan \frac{\phi \pi}{\sqrt{\frac{E_o}{E}}} \zeta \tan \phi \pi \left(\frac{1}{2} - \zeta\right) = 1 \quad \ldots\ldots\ldots\ldots\ldots\ldots (5)$$

in which ϕ^2 is equal to σ_{cr}/σ_e; σ_{cr} is the critical buckling stress; and ζ represents the parameter specifying the extent of yielded zone (Fig. 2(a)).

For given values of E_o/E and ζ, values of ϕ can be derived by trial and error. As buckling occurs within the plastic range, that is, the critical stress σ_{cr} is equal to the yield stress σ_o, the slenderness ratio l/r can be computed as:

$$\sigma_{cr} = \sigma_o = \phi^2 \sigma_e = \frac{\phi^2 \pi^2 E}{\left(\frac{l}{r}\right)^2} \quad \ldots\ldots\ldots\ldots\ldots\ldots (6a)$$

[7] "Theory of Elastic Stability," by S. Timoshenko, McGraw-Hill Book Co., Inc., New York, 1936, p. 128.

or

$$\left(\frac{l}{r}\right)^2 = \phi^2 \frac{\pi^2 E}{\sigma_o} \quad \ldots\ldots\ldots\ldots\ldots\ldots (6b)$$

The shortening of the column, Δl, is given by:

$$\Delta l = \epsilon_f (1 - 2\zeta) l + 2 \epsilon_o \zeta l \quad \ldots\ldots\ldots\ldots\ldots (7a)$$

and the average strain at which buckling occurs by:

$$\epsilon_{cr} = \frac{\Delta l}{l} = (1 - 2\zeta) \epsilon_f + 2 \zeta \epsilon_o \quad \ldots\ldots\ldots\ldots\ldots (7b)$$

Numerical results for Eq. 7(b), shown in Fig. 2, curve a, are derived on the basis of the following material constants: E = 30,000 kips per sq in.; E_o = 800

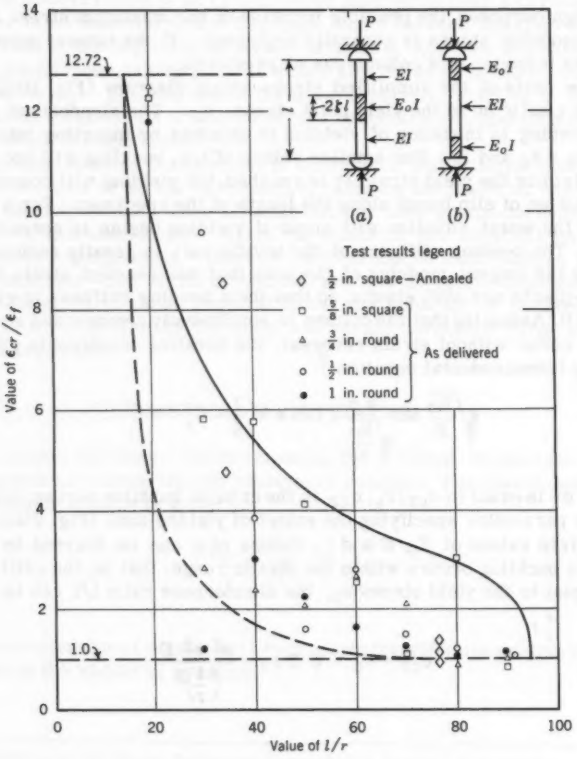


FIG. 2.—COMPARISON OF THEORETICAL CURVES WITH RESULTS OF MODEL COLUMN TESTS

kips per sq in.; $\epsilon_f = 1.1 \times 10^{-3}$; $\epsilon_o = 14 \times 10^{-3}$; and $\sigma_o = 33$ kips per sq in. The yield stress, σ_o, is reached for a slenderness ratio $l/r = 94.9$, the corresponding strain being the yield strain ϵ_f. For smaller slenderness ratios, l/r, the buckling stress σ_{cr} remains constant at the yield stress level. Buckling will occur only after the yielded zone at the center has spread over a length $2\zeta l$, resulting in a great reduction of the bending stiffness over this section.

The average critical strain changes little at first with the decreasing l/r-value, but it increases rapidly for values of l/r smaller than 30. For $l/r = 15.4$, the entire length is strain-hardened before buckling occurs. If l/r is further reduced, the critical stress increases above the yield stress σ_o. All material being strain-hardened, the tangent modulus E_t for the entire length is given by the slope of the stress-strain curve in the strain-hardening range.

Another assumption is that yielding spreads symmetrically from both ends. The corresponding curve b in Fig. 2 is above the previously derived curve a. This reasoning is substantiated by the results of 37 tests on small model columns, plotted in Fig. 2. The average yield stress of the steel used was approximately 35 kips per sq in. No records of the strain-hardening strain, ϵ_o, and the strain-hardening modulus, E_o, are available. Almost all test points lie between the two theoretically-derived curves. The actual yield pattern may occur anywhere between the two extreme cases discussed above.

The experimental indications, however, are that strains larger than the yield strain, ϵ_f, can be reached without buckling. For sufficiently small l/r-values, the point of strain-hardening, ϵ_o, can be reached and even exceeded. Corresponding test results will be given in a subsequent section.

If theoretical predictions, based on Eqs. 1 and 2 and on a tangent modulus E_t derived from a coupon stress-strain diagram, are compared to the actual behavior of structural steel columns, such as WF-sections and built-up members, a discrepancy is observed in the intermediate column range $30 \leq l/r \leq 110$, the theoretical predictions always being too high. This situation has generally been attributed to such causes as initial imperfections and accidental end eccentricities. Bleich[4] introduced an "effective" coefficient (E_t/E) below the actual value of E_t/E, based on a coupon stress-strain curve, in order to preserve the applicability of Eq. 2 to inelastic buckling. However, recent theoretical and experimental investigations explained the situation by demonstrating that this discrepancy was due to the presence of residual stresses.[8,9,10] The proportional limit of an axially loaded column is reached when the sum of the applied stress, P/A, and the maximum compressive residual stress reaches yielding. The subsequent behavior of the column depends on the distribution of the residual stresses and the direction of buckling—that is, buckling about a weak or strong axis. For l/r approaching approximately 15, the strain-hardening range is reached and the influence of residual stresses is completely wiped out. For values of l/r smaller than 15, the buckling load is governed only by the tangent modulus, E_t.

Inelastic Plate Buckling Under Uniform Compression.—In the previous section, the possibility of a column buckling at stresses above the yield stress, σ_o,

[8] "The Influence of Residual Stress on the Instability of Columns," by A. W. Huber, thesis presented to Lehigh Univ., in 1956, in partial fulfillment of the requirements for the degree of Doctor of Philosophy.

[9] "Residual Stress and the Compressive Strength of Steel," by A. W. Huber and L. S. Beedle, Welding Journal, Vol. 30, No. 12, December, 1954, pp. 589S–614S.

[10] "Residual Stress and the Yield Strength of Steel Beams," by C. H. Young, L. S. Beedle, and B. G. Johnston, Welding Journal, Vol. 31, No. 4, April, 1952, pp. 205S–229S.

was shown. It can therefore be assumed that the same holds true for plates. The object of the following analysis is to derive a plate-buckling equation that is applicable to the strain-hardening range. The behavior of plates that buckle in the intermediate range between the proportional limit (the sum of applied and residual stress equal to yield stress) and the strain-hardening range is governed by the presence and distribution of residual stresses. Although no direct solution of this problem has been developed, a reasonable transition curve will be proposed.

During yielding the material changes its physical properties so that at strain-hardening the initially isotropic material is orthotropic—that is, the properties are direction-dependent. In the case of plane stress, the stress and strain relations of the material can be expressed in the following general form:

$$d\epsilon_x = \frac{1}{E_x} d\sigma_x - \frac{\nu_y}{E_y} d\sigma_y \quad \ldots\ldots\ldots\ldots\ldots\ldots (8a)$$

$$d\epsilon_y = -\frac{\nu_x}{E_x} d\sigma_x + \frac{1}{E_y} d\sigma_y \quad \ldots\ldots\ldots\ldots\ldots\ldots (8b)$$

and

$$d\gamma_{xy} = \frac{1}{G_t} d\tau_{xy} \quad \ldots\ldots\ldots\ldots\ldots\ldots (8c)$$

in which γ is the shear strain; σ represents the normal stress; τ denotes the shear stress; E_x and E_y are the tangent moduli in x and y-directions; G_t is the tangent shear modulus; and ν_x and ν_y represent coefficients of dilatation for increases in σ_x and σ_y. If Eqs. 8(a), (b), and (c) are valid for the entire plate cross section, the expressions for the bending and twisting moments in terms of the transverse plate deflection, w, become:

$$M_x = -D_x I\left(\frac{\partial^2 w}{\partial x^2} + \nu_y \frac{\partial^2 w}{\partial x^2}\right) \quad \ldots\ldots\ldots\ldots\ldots\ldots (9a)$$

$$M_y = -D_y I\left(\frac{\partial^2 w}{\partial y^2} + \nu_x \frac{\partial^2 w}{\partial x^2}\right) \quad \ldots\ldots\ldots\ldots\ldots\ldots (9b)$$

and

$$M_{xy} = -2 G_t I \frac{\partial^2 w}{\partial x \partial y} \quad \ldots\ldots\ldots\ldots\ldots\ldots (9c)$$

in which the moment of inertia $I = t^3/12$; t is the plate thickness; $D_x = E_x/1 - \nu_x \nu_y$; and $D_y = E_y/1 - \nu_x \nu_y$. Eqs. 9(a), (b), and (c) imply that buckling occurs without strain reversal. From these relationships, the following general expressions for the buckling strength of uniformly compressed, rectangular plates is derived:[5]

1. Loaded edges $x = 0$ and $x = l_p$ are hinged, unloaded edge $y = 0$ is hinged, and unloaded edge $y = b_1$ is free (Fig. 3(a)). Therefore,

$$\sigma_{cr} = \left(\frac{t}{b_1}\right)^2 \left[\frac{\pi^2}{12} D_x \left(\frac{b_1}{l_p}\right)^2 + G_t\right] \quad \ldots\ldots\ldots\ldots\ldots\ldots (10)$$

in which b_1 represents the width of plate; and l_p is the length of plate or half-wave length. For a long plate, the first term can be neglected and the buckling stress becomes:

$$\sigma_{cr} = \left(\frac{t}{b_1}\right)^2 G_t \quad \ldots\ldots\ldots\ldots\ldots\ldots (11)$$

2. Loaded edges $x = 0$ and $x = l_p$ are hinged, unloaded edge $y = 0$ in fixed and unloaded edge $y = b_1$ is free. The minimum value of the buckling stress occurs when the length-to-width ratio is

$$\frac{l_p}{b_1} = 1.46 \sqrt[4]{\frac{D_x}{D_y}} \quad \ldots\ldots\ldots\ldots\ldots\ldots (12)$$

Then,

$$\sigma_{cr} = \left(\frac{t}{b_1}\right)^2 \left[0.769 \sqrt{D_x D_y} - 0.270 \left(D_{xy} + D_{yx}\right) + 1.712 G_t\right] \quad \ldots (13)$$

in which $D_{xy} = \nu_y D_x$ and $D_{yx} = \nu_x D_y$.

3. Loaded edges $x = 0$ and $x = l_p$ are hinged, and unloaded edges $y = +b_2/2$ are hinged (Fig. 3(b)). The minimum value of the buckling stress is obtained for the following value of the length-to-width ratio:

$$\frac{l}{b_2} = \sqrt[4]{\frac{D_x}{D_y}} \quad \ldots\ldots\ldots\ldots\ldots\ldots (14)$$

in which b_2 is the width of plate supported along all four edges. Then,

$$\sigma_{cr} = \frac{\pi^2}{12} \left(\frac{\pi^2}{b_2}\right)^2 \left[2 \sqrt{D_x D_y} + D_{xy} + D_{yx} + 4 G_t\right] \quad \ldots\ldots (15)$$

4. Loaded edges $x = 0$ and $x = l_p$ are hinged, and unloaded edges $y = +b_2/2$, are fixed. The minimum value of the buckling stress is obtained for

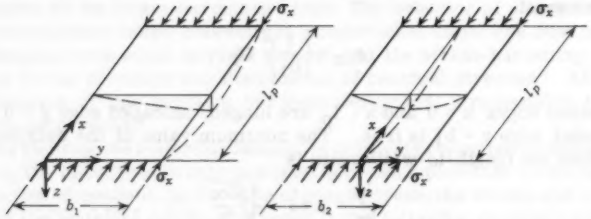
$$\frac{l}{b_2} = 0.66 \sqrt[4]{\frac{D_x}{D_y}} \quad \ldots\ldots\ldots\ldots\ldots\ldots (16)$$

Then

$$\sigma_{cr} = \frac{\pi^2}{12} \left(\frac{t}{b_2}\right)^2 \left[4.554 \sqrt{D_x D_y} + 1.237 \left(D_{xy} + D_{yx}\right) + 4.943 G_t\right] \quad \ldots (17)$$

Several theories of plasticity are available for the determination of the moduli E_x, E_y, ν_x, ν_y, and G_t. The theoretical predictions applied to the plate buckling problem are summarized in Table 1. The secant modulus $E_{sec} = \sigma/\epsilon$; ν represents Poisson's ratio; and the tangent modulus $E_t = \partial\sigma/\partial\epsilon$. There are significant discrepancies between these theories. According to the mathematical theory of plasticity, the stress-strain relations should be of the incremental type. Only the stress-strain law used by George H. Handelman and William Prager,[11] satisfies this condition. Therefore, all theories but this one may be discarded.

[11] "Plastic Buckling of a Rectangular Plate under Edge Thrusts," by G. H. Handelman and W. Prager, Technical Note No. 1530, National Advisory Committee for Aeronautics, Washington, D. C., August, 1948.



(*a*) PLATE WITH ONE EDGE FREE

(*b*) PLATE SUPPORTED ALONG ALL FOUR EDGES

FIG. 3.—BUCKLING STRENGTH OF PLATES

TABLE 1.—COMPARISON OF MODULI AS PREDICTED BY DIFFERENT THEORIES

Theory (1)	E_x (2)	E_y (3)	G_t (4)	ν_x (5)	ν_y (6)
Bleich[a]	E_t	E	$\frac{\sqrt{E\,E_t}}{2(1+\nu)}$	$\nu\sqrt{\frac{E_t}{E}}$	$\nu\sqrt{\frac{E}{E_t}}$
Kaufmann[b]	E_t	E	$\frac{E\,E_t}{(1+\nu)\,(E+E_t)}$	ν	ν
Bijlaard[c] Ilyushin[d] Stowell[c]	E_t	$\frac{E_t}{\frac{1}{4}+\frac{3}{4}\frac{E_t}{E_{sec}}}$	$\frac{E_{sec}}{3}$	$\frac{1}{2}$	$\frac{1}{\frac{1}{2}+\frac{3}{2}\frac{E_t}{E_{sec}}}$
Handelman and Prager[f]	E_t	$\frac{4EE_t}{E+3\,E_t}$	$\frac{E}{2(1+\nu)}$	$\frac{E_t(2\nu-1)+E}{2E}$	$\frac{2\left[E_t(2\nu-1)+E\right]}{E+3\,E_t}$

[a] "Buckling Strength of Metal Structures," by F. Bleich, McGraw-Hill Book Co., Inc., New York, N.Y., 1952.

[b] "Bemerkungen zur Stabilitat Dunnwandiger Kreiszylindrischer Schalen Oberhalb der Proportionalitats Grenze," by W. Kaufmann, Ingenieur-Archiv, Vol. VI, No. 6, 1935.

[c] "Some Contributions to the Theory of Elastic and Plastic Stability," by P. P. Bijlaard, Publications, International Assoc. for Bridge and Structural Engrg., Vol. VIII, 1947.

[d] "Stability of Plates and Shells Beyond the Proportional Limit," by A. A. Ilyushin, Technical Memorandum 1116, NACA, October, 1947.

[e] "A Unified Theory of Plastic Buckling of Columns and Plates," by E. Z. Stowell, Report 898, NACA, 1948.

[f] "Plastic Buckling of a Rectangular Plate with Edge Thrust," by G. H. Handelman and W. Praeger, Technical Note 1530, 1948.

Although the stress-strain law of Handelman and Prager, with the second invariant of the deviatoric stress tensor as the loading function, has been verified experimentally by combined compression and torsion tests on tubes of mild steel stressed into the strain-hardening range, it cannot be applied without modification to the plate buckling problem. E. T. Onat and Daniel C. Drucker,[12] F. ASCE, stated that the Handelman—Prager theory is unable to predict the buckling of actual plates because of the influence of unavoidable initial imperfections.

It has been shown[5] how effective values of the moduli can be obtained from an incremental stress-strain relationship. From the stress-strain curve for the strain-hardening range of mild steel,

$$\epsilon - \epsilon_o = \frac{\sigma - \sigma_o}{E_o} + K\left(\frac{\sigma - \sigma_o}{E_o}\right)^m \quad \ldots\ldots\ldots\ldots (18)$$

with E_o = 900 kips per sq in.; K = 21; and m = 2, the following values of the moduli were found to be applicable:[5] D_x = 3,000 kips per sq in.; D_y = 32,800 kips per sq in.; $D_{xy} = \nu_y D_x = \nu_x D_y$ = 8,100 kips per sq in.; and G_t = 2,400 kips per sq in.

The developed expressions for the buckling strength of orthotropic plates (Eqs. 10, 13, 15, and 17) can be applied only if all material is strained into the strain-hardening range ($\epsilon \geq \epsilon_o$). In the intermediate range, transition curves can be developed as in the case of column buckling (Fig. 2).

Consider a flange of length 2 l, with the loaded edges x = 0 and x = 2 l fixed, the unloaded edge y = 0 hinged, and the unloaded edge y = b free. This example has been chosen as a basis of comparison of the theory with the results of tests on plates with these boundary conditions. For the simplified stress-strain curve of Fig. 1(b), the elastic solution is valid for $\sigma_{cr} < \sigma_o$, and is obtained from Eq. 10 by substituting the elastic values of the moduli. Thus,

$$\sigma_{cr} = \left(\frac{t}{b_1}\right)^2 \left[\frac{\pi^2 E}{12\,(1 - \nu^2)} \left(\frac{b_1}{l}\right) + G\right] \quad \ldots\ldots\ldots\ldots (19)$$

If the geometry of the specimen, given by b/t and b/l, is such that σ_{cr} (Eq. 19) would exceed the yield stress, σ_o, yielding will occur before the plate buckles, the stress remaining at the yield value σ_o. To find a solution for this case, it is necessary to assume a certain distribution of the strain-hardened zones—for example, yielding begins at the ends and spreads toward the middle. This assumption seems to be reasonable in view of the fixed-end restraints, and has been observed during tests.

The middle section, being still elastic, is practically rigid compared with the yielded zone of length ζ l. Assuming that only the latter will deform,

$$\sigma_{cr} = \sigma_o = \left(\frac{t}{b_1}\right)^2 \left[\frac{\pi^2 D_x}{12} \left(\frac{b_1}{\zeta l}\right)^2 + G_t\right] \quad \ldots\ldots\ldots\ldots (20)$$

The corresponding average critical strain is

$$\epsilon_{cr} = (1 - \zeta)\,\epsilon_f + \zeta\,\epsilon_o \quad \ldots\ldots\ldots\ldots\ldots\ldots (21)$$

---

[12] "Inelastic Instability and Incremental Theories of Plasticity," by E. T. Onat and D. C. Drucker, Journal of the Aeronautical Sciences, Vol. 20, No. 3, 1953.

Eqs. 20 and 21 are applicable to plate elements that are free of residual stresses, such as annealed specimens. However, delivered specimens, in general, contain residual stresses of considerable magnitude in order that partial yielding will set in at an applied stress considerably below the yield stress. In the following, a more realistic approach to the range $\sigma_p < \sigma_{cr} < \sigma_o$ will be examined. The elastic solution is valid only up to a limiting stress, σ_p. The magnitude of σ_p is determined in order that the sum of the applied stress, σ_p, and the maximum residual compressive stress, σ_R, equals the yield stress σ_o. Hence, the stress σ_p corresponds to the effective proportional limit of the specimen.

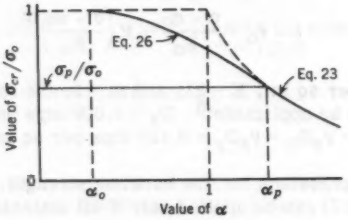


FIG. 4.—BUCKLING STRENGTH OF COLUMNS AND PLATES

Buckling at Stresses Below the Yield Stress.—The elastic buckling stress of a perfectly plane plate of isotropic material, subjected to forces acting in its plane, is given by:

$$\sigma_e = k \frac{\pi^2 E}{12\left(1 - \nu^2\right)}\left(\frac{t}{b}\right)^2 \quad \ldots\ldots\ldots\ldots\ldots\ldots (22)$$

in which k is the plate buckling coefficient.

Eq. 22 and Eq. 1, the expressions for the elastic buckling stress of a column, can be written in a dimensionless form:

$$\frac{\sigma_e}{\sigma_o} = \frac{1}{\alpha^2} \quad \ldots\ldots\ldots\ldots\ldots\ldots\ldots\ldots (23)$$

but for a column,

$$\alpha = \frac{1}{\pi r}\sqrt{\frac{\sigma_o}{E}} \quad \ldots\ldots\ldots\ldots\ldots\ldots\ldots (24)$$

and for a plate,

$$\alpha = \frac{1}{\pi t}\sqrt{\frac{12\,\sigma_o\,(1 - \nu^2)}{k\,E}} \quad \ldots\ldots\ldots\ldots\ldots (25)$$

Eq. 23 is valid for values of α larger than a limiting value α_p, as shown in Fig. 4, the dimensionless representation of the buckling strength of columns and plates. In Fig. 4, α_o is equal to the value of α at the point of strain-hardening and α_p is the value of α at the proportional limit. The corresponding limiting stress is σ_p. As indicated, the sum of this limiting stress and the maximum residual stress equals the yield stress σ_o. From this point, σ_p/σ_o

and α_p, a transition curve must be followed to the point at which the buckling stress equals the yield stress, $\sigma_{cr}/\sigma_o = 1$ and α_o. If a specimen reaches this point, all its material has been yielded and has reached the strain-hardening range. The transition curve can generally be taken as

$$\sigma_{cr}/\sigma_o = 1 - (1 - \left(\frac{\sigma_p}{\sigma_o}\right)\left(\frac{\alpha - \alpha_o}{\alpha_p - \alpha_o}\right)^n \quad \ldots\ldots\ldots\ldots (26)$$

The value of α_o for a column is relatively small and the influence of strain-hardening is therefore generally neglected by taking $\alpha_o = 0$. It was shown by Huber[7] that the shape of the transition curve for WF columns depends on the distribution of the residual stresses and the axis (weak or strong) about which the column buckles. The magnitude of the residuals determines the value of σ_p/σ_o. Actual measurements of residual stresses in WF shapes have furnished high values. To be conservative, σ_p/σ_o for most WF shapes should be taken as being equal to 0.5.

For WF columns the influence of residual stresses is most pronounced if buckling takes place about the weak axis. The transition curve was found to be approximately a straight line ($n = 1$ and $\alpha_o = 0$). When the column fails by bending about the strong axis, a quadratic parabola ($n = 2$ and $\alpha_o = 0$), is a good approximation of the transition curve.

For plate buckling, the influence of residual stresses is less severe because the buckling stress is dependent not only on the modulus E_x in the direction of the compressive loads, but also on the modulus E_y in the transverse direction and the shearing modulus G_t (Eq. 8, and Eqs. 10 to 18). Yielding affects G_t to a lesser degree than E_x. This influence can be taken into account through a higher value of n. However, the transition curve given by Eq. 26 can at most be tangent to the elastic solution given by Eq. 23. From this condition the limiting value of n is found:

$$n_{max} = \frac{2\left(\alpha_p - \alpha_o\right)}{\left(\alpha_p{}^2 - 1\right)} \quad \ldots\ldots\ldots\ldots\ldots (27)$$

It is suggested that this value be used for all cases of plate buckling.

Finally, the problem remains to determine the values of α_p and α_o. Eq. 23 gives the value of α_p by substituting $\sigma_e = \sigma_p$, in which σ_p is the effective proportional limit. For structural wide-flange shapes, it is conservative to take $\sigma_p/\sigma_c = 0.5$—thus, $\alpha_p = \sqrt{2}$. The following values of α_o are determined from Eqs. 2, 11, 13, 15, and 17, respectively, by substituting the given values of the moduli. The corresponding values of l/r, b_1/t, or b_2/t are given in parenthesis for $\sigma_o = 36$ kips per sq in.

Columns	$\alpha_o = 0.173$	$(l/r = 15.7)$
Long hinged flanges	$\alpha_o = 0.455$	$(b_1/t = 8.15)$
Fixed flanges.	$\alpha_o = 0.461$	$(b_1/t = 14.3)$
Hinged webs	$\alpha_o = 0.588$	$(b_2/t = 32.3)$
Fixed webs	$\alpha_o = 0.579$	$(b_2/t = 42.0)$

This suggests that the values of α_o depend only on the type of compression element (column, flange, or web plate), and are nearly independent of the amount of restraint. The problem can therefore be simplified by taking for columns, $\alpha_o = 0.17$; for flanges (plates with one free edge), $\alpha_o = 0.46$; and for webs (plates

supported along all four edges, $\alpha_0 = 0.58$. These values are used subsequently in Fig. 19 in which comparison to test results is made.

Inelastic Plate Buckling under Combined Bending and Compression.—An extension of the previous considerations to cases of plates subjected to bending and axial load is of practical importance. The web of a WF-beam subjected to a bending moment, M, and an axial load, P, presents such a case. Depending

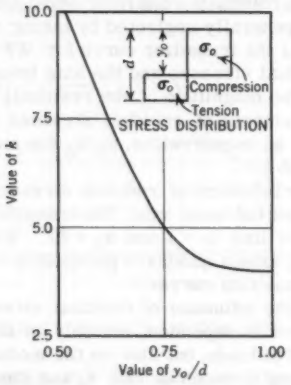


FIG. 5.—PLATE COEFFICIENT OF WEBS

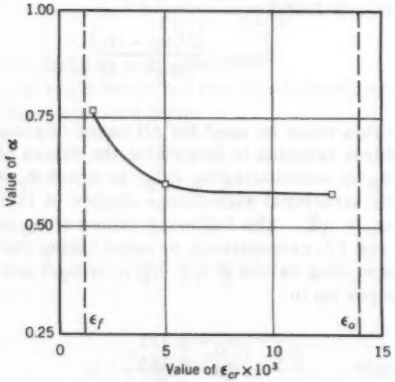


FIG. 6.—EXPERIMENTALLY DETERMINED VALUES OF α

on the ratio of P/P_0, P_0 being the yield load of the axially-loaded member and equal to $\sigma_0 A$, the neutral axis may lie inside or outside of the web.

The plate buckling coefficient, k, must first be determined. The minimum values of k for a stress distribution of a fully plastified WF section subjected to axial load and moment are shown in Fig. 5. In this figure, d corresponds to

the depth of the web, and y_o fixes the position of the neutral axis. The values were determined by equating the work of the external forces to the dissipation of the internal energy at the moment of buckling, using the moduli given under the heading, "Inelastic Plate Buckling Under Uniform Compression."

The strain, ϵ_{cr}, at which buckling of the web plate occurs, and the corresponding depth to thickness ratio, d/t, is important. For a solution of this problem, test results are described subsequently. Fig. 6 shows experimentally determined values of α as a function of the critical strain ϵ_{cr} for uniformly compressed webs. Using depth d instead of width b in Eq. 25, the parameter α is defined by:

$$\alpha = \frac{d}{\pi t}\sqrt{\frac{12\,\sigma_o\,(1-\nu^2)}{k\,E}} \quad \ldots\ldots\ldots\ldots\ldots\ldots (28)$$

and is hence proportional to the d/t ratio. The maximum strain of the compression flange is taken as ϵ_m. As the strain varies linearly over the depth of the section, the mean strain of the compression zone in the web is $\epsilon_m/2$. Using this latter value in Fig. 6, the following values of α are found:

ϵ_m/ϵ_f	α
12	0.58
8	0.60
4	0.69

The resulting curves for the critical d_f/t-ratios are plotted in Fig. 7 for σ_o = 33 kips per sq in. The area of the web is represented by A_w, t is the web thickness, d_f is the distance between the center plane of the flanges.

Values of d_f corresponding to σ_o different from 33 kips per sq in. are obtained by multiplying d_f/t by $\sqrt{33/\sigma_o}$.

EXPERIMENTAL INVESTIGATION

Compression Tests on Short Rectangular Columns.—It was stated previously that buckling of columns at stresses above the yield stress should be permissible without special precautions to prevent buckling at the yield stress. To verify this statement experimentally, a number of compression tests on short model columns of rectangular cross section were performed. The dimensions of the specimens, cut from the flange of an 8WF40 section (ASTM A-7 steel), were chosen so that buckling in the strain-hardening range could be expected. Table 2 shows the dimensions of the short columns, in which $l/r = L_c/2r$, the effective slenderness ratio (test conditions simulate fixed ends); L_c is the length of the specimen and the radius of gyration, $r = \frac{t}{\sqrt{12}}$. The columns were placed flat-ended in a hydraulic testing machine. During the tests, simultaneous load, strain, and lateral deflection readings were taken.

The maximum loads divided by the area are plotted in Fig. 8 and compared with the tangent-modulus and reduced-modulus loads, confirming the prediction that the maximum load lies between the tangent and reduced-modulus load. The behavior of the columns (Fig. 9) shows the lateral deflection of the column as a function of the strain. The curves demonstrate that the columns can reach the strain-hardening range without deflecting excessively. The critical strains

corresponding to the tangent-modulus loads are indicated by arrows. At these points, the deflections begin to increase at an accelerated rate, confirming that the tangent modulus load is the load at which bending commences.

Compression Tests on Angles.— Next in the experimental program was the verification of the inelastic plate buckling theory. For this purpose, a number

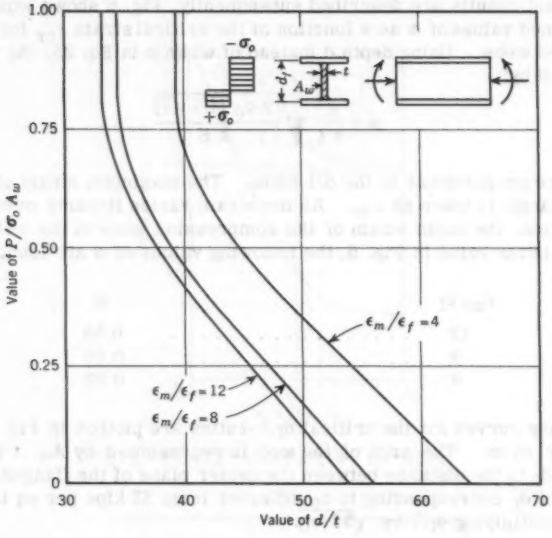


FIG. 7.—ALLOWABLE d/t_w RATIOS OF WEBS OF FULLY PLASTIFIED SECTIONS

TABLE 2.—DIMENSIONS OF SHORT COLUMNS

Specimen (1)	Width, in inches (2)	Thickness, in inches (3)	Length, in inches (4)	l/r (5)
C2	0.745	0.544	2.80	8.9
C3	0.745	0.543	3.20	10.2
C4	0.745	0.543	3.65	11.6
C5	0.745	0.545	4.33	13.9
C6	0.745	0.545	4.80	15.3
C7	0.750	0.527	5.65	18.9
C8	0.750	0.527	6.90	23.4

of compression tests on angles were performed. When buckling torsionally, the flanges of an equilateral angle act as two plates, hinges along the heel and free along the outstanding edge. The loaded ends of the angle columns were fixed in the testing machine against rotation. The dimensions of all specimens are given in Table 3. They were machined from a 6-by-6-by-$\frac{1}{8}$ (14.9 lb) angle,

ASTM A-7 steel, by reducing the width of the leg to the desired dimension, b. Table 3 indicates that six specimens were tested after complete annealing, and two specimens were in the "as-delivered" state. Material properties obtained from coupon tests are summarized in Table 4. All coupons were tested in a 60,000-lb hydraulic machine, the valve opening corresponding to a testing speed of $1\,\mu$ in. per in. per sec in the elastic range.

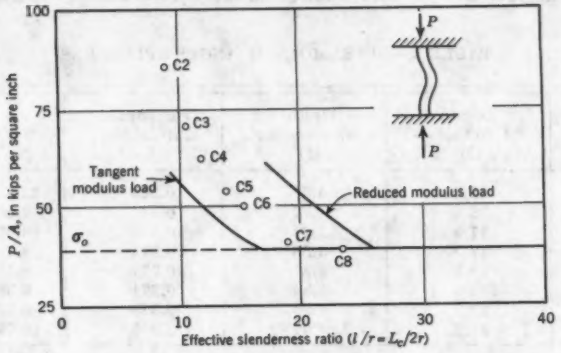


FIG. 8.—COMPARISON OF MAXIMUM LOADS WITH TANGENT MODULUS AND REDUCED-MODULUS LOADS

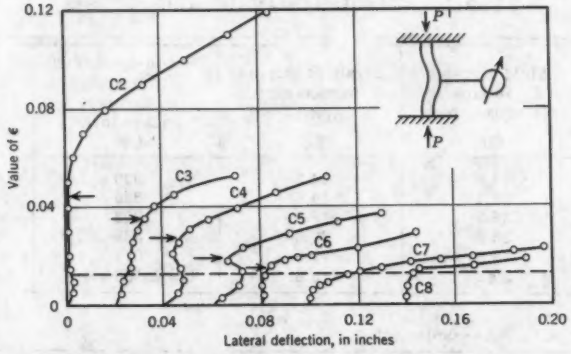


FIG. 9.—LATERAL DEFLECTION OF SHORT COLUMNS

Fig. 10 shows the obtained stress versus average axial strain curves. The angles of lateral rotation of the center section, θ, were measured, and are plotted as a function of the average strain (Fig. 11). The numbers shown in parentheses are values of b/t. In both Fig. 10 and 11, the experimentally determined critical strains are indicated by arrows. The critical strain is defined as the strain at which the rotation begins to increase more rapidly than it did initially.

Specimens A41 and A42 did not buckle torsionally, but failed by bending about the weak axis. Buckling occurred in the strain-hardening range, providing that buckling does not necessarily take place at the yield stress. The results of all tests on angles are summarized in Table 5.

The theoretical solution for the strain-hardening range is given by Eq. 10, and for the yielding range by Eqs. 20 and 21. Fig. 12 shows a plot of ζ versus b_1/t as obtained from Eq. 20 for $l_p/b_1 = 2.65$. Because elastic deformations have been neglected in the derivation of Eq. 20, $b_1/t = \infty$ for $\zeta = 0$ (rigid-plastic

TABLE 3.—DIMENSIONS OF ANGLE SPECIMENS

Specimen (1)	Length 2 l, in inches (2)	Width b, in inches (3)	Thickness t, in inches (4)	b/t (5)	2 l/b (6)
A21[a]	25.0	4.87	0.383	12.70	5.14
A22[a]	25.0	4.79	0.381	12.60	5.21
A31[a]	17.9	3.27	0.370	8.85	5.48
A32[a]	17.9	3.28	0.374	8.79	5.46
A41[a]	12.5	2.31	0.377	6.13	5.41
A42[a]	12.5	2.34	0.371	6.36	5.35
A33[b]	17.5	3.30	0.378	8.73	5.30
A51[b]	21.2	4.07	0.380	10.70	5.21

[a] Annealed. [b] As- delivered.

TABLE 4.—RESULTS OF ANGLE COUPON TESTS

Coupon (1)	Yield stress, σ_0, in kips per square inch (2)	Strain at Strain-hardening, ϵ_0, x 10^3 (3)	Strain-hardening Modulus, E_0, in kips per square inch (4)	Type of loading (5)
C1[a]	37.6	14.3	906	compression
C2[a]	35.1	14.6	845	compression
T1[a]	36.8	18.5	903	tension
T2[a]	38.2	20.0	869	tension
T3[b]	40.2	9.5	877	tension
T4[b]	39.9	15.6	1,160	tension

[a] Annealed. [b] As- delivered.

solution). From Eq. 19 it follows that for $\zeta = 0$, $b_1/t = 20.7$. Knowing the rigid-plastic solution and the point for $\zeta = 0$, corresponding to the limit of the elastic solutions, the elastic-plastic solution is sketched as a dotted line (Fig. 12). The critical strain can then be determined from Eq. 21.

The obtained ϵ_{cr} versus (b/t)-curves are compared with test results in Fig. 13. The theoretical curves for $\sigma = 36$ kips per sq in. describe adequately the behavior of the test specimens.

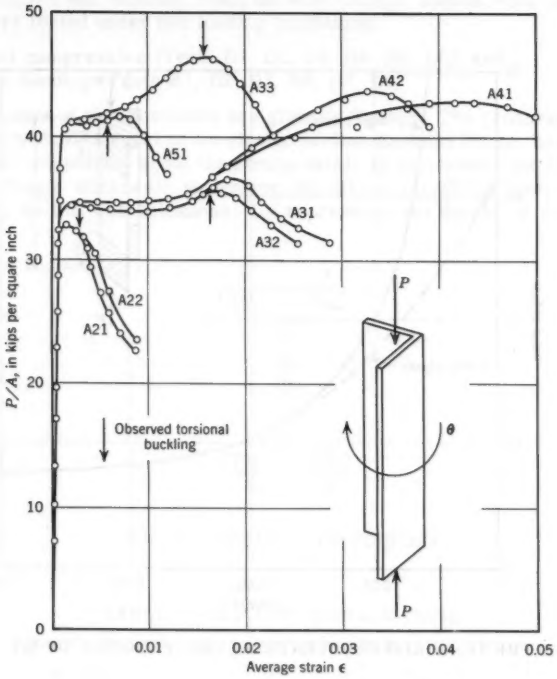


FIG. 10.—RESULTS OF ANGLE COMPRESSION TESTS

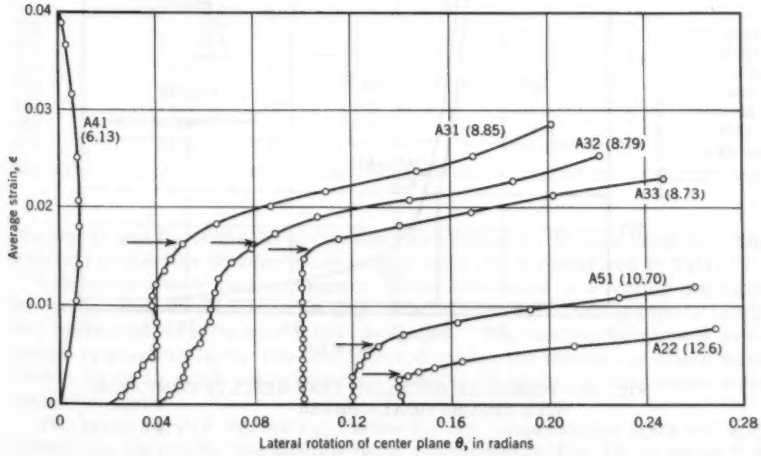


FIG. 11.—LATERAL ROTATION OF ANGLE SPECIMENS

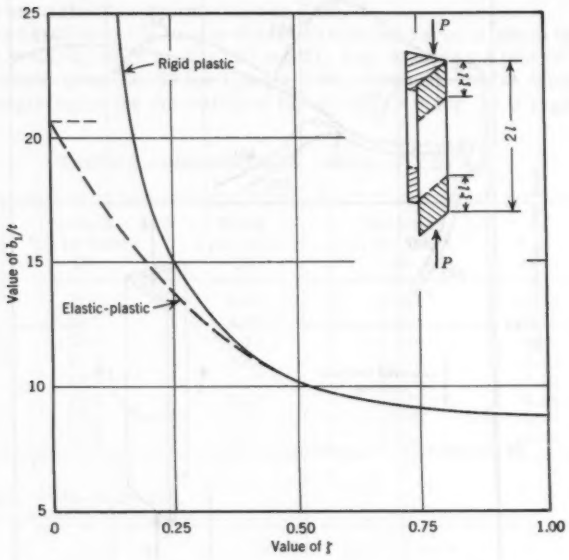


FIG. 12.—YIELD PENETRATION ζ AS A FUNCTION OF b/t

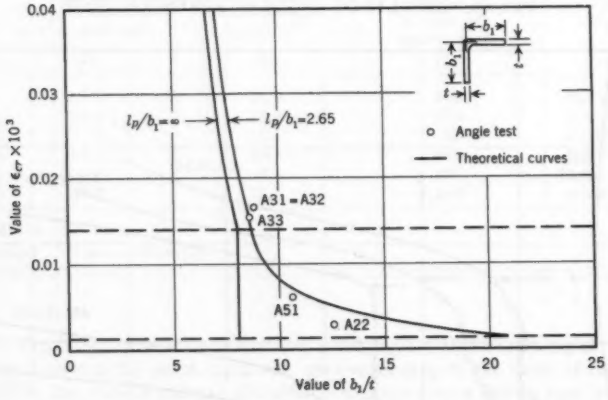


FIG. 13.—TORSIONAL BUCKLING TEST RESULTS COMPARED WITH THEORETICAL CURVES

Compression and Bending Tests on Wide-Flange Shapes.—Six wide-flange shapes were tested under two loading conditions:

1. Axial compression (Tests D1, D2, D3, D4, D5, D6), and
2. Pure bending (Tests B1, B2, B3, B4, B5, B6).

The dimensions of all specimens are given in Table 6. The cross-section area is denoted by A; Z is equal to the plastic section modulus (twice the static moment of half the section about the strong axis); 2b represents the flange width and t_f the flange thickness; d_f denotes the distance between center planes of flanges; t_w is the web thickness; L_c represents the length of compression

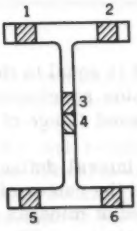


FIG. 14.—LOCATION OF COUPONS

TABLE 5.—RESULTS OF ANGLE TESTS

Test (1)	σ_o, in kips per square inch (2)	$\epsilon_{cr} \times 10^3$ (3)	σ_{cr}, in kips per square inch (4)	Type of Buckling (5)
A22	. . .	3.0	32.2	torsional
A31	34.9	16.5	35.8	torsional
A32	34.6	16.5	35.6	torsional
A41	35.3	. . .	. . .	bending
A42	34.1	. . .	. . .	bending
A33	41.3	16.0	46.4	torsional
A51	41.0	6.0	41.2	torsional

specimen; and L_b is the length of specimen subjected to pure bending. The material properties obtained from coupon tests are summarized in Table 7.

The compression specimens were placed flat-ended in a testing machine, the length being divided in three gage lengths over which the change in length was measured directly with 0.0001 in. gages. The bending specimens were loaded symmetrically by two concentrated loads, the location of which were chosen so as to avoid shear failure. Changes in length of the flanges were measured again.

The resulting P/A versus ϵ_{av} curves for the compressions tests and M/Z versus ϵ_{av} curves for the bending tests are plotted in Fig. 15, in which P is

TABLE 6.—DIMENSIONS

Specimen (1)	Shape (2)	A, in square inches (3)	Z, in cubic inches (4)	2b, in inches (5)
B1, D1	10WF33	9.66	38.56	7.95
B2, D2	8WF24	6.83	22.56	6.55
B3, D3	10WF39	11.34	45.63	8.02
B4, D4	12WF50	14.25	70.28	8.18
B5, D5	8WF35	10.00	33.68	8.08
B6, D6	10WF21	5.84	22.45	5.77

equal to the compressive load, M is equal to the bending moment and ϵ_{av} is the average strain of the compression specimens in Fig. 15(a) and the average strain at center of the compressed flange of the bending specimens in Fig. 15(b).

With the aid of a dial gage, lateral deflection measurements were taken along the edges of the flanges and the center of the webs. For the bending tests the lateral rotation was measured at midspan of the beam. The loading points were supported against lateral rotation. The observations of web deflection, flange buckling, and lateral rotation from test B3 are plotted in Fig. 16 as a typical example. From these curves, the critical strains are obtained, as indicated by arrows in Fig. 15. As mentioned previously, the critical strain is defined as the average strain at which the deflection begins to increase more rapidly than it did initially. The results of all tests are summarized in Table 8.

The results of those tests in which flange buckling was predominant are shown in Fig. 17(a). The results of tests D4 and D6 are omitted because web buckling occurred first and caused premature flange buckling. Specimen B4 did not develop a major flange buckle but failed by lateral-torsional buckling. This result is eliminated from Fig. 17(a). The critical strains are plotted as a function of b/t_f and are compared with theoretical solutions[5] for different values of the coefficient of restraint, β. The theoretical curves are for $\sigma_o = 36$ kips per sq ft. This coefficient represents the restraints provided by the web to the flange. In case of elastic restraint, in which ψ represents moment per unit length required for a unit rotation, the coefficient of restraint becomes

$$\beta = \frac{\psi b}{2 D_y I} \quad \ldots\ldots\ldots\ldots\ldots\ldots (29)$$

The test results show that β has a value of approximately 0.01.

For the cases in which web buckling occurred first (tests D4 and D6), or simultaneously with flange buckling (test D2), the results are plotted in Fig. 17(b) and are compared with the theoretical solution given by Eqs. 15 and 17. The theoretical curves give a good description of the actual behavior of flanges and webs.

Some examples of typical wide-flange specimens after testing are shown in Fig. 18. Specimen D6 failed by web buckling after just reaching the yield point stress. The yielded material is concentrated at the top of the specimen. Simultaneous web and flange buckling caused specimen D2 to fail just after being completely strain-hardened, whereas specimen D5 failed by flange buckling in

OF WF SPECIMENS

t_f, in inches (6)	d_f, in inches (7)	t_w, in inches (8)	L_c, in inches (9)	L_b, in inches (10)	b/t_f (11)	d_f/t_w (12)
0.429	9.37	0.294	32	32	9.2	31.9
0.383	7.63	0.236	26	26	8.6	32.3
0.512	9.37	0.328	32	32	7.8	28.6
0.620	11.57	0.351	32	32	6.6	33.0
0.476	7.65	0.308	32	32	8.5	24.8
0.318	9.56	0.232	23	26	9.1	40.9

the strain-hardening range. Of the bending specimens, B2 and B6 failed because of flange buckling, but B4 buckled laterally without developing a flange buckle.

Summary of Test Results.—All test results are summarized in Fig. 19, showing σ_{cr}/σ_0 as a function of the dimensionless parameter α. The theoretical curves are curve (a) for column buckling, curve (b) for hinged plate with one unloaded edge unsupported, and curve (c) for hinged plate supported along all four edges. The difference in the behavior of columns, flanges, and webs is shown. The values of α for which the strain-hardening range can be reached are confirmed by the test results and can be taken as follows:

Type of Buckling	Value of α
Column	0.17
Flange	0.46
Web	0.58

For flanges and webs, the shape of the transition curves (the plotted curves correspond to the maximum value of the exponent n; Eq. 27) should be considered as reasonable interpolations in the absence of sufficient test results in this particular region. Considerable experimental and theoretical data are available[7] for the transition curve for the columns.

RECOMMENDED GEOMETRY OF WIDE-FLANGE SHAPES IN PLASTIC DESIGN

Flanges.—The following recommendations are based directly on the theoretical and experimental investigation. Flanges of WF shapes can be strained into the strain-hardening range if $\alpha \leq 0.46$. This is generally a sufficient requirement for the development of plastic hinges, because buckling is then not accompanied by a sudden drop of the load (see results of tests A31, A32, A33, D2, and B2 in Figs. 10 and 15 respectively). Consequently, the following recommendation can be given: The ratio of the outstanding width to the thickness of flanges, b/t_f, shall not exceed the following values depending on the value of the yield stress, σ_0: For $\sigma_0 = 33$ kips per sq in., $b/t_f \leq 8.7$; and for $\sigma_0 = 36$ kips per sq in., $b/t_f \leq 8.3$.

Uniformly Compressed Webs.—The results of compression tests on WF shapes failing by web buckling showed that for $\alpha = 0.77$ (test D6) the yield stress

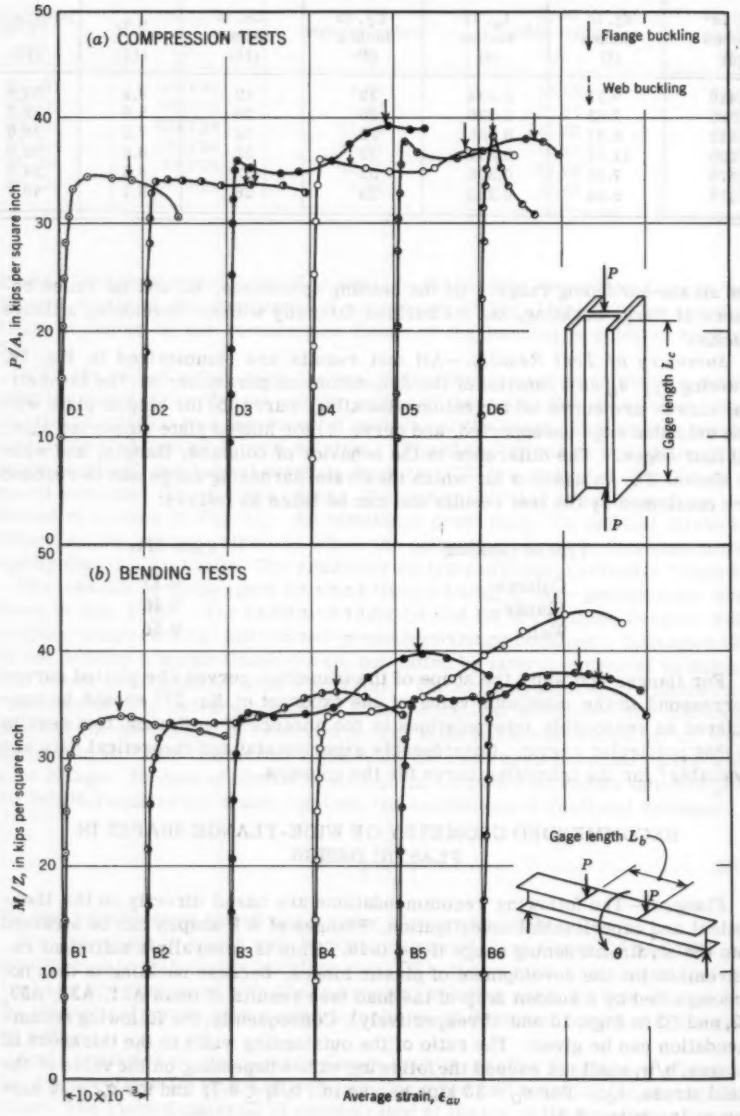


FIG. 15.—RESULTS OF COMPRESSION AND BENDING TESTS

TABLE 7.—RESULTS OF COUPON TESTS

Coupon	Section	Buckling Tests	Location[a]	Yield stress, σ_o, in kips per square inch	Strain at Strain-hardening, ϵ_o, x 10^3	Strain-hardening, Modulus, E_o, in kips per square inch	Type of Location
(1)	(2)	(3)	(4)	(5)	(6)	(7)	(8)
T6			1	35.5	16.5	675	tension
T7	10WF33	B1-D1	5	35.0	14.7	750	tension
C14			2	40.0	14.5	855	compression
C15			6	37.0	13.8	805	compression
T21			1	35.4	18.4	530	tension
T22	8WF24	B2-D2	2	35.6	18.0	600	tension
T23			3	36.3	19.3	470	tension
T31			1	35.6	14.3	525	tension
T32	10WF39	B3-D3	2	36.8	18.9	580	tension
T33			3	37.8	16.3	580	tension
T41			1	37.1	18.0	500	tension
T42	12WF50	B4-D4	2	36.9	18.1	530	tension
T43			3	39.4	15.9	580	tension
T51			1	37.6	16.9	560	tension
T52	8WF35	B5-D5	2	37.3	16.6	465	tension
T53			3	39.9	19.6	600	tension
T61			1	38.0	20.8	520	tension
T62	10WF21	B6-D6	2	34.2	23.4	570	tension
T63			3	44.2	23.6	490	tension

[a] The coupon locations are given in Fig. 14.

TABLE 8.—RESULTS OF WF TESTS

Test	σ_o, in kips per square inch	ϵ_{cr} x 10^3		σ_{cr}, in kips per square inch		Flange l/b	Web l/d	Type of Buckling
		Flange	Web	Flange	Web			
(1)	(2)	(3)	(4)	(5)	(6)	(7)	(8)	(9)
D1	34.4	8.5	8.5	34.2	34.2	1.8	0.56	flange
D2	34.0	13.5	12.7	34.0	34.0	1.5	0.50	flange & web
D3	35.2	19.0	19.0	39.0	39.0	1.5	0.46	flange
D4	35.0	18.5	5.0	36.8	35.4	1.5	0.55	web
D5	36.6	17.0	17.0	38.0	38.0	2.1	0.56	flange
D6	38.0	4.3	1.6	33.8	37.2	. . .	0.54	web
B1	. . .	7.0	. . .	. . .	. . .	2.4	. . .	flange
B2	. . .	23.0	. . .	. . .	. . .	2.0	. . .	flange & lateral
B3	. . .	22.5	. . .	. . .	. . .	2.2	. . .	flange & lateral
B4	. . .	29.0	. . .	. . .	. . .	. . .	. . .	lateral
B5	. . .	22.0	. . .	. . .	. . .	2.0	. . .	flange & lateral
B6	. . .	14.0	. . .	. . .	. . .	2.4	. . .	flange & lateral

can just be reached, and for $\alpha = 0.57$ (test D2) the section can be uniformly compressed up to the strain-hardening range. For a section subjected to axial load only, the first attainment of the yield stress is generally a sufficient requirement. In this case, therefore, the following recommendation can be given: If a section is subjected to an axial load only, the ratio of the distance between

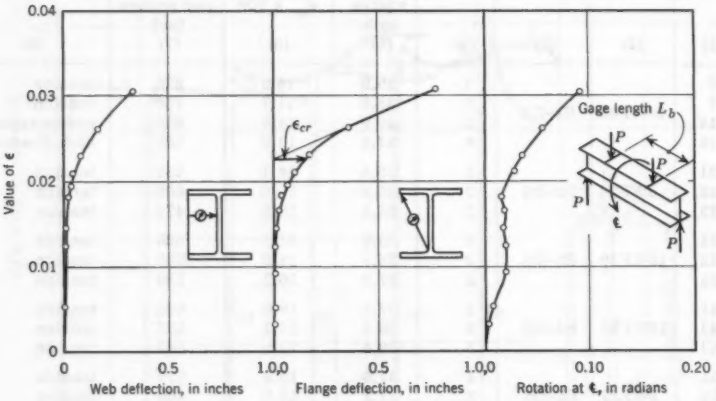


FIG. 16.—CURVES FOR LATERAL WEB AND FLANGE DEFLECTIONS AND LATERAL ROTATION

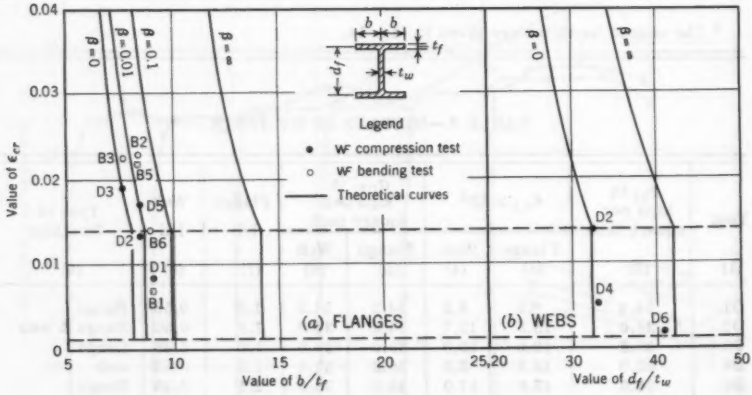
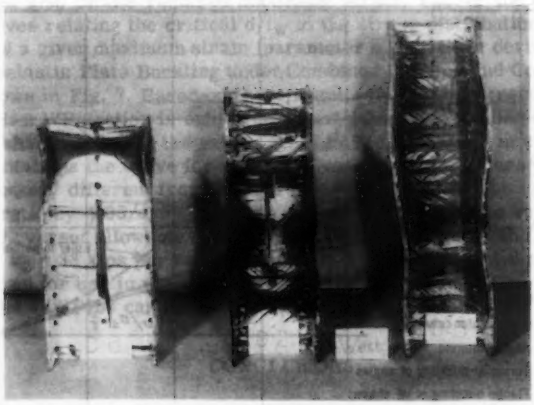


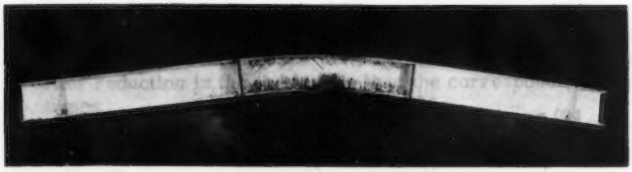
FIG. 17.—BUCKLING OF FLANGES AND WEBS OF WF SHAPES

the center planes of the flanges over the thickness of the web, d/t_w, shall not exceed the following values depending on the magnitude of the yield stress σ_0: for $\sigma_0 = 33$ kips per sq in., $d/t_w \leq 44$; and for $\sigma_0 = 36$ kips per sq in., $d/t_w \leq 42$.

Webs in Compression and Bending.—Wide-flange members subjected to axial load, P, and bending moment, M, may be required to deform plastically.



(*a*) SPECIMEN D6 (*b*) SPECIMEN D2 (*c*) SPECIMEN D5



(*d*) SPECIMEN B2



(*e*) SPECIMEN B5



(*f*) SPECIMEN B4

FIG. 18.—WIDE-FLANGE SPECIMENS AFTER TESTING

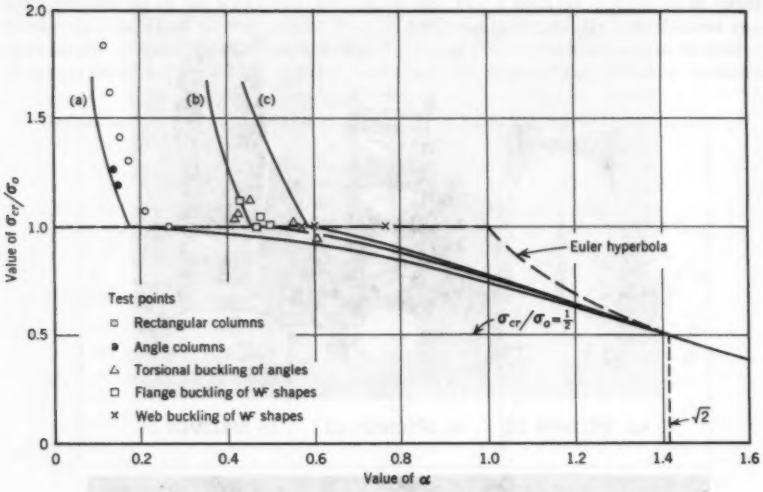


FIG. 19.—SUMMARY OF TEST RESULTS AND THEORY

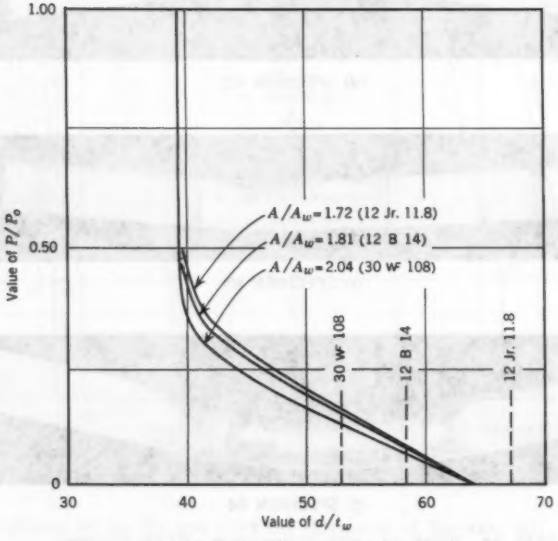


FIG. 20.—ALLOWABLE d/t_w OF THREE DEEP SECTIONS

The critical depth to thickness ratio, d/t_w, depends not only on the stress distribution but also on the required maximum strain, ϵ_m, of the compression flange. Curves relating the critical d/t_w to the stress distribution (parameter $p/\sigma_o A_w$) and a given maximum strain (parameter ϵ_m/ϵ_f) were derived under the heading "Inelastic Plate Buckling under Combined Bending and Compression," and are shown in Fig. 7. Based on these results the following recommendation is made: If a WF section is subjected to axial load and bending moment, the d/t_w ratio shall not exceed the values given in Fig. 7. Except in cases requiring large rotations the curve for $\epsilon_m/\epsilon_f = 4$ can be used. Values of d/t_w for a yield stress, σ_o, different from 33 kips per sq in., may be obtained by multiplying the ratio by $\sqrt{33/\sigma_o}$. From the curves of Fig. 7, three specific examples of P/P_o versus allowable (d/t_w)-ratios were investigated and are shown in Fig. 20 for $\sigma_o = 33$ kips per sq in. and $\epsilon_m/\epsilon_f = 4$. The 12Jr.11.8 section is not recommended for use in plastic design, the 12B14 section can be used if P/P_o 0.08, and the 36WF108 can be used if $P/P_o \leq 0.135$.

CONCLUSIONS

Columns and plates of structural steel can be compressed beyond the yield stress level and even into the strain-hardening range, provided certain geometric conditions are met. After a presentation of the discontinuous yielding process of structural steel, the values of these geometric conditions such as slenderness ratio l/r for columns and width-thickness ratio for plates were derived theoretically. Plates reach the strain-hardening range with a relatively smaller reduction in the (b/t)-ratio than the corresponding reduction in l/r for columns.

The findings were substantiated by a series of tests on rectangular bars in axial compression, on angles, and WF sections in compression, and on WF members in bending.

The results are used to specify the geometric cross-section proportions of WF beams so that these members may develop large plastic deformations without local buckling and a consequent fall-off in load. These latter requirements are essential for a successful application of plastic design methods.

ACKNOWLEDGMENTS

This investigation has been performed as part of the project "Welded Continuous Frames and Their Components" at the Fritz Engineering Laboratory, Lehigh University, Bethlehem, Pa.

The project was sponsored jointly by the Welding Research Council and the Department of the Navy, with funds furnished by the American Institute of Steel Construction, the American Iron and Steel Institute, the Column Research Council (Advisory), the Office of Naval Research, the Bureau of Ships, and the Bureau of Yards and Docks.

Mr. Paul C. Paris, A. M. ASCE, kindly supplied the test results shown in Fig. 2. The tests were performed by him and Dr. Thomas A. Hunter at the University of Michigan, Ann Arbor, under the direction of Prof. John A. Van den Broek.

The assistance of numerous Fritz Laboratory staff members throughout the investigation is greatfully acknowledged.

APPENDIX I. NOTATION

The following symbols, adapted for use in the paper and for the guidance of discussers, conform essentially with "American Standard Letter Symbols for Structural Analysis" (ASA Z10.8-1949), prepared by a committee of the American Standards Association with Society representation, and approved by the Association in 1949:

A = area:

A_w = area of web;

b_1 = width of plate with one free edge:

b_2 = width of plate supported along all four edges;

$D_x = \dfrac{E_x}{1 - \nu_x \nu_y}$;

$D_y = \dfrac{E_y}{1 - \nu_x \nu_y}$;

$D_{xy} = \nu_y D_x$;

$D_{yx} = \nu_x D_y$;

d = depth of web;

d_f = distance between center planes of flanges;

E = modulus of elasticity:

E_o = strain-hardening modulus;

E_r = reduced modulus;

E_{sec} = secant modulus = σ/ϵ

E_t = tangent modulus = $\dfrac{d\sigma}{d\epsilon}$;

E_x = tangent modulus in x-direction;

E_y = tangent modulus in y-direction;

G = modulus of elasticity in shear;

G_t = tangent modulus in shear;

I = moment of inertia;

K = coefficient in Eq. 18;

k = plate buckling coefficient;

L = length of column;

L_b = length of WF specimen subjected to pure bending;

L_c = length of WF compression specimen;

l = effective length of column;

l_p = half-wave length of buckled shape;

M = bending moment:

M_x = bending moment per unit width of plate in x-direction;

M_y = bending moment per unit width of plate in y-direction;

M_{xy} = torsional moment per unit width of plate;

m = exponent in Eq. 18;

n = exponent in Eq. 26;

n_{max} = maximum value of n defined by Eq. 27;

P = axial load;

P_o = $\sigma_o A$ = yield load;

r = radius of gyration;

t = thickness:

t_f = flange thickness;

t_w = web thickness;

w = plate deflection;

x = coordinate;

y_o = distance between neutral axis and compression flange;

Z = plastic section modulus;

α = dimensionless coefficient defined by Eqs. 24 and 25;

α_o = value of α at point of strain-hardening;

α_p = value of α at proportional limit;

β = coefficient of restraint;

γ = shear strain;

Δl = shortening of column;

ϵ = normal strain:

ϵ_{av} = average strain;

ϵ_{cr} = critical strain;

ϵ_f = yield strain;

ϵ_m = maximum strain of compression flange;

ϵ_o = strain at beginning of strain hardening;

ζ = coefficient determining extent of yielding;

θ = angle of lateral rotation;

ν = Poisson's ratio;

ν_x = coefficient of dilatation for stress increment in x-direction;

ν_y = coefficient of dilatation for stress increment in y-direction;

σ = normal stress:

σ_{cr} = critical (buckling) stress;

σ_e = elastic buckling stress;

σ_p = stress corresponding to limit of validity of elastic solution;

σ_o = yield stress;

σ_R = residual stress;

σ_r = reduced-modulus stress;

σ_t = tangent-modulus stress;

τ = shear stress;

ψ = edge moment per unit length to produce unit rotation of edge; and

ϕ = $\sqrt{G_{cr}/\sigma_e}$.

DISCUSSION

PAUL P. BIJLAARD,[13] F. ASCE.—The authors state in their dealings with buckling of structural steel plates in the horizontal part of the stress-strain diagram that from the mathematical theory of plasticity, the stress-strain relations should be of the incremental type, and that only the stress-strain law used by Handelman and Prager satisfies this condition, so that all other theories can be discarded. They refer to tests on combined compression and torsion on tubes of mild steel in the horizontal part of the stress-strain diagram that confirm the stress-strain laws of simple flow theory. They then derive formulas that apply to this special case, for which they refer mainly to another paper.[14]

---

[13] Prof. of Mechanics, Cornell Univ., Ithaca, N. Y.

[14] "Plate Buckling in the Strain-Hardening Range," by G. Haaijer, Transactions, ASCE, Vol. 124, 1959, pp. 117–148.

It can be shown that the authors' theoretical results are based on the writer's theory, as published in various papers.[15,16,17,18,19,20,21] The writer's theory, as also stated elsewhere,[22] includes both deformation and incremental theory. The stress-strain relations for simple flow theory, derived by George H. Handelman and William Prager, F. ASCE, in 1948, follow directly from the writer's theory, published in 1938. This is seen from the writer's papers[23,24] by assuming $e = \epsilon_p/\epsilon_e = 0$, in which ϵ_p and ϵ_e are the equivalent plastic and elastic strains at incipient buckling, and selecting the special case of uniaxial compression dealt with by G. H. Handelman and W. Prager ($\beta = 0$) or, with other notations, for $E_s/E = 1$, in which E_s is the secant modulus at incipient buckling.[19,20,21] In papers published before 1942, the writer's showed that deformation theory gave a lower bound for the buckling stress, admitting the possibility that for structural steel this might slightly underestimate the buckling stress.[25] For buckling below the yield point, the only case that had to be considered for structural steel, ϵ_p, was small, and, hence, e is small, so that incremental or flow theory gave only slightly higher results. Using deformation theory, the resulting buckling stresses were much higher than accorded to E. Chwalla's[26] theory (using the same plastic reduction factor for plates as for columns), which at that time (1938) in Europe was assumed to be right. It was also shown by experiments by C. E. Chase on steel plates that buckling at the yield point was in agreement with incremental theory.[27]

---

15 "A Theory of Plastic Buckling with its Application to Geophysics," by P. P. Bijlaard, Proceedings, Royal Netherlands Academy of Sciences, Amsterdam, Vol. 41, No. 5, 1938, pp. 468–480.

16 "A Theory of Plastic Stability and its Application to Thin Plates of Structural Steel," by P. P. Bijlaard, Proceedings, Royal Netherlands Academy of Sciences, Amsterdam, Vol. 41, No. 7, 1938, pp. 731–743.

17 "Theory of the Plastic Stability of Thin Plates," by P. P. Bijlaard, Publications Internatl. Assn. for Bridge and Structural Engrs., Zürich, Vol. 6, 1940–1941, pp. 45–69.

18 "Some Contributions to the Theory of Elastic and Plastic Stability," by P. P. Bijlaard, Publications Internatl. Assn. for Bridge and Structural Engrs., Zürich, Vol. 8, 1947, pp. 17–80.

19 "Theory and Tests on the Plastic Stability of Plates and Shells," by P. P. Bijlaard, Journal of the Aeronautical Sciences, Vol. 16, No. 9, 1949, pp. 529–541.

20 "On the Plastic Buckling of Plates According to the Flow Theory," by P. P. Bijlaard, Journal of the Aeronautical Sciences, Vol. 17, No. 12, 1950, pp. 810–811.

21 "Theory of Plastic Buckling of Plates and Application to Simple Supported Plates Subjected to Bending or Eccentric Compression in their Plane," by P. P. Bijlaard, Journal of Applied Mechanics," Vol. 23, No. 1, 1956, pp. 27–34.

22 "Handbook of Structural Stability, Part I—Buckling of Flat Plates," by G. Gerard and H. Becker, National Advisory Committee for Aeronautics Technical Note 3781, July, 1957.

23 "A Theory of Plastic Buckling with its Application to Geophysics," by P. P. Bijlaard, Proceedings, Royal Netherlands Academy of Sciences, Amsterdam, Vol. 41, No. 5, 1938, p. 480.

24 "A Theory of Plastic Stability and its Application to Thin Plates of Structural Steel;" by P. P. Bijlaard, Proceedings, Royal Netherlands Academy of Sciences, Amsterdam, Vol. 41, No. 7, 1938, p. 733.

25 Ibid., pp. 733–734.

26 "Report on the 2nd Internat'l Congress for Bridges and Structural Engineering, Vienna," by E. Chwalla, 1928, pp. 321–322.

27 "A Theory of Plastic Stability and its Application to Thin Plates of Structural Steel," by P. P. Bijlaard, Proceedings, Royal Netherlands Academy of Sciences, Amsterdam, Vol. 41, No. 7, 1938, p. 740.

In papers published after 1946 the writer concluded[18] from new tests by C. F. Kollbrunner[28] on aluminum alloy plates that, using deformation theory, the theoretical results were in agreement with these experiments. The theory was developed further for aircraft structures[19] and showed agreement with tests by the National Advisory Committee for Aeronautics (NACA) and others.[21] The theory is now used generally in aircraft design,[29,30] sometimes with E. Z. Stowell's simplification (Poisson's ratio in the elastic range is 0.5).[22]

In certain cases the deformation theory will lead to impossible results.[31] This does not mean that in the special case of buckling in which the ratio between stress components changes smoothly, the actual behavior cannot be similar to that which would follow from the deformation theory—although it may be different in cases other than buckling—that is, for nonlinear behavior. This behavior, which is in accordance with buckling tests on aluminum alloys, can be explained.[19,21] It does not conflict with the theory of plasticity.[32] It places the general behavior between deformation and simple flow (incremental) theories.[19,20] Although in the United States the flow theory is used for problems other than buckling, in Russia the deformation theory is used. The slip theory of S. B. Batdorf and Bernard Budiansky, M. ASCE, which is sound theoretically but was not confirmed completely by nonbuckling tests on compressed and twisted tubes, in the case of buckling also reduces to deformation theory.[33] The actual behavior of a polycrystalline metal under all kinds of stress variations could be predicted only by a theory based on such causes as the interaction of its dislocations and flaws. This theory does not exist, but as explained[19,21] for the special case of buckling of materials such as aluminum, magnesium, titanium alloys, and high-strength steels, and in an approximate way, also for mild steel below the yield point, the behavior is similar to that according to deformation theory (but may be generally incremental). As was shown[34] for aluminum the assumption of eccentricities, as suggested by E. T. Onat and Daniel C. Drucker,[35] F. ASCE, does not lead to an agreement between simple flow theory and buckling tests.

However, as observed elsewhere,[36] it is understandable that in the horizontal part of the stress-strain diagram of mild steel, which is considered by

---

28 "Das Ausbeulen der auf einseitigen, gleichmässig verteilten Druck beanspruchten Platten im elastischen und plastischen Bereich," by C. F. Kollbrunner, Mitt. a. d. Institut für Baustatik a. d. E.T.H., Zürich, No. 17, 1946.

29 "Plasticity Coefficients for the Plastic Buckling of Plates and Shells," by A. Krivetsky, Journal of the Aeronautical Sciences, Vol. 22, No. 6, 1955, pp. 432-435.

30 "Inelastic Buckling—From the Designer's Viewpoint," by E. E. Sechler, Journal of the Aeronautical Sciences, Vol. 23, No. 5, 1956, pp. 500-506.

31 "A Theory of Plastic Stability and its Application to Thin Plates of Structural Steel," by P. P. Bijlaard, Proceedings, Royal Netherlands Academy of Sciences, Amsterdam, Vol. 41, No. 7, 1938, p. 734.

32 "A Discussion of the Theories of Plasticity," by D. C. Drucker, Journal of the Aeronautical Sciences, Vol. 16, No. 9, 1949, pp. 567-568.

33 "Theories of Plastic Buckling," by S. B. Batdorf, Journal of the Aeronautical Sciences, Vol. 16, No. 7, 1949, pp. 405-408.

34 "On Theories of Plasticity and the Plastic Stability of Cruciform Sections," by P. P. Bijlaard and H. A. B. Wiseman, Journal of the Aeronautical Sciences, Vol. 20, No. 11, 1953, pp. 787-788.

35 "Inelastic Instability and Incremental Theories of Plasticity," by E. T. Onat and D. C. Drucker, Journal of the Aeronautical Sciences, Vol. 20, No. 3, 1953, pp. 181-186.

36 "Buckling of Columns, with Special Attention to Eccentricity, Plasticity and Local Buckling," by P. P. Bijlaard, Proceedings, 7th Technical Session of the Column Research Council, 1958, p. 55.

the authors, the behavior is close to simple flow (incremental) theory. The writer's explanation of the behavior of aluminum alloys[19,21] is based on the fact that, due to unavoidable small eccentricities or due to F. R. Shanley's principle of simultaneous action, the buckling stress increases during buckling. In the horizontal part of the stress-strain diagram this increase is impossible, so that the same case occurs as in a tube which, after being subjected to compression, is twisted while keeping the compressive stress constant. In this case, as follows from the authors' tests and also from earlier tests by K. Hohensmer and W. Prager[37] the material behaves in accordance with incremental theory. Hence, here the writer's theory applies, with e = 0 or $E_s/E = 1$.

The authors assume that in this horizontal part of the stress-strain diagram, the entire cross section behaves in a plastic way at buckling, based on a proof given elsewhere.[14] This has already been proved in a similar way by the writer.[38,39] This proof cannot be derived from F. R. Shanley's principle, because in the present case the direct stress does not increase during buckling.

The authors have said that until now it was assumed that at the yield stress a plate has no rigidity against buckling. The writer's theory on the plastic buckling of plates was actually developed with the purpose of showing that at the yield stress a plate still has considerable rigidity against buckling.[15,19,40]

For the basic equations (Eq. 9 and following) the authors could have used the writer's constants: $D_x = E\,A$; $D_y = E\,D$; $H = E\,(B + 2F)$; $D_{xy} = D_{yx} = E\,B$; and $G_t = E\,F$. The values A, B, D, and F, where in the present case e = 0 or E_s/E is one, can be obtained[19] as functions of E, E_t, ρ_1, ρ_2, and Poisson's ratio, ν, in the elastic range. In the authors' notations $\rho_1 = \sigma_x$ and $\rho_2 = \sigma_y$. Their value, $G_t = d\tau/d\gamma = 2{,}400$ kips per sq in., was obtained elsewhere.[41] Consequently,[42]

$$F = \frac{3}{4J_2}\left(\frac{1}{E_t} - \frac{1}{E}\right) \qquad (30)$$

Hence,[41]

$$\frac{d\gamma}{d\tau} = \frac{2\,(1+\nu)}{E} + 4F\tau^2 = \frac{2(1+\nu)}{E} + \frac{3}{J_2}\,\frac{E - E_t}{E\,E_t}\,\tau^2 \qquad (31)$$

Eq. 31 also appears elsewhere,[43]

$$\frac{\partial\gamma}{\partial\tau} = \frac{\partial\gamma_e}{\partial\tau} + \frac{\partial\gamma_p}{\partial\tau} = \frac{1}{G} + \frac{1}{G_p} + \frac{3\tau^2}{\sigma^2 G_p}\left(\frac{E_p}{\tan\phi}\right) - 1 \qquad (32)$$

---

37 "Beitrag zur Mechanik des bildsamen Verhaltens von Flusstahl," by K. Hohenemser und W. Prager, Zeitschrift für angewandte Mathematik und Mechanik, Vol. 12, 1932, pp. 1-14.

38 "A Theory of Plastic Buckling with its Application to Geophysics," by P. P. Bijlaard, Proceedings, Royal Netherlands Academy of Sciences, Amsterdam, Vol. 41, No. 5, 1938, p. 476.

39 "Theory of the Plastic Stability of Thin Plates," by P. P. Bijlaard, Publications Internatl. Assn. for Bridge and Structural Engrg., Zürich, Vol. 6, 1940-1941, p. 52.

40 "Some Remarks on Chapter IX and Some Other Items in Bleich 'Buckling Strength of Metal Structures'," by P. P. Bijlaard, Report, Column Research Council, 1952.

41 "Plate Buckling in the Strain-Hardening Range," by G. Haaijer, Transactions, ASCE, Vol. 124, 1959, Eqs. 49, 50.

42 Ibid., Eq. 39.

43 "Some Contributions to the Theory of Elastic and Plastic Stability," by P. P. Bijlaard, Publications Internatl. Assn. for Bridge and Structural Engrg., Zürich, Vol. 8, 1947, Eqs. 10, 18.

whereas in the authors' notations,[44]

$$E_p/G_p = 3;\ \sigma^2 = \frac{3}{2} S_1^2 = 3J_2;\ \text{and}\ \tan\phi = \frac{E\,E_t}{E - E_t}.$$

In the present case, $e = E/E_p = 0$, or $E_p = G_p = \infty$, so that

$$\frac{\partial\gamma}{\partial\tau} = \frac{1}{G} + \frac{9\tau^2}{3J_2}\frac{E - E_t}{E\,E_t} = \frac{2(1+\nu)}{E} + \frac{3}{J_2}\frac{E - E_t}{E\,E_t}\tau^2 \quad \ldots\ldots\ldots (33)$$

which is identical to Eq. 31. In the same way other equations,[45] from which the authors' values D_x, D_y and D_{xy} are computed, are identical to the writer's equations.[46]

Reference is made to Eqs. 10 to 17 which could have been obtained directly from another source,[47] in which the plastic reduction factors, η, are given, and have to be multiplied by the elastic buckling stress, σ_e, to obtain the plastic buckling stresses, σ_{cr}. This would have avoided the errors that occur in case 2.

Cases 1, 3, and 4 will be considered using another source.[48]

1. Loaded edges $x = 0$ and $x = l$ are hinged, unloaded edge $y = 0$ are hinged, and unloaded edge $y = b$ is free. With $\nu = 0.3$

$$\sigma_{cr} = \eta\sigma_e = 2.6\ F\ G\left(\frac{t}{b}\right)^2 = 2.6\ F\ \frac{E}{2.6}\left(\frac{t}{r}\right)^2 = G_t\left(\frac{t}{r}\right)^2 \quad \ldots\ldots (34)$$

in accordance with Eq. 11. The more general Eq. 10 is to be found elsewhere.[49]

2. Loaded edges $x = 0$ and $x = l$ are hinged, and unloaded edges $y = +\,d/2$ are hinged.

$$\sigma_{cr} = \eta\sigma_e = 0.455\left(\sqrt{AD} + B + 2F\right)\frac{4\pi^2 E}{12\left(1 - \nu^2\right)}\left(\frac{t}{d}\right)^2$$

$$= \frac{\pi^2}{12}\left(\frac{t}{d}\right)^2\left(2\sqrt{D_x D_y} + 2D_{xy} + 4G_t\right) \quad \ldots\ldots\ldots\ldots (35)$$

in accordance with Eq. 15, because $D_{yx} = D_{xy}$.

3. The unloaded edges $y = \pm\, d/2$ are fixed.

$$\sigma_{cr} = \eta\sigma_e = \left[0.598\sqrt{AD} + 0.312\,(B + 2F)\right]\frac{6.99\,\pi^2 E}{12\left(1 - \nu^2\right)}\left(\frac{t}{d}\right)^2$$

$$= \frac{\pi^2}{12}\left(\frac{t}{d}\right)^2\left[4.60\sqrt{D_x D_y} + 2.40\left(D_{xy} + 2G_t\right)\right] \quad \ldots\ldots\ldots (36)$$

which is practically in accordance with Eq. 17.

---

44 "Theory and Tests on the Plastic Stability of Plates and Shells," by P. P. Bijlaard, Journal of the Aeronautical Sciences, Vol. 16, No. 9, 1949, p. 536.

45 "Plate Buckling in the Strain-Hardening Range," by G. Haaijer, Transactions, ASCE, Vol. 124, 1959, Eqs. 51, 52.

46 "Some Contributions to the Theory of Elastic and Plastic Stability," by P. P. Bijlaard, Publications Internatl. Assn. for Bridge and Structural Engrg., Zürich, Vol. 8, 1947, Eqs. 19.

47 "Theory and Tests on the Plastic Stability of Plates and Shells," by P. P. Bijlaard, Journal of the Aeronautical Sciences, Vol. 16, No. 9, 1949, Table 5.

48 Ibid.

49 "Some Contributions to the Theory of Elastic and Plastic Stability," by P. P. Bijlaard, Publications, Internatl. Assn. for Bridge and Structural Engrg., Zürich, Vol. 8, 1947, Eq. 34.

4. Unloaded edge y = 0 is fixed, and unloaded edge y = b is free.

$$\sigma_{cr} = \eta\sigma_e = 0.473\left(\sqrt{AD} + 2.97\ F - 0.405\ B\right)\frac{1.28\pi^2\ E}{12\left(1 - \nu^2\right)}\left(\frac{t}{d}\right)^2$$

$$= \left(\frac{t}{d}\right)^2 = \left(0.546\ \sqrt{D_x\ D_y} - 0.221\ D_{xy} + 1.62\ G_t\right) \ldots\ldots\ldots (37)$$

In contrast, the authors obtain in their Eq. 13,

$$\sigma_{cr} = \left(\frac{t}{d}\right)^2\left(0.769\ \sqrt{D_x\ D_y} - 0.54\ D_{xy} + 1.712\ G_t\right) \ldots\ldots\ldots (38)$$

which is similar to another form of this equation.[50] It is obvious that Eq. 13 must be in error, because in the elastic range it does not reduce to the elastic buckling stress,

$$\sigma_{cr} = 1.28\ \frac{\pi^2\ N}{d^2 t} = 1.16\ E\left(\frac{t}{d}\right)^2 \ldots\ldots\ldots\ldots (39)$$

In the elastic range $D_x = D_y = E/\left(1 - \nu^2\right)$, $D_{xy} = E\nu/\left(1 - \nu^2\right)$, and $G_t = G = E/(2 + 2\nu)$, so that, with $\nu = 0.3$, Eq. 13 yields $\sigma_{cr} = 1.325\ E\left(\frac{t}{d}\right)^2$.

The authors' method of computation, requiring the assumption of unknown eccentricities for determining the buckling stress or critical strain, is somewhat arbitrary. For example, their value G_t = 2,400 kips per sq in. is based on another source,[51] from which G_t could have been chosen as well as 1,500 or 3,000 kips per sq in. Their method is therefore not useful for predicting the critical strains, but their results have to be based on tests. The authors should be complimented on their careful and important experiments, on which their selection of the values for G_t, D_x, D_y, and D_{xy} is mainly based.

GEERHARD HAAIJER,[52] M. ASCE, and BRUNO THÜRLIMANN,[53] M. ASCE.—Mr. Bijlaard is correct in pointing out that Eq. 13 does not reduce to the elastic buckling stress when the elastic moduli are substituted. Eq. 13 was derived for the strain-hardening range of mild steel.[5] In the strain-hardening range, Mr. Bijlaard's formula gives slightly larger values for the critical stress than does Eq. 13. Because of the small value of the tangent modulus, however, the differences in critical strain values would be considerable.

Furthermore, Mr. Bijlaard's discussion corrects the statement made by the writers that his theory is of the deformation type. Although his theory, as it is used today in aircraft design, is a deformation theory, the complete theory as published in 1938 includes both deformation and incremental theory.

Mr. Bijlaard has been able to reduce all subsequent contributions to inelastic plate buckling, such as the papers by Ilyushin,[54] Stowell,[55] Handelman-Prager,[10] and the one by the writers, to his original theory.

---

[50] "Plate Buckling in the Strain-Hardening Range," by G. Haaijer, Transactions, ASCE, Vol. 124, 1959, Eq. 15.

[51] Ibid., Fig. 10.

[52] Research Engr., Applied Research Lab., U. S. Steel Corp., Monroeville, Pa.

[53] Prof. of Structural Engrg., Swiss Federal Inst. of Technology, Zurich, Switzerland.

[54] "Stability of Plates and Shells Beyond the Proportional Limit," by A. A. Ilyushin, National Advisory Committee for Aeronautics Technical Memorandum 116, October 1947.

[55] "A Unified Theory of Plastic Buckling of Columns and Plates," by E. Z. Stowell, National Advisory Committee for Aeronautics Report No. 898, 1948.

Concerning the writers' paper, it may be well to quote Mr. Bijlaard's own statement presented at the Annual Meeting of the Column Research Council, May, 1957.[36]

> "The writer's theory" [Mr. Bijlaard's theory] "of plastic buckling of plates is in excellent agreement with test results with aluminum plates. It is also in good agreement with tests on structural steel for small plastic deformations as occur below the yield stress. However, in the horizontal part of the stress strain diagram at the yield stress where the material flows in layers and this behaves discontinuously, in contrast with the continuous behavior assumed in the theory, it obviously does not apply and is too conservative, as was pointed out for columns in reference 16. This was taken into account by using the requirements $b/t < 8.5$ and 34 from reference 8 for hinged flanges and plates where large strains at the yield stress are necessary."[56,57]

References 16 and 8 in the quoted material correspond to footnotes 54, 55 given herein.

This statement implies that Mr. Bijlaard himself did not feel that his theory would be extended to the case treated by the writers in their paper.

Instead of starting from a general theory of plasticity, the writers determined expressions for the plate buckling stresses based on orthotropic behavior of the material. Agreement should exist between these expressions and others based on plastic reduction factors that imply proper orthotropic behavior. The advantage of giving general expressions for the buckling strength of orthotropic plates was to indicate clearly the influence of the various stiffness factors that are involved. This approach enabled the writers to show the source of differences in the buckling stresses predicted by various theories (see Table 1).

The writers sincerely appreciate Mr. Bijlaard's careful review and discussion of their paper.

---

[56] "Exact Computation for the Buckling of the Webs of Truss Members Used in Bridge Building," by P. P. Bijlaard, De Ingenieur in Nederlands Indie, No. 2, 1939, pp. 1,17–1,23.

[57] "Plastic Design in Structural Steel," by L. S. Beedle, B. Thürlimann, and R. L. Ketter, A.I.S.C., New York, N. Y., September, 1955.

AMERICAN SOCIETY OF CIVIL ENGINEERS

Founded November 5, 1852

TRANSACTIONS

Paper No. 3024

HYDRAULIC DESIGN OF COLUMBIA RIVER NAVIGATION LOCKS

By George C. Richardson,[1] and Marvin J. Webster,[2] Fellows, ASCE

SYNOPSIS

Some of the highest lift navigation locks in the world are located on the Columbia River Basin Projects. Locks at McNary Dam on the Columbia River, near Plymouth, Ore.-Wash., and The Dalles Dam on the Columbia River, near Dalles, Ore.-Wash., have maximum lifts of 92 and 90.5 ft, respectively. These will be exceeded for a brief period by the new Wilson lock on the Tennessee River near Sheffield, Ala., which will have a lift of 101 ft. The Ice Harbor lock near Pasco, Wash., on the Snake River, the main tributary of the Columbia River, will have a maximum lift of 103 ft when completed in 1961. This in turn will be exceeded by the John Day Lock on the Columbia River, near Arlington, Ore.-Wash., scheduled for completion in 1966, which will have a maximum lift of 113 ft. Many recently developed improvements are incorporated in the design of the hydraulic systems for these locks. As a result of the increased lock lifts, the rapidly expanding volume of traffic and the demands of the navigation interests, the designers have been forced to develop many of these improvements, frequently with the aid of hydraulic model studies. The tremendous improvements in the filling systems are reflected by the almost complete lack of turbulence in the lock chambers of McNary and The Dalles locks, as compared to the very turbulent condition in the Bonneville lock on the Columbia River, near Portland, Ore. The model studies indicate that even less turbulence will occur in the Ice Harbor lock.

INTRODUCTION

The Columbia River has a project depth of 35 ft from its mouth to the mouth of the Willamette River near Portland, Oregon, and 30 ft to Vancouver, Wash-

Note.—Published, essentially as printed here, in September, 1958, in the Journal of the Waterways and Harbors Division, as Proceedings Paper 1773. Positions and titles given are those in effect when the paper was approved for publication in Transactions.

[1] Chf., Hydr. Design Sect., Corps of Engrs., City-County Airport, Walla Walla, Wash.

[2] Chf., Hydr. Sect., Corps of Engrs., Pittock Block, Portland, Ore.

ington. The project depth from Vancouver to Bonneville is 27 ft, but, the channel has not been maintained to this depth. The depth of the pool above Bonneville Dam to The Dalles Dam is 30 ft or more. Although the navigation lock at Bonneville was designed and built to accommodate ocean-going vessels, traffic upstream from Vancouver has been limited to barge tows.

This paper is limited to a brief description of the hydraulic systems of the navigation locks at Bonneville, McNary, The Dalles, and Ice Harbor, to a comparison of the approaches to the Bonneville, McNary, and The Dalles locks, and to a few problems encountered during their operation. Bonneville lock was placed in operation in 1938, McNary in 1953, and The Dalles in 1957. The Ice Harbor lock is scheduled to be ready for river traffic in 1961. Locations of these projects are shown in Fig. 1, and data on existing and proposed locks in the Columbia River Basin are given in Table 1.

BONNEVILLE NAVIGATION LOCK

Bonneville Dam is situated approximately 146 miles upstream from the mouth of the Columbia River. The navigation lock, on the Oregon side, is 76 ft wide, has a usable length of 500 ft and a depth of 24 ft over the lower sill at normal low water. The normal lift of the lock is approximately 58 ft, but the lift can vary from 66.5 ft at low water to 30 ft at extreme high water.

The hydraulic system shown in Fig. 2(a) is similar in design to the first Keokuk lock on the Mississippi River, near Keokuk, Iowa, and to the locks in the Panama Canal. The lock chamber fills and empties through circular openings in the floor of the chamber. Water enters the lock from the powerhouse forebay through two intakes in the river side of the north or river wall. The two intake culverts, each equipped with a 7.0-ft by 11.5-ft tainter valve, lead into a 14-ft-diam longitudinal central culvert beneath the floor of the lock with branches leading to 41 ports, each 4 ft in diameter. The total area of the lock chamber ports is 515 sq ft and the ratio of port area to culvert area at the filling valves is 3.2 to 1. The lock empties through the same culvert system leading to two 7.0-ft by 11.5-ft tainter valves near the downstream end of the lock. The water discharges into the lower pool through five 6.0-ft by 7.0-ft vertical ports located immediately downstream from the miter gates. The lock chamber is equipped with three floating mooring bits in each wall.

There is extreme turbulence in the lock chamber during filling with normal operation of the filling valves as shown in Fig. 3. The valves, of the conventional tainter type with skin plates facing upstream, were designed to open in 2.3 min. Considerable air enters the lock through vortices at the intakes and through the valve shafts. To reduce turbulence in the lock chamber when locking all types of traffic, the filling valves are opened to the 1/4 position and the chamber filled to approximately El 30. The valves are then opened to the 1/2 position and the chamber filled to approximately El 40, after which time the valves are fully opened. (Normal tailwater is El 14.) This increases the filling time for the normal lift of 58 ft from 11.5 min to almost 15 min.

The emptying valves, also conventional tainter type, are opened to full open position in 2.3 min. Flow from the large vertical discharge ports shoots several feet above tailwater, causing a reduction in the effective head. Emptying time is 13.3 min for normal operation with a head of 58 ft, approximately 2 min longer than the filling time. The violent action of the water during emptying washes sand and gravel against the downstream side of the miter gates, which

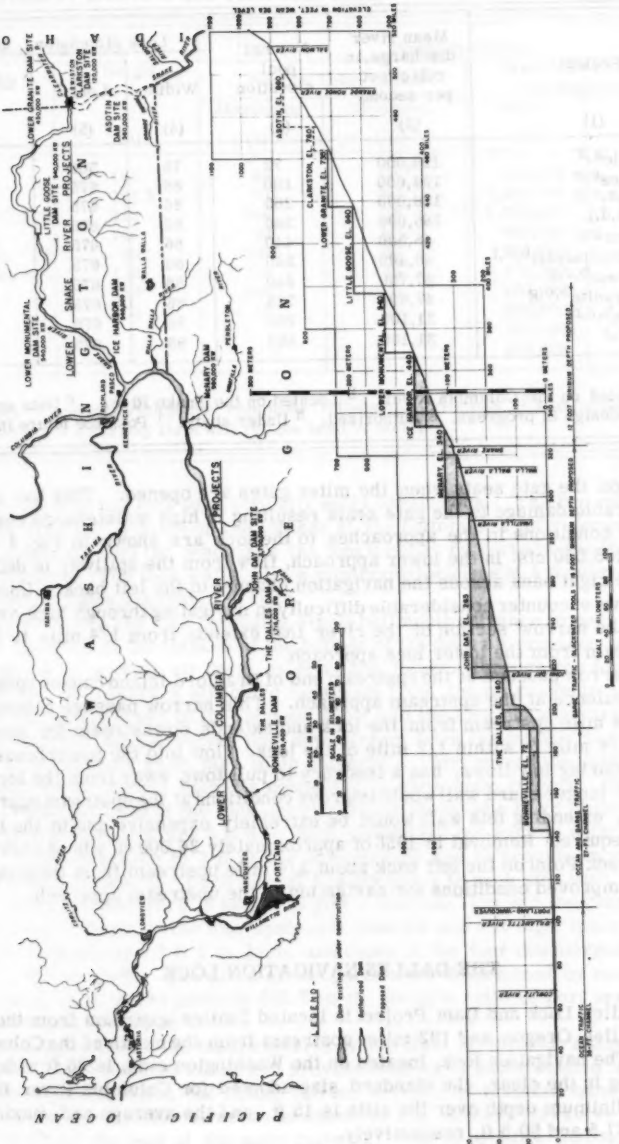


FIG. 1.—COLUMBIA RIVER BASIN PROJECTS

TABLE 1.—NAVIGATION AND POWER

Project	Mean river discharge, in cubic feet per second	Normal pool elevation	Lock dimensions, in feet		
			Width	Length	Maximum lift
(1)	(2)	(3)	(4)	(5)	(6)
Bonneville[a,d]	199,000	72	76	500	66.5
The Dalles[a,e]	194,000	160	86	675	90.5
John Day[a,c,e]	188,000	265	86	675	113
McNary[a,d,j]	185,000	340	86	675	92
Ice Harbor[b,e]	48,500	440	86	675	103
Lower Monumental[b,c,f]	48,400	540	86	675	103
Little Goose[b,c,g]	47,700	640	86	675	103
Lower Granite[b,c,g]	47,600	735	86	675	98
Clarkston[b,c,h]	31,100	760	86	675	48
Asotin[b,c,h]	31,100	860	86	675	103

[a] Located on the Columbia River. [b] Located on the Snake River. [c] Data are preliminary design in progress. [g] Authorized. [h] Under study. [i] Possible future increase

deposit on the gate seats when the miter gates are opened. This has caused considerable damage to the gate seals resulting in high maintenance costs.

Flow conditions in the approaches to the lock are shown in Fig. 4 with a flow of 185,000 cfs. In the lower approach, flow from the spillway is deflected from the right bank across the navigation channel to the left bank. Upstream bound tows encounter considerable difficulty in navigating through high-velocity flow in the narrow section of the river that extends from 1/4 mile to 1 mile downstream from the lower lock approach.

The narrow passage at the upstream end of Bradford Island causes considerable turbulence at the upstream approach. This narrow passage commences about 3/4 mile upstream from the lock and extends downstream for approximately 1/4 mile to within 1/2 mile of the lock. Flow into the powerhouse, especially during low flows, has a tendency to pull tows away from the lock entrance. A longer guard wall would improve conditions at the upstream approach. However, extending this wall would be extremely expensive due to the height of wall required. Removal in 1958 of approximately 26,000 cu yds of rock from Eagle Creek Point on the left bank about 3/4 mile upstream from the lock only slightly improved conditions for navigation in the upstream approach.

THE DALLES NAVIGATION LOCK

The Dalles Lock and Dam Project is located 3 miles upstream from the city of The Dalles, Oregon, and 192 miles upstream from the mouth of the Columbia River. The navigation lock, located on the Washington side, is 86 ft wide and 675 ft long in the clear, the standard size adopted for Columbia River Basin locks. Minimum depth over the sills is 15 ft, and the average and maximum lifts are 87.5 and 90.5 ft, respectively.

The hydraulic system for the lock is shown in Fig. 5. It was necessary to vary the design somewhat from the conventional hydraulic system because of

FACILITIES AT EXISTING AND PROPOSED DAMS

Lower lock gates		Power facilities			
Type	Height, in feet	Normal head, in feet		Installed capacity, in kilowatt hours	
		Maximum	Minimum	Initial	Ultimate
(7)	(8)	(9)	(10)	(11)	(12)
Miter	102	68	26	518,000	1,000,000[i]
Miter	107.5	91	60	1,092,000	1,716,000
Vertical Lift	113	104	78	1,080,000	2,700,000
Miter	106	92	62	980,000	1,400,000[i]
Vertical Lift	89	102	77	270,000	540,000
Vertical Lift	112	100	75	270,000	540,000
	119	100	85	270,000	540,000
	101	85	59	225,000	450,000
				120,000	160,000
				360,000	450,000

liminary. [d] Initial development complete. [e] Under construction. [f] Authorized and preconsidered. [j] John Day Dam will reduce head at McNary.

the location of the lock in practically solid basalt rock. The two major variations were the location of the intakes at the bottom of a pit riverward of the lock entrance, and the placing of the longitudinal culverts in the floor of the lock chamber. The lock walls, with a minimum thickness of 4 ft, were anchored to vertical faces excavated in rock.

Water enters the lock through a single bellmouth entrance in each main culvert. Location of the intakes at the bottom of the deep pit provides ample submergence to prevent air from entering the intakes through the formation of vortices. A trashrack structure upstream from the pit prevents trash from entering the approach to the intakes. Flow into the lock chamber is controlled with reversed tainter valves just downstream from the intakes in each of the two 12-ft-wide by 14-ft-high main culverts. Flow enters the lock chamber through seven lateral culverts connected to each main culvert. The lateral culverts in the floor of the lock are grouped in the middle third of the chamber. The lateral culverts are 5 ft 6 in. high throughout but vary in width from 5 ft 6 in. at the entrance to 2 ft at the downstream end to provide more uniform flow from the lateral. Each lateral has six ports in each side wall. All ports are 16 in. wide but vary in height to give a uniform flow into the chamber during filling. Ports in the four upstream laterals are 4 ft high, those in the six center laterals are 3 ft 1 in. high, and those in the four downstream laterals are 1 ft 9 in. high. The sizes of the ports were determined by model study. The total area of the ports is 663.8 sq ft, giving a ratio of port area to main culvert area of 1.98 to 1.

Although placing the main culverts in the floor of the lock chamber saved considerable rock excavation and provided sufficient submergence to eliminate negative pressures at the filling valves, it required a double bend at the entrances to the lateral culverts. As shown in Fig. 6, these entrances extend the full width of the roof of the main culverts. There is little turbulence in the lock chamber during filling. The lock chamber is equipped with four floating mooring bits in each wall.

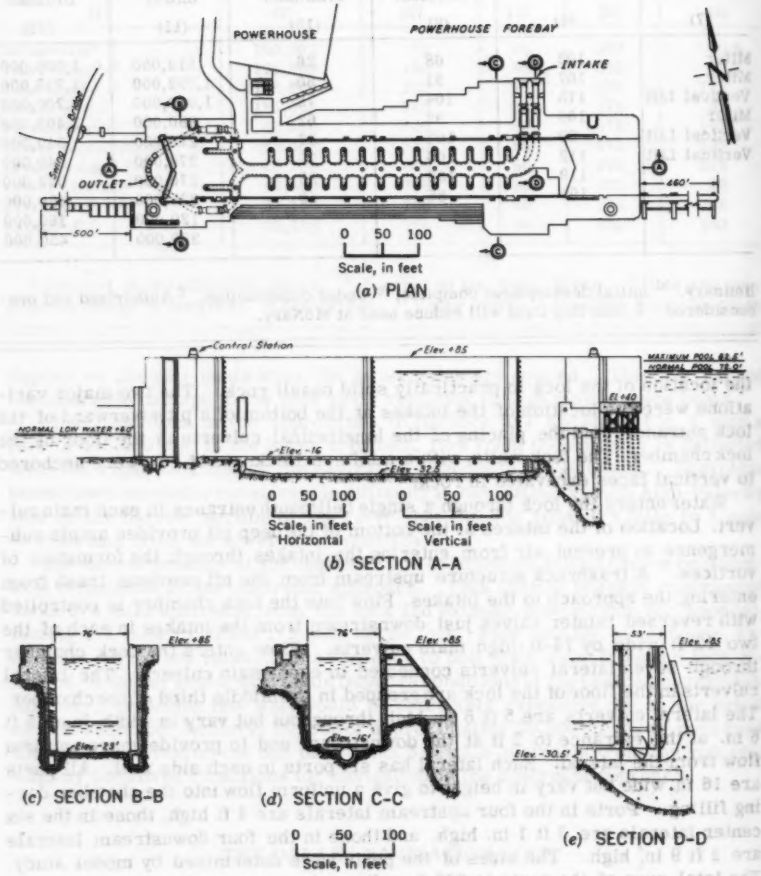


FIG. 2.—BONNEVILLE DAM NAVIGATION LOCK



FIG. 3.—TURBULENCE IN BONNEVILLE LOCK DURING FILLING



FIG. 4.—BONNEVILLE DAM

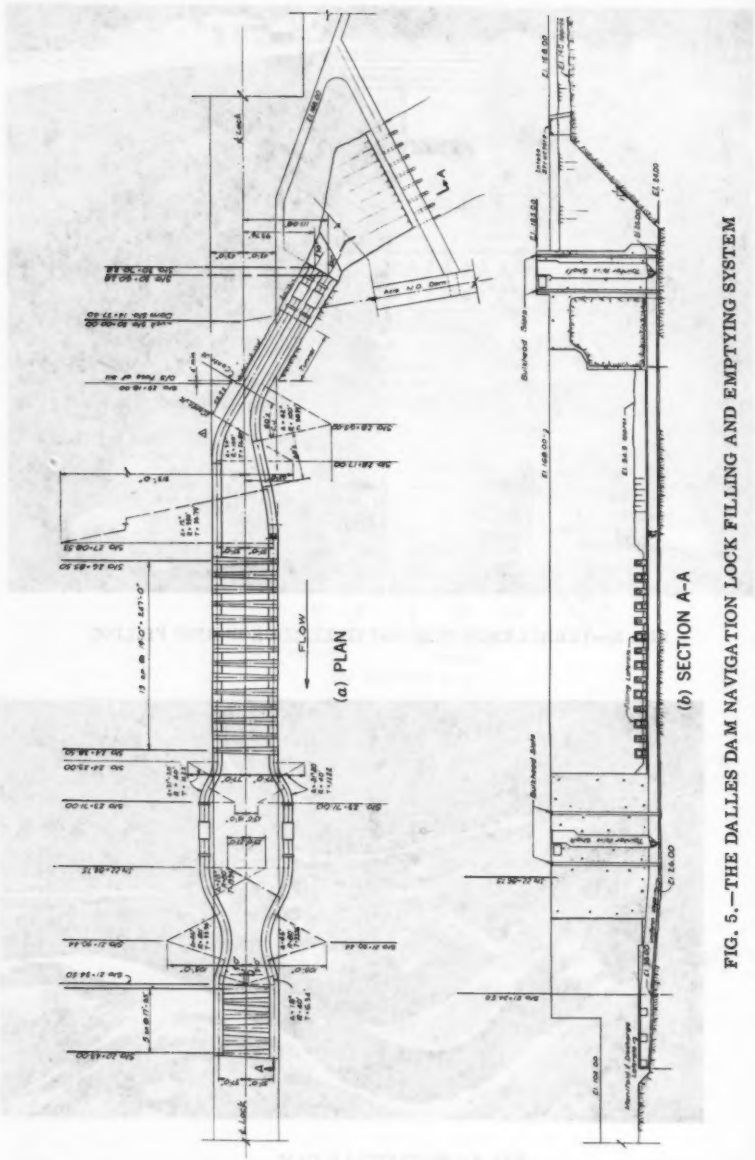


FIG. 5.—THE DALLES DAM NAVIGATION LOCK FILLING AND EMPTYING SYSTEM

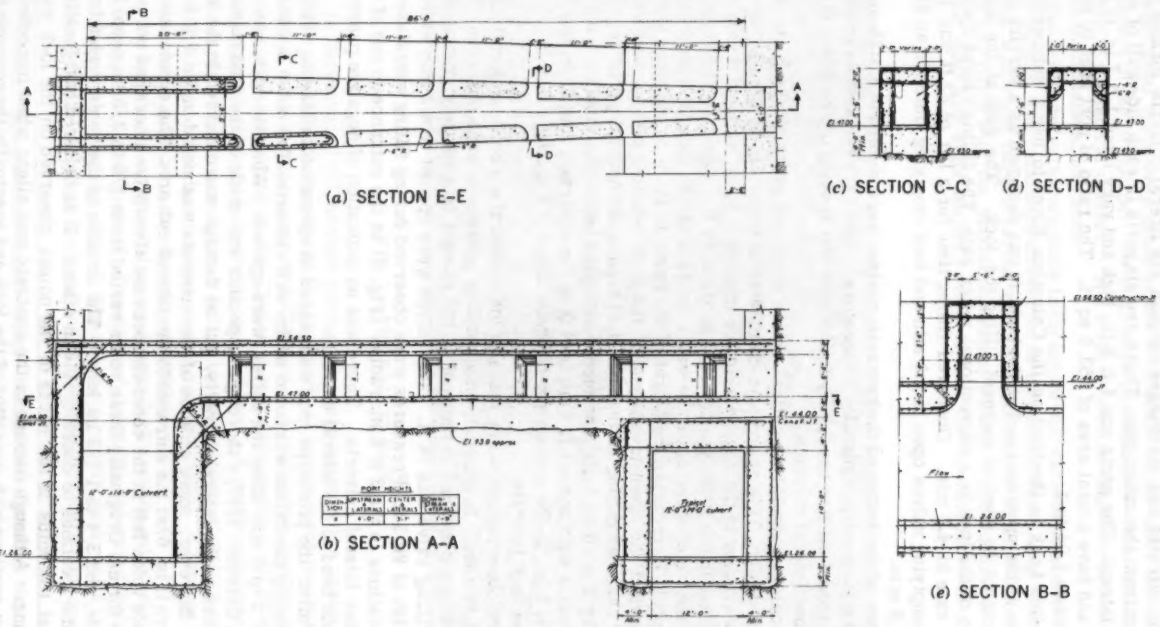


FIG. 6.—THE DALLES DAM NAVIGATION LOCK FILLING LATERALS AND CULVERT

Flow from the lock during emptying is controlled by reversed tainter valves in the main culverts and discharges through six lateral culverts located just downstream from the miter gate. There are six ports in each side wall of each discharge lateral. The ports are 4 ft 8 in. high and vary from 1 ft 7 in. to 2 ft 3 in. wide and have a total area of 653.5 sq ft. The ratio of port area to main culvert area is 1.94 to 1.

The Dalles Lock is the first on the Columbia River to use a submergible tainter gate at the upstream end of the lock. It was designed as a service gate only and cannot be used to augment filling the lock. The gate at the downstream end of the lock is a conventional miter gate. The filling valves open at a uniform rate in 4.2 min. Observed filling time for a lift of 82 ft was 10.7 min. The emptying valves open in 2.1 min and lock emptying time for an 82-ft head is 11.5 min.

All phases of the design of the hydraulic system were studied in a 1:25-scale model at the Bonneville Hydraulic Laboratory. Several revisions were made during the model studies especially in the size and spacing of the ports in the lock chamber lateral culverts.

The model indicated that vortical action occurred at the intake ports with the original design. This action was eliminated in the model by simulating additional excavation in the approach to the intakes. Some vortical action has been observed in the prototype for lifts to about 85 ft. However the action is slight and does not occur until the water surface in the lock is within 5 ft of the upper pool. Decreasing the height of the ports in the lock chamber lateral culverts toward the downstream end of the lock resulted in less turbulence in the lock chamber during filling. In the original design, all ports were 1 ft 4 in. wide by 2 ft 10 in. high. The model indicated better distribution from the lateral culverts with ports 1 ft 4 in. by 4 ft in the upstream four laterals, 1 ft 4 in. by 3 ft 1 in. in the center six laterals and 1 ft 4 in. by 1 ft 9 in. in the downstream four laterals.

Pressure observations were made in the model at all critical locations in the culvert system. In general, only positive pressures were observed. The lowest pressure observed in the roof of the culvert immediately downstream from the filling valve was +4 ft. The valves were opened in 4.2 min with the maximum lift of 90.5 ft. Pressures were observed during filling operations at several locations in the 3 ft 6 in. radius (Fig. 6) in the entrance to one of the lock chamber lateral culverts. There was no indication of negative pressure in the double bend to the lateral culverts.

Shortly after the prototype lock was placed in operation in March, 1957, a noise indicating cavitation was noted in the wall culverts. The noise lasted for a period of 2 to 3 min after the valves were opened. When the lock was unwatered in October, 1957, a thorough inspection was made of the wall culverts and entrances to the lateral culverts, but no damage was observed in the wall culverts. However, some erosion of the concrete was noted in the 3 ft 6 in. radius curve (Fig. 6) at the entrance to the lateral culverts. The erosion started in surface voids left in the concrete, because absorptive liners had not been used in the forms. Originally these voids varied from 1/8 to 3/8 in. deep, 1/2 to 1 in. wide, and 3/4 to 1 1/2 in. long. The erosion of the voids varied from none in some locations to considerable in others. It is believed that localized cavitation at the voids is the cause of the noises observed on the lock walls during filling. Although damage to the concrete was slight when inspected in 1957, it may continue with operation of the lock and eventually the concrete entrances to the lateral culverts may have to be replaced. Absorptive form liners

would have eliminated the surface voids and their use is highly recommended at similar locations in future locks.

Additional tests were made in the 1:25 scale model after the damage was observed in the prototype. Several more piezometers were added at the entrance to the lateral culvert. The tests showed no negative pressures at any point in the lateral entrance.

Hawser force tests were made in the model with various numbers of standard-size barges. The maximum hawser force measured was a longitudinal force of 8 tons with eight barges having a total displacement of 11,040 tons when the lock was filled with the maximum head of 90.5 ft. The maximum transverse force, also with eight barges, was 4 tons at the downstream end of the barge tow.



FIG. 7.—THE DALLES DAM

In December, 1957, hawser force tests were made in the prototype locks at McNary and The Dalles Dams.[3] Longitudinal forces were measured on a tow having a total displacement of 2,780 tons. A maximum longitudinal force of 3.2 tons was measured at The Dalles during filling with a lift of 84.6 ft. The maximum force during emptying was 1.1 ton. A maximum force of 2.8 tons was measured in the model in a filling test simulating prototype conditions for satisfactory correlation between model and prototype. A hawser test was not made in the model for an emptying operation.

The approaches to The Dalles navigation lock provide satisfactory conditions for navigation. The general alinement of the guide and guard walls are shown in the aerial photograph, Fig. 7. The concrete gravity guide walls are in straight alinement with and are a continuation of the right lock wall. The upstream guide

[3] Report: "Hawser Force Measurements—The Dalles and McNary Navigation Locks," Bonneville Hydraulic Loaboratory, March 31, 1958.

wall extends 686 ft upstream from the upper lock gate. The downstream guide wall extends 1020 ft downstream from the miter gate.

The alinements of the guard walls were based on studies in a 1:80-scale river model at the Bonneville Hydraulic Laboratory. The upstream guard wall is of concrete gravity construction, extends approximately 1165 ft upstream from the upper lock gate, and is flared to a width of 307 ft at the upstream end of the approach to provide easy access to the lock. The downstream guard wall is of rock fill construction and flares to a protected channel width of 250 ft at a point 645 ft downstream from the miter gate. The guard wall extends a total distance of 1320 ft downstream from the miter gate.

The upper limit of navigation at The Dalles Dam is 800,000 cfs. Model tests indicate maximum velocities of 6 to 7 fps at the upstream end of the upper guard wall and 6 to 8 fps at the downstream end of the lower guard wall for this discharge.

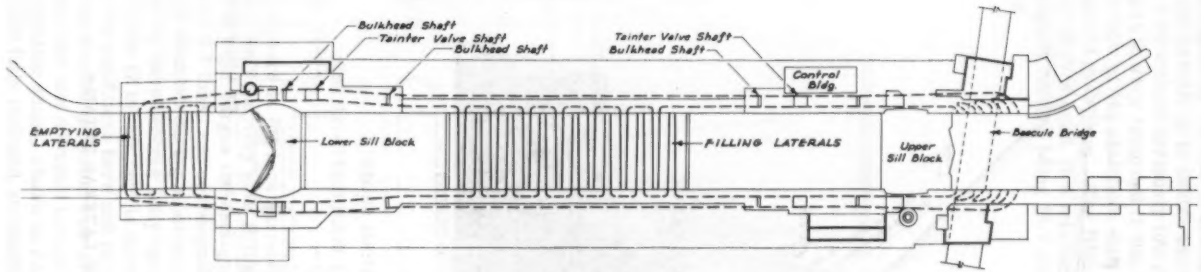
McNARY NAVIGATION LOCK

The first lock conforming to the now accepted standard size (86 by 675 ft) for Columbia River Basin locks was constructed at McNary Dam, 292 miles above the river's mouth. It is situated at the foot of the former Umatilla rapids, 2.5 miles above Umatilla, Ore. It provides slack-water navigation 36 miles upstream to Pasco and Kennewick, Wash. and 10 miles up the Snake River to Ice Harbor Dam. The lock was placed in operation in 1953 under normal pool elevation and has a maximum design lift of 92 ft. At that time it was the highest single-lift lock in operation, now (1960) surpassed by the new Wilson Lock in the T.V.A.

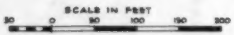
Filling the lock is accomplished by means of a bottom-lateral system, as shown in Fig. 8. The wall culverts are 11 by 12 ft in size, the intakes consist of four 11 ft 6 in. by 14 ft 9 in. openings in each wall immediately above the sill block. Both filling and emptying valves are reversed tainter valves, as seen on Fig. 9. There are seven lateral culverts extending from each wall culvert, each of which has 12 ports 1 ft 2 in. by 2 ft 6 in. (see Fig. 10). The entire lateral system is located in the central third of the lock chamber. The laterals are 5 ft by 5 ft at the entrance, tapering uniformly by 2 ft by 5 ft. The ratio of total port area to culvert area is 1.86 to 1.

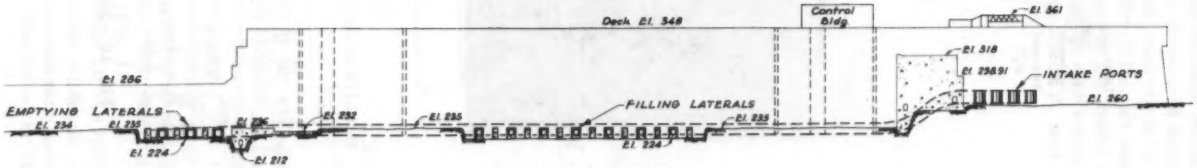
The emptying system consists of a continuation of the 11 by 12 ft culverts into the downstream approach walls, where three laterals from each culvert extend into the floor of the approach channel. Each discharge lateral is tapered from 8 ft by 8 ft to 2 ft by 8 ft in section and includes 16 ports of constant height, 2 ft 6 in., and of a width varying from 1 ft 11 in. to 1 ft 5 in.

When design was initiated on McNary the approved lock size was 86 ft by 500 ft and initial design and model studies were based on these dimensions. When the decision was made to use the 675 ft length, little time was left to complete model studies. For that reason construction had already started before all the model studies were performed. As a result, one undesirable characteristic was revealed that could have been prevented had time permitted. This was the presence of low pressures on the roof of the culvert below the filling valves, pressures well down in the cavitation range with a valve opening time of 4 min. To alleviate the low pressures a nonuniform valve opening schedule was developed whereby the valve is opened rapidly 2 ft, and then slowly opened until the lock has partially filled, and then is opened rapidly



(a) PLAN





(b) VERTICAL SECTION

FIG. 8.—McNARY LOCK

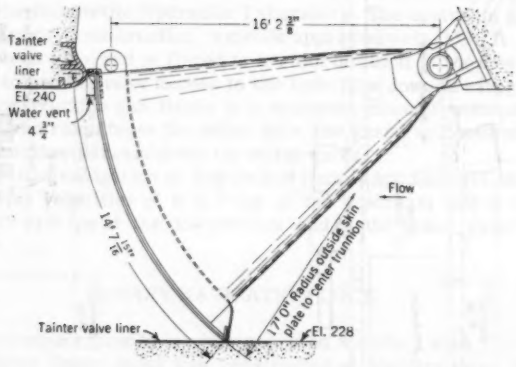


FIG. 9.—McNARY LOCK VALVE

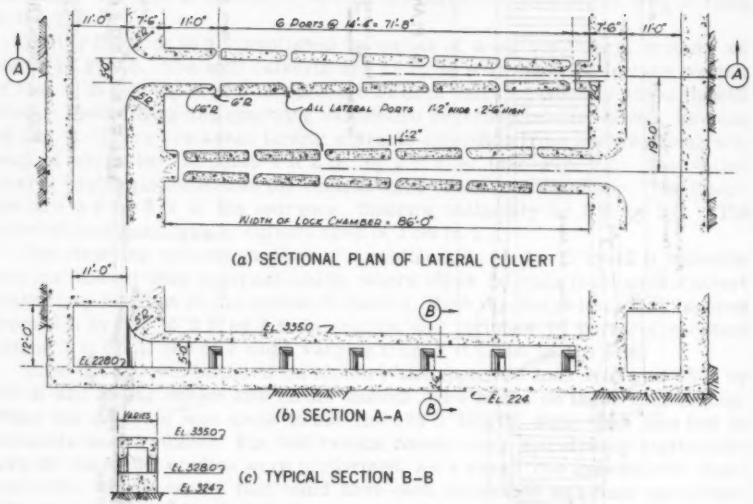


FIG. 10.—McNARY LOCK FILLING LATERAL DETAILS

again, requiring 7.5 min to become fully open. In this way enough back pressure can be built up to enable the valve to pass through the most critical range (near 7 ft) without seriously low pressures. Even so, pressures equivalent to minus 15 ft were recorded in the model. This was assumed not to be dangerous in view of the stainless-clad plate liner below the valve, an assumption that proved to be true. The filling time as determined in the model was 16.1 min for 92 ft of head, 15.4 min for 82 ft, and 14.1 for 63 ft. The emptying time was slightly faster, being 15.7 min for 92 ft, 15,2 min for 82 ft, and 14.1 min at 63 ft.



FIG. 11.—TURBULENCE IN McNARY LOCK DURING FILLING

Turbulence in the lock chamber has been slight, due to the well-distributed flow and the relatively slow filling time. With the lock chamber at its full capacity of eight barges the maximum hawser force, as measured in the model, was only 3.3 tons, and correspondingly less with small tows. Fig. 11 shows the lock chamber during a normal filling operation, immediately after the filling valves have become fully open, the condition producing maximum turbulence. One 12 in. air vent is open at each filling valve. Note the contrast between the conditions here and in the Bonneville lock (Fig. 3).

Considerable attention was given to the proper shape for the filling valve in order that low downpull forces could be combined with minimum vibration. The resulting shape, shown in Fig. 9, incorporates an upstream convex skinplate with fully inclosed, streamlined trunnion arms. The valves at The Dalles

have the same shape, as will those at Ice Harbor and John Day Locks. Because McNary is the first of the high lift locks to use a bottom lateral system, much interest has been shown in its operation, which, on the whole, has been good. When it was first put into service, some fear was expressed by observers that certain loud noises emanating from the valve and bulkhead shafts were indicative of damage to the valves. These noises, which seem to be acoustic phenomena associated with the formation of the hydraulic jump in the culverts during valve opening periods, have proved to be harmless, because no damage to valve, liner or machinery has appeared. It has been found that much of the sound can be reduced by opening one of six 12-in. air vents below each filling valve.

An extensive prototype testing program has been carried on by the Walla Walla District in conjunction with the Waterways Experiment Station and the Bonneville Hydraulic Laboratory. In October and November, 1955[4] pressures in the filling and emptying culverts were measured by a system of 50 piezometers that had been installed at the time of construction. In general there was good correlation between the model and prototype measurements. In addition, filling and emptying curves were obtained, overtravel and undertravel observed and the effect of varying valve opening curves studied. It was noted that the lock filled approximately 1 min faster and emptied 2½ min faster than the model. This difference has been noted on other locks and is believed to be caused by the inability of a small scale model to reproduce friction losses accurately.

In November, 1957 pressure cells were installed in the roof of the culvert near one filling valve, accelerometers were placed on the valve and lock wall and air-water probes set in the culvert roof. Air-mercury manometers were also attached to the piezometers adjacent to the pressure cells. The purpose of this installation was to learn more about the nature of the pounding noises coming from the culverts. At this time the mass of information obtained from these tests has not been analyzed. As mentioned in the consideration of The Dalles Dam, hawser force tests were made in the prototype in December, 1957. With the same tow of 2,780 tons used at The Dalles, a maximum longitudinal force of 1.7 tons was measured in the McNary Lock with a head of 87.9 ft.

The aerial view in Fig. 12 shows the relationship of the lock and its approaches to the adjacent structures. The upstream guard wall extends for 1,590 ft from the upper lock gate and the downstream wall 1,675 ft from the lower gate. In addition, a concrete moorage wall parallels the lower guard wall on the land side of the channel, which is 250 ft wide at this point. Although extreme turbulence is formed over the discharge laterals during the emptying of the lock, conditions downstream where entering tows must wait are quite acceptable.

ICE HARBOR NAVIGATION LOCK

Ice Harbor Dam is located at the head of the McNary pool on the Snake River, 10 miles from its mouth, near Pasco, Wash. First-stage construction, which includes the powerhouse, seven of the ten spillway bays and the south abutment was completed early in 1959. Construction of the navigation lock and the remainder of the north shore structures was commenced soon after the second-step cofferdam was completed after the high water of 1959. The lock is scheduled to be put in operation late in 1961.

[4] "Report on Model-Prototype Conformity, McNary Dam Navigation Lock," U. S. Army Engr. Dist., Walla Walla, Wash., March, 1958.



FIG. 12.—McNARY DAM

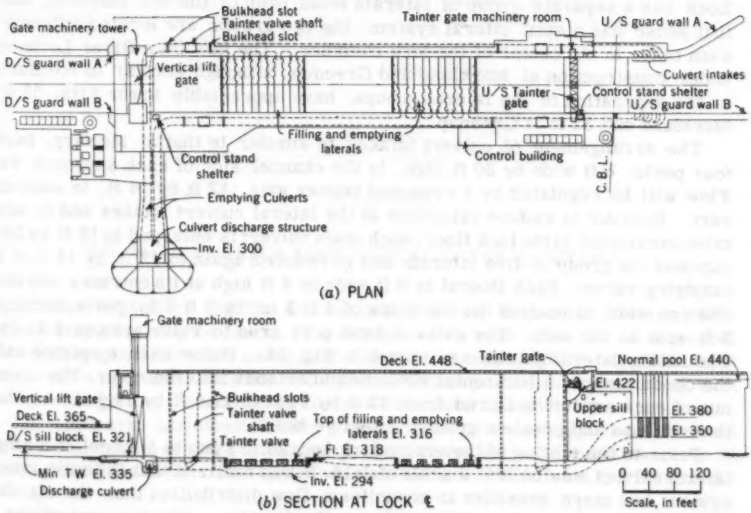


FIG. 13.—ICE HARBOR LOCK

With McNary pool at its normal elevation of 340, and average flow conditions in the Snake, maximum lifts up to 100 ft can be expected annually. Were the McNary reservoir to be drawn down to its minimum operating level, El 335, and nothing released from Ice Harbor, an absolute maximum of 105 ft could occur. However, this would require a rather unlikely combination of circumstances, and for design purposes a head of 103 ft has been used, exceeding both The Dalles and McNary.

A 1:25 scale model of the lock was tested at the Bonneville Hydraulic Laboratory. The final design is that shown on Figs. 13 and 14.

The plan dimensions of the lock are standard, 86 by 675 ft, but several unusual features warrant attention. First, the downstream lock gate is a vertical lift gage, 86 by 89 ft, the top of which seats against a concrete box girder which forms the service bridge across the lock. The capability of such a gate being opened under slight head (up to approximately 3 ft) permits the use of a river discharge system, which is the second feature of special interest. Heretofore designers of Columbia River locks had been faced with the problem of the difference in water surface between the river proper and the downstream lock approach (as much as 2 ft in McNary). This condition necessitated the use of a lock discharge system in the lock approach because a conventional miter gate could not open against a head greater than 9 to 12 in. The filling system is the split-lateral variation of a bottom lateral system. In this arrangement each of the two main culverts has five lateral culverts in the lock floor (Fig. 13). However, instead of the laterals interlacing as at McNary and The Dalles, one set of five is located in the central third of the upstream half of the lock and the other five in the central third of the downstream half. In this way the magnitude of the longitudinal surge is reduced greatly, with resultant lower hawser forces. It is believed that Ice Harbor is the first high lift lock in this country to use the split lateral system in this fashion. Although the new Wilson Lock has a separate group of laterals from each of the two culverts, and in that sense has a split lateral system, the two groups are located adjacent to each other in the center of the lock chamber. The new Ohio River Locks now under construction at Markland and Greenup, although similar to Ice Harbor in the separation of the lateral groups, have appreciably lower lifts, 35 ft at Markland and 32 ft at Greenup.

The arrangement of culvert intakes is similar to that at McNary, having four ports, 8 ft wide by 30 ft high, in the channel side of each approach wall. Flow will be regulated by a reversed tainter gate, 12 ft by 14 ft, in each culvert. In order to reduce velocities at the lateral culvert intakes and to minimize excavation in the lock floor, each main culvert is enlarged to 12 ft by 20 ft, opposite its group of five laterals and is reduced again to 12 ft by 14 ft at the emptying valves. Each lateral is 8 ft wide by 4 ft high at its entrance and steps down in width at each of the six pairs of 1 ft 3 in. by 2 ft 6 in. ports, becoming 3 ft wide at the end. The ratio of total port area to valve area is 1.11 to 1. The filling lateral details are shown in Fig. 14. Below each emptying valve the conduit makes a horizontal 90° bend and extends into the river. The terminus of each conduit is flared from 12 ft by 14 ft to 17.4 ft by 19.4 ft to reduce the exit loss and create a greater effective head.

Prior to the testing of the entire lock hydraulic system a model of a single lateral culvert was built at a scale of 1:16. It was realized that the split-lateral system was more sensitive to nonuniform flow distribution than the standard bottom laterals, which are somewhat self adjusting. Many combinations of

flow and port arrangements were tried in this model, and it was found that to obtain the optimum flow distribution a different design for each lateral would be required. In the interests of simplicity a single design was selected to be common to all laterals. The differences in flow distribution between the selected design and various designs giving nearly uniform flow were felt to be negligible, and indeed proved to be so when installed in the general model.

The model results were gratifying. Even with the small port-to-culvert ratio of 1.11:1, the lock fills in 11.8 min with a lift of 103 ft and with a constant speed valve time of 4 min. It empties in 13 min with a valve time of 2.2 min.

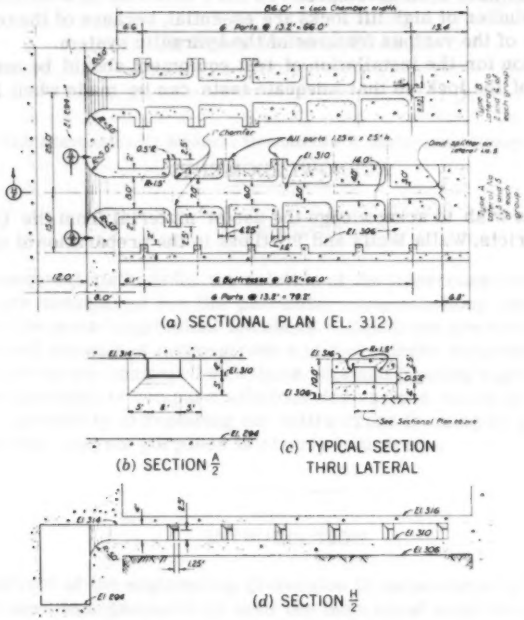


FIG. 14.—ICE HARBOR LOCK TYPICAL LATERAL DETAILS

Experience at McNary and The Dalles indicates that the actual prototype filling and emptying may be faster. Pressures on the roof below the filling valve are slightly positive when using both valves and only slightly negative under single valve operation with the 103 ft lift. Hawser pull tests indicate that with an eight-barge tow the maximum force will be less than five tons.

The upstream and downstream guard walls are relatively short because the general model of the Ice Harbor project revealed no adverse currents at either end of the lock. The upstream wall extends 680 ft from the face of the

upper lock gate and the downstream wall 700 ft from the lower gate. Because the lock empties directly into the river there will be no flow in the lower approach and hence no velocity. The guide walls will be of concrete.

CONCLUSIONS

1. Since the construction of Bonneville Lock and Dam extensive improvements have been made in lock design.
2. High single lift locks introduce problems of low pressures in the culverts and high hawser forces in the lock chamber. Methods of overcoming these problems have been developed.
3. Model studies of high lift locks are essential, because of the complicated inter-relation of the various features of the hydraulic system.
4. Provision for the installation of test equipment should be made during construction of the lock so that adequate tests can be made when it is put in operation.

ACKNOWLEDGMENTS

The authors wish to acknowledge the use of material from the U. S. Army Engineer Districts, Walla Walla and Portland, in the preparation of this paper.

AMERICAN SOCIETY OF CIVIL ENGINEERS

Founded November 5, 1852

TRANSACTIONS

Paper No. 3025

NUMERICAL SOLUTIONS FOR INTERCONNECTED BRIDGE GIRDERS

By Henry Malter,[1] F. ASCE

With Discussion by Messrs. Dronnadula V. Reddy; and Henry Malter

SYNOPSIS

Two numerical methods for the solution of the interconnected bridge girder problem are considered for the particular case involving infinite torsional rigidity of the main longitudinal members. Equations are developed for both deflection and moment of a two-girder and four-girder structure, and results from both cases are compared with those obtained by using rigorous equations. Tables are included to compare solutions for various values of relative stiffness. The possibility of replacing the entire cross framing by a single-center diaphragm for analysis purposes is clearly indicated.

INTRODUCTION

The interest of the engineering profession in the problem of interconnected bridge girders is engendered by both the theoretical aspects of the problem, and by the practical application of the results to the expanding highway program in the United States and throughout the world. Various theoretical solutions to the general problem have been proposed in recent years, including moment distribution,[2] anisotropic plates,[3] and a method employing a Fourier

Note.—Published, essentially as printed here, in October, 1958, in the Journal of the Structural Division, as Proceedings Paper 1815. Positions and titles given are those in effect when the paper or discussion was approved for publication in Transactions.

1 Prof. of Civil Engrg., Univ. of Illinois, Urbana, Ill.

2 "A Distribution Procedure for the Analysis of Slabs Continuous over Flexible Beams," by N. M. Newmark, Bulletin No. 304, Engrg. Experiment Sta., Univ. of Illinois, Urbana, Ill., 1938.

3 "Deflections in Gridworks and Slabs," by W. W. Ewell, S. Okubo, and J. I. Abrams, Transactions, ASCE, Vol. 117, 1952.

series loading.[4] In addition, many experimental and test results have been recorded in engineering literature. A comprehensive survey of the various aspects of the problem appears in an article by Chester P. Siess, F. ASCE, and Anestis S. Veletsos, A. M. ASCE,[5] and a complete bibliography of recent articles appears in a discussion article by Z. S. Makowski.[6]

The general problem consists of a series of simply supported or continuous main longitudinal girders, interconnected by either a slab or a series of diaphragms, or both. A load placed on any one of the girders results in deflections of the adjacent beams of the structure as well as of the loaded girder. Part of the load is thus transmitted through the diaphragms or slab to the other beams.

The two limiting conditions for the general solution of this problem are (1) negligible torsional rigidity of the longitudinal beams, and (2) infinite torsional rigidity of the longitudinal beams. The first condition, at present the more important of the two from a practical viewpoint, includes the usual I-beam type of bridge with a concrete deck slab. The second condition is encountered in a bridge consisting of heavy concrete girders that are able to resist rotation.

This paper considers only a limited aspect of the problem, that is, numerical methods for the solution of condition (2). The applicability of a particular solution to a specific problem is largely a matter of interpretation of the behavior of the structure under consideration, and is somewhat indefinite. Any practical conclusions must be governed to a great extent by experimental results and observations on full-scale bridges, and no effort to consider the applicability of any particular solution will be undertaken in this paper.

A solution for the problem being considered has been obtained by Alfred J. S. Pippard,[7] F. ASCE, and by Miklos Hetenyi,[8] F. ASCE, both employing similar methods, and basing their derivations on a rigorous solution of the differential equations pertaining to the problem. Pippard has tabulated the solutions for two, three, and four-girder structures, and the results obtained by the approximate methods will be compared with those obtained from a substitution in the Pippard equations.

Although the numerical methods used emphasize only one particular problem, that of a concentrated load at the center of one of the longitudinals, it should be realized that this is done merely for ease of comparison with the results obtained by Pippard's more rigorous method. Also, this is usually the more critical case, and is therefore of greater importance. The method used is just as applicable to distributed loadings or to concentrated loads not centrally placed. The ease of numerical solutions for particular cases will be obvious, although general formulas may also be derived, as will be done for several cases.

---

[4] "Load Distribution in Highway Bridge Decks," by A. W. Hendry and L. G. Jaeger, Transactions, ASCE, Vol. 123, 1958, pp. 1214-1244.

[5] "Distribution of Loads to Girders in Slab and Girder Bridges," by C. P. Siess and A. A. Veletsos, Report No. 14-B, Highway Research Bd., Natl. Research Council, Washington, D. C., 1953.

[6] Discussion by Z. S. Makowski of "Distribution of Loads on Bridge Decks," A. M. Lount, Proceedings Paper 1303, July 1957, in Proceedings Paper 1522, January, 1958.

[7] "Studies in Elastic Structures," by A. J. S. Pippard, Edward Arnold and Co., London, 1952, pp. 96-110.

[8] "Beams on Elastic Foundations," by M. Hetenyi, The Univ. of Michigan Press, Ann Arbor, Mich., 1946.

The various aspects of the problem can be understood by considering a two-girder bridge in which the connecting members are either a series of diaphragms or a concrete deck slab. The stiffness of the main members is designated as E I, and the stiffness of the cross members per unit length of the structure as $E I_c$. This latter term may be obtained by assuming any cross member as being distributed uniformly over a cross member spacing, and adding to this the stiffness of the slab per unit length. A load applied to any one girder results in deflections along the length of the structure that are different for each beam.

To enable ease of comparison between the various methods, only symmetrical structures are considered. However, once the technique is understood, it will be obvious that no restrictions are placed on the type of problem that may be handled. Unsymmetrical structures, as well as beams of varying moments of inertia, can be handled in the manner outlined for the symmetrical system. It should be remembered that the condition of infinite torsional rigidity of the main girders is the case being considered.

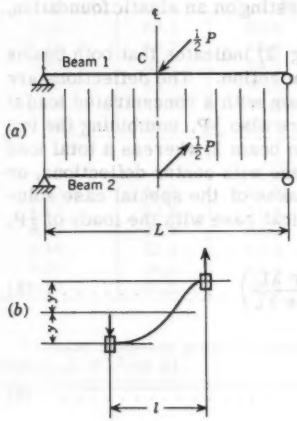


FIG. 1

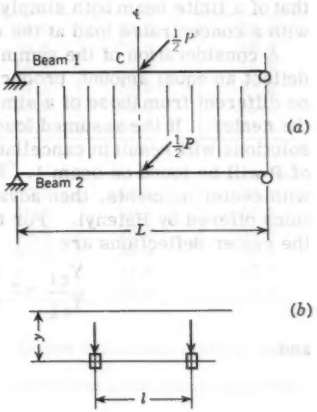


FIG. 2

Notation.—The letter symbols adopted for use in this paper are defined where they first appear, in the illustrations or in the text, and are arranged alphabetically, for convenience of reference, in the Appendix.

RIGOROUS METHOD

The general problem could be solved directly. However, for cases involving symmetry, as is assumed herein $(E I_1 = E I_2)$, it is often preferable to utilize the familiar symmetrical and antisymmetrical load systems, combining the results obtained. Thus, if two antisymmetrical loads, each of ½P, are applied at the centers of beams 1 and 2 (Fig. 1), the resulting total deflection of 2 y between the beams will be observed, in which y is the deflection of each

beam from its initial position. This total deflection of 2 y will produce in the cross beam a shear of

$$w = \frac{12\ E\ I_c}{l^3}\ 2\ y \quad \ldots\ldots\ldots\ldots\ldots\ldots \quad (1)$$

in which w is the shear per unit length of the structure, and l represents the spacing of the main members. This shear now appears as a distributed load on the main girders, acting upward on girder 1 and downward on girder 2. Inasmuch as this distributed load is a function of deflection, it may be recognized as an elastic foundation reaction. The equation for its solution is

$$\frac{d^4\ y}{d\ x^4} = -\left(\frac{12\ E\ I_c}{l^3\ E\ I}\right)2\ y = -2\ K\ y \quad \ldots\ldots\ldots\ldots\ldots \quad (2)$$

in which K is substituted for the term in the parenthesis, and the spring constant r may be defined by $r = 2\ K\ E\ I$. A solution to this problem may be obtained easily by recognizing it as one of the special cases considered by Hetenyi,[8] that of a finite beam both simply supported and resting on an elastic foundation, with a concentrated load at the center.

A consideration of the symmetrical case (Fig. 2) indicates that both beams deflect an equal amount, producing no diaphragm action. The deflections are no different from those of a simply supported beam with a concentrated load at the center. If the assumed loads in this case are also $\frac{1}{2}P$, combining the two solutions will result in cancellation of the load on beam 2, whereas a total load of P will be found on beam 1. If the concern were with center deflections, or with center moments, then advantage could be taken of the special case solutions offered by Hetenyi. For the antisymmetrical case with the loads of $\frac{1}{2}P$, the center deflections are

$$\frac{Y_{c1}}{Y_{c2}} = \pm\frac{P\lambda}{4r}\left(\frac{\sinh \lambda L - \sin \lambda L}{\cosh \lambda L + \cos \lambda L}\right) \quad \ldots\ldots\ldots\ldots \quad (3)$$

and

$$\lambda = \sqrt[4]{\frac{r}{4\ EI}} \quad \ldots\ldots\ldots\ldots\ldots\ldots \quad (4)$$

using the plus sign for the downward deflection of beam 1, and the minus sign for the upward deflection of beam 2.

For the symmetrical case, with loads of $\frac{1}{2}P$, the deflections of both beams are the same, each one being equal to $PL^3/96\ EI$, in which L is the span length.

Combining the two cases produces a total center deflection of

$$\frac{Y_{c1}}{Y_{c2}} = \frac{P\ L^3}{48\ EI}\left[\frac{1}{2} \pm \frac{48\ EI}{L^3} \cdot \frac{\lambda}{4r}\left(\frac{\sinh \lambda L - \sin \lambda L}{\cosh \lambda L + \cos \lambda L}\right)\right] \ldots\ldots \quad (5)$$

The plus sign is used for beam 1, now loaded with a concentrated load of P, and the minus sign is used for unloaded beam 2. Because $K = 2\ \lambda^4$, Eq. 5 can be simplified to a final form of

$$\frac{Y_{c1}}{Y_{c2}}\ \frac{C_1}{C_2} = \frac{P\ L^3}{48\ EI}\left[\frac{1}{2} \pm \frac{3}{\lambda^3\ L^3}\left(\frac{\sinh \lambda L - \sin \lambda L}{\cosh \lambda L + \cos \lambda L}\right)\right] \ldots\ldots \quad (6)$$

It will be recognized that Eq. 6 is similar to the equation obtained by Pippard,[7] but with the trigonometric terms omitted. The influence of these latter terms is at all times small when λL is large, and their omission results in small errors. This is evident from the fact that the values of the terms in the parenthesis are 1.08, 1.05, and 1.01 for λL values of 3, 4, and 5 respectively.

To obtain center moments, reference is again made to the special problems solutions offered by Hetenyi,[8] but this time using the equation for center moment. In a manner similar to that previously outlined for deflections, the

TABLE 1.—COMPARATIVE RESULTS FOR A TWO-GIRDER STRUCTURE

Relative stiffness, K, in 10^{-8} inches^4 (1)	Pippard method (2)	Diaphragm method (3)	Finite difference method (4)	Pippard method (5)	Diaphragm method (6)	Finite difference method (7)
	L = 600 inches			L = 1000 inches		
(a) Center moments[a]						
1.40	59.1	58.6	59.4	55.5	57.6	56.4
1.10	59.7	58.8	59.9	55.8	57.6	56.6
0.80	60.5	59.4	60.8	56.3	57.6	56.7
0.50	61.8	60.4	62.2	57.1	58.0	57.2
0.20	65.5	64.2	66.5	58.9	58.5	59.1
0.10	70.2	68.9	70.9	60.5	59.7	61.2
(b) Center deflections[b]						
1.40	51.8	51.3	51.8	50.3	50.2	50.3
1.10	52.5	51.6	52.1	50.4	50.2	50.3
0.80	52.8	52.2	52.8	50.6	50.3	50.5
0.50	53.9	53.5	54.1	50.8	50.5	50.8
0.20	58.4	57.8	58.2	51.7	51.2	51.7
0.10	64.2	63.5	63.6	52.8	52.3	52.8

[a] Center moments given as percentage of PL/4. [b] Center deflections given as percentage of $PL^3/48$ EI.

following final form for center moments is obtained:

$$\frac{M_{c1}}{M_{c2}} = \frac{PL}{4}\left[\frac{1}{2} \pm \frac{1}{2\lambda L}\left(\frac{\sinh \lambda L + \sin \lambda L}{\cosh \lambda L + \cos \lambda L}\right)\right] \quad \ldots\ldots\ldots \quad (7)$$

The trigonometric terms may again be ignored for large values of λL. The values of the terms in the parenthesis are 1.12, 1.00, 0.982, and 1.00 for λL-values of 3, 4, 5, and 6 respectively.

Eqs. 6 and 7 have been used to obtain both center deflections and center moments for various values of relative stiffness K. The results are compared in Table 1 with those obtained by other methods. In all cases, the results are shown as percentages of total deflection $PL^3/48$ EI, or of total moment PL/4.

A rigorous solution for a four-girder bridge will not be attempted. However, using the formulas provided by Pippard[7] for this case, the results for both deflections and moments for the various girders have been tabulated for

different values of K, and are included in Table 2, in which they are compared with the results obtained by each of the approximate methods outlined.

CENTER DIAPHRAGM METHOD

The center diaphragm method presupposes that the entire cross-diaphragm stiffness, whether continuous in the form of a slab or consisting of distinct cross beams, may be replaced by three concentrated diaphragms, one at the

TABLE 2.—COMPARATIVE RESULTS FOR A FOUR-GIRDER STRUCTURE

Relative stiffness, K, in 10^{-8} inches^4 (1)	Pippard method (2)				Diaphragm method (3)				Finite difference method (4)			
	(a) Center moments[a,b]											
	M_{C1}	M_{C2}	M_{C3}	M_{C4}	M_{C1}	M_{C2}	M_{C3}	M_{C4}	M_{C1}	M_{C2}	M_{C3}	M_{C4}
1.40	34.8	29.3	24.3	11.6	33.2	29.4	25.4	12.0	35.0	29.2	25.4	10.4
1.10	35.9	29.1	23.7	11.3	34.2	29.5	24.6	11.8	37.0	29.6	23.0	10.4
.80	37.6	28.7	22.9	10.8	36.1	29.7	23.5	10.7	39.0	29.6	21.6	9.7
.50	40.1	28.1	21.7	10.1	39.4	30.1	21.1	9.4	43.0	28.7	19.6	8.8
.20	46.2	26.8	18.6	8.4	49.0	30.4	15.2	5.4	52.5	28.0	14.5	4.9
.10	51.6	25.7	15.9	6.8	59.2	28.3	9.7	2.8	62.0	26.2	9.4	2.2
	(b) Center deflections[a,c]											
	Y_{C1}	Y_{E2}	Y_{E3}	Y_{C4}	Y_{C1}	Y_{E2}	Y_{E3}	Y_{C4}	Y_{C1}	Y_{E2}	Y_{E3}	Y_{C4}
1.40	22.2	34.0	29.6	14.2	21.4	34.5	29.9	14.2	22.4	34.2	29.2	14.0
1.10	23.3	34.1	28.9	13.7	22.6	34.7	28.9	13.6	23.6	34.3	28.5	13.4
.80	25.1	34.3	27.7	12.9	24.6	35.1	27.7	12.6	25.4	34.5	27.3	12.6
.50	28.6	34.9	25.3	11.2	28.4	35.6	25.0	10.8	29.3	35.2	25.0	11.0
.20	40.5	36.3	17.3	5.9	40.0	35.6	17.8	6.5	40.2	34.9	17.9	6.8
.10	56.5	38.4	6.6	--	52.0	33.2	11.4	3.2	51.3	32.4	12.2	4.2

[a] The load is placed on beam 1, L = 600 inches and n = $\frac{1}{2}$. [b] Center moment given as percentage of PL/4. [c] Center deflections given as percentage of $PL^3/48$ EnI for beams 1 and 4, and $PL^3/48$ EI for beams 2 and 3.

center, and one at each end. The center diaphragm will have a stiffness of h EI_c, and the end diaphragms a stiffness of $\frac{1}{2}$h EI_c, in which EI_c is the cross stiffness per unit length of the structure, and the subdivision spacing, h, is in this case $\frac{1}{2}$L. Because the ends of the beams do not deflect, the end diaphragms are consequently of no factor in the analysis, and will hereafter be omitted.

Two-Girder Structure.—The conditions for the case of antisymmetrical loading, with loads of $\frac{1}{2}$P, are shown in Fig. 3. The shear in the cross girder at the center is

$$V_c = \frac{12\ EI_c}{l^3} \cdot 2Y_c h \quad \ldots\ldots\ldots\ldots\ldots\ldots \quad (8)$$

in which Y_c represents the deflection of the structure from its original position at point C. This shear appears as concentrated loads in Fig. 3(c), and the center deflection of beam 1 is

$$Y_{c1} = \frac{PL^3}{96\ EI} - \left(\frac{12\ EI_c}{l^3} \cdot \frac{1}{EI}\right)\frac{2Y_{ch}\ L^3}{48} \quad \ldots\ldots\ldots\ldots (9)$$

whereas the deflection of beam 2 is the second term only and uses a plus sign. In Eq. 9, substituting K for the term in parentheses, and $\frac{1}{2}L$ for h, and using the term ϕ for $KL^4/96$, results in

$$Y_c = \frac{PL^3}{96\ EI}\left(\frac{1}{1 + 2\phi}\right) \quad \ldots\ldots\ldots\ldots\ldots\ldots (10)$$

For the symmetrical case, the deflection of each beam is $PL^3/96\ EI$. In combining the two cases, the final deflection becomes

$$\frac{Y_{c1}}{Y_{c2}} = \frac{PL^3}{48\ EI}\left[\frac{1}{2} \pm \frac{1}{2}\left(\frac{1}{1 + 2\phi}\right)\right] \quad \ldots\ldots\ldots\ldots\ldots (11)$$

In obtaining center moments by this approximate method, it was observed that for both concentrated center loads and for triangular loadings, the deflections at the quarter points of simply supported beams is approximately 70% of the center deflection. For a diaphragm spacing of $h = \frac{1}{4}L$, the shear in the center diaphragm becomes:

$$V_c = \frac{12\ EI_c}{l^3}\frac{L}{4}\left(Y_{c1} - Y_{c2}\right) \quad \ldots\ldots\ldots\ldots\ldots (12)$$

for a beam loaded with a load P on beam 1. Substituting this value for previously found $(Y_{c1} - Y_{c2})$, the shear becomes

$$V_c = \frac{P\phi}{2}\left(\frac{1}{1 + 2\phi}\right) \quad \ldots\ldots\ldots\ldots\ldots\ldots (13)$$

The concentrations due to the diaphragms at the quarter points are 70% of Eq. 13, and the conditions are shown in Fig. 4. For this loading the center moments are

$$M_C = \frac{L}{4}\left(-V_{\frac{1}{4}} - V_{\frac{1}{2}} + P\right) \quad \ldots\ldots\ldots\ldots\ldots (14)$$

and the final center moments are

$$\frac{M_{c1}}{M_{c2}} = \frac{PL}{4}\left[\frac{1}{2} \pm \frac{1}{2} \mp \frac{1.70\ \phi}{2}\left(\frac{1}{1 + 2\phi}\right)\right] \quad \ldots\ldots\ldots\ldots (15)$$

Results for both deflections and moments are given in Table I.

Four-Girder Structure: Load on Beam 1.—The effectiveness of the approximate method will be demonstrated by its application to a four-girder structure (Fig. 5). To make the problem general, it is assumed that the inner girders are each of stiffness EI, whereas the two outer girders are assumed to have a stiffness of E nI, in which n is the ratio of EI_1/EI_2. The unit stiffness

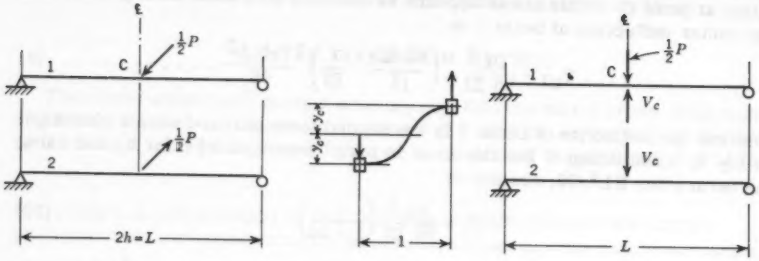


FIG. 3

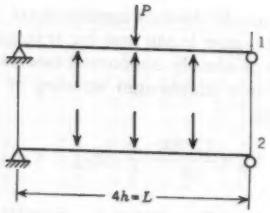


FIG. 4

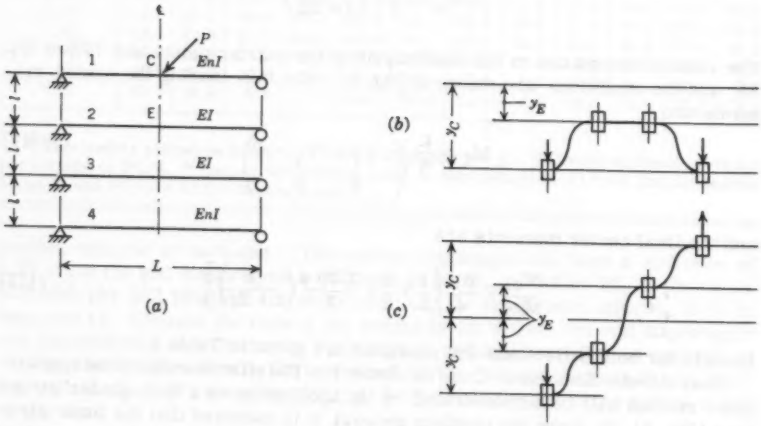


FIG. 5

of the cross members is EI_c, and the value of the relative stiffness will be defined as the ratio $12\ EI_c/l^3\ E\ nI$, thus identifying it with the outer girder. The symbol K is used again for relative stiffness. (This definition is the same as that employed in the two-girder case for which n = 1). For this example two solutions will be required, the first with a load P on girder 1, and a second general solution with a load P on girder 2.

The method used is similar to that used for the two-girder structure. However, for each of the two cases, symmetrical and anti-symmetrical, two sets of simultaneous equations are required to find the two unknown deflections, Y_C and Y_E. The situation for the symmetrical loads is shown in Fig. 5(b), and the deflections at points C and E are

$$Y_C = \frac{PL^3}{96\ E\ n\ I} - \frac{12\ EI_c}{l^3}\ \frac{L}{2}\ (Y_C - Y_E)\ \frac{L^3}{48\ E\ nI} \quad \ldots\ldots\ldots (16)$$

and

$$E = \frac{12\ EI_c}{l^3}\ \frac{L}{2}\ (Y_C = Y_E)\ \frac{L^3}{48\ EI} \quad \ldots\ldots\ldots\ldots (17)$$

Substituting for K and ϕ, and solving, will give for the symmetrical case

$$Y_C = \frac{PL^3}{96\ E\ nI}\left(\frac{1 + n\ \phi}{1 + \phi + n\ \phi}\right) \quad \ldots\ldots\ldots\ldots (18)$$

and

$$Y_E = \frac{PL^3}{96\ E\ nI}\left(\frac{n\ \phi}{X}\right) \quad \ldots\ldots\ldots\ldots (19)$$

in which X has been substituted for the term $(1 + \phi + n\ \phi)$ appearing in the denominator.

The beam positions for the antisymmetrical case are shown in Fig. 5(c). The loading condition for beam 1 is the same as that for the symmetrical case, and its equation is the same Eqs. 18 and 19. However, the conditions for beam 2 are different. The resulting equations after substitutions are

$$Y_C = \frac{PL^3}{96\ E\ nI} - \phi\ (Y_C - Y_E) \quad \ldots\ldots\ldots\ldots (20)$$

and

$$Y_E = n\ \phi\ (Y_C - Y_E) - n\ \phi\ (2Y_E) \quad \ldots\ldots\ldots\ldots (21)$$

A solution of Eq. 20 and 21 gives

$$Y_C = \frac{PL^3}{96\ E\ nI}\left[\frac{1 + 3\ n\ \phi}{(1 + \phi)\ (1 + 3n\ \phi) - n\ \phi^2}\right] \quad \ldots\ldots\ldots (22)$$

and

$$Y_E = \frac{PL^3}{96\ E\ nI}\left(\frac{n\ \phi}{Y}\right) \quad \ldots\ldots\ldots\ldots (23)$$

in which Y has been substituted for the term $(1 + \phi)\ (1 + 3n\ \phi) - n\ \phi^2$.

Combining both cases results in the solution for deflections caused by a load P on beam 1. These deflections are

$$\frac{Y_{c1}}{Y_{c4}} = \frac{PL^3}{96\,E\,nI}\left(\frac{1+n\,\phi}{X} \pm \frac{1+3n\,\phi}{Y}\right) \quad \ldots\ldots\ldots\ldots (24)$$

and

$$\frac{Y_{E2}}{Y_{E3}} = \frac{PL^3}{96\,E\,nI}\left(\frac{n\,\phi}{X} \pm \frac{n\,\phi}{Y}\right) \quad \ldots\ldots\ldots\ldots\ldots (25)$$

To obtain moments by this method, it is again assumed that the quarter-point deflections are 70% of the center deflections. The shear in the diaphragms, now assumed to exist both at the quarter points as well as at the center, is a direct result of the difference in deflection of adjacent beams. These differences are

$$(Y_{c1} - Y_{E2}) = \frac{PL^3}{96\,E\,nI}\left(\frac{1}{X} + \frac{1+2n\,\phi}{Y}\right) \quad \ldots\ldots\ldots\ldots (26)$$

$$(Y_{E2} - Y_{E3}) = \frac{PL^3}{96\,E\,nI}\left(\frac{2n\,\phi}{Y}\right) \quad \ldots\ldots\ldots\ldots\ldots (27)$$

and

$$(Y_{E3} - Y_{C4}) = \frac{PL^3}{96\,E\,nI}\left(\frac{-1}{X} + \frac{1+2n\,\phi}{Y}\right) \quad \ldots\ldots\ldots\ldots (28)$$

The concentrated loads produced at any point are $P_X = \frac{P\,\phi}{4}(\,)$ and the terms in parentheses are given in Eqs. 26, 27, and 28.

For this type of loading, the final form of the equations for center moment are

$$\frac{M_{C1}}{M_{C4}} = \frac{PL}{4}\left[\frac{1}{2} \pm \frac{1}{2} - \frac{1.70\,\phi}{4}\left(\frac{1}{X} \pm \frac{1+2n\,\phi}{Y}\right)\right] \quad \ldots\ldots\ldots\ldots (29)$$

and

$$\frac{M_{C2}}{M_{C3}} = \frac{PL}{4}\left[\frac{1.70\,\phi}{4}\left(\frac{1}{X} \pm \frac{1}{Y}\right)\right] \quad \ldots\ldots\ldots\ldots\ldots (30)$$

Results from the use of Eqs. 29 and 30, as well as from the equations for deflections, have been tabulated in Table 2 in which they may be compared with the results of the other methods.

Four-Girder Structure: Load on Beam 2.— For beam 2 loaded, a similar method could be employed, resulting in the following equations:

$$\frac{Y_{C1}}{Y_{C4}} = \frac{PL^3}{96\,EI}\left(\frac{\phi}{X} \pm \frac{\phi}{Y}\right) \quad \ldots\ldots\ldots\ldots\ldots (31)$$

$$\frac{Y_{E2}}{Y_{E3}} = \frac{PL^3}{96\,EI}\left(\frac{1+\phi}{X} \pm \frac{1+\phi}{Y}\right) \quad \ldots\ldots\ldots\ldots\ldots (32)$$

$$\frac{M_{C1}}{M_{C4}} = \frac{PL}{4}\left[\frac{1.70\,n\,\phi}{4}\left(\frac{1}{X} \pm \frac{1}{Y}\right)\right] \quad \ldots\ldots\ldots\ldots\ldots (33)$$

and

$$\frac{M_{C2}}{M_{C3}} = \frac{PL}{4}\left\{\frac{1}{2} \pm \frac{1}{2} - \frac{1.70\, n\, \phi}{4}\left[\frac{1}{X} \pm \frac{1 + 2\,(1 + \phi)}{Y}\right]\right\} \quad \ldots\ldots (34)$$

FINITE DIFFERENCE METHOD

Eq. 35 is used for the solution of beam deflection problems;

$$\frac{d^4y}{dx^4} = -\frac{w}{E\,I} \quad \ldots\ldots (35)$$

As in many problems involving differential equations, it has been found that difference operators may be substituted for the differential operators. Using the "molecule notation for central difference operators,"[9] the fourth difference operator is

$$\frac{\Delta_4}{\Delta x^4} = \frac{1}{h^4}\,(1,\ -4,\ +6,\ -4,\ 1) \quad \ldots\ldots (36)$$

Only the application of the finite difference operation to the present problem will be emphasized.

A beam resting on an elastic foundation and subjected to vertical forces will be deflected in some manner, and result in foundation pressures that vary along the length of the beam. This foundation pressure that is a continuous function may be replaced by a set of concentrations at the various subdivision points of the beam. The concentrations may be represented in several ways. First, a "stepped" variation may be assumed (Fig. 6(a)), resulting in subgrade reactions of $r\,h\,Y_B$, $r\,h\,Y_C$, etc., in which r is the subgrade modulus, h is the length of the subdivision, and Y_B, Y_C, Y_D are the deflections of the beam at the points designated. Using a "straight line" variation (Fig. 6(b)) would result in a more accurate form of concentration $(B + 4C = D)\,r\,h/6$, but would require more labor. The parabolic formula suggested by Nathan M. Newmark, F. ASCE, for his numerical integration process,[10] could be used to give concentrations of the form $(Y_A + 10\,Y_B + Y_C)r\,h/12$. The simplest method is the "stepped" method, and it will be used herein.

Correction Factor.—Before considering any bridge structure, a set of correction factors should be obtained for later use. These can be found through solution by the finite difference method of a simply supported beam divided into four subdivisions, and having a load P at the center (Fig. 7). To obtain the unknown deflections at B and C, one fictitious point is required in the first equation. The following two simultaneous equations are set up

$$-Y_B - 4Y_A + 6\,Y_B - 4Y_C + Y_B = 0 \quad \ldots\ldots (37)$$

and

$$-8Y_B + 6\,Y_C = \frac{P\,h^3}{E\,I} \quad \ldots\ldots (38)$$

---

9 "Numerical Methods in Engineering," by M. G. Salvadori and M. L. Baron, Prentice Hall Inc., New York, N. Y., 1952, p. 69.

10 "Numerical Procedure for Computing Deflections, Moments and Buckling Loads," by N. M. Newmark, Transactions, ASCE, Vol. 108, 1943, pp. 1161-1188.

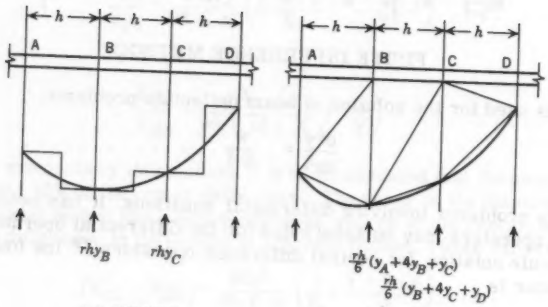


FIG. 6

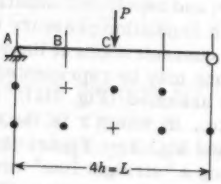


FIG. 7

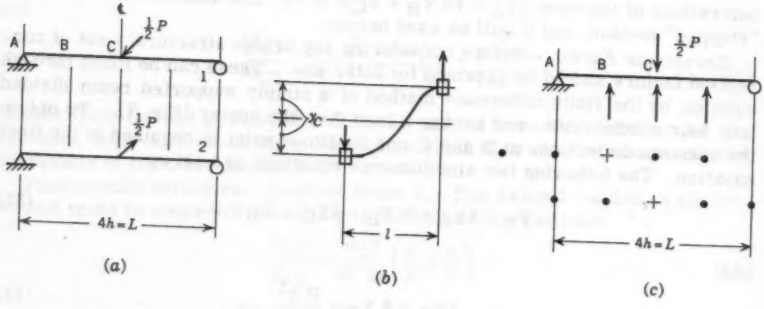


FIG. 8

in which P/h has been substituted for w at point C. Because the deflection at point A is zero, a solution of these equations can be obtained easily, and produces the following deflections:

$$Y_B = \frac{P\,L^3}{64\,E\,I} \quad \ldots\ldots\ldots\ldots\ldots\ldots (39)$$

and

$$Y_C = \frac{3\,P\,L^3}{128\,E\,I} \quad \ldots\ldots\ldots\ldots\ldots\ldots (40)$$

These values are approximately 11% too large, an error that is inherent in the use of the four-division spacing together with the stepped distribution diagram. The correct values should be

$$Y_B = \frac{11}{16}\,\frac{P\,L^3}{48\,E\,I} \quad \ldots\ldots\ldots\ldots\ldots\ldots (41)$$

and

$$Y_C = \frac{P\,L^3}{48\,E\,I} \quad \ldots\ldots\ldots\ldots\ldots\ldots (42)$$

In the solutions to be derived subsequently, similar errors will occur, and they can be corrected by substituting $\frac{11}{16}\,\frac{1}{48}$ for $\frac{1}{64}$, and $\frac{1}{48}$ for $\frac{3}{128}$.

Two-Girder Structure.—In the two-girder structure (Fig. 8), it is assumed that the entire cross framing is concentrated in the evenly-spaced diaphragms at the quarter points and at the center. When the structure is loaded with a set of antisymmetric loads, the shear in the diaphragms, and concentrations at the division points are

$$V_B = \frac{12\,E\,I_c}{l^3}\,(2h\,Y_B) = 2\,k\,h\,Y_B\,E\,I \quad \ldots\ldots\ldots\ldots (43)$$

and

$$V_C = 2\,k\,h\,Y_C\,E\,I \quad \ldots\ldots\ldots\ldots\ldots\ldots (44)$$

The structure has two unknown deflections, Y_B and Y_C, and consequently two simultaneous equations are required. These are

$$-Y_B - 4Y_A + 6Y_B - 4Y_C + Y_B = -2\,K\,h^4\,Y_B \quad \ldots\ldots\ldots (45)$$

and

$$-8Y_B + 6Y_C = -2\,K\,h^4\,Y_C + \frac{P\,h^3}{E\,I} \quad \ldots\ldots\ldots\ldots (46)$$

Replacing $Kh^4 = KL^4/256$ by N, and recognizing that the deflection at A is zero, Eqs. 45 and 46 become

$$6Y_B - 4Y_C = -2N\,Y_B \quad \ldots\ldots\ldots\ldots\ldots\ldots (47)$$

$$-8Y_B + 6Y_C = -2N\,Y_C + \frac{P\,h^3}{E\,I} \quad \ldots\ldots\ldots\ldots (48)$$

A solution of these two equations results in the deflections

$$Y_B = \frac{P\,L^3}{64\,E\,I}\left\{\frac{1}{2}\left[\frac{1}{(3+N)^2 - 8}\right]\right\} \quad \ldots\ldots\ldots\ldots (49)$$

and

$$Y_C = \frac{3\,P\,L^3}{128\,E\,I}\left[\frac{1}{6}\left(\frac{3+N}{Z}\right)\right] \quad \ldots\ldots\ldots\ldots (50)$$

in which Z has been substituted for the term $(3 + N)^2 - 8$ appearing in the denominator. It is obvious that the terms 1/64 and 3/128 are in error and should be replaced by the correct values as previously outlined.

For the symmetrical case, loads of $\frac{1}{2}$P placed at the center of each girder result in deflections of

$$Y_B = \frac{11}{16}\,\frac{P\,L^3}{96\,E\,I} \quad \ldots\ldots\ldots\ldots (51)$$

and

$$Y_C = \frac{P\,L^3}{96\,E\,I} \quad \ldots\ldots\ldots\ldots (52)$$

The combined values are

$$\frac{Y_{B1}}{Y_{B2}} = \frac{11}{16}\,\frac{P\,L^3}{48\,E\,I}\left[\frac{1}{2} \pm \frac{1}{2}\left(\frac{1}{Z}\right)\right] \quad \ldots\ldots\ldots\ldots (53)$$

and

$$\frac{Y_{C1}}{Y_{C2}} = \frac{P\,L^3}{48\,E\,I}\left[\frac{1}{2} \pm \frac{1}{6}\left(\frac{3+N}{2}\right)\right] \quad \ldots\ldots\ldots\ldots (54)$$

Once the deflections have been determined, these values may be translated into loads at the quarter points and at the center. For the antisymmetrical case these loads simplify to

$$P_B = P\,N\left[\frac{11}{12}\left(\frac{1}{Z}\right)\right] \quad \ldots\ldots\ldots\ldots (55)$$

and

$$P_C = P\,N\left[\frac{4}{9}\left(\frac{3+N}{2}\right)\right] \quad \ldots\ldots\ldots\ldots (56)$$

The combined value is

$$P_B + P_C = P\,N\left(\frac{2.25 + 0.444\,N}{Z}\right) \quad \ldots\ldots\ldots\ldots (57)$$

For the symmetrical case the center moments are P L/8, and combining both cases results in the final form of the equation for the moment:

$$\frac{M_{C1}}{M_{C2}} = \frac{P\,L}{4}\left[\frac{1}{2} \pm \frac{1}{2} + N\left(\frac{2.25 + 0.444\,N}{Z}\right)\right] \quad \ldots\ldots\ldots (58)$$

The results for both center deflections, and for center moments for various values of relative stiffness, K, are recorded in Table 1, in which the close agreement with the other methods is evident.

Four-Girder Structure: Load on Beam 1.—A solution of the four-girder problem by the finite difference method does not lend itself readily to the setting up of simple formulas. However, individual cases of particular relative stiffness can be solved easily through the solution of four simultaneous equations each for the symmetrical and antisymmetrical case.

The structure to be considered (Fig. 9) has E I as the stiffness of the inner girders, and E n I as the stiffness of the outer girders. Diaphragms are assumed to be located at the quarter points as well as at the center, and the four

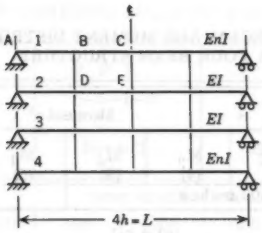


FIG. 9

unknown deflections are Y_B, Y_C, Y_D, and Y_E. For symmetrical loading the equations required are

$$6Y_B - 4Y_C = -N(Y_B - Y_D) \quad \ldots\ldots\ldots\ldots\ldots (59)$$

$$-8Y_B + 6Y_C = -N(Y_C - Y_E) + \frac{P\,h^3}{2\,Y_E\,n\,I} \quad \ldots\ldots\ldots (60)$$

$$6Y_D - 4Y_E = n\,N(Y_B - Y_D) \quad \ldots\ldots\ldots\ldots\ldots (61)$$

and

$$-8Y_D + 6Y_E = n\,N(Y_C - Y_E) \quad \ldots\ldots\ldots\ldots\ldots (62)$$

For the antisymmetrical case the four equations are

$$6Y_B - 4Y_C = -N(Y_B - Y_D) \quad \ldots\ldots\ldots\ldots\ldots (63)$$

$$-8Y_B + 6Y_C = -N(Y_C - Y_E) + \frac{P\,h^3}{2\,Y_E\,n\,I} \quad \ldots\ldots\ldots (64)$$

$$6Y_D - 4Y_E = nN(Y_B - Y_D) - nN\,(2\,Y_D) \quad \ldots\ldots\ldots (65)$$

and

$$-8Y_D + 6Y_E = nN(Y_C - Y_E) - nN(2\,Y_E) \quad \ldots\ldots\ldots (66)$$

Solutions of these equations give the deflections, and once the deflections have been determined, the moments are easily arrived at. Solutions of Eqs. 59 to 66 for both deflection and moment have been tabulated for various values of K in Table 2, and may be compared with the results of the other methods.

TABLES

To indicate the accuracy that can be obtained by the approximate methods, Tables 1 and 2 have been prepared to show comparative results for both moments and deflections. Table 1 shows results for two-girder structures 600 in.

TABLE 3.—PERCENTAGE MOMENT DISTRIBUTION FOR A FOUR BEAM STRUCTURE

Relative stiffness, K, in 10^{-8} inches^4 (1)	Moments[a]							
	M_1 (2)	M_2 (3)	M_3 (4)	M_4 (5)	M_1 (6)	M_2 (7)	M_3 (8)	M_4 (9)
	L = 600 inches				L = 1000 inches			
	(a) n = 1							
	Moments due to load placed on beam 1							
1.40	41.3	22.0	18.8	17.8	34.8	23.2	21.3	20.7
1.10	42.3	21.8	18.5	17.3	35.4	23.1	21.1	20.4
0.80	43.8	21.6	18.0	16.7	36.3	22.9	20.8	20.0
0.50	46.1	21.1	17.1	15.8	37.6	22.7	20.2	19.4
0.20	51.5	20.1	15.1	13.2	41.0	22.0	19.0	17.9
	Moments due to load placed on beam 2							
1.40	22.0	38.3	20.8	18.8	23.2	33.0	22.5	21.3
1.10	21.8	39.0	20.6	18.5	23.1	33.4	22.4	21.1
.80	21.6	40.1	20.4	18.0	22.9	34.0	22.2	20.8
.50	21.1	42.2	19.7	17.1	22.7	35.3	21.8	20.2
.20	20.1	46.4	18.4	15.1	22.0	37.9	21.0	19.0
	(b) n = $\frac{1}{2}$							
	Moments due to load placed on beam 1							
1.40	34.8	29.3	24.3	11.6	27.5	30.9	28.0	13.6
1.10	35.9	29.1	23.7	11.3	28.2	30.8	27.6	13.4
.80	37.6	28.7	22.9	10.8	29.1	30.5	27.1	13.2
.50	40.1	28.1	21.7	10.1	30.7	30.2	26.3	12.7
.20	46.2	26.8	18.6	8.4	34.3	29.4	24.6	11.7
	Moments due to load placed on beam 2							
1.40	14.7	47.0	26.2	12.1	15.4	41.5	29.1	14.0
1.10	14.6	47.8	25.8	11.8	15.4	42.0	28.8	13.8
.80	14.3	49.0	25.2	11.5	15.2	42.8	28.4	13.6
.50	14.1	50.9	24.1	10.8	15.1	43.9	27.8	13.2
.20	13.4	55.6	21.8	9.3	14.7	46.6	26.4	12.3

[a] Moments given as a percentage of PL/4.

and 1,000 in. long. For the two-girder structure, both longitudinals have the same stiffness.

Table 2 shows the distribution of moment and deflection on a four-girder structure with a load only on beam 1. The ratio of outer to inner girder stiffness is $\frac{1}{2}$. The moments appearing on each beam are shown as percentages of the maximum value P L/4. For deflections, the values shown are percentages of $P L^3/48 E n I$ for the outer girders, and of $P L^3/48 E I$ for the inner girders. It should be noted that in Table 2, column 2, the use of the Pippard formulas for K-values as low as 0.10×10^{-8} is not recommended. For this low value $\lambda L = 2.64$ and a correction factor is required.

Tables 3 and 4 have been prepared, using the Pippard formulas, to indicate the general trend in obtainable results. However, either of the approximate

TABLE 4.—MOMENTS FOR COMBINED LOADS ON A FOUR BEAM STRUCTURE

Relative stiffness, K, in 10^{-8} inches^4	P P P I—I—I—I * Beam 1 (2)		P P P I—I—I—I * Beam 2 (3)		P 2P 2P I—I—I—I * Beam 1 (4)		$\frac{1}{2}$P P P I—I—I—I * Beam 2 (5)	
	Span length, L, in inches							
	600	1000	600	1000	600	1000	600	1000
(1)	Moments,[a] in							
1.40	82.1	79.3	81.1	78.7	88.3	86.3	87.9	86.1
1.10	82.6	79.6	81.4	78.9	88.7	86.6	88.2	86.2
0.80	83.0	80.0	82.1	79.1	89.1	86.9	88.6	86.5
0.50	84.3	80.5	83.0	79.8	89.9	87.3	89.1	86.8
0.20	86.7	82.0	84.9	80.9	91.6	88.3	90.8	87.7

[a] Moments shown as percentage of PL/4 for beam indicated with loads on beams 1, 2, and 3 of structure.

methods might have been used. Both Tables 3 and 4 apply to four-girder structures, both 600 in. and 1,000 in. long, and having n-values of both $\frac{1}{2}$ and 1. For each structure, two sets of results have been obtained, first with the load placed on beam 1, and then with the load placed on beam 2. Table 3 shows the moment percentage appearing on each beam for the various cases considered.

If each girder of the structure is given a maximum load at the center, then the value of the moment in each girder will be 100% of P L/4. However, normal spacing often precludes the possibility of loading all four girders at the same time. Assuming that only three of the girders are fully loaded, the moments are combined for each case, and the total moments are shown in Table 4. Columns 2 and 3 of Table 4 show the moments when load P is applied to beams 1, 2, and 3, column 4 indicates the moments when load P is applied to beam 1 and load 2 P is applied to beams 2 and 3. The moments given in column 5 result when $\frac{1}{2}$P is applied to beam 1 and load P is applied to beams 2 and 3. In Table 4, n = 1 for columns 2 and 3. For the case of n = $\frac{1}{2}$ (columns 4 and 5), it was assumed that the load appearing on each girder was the maximum design load, and the inner girders were given twice the load of the outer girder. Two sets of combined maximum values were obtained, one for beam 1, and a second

set for beam 2. The maximum obtainable moment is between 80% to 90% of that on a fully-loaded structure, or on a structure for which each beam is assumed to carry its own load.

The Pippard formulas used for the various structures considered are lengthy and will not be reproduced here. They may be found elsewhere.[11]

CONCLUSIONS

The results obtained indicate the validity of the simple numerical methods outlined. For the type of structure examined, the possibility of replacing the entire cross framing by a single center diaphragm for analysis purposes is clearly indicated. Where interconnected girders are employed, that preclude the possibility of all girders being fully loaded at the same time, distinct savings are indicated.

APPENDIX. NOTATION

The following symbols, adapted for use in this paper and for the guidance of discussers, conform essentially with the "American Standard Letter Symbols for Structural Analysis" (ASA Z10.8-1949) prepared by a committee of the American Standards Association with Society representation, and approved by the Association in 1949:

- E = modulus of elasticity;
- EI_1 = stiffness of girder 1;
- EI_2 = stiffness of girder 2;
- EI_c = stiffness of cross framing per unit length of structure;
- h = length of subdivision;
- I = moment of inertia;
- K = relative stiffness = $12\ E\ I_c/l^3\ E\ n\ I$;
- L = span length;
- l = distance between main girders;
- M_c = center moment of a designated beam;
- N = $K\ L^4/256$;
- n = ratio of $E\ I_1/E\ I_2$ in a four girder structure;
- P = concentrated load applied at center span;
- P_x = concentrated load at any point;
- r = spring constant = $2\ K\ E\ I$
- V = shear in cross girder;

V_c = shear in the center diaphragm;

w = shear per unit length;

X = $(1 + \phi + n\phi)$;

Y = $(1 + \phi)(1 + 3n\phi) - n\phi^2$;

y = deflection of a beam from its initial position;

y_{C1} = deflection of beam 1 at point C;

y_{C2} = deflection of beam 2 at point C;

Z = $(3 + n)^2 - 8$;

ϕ = $KL^4/96$; and

λ = $\sqrt[4]{r/4EI}$.

DISCUSSION

DRONNADULA V. REDDY.[11]—Mr. Malter's paper is confined to numerical methods of analysis for interconnected beam systems with the following two assumptions: (1) Infinite torsional rigidity of the longitudinal girders and (2) external torques preventing rotation. As shown by the author, Alfred J. S. Pippard and John P. A. De Waele[12] made the same assumptions for their solution by differential equations. These assumptions are difficult to satisfy in practice. In reinforced concrete T-beam bridges, the girders may justifiably be assumed to possess infinite torsional rigidity, but in the case of simply supported ends, there is nothing to prevent rotation.

Consider the transverse profile of the 3-girder bridge, shown in Fig. 10. From slope deflection relationships the moment in transverse medium 1-2 per unit length is

$$M_{12} = \frac{6\,N\,E\,I_c}{l^2 L}\left(y_2 - y_1 - \frac{2}{3}\,l\theta_1\right) \quad \ldots\ldots\ldots\ldots (67)$$

in which $E\,I_c$ is the flexural rigidity of a transversal; N is equal to the number of transversals; L represents the span of the bridge; l is the spacing of longitudinals; y_1 and y_2 are deflections of longitudinals Nos. 1 and 2; and θ_1 denotes the rotation of longitudinal No. 1.

The moment M_{12} has to be balanced by moments in the longitudinal No. 1. The balancing moments in the longitudinal can be induced if there is a relative twist in it, or if external constraints provide the necessary restraint. There is no relative twist in a longitudinal with infinite torsional rigidity, and, therefore, it rotates as a rigid body. When the ends are simply supported, there are no restraints preventing rotation except the transversals, which have to

[11] Research Student, Dept. of Bldg. Science, Univ. of Liverpool, Liverpool, England.

[12] "The loading of Interconnected Bridge Girders," by A. J. S. Pippard and J. P. A. De Waele, Journal, Inst. C. E., Vol. 10, No. 1, 1938.

be very stiff to provide sufficient rotational restraint. From the values plotted by Arnold W. Hendry and Leslie G. Jaeger,[13] the minimum value of K for this condition is found to be 22.7 X 10^{-8} for a four-girder bridge loaded on the outer girder. Mr. Malter's values of K are much less than this amount. The percentage moment values obtained from analysis of the four-girder grid loaded on the outer longitudinal, assuming infinite torsional rigidity in the longitudinals with no rotation, and with rigid-body rotation, are plotted in Fig. 11. The span length is 600 in. The values have been obtained from the plotted results of Hendry and Jaeger. The Malter's values are also shown for comparison. For the case considered by the author, the results show good agreement with the Hendry-Jaeger values. However, there is considerable difference in moment proportions between the conditions of 'no rotation' and 'rotation'. Even when the errors in longitudinal moments are small, the moments in the transverse members may be considerably overestimated by assuming no rotation in the main girders.

The observation of 70% deflection at quarter points derives from the fact that a beam under symmetrical loading deflects almost exactly into a sinusoidal profile (first harmonic). However, the author does not refer to it in this manner.

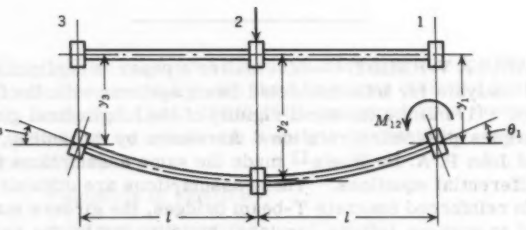


FIG. 10.—TRANSVERSE PROFILE OF A 3-GIRDER GRID

The method of representing the pressure of an elastic foundation by means of a series of redundant reactions, and setting up a system of simultaneous equations in terms of the pressure ordinates and the elastic constants of the beam and foundation, was described first by Zusse Levinton.[14] In a discussion of Levinton's paper, Joseph Gold[15] suggested the finite difference method of solution. This method has been applied in some numerical examples by Mr. Malter.[16] The number of equations becomes large for unsymmetrical loading and the approximations in computing the areas of pressure diagrams of the elastic foundations may cause appreciable errors in the case of ill-conditioned equations. Also, small errors in deflection lead to large errors in moment

13 "The Analysis of Grid Frameworks and Related Structures," by A. W. Hendry and L. G. Jaeger, Chatto and Windus, London, 1958.

14 "Elastic Foundations Analysed by the Method of Redundant Reactions," by Z. Levinton, Transactions, ASCE, Vol. 114, 1949, pp. 40–52.

15 Discussion by J. Gold of "Elastic Foundations Analysed by the Method of Redundant Reactions," ibid., pp. 64–70.

16 "Numerical Solutions for Beams on Elastic Foundations," by H. Malter, Proceedings Paper 1562, ASCE, March, 1958.

values, particularly in the transversals. The method of using correction factors to reduce the error caused by using finite differences instead of infinitesimals is to be commended. It is simpler than the application of generalized extrapolation procedures described by L. F. Richardson.[17] However, the writer cannot agree with the use of the same correction factors in all the longitudinals that assumes similar forms of deformation. It is convenient to examine the shapes of deflected profiles from the viewpoint of harmonic analysis. The loaded girder deforms almost exactly into a profile given by the superposition

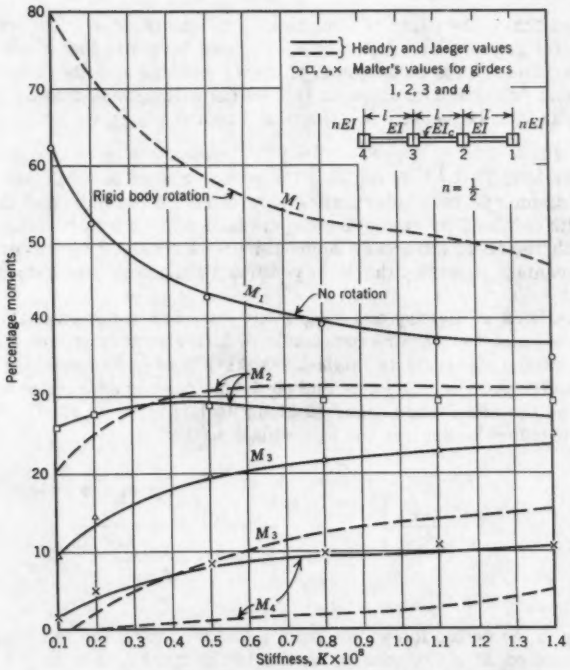


FIG. 11.—PERCENTAGE MOMENT DISTRIBUTION

of a first and a third harmonic, but the unloaded girders deform into profiles represented by first harmonics only. Whereas the errors caused by using the same correction factors in all longitudinals may not be serious for symmetrical loading, they may become appreciable for unsymmetrical loads.

---

17 "The Approximate Arithmetical Solution by Finite Differences of Physical Problems Involving Differential Equations," by L. F. Richardson, Philosophical Transactions, Royal Soc. of London, Series A, Vol. 210, 1911, pp. 307–357.

Mr. Malter replaces the entire transverse system by three evenly-spaced diaphragms at the quarter points and the center. Because each diaphragm represents the transverse medium for a quarter of the span, only three-quarters of the whole span is accounted for. If the outer diaphragm were assumed to be at the sixth points, then each diaphragm would replace the transverse medium for a third of the span.

By the statement in the Introduction,

> "Any practical conclusions must be governed to a great extent by experimental results and observations on full-scale bridges, and no effort to consider the applicability of any particular solution will be undertaken in this paper,"

the author limits the paper to analytical procedures only. The writer would like to refer readers to a paper by Hendry and Jaeger[18] that gives a comprehensive account of the comparison of theory with the results of tests on large models and full-sized bridges at the Building Research Station at Watford, England, and the University of Illinois at Urbana.

HENRY MALTER,[19] F. ASCE.—The writer wishes to thank Mr. Reddy for his discussion. Of particular interest were the curves indicated in Fig. 11 of the results obtained by employing the methods of Hendry and Jaeger as compared with the finite difference approximations obtained by the writer. The good agreement shown by the totally different methods was informative and gratifying.

The methods of Hendry and Jaeger are based on a series analysis, and it might be of value to compare the results of a straightforward series approach with that of the approximate method. Miklos Hetenyi[20] examines the series solution to the problem of a concentrated load resting on a beam with simple supports at the ends, and supported along its length by an elastic foundation. For this problem he derives the following equation:

$$y = \frac{2\,PL^3}{\pi^4\,E\,I} \sum_{m=1}^{\alpha} \frac{\sin\frac{m\pi c}{L}\sin\frac{m\pi x}{L}}{m^4 + \frac{r\,L^4}{m^4\,E\,I}} \qquad \ldots\ldots\ldots (68)$$

in which y is the deflection at any point x distance from the left support; P is the load applied at c distance from the left support and m may take on the values 1, 2, 3 .... Eq. 68 may be compared with the equation for deflection employed in the derivation of Eq. 11.

$$Y_C = \frac{P\,L^3}{96\,E\,I}\left(\frac{1}{1+2\,\phi}\right) \qquad \ldots\ldots\ldots\ldots\ldots (69)$$

---

18 "Load Distribution in Highway Bridge Decks," by A. W. Hendry and L. G. Jaeger, Transactions, ASCE, Vol. 123, 1958, pp. 1214-1241.

19 Prof., Civ. Engrg., Univ. of Illinois, Urbana, Ill.

20 "Beams on Elastic Foundations," by M. Hetenyi, the Univ. of Michigan Press, Ann Arbor, Michigan, 1946; p. 76.

Substituting values for ϕ, and changing 1/2 P to P, this equation becomes, for the load P at the center of the beam,

$$Y_C = \frac{P L^3}{48 E I}\left(\frac{1}{1 + \frac{r L^4}{96 E I}}\right) \quad \ldots\ldots\ldots\ldots\ldots\ldots (70)$$

This will be recognized as the first term of the series solution derived by Hetenyi,[20] with 96 being substituted for $\pi 4$.

The description by Mr. Reddy of the various conditions of torsional rigidity that may be encountered are essentially correct. However, it is felt that in the condition of a heavy end diaphragm in concrete beam or box girder type of construction, the case of infinite torsional rigidity with no rotation might be encountered.

Regarding the spacing of the diaphragms, whether at the quarter or the sixth points, it is questionable whether one would be more accurate than the other in approximating a distributed slab. The quarter-point spacing in reality results in five diaphragms being employed, the two end diaphragms having no effect on the computations inasmuch as no deflections occur at the supports. Also, using the quarter-point diaphragms simplifies the calculations.

AMERICAN SOCIETY OF CIVIL ENGINEERS

Founded November 5, 1852

TRANSACTIONS

Paper No. 3026

SELECTION OF DESIGN WAVE FOR OFFSHORE STRUCTURES

By Charles L. Bretschneider,[1] M. ASCE

With Discussion by Messrs. J. E. Chappelear; and Charles L. Bretschneider

SYNOPSIS

Methods are presented for selecting the design wave, crest elevation, wave length, and maximum horizontal particle velocity at the crest for offshore structures. Wave data from various sources, supplemented by a limited amount of wave theory required for the development of generalized graphs, are given in Appendix I.

INTRODUCTION

Methods of predicting maximum waves for hurricane design-wave problems have been presented elsewhere.[2,3] In regard to the design of both offshore structures and coastal structures, it is important to realize a design-wave height, period, crest elevation, and wave length. In many cases there may be a number of waves for selection. For the design of an offshore platform supported by piling, it is necessary that the underside of the deck clear the crest of the wave. The wave length and surface profile are important when computing total forces and overturning moments induced by the wave on a

Note.—Published, essentially as printed here, in March, 1958, in the Journal of the Waterways and Harbors Division, as Proceedings Paper 1568. Positions and titles given are those in effect when the paper or discussion was approved for publication in Transactions.

[1] Hydr. Engr. Beach Erosion Bd., Corps of Engrs., Washington, D.C.

[2] "Surface Waves and Offshore Structures: The Design Wave in Deep or Shallow Water, Storm Tide, and Forces on Vertical Piling and Large Submerged Objects," by O. R. Reid and C. L. Bretschneider, Technical Report, Texas A. & M. Research Foundation, Coll. Sta., Tex., October, 1953.

[3] "Hurricane Design-Wave Practices," by C. K. Bretschneider, Transactions, ASCE, Vol. 124, 1959, pp. 39-62.

series of supporting piles. The maximum horizontal particle velocity at the crest provides a check against the wave theory used to compute the internal velocity field.

The selection of the design wave consists of the following steps:

1. Calibration
   a. Storm surge formulas
   b. Wave forecasting formulas and techniques
2. Frequency study
   a. Wave statistics
   b. Hurricane frequency study
3. Predictions for design
   a. Storm surge
   b. Significant wave height and period
   c. Maximum wave height and corresponding wave period
   d. Crest elevation of maximum wave
   e. Wave length of maximum wave

Each of these steps will be discussed subsequently.

Notation.—The letter symbols adapted for use in this paper are defined where they first appear, and are arranged alphabetically, for convenience of reference, in Appendix II.

CALIBRATION

It is necessary to calibrate storm surge prediction formulas and techniques to take into account deviations between observed and predicted high water levels. This is particularly evident in and near coastal areas in which irregularities in both bottom topography and coastal features play an important role in modification of storm surges.

Methods of predicting storm surges on the open coast have been presented by Robert D. Reid[4] and John C. Freeman et al.[5] In using any method, storm surge hydrographs should be used for calibration when they are available, such that when they are applied to the design storm, a reasonable estimate of storm surge is obtained. This requires an analysis of all past hurricanes, where such data are available. In those cases in which no data are available, data from a nearby and similar location may be used. As a first approximation to the solution of the storm surge, the method proposed by Reid[4] may be used directly.

Calibration of wave forecasting formulas and techniques is also necessary to account for variabilities in individual techniques and locations. A number of methods are available for predicting waves in both deep and shallow water. In the case of deep water there are four methods generally used: the Sverdrump-Munk-Bretschneider method,[6] the Pierson-Neumann-James

[4] "Approximate Response of Water Level on a Sloping Shelf to a Wind Fetch which Moves Towards Shore," by R. O. Reid, Technical Memorandum No. 83, Beach Erosion Bd., Corps of Engrs., U.S. Dept. of the Army, June, 1956.

[5] "The Bathystrophic Storm Tide," by John C. Freeman, Jr., Ledolph Baer, and Glen H. Jung, presented at the 150th Natl. Meeting of the Amer. Meteorological Soc., January 28-31, 1957, New York, N.Y. Journal of Marine Research, Vol. 16, No. 1, pp. 12-22, 1957.

[6] "Revised Wave Forecasting Relationships," by C. L. Bretschneider, Proceedings, 2d Conf. on Coastal Engrg., Council of Wave Research, Engineering Foundation, Berkeley, California, 1952.

method,[7] the Darbyshire method,[8] and the Suthon-Braceline method.[9] All of these methods have incorporated inherent characteristics associated with both the procurement of data from various locations, and with the method of analysis and interpretation of these data by the individual contributors. An objective verification study of the forementioned methods was made by H. U. Roll,[10] and the general conclusion was that each method works best for the particular region from which the principal data were obtained. Perhaps even better verification might have been obtained if the individual contributors had made the forecast, each using his own methods and techniques. The graphical approach methods, utilized by Basil W. Wilson,[11] should be useful for calibration purposes.

There exist two methods for predicting wind waves in shallow water, presented by J. Th. Thijsse[12] and Bretschneider.[13] Each gives reasonably consistent results for shallow water of constant depth. The Bretschneider method,[14] extended to the Continental Shelf, is calibrated, based on hurricane wind and wave data from Lake Okeechobee, Florida,[15] and some ordinary wind wave data from the Gulf of Mexico.[16] Although this method is used to predict hurricane waves over the Continental Shelf, improvements in the techniques can be expected when hurricane wave data become available from the Continental Shelf for a refined calibration. An example of computations showing the use of this method is given elsewhere.[3]

FREQUENCY STUDY

By use of the wave hindcasting techniques, data have been compiled on wave statistics for various locations along the United States shores. The data, summarized in various Beach Erosion Board Technical Memoranda,[17] are given

---

7 "Practical Methods for Observing and Forecasting Ocean Waves by Means of Wave Spectra and Statistics," by W. J. Pierson, Jr., Gerhard Neumann, and R. W. James, No. 603, Hydrographic Office, 1955.

8 "An Investigation of Storm Waves in the North Atlantic Ocean," by J. Darbyshire, Proceedings, Royal Soc. of London, Series A230, 1955.

9 "The Forecasting of Sea and Swell Waves," by Comdr. C. T. Suthons, Naval Met. Branch, Memorandum No. 135/45, U.S. Hydrographic Dept., 1955.

10 "Forecasting Surface Gravity Waves," by H. U. Roll, Conf. on Long Waves and Storm Surges, Natl. Inst. of Oceanography, Wormley, England, May, 1957.

11 "Graphical Approach to the Forecasting of Waves in Moving Fetches," by B. W. Wilson, Technical Memorandum No. 73, Beach Erosion Bd., Corps of Engrs., U.S. Dept. of the Army, Washington, D.C., April, 1955.

12 "Growth of Wind-Generated Waves and Energy Transfer," by J. Th. Thijsse, Circular 521: Gravity Waves, Natl. Bur. of Standards, Washington, D.C., 1952, pp. 281-287.

13 "Generation of Wind Waves in Shallow Water," by C. L. Bretschneider, Technical Memorandum No. 51, Beach Erosion Bd., U.S. Army Corps of Engrs., Washington, D.C., 1954.

14 "Wave Forecasting Relationships for the Gulf of Mexico," by C. L. Bretschneider, Technical Memorandum No. 84, Beach Erosion Bd., U.S. Army Corps of Engrs., Washington, D.C., December, 1956.

15 "Project CWI - 167: Waves and Wind Tides in Inland Waters; Lake Okeechobee, Florida," Project Bulletin No. 5, Hurricane Data, Corps of Engrs., U.S. Army, Office of the Dist. Engr., Jacksonville, Fla., October, 1950.

16 "Field Investigation of Wave Energy Loss in Shallow Water Ocean Waves," by C. L. Bretschneider, Technical Memorandum No. 46, Beach Erosion Bd., U.S. Army Corps of Engrs., Washington, D.C., September, 1954.

17 Technical Memoranda Nos. 36, 37, 38, 55, 57, 85, 86, 87, 88, 89, and 98, Beach Erosion Bd., Corps of Engrs., U.S. Dept. of the Army, Washington, D.C.

in terms of the significant height and period. The importance of these wave statistics can be considered for certain design problems other than offshore structures, and for planning marine operations where hurricanes are not a menace. It must be emphasized that the maximum wave may be as much as 1.87 times the significant height.

To date (1960), little information is available on the frequency of hurricane waves, as far as actual observations are concerned. However, hurricane wave statistics for the deep water of the Gulf of Mexico have been compiled recently by Basil W. Wilson,[18] using the graphical approach to wave forecasting.[11] For most design problems these data must be brought across the Continental Shelf, taking bottom friction and refraction into account as further generation takes place. This report[18] might be a source for obtaining the design wave for locations in the Gulf of Mexico.

TABLE 1.—FREQUENCY OF 17 HURRICANES BETWEEN CAPE HATTERAS AND JACKSONVILLE (1893-1955)

Hurricane (1)	Date (2)	R[a], in nautical miles (3)	Δp[a], in inches of mercury (4)	RΔP (5)	f, in percentage (6)
1	9/31/99	110	1.22	134.2	2.94
2	10/15/54	36	2.31	83.2	8.82
3	9/19/55	50	1.46	73.0	14.71
4	8/12/55	45	1.40	63.0	20.59
5	12/ 2/25	54	1.02	55.1	26.47
6	8/27/93	34	1.64	50.8	32.35
7	9/13/13	39	1.16	45.2	38.23
8	9/ 2/98	32	1.40	44.8	44.12
9	8/17/55	45	0.82	36.9	50.00
10	9/17/06	37	0.99	36.6	55.88
11	9/13/93	23	1.59	36.5	61.76
12	8/11/40	27	1.19	32.1	67.64
13	8/28/11	27	1.05	28.4	73.53
14	8/14/53	30	0.79	23.7	79.41
15	10/15/47	12	1.38	16.6	85.29
16	8/11/14	19.5	0.76	14.8	91.17
17	8/30/52	20	0.95	11.4	97.05

[a] Values R and ΔP were furnished by Hydrometeorological Section, U.S. Weather Bureau.

The selection of the design wave can be obtained by use of an alternate method, wherein the design storm is first selected. This method consists of a frequency study of all hurricanes and other major storms passing a given length of coastline. Generally, a 300 to 400-mi section of coastline is selected in order to obtain a sufficient number of hurricanes for a frequency study. The frequency study is then normalized in terms of 100 mi of coastline. For example, consider the hurricanes of record that entered the United States

[18] "Hurricane Wave Statistics for the Gulf of Mexico," by B. W. Wilson, Technical Memorandum No. 98, Beach Erosion Bd., Corps of Engrs., U.S. Dept. of the Army, Washington, D.C.

coast between Jacksonville, Florida and Cape Hatteras, North Carolina, a distance of close to 430 nautical miles. Between 1893 and 1955, 17 hurricanes entered this part of the coast. Insufficient data are available for hurricanes occurring before 1893. These 17 hurricanes are summarized in Table 1 in descending order of the Energy Index, RΔp, in which R is the radius of maximum wind in nautical miles, and Δp represents the pressure anomaly at the center of the hurricane from normal pressure. The frequency of occurrence of the hurricanes is obtained by use of the Beard's formula;[3]

$$f = \frac{100\ n - \frac{1}{2}}{M} \quad \ldots\ldots\ldots\ldots\ldots\ldots \quad (1)$$

in which f represents the percentage of occurrence; n denotes the order of RΔp (1 to 17); and M is the total number of hurricanes (17).

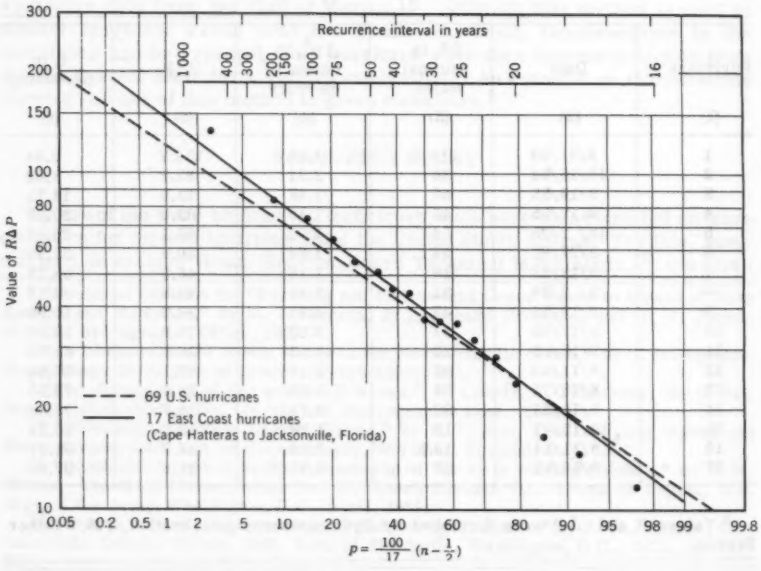


FIG. 1.—FREQUENCY OF HURRICANE RΔP VERSUS PERCENTAGE OF OCCURRENCE

The information from Table 1 is plotted on the log-probability graph in Fig. 1. The term p represents the percent probability that RΔp is equal to or exceeded, and n is the number order of RΔp beginning with the largest value of RΔp. It is seen that the intensity along this part of the coast is slightly greater than for the United States as a whole, as given by Reid.[19]

19 "Surface Waves and Offshore Structures: The Design Wave in Deep or Shallow Water, Storm Tide, and Forces on Vertical Piling and Large Submerged Objects," by O. R. Reid and C. L. Bretschneider, Technical Report, Texas A. & M. Research Foundation, Coll. Sta., Tex., October, 1953, Fig. 7.

Because 17 hurricanes entered a 430-mi section of coast in 62 yr, $\frac{62}{17} \times \frac{430}{100} = 15.7$ yr is the hurricane recurrence interval. Therefore, the center of a hurricane will generally enter a 100-mi section of the east coast between Cape Hatteras and Jacksonville once in 15.7 yr. The recurrence interval, in years, for any particular strength of storm for Fig. 1, is obtained from

$$I = \frac{15.7}{f} 100 \quad \ldots\ldots\ldots\ldots\ldots\ldots \quad (2)$$

and

$$f = \frac{1570}{I} \quad \ldots\ldots\ldots\ldots\ldots\ldots \quad (3)$$

Fig. 1 can be used to obtain the Energy Index $R\Delta p$ for a particular recurrence interval. Thus, for I = 100 yr, f = 1570/100 = 15.7%, and from Fig. 1,

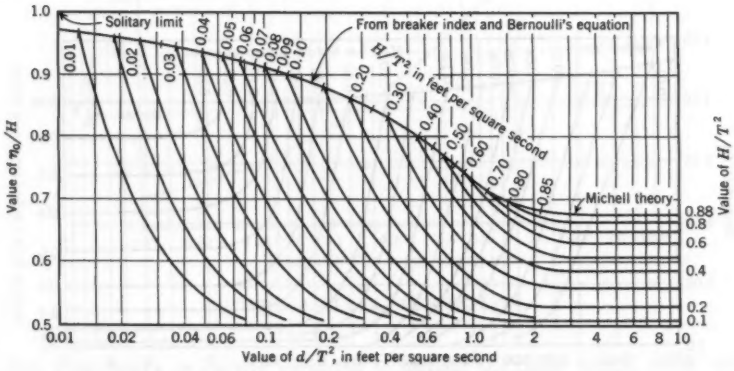


FIG. 2.—RATIO OF CREST ELEVATION ABOVE STILL WATER TO WAVE HEIGHT

$R\Delta p = 69$. From Table 1 it is seen that the radius of maximum wind will be between 45 and 50 nautical miles and Δp between 1.46 and 1.40 in. of mercury. Further investigations reveal that such a hurricane may have a forward speed V_F between 7 and 14 knots.[20] Hence the design storm is selected for a recurrence interval of one in 100 yr per 100 mi of coast; and R = 48 nautical miles, Δp = 1.44 inches of mercury, $R\Delta p = 69$, and V_F = 10.5 knots.

DESIGN WAVE PREDICTIONS

Once the design storm has been determined and the prediction equation calibrated, computations are made for storm surge and significant waves. An example has been worked out[3] based on Hurricane Hazel of October 15, 1954.

20 "Surface Waves and Offshore Structures: The Design Wave in Deep or Shallow Water, Storm Tide, and Forces on Vertical Piling and Large Submerged Objects," by O. R. Reid and C. L. Bretschneider, Technical Report, Texas A. & M. Research Foundation, Coll. Sta., Tex., October, 1953, Table 1.

For this example, $R\Delta p = 83.2$, corresponding to f = 9.0% from Fig. 1. The recurrence interval in years per 100 miles of coast is I = 1570/9 = 175 yr. In this example it was found that for a mean low water depth, d_o = 74 ft, the total water depth with surge applied d = 85.3, the maximum wave height H_{max} = 39.6 ft and the wave period T = 11.63 sec.

The crest elevation above d = 85.3 ft is obtained by use of Fig. 2. (See Appendix I for development of Figs. 2, 3, and 5.) Compute $H/T^2 = .293$ and $d/T^2 = .63$, and read $\eta_o/H = .69$ from Fig. 2. Hence $\eta_o = (39.6)(.69) = 27.3$ ft, and the crest elevation will be 85.3 + 27.3 = 112.6 ft above sea bottom. In Fig. 2, H represents the wave height in feet, d denotes the still water depth in feet, and η_o is the crest elevation above still water in feet. The isolines are cross interpolations from Figs. 11 and 12.

The wave length is obtained from

$$L = \left(\frac{L}{L_A}\right) \frac{gT^2}{2\pi} \tanh \frac{2\pi d}{L_A} \quad \ldots\ldots\ldots\ldots\ldots\ldots (4)$$

in which L_A is the Airy wave length, L/L_A is a correction factor for wave steepness and is obtained by use of Fig. 3, and h is the trough elevation above

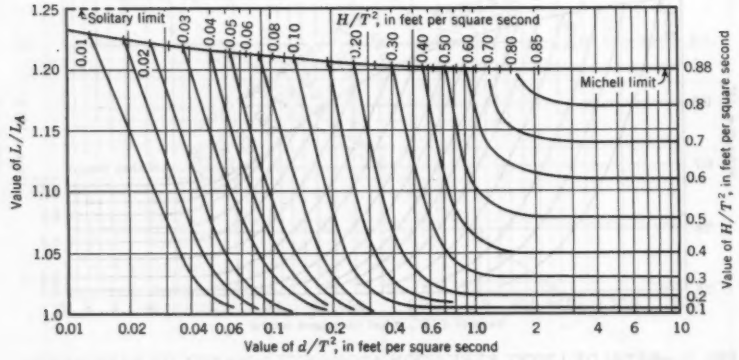


FIG. 3.—CORRECTION FACTOR FOR WAVE LENGTH DUE TO STEEPNESS

bottom. The deep water Airy wave length $L_o = gT^2/2\pi = 5.12\ T^2 = 693$ ft when the acceleration of gravity g = 32.16 ft per sq sec and $\pi = 3.1416$. Computing $d/L_o = \frac{85.3}{693} = .123$ and from Wiegel's[21] tables, $\frac{L_A}{L_o} = \tanh \frac{2\pi d}{L_A} = .7656$. The solution of L_A/L_o is given in Fig. 4 in terms of d/T^2 and is equal to 0.77. From Fig. 3 for $d/T^2 = .63$ and $H/T^2 = .293$ read $L/L_A = 1.06$.

Thus, L = 1.06 (693)(.77) = 565 ft. The wave celerity C = L/T = 565/11.63 = 48.5 ft per sec.

---

21 "Tables of the Functions d/L and d/L_o," by R. L. Wiegel, Report No. H.E.-116-265, Dept. of Engrg., Univ. of California, Berkeley, Calif., January, 1948.

The maximum horizontal particle velocity at the crest u_{max} can be obtained from Fig. 5. Compute,

$$\frac{2g\,\eta_o}{C^2} = \frac{(64.4)(27.3)}{C^2} = .75$$

From Fig. 5 read $u_{max}/C = 0.5$. Thus $u_{max} = 0.5\,(48) = 24$ ft per sec.

It is interesting to compare these values with those obtained by use of the Airy[22,23] wave theory, wherein $\eta_o = \frac{H}{2} = (39.6)/2 = 19.8$ ft, or 7.5 ft lower than that given for this example. The Airy wave length is $L_A = 693\ (.7656) = 531$ ft, or 32 ft shorter. The wave speed is $C = L/T = 45.6$ ft per sec. The maximum horizontal particle velocity is given by $u_{max} = \frac{gH}{2C} = 13.8$ ft per sec.

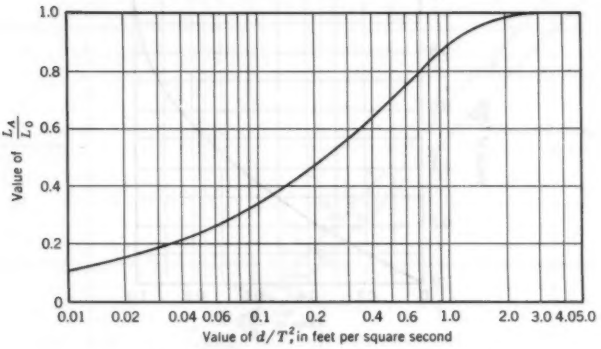


FIG. 4.—L_A/L_o VERSUS d/T^2

The Airy theory is usually extended to include the finite height, from which u_{max} is given by

$$u_{max} = \frac{\pi H}{T} \frac{\cosh \frac{2\pi\,(d + .5H)}{L}}{\sinh \frac{2\pi d}{L}} \qquad \ldots\ldots\ldots\ldots\ldots (5)$$

and is equal to 17.0 fps, 40% less than that obtained by use of Bernoulli's equation (Fig. 5). Because the force on a pile is proportional to the velocity squared, $(24/17)^2 = 2.0$ is the ratio of maximum crest force obtained by the two methods, assuming the same drag coefficient in either case.

22 "On Tides and Waves," by G. B. Airy, Encyclopedia Metropolitana, Vol. 5 (Mixed Science), London, 1845, pp. 241-396.

23 "Hydrodynamics," by Horace Lamb, Dover Pub., New York, 6th Ed., 1945.

Thus, if the Airy wave theory is used for design conditions, an added safety factor is mandatory for both the crest elevations and the velocity and acceleration fields. Use of the Airy theory in the forementioned sense is not a recommended practice.

APPLICATION TO HURRICANE WIND WAVES

The preceding discussion is applicable to regular and simple waves, unaffected by strong winds. Figs. 2 and 3 do not take into account any change in wave characteristics due to strong winds. This can best be studied by use of empirical data. Hurricane wave data from Lake Okeechobee, Florida,[15] have been analyzed for H, T, d, and η_0 (Table 4). Fig. 2, with the aid of H/T^2 and d/T^2 computed from Table 4, was used to obtain the predicted value of η_0

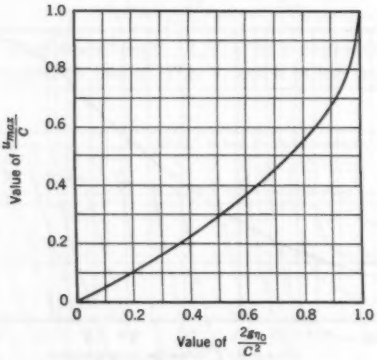


FIG. 5.—MAXIMUM HORIZONTAL PARTICLE VELOCITY AT CREST

also presented in Table 4. Fig. 6 is a comparison between observed η_0 and predicted η_0. The equation of regression line is

$$(\eta_0)_{ob} = .052 + 1.045\ (\eta_0)_{pr} \quad \ldots\ldots\ldots\ldots \quad (6)$$

in which $(\eta_0)_{ob}$ and $(\eta_0)_{pr}$ are the observed and predicted crest elevations respectively, and the correlation coefficient r = .958. In Fig. 6 the predictions were obtained by use of Fig. 2. Much of the scatter is due to the inability of obtaining exactly H, T, and d, and long run averages are more significant. Even under controlled laboratory conditions a considerable scatter of individual data is experienced. The regression line of observed η_0 to predicted η_0 has an intercept at .052 and a slope of 1.045 as determined by the least squares techniques. If it is assumed that Fig. 2 is correct for waves unaffected by wind, then the effect of hurricane winds is to increase on long run averages the crest elevation above still water by approximately 5%. Be-

cause of the scatter of data, perhaps a 10% increase in some cases is justified for the design wave. This, of course, needs further study, using possible wave data of the Gulf of Mexico.

CONCLUSIONS

This paper represents a method of obtaining for the design wave height, the crest elevation, wave length, and maximum horizontal particle velocity at the crest of the design wave, and is intended to supplement information presented elsewhere.[2,3]

Two generalized graphs are prepared using wave theory, Bernoulli's equation, and wave data. Fig. 2 is for obtaining the crest elevation and Fig. 3 for

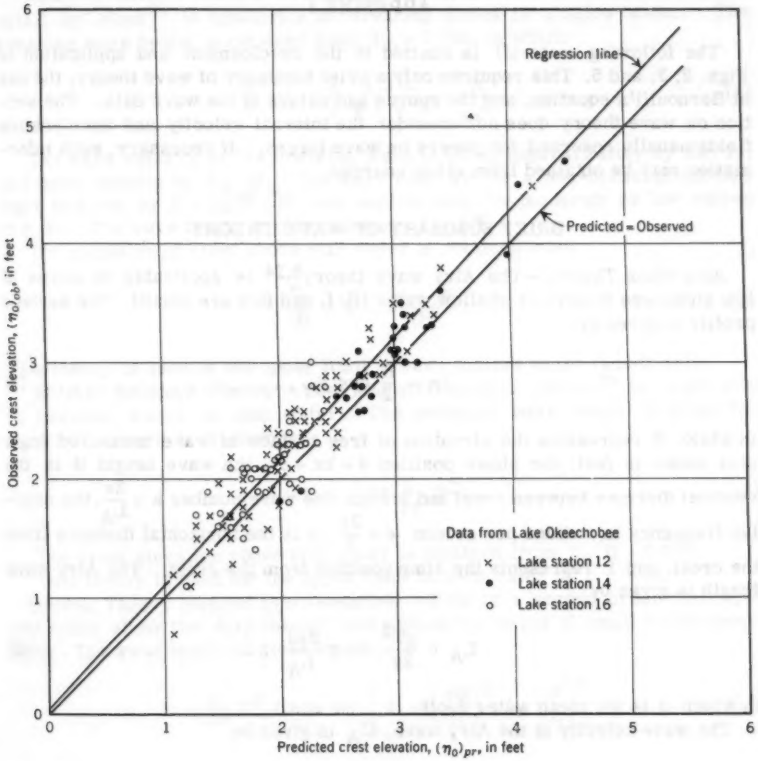


FIG. 6.—COMPARISON BETWEEN OBSERVED AND PREDICTED CREST ELEVATION ABOVE STILL WATER

obtaining the wave length of the design wave. Fig. 5 can be used in conjunction with Figs. 2 and 3 for predicting the maximum horizontal particle velocity at the crest. The effect of hurricane winds has been considered. Based on Lake Okeechobee hurricane wave data, it was found that the crest elevations were approximately 5% greater than those predicted by Fig. 2. The scatter of data

shows that perhaps a 10% increase may be justified, but this needs further investigation of larger hurricane waves, such as might be found in the Gulf of Mexico.

ACKNOWLEDGMENTS

The author extends his appreciation to the Beach Erosion Board for sponsoring personnel and time used in the preparation of this paper, to Francis W. Kellum for computations, Verner E. Dahlin for drafting. Credit is also extended to Robert O. Reid[2] who initiated much of the original work.

APPENDIX I

The following material is limited to the development and application of Figs. 2, 3, and 5. This requires only a brief summary of wave theory, the use of Bernoulli's equation, and the source and nature of the wave data. The section on wave theory does not consider the internal velocity and acceleration fields usually reserved for papers on wave forces. If necessary, such information may be obtained from other sources.

BRIEF SUMMARY OF WAVE THEORY

Airy Wave Theory.—The Airy wave theory[5,24] is applicable to waves of low steepness in deep or shallow water (H/L and H/d are small). The surface profile is given by

$$\eta = \frac{H}{2} \cos \theta \quad \ldots\ldots\ldots\ldots\ldots\ldots \quad (7)$$

in which η represents the elevation of free surface of wave measured from still water in feet, the phase position $\theta = kx - \sigma t$, the wave height H is the vertical distance between crest and trough, the wave number $k = \frac{2\pi}{L_A}$, the angular frequency in radians per second $\omega = \frac{2\pi}{T}$, x is the horizontal distance from the crest, and t represents the time position from the crest. The Airy wave length is given by

$$L_A = \frac{gT^2}{2\pi} \tanh \frac{2\pi d}{L_A} \quad \ldots\ldots\ldots\ldots\ldots\ldots \quad (8)$$

in which d is the mean water depth.

The wave celerity of the Airy wave, C_A is given by

$$C_A = \frac{L_A}{T} \quad \ldots\ldots\ldots\ldots\ldots\ldots \quad (9)$$

The Airy theory is used for the lower boundary limit (Figs. 2 and 3) in the field of wave theories.

---

24 "A Study of Progressive Oscillatory Waves in Water," by Martin A. Mason, Technical Report No. 1, Beach Erosion Bd., Office of the Ch. of Engrs., Washington, D.C., 1948.

Solitary Wave Theory (for breaking waves).—The solitary theory for non-breaking waves will not be discussed. The highest wave in shallow water is governed by the solitary wave theory[25] and is a wave of elevation entirely. The height of the breaking wave is obtained from $H_b = 0.78d$.

The celerity of the breaking wave is given by

$$C_b = \sqrt{2g\,H_b} \quad \ldots\ldots\ldots\ldots\ldots\ldots (10)$$

The crest of the breaking wave is cusp shaped with an angle of 120° and the crest elevation $\eta_o/H = 1.0$. This theory is used for the upper boundary limit for $d/L \to 0$.

Modified Solitary Theory.—The modified solitary theory discussed in great detail by Munk[25] is applicable to breaking waves in shallow water. The breaking wave height is obtained from $H_b = 0.78h$, in which

$$\frac{d}{h} = 1 + \frac{4}{3}\sqrt{\frac{3\,h}{h+H}\cdot\frac{H}{gT^2}} \quad \ldots\ldots\ldots\ldots\ldots\ldots (11)$$

The wave celerity of the breaking wave is given approximately by Eq. 10, and more exactly by Eq. 26. The wave celerity for a non-breaking solitary wave is given by $C = \sqrt{g(H+h)}$, and applies only for moderate or low values of h/H. The wave length is obtained from $L = CT$.

The elevation of crest above still water is obtained from

$$\frac{\eta_o}{H} = 1 - \frac{(d-h)}{(H)} \quad \ldots\ldots\ldots\ldots\ldots\ldots (12)$$

This theory is used as the upper limit in very shallow water (small d/L).

Michell-Havelock Theory.—The Michell-Havelock theory[26] is applicable to breaking waves in deep water. The breaking wave height is given by, $H_b = L/7$, where L is given by

$$L = 1.20\,\frac{g}{2\pi}\,T^2 \quad \ldots\ldots\ldots\ldots\ldots\ldots (13)$$

The crest elevation above still water is obtained from $\eta_o/H = 0.676$.

This theory is used for the upper limit in deep water (d/L = 0.5).

Strokes Theory (second approximation).—This is a second order theory,[27] one order above the Airy theory, and applies for waves of small finite steepness. The wave length is given by

$$L = \frac{g}{2\pi}\,T^2\,(\tanh kd)\left[1 + \left(\frac{\pi H}{L}\right)^2 f_1\left(\frac{d}{L}\right)\right] \quad \ldots\ldots\ldots (14)$$

---

25 "Solitary Wave Theory," by W. H. Munk, Annals, New York Academy of Sciences, Vol. 51, New York, May 13, 1949, pp. 376-424.

26 "On the Highest Waves in Water," by J. H. Michell, Philosophical Magazine, Vol. 36, No. 5, 1893, pp. 430-435.

27 "On the Theory of Oscillatory Waves," by G. G. Stokes, Transactions, Cambridge Philosophical Soc., Vol. 8, pp. 441-455, 1847.

in which

$$f_1\left(\frac{d}{L}\right) = \frac{5 + 2\cosh 2kd + 2(\cosh 2kd)^2}{8[\sinh kd]^4} \quad \ldots\ldots\ldots (15)$$

The surface profile is given by

$$\eta/H = \frac{1}{2}\left[\cos\theta + \frac{1}{2}\frac{\pi H}{L} f_2(d/L)\cos 2\theta\right] \quad \ldots\ldots\ldots (16)$$

in which

$$f_2(d/L) = \frac{1}{2}\frac{(\cosh kd)(2 + \cosh 2kd)}{[\sinh kd]^3} \quad \ldots\ldots\ldots (17)$$

The elevation of crest η_o above still water is obtained from Eq. 16 for $\theta = 0$. This theory is used next to the boundary of the Airy theory.

Stokes Theory (third approximation for deep water).—The third approximation for deep water has a surface profile given by

$$\eta/H = \cos\theta + \frac{\pi A}{L}\cos 2\theta + \frac{3}{2}\left(\frac{\pi A}{L}\right)^2 \cos 3\theta \quad \ldots\ldots\ldots (18)$$

in which the wave amplitude above still water a is related to half the wave height $a_o = \frac{H}{2}$ according to Keulegan[28]

$$a_o = a\left[1 + \frac{3}{2}\left(\frac{\pi A}{L}\right)^2\right] \quad \ldots\ldots\ldots\ldots\ldots (19)$$

and the celerity is given by

$$C^2 = \frac{gL}{2\pi}\left[1 + \left(\frac{2\pi a}{L}\right)^2\right] \quad \ldots\ldots\ldots\ldots\ldots (20)$$

This theory is used as the boundary for deep water with waves of finite height, but is adjusted slightly as H/L approached 1/7.

The solution of Eqs. 19 and 20 is given in Table 2. Eq. 18 for η_o/H breaks down sooner than Eq. 20, and is adjusted by use of wave data.

The previous theories are used, together with wave data, to prepare graphs for determining wave characteristics for most design waves. The Cnoidal wave theory might also be mentioned, since it represents waves in the intermediate zone between Stokian and solitary waves. However, this theory is somewhat difficult to use in its present form, and can be replaced by wave data as far as Figs. 2 and 3 are concerned.

APPLICATION OF BERNOULLI'S EQUATION

Wave data with the aid of Bernoulli's equation can be used to obtain best fit numerical relationships for wave characteristics in the intermediate zone in

[28] "Wave Motion," by G. H. Keulegan, Engineering Hydraulics, Proceedings, 4th Hydr. Conf., Iowa Inst. of Hydr. Research, June, 1949, pp. 711-768, Chapter II.

which no simple wave theory exists. The problem of wave motion can be reduced to one of steady state by use of the Rayleigh principle wherein a steady current equal to the wave celerity is superimposed thereon in an opposite direction to wave motion. The free surface profile then becomes a streamline. The pressure along this streamline is constant atmospheric, or in reference to the atmosphere is zero. Using the mean water depth as a reference and applying Bernoulli's equation along the free surface of the now stationary wave, Eq. 21 is obtained.

$$\left[\frac{u_s - C}{C}\right]^2 + \left[\frac{w_s}{C}\right]^2 + \frac{2g\eta}{C^2} = K \quad \ldots\ldots\ldots\ldots (21)$$

in which $(u_s - C)$ is the horizontal particle velocity along the free wave surface in the moving coordinate system in ft per sec, u_s represents the horizontal particle velocity along the free wave surface in the stationary coordinate system in ft per sec, C denotes the wave speed in ft per sec, w_s is equal to the vertical particle velocity at the free surface in ft per sec, η represents the

TABLE 2.—SOLUTION OF STOKES THIRD APPROXIMATION FOR WAVE LENGTH IN DEEP WATER

a_o/a (1)	H/L (2)	L/L_A (3)	H/T^2, in feet per square second (4)
1.01	.0524	1.027	.275
1.02	.0748	1.054	.397
1.03	.0925	1.083	.513
1.04	.1079	1.112	.614
1.05	.1217	1.141	.711
1.06	.1346	1.172	.808
1.07	.1468	1.203	.900

elevation of free surface measured from still water (positive above and negative below still water) in feet, and K is the constant of Bernoulli's equation.

The absolute velocity V_a, is obtained from

$$V_a^2 = (u_s - C)^2 + w_s^2 \quad \ldots\ldots\ldots\ldots\ldots (22)$$

The constant, K, can be evaluated at any number of known positions of the free surface. For this purpose, the constant will be evaluated at still water, where $\eta = 0$. At this point $u_s = 0$, but w_s has a finite value which will be termed w_m, not necessarily the maximum vertical particle velocity. Hence the constant becomes

$$K = 1 + \left(\frac{w_m}{C}\right)^2 \quad \ldots\ldots\ldots\ldots\ldots (23)$$

Thus

$$\left[\frac{u_s - C}{C}\right]^2 + \left[\frac{w_s}{C}\right]^2 + \frac{2g\eta}{C^2} = 1 + \left(\frac{w_m}{C}\right)^2 \quad \ldots\ldots\ldots (24)$$

Eq. 24 relates the surface profile to the wave celerity, horizontal particle velocity u_s and w_m.

The crest elevation η_o above still water can be determined, since at $\theta = 0$, $u_s = u_o$ (the horizontal particle velocity at the crest) and $w_s = 0$, from which

$$2g\ \eta_o = 2\ u_o C - u_o^2 + w_m^2 \quad \ldots\ldots\ldots\ldots (25)$$

Breaking Waves.—For the special case of breaking waves, deep or shallow, $u_o = C = C_b$ and $\eta_o = \eta_b$, the crest elevation of breaking waves above still water. Thus

$$C_b^2 = 2g\ \eta_b - w_m^2 \quad \ldots\ldots\ldots\ldots\ldots\ldots (26)$$

Eq. 26 can be written in the following form:

$$\frac{\eta_b/H}{(L/L_A)^2} = \frac{g}{8\pi^2} \frac{\left(\tanh \frac{2\pi d}{L_A}\right)^2}{H/T^2} \left[1 + \left(\frac{w_m}{C_b}\right)^2\right] \quad \ldots\ldots\ldots (27)$$

in which L_A is the Airy wave length given by Eq. 8.

For the special case of the solitary breaker in shallow water, $\eta_b/H = 1.0$, $w_m^2 = 0$, $\tanh \frac{2\pi d}{L_A} \to \frac{2\pi d}{L_A}$ and $H/d = .78$, whence from Eq. 27, $L/L_A = 1.25$.

For the special case of the highest wave in deep water, according to the Michell Theory, $\eta_b/H = .676$, $L/L_A = 1.20$, and $H/L = 1/7$ and because $\tanh \frac{2\pi d}{L} \to 1.0$, whence from Eq. 27, $\left(\frac{w_m}{C_b}\right)^2 = .0113$.

If it is assumed that $\left(\frac{w_m}{C_b}\right)^2$ varies from 0 in shallow water to a maximum of .0113 in deep water, then its contribution in Eq. 27 is negligible for all breaking waves.

Thus for all breaking waves

$$C_b = \sqrt{2g\ \eta_b} \quad \ldots\ldots\ldots\ldots\ldots\ldots (28)$$

Maximum Horizontal Particle Velocity.—The maximum horizontal particle velocity, u_{max}, occurs at the crest position $\theta = 0$ ($u_{max} = u_o$, and $\eta = \eta_o$). Therefore u_{max} can be investigated by use of Bernoulli's equation, provided η_o and L have previously been determined, using Figs. 2 and 3, respectively. Solving Eq. 25 for u_{max}/C,

$$\frac{u_{max}}{C} = 1 - \sqrt{1 - \frac{2g\ \eta_o}{C^2} + \left(\frac{w_m}{C}\right)^2} \quad \ldots\ldots\ldots (29)$$

For all breaking waves deep or shallow water w_m/C^2 can be neglected. This is also probably true for all non-breaking waves. Thus,

$$\frac{u_{max}}{C} = 1 - \sqrt{1 - \frac{2g\,\eta_o}{C^2}} \quad \ldots\ldots\ldots\ldots\ldots (30)$$

u_{max} can never be greater than given by the approximation in Eq. 30.

Eq. 30 may be investigated for the Airy Wave Theory (H/L being small). If H/L is small, $\eta_o = \frac{H}{2}$ and $gH/C^2 \ll 1.0$. Hence an expansion of Eq. 30 by the binominal theorem leads to $u_{max} = \frac{gH}{2C}$

$$u_{max} = \frac{gH}{2C} \quad \ldots\ldots\ldots\ldots\ldots\ldots (31)$$

which is the same as that predicted from the Airy theory for a small value of H/L. Considering Eq. 29, for the Airy wave theory, $(w_m)^2 = (u_{max})^2$ and Eq. 31 is obtained exactly. Thus, Eq. 30 is a good approximation for obtaining the maximum horizontal particle velocity at the crest. The solution of Eq. 30 is given in Fig. 5.

TABLE 3.—SUMMARY OF OBSERVATIONS OF DEPTH OF BREAKING LOCATION

Location of observations (1)	Number of Average Observations (2)	H/T^2, in feet per square sec (3)	d/T^2, in feet per square sec (4)
Estero Bay	244	.026	.034
SIO Daily	238	.041	.053
SIO Leica	56	.067	.081
WHOI	17	.072	.079
Berkeley Tank	2	.123	.157
B.E.B. Tank	27	.205	.267
Lake Superior	134	.358	.558

SOURCE AND NATURE OF WAVE DATA

Wave data used in this paper consists of both breaking and non-breaking waves. Breaking waves from various sources have been summarized by Munk[25] in terms of H_b/L_o, and d/H_b, where the deep water Airy wave length $L_o = \frac{g}{2\pi} T^2$. This information in terms of H_b/T^2 and d/T^2 is given in Table 3.

The information given in Table 3 is presented in Fig. 7 for H/T^2 versus d/T^2. At the far right of Fig. 7 are two points representing wind waves obtained in the Berkeley tank by Bretschneider and Rice.[29] Data from Danel,[30]

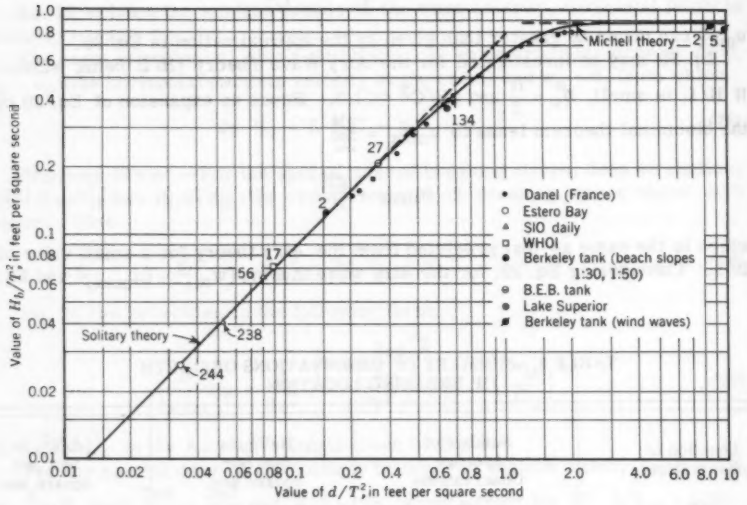


FIG. 7.—BREAKING INDEX CURVE

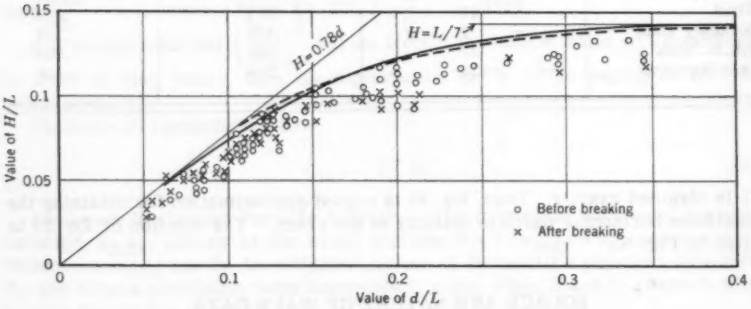


FIG. 8.—H/L VERSUS d/L FOR MAXIMUM WAVES

29 "The Generation and Decay of Wind Waves in a Sixty-foot Channel," by C. L. Bretschneider and E. K. Rice, Technical Report HE-116-327, Inst. of Engrg. Research, Univ. of California, Berkeley, Calif., July, 1951.

30 "On the Limiting Clopotis," by Pierre Danel, Circular 521: Gravity Waves, Natl. Bur. of Standards, U.S. Dept. of Commerce, Washington, D.C., November 28, 1952, pp. 35–45, Chapter 6.

originally given in terms of H/L and d/L, but transformed approximately to H/T^2 and d/T^2 are also shown in Fig. 3. The lower portion of the curve is governed by the solitary theory (H = .78d) and the deep water portion by the Michell theory ($H/L = 1/7$, or $H/T^2 = .88$). The transition is governed by wave observations, imposing Bernoulli's equation and the other figures to be discussed. The numbers beside the plotted points designate the number of waves averaged.

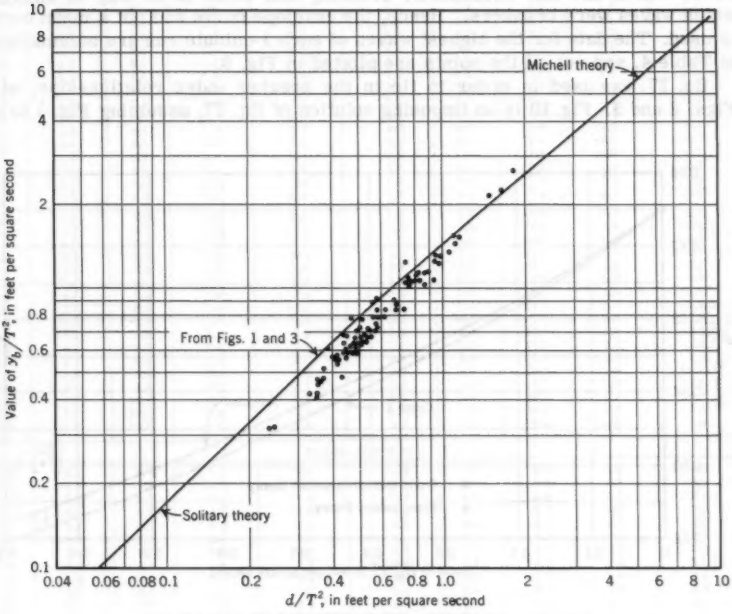


FIG. 9.—BREAKING WAVE CREST ELEVATION

Fig. 8 is the breaking index curve in terms of H/L versus d/L and is similar to that of Fig. 7. The dashed curve is the relationship given by Danel[30] and corresponds to

$$H/L = 1/7 \tanh \frac{2\pi d}{L} \quad \ldots\ldots\ldots\ldots\ldots (32)$$

At approximately d/L = 0.1 the curve by Danel intersects and crosses the solitary limit H = .78d. The solid curve is a continuous curve from d/L = 0 to d/L = deep water, and is based on the imposing solution of Bernoulli's equation using Figs. 3, 7, and 10.

Fig. 9 is a plot of the breaking crest elevation above bottom Y_b/T^2 versus d/T^2. The data indicated by dots was obtained from Lake Okeechobee, Florida. This curve is obtained by use of Figs. 2 and 7 of the text, and

$$\frac{Y_b}{T^2} = \frac{d}{T^2} + \frac{\eta_o}{H}\frac{H}{T^2} \quad \ldots\ldots\ldots\ldots\ldots\ldots (33)$$

The data consists of maximum waves of the October 17-18, 1950 hurricane.[15] These waves are not necessarily breaking and there is no way of knowing which waves were breakers. Hence, the envelope curve and not a mean curve is used. The data for the highest waves of each 1-minute run are summarized in Table 4, and not all the points are plotted in Fig. 9.

Eq. 27 was used in order to tie in the breaker index relationships, with Figs. 2 and 3. Fig. 10 is an imposing solution of Eq. 27, assuming Fig. 7 to be

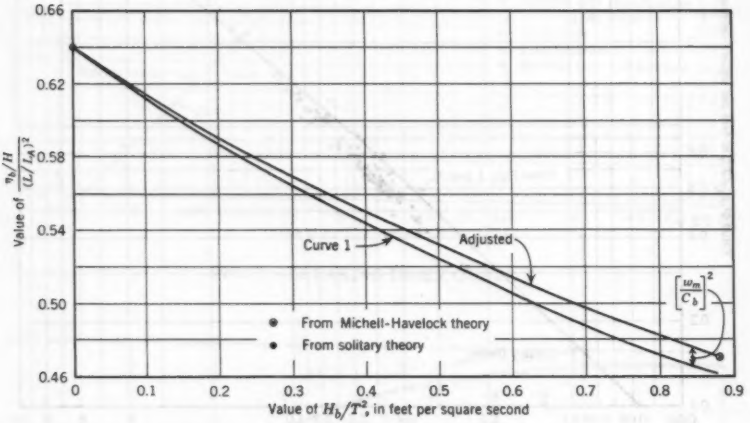


FIG. 10.—SOLUTION OF BERNOULLI'S EQUATION

correct, and assuming $(w_m/C_b)^2$ shown by Fig. 10 varies as shown from 0 at $H_b/T^2 = d/T^2 = 0$, to .0113 at deep water, $H/T^2 = .88$. Curve 1 represents

$$\frac{\eta_b/H}{(L/L_A)^2} = \frac{g}{8\pi^2}\,\frac{\left[\tanh\frac{2\pi d}{L_A}\right]^2}{H/T^2}$$

Therefore it would have made little difference in the final results if $(w_m/C_b)^2 = 0$ had been assumed for all breaking waves. Assuming Figs. 8 and 10 to be correct permits determination of L/L_A as a function of either d/T^2 or H/T^2, and hence the determination of η_b/H for all breaking waves in the transition zone. Perhaps other representations of Figs. 8 and 10 could have been made, thus altering each of the corresponding figures. However, there is one best solution which gives the most accurate overall relationships. A trial and

TABLE 4.—HURRICANE WAVE DATA LAKE OKEECHOBEE, FLORIDA

H, in feet	T, in seconds	d, in feet	η_0, in feet		H, in feet	T, in seconds	d, in feet	η_0, in feet	
			Observed	Predicted				Observed	Predicted
(1)	(2)	(3)	(4)	(5)	(6)	(7)	(8)	(9)	(10)
				(a) Lake Station 12					
2.7	2.6	8.8	2.0	1.7	3.1	2.5	8.2	2.1	2.0
2.6	2.8	8.6	2.1	1.7	3.2	3.0	8.1	2.6	2.1
2.2	3.2	8.6	1.5	1.3	4.3	2.9	8.1	3.1	3.1
2.3	2.7	8.6	1.4	1.4	3.4	3.2	8.1	2.8	2.3
2.2	3.5	8.5	1.2	1.3	3.5	2.9	8.1	2.5	2.4
1.8	3.4	8.5	1.2	1.1	3.9	3.0	8.1	2.9	2.7
2.4	2.7	8.5	1.6	1.5	2.2	3.0	8.0	1.7	1.4
2.7	3.2	8.6	1.6	1.7	2.8	3.8	7.7	2.1	1.8
1.9	3.7	8.6	.7	1.1	3.1	3.7	7.7	2.3	2.1
3.6	2.6	8.6	2.9	2.4	3.9	3.8	7.7	3.3	2.8
2.6	3.0	8.5	1.7	1.6	5.3	4.0	7.7	4.5	4.2
2.5	3.0	8.5	1.3	1.6	4.5	3.2	7.7	3.5	3.3
2.9	2.8	8.5	2.2	1.9	3.2	3.2	7.7	2.4	2.2
2.2	2.8	8.4	1.6	1.3	3.9	3.7	7.7	2.9	2.8
3.2	2.9	8.4	2.1	2.1	4.3	3.0	7.6	3.4	3.1
2.6	2.9	8.4	1.7	1.7	4.7	2.6	7.6	3.8	3.4
3.6	3.7	8.3	2.3	2.5	4.1	3.0	7.6	3.5	3.0
3.5	3.5	8.3	2.4	2.4	3.2	3.0	7.6	2.5	2.2
2.7	3.5	8.3	1.8	1.7	3.9	3.1	7.6	3.2	2.8
3.0	3.7	8.3	2.3	2.0	2.8	4.1	7.6	1.8	1.9
2.6	2.6	8.3	2.2	1.6	2.8	2.4	7.9	2.4	2.0
3.2	2.8	8.0	2.6	2.1	2.8	3.7	10.8	2.0	1.7
2.0	4.7	8.0	1.1	1.2	3.5	3.5	10.6	2.6	2.2
2.9	4.8	8.8	1.6	1.9	3.7	4.9	10.6	2.4	2.5
3.2	4.7	8.8	2.1	2.1	3.0	3.1	10.4	2.4	1.9
2.9	3.4	8.8	1.9	1.8	3.1	3.8	10.4	1.8	2.0
3.3	3.0	9.2	2.1	2.1	3.7	4.4	10.3	2.9	2.5
3.2	4.2	9.5	1.9	2.1	2.8	3.8	10.3	1.8	1.7
3.7	3.7	9.5	2.6	2.5	2.5	3.9	10.3	1.7	1.5
3.3	3.0	9.6	2.5	2.1	2.7	4.0	10.3	1.7	1.6
4.2	4.3	9.6	3.0	2.9	3.9	3.4	10.3	3.0	2.6
3.2	4.1	9.6	2.4	2.1	2.5	3.2	10.3	2.0	1.5
3.6	3.7	9.6	2.7	2.4	3.0	4.6	10.2	1.9	1.9
3.2	3.3	9.6	2.3	2.0	2.7	4.3	10.2	1.9	1.6
3.3	3.7	9.6	2.5	2.1	3.7	3.9	10.2	2.8	2.5
3.8	3.6	10.4	2.6	2.5	2.8	3.9	10.2	1.9	1.7
3.2	3.7	10.4	2.3	2.0	3.5	2.9	10.0	2.5	2.3
2.6	5.0	10.8	1.5	1.6	3.1	3.4	10.0	2.1	1.9
				(b) Lake Station 14					
4.3	2.8	8.6	3.1	3.0	4.3	3.7	9.3	3.3	3.0
3.9	3.8	8.7	3.1	2.7	4.5	4.8	9.5	3.3	3.3
2.9	3.5	8.7	1.9	1.8	4.4	4.1	9.6	3.3	3.1
3.8	3.4	8.7	2.7	2.6	4.4	2.7	9.7	3.2	3.0
4.1	3.2	8.7	2.9	2.8	6.0	3.3	9.7	4.7	4.5
4.1	3.9	8.8	2.7	2.8	4.0	3.8	9.7	2.9	2.7
4.1	3.2	8.9	2.6	2.8	4.8	3.4	9.7	3.6	3.4
3.9	3.7	8.9	2.8	2.7	4.4	4.2	9.7	3.4	3.1
3.4	3.4	8.9	1.9	2.2	3.1	3.6	9.7	1.8	2.0
3.5	2.7	8.9	2.3	2.3	5.3	5.0	9.7	3.9	4.0
3.9	3.7	9.0	2.8	2.7	4.5	4.7	9.5	3.0	3.2
4.6	2.2	9.0	3.5	3.1	4.5	5.1	9.3	3.3	3.3
3.7	2.4	8.9	2.7	2.5	5.7	3.0	9.4	4.5	4.1
3.9	3.6	8.9	2.6	2.7	4.4	2.4	9.4	3.1	3.0
4.3	2.9	9.3	3.1	3.0	4.5	3.2	9.5	3.0	3.1
				(c) Lake Station 16					
3.3	3.8	8.7	2.0	2.2	2.6	4.7	9.5	2.1	1.6
3.5	2.9	8.7	2.3	2.3	2.5	3.3	9.6	1.7	1.5
2.3	3.7	8.9	1.9	1.4	2.9	4.3	9.6	1.9	1.9
3.1	3.9	8.9	2.2	2.0	2.8	3.5	9.6	2.1	1.8
2.7	3.7	9.0	2.1	1.7	2.8	3.7	9.6	1.9	1.8
2.3	4.9	9.0	2.3	2.2	2.1	3.8	9.6	1.7	1.3
3.6	4.0	9.3	2.8	2.4	2.9	5.4	9.7	2.1	1.7
3.2	3.0	9.3	2.2	2.0	3.2	4.0	9.7	2.2	2.0
3.5	3.9	9.3	1.9	2.3	2.1	4.9	9.7	1.1	1.2
2.5	4.2	9.3	1.4	1.8	3.6	4.5	9.7	2.6	2.4
2.5	4.0	9.4	1.7	1.7	3.5	2.7	9.7	3.0	2.3
3.2	3.4	9.3	2.2	2.0	3.3	3.4	9.7	2.5	2.1
2.5	4.1	9.3	1.5	1.7	3.0	4.4	9.7	2.1	1.9
3.0	3.4	9.3	2.1	1.9	3.5	3.6	9.7	2.8	2.3
2.5	3.7	9.2	1.6	1.5	3.4	3.4	10.0	2.3	2.2
2.6	3.9	9.3	1.7	1.6	3.1	4.8	10.0	2.3	2.0
2.6	3.7	9.3	1.6	1.6	3.3	3.0	10.0	2.4	2.1
3.2	3.3	9.3	2.2	2.0	2.7	3.3	10.0	1.8	1.7
3.8	4.0	9.3	1.9	1.8	2.8	4.6	10.0	2.1	1.7
2.7	4.7	9.3	2.1	1.7	2.9	3.2	9.7	2.0	1.8
3.2	4.8	9.5	2.2	2.0	3.3	3.2	9.3	1.9	2.1
3.2	4.4	9.5	2.3	2.1	3.2	4.4	9.3	1.8	2.1
2.9	4.8	9.5	2.1	1.8					

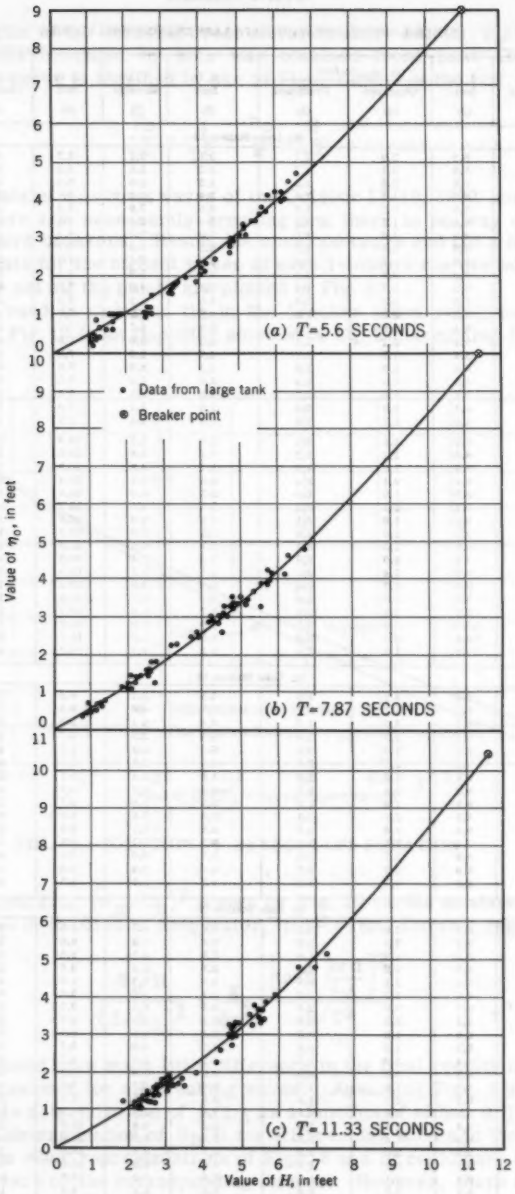


FIG. 11.—η_0 VERSUS H

error process was used to obtain this solution. In addition, use was made of the non-breaking waves.

Fig. 11 indicates wave data for non-breaking waves obtained in the large tank of the Beach Erosion Board. The depth of the water was 15 ft. Three wave periods, T = 5.6 sec, 7.87 sec, and 11.33 sec, were tested for a wide

TABLE 5.—SUMMARY OF WAVE DATA

(a) T = 5.6 Seconds				(b) T = 7.87 Seconds				(c) T = 11.33 Seconds			
Highest Wave		Lowest Wave		Highest Wave		Lowest Wave		Highest Wave		Lowest Wave	
H, in feet	η_o, in feet	H, in feet	η_o, in feet	H, in feet	η_o, in feet	H, in feet	η_o, in feet	H, in feet	η_o, in feet	H, in feet	η_o, in feet
(1)	(2)	(3)	(4)	(5)	(6)	(7)	(8)	(9)	(10)	(11)	(12)
6.18	4.04	5.45	3.48	5.82	3.85	5.45	3.65	6.57	4.79	4.70	2.72
6.35	4.52	5.72	3.85	5.90	3.93	5.30	3.48	7.00	4.80	4.88	3.29
6.20	4.04	5.45	3.48	5.85	3.85	5.27	3.36	5.37	3.79	4.82	3.29
6.18	4.23	5.52	3.67	5.67	3.85	5.09	3.48	5.26	3.48	4.73	3.12
6.20	4.04	5.45	3.47	5.86	4.22	5.62	3.24	7.31	5.18	5.26	3.28
6.35	4.52	5.66	3.85	6.36	4.60	4.70	3.10	5.65	3.85	4.89	3.29
6.02	4.23	5.45	3.48	6.75	4.80	4.84	3.29	5.45	3.66	4.43	2.61
6.56	4.79	5.80	4.19	6.26	4.13	4.89	3.33	5.55	3.66	4.31	3.29
4.86	2.82	3.98	2.40	5.92	4.13	4.85	3.29	5.45	3.48	4.75	3.03
5.12	3.38	3.98	2.35	4.88	3.27	4.55	3.10	5.52	3.37	4.79	2.95
5.06	3.11	4.04	2.22	5.00	3.33	4.50	2.81	5.90	4.04	4.72	3.29
5.15	3.34	4.42	2.44	4.89	3.48	4.60	2.57	5.45	3.66	4.82	2.95
4.87	2.67	4.09	2.06	4.68	3.10	3.99	2.63	5.49	3.29	4.70	2.93
4.85	2.82	3.94	1.88	4.70	3.25	3.98	2.48	2.87	1.66	2.25	1.18
4.87	2.92	4.15	2.16	4.25	2.91	3.76	2.48	2.95	1.79	2.35	1.22
5.22	3.10	4.15	2.35	4.27	2.93	3.36	2.28	3.06	1.79	2.14	1.05
3.29	1.60	2.63	1.22	4.31	2.92	3.38	2.26	2.63	1.41	2.18	1.15
3.22	1.60	2.57	1.08	2.63	1.60	2.39	1.43	2.82	1.79	1.79	1.22
3.34	1.74	2.63	1.22	2.61	1.58	2.16	1.41	2.72	1.41	2.23	1.22
3.38	1.78	2.72	1.03	2.76	1.79	2.28	1.41	2.78	1.60	2.29	1.05
3.66	1.98	2.54	.94	2.80	1.29	2.24	1.22	3.08	1.79	2.49	1.41
3.47	1.88	2.64	1.04	2.78	1.79	2.16	1.04	2.78	1.54	2.12	1.03
3.25	1.60	2.44	1.04	2.63	1.41	2.09	1.04	2.96	1.75	2.34	1.32
3.38	1.74	2.76	1.50	2.65	1.62	2.11	1.22	2.98	1.60	2.44	1.41
1.67	1.03	1.24	.85	2.59	1.50	1.95	1.05	3.00	1.60	2.51	1.22
1.69	1.06	1.26	.39	1.26	.66	.92	.38	3.26	1.65	2.44	1.22
1.69	.66	1.19	.33	1.43	.72	.98	.66	3.38	1.80	2.68	1.22
1.69	.83	1.30	.66	1.32	.68	1.09	.57	3.04	1.82	2.42	1.22
1.82	1.04	1.18	.28	1.24	.51	.98	.47	3.42	1.60	2.25	1.22
1.67	1.04	1.17	.47	1.35	.66	1.09	.47	3.02	1.58	2.25	1.03
1.73	1.04	1.09	.47	1.34	.70	.99	.47	3.72	1.97	2.46	1.48
1.51	.66	1.30	.47	1.34	.68	1.04	.47	2.93	1.56	2.52	1.22
								2.94	1.60	2.28	1.03
								3.13	1.62	2.52	1.22
								3.00	1.60	2.62	1.22

range in wave heights. Each wave record was 15 min in duration and the highest and the lowest individual wave of each record was determined. These data are summarized in Table 5 according to the highest and the lowest wave of each record. The termination point of the curves of Fig. 11 is obtained by the breaking index curve of Fig. 7. These data are truly in the intermediate zone of d/T^2 and H/T^2.

Fig. 12 is a plot of data of η_o/H versus H/T^2 for deep water waves obtained in the small tank of the Beach Erosion Board, and reported by Mason.[24] The numbers beside the points indicate the number of waves averaged and the letters in parenthesis correspond to the listing of data summarized in Table 6. Since these are deep water data the variable d/T^2 is eliminated. However, the wave period, T, was different under each test run, so that the plot is given in terms of η_o/H versus H/T^2. The breaking point corresponds to the Michell Theory, $\eta_o/H = .676$ and $H/T^2 = .88$.

Using cross plots of Figs. 11 and 12 and Figs. 7 and 8, it is possible to construct the generalized graph of η_o/H (Fig. 2). The graph of η_o/H versus d/T^2 with isolines of H/T^2, are tied together as best fit relationships using wave theory, Bernoulli's equation and wave data. Table 7 represents the final selected values of the breaking wave characteristics.

In Fig. 3 the envelope curve of L/L_A is related to the breaker index curve in Fig. 7, Bernoulli's equation in Fig. 10, and the envelope curve of η_o/H in Fig. 2. These are terminating points. The starting point for low but finite steepness is given by Stokes' theory (Eq. 14). For waves of finite height in deep water, Stokes' third approximation is used (Eqs. 19 and 20). The values

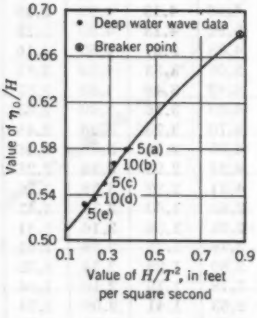


FIG. 12.—η_o/H VERSUS H/T^2

given in Table 2 are slightly adjusted such that $L/L_A = 1.20$ at $H/T^2 = .88$. These are used to obtain the isolines of H/T^2 at the far right of Fig. 3. To obtain the continuation of these isolines of H/T^2 to the breaking limit established along the envelope curve, Fig. 2 might be used and Eq. 24 solved for non-breaking waves. This would require the knowledge of the horizontal particle velocity at the crest, because $u_o \neq C$ for non-breaking waves. At present (1960) there is no suitable wave theory for obtaining u_o for large non-breaking waves. However, a velocity field can be assumed based on an approximation of wave theory, using Figs. 2 and 3 as first approximations, and employing relaxation techniques to obtain the complete picture. Such a procedure has been set up by John Chappelear[31] in case of the solitary theory. The isolines of H/T^2 in Fig. 3 have been assumed as shown, but have not been

31 "An Investigation of the Solitary Wave," by J. E. Chappelear, Transactions, American Geophysical Union, Vol. 37, No. 6, December 1956, pp. 726-734.

TABLE 6.—SUMMARY OF DATA USED IN FIG. 12

Run (1)	H, in feet (2)	T, in seconds (3)	H/T^2 (4)	η_o/H (5)
		(a) 5 waves averaged		
1	.293	.850	.406	.543
1	.279	.850	.387	.548
18	.272	.847	.378	.585
3	.264	.848	.367	.610
1	.259	.850	.359	.602
Average			.379	.578
		(b) 10 waves averaged		
18	.249	.847	.347	.570
13	.236	.848	.328	.533
18	.236	.847	.328	.610
4	.234	.860	.316	.556
4	.233	.860	.315	.579
13	.225	.848	.313	.587
23	.305	.988	.311	.587
4	.223	.860	.302	.548
23	.296	.988	.302	.571
23	.287	.988	.293	.540
Average			.323	.567
		(c) 5 waves averaged		
19	.203	.842	.286	.589
19	.196	.842	.276	.541
19	.192	.842	.270	.542
22	.178	.843	.251	.539
2	.248	1.003	.248	.581
Average			.275	.550
		(d) 10 waves averaged		
2	.242	1.003	.242	.538
14	.226	.969	.241	.487
22	.170	.843	.240	.530
14	.218	.969	.233	.550
14	.214	.969	.228	.509
5	.217	.985	.225	.535
2	.220	1.003	.220	.563
22	.155	.843	.218	.555
5	.207	.985	.214	.522
17	.192	.966	.204	.551
Average			.231	.537
		(e) 5 waves averaged		
17	.190	.966	.203	.516
5	.195	.985	.202	.543
17	.186	.966	.198	.506
20	.176	.996	.178	.547
20	.161	.996	.162	.528
Average			.197	.532

checked and adjusted according to relaxation techniques. It is believed that the assumed isolines of H/T^2 of Fig. 3 are sufficiently accurate for design purposes, but if greater accuracy is required the work by Chappelear[29] may be referred to. Hence the design wave length is given by

$$L = \left(\frac{L}{L_A}\right) \frac{gT^2}{2\pi} \tanh \frac{2\pi d}{L_A} \quad \ldots\ldots\ldots\ldots\ldots\ldots (34)$$

Fig. 5 is used to predict the maximum horizontal particle velocity at the crest, the accuracy of which depends on the accuracy of Figs. 2 and 3.

TABLE 7.—SUMMARY OF BREAKING INDEX RELATIONSHIPS

d/T^2	H/T^2	H/d	d/L_A	H/L_A	L_A/L_o	$\frac{\eta_b/H}{(L/L_A)^2}$ Approx.[a]	$\frac{\eta_b/H}{(L/L_A)^2}$ Adjusted[b]	η_b/H	L/L_A	d/L	H/L	Y_b/T^2
(1)	(2)	(3)	(4)	(5)	(7)	(8)	(9)	(10)	(11)	(12)	(13)	(14)
0	0	.780	0	0	.1106	.6410	.641	1.000	1.249	0	0	
.01	.0078	.780	.0177	.0138	.1106	.6383	.639	.970	1.232	.0144	.0112	.0178
.02	.0156	.779	.0251	.0195	.1561	.6357	.637	.957	1.227	.0205	.0159	.0349
.03	.0233	.778	.0307	.0239	.1907	.6352	.636	.951	1.223	.0251	.0195	.0522
.04	.0311	.777	.0356	.0276	.2197	.6317	.634	.941	1.219	.0292	.0226	.0693
.05	.0389	.777	.0399	.0310	.2452	.6291	.631	.934	1.217	.0328	.0255	.0863
.06	.0466	.776	.0438	.0340	.2679	.6266	.628	.926	1.214	.0361	.0280	.1032
.08	.0620	.775	.0507	.0393	.3081	.6231	.624	.918	1.213	.0418	.0324	.1369
.10	.0774	.774	.0569	.0440	.3431	.6190	.621	.911	1.212	.0469	.0363	.1706
.15	.1154	.770	.0705	.0542	.4158	.6098	.611	.896	1.210	.0583	.0448	.2534
.20	.1532	.766	.0823	.0630	.4753	.6002	.601	.877	1.208	.0681	.0522	.3344
.25	.1900	.760	.0930	.0707	.5253	.5911	.593	.865	1.207	.0771	.0586	.4144
.30	.2266	.755	.1029	.0777	.5695	.5826	.585	.852	1.207	.0853	.0644	.4931
.35	.2622	.749	.1123	.0841	.6083	.5744	.578	.842	1.206	.0931	.0697	.5708
.40	.2973	.743	.1215	.0903	.6432	.5664	.570	.829	1.206	.1007	.0749	.6465
.45	.3312	.736	.1303	.0959	.6745	.5591	.564	.819	1.205	.1081	.0796	.7213
.50	.3645	.729	.1389	.1013	.7031	.5520	.557	.808	1.204	.1154	.0841	.7945
.60	.4274	.712	.1557	.1109	.7535	.5407	.548	.794	1.203	.1294	.0922	.9394
.70	.4864	.695	.1721	.1196	.7941	.5277	.534	.776	1.202	.1432	.0995	1.0774
.80	.5404	.675	.1884	.1273	.8289	.5175	.525	.756	1.200	.1570	.1061	1.2065
1.00	.6339	.634	.2211	.1402	.8832	.5008	.510	.732	1.198	.1846	.1170	1.4640
1.20	.7075	.590	.2544	.1500	.9215	.4885	.497	.712	1.197	.2125	.1253	1.7037
1.40	.7628	.545	.2883	.1571	.9482	.4797	.489	.700	1.197	.2409	.1312	1.9340
1.60	.8025	.502	.3234	.1622	.9662	.4735	.483	.693	1.197	.2702	.1355	2.1641
2.00	.8492	.425	.3960	.1681	.9847	.4647	.476	.684	1.198	.3306	.1403	2.5809
2.40	.8691	.362	.4712	.1706	.9947	.4633	.474	.682	1.199	.3930	.1423	2.9927
3.00	.8770	.292	.5867	.1713	.9987	.4629	.473	.681	1.200	.4889	.1427	3.5924
5.12	.8800	.172	1.0000	.1720	1.0000	.4625	.470	.677	1.200	.8333	.1428	5.7184

[a] First approximation Fig. 10 (Curve 1). [b] Adjusted Fig. 10.

APPENDIX II. NOTATION

The following symbols, adapted for use in the paper and for the guidance of discussers, conform essentially with "American Standard Letter Symbols for Hydraulics" (ASA Y10.2-1958) prepared by a committee of the American Standards Association with Society representation, and approved by the Association in 1942:

a = wave amplitude above still water;

a_o = $H/2$, half the wave height;

b = used as a subscript to denote a breaking wave;

C = wave celerity;

C_A = wave celerity of the Airy wave;

C_B = wave celerity of breaking waves;

d = depth of water;

d_o = mean low water depth;

f = frequency of occurrence;

g = acceleration of gravity;

h = trough elevation above bottom;

H = wave height;

H_b = breaking wave height;

H_{max} = maximum wave height;

I = recurrence interval;

k = $2\pi/L$, wave number;

K = constant in Bernoulli's equation;

L = wave length;

L_o = deep water Airy wave length;

L_A = Airy wave length;

R = radius of maximum wind;

t = time position from the crest;

T = wave period;

u_s = horizontal particle velocity along the free surface of gravity wave in the stationary coordinate system;

u_o = horizontal particle velocity at crest ($\theta = 0$);

u_{max} = maximum horizontal particle velocity at the crest;

V_a = absolute particle velocity;

V_F = forward speed of hurricane;

w_s = vertical particle velocity;

w_m = particle velocity at still water elevation at the free surface;

x = horizontal distance from the crest;

y_b = crest elevation above bottom; breaking waves;

π = 3.1416;

ω = angular frequency;

η = elevation of free surface of wave measured from still water;

η_o = crest elevation above still water;

η_b = crest elevation of breaking wave above still water;

θ = phase position;

μ = total number of hurricanes;

Δp = pressure anomaly at center of hurricane from normal pressure;

p = probability that a given value of $R\Delta p$ will be equal to or exceeded;

n = order of $R\Delta p$ beginning with n=1 for largest value of $R\Delta p$;

$(\eta_o)_{ob}$ = observed crest elevations; and

$(\eta_o)_{pr}$ = predicted crest elevation

DISCUSSION

J. E. CHAPPELEAR.[32]—It is surprising that most of the curves presented as extrapolation of limiting cases, that is, deep and shallow water theories,

TABLE 8.—COMPUTED VALUES USED IN FIGS. 13, 14 AND 15

H/L (1)	d/L (2)	y_b/T^2, in feet per second (3)	d/T^2, in feet per second (4)	H/T^2, in feet per second (5)
.0579	.0666	.3521	.1990	.1729
.0636	.0775	.4297	.2524	.2074
.0696	.0885	.5144	.3111	.2444
.0755	.0996	.6038	.3735	.2834
.0921	.1328	.8918	.5822	.4038
.1059	.1659	1.191	.8098	.5171
.1167	.1988	1.484	1.0449	.6134
.1246	.2314	1.764	1.280	.6894
.1303	.2638	2.027	1.511	.7461
.1343	.2961	2.277	1.736	.7876
.1370	.3282	2.513	1.956	.8163
.1427	.6471	4.578	3.986	.8787
.1431	.9655	6.541	5.947	.8797

supplemented by a considerable amount of empirical data, agree with the theoretical computations of the properties of the highest wave recently made by the writer,[33] following the suggestion of Michell[34] in his original paper. The surprise is not that the experiments agree with the theory but rather vice versa. The theoretical computations were intended as a rough guide for computational purposes, and as a computation aid for wave properties as yet unmeasured. Table 8 gives computed numerical values corresponding to Figs. 13, 14,

[32] Shell Development Co., Houston, Tex.

[33] "On the Theory of the Highest Waves," Technical Memorandum No. 116, Beach Erosion Bd., Corps of Engrs., U. S. Dept. of the Army, Washington, D. C., July, 1959.

[34] "On the Highest Waves in Water," by J. H. Michell, Phil. Mag., Vol. 36, No. 5, 1893, pp. 430–435.

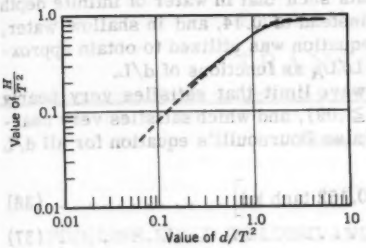


FIG. 13.—BREAKING INDEX CURVE

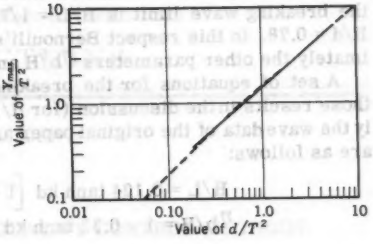


FIG. 14.—BREAKING WAVE CREST ELEVATION

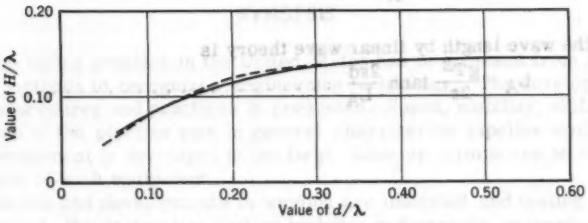


FIG. 15.—H/λ VERSUS d/λ FOR MAXIMUM WAVES

and 15. If these points are plotted on the figures in the original paper, the agreement is interesting.

CHARLES L. BRETSCHNEIDER,[35] M. ASCE.—The results presented by J. E. Chappelear for the breaking index relations between H/L and d/L are of interest. His values are in close agreement with those of the paper for $d/L \geq .09$, but for $d/L < .09$ the agreement is not as good. His d/L-values are in close agreement with the equation given by Miche.[36]

$$H/L = 0.14 \tanh kd \quad \ldots\ldots\ldots\ldots \quad (35)$$

in which $k = 2\pi/L$.

Eq. 35 tends to fail for $d/L < .09$ if the solitary wave theory is accepted as the upper limit for breaking waves in shallow water. According to the solitary wave theory for shallow water the breaking wave limit is H/d = 0.78.

For shallow water tanh kd tends to $kd = \frac{2\pi d}{L}$, whence from Eq. 35, $H/d = 0.14(2\pi) = 0.88$ is obtained. This predicts the breaking wave height 13% greater than that given by the solitary wave theory (H/d = 0.78). An attempt was made

35 Hydr. Engr. (Research), Beach Erosion Board, Corps of Engrs., U.S. Dept. of the Army, Wash., D. C.

36 "Movements ondulatoires de la mer en profondeur constante on decroissante," by M. Miche, Ann. des Ponts et Chausees, tome 114, 1944.

in the original paper to utilize Eq. 35 as a guide, with particular emphasis on Bernoulli's equation and also on wave data such that in water of infinite depth the breaking wave limit is $H/L = 1/7$, instead of 0.14, and in shallow water, $H/d = 0.78$. In this respect Bernoulli's equation was utilized to obtain approximately the other parameters η_b/H and L/L_A as functions of d/L.

A set of equations for the breaking wave limit that satisfies very nearly those results in the discussion (for $d/L \geq .09$), and which satisfies very nearly the wave data of the original paper and also Bournoulli's equation for all d/L are as follows:

$$H/L = 0.124 \tanh kd \left[1 + 0.152 \tanh kd\right] \quad (36)$$

$$\eta_b/H = 1 - 0.32 \tanh kd \quad (37)$$

and

$$L/L_A = 1.56 \frac{\tanh kd}{\tanh \frac{2\pi d}{L_A}} \left[1 - 0.177 \tanh kd - 0.059 (\tanh kd)^2\right] \quad (38)$$

in which the wave length by linear wave theory is

$$L_A = \frac{gT^2}{2\pi} \tanh \frac{2\pi d}{L_A} \quad (39)$$

AMERICAN SOCIETY OF CIVIL ENGINEERS

Founded November 5, 1852

TRANSACTIONS

Paper No. 3027

PIPELINE FIELD WELDING AND QUALITY CONTROL METHODS

By Armand G. Barkow,[1]

SYNOPSIS

Pipeline laying practice in the United States has progressed from field experience methods to recognized engineering technology. The development of pipeline procedures and practices is presented. Speed, mobility, skill and inventiveness of the pipeline men in general characterize pipeline work. Most pipeline equipment is developed in the field. Line-up clamps are an outstanding example of such equipment.

Procedures and developments in welding are indicated and testing methods are described. Nondestructive testing includes radiography, magnetic, supersonic, dye penetrant, and pressure testing. Radiographic inspection has helped greatly to improve welding.

Technical investigations into new materials and processes present a real challenge to the engineering profession. Codes and standards control all phases of pipeline work from the material being used to the installation of the line.

INTRODUCTION

The pipeline industry began as an outgrowth of the necessity to transport petroleum liquids and gases from the wellhead to the market. Originally pipelines were laid without the help of elaborate engineering studies and depended on the experience of the construction men. Organized engineering practices in this field have brought about a realization that pipelining has changed from an art to a science. The sheer brawn and individual know-how of the "spread" man has been replaced by such recognized engineering practices as accurate aerial and ground surveys; scientific studies of terrain, soil, and rock conditions; weather and water data as gathered by the Weather Bureau, United States Department of Commerce (USWB); and consideration of design conditions.

Note.—Published, essentially as printed here, in June, 1958, in the Journal of the Pipeline Division, as Proceedings Paper 1673. Positions and titles given are those in effect when the paper was approved for publication in Transactions.

[1] Supt. of Inspection, Natural Gas Pipeline Co. of America, Chicago, Ill.

Material is no longer just pipe and fittings. Field work is no longer just welding, coating, and lowering into a ditch. Pipe and fittings are purchased in accordance with well-developed standards and based on predetermined desired properties in accordance with operating demands. Pipeline construction is controlled not only by individual specifications but by recognized codes and standards. Welding, as one of the prime functions, is served by a specific standard, designed to produce the highest quality workmanship consistent with economic practices. This standard[2] has been used widely for construction of pipelines in the United States as well as in Europe and Asia.

This standard covers all phases of welding as well as physical and nondestructive testing of welds. Because this standard might be considered the primer of pipeline construction, it will be used as the basis of this paper.

HISTORY

Pipelines as a method of transportation are frequently considered something entirely new. However, gas was transmitted through pipelines in 400 B. C., when the Chinese brought gas from "burning springs" through bamboo logs to the sea coast to evaporate salt water. In 1821 the United States acquired its first pipeline, a hollow log-line from Canadaway Creek to nearby houses in Fredonia, N. Y. The first industrial use of natural gas, to evaporate salt brine, was at Centerville, Pa., in 1840. By the time the first iron pipeline was laid in 1872, gas had been discovered in various parts of Pennsylvania and Kansas. By 1884, Pittsburgh, Pa., had 335 mi of gas distribution system and supplied 250 million cfd.

The first high pressure, long distance line was built in 1891 from Greentown, Ind., to Chicago, Ill. The distance was 120 mi and it operated at 525 psi.

By 1900 natural gas had been discovered in seventeen states with production valued at more than $25,000,000. By 1909 a number of pipelines had been put into operation. Among them were a 16-in. line to Joplin, Mo., and a 183 mi, 20-in. line from West Virginia to Cincinnati, O. The first application of oxy-acetylene welding of pipelines on an 11 mi line to Philadelphia, Pa., occurred in 1911. In 1926 the era of long distance, large diameter, high pressure pipelines began, with the completion of a 22-in., 170 mi line to Baton Rouge, La., that operated at 350 psi. The following year 1927 saw the advent of lines of high strength, large diameter, electric welded pipe. This large diameter pipe, with comparatively light wall, made long distance lines economically feasible. Pipelines then extended to all parts of the United States. In 1931 two long distance lines were completed. The 900 mi line ran from the Panhandle field in Texas to Chicago, and an equally long line extended from the same area to Muncie, Ind., and later to Detroit, Mich.

The depression of the 1930's slowed industrial expansion, but World War II saw the building of the now famous "Little and Big Inch" lines and many other mammoth lines, including an 1840 mi line from Texas to New York. In 1960 there were more miles of pipelines than railroads.

It was noted previously that acetylene welding was introduced into pipeline work in 1911. Electric welding was first introduced in 1922 on a short line laid at Caney, Kan. Although this line proved faulty welding improved rapidly, and by 1928 a 169 mi line was welded electrically by advanced pipeline technique.

[2] API Std. 1104, 6th Ed., August, 1959, Standard for Field Welding of Pipelines, API-AGA Joint Committee on Oil and Gas Pipeline Field Welding Practices.

By 1930 the shielded electrode was being used. Soon many of the old "gas welding" ideas disappeared. First, the back-up ring was eliminated. Then roll welding (Fig. 1) was succeeded by stove-pipe welding, in which one joint after another was welded to make mile-long strings, rather than three or four joint strings.

Welding has gradually improved until in 1960 modern equipment and quality control are prevelant. Such control includes the use of radiography and other nondestructive methods that will be considered subsequently.

WELDING

In modern pipeline welding, acetylene still finds its use in small diameter, thin wall pipe, such as are used around pumping or compressor stations, meter settings, and similar work. Its most important function is in the cutting torch, where it still is an indispensable tool. With high strength, alloy steels and with all-weather work, acetylene is finding a new field in preheating. With a slightly oxidizing flame it does not leave a carbon deposit on the beveled face, thus leaving a clean surface with which to work. Acetylene has been used as the heating unit for a flash butt weld in experimental work, but this process has not been developed to practical application.

Manual electric arc welding using the common shielded electrodes of the all positions E6010 and E7010 classification is the general practice in field welding today. However, field welding itself is not "common" and it may still be regarded as an art. Field welding is quite different from ordinary pipe welding. Two important features in field-welding techniques are most obvious differences. First, the field welder uses a stationary downhill method starting at the top of the pipe and working downward. Second, arc amperage is considerable higher than is normally used and, consequently, the speed is considerably greater.

With all these contradictions to ordinary welding technique, the finished weld (Fig. 2) is equal to and, in many cases, superior to shop welding. In addition to these radical changes in technique, field welding practice has developed a unique production method that permits greater mobility of the welding crew. Field welding is divided into three stages, each complimenting the other. The first group of welders, referred to as stringer bead welders, consists of either two, three, or four welders who do nothing but lay in the first bead, a stringer bead of 30-in. or 36-in. pipe. Usually two of the welders are right-handed and two are left-handed, so that the work may be done with machine-like precision.

The line-up crew compliments the stringer bead welders. These men line up the joint to a precise gap between the two pipes and clamp the pipe tight with an internal line-up clamp. The gap may range from dime to nickle width, depending on the welder's choice. Dime-width is used most frequently.

The welder's helpers clean the bevels before the welding actually starts and also clean between beads. Cleaning is not simply another chore that can be done as a step in the procedure. A great deal of weld quality depends on the thoroughness of cleaning and preparation between passes. Many inferior welds could be saved by proper preparation. A little chipping of holes or high spots, a few extra jabs of ice picks in undercuts and slag pockets, a little grinding, and a little more care will save hundreds of dollars for the contractor in the salvage of potentially inferior welds. Speed is a commendable asset in pipeline welding, but haste in cleaning makes waste.



FIG. 1.—ROLL WELDING USING ACETYLINE TORCH



FIG. 2.—COMPLETED GIRTH WELD

Tack welds are not used, but step welding is common practice. Here the welders use one-rod length beads, working in opposite quarters and step upward or downward depending on the side being welded. To clarify this method, the procedure of a two-man crew might be considered. One welder will start at approximately 1 o'clock on the periphery and weld to 3 o'clock. (The times are pipeline jargon for locating points on the periphery of a girth seam.) In the meantime, the other welder is welding from 8 o'clock to 6 o'clock. The first will then weld from 4 o'clock to 6 o'clock making sure of a good bottom lap, while the second welds from 12 o'clock to 10 o'clock. Finally both welders will finish the sides.

Such a procedure is used to minimize shrinkage and prevent closing of the welding gap. This whole procedure, from lining-up a joint to completion of the stringer bead, takes far less time than it has taken to describe it.

A good stringer bead welder will make a weld with a smooth, even internal bead approximately $\frac{1}{16}$ in. high and approximately $\frac{5}{16}$ in. wide. The bead will be so smooth that it will seem as if the bead was put in from the opposite side. Stringer bead welders are top hands and are recognized as such by the welding fraternity.

The welder must respond instantly to any fluctuation in arc voltage and most stringer bead welders can do that almost with the accuracy of an electronic control. Stringer bead welding rate is between 20 in. per min and 30 in. per min.

A second group of expert welders now begin work—the hot pass welders. They, too, work in groups of two or four, usually two to a weld, leapfrogging each other. Like the stringer bead welders, they work at high rates of speed. This crew puts in the second pass and thus builds the weld to a self-sustaining strength. The hot pass crew immediately follows the stringer bead crew so that the weld does not have an opportunity to cool, thereby taking advantage of the residual welding heat. This second pass not only strengthens the weld with added metal but repairs any gaps or windows left by the stringer bead men. The heat of the second metal application also produces a stress-relieving heat treatment in the first-pass metal deposit that prevents cracking and reduces welding stress. This crew leaves the weld with a solid foundation for its completion. The third crew of finish welders follows further behind and actually finishes the weld.

Typical field-welding procedure calls for one bead for each $\frac{1}{8}$ in. of metal thickness, plus the root and cover pass. Thus, a typical $\frac{1}{2}$ in. wall pipe would require five passes. Frequently an extra stripper pass is used on both sides to help fill the groove. This stripper pass usually runs from 2 o'clock to 4 o'clock and from 10 o'clock to 8 o'clock. It is made before the final cover pass.

In discussing the technique of pipeline welding, it is essential to consider the welding generator. Commonly used generators are either gasoline or diesel driven, portable D. C. welders of 300 amp rating. Arc current and stability require smooth, constant, and instantaneous action. Thus, weld quality actually starts at the generator, which is the starting point of weld inspection. The welding inspector checks the generators frequently and has the authority to remove a machine from the line as readily as he would an unsatisfactory welder. Pipeline welding is probably the only welding method that condones the practice of mixing electrodes for carbon steel welds. In pipeline welding the E6010 type rod is used for the stringer bead because of its greater ductility under movement of the pipe. The E7010 type electrode is used for the remaining

passes to secure desired strength. The cover pass may be made with an E6010 electrode to improve appearance and contour. This practice of mixing electrodes was started by pipeline welders through field tests and research so that the most advantageous physical properties could be produced in each layer of weld metal. These properties include ductility at the root, strength in the body, and smoothness in the cover.

In contrast to power-piping welding, and shop fabrications of piping, the two outstanding features of field welding are the downhill method and the comparatively narrow weld. Downhill welding, that is, starting at the top in a stationary work position and working around the pipe to the bottom, allows for greater arc speed in a narrower groove. A very short arc is maintained and the root pass is made by burning through the adjoining lips in such a manner that the puddle fills the gap to produce a full, smooth, inside bead. A high degree of skill is required to proceed at a rate of speed that will maintain the opening and puddle relationship in such a manner that no arc break results. Such a break would cause a window or a lack of full penetration.

Completely automatic welding for girth welds of pipelines, with the pipe in a stationary position, has not been successfully achieved as yet (1960). Numerous attempts have been and are being made to adopt automatic welding but there does not yet (1960) exist, for cross country welding, an automatic process with the necessary speed and flexibility comparable to that obtained by the manual procedure.

About 1947 a pressure butt welding method was developed in which the ends of the pipe were heated with gas flames to an advanced plastic state. The pipe then was "bumped" together to achieve fusion. The unsolved problem with this method was the holding of the pipe in proper alinement during the bumping process.

Submerged arc welding, successfully used for the longitudinal seam, is being widely adopted to "rail head welding"—a method of butt welding two joints of pipe at a central location before stringing. This method has a fairly successful history and does speed progress in the field because the same number of field welds will give twice the pipeline progress.

The most recent development in this field is a submerged arc process (Fig. 3) in which the outside beads are welded first with use of a relatively heavy bead. The inside bead then is made by the same process, using an automatic head held by a boom and manually guided by an operator riding the boom. Although this is the first fully automatic machine-made girth weld, this process is still applicable only to double jointing.

A great deal of experimental work is being done in this field, particularly in view of the shortage of fully experienced stringer bead welders. A process that may hold the answer is the shielded inert gas metal arc process which is finding widespread application in other fields of welding. There have been no actual field trials made with this process although it has been used successfully for prefabricated pipe welding in fabricator plants.

Welding electrodes, other than those mentioned previously, are being investigated for possible application. Among the latest developments in this field are the low-hydrogen iron powder contact electrodes. The need for a control of notch sensitivity and under-bead cracking makes the use of low hydrogen electrodes very desirable. The low-hydrogen iron powder contact electrodes find some application where downhand welding can be used. This is particularly true in the welding of sleeves, saddles, pads, and other pipeline attachments.

Based on the active research in the field, it is evident that pipeline welding is a living, dynamic science, and that great strides toward improved welding are imminent.

INTERNAL LINEUP

Pipeline equipment is frequently developed by a practical field man and as such has been "engineered" by nonengineers. Improvements and refinements

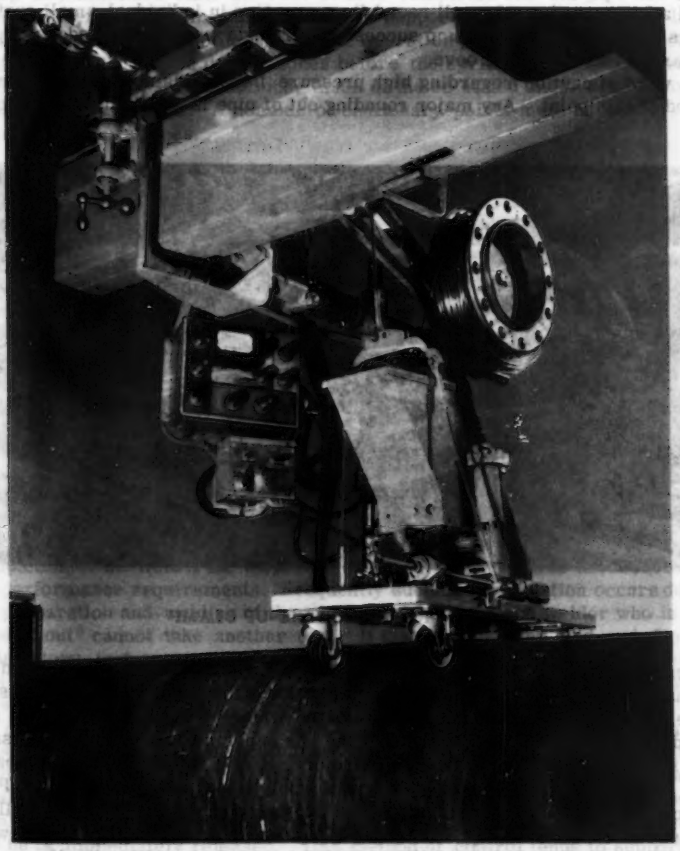


FIG. 3.—SUBMERGED ARC PROCESS APPARATUS

have been added by trained equipment engineers after the basic developments were proven in actual usage.

One of the most ingenious of these tools, and one that added greatly to the improvement of welding, is the internal line up clamp. The internal line up clamp is an expanding device that is fitted under the mating ends of the pipes and holds them firmly in place for welding. The two advantage of this device is that it eliminates the need for tack welds and helps level the mating edges, thus minimizing miss-match. The earliest model was a hand-cranked device in which a screw and lever arm forced shoe segments against the pipe inner surface.

Later developments introduced electric motive power, hydraulic pressure, and pneumatic power (Fig. 4). The shoes also developed from a simple split band a large number of small round fingers acting in individual small surface areas. The latest (1959) clamp successfully rounds out adjoining edges to give a near perfect welding groove.

A word of caution regarding high pressure line-up clamps should be mentioned at this point. Any major rounding out of pipe in the field, where a per-



FIG. 4.—PNEUMATIC LINE-UP CLAMP

menent set cannot be achieved to hold this roundness, produces a locked-up mechanical strain in the stringer bead in addition to the normal welding stresses. In welding the second bead the strength of the stringer bead momentarily is reduced to a very low level, at which time the superimposed bending stresses may instigate root bead cracks. Therefore, it is a fallacy to believe that a pipe does not have to be perfectly round when it leaves the pipe mill. Pipe will crush slightly during shipment, but out-of-roundness at the pipe mill is almost inexcusable. Very little pipe in pipeline use has a diameter-to-wall ratio of a degree such that it will not maintain roundness within itself.

In regard to the line-up clamp, and particularly to its use in welding of large-diameter line pipe, another hazard must be considered. As noted previously, the line-up clamp does set up a strain in the pipe wall. Releasing the pressure causes a spring back. It has been noted that weld metal has comparatively little strength until it has cooled below the critical temperature. It

may be noted that metal of line pipe composition passes through a second critical stage at approximately 600° F, known as the blue brittle range. Knowing these facts it can be readily seen that superimposed loads during these transition periods can instigate fractures. The external load caused by lowering pipe onto skids after welding, added to the locked-up stresses caused by reforming out-of-roundness pipe, may be sufficient to cause fissures in those sections of a weld metal that have not passed through the transition temperature ranges.

Based on these facts, it is recommended that the tension of the line-up clamp be maintained until the root bead is completed and the pipe has been rested properly. The line-up clamp lends support against the shock of landing the pipe, and the time interval of the operation permits all sections of the weld to pass through the danger zones before the spring back load is affected.

By observing these precautions, much of the so called under bead cracking trouble can be avoided. A number of cautionary points must be observed in sound welding practices.

QUALIFICATION OF PROCESS AND WELDERS

Pipeline welding follows the methods of qualification that have been established[3]. Because the essential factors of pipeline welding vary from normal, procedure qualification is based on pipe size, wall thickness, bevel design, climatic conditions, and similar items, rather than material groups, as specified in other standards. Pipeline procedures recognize only two groups of materials, both of which normally would fall into AWS classification P-1. Normally one position is used in all qualification procedures. This is the horizontal stationary, in which the weld groove is actually vertical and all positions are encountered.

Welder qualification is by far the most important consideration, because the pipeline welder is naturally more on his own in actual production. Although pipeline welding is divided into three separate operations, as described previously, each welder is qualified on a complete weld.

A welder's technique is observed and the test may be terminated before completion of the weld if the inspector feels that the weld does not meet standard performance requirements. Frequently such disqualification occurs during the preparation and welding of the root or second bead. A welder who is thus "looked out" cannot take another test. If the weld is completed and "looks" satisfactory, test coupons are cut from its periphery and subjected to tension, root and face bend, and nick-break tests. Failure of test specimens having physical properties greater than the minimum required or defects less than the maximum permitted by the limits of acceptability of the standard[4] may not cause disqualification, but most often one specimen failure is sufficient for disqualification, and only rarely is a welder given a second chance. Welds also are cut periodically from the actual line and tested as described previously. A failure of any one specimen terminates the welder's qualification for the job and he is immediately released. This method of control tends to support the quality of each weld.

This practice is probably the chief difference between shop quality control and field quality control and makes the welder solely responsible for the

[3] API Std. 1104, Standard for Field Welding of Pipelines.
[4] API Std. 1104, Part II, Standards of Acceptability.

quality of his welding. With such a practice it is little wonder that all welders must be specialists in pipeline welding. Inexperienced pipeline welders seldom, if ever, can fit into a pipeline spread. A special pipeline welders' union local has been set up for pipeline welders operating all over the United States. This union takes precedence over all other welder unions, thus giving free reign to welders passing from one locally controlled union district to another.

NONDESTRUCTIVE TESTING

The quality of pipeline welding is controlled by the much more searching methods of nondestructive testing. Desirable improvement in weld quality was achieved when radiography, both X-ray and gamma-ray, was adapted to field conditions. When X-ray was first considered, the equipment was unwieldy and most X-ray engineers did not consider its use feasible. However, equipment meeting the requirements for pipeline application was developed on a principle far removed from that then in use.

The X-ray tube and necessary electrical compliment were made smaller without reducing the power. The whole appartus, with the exception of the controls, was incased in a "pig" or casing. This pig then was mounted on a carrier, and with a power tractor attached, it was ready to be run inside pipe 20 in. and larger in diameter. Later models were made to go into pipe 12 in. in diameter. Sundry, and often ingenious, appurtenances made it possible for the pig to travel as much as $\frac{1}{4}$ mi through a solidly welded line, stopping to radiograph each weld and then coming back out again. As isotopes became available, they also were adapted to pipeline radiography. The isotopes of cobalt, iridium, and later cesium have all been used. Other isotopes also are being examined for possible use.

The processing laboratory as well as the radiographic equipment has been taken to the construction location. The dark room, developing tanks, washing and film drying appartus and power plant is mounted on a truck for portability, and follows in line of progression immediately behind the welders.

Soon after the weld is completed, the welding inspector can look at the developed film and instigate necessary corrections. A pattern of defects so poor welding procedure can be discovered and corrected before reaching a serious condition that would cause rejection of welds.

Recognizing the value of radiography, standards have been developed covering radiographic technique, film processing, radiation safety, interpretations of film, and acceptability limits for defects.[5] Although all welds are not perfect, homogeneous, and free of inclusions and voids, neither is the steel plate of the pipe body. It is recognized that all defects are not harmful to the same degree and that a certain amount of discontinuity can be tolerated. Therefore, limits in tolerable defect sizes and distribution have been developed. Defects of a greater magnitude may be repaired if it is possible and economically feasible to do so, or the entire weld may be removed from the line.

The application of radiographic examination to welding has been phenomenal in the improvement of weld quality. As an example, one line of several hundred miles was laid before radiographic control was used, and weld leaks were found on an average of 1 per mile. In one section of 30 mi or 40 mi an even

[5] API Std. 1104, Part III, Radiographic Procedure.

greater concentration occurred. On another line of 1,400 mi, using approximately 25% radiographic coverage, only six defects were found. This would tend to prove that thorough radiographic coverage is worth the additional cost.

Nondestructive testing is not confined to radiographic coverage alone. Magnetic inspection, ultrasonic inspection, dye-penetrant inspection, and pressure testing are playing increasingly greater parts in proving a pipeline before it is placed into service.

Recent developments in magnetic inspection and field tests of this method indicate that major defects can be detected even if they are not visible or are subsurface. Whereas this method is not as conclusive as radiographic inspection, it has the advantage of greater ease in application and greater speed of determination of results. Using magnetic powder, the defect indications are located at the exact location of the defective weld being examined. The indications can be preserved by transfer to an adhesive belt, thus producing a record similar to radiographic film. This application is still in an embryo stage, but it does have a bright potential and may compensate for its disadvantages by a greater coverage.

Ultrasonic inspection likewise has a potential use in weld inspection, but has not been developed for a truly successful pipeline application. However, it does find an advantageous application in determination of pipe wall soundness and pipe wall thickness before installation of branch taps and before other welding is started on pipelines while under service pressure. This method can find laminations and dangerous conditions before the welder strikes an arc to the pipe.

It therefore provides a safety factor for pipeline personnel that has met with phenomenal acceptance in this particular operation. Ultrasonic inspection similarly has been useful in the examination of piston shafts, crank shafts, fly wheels, and other engine equipment, in which defects have been detected before actual equipment failure occurred.

Dye-penetrants have been used in all types of inspection. Because of simplicity of application and rapid production of results, this method frequently is used in conjunction with repair welding to locate surface defects or to determine if defects have been completely removed by grinding and chipping.

Pressure testing, either hydraulic or pneumatic, is the reliable proof test of any welded enclosure. It is being used in the final testing of cross-country pipelines, even when other methods of nondestructive testing have been employed.

NEW DEVELOPMENTS

Pipelines are continually stretching from new oil and gas fields in mountains, under the oceans, in the north, and in tropical jungles, to markets in all cities of the nation. The large diameter pipe of the 1930's is paralleled by even larger lines, and the vast deliveries of today have only scratched the surface of the potential market. Pipeline transportation has unlimited potentials for development.

What materials does the future hold? The low alloy, high strength steels already are becoming part of the picture. Materials having high corrosion resistance definitely are needed for transportation of corrosive materials. Materials with minimum yield strengths of 100,000 psi are in the planning stage. Non-ferrous alloys, such as aluminum, are being used experimentally. Plastics have appeared on the scene. Stainless clad steel may offer some advantages. Thus, it can be seen that a wide variety of materials are, or will be, available.

FIG. 5.—WELD DEFECTS: INDICATION AND THEORY

These new materials will require new construction methods, welding procedures, handling, and coating equipment. They will present challenging engineering problems, investigations, and acceptance studies. Future increased requirements for construction speed means more automatic equipment, more automatic welding, and more stringent quality control. The requirements for improved welding procedures will result in the development of new welding techniques, new welding processes, new types of electrodes and many new problems. All of these improvements are being studied by pipeline engineers and are being adopted as fast as they can be proven. The demands of the industry present real challenges to the engineering profession and the challenges are rapidly being met because of the joint interest of engineering organizations.

CODES AND STANDARDS

A growing industry must control itself to prevent disorganization. The pipeline industry realized this and through various available agencies has set up standardization committees to develop codes that promote reasonable safety standards to be followed in construction and operation.

Most all pipe is manufactured in accordance with either API Std. 5L for carbon steel line pipe or API Std. 5LX for high strength line pipe. These standards specify the chemical and physical properties of various grades of steel skelp and seamless pipe. They also control manufacturing processes and specify quality control practices. They set forth test standards and limits of acceptability. Finally they provide a recognized identification mark.

Welding controls are based on API Std. 1104, that gives detailed instruction on development of procedures, testing of welders, design and welding practices, nondestructive testing, and limits of acceptability. It is actually the field bible in pipeline welding, and has gained world wide recognition. Construction is based on ASA Std. B 31.8. This standard guides the designer as well as field construction crews toward the building of safer, more economical pipelines and facilities. The standard covers all phases of construction and incorporates all other applicable standards and specifications.

The one outstanding feature of all these standards is that they were written by practical operating engineers interested in all phases of pipelining. They represent experience, knowledge, and understanding. They are factual statements that can be applied to construction and have been field tested. They are practical and yet conservative. They are authoritative to the point at which they have been accepted in legislative codes of state regulatory bodies.

CONCLUSIONS

It has been demonstrated that pipelining is a lusty industry—one that is growing more rapidly than any other form of transportation. Pipelining started with only a practical knowledge, adopted engineering principles, technical developments and scientific practices as it developed, and now has gained the respect and admiration of large engineering groups.

AMERICAN SOCIETY OF CIVIL ENGINEERS

Founded November 5, 1852

TRANSACTIONS

Paper No. 3028

MOMENTS IN BEAMS BY THE METHOD OF PARTIAL MOMENTS

By Harry Posner,[1] F. ASCE

With Discussion by Messrs. William S. Walker and Joseph T. Kolibal; Anatol A. Eremin; Lembit Kald; and Harry Posner

SYNOPSIS

This paper presents a method of obtaining moments in restrained or continuous beams by first solving for the moments at each support while placing the load on only one span at a time (partial moments). Then by combining these moments in a prescribed manner, the moments at each support with all the spans loaded are obtained (total moments). Both analytical and geographical solutions are presented.

INTRODUCTION

Much attention has been devoted in engineering literature to the matter of devising methods for obtaining moments in restrained or continuous beams that are simpler and less time-consuming than the methods of the theory of three moments, slope deflection, or similar methods. In 1925, a graphical solution, the method of conjugate points,[2] appeared and in 1930 an analytical solution, the method of distributing fixed-end moments,[3] was presented. The method described in this paper is called, by the writer, the method of partial moments. The solution of the partial moments may be performed either analytically or graphically, as will be shown.

Note.—Published, essentially as printed here, in March, 1958, in the Journal of the Structural Division, as Proceedings Paper 1567. Positions and titles given are those in effect when the paper or discussion was approved for publication in Transactions.

1 Partner, Briggs, Blitman & Posner, New Rochelle, N. Y.

2 "The Method of Conjugate Points," by L. N. Mishkian and D. B. Steinman, Proceedings, ASCE, October, 1925.

3 "The Method of Distributing Fixed-End Moments," by Hardy Cross, Proceedings, ASCE, May, 1930.

Several advantages may be claimed for the method of partial moments. The method is less time-consuming than the older methods, particularly when more than 4 spans are involved, and when several trial loadings are to be investigated. In addition, the method is less subject to errors because its application is self-checking. It does not require the use of computing machines because the ordinary use of slide-rule work in common practice gives results, well within the limits of required accuracy in practical work.

GENERAL DESCRIPTION OF METHOD

The continuous beam is divided into as many units as there are spans in the beam. Each unit includes 3 spans, 4 points of support, and free ends, the load-

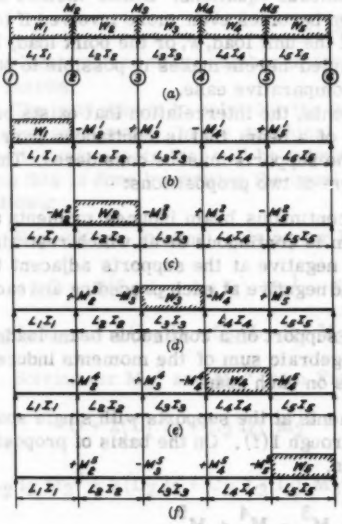


FIG. 1.—UNIFORM LOADING ON FIVE SPANS, SIX POINTS OF SUPPORT

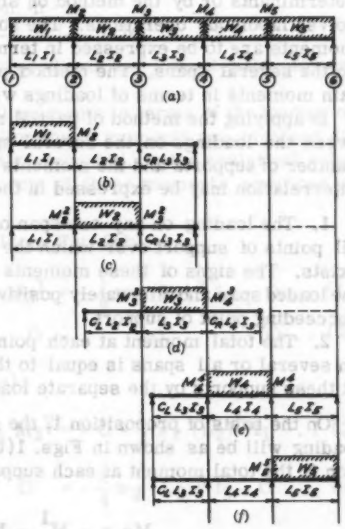


FIG. 2.—UNIFORM LOADING ON THREE SPANS, FOUR POINTS OF SUPPORT

ing being on 1 span only. The moments at the supports, adjacent to the loaded span only, are solved for and are referred to as partial moments. The partial moments are then combined to give the total moments at the supports of the continuous beam.

BASIC PRINCIPLES AND METHOD OF PROCEDURE

Fig. 1(a) represents a continuous beam comprising 5 spans and 6 points of support with the ends of the beam simply supported. The usual equations of

condition of the theorem of three moments may be written as

$$O + 2(L_1 I_2 + L_2 I_1) M_2 + L_2 I_1 M_3 = -\frac{1}{4} w_1 (L_1)^3 I_2 - \frac{1}{4} w_2 (L_2)^3 I_1$$

$$L_2 I_3 M_2 + 2(L_2 I_3 + L_3 I_2) M_3 + L_3 I_2 M_4 = -\frac{1}{4} w_2 (L_2)^3 I_3 - \frac{1}{4} w_3 (L_3)^3 I_2$$

$$L_3 I_4 M_3 + 2(L_3 I_4 + L_4 I_3) M_4 + L_4 I_3 M_5 = -\frac{1}{4} w_3 (L_3)^3 I_4 - \frac{1}{4} w_4 (L_4)^3 I_3$$

$$L_4 I_5 M_4 + 2(L_4 I_5 + L_5 I_4) M_5 + O = -\frac{1}{4} w_4 (L_4)^3 I_5 - \frac{1}{4} w_5 (L_5)^3 I_4$$

in which L is the length of the span, M is the moment, w is the weight per linear foot on the span, and I denotes the moment of inertia. The subscripts refer to the corresponding span. These equations may be solved by either the method of determinants or by the method of simultaneous equations. Either method involves laborious operations. The solution becomes even more involved if the moments are to be expressed in terms of the unit load, w, or the point load, P, on the several spans. The method presented herein makes it possible to obtain moments in terms of loadings with comparative ease.

In applying the method of partial moments, the interrelation that exists between the loadings on the several spans of a beam that is continuous over a number of supports and the moments at the supports must be considered. This interrelation may be expressed in the form of two propositions:

1. The loading on any one span of a continuous beam induces moments at all points of support over which the beam is continuous or at which restraint exists. The signs of these moments are negative at the supports adjacent to the loaded span and alternately positive and negative at each preceding and each succeeding point of support.
2. The total moment at each point of support of a continuous beam loaded on several or all spans is equal to the algebraic sum of the moments induced at these supports by the separate loadings on each span.

On the basis of proposition 1, the moments at the supports with single span loading will be as shown in Figs. 1(b) through 1(f). On the basis of proposition 2, the total moment at each support is,

$$M_2 = -M_2^1 - M_2^2 + M_2^3 - M_2^4 + M_2^5$$

$$M_3 = +M_3^1 - M_3^2 - M_3^3 + M_3^4 - M_3^5$$

$$M_4 = -M_4^1 + M_4^2 - M_4^3 - M_4^4 + M_4^5$$

$$M_5 = +M_5^1 - M_5^2 + M_5^3 - M_5^4 - M_5^5$$

In designating these moments the superscripts refer to the loaded span that induces the moments, whereas the subscripts refer to the supports at which the moments are obtained. It is not necessary to solve for the moments at every

support for each loaded span. It is sufficient merely to solve for the moments at the supports adjacent to the loaded span and then to make the summation in a manner that will be explained subsequently.

Fig. 2(a) represents the beam shown in Fig. 1(a). Figs. 2(b) to 2(f) differ from Figs. 1(b) to 1(f) in that Figs. 2(b) to 2(f) each include 3 spans and 4 points of support instead of 5 spans and 6 points of support. The length of the end spans $C_L L_2$, $C_L L_3$, $C_R L_3$ and $C_R L_4$ must be such as to make the moments indicated in Figs. 2(b) to 2(f) equal in magnitude to the corresponding moments in Figs. 1(b) to 1(f) respectively. These moments will be referred to hereafter as partial moments. The general expressions for the end span factors C_R and C_L are

$$C_R = 1 - \frac{L_n\ I_{n+1}}{4\left(L_n\ I_{n+1} + L_{n+1}\ I_n\right)}$$

and,

$$C_L = 1 - \frac{L_n\ I_{n-1}}{4\left(L_n\ I_{n-1} + L_{n-1}\ I_n\right)}$$

in which n refers to the number of the shortened span and I denotes the moment of inertia.

The next step is to solve for the partial moments in terms of the loading on the several spans. In the graphical solution these moments are obtained directly from charts that will be subsequently presented. In the analytical solution this is done by writing the usual theorem of three moments equations as follows:

For uniform loading; solving for M_2^1 from Fig. 2(b):

$$0 + 2\left(L_1 I_2 + L_2 I_1\right) M_2^1 + L_2 I_1 M_3^1 = -\frac{1}{4} w_1 (L_1)^3 I_2 - 0 \quad . . (1)$$

$$L_2 I_3 M_2^1 + 2\left(L_2 I_3 + C_R L_3 I_2\right) M_3^1 + 0 = - 0 - 0 \quad . . (2)$$

Solving for M_2^2 and M_3^2 from Fig. 2(c):

$$0 + 2\left(L_1 I_2 + L_2 I_1\right) M_2^2 + L_2 I_1 M_3^2 = - 0 - \frac{1}{4} w_2 (L_2)^3 I_1 \quad . . (3)$$

$$L_2 I_3 M_2^2 + 2\left(L_2 I_3 + C_R L_3 I_2\right) M_3^2 + 0 = -\frac{1}{4} w_2 (L_2)^3 I_3 - 0 \quad . . (4)$$

Solving for M_3^3 and M_4^3 from Fig. 2(d):

$$0 + 2\left(C_L L_2 I_3 + L_3 I_2\right) M_3^3 + L_3 I_2 M_4^3 = - 0 - \frac{1}{4} w_3 (L_3)^3 I_2 \quad . . (5)$$

$$L_3 I_4 M_3^3 + 2\left(L_3 I_4 + C_R L_4 I_3\right) M_4^3 + 0 = -\frac{1}{4} w_3 (L_3)^3 I_4 - 0 \quad . . (6)$$

Solving for M_4^4 and M_5^4 from Fig. 2(e):

$$0 + 2\left(C_L L_3 I_4 + L_4 I_3\right) M_4^4 + L_4 I_3 M_5^4 = - 0 - \frac{1}{4} w_4 (L_4)^3 I_3 \quad . . (7)$$

$$L_4 I_5 M_4^4 + 2\left(L_4 I_5 + L_5 I_4\right) M_5^4 + 0 = -\frac{1}{4} w_4 (L_4)^3 I_5 - 0 \quad . . . . . (8)$$

Solving for M_5^5 from Fig. 2(f):

$$O + 2(C_L\ L_3\ I_4 + L_4\ I_3)\ M_5^4 + L_4\ I_3\ M_5^5 = -\ O - O \quad \ldots\ldots\ (9)$$

$$L_4\ I_5\ M_5^4 + 2(L_4\ I_5 + L_5\ I_4)\ M_5^5 + \quad O = -\frac{1}{4} w_5\ (L_5)^3\ I_4 \quad \ldots\ldots\ (10)$$

For concentrated loading; solving for M_2^1 from Fig. 3(b):

$$O + 2(L_1\ I_2 + L_2\ I_1)\ M_2^1 + L_2\ I_1\ M_3^1$$

$$= -\ P'_1\ (L_1)^2\ I_2\ K'_A - P''_1\ (L_1)^2\ I_2\ K''_A - O \quad \ldots\ldots\ (11)$$

$$L_2\ I_3\ M_2^1 + 2(L_2\ I_3 + C_R\ L_3\ I_2)\ M_3^1 + O = -\ O - O - O \quad \ldots\ldots\ (12)$$

Solving for M_2^2 and M_3^2 from Fig. 3(c):

$$O + 2(L_1\ I_2 + L_2\ I_1)\ M_2^2 + L_2\ I_1\ M_3^2$$

$$= -\ O - P'_2\ (L_2)^2\ I_1\ K'_B - P''_2\ (L_2)^2\ I_1\ K''_B \quad \ldots\ldots\ (13)$$

$$L_2\ I_3\ M_2^2 + 2(L_2\ I_3 + C_R\ L_3\ I_2)\ M_3^2 + O$$

$$= -\ P'_2\ (L_2)^2\ I_3\ K'_A - P''_2\ (L_2)^2\ I_3\ K''_A - O \quad \ldots\ldots\ (14)$$

Solving for M_3^3 and M_4^3 from Fig. 3(d):

$$O + 2(C_L\ L_2\ I_3 + L_3\ I_2)\ M_3^3 + L_3\ I_2\ M_4^3$$

$$= -\ O - P'_3\ (L_3)^2\ I_2\ K'_B - P''_3\ (L_3)^2\ I_2\ K''_B \quad \ldots\ldots\ (15)$$

$$L_3\ I_4\ M_3^3 + 2(L_3\ I_4 + C_R\ L_4\ I_3)\ M_4^3 + O$$

$$= -\ P'_3\ (L_3)^2\ I_4\ K'_A - P''_3\ (L_3)^2\ I_4\ K''_A - O \quad \ldots\ldots\ (16)$$

Solving for M_4^4 and M_5^4 from Fig. 3(e):

$$O + 2(C_2\ L_3\ I_1 + L_4\ I_3)\ M_4^4 + L_4\ I_3\ M_5^4$$

$$= -\ O - P'_4\ (L_4)^2\ I_3\ K'_B - P''_4\ (L_4)^2\ I_3\ K''_B \quad \ldots\ldots\ (17)$$

$$L_4\ I_3\ M_4^4 + 2(L_4\ I_5 + L_5\ I_4)\ M_5^4 + O$$

$$= -\ P'_4\ (L_4)^2\ I_5\ K'_A - P''_4\ (L_4)^2\ I_5\ K''_A - O \quad \ldots\ldots\ (18)$$

Solving for M_5^5 from Fig. 3(f):

$$O + 2(C_L\ L_3\ I_4 + L_4\ I_3)\ M_5^4 + L_4\ I_3\ M_5^5 = -\ O - O - O \quad \ldots\ldots\ (19)$$

$$L_4 I_5 M_5^4 + 2(L_4 I_5 + L_5 I_4) M_5^5 + O$$

$$= - O - P'_5 (L_5)^2 I_4 K'_B - P''_5 (L_5)^2 I_4 K''_B \quad \ldots\ldots\ldots\ldots\ldots\ldots \quad (20)$$

In the preceding equations $K'_A = \left[k' - (k')^3\right]$, $K''_A = \left[k'' - (k'')^3\right]$

$K'_B = \left[2k' - 3(k')^2 + (k')^3\right]$, and $K''_B = \left[2k'' - 3(k'')^2 + (k'')^3\right]$, in which k' and k'' are varying percentages of the length L.

Having obtained the partial moments the next step is the determination of the moments at every support over which the beam is continuous in terms of

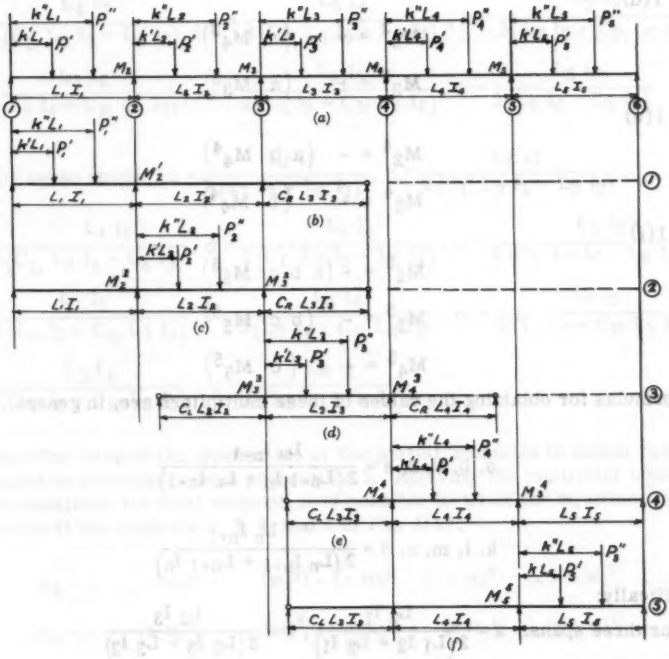


FIG. 3.—CONCENTRATED LOADING

the partial moments. This is done by multiplying the partial moments by certain coefficients or mutipliers, being careful to give them the proper signs in accordance with proposition 1. These multipliers will be designated by the letters a through e when expressing moments at given supports in terms of the moment at a succeeding support, and the letters k through o when expressing moments at given supports in terms of the moment at a preceding support.

Thus, referring to

Fig. 1(b)

$$M_5^1 = +(k\ l\ m\ M_2^1)$$
$$M_4^1 = -(k\ l\ M_2^1)$$
$$M_3^1 = +(k\ M_2^1)$$

Fig. 1(c)

$$M_5^2 = -(l\ m\ M_3^2)$$
$$M_4^2 = +(l\ M_3^2)$$

Fig. 1(d)

$$M_5^3 = +(m\ M_4^3)$$
$$M_2^3 = +(a\ M_3^3)$$

Fig. 1(e)

$$M_2^4 = -(a\ b\ M_4^4)$$
$$M_3^4 = +(b\ M_4^4)$$

Fig. 1(f)

$$M_2^5 = +(a\ b\ c\ M_5^5)$$
$$M_3^5 = -(b\ c\ M_5^5)$$
$$M_4^5 = +(c\ M_5^5)$$

Formulas for obtaining the values of these multipliers are, in general,

$$a, b, c, d, e = \frac{L_n I_{n-1}}{2(L_{n-1} I_n + L_n I_{n-1})}$$

and,

$$k, l, m, n, o = \frac{L_n I_{n+1}}{2(L_n I_{n+1} + L_{n+1} I_n)}$$

Specifically:

For three spans: $a = \frac{L_2 I_1}{2(L_1 I_2 + L_2 I_1)}$, $k = \frac{L_2 I_3}{2(L_2 I_3 + L_3 I_2)}$

For four spans: $a = \frac{L_2 I_2}{2(L_1 I_2 + L_2 I_1)}$, $b = \frac{L_3 I_2}{2(C_L L_2 I_3 + L_3 I_2)}$

$k = \frac{L_2 I_3}{2(L_2 I_3 + C_R L_3 I_2)}$, $l = \frac{L_3 I_4}{2(L_3 I_4 + L_4 I_3)}$

For five spans: $a = \frac{L_2 I_1}{2(L_1 I_2 + L_2 I_1)}$, $b = \frac{L_3 I_2}{2(C_L L_2 I_3 + L_3 I_2)}$,

$c = \frac{L_4 I_3}{2(C_L L_3 I_4 + L_4 I_3)}$, $k = \frac{L_2 I_3}{2(L_2 I_3 + C_R L_3 I_2)}$, $l = \frac{L_3 I_4}{2(L_3 I_4 + C_R L_4 I_3)}$,

$m = \frac{L_4 I_5}{2(L_4 I_5 + L_5 I_4)}$

For six spans: $a = \frac{L_2 L_1}{2(L_1 I_2 + L_2 I_1)}$, $b = \frac{L_3 I_2}{2(C_L L_2 I_3 + L_3 I_2)}$,

$c = \frac{L_4 I_3}{2(C_L L_3 I_4 + L_4 I_3)}$, $d = \frac{L_5 I_4}{2(C_L L_4 I_5 + L_5 I_4)}$, $k = \frac{L_2 I_3}{2(L_2 I_3 + C_R L_3 I_2)}$,

$l = \frac{L_3 I_4}{2(L_3 I_4 + C_R L_4 I_3)}$, $m = \frac{L_4 I_5}{2(L_4 I_5 + C_R L_5 I_4)}$, $n = \frac{L_5 I_6}{2(L_5 I_6 + L_6 I_5)}$

For seven spans: $a = \frac{L_2 I_1}{2(L_1 I_2 + L_2 I_1)}$, $b = \frac{L_3 I_2}{2(C_L L_2 I_3 + L_3 I_2)}$,

$c = \frac{L_4 I_3}{2(C_L L_3 I_4 + L_4 I_3)}$, $d = \frac{L_5 I_4}{2(C_L L_4 I_5 + L_5 I_4)}$, $e = \frac{L_6 I_5}{2(C_L L_5 I_6 + L_6 I_5)}$,

$k = \frac{L_2 I_3}{2(L_2 I_3 + C_R L_3 I_2)}$, $l = \frac{L_3 I_4}{2(L_3 I_4 + C_R L_4 I_3)}$, $m = \frac{L_4 I_5}{2(L_4 I_5 + C_R L_5 I_4)}$,

$n = \frac{L_5 I_6}{2(L_5 I_6 + C_R L_6 I_5)}$, $o = \frac{L_6 I_7}{2(L_6 I_7 + L_7 I_6)}$

The final step is the summation of the partial moments to obtain the total moments in accordance with proposition 2. Applying the multiplier equations to the equations for total moment, it is possible to write the equations for the moments at the supports 2, 3, 4, and 5 in Fig. 1(a).

$$M_2 = - (M_2^1) - (M_2^2) + (a\ M_3^3) - (a\ b\ M_4^4) + (a\ b\ c\ M_5^5) \quad .. \quad (21)$$

$$M_3 = + (k\ M_2^1) - (M_3^2) - (M_3^3) + (b\ M_4^4) - (b\ c\ M_5^5) \quad .. \quad (22)$$

$$M_4 = - (k\ l\ M_2^1) + (l\ M_3^2) - (M_4^3) - (M_4^4) + (c\ M_5^5) \quad .. \quad (23)$$

$$M_5 = + (k\ l\ m\ M_2^1) - (l\ m\ M_3^2) + (m\ M_4^3) - (M_5^4) - (M_5^5) \quad .. \quad (24)$$

Eqs. 21 to 24 give values of the moments at the supports precisely the same as do the equations of the theorem of three moments but the amount of time and labor involved is greatly reduced. This is especially true if the moments are to be expressed in terms of the loadings on the spans.

The summation of partial moments for various size spans is as follows:

For three spans,

$$M_2 = - M_2^1 - M_2^2 + (a)M_3^3$$

$$M_3 = + (k)M_2^1 - M_3^2 - M_3^3$$

For four spans,

$$M_2 = - M_2^1 - M_2^2 + (a)M_3^3 - (a)(b)M_4^4$$

$$M_3 = + (k)M_2^1 - M_3^2 - M_3^3 + (b)M_4^4$$

$$M_4 = - (k)(l)M_2^1 + (l)M_3^2 - M_4^3 - M_4^4$$

For six spans,

$$M_2 = - M_2^1 - M_2^2 + (a)M_3^3 - (a)(b)M_4^4 + (a)(b)(c)M_5^5 - (a)(b)(c)(d)M_6^6$$

$$M_3 = + (k)M_2^1 - M_3^2 - M_3^3 + (b)M_4^4 - (b)(c)M_5^5 + (b)(c)(d)M_6^6$$

$$M_4 = - (k)(l)M_2^1 + (l)M_3^2 - M_4^3 - M_4^4 + (c)M_5^5 - (c)(d)M_6^6$$

$$M_5 = + (k)(l)(m)M_2^1 - (l)(m)M_3^2 + (m)M_4^3 - (m)M_5^4 - M_5^5 + (d)M_6^6$$

$$M_6 = - (k)(l)(m)(n)M_2^1 + (l)(m)(n)M_3^2 - (m)(n)M_4^3 + (n)M_5^4 - M_6^5 - M_6^6$$

ANALYTICAL SOLUTION OF ILLUSTRATIVE PROBLEMS

The solution of the illustrative problems will be given in full detail, listing every step from the method of obtaining the constants C_R and C_L, and the multipliers, to the combination of these multipliers in the summation of the partial moments. In actual practice, it will be found that a number of short cuts can be used in obtaining and applying these factors without materially affecting the accuracy of the results. A list of short cuts is given following the illustrative problems.

Illustrative Problem Number 1.— Uniform loading problem solved in terms of w (Fig. 2(a)).

For all uniform loading problems sovled in terms of w let spans $L_1 = L_5 = 18$ ft; $L_2 = L_4 = 24$ ft; $L_3 = 30$ ft. Let $I_1 = I_5 = 1000$ in.^{4}; $I_2 = I_4 = 2000$ in.^{4}; $I_3 = 3000$ in.^{4} and let the loading on $L_1 = w_1$; $L_2 = w_2$; $L_3 = w_3$; $L_4 = w_4$; $L_5 = w_5$.

Subdivision of Beams: $C_L L_2 = 21.60$ ft; $C_L L_3 = 26.55$ ft; $C_R L_3 = 26.55$ ft; $C_R L_4 = 21.60$ ft.

Partial Moments: Applying Eqs. 1 to 10, then for Fig. 2(b) $M_2^1 = 25.76 w_1$; for Fig. 2(c) $M_2^2 = 21.95 w_2$ and $M_3^2 = 35.70 w_2$; for Fig. 2(d) M_3^3 and $M_4^3 = 43.65 w_3$; for Fig. 2(e) $M_4^4 = 35.70 w_4$ and $M_5^4 = 21.95 w_4$; and for Fig. 2(f) $M_5^5 = 25.76 w_5$.

Summation of Partial Moments: From the equations for multipliers for 5 spans, a = 0.20, b = 0.24, c = 0.29; k = 0.29, l = 0.24, and m = 0.20. Following the method of summation of partial moments previously given and reducing to

obtain the total moments at the supports in terms of w,

$$M_2 = -25.76\,w_1 - 21.95\,w_2 + 8.73\,w_3 - 1.72\,w_4 + .36\,w_5$$

$$M_3 = +7.50\,w_1 - 35.70\,w_2 - 43.65\,w_3 + 8.60\,w_4 - 1.80\,w_5$$

$$M_4 = -1.80\,w_1 + 8.60\,w_2 - 43.65\,w_3 - 35.70\,w_4 + 7.50\,w_5$$

$$M_5 = +.36\,w_1 - 1.72\,w_2 + 8.73\,w_3 - 21.95\,w_4 - 25.76\,w_5$$

If the loading on any one of the 5 spans is changed it is necessary to only substitute the new value of w (w is 0 where loading is omitted) into the preceding equations to get the new moments. Therein lies the advantage of solving in terms of the loading w.

Illustrative Problem Number 2.—A concentrated loading problem solved in terms of P. For all concentrated loading problems let spans $L_1 = L_5 = 18.0$ ft; $L_2 = L_4 = 24.0$ ft, $L_3 = 30$ ft, let $I_1 = I_5 = 1000$ in.^{4}; $I_2 = I_4 = 2000$ in.^{4}; $I_3 = 3000$ in.^{4}, and let loading on $L_1 = P_1'$ and P_1''; $L_2 = P_2'$ and P_2''; $L_3 = P_3'$ and P_3''; $L_4 = P_4'$ and P_4''; $L_5 = P_5'$ and P_5''. In Fig. 3(b), $k' = 0.278$ and $k'' = 0.611$. In Fig. 3(c), $k' = 0.291$ and $k'' = 0.541$. In Fig. 3(d), $k' = 0.267$ and $k'' = 0.600$. In Fig. 3(e), $k' = 0.375$ and $k'' = 0.625$. In Fig. 3(f), $k' = 0.444$ and $k'' = 0.777$.

Subdivision of Beams: $C_L L_2 = 21.60$ ft, $C_L L_3 = 26.55$ ft, $C_R L_3 = 26.55$ ft, $C_R L_4 = 21.60$ ft.

Partial Moments: Applying Eq. 11 to Eq. 20, then for Fig. 3(b) $M_2^1 = 1.48\,P_1' + 2.20\,P_1''$, for Fig. 3(c) $M_2^2 = 1.40\,P_2' + 1.32\,P_2''$; $M_3^2 = 1.47\,P_2' + 2.26\,P_2''$, for Fig. 3(d) $M_3^3 = 2.07\,P_3' + 1.90\,P_3''$; $M_4^3 = 1.35\,P_3' + 2.32\,P_3''$; for Fig. 3(e) $M_4^4 = 2.31\,P_4' + 1.81\,P_4''$; $M_5^4 = 1.12\,P_4' + 1.49\,P_4''$; for Fig. 3(f) $M_5^5 = 2.20\,P_5' + 1.23\,P_5''$.

Summation of Partial Moments: From the equations for multipliers for 5 spans, $a = 0.20$, $b = 0.24$, $c = 0.29$, $k = 0.29$, $l = 0.24$, $m = 0.20$. Following the method of summation of partial moments previously given and reducing to obtain total moments at the supports in terms of P,

$$M_2 = -1.48\,P_1' - 2.20\,P_1'' - 1.40\,P_2' - 1.32\,P_2'' + 0.41\,P_3' + 0.38\,P_3'' - 0.11\,P_4' - 0.09\,P_4'' + 0.03\,P_5' + 0.02\,P_5''$$

$$M_3 = +0.43\,P_1' + 0.64\,P_1'' - 1.47\,P_2' - 2.26\,P_2'' - 2.07\,P_3' - 1.90\,P_3'' + 0.55\,P_4' + 0.43\,P_4'' - 0.15\,P_5' - 0.09\,P_5''$$

$$M_4 = -0.10\,P_1' - 0.15\,P_1'' + 0.35\,P_2' + 0.54\,P_2'' - 1.35\,P_3' - 2.32\,P_3'' - 2.31\,P_4' - 1.81\,P_4'' + 0.64\,P_5' + 0.36\,P_5''$$

$$M_5 = +0.02\,P_1' + 0.03\,P_1'' - 0.07\,P_2' - 0.10\,P_2'' + 0.27\,P_3' + 0.46\,P_3'' - 1.12\,P_4' - 1.49\,P_4'' - 2.20\,P_5' - 1.23\,P_5''$$

If the loading on any one of the 5 spans is changed it is necessary only to substitute the new value of P (P is where loading is omitted) into the preceding

equations to get the new moments. Therein lies the advantage of solving in terms of the loading P.

GRAPHICAL SOLUTION OF ILLUSTRATIVE PROBLEMS

In the analytical solution the partial moments were obtained by applying the theorem of three moments to each subdivided beam having 3 spans, ends simply supported and loaded on 1 span only. In the graphical solution the partial moments will be obtained from the graphs given on Figs. 4 through 7.

In their construction, the graphs are similar to, but are not identical with, those given by J. A. L. Waddell.[4] Furthermore, the graphs developed by the writer are applicable to both concentrated and uniform loading, whereas Waddell's graphs are applicable to uniform loading only.

The solution of the illustrative problems to follow will describe the method in detail. As explained in the case of the analytical solution, a number of short cuts are available to the engineer using this method in actual practice.

Illustrative Problem Number 1.—Uniform loading problem solved in terms of w.

Subdivision of Beams: $C_L L_2 = 21.60$ ft; $C_L L_3 = 26.55$ ft; $C_R L_3 = 26.55$ ft; $C_R L_4 = 21.60$ ft.

Partial Moments: $f_1 = \frac{L_2 I_1}{L_1 I_2}$ and $f_2 = \frac{L_2 I_3}{L_3 I_2}$, in which L_1, L_2 and L_3 are as indicated in Figs. 4 and 5. Thus, for Fig. 2(b), $f_1 = 0.67$ and $f_2 = 1.36$; for Fig. 2(c), $f_1 = 0.67$ and $f_2 = 1.36$; for Fig. 2(d), $f_1 = 0.93$ and $f_2 = 0.93$; for Fig. 2(e), $f_1 = 1.36$ and $f_2 = 0.67$; and for Fig. 2(f), $f_1 = 1.36$, and $f_2 = 0.67$.

Curves A and B give the coefficients A and B which enter the expression for moments $Aw_n(L_n)^2$ and $Bw_n(L_n)^2$. In the end spans, coefficient A applies to the moment at the right support and coefficient B to the moment at the left support. In the intermediate spans, coefficient A applies to the moment at the left support and coefficient B to the moment at the right support (Figs. 4 and 5).

To read the curves, enter the abscissas with the value of f_1, up vertically to curves A or B to an intersection with the corresponding value of f_2, then to the left or right, where the coefficients A or B are read. Thus, read for Fig. 2(b), A = .0795; for Fig. 2(c), A = .0380 and B = .0620; for Fig. 2(d), A = .0485 and B = .0485; for Fig. 2(e), A = .0620 and B = .0380; for Fig. 2(f), B = .0795.

Writing partial moments yields, for Fig. 2(b), $M_2^1 = .0795\, w_1(L_1)^2 = 25.76\, w_1$; for Fig. 2(c), $M_2^2 = .0380\, w_2(L_2)^2 = 21.95\, w_2$; $M_3^2 = .0620\, w_2(L_2)^2 = 35.70\, w_2$; for Fig. 2(d), $M_3^3 = .0485\, w_3(L_3)^2 = 43.65\, w_3$; $M_4^3 = .0485\, w_3(L_3)^2 = 43.65\, w_3$; for Fig. 2(e), $M_4^4 = .0620\, w_4(L_4)^2 = 35.70\, w_4$; $M_5^4 = .0380\, w_4(L_4)^2 = 21.95\, w_4$; and for Fig. 2(f), $M_5^5 = .0795\, w_5(L_5)^2 = 25.76\, w_5$.

Summation of partial moments is accomplished by first determining the multipliers as previously shown. From this method, a = 0.20; b = 0.24; c = 0.29; k = 0.29; l = 0.24; m = 0.20. Then the method of summation of partial moments as previously given is carried out and reduction is accomplished to obtain total moments at the supports in terms of w.

---

[4] "Bridge Engineering," by J. A. L. Waddell, John Wiley & Sons, Inc., 1916, Vol. I.

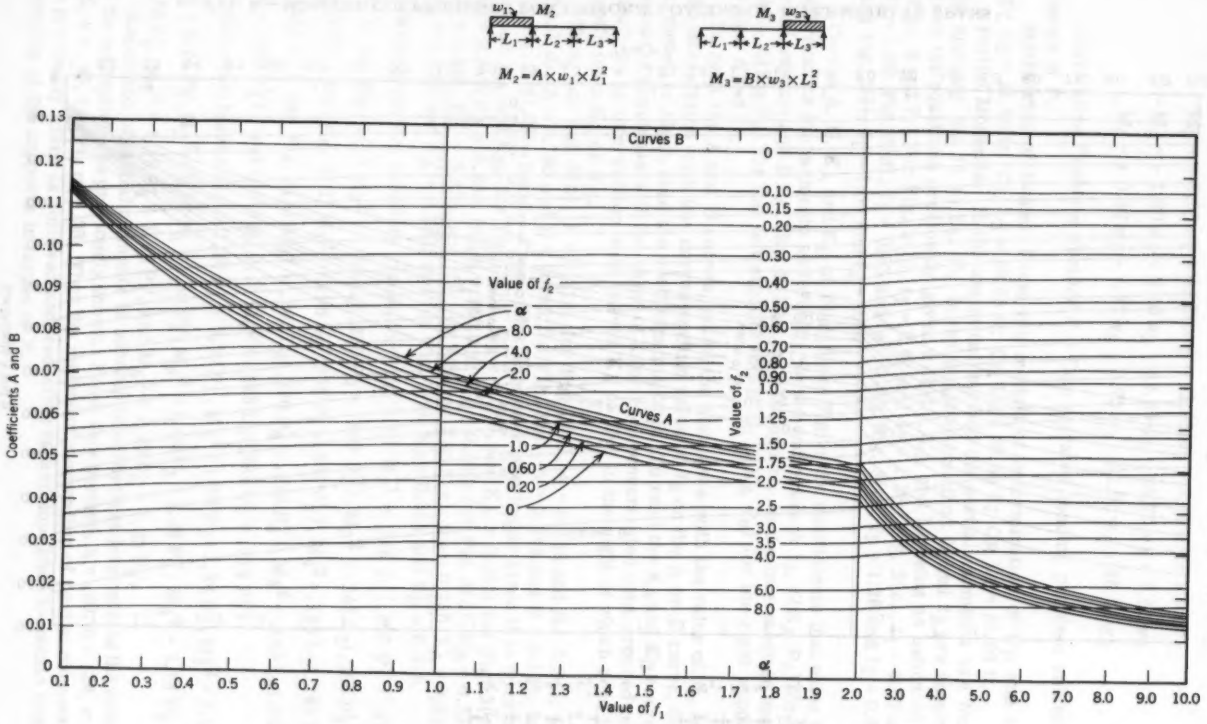


FIG. 4.—MOMENT COEFFICIENTS FOR UNIFORM LOADING OF END SPANS

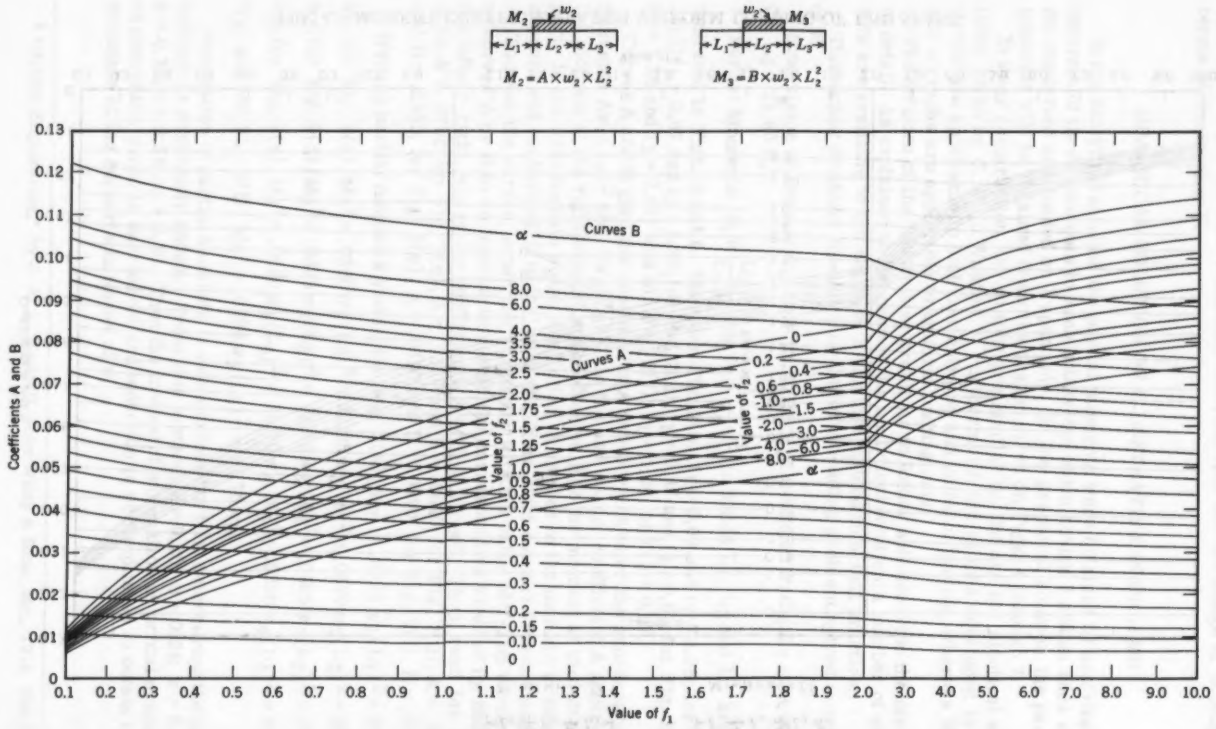


FIG. 5.—MOMENT COEFFICIENTS FOR UNIFORM LOADING OF INTERMEDIATE SPANS

$$M_2 = -25.76w_1 - 21.95w_2 + 8.73w_3 - 1.72w_4 + 0.36w_5$$

$$M_3 = +7.50w_1 - 35.70w_2 - 43.65w_3 + 8.60w_4 - 1.80w_5$$

$$M_4 = -1.80w_1 + 8.60w_2 - 43.65w_3 - 35.70w_4 + 7.50w_5$$

$$M_5 = +0.36w_1 - 1.72w_2 + 8.73w_3 - 21.95w_4 - 25.76w_5$$

Illustrative Problem Number 2.— Concentrated loading problem solved in terms of P.

Subdivision of Beam: From the method of determination of C_R and C_L, $C_L L_2 = 21.60$ ft; $C_L L_3 = 26.55$ ft; $C_R L_3 = 26.55$ ft; $C_R L_4 = 21.60$ ft.

Partial Moments: In the analytical method the partial moments are found by applying Eq. 11 to Eq. 20. In the graphical method f_1 and f_2 are obtained from the equations previously given with L_1, L_2, and L_3 being as indicated on Figs. 6 and 7. For Fig. 3(b), $f_1 = 0.67$ and $f_2 = 1.36$; Fig. 3(c), $f_1 = 0.67$ and $f_2 = 1.36$; Fig. 3(d), $f_1 = 0.93$ and $f_2 = 0.93$; Fig. 3(e), $f_1 = 1.36$ and $f_2 = 0.67$; and Fig. 3(f), $f_1 = 1.36$ and $f_2 = 0.67$.

Curves A, B, K_A and K_B of Figs. 6 and 7 give the coefficients that enter the expressions for moments as follows: In the end spans $A L_n \Sigma(K_A P_n)$ for the right support and $B L_n \Sigma(K_B P_n)$ for the left support. In the intermediate spans $A L_n \Sigma(K_B P_n)$ for the left support and $B L_n \Sigma(K_A P_n)$ for the right support (Figs. 6 and 7).

To read the A and B curves, enter the abscissas with the value of f_1, find the intersection with the corresponding value of f_2 on the A or B curve, then at the left or right, read the coefficients A or B. To read the K_A and K_B curves, enter the abscissas with the value of k for each concentrated load, proceed vertically to an intersection with curves K_A or K_B, to the right of which read the coefficients K_A or K_B.

Thus, for Fig. 3(b), A = 0.318, for Fig. 3(c), A = 0.155 and B = 0.245; for Fig. 3(d), A = 0.195 and B = 0.195; for Fig. 3(e), A = 0.245 and B = 0.155; and for Fig. 3(f), B = 0.318. From the values of k previously given it is possible to read K_A and K_B, for Fig. 3(b), $K'_A = 0.260$, and $K''_A = 0.385$; for Fig. 3(c), $K'_B = 0.350$, $K'_A = 0.265$. $K''_B = 0.360$, and $K''_A = 0.380$; for Fig. 3(d), $K'_B = 0.335$, $K'_A = 0.245$, $K''_B = 0.335$, and $K''_A = 0.385$ for Fig. 3(e), $K'_B = 0.380$, $K'_A = 0.320$, $K''_B = 0.320$, and $K''_A = 0.380$; and for Fig. 3(f), $K'_B + 0.385$ and $K''_B = 0.215$.

Writing partial moments yields, for Fig. 3(b) $M_2{}^1 = .318\, L_1(.260\, P'_1 + .385\, P''_1)$; for Fig. 3(c) $M_2{}^2 = .155\, L_2(.350\, P'_2 + .360\, P''_2)$, $M_3{}^2 = .245\, L_2(.265\, P'_2 + .380\, P''_2)$; for Fig. 3(d) $M_3{}^3 = .195\, L_3(.335\, P'_3 + .335\, P'_3)$, $M_4{}^3 = .195\, L_3(.245\, P'_3 + .385\, P''_3)$ for Fig. 3(e) $M_4{}^4 = .245\, L_4(.380\, P'_4 + .320\, P''_4)$, $M_5{}^4 = .155\, L_4(.320\, P'_4 + .380\, P''_4)$ and for Fig. 3(f) $M_5{}^5 = .318\, L_5(.385\, P'_5 + .215\, P''_5)$.

Reduction leaves $M_2{}^1 = 1.48\, P'_1 + 2.20\, P''_1$, $M_2{}^2 = 1.30\, P'_2 + 1.34\, P''_2$, $M_3{}^2 = 1.57\, P'_2 + 2.24\, P''_2$, $M_3{}^3 = 1.96\, P'_3 + 1.96\, P''_3$, $M_4{}^3 = 1.46\, P'_3 + 2.26\, P''_3$, $M_4{}^4 = 2.24\, P'_4 + 1.88\, P''_4$, $M_5{}^4 = 1.19\, P'_4 + 1.42\, P''_4$, and $M_5{}^5 = 2.20\, P'_5 + 1.23\, P''_5$.

Summation of partial moments is accomplished by first determining the value of the multipliers as previously shown. From this method, a = .20, b = .24, c = .29, k = .29, l = .24, m = .20. Then the method of summation of partial moments as previously given is followed and reduction is accomplished to obtain total moments at the supports in terms of P.

FIG. 5.—MOMENT COEFFICIENTS FOR UNIFORM LOADING OF INTERMEDIATE SPANS

$$M_2 = -1.48 P'_2 - 2.20 P''_1 - 1.30 P'_2 - 1.34 P''_2 + 0.39 P'_3 + 0.39 P''_3 - 0.11 P'_4 - 0.09 P''_4 + 0.03 P'_5 + 0.02 P''_5$$

$$M_3 = +0.43 P'_1 + 0.64 P''_1 - 1.57 P'_2 - 2.24 P''_2 - 1.96 P'_3 - 1.96 P''_3 + 0.54 P'_4 + 0.45 P''_4 - 0.15 P'_5 - 0.09 P''_5$$

$$M_4 = -0.10 P'_1 - 0.15 P''_1 + 0.38 P'_2 + 0.54 P''_2 - 1.46 P'_3 - 2.26 P''_3 - 2.24 P'_4 - 1.88 P''_4 + 0.64 P'_5 + 0.36 P''_5$$

$$M_5 = +0.02 P'_1 + 0.03 P''_1 - 0.08 P'_2 - 0.11 P''_2 + 0.29 P'_3 + 0.45 P''_3 - 1.19 P'_4 - 1.42 P''_4 - 2.20 P'_5 - 1.23 P''_5$$

SHORT CUTS IN METHOD OF PARTIAL MOMENTS

The following short cuts may be used if a lesser degree of accuracy in the results obtained is deemed justified by the engineer.

An examination of the equations for C_R and C_L indicates that if the lengths of all the spans are equal and the moments of inertia of all the beams are equal, then $C_R = C_L = 0.875(7/8)$. It will be noted from the illustrative problems that for spans of unequal length and for beams having different moments of inertia, these constants vary from 0.885 to 0.900. It is therefore apparent that a value of $0.875(7/8)$ for both C_R and C_L may be used without a material loss of accuracy in the results. However, in extreme cases of variation in span lengths and moments of inertia, the value of these constants may vary from 0.75 to 1.00.

An examination of the equations for the values of the multipliers indicates that if the spans are equal in length and the moments of inertia of the beam for all the spans are also equal, then each of the multipliers will be equal to 0.25 (1/4). On the other hand, the illustrative problems show that when the span lengths and moments of inertia are not equal, the values of the multipliers vary from 0.20 to 0.29. The error resulting from neglecting this variation in the values of the multipliers is appreciable. Using the value of $0.25(1/4)$ for all the multipliers in the example problems, $a = 1/4$, $a \times b = 1/16$, $a \times b \times c = 1/64$, whereas, using the correct values of the multipliers, $a = 1/5$, $a \times b = 1/21$, $a \times b \times c = 1/72$. The engineer's judgment must guide him in the choice of this short-cut.

If more than 5 spans are involved in the summation of partial moments, time and labor may be saved without any material sacrifice of accuracy if the terms involving more than 3 multipliers are neglected. Thus, referring to the summation of partial moments for various size spans that was previously noted, in the 6-span beam the terms $a \times b \times c \times d\ M_6^6$ (For M_2) and $k \times l \times m \times n\ M_2^1$ (For M_6) may be disregarded and in the 7-span beam the terms $a \times b \times c \times d\ M_6^6$ (For M_2); $a \times b \times c \times d \times e\ M_7^7$ (For M_2); $b \times c \times d \times e\ M_7^7$ (For M_3); $k \times l \times m \times n\ M_2^1$ (For M_6); $k \times l \times m \times n \times o\ M_2^1$ (For M_7) and $l \times m \times n \times o\ M_3^2$ (For M_7) may be disregarded.

CORRECTION FOR THE GRAPHICAL SOLUTION

It will be noted that the partial moments obtained by the graphical method do not quite agree with those obtained by the analytical method. However, the

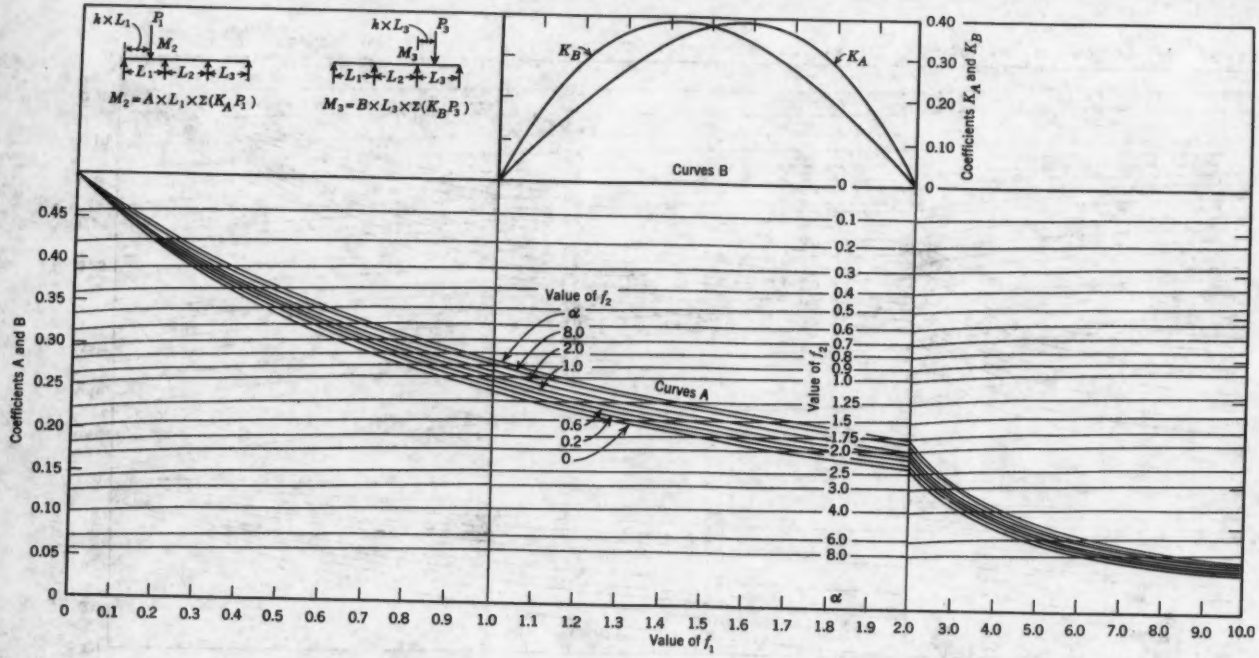


FIG. 6.—MOMENT COEFFICIENTS FOR CONCENTRATED LOADINGS OF END SPAN

FIG. 7.—MOMENT COEFFICIENTS FOR CONCENTRATED LOADING OF INTERMEDIATE SPANS

resultant error in the total moments due to this discrepancy is very small and may be safely neglected. As a matter of record, however, the nature of and the method of correcting this error will be explained.

Due to the mechanics of construction of the A and B curves for concentrated loading (Figs. 6 and 7) a small correction must be applied to the partial moments in the intermediate spans (Figs. 3(c) to 3(e)). The correction $(K_B - K_A)\Delta k$ is to be applied to moments at the left support and $(K_A - K_B)\Delta k$ is to be applied to moments at the right support.

To read the curves Δk (Fig. 7) the abscissa is entered with the value f_1, the intersection with the corresponding value of f_2 is located, and the coefficients Δk is read to the left for f_1 less than 2.0 and to the right for f_1 greater than 2.0. Thus, the value of Δk turns out to be 1.2 for all cases of Fig. 3. For loads P', in Figs. 3(c), 3(d), and 3(e) respectively at the left support $(K'_B - K'_A)\Delta k$ is equal to +0.085 x 1.2, +0.090 x 1.2, and +0.060 x 1.2 and at the right support $(K'_A - K'_B)\Delta k$ is equal to - 0.085 x 1.2, -0.090 x 1.2, and -0.060 x 1.2. For loads P'', in Figs. 3(c), 3(d), and 3(e) respectively at the left support $(K''_B - K''_A)\Delta k$ is equal to -0.020 x 1.2, -0.050 x 1.2, and -0.060 x 1.2 and at the right support $(K''_A - K''_B)\Delta k$ is equal to +0.020 x 1.2, +0.050 x 1.2, and +0.060 x 1.2.

Applying these corrections to the partial moments yields $M_2^1 = 1.48\,P'_1 + 2.20\,P''_1$ (no corrections), $M_2^2 = (1.30 + .10)\,P'_2 + (1.34 - .02)\,P''_2$; $M_3^2 = (1.57 - .10)\,P'_2 + (2.24 + .02)\,P''_2$; $M_3^3 = (1.96 + .11)\,P'_3 + (1.96 - .06)\,P''_3$; $M_4^3 = (1.46 - .11)\,P'_3 + (2.26 + .06)\,P''_3$; $M_4^4 = (2.24 + .07)\,P'_4 + (1.88 - .07)\,P''_4$; $M_5^5 = (1.19 - .07)\,P'_4 + (1.42 + .07)\,P''_4$; and $M_5^5 = 2.20\,P'_5 + 1.23\,P''_5$ (no corrections).

Reductions leaves $M_2^1 = 1.48\,P'_1 + 2.20\,P''_1$ $M_2^2 = 1.40\,P'_2 + 1.32\,P''_2$ $M_3^2 = 1.47\,P'_2 + 2.26\,P''_2$; $M_3^3 = 2.07\,P'_3 + 1.90\,P''_3$; $M_4^3 = 1.35\,P'_3 + 2.32\,P''_3$; $M_4^4 = 2.31\,P'_4 + 1.81\,P''_4$; $M_5^4 = 1.12\,P'_4 + 1.49\,P''_4$; and $M_5^5 = 2.20\,P'_5 + 1.23\,P''_5$. Determining the multipliers and summing the partial moments yields the corrected total moments.

SPECIAL CASES

The method of partial moments is applicable to many special cases. Some of these are given in Fig. 8, in which F.E. designates fixed end.

1. One span, one end fixed.—Add one imaginary span $(L_0 = 0)$ at the fixed end and another at the free end $(L_2 = \infty\,(\text{infinity}))$, then proceed as for a 3-span beam.

2. One span, both ends fixed.—Add imaginary span $L_0 = 0$ at one end and $L_2 = 0$ at the other end, then proceed as for a 3-span beam.

3. Two spans, ends free.—Add one imaginary span $L_3 = \infty$, then proceed as for a 3-span beam.

4. Two spans, one end fixed.—Add one imaginary span $L_3 = 0$, then proceed as for a 3-span beam.

5. Two spans, both ends fixed.—Add imaginary spans $L_0 = 0$ at one end and $L_3 = 0$ at the other end, then proceed as for a 4-span beam.

6. n number of spans, one end fixed.—Add one imaginary span $L_{n+1} = 0$ at the fixed end, then proceed as in the normal case.

7. n number of spans, both ends fixed.—Add imaginary spans $L_0 = 0$ and $L_{n+1} = 0$ at each end, then proceed as in the normal case.

8. n number of spans, with cantilevers at one end or both ends.—Proceed as in the normal case. Use the cantilever moments as partial moments $M_1{}^c$ and $M^c{}_{n+1}$ in writing the summation of partial moments. M_1 and M_{n+1} are equal to $P(L_c)$.

MOMENTS AND SHEARS

Moments.—In the foregoing matter a method has been developed for obtaining the moments at the supports of a continuous beam. Once these moments have

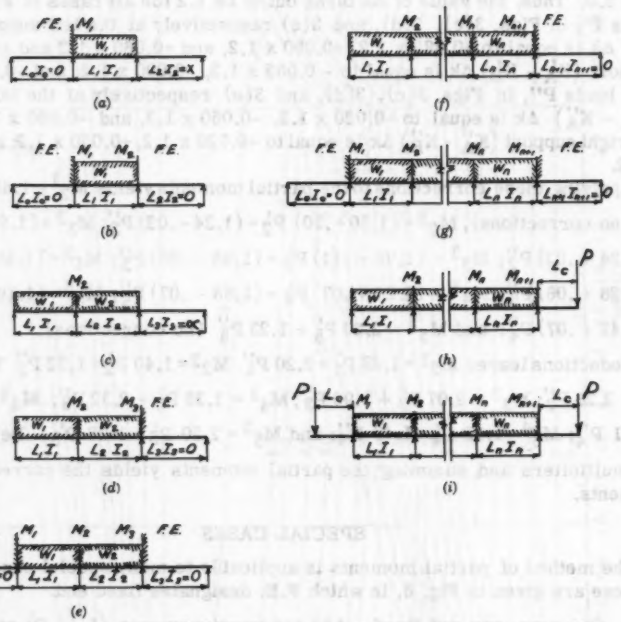


FIG. 8.—SPECIAL CASES FOR APPLICATION OF METHOD OF PARTIAL MOMENTS

been found, the moments at any point in the beam and the shears and reactions at the supports can be readily arrived at.

For any given span, AB, in which fixing moments M_a and M_b are found to exist at points A and B respectively, the moments at any point x distance from B will be

$$M = M_1 + M_b + (M_a - M_b)\frac{x}{L} \quad \ldots\ldots\ldots\ldots\ldots\ldots \quad (25)$$

in which M_1 is the bending moment for a freely supported beam of the same span at a distance x from B and M_a and M_b are the moments at the supports A and B respectively.

Shears.—The shear at either end of any span, must be increased or decreased by an amount that is found by dividing the difference of the moments at the extremities of any span by the span length itself.

In Fig. 9, the shears may be written as

$$V_2 = P_2\left(\frac{L_2 - kL_2}{L_2}\right) - \frac{M_2 - M_3}{L_2} \quad \ldots\ldots\ldots\ldots\ldots\ldots \quad (26)$$

$$V_3^1 = P_2\left(\frac{kL_2}{L_2}\right) + \frac{M_2 - M_3}{L_2} \quad \ldots\ldots\ldots\ldots\ldots\ldots \quad (27)$$

$$V_3 = P_3\left(\frac{L_3 - kL_3}{L_3}\right) - \frac{M_3 - M_4}{L_3} \quad \ldots\ldots\ldots\ldots\ldots\ldots \quad (28)$$

$$V_4^1 = P_3\left(\frac{kL_3}{L_3}\right) + \frac{M_3 - M_4}{L_3} \quad \ldots\ldots\ldots\ldots\ldots\ldots \quad (29)$$

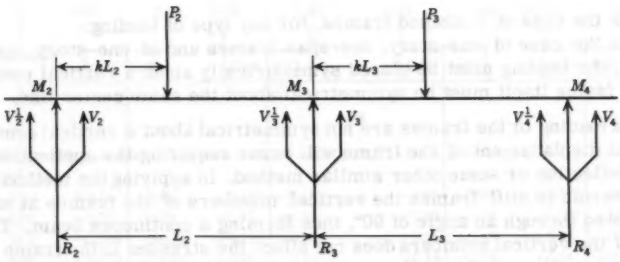


FIG. 9.—MOMENT, SHEAR AND REACTION DETERMINATIONS

It is important to note the sign before the fractions $\frac{M_2 - M_3}{L_2}$ and $\frac{M_3 - M_4}{L_3}$. The reason for the different signs is to be found in the fact that, although in Fig. 9 the moments M_2 and M_3 have opposite signs to those caused by the loadings P_2 and P_3, in Eq. 25 the three component moments are given the same sign.

Another method for obtaining the shears is to take moments about either end of the spans L_2 and L_3 in Fig. 9. Thus, taking moments about the right end of L_2,

$$V_2\,(L_2) - \Sigma P_2\left(\frac{L_2 - kL_2}{L_2}\right) + M_2 = M_3 \quad \ldots\ldots\ldots\ldots \quad (30)$$

While taking moments about the left end of L_2,

$$V_3^1\,(L_2) - \Sigma P_2\left(\frac{kL_2}{L_2}\right) + M_3 = M_2 \quad \ldots\ldots\ldots \quad (31)$$

Taking moments about the right end of L_3,

$$V_3 (L_3) - \Sigma P_3 \left(\frac{L_3 - k L_3}{L_3} \right) + M_3 = M_4 \quad \ldots\ldots\ldots \quad (32)$$

and taking moments about the left end of L_3,

$$V_4^1 (L_3) - \Sigma P_3 \left(\frac{k L_3}{L_3} \right) + M_4 = M_3 \quad \ldots\ldots\ldots\ldots \quad (33)$$

These equations reduce to Eqs. 26 through 29.

Thus it will be seen that by the aid of Eq. 25 the moments at any point of a continuous beam may be determined. Similarly, by the aid of Eqs. 26 through 29, the shears at any support may be determined. The reaction at any support is equal to the sum of the shears at that point. Thus, in Fig. 9, $R_2 = V_2^1 + V_2$; $R_3 = V_3^1 + V_3$; and $V_4^1 + V_4$.

STIFF FRAMES

The method of partial moments may be applied to stiff frames under the following conditions:

1. In the case of L-shaped frames, for any type of loading.
2. In the case of one-story, one-span frames and of one-story, multispan frames, the loading must be placed symmetrically about a vertical center line and the frame itself must be symmetrical about the same center line.

If the loading or the frames are not symmetrical about a vertical center line, a lateral displacement of the frame will occur requiring the application of the slope-deflection or some other similar method. In applying the method of partial moments to stiff frames the vertical members of the frames at each end are rotated through an angle of 90°, thus forming a continuous beam. This rotation of the vertical members does not affect the stresses in the frame as long as the connections between the vertical and the horizontal members remain rigid.

CONCLUSIONS

The main purpose of this paper is to offer the practicing engineer an authentic and at the same time a labor saving method for solving problems involving multispan continuous beams. This is accomplished by making available to him a definite pattern of procedure which can be followed at once without the necessity of setting up equations or of making special graphical constructions for every new problem that comes up.

It has a further advantage in that it permits the engineer to express the moments at the supports in terms of the loading W or P. This feature is extremely important as a time saver when trial loading tests are involved and its importance increases as the number of spans in the continuous beam is increased.

The method is readily open to visual control and can be easily checked at the several steps of computation as the work progresses. It is unnecessary to employ elaborate computing devices because the use of slide-rule work in common practice gives results well within the limits of required accuracy.

DISCUSSION

WILLIAM S. WALKER,[5] M. ASCE, and JOSEPH T. KOLIBAL[6]—Mr. Posner is to be commended for his excellent presentation of the theory of partial moments and the graphs that aid the rapid solution of problems by this method. However, it is pointed out that there are several methods of direct moment distribution available whereby, in a matter of minutes, the final moment and carryover factors can be computed by a simple routine arithmetical process independent of the loading. One such method has been used by the writers successfully for the past ten years. It is called the method of partial fixities. The author's beam, Fig. 2(a), is solved by this method in Fig. 10.

In a total time of 15 min by a routine arithmetical process it is possible to compute, by slide-rule:

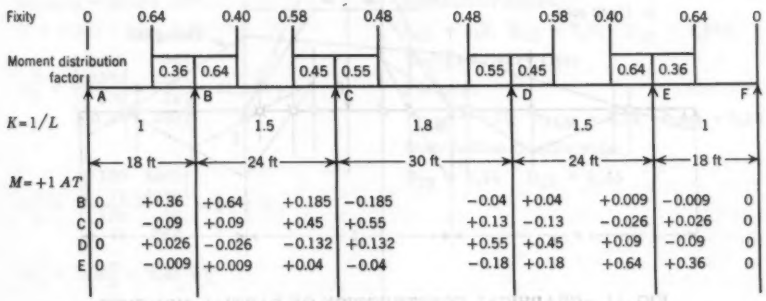


FIG. 10.—PARTIAL FIXITIES METHOD

1. The true joint fixities and final moment distribution factors at each joint.
2. The final distributed moment at each joint due to the application of a unit moment at each support.

All that remains to be done is to use the distributed moments, as recorded, for a moment of unity in order to obtain the support moments for any fixed end moment. The fixed end moments for any loading condition are well known. No graphs are needed. Moreover, the theory is perfectly general and applies to any condition of end support: fixed, cantilever, or partially fixed. For example, suppose that the loading in span C-D (Fig. 1) is such that the fixed end moment at C, $M_{C\text{-}D}$ is -1000 ft-kips, and at D, $M_{D\text{-}C}$, = 500 ft-kips. The final moment at support B, ($M_{B\text{-}C}$), from Fig. 10, is

$$M_{B\text{-}C} = +0.09\ (+1000) - 0.026\ (-500) = +103\ \text{ft-kips}.$$

[5] Sales Engr., Detroit Steel Products Co., Pittsburgh, Pa.
[6] Structural Engr., Pittsburgh, Pa.

ANATOL A. EREMIN,[7] M. ASCE.—Mr. Posner has shown the simplified method of moment distribution with summation of the partial moments in the continuous beam. Two methods of computing the partial moments have been shown; that is, by algebraic formulas and by the graphical method with the graphs bending moments, computed for uniformly distributed loading and concentrated unit forces.

The moment distribution method presented by the author has two advantages: It is simple for visual control and it can be checked in the separate steps of computation. The graphical construction of the partial moments can also be performed directly with the simple bending-moment diagram on the loaded span, as shown in Fig. 11. For span a, L = 90 ft, for span b, L = 75 ft, for span c, L = 60 ft, and I = 1.0 for all spans. The characteristic points on the beam in Fig. 11 are determined by the graphical construction termed three-

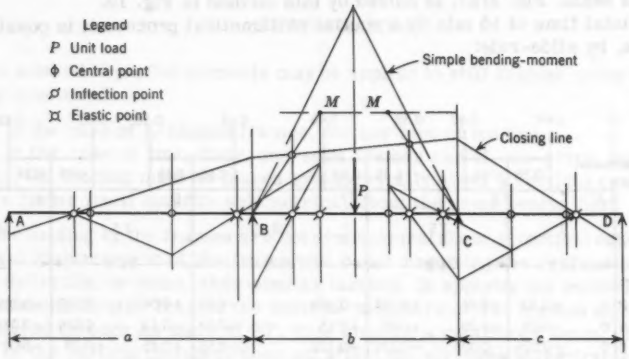


FIG. 11.—GRAPHICAL CONSTRUCTION OF PARTIAL MOMENTS

line polygon.[8,9] Lines MB and MC, drawn through the central moments and points of supports, intersect the inflection point-verticals at points on the bending moment closing line (Fig. 11).

For the loading given in Fig. 2 the partial moments can be performed by summation in the same manner as shown by the author. The bending-moment graphs shown by the author will not be required with the graphical construction in Fig. 11. The method of moment distribution using partial moments, should result in savings of time and effort. The author is to be complimented for his valuable paper.

---

[7] Assoc. Bridge Engr., Bridge Dept. Div. of Highways, State Dept. of Public Works, Sacramento, Calif.

[8] "Simplified Graphical Distribution of Bending Moments," by A. A. Eremin, Published by the author, A. A. Eremin, 1948.

[9] Discussion by A. A. Eremin of "Continuous Arches and Bents Analyzed by Column Analogy," by T. M. Yu, Transactions, ASCE, Vol. 115, 1950, p. 630.

LEMBIT KALD,[10] M. ASCE.—No single method or procedure of computation is equally suited for all types of problems encountered in the analysis of indeterminate structures. On the other hand, if a new method is to be of value, there must be an area in which the new method is superior to existing methods.

ANALYSIS BY THE METHOD OF PARTIAL MOMENTS

$L_1I_2 = L_5I_4 = 36 \times 10^3$

$L_2I_1 = L_4I_5 = 24 \times 10^3$

$L_2I_3 = L_4I_3 = 72 \times 10^3$

$L_3I_2 = L_3I_4 = 60 \times 10^3$

$C_R = 0.886$

$2(L_1I_2 + L_2I_1) = 120 \times 10^3$

$2(L_2I_3 + C_RL_3I_2) = 250 \times 10^3$

$1/4\ W_2(L_2)^3\ I_1 = 3460 \times 10^3\ W_2$

$1/4\ W_2\ (L_2)^3\ I_3 = 10370 \times 10^3\ W_2$

$C_RL_4I_3 = 63.8 \times 10^3$

$L = 0.24; \quad m = 0.20$

$$M_2^2 = \frac{\begin{vmatrix} 3460 & 24 \\ 10370 & 250 \end{vmatrix}}{\begin{vmatrix} 120 & 24 \\ 72 & 250 \end{vmatrix}} = 21.8\ W_2$$

$$M_3^2 = \frac{\begin{vmatrix} 120 & 3460 \\ 72 & 10370 \end{vmatrix}}{\begin{vmatrix} 120 & 24 \\ 72 & 250 \end{vmatrix}} = 35.2\ W_2$$

$M_4^2 = L\ M_3^2 = 8.45\ W_2$

$M_5^2 = m\text{-}M_4^2 = 1.69\ W_2$

ANALYSIS BY THE METHOD OF MOMENT DISTRIBUTION

Fixed End Moment: $48\ W_2$

Stiffness Factors:

$K_{12} = 55.6; \quad K_{23} = 83.3; \quad K_{34} = 100$

In Terms of Relative Stiffness:

$K_{12} = 1.0; \quad K_{23} = 1.5; \quad K_{34} = 1.8;$

Modified Stiffness Factors:

$K_{21M} = 0.75; \quad K_{23M} = 1.315$

$K_{32M} = 1.25; \quad K_{34M} = 1.535$

Restraint Factors:

$R_{23} = 1.5; \quad R_{32} = 2.02; \quad R_{34} = 1.694;$

Modified Carry Over Factors:

$\gamma_{23M} = 0.29; \quad \gamma_{34M} = 0.24; \quad \gamma_{32M} = 0.20$

Distribution Coefficients:

$D_{23} = 0.64 \quad D_{32} = 0.45$

Moment Distribution:

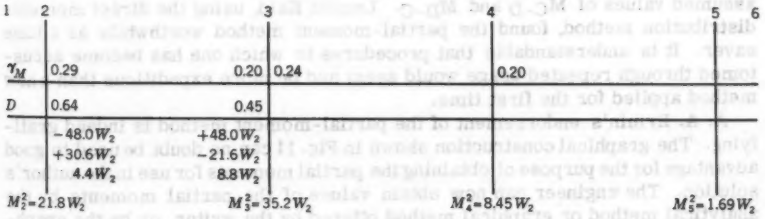


FIG. 12

[10] Chf. Structural Engr., Leonard S. Wegman Co., Engrs., New York, N. Y.

On the basis of this criterion, Mr. Posner's method of partial moments is a valuable contribution to the store of tools for the analysis of continuous beams. The method of partial moments is superior to existing methods of analysis for continuous beams if:

1. Moment of inertia of the beam is constant within each span, but varies from span to span.
2. The loading varies substantially from span to span, or the purpose of analysis is to determine the effect of varying the load on 1 span.

To solve problems of the aforementioned type most efficiently by existing methods, a method of direct moment distribution[11] should be used. In order to compare the amount of work involved in solving such a problem by the method of partial moments and by the method of moment distribution, the beam shown in Fig. 1(c) is analysed by both methods in Fig. 12. In the left hand portion of Fig. 12 the moments M_2^2 and M_3^2 are calculated by solving the simultaneous Eqs. 16 and 17 in Mr. Posner's paper. First the coefficients of the unknown moments are computed, then the moments are solved by determinants.[12]

Considering each multiplication, summation, or division as one operation, 40 operations are required to solve the problem by the method of partial moments, and 48 operations are required to solve the problem by the method of direct distribution.

The author is to be commended for the clear presentation of his method of analysis.

HARRY POSNER[13] F. ASCE.—The writer is thankful to the engineers who have discussed his paper, and who have taken the time to test a new method of approach to the analysis of continuous beams in order to appraise its value in practical application.

Messrs. Walker and Kolibal feel that the application of the direct moment-distribution method, which they had been using for a number of years, gives results more quickly than the proposed method. It is regrettable that they did not carry their computations to a point at which the moments are expressed in terms of the loading "W", but have instead applied their constants to arbitrarily assumed values of $M_{C\text{-}D}$ and $M_{D\text{-}C}$. Lembit Kald, using the direct moment-distribution method, found the partial-moment method worthwhile as a time saver. It is understandable that procedures to which one has become accustomed through repeated usage would seem and be more expeditious than a new method applied for the first time.

A. A. Ermin's endorsement of the partial-moment method is indeed gratifying. The graphical construction shown in Fig. 11 can no doubt be used to good advantage for the purpose of obtaining the partial moments for use in the author's solution. The engineer can now obtain values of the partial moments by the analytical method or graphical method offered by the writer, or by the graphical construction offered by Mr. Eremin. In the final analysis, it will be the task of the engineer at work to make his choice of tools when he is faced with solving this type of problem.

---

11 "A Direct Method of Moment Distribution," by T. Y. Lin, Transactions, ASCE, Vol. 102, 1937, pp. 561-605.

12 "Mathematical Solution of Engineering Problems," by Salvadori and Miller, McGraw-Hill, First Edition, Chapter IV.

13 Partner, Briggs, Blitman & Posner, New Rochelle, N. Y.

The writer feels particularly indebted to Lembit Kald for taking pains to set up the solution of a problem in two parallel columns, one for the writer's method of partial moments, and the other for the direct moment-distribution method now in general use in one form or another. That he found the writer's method, using the analytical solution, attractive and time saving is very encouraging. It is understandable that a certain amount of resistance must be overcome to launch any new and unfamiliar method or procedure.

It is hoped that the proposed method will contribute something of value to the busy engineer. In his own practice the writer has used the method of partial moments for many years and has found it to be extremely useful. This is particularly true in dealing with problems involving trial loading investigations. The greater the number of spans covered by the continuous beam, the more time-saving the method becomes. The ease with which the answer can be expressed in terms of the uniform loading, W, or the concentrated loading P, adds to the usefulness of the proposed method.

AMERICAN SOCIETY OF CIVIL ENGINEERS

Founded November 5, 1852

TRANSACTIONS

Paper No. 3029

SELF-AERATED FLOW IN OPEN CHANNELS

By Lorenz G. Straub,[1] F. ASCE, and
Alvin G. Anderson,[2] M. ASCE

With Discussion by Messrs. Michele Viparelli; and Lorenz G. Straub and Alvin G. Anderson

SYNOPSIS

Measurements of distribution of air concentration in self-aerated flows are presented. The experiments were made in a rough channel of sand-grain type surface at various slopes and discharges, and the data were used as a basis for study of the mechanism of entrainment of air and to relate the air content and distribution to the characteristics of the flow. The analysis of the data shows that the air distribution can be adequately described by relationships based on a simplified concept of turbulent transport and thus are functions of the flow characteristics. The maximum depth and the mean velocity are both shown to increase above those of a corresponding nonaerated flow.

INTRODUCTION

A characteristic of high-velocity, open-channel flow is the phenomenon of self-aeration in which atmospheric air is insufflated into and mixed with the flow to create the appearance of "white water" with its violently agitated and ill-defined free surface. This condition is frequently observed in flows down steep chutes and spillways.

Note.—Published, essentially as printed here, in December, 1958, in the Journal of the Hydraulics Division, as Proceedings Paper 1890. Positions and titles given are those in effect when the paper on discussion was approved for publication in Transactions.

[1] Dir., St. Anthony Falls Hydr. Lab.; Prof. and Head, Dept. of Civ. Engrg., Univ. of Minnesota, Minneapolis, Minn.

[2] Prof. of Hydromechanics, St. Anthony Falls Hydr. Lab., Univ. of Minnesota, Minneapolis, Minn.

It has been reasonably well established by several observers [3,4,5,6,7], that for flows over a spillway from a quiescent reservoir, incipient aeration does not occur on the slope until a point or region is reached at which the boundary layer thickness is equal to the depth. The characteristic roughening of the water surface immediately upstream of the appearance of white water can be readily observed in such occurrences. With increasing initial water depths, the points where the surface roughening and the white water occur move downstream along with the intersection of the boundary layer with the water surface. These considerations suggest that the aeration phenomena are related to the conditions of turbulence in the flow. Examination of such flows by means of high-speed photography indicates that the upper boundary of the flow is rather ill-defined. It consists of a zone that appears white because of entrained air, while above this zone a spray of water droplets occurs moving more or less parallel to the flow and below which is a region of discrete air bubbles suspended in the fluid. Other investigators have described air-entrained flow as being made up of air bubbles entrained in water in the lower levels and water particles in the air in the upper regions. This concept is further emphasized by measurements of the air concentration distribution [8,9,10], which show that the air concentration increases continuously from the bed, exhibiting a smooth transition from a finite value near the bed to a maximum value of 100% at the free surface which value is approached asymptotically.

The results of systematic experiments on distribution of air in self-aerated flows in a channel set at various slopes and operated at various discharges are presented. A provisional analysis is made of the data with respect to air distribution in a vertical section transverse to the direction of flow with a view of arriving at empirical relationships between concentration parameters and the flow characteristics.

EXPERIMENTS AND RESULTS

Apparatus.—The experiments were undertaken in a channel 50 ft long, 1.5 ft wide, and 1 ft deep, and adjustable to any slope from horizontal to nearly vertical. The width was chosen so that for ordinary flows sidewall effects due to growth of the sidewall boundary layer and air entrainment along the sides could be avoided in the central part of the cross section. Earlier measurements of air concentration and velocity in a transverse section at the end of the flume,[8] demonstrated that the width was adequate to make the flow two-dimensional in the center part. The flow was obtained by gravity from the laboratory main

3 "Entrainment of Air in Swiftly Flowing Water," by E. W. Lane, Civil Engineering, Vol. 9, No. 2, 1939, pp. 88-91.

4 "Air Entrainment on Spillway Faces," by G. H. Hickox, Civil Engineering, Vol. 15, No. 12, 1945, pp. 562-563.

5 "Etude de la mise en regime des ecoulements sur les ouvrages a forte pente," by G. Halbronn, La Houille Blanche, No. 1, 1952, pp. 21-40.

6 Ibid., No. 3, pp. 347-371.

7 Ibid., No. 5, pp. 702-722.

8 "Studies of Air Entrainment in Open-Channel Flows," by L. G. Straub and O. P. Lamb, Transactions, ASCE, Vol. 121, 1956, pp. 30-44.

9 "Air Entrainment in Steeply Sloping Flumes," by G. Halbronn and G. Cohen de Lara, Proceedings, Minnesota International Hydr. Convention, Minneapolis, Minn., September, 1953, pp. 455-466.

10 "Flow in a Flume with 1:1 Slope," by M. Viparelli, Proceedings, Minnesota International Hydr. Convention, Minneapolis, Minn., September, 1953, pp. 415-423.

supply flume through two feed lines and controlled by hydraulically-operated valves. The water reached the inlet of the flume through hollow support members and through a rectangular conduit on the underside of the channel. Fig. 1 shows the channel and appurtenances. A control panel separate from the channel contained the actuating components for the hydraulic system and the indicators for the slope, gate opening, and discharge settings.

At the inlet the flow is guided through two 90° vaned bends and a contraction. The inlet gate itself is cantilevered from its mounting at the top of the flume so that there are no slots or guides to disturb the flow. Further guidance is provided by a lip attached to the bottom of the gate and extending inward to further contract the flow. Therefore, the gate opening corresponds to the depth of flow at the upstream end of the channel. The maximum gate opening is 0.5 ft. Pitot



FIG. 1.—VARIABLE SLOPE CHANNEL FOR AIR-ENTRAINMENT EXPERIMENTS



FIG. 2.—PROBES FOR AIR-CONCENTRATION METER

measurements of the flow just downstream of the inlet with a 0.25-ft gate opening showed no deviation greater than 2% from the mean velocity except in the bottom corners where slightly smaller velocities were encountered.

The air-entrainment process was intensified by the installation of artificial roughness on the channel bed that was considerably rougher than the painted steel sidewalls of the channel itself. The material used for the roughness was a commercial nonslip fabric coated with granular particles. The particles, whose mean size was 0.028 in., had a mean spacing of 0.039 in. and were embedded in a mastic.

The discharge rate was measured by two calibrated pitot cylinders mounted in the supply lines and leading to differential gages mounted on the control

panel. Each discharge meter was calibrated separately for flows from 1/2 to 10 cfs with an accuracy of the order of 1%.

The electrical air-concentration measuring instrument has been fully described in an earlier report.[11] The method consists basically of a measurement of the difference between the conductivity of a mixture of air and water and the conductivity of the ambient water alone. A strut supporting a pair of probes is combined with the electrical circuit so that the air-concentration measurements may be made in a small region of the flow. The probes were 1/4 in. wide and 1/4 in. apart. The instrument is direct reading, and the relation between conductivity and air concentration can be determined analytically. The strut holding the probes is arranged so that it is possible to traverse the flow cross section both vertically and laterally. The instrument is limited to measurements not closer than 0.02 ft from the walls because of current deflections by the walls at lesser distances. Because the measurements of the air concentration depend on the resistance or specific sensitivity of the suspending water, the meter was zeroed in water continually circulated from the test channel through a deaerating tank, thus providing water of the same character as that in the flume. Oscilloscope measurements show a rapidly fluctuating current between the probes. Because the meter could not follow these rapid fluctuations, the value read on the meter represented an average value. This average compared well with results obtained by means of a mechanical sampler previously developed and which was not subject to the same averaging problems. Fig. 2 shows the probes and strut supports for the air-concentration meter.

Some of the experimental runs also required taking velocity traverses in verticals through the aerated flows. The instrumentation for making these observations had been previously described[12] in some datail. It consists essentially of a device for timing the travel of minute salt-water cloudlets injected into the air-water mixture. The operating principle of the velocity meter consists basically of marking a small element of flowing mixture and then recording the time interval required for this marked element to traverse a fixed distance. The marking is accomplished by making a diminutive part of flowing water more highly conductive to electrical current by injecting a small amount of salt solution into the stream. The passage of this ionized cloudlet is then detected by electrodes at stations fixed 3 in. apart in the flow path. The injections were made at a speed of approximately 20 per sec with individual injections of approximately 0.03 cu cm of 6% saline solution injected in approximately 1/600 sec. The accuracy of the air-concentration meter and the velocity meter was checked by comparing the measured water rate entering the channel with the integrated flow determined by the velocity traverses and the air-concentration traverses over the channel cross section.

Experimental Data.—For the air-distribution measurements described in this report, the channel slope S and water discharge, Q, were varied independently. Experiments were made for slopes of 7.5, 15, 22.5, 30, 37.5, 45, 60, and 75 degrees. For each slope, measurements of air concentration were made for total-water discharges, Q, from 2.2 to 9.6 cfs and for some slopes up to 15.0 cfs.

The measurements were made at Station 45 (45 ft from the inlet) in a vertical centerline plane. Readings were taken at 0.01-ft intervals on a line normal

11 "An Electrical Method for Measuring Air Concentration in Flowing Air-Water Mixtures," by O. P. Lamb and J. M. Killen, Technical Paper No. 10, Series B, St. Anthony Falls Hydr. Lab., Univ. of Minnesota, March, 1952.

12 "Velocity Measurement of Air-Water Mixtures," by L. G. Straub, J. M. Killen, and O. P. Lamb, Transactions, ASCE, Vol. 119, 1954, pp. 207-220.

to the channel bottom with the lowest point 0.02 ft from the bed and the uppermost point where the probes were completely out of the flow and the meter registered zero water concentration. The concentration profile was obtained for each slope and each water discharge after the channel had been adjusted for equilibrium conditions. For this purpose equilibrium flow was considered to be that condition of the flow of the air-water mixture for which the air-concentration distribution was the same at two sections 10 ft apart along the channel. This condition could be obtained by the adjustment of the initial depth of flow through control of the inlet-gate opening. Repeated measurements of the profiles were made at the two sections for different gate openings until the two air-concentration profiles were similar. Comparisons were made of the concentration at corresponding distances normal to the bed. A typical comparison of the profiles at the two stations for equilibrium flow is shown in Fig. 3.

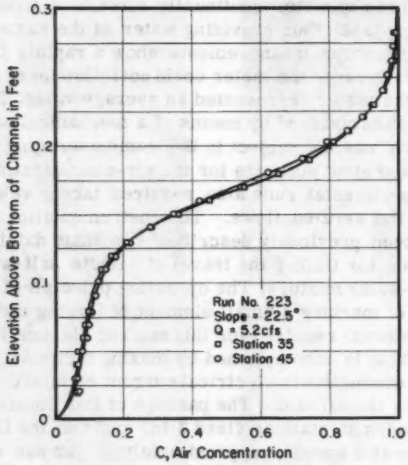


FIG. 3.—COMPARISON OF AIR-CONCENTRATION PROFILES

The results of the experiments in the form of measured concentrations for each slope and discharge have been tabulated elsewhere.[13] Table 1 is a sample of these measured concentrations. A sample tabulation of computed parameters is given in Table 2. A more detailed tabulation has been presented elsewhere.[14]

The air concentration C is defined as the ratio of the volume of air per unit volume of air and water as measured by the concentration-meter probes. It is assumed that the concentration as measured represents the average value of the concentration in the region described by the probes of the concentration

13 "Experiments on Self-Aerated Flow in Open Channels," by L. G. Straub and A. G. Anderson, Proceedings Paper 1890, ASCE, 1958, pp. 28-31.

14 Ibid., pp. 32-35.

TABLE 1.—AIR CONCENTRATION DISTRIBUTION FOR VARIOUS DISCHARGES AND SLOPES

Distance from channel bed, y, in feet	Discharge, Q, in cubic feet per second																				
	2.2	3.2	4.2	5.2	6.4	7.2	8.2	9.6	11.2	12.1	12.8	2.2	3.2	4.2	5.2	6.4	7.2	8.2	9.6	11.2	12.8	15.0
	(a) 7.5° Slope											(e) 37.5° Slope										
0.05	0.01	0.02	0.02	0.02	0.02	0.02	0.02	0.02	...	...	...	0.46	0.43	0.42	0.42	0.33	0.33	0.29	0.23	0.22	0.20	0.15
0.10	0.13	0.01	0.02	0.02	0.02	0.02	0.02	0.02	...	...	...	0.73	0.58	0.52	0.49	0.41	0.38	0.34	0.29	0.28	0.24	0.19
0.15	0.92	0.22	0.06	0.02	0.02	0.02	0.02	0.02	...	...	...	0.93	0.81	0.69	0.60	0.50	0.45	0.42	0.36	0.33	0.29	0.24
0.20	...	0.94	0.54	0.19	0.04	0.03	0.02	0.02	...	...	...	0.995	0.95	0.87	0.77	0.70	0.58	0.53	0.45	0.39	0.36	0.29
0.25	...	...	0.99	0.82	0.41	0.24	0.07	0.03	...	...	...	...	...	0.97	0.91	0.86	0.76	0.72	0.64	0.53	0.47	0.38
0.30	...	...	...	...	0.93	0.81	0.51	0.21	...	...	...	...	...	...	0.98	0.95	0.90	0.87	0.81	0.73	0.64	0.55
0.35	...	...	...	...	...	0.99	0.93	0.72	...	...	...	...	...	...	...	0.995	0.975	0.95	...	...	0.80	0.75
0.40	...	...	...	...	...	...	...	0.96	...	...	...	...	...	...	...	...	...	0.99	0.98	0.94	0.90	0.88
	(b) 15.0° Slope											(f) 45.0° Slope										
0.05	0.03	0.04	0.04	0.05	0.06	0.04	0.04	0.03	...	...	...	0.53	0.53	0.51	0.52	0.51	0.45	0.42	0.37	0.32	0.24	0.13
0.10	0.45	0.13	0.09	0.08	0.09	0.07	0.06	0.04	...	...	...	0.76	0.67	0.59	0.57	0.55	0.54	0.48	0.42	0.37	0.30	0.17
0.15	0.98	0.76	0.40	0.23	0.15	0.12	0.09	0.06	...	...	...	0.95	0.85	0.74	0.66	0.61	0.57	0.52	0.47	0.41	0.34	0.22
0.20	...	0.99	0.91	0.74	0.46	0.33	0.23	0.14	...	...	...	...	0.96	0.89	0.80	0.72	0.68	0.60	0.54	0.49	0.41	0.29
0.25	...	...	...	0.98	0.87	0.79	0.61	0.36	...	...	...	...	...	0.96	0.91	0.85	0.82	0.75	0.66	0.62	0.54	0.44
0.30	...	...	...	...	0.99	0.96	0.90	0.76	...	...	...	...	...	...	0.97	0.94	0.92	0.87	0.80	0.75	0.73	0.66
0.35	...	...	...	...	...	...	0.99	0.95	...	...	...	...	...	...	...	0.98	0.97	0.95	0.90	0.88	0.86	0.82
0.40	...	...	...	...	...	...	...	...	...	...	...	...	...	...	...	...	...	0.98	0.97	0.96	0.94	0.94
	(c) 22.5° Slope											(g) 60.0° Slope										
0.05	0.11	0.09	0.10	0.08	0.09	0.07	0.06	0.05	...	...	0.03	0.65	0.61	0.61	0.59	0.59	0.56	0.54	0.51	...	...	...
0.10	0.62	0.29	0.22	0.13	0.14	0.11	0.09	0.07	...	...	0.04	0.84	0.72	0.68	0.65	0.65	0.62	0.59	0.56	...	...	...
0.15	0.98	0.83	0.66	0.35	0.25	0.21	0.15	0.13	...	...	0.07	0.96	0.87	0.78	0.74	0.70	0.67	0.63	0.59	...	...	...
0.20	...	0.99	0.94	0.79	0.60	0.46	0.35	0.25	...	...	0.12	...	0.95	0.90	0.84	0.77	0.74	0.68	0.64	...	...	...
0.25	...	...	...	0.97	0.87	0.81	0.70	0.54	...	...	0.24	...	0.995	0.97	0.93	0.85	0.82	0.76	0.72	...	...	...
0.30	...	...	...	...	0.98	0.96	0.90	0.83	...	...	0.53	...	...	...	0.98	0.93	0.89	0.85	0.82	...	...	...
0.35	...	...	...	...	...	0.99	0.99	0.95	...	...	0.82	...	...	...	0.995	0.97	0.95	0.92	0.89	...	...	...
0.40	...	...	...	...	...	...	...	0.99	...	...	0.94	...	...	...	...	0.995	0.98	0.96	0.95	...	...	...
	(d) 30.0° Slope											(h) 75.0° Slope										
0.05	0.24	0.22	0.20	0.20	0.16	0.17	0.15	0.12	0.12	0.09	0.12	0.69	0.72	0.69	...	...	...	...	...	...	...	...
0.10	0.70	0.43	0.34	0.28	0.23	0.22	0.19	0.16	0.15	0.12	0.15	0.83	0.79	0.73	0.70	0.70	0.68	0.67	0.65	...	...	...
0.15	0.97	0.82	0.69	0.51	0.38	0.33	0.27	0.23	0.20	0.16	0.19	0.94	0.89	0.78	...	...	...	...	...	...	...	...
0.20	...	0.99	0.94	0.83	0.70	0.59	0.49	0.39	0.31	0.25	0.26	0.98	0.95	0.85	0.82	0.76	0.75	0.72	0.69	...	...	...
0.25	...	...	...	0.98	0.92	0.85	0.78	0.67	0.54	0.45	0.43	....	0.98	0.93	...	...	...	...	...	...	...	...
0.30	...	...	...	...	...	0.98	0.94	0.88	0.79	0.71	0.66	...	0.995	0.97	0.93	0.88	0.87	0.84	0.81	...	...	...
0.35	...	...	...	...	...	...	0.995	0.98	0.93	0.90	0.85	...	...	0.99	...	...	...	...	...	...	...	...
0.40	...	...	...	...	...	...	...	...	0.99	0.98	0.95	...	...	...	0.99	0.96	0.97	0.95	0.94	...	...	...

TABLE 2.—SUMMARY OF EXPERIMENTAL MEASUREMENTS OF ROUGH CHANNEL

Run	Temperature	Q	$\bar{d}$	d_a	d_T	$\bar{d}d_T^{1/2}$	$q/g^{1/2}$	$\bar{C}$	$\bar{C}_T$	C_T	C_1	$\bar{V}$	V_s	$V_s/d_T^{2/3}$	R x 10^{-5}	s		$\bar{V}/V_m$
							(a) 17.5° Slope											
200	22.3	2.2	0.1209	0.169	0.120	0.0418	4.06	0.285	0.054	0.45	0.006	12.13	0.710	2.92	5.65	1.920	0.022	1.059
202	0	4.2	0.1937	0.260	0.197	0.0860	7.75	0.255	0.070	0.50	0.005	14.45	0.909	3.66	5.91	2.150	0.024	1.017
204	0	6.4	0.2515	0.329	0.257	0.1274	11.80	0.236	0.065	0.50	0.005	16.95	1.039	3.56	9.05	1.900	0.031	1.034
206	0	9.2	0.2943	0.380	0.296	0.1605	15.10	0.225	0.059	0.48	0.004	19.55	1.119	3.51	11.46	1.750	0.035	1.036
							(b) 15.0° Slope											
210	21.0	2.2	0.1010	0.115	0.102	0.0322	2.88	0.348	0.090	0.50	0.031	14.50	0.923	4.41	5.58	1.355	0.023	1.018
212	0	4.2	0.1514	0.234	0.157	0.0600	5.50	0.353	0.114	0.50	0.060	18.50	1.144	3.92	6.03	0.785	0.033	1.036
214	0	6.4	0.1937	0.303	0.200	0.0866	8.37	0.361	0.125	0.46	0.083	22.0	1.292	3.77	9.14	0.527	0.045	1.073
216	0	9.2	0.2275	0.338	0.233	0.1097	10.73	0.327	0.113	0.48	0.067	24.0	1.396	3.63	11.59	0.630	0.049	1.074
							(c) 22.5° Slope											
220	19.6	2.2	0.0886	0.159	0.095	0.0273	2.37	0.443	0.167	0.55	0.107	16.55	1.081	5.19	5.71	0.693	0.028	1.013
222	0	4.2	0.1356	0.243	0.145	0.0517	4.53	0.441	0.172	0.52	0.123	20.6	1.338	4.84	6.21	0.507	0.041	1.015
224	0	6.4	0.1763	0.310	0.190	0.0768	6.90	0.431	0.175	0.50	0.140	24.1	1.530	4.62	9.54	0.388	0.052	1.028
226	0.1	9.2	0.2116	0.351	0.288	0.1009	8.85	0.396	0.157	0.53	0.107	25.8	1.676	4.49	12.20	0.547	0.058	1.014
							(d) 30.0° Slope											
230	21.0	2.2	0.0760	0.165	0.087	0.0224	2.07	0.540	0.261	0.55	0.222	19.30	1.182	6.00	6.33	0.326	0.035	1.078
232	0	4.2	0.1125	0.236	0.129	0.0419	3.96	0.527	0.263	0.61	0.245	24.9	1.494	5.55	7.18	0.345	0.041	1.029
234	1.2	6.4	0.1530	0.303	0.163	0.0655	6.03	0.495	0.255	0.58	0.213	27.9	1.715	5.31	11.04	0.366	0.052	1.094
236	0.2	9.2	0.1808	0.348	0.220	0.0848	7.72	0.480	0.254	0.61	0.200	30.2	1.880	5.16	13.83	0.420	0.058	1.066
							(e) 37.5° Slope											
240½	19.6	2.2	0.0605	0.196	0.085	0.0176	1.86	0.695	0.454	0.63	0.431	24.2	1.292	6.66	7.49	0.184	0.048	1.270
242	16.8	4.2	0.0922	0.291	0.148	0.0355	3.59	0.683	0.480	0.68	0.462	30.3	1.706	6.09	15.23	0.142	0.061	1.267
244	5.0	6.4	0.1317	0.361	0.195	0.0562	5.46	0.635	0.417	0.68	0.402	32.3	1.955	5.82	15.40	0.177	0.073	1.186
246	9.3	9.2	0.1636	0.413	0.227	0.0780	7.01	0.603	0.381	0.63	0.363	33.4	2.11	5.67	21.0	0.192	0.081	1.125
							(f) 45° Slope											
250½	18.6	2.2	0.0530	0.188	0.090	0.0159	1.74	0.718	0.524	0.71	0.510	27.7	1.430	7.10	8.80	0.140	0.046	1.378
252	12.8	4.2	0.0791	0.303	0.151	0.0307	3.33	0.739	0.560	0.75	0.550	35.4	1.852	6.52	16.31	0.113	0.060	1.427
254	12.9	6.4	0.1065	0.376	0.205	0.0482	5.07	0.718	0.560	0.72	0.556	40.0	2.16	6.21	25.3	0.092	0.079	1.389
256	12.1	9.2	0.1361	0.422	0.240	0.0667	6.50	0.677	0.505	0.72	0.490	40.1	2.34	6.06	29.0	0.122	0.080	1.289
							(g) 60° Slope											
261	19.8	2.2	0.0397	0.190	0.085	0.0116	1.56	0.791	0.628	0.78	0.613	37.0	1.539	7.93	11.50	0.107	0.053	1.737
263	15.0	4.2	0.0648	0.290	0.160	0.0259	3.01	0.777	0.654	0.80	0.645	43.2	2.11	7.15	24.1	0.091	0.061	1.636
265	15.6	6.4	0.0887	0.369	0.220	0.0416	4.59	0.772	0.659	0.81	0.657	48.2	2.49	6.84	37.6	0.0806	0.090	1.570
267	19.8	9.2	0.1163	0.476	0.260	0.0693	5.88	0.756	0.628	0.78	0.610	47.0	2.69	6.59	44.0	0.087	0.098	1.424
							(h) 75° Slope											
270	19.8	2.2	0.0362	0.212	0.100	0.0121	1.49	0.820	0.699	0.83	0.690	38.4	1.767	8.18	14.32	0.093	0.060	1.730
272	22.0	4.2	0.0618	0.333	0.200	0.0275	2.85	0.814	0.733	0.85	0.730	45.4	2.50	7.30	34.6	0.063	0.084	1.654
274	21.3	6.4	0.0874	0.501	0.250	0.0457	4.35	0.823	0.711	0.82	0.715	48.9	2.79	7.03	46.1	0.050	0.125	1.547
276	20.9	9.2	0.1015	0.500	0.270	0.0326	5.56	0.797	0.691	0.81	0.687	53.8	2.90	6.93	54.4	0.0506	0.118	1.555

meter and is applicable to the midpoint of the probes. Essentially continuous curves of air concentration with respect to distance normal to the bed were obtained for each experiment. The concentration increases gradually from the bed, more rapidly in the central region and then more slowly in the upper region, apparently asymptotically approaching the limit of 100% air concentration, as is shown in Fig. 3, and subsequently in Fig. 7. It appears that the complete curve is comprised of two parts that have basically different characteristics. Although there is no sharp demarcation between the two parts, the curves tend to support the description that in the lower regions of the stream air bubbles are suspended in water, while the upper regions consist of water droplets in air. The existence of these water droplets can readily be detected by holding one's hand just above the main flow.

Because there is no definite upper boundary to the air-entrained flow in an open channel, questions of the definition of the linear dimensions of the flow arise. A number of different depth parameters related to the air concentration and distribution may be defined, each having particular applications in describing the bulk-flow conditions. These depth parameters may be described as follows:

1. A depth $\bar{d}$ is used to represent a mean depth of flow that would exist if all of the entrained air were removed up to the highest point where water is found. It therefore corresponds to the depth of a nonaerated flow of a given discharge with a velocity equal to that of the entrained flow and is defined as

$$\bar{d} = \int_0^\infty (1-C)\,dy \quad \ldots\ldots\ldots\ldots\ldots\ldots\ldots\ldots (1)$$

in which y is the normal distance from the bed and C is the concentration of air as a function of y. The value of $\bar{d}$ can be approximated with sufficient accuracy by a summation of the products of the water concentrations and their corresponding incremental depths.

2. An upper boundary of the air-entrained flow or an upper depth d_u may be defined as the value of y where the air concentration has some arbitrarily prescribed value. For some purposes, such as determining the mean depth, and because of the asymptotic nature of the curve, it is convenient to define d_u as that value of y where the air concentration C is 0.99. Other depths may be similarly defined. One such depth has previously been defined[6] as that corresponding to the value of y where the air concentration is C = 0.95. This arbitrarily was chosen as a depth where the concentration of air could be reliably measured and included from 98% to 99% of all the water and consequently represented an upper limit for the water.

3. A third depth parameter may be defined on the basis of the air-concentration distribution as that depth d_T representing the value of y where the transition from the distribution in the lower regions to that in the upper regions occurs. Its value would then depend on the characteristics of the channel as well as the air distribution. This depth parameter will be discussed in detail subsequently.

The mean air concentration in the vertical can also be defined in different ways depending upon the particular application. The mean concentration over the whole range of concentrations measured is defined as

$$\bar{C} = \frac{1}{d_u} \int_0^{d_u} C\,dy \quad \ldots\ldots\ldots\ldots\ldots\ldots\ldots\ldots (2)$$

in which $\bar{C}$ is the mean concentration of the entire flow and d_u is the so-called upper limit where the concentration is 0.99. Another mean concentration, $\bar{C}_T$, is defined as the mean concentration in the region below the transition depth $y = d_T$ and applies to that air being transported by the flow.

$$\bar{C}_T = \frac{1}{d_T} \int_0^{d_T} C dy \quad \ldots\ldots\ldots\ldots\ldots\ldots (3)$$

Dimensional plots of $\bar{d}$, d_u, and d_T for the various discharges and for each slope are presented in Fig. 4 to indicate the range of values as determined from the concentration data. In Fig. 4 (c) the mean depth $\bar{d}$ varies with discharge and slope in much the same manner as nonaerated flow. The mean depth increases regularly with the discharge and decreases with the slope. The data for the upper limit d_u (Fig. 4 (a)) indicate that for a given discharge, d_u tends to decrease at first and then to increase as the slope increases. Consequently, the maximum depth tends to be nearly the same for corresponding discharge rates on the various lower slopes. It appears that the increased depth due to aeration increases with both slope and discharge. However, in combination with the mean depth, which decreases with slope and increases with discharge, the upper limit tends to decrease and then increase as the slope increases. As a result, over a considerable range of slopes (15° to 30°), the upper limit is essentially the same and depends only on discharge. A similar situation exists in regard to d_T (Fig. 4 (b)) in that it also shows a tendency to decrease gradually and then to increase gradually as the slope increases. Consequently, the range of variation of d_T for any given discharge is relatively little over a wide range in slopes.

The mean concentration $\bar{C}$ for the entire flow and $\bar{C}_T$, the mean concentration in the region below d_T, have been plotted in Figs. 5 (c) and 5 (b) in terms of the discharge and for each slope It is interesting to note that the mean concentration for the entire flow is nearly constant for a quite wide range of discharges but increases considerably with the slope. The mean concentration $\bar{C}_T$ for the region below d_T has similar characteristics. In Fig. 5 (a) the concentration C_T at the transition depth is plotted. This concentration varies but little with the depth but increases with the channel slope.

ANALYSIS OF THE DATA

Distribution of Air in Aerated Flow.—A qualitative concept of air-entrainment phenomena has been established with the aid of the air-concentration determinations made transverse to the direction of self-aerated flows, high-speed photographs and motion pictures of the flow, and other similar information. Since it has been shown that aeration of flows on a steep slope begins in a region where the boundary layer generated by the channel bed has reached the water surface, it is to be presumed that aeration depends primarily on the turbulence intensity of the flow. Aeration appears to occur when the transverse velocities of turbulence are sufficiently strong near the air-water interface to cause clumps of water to break through the surface into the air and then fall back by gravity into the flowing stream. This breaking away of clumps of water from the main stream and the falling back into the stream with attendant splashing and breaking into a heterogeneous spray of globules and droplets is associated with the insufflation of air into the stream. It occurs particularly with water flow at high

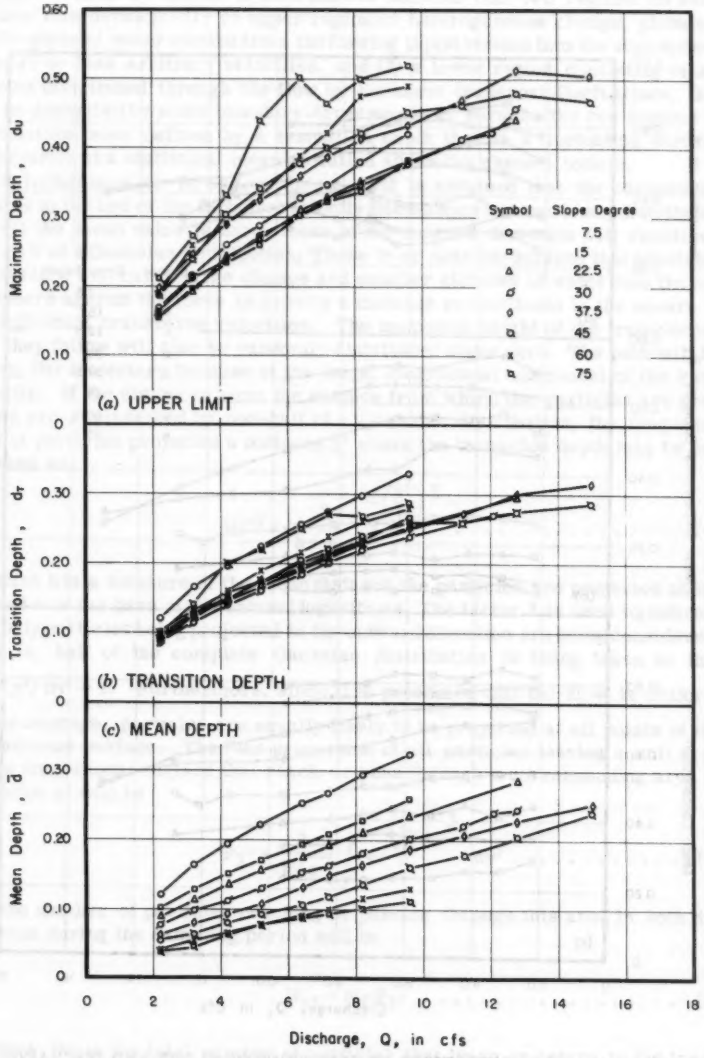


FIG. 4.—DEPTHS OF AERATED FLOW AS A FUNCTION OF DISCHARGE

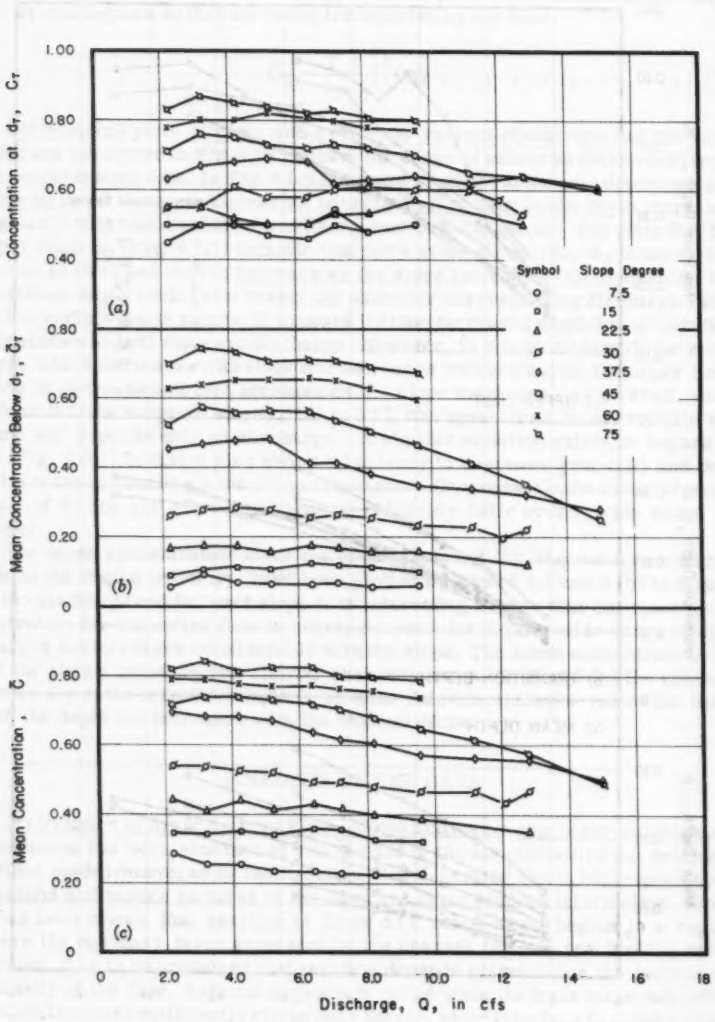


FIG. 5.—AIR CONCENTRATIONS AS FUNCTIONS OF SLOPE AND DISCHARGE

velocities on steep slopes. The air carried back is then distributed throughout the flow by turbulent transfer.

Observations by means of instruments indicate that two regions on self-aerated flow develop: (1) an upper region of heterogeneous clumps, globules, and droplets of water ejected from the flowing liquid stream into the atmosphere at more or less arbitrary velocities, and (2) a lower region consisting of air bubbles distributed through the flow by turbulent transport fluctuations, that can be described by some boundary-layer equation. Between the two regions is a transition zone defined by a transition depth that is a fluctuating surface necessarily at a statistical mean elevation above the channel bottom.

Distribution of Air in Upper Region.—If it is assumed that the components normal to the bed of the turbulent velocity fluctuations are randomly distributed so that the mean value is zero, those in the outward direction will constitute one-half of a Gaussian distribution. Those in or near the surface that penetrate the surface will carry large clumps and smaller globules of water into the atmosphere against the force of gravity a distance proportional to the square of the individual transverse velocities. The maximum height of the trajectories that they follow will also be randomly distributed about zero. The path will be a long, flat trajectory because of the large, longitudinal component of the local velocity. If the distances from the surface from which the particles are projected are represented by one-half of a Gaussian distribution, the frequency f(y') of particles projected a distance y' above the transition depth may be expressed as

$$f(y') = \frac{2}{h\sqrt{\pi}} e^{-\left(\frac{y'}{h}\right)^2} \quad \ldots\ldots\ldots\ldots\ldots\ldots (4)$$

in which h is a measure of the mean distance the particles are projected above d_T and e is the base of the natural logarithms. The factor 2 is used to indicate that only particles being projected in the outward direction are being considered. That is, half of the complete Gaussian distribution is being taken so that $\int_0^\infty f(y')\, dy' = 1$. Furthermore, since it is presumed that the flow is uniform on the average, particles are equally likely to be projected at all points of the transitional surface. Then the proportion of all particles leaving a unit area of the transitional surface that reach or pass through a corresponding area at elevation y' will be

$$P_{y'} = \frac{2}{h\sqrt{\pi}} \int_{y'}^{\infty} e^{-\left(\frac{y'}{h}\right)^2} dy' \quad \ldots\ldots\ldots\ldots (5)$$

and the number of particles reaching or passing through this area in both directions during the sampling period will be

$$N_{y'} = N_T P_{y'} \quad \ldots\ldots\ldots\ldots\ldots\ldots (6)$$

in which N_T is the total number of particles that leave or return to the transition surface per unit area during the sampling period. The average number of particles of water that reach or pass through any horizontal area per unit time may be assumed proportional to the average concentration of water particles. Therefore, using Eqs. 5 and 6, the air concentration at any distance y'

above the transition level in terms of the concentration at the transition level, C_T, and the representative height, h, is

$$\frac{1-C}{1-C_T} = \frac{2}{h\sqrt{\pi}} \int_{y'}^{\infty} e^{-\left(\frac{y'}{h}\right)^2} dy' \quad \ldots\ldots\ldots\ldots (7)$$

Eq. 7 is, of course, the cumulative Gaussian probability curve and is applicable to the aeration phenomenon only for $y' > 0$. The gradient of the concentration from Eq. 7 is

$$\frac{dC}{dy} = \frac{2(1-C_T)}{h\sqrt{\pi}} e^{-\left(\frac{y'}{h}\right)^2} \quad \ldots\ldots\ldots\ldots\ldots (8)$$

and when $y' = 0$, $\frac{dC}{dy}$ is a maximum whose value is

$$\left(\frac{dC}{dy}\right)_{max} = \frac{2(1-C_T)}{h\sqrt{\pi}} \quad \ldots\ldots\ldots\ldots\ldots (9)$$

and occurs where the concentration is C_T and the depth is d_T.

The constants C_T and h are properties of the flow related to the intensity of the turbulence in the neighborhood of d_T. This, in turn, is probably dependent on the velocity and roughness of the channel.

Distribution of Air in Lower Region.—The air entrained at the transition surface by the turbulent fluctuations is then distributed throughout the flow in the region below d_T by the turbulence in the stream resulting in a statistical equilibrium between the bouyancy of the air and the concentration gradient. Such equilibrium is described by

$$-C V_b + \epsilon_b \frac{dC}{dy} = 0 \quad \ldots\ldots\ldots\ldots\ldots (10)$$

in which C is the air concentration at a normal distance y from the bed. The rising velocity of the air bubbles, V_b, is considered as being negative, and ϵ_b is a mixing parameter for the air-bubble transfer. In aerated flows the value of ϵ_b as a function of y unknown, and a number of assumptions as to the form of the function can be made. However, it may be presumed that the air bubbles are transported in the same manner as momentum, and it appears reasonable as an approximation to assume ϵ_b to be proportional to ϵ_m, the momentum mixing parameter, as is done in the case of transport of other substances such as sediment. In open channels in the non-aerated condition where the shear is linearly distributed from zero at the surface to a maximum at the bed and the velocity profile is considered to be logarithmic throughout the depth of flow, it has been shown[15] that ϵ_m has a parabolic form being zero at the surface and at the bed with a maximum at the centerline and can be expressed in the form

$$\epsilon_b = \beta k \sqrt{\tau_0/\rho} \left(\frac{d_T - y}{d_T}\right) y \quad \ldots\ldots\ldots\ldots (11)$$

15 "Transportation of Suspended Sediment by Water," by V. A. Vanoni, Transactions, ASCE, Vol. 111, 1946, pp. 67-113.

in which $\sqrt{\tau_0/\rho} = V_s$, the shear velocity, τ_0 is the boundary shear at the bed, ρ is the density of the fluid, β is a proportionality factor in $\epsilon_b = \beta \epsilon_m$, and k is the Karman universal constant. In the case of transport in a closed channel, however, the shear at the upper boundary is not zero and the maximum velocity occurs at a point between the upper and lower boundary, at which point the shear is also zero. This requires that ϵ_m also be zero at this point and that the distribution of ϵ_m consists of two parabolas having zero at the bed, the point where the maximum velocity occurs, and at the upper boundary, and maximum values at intermediate points above and below the point of maximum velocity. It has been shown,[16] however, that suspended matter is actually transported transversely across the level of zero mixing coefficient, and it has been suggested that the mixing coefficient be considered constant in this region. Because it is likely that the vertical transport of suspended matter depends only on the transverse velocity fluctuations in the vertical direction, such transport may well occur even if the correlation between the vertical and longitudinal fluctuations approaches zero.

Measurements of velocity distribution in aerated flows show[8,9] that the velocity tends to decrease as the upper limit of the flow is approached and that the maximum occurs well down in the flow proper. This implies that a shear is developed in the transition zone. A plausible explanation for such a shear is the change in momentum engendered by the return of water clumps and droplets to the flow at the end of their trajectory through the atmosphere above d_T. In the course of that trajectory, they suffer a loss of velocity due to atmospheric drag on the mass. The shear developed at d_T is analogous to an upper boundary and a distribution of the type found for closed channels might be expected.

The complex distribution found for closed channels may be approximated by a parabolic distribution over the entire region below d_T, with the maximum value incorporated in the factor β. This approximation is equivalent to assuming a distribution for ϵ_b as given by Eq. 11. Substituting the value of ϵ_b, given in Eq. 11 into Eq. 10,

$$CV_b = \beta k \sqrt{\tau_0/\rho} \left(\frac{d_T - y}{d_T}\right) y \frac{dC}{dy} \quad \ldots\ldots\ldots\ldots (12)$$

which upon integration, assuming that V_b is independent of y, is

$$C = C_1 \left(\frac{y}{d_T - y}\right)^z \quad \ldots\ldots\ldots\ldots\ldots (13)$$

in which

$$z = \frac{V_b}{\beta k \sqrt{\tau_0/\rho}} = \frac{V_b}{\beta k V_s} \quad \ldots\ldots\ldots\ldots (14)$$

and C_1 is a constant whose value is the concentration at $y = \frac{d_T}{2}$.

Application to Experimental Data.—The use of Eqs. 7 and 13 as a description of the air-concentration distribution characteristics depends on the degree to

16 "Turbulent Transfer Mechanism and Suspended Sediment in Closed Channels," by H. M. Ismail, Transactions, ASCE, Vol. 117, 1952, pp. 409–446.

which they fit the experimental data. Two factors having a bearing on this are the form of the equation and the magnitude of the constants. Whether or not the form of the equations is reasonably correct depends on the extent that the assumptions made approximate the actual mechanism in their development. The constants involved depend on the intensity of the turbulence and at the present cannot be determined analytically, but must be evaluated empirically from systematic experimentation.

Eq. 9 permits the determination of the transition depth d_T and the concentration C_T at that depth. From a plot of the concentrations in terms of the normal distance from the bed, the point where the gradient dC/dy is a maximum was graphically located, as shown in Fig. 6 (a). The corresponding values of d_T and C_T are noted. Using this value of C_T, the ratio $\frac{(1-C)}{2(1-C_T)}$ was plotted as a function of y on probability paper, on which a cumulative Gaussian distribution plots as a straight line. The value of h, or rather the value of σ, the standard deviation of the distribution, wherein $h = \sigma\sqrt{2}$, is obtained from the slope of this straight line. Alternately, h can be determined directly from Eq. 9 by evaluating the gradient at the point where dC/dy is a maximum and inserting the value of C_T obtained for that point. Fig. 6 (b) shows a plot of the concentrations in the upper region of the flow plotted in this manner with the standard deviation indicated. It is apparent from this plot that the concentrations possess a cumulative Gaussian distribution.

In the region of flow below d_T, Eq. 13 indicated that the concentration C is a function of $\frac{y}{d_T-y}$ which, when plotted logarithmically, results in a straight line whose slope is equal to the exponent z, and C_1 is the value of C at $\frac{y}{d_T-y} = 1$. The concentration data for the experiment have been plotted in this manner in Fig. 6 (c) to show the degree of agreement with the form of Eq. 13 and to indicate the evaluation of C_1 and z. Inasmuch as C approaches infinity as y approaches d_T, the experimental data must depart from the curve for the larger values of $\frac{y}{d_T - y}$, but in this case the data agree with the curve up to $\frac{y}{d_T} \approx 0.9$.

The straight lines drawn through the data in Figs. 6 (b) and (c) have been transposed to the original plot in Fig. 6 (a) to show the characteristics of the curves on the arithmetic scales. Eqs. 7 and 13 have also been plotted with the data for a number of typical experiments using various discharges and slopes shown in Fig. 7 for purposes of comparison. Because of the character of Eq. 13 in the neighborhood of $y = d_T$, the two curves are connected by a transition to pass from one curve to the other.

Relation of Parameters of Flow Conditions.—Based on the foregoing analysis of the aeration phenomenon, a number of parameters were developed as being descriptive of both the magnitude and the distribution of the air. These parameters varied with the flow conditions such as the channel slope and discharge, which in turn, along with the roughness characteristics of the channel, govern intensity and scale of the generated turbulence. The flow turbulence is created initially at the bed by the wakes and eddies formed by the flow over the roughness elements and the turbulent eddies are then diffused upward into the flow stream. The intensity of turbulence at the transitional surface that appears to be paramount in the aeration process should then depend on both the initial generation and the depth of the mixture to the transitional surface. The intensity of the turbulence is related to the boundary shear τ_0 on the bed, which can

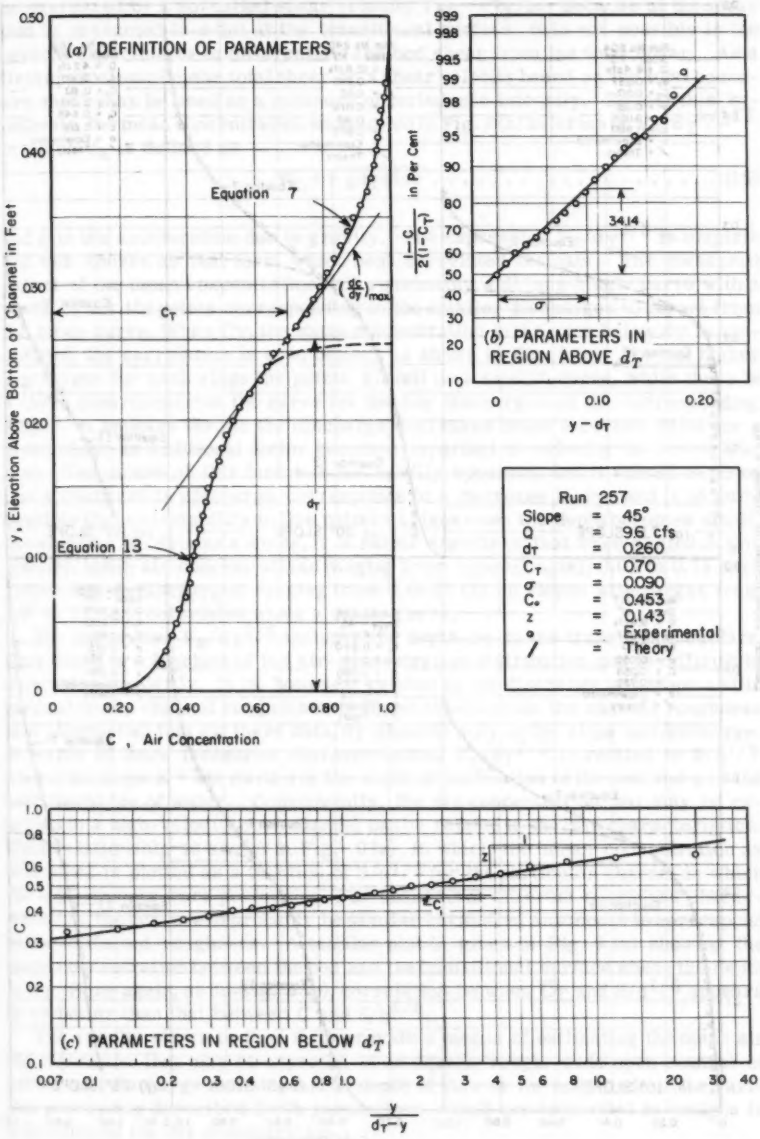


FIG. 6.—DETERMINATION OF AIR-CONCENTRATION DISTRIBUTION PARAMETERS

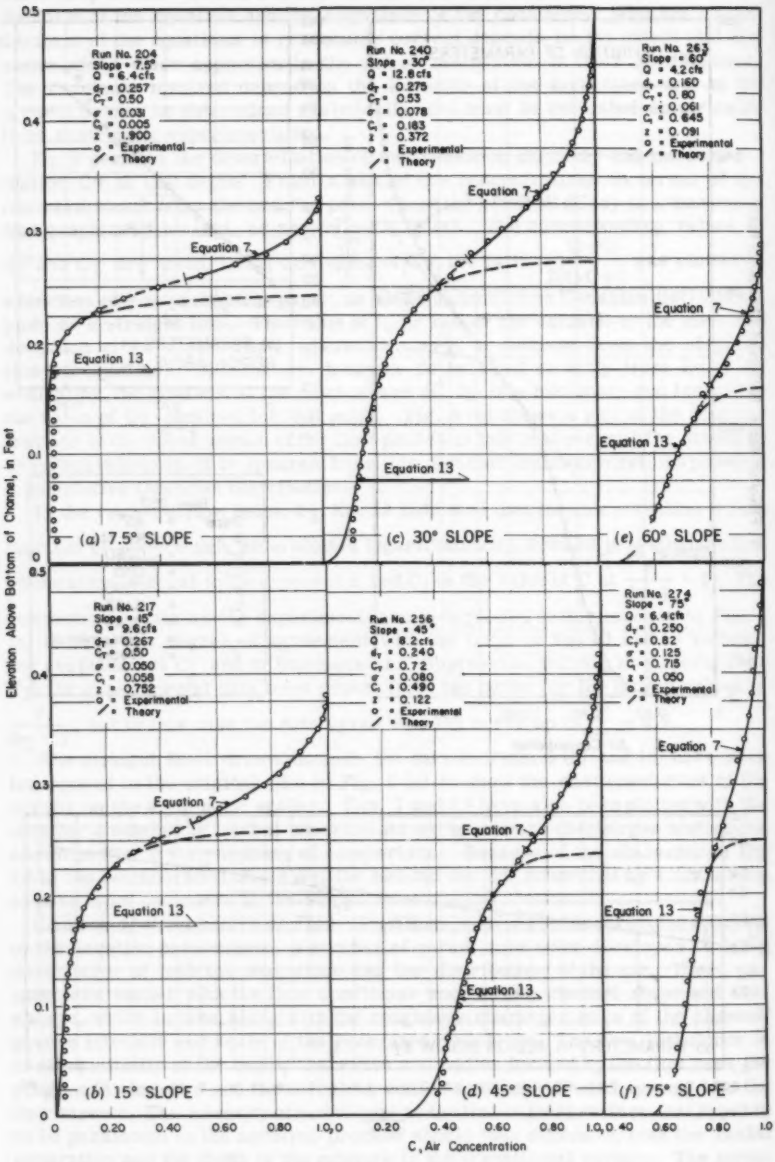


FIG. 7.—COMPARISON OF MEASURED CONCENTRATIONS WITH THEORETICAL EQUATIONS FOR VARIOUS SLOPES

be expressed by a so-called shear velocity $V_{sb} = \sqrt{\tau_0/\rho}$. Because of the shear that is presumed to exist at the transitional surface, it is not possible in the present experiments to differentiate the bed shear from the total shear. As a first approximation, the total shear or a shear velocity based on the total boundary shear may be used as a measure of turbulence intensity. To test this hypothesis, the mean concentration was plotted in Fig. 8 (a) in terms of $V_S/d_T^{2/3}$[13] in which V_S is defined as

$$V_S = \sqrt{g d_T \sin\alpha} \quad \ldots\ldots\ldots\ldots\ldots\ldots \quad (15)$$

and g is the acceleration due to gravity. The expression $V_S/d_T^{2/3}$ is empiri- and was chosen as that form which best correlated the data. The measured values of the mean concentration fall reasonably well on a single curve with a tendency for the points corresponding to the smaller discharges to depart from the mean curve. When C_T, the mean concentration in the area below d_T is considered, the correlation is even better, as shown in Fig. 8 (b). For the higher discharges for each slope the points all fall on a smooth curve, while there is a clear departure from the curve for the low discharges on the corresponding slopes. It appears that as the discharge decreases below a certain value for a given slope, an additional factor becomes important in reducing the concentration. The nature of this factor is not readily apparent, but it should be noted that a decrease in discharge corresponds to a decrease in d_T, and it is quite possible that an instability in flow pattern arises when the depth becomes small. Considering the data as a whole, it is rather significant that when plotted in this manner, mean air concentrations ranging from approximately 0.05 to 0.75 corresponding to discharges ranging from 4 to 15 cfs on slopes with ranges from 7.5° to 75° are correlated along a single curve.

The parameter $V_S/d_T^{2/3}$ includes the depth d_T to the transitional surface. This depth is a function of the air-concentration distribution and is difficult to determine explicitly. It is, however, related to the discharge and slope and in general to the channel roughness. In these experiments the channel roughness is a constant so that for these data, d_T depends only on the slope and discharge. In terms of these measured characteristics, $V_S/d_T^{2/3}$ is related to $S/q^{1/5}$ where the slope $S = \sin\alpha$ and α is the angle of inclination of the bed and q is the unit discharge of water. Consequently, the air concentration that may be expected in a high-velocity open channel can be related to the flow characteristics. This relationship is shown in Fig. 9 (a), in which the mean concentration as measured is plotted as a function of $S/q^{1/5}$ for the particular channel in which the experiments were performed. For channels of different roughness characteristics, the curve will probably be similar but shifted an amount to correspond to the different roughness. A similar plot is given in Fig. 9 (b) showing the mean concentration between the bed and the transitional surface where the depth is d_T. Here again, as in Fig. 8 (b), correlation between $\bar{C}_T$ and $S/q^{1/5}$ appears to be better than that between $\bar{C}$ and $S/q^{1/5}$.

The results shown in Fig. 9 (b) provide a means of estimating the mean air concentration that may be expected in an equally rough, wide open channel of known unit discharge and slope. The depth of flow or the magnitude of the various previously described depth parameters, which are important in design, is a function of the air concentration.

Effect of Entrained Air on the Flow.—It was suggested previously that the air insufflated into the flow is distributed throughout the flow by turbulent transport. The entrained air has the effect of changing the flow from one of water alone to

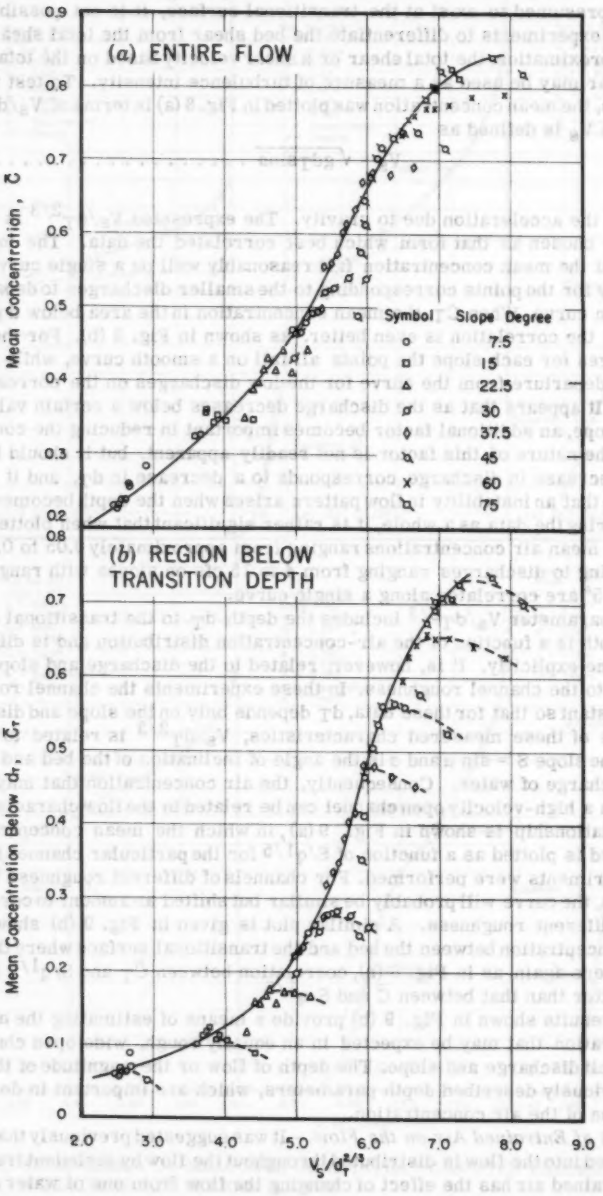


FIG. 8.—MEAN CONCENTRATION AS A FUNCTION OF $V_s/d_t^{2/3}$

the flow of a mixture of air and water. Several characteristic depths were defined, such as d_u to represent the uppermost extent of the water particles projected from the flow, $\bar{d}$ to represent the depth of flow of the water alone, and d_T to represent a new equilibrium depth brought about by the presence of air in the flow. For design purposes, it is of considerable importance to know how

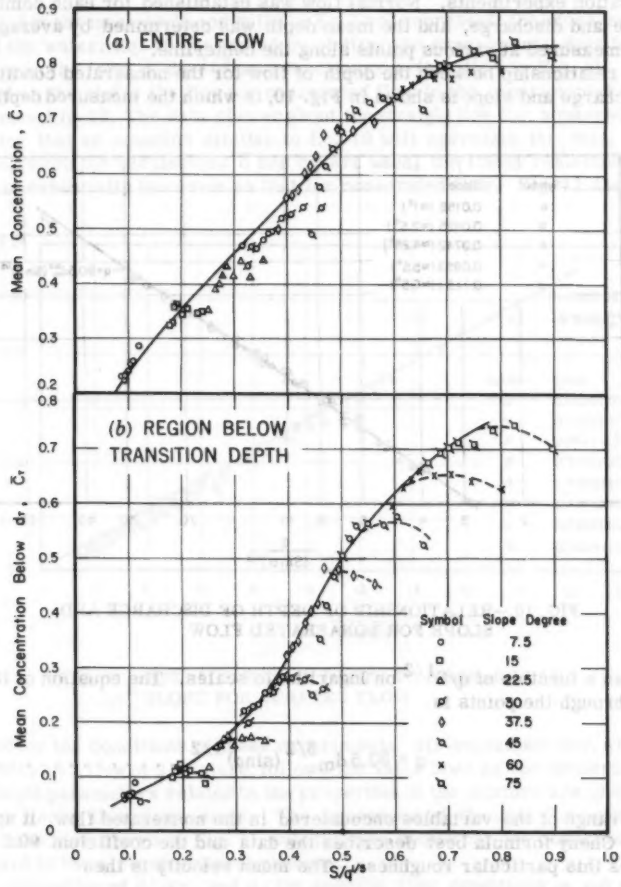


FIG. 9.—MEAN CONCENTRATION AS A FUNCTION OF $S/q^{1/5}$

these parameters and the actual flow velocity are related to the bulk flow properties or what differences might be expected in these parameters in relation to a corresponding nonaerated flow for which the depth may be computed by means of well-established flow formulas such as the Manning or Chezy formula.

In order to investigate such a relationship, tests were performed in the experimental channel to establish the resistance of the channel to nonaerated flow,—that is, flow of water alone. The slope was decreased so that for comparable discharges the flow would be nonaerated. These slopes ranged from approximately 1° to a maximum of approximately 6.5°, above which aeration was observed to occur. The discharges were in the same range as those used in the aeration experiments. Normal flow was established for each combination of slope and discharge, and the mean depth was determined by averaging the depths measured at various points along the centerline.

The relationship between the depth of flow for the nonaerated condition and the discharge and slope is shown in Fig. 10, in which the measured depth d_m is

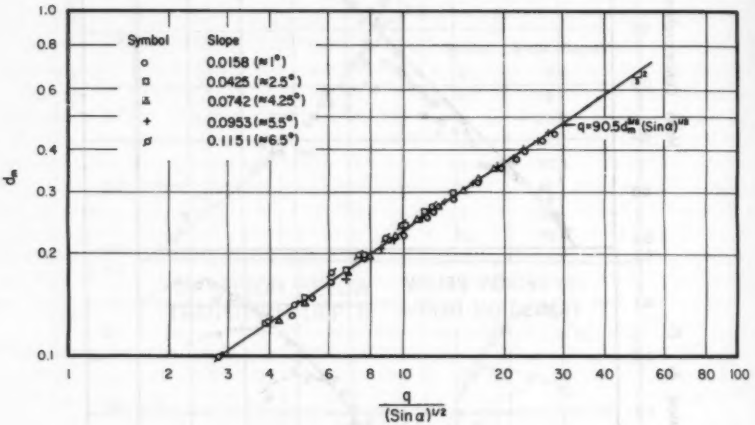


FIG. 10.—RELATIONSHIP OF DEPTH OF DISCHARGE AND SLOPE FOR NONAERATED FLOW

plotted as a function of $q/S^{1/2}$ on logarithmic scales. The equation of the line drawn through the points is

$$q = 90.5\, d_m^{3/2} (\sin\alpha)^{1/2} \quad \ldots\ldots\ldots\ldots\ldots (16)$$

For the range of the variables encountered in the nonaerated flow, it appears that the Chezy formula best describes the data and the coefficient 90.5 characterizes this particular roughness. The mean velocity is then

$$V_m = 90.5\, d_m^{1/2} (\sin\alpha)^{1/2} \quad \ldots\ldots\ldots\ldots\ldots (17)$$

If it were assumed that the same type of flow equation applied to aerated flow, the mean velocity of the air-water mixture flowing at a depth d_T is

$$\bar{V} = C d_T^{1/2} (\sin\alpha)^{1/2} \quad \ldots\ldots\ldots\ldots\ldots (18)$$

in which $\bar{V}$ is the mean velocity of the air-water mixture and C is the Chezy coefficient. Assuming that the velocity of the air and water components are equal, then Eq. 18 can be written in terms of the water discharge, as

$$q = C(\bar{d})(d_T)^{1/2}(\sin\alpha)^{1/2} \quad \ldots\ldots\ldots\ldots (19)$$

in which $\bar{d}$ is the mean depth computed by Eq. 1 and represents the cross-sectional area of the water. Eq. 19 was tested by plotting the experimental data for aerated flow in the form $\bar{d}\ d_T^{1/2}$ as a function of $q/(\sin\alpha)^{1/2}$ in Fig. 11. Superimposed on the plot is the line for nonaerated flow in the experimental channel taken from Fig. 10. The data cluster about the straight line for nonaerated flow, indicating that an equation similar to Eq. 19 will correlate the data, and in addition, when the parameters $\bar{d}$ and d_T are used, the Chezy resistance coefficient is essentially the same as that for nonaerated flow. Fig. 11 shows that

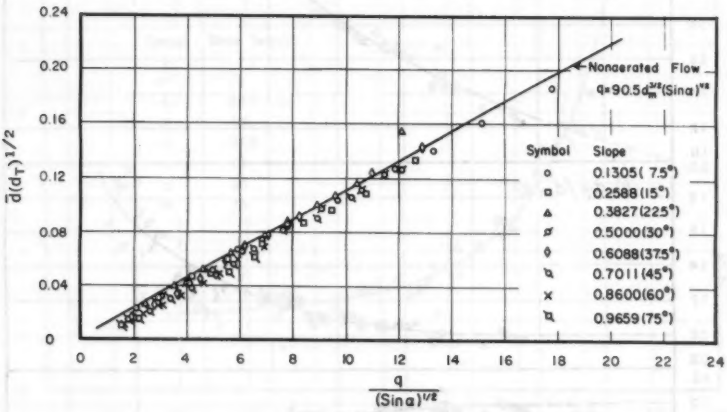


FIG. 11.—RELATIONSHIP OF DEPTH TO DISCHARGE AND SLOPE FOR AERATED FLOW

at least for the conditions of these experiments, air-entrained flow, when considered to be a flow of a mixture, follows the same laws as for nonaerated flow when depth parameters related to the properties of the mixture are used to define the linear flow dimensions. The agreement of the data for aerated and nonaerated flow shown in Fig. 11 substantiate somewhat the deductions made in regard to the air-entrainment process.

An evaluation of $\bar{d}$, d_T, and d_u for specific flow conditions is not possible from Fig. 11. A clearer idea of the changes in these parameters will be obtained if they are compared with the depth, d_m, computed in the usual manner, using Eq. 16 which includes for this channel the Chezy coefficient of 90.5. It is the depth at which the water would flow in this channel at the given discharge and slope assuming no air entrainment. The ratios d_u/d_m, d_T/d_m, and $\bar{d}/d_m$ as functions of mean air concentration are plotted in Fig. 12. In all cases, of course, the ratios approach unity as the mean concentration approaches zero.

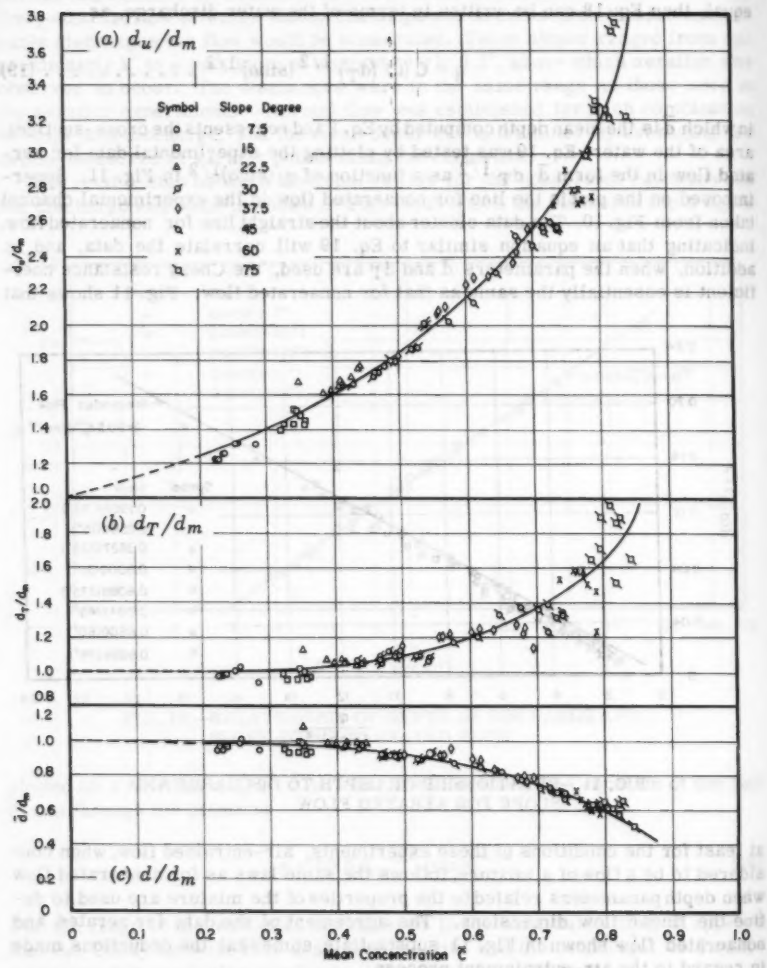


FIG. 12.—INFLUENCE OF AIR CONCENTRATION OF DEPTHS OF AERATED FLOW RELATIVE TO CORRESPONDING NONAERATED FLOW

That is, for water flow only, $d_u = \bar{d} = d_T = d_m$. As the mean air concentration increases, the ratios depart from unity in such a way that as $\bar{C}$ approaches 1.0, $\bar{d}$ becomes small, while d_u and d_T necessarily increase.

The upper limit of the spray d_u increases considerably with increased air concentration. This in turn means an increase in the turbulence intensity to project water particles farther into the atmosphere. For the highest concentrations measured, the value of d_u is nearly four times as large as the nonaerated depth for a corresponding discharge and slope. The transition depth, as might be expected, also increases relative to the computed depth, because increasing concentration bulks the flow and makes the effective depth greater. On the other hand, the mean depth decreases with increasing concentration. It appears from Fig. 12 that concentration has relatively little effect on d_T and $\bar{d}$ until the air concentrations are greater than approximately 50%. For the

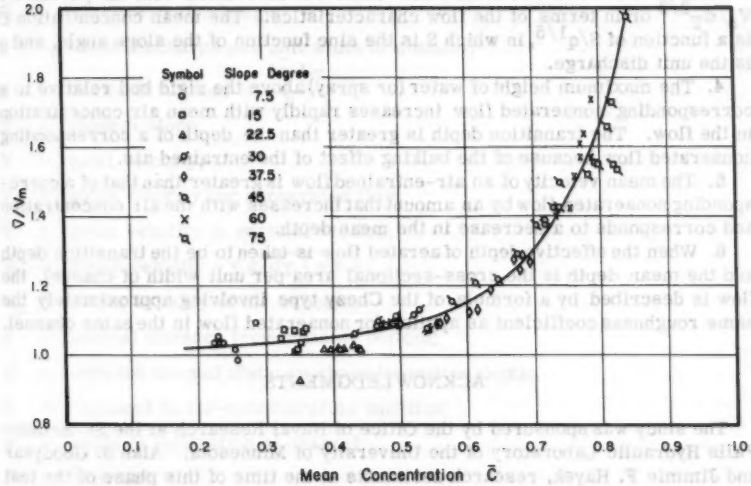


FIG. 13.—INFLUENCE OF AIR CONCENTRATION OF VELOCITY OF AERATED FLOW RELATIVE TO CORRESPONDING NONAERATED FLOW

slopes where the air concentrations were the greatest (being approximately 85%), $\bar{d}$ was reduced to one-half of d_m, while d_T was nearly twice as large as d_m.

The decrease in $\bar{d}$ with increase in mean air concentration implies a corresponding increase in the mean water velocity above that computed on the basis of d_m, because $\bar{d}$ is the cross-sectional area of the water flow. The trend of the mean water velocity in terms of the nonaerated velocity in this channel is shown in Fig. 13. Again, the velocity of aerated flow is about the same as that of a corresponding nonaerated flow until the mean concentration is in the neighborhood of 50%. It then increases rather rapidly.

CONCLUSIONS

1. Self-aerated, high-velocity, open-channel flow appears to consist of two distinct phases: an upper region consisting primarily of independent droplets and larger agglomerations of water that move independently of the stream proper, and a lower region in which discrete air bubbles are suspended in a turbulent stream and are distributed by the mechanism of turbulence.

2. In the upper region, the distribution of water-air agglomerate and droplets can be adequately described by the Gaussian cumulative probability equation, the constants of which are properties of the flow conditions. In the lower region, the distribution of the air agrees closely with an equation for turbulent mixing based on an approximation for the distribution of the mixing parameter.

3. The magnitude of the entrained air concentrations apparently depends on the intensity of turbulent fluctuations generated at the rigid bed and the depth of flow. The mean concentration could be correlated with the parameter $V_s/d_T^{2/3}$ or in terms of the flow characteristics. The mean concentration $\bar{C}$ is a function of $S/q^{1/5}$, in which S is the sine function of the slope angle, and q is the unit discharge.

4. The maximum height of water (or spray) above the rigid bed relative to a corresponding nonaerated flow increases rapidly with mean air concentration in the flow. The transition depth is greater than the depth of a corresponding nonaerated flow because of the bulking effect of the entrained air.

5. The mean velocity of an air-entrained flow is greater than that of a corresponding nonaerated flow by an amount that increases with the air concentration and corresponds to a decrease in the mean depth.

6. When the effective depth of aerated flow is taken to be the transition depth and the mean depth is the cross-sectional area per unit width of channel, the flow is described by a formula of the Chezy type involving approximately the same roughness coefficient as applies for nonaerated flow in the same channel.

ACKNOWLEDGMENTS

The study was sponsored by the Office of Naval Research at the St. Anthony Falls Hydraulic Laboratory of the University of Minnesota. Alan S. Goodyear and Jimmie F. Hayek, research assistants at the time of this phase of the test program, assisted in the collection and analysis of the data.

APPENDIX. NOTATION

C = Concentration, ratio of volume of air to volume of air plus water;

$\bar{C}$ = mean concentration in vertical section;

C_1 = concentration at point $y = d_T/2$;

$\bar{C}_T$ = mean air concentration in region between lower boundary and d_T;

C_T = concentration at transition depth $y = d_T$;

$\bar{d}$ = mean depth of flow;

d_u = upper limit of flow or value of y when $C = 0.99$;

d_T = transition depth between upper and lower regions of flow;

d_m = mean measured depth in nonaerated flow;

e = base of the natural logarithms;

g = acceleration due to gravity;

h = mean height to which water particles are projected above d_T;

k = Von Karman universal constant for velocity distribution;

$N_{y'}$ = number of particles reaching or passing through a horizontal area a distance y' above transition depth d_T;

N_T = number of particles that leave or return to an area at the transition depth;

$P_{y'}$ = proportion of all particles leaving area at transition depth that reach or pass through horizontal area at y' above transition depth;

Q = total-water discharge;

q = water discharge per unit width of channel;

R = Reynolds number = $\frac{4\bar{V}d_T}{\nu}$;

S = channel slope;

V = local velocity;

V_m = mean velocity for nonaerated flow;

$\bar{V}$ = mean velocity in vertical section;

V_s = shear velocity = $\sqrt{g(d_T)\sin\alpha}$;

V_b = rising velocity of air bubbles;

y = normal distance from channel bottom;

y' = outward normal distance above transition depth;

z = exponent in air-concentration equation;

α = angle of inclination of channel;

β = constant;

ϵ_b = mixing coefficient for air bubbles in turbulent flow;

ϵ_m = mixing coefficient for momentum transfer;

ν = kinematic viscosity of water;

ρ = density of water;

σ = standard deviation of air distribution above d_T;

τ = shear force; and

τ_0 = boundary shear force.

DISCUSSION

MICHELE VIPARELLI.[17]—In 1943, many data collected on big hydraulic structures were published in an article on steep channels, and it was stated[18] that laboratory research on models would have been of small interest only because the laws of similitude are not valid for air entrainment. Now it can be seen that the laboratory research in Minnesota, the results of which are presented by the authors, and research in Naples, the results of which were given by the writer,[19,20] not only succeeded in realizing new methods of measurements, but made clear the nature of the phenomenon. General conclusions for prototype design were also deduced.

In Minnesota, recourse has been made to an electric apparatus for measuring air concentration, C, and to an electric and chemical apparatus for recording instantaneous velocities in a given point of the air and water flow. The local average velocity, V, was obtained through a statistical analysis of recorded data.

In Naples the quantities measured were the dynamic pressure δ on the tip of a pitot tube, the discharge, Q_s, of the water only, through a vertical strip of unit width, and the discharges of air and water siphoned from a point of the current. For this aim, three simple hydraulic instruments were used: the common pitot tube, the open sampler, and the closed sampler.

The open sampler, disposed at distance y from the bottom, collects the water discharge Q_s (y) of the current above y. The ratio $q = \frac{\Delta Q_s}{\Delta y}$ gives the water discharge at elevation y, through an elementary unit area, whose normal is in the direction of the flow. The unit water discharge, q, has the dimension of a velocity and agrees with the average local velocity, V, in a water flow.

The quantity $\sqrt{2\,g\delta}$ was found to depend on the values of $\sqrt{V\,q}$ according to a linear law. In a current of water only, $v = q = \sqrt{2\,g\delta}$.

In the closed sampler, air and water siphoned from the current became separated and their volumes were measured. The ratio of air volume to the volume of air plus water clearly depends on the air concentration in the point of measurement. However, that ratio depends also on the shape of the tip of pipe through which air and water are sucked from the current, and on the depression in the closed sampler.

After many trials using the closed sampler, a tip was adopted with a hole opened toward the direction of the movement, similar to the tip of a simple pitot tube. The depression in the sampler was made to assume different values, in order to obtain that value for which the water discharge through the hole of the tip was equal to q w, in which w is the area of the hole and q the value of the corresponding unit discharge. The ratio of air volume to the volume of air plus water so collected in the closed sampler was interpreted as

17 Prof. Ing., Inst. of Hydr. and Hydr. Constr., Naples Univ., Naples, Italy.

18 "Open Channel Flow at High Velocity," by L. Standish Hall, Transactions, ASCE, Vol. 108, 1943, pp. 1394–1434.

19 "Fast Water Flow in Steep Channel," by M. Viparelli, I.A.H.R. Convention, Lisbon, 1957.

20 "Correnti Rapide," by M. Viparelli, L'Energia Elettrica, Milan, July, 1958.

the ratio C_t of air discharge to that of air plus water through the unit area. In effect, when the water discharge through the hole is equal to q w, the flow in the point of measurement is not, or almost not, disturbed.

Hence for a flow of air and water it can be written as

$$q = \frac{1}{1 + C_t} V \quad \ldots\ldots\ldots\ldots\ldots\ldots\ldots (20)$$

When C_t is not large, air concentrations, C, of the authors, and C_t are absolutely different. Values of C, obtained by means of an electrical apparatus, depend on air concentration in a plain parallel to the flow, while those of C_t depend on the air discharge through unit area of cross section. In effect, the writer tried to measure air concentrations by means of an electric apparatus, and obtained much larger values than those measured by means of the closed sampler, according to the method explained above.

The authors and the writer have both admitted that particles of water are projected randomly from the transition surface in the overlying region. The measured air concentration, C, depends on the average number of particles of water that reach or pass through any area parallel to the bottom per unit time at elevation $y' = y - d_T$ (the authors define d_T as the transition depth). The parallel water concentration is measured by 1 - C, at least for values of C that are not too large. The authors have found that 1 - C depends on y', according to the cumulative Gaussian probability curve.

The writer admitted that the water particles above the transition preserve a constant average velocity. In this case, Q_s (y') resulting by the product of average velocity for the number of water particles that pass through a unit normal strip above y' must be distributed according to the cumulative Gaussian probability curve. Experimental data confirm that Q_s (y') is distributed according to the cumulative Gaussian curve.

As Q_s and C depend on y' according to the same rule, the conclusions of the authors on water distribution give new proof of the hypothesis made by the writer that the average velocity of water particles above the transition surface assumes a constant value along a normal to the bottom. The other proof was deduced by the writer from the law by which Pitot's data depend on the unit discharge q.

The authors indicate that the velocity of flow, measured by means of the chemical-electrical apparatus already mentioned, decreases above the transition depth. As the values of measured velocities are not given, the writer thinks that the observed decrease of velocity should be very small. In this case, data referring to upper layers collected in both researches may be considered thoroughly compatible among them.

The different meanings of C and C_t should merit an investigation. The dependence of the one on the other may illuminate the relation between the average local velocities and the random velocity components of turbulence.

In the present case it can be stated that values of parallel concentration C are scarcely useful in computations referring to water discharge and mean velocity. They can be misleading, because in lower layers the transverse concentration C_t is always much smaller than C. In the Naples research, C_t was found to vary below the transition depth from less than 0.001 for a 11° slope to 0.2% + 0.3% for a 23° slope and 2% + 3% for a 45° slope. According to these values of C_t, the measured values of $\sqrt{2\,g\delta}$, q, and V are practically equal in lower layers, at least for a slope of less than 45° (in Naples the largest slope given to the experimental flume was 45°).

Other results of interest obtained in Naples are the following:

In the lower layers the velocity distribution follows the logarithmic law valid for smooth walls if the channel walls are smooth, and the law valid for rough walls in other cases.

The depth of transition d_T can be assumed as the height of the part of current that contributes to overcome the resistances.

The unit water discharge, q, at elevation y' above the transition surface is given by the product: number by velocity of water particles, reaching and not surpassing that elevation. The velocity which does not vary with y' is equal to the maximum velocity U of the flow along y'. Consequently, q, like the number of water particles, is distributed according to a Gaussian law. Precisely, it is

$$q = U\, e^{-1/2 \left(\frac{2g\, y'}{\delta U^2} \right)^2} \quad \ldots\ldots\ldots\ldots\ldots\ldots (21)$$

in which the standard deviation δ was found to depend on the roughness of walls. In effect, δ varies from 0.0020 for smooth walls to 0.0040 for very rough walls.

For $y' = y - d_T = 0$, the total water discharge Q_s (0) through a transverse strip in the upper layers is

$$Q_s(0) = 0.5 \sqrt{2\pi}\ \delta\ \frac{U^3}{2g} \quad \ldots\ldots\ldots\ldots\ldots\ldots (22)$$

From the foregoing results, the writer was encouraged to draw more general conclusions than the authors did, also because the examination of data gathered by Nitchiporovich[21] on the Gizeldon chute presented evidence that results of laboratory research were confirmed by tests on a prototype.

In the lower layers, where water flows with air bubbles in suspension, the average velocity can be computed with the same equations used in computations referring to currents of pure water, at least for a slope equal to or less than 45°. In these equations, cross section, wetted perimeter, and hydraulic radius are to be computed below the transition surface, because the weight of water particles dispersed in the air does not contribute to overcome the resistance at the walls.

To contain the flow above transition surface the wall of steep channels must be raised adding to d_T a height $\frac{c\delta U^2}{2g}$, in which U is the velocity of flow at the transition surface, δ represents the standard deviation, and c a constant of proportionality. It is convenient to give U the value of the maximum velocity in the section, computed according to the knowledge on uniform flow in open channels.

The constant c cannot be given once and for all, but must be assigned for each case. In effect, because water drops are distributed according to the Gaussian law, they can reach increasing heights but in decreasing numbers. Therefore, the opportunity of elevating less or more the wall depends on the inconveniences that water drops can cause.

The total water discharge is

$$Q = rv + b\ 0.5 \sqrt{2\pi}\ \delta\ \frac{U^3}{2g} \quad \ldots\ldots\ldots\ldots\ldots\ldots (23)$$

---

21 "Rezultati ispitivanyi bistrotoka Gizeldonskoy gidrostanciyi," by A. A. Nitchiprovich, Gidrotehniceskoe Stroiteljstvo, No. 5, 1934.

in which r is the area of the hydraulic section below d_T, and b is the breadth of the channel at transition surface.

These conclusions are acceptable if the flow in the steep channel is regular. However, it is necessary to not forget that transversal waves and irregularities in the flow can easily appear and make not enough high the training walls.

LORENZ G. STRAUB,[24] F. ASCE and ALVIN G. ANDERSON,[25] M. ASCE.—All of the data and conclusions as to the mechanism of transport of entrained air were based on measurements of air concentration for various flows and slopes. The mean depth $\bar{d}$ and transition depth d_T, were defined in terms of the air concentration distribution. Knowing the water discharge and the mean depth which implies the area per unit width of water flow, the mean velocity may be computed as was shown in Table 2.

The concept of the transition depth, d_T, defined from the shape of the air concentration distribution curve provided a means of establishing the depth at which the mixture of air and water flowed as an open channel flow subject to the usual laws of open channel flow. If the channel is hydraulically rough so that the friction coefficient is independent of the mixture Reynolds number, the resistance coefficient of the aerated flow should be the same as that for nonaerated flow. This assumption was tested by making experiments in the same channel under nonaerated conditions and comparing the results. The comparison showed that for rough channel used in the present experiments the resistance coefficient was essentially the same for both aerated and nonaerated flow when the depth of the aerated flow is defined as d_T. The graphical comparison is shown in Fig. 11.

With this agreement in resistance coefficients it was possible to compute the velocity and depth of nonaerated flow having the same water discharges and slopes as the aerated flows used in the experiments. Figs. 12 and 13 show the ratios of the aerated depths $\bar{d}$, d, and d_u to the computed depth for an equivalent nonaerated flow d_m, as well as the ratio of the mean velocity for aerated flow to the mean velocity of an equivalent nonaerated flow.

Because the mean velocity of the aerated flow was computed from the water discharge divided by the mean depth $\bar{d}$ as determined from the air concentration distribution curve, it appeared desirable to make an independent measurement of the velocity in the aerated flow to compare with the computed value. For this purpose velocity and air concentration measurements were made for several aerated flows, from which the mean velocity of the water could be determined. The mean water velocity was expressed as

$$\overline{V} = \frac{\sum_0^{d_u} (1 - C)\, V \Delta y}{\sum_0^{d_u} (1 - C)\, \Delta y} \quad \ldots\ldots\ldots\ldots (24)$$

---

[24] Dir., St. Anthony Falls Hydr. Lab., Prof. and Head, Dept. of Civ. Engrg., Univ. of Minn., Minneapolis, Minn.

[25] Prof. of Hydromechanics, St. Anthony Falls Hydr. Lab., Univ. of Minn., Minneapolis, Minn.

in which V is the local velocity and C is the air concentration at elevation y normal to the bed.

The mean velocity for an open channel flow for the same discharge and slope was computed in accordance with Eqs. 16 and 17 just as though no air were entrained. The ratio of this velocity V_m and the mean velocity for the equivalent air entrained flow was determined and plotted in Fig. 13, which is reproduced with the new points added to it as Fig. 14. The agreement of velocity ratio based on velocity measurements and that based on air concentration measurements is remarkably good.

The computation of the normal nonaerated elements of open channel flow in a particular application forms a base from which the elements pertaining to aerated flow depart as a consequence of the entrained air. The data and curves given in Figs. 9(a), 12 and 13 form the basis for estimating the depths and mean

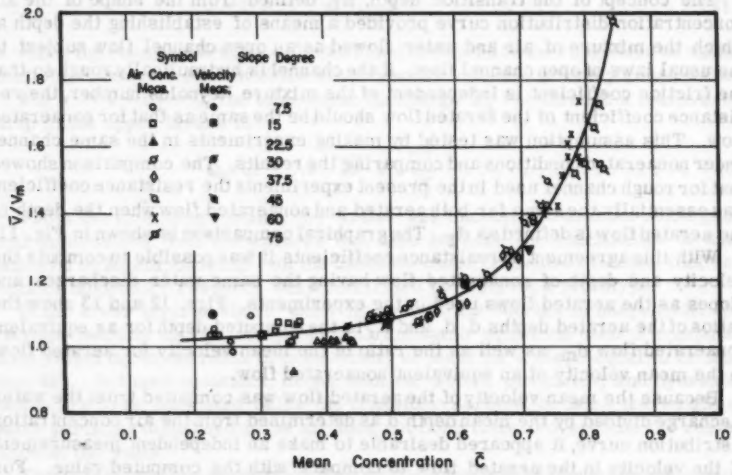


FIG. 14.—COMPARISON OF MEAN VELOCITY OF AIR ENTRAINED FLOW FROM VELOCITY MEASUREMENTS AND FROM AIR CONCENTRATION DISTRIBUTION

velocity in a steep channel of equal roughness on which air entrainment will occur. The value of the Manning n for the experimental channel varies from approximately 0.012 to 0.016, depending on the depth of flow, so that the channel roughness corresponds approximately to a surface roughness such as may be found in practice. In a particular instance of flow on a steep channel, the water discharge and slope are known. Thus, $S/q^{1/5}$ can be computed, in which S is the sine of the slope angle. The application of this value to the curve in Fig. 9(2) will supply an estimate of the expected mean air concentration. Entering Figs. 12 and 13 with this mean air concentration will yield the various depths and the mean velocity of the stabilized air entrained flow in terms of the equivalent depth and mean velocity computed in the usual way as though the flow were not aerated.

AMERICAN SOCIETY OF CIVIL ENGINEERS

Founded November 5, 1852

TRANSACTIONS

Paper No. 3030

LOWER-COST CANAL LINING PRACTICE

By Richard J. Willson,[1] F. ASCE

With Discussion by Messrs. Frederick L. Hotes; and Richard J. Willson

SYNOPSIS

Seepage through canals and laterals, that causes loss of valuable water and water-logging of valuable farm lands, is an important problem that can best be dealt with by some manner of canal lining. This paper examines the various types of linings available. The commonly used types of canal linings are described and their respective advantages, disadvantages, and limitations are enumerated. Experimental linings, whose usefulness is still being considered, and more recent developments that are thought to be of significant interest to the field, are described herein.

INTRODUCTION

With the present growth of the western United States, that constitutes the sphere of activity of the Bureau of Reclamation, Department of the Interior (USBR), water is rapidly becoming the most critically deficient resource of the area. In recent meetings of the American Society of Civil Engineers and other similar organizations, much thought has been given to nation-wide, and world-wide water conservation. In addition to the principal problem of conserving water lost in transit from unlined canals, the water lost by seepage from waterways creates another problem on some irrigation projects. Good farm land lying below canals and laterals is water-logged by the seepage and many acres of land are thereby unavailable for cultivation.

Note.—Published essentially as printed here, in April, 1958, in the Journal of the Irrigation and Drainage Division, as Proceedings Paper 1589. Positions and titles given are those in effect when the paper or discussion was approved for publication in Transactions.

[1] Engr., Bur. of Reclam., U. S. Dept. of the Interior, Denver, Colo.

One method of saving water and reducing seepage is to be sure that as little as possible escapes in transit to the reservoirs, irrigated land, or other points of use. The solution to this problem is to be certain that conveyance systems are as water-tight as it is economically possible to make them. Lining seems to best meet this criterion.

Lining waterways has been a two-fold benefit on USBR projects. Water has been saved and the amount of drainage construction necessary in reclaiming good, fertile, crop-producing acres has been reduced. On some projects the previously constructed drains have been filled, and the recovered land is being utilized for crops, as a result of the decrease in seepage due to canal or lateral lining. Lining of course will not eliminate all drains, nor is lining less expensive than drain construction in many instances.

It has been a general policy of the USBR, during initial construction, to line only those canals and laterals where it was quite certain that there would be excessive leakage or where the safety of the canal, its structures, and the adjacent land is essential. Where there is a reasonable chance that the channel will function satisfactorily without lining, the lining has been omitted. If it later develops that lining is required, it is done as supplemental construction. Experience has proved this policy to be a sound one economically.

In the past, silt, earth blankets, and concrete linings have been primarily relied upon to reduce the water losses from waterways. Shotcrete also was used extensively as a lining material, primarily in the south and southwest. Silting and loose earth blankets are not costly, and have been successful in reducing losses to a point at which these losses can be tolerated, but generally they have been only of temporary benefit. The more reliable linings have generally been constructed of concrete or shotcrete, many of which are reinforced. However, these materials are expensive. As a matter of fact, costs to provide permanent relief would have made the construction of some projects infeasible and the rehabilitation or protection of existing projects an impossible burden to the project water users.

THE LOWER-COST CANAL LINING PROGRAM

In 1946, the USBR, recognizing the continuing need for conserving valuable irrigation water, made a concerted effort to reduce canal lining costs. A committee was appointed and a lower-cost canal lining program was initiated. The program was, and continues to be, one of laboratory and field study, field installation, and field evaluation. This last gains importance with time, because the overall cost of a successful lining must include the cost of maintenance or replacement.

A number of materials have been studied under the program and have been adapted for lining purposes. Resourceful contractors have been especially helpful in assisting in the design of new equipment and procedures for adapting these materials to present-day construction methods. Manufacturers have been most helpful in the development or improvement of new materials. The designers also have contributed to the development of lower-cost linings. In the case of concrete linings, savings have been effected by eliminating reinforcement steel and permitting greater tolerances in alinement, grade, and surface finish.

The variety of materials studied is presented in Table 1. This total, because the program was initiated in 1946, comes to more than 40,000,000 sq yd

of lower-cost type linings that have been placed in approximately 1,700 miles of canals and laterals on USBR projects as of 1960. One of the most important facts learned is that no single lining is suitable for all conditions encountered.

COMMONLY USED LININGS

On a volume basis concrete still continues to lead the field as a canal lining material. Linings of concrete, buried, hot applied asphalt membrane, thick compacted-earth, shotcrete, bentonite membranes, earth blankets, and asphaltic concrete represent approximately 99% of the lower-cost type linings placed from 1946 to 1960.

TABLE 1.—CANAL LININGS PLACED[b]

Type of Lining[a]	Quantity	
	Square Yards	Miles
Unreinforced Concrete	20,635,946	741.0
Shotcrete	1,803,975	145.8
Asphalt:		
Asphaltic Concrete	334,474	46.6
Buried Asphaltic Membranes:		
Hot-applied (sprayed)	7,000,000	330.0
Prefabricated	23,299	2.1
Asphalt Macadam	14,037	1.1
Prime Asphalt Membrane	88,428	10.6
Earth:		
Thin Compacted (Less than 12" thick)	3,424,436	148.0
Thick Compacted (12" thick or more)	5,845,742	207.9
Loose Earth	874,345	14.0
Bentonite:		
Raw or Processed Membrane	257,384	17.0
Bentonite-soil Membranes	6,080	0.8
Mixed-in-place	24,664	1.8
Soil-Cement:		
Standard	69,020	8.0
Plastic	10,018	1.1
Miscellaneous	22,399	2.5

[a] This tabulation does not include reinforced concrete.
[b] As of 1960.

From continued evaluation during this period, it has been found that these linings, with the possible exception of loose earth, have been quite efficient in reducing seepage, and are the types of linings that have given best service with a minimum of maintenance. Specifications have been developed for the construction of these linings. A continuing effort is being made to improve the specifications, the materials being used, and the methods of construction and maintenance.

Unreinforced Concrete Linings.—Unreinforced concrete is generally placed in the larger canals by means of rail-guided slip-forms, similar to that shown

in Fig. 1. This type of slip-form is not entirely new to the placement of unreinforced concrete, and similar devices are adaptable to the placement of reinforced concrete. The development of a subgrade-guided slip-form has made the lining of small canals and laterals with unreinforced concrete economically feasible.

The placement of concrete lining by subgrade-guided slip-forms becomes less practical as the cross-sectional area of the canal exceeds 50 sq ft to 60 sq ft. Probably the maximum size canal economically feasible for lining in this manner is one in which the area does not exceed 100 sq ft.

Although the rate of placement of concrete by a subgrade-guided slip-form will vary considerably due to many factors, the controlling factor, in most instances, has been the rate at which concrete can be supplied to the slip-form. As in the case of any concrete structure, the subgrade conditions upon which the concrete lining is placed is of considerable importance. The subgrade should be well consolidated or, if backfilling is necessary, the material used should be well graded to prevent its piping.

Concrete linings placed over expansive clays also have created problems. The clay must be removed and replaced with sandy or gravelly material, free of clay, before placing the concrete lining or, preferably, another type of lining should be used. An attempt should be made to avoid placement of concrete linings in a location in which they will be subjected to a high external hydrostatic pressure or in which the pressure, coupled with subsequent freezing and thawing, could result in heaving by the subgrade soils.

It has been found that construction joints, or dummy-groove control joints, in concrete linings, aid in controlling and reducing the number of cracks and the amount of spalling that subsequently occurs.

Hot-Applied, Buried, Asphaltic Membranes.—Buried, asphalt membranes evolved from earlier unsuccessful surface linings of asphalt applied to the subgrade of a canal or lateral. Asphalt membranes need protection from the sun, from the weather, and from mechanical injury such as livestock traffic.

With reference to Fig. 2, the buried asphalt membrane lining consists of a layer of asphalt, approximately 1/4-in. thick, sprayed at high temperature to form a waterproof barrier. This membrane is held in place and protected by a cover layer of earth or earth and gravel, the thickness of which is dependent upon the size of the canal, and its operating characteristics. The cover must be erosion resistant. Practice in the construction of buried asphaltic membrane linings is to provide a fillet, or rounded section, at the toe of the side slopes. The long radius fillet of the curved section should have a tangent length equal to one-half the membrane slope length or one-half the base width, whichever is the smaller.

Side-slopes no steeper than 2 on 1 are favored for buried, hot-applied asphaltic membrane linings, because of erosion and beaching action. Although slopes steeper than 2 on 1 have been used in some of the earlier installations, it has been noted that, generally, they are now approaching 2 on 1, regardless of the angularity of the cover material. The traffic of livestock, that, in open range, enter the canals for water or cross them going to and from pasture, affect the stability of cover material on the slopes. The sloughing of the cover material down the side slopes can be controlled by using less sandy cover materials.

Although many types of asphalt have been used experimentally, it has been found that a membrane composed of a catalytically-blown asphalt has given

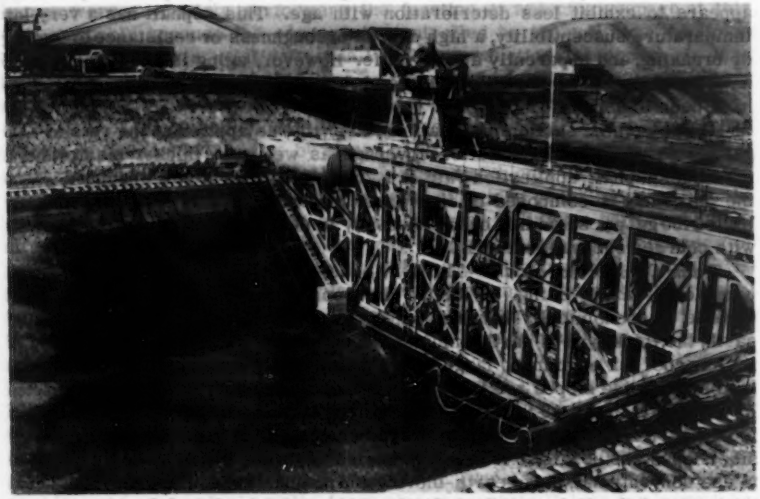


FIG. 1.—RAIL GUIDED SLIP-FORM

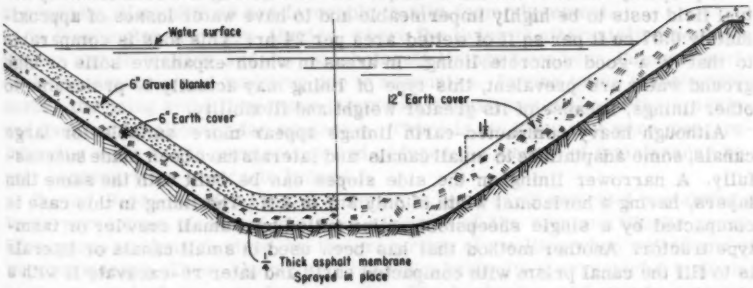


FIG. 2.—BURIED ASPHALT MEMBRANE CANAL LINING

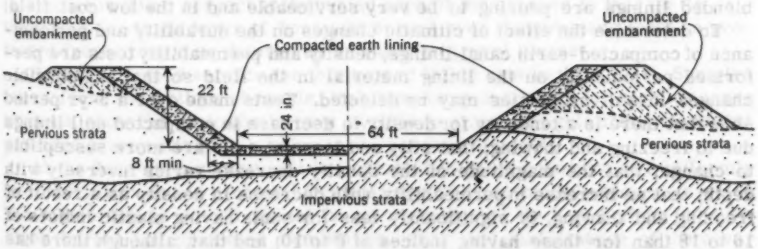


FIG. 3.—TYPICAL CROSS-SECTION OF HEAVY COMPACTED EARTH LINING

best results. Asphalt in which the catalyst has been phosphorous pentoxide appears to exhibit less deterioration with age. This asphalt has a very low temperature susceptibility, a high degree of toughness or resistance to tearing or breaking, and apparently a longer life. However, aging is not considered to have contributed to failure of the membranes thus far, although come linings have been in service 12 yr.

In many of the earlier installations, asphalt was applied at the rate of 1.00 gal per sq yd. To insure better coverage as well as a thicker membrane, a minimum asphalt-application rate of 1.25 gal per sq yd is now specified where the subgrade is composed of fine grain materials and is relatively smooth. Up to 1.50 gal per sq yd has been necessary in securing an adequate membrane with courser subgrade materials.

Thick Compacted Earth.—Third in order of volume placed is the "thick compacted-earth" lining. With the development of construction equipment capable of economically hauling, placing, and compacting large quantities of earth, the thick type of earth lining has been used more extensively because of its low cost for medium to large size canals. In this type of lining, Fig. 3, the bottom and side slopes are built up with selected impervious soils compacted in horizontal layers 6 in. thick. The bottom thickness on USBR installations is usually 2 ft, but varies with the requirements of the job. The layers on the side slopes are usually 6 ft to 8 ft in horizontal width, which makes it possible to use conventional, large earth-moving and compaction equipment. The actual thickness of the lining on the side slopes is approximately 3 ft, as measured perpendicularly to the subgrade slopes.

A properly-constructed thick compacted-earth lining has been found by actual field tests to be highly impermeable and to have water losses of approximately 0.07 cu ft per sq ft of wetted area per 24 hr. This loss is comparable to that of a good concrete lining. In areas in which expansive soils or high ground water are prevalent, this type of lining may actually be preferable to other linings, because of its greater weight and flexibility.

Although heavy compacted-earth linings appear more suitable for large canals, some adaptations to small canals and laterals have been made successfully. A narrower lining on the side slopes can be built with the same thin layers, having a horizontal width of only 3 ft to 4 ft. The lining in this case is compacted by a single sheepsfoot roller pulled by a small crawler or farm-type tractor. Another method that has been used in small canals or laterals is to fill the canal prism with compacted earth and later re-excavate it with a plow-type ditcher.

To overcome an absence of suitable compaction material on some projects, a finer soil is blended with the sandy and gravelly subgrade material. These blended linings are proving to be very serviceable and in the low cost field.

To determine the effect of climatic changes on the durability and performance of compacted-earth canal linings, density and permeability tests are performed periodically on the lining material in the field so that any possible changes in soil properties may be detected. Tests made over a 5-yr period show that there is a tendency for density to decrease in compacted soil linings due to freezing and thawing; that silty and loessial soils are more susceptible to change; that the magnitude of the density decrease varies inversely with depth; that an increase in permeability, with decrease in density as a result of freezing and thawing, is significantly less for souls having plastic indices of 16 to 18 than for those having indices of 8 to 10; and that, although there has

been a decrease in soil density in some of the more susceptible materials, the linings were adequately performing the function of reducing seepage at this time, probably because the seepage is controlled by the soil near the lining bottom where only a relatively small density reduction has occurred. It is known that clay linings of this type on one project in Wyoming have been in service 15 yr to 20 yr without material decrease in density.

Shotcrete Linings.—Shotcrete is a portland cement mortar applied through a hose to the canal subgrade by means of an air jet. The mortar consists of approximately 1 part cement to 4½ parts of sand with only enough water to secure proper placement, but enough to avoid sloughing of the mortar from the side slopes. The shotcrete process is well adapted to lining a canal to any desired shape or lining thickness, and may be used on irregular subgrades or rock cuts or as an economical method for repairing concrete linings. The small size and portability of the placing equipment make the method very useful for small or widely scattered jobs. The mortar layer in USBR work is usually 1½-in. to 2-in. thick. Careful control to secure a uniform lining thickness is especially important.

Shotcrete linings have given satisfactory service in many installations for 20 yr or more in cases where the temperature variation is not extreme, or where water can be kept in the canals for the entire year to reduce temperature variations, or where the subgrade material is stable. In northern climates shotcrete linings have not been so successful. They are not considered as desirable or as economical as slip-form-placed concrete linings for large jobs. The rate of placement is very slow compared to slip-form concrete operations. A layer of shotcrete from 1½-in. to 2-in. thick usually costs as much as 2-in. of concrete, if conditions are favorable to slip-form placement.

In Washington and New Mexico, where the lining is alternately exposed to the sun and to wetting and drying, shotcrete linings have been damaged seriously by cracking and buckling due to expansion. Sawing joints transversely across the lining and filling these joints with asphalt has relieved the cracking and buckling by allowing for expansion. There is evidence that wire mesh reinforcing adds to the permanence and reduces the amount of maintenance repair necessary for shotcrete linings.

Buried Bentonite Membranes.—Bentonite is an earth material containing a large percentage of one of the clay minerals of the montmorillonite group. This group is characterized by the properties of swelling when wetted and of imperviousness. These characteristics make bentonite a very useful material in the control of seepage from canals. The bentonite used may be a pit run product that is screened to remove larger chunks, or it may be the commercially-processed dried, granular, or powdered form. The buried bentonite membrane is similar in some respect to the buried asphalt membranes in that the 1½-in.-thick to 2-in.-thick layer of bentonite spread over the subgrade must be protected from erosion or damage by an earth or gravel blanket.

Records of good service for this type of lining date back to 1941. Samples taken from the bottom of canals, that have been in service for eight or more seasons, show the bentonite to have swelled to a compact gelatinous mass that provides a very effective barrier to the passage of water.

At the time of construction it is important to spread the bentonite uniformly over the subgrade and protect it from damage by a cover. Side-slopes on which the membrane is placed should be no steeper than the 2 on 1 slope used for other buried and protected membranes. Care and maintenance of the cover are equally important.

Loose Earth Blankets.—This type of lining is mentioned herein only because it is one of the types of linings used, in volume, by the USBR because of its low cost, or its convenience in an emergency. These very inexpensive linings consist of a loose (uncompacted) blanket of selected fine-grained soil dumped in the canal and spread over the bottom and side slopes. Unprotected by gravel the loose-earth linings are subject to erosion and severe damage from maintenance. The records generally indicate that the linings have not been permanent or efficient in reducing seepage over long periods of time. Often, a more permanent lining is installed as soon as the irrigation season permits or funds can be made available.

Asphaltic Concrete.—The hot-mix type of asphaltic concrete, that has long been used to such good advantage for street and highway paving, was given early consideration to determine its possibilities as a satisfactory, low-cost canal lining material. It is particularly well adapted to smaller canals and laterals, which, like unreinforced concrete linings in similar locations, permits the use of an inexpensive subgrade-guided slip-form.

The first cost of this lining is approximately the same as Portland cement concrete placed by slip-form methods. The linings of this type have given good service on the USBR's Yakima Project in Washington and Owyhee Project in Oregon and Idaho for 12 yr to 18 yr. Not only are there some types of weeds that can penetrate asphaltic concrete, but some plant growth appears to actually be promoted by the heat-absorbing property of the black surface. For this reason treatment of the subgrade with a soil sterilant prior to placement of the lining is advisable.

The asphaltic concrete lining is also characterized by uniformly spaced shrinkage cracks that continue to develop for some time. They are preferably repaired with hot asphalt.

A considerably harder asphalt is now (1960) specified in hot-mix linings to obtain better resistance to water erosion and weed puncture. Also, laboratory studies, utilizing rubberized paving grade asphalt cements, indicate that more workable and probably more stable and dense asphaltic concrete linings can be constructed with this type of binder.

EXPERIMENTAL LININGS

Several other types of linings and lining materials have been tested, as shown in Table 1. These are considered to be in an experimental state and are being evaluated. They include prefabricated asphalt membranes, asphalt macadams, prime-asphalt membranes, asphalt-emulsion concrete, asphalt-emulsion sand-mortars placed pneumatically, thin-compacted earth, bentonite-soil mixtures, soil-cement, plastics, and chemicals. Chemicals, asphalts, and other materials also are being studied in soil-stability tests. Asphalt has been used to underseal concrete linings.

Prefabricated Asphaltic Membranes.—Probably one of the most important developments as a convenience in the placement of the lining on small laterals is the buried, lightweight, prefabricated, asphaltic membrane. It can be installed by unskilled labor and a minimum of equipment. Several manufacturers are now producing the relatively thin, 1/8-in. to 1/4-in. thick, prefabricated asphaltic material and a prefabricated asphaltic sheet that is 1/2-in. or more in thickness. The latter is designed for use as an exposed membrane, but USBR experience with this thicker material is limited. Several trial instal-

lations have been made and in the southwest the material appears to be standing up well after 8 yr.

Tests made upon samples of the thinner, buried-prefabricated material, obtained from field installations, indicate the thinner prefabs should probably be at least 3/16-in.-thick or 1/4-in.-thick.

Asphalt Macadams.—Field Experiments indicate that it is not economically feasible to make the asphalt macadam linings watertight for extended periods. Large quantities of asphalt are required during construction and continued maintenance is necessary to fill cracks and voids that develop during exposure and accompanying shrinkage. Several trial installations have been made in which the macadam has been placed over an asphalt membrane. This procedure provides a more watertight lining; however, the practicability of using the macadam for a cover of a buried membrane is offset by the less expensive use of earth or gravel cover materials.

Prime Asphalt Membranes.—Prime-membranes that were actually the forerunner of present buried asphalt membrane linings are no longer considered a potential low-cost lining. They were constructed by first priming or penetrating the soil with a light fuel oil or distillate and then placing an asphalt membrane over the soil to stabilize it. Prime-membranes proved to be expensive to construct and maintain, were easily damaged by sun and weather, and were subject to injury by livestock and necessary canal maintenance operations.

Thin Compacted Earth.—Thin compacted earth linings have not been used widely due to the relatively high cost of side-slope compaction, and the danger of removal by scour or during canal cleaning operations. There is also the problem of loss of density of thin compacted earth upon freezing and thawing in the northern climates. Generally, linings of this type have given best results when provided with a gravel cover to prevent erosion and scour.

Bentonite-soil Mixtures.—Bentonite has been mixed with sandy, and gravelly materials by either spreading the premixed material over the canal perimeter or spreading the bentonite on the subgrade and mixing it with a disk or plow into the subgrade material. This method has been effective when the material is well compacted and where sufficient bentonite has been used to fill the voids of the sands and gravels. This has required from 5% to 25% bentonite with the result, in essence, being a blended compacted earth lining. Placing this type of lining on the side-slopes by mechanical means is extremely difficult, and hand placement costs make this method too expensive in the United States.

Soil-Cement.—Soil-cement linings of the standard type have not been too successful. They are not as weather resistant as concrete and securing adequate compaction of the material, when placed on the side-slopes, is a problem. In an attempt to secure better compaction and higher densities from a 5-in.-thick soil-cement lining, an experiment was made on the Columbia Basin project in the fall of 1956. An attempt was made to provide a greater density by longitudinal rolling with heavier rollers. This lining is being observed.

Plastic soil-cement linings, as compared with the standard type, have been most successful in the southwestern states. These plastic soil-cement linings were actually lean portland cement mortar linings.

Soil-cement offers possibilities for use as a canal lining material in localities in which subgrade soils or those soils adjacent to the canal are of a sandy nature and other suitable lining materials are not readily available. Placement of the plastic type by slip-form reduces cost.

Asphalt-Emulsion Concrete.—The cold-mixed asphalt linings are similar to the hot-mixed in that well-graded aggregate and asphalt are mixed together and compacted in place. The curing of linings of this type requires time and favorable weathering conditions. Some of the mixes tend to remain soft indefinitely, whereas others contract in curing, thereby creating cracks that must later be filled. Cold mixes tend to exhibit low erosion resistance and low stability for an appreciable period of time after placement. In general, hot mixes are preferable to cold mixes and the cost of placement per square yard is about the same. New asphaltic emulsions are being tested.

Pneumatically Applied Asphalt-Sand Linings.—Like shotcrete, mixtures of asphalt and sand have also been placed pneumatically. The method is particularly advantageous in covering exceptionally rough or irregular surfaces where use of a slip-form is impractical. The slow rate of application, relatively high cost, and low-erosion resistance of the completed surfaces are presently unfavorable to the use of this material as a lining.

Asphalt Undersealing of Concrete Linings.—The undersealing of old concrete linings with asphalt, although not strictly a lining in itself, is important as a method of rehabilitation. Hot asphalt-cement, pumped under the lining at moderate pressures, often travels 40 ft, filling voids, joints, and water channels, re-establishing the subgrade support, and minimizing leakage without any appreciable lifting of the lining.

MORE RECENT DEVELOPMENTS

Some of the more recent developments upon which studies are now (1960) underway, are: the resurfacing and repair of concrete linings; the development of improved crack sealants; the study of chemical and sediment sealants, cast-in-place concrete pipe, that is not a lining but an alternative for lining; the underwater application of asphalt sheets where water cannot be taken out of a canal to install a lining; and methods of determining the location and amount of seepage.

Repair of Concrete Linings.—There is a need for a less costly and more satisfactory method of repairing or resurfacing deteriorated or surface eroded concrete linings on many of the USBR projects. Portland-cement concrete linings have been successfully repaired in the bottom of canals with asphaltic concrete. These repairs have performed well over a period of 10 to 12 yr. However, repairing the side-slopes where compaction to secure density is difficult has been a problem. An attempt is being made to secure better compaction and to develop new adhesives to help bond the asphalt repair to the old concrete surface.

Also, 1/4-in.-thick to 1/2-in.-thick prefabricated asphalt sheets have been used to repair concrete surfaces. An installation of this material made in 1955 is shown in Fig. 4.

Sediment Linings.—The puddling and printing of new unlined canals with sediment is an accepted practice in reducing seepage losses from canal systems. A natural sealing of operating canals occurs if considerable sediment is carried by the water in the canal. If the water carried by the canal is relatively clear, sediments have been added artificially.

The sealing of canals and laterals with sediment has ranged from being unsuccessful on many USBR projects, through being moderately successful for a limited time on some, to being outstandingly successful over a period of years

on a relatively few. Sealing with sediment has been found to be more effective and permanent where gravel blankets had been placed over the canal perimeter to trap and hold the sediment. Although there are other factors that should be considered, the effectiveness of the sediment in reducing seepage appears to depend mainly on the following factors: the suitability of the sediment; the velocity of the water flowing in the canal; the type and amount of sediment carried by the flowing water; and the structure of the soils in which the canal is constructed and through which the seepage occurs.

A natural layer of sediment, deposited on the wetted perimeter of a canal constructed in fine sandy soil, reduced the seepage for a short reach from 5.0 cfs to 0.5 cfs until it was scoured and eroded by clearer water flowing through the canal. Apparently, little permanent benefit can be achieved from such sediment layers unless the sediment penetrates the voids in the subgrade material to sufficient depth to be protected from removal by scour, erosion or mechanical means.

Because sedimenting is not costly and because it does offer possibilities under certain conditions, a cooperative study between the USBR and Colorado State University, Fort Collins, Colorado, was initiated in July, 1953. This

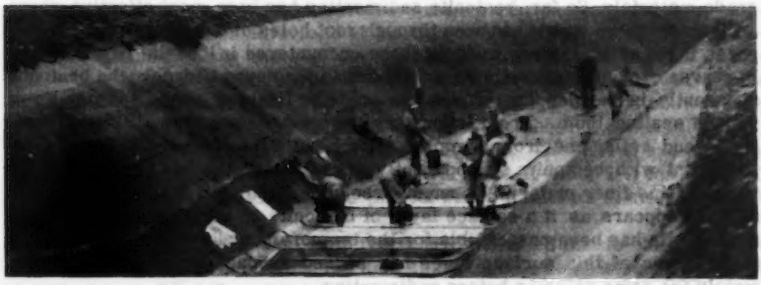


FIG. 4.—INSTALLATION OF PREFABRICATED ASPHALT SHEETS IN REPAIR OF CONCRETE LININGS.

study was to investigate the possibilities of sediment sealing in more detail and determine the conditions under which the process could be expected to be successful.

After considering several types of sediment, a high-swelling type of bentonite was chosen as the sedimenting agent for the following reasons: its chemical and physical uniformity as compared with other types of natural clays; its high colloidal yield; its ability to expand upon becoming wet; and its availability, at lower cost, in the general area in which the first tests were made as compared with other types of materials.

Because the chemical nature of the water and the subgrade materials of the canal affect the stability of the suspensions, efforts have been directed toward securing stable suspensions of the colloids in the canal water by using dispersing agents. Field trials in small canals and laterals and laboratory tests have been made to the depth of penetration of the colloids into the voids of various types of subgrade materials, the permanence of the seal provided by the colloids.

The bentonite used usually has been a commercially processed, dried, ground, and screened product. In the field trials the bentonite usually has been mixed with the canal water and a dispersing agent in a high velocity air-water jet. The mixed slurry of bentonite, dispersant and water is then generally placed into a retaining pond where the non-colloidal and foreign particles have been permitted to settle. From the pond, the slurry has been drawn or pumped into the water flowing in the canal to secure a bentonite concentration of approximately 1% by volume. The mixture then has been allowed to flow down the canal, carrying the colloidal material into place.

Temporary reduction in seepage has been accomplished in field trials made by the USBR in several types of subgrade materials where the sealing has been attempted. Colorado State University, in other field trials, reports somewhat better and more lasting results, provided the bentonite or other clay that settles on the surface of the wetted perimeter of a canal is harrowed or disced into the subgrade materials. The temporary reduction poses the economic question of whether the value of water saved justifies repeated sedimenting or whether, over a period of years, a more permanent conventional lining would be less costly.

The amount of seepage reduction has varied with the character of the subgrade materials. So far, bentonite sedimenting has been most effective where seepage from the canals has been through root holes or other secondary macro pores in the soil structure, such as those encountered in loessial types of soil. In coarse sandy and gravelly materials and in fractured bedrock, the bentonite apparently is carried on through the voids or fissures by the seepage water without sealing them. From laboratory tests made upon typical finer grained sands and soils, and from samples of such soils taken from the canals after treatment with bentonite, it apparently has not been possible to penetrate the voids of this finer material to any appreciable depth with the colloidal bentonite. It appears as if a surface layer of bentonite on the wetted perimeter of the laterals has been responsible for the temporary reduction in seepage, and that erosion of this surface layer has caused seepage to return to approximately the same value as before sedimenting.

Monolithically Unreinforced Cast-in-Place Concrete Pipe.—On several projects, monolithically, unreinforced, cast-in-place concrete pipe has been installed. This pipe and other similar pipe has been used by private irrigation districts in California and has a good record of serviceability. The limitations of this pipe cause it to be used primarily to replace small laterals and lateral distribution systems having hydrostatic heads of about 15 ft maximum.

The cost of this and other types of concrete pipe compared to the placement of linings in open canals, has been high and has been one reason for their limited application. Data from recent (1959) installations indicate that cast-in-place pipe, 30 in. to 48 in. in diameter, costs less than precast pipe and may actually be competitive with concrete slip-form linings under favorable conditions.

The special machine used to construct this type of pipe operates in a previously excavated trench and pulls itself forward by a winch and cable anchored several hundred feet away in the bottom of the trench. Arch forms to support the top of the pipe are fed into the machine as the work progresses and a man inside of the pipe places shoring to hold the forms in place.

Plastic Linings.—Originally the use of plastics as a canal lining material was limited because of cost. In addition, many plastics tested were easily punctured and some types disintegrated rapidly upon exposure. Plastics do

have a high resistance to rupture and rot, and some placed as buried membranes in 1955 are performing well (1960).

Lower production costs now make it possible to obtain plastic materials for canal linings that are competitive cost-wise with hot-sprayed and prefabricated asphaltic materials. The most promising plastics tested appear to be the polyvinyl and polyethelene films and these have been used so far in several experimental installations made by the USBR and others.

Plastics presently available appear to hold more promise as a lining material if used as a buried membrane. Most of the recent installations have been made in that manner, providing a cover of earth and/or gravel to protect the plastic film from weathering, erosion, livestock traffic and necessary canal maintenance operations.

Plastic film, even of 1-1/2-mil thickness, is essentially a watertight material; however, film less than 6-to-8-mils in thickness has low puncture resistance and is easily damaged in handling and when placed over rough subgrade and covered with angular materials. Ordinary weed growth has not penetrated plastic film of the thickness used in experimental installations, but thinner films tested in laboratories have been penetrated by the more hardy weeds.

One advantage of the plastic film is its lightweight per unit area, permitting shipment long distances without excessive transportation costs and easy handling on the job. Another advantage of more recent development is the fabrication of the film into long and wide sheets, making it possible to provide a one-piece covering for some relatively large laterals. The film is now available in most any width or length. The size sheet that can be handled conveniently during placement is the controlling factor. A single sheet of 8-mil (0.008-in.) thick, black-pigmented, polyvinyl film, 17-ft wide, 400-ft long and weighing 350 lb was accordian-folded into a cardboard box 4-ft wide, 6-ft long and 1-ft deep. It was unfolded, handled, and placed with a minimum of effort to line a lateral.

Like asphaltic membranes, field trials have indicated that to obtain a stable buried plastic membrane lining, the side slopes should be no steeper than 2 on 1 with slopes of 2-1/2 on 1 being preferred.

Underwater Installation of Asphalt Sheets.—There are hundreds of miles of unlined canals and laterals on projects in Arizona and California that must be kept in service for the entire year. Accordingly, the water cannot be taken out of the canals long enough to place a conventional type lining. A means of lining the canals and laterals without removing the water has been a real problem. A new approach to the problem was the underwater installation of 1/2-in. thick prefabricated asphalt sheets.

The canal in which the installation was made was 30 ft wide. At the time of installation the water flowing in the canal was from 3½ ft to 4½ ft deep with velocities varying between 1.0 cfs and 3.0 cfs. Although several methods of installation were tried, the most successful consisted of fabricating a panel of asphalt sheets, starting from the top of the canal bank, down the slope and out onto a barge. The barge was then pulled laterally across the canal and the fabricated panel allowed to drop into the water. A similar operation from the opposite bank left a lapped center joint that was expected to seal when lapped over the mastic along the outer edge of the first panel placed. Some difficulty was experienced in sinking the panel because of the current, and weighted rollers were used in overcoming this difficulty. Following the installation, the canal was emptied of water and inspected. The inspection of this test installation revealed that all transverse joints to the water line were satisfactorily

and effectively made, and that of the several types of mastic used in making the joints below water, a hot-melt asphalt seemed best. However, difficulty was encountered in securing a good joint between the two panels placed from opposite sides of the bank. It it possible that a large air-driven stapler for the building trade that would require only minor modification could be used to stitch the two panels together to assist in making the longitudinal joint in the middle of the canal and elsewhere if needed. Development work remains to be done, particularly in finding a fully satisfactory adhesive and fastening process for bonding the sheets together.

CONCLUSIONS

The lower-cost canal lining program outlined in this paper has been instrumental in bringing about lower costs and improved linings. Some results of this program are evident in almost every project the USBR has built in recent years. Not only have costs been reduced but more linings have been installed and, as a result, more water and land has been saved. There is much that needs to be done. There is need to keep abreast of new developments in plastics and chemicals, particularly in the possible use of chemicals as sealants and soil stabilizers.

Most of the linings installed have a definite place in a program of this nature and have accomplished the purpose for which they were installed. Some have either proven to be too costly for large-scale installation, have not given satisfactory performance, or, although low in first cost, have required excessive maintenance. The most successful linings will be evaluated not only on the basis of first cost, but also for the cost of maintenance and useful life.

DISCUSSION

FREDERICK L. HOTES,[2] F. ASCE.—The leadership and contributions of the USBR in connection with the development of lower-cost canal linings are recognized throughout the world. It is in this direction that some of the greatest improvements have been made, and can continue to be made, in irrigation engineering. Low-cost canal linings mean not only conservation of water and reduced drainage problems, but may also mean lower annual costs, considering both initial costs and maintenance charges.

Another important factor, particularly as regards secondary systems, is the conservation of land, and the ease and increased flexibility of farming operations that can be achieved by the use of concrete pipe distribution systems. The author has mentioned briefly the use of monolithically cast-in-place concrete pipe in this regard. A similar type of pipe is the cast-in-place concrete pipe constructed in two parts. Both of these types of pipes are unreinforced. They have been used for many years in California, particularly by the Turlock Irrigation District in the San Joaquin Valley. This district is reported[3] to

[2] Mgr., San Francisco Area Office, Engineering-Science Inc., Oakland, Calif.

[3] "Monolithic Concrete Pipe," Western Construction News, Vol. 21, February, 1946, p. 83.

have successfully installed more than 200 mi of two-part type pipe, with a saving of 0.6 acre of land per 1,000 ft length of lateral, as compared to open ditches of the same capacity.

Approximate prices per linear foot in 1954 in the Turlock area for two-part pipe, including cost of excavation, backfill, and leveling, were $1.60 for 30-in. pipe (all pipe sizes refer to inside diameter), $2.00 for 36-in pipe, and $2.90 for 42-in. pipe.

These prices reflect conditions in which the contractors have had several years of experience in this type of work for the Turlock Irrigation District. Many of these pipes have been in successful operation for several years.

In the opinion of the writer, the economy and advantages of such pipes merit more consideration for their use in distribution sytsems than they have received in the past.

RICHARD J. WILLSON,[4] F. ASCE.—The economy and advantage of using unreinforced, monolithically cast-in-place concrete pipe in lieu of canal linings should be considered, as suggested by Mr. Hotes, particularly for small or secondary irrigation carriage and distribution systems. The miles of two-part type cast-in-place concrete conduit placed by the Turlock Irrigation District to serve lands in the San Joaquin Valley of California are reported to be serving very well. The installation by the Salt River Valley Water Users' Association on the Salt River Project, Arizona, of more than 21 mi of 30-in. diameter, 42-in.-diameter, unreinforced, cast-in-place, monolithic pipe of the no-joint type, has been reported[5] on.

Since this report[4] many additional miles of this type of pipe have been constructed by the Salt River Valley Water Users' Association, as a replacement for deteriorated conventional canal linings, for enclosing open ditches in urban areas, and in lieu of linings in unlined reaches of other laterals. In addition to the 30-in.-diameter and 42-in.-diameter pipe, several miles of 36-in.-diameter and 48-in.-diameter pipe has been constructed, and it is understood that a machine now has been purchased to construct 54-in.-diameter conduit. The average cost per lineal foot for constructing the pipe by project forces has been: 30-in.-diameter-$4.03, 36-in.-$4.84, 42-in.-$5.69 and 48-in.-$6.06. The cost will vary with subgrade conditions and other preparatory factors encountered incidental to the installation of the pipe.

Approximately 2,000 ft of 30-in. conduit and 1,300 ft of 48-in. conduit of the no-joint type also was placed experimentally in 1954 on the Orland Project in Northern California. Experience with the cast-in-place concrete conduit in central Arizona and northern California areas has been very satisfactory. It is believed the climate and soil condition on these projects are almost ideal for this type of construction and that these conditions are important in considering the use of either the two-part or no-joint type of pipe. Temperate climate and cohesive soils that will stand almost vertically for trench excavation are believed essential to the economical and possibly to the successful construction of this type of conduit. In unconsolidated and noncohesive soils and under severe climatic conditions the acceptability and practicability of the pipe is still to be determined.

---

[4] Engr., Bur. of Reclam., U. S. Dept. of the Interior, Denver, Colo.

[5] "Slip-Formed Concrete Pipe: What has been Learned in Arizona," by H. Shipley, Asst. Genl. Mgr., Salt River Project, Phoenix, Ariz., Western Construction News, Vol. 32, No. 11, November, 1957.

A close examination of the interior of the no-joint pipe on the Salt River Project, the first of which was placed in 1955, has not been possible because of its being in constant use. However, there has been little evidence of leakage or cracks. An evaluation was made in 1957 of the 30-in no-joint pipe placed on the Orland Project and tests to determine the leakage in a section of pipe were conducted. The indicated losses were approximately 0.5%, based upon a designed capacity of 10 cfs. The leakage was primarily from construction joint cracks at the junction of the conduit with the headworks and outlet structures. Provisions have been made for sealing these leaking joints and additional tests will be conducted as operating conditions permit.

Internal hydraulic pressure and external loading to which this pipe should be subjected also is a factor to be considered. Tests made on the Salt River Valley Project[5] and on the Orland Project indicate the capability of the pipe to withstand more stress than the internal hydraulic pressure equivalent of 8-ft to 15-ft of head that the installed pipe has been subjected to during normal operation. On the Salt River Project, the no-joint pipe is being used in urban and rural areas, whereas conventional precast concrete pipe is being specified for use in locations subject to external loading and shock, such as that encountered under streets and highways.

AMERICAN SOCIETY OF CIVIL ENGINEERS

Founded November 5, 1852

TRANSACTIONS

Paper No. 3031

EARTHQUAKE RESPONSE OF ELEVATED TANKS AND VESSELS

By Donald F. Moran,[1] and James A. Cheney,[2] A. M. ASCE

With Discussion by Messrs. A. A. Eremin; and Donald F. Moran and James A. Cheney

SYNOPSIS

Earthquakes in the western United States, that occurred in the 1940's and early 1950's, while not being as severe as can reasonably be expected to occur, have provided the first tests of many structures specifically designed to resist earthquake forces. Engineering studies of these shocks have provided valuable data.

Research has provided methods of estimating stresses in simple structures due to actual earthquake motion. A method of analysis is examined wherein minor damage to elevated water tank towers and refinery vessels can be satisfactorily explained.

INTRODUCTION

Earthquakes in the western United States have provided data[3,4] on damage to earthquake-resistive elevated water storage tanks and refinery-type structures. This damage, although slight, indicates some weaknesses in present methods of analysis.

Note.—Published, essentially as printed here, in March, 1958, in the Journal of the Structural Division, as Proceedings Paper 1563. Positions and titles given are those in effect when the paper or discussion was approved for publication in Transactions.

[1] Chief Struct. Engr., Quinton Engineers Ltd., Los Angeles, Calif.

[2] Head, XA Strength, Missile and Space Div., Lockheed Aircraft Corp., Sunnyvale, Calif.

[3] "An Engineering Study of the Southern California Earthquake of July 21, 1952, and its Aftershocks," by Karl V. Steinbrugge and Donald F. Moran, Bulletin, Seismological Society of America, Vol. 44, No. 2B April, 1954.

[4] "Proceedings of the Symposium on Earthquake and Blast Effects on Structures," of Earthquake Engrg. Research Inst., Univ. of California, June, 1952.

Because these particular types of structures can be treated, relatively easily, as dynamic structures, the authors have chosen them as examples. These examples are studied by being mathematically subjected to actual loadings as indicated by instrument records of strong shocks in the 1940's and 1950's including those in which they suffered damage. All counties and cities indicated in this paper are in California.

FACTORS INVOLVED

Earthquake Spectra.—Research, using an electric analog computer to analyse strong motion accelerogram records, has produced spectra that can be

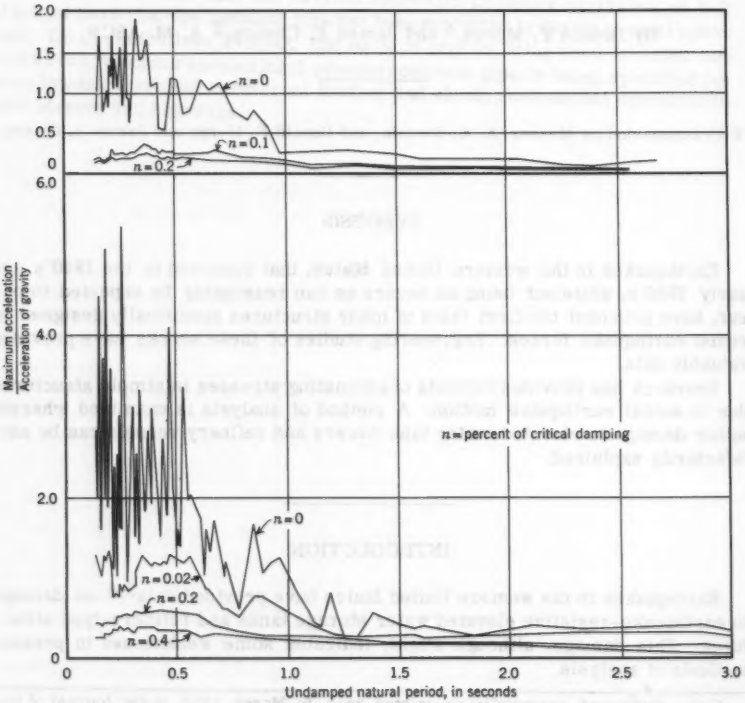


FIG. 1.—ACCELERATION SPECTRA

used to predict[5] stresses in structures when subjected to actual earthquake motion. Briefly, the earthquake spectrum is a plot of the maximum response

5 "Spectrum Analysis of Strong-Motion Earthquakes," by G. W. Housner, R. R. Martel, and J. L. Alford, Bulletin, Seismological Society of America, Vol. 43, No. 2, April, 1953.

of a simple oscillator versus the period of the oscillator when subjected to actual ground motion at a particular location in a particular earthquake. Various percentages of critical damping of the oscillator can be introduced in the spectrum, and, as shown in Fig. 1, relatively small amounts reduce the structural response sharply. Fig. 1 shows acceleration spectra and the maximum acceleration for two different earthquakes with respect to gravity versus the oscillator period for various percentages of critical damping. These spectra are plotted for only one direction at each location, although two are generally made for two directions, 90° apart. The upper spectra is for the Taft earthquake of July 21, 1952 while the lower spectra is for the El Centro earthquake of May 18, 1940.

Damping.—Tests have shown that percentages of critical viscous damping for various types of construction are approximately one to five for elevated

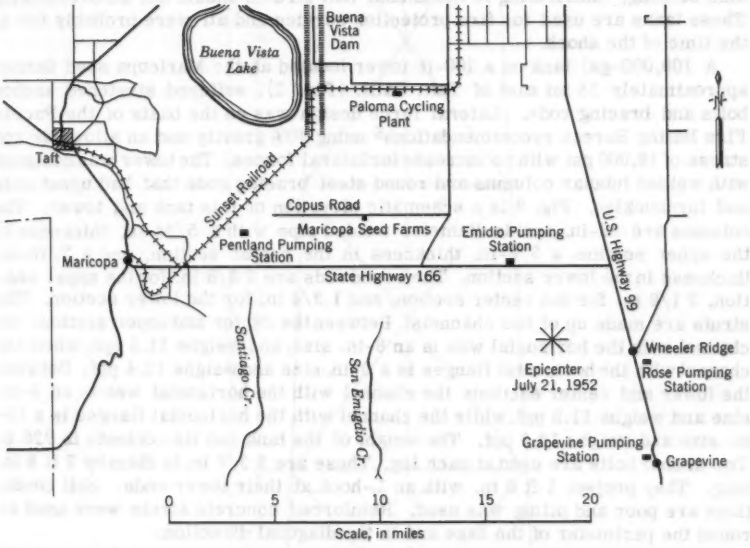


FIG. 2.—EARTHQUAKE LOCALE

water tank towers,[6] one-half to one for unlined self-supporting welded steel stacks[7] and one to one and a half for the same type of stacks lined with gunite.

For elevated tank towers, the damping was found to be decreased by tightening the rods and strengthening the towers. Welded steel stacks apparently have smaller damping than riveted types and, presumably, the use of fire brick lining would increase the damping, but there is a lack of data to substantiate this.

[6] "Earthquake Investigations in California 1934–1935," Special Publication 201, U. S. Dept. of Commerce, Coast and Geodetic Survey, 1936.

[7] "The Vibration of Steel Stacks," by Walter Dickey and Glenn B. Woodruff, Proceedings - Separate 540, ASCE, November, 1954.

ELEVATED WATER TANK TOWERS

Experience with elevated tank towers and refinery-type structures in the California earthquake of July 21, 1952, indicates[3] that the type of damage exhibited can be explained when it is realized that these structures have relatively low percentages of critical damping and practically no secondary lateral force resisting elements.

Five of eleven elevated water tanks, that had been designed to resist earthquakes, suffered stretching of their anchor bolts in the Kern County area. While two showed evidences of slightly stretched rods. Slight anchor bolt stretching was also noted on one earthquake resistive tank in Eureka, after the earthquake of December 21, 1954.

All of the above tanks have four legs and are generally of welded construction with very thick base plates. The possibility of prying action, due to column bending, contributing to the anchor bolt stretch should not be overlooked. These tanks are used for fire protection service and all were probably full at the time of the shock.

A 100,000-gal tank on a 100-ft tower located at the Maricopa seed farms, approximately 15 mi east of Taft, Calif. (Fig. 2), suffered stretched anchor bolts and bracing rods. Lateral force design was on the basis of the Pacific Fire Rating Bureau recommendations[8] using 10% gravity and an allowable rod stress of 18,000 psi with no increase for lateral forces. The tower was designed with welded tubular columns and round steel bracing rods that had upset ends and turnbuckles. Fig. 3 is a schematic elevation of this tank and tower. The columns are 22-in. inside diameter welded pipe with a 5/16-in. thickness in the upper section, a 3/8-in. thickness in the center section, and a 7/16-in. thickness in the lower section. The round rods are 2 3/8 in. for the upper section, 2 1/8 in. for the center section, and 1 3/4 in. for the lower section. The struts are made up of two channels. Between the center and upper sections the channel with the horizontal web is an 8-in. size, and weighs 11.5 ppf, while the channel with the horizontal flanges is a 9-in. size and weighs 13.4 ppf. Between the lower and center sections the channel with the horizontal web is an 8-in. size and weighs 11.5 ppf, while the channel with the horizontal flanges is a 10-in. size and weighs 15.3 ppf. The weight of the tank and its contents is 926 k. Two anchor bolts are used at each leg. These are 1 3/4 in. in diam by 7 ft 6 in. long. They project 1 ft 6 in. with an L-hook at their lower ends. Soil conditions are poor and piling was used. Reinforced concrete struts were used around the perimeter of the base and in the diagonal direction.

This structure, for purposes of analysis, may be considered as a single mass concentrated at the center of gravity of the tank and supported by a weightless elastic frame. For this type of structure, one degree of freedom can be assumed and the free period computed[9] from

$$T = 2\pi\sqrt{\frac{\delta_{st}}{g}} \quad \ldots\ldots\ldots\ldots\ldots\ldots\ldots\ldots (1)$$

in which T is the free period in seconds; δ_{st} denotes the deflection, in feet, of the top of the tower under a static horizontal force equal to its own weight; and g is the acceleration of gravity in fps.

8 "Recommendations, Earthquake Resistive Design of Buildings, Structures and Tank Towers," by H. M. Engle and J. E. Shield, revised and reprinted by Pacific Fire Rating Bureau, 1950.

9 "Earthquake Investigations in California 1934–1935," Special Publication 201, U. S. Dept. of Commerce, Coast and Geodetic Survey, 1936, p. 112.

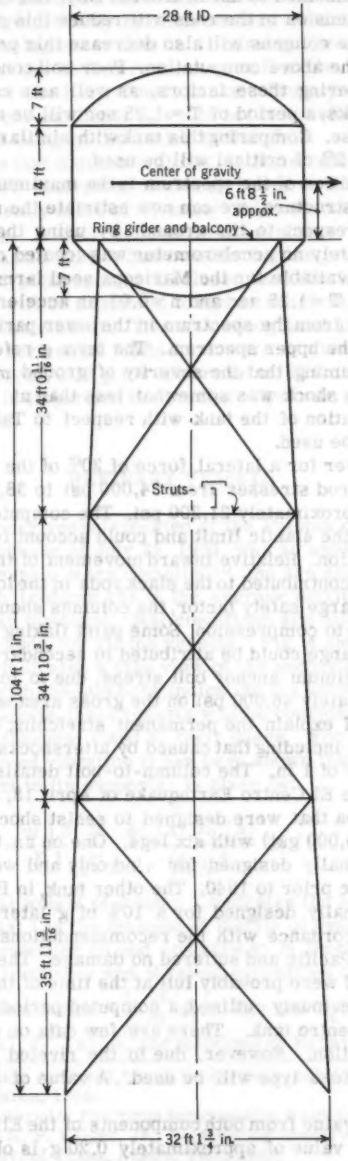


FIG. 3.—SCHEMATIC ELEVATION OF TANK AND TOWER

If the rods are assumed to act in tension only, the computed period T = 1.4 sec. However, pretension in the rods will reduce this period somewhat. Secondary bending in the columns will also decrease this period as all joints were assumed hinged in the above computation. Poor soil conditions should lengthen the period. Considering these factors, as well as a comparison with actual tests on similar tanks, a period of T = 1.25 sec will be assumed as being more nearly the actual case. Comparing this tank with similar tanks which have been tested,[6] damping of 2% of critical will be used.

Because the definition of the spectrum is the maximum response of a single degree of freedom structure, we can now estimate the maximum acceleration of this tank, with respect to the ground, by using the acceleration spectra (Fig. 1). Unfortunately no accelerometer was located closer than Taft and no actual spectra are available for the Maricopa seed farms area.

Using a period of T = 1.25 sec and n = 0.02, an acceleration of approximately 0.30 g can be picked from the spectrum in the lower part of Fig. 1, and approximately 0.12 g from the upper spectrum. The term g refers to the acceleration due to gravity. Assuming that the severity of ground motion at the epicenter of the July 21, 1952, shock was somewhat less than at El Centro in 1940, and considering the location of the tank with respect to Taft and the epicenter, a value of 0.20 g will be used.

Analyzing the tower for a lateral force of 20% of the weight of the tank and contents, results in rod stresses from 34,000 psi to 38,000 psi and maximum column stress of approximately 21,200 psi. The computed rod stresses are in the neighborhood of the elastic limit and could account for some small amount of permanent elongation. Relative inward movement of the column bases during the earthquake also contributed to the slack rods in the lower panel. Considering their relatively large safety factor, the columns should not and did not show signs of distress due to compression. Some paint flaking at welded joints where plate thicknesses change could be attributed to secondary bending.

However, the maximum anchor bolt stress, due to forces in a diagonal direction, is approximately 46,000 psi on the gross area which is well above the yield point and could explain the permanent stretching of these bolts. Maximum total elongation including that caused by aftershocks as late as January 12, 1954, is on the order of 1 in. The column-to-bolt details were also deformed.

At the time of the El Centro Earthquake of April 18, 1940, there were only two tanks in that area that were designed to resist shock. These tanks were relatively large (250,000 gal) with six legs. One on an 80-ft tower located in El Centro was originally designed for wind only and was subsequently reinforced for earthquake prior to 1940. The other tank, in Brawley, is on a 120-ft tower and was originally designed for a 10% of g lateral force. Both tanks were designed in accordance with the recommendations of the Board of Fire Underwriters of the Pacific and suffered no damage. These tanks are used for city water supply and were probably full at the time of the shock.

Using methods previously outlined, a computed period T = 1.20 sec was arrived at for the El Centro tank. There are few data on damping for this size and type of construction. However, due to the riveted construction, a value higher than for a welded type will be used. A value of 5% of critical will be assumed.

Using an average value from both components of the El Centro spectra (lower part of Fig. 1), a value of approximately 0.20 g is obtained and computed stresses for the rods are 27,700 psi to 28,500 psi. Anchor bolt stresses are approximately 50,000 psi on the gross section.

When considering the above stresses the absence of damage can be explained by the fact that there are probably more secondary unconsidered resisting elements present in a six-leg tower than in a four-leg tower. Another factor is that the base details on the El Centro tank were flexible when compared with the rigid welded type of the Kern County tanks. The prying action of the column base plate, due to column bending, would not be as effective on the El Centro tank due to the bolt being in the center of the plate.

The results indicate that moderate allowable rod stresses of 18,000 psi with no seismic increase are desirable. A design based on 20,000 psi plus a one-third increase as presently allowed by many codes would have resulted in excessive rod stretching. Anchor bolts should be proportioned so as to deep stresses within the elastic limit when considering the probable lateral loads.

An examination of typical spectra discloses that shorter towers with relatively shorter periods will be subjected to higher accelerations in the same location and during the same shock. This was recognized as early as 1935 when recommendations for horizontal loads for towers on firm ground were 0.10 g for towers of 75 ft or over, 0.12 g for towers from 50 ft to 75 ft, and 0.15 g for towers under 50 ft. It is important to note that a dynamic analysis supports the observed performance.

REFINERY VESSELS

Damage to tall slender vessels located at the Paloma cycling plant (Fig. 2) in the California earthquake of July 21, 1952, was as shown in Fig. 4.

Data on various vessels were compiled[10] and are shown in Table 1. The measured bolt stretch (column 16) is the average maximum that usually occurred in the northeast quadrant. Soil conditions are only fair at Paloma and spread footings were used for all the vessels. Fig. 4 shows details of a typical vessel. Fig. 4(b) indicates a plan view of the anchor bolt stretch due to the July 21, 1952 shock, with the numbers indicating the amount of stretch.

For purposes of analysis, these vessels will be considered as uniform beams (with constant wall thickness) fixed at their bases. For a continuous uniform beam subjected to forced vibration it has been shown that the deflection, y, of any point (with respect to its supports) is given by:

$$y\,(x, t) = \frac{W\,L^3}{E\,I} \sum_{i=1}^{\infty} \frac{\phi_i\,(x)\;K_i\,(x)}{(\beta_i\,l)^4}\;D_i\,(t) \quad \ldots\ldots\ldots\ldots\ldots\ldots \quad (2)$$

in which W is the total weight of beam; l indicates the length of beam; E denotes Young's modulus; I is the moment of inertia of beam; $\phi_i(x)$ is the characteristic function depending on end conditions; β_i denotes the characteristic number depending on frequency and physical properties of the beam; $K_i(x)$ indicates the participation factor $= \frac{1}{L}\int_0^L \phi_i(x)\,dx$; and $D_i(t)$ is the dynamic load factor. Values of $\phi_i(x)$, $\phi_i''(x)$, β_i, and solutions of K_i have been tabulated[11,12]

10 "Earthquake Damage Analyzed," by E. O. Bergman and Noel Owen, Petroleum Refiner, Vol. 33, No. 3, March, 1954.

11 "Tables of Characteristic Functions Representing Normal Modes of Vibration of a Beam," by D. Young and R. P. Felgar, Jr., Engineering Research Series No. 44, Bureau of Engrg. Research, Univ. of Texas, Austin, Tex., 1949.

12 "Formulas for Integrals Containing Characteristic Functions of a Vibrating Beam," by R. P. Felgar, Jr., Circular No. 14, Bureau of Engrg. Research, Univ. of Texas, Austin, Tex., 1950.

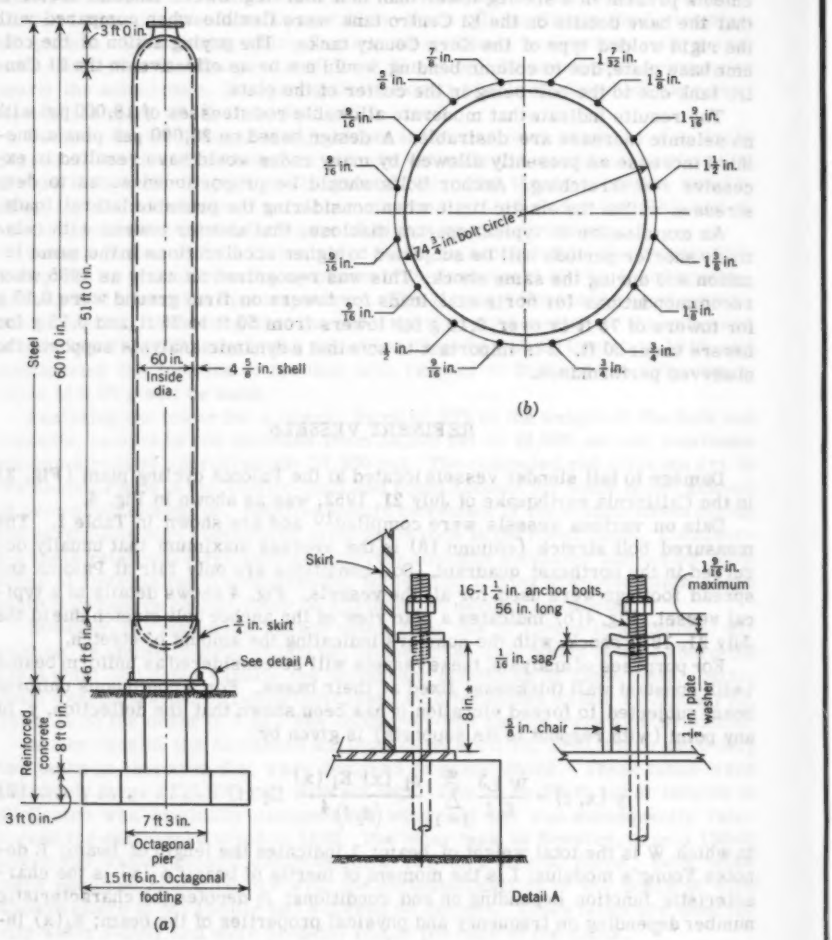


FIG. 4.—PROCESSING TOWER AND SHOCK EFFECT

TABLE 1.—FRACTIONATOR COLUMN PROPERTIES

Vessel									Anchor Bolts						
Tower Number	Inside Diameter in inches	Height, in feet	Shell Thickness, in inches	Skirt Thickness, in inches	Weight of Vessel, in Kips		Height to[a] center at gravity, feet		Number	Diameter, in inches	Type[b]	Area, in Square inches		Bolt Circle, in inches	Bolt Stretch, in inches
					Empty	Operating	Empty	Operating				Gross	Net		
(1)	(2)	(3)	(4)	(5)	(6)	(7)	(8)	(9)	(10)	(11)	(12)	(13)	(14)	(15)	(16)
C 1	60	60	4 5/8	3/4	203	211	30.3	30.0	16	1 1/4	L56	19.62	14.86	14 3/4	1 1/2 - 1 3/4
C 4	66	59	7/16	3/8	52	62	31.5	29.3	12	1 1/4	J51	14.72	11.15	71 7/8	1/8 - 3/16
C 5	54	68	1/4	3/8	29	36	35.0	33.0	16	1 1/4	J51	19.62	14.86	59 3/4	1/16 - 1/8
C 6	78	104	1	5/8	141	160	55.5	54.5	16	1 3/4	J70	38.50	31.70	85 1/2	0 - 1/16
C 7	66	97	1 1/16	5/8	111	123	49.5	48.2	16	1 3/4	J70	38.50	31.70	73 1/8	0
C 8	36	48	3/8	3/8	16	18	25.5	24.7	8	1 1/2	J58	14.14	11.24	41 3/4	0 - 1/16
C 9	48	97	7/16	1/2	50	57	49.4	48.0	16	1 3/4	J72	38.50	31.70	54 1/2	0 - 1/16
C60	78	84	2 1/4	1/2	203	225	43.3	42.0	16	1 3/4	J45	38.50	31.70	88	5/8 - 3/4
C64	108	80	1	1/2	162	223	43.3	39.0	20	1 1/4	L53	24.54	18.58	115	1/2 - 5/8
C66	60	105	7/8	1/2	109	120	49.0	48.5	12	2	J60	37.70	31.80	67 1/2	1/8 - 3/16
C67	42	54	1 1/16	3/8	35	39	31.0	30.0	8	1 1/2	J45	14.14	11.24	49	3/8 - 1/2
C68	42	94	7/16	1/2	39	46	50.0	47.0	12	2	J60	37.70	31.80	49	0 - 1/8

[a] Height to center of gravity is above base ring.
[b] The letter refers to the shape and the number indicates the length in inches.

for uniform beams with various end conditions. All of the preceding terms except the dynamic load factor are functions of the physical and dynamic properties of the beam and are independent of the forced vibration.

For earthquake motion, the dynamic load factor is obtainable for each mode from the acceleration spectrum and represents the effect of actual earthquake ground motion on the vibration of the beam.

Thus, if we know or can estimate the physical and dynamic properties of the structure, then, by using the spectrum for any particular location and earthquake, we can estimate what the maximum response would have been at that location in terms of deflections. In the same respect by differentiating Eq. 2,

$$M(x,t) = W l \sum_{i=1}^{\infty} \frac{\phi_i''(x)}{(\beta_i l)^2} K_i D_i(t) \quad \ldots\ldots\ldots\ldots (3)$$

in which $M(x,t)$ is the maximum moment at any point, and

$$V(x,t) = W \sum_{i=1}^{\infty} \frac{\phi_i'''(x)}{\beta_i l} K_i D_i(t) \quad \ldots\ldots\ldots\ldots (4)$$

in which $v(x,t)$ is the maximum shear at any point.

The maximum response assumes the worst condition of all modes of vibration being additive and is on the conservative side. Generally, only the first two or three modes need be considered. Using Eq. 3, the maximum base moment will be computed for the vessels, considering the first two modes only. The weight w used will be the operating weight as given in column 7 of Table 1.

Assuming a clamped-free condition (similar to a cantilever beam) the various values[11] for the clamped end or base are, first Mode: $(\beta_1 l)^2 = 3.52$, $\phi_1'' = 2.0$, $K_1 = 0.79$, $\frac{\phi_1'' K_1}{(\beta_1 l)^2} = 0.45$, and second Mode: $(\beta_2 l)^2 = 22.03$, $\phi_2'' = 2.0$, $K_2 = 0.435$, and $\frac{\phi_2'' K_2}{(\beta_2 l)^2} = 0.04$, in which the subscript refers to the first or second mode.

In order to pick the proper dynamic load factor, $D_i(t)$, from the spectrum, we must know the period, T, and the percentage of critical damping. The period t for each mode can be computed from:

$$T_i = \frac{2\pi}{\omega_i} \quad \ldots\ldots\ldots\ldots (5)$$

in which ω_i, the angular velocity, $= \beta_i^2 \sqrt{\frac{EI}{m}}$ in which m is the mass per unit length.

From Eq. 5 the periods shown in Table 2 have been computed. In order to arrive at these values the following factors must be evaluated (assumptions made in computations for Table 2 are also indicated):

1. Initial tension in the anchor bolts. None was assumed.
2. The cross-sectional area of the bolt to be used; net area, gross area, or something between these two values. Gross areas were used.

3. The amount of the operating liquid to be included in figuring the weight.

4. The effect of vertical acceleration. The July 21, 1952, shock was characterized by considerable vertical acceleration due probably to the combination of vertical and horizontal faulting. This factor was neglected.

5. The percentage of damping. This undoubtedly varies among the various vessels due to differences in contents, insulation, and foundations. A value of 2% of critical for all was used to arrive at the dynamic load factor in Table 2.

6. The effect of impact after initial stretch of anchor bolts. This was neglected.

Again we are faced with the problem of not having spectra available for the earthquake area. The dynamic load factors $D_i(t)$ shown in Table 2 were arrived at by assuming the motion at Paloma to be represented by roughly the

TABLE 2

To vol.	Period, Ti in seconds		Dynamic Load Factor, Di(t)		Maximum Base Moment M, in foot = kips x 10^3
Number	First Mode	Second Mode	First Mode	Second Mode	
(1)	(2)	(3)	(4)	(5)	(6)
C 1	.22	.04	0.5	0.5	3.11
C 4	.35	.06	0.4	0.5	0.73
C 5	.71	.05	0.4	0.5	0.49
C 6	.69	.11	0.4	0.5	3.33
C 7	.69	.11	0.4	0.5	2.38
C 8	.38	.06	0.5	0.5	0.21
C 9	1.16	.19	0.25	0.5	0.73
C60	.50	.09	0.5	0.5	4.63
C64	.34	.05	0.5	0.5	4.38
C66	.95	.15	0.3	0.5	1.95
C67	.31	.05	0.5	0.5	0.52
C68	1.21	.20	0.15	0.5	0.38

average value of Taft spectrum and two thirds the value of El Centro spectrum (upper and lower parts, respectively of Fig. 1). However, the actual magnitude of $D_i(t)$ is not as important here as are its comparative values for the various vessels. Combining the various factors as indicated by Eq. 3 gives the values of base moments M shown in Table 2.

Fig. 5 is a plot of observed average maximum bolt stretch versus computed stress using the base moment M and the gross area of the bolts. The dashed line in Fig. 5 represents an approximately average value of the various points and indicates only minor stretching that would result if the computed stresses are held in the neighborhood of the elastic limit. For computed stresses above the elastic limit, the observed stretch increases sharply.

Considering the assumptions made, the relation between the observed bolt stretch and the computed stress is striking. This relation provides ample evidence to warrant dynamic analysis when designing similar structures instead of using the same static factor for all. Allowable stresses, in this analysis, can approach the yield point when the maximum response expected is used, because all modes would not peak together. Maximum values for deflections, moments, and shears at any location along a uniform beam with various end conditions can be computed using this method.

Many additional records of strong shocks, particularly on various types of soils, are necessary in order to provide the engineer with spectra which can be assumed as reasonable maxima to be expected for any particular location.

CONCLUSIONS

In the future dynamic considerations will undoubtedly result in a more economical use of materials and members in tall structures by considering their action under actual predicted ground motions. However, present dynamic methods, even when applied to very simple structures, are extremely complicated for the average design office. Oversimplification of dynamic analysis when applied to buildings may result in dangerous errors due to the number of necessary assumptions which must be made.

Realistic lateral force factors and allowable stresses for buildings based on observed damage should not be discarded in favor of a pure dynamic analysis until more data are available.

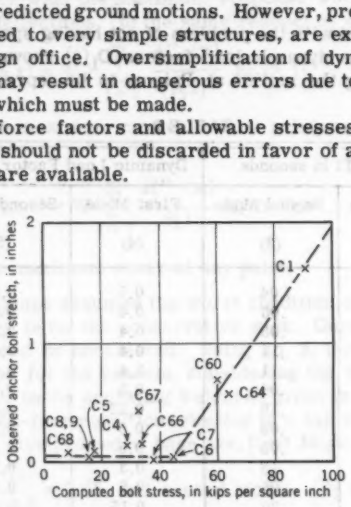


FIG. 5.—RELATIONSHIP OF COMPUTED STRESS TO BOLT STRETCH

Relatively simple structures, such as elevated tank towers, refinery vessels, stacks and simple framed towers can be investigated dynamically, using methods shown in this paper, to predict actual damage.

ACKNOWLEDGMENTS

Harold M. Engle, F. ASCE, Con. Structural Engr., and Karl V. Steinbrugge, F. ASCE, Structural Engr., Pacific Fire Rating Bureau, by virtue of their experience in seismic design and investigation of earthquake damage have offered valuable suggestions in the preparation of this paper.

C. Martin Duke, F. ASCE, Univ. of California at Los Angeles, contributed by reading the manuscript and offering valuable suggestions.

Vincent R. Bush, M. ASCE, and John D. B. Allison, M. ASCE, Structural Engrs for the Pacific Fire Rating Bureau, have also contributed by checking data and computations.

DISCUSSION

A. A. EREMIN,[13] M. ASCE.—The authors of this paper have made a valuable contribution by analyzing the stresses and damages in water tank towers and refining vessels caused by earthquake shocks in California. The stresses and strains computed with the assumed dynamic forces, according to the spectra in Fig. 1 are in close agreement with those which have caused damages in these structures. However, in the paper it was stated that "oversimplification of dynamic analysis *** may result in dangerous errors." The purpose of research has always been to find more exact interpretations and to reduce oversimplifications.

In California all structures located in the vicinity of fault lines are analyzed for the effect of earthquake shocks. Seismic stresses in bridges are computed with the assumed horizontal force V,[14] which is

$$V = C\,W \qquad \ldots\ldots\ldots\ldots\ldots\ldots\ldots\ldots (6)$$

in which W is the dead load weight of the structure and C is a coefficient equal to 0.02 for the rock foundation, 0.04 for a spread footing, and 0.06 for pile foundations. Force V acts in any direction and is applied at the centroid of the dead load weights.

Only minor damage to the anchor bolts in bridges have been reported during the earthquake shocks in California in the 1950's. However, it may be stated that improvement in the analysis of seismic forces in bridges may result in a more economical use of materials.

In a more exact analysis of seismic forces the spectra shown in Fig. 1 would perhaps include the effect of various foundation soil conditions. Furthermore, the dynamic stresses in water tank towers should consider impact forces caused by the mass of water in the tanks.

In refining vessels considerable effect on the stresses in the anchor bolts may be produced by transverse vibration of the circular section of the vessels.

Regarding increaded horizontal load coefficients in the lower water tank towers, the authors refer to the higher acceleration stresses at the 2% of damping. Similar effect on the stresses in water tank towers may also be explained by the higher vibration frequency in the lower towers.

Because examination of dynamic forces in structures is quite timely, the authors deserve praise for their paper.

DONALD F. MORAN,[15] and JAMES A. CHENEY,[16] MEMBERS, ASCE.—The authors are indebted to the discussion by Mr. Eremin. It is true that soil conditions should be considered when applying spectral response to any particular location. Unfortunately, little exact information is available on the effects of

---

[13] Assoc. Bridge Engr., Bridge Dept., Div. of Highways, State Dept. of Public Works, Sacramento, Calif.

[14] "Highway and Railroad Bridges," by A. A. Eremin, Sacramento, Calif., 1956.

[15] Chf. Structural Engr., Quinton Engrs., Ltd., Los Angeles, Calif.

[16] Head, XA Strength, Missile and Space Div., Lockheed Aircraft Corp., Sunnyvale, Calif.

various soil conditions on the spectra. This is due to the fact that accelerograph instruments are generally located on relatively good soils or rock.

Furthermore, soil conditions affect the periods of structures and consequently their response to a particular earthquake. Here again, little quantitative information is available.

Dynamic forces of water in elevated water tanks have been considered in vibration studies.[6] Close agreement was obtained between measured and computed periods when the tanks were nearly full, which is a critical condition for seismic loading. Also, a full condition usually exists for these tanks as they are generally used for fire protection purposes.

AMERICAN SOCIETY OF CIVIL ENGINEERS

Founded November 5, 1852

TRANSACTIONS

Paper No. 3032

HYDRAULIC PROBLEM SOLUTION ON ELECTRONIC COMPUTERS

By Edward A. Lawler[1] and Frank V. Druml[2]

SYNOPSIS

Applications on three types of electronic computers are presented demonstrating the wide range of problems readily solved by these modern tools. Tedious, cumbersome, conventional methods of solution are replaced by quicker and frequently more accurate methods, thus making more efficient use of the engineer for truly engineering problems.

INTRODUCTION

Economical use of electronic computers becomes justified only in those instances in which the problem solved falls into one of more of these categories: (a) complex problems not readily solvable by conventional methods, (b) repetitive problems, not necessarily complex, and (c) problems neither complex nor repetitive, but those in which even a small saving in time or personnel may be important. Group (a) may be problems such as the solution of simultaneous equations, group (b) problems such as unit hydrograph computations, and (c) flood routing problems in which predictions are used to determine the schedule of flood control projects.

The Ohio River Division of the Corps of Engineers has used three computers for the solution of hydraulic problems. Typical applications on each computer will be given. They represent in each case only a few of the problems solved readily by electronic computers.

Note.—Published, essentially as printed here, in January, 1958, in the Journal of the Waterways and Harbors Division, as Proceedings Paper 1515. Positions and titles given are those in effect when the paper was approved for publication in Transactions.

[1] Ohio River Div., Corps of Engrs., Cincinnati, Ohio.

[2] Louisville Dist., Corps of Engrs., Louisville, Ky.

APPLICATIONS

Univac I.—The Remington-Rand Univac I, a large high speed digital computer, although not the most modern, largest, or speediest machine available, may be considered representative of its class.

A program was established to formulate a method of solution for the partial differential equations[3] expressing the fundamental law of unsteady flow. The equations

$$H_x + \frac{V}{g} V_x + \frac{1}{g} V_t + \frac{V^2}{C^2 R} = 0 \quad \ldots\ldots\ldots\ldots \quad (1)$$

and

$$A V_x + V A_x + B H_t = 0 \quad \ldots\ldots\ldots\ldots\ldots \quad (2)$$

for solution by numerical methods may be written as

$$V_t + V V_x + g H_x = - G V|V| \quad \ldots\ldots\ldots\ldots \quad (3)$$

$$(V A)_x + B H_t = Q \quad \ldots\ldots\ldots\ldots\ldots \quad (4)$$

in which H denotes elevation of water surface, V represents velocity, A is the cross-sectional area of the stream, B denotes the surface width of the stream, G is a friction function, Q is equal to local inflow per unit length of the river, C is the Chézy Coefficient and g represents the acceleration of gravity. Subscripts t and x denote the derivative of the variable with respect to time and distance along the stream respectively. The friction function $G = \frac{gn^2}{(1.486)^2 R^{\frac{4}{3}}}$, in which n is Mannings n, and R is the hydraulic radius.

Replacing the derivatives by difference quotients transforms the equations into a system of difference equations. The integration of Eq. 3 and Eq. 4 can be performed if the coefficients A, B, G and Q (here including tributary inflow) are known and boundary conditions are established at end points.

Three problems were presented for solution: (a) movement of a flood wave in a river channel, (b) movement of a flood wave at the junction of two tributaries, and (c) movement of a flood wave in a long narrow reservoir. In general the same system of difference equations and method of solution was employed in all three problems.

The river channel chosen for the first problem was the 375 mi reach of the Ohio River from Wheeling, W. Va., to Cincinnati, Ohio. Coefficients A, B and G were computed empirically from available records and boundary conditions prescribed at Wheeling were observed stage and discharge data. Boundary conditions at Cincinnati were prescribed as a rating curve. Local runoff and tributary contribution as observed were assumed known. Reproduction of the 1945 flood hydrographs at key points on the Ohio appears in Fig. 1. For comparative purposes both observed and computed hydrographs are shown. Solution by the method of finite differences implies the determination of approximate solutions of the differential equations in a discrete net of points in an x, t plane. Use was made of a staggered net, wherein $2x = 10$ mi and $t = 9$ min. Solution time, excluding coding of basic data, editing of results and input and output time, is 30 min for each 24 hr period, or 6-3/4 hr for 13-1/2 days.

The junction chosen was the confluence of the Ohio and Mississippi Rivers at Cairo, Illinois. Boundary conditions were established at Metropolis, Illinois,

[3] "The Hydraulics of Flood Wave Movements in Rivers," by H. A. Thomas, Engineering Bulletin, Carnegie Inst. of Tech., 1934.

on the Ohio and Thebes, Illinois, on the Upper Mississippi, each approximately 40 mi above the confluence and at Hickman, Kentucky, on the Lower Mississippi approximately 40 mi below Cairo. During the computations certain equalities are requirements of the solution, such as: the sum of the flows from the Ohio Branch and the Mississippi Branch flowing into the junction must equal the flow out of the junction; at the junction, elevation in all three branches must be identical. Fig. 2 shows the routing of the January 1947 flood, observed and computed hydrographs being plotted. Computing time, excluding coding of basic data, time of input, output and editing, is approximately 3½ hr for 20 days.

The long narrow reservoir chosen in the example was Kentucky Reservoir on the Lower Tennessee River. The reservoir is 184 mi in length, extending

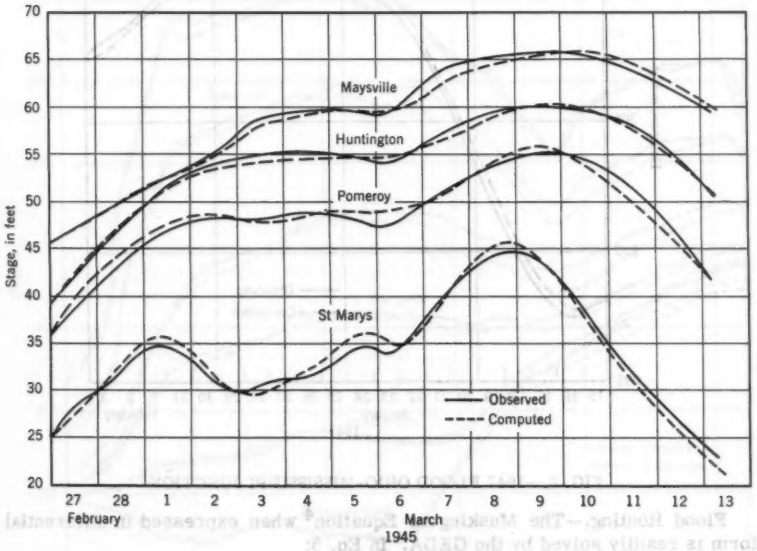


FIG. 1.—1945 FLOOD OHIO RIVER

from Kentucky Dam to Pickwick Landing Dam. Boundary conditions were established at both ends of the reservoir in terms of discharge because both inflow at head of the reservoir and outflow at the lower end are fully controlled. Local and tributary inflow were assumed known. The 1948 and 1950 floods were routed through the reservoir. Results of the 1950 routing are shown on Fig. 3, with observed data plotted for comparative purposes. The 1948 flood computations extended only until the date of February 1948, at which time the rate of change of elevation exceeded the limits of the method adopted. A modification in the method will eliminate this difficulty. Time of solution, again excluding coding time, time of input, output and editing, is approximately 12 min for each day, or 4 hr for 20 days.

Goodyear Electronic Differential Analyser.—The Goodyear Electronic Differential Analyser or "GEDA" is a high quality analyser or analog employing high gain operational amplifiers. Procured originally for flood routing problems, it has been used for the solution of other problems, several of which will be described.

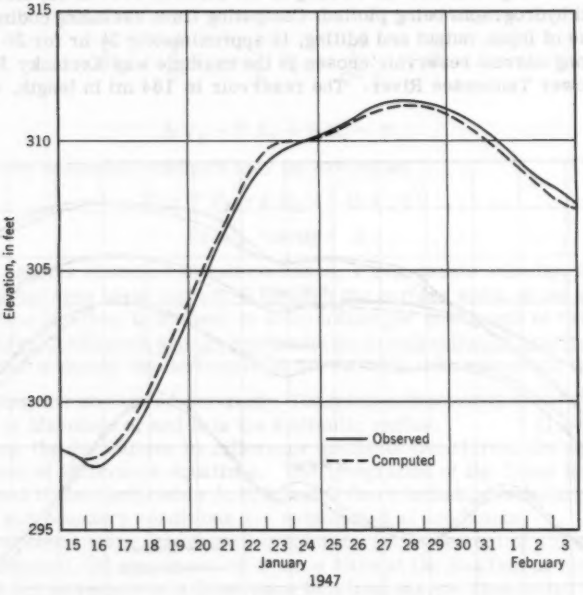


FIG. 2.—1947 FLOOD OHIO-MISSISSIPPI JUNCTION

Flood Routing.—The Muskingum Equation[4] when expressed in differential form is readily solved by the GEDA. In Eq. 5:

$$\frac{dO}{dt} = C_0 (I - O) - C_1 \frac{d\,I}{d\,t} \quad \ldots\ldots\ldots\ldots\ldots \quad (5)$$

I and O are instantaneous values of inflow and outflow and coefficients

$$C_0 = f_1 (O) = \frac{1}{K (1 - x)} \quad \ldots\ldots\ldots\ldots\ldots \quad (6)$$

$$C_1 = f_2 (O) = \frac{x}{1 - x} \quad \ldots\ldots\ldots\ldots\ldots \quad (7)$$

in which K and X, determined empirically, express the characteristics of prismatic and wedge storage respectively in a river channel as functions of outflow. In the solution by GEDA the known or predicted inflow hydrograph is

4 "Flood Control," Engineering Construction Text X-156, Engineer School, Corps of Engrs., U. S. Dept. of the Army, 1946, p. 151.

introduced into the computer by a curve follower. Coefficients C_0 and C_1 are developed by function generators from continuously computed values of outflow. Initial value of outflow is introduced as an initial condition. The computer continuously computes the rate of change of outflow and when integrated and recorded, results in a continuous hydrograph of outflow. The patch diagram, showing how the various computer components are interconnected to satisfy the equation, is shown in Fig. 4. Fig. 5(a) is a recording of the routing of the 1937 flood through the St. Marys-Pomeroy reach of the Ohio River. Total in-

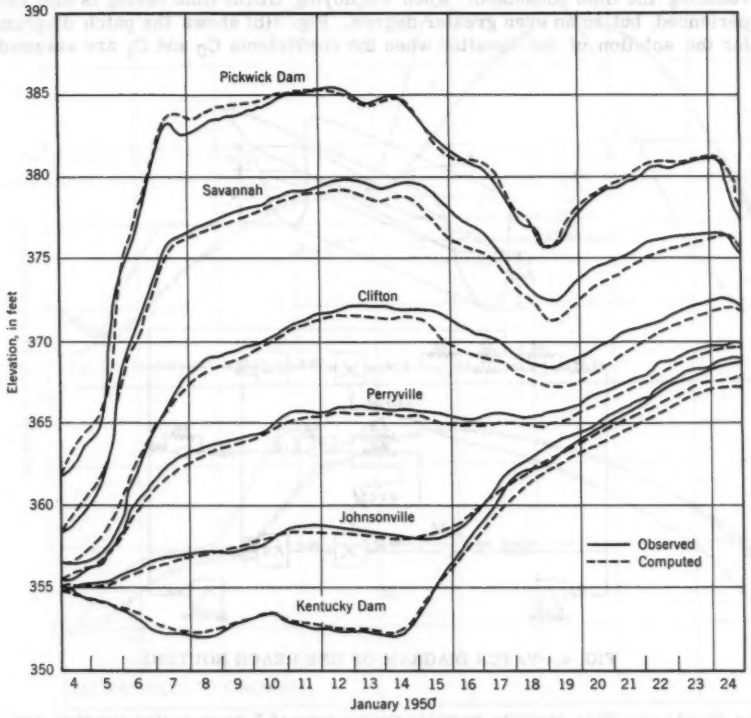


FIG. 3.—1950 FLOOD KENTUCKY DAM

flow into the reach, observed outflow, and arithmetical solution using finite time periods of one half day are also plotted for comparative purposes. Fig. 5(b) shows plottings for the 1937 flood through the Maysville-Cincinnati reach of the Ohio River. Fig. 6 is a plotting of the C_0 and C_1, functions of O for Ohio River from Wheeling to St. Marys.

Multiple reach routing can be accomplished by cascading. Because the outflow from the first reach becomes a portion of the inflow for the next reach, it is combined with the local and tributary inflow in the second reach by the

use of a second curve follower and a summing amplifier. Fig. 7(a) shows the patch diagram for two reaches. Time of solution may be varied considerably, depending on the time scale chosen. The time scale of 5 sec for 1 day has been found convenient. Time of solution for a 20 day flood, including setting of function generators, mounting of hydrographs, and so forth, is approximately 10 min. Computer running time is 100 sec and solution by conventional methods is about 2 hr.

Simplification of the equation is frequently feasible, with such simplification, when computations are made on desk computer or by slide rule, materially reducing the time consumed. When employing GEDA time saving is also experienced, but to an even greater degree. Fig. 7(b) shows the patch diagram for the solution of the equation when the coefficients C_0 and C_1 are assumed

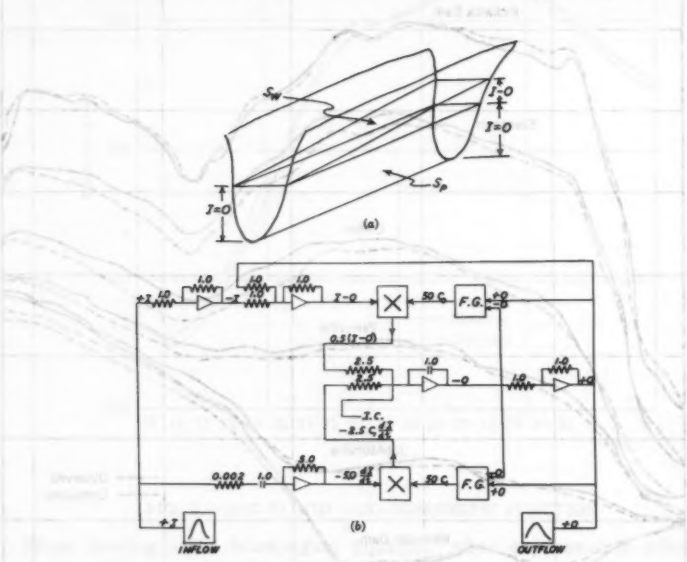


FIG. 4.—PATCH DIAGRAM OF ONE REACH ROUTING

as constants. This circuity permits the routing of 3 consecutive reaches concurrently. The time of solution, including mounting of charts, setting of coefficients etc., for a 20 day flood is approximately 5 min. Comparable time using conventional methods is approximately 3½ to 4 hr.

In determining the benefits resulting from regulation of floods by reservoirs, a choice of several methods is available. One method is to route the reductions, or the differences, plus and minus, between the natural and modified inflow hydrographs, and applying the routed reductions to the natural outflow hydrograph. Another method is to route the natural hydrograph and the modified hydrograph. Either of these methods can be employed on GEDA with ease. Fig. 7(c) shows the patch diagram for routing reservoir reductions thru 5 reaches, using 2 constant coefficients for each reach.

In certain studies the effects resulting from reservoir regulations are desired at a point several reaches below the initial inflow point. Fig. 7(d) shows a patch diagram for such a solution. Nine consecutive reaches are routed and the results may be recorded at any or all of the nine outflow points. This represents the circuit for routing the effects of the Pittsburgh District Reservoirs from Wheeling, W. Va. to Metropolis, Ill. near the mouth of the Ohio, a distance of almost 900 miles. Fig. 8 shows a typical recording. Reductions at

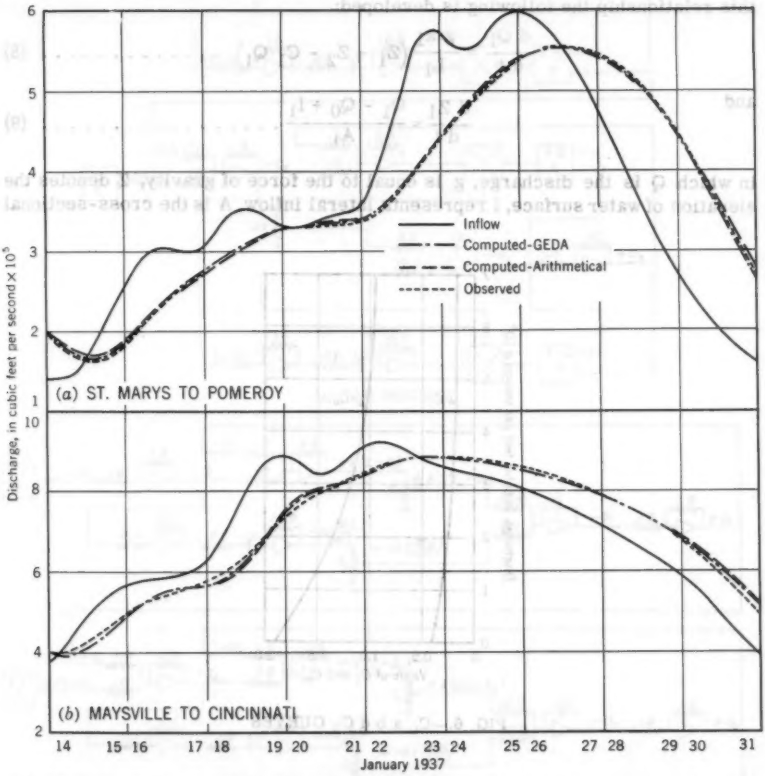


FIG. 5.—OHIO RIVER FLOOD ROUTING

Wheeling, W. Va. and all nine outflow points were recorded. Time of solution is approximately 10 min, computer running time for this flood of 40 days being 40 sec. Time required by conventional methods is not less than 8 hr.

Surges in Sewers.—At local protection projects, in which gravity flow in sewers is interrupted during flood periods and pumping is required, the surges resulting from modification of pump operation or power failure must be evaluated. Compatable surge range, sump and surge chambers must be determined,

particularly with respect to economic considerations. A typical system is shown in Fig. 9. Riser 1 is the pump sump and risers 2 to 5 surge chambers or storage areas in the system. Riser 6, shown as constant level reservoir, is the balance of the system, at such a distance as to have little or no effect on surges in the pump sump. I_2 to I_5 are lateral inflow points.

From the law of motion it can be shown that if an unbalanced head is applied to a mass of water of cross-sectional area a and length L the resulting change in velocity will be gh/L and rate of change of discharge will be gha/L. From this relationship the following is developed:

$$\frac{d\,Q_1}{d\,t} = \frac{g\,a_1}{L_1}\left(Z_1 - Z_2 - C_1\,Q_1\right) \quad \ldots\ldots\ldots\ldots \quad (8)$$

and

$$\frac{d\,Z_1}{d\,t} = \frac{Q_1 - Q_0 + I_1}{A_1} \quad \ldots\ldots\ldots\ldots\ldots\ldots \quad (9)$$

in which Q is the discharge, g is equal to the force of gravity, Z denotes the elevation of water surface, I represents lateral inflow, A is the cross-sectional

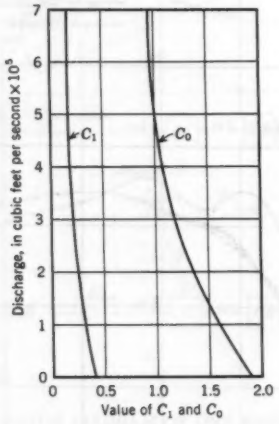
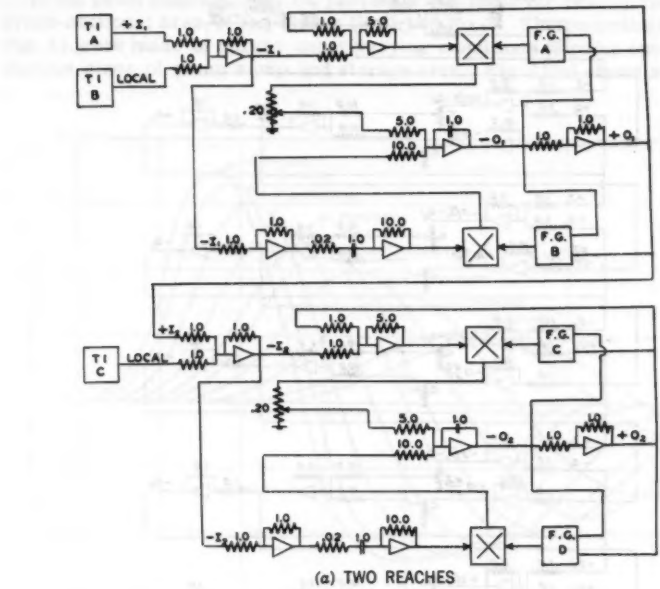


FIG. 6.—C_0 a b d C_1 CURVES

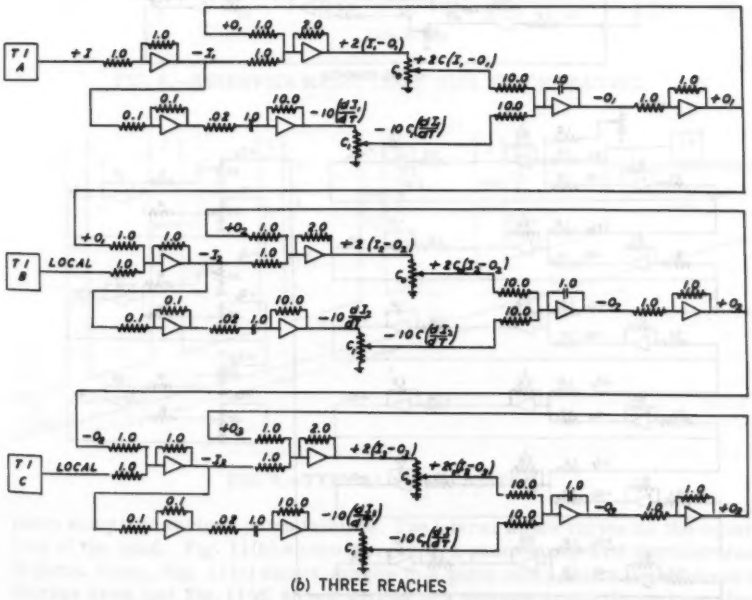
area of riser, a denotes the cross-sectional area of sewer, L represents the length of sewer section, and C is the hydraulic loss factor, defined such that CQ is total loss in sewer section.

Subscripts in equations refer to numbered sections. Pertinent data are given in Tables 1 and 2. In the solution the following assumptions were made:

1. Head loss in sewer sections varies linearly with rate of flow.
2. Lateral inflow varies as square root of head.
3. The section shown as constant level reservoir (Fig. 9) is the balance of the system at a distance greater than 24,415 ft from sump, and elevation is assumed to be constant. Elevation in this section is taken as reference datum.

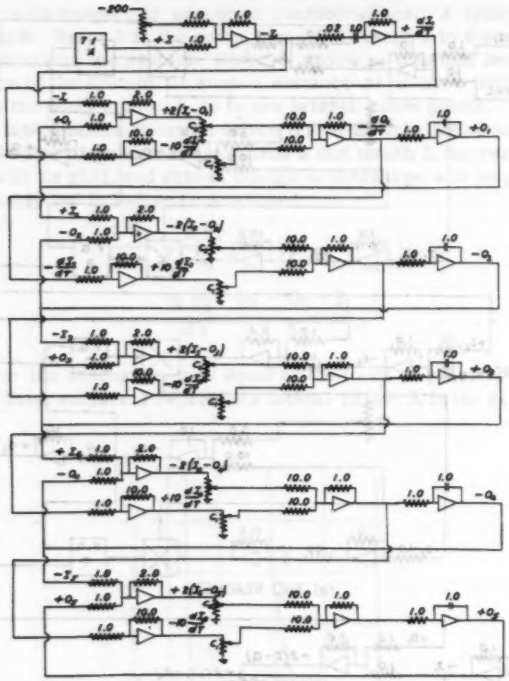


(a) TWO REACHES

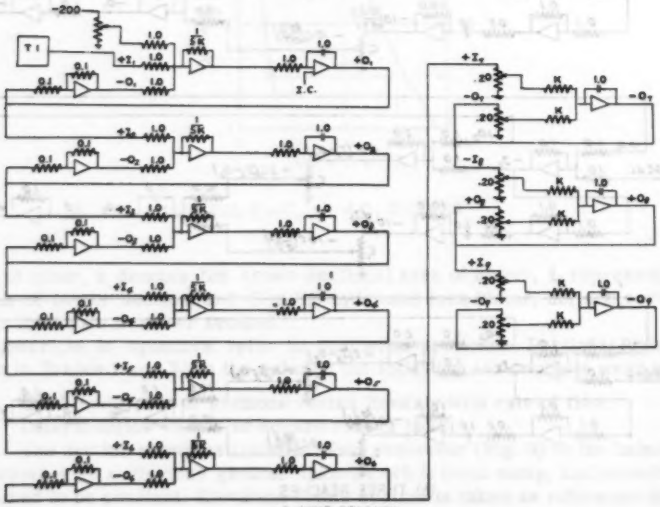


(b) THREE REACHES

FIG. 7(a,b).—PATCH DIAGRAMS FOR TWO, THREE, FIVE AND NINE REACH ROUTINGS



(c) FIVE REACHES



(d) NINE REACHES

FIG. 7(c,d).—PATCH DIAGRAMS FOR TWO, THREE, FIVE AND NINE REACH ROUTINGS

In the patch diagram, Fig. 10, provision was made for readily changing the cross-sectional area of the risers No. 1 and No. 2. The recordings shown in Fig. 11 were made of surges under varying conditions of pump operation and various sizes of pump sump and storage area. Fig. 11(a) shows surges in a

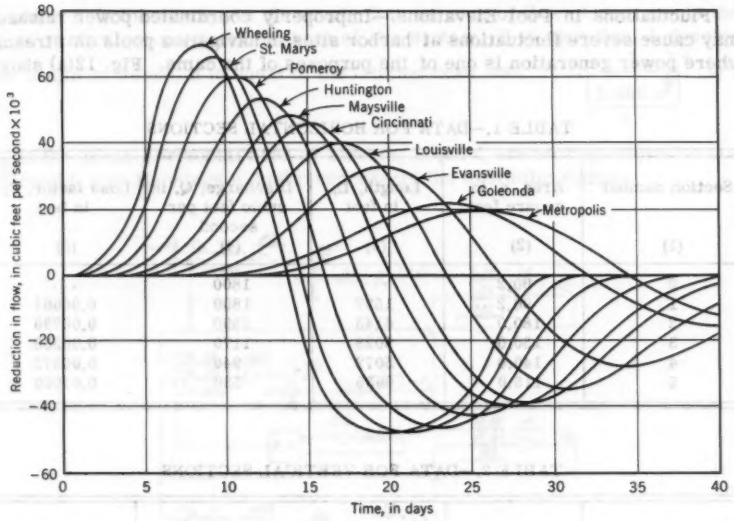


FIG. 8.—RESERVOIR REDUCTIONS, NINE REACH ROUTING.

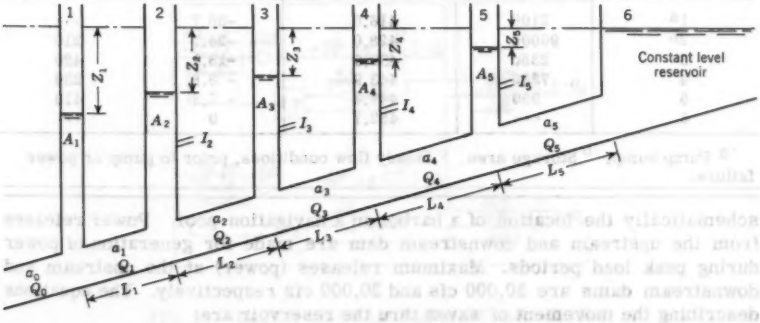


FIG. 9.—TYPICAL SEWER SYSTEM

pump sump with various pump failures. The lateral inflow varies as the square root of the head. Fig. 11(b) shows surges in a pump sump with various sizes of pump sump, Fig. 11(c) shows surges in a pump sump with various sizes of storage area, and Fig. 11(d) shows surges in a storage area with various sizes

of storage area. In Figs. 11(b), (c), and (d) surges were caused by complete failure.

The time scale chosen was 1 sec in solution equal to 10 sec in problem. Time of each recording of 800 sec was therefore 80 sec. It is conservatively estimated that the time saving, as compared to conventional methods, is in the order of 400 to 1.

Fluctuations in Pool Elevations.—Improperly coordinated power releases may cause severe fluctuations at harbor sites in navigation pools on streams where power generation is one of the purposes of the dams. Fig. 12(a) shows

TABLE 1.—DATA FOR HORIZONTAL SECTIONS

Section number (1)	Area, a, in square feet (2)	Length, L, in feet (3)	Discharge, Q, in cubic feet per second (4)	Loss factor, C, in feet (5)
0	90.2	...	1800	...
1	90.2	1537	1800	0.00667
2	180.0	6143	1590	0.00730
3	150.0	5028	1170	0.00368
4	140.0	5072	940	0.00372
5	115.0	6635	530	0.01000

TABLE 2.—DATA FOR VERTICAL SECTIONS

Riser number (1)	Area, A, in square feet (2)	Water surface elevation,[c] in feet above sea level (3)	Head, Z,[c] in feet (4)	Lateral inflow, I,[c] in cubic feet per second (5)
1[a]	2100	416.0	-36.7	...
2[b]	90000	428.0	-24.7	210
3	2350	439.6	-13.1	420
4	7350	443.9	- 8.8	230
5	350	447.4	- 5.3	410
6	...	452.7	0	...

[a] Pump sump. [b] Storage area. [c] Steady flow conditions, prior to pump or power failure.

schematically the location of a harbor in a navigation pool. Power releases from the upstream and downstream dam are made for generation of power during peak load periods. Maximum releases (power) at the upstream and downstream dams are 30,000 cfs and 20,000 cfs respectively. The equations describing the movement of waves thru the reservoir are:

$$\frac{d S_{1-2}}{d t} = Q_1 - Q_2 \quad \ldots\ldots\ldots\ldots\ldots\ldots (10)$$

$$\frac{d H_2}{d t} = \frac{Q_1 - Q_3}{A_{h\,1-3}} \quad \ldots\ldots\ldots\ldots\ldots\ldots (11)$$

$$\frac{d\,Q_2}{d\,t} = \frac{g\,A_2}{L_2}\,(H_1 - H_3 - h_2) \quad \ldots\ldots\ldots\ldots\ldots\ldots (12)$$

and

$$\frac{H_1 + H_2}{2} = B\,S_{1-2} + C \quad \ldots\ldots\ldots\ldots\ldots\ldots (13)$$

in which S is the storage in the reach; Q is the rate of flow; A represents the mean vertical cross-sectional area of the stream; H is elevation, L denotes the length of reach, h is equal to the friction head loss $= L\left(\frac{1}{\frac{1.486\ r^{\frac{2}{3}}}{n}}\right)^2 Q^2$;

A_h is the mean horizontal area of stream; B and C are storage elevation coefficients; n is Mannings n; and r represents the hydraulic radius.

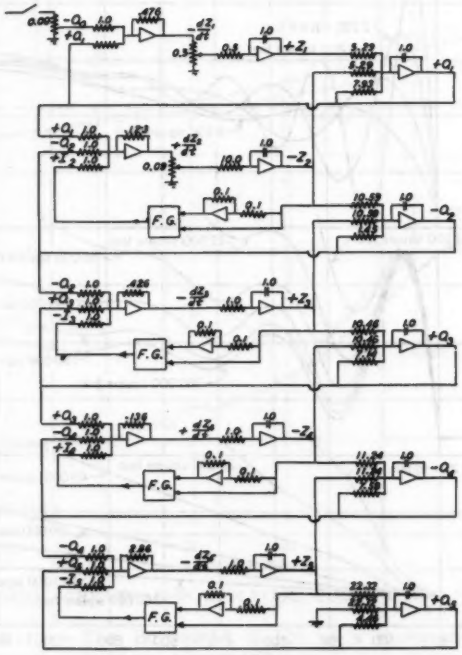


FIG. 10.—PATCH DIAGRAM FOR A SEWER SYSTEM

Subscripts relate to the sections under consideration. Boundary conditions of discharge are known or assumed. The patch diagram is given in Fig. 12(b).

Trial runs were made with various schedules of release covering the range normally anticipated. The fluctuations at the harbor site resulting from each

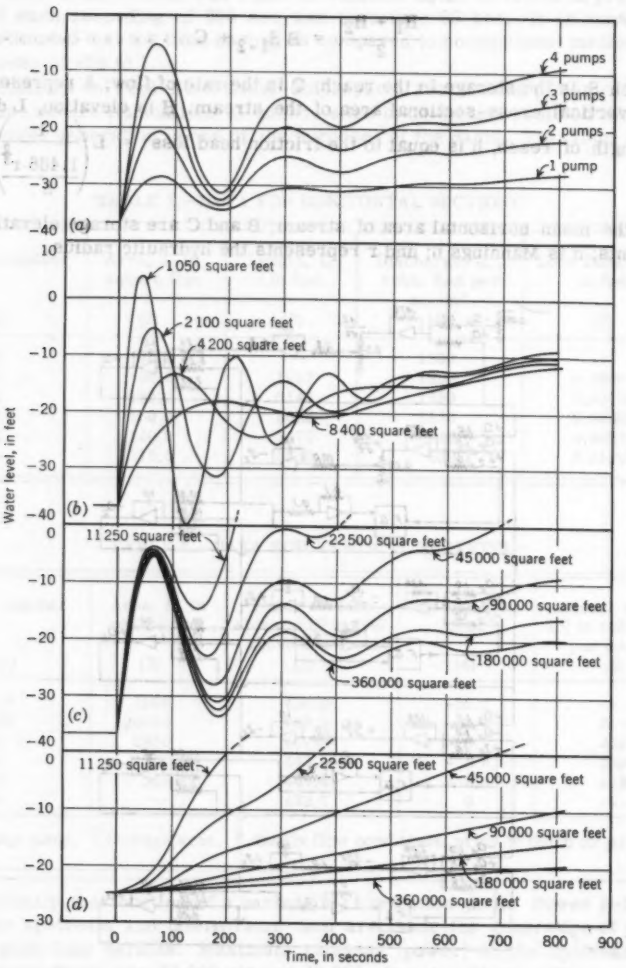


FIG. 11.—SOLUTION OF SEWER SYSTEM SURGES

schedule was recorded. Fig. 13 shows the recordings, the number associated with each being the schedule listed in Table 3. It is estimated that the time saving ratio between GEDA solution and conventional methods is approximately 100 to 1. Limitations in components required certain simplifying assumptions and limited the number of sections to five. Additional components would produce solutions on which a greater degree of confidence could be placed. However, it is believed that the results obtained are quite indicative.

Among the additional problems that have been solved on the Ohio River Division by the GEDA are the analysis of siphon air vents and the analysis of fluctuation hydro power surge chambers.

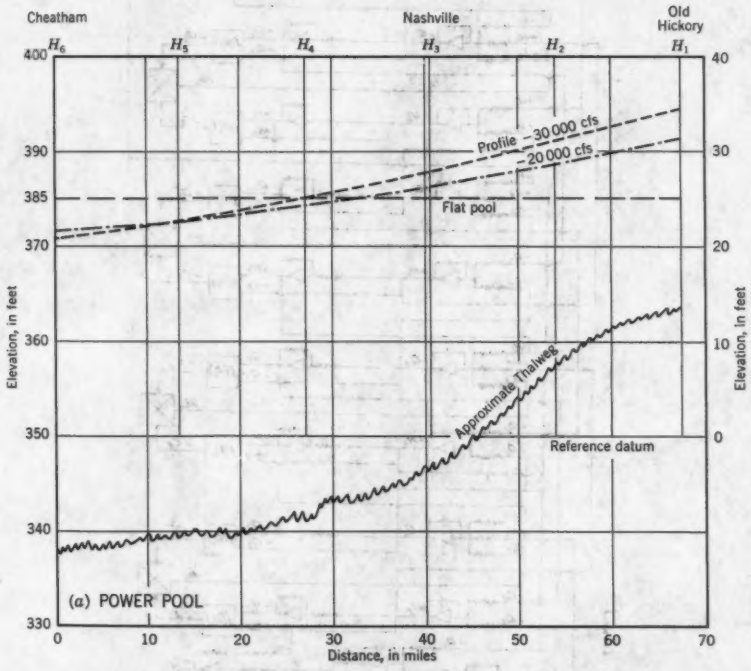
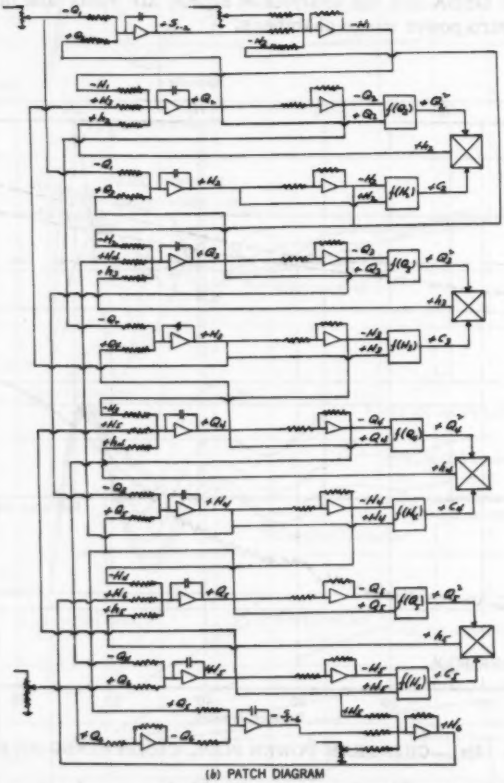


FIG. 12(a).—CHEATHAM POWER POOL, CUMBERLAND RIVER

Burroughs E-101.—The Burroughs E-101 is a moderate speed, small size digital computer. Data are entered by means of an eleven digit keyboard, similar to a desk computer, or by paper tape. The computer is externally programed by means of 8 pinboards, each having 16 instructions. One hundred words of memory are provided on a magnetic drum, each word consisting of 12 decimal digits plus sign. Printed output is on 16 in. 10 column paper, in accordance with any desired format. Tape input and output is obtainable as an optional accessory as is also an expanded memory of 120 additional words. Procured primarily for unit hydrograph computations this computer is being used for solution of a widely expanding range of problems.

Unit Hydrograph Computations.—In connection with determining the flows from historical storm patterns, in place or transposed, computations must begin with rainfall data. The unit hydrograph[5,6] describes the time distribution of flow from a given drainage area resulting from an effective rainfall of one inch for some unit of time duration. Expressed in terms of flow, the ordinates when applied to successive storm rainfalls produce the flows resulting from those rainfall amounts. The number of ordinates may vary from as few as 4



(b) PATCH DIAGRAM

FIG. 12(b).—CHEATHAM POWER POOL, CUMBERLAND RIVER

or 5 to as many as 30 or more, depending upon the drainage characteristics of the area. It is readily seen that determining flows for a storm or combination of storms having numerous rainfall periods will require many arithmetical operations.

5 "Stream Flow from Rainfall by the Unit Graph Method," by L. K. Sherman, Engineering News Record, Vol. 108, 1932, pp. 501–505.

6 "Synthetic Unit Graphs," by F. F. Snyder, Transactions, Am. Geophysical Union, Vol. 19, Part I, 1938, pp. 447–454.

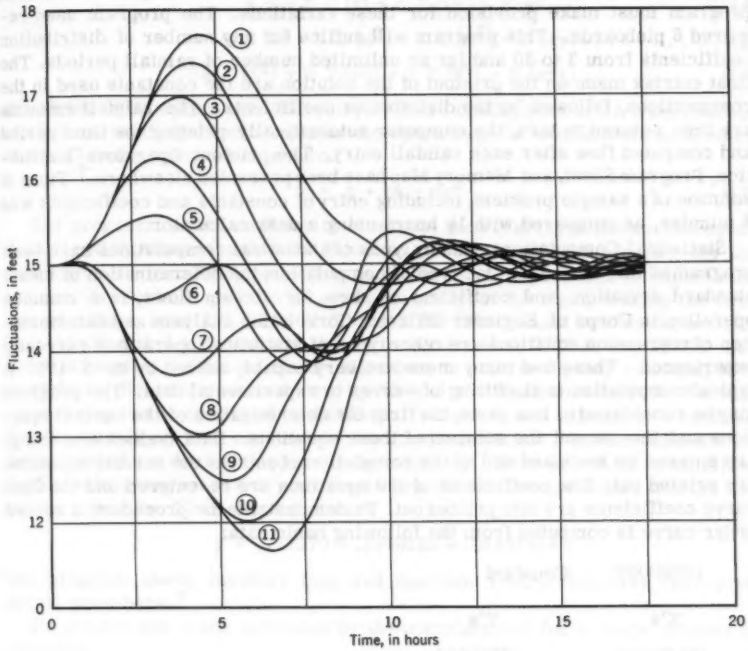


FIG. 13.—POWER POOL FLUCTUATIONS.

TABLE 3.—DATA IN FIG. 13

Curve Number (1)	Hours of Release	
	Old Hickory (2)	Cheatham (3)
1	0 - 4	4 - 10
2	0 - 4	5 - 9
3	0 - 4	2 - 8
4	0 - 4	1 - 7
5	0 - 4	0 - 6
6	1 - 5	0 - 6
7	2 - 6	0 - 6
8	3 - 7	0 - 6
9	4 - 8	0 - 6
10	5 - 9	0 - 6
11	6 - 10	0 - 6

Since the number of rainfall periods and the number of ordinates (in the program called distribution coefficients) vary over wide ranges an efficient program must make provision for these variations. The program used required 6 pinboards. This program will suffice for any number of distribution coefficients from 3 to 30 and for an unlimited number of rainfall periods. The first entries made on the printout of the solution are the constants used in the computations, followed by the distribution coefficients. The rainfall amounts are then entered in turn, the computer automatically printing the time period and computed flow after each rainfall entry. The printout Operators Instruction, Program Sheet, and Memory Map have been presented elsewhere.[7] Time of solution of a sample problem, including entry of constants and coefficients was 6 minutes, as compared with 1½ hours using a desk calculator.

Statistical Computations.—Many types of statistical computations have been programed for the E-101. One type of computation, the determination of mean, standard deviation, and coefficient of skew for stream flows, is a common operation in Corps of Engineer Offices. Correlation analysis and determination of regression equations are other types of statistical operations currently experienced. These and many more are very capably solved by the E-101. A typical computation is the fitting of curves to experimental data. The program may be considered in two parts, the first the determination of the normal equations and the second the solution of these equations. Data (values of x and y) are entered by keyboard and at the completion of entries the normal equations are printed out. The coefficients of the equations are re-entered and the final curve coefficients are then printed out. To demonstrate the procedure a second order curve is computed from the following basic data:

10000000	Constant
X's	Y's
00000000	7370000
10000000	5720000
20000000	4900000
30000000	4450000
40000000	4220000
50000000	4140000
60000000	4100000

a's	b's	c's	d's
70000000	210000000	910000000	34900000
210000000	910000000	4410000000	91050000
910000000	4410000000	22750000000	383990000

Rationalized

a's	b's	c's	d's
70000000	210000000	910000000	34900000-
21000000	91000000	441000000	9105000-
9100000	44100000	227500000	3839900-
717370128	135817828-	14511904	
a	b	c	

[7] "Hydraulic Problem Solution on Electronic Computers," by E. A. Lawler and F. V. Druml, Proceedings Paper 1515, ASCE, January, 1958, pp. 30–33.

The coefficients for the normal equations

$$a\,N + b\,\Sigma\,(x) + c\,\Sigma\,(x^2) = \Sigma\,(y) \quad \ldots\ldots\ldots\ldots (14)$$

$$a\,\Sigma\,(x) + b\,\Sigma\,(x^2) + c\,\Sigma\,(x^3) = \Sigma\,(xy) \quad \ldots\ldots\ldots\ldots (15)$$

$$a\,\Sigma\,(x^2) + b\,\Sigma\,(x^3) + c\,\Sigma\,(x^4) = \Sigma\,(x^2y) \quad \ldots\ldots\ldots\ldots (16)$$

are shown in this print out. Re-entry of these coefficients after transposition of right term of equation completes the operation, the coefficients a, b, and c of Eq. 17 being print out as shown.

$$y = c + bx + ax^2 \quad \ldots\ldots\ldots\ldots\ldots\ldots (17)$$

The program could be written to eliminate the re-entry of the normal equations for simultaneous solution. However, to obtain greater accuracy for the final curve a normalizing procedure is followed. For purposes of explanation assume the decimal point to be seven places from the right, making the first row of values read 7.0, 21.0, 91.0, and 3.49. The second row would be 21.0, 91.0, 441.0, and 9.105, and the third row 91.0, 441.0, 2275.0, and 38.39. Because it is permissable to divide all values in any row by any constant, it is feasible to divide the second row by 10 and the third row by 100. Further normalizing can be employed by dividing all values in any column by a constant and then applying that constant to the final coefficient. In this instance the latter procedure does not appear to be indicated. Re-entry of the normalized coefficients by keyboard entry accomplishes the final computations and the coefficients for Eq. 17 as printed out are

$$y = .717370 - .135818x + .014512x^2$$

The program sheet, memory map and operator instruction have been presented elsewhere.[8]

Programs are made available by the manufacturer for a large number of problems.

CONCLUSIONS

Electronic computers, large or small, analog or digital, now quite generally available, are usable tools. Their accuracy, speed and computing capabilities allow engineers to evaluate more complex relationships and to eliminate tedious highly repetitive operations. The engineer of the future should recognize the value and employ the capabilities of these modern-day tools.

---

[8] "Hydraulic Problem Solution on Electronic Computers," by E. A. Lawler and F. V. Druml, Proceedings Paper 1515, ASCE, January, 1958, pp. 36–38.

AMERICAN SOCIETY OF CIVIL ENGINEERS

Founded November 5, 1852

TRANSACTIONS

Paper No. 3033

CONTAINMENT SPHERE FOR DRESDEN STATION

By Leonard P. Zick,[1] M. ASCE, James T. Dunn,[2] A. M. ASCE, and James B. Maher[3]

SYNOPSIS

The unusual problems encountered in fabricating and erecting a self-supporting leak-tight spherical pressure vessel 190 ft in diameter are presented. Special features that make this 29.5-psig pressure vessel usable as a containment housing around a nuclear power plant include a dual support system, access locks, and unusual shell penetrations.

INTRODUCTION

Design considerations for the Dresden Nuclear Power Station determined that a 190-ft-diam steel, spherical pressure vessel most nearly met the many factors that had to be considered in providing containment for this particular nuclear reactor and associated auxiliaries. Extensive studies[4] were made by others before deciding on this type of shell and determining the design pressure conditions on it.

The specifications required that the subcontractor be entirely responsible for the design, procurement, fabrication, erection, inspection, and testing of the spherical pressure enclosure and its appurtenances, so as to meet the specifications and to produce a vessel of the highest integrity, suitable in every way for containing all gases and vapors under the following conditions:

1. The spherical pressure enclosure is to house a nuclear reactor and miscellaneous appurtenances of a 180,000-kw nuclear power plant.[5] It will nor-

Note.—Published essentially as printed here, in April, 1958, in the Journal of the Power Division, as Proceedings Paper 1601. Positions and titles given are those in effect when the paper was approved for publication in Transactions.

[1] Research Engr., Chicago Bridge and Iron Co., Chicago, Ill.

[2] Civ. Engr., Chicago Bridge and Iron Co., Philadelphia, Pa.

[3] Mech. Engr., Chicago Bridge and Iron Co., Chicago, Ill.

[4] "The Dresden Nuclear Power Station," by Wolcott, et al, Paper No. 56-A-169, ASME.

[5] "Design Features of the Dresden Nuclear Power Station," by J. E. Love, C. S. Darrow, and B. H. Randolph, Transactions, ASCE, Vol. 124, 1959, pp. 617-632.

mally not be under internal pressure. In the case of certain accidents or malfunction of the power plant, the structure will be subjected to an internal pressure and a coincident internal temperature rise. Due to the great potential hazard to the environs from radioactive material the highest degree of integrity is demanded of the spherical pressure enclosure throughout the entire life of the plant. All portions and details subject to vessel pressure will have at least as great a margin of safety as the structure as a whole.

2. The spherical enclosure will be based on design conditions as follows:

a. Design internal pressure is to be 29.5 psig accompanied by a design temperature rise of 250° F.

b. The large-diameter, relatively thin spherical enclosure is to be self-supporting and capable of safely resisting all dead and live loads, and in addition should be capable of resisting a minimum external pressure of 1 psig, together with the effect of all dead loads.

This paper deals with the designing, fabricating, erecting, and testing of this 190-ft-diam, self-supporting, leak-tight sphere. The operating conditions for the spherical enclosure are similar to those of existing power plant buildings, except that the sphere must always be ready to act as a pressure vessel. During operation, access for personnel and equipment into the sphere is provided by three locks so arranged that one door is always sealed.

SPHERICAL SHELL

The specifications require that this spherical pressure vessel meet the ASME Boiler and Pressure Vessel Code, latest edition, including addenda and Code Cases: Section II, Material Specifications; Section VIII, Unfired Pressure Vessels; and Section IX, Welding Qualifications. The specifications were written before the Code was modified to precisely cover this unusual type of pressure vessel. Since that time pertinent code cases have been passed that now make it possible to stamp this vessel.

Case No. 1224-1 defines this type of vessel: "*Containment Vessels* are those outer vessels which enclose the reactor vessel or portions of the primary coolant circuit or both. The containment vessels are not normally pressurized and are built to contain the lethal radioactive substance that may be released in case of an accident or failure of the reactor vessel or the primary coolant circuit or both."

Case No. 1226-3 recognizes the fact that this type of vessel cannot usually be stress-relieved after completion, as required by Section VIII for vessels containing lethal substances. This case provides alternatives in lieu of stress-relief of the completed vessel:

1. The plates and forgings must conform to specifications A300 and A350, respectively. These and other materials and the construction must meet certain impact test requirements. Keyhole Charpy values of at least 15 ft-lb at a testing temperature of minus 50° F are required.

2. All doors, nozzles, and opening frames must be preassembled into shell plates and stress-relieved as complete assemblies for butt-welding into the shell.

3. Special consideration must be given to make the design of the reinforcement for large openings (over 40 inches in diam for this vessel diameter) as strong as the shell.

4. Butt-welds in shells thicker than 1 1/4 in. must be preheated to 200° F during welding, and welds thicker than 1 1/2 in. require stress-relief.

5. Shell joints must be double welded butt-joints and must be fully radiographed. All welds, such as those around nozzles and opening frames, that cannot be radiographed must be examined for cracks by the magnetic particle or the fluid penetrant method of inspection.

6. Mandatory corrosion allowance in the code for air, steam, or water service does not apply to containment vessels. This vessel can be maintained or protected like other steel buildings.

Case No. 1235 recognizes the hazardous character of the material that might be released and specifies that pressure relief devices are not required.

Fig. 1 shows features of the sphere. The dimensions of these features are as follows: the head of the upper hemisphere consists of three plates, 1.25 in. thick; course a contains thirty plates, 1.25 in. thick; course b contains forty-

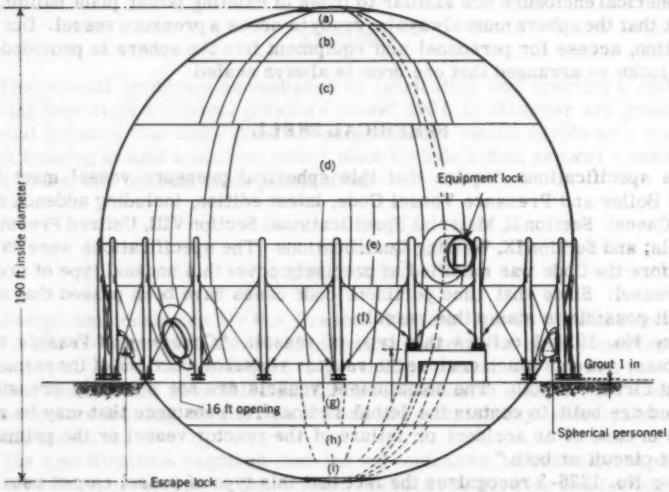


FIG. 1.—ELEVATION VIEW OF SPHERE

two plates, 1.25 in. thick; course c contains fifty-four plates, 1.27 in. thick; course d contains sixty plates, 1.28 in. thick; course e, at the equator, contains sixty plates, 1.31 in. thick; course f contains sixty plates, 1.36 in. thick; course g contains fifty-four plates, 1.40 in. thick; course h contains forty-two plates 1.25 in. thick; course i contains thirty plates, 1.27 in. thick and the head of the lower hemisphere consists of three plates, 1.27 in. thick. The twenty columns are 24 5/8 in. diameter by 5/16 in. thick for the long columns, and 24 5/8 in. diameter by 3/8 in. thick for the short columns.

The sphere is supported entirely on the columns without any internal or external bracing during the first pressure test. For this condition the plate thicknesses in the bottom hemisphere could be approximately the same thickness as their counterparts in the upper hemisphere. However, after satisfactory completion of the first tests the lower part of the sphere will be embedded.

Note that the plate thicknesses increase from 1.25 in. at the top to 1.40 in. for the course at the embedment. These thicknesses are determined by combining the internal pressure stress with the stress due to dead and live loads.

Usually, the maximum membrane stress is tension in the circumferential direction. If the sphere is cut on a horizontal plane, the stress on the cut edge due to dead loads is compression. In a sphere, these compressive stresses are balanced by tension stresses in the circumferential direction. After embedment, the internal pressure causes the sphere to rise at the equator, thus relieving the load on the columns, and transferring the entire weight to the spherical shell.

The supports and dead loads are such that the upper 1 1/4-in.-thick plates govern the ability of the sphere to resist external pressure. The code rules indicate that a 1 1/4-in.-thick sphere with a 95-ft radius could safely resist a working external pressure of slightly more than 2 psig. Deducting the effect of the dead loads, including the weight of the structure, leaves slightly less than 1 1/2 psig allowable external pressure. This exceeds the specification requirement of 1 psig.

TABLE 1.—MEMBRANE STRESSES

Type of Load	Stresses in Pounds per Square Inch	
	Circumferential	Meridianal
Internal Pressure (29.5 psig)	12,000	12,000
Dead Load	1,250	-1,050
Combined Load	13,250	10,950
110 mile per hour wind (leeward side)	100	-100
3.3% Earthquake factor (leeward side)	50	-50

During erection, this thin, self-supporting shell is very limber and requires special support. Once the sphere is completed and embedded in its permanent foundation, it becomes very stable against wind or earthquake forces. The stresses caused by the dead and live loads and by natural forces, such as wind, snow, and earthquakes, are small because of the shell thickness required to resist the pressure stresses. Table 1 gives a summary of the membrane stresses immediately above grade in a 1.40-in. shell.

When combined, as required by the specifications, the maximum membrane stress at all points is less than the code allowable of 13,500 psi. This allowable is based upon a 60,000-psi minimum tensile strength steel. A factor of safety of four is used to obtain a stress value of 15,000 psi, and this is further reduced by multiplying by 90% as required by the code for 100% radiographed joints.

FABRICATION

The steel plates used for the shell and all other pressure parts meet ASTM Specifications A201 Grade B Firebox Quality and are heat-treated (normalized)

to ASTM A300 specifications, with keyhole Charpy impact tests taken at minus 50° F. The stress in a sphere under pressure is nearly uniform and the transverse Charpy values will be lower than the longitudinal. Therefore, three impact specimens are taken transverse to the direction of rolling for each plate as rolled. If the average of these tests is less than 15 ft-lb, the plate will be rejected.

Where plate material cannot be used, equivalent material in the pipe, tube, or forging specifications will be used. Heat-treated plates were available only from mills in the eastern United States. Because of this, the fabrication of the heat-treated steel, that represents more than 95% of the tonnage, was done in Greenville, Pa. The fabrication of the tower, ladders, and other equipment, A283 Grade C and A7 steel not requiring heat treatment, was done in Chicago, Ill.

Great care is exercised in the fabrication of the plates used in the construction of the sphere. The plates are gaged and carefully inspected for laminations and surface defects. Wherever possible, defects are repaired using careful procedures approved by the inspector, or, if this is not possible or practical, the plates are rejected. The plates are formed using a hydraulic press. All plates are treated by a pickling process, which consists of immersing the plates in baths of sulphuric acid, wash water, and phosphoric acid. The plates, except for the surface immediately adjacent to the edges prepared for welding, are given a shop coat of paint immediately after pickling. Because mill scale seems to be a special problem with thick normalized plates, considerable time is spent removing it from the plates.

Nearly all of the shell penetrations and all of the column stubs are shop welded to shell plate sections. The same careful welding procedures that are used in field erection are used also in the shop. Each of these shell plates, that involves having other parts welded to it, is thermally stress-relieved in a shop furnace.

The three locks are completely assembled in the shop. Two of these locks are welded into complete units that include the adjacent shell and its reinforcement. The completed units are shipped in one piece to the field. Because the third lock is larger it is welded into four separate sections. These are shipped individually to the field, for final assembly.

SUPPORTS

The sphere is supported during erection by twenty 24-in. diam tubular columns braced by diagonal rods. The columns are supported by individual concrete piers resting on sandstone. The lower column sections are erected first, and are followed by erection of the equator plates that have column stubs attached to every third plate (Fig. 2).

Two columns are shorter than the others because of a concrete shielding tunnel surrounding the main steam lines. These two columns are supported by the tunnel, and are slightly heavier than the others because they carry the load of the equipment lock located midway between them. These columns are designed to carry 417 kips dead load plus 62 kips from an assumed wind load of 110 mph. During the overload air test, an additional load of 29 kips is imposed on each column by the 580,000 lbs of air that are pumped into the vessel. The long columns are designed to carry 348 kips dead load plus 62 kips wind load. They also support an additional 29 kips during the air test.

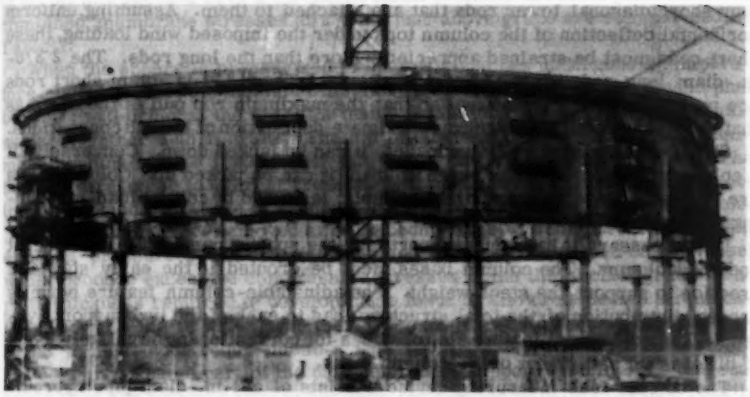


FIG. 2.—EQUATOR COURSE ON TUBULAR COLUMNS

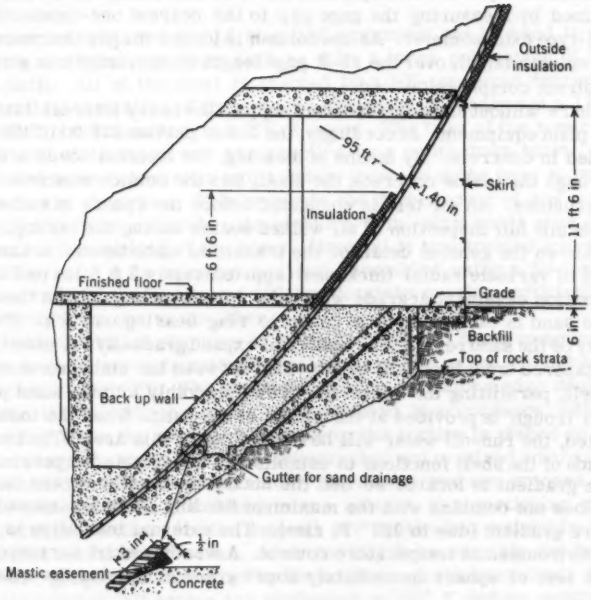


FIG. 3.—TRANSITION EMBEDMENT AT GRADE

Having two short columns requires special consideration in designing the four short diagonal tower rods that are attached to them. Assuming uniform horizontal deflection of the column tops under the imposed wind loading, these short rods must be strained appreciably more than the long rods. The 2 3/8-in.-diam long rods are made of A7 material. The 1 3/4-in.-diam short rods are made of high strength steel so that the maximum rod pull is the same as that of the long rods, permitting approximate duplication of the end connections.

Should a column become overloaded, it can be jacked down. Conversely, if a column is not carrying its share of load, it can be jacked up. Column loads are evaluated by indicators on the hydraulic jacks and by column load-measuring devices.

It is necessary to have dual supports for the sphere, namely the embedment and the columns. The column bases must be grouted in the early stages of erection to support the steel weight. The adjustable-column feature permits proper distribution of the total structure load to each of the two support systems. The adjustment feature also provides for correction in the unlikely event of differential settlement of the column piers.

The column load-measuring device consists of a 2-in.-diam pipe approximately 19 ft long fixed to the column at the top end, and free but guided at the bottom. A stainless steel stud is attached to the bottom end of the pipe and a similar stud is attached directly below it to a bracket on the column. A gage gap of approximately 6 3/8 in. separates the two. The change in the gage length is determined by measuring the gage gap to the nearest one-thousandth inch with a dial-type extensometer. As the column is loaded the gap decreases. The change in column length over the 19-ft gage length is converted into stress and then into direct compression load.

The sphere without embedment cannot support the heavy internal loads from the power plant equipment. Accordingly, the lower portion (39 ft) of the sphere is embedded in concrete. By means of bearing, the internal loads are transferred through the inside concrete, the shell, and the outside concrete into the rock substructure. An air test is conducted before the sphere is embedded in order to permit full inspection of all welded seams during the testing.

Fig. 3 shows the general detail of the transition embedment. A sand pad 8 ft deep and of variable radial thickness (approximately 2 ft 6 in. to 4 ft) provides transition easement at grade where the sphere emerges from the embedment. The sand is backed up by a concrete ring bearing on rock. The compressibility of the sand permits the sphere to expand gradually. A mastic easement or a tapered transition will be provided between the embedment concrete and the shell, permitting the vessel to "grow" smoothly into the sand pad.

A drain trough is provided at the bottom of the sand. When the installation is completed, the run-off water will be flashed out of this area. The insulation on the inside of the shell functions to establish an acceptable temperature gradient. The gradient is located so that the maximum bending stress caused by pressure does not combine with the maximum bending stresses caused by the temperature gradient (due to 250° F. rise). The external insulation is principally for environmental temperature control. A weather skirt surrounding the 12 vertical feet of sphere immediately above grade completes the outside insulation.

The theoretical radial growth of the sphere due to 29.5-psig internal pressure is 0.33 in. and a 250° F temperature rise increases this to 2.24 in. Realization of this growth confirms the need for special embedment considerations at grade. The restraint at grade is similar to the restraint of the bottom

of an oil storage tank or of a circumferential stiffener around a penstock. The combined membrane stresses at a joint just above grade are summarized in Table 1.

When the sphere is pressurized to 29.5 psig and has undergone a temperature rise of 250° F, the maximum meridianal combined stress (membrane plus bending) will occur at the top of the inside insulation (21,250 psi on the outside surface) rather than at grade. The top of the insulation is the point of maximum bending stress (±9,655 psi) due to the 250° F temperature rise. The bending stress due to internal pressure is a maximum (±2,260 psi) at the bottom of the sand pad where the bending stress due to temperature is negligible.

If the columns were removed after embedment, as was considered, the 1-psig external pressure requirement superimposed on the dead load of the vessel would produce excessive compressive stresses in the thin shell at grade. The plate thickness required to develop these loads at allowable design stress exceeded 1 1/2 in., in which case the welded seams would require field stress-relief to meet code requirements. This would be impractical, and therefore the columns became part of the dual permanent support system. The diagonal tower rods are removed after embedment because the structure can then readily develop the lateral shear loads.

FIELD ERECTION

Whereas a certain amount of standard equipment can be used to advantage in erecting a special structure such as this, a large percentage of it must be custom-built. All of the steel is erected by a 100-ton guyed derrick, located on the vertical centerline of the sphere. The derrick consists of a 170-ft mast and a 135-ft boom mounted on a 210-ft tower. The base of the tower was 40 ft below grade. Hoisting power was supplied by a multi-drum hoist. The four-post derrick tower converges into a double trunnion at the base to provide end rotation in any direction. This prevents the development of any end moment that might otherwise exist when the eight 2 1/4-in.-diam cable guys are developing the horizontal load of the boom. Material is transported into an assembly yard by rail. It is unloaded and sub-assembled using a 50-ton derrick. The boom radii of the 50-ton and 100-ton derricks overlap sufficiently to pass lifts directly from one to the other.

Several individual shell plates as large as 10 ft by 35 ft and weighing as much as 10 tons each, are automatically welded together on the ground and hoisted into place in a single lift. The automatic welding is performed on double acting, adjustable tables. All the seams are preheated in accordance with code requirements. When the welding is complete, the section is placed on a stationary table where the welds are 100% radiographed and repaired where necessary. The automatic welding is performed by the submerged arc process. After the multiple-plate sections are fitted to one another in a particular course, the joints between sections (radial seams) are double-butt welded by hand using the shielded metal-arc process. After welding from one side, the back side is carbon-arc gouged and inspected by the magnetic particle method. As with the automatic welding, all seams are preheated to 250° F before welding is done, and the completed weld is 100% radiographed. Erection is performed from the equator to the bottom and then from the equator to the top. The horizontal welds between courses (girth seams) are also hand-welded. All hand welds are made using low hydrogen electrodes.

To assure the vessel being built to a truly spherical contour, the equator course is held round by a spider ring supported off the derrick tower. The subsequent courses, erected below the equator, are suspended back to the tower by hangers of predetermined length. During erection, the partly completed upper hemisphere has a tendency to lay in from its own dead weight and may be further pushed inward by wind loading. The courses above the equator are, therefore, supported from the tower by hogged booms of predetermined length.

This dimensional control and periodic tape checks insure that the vessel will be built to a constant spherical radius. The code states that the inner surface of this vessel shall not deviate from the specified shape by more than 1.25% of the inside diameter. This gives a permissible "out of roundness" of 28.5 in., which is several times greater than that anticipated. To control local shell contour, the specifications require checking the curvature with a 15-ft template. When this template is entirely on a single plate and no closer than 12 in. to a welded seam, the permissible deviation of the plate from the template is 0.50 in. When the template is placed across one or more welded seams the deviation shall not exceed 1.00 in., after allowance for any weld reinforcement.

There are 492 individual shell plates in the sphere and approximately 17,200 ft (3 1/4 miles) of welded seam. The geometric volume is 3,600,000 cu ft and the surface area is 113,400 sq ft (2 1/2 acres). The completed vessel weighs approximately 3,500 tons.

The required stress-relief of penetration weldments is performed in the shop on all but the 16-ft diameter equipment opening. The 26-ft-7-in. over-all diameter of this weldment precludes built-up shipment, and thus requires a special field stress-relieving furnace. The complete assembly, including the cover, was heated to 1150° F minimum for a holding time of three hours and then cooled down at a prescribed rate.

PENETRATIONS

There are a total of 132 permanent shell penetrations ranging in size from 1/2 in. to 16 ft in diameter. Various connecting lines between equipment inside of the sphere and the power plant buildings pass through these penetrations. Expansion joints are installed in certain connecting lines to provide flexibility and to reduce loads on the sphere resulting from movements of the piping.

All corner welds joining necks to the shell and reinforcing plates are full fusion welds. The detail of a typical penetration weld is shown in Fig. 4. At least one end of each penetration is prepared for welding to the connecting line or expansion joint. The connecting welds are made after the sphere has passed the first test. Temporary test covers are used to blank off these penetrations during the first air test.

Three of the major penetrations are air locks. The largest and most difficult opening to provide was the 16-ft-diam permanent bolted opening. It is centered approximately 17.5 ft above grade so that it does not complicate the stress pattern at grade. All of the penetrations are purposely located outside the area just above and below grade. Considerable thought was given as to how the 16-ft-diam opening could best be provided. The problem was resolved into four basic phases. These were: Design of the shell reinforcement and cover to satisfy code material and stress-relief requirements of the code; procurement of special materials; development of the gasket, seal weld, and bolting details; and development of an inside cover handling device. Fig. 5 shows the

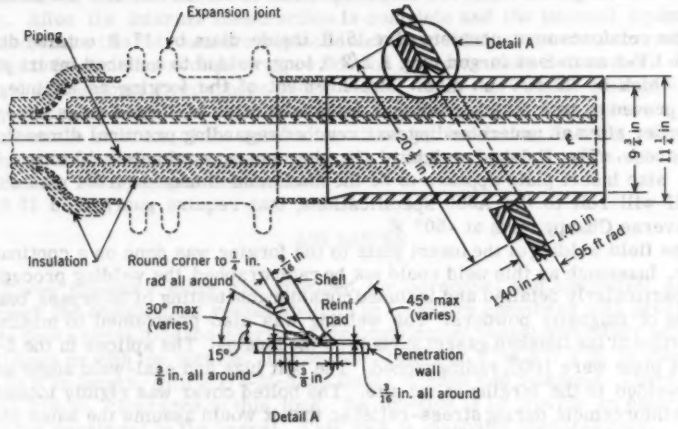


FIG. 4.—TYPICAL PENETRATION DETAIL

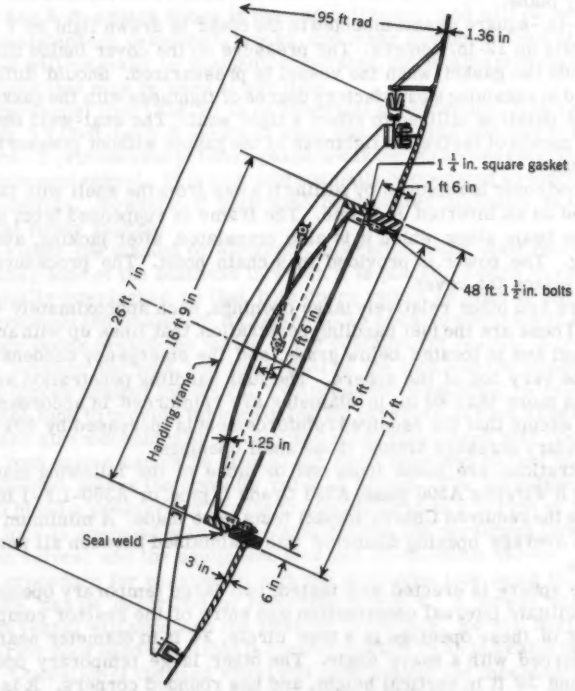


FIG. 5.—SECTION THROUGH 16-FT-DIAMETER OPENING

general arrangment of the reinforcement, the bolted cover, and the handling device.

The reinforcement consists of a 16-ft inside diam by 17-ft outside diam. A350-LF-1 seamless forged ring 1 1/2 ft long, welded to a dished insert plate 3-in.-thick-by-26-ft-7-in. diam. Procurement of the forging as an integral ring proved to be a major problem. A manufacturer of forged rings accepted the order after an understanding was reached regarding practical dimensional tolerances. The finished weight of the ring was approximately 10 tons. The 3-in. size insert plate appears to be the maximum thickness A201 plates that a mill will roll to the A300 specifications, that require guaranteed 15 ft-lb transverse Charpy tests at -50° F.

The field welding of the insert plate to the forging was done on a continuous basis. Inasmuch as this weld could not be radiographed, the welding procedure was particularly detailed and included considerable testing of interpass beads, by use of magnetic powders. The welding was also programed to minimize distortion of the finished gasket surface on the forging. The splices in the 3-in. insert plate were 100% radiographed. The bolt lugs and seal-weld angle were also welded to the forging at the site. The bolted cover was rigidly locked to the reinforcement during stress-relief so that it would assume the same plane as the ring should the ring distort. The completed reinforcement weldment and cover were satisfactorily field stress-relieved and the gasket faces remained remarkably plane.

A 1 1/4-in.-square gasket mounted in the cover is drawn tight by 1 1/2-in.-diam eyebolts on 12-in. centers. The pressure on the cover inside the sphere further loads the gasket when the vessel is pressurized. Should difficulty be experienced in obtaining a satisfactory degree of tightness with the gasket alone, a seal-weld detail is utilized to effect a tight seal. The seal-weld detail also provides a means of testing the tightness of the gasket without pressurizing the entire sphere.

The bolted cover is removed by pulling it away from the shell with jacks that are mounted on an inverted A-frame. The frame is suspended from an overhead trolley beam along which it is also translated, after jacking, away from the opening. The power is provided by a chain hoist. The procedure is reversed to replace the cover.

There are two other relatively large openings, each approximately 40 in. in diameter. These are the fuel handling penetration, that lines up with an underground tunnel and is located below grade, and the emergency condenser vent, that is at the very top of the sphere. The fuel handling penetration and other penetrations more than 40 in. in diameter are reinforced in accordance with code rules, except that the required reinforcement is increased by 40% to minimize secondary stresses around these shell openings.

All penetrations are made from one or more of the following materials: A201 Grade B Firebox A300 plate, A333 Grade C pipe, or A350-LF-1 forgings. In each case the required Charpy impact tests were made. A minimum spacing of twice the average opening diameter was maintained between all permanent penetrations.

After the sphere is erected and tested, two large temporary openings will be cut to facilitate internal construction and entry of the reactor components. The smaller of these openings is a true circle, 24 ft in diameter near grade, and is reinforced with a heavy angle. The other large temporary opening is 22 ft wide and 29 ft in vertical height, and has rounded corners. It is also at grade and is reinforced completely along all edges. This opening is cut after

embedment, whereas the 24-ft-diam opening is cut immediately after the first test. After the internal construction is complete and the internal equipment placed, these two cut-outs are replaced and their reinforcements removed.

Scaffold attachment clips are provided on approximately 8-ft centers on the inside of the upper hemisphere of the vessel. Also, an outside stairway from the equipment lock to the top of the sphere is provided. Various studs are provided on the exterior of the sphere for attaching insulation, flashing, and drain troughs among other appurtenances. All attachment-welds to the sphere are made with low hydrogen electrodes.

AIR LOCKS

Three pressure locks are provided for personnel and equipment access through the containment vessel shell. The locks are chambers with pressure-tight doors connecting the interior of the containment vessel with either adjacent buildings or with the outside. The escape lock (Fig. 6) is 4 ft 9 in. in diameter by 10 ft in length, with 2 1/2-ft-diam doors in each end bulkhead. There is 8-ft-11 3/4-in. clearance in this lock. Its function is to provide an emergency exit for personnel in the vessel. This lock is manually operated only.

The equipment lock (Fig. 7) varies in diameter from 11 ft at the center to 12 ft at the interior to 14 ft at the exterior, and provides 29 ft 1/2-in. clearance. It has 8-ft-square doors in the end bulkheads, and will be used for passage of maintenance personnel, trucks, and other equipment into or out of the vessel. It will normally be pushbutton operated, but is also provided with manual controls that may be used at any time.

The personnel lock (Fig. 8) is of spherical construction. It is 12 ft in diameter with 2 1/2-ft-by-6-ft doors in each end bulkhead and has 8-ft-2 1/4-in. clearance. It provides the primary passageway for personnel entering or leaving the containment vessel. This lock will normally be operated by electrical push-button controls. However, it may also be operated manually in the event of electrical power failure.

With either the manual or electrical operation, each door can be operated from either side of the bulkhead in which it is placed. Doors in each lock are mechanically interlocked so that both doors cannot be open at the same time. In the personnel and equipment locks, the doors are also electrically interlocked. Each door opens toward the inside of the containment vessel. A pressure difference between the lock and the vessel or the lock and the atmosphere, will produce forces against the doors. Two pressure-equalizing valves are installed in each lock to provide for equalizing the pressure across either door. The valves are also mechanically interlocked and synchronized with door operation so that both valves cannot be open at the same time and so that one door cannot be opened unless the opposite valve is closed. The plug-type valves are sized to bleed a pressure of 20 psig to atmospheric in a period of 15 sec. The escape lock is equipped with 2-in.-diam valves, the personnel lock has 2 1/2-in.-diam valves; and the equipment lock has 10-in.-diam valves.

The procedure for passing through the personnel lock using the hand wheel operators, can be described by referring to Fig. 8. A person wishing to exit from the vessel will approach the interior of the lock. He will begin to operate the interior door hand wheel that is clearly marked by an indicator in contrasting colors. Operation of the hand wheel will first engage the mechanical interlock. This mechanism locks the hand wheels that control the opposite or exterior

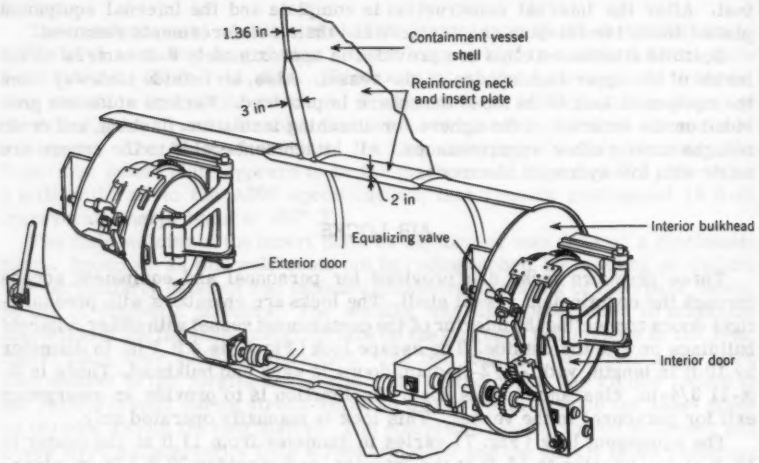


FIG. 6.—ESCAPE LOCK

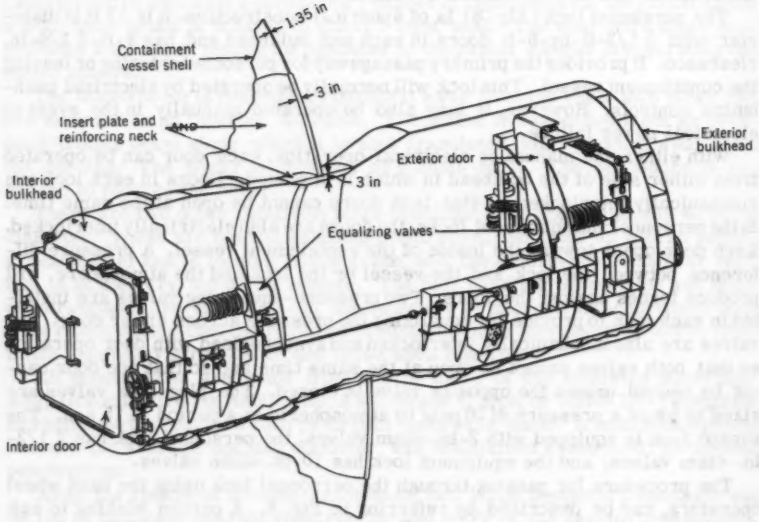


FIG. 7.—EQUIPMENT LOCK

door. Thus, from this time until the interior door and valve are again sealed, the exterior door and valve are locked in the pressure-tight position. As the hand wheel is rotated, the interior equalizing valve is opened. This equalizes the pressure in the lock with that in the vessel. Further rotation of the hand wheel will perform the third function, that is, the unseating of the door from its gasket. The door is mechanically pushed out a sufficient distance to provide a space between the door tongue and the rubber gasket. This space furnishes an additional means of pressure equalization across the door. The final operation accomplished by continuous rotation of the hand wheel is the opening of the door. Because the door is free-wheeling, one can either pull the door open by the handle on the door, or swing the door remotely with the hand wheel.

Before gaining access to the adjacent building, one must close the interior door after passing into the lock, pass through the lock, and open the exterior

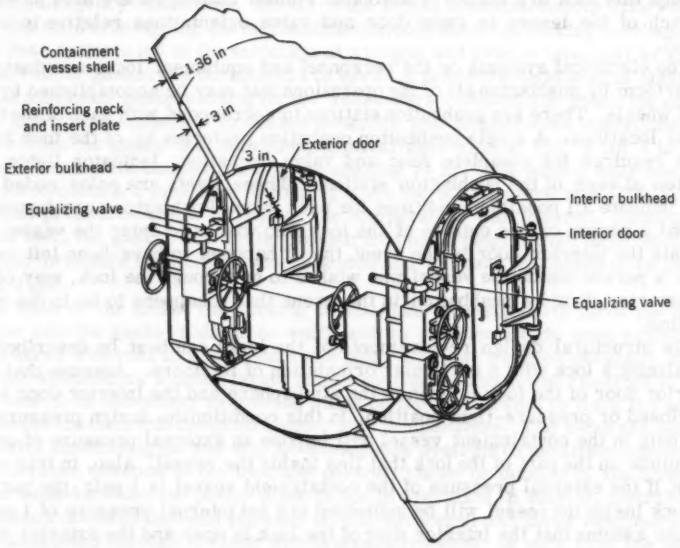


FIG. 8.—PERSONNEL LOCK

door. Operation of the interior door hand wheel inside the lock will reverse the four steps described previously. The interior door and equalizing valve will be in the fully closed and sealed position before the interlock is returned to the position at which the exterior door hand wheels are unlocked.

If the exterior door were inadvertently left in the open position, the interlock would be engaged. Thus, the interior door hand wheels could not be operated. However, it will be noted that two hand wheels are provided on the vessel side of the interior bulkhead. The extra hand wheel is provided for emergency and will perform the four operations on the exterior door. If the exterior door is open at a time at which quick exit from the containment vessel is necessary, it can be swung shut on its hinges, the door and valve sealed, and the

interlock returned to a position that will allow operation of the interior door. This feature protects personnel in the vessel against the possibility of being locked in. Entering the vessel through the lock involves the same operation.

The escape lock and the equipment lock have the same features of interlocking, equalizing valve and door seating, and door swinging as the personnel lock, with one exception. The hand wheel operation on the equipment lock is provided by an electric motor drive rather than by swinging the door on its hinges. The door is free-wheeling and can also be swung by hand. The additional hand wheel on the vessel side of the interior bulkhead for remote operation of the exterior door is not provided on the equipment lock.

Pointer indicators at each hand wheel on the two large locks, indicate the various positions of the doors and equalizing valves. In the escape lock, each hand lever is swung through a total arc of 120° to perform all four operating functions on one door. A person can perform all functions necessary to pass through this lock in a matter of seconds. Pointer indicators are also provided on each of the levers to show door and valve orientations relative to lever travel.

The electrical systems on the personnel and equipment locks are designed to perform by pushbutton all of the operations that may be accomplished by the hand wheels. There are pushbutton stations to correspond with each of the hand wheel locations. A single pushbutton operation performs all of the four functions required for complete door and valve operation. Indicator lights are located at each of the pushbutton stations. These lights are color coded and they indicate all possible conditions for each door. Pushbuttons are furnished so that a person on the outside of the lock who wishes to enter the vessel can operate the interior door in the event that it happens to have been left open. Also, a person inside the vessel who wishes to go through the lock, may close the exterior door by pushbutton in the event that it happens to be in the open position.

The structural design requirements of the locks can best be described by visualizing a lock with a particular orientation of its doors. Assume that the exterior door of the lock is open to the atmosphere and the interior door is in the closed or pressure-tight position. In this condition the design pressure of 29.5 psig in the containment vessel will impose an external pressure of equal magnitude on the part of the lock that lies inside the vessel. Also, in this condition, if the external pressure of the containment vessel is 1 psig, the part of the lock inside the vessel will be subjected to a net internal pressure of 1 psig.

Also assume that the interior door of the lock is open and the exterior door is in the closed or pressure-tight position. In this case, that part of the lock lying outside the containment vessel will be subjected to the same pressure as may exist in the containment vessel itself. The various design pressures described in these conditions produce membrane and bending stresses in the lock's shells, doors, and end bulkheads. Certain stresses resulting from dead and live loads in the lock are superimposed on stresses due to pressure alone.

Each lock is supported entirely by the containment vessel shell. The parts of the lock that lie inside and outside the vessel are cantilevered from the part actually built into the shell. To insert the lock assembly in the containment-vessel shell, it is necessary to cut large holes in the shell plates. These cut-outs are reinforced to maintain the continuity of membrane action in the shell. The reinforcing is also designed to distribute the lock's dead and live loads over a large area of vessel shell.

The advantage of having the doors swing open toward the inside of the vessel is that the design pressure of 29.5 psig will furnish a gasket-seating force on either the interior door or the exterior door if the pressure is allowed to build up in the lock. The sealing mechanism is not required to hold the door in a pressure-tight position against the high-pressure load. This provides an additional safety feature and lessens the mechanical advantage requirement of the mechanism. The door-locking mechanism is designed to hold the door in a pressure tight position against a pressure of 2 psig. With both doors in the sealed position, and when pressure in the vessel is atmospheric, the lock may be pressurized to an internal pressure of 2 psig.

The principal requirement for the locking mechanism and the seal is that it must be possible to obtain a pressure-tight seal with a minimum of manual handle effort in the shortest possible time. Operation of levers or hand wheels must be simple and quick in order to minimize possibility of confusion or delay in emergency conditions. On all of the locks, a manual handle effort of 20 lbs was used in designing the mechanical components of the locking mechanism.

These criteria led to the selection of a tongue and groove type seal in which a soft rubber gasket (40 durometer) is used. A pressure-tight seal is obtained with a minimum gasket seating force. Tests were conducted in which the actual seal detail was subjected to design pressure and temperature conditions. In these tests the gasket and surrounding metal were held at 350° F for 4 hr and cooled to ambient temperature in the ensuing 24 hr. The gasket seal was required to contain a pressure of 37 psig when the temperature was 350° F, and various pressures below 37 psig as the temperature was lowered. Subsequent to the test, the gasket was again pressurized to 37 psig. Seven days later the 37 psig pressure application was repeated and the seal was found to be pressure-tight.

In each of the locks, the locking mechanism is designed to force the door tongue into the gasket a distance sufficient to produce a tight seal against an internal or external lock pressure of 2 psig. Because a higher pressure in the vessel will produce a much larger gasket seating load than that required to seal the door, it is necessary to provide stops on the door frame to limit the penetration of the door into the gasket under high temperature. The locks are equipped with electric lights and will have telephone systems to facilitate conversation between persons in the lock and persons inside or outside of the containment vessel. When the power plant is not in operation, it may be desirable to have both doors in the open position so that personnel and large equipment can be transported through the lock with comparative ease. In each lock, the interlock can be violated so that it is possible to have both doors open simultaneously. Special tools and procedures are required, so that the interlock can be violated only by specific authorization of the plant management.

The live load used in the design of the floor plate in the personnel lock is 100 psf. The spherical or multisphere construction principal used in this lock has economic and design advantages over a cylindrical lock. This is because the lock is located in the shell at a considerable distance below the equator of the sphere. The included angle between the horizontal axis of the lock and a radial line drawn through the shell at the lock is approximately 24°. The intersection of a spherical lock with the spherical vessel is a circle. The circular cutout, with its reinforcing detail, provides a scheme that can be fabricated more accurately and that provides a more uniform stress distribution than would exist for an elliptical cutout required for a cylinder of the same diameter.

The floor in the equipment lock is designed to support truck wheel loads of 10 tons per axle with the truck axles being 10 ft apart. The outside dimensions of the door are greater than the frame in the bulkheads. Removable floor sections are provided in the area immediately in front of the exterior door and because the truck will pass through the lock at infrequent intervals, the removable floor sections can be stored and installed only when necessary. There is a sub-floor under the removable sections that makes it possible to use the lock and operate the exterior door in the normal manner, except when transferring the truck through the lock.

It is extremely unlikely that, under any operating conditions, the truck will be in the equipment lock coincident with the application of design pressures. For this reason, the net stresses that result in a combination of stresses produced by the heavy truck loads with stresses produced by design pressures, are not required to be within the code allowable stresses.

INSPECTION AND TESTING

When it was evident that the ASME through its Boiler and Pressure Vessel Code, had decided on code cases that permitted the building and stamping of this type of vessel to Code requirements, insurance inspectors were hired to follow the work both in the shop and in the field. All of the hand welds are inspected at least four different times. The butt welds are inspected using magnetic particle inspection after arc-air gouging the back side of the first side welded. The completed butt weld is fully radiographed. It is inspected with soapsuds both before and after the overload test. All of the corner and fillet welds that cannot be radiographed are inspected using the magnetic particle method after, and in some cases during welding. These welds are also tested using soapsuds both before and after the overload test and, in addition, are inspected again using the magnetic particle method after the overload test.

Because the vessel is not capable of supporting a hydrostatic test, the standard pneumatic test specified by the code of 1 1/4 times the working pressure will be applied to the vessel. After the vessel has been erected on the 20 tubular columns, the lower part is held at least 2 1/2 ft above the rock excavation. The first pneumatic test is made while the vessel is supported in this manner so that the entire shell can be inspected.

All welds and seals will be inspected for leaks using a soap bubble test while the sphere is under a pneumatic pressure of 5 psig. The test is started with the inner door of each of the locks closed and the outer doors open. After inspecting the inner bulkhead and doors, the outer doors are closed. Then the locks are pressurized and the outer bulkheads, doors and the shell of the lock are inspected for leaks. If no leaks are found the pressure will be raised to 37 psig and then lowered to the design pressure of 29.5 psig. The soap bubble inspection is then repeated, during which time any increase in pressure due to an atmospheric increase in temperature will be bled off so that the design pressure is not exceeded. Because of the potential risk involved, no one is allowed on or near the sphere during the overload test. With the pressure at approximately the design pressure, a leakage rate test will be conducted over a 48-hr period. After this holding time, the air is released and the welded openings are inspected both inside and outside using magnetic particle inspection.

After cutting the temporary openings, no work is done on the spherical pressure vessel until the internal equipment has been installed. When this work is

completed, the temporary openings are rewelded and these seams are inspected to the same degree as the original shell seams.

Although the loads on the structure will normally be small during operation of the Dresden Nuclear Power Station, the column load measuring devices will be available to provide a check on the uniformity of the column loads and the elevation of the equator as a check on the remote possibility of unequal settlement. The locks will be tested to 2 psig and inspected using soapsuds in the shop. This tightness test may be used periodically to check the lock door seals and bulkhead connections without necessitating the pressurization of the entire vessel.

CONCLUSIONS

Careful design and planning make it possible to fabricate, erect and test a self-supporting, leak-tight spherical containment enclosure as large as 190 ft in diameter.

A dual support system is advantageous because it permits easy erection and inspection and after embedment provides for carrying extremely heavy internal loads direct to the foundation.

Ready access and escape for personnel (and equipment) is provided through locks that maintain the integrity of the containment philosophy.

Both permanent and temporary penetrations are required and both require careful attention to insure their integrity.

AMERICAN SOCIETY OF CIVIL ENGINEERS

Founded November 5, 1852

TRANSACTIONS

Paper No. 3034

WELDED PIPELINE BRANCH CONNECTIONS

By Everett C. Rodabaugh[1] and Henry H. George[2]

SYNOPSIS

Pipeline branch connections are designed on an empirical basis because no suitable theoretical analysis is available. Code requirements, loadings, and field failures are described. Test data on pressure and external loadings, both static and cyclic, are presented.

INTRODUCTION

When an opening is cut into a pipe, the uniform distribution of stress under pressure is interrupted. The resulting stresses around the opening are significantly higher than those in uncut pipe. Accordingly, when this opening is made for branch connection, reinforcement is required to obtain strength equal to that of the uncut pipe and to provide for external loadings that may be imposed through the branch pipe.

As yet (1958) there is no theoretical analysis for the strength of pipeline branch connections, the problem being extremely complex due not only to the shape of the structure but also due to the presence of four independent variables—the diameters and thicknesses of the run and branch pipes. Consideration of laterals adds another variable, the lateral angle. Accordingly, the design of branch connections is based entirely on empirical rules derived from experience and tests. The empirical rules generally used for the reinforcement of fabricated branch connections in pipelines are given by the American

Note.—Published, essentially as printed here, in March, 1957, in the Journal of the Pipeline Division as Proceedings Paper 1193. Positions and titles given are those in effect when the paper was approved for publication in Transactions.

[1] Sr. Research Engr., Tube Turns, a Division of National Cylinder Gas Co., Louisville, Ky.

[2] Mgr. of Research Sect., Tube Turns, a Division of National Cylinder Gas Co., Louisville, Ky.

Standards Association[3,4] (ASA) and the American Society of Mechanical Engineers[5,6] (ASME).

Brief examinations of loadings, code requirements, and field failures of branch connections are presented herein. Rather extensive test data have been accumulated and are reviewed and correlated with code requirements and field experience. The results of the test data and field experience are then summarized.

LOADING ON BRANCH CONNECTIONS

The types of loadings that may be applied to a branch connection are illustrated in Fig. 1. In Fig. 1, F_{Ab} is an axial force, M denotes the twisting moment, M_{Bi} is the in-plane bending moment, M_{Bo} represents the out-of-plane bending moment, P is the internal pressure, and F_{Ar} denotes the end thrust due to the internal pressure. In field service a combination of these loads will be applied.

The internal load, that is, the pressure, exerts a uniform load normal to the pipe walls. This load may be negative in the case of vacuum service. The end thrusts caused by the pressure may or may not be present, depending on how the pipes are anchored adjacent to the intersection. The internal pressure may vary because of change in flow rate, intermittent service, or pulsations set up by the pump or line resonance.

The external loads have been classified as bending, twisting, and axial, with bending being further subdivided into "in-plane" and "out-plane." In service, the bending load may be between these planes. For analytical purposes, however, the actual bending load may be separated into its in-plane and out-of-plane components. Static external loads are imposed by the unsupported weight of the piping, installation misalinement, foundation or support settlement, and similar factors. Cyclic external loads may be present due to cyclic temperature changes producing variations in the pipeline length and corresponding variations in loads on the branch connection and mechanical vibrations of the branch line.

CODE REQUIREMENTS

Rules for reinforcement of fabricated branch connections, primarily from the standpoint of providing adequate internal pressure strength, are available able[3,4,5,6].

The basic concept of reinforcement of branch connections is illustrated in Fig. 2, in which

$$A_{Rr} = d\,t \quad \ldots\ldots\ldots\ldots\ldots\ldots \quad (1)$$

and

$$A_{Ra} = A_1 + A_2 + A_3 \quad \ldots\ldots\ldots\ldots\ldots \quad (2)$$

---

[3] ASA Code for Pressure Piping, Section 6, "Fabrication Details."

[4] ASA Code for Pressure Piping, Section 8, Paragraph 831.4, "Reinforcement of Welded Branch Connections."

[5] ASME Unfired Pressure Vessel Code, Paragraphs UG-36 to UG-46, "Openings and Reinforcements."

[6] ASME Power Boiler Code, Paragraph PO268, "Openings and Reinforcements."

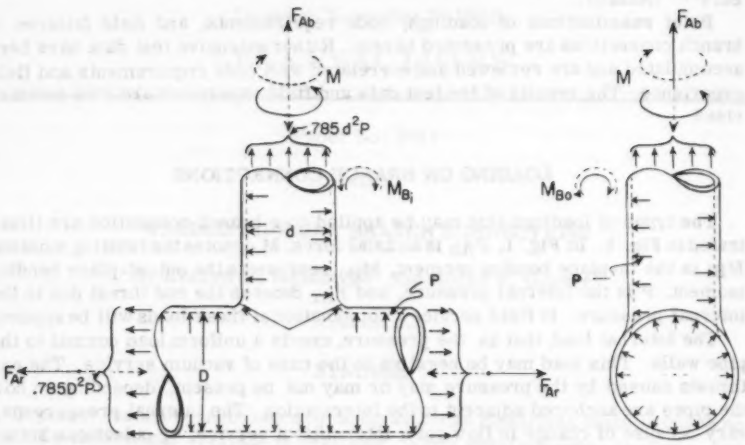


FIG. 1.—LOADINGS ON A PIPELINE BRANCH CONNECTION

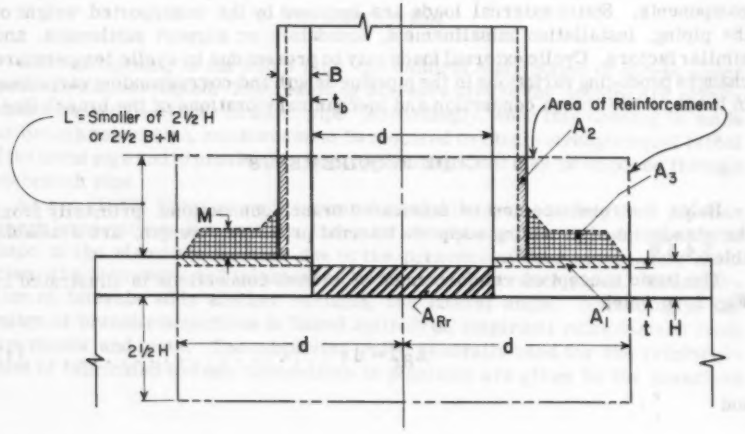


FIG. 2.—TYPICAL REINFORCING REQUIREMENTS

in which A_{Rr} is the area of reinforcement required and A_{Ra} is the area of reinforcement available. Essentially, these rules require that the metal in the run-pipe, cut out by the opening, must be fully replaced by extra metal placed within a zone close to the opening. Details of reinforcement requirements and restrictions on the opening size, ratio of opening to header size, and angle between header and branch, vary with the specific code. All of the codes state that their rules are intended to provide reinforcement for internal pressure. External loadings are not evaluated, or are assumed to be those normally applied to such connections. Special consideration where the external loads are unusually high or cyclic is required; special care is also required where the pressure may be cyclic.

Branch connections termed steel butt-welding fittings are covered by a code of ASA[7]. In this standard adequate strength of the fittings is assured by proof tests. The standard requirements that actual bursting pressure of the fittings must be at least equal to the computed bursting pressure of the seamless pipe of the size, schedule number (wall thickness), and material designated by the marking on the fitting. Manufacturers of such steel butt-welding fittings run numerous hydrostatic tests on their pipe fittings to be sure that their design meets this requirement.

FIELD FAILURES AND THEIR CAUSES

Several failures of saddle-reinforced branch connections on gas and oil transmission lines have been reported. Another type of field failure commonly encountered involves a small branch connection to a relatively large run pipe, reinforced by pads or saddles, or, in some cases, unreinforced. Mechanical vibration or movement of the branch pipe with respect to the run has caused failures of such connections. This type of branch connection formerly gave considerable trouble in steam power plants. However, experienced pipe designers in that field now recognize the inherent high stress conditions in such connections and design small branch pipes of XXS or Sch. 160 wall thickness and, in some instances, maintain a certain minimum diameter for small branch connections. (Wall thickness designations "XXS" and "Sch. 160" refer to heavy-wall pipe in accordance with ASA Standard B36.10, "Wrought-Steel and Wrought-Iron Pipe.")

The field failures generally involved connections that were adequately reinforced according to code rules. Furthermore, hydrostatic tests on similar branch connections would indicate that the connections were adequately designed for the operating pressure. Because field failures have occurred at normal operating pressures, it appears that such field failures of branch connections are not usually due to static pressure load but are probably due to cyclic internal pressure, excessive static external loads, or cyclic external loads.

In considering the possible causes of field failures, other factors besides loads must be considered. A fabricated branch connection involves considerable manual welding which introduces the welding quality as a factor. The weld around the intersection between the run and branch pipes is rather difficult to make with consistently good quality, even for an experienced pipe welder. The ends of the branch pipe or the edge of the hole in the run pipe must be carefully beveled if a full-penetration weld is to be obtained. In welding a pad or saddle-type reinforcement, the fillet weld between the edge of the pad or saddle and

[7] ASA Code for Steel Butt-Welding Fittings, ASA B16. 9.

the pipe can result in an undercut at the toe of the fillet weld in the run pipe, and as will be shown subsequently, this is a frequent location for failure in such reinforced connections.

Another factor in welding is the possibility of starting cracks by welding. It is known that, in the case of steels rather high in carbon and manganese that are welded at low ambient temperatures in a constrained position, welding may start cracks either in the weld metal itself or in the adjacent base material. Although the writers are not aware of any field failures directly attributable to weld-associated cracking, it cannot be entirely ruled out as a possible contributor to field failures. Other factors that may influence or cause field failures are corrosion, and, at high temperatures, creep or graphitization.

STATIC PRESSURE TESTS

Static pressure tests may be briefly described as tests wherein the pressure is gradually increased until the branch connection fails by yielding and rupture. In conjunction with these static tests, additional information is gained by measuring the strains at critical locations as functions of the pressure. These strains, which may be measured by electrical resistance or mechanical strain gages or by brittle coating, may then be converted to stresses and compared with allowable stresses for the material under static or cyclic loading conditions. Either strains or over-all dimentional changes may be plotted against the applied pressure to determine the pressure corresponding to yielding. In the case of a complex shape such as a branch connection, however, the practical significance of yielding has not been evaluated.

It is impossible to describe and give herein the results of all of the static pressure tests that have been performed on branch connections. References to such test data are given in the Appendix.

Unreinforced Branch Connections.—An unreinforced branch connection is defined as a branch connection made by welding a branch pipe to the opening in run pipe without the provision of additional reinforcement. It is possible that such a connection may be fully reinforced according to code rules. This occurs where the branch pipe is very thick in relation to its diameter. Also, if the run pipe is twice as thick as is required to hold the design pressure, the branch connection is generally fully reinforced for the design pressure according to code rules.

Fig. 3(a) and (b) show failures produced by hydrostatic tests to rupture, that is, burst tests. The left hand photographs show failures in the crotch of the intersection, which is the more normal location of the rupture. However, rupture often occurs at the sides as shown by the right-hand photographs—the intersection weld being a weak point. In Table 1 the results of a number of typical burst tests of unreinforced branch connections are presented. The crotch is the area where the branch joins the run pipe at an angle α. The angle α is the angle made by the branch joining the run pipe while the "side" refers to the side intersection of branch and run pipe.

Based on hydrostatic burst tests of unreinforced tees and laterals, an empirical formula for the strength of such branch connections has been developed:

$$\frac{P_a}{P_c} = 1 - \frac{d}{d_r}\left(1 - 0.7\, e \sin^{1.5}\alpha\right) \quad \ldots\ldots\ldots\ldots (3)$$

in which P_a is the burst strength of branch connection, in pounds per square inch, P_c denotes the burst strength of uncut pipe of the same outside diameter and wall thickness as the run of the branch connection, in pounds per square inch; d is the inside diameter of the branch in inches; d_r represents the inside diameter of the run in inches; e is the weld efficiency (e = 0.8 for field welding and e = 1.0 for shop welding); and α denotes the angle between the run and the branch (acute angle for laterals).

In addition to hydrostatic tests to rupture, a number of tests have been made on unreinforced branch connections in which stresses around the branch were determined by the use of strain gages. As might be expected, stresses in an unreinforced branch connection are highest at the junction between the branch

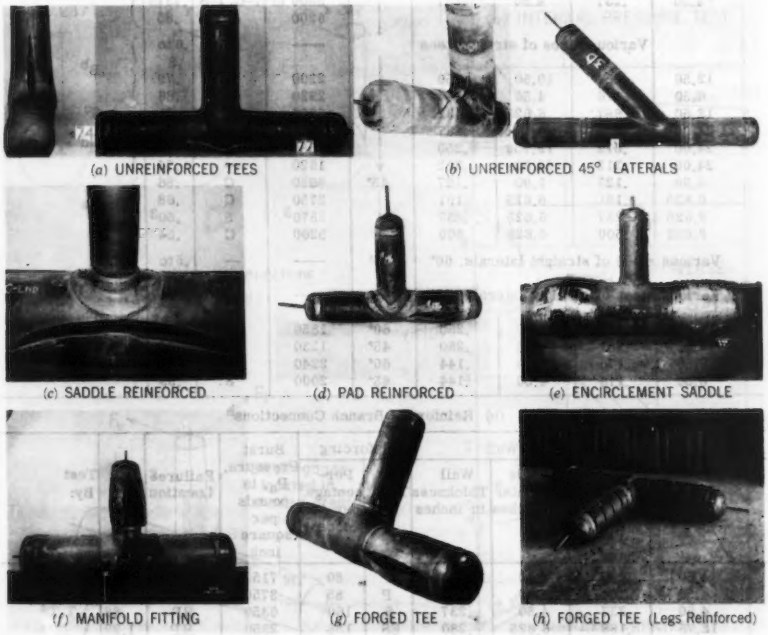


FIG. 3.—FAILURES IN STATIC PRESSURE TESTS

and run pipe, the stresses rapidly decreasing with the distance from the intersection. Variation of stresses around the intersection of three unreinforced branch connections are shown in Fig 4.[8] In Fig. 4 the ratios of maximum measured stresses, S_{max}, to the nominal computed stresses, S_{nom}, are plotted against the position around the intersection. In Fig. 4(a)

$$S_{nom} = \frac{pd}{2t} \quad \ldots\ldots\ldots\ldots\ldots\ldots\ldots\ldots (4)$$

[8] "How Stresses are Affected by Branch Connections," by E. D. Abraham and G. M. McClure, Pipeline Industry, Sept., 1954.

TABLE 1.—TYPICAL BURST TEST RESULTS

(a) Unreinforced Branch Connections

Run		Wall			Burst Pressure, P_a, in pounds per square inch	Failure[g] Location	$\frac{P_a}{P_c}$	Test By:
Outside Diameter in inches	Wall Thickness in inches	Outside Diameter in inches	Wall Thickness in inches	Angle, in inches				
4.50	.237	1.315	.133	90°	6350	RP	1.0	
4.50	.237	2.375	.154		6175	C	.97	
4.50	.237	3.50	.216		6100	S	.96	T.T[a]
4.50	.237	4.50	.237		5300	C	.83	
[f]4.50	.237	4.50	.237		5300 to 6200	7-C, 1-S	.73 to .85	
Various sizes of straight tees					-----	--	.6 to .8	B[b]
12.50	.281	10.50	.250		2200	S	.79	
6.50	.176	4.50	.144		2920	S	.86	
12.50	.687	6.625	.432		5850	C	.91	S[c]
24.00	.312	4.50	.237		1970	C	.90	
24.00	.312	12.750	.250		1580	C	.72	A.M[d]
24.00	.312	24.00	.312		1620	--	.74	
1.90	.127	1.90	.127	45°	8050	C	.86	
6.625	.191	6.625	.191		2750	C	.68	T.T[a]
6.625	.237	6.625	.237		2570[3]	S	.50[3]	
6.625	.500	6.625	.500		5200	C	.54	
Various sizes of straight laterals, 60°				60°	-----	--	.5 to .7	
Various sizes of straight laterals, 45°				45°	-----	--	.4 to .6	B[b]
12.50	.281	10.50	.250	60°	1850	S	.66	
12.50	.281	10.50	.250	45°	1230	S	.44	
6.50	.176	4.50	.144	60°	2240	S	.66	
6.50	.176	4.50	.144	45°	2000	S	.59	

(b) Reinforced Branch Connections[h]

Run		Wall		Reinforcing		Burst Pressure, P_a, in pounds per square inch	Failure[g] Location	$\frac{P_a}{P_c}$	Test By:
Outside Diameter in inches	Wall Thickness in inches	Outside Diameter in inches	Wall Thickness in inches	Type[i]	Percentage per ASA code				
4.50	.237	4.50	.237	P	80	7150	RP	.98	
4.50	.134	4.50	.134	P	85	3750	BP	.91	
4.50	.237	4.50	.237	S	160	6350	RP	.88	T.T[a]
12.75	.188	6.625	.280	ES	155	2350	RP	1.22	
22.00	.312	10.75	.500	S	160	2100	RP	.99	
6.50	.250	6.50	.250	P	85	4800	RP	.92	B[b]
8.625	.500	8.625	.500	P	110	8750	RP	.99	S[c]
30.00	.344	16.00	.375	S	100	1990	RP	1.08	
30.00	.344	16.00	.375	P	105	1865	RP	1.01	
30.00	.500	16.00	.375	S	85	2310	RP	.93	
30.00	.500	16.00	.375	P	105	2490	RP	1.00	B.H[e]
30.00	.344	16.00	.375	S	70	1640	RP	1.00	
30.00	.344	16.00	.375	ES	120	2060	C	1.12	

[a] Tube Turns.
[b] Bibliography reference (1).
[c] Bibliography reference (2).
[d] Bibliography reference (3).
[e] Bibliography reference (4).
[f] Range of eight tests.
[g] RP run pipe; BP branch pipe; C crotch; S side.
[h] All Tests on straight tees.
[i] P pad; S saddle; ES encirclement saddle.

and in Fig. 4(b) and (c)

$$S_{nom} = \frac{M}{Z_b} \quad \ldots\ldots\ldots\ldots\ldots\ldots\ldots\ldots (5)$$

in which Z_b denotes the section modulus of the branch pipe.

In the absence of a theoretical analysis, it is difficult to draw any general deductions as to stresses in unreinforced branch connections. It should be noted that stresses determined by strain-gage measurements are valid only while the structure behaves elastically. In particular, the stresses so obtained do not necessarily give any information as to the bursting pressure of the connection.

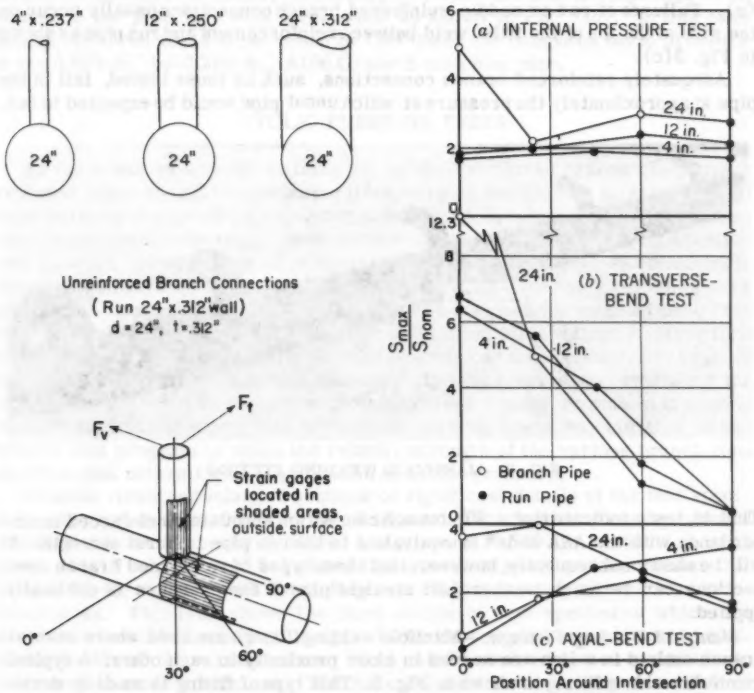


FIG. 4.—STRESSES IN AN UNREINFORCED BRANCH CONNECTION

For example, the strain-gage measurements of the 24-in.-by-24-in. fabricated unreinforced branch connection indicated a maximum stress that was approximately five times the stress in the run pipe at locations remote from the branch connection. However, this particular branch connection, when subjected to a burst test, had approximately 75% of the strength of the run pipe or a "stress ratio," at the burst pressure, of only 1.33 rather than 5. This difference is due to the fact that when a branch connection is fabricated from a ductile material, the material can yield and readjust to a more favorable shape before breaking. On the other hand, when loads are applied cyclically the stresses indicated

by strain gages are significant. As will be noted subsequently an approximate correlation exists between static strain-gage measurements with the number of cycles to failure and failure location in cyclic pressure tests.

Fabricated Reinforced Branch Connections.—A fabricated reinforced branch connection is defined herein as a branch connection that has additional reinforcement components placed around the branch outlet. These reinforcement components usually consist of saddles, pads, encirclement sleeves, or combinations thereof. In Table 1(b) the results of a number of typical burst tests of reinforced branch corrections are presented. Percentage of reinforcing refers to that percentage required to make the intersection equal in strength to the run pipe in accordance with the American Standard Code for Pressure Piping, ASA B 31.1 - 1955 Paragraph 639. Typical failures are shown in Fig. 3(c), (d), and (e). Failures of pad or saddle-reinforced branch connections usually occur on the side at the toe of the fillet weld between reinforcement and run pipe as shown in Fig. 3(c).

Adequately reinforced branch connections, such as those tested, fail in the pipe at approximately the pressure at which uncut pipe would be expected to fail.

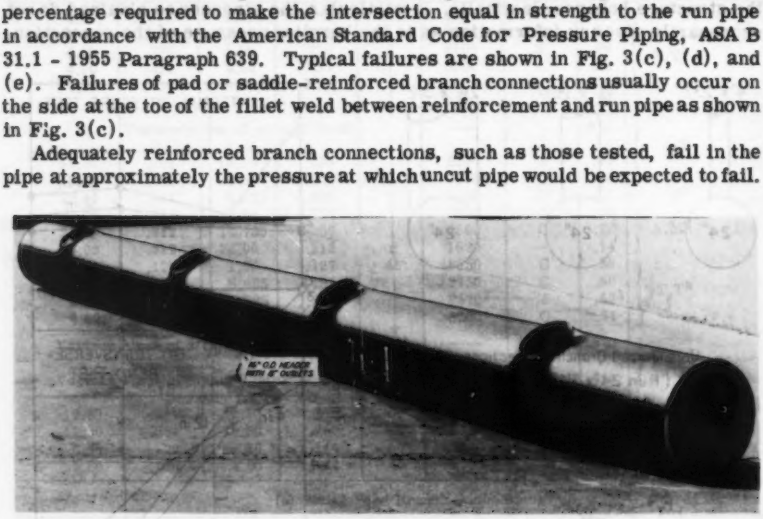


FIG. 5.—MANIFOLD WELDING FITTING

That is, tests indicate that a 90° branch connection adequately reinforced in accordance with the ASA code[4] is equivalent to the run pipe in burst strength. It will be shown subsequently, however, that these types of reinforced branch connections can be much weaker than straight pipe if the pressure is cyclically applied.

Manifold Welding Fittings.—Manifold welding fittings are used where several branch outlets in a line are needed in close proximity to each other. A typical manifold welding fitting is shown in Fig. 5. This type of fitting is made by drawing one or more branch outlets in a section of run or header pipe, the header pipe being considerably thicker than required for uncut pipe. In this design the reinforcement is integral with the fitting. Welding of the branch to the run is accomplished by means of relatively simple circumferential butt weld, thus avoiding the welding difficulties inherent in the complex branch-to-run pipe weld encountered in fabricated branch connections.

The failure resulting from a burst test of a section of a typical manifold fitting is shown in Fig. 3(f). In this particular case the branch pipe was the weakest member. This manifold fitting, a 10-in.-by-6-in. size was designed to be equal in burst strength to a 10-in.-by-0.500-in., A106 Grade B run pipe. The burst pressure was 5,810 psi which is 1.41 times the computed burst pressure of the

equivalent pipe, thereby proving the adequacy of the reinforcement in accordance with ASA requirements.

Butt-Welding Forged Tees.—Butt-welding tees are forged in a manner causing a preferential increase in wall thickness at the locations of highest stress. In addition, the barrel shape of the run and the large crotch radii combine to minimize stress concentrations from either pressure or external bending loads. The failure resulting from a burst test of a typical forged tee is shown in Fig. 3(g). Because the tee is designed to be stronger than the matching pipe, failure occurred in the run pipe in this particular case at a pressure to 2,600 psi which is 1.19 times the computed burst pressure of the 18-in.-by-0.375-in. A106 Grade B matching pipe. In order to obtain information on the burst strength of the forged tee itself, it is usually necessary to either use heavier pipe legs or to reinforce the pipe legs with steel bands as shown in Fig. 3(h). In this case failure occurred at 5,950 psi which is 1.34 times the computed burst pressure of the 6.625-in.-by-0.280-in., A106 Grade B matching pipe.

CYCLIC PRESSURE TESTS

As the result of several failures of saddle-reinforced branch connections reported in gas and oil transmission lines, serious thought was directed toward improving the design of the reinforcement of such openings. Because failures usually occurred at the toe of the weld between the saddle and run pipe, attention was directed toward a type of reinforcement which would completely encircle the run pipe. Several varieties of these encirclement-type reinforcements were proposed.[4] Some of these reinforcements were designed for application to "hot tap" connections, wherein a branch connection is installed without stopping flow through the main pipeline. These reinforcements can also be used for normally constructed branch connections. To assist pipeline operators in evaluating the respective merits of these new encirclement-type reinforcements, and to generally evaluate the strength of branch connections, there was initiated an extensive test program in which the relative strength of the various branch connections was determined by application of cyclic pressure.

General views and enlarged sections of significant details of the test specimens are given in Figs. 6 and 7. Fig. 6 shows the first series of test specimens which all involve 22-in.-by-5/16-in. run pipe and 10.750-in.-by-50-in. branch pipes. Fig. 7(a), (b), and (c) shows the second series of test specimens that involve 24-in. run pipe with 4-in., 8-in., or 12-in. branches with various reinforcements. Fig. 7(d) shows the third series of test specimens which are sections of manifold welding fittings. In the first series approximately half-scale models of the variants shown were constructed and tested in addition to tests on full-scale specimens. The material used in the models was different from the full-scale specimens only in that the run pipe was A106 Grade B pipe instead of API-5LX-52 pipe, with a Grade B cap. The sections shown in Fig. 6 are as follows:

a. rolled and welded pipe, typical of run pipe for all variants;
b. unreinforced intersection, branch attachment typical except for variants i and j;
c. ordinary saddle, saddle superimposed on unreinforced intersection;
d. encirclement sleeve, half cylinders joined by top welding along sides;
e. encirclement sleeve and saddle, same as d except for addition of saddle;
f. encirclement saddle, welded, halves are butt-welded at crotch and lap-welded at back;

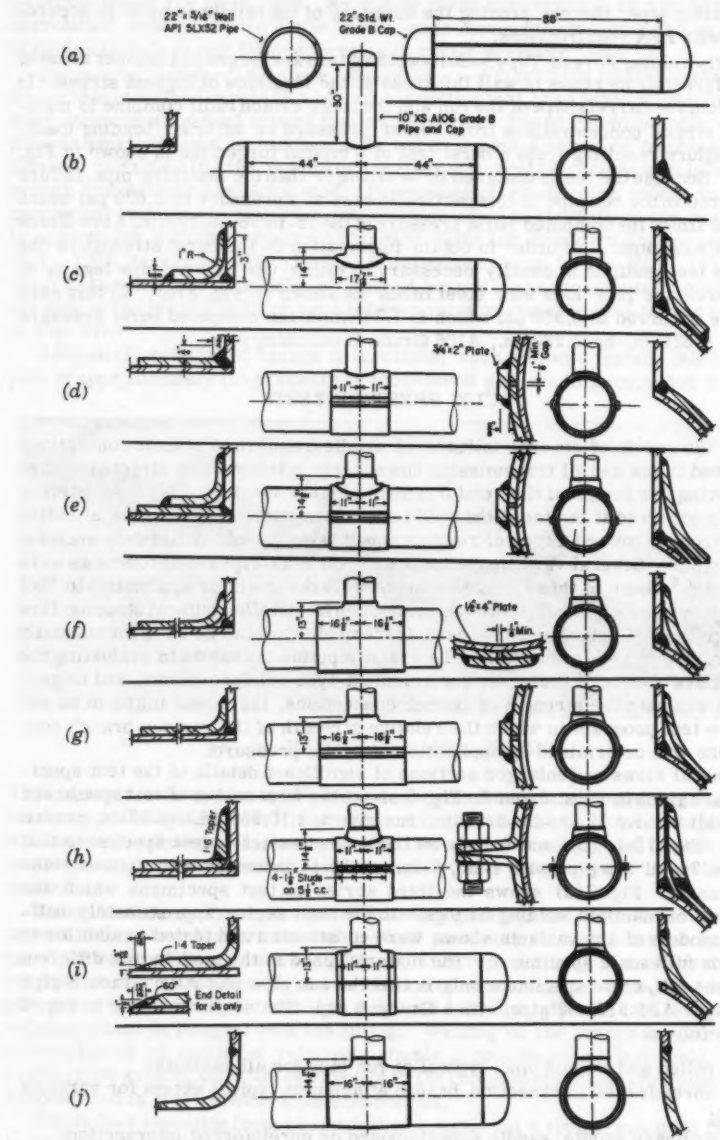


FIG. 6.—SPECIMENS FOR CYCLIC PRESSURE TESTS, SERIES 1

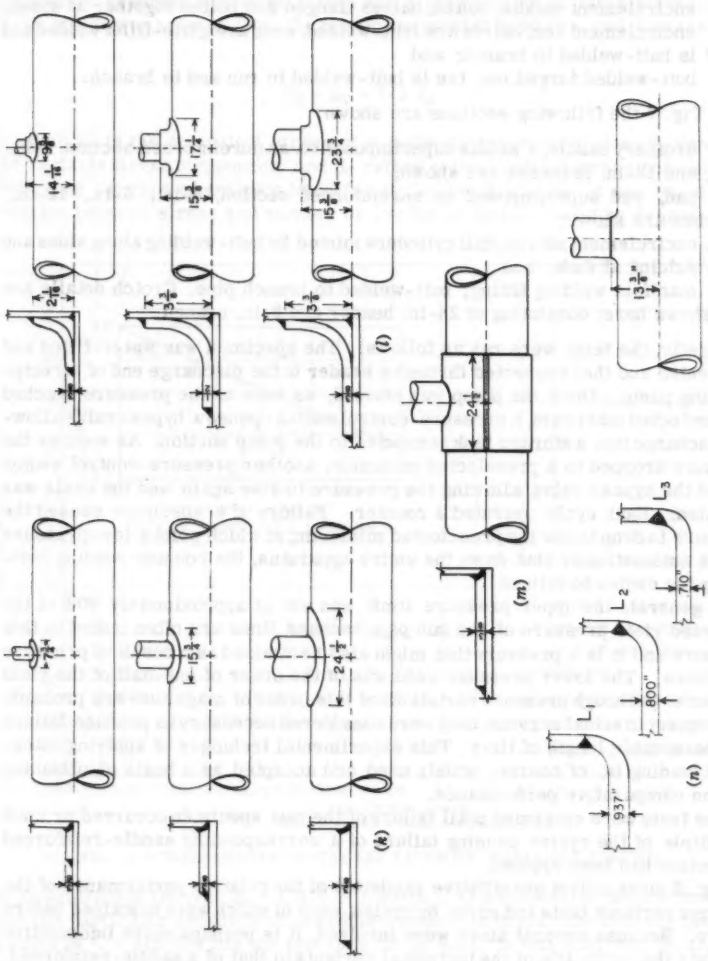


FIG. 7.—SPECIMENS FOR CYCLIC PRESSURE TESTS, SERIES 2 AND 3

g. encirclement saddle, welded, same as f except that the halves are lap-welded along the sides;

h. encirclement saddle, bolted, halves flanged and bolted together at sides;

i. encirclement tee, halves are butt-welded, ends are girth-fillet welded and outlet is butt-welded to branch; and

j. butt-welded forged tee, tee is butt-welded to run and to branch.

In Fig. 7 the following sections are shown:

k. ordinary saddle, a saddle superimposed on an unreinforced section, 4-in., 8-in., and 12-in. branches are shown;

l. pad, pad superimposed on unreinforced section, 4-in., 8-in., 12-in., branches are shown;

m. encirclement sleeve, half cylinders jointed by butt-welding along sides and fillet-welding at ends; and

n. manifold welding fitting; butt-welded to branch pipe. Crotch details are also shown here, consisting of 24-in. header and 8-in. branch.

Briefly, the tests were run as follows: The specimen was water-filled and air-vented and then connected through a header to the discharge end of a reciprocating pump. Once the pump was started, as soon as the pressure reached a preselected maximum, a pressure-control switch opened a bypass valve allowing discharge into a storage tank connected to the pump suction. As soon as the pressure dropped to a preselected minimum, another pressure-control switch closed the bypass valve allowing the pressure to rise again and the cycle was repeated. Each cycle operated a counter. Failure of a specimen caused the pressure to drop below the preselected minimum, at which point a low-pressure switch automatically shut down the entire apparatus, the counter reading indicating the cycles to failure.

In general, the upper pressure limit was set at approximately 90% of the computed yield pressure of the run pipe because lines are often tested to this pressure and it is a pressure that might also be attained as a result of pressure pulsations. The lower pressure used was of the order of one-half of the yield pressure. Although pressure variations of this order of magnitude are probably not frequent in actual service, they were considered necessary to produce failure in a reasonable length of time. This experimental technique of applying intensified loading is, of course, widely used and accepted as a basis of obtaining data on comparative performance.

The tests were continued until failure of the test specimen occurred or until a multiple of the cycles causing failure of a corresponding saddle-reinforced connection had been applied.

Fig. 8 gives a first quantitative yardstick of the relative performance of the different variants tests and given by cycles, each of which were sustained before failure. Because several sizes were involved, it is perhaps more informative to relate the cyclic life of the individual variants to that of a saddle-reinforced branch connection. The saddle-reinforced connection was chosen as a basis for evaluation because it was the type that had occasionally failed. Thus, this type of reinforcement may be considered a borderline design. Branch connections that are significantly superior to the saddle-reinforced design would presumably be adequate under field conditions. Those connections that are significantly inferior to the saddle-reinforced design might be expected to fail under severe field service conditions.

In order to generalize the available test data on saddle-reinforced branch connections, a plot of equivalent stress versus cycles to failure was constructed

as shown in Fig. 8. The cyclic pressure tests may be considered as applying a mean stress on which a cyclic stress is superimposed. The relation between completely reversed cycles of stress and a combination of mean stress plus cyclic stress was adopted from the relation suggested by Moore and Kommers.[9]

$$S_e = S_v + 1/3\ S_c \quad \ldots\ldots\ldots\ldots\ldots\ldots\ldots (6)$$

in which S_e is the equivalent stress of completely reversed cycles; S_v denotes the variable stress component; and S_c refers to the constant stress component. Following the type of analysis used for cyclic bending tests, it was found that relation between stress and number of cycles-to-failure could be represented

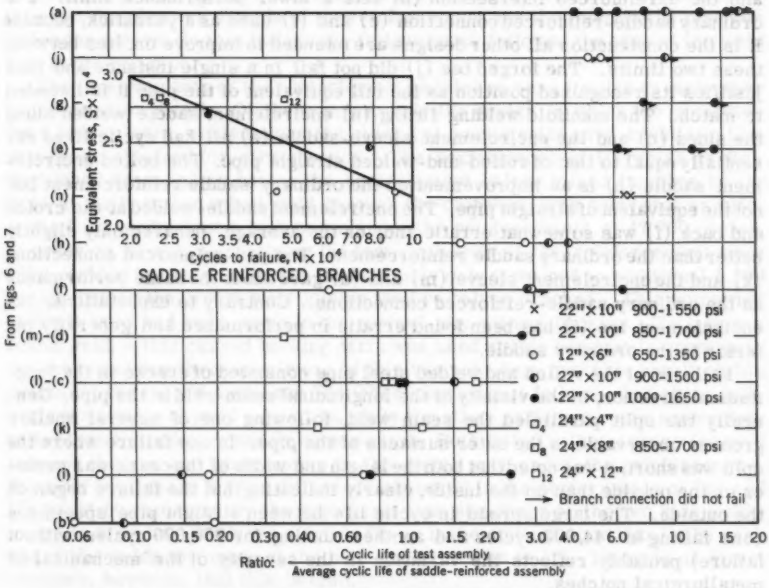


FIG. 8.—COMPARISON OF CYCLIC LIVES OF VARIANTS TESTED

by an equation of the type $S_e = CN^{-0.2}$ in which C is a constant to be determined. For the particular proportions of saddle-reinforced branch connections tested, a value of C = 216,000 fits the test data fairly well. In this analysis, S_v and S_c were computed as nominal membrane stresses in the run pipe.

Of the seven saddle-reinforced connections tested, five are roughly geometrically similar. The other two (the 24-in.-by-4-in. and 24-in.-by-8-in.) specimens because they involve a smaller ratio of branch to run size, would not be expected to fall on the same S-N curve as the other five specimens. It was found, however, that the diagonal line on the S-N graph on Fig. 8 fairly well represents the data for all seven specimens. Apparently the controlling factor

9 "Textbook of Materials of Engineering," by H. F. Moore, McGraw-Hill Book Co., Inc., New York, N. Y., 1941, p. 57.

is the discontinuity at the edge of the saddle-to-run pipe weld, because failure consistently occurred there. The geometry of the rest of the construction, at least over a limited range, apparently has little influence over the controlling stress. This hypothesis is somewhat supported by the pad-reinforced connection tests, that failed at the same location at approximately the same number of cycles. However, the generalizations are based on rather limited data and extrapolations to shapes or proportions radically different than those tested may not be justified. Having established a reference line for saddles, the relative life of various types of branch connections are then as shown in Fig. 8, in which the different types of branch connections are arranged in order of decreasing life.

As anticipated, the straight pipe (a) lends itself well as an upper aim point and the unreinforced intersection (b) sets a lower performance limit. The ordinary saddle-reinforced connection (c) and (l) used as a yardstick, because it is the construction all other designs are intended to improve on, lies between these two limits. The forged tee (j) did not fail in a single instance and thus justifies its recognized position as the full equivalent of the pipe it is intended to match. The manifold welding fitting (n) encirclement saddle welded along the sides (c) and the encirclement sleeve-saddle (e) all had cyclic lives essentially equal to that of rolled-and-welded straight pipe. The bolted encirclement saddle (h) is an improvement on the ordinary saddle reinforcement but not the equivalent of straight pipe. The encirclement saddle-welded at the crotch and back (f) was somewhat erratic and, on the average, behaved only slightly better than the ordinary saddle reinforcement. The pad-reinforced connections (k) and the encirclement sleeve (m) and (d) gave about the same performance as the ordinary saddle-reinforced connections. Contrary to expectations, the encirclement tee (i) has been found erratic in performance and generally inferior to the ordinary saddle.

Failures of the rolled and welded steel pipe consisted of cracks in the longitudinal direction, in the vicinity of the longitudinal seam weld in the pipe. Generally the split paralleled the seam weld, following one of several shallow grooves observable in the outer surfaces of the pipe. In one failure where the split was short, it was noted that both the length and width of the crack was greater on the outside than on the inside, clearly indicating that the failure began on the outside. The large spread in cyclic life between straight pipe specimens (one failing at 144,000 cycles and another running for 900,000 cycles without failure) probably reflects the variation in the severity of the mechanical or metallurgical notches.

The unreinforced connections failed either by cracking across the weld in the crotch, or along it at the side, both types of failure being experienced simultaneously in one assembly. This is in accord with strain gage test results obtained by other investigators. For connections where the branch size is one-half that of the run or less, the maximum stresses are nearly uniform around the perimeter of the intersection with only the direction changing.

In case of the connection reinforced with an ordinary saddle, (c) the run pipe invariably split along the side at the edge of the saddle. A fatigue crack begins at the location of marked change in section at the toe of the attachment weld, which discontinuity in some instances may be accentuated by undercutting during welding. Noticeable change in texture of the cracked face indicated how far the fatigue crack progressed inwardly through the wall before this was weakened so that the specimen burst open, being no longer able to sustain the internal pressure.

The pad-reinforced connections failed in the same manner as the saddle-reinforced connections. The encirclement-sleeve reinforced connection (d) failed by splitting through the crotch. Both the test variant itself and the failure location bear close resemblance to the unreinforced intersection. By the approximate correlation between stress and cycles to failure suggested by Eq. 6, to follow a comparison of cycles to failure of the sleeve-reinforced connections with the unreinforced connections implies that 1/2-in.-thick sleeve in the 22-in.-by-10-in. assembly served to reduce the controlling stress to 55% of the value without this reinforcement. Similarly the 3/8-in.-thick sleeve on the 24-in.-by-12-in. assembly reduced the stress to 75% of the value without reinforcement. These would appear to be reasonable estimates of the reinforcing effect of the sleeves.

The sleeve-and-saddle reinforcement gave excellent results. Two specimens failed in the pipe run outside of the reinforcement and the third in the pipe run under the sleeve. In this failure the fatigue crack followed the edge of the weld line in the run pipe.

The three variants of the encirclement saddle are very similar to each other in intersection detail. Of these three, only the design in which the encirclement halves were welded along the sides (g) consistently gave results in line with those obtained for straight pipe. The performance of (f) which is distinguished from (g) by having the encirclement halves joined together by lap weld at the back and a butt weld through the crotches, was somewhat erratic. In the first model test a leak began under the reinforcement at 47,200 cycles. In order to be able to continue the test, both ends of the reinforcement were fillet-welded to the run pipe but the assembly only sustained an additional 5,500 cycles before the crotch weld joining the two halves cracked. This somewhat difficult weld had been made in the normal way without backing. To insure a sound weld, a thin curved backing strip was used at this location in constructing the remaining three specimens of this variant. As a probable result of this provision, the second model ran 264,000 cycles without failure. One of the full-scale specimens showed a fair life, while the other performed only moderately better than the ordinary saddle construction. Both failed in the intersection weld between the run and branch pipe, in the crotch area under the reinforcement. Possibly the reason for the difference observed in the performance of (g) and (f) might be explained by the hypothesis that shrinkage of the two side welds in (g) in some way produces a better fit-up in the critical zone than is the case where the welds are made at the back and crotch as in (f). There is no direct evidence, however, that this is true.

The bolted variant (h) provided moderate but consistent improvement over the ordinary saddle construction. As in the other types of encirclement reinforcements, failure occurred in the intersection weld in the crotch area. With the thought that close contact of the saddle with the branch-to-run intersection weld might have a beneficial effect, intentional variables in the detailed fit-up in this location were introduced, but no marked effect on relative life of the different specimens was produced. This design evolved from the thought that bolts should provide an excellent means of bringing the reinforcement into forceable contact close to the critical intersection weld. In addition, there is no welding against the run pipe such as that which occurs where the sleeve halves are joined by a butt weld. In the design actually tested however, the bolts were placed too far from the shell and the bolting flanges were too light. Improvements in detail of this design might improve its performance so as to be comparable with that of straight pipe.

The encirclement tee (i) is basically different from the reinforcements previously examined in that the reinforcing member directly carries the internal pressure. The branch pipe is butt-welded to the reinforcement and is not welded to the run pipe. This type of branch connection gave unexpectedly poor results. With the exception of the initial failure in the first model, where the butt weld joining the two halves cracked in only 6,500 cycles, all failures occurred in the fillet welds between the tee and run pipes. The location in all except one instance was directly in line with the crotch. The cracks ran in a circumferential direction and apparently started at the root of the fillet weld.

The encirclement tee assemblies, including the fillet welds in all but the last specimen, had been proportioned to parallel the assembly used by Del Buono, Vissat and Williams[10] in their exhaustive and evidently very carefully conducted strain gage tests. It is noteworthy that failure in the cyclic pressure tests occurred in the precise location where these investigators had obtained the highest strains, and that the crack closely resembled that found by them on sectioning through the crotch plane after bursting their test assembly.

Because the fillet weld quite obviously constituted a point of weakness, it was thought that the performance of this design could be improved by increasing the weld size. Accordingly, a special test assembly was made by using what was considered a maximum practical weld size. The weld leg dimension was increased by more than 50% and the tee end was machined with a reverse bevel of 60° and a 3/16-in. root radius. This resulted in an increase of more than 150% in the amount of weld metal deposited. This design with a heavier weld lasted 3 ¼ times as long as one with the original weld proportions tested under otherwise identical conditions. This specimen, however, still had a cyclic life only slightly better than a corresponding saddle-reinforced connection.

Forged tee and manifold-welding fittings are basically different from the preceding variants in that they cannot be used for hot tap connection. In none of the three specimens of the forged tee did failure occur in the tee itself. The two model tests were run to a large multiple of the cycles causing failure in a corresponding ordinary saddle-reinforced connection. In the full-scale specimen the test was terminated by failure of the run pipe, with the tee left unharmed. It is apparent that the integral reinforcement, large crotch radii, preferential thickening in highly stressed areas and gradual change in wall thickness make the forged tee the full equivalent of the pipe it is designed to match.

Although the manifold-welding fittings performed well, they were not equal to the forged tees. All three manifold-welding fittings had a cyclic life of the same order as that obtained for straight pipe. The failures consisted of cracks in the crotch area. It was not expected that the manifold welding fittings would be as good as the forged tees because they do not have the generous crotch radii and preferential thickening in highly stressed areas obtained with forged tees.

It is possible to correlate the results of the cyclic-pressure tests with the strain-gage tests. In the series 2 tests, where the specimens had been used for strain-gage tests prior to the cyclic pressure tests, all seven specimens failed in locations at or near the points of maximum measured stress. As was demonstrated earlier, failures of the encirclement tees (i) occurred at the location of maximum measured stress. A rough correlation between stresses and cycles to failure was also observed. Because strain gages do not measure the effect of local notches, such as weld defects or undercutting, it would not be expected

[10] "Design of Hot Tap Tee Connections in High-Pressure Pipe Lines," by A. J. Del Buono, P. L. Vissat, and F. S. G. Williams, Paper No. 53-PET-31, ASME, 1953.

that good correlation between stress measured by strain gages, and cycles to failure would necessarily exist.

Although all of the reinforced-fabricated branch connections used in the cyclic-pressure tests were more than 100% reinforced, based on the ASA code for Pressure Piping Rules, these connections were not all equal to the longitudinally welded straight pipe in cyclic life. Accordingly, while it was concluded the 90° fabricated branch connections, reinforced by the ASA rules, were equal to straight pipe in burst strength, the same conclusion cannot be drawn for cyclically applied pressure.

EXTERNAL LOADS

Static External Load.—A test was made in which a combination of static internal pressure and static out-of-plane bending load was applied to produce rupture. In this test, a 22-in.-by-10-in. saddle-reinforced branch connection, constructed as shown in Fig. 6(c) was pressurized with water to 1,200 psi. An out-of-plane bending force was then applied and gradually increased until failure occurred at a bending moment of 300,000 ft-lb. The pressure corresponded to a circumferential stress in the run pipe of approximately 72% of its yield strength. The bending moment at failure gives a computed maximum stress in the branch pipe of 73,000 psi. Before failure occurred, the bending force bent the branch 15° from its original position. This test indicates that very large static-bending loads can be carried by a reinforced branch connection. Stresses resulting from static bending moments are shown in Fig. 4.

Cyclic External Loads.—Cyclic-bending tests[11] in which approximately one hundred different branch connections were subjected to cyclic bending loads to failure were run using the test machine shown in Fig. 9. In these tests, one end of the assembly was anchored rigidly and the other, a hinged end, was forced to deflect cyclically through a given amplitude maintained by the machine's eccentric setting. The specimens were subjected to individual load-deflection calibrations. Filled with water to provide a ready means of detecting failure, the specimens were flexed cyclically through a predetermined amplitude until a leak of the water signalled a crack through the entire wall. This was done at several amplitudes for each type of specimen so that upon completion of tests a plot of stress against cycles-to-failure (S-N curve) could be constructed. The stress is the nominal stress in corresponding size and wall thickness straight pipe computed by the ordinary beam formula:

$$S = \frac{FL}{Z_p} \quad \ldots\ldots\ldots\ldots\ldots\ldots\ldots\ldots (7)$$

in which S is the nominal bending stress, in pounds per square inch; F denotes the applied load, obtained from load-deflection calibration; L refers to the level arm from point of load application to point of failure; and Z is the section modulus of corresponding straight pipe.

Details of reinforced test specimens are shown in Table 2. In Table 2, specimen 1 is run-thickened, specimen 2 is branch-thickened, specimens 3 and 8 are saddle-reinforced, specimens 4, 5, and 6 use reinforcing pads, and specimen 7 uses triform reinforcing. Specimens 1 through 4 use fittings designed

11 "Fatigue Tests of Piping Components," by A. R. C. Markl, Transactions, ASME, Vol. 74, No. 3, 1951.

to match 4-in. standard weight pipe and their run and branch are 0.237 in. thick except where noted. The pad of specimen 4, is 0.237 in., that of specimen 5 is 0.120 in. thick and that of specimen 6 is 0.312 in. thick. The ribs of the triform reinforcing are 1 3/4 in. by 3/8 in. The run pipe of specimen 8 is 12.75 in. by 0.188 in. while its branch pipe is 4.50 in. by 0.169 in. In addition, various designs of forged butt-welded tees and unreinforced straight fabricated branch connections with dimensions as indicated on Figs. 10, 11, 12, and 13 were tested. Results of these tests as S-N plots are shown in these figures along with the results of bending fatigue tests by J. S. Blair.[12] Photographs of typical failures are shown in Fig. 14.

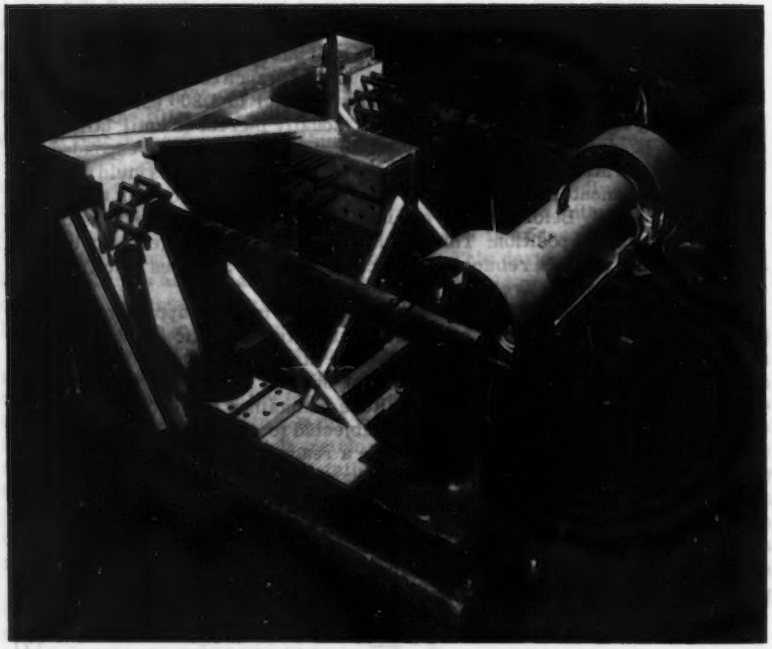


FIG. 9.—FATIGUE TEST MACHINE FOR IN-PLANE BENDING TEST

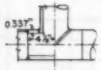
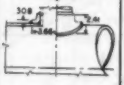
Tests conducted by Blair were run with static internal pressure applied to the connections while the cyclic-bending loads were applied. Accordingly, in these tests, there was a constant stress due to pressure as well as cyclic stresses due to bending. For these specimens an arrow pointing upward is shown, with the tip of the arrow indicating the equivalent stress for complete reversal in accordance with Eq. 6.

It is pertinent to note the location of failures in the forged tee, indicating the areas of highest stress. It is in this highly-stressed area where the intersection

12 "Reinforcement of Branch Pieces," by J. S. Blair, Engineering, London, 1946.

weld of a fabricated branch connection is located. Because it is practically impossible to make such an intersection weld without some defects and notches, such fabricated connections, even though heavier than the seamless forged tee, are liable to premature fatigue failure due to the stress concentrations caused by weld irregularities. Pad-reinforced intersections also failed along the intersection weld. In the case of the saddle-reinforced connections, the saddle was

TABLE 2.—REINFORCED CONNECTIONS IN CYCLIC BENDING TESTS

Specimen Number	Specimen	Percent[a] Reinforcing	Stress Intensification Factor, (i)			Computed Test Average
			Computed	By Test		
				in-plane	out-of-plane	
1		50	2.84	2.15	---	1.32
2		20	2.84	2.15	---	1.32
3		190	1.18	1.10	1.08	1.08
4		75	1.97	1.78	1.83	1.09
5		90	3.17	2.21	2.43	1.37
6		95	2.16	2.58	---	0.84
7		---	---	2.30	2.85	---
8		130	3.70	1.19	4.18	1.37

[a] Percent of reinforcing required to make intersection equal in internal pressure strength to the run pipe in accordance with ASA B31.1-1955 Para. 639.

able to support the intersection weld. Thus, the failure location was transferred to the outer edge of the saddle at the toe of the fillet weld between saddle and pipe. In this location, unless care is used, fillet welding can cause an undercut into the run or branch pipe, thereby creating an additional notch in a highly-stressed area. The welding of these test specimens was done with great care under ideal shop conditions. Carelessly made welds or poor welding conditions may produce an adverse affect on the fatigue life.

Similar bending fatigue tests were run on circumferentially butt-welded straight pipe and the results of these tests were also plotted on an S-N graph. The relative strengths of the various types of branch connections were evaluated in relation to the strength of such butt-welded pipe. It was found that the test data could be reasonably well represented by the formula:

$$iS = 245{,}000\ N^{0.2} \quad \ldots\ldots\ldots\ldots\ldots\ldots\ (8)$$

in which i, the stress intensification factor, is equal to unity for circumferentially butt-welded straight pipe.

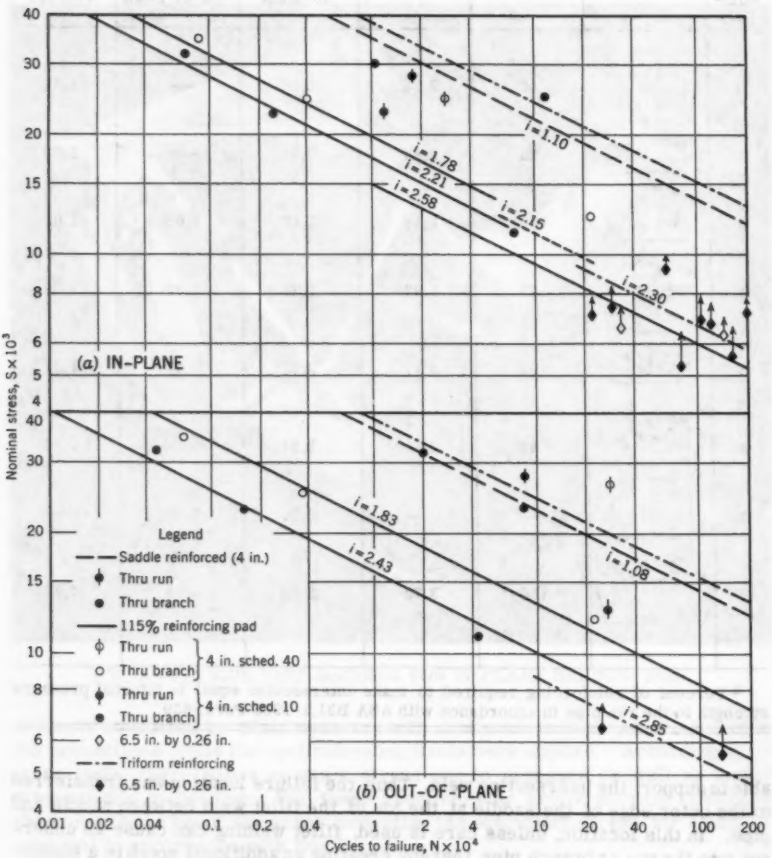


FIG. 10.—STRESS-CYCLE RELATIONSHIPS FOR REINFORCED INTERSECTION

The values of the stress-intensification factors in relation to butt-welded pipe are shown in Figs. 10, 11, 12, and 13. In attempting to evaluate and generalize these test results, it was noted that failures in forged tees were analogous in location and direction to those failures occurring in elbows or curved pipe submitted to the same type of fatigue test. Based on the fact that stresses in curved pipe can be readily evaluated by theoretical methods, the theory of curved

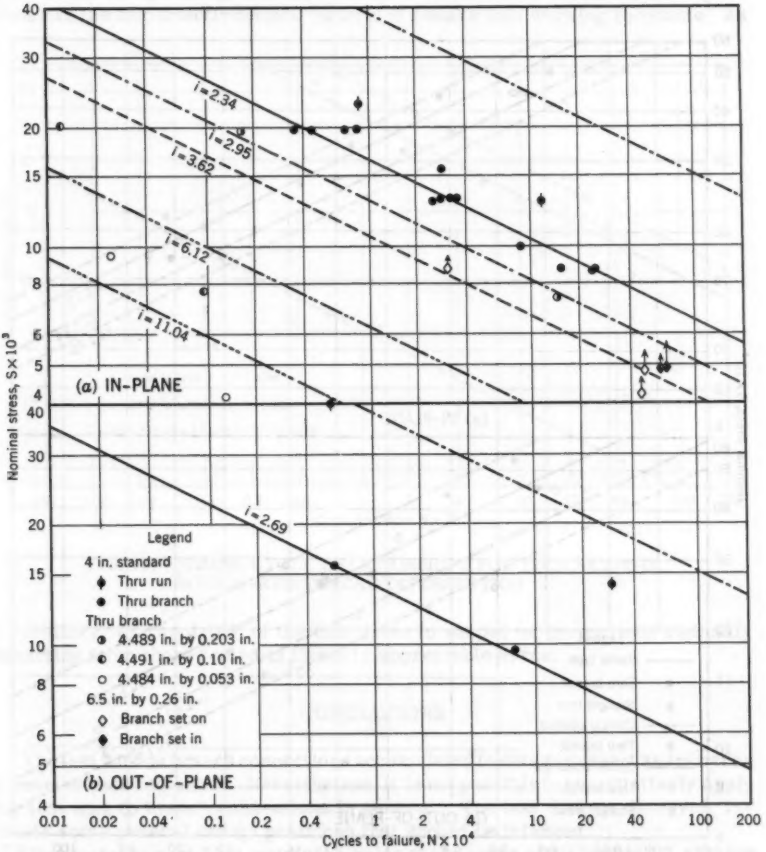


FIG. 11.—STRESS-CYCLE RELATIONSHIPS FOR UNREINFORCED INTERSECTION

pipe was used as a basis for generalizing the experimental fatigue life data on branch connections. This leads to the formula for stress intensification factor,

$$i = \frac{0.9}{h^{2/3}} \geqq 1.0$$

in which h is derived from the following formulas, in which T is the thickness of the saddle or the pad, and r is the radius of the run pipe.

a. For a full-size welding tee per ASA B 16.9, $h = (4.4)\ t/4$.

b. For a full-size pad or saddle-reinforced fabricated tee, $h = \left(1 + \frac{T}{2t}\right)^{5/2} \frac{t}{r}$.

However, when T exceeds 1.5 t, then $h = 4.05\ \frac{t}{r}$.

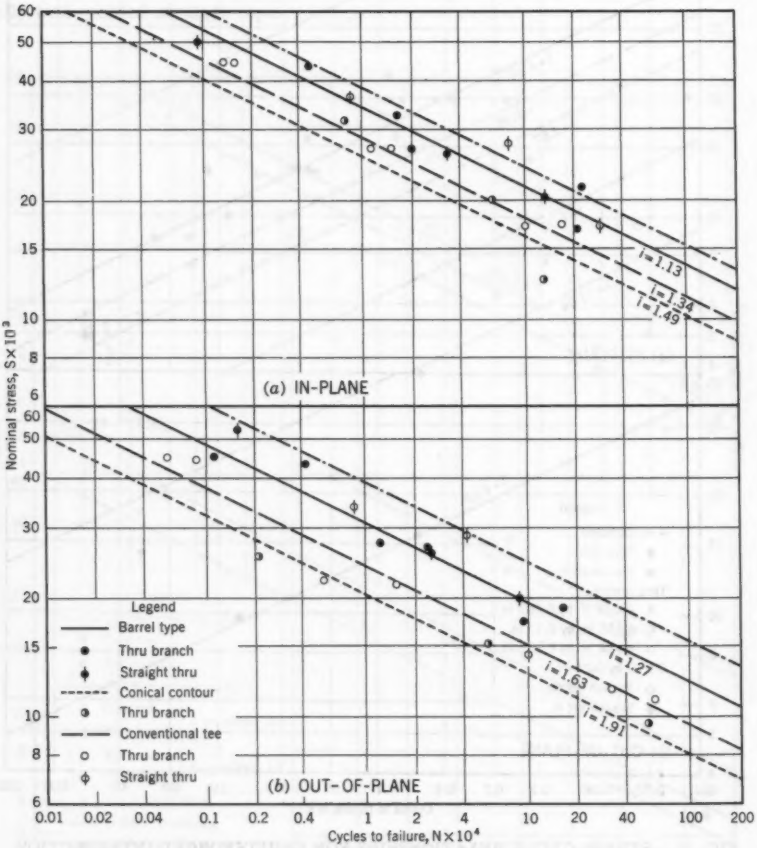


FIG. 12.—STRESS-CYCLE RELATIONSHIPS FOR FORGED WELDING TEE

c. For a full-size, unreinforced, fabricated tee, $h = t/r$.

All of the preceding formulas may be used for reducing outlet tees, in the absence of directly applicable data.

The stress-intensification factors based on these tests have been incorporated in the American Standard Code for Pressure Piping, along with factors derived from similar tests on other piping components such as elbows, mitres, and flanged joints.

Each of the individual cyclic bending tests represents a considerable expenditure of labor, hence the number of specimens and variants were necessarily limited. Accordingly, the generalizations derived are based on rather limited data. Only the pressing need for design information induced the attempt to translate the imperfectly defined pattern of results into working constants. As

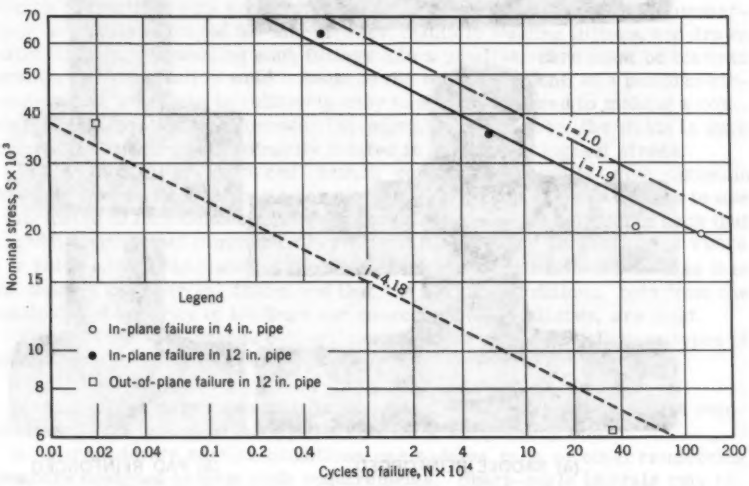


FIG. 13.—STRESS-CYCLE RELATIONSHIPS FOR 12-IN.-BY-4-IN. SADDLE-REINFORCED INTERSECTION

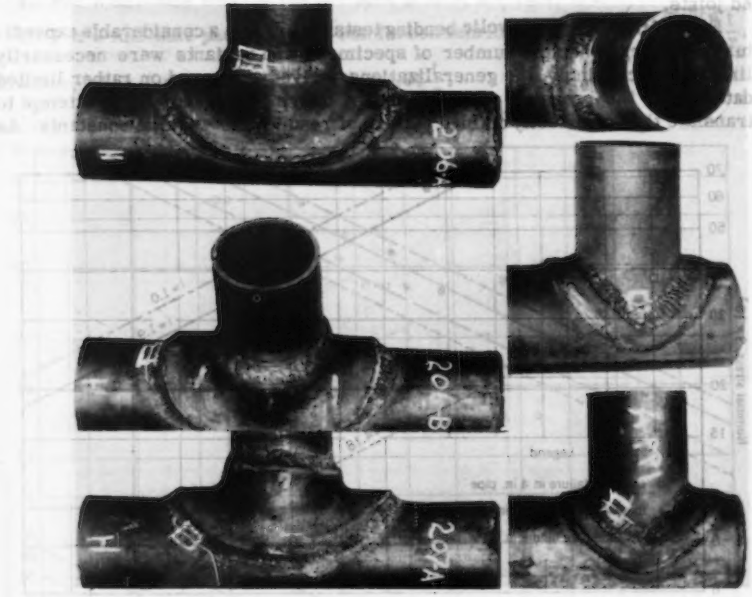
a corollary, extrapolation of the data given to shapes or proportions radically departing from those tested is liable to appreciable error.

CONCLUSIONS

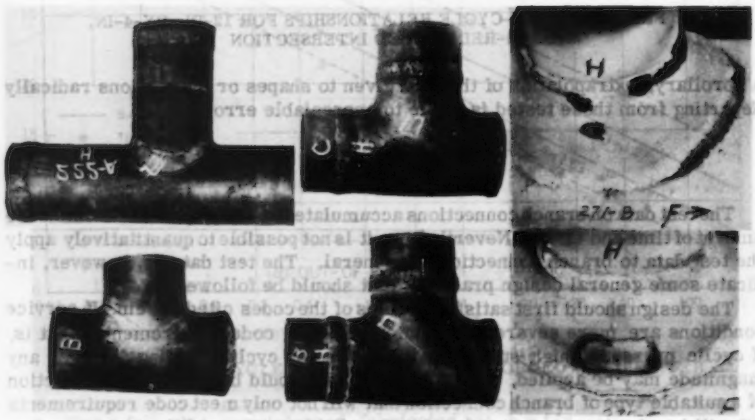
The test data on branch connections accumulated to date represent an immense amount of time and effort. Nevertheless, it is not possible to quantitatively apply the test data to branch connections in general. The test data do, however, indicate some general design practices that should be followed.

The design should first satisfy the rules of the codes cited herein. If service conditions are more severe than contemplated in code requirements, that is, if cyclic pressure, high static bending loads, or cyclic bending loads of any magnitude may be applied, then consideration should be given to the selection of a suitable type of branch connection that will not only meet code requirements but will be of optimum design for the expected service conditions.

In an optimum design, one must balance the first cost of the installation against the possibilities of failure and the consequence of such a failure. In some pipelines, that may be shut down with little effect on associated processes, a failure



(a) SADDLE REINFORCED (b) PAD REINFORCED



(c) UNREINFORCED AND FORGED TEES (d) SADDLE REINFORCED

FIG. 14.—FAILURES IN CYCLIC BENDING TEST

may mean only the necessity of replacing the failed component. In other pipelines, however, a forced shutdown may be extremely costly. Failure of lines carrying lethal or inflammable fluids or gases at high pressure may result in great economic loss and hazard to life.

The test data and field experience all tend to indicate that branch connections with integral reinforcing, large intersection radii, gradual changes in wall thickness, and preferential thickening in highly-stressed areas will give optimum strength. It is not surprising that this should be true of branch connections. Parallel experience with machine design has led to the use of generous radii and gradual thickness changes to reduce the possibility of fatigue failures. Branch connections with such characteristics in varying degrees are commercially available as forged tee and crosses, manifold welding fittings, and drawn outlet laterals. In welding such fittings into a pipeline, care must be taken to obtain a full-penetration weld. Because the welding is done in a uniform circumferential joint, this is relatively easy to do as compared to making a complicated intersection weld between two pipes. Furthermore, the welds in such integral fittings are not ordinarily located in the area of highest stress.

While integrally-reinforced branch connections usually give optimum strength, there are occasions where it is either necessary or desirable to use a fabricated branch connection. Such occasions are when the size is such that forged fittings are not commerically available for "hot-tap" connections or where it is believed that the installed cost of a fabricated connection will be less than that using a commercial fitting and that the service conditions, both from the standpoint of severity of loadings and consequences of failures, are mild.

Where fabricated branch connections are to be used, the following types of construction are recommended:

a. For severe service conditions, use a complete encirclement type of reinforcement such as one of the types shown to be adequate by test.

b. For moderate service conditions, use saddles, pads, or other reinforcing members designed to meet code requirements. Sharp-angle laterals may require more reinforcing than implied by code requirements.

c. For mild service conditions, code requirements may be met by "unreinforced connections." However, extreme caution should be used to assure that substantial external loadings will not be applied, even though the pressure is of a low order.

In constructing fabricated branch connections, great care must be taken with welding in order to assure adequate service life. In making the branch-to-run pipe intersection weld, the ends of the branch should be properly shaped and beveled, or the opening in the run pipe shaped and beveled, so that full penetration of the weld can be obtained. Lack of penetration of this weld not only produces a severe mechanical notch in a highly-stressed location but also leaves a crevice that is ideal for promoting cell-type corrosion, should the fluid have any tendency toward this type of corrosion with the particular metal used in constructing the pipeline. The fillet weld between a reinforcing member, such as a saddle or pad, and the run pipe must also be carefully made to avoid undercutting into the run pipe at the toe of the fillet weld.

APPENDIX I. NOTATION

A_{Ra} = area of reinforcement available;

A_{Rr} = area of reinforcement required;

d = inside diameter of branch;

d_r = inside diameter of run pipe;

e = weld efficiency;

F_{Ab} = axial force;

F_{Ar} = end thrust due to internal pressure;

M = twisting moment;

M_{Bi} = in-plane bending moment;

M_{Bo} = out-of-plane bending moment;

F = applied load;

P_a = burst strength of branch connection;

P_c = burst strength of unreinforced pipe of same outside diameter and wall thickness;

p = internal pressure;

S = nominal bending stress;

S_c = constant stress component;

S_e = equivalent stress for completely reversed cycles;

S_{max} = maximum measured stress;

S_{nom} = nominal computed stresses;

S_v = variable stress component;

t = thickness of pipe;

Z_b = section modulus of the branch pipe in a branch connection;

Z_p = section modulus of pipe; and

α = angle between run and branch.

APPENDIX II. BIBLIOGRAPHY

(1) "Bursting Pressure Tests of Welded Pipe Headers," by Eric R. Seabloom, The Valve World, July-August, 1941.

(2) "Welded Tee Connections," by A. G. Barkow and R. A. Huseby, Welding Research Council Bulletin Series, No. 22, May, 1955.

(3) "Pressure-Pulsation Tests of Branch Connections to Large-Diameter Pipe," by A. R. C. Markl, H. H. George, and E. C. Rodabaugh, Transmission and Storage Conference, Paper GSTS-55-3, American Gas Assn. Gas Supply, Pittsburgh, Pa., May 9-10, 1955.

(4) "Stresses in Branch Connections," Report of the Supervising Committee for Pipeline Project NG-11, American Gas Assn., Inc., 1956.

(5) "Effect of Openings in Pressure Vessels," by J. H. Taylor and E. O. Waters, Transactions, Vol. 56, 1934, pp. 119-140.

(6) "Investigations of Stress Conditions in a Full-Size Welded Branch Connection," by F. L. Everett and A. McCutchan, Transactions, Vol. 60, No. 5 ASME, July, 1938, pp. 399-410.

(7) "Bursting Pressure Tests of Welded Pipe Headers Show Need for Nozzle Reinforcements," by E. R. Seabloom, Valve World, July-August, 1941.

(8) "Design of Fabricated Plate Steel Tees, Laterals and Wyes of Large Diameters for the Pressure Aqueduct of the Boston Metropolitan District Water Supply Commission," by C. J. Ginder and E. B. Cobb, Boston Society of Civil Engineers, Vol. 28, 1941.

(9) "Strengthening of Circular Holes in Plates Under Edge Loads," by L. Beskin, Journal of Applied Mechanics, September, 1944.

(10) "Stresses in a Cylindrical Shell Due to Nozzle or Pipe Connection," by G. J. Schoessow and L. F. Kooistra, Transactions, ASCE, Vol. 110, 1945.

(11) "Reinforcement of Branch Pieces," by J. S. Blair, Engineering, Vol. 162, London, July 5, 1946.

(12) Ibid., September 6.

(13) Ibid., November 29.

(14) Ibid., December 6.

(15) Ibid., December 13.

(16) Ibid., December 20.

(17) Ibid., December 27.

(18) "Experimental and Analytical Determinations of the Stress Systems in a Welded Pressure Vessel," British Welding Assn.

(19) "Analysis of Experimental Data Regarding Certain Design Features of Pressure Vessels," by G. J. Schoessow and E. A. Brooks, Transactions, ASME, July, 1950.

(20) "Fatigue Tests of Piping Components," by A. R. C. Markl, Transactions, Vol. 74, No. 3, ASME, April, 1952.

(21) "Design of Hot Tap Connections in High Pressure Pipelines," by A. J. Del Buono, P. L. Vissat and F. G. Williams, presented at the ASME Petroleum Conference, Houston, Tex., September 28-30, 1953.

(22) "Deformations and Stresses in Circular Cylindrical Shells Caused by Pipe Attachments," by N. J. Hoff, J. Kempner, S. V. Nordo, and F. V. Pohle, Report KAPL 921, 922, 923, 924, 925, and 1025, Knolls Atomic Power Laboratory, November, 1953.

(23) "Researches on Welded Pressure Vessels and Pipelines," by N. Gross, British Welding Journal, April, 1954.

(24) "Stress Analysis of Split Tee Welded Sleeve Reinforcement of Welding Branch Connection for Hot Tapping," Report by the Ladish Co., Metallurgical Dept., November 1, 1954.

(25) "Stresses from Radial Loads in Cylindrical Pressure Vessels," by P. P. Bijlaard, Welding Research Supplement of The Welding Journal, Vol. 33, December, 1954.

(26) Ibid., December, 1955.

(27) "Welded Tee Connections," by A. G. Barkow and R. A. Huseby, Welding Research Council Bulletin Series, No. 22, May, 1955.

(28) "Investigation of Static and Fatigue Resistance of Model Pressure Vessels," by J. Dubuc and G. Welter, The Welding Journal, July, 1956. Complete paper, "Fatigue Resistance of Simulated Nozzles in Model Pressure Vessels," Welding Research Council, Research Report, Vol. 22, 1957, pp. 271-274.

AMERICAN SOCIETY OF CIVIL ENGINEERS

Founded November 5, 1852

TRANSACTIONS

Paper No. 3035

THE COLUMBIA RIVER CONTROLLED

By Louis H. Foote,[1] F. ASCE

With Discussion by Messrs. Roy F. Bessey; and Louis H. Foote

SYNOPSIS

Continued planning is under way by the Corps of Engineers for development of the water resources of the Columbia River Basin. These studies will take cognizance of changed conditions and needs since the Corps' comprehensive report of 1948. This paper outlines these changes and the problems being encountered in providing an extended long-range plan for resource development.

Engineers of today recognize that as life becomes more complicated, so do the problems of planning for the future. There can be no final long-range plan. All plans that project into the future must be flexible, and engineers must be prepared to adjust changing conditions. Because perfect insight into the future is not possible, planning becomes an art rather than a science, and, with the passing of time, engineers must alter their sights and reconsider.

It was only 25 or 30 years ago that engineers first undertook to lay out a long-range plan for the Columbia River. Many of today's projects were proposed in the first Columbia River "308" Report[2] written in 1930 and 1931, The 10-dam plan recommended in 1932 by the Board of Engineers for Rivers and Harbors for ultimate development of the main Columbia River is essentially the plan in use today. In 1947 and 1948 a review report[3] was written on comprehensive planning for the Columbia River Basin. Further developments

Note.—Published, essentially as printed here, in January, 1958, in the Journal of the Waterways and Harbors Division, as Proceedings Paper 1514. Positions and titles given are those in effect when the paper or discussion was approved for publication in Transactions.

[1] Brig. Gen., Div. Engr., U. S. Army Engr. Div., North Pacific, Corps of Engrs., Portland, Ore.

[2] H. D. 103, 73d Congress, 1st Session.

[3] H. D. 531, 81st Congress, 2d Session.

were recommended in the light of conditions appraised at that time and another step forward was taken. Today, (1958) another appraisal is being made of the resources of the basin, and based on the new findings, the plans of the past will be realigned again for the future.

Present concepts of water resource planning for the Columbia River are slightly different than they were in the past. However, in many cases the changes have been so gradual that they are frequently overlooked, and engineers continue to analyze problems with the old yardstick. A brief summary of these changes should make them more apparent.

The most important economical use of water resources is for the generation of hydroelectric power. Even the early studies recognized the tremendous power potential of the Columbia River. However, the earliest estimates of future load were generally conservative. Fig. 1 shows the basin load estimates

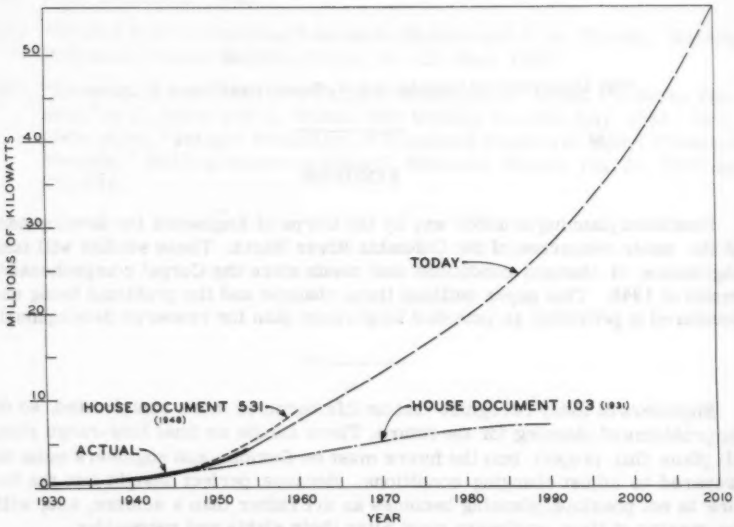


FIG. 1.—COMPARISON OF POWER LOAD ESTIMATES

contained in the 1931 and 1948 reports, together with the November 1956 estimate prepared jointly by the Federal Power Commission and the Bonneville Power Administration, and which has been accepted for the Corps of Engineers' current review report. Whereas there has been a great change in thinking since 1931, the major change since 1948 has been an extension of previous ideas. In 1931 it was certain there was adequate hydro power potential to meet the future load that was expected to stop increasing in approximately 1990. In 1948 the problem was again presented, but it was considered that insufficient hydro generation, necessitating the use of thermal power, would occur so far in the future that it would have little bearing on the economics of the projects being recommended at that time. However, with this eventuality in mind, space for future units was provided.

Fig. 2 gives a forecast of average annual energy requirements for the Pacific Northwest and shows the probable capabilities of obtainable, economic hydro generation and how the future load beyond that amount probably will be met with steam, both fossil-fuel fired and atomic. This situation, that appears inevitable now, requires several changes in the power approach.

In 1948 the basic concept for power analysis was an all-hydro system with only incidental small amounts of the more expensive thermal energy used during breakdowns, extreme critical peaking conditions, and similar emergencies. The basic problem was consequently one of providing enough peaking capacity and energy to meet the critical-period requirements. Storage was needed to

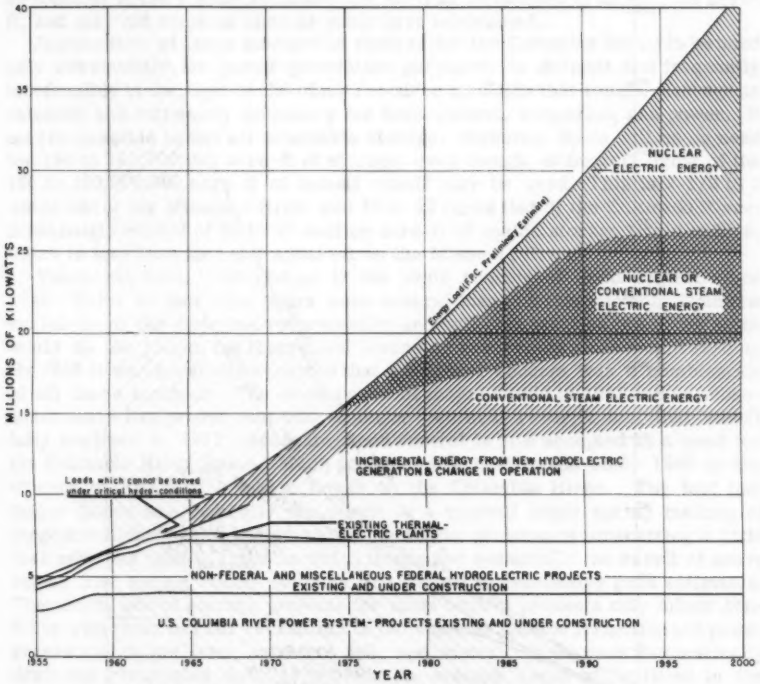


FIG. 2.—PACIFIC NORTHWEST LONG RANGE OUTLOOK

bridge this critical period. Extra generation obtainable during better than critical water conditions is the interruptible and secondary power available in any hydro system.

Fig. 3 shows how thermal generation will enter the present hydro system. The chart should be considered more demonstrative than factual because the data used to plot the curves are tentative estimates. The lower shaded area represents hydro energy and the shaded area just above it represents thermal energy. The average load estimate corresponds to the curve of average annual energy shown in Fig. 2. The cross-hatched areas represent peaking capacity, hydro and thermal, with the top line representing the estimated system

total peak requirement corresponding to the average annual energy forecast.

There are three general periods reflected in Fig. 3. First, the essentially all-hydro period up to sometime after 1975, at which time all of the obtainable economic hydro projects are assumed completed. At this point, increasing amounts of thermal generation must be added to meet the growing energy requirements. Additional units will be added at the hydro plants for capacity, and every effort will be made to utilize all water resources. Storage will be

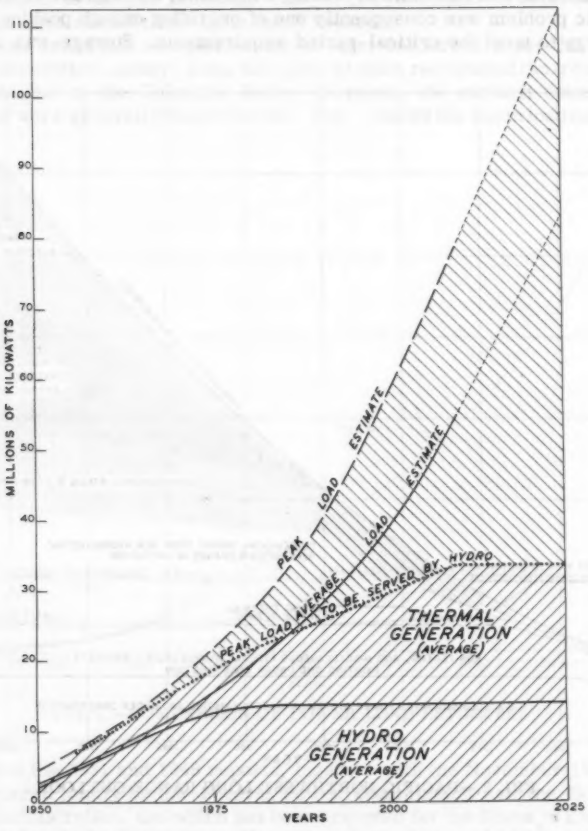


FIG. 3.—CHANGE FROM HYDRO SYSTEM TO THERMAL-HYDRO SYSTEM

used as much in the second period as in the first, and possibly more, because the load will be so great that it will be economical to use all refillable storage every year for steam replacement energy. Storage drawdown is frequently stopped after the peak has been met, and the reservoir is then refilled up to flood control limitations, even though it is known that water will be spilled later on.

The second period will end sometime after the year 2000, when no more capacity can be installed at hydro projects. This will be fixed by operational limitations, as well as by physical and economic considerations. After this time thermal generation will be required for both capacity and energy. The peaking requirements will be so great that the cheaper capacity sources must be fully utilized, and great care be taken to insure a full head at all the storage projects every year during the winter season when maximum capacity is required. Storage will be spaced judiciously, and its need and use will be somewhat less than before. This last period is frequently referred to as having an important bearing on the need for, and the economics of storage for power. It represents a major change in the storage concept, but it will still be possible to use a substantial amount, such as 20,000,000 to 25,000,000 acre-ft, and may not come as soon as some have envisioned.

Justification of large amounts of storage for the Columbia Basin, to be used only infrequently for power generation purposes, is difficult and frequently indefensible in the light of the other resource conflicts that result. Storage is valuable and extremely necessary for flood control, irrigation, and power. It may be possible to use all obtainable storage. However, there will ne no need for 150 to 180,000,000 acre-ft of storage, even though, ultimately, most of the 150 to 180,000,000 acre-ft of annual runoff may be used. This is 2-1/2 to 3 times that of the Missouri River and 10 to 12 times that of the Colorado River. In the neighborhood of 30 to 40 million acre-ft of usable storage would suffice, which is less than that now apparent on the Missouri River.

There has been little change in the basic concept of flood control since 1948. Prior to that time there were several ideas on this subject. Opinions varied from the view that reforestation and soil conservation practices alone would do the job, to the theory that levees or reservoirs alone would suffice. By 1948 it was generally accepted that the proper concept was a combination of all these methods. The occurrence of major floods in 1948 and in subsequent years has proven that this condition can still recur, a fact that wasn't fully realized in 1931. Adequate flood control is now accepted as a must for the Columbia River Basin. Much progress has been made since 1948 in the science of forecasting major floods on the Columbia River. The fact that major floods are basically the result of a general rapid spring melting of large accumulations of winter snows makes the problem of forecasting a little less nebulous than in areas in which floods are essentially the result of heavy rains. The spring runoff volumes are subject to reasonably good estimates. Therefore, use of storage projects for flood control presents only minor conflicts with their use for recreation in the summer and for irrigation and power generation in the later summer, fall, and winter. These uses automatically draw the reservoirs down to provide the storage space to be filled in the spring flood-control operation.

Although the goals that were established in 1948 are valid today, they are, unfortunately, still unattainable. Of the 21 million acre-ft of storage in the Main Control Plan that were found necessary to control the 1894 flood, there are only 5,190,000 acre-ft existing today that can be used. The present outlook is that only an additional 4,700,000 acre-ft will be achieved in the immediately prospective future.

Table 1 shows the flood control storage of the Main Control Plan of H. D. 531 distributed by major basins. The storage available for flood control use totals approximately 27,000,000 acre-ft. Similarly, the amount of storage used in that Main Control Plan for control of the 1894 flood to 800,000 cfs at The

Dalles totals approximately 21,000,000 acre-ft. Table 2 shows the present status of the Main Control Plan in storage usable at site. In addition to that which is existing or in reasonably immediate prospect, more than twice as much usable storage is needed to control the 1894 flood to 800,000 cfs. The changed conditions previously mentioned have interfered with completion of that Main Control Plan. A new appraisal and a new Main Control Plan will be required if flood control is to be achieved.

Table 3 shows possible additional storage projects that are available. The 9 million acre-ft in Table 3 (a) and (b) would be adequate, assuming the depleted flows estimated by 1985. A little more storage will be needed until that time. The question arises of whether it will be possible to achieve all eleven

TABLE 1.—MAIN CONTROL PLAN FLOOD CONTROL STORAGE[a]

Basin (1)	Project (2)	Stream (3)	Total Storage Available for Flood Control, in acre feet (4)	Storage used to Control 1894 Flood, in acre feet (5)
Kootenai	Libby	Kootenai River	4,250,000	3,900,000
Clark Fork	Glacier View	NF Flathead	3,160,000	1,800,000
	Hungry Horse	SF Flathead	2,980,000	2,100,000
	Subtotal		6,140,000	3,900,000
Snake	Palisades	Snake	1,200,000	1,200,000
	Cascade	Payette	650,000	160,000
	Garden Valley	Payette	1,250,000	300,000
	Anderson Ranch	Boise	420,000	
	Arrowrock	Boise	285,000	230,000
	Lucky Peak	Boise	295,000	
	Hells Canyon	Snake	3,280,000	2,600,000
	Subtotal		7,380,000	4,490,000
Columbia	Grand Coulee	Columbia	5,120,000	5,100,000
	Priest Rapids	Columbia	2,100,000	2,100,000
	John Day	Columbia	2,000,000	1,400,000
	Subtotal		9,220,000	8,600,000
	Total		26,990,000	20,890,000

[a] From H. D. 531, 81st Congress, 2d Session.

projects listed. It is probable that one or more of the controversial projects shown in Table 3 (c) will be required.

There has been a problem as to where the storage should be located. Fig. 4 shows the source of the three major floods most familiar to the region. There is a great similarity in the three diagrams. The total "pie" represents the observed volumes in each case passing The Dalles during the flood control

period. These total volumes for comparison are as follows:

a. 1894 72,300,000 acre-ft, the largest flood of record
b. 1948 57,800,000 acre-ft, the third largest
c. 1956 41,000,000 acre-ft, the eleventh largest, that could have been the fourth largest without the flood control operations that were carried out with existing storage.

TABLE 2.--PRESENT STATUS MAIN CONTROL PLAN STORAGE

Project (1)	Flood Control Storage usable at site to control 1894 Flood	
	Main Control Plan, in acre feet (2)	Present Outlook, in acre feet (3)
(a) Existing		
Hungry Horse	2,100,000	2,100,000
Grand Coulee	1,240,000[a]	1,500,000[b]
Palisades	1,200,000[c]	1,200,000[c]
Payette & Boise Rivers	390,000	390,000
Subtotal	4,930,000	5,190,000
(b) Additional proposed		
Grand Coulee (increase)	3,860,000	2,700,000[e]
Glacier View	1,800,000	---- [f]
Libby	3,900,000[g]	---- [g]
Priest Rapids	2,100,000	500,000[h]
John Day	1,400,000[d]	500,000[i]
Payette & Boise Rivers	300,000	---- [j]
Hells Canyon	2,600,000	1,000,000[k]
Subtotal	15,960,000	4,700,000
Total	20,890,000	9,890,000

[a] Amount formerly usable without use of outlets.
[b] Fully usable in 1956 and assumed to be available subsequently through use of 38 of 40 outlets in two top tiers but without additional upstream storage.
[c] Operable for storage in 1957.
[d] 2,000,000 acre feet was available for use as required.
[e] With 60 outlets. Full increase to presently estimated capacity of 5,230,000 acre feet not effective until other major storage above Grand Coulee is developed.
[f] Not recommended because of objections by recreation and wildlife interests.
[g] Authorized but construction delayed pending completion of negotiations with Canada. Current plan (Mile 217) provides for 5,010,000 acre feet of usable storage.
[h] Alternate 2-dam plan of Grant County PUD #2 would provide only 500,000 acre feet.
[i] Authorized but because of objections to surcharge storage, recommended modification to provide 500,000 acre feet submitted to Congress.
[j] Recommended Garden Valley project, Payette River, not authorized.
[k] Not authorized. Alternate Brownlee project would provide 1,000,000 acre feet. Pending Pleasant Valley project would provide additional 500,000 acre feet.

Fig. 5 (a) is an "exploded pie" for the 1894 flood. The control period is shown in Fig. 5 (b). The portions of each contribution that would be controlled by the storages in one of the prospective systems, assuming 1985 conditions

are shown. Actually, the system consists of the present outlook storage of 9,890,000 acre-ft shown on Table 1, the recommended Clearwater projects of 3,730,000 acre-ft, and the 5,290,000 acre-ft of storage under active study, shown on Table 3. The system thus totals 18,910,000 acre-ft of at-site stor-

TABLE 3.—POSSIBLE ADDITIONAL FLOOD CONTROL STORAGE[a]

PROJECT (1)	STREAM (2)	Total Storage Available, in acre feet (3)	Usable for control 1894 flood to 800,000 cubic feet per second at the Dalles, in acre feet (4)
(a) Previously recommended			
Bruces Eddy	NF Clearwater	1,430,000	1,430,000
Penny Cliffs	MF Clearwater	2,300,000	2,300,000
TOTAL		3,730,000	3,730,000
(b) Under active study			
Long Meadows	Yaak River	400,000	400,000
Spruce Park	MF Flathead	300,000	300,000
Flathead Lake Outlet	Flathead	500,000	500,000
Buffalo Rapids	Flathead	670,000	670,000
Ninemile Prairie	Blackfoot	960,000	720,000
Enaville	Coeur d'Alene	700,000	600,000
Wenaha	Grande Ronde	1,000,000	1,000,000
Garden Valley	Payette	1,250,000	600,000[b]
Pleasant Valley	Snake	500,000	500,000
TOTAL		6,280,000	5,290,000
(c) Others[c]			
Chiwawa	Wenatchee	150,000	150,000
Paradise	Clark Fork	4,080,000	4,080,000
Libby	Kootenai	5,010,000[d]	5,010,000[d]
Mica Creek	Columbia in Canada	11,700,000	7,670,000
Arrow Lakes	Columbia in Canada	3,030,000	1,200,000
Smoky Range	NF Flathead	1,500,000	1,500,000
Nez Perce (1490)	Snake	4,120,000	4,120,000
High Mountain Sheep (1490)	Snake	1,600,000	1,300,000

[a] Based on studies to April 1957, preliminary data.

[b] Garden Valley shown operated for downstream flood control. Only 300,000 acre-feet used, in H. D. 531 operated for local flood control with incidental downstream benefits. Similar operation will also increase usable storages at Cascade Reservoir from 160,000 acre-feet to 300,000 acre-feet. Additional 30,000 acre-feet assumed used at Deadwood Reservoir.

[c] Assumed in alternate systems.

[d] Libby data based on project at Mile 217.0. Modified project since H. D. 531.

age usable for control of this flood. To this was added an equivalent of approximately 2 million acre-ft to represent the irrigation depletions now forecast for 1985.

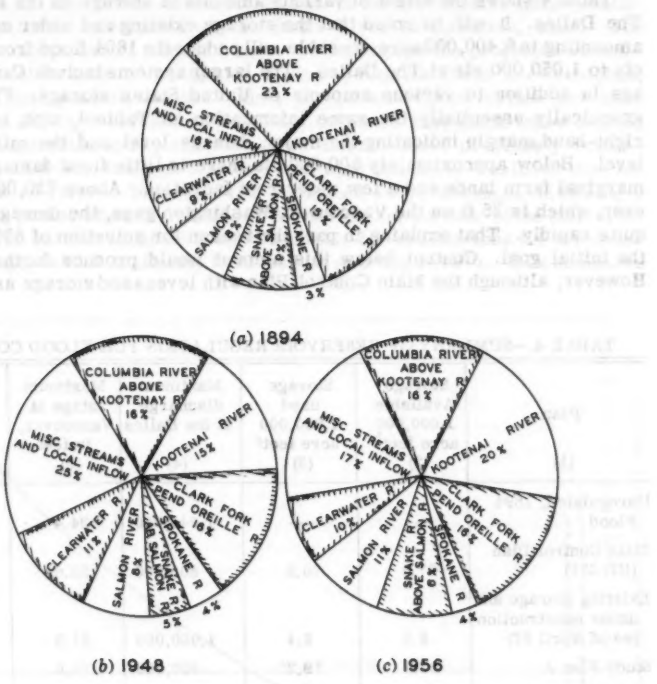


FIG. 4.—SOURCE OF MAJOR FLOODS

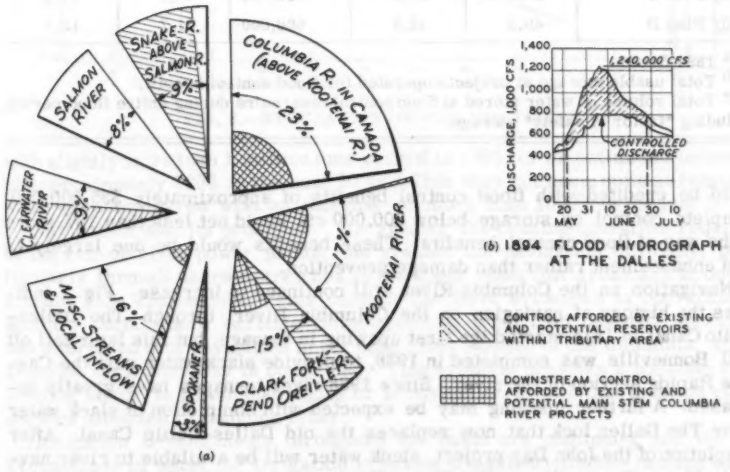


FIG. 5.—1894 FLOOD

Table 4 shows the effect of various amounts of storage on the 1894 flood at The Dalles. It will be noted that the storage existing and under construction, amounting to 6,400,000 acre-ft usable will reduce the 1894 flood from 1,240,000 cfs to 1,050,000 cfs at The Dalles. The larger systems include Canadian storage in addition to various amounts of United States storage. Fig. 6 shows graphically essentially the same information as Table 4, with, however, the right-hand margin indicating the major damage level and the minor damage level. Below approximately 500,000 cfs there is little flood damage except to marginal farm lands and a few waterfront facilities. Above 730,000 cfs, however, which is 25 ft on the Vancouver, Washington gage, the damage increases quite rapidly. That explains in part the reason for selection of 800,000 cfs as the initial goal. Control below this amount would produce further benefits. However, although the Main Control Plan with levees and storage as envisioned

TABLE 4.—SUMMARY OF RESERVOIR REGULATION FOR FLOOD CONTROL[a]

Plan (1)	Storage Available 1,000,000 acre feet[b] (2)	Storage used 1,000,000 acre feet[c] (3)	Maximum discharge at the Dalles (4)	Maximum stage at Vancouver, in feet (5)	Total stage reduction, in feet (6)
Unregulated, 1894 Flood	---	---	1,240,000	34.4	---
Main Control Plan (HD 531)	27.0	20.9	800,000	26.6	7.8
Existing storage and under construction (as of April 57)	8.5	6.4	1,050,000	31.3	3.1
Study Plan A	22.2	19.2	800,000	26.6	7.8
Study Plan B	28.4	25.3	690,000	24.0	10.4
Study Plan C	34.5	31.6	610,000	22.0	12.4
Study Plan D	49.2	38.9	600,000	21.7	12.7

[a] 1894 flood.
[b] Total usable storage at projects operated for flood control benefit.
[c] Total volume of water stored at flood control reservoirs during entire flood period, including "factor of safety" storage.

could be credited with flood control benefits of approximately $35,000,000, complete control by storage below 800,000 cfs would net less than 10% more in the way of flood control benefits. These benefits would be due largely to land enhancement rather than damage prevention.

Navigation on the Columbia River still continues to increase. Fig. 7 indicates the history of naviagion on the Columbia River, through The Dalles-Celilo Canal in 1915 started the first upswing in tonnage, but this later fell off until Bonneville was completed in 1938, to provide slack water past the Cascade Rapids section of the river. Since 1938 river tonnages have greatly increased. A further upswing may be expected with completion of slack water above The Dalles lock that now replaces the old Dalles-Celilo Canal. After completion of the John Day project, slack water will be available to river navigation from Bonneville to the Pasco-Kennewick area on McNary pool. Ice

Harbor Dam is now under construction and in the foreseeable future slack-water navigation is anticipated up the Snake River to Lewiston, Idaho. The navigation concept hasn't changed since 1948 although the projected viewencourages consideration of navigation up the Columbia River to Wenatchee, Washington, and possibly beyond. Also, the possibility of further low head dams on the Snake River above Lewiston indicates that slack water may be extended on upstream to replace open river improvement previously recommended. In 1948 the tonnage forecast was approximately 5 million tons for this stretch of river. This was the estimated 50-yr average, following a development period after completion of the navigation portion of the Main Control Plan. The current estimate is approximately 7.5 million tons for a similar 50-yr average, but for a slightly later period starting in 1975. This compares

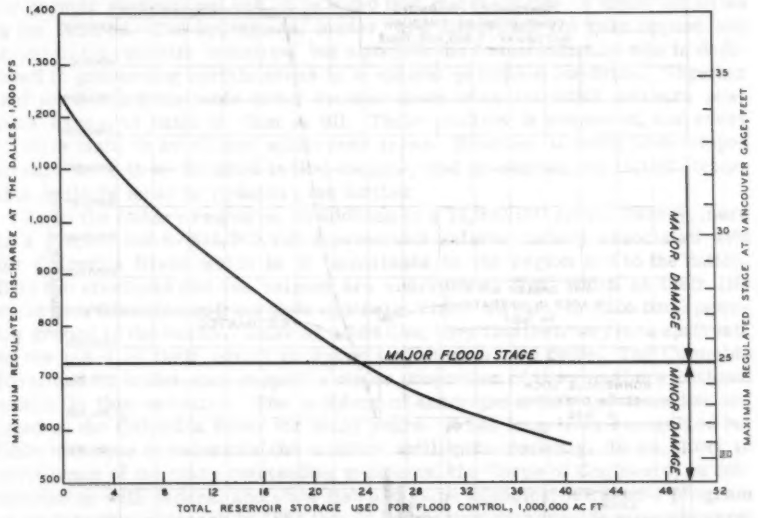


FIG. 6.—REGULATION OF THE 1894 FLOOD

with slightly more than 1 million tons passed in 1955, or an estimated increase of approximately 700% in the next 50 yr. This does not seem quite so remarkable when compared with an increase of more than 1000% in the last 20 yr.

Navigation has its problems. The greater the peaking operation required at the run-of-river power plants, the greater the navigation difficulty, particularly through narrow stretches in the upper reservoir areas and at downstream lock approaches. This conflict has been evidenced in operation of McNary Dam, where variable flows resulting from load factored operation has interfered with navigation in the open river stretch of the Columbia, which remains until John Day is completed. This problem presents a possible controlling factor in power operations or in navigation growth that must be given serious attention in planning today.

Irrigation developments throughout the basin are continuing and the increased use of water for irrigation is having a marked influence in many ways. In 1948, a careful study was made of future irrigation potentials to take into

account in all power studies the effect of future upstream depletions. Future depletions were estimated liberally in order to be conservative in the estimate of future power benefits from downstream projects. That was not necessarily a new concept in 1948, but it was not a factor commonly applied before. The horizon has been extended further into the future with the result that today the estimated future depletions are greater for the projects now being considered.

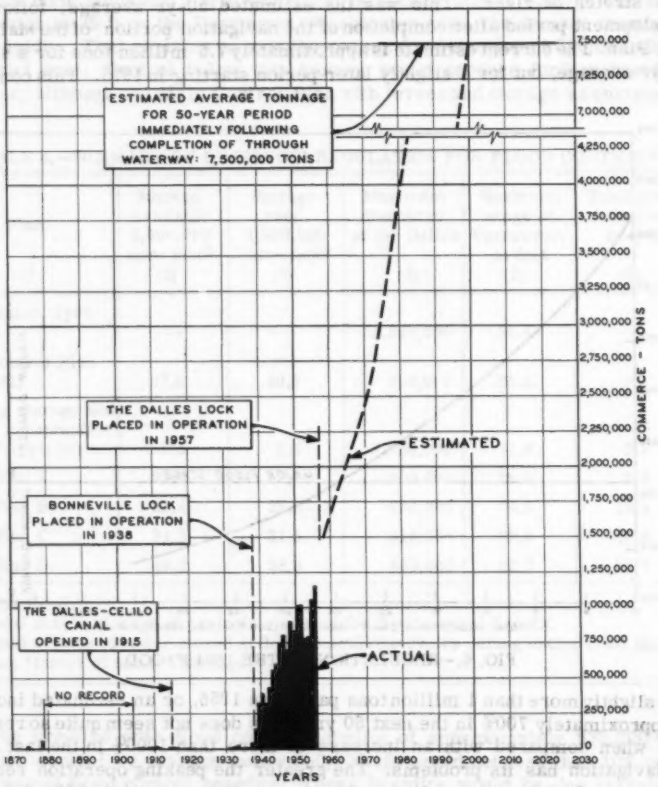


FIG. 7.--COMMERCE THROUGH THE DALLES-CELILO CANAL

There has been a tremendous upswing of interest in the matter of recreation since 1948. This is being evidenced not only locally, in connection with individual projects, but also at the congressional level where legislation has been under consideration to establish a national policy with respect to recreation. In 1948 recreation needs and values were considered but there was a lack of local interest in this area, in which there are so many recreational opportunities. Today, however, there is a serious interest not only in the

preservation of present recreational opportunities but also in developing new opportunities. This interest is shared by both sportsmen and conservation groups, and becomes very strong when the infringement of man-made dams and reservoirs on natural conditions is involved. As more and more leisure time becomes available for recreational activities and the need for increased development of water resources becomes greater, the conflict becomes critical. Comprehensive studies being conducted include serious attention to the matter of recreation. The National Park Service has agreed to undertake a recreational study in connection with each project considered and the Corps of Engineers'[4] report is comprehensive in this field also.

The pressure of civilization is forcing the development of water resources farther and farther upstream and wild, natural areas are now threatened by dams and reservoirs. Considering the problem of providing more facilities for greater recreational use, it is found that increased use of these facilities is not desired. The sportsman, hunter, and fisherman not only oppose any threat to the wildlife resource, but also join the conservationist who is dedicated to preserving certain areas in a natural primitive condition. Together they present a formidable factor because there is no remedial measure possible except to build no dam at all. Their position is respected, and every effort is made to avoid true wilderness areas. However, if every undeveloped stream were to be included in that category and preserved, the list of obtainable projects must be reduced even further.

As to the fishery resource, in addition to a $5,000,000 sports fishery, there is a $10,000,000 to $15,000,000 commercial salmon fishery associated with the Columbia River which is of importance to the region and to the nation. Both the steelhead and the salmon are anadromous fish, which in their life cycle pass downstream from their upstream river, stream, or lake bed spawning ground to the ocean. Later as adult fish, they find their way back upstream to the place of their origin to spawn and start a new cycle. The Columbia River and its tributaries support a major proportion of the remaining national wealth in this resource. The problem of anadromous fish and dams has existed on the Columbia River for many years. It has long been recognized but little was done to reconcile the conflict until quite recently. In an effort to solve some of the many outstanding problems, the Corps of Engineers, in collaboration with federal and state fish and game agencies, initiated a program of engineering research in 1953 that is now beginning to provide some answers.

Specifically, the Corps of Engineers' Fisheries Engineering Research program was designed to find less expensive and better means of passing fish both upstream and downstream over dams. Although the fish-passage facilities at Bonneville and McNary dams are proving generally satisfactory, research indicates that the ladders could be made steeper and narrower and still be adequate. In addition to economies in construction cost, there can be a saving in the amount of water that would bypass the turbines, providing a saving in operating costs at existing as well as future projects. Research also offers prospects of finding means of guiding downstream migrants away from spillway and turbine hazards and into facilities for handling the fingerlings safely downstream. Another prospective achievement is the proving out of artificial spawning grounds for salmon and steelhead. If artificial spawning areas can be constructed to effectively and economically provide replacement for natural spawning areas flooded by dams, another obstacle will be removed.

[4] Report on Water Resource Development of the Columbia River Basin, 1960.

Hatcheries, as a solution for lost spawning grounds, are not only expensive but unreliable when it comes to maintaining an important fish run.

The foregoing covers the major water uses except for water supply and pollution abatement. With the continued population growth and increased water requirement, the need for domestic and industrial water supply has become as serious in many parts of the country as the agricultural requirements. Similarly, the problem of pollution abatement has multiplied as the quantities of stream flows decrease and the amounts of industrial waste increase. Fortunately, the Columbia Basin has few problem areas of this nature, either at the present time or expected in the immediate future. This problem has been emphasized by the recent drought of the Southwest, and careful attention will be given to the matter in the current comprehensive review report,[5] with the assistance of the Public Health Service.

An additional element of the Columbia River problem, involving as much national policy as engineering, is the Canadian aspect. Approximately 15% of the headwater drainage area of the Columbia River lies in British Columbia. From this area comes approximately 29% of the average annual runoff of the river at its mouth. Consequently, major water use developments in Canada could have a material bearing on developments downstream in the United States. In 1948, there was little active interest in Canada for early utilization of the water resources of the Columbia River but since that time an active interest has developed. Largely prompted by an inquiry of the International Joint Commission relative to the Libby project, but intensified by the comparison of economic growth in Canada with that of the United States resulting from large amounts of low cost power, interest in Canada in a comprehensive plan for maximum resources development has grown to possibly exceed that in the United States' portion of the basin. At the present time the Canadian Federal Government, the Provincial Government, and both public and private utility interests of British Columbia are exploring, estimating, and actively studying various project potentials. United States groups are also interested in working out a procedure whereby they could profit from their Canadian investment within the United States.

Canadian planning is of serious concern to the United States because of the effects on downstream projects. One of the plans under active study[5] involves the diversion of the Kootenay River at Canal Flats, directing all the Kootenay River runoff above that point, a runoff of approximately 2 million acre-ft annually, down the Columbia River in Canada, rather than down the Kootenai River through Libby and the other potential head developments within the United States. From the Canadian point of view that would be a far better plan, but from the United States point of view, many millions of kilowatt hours would be lost. The question is, which solution is best from the over-all point of view, and then how should the loser be compensated.

Another plan, involving diversion in Canada from the Columbia River into the Fraser River Basin, would mean a complete annual loss of some 15 million acre-ft of water to the United States through all its main stem plants, Grand Coulee and downstream. Although this proposal appears possible from an engineering standpoint, and possibly attractive from the economic viewpoint of Canada, it may not prove entirely practicable.

The major international problem will be the adjustment of costs and benefits. Any regulation in Canada will benefit the United States, provided that the

[5] 1959 Report by the International Columbia River Engineering Board to the International Joint Commission.

water is not lost entirely, and coordinated operation of the projects of the two countries would result in a greater benefit. In order to be equitable, Canada and the United States should share these downstream benefits. The question is, how much benefit to each. Engineering will play its part in estimating the values involved, but the final decision probably will be made by others after many factors have been considered. Until this is done, the final economic picture for the United States projects remains undecided. Yet development must continue because power and the flood control are needed.

Thus planning must proceed and the Columbia River must be controlled. If the maximum return is to be realized at a minimum cost, both in dollars and other resource values, all the engineering science available, as well as good judgment, must be employed. Realizing the magnitude of the task and the great responsibility it imposes, the Corps of Engineers has used the best talent available throughout the region and the country in preparing its report.[4] The Corps' procedures have been likened to a "fish bowl" operation, because everyone was invited to observe and express opinions. All interested Federal and State agencies participated. The Bureau of Reclamation actually took over a large share of the detailed project studies. Private power and public power people from both the administrative and the operational level were represented on the Corps' advisory committees, as were navigation and other interests. There was a board of engineering consultants from other parts of the nation. This was a departure from previous custom, and whereas many complications and problems were added by reason of the extra persons employed, engineers who are familiar with this type of work will recognize that in this increasingly complicated world many things must be considered other than straight engineering on a technical level.

CONCLUSIONS

Comprehensive planning is needed and it is obvious, in spite of the fact that changes are almost inevitable, that long-range planning must continue if the Columbia River is to be controlled effectively and to the maximum practicable advantage. The major water plan for the Columbia River as developed in recent studies is a product of that type of planning. It provides a valuable guide to meet the flood control, navigation, power, and other water resource needs of the basin, regardless of the outcome of concurrent studies being made of the Canadian water resource potentialities.

DISCUSSION

ROY T. BESSEY,[7] M. ASCE.—The 1948 report[8] of the Corps of Engineers represented a considerable step forward from the 1932 report[9] in concepts of comprehensive, multiple-purpose development of a major river basin. Ideally,

[7] Consultant, Resources and Regional Planning, Portland, Ore.
[8] H. D. 531, 81st Congress, 2d Session, Columbia River and Tributaries.
[9] H. D. 103, 73d Congress, 1st Session, Columbia River and Tributaries.

the result of the 1958 report should present another forward step, with new emphasis on full development and use of resources.

A plan for full development faces a number of evident hazards in the form of opposition to various elements by the interests affected, as well as in proposals for piecemeal or limited-purpose development. These opposing forces can cut deeply into the heart of a comprehensive, rational, and widely beneficial plan.

Yet the need of full development of basic river basin resources is greater than ever. In the face of rapidly expanding population, of rising living standards, and of the growing material, economic, and social needs of a highly productive economy, our resource base must be strenthened and widened and our natural resources conserved and used to the fullest. This is reason enough for a full development plan. But such a conclusion should be inevitable in view of a continuing, long-run world crisis in which our strength and leadership in the scientific development and use of resources is a matter of great moment both at home and abroad. It is emphasized by an increasing knowledge of strong advances in the technology and development of vast river basins and other resources, by other nations.

It will be evident, as the author implies, that problems of planning and development call for more than the best available engineering science. The problems of economics, of negotiation, of legislation, of organization, and cooperation—of political science particularly—should be apparent also.

The case for the full development of the Columbia River system is especially strong. The Columbia is the nation's greatest power streams and has one of the largest water supply potentials. It has outstanding navigation potentials, particularly as far as the west is concerned. The resources of the Columbia are thus of truly large national consequence, and their full development and contribution toward meeting the needs of the national economy and of our defense and security are distinctly in the general interest.

Public Interest and Need, Basic Principles and Policy.—The national and public interests involved demand the rigorous application of well-established principles of conservation and development, and the firm establishment of the best feasible plan and program of development.

The wise use of national resources is linked inseparably with underlying purposes of human enterprise, security, and well-being. Development of these resources should make a maximum contribution to the growing material needs of the nation. They should make their vital contributions to pressing regional and local needs for expanded and diversified economic opportunity, both for purposes of relieving recession and stabilizing employment through construction and related industry in the immediate situation and of strengthening the industrial and general economic base for the longer run.

The hard-won principles of wise and full conservation and use of resources, of comprehensive and coordinated, multiple-purpose, basin-wide development, of maximum net benefit and wide distribution of benefits, should be applied to the feasible limit.

Coordinated Main Control Plan.—A coordinated main control plan providing maximum feasible storage and regulation of flow is required. This is the key to achieving maximum benefits, well distributed among multiple uses and geographic areas. The high sights of the 1948 plan, in its current and ensuing phases, should not be lowered. The goals of the plan for the next two decades should include well located and distributed storage capacity, that will reduce the flow of an 1894-volume flood to approximately half or not over 600,000 cfs.

at The Dalles. It should provide maximum at site and downstream power, to insure adequate water supplies in quantity and quality for rapidly expanding industrial, agricultural, municipal, and domestic uses, and to provide other material benefits.

The gross and net benefits of strategically-located, large-capacity, up-river storages of a main control plan, such as the large Hells Canyon, Nez Perce, Paradise, Libby, and Canadian projects, are greatly superior in scope and economy to the limited-purpose and limited-scope projects that would bar development of the larger projects and result in permanent losses of resources, project, and program capabilities and benefits. Such key projects are essential to attainment of optimum river regulation and should be included in the ultimate and immediate programs.

Individual and Combined Aspects of Development.—Some aspects of development aims and criteria that should be especially stressed are:

Water Storage.—The retention of excess flows and release at more favorable times is a fundamental purpose and procedure in river system development and utilization. The uses of storage in flood control, power production, and water supply are readily apparent. On the Columbia River, where floods are primarily of the more predictable snow-melt type, the conflicts among storage uses are relatively minor. The uses for flood control and power are quite complementary and mutually supporting. The main burden of establishing feasibility of storage development rests on both of these needs. Adequate storage capacity is the key to a comprehensive and effective main control plan with a balanced upstream and downstream development in which feasibility of each is enhanced by the other. Under the circumstances, it is desirable to aim at the highest feasible level of storage development.

Power.—The vital and rapidly expanding energy needs of the national economy exert great pressure for the most complete and economical development of the water-power resources of the Pacific Northwest. The importance of abundant electrical energy at lowest practicable cost can hardly be overstated, nor can the use of the Columbia River's full potentials. Obviously, that full potential in maximum output and low unit cost connot be attained if the at site and downstream values of upstream projects go unrealized.

Under the anticipated load growth of the next two decades power requirements will pass beyond the combined power capacity of all feasible hydro projects. Because the unit costs of such hydro power will be less than that of thermal power, all feasible hydro should be developed; not to do this would be a waste of a continuing, self-replenishing resource.

Due to economies of large scale, multiple-purpose development, hydraulic and electric integration, and of public financing, the lower unit cost of power from the large Federal projects should also be considered for its spiraling and cumulative effects. The lower cost will induce higher usage and economic activity, raising rate of load growth, and increasing power benefits. The low energy cost is crucial in the location and establishment of certain heavy industrial plants because their primary effects in economic expansion and diversification are needed in the region.

Therefore, it is suggested that load estimates for power development can be too conservative and tend to inhibit full and timely development. One way to avoid power shortage is to hold growth down and to fail to meet the need.

Although power benefits do not stand alone and must be considered in conjunction with other multiple benefits of a coordinated plan, they are largest

among individual benefits in monetary and economic terms. The economic returns from high-volume, low-cost power—in added industrial development and diversity, in raised production, income and living levels, and in increased strength, balance and security in local, regional and national economies—are very great and broadly proportionate with the volume and economy of the power made available.

Flood Control.—With dependence primarily on upstream storage (on Columbia and up-river tributaries and on the Willamette) and secondarily upon local levee systems, flood control is essential for protection of life, property, and productivity, and for effective use of strategic and highly-valuable lowland areas for their best economic purposes. Full weight must be given, of course, to the direct and indirect, measurable and unmeasurable human values of flood control, to the savings in human life and welfare, in individual and family well being, and the prevention of losses and dislocations in industry, service and community activities, and in production and income.

Navigation.—Development of the west's outstanding seaway and inland waterway reaching far into the interior, with maximum feasible geographic extension and channel and lock improvement to highest practicable standards, is essential to realization of economic potentials of the river system and the region. It will provide a material contribution to the national economy.

Water Supply.—Water supply enhancement and security, in one of the nation's top-ranking resources, is necessary to meet widely-recognized and growing needs, particularly for crucial demands of industry, but also for vital agricultural, municipal, and domestic requirements.

Combined Uses.—The strategic combination of navigation, abundant and low-cost power, and adequate water supplies, coupled with local port, terminal, and industrial district improvements, should be given full and coordinate consideration in a basic plan and program. Flood control combines with these strategic elements in enhancing the developmental values inherent in the waters and waterfronts of main-stem areas.

Irrigation.—Irrigation that can be provided through the development of the Columbia River is of primary importance. It is essential that the maximum feasible acreage be developed to meet the expanding food and fiber needs of a growing west and nation. The new crop land is needed, in spite of increasing efficiency of production, to meet requirements of an expanding population coupled with substantial withdrawals of crop land areas for various special purposes, including those of urban, industrial, transport, and military usage, as well as for reasons of agricultural submarginality.

Fisheries.—Fisheries are of importance not only because of the positive economic and social values in the Columbia system, but because of the deterrent effect of fishery problems and controversies upon a full and timely multiple-purpose development of the rivers. It is highly desirable that the fishery aspect be considered from a progressive and developmental, and not merely a protective standpoint. An entirely adequate and fully integrated attack on the fishery part of the development problem has not been previously attained. Essential fishery research, planning, and improvement work has tended to lag behind in the procession of river project development. There is need for a new initiative in picking up neglected opportunities for extending the fisheries' capabilities both as to area and volume. The solution of the problem of passage at high dams is particularly pressing from the standpoint of fish resource protection. It may also open, or even reopen, long river reaches for fish production. Fishery research, planning, and experimental work should be stepped up to proceed in advance of prospective river changes. Fishery improvement

should proceed in close concert with river development works if maximum values are to be obtained in fishery and general development.

Other beneficial water uses mentioned by the author, including watershed management, recreation, and wildlife, are not discounted in any sense. They are of great and growing economic and social significance and should be considered as primary objects and benefits in both immediate and long-range plans and programs of development.

Project area planning is a field in which a larger and better coordinated effort would pay extra dividends in project and program benefits. A major river development project will be of greatest value and will have assurance of successful consummation if its integral nature and close relationship to its environment are preserved, if all of the mutually supporting uses are developed to the fullest, included in plan and authorization, and carried out in coordination.

In this field responsibility and leadership must be shared among federal, state, and local agencies. Coordinated project, land, community, and utility planning should proceed, with project planning and development, with the view of minimizing inevitable dislocations and reaping maximum benefits in timely and orderly re-establishment and establishment of farms, industries, homes, communities, transportation, electric utilities, governmental services, and other facilities and activities affected.

In this connection, preliminary draft legislation for the large Paradise project on the Clark Fork of the Columbia would make interesting and innovating provisions for area replanning under federal sponsorship. Past joint investigations[10] and planning activities headed by the Bureau of Reclamation in connection with its Columbia Basin project provide a useful precedent.

Coordination of Effort.—The difficulties in putting and holding together a complex plan and program are great. This is a condition that is widely recognized as a result of long and varied experience in the Columbia and other basins. Accordingly, it is suggested that special attention be given to problems and needs of organization and procedure and other ways and means for coordination of effort in planning and programing, public information and cooperation, legislation and authorization, appropriation and finance, and construction and operation aspects and stages of development.

Federal Aims and Responsibilities.—A Federal purpose and responsibility for the wise conservation, development, and management of national resources, for most effective improvement of major river systems with maximum aims in beneficial use for all purposes, shows clearly in the constitutional, legislative and policy background of river basin investigations and planning, such as that presented by the author. In the present crucial situation, with its clear need for expansion in resource base and with a momentous review of the comprehensive plan for the Columbia system coming under executive and legislative consideration, the Corps of Engineers clearly holds a responsibility for drawing the best, the most comprehensive, and most effective development plan possible.

LOUIS H. FOOTE,[11] F. ASCE.—Bessey submits a stimulating supplement to the original paper that evidences the deep interest and concern of informed individuals in adequate planning for the development and use of the water resources of the Columbia River Basin. The argument for full development of

---

10 U. S. Bureau of Reclamation, Columbia Basin Joint Investigations, (a series of reports on planning problems of the project and project area, circa, 1941, et seq.)

11 Brig. Genl., U. S. Army (Retired), Cons. Engr., Forest Grove, Ore.

the Columbia River resource for maximum multiple use benefits is most convincing. However, the planner must evaluate all of the factors involved in the problem of Columbia River development, regardless of their nature, to determine what constitutes full development. Only by this process can an economically sound plan be evolved that will assure optimum tangible benefits. A plan based on an exclusively theoretical study would, regardless of its excellence, be of only academic interest and value.

AMERICAN SOCIETY OF CIVIL ENGINEERS

Founded November 5, 1852

TRANSACTIONS

Paper No. 3036

STRENGTH OF REINFORCED CONCRETE BEAMS

By Sidney A. Guralnick,[1] M. ASCE

With Discussion by Messrs. Henry J. Cowan; Robert F. Warner; Béla Goschy and George Balázs; Kuang-Han Chu; and Sidney A. Guralnick

SYNOPSIS

Shear failure of concrete beams is recognized as the failure under combined compression and shear of the concrete above a diagonal crack. Rational interaction equations for the failure of plain concrete under this stress combination are developed on the basis of Mohr's failure theory. For the equations to be applicable, the strength of the particular concrete in direct compression as well as in direct tension must be known. The latter is determined satisfactorily from the modulus of rupture. The equations are used to develop a rational theory of shear strength of beams without web reinforcement.

It is the object of this paper to examine some basic aspects of the problem of shear strength of reinforced concrete beams with a view toward establishing a general shear-strength theory. In particular, a theory is developed for the shear strength of beams with plain webs that is based on the material's properties and geometry of the beam. The theory is considered to have possibilities for extension to the case of beams having reinforced webs. Test results from twenty-one beams with plain webs and eight beams having vertical stirrups as web reinforcement were compared with values for ultimate strength predicted by the theory developed herein.

INTRODUCTION

Recent interest in ultimate-load methods of design both in the United States and abroad has led researchers to re-examine problems connected with the

Note.—Published, essentially as printed here, in January, 1959, in the Journal of the Structural Division, as Proceedings Paper 1909. Positions and titles given are those in effect when the paper was approved for publication in Transactions.

[1] Asst. Prof., Dept. of Civ. Engrg., Illinois Inst. of Tech., Chicago, Ill.

ultimate strength of reinforced concrete beams. The problem of predicting the behavior and load at failure of reinforced concrete beams that fail in flexure has been mostly solved. Such is not the case with regard to beams that fail in shear. A number of recent papers[2,3,4,5,6,7,8,9,10,11,12] on this subject have explored various aspects of this problem; however, a definitive general solution remains to be attained.

Notation.—The letter symbols adopted for use in this paper are defined where they first appear and are arranged alphabetically, for convenience of reference, in the Appendix.

RELATED PROPERTIES OF MATERIALS OF PLAIN CONCRETE

General.—Failure in shear of a reinforced concrete beam is assumed to occur in two stages. First, an inclined crack or cracks form in the web of the beam (such as zone A of the beam of Fig. 1(a) either as a continuation of existing flexural cracks or independent of any existing cracks. These inclined cracks are usually termed diagonal-tension cracks. Second, a region of the compression concrete immediately above a diagonal-tension crack (such as zone B of the beam of Fig. 1(a) fails either by crushing or by a prolongation of a diagonal-tension crack entirely through it, causing a sudden destruction of the carrying capacity of the beam. Considering a beam with plain web, such as the one shown in Fig. 1(a), the distribution of forces at failure in shear is assumed to be as given in Fig. 1(b). It may be observed from Fig. 1(b) that the concrete of zone B is subjected to a combination of shearing and compressive forces. Furthermore, the load causing destruction of the beam in shear is seen to be determined by the resistance of the plain concrete of zone B to a stress pattern consisting of a combination of shearing and normal compressive stresses.

Strength of Plain Concrete Subjected to Biaxial Stress.—The question of the strength of plain concrete subjected to a biaxial or triaxial stress field has

---

2 "Diagonal Tension Strength of Reinforced Concrete Tee Beams with Varying Shear Span," by A. F. Al-Alusi, Journal, A.C.I., Vol. 28, May, 1957.

3 "Diagonal Tension in Reinforced Concrete Beams," by Arthur P. Clark, Ibid., Vol. 23, October, 1951.

4 "Effect of Moment-Shear Ratio on Diagonal Tension Cracking and Strength in Shear of Reinforced Concrete Beams," by A. Feldman and C. P. Siess, Civil Engineering-Studies Structural Research Series, No. 107, Univ. of Illinois, Urbana, Ill., June, 1955.

5 "Some Implications of Recent Diagonal Tension Tests," by P. M. Ferguson, Journal, A.C.I. Vol. 28, August, 1956.

6 "The Ultimate Strength of Reinforced Concrete Beams in Shear," by Royston Jones, Magazine of Concrete Research, Vol. 8, England, August, 1956, pp. 69-84.

7 "Strength in Shear of Reinforced Concrete Beams," by A. Laupa, C. P. Siess, and N. M. Newmark, Bulletin No. 428, Engrg. Experiment Sta., Univ. of Illinois, Urbana, Ill., March, 1955.

8 "Shear Strength of Reinforced Concrete Beams," by K. G. Moody, et al., Journal, A.C.I., Vol. 26, December, 1954, pt. 1.

9 Ibid., Vol. 26, January, 1955, pt. 2.

10 Ibid., Vol. 26, February, 1955, pt. 3.

11 Ibid., Vol. 26, March, 1955, pt. 4.

12 "An Investigation of the Strength of Welded Stirrups in Reinforced Concrete Beams," by O. Moretto, Ibid., Vol. 17, November, 1945.

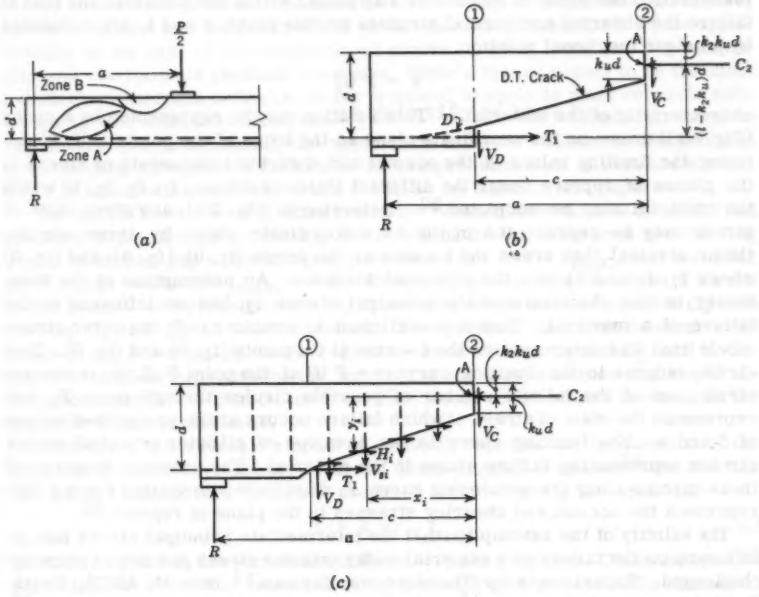


FIG. 1.—FAILURE OF REINFORCED CONCRETE BEAM

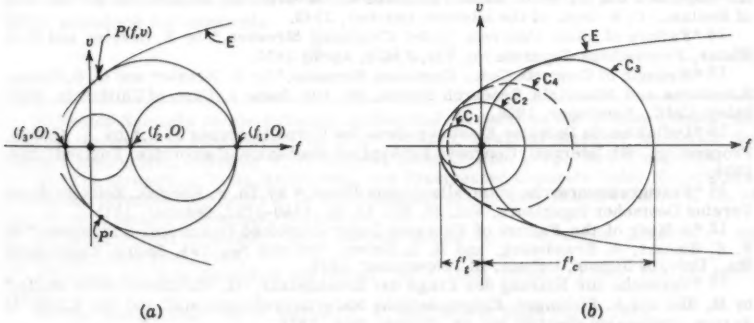


FIG. 2.—DEVELOPMENT OF ENVELOPE FOR MOHR'S CIRCLE

been investigated by numerous researchers.[13,14,15,16,17,18,19] One of the earliest theories developed was Mohr's rupture theory.[20] The basic postulate of Mohr's theory is that failure occurs by sliding or slipping on a definite plane (called the plane of rupture or slip plane) within the material and that at failure the shearing and normal stresses on this plane, v and f, are connected by a unique functional relation,

$$v = F(f)$$

characteristic of the material.[21] This relation may be represented by a curve (Fig. 2(a)) drawn on the coordinate plane as the locus of the points P (f, v) defining the limiting values of the normal and shearing components of stress in the planes of rupture under the different states of stress, f_1, f_2, f_3, to which the material may be subjected.[20] Referring to Fig. 2(a), any given state of stress may be represented in the f - v coordinate plane by three circles (Mohr circles) that cross the f - axis at the points $(f_1, 0)$, $(f_2, 0)$, and $(f_3, 0)$ where f_1, f_2 and f_3 are the principal stresses. An assumption of the Mohr theory is that the intermediate principal stress, f_2, has no influence on the failure of a material. Thus it is sufficient to consider only the outer stress circle that has intercepts on the f - axis at the points $(f_1, 0)$ and $(f_3, 0)$. This circle, tangent to the limiting curve $v = F(f)$ at the point P (f, v), is the one circle, out of the infinite number of possible circles through point P, that represents the state of stress at which failure occurs at the prescribed values of f and v. The limiting curve is the envelope of all outer principal stress circles representing failure states in the material. The points of tangency of these circles along the enveloping curve, E, must have coordinates f and v that represent the normal and shearing stresses in the plane of rupture.[20]

The validity of the assumption that the intermediate principal stress has no influence on the failure of a material under triaxial stress has been seriously challenged. Experiments by Theodore von Karman,[17] Hon. M. ASCE, Frank G. Richart, F. ASCE, et al.,[18] and Mirko Ros, F. ASCE, and A. Eichinger[19]

---

13 "Shearing Strength of Concrete Under High Triaxial Stress—Computation of Mohr's Envelope as a Curve," by G. Balmer, Structural Research Lab. Report, No. SP-23, Bur. of Reclam., U. S. Dept. of the Interior, October, 1949.

14 "Failure of Plain Concrete Under Combined Stresses," by B. Bresler and K. S. Pister, Proceedings-Separate No. 674, ASCE, April, 1955.

15 "Strength of Concrete Under Combined Stresses," by B. Bresler and K. S. Pister, Structures and Materials Research Series, No. 100, Issue 1, Univ. of California, Berkeley, Calif., November, 1956.

16 "Definition du Domaine Elastique dans les Corps Isotropes . . . ," by A. Caquot, Proceedings, 4th Internatl. Congress for Applied Mechanics, Cambridge, England, July, 1934.

17 "Festigkeitsversuche unter allseitigem Druck," by Th. v. Kármán, Zeitschrift des Vereins Deutscher Ingenieure, Vol. 55, No. 42, pp. 1749-1757, October, 1911.

18 "A Study of the Failure of Concrete Under Combined Compressive Stresses," by F. E. Richart, A. Brandtzaeg, and R. L. Brown, Bulletin No. 195, Engrg. Experiment Sta., Univ. of Illinois, Urbana, Ill., November, 1928.

19 "Versuche zur Klarung der Frage der Bruchgefahr. II, Nichtmetallische Stoffe," by M. Rôs and A. Eichinger, Eidgenossische Materialprufungsanstalt and der E.T.H. in Zurich, Diskussion sbericht No. 28, Zurich, June, 1928.

20 "Theory of Flow and Fracture of Solids," by A. Nadai, Vol. 1, 2d Ed., McGraw-Hill Book Co., Inc., New York, 1950.

21 "Elasticity, Fracture, and Flow," by J. C. Jaeger, John Wiley and Sons, Inc., New York, 1956.

among others, have shown that failure in brittle materials, such as marble and concrete, subjected to triaxial compression is definitely influenced by the magnitude of the intermediate principal stress. Although the use of Mohr's theory in the case of three-dimensional stress is open to question, no experimental evidence has been uncovered so far that would cast doubt on its applicability to the case of two-dimensional stress. Indeed, from both the simplicity and clarity of its physical reasoning, Mohr's theory seems to be the most satisfactory strength criterion so far proposed to apply to plain concrete subjected to two-dimensional stress.[13,22,16,23,24,25,26,27] Since stresses in beams are two-dimensional, the application of Mohr's theory to the problem of predicting stresses at failure in the compression zone of reinforced concrete beams seems reasonable and it will be so taken in this paper.

The normal and shearing stresses in the compression zone of a reinforced concrete beam usually vary along the length of the beam between two limiting states of stress, one extreme being pure shear ($f = 0$, $v = v_{max}$), and the other pure compression ($f = f_{max}$, $v = 0$). Referring to Fig. 2(b) the state of stress in the beam's compression zone is, in general, represented by circle C_4 with circles C_2 and C_3 as limiting cases. The problem then is to determine the shape of the envelope, E, in the region between circles C_2 and C_3, and to determine relationships between the normal and shearing stresses that would allow prediction of the load on the beam that would cause failure to occur in the concrete compression zone.

There is a considerable amount of research reported on the question of the shape of the Mohr envelope for concrete. Mohr himself proposed[28] the straight line as an envelope. A. Caquot[16] proposed a curve having the equation

$$f = k v^{\gamma} - f_o \quad \ldots\ldots\ldots\ldots\ldots\ldots \quad (1)$$

in which K, γ and f_o are experimentally determined constants. Glenn Balmer,[13] reporting the results of research at the United States Bureau of Reclamation, Department of the Interior (USBR), gives equations of similar form connecting the principal stresses that were obtained by a least squares analysis of his test data compiled from more than 50 specimens: $f_3 = 0.0051\ f_1^{1.37} - 430$ for 28-day-old concrete, and $f_3 = 0.0074\ f_1^{1.33} - 480$ for 90-day-old concrete. P. Pernot[26] proposes an equation of the form of a semi-cubical parabola for the Mohr envelope for concrete

$$v^3 = k'f^2 + k'' \quad \ldots\ldots\ldots\ldots\ldots\ldots \quad (2)$$

---

22 "Some Remarks on the Influence of Residual Stresses on the Brittle, Plastic, and Fatigue Behavior of Structures," by P. P. Bijlaard, Residual Stresses in Metals and Metal Construction, edited by W. R. Osgood, Reinhold Pub. Corp., New York, 1954.

23 "The Strength of Plain, Reinforced, and Prestressed Concrete Under the Action of Combined Stresses," by Henry J. Cowan, Magazine of Concrete Research, Vol. 5, No. 14, pp. 75-86, England, December, 1953.

24 "Prestressed Concrete," by Y. Guyon, edited by W. M. Johns, John Wiley and Sons, Inc., New York, 1953.

25 "Uber der Scherfestigkeit des Betons," by A. Leon, Beton u. Eisen, Vol. 34, April, 1935.

26 "Le Beton Arme," by P. Pernot, J. B. Bailliere et Fils, Paris, 1954.

27 "Drillung (Torsion), Schub, und Scheren im Stahlbeton-Bau," by Ernst Rausch, Dritte, Neubearbeitete und erweiterte Auflage Vertrieb: Deutscher Ingenieur—Verlang-cmbh, Dusseldorf, 1953.

28 "Strength of Materials," by S. Timoshenko, D. Van Nostrand Co., Inc., New York, 1956, pts. 1 and 2.

in which k' and k'' are other experimentally determined constants. Allen Leon,[25] A.M. ASCE, advocates the use of a simple parabola for the same purpose:

$$v^2 = e f + e' \ldots\ldots\ldots\ldots\ldots\ldots \quad (3)$$

in which e and e' are experimentally determined constants. In all of these equations it is necessary to evaluate at least two parameters in terms of physical properties of the material obtained from tests. In the case of the concrete in the compression zone of a beam it has been shown that the limiting stress circles are those of pure shear and pure compression. Consequently, it seems logical to try to base the Mohr envelope equation on the pure shear and pure compression strength of the concrete as determined by tests. The drawback to this approach is the difficulty, if not impossibility, of devising a

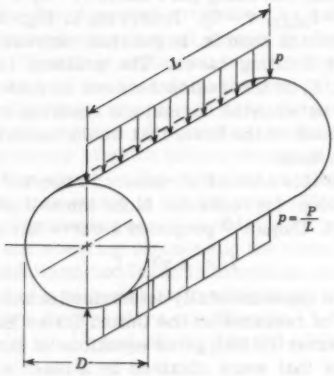


FIG. 3.—AZAKAWA SPLITTING TEST

procedure for making a pure shear test on a specimen of plain concrete. The only satisfactory procedure proposed so far consists of subjecting a specimen in the shape of a long, thin, hollow cylinder to torsional loading. Obviously, this procedure is unsuitable for the needs of construction practice in which it is required that large numbers of samples be tested with the simplest possible equipment, preferably portable, operated by semi-skilled or sub-professional personnel. In order to overcome this difficulty the researchers previously cited, among others, have proposed the use of the uniaxial tension test in place of the pure shear test. Thus, it is concluded that the two physical constants of concrete that are to be used in determining an equation for Mohr's envelope are the tensile strength and the compressive strength.

Tensile Strength of Plain Concrete.—As yet no entirely satisfactory procedure has been devised for obtaining the tensile strength of a plain concrete specimen. The specimen either fails in the grips, or the procedure is so complicated and costly that it is not suitable for adoption by the construction

industry. In order to avoid these two problems, indirect tensile tests have been devised. The most recent of these is the Azakawa splitting test.[29] This test consists in loading a standard cylindrical specimen on its side as shown in Fig. 3 and in obtaining the tensile strength as

$$f_t = \frac{2P}{\pi D L}$$

in which P is the total load at rupture, D is the diameter and L the length of the specimen. This test may be performed in the same testing machine and on the same size cylindrical specimens as used in the standard compression test. The only difficulty lies in the requirements that the sides of the specimen must be perfectly straight and parallel, as must be the loading plates of the testing machine. These requirements probably make this test unsuitable for field practice, but it still remains a very useful research technique.

The oldest, simplest, and hitherto most widely accepted indirect method for evaluating tensile strength of concrete is the flexural modulus of rupture test (A.S.T.M. Standard C-78). The procedure consists in subjecting a plain concrete prism of square cross section and a length equal to three times its width to beam type loading at its third points. Such specimens fail in tension when the stress in the most highly stressed tensile fiber reaches the ultimate strength of concrete in tension. The so-called flexural modulus of rupture is the maximum tensile stress at the failure load calculated by the formula

$$f_r = \frac{M}{Z} \quad \ldots\ldots\ldots\ldots\ldots\ldots \quad (4)$$

in which M is the bending moment and Z is the section modulus. This formula is based on the assumption of a straight-line stress-strain diagram. It is well known that the tensile stress-strain diagram for concrete is not a straight line up to the point of failure, but is curved and closely resembles a scaled-down version of the compressive stress-strain diagram.[30] Consequently, the quantity f_r considerably overestimates the true ultimate stress at the outer fiber because no assumption of plastic redistribution of stresses is made in the derivation of Eq. 4. Fortunately, there seems to be a simple relationship connecting the flexural modulus of rupture, f_r, and the true tensile strength, f_t. This relation is of the form

$$f_r = e_1 f'_t$$

with e_1 of the range, 1.8 to 2.2. The constant e_1 is influenced by the type of loading, shape of the specimen and type of concrete.[29,31,32] However, for the usual 6-in.-by-6-in.-by-18-in. specimen subject to third-point loading (that will be termed the standard flexural test), and for the usual concretes found in

---

29 "Tension Test Method for Concretes," by Tsueno Azakawa, Bulletin No. 16, Union of Testing and Research Labs. for Materials and Structures, November, 1953, Paris.

30 "Tensile and other Properties of Concrete Made with Various Types of Cements," by L. Schuman and J. Tucker, Journal of Research, Natl. Bur. of Standards, U. S. Dept. of Commerce, Washington, D. C., Vol. 31, August, 1943.

31 "Compression, Flexure, and Tension Tests of Plain Concrete," by H. F. Gonnerman and E. C. Shuman, Proceedings, A.S.T.M., Vol. 28, 1928, pt. II.

32 "The Effect of Several Mechanical Features of Testing on the Determination of the Flexual Strength of Plain Concrete," by T. F. Willis and F. N. Wray, Proceedings, A.S.T.M., Vol. 28, 1928, pt. II.

construction practice in the United States, e_1 may be taken as approximately 2.0. Then the previous equation becomes

$$f_r = 2.0\, f'_t$$

From investigation made by the writer,[33] it has been found that the usual approximation

$$f'_t = \frac{1}{10} f'_c$$

is not generally applicable. If one defines the ratio of tensile to compressive strength of a given concrete as $\alpha = f'_t/f'_c$, the extreme range of α can be[24] from 1/30 to 1/8. For usual concretes (say from 2000 psi to 6000 psi), the range of α is from 1/16 to 1/10. This indicates that tensile strength, f'_t, is an independent property of the material and should be just as much a part of concrete theory as the cylinder compressive strength, f'_c.

The major premises of this paper can be summarized as follows:

1. Mohr's strength theory is assumed to be applicable to the problem of predicting the combination of normal and shearing stresses that will cause rupture in the concrete of the compression zone of a reinforced concrete beam.
2. The two physical properties of concrete that are sufficient to determine the Mohr envelope are the compressive strength, f'_c, and the tensile strength, f'_t.
3. Tensile strength may be evaluated satisfactorily by means of the modulus of rupture test, and if the standard flexural test is employed, the relation between f_r and f'_t may be taken as $f_r = 2.0\, f'_t$. This approach is different from previous practice in the United States in that it is predicated on specifying not only the compressive strength, but also the tensile strength of concrete.

Derivation of an Interaction Equation for Predicting the Strength of Plain Concrete Subjected To Shearing and Compressive Stresses.—The problem now remaining is to ascertain the shape of the Mohr envelope in the region between the circle of pure tension and the circle of pure compression. Specifying a shape of the envelope in this region leads directly to the specification of a value for the pure shear strength, v'_c, and to relationships that govern the interaction of shearing and normal stresses at rupture for states of stress that lie in the region under consideration.

It was mentioned previously that the shape of the envelope may be assumed as given by either Eqs. 1, 2 or 3. The curves of any of these equations in the region between circles C_1 and C_3 of Fig. 2(b) are so flat that it appears justifiable to assume that the envelope in this region may be approximated by two straight lines tangent to the circles C_1 and C_3 (i.e. curve E of Fig. 4). It can be seen from Fig. 4 that this approximation is somewhat conservative because the curves of any of the three equations given lie outside the envelope E, formed by the two straight lines in the region between circles C_1 and C_3. This same approximation of the Mohr envelope by two straight lines has been used also by Henry J. Cowan[23] and Ernest Rausch.[27] It should be noted that a straight line approximation of the Mohr envelope is definitely not valid for states of stress that are represented by circles, such as C_5, that lie outside the range between circles C_1 and C_3, because the true envelope is probably similar to curve E' in Fig. 4, instead of the approximation denoted E in that figure.

---

[33] "Some Basic Aspects of the Problem of Shear Strength of Reinforced Concrete Beams," by S. A. Guralnick, thesis presented to Cornell Univ., at Ithaca, New York, in 1958, in partial fulfilment of the requirements for the degree of Doctor of Philosophy.

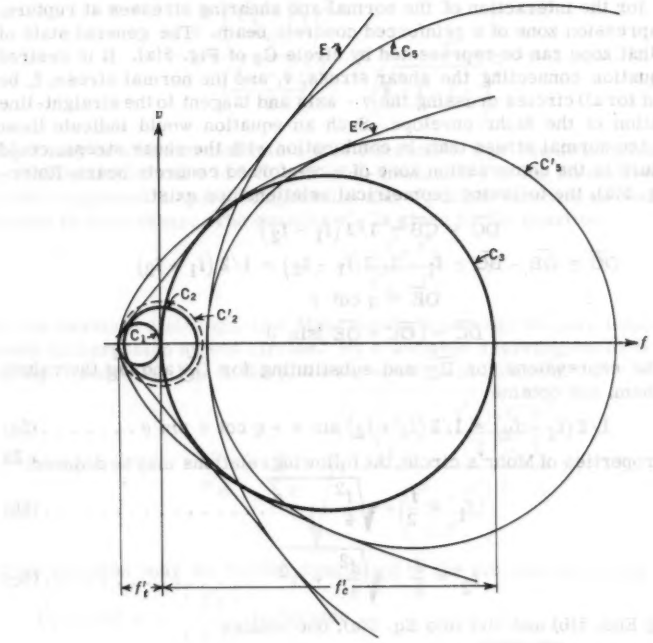


FIG. 4.—POSSIBLE ENVELOPES FOR MOHR'S CIRCLES

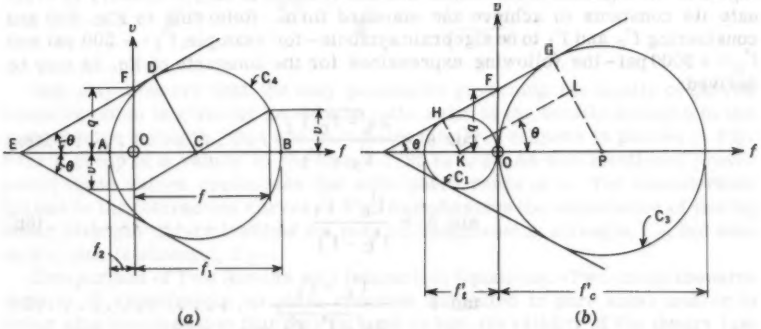


FIG. 5.—GEOMETRICAL RELATIONSHIPS FOR STRAIGHT LINE APPROXIMATION OF MOHR ENVELOPE

If the shape of the Mohr envelope in the region between circles C_1 and C_3 of Fig. 4 is taken to be a straight line, a simple analytic expression may be developed for the interaction of the normal and shearing stresses at rupture, in the compression zone of a reinforced concrete beam. The general state of stress in that zone can be represented by circle C_4 of Fig. 5(a). It is desired that an equation connecting the shear stress, v, and the normal stress, f, be determined for all circles crossing the v - axis and tangent to the straight-line approximation of the Mohr envelope. Such an equation would indicate those values for the normal stress that, in combination with the shear stress, could cause rupture in the compression zone of a reinforced concrete beam. Referring to Fig. 5(a), the following geometrical relationships exist:

$$\overline{DC} = \overline{CB} = 1/2\,(f_1 - f_2)$$

$$\overline{OC} = \overline{OB} - \overline{BC} = f_1 - 1/2\,(f_1 - f_2) = 1/2\,(f_1 + f_2)$$

$$\overline{OE} = q \cot \theta$$

$$\overline{DC} = (\overline{OC} + \overline{OE}) \sin \theta$$

Equating the expressions for $\overline{DC}$ and substituting for $\overline{OC}$ and $\overline{OE}$ the values given for them, one obtains

$$1/2\,(f_1 - f_2) = 1/2\,(f_1 + f_2) \sin \theta + q \cot \theta \sin \theta \quad \ldots\ldots\ldots (5a)$$

From the properties of Mohr's circle, the following relations may be deduced:[28]

$$f_1 = \frac{f}{2} + \sqrt{\frac{f^2}{4} + v^2} \quad \ldots\ldots\ldots\ldots\ldots (5b)$$

$$f_2 = \frac{f}{2} - \sqrt{\frac{f^2}{4} + v^2} \quad \ldots\ldots\ldots\ldots\ldots (5c)$$

Substituting Eqs. 5(b) and 5(c) into Eq. 5(a), one obtains

$$\sqrt{\frac{f^2}{4} + v^2} - 1/2\, f \sin \theta = q \cot \theta \sin \theta \quad \ldots\ldots\ldots (5d)$$

Eq. 5d is the equation of an ellipse in f and v, and it is only necessary to evaluate its constants to achieve the standard form. Referring to Fig. 5(b) and considering f'_c and f'_t to be algebraic symbols—for example, $f'_t = -300$ psi and $f'_c = +3000$ psi—the following expressions for the constants of Eq. 5d may be derived:

$$\cos \theta = \frac{2\sqrt{-f'_c f'_t}}{f'_c - f'_t} \quad \ldots\ldots\ldots\ldots\ldots (6a)$$

$$\sin \theta = \frac{f'_c + f'_t}{f'_c - f'_t} \quad \ldots\ldots\ldots\ldots\ldots (6b)$$

$$\tan \theta = \frac{f'_c + f'_t}{2\sqrt{-f'_c f'_t}} \quad \ldots\ldots\ldots\ldots\ldots (6c)$$

and

$$q = \frac{\sqrt{-f'_c f'_t}}{2} \quad \ldots\ldots\ldots\ldots\ldots (6d)$$

On substituting these constants into Eq. 5(d) and by suitable rearrangement of

terms, one obtains the standard form of the equation of an ellipse with variables v and f as

$$\frac{f - \left(\frac{f'_c + f'_t}{2}\right)^2}{\left(\frac{f'_c - f'_t}{2}\right)^2} + \frac{v^2}{\left(\sqrt{-f'_c f'_t}/2\right)^2} = 1 \quad \ldots\ldots\ldots\ldots (7)$$

Eq. 7 may be transformed into a true interaction type equation by changing the variables from f and v to f/f'_c and v/v'_c in which f'_c is the strength of the concrete subjected to pure compression and v'_c is the strength of concrete subjected to pure shear. The quantity v'_c is given by the equation

$$v'_c = \frac{-f'_c f'_t}{f'_c - f'_t} \quad \ldots\ldots\ldots\ldots\ldots\ldots (8)$$

if one assumes a straight-line Mohr envelope between the pure tension and the pure compression stress circles. By a suitable rearrangement of the terms of Eq. 7 and using Eq. 8, the following equation is obtained:

$$\frac{v}{v'_c} = \frac{q}{v'_c}\sqrt{1 - \frac{\left(\frac{f}{f'_c} - \frac{f'_c + f'_t}{2f'_c}\right)^2}{\left(\frac{f'_c - f'_t}{2f'_c}\right)^2}} \quad \ldots\ldots\ldots\ldots (9a)$$

This equation may be further simplified by the introduction of the constant $\alpha = -f'_t/f'_c$ or $\alpha = \frac{|f'_t|}{|f'_c|}$ to become

$$\frac{v}{v'_c} = \frac{(1+\alpha)\sqrt{\alpha}}{2\alpha}\sqrt{1 - \frac{\left(\frac{f}{f'_c} - \frac{1-\alpha}{2}\right)^2}{\left(\frac{1+\alpha}{2}\right)^2}} \quad \ldots\ldots\ldots\ldots (9b)$$

One may observe that the only parameter governing the family of curves whose equation is given by Eq. 9(b) is α, the ratio of the tensile strength to the compressive strength. This one parameter family of ellipses is plotted in Fig. 6 for a group of α values in the range 1/25 to 1/8. As was mentioned previously, these values encompass the anticipated range of α. The considerable spread in the interaction curves of Fig. 6 emphasizes the importance of basing shear strength determinations not only on compression strength, f'_c, but also on the tensile strength, f'_t.

Comparison of Test Results with Interaction Equations.—Two comprehensive reports of experiments on plain concrete subjected to pure shear and/or to shear plus compression that may be used to test the validity of the theory just developed are those of Herbert J. Gilkey,[34] F. ASCE, and of Boris Bresler, M. ASCE, and Karl S. Pister,[14,15] M. ASCE.

[34] Discussion by H. J. Gilkey of "Experiments with Concrete in Torsion," by Paul Anderson, Transactions, ASCE, Vol. 100, 1935, p. 960.

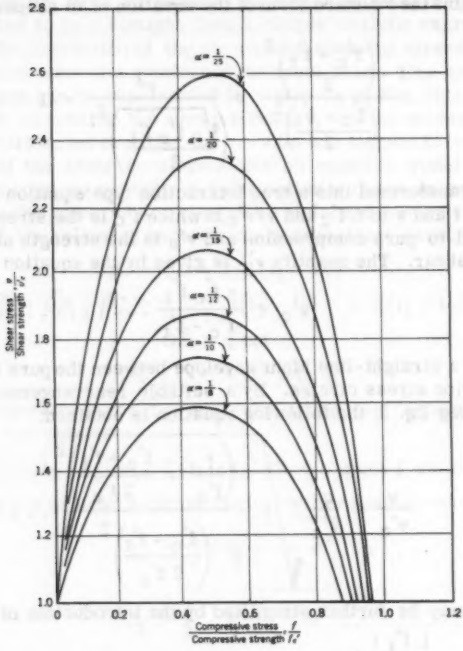


FIG. 6.—THEORETICAL CURVES FOR THE SHEAR-COMPRESSION STRENGTH OF PLAIN CONCRETE

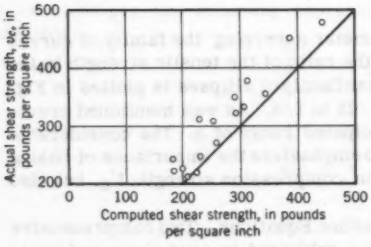


FIG. 7.—COMPARISON OF SHEAR STRENGTH OF PLAIN CONCRETE SPECIMENS WITH COMPUTED SHEAR STRENGTH

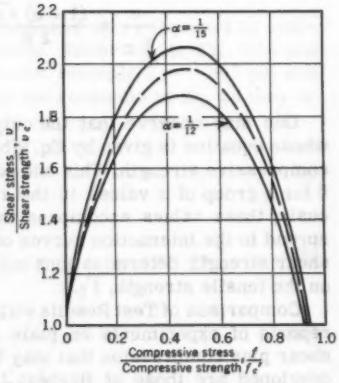


FIG. 8.—COMPARISON OF THEORETICAL CURVES WITH AN EMPIRICAL CURVE

The investigation reported by Gilkey contained data from a number of compression, flexure, tension, and torsion tests on plain concrete specimens. The torsion tests were performed on solid cylindrical specimens and yielded data on the behavior of plain concrete subjected to a pure shear state of stress. This data on shear strength at failure, v'_c, has been compared with predicted values for shear strength computed by means of Eq. 8. This comparison is given in Fig. 7, in which v'_c is the actual shear stress at failure[34] for a particular specimen and v''_c is the predicted shear stress at failure computed by means of Eq. 8. It is apparent from Fig. 7 that the values for shear strength predicted by Eq. 8 are in reasonable agreement with the test results and are conservative, which, in view of the many uncertainties inherent in the problem, is not prejudicial to the theory.

Bresler and Pister's series of tests were on hollow cylindrical specimens subjected to a combination of axial and torsional loading. They have proposed the following empirical equation as giving a lower limit for their test points:

$$\frac{v}{f'_c} = 0.1\sqrt{0.622 + 7.86\,\frac{f}{f'_c} - 8.46\left(\frac{f}{f'_c}\right)^2} \quad \ldots\ldots\ldots (10)$$

This empirical equation can be compared with the theoretical interaction equation (Eq. 9(b)) by making certain transformations. Bresler and Pister found that the pure shear strength of their specimens could be described by the empirical equation

$$v'_c = 0.079\, f'_c \quad \ldots\ldots\ldots\ldots\ldots\ldots (11)$$

If both sides of Eq. 10 are multiplied by the quantity f'_c/v'_c and the value of v'_c given by Eq. 11 is used on the right-hand side of Eq. 10, then the following equation results:

$$\frac{v}{v'_c} = 1.265\sqrt{0.622 + 7.86\,\frac{f}{f'_c} - 8.46\left(\frac{f}{f'_c}\right)^2} \quad \ldots\ldots\ldots (12)$$

A curve representing this equation is shown dashed in Fig. 8. The "interaction" curves for values of α equal to 1/12 and 1/15 have also been drawn in this figure for purposes of comparison. It can be seen that the curve of Eq. 12 lies exactly midway between the two theoretical interaction curves. Since the average ratio, α, of the tensile to compressive strength of the concretes used in the Bresler-Pister report is 1/13.4 or midway between the values of 1/12 and 1/15, the test curve is seen to be in satisfactory agreement with theory.

In view of the reasonable agreement between experiment and theory for the specimens cited it is concluded that the "interaction" equation (Eq. 9(b)) developed in this paper reasonably and conservatively describes the behavior of a plain concrete member subjected to a combination of shearing and compressive normal stresses in a two-dimensional state of stress.

ELEMENTS OF A THEORY FOR THE SHEAR STRENGTH OF REINFORCED CONCRETE BEAMS

General.—Failure in shear in reinforced concrete beams of normal proportions occurs in two stages. First, an inclined crack or cracks, usually called

diagonal-tension cracks, form in the web of the beam in a zone such as zone A of Fig. 1(a) at a load below the ultimate. This crack or cracks may form at the top of an existing vertical flexural crack or independent of any flexural cracks. Such cracks usually extend themselves at both ends as loading on the beam increases. The second and ultimate stage occurs when the compression concrete immediately above a diagonal-tension crack (zone B of Fig. 1(a)) fails. Failure of the compression concrete may take the form of the shear-compression failure in which only simple crushing is apparent in the compression zone, or it may take the form of the diagonal-tension failure, which occurs by prolongation of the diagonal-tension crack entirely through the compression zone and from bottom to top of the beam. No distinction will be made herein between a diagonal-tension and a shear-compression failure. Both types of failure are considered to be one and the same, except that they exhibit different modes of rupture of the compression concrete in the critical zone above a diagonal-tension crack or cracks. That is, both types of failure are really only different manifestations of a failure in the compression concrete. This failure is governed by the interaction equation developed in the preceding section.

In beams without web reinforcement, the diagonal-tension crack causing failure may, on reaching the level of the longitudinal steel, turn to a horizontal plane and result in a phenomenon known as a splitting failure (line D of Fig. 1 (b)). It is assumed herein that this is a secondary effect and that the shear carried by the longitudinal steel (V_D in Fig. 1(b)) may be neglected in computing the shear resistance of a reinforced concrete beam.

The basic assumptions made in this paper in regard to beams failing in shear are:

1. Failure in shear cannot occur before the formation of the first diagonal-tension crack.
2. Diagonal-tension cracking is governed by the maximum shearing stress occurring in the web of the uncracked beam (that is, considering the full cross-section as resisting the shear).
3. Rupture of the compression concrete in the critical zone immediately above a diagonal-tension crack is governed by the interaction formula, Eq. 9 (b), which is based on Mohr's rupture theory.
4. The average shear stress in the critical compression zone at failure can be taken as

$$v = \frac{V_c}{b\, k_u\, d} \qquad \ldots\ldots\ldots\ldots\ldots\ldots (13)$$

because the concrete below the neutral plane cannot sustain shear stresses at ultimate load in view of the presence of numerous flexural-tension cracks. In this equation V_c is the resisting shear supplied by the compression concrete and k_u is the ratio of depth of neutral axis to effective depth at failure in flexure.

5. The normal stress distribution in the critical compression zone is assumed to be as given in Fig. 9 with the constants k_1, k_2 and k_3 given by the following equations:[35]

---

35 "Concrete Stress Distribution in Ultimate Strength Design," by E. Hognestad, N. W. Hanson, and D. McHenry, Journal, A.C.I., Vol. 27, December, 1955.

$$k_1 = 0.94 - \frac{f'_c}{26{,}000}$$

$$k_2 = 0.50 - \frac{f'_c}{80{,}000}$$

$$k_3 = \frac{3900 + 0.35}{3900 + 0.82\, f'_c - \frac{f'_c}{26{,}000}}$$

Formation of the First Diagonal-Tension Crack.—Because a shear failure by definition cannot occur before the formation of the first diagonal-tension crack, it is necessary to have some means for predicting the shear, V_{cr}, at which that crack forms. One way to approach this problem is to argue that the shearing stress that causes the first diagonal-tension crack to form is that stress, based on the gross concrete section, at which failure in pure shear would occur according to Mohr's rupture theory. This assumption is fairly justifiable in most cases because very little tension cracking occurs to damage the beam before the first diagonal-tension crack appears. The equation for the shearing stress, v_{cr}, that causes the first diagonal-tension crack to appear can be taken as

$$v_{cr} = \frac{V_{cr}\, Q_{max}}{I_{gr}\, b}$$

which gives

$$V_{cr} = \frac{v'_c\, I_{gr}\, b}{Q_{max}}$$

in which Q_{max} is the first moment, based on the gross concrete section, of the cross-sectional area lying above or below the centroidal axis; I_{gr} is the moment of inertia of the gross concrete area; and b is the thickness of the beam web at the centroidal axis. The shear stress, v'_c, is the predicted stress at failure of a plain concrete member subjected to pure shear. This stress may be predicted according to Eq. 8 based on Mohr's theory. One may expect that the shear, V_{cr}, causing the first diagonal-tension crack will be conservatively predicted by the preceding equation since it was shown previously that Eq. 8 is also on the conservative side.

Beams with Plain Webs.—Considering the free body diagram of Fig. 1(b), the equation for the compressive force, C, is:

$$C = \frac{M}{(1 - k_2\, k_u)\, d} \quad \ldots\ldots\ldots\ldots\ldots\ldots \quad (14a)$$

Defining f to be the average compressive stress over the cross-section, then

$$C = f\, b\, k_u\, d \quad \ldots\ldots\ldots\ldots\ldots\ldots \quad (14b)$$

and equating C given by Eqs. 13(a) and 13(b), and solving for f, one obtains:

$$f = \frac{M}{b\, d^2} \cdot \frac{1}{k_u\,(1 - k_2\, k_u)} \quad \ldots\ldots\ldots\ldots\ldots\ldots \quad (15a)$$

The average shear stress at failure is given by the Eq. 13 which can be solved for k_u as $k_u = \frac{V}{v\, b\, d}$. One of the k_u's in Eq. 15 may be replaced by this expression to yield the equation:

$$f = v \frac{M}{V d} \cdot \frac{1}{1 - k_2 k_u} \quad \text{(15b)}$$

which may be further transformed by introducing the constants f'_c and v'_c as:

$$\frac{v}{v'_c} = \frac{f}{f'_c} \cdot \frac{1 - k_2 k_u}{M/V d} \cdot \frac{f'_c}{v'_c} \quad \text{(15c)}$$

Defining a new constant K_p as

$$K_p = \frac{1 - k_2 k_u}{M/V d} \cdot \frac{f'_c}{v'_c}$$

and substituting it in Eq. 15(c) one obtains the equation:

$$\frac{v}{v'_c} = K_p \frac{f}{f'_c} \quad \text{(16)}$$

Thus for a given value of K_p a straight line relation between the two quantities v/v'_c and f/f'_c is obtained that can be combined with the interaction equations to yield information on the shear strength of reinforced concrete beams. A procedure that may be used to predict the shear strength of a given beam is as follows:

1. Compute the constant K_p using the materials' properties and proportions of the given beam.
2. Plot the straight-line graph of Eq. 16 on the interaction-curve diagram (Fig. 10).
3. Select the interaction curve that has the same ratio of tensile to compressive strength, α, as the concrete of the given beam, and obtain the coordinates of the point of intersection of the straight-line graph of Eq. 16 with the proper interaction curve. The coordinates of the point of intersection are the ratios v/v'_c and f/f'_c, which give the average stresses on the critical compression zone in the beam at failure. Once the ratio v/v'_c is known, one can easily compute the maximum shear stress, v, that the critical compression zone can resist by using Eq. 8 and the corresponding shear force from Eq. 13.

It has been tacitly assumed in the foregoing development that the maximum normal stresses in the critical compression zone are high enough to be in the inelastic or plastic range, thus giving rise to the stress distribution of Fig. 9. If, on obtaining the coordinates of the point of intersection, P, on Fig. 10 for a given beam, it is found that the ratio f/f'_c is less than approximately 0.5 to 0.7, an elastic (that is, triangular) distribution of normal stresses in the critical compression zone must be assumed. In such a case a derivation entirely similar to the aforementioned could be performed and would result in the following equations:

$$\frac{v}{v'_c} = K_e \frac{f}{f'_c} \quad \text{(17)}$$

in which

$$K_e = \frac{j}{M/V d} \cdot \frac{f'_c}{v'_c}$$

in which j is the ratio of arm length of internal couple of flexural resisting moment to effective depth. In most cases, however, K_e and K_p are very close in magnitude, so much so that differences in the ratios v/v'_c and f/f'_c obtained

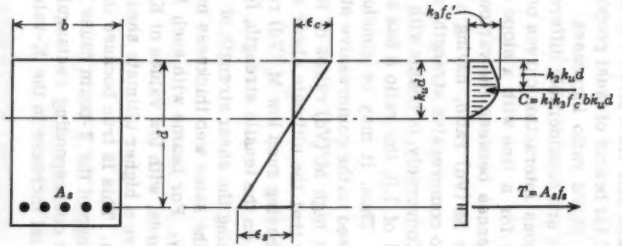


FIG. 9.—ASSUMED DISTRIBUTION OF FLEXURAL STRESSES IN A REINFORCED CONCRETE BEAM AT FAILURE

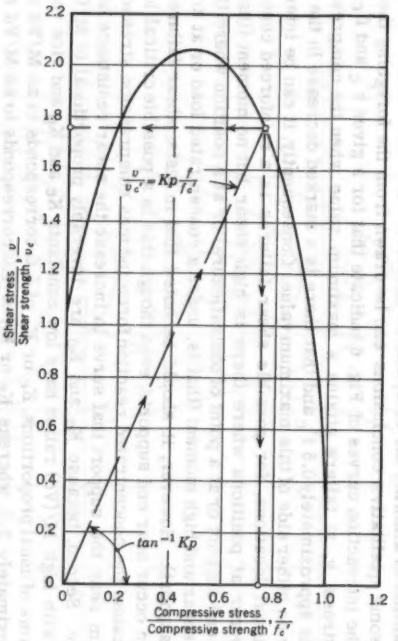


FIG. 10.—USE OF INTERACTION CURVE DIAGRAM TO PREDICT SHEAR

by using the two different constants K_e and K_p for the same beam are not more than 5% of the respective values. Consequently, for design purposes, the refinement of using K_e to make a second trial computation, when K_p was used originally is usually not justified.

In addition to allowing the computation of failure loads for beams failing in shear, some qualitative conclusions can be drawn from the foregoing theory. First, the interaction curves of Fig. 6 indicate that for a given v'_c and f'_c the shear stress, v, at failure attains a maximum value when the compressive stress is approximately 0.5 f'_c and that there is a marked decrease in the values of v on either side of this maximum value. Consequently, it can be inferred that critical locations, for possible shear failures in a reinforced concrete beam, occur at positions where there is high shear but no moment (that is, near an end support or at a point of contraflexure) or at a position where there is high shear and high moment (that is, under a concentrated load or at an interior support). However, it should be noted that in tests, shear failures do not often occur near end supports, even though this is a possible critical location, because the concentrated reaction force induces compression stresses in the beam near the support that serve to increase the shear resistance of the concrete. Second, because K_e and K_p are inversely proportional to M/(Vd), beams with high M/(Vd) ratios have low constants K_e and K_p and vice versa. For beams of usual proportions, K_e or K_p of 5.0 corresponds to an M/Vd ratio of approximately 3.0, whereas K_e or K_p of 1.0 corresponds to an M/Vd ratio of approximately 8.0. From Fig. 11 it may be seen that beams with K values of approximately 4.0 to 5.2 have the highest shear stress ratios, v/v'_c, at rupture, whereas beams that have K values less than 4.0 have correspondingly lower v/v'_c ratios. This means that for a given v'_c, above a certain low value of M/(Vd) (approximately 3.0 for beams of usual proportions) the shear stress at failure decreases as the M/Vd ratio increases. Finally, it may also be seen from Fig. 11 that there are considerable differences between the points of intersection with the various interaction curves of a line with a slope of K equal to 3.0 or 4.0, whereas for a line with a slope of K equal to 1.0 or less there are hardly any differences between the various points of intersection. Thus, for beams with a low M/(Vd) ratio, having a K value of 3.0 to 4.0 or larger, the ratio of tensile to compressive strength, α, has a strong influence on ultimate shear strength. Conversely, in beams with high M/Vd ratios having K values in the neighborhood of 1.0, the ratio α has an insignificant influence on ultimate shear strength. Thus, it may be concluded that ultimate shear strength theories that are based on the compressive strength of concrete alone may be valid for beams with high M/(Vd) ratios of the order of 6.5 to 7.0 or larger. However, it is clear that the ultimate shear strengths cannot be adequately predicted for beams having such low M/(Vd) ratios as from 3.0 to 6.5. For such beams information on the tensile strength, f'_t, is essential.

Some conclusions concerning the shear strength of T-beams relative to that of rectangular beams having the same web thickness may also be drawn on the basis of the foregoing theory. For beams with such high M/(Vd) ratios as in excess of 6.0, or, in other words, with low values of K_e or K_p (for example, K = 1.0), the T-beam should have a higher ultimate shear strength than the corresponding rectangular beam. This is true because the smaller normal compression stresses in the flange of the T-beam cause its K-value to be somewhat larger than that of the corresponding rectangular beam. It is obvious from Fig. 11 that a substantial increase in the K-value (say from 1.0 to 1.3)

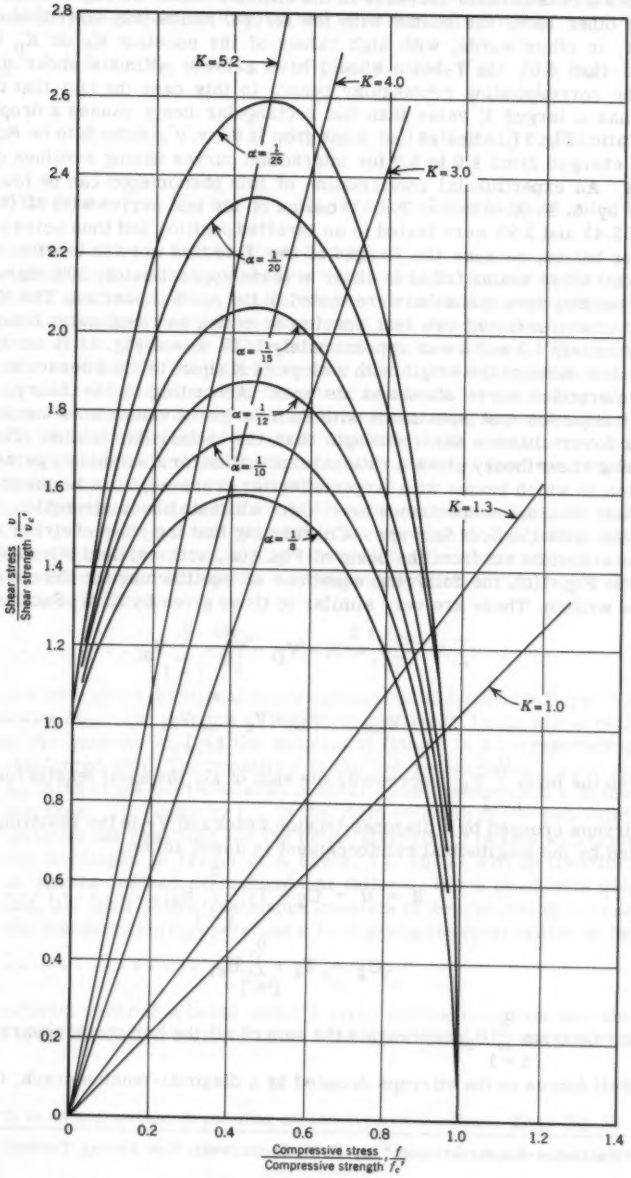


FIG. 11.—SHEAR STRESS RATIOS APPLIED TO INTERACTION CURVES

produces a considerable increase in the ultimate shear strength of the beam. On the other hand, for beams with low M/(Vd) ratios (say M/(Vd) less than 4.0) or, in other words, with high values of the constant K_e or K_p (say K greater than 4.0), the T-beam should have a lower ultimate shear strength than the corresponding rectangular beam. In this case the fact that the T-beam has a larger K value than the rectangular beam causes a drop in the v/v'_c ratio. Fig. 11 indicates that some drop in the v/v'_c ratio is to be expected if K is changed from 4.0 to 5.2 for interaction curves having α-values of 1/15 or less. An experimental confirmation of this phenomenon can be found in a report by A. F. Al-Alusi.[2] Two T-beams of his test series with M/(Vd) ratios of 3.45 and 3.96 were tested in an inverted position and thus acted as rectangular beams, because the flanges of the T-beams were in tension. It was found that these beams failed in shear at loads approximately 30% higher than corresponding specimens that were tested in the normal position. The K-value for the aforementioned two test specimens acting as rectangular beams was approximately 4.0 and α was approximately 1/15. From Fig. 11 it can be seen that a line through the origin with a slope of K equal to 4.0 intersects the α = 1/15 interaction curve almost at its apex. According to the theory, the T-beam companion test specimens with their larger K values must necessarily have a lower ultimate shear strength than the rectangular beams. Thus, the foregoing shear theory gives a rational explanation for a seemingly paradoxical situation, in which beams with larger effective cross-sections in compression than their companion specimens have lower ultimate shear strengths.

Beams with Vertical Stirrups.—Considering that the state of stress at failure on a section cut from the beam of Fig. 1(a), with vertical stirrups, is as given in Fig. 1(c), the following equations of equilibrium for the cut section may be written. These are very similar to those given by K. W. Sachnowski[36]

$$\sum V = 0 = R - V_D - V_c - \sum_{i=1}^{n} V_{si} \quad \ldots\ldots\ldots \quad (18a)$$

or,

$$R = V_{tot} = V_D + V_c + \sum_{i=1}^{n} V_{si} \quad \ldots\ldots\ldots\ldots \quad (18b)$$

in which the term $\sum_{i=1}^{n} V_{si}$ represents the sum of all the axial tensile forces in the stirrups crossed by a diagonal-tension crack and V_D is the resisting shear supplied by the longitudinal reinforcement in dowel action.

$$\sum H = 0 = C_2 - T_1 - \sum_{i=1}^{n} H_{si} \quad \ldots\ldots\ldots\ldots \quad (19a)$$

or

$$C_2 = T_1 + \sum_{i=1}^{n} H_{si} \quad \ldots\ldots\ldots\ldots\ldots \quad (19b)$$

in which the term $\sum_{i=1}^{n} H_{si}$ represents the sum of all the horizontal shearing (that is, dowel) forces on the stirrups crossed by a diagonal-tension crack, C is the

36 "Stahlbeton-Konstruktionen," by K. W. Sachnowski, Veb Verlag Technik, Berlin, 1956.

total compressive force acting on the cross-section of a beam, and T is the tensile force acting on main longitudinal tensile reinforcement.

$$\sum M_A = 0 = R\,a - V_D\,c - T_1\left(1 - k_2\,k_u\right)d - \sum_{i=1}^{n} x_i\,V_{si} - \sum_{i=1}^{n} y_i\,H_{si} \quad \ldots (20a)$$

or,

$$R\,a = M_2 = V_D\,c + T_1\left(1 - k_2\,k_u\right)d + \sum_{i=1}^{n} x_i\,V_{si} + \sum_{i=1}^{n} y_i\,H_{si} \quad \ldots (20b)$$

in which the terms $\sum_{i=1}^{n} x_i\,V_{si}$ and $\sum_{i=1}^{n} y_i\,H_{si}$ are the moments about point A of the stirrup axial and dowel forces respectively.

The aforementioned equations are insufficient in number to determine all the unknown quantities. Thus, explicit expressions for the contributions of the stirrups, longitudinal tensile reinforcement, and compression concrete area to the total shear resistance of the beam cannot be obtained. There is as yet little data reported in the literature that would enable the formulation of the requisite number of additional conditions or equations for computing the pertinent unknowns. Royston Jones[6] has made an interesting experimental attempt to determine the distribution of shear resistance in a reinforced concrete beam between longitudinal steel, stirrups, and concrete. However, his investigation is merely a beginning to the problem.

In view of the lack of data that would allow one to pursue the basic approach, as outlined previously, it was decided to use an empirical equation developed in the Laupa-Siess-Newmark report[7] that relates the shear strength of beams with web reinforcement to that of a corresponding beam without web reinforcement. This equation is

$$\frac{M_{sw}}{M_s} = 1 + \frac{2\,r\,f_{yw}}{10^3} \quad \ldots (21)$$

and it has been given additional experimental confirmation by Royston Jones.[6] The quantity M_s is the moment at failure in shear of a beam with a plain web, whereas the quantity M_{sw} is the moment at failure in a corresponding beam with a reinforced web. The quantity r is the web reinforcement ratio $A_v/(bs)$, where A_v is the cross-sectional area of shear reinforcement and s is the spacing of stirrups. The quantity f_{yw} is the yield strength of the web reinforcing steel. Because the equations for the shear strength of beams with plain webs have been developed in terms of a shear, V_c, Eq. 21 will be transformed in terms of shears instead of moments at failure. For a beam with web reinforcement, the total shear resistance consists of a term giving the contribution of the compression concrete and a term giving the contribution of the stirrups

$$V_{tot} = V_c + V_s$$

The maximum shear in a beam under a given loading condition can always be related to the maximum moment in the beam by a simple linear relation of the form

$$M = m\,V$$

in which m is a constant depending on the type of loading. Then Eq. 21 can be

transformed to

$$\frac{M_{sw}}{M_s} = \frac{m\,V_{tot}}{m\,V_c} = 1 + \frac{2\,r\,f_{yw}}{10^3}$$

or,

$$V_{tot} = \left(1 + \frac{2\,r\,f_{yw}}{10^3}\right) V_c \quad \ldots\ldots\ldots\ldots\ldots\ldots (22)$$

Using Eq. 22 and the previous definition of V_{tot} one can obtain an expression for the contribution of the stirrups to the total shear resistance of the beam as

$$V_c + V_s = \left(1 + \frac{2\,r\,f_{yw}}{10^3}\right) V_c$$

which leaves

$$V_s = \frac{2\,r\,f_{yw}}{10^3}\, V_c \quad \ldots\ldots\ldots\ldots\ldots\ldots (23)$$

Thus, according to Eq. 23, the contribution of the stirrups to shear resistance, V_s, is a function of the contribution of the compression concrete, V_c, and a parameter relating to the amount and yield strength of the web steel.

Applicability of the Theoretical Developments to Practical Beam Design.— Treating the case of the beam with plain web first, it may be observed that a triple criterion for failure has been developed. The shear V_{cr} at the appearance of the first diagonal-tension cracks, the shear V_f corresponding to a failure in flexure, and the shear V_c corresponding to a failure of the compression concrete above a diagonal-tension crack, must all be known before the mode of failure and the ultimate load may be predicted. The various possible modes of failure in terms of these three computed shears are:

1. $V_f > V_c > V_{cr}$. In this case failure in shear occurs after the formation of a diagonal-tension crack. The failure is an undesirable type from the standpoint of structural safety because it may occur suddenly. However, there is some warning of structural distress in the beam in view of the prior appearance of the diagonal-tension crack.

2. $V_{cr} > V_f > V_c$. In this case failure occurs by flexure because the diagonal-tension crack never has an opportunity to form, and substantially the whole cross section of the beam resists shear, so that V_c has no meaning. This case is, in effect, identical to the cases in which $V_c > V_{cr} > V_f$ or $V_{cr} > V_c > V_f$, in which it is clearly evident that failure is by flexure. In beams of usual proportions, flexural failures occur by yielding of the tensile reinforcement and are gradual, thus giving adequate warning of distress.

3. $V_f > V_{cr} > V_c$. In this case a very sudden failure in shear occurs when the external shear reaches a value V_{cr} and a diagonal-tension crack forms, leading to immediate shear failure. This mode of failure is undesirable because no warning of distress is present prior to actual failure. The suddenness of this mode of failure is due to the fact that V_c will be exceeded before V_{cr} has been reached. Thus, as soon as V_{cr} is reached and a diagonal-tension crack forms, the shear resistance of the beam drops to the value V_c and collapse occurs at once.

4. $V_c > V_f > V_{cr}$. In this case failure occurs by flexure, as in case 2, the only difference being that failure is preceded by the formation of a diagonal-tension crack. This mode of failure has the same desirable features as those of case 2.

For beams with web reinforcing, the problem of predicting the mode of failure and the ultimate load is somewhat simpler. This is so because in beams with reinforced webs the shear V_{cr} at the appearance of the first diagonal-tension crack is usually considerably below the ultimate shear. Hence, diagonal cracks occur before the ultimate shear is reached, except of course, in beams that are unusually weak in flexure, and thus V_{cr} plays no role in determining the mode of failure. In beams with reinforced webs, it is sufficient to compute V_{tot} by Eq. 22 and V_f from the ultimate flexural strength and compare the two results. If V_{tot} is greater than V_f, then the beam may be expected to fail in flexure with an ultimate shear equal to V_f. If the opposite is true then one may expect a shear failure with an ultimate shear equal to V_{tot}.

In the derivation of the various expressions for shear strength given herein, it has been tacitly assumed that stresses in beams at failure may be computed by the simple expressions of Eqs. 13 and 15(a). There is a limitation to the applicability of these equations that must necessarily carry over to the expressions that have been developed for predicting shear strength. The limitation occurs when a structural member passes from the category of a beam (that is, it carries load primarily in flexure) to the category of a diaphragm (that is, it carries load primarily in shear or in direct compression). The proportions and the manner of loading determine whether a structural member acts as a beam or as a diaphragm. Because the proportions of the member and the manner of its loading influence the ratio of shear and moment occurring in the member, it is possible to use a nondimensional quantity such as the M/(Vd) ratio as an index in determining whether the member is in the diaphragm or in the beam category. Members with a very low M/(Vd) ratio fall into the diaphragm category, whereas those with high M/(Vd) ratios fall into the beam category. For homogeneous, isotropic, elastic members, Chow, Conway, and Winter[37] have shown that a significant divergence between stresses, computed by means of the more exact approach afforded by the theory of elasticity and the conventional beam theory, occurs for a M/(Vd) ratio of one or less. That is, elastic structural members with M/(Vd) ratios of one or less are definitely in the diaphragm category. Although reinforced concrete beams can hardly be approached from the standpoint of the theory of elasticity, it has been shown by Armas Laupa, M. ASCE, Chester P. Siess, F. ASCE, Nathan M. Newmark,[7] F. ASCE, that a reinforced concrete flexural member with a M/(Vd) ratio of 2.0 to 2.5 may still be in the diaphragm category. In order to compensate for the effects of the loads and the reactions, which in most practical cases are distributed over a length of the beam of nearly the same order of magnitude as the depth, it seems wise to put a lower limit on the applicability of the equations developed in this paper. The theories developed herein are believed to apply solely to beams or parts of beams in which the M/(Vd) ratio is equal to or exceeds 3.0. This is not a serious limitation for practical design purposes because most beams in usual construction work have M/(Vd) ratios that exceed 3.0 by a considerable margin.

COMPARISON OF SELECTED TEST RESULTS WITH COMPUTED VALUES

According to the theory developed in this paper, it is necessary to know the tensile strength, or usually the modulus of rupture, as well as the compressive

37 "Stresses in Deep Beams," by Li Chow, Harry Conway, and George Winter, Transactions, ASCE, Vol. 118, 1953, pp. 686-702.

strength of the concrete of a beam before a prediction of its ultimate shear strength can be made. Accordingly, the test results evaluated herein are limited either to beam tests in which modulus of rupture data was available, or to beam tests for which the modulus of rupture could be inferred to a reasonable degree of certainty.

The pertinent properties of the beam specimens evaluated[38,39,4,40] appear in Table 1. The first two beams listed are from Bell,[38] the next four are from Brungraber,[39] the next seven are from Feldman and Siess,[4] and the rest are from the author.[40] There are twenty-nine beams in all, twenty-one of which are simply-supported (designated S in column 1) whereas the other eight are restrained beams (designated R). The "restrained" beams were statically-determinate beams that were provided with a loaded overhang at one end thus inducing moment and shear at one support to simulate the condition at an interior support in a continuous beam. Thirteen of the simple beams had rectangular cross sections and plain webs whereas the remaining eight were T-beams (designated T) provided with vertical stirrups. These eight specimens were retests of relatively undamaged portions of eight restrained beams tested in another investigation.[40] All eight restrained beams were T-beams provided with vertical stirrups and loaded by two concentrated forces. The beam specimens ranged in span from 6.33 ft to 17.00 ft and in M/(Vd) ratio from 2.01 to 8.65. Concrete compressive strengths for the specimens were in the range from 2440 psi to 5320 psi, the moduli of rupture ranged from 310 psi to 573 psi and the yield strengths of the reinforcement ranged from 37.5 ksi to 87.7 ksi.

Table 2 gives a comparison of test results with computed values based on the theory previously developed. The beam numbers of Table 2 match the corresponding beam number of Table 1. The actual shear at failure, V_u, and the actual type of failure are to be compared with the computed shear at failure, V', and the predicted type of failure. The quantity V' was taken as the smaller of the two computed ultimate strengths, V_f and V_{tot}, that were computed on the basis of flexural failure and of shear failure respectively. The predicted type of failure, column 11, was obtained by predicting that the specimen would fail in shear if its computed shear strength, column 10, was found to be less than its computed flexural strength, column 4, and vice versa. Column 13 gives the percent error between the computed value, column 12, and the actual shear at failure, column 2.

It may be observed from Table 2 that the mode of failure of the simply-supported beams is correctly predicted in every case but one. There are two beams shown in Table 2, S-7 and S-19T, that have very large percent errors (47.9 and 48.6 respectively). Beam S-19T was one of the eight retest specimens, and it may have been so badly damaged during the initial test that its carrying capacity was seriously impaired. The shear strength of this beam was checked against values computed by two other theories and it was found that V_u was again very low by comparison. Beam S-7 had a M/(Vd) ratio of

---

38 "Ultimate Shear Strength of Reinforced Concrete Beams," by R. B. Bell, thesis presented to Cornell Univ., at Ithaca, in 1956, in partial fulfilment of the requirements for the degree of Master of Science.

39 "Ultimate Strength in Shear of Reinforced Concrete Beams," by R. J. Brungraber, thesis presented to Cornell Univ., at Ithaca, in 1956, in partial fulfilment of the requirements for the degree of Master of Science.

40 "An Investigation of High-Strength, Deformed Steel Bars for Concrete Reinforcement," by S. A. Guralnick, Report No. TSR 4730-7146, Cornell Univ., Ithaca, N. Y., 1957.

TABLE 1.--PROPERTIES OF BEAM SPECIMENS

Beam Number	Span Length of Beam, L, in feet	Width, b, in inches	Effective Depth, d, in inches	M/(Vd)	Compressive Stress, f'_c, in pounds per square inch	Modulus of Rupture, f_r, in pounds per square inch	Yield Strength of Longitudinal Steel, f_y, in kips per square	Longitudinal Reinforcement	Longitudinal Reinforcement Ratio, P	Web Reinforcement	Web Reinforcement Ratio, r
(1)	(2)	(3)	(4)	(5)	(6)	(7)	(8)	(9)	(10)	(11)	(12)
S-1	7.50	4.5	6.13	5.23	4810	451	52.8	2 No. 6	.0320	—	—
S-2	7.50	4.5	6.13	5.23	4810	451	53.7	2 No. 6	.0320	—	—
S-3	15.00	7.0	11.94	7.54	3140	471	37.5	2 No. 9	.0239	—	—
S-4[b]	15.00	7.0	11.94	7.54	3140	471	37.5	2 No. 9	.0239	—	—
S-5	17.00	7.0	11.97	8.65	4020	528	50.7	2 No. 11[a]	.0378	—	—
S-6[b]	17.00	7.0	11.97	8.65	4020	528	50.7	2 No. 11[a]	.0378	—	—
S-7	6.33	7.0	9.94	2.01	3050	395	44.0	2 No. 9[a]	.0336	—	—
S-8	8.00	7.0	9.94	3.02	3120	401	45.0	2 No. 9[a]	.0336	—	—
S-9	8.00	7.0	9.94	3.02	5320	573	41.0	2 No. 9[a]	.0336	—	—
S-10	9.67	6.0	9.94	4.02	4060	478	45.0	2 No. 9[a]	.0336	—	—
S-11	11.33	7.0	9.94	5.03	3740	453	44.0	2 No. 9[a]	.0336	—	—
S-12	13.00	7.0	9.94	6.04	4050	477	48.0	2 No. 9[a]	.0336	—	—
S-13	14.67	7.0	9.94	7.04	4440	508	46.0	2 No. 9[a]	.0336	—	—
S-14T[c]	8.0	23.0	11.81	3.05	3230	315	87.7	2 No. 7; 2 No. 6	.0077	No. 4 @ 3 1/2	.0163
S-15T	8.0	23.0	12.05	2.99	2620	330	87.7	2 No. 7; 2 No. 6	.0075	No. 2 @ 5 3/4	.0025
S-16T	8.0	23.0	11.81	3.05	2440	310	84.6	2 No. 7	.0044	No. 4 @ 3 1/2	.0163
S-17T	8.0	23.0	12.12	2.97	2440	310	84.6	2 No. 7	.0043	No. 2 @ 5 3/4	.0025
S-18T	8.0	23.0	11.78	3.06	4930	470	83.9	2 No. 7; 2 No. 10	.0138	No. 4 @ 3 1/2	.0163
S-19T	8.0	23.0	12.19	2.95	4930	470	83.9	2 No. 7; 2 No. 10	.0133	No. 2 @ 5 3/4	.0025
S-20T	8.0	23.0	11.81	3.05	4930	470	87.7	2 No. 7; 2 No. 6	.0077	No. 4 @ 3 1/2	.0163
S-21T	8.0	23.0	12.05	2.99	4930	470	87.7	2 No. 7; 2 No. 6	.0075	No. 2 @ 5 3/4	.0025
R-22T	8.0	23.0	11.81	3.05	3230	315	87.7	2 No. 7; 2 No. 6	.0077	No. 4 @ 3 1/2	.0163
R-23T	8.0	23.0	12.05	2.99	2620	330	87.7	2 No. 7; 2 No. 6	.0075	No. 2 @ 5 3/4	.0025
R-24T	8.0	23.0	11.81	3.05	2440	310	84.6	2 No. 7	.0044	No. 4 @ 3 1/2	.0163
R-25T	12.0	23.0	12.12	2.97	2440	310	84.6	2 No. 7	.0043	No. 2 @ 5 3/4	.0025
R-26T	8.0	23.0	11.78	3.06	5520	486	83.9	2 No. 7; 2 No. 10	.0138	No. 4 @ 3 1/2	.0163
R-27T	8.0	23.0	12.19	2.95	5520	486	83.9	2 No. 7; 2 No. 10	.0133	No. 2 @ 5 3/4	.0025
R-28T	8.0	23.0	11.81	3.05	5520	486	87.7	2 No. 7; 2 No. 6	.0077	No. 4 @ 3 1/2	.0163
R-29T	8.0	23.0	12.05	2.99	5520	486	87.7	2 No. 7; 2 No. 6	.0075	No. 2 @ 5 3/4	.0025

[a] Violates ACI code.
[b] Loaded through column stub.
[c] Stem width of all T-beams is b^1 = 7.0 in., flange width b is given in (3).

TABLE 2.—COMPARISON OF BEAM TEST RESULTS THEORY

	Test Results		Results of Computations									
Beam Number	Shear at Fail- V_u, in Kips	Type of failure[a]	Shear in flexure V_f, in Kips	Shear to cause diagonal tension crack, V_{cr}, in Kips	Ratio of tensile to compressive strength, g	K_p	Resisting Shear of compression Concrete, V_c in Kips	$\frac{1 + 2rf_{yw}}{10^3}$	Total shear resistance, V_{tot}, in Kips	Predicted[a] type of failure	Predicted shear at failure, V', in Kips	Percent Error
(1)	(2)	(3)	(4)	(5)	(6)	(7)	(8)	(9)	(10)	(11)	(12)	(13)
S- 1	6.45	SC	6.94	4.86	1/21.0	3.32	6.62	1.00	6.62	S	6.62	- 2.6
S- 2	6.00	SC	7.03	4.86	1/21.0	3.32	6.73	1.00	6.73	S	6.73	-12.1
S- 3	9.35	F	8.93	14.31	1/13.0	1.71	5.85	1.00	5.85	F	8.93	+15.2
S- 4	9.25	F	8.93	14.31	1/13.0	1.71	5.85	1.00	5.85	F	8.93	+14.3
S- 5	13.30	FC	15.39	16.20	1/15.0	1.57	9.90	1.00	9.90	F	15.39	-15.7
S- 6	13.65	FC	15.39	16.20	1/15.0	1.57	9.90	1.00	9.90	F	15.39	-12.7
S- 7	26.10	SC	31.55	8.93	1/15.3	5.89	13.59	1.00	13.59	S	13.59	+47.9[b]
S- 8	17.00	SC	21.42	9.07	1/15.5	3.93	14.32	1.00	14.32	S	14.32	+15.7
S- 9	18.00	SC	22.63	13.06	1/18.6	5.40	14.08	1.00	14.08	S	14.08	+21.7
S-10	12.00	SC & DT	17.26	10.85	1/17.0	3.45	14.40	1.00	14.40	S	14.40	-20.0
S-11	11.50	DT	13.34	10.27	1/16.5	2.66	12.60	1.00	12.60	S	12.60	- 9.6
S-12	11.50	DT	12.03	10.85	1/17.0	2.24	12.97	1.00	12.97	F	12.97	-12.8
S-13	10.50	F	10.23	11.52	1/17.4	2.05	11.65	1.00	11.65	F	10.23	+ 2.6
S-14T	60.10	F	52.53	—	1/20.0	5.37	25.53	2.48	63.31	F	52.53	+12.6
S-15T	37.60	DT	52.39	—	1/16.0	4.85	27.24	1.56	42.49	S	42.49	-13.0
S-16T	42.60	F	30.47	—	1/16.0	5.01	14.99	2.48	37.18	F	30.47	+28.5
S-17T	31.50	DT	31.39	—	1/16.0	5.16	15.03	1.56	23.45	S	23.45	+25.6
S-18T	92.60	SC & F	87.03	—	1/21.0	6.12	48.63	2.48	120.60	F	87.03	+ 6.0
S-19T	50.60	SC	90.67	—	1/21.0	6.38	48.21	1.56	75.21	S	75.21	-48.6
S-20T	63.40	F	54.56	—	1/21.0	6.58	28.21	2.48	69.96	F	54.56	+13.9
S-21T	48.90	DT	55.89	—	1/21.0	6.74	27.80	1.56	43.37	S	43.37	+11.3
R-22T	58.00	DT	52.53	—	1/20.5	5.30	16.04	2.48	39.78	S	39.78	+31.4
R-23T	30.80	DT	52.44	—	1/16.0	4.19	15.32	1.56	23.90	S	23.90	+22.4
R-24T	44.20	DT	30.47	—	1/15.8	4.03	14.29	2.48	35.44	F	30.47	+31.1
R-25T	25.40	DT	31.39	—	1/15.8	4.14	14.76	1.56	23.03	S	23.03	+ 9.3
R-26T	91.20	DT	88.58	—	1/22.7	5.99	24.81	2.48	61.53	S	61.53	+32.5
R-27T	40.80	DT	92.33	—	1/22.7	6.21	25.67	1.56	40.05	S	40.05	+ 1.8
R-28T	71.00	DT & FT	55.17	—	1/22.7	6.04	24.40	2.48	60.51	F	55.17	+22.3
R-29T	40.50	DT	56.33	—	1/22.7	6.18	24.89	1.56	38.83	S	58.83	+ 4.1

[a] S denotes a shear failure, SC a shear compression failure, DT a diagonal tension failure, F a flexural failure, and FC a flexural compression failure.
[b] M/(Vd) ratio for this beam is less than 3, causing the theory to be inapplicable.

2.01, and was consequently in the diaphragm category so that the theory developed herein is inapplicable. It is interesting to observe that the theory considerably underestimates the failure shear in this case. This is to be expected considering the large restraints imposed on the concrete by the reaction and load forces. This same phenomenon occurs in the case of restrained beams. Therefore, beams S-7 and S-19T will be eliminated from an analysis of the data.

Fig. 12(a) is a comparison chart for the computed shear at failure versus the actual ultimate shear for the simply-supported beams. In this chart, points that fall above the 45°-line are conservative whereas those that fall below are not conservative. Agreement between tests and theory is seen to be satisfactory and deviations are mostly on the conservative side. In spite of the small size of the sample, a statistical evaluation of these tests has been made. It resulted in a coefficient of correlation of 0.986, a mean value of the test to theory ratio of 1.025, and a standard deviation of 0.145. These values can be regarded as indicative of satisfactory agreement.

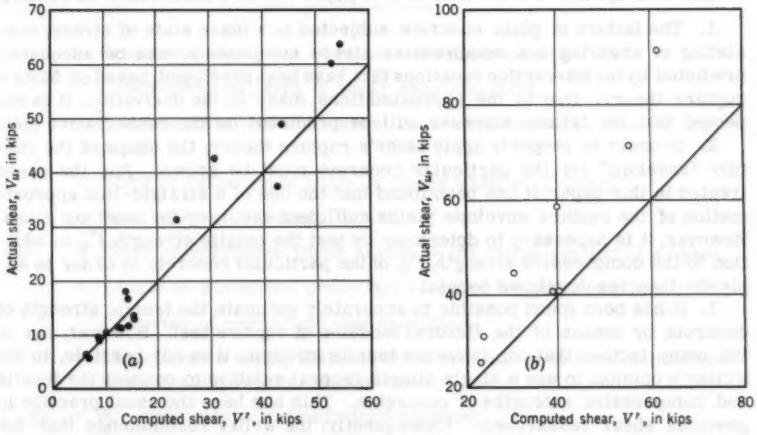


FIG. 12.—COMPARISON OF ULTIMATE SHEAR WITH COMPUTED SHEAR

Fig. 12(b) is a comparison chart for the eight restrained beams. Three of the beams show agreement between test and theory, whereas the remaining five err considerably on the conservative side. One explanation for the large deviation between test and theory in these beams is the fact that the critical zones for shear or flexural failure occurred at the face of the interior support, with the attendant extra restraint afforded by the reaction force. Due to the small size of the sample and the fact that there were no duplicate specimens, it is not possible to undertake statistical computations. Therefore, in regard to restrained beams having an M/(Vd) ratio of 3.0 or larger, the only conclu-

sion justifiable on the basis of the evidence presented is that the theory developed herein appears to be applicable and that the errors that may occur through its application will most probably be on the conservative side.

CONCLUSIONS

It has been found, by comparison with numerous test results, that Mohr's rupture theory is adequate in predicting failure stresses for cases of plain concrete subjected to a state of plane stress consisting of shearing and compressive stress. Equations based on Mohr's theory have been developed that express the interaction of the shearing and compressive stresses at failure. Because it has been recognized that failure in shear is essentially a failure of the concrete above a diagonal crack, the problem of predicting the ultimate load of beams failing in shear has been approached by applying the interaction equations developed for plain concrete. A failure theory for beams with plain webs has been developed and a very tentative extension to beams with vertical stirrups has been made. Test data from twenty-nine beams has been used to check the validity of the theory.

The findings and conclusions of this paper can be summarized as follows:

1. The failure of plain concrete subjected to a plane state of stress, consisting of shearing and compressive stress components, can be adequately predicted by the interaction equations that have been developed, based on Mohr's rupture theory. Due to the approximations made in the derivation, it is expected that the failure stresses will be predicted on the conservative side.

2. In order to properly apply Mohr's rupture theory, the shape of the rupture "envelope" for the particular concrete must be known. For the cases treated in this paper, it has been found that the use of a straight-line approximation of the rupture envelope yields sufficient accuracy for most purposes. However, it is necessary to determine by test the tensile strength, f'_t, in addition to the compressive strength, f'_c, of the particular concrete in order to apply the theories developed herein.

3. It has been found possible to accurately estimate the tensile strength of concrete by means of the flexural modulus of rupture test. However, due to the many factors that can influence tensile strength, it is not possible, in the writer's opinion, to use a single simple general relation to connect the tensile and compressive strengths of concretes. This has been the usual practice in previous shear researches. Consequently, the writer recommends that the flexural modulus of rupture test be adopted along with the cylinder compression test as standard practice for the determination of the relevant properties of concrete used in flexural members.

4. It has been found possible to develop a rational theory to predict the shear strength of beams with plain webs based on the interaction curves developed for plain concrete, and employing a triple criterion for failure. These consist of the shear at the appearance of the first diagonal tension crack, the shear at failure of the critical compression zone above a diagonal-tension crack subjected to compressive and shearing stresses, and the shear corresponding to a flexural failure. The relative magnitude of these three shear forces determines the mode of failure, and permits the prediction of failure load.

5. Due to lack of experimental measurements of the relative contributions of the concrete, the longitudinal and the web reinforcement to the shear resistance of a beam, it has not been found possible to develop a rational theory for

predicting the shear strength of beams with web reinforcement. Recourse was made to an empirical relation developed by Laupa, Siess, and Newmark[7] that connects the shear strength of beams with plain webs with that of beams with reinforced webs.

6. The theory in its present form is not applicable to beams in the diaphragm category (beams that have an M/(Vd) ratio of 3.0 or less).

7. Experimental evidence, though limited, seems to give satisfactory confirmation to the fundamental interaction equations as well as to the theory of shear strength of beams based on them.

This paper does not presume to give a final practical answer to the problem of shear strength of reinforced concrete beams. However, it is hoped that the theories developed herein do provide a rational, basic point of departure for future work in the field.

APPENDIX.—NOTATION

A_s = Cross-sectional area of tension reinforcement;

A_v = Cross-sectional area of shear reinforcement;

a = Distance from plane of nearest concentrated load to plane of support;

b = Width of rectangular beam or flange width of T-beam;

b' = Stem width of T-beam;

C, C_2 = Total compressive force acting on the cross-section of a beam;

c = Length of horizontal projection of major diagonal-tension crack;

D = Diameter of cylindrical test specimen;

d = The effective depth, distance from centroid of tension reinforcement to compression edge of beam;

e, e', e_1 = An experimentally determined constant;

f = Normal stress acting on a given plane of a stressed element;

f_1, f_2, f_3 = Principal normal stresses;

f'_c = Compressive strength of concrete;

f_r = Flexural tensile strength of concrete or modulus of rupture;

f_s = Tensile stress in longitudinal reinforcing steel;

fy = Yield strength of the longitudinal reinforcing steel;

f_{yw} = Yield strength of the web reinforcing steel;

H = Horizontal force acting on a given cross-section of a beam;

H_{s1}, H_{s2} = Horizontal dowel force acting on a given vertical stirrup;

I = Moment of inertia;

I_{gr} = Moment of inertia of the gross concrete section;

j = Ratio of arm length of internal couple of flexural resisting moment to effective depth;

K_e, K_p = Constants which relate the shearing and compressive stresses in the "compression zone" of a reinforced concrete beam;

k, k', k'' = An experimentally determined constant;

k_1, k_2, k_3 = Constants which define the flexural compressive stress distribution in the inelastic range;

k_u = Ratio of depth of neutral axis to effective depth at failure in flexure;

L = Span length of beam;

M = Bending moment;

M_s = Moment at failure in shear of a beam with plain web;

M_{sw} = Moment at failure in shear of a beam with web reinforcement;

p = Longitudinal reinforcement ratio = $\frac{A_s}{bd}$;

Q = First statical moment of the area;

R = Reaction force at the support of a beam;

r = Web reinforcement ratio = $\frac{A_v}{bs}$;

s = Spacing of stirrups;

T, T_1 = Tensile force acting on main longitudinal tensile reinforcement;

V = Shear acting on a given cross-section of a beam;

V_c = Resisting shear supplied by the compression concrete;

V_{cr} = Shear at which the first diagonal-tension crack forms;

V_D = Resisting shear supplied by the longitudinal reinforcement in dowel action;

V_f = Calculated shear at failure in a beam expected to fail in flexure;

V_s = Resisting Shear supplied by the web reinforcement;

V_{s1}, V_{s2} = Tensile force acting on a given stirrup;

V_{tot} = Calculated total shear resistance of a beam expected to fail in shear;

V_u = Measured shear at failure in a beam test;

V' = Predicted shear at failure in a beam test;

v = Shear stress acting on a given plane of a stressed element;

v_c = Actual shear stress at failure of a material subjected to a "pure shear" state of stress;

v_c' = Predicted shear stress at failure of a material subjected to a "pure shear" state of stress;

Z = The section modulus;

α = Ratio of tensile to compressive strength of a given concrete;

γ = An experimentally determined constant;

ϵ_c = Compressive strain in concrete; and

ϵ_s = Tensile strain in longitudinal reinforcing steel.

DISCUSSION

HENRY J. COWAN,[41] M. ASCE.—The problem of combined bending and transverse shear, although more important in practice, presents greater difficulties than the related problem of combined bending and torsion. This is mainly because it is much easier to separate the effect of bending in the case of torsion. It is gratifying, if not unexpected, to find that the author obtained results for shear similar to those previously obtained for torsion by U. Nylander[42] and later by S. Armstrong and the writer.[43]

The writer finds himself in agreement with the author's statement that the tensile strength and compressive strength of concrete are two separate physical constants of the material. However, this would suggest to the writer the use of two separate failure criteria. Although the author refers to the writer's work[23] and uses similar examples, the writer did in fact use two failure criteria. These were the maximum stress criterion for primary tension failure and the Mohr criterion for primary compression failure. The effect of using only the Mohr criterion becomes apparent if one refers to Fig. 5(b), which is grossly out of scale for the range of values of α given by the author. The author's footnote suggests a ratio of f'_c/f'_s equal to 10, where as the figure shows a ratio of only 2.8. For a ratio of 10, the angle θ would be very much larger. Assuming that a straight line envelope with a constant angle of inclination is to be used for the entire range of stress combinations investigated by the author, it is difficult to reconcile this angle with the work of Balmer[13] or the earlier work of F. B. Richart, A. Brandtzaeg, and R. L. Brown.[44] It seems to the writer that the angle θ requires adjustment. This would alter the curves in Fig. 11, although it would not make a fundamental difference to the author's conclusions.

---

41 Prof. and Head of Dept. of Arch. Science, Univ. of Sydney, Sydney, Australia.

42 "Vridning och vridningsinspänning vid betongkonstruktioner," by H. Nylander, States Kommittee för Buggnadsforskning, Meddelanden 3, Stockholm, 1945, p. 138.

43 "Experiments on the strength of reinforced and prestressed concrete beams and of concrete-cased steel joints in combined bending and torsion," by H. J. Cowan and S. Armstrong, Magazine of Concrete Research, Vol. 7, No. 19, 1955, pp. 3-20.

44 "A study of the failure of concrete under combined compressive stresses," by F. E. Richart, A. Brandtzaeg, and R. L. Brown, Bulletin No. 185, Engrg. Experiment Sta., Univ. of Illinois, Urbana, Ill., 1928, p. 104.

ROBERT F. WARNER.[45]—The author's application of the Mohr failure theory to the concrete in the stress block above the inclined crack is a useful contribution to the understanding of the shear compression failure that is commonly observed in laboratory tests. It is interesting to note that in an independent investigation Rene E. Walther[46] also used the Mohr failure theory to obtain the critical stresses above the inclined crack. The author's treatment is more general that Walther's in that it takes into account variations in the ratio of the tensile to compressive strength of concrete.

In dealing specifically with the shearing strength of concrete beams, however, the author has made an omission that severely restricts the usefulness of the theory. He does not state a compatibility condition in his paper, and hence gives no indication of how the depth of the neutral axis at failure, defined by the dimensionless parameter k_u, is to be determined. This quantity occurs explicitly in Eq. 13 and in the author's definition of the constant K_p.

Probably there would be no great error involved in letting $(1 - k_2k_u) = 0.9$ in the equation for K_p in order to avoid the use of a specific k_u value, but in Eq. 13, where any error in k_u will cause a proportional error in V_c, the ultimate shearing force resisted by the section, no such approximation can be used.

Although it is not explicitly stated in the paper, the author appears to have avoided using a compatibility condition in the table of computations (Table 2) by assuming that the longitudinal reinforcing steel has yielded at the time of failure. This assumption which was made also by Boris Bresler, M. ASCE, and Karl S. Pister,[47] M. ASCE, is unjustified. If the steel reaches yield, the flexural strength of the beam has been achieved and the problem of premature shear failure does not arise. Bresler and Pister foresaw this objection and showed that their computed values for shearing strength, based on the assumption of yielding in the steel, were significantly lower than the computed flexural strengths. This is not a justification for the assumption of yielding in the steel, an assumption that is contrary to the experimental evidence of many shear tests. It is an indication, however, that there is a second compensating error in the formulation of the theory.

The problem of finding a rational compatibility condition for the failure region appears to be the one major obstacle to a satisfactory theory for the shear compressive strength of prestressed and reinforced concrete beams. A promising approach has been made by Walther,[46] who stipulates a shear-rotation about the neutral axis, coupled with a pull-out effect of the longitudinal steel relative to the surrounding concrete. However, the present formulation of this theory does not correlate test data as well as the purely empirical approach suggested by Mete A. Sozen,[48] A. M. ASCE.

The writer feels it is important that the shear-compression failure should not be considered the only shearing type of failure that can occur in prestressed and reinforced concrete beams. Phil M. Ferguson[49] has already demonstrated experimentally that the shear strength of a beam, when loaded through

---

45 Research Assoc. in Civ. Engrg., Lehigh Univ., Bethlehem, Penn.

46 "The Shear Strength of Prestressed Concrete Beams," by Rene E. Walther, Paper No. 9, 3d Cong. of the Federation Internationale de la Preconstrainte, Session 1, Berlin, 1958.

47 "Strength of Concrete Under Combined Stresses," by B. Bresler and K. Pister, Journal, A.C.I., September, 1958.

48 "Strength in Shear of Prestressed Concrete Beams Without Web Reinforcement," by M. A. Sozen, thesis presented to the Univ. of Illinois at Urbana, in 1957, in partial fulfillment of the requirements for the degree of Doctor of Philosophy.

49 "Some Implications of Recent Diagonal Tension Tests," by Phil M. Ferguson, Journal, A.C.I., August, 1956.

side stubs, can be as low as 37% of its strength when loaded on the top surface of the concrete. Whether failure will be in shear compression or diagonal tension when moving point loads, distributed loads, side shear loads, and other practical loading conditions are involved, can only be determined by more tests in which the loading conditions are varied. It is quite possible that the shear compression failure occurs only under conditions similar to those existing in the typical laboratory shear tests, in which stationary point loads are applied to the top surface of the beam. More research work is urgently required in this area to determine the proper limitations to the use of the concept of shear compression failure.

BÉLA GOSCHY[50] AND GEORGE BALÁZS.[51]—The author has proposed applying Mohr's failure theory to determine the rupture condition in the compression zone of reinforced concrete beams subjected to bending and shear. Although the application of Mohr's fracture theory for concrete has been widely criticized, the investigations of Bresler and Pister,[14,15,47] proved its validity. According to Mohr's theory the relation between shear and compression stress in the state of rupture can be expressed as

$$v = \frac{f_c 1}{1+\alpha}\sqrt{\alpha^2 + (1-\alpha)\,\alpha\,\frac{f}{f'_c} - \alpha\,\frac{f^2}{(f'_c)^2}}$$

$$= \frac{\alpha f'_c}{1+\alpha}\sqrt{1 + \frac{(1-\alpha)}{\alpha}\,\frac{f}{f'_c} - \frac{1}{\alpha}\,\frac{f^2}{(f'_c)^2}} \quad \ldots\ldots\ldots\ldots (24)$$

That is another form of the Eq. 9(b). By considering the results of Bresler and Pister that can be formulated with a good approximation as

$$\left[\frac{f_1}{f'_c}\right] + \frac{f_2}{\alpha f'_c} = 1 \quad \ldots\ldots\ldots\ldots\ldots\ldots (25)$$

and substituting $f_1 = f$ and $f_2 = -\frac{f}{2} + \sqrt{\frac{f^2}{4} + v^2}$ one obtains:

$$v = \alpha f'_c\sqrt{1 + \frac{1-2\alpha}{\alpha}\,\frac{f}{f'_c} - \frac{1-\alpha}{\alpha}\,\frac{f^2}{(f'_c)^2}} \quad \ldots\ldots\ldots\ldots (26)$$

The difference between Eqs. 24 and 26 from different values of α is less than 10%.

For a more complete view of the problem it must be mentioned that Eq. 24 can be deduced by introducing the idea of the reduced stress, f_p as well.

According to Mohr's theory the value of the reduced stress is

$$f_p = f_1 - \alpha f_3 = \frac{1-\alpha}{2} f + \frac{1+}{2}\,\alpha\sqrt{f^2 + 4v^2} \quad \ldots\ldots\ldots\ldots (27a)$$

Fig. 13 shows the distribution of the reduced stress (b), the compressive

[50] Civ. Engr., Budapest, Hungary.
[51] Asst. of Civ. Engrg., Univ. of Budapest, Budapest, Hungary.

stress (c), and the shear stress (d). From Eq. 27(a), v can be expressed as

$$v = \frac{f_p}{1+\alpha}\sqrt{1-(1-\alpha)\frac{f}{f_p}-\alpha\frac{f^2}{f_p^2}}$$

and for $f = \frac{f'_c}{y_o}\,y$ the corresponding value of f_p is

$$f_p = \alpha f'_c + \frac{f'_c - \alpha f'_c}{y_o}\,y \quad \ldots\ldots\ldots\ldots \quad (27b)$$

By elimination of the parameter y/y_o one obtains Eq. 24.

The average shear stress in the compression zone can be discussed not only based on its degree of approximation but also on its universal validity. Using other stress distribution theories, such as those of Westergard, square

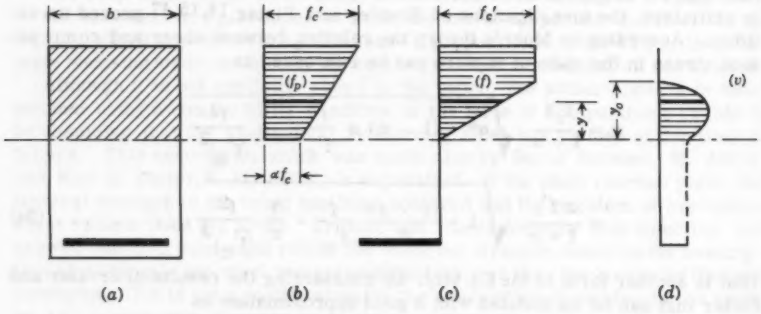


FIG. 13.—STRESS DISTRIBUTION FOR REINFORCED CONCRETE BEAM

shape shear stress as in the compression zone, resulting from rupture, is impossible, and the assumption of diagonal cracks does not give any results for the failure shear. It is much more adequate to determine the failure shear,

$$Q_{max} = \int_0^{y_o} v\,b\,\alpha\,y$$

in which the function of v is given by Eq. 24 with the substitution of $\frac{f}{f'_c} = \frac{y}{y_o}$ (Fig. 13).

The shear distribution below the neutral plane is not a question of cracks but is dependent only on the connection between steel and concrete. When slip is impossible the shear-stress distribution extends to the reinforcements.

KUANG-HAN CHU,[52] F. ASCE.—Although being more of a practical designer, and not an expert in this field, the writer has seen too many empirical formulas in various publications that make no sense because of their lack of physical meaning. The author's paper is one of the few that offer a rational approach. However, the following points need clarification.

a. Why is v_c^1 used to predict the occurrence of the first diagonal-tension crack? This question is based on the following considerations: (1) Diagonal

[52] Assoc. Prof., Civ. Engrg. Dept., Illinois Inst. of Technology, Chicago, Ill.

tension cracks are actually caused by diagonal tension, not by shear; (2) It has been stated in many books and papers that the shearing strength of concrete is greater than its tensile strength; and (3) Although shearing stress is usually computed as a measure of the diagonal tension stress, the actual governing factor should be the tensile strength, not the pure shear strength. Thus, it is not clear to the writer why the pure shear strength is used instead of the tensile strength. Also, in beams in which the combinations of shear and tension exist, why not use the shear strength corresponding to the particular tensile stress as determined by the Mohr circle envelope?

b. The Mohr circle properly determines the stress at a point. However, in the paper, the average stress is used. The writer wonders whether this is rigorously correct.

c. The derivations of the constants K_p and K_e are based on the assumptions that the beam either developed the ultimate strength or is still in the elastic range. Is there any possibility that the beam section is partly elastic and partly plastic? The author pointed out the K_p and K_e differ by no more than 5%. This is probably true for rectangular sections, but it is not necessarily true for other kinds of cross-sections, such as circular sections used for rigid-frame legs.

SIDNEY A. GURALNICK,[53] M. ASCE.—The writer would like to thank Messrs. Chu, Warner, Cowan, Goschy and Balazas for the time and effort they have expended in writing discussions of his paper. The comments made in these discussions form a significant contribution to the value of the paper.

Mr. Chu has raised three questions of considerable importance and an attempt to answer them follows.

In answer to the question of why v'_c was used to predict the occurrence of the first diagonal tension crack, it can be said that although pure shear failure in plain concrete is almost always observed as a diagonal-tension rupture, it is correct to use the maximum shear stress, v'_c, which corresponds to the failure state of stress, to describe this pure shear. Actually v'_c is simply the radius of the pure shear stress circle at failure. As has been stated by Bijlaard[22] and others, the radius of the pure shear stress circle must be equal in magnitude to the diameter of the pure tension stress circle in plain concrete. However, if a straight-line approximation of the Mohr envelope is adopted, the magnitude of the maximum shear stress at failure for an element subjected to a pure shear state of stress is given by a geometrically-derived relationship (Eq. 8). The magnitude of v'_c given by this equation is always less than the magnitude of the pure tensile strength. Therefore Eq. 8 represents a conservative estimate of the pure shear strength of plain concrete as was previously demonstrated.

The second question concerns the use of average stresses. The average normal and average shear stresses were used in the author's derivations because it is impossible, at the present state of knowledge, to predict the exact stresses in the compression zone of the beam after flexural tension and diagonal tension cracking have occurred. Consequently, recourse was made to the average stresses, even though it was recognized that Mohr's circle properly refers to the state of stress at a point. Because the normal and shear stress distributions are convex outward in most cases, there is probably not

[53] Asst. Prof., Dept. of Civ. Engrg., Illinois Inst. of Tech., Chicago, Ill.

a great deal of difference between the average and the maximum stress. Furthermore, it is quite likely that the maximum normal stress will occur at a level other than that at which the maximum shear stress occurs. Therefore, the location within the compression zone at which the combination of normal stress and shear stress is such as to cause failure will very probably be one at which either one or both of the stress components are lower than their respective maximum values. Thus the lack of exactness inherent in using the average stresses is probably quite low.

The third question raised concerned the applicability of the theories presented to the case of a beam section subjected to a partly elastic and partly inelastic stress distribution. In other words, is the theory applicable if the maximum compressive stress at failure is expected to be somewhere in the range between 50% and 100% of f'_c? The writer believes that his theory is applicable in such cases if one can correctly compute the quantity k_u. As was pointed out by Mr. Warner, it is necessary to use a compatibility condition to obtain an analytical expression for k_u. Unfortunately, an explicit compatability condition that can be used in predicting shear strength is yet to be definitively established. If and when such a compatibility relation is established it can easily be incorporated into the author's theory. In view of the present lack of an explicit compatibility relation, an estimate of k_u when it is expected that the compressive stress at failure will lie in the range between 50% and 100% of f'_c must somehow be made. One way to estimate k_u for this case is to assume that the stress in the tension steel is at the yield point and k_u is given by the equation from flexural strength analysis

$$k_u = \frac{1}{k_1 k_3} - \frac{p f_y}{f'_c}$$

in which k_1 and k_3 are given by the author's equations. The minimum, and therefore the most conservative value for k_u will result if one uses this procedure. In reviewing the restrained beams given in Table 1, a slightly different approach was used in computing k_u. Since large amounts of compression reinforcement were present in all the restrained beams, the most conservative estimate of k_u resulted if k_u was computed by

$$k_u = \frac{\epsilon_u}{\epsilon_u + \epsilon_y}$$

in which ϵ_y is the yield strain of the longitudinal tensile reinforcement and ϵ_u is the ultimate compression strain for plain concrete. The value of ϵ_u was obtained from the equation given by Hognestad, Hanson, and McHenry[35] as

$$\epsilon_u = 0.004 - \frac{f'_c}{6.5 \times 10^6}$$

The writer fully agrees with Mr. Warner that further theoretical and experimental studies are needed in regard to the problem of formulating a rational compatibility condition for shear failure. Furthermore, he is aware of the pressing need for studies of the behavior of beams loaded through side stubs because these more closely represent the conditions to be found in actual cast in place structures than do the typical top surface loaded laboratory test specimen.

The constructive evaluation of the author's work by Mr. Cowan is most appreciated. It is very gratifying that he finds so many areas of agreement with the author's arguments. The one area of apparent disagreement concerning failure criteria is more one of semantics than one of physical principle. Mr. Cowan argues that if the tensile and compressive strength of concrete are two separate physical constants of the material, then two separate failure criteria must be used. In the writer's opinion, this is just another way of stating that at least two physical constants are necessary to completely specify the envelope of circles representing failure states of stress (that is the rupture envelope or intrinsic curve) and, in the case of plain concrete, these physical constants are the tensile and the compressive strengths. Mr. Cowan's dual failure criterion differs from the author's failure criterion only in the details concerning the method of specifying the exact shape of the rupture envelope. Results obtained from either approach should be comparable.

It is unfortunate that Mr. Cowan misinterpreted Fig. 5(b), thus leading him to conclude that there was a great physical difference between his and the author's failure criteria. Fig. 8(b) was deliberately not drawn to scale because its sole purpose was to show the various geometrical quantities and relations used in the development of Eq. 9(b). No single fixed value of the angle θ was used in the author's work, as erroneously assumed by Mr. Cowan. Angle θ was treated as a perfectly general quantity whose functional relations were given by the author. Perhaps a more meaningful relation for angle θ results if one transforms these relations by the substitution $\alpha = f'_t/f'_c$ to obtain

$$\sin \theta = \frac{1 - \alpha}{1 + \alpha}$$

From this equation it is obvious that as the ratio of tensile to compressive strength, α, decreases, angle θ increases. Thus it is seen that, contrary to Mr. Cowan's implications, no significant disparity exists between the author's work and that of Balmer[13] or Richart, Brandtzaeg, and Brown.[18]

Many thanks are due Messrs. Goschy and Balazas for their independent verification of the Eq. 9(b) which is so central to the entire theory of shear strength presented. Their use of the concept of reduced stress is interesting and may have important applications in building code provisions and design procedures if the theories presented in this paper gain wider acceptance. It is believed that the questions raised in their remarks are fully answered elsewhere in this discussion.

In view of the questions concerning certain of the assumptions made by the author and as check on the validity of his theory, a further analysis is presented of the shear strength of beams reinforced with vertical stirrups. Eq. 22, which is based on an empirical expression developed by Laupa, Siess and Newmark,[7] gives the total shear resistance, V_{tot}, of a beam reinforced with vertical stirrups. An analytic expression for V_{tot} that is very similar in form to Eq. 22 will be derived.

Considering the free-body diagram of a portion of a beam reinforced with vertical stirrups shown in Fig. 14, the following assumptions may be made:

1. For the purposes of computing ultimate strength, only the stirrups crossed by a diagonal-tension crack are effective in contributing to the shear resistance of the beam.

2. At failure the stress in the stirrups crossed by a diagonal-tension crack is equal to the yield stress of the steel.

If the free-body diagram shown in Fig. 14 is in equilibrium, then

$$R = V_{tot} = V_c + V_s \quad \ldots\ldots\ldots\ldots\ldots\ldots (28)$$

in which V_c is the contribution to the shear resistance of the concrete and V_s that of the stirrups. V_s may also be written as

$$V_s = \sum_{i=1}^{n} V_{si} = n A_v f_{yw} \quad \ldots\ldots\ldots\ldots\ldots (29)$$

in which A_v is the cross-sectional area of shear reinforcement. If the stirrups in the region crossed by a diagonal-tension crack are equally spaced, then

$$n = \frac{c}{s}$$

in which

$$c = (1 - k_u)\, d \cot \beta$$

and s is the spacing of the stirrups from Fig. 14 therefore,

$$n = \frac{(1 - k_u)\, d \cot \beta}{s} \quad \ldots\ldots\ldots\ldots\ldots\ldots (30)$$

Substituting this n into Eq. 29 an equation for V_s is obtained as

$$V_s = \frac{(1 - k_u)\, d \cot \beta}{s} A_v f_{yw} \quad \ldots\ldots\ldots\ldots (31a)$$

or

$$V_s = \left[(1 - k_u)\, b\, d \cot \beta\right] r f_{yw} \quad \ldots\ldots\ldots\ldots (31b)$$

in which

$$r = \frac{A_v}{b s}$$

If the right-hand side of Eq. 31(b) is multiplied by the ratio $V_c/(bk_u dv_c)$ which is equal to unity, the equation for V_s becomes

$$V_s = \frac{1 - k_u}{k_u} \cdot \frac{\cot \beta}{v_c} r f_{yw} V_c \quad \ldots\ldots\ldots\ldots (32)$$

If the angle β is less than 45°, cot β is greater than unity. Angle β is greater than 45° only if the M/(Vd) ratio is less than about 2.5. Therefore, a conservative estimate of V_s results if cot β is set equal to unity in Eq. 32. If this is done Eq. 32 becomes

$$V_s = \frac{1 - k_u}{k_u} \cdot \frac{r f_{yw}}{v_c} V_c \quad \ldots\ldots\ldots\ldots (33)$$

Substitution of this value of V_s into Eq. 28 yields an equation for the shear resistance of a reinforced concrete beam

$$V_{tot} = \left(1 + \frac{1 - k_u}{k_u} \cdot \frac{r f_{yw}}{v_c}\right) V_c \quad \text{(34a)}$$

Eq. 34 is seen to be remarkably similar to the empirically derived Eq. 22 $V_{tot} = \left(1 + \frac{2 r f_{yw}}{10^3}\right) V_c$ One obvious advantage of Eq. 34 over Eq. 22 is that it is dimensionally correct.

Eq. 34 may be further simplified by substituting for the ratio $(1 - k_u)/k_u$ the quantity γ. If this is done the equation becomes

$$V_{tot} = \left(1 + \gamma \frac{r f_{yw}}{v_c}\right) V_c \quad \text{(34b)}$$

In the usual case k_u is less than 0.5 and therefore a conservative value for γ is unity. In those unusual cases in which k_u exceeds 0.5, Eq. 34 must be used to compute shear resistance.

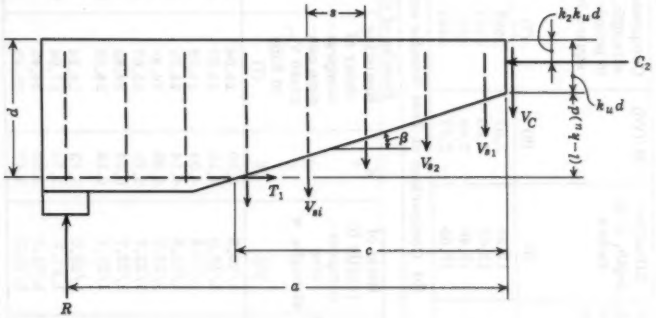


FIG. 14.—FREE BODY DIAGRAM OF BEAM WITH VERTICAL STIRRUPS

Ultimate strengths of the restrained beams reported in Table 2 are compared with values of shear strength predicted by Eq. 34(a) to demonstrate the validity of this equation. The results of this comparison of test and theory are reported in Table 3(b). In addition, a comparison of test and theory for four new beam specimens, whose properties are given in Table 3(a), are also reported in Table 3(b). These specimens are designated as series-M beams. Beams 30M and 33M had plain webs whereas the other ten beams reported in Table 3 had web reinforcement consisting of equally speced vertical stirrups.

It may be observed in Table 3 that the theory correctly predicts the mode of failure in all but one case. The exception is beam R-24T which had a low computed flexural strength, V_f. Beams 31M and 33M which failed in flexure also had low computed flexural strengths. This underestimation of flexural strength occurred because the tensile reinforcing steel used, which was high-strength alloy steel deformed bars having a nominal yield point of 80,000 psi,

TABLE 3.—DEMONSTRATION OF VALIDITY OF EQ. 34(a)

(a) Properties of Series—M Specimens

Beam Number	Span Length, L, in feet	Flange width, b, in inches	Stem width, b^1, in inches	Effective depth, d, in inches	M/(Vd)	Compressive strength, f'_c, in pounds per square inch	Modulus of rupture, f_r, in pounds per square inch	Yield strength of longitudinal steel, f_y, in Kips per square inch	Longitudinal reinforcement	Web reinforcement
(1)	(2)	(3)	(4)	(5)	(6)	(7)	(8)	(9)	(10)	(11)
30M	12.0	23.0	7.0	12.55	2.87	3898	390	92.2	2 No. 7; 2 No. 6	——
31M				12.63	2.85	3237	366	103.1	4 No. 5	No. @3 1/2
32M				12.46	2.89	4862	455	83.7	2 No. 7; 2 No. 10	——
33M				12.55	2.87	4493	461	92.2	2 No. 7; 2 No. 6	No. @3 1/2

(b) Comparison of Test Results with Theory

Beam Number	Test Results		Results of Computation									
	Shear at failure, V_u, in Kips	Type[a] of failure	Shear in flexure failure, V_f, in Kips	Ratio of tensile to compressive strength, α	K_p	Resisting shear of compression concrete V_c, in Kips	$\frac{rF_{yw}}{v_c}$	γ	Total shear resistance, V_{tot}, in Kips	Predicted[a] type of failure	Predicted shear at failure, V^1, in Kips	Percent error
(1)	(2)	(3)	(4)	(5)	(6)	(7)	(8)	(9)	(10)	(11)	(12)	(13)
R-22T	58.0	DT	52.53	1/20.5	5.30	16.04	2.081	0.835	43.92	S	43.92	+24.3
R-23T	30.8	DT	52.44	1/16.0	4.19	15.32	0.851	0.814	25.94	S	25.94	+15.8
R-24T	44.2	DT	30.47	1/15.8	4.03	14.29	2.406	0.783	41.21	F	30.47	+31.0
R-25T	25.4	DT	31.39	1/15.8	4.14	14.76	0.903	0.783	25.20	S	25.20	+ 0.8
R-26T	91.2	DT	88.58	1/22.7	5.99	24.81	1.293	0.904	53.81	S	53.81	+41.0
R-27T	40.8	DT	92.33	1/22.7	6.21	25.67	0.489	0.904	37.02	S	37.02	+ 9.3
R-28T	71.0	DT & F	55.17	1/22.7	6.04	24.40	1.293	0.942	54.12	S	54.12	+23.8
R-29T	40.5	DT	56.33	1/22.7	6.18	24.89	0.489	0.942	36.36	S	36.36	+10.2
30M	19.1	DT	59.90	1/20.0	5.73	18.24	—	—	18.24	S	18.24	+ 4.5
31M	53.3	F	41.20	1.17.7	5.04	17.04	2.320	0.984	55.94	F	41.20	+22.7
32M	22.7	DT	93.30	1/21.3	5.89	24.45	—	—	24.45	S	24.45	- 7.7
33M	77.9	F	60.60	1/19.5	5.47	23.43	1.763	0.931	61.01	F	60.60	+22.2

[a] S denotes a shear failure, F a flexural failure, DT a diagonal tension failure.

had
im
tio
fai
ste

13
the
tes
thi
co
fec
be
the

had little or no yield plateau and entered the strain hardening range almost immediately upon reaching its yield stress. The flexural strength computations were simply based on attaining the yield stress in the tensile steel at failure and they did not reflect any extra strength that might occur if tensile steel stresses progressed into the strain hardening range.

Considering all beams other than the three mentioned previously, column 13 of Table 3(b) shows that the theory is conservative in all but one case. Furthermore, in six of the beams that failed in shear, the percent error between test and theory was confined to a range of -7.7% to +15.8%. In the remaining three beams the percent error is rather high. Because the theory errs on the conservative side in these cases, and because these results may have been affected by errors in experimental technique, it is believed that these last three beams do not cast any serious doubt on the general validity of the author's theories.

AMERICAN SOCIETY OF CIVIL ENGINEERS

Founded November 5, 1852

TRANSACTIONS

Paper No. 3037

ELECTRIC PIPELINE FOR HIGH-VISCOSITY FUEL

By Albert G. Purdue[1]

SYNOPSIS

The use of vacuum still bottoms as primary energy source in a thermal generating station is described. Emphasis is placed on the method of pipeline transport of this material from a nearby refinery to the 100,000 kw Central Sur Station of the Puerto Rico Water Resources Authority at Guayanilla, Puerto Rico.

FOREWORD

A modern electrical generating facility has recently been constructed (1959) on the south coast of Puerto Rico by the Autoridad de las Fuentes Fluviales (Water Resources Authority). The primary energy source for this 100,000 kw installation is vacuum still bottoms used as high viscosity (HiVis) fuel. This material was formerly regarded as too viscous at readily maintainable temperatures for pipeline transport to an outside consumer. The determination of the Autoridad to make the most efficient use of available resources has resulted in the design of an automatic, high-temperature delivery system to supply HiVis to their steam generators. This pioneer venture has shown that a large thermal potential, that until now has been employed inefficiently, can be made available by advanced techniques of fuel handling and storage. The following description of the installation will be of special significance to those concerned with the most effective use of petroleum resources for power generation.

INSTALLATION

It is a safe prediction that the demand for thermally-generated electric power will continue its present rise into the next decade and beyond. The

Note.—Published, essentially as printed here, in May, 1959, in the Journal of the Pipeline Division, as Proceedings Paper 2038. Positions and titles given are those in effect when the paper was approved for publication in Transactions.

[1] President, Fluid Systems, Inc., New Haven, Conn.

most optimistic forecasts for the future of synthetic energy sources only give further reason to believe that natural petroleum fuels will carry the base load of the world's energy requirements for years to come. This predictable increase, coupled with changing world conditions which may result in a redistribution of petroleum reserves, makes it imperative that ways be found for obtaining the maximum energy usage from each barrel of crude oil produced.

The demand for lighter distillates, for high-quality, special-purpose gas and liquid fuels, will continue to increase. From the standpoint of refinery economics, it is especially important that these constituents be extracted with the greatest yield possible. If a refinery could do nothing but convert every barrel of crude oil into a barrel of fuel oil to be sold at market prices, an over-all loss would result. The lighter distillates must be of sufficient quantity to offset this loss and to show a profit.

These two demands, the need for more thermal power and the market for lighter distillates, are somewhat in conflict. The reasoning behind this statement is as follows. Most existing power generators that burn liquid fuel use a product that can be stored in tanks and pumped through delivery lines at moderate temperatures. When, however, the maximum yield of volatile hydrocarbons is extracted from crude oil, the viscosity of the residue becomes so high that it can neither be stored nor pumped at moderate temperatures and so it is not directly usable by a majority of existing facilities for power generation. In fact, when the distillation process is carried to the extreme yield point, the residue is a tarry solid at ambient temperatures. This material, variously called tar pitch, vacuum still bottoms, or HiVis fuel, is all but unmanageable by the usual techniques for fuel handling and storage. Bottoms used as high viscosity fuel will be called HiVis hereafter.

HiVis represents a very considerable fraction of each barrel of crude oil, 20% to 30%, depending on the source of crude and the fractionation process. Its physical properties cannot be specified precisely because they vary according to the throughput schedules of the refinery. Whereas a liquification temperature of approximately 250° F is typical, and the material usually flows readily at approximately 350° F, it can only be burned at the still higher temperatures of approximately 450° F. The following data, taken from tests on a particular sample of HiVis, show the general variation of viscosity:

Temperature in ° F	Seconds Saybolt Universal Viscosity
122	12,000,000
250	12,000
300	2,000
350	540
400	280
450	150

HiVis are high in sulfur content but are not chemically active or corrosive below 500° F. The free carbon content is high (15% to 25% may be a typical range) but, as ordinarily produced, it is free from particle aggregates and nozzle-blocking dirt. A high flash-point permits safe handling at the temperatures at which the material can be pumped.

The significant property of HiVis is that it is a good fuel. On a pound-for-pound basis, HiVis has a heating value not inferior to that of the bunker oils in general use and its luminosity characteristics contribute to a high generator efficiency. The problem is to deliver this highly variable material to the burner nozzles in useable condition. The absence of a generally serviceable solution to the transport problem limits the use of HiVis fuel.

Dispositions made of the large heat potential of HiVis are often unsatisfactory from both the short-range and the long-range points of view. At times it has been regarded as a pure waste produce to be disposed wherever it would not create a pollution problem. This may be satisfactory from the standpoint of a specific refinery operation but can hardly be considered a general solution. Another possible non-fuel use for HiVis includes blending it into surfacing materials. This offsets production costs but is not an efficient use of thermal potential. A common solution involves the blending of vacuum-still bottoms into lighter distillation products in such a proportion that the result is not below grade for fuels that can be handled by standard burner equipment. However, an undesirable restriction on the operating decisions of a refinery arises. The distribution of products, ideally determined by relative demands, must be determined instead by what is available.

It would be advantageous to have a direct use for HiVis in whatever quantity it was available. The sale on a Btu basis would represent the greatest value to both supplier and consumer. The additional degree of freedom in refinery management would leave it free to respond to market demands. It appears most desirable to find solutions to handling and storage problems in order to use the superior qualities of this fuel.

HANDLING AND STORAGE

If a large potential consumer of HiVis is located in the vicinity of a petroleum refinery, it becomes worthwhile to consider the possibility of piping the hot fuel directly to the user. The important consideration is the distance between facilities. Whereas a short run of 450° F-to-500° F pipeline presents no insurmountable problems, a run of even moderate distance is beset with difficulties. In order to determine the problems to be solved the requirements on the line must be considered.

Because HiVis is produced continuously with little or no storage available at the producer's end, the line must be completely reliable. The material delivered may vary over wide ranges in its thermal characteristics. The line must maintain constant flow conditions regardless of these variations and must be equally adaptable to conditions of flow and non-flow. Whatever the temperature and rate of delivery, the line must maintain its pumping ability for the full length of the run. Finally, the line must have sufficient reserve capacity to recover the complete handling facility following a freeze-up and to attain its pumping ability within a reasonable length of time. These requirements are expensive and difficult to meet when approached by ordinary techniques suited to less demanding materials.

The proximate location of a refinery and the generator encountered in the construction of the Central Sur Generating Station made it adaptable to the use of HiVis. The potential supplier was a refinery located approximately a mile from the generator site. This refinery has sufficient HiVis output to serve as primary fuel for the normal 100,000 kw load on the station and can also supply

alternate fuels in any needed quantity. Accordingly, the station was designed to burn any combination of HiVis and bunker C oil.

Fig. 1 shows the station under construction in the foreground and the refinery in the distance. Immediately behind the station is the 150 kv switchyard that feeds the integrated network serving the growing domestic and industrial needs of the island.

The arrows in Fig. 1 indicate the course of the fuel line feeding the four storage tanks in the right foreground and the pumping area delivering HiVis to the station. Construction and operation of a pipeline by ordinary techniques would be quite difficult. Therefore it was necessary to use an electrically heated line.

The thermal electric line was developed for heated pipeline transportation of high viscous materials. In solving the problem of electrically heating a



FIG. 1.—FACILITIES LINKED BY PIPELINE

pipeline, the electric line principle uses the reactance of the pipe itself to transform electrical energy into heat that can be regulated closely. By governing the energy inflow rate to balance exactly the rate of thermal loss, fluid flow conditions are brought close to the ideal. By maintaining a constant temperature along the length of the pipe, thermal exchanges between the fluid and the pipe wall are minimized, and flow conditions and load on the pumping station are held constant. Because the proper conditions of energy supply can be attained in practice, it is clear that the principle under examination is physically sound.

One of the foremost advantages of this method is that standard schedule piping can be heated with readily available values of currents and voltages. Other positive values are found when alternative methods of achieving the same result are studied. For example, a comparison between the electrically heated line and a steam-jacketed line indicates the purely mechanical advantages of the electrical system. It is required that the entire line be recoverable in case of freeze-up. This implies a large allowance for thermal expansion and, if a jacket were used, provision for differential expansion of jacket and conductor must be included. Operation at temperatures up to 500° F implies a fair pressure and the requirement for rapid recovery requires a large circulating steam capacity. Obviously the materials and engineering cost for a steam line of any length will be high. The electric line in the same service, on the other hand, will have provisions for large expansion, consisting of sizable expansion bends, but otherwise will be insulated, standard schedule piping.

The electric line compares even more favorably in the comparison of thermal efficiency. Because only part of the superheat of the steam is useful, it is imperative that the condensate be returned with minimal heat loss. This is another line at fair pressure and temperature. Of course, the electric line counterpart also requires a return. However, a moderate cross section of copper or aluminum will return currents of the required magnitude with negligible loss.

The whole cross section of the thermal electric line consists of fluid, pipe, and the covering serving as both thermal and electrical insulation. Only moderate electrical potentials are required for pipe-heating, the insulation used for off-ground purposes only. The resultant diameter and surface area per unit length are small as compared with a steam line. So are the direct thermal losses to the atmosphere, because both convective and radiant losses vary with area.

The prior statements are useful in establishing the merits of a working principle. However, from a practical viewpoint the fact that the electrically heated line is a highly developed engineering method and not an abstract principle is more important.

DESIGN OF THE SYSTEM

The design of a complete system is undertaken in the following sequence.

1. The heating requirements for each part of the system—transmission, storage, and end-use segments—is determined working from preliminary design data and the over-all performance specifications for the transport and storage systems. On the basis of these findings the system is analyzed into parts that are to be temperature-controlled and energized separately. This division is governed partly by mechanical considerations and partly by the desire to work within certain ranges of supply voltages and currents.

2. A mechanical design is drawn up, a large part of the problems of detailing having been solved in advance by designs for insulating and isolating hardware that are made adaptable to any likely combination of temperature and pressure conditions and offer predictable electrical performance.

3. The reactances of parts of the system are computed using tables of empirical data compiled from research on a variety of pipe materials, their configurations, and the variations in their characteristics over the involved temperature ranges.

4. An electrical supply system is synthesized with regard for reliability, safety, and freedom from overhead cost. The central idea is to attain automation of operation so that the final system adapts to all flow or non-flow conditions and to any ambient variations without attention from operating personnel. Other important objectives include the accessible grouping of all existing controls and the arrangement of the electrical system for simple and complete inspection. In addition, full provision is made for protection of electrical equipment in case of unforseeable damage to any part of the system.

5. The last step is especially critical. The design and supply of compatible apparatus is reviewed by on-the-job engineers to insure a fully functional system from the beginning. This has frequently resulted in avoiding costly

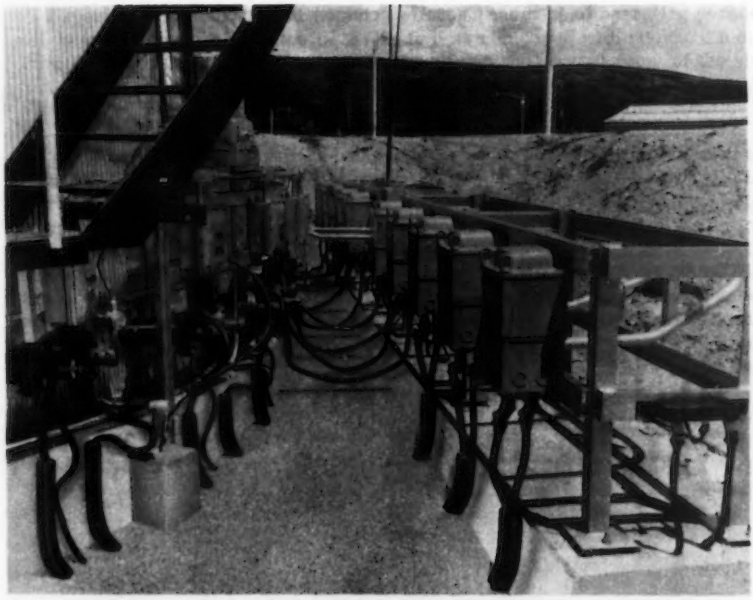


FIG. 2.—VIEW OF TANK BASE SHOWING HEATING ARRANGEMENT

errors by construction personnel, many of whom fail to appreciate the dual role of fluid conduction and current conduction in a single element. There is no substitute for the experience and instruction that highly-trained field engineers can offer in the course of construction. The result of this policy is that thermal electric systems work on schedule avoiding expensive delays in operation.

CONSTRUCTION FEATURES

It is beyond the scope of this paper to describe the construction of the electric system in detail, but some of the salient features of the Puerto Rican installation are worthy of mention.

Power is supplied to the pipe and storage elements by a total of seventy-five energizing units, thirty-four of which are supplied to the tanks, the rest distributed along the length of the run. Each energizer is post-mounted with its thermostatic control element. The primaries of the energizers are supplied with 480 v, 60-cycle current by underground conduit. The main power is furnished by a small substation and a switch panel from which energizers may be controlled individually or in banks. This substation is normally operated at a fraction of its rating because of the cyclical function of the energizers. It has sufficient reserve capacity to ensure "start-up" from a frozen condition.

The heating of the storage tanks was an important part in this operation. Three 180,000-gal tanks and one of 70,000 gal are held at 450° F so that full



FIG. 3.—CONTROL ROOM OF CENTRAL SUR POWER STATION

flow at burning temperature is available immediately. Heating elements and energizers here are controlled individually. The tanks are heated by nichrome resistance elements inserted through nozzles which extend through the tank wall, into heating coils of 2-1/2 in. Schedule 40 steel pipe supported 1 ft above the tank bottom. There are ten coils in each of the larger storage units and four in the smaller. Fig. 2 shows the arrangement of energizers and thermostat switches applied to the tanks. Coil terminals, insulated by special hardware are seen protruding through the tank wall. Above the coil terminals on the tank wall are the explosion-proof thermostat control boxes. Each of the energizer units on the framework at the right in Fig. 2 supplies current to one of the independent heating coils. The assembly permits electrical feed through the tank wall without metallic contact and has proven itself in many

kinds of service. This internal arrangement of heating elements results in a uniform temperature distribution within the tank, with exact control of the skin temperature of the coils, not influenced by surrounding fuel temperature. The electric line apparatus can be designed to meet any combination of safety regulations and introduce no electrical hazard in a similar situation.

HiVis are taken from the storage units by three pumps for a delivery capacity of 200 gpm. The pump bodies, maintained at 350° F by means of radiant heaters, are small units because they are only required to offset minor losses. The control of temperature is achieved by cycle timers.

The HiVis control piping inside the station is essentially that of the low-temperature alternate fuel. In this part of the installation, energizers are grouped "below deck" to reduce congestion in working areas, and, as in the case of the pumps, radiant heaters are used for temperature maintenance of control valves.

Experience has shown that no extra effort on the part of operating personnel is occasioned by the use of HiVis fuel as compared with standard fuels. Fuel changeover is accomplished with ease from the control room of the station. The control room is shown in Fig. 3. The television panel enables the engineer to observe several functions of the system including the condition of the fires by direct view into the furnaces.

The combination of facilities described herein is a significant factor in the industiral and economic life of Puerto Rico. There is an acute population problem and resulting need for industrial growth in this territory. The Water Resources Authority has planned and carried out full utilization of the hydroelectric potential of the island. Having borne the responsibility for foreseeing the future power needs of their country, it was realized at an early date that the base load must fall eventually on thermal generation. Wise planning has resulted in a sufficient supply of energy for those large enterprises that find the island location advantageous. The Central Sur Power station is the latest addition to the well-balanced power structure of the island.

AMERICAN SOCIETY OF CIVIL ENGINEERS

Founded November 5, 1852

TRANSACTIONS

Paper No. 3038

WATER FORCES ON ACCELERATED CYLINDERS

by Alan D. K. Laird,[1] Charles A. Johnson,[2] and Robert W. Walker[3]

SYNOPSIS

The economical design of fixed structures immersed in ocean waves or other oscillating fluid masses is handicapped by an insufficiency of data. Statistical studies based on wave records collected in many parts of the world provide an estimate of the heights and steepnesses of waves which may be expected at a given site during a specific period of years. From these wave parameters and the depth of the water, the designer must compute the forces on the structures.

This paper deals with the forces exerted by water on an immersed, horizontally mounted, circular cylinder, which was moved in a horizontal direction normal to its long axis. The accelerations and velocities were in the range common to ocean waves. Both constant and variable linear accelerations and decelerations were used to discover possible effects of acceleration and rates of change of acceleration. Three diameters were used to cover the range of Reynolds numbers from the Karman vortex region through the boundary layer transition region. The regions of overlapping of the data permitted observation of the effects of diameter at constant Reynolds number. By towing another similar cylinder parallel to the test cylinder, some of the effects of a neighboring cylinder were investigated.

INTRODUCTION

Measurements of the forces of waves on structures of many shapes and configurations have been made on models in the laboratory and in the ocean. A

Note.—Published, essentially as printed here, in March, 1959, in the Journal of the Waterways Division, as Proceedings Paper 1297. Positions and titles given are those in effect when the paper was approved for publication in Transactions.

[1] Prof. of Mech. Engrg., Univ. of California, Berkeley, Calif.

[2] Research Asst., Inst. of Engrg. Research, Univ. of California, Berkeley, Calif.

[3] Research Asst., Univ. of California, Berkeley, Calif. Presently: Design Engr., Caterpillar Tractor Co., Peoria, Ill.

semi-empirical method has been developed[4] for the prediction of forces induced by waves in moderately deep water. Data from vertical circular cylinders have been reported.[5] These data, when measured against the corresponding semi-empirical predictions, suggests that some important factors are missing from this method of prediction. It is typical of much published data that, in many cases, the forces exerted by the majority of the waves could be predicted by the semi-empirical method. However, in a significant number of cases, the predicted forces were as much as three times too large or too small. These numerous failures of the analytical method based on the currently (1959) recognized phenomena indicated the existence of undiscovered phenomena in the interaction of waves and piling.

Water depth at the ocean test site was of the order of one-tenth of the wave length. The records of the shapes of the waves showed deviations from those predicted by the corresponding wave theories. These deviations could be attributed to irregularities of the bottom, to the superposition of small waves on larger waves, to the neighboring piling and to imperfections of the theory. In the majority of cases, the force records agreed within 30% with those predicted from the theory. Many of the small deviations synchronized with the deviations of the wave shapes, indicating small effects caused by small deviations of the actual from the theoretical. Many of the waves were short crested rather than long crested as specified by the theory, but no consequent large effects were detected. The large deviations did not appear to result from any of the observed discrepancies. Previous laboratory studies had shown that the pile-spacing was large enough so that the shapes and sizes of the waves were not appreciably affected. The effect of the pile-spacing on the forces on the piles was not investigated. In the semi-empirical method, it was assumed that the magnitude, direction and rate of change of acceleration do not affect the drag coefficient. No data were available to check these assumptions.

Research was initiated to test the validity of the semi-empirical method under controlled conditions and to discover which of the variables that had previously been neglected were actually important. The part of this research which dealt with the effects of accelerations produced by essentially constant driving forces has been previously summarized.[6] Half-inch and one-inch horizontal cylinders were accelerated vertically through water from their rest positions. This work showed no large deviations up to accelerations of 4 ft per sec^2 and velocities of 1.5 fps. The effects of spacing and of other types of accelerations upon circular cylinders remained to be investigated.

EXPERIMENTAL EQUIPMENT

The experiments were performed in a 200-ft-by-8-ft towing tank. The cylinders were of smooth aluminum with hemispherical ends. The surface condition was held constant by coating the cylinders with white petroleum jelly. The overall length of all the cylinders was 39 in. while the diameters were 1.25 in., 2.33 in., and 4.47 in. The resulting length to diameter ratios were

---

4 "The Force Exerted by Surface Waves on Piles," by J. R. Morison, et al, Technical Paper 2846, Journal of Petroleum Technology, AIMME, Vol. 2, No. 5, 1950.

5 "Ocean Wave Forces on Circular Cylindrical Piles," by W. L. Wiegel, K. E. Beebe, and James Moon, Proceedings Paper 1199, ASCE, April, 1957.

6 "Fluid Resistance to Cylinders in Accelerated Motion," by S. Russell Keim, Proceedings Paper 1113, ASCE, December, 1956.

31.2, 16.7 and 8.72. In Fig. 1 the apparatus for the tests on the larger cylinders is shown diagrammatically. For the larger cylinders, the water-depth was 48 in. The cylinder-top to water-surface distance was 13 in.

The cylinders were supported by 1/4 in. diam horizontal stings in the wake of the cylinders just inboard from their hemispherical ends. The vertical struts of 0.25 in. by 1.5 in. steel were about 2.5 in. behind the cylinders. The upper ends of the struts were thickened to accommodate an SR-4 strain gauge bridge

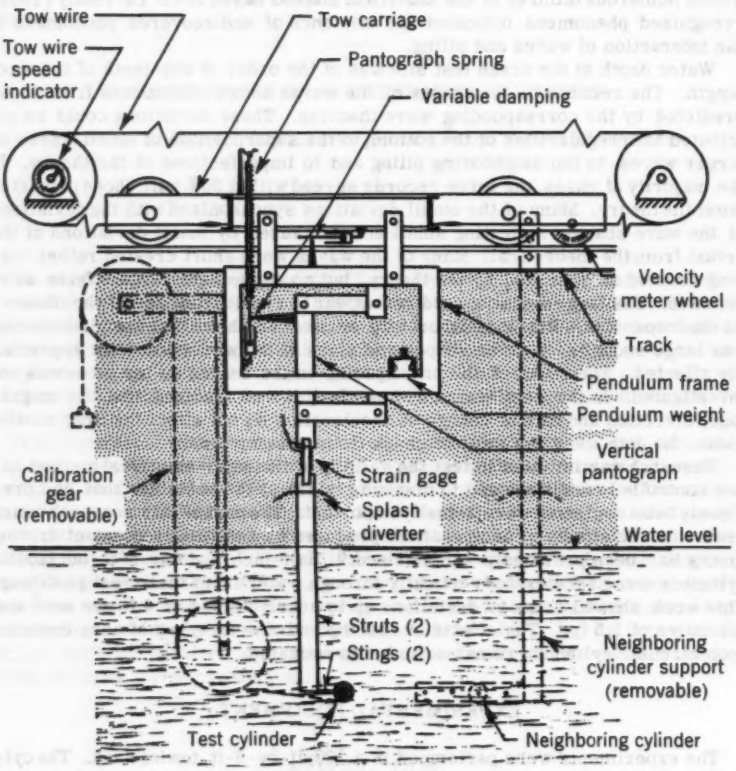


FIG. 1.—EXPERIMENTAL APPARATUS

which served as a force meter. The output of the bridge was recorded by an oscillograph at a tape speed of 50 mm per sec.

The struts were attached to a pantograph and its load, consisting of the test cylinder and its supports, was borne by two vertical soft-coil springs attached to the tow-carriage frame. Adjustable damping was provided by a piston in an oil filled cylinder with a valved bypass. The pantograph was attached to a horizontal pendulum which was hung from the tow carriage by four links pivoted

on ball bearings. Adjustable damping was provided. Weights placed on the pendulum-frame reduced deflections caused by the cylinder drag. The pendulum effectively reduced transmission of disturbances from the wire to the cylinder. During preliminary test, the pantograph insolated the cylinders from vertical vibrations of the tow carriage. It was found that these vibrations were negligible and since the vertical forces on the cylinders caused objectionable vibrations, the pantograph was inactivated by clamping it to the horizontal pendulum during test runs.

When a neighboring cylinder was to be used, a support was bolted to the front of the tow-carriage. The position of the neighboring cylinder was varied by selecting convenient bolt-holes in the support. These supports were at the ends of the neighboring cylinder that was nearly the same diameter as the test cylinder and approximately 9 in. longer.

The force-meter was calibrated at 1 hr to 3 hr intervals by applying a known horizontal force at the midpoint of the test cylinder, by means of a wire. The wire was led over two pulleys, as shown in Fig. 1, so that weights could be suspended from a hook at the other end of the wire.

The controls were modified so that constant linear accelerations and decelerations to 0.3 g could be maintained for arbitrary periods compatible with the tank length and with chosen maximum velocities up to 22 fps. The voltage output of the speed control generator was a linear function of the velocity of the carriage. This voltage was recorded continuously on the oscillograph tape. During most runs, the velocity-trace was calibrated by simultaneously recording the velocity during the uniform part of the motion on a velocity-meter which counted the revolutions of a calibrated wheel attached to the tow carriage and running on the same track.

The natural frequencies of the components of the system in their possible modes of vibration were measured. The modes were separated by means of a 2 g accelerometer fastened to the component in the desired direction. The simultaneous traces of the accelerometer and the force-meter were used to estimate the magnitudes of transmitted vibrations under the test conditions. The drag forces on the struts alone during uniform and accelerated motions were measured.

The effect of length to diameter ratio was checked by a preliminary set of experiments with 2.33 in. diam cylinders over the complete range of speeds and accelerations used for the principal tests. The ratios used were 9.02, 12.9, and 16.7.

METHOD OF ANALYSIS

The forces of the water on the test cylinder during a run can be represented[7] in terms of a resistance coefficient, C, defined by

$$D_T = C\,A\,\rho\,\frac{V^2}{2} \qquad (1)$$

in which D_T is the total drag, A is the area of a diametral cross section of the cylinder, ρ is the fluid density, and V is the velocity of the cylinder, relative

[7] "Forces on Cylinders and Plates in an Oscillating Fluid," by G. H. Keulegan and L. H. Carpenter, Report 4821, National Bureau of Standards, September, 1956.

to the water. Much of the available resistance coefficient data has been summarized[8] and correlated with the acceleration modulus, aD/V^2.

According to the semi-empirical method, the resistance can be separated into a drag force which is due to velocity effects, and an inertia force caused by the acceleration of the surrounding water. These are C_M,

$$\text{Drag force} = C_D A \rho \frac{V^2}{2} \quad \ldots\ldots\ldots\ldots\ldots\ldots\ldots\ldots\ldots\ldots (2)$$

$$\text{Inertia force} = C_M m a \quad \ldots\ldots\ldots\ldots\ldots\ldots\ldots\ldots\ldots\ldots (3)$$

in which a is the acceleration and m the mass of the water displaced by the cylinder, C_D is the drag coefficient and C_M the inertia coefficient. This method of analysis implied that the drag and the inertia effects are without appreciable mutual interference, so that they are additive. It also requires a knowledge of the variation of C_D and C_M with the flow conditions. This method has been previously amplified.[7] In the analysis of the present paper, because the variation of C_M is practically unknown, it was assumed constant and equal to unity, as predicted by simple hydrodynamic theory. This simplification has the effect of including in C_D the deviations of C_M from unity.

The velocity-meter and force-meter records were transferred to rectangular coordinates as shown in Fig. 4. The existence of constant acceleration was indicated by a straight portion of the velocity curve. The slope of the velocity curve at any time was equal to the acceleration. The drag and inertia forces on the struts and stings (Fig. 1) were subtracted from all the force records. It was assumed that the struts experienced the same drag at a given velocity during accelerated motion as during uniform motion. The change in drag on the struts caused by the presence of the wake of the cylinder was assumed negligible. The inertia force of the water acting on the struts were neglected. The coefficients for all cylinders were corrected to infinite length to diameter ratio, L/D, by means of factors given elsewhere.[9] The principal test conditions are listed in Table 1.

TEST RESULTS

The infinite-cylinder drag coefficients, C_D, are shown as a function of Reynolds number in Figs. 2(a), (b) and (c), for the test cylinders alone. In Figs. 2(a), (b) and (c) the diameters are 1.25 in. 2.33 in. and 4.77 in. and the L/D correction factors are 1.26, 1.36, and 1.53, respectively. The lengths were all 39 in. The data of the two larger cylinders, 2(b) and (c), pass through the transition from laminar to turbulent boundary layers. It should be noted that although the drag coefficient correction from finite to infinite length cylinders is not valid beyond the transition velocity, it was used in this paper for want of a better correction.

The insensitivity of the drag coefficients to changes in acceleration is an important result. The larger the cylinder, the greater was the tendency for the drag coefficients during deceleration to deviate from those during acceleration. This may be due to diameter or to length to diameter ratio effects.

---

[8] "Re-Analysis of Existing Wave Force Data on Model Piles," by R. C. Crooke, Technical Memorandum 71, U. S. Army, Corps of Engrs., Beach Erosion Bd., April, 1955.

[9] "Ergebnisse der aerodynamischen versuchsanstalt zu gottingen," by C. Wieselberger and C. Betz, Vol. 2, R. Oldenbourg, Berlin, 1923, p. 26.

The infinite-length drag coefficients for the three sizes of cylinders in Fig. 2 during acceleration and uniform motion agree with the accepted values for Reynolds numbers below transition. The grouping of the constant acceleration points results from computing at a few arbitrarily chosen velocities for the sake of economy and clarity of presentation. Had more velocities been chosen, more similar groups would have resulted. The frequencies of the occurrence of points are shown by the numbers beside them, unity having been omitted. Reliable data at velocities below 3 fps were difficult to obtain at reasonable accelerations because of starting disturbances such as shown in Fig. 4 for run 125 during the first half second. In Figs. 2(a), (b) and (c), the scatter is larger at the lower velocities because of the relatively larger inaccuracies in calibration, measurement, and computation. During deceleration there appeared to be a diameter effect, or length to diameter ratio effect, which caused the

TABLE 1.—RANGES OF VARIABLES

Number	Diameter, inches		Length-to-Diameter Ratio	Reynolds' Number x 10-41	Acceleration, in feet per second squared	Centerline Distance, inches	
	Test Cylinder	Neighboring Cylinder				Vertical	Horizontal
a) Cylinder without neighbor							
1	1.25	---	31.2	2.5 to 82	-23 to 10	---	---
2	2.33	---	16.7	2.7 to 31	-5 to 6	---	---
3	4.47	---	8.72	2.7 to 41	-4 to 5	---	---
b) Cylinder with leading parallel neighbor							
1.	2.33	2.37		1.7 to 21	1.5 to 3.6	0 1.38 2	6.0 8.1 5.7 9.0 9.1 11.0 13.0
2.	4.47	4.50		3.3 to 28	1.2 to 2.3	0 2.63	9.0 15.0 15.0 15.0

drag coefficients to be higher for larger diameters at the lower velocities. If the coefficient of mass were taken as zero, then the coefficient of resistance would be the coefficient of drag.

For run 107 the deceleration points shown in Fig. 2(c) below a Reynolds number of 10^5, correspond to the points in Fig. 3 for the same run at values of aD/V^2 less than -1.3. It can be seen that these resistance coefficients are much closer to the uniform motion and acceleration drag coefficients than are the deceleration drag coefficients. This fact suggests that the mass coefficient may be closer to zero than to unity during deceleration in this range of Reynolds numbers. The deceleration points in Fig. 2(b), at Reynolds numbers less than 10^5, correspond, approximately, to the points in Fig. 3 at aD/V^2 values between -0.02 and -0.09. It appears that more research would be necessary

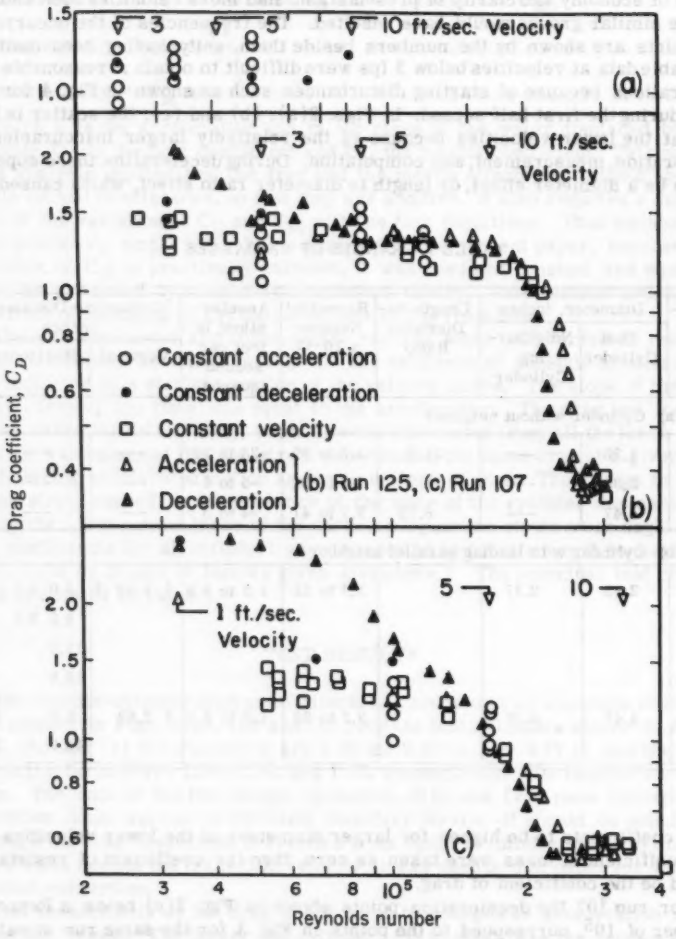


FIG. 2.—RELATIONSHIP BETWEEN INFINITE CYLINDER DRAG COEFFICIENT AND ACCELERATION MODULUS

to explain the high values of drag coefficient below a Reynolds number of approximately 10^5, and the low values above about 1.8×10^5 during deceleration.

The boundary layer transition in Figs. 2(b) and 2(c) appears early for infinitely long smooth cylinders. This probably reflects the finite length of the cylinder, the flexibility of the supports and the disturbances in the water.

During some of the fast runs of the 4.47 in. cylinder, surface waves up to 4 in. high followed 10 in. behind the cylinder. It was estimated,[10] approximately, that such a wave would cause a maximum overestimate of the resistance coefficient of less than 3%. Because this was less than the general scatter it was neglected.

The velocity meter was separated from the cylinder by the towing wire which produced a negligible maximum error in carriage position of 0.03 in. After each run, long period waves were damped out very slowly so that it was impractical to wait for the waves to stop before the next run. Consequently, runs were started in the 2 sec or 3 sec that the water was practically motionless in the nodes of the waves. There was some chance that the start of a run would not be at a node. The nodes did not last during the whole of most runs, so that these long waves could cause errors in velocity of as much as 1 fps for fast runs and large cylinders. There is a possibility that the large drag coefficients during deceleration are caused by these wave induced velocities. It is improbable, however, that such errors would always be towards higher values as shown in Figs. 2(b) and 2(c). There were undoubtedly other disturbances in the tank, such as large eddies, which could have contributed to the general scatter of the data.

As a test of the applicability of correction factors previously mentioned[9] for conversion of data from finite to infinite cylinders, the drag coefficients for the three lengths of 2.33 in. diameter cylinders were corrected to infinite lengths by these factors. All three sets of values were within the range of accepted values below the transition Reynolds number. However, through transition and above, more research is needed to establish correction factors.

Unity was used as the value of the inertia coefficient, C_M, because of the simplicity of the computations and because its actual values were practically unknown. If the acceleration and the drag coefficient during part of a run were constant, the mass coefficient could be computed from the force-time curve. This would be an attractive method if precise data were available. Many values of C_M were computed from selected curves, but different pairs of selected points on the same curve gave different values of C_M. Most of the values were below unity and tended to decrease and become negative at increasing values of time, because C_D was not constant but decreased as the Reynolds number approached the transition value. It is probable that the actual values of C_M were close to unity. It is apparent that deviations of C_M from unity had little effect on the acceleration and uniform motion results over the range of variables of the present research, and the analysis of Eq. 2 and 3 is adequate for these cases.

Another interesting result of this research is the demonstration in Fig. 3 that the acceleration modulus, aD/V^2, in which a is the acceleration, D the projected diameter and V the velocity, does not correlate resistance coefficients, C, in the region of small values of the modulus. It is particularly impotent near the boundary layer transition. The dash-dot line in the center of

10 "Hydrodynamics," by H. Lamb, Dover Publications, New York, 1945, p. 417.

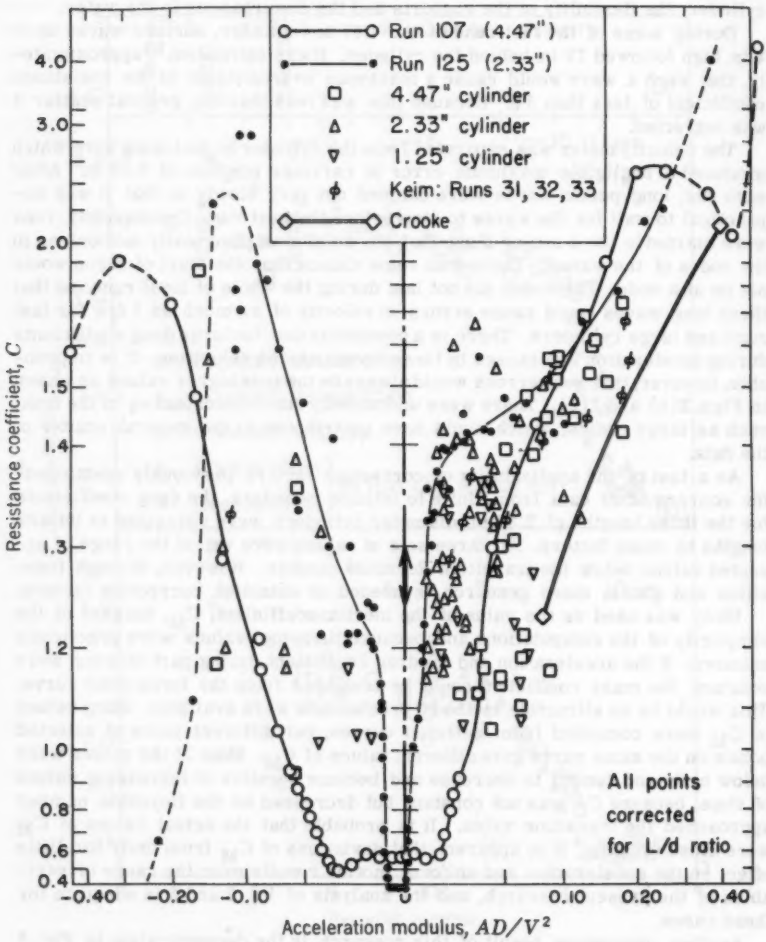


FIG. 3.—RELATIONSHIP BETWEEN INFINITE CYLINDER RESISTANCE COEFFICIENT AND ACCELERATION MODULUS

Fig. 3 is the zero value for uniform motion and the arrow in it is the approximate uniform motion value below transition. The coordinates in Fig. 3 were distorted for the sake of clarity. The data from the three sizes of cylinders scatter widely about the proposed line given by R. C. Crooke,[8] at these low values of the modulus. For all non-zero values of acceleration, the boundary layer must pass through transition twice as the acceleration modulus goes from large positive values through zero to large negative values. The magnitude of the acceleration modulus at which transition will occur depends mostly on the diameter, acceleration, and velocity, but, also on the roughness and fluid disturbances. By proper choice of variables, therefore, transition could be induced at almost any value of the modulus. Since the resistance coefficient reflects the change in drag coefficient, the correlation of C by the acceleration modulus is not possible where transition occurs.

A continuous set of values for each of the 2.33 and the 4.47 inch cylinders from near rest through positive, zero, and negative accelerations to near rest is shown for Runs 125 and 107 respectively. The value of C for uniform velocity (acceleration modulus zero) for the larger cylinder is higher because of the over-correction for the length to diameter ratio at speeds beyond the transition speed. Because both runs started and ended with relatively large accelerations, the resistance coefficients have very large positive values near starting and very large negative values near stopping. The degree of scatter is large when the velocities are 1 fps or less. Consequently, the curves are shown dotted to indicate trends rather than exact values.

Below the transition range, the uniform motion value of the resistance coefficient is approximately 1.25 to 1.30. Because the acceleration modulus does not correlate data in the Reynolds number range in this work, and because they were taken from runs at different accelerations, speeds and diameters, the remainder of the points in Fig. 3 appear to be unrelated.

In Fig. 4 examples of typical velocity and force traces are represented for three runs during acceleration, uniform motion and deceleration. These curves, from which small fluctuations have been excluded, show typical variations of force as functions of time and velocity in the present research. They may be used as rough models for corresponding ocean waves. The solid lines in Fig. 4 are for the 2.33 in. cylinder, whereas the dotted lines are for the 4.47 in. cylinder. The heavier of these lines designate the force values while the lighter lines designate velocity values. The higher set of velocity and force curves for the 2.33 in. cylinder (run 125) shows clearly the effect of boundary layer transition. Because of boundary layer transition on the faster 4.47 in. cylinder (run 108), its force trace is lower than that of the lower of the 2.33 in. cylinders (run 218). In each curve the inertia effects are evident in the increased force during acceleration over the force during deceleration at the same velocity. Typical force fluctuations from the uniform velocity sections of runs 218 and 108 are shown enlarged in Figs. 5(a) and 5(b) respectively.

Runs 108 and 125 have about the same maximum Reynolds numbers, 3.18 and 3.02×10^5 respectively. Run 108 was practically the same as run 107. Consequently, Fig. 4 shows the force-time-velocity relationships, Fig. 3 the resistance coefficient-acceleration modulus variations and Figs. 2(b) and 2(c) the drag coefficient-Reynolds number variations for runs 107, 108, and 125. It can be seen that the maximum Reynolds number does not completely specify the shape of the curves. The effects of transition and acceleration are particularly noticeable in Fig. 4. Run 218 for the 2.33 in. cylinder was a little slower than run 108 for the 4.47 inch cylinder, but the forces were higher over most of the run because run 218 was below transition.

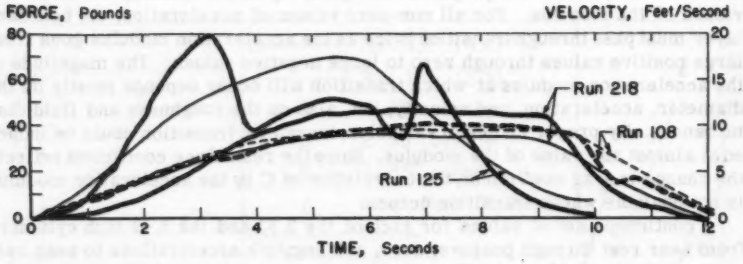


FIG. 4.—TYPICAL FORCES AND VELOCITIES AS FUNCTIONS OF TIME

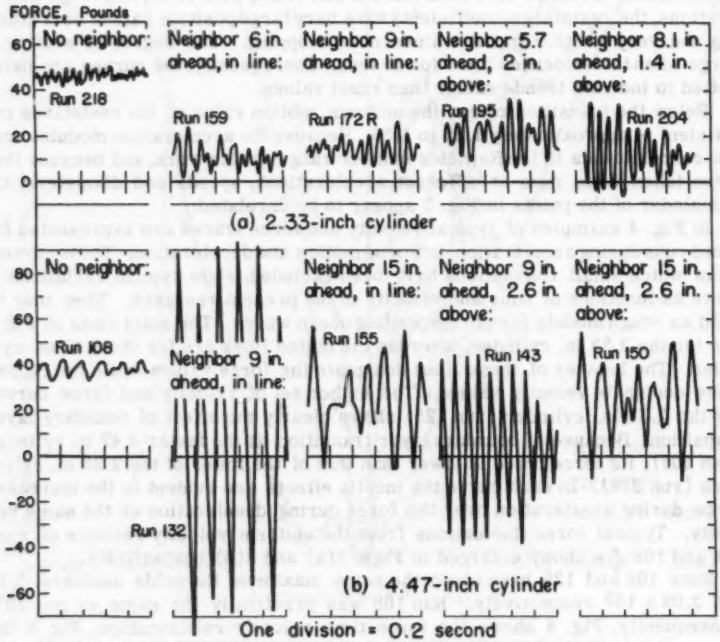


FIG. 5.—UNIFORM MOTION DRAG FORCES FOR CYLINDERS

The typical changes in the drag force traces when a neighboring cylinder is introduced are shown in Figs. 5(a) and 5(b). Fig. 5(a), shows the reduction of the mean force, or sheltering, by the neighboring cylinder. Differences in spacing of the cylinders cause differences in mean force and in fluctuating force. In Fig. 5(b), the sheltering and the fluctuations are seen to be more pronounced for the 4.47 in. cylinder than for the 2.33 in. cylinder.

In most runs, the fluctuations were absent for the single cylinders during rapid acceleration and deceleration. The fluctuations appeared to be due to the interaction of the forces caused by the nearly periodic shedding of eddies during uniform motion, and the elastic forces of the strain bars. Similar behavior of smokestacks and of iron bars has been reported.[11,12]

By means of the accelerometer, it was demonstrated that no measurable horizontal vibration was transmitted from the tow-wire or carriage to the horizontal pendulum. Direct measurement of vertical vibrations of the cylinder was not attempted because it was submerged. On the basis of the cylinder and the displaced water, being a weight on the end of the quarter inch stings, acting as cantilevers, the computed natural period for the vertical vibrations was 0.065 secs for the 2.33 in., and 0.092 secs for the 4.47 in. cylinder. The force meter did not respond to transverse horizontal forces, and was ten times as sensitive to forces in the direction of motion as in the vertical transverse direction. The torsional vibrations about a vertical axis, and vibrations in the direction of motion of the 2.33 in. cylinder had measured natural periods of approximately 0.13 sec. These torsional vibrations and vibrations in the direction of motion of the 4.47 in. cylinders had periods of 0.15 and 0.18 respectively, when the cylinder was stopped. After rapid decelerations of the 4.47 in. cylinder, the vibrations in the direction of motion frequently had a period of 0.16 secs.

The measured periods of vibration of the cylinders during uniform motion were recorded. For comparison, the approximate periods of shedding eddy pairs were also tabulated. These values were based on a Strouhal number of 0.186 for Reynolds numbers below 10^5 and 0.200 for higher Reynolds numbers at which the Strouhal number is more uncertain. From a consideration of the flow patterns about cylinders, one might expect a transverse force, or lift force, from eddies at the frequency of shedding-pairs. Each change in direction of the lift force should cause a force in the direction of motion, so that the frequency of the fluctuations in this force would be that of shedding alternate single eddies. It may be, however, that, if transverse vibrations at some preferred frequency would have large enough amplitudes, eddy pairs would be shed at this frequency. If the vibration were in the direction of motion, one might expect a tendency toward shedding either single alternate eddies or simultaneous pairs.

These periods showed practically no agreement with the periods estimated from Strouhal numbers at either full or half periods. The periods for the single 2.33 in. cylinder are predominantly near 0.06 sec, which probably corresponds to the vertical vibration. The less frequent and generally smaller vibrations between 0.15 and 0.17 secs may be due to the vibrations in the direction of motion. For the single 4.47 in. cylinder, the principal period, 0.18, is

11 "The Wind Induced Vibration of Cylindrical Structures," by J. Penzien, Proceedings Paper 1141, ASCE, January, 1957.

12 "Flow About a Pair of Adjacent, Parallel Cylinders Normal to a Stream: Theoretical Analysis," by L. Landweber, Report 485, U.S. Navy, The David W. Taylor Model Basin, July, 1942.

that of the natural vibration in the direction of motion. The recorded periods of approximately 0.08 secs may correspond to the natural period of the vertical vibrations of the frame of the car. During run 126 of the 4.47 in. cylinder, the period was 0.075 and after approximately 3 secs, the stings broke due to fatigue. Consequently, it would appear that vertical vibrations of the stings had occurred frequently throughout the runs. During run 132 the frame of the carriage appeared to vibrate with an amplitude of over 1/2 in. At the same time, the carriage wheels were periodically lifted clear of the track due to the forces from the test cylinder and its neighbor. The total weight of the carriage and its load was estimated at 450 lbs. Apparently the lift forces were comparable to the drag forces. Further research to measure the lift forces and to determine the eddy patterns and the reasons for the observed periods would be desirable.

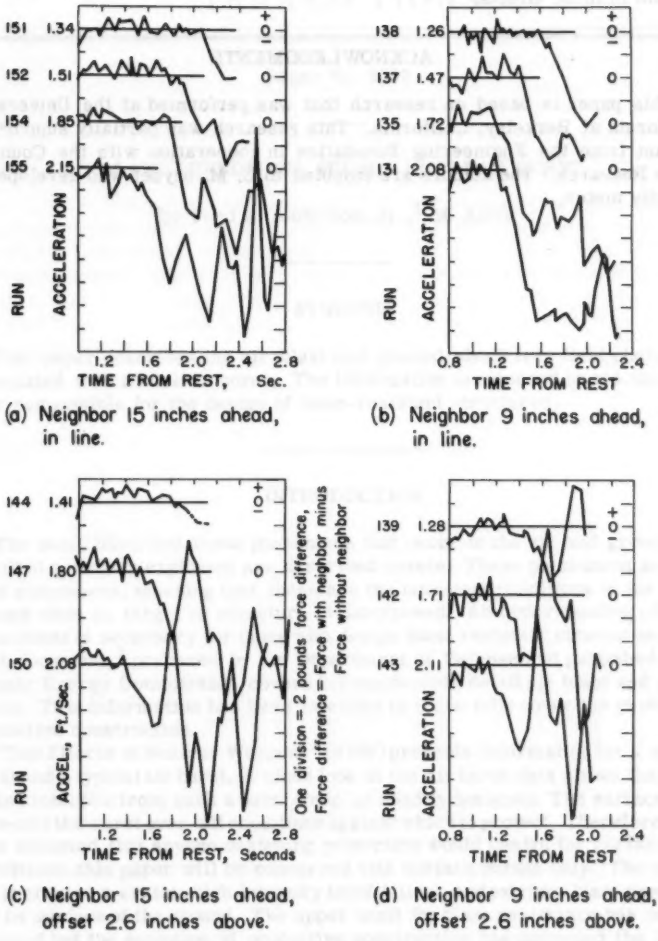
In Fig. 6, effects of a neighboring cylinder during constant acceleration are shown for the 4.47 in. cylinder. These curves, were obtained by subtracting the computed forces, at the corresponding acceleration and velocities for the cylinder alone, from the measured forces during acceleration. It is evident that increased acceleration caused earlier onset of the sheltering effect. A corresponding increase in the magnitude of the sheltering and in the violence of the fluctuating forces occurred. During acceleration, the violence of the fluctuation was greater for the offset cylinders than for the cylinders in line. Similar results were obtained with the 2.33 in. cylinders, although in general the fluctuations were less severe.

The increase of resistance force with time during constant acceleration is given in Fig. 4 for cylinders without neighbors. In Fig. 6, the first portion of each curve that oscillates about zero represents similar behavior, but with somewhat more vibration. The sudden decrease of values shows the onset of the influence of a parallel neighbor leading the test cylinder. It is believed that the arrival of a shed-eddy, or eddies, at the test cylinder changed the flow about it and reduced the mean force. The subsequent arrival of more eddies caused changes in the flow pattern that resulted in large fluctuations in the resistance force. Evidently, eddies from offset neighboring cylinders affected the following cylinder differently than did eddies from cylinders directly ahead. These traces might be likened to what would be expected during the corresponding motion of water during the crest half of the wave action. There is an essential difference in the two systems, however, since the water in the wave would have been disturbed by eddies that were shed by the pair into the water during the latter part of the trough-half of the preceding wave. During deceleration of the towed cylinder there was no return of the resistance force to that of a cylinder alone. That is, the sheltering continued throughout deceleration.

CONCLUSIONS

From the test conditions of this research the following conclusions may be drawn:

1. Drag coefficients for accelerated and uniform motion agreed with the corresponding accepted values for uniform motion.
2. During deceleration there was strong evidence of deviation of the drag coefficient from the accepted values for uniform motion.
3. The acceleration modulus, aD/V^2, did not correlate the resistance coefficient near boundary layer transition.



(a) Neighbor 15 inches ahead, in line.

(b) Neighbor 9 inches ahead, in line.

(c) Neighbor 15 inches ahead, offset 2.6 inches above.

(d) Neighbor 9 inches ahead, offset 2.6 inches above.

FIG. 6.—EFFECT OF NEIGHBORING CYLINDER ON FORCE EXERTED BY TEST CYLINDER

4. Some irregularities in wave force records may have been due to transition and acceleration effects.

5. The presence of a neighboring cylinder caused reductions of resistance and large fluctuations in the resistance and lift forces. The spacing was improtant in these effects.

ACKNOWLEDGMENTS

This paper is based on research that was performed at the University of California at Berkeley, California. This research was partially supported by a grant from the Engineering Foundation in cooperation with the Council on Wave Research. The authors are indebted to C. M. Snyder who developed the velocity meter.

AMERICAN SOCIETY OF CIVIL ENGINEERS

Founded November 5, 1852

TRANSACTIONS

Paper No. 3039

BLAST PHENOMENA FROM A NUCLEAR BURST

By Ferd E. Anderson, Jr.,[1] M. ASCE

SYNOPSIS

This paper describes the air blast and ground-shock free field phenomena associated with a nuclear burst. The information is intended to aid the engineer responsible for the design of blast-resistant structures.

INTRODUCTION

The basic blast and shock phenomena that occur in the air and ground as a result of a nuclear explosion are described herein. These phenomena are free field phenomena, meaning that these are the transient conditions in the air or ground when no target or structure is interposed. An understanding of these phenomena is necessary for those who design blast resistant structures.

A document,[2] prepared by the Department of Defense and published by the Atomic Energy Commission, covers in considerable detail air blast and ground shock. This information has been extended to more fully cover the problem of protective construction.

"The Effects of Nuclear Weapons" (ENW) presents information for a surface burst and a typical air burst. A close look at the air burst data shows that complete protection from such a burst could be readily designed. The surface burst presents the worst over-all conditions against which to protect. Therefore, since it is assumed that anyone designing protection would design for surface burst conditions, this paper will be concerned with surface bursts only. The surface burst creates a crater, high intensity local fallout, and extreme blast pressures on the surface of the ground. The upper limit for blast resistance has not been reached but the evolution of protective construction has exceeded the 100-psi

Note.—Published, essentially as printed here, in November, 1958, in the Journal of the Structural Division, as Proceedings Paper 1836. Positions and titles given are those in effect when the paper was approved for publication in Transactions.

[1] Maj., U.S. Army Constr. Agency France, A.P.O. 122, c/o Postmaster, New York, N. Y.

[2] "The Effects of Nuclear Weapons," edited by Samuel Glasstone, Supt. of Documents, U. S. Govt. Printing Office, Washington, D. C., June, 1957.

level. Surface burst craters are described fully elsewhere,[2] and fallout protection is not within the scope of this paper.

SURFACE BURSTS

The ENW information on surface burst air-blast pressures extends to 100 psi for both peak overpressure, p, and peak dynamic pressures, q. Overpressure is the transient (pseudo-static) pressure exceeding the ambient atmospheric pressure. Dynamic pressure is the pressure that results from the mass flow of the air behind the shock front and is customarily defined as

$$q = \frac{1}{2}\rho\mu^2 \quad \ldots\ldots\ldots\ldots\ldots\ldots (1)$$

in which ρ represents the air density and μ is the air particle velocity. The peak values versus distance of both of these pressures are indicated in Fig. 1, from 1 to 1,000 psi for 1 KT. One kiloton is used as a base point for the expression of most blast phenomena because values for other weapon sizes can

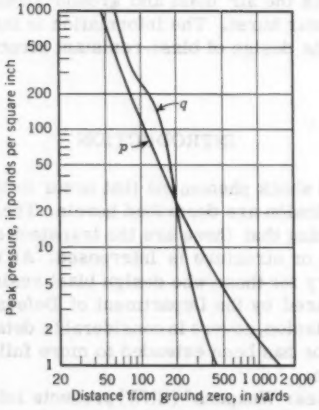


FIG. 1.—PEAK PRESSURE VERSUS DISTANCE, 1 kt SURFACE BURST

be obtained by applying cube root scaling procedures. The distance at which a given peak pressure is obtained is proportional to the cube root of the weapon yield.

At a given distance the pressure-time relationship is generally expressed as shown in Fig. 2(a). The equations for overpressure, p(t), and dynamic pressure, q(t), are

$$p(t) = p\left(1 - \frac{t}{t_+}\right) e^{-t/t_+} \quad \ldots\ldots\ldots\ldots\ldots (2)$$

and

$$q(t) = q\left(1 - \frac{t}{t_+}\right)^2 e^{-2t/t_+} \quad \ldots\ldots\ldots\ldots\ldots (3)$$

These equations of decay apply to relatively low pressures of 10 to 20 psi overpressure. Descriptions of the theoretical wave shapes for high pressures have been presented elsewhere.[3]

Experience has shown that when the overpressure from a surface burst is greater than 20 psi or 30 psi, or at distances less than 200 yd for 1 KT, the turbulence existing in the blast wave has caused the overpressure-time p(t) and dynamic-pressure-time q(t) functions to deviate from the ideal or theoretical-type blast waves shown in Fig. 2(a) and approach the pressure-time function shown in Fig. 2(b).

Approximate values of the rise time, t_r, for 1 KT are 3 to 5 m sec. The values of t_r are expected to scale as the cube root of the weapon yield. Therefore, for megaton range weapons, the rise times may be of the order of 50 to 100 m sec. The rise time will reduce any reflections of the overpressure of such a shock wave striking a structure surface to less than the reflected values obtained from a shock wave with an instantaneous rise time[4] (Fig. 2(a)). However, the dynamic pressures have increased in this region to approximately twice the theoretical value. Fig. 1 shows this as a hump in the q-curve. These irregularities do not seem to exist at overpressure levels of more than 200 psi for a surface burst.

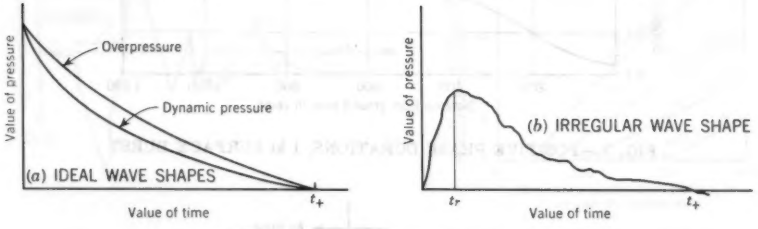


FIG. 2.—WAVE SHAPES

The positive phase durations (t_+) for a 1-KT surface burst are given in Fig. 3. The shock front velocity is given elsewhere.[5]

The durations are proportional to $W^{1/3}$ at distances proportional to $W^{1/3}$. The distance at which a given shock front velocity occurs is proportional to $W^{1/3}$. During the negative phase of the blast wave the overpressures become less than atmospheric and the dynamic pressures reverse direction, the winds now blowing toward ground zero. The maximum negative overpressure that can be obtained is approximately 4 psi below atmospheric. In some cases this may be important in structure design. The reversed dynamic pressures are small and can be ignored.

Earth stresses, accelerations, and displacements occur as a result of direct ground shock and air-blast induced ground shock. The direct ground shock is defined as the shock wave that travels entirely through the ground from the point of detonation on the surface to the point of interest at some distance from the burst. The air-blast induced ground shock is the ground shock set up at some

3 "Numerical Solution of Spherical Blast Waves," by H. L. Brode, Journal of Applied Physics, 1955, 26, 766.

4 "The Effects of Nuclear Weapons," edited by Samuel Glasstone, Supt. of Documents, U. S. Govt. Printing Office, Washington, D. C., June, 1957, p. 100, par. 3.81.

5 Ibid., p. 99, first equation.

distance from the burst by the air-blast overpressures traveling over the ground above the point of interest. The problem of evaluating stresses, accelerations, and displacements presents considerable difficulty. The effects of depth of measurement, type of soil, and weapon size are major uncertainties. Therefore, although air-blast phenomena are known to an accuracy of approximately ±25%, the ground-shock phenomena may be inaccurate by a factor of 2 or 3.

From high yield (megaton) surface bursts, where the point of interest in the ground is at a depth of less than 50 ft, the air-blast induced ground shock will predominate over the direct ground shock in producing stresses, accelerations, and displacements at distances from ground zero where air overpressures are less than 300 psi. Assuming that the region of interest is above a 50-ft depth and at pressures less than 300 psi for megation bursts, it is further assumed than that the direct ground shock can usually be ignored. At overpressures of 100 psi, the direct ground shock will be of little or no importance.

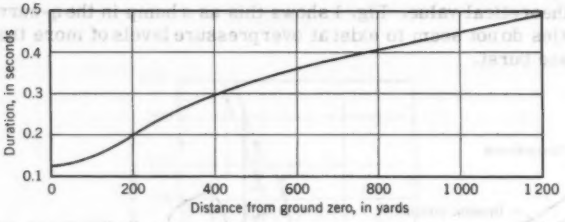


FIG. 3.—POSITIVE PHASE DURATIONS, 1 kt SURFACE BURST

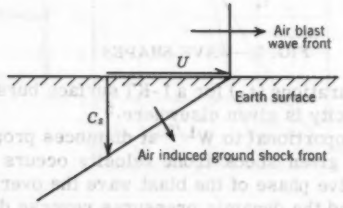


FIG. 4.—AIR-INDUCED GROUND SHOCK PROPAGATION

The direction of propagation of the air-induced ground shock is related to the velocity of the airblast wave and the vertical seismic velocity of the soil. Fig. 4 shows the air-induced ground shock propagation, in which U is the air blast wave front velocity and C_g is the vertical seismic velocity.

Although the maximum stress is not perpendicular to the shock front, this representation does indicate the sequence in which an underground structure will be loaded. The vertical stresses in the soil are equal to the air-blast overpressure at the surface and can be considered as not attenuated to a depth of 50 ft. At some depth (unknown but probably greater than 50 ft) attenuation does become significant. Horizontal stresses may be as low as 15% of the air-blast pressures in loose, dry soil, approximately 50% in moist soil, and approach 100% in saturated soils. It is recommended that 50% be used for soils above

the water table and 100% in soil below the water table. The rise times of the earth stresses will be increased over the rise time of the air-blast overpressure as depth is increased.

Accompanying the ground shock are accelerations that have been measured in the vertical and horizontal (lateral and radial) directions. Vertical accelerations at a 10-ft depth are related to the surface air blast pressures by

$$A_{10} = .053\ p^{1.2} \quad \ldots\ldots\ldots\ldots\ldots\ldots\ldots (4)$$

in which A_{10} is equal to the peak vertical acceleration at a 10-ft depth in units of the acceleration of gravity, g, and p is the surface air blast overpressure in psi.

The attenuation with depth of the vertical accelerations is given as

$$A_y = \frac{A_{10}\sqrt{10}}{\sqrt{y}} \quad \ldots\ldots\ldots\ldots\ldots\ldots\ldots (5)$$

in which A represents the peak vertical acceleration at a depth greater than 10 ft and y is the depth >10, in feet, of the point of measurement.

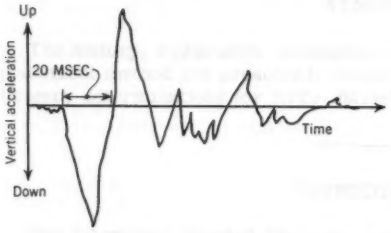


FIG. 5.—ACCELERATION VERSUS TIME RECORD

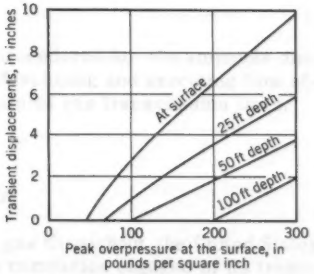


FIG. 6.—TRANSIENT VERTICAL SOIL DISPLACEMENTS

Horizontal accelerations are evaluated at a point as 70% of the vertical accelerations. These peak accelerations are spikes on an erratic acceleration versus time function in which the spikes have durations of approximately 20 m sec. A typical acceleration versus time record is shown in Fig. 5.

Displacements of the soil, both transient and permanent, are expected to vary considerably with soil type and water content of the soil. For compressible dry soils, representing soils in which the greatest displacements will occur, at 300 psi the surface will have a permanent vertical displacement of approximately 4 in. At approximately 50 psi noticeable displacements cease to exist. The transient displacements are approximately three times the permanent displacements. The displacements decrease with increasing depth so that at 300 psi there are essentially no displacements at a depth of 150 ft. Fig. 6 shows the transient vertical soil displacements.

The difference in maximum transient displacements does not represent the maximum relative displacements between two depths because the maximum at each depth occurs at a slightly different time. Therefore, the maximum relative displacement between two points may approach the maximum transient displacement of the shallower point.

The paper has presented blast and shock data as evaluated in 1958. Continued research and analysis of test data is providing refinements to the evaluation. There was a considerable bulk of test data that had been analyzed in only a preliminary way at the time of this writing. In addition, the use of shock tubes, wind tunnels, and high explosive tests continue to provide better correlation between the phenomena described and the loading and response of structures subjected to such phenomena. Subjects under study were (1) effects of varied topography on the blast wave, (2) blast wave conditions within the built-up area of a city, (3) loading from high dynamic pressures on streamlined structural shapes, and (4) underground phenomena and loading.

AMERICAN SOCIETY OF CIVIL ENGINEERS

Founded November 5, 1852

TRANSACTIONS

Paper No. 3040

FLOW TESTING BY AMMONIA DISPLACEMENT

By Jack N. White[1] and Thomas Thawley[2]

SYNOPSIS

The history, equipment, techniques, and procedures for the ammonia displacement method are presented, as used in developing and executing flow efficiency determinations for large-diameter natural gas transmission lines.

INTRODUCTION

The increasing demand for more natural gas throughout the United States has taxed the capacity of most of the pipeline companies engaged in its transportation. With the rising cost of labor and pipeline materials, it is of paramount importance that the designed capacity of existing systems be increased, or at least maintained.

With the growth of transmission companies, and consequent expanding knowledge in the field, it has become apparent that large-diameter pipelines have a characteristic efficiency for the flow of natural gas. This efficiency combines the effects of internal roughness of the steel pipe, the bends and fittings in the line, and the accumulation of lubricating oil and other material on the walls of the pipe.

It is common practice to clean newly-constructed pipelines thoroughly to attain highest efficiencies. Under these conditions it is not unusual to have initial flow efficiencies of 92% to 97%, depending on the smoothness of the line and the equation used to predict the efficiency.

Pipelines that have been in service for some years present a somewhat different problem. Although natural gas is transmitted in an essentially dehydrated state, there are minute droplets of water and distillate still entrained in the flowing gas stream. Over a period of time these entrained liquids coat the

Note.—Published, essentially as printed here, in January, 1959, in the Journal of the Pipeline Division, as Proceedings Paper 1905. Positions and titles given are those in effect when the paper was approved for publication in Transactions.

[1] Supt., Pipeline Section, Panhandle Eastern Pipeline Co., Kansas City, Mo.

[2] Engrg., Pipeline Section, Panhandle Eastern Pipeline Co., Kansas City, Mo.

internal walls of the pipe and collect at the low points of the line, restricting the flow.

Carry-over of compressor station lubricating oils is another cause of contamination. It becomes the responsibility of the operating section of the transmission companies to so maintain transmission pipelines that the dissipation of compression energy is kept to a minimum. The efficiency of the line is checked periodically and the trend of the decreasing efficiencies noted to determine when the line should be cleaned to bring it back to its design or initial efficiency—a purely economic measure.

For each 5% flow-efficiency decrease below the design efficiency, approximately 13% of the original line would require looping to restore it to original capacity. This means a 5% reduction in flow efficiency for an existing 100-mi, 30-in. pipeline would require 13 mi of 30-in. loop, at a cost of approximately $1,100,000 to permit the original volume of gas to flow under the original pressure conditions. When this price is compared to the $20,000 estimate required to clean and restore the pipeline to its original capacity, the importance of flow efficiency is apparent.

The operator's problem was the accurate measurement of the flow efficiency of an existing line. Over all flow efficiency, E, is defined as the ratio of the measured throughput for any one section of pipeline to the theoretical throughput of the same section under the same flowing conditions of pressure and temperature.

MEASUREMENT OF RATE OF FLOW

Several formulas used today that define the theoretical flow conditions in the pipeline include the Weymouth Formula, Panhandle "A", and the Modified Panhandle Formula. It is not the writers' purpose to evaluate existing formulas. The consistent use of one formula for design purposes and for determination of theoretical capacities establishes a valid basis for comparison to the actual measured throughput of the same system. This comparison determines the over all flow efficiency of a system.

Throughout the history of the gas industry, basically three methods have been used in an attempt to measure the actual rate of flow within a test section. The most obvious method is the use of orifice meters in the flowing gas stream when orifice meters are in the test section. However, an orifice meter section is not found normally in the line to be tested.

Early in the 1940's experiments were conducted using portable pitot tubes that were inserted in the main line. The use of these pitot tubes was discontinued because the results recorded could not be readily reproduced.

Late in the 1940's the possibility of measuring the actual rate of flow by timing the travel of an injected substance between two points was investigated. First attempts, using an odorant, were unsuccessful. Field hands assigned to each gate-setting were to sniff the gas bled off through a blow-off and call in as soon as the odorant was detected. Naturally, the men should have detected the odorant in succession as the gas flowed downstream. Such was not the case. After a waiting period, the fifth downstream station reported a "sniff" detection and almost immediately, all stations reported likewise.

The injection of anhydrous ammonia and detection by chemical indication was then inaugurated with encouraging results. The techniques of procedures

for the ammonia displacement method have since been refined to the point that a high degree of accuracy can be attained.

OPERATIONAL PHASES

The following examination of the operational phases of flow testing with emphasis on techniques and procedures and actual field conditions encountered during flow tests is similar to a method that has been described elsewhere.[3]

The object of a flow test is the collection of certain necessary data under controlled conditions. The data collected must be sufficient to solve for the theoretical throughput of a given section and the actual throughput of the same section.

The following information must be gathered:

Data	Tolerance
D = inside pipe diameter	Commercial
$h_2 - h_1$ = elevation change	$\pm$ 2.50 ft
L = length of section	$\pm$ 0.000 mi
P_1 = upstream pressure, psig	$\pm$ 0.100 psi
P_2 = downstream pressure, psig	$\pm$ 0.100 psi
P_a = atmospheric pressure psia	$\pm$ 0.050 psi
T_a = flowing gas temperature, degrees absolute	$\pm$ 0.500°
G = gas gravity	$\pm$ 0.001%
Z = compressibility	$\pm$ 0.005%
t = ammonia travel time	$\pm$ 0.500 sec

The first three items are fixed physical characteristics of the section being tested. The data for the last seven must, therefore, be measured in the field during the course of the test. The theoretical throughput is determined using the data in the adopted flow formula. By applying the same flowing conditions to the physical characteristics of the section, the corrected volume of gas in the section may be determined. This volume, factored by the time that it takes a slug of ammonia to travel between the sections, produces the actual rate of flow.

There are several important considerations to be made in selecting the pipeline section that will constitute the field set-up. Because all flow formulas are based on stable flowing conditions, it is mandatory that the test section be selected to provide the physical conditions most conducive to steady-state flow. It is difficult, even under ideal operations, to maintain a stable flow pattern in any given point for a long period of time. This is probably the most common source of error. Proper selection of a test section will, however, reduce

[3] "Pipeline Flow Efficiency Testing," by R. F. Bukacek and R. T. Ellington, Oil and Gas Journal, Vol. 55, Nos. 37, 38, 39, 1957.

the fluctuations to a minimum. The following precautions must be taken into account:

1. The section selected must be long enough to prevent human error in reading pressures from becoming a major factor. A measurement error of 1/10 of a psi in the pressure drop (that would occur, for instance, in 1,000 ft of pipe), would be of serious proportions. However, if the 1/10-psi error were applied to the pressure drop in a section 10 mi long, the magnitude of the error becomes acceptably small. An unrestricted section between 5 and 15 miles in length gives reasonable accuracy.
2. There should be no orifice plates or valves in the line between the points of the test section.
3. There should be no major pipe junctions near the point where pressure is recorded.
4. The elevation change between the points must be readily determinable.
5. There should be no multiple sections, such as river crossings, between the end points.
6. The pipe should be cleared of removable drip fluids.
7. The test section should be far enough away from compressor stations to avoid pressure pulsations.
8. The section should be sufficiently downstream from compressor stations to avoid the extreme temperature changes found in the flowing gas stream immediately adjacent to the station discharge.
9. Main-line taps should be avoided that supply market areas subject to short duration pull-down.
10. The end points of the test section should be accessible and should provide suitable appurtenances for the installation of injection and detection equipment and dead weights.

If all these conditions can be met and the upstream and downstream compressor stations are able to maintain constant discharge and suction pressures on the line for several hours preceding the test, then stable flow in the test section is approached closely.

The equipment required to inject and detect the ammonia can be shop-fabricated with ease. The basic injection equipment consists of a pressure tank, connecting tubing, ammonia bottle and insert staff, plus standard steel valves and fittings.

The operation of the injection system is quite simple. The ammonia bottle is loaded with 3 to 5 lb of anhydrous ammonia and placed atop the riser staff. The high-pressure tank is pressured with gas from the line and water is pumped into the tank to increase the gas pressure to approximately 200 lb above the line pressure. The same thing can be accomplished with a cylinder of nitrogen or any other inert gas. It is convenient to attach a pressure gage to the tank so that the pressure may be observed. The high-pressure tank is then connected to the ammonia bottle through high-pressure hose or tubing. All valves between the pressure tank and the gas stream are then opened except the one gate valve immediately downstream of the ammonia bottle. The ammonia slug is then ready to be injected into the line. The final step consists of opening the last gate valve rapidly and simultaneously starting a stop watch to record the travel time of a slug between the injection point and the detection point.

The equipment required for detection is simpler: A 1/4-in. extra-heavy pipe staff, a section of 1/4-in. pipe fitted with a tee and gate valve leading to

atmosphere, and a needle valve leading from the branch of the "T" to two rubber hoses. Gas is, therefore, directed from the pipeline through the staff, to test tubes containing the reagent.

It is quite convenient to fabricate a small hand-carried stand to hold the test tubes and chemical agents required for the detection of the ammonia slug. The case can be mounted on or adjacent to the riser for ease of handling.

Operation of the detection equipment is also uncomplicated. After assembling the apparatus, each test tube is filled with approximately 30 cu cm of distilled water to which is added one or two drops of 1% phenolphthalein solution. The test reagent is a clear, colorless liquid in its uncontaminated state. To insure sufficient flow of main-line gas to the test reagent, all valves in the vertical part of the detection staff are opened permitting the main-line pressure to vent to atmosphere. The free end of the rubber tubing is inserted into the test tube just beneath the surface of the reagent. The needle valve is adjusted so that the gas bubbles vigorously through the reagent. At the arrival of the ammonia charge, indicated by a pink coloration of the phenophthalein solution, the stopwatch at the detection point is stopped, thereby determining the time that has elapsed between ammonia injection and ammonia detection. The watch that was started at the time of injection may be transported to the detection end and stopped at the time of detection or the time of injection may be transferred to another watch at the detection point.

Main-line pressures are recorded at four locations on the section between compressor stations: the discharge fire gate of the upstream station, the injection point, the detection point, and the suction fire gate of the downstream station. Calibrated dead-weight gages are used to measure the pressure at each location. The readings and recordings of pressure are begun one or two hours before the injection of ammonia and continue at five to ten minute intervals throughout the test. The reading of pressures before the injection of ammonia indicates the stability of the flow in the section to be tested. If the pressures are constant at each location, it is reasonable to assume that the flow of gas in the entire section is stable.

It is the practice of compressor engine operators to control the discharge pressure at the upstream station and the suction pressure at the downstream station by monitoring a dead-weight gage set up in the engine room. In this way, small changes in discharge pressure are discovered immediately and can be corrected without inducing large pressure variations in the main line.

Temperature wells are installed at each main-line gate setting to compute the mean temperature of the flowing gas. The thermometers that were inserted in each well before the tests are picked up on the day of the flow test and the temperature at each location is recorded and plotted during the test. These temperatures are, in reality, the temperature of the outside wall of the transmission pipeline. A negligible difference exists between the flowing gas temperature on the inside wall of the pipeline and the temperature measured in the thermometer well.

The gravity of the flowing gas must be accurately measured either by portable gravitometers or at a fixed gravitometer station. Supercompressibility of the gas should be determined through direct measurements with one of the several pieces of apparatus available for that purpose.

Successful flow testing is dependent on detailed planning, proper coordination and complete cooperation of the several operating sections of the pipeline company. Dispatching personnel must be fully cognizant of the requirements

and importance of the test. They must be given sufficient beforehand notice so that they may stabilize their load pattern throughout the system to attain a steady-state flow easily.

Compressor station personnel must maintain close control of the compressor engines so as to govern discharge and suction pressure as closely as possible. A 6-to-8-hr period is required to attain the steady flow and to conduct the test. If flow tests are to be conducted in or near the gathering system, caution must be taken to insure that wells are not turned off or on during the course of the test.

The tests described herein were scheduled for Tuesday, Wednesday and Thursday, and planned so that the first ammonia injection occurred at or just after 9 a. m. In this way, cutbacks that occur on Friday in anticipation of reduced weekend sales and build-ups that occur late Sunday and Monday to supply the weekday sales, are avoided.

A series of flow tests are conducted in the fall of the year to forecast heavy winter market demands and capabilities. Thus, up-to-date efficiencies are available during the peak load period. However, inclement weather remains the chief obstacle for flow testing during this season.

The major sources of error in making any flow test include: (1) Pressure measurement; (2) incorrect communication of the time; (3) neglect in correcting elevational changes; (4) unstablized flow; (5) failure to correct the dead weight; and (6) the use of an incorrect length of line in computing the ammonia run.

It is not uncommon to fail to add the 5 lbs, the weight of the table, to the dead weight reading, or to add the weights on the table incorrectly. An error of one minute is often made in communicating the time ahead of the detection point. Elevation corrections are necessary in most cases.

Line stability is essential for consistent results. All dead weights do not read the same and correction should be made to a standard dead-weight tester. Dead weights can differ as much as a pound and a half at full scale. To make this correction, it is only necessary to calibrate each of the dead weights and compare it with some standard. Relative, not individual readings are important. A reading can be a half-pound off, providing that this is consistent throughout and that the same dead weight is used as a standard.

Some errors may be eliminated by running two slugs of ammonia at 30-min intervals, to determine the steadiness of the flow. If the flow is stable the answer obtained will be nearly the same. The use of the correct length of line in the test section is readily apparent.

The most important uses of the results of the flow test are: (1) Design of future facilities; (2) dispatching; (3) flow study; and (4) determining whether the line needs to be cleaned.

Efficiencies used for flow studies and dispatching should not contain elevation corrections. For these purposes a dispatcher or engineer is interested in the amount of gas that can actually pass through the line with changes in elevation and not how much can pass through the line if these changes in elevation were not present. Consideration should also be given to pressure drops in yard piping, if present.

Corrections in elevation are important in determining whether a line should be cleaned. Determine the efficiency of the entire line between two compressor stations and compare the results with the previous test. If a decrease is indicated, then determine the efficiency of the individual sections between the gate

settings to see whether the low efficiency is due to the entire line or one or two sections. With this method, relative results are important. If the same error is made each time, the relative results will not be affected. The trend of efficiencies from year to year, and not on individual tests, is emphasized.

The ammonia displacement method is economical and adaptable to most pipeline systems. It permits a high degree of accuracy under field conditions, and in the opinion of the writer, is the best method yet developed.

CONCLUSIONS

1. Flow testing large diameter natural gas transmission lines by ammonia displacement is an accurate and economical approach to determine pipeline efficiency.

2. Equipment required to inject and detect the ammonia can be easily fabricated and assembled in an operational type pipeline maintenance shop.

3. The ammonia displacement method is adaptable to most pipeline systems and a high degree of accuracy under field conditions can be achieved easily with planning and cooperation of the operating personnel.

AMERICAN SOCIETY OF CIVIL ENGINEERS

Founded November 5, 1852

TRANSACTIONS

Paper No. 3041

COMPACTED CLAY

A SYMPOSIUM

PAGE

STRUCTURE

By T. William Lambe, F. ASCE 682

WITH DISCUSSION BY MESSRS. D. Hugh Trollope; B. P. Warkentin and Raymond N. Y. Yong; Gerald A. Leonards; D. P. Krynine; Dean R. Freitag; and T. William Lambe 706

ENGINEERING BEHAVIOR

By T. William Lambe, F. ASCE 718

WITH DISCUSSION BY MESSRS. Alfred C. Scheer; Raymond N. Y. Yong and B. P. Warkentin; J. MacNeil Turnbull; José A. Jiménez Salas; D. Hugh Trollope; and T. William Lambe. 741

COMPACTED CLAY: STRUCTURE

By T. William Lambe,[1] F. ASCE

With Discussion by Messrs. D. Hugh Trollope; B. P. Warkentin and Raymond N. Y. Yong; Gerald A. Leonards; D. P. Krynine; Dean R. Freitag; and T. William Lambe

SYNOPSIS

This paper describes the nature of clay structure, a term referring to the arrangement of particles and the electrical forces acting between them. The effects of forces and environmental factors on this structure are inferred from the principles of colloid chemistry and crystal chemistry.

INTRODUCTION

The nature and engineering significance of the structure of compacted clay are treated in this and in the subsequent paper. This paper describes the nature of clay structure; the second paper uses the concepts presented herein to explain the fundamentals of the engineering behavior of clay.

In this paper, the term "structure" means the arrangement of soil particles and the electrical forces acting between adjacent particles. The structure of a clay determines its properties. The engineer must, therefore, consider structure in order to understand the fundamentals of soil behavior. He needs an understanding of structure especially if he tries to predict the effects on soil properties of time, pressure, and changes in environmental conditions. The increasing study of soil structure indicates a growing recognition of the importance of structure.

The term "structure" was initially limited to the arrangement of soil particles. The inclusion of electrical forces as a component of structure seems necessary. Progress on elucidating the force component of structure has been made only in recent years, primarily because the underlying sciences—colloid chemistry and crystal chemistry—are relatively young. The importance of the arrangement of soil particles, however, was recognized many years ago (1), (2), (3).[2] Juud Hvorslev, F. ASCE (3), postulated the effect of one-dimensional compression on the alinement of clay platelets. The measurements described herein show Hvorslev's hypotheses were correct.

Note.—Published, essentially as printed here, in May, 1958, in the Journal of the Soil Mechanics and Foundations Division, as Proceedings Paper 1654. Positions and titles given are those in effect when the paper or discussion was approved for publication in Transactions.

[1] Prof. and Head, Dept. of Soil Engrg., Massachussets Inst. of Technology, Cambridge, Mass.

[2] Numerals in parentheses—thus, (1)—refer to corresponding references in the Bibliography (Appendix).

Studies on compacted clay can be of immediate practical value as well as of value to the basic understanding of the behavior of fine-grained soils. Compacted clays, both with and without added stabilizers, are being used increasingly in engineering works. Plastic clays are, for example, being placed in earth dams and highway subgrades more often than in the past, sometimes by choice and sometimes by necessity. As the use of and severity of imposed loads on compacted clay increase, the need for a better understanding of the properties of the clay becomes greater.

This series of papers should help answer the important question, "should a fine-grained soil be compacted wet or dry of optimum moisture content?" Some of the effects of molding water on the behavior of a soil will be demonstrated. It will be shown that the best placement moisture for a given soil depends on the properties desired in a particular problem.

As will be shown there are fundamental similarities between the structures of compacted and natural clays. Studies on compacted clays can, therefore, improve our knowledge of naturally sedimented clays. There are experimental advantages to using compacted instead of natural clays for studying the fundamental properties of clays.

Although the following material deals primarily with clays, most of the concepts hold also for soils containing silt or clay. Colloidal phenomena are, of course, less important in soils of low or no plasticity. This paper is limited to inorganic soil components.

As will be noted, several facets of structure are not fully understood. It is not the intent, therefore, to present this material as the final "word," but rather as a stimulant, and, hopefully, a guide to further studies on this complex subject.

AGGREGATION AND DISPERSION OF SOIL PARTICLES

Electrical Forces.—Many groups of scientists, especially colloid chemists and crystal chemists, have given much thought to the electrical forces acting between atoms (4),(5),(6),(7). Also, the writer has presented a short description of some of these forces (8). These forces fall into three categories: Primary valence bonds, hydrogen bonds, and secondary valence forces.

Primary valence bonds, which are the strongest, hold atoms together in the basic mineral units. The three most important bonds to the soil mineralogist are the ionic (an exchange of electrons by the linked atoms), the covalent (sharing of electrons by the linked atoms), and the heterpolar (in effect, part ionic and part covalent, because it results from an unequal sharing of electrons by the linked atoms). Some crystal chemists do not recognize the heterpolar bonds as a separate type but merely a mixture of ionic and covalent bonds. The bonds linking silicon and oxygen atoms in the silicate minerals are heterpolar, that is, 50% ionic and 50% covalent. Since the ionic and heterpolar bonds bring about atomic groups that are not electrically symmetrical, they act like magnets. This electrical nature of the soil minerals is most important, as shall be seen.

The hydrogen bond occurs when an atom of hydrogen is strongly attracted by two other atoms; hydrogen bonds are only important when oxygen, nitrogen, or fluorine atoms are present. The best example of the hydrogen bond is the linkage between water molecules. Attracted to the oxygen atoms in neighboring water molecules, each hydrogen atom links its water molecules to others.

The hydrogen bond is considerably weaker than primary valence bonds. It operates not only in water but also in other areas of interest to the soil engineer. It is the main linkage between the basic units of certain minerals, the most important of which is kaolinite.

The primary valence and hydrogen bonds are both too strong to be broken by the stresses an engineer would normally apply to a soil system. This is not true, however, of the secondary valence forces, which are much weaker than the other two. Another difference between the secondary valence forces and the other two types is the fact that secondary valence forces can act over relatively large distances.

The secondary valence forces (also called van der Waals forces) between units of matter arise from electrical moments existing within the units. They are quite similar to those acting between two short bar magnets. In certain relative positions the magnets repel each other and in others, they attract. Because there are more attractive positions than there are repulsive positions, the net effect is attraction. In a similar fashion the net effect of secondary valence forces is attraction.

Because of the nonsymmetrical distribution of electrons in the silicate crystals (arising from the heterpolar bonds), these crystals act as a large number of dipoles. They can attract other dipoles, the most important being water. The nonsymmetrical configuration of the water molecule makes it dipolar.

The water molecule is a permanent dipole because its polar nature arises from the position of the atoms in the molecule. Other kinds of dipoles are induced and statistical. When a normally symmetrical molecule is placed in an electric field it becomes polar. The electric field can cause a nonpolar unit to become an induced dipole.

Because the electrons in an atom are not stationary but vibrating, they periodically assume unsymmetrical positions. Symmetrical molecules periodically become polar, that is, statistical dipoles.

These secondary valence forces are of vital concern to the soil engineer, because they contribute to clay strength and cause soils to hold water. Much of the remaining material contained herein is concerned with these important electrical forces.

Another type of primary valence linkage that must be considered is the electrostatic attraction or repulsion of electrically charged units of matter. The negatively charged soil particle attracts cations, cations and anions attract each other, cations repel each other, and anions repel each other. Those electrostatic forces are similar to primary valence bonds in that they involve units with net electrical charges. They can, however, act over much larger distances than can ionic bonds.

In summary, the main importance to the soil engineer of primary valence and hydrogen bonds is that they are the seat of electrical forces. Of much more concern to the engineer are secondary valence and electrostatic forces, because they are greatly influenced by applied stresses and by changes in the nature of the soil-water system.

Colloid Stability.—Electrical forces of the types previously described act between all adjacent soil particles. They become important only when they are large in comparison to the forces related to mass. Because the electrical forces act only near the particle surface, and since many of them result from discontinuities at or near the surface, they are significant when surface area per mass, that is, specific surface, is high. When a particle has a specific surface large enough to cause the electrical forces to dominate the mass forces,

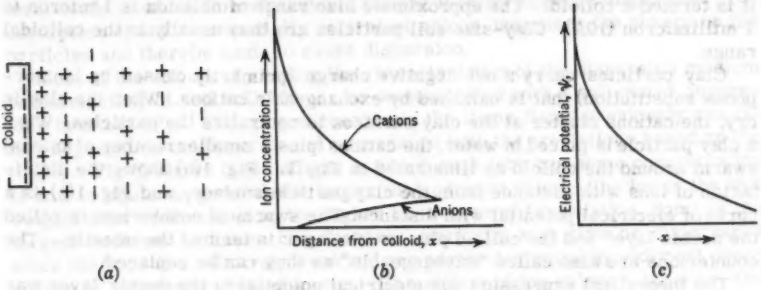


FIG. 1.—DIFFUSE DOUBLE LAYER

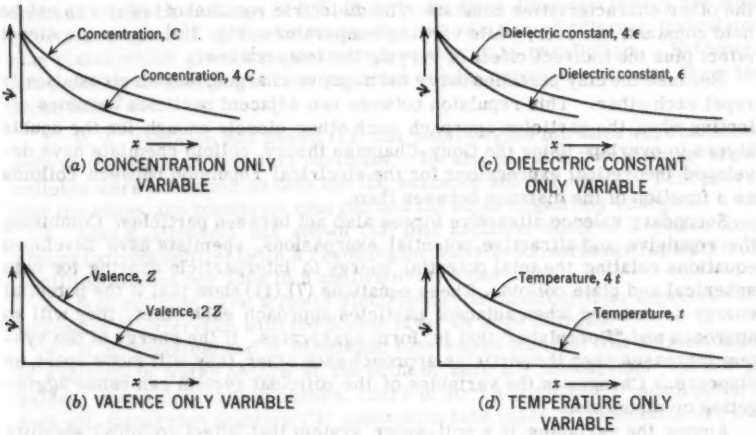


FIG. 2.—EFFECTS OF CHANGES IN SYSTEM PROPERTIES ON DIFFUSE DOUBLE LAYER

it is termed a colloid. The approximate size range of colloids is 1 micron to 1 millimicron (10A). Clay-size soil particles are thus usually in the colloidal range.

Clay particles carry a net negative charge (primarily caused by isomorphous substitution) that is balanced by exchangeable cations. When the clay is dry, the cations cluster at the clay surfaces to neutralize the particles. When a clay particle is placed in water, the cations (plus a smaller number of anions) swarm around the colloid as illustrated in Fig. 1. Fig. 1(b) shows the distribution of ions with distance from the clay particle surface, and Fig. 1(c) is a curve of electrical potential with distance. The swarm of counterions is called the double layer and the colloid plus double layer is termed the micelle. The counterions are also called "exchangeable" as they can be replaced.

The theoretical expression for electrical potential in the double layer was developed independently by G. Gouy (9) and D. L. Chapman (10) and is often termed the Gouy-Chapman theory. This theory shows how the potential-distance curve, that is, double layer, varies with characteristics of the dispersion medium. These effects are illustrated in Fig. 2. Figs. 2(a) through 2(d) show the effect on the double layer of varying only the characteristic noted while holding the other characteristics constant. The dielectric constant of water can not be held constant, however, while varying temperature. Fig. 2(e) shows the direct effect plus the indirect effect of varying the temperature.

Because the clay particles carry net negative charges, they electrostatically repel each other. This repulsion between two adjacent particles becomes effective when the particles approach each other closely enough for the double layers to overlap. Using the Gouy-Chapman theory, colloid chemists have developed theoretical expressions for the electrical repulsion between colloids as a function of the distance between them.

Secondary valence attractive forces also act between particles. Combining the repulsive and attractive potential expressions, chemists have developed equations relating the total potential energy to interparticle spacing for both spherical and plate colloids. These equations (7),(11) show that if the potential energy is reduced when adjacent particles approach each other, they will so approach and "flocculate," that is, form aggregates. If the energy of the system increases when the particles approach each other, they will move apart, or disperse. Changes in the variables of the colloidal system can cause aggregation or dispersion.

Among the variables in a soil-water system that affect colloidal stability are (a) electrolyte concentration; (b) ion valence; (c) dielectric constant; (d) temperature; (e) size of hydrated ion; (f) pH; and (g) anion adsorption.

The Gouy-Chapman theory states, in general terms, that a tendency toward flocculation is usually caused by increasing electrolyte concentration, ion valence, and temperature; and decreasing dielectric constant, size of hydrated ion, pH, and anion adsorption.

The influence of the first four variables follows from the Gouy-Chapman theory of the diffuse double layer, as a decrease in the double-layer thickness reduces the electrical repulsion, which, in turn, causes a tendency toward flocculation. The smaller an ion plus its "shell" of hydration water, the closer it can approach the colloidal surface—thus the smaller the hydrated ion, the smaller the double layer, and the more likely is flocculation.

The pH of the pore fluid affects the net negative charge on a soil particle by altering the extent of dissociation of OH^- groups on the edges of the particle. High pH encourages the dissociation and increases the net charge, thus

expanding the double layer, low pH does the reverse. Lowering the pH, therefore, tends to cause flocculation and raising it tends to cause dispersion. The adsorption of anions, especially polyvalent anions, increases the charge on the particles and thereby tends to cause dispersion.

Most of the effects of varying the characteristics of the dispersion medium on the stability of soil colloids can be demonstrated with a soil-water suspension in a test tube. Changing successively the items listed previously can affect aggregation or dispersion in accordance with the predictions based on the theory. Fig. 3 shows these effects in which each tube has some concentration of soil in liquid. In general, the larger the sediment volume (the lower the unit weight) after sedimentation, the higher the degree of flocculation. Some of the largest sediment volumes can decrease markedly with time or disturbance since the flocs are relatively weak and are partly destroyed by sediment overburden or externally applied forces. The effects of ion valency, ion size, and pH are complicated by ion-exchange reactions.

Non-Salt Flocculation.—The Gouy-Chapman theory assumes that the colloid charge is spread uniformly over the entire colloid surface. This implies that the edges of the soil platelets carry the same charge as the flat surfaces or that the ratio of edge area to plate area is small. This ratio is not always small as it can be as large at 1/5. If, as in the Gouy-Chapman theory, the edge effects are ignored, it can be shown that the position of adjacent flocculated clay plates which gives the minimum free energy is parallelism. Evidence, however, that the edges of clay particles can be oppositely charged from the faces follows:

1. P. A. Thiessen has shown (12) that negative gold micelles were adsorbed only at the edges of kaolinite particles. He also showed that positive silver colloids were adsorbed on both the flat surfaces and the edges. This proves that the edges are positively charged and the faces negatively charged.
2. Alan S. Michaels has shown (13) that kaolinite adsorbs negative ionic groups (polyphosphates) with a resulting increase in ion exchange capacity from 2 milliequivalent per 100g to 5 milliequivalent per 100g.
3. Soil colloids have a lower electrophoretic mobility than expected (14), indicating interference with the double layer by edge charges.
4. R. K. Schofield and H. R. Samson have shown (15),(16) that deflocculation of kaolinite in water occurs at the point of zero Cl^- adsorption. At low pH values, where flocculation occurs, there is strong positive Cl^- adsorption; at high pH, dispersion negative Cl^- adsorption take place. These facts are evidence of edge-to-face flocculation.

There are also indications that flocculated sediments are not composed of plates in a parallel array:

1. A flocculated sediment is very loose, that is, it has a low density. This means that the colloids cannot be packed in a parallel arrangement as this efficient packing would give a high density.
2. R. Fahn, A. Weiss, and U. Hofmann proved (17) that montmorillonite particles in a thixotropic gel were in contact. They removed the water from the gel by quick freezing followed by sublimation. The removal of water by this means left a rigid structure of essentially the same volume as the gel. Such a porous structure could hardly be obtained from parallel particles.

The inescapable conclusions are therefore: (a) The edges of clay particles can carry a charge opposite to that of the faces, and (b) flocculated sediments are not composed entirely of parallel particles. Two types of flocculation, salt

type with an orientation approaching parallelism, and a non-salt type with an orientation approaching a perpendicular array, can exist. These orientations and a dispersed orientation are illustrated in Fig. 4.

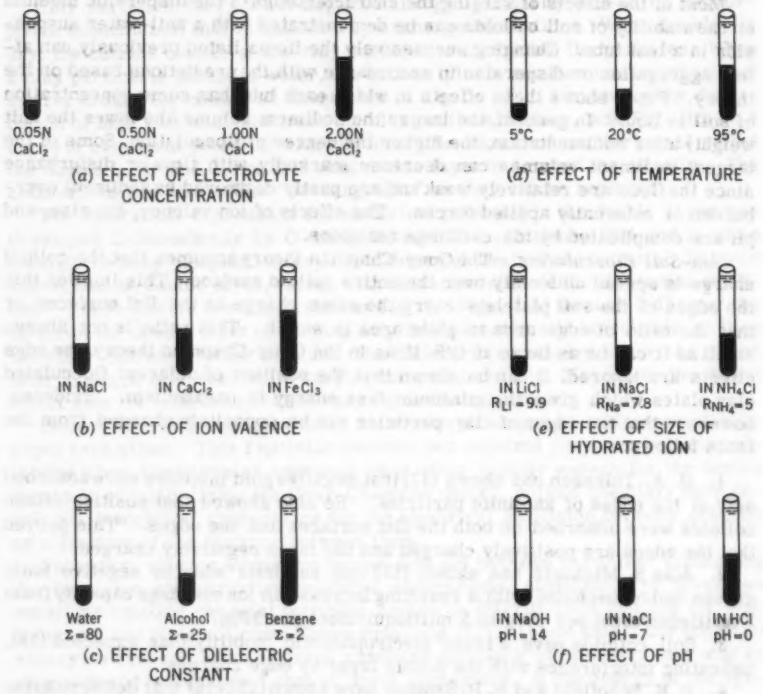


FIG. 3.—EFFECTS OF SYSTEM CHARACTERISTICS ON SOIL SEDIMENT



FIG. 4.—SEDIMENT STRUCTURES

The presence of both types of flocculation in the same colloidal system can be demonstrated with kaolinite in water. As Fig. 5 illustrates, pure kaolinite in distilled water flocculates by the edge-to-face mechanism to give a very

loose sediment. The addition of a small amount of electrolyte results in dispersion, whereas further salt results in salt-flocculation. Adding salt to the system increases the concentration of anions that gather at the edges of the particles. Because of this anion concentration the positive charge of the particle is effective over a smaller distance, and thus its ends are less able to cause flocculation. The same neutralization can be obtained with small negatively charged particles, for example, montmorillonoids (16). The use of the principle of streaming birefringence shows a higher degree of particle parallelism with salt than with non-salt flocculation. Shaking a suspension of particles with a high degree of parallelism will cause a streaked or nonhomogeneous appearance. This appearance is due to the reflection of light from a large number of particles at the same orientation.

Limitations of Colloid Theory in Soil Masses.—The soil engineer is almost always concerned with large masses of natural soil rather than with very dilute

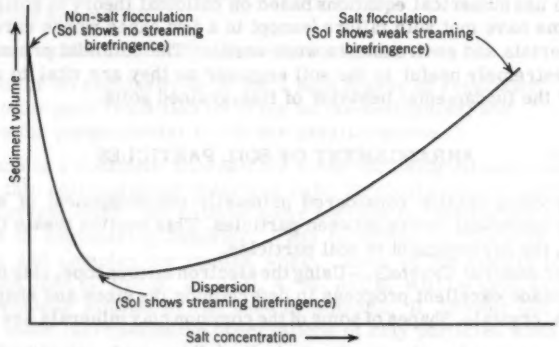


FIG. 5.—FLOCCULATION AND DISPERSION OF KAOLINITE IN WATER

suspensions of colloids. There are, therefore, several important factors neglected in colloidal theories which he must consider. These factors are in addition to the assumptions of the characteristics of individual colloids made in the theories, such as uniform surface charge, ions as point charges, and similar assumptions. These factors are:

1. Particle Size and Shape.—The particles in a natural soil are not all of the same size and shape as the theories assume. Nearly all soils contain particles of many shapes and many sizes. Most soils contain more than one mineral and several impurities. Silt-size particles occur in most plastic soils, and these nonplate-shaped particles affect the arrangements of the plate-shaped particles. Colloidal phenomena are much less important in silt than in clay-size particles.

2. Soil Concentration.—The concentration of mineral matter in soil fluid is much higher than assumed—in fact, most natural inorganic soils contain far more mineral matter than water. There is considerable physical and electrical interference among neighboring particles. The theory of colloid interaction should consider many particles, not simply two adjacent ones.

3. Interparticle Spacing.—The average interparticle spacings in a natural soil are the lower limit of validity for colloidal theory. When particles are

almost touching, that is, less than 10A apart, forces not considered by the Gouy-Chapman theory operate.

4. Applied Forces.—Most clay-size particles are, indeed, colloidal when they are in dilute suspensions. In large clay masses, however, there are very important forces which are external in origin. Although the mass of an isolated clay particle results in a force that is inconsequential relative to the colloidal forces acting, the accumulated effect of overburden in a natural deposit is not inconsequential. The various other intergranular forces that the soil engineer encounters, such as those occurring from overlying structures or from moving water, can be of great importance in determining the behavior of clay. The force system acting between soil particles is influenced not only by the forces arising from the nature of particles but also by those arising from noncompositional sources. Colloid theories usually consider only the former.

Because of these four factors, plus other less important ones, the various attempts to use numerical equations based on colloidal theory in soil engineering problems have met with failure (except in a few cases where carefully selected materials and environments were used). The colloidal principles are, however, extremely useful to the soil engineer as they are vital to an understanding of the fundamental behavior of fine-grained soils.

ARRANGEMENT OF SOIL PARTICLES

The preceding section considered primarily one component of structure; namely, the electrical forces between particles. This section treats the second component, the arrangement of soil particles.

Shapes of Mineral Crystals.—Using the electron microscope, clay mineralogists have made excellent progress in determining the sizes and shapes of the clay mineral crystals. Shapes of some of the common clay minerals are (18), (19):

kaolinite	sheets (often regular hexagonal sheets)
halloysite	tubes of curled sheets
montmorillonite	flaky sheets
nontronite	laths
illite	irregular flaky sheets
attapulgite	narrow fibers
chlorite	sheets
vermiculite	sheets

Thus, none of the mineral particles that contribute nearly all of the plasticity to natural clays are equidimensional—they are usually sheets or plates and sometimes rods or laths.

The other minerals (quartz, feldspars, carbonates, and oxides) common in natural clays are irregularly shaped, but their particles are usually not far from equidimensional. These particles can be considered, with reasonable accuracy, as rough-edged shapes approaching spheres.

Possible Arrangements of Particles.—Because the sizes and shapes of particles in a natural clay vary, and especially since the most important particles are far from equidimensional, there are many possible arrangements of particles. Very irregular and very complex patterns are possible. The patterns of arrangements are less complex in compacted clays than in sedimentary clays, because stratifications are less important. Sedimentary clays usually have

layers of different-sized particles resulting from different conditions of deposition. Layering between the compaction lifts and variation of soil due to changes in the characteristics of borrow do, of course, occur. They are, however, of much less importance to structure than are the sedimentation stratifications in natural clays.

James K. Mitchell, A. M. ASCE, worked out (20) a semiquantitative system for describing a particle arrangement, or fabric. The items in his system are:

1. Texture
   a. Regularity of components; and
   b. Transition between components
2. Particle Orientation
   a. Within small areas, that is $<1500\mu$;
   b. Within large areas, that is $>1500\mu$; and
   c. Clay around silt.

Mitchell used scales to describe these factors, as

a. Zero for no regularity to 90 for a high degree of regularity;
b. Zero for poor transition to 90 for no discontinuities; and
c. Zero for perpendicular to 100 for parallel plates.

By means of a complete microscopic study, including measurements of extinction of thin sections under polarized light, Mitchell assigned numbers to the fabric of several clays. He enjoyed some success in relating his fabric measurements to engineering behavior. His technique is, however, too time-consuming and complex for routine work. Some of the results obtained by Mitchell and John G. Pacey, Jr. (21), A. M. ASCE, will be used subsequently. Using a technique similar to that used by Mitchell, R. Brewer and A. D. Haldane have made (22) qualitative observations of clay particles when sands are permeated with clay suspensions. In general, the clay plates oriented themselves into positions parallel to the sand surfaces.

In this paper descriptions of the arrangement component of structure will refer only to the orientation and spacing of adjacent particles. This simplification of Mitchell's complete description of particle orientation is justified, especially in compacted clays, because arrangement will be used as a concept only for qualitative purposes.

Arrangements of Particles Occurring in Soils.—The arrangement of silt-sized particles can be, and has been, easily determined by means of a microscopic examination. Where there is convincing indirect evidence on the orientation of individual clay-sized particles (a few microns and smaller), no direct measurements have been made. The preparation of clays for examination with an electron microscope in most techniques destroys the structure in a natural soil—in fact, some think that the severe pretreatment (especially drying) given specimens for the electron microscope actually changes the size and shape of some clay crystals, for example, nontronite. Some of the replica techniques may give reliable electron photomicrographs of soil without disturbing the structure. The limitation of microscope resolution prevented Mitchell from making reliable determinations of particle orientation in zones smaller than 10 microns wide. He had to assume, therefore, that the orientations he measured within aggregates 10 microns and larger in size existed between individual

particles. His work on specially prepared specimens of known particle orientation indicate his technique does give correct results. His and Pacey's data on natural soils are most likely correct.

In the preceding section, it was seen that the particle orientation resulting from the flocculation of a sol approached a perpendicular array and that from the settling of a dispersed sol tended to a parallel array. Certainly non-salt flocculation gives a perpendicular orientation and salt flocculation gives a random orientation with individual particles tending to be parallel. The fact that a much denser deposit results from the sedimentation of a dispersed sediment than of a flocculated one proves that the particle packing in a dispersed sediment is much more efficient in a more nearly parallel array.

It has been pointed out that the soil engineer cannot neglect mass forces in the soil systems with which he works. In these soil systems, the terms "dispersed" and "flocculated" have slightly different meanings from those given them by the colloid chemist. To the soil engineer, a dispersed soil is one in which the net electrical forces between adjacent particles were repulsion at the time of deposition, and a flocculated soil is one in which the electrical forces were attraction during deposition. This concept is very important.

When a deposit of dispersed soil is being formed by compaction or by sedimentation, the particles can slide past one another to positions giving a very efficient packing. Flocculating particles stick to one another when they approach each other, and mechanical manipulation is much less effective in arranging particles.

Although the soil particles in a dispersed sediment are colloids, they are essentially in contact—not far apart as the term dispersed implies. The reasons for this have been presented: Externally applied forces, as well as electrical forces, are important. The use of dispersion and flocculation in this sense (which the colloid chemist might question), may not be wise—it is, however, widespread. As long as it is understood that a dispersed sediment implies interparticle electrical repulsion, and a flocculated sediment interparticle electrical attraction, the confusion should be minor.

Even though the particles in a flocculated sediment are nonparallel at the time of deposit formation, they can be made to assume a parallel array. The most obvious way to rearrange particles is through the application of a pressure. A parallel arrangement of particles in a flocculated deposit can result from one-dimensional consolidation under a very high pressure. Later sections examine changes in particle orientation that can occur after deposition.

NATURE OF WATER IN CLAY

The influence of water on the behavior of clay is tremendous. Karl Terzaghi, Hon. M. ASCE (1), pointed out the importance of water in clay in his early work and nearly every investigator since has confirmed it. Of concern to the soil engineer are the amount of water; the nature of water (how strongly held by the soil, electrolyte type and concentration); and the stresses in the water. Even though much study has been devoted to clay water, knowledge of it is limited in extent and not well supported by experimental data.

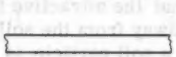
Water is held to a clay particle by a force that decreases in magnitude as the distance from the particle surface increases. A rough approximation of the attractive force between soil and water as a function of distance is given by the electrical potential-distance plot, shown in Fig. 1. That is, all of the

water in the double layer is attracted to the soil particle. The force-distance plot is a smooth curve with no sharp discontinuities, and it can be expanded and compressed by altering the system characteristics presented under the heading "Aggregation and Dispersion of Soil Particles," or by altering the intergranular pressure. Applying an intergranular stress to adjacent colloids reduces the spacing of the colloids and the double layers are reduced.

The soil-water attractive force consists basically of two components, namely:

1. Attraction of the dipolar water to the electrically charged soil; and
2. Attraction of the dipolar water to the cations in the double layer, the cations in turn being attracted to the soil.

The mineral crystal carries net electrical charges, resulting from isomorphous substitution, and also local charges, resulting from the heterpolar bonds holding the mineral atoms together, and from local discontinuities. Anion adsorption also contributes to the charge of the crystal. The water very near the soil is strongly held by these electrical charges on the soil. The water anywhere in the double layer is attracted by an induction type of force since the entire double layer is an electric field.



(*a*) TYPICAL MONTMORILLONITE PARTICLE
1000 A BY 10 A THICK

(*b*) TYPICAL KAOLINITE PARTICLE
1μ BY 0.10μ THICK
(10000 A BY 1000 A THICK)

FIG. 6.—CLAY PARTICLES

Further away from the colloid surface, the cations become fewer (Fig. 1(b)) and the soil-cation linkage weaker. The force thus holding the cation hydration water to the soil is related to the potential in the double layer.

On the basis of the relative magnitude of force between water and soil, the water in a clay can be more or less arbitrarily divided into three types—adsorbed water, double layer water and free water. Within the crystal lattices of some minerals exist OH^- groups. If these minerals are heated to 600 or 700° C, these OH^- groups undergo condensation polymerization, which reaction produces water. Because the OH^- groups, sometimes called "structural water," do not exist as water in the minerals, they are not considered here as "water." The adsorbed water is that which is strongly held by the soil, the double layer water is all the water attracted to the soil, and free water is water that is not attracted to the soil at all. Adsorbed water is, therefore, the innermost part of the double layer water. Although this classification of water is accepted by some, many others use "adsorbed" to describe all of the double layer water.

In Fig. 6 are shown, to scale, extremes of the most common plastic soil minerals, namely, kaolinite and montmorillonite. Fig. 7 shows approximately the extent of adsorbed and double layer water on these particles when they are isolated and have free access to water. (Each is to scale with its dimensions given. The scale in Fig. 7(a) is different from that in Fig. 7(b)). Fig. 7 gives

some idea of the amounts of tightly and loosely held water around the soil particles.

Heat of wetting data by I. Th. Rosenqvist (22), permeability data by Michaels and C. S. Lin (23) and sorption data by R. T. Martin (24) all show that the strongly-held water is only a few molecules thick, of the order of 10A. The force required to pull this adsorbed water off the mineral surface is prodigious —varying from 100 atmospheres for the outside water molecules to 10,000 atmospheres for the closest molecules. As the charge density on kaolinite is approximately twice that on montmorillonite, there is a thicker layer of adsorbed water on kaolinite. The amount of adsorbed water expressed as a percentage of mineral weight is, however, much greater on montmorillonite as its specific surface is greater.

The adsorbed layer is approximately the same thickness as the Stern Layer in the Gouy-Chapman colloid theory. The concentration of exchangeable ions in this layer is very high, approximately 70% of the divalent exchangeable ions and 40% of the monovalent ions. Martin has described (24) in detail the adsorbed layer on kaolinite. He gives the magnitudes of forces existing between water and soil, and the orientations and locations of the water molecules.

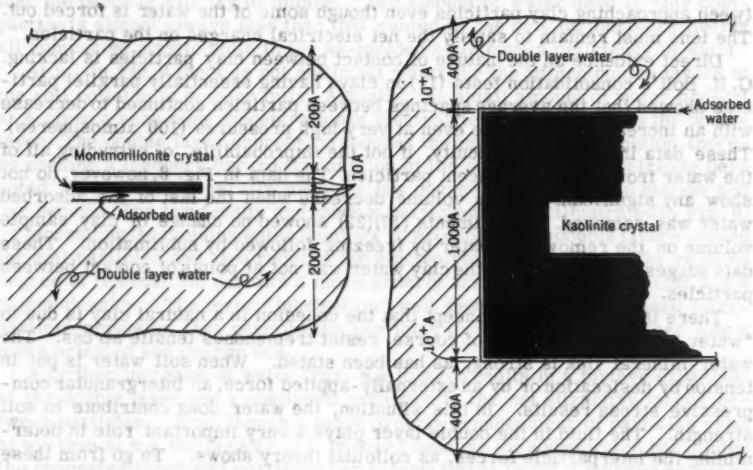
As with the adsorbed water, the double layer water is thicker on kaolinite than on montmorillonite because of the higher charge density on kaolinite. The dimensions given in Fig. 7 indicate that essentially all of the pore water in a clay under normal field conditions is within the double layer.

It is important to realize that the attractive forces in the double layer are forces required to pull water away from the soil. The force required to move water parallel to the sides of a soil particle is much less than the force required to remove, without replacement, the double layer water. When water flows through clay all but the adsorbed water moves, for example. This fact has led to the concept of double layer water as a "two-dimensional liquid." Another concept useful to the soil engineer is that of "mushy" particle for the soil plus its water. The thickness of water film obviously depends to a tremendous extent on the system characteristics and the intergranular pressure—and time. The movement of water nearest the surface of the particle takes considerable time since it is a diffusion process.

Because the double layer water is electrically attracted to the soil particle, its behavior is unlike that of free water. Many have postulated that the density, viscosity, and other characteristics are different from normal water. Phillip F. Low has presented (25) convincing experimental evidence that the density of the double layer decreases as the soil surface is approached. The effective viscosity of the double layer must be greater than free water. Unfortunately there are few experimental data (such as Low's) on the nature of clay water.

The controversy as to whether or not particles in a clay are in mineral-to-mineral contact has not yet been settled. The writer's opinion on this question is summarized herewith:

Approaching clay particles first "contact" each other when their double layers interact. The change of interparticle spacing depends on the force system (as examined in the following paper). When the interparticle spacing has been reduced to a distance of approximately 20A, all of the water between the particles is tightly held. With sufficient externally-applied effective stress, or sufficient time, or sufficient water removal (for example, desiccation) much (all, in the case of desiccation) of the tightly-held water can be extruded or removed. The surfaces of clay minerals usually contain rough spots that are greater than approximately 7A. Thus, the extrusion by intergranular pressure



(*b*) TYPICAL MONTMORILLONITE PARTICLE 1000 A BY 10 A

(*a*) TYPICAL KAOLINITE PARTICLE 10000 A BY 1000 A

FIG. 7.—CLAY WATER

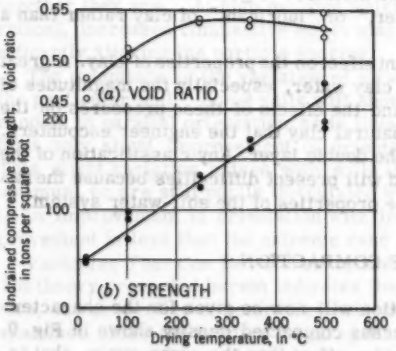


FIG. 8.—STRENGTH OF DRIED BOSTON BLUE CLAY

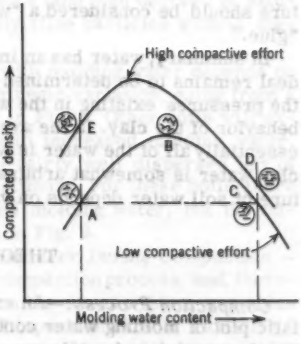


FIG. 9.—EFFECTS OF COMPACTION ON STRUCTURE

of all the interparticle water is impossible, although there might be isolated areas of mineral-to-mineral contact. The exchangeable ions also remain between approaching clay particles even though some of the water is forced out. The ions must remain to satisfy the net electrical charges on the particles.

Direct evidence on the nature of contact between clay particles is lacking. G. H. Bolt's consolidation tests (11)on clays having essentially parallel particles showed that the average spacings between particles continued to decrease with an increase in pressure even at very high pressures (100 atmospheres). These data indicate the difficulty, if not the improbability, of extruding all of the water from between adjacent particles. The data in Fig. 8, however, do not show any significant sample volume decrease when the last of the adsorbed water was removed. Experiments (17)(22) showed no change of clay sample volume on the removal of water by freezing followed by sublimation. These data suggest that the last of the clay water was not at points of contact between particles.

There is a widely-held concept that the cohesion in a natural clay is due to "water bonds." Water can, of course, resist tremendous tensile stress. The water-mineral link is strong, as has been stated. When soil water is put in tension by desiccation or by an externally-applied force, an intergranular compressive stress results. In this situation, the water does contribute to soil strength. The fluid in the double layer plays a very important role in determining the interparticle forces, as colloidal theory shows. To go from these facts, however, to the belief that water bonds are the sole source of cohesion in clay is unwarranted.

The limitations of the water-bond concept are indicated by the fact that the maximum cohesion a clay ever possesses occurs when the clay is dry, containing no water.

Presented in Fig. 8 are the results of a series of tests on remolded Boston blue clay which show that an increase in strength occurs with higher drying temperatures. One can not attribute the strength of the dry clay to "adsorbed moisture," because all of the adsorbed moisture is gone at 200° C. Soil moisture should be considered a "weakener," or "lubricant" of clay rather than a "glue."

In summary, water has an important effect on the properties of clay. A great deal remains to be determined about clay water, especially the magnitudes of the pressures existing in the water and the effects of these pressures on the behavior of the clay. In the average natural clay that the engineer encounters, essentially all of the water is within the double layer. Any classification of the clay water is somewhat arbitrary and will present difficulties because the nature of soil water depends on variable properties of the soil-water system.

THEORY OF COMPACTION

Compaction Process.—An explanation will now be given for the characteristic plot of molding water content versus compacted density shown in Fig. 9. The lower plot is for a lower compactive effort than the upper curve, that is, the lower could represent standard and the upper modified American Association of State Highway Officials (AASHO) compaction effort.

First, however, the concept of water deficiency needs to be presented. This concept recognizes that any given soil particle under any given state of stresses requires a certain amount of water to develop fully its double layer. The

difference between this needed water and the existing water is deficient water that the particle will try to imbibe. The amount of water used in clay compaction is almost always less than that wanted by the soil; furthermore, nearly all compacted plastic soils in the as-molded state have a deficiency in water.

At w_A in Fig. 9 there is not sufficient water for the diffuse double layers of the soil colloids to develop fully. Actually, the small amount of water present at A gives a very high concentration of electrolyte which depresses the double layer. The double layer depression reduces the interparticle repulsion, thereby causing a tendency toward flocculation of the colloids. As has already been noted, flocculation generally means a low degree of particle orientation and low density. The low density and random particle array is illustrated in Fig. 9.

Increasing the molding water from w_A to w_B expands the double layers around the soil particles and also reduces the electrolyte concentration. The reduced degree of flocculation permits a more orderly arrangement of particles and a higher density. The term "lubrication" well describes the increased interparticle repulsion that permits the particles to slide past each other into a more oriented and denser bed.

A further increase of water from w_B to w_C results in a further expansion of the double layer and a continued reduction in the net attractive forces between particles. Even though a more orderly arrangement of particles exist at w_C than at w_B, the density of C is lower because the added water has diluted the concentration of soil particles per volume (there is not a marked decrease in air content from B to C as there was from A to B).

Because of the water deficiency, the water present is subjected to tension as the colloids try to draw water from outside. Because there is less water at w_A than w_B or w_C, the water deficiency, and thus pore-water tension is greater at w_A.

Fig. 9 also illustrates what happens to soil structure when the compactive effort, and thus compacted density, are increased. The greater the input of work, the more nearly parallel are the clay particles, and, usually, the closer together they are. At high molding water contents (and high degrees of saturation), increased compactive effort may merely aline particles without significantly altering the particle spacing.

The magnitude of the variation of structure with molding water depends on the particular soil. Some soils will show an extreme variation, going from a random to parallel orientation, as is illustrated in Fig. 9. Other soils will exhibit only slight improvement of orientation with increased molding water. This slight variation arises with soils that are fairly well dispersed dry of optimum, or are still partly flocculated wet of optimum. For these soils, there is an improvement in orientation with increased molding water; but the improvement is less than the extreme case shown in Fig. 9.

Variables That Can Be Altered by the Soil Engineer During Compaction.— The theory presented herein indicates that the compaction process, and, therefore, the properties of compacted soil depend on the seven system variables examined under the heading "Aggregation and Dispersion of Soil Particles," and also on other factors to be presented subsequently. Many of these variables cannot feasibly be altered or controlled by the soil engineer on a given job. In such cases, he can use the theory to predict the effects of changes brought about by nature.

The soil engineer can, however, alter several variables during a given set of boundary conditions. These variables are:

1. Type of Compaction.—Little is known on how the type of compaction influences the fundamental components of structure listed in the preceding section. Dynamic compaction gives a different product from static compaction (26)(27)(28)—how and why are not clearly understood. The time and area of contact between compacting element and soil are apparently important variables.

2. Amount of Compaction.—For any method of compaction and any clay at a given water content, the greater the compactive work employed, the greater is the density (particles closer together) and the better, usually, the particle orientation that occur. Although increased compactive effort usually gives greater strength, it can, of course, give lower strength.

3. Amount of Water.—The more the water added, other variables being constant, the greater is the repulsion between particles. Thus, water weakens, or lubricates clay.

4. Additives.—The rheology of a soil-water-air system being compacted can be sharply changed with additives. Dispersants, in effect acting as additional water, reduce net interparticle attractive forces. These chemicals reduce optimum water content and increase maximum compacted density. Aggregants do the reverse of dispersants—by increasing flocculation, they raise optimum water content and reduce the maximum density. Dispersants permit a higher degree of particle orientation, while aggregants result in a more random array. Other types of additives can affect the compaction process.

Measurements of Structure.—Using Mitchell's technique, Pacey (21) measured particle orientation as a function of molding water content on compacted Boston blue clay. His data presented in Fig. 10 agree with the present theory, namely that the more the molding water and the greater the density, the more nearly parallel are the clay particles. Pacey ran his tests in a miniature mold. Curves 1 in Fig. 10 were obtained by using a compactive effort approximating standard AASHO and curves 2, by using modified AASHO.

Direct measurements (as made by Mitchell and Pacey) of particle orientations within a clay are valuable data. Because such measurements are, unfortunately, difficult to take, a simple method of determining particle orientation is greatly needed. Possibly the amount of shrinkage upon drying could be used as a measure of average orientation. Any given soil with parallel particles should undergo more volume reduction upon drying than the same soil with its particles in a random array.

Fig. 11 shows the effect of oven drying on the void ratio as measured by Pacey on Boston blue clay (shrinkage of the compacted soil represented by curve 1 in Fig. 10). Fig. 12 shows shrinkage data obtained by Isaac Tiles (29) on compacted kaolinite. In Fig. 13 are plotted Pacey's data to show the relationship between particle orientation at the start of drying versus the amount of shrinkage from drying at 105° C. Figs. 11, 12, and 13 show that the more nearly parallel the particles are, the greater the shrinkage of the soil upon drying.

A slaking test may give some qualitative indications of the electrical forces between particles. A clay in which the individual particles possess high net attractive electrical forces would resist water attack better than one in which the particles have net repulsive forces between them. The hope that a slaking test might be a useful structure indicator was supported by the fact that a sample of dispersed clay was found to slake before a sample of the same clay having a flocculated structure. Interpretation of slaking tests can be complicated by the effect of structure on permeability. Water gets into a dispersed

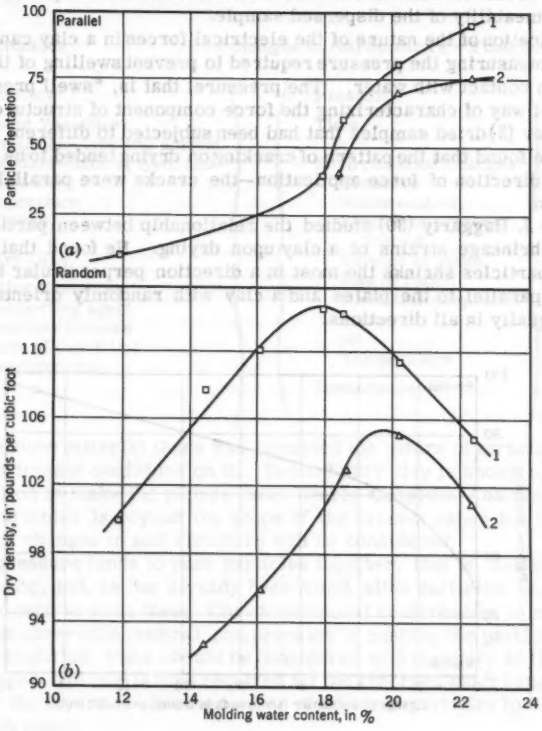


FIG. 10.—ORIENTATION VERSUS WATER CONTENT FOR BOSTON BLUE CLAY

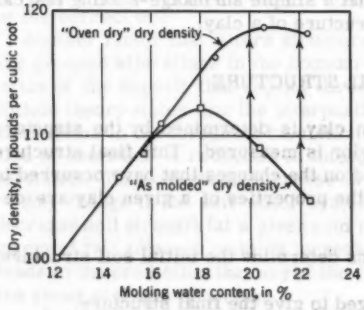


FIG. 11.—DRY DENSITY VERSUS MOLDING WATER CONTENT FOR BOSTON BLUE CLAY

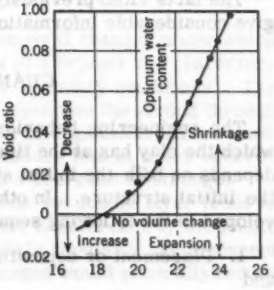


FIG. 12.—EFFECT OF OVEN DRYING ON VOID RATIO OF COMPACTED KAOLINITE

sample at a slower rate than it does into a flocculated sample because of the lower permeability of the dispersed sample.

An indication of the nature of the electrical forces in a clay can also be obtained by measuring the pressure required to prevent swelling of the clay when it is put in contact with water. The pressure, that is, "swell pressure," may be a useful way of characterizing the force component of structure.

Hvorslev (3) dried samples that had been subjected to different loading conditions. He found that the pattern of cracking on drying tended to be perpendicular to the direction of force application—the cracks were parallel to particle orientation.

George J. Haggarty (30) studied the relationship between particle orientation and shrinkage strains of a clay upon drying. He found that a clay with oriented particles shrinks the most in a direction perpendicular to the plates and least parallel to the plates and a clay with randomly oriented particles shrinks equally in all directions.

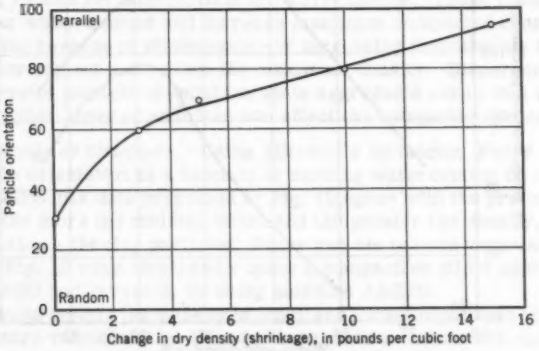


FIG. 13.—ORIENTATION VERSUS SHRINKAGE FOR COMPACTED BOSTON BLUE CLAY

The facts cited previously indicate that a simple shrinkage-slaking test can give considerable information on the structure of a clay.

CHANGES IN SOIL STRUCTURE

The engineering behavior of a given clay is determined by the structure which the clay has at the time the behavior is measured. This final structure depends on both the initial structure and on the changes that have occurred to the initial structure. In other words, the properties of a given clay are developed in the following sequence:

1. Placement or deposition conditions determine the initial soil structure; and
2. The initial soil structure is changed to give the final structure.

This development is shown by:

Initial Soil Structure + Changes in Soil Structure = Final Soil Structure

Compacted Clay Placement Variables Compaction—type and amount Pore fluid—nature, type, and amount Temperature Additives			Pressure Time Environmental Changes Pressure Water content Electolyte concentration Valence of cation Size of cation Dielectric properties Anion pH Temperature Disturbance	
Sedimentary Clay Deposition Variables Transporting agent Deposition process Nature of deposition environment	+			= Final Soil Structure

In the previous material there was examined the nature of structure and the effects of placement conditions on it. Sedimentary clay is shown in the foregoing tabulation to make the picture more nearly complete. An examination of deposition variables is beyond the scope of the present paper but the causes and effects of changes in soil structure will be considered.

Normal pressure tends to push particles together, that is, decrease interparticle spacing, and, as has already been noted, aline particles. Shear deformations also tend to aline them. One-dimensional compression is much more effective than three-dimensional compression in pushing the particles toward a parallel orientation. Time should be considered with pressure as they usually go hand-in-hand. Not only is time required for the adsorbed water to be extruded, but also for the layers of adsorbed water of adjacent particles to slide in relation to each other.

H. Bolton Seed, M. ASCE, has shown (31) that repetitive load applications caused a significant increase in the strength of a compacted silty clay. This strength increase was in addition to that caused by aging. Seed attributed the strength increase to an alteration in soil structure. This explanation seems to be the correct one.

Another factor that alters structure is environmental change, under which are grouped alterations in the boundary conditions of a deposit and characteristics of the deposit that depend directly on these boundary conditions. The colloid theory states that the interparticle forces depend on the second through ninth items in the foregoing tabulation. Changes in intergranular stress must also be included. A reduction in intergranular pressure lets in water between particles. This causes an increase in volume and a decrease in strength.

Any change in the soil-water system that expands the double layer tends to decrease soil strength (at a given void ratio), because interference by the double layers of two adjacent colloids increases interparticle repulsion. This concept leads to the prediction that any of the following changes would generally reduce the shear strength of a clay:

1. Reduction of electrolyte concentration;
2. Cation exchange from high to low valence (for example, Ca^{++} to Na^{+});

3. Adsorption of anions (phosphate);
4. Exchange from a cation of small hydrated radius to a cation of large hydrated radius (Na^+ to Li^+);
5. Increase of dielectric constant of pore fluid;
6. Increase of pH of pore fluid;
7. Decrease of temperature; and
8. Increase in water content.

The influence of some of these eight changes has been investigated. Some Norwegian engineers have, for example, conclusively shown (32)(33)(34) that a reduction of electrolyte by leaching can reduce both the undisturbed and remolded shear strengths. The reduction of strength resulting from an increase in moisture is well known. The effect of some of the other changes, for example, temperature, has yet to be thoroughly investigated.

Disturbance can change particle arrangement and interparticle forces. Particles that have been pushed into contact during years or, of more importance, during eons of high pressure can be separated by remolding or even less severe disturbance, for example, deformations from applied stresses. Experiments by ceramists have shown that extrusion tends to aline particles. Mitchell proved (20) with measurements that not only remolding, but even shear strains, arranges particles in a parallel array.

There are several results of the changes in soil structure listed and described previously that are of considerable importance to the soil engineer. Among these are sensitivity, strength loss with time, strength gain with time (thixotropy), creep, secondary compression, and loss of strength with strain past peak strength.

Sensitivity is caused by a structure change on remolding. That is, the structure that will be formed by a thorough working (which will thus determine the remolded strength) must be unlike that which existed prior to the disturbance (that will determine the undisturbed strength). A change of the structure of the clay from what it was at deposit formation to what it is at time of test is necessary for the clay to be sensitive. Factors causing such a structure change fall into two groups:

1. Time and pressure that push particles into alinements and spacings not obtainable by remolding; and
2. Environmental changes from the time of deposition to the time of test that tend to increase interparticle repulsion such as the eight listed previously.

The three factors most important in developing sensitivity in natural clays are probably time, pressure, and the reduction of electrolyte concentration in the pore fluid. Well known research at the Norwegian Geotechnical Institute (32)(33)(34) has proved the importance of electrolyte reduction in producing sensitivity. Any of the factors, however, can cause sensitivity. This fact is emphasized by the following test data on Boston blue clay:

	Undisturbed strength, in pounds per square foot	Remolded strength, in pounds per square foot
Clay leached with water	450	41
Clay leached with $Na_6P_4O_{13}$	220	0

Leaching the saturated clay (at constant volume) with the sodium polyphosphate permitted ion exchange Na^+ for Ca^{++}, and anion adsorption, that is,

phosphate. These two factors changed the sensitivity from eleven to infinity. This tremendous increase in sensitivity occurred even though there was an increase in electrolyte concentration and little change in the other factors.

The reduction of electrolyte concentration is very widespread as it has occurred in nearly all natural clays laid down in a marine environment. (The average marine clay was originally deposited in water containing approximately 35 g of salt per liter and the clay water contains, after leaching with ground water, approximately 5 g of salt per liter). This is of little importance to the development of sensitivity of compacted clays. The important factors for man-placed clays are probably water pick-up, time, and pressure. Samples compacted dry of optimum have structures that are more greatly changed than those of wet compacted samples. Sensitivity is much more likely, therefore, in clay compacted dry of optimum than it is in clay compacted wet of optimum.

Strength loss with time can be caused by an increase in moisture that increases interparticle repulsion. The increase in moisture could be the result of a change in ground-water conditions or a reduction in intergranular pressure. The leaching data on the Boston blue clay, showing a 50% reduction in undisturbed strength, indicate that significant strength loss can occur from changes in environment. Disturbance can also be a source of strength loss. In compacted clays, however, especially those compacted dry of optimum, moisture increase would appear to be the most important cause of strength loss. Strength loss with time usually implies an increase in sensitivity.

Strength gain with time results from the same factors as those causing strength loss, except that the changes are in the opposite direction. Pressure, time, moisture reduction, electrolyte increase, ion exchange from low to high valence, pH decrease, temperature increase, all strengthen soil. Thixotropy experiments have been conducted in which attempts have been made to hold all factors other than time constant. The strength gains measured can be explained solely by the time required for particles to arrange themselves into an equilibrium array under even the small pressures acting. Imperfect control of the other factors, however (moisture decrease, ion exchange, temperature change, and so forth) may well have had an effect on the soil strengths measured.

Creep probably results from particle realinement and greater interparticle spacing. We have already noted that strains aline particles. Deformations tend to push particles apart at points of contact, permitting water to enter. Clay sheared in triaxial tests in which the water content of the entire specimen was held constant have shown an increase in moisture content in the failure zone and a decrease in the end or "dead" zones.

Secondary compression results from changes in particle orientations and spacings that occur as tightly-held water molecules on one particle are slid past those on another particle or as some of this water is extruded from contact areas.

Loss of strength past peak strength is caused by changes in orientations and spacings of soil particles. This loss of strength will, of course, be larger in those soils that have structures sensitive to disturbance.

Because of the similarities in causes, the following results of changes in structure might well go together—sensitivity, creep, and loss of strength with strain past peak strength.

The presentation herein applies in general to both naturally-made and man-made deposits. The factors important to the development of properties in compacted clays, however, are different from those in natural clays. In the subse-

quent paper there are presented the effects of some of these factors on compacted clays.

CONCLUSIONS

This paper has described the nature of clay structure, a term referring to the arrangement of particles and the electrical forces acting between them. The effects of forces and environmental factors on structure are inferred from the principles of colloid chemistry and crystal chemistry.

The theoretical considerations presented herein throw considerable light on the fundamental nature of clay-water systems. These considerations plus available experimental data fall short, however, of furnishing a complete understanding of clay-water systems. Some of the topics needing study are noted in the following paper.

APPENDIX. BIBLIOGRAPHY

1. "Erdbaumechanik," by Karl Terzaghi, F. Deuticke, Vienna, 1925.
2. "The Structure of Clay and Its Importance in Foundation Engineering," by A. Casagrande, Journal of BSCE, April, 1932.
3. "The Shearing Resistance of Remolded Cohesive Soils," by Juul Hvorslev, Proceedings, Soils and Foundation Conference, U. S. Engrg. Dept., Boston, Mass., June, 1938.
4. "Crystal Chemistry," by R. C. Evans, Cambridge Univ. Press, 1948.
5. "The Nature of the Chemical Bond," by Linus Pauling, Cornell Univ. Press, 1951.
6. "The Structure of Matter," by F. O. Rice and E. Teller, John Wiley & Sons, Inc., 1949.
7. "Colloid Science, I, Irreversible Systems," by H. R. Kruyt, Elsevier Publishing Co., New York, N. Y., 1952, p. 195.
8. "Structure of Inorganic Soil," by T. William Lambe, Proceedings-Separate 315, ASCE, October, 1953.
9. "Constitution of the Electric Charge at the Surface of an Electrolyte," by G. J. Gouy, Journ. de Physique, Vol. 4, No. 9, June, 1910.
10. "A Contribution to the Theory of Electrocapillarity," by D. L. Chapman, Philosophical Magazine and Journal of Science, Sixth Series, Vol. 25, 1913.
11. "Analysis of the Validity of the Gouy-Chapman Theory of the Electric Double Layer," by G. H. Bolt, Journal of Colloid Science, Vol. 10, 1955, p. 206.
12. "Wechselseitige Adsorption von Kolloiden," by P. A. Theissen, Zeitschrift fur Elektronchemie, Vol. 48, 1942, p. 675.

13. "Mechanism of Deflocculation of Clays by Condensed Alkali Phosphates," by Alan S. Michaels, Industry and Engineering Chemistry, Vol. 50, No. 6, 1958.

14. "The Stabilization of Montmorillonite Soils by Chemical Treatment," by H. van Olphen, Recueil Des Travaux Chimiques Des Pays-Bas, Amsterdam, September and October, 1950.

15. "The Deflocculation of Kaolinite Suspensions and the Accompanying Change-Over from Positive to Negative Chloride Adsorption," by R. K. Schofield and H. R. Samson, Clay Minerals Bulletin, Vol. 2, No. 9, British Mineralogical Soc., July, 1953.

16. "Flocculations of Kaolinite Due to the Attraction of Oppositely Charged Crystal Faces," by R. K. Schofield and H. R. Samson, Discussion of the Faraday Society, No. 18, London, 1954.

17. "Thixotropy in Clays," by R. Fahn, A. Weiss, and U. Hofmann, Berichte der Deutsche Keramischen Gesellschaft, Vol. 30, 1953, p. 21.

18. "Reference Clay Minerals," API, Research Project 49, Columbia Univ., New York, N. Y., 1951.

19. "Clays and Clay Minerals," Publication 395, Nat. Acad. of Science and Nat. Research Council, Washington, D. C., 1955.

20. "The Importance of Structure to the Engineering Behavior of Clay," by James K. Mitchell, thesis presented to Massachusetts Institute of Technology, at Cambridge, in 1956, in partial fulfillment of the requirements for the degree of Doctor of Science.

21. "The Structure of Compacted Soils," by John G. Pacey, Jr., thesis presented to Massachusetts Institute of Technology, at Cambridge, in 1956, in partial fulfillment of the requirements for the degree of Master of Science.

22. "Soil Properties and their Measurements," by I. Th. Rosenqvist, Proceedings, 4th International Soils Conference.

23. "Effects of Counter Electro-Osmosis and Sodium Ion Exchange on the Permeability of Kaolinite," by A. S. Michaels and C. S. Lin, Industry and Engineering Chemistry, Vol. 47, No. 6, Amer. Chem. Soc., Washington, D. C., 1955.

24. "Water Vapor Sorption on Kaolinite: Hysteresis," by R. T. Martin, Clays and Clay Minerals, Nat. Acad. of Science and Nat. Research Council, 1957.

25. "Movement and Equilibrium of Water in Soil Systems as Affected by Soil-Water Forces," by P. F. Low, Highway Research Board Meeting, January, 1958.

26. "Development of CBR Flexible Pavement Design Method for Airfields, A Symposium," Transactions, ASCE, Vol. 115, 1950, p. 453.

27. "The Effect of Compaction Method on the Stability and Swell Pressure Characteristics of Soil," by H. B. Seed, R. Lundgren, and C. K. Chan, Highway Research Board, 1954.

28. "Some Relationships Between Density and Stability of Subgrade Soils," by H. B. Seed and C. L. Monismith, Highway Research Board, 1954.

29. "Shrinkage and Strength of Compacted Sand-Clay Mixtures," by I. Tiles, thesis presented to Massachusetts Institute of Technology, at Cambridge, in 1956, in partial fulfillment of the requirements for the degree of Master of Science.

30. "Measurement of Shrinkage Strains in Clays," by G. J. Haggarty, thesis presented to Massachusetts Institute of Technology, at Cambridge, in 1957, in partial fulfillment of the requirements for the degree of Master of Science.

31. "Increased Resistance to Deformation of Clay Caused by Repeated Loading," by H. B. Seed, R. L. McNeill and J. de Guenin, Transactions, ASCE, Vol. 125, 1960, pp. 141-165.

32. "Geotechnical Properties of Norwegian Marine Clays," by L. Bjerrum, Publication No. 4, Norwegian Geotechnical Inst., Oslo, 1954.

33. "Investigations in the Clay-Electrolyte-Water System," by I. Th. Rosenqvist, Publication No. 9, Norwegian Geotechnical Inst., Oslo, 1955.

34. "Some Experiments with Artificially Sedimented Clays," by L. Bjerrum and I. Th. Rosenqvist, Publication No. 25, Norwegian Geotechnical Inst., Oslo, 1957.

DISCUSSION

D. HUGH TROLLOPE,[3] M. ASCE.—There can be no doubt that the intercolloid electrical forces are most important in determining the arrangement and subsequent behavior of clay structures. In particular the author's emphasis on the dominating effect of environmental conditions during deposition or formation of the structure is to be endorsed. At the present time it appears to be reasonable to assume that, arising from the electrical nature of colloid activity, either a net repulsive or a net attractive force is developed between proximate clay particles. The author has identified this net interparticle force with the salt content of the pore fluid and has suggested the terms salt-flocculation and non-salt-flocculation to describe the resulting arrangements. However, the theoretical background on which this is based derives from a study of dilute colloid suspensions. In engineering soils we are mostly concerned with much denser suspensions and it seems likely that other factors will contribute to structural arrangement. In a recent study[4] the writer has attempted to show that external forces contribute markedly to the nature of structurally possible clay particle arrangements, and also as the author recognizes, a moisture deficiency can produce equivalent salt conditions in a soil without altering the total salt content. It is for these reasons that the writer feels that the terms salt and non-salt flocculation may be too restrictive in the descriptive sense.

[3] Reader in Civ. Engrg., Univ. of Melbourne, Melbourne, Australia.

[4] "Soil Structure and the Step-Strain Phenomenon," by D. H. Trollope and C. K. Chan, Proceedings Paper 2431, ASCE, April, 1960.

From an analysis of two-dimensional models[4] the writer would suggest as alternatives the relevant geometric terms—triangular for salt flocculation and rhombic for non-salt flocculation. Even these terms avoid the complications of three dimensional geometry so that tetrahedral and rhombohedral respectively may be more suitable and form a useful link with established crystal geometry.

BENNO P. WARKENTIN,[5] and RAYMOND N. Y. YONG,[6] A. M. ASCE.—From diffuse double layer theory, one would predict that there would be only a small influence of surface charge density on the thickness of the diffuse ion layer or of the corresponding water layer. In the development of the theory, the second integration of the combined Poisson-Boltzmann equation requires, in the boundary condition, a specification of either charge or potential at the surface. In clays where the surface charge rather than the surface potential can be considered constant, this condition is usually specified from the requirement of over-all electroneutrality, that the surface charge is equal and opposite to the space charge. Theoretically it would be just as satisfactory to fix the surface potential instead of the surface charge. Mathematically the problem is solved by setting the potential equal to infinity at some plane inside the clay surface and solving the relation between potential and distance from this plane. The distance between this plane of infinite potential and the clay surface is determined from the relationship between potential and space charge, from the conditions that the space charge must equal the surface charge. The surface charge for clay is taken from the measured cation exchange capacity. This distance turns out to be $x_o = \frac{4}{v\Gamma\beta}$ (Schofield),[7] in which v represents the valence of cation; Γ denotes the surface charge density; and β is a constant at constant temperature and dielectric constant.

The influence of charge on the diffuse ion layer then is x_o. The maximum value encountered for the three types of clay, kaolinite, illite, and montmorillonite is 4 Å for Na-montmorillonite. The higher the charge density and the higher the valence of the cations, the smaller is the value of x_o which must be subtracted, and therefore the larger is the diffuse layer thickness. But this is only a small percentage of the total thickness in saturated clays.

The repulsion between clay particles may not be an electrostatic repulsion between the negatively charged units. Because only a small error is introduced by the usual assumption that the diffuse layer of cations per unit area of surface which supports it, fully neutralizes that surface charge (Childs),[8] such a system then might have an electrical net attractive force. Langmuir[9] has, indeed, considered that the attractive force in such a system is due to the cations. This may be more acceptable than postulating van der Waal's forces of attraction. For interaction between the relatively large clay particles there is reasonable doubt whether van der Waal's forces extend to distances of 100 Å.

---

[5] Asst. Prof., Dept. of Agric. Physics, Macdonald College, McGill Univ., Montreal, Canada.

[6] Asst. Prof., Dept. of Civ. Engrg., McGill Univ., Montreal, Canada.

[7] "Ionic Forces in Thick Films of Liquid between Charged Surfaces," by R. K. Schofield, Transactions, Faraday Soc., Vol. 42B, London, 1946, pp. 219–225.

[8] "The Space Charge in the Gouy Layer between Two Plane Parallel Nonconducting Particles," by E. C. Childs, Transactions, Faraday Soc., Vol. 50, London, 1954, pp. 1356–1362.

[9] "The Role of Attractive and Repulsive Forces in the Formation of Tactoids, Thixotropic Gels, Protein Crystals, and Coacervates," by Irving Langmuir, Journal, Chemical Physics, Vol. 6, 1938, pp. 873–896.

Therefore, a repulsion due to osmotic pressure may be the fundamental way of looking at repulsion between negatively charged clay particles. Alternatively it can be considered as an interaction of diffuse ion layers with an excess, at the point midway between the plates, of hydrostatic pressure over the electrostatic pressure resulting from the force of the space charge.

The term double layer is used in different ways in the literature. It was first applied to those colloidal sols that became charged by attracting a layer of ions to the surface. The second layer is composed of the ions held at some average distance from the surface. The diffuse double layer consists then of an inner layer of ions and an outer diffuse layer. In clays where much of the charge arises within the colloidal crystal, there is really only one layer of ions, that is, the diffuse one. However, the nomenclature has been carried over and is now used in papers on electrochemical studies of the diffuse layer. It might be preferable not to use the term double layer, but if it is used, the layers referred to should be specified as the author has done. Any charge on the clay crystal surface due to OH^- groups corresponds more closely to the systems where "double layer" would be appropriate.

The author has clearly defined his use of the term flocculation and dispersion. This is not questioned, but the applicability of the classical concept of flocculation may be discussed. The term was defined from experience with inorganic sols which at a fairly definite salt concentration show a clearly defined and largely irreversible flocculation or coagulation. Disturbing such a system hastens flocculation. The flocculation concentration of an As_2S_3 sol can be determined by adding various salt concentrations, and shaking after several hours. On shaking, a rapid flocculation takes place above a certain salt concentration. These flocculated sols cannot be dispersed by further shaking. With clay suspensions, especially high swelling clays, there is no unique property change that defines flocculation. Shaking breaks up any flocs. One criterion for flocculation is the appearance of a clear layer of supernatant liquid under certain specified conditions, but the formation of loosely-bound floc units and changes in viscosity can be demonstrated at lower salt concentration.

There need be no force of attraction involved in what is designated as "flocculation" of clay suspensions. As the force of repulsion is decreased by decreasing the thickness of the diffuse ion layer, the particles approach each other more closely and act in unison to settle slowly. Any interaction that has been demonstrated in dilute clay suspensions is weak, and does not resemble the van der Waal's forces. There need be no unique point at which clay particles are attracted to each other and no net force of attraction. For a sol of As_2S_3 containing sufficient electrolyte for flocculation, a net force of attraction exists and leads to small interparticle distances that are irreversible. Such a situation does not exist in flocculated dilute clay suspensions.

There is little evidence from studies of concentrated clay pastes that there is a point of abrupt change from repulsion between particles to attraction between particles. Rather there is a continuous transition as repulsion decreases and random orientation increases. Measurements have shown that there is no discontinuity in measured swelling pressures of Na-montmorillonite in solution from 0.0001 to 0.1 N NaCl and there is no evidence of a force of attraction. The suspension in 0.1 N NaCl would be considered flocculated. There is also little difference in the water content at a given pressure of a flocculated or of a dispersed slurry during the initial compression. These data are admittedly only for Na-saturated montmorillonite. The observation that the swelling of

Ca-montmorillonite is lower than the computed from osmotic forces does not prove that a force of attraction, specifically one of van der Waal's type is present. Many of the forces holding natural clays together may be due to "cementing" substance, such as iron, organic materials, carbonates, or aluminum and silicate compounds.

GERALD A. LEONARDS,[10] M. ASCE.—Potential benefits to soil mechanics and its applications of the physico-chemical approach to soil structure are virtually unlimited. The rapidity with which significant advances are being made make it difficult to assimilate this new knowledge and to assess its practical utility. Accordingly, the paper by the author which presents these new developments with unusual clarity, is particularly welcome at this time. It is worthy of careful study by the entire profession.

An important factor not considered by the author—or, for that matter, in soil mechanics literature—are the properties of water itself. It has been demonstrated by J. O. Bernal and R. H. Fowler,[11] S. Katzoff,[12] and others,[13] from X-ray diffraction and infra-red absorption measurements that liquid water molecules can exist in a variety of quasi-crystalline states. N. Lavergne and W. Drost-Hansen[14] summarized and called attention to the discontinuities in slope (or "kinks") observed in the temperature dependence of many properties of liquid water, such as compressibility, index of refraction, specific heat, and thermal expansion. These discontinuities in slope were attributed to breakdown of water structure, which seems to occur approximately at regular temperature intervals (near 15°, 30°, 45°, and 60° C). Drost-Hansen[15] showed that biological temperature optima lie between the temperatures at which breakdown in water structure occurs; for example, 37° C for mammals (halfway between 30° and 45° C), 22° to 23° C for bacteria found in soil, and 52° to 55° C for many of the thermophilic bacteria. Conversely, critical survival temperatures are near the points of discontinuities, as is the case in the pasturization of milk. Under certain conditions the structure of liquid water can be ice-like, as evidenced by observed frost damage to corn at temperatures above 40° F, and the development of a solid precipitate in natural gas lines at temperatures above 60° F. Thus, the structure of bulk water has important practical consequences; it may be expected that water structure would play an equally important role in the behavior of soil-water systems.

Phenomena observed in freezing experiments illustrate the need for considering water structure as an important element of soil structure. E. N. Dorsey[16] found that electrolytes have a negligible effect on the supercooling of

---

10 Prof. of Soil Mechanics, Purdue University, Lafayette, Ind.

11 "Theory of Water and Ionic Solutions with Particular Reference to Hydrogen and Hydroxyl Ions," by J. O. Bernal and R. H. Fowler, Journal of Chemical Physics, Vol. 1, 1933, pp. 515-548.

12 "Studies of the Molecular Arrangement in Liquids," by S. Katzoff, Journal of Chemical Physics, Vol. 2, 1934, pp. 841-851.

13 "Water," by S. M. Buswell and W. H. Rodebush, Scientific American, Vol. 194, No. 4, 1956, pp. 77-89.

14 "Discontinuities in Slope of the Temperature Dependence of the Thermal Expansion of Water," by N. Lavergne and W. Drost-Hansen, Naturwissenschaften, Vol. 43, 1956, p. 511.

15 "Temperature Anomalies and Biological Temperature Optima in the Process of Evolution," by W. Drost-Hansen, Naturwissenschaften, Vol. 43, 1956, p. 512.

16 "The Freezing of Supercooled Water," by E. N. Dorsey, Transactions, Am. Phil. Soc., Vol. 38, 1948, pp. 248-328.

water. T. F. Buehrer and M. S. Rose[17] determined the amount of unfrozen water at -6° C in Pima Clay saturated with different cations. Their data clearly show that the percentage of unfrozen water is sensibly independent of cation concentration and valence (see Table 1). These results could hardly be anticipated from the Gouy-Chapman theory. Working with compacted clay (LL = 75, PI = 50, dry unit weight 91 lb per cu ft, water content = 28%) C. W. Lovell[18] found over 55% of the soil water remained unfrozen at a temperature of -24° C. It is the writer's opinion that a freezing point depression of this magnitude can be explained only in terms of a strongly developed water structure in the vicinity of clay particles. In this case, however, the water structure must surely be very different from that of ice to remain unfrozen at -24° C.

Striking evidence of the development and significance of water structure are obtained from diffusion experiments. Rosenqvist[19] found that the diffusion coefficient of heavy water through clay-water systems, corrected for the presence of clay particles, was less than 10% of the value obtained by J. H. Wang[20] for bulk water. Wang[21] measured the self-diffusion of heavy water in aqueous solutions of electrolytes and found that certain solutes increased the diffusion coefficient. Wang attributed the increase to a breakdown of water structure.

TABLE 1.—UNFROZEN WATER IN PIMA CLAY

Cation (1)	Electric potential, in volts (2)	Unfrozen water per gram ion of cation moles (3)	Unfrozen water per 100 grams of clay moles (4)
Ca^{++}	1.90	93	24
Cu^{++}	2.08	114	33
Mg^{++}	2.56	100	37
NH_4^+	0.70	42	39
K^+	0.75	41	36
Na^+	1.02	49	38

The phenomenon becomes more pronounced when the effect of varying the concentration of the electrolyte is considered (see Fig. 14). As the electrolyte concentration increases, the diffusion coefficient increases, and then decreases at higher concentrations. It is the writer's opinion that at low concentrations the water structure is disrupted, thereby increasing the diffusion rate; at higher concentrations a new structure is formed, resulting in a reduction in diffusion rate.

17 "Studies in Soil Structure V: Bound Water in Normal and Puddled Soils," by T. F. Buehrer and M. S. Rose, Technical Bulletin No. 100, Arizona Agri. Experiment Station, 1943.

18 "Temperature Effects on Phase Composition and Strength of Partially Frozen Soil," by C. W. Lovell, Bulletin 168, Highway Research Board, 1957, pp. 74-95.

19 "Investigations in the Clay-Electrolyte-Water System," by I. Th. Rosenqvist, Publication No. 9, Norwegian Geotechnical Inst., Oslo, 1955.

20 "Self-Diffusion and Structure of Liquid Water with 0 as a Tracer," by J. H. Wang, Journal, Am. Chem. Soc., Vol. 73, 1951, pp. 4181-4183.

21 "The Effect of Ions on the Self-Diffusion and Structure of Water in Aqueous Electrolytic Solutions," by J. H. Wang, Journal of Physical Chemistry, Vol. 58, 1954, pp. 686-692.

D. F. Anderson and P. F. Low[22] showed that the density of soil water decreased (for a given temperature) at distances from the clay particles less than approximately 80 Angstroms. The smaller the distance from the clay particle surfaces, the greater the reduction in density. The high internal pressures believed to exist in the water at such small distances from the particle surfaces should tend to cause an increase in density. However, the ordered water structure apparently more than compensates for the effects of its compressibility.

Much additional evidence of the significance of water structure can be cited,[23,24] but the data presented suffice to show that the concept of water structure (orientation of water molecules) may be as important as that of particle orientation, and can hardly be neglected in the over-all concept of soil structure.

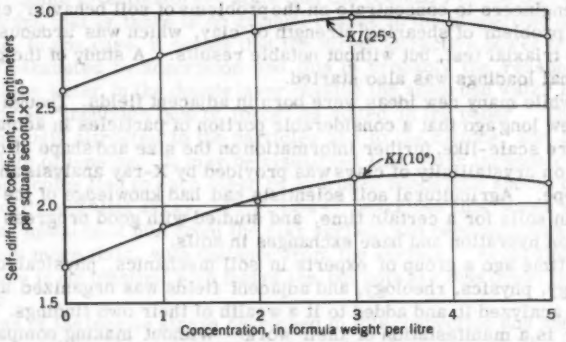


FIG. 14.—VARIATION OF THE SELF-DIFFUSION COEFFICIENT OF WATER IN SOLUTIONS OF POSTASSIUM-IODIDE

The author's explanations of such phenomena as strength gain with time, creep, secondary compression, and loss of strength past the peak strength are considered as simplifications intended to show the generality of the physico-chemical approach. The writer is of the opinion that these phenomena are more complex than the author's explanations suggest.

The author has listed reduction in temperature among the factors contributing to reduced shear strength in clays. The writer is aware of only three records on the relationship between temperature and shearing resistance of clays; C. A. Hogentogler and E. A. Willis,[25] Rosenqvist,[19] and Trask and J. E. H. Close.[26] All three report an increase in strength with decrease in temperature. Fig. 14 shows that a reduction in temperature reduces the self-diffusion

22 "The Density of Water Absorbed by Lithium-, Sodium-, and Potassium-Bentonite," by D. F. Anderson and P. F. Low, Proceedings, Soil Science Soc. of America, Vol. 22, No. 2, 1958, pp. 99–103.

23 "The Variation in the Structure of Water in Ionic Solutions," by G. W. Stewart, Journal of Chemical Physics, Vol. 7, 1939, pp. 869–877.

24 Ibid., Vol. 11, 1943, pp. 72–74.

25 "Stabilized Soil Roads," by C. A. Hogentogler and E. A. Willis, Public Roads, Vol. 17, No. 3, 1936, pp. 45–65.

26 "Effect of Clay Content on Strength of Soils," by P. D. Trask and J. E. H. Close, Proceedings, 6th Conf. on Coastal Engineering.

coefficient significantly, which is indicative of a more strongly developed water structure and probably greater shear strength.

D. P. KRYNINE,[27] F. ASCE.—In 1918 or thereabouts, the old Rankine and Coulomb formulas were practically the only ones at hand for the use of soil engineers. When Terzaghi published his "Erdbaumechanik," the present day soil mechanics was started.[28]

Since that time the writer has witnessed two revolutions, or, more precisely, two periods of unusually intense activity and creation of new efficient ideas in the province of soil mechanics. The first revolutionary period lasted several years after 1925, when Terzaghi presented his ideas and other engineers, inspired by his work, published numerous papers and discussions. In the subsequent decade or so the engineering mind was preoccupied mostly with the improvement of sampling and testing. Later, wartime conditions did not permit soil engineers to concentrate on the problems of soil behavior, except perhaps the problem of shearing strength of clay, which was arduously studied using the triaxial test, but without notable results. A study of the problem of repetitional loadings was also started.

Meanwhile many new ideas were born in adjacent fields. Though soil engineers knew long ago that a considerable portion of particles in actual clay deposits were scale-like, further information on the size and shape of clay particles, and on crystallinity of clays was provided by X-ray analysis and electron microscope. Agricultural soil scientists had had knowledge of the electrical charges in soils for a certain time, and studied with good progress the problems of ion hydration and base exchanges in soils.

Some time ago a group of experts in soil mechanics, physical chemistry, mineralogy, physics, rheology, and adjacent fields was organized and studied material, analyzed it, and added to it a wealth of their own findings. The present paper is a manifestation of their work. Without making comparisons or drawing parallels, the writer wishes to state his belief that this paper, with the previous works by the same author, is the beginning of another significant revolution in soil mechanics. Whereas at the present time in considering clay we look separately at the clay particles and at the soil water, the new outlook consists in looking into the inseparable team "clay platelets—water," into the orientation of the particles and into the particles themselves.

The following remarks are not intended to oppose the views of the author, but to merely clarify some questionable points or to ask for, or provide some additional information.

Flocculated and Dispersed Clay Structure.—To an attentive reader of the paper the difference between the flocculated and dispersed structure is quite clear. But it will be difficult to explain to the average engineer or student that the dispersed structure means smaller pore volume and greater dry density of the soil, as compared with the flocculated one. Perhaps it would be better to substitute the term "dense" or some other adequate term for "dispersed" structure.

If the faces of a clay particle are charged negatively, there should be both positive and negative charges at the edges. Because of a possible anion concentration at the particle ends, the total positive charge at the particle end should

---

27 Cons. Engr., Berkeley, Calif.

28 "Erdbaumechanik, auf boden-physikalischer Grundlage," by Karl Terzaghi, Dauticke, Leipzig, 1925.

be weak, and so is the structure thus formed. Isomorphous substitution should contribute to this weakness.

The writer has always been of the opinion that marine clays have larger pores than fresh-water clays. The impression produced by Fig. 4 is not in accordance with this opinion. If the latter is correct, it would be advisable to decrease the whole Fig. 4(b) in order to make the thickness of the particles identical in both Fig. 4(a) and (b).

Diffuse Double Layer.—This concept was originally advanced by the German physicist Hermann Helmholtz (1821-1894) and subsequently was given various interpretations by different authors. That one given in this paper seems to be the clearest of those the writer knows. The author states that (1) there is adsorbed water (thickness about 10A) strongly held by the clay particles; (2) the cations are attracted to the clay; (3) water in the double layer is attracted by the cations. Some investigators[29] state that the boundary of the thin absorbed layer is abrupt, that is, there is no gradual change in the properties of the absorbed fluid. In any case, it seems that the direct attractive power of the clay particle is exhausted by adsorption and this is probably the reason why the cations and the water in the double layer outside the adsorbed water layer are attracted by an "induction type of force" as stated in the paper. Thus water is simultaneously attracted to the particles and to the cations, and therefore is in the state of tension. It may be visualized that water threads consisting of water molecules tied to each other by hydrogen bonds thus should be placed in a practically parallel array. P. F. Low[25] describes this water structure as extending upwards of 60A from the clay surface and becoming less regular, and probably more fluid, with distance from the surface. According to Low, this structure is not identical with that of ice, but both are less dense than "normal" water.

The value of the tensile stress developed in this connection and hence some possible volumetric changes in water depends, of course, on the hydration characteristics of the cations. It appears, therefore, that by using the base exchange process, the water level in a laboratory vessel containing dense clay suspension can be made to fluctuate, though on microscopically small vertical distances. Existence of holes in water is inconceivable. However, in reviewing old literature the writer ran into such terminology.[30]

Some Soil-Water Concepts Interrelated.—In connection with the diffuse double layer, the writer believes that the following three soil-water concepts should be in some way interrelated and on some occasions even identical; (1) plastic limit; (2) optimum moisture content; (3) not fully developed diffuse double layer. Obviously, both the plastic limit and the optimum moisture content depend on the hydration characteristic of the cations in the double layer. It seems also that plasticity and thixotropy are related phenomena.

Contact Conditions.—When the clay crystals are not in contact, the surface of the adsorbed layer is not necessarily an exact replica of the surface of the crystal; probably it is smooth. When, under pressure, two crystals come in close contact, the two adsorbed layers will form a continuous water envelope in which the two crystals will be suspended, so to speak. If, according to Bolt,[31] a pressure of 100 atmospheres is not sufficient to make two crystals touch each

---

29 "Problems of Geotechnics," by B. V. Deriagin, State Railroad Publishing House, Moscow, 1956. (in Russian)

30 Comptes Rendus, Acad. Sci. Paris, Vol. 187, 1928, p. 718.

31 "Physical-Chemical Analysis of the Compressibility of Pure Clay," by G. H. Bolt, Geotechnique, Vol. 6, June, 1956, pp. 86-93.

other, clay crystals under engineering structures are never in immediate contact because no such soil pressures as 100 tons per sq ft or so exist in practice. This point of view needs criticism and additional study, however.

Slaking Test as a Measure of Structure.—The difference in behavior between a dispersed and a flocculated sample of the same clay in a slaking test can be easily explained on the basis of the author's theories. The following may be added, however, Kaolinite, halloysite, and many mica clays defy penetration of water and remain intact when submerged, nor does sodium bentonite disintegrate in water.[32] Expandable clays (for example, montmorillonites) disintegrate in water rapidly.

Electrical Forces and Thixotropy.—Inclusion of electrical forces as a component of the clay structure is a very desirable feature of the author's theory of clay structure. The writer suspects that the electrical forces appear in clay in the presence of any polar liquid; so far as water is concerned, this is a well known fact. Furthermore, the electrical forces that participate in the building of a clay structure, are, at least partially, responsible for the regain in strength (thixotropy) of damaged (for example, compacted) clay. In this connection the writer wishes to quote N. J. Denisov and P. A. Rehbinder.[33] "Sediments of clay powder are denser in gasoline than in water but at the same time weaker mechanically and exhibit no thixotropy. In water, on the other hand, they do form thixotropic structures." Because the phenomenon of thixotropy is not developed in gasoline and probably in other non-polar liquids thixotropy is not an intrinsic property of clay. On the other hand, since all compacted clays contain dipolar water, they are all thixotropic, presumably to variable degrees.

The paper presented the results of fundamental research in the structure of clays. The fundamental research data are ably interwoven with engineering applications, particularly in the field of compaction. In all justice, this is an outstanding engineering paper, and its reading should be recommended to all civil engineers. Particularly this paper is a "must" for soil and foundation engineers if they do not want to lag behind the times in the new soil mechanics era.

DEAN R. FREITAG,[34] A. M. ASCE.—To the average civil engineer many of the terms and concepts employed in this paper are strange to the ears, and often the full implication of a new concept is difficult to comprehend. In this respect the writer would appreciate a more detailed discussion of the data presented in Fig. 8 of the paper. The author states that at approximately 200° C all the adsorbed moisture has left the clay and also at that temperature his void ratio data imply that the soil particles no longer tend to come closer together. In spite of these facts the strength of the soil continues to increase in proportion to the drying temperature. How does this occur?

In several instances Mr. Lambe uses measurements of the shrinkage or swell of compacted soil samples as a means of demonstrating structural differences. In all cases the volume changes are measured relative to the as-compacted volume. Although such measurements graphically portray the state

---

32 "Physical-Chemical Properties and Engineering Performance of Clays," by R. C. Mielenz and M. E. King, Clay and Clay Technology, Calif. Div. Mines Bull. 169, 1955.

33 "On Colloid-chemical nature of cohesion in argillaceous rocks," by N. J. Denisov and P. A. Rehbinder, Doklady (reports), Acad. Science USSR, Vol. 54, Moscow, 1946, p. 519.

34 Chf., Soils Stabilization Sect., Embankment and Foundation Branch, Soils Div., U. S. Army Engr., Waterways Experiment Sta., Vicksburg, Miss.

of compaction of the various specimens, the writer wonders if they can be considered a valid indication of structure. It would seem that a more interesting and revealing approach would be to consider the over-all capacity of the soil to undergo volume changes. This approach has been followed by the writer in analyzing the data shown in Fig. 15. These data were collected during the course of tests conducted for another purpose and are not as precise and complete as could be desired but are believed to be adequate to support the discussion.

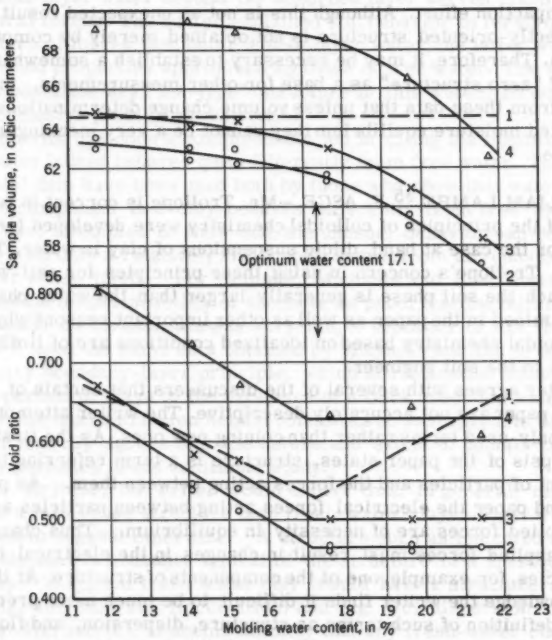


FIG. 15.—VOLUME-VOID RATIO DATA FOR VICKSBURG LOESS.

To obtain these data the various specimens were first dried from the as-compacted state (line 1) to equilibrium at 50% relative humidity (line 2). Next, half of the specimens were allowed to adsorb water from air at 100% relative humidity (line 3) and the remainder were wetted by capillary rise (line 4). The specimens represented by line 4 achieved an average degree of saturation ranging from about 92% for the lowest molding water content to about 88% for the highest molding water content. All specimens had been removed from the molds immediately after molding and were not confined in any way during the test sequence.

It is evident that, based on the as-compacted condition, shrinkage upon drying predominates on the wet side of optimum water content while swelling is most pronounced on the dry side of optimum. There is, however, very little difference in the over-all volume change, particularly when the volume changes are considered in terms of a unit of soil as in the void ratio data plot. If void ratio can be considered an indication, it would appear from these data that,

after the initial drying at least, all of the wet side specimens had essentially the same structure. This is not true on the dry side. Thus it should be possible to evaluate the structure of a dry side specimen by a comparison of its void ratio with that of a wet side specimen in a comparable state of moisture equilibrium.

However, data from a few specimens compacted at water contents higher than optimum and using both higher and lower compactive efforts (that is, a greater and a lesser number of applications of the compacting loading) indicate that a lower void ratio is obtained (at an equilibrium water content) by increasing the compaction effort. Although this is not an unexpected result it implies that a perfectly-oriented structure is not obtained merely by compacting wet of optimum. Therefore, it may be necessary to establish a somewhat arbitrary standard of "zero structure" as a base for other measurements. In any event it appears from these data that unless volume change determinations are made at a specified moisture equilibrium they cannot be a very meaningful measure of structure.

T. WILLIAM LAMBE,[35] F. ASCE.—Mr. Trollope is correct in pointing out that most of the principles of colloidal chemistry were developed for the dilute sols and, for the case at hand, dilute suspensions of clay in water. The writer shares Mr. Trollope's concern in using these principles for soil-water systems in which the soil phase is generally larger than the water phase. This point is examined in the paper as well as other important reasons why the theories of colloidal chemistry based on idealized conditions are of limited quantitative value to the soil engineer.

The writer agrees with several of the discussers that certain of the terms used in the paper are not accurately descriptive. The writer attempted to employ commonly-used terms rather than coining new ones. As the first sentence of the synopsis of the paper states, structure is a term referring both to the arrangement of particles and the forces acting between them. As pointed out in the second paper the electrical forces acting between particles and the externally applied forces are of necessity in equilibrium. Thus changes in the externally applied forces must result in changes in the electrical forces between particles, for example, one of the components of structure. At the present state of knowledge the writer finds it difficult to be much more precise in the numerical definition of such terms as structure, dispersion, and flocculation. It is hoped that further knowledge will permit this improvement, and a selection of better terms.

Mr. Warkentin and Mr. Yong feel that there is no need for an electrical attraction to exist for soil particles to flocculate in a clay-water suspension. The writer cannot accept this view. In fact, are not the discussers implying a net force of attraction when they state that ". . . the particles approach each other more closely and act in unison . . ."?

Mr. Warkentin and Mr. Yong are correct in suggesting that cementing substances may help hold the particles together in natural clays. The writer has presented elsewhere[36] experimental evidence on the cementation of fines in natural clays by iron oxides, carbonates, and organic matter.

Mr. Leonards takes exception to the relatively minor role the writer gives to any unusual structure of soil water. The paper uses the term "double layer water" in a general sense to cover all water acted on by significant attractive

35 Prof. and Head, Soil Engrg., Massachusetts Inst. of Technology, Cambridge, Mass.
36 "Composition and Engineering Properties of Soil IV," by T. William Lambe and R. T. Martin, Highway Research Board, January, 1956.

forces from the soil. The innermost part, and most strongly held part, of the double layer water is termed "adsorbed water" (see Fig. 7). The molecules of adsorbed water are undoubtedly oriented, those in the water farther from the soil to a less degree.

The writer feels that adsorbed water has physical and chemical properties unlike free water as would exist in a beaker of water. It, for example, appears to be more viscous than free water. This adsorbed water plays an important role in such phenomena as secondary compression and creep.

The double layer water beyond the adsorbed layer serves mainly to transmit electrical forces. The writer explained soil behavior in terms of adsorbed water, electrical forces, and outer double layer water; the latter water having a structure and properties approximating those of free water. The writer sees no need to postulate any "ice-type" structure in this water; he does not feel there is conclusive proof of its existence.

Mr. Leonards has done a commendable job in citing the literature to show that soil water indeed behaves quite differently from free water. The available experimental data have been used both by those who show that water plus ions as a single component in a clay behaves differently from free water and by those who have attempted to show that the unusual behavior can be explained by the ions with only a relatively small contribution from any unusual structure of the water phase itself. For example, Michaels and Lin[37] interpret their experiments on the permeability of kaolinite as proof that the thickness of immobilized water on the kaolinite was very thin, of the order of 10Å. Mr. Werner E. Schmid[38] used the same data obtained by Michaels and Lin to help support his stationary boundary-layer principle, which attributes the unusual permeability properties of clays to the existence of a thick adsorbed water layer.

Mr. Krynine has contributed helpful comments on several parts of the paper. The writer heartily agrees that the nature and extent of contact between adjacent clay particles needs additional study.

Like Mr. Krynine, the writer would expect that, in general, marine clays would have a less dense structure than fresh-water clays. Figs. 4 and 5 were not intended to suggest otherwise. A structure such as indicated in Fig. 4(a) (salt flocculation) is probably typical of the structure of a freshly deposited marine clay. A typical fresh water clay should have a structure somewhere between Fig. 4(b) (non-salt flocculation) and Fig. 4(c) (dispersion) or even between Figs. 4(a) and (c). It seems unlikely that any fresh-water clay would be deposited in such pure water as to permit an arrangement consisting entirely of edge-to-face flocculation as shown in Fig. 4(b) and at the far left in Fig. 5.

The writer suggested shrinkage upon drying as a crude and easily obtained measure of structure. Mr. Freitag's procedure of measuring shrinkage to a given relative humidity and then measuring expansion under controlled conditions certainly gives more information than a simple shrinkage measurement. Mr. Freitag's method is, unfortunately, very time-consuming.

In conclusion the writer would like to express his appreciation to those who prepared and submitted discussions to his paper.

---

37 "The Permeability of Kaolinite," by A. S. Michaels and C. S. Lin, Industry and Engineering Chemistry, Vol. 46, June, 1954.

38 "The Permeability of Soils and the Concept of a Stationary Boundary-Layer," by Werner E. Schmid, Presented before the 60th annual meeting of the A.S.T.M., Atlantic City, N. J., 1957.

COMPACTED CLAY: ENGINEERING BEHAVIOR

By T. William Lambe,[1] F. ASCE

With Discussion by Messrs. Alfred C. Scheer; Raymond N. Y. Yong and B. P. Warkentin; J. MacNeil Turnbull; José A. Jiménez Salas; D. Hugh Trollope; and T. William Lambe

SYNOPSIS

This paper employs the principles of colloid chemistry and crystal chemistry to give a physical explanation of the engineering behavior of compacted clay. The relationships between clay structure and behavior are described and then illustrated with experimental data.

INTRODUCTION

The theoretical principles describing the structure of compacted clay and predicting the factors affecting it are employed herein to give a physical explanation of the engineering behavior of clay.

The concepts are often neither as definite nor as complete as would be desired. Improvements (and probably corrections) to these concepts will result from research on the fundamentals of clay behavior that is being conducted in a number of soil laboratories. Contributions to the understanding of clay properties can be anticipated from both soil scientists and soil engineers.

PERMEABILITY OF COMPACTED CLAY

Importance of Permeability Studies on Clay.—The permeability of a soil is one of its three important and fundamental[2] properties, compressibility and strength being the other two. Permeability enters into problems of seepage, settlement and stability. In the core of an earth dam, for example, the rate of leakage, rate of settlement, and rate of strength build-up all vary directly with the permeability.

Permeability studies on clays not only are valuable for use in practical engineering problems, but are also helpful in fundamental research on the nature

Note.—Published, essentially as printed here, in May, 1958, in the Journal of the Soil Mechanics and Foundations Division, as Proceedings Paper 1655. Positions and titles given are those in effect when the paper or discussion was approved for publication in Transactions.

[1] Prof. and Head, Dept. of Soil Engrg., Massachusetts Inst. of Technology, Cambridge, Mass.

[2] "Effects of Counter Electro-Osmosis and Sodium Ion Exchange on the Permeability of Kaolinite," by Alan S. Michaels and C. S. Lin, Industrial and Engineering Chemistry, 1955.

of clays. Michaels and Lin[2] used permeability tests to study the nature of water in kaolinites.

Factors Affecting Permeability.—In an earlier paper the factors affecting the permeability of fine grained soils were examined.[3] The factors treated were: soil composition, characteristics of permeant, void ratio, degree of saturation, and structure. For a given soil and permeant, that is, first two factors constant, the relationship between permeability and the other factors is expressed by the Kozeny-Carman equation,

$$K = \frac{1}{k_o S^2} \frac{e^3}{1+e} \quad \ldots\ldots\ldots\ldots\ldots\ldots (1)$$

in which K represents the absolute permeability, k_o is a constant depending on pore shape and tortuosity of flow, S denotes the specific surface, and e is the void ratio. The Kozeny-Carman equation does not consider variations in degree of saturation.

A liberal interpretation of the Kozeny-Carman equation might make $k_o S^2$ a term indicating the tortuosity of flow or actually the orientation of soil particles. This orientation component of structure is the important component as far as permeability is concerned. The orientation term is,

$$k_o S^2 = \frac{1}{K} \frac{e^3}{1+e} \quad \ldots\ldots\ldots\ldots\ldots\ldots (2)$$

Previous work[3,4] has proved that the structure of a soil has a very large effect on its permeability. The following section examines the effect of the structure of compacted clay on permeability.

Effect of Structure on Permeability.—Test data from permeability tests on two soils will be used to describe the effect of structure on permeability. The data, shown in Figs. 1 and 2, were obtained on samples first compacted and then subjected to flow until a steady-state case existed. The tests on the Jamaica soil (Fig. 1) were run in such a way that the soil could change volume during permeation, the Siburua clay (Fig. 2) was permitted to densify but not expand. Changes in moisture and density that occurred during flow are shown in Figs. 1(b) and 2(b). The values of permeabilities plotted in Figs. 1(a) and 2(a) are those at equilibrium.

A comparison of permeabilities for dry-side compaction with those for wet-side is shown in Table 1.

This comparison shows a much higher permeability for a soil compacted dry of optimum than for the soil compacted wet of optimum. Since the sample compacted dry of optimum has more random orientation, it has more large pores than does the sample with more nearly parallel arrangement obtained from wet-side compaction. The larger the individual pores for any given total total pore area, the greater is the flow, since the permeability varies as a power function of opening size.

It has been shown that the $k_o S^2$ structure term in the Kozeny-Carman equation gives a good measure of soil structure or, particle orientation. In other words, the more nearly parallel the clay plates, the smaller is the average void available for flow and the more tortuous the flow. Fig. 3 is a plot of $k_o S^2$

---

3 "The Permeability of Compacted Fine Grained Soils," by William T. Lambe, ASTM, 1955.

4 "The Permeability of Kaolinite," by Alan S. Michaels and C. S. Lin, Industrial Engineering Chemistry, Vol. 46, 1954, p. 1239.

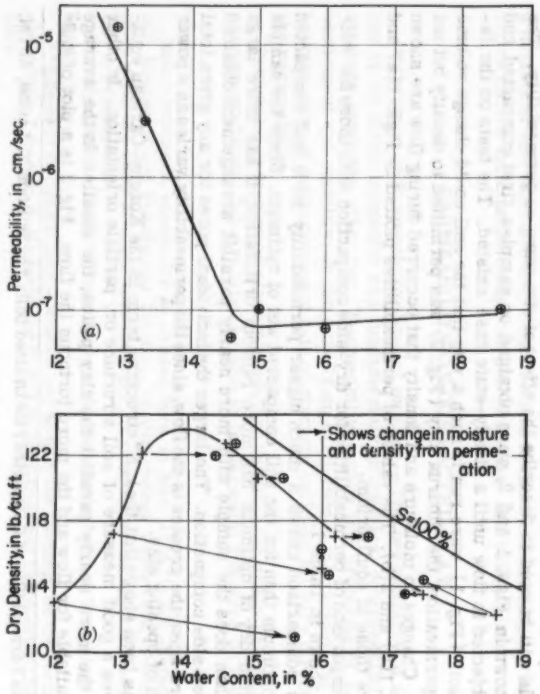


FIG. 1.—COMPACTION-PERMEABILITY TESTS ON JAMAICA SANDY CLAY

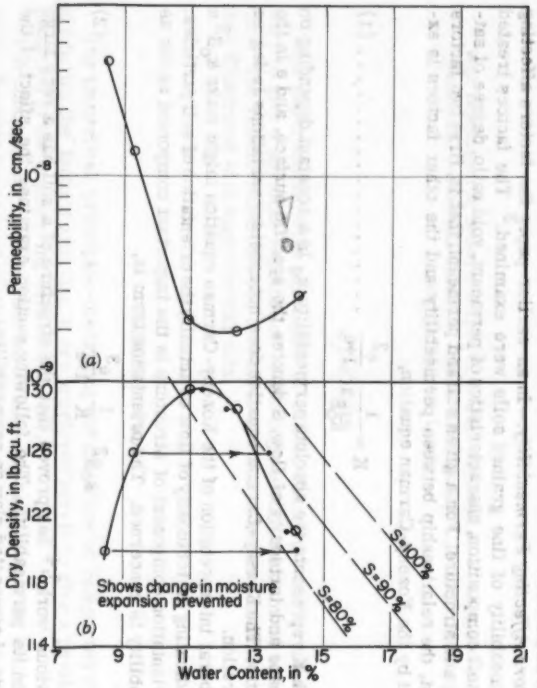


FIG. 2.—COMPACTION-PERMEABILITY TESTS ON SIBURUA CLAY

versus molding water content for the data (Fig. 2) on the Siburua clay. It shows that the reduced permeability with increased molding moisture content can well be explained by particle orientation. The larger the repulsive electrical forces

TABLE 1.—COMPARISON OF PERMEABILITIES

Soil (1)	Dry density, in pounds per cubic foot (2)	Molding moisture (3)	Permeability, in centimeters per second (4)
Jamaica soil	116	dry of optimum	1.4×10^{-5}
	116	wet of optimum	8.0×10^{-5}
Siburua clay	122	dry of optimum	3.0×10^{-8}
	122	wet of optimum	2.5×10^{-9}

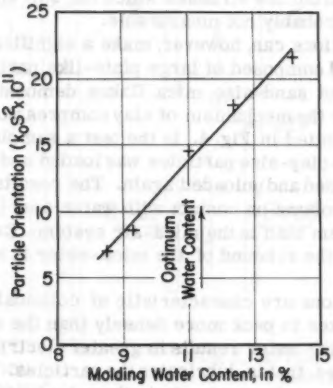


FIG. 3.—PARTICLE ORIENTATION VERSUS MOLDING WATER

between particles at the time of compaction the lower is the permeability of the resulting soil.

COMPRESSION AND EXPANSION OF COMPACTED CLAY

Components of Volume Change.—If a clay is subjected to an "all around" pressure with drainage permitted, it compresses; upon load release, it usually

expands. These volume changes in clay are due to one or more of the five following components: (1) Gas—change of volume or amount; (2) particle diminution; (3) particle deformation; (4) particle rearrangement; and (5) change in size of michelle.

Gas can contribute to a volume decrease in a soil either by compressing, because of an increase in pressure, or by going into solution in the pore water because of a greater pressure or a lower temperature. On the other hand, it can contribute to a volume increase by expanding under a load release or by coming out of solution of the pore fluid when the pressure is reduced or the temperature raised. Volume changes of fine-grained soils caused by gas are complex and not well understood. This component will be excluded from the following examination of volume change.

Whereas Components 2 and 3 (particle diminution and particle deformation) undoubtedly occur in certain soils, they are probably insignificant in clays. The contact area in granular soils is so small that the usual stresses are large enough to crush unsound mineral (or rock) aggregates or to deform them elastically. The particles of such friable materials as caliche or weathered granite often decrease in size during laboratory or field compactions. The amount and type of contact area in clays, however, is such that particle crushing or elastic deformation from the stresses which the soil engineer would normally apply to the soil is probably not measurable.

Particle deformations can, however, make a significant contribution to volume changes in a soil composed of large plate-like particles. Loading and unloading a dry mass of sand-size mica flakes demonstrates this. To us this experiment to deduce the mechanism of clay compression is not wise, as shown by the test results plotted in Fig. 4. In the test a sample of dry mica (muscovite) having silt-and-clay-size particles was loaded and unloaded, leached with water, and finally loaded and unloaded again. The results show: (1) A marked decrease in sample volume on contact with water, and, (2) a larger rebound in the mica-water system than in the mica-air system. Expressed as a percentage of compression, the rebound of the mica-water is more than twice that of the mica-air.

Both of these actions are characteristic of colloidal behavior. The water permits the mica flakes to pack more densely than the air does. Because it is more polar than air, the water results in greater electrical repulsions between adjacent mica particles, that is, lubricates the particles. Since there are greater interparticle repulsions when water is in the mica pores than when air is, the greater expansion upon load release is to be expected.

This compression test shows that merely reducing the particle size of the mica introduces colloidal phenomena. With clay particles (which have relatively large electrical surface potentials) colloidal phenomena are much more important than with the mica flakes (which have low potentials).

The rearrangement of soil particles from a random array to a more orderly array contributes to compression. There are convincing data[5,6] that one-dimensional compression tends to aline particles. The sudden decrease in volume

---

5 "The Shearing Resistance of Remolded Cohesive Soils," by Juul Hvorslev, Proceedings, Soils and Foundation Conference, U. S. Engrg. Dept., Boston, Mass., June, 1938.

6 "The Improtance of Structure to the Engineering Behavior of Clay," by James K. Mitchell, thesis presented to Massachusetts Inst. of Technology at Cambridge, in 1956, in partial fulfillment of the requirements for the degree of Doctor of Science.

shown in Fig. 4, when the water permeated the mica sample is due to a rearrangement of mica particles. Volume decreases caused by the rearrangement of particles are essentially nonrecoverable. When the volume increases from other causes, some minor changes, of course, occur in particle orientation.

In most clays Component 5, changes in size of soil micelle, that is, soil mineral particle plus double layer water (including adsorbed water, is an important contributor to compression upon pressure application and is almost the sole cause of rebound upon load reduction. The influence of this component is illustrated by Fig. 5, showing two adjacent soil colloids and the relationship (Fig. 5(c)) between spacing and total potential energy.

At equilibrium the externally derived intergranular pressure (consider the colloids as having unit areas) $\bar{\sigma}$ plus the electrical attraction between the particles equals the electrostatic repulsion. The spacing 2d is the one that brings about equilibrium for this force system.

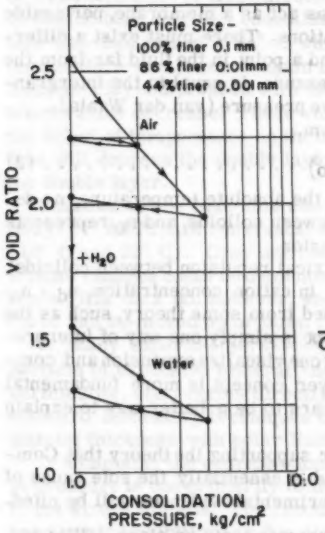


FIG. 4.—COMPRESSION OF MUSCOVITE

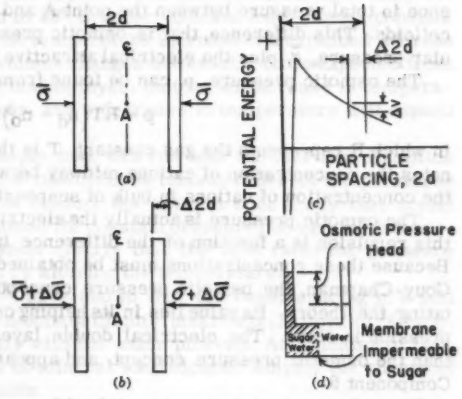


FIG. 5.—INTERPARTICLE SPACING AS FUNCTION OF FORCES

If we add an increment of intergranular pressure, $\Delta\bar{\sigma}$, as shown in Fig. 5(b) the forces are not in equilibrium until the intercolloid spacing is reduced by Δ2d requires an input of work equal to ΔV; in other words, the net repulsive force between the colloids have increased $\Delta\bar{\sigma}$. If $\Delta\bar{\sigma}$ is removed, the colloids will move apart a distance of Δ2d, because force and spacing are uniquely related.

The compression and expansion of colloids which has just been explained in terms of the Gouy-Chapman double layer theory can also be considered in terms

of osmotic pressure. Fig. 5(d) shows the classic demonstration of osmotic pressure. On the left of a membrane, which is permeable to water molecules but impermeable to sugar molecules, is a sugar solution, and on the right is pure water. The column of fluid in the sugar solution is higher than that in the water, the difference being the osmotic pressure. One way to look at the phenomenon is to consider the water pressure on both sides of the membrane as equal. To the water pressure on the left must be added the pressure of the sugar molecules which are held back by the membrane. Thus, the total pressure on the left, made up of water pressure plus sugar "pressure," is greater than that on the right by an amount equal to the sugar pressure, that is, osmotic pressure.

The two particles shown in Fig. 5 present a similar situation to the model in Fig. 5(d). The electrical charges on the colloids keep the cations between the particles from moving freely to the bulk of the suspension to equalize the concentrations of cations. The colloid charges act as a membrane, permeable to water and impermeable to double layer cations. There must exist a difference in total pressure between the point A and a point in the fluid far from the colloids. This difference, that is, osmotic pressure, is equal to the intergranular pressure, $\bar{\sigma}$, plus the electrical attractive pressure (van der Waals).

The osmotic pressure, p, can be found from,

$$p = RT(n_d - n_o) \quad \ldots\ldots\ldots\ldots\ldots\ldots (3)$$

in which R represents the gas constant, T is the absolute temperature, n_d denotes the concentration of cations midway between colloids, and n_o represents the concentration of cations in bulk of suspension.

The osmotic pressure is actually the electrical repulsion between colloids; this repulsion is a function of the difference in cation concentration, $n_d - n_o$. Because these concentrations must be obtained from some theory, such as the Gouy-Chapman, the osmotic pressure concept is simply one way of interpretating the theory. Its value lies in its helping one visualize expansion and compression in clays. The electrical double layer concept is more fundamental than the osmotic pressure concept, and appears to be a better way to explain Component 5.

There is convincing experimental evidence supporting the theory that Component 5 contributes to clay compression and is essentially the sole cause of clay expansion. Four of these confirming experimental evidences will be cited.

1. Bolt and Miller[7] and Bolt[8] ran compression tests on clays (illite and montmorillonite) with various electrolyte concentrations in the pore fluids. After a few cycles of loading and unloading to minimize particle rearrangement in later runs, they found a reversible void ratio-pressure curve, that is, rebound equalled compression. The void ratio-pressure curves were completely understandable in terms of the Gouy-Chapman theory; for example, whenever salt was added to depress the double layer, less compression and rebound resulted. Later work (Warkentin, Bolt, and Miller, 1957) compared experimental compression data with plots computed from colloidal theory. Excellent agreement between theory and tests was obtained from solium-montmorillonite, after a couple of load-unload cycles had made the particles parallel. Warkentin,

---

7 "Compression Studies of Illite Suspensions," by G. H. Bolt and R. D. Miller, Soil Science Proc., Vol. 19, 1955, pp. 285-288.

8 "Physical-Chemical Analysis of the Compressibility of Pure Clay," by G. H. Bolt, Geo. Technique, Vol. 6, No. 2, June, 1956, pp. 86-93.

et al., assumed for the dispersed systems with which they worked that the electrical attraction between particles was zero, that is, the swell pressure equalled the electrical repulsion. This assumption did not prove to be true with calcium-montmorillonite; the measured values of swelling pressure ($\bar{\sigma}$) were much greater than computed repulsion (R). To assume that the electrical attraction, A, equals zero in the soil systems with which the engineer usually works seems unjustified.

2. The work of Charles C. Ladd, A. M. ASCE,[9] described in the next section of this paper, showed that the swelling of compacted clay can be explained completely by Component 5. Changing the electrolyte in the water available for imbibition, he was able to alter the measure swelling as had been theoretically predicted.

3. To check the belief that Component 5 was the cause of clay expansion, a test was conducted in which the effect of temperature was investigated. A sample of Boston blue clay was consolidated at a temperature of 20° C; the temperature was then raised to 41° C while the load was held constant; and finally the temperature was lowered again to 20° C under constant load. Under constant load, the clay compressed with the temperature increase and expanded with the temperature decrease. These volume changes are exactly those expected from the effect of temperature on the double layer, that is, an increase in temperature will depress the double layer, and a decrease in temperature will expand the double layer.

Unknown at the time this simple test was run was the fact that Hamilton Gray[10] F. ASCE, had run standard consolidation tests at different temperatures (10° C and 22° C). Gray did not conduct his tests in such a way that actual volume changes could be determined for constant pressure but varying temperature. His data do, however, show clearly that the void ratio-log pressure curve can be moved up or down by altering the temperature.

4. Many experimenters[11,12] have shown that the basal spacing in a soil particle of expansive mineral (montmorillonite, nontronite, halloysite ($4H_2O$), vermiculite, etc.) varies directly with the water pick-up. As a matter of fact, standard laboratory techniques of mineral identification employ the change of platelet thickness with polar fluids.

In summary, the compression of saturated clay resulting from an increase in pressure is due primarily to the reorientation of particles and to a decrease in the size of micells. The rebound or expansion on load release (also swelling upon water imbibition) is due almost entirely to an increase in the size of the micille. This theory leads us to predict that any change in the system variables, listed under the heading "Permeability of Compacted Clay," that changes the double layer can change the compression-expansion characteristics of the clay.

Effect of One-Dimensional Compression on Structure.—Figure 6 illustrates the effects of one-dimensional compression on the structure of clays. If the

---

[9] "Swelling of Compacted Clay," by C. C. Ladd, thesis presented to Massachusetts Inst. of Technology, at Cambridge, in 1957, in partial fulfillment of the requirements for the degree of Master of Science.

[10] "Structure of Inorganic Soil," by T. William Lambe, Proceedings-Separate 315, ASCE, October, 1953.

[11] "Final Report, Soil Solidification Research Vol. II—Fundamental Properties, Clay-Water Systems," Cornell Univ., Ithaca, New York, 1951.

[12] "The Swelling of Montmorillonite," by K. Norrish, Faraday Society, Discussion No. 18, 1954.

effects of long periods of time on clay deposits are ignored, both natural and compacted clays can be treated in the same presentation. A sample of clay compacted dry of optimum and a natural clay would both tend toward a random orientation of particles. A sample compacted wet of optimum or a sample of natural clay which is remolded would both tend toward a parallel orientation.

Fig. 6(a) shows what would happen to the particle orientations under a one-dimensional compression. The orientations in the circles show that a load tends to aline the particles in a parallel array. In the case of the remolded or wet-side compacted clay in which the particles are already parallel, a load merely brings them closer together.

Fig. 6(b) suggests what would happen to particle orientations under very high pressures. For the dry-side compacted sample the pressure orients the particles normal to the direction of compression and decreases the spacing between them. For the wet-side compacted clay in which the particles are already oriented the pressure reduces the spacing between particles. Theoretically, a large enough pressure would make the structure of the wet-side compacted sample identical to that of the dry-side compacted sample. Upon load

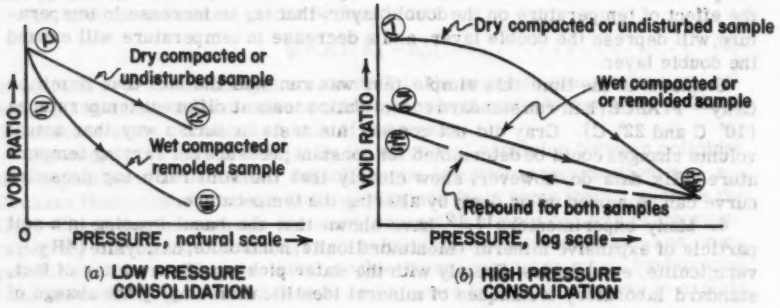


FIG. 6.—EFFECT OF ONE DIMENSIONAL COMPRESSION ON STRUCTURE

release from this pressure the two samples would follow the same rebound. During rebound the spacing between particles increases, but only negligible changes in orientation occur.

Effect of Molding Water on Compressibility Characteristics of Compacted Clay.—As was shown in Fig. 5, for any given pressure system there is an equilibrium, that is, an equilibrium amount of water which the clay will absorb. If a sample of clay is compacted at a moisture content less than the equilibrium water content of the clay, the clay will try to draw in more water to satisfy its double layer requirements. If an outside source of water is not available, capillary menisci will develop and tensions in the pore water will result. The pore water tension will create an intergranular pressure of equal magnitude to satisfy the double layer of the soil colloid, that is, since there is no water to satisfy the colloid under a small intergranular pressure, the intergranular pressure increases to reduce the amount of moisture necessary for equilibrium.

When two samples at the same density, one compacted dry of optimum and one compacted wet of optimum, are compared, it is evident that the sample

compacted dry of optimum must adsorb more moisture to come into equilibrium than the sample on the wet side. This well-known fact is illustrated in Figs. 1 and 2 and Fig. 13 shown subsequently.

In Fig. 13(c) both the compaction curve as molded (by the solid line) and the moisture-density curve after soaking (by the dashed line) has been permitted. It can be seen that a sample compacted dry of optimum picks up more moisture and swells more than does a sample of the same density compacted wet of optimum. If sufficient time were allowed the dashed curve might eventually become a straight line.

The effect of molding water on swelling behavior can also be illustrated by tests in which are measured the pressures required to prevent samples from swelling when given access to water. Such tests were run on Boston blue clay. One sample was compacted dry of optimum to a density of 108.6 lb per cu ft and another was compacted wet of optimum with the same effort to the same density. A pressure of 1.01 kg per sq cm was required to prevent the dry-side sample from swelling and 0.12 kg per sq cm to prevent the wet-side sample from swelling.

As Fig. 6 indicates, the amount of compression that occurs under a increment of load when the pressure is small will cause a greater settlement on a wet-side compacted sample than on a dry-side compacted sample, if they are both initially saturated and at the same void ratio. On the sample compacted wet of optimum no work is required to orient the particles; extra pressure is required to do this on the flocculated structure.

Fig. 6(b) shows that under higher pressures the slope of the void ratio-log pressure curve is steeper for the dry-side than for the wet-side sample. In other words, when the pressure is large enough to cause particle reorientations, greater volume change per increment of pressure results than when no orientation changes are taking place.

Fig. 6(b) also shows that there is a certain pressure required to start significant changes in particle orientations. This pressure might be interpreted as the preconsolidation load on the compacted sample. This "equivalent preconsolidation pressure," however, is not necessarily caused by a pressure or its equivalent in compactive effort. The theory would indicate, for example, that the longer the dry-side compacted sample had remained under load, the higher would be the so-called preconsolidation pressure. This pressure would also depend on the characteristics of the pore fluid. In other words, time and chemical changes can give a shape to the consolidation curve of a compacted clay and possibly a natural clay which would normally be interpreted as a preconsolidation pressure. The effects on other properties of the sample may be different when the change of slope in the void ratio-pressure curve is caused by chemical factors or time rather than by pressure.

SHEAR STRENGTH OF COMPACTED CLAY

Forces Between Particles.—The shear strength of a soil can be thought of as made up of a granular-type strength plus a colloidal-type strength. The strength of a clean sand, for example, would be of the granular type and that of a plastic clay of the colloidal type. A soil of both colloids and granular particles would have both types of strength. The nature of granular strength, which is comparatively well-known, is outside the scope of this paper and it is not considered herein.

The first step in a study of the shear strength of two adjacent colloids is to consider the entire force system. There are four horizontal forces (if unit area is assumed, force and stress can be used interchangeably) which can act between the adjacent colloids shown in Fig. 7, which are: (1) $\bar{\sigma}$ = the externally applied intergranular stress; (2) A = the electrical attraction; (3) R = the electrical repulsion; and (4) I = the steric or geometric interaction, that is, contact pressure.

The intergranular stress, also called the effective stress, is derived from some other source than electrical stresses originating within the particles. It is usually the most fundamental stress the soil engineer can measure or compute. Under certain conditions it is equal to the total applied normal stress minus the pore water stress.

The stress A is derived primarily from van der Waals forces. It can act over large distances of more than 100A. There can be other components in A, for example, the electrostatic attraction occurring in non-salt flocculation.

The stress R arises primarily from the electrostatic repulsion between clay particles, which carry net negative charges. R is very sensitive to the nature of the soil water system. Changes in R bring about changes in the degree of flocculation or dispersion of colloids.

The contact pressure I, like R, is a repulsive stress. It acts only, of course, when the adjacent particles are in contact. The contact can be either between mineral surfaces or between molecules of tightly-held water. The stress I is electrical in nature, but can be caused by forces originating either within the particles or outside them.

Equilibrium conditions require (a) for dispersed particles, $\bar{\sigma} + A = R$; and (b) for particles in contact, $\bar{\sigma} + A = R + I$.

Factors Influencing Shear Strength.—The shear strength of a clay is completely determined by the electrical forces acting between the particles, that is, A, R and I. The electrical forces are thus the primary cause of strength. The four factors, particle spacing, particle orientation, externally applied stresses, and characteristics of soil-water system, which determine the electrical forces are secondary causes of shear strength. These five causes are examined as follows:

1. Electrical Forces. The electrical forces between clay plates are a function of particle displacement in a direction parallel to the particles, as well as a function of displacement perpendicular to the particles. The greater A and I, the greater is the shear strength; the greater R, the lower the shear strength.

2. Spacing of the Particles. The closer two clay particles, the greater are all of the electrical forces. If two clay particles are spaced some distance apart (that is, where I = 0), the effect of a reduction in spacing on the shear strength would depend on whether the net increase in attraction is positive or negative. At the close interparticle spacings that exist in the typical natural or compacted clays, a decrease in spacing results in an increase in I. This increases the shear strength. Because increasing the externally applied intergranular pressure reduces the spacing, it increases the shear strength. This reasoning supports the well-known fact in soil engineering that, other things being equal, the denser the soil (the closer the average particle spacing), the greater the shear strength.[13,14]

---

[13] "Strength of Natural Clays," by P. C. Rutledge, Presented at the October, 1958 Meeting of ASCE.

[14] "Strength Characteristics of Compacted Clay," by G. A. Leonards, Transactions, ASCE, 1955.

3. Orientation of Particles. For a given average particle spacing (given void ratio), the more nearly parallel the adjacent particles are, the weaker the soil. Fig. 8(a) and 8(b) show two adjacent colloids with the same average spacing Δ. The total of I plus net electrical attractive force between the adjacent particles is greater in Fig. 8(b) than in Fig. 8(a). Therefore, the shear stress required to slide the particles relative to each other is greater for the situation pictured in Fig. 8(b) than for that in Fig. 8(a). Since the sum of I and the net attractive force between the particles varies inversely with a power function of the spacing, tilting the two particles in Fig. 8(a) to the position in Fig. 8(b) results in a greater increase of I plus net attractive force on the right side of the particles that is lost on the left side.

The foregoing examination of forces and strength treated only particles that are parallel or approximately parallel. This is the most common arrangement of adjacent soil colloids since it is the one which exists among dispersed particles or particles which have been flocculated with a salt type of flocculation. If two particles are perpendicular to each other as happens in nonsalt flocculation (Fig. 8(c)) they resist displacement more than do the same two particles with the same average spacing but parallel as shown in Fig. 8(d). With nonsalt flocculation edge-to-face electrical attraction is an additional component.

When a sufficiently large shear stress is applied to the system in Fig. 8(c), it rotates the particle in such a way that the orientation tends to become parallel. Experimental evidence of this tendency has already been cited. This realinement explains why the ultimate strength of a dry-side compacted sample (or an undisturbed clay sample) approaches the ultimate strength of a sample compacted wet of optimum but to the same density (for remolded sample).

The effects of particle orientation can be summarized as follows: For any given void ratio and, therefore, given average particle spacing, the more nearly parallel the particles are, the weaker the soil is.

4. Applied Stresses. A change in externally applied intergranular pressure results in a change in spacing and or orientation which alters the electrical forces between the particles and so affects the shear strength. For particles in contact with each other, a change in the intergranular pressure affects the contact pressure between particles and thus the shear strength. The stress in the pore fluid is not a primary variable of the shear strength of the soil, but rather a factor which helps determine the intergranular stress between the particles. When the degree of saturation is 100%, negative water tensions cause intergranular pressures of equal magnitude. This is probably true also for partially saturated soils in which the degree of saturation is high. Research is needed, however, on the transmission of pore water tensions to intergranular pressures in partially saturated soils.

The stress in the pore fluid can come from several sources:

a. Hydrostatic pressure due to the weight of overlying water.

b. Seepage: When particles in a saturated soil move closer to each other because they are subjected to a pressure, moisture must flow out and until an equilibrium condition exists there is an excess pressure in the water. The opposite takes place when the particles move apart.

c. Shortage of double layer water: As has been noted, if the spacing of the colloids is such that they cannot develop completely their double layers, they will swell if there is water available. If there is no water available, they will throw tension into the pore water, thus increasing intergranular pressure to hold the particles to the given spacing.

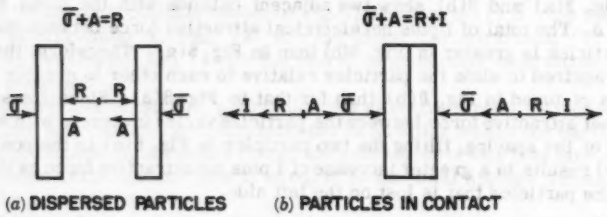


FIG. 7.—FORCES BETWEEN ADJACENT PARTICLES

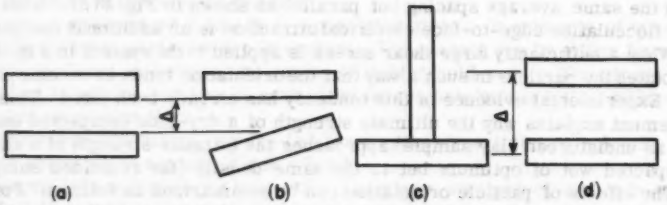


FIG. 8.—CHANGES IN PARTICLE ORIENTATIONS

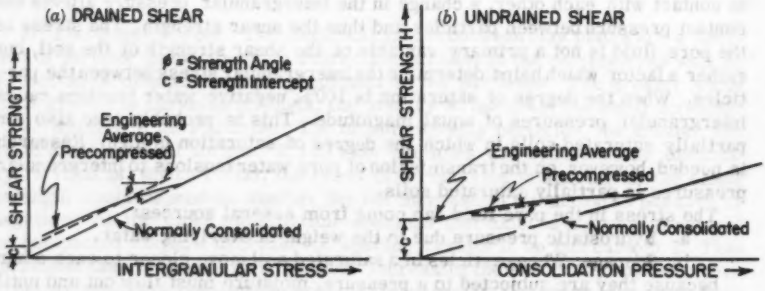


FIG. 9.—ENVELOPES FOR DRAINED AND UNDRAINED SHEAR

Water deficiency in soils has been treated in detail by Aitchison.[15] He used the terms "quasi-saturated" and "unsaturated" to describe soils in which the pore pressure is negative. "Quasi-saturated" soils have all their voids filled with water; "unsaturated" soils contain air. Aitchison lists a number of causes of water deficiency in soils.

5. Characteristics of the Soil-Water System. The effects which the variables in the soil-water system have on the electrical forces between particles are discussed under the heading Permeability of Compacted Clay. Any expansion of the double layers increases the electrical repulsive force between adjacent particles.

The attractive forces between particles are seldom altered by colloidal phenomena. Percolating waters can, however, deposit cementing agents, of which the most important are carbonates and iron oxides.

Cohesion and Friction.—The results of soil strength tests are usually plotted as shear strength versus normal pressure[16] as shown in Fig. 9(a) for drained shear or for undrained shear with measured pore pressures, and in Fig. 9(b) for consolidated undrained shear without measured pore pressures. Drained shear strength is taken as the shear stress on the plane of maximum stress obliquity at the strain required to develop maximum obliquity. Undrained shear strength is taken as $P_{max}/2A \cos \phi$ $\left(\text{about } .43 \frac{P_{max}}{A}\right)$ or simply $P_{max}/2A$.

In Fig. 9, the following legend is used: dashed line for normally consolidated clay; solid line for precompressed clay; dotted line for straight line representation of shear strength for use in engineering analyses.

The terms "cohesion" and "friction angle" have been used in various ways to describe the strength envelopes. One common use is to name the parameters of the engineering approximation as, strength = cohesion + $\bar{\sigma}$ tangent of the friction angle, or

$$s = c + \bar{\sigma} \tan \phi \quad \ldots\ldots\ldots\ldots\ldots\ldots (4)$$

Eq. 4 (Coulomb equation) is very useful to the soil engineer. While its use is completely sound, the selection of "cohesion" for c and "friction angle" for ϕ is most unfortunate. There is little in the strength envelopes to indicate the mechanism of shear strength development as the terms "cohesion" and "friction" imply. There is, moreover, no standard test that can identify the contributing fundamental components of clay shear strength.

This unnecessary confusion can easily be avoided by using c equal to the strength intercept, and ϕ as the strength angle.

Fig. 9 shows that precompression strengthens soils. As noted in earlier parts of this paper, a consolidating pressure alines particles and reduces the spacings between them. When the confining pressure is reduced, the orientation of particles remains essentially unchanged.

The permanence of the effect of precompression on particle spacing depends on the electrical nature of the system. Particles represented by curve 1 of the

---

15 "The Nature, Extent and Engineering Significance of the Conditions of Unsaturation in Soils Within the Australian Environment," by M. E. Aitchison, thesis presented to the University of Melbourne, at Melbourne, Australia, in 1956, in partial fulfillment of the requirements for the degree of Doctor of Philosophy.

16 "The Structure of Compacted Soils," by John G. Pacey, Jr., thesis presented to Massachusetts Inst. of Technology, at Cambridge, in 1956, in partial fulfillment of the requirements for the degree of Master of Science.

energy-distance plots in Fig. 10 gain net electrical attraction with reduced spacing. At least part of the strength increase from compression for a soil represented by curve 1 should, therefore, remain upon load release. The same should be true for spacings less than x in curve 2. The reduced spacings caused by precompression on particles represented by curve 2 at distances greater than x should be temporary, because swelling would accompany load release.

This reasoning leads to an interesting prediction, namely: A clay with parallel particles and net electrical repulsion (a remolded, swelling clay tends to meet this requirement) should have the same drained strength envelope regardless of precompression.

As one can imagine, the effects of time are very important in the phenomena just described. The theory, of course, assumes equilibrium conditions and further assumes that other time effects (thixotropic strength-regain, primarily) are constant for all the various strength measurements.

Because compression results in a volume decrease that is not completely recoverable upon load release, precompression has a much larger effect upon undrained shear strength that upon drained strength. The fact that the void ratio of a precompressed sample at a given intergranular pressure is lower than that of a normally consolidated sample of the same clay at the same pressure means that smaller positive pore water pressures are developed during undrained shear.

Effect of Compaction Conditions on Strength.—

1. As Molded Strength.—Fig. 11 presents compaction and strength data on Boston blue clay.[16] The tests were made using a miniature compaction mold and the following compactive efforts were used: Curves 1 - 40 lb tamp, 3 layers of 25 tamps; curves 2 - 40 lb tamp, 5 layers of 25 tamps; and curves 3 - 80 lb tamp, 3 layers of 25 tamps. The data, typical of undrained, as-molded strengths of compacted clay, illustrate the following facts:

a. Increased compactive effort, dry of optimum, increases strength.

b. Increased compactive effort, wet of optimum, can result in a gain or loss of strength, and the effect is small.

c. For the same compactive effort and same compacted density, dry-side compaction gives a higher strength than does wet-side compaction.

These three well-known facts[17] can be explained by the compaction theory. Comparing samples compacted at the same moisture dry of optimum but to different densities A and E in Fig. 9 of the companion paper, it can be seen that

a. A has a more random particle orientation than E.

b. E has closer particle spacing than A.

The reduction of particle spacing in E more than offsets the improvement of orientation; going from A to E results in an increase of strength.

Going from C to D improves the orientation, which takes away strength, but makes the interparticle spacing smaller, giving strength. Unlike the difference between A and E, the decrease in the spacing of particles (that is, increase in density) is relatively small. The two effects are of the same magnitude and so either a net gain or a net loss of strength can occur.

Sample A is much stronger than C for three reasons: (1) The orientations at A are more random; (2) there are lower pore water pressures (higher negative pressures) at A than at C; and (3) the electrical repulsions at A are lower because of the greater water deficiency.

---

17 "Stabilization of Materials by Compaction," by W. J. Turnbull and Charles R. Foster, Transactions, ASCE, Vol. 123, 1958, pp. 1-26.

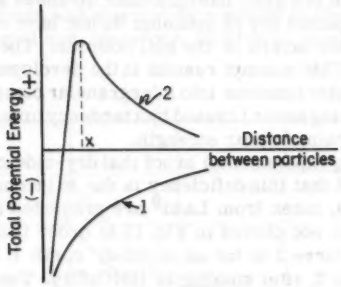


FIG. 10.—ENERGY-DISTANCE CURVES FOR TWO ADJACENT COLLOIDS

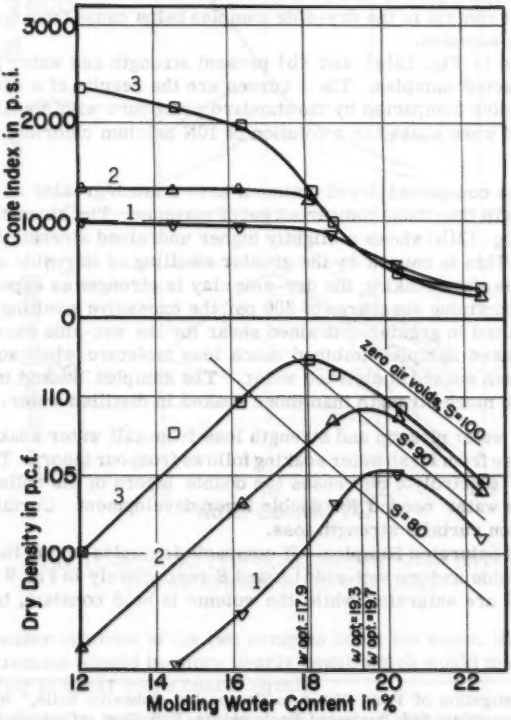


FIG. 11.—CONE INDEX AND DRY DENSITY VERSUS MOLDING WATER CONTENT FOR BOSTON BLUE CLAY

There is substantial direct and indirect evidence[18] that clays compacted dry of optimum usually have negative pore water pressures. These negative water pressures result in higher intergranular stresses and, therefore, higher strength. Clays compacted dry of optimum do not have sufficient moisture to develop fully the double layers of the soil colloids. The colloids try to draw in the needed water. This attempt results in the development of capillary memisci that transfer water tensions into intergranular compression. Pore water tensions developed during shear (caused by a tendency toward a volume increase) also increase the undrained shear strength.

There is convincing experimental proof that dry-side compacted clays have a water deficiency and that this deficiency is due to incomplete development of the double layer. Data, taken from Ladd[9] are presented in Fig. 12. Many experimental points were not plotted in Fig. 12 in order that the trends might be more clearly seen. Curve 3 is for as-molded; curve 1, after soaking in distilled water; and curve 2, after soaking in 10N$CaCl_2$. The curves in Fig. 12(c) show the density-water content curve as molded and after the samples had been soaked in a mold while subjected to a surcharge of 200 psf. The sloping lines with the arrow heads show the changes of various points due to soaking. These curves show two typical characteristics of such tests, namely, that dry-side compacted samples pick up more water and swell more than wet-side samples. The higher air content in the dry-side samples helps cause them to swell more than wet-side samples.

The curves in Fig. 12(a) and (b) present strength and water pick-up data for the compacted samples. The 1 curves are the results of a series of tests in which samples compacted by the standard procedure with distilled water as the pore fluid were soaked in a solution of 10N calcium chloride. The curves show:

1. Samples compacted dry of optimum have a much greater as-molded undrained strength than those compacted wet of optimum. The strengths of soaked samples in Fig. 12(b) shows a slightly higher undrained strength for wet-side compaction. This is caused by the greater swelling of dry-side samples. At equal densities after soaking, the dry-side clay is stronger as expected. Under the very low confining surcharge of 200 psf, the excessive swelling of dry-side samples resulted in greater undrained shear for the wet-side samples.
2. The soaked samples imbibed much less moisture when soaked in salt water than when soaked in distilled water. The samples soaked in salt water retained much more strength than those soaked in distilled water.

The lower water pick-up and strength loss from salt water soaking in comparison to those from fresh water soaking follows from our theory. The increase in pore water electrolyte depresses the double layers of the colloids, that is, it reduces the water needed for double layer development. Curtailing double layer expansion curtails strength loss.

Strength of Saturated Samples.—If compacted samples having the same density, one dry-side and one wet-side (A and E respectively in Fig. 9 of the companion paper) are saturated while the volume is held constant, the dry-side

---

18 "An Investigation of Pore Water in Compacted Cohesive Soils," by J. W. Hilf, Technical Memorandum 654, Bureau of Reclamation, U.S. Dept. of the Interior, Denver, Colo., October, 1956.

sample should be stronger than the wet-side sample, but the strength difference should be reduced by the saturation. After saturation at constant volume:

a. The water contents and electrolyte contents in the pore fluids of the two samples should be equal and, therefore, electrical repulsions should be more nearly equal.

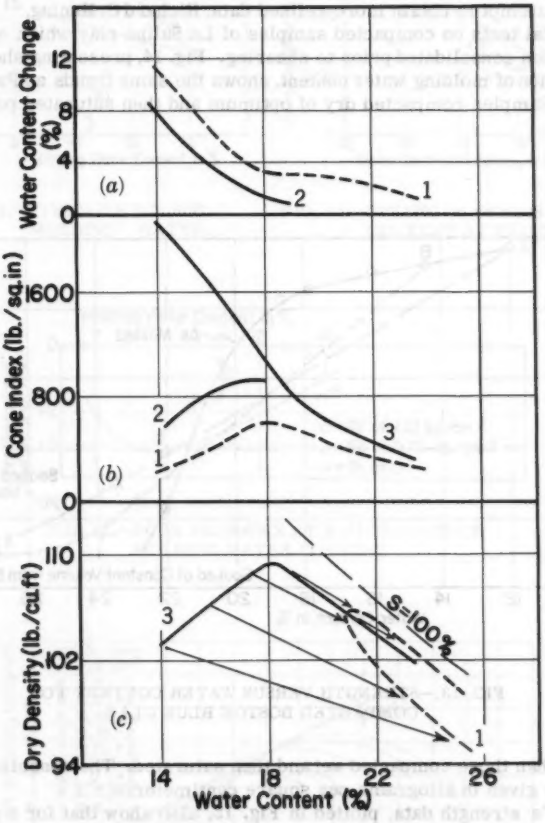


FIG. 12.—COMPACTION-SOAKING-STRENGTH DATA FOR VICKSBURG BUCKSHOT CLAY

b. The water contents of the two samples being the same, the double layer water deficiencies should be more nearly equal, which would make pore water tensions prior to shear more nearly equal.

The orientation at A would still be more random than at C, and the strength at A should, therefore, still be greater than at C. Sample A, being less com-

pressible than C, will develop smaller positive pore water pressures during undrained shear.

Fig. 13 (from Pacey[16]) shows that samples compacted dry of optimum and then soaked at approximately constant volume have higher shear strengths than samples compacted wet of optimum. Pacey's data were obtained from a cone penetration test. If free swelling, or even partial swelling, is permitted, the wet compacted clay may have higher undrained strength.[19,20]

In an attempt to obtain more refined data, Richard C. Huning,[21] A. M. ASCE, ran triaxial tests on compacted samples of La Salina clay which were saturated and then consolidated prior to shearing. Fig. 14, presenting shear strength as a function of molding water content, shows the same trends as Pacey's work, namely: Samples compacted dry of optimum and then saturated possess more

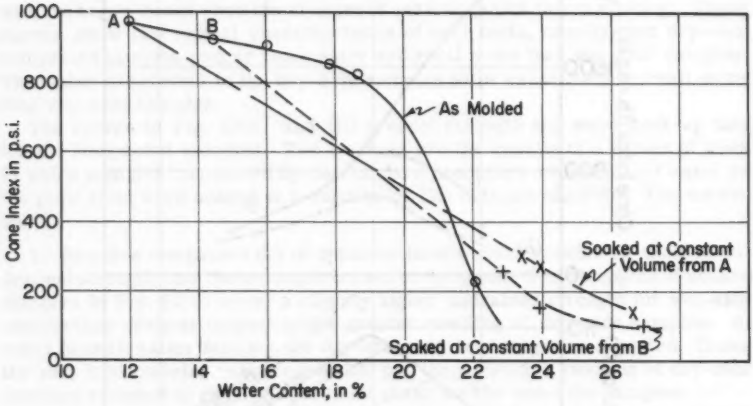


FIG. 13.—STRENGTH VERSUS WATER CONTENT FOR COMPACTED BOSTON BLUE CLAY

strength than those compacted wet and then saturated. The consolidation pressure σ_c is given in kilograms per square centimeter.

Huning's strength data, plotted in Fig. 15, also show that for a given water content at failure, higher strength results from dry-side compaction.

The data in Figs. 14 and 15 were obtained from undrained triaxial tests in which pore water pressures were measured. The measured pore pressures,

19 "Development of CBR Flexible Pavement Design Method for Airfields, A Symposium," Transactions, Vol. 115, ASCE, 1950, p. 453.

20 "Some Relationships Between Density and Stability of Subgrade Soils," by H. B. Seed and Carl L. Monismith, Highway Research Board, 1954.

21 "The Effect of Structure on the Strength of Compacted Soil," by R. C. Huning, thesis presented to Massachusetts Inst. of Technology, at Cambridge, in 1957, in partial fulfillment of the requirements for the degree of Master of Science.

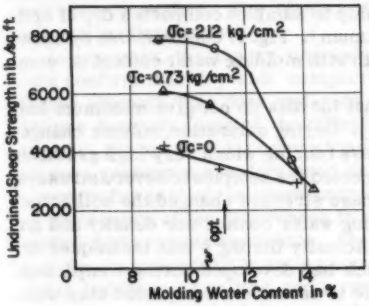


FIG. 14.—STRENGTH VERSUS MOLDING WATER

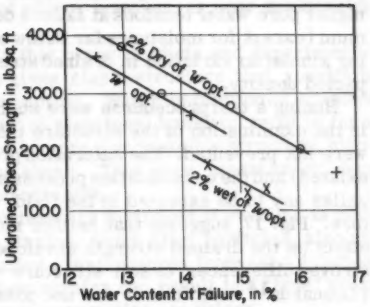


FIG. 15.—STRENGTH VERSUS WATER CONTENT AT FAILURE

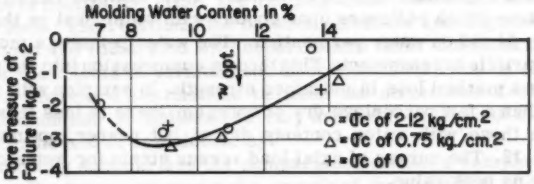


FIG. 16.—PORE PRESSURE AT FAILURE VERSUS MOLDING WATER CONTENT

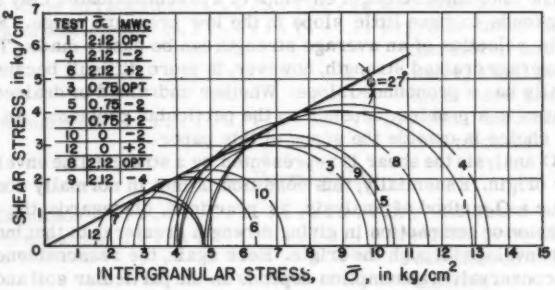


FIG. 17.—STRENGTH ENVELOPE FOR LA SALINA CLAY

all tensions, shown in Fig. 16, indicate that the strength-intergranular stress plots will not differ very much for the various compaction water contents since higher pore water tensions at failure develop in samples compacted dry of optimum (except for moistures far below optimum). Fig. 17 confirms this by showing almost no variation in drained strength with molding water content or compacted density.

Huning's test procedures were such that the data do not give maximum help in the examination of the structure theory. During saturation, volume changes were not prevented. The saturation process (during which very high gradients existed) and the consolidation process subjected the samples to severe stresses, unlike any to be expected in the field. These stresses changed the soil structure. Fig. 17, suggests that neither molding water content nor density had any effect on the drained strength envelope. Actually Huning's test techniques destroyed differences in soil structure which had developed during compaction. (Leonards[14] noted that it was not possible to saturate a compacted clay without disturbing the structure.) For example, the densest samples swelled the most, thus wiping out the benefits of high density. Further tests are needed to show clearly the effect of compaction on drained shear strength.

Samples compacted dry of optimum have much steeper stress-strain curves than samples compacted wet (Seed and Monismith[19]). In fact, samples compacted far below optimum tend to be brittle. Such samples can have a metastable structure which collapses upon contact with water, just as the air-mica system (Fig. 4) did on water permeation. The water permits a more orderly and denser particle arrangement. This throws compression into the pore water and produces a marked loss in undrained strength. In samples with water contents more than a few percentage dry of optimum, there is less tension developed than in those with water contents dry of, but nearer, optimum; this is shown in Fig. 16. The curves of axial load versus strain for wet-side samples usually show no peak value.

In recent years there has been much controversy as to whether ϕ or c or either one ought to be taken as zero in stability analysis. A $\phi = 0$ analysis really amounts to using a constant, that is, average value of shear strength for the entire trial failure surface being considered. This, of course, greatly simplifies the stability computations and is just as accurate as is the selection of strength. The undrained strength envelope of a preconsolidated clay or a compacted clay tends to have little slope in the low pressure range. For such a condition, the selection of an average strength can be easily made. The selection of an average drained strength, however, is more difficult because the envelope usually has a pronounced slope. Whether undrained or drained strength should be used in a problem depends on the particular problem. An examination of this choice is outside the scope of this paper.

In a $c = 0$ analysis the shear is represented by a straight line envelope going through the origin. Essentially, this condition is met in normally consolidated clays. The $c = 0$ method of analysis, as practiced, disregards the effects of precompression or compaction in giving strength greater than that indicated by the straight envelope through the origin. Here again, the reasonableness of this severe and conservative assumption depends on the particular soil and problem at hand. More understanding on the permanence of the effects of precompression and compaction are certainly needed.

The proper selection of the shear strength (or components in the Coulomb equation for strength) depends on the soil and problem at hand. This selection

can be difficult and involves certain assumptions. The use of a horizontal envelope ($\phi = 0$) or straight envelope through the origin ($c = 0$) can be correct and very convenient. The blanket use of either, however, is poor engineering and can be disastrous.

In summary, the theory expounded in this paper predicts and experimental data confirm that dry-side compaction gives clay a structure that results in higher strength than does wet-side compaction. Water imbibition at constant volume destroys some of the differences in structure; however, most of them remain. Since wet-side compaction gives a more compressible structure, higher pore pressures are developed during shear. This pore pressure build-up accounts for part of the lower undrained strength.

Even more of the differences in structure are destroyed if swelling is permitted during water imbibition. Shear strains, which aline particles, also affect the structure built in during compaction. Disturbances from consolidation, water imbibition, swelling, and large shear strains can result in a "true" shear strength envelope which has no relation to compaction conditions.

CONCLUSIONS

A mechanistic picture of the process of clay compaction has been presented. The effects of compactive effort and molding water content on the soil structure are described. The relationships between structure and engineering behavior are examined and illustrated with experimental data. Colloidal theory is used to present the effects of environment on soil structure and on changes in soil structure. There are similarities between the structures of clay compacted dry of optimum and of undisturbed clay and between those of clay compacted wet of optimum and of remolded clay.

The following summarizes the comparison between a sample compacted to a given density dry of optimum and a sample of the same clay compacted to the same density at a water content wet of optimum.

Property	Comparison
1. Structure	
A. Particle Arrangement	Dry-Side more random.
B. Water Deficiency	Dry-Side more deficiency, therefore, imbibe more water, swell more, have lower pore pressure.
C. Permanence	Dry-Side structure sensitive to change.
2. Permeability	
A. Magnitude	Dry-Side more permeable.
B. Permanence	Dry-Side permeability reduced much more by permeation.
3. Compressibility	
A. Magnitude	Wet-Side more compressible in low pressure range, dry-side in high pressure range.

B. Rate . . . . . Dry-Side consolidates more rapidly.
C. Rebound . . . . . Wet-Side rebound per compression greater.

4. Strength

A. As Molded
Undrained . . . . . Dry-Side much higher.
Drained . . . . . Dry-Side somewhat higher.
B. After Saturation
Undrained . . . . . Dry-Side somewhat higher if swelling prevented; wet-side can be higher if swelling permitted.
Drained . . . . . Dry-Side about the same or slightly greater.
C. Pore Water Pressure at Failure . . . . . Wet-Side higher.
D. Stress-Strain Modulus . . . . . Dry-Side much greater.
E. Sensitivity . . . . . Dry-Side more apt to be sensitive.

The answer to the question "which is better, dry-side or wet-side compaction?" depends on the soil and problem involved. For example: (1) A low clay dam on a compressible foundation should be compacted wet. (2) A high highway clay fill to be built very rapidly on a good foundation should be compacted dry.

This paper has, of necessity, neglected factors which could be important, namely:

1. The effects of silt and sand particles.
2. The effects of chemical reactions in the soil which result in new products, especially cementing agents.
3. Certain electrical forces which can act between particles at close spacing.

These factors would not have any fundamental effects on the theories presented, but would influence the magnitude of the trends postulated.

The experimental data presented in this paper are typical of the results obtained from many tests run during the past few years. Limitations of space prevented inclusion of more of these data and also prevented an examination, in the light of the theoretical concepts given by this paper, of some of the published data by other soil engineers.

This paper is not intended to be the last word, but rather an over-all guide to the understanding of the behavior of fine-grained soils, especially compacted clays. Several topics presented in this paper need critical theoretical and experimental study; among them are:

1. Soil Moisture—nature of the moisture near the clay particles, especially the effect of time on its behavior.

2. Pore Pressures—a study of pore pressures in clay, especially partially saturated clays, to determine such things as the minimum degree of saturation at which pore pressures can be measured and the range of validity of the expression, Total = intergranular + neutral pressure.

3. Strength—a very detailed mechanistic picture of shear strength of clay and of clay containing silt and sand particles. An experimental study of the variation of strength with changes in the factors discussed under the heading Factors Influencing Shear Strength.

4. Environmental Changes—an investigation of the effect of changes in the characteristics of the soil-water system (temperature, etc.) on soil structure and the effect of changes in soil structure.

5. Soil Structure—further correlations of structure with behavior; development of simple test to determine structure.

6. Type of Compaction—the effects of compaction type on structure and behavior should be studied first in the laboratory and then in the field. The development of more convenient and more representative laboratory compaction tests could result. Better field compaction techniques would result.

Much of the compaction of clay today is a fairly crude and yet expensive operation. The designer of clay embankments is faced with many unknowns. The development of knowledge about compacted clay can result in more economical designs and cheaper unit field compaction. An understanding of the fundamentals of compacted clay can greatly increase the likelihood of finding chemical additives which can be widely and economically used to improve the properties of clay.

ACKNOWLEDGEMENTS

The author is happy to acknowledge the help of many in obtaining and in presenting the information in this paper. The results of the author's research students John G. Pacey, Issac Tiles, Richard C. Huning, Harold W. Olsen, George G. Haggarty, and Dr. James K. Mitchell have been used.

Staff members in the M.I.T. Soil Engineering Division John M. de Souza, Richard Harkness, Oliver H. Gilbert, Jr., Thomas J. Lambie, Za C. Moh, Peter S. Parsonson, and James E. Roberts and particularly Charles C. Ladd have contributed to this paper.

Also assisting in the study were A. S. Michaels, R. Torrence Martin, and Robert V. Whitman.

DISCUSSION

ALFRED C. SCHEER,[21] M. ASCE.—One factor that might be worthy of some further consideration, in connection with permeability, is the nonisotropic character of compacted clay.

The treatment of permeability in the early part of the paper is written as though compacted clay specimens were isotropic, with respect to permeability. No mention is made of the direction of permeability measurements. Were the permeabilities reported in Fig. 1 and Fig. 2 measured horizontally or vertically? Also Eqs. 1 and 2 are presented without any mention of the direction of flow. Both K and k_0 would be different for different directions of flow.

The extent and nature of the differences in permeability in different directions would seem to be a matter of considerable importance in studies of this type, especially in cases where the clay platelets tend to be oriented with their faces parallel.

[21] Assoc. Prof. of Civ. Engrg., Montana State College, Bozeman, Mont.

RAYMOND N. Y. YONG,[22] A.M., ASCE, AND BENNO P. WARKENTIN,[23]—The author examines the influence of temperature on electric potential, and in Fig. 2 shows that the diffuse ion-layer expands or increases in thickness with an increase in temperature. The thickness of this layer is usually specified as the distance over which the potential drops to some fraction of the potential at the surface (1/e if 1/K is considered the diffuse ion-layer thickness, Kruyt[24]). The compaction results, however, show that the clay compressed with an increase and expanded with a decrease in temperature. This appears to be opposite to that predicted theory, which considers expansion due to an increase in thickness of the diffuse ion-layer.

Gray's[25] results on the consolidation of fine-grained soil, wherein an increase in temperature resulted in a steeper secondary compression curve, seem to indicate that more water is extruded from the contact areas at a higher temperature. If the concept of three types of water, that is, bound water, diffuse ion-layer water, and free water is adhered to, this would seem

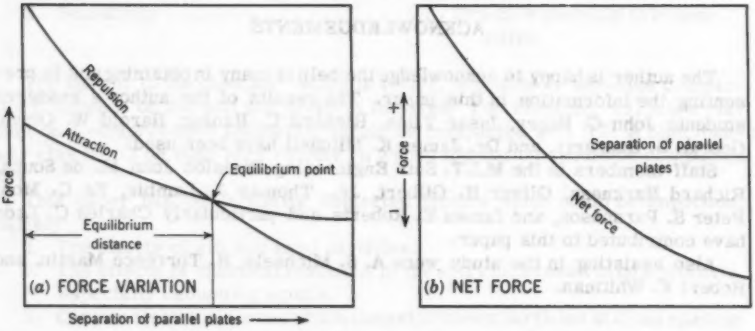


FIG. 18.—FORCE VARIATION AND NET FORCE VERSUS SEPARATION OF PARALLEL PLATES

to be at odds with theory where diffuse ion-layer expands with temperature, resulting in less free water. This assumes that the water extruded is free water. If free water is not available for expansion of the diffuse ion-layer such expansion would cause a resultant expansion in the soil mass. Considering available free water, the greater the expansion of the diffuse ion-layer, the less would be the amount of available free water.

However, as stated, this expansion of the diffuse ion-layer tends to decrease soil strength which may offset the effects of the reduction of available

---

22 Asst. Prof., Dept. of Civ. Engrg., McGill Univ., Montreal, Canada.

23 Asst. Prof., Dept. of Agric. Physics, Macdonald College, McGill Univ., Montreal, Canada.

24 "Colloid Science," I, "Irreversible Systems," by H. R. Kruyt, Elsevier Publishing Co., New York, 1952.

25 "Progress Report on Research on the Consolidation of Fine-Grained Soils," by Hamilton Gray, Proceedings, Int. Conv. on Soil Mechanics and Foundation Engrg., Vol. 2, Harvard Univ., 1936, pp. 138-141.

free water. It is also stated that soil strength, which is decreased by an expansion of the diffuse ion-layer, decreases with a decrease in temperature. From theoretical reasoning, with a contraction of the diffuse ion-layer as a result of temperature decrease, soil strength should increase.

If a net force of attraction or of repulsion between particles were present, and if this net resultant force could be separated into individual forces of attraction and of repulsion, then they could be represented as shown in Fig. 18(a). The schematic diagram appears to indicate that without any external force an equilibrium condition could be reached where the attractive forces would balance the forces of repulsion. This equilibrium condition would then establish an equilibrium distance between parallel particles. Any separation other than this equilibrium distance would result in a net force of attraction or of repulsion as the case may be. It is generally agreed that since only net forces can be measured it may not be correct to indicate a separate curve for the force of repulsion and another for the force of attraction, and that a more accurate presentation would be a graph showing only the net force (see Fig. 18(b)).

J. MacNEIL TURNBULL,[26] A.M. ASCE.—There are several points on which the author's conclusions are at variance with those of the writer.

Effect of Structure on Permeability.—Neither of the two soils, Figs. 1 and 2, are true clays. This is indicated by the low optimum moisture content and the high dry density. Because these soils would not contain any appreciable proportions of the true clay minerals they appear to be ill-chosen for inclusion as proof of any properties of clays. Because a soil contains more than 30% of particles finer than 0.005 mm. does not imply that it will have any of the properties of a clay. The writer pays more attention to the minimum size of particle in the soil, and the proportion of colloids. Because at any time a colloid content of 30% may consist of silica and be quite useless in a reservoir embankment, hand tests are frequently used to check the results of the mechanical analysis.

Components of Volume Change: Confirming Experimental Evidence (3).—Is not the noted effect of temperature change largely due to the change in the viscosity of the water? The latter decreases considerably with a temperature rise of 21° C, and would enable the removal of more water from the specimen under a constant load, with a resulting increase in the consolidation. On decreasing the temperature the viscosity of the water increases, and because the actual amount of consolidation for that particular load has been artificially increased by the induced removal of more water than required for equilibrium at a lower temperature, the soil will slowly expand.

Effect of Molding Water on Compressibility Characteristics of Compacted Clay.—What tempering time was given to the soil after the addition of water and mixing before proceeding to make the compaction test? The testing of clays can be quite misleading unless adequate attention is given to the proper tempering of the soil. The writer's practise for clayey soils after addition of water to air-dry soil and thorough mixing, is to leave it to temper in sealed jars for at least two weeks before proceeding with compaction and Atterberg Limit tests. At times this has to be extended to three weeks. Unless this is

---

[26] Deputy Supt. of Testing, State Rivers and Water Supply Comm., Melbourne, Victoria, Australia.

done the clay will not be in its natural state, and a change of 2.5% in the optimum moisture content can easily result. For one soil the optimum moisture content was changed from 30.7% at 88.2 lb per cu ft dry density after tempering for one week, to 28.2% and 91.7 lb per cu ft after three weeks This was ascribed to the entry of the water into the crystal lattice, providing a more flexible particle with better compaction characteristics, and the removal of water from the surface of the particles where it only hindered compaction. The portion of the curve on the wet leg above 31.5% was common to both tempering periods.

Cohesion and Friction.—The writer is pleased that the author has chosen to avoid the confusion arising from the practice of calling the strength intercept C "cohesion" and the strength angle ϕ "internal friction." However, five comments are applicable here:

(1) The normal stresses of Fig. 9 obviously include capillary normal stress (negative pore water pressures), because the normally consolidated curves pass through the origin. The presence of capillary normal stress, which is a real stress, is easily demonstrated by comparison of the strength envelopes of specimens having the same dry density but different moisture contents. The precompressed curve should be straight lines, any departure therefrom being due to errors in the testing technique, such as, too long an interval between the unloading from the preconsolidation stress and the end of the test, or testing the specimen under too small an applied normal stress. Both procedures permit an expansion of the soil with a consequent reduction in strength. Keeping the rate of strain to not less than 0.30 in per hr, and the applied normal stress to not less than 25% of the precompression stress will reduce this risk. At the same time it is necessary for the effect of these fast rates of strain to be evaluated before the true shearing resistance can be determined. Undisturbed samples, for the same reason, should always be tested under applied normal stresses greater than their preconsolidation stress to determine their true normally consolidated shear strength envelope.

(2) From the appearance of the precompressed curves in Fig. 9 it would appear that the specimens had been tested very close to the origin. This would not be practicable with clays owing to their large capillary forces. Particularly unfortunate are the curves marked "Engineering average," which should intercept the normally consolidated curve at the preconsolidation stress. The latter property has often led to the discovery of an erratic test result at the preconsolidation stress.

(3) The statement that "there is no standard test which can identify the contributing fundamental components of clay shear strength" overlooks the fact that this has been done in this laboratory for many years.[27,28] The determination of the true values of all soil characteristics is considered to be essential for the intelligent selection of design values, and to provide a reliable picture of the soil.

(4) Tests to determine the true cohesion and the true internal friction of a compacted clay have demonstrated that, for the same dry density at different moisture contents, the true cohesion is the same at the same total normal stress (capillary + applied normal stresses) as shown in Fig. 19. The true

---

27 "Handbook of Methods of Testing Soils," by J. MacNeil Turnbull, Govt. Printer, distributed by Tait Book Co., 1945.

28 "Shearing Resistance of Soils," by J. MacNeil Turnbull, Proceedings, 1st Australia-New Zealand Conf. on Soil Mechanics and Foundation Engrg., 1952, pp. 48-81.

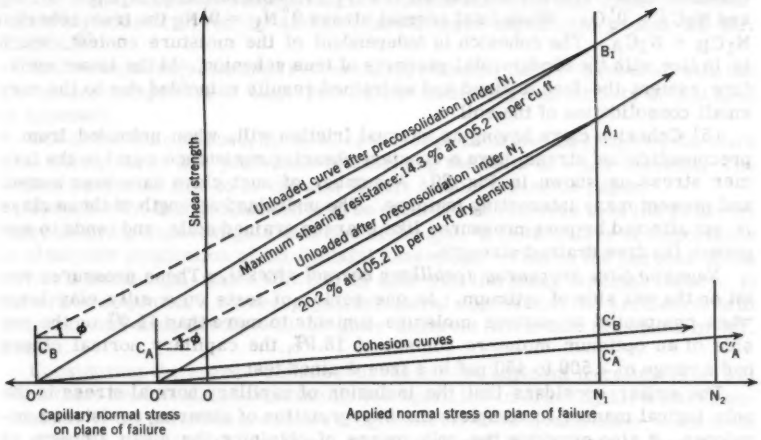


FIG. 19.—DRAINED TESTS OF UNLIMITED DURATION

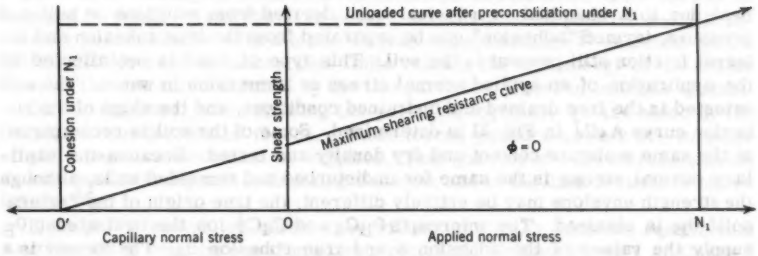


FIG. 20.—DRAINED TESTS ON PURELY COHESIVE SOILS

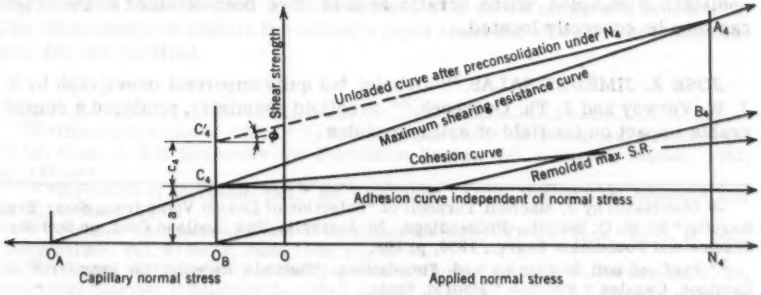


FIG. 21.—DRAINED SHEARING RESISTANCE OF ADHESIVE SOILS

cohesion under applied normal stress N_1 is represented by $N_1C_B' = 0'' C_B$ and $N_1'C_A' = 0' C_A$. When total normal stress $0''N_1 = 0'N_2$ the true cohesion $N_1C_B = N_2C_A$. The cohesion is independent of the moisture content, which is in line with the fundamental property of true cohesion. At the lower moisture content the free drained and undrained results coincided due to the very small consolidation of the soil.

(5) Cohesive clays having no internal friction will, when unloaded from a preconsolidation stress, have a constant shearing resistance equal to the former stress as shown in Fig. 20. A number of such clays have been tested, and present many interesting features. The undrained strength of these clays is not affected by pore pressures like coarser grained soils, and tends to approach the free drained strength.

Negative pore pressures (capillary normal stress).—These pressures exist on the wet side of optimum. In one series of tests on a silty clay loam when compacted at various moisture contents to more than 11.0% on the wet side of an optimum moisture content of 18.9%, the capillary normal stress had a range of 2,500 to 450 psf in a free drained test.

The writer considers that the inclusion of capillary normal stress is the only logical manner to complete the interpretation of shearing resistance envelopes. It also provides the only means of obtaining the mean strength of mixtures of different soils.[29]

In conclusion, a description of the writer's method of determining the value of the shearing resistance of cemented soils may be of interest. The component due to a chemical or physical bond derived from solutions or heat and pressure, termed "adhesion" can be separated from the true cohesion and internal friction still present in the soil. This type of bond is not affected by the application of an applied normal stress or immersion in water. The soil is tested in the free drained and undrained conditions, and the slope of the cohesion curve A_4C_4' in Fig. 21 is determined. Some of the soil is recompacted at the same moisture content and dry density and tested. Because the capillary normal stress is the same for undisturbed and remolded soils, although the strength envelope may be entirely different, the true origin of the "natural soil" 0_B is obtained. The intercepts 0_BC_4 and C_4C_4' on the ordinate at 0_B supply the values of the adhesion a and true cohesion c_4. The former is a constant under all normal stresses, while the latter will vary with the normal stress, the value c_4 applying to the applied normal stress $0N_4$ only. In the absence of adhesion the technique has proved of much assistance when testing undisturbed samples where erratic results have been obtained as the origin can then be correctly located.

JOSÉ A. JIMÉNEZ SALAS.[30]—A brief, but quite important monograph by E. J. W. Verwey and J. Th. Overbeek,[31] on colloid chemistry, produced a considerable impact on the field of soil mechanics.

---

29 Discussion by J. MacNeil Turnbull of "Selection of Design Value from Shear Test Results," by M. G. Speedie, Proceedings, 2d Australia-New Zealand Conf. on Soil Mechanics and Foundation Engrg., 1956, p. 108.

30 Prof. of Soil Mechanics and Foundations, "Escuela Especial de Ingenieros de Caminos, Canales y Puertos," Madrid, Spain.

31 "Theory of the Stability of the Lyophobic Colloids," by E. J. W. Verwey and J. Th. Overbeek, Elsevier Publishing Co., 1948.

The writer is partly responsible for a paper following this impact[32] which was very soon followed by another, much more significant paper, by Mr. Lambe.[33]

Since then, several eminent researchers, including Bolt,[34] have dealt with the mechanical properties of clay, proving the feasibility and fertility of this kind of approach.

Due to the time elapsed, the need arose for publication that gathered the work done during these last years, and establishing the basis of a new doctrine. The writer interprets this to be the aim of Mr. Lambe's current paper.

Undoubtedly, this publication is to be studied and referred to in the future by those desiring to investigate this line of thought. It is therefore of importance to clear this publication of all doubtful assertions. This is the purpose of the writer's comments, which will mainly deal with the shear strength theory. In the writer's opinion, a correct physicochemical approach of the problem is still missing, and undoubtedly will be quite different from that presented by Mr. Lambe.

Considering the energy-distance curves for two adjacent micelles (Fig. 10) when these two micelles are infinitely far apart, the interacting forces are nonexistent. If the particles are drawn progressively toward each other, work must be supplied (positive or negative), which is stored in the form of free or potential energy.

Considering first the case of dispersed particles, when the particles draw near, it is necessary to overcome the electrical repulsion R. The work to be supplied is positive, and the free energy accumulated is positive too. It increases in accordance with a more or less exponential law[35] and ends with a finite value for zero distance. This finite value is the free energy of the double layer of the system constituted by the two particles, joined in intimate contact.

On the contrary, when drawing the particles together, we are aided by the attractive van der Waals' forces. These forces produce a work or, in other words, a negative work must be supplied. This quantity of work increases more or less quadratically with decreasing distance, and in the limit it tends to minus infinity.[36]

If the particles are left alone, they will automatically adopt an equilibrium position, which must be one of minimum potential. Neither Curve 1 or Curve 2 in Fig. 10 show a potential minimum, so that there cannot be any equilibrium position. In the system represented by Curve 1, the particles will spontaneously draw near, releasing the greatest possible part of their free energy, until they reach a close contact, and the system will not be dispersed any longer. The considerations made in the author's paper about the effects of precompression are not justified.

---

[32] "Compressibility of Clays," by J. A. J. Salas and J. M. Serratosa, Proceedings, 3d Int. Conf. on Soil Mechanics and Foundation Engrg., Vol. I, Zurich, August, 1953, pp. 192–198.

[33] "Structure of Inorganic Soil," by T. William Lambe, Proceedings-Separate 315, ASCE, October, 1953.

[34] "Physico-Chemical Analysis of the Compressibility of Pure Clays," by G. H. Bolt, Geotechnique, Vol. 6, No. 2, June, 1956, pp. 86–93.

[35] "Theory of the Stability of the Lyophobic Colloids," by E. J. W. Verwey and J. Th. Overbeek, Elsevier Publishing Co., 1948, p. 95.

[36] "Theory of the Stability of the Lyophobic Colloids," by E. J. W. Verwey and J. Th. Overbeek, Elsevier Publishing Co., 1948, p. 101.

In the case of Curve 2, it can be assumed that particles are separated by a distance smaller than x. The particles will likewise tend to reach close contact. But in the event that the distance is greater than x, the particles will tend to separate more and more. This is the case of a colloidal suspension. Point x represents an "energy barrier" that the particles cannot tresspass without the the aid of an external force.

A particular case is that corresponding to distance x. The derivative of potential with respect to distance is zero, that is, the attractive and repulsive forces are equal. This is an equilibrium position, but one of perfect instability. A movement in any sense will release energy. This is an impossible position, because it corresponds to a maximum of potential. On the contrary, if there were a minimum of potential, it would be necessary to supply work to displace the particle from its equilibrium position, and this would be stable.

However, there are two factors that affect the phenomenon, and that are not directly reflected on Fig. 10. First: The laws of attraction and repulsion change for very small distances between particles; steric interaction I, as it has been called by Mr. Lambe, makes its appearance. Second: In many cases, there is a potential minimum, a shallow one, at the right zone of curves of type 2. This shallow minimum corresponds to a thixotropic gel, and represents the distance at which the particles arrange themselves in a soil deposited in a slow and quiet manner.

Therefore, in accordance with the laws of attraction and repulsion, the soil adopts an equilibrium state by itself, which sometimes is a single one (perfect coagulation in curves of type 1), and other times is double (perfect coagulation or thixotropic coagulation, at either side of the energy barrier, in curves of type 2). Soils cannot be displaced from this equilibrium position, except for the action of an external force.

This action can be moisture deficiency (insufficient liquid contents for development of a complete double layer). But we will now deal with the case when the external force is a mechanical one.

This force, if a compression, plays the role of an attractive force, and its potential is negative for decreasing distances. If it is established that the force is independent of the distance (a very common case), the curve representative of its potential is a straight line.

Now, adding this new potential to the two potentials previously mentioned a new curve for the total potential is obtained. This potential curve has a new minimum, that corresponds to a smaller distance between particles, as it could be reasonably expected. The construction of the new curve, as well as the determination of the new minimum, are shown on Fig. 22. It can be seen that, for a certain value, the minimum becomes an inflexion point, with horizontal tangent (P_4). This corresponds to the crossing of a new "energy barrier." It could also be seen that the distance corresponding to this energy barrier varies with the form of the external force potential curve, which can be other than a straight line.

Fig. 22 also shows an "external pressure-distance" curve, similar to a consolidated curve, computed from the potential-distance curve.

Now we consider the shear strength problem, and examine position of shear strength in Fig. 22.

It can be assumed that shear strength is proportional to the force required to produce a certain deformation, but this would be rigidity, not strength. Certain considerations, that the writer will explain in detail subsequently, lead him to relate shear strength with the quantity of energy (ΔP in Fig. 22) required to

bring the soil from its equilibrium position to the shallow minimum, representative of thixotropical coagulation. This energy increases with decreasing distance, that is, with increasing external force. The curve "external pressure-ΔP" is also shown on Fig. 22.

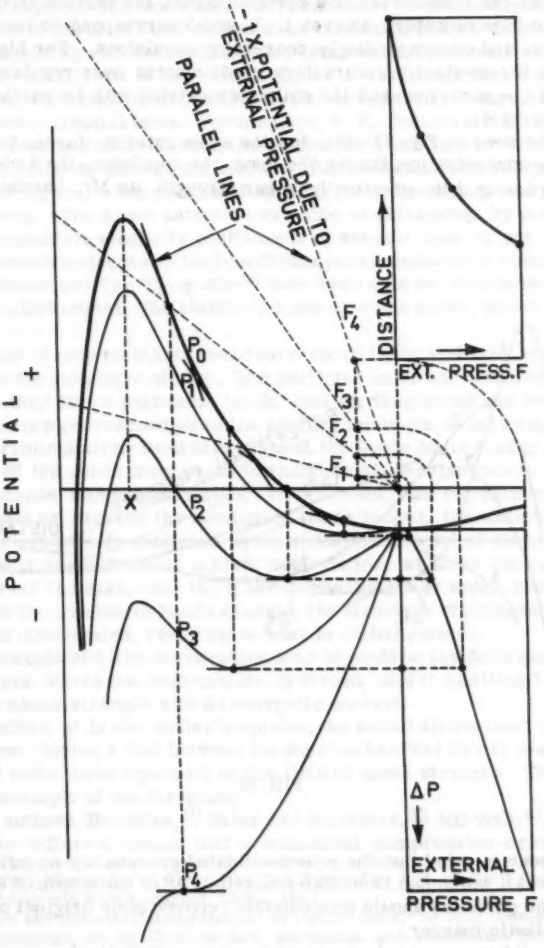


FIG. 22

In this light, the assertion posed in Mr. Lambe's paper under the heading, "Factors Influencing Shear Strength," that "the greater the attractive force, the greater the shear strength, the greater the repulsive forces, the lower the shear strength," is not very clear. As a matter of fact, the greater the external

force, the greater the repulsive forces, since an equilibrium must be reached but the shear strength will be greater too, and not lower.

Probably, Mr. Lambe's assertion must be interpreted in another sense: If the electrical forces are altered so that the repulsive force diminishes, the shear strength increases for a given external pressure. Fig. 23 represents the potential-distance curves of a certain colloid, for various electrolyte concentrations in pore water. Curves 1, 2, and 3 correspond to increasing concentrations, and correspondingly decreasing repulsions. For higher concentrations of the electrolyte, attraction predominates over repulsion for every position of the particles, and the colloid coagulates with its particles in close contact (curve 4).

It can be seen in Fig. 23 that, for the same external force, the higher the electrolyte concentration, that is, the lower the repulsion—the higher ΔP,—and let us suppose that the greater the shear strength, as Mr. Lambe advanced in his paper.

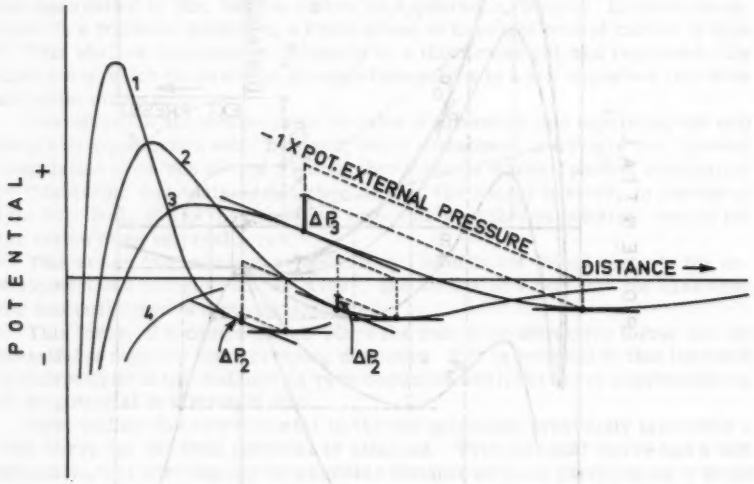


FIG. 23

Let us bear in mind that the preconsolidated process has no influence whatsoever upon all which has been stated hereto. After the action of a force disappears, the particles should immediately recover their original position in a perfectly elastic manner.

Preconsolidation can only be considered in a statistical manner. To each external pressure, there will correspond a determined number of particles which, due to their special positions, will pass the energy barrier in an irreversible manner. The higher the external pressure, the higher their number will be. The irreversible orientation changes can give a statistical account of preconsolidation phenomena.

Now, considering the process of shear itself, the general lines stated by Tan Tjong Kie[37] will be followed, although Kie gives much less importance than the writer to the physicochemical part of this phenomenon.

Clay, for the consistencies for which application of these theories can be imagined, does not break as a brittle solid, but flows like a viscoelastic material. Some recent experiments are sufficiently conclusive to demonstrate that there exists an elastic limit, or first deformation threshold, before which the deformation is completely recoverable, and clay behaves as a perfectly elastic solid. The elasticity coefficient is very much higher at this stage than the elasticity coefficients or deformation moduli ordinarily encountered in consolidation tests and unconfined or triaxial tests. For instance, N. H. Denisov and B. F. Reltov[38] mention the case that clay masses, the deformation modulus or which does not exceed some 1,000 kg per sq cm, show elasticity coefficients of up to 20,000-30,000 kg per sq cm, when computed starting from the propagation velocity of seismic waves. The same authors were able to determine, by means of vibratory plastometer, elasticity coefficients of several time kg per sq cm, in clay pastes which under static load conditions purely behaved as viscous liquids. Likewise, Geuze and Tan Tjong-Kie[39] have been able to determine, by means of a special plastometer, the elasticity limit of some clays, under static load conditions.

This range of true elasticity could correspond to the stresses which are not able to alter the structure of clay. The particles move one with respect to the others, but they do not lose their bonds, that is, they do not get farther apart than the distance corresponding to the shallow minimum of potential.

But, after the elasticity limit is surpassed, the bonds begin sliding and breaking. Some of the bonds form again instantaneously in other points, due to the attractive forces between particles. In the event that the number of bonds created equals or exceeds the number of bonds broken, the material remains unaltered or practically unaltered, from a statistical point of view, in spite of the fact that it has undergone a great deformation, which is not recoverable.

If this is not the case, that is, if the number of bonds which break is much greater than the number of bonds created, the structure disintegrates, the deformation is accelerated, resulting in what is called rupture.

It is thus explained why the breaking load depends on the deformation speed, in those cases where the deformation is forced, and it justifies the writer's correlating shear strength with an energetic concept.

Nevertheless, it is the writer's opinion, as stated above, that we still are very far from finding a link between the physicochemical theory and the actual behavior of soils, most specially on the field of shear strength. The following case is an example of the foregoing.

Several authors, Hvorslev,[40] Salas and Serratosa,[32] Mitchell,[41] have demonstrated by different means that a monoaxial compression orientates clay

37 "Structure Mechanics of Clays," by Tan Tjong-Kie, Inst. of Civil Engrg. and Architecture, Academia Sinica, Harbin, China, 1957.

38 "Elastic and Structural Reformations of Clayey Soils," by N. H. Denisov and B. F. Reltov, Proceedings, 4th Int. Conf. on Soil Mechanics and Foundation Engrg., Vol. I, London, 1957, pp. 17-21.

39 "The Mechanical Behavior of Clays," by E. C. W. A. Geuze and Tan Tjong-Kie, 2d Int. Cong. on Rheology, London, 1953, pp. 247-259.

40 "The Shearing Resistance of Remolded Cohesive Soils," by J. Hvorslev, Proceedings, Soils and Foundation Conf., U. S. Engr. Dept., Boston, Mass., June, 1938.

41 "The Importance of Structure to the Engineering Behavior of Clays," by J. K. Mitchell, thesis presented to Massachusetts Inst. of Technology, at Cambridge, in 1956, in partial fulfillment of the requirements for the degree of Doctor of Science.

particles in a direction at right angles to the force direction. By imagining clay thus oriented, it is not too easy to see what shear strength the clay will show in the direction of the orientation, but, admitting its existence, it seems that it has to be lower than that perpendicular to the orientation, since in this direction it will be necessary to entirely disorganize the structure. Thus it can easily be demonstrated that the inclination of the shear planes must be entirely different (greater than 45° with respect to the direction of the force applied) from those observed in practice, which proves how far theory is still from reality.

However, a case can be pointed out where theory can aid to interpret a fact observed. Parallel orientation results in anisotropy as far as cohesion is concerned, this cohesion being smaller in the orientated direction.

At the initial moment of failure, the shear planes have a certain inclination as a result of the joint action of cohesion and friction (which with difficulty can be accounted for in physicochemical theory, in the case of parallel orientation). But, after failure is started, the particles orient themselves in the direction of flow, resulting in an orientation more complete even than that due to monoaxial compression. This results in a new pattern of anisotropy which determines the rotation of the shear plane, tending towards 45°, according as the shear test progresses. The fact that the shear plane rotates in said direction has been observed by others.[42]

The anisotropy due to the orientation of the particles should also become apparent under other circumstances. Thus, it can be stated that the inclination angle of the failure plane in soils compacted on the wet side should be other than in soils compacted on the dry side, which might be useful as a suggestion for further research.

Finally, the writer would like to know whether the test conducted heating and cooling a sample of Boston blue clay, was carried out on a perfectly saturated sample. Salas and Serratosa[43] conducted a similar test on nonsaturated clay samples, obtaining similar results, but they explained these results by the variation of capillary potential with temperature.

Through all these remarks, the writer does not at all intend to minimize the importance of Mr. Lambe's work, but he wishes to banish the feeling that the physicochemical theory has already solved the fundamental problems of soil behavior. At the present time, we should rather limit ourselves to point out that this is a brilliant way, and encourage researchers to follow it, in the hope that some day it will be possible to reach positive results in the solution of said problems.

On the other hand, this way is only useful to study "clay paste." However, a large part of soil behavior is due to the "Macromechanics" of clay aggregates and of clay-coarse particle aggregates[44] for the study of which theoretical ideas in the field of pure mechanics are required. This is the reason why some researchers[32, 33] have worked with extremely pure clay, in order to avoid the interference of these aggregation phenomena. These researchers did not pre-

---

42 "Experimental Determination of the True Cohesion and True Angle of Internal Friction in Clays," by R. E. Gibson, Proceedings, 3d Int. Conf. on Soil Mechanics and Foundations Engrg., Vol. I, Zurich, August, 1953, pp. 126–130.

43 "Foundations on Swelling Clays," by J. A. J. Salas and J. M. Serratosa, Proceedings, 4th Int. Conf. on Soil Mechanics and Foundation Engrg., Vol. I, London, 1957, pp. 424–428.

44 "Correspondence to the Secretary of the Inst. of Civ. Engrg.," by Karl Terzaghi, Geotechnique, Vol. 6, No. 4, December, 1956, pp. 191–192.

tend that the results of their tests be representative, in a general manner, of the behavior of the natural soils that the engineer must face, although these tests afforded basic facts for the interpretation of such behavior.

D. HUGH TROLLOPE,[45] A.M. ASCE.—In focusing attention on the reorientation of colloid particles associated with shear strain, the author has contributed to one of the most valuable fundamental concepts of particle behavior. Indeed there is limited visual evidence that some degree of reorientation is associated with shear deformation of all platey particles and that in the case of clay colloids the electrical interactions merely modify the resulting particle dispositions.

Consideration of the equilibrium conditions of the disperse system leads to some interesting conclusions. If, as is assumed in the theory under discussion, a net attractive force can exist between platelets in a disperse array, then this arrangement can have only one stable condition; that when all parallel particles are in full contact. The individual particles must come together and coalesce, and it follows that external forces can have no effect on the resulting structure. The author has introduced the additional term Contact Interaction I in Fig. 7, which presumably would provide the resistance to this complete merger of disperse particles, but it is not related to any physical quantity. In the writer's opinion the need to introduce some term such as Contact Interaction indicates that existing theory does not fully explain the interparticle behavior in dense suspensions of clay colloids. The net force between colloids is dependent on factors other than the electrostatic repulsions of the diffuse double layers and the attractions attributed to the long range Van der Waals forces. It appears that the laws governing contact interaction are likely to be of real importance in arriving at a fuller understanding of the true effective stress with respect to shear strength phenomena.

Following a study of the behavior of saturated clay soils under isotropic three-dimensional consolidation, the writer's colleague R. H. G. Parry[46] has recently suggested that the net interparticle electrical forces are not necessarily a unique function of interparticle spacing. An illustration of this is given in the case of the characteristic consolidation (p/e)-curve where differing values of the consolidating pressure are required to maintain a selected value of the void ratio depending on the degree of overconsolidation. Whereas even under isotropic stress conditions this can be visualised as being associated with progressive reorientation of unsymmetrically arranged particles, this in itself does not appear to be sufficient to account for the experimental observations. Is it possible that contact interaction is only called into play when particles tend to approach each other more closely? A conceivable hypothesis to account for this would be that the water molecules and associated ions in the diffuse double layers, like the colloid particles themselves, are subject to reorientation under the consolidating influence of external forces and that this process is, at least partly, irreversible.

It is perhaps inappropriate at the present time to ask the author to elaborate on contact interaction, but it does appear to be of considerable importance and his views on this would be most welcome.

---

[45] Reader in Civ. Engrg., Univ. of Melbourne, Melbourne, Australia.

[46] "The Role of Latent Interparticle Forces in the Behaviour of Clay," by R. H. G. Parry, Interparticle Forces in Clay-Water-Electrolyte Systems: A Symposium, Commonwealth Scientific and Industrial Research Organization, Melbourne, 1960.

T. WILLIAM LAMBE,[47] F. ASCE.—Mr. Scheer wonders about the differences in horizontal and vertical permeability as a function of structure. As one would suppose, the flocculated structure shows permeability in all directions approximately equal. Upon particle orientation, the permeability of a soil becomes nonisotropic with the permeability being less for flow perpendicular to the long axis of the plates than for flow parallel. In other words, one dimensional compression in the vertical direction will line the particles horizontally; the ratio of horizontal to vertical permeability will increase.

The writer had hoped to use this concept to measure particle orientation in a soil mass by the ratio of vertical to horizontal permeability. While the concept is apparently sound, the differences in permeability with direction are usually relatively small (typical ratio values of 2 or 3). This fact along with others indicates that a high degree of particle alinement can occur in zones, with different alinements between zones, that is, random oriented packets of parallel particles.

Mr. Yong and Mr. Warkentin feel a decrease in temperature theoretically causes a compression of the double layer and thus a decrease in interparticle repulsion. The formulas and plots presented by Overbeek[48] agree with the writer's statement that a decrease in temperature causes an increase in repulsion. These formulas were derived for colloids having surface charges considerably lower than exist on typical clay particles. Formulas derived by G. H. Bolt[49] indeed show the trend stated by Yong and Warkentin. Bolt's formulas, as do Overbeek's, neglect soil-water interaction, non-Coulombic electrical repulsion, etc., as pointed out by P. F. Low.[50]

The experimental facts, however, support the writer's original statement. Two of these facts are:

1. Heating a clay-water sol tends to cause flocculation.
2. Cooling a saturated clay (with access to water) causes an expansion.

Both of these facts indicate cooling causes a net increase in electrical repulsion.

Based on the apparent fact that cooling increases repulsion, the writer was led to predict a reduction in shear strength. As noted in Fig. 7 there exists an equilibrium of forces between adjacent particles. Increasing R at constant volume results in an increase in $\bar{\sigma}$; increasing R at constant $\bar{\sigma}$ results in a sample expansion with a resulting decrease in R. Test results bear out each of these statements. The effect of a temperature change on shear strength is not easily inferred in either case. Tests to measure the effects of temperature changes on strength are now in progress.

Mr. Turnbull of Australia has raised objections that need examination. He states that the two soils for which permeability data are presented in Figs. 1 and 2 are not "true clays" and ". . . would not contain any appreciable proportions of true clay minerals . . .". Both soils behave as clays and both

---

[47] Prof. and Head, Dept. of Soil Engrg., Massachusetts Inst. of Technology, Cambridge, Mass.

[48] "Colloid Science, I, Irreversible Systems," by H. R. Kruyt, Elsevier Publishing Co., New York, 1952, p. 195.

[49] "Analysis of the Validity of the Gouy-Chapman Theory of the Electric Double Layer," by G. H. Bolt, Jour. Colloid Science, 1955.

[50] "Movement and Equilibrium of Water in Soil Systems as Affected by Soil-Water Forces," by P. F. Low, Highway Research Board Meeting, January, 1958.

contain "true" clay minerals; both, however, contain silt and sand-size particles. The Jamaica soil termed by the writer as "sandy clay" contains about 10% kaolinite; the Siburua clay contains about 50% of "true" clay minerals—illite, montmorillonite, and kaolinite in equal portions. The permeability of a soil is determined largely by the finer particles rather than the coarser ones. A prepared mixture of 10% montmorillonite clay and 90% sand will have a permeability much closer to that of 100% montmorillonite than to that of 100% sand.

Mr. Turnbull has used the optimum water content as an indication of the behavior of a clay. The unsoundness of this procedure is clearly shown by the test data[51] in Table 2.

These data should suggest caution to Mr. Turnbull in the broad use of optimum water content values.

The compaction tests employed the procedure described elsewhere[52] and tempering was use.

Mr. Turnbull and the writer are apparently far apart on their concepts of shear strength. Much of the difference may reside in lack of conformity on the meaning of terms. A complete answer to all of Mr. Turnbull's objections

TABLE 2.—OPTIMUM WATER CONTENT

Clay	Plastic Limit, %	Plasticity Index, %	Optimum Water, % (Proctor Compaction)
Na Montmorillonite	54	650	22
Fe Montmorillonite	75	220	29
Na Illite	53	63	25
Fe Illite	49	59	27
Na Kaolinite	32	21	17
Fe Kaolinite	37	22	21
Attapulgite	150	130	66

to the paper would have to be preceded by an agreement of definitions. In Fig. 9 the stress plotted on the horizontal axis is "intergranular" or "effective" stress, which is equal to the combined pressure minus the pore pressure. This definition of stresses is widely accepted. Any capillary pressures would have been properly accounted for.

Mr. Turnbull is correct in stating that clay compacted wet of optimum can have negative pore water pressures. The writer stated that the pore water tensions dry of optimum would be greater than those for compaction wet of optimum. That this can be true is shown by the following experimental data:

2% dry of optimum; pore pressure = 0.4 kg per cm^{sq}
Optimum; pore pressure = -0.3 kg per cm^{sq}
2% wet of optimum; pore pressure = -0.1 kg per cm^{sq}
and atmosphere pressure is taken as zero.

51 "Final Report Soil Solidification Research," Cornell Univ. Ithaca, N. Y., September, 1951.

52 "Soil Testing for Engineers," by T. William Lambe, John Wiley and Sons, 1951.

In view of Mr. Salas' pioneering work on soil structure, his discussion merits study. The writer readily agrees that physiochemical theory has not completely solved the fundamental problems of soil behavior. In fact the companion paper started with, "as will be noted, several facets of structure are not fully understood. It is not the intent, therefore, to present this material as the final work, but rather as a stimulant, and, hopefully, a guide to further studies on this complex subject."

Mr. Salas apparently differs from the writer's view that sufficient pressure and time can transform a clay into a system that will not disperse. The writer considers a true compaction shale an example of just this phenomenon.

The colloidal theory was presented as a general guide. It has been stated that there are "***several important factors neglected in colloidal theories***." Also stated was "***attempts to use numerical equations based on colloidal theory in soil engineering problems have met with failure***." The writer, as does Mr. Trollope, doubts that theories developed for particles far apart can be numerically used for the close spaced particles occurring in the typical natural soil.

Mr. Salas has presented an interesting approach to soil structure which is based entirely on energies rather than on energies and forces. The writer would feel that the force approach, as used in the paper, is superior, especially for natural clays, since it better allows one to consider forces (such as to edge-to-face linkage) which are ignored in the colloidal theories.

The writer agrees with Mr. Salas that the inclusion of a statistical concept with the principles of structure is helpful.

The writer strongly endorses Mr. Trollope's view on the importance of contact interaction.

In conclusion the writer expresses appreciation to those who prepared discussions to his paper. They have emphasized both the importance and the incomplete state of knowledge on the subject.

AMERICAN SOCIETY OF CIVIL ENGINEERS

Founded November 5, 1852

TRANSACTIONS

Paper No. 3042

NUMERICAL SOLUTIONS FOR BEAMS ON ELASTIC FOUNDATIONS

By Henry Malter,[1] F. ASCE

With Discussion by Messrs. Norman J. Ryker, Jr.; Alexander Dodge; Lymon C. Reese; Victor R. Bergman; and Henry Malter

SYNOPSIS

Two numerical methods for the solution of beams on elastic foundations are considered. The first, based on the Newmark method, is a step-by-step integration process. The second method, using finite difference equations, obtains a solution by means of a set of simultaneous equations. Examples are solved, and comparisons are made between the results obtained using various approximate methods as well as rigorous methods.

INTRODUCTION

Beams on elastic foundations confront the analyst with three phases to each problem. The first phase, the most important one, is concerned with the basic assumptions of the behavior of the structure—the type of foundation. The second phase is that of the selection of the constants needed—modulus of elasticity, moment of inertia, foundation modulus. The last phase of the problem consists of the mathematical manipulation of the information obtained from the first and second phases. This paper is concerned with only the mathematical manipulation. The mathematical methods may be either rigorous or approximate. The approximate methods may be either graphical or numerical. A numerical method was employed by Zusse Levinton, F. ASCE,[2] whereas E. P. Popov, F.

Note.—Published, essentially as printed here, in March, 1958, in the Journal of the Structural Division, as Proceedings Paper 1562. Positions and titles given are those in effect when the paper or discussion was approved for publication in Transactions.

[1] Prof. of Civil Engrg., Univ. of Illinois, Urbana, Ill.

[2] "Elastic Foundations Analyzed by the Method of Redundant Reactions," by Zusse Levinton, Transactions, ASCE, Vol. 114, 1949, pp. 40–52.

ASCE,[3] used a graphical method to obtain approximate solutions. Two numerical methods are employed herein and the results are compared with results obtained by other methods, both approximate and rigorous.

Two assumptions may be made regarding the type of foundation encountered. The more general assumption is that of an elastic-solid involving complete continuity. This type of problem, however, does not lend itself easily to mathematical solution, and is not considered herein.

A type of elastic foundation that does lend itself easily to approximate solution is known as a Winkler foundation. This type is characterized by the fact that at every point the pressure in the foundation is proportional to the deflection occurring at that point, and is unaffected by deflections at adjacent points. This idealized foundation may be thought of as consisting of a series of independent springs. This subject has been examined by Miklos Hetenyi,[4] F. ASCE. Popov has a summary[3] of the problem, and in addition has a lengthy bibliography of Russian and the German works on the subject.

A rigorous method should be sought at all times. Hetenyi has collected information in order to simplify the solution for various conditions of foundation and of loading by rigorous methods. However, despite the simplifications, and despite the use of derived formulas, as well as the use of prepared tables, it is soon evident that a great deal of time and labor is required for all but the simplest type of problem.

An assumption that a Winkler type foundation is applicable leads to the first approximation. A second set of approximations exists as to the values of the various constants employed. After having accepted and recognized these approximations, the designer is confronted with the choice of whether to employ a rigorous or approximate mathematical manipulation. Recognizing the nature of the overall problem, it is often preferable to use an approximate method to quickly obtain a solution. A solution obtained by an approximate method may in actuality be no further from a true and exact solution than one derived by a rigorous method.

Two numerical methods are described, both of which are based on the relationship between moment area and angle change. In the first, using the Newmark method,[5] a step by step method of numerical integration is used. In the second, using the finite difference method, a series of simultaneous equations is solved. Both methods are rapid and general, although the finite difference method seems to be less time consuming.

One should not be tempted by ease of mathematical manipulation to apply the fore-mentioned methods without careful consideration of the limits put on these methods by any problem encountered. Where the supporting media is water, or elastic beams, or even piles driven to a solid supporting material, direct application may be found of a Winkler type of foundation. Where soil is

---

[3] "Successive Approximations for Beams on an Elastic Foundation," by E. P. Popov, Transactions, ASCE, Vol. 116, 1951, pp. 1083-1095.

[4] "Beams on Elastic Foundations," by Miklos Hetenyi, The University of Michigan Press, Ann Arbor, Mich., 1946.

[5] "Numerical Procedure for Computing Deflections, Moments, and Buckling Loads," by N. M. Newmark, Transactions, ASCE, Vol. 108, pp. 1161-1234.

the supporting media, there is no substitute for a good knowledge of soil mechanics, and any method of solution must be employed with careful reference to soil mechanics.

NEWMARK METHOD

A general knowledge of the Newmark method is assumed, and the details will be only briefly reviewed. Foundation problems may consist of concentrated loads, single point spring reactions, distributed loadings, and distributed foundation reactions. In a step-by-step procedure the distributed loadings and distributed foundation reactions are converted into concentrations at the subdivisions selected. The use of concentrations introduces an error inherent in the system. Increasing the number of divisions reduces this error, but increases the amount of work. In the problems to be considered the subdivisions will be made equal to each other. This is not necessary, but further simplifies the arithmetic of the process through the use of the common multiplier involving the length of the subdivision, h.

A suggested method for changing distributed loads to concentrations is indicated in Fig. 1, in which $R_A = \frac{h}{24}(7A + 6B - C)$; $R_B = \frac{h}{12}(A + 10B + C)$; and $R_C = \frac{h}{24}(7C + 6B - A)$. These formulas, which were utilized by Newmark, assume that the loading curves are parabolic and continuous, and are applicable for the examples used in this paper. For other types of problems straight line formulas may be used, or account taken of discontinuities.

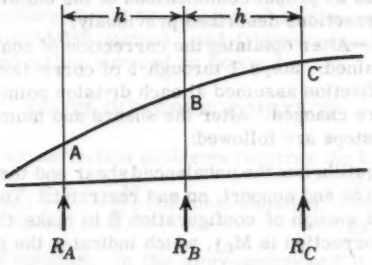


FIG. 1.—DISTRIBUTED LOADS CONVERTED TO CONCENTRATED

The numerical procedure to be outlined is a method of arithmetical integration based on the relationships $dV = P\,dx$, $dM = V\,dx$, $\alpha = \frac{M}{EI}$, $d\phi = \alpha\,dx$, and $dy = \phi\,dx$, in which P is the concentrated load, q is the distributed load, V is the shearing force, M is the moment of force, α is the angle change due to the load, ϕ is the slope of the beam due to the angle change, y is the deflection of the beam, E is the modulus of elasticity, and I is the moment of inertia. The positive values of these terms, as used herein, will be upward for P, upward force on left of section for V, compression in upper fiber for M, angle change α which causes an increase in slope, slope ϕ that is downward to the right, deflection y that is downward, and coordinates that add to the right. Values for distributed loading will be designated by the terms q and α whereas the concentrated loadings will be shown as q and α.

Correction Configurations.—Before beginning an analysis with given loadings, a set of correction configurations must be established. These will be required subsequently in the general solution. The correction configurations will

be derived from two sets of corrections introduced into the problem. The first correction involves a uniform deflection, and the second a uniform rotation. These configurations are obtained as follows:

1. Assume a uniform deflection at each panel point of the beam.
2. Using the assumed deflections determine the resisting pressures, q, at each panel point.
3. Change distributed reactions to concentrations.
4. Assuming zero reaction at the left support, determine the shear along the beam by adding successively the various concentrations. There will usually be an unbalanced shear at the extreme right.
5. Assuming zero moment at the left support, determine the moments along the beam by adding the various shears successively. There will usually be an unbalanced moment at the extreme right of the beam.

A uniform rotation of the beam is now assumed. Any point may be considered a center of rotation, but for convenience assume the center of the beam as the center of rotation. The uniform rotation will result in a set of deflections that are used, repeating the forementioned process, again obtaining an unbalanced shear and unbalanced moment at the right end of the beam.

Two correction configurations will be required for the general problem. The first, configuration A, should have zero unbalanced end shear, but will have some unbalanced moment. The second, configuration B, should have zero unbalanced end moment, but will have some unbalanced shear. Both configurations may be obtained by proper combinations of the uniform deflection and the uniform rotation corrections described previously.

General Solution.—After obtaining the correction of configurations, the general solution is obtained. Steps 1 through 5 of correction configurations are followed. With a deflection assumed at each division point, the distributed resisting pressures are changed. After the shears and moments along the beam are obtained, these steps are followed:

6. For static equilibrium the unbalanced shear and the unbalanced moment should both be zero (no end support, no end restraint.) To account for the unbalanced shear, add enough of configuration B to make the unbalanced shear zero. This line of correction is M_{c1}, which indicates the first correction moment.
7. To satisfy the condition of no end restraint, add enough of configuration A to make the end moment zero. This line of correction is M_{c2}, which indicates the second correction moment.
8. $M + M_{c1} + M_{c2} = M_a$. The values of M_a thus obtained correspond to a definite deflection of the beam that produces static equilibrium. The moment values, M_a, are the panel point values of a distributed moment along the beam.
9. The distributed moment along the beam results in a concentrated angle change at each panel point α.
10. Assuming a slope at the left end, proceed to find the slope, ϕ, at all other points.
11. Assuming a deflection at the left end, proceed to find the deflections along the beam by adding successively the slopes encountered.
12. Change y to y' by multiplying all values of y by a common multiplier to convert the values of the deflections to inches or to some other convenient unit.
13. Using the values of y' obtained, proceed as in steps 1 to 11 to obtain a value for M_0.

This completes one cycle of computations. The cycle consisted of assuming a set of deflections, computing shears and moments, and correcting the moments, and therefore the assumed deflections, to bring the beam into static consistency. The statically consistent moment M_a is then applied to the beam, and the deflection of the beam determined, again bringing it into static consistency. The resulting deflections correspond to a set of moments. If these final moments, M_o, are not identical with those of the originally corrected moments M_a, and they will rarely be even in close agreement after one cycle, a second cycle of computations must be started. It is often found that M_o is a better assumption than M_a was, and should now be used as a new starting point in the second cycle. The agreement after each cycle should be much closer than the preceeding until after several cycles, sufficient agreement is found between M_a and M_o to warrant an acceptance of the results. When sufficient accuracy has been obtained, the q line of the last cycle should be corrected using the same percentages used in the correction of the final moments, and thus a q corrected line established.

The rapidity of convergence is a function of the relationship of the relative stiffness of the beam (E I) and that of the foundation modulus (spring value). Where the beam is much stiffer than the foundation, convergence is rapid, in which case "M_o" is always a better approximation than M_a. When the relationship is reversed, divergence will occur, and the problem cannot be solved by ordinary means. For the intermediate case of the spring constant being equal to or close to the critical spring constant, convergence is slow, and the average of M_a and M_o should be used as the new value of assumed moment.

The outlined procedure should be recognized as a numerical systematization of the Vianello-Stodola[6] method, and follows essentially by numerical methods the graphical outline pursued by Popov.[3]

FINITE DIFFERENCE METHOD

The solution of beam deflection problems requires the following set of equations; $\frac{dy}{dx} = \phi$ the slope; $\frac{d^2y}{dx^2} = \frac{M}{E\,I}$, moment equation; $\frac{d^3y}{dx^3} = \frac{V}{E\,I}$, shear equation; $\frac{d^4y}{dx^4} = \frac{w}{E\,I}$, load equation. In the afore-mentioned it should be remembered that both E and I must be constant quantities for general use. With the moment of inertia, I, variable, as it often is, the moment term is applicable, but the shear and load equations become more complicated.

As in many problems involving differential equations, it has been found that difference operators may be substituted for the differential operators. Using the "molecule notation for central difference operators"[7] one obtains the following:

$$\frac{\Delta}{\Delta x} = \frac{1}{2\,h}\,(-1,\ 0,\ +1) \qquad \frac{\Delta^3}{\Delta x^3} = \frac{1}{2h^3}\,(-1,2,0,-2,1)$$

$$\frac{\Delta^2}{\Delta x^2} = \frac{1}{h^2}\,(1,\ -2,\ 1) \qquad \frac{\Delta^4}{\Delta x^4} = \frac{1}{h^4}\,(1,-4,\ 6,\ -4,\ 1)$$

6 "Buckling Strength of Metal Structures," by F. Bleich, McGraw Hill Book Co., Inc., New York, 1952, p. 81.

7 "Numerical Methods in Engineering," by M. G. Salvadori and M. L. Baron, Prentice-Hall Inc., 1952, p. 69.

These difference operators may be used in various ways for the solution of elastic foundation problems.

A beam supported along its entire length by an elastic medium and subjected to vertical forces, will be deflected in some manner, and will result in a foundation pressure that will vary along the length of the beam. This foundation pressure, that is most likely a smooth continuous function, may be represented in various ways. First, one may assume a stepped variation resulting in the subgrade reactions in Fig. 2(a) in which k is the foundation modulus, h is the length of the subdivision, and the letters A, B, C, and so forth are the deflections of the beam at the various subdivisions. Using a straight line variation would result in the more accurate form of concentrations shown in Fig. 2(b), but would require more labor. The parabolic formula suggested by Newmark for his numerical integration process could be used to give concentrations of the form $\frac{kh}{12}(A + 10B + C)$. The simplest method to use is the stepped method, and it is the one that will be used in the solution of the examples to follow.

The most convenient formula to use in the solution of elastic beam problems is the moment equation. In difference notation this becomes $\frac{1}{h^2}(A - 2B + C) = \frac{M_B}{EI}$, $\frac{1}{h^2}(B - 2C + D) = \frac{M_C}{EI}$, and so forth. The moment at the point under consideration may be found by including all of the given loads as well as

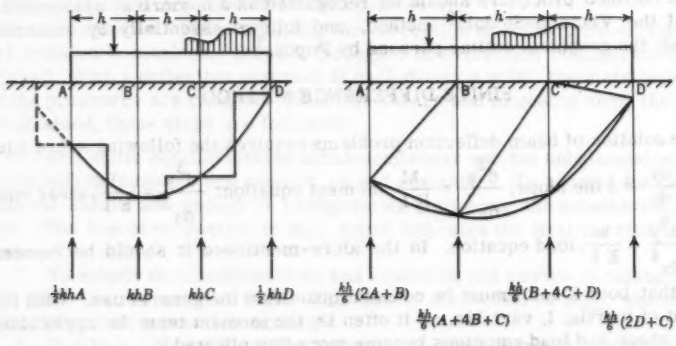


FIG. 2.—FOUNDATION PRESSURE CONCENTRATION

the unknown foundation concentrations either to the left of the point, or to the right. Thus, considering the simple problem of a beam supporting a single concentrated load and resting on a elastic foundation, Fig. 3(a), it can be seen that the values of the moments at point B will be

$$M_B = -\frac{1}{2}kh^2A + Ph \qquad \text{(left)}$$

$$M_B = -\frac{1}{2}kh^2C \qquad \text{(right)}$$

The three simultaneous equations needed to solve this problem would be obtained by using the moment at B from the left, the moment at B from the right, and

the ΣV equals zero. Any consistent sign convention may be employed. The three resulting equations would be

$$A - 2B + C = -\frac{k h^4}{E I}\left(\frac{1}{2}A\right) + \frac{P h^3}{E I}$$

$$A - 2B + C = -\frac{k h^4}{E I}\left(\frac{1}{2}C\right)$$

$$\frac{1}{2}A + B + \frac{1}{2}C = \frac{P}{k h}$$

A solution of these equations should give the deflections directly, and from the deflections the foundation pressures could be obtained. It should be noted that the first two equations imply zero moment and zero shear at both ends of the beam. Combined with the third equation, one can see that the laws of statics must be satisfied. The forementioned method is similar to that used by Joseph Gold, J. M. ASCE.[8]

A method, not recommended, but of interest for its theoretical implications would be one involving the use of the fourth difference equation. This equation, having five terms, requires the same number of subdivision points (Fig. 3(b). Fictitious points at each end may be used, and can be derived from the fact

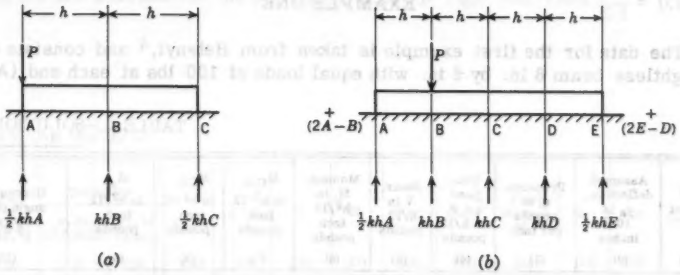


FIG. 3.—BEAMS SUPPORTING SINGLE CONCENTRATED LOADS

that the moment at the end of the beam is zero, thus obtaining the relationship for the left fictitious point of $B' - 2A + B = 0$, that leaves $B' = 2A - B$. This method, however, does not lend itself easily to the solution of problems involving variable moment of inertia, and will generally be more laborious than that method using the second order equations. To indicate the method, the five simultaneous equations that would be required to solve the problem of Fig. 3(b) would be

$$(2A - B) - 4A + 6B - 4C + D = -\frac{k h^4}{E I}(B) + \frac{h^4}{E I}\left(\frac{P}{h}\right)$$

$$A - 4B + 6C - 4D + E = -\frac{k h^4}{E I}(C)$$

$$B - 4C + 6D - 4E + (2E - D) = -\frac{k h^4}{E I}(D)$$

$$\frac{1}{2}A + B + C + D + \frac{1}{2}E = \frac{P}{k h}$$

$$A - 2B + C = -\frac{k h^4}{E I}\left(\frac{1}{2}A\right)$$

[8] Discussion by Joseph Gold, of "Elastic Foundations Analyzed by the Method of Redundant Reactions," by Z. Levinton, Transactions, ASCE, Vol. 114, 1949, pp. 64-70.

Recognizing that the $\frac{P}{h}$ term is the distributed equivalent of the concentrated load P, the first three equations are straightforward. The fourth implies that $\Sigma V = 0$. Inasmuch as the two fictitious terms used imply no external moment, one additional equation is required to eliminate the possibility of end shear. The fifth equation assumes zero end shear at the left end, and in consequence, zero shear at both ends. Thus, the laws of statics are satisfied. This method may at times be useful, although it is not recommended for general use.

The application of both numerical methods to the solution of various examples can best be shown by the solution of the same set of problems that were used by Popov.[3] These problems show the application of this method to various types of problems. The first uses a variable foundation modulus. The second is symmetrical, but with varying moment of inertia. The third involves unsymmetrical loading. A fourth example has been added to demonstrate the handling of concentrated moments. All four examples will be solved by the finite difference method, whereas only the first and second will be solved by the Newmark method.

EXAMPLE ONE

The data for the first example is taken from Hetenyi,[4] and consists of a weightless beam 8 in. by 6 in. with equal loads of 100 lbs at each end (A for

TABLE 1.—SOLUTION BY

Point	Assumed deflection, y_a in 10^{-3} inches	Pressure, q, in pounds per inch	Total Load q + P, in h/12 pounds	Shear, V in h/12 pounds	Moment, M_z in $h^2/12$ inch pounds	M_{C1}, in $h^2/12$ inch pounds	M_{C2}, in $h^2/12$ inch pounds	M_B, in $h^2/12$ inch pounds	Concentrated angle change, α, in $h^3/144EI$
(1)	(2)	(3)	(4)	(5)	(6)	(7)	(8)	(9)	(10)
(a) First Cycle - Example 1									
A	+ 6	+4.20	-14.25	-14.3	0	0	0	0	—
B	+ 1	+0.50	+10.10	- 4.2	-14.3	- 6.9	+ 4.2	-17.0	+188
C	+ 3	+0.90	+10.50	+ 6.4	-18.5	-10.8	+10.0	-19.3	+209
D	+10	+1.00	-24.05	-17.6	-12.1	0	-12.1	0	—
(b) Second Cycle - Example 1									
A	—	—	—	—	—	—	—	—	—
B	—	—	—	—	—	—	—	-15.3	+171
C	—	—	—	—	—	—	—	-16.0	+195
D	—	—	—	—	—	—	—	—	—
(c) First Cycle - Example 2									
	in feet	in kips per foot	kips	kips	foot kips	M_0 in foot kips		foot kips	α, in $h^2/12EI$	$\overline{\alpha}$, in $h^3/144EI$
A^1	+1	+3	+ 24	+ 24	0	0		0	0	—
B^1	+2	+6	+ 72	+ 96	+ 24	-12.5		+ 11.5	-5.12	- 70.8
C^1	+3	+9	+105	+201	+120	-50		+ 70	(-13.1)	-260
D^1	+3	+9	-252	+150	+321	-112		+209	-39.2	-418

[a] Computed following third cycle.

left end, D for right end). The constants for the beam are $E = 2.5 \times 10^6$ psi and $I = 144$ in.^{4} The foundation modulus is assumed to vary linearly from 87.5 lbs per cu in at the left end to 12.5 lbs per cu in. at the right end, or from 700 lbs per lineal in. at the left end, to 100 lbs per lineal in. at the right end. The beam has three divisions at 40 in., producing, a total length of 120 in. The points of the center division are B at left center and C at right center.

To estimate the order of magnitude for the initial assumption of beam deflection to be used in the Newmark method, it can be seen that with an average uniform foundation modulus of 50 lbs per cu in., and a rigid beam, that the average deflection would be 0.004 in. Obviously the deflection should be greater under the loads, and greater at the right end than at the left. The initial assumed deflections are as shown in Table 1. Because the agreement between M_a and M_o at the end of the first cycle is not sufficient, a second cycle was run. Because sufficient accuracy was obtained, the foundation pressures were computed for this last cycle. In Table 2 there is shown the computations for the correction configurations required for the examples using the Newmark method.

The solution by the finite difference method can also be shown for this example. A stepped varying foundation modulus is used with 650 lbs per lineal in. at the left end, and 150 lbs per lineal in. at the right end. Then $\frac{h^4}{EI} = 0.0071$

NEWMARK METHOD

Slope, ϕ, in $h^3/144EI$	Deflection y, in $h^4/144EI$	Deflection y^1, in inches	q	$\bar{q} + P$	V	M	M_{C1}	M_{C2}	Final Moment, M_o	q_{C1}	q_{C2}	Final Pressure, q_o
(11)	(12)	(13)	(14)	(15)	(16)	(17)	(18)	(19)	(20)	(21)	(22)	(23)
-188	+ 188	+0.928	+6.51	- 7.22	- 7.22	0	0	0	0	—	—	—
0	0	0	0	+ 6.51	- 0.71	- 7.22	-10.25	+ 2.66	-14.81	—	—	—
+209	0	0	0	+ 1.03	+ 0.32	- 7.93	-16.08	+ 6.32	-17.69	—	—	—
—	+ 209	+1.03	+1.03	-- 5.40	-26.08	- 7.61	0	+ 7.61	0	—	—	—
-171	+ 171	+0.846	+5.92	- 9.27	- 9.27	0	0	0	0	-3.44	+1.35	+3.83
0	0	0	0	+ 5.92	- 3.35	- 9.27	-11.40	+ 5.25	-15.42	+0.62	+0.10	+0.72
+195	0	0	0	+ 0.97	- 2.38	-12.62	-17.80	+12.48	-17.94	+2.23	-0.45	+1.78
—	+ 195	+0.966	+0.966	-26.62	-29.00	-15.00	0	+12.04	0	+1.36	-0.32	+2.00
							M_C			q^a	$q_c{}^a$	$q_o{}^a$
+540	0	0	0	3.34	+ 3.3	0	0	0	0	0	+2.46	+2.46
+469	+ 540	+0.540	+1.62	+19.2	+22.5	+ 3.3	+ 16.7	+20.0	+1.90	+2.46	+4.36
+209	+1009	+1.009	+3.03	+35.6	+58.1	+25.8	+ 67.0	+92.8	+3.46	+2.46	+5.92
—	+1218	+1.218	+3.65	-317.4	-201	+83.9	+151.0	+234.9	+4.16	+2.46	+6.62

and $\frac{Ph^3}{EI} = 0.0178$. The resulting equations are as follows:

$$A - 2B + C = -\frac{kh^4}{EI}\left(\frac{1}{2}A\right) + \frac{Ph^3}{EI}$$

$$B - 2C + D = -(A + B) + \frac{2Ph^3}{EI}$$

$$B - 2C + D = -\left(\frac{1}{2}D\right) + \frac{Ph^3}{EI}$$

$$3.25A + 5B + 3C + .75D = \frac{2P}{h} \times 10^{-2}$$

TABLE 2.—CORRECTION CONFIGURATIONS

Point	Assumed Deflection y_a, in 10^{-2} inches	Resisting Pressure, q, in pounds per inch	Concentrated Pressure q, in $\frac{h}{12}$ pounds	Shear V, in $\frac{h}{12}$ pounds	Moment M, in $\frac{h^2}{12}$ inch pounds
a) Example 1 - Uniform Deflection - D					
A	+1	+7	+38	+ 38	0
B	+1	+5	+60	+ 98	+ 38
C	+1	+3	+36	+134	+136
D	+1	+1	+10	+144	+270
Uniform Rotation - C					
A	+3	+21	+90	+ 90	0
B	+1	+ 5	+68	+158	90
C	-1	- 3	-28	+130	+248
D	-3	- 3	-22	+108	+378
Correction A (C-0.76D)					
A	—	+15.75	—	—	0
B	—	+ 1.25	—	—	+ 61.5
C	—	- 5.25	—	—	+146.0
D	—	- 3.75	—	0	+175.5
Correction B (C-1.40D)					
A	—	+11.20	—	—	0
B	—	- 2.00	—	—	+ 36.8
C	—	- 7.20	—	—	+ 57.6
D	—	- 4.40	—	-93.6	0
Example 2 - Uniform Deflection - Correction A					
	10^{-2} feet	kips per foot	kips x h/12	kips x h/12	$\frac{h^2}{12}$ foot kips
A^1	+1	+3	+18	+ 18	0
B^1	+1	+3	+36	+ 54	+ 18
C^1	+1	+3	+36	+ 90	+ 72
D^1	+1	+3	+36	+216	+162

Solution of these equations yields the deflections directly. A is 0.478 by 10^{-2} in., B is 0.138 by 10^{-2} in., C is 0.504 by 10^{-2} in. and D is 1.74 by 10^{-2} in. From these values foundation pressures in lbs. per inch can be attained as 3.35 for A, .69 for B, 1.51 for C and 1.74 for D.

EXAMPLE TWO

This example is one taken from those solved by Popov, and consists of a continuous concrete footing having a cross section as shown in Fig. 4(a), and loaded with a line load of 150 kips per ft. The weight of the footing is neglected. The pertinent values are E = 432,000 kips per sq ft, and the foundation modulus is 300 kips per cu ft. The moment of inertia is a function of the beam depth and varies along the length of the beam.

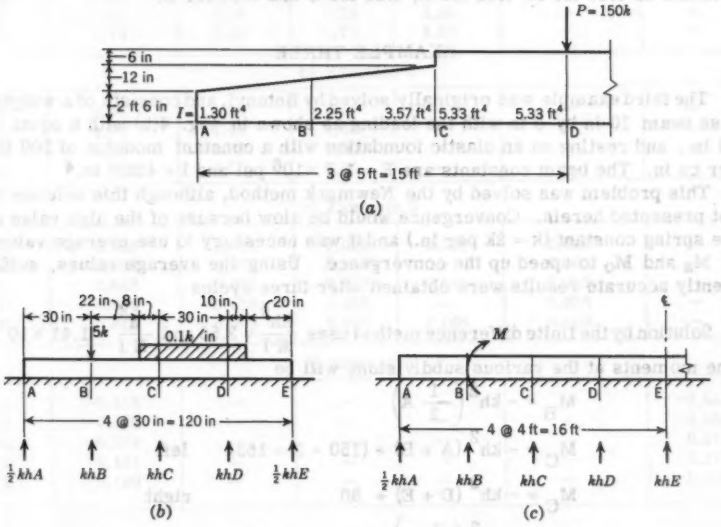


FIG. 4.—BEAMS USED IN SAMPLE PROBLEMS

In this problem advantage is taken of the symmetry, and only one correction configuration is employed for the Newmark solution, that for shear. The discontinuity at point C in the value of the moment of inertia involved a process of obtaining concentrated angle changes on each side of the point, and then adding both of them to obtain the total angle change at the point. After three cycles a comparison of the M_a and the M_o values indicated sufficient accuracy and the values of the foundation pressures were computed from values of M_o for A, B, C and D of 0, +18.7, + 89.4 and +230.4 respectively as shown in Table 1.

The finite difference solution is obtained from previous data and the equations $\frac{kh^4}{E} = 0.434$ and $\frac{3}{2kh} = 1 \times 10^{-3}$. For this method an average value of

moment of inertia was used at the point of discontinuity. The resulting equations are as follows:

$$A - 2B + C = -\frac{0.434}{2.25}\left(\frac{1}{2}A\right)$$

$$B - 2C + D = -\frac{0.434}{4.23}(A + B)$$

$$C - 2D + C = -\frac{0.434}{5.33}(1.5A + 2B + C)$$

$$A + 4B + 2C + 2D = \frac{3P}{2kh} \text{ (Simpsons Rule)}$$

Solution of these equations yields the deflections directly. These values are, in P multiplied by 10^{-3} feet, 0.0590 for A, 0.0975 for B, 0.130 for C, and 0.147 for D. From these values, foundation pressures in kips per ft can be attained as 2.66 for A, 4.38 for B, 5.85 for C and 6.62 for D.

EXAMPLE THREE

The third example was originally solved by Hetenyi, and consists of a weightless beam 10 in by 8 in with the loading as shown in Fig. 4(b) with h equal to 30 in., and resting on an elastic foundation with a constant modulus of 200 lbs per cu in. The beam constants are $E = 1.5 \times 10^6$ psi and $I = 426.7$ in.^{4}

This problem was solved by the Newmark method, although this solution is not presented herein. Convergence would be slow because of the high value of the spring constant (k = 2k per in.) and it was necessary to use average values of M_a and M_o to speed up the convergence. Using the average values, sufficiently accurate results were obtained after three cycles.

Solution by the finite difference method uses $\frac{kh^4}{EI} = 2.53$ and $\frac{h^2}{EI} = 1.41 \times 10^{-3}$

The moments at the various subdivisions will be

$$M_B = -kh^2\left(\frac{1}{2}A\right)$$

$$M_C = -kh^2(A + B) + (150 - 3 = 153) \quad \text{left}$$

$$M_C = -kh^2(D + E) + 80 \quad \text{right}$$

$$M_D = -kh^2\left(\frac{1}{2}E\right) + 5$$

The resulting equations are as follows:

$$A - 2B + C = -\frac{kh^4}{EI}\left(\frac{1}{2}A\right)$$

$$B - 2C + D = -(A + B) + \frac{h^2}{EI}(153)$$

$$B - 2C + D = -(D + E) + (80)$$

$$C - 2D + E = -\left(\frac{1}{2}E\right) + (5)$$

$$\frac{1}{2}A + B + C + D + \frac{1}{2}E = \frac{1}{kh}(5 + 4.8 = 9.8)$$

Solution of these equations yield the deflections directly, as 0.029 in. for A, 0.058 in. for B, 0.049 in. for C, 0.035 in. for D and 0.011 in. at E.

This example was also solved by the finite difference method using the more accurate straight line formulas $\frac{h}{6}(A + 4B + C)$. A comparison of the various

TABLE 3.—COMPARISON OF METHODS

Point	Finite Difference	Newmark Method	Popov	Hetanyi	Finite Difference[a]	Rigorous Method
			a) Example 1			
A	3.35	3.83	3.54	3.62	—	—
B	0.69	0.72	0.73	0.57	—	—
C	1.51	1.78	1.70	1.65	—	—
D	1.74	2.00	1.79	1.89	—	—
			b) Example 2			
A	2.66	2.50	2.70	—	—	—
B	4.38	4.40	4.50	—	—	—
C	5.85	5.90	5.90	—	—	—
D	6.62	6.70	6.50	—	—	—
			c) Example 3			
A	0.029	0.021	0.029	0.030	0.023	—
B	0.058	0.056	0.057	—	0.061	—
C	0.049	0.052	0.053	0.052	0.053	—
D	0.035	0.034	0.033	—	0.036	—
E	0.011	0.005	0.007	0.006	0.006	—
			d) Example 4			
A	-0.418	—	—	—	—	-0.432
B	-0.130	—	—	—	—	-0.138
C	0.078	—	—	—	—	0.078
D	0.171	—	—	—	—	0.172
E	0.190	—	—	—	—	0.188

[a] Using h/6 (A + 4B + C) - straight line variation for foundation pressure.

results is shown in Table 3. For most purposes sufficient accuracy is obtained by any of the approximate methods, although the finite difference method that was outlined is the least time consuming.

EXAMPLE FOUR

This final example has been added to indicate a method of handling concentrated moments. The sketch shown in Fig. 4(c) represents any type of beam resting on an elastic foundation, and with dimensions to give values of E = 300,000 k per sq ft, and I = 20 ft.^{4} The beam is symmetrically loaded with two equal concentrated moments, one clockwise, the other counter clockwise. The foundation modulus is 6000 kips per lineal ft, and it is assumed that the foundation

can take negative loads. (This would merely mean a reduction in the pressure caused by any direct loads). Using $\frac{kh^4}{EI} = 0.256$ and $\frac{h^2}{EI} = 0.267 \times 10^{-5}$ the resulting equations are as follows:

$$A - 2B + C = -\frac{kh^4}{EI}\left(\frac{1}{2}A\right) - \frac{h^2}{EI}\left(\frac{1}{2}M\right)$$

$$B - 2C + D = -(A + B) - (M)$$

$$C - 2D + E = -\left(\frac{3}{2}A + 2B + C\right) - (M)$$

$$D - 2E + D = -(2A + 3B + 2C + D) - (M)$$

$$\frac{1}{2}A + B + C + D + \frac{1}{2}E = 0$$

Remembering that bending in a beam is a direct result of moment area (angle change), the justification for the 1/2 M in the first equation is recognized. This is an average value of the moment area between A and C.

CONCLUSIONS

Solutions to elastic foundation problems have long been avoided by the civil engineer, as too laborious and too time consuming. Rigorous solutions are available, but invariably involve the use of hyperbolic trigonometric functions, and prepared hyperbolic function tables.

This paper indicates the ease with which approximate solutions may be obtained through the use of simple numerical procedures. Various complexities of loading, beam structure, or foundation variation may be handled with no more difficulty than that employed in simple cases. The reliability of any of the methods discussed can be seen from the proximity of the results obtained as indicated in Table 3.

DISCUSSION

NORMAN J. RYKER, JR.[9]—In this paper the author has outlined, in excellent detail, two numerical methods for solution of beams on elastic foundation. The paper will undoubtedly increase the popularity of the successive approximation methods for the solution of these problems. The earlier work of Popov[3] dealt primarily with the graphical solutions and therefore may have had limited acceptance by those who dislike graphics, an attitude apparently growing in popularity. Popov did mention that his computations could be set up in tabular form.

The second innovation by the author, and one that can contribute greatly to rapid convergence for long flexible beams, is the initial assumption of an approximate deflected shape rather than the rigid shape. Contrary to the author's

[9] Preliminary Design Engr., Missile Div., North American Aviation, Inc., Downey, Calif.

statement, however, the successive approximation method using the Newmark type of solution is not restricted to relatively short beams. It is the purpose of the writer to present a method[10] that will assure convergent solutions for very long beams on elastic foundations.

In general, the method proposed by Malter will provide a convergent solution as long as $\lambda L = 3$, in which L is the length of the beam and $\lambda^4 = k/4EL$. For beams of greater length a convergence factor may be used to obtain a convergent solution. The general procedure is as follows:

1. Assume an original deflected shape and place the beam in equilibrium with the applied loads and moments by rigid beam deflection and rotation. Let the balanced beam shape be denoted by y_o.
2. Using the resulting foundation pressures and the applied loads, compute the new deflected shape by any convenient method. Add rigid beam deflections and rotations so that there is no net load or moment on the beam (remove all applied loads). Let this deflected shape be denoted by δ_1.
3. Apply the foundation pressures of δ_1 as loads on the beam and compute a new deflected shape. Adjust as in step 2 and let this shape be denoted by δ_2.
4. Compute the quantity $r = \frac{\delta_1}{\delta_1 - \delta_2}$ at each panel point of the beam, and average for the entire beam.
5. The final shape is then:

$$y = y_o + \delta_1 + r\,\delta_2 \quad \ldots\ldots\ldots\ldots\ldots\ldots \quad (1)$$

6. If the quantity $r\,\delta_2$ is large or if the convergence factor r varies greatly along the beam repeat the preceeding steps.

The development of this procedure is quite simple. In successive approximation methods the solution can be represented as:

$$y = y_o + \delta_1 + \delta_2 + \ldots.$$

in which y_o, the original assumed shape, balances all applied loads and δ_1, δ_2, and so forth, that are corrections to this shape, are in static equilibrium without applied loads. As long as δ_n and all successive δ_n's are similar in shape then

$$r\,\delta_n = \delta_n + \delta_{n+1} + \delta_{n+2} + \ldots$$

and

$$y = y_o + \delta_1 + \ldots + r\,\delta_n$$

To minimize computations it is proposed that only the first and second cycles be used to compute the quantity r even though these shapes generally are not similar.

From first cycle $\quad y = y_o + r\,\delta_1$

From second cycle $\quad y = y_o + \delta_1 + r\,\delta_2$

10 "An Approximate Numerical Method for Analysis of Stiffened Cylinders, Conical Shells and Domes," by N. J. Ryker, Jr., thesis presented to the University of California, at Berkeley, in 1951, in partial fulfilment of the requirements for the degree of Master of Science in civil engineering.

Equating these two quantities, the convergence factor in step 4 is obtained.

The validity of this procedure is dependent upon the similarity of δ_1 and δ_2, and because in general they will not be similar, the second of these two equations will more closely approximate the true shape.

Jacob Karol,[11] F. ASCE, suggested using:

$$r = \frac{R_1}{R_1 + R_2} \quad \ldots\ldots\ldots\ldots\ldots\ldots \quad (2)$$

in which R_1 is the total reaction under δ_1, if the ends of the shape δ_1 are placed at the surface of the foundation; and R_2 is the total reaction under δ_2, if the ends of the shape δ_2 are placed at the surface of the foundation.

This equation is based upon the end pressures of δ_1 and δ_2 because for a constant foundation modulus

$$R_1 = \left[\frac{(q_1)_{x=0} + (q_1)_{x=L}}{2}\right] L \quad \ldots\ldots\ldots\ldots\ldots\ldots \quad (3)$$

in which q_1 is the foundation pressure for δ_1. Eq. 2 fails to give a convergent solution in some cases that the writer's method does, because it is based solely upon the end values.

V. A. Plumb,[12] in a concurrent development of a convergence factor similar to Karol's, continued his successive approximation process until the ratios of successive differences were a constant. However, in the case of beams of $\lambda L = 6$ the procedure must be repeated for at least four cycles and requires the use of from six to ten significant numbers because the answer is on the order of $10^{-4}\ \delta_4$.

The general procedure outlined herein can be applied directly to the procedures outlined by the author, the principal difference being that δ_1 and δ_2 are not obtained directly.

1. Follow Malter's steps 1 through 13 and then using the computed M_o repeat steps 9 through 12.
2. Correct the original assumed deflected shape y_a and the two successive values y to place them in equilibrium with the applied loads using Malter's correction configurations. Let these successive values be y_o, y_1, and y_2.
3. Compute $\delta_1 = y_1 - y_o$ and $\delta_2 = y_2 - y_1$.

To demonstrate this procedure, consider the first problem presented by the author. The first cycle remains as shown. However, the actual computed values of M_o must be used to initiate the second cycle from which the deflection, shears, and moments shown in Table 4 were computed. In this table

$$y^v C_1 = -\left(\frac{29.9}{96.6}\right) y_B;\ y^1 C_2 = \left(\frac{17.29}{175.5}\right) y_A;\ y_2$$

$$= y + y^1 e_1 + y^2 C_2;\ \delta_1 = y_1 - y_o \text{ and } \delta_2 = y_2 - y_1.$$

---

11 Discussion by J. Karol of "Successive Approximations for Beams on Elastic Foundation," by E. P. Popov, Transactions, ASCE, Vol. 116, 1951, pp. 1101-1103.

12 "Approximate Methods of Analysis of Beams and Circular Plates on an Elastic Foundation," by V.A. Plumb, thesis presented to the University of California, at Berkeley, in partial fulfilment of the requirements for the degree of Master of Science in civil engineering.

After the moment and shear at the end of the beam were computed, equal and opposite moments and shears were applied to balance the deflected beam. The rigid deflections of Malter's correction configurations for shear(y_B) and moment(y_A)were added to y^1, producing y_2. Similar corrections were computed for y_A and y^1 in the first cycle producing y_o and y_1 respectively. From the differences, the convergence factor r was computed. The variation of r along the beam indicates that δ_1 and δ_2 are not similar, but the average value of r = 0.788 produces better agreement with Hetenyi's[13] solution than does y_2.

TABLE 4.–SOLUTION AND COMPARISON FOR EXAMPLE ONE

Functions	Points A	B	C	D
	(a) Second Cycle			
M_o, in $\frac{h^2}{12}$ inch pounds	0	-14.81	-17.69	0
y', in 10^{-2} inches	+0.819	0	0	+0.947
V, in $\frac{h}{12}$ pounds	-9.90	-4.17	-3.22	-29.9
M, in $\frac{h^2}{12}$ inch pounds	0	-9.90	-14.07	-17.29
y' C_1	-0.512	+0.128	+0.769	+1.281
y' C_2	+0.221	+0.025	-0.172	- 0.369
	(b) Balanced Deflections			
y_2	+0.528	+0.153	+0.597	+1.859
y_1	+0.580	+0.123	+0.594	+1.982
y_o	+0.454	+0.193	+0.629	+1.393
δ_1	+0.126	-0.070	-0.035	+0.589
δ_2	-0.052	+0.030	+0.003	-1.23
r	+0.708	+0.700	+0.920	+0.826
	(c) Deflection Valves			
Ryker	0.539	0.147	0.596	+1.885
Malter	0.528	0.153	0.597	+1.859
Hetenyi	0.517	0.114	0.53	+1.89

It is apparent from the values of y_2 and y_1, that, because of the idealization of the beam, the solution will never exactly coincide with Hetenyi's solution.

A better example of the rapid convergence is supplied by Malter's second example. In this case, using one cycle of the general procedure (that is equivalent to two cycles of Malter's procedure) and an average convergence factor of 0.710 results were obtained which were equivalent to Malter's three cycles. After two cycles the writer obtained foundation pressure values, in pounds per ft, of 2.5 for A, 4.4 for B, 5.9 for C, and 6.63 for D. Reference to table 3 will indicate the proximity of these values with those obtained by Malter and Hetenyi.

[13] "Beams on Elastic Foundation," by Miklos Hetenyi, The University of Michigan Press, Ann Arbor, Mich., 1946.

In Malter's third example convergence was less rapid because of the extreme flexibility of the beam. An original shape was assumed which seemed consistent with the applied loading and this was balanced producing the original shape y_o. After two cycles the convergence factor and a resulting shape were computed. Another cycle was computed because of the wide variation in the factor, and the result of this cycle produced a maximum deflection of .057 in. that is comparable to the value of 0.056 in. shown by Malter. It is interesting to note that Malter could only obtain the solution to the problem by averaging the results which is equivalent to using a convergence factor of 0.5. In the case of the writer's solution after two cycles the computed average convergence factor was 0.55.

In extending the method to very long beams,[10] a comparison was made between this numerical procedure and the exact solution for centrally loaded beams of $\lambda L = 8$. In this comparison the maximum error in deflection at the end of the beam after two cycles of the general procedure (equivalent to four cycles of actual deflection computation) was less than 5% of the maximum deflection. The maximum moment was idential to the moment computed by Hetenyi's method. Without the use of the convergent factor the successive approximation solution was rapidly divergent. The computed value of the convergence factor was .083 indicating that an averaging technique would also be unsatisfactory.

The writer's purpose was to show that the use of a convergence factor enables one to obtain convergent solutions by successive approximations for beams lengths of all practical interest, that is, beams with a free length beyond the applied load or a restraint of not more than $\lambda L = 4$. As shown by Hetenyi[4] there is no appreciable effect on the beam at greater distances. Longer beams can be handled by assuming a free beam length of $\lambda L = 4$ for analysis and assuming the rest of the beam is unstressed and undeflected. This will generally result in errors no greater than 5% of the maximum values.

ALEXANDER DODGE,[14] F. ASCE.—The author gives numerical solutions for beams on elastic foundations by two approximate methods and compares the results with those obtained by the rigorous method. These types of problems have been avoided because their solution has been thought to involve a cumbersome and time-consuming analysis. The author should be commended for demonstrating the ease with which an approximate solution of a problem can be obtained by the finite difference method.

In his introduction the author states that "a 'rigorous' method should be sought at all times," and that "recognizing the nature of the overall problem, it is often preferable to use an approximate method to obtain quickly a solution. A solution obtained by an approximate method may in actuality be no further from a true and exact solution than one derived by a rigorous method." From past experience in this field the writer believes that an approximate solution is more than ample in all but a few cases. Precision in computations is justified when a purely academical approach to a problem is desired, when the establishment of certain assumptions must be verified, when an independent check or comparison with some other exact method is sought, or when thorough working knowledge of the subject is required. In practice one is guided by design codes, manuals, specifications, and more often by exactly prescribed procedures, formulas and coefficients. The problem of beams on elastic foundation is no different, and the writer will try to show how solutions of such problems can be made quickly by charts.

---

[14] Consultant, Design Branch, Corps of Engrs., Portland, Ore.

Exact Solution.—The oldest theory of bending a beam on elastic foundation was for the Windler foundation described by the author. Application of the theory was demonstrated by Stephan P. Timoshenko[15] in whose nomenclature the deflection equation of a bar of infinite length on an elastic foundation can be represented by the equation:

$$y = e^{\beta x}(A \cos \beta x + B \sin \beta x) + e^{-\beta x}(C \cos \beta x + D \sin \beta x) \ldots (4)$$

in which $\beta = \sqrt[4]{\frac{k}{4EI}}$, k is the modulus of foundation and A, B, C, and D are the constants of integration.

This method of solution has been available to the engineering profession for at least 30 yr, but to the writer's knowledge its use has been neglected, probably because its universality was not readily recognized nor properly appreciated. Applying this method to a bar of finite length βb, loaded at the far end from the origin of coordinates with downward load P and counterclockwise moment M, and integrating within definite limits, the following equations in which βx is any distance along this beam will result:

$$M_{\beta x = 0} = 0 \ldots\ldots\ldots\ldots\ldots B = D \ldots\ldots\ldots\ldots\ldots (4a)$$

$$M_{\beta x} = 2EI\beta^2[A\mu + B(\theta - \eta) - C\omega] \ldots\ldots\ldots\ldots\ldots (4b)$$

$$M_{\beta b} = M = 2EI\beta^2[A\mu + B(\theta - \eta) - C\omega] \ldots\ldots\ldots\ldots\ldots (4c)$$

$$S_{\beta x} = 2EI\beta^3[A\epsilon - B(\gamma + \phi) - C\psi] \ldots\ldots\ldots\ldots\ldots (5a)$$

$$S_{\beta x = 0} = 0 \ldots\ldots\ldots\ldots\ldots A + 2B + C = 0 \ldots\ldots\ldots\ldots\ldots (5b)$$

$$S_{\beta b} = P = 2EI\beta^3[A\epsilon - B(\gamma + \phi) - C\psi] \ldots\ldots\ldots\ldots\ldots (5c)$$

$$y = A\eta + B(\mu + \omega) + C\theta \ldots\ldots\ldots\ldots\ldots (6)$$

$$\frac{dy}{dx} = \beta(A\gamma + B(\epsilon + \psi) - C\phi) \ldots\ldots\ldots\ldots\ldots (7)$$

Where,

$\mu = e^{\beta x} \sin \beta x$, $\eta = e^{\beta x} \cos \beta x$, $\theta = e^{-\beta x} \cos \beta x$, $\omega = e^{-\beta x} \sin \beta x$,

$\phi = \theta + \omega$, $\psi = \theta - \omega$, $\gamma = \eta - \mu$, $\epsilon = \eta + \mu$

Positive moment indicates tension on the bottom, positive shear indicates that the left part of the beam tends to go up, positive deflection is downward and positive slope is clockwise. Exponential and circular function being available in many engineering handbooks, the constants of integration A, B, and C can be readily determined from the Eqs. 4(c), 5(b) and 5(c). Applying these notations to the author's Example 1, using stepped foundation modulus, the following beam constants will be obtained:

---

15 "Strength of Materials," by S. Timoshenko, Part II, D. Van Nostrand Co., Inc., 1930, p. 402.

TABLE 5.—BEAM CONSTANTS

Item	Values of Foundation Modulus			
	650	500	300	150
β	.0259	.0243	.0214	.01797
b	20	40	40	20
βb	.518	.972	.856	.3594

Considering the end load P = 100 lbs and the end moment M = 1000 in.-lbs as separate problems and solving Eqs. 4(c), 5(b) and 5(c) for each segment of the beam, the resulting values of end deflections and slopes will be as shown in Table 6.

TABLE 6.—END DEFLECTIONS AND SLOPES OF BEAM SEGMENTS

Segment	Point	P = 100 pounds		M = 1000 inch-pounds	
		y	$\frac{dy}{dx}$	y	$\frac{dy}{dx}$
A-B	A	- .015 417	.002 311 4	.023 114	- .002 307 7
	B	.030 886	.002 320 7	- .023 207	- .002 335 5
C-D	C	- .009 832 2	.000 733 22	.007 332 2	- .000 359 28
	D	.020 085	.000 770 03	- .007 700 3	- .000 414 56
E-F	E	- .016 429	.001 228 0	.012 280	- .000 606 64
	F	.033 280	.001 264 9	- .012 649	- .000 662 03
G-H	G	- .066 578	.009 985 7	.099 857	- .009 982 0
	H	.133 210	.009 994 9	- .099 949	- .010 009 7

Knowing the end slopes and deflections of the beam segments due to unit loads, continuity of the beam is restored in the usual manner by introducing unknown (interacting) shears (S) and moments (M), as shown in Table 7, and by equating the final slopes and deflection at common points BC, DE, and FG. There will then be six equations:

$$\Delta_B - \Delta_C = 0 = +.050971S_1 + .0155067M_1 + .00983228_2 + .0073322M_2 - .15417$$

$$\Delta_D - \Delta_E = 0 = +.009832S_1 - .0073322M_1 + .05336S_2 - .0049487M_2 + .016429S_3 + .012280M_3$$

$$\Delta_F - \Delta_G = 0 = + .016429S_2 - .012280M_2 + .166490S_3 - .087300M_3$$

$$\phi_B - \phi_C = 0 = +.00155067S_1 + .00275006M_1 - .0007332S_2 - .00035928M_2 - .0023114$$

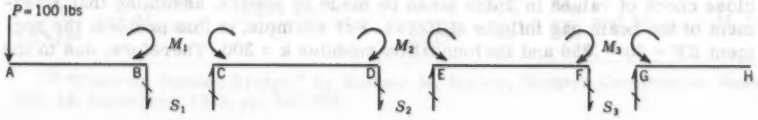
$$\phi_D - \phi_E = 0 = +.00073222S_1 - .00035928M_1 - .0004987S_2 + .00107659M_2 - .001228S_3 - .00060664M_3$$

$$\phi_F - \phi_G = 0 = + .001228S_2 - .00060664M_2 - .00873083 + .01067173M_3$$

in which Δ and ϕ are final deflections and slopes at the point indicated by a subscript.

TABLE 7.—BEAM SLOPES AND FOUNDATION PRESSURE DEFLECTIONS

Point	End Slope, in Radians	End Deflection, in inches	Final Deflections				Foundation Pressure, in pounds per square inch
			Due to $P_A = 100$	Due to $P_H = 100$	Due to $P_A = 100$ and $P_H = 100$		
					Exact	Approximate	
A	$-.0023207$ $+.0023114S_1$ $+.0023077M_1$	$+.030886$ $-.015417S_1$ $-.023114M_1$	0.00855	-0.002482	0.006068	0.005	3.94
B	$-.0023114$ $+.0023207S_1$ $+.0023355M_1$	$-.015417$ $+.030886S_1$ $+.023207M_1$	.004538	- .001518	.003020	.00346	1.96
C	$+.00077003S_1$ $-.00041456M_1$ $+.00073322S_2$ $+.00035928M_2$	$-.020085S_1$ $+.0077003M_1$ $-.0098322S_2$ $-.0073322M_2$	.004539	- .001518	.003021	—	1.51
D	$+.00077003S_2$ $+.00041456M_2$ $+.00073322S_1$ $-.00035928M_1$	$+.020085S_1$ $+.0077003M_2$ $+.0098322S_1$ $-.0073322M_1$	- .000164	.002120	.001956	.00260	0.98
E	$+.0012649S_2$ $-.00066203M_2$ $+.0012280S_3$ $+.00060664M_3$	$-.033280S_2$ $+.012649M_2$ $-.016429S_3$ $-.012280M_3$	- .000165	.002116	.001951	—	0.59
F	$+.0012649S_3$ $+.00066203M_3$ $+.0012280S_2$ $-.00060664M_2$	$+.033280S_3$ $+.012649M_3$ $+.016429S_2$ $-.012280M_2$	- .00188	.01227	.010389	—	3.1
G	$+.0099949S_3$ $-.0100097M_3$	$-.133210S_3$ $+.099949M_3$	- .0018	.01231	.010432	.01026	1.55
H	$+.0099857S_3$ $-.0099820M_3$	$+.066578S_3$ $-.099857M_3$	- .00249	.019873	.017383	.0149	2.61



Solution of these equations, as well as similar equations due to load P_H = 100 lbs, yields the values given in Table 8. Values for intermediate points of a segment may be found, if necessary, by substitution of the proper βx values in Eqs. 4(b) and 5(a). Solution of equations for both loads or for any number of loads at different points of the beam can be made at once, but in studies as well as in practical designs, solution for a unit load or moment is more valuable.

Unless one is interested in the mechanics of all operations performed in solution of this problem, there is no justification for presenting such computations. The validity of the solution can be verified simply by computing the moment of the $\frac{M}{EI}$ diagram for the loads equal to the foundation pressures shown in Table 7. When a plot of such values (deflections from the end tangent) coincides with deflections shown in the same table, and if the area of the foundation pressures is equal to the superimposed loads, and moment equilibrium is satisfied, veracity of the solution is established. It was found that

TABLE 8.—BEAM SHEARS AND MOMENTS

Item	Exact Solution			Approximate Solution		
	P_A = 100 pounds	P_H = 100 pounds	$P_A + P_H$	P_A = 100 pounds	P_H = 100 pounds	$P_A + P_H$
S_1	- 16.0	- 26.0	- 42	- 18.6	- 27.9	- 46.5
M_1	1073	281	1354	1111	308	1419
S_2	20.4	- 26.8	- 6.4	21.2	26.2	- 4
M_2	675	1574	2249	730	1679	2409
S_3	6.6	51.9	58.5	7.4	55	62.4
M_3	69	1481	1550	78	1515	1593

these conditions are entirely satisfied. In this respect problems on elastic supports are easier and faster to verify than solution of other indeterminate structures. It should be noted that when deflections are computed on the assumption of a stepped modulus of foundation, this modulus must also be used to evaluate foundation pressures, and the foundation pressures so determined must be used to establish validity of the solution. Failure to observe this procedure will lead to inequalities in equations of statics $\sum V = 0$ and $\sum M = 0$, and also may give quite a large disparity in elastic curves. Therefore, from a theoretical standpoint, deflections at points A and D by finite difference method in Table 3 should be 3.11 and 2.62 instead of 3.35 and 1.74 as shown, respectively. From a practical standpoint such a refinement may be immaterial.

In the progress of work, it is well to remember and observe that such other controlling conditions as slope due to unit load equals deflection due to unit moment, or Maxwell's law of reciprocal deflections, are satisfied. (Observe the values in Tables 6 and 7 in this respect.) Moreover, a sufficiently close check of values in Table 6 can be made by statics, assuming that a segment of the beam has infinite stiffness. For example, in this problem the segment EF = βb = .856 and the foundation modulus k = 300. Therefore, due to the

end load, P = 100 lbs, $\frac{4P}{3} = \frac{k\, y_E \times 40 \times 2}{2 \times 3}$, and the deflections

$$y_E = .0333, \quad y_F = \frac{1}{2} y_E = .01667$$

the slope is

$$-\frac{1.5}{40} y_E = -.00125 \text{ radians}$$

Similarly, due to the end moment,

$$M = 1000 \text{ in-lbs}, \quad \frac{M \times 3}{40 \times 2} = \frac{k\, y_E \times 40}{2 \times 2}$$

the deflection,

$$y_E = y_F = .0125 \text{ in.}$$

and the slope

$$S = \frac{2\, y_E}{40} = .000625 \text{ radians.}$$

Once the method is understood, it will be realized how much tedious, subprofessional work is involved in performing a series of similar computations. The description of such a method is given here as a reminiscence of analysis developed for the design[16] of the Lake Washington Floating Bridge in Seattle, Washington. Determination of the maximum length of an individual unit and the maximum number of units that could be rigidly connected in a continuous structure were sought. Without precedent in design of such bridges, pioneering in analysis started by the method recommended above for checking validity of solutions. Realizing that water was a perfect Winkler's foundation,[11] deflections of the unit were assumed and corrected until the assumed deflections came into close agreement with computed deflections after conditions of static equilibrium were satisfied. When a continuous bridge of approximately 1000 ft in length was analyzed, it was evident that for such length the maximum live load and temperature stresses were practically the same as for a bridge of infinite length. For these reasons all units were rigidly connected by prestressing and grouting into one continuous structure approximately 6500 ft long. Continuity has been interrupted only by the movable, telescoping span required by navigation. This 378-ft span was connected to the east part of the bridge by a hinged joint, and to the west part by two sets of vertical rollers. To determine statically indeterminate reactions at the rollers and the hinge by the hit and miss method, as well as to derive the load distribution on the transition span of variable moment of inertia, was too laborious a job. For these reasons the exact method presented herein was developed, after which influence lines for the previously mentioned reactions were easily determined. The performance of the bridge after two decades of service stands as testimony to the validity of the analysis.

Later, as more applications of the method were made to various structures, the data on deflections, slopes and moments of beams of finite length were accumulated and compared with the maximum values of the respective functions computed for a unit load or moment acting at the end of a semi-infinitely long bar of the same EI. For beams of semi-infinite length[15] $y_o = \frac{P_o}{2EI\beta^3}$, $\frac{dy_o}{dx} = -\frac{P_o}{2EI\beta^2}$ and $M_{max} = -\frac{.3224\, P_o}{\beta}$ or $y_o = \frac{-M_o}{2EI\beta^2}$, $\frac{dy_o}{dx} = \frac{M_o}{EI\beta}$ and $M_{max} = M_o$ in

16 "Concrete Pontoon Bridge," by Holmer M. Hadley, Western Construction News, Vol. 14, September, 1939, pp. 293-298.

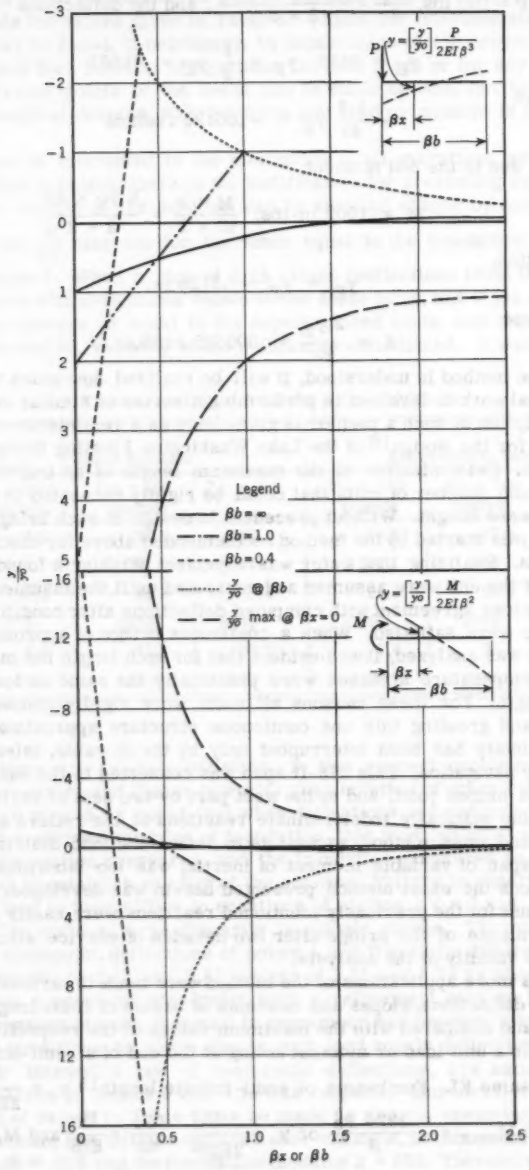


FIG. 5.—DEFLECTION RATIOS FOR END LOADED BEAMS

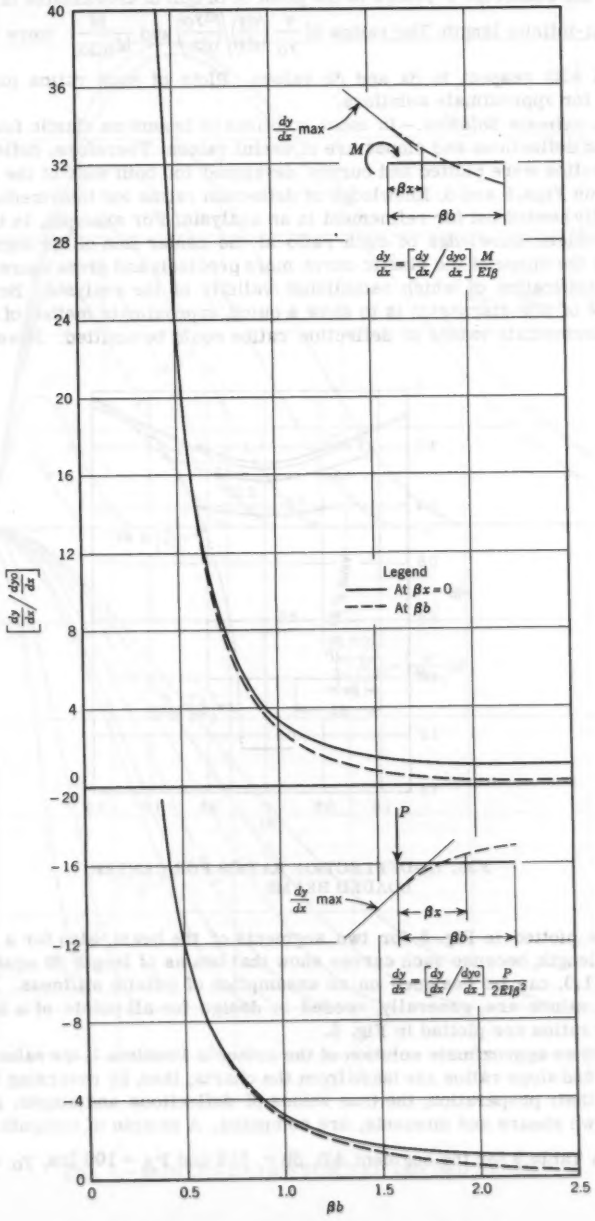


FIG. 6.—SLOPE RATIOS FOR END LOADED BEAMS

which the subscript o refers to the point of origin of coordinates of the beam of semi-infinite length. The ratios of $\frac{y}{y_o}\left(\frac{dy}{dy}\right)\Big/\left(\frac{dy_o}{dx}\right)$ and $\frac{M}{M_{max}}$ were found and plotted with respect to βx and βb values. Plots of such ratios provide the means for approximate solutions.

Approximate Solution.—In most solutions of beams on elastic foundations, only end deflections and slopes are of useful values. Therefore, deflection and slope ratios were plotted and curves developed for both ends of the beams as shown on Figs. 5 and 6. Knowledge of deflection ratios for intermediate points is hardly needed but for refinement in an analysis. For example, in the previous problem, knowledge of such ratio at the center line of the segment C-D defines the shape of the elastic curve more precisely and gives more accurate data, verification of which establishes validity of the analysis. Because the purpose of this discussion is to show a quick, approximate method of an analysis, intermediate values of deflection ratios could be omitted. Nevertheless,

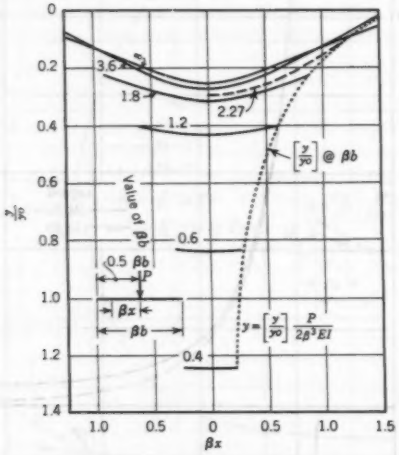


FIG. 7.—DEFLECTION RATIOS FOR CENTER LOADED BEAMS

they are plotted in Fig. 5 for two segments of the beam, also for a beam of infinite length, because such curves show that beams of length βb equal to 0.5, or even 1.0, can be designed on an assumption of infinite stiffness. Because moment values are, generally, needed in design for all points of a beam, all moment ratios are plotted in Fig. 8.

To get an approximate solution of the author's Problem 1, the values of deflection and slope ratios are taken from the charts; then, by reversing the process of their preparation, the true values of deflections and slopes, in terms of unknown shears and moments, are computed. A sample of computations is shown in Table 9 for the segment AB, $\beta b = .518$ and $P_A = 100$ lbs, y_o and $\frac{dy_o}{dx}$

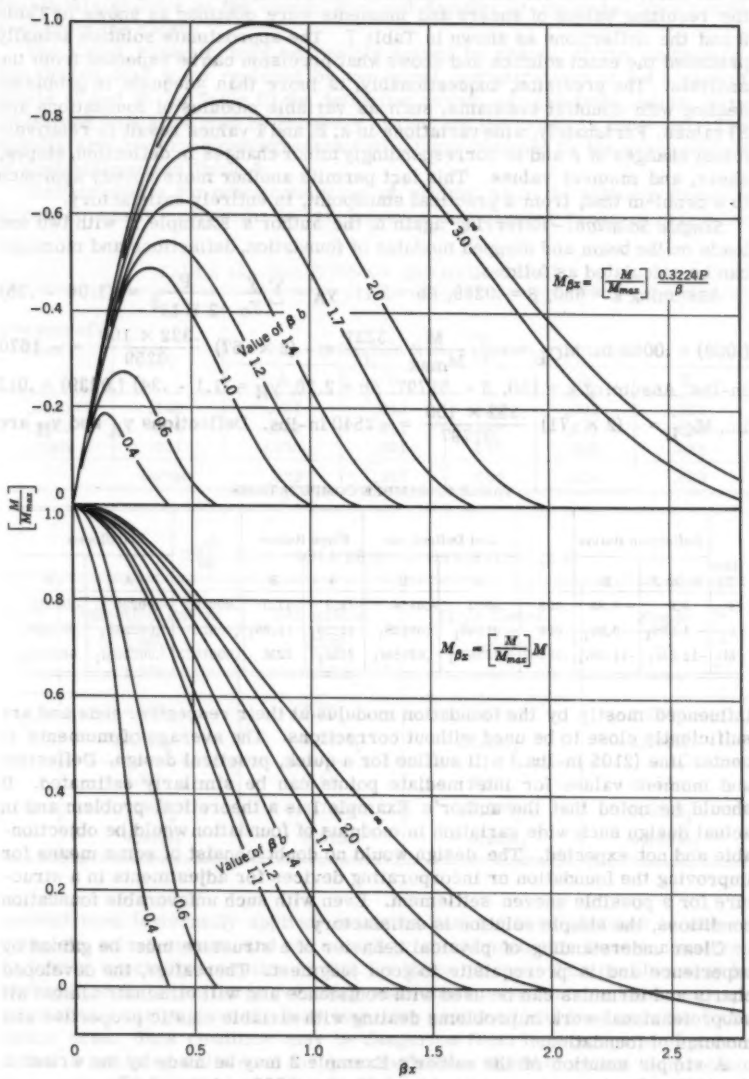


FIG. 8.—MOMENT RATIOS FOR END LOADED BEAMS

are computed from the equations for beams of semi-infinite length. Proceeding in the same manner for other segments, composing and solving six equations, the resulting values of shears and moments were obtained as shown in Table 8 and the deflections as shown in Table 7. The approximate solution actually preceded the exact solution and shows what precision can be expected from the analysis. The precision, unquestionably, is more than adequate in problems dealing with doubtful constants, such as variable modulus of foundations and EI values. Fortunately, wide variations in k, E, and I values result in relatively minor changes of β and in correspondingly minor changes in deflection, slopes, shear, and moment values. This fact permits another more speedy approach to a problem that, from a practical standpoint, is entirely satisfactory.

Simple Solution.—Referring again to the author's Example 1, with two end loads on the beam and stepped modulus of foundation, deflections and moments can be calculated as follows:

Assuming k = 650, β = .0259, βb = 3.11. $y_A = \sum \frac{y}{y_o} \frac{P}{2 E I \beta^3}$ = (1.04 - .25) (.008) = .0063 in. $M_{C_L} = - \sum \frac{M}{M_{max}} \frac{.322P}{\beta}$ = - (2 × .67) $\frac{.322 \times 100}{.0259}$ = - 1670 in-lbs. Assuming k = 150, β = .01797, βb = 2.16, y_H = (1.1 - .34) (.0239) = .018 in., M_{C_L} = - (2 × .71) $\frac{.322 \times 100}{.01797}$ = - 2540 in-lbs. Deflections y_A and y_H are

TABLE 9.—SAMPLE COMPUTATIONS

Due To	Deflection Ratios		y_o	End Deflections		Slope Ratios		$\frac{dy_o}{dx}$	End Slopes	
	Point A	B		A	B	A	B		A	B
P_A	3.9	- 1.93	.008	.0312	-.0154	-11.3	-11.3	.000207	-.00235	-.00235
S_1	- $1.93S_1$	$3.9S_1$	.008	-.0154S_1	.0312S_1	$11.3S_1$	$11.3S_1$	.000207	.00235S_1	.00235S_1
M_1	-$11.3M_1$	-$11.3M_1$	.00207	-.0235M_1	.0235M_1	$22M_1$	22M	.0001073	.00235M_1	.00235M_1

influenced mostly by the foundation modulus at their respective ends and are sufficiently close to be used without corrections. The average of moments at center line (2105 in-lbs.) will suffice for a quick, practical design. Deflection and moment values for intermediate points can be similarly estimated. It should be noted that the author's Example 1 is a theoretical problem and in actual design such wide variation in modulus of foundation would be objectionable and not expected. The design would no doubt consist of some means for improving the foundation or incorporating devices for adjustments in a structure for a possible uneven settlement. Even with such unfavorable foundation conditions, the simple solution is satisfactory.

Clear understanding of physical behavior of a structure must be gained by experience and is prerequisite to good judgment. Thereafter, the developed charts and formulas can be used with confidence and will eliminate almost all subprofessional work in problems dealing with variable elastic properties and modulus of foundation.

A simple solution of the author's Example 2 may be made by the writer's chart, Fig. 7. Assuming constant I = 5.33, β = .0755 and βb = 2.27.

$$y_{C_L} = (0.293) \frac{P}{2 E I \beta^3} = .0221 = .148 \times 10^{-3} P, \text{ ft}$$

$$y_A = (0.113) \left(\frac{P}{2 E I \beta^3} \right) = .00855 = .057 \times 10^{-3} P, \text{ ft}$$

Due to greater flexibility of the beam toward the ends, actual deflections will be slightly greater at the center line and smaller at the ends. This can be seen from the chart.

The third example may be readily solved by charts, if the uniformly-distributed load were replaced by two equal concentrations of 2.4 k each at points C and D. In Table 10 the deflection ratios, as read from charts, were multiplied on a slide rule by proper y_o value and the products recorded. The results are in very close agreement with those obtained by the exact method of analysis given in Table 3.

Similar charts for other conditions of loading, as in the author's Example 4, can be easily prepared. So far, however, a sufficient range of ratios for

TABLE 10.—SOLUTION OF EXAMPLE THREE

Position of Load	y_o	Deflection Ratios times y_o, in inches				
		A	B	C	D	E
.25βb	.148	.037	.043	.021	.003	-.010
.50βb	.071	-.003	.011	.019	.011	-.003
.75βb	.071	-.005	.001	.010	.020	.018
Sums		.029	.055	.050	.034	.005

TABLE 11.—SOLUTION OF EXAMPLE FOUR

Point	Deflection Ratios	Deflections	Slope Ratios	Slopes
A	$-2.0S_1$	$-8.32S_1$	—	—
	$-11.8M_1$	$-6.20M_1$	—	—
B	$4.02S_1$	$16.7S_1$	$11.9S_1$	$6.23S_1$
	$11.9M_1$	$6.23M_1$	$23.5M_1$	$3.09M_1$
(B)	-0.97	-0.51	0.95	0.125
	$0.90S_1$	$-3.74S_1$	$0.97S_1$	$0.510S_1$
	$0.97M_1$	$0.51M_1$	$-0.95M_1$	$0.125M_1$

concentrated (externally applied) moments has not been obtained to draw a complete set of curves, and not enough practical problems were encountered to justify special preparation of data for these curves. This problem may be exemplified by a cantilever retaining wall where a concentrated moment, applied at an interior point of a base slab, may produce local tension in the foundation area. This condition may be dangerous from the standpoint of percolation in retaining walls used for dam abutments. Whether or not the problem is a case of symmetry, the distribution of base pressures in such walls can be easily determined from two linear equations in two unknowns, S_1 and M_1, at the point of application of an external moment. The basic data for solution of the author's Example 4 are: $\beta = .126$, $\beta b = 4.02$, Moment at $\beta x = .50$, $y_o = 4.16 \times 10^{-5} P_o$, $y_o = .525 \times 10^{-5} M_o$, $\frac{dy_o}{dx} = .525 \times 10^{-5} P_o$, and $\frac{dy_o}{dx} = .132$

$\times 10^{-5}M_0$. The deflection and slope ratios, as taken from charts, and the corresponding deflections and slopes for the two segments of the beam A-B = .50 and B-(A) = 3.52, as computed in Table 11, result in two equations in terms of the unknowns S, and M, at points B and (B). $\Delta_B - \Delta_{(B)} = 20.44S_1 + 5.72M_1 + .51 = 0$, $\phi_B - \phi_{(B)} = 5.72S_1 + 3.214M_1 - .125 = 0$.

Solution of the equations and substitution yield the following values of deflection: $\Delta_A = -.44 \times 10^{-5}M$, $\Delta_B = -.15 \times 10^{-5}M$ and $\Delta_E = .198 \times 10^{-5}M$. It can be seen from the charts that the total length and the distance between the loads are such that sufficiently close results can be obtained considering the beam to be of semi-infinite length. The resulting values will be $\Delta_A = -.81 \times .525 = -.428$, $\Delta_B = -.28 \times .525 = -.147$ and $\Delta_E = 2 \times .185 \times .525 = .194$.

The charts presented with this discussion give the simplest and quickest method of solution of beams on elastic foundations and will suffice for practical problems. There is no doubt that a set of similar charts to cover a range of beams with variable elastic properties and modulus of foundation will be available to designers, and that solutions of beams on elastic foundation will become as common a problem as solutions of other indeterminate structures.

LYMON C. REESE,[17] M. ASCE.—The problem examined by Malter is encountered in the design of laterally-loaded piles. Sol Gleser,[18] F. ASCE, has proposed a numerical method for computing stresses in soil-supported structures based on the fourth difference equation. This discussion proposes to apply the Gleser method to solve Example 1 of the author's paper. A representation of the problem posed in Example 1 is shown in Fig. 9.

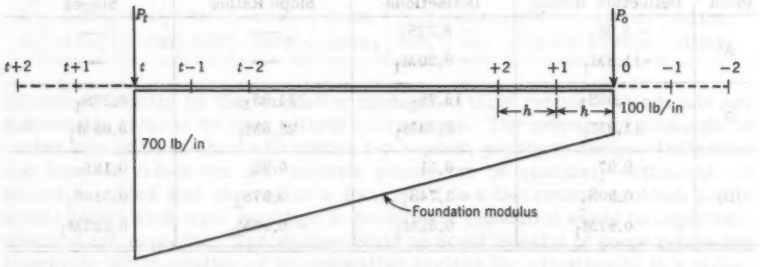


FIG. 9.—SUBDIVISION OF BEAMS FOR DIFFERENCE EQUATION SOLUTIONS

The beam is divided into a number of increments of equal length such that $h = \frac{L}{n}$. The fourth difference equation, where y_m is the deflection of the beam at point m, is

$$y_{m-2} - 4y_{m-1} + 6y_m - 4y_{m+1} + y_{m+2} = \frac{k_m}{EI}\left(\frac{L}{n}\right)^4 y_m \quad \ldots \ldots (8)$$

---

17 Prof. of Civ. Engrg., Univ. of Texas, Austin, Tex.

18 "Lateral Load Tests on Vertical Fixed-Head and Free-Head Piles," by Sol M. Gleser, Symposium on Lateral Load Tests on Piles, ASTM Special Technical Publication No. 154, 1953.

Considering the laterally loaded pile for the moment, both the shear and moment at the pile tip (at Point 0) are equal to zero, or

$$-y_2 + 2y_1 - 2y_{-1} + y_{-2} = 0 \quad \ldots\ldots\ldots\ldots \quad (9a)$$

and

$$y_1 - 2y_0 + y_{-1} = 0 \quad \ldots\ldots\ldots\ldots\ldots \quad (9b)$$

Using Eqs. 8, 9a, and 9b, one may start at the pile tip and eliminate the y_{-1} and y_{-2} terms. Successive points up the pile are considered and an expression is derived, as follows:

$$y_m = -B_{2m}\, y_{m+2} + B_{2m+1}\, y_{m+1} \quad \ldots\ldots\ldots\ldots \quad (10)$$

in which $$B_{2m} = \frac{1}{6 + A_m - B_{2m-4} - B_{2m-1}\left(4 - B_{2m-3}\right)}, \quad \ldots \quad (11a)$$

$$B_{2m+1} = B_{2m}\left(4 - B_{2m-1}\right) \quad \ldots\ldots\ldots\ldots \quad (11b)$$

and

$$A_m = \frac{k_m}{EI}\left(\frac{L}{n}\right)^4 \quad \ldots\ldots\ldots\ldots \quad (11c)$$

Eqs. 11(a) and 11(b) hold for all the B-values with the exceptions of $B_0 = \frac{2}{A_0 + 2}$, $B_1 = 2B_0$ and $B_2 = \frac{1}{5 + A_1 - 2B_1}$.

In the case of the beam, (Fig. 9) Example 1 in the author's paper, the boundary conditions at Point 0 are given by Eq. 9(b):

$$-y_2 + 2y_1 - 2y_{-1} + y_{-2} = \frac{2P_0\left(\frac{L}{n}\right)^3}{EI} \quad \ldots\ldots\ldots \quad (12)$$

Using Eq. 12 instead of Eq. 9(a) and proceeding as before, a general expression for y_m is determined as,

$$y_m = -B_{2m}\, y_{m+2} + B_{2m+1}\, y_{m+1} - D_m \quad \ldots\ldots\ldots \quad (13)$$

in which $$D_m = \left(4 - B_{2m-3}\right) D_{m-1} - D_{m-2}\, B_{2m}$$

and all other terms are defined as before. The equation for D_m holds for all D-values with the exception of $D_0 = -\frac{2P_0\left(\frac{L}{n}\right)^3}{EI\left(A_0 + 2\right)}$ and $D_1 = 2D_0B_2$

Using the equation for D_m and the boundary conditions at the other end of the beam, point t, one may compute expressions for the deflections, as follows:

$$y_{t+2} = C_1\, B_{2t+1} y_{t+1} - C_1 y_t - C_1 D_t \quad \ldots\ldots\ldots \quad (14a)$$

$$y_{t+1} = \frac{\left(2 - B_{2t-1}\right) y_t + D_{t-1}}{1 - B_{2t-2}} \quad \ldots\ldots\ldots\ldots \quad (14b)$$

$$y_t = \frac{\left[E_1 - C_1 D_t - \left(2 - B_{2t-3}\right) D_{t-1} + D_{t-2}\right]\left[1 - B_{2t-2}\right] + C_2 D_{t-1}}{C_3\left(1 - B_{2t-2}\right) - C_2\left(2 - B_{2t-1}\right)} \quad \ldots \quad (14c)$$

in which $C_1 = \frac{1}{B_{2t}}$, $C_2 = C_1 B_{2t+1} - 2 - B_{2t-2} (2 - B_{2t-3})$, $C_3 = C_1 - B_{2t-4} - B_{2t-1} (2-B_{2t-3})$ and $E_1 = \frac{2P_t}{EI} \left(\frac{L}{n}\right)^3$

This completes the derivation of the necessary equations. The solution is made by first computing A, B, D, C, and E-values; then the y-values at one end of the beam may be computed by using Eqs. 14(a) through 14(c). Finally, Equation 13 can be used to compute other y-values.

The Gleser method was used to solve the problem posed in Example 1, with h taken as 10 in or n taken as 12. The results are shown in Table 12. Points 0, 4, 8, and 12 correspond to the author's points D, C, B, and A, respectively.

TABLE 12.—GLESER-METHOD SOLUTION

Point	Deflection y, in inches	Pressure q, in pounds per inch
0	0.01918	1.92
1	.01525	2.29
2	.01158	2.32
3	.00834	2.09
4	.00567	1.70
5	.00362	1.27
6	.00222	0.89
7	.00145	0.65
8	.00126	0.63
9	.00160	0.88
10	.00239	1.43
11	.00353	2.29
12	.00487	3.41

The author is correct when he states that a method using the fourth difference equation cannot be applied readily to problems involving variable moments of inertia, but the writer and a colleague have formulated the compatibility equations for the Gleser method that are necessary in solving the problem of the laterally-loaded pile where there is an abrupt change in moment of inertia of the pile.

The Gleser method is particularly adaptable for use on a high-speed digital computer. For a laterally-loaded pile made of three sections, each with a different moment of inertia, a difference equation solution in which 50 points are used along the pile, can be obtained in approximately 3 min on a medium-sized digital computer.

It is ture that more accurate solutions than those indicated by the author are seldom needed, because the foundation modulus ordinarily cannot be obtained very accurately. However, with regard to the laterally loaded pile, research has been done[19] and is continuing[20] that should allow the soil modulus to be obtained with reasonable accuracy.

19 "Soil Modulus of Laterally Loaded Piles," by Bramlette McClelland and John A. Focht, Jr., Proceedings Paper 1081, ASCE, October, 1956.

20 "Procedures and Instrumentation for Tests on a Laterally Loaded Pile," by Hudson Matlock and E. A. Ripperger, Proceedings, 8th Texas Conf. on Soil Mech. and Foundation Engrg., The Univ. of Texas, Austin, 1956.

VICTOR R. BERGMAN,[21] M. ASCE.—There can be no argument with Mr. Malter's decision to deal exclusively with the mathematical manipulations involved in the solutions. Whereas Mr. Malter states that the phase covered in his work is only one aspect of a three-part problem, designing engineers must often face the problem[22] in its entirety.

In his concise presentation of the application of numerical methods to the solution of beams on the Winkler foundation, Mr. Malter has furnished two references for further study of the finite-difference method. This technique, as applied to the problem considered, is of such beautiful simplicity that consultation of references is unnecessary. The only feature of the procedure that may

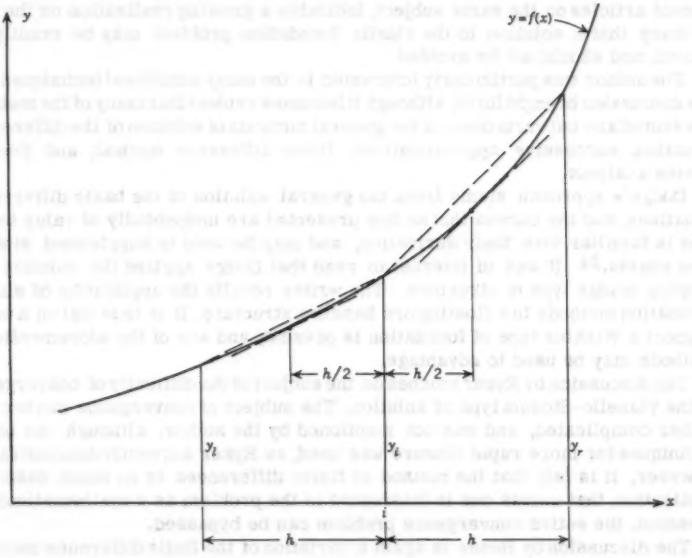


FIG. 10.—DERIVATION OF FINITE DIFFERENCE APPROXIMATION

prove unfamiliar to the structural analyst is the replacement of the second derivative in the familiar beam equation, $d^2y/dx^2 = M/EI$, by its finite-difference approximation,

$$\frac{y_r - 2y_i + y_l}{h^2}$$

A simple derivation of this approximate expression is offered in Fig. 10. At $x = i - h/2$, $dy/dx = \frac{y_i - y_l}{h}$. At $x = i + h/2$, $dy/dx = \frac{y_r - y_i}{h}$. The change of

21 Vice-Pres., Godwin Constr. Co., New York, N. Y.

22 "Evaluation of Coefficients of Subgrade Reaction," by K. Terzaghi, Geotechnique, Vol. 5, No. 4, December, 1955, pp. 297-326.

slope between $x = i - (h/2)$ and $x = i + (h/2)$ is approximately $\frac{y_r - y_i}{h} - \frac{y_i - y_l}{h} = \frac{y_r - 2y_i + y_l}{h}$, and the rate of change at slope at $x = i$ is

$$\frac{d^2y}{dx^2} \cong \left(\frac{y_r - 2y_i + y_l}{h}\right) \Big/ h \cong \frac{y_r - 2y_i + y_l}{h^2}$$

HENRY MALTER,[23] M. ASCE.—The writer wishes to thank those who participated in the discussion of this paper. The interest in the subject, as made evident by the response to the particular article, as well as to the many other recent articles on the same subject, indicates a growing realization on the part of many that a solution to the elastic foundation problem may be readily obtained, and should not be avoided.

The author was particularly interested in the many additional techniques that the discussion brought forth, although it becomes evident that many of the methods presented are but variations of the general methods of solution of the differential equation, successive approximations, finite difference method, and Fourier Series analysis.

Dodge's approach stems from the general solution of the basic differential equations, and the curves that he has presented are undoubtedly of value to one who is familiar with their derivation, and may be used to supplement similar type charts.[24] It was of interest to read that Dodge applied the solution to a floating bridge type of structure. The writer recalls the application of elastic foundation methods to a floating ore handling structure. It is true that on a water support a Winkler type of foundation is present, and any of the aforementioned methods may be used to advantage.

The discussion by Ryker touches on the subject of the difficulty of convergence of the Vianello-Stodola type of solution. The subject of convergence can become rather complicated, and was not mentioned by the author, although one of the techniques for more rapid closure was used, as Ryker correctly demonstrated. However, it is felt that the method of finite differences is so much easier in application, that unless one is interested in the problem as a mathematical digression, the entire convergence problem can be bypassed.

The discussion by Reese is again a variation of the finite difference method, and one that Reese emphasizes may be easily applied through the use of a digital computer. Although it is recognized that the American engineering profession is at present very digital computer conscious, it should be remembered that there are many engineers, in both the United States and in foreign countries, who may never have access to this latest engineering device. It should be emphasized that the entire set of computations for the author's original paper were performed with nothing more than a 10-in. slide rule.

The reference mentioned by Bergman was deliberately omitted from the author's original article in an attempt to re-emphasize the application of these techniques to building foundations where they rarely belong. It is unfortunate that this phase of engineering knowledge is entitled "Beams on Elastic Foundations." A substitution of the word "springs" for the word "foundations," would separate it from building foundations, and relegate it to the Winkler type

---

23 Prof. of Civ. Engrg., Univ. of Illinois, Urbana, Ill.

24 "Advanced Mechanics of Materials," by F. B. Seely and J. O. Smith, John Wiley and Sons, New York, 1952.

of support, where it properly belongs. An approach to this phase of the subject may be obtained in a discussion[25] to the original article by Popov.

25 Discussion by W. E. Hanson of "Successive Approximations for Beams on an Elastic Foundation," by E. P. Popov, Proceedings, ASCE, Vol. 77, April, 1951.

AMERICAN SOCIETY OF CIVIL ENGINEERS

Founded November 5, 1852

TRANSACTIONS

Paper No. 3043

UNDERSEEPAGE CONTROL AT FORT RANDALL DAM

By Stanley T. Thorfinnson,[1] M. ASCE

SYNOPSIS

The relief well system installed to control underseepage beneath Fort Randall Dam is described. Data are presented on the field investigations made, the design of the wells and the performance of the completed system.

INTRODUCTION

Fort Randall Dam is located on the Missouri River in southeastern South Dakota, as shown in Fig. 1. It is an integral part of the Pick-Sloan Plan for Missouri River development. The dam is a multi-purpose project furnishing flood control and navigation storage, generating 320,000 kw of power and providing recreational facilities. Construction of the dam was begun in 1946 and it was completed in 1955.

Control of underseepage in the valley alluvium beneath the dam was provided by an impervious upstream blanket and a system of relief wells at the downstream toe of the main impervious embankment. Several other installations at various structures, not considered within the scope of this paper, were made to control underseepage during and subsequent to construction. These installations included vertical drains to control uplift in the Niobrara chalk beneath the spillway crest structure; relief wells to control uplift pressures in the

Note.—Published, essentially as printed here, in February, 1959, in the Journal of the Soil Mechanics and Foundations Division, as Proceedings Paper 1936. Positions and titles given are those in effect when the paper was approved for publication in Transactions.

[1] Chf, Special Studies & Foundation Design Unit, F & M Branch, Engrg. Div., Omaha Dist., U. S. Army Engr. Dist., Omaha, Nebr.

Codell sandstone beneath the spillway and outlet works stilling basins; and drains to control seepage through the Niobrara chalk surrounding the power and flood control tunnels.

GENERAL PLAN

A plan showing the dam and pertinent structures is shown on Fig. 2. The power and flood-control structures as well as the spillway are located on the left abutment. The dam is of rolled earth construction, extending across the valley approximately 10,000 ft to the right abutment. The maximum height of



FIG. 1.—LOCATION MAP

the dam is 160 ft, the crest width is 60 ft, and the maximum width at the base, including the upstream impervious blanket and the downstream chalk berm is 5,000 ft. Approximately 28,000,000 cu yd of impervious fill and 22,000,000 cu yd of chalk berm were utilized in its construction. The majority of the impervious fill was obtained from excavation for the structures in the left abutment

glacial tills supplemented by loess material borrowed from the right bank. The chalk was obtained from required excavation on the left bank.

The geologic profile on the centerline of the dam shown in Fig. 3 presents a general picture of the geology at the dam site. The bedrock encountered at the site in descending order consists of the Pierre shale, Niobrara chalk, Carlile

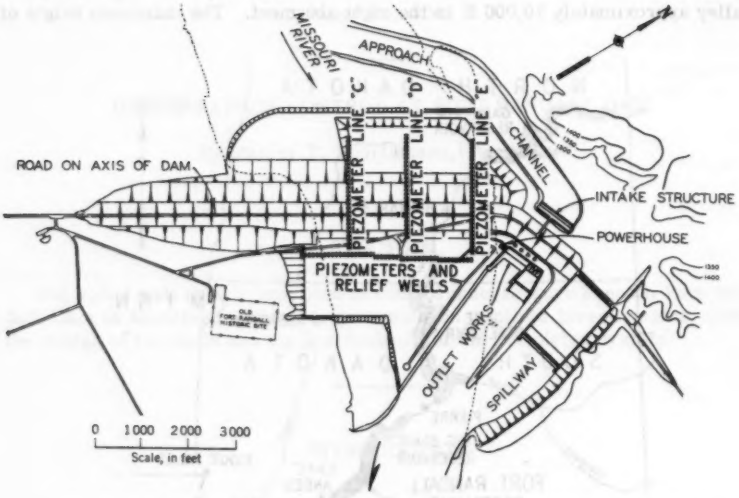


FIG. 2.—GENERAL PLAN

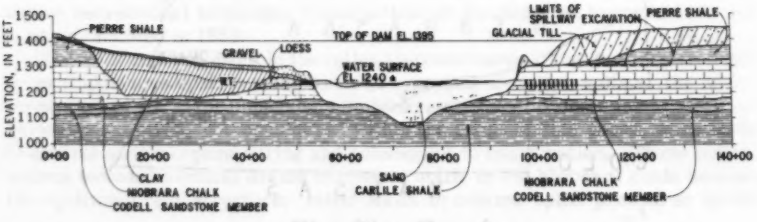


FIG. 3.—GEOLOGIC PROFILE ON AXIS OF DAM

shale, and Green horn Limestone. The outlet works, powerhouse and spillway structures were located on the left abutment to take advantage of the relatively high elevation of the Niobrara chalk as a foundation material and as a tunneling medium for the power and flood-control tunnels.

The river valley is approximately 8,000 ft wide at the site, 4,000 ft of which is occupied by the existing river channel adjacent to the left abutment. The

remaining 4,000 ft consists of a river terrace. The surface of the terrain on the right abutment rises abruptly 60 ft adjacent to the river and then slopes gently upward toward the hills south of the river. The overburden material on the left abutment is a glacial drift deposit reaching depths of 100 ft. The river is underlain by alluvial sand deposits reaching a maximum depth of 150 ft. A deposit of loess soil, reaching a maximum depth of 50 ft, caps the right terrace adjacent to the river. The loess is underlain by a deposit of poorly consolidated clays which reaches maximum depths of 130 ft in an old buried channel of the river.

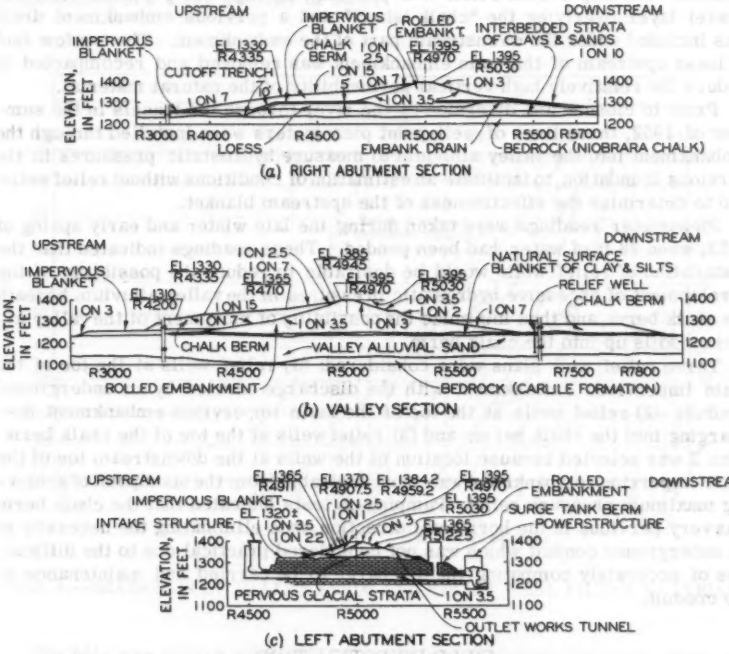


FIG. 4.—EMBANKMENT SECTIONS

Adjacent to the river the clay deposits are thin and are underlain by pervious sands and gravels that overlay a relatively high "chalk island" between the old buried channel and the river.

Typical embankment sections are shown in Fig. 4. On the left abutment (Fig. 4(c)) the embankment consists in part of in-place glacial till and in part of rolled earth fill. An upstream impervious zone with a shallow cutoff trench into the chalk and a downstream toe drain were provided in view of the existence of some relatively pervious layers of sand and gravel in the glacial till. The upstream slopes are protected from wave action by dumped riprap. The

valley section of the dam consists of an impervious main embankment flanked by chalk berms with an impervious blanket extending upstream beneath the chalk berm. Valley alluvium exposed in the side slopes and bottom of the outlet works approach channel were also blanketed to maintain the integrity of the "upstream blanket." The upstream chalk berm was constructed with flat beach slopes in lieu of hard rock riprap for wave protection in the range of pool fluctuation.

The embankment section on the right abutment (Fig. 4(a)) consists of an impervious main embankment with an upstream chalk berm. The thick deposit of loess was removed beneath the main embankment of minimize differential settlement. An impervious cutoff was provided through the pervious sand and gravel layer overlying the "chalk island" and a pervious embankment drain was included under the downstream part of the embankment. The top few feet of loess upstream of the main embankment was removed and recompacted to reduce the relatively high vertical permeability of the natural material.

Prior to closure and diversion of the river through the tunnels in the summer of 1952, three lines of well-point piezometers were installed through the embankment into the valley alluvium to measure hydrostatic pressures in the pervious foundation, to facilitate an estimation of conditions without relief wells, and to determine the effectiveness of the upstream blanket.

Piezometer readings were taken during the late winter and early spring of 1953, when 28 ft of water had been ponded. These readings indicated that the installation of relief wells would be desirable to reduce the possibility of the development of excessive hydrostatic pressures in the valley alluvium beneath the chalk berm, and thus minimize the possibility of movement of the valley alluvium soils up into the chalk berm.

Three relief well plans were considered: (1) relief wells at the toe of the main impervious embankment with the discharge carried by an underground conduit; (2) relief wells at the toe of the main impervious embankment discharging into the chalk berm; and (3) relief wells at the toe of the chalk berm. Plan 2 was selected because location of the wells at the downstream toe of the main impervious embankment was most desirable from the standpoint of achieving maximum pressure relief. Pumping-in tests indicated that the chalk berm was very pervious in the horizontal direction, thus eliminating the necessity of an underground conduit which was not considered practical due to the difficulties of accurately computing the discharge to be carried and maintenance of the conduit.

FIELD INVESTIGATIONS

The foundation soils in the area of the relief well installation are generally water-deposited sands and gravels with some clay at the surface between stations 80 + 00 to 87 + 00. The sand varies in thickness across the river bottom from a relatively shallow depth adjacent to the abutments to a maximum thickness of 150 ft. The upper part of valley alluvium consists primarily of fine to medium sands. The sands become somewhat coarser and in part gravelly with increasing depth, but the fine-to-medium sands still predominate. Occasional small seams of silty sands, chalk and lignite float are encountered. Ranges in gradation of the valley sands are shown on Fig. 5. Records from previous pumping tests in the valley sands indicated a coefficient of permeability in the

horizontal direction of approximately 0.002 fps. These pumping tests also indicated the existence of two distinct aquifers, separated by a relatively impervious layer of clay. However, numerous borings made in the alluvium indicated that the clay layer was not continuous.

A drilling and pumping-in test was conducted in the chalk berm to determine (1) whether the dumped chalk material could be drilled with a large diameter bit; (2) whether the walls of the hole would stand without casting; (3) the quantity of gravel that could be flushed into the voids in the chalk berm adjacent to the hole; (4) the resistance of flow of water out of the well screen; and (5) the amount of settlement and caving that might occur in the vicinity of the well due to movement of a large quantity of water.

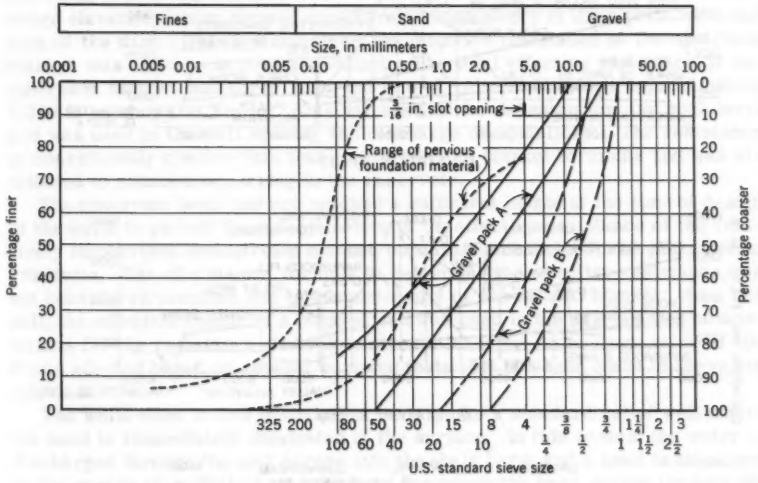


FIG. 5.—GRADATION OF VALLEY SANDS AND RELIEF WELL FILTER MATERIALS

The hole was drilled with a 39-in. auger bit. Although the chalk berm had been placed by dumping in 10-ft lifts, the hole remained open to its full depth of approximately 50 ft. The average rate of drilling was 0.1 ft in 7 min of actual drilling time. The hole was cased with 35-in. diam casing. A 27.5-ft length of length of 6+ in. screen consisting of slotted metal pipe was centered and set to the bottom of the hole. The 1/4 in.-wide slots cut parallel to the axis of the pipe were 2 ft long and overlapped 4 in. Seven slots were cut around the circumference of the pipe. An 8-in. riser pipe extending to the surface of the berm was split and welded to the slotted pipe to form a water-tight joint.

The annular space between the screen and the chalk was gravel-packed by flushing the gravel down a 3-in. pipe, and by withdrawing the 35-in. casing as the gravel level rose. A total of 36 cu yd of gravel was used, approximately 21 of which were flushed into voids in the chalk berm adjacent to the hole. Water was pumped down the hole at an average rate of 232 gpm for 107 hours during

the gravel-packing operation. Subsequent to completion of the gravel-packing, water was pumped into the well screen at the rate of 430 gpm for a period of approximately 19 hr. No appreciable head was built up in the screen during the test.

RELIEF WELL DESIGN

For the purpose of computing well spacing it was assumed that hydrostatic uplift would be resisted only by the weight of a saturated impervious blanket

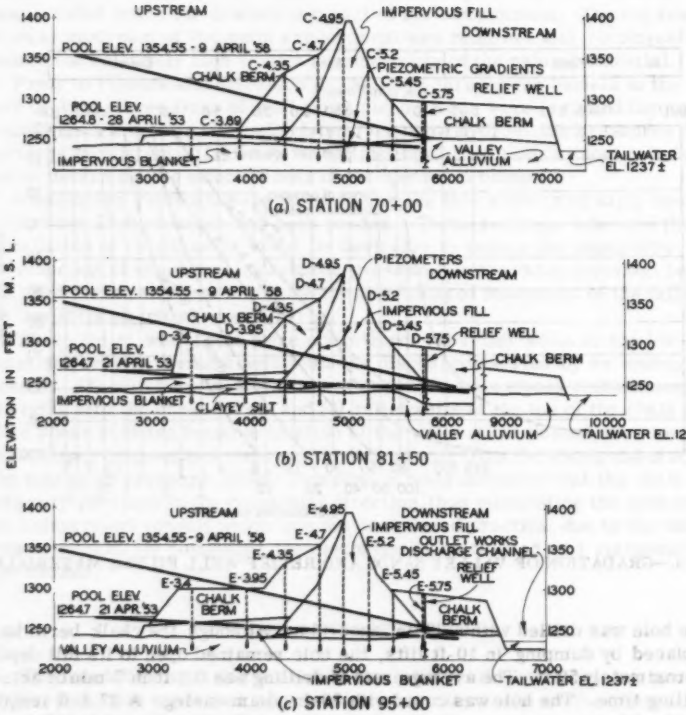


FIG. 6.—PIEZOMETRIC GRADIENTS IN FOUNDATION SANDS

5 ft thick and of uniform extent across the valley. This assumption was not fully born out by the logs of borings, but was considered justified in view of the uniformity across the valley indicated by the piezometer observations. In areas where the borings did not indicate the existence of the impervious blanket, stratification in the upper part of the valley sands apparently acted as a blanket in resisting upward flow. The weight of the chalk berm was not considered as

resisting upward flow or as resisting the uplift pressures as it was assumed that piping could occur in the large voids in the dumped chalk. Based on a unit weight of saturated blanket material of 115 lb per cu ft and a factor of safety of 1.0, the maximum allowable uplift pressure at the base of the blanket was computed to be 9.2 ft of water.

Fig. 2 shows three lines of well-point piezometer tubes installed in the pervious valley alluvium normal to the axis of the dam to measure hydrostatic foundation pressures. The piezometers penetrated the main embankment and the upstream and downstream chalk berms. Embankment sections showing the three lines of piezometers are indicated in Figs. 6 and 7. Typical piezometric observations made in the design period are also shown. The effective resistance of the impervious upstream blanket was determined by extending the piezometric gradient upstream until it intersected the water surface in the pool. The ratio of piezometric head to the total head in the pool, referenced to a tailwater elevation datum, showed considerable consistency in lines parallel to the axis of the dam. This indicated that the effective resistance of the upstream blanket was uniform across the valley. The total effective resistance of the upstream blanket measured from the line of relief wells, was approximately 3,200 ft as shown in Fig. 6. This value would be the same for any pool level and was used in the well spacing and discharge computations. The resistance is considerably greater than that computed from blanket formulas and was attributed to siltation occurring in the reservoir.

The reservoir level had not reached a sufficient height at the time of design of the wells to permit the determination of the effective resistance of the relatively impervious downstream blanket beneath the chalk berm by piezometric gradients. Use of a blanket formula to determine the effective resistance was not considered justified due to nonuniformity of the natural blanket. As a result, the effective radius of a pumped well was used in the well spacing computations for the resistance of the downstream blanket. An average value of 400 ft was adopted based on several pumping tests that had been made in the valley alluvium.

The wells used in this installation were unlike a standard relief well where the head is immediately dissipated at the surface. In this system the water is discharged through the well screen into the chalk berm and a head is developed in the screen of sufficient magnitude to overcome the head losses through the slots. The amount of head loss was computed considering the slots as free-flowing submerged orifices. The degree of clogging of the slot openings could only be approximated and the conservative assumption was made that only 25% of the slot openings were effective. Considering a well screen with 30 sq in. of slot opening per linear foot, an orifice discharge coefficient of 0.61, and assuming the slot openings 25% effective, the head loss was computed using the following equation:

$$h_x = \left(5.89 Q_w\right)^{2/3} \quad \ldots\ldots\ldots\ldots\ldots\ldots \quad (1)$$

in which Q_w is the total well discharge. For the purpose of design computations the screen entrance and riser loss and the head built up in the chalk berm were considered negligible.

Fig. 7 is a cross section of the dam showing the symbols used in computing the well spacing for fully penetrating and partly penetrating wells. The term Z_b represents the thickness of the relatively impervious downstream blanket; D is the thickness of the pervious substratum; Z_w is equal to the depth of proposed relief well; H denotes the total head; P_a is the mean potential over plane

of wells; and P_m is the surface potential at midpoint between partly penetrating wells. The head loss due to flow out of the well screen into the chalk berm is represented by H_x, the total head loss from source to line of wells H_1 is $H - (P_a - h_x)$; d represents the effective resistance upstream of the line of wells; X_d is equal to the effective resistance downstream of the line of wells; the net potential gradient producing discharge from wells S is $S_u - S_d$; a denotes the well spacing; the potential midway between fully penetrating wells in excess of the average potential over the plane h3 is 0.11 a S; K_f denotes the horizontal permeability of pervious substratum; the discharge of well Q_w is K_f D a S; and r_w represents the radius of the proposed well.

Relief wells that fully penetrated the valley alluvium were installed at all locations except in the center of the valley section where the bedrock is at a considerable depth. The well spacing for fully penetrating wells was computed by the method developed by P. T. Bennett.[2] The well spacing was computed so that the maximum head midway between the wells would not exceed the aforementioned allowable uplift pressure. Although the well spacing was computed

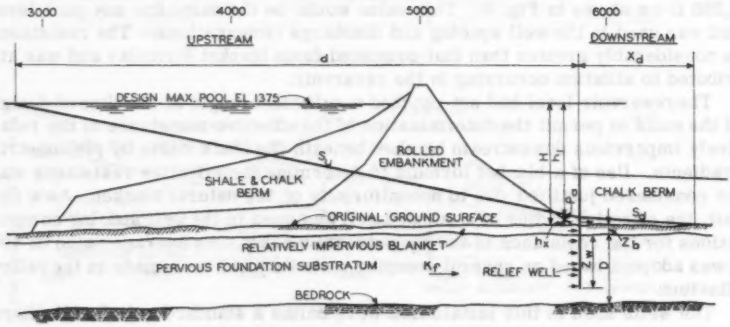


FIG. 7.—CROSS SECTION OF DAM

for fully penetrating wells, they were stopped 10 ft above bedrock due to the existence of a boulder layer immediately overlying the bedrock.

Computation for Partly Penetrating Well.—The fully penetrating well formula is as follows:

$$P_a = \left(\frac{a}{2\pi} \log_e \frac{a}{2\pi r_w}\right) S = FS \quad \ldots\ldots\ldots\ldots \quad (2)$$

The average original ground surface elevation is 1235, the average bedrock elevation is 1165, the total head H is 140 ft, and the thickness of pervious substratum D is 65 ft. Assuming the well spacing a and a value for $P_a + h_x$ (Fig. 7), the total uplift is computed by trial and error. The total uplift $P_a + h_x + h3$

[2] Comments on the Design of Relief Wells," by P. T. Bennett, from "Conference on Control of Underseepage," Waterways Experiment Sta., Vicksburg, Miss., 1945.

≦ allowable uplift. Assume a = 100, then

	1st Trial	2nd Trial
$P_a + h_x$ (assumed)	3.2	3.7
h_1	136.8	136.3
S_r	0.0428	0.0426
S_1	0.0080	0.0093
S	0.0348	0.0333
Q_w (in cfs.)	0.45	0.43
h_x	1.95	1.89
$P_a = F\,S = 55\,S$	1.91	1.83
$P_a + h_x$	3.86	3.72
h_3	0.38	0.37
$h_x + P_a + h_3$	4.24	4.09

The computed value for $P_a + h_x$ corresponds to the assumed values in the second trial and the total computed potential $h_x + P_a + h_3$ is slightly less than the allowable value, therefore the well spacing of 100 ft is adequate.

Partly penetrating relief wells, penetrating to El 1150 or approximately 60% of the depth of the valley alluvium were used in the center of the valley section where bedrock is at considerable depth. For the purpose of well spacing computations, the valley alluvium was assumed to be 16 times more permeable in the horizontal direction than vertically. The depth of well and the permeability were transformed by the relationship $\sqrt{K_f/K_v}$.

Computation for Fully Penetrating Well.—The well spacing was computed using the partial penetration multiple well spacing equations developed by P. T. Bennett.[3] The mean potential equation is

$$P_a = \left[\frac{a\,D^1}{2\pi\,Z_w^1} \log_e \frac{a}{2^1 - \left(\frac{D^1}{a} - 1\right)\left(1 - \frac{Z_w^1}{D^1}\right)\pi\,f_w} \right] S \quad \ldots\ldots (3)$$

The midpoint potential equation is

$$P_M = \left[\frac{a\,D^1}{2\pi\,Z_w^1} \log_e \frac{a}{2\left(\frac{1 - Z_w^1}{D^1}\right)\pi\,r_w} \right] S \quad \ldots\ldots\ldots (4)$$

The average ground surface elevation is 1238, the average bedrock elevation is 1080, the bottom of well elevation is 1150, H = 137 ft, D = 65 ft, transformed D^1 = 612 ft, Z_w = 33 ft, and transformed Z_w^1 = 332 ft.

[3] Discussion by P. T. Bennett of "Relief Well for Dams and Levees," by W. J. Turnbull and C. I. Mansur, Transactions, ASCE, Vol. 119, 1954, p. 862.

Assume the well spacing a and a value for $P_a + h_x$ and compute total uplift, using the transformed depths and permeability by trial and error. Total uplift $P_M + h_x \leq$ allowable uplift.

	1st Trial	2nd Trial	3rd Trial
a (assumed)	100.0	100.0	70.0
$P_a + h_x$ (assumed)	6.0	6.4	5.4
h_1	131.0	130.6	131.6
S_r	0.0409	0.0408	0.0411
S_1	0.0150	0.0160	0.0135
S	0.0259	0.0248	0.0276
Q_w	0.79	0.76	0.59
h_x	2.79	2.71	2.30
P_a	3.83	3.70	3.14
$P_a + h_x$	6.62	6.41	5.44
P_M	---	2.80	1.95
$P_M + h_x$	---	5.51	4.25

The computed value for $P_a + h_x$ corresponds to the assumed value in the second trial. However, the total computed potential, $P_M + h_x$, is greater than the allowable value. Therefore, the spacing of 100 ft is inadequate. The computed value for $P_a + h_x$ corresponds to the assumed value in the third trial and the total computed potential $P_M + h_x$ is approximately equal to the allowable value, therefore the spacing of 70 ft is adequate.

A typical relief well is shown on Fig. 8. Discharge computations indicated that an 8-in. inside diameter screen and riser pipe would provide adequate capacity to carry the flow without excessive head loss. Treated wooden well screens and riser pipes were chosen for their advantages of low cost and long life as long as the wood is immersed. The well screen pipe was slotted with 3/16-in. slots of such spacing and length to provide a minimum of 30 sq in. of clear slot opening per linear foot of screen. The screen section is continuous through the valley alluvium and well up into the chalk berm.

The range of gradation of the filter material for that part of the well in the valley alluvium is designated as gravel pack "A" and is shown on Fig. 5, together with gradation curves for the limiting sizes of the pervious valley alluvium. The gradation of gravel pack "A" was based on standard Corps of Engineers procedure. A minimum thickness of gravel pack of 6 in. was provided between the well screen and the foundation material. The wells were surged by intermittent pumping to develop and stabilize the gravel pack. Normally the surging would have been accomplished using a plunger, but a plunger was not considered feasible in this system as the water table was within the screen portion of the well which would have resulted in loss of surging action and the screen might have been damaged. The top of gravel pack "A" was extended 1 ft above the top of the valley alluvium to allow for settlement in the gravel pack and thus insure that the coarser gravel pack "B" did not come in contact with the valley sands.

A thick gravel pack, designated as gravel pack "B" on Fig. 5 was provided in the chalk berm portion of the well. This gravel pack does not act as a filter because the direction of flow in the chalk portion of the well is out of the well screen and into the chalk berm. The selected gradation gave a gravel of fairly uniform size that would pass the flow from the well with a minimum head loss and that was free of fine material that might choke the voids in the chalk.

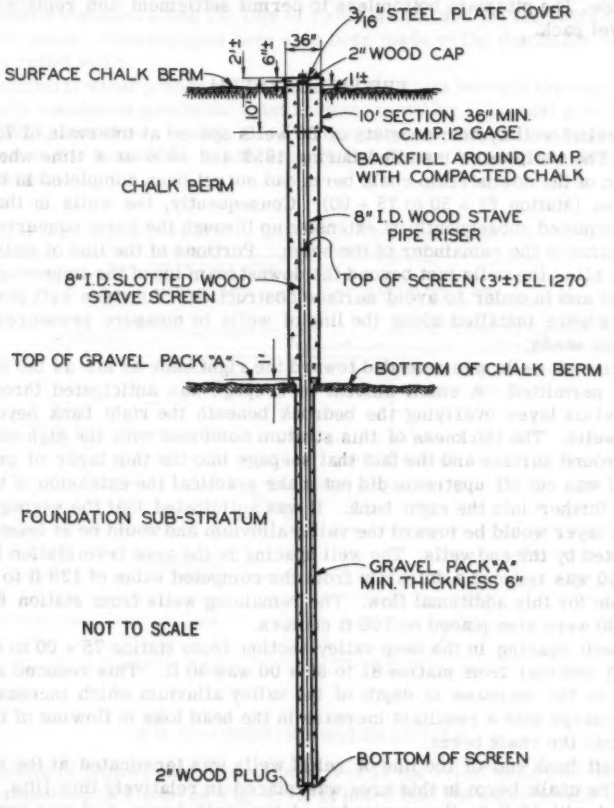


FIG. 8.—RELIEF WELL

The added thickness of gravel pack "B" was provided in order to (1) reduce the danger of bridging in the gravel pack as settlement of the pack occurred which would probably be increased by movement of filter material into the chalk berm; and (2) to protect the wood stave screen and riser pipe from the

heat that may be generated by the oxidation and combustion of the fine disseminated iron pyrite in the chalk. Gravel pack "B" was extended to the surface to facilitate replacement of gravel lost by settlement.

Each well was fitted with a corrugated metal well pit and cover to protect the well and prevent caving of the chalk berm at the surface. The cover was designed to provide a tight fit to minimize drying out of the wood pipe. The well pits were extended 2 ft above the finished surface of the chalk berm and supported by compacting the chalk into the corrugations on the outer surface of the pipe. The pits were bottomless to permit settlement and replacement of the gravel pack.

THE WELL SYSTEM

The relief well system consists of 36 wells spaced at intervals of 70 ft and 100 ft. The wells were installed during 1953 and 1954 at a time when construction of the downstream chalk berm had not yet been completed in the closure area (station 61 + 50 to 75 + 00). Consequently, the wells in that area were completed subsequently by extension up through the berm concurrent with construction of the remainder of the berm. Portions of the line of wells were offset to place the wells just beyond the downstream toe of the impervious embankment and in order to avoid surface obstruction. Fourteen well point piezometers were installed along the line of wells to measure pressures in the foundation sands.

The line of wells was extended toward the right bank as far as the depth of bedrock permitted. A small amount of seepage was anticipated through the thin pervious layer overlying the bedrock beneath the right bank beyond the line of wells. The thickness of this stratum combined with the high elevation of the ground surface and the fact that seepage into the thin layer of pervious material was cut off upstream did not make practical the extension of the line of wells further into the right bank. It was anticipated that the seepage from this thin layer would be toward the valley alluvium and would be at least partly intercepted by the end wells. The well spacing in the area from station 61 + 50 to 65 + 50 was reduced arbitrarily from the computed value of 120 ft to 100 ft to provide for this additional flow. The remaining wells from station 65 + 50 to 75 + 00 were also placed on 100 ft centers.

The well spacing in the deep valley section from station 75 + 00 to 81 + 00 was 70 ft and that from station 81 to 85 + 00 was 80 ft. This reduced spacing was due to the increase in depth of the valley alluvium which increased the well discharge with a resultant increase in the head loss in flow out of the well screen into the chalk berm.

The left bank end of the line of relief wells was terminated at the switchyard. The chalk berm in this area was placed in relatively thin lifts, 3 ft as compared with 10 ft in the remainder of the chalk berm, and was somewhat compacted by the passage of hauling equipment. It was assumed that this part of the chalk berm was therefore more impervious and might not satisfactorily conduct the flow away from the wells. The possibility also existed that flow through the chalk might cause settlement with resultant damage to the structure

and electrical installations in the switchyard area. The discharge channel slope of the switchyard area was provided with riprap and a filter for a sufficient distance downstream to provide a means of controlled pressure relief.

OBSERVATIONS SUBSEQUENT TO CONSTRUCTION

Periodic observations have been made of the piezometric pressures in the valley alluvium beneath the dam as measured by (1) the water levels in the lines of piezometers normal to the axis of the dam; (2) the water levels in the piezometers installed along the line of relief wells; and (3) the water levels in the relief wells. Observations have also been made of the discharge of the individual relief wells.

Piezometric water pressures in the valley alluvium beneath the dam indicate that fairly consistent gradients exist across the valley. Typical gradients for April, 1958, are shown on Fig. 6. Furthermore, no excessive pressures are indicated in the foundation sands beneath the dam or beneath the downstream chalk berm.

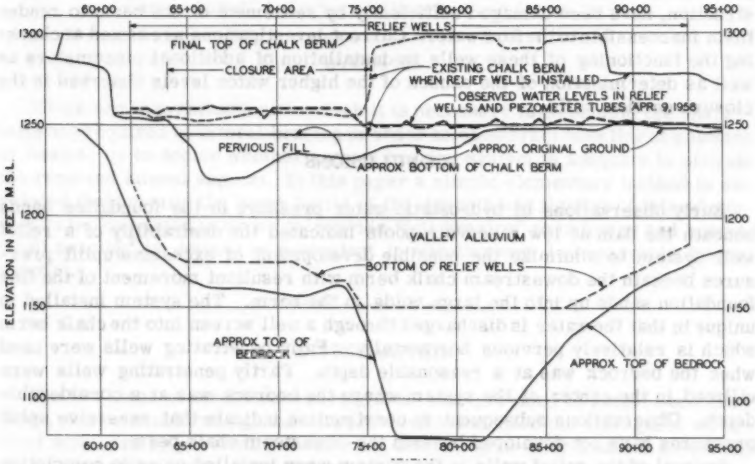


FIG. 9.—OBSERVED WATER LEVELS

A profile of typical water levels observed in the relief wells and intermediate piezometers is shown on Fig. 9. It is noted that the water levels in the relief wells in the closure area are consistently approximately 7 ft higher than the levels observed in the remainder of the wells. The piezometers in the closure area have generally indicated pressures approximately 7 ft lower than those observed at the wells as compared with those observed elsewhere along the line of wells. The cause of the higher water levels observed in the closure area relief wells and the difference between the levels observed in the wells and those in the intermediate piezometers has not been determined. Several factors that may have a bearing include (1) the absence of a natural blanket overlying the valley alluvium in the closure area; (2) the substantial depth of relatively clean dredged sand fill placed in the river channel in this area; (3)

the fact that the lower part of the chalk berm in the closure area consisted of more finely broken-up material with less voids than elsewhere along the line of wells which could result in less flow out of the wells with a resultant build up of head in the wells; and (4) the possible existence of two separate aquifers in this area with higher pressures existing in the lower aquifer, which would be penetrated by the relatively deep relief wells but might not be by the shallower piezometer tubes. The existence of the relatively compact impervious layer at the base of the chalk berm reduces the possibility of movement of the underlying valley sand up into the chalk berm. The higher head observed in this area has not been detrimental. No excessive seepage has been observed at the downstream toe of the chalk berm in this area nor is any local subsidence of the chalk berm in evidence.

Observed discharges from the individual relief wells have been somewhat erratic but have shown a trend toward decreased flow. This trend is due probably to reduced efficiency of the wells and to an increasing effectiveness of the upstream blanket due to siltation in the reservoir.

Some of the wells, particularly in the closure section where the wells were installed when the berm was at a low level and extended concurrent with construction, have been damaged sufficiently by settlement of the berm to render them inaccessible to the flow water. Current investigations are aimed at checking the functioning of these wells by installation of additional piezometers as well as determination of the causes of the higher water levels observed in the closure section wells.

CONCLUSIONS

Early observations of hydrostatic water pressure in the foundation sands beneath the dam at low reservoir pools indicated the desirability of a relief well system to minimize the possible development of excessive uplift pressures beneath the downstream chalk berm with resultant movement of the fine foundation sands up into the large voids in the berm. The system installed is unique in that the water is discharged through a well screen into the chalk berm which is relatively pervious horizontally. Fully penetrating wells were used when the bedrock was at a reasonable depth. Partly penetrating wells were utilized in the center of the system where the bedrock was at a considerable depth. Observations subsequent to construction indicate that excessive uplift pressures have not developed beneath the downsteam chalk berm.

Several of the relief wells in the system were installed prior to completion of the surrounding chalk berm and extended concurrent with completion of the berm. The wells suffered damage due to settlement of the berm. The possibility of damage to the wells due to settlement should be carefully considered in any future installation of this type.

AMERICAN SOCIETY OF CIVIL ENGINEERS

Founded November 5, 1852

TRANSACTIONS

Paper No. 3044

LATERAL BRACING OF COLUMNS AND BEAMS

George Winter,[1] F. ASCE

With Discussion by Messrs. Anthony A. Chibaro; Giles G. Green; Bruce G. Johnston; Marvin A. Larson; William Zuk; and George Winter

SYNOPSIS

There are many situations in which it is necessary to determine the characteristics required of lateral bracing in order to counteract buckling of columns or beams, or to decide whether a given bracing system is adequate to provide the required lateral support. In this paper a simple elementary method is developed that permits the lower limits of the strength and rigidity of lateral support to be computed in order to provide "full bracing" to columns and beams. "Full bracing" is defined as equivalent in effectiveness to immovable lateral support.

INTRODUCTION

The two kinds of structural bracing are: that provided to resist secondary loads, such as windbracing, and that provided to increase the strength of structural members by preventing them from deforming in their weakest direction. This paper refers only to the latter kind of bracing. Here, again, there are two different types of problems. The first of these is bracing applied to counteract stable but detrimental types of deformation. As examples one might mention beams of channel or Z-shape, loaded in the plane of the web. Such beams, unless properly braced, twist and deflect sideways with consequent loss of strength.[2,3] The second such problem is in regard to bracing applied to prevent buckling in the weakest direction, and thereby to increase the usable strength

Note.—Published, essentially as printed here, in March, 1958, in the Journal of the Structural Division, as Proceedings Paper 1561. Positions and titles given are those in effect when the paper or discussion was approved for publication in Transactions.

[1] Prof. and Head, Dept. of Struct. Engrg., Cornell Univ., Ithaca, N. Y.

[2] "Performance of Laterally Loaded Channel Beams," by George Winter, Warner Lansing, and R. B. McCalley, Research, Engineering Structures Supplement, Colston Papers, Vol. II, London, 1949, p. 179.

[3] "Unsymmetrical Bending of Beams with and Without Lateral Bracing," by Lev Zetlin and George Winter, Proceedings Paper 774, ASCE, August, 1955.

of the member. It is this last kind, bracing against buckling, that is the subject of the present investigation.

To resist secondary loads, and to counteract stable but detrimental deformations, it is only necessary to provide bracing of sufficient strength. Given the loads, there is no basic difficulty in computing the internal forces in the bracing system and to dimension it accordingly. In contrast, for bracing against buckling to be effective, it must possess not only the requisite strength but also a definite minimum rigidity. As will be seen, neither the requisite strength nor the necessary rigidity can be computed uniquely except on the basis of assumed imperfections of shape or loading of the member to be braced.

Mention of a few frequent problems of such bracing will show the variety of such situations. To prevent buckling of the compression chord of a roof truss out of its plane, is the strength and rigidity of the roof proper sufficient (steel roof deck, or other planking adequately connected to form a diaphragm), or must special bracing members be provided. For a laced wall column in a mill building, where the outer leg is adequately braced in the plane of the wall, how must horizontal braces be positioned and dimensioned to prevent buckling, parallel to the wall, of the free-standing inner leg. In order for a beam or girder to be fully braced, must its compression chord be embedded in a concrete floor slab. If not, what is the required minimum strength and rigidity of the floor system to provide full bracing. These few cases will suffice to show the problem of bracing against buckling.

Notation.— The letter symbols adopted for use in this paper are defined where they first appear, in the illustrations or in the text, and are arranged alphabetically for convenience of reference, in the Appendix.

CHARACTERISTICS OF EFFECTIVE BRACING

Bracing of this type is of considerable consequence because very large increases in carrying capacity can be achieved by very light and inexpensive bracing. This will be illustrated by selected results from a series of tests that have been reported[4] in detail.

Specimens consisted of two channels cold-formed of 16—gage sheet steel and spot welded back-to-back to form an I-shape 4 in. deep and 2 in. wide. They were tested as columns 12 ft 3 in. long between knife edges. Whereas one of the columns was tested unbraced, for the other identical specimens intermediate bracing was provided at equidistant points. This bracing, at each point, consisted of two strips of thin, 10-ply cardboard, 3/4 in. wide and 2 in. or 15 in. long whose combined tensile strength was 103 lb per pair. Fig. 1 shows one of the studs under test, with four pairs of strips in place, the right part a portion of a failed specimen with two pairs of broken cardboard strips. (These photos happen to show tests where the strips were 1.5 in. wide.) Table 1 gives a representative selection of test results.

These results qualitatively illustrate a number of important points:

1. In these tests the usable strength of the columns could be increased as much as fifteen times by using bracing as weak as that provided by the described cardboard strips.

---

4 "Light Gage Steel Columns in Wall-Braced Panels," by G. G. Green, George Winter, and T. R. Cuykendall, Bulletin No. 35/2, Engrg. Experiment Sta., Cornell Univ., Ithaca, N. Y.

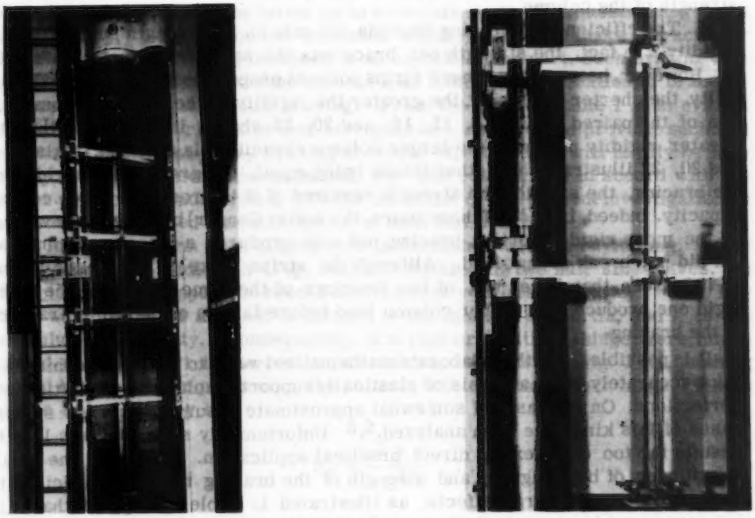


FIG. 1.—TEST OF STEEL STUD BRACED BY CARDBOARD STRIPS

TABLE 1.—TESTS ON CARDBOARD BRACED LIGHT GAGE STEEL COLUMNS.

Test[b]	Cardboard Strips		Measured Ultimate Load, in pounds	Brace Strength, in Percent of Column Strength	Failure[a]
	Number of Pairs	Length, inches			
0	0	—	1098	—	—
4	1	15	4650	2.2	column buckled
8	2	15	8600	1.2	strips broke
9	2	4	9900	1.0	column buckled
15	3	15	10,450	1.0	strips broke
16	3	2	15,200	0.7	strips broke
20	4	15	11,600	0.9	strips broke
22	4	2	17,000	0.6	column buckled

[a] When failure occurred by buckling, the bracing strips remained intact.
[b] Test numbers agree with those used by Green, Winter, and Cuykendall.

2. In those tests in which column failure was accompanied by fracture of the bracing strips, the strength of one brace was of the order of only 1% of the strength of the column.

3. The efficiency of bracing depends not only on its strength but also on its rigidity. In fact, the strength per brace was the same in all these tests, 103 lb. However, because the longer strips possess proportionately larger extensibility, the shorter the strips, the greater the rigidity of the bracing. Comparison of the paired tests 8, 9; 15, 16; and 20, 22 shows, in each case, that the greater rigidity produced the larger column capacity. In addition, tests 8, 9 and 20, 22 illustrate that, other things being equal, the greater the rigidity of the bracing, the smaller the strength required of it to produce a given column capacity. Indeed, in each of these pairs, the softer (longer) bracing broke whereas the more rigid (shorter) bracing not only produced a larger column load but did not break at that load. Although the strips broke in both tests 15 and 16 it is seen that here, too, of two bracings of the same strength, the more rigid one produced the higher column load before failure occurred by fracture of the bracing.

It is possible, in rather elaborate mathematical ways, to investigate this situation accurately by an analysis of elastically supported columns with initial imperfections. On the basis of somewhat approximate assumptions a few special cases of this kind have been analyzed.[5,6] Unfortunately such analyses lead to results far too complex for direct practical application. However, the small magnitudes of both rigidity and strength of the bracing that are sufficient to produce extremely large effects, as illustrated in Table 1, suggest that it is not necessary to compute these two characteristics with great accuracy. Instead, it is sufficient and practical, to devise a simple method which permits: (1) Computing a safe lower limit, rather than an exact value, of the necessary rigidity of the bracing such that the strength of the braced member will attain its maximum possible value; and (2) determining a safe, lower limit, rather than an exact value, of the strength required of a bracing of rigidity equal to or larger than that so computed.

POINT-BRACED COLUMNS

Analysis.—As an acceptable approximation, the performance of practical means of bracing can be regarded as elastic. Consequently, for ideal columns (straight, concentrically loaded, and so forth) the well established theory of columns on elastic supports permits one, for a given column, to determine[4, 6,7] the relation between support rigidity (spring constant) and column load, at least for simple cases of equidistant supports. These investigations give no information on required strength of support, because for such ideal conditions, the reaction at the support is zero up to the moment of buckling, and indeterminate when buckling occurs.

---

5 "Lateral Bracing Forces on Beams and Columns," by W. Zuk, Proceedings Paper 1032, ASCE, July, 1956.

6 "Theory of Elastic Stability," by S. Timoshenko, McGraw-Hill Book Co., Inc., New York, 1936.

7 "Lateral Buckling of Elastically Braced Columns," by G. G. Green, thesis presented to Cornell University, at Ithaca, in 1948, in partial fulfilment of the requirements for the degree of Doctor of Philosophy.

However, for most design situations the question is not that of determining the buckling load for a given rigidity of support. The former more or less steadily increases with the latter up to a certain limit. The question is, much more simply, to determine the minimum rigidity that will make the actually elastic bracing equivalent, in effect, to an unyielding support. Such bracing will evidently produce the maximum column load for the given location of brace or braces and will be called full bracing. From the data of Table 1 it is evident that relatively low rigidities and strengths are required to provide such full bracing. Consequently, any bracing of lesser effectiveness will hardly be less costly, and is therefore uneconomical. For this reason, and in accord with the points previously enumerated, it is the main aim of the present investigation to compute the required characteristics of such full bracing.

If an ideal column with hinged ends is furnished with an unyielding, knife-edge support at midlength (Fig. 2 (a)), it buckles in two half sine-waves. At the intermediate support the second derivative of y with respect to x $y'' = -M/EI = 0$, in which M is the moment of force, I is the moment of inertia, and E is the modulus of elasticity. Consequently, if a real or fictitious hinge were introduced at the support in the continuous column, as shown in Fig. 2 (b), nothing would be changed. In particular, the column, with or without such hinge, buckles at the Euler-Shanley load

$$P_e = \frac{\pi^2 E I}{L^2} \quad \ldots\ldots\ldots\ldots\ldots\ldots (1)$$

in which L is the unbraced length of the column, P_e is the column load and where, in the elastic domain, E is Young's modulus and in the plastic domain it is the tangent modulus.

If this ideal column is braced by an elastic support and if this support is rigid enough to provide full bracing, the column buckles in exactly the same manner as for unyielding support, and again a fictitious hinge can be introduced at the support (Fig. 2 (c)).

To obtain information for practical design of bracing it is now necessary to investigate real columns. This is necessary because, as previously mentioned, the theory of ideal columns would indicate that supports of infinitesimally small strength are sufficient, which is evidently not a permissible idealization and is at variance with the information of Table 1. Also, as will become apparent, the minimum rigidities computed for full bracing of ideal columns are not sufficient to achieve full bracing of real, that is, imperfect columns. To simplify analysis it will be assumed that actual column imperfections (eccentricity, curvature, and so forth) can be represented by an equivalent, initial crookedness or bow, whose amplitude d_o is small as compared to L.

Such a column, with single elastic support, is shown in Fig. 2 (d). As the column is loaded, the elastic brace with spring constant k deflects together with the column as is shown in broken lines, with a consequent support reaction $F = k\,d$. If full bracing is provided, final failure occurs at a load equal, or almost equal, to P_e, at which load the column snaps into the two-half-wave mode shown solidly. In this case, as before, a fictitious hinge can be introduced at the support with negligible error.

Taking moments about this hinge $M = \frac{F\,L}{2} - P_e\,(d_o + d) = 0$. Introducing $F = k\,d$ one obtains the spring constant required to produce full bracing:

$$k_{req} = \frac{2\,P_e}{L}\left[(d_o/d) + 1\right] \quad \ldots\ldots\ldots\ldots\ldots (2)$$

For an ideal column $d_o = 0$ and one has

$$k_{id} = \frac{2\,P_e}{L} = \frac{2\,\pi^2\,E\,I}{L^3} \quad \ldots\ldots\ldots\ldots\ldots (3)$$

This value is identical with that given by the exact theory of elastically supported columns, for that amount of rigidity that is required to make an elastic support

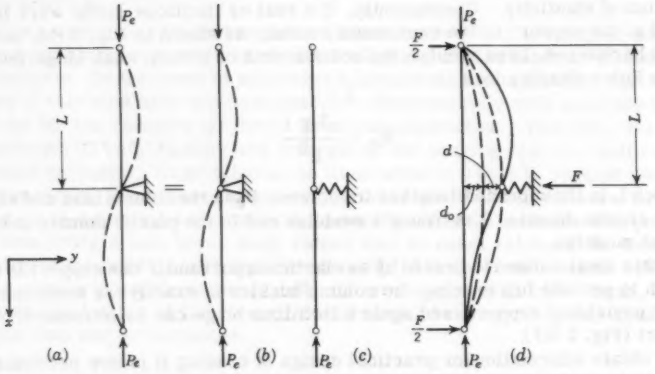


FIG. 2.—IDEAL COLUMN WITH KNIFE EDGED AND ELASTIC SUPPORT

as effective as an unyielding support. It will be observed that the rigidity required to produce full bracing in imperfect columns (Eq. 2) exceeds that required for the ideal column (Eq. 3). The larger the imperfection d_o, the more this is so.

If one knows or estimates the initial imperfection d_o (being guided, for instance, by specified tolerances for crookedness) and if one stipulates the maximum permissible deflection, d, immediately preceding failure, (for example $d = L/500$, conservatively), one can then compute the required spring constant k_{req}, which is a measure of the rigidity of the bracing.

The required strength of bracing (S) is equal to the reaction F at, or immediately preceding, buckling, that is,

$$S_{req} = k_{req}\,d = \frac{2\,P_e}{L}\,(d_o + d) = k_{id}\,(d_o + d) \quad \ldots\ldots\ldots (4)$$

It can now be said that "full bracing" has been provided if $k_{act} \geqq k_{req}$ and $S_{act} \geqq S_{req}$.

Columns with two and three equal and equidistant supports will be considered briefly, whereupon certain generalizations will become apparent. A column with two equidistant supports, when loaded with P_e so that fictitious hinges can be assumed at these supports, could buckle in one of the two modes shown on Fig. 3 (a) or 3 (b). To decide which of these modes is more unfavorable, that is, which requires the larger support rigidity, k, the case of the ideal column will be investigated first. From Fig. 3 (a) $F\,L - P_e d = 0$ which, with $F = k_{id} d$ gives $k_{id} = \frac{P_e}{L}$. On the other hand, from Fig. 3 (b) $\frac{F}{3} L - P_e\, d = 0$ which, with $F = k_{id} d$ gives

$$k_{id} = \frac{3\ P_e}{L} \quad \ldots\ldots\ldots\ldots\ldots\ldots (5)$$

It is seen that k_{id} for the mode of Fig. 3 (b) exceeds considerably that for Fig. 3 (a). This means that if k actually had only the value given for Fig. 3 (a), then the column could not reach the value P_e and buckle in the mode of Fig. 3 (a), because at some lower load it would snap into and buckle in the mode of Fig. 3 (b). It is, consequently, the latter mode that governs and determines the magnitude of k_{id}. The truth of this can also be shown by simple energy considerations or from the complete theory of elastically supported columns summarized in the Appendix. (The method of fictitious hinges for finding k_{id} for full bracing of ideal columns has been used by Fr. Bleich.[8])

To obtain values for k_{req} and S_{req} it is now necessary, as in the previous case, to assume an initially curved shape. Because the ideal column buckles according to Fig. 3 (b), it is evidently most unfavorable if the initial shape happens to be affine to this buckling shape. It is improbable that a fabricated column will be bowed exactly in such a symmetrical S-shape. Making such a simplifying assumption is, therefore, on the conservative side.

Assuming the initial and final shape of Fig. 3 (c), which, for simplicity, only the chords connecting the hinges have been shown instead of the curved column, one has $\frac{F}{3} L - P_e \left(d_o + d\right) = 0$ and $F = k_{req} d$. Then,

$$k_{req} = \frac{3\ P_e}{L} \left[\left(d_o/d\right) + 1\right] \quad \ldots\ldots\ldots\ldots\ldots (6)$$

and,

$$S_{req} = \frac{3\ P_e}{L} \left(d_o + d\right) = k_{id} \left(d_o + d\right) \quad \ldots\ldots\ldots\ldots (7)$$

in view of Eq. 4.

Finally, for three intermediate supports it can be shown similarly that of the three possible modes again the zigzag shape in which consecutive supports are displaced in opposite directions requires the largest rigidity of support. This situation is shown schematically in Fig. 4. It is assumed that k is the same for all three supports, but this does not mean that the deflections, d, are the same. Taking moments about hinge a of the forces acting on spans 1 and 2,

8 "Stahlhochbauten," by F. Bleich and Springer, Vol. 1, Berlin, 1932, p. 182.

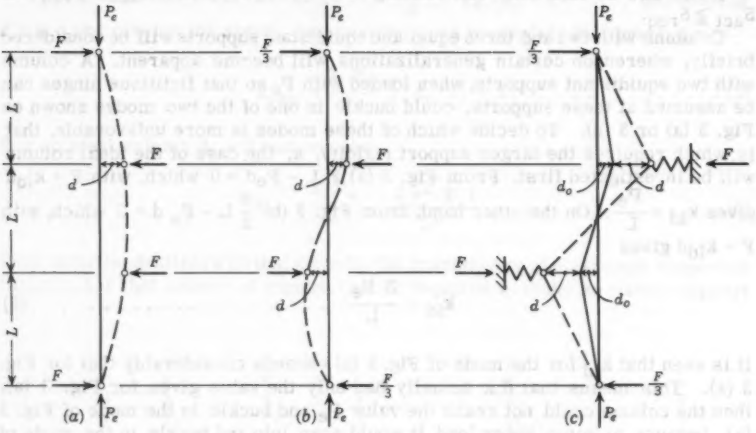


FIG. 3.—COLUMN WITH TWO EQUIDISTANT SUPPORTS

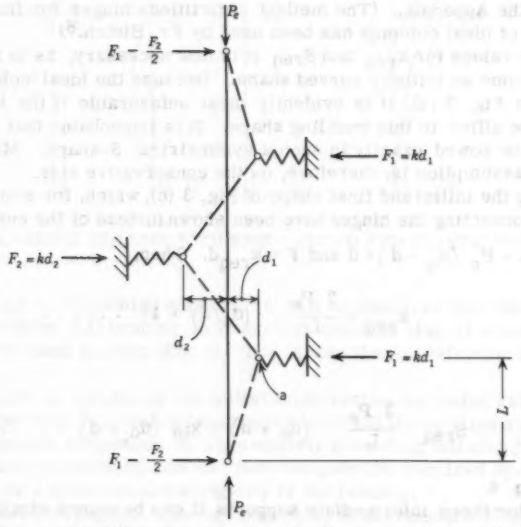


FIG. 4.—COLUMN WITH THREE INTERMEDIATE SUPPORTS

respectively, $P_e\, d_1 - \left[F_1 - (F_2/2)\right]L = 0$ and $P_e(d_1 + d_2) + (F_2/2)L = 0$. Introducing $F_1 = k_{id} d_1$ and $F_2 = k_{id} d_2$, the simultaneous solution of these two equations gives a quadratic equation whose larger root is

$$k_{id} = \frac{3.41\ P_e}{L} \quad \ldots\ldots\ldots\ldots\ldots\ldots (8)$$

If this value is substituted in either of the two equations, one finds $d_2 = \sqrt{2}\, d_1$ which defines the ratio of the two deflections in the natural buckling mode.

If, for the same reasons as in the preceding case, one assumes the shape of the initially bowed column to be affine to this buckling mode, that is, if $d_{o2} = \sqrt{2}\, d_{o1}$, then the moment equations about the same hinge a in this column results in

$$k_{req} = \frac{3.41\ P_e}{L}\left[\left(d_{o1}/d_1\right) + 1\right] = \frac{3.41\ P_e}{L}\left[\left(d_{o2}/d_2\right) + 1\right] \quad \ldots\ldots (9)$$

$$S_{1\,req} = \frac{3.41\ P_e}{L}\left(d_{o1} + d_1\right) = k_{id}\left(d_{o1} + d_1\right) \quad \ldots\ldots (10)$$

$$S_{2\,req} = \frac{3.41\ P_e}{L}\left(\sqrt{2}\, d_{o1} + 2\, d_1\right) = k_{id}\left(d_{o2} + d_2\right) \quad \ldots\ldots (11)$$

Summary and Application.—To summarize, it was found that for n number of equally spaced, equally rigid braces the values of k_{id} are as given as follows:

n	1	2	3	4
k_{id} =	$\frac{2\ P_e}{L}$	$\frac{3\ P_e}{L}$	$\frac{3.41\ P_e}{L}$	$\frac{3.63\ P_e}{L}$

These values agree identically with the rigorous theory of elastically supported columns. In fact, the value shown for n = 4, which has not been computed herein, has been taken directly from that theory.

Furthermore, in each of the analyzed cases it was found that for the initially bowed column

$$k_{req} = k_{id}\left[\left(d_o/d\right) + 1\right] \quad \ldots\ldots\ldots\ldots (12)$$

$$S_{req} = k_{req}\, d = k_{id}\left(d_o + d\right) \quad \ldots\ldots\ldots\ldots (13)$$

When the actual rigidity of bracing exceeds the required minimum value $(k_{act} > k_{req})$, as will usually be the case, then the deflection at a load almost equal to that which causes buckling between braces is found by substituting k_{act} for k_{req}. Thus,

$$d = d_o \frac{k_{id}}{k_{act} - k_{id}} \quad \ldots\ldots\ldots\ldots (14)$$

and, in this case, the required strength of the brace is

$$S_{req} = k_{act}\, d = d_o \frac{k_{id}}{1 - (k_{id}/k_{act})} \quad \ldots\ldots\ldots (15)$$

Eq. 12 indicates that it is not sufficient to provide bracing of rigidity k_{id} as is sometimes maintained, because in that case, the slightest initial crookedness d_o would require bracing of infinitely large strength in order for buckling not to occur below the stipulated value P_e.

These equations and values have been derived for prismatic columns with equally spaced and equal braces. This was done primarily for simplicity and also in order to demonstrate the relation of this approach to the exact theory of elastically supported columns. By the same simple means of writing moment equations about the fictitious hinges at the braces it is also possible to analyze the required bracing for columns with unequally spaced supports or with cross-sections that differ in the individual spans. In this case it is merely necessary to introduce for each portion between braces its appropriate P_e depending on the length and cross-section of that portion.

In these cases of continuous columns the characteristics of the bracing so computed are not exact but satisfy the stipulations specified early in this paper to the effect that lower limits rather than precise values of these characteristics are desired. The method is equally applicable to the case of non-continuous columns, that is, to members that at the brace locations are spliced or otherwise connected in a manner approaching a hinge. In fact, because hinges have been assumed at these locations, the analytical results are, if anything, more accurate for these discontinuous cases than for continuous columns.

The required bracing characteristics have been seen to depend, among other things, on the assumed initial bow d_o and on the additional deflection, d, deemed permissible under a load just below the buckling load, P_e. In design work, P_e can be determined from Eq. 1. This becomes difficult when L/r is less than approximately 100, because in that case the variable tangent modulus must be used. Instead, it is satisfactory in all cases to determine P_e as the allowable load multiplied by the safety factor for columns used in the particular design code (approximately 1.9 to 2.0 in the American Institute of Steel Construction (AISC) specification). The value of the imperfection d_o eventually might be specified in codes. Lacking such provisions one can be governed by permissible tolerances. Thus, in various parts of the "Steel Construction Manual" of the AISC tolerances for columns and other compression members being crooked and being out-of-plumb vary from 1/500 to 1/1000 of the length. Assuming additional imperfections, such as eccentricities, it would seem consistent and realistic to specify d as about twice the value, which would be 1/250 to 1/500 of the length depending on the particular type of member. As regards the additional deflection, d, a rigorous requirement would be to make it equal to the assumed value of d_o. Because d is the deflection at incipient failure, this would mean that the deflection under design load would be less than half this value.

Practically, then, for a column of given characteristics and with given location of braces, one determines P_e and one specifies d_o and d from some such considerations as just shown. Then one chooses a k_{id} to match the number of braces, and from Eqs. 12 and 13 one chooses the required rigidity of the bracing and the required strength if the actual rigidity happens to be equal to the required value of rigidity. In most cases the actual rigidity will exceed this value

$(k_{act} > k_{req})$, so that correspondingly smaller actual deflections and required strengths are found from Eq. 15.

CONTINUOUSLY BRACED COMPRESSION MEMBERS

In contrast to members braced at definite intervals there are cases where elastic (or near-elastic) support against buckling is provided continuously along the entire length of the member. A case in point was mentioned in the introduction, namely the compression chord of a roof truss that, without purlins, carries roofing spanning directly from truss to truss. A similar case concerns the bracing effect on the compression chord of open web joists obtained from the floor supported by the joist. As will be seen later, probably the most important application concerns the problem of laternal support for beams and girders.

It is not possible to treat this case by basic methods as elementary as those for point-support. However, the results[6] of the well-established theory of columns on continuous elastic foundation can be approximated by convenient, algebraic expressions which will permit formulating requirements for such bracing in very simple terms.

An ideal elastic column on a continuous, elastic foundation buckles into m number of half-waves, in which the number m depends on the relative rigidities of the column and the foundation, and is obtained from the relation

$$m^2 (m + 1)^2 = \frac{\beta_{id} L^4}{\pi^4 E I} \quad \ldots\ldots\ldots\ldots\ldots (16)$$

in which β is the modulus of the elastic foundation, and the subscript id indicates that the equation refers to the case of the ideal column. The load at which such buckling occurs is given by

$$P_{cr} = P_E m^2 + \frac{\beta_{id} L^2}{\pi^2 m^2} \quad \ldots\ldots\ldots\ldots\ldots (17a)$$

in which $P_E = \pi^2 EI/L^2$, and is the Euler load of the same column without elastic support. For one extreme, namely for small values of β_{id}, the column bends into one half-wave and from Eq. 17 (a), in non-dimensional terms

$$\frac{P_{cr}}{P_E} = 1 + \frac{\beta_{id} L^2}{\pi^2 P_E} \quad \ldots\ldots\ldots\ldots\ldots (17b)$$

At the other extreme, namely for very large values of β_{id}, the number m becomes so large that 1 (unity) can be neglected compared to it. Hence, an asymptotic relation for large m is obtained from Eq. 16, namely $m \rightarrow \frac{L}{\pi} \sqrt[4]{\frac{\beta_{id}}{EI}}$. For very high foundation rigidity, substitution of this expression in Eq. 17 (a) gives the asymptotic value of the critical load, in non-dimensional terms

$$\frac{P_{cr}}{P_E} \rightarrow \frac{2}{\pi} \sqrt{\frac{\beta_{id} L^2}{P_E}} \quad \ldots\ldots\ldots\ldots (17c)$$

For the values of m other than 1, or large as compared to 1, an exact value of the critical load can only be obtained by tediously computing m from Eq. 16 and substituting in Eq. 17 (a).

However, the critical load for any value of β_{id} and, consequently, of any m can be obtained with entirely satisfactory approximation from,

$$\frac{P_{cr}}{P_E} = 1 + \frac{\beta_{id} L^2}{\pi^2 P_E} \quad \text{for } 0 < \frac{\beta_{id} L^2}{P_E} \leqq 30 \quad \ldots\ldots (18)$$

and,

$$\frac{P_{cr}}{P_E} = 0.6 + \frac{2}{\pi}\sqrt{\frac{\beta_{id} L^2}{P_E}} \quad \text{for } \frac{\beta_{id} L^2}{P_E} \geqq 30 \quad \ldots\ldots (19)$$

It will be recognized that Eq. 18 is identical with the exact Eq. 17(b) (for small values of β_{id}) and that for large values of β_{id} Eq. 17(c) is the asymptotic value of Eq. 19, as it ought to be. Numerical computation shows that the error in determining P_{cr} from Eqs. 18 or 19 is in most cases extremely small and at the worst never exceeds $\pm$ 8% (see Appendix).

By inversion one obtains the following relations which will be useful:

$$\frac{\beta_{id} L^2}{P_E} = \pi^2 \left(\frac{P_{cr}}{P_E} - 1\right) \quad \text{for } 0 < \frac{\beta_{id} L^2}{P_E} \leqq 30 \quad \ldots\ldots (20)$$

$$\frac{\beta_{id} L^2}{P_E} = \frac{\pi^2}{4}\left(\frac{P_{cr}}{P_E} - 0.6\right)^2 \quad \text{for } \frac{\beta_{id} L^2}{P_E} \geqq 30 \quad \ldots\ldots (21)$$

By analogy with Eqs. 12 and 14, which have been derived for point-supported columns, it will now be assumed without proof that for imperfect columns with continuous elastic support similar relations hold:

$$\beta_{req} = \beta_{id}\left(d_o/d + 1\right) \quad \ldots\ldots\ldots\ldots\ldots (22)$$

or by inversion

$$d = d_o \frac{\beta_{id}}{\beta_{act} - \beta_{id}} \quad \ldots\ldots\ldots\ldots\ldots (23)$$

These relations assume, as in the case of point support, that the initial shape of amplitude d_o is affine with the buckling shape. The relations are obviously exact in the limiting cases when $\beta_{act} = \infty$ (immovable support) or when $\beta_{act} = \beta_{id}$. For intermediate values the relations are conservative since complete affinity of the initial with the buckling shape is improbable.

With these relations one then obtains the strengths required per unit length of continuous bracing from the following equations. When $\beta_{act} = \beta_{id}$

$$s_{req} = \beta_{req}\, d = \beta_{id}\left(d_o + d\right) \quad \ldots\ldots\ldots\ldots (24)$$

and when $\beta_{act} > \beta_{id}$

$$s_{req} = \beta_{act}\, d = d_o \frac{\beta_{id}}{1 - (\beta_{id}/\beta_{act})} \quad \ldots\ldots\ldots\ldots (25)$$

As can be seen these equations are comparable to Eqs. 13 and 15.

Example.—The four-panel top chord of a triangular roof truss is 20 ft long and consists of two lipped, cold-formed $3\frac{1}{2}$ x 4 in., 12 gage channels, connected back-to-back. The relevant properties[9] are: A = 1.69, r_x = 1.38, r_y = 1.06, I_y = 1.90 (all in inch units). The truss is perpendicularly braced only at mid-span and carries a roof deck that spans directly between adjacent trusses, without purlins. The deck is suitably connected to form a diaphragm that serves to brace the top chord against buckling perpendicular to the plane of the truss. What are the required characteristics of this continuous bracing? For simplicity bending between panel points due to the uniform roof load will be neglected.

In the plane of the truss, $L/r_x = 60/1.38 = 43.5$. For this value the allowable compression stress, by AISI Specification, is 14.5 ksi. The safety factor for columns in that specification is 2.17 so that the specified ultimate load of the top chord is $P_{ult} = 2.17 \times 14.5 \times 1.69 = 53.1$ k. The Euler load of that chord for buckling out of the plane of the truss is $P_E = \pi^2 \times 29.5 \times 10^3 \times (1.90/240^2) = 9.6$ k. For the bracing to be adequate, the buckling perpendicular to the truss should not occur at a load below that for buckling in the plane of the truss, that is $P_{cr} = P_{ult} = 53.1$ k.

Assuming an initial imperfection $d_o = L/500 = 240/500 = 0.48$ in. and a maximum permissible additional deflection of the same amount immediately before failure (both deflections being perpendicular to the truss), one has from Eq. 21 $\frac{\beta_{id} L^2}{P_E} = \frac{\pi^2}{4} \left(\frac{53.1}{9.6} - 0.6\right)^2 = 60.0 > 30$. Thus, this solution is satisfactory and, $\beta_{id} = \frac{60.0 \times 9600}{(240)^2} = 10.0$ lb per in per in. Then, from Eq. 22 $\beta_{req} = 10.0\left(\frac{0.48}{0.48} + 1\right) = 20.0$ lb per in per in. For this value β, and from Eq. 24, the required strength of bracing $s_{req} = 20.0 \times 0.48 = 9.6$ lb per in = 115 lb per ft. Usually the actual rigidity will exceed the required value considerably. If, for example, $\beta_{act} = 100$ lb per in per in, then from Eq. 25 $s_{req} = 0.48 \frac{10.0}{1 - (10/100)} = 5.33$ lb per in = 64 lb per ft.

It is seen that very low values of both rigidity and strength of the diaphragm bracing suffice to stiffen the chord adequately. It should be noted that the very light bracing required in this case is due in part to the favorable relation of r_y to r_x. For less favorable ratios a stronger and stiffer bracing would be needed as can easily be checked by substituting for the top chord a pair of plain channels (without lips) of equal x-axis properties.

LATERAL BRACING OF BEAMS AND GIRDERS

The bracing of compression members is mostly achieved by bracing systems especially provided for the purpose, even though the preceding example shows

9 "Light Gauge Cold-Formed Steel Design Manual," Amer. Iron & Steel Inst., New York, N. Y., 1956, Table 4, p. 72.

a frequent exception from this situation. In contrast, for beams and girders the most frequent problem is that of deciding whether portions of the structure provided for other purposes give adequate, or full lateral support. Thus, it is sometimes maintained that for a floor to furnish adequate bracing to the beam on which it rests, the compression flange of that beam must be embedded in a concrete slab. The moderate required values of strength and rigidity shown so far suggest that systems weaker than actual embedment in concrete, such as floors or roofs made of a variety of prefabricated elements of lesser rigidity than cast in place concrete slabs may suffice for adequate lateral bracing of beams. Therefore, it is desirable to develop a simple method for deciding whether a lateral system whose characteristics are known with reasonable accuracy provides sufficient bracing for a beam of given properties.

The analysis of the torsional-flexural buckling of ideal beams is considerably more involved than that of the simple, flexural buckling of columns. An analysis of such buckling for elastically supported beams has been developed[5] only for a few special cases and is too complex for design use. However, for determining safe lower limits, rather than exact values, of the required bracing characteristics, as is the stated purpose of this investigation, conservative approximations can be introduced that lead to satisfactorily simple solutions.

It is known[10] that a beam is more stable against lateral buckling than is its compression portion if regarded as an independent strut free to buckle in the direction perpendicular to the plane of the loads. This can be understood qualitatively if one considers that the tension portion resists lateral bending and that, in addition, the torsional rigidity counteracts the twist which accompanies lateral beam-buckling. Consequently, these two influences reduce the buckling tendency of the compression portion and increase its stability as compared to that of the identical but isolated compression member. At the same time numerical computations show that the total force in the compression portion of beams at the instant of lateral buckling, while it is larger than the Euler column load of that portion when isolated, is still of the same order of magnitude. Consequently, if bracing is dimensioned so that it is adequate for the compression portion, assumed to be "cut off" from the tension portion, such bracing obviously will also be adequate, with some added safety, for the actual beam. This added safety, moreover, is hardly economically wasteful because the stability of the beam does not exceed that of the compression portion by a very sizable amount and because relatively weak bracing suffices for full effectiveness.

The following discussion is restricted to I-shaped beams. Rectangular or double-web beams (such as U- or hat-shapes) are so stable that no lateral bracing is required for almost any practical dimensions even though this is not explicitly recognized in some existing design specifications.

It is proposed, then, that bracing requirements for beams and girders be computed in the following manner:

1. Determine the total compression force of the fully braced beam when the allowable stress multiplied by the safety factor is reached in the outer fiber of the beam so braced (incipient failure).

2. By the methods previously developed determine the required characteristics for bracing against column buckling perpendicular to the plane of the loads

---

10 "Strength of Slender Beams," by G. Winter, Transactions, ASCE, Vol. 109, 1944, p. 1321.

of the compression portion alone, considered as isolated from the tension portion and as loaded by the above force.

Example.—Determine the bracing characteristics for an 18 WF 50 beam of 30 ft span, uniformly loaded by the floor which it carries, using the AISC Specification (1949). For this beam $I_y = 37.2$ in^4; $d/bt = 4.22$ in^{-1}; flange area $(A_f) = 4.27$ in^2; area of half-web $(A_w) = 3.02$ in^2. Without lateral bracing the allowable stress for this beam if 7.88 ksi which is less than 40% of that for the fully braced condition (20 ksi).

At incipient failure, with the AISC nominal safety factor of 1.65, the outer fiber stress of the braced beam is 1.65 x 20 = 33 ksi. (that is the yield point of ASTM A-7 steel). The total compression force is computed from the usual linear distribution of bending stresses. Neglecting the small difference between the stress at the outer and the inner fiber of the flange, $P_{ult} = 33 \times 4.27 + (33/2) \times 3.02 = 191$ k. The Euler load for the compression half of the beam is $P_E = \pi^2 \times 29.5 \times 10^3 \times (37.2/2) / 360^2 = 41.8$ k. Proceeding now exactly as in the case of the preceding example one finds, assuming $d_o = d = L/500/0.72$ in, $\beta_{id} = 12.5$ lb per in per in; $\beta_{req} = 25$ lb per in per in and for the case that $\beta_{act} = \beta_{req}$ then $s_{req} = 18$ lb per in = 216 lb per ft. The rigidity of even quite flexible floor systems is likely to exceed β_{req} considerably. For example, if one assumes $\beta_{act} = 200$ lb per in per in one obtains $s_{req} = 9.6$ lb per in = 115 lb per ft. These, then, are the characteristics which assure bracing adequate for the unreduced bending stress of 20 ksi to be permissible, instead of 7.88 ksi for the case of no, or inadequate, bracing.

A uniformly distributed load of 1280 lb per ft is required to develop this permissible stress or, to put it differently, a load of 1.65 x 1280 = 2120 lb per ft will produce that state of incipient failure or extreme fiber yielding for which the bracing has been proportioned. It is seen that the required lateral support, s_{req}, in this example does not exceed 10% of the vertical load. Hence, mere friction between the top of the beam and the floor which rests on it would suffice to develop the force required for lateral bracing. Although this is not to suggest that such friction should actually be relied upon, the weakest connection which is practically feasible, say 1/2 in bolts at 3 ft spacing along the span, would develop a multiple of the required holding force.

SAMPLE CHARACTERISTICS OF A FLOOR SYSTEM

From 1956 to 1959 a sizable number of tests were made at Cornell University, at Ithaca, by A. H. Nilson on full-size cellular steel panel floors to ascertain their effectiveness as diaphragms, primarily for wind and earthquake bracing. The characteristics measured in these tests are, of course, the same ones which matter if such floors are to act as bracing for the supporting beams. To give some indication of actual values of horizontal strength and rigidity for floors of this kind it will suffice to quote and interpret the results of one of the weakest systems tested in that series.

Omitting irrelevant details, the test set-up is schematically shown in plan on Fig. 5(a). Three panels of steel framework, 10 ft by 12 ft each, were erected in the laboratory. Eight short stub columns, all placed on rollers, carried the shown system of beams (12 WF 27 longitudinally and 10 WF 21 transversely). The two outer transverse beams were anchored at their ends A and D. Hydraulic

jacks with load cells were placed at B and C to apply horizontal forces to the inner transverse beams. Horizontal deflections were measured at E and F. Because the longitudinal beams were not continuous across the columns, the framework itself was so flexible horizontally that by pushing at B or C by hand a deflection of an inch and more could easily be produced. Cellular steel floor panels of one of the widely used makes were then erected, simulating standard practice. The individual panels, 2 ft wide, are shown in dashed lines. These panels

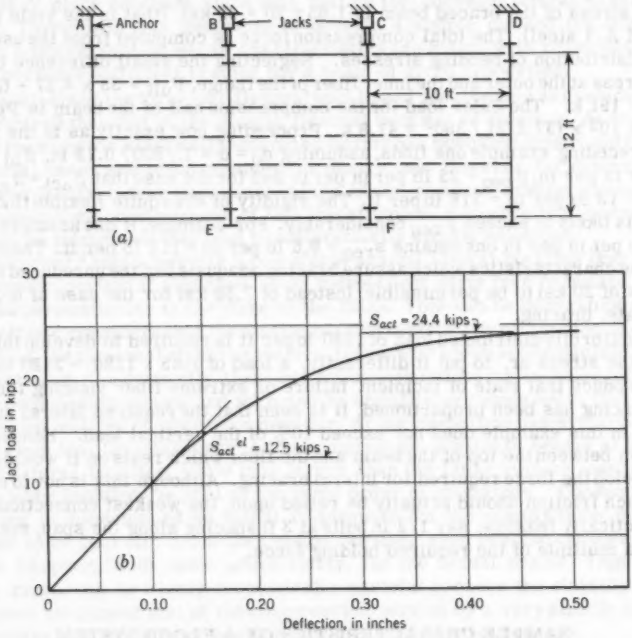


FIG. 5.—FULL SCALE TEST ON CELLULAR STEEL FLOOR

were 3 in deep, of 16 gage steel, and were welded to the beams. In the particular test being discussed, adjacent panels, along their hook joints, were connected to each other by crimping at 2 ft intervals by means of a clinching tool. Tests have shown that diaphragms of this type, together with the surrounding beams, act somewhat like plate girders, and develop considerable horizontal strength and rigidity.

Loads on jacks B and C were kept equal throughout the test, and horizontal deflections at E and F proved equal within a few thousandths of an inch. The load-deflection diagram is given on Fig. 5(b). It is seen that it is practically linear up to a load, per jack, of 12,500 lb, at which load the deflection was 0.125 in. Consequently, over the linear range the spring constant was k_{act} = 100,000 lb per in. The diaphragm failed under a horizontal load per jack, S_{act} = 24,400

lb. Even if, conservatively, one were to define the useful strength as the limit of the elastic range, one would have S^{el}_{act} = 12,500 lb.

When, in another test, the usual $2\frac{1}{2}$ in. concrete fill was applied over the steel deck, the rigidity increased to k_{act} = 1,150,000 lb per in, the ultimate strength to S_{act} = 57,000 lb, and the limit of the elastic range to S^{el}_{act} = 24,000 lb.

To see the significance of these values, a floor system will be assumed identical with that tested, except that a 30 ft girder from A to D will be assumed to carry the transverse beams BE and CF without intermediate support (on a 30 ft span) and that similar transverse beams frame into that girder from the other side. A simple check will show that the 18 WF 50 section of the preceding example is then satisfactory to carry, for such a system, a total floor load of 100 psf.

The girder, then, is stiffened at B and C by the transverse beams which, in turn, are supported against motion in direction of their axes by the strength and rigidity of the diaphragm formed by the panels which they support. The unsupported length of the girder is now reduced to 10 ft, resulting in $Ld/bt = 507 < 600$, so that by present AISC specifications the unreduced stress of 20,000 psi is permissible. Making use of the data of the preceding example, the girder is then to be braced for a force $P_{ult} = P_e = 191$ k. From the previously tabulated formulas for k_{id}, for n = 2, $k_{id} = (3 \times 191{,}000)/120 = 4770$ lb per in. Assuming again $d_o = d = L/500 = 360/500 = 0.72$ in, one has from Eq. 12 $_{req} = 4770$ $[(0.72/0.72 + 1)] = 9540$ lb per in and if, by chance, $k_{act} = k_{req}$, then from Eq. 13 $S_{req} = 9540 \times 0.72 = 6860$ lb. However, the actually measured rigidity was $k_{act} = 100{,}000$ lb per in so that, from Eq. 15, for this rigidity $S_{req} = 0.72 \dfrac{4770}{1 - (4770/100{,}000)} = 3620$ lb.

A comparison of these required values with the corresponding quantities obtained in the test with bare deck shows that the actual rigidity (k) was approximately ten times the required amount, and the actual usable strength S^{el}_{act} approximately three and five tenths times the required amount. It is seen, then, that this laterally relatively weak and flexible floor system supplies a multiple of the support required in this example for full lateral bracing. An even greater reserve is obtained after the usual concrete fill has been applied.

It should be observed that all the foregoing determinations have been made for the state of incipient failure, rather than for design loads. This is necessary because some of the involved phenomena are non-linear. It follows from this that the required bracing characteristics, so computed, already involve a safety factor which is, in fact, greater than that implied in the pertinent general design specification. This is so because the proposed analysis, as repeatedly emphasized, is based on a number of conservative assumptions. Hence the computed, required properties (k_{req}, S_{req}, and so forth) refer to the actual minimal requisite values and are not in need of further multiplication by a safety factor.

RESERVATIONS AND LIMITATIONS

It has been suggested that the equivalent initial crookedness, duly related to applicable straightness tolerances, might be assumed of the order of L/250 to L/500 and that the additional deflection under a load just below failure might,

conservatively, be taken as equal to this amount. The three numerical examples have been computed on that basis. Whereas it is believed that these quantities are reasonable, it is evident that they should be related to imperfections and, implicitly, to safety factors assumed in the relevant design specifications. The quoted, specific values should, therefore, be understood rather as samples subject to more detailed determination by those responsible for the design specification.

The proposed method for bracing of beams and girders utilizes the proposition that a beam is more stable than its compression portion if the latter were isolated from the rest of the member. Although, this is true in the majority of cases, contrary situations may exist,[10,11] for instance, when the center of gravity of the load is located at a level very considerably above the top flange of the beam (As an illustration, consider the unlikely case of an entirely detached brick wall supported on the top flange of an unbraced girder.) In these cases, for the same reasons as stated, the usual, simplified design code provisions for lateral buckling are also inapplicable.

For the time being the proposed method should be applied only in connection with elastic design, because it has been developed to provide adequate support up to loads which cause either incipient yielding or buckling in a plane perpendicular to the bracing. It is known,[12] in regard to plastic design of steel structures, that the ultimate loads predicted by that method will not be reached unless the structures are adequately braced at least at those locations where yield hinges form. This condition is not included in the foregoing development. Hence, when applied to plastic design the proposed method of bracing analysis may require modifications which are not a subject of this paper.

CONCLUSIONS

Experimental evidence has been cited to show that very light lateral bracing (small strength and small rigidity) suffices to produce very large gains in carrying capacities of columns and beams.

A simplified analysis of initially imperfect columns with one or more intermediate supports leads to a method which permits analysis by the simplest of computations to determine lower limits for the strength and rigidity required to produce full bracing. By using two simple equations to express the results of the rigorous theory of columns on elastic foundations, a similarly simple method has been developed for determining the bracing characteristics for cases of continuous lateral support.

By an approximate method, which errs on the conservative side, the problem of laterally supported beams is reduced to that of laterally supported columns. By this means a simple procedure is developed for determining minimum characteristics for lateral support of beams and girders.

Sample computations and comparison with bracing characteristics determined in full-size tests on a light floor system show that for beams and girders lateral

---

11 "Lateral Stability of Unsymmetrical I-beams and Trusses in Bending," by G. Winter, Transactions, ASCE, Vol. 108, 1943, p. 247.

12 "Behavior of Welded Single-Span Frames under Combined Loading," by C. G. Schilling, F. W. Schutz, Jr., and L. S. Beedle, Welding Research (Welding Journal, Vol. 35), 1956, p. 234.

support much lighter than that provided by flange embedment in a concrete floor is generally adequate to furnish sufficient bracing.

APPENDIX

Throughout this paper repeated reference has been made to the results of the rigorous analysis of ideal columns on elastic supports. To elaborate briefly on those features, these results are given here in a graphical non-dimensional presentation,[4,7] (Fig. 6). The value P_E used in the non-dimensional abscissa is the Euler load of the identical, full length column without intermediate supports. Consequently, this definition is identical in the elastic range with P_E as used before for continuous support in Eqs. 17 to 19. For point support, the value P_e, (Eq. 1,) had been referred to the free length between supports. Hence, for n number of intermediate equidistant point supports the relation between P_e and P_E is

$$P_e = P_E (n + 1)^2 \quad \ldots\ldots\ldots\ldots\ldots\ldots (26)$$

For a column elastically supported at n equidistant points it is seen that the critical buckling load increases with increasing support rigidity k. For very low

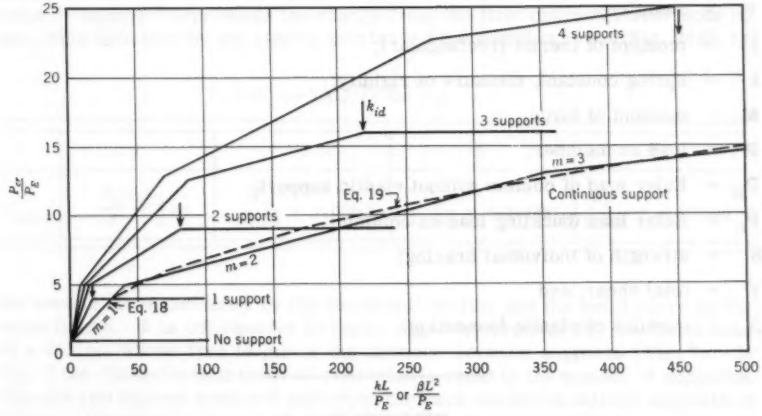


FIG. 6.—CRITICAL LOADS FOR ELASTICALLY SUPPORTED COLUMNS

values of k the column buckles in a single half-wave (m = 1). The larger k is, the larger the number, m, of half-waves and the larger P_{cr} is, up to that value of k at which the number of half-waves becomes equal to the number of free lengths between point-supports, (i.e. $m_{max} = n + 1$). For any magnitude of k equal to or larger than this particular value the column buckles as if it were held immovably at the intermediate supports, in the manner shown on Fig. 2 for n = 1. For such elastic support, then, the ideal column has attained its maximum possible carrying capacity, which represents full bracing by the definition of this paper. These particular minimum values of k which produce full bracing by the rigorous theory are identical with those values k_{id} previously tabulated, which have been determined by elementary means in this study. They are shown on Fig. 6.

For continuous, elastic foundation the solid curve of Fig. 6 gives the results of the rigorous theory and indicates, again, that as the rigidity of the foundation increases, so does the number of half-waves m as well as the theoretical buckling load P_{cr}. Of the two expressions Eqs. 18 and 19 used in this study to represent the relationship between P_{cr} and β_{id}, Eq. 18 is identical with the exact relation over this range. The second, approximate expression, Eq. 19, is shown by the broken curve. Entirely satisfactory agreement for engineering purposes, is seen to be obtained throughout, with maximum deviations of about $\pm$ 8% confined to a few short regions.

APPENDIX. NOTATION

d = amplitude of movement of member under load;

d_o = amplitude of bow in "real" member;

E = modulus of elasticity;

F = reaction;

I = moment of inertia (rectangular);

k = spring constant, measure of rigidity;

M = moment of force;

P = load on member;

P_E = Euler load of column without elastic support;

P_e = Euler load (buckling load on column);

S = strength of individual bracing;

V = total shear; and

β = modulus of elastic foundation.

DISCUSSION

ANTHONY A. CHIBARO[13] F. ASCE.—The author deserves praise for clearly presenting, in simple terms, solutions of a number of problems encountered in the proportioning of lateral bracing. Although the approach is not new, he has skillfully extended its application considerably, and presented the profession with a much needed design method.

The writer found it relatively simple to compute the value of $k_{id} = \frac{3.63\ P_e}{L}$ for the case n = 4, given in the tabulations of k_{id}, by using the author's method.

[13] Struct. Engr., Jackson & Moreland, Inc., Boston, Mass.

GILES G. GREEN[14], M. ASCE.—The author has presented a clear step by step derivation of the required stiffness and strength of the bracing for compression members with elastic lateral supports. The required stiffness and strength of the lateral bracing is a function of the critical column load, the column, length, (d_o), the assumed initial bow of the column, and (d) the additional deflection under load. The latter two quantities are related for unsupported columns and for point braced columns with elastic lateral supports by the expression

$$d = \frac{Pd_o}{P_{cr}-P} \quad \ldots\ldots\ldots\ldots\ldots\ldots \quad (27)$$

where P is any load less than the critical value, P_{cr}. Allowance is made for the effect of the lateral bracing in increasing the critical column load. The initial shape of the column causes the greatest load on the lateral bracing when it is similar to the characteristic mode of distortion equal to the number of equally spaced concentrated supports. The strength and rigidity of the lateral supports for optimum efficiency should be sufficient to cause the column to buckle in a characteristic mode of distortion, which is one greater than the number of such supports. That is, there should be a node at each support as shown by Fig. 2(d). Fig. 6 shows the change in the mode of distortion with increase in the stiffness of the lateral support. Thus, the break in the curve labeled "1 support" represents the change from the first characteristic mode of distortion indicated by the sloping portion and the dotted curve of Fig. 2(d), to

TABLE 2.—VALUES OF P_{cr}

n	1	2	3	4
P_{cr}	$\frac{P_e}{4} + \frac{3}{8}kL$	$\frac{P_e}{2.14} + 0.178kL$	$\frac{P_e}{1.555} + 0.1044kL$	$\frac{P_e}{1.308} + 0.0649kL$

the second mode indicated by the horizontal portion and the solid curve of the same figure. It is informative to replot Fig. 6 in terms of P_e, the Euler load of a column whose free length is the distance between supports (Fig. 7). In Fig. 7 the characteristic mode of distortion is equal to the number of supports. Only the two highest modes of distortion for each number of lateral supports is drawn. The sloping portion of each curve may be approximated by a straight line with an equation as shown in Table 2, where n is both the number of supports and the characteristic mode of distortion.

The limiting value of P_{cr} in each case is P_e. These values may be used to compute d at the point of lateral support from the above expression. This is for d in terms of P, d_o and P_{cr}, but only for values of k such that $P_{cr} < P_e$, that is, for values of k less than k_{id}. As P approaches P_{cr}, d becomes infinite, indicating failure of the bracing simultaneously with failure of the column. However, as k exceeds k_{id} and the column buckles in the next higher mode of distortion, at a load $P_{cr} = P_e$, d refers to the amplitude of the bowing curve of that higher mode which then occurs midway between the points of lateral support. Practically, in the design of the lateral bracing, the suggestion that d be made

[14] Struct. Engr., Hardesty and Hanover, New York, N. Y.

equal to the assumed value of d_o seems conservative when the lateral bracing is stiff enough to cause a node. If the lateral bracing is more flexible than this requirement, the deflection under load should be computed as previously indicated.

As an example of the use of the above relationships, a channel column will be investigated. This column consists of a 12 in.-30 lb channel 30 ft-long braced against buckling about its minor axis by the beam action of two pairs of $3\frac{1}{2}$ x $3\frac{1}{2}$

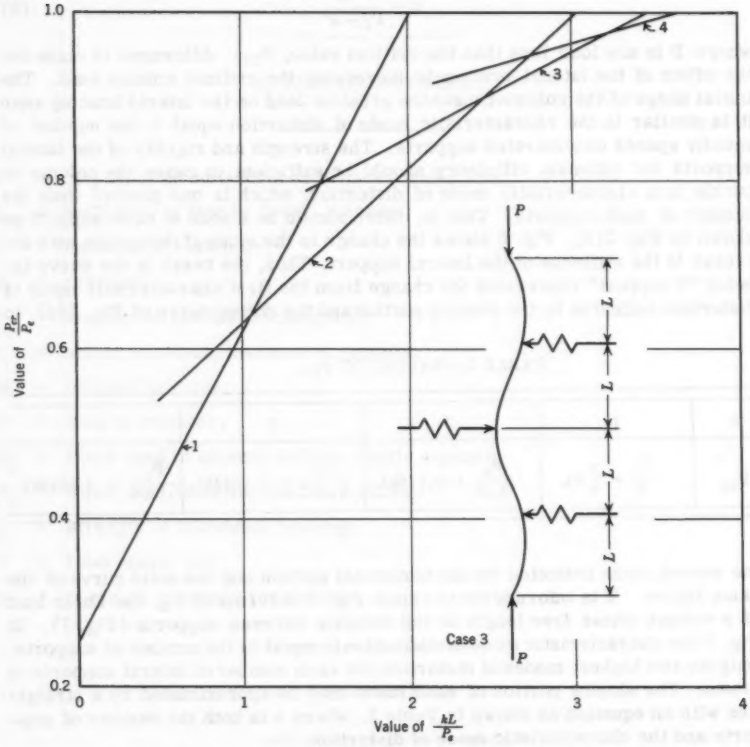


FIG. 7.—REPLOT OF FIG. 6 IN TERMS OF P_e

x 3/8 angles 9 ft-long, bracing the column at its third points. An illustration of the use of such construction is the compressed diagonal of a lattice truss or, in the case of a single brace, in the intersecting lateral bracing of a bridge. $L/R_{1-1} = 120/0.77 = 155.5$ $L/R_{2-2} = 360/4.28 = 84$. Thus 155.5 controls. For $L/R = 155.5$, F_c allow. = 6310 p.s.i. (AISC Hbk., p. 210) $P_{des} = 630 \times 8.79$ sq

in. = 55,500 lb P_{ult} = 1.9 x 55,500 = 105,500 lb $P_e = \frac{\pi^2 \times 3 \times 10^7 \times 5.2}{120^2}$

= 106,700 lb $k_{id} = \frac{3P_e}{L} = \frac{3 \times 106,700}{120}$ = 2670 lb per in. d_o = 1/1000 x length

$= \frac{360}{1000} = 0.36$ The value of k furnished by two angles 3½ x 3½ x 3/8 x 9 ft long

is $\frac{48\ EI}{L^3} = \frac{48 \times 3 \times 10^7 \times 2 \times 2.9}{9 \times 12^3}$ = 6620 lb per in. = k_{act}. Since $k_{req} = k_{id}\left(\frac{d_o}{d} + 1\right)$ then, $k_{req} = 2670\left(\frac{0.36}{0.36} + 1\right)$ = 5340 lb per in. Thus $k_{act} > k_{req}$ and

$S_{req} = k_{act}\ d = 6620 \times 0.36 = 2390$ lb.

$$(f_t)_{ult} = \frac{M}{S} = \frac{2390 \times 9 \times 12}{4 \times (2 \times 1.2)} = 26,900 \text{ psi} < 33,000 \text{ psi}$$

It is seen from the above computations that in order for the column to be adequately braced about its minor axis at the third points, a certain spring constant of the supports, k_{req}, is needed. This quantity is computed and compared with that actually supplied to see that the bracing is stiff enough. With the effective length of the column about its minor axis now one third the total length, the ultimate load is then computed from the AISC column formula multiplied by 1.9, the approximate factor of safety. Taking the initial crookedness of the column as 0.001 for its length, the required strength of the bracing, S_{req}, is then computed. Because this force is found to cause a stress in the bracing less than its yield point stress, the bracing is strong enough to withstand the forces induced in it by the action of the ultimate column load.

In the event that the lateral bracing is not stiff enough to cause a mode at the point of support, it can still be utilized to increase the strength of the column. Thus, in the afore-mentioned example, if the bracing angles were 14 ft-long,

$$k_{act} = \frac{48 \times 3 \times 10^7 \times 2 \times 2.9}{(14 \times 12)^3} = 1760 \text{ lb per in.}$$

this is less than k_{id}, so $P_{cr} < P_e$, $P_{cr} = (P_e/2.14) + 0.178\ kL = (106,700/2.14) + 0.178 \times 1760 \times 120$, P_{cr} = 87,500 lb.

At the yield point, the bracing can withstand a force computed from $33,000 = \frac{S \times 14 \times 12}{4\ (2 \times 1.2)}$ from which S = 1880 lb and $d = \frac{1880}{1760} = 1.07$ in. In order to obtain the load on the column causing this lateral deflection, solve Eq. 20 as $1.07 = \frac{P \times 0.36}{87,500 - P}$, from which P = 65,500 lb. However, this load would cause an excessive column stress due to the large lateral deflection. Therefore the ultimate column load in this instance would be determined by column stress as follows: $33,000 = \frac{P}{A} + \frac{P}{S} \times \frac{Pd_o}{P_{cr} - P}$ from which P = 62,000 lb. Thus, P_{allow} = P/1.9 = 62,000/1.9 = 32,600 lb.

Although this column load is less than that permitted if the bracing were sufficiently rigid, it is considerably greater than that of the unbraced column.

BRUCE G. JOHNSTON,[15] F. ASCE.—This paper is an important contribution to a subject about which little has been written, in spite of the fact that it has been an area in which information has been needed by engineers for many years. The author is to be congratulated on the well balanced combination of tests, intuitive judgment, and analysis that are combined with a practical approach to the design problem.

The writer was particularly interested in the statement in the last paragraph of the section on lateral bracing of beams and girders, which reads, "Hence, mere friction between the top of beam and the floor which rests on it would suffice to develop the force required for lateral bracing." This statement is apt to be taken out of context by engineers who, perhaps quite rightly, would like to rely solely on friction for lateral support. However, the author qualifies this statement in the following sentence so as not to commit himself definitely to the implied conclusion. It would be desirable to pin this matter down more definitely. The matter of what does constitute minimum requirement for lateral support seems still to be left open. Is it, in fact, permissible to rely only on friction? Does the type of floor have anything to do with the problem? For example, some beams may support timber planking or lightweight open metal grid. Is the friction in this case sufficient? Does the matter of dynamic or vibratory loads affect the problem? In the latter case it might well be argued that when, due to vibration, the friction is absent the load also is simultaneously absent. The writer does not contest the correctness of the author's conclusion but in view of the fact that engineering teachers have been recommending flange embedment in concrete as a minimum for top flange lateral support of beams this question needs a little further elaboration.

The writer wishes to emphasize the importance of this matter in relation to current engineering practice and the recommendations that are given in most texts on design.

MARVIN A. LARSON,[16] F. ASCE.—This paper treats a subject on which but meager information is available in a form to be of aid to the practical designer. Our present design specifications give empirical rules for the design of members which are either laterally braced or unbraced, but are of little assistance in prescribing just what constitutes adequate lateral bracing. Winter has explored this matter with regard to several problems involving the lateral buckling of compression members and compression elements of flexural members, and has shown rather simple procedures for determining whether the lateral support requirements, both as to strength and stiffness are met.

The principal deficiency of the paper is the implicit assumption that the relationships derived are directly applicable to problems commonly encountered in the design of practical structures. Actually, such is not the case, and some modifications of the procedure must be made to prevent erroneous results from being obtained. It will be shown that even with the specific examples used by the author, the true condition is at considerable variance with that stated, and in some instances even in direct opposition.

---

[15] Prof. of Struct. Engrg., Civ. Engrg. Dept., Univ. of Michigan, Ann Arbor, Mich.
[16] Prin. Struct. Engr., San Francisco, Calif.

The member described by the author is considered to be laterally supported at one or more points along its length through elastic members connected at the far end to a point considered fixed in space relative to the two ends of the primary member under consideration. This situation is, for practical purposes, achieved under the conditions of the laboratory test described. In this test the flexible sheet steel column was braced to the massive, rigid frame of the testing machine. In an actual structure, this situation might occur occasionally, as where a flexible beam or column may run parallel and adjacent to a relatively stiff and massive masonry wall to which it is attached at intervals. However, in the majority of cases, such as the columns of a long mill-type building, parallel beams of a floor system above the first floor of a building, and the upper chords of roof trusses, such a fixed point is not conveniently available for the attachment of bracing. In actual practice, bracing is most commonly effected by interconnecting various members of the structure (each of which may have little lateral stiffness by itself) in such a manner as to provide, by combined action, greater resistance to buckling than is provided by the sum of the individual members acting independently.

The floor system described by the author, composed of two 18WF50 beams of 30 ft span and 12 ft spacing supporting a 16 gage cellular steel deck, will illustrate the significance of the support conditions. Using all dimensions and physical properties as in the original, this assembly is loaded as shown in Fig. 8(a). From the original load-deflection curve, to produce deflections of 0.01 in. at points E and F, with both points moving in the same direction, jack loads of 1.0 kip each will be required at points B and C. Assigning this entire force to shear deformation stresses induced in the steel deck, we perceive that a total shear force of 1.0 kip is induced in the deck between points A and B, and likewise a shear force of equal magnitude but opposite sense between points C and D. The steel deck between points B and C is undeformed, hence develops no shear stresses.

Now load the same structural system as in Fig. 8(b), this time applying loads so as to produce deflections of 0.01 in. at both points E and F, but in opposite directions. Again, total shear forces of 1.0 kip will be developed in the end panels AB and CD, but this time of like sense. In addition, the center panel of steel deck, from B to C, will be subjected to a shear deformation twice as great as the end panels. Hence, the center panel will develop a shear force of 2.0 kips of a sense opposite to that of the end panels. The jacking loads required to produce the deformation shown in Fig. 8(b) are 3.0 kips each at points B and C.

The implications of these figures are immediately apparent. In all relationships developed in the paper, the lateral restraining force on a member at a point of lateral support was assumed to be a function of the lateral displacement of that point only, and independent of the lateral displacement of any other point on the member. In the present instance, such is not the case. The author, proceeding from a loading condition as shown in Fig. 8(a) derived an equivalent support regidity of 100,000 lb per in, and then assumed that this applied also to conditions as shown in Fig. 8(b). Actually, for Fig. 8(b) the support regidity is 300,000 lb per in.

Because the action of a diaphragm in restraining lateral buckling is not properly represented by the equivalent elastic supports used by the author in deriving buckling equations, it will be necessary to start anew to develop relationships expressing the criteria for stability against lateral buckling. We

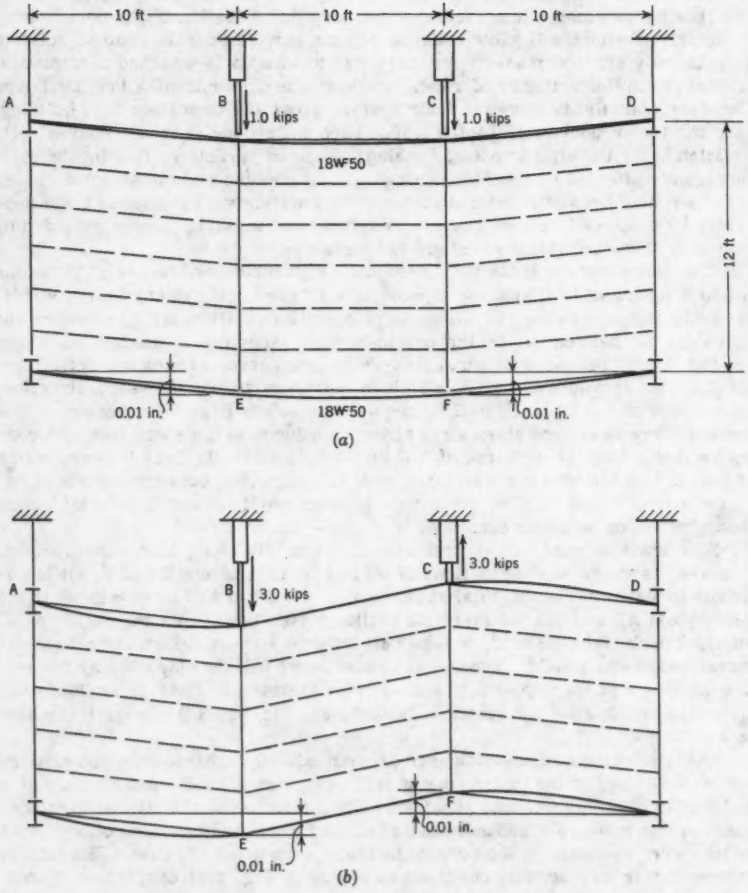


FIG. 8.—FLOOR SYSTEM SUBJECTED TO SYMMETRIC AND ANTI-SYMMETRIC SHEAR LOADS

must first recognize that the stabilizing force developed at a point is a function of the deflection not only of the point of attachment being considered, but of the deflection of adjacent points of lateral bracing as well. It will be convenient to express the resistance of the diaphragm to shear deformation as a function, γ, which is the total shear force required to produce a shear deformation of one radian. Thus, continuing with the same structure as before, a shear force of 1.0 kip produced a deformation of 0.01 in. in a length of 120 in., and γ is equal to 12,000 kips per radian.

Let us consider the beams and deck of Fig. 8(a) to be a part of a continuous floor system such that each beam receives the benefit of the bracing effect of a full 12 ft width of steel deck. If we consider only the compression elements of the beam, and assume that this compression is introduced by means of concentrated compressive forces on the ends of the beam, that it is an ideal member (no end eccentricity or initial crookedness), and that the loading has reached the critical buckling stage, the condition of the member can be represented by Fig. 9, in which all properties are expressed in general terms. Deflections at points B and C have purposely been shown as unequal.

The shear forces developed in the several panels of the diaphragm are $V_{AB} = \gamma d_B/L$, $V_{BC} = \gamma(d_c - d_B)/L$, and $V_{CD} = -\gamma d_c/L$. From which the lateral forces can be obtained as $F_A = \gamma d_B/L$, $F_B = \gamma d_B/L - \gamma(d_c - d_B)/L = \gamma 2d_B - d_c)/L$, $F_C = \gamma(d_c - d_B)/L + \gamma d_c/L = \gamma(-d_B + 2d_c)/L$, and $F_D = \gamma d_c/L$. All forces and deflections are positive, as shown in Fig. 9.

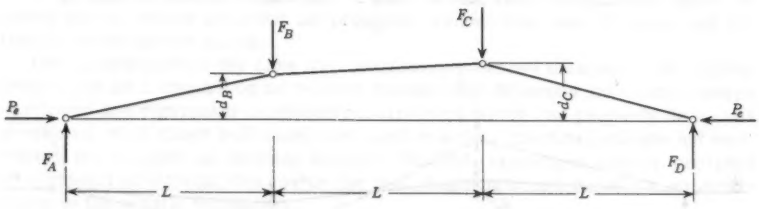


FIG. 9.—IDEAL COMPRESSION MEMBER, POINT SUPPORTED AGAINST LATERAL BUCKLING. CRITICAL BUCKLING STAGE

The relationship between the buckling load and the diaphragm stiffness can be immediately obtained by summing the moments about point B of forces applied at A, as

$$d_B P_e - L(\gamma d_B/L) = 0; \text{ Thus, } \gamma_{id} = P_e \quad \ldots\ldots\ldots\ldots (28a)$$

Likewise, a summing moments about point C of forces applied at D,

$$d_c P_e - L(\gamma d_c/L) = 0, \text{ and again } \gamma_{id} = P_e \quad \ldots\ldots\ldots\ldots (28b)$$

It should be noted that the required diaphragm stiffness has been obtained without the necessity of assuming any relationship between the deflections at points B and C. A careful check will reveal that all forces are in balance, both internally and externally. This means that there are no compatibility conditions to be satisfied by the deflections at B and C. The condition shown in Fig. 9 is a stable stage of buckling. The buckling load is the same whether points B

and C deflect in the same direction, in opposite directions, equal distances or unequal distances, or one or the other remains at the neutral position. In addition, if the member were extended by the addition of successive increments of length (L) to four, five, or more spans, the required shear stiffness would retain the same value of $\gamma_{id} = P_e$ and the deflection of each of the points of support would remain independent of the others.

For an ideal column or beam and for equal spacing of points of support we are freed from the necessity of considering symmetrical, asymmetrical or zig-zag modes of buckling. The total length of the member and number of intermediate supports is immaterial. A series of coefficients such as the authos's k_{id} tabulations is not needed. The required diaphragm stiffness to prevent buckling at the points of lateral support, Eqs. 28(a) and 28(b) is independent of the mode of buckling or the number of panels in the bracing system, but is uniquely determined by the length of a panel between points of lateral support and the critical buckling load of the column associated with this length.

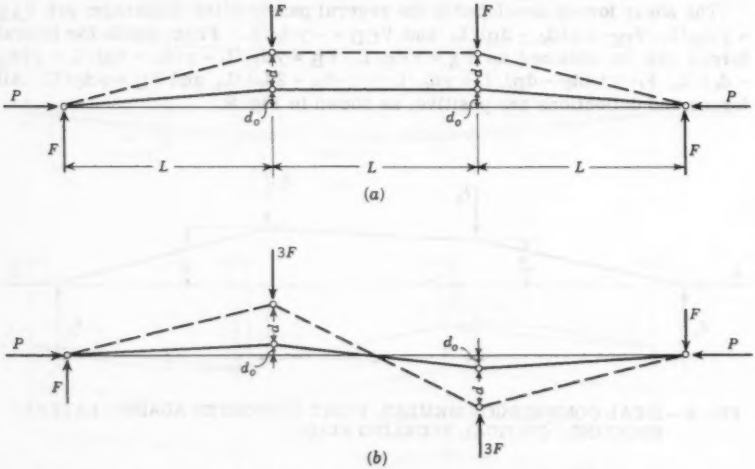


FIG. 10.—IMPERFECT COMPRESSION MEMBER, POINT SUPPORTED AGAINST LATERAL BUCKLING.

Let us now turn to consideration of an imperfect compression member, as represented by Fig. 10(a). The required strength and stiffness of the diaphragm can be obtained as follows:

$$F = \gamma(d/L) = \left[P\left(d + d_o\right)\right]/L = S_{req} \quad \ldots\ldots\ldots\ldots (29)$$

$$\gamma_{req} = S_{req}/d = P\left(\frac{d + d_o}{d}\right) \quad \ldots\ldots\ldots\ldots\ldots\ldots (30)$$

Again, let us consider a member with initial imperfections as shown in Fig. 10b. For this case, the required strength and stiffness are the same as equations 22 and 23. We now see that whereas the mode of buckling is influenced

by the nature of the initial imperfections, the required strength or stiffness of the diaphragm is not, as long as the initial deflections d_o are the same in either case. If we add the practical consideration that the magnitude of the initial deflection will in all probability be less for Fig. 10(b) than for Fig. 10(a), then the latter form of buckling is the more likely.

A re-evaluation of the adequacy of the diaphragm to furnish lateral bracing or the author's 18WF50 beam is as follows: $\gamma_{id} = P = 191$ kips per / radian. Assuming $d_o = d = 3L/500 = 360/500 = 0.72$, $\gamma_{req} = 191 \times \left(\frac{0.72 + 0.72}{0.72}\right)$ = 382 kips per radian. If $\gamma_{act} = \gamma_{req}$, then $S_{req} = 191 \times (0.72 + 0.72/120) = 2.3$ kips.

If the actual stiffness furnished by the diaphragm is greater than required to restrain the lateral deflection to the specified manimum value, then the actual deflection and the required strength will be given by the equations

$$d = \frac{P}{\gamma_{act} - P} d_o \quad \ldots\ldots\ldots\ldots\ldots\ldots (31)$$

$$S_{req} = \gamma_{act}\, d/L \; S_{req} = \frac{\gamma_{act}\, P}{\gamma_{act} - P}\left(\frac{d_o}{L}\right) \quad \ldots\ldots\ldots\ldots (32)$$

In the present case, γ has the value of 12,000 kips per radian, from which $d = \frac{191}{12{,}000 - 191} \times 0.72 = 0.0117$ in. and $S_{req} = 1.17$ kips. The steel deck actually furnishes a stiffness of 12,000 kips per radian and a strength at the elastic limit of approximately 12.5 kips. These values are respectively, about 30 times and 11 times as great as required, rather than the 10 times and 3.5 times, as the author states.

Let us now turn to the case of a continuously braced member. The author treats this as a column on an elastic foundation. Whereas the relationships developed are rigorously correct for a structure which can properly be so represented, such cases will rarely be found in actual practice, and are not necessary for an adequate bracing system. Instead, bracing is usually provided by a system of internal ties, or by the roof diaphragm, and these are not analogous to the elastic foundation.

It might be noted that the author's equation for the asymptotic value of the critical load in non-dimensional terms is not stated in its simplest and most useful form. Let L be the length between nodes of the buckled compression member, rather than the overall length The buckling load then is given by Eq. 14, which is re-written here as

$$P_{cr} = \frac{\pi^2 E I}{L^2} + \frac{\beta L^2}{\pi^2} \quad \ldots\ldots\ldots\ldots\ldots\ldots (33)$$

Now, if we omit consideration of end conditions, we can find a buckling length L', for which the buckling load given by Eq. 26 is a minimum. This is

$$L' = \pi \sqrt[4]{(E I)/\beta} \quad \ldots\ldots\ldots\ldots\ldots\ldots (34)$$

And for this buckling length (L'), the minimum critical buckling load is

$$P' = 2 \sqrt{E I \beta} \quad \ldots\ldots\ldots\ldots\ldots\ldots (35)$$

The general procedure then for computing the critical buckling load is:

1. Compute L' from Eq. 34.

2. Compare L' with the over-all length of the member Determine closest lengths L_1 and L_2, larger and smaller than L' into which the over-all length is evenly divisible.

3. Evaluate Eq. 33 for both lengths L_1 and L_2. The lesser of these is the critical buckling load.

4. If L' is small compared with the over-all length, or if it differs by but a small amount from L_1 or L_2, the critical buckling load will be given, with only slight error, by Eq. 35.

As an example of the use of the forementioned procedure, the following is given. A column on an elastic foundation has an over-all length between pin-connected ends of 100 in. EI is 2500 lb-in.^{2}, and β is 1 lb per in. per in. What is the buckling load for the column?

From Eq. 34 L' = 22.2 in. From Eq. 35 P' = 100 lb. We next find L_1 = 100 in./5 = 20 in. < 22.2 in. and L_2 = 100 in. /4 = 25 in. > 22.2 in. Eq. 33 gives L_1 = 20 in, P_1 = 61.7 + 40.6 = 102.3 lb and L_2 = 25 in, P_2 = 39.4 + 63.2 = 102.6 lb. Certainly there is nothing tedious about the computations. Moreover, the value from Eq. 35 is not only acceptably close to the true value, but on the conservative side.

Consider a series of columns of length L, bending stiffness EI, braced against buckling in their weak direction by a continuous diaphragm, such as a steel roof deck, with a shearing stiffness γ. Isolate one column and its associated width of diaphragm as in Fig. 11(a). Assume an initial crookedness which for mathematical convenience is expressed as $Y_o = d_o \sin \frac{\pi x}{L}$. Apply end loads P to the column such that the column buckles laterally a slight distance from its initial position. Use coordinate axes as shown, except that y distances are measured from the initial centerline of the column before application of loads.

If an elemental segment of the column and attached diaphragm is isolated, forces as in Fig. 11(b) will be found to be acting. These can be evaluated in terms of the geometry and physical properties as follows:

$$M = - E I \left({}^{d^2y}/_{dx^2} \right)$$

$$dM = - E I \left({}^{d^3y}/_{dx^3} \right) dx$$

$$V = \gamma \, {}^{dy}/_{dx}$$

Applying the principles of statics to the forces on the element, $dM = P \left(dy + \frac{\pi}{L} d. \cos \frac{\pi x}{L} dx \right) - V dx$ which leads to the differential equation $- E I \, {}^{d^3y}/_{dx^3} = P \, {}^{dy}/_{dx} + P \frac{\pi}{L} d. \cos \frac{\pi x}{L} - \gamma \, {}^{dy}/_{dx}$. This is easily solved to yield the particular solution

$$y = \frac{P d_o}{(\pi^2 E I)/L^2 - (P - \gamma)} \sin \frac{\pi x}{L} \quad \ldots\ldots\ldots\ldots (36)$$

$${}^{dy}/_{dx} = \frac{P d_o}{(\pi^2 E I)/L^2 - (P - \gamma)} \frac{\pi}{L} \cos \frac{\pi x}{L} \quad \ldots\ldots\ldots (37)$$

Substituting d for y and L/2 for x, provides

$$d = \frac{P\, d_o}{(\pi^2 (E\, I)/L^2 - (P - \gamma)}$$

Noting that $(\pi^2 (E\, I)/L^2$ is the Euler buckling load, for which we make the substitution P_e, the equation can be rearranged in the form

$$P = (P_e + \gamma) \frac{d}{d + d_o} \quad \ldots\ldots\ldots\ldots\ldots\ldots (39)$$

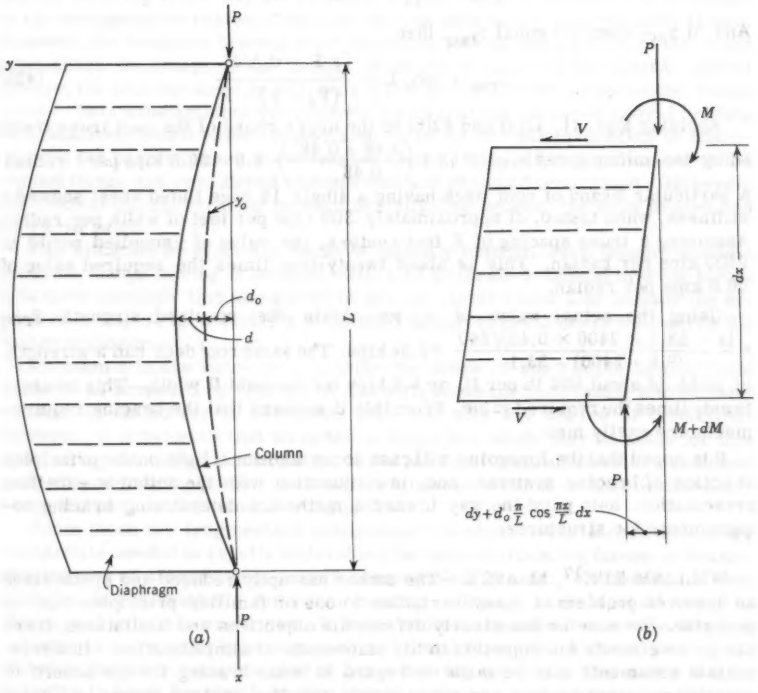


FIG. 11.—IMPERFECT COMPRESSION MEMBER, CONTINUOUSLY SUPPORTED AGAINST LATERAL BUCKLING

From Eq. 39(12) we can obtain the equation for the buckling load on an ideal column by setting d_o equal to zero, which gives

$$P_{er} = P_e + \gamma \quad \ldots\ldots\ldots\ldots\ldots\ldots (40)$$

For the practical case of the imperfect column, we can solve Eq. 39 for the required value of γ

$$\gamma_{req} = P\left(\frac{d + d_o}{d}\right) - P_e \quad \ldots\ldots\ldots\ldots\ldots\ldots (41)$$

The maximum shear stress occurs at the supports. Setting $x = 0$ in Eq. 37, and substituting d from Eq. 38 gives $dy/dx = \frac{(\pi d)}{L}$. If γ_{act} is exactly equal to γ_{req}, then

$$S_{req} = P\frac{\pi}{L}(d + d_o) - P_e\frac{\pi}{L}d \qquad (42a)$$

And, if γ_{act} does not equal γ_{req}, then

$$S_{req} = \pi d\gamma/L = \frac{(\pi P \gamma d_o)/L}{(P_e + \gamma) - P} \qquad (42b)$$

Applying Eqs. 41, 42(a) and 42(b) to the upper chord of the roof truss treated by the author gives $\gamma_{req} = 53.1\left(\frac{0.48 + 0.48}{0.48}\right) - 9.6 = 96.6$ kips per / radian

A particular brand of roof deck having a single 18 gage fluted sheet showed a stiffness, when tested, of approximately 300 kips per feet of width per radian. Assuming a truss spacing of 8 feet centers, the value of γ supplied would be 2400 kips per radian. This is about twenty-five times the required value of 96.6 kips per radian.

Using the actual value of γ we obtain the required strength $S_{req} = \frac{(\pi \times 53.1 \times 2400 \times 0.48)/240}{(9.6 + 2400) - 53.1} = 0.34$ kips. The same roof deck had a strength, at yield, of about 800 lb per ft, or 6.4 kips for an eight ft width. This is about twenty times the required value. From this it appears that the bracing requirements are easily met.

It is hoped that the foregoing will cast some additional light on the principles of action of bracing systems, and, in conjunction with the author's excellent presentation, help point the way toward a method of determining bracing requirements for structures.

WILLIAM ZUK[17], M. ASCE.—The author has aptly reduced and synthesized an involved problem of many variables to one of familiar principles easy to perceive. Because he has clearly defined his objectives and limitations, there can be no grounds for objection to his statements of simplification. However, certain comments may be made in regard to beam bracing for the benefit of practicing engineers who are not familiar with the involved theory of lateral buckling but who are concerned with safe, economical bracing. These comments are thus not intended for the author, who is quite aware of these facts already. The section on column bracing is neatly treated, so that all comments in this discussion apply only to beams.

Professor Winter's approximate analysis of beam bracing conservatively assumes the compression flange to stand alone in the lateral direction and thus to act as a column. Several limitations of this assumption suggest themselves where the approximate theory would be inadequate. The following are several such situations:

[17] Prof. of Civ. Engrg., Univ. of Virginia, Charlottesville, Va.

a. Beams whose bracing is not in the plane of the compression flange as in the case of tie rods and knee braces in a through plate girder bridge.

b. Beams with an initial torsional twist, with or without a bow in the compression flange.

c. Beams in which the compression flange force changes magnitude between points of bracing, particularly for beams whose flange stress changes from compression to tension as beams with an overhang.

The writer has presented an investigation[18] in which the required force on I-beams is presented for bracing positioned at any level on the beam, taking into account the torsional-flexure behavior. The results show that the full lateral buckling value may be obtained for the beam if the brace is anywhere in the compression region, from the neutral axis to the compression flange. However, the required bracing force becomes less as the position of the brace approaches the compression flange. Even for a brace at the neutral axis of flexure, the bracing force is still only a few percent of the compression flange force. This substantiates the author's views that the required lateral bracing is a relatively small value. It may also be noted that partial bracing is attained even for beams braced at the tension flange. Normally beams braced at the tension flange are considered unsupported and designed accordingly. However, the critical lateral buckling moment actually lies between the fully braced and unbraced value.

The situation in which the beam is initially twisted, even though no compression flange bowing is present, will also generate a lateral bracing force. It is quite possible that an equivalent bowing factor could also include the effects of twist, so that Winter's simplified design criteria could well serve the design engineer.

Situation c is one which falls outside the scope of any simple approximate analysis as proposed by Winter. A more rigorous method, taking into account torsion, is called for to solve this situation with any degree of reliability. However, it is believed that an order of magnitude study may be made for this case, using the author's procedure, if the points of contraflexure are assumed as fictitious bracing points, with the buckling value based on this distance between the real or fictitious bracing points.

From these few fragmentary comments, it is obvious that a good deal more research is needed to exactly understand the nature of bracing forces on beams, and trusses of straight and curved compression chords. No conclusive test evidence is yet available for beam bracing, although some special cases of theoretical solutions are known. It is the writer's opinion that column bracing behavior is now on fairly sure ground and that future efforts should be concentrated on the more complex case of beam bracing behavior. The author's contribution to beam bracing behavior stands analogous to the lateral beam buckling criteria of $\frac{L}{b} < 40$ of former years based on a freed compression flange, in relation to the present more exact criteria of $\frac{Ld}{bt} < 600$ based on torsion-flexure. The contribution is a valuable one, but perhaps not a final one.

---

[18] "Lateral Bracing Forces on Beams and Columns," by W. Zuk, Proceedings Paper 1032, ASCE, July, 1956.

GEORGE WINTER,[19] F. ASCE.—The lively response to the paper is appreciated by the writer, who welcomes the fact that two of the discussions considerably extend the range of the methods he has proposed.

G. G. Green's contribution supplements the information developed by the writer in that it permits one to compute the load capacity of a column if the bracing system supplies less than full bracing. In this case use must be made of the detailed theory of elastically supported columns, as in the form presented in Fig. 6 of the writer's paper. (That figure, as stated by the author, was taken from a paper of which Green was a co-author while doing graduate work at Cornell University.) Mr. Green has chosen only to replot the last of the various sloping portions of the respective curves given on the writer's Fig. 6. In order to use Mr. Green's method for all possible values of $k_{act} < k_{req}$, it is necessary to have the complete information on elastically supported column for the entire range from $k_{act} = 0$ to $k_{act} = k_{req}$. This information is contained in the writer's Fig. 6 and is given elsewhere greater detail and with sufficient accuracy for design purposes.

Mr. Green's method for less than full bracing, as shown in the second part of his numerical example, can be stated in general terms: Given the column, point-supported at n number of points, and the value k of these elastic supports.

1. Compute the actual strength S_{act} of each of the braces, that is the maximum reaction from the column which it can withstand.

2. From S_{act}, compute the maximum deflection $(d_{max} = S_{max}/k)$ to which the brace can be subjected without failure.

3. For the given k and the given column dimensions, find the critical load P_{cr} of the ideal elastically supported column. This can be done approximately from the writer's Fig. 6, and with better accuracy from the previously mentioned reference.

4. The maximum load on the column, P_{max}, is now determined from the requirement that the bracing deflection caused by this load shall not exceed d_{max} as determined in step 2. For this purpose the first equation in Green's contribution is utilized which, in terms of the present notation, is $d_{max} = d_o \frac{P_{max}}{P_{cr} - P_{max}}$. From this it follows that $P_{max} = P_{cr} \frac{d_o}{d_o + d_{max}}$. The allowable load is then obtained by dividing P_{max} by the safety factor, as indicated in Green's example.

It should be noted that the equation $d = d_o P/(P_{cr} - P)$, utilized by Mr. Green as indicated in step (4) has not, to the writer's knowledge, been rigorously proved for elastically supported columns. However, apart from being a close approximation in most elastic stability phenomena, its applicability to elastically supported columns has been demonstrated by some twenty eight tests reported[4] that cover a wide range of variables.

It is interesting to note the following from Green's numerical example: The channel column, when fully braced according to the writer's requirements, would have an allowable load of 55,500 lbs, as shown in the first part of his example. Green shows that if the bracing which is actually furnished has a stiffness as small as one-third of that required for full bracing, the allowable load is only reduced to 34,500 lb, or to 62% of the fully braced value. It is

---

[19] Prof. and Head, Dept. of Struct. Engrg., Cornell Univ., Ithaca, N. Y.

seen, however, that deflections in this partially braced column are very considerably larger than when fully braced. Thus, while the fully braced column in Mr. Green's example, under its capacity load P_{ult} = 105,500 lbs has a deflection of only 0.36 in. or 1/1000 of its length, the partially braced column under its much smaller capacity load of 65,500 lbs has a deflection of 1.07 in. This is three times the previous value, or 1/340 of the column length. For this reason, when using Green's method for partially braced columns, the following step should be added:

5. Check whether the section of the column is capable of simultaneously supporting without failure the axial load P_{max} and the bending moment $M_{max} = P_{max}d_{max}$.

It is believed that Green's example shows the advantage of the writer's proposal to design for full bracing. This is seen to result not only in a stronger but also in a much more rigid column. It is for this condition that the writer has developed his simple method. Green's complimentary approach permits one to ascertain the effect of partial bracing with relative simplicity, if such partial bracing is encountered in some special situation, such as when checking an existing structure.

M. A. Larson extends the scope of the writer's investigation in another direction. He points out that in many cases bracing to compression members or flanges is often provided in a manner different from that analyzed in the paper. In the paper, support was furnished by the equivalent of elastic springs acting independent of each other. Larson points out that if bracing is provided by rigid diaphragms (floors or roofs) spanning parallel to the members to be braced and supported at the ends by shear walls or other rigid parts of the structure, then a different kind of action ensues. Such a system is schematically represented by Fig. 5, or Larson's analogous Fig. 8, (the jacks at B and C being removed). The 18 WF 50 girder AD carries the floor beams BE and CF. These, in turn, support the cellular steel decking which is interconnected to form a rigid diaphragm and is attached at its ends to the shear walls which pass through A and D. It is evident that the top flange of the girder can buckle only if the entire diaphragm distorts as shown by Larson. This case indeed appears to be somewhat different from the writer's spring supports (see Figs. 2 through 4), but can be readily reduced to it. Larson simplifies his system for purposes of analysis by assuming that the diaphragm's entire resistance to distortion is furnished by its shear rigidity. In numerous diaphragm tests at Cornell University that share of the total deflections which was caused by shear distortion varied from about two-thirds to five-sixths of the total deflections, the rest being due to flexure of the deck plus marginal members acting as a plate girder. Therefore, the assumption of assigning the entire deformation to shear is reasonably justified.

Larson implies that, by far, the most frequent type of actual bracing is of this shear diaphragm variety, and the writer's "elastic braces connected at the far ends to points fixed in space" hardly occur in actual structures. The writer is aware that on the west coast of the United States, in view of seismic requirements, rigid shear diaphragms are almost universally used for floors and roofs. Under these conditions it is evidently most economical to use these same diaphragms also for bracing against buckling. However, in non-seismic construction, roof elements (such as standard steel roof decks, gypsum or

concrete plank) are not usually connected to form rigid diaphragms. Bracing in mill-type buildings is then furnished by providing braced bays every so often and by bracing compression members in the other bays. That is, top chords or top flanges of roof trusses or girders, are connected to these braced bays along specified lines, such as by purlin struts. The same kind of bracing is furnished for the columns in regard to buckling in the direction of the non-rigidly sheathed walls, by connecting girts or similar longitudinal bracing members to the braced bays. Because the rigidity of the braced bay is very large as compared to that of the members to be braced, the writer's independent spring supports are closely approximated and his method permits the dimensioning of the bracing members just mentioned. Numerous other such situations occur, such as the inner leg of a mill building column mentioned in the writer's introduction. The conclusion to be drawn is that both Larson's and the writer's bracing systems occur, depending upon the specific situation.

Referring to Fig. 3(b) it is seen that the shear distortion in the two exterior spans is d/L and in the interior span is 2d/L. Consequently, using Larsen's shear rigidity γ, the shear forces in the corresponding portions of the diaphragm are

$$V_{ext} = \gamma\,(d/L) \quad \ldots\ldots\ldots\ldots\ldots \quad (43a)$$

$$V_{int} = 2\,\gamma\,(d/L) \quad \ldots\ldots\ldots\ldots\ldots \quad (43b)$$

From this it is seen that the reactions between girder and floor beam are

$$F = 3\,\gamma\,(d/L) \quad \ldots\ldots\ldots\ldots\ldots \quad (44a)$$

in terms of Larson's shear rigidity γ, while the same force is

$$F = k\,d \quad \ldots\ldots\ldots\ldots\ldots \quad (44b)$$

in terms of the writer's spring constant k. Hence, if bracing is provided by the shear rigidity of the diaphragm rather than by exterior, elastic bracing members, then for the buckling mode of Fig. 3(b), equating the two above expressions for F, yields

$$\gamma = k(L/3) \quad \ldots\ldots\ldots\ldots\ldots \quad (45a)$$

which, for the case at hand, gives the relation between Larson's γ and the writer's k. For the buckling mode of Fig. 3(a), similar simple reasoning leads to

$$\gamma = kL \quad \ldots\ldots\ldots\ldots\ldots \quad (45b)$$

For the latter case it was found that $k_{id} = P_e/L$ and for the former $k_{id} = 3P/L$. If these values are substituted, respectively, in Eqs. 45(a) and 45(b), one obtains for both cases

$$\gamma_{id} = P_e \quad \ldots\ldots\ldots\ldots\ldots \quad (46)$$

which is identical with Mr. Larson's Eq. 28. In fact, Larson's general statement that the shear rigidity γ_{id} is independent of both the number of spans and the buckling mode appears to be correct, as is easily checked in the aforementioned manner for other cases.

However, his statement that the buckling mode is also irrelevant in regard to the required strength of the bracing system is erroneous, as is easily demonstrated by the same example. It is first necessary to specify what is meant

by "strength" in the case at hand. For the given system to function adequately, the shear strength of the diaphragm proper, and the strength of the connections between floor beams and girder must be adequate, both individually and separately. Neither of these is identical with the quantity S_{req} computed, but not defined, by Larson. For the present purposes call V_{req} the shear strength of the diaphragm and as before in the writer's paper, S_{req} the strength of the beam-to-girder connection.

Then, for the case of the initially distorted top flange one obtains, for both Figs. 10(a) and 10(b) γ_{req} = 382 kips per radian using either Larson's method or the writer's values and Eqs. 45(a) and 45(b). The maximum shear force on the diaphragm is now obtained by substituting this value in Eq. 43(b) which gives V_{req} = 4.58 kips. The maximum required connection strength is obtained by substituting γ_{req} in Eq. 44(b) for the interior reaction F, which gives S_{req} = 6.86 kips. This is identical with the writer's original value for the case of $k_{act} = k_{req}$ (or in Mr. Larson's terms, $\gamma_{act} = \gamma_{req}$). Neither of these values checks with Mr. Larson's S_{req} = 2.3 kips.

If instead of the mode of Fig. 10(b) that of Fig. 10(a) is investigated, similar elementary computation shows that one-half the above value would have been obtained for V_{req} and one-third for S_{req}. Whereas the two result in the same required shear rigidity, as defined by Larson, only the mode of Fig. 10(b) results in the maximum, and therefore the governing, strength requirements for the bracing system. It is thus seen that the investigation of the correct buckling mode is just as necessary for bracing by shear diaphragms as for bracing by elastic springs.

It is not maintained that the afore-mentioned solves the general problem of shear diaphragm bracing. In particular, Larson's Eq. 28(a) is intriguing in its simplicity. Also, cases of three and more interior supports may not as easily reduce to the corresponding cases of spring supports. Finally, it admitted that the way in which the writer used the quoted results of the diaphragm test to derive k_{act} = 100,000 lb per in. for his numerical example may have been excessively conservative for the given buckling mode.

In regard to continuous support, Mr. Larson first proposes a different method for finding P_{cr} in conformity with classical theory. Whether one prefers Larson's or the writer's method, or whether one prefers to use a curve such as on the writer's Fig. 6, is a matter of taste, since all three methods are simple and give identical answers within engineering accuracy.

In contrast to the point-supported case, Mr. Larson's analysis of a compression member continuously supported in a medium which possesses only shear rigidity is very interesting indeed and leads to results of great simplicity and relevance. Whereas the writer has not checked all the ramifications of this problem, he believes the method to be correct and thinks that this portion represents the main contribution of Larson's discussion.

In passing, the writer wishes to draw attention to the lack of published data on strength and rigidity of diaphragms, particularly those made up of cellular steel panels and of steel roof decks. A tremendous amount of full-scale testing of such diaphragms has been done in recent years. The fact that all these tests were made on proprietary products, so far has prevented making the results available to the profession at large. The present investigation (both Larson's contribution and the original paper) show to what extent such data are needed for intelligent and economical design. Some way ought to be found to make these data available to the profession in a form which would be useful for design without violating justified, competitive proprietary interests.

B. G. Johnston's complimentary remarks are greatly appreciated. He invites the writer's additional comments on a specific question, namely, to what extent, if any, mere friction between a floor and the supporting beam should be relied upon to provide lateral support to the beam and, at the other extreme, what justification there is, if any, in the frequent textbook statement that flange embedment in concrete is the minimum requirement for acceptable lateral support.

The writer's numerical example of an 18 WF 50 girder of 30 ft span shows, as stated in the paper, that "mere friction would suffice to develop the force required for lateral bracing" for the loads and dimensions of this specific example. The very next sentence, however, reads; "This is not to suggest that such friction should actually be relied on. . ." and goes on to indicate one of several minimum shear key measures which will provide more than adequate support even for zero friction. It is clear that the proposed method of computing lateral support requirements must be used in conjunction with, rather than as a substitute for engineering judgement. This means that the action of each bracing system must be correctly reflected. For instance, the timber planking mentioned by Mr. Johnston will ordinarily not be interconnected to form a rigid diaphragm and, therefore, may not have any bracing value of its own, in contrast to a monolithic concrete floor. On the other hand it is believed that the proposed method is sufficiently reliable to answer Mr. Johnston's questions.

The analysis as presented definitely shows that adequate lateral support is easily obtained by measures much less restrictive than the embedment of the flange in concrete. That textbook statement was an acceptable and conservative advice as long as no positive, quantitative information was available, but should be discarded as excessively restrictive. On the other hand, as indicated by the two previous quotations, the writer would not rely on frictions alone even if computation indicates this to be adequate. He would provide a minimum of shear connections, in conformity with calculations, by whatever means appear most economical in the given case, such as welded studs, light bolts, special clips, or nailing where such is possible (as in many light-gage steel shapes).

Mr. William Zuk lists a number of special situations for which he would wish more accurate methods used than those proposed by the writer. He points out that theoretical analyses of some of them was given in his own paper, but generally in a form too complex or too special for design use. He concludes by saying that "The contribution is a valuable one, but perhaps not a final one". The writer would like to add that no contribution is ever final and that it is precisely this fact which makes for the zest in research as an occupation.

It is repeatedly stated in the paper that the writer's sole purpose was to develop a reliable approximate method sufficiently simple for the usual design purposes. To take an analogy, there are many situations in which the presently accepted parameter $\left(\frac{Ld}{bt}\right)$ for lateral buckling is inapplicable or misleading. Yet it is valuable if used with discretion, and is a better crutch than we have had before. It is hoped that the present paper, likewise, will be found to be a better crutch than we have had before. The writer fully agrees with Mr. Zuk that this should in no way stop further and more refined research into the various phases of the bracing problem. He also agrees that his methods were never intended to apply to the problem of compression chords or flanges

of open through bridges (such as pony truss bridges), except possibly as approximations in the preliminary design. A considerable, and very adequate, body of literature exists on this special, important problem.

A. Chibaro's remarks are much appreciated. In a personal communication Mr. F. E. Fahy, asks the following:

> "In dealing with cases of multiple support (such as in Figs. 3 to 4) or of continuous support, should not the value of the initial amplitude (d_o) to be used in computing the required strength of the restraining means, be that for the half wave of the buckled shape or column? This is as illustrated in Figs. 3(c) and 4. The problem arises in dealing with a long strut that is initially bowed in a single half wave of considerable amplitude. A slender strut with an overall length of 20 ft might conceivably have an initial deflection at its mid-point (d_o in Fig. 20) of something like 3/4 in.. However, if it is supported at several points as in Figs. 3(c) and 4, should not the value of d_o used in Eqs. 12 and 18 be some appropriate fraction of the total 3/4 in. amplitude?"

This question is really outside the writer's competence, because its answer depends more on rolling, fabrication and erection practices than on analytical considerations. For multiple support the most unfavorable and analytically most convenient assumption has been made that the initial distortion is affine to the buckling shape. It was stated that this is an assumption of low probability and, therefore, quite conservative. If it were true that long struts are likely to be bowed initially only in a single half wave, as implied by Fahy, it would evidently be justified to take an appropriate fraction of the total amplitude for d_o in a case of multiple support. On the other hand, straightness tolerances usually are so worded that they do not rule out S-shaped members with maximum amplitudes at one or both crests equal to the full tolerance. In testing as-received, rolled members the writer has repeatedly found them to be S-shaped, although their amount of crookedness has rarely approached the value of the full straightness tolerance. Also, in fabrication and erection, additional crookednesses of single or multiple wave shape are likely to be superposed on those of the member as-rolled.

This emphasizes the fact that, as design procedures are being refined, greater attention is needed to tolerances of shape, and that this is a matter for those responsible for design specifications and codes, as repeatedly indicated in the paper. Pending such determinations, engineers connected with rolling, fabricating and erecting, as Fahy himself, are better able than the writer to judge what conditions are likely to be obtained in the finished structure.

It is evident from the analysis presented in the paper that for multiple support the required strength of the bracing is considerably less if the initial shape is a half-wave of amplitude d_o than if it is a multiple wave curve affine to the buckling mode, with the same amplitude, d_o. If the writer were to use his method for design, without appropriate guidance by codes, he would, therefore, use for the determination of d_o the total length of the member divided by the number of intermediate supports (i.e. $3L/2$ for Fig. 3(c), $4L/3$ for Fig. 4, etc.). Taking this length as basis, he would then determine d_o as two to three times the straightness tolerance stipulated for that length in the pertinent design code or specification. The taking of such a multiple appears necessary to account for the possibility of actually having S-shaped members, for the additional influence of possible eccentricities, and for such other imperfections of alignment as may be caused in fabrication and erection.

AMERICAN SOCIETY OF CIVIL ENGINEERS

Founded November 5, 1852

TRANSACTIONS

Paper No. 3045

TORQUE-LOADED CONTINUOUS BEAMS OF PROFILE SECTION

By Donovan H. Young[1] and John F. Brahtz,[2] M. ASCE

SYNOPSIS

If a beam of thin profile section is continuous over several supports and subjected to transverse loads that do not occur on the shear-center axis, it will undergo torsion as well as bending. Beginning with the general theory of nonuniform torsion for such bars, expressions for the angle of twist, ϕ, along the bar are written for two consecutive spans. From these expressions, a single recurrence-type of formula is derived which involves, as unknowns, only the three quantities of ϕ''_n, ϕ''_{n+1}, ϕ''_{n+2}, at three consecutive supports. This recurrence formula is somewhat analogous to the three-moment equation and greatly simplifies the analysis of the torsional behavior of a continuous beam subjected to eccentrically applied transverse loads. Its application to the case of a two-span beam is shown by an example and an experimental study of this two-span case is described. The results of this experiment are in very good agreement with the theory.

THEORY

Consider, in Fig. 1, the case of a continuous beam of thin-walled open profile section subjected to the action of various transverse loads. Each load can be replaced by a parallel load applied on the shear-center axis, z, and a torque. The loads on the shear-center axis only produce bending and the corresponding stresses and deflections can be easily found from the theory of bending of continuous beams. The main purpose of this paper is to develop a general method of finding the stresses and deformations produced by the torques. This can be done by using the general theory of nonuniform torsion of bars of thin walled

Note.—Published, essentially as printed here, in April, 1959, in the Journal of the Engineering Mechanics Division, as Proceedings Paper 1992. Positions and titles given are those in effect when the paper was approved for publication in Transactions.

[1] Prof. of Civ. Engrg., Stanford Univ., Stanford, Calif.

[2] Dir. of Engr., J. H. Pomeroy & Co., Los Angeles, Calif.

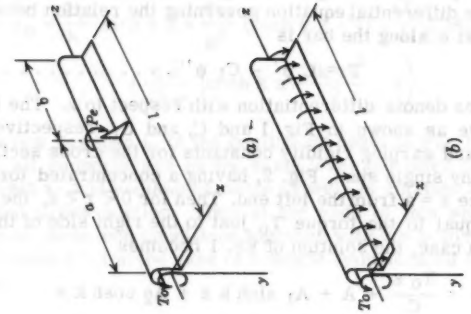


FIG. 2.—SINGLE SPAN WITH TORQUE LOADING

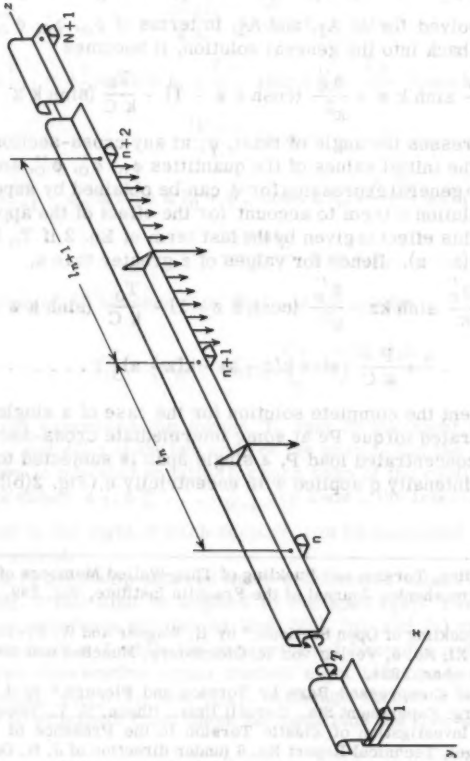


FIG. 1.—CONTINUOUS BEAM OF THIN-WALLED OPEN PROFILE SECTION

open section that has been developed.[3,4] Such treatment will be simplified if the effect of bending stresses, δ_z, on the torsional rigidity of the bar is neglected.[5,6] Then the differential equation governing the relation between torque T and angle of twist ϕ along the bar is

$$T = C\phi' - C_1\phi''' \quad \ldots\ldots\ldots\ldots\ldots\ldots \quad (1)$$

wherein the primes denote differentiation with respect to z. The torque T is considered positive as shown in Fig. 1 and C, and C_1, respectively, are the torsional rigidity and warping rigidity constants for the cross section.

Consider now any single span, Fig. 2, having a concentrated torque Pe applied at the distance z = a from the left end. Then for $0 \leq z \leq a$, the torque, T, is constant and equal to the torque T_0 just to the right side of the left-hand support. For such case, the solution of Eq. 1 becomes

$$\phi = \frac{T_0 z}{C} + A + A_1 \sinh k z + A_2 \cosh k z$$

in which $k^2 = C/C_1$ and A, A_1, and A_2 are constants of integration. For z = 0, this solution gives $\phi_0 = A + A_2$, $\phi'_0 = \frac{T_0}{C} + k A_1$, and $\phi''_0 = k^2 A_2$. When these expressions are solved for A, A_1, and A_2, in terms of ϕ_0, ϕ'_0, ϕ''_0, and these values substituted back into the general solution, it becomes

$$\phi = \phi_0 + \frac{\phi'_0}{k}\sinh k z + \frac{\phi''_0}{k^2}(\cosh k z - 1) - \frac{T_0}{k C}(\sinh k z - k z) \ldots (2)$$

This equation expresses the angle of twist, ϕ, at any cross-section, at z distance in terms of the initial values of the quantities ϕ_0, ϕ'_0, ϕ''_0, and T_0.

For $a \leq z \leq l$, the general expression for ϕ can be obtained by superimposing on the previous solution a term to account for the effect of the applied torque Pe beyond z = a. This effect is given by the last term of Eq. 2 if T_0 is replaced by (- Pe) and z by (z - a). Hence for values of z greater than a,

$$\phi = \phi_0 + \frac{\phi'_0}{k}\sinh kz + \frac{\phi''_0}{k^2}(\cosh k z - 1) - \frac{T_0}{k C}(\sinh k z - k z) + \frac{P e}{k C}\left[\sinh k(z - a) - k(z - a)\right] \ldots\ldots\ldots\ldots, \quad (3)$$

Eqs. 2 and 3 represent the complete solution for the case of a single span subjected to a concentrated torque Pe at some intermediate cross-section.

If, instead of a concentrated load P, a single span is subjected to uniformly distributed load of intensity q applied with eccentricity e (Fig. 2(b)) the torque

---

3 "Theory of Bending, Torsion and Buckling of Thin-Walled Members of Open Cross Section," by S. P. Timoshenko, Journal of the Franklin Institute, Vol. 239, March-May, 1945.

4 "Torsion and Buckling of Open Sections," by H. Wagner and W. Pretschner, Luftfahrtforschung, Vol. XI, No. 6, Verlag von R. Oldenbourg, Munchen und Berlin (NACA, T.M., No. 784), December, 1934.

5 "The Buckling of Compressed Bars by Torsion and Flexure," by J. N. Goodier, Bulletin No. 27, Engrg. Experiment Sta., Cornell Univ., Ithaca, N. Y., December, 1941.

6 "Experimental Investigation of Elastic Torsion in the Presence of Initial Axial Stress," by H. L. Engel, Technical Report No. 6 (under direction of J. N. Goodier), Div. of Engrg. Mechanics, Stanford Univ., Stanford, Calif., January, 1950.

$T = T_o - q\ e\ z$, in which T_o is the torque at the left end of the span taken as the origin of z. With this value of T, integration of Eq. 1 gives

$$\phi = \phi_o + \frac{\phi'_o}{k} \sinh k\ z + \frac{\phi''_o}{k^2} (\cosh k\ z - 1) - \frac{T_o}{k\ C} (\sinh k\ z - k\ z) + \frac{q\ e}{k^2\ C} \left(\cosh k\ z - \frac{(k\ z)^2}{2} - 1\right) \quad \ldots\ldots\ldots\ldots \quad (4)$$

Consider now any span l_n of the continuous beam in Fig. 1 in which it is assumed that all supports are on the same level and offer no more constraint than to prevent x- and y-displacements as well as rotation about the z-axis of the supported cross-section. Then at the ends of this span, $\phi_n = \phi_{n+1} = 0$. Substitution of these end conditions together with $z = l_n$ into Eq. 3 and its derivatives, ϕ' and ϕ'', for the case of a single concentrated torque $(Pe)_n$ on the span, yields

$$0 = \frac{\phi'_n}{k} \sinh k\ l_n + \frac{\phi''_n}{k^2} (\cosh k\ l_n - 1) - \frac{T_n}{k\ C} (\sinh k\ l_n - k\ l_n) + \frac{(P\ e)_n}{k\ C} (\sinh k\ b_n - k\ b_n) \quad \ldots\ldots\ldots\ldots \quad (5a)$$

$$\phi'_{n+1} = \phi'_n \cosh k\ l_n + \frac{\phi''_n}{k} \sinh k\ l_n - \frac{T_n}{C} (\cosh k\ l_n - 1) + \frac{(P\ e)_n}{C} (\cosh k\ b_n - 1) \quad \ldots\ldots\ldots\ldots \quad (5b)$$

$$\phi''_{n+1} = \phi'_n\ k \sinh k\ l_n + \phi''_n \cosh k\ l_n - \frac{k\ T_n}{C} \sinh k\ l_n + \frac{k(P\ e)_n}{C} \sinh k\ b_n \quad \ldots\ldots\ldots\ldots \quad (5c)$$

Elimination of ϕ'_n between Eqs. 5(a) and 5(c) yields

$$T_n = (\phi''_n - \phi''_{n+1}) \frac{C_1}{l_n} + \frac{(P\ e)_n b_n}{l_n} \quad \ldots\ldots\ldots\ldots \quad (6)$$

This equation expresses the torque T_n just to the right of the support n in terms of ϕ''_n and ϕ''_{n+1} at the two ends of the span l_n and the applied torque load $(P\ e)_n$. There is one such equation for each span of the continuous beam. Thus when all the values $\phi''_1, \phi''_2, \ldots \phi''_{N+1}$ are known, the internal torques $T_1, T_2, \ldots T_N$, just to the right of each support, can be computed from Eq. 6 and the problem is solved.

To find a relationship between three consecutive values ϕ''_n, ϕ''_{n+2}, at three supports, Eq. 3 can also be applied to the span l_{n+1}. This will give another set of three equations similar to Eqs. 5(a), (b), and (c) except that the subscript n becomes n+1 while the subscript n+1 becomes n+2. These six equations for two consecutive spans contain eight unknowns, namely, $\phi''_n, \phi''_{n+1}, \phi''_{n+2}, \phi'_n, \phi'_{n+1}, \phi'_{n+2}, T_n$, and T_{n+1}. Although this is a tedious operation, it is possible to eliminate from these six equations the five unknowns ϕ'_n, ϕ'_{n+1},

ϕ'_{n+2}, T_n, and T_{n+1}. This leaves an equation expressing the desired relationship between ϕ''_n, ϕ''_{n+1}, and ϕ''_{n+2} at three supports

$$\left[\xi(k\,l_n)\right]\phi''_n + \left[\eta(k\,l_n) + \eta(k\,l_{n+1})\right]\phi''_{n+1} + \left[\xi(k\,l_{n+1})\right]\phi''_{n+2} = \left[\psi\left(\frac{a_n}{l_n}, k\,l_n\right)\right]\frac{k(P\,e)_n}{C} + \left[\psi\left(\frac{b_{n+1}}{l_{n+1}}, k\,l_{n+1}\right)\right]\frac{k(P\,e)_{n+1}}{C} \quad \ldots\ldots (7)$$

in which the functions ξ, η, ψ, depend only on the physical dimensions of the beam and the placement of the loads. These functions are defined as

$$\xi(k\,l) = \frac{1}{k\,l} - \frac{1}{\sinh k\,l} \quad \ldots\ldots (8a)$$

$$\eta(k\,l) = \frac{1}{\tanh k\,l} - \frac{1}{k\,l} \quad \ldots\ldots (8b)$$

$$\psi\left(\frac{a}{l}, k\,l\right) = \frac{a}{l} - \frac{\sinh k\,a}{\sinh k\,l} \quad \ldots\ldots (8c)$$

Eq. 7 is a recurrence-type of formula that may be written once for each pair of consecutive spans throughout the continuous beam. Thus, its application to a beam subjected to various applied torque loads is somewhat analogous to that of the three-moment equation used in the analysis of continuous beams subjected to bending loads. In the case of a beam on N+1 supports and having N spans, Eq. 7 can be written N-1 times. This gives a system of N-1 linear equations involving the N+1 unknowns $\phi''_1, \phi''_2, \ldots \phi''_{N+1}$. If the cross-sections at the two extreme ends of the beam are free to warp, then $\phi''_1 = \phi''_{N+1} = 0$ and Eq. 7 is sufficient to determine $\phi''_2, \phi''_3, \ldots \phi''_N$. As soon as these values are known, the internal torques $T_1, T_2, \ldots T_N$ can be found from Eq. 6 and the problem is solved.

If the extreme left end of the beam is built-in so that warping of that cross-section is prevented, the value of ϕ''_1 is not known but instead, as a condition of constraint against warping, $\phi'_1 = 0$. The simplest way to handle this situation is as follows:

Imagine a mirror at the built-in end which reflects the span l_1 and its torque load $(P\,e)_1$ as shown in Fig. 3. Then the reflected span l_1 and the actual span l_1 represent two consecutive spans for which the plane AA is a plane of symmetry. From this it follows that the condition $\phi'_1 = 0$ will be satisfied. Thus, Eq. 7 may be written for these two consecutive spans yielding an additional equation to match the additional unknown ϕ''_1. In applying Eq. 7 to the fictitious situation in Fig. 3, it must be noted that b_1 should be substituted for both a_n and b_{n+1}, while l_1 is substituted for both l_n and l_{n+1}. The same procedure may be used if the extreme right end of the beam is built-in.

Thus far, only the case of a continuous beam subjected to eccentrically applied concentrated forces has been treated. The case of uniformly distributed load of intensity q applied with eccentricity e from the shear-center axis (Fig. 2(b)) can be treated in the same way, using the general solution represented by Eq. 4, In this case, the recurrence formula, analogous to Eq. 7, becomes

$$\left[\xi(k\,l_n)\right]\phi''_n + \eta(k\,l_n) + \eta(k\,l_{n+1})\,\phi''_{n+1} + \xi(k\,l_{n+1})\,\phi''_{n+2} = \left[\zeta(k\,l_n)\right](q\,e)_n + \left[\zeta(k\,l_{n+1})\right](q\,e)_{n+1} \quad \ldots\ldots (9)$$

where $\xi(k\,l)$ and $\eta(k\,l)$ are the same functions already introduced in Eqs. 8 (a) and (b) and the new function $\zeta(k\,l)$ is

$$\zeta(k\,l) = \frac{k\,l}{2} - \tanh\frac{k\,l}{2} \quad \ldots\ldots\ldots\ldots\ldots (10)$$

For this case, the torque T_n just to the right of the support n is

$$T_n = \frac{C_1}{l_n}\left[\phi''_n - \phi''_{n+1}\right] + \frac{(q\,e)_n\,l_n}{2} \quad \ldots\ldots\ldots\ldots (11)$$

thus being analogous to Eq. 6. Eqs. 9 and 11 are sufficient to handle the case of a continuous beam under the action of uniformly distributed load.

If there are several concentrated loads in any one span, or both concentrated loads and uniformly distributed load, it is only necessary to superimpose the appropriate right-hand members of Eqs. 7 and 9 and, likewise, the load terms in Eqs. 6 and 11.

To facilitate the use of the recurrence formula (Eqs. 7 or 9), the functions ξ, η, ζ, and ψ, defined by Eq. 8(a), (b) and (c) and Eq. 10, are recorded in Table 1 for a range of values of k l from 0 to 5.0.

EXPERIMENTAL VERIFICATION

As an experimental check on the foregoing theory, a simple test was made on a two-span beam in which each span was 35-in.-long. In this test, an eccentric transverse load P_1 was applied to a small pulley at the middle of span 1 and the corresponding angle of rotation ϕ was measured at the middle of span 2 by means of a reflected light-beam. The specimen used for this test was an aluminum alloy beam 70 in. long and having the balanced Z-section shown in Fig. 4. Free warping conditions at the supports were attained by using roller-type bearings oriented so as to prevent both rotation and lateral displacement of the supported cross-section in its plane while allowing complete freedom for longitudinal strain. For a load P_1 = 10 lb. applied with eccentricity e = 2.603 in. in span 1, the measured value of ϕ in span 2 was - 0.0071 radians as compared with a computed value of - 0.00779 radians.

Numerical Computations.—In computing ϕ, the following data is given: Aluminum alloy, with a Young's modulus $E = 10.5(10)^6$ psi, and a modulus of elasticity in shear $G = 4.0(10)^6$ psi; length m of center-line of cross-section (Fig. 4) $m = 1.319 + 0.2595 \times 2 + 0.919 \times 2 = 3.676$ in.; torsional rigidity constant $C = \frac{1}{3}\,m\,t^3\,G = \frac{1}{3}\,(3.676)\,(0.081)^3 \times 4.0\,(10)^6 = 2605$ lb.-in.^{2}; warping rigidity constant $C_1 = \frac{E\,t\,b^2}{12\,m}\left[4\,d^3\,(d + 4\,b + 2\,h) + 12\,h\,d^2\,(b + h) + 2\,h^2\,d\,(2\,b + 3\,h) + h^2\,b\,(b + 2\,h)\right]$. So that $C_1 = 16284\,[0.4594 + 2.385 + 5.232 + 5.687] = 224100$ lb.-in.^{4} With C and C_1 determined, $k = \sqrt{C/C_1} = \sqrt{0.01162} = 0.1078$ in.$^{-1}$. Thus, from $l_1 = l_2 = 35$ in., $k\,l_1 = k\,l_2 = 3.773$.

For $k\,l = 3.773$ and $a/l = 0.50$, Table 1 gives $\xi = 0.2191$, $\eta = 0.7357$, and $\psi = 0.3516$. Then with $\phi''_1 = \phi''_3 = 0$, Eq. 7 becomes $0 + [0.7357 + 0.7357]\,\phi''_2 + 0 = 0.3516\left(\frac{0.1078}{2605}\right)(P\,e)_1$, from which $\phi''_2 = 0.00000989(P\,e)_1$.

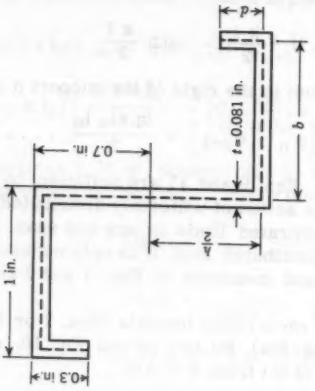


FIG. 4.—Z-SECTION TESTED

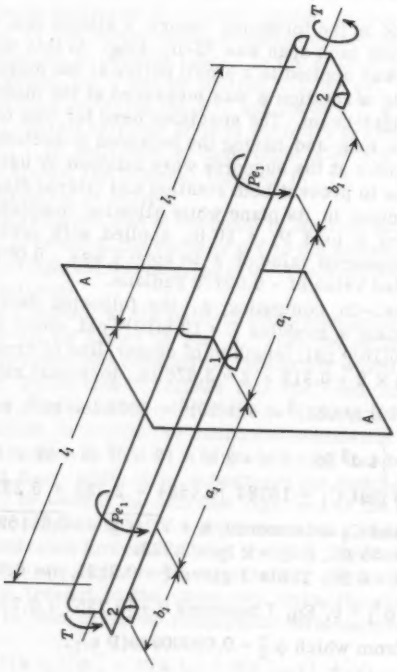


FIG. 3.—REFLECTION OF SPAN AND ITS TORQUE LOAD

TABLE 1.—FUNCTIONS FOR USE IN RECURRENCE FORMULAS

kl	ξ	η	ζ	ψ a/l = 1/4	ψ a/l = 1/2	ψ a/l = 3/4
0.00	0.0000	0.0000	0.0000	0.0000	0.0000	0.0000
0.10	0.0166	0.0333	0.0000	0.0004	0.0006	0.0005
0.20	0.0332	0.0665	0.0003	0.0016	0.0029	0.0022
0.30	0.0494	0.0994	0.0011	0.0035	0.0056	0.0049
0.40	0.0654	0.1319	0.0026	0.0061	0.0098	0.0086
0.50	0.0810	0.1640	0.0051	0.0095	0.0152	0.0134
0.60	0.0960	0.1953	0.0087	0.0135	0.0217	0.0191
0.70	0.1103	0.2260	0.0136	0.0181	0.0291	0.0257
0.80	0.1240	0.2559	0.0200	0.0233	0.0375	0.0331
0.90	0.1369	0.2850	0.0281	0.0290	0.0467	0.0414
1.00	0.1491	0.3130	0.0379	0.0350	0.0566	0.0503
1.10	0.1604	0.3401	0.0495	0.0415	0.0671	0.0598
1.20	0.1708	0.3662	0.0630	0.0483	0.0782	0.0699
1.30	0.1804	0.3913	0.0783	0.0553	0.0898	0.0805
1.40	0.1892	0.4151	0.0956	0.0629	0.1016	0.0916
1.50	0.1971	0.4381	0.1148	0.0697	0.1138	0.1029
1.60	0.2040	0.4600	0.1360	0.0771	0.1262	0.1146
1.70	0.2102	0.4809	0.1589	0.0845	0.1386	0.1265
1.80	0.2157	0.5006	0.1837	0.0918	0.1511	0.1385
1.90	0.2203	0.5195	0.2102	0.0991	0.1636	0.1507
2.00	0.2243	0.5373	0.2384	0.1063	0.1760	0.1629
2.10	0.2276	0.5542	0.2682	0.1134	0.1882	0.1752
2.20	0.2301	0.5704	0.2995	0.1203	0.2003	0.1874
2.30	0.2322	0.5855	0.3322	0.1270	0.2122	0.1996
2.40	0.2338	0.5999	0.3663	0.1335	0.2239	0.2118
2.50	0.2347	0.6136	0.4017	0.1398	0.2352	0.2238
2.60	0.2352	0.6265	0.4383	0.1459	0.2463	0.2357
2.70	0.2354	0.6387	0.4759	0.1518	0.2571	0.2474
2.80	0.2350	0.6503	0.5146	0.1574	0.2675	0.2590
2.90	0.2344	0.6613	0.5543	0.1628	0.2777	0.2705
3.00	0.2335	0.6717	0.5948	0.1679	0.2875	0.2817
3.10	0.2323	0.6815	0.6362	0.1728	0.2969	0.2928
3.20	0.2310	0.6908	0.6783	0.1775	0.3060	0.3036
3.30	0.2291	0.6997	0.7211	0.1819	0.3148	0.3143
3.40	0.2273	0.7081	0.7646	0.1861	0.3232	0.3247
3.50	0.2253	0.7161	0.8086	0.1901	0.3313	0.3349
3.60	0.2231	0.7237	0.8532	0.1939	0.3391	0.3450
3.70	0.2208	0.7309	0.8982	0.1974	0.3466	0.3548
3.80	0.2184	0.7378	0.9438	0.2008	0.3537	0.3644
3.90	0.2159	0.7444	0.9897	0.2040	0.3605	0.3737
4.00	0.2134	0.7507	1.0360	0.2069	0.3671	0.3829
4.10	0.2107	0.7566	1.0826	0.2097	0.3734	0.3919
4.20	0.2081	0.7623	1.1295	0.2124	0.3794	0.4006
4.30	0.2055	0.7678	1.1768	0.2149	0.3851	0.4092
4.40	0.2027	0.7730	1.2243	0.2172	0.3905	0.4175
4.50	0.2000	0.7780	1.2720	0.2194	0.3958	0.4257
4.60	0.1973	0.7828	1.3199	0.2214	0.4007	0.4337
4.70	0.1946	0.7874	1.3680	0.2234	0.4055	0.4414
4.80	0.1918	0.7918	1.4163	0.2252	0.4100	0.4490
4.90	0.1892	0.7960	1.4648	0.2268	0.4143	0.4564
5.00	0.1865	0.8001	1.5134	0.2284	0.4185	0.4636

Eq. 6 applied to span 2 now gives

$$T_2 = [0.00000989 - 0] \frac{224100}{35} (P\,e)_1 = 0.0633(P\,e)_1.$$

Elimination of ϕ'_n between Eqs. 5(a) and 5(b), after replacing T_n by its value derived from Eq. 6, gives

$$\phi'_{n+1} = \frac{\phi''_n}{k} \left[\xi(k\,l_n)\right] + \frac{\phi''_{n+1}}{k} \left[\eta(k\,l_n)\right] - \frac{(P\,e)_n}{C} \left[\psi\left(\frac{a_n}{l_n}, k\,l_n\right)\right].$$

Applied to the two-span problem being investigated, this becomes

$$\phi'_2 = \frac{\phi''_2}{k} \left[\eta(k\,l_1)\right] - \frac{(P\,e)_1}{C} \left[\psi\left(\frac{a_1}{l_1}, k\,l_1\right)\right].$$

Substitution of the value of ϕ''_2 previously found, together with η and Ψ, gives

$$\phi'_2 = \frac{9.89(P\,e)_1}{0.1078(10)^6} (0.7357) - \frac{(P\,e)_1}{2605} (0.3516) = -0.0000675(P\,e)_1.$$

Finally, the angle of twist at the mid-point of span 2 is obtained from Eq. 2 which, for $z = l/2$, becomes

$$\phi = 0 + \frac{\phi'_2}{k} \sinh \frac{k\,l_2}{2} + \frac{\phi''_2}{k^2} \left(\cosh \frac{k\,l_2}{2} - 1\right) - \frac{T_2}{k\,C} \left(\sinh \frac{k\,l_2}{2} - \frac{k\,l_2}{2}\right).$$

With the values of ϕ'_2, ϕ''_2, and T_2, already found, this gives

$$\phi = (-0.002015 + 0.002016 - 0.0003003)(P\,e)_1 = -0.0002993(P\,e)_1.$$

For $P_1 = 10$ lb. and $e = 2.603$ in.,

$$\phi = -0.0002993 \times 26.03 = -0.00779 \text{ radians.}$$

CONCLUSIONS

The recurrence formulas, Eqs. 7 and 9, constitute the essence of the paper and furnish a basis for the analysis of continuous beams of thin walled open cross section subjected to torque loading. Their use, augmented by the tabulated values of the functions ξ, η, ζ, and ψ, will considerably reduce the amount of labor involved in such an analysis. Since beams of thin walled open cross section are coming into more common use, it is hoped that the procedure may be of help to designers confronted with this problem.

AMERICAN SOCIETY OF CIVIL ENGINEERS

Founded November 5, 1852

TRANSACTIONS

Paper No. 3046

FORCES INDUCED ON A LARGE VESSEL BY SURGE

By John T. O'Brien,[1] F. ASCE and David I. Kuchenreuther,[2] A. M. ASCE

With Discussion by Messrs. Basil W. Wilson; and J. T. O'Brien and D. I. Kuchenreuther

SYNOPSIS

Field measurements are presented for forces of up to 40,000 lb as induced by two predominant standing waves. The waves with 1-min and 2 1/2-min periods produced water surface slopes of up to 0.0015 in the lines of the ship *USS Norton Sound* (AVM-1) of 12,000 long tons. The ship was moored alongside by unusually taut lines at Port Hueneme, California, and close to a node of the shorter wave. The two waves acted simultaneously to produce only significant surge. Tight lines tend to reduce the inertial force.

The excitation in surge is defined by the product of the slope of the water surface and the weight of the ship. Restoring forces of up to 30,000 lb in surge as computed on this basis are approximately one-third greater than those measured. In no case was it considered that resonance was encountered.

INTRODUCTION

Notation.—The letter symbols adopted for use in this paper are defined where they first appear, in the illustrations or in the text, and are arranged alphabetically, for convenience of reference, in the Appendix.

Note.—Published, essentially as printed here, in March, 1958, in the Journal of the Waterways and Harbors Division, as Proceedings Paper 1571. Positions and titles given are those in effect when the paper or discussion was approved for publication in Transactions.

[1] Dir., Harbor Div., U.S. Naval Civ. Engrg. Lab., Bureau of Yards and Docks, Dept. of the Navy, Port Hueneme, Calif.

[2] Hydr. Engr., U.S. Naval Civ. Engrg. Lab., Bureau of Yards and Docks, Dept. of the Navy, Port Hueneme, Calif.

The reaction of a moored ship subjected in surge to the excitation produced by standing waves has been considered systematically at least since Robert T. Knapp and Vito A. Vanoni,[3] F. ASCE, and Robert E. Carr.[4] Carr likened the moored ship oscillating against the restoring force of its lines to that of a mass oscillating with an initial velocity against the restoring action of two linear springs with a clearance or gap, where the period of oscillation depends not only on the spring factor but also on the magnitude of the gap and the initial conditions. It is postulated that when the computed value of this period tends to coincide with that of the exciting wave than a condition of resonance is produced with relatively high mooring forces.

Basil W. Wilson,[5] M. ASCE, derived an expression for the periodicity, T_n, of the longitudinal oscillation of a moored ship of mass m at resonance with the exciting standing wave in water of depth d. When rearranged, Wilson's expression appears to be that for the natural period of oscillation of a nonlinear spring-suspended mass $T_n = 2\pi(m/k)^{1/2}$, multiplied by a factor that expresses the nonlinearity of the system and the amplitude, A, of the standing wave in the ship's basin $(mgA^2/kd)^c$, in which $c = (1-n)/2(1+n)$.

The numerical exponent used with mooring ropes is n, and g is the acceleration due to gravity. The spring factor, k, for the lines collectively is equal to D N/4, where D is the spring factor for a representative line, and N is the total number of lines. The spring factor, k, has the unusual dimension of force per (movement to the nth power). When the lines become significantly taut (n = 1 and k has usual dimensions), the second factor becomes equal to unity, the spring factor becomes linear, and Wilson's general expression becomes that for a simple system. Wilson also showed that T_n was related to the initial tension in the lines and demonstrated that the maximum force in surge to be expected in the moorings as a whole was related inversely to this period and directly to the weight of the ship, W, and the characteristics of the standing wave, $2\pi WA/T_n(gd)^{1/2}$. G. W. R. Deacon, R. C. H. Russel, and J. E. G. Palmer[6] stated that this expression can be shown to be that for the maximum force on the ship if the cables are all tight, the ship is held stationary, and the virtual mass of the ship is neglected.

Robert L. Wiegel, et al.,[7] measured the mooring forces induced by short laboratory type "wind" waves on five moored ship models. No particular analytical treatment was made of the results. The conclusions reached were that the importance of initial tension as a factor in the explanation of maximum forces had been demonstrated, all of the systems were found to have nonlinear load-movement characteristics, in most cases mooring forces reach their maximum during the passage of only the second or third wave, and any satisfactory analytical treatment of the problem must include coupled motions.

---

3 "Wave and Surge Study for Navy Operating Base, Terminal Island, California," by R. T. Knapp and V. A. Vanoni, Report under contract NOy-8522 with the Bureau of Yards and Docks, California Inst. of Technology, January, 1945.

4 "Memo on Waves in Los Angeles Harbor associated with the Alaskan Earthquake of April 1, 1946," by R. E. Carr, Report under contract NOy-13116 with the Bureau of Yards and Docks, April, 1947.

5 "Ship Response to Range Action in Harbor Basins," by B. W. Wilson, Transactions, ASCE, Vol. 116, 1951, pp. 1129-1157.

6 "Origin and Effect of Long Period Waves in Ports," by G. W. R. Deacon, R. C. H. Russel, and J. E. G. Palmer, Communication 1, Section 2, Proceedings, 19th International Navigation Congress, London, 1957.

7 "Model Study of Ship Mooring Forces; Final Report," by R. L. Wiegel, R. A. Dilley, R. W. Clough, and J. B. Williams, Series 92, Wave Research Lab., Univ. of California, part of contract NOy-73264 with the Bureau of Yards and Docks, August, 1956.

On the basis that the theory advanced by Wilson[5] ". . .is so unamenable to analysis that approximations have to be made which spoil its many virtues. . ," Deacon, et al.,[6] presented simpler methods for estimating the line tensions for the case of a ship with lines that periodically go slack. When such a ship is released from rest at an instant when the standing-wave-excited water particles are also at rest, it was indicated by use of simple mechanics that the maximum force required to hold the ship stationary is that given by Wilson[5] and presented herein, multiplied by the factor 1.5. Like Wilson, the desirability of tight cables as a means of reducing the mooring forces was also cited. W. C. Q. Joosting[8] states that while the forces that excite a moored ship can be considered sinusoidal, the mooring system generally does not have linear extension characteristics, so that no actual resonance can be expected, and the general behavior should be examined on the basis of forced oscillations. Also, some anomalies in Wilson's theory were found when applying it to an important case. On the basis of the familiar equation for the forced vibration of a damped spring-suspended mass, Joosting evolves an expression for the longitudinal movement of a moored ship in which the inertia force on the ship is taken to be the product of the mass of the ship and the difference between the acceleration of the water and the acceleration of the ship. Deacon, Russel and Palmer,[6] have objected to the use of the same reasoning by Wilson.[5]

An exceptional analytical study of the forces and movements induced by ocean waves on a large floating platform moored in approximately 12,000 ft of water in the ocean 300 miles offshore was undertaken[9] in which use was made of basic hydrodynamic theory to compute the forces and movements induced by the deep water waves. It appears that a significant restraining force was considered to be present at all times so that, as in this study, it was not necessary to cope with the problem posed by periodically slack moorings.

ANALYTICAL CONSIDERATIONS

The condition of force equilibrium on a moored ship in surge, based on the damped motion of a simple spring-suspended mass under the action of a periodic disturbing force is considered to be

$$\text{inertial} + \text{damping} + \text{restoring} + \text{excitation} = 0 \quad \ldots\ldots\ldots (1)$$

From a consideration of basic hydrodynamic theory the inertial reaction is considered to be made up of two parts, that of the ship and that of the hydrodynamic mass of the ship. This can be expressed as inertia force = $m(1+C_m)\, d^2x/dt^2$, in which C_m represents the inertial coefficient (ratio of hydrodynamic mass to displaced mass) and d^2x/dt^2 is the acceleration of the ship in the surge direction and equal to $\ddot{x}$. In most cases, $(1+C_m)$ is written as C_M so that

$$\text{inertia force} = C_M\, m\ddot{x} \quad \ldots\ldots\ldots\ldots\ldots\ldots (2)$$

in which C_M is termed a mass factor.

The damping reaction is based on the expression

$$\text{damping force} = \frac{C_d\, A_s \rho \left(\frac{dx}{dt}\right)^2}{2} \quad \ldots\ldots\ldots\ldots\ldots (3)$$

---

8 "Investigation into Long Period Waves in Ports," by W. C. Q. Joosting, Communication 1, Section 2, Proceedings, 19th International Navigation Congress, London, 1957.

9 "Feasibility Report on Continental Defense Stations," Copper & Steel Industries, Inc., report prepared for Massachussetts Inst. of Technology, 1956.

in which C_d is a drag coefficient experimentally derived where form is considered, A_s is the projected underwater area of the ship for form drag and the wetted area of the ship for frictional drag, dx/dt represents the speed of the ship in the surge direction and is equal to $\dot{x}$, and ρ denotes the density of sea water.

With cables that are always significantly taut, the restoring reaction consists significantly of that due to the elasticity of the cables where by the application of Hooke's Law (total elongation = $Pl_m/A_l E$)

$$\text{restoring force} = \sum \left[\text{total elongation} \left(\cos\alpha_i \cos\beta_i \right) \right] A_{li} \frac{E_i}{l_{mi}} \quad \ldots (4)$$

in which i represents an item number, α is the angle between the mooring line and the horizontal, β denotes the angle between the horizontal projection of the mooring line and the face of the wharf (the x-axis), P is equal to the total force in a mooring line, and l_m is the length of a mooring line.

When there is significant slack in the moorings, as in the usual case, then the restoring force is no longer given completely by Eq. 4, but rather by one of the type given by Wilson:[5]

$$\text{restoring force} = \sum k_i \, (\text{surge movement}) \, n_i \quad \ldots\ldots\ldots (5)$$

in which k is the spring factor for a single mooring line.

This function must be obtained through a consideration of Eq. 4 and the characteristics of the moorings in the case of resilient but significantly weightless lines such as ropes. The catenary equation should be used in the case of very heavy but significantly nonresilient moorings such as chains.

From a consideration of basic hydrodynamics the excitation force is that obtained by integrating the proper components of the wave-induced pressure over the wetted surface of the ship. It is beyond the scope of this paper to attempt to accomplish this analytically. However, as an approximation for waves much longer than the ship, Joosting[8] and others[10] consider the excitation to be that due to a ship sliding up and down a sloping water surface such that

$$\text{excitation force} = m\,g\,\frac{dz}{dx} \quad \ldots\ldots\ldots\ldots\ldots (6a)$$

and

$$\text{excitation force} = m\,g \left(\frac{2\pi A}{L} \right) \left(\sin \frac{2\pi t}{L} \right) \quad \ldots\ldots\ldots (6b)$$

in which dz/dx represents the slope of the water surface in the surge direction, and A is the amplitude of the exciting wave, L denotes the length of a wave, and T is equal to the period of oscillation. Eq. 6b assumes that there is no appreciable trim of the ship as it oscillates in surge. This assumption seems adequate for many cases because the standing waves and combinations thereof ordinarily active in harbors are of low amplitude even though very long.

If the relationships $L = T(g\,d)^{1/2}$ and $m\,g = W$ are used in Eq. 6b, it becomes

$$\text{excitation force} = \left(2\pi \frac{WA}{T} (g\,d)^{1/2} \right) \left(\sin \frac{2\pi t}{T} \right) \quad \ldots\ldots\ldots (6c)$$

When the time $t = T/4$ or $3T/4$ (extremes of the oscillations) the sine term

---

10 "Estimation of Forces Action on a Floating Vessel in a Channel of Finite Depth due to Traveling Waves," David Taylor Model Basin, Memo from C.O. & Director DTMB to Chief, Bureau of Ships, U. S. Dept. of the Navy, A-11/Hydro (596:EYH:lf), 1954.

becomes unity and Eq. 6c reduces to that given by Wilson for the maximum tension in the lines as referred to under the heading "Introduction."

In an environment of standing waves, it is well to consider that moored ships will be subject to a maximum variation in water level which is that produced by the sum of the various standing waves. Thus, a computation of the slope of the water surface by an expression such as that contained in Eq. 6(b) is not likely to give accurate results, because this equation considers only one wave (and that of strictly sinusoidal form) while it is probable that in most cases two or more waves will be active.

TEST FACILITIES AND PROCEDURES

The investigation was conducted in a virtually closed basin, (Fig. 1) approximately 1,900 ft long, 280 ft wide, and 32 ft deep at mean lower low water (MLLW), where the tidal variation was approximately 4 ft.

The ship used in the study was the USS Norton Sound (AVM-1) which has its home port in Port Hueneme, Calif. It was selected for the study because it is berthed conveniently close to the U.S. Naval Civil Engineering Laboratory, and because the harbor of Port Hueneme contains a system of standing waves that induce interesting if not high-level mooring forces. The following are characteristics of the ship at the time of the study:

Over-all length	540	ft
Extreme beam length	72	ft
Projected area above water line		
side	31,000	sq ft
end	5,100	sq ft
Displacement	12,000	long tons
	26,880,000	lb
Mass	835,000	slugs
Projected area below water line		
side	10,800	sq ft
end	1,150	sq ft
Draft	20	ft
Wetted area	40,000	sq ft

Because the basin is part of the harbor as a whole, where the water in both is excited by waves from the ocean, it is apparent that more than one wave system is likely to be active in the basin at any given time. This is in fact the case, because standing waves with periods of approximately 1, 2 1/2 and 12 1/2 min are known to be active. The ship was moored alongside wharf No. 2 (Fig. 1) and near the node of the wave with 1 min period.

Water-level variations were measured at two points, one near the bow and the other near the stern of the ship (Fig. 1), by means of pressure pickups as described by Knapp[11] placed on the bottom of the basin. The variations due to the long-period waves encountered were indicated directly by the output of these pickups, whereas it is recognized that this is not the case with those of shorter period usually referred to as wind waves. The variations induced by these long-period waves are important, because as determinants of the significant slope of the water surface, they evaluate the major parameter in the expression for the ship excitation (Eq. 6a).

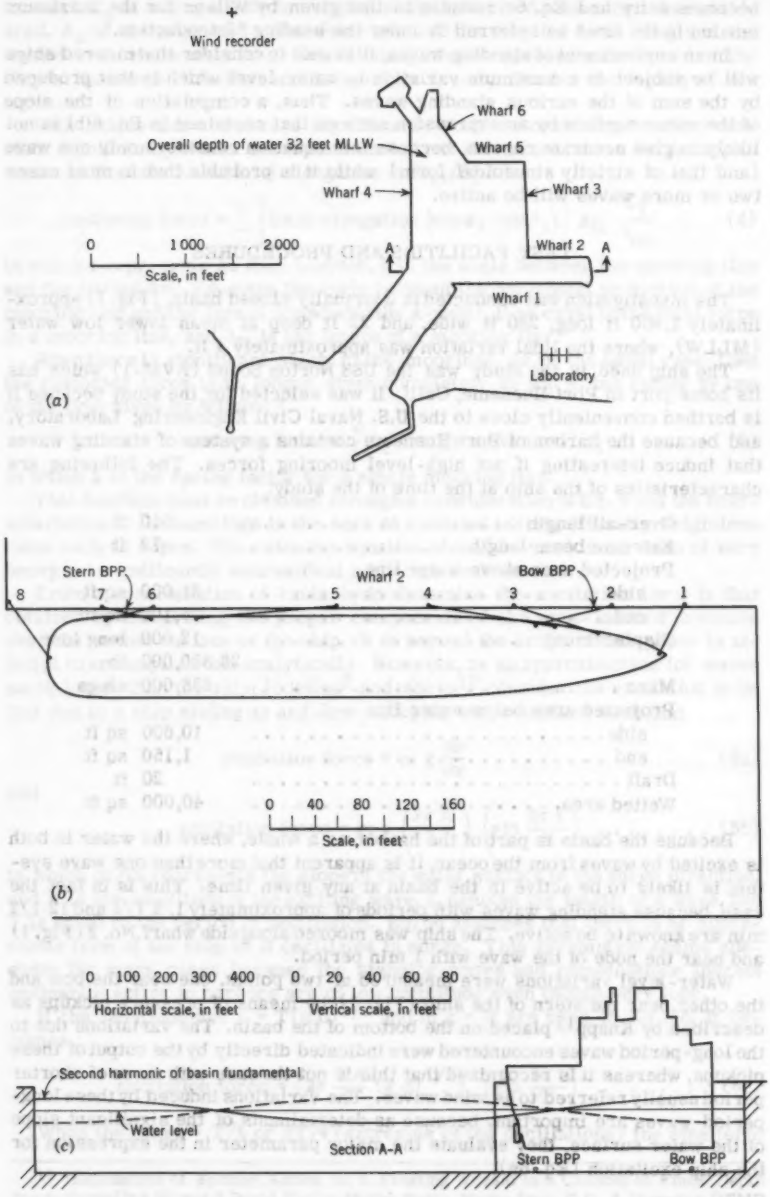


FIG. 1.—HARBOR AND BASIN, WITH THE SHIP AS MOORED DURING THE STUDY

In some cases only the stern water-level pickup was available because of malfunctioning of the other. However, on the basis of trends established with data from two pickups, it was possible to obtain a reasonable approximation to the slope of the water surface from the water-level variation at the single location.

The ship restraints consisted of seven manila ropes varying in circumference from 8 to 12 in. and one spring-lay cable of 1 1/2-in. diam. A portside profile of the ship showing the mooring lines is given in Fig. 2. The lines have characteristics as given in Table 1.

The data presented in Table 1 are the result in part of measurements made in the field at various tide levels. The results presented therein have been reduced to a common tide level of 4.8 ft mean lower low water (MLLW) on November 18, 1954. Initial tension is a variable depending on the ship's crew and tide level.

TABLE 1.—CHARACTERISTICS OF THE SHIPS MOORINGS

Line[a] (1)	Point[b] of line attachment to ship, in feet (2)	Initial tension, in Kips (3)	l_m, in feet (4)	α (5)	β (6)	x, in feet (7)	y, in feet (8)	z, in feet (9)	r, in feet (10)	r_1, in feet (11)	z_1, in feet (12)
1	536.0	0	51.5	32°-00'	59°-20'	21.5	36.2	26.4	42.1	49.6	35.2
2	428.0	2.0	72.0	17°-00'	12°-26'	67.0	14.5	20.8	68.6	71.8	29.6
3	482.0	3.0	79.3	16°-50'	13°-05'	73.8	17.0	22.8	75.7	79.1	31.6
4	444.0	15.0	117.0	10°-53'	5°-04'	114.5	9.6	24.0	114.9	117.0	32.8
5	130.0	16.0	124.0	5°-03'	0°-20'	124.0	6.5	13.2	123.0	124.0	22.0
6	50.0	0	47.4	14°-32'	11°-45'	42.1	8.9	10.9	43.0	44.4	19.7
7	90.0	0	44.0	14°-18'	9°-56'	40.3	7.0	10.2	40.9	42.2	19.0
8	0	0	63.0	12°-30'	55°-10'	34.5	49.6	14.2	60.4	61.9	23.0

[a] See Fig. 2. [b] Measured horizontally along center line of ship from stern.

The symbols listed in Table 1, columns 4 to 12, are shown in Fig. 2(b), (c), and (d); in which x represents the horizontal distance along the axis parallel to the wharf (surge), y denotes the horizontal distance along the axis normal to the wharf (sway), z is the vertical distance along the axis normal to the water surface (heave), r is equal to the length of the horizontal projection of a mooring line, r_1 denotes the straight line distance between extremities of a mooring line, and z_1 is the vertical distance to the water surface from point of attachment of line to ship.

The lines listed in column 1 are shown in Fig. 2(a). Lines 1, 2, 3, 6, and 7 are three parts 8-in. manila and line 8 is three parts 1 1/2-in. spring lay (steel and manila). Line 4 is two parts 12-in. manila for 20 ft from the ship, one part 12-in. manila for the next 77 ft, and two parts 1-in. diam steel cable for the remaining 20 ft. Line 5 is two parts 12-in. manila for 49 ft from the ship, one part double 12-in. manila for the next 65 ft, and two parts 1-in. steel cable for the remaining 10 ft.

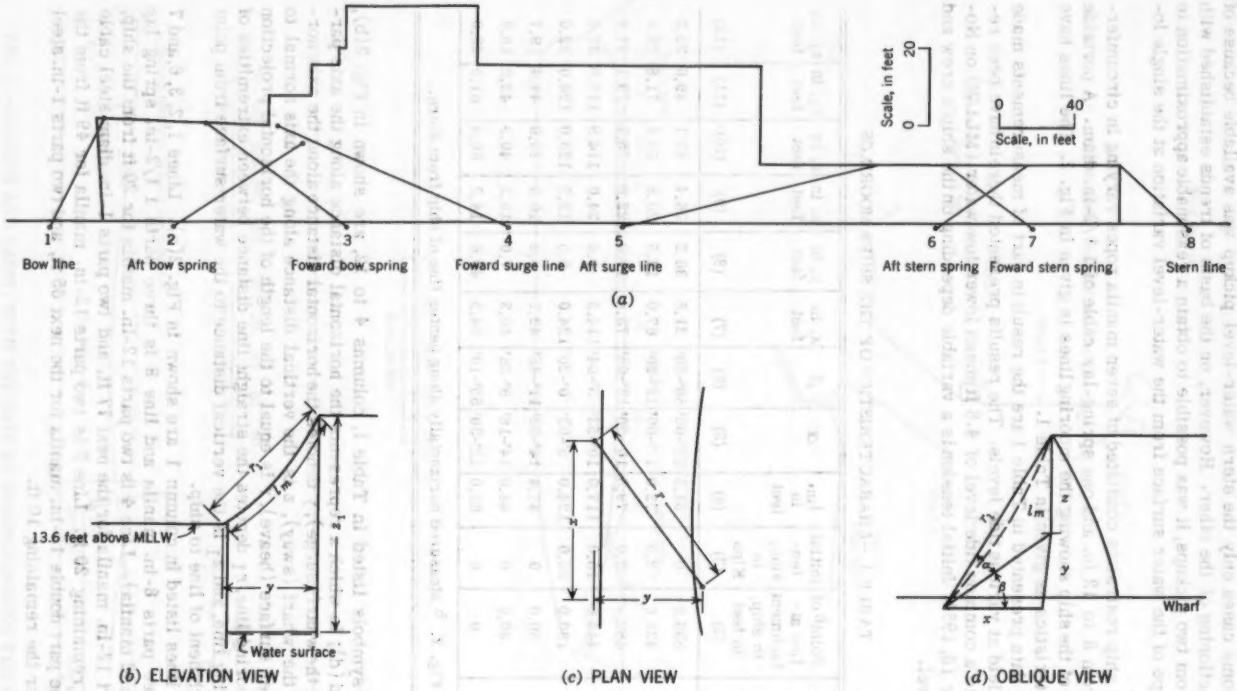


FIG. 2.—PORTSIDE PROFILE OF THE SHIP SHOWING MOORING LINES

The two surge lines were always kept taut, an unusual circumstance, and one that served to ease the task of reducing the force data, because it assured that a significant restoring force, later shown to vary almost linearly with movement, would be present at all times. This eliminated consideration of an unrestrained "run" of the ship as would have been the case if all the lines periodically went slack.

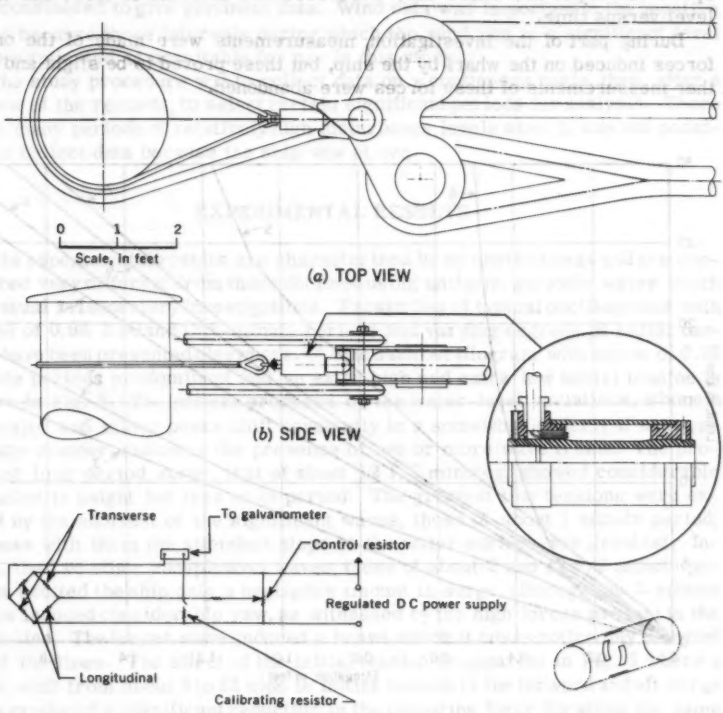


FIG. 3.—TENSION FORCE PICKUP AS USED IN THE SHIP'S LINES

Mooring forces were measured on a continuous basis by means of dynomometers of the tube-strain-gage type incorporated directly into the lines (Fig. 3). Because the incorporation procedure involved a line handling effort slightly over and above that required normally, it was generally only on weekends, when the ship was not to sea, or at other infrequent periods of inactivity, that it was possible to activate the dynamometers and collect force data.

Data on the relationship between loads in the mooring lines and their elongation were obtained by special measurements, some of which were made in place.

Fig. 4 shows the variation of elongation with load for all of the ships lines. It will be noted that in most cases the relationship is linear where the data presented represent the mean of a number of data points that in many cases showed significant scatter due in part to hysteresis effects.

The outputs of the dynamometers and water-level pickups were transmitted through cables to a photographic-type oscillograph operating at a slow paper speed (12 in per hr) where they were recorded in terms of force and water level versus time.

During part of the investigation, measurements were made of the on-off forces induced on the wharf by the ship, but these proved to be slight and further measurements of these forces were abandoned.

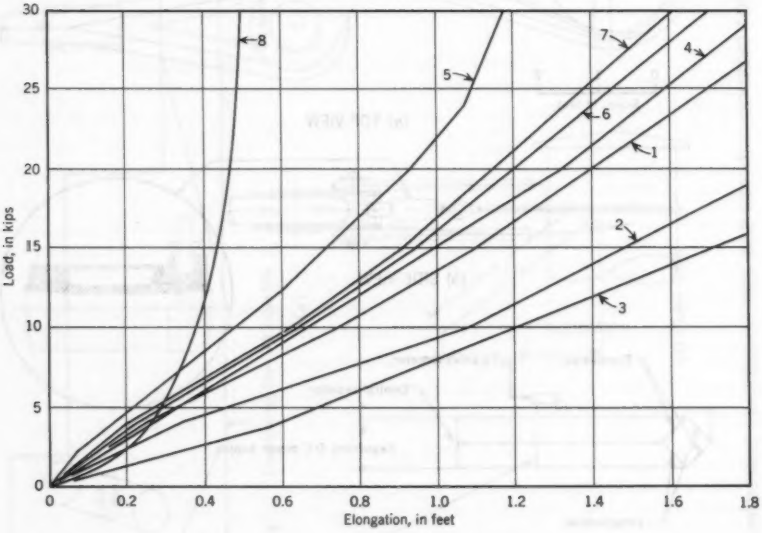


FIG. 4.—VARIATION OF ELONGATION WITH LOAD FOR ALL OF THE SHIP'S LINES

It was considered that if ship movements were to be measured it would have to be on a continuous basis in order to permit selection of those intervals that seemed likely amenable to analysis. Because a proper pickup of this type for the relatively small movements involved was not available (that outlined by Knapp[11] was found too insensitive) and ordinary survey methods were considered too laborious and expensive, direct measurement of ship motion was not attempted. The determination was made analytically on the basis of the computed elongations of the surge lines.

11 "Wave Produced Motion of Moored Ships," by R. T. Knapp, Proceedings, 2d Conference on Coastal Engrg., Council on Wave Research, Univ. of California, 1952.

No attempt was made to measure the water currents mechanically, because no proper meter of the continuous type considered necessary was available. Those utilizing propellers and drag spheres proved inadequate. Data from floats placed in the area indicated that undirectional currents, including those caused by tides, were insignificant.

Wind speed and direction were obtained by means of a recording selsyn-type annemograph that, although approximately one-half mile northwest of the ship, was considered to give pertinent data. Wind data was important in the negative sense because those intervals during which the wind was at a significant level were eliminated as unsuitable for use in this study.

The study procedure was to collect data on a continuous basis, then, after a review of the records, to select certain significant periods for analysis. There were many periods of relatively high disturbance levels when it was not possible to collect data because the ship was at sea.

EXPERIMENTAL RESULTS

The experimental results are characterized by an unsteadiness and are considered very different from those obtained using uniform, periodic waves which are usual in laboratory investigations. Facsimiles of typical oscillograms with waves of 0.98, 2.50 and 12.5-minute periods and varying degrees of initial tension have been presented elsewhere.[12] One such oscillogram with waves of 0.98 minute periods predominant and an extra high and extra low initial tension is shown in Fig. 5. The pattern produced by the water-level variations, wherein the major and minor peaks shift constantly in a somewhat orderly if not systematic manner, indicates the presence of two or more wave trains. The prominent long period surge, that of about 12 1/2 minutes, showed considerable variation in height but less so in period. The greatest line tensions were excited by the shortest of the significant waves, those of about 1 minute period, because with them the attendent slope of the water surface was greatest. Indeed, the two other conspicuous waves, those of about 2 and 12 1/2 minute periods, excited the ship only a negligible amount in surge, although the 2-minute waves induced considerable yaw, as witnessed by the high forces present in the stern line. The longer wave induced a heave which at times noticeably affected all of the lines. The effect of the initial tension is apparent in Fig. 5 where a quick shift from about 3 to 22 kips in initial tension in the forward and aft surge lines produced a significant reduction in the restoring force for about the same excitation.

It is also apparent[12] that the variations in water level near the bow and stern of the ship due to the standing wave with a 1-min period are 90° out of phase with each other. This is indicative of the fact that the center of the ship is near a node of this standing wave (Fig. 1(c)). This is a fortunate circumstance from a research viewpoint and to a considerable extent influenced the decision to use this ship for the study. The wave spectrum in the basin was dominated[11] by waves with periods of approximately 1, 2 1/2 and 12 1/2 min. It is not known whether or not such long-period waves, assumed to be of the standing type, are periodic. It is considered that the various basins in any harbor can respond naturally only in a periodic manner depending on their geometrical characteristics. However, it is thought that their excitation is not periodic, because it is produced by ocean waves.

[12] "Forces Induced on a Large Vessel by Surge," Proceedings Paper 1571, ASCE, March, 1958, pp. 12-16.

To bring order to the results, the period, T_n, of the free oscillation of the water in pertinent basins of length l_b was computed using the expression $T = B\, l_b/n'\, (gd)^{1/2}$ in which n' has a value of 1, 2, 3, and so forth, for a closed basin, and 1, 3, 5, and so forth, for an open basin, and B has a value of 2 and 4 for closed and open basins respectively. These computations indicate that the fundamental and second harmonic for basin oscillation are 1.96 and 0.98 min respectively, while the fundamental and third harmonic for the harbor as a whole are 7.50 and 2.50 min respectively, the second harmonic being supressed

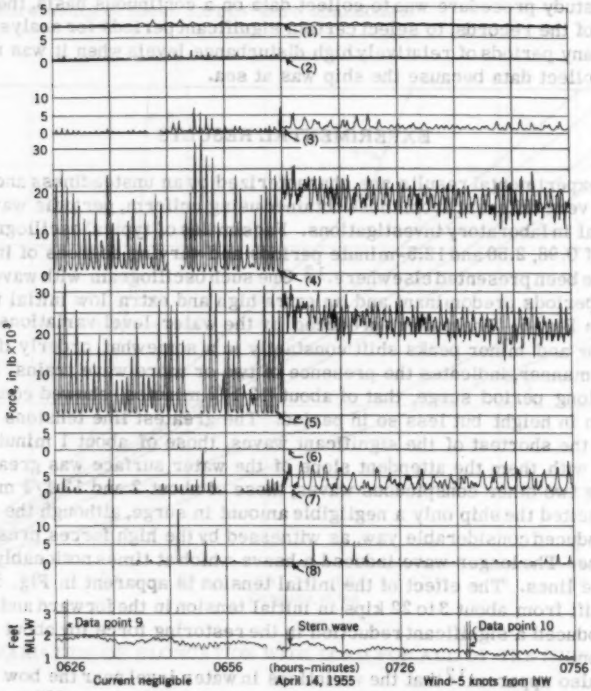


FIG. 5.—FACSIMILE OF AN OSCILLOGRAM

entirely. Such computations do not seem to explain the source of the prominent wave with a period of 12 1/2-min in Norton Sound slip. As speculated by O'Brien,[13] it may be the result of the oscillation of water over the very deep submarine canyon which fronts the harbor, or of coupling between the oscillations in the various basins of the harbor. No investigation specifically intended to determine the origin of this wave is known to have been made.

13 "Waves in and around Port Hueneme, California associated with the tsunami of 9 March 1957," by J. T. O'Brien, Report LR-R-015, U.S. Naval Civ. Engrg. Research and Evaluation Lab., April 9, 1957.

In a study of the wave environment, a part of the water-level oscillogram obtained from the bottom pressure pickup near the stern of the ship was reduced to eliminate the effects of tide and the 12 1/2-min wave. It was then analyzed using the method of residuation as originated by G. Chrystal[14] and replotted in Fig. 6. This procedure involves the offsetting of the traces by a certain increment of time to induce cancellation of certain components. The original record was residuated first with respect to the 2.50-min wave to expose the 0.98-min wave and then vice versa, so that the result is two separate traces of water level versus time in which the waves of 0.98 and 2.50-min periods are respectively predominant. It will be noted in Fig. 6 that the maximum amplitude of the 2.50-min wave (0.10 ft) is approximately double that of

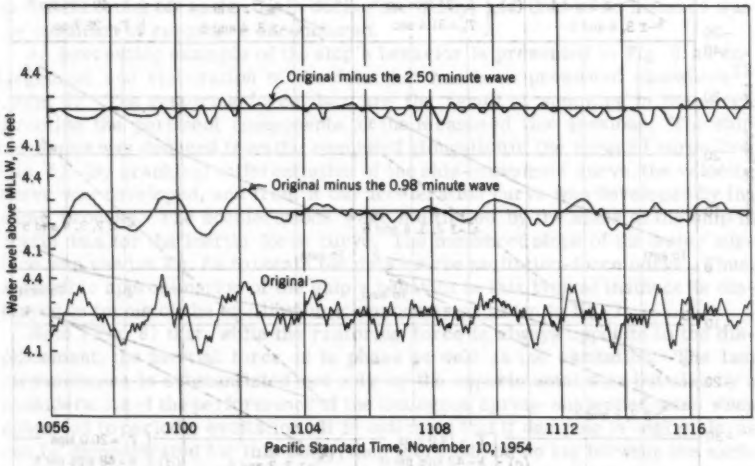


FIG. 6.—RESULTS OF APPLYING THE RESIDUATION TECHNIQUE

the 0.98-min wave. From the geometry of the harbor it is apparent that the crest of the 2.50-min wave as the third harmonic of the fundamental oscillation of the water in the harbor as a whole is likely to be somewhat oblique to the long axis of the basin. The noticeable tendency of the ship to yaw when such a wave is predominant may be explained on this basis. It is probable that a wave with the fundamental period of the basin (approximately 1.96-min) is also present, but to a minor extent for it was not exposed by the residuation technique. This may have been due to the tendency toward accumulated errors inherent in the technique.

14 "On the hydrodynamic theory of seiches," by G. Chrystal, Transactions, Royal Soc. of Edinburgh, Vol. 41, pp. 1904-1905, Pt. III.

The ship movement was resisted at all times by at least the two surge lines, No. 4 and No. 5, which were kept taut so that their tension never became less than one kip. This is indicated in Fig. 7 which presents restoring force, the surge component of the individual line tensions, as a function of surge. Movements of 1/2 ft that result in restoring forces of approximately 20 kips are indicated.

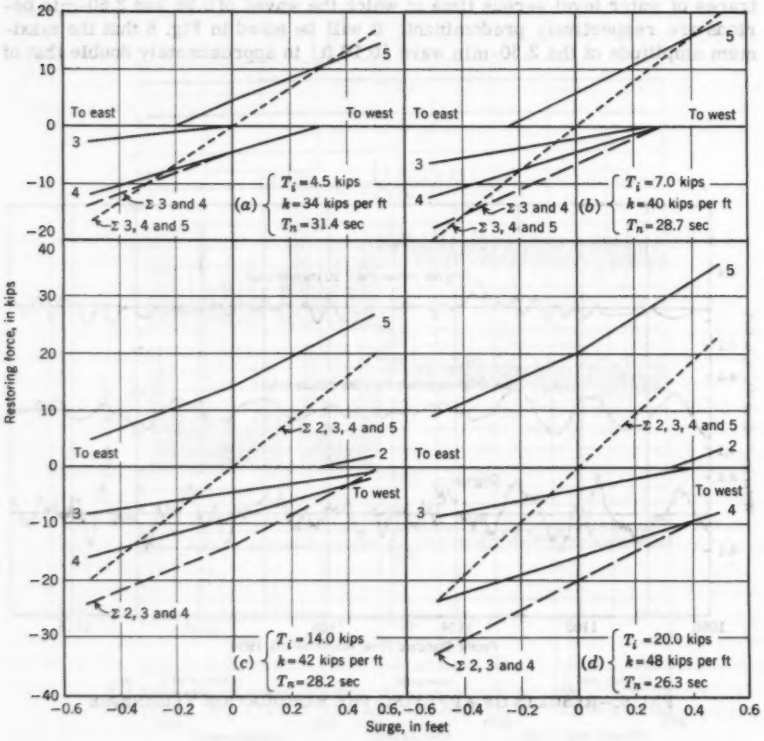


FIG. 7.—VARIATION OF COMPUTED RESTORING FORCE WITH SHIP MOVEMENT IN SURGE

As a standard operation, the tension in the lines for any given tide level was varied as desired by the ship's crew changing the length of the aft surge line (No. 5). This operation caused the ship to move and thus altered the tension in all the lines. This is illustrated in Fig. 5 where an increase in the initial tension of 20 kips in the aft surge line (No. 5) caused the forward bow spring line (No. 3) and the forward stern spring (No. 7) to become more active and to operate with the forward surge line (No. 4) which was always active. In the case cited there was a slight decrease in the slackness of the remaining lines

but not enough to induce significant tensions. Only in rare cases was the length of any line, other than the aft surge, altered.

When the ship yawed considerably, as it did frequently when 2 1/2-min waves were predominant, then the stern line (No. 8) was loaded on the order of 20 kips. Such intervals were not analyzed because enough difficulty was encountered in dealing with significant surge movements without attempting to cope with those involving obvious coupling.

Analysis of the experimental data (Fig. 7) shows that the relationship between restoring force and ship movement was continuous and sensibly linear in all significant cases. The factor expressing this relationship, designated k, was found to vary from 34 to 48 kips per ft as a function of the initial tension, T_i, where a value of approximately 40 kips per ft seems to cover all cases adequately. Substitution of this value of k in the familiar expression for the natural period T_n of the undamped oscillation of a simple spring-suspended mass $(T_n = 2\pi\,(m/k)^{1/2})$ gives a value for T_n of approximately 30 sec. It is obvious that this is considerably less than the period of the significant standing waves encountered in the basin during the study, and thus in no instance was the condition of resonance encountered.

An interesting example of the ship's behavior is presented in Fig. 8, an enlargement and elaboration of the data that has been presented elsewhere[12] (point 8). The restoring-force data are the result of summing in the surge direction the pertinent components of the measured line tensions. The ship movement was deduced from the computed elongation of the forward surge line (No. 5). By graphical differentiation of the ship-movement curve, the velocity curve was developed, and from it the acceleration curve was developed by the same process. The accelerations were multiplied by the mass of the ship to obtain data for the inertia-force curve. The measured slope of the water surface was used in Eq. 6a to obtain the data for the excitation-force curve. Thus, a sensible approximation of the ship's behavior in this typical instance is displayed in terms of the equilibrium components as given in Eq. 1.

Note (Fig. 8) that, while the restoring force is always opposite to the displacement, the inertial force is in phase as well as the excitation. The last circumstance is substantiated not only by the experimental data but also by a consideration of the performance of the analogous spring-suspended mass when subjected to periodic excitation. It is indicated that if damping is negligible, as can be demonstrated for this study, then there can be no lag between the excitation and the displacement.

In reviewing the effect of damping it will be assumed that viscous damping is dominant, and of this, the part due to skin friction is negligible, because forces of less than 1 lb are computed from the expression given by Schlichting[15] for a flat plate in longitudinal flow. That due to wave generation by the ship is also negligible. This leaves only the drag due to flow separation (form drag) to be considered.

In Eq. 3 it would appear that the drag coefficient, C_d, should not be taken as greater than approximately 1.0, because for a circular cylinder with axis in the flow direction, Hunter Rouse[16] gives a value for the coefficient of 0.90 for a condition where the Reynolds number R is greater than 10^3 and the length-to-diameter ratio is 20. The Reynolds number R for this study is approximately

---

15 "Boundary layer theory," by H. Schlighting, NACA Technical Memorandum 1217, 1949, p. 51.

16 "Elementary Mechanics of Fluids," by H. Rouse, John Wiley & Sons, Inc., New York, N. Y., 1946.

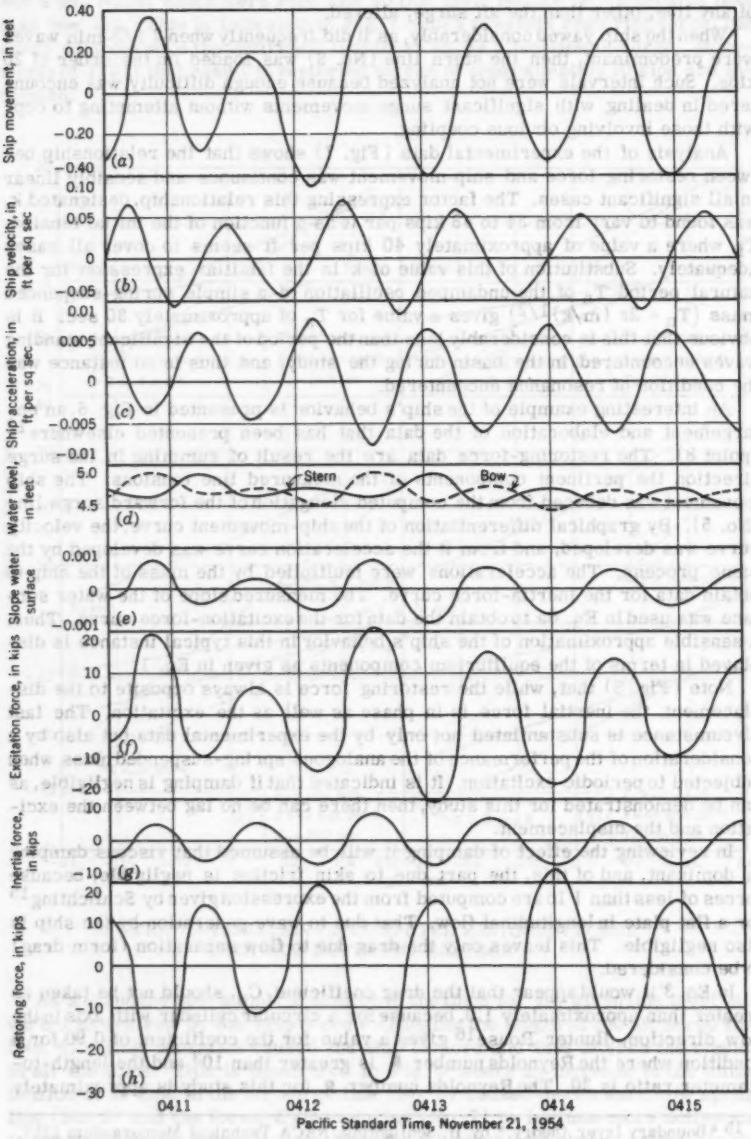


FIG. 8.—VARIATION OF MEASURED RESTORING FORCE AND COMPUTED INERTIA AND EXCITATION FORCES WITH TIME

10^6 based on the maximum particle velocity and the ship's beam. The length-to-beam ratio is approximately 7.

The value of $\dot{x}$ to be used in Eq. 3 can be estimated on the assumption that the ship is stationary and subject to a standing wave of 1/4 ft amplitude. In this case the maximum particle speed, V_m, computed from the relationship $V_m = A\,(g/d)^{1/2}$ is 0.25 feet per sec. From Eq. 3, with the values of C_d and V_m as computed substituted with 1,150 sq ft for the underwater projected end area of the ship, a value is obtained for the damping force of less than 100 lb, which is considered negligible.

At a number of points of maximum acceleration (the extremes of ship movement) the mass factor, C_M, was evaluated using Eq. 1 and the data presented in Fig. 8. For accelerations on the order of 0.007 fps per sec, the factor was found to vary between 1.0 and 1.2. The definition from the oscillograms of the slope of the water surface, the controlling parameter in the expression for the excitation force, was found to be critical in the evaluation of C_M. Treatment of a second situation, similar to that illustrated in Fig. 8, resulted in similar values for C_M. These values seemed close enough to unity to permit C_M to be so considered and thus effectively to eliminate it as a significant factor.

The measured maximum values of the restoring forces as a function of the water surface slope are compared in Fig. 9 (initial tension = 15 to 22 kips) and Table 2 with maximum values of such forces computed on the basis of Eq. 1. The measured values of the slopes of the water surface were used on the basis of readings from both stern and bow pickups. In two of the ten cases where the stern pickup only was active, this slope was deduced from the relationship between maximum water-level variation near the stern and the slope as determined from data collected when both water level pickups were active. The ship movement was deduced from a consideration of the elongation of the two surge lines on the basis of the particular loads measured in them.

Values for the maximum acceleration in the Table 2 computations were obtained by assuming the ship to be oscillating in simple harmonic motion at a constant circular frequency, ω, and amplitude, A_m, so that the maximum acceleration was equal to $A_m\omega^2$. That this method of obtaining the acceleration is not entirely accurate is indicated by considering the situation which existed on November 21, 1954, at 4 hr 12 min 36 sec (point number 8 in Table 2 and Fig. 8) where the acceleration as computed is 0.0057 fps per sec while that obtained by graphical differentiation of the ship-movement curve is 0.0075 fps per sec. While the difference of 30% based on the computed value of the acceleration is considerable, the effect on the restoring force will not be nearly as great (a change of 1.5 kips in a total of 38.0 kips) because in this case inertia is not predominant. It is considered that, notwithstanding the differences cited, the approach presented in Table 2 should be viewed with interest in an engineering field where, at present, estimates, especially of the forces induced by waves, to within 100% or so of the true value frequently are welcomed.

It will be noted (Fig. 9) that the measured values of the restoring forces are three-quarters of those computed. This circumstance may be due in large part to the liberties taken with the actual mechanics in the computation of the acceleration and the equally approximate measures taken to obtain the ship movement.

When the ship was tied relatively loosely, as it was in the situations designated numbers 1 and 9 in Table 2, it was apparent from the analysis of the data that the ship tended to possess a considerable inertia force that, when added to that of the excitation, required restoring forces that were relatively large (20 to 30 kips).

TABLE 2.—COMPUTATION OF RESTORING FORCE ON BASIS OF MEASURED SLOPE OF WATER SURFACE AND SHIP MOVEMENTS INFERRED FROM CHANGES IN TENSION IN AFT SURGE LINE.

Data measured	Point									
	1	2	3	4	5	6	7	8	9	10
Year	1954	1954	1954	1954	1954	1954	1954	1954	1955	1955
Day and month	10 Nov.	19 Nov.	20 Nov.	20 Nov.	20 Nov.	20 Nov.	20 Nov.	21 Nov.	14 Apr.	14 Apr.
Hour	11	18	17	19	20	20	20	04	06	07
Water level, in feet[d]										
Trough at bow	. . . [a]	3.90	4.05	3.50	3.80	3.80	3.65	4.90	. . . [a]	. . . [a]
Trough at stern	3.35	3.50	3.70	3.60	3.40	3.45	3.30	4.40	1.70	1.20
Trough : B-S	. . . [a]	0.40	0.35	0.10	0.40	0.35	0.35	0.50	. . .	. . .
Slope : (B-S)/410[c]	0.00063[b]	0.00098	0.00086	0.00024	0.00098	0.00085	0.00085	0.00122	0.00050[b]	0.00052[b]
Crest at bow	. . . [a]	3.20	3.65	4.10	3.35	3.50	3.10	4.40	. . . [a]	. . . [a]
Crest at stern	3.55	3.70	3.85	3.95	3.55	3.75	3.55	4.80	1.85	1.36
Crest : B-S	. . .	0.50	0.20	0.20	0.20	0.25	0.45	0.40	. . .	. . .
Slope : (B-S)/410[c]	0.00040[b]	0.00122	0.00049	0.00048	0.00049	0.00061	0.00110	0.00098	0.00030[b]	0.00032[b]
Height of oscillation, in feet[d]										
Bow : trough - crest	. . . [a]	0.70	0.40	0.60	0.45	0.30	0.55	0.50	. . . [a]	. . . [a]
Stern : trough - crest	0.20	0.20	0.15	0.35	0.15	0.30	0.25	0.40	0.15	0.16
Time of oscillation, in minutes and seconds										
Trough : B and S	15:33	15:00	48:47	04:45	03:54	07;24	14:25	12:36	28:00	37:30
Crest : B and S	15:57	15:24	48:18	06:00	03:30	07:00	14:00	12:09	27:36	37:54
Difference : T/2	:24	:24	:29	1:15	:24	:24	:25	:27	:24	:24
Inertial force										
T, in sec per cycle	:48	:48	:58	:150	:48	:48	:50	:54	:48	:48
ω, in cycles per sec	0.131	0.131	0.108	0.042	0.131	0.131	0.126	0.116	0.131	0.131
ω^2 in $(C/S)^2$	0.0172	0.0172	0.0117	0.0018	0.0172	0.0172	0.0158	0.0135	0.0172	0.0172
At trough : $\ddot{x} = d\omega^2$	0.0124	0.0075	0.0046	0.0004	0.0066	0.0069	0.0063	0.0057	0.0183	0.0019
: force = m $\ddot{x}$ in kips	10.4	6.3	3.9	0.34	5.5	5.8	5.3	4.8	15.4	1.6
At crest : $\ddot{x} = d\omega^2$	0.0172	.0097	0.0047	0.0004	0.0077	0.00064	0.0104	0.0056	0.0217	0.0024
force = m $\ddot{x}$	14.5	8.1	3.9	0.34	6.5	5.4	8.7	4.7	18.7	2.0

Movement of ship												
	#5	#4								#5	#4	
Initial condition: tension, in Kips	6.0	6.0	12.7	15.5	13.0	15.0	15.0	15.0	16.5	3.5	3.5	22.0
: elongation, in feet	0.28	0.40	0.62	0.75	0.63	0.72	0.72	0.72	0.78	0.14	0.24	1.00
At trough : tension, in Kips	21.5	0.5	23.5	28.3	8.0	25.2	26.5	25.1	32.0	32.0	0.5	26.0
: elongation, in feet	1.00	...	1.06	1.14	0.38	1.10	1.12	1.10	1.20	1.20	...	1.11
At crest : tension, in Kips	0.5	21.5	2.0	7.5	21.0	6.0	7.5	2.0	7.8	8.4	25.0	18.5
: elongation, in feet	...	1.40	0.06	0.35	0.97	0.35	0.35	0.06	0.37	...	1.50	0.86
Difference in elongation												
tr. - initial, in feet	0.72		0.44	0.39	0.25	0.38	0.40	0.40	0.42	1.06		0.11
cr. - initial, in feet	1.00		0.57	0.40	0.24	0.45	0.37	0.66	0.41	1.26		0.14
Excitation force, in Kips												
Trough : slope w.s. x W	17.0		26.4	23.1	6.5	26.4	22.9	22.8	32.8	13.5		14.0
Crest : slope w.s. x W	10.8		32.8	13.2	12.9	13.2	16.5	29.4	26.4	8.1		8.6
Computed restoring force, in Kips												
Trough : - excitation - m $\ddot{x}$	27.4		32.7	27.0	6.8	31.9	28.7	28.1	37.6	28.9		15.6
Crest : - excitation - m $\ddot{x}$	25.3		40.9	17.1	13.3	19.7	21.9	38.1	31.1	26.8		10.6
Measured restoring force, in Kips												
Trough	21.0		17.8	23.4	9.0	20.8	21.8	19.8	27.6	32.0		11.0
Crest	21.0		34.3	16.4	13.0	17.4	14.2	25.0	19.3	30.7		7.5

[a] Not measured. [b] Obtained from plot of measured slope versus height of water level oscillation at the stern.
[c] 410 feet is equal to the distance between bottom pressure pickups at the bow and stern of the ship.
[d] B represents the bow, S denotes the stern, tr. represents the trough, cr. denotes the crest, and w.s. is the water surface.

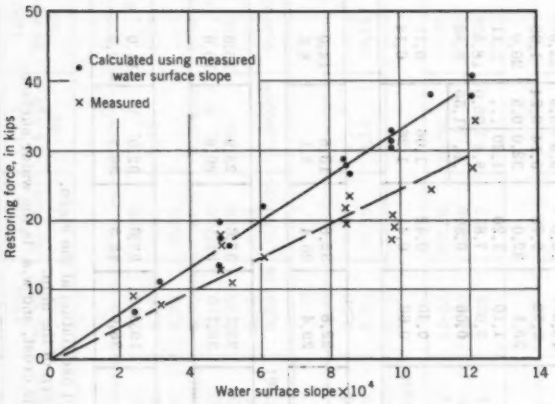


FIG. 9.—VARIATION OF RESTORING FORCE WITH SLOPE OF WATER SURFACE

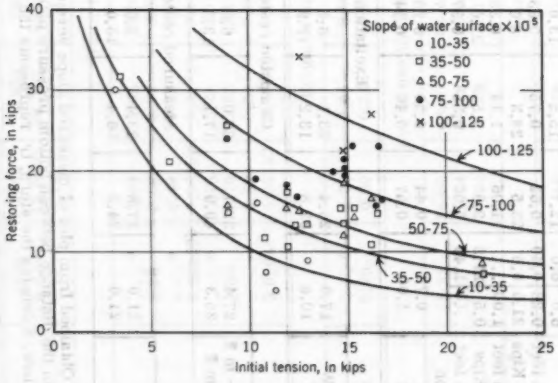


FIG. 10.—VARIATION OF RESTORING FORCE WITH INITIAL TENSION FOR VARIOUS WATER SURFACE SLOPES

It is apparent from a review of the data in Fig. 9 that for any given mooring condition the slope of the oscillating water surface is the dominant parameter and one with which the restoring force seems to vary almost linearly.

On the basis of limited data with considerable scatter, an attempt was made to demonstrate this further by presenting (Fig. 10) the restoring force as a function of initial tension with the various slopes of the water surface encountered drawn as contours in the body of the data. It is apparent that an inverse relationship exists for any particular water-surface slope so that it is possible to substantiate a conclusion arrived at by Wilson[5] and Deacon et al.[6] among others, that tight lines tend to reduce the restoring force required.

A designer concerned with the indirect determination of the restoring force for nonresonant cases for a ship moored with taut lines in long waves, could cope with the deduction of sensible values for the inertial term in Eq. 1 on the basis of a reasonable estimate of the elongation of the ship's lines and the amplitude of the water particle movement. However, the designer would have difficulty in obtaining a value for the excitation with the same degree of confidence. The reason for this lies in the difficulties inherent in the computations of the slope of a water surface which is likely to be disturbed by two or more waves.

CONCLUSIONS

The following conclusions are drawn from this study of the 12,000-ton ship berthed with unusually taut lines in a standing wave environment in a harbor near the node of one of two significant standing waves. The significant movements, those of up to 1 ft induced by water surface oscillations at periods of 1 and 2 1/2 min with slopes up to 0.0015 were only in surge.

1. The restoring force for initial line tensions of approximately 20 kips varied directly with the slope of the water surface, being approximately 10 and 30 kips at slopes of .0004 and .0012 respectively.

2. Restoring force varied inversely with initial tension for any particular water surface slope, such that with a slope of .0007 this force was 20 and 10 kips for initial tensions of 10 and 25 kips respectively.

3. Tight lines tended to reduce the restoring force required to resist any particular excitation force, because the inertia force was thereby reduced.

4. Measured values of the restoring force were found to be approximately three-quarters of those computed on the basis of the slope of the water surface and simple harmonic motion.

5. The excitation can be considered to be represented significantly as the product of the slope of the water surface and the weight of the ship.

6. The maximum inertial force, the product of mass and acceleration, can be computed to a sensible degree of accuracy by considering the ship to be oscillating in simple harmonic motion. The value of the maximum acceleration is equal to the product of the amplitude of the ship motion, deduced from the elongation of the lines as computed on the basis of the forces measured in them, and the square of the frequency of the oscillation deduced from that of the water surface.

7. The restoring force can be considered as the sum of the inertia and excitation forces where damping and the added mass effect are neglected.

8. A satisfactory estimate for the natural period of oscillation of the moored ship can be obtained by considering this to be analogous to the natural period

of the undamped oscillation of a spring-suspended mass. A sensible value for the spring factor required can be obtained by linearizing the relationship between restoring force and ship movement.

ACKNOWLEDGMENTS

Appreciation is expressed to the U. S. Naval Civil Engineering Laboratory of the Bureau of Yards and Docks of the Department of the Navy for permission to publish this paper and to the officers and men of the *USS Norton Sound* for their cooperation and assistance.

APPENDIX.—NOTATION

The following symbols have been adopted for use in the paper and are presented herewith for the guidance of discussers:

A = amplitude of wave, one-half vertical distance crest to trough;

A_m = amplitude of ship movement;

A_s = projected underwater area of ship;

A_l = cross-sectional area of a mooring line; wetted area of a ship;

B = constant in the expression for natural period of oscillation of basins;

D = spring factor for representative mooring line;

C_d = coefficient of drag;

C_m = coefficient of mass;

C_M = mass factor;

c = $(1-n)/2(1+n)$;

d = depth of water;

E = Young's modulus of elasticity;

g = acceleration due to gravity;

i = item number;

k = spring factor;

l_m = length of a mooring line;

l_b = length of a basin;

L = length of a wave;

m = static mass of a ship;

N = total number of mooring lines;

R = Reynolds number;

n = numerical exponent used with mooring ropes;

n' = integer defining harmonic order and nodality of an oscillation in a closed and open basin;

P = total force in a mooring line;

r = length of the horizontal projection of a mooring line;

r_1 = straight line distance between extremities of a mooring line;

t = time;

T = period of oscillation;

T_i = initial tension;

T_n = natural period of oscillation of a system;

V_m = maximum speed of water-wave-excited particles;

W = weight of a ship;

x = horizontal distance along the axis parallel to the wharf (surge);

y = horizontal distance along the axis normal to the wharf (sway);

z = vertical distance along the axis normal to the water surface (heave);

z_1 = vertical distance to the water surface from point of attachment of line to ship;

α = angle between mooring line and horizontal;

β = angle between horizontal projection of the mooring line and the face of the wharf (the x axis);

ω = $2\pi/T$ = circular frequency;

π = 3.1416;

ρ = density of sea water;

dx/dt = $\dot{x}$ = speed of ship in surge; and

d^2x/dt^2 = $\ddot{x}$ = acceleration of ship in surge;

DISCUSSION

BASIL W. WILSON[17], F. ASCE.—The authors' paper is of considerable interest and value as a contribution to the literature on ship mooring forces and the more general problem of surging in harbors. In referring to the writer's paper[5] the authors have recorded that the essential result for the period of longitudinal oscillation in surge of a moored ship, as obtained therein, is expressible in the form

$$T_n = 2\pi\left(\frac{m}{k}\right)^{1/2}\left(\frac{mgA^2}{kd}\right)^{j/2} \quad \ldots\ldots\ldots\ldots\ldots (7)$$

in which $k = DN/4$ and $j = (1 - n)/(1 + n)$. This interesting analogy to the simple

[17] Prof., Engineering Oceanography, Agri. and Mech. College of Texas, College Station, Tex.

statement for an undamped, linear oscillating system, could perhaps have been more easily drawn by writing

$$T_n = 2\pi\left(\frac{m}{k'}\right)^{1/2} \quad \ldots\ldots\ldots\ldots\ldots\ldots \quad (8)$$

in which k' is a nonlinear spring factor given by

$$k' = \frac{ND}{4}\left(\frac{NDd}{4mgA^2}\right)^j \quad \ldots\ldots\ldots\ldots\ldots\ldots \quad (9)$$

The authors have further stated that the writer's result for the maximum total force in the moorings (R_{max}) reduced to

$$R_{max} = \frac{2\pi\ WA}{T_n\sqrt{gd}} \quad \ldots\ldots\ldots\ldots\ldots\ldots \quad (10)$$

which Russell's[6] explains as exactly equivalent to the maximum force in the cables if the latter are tight, the ship held stationary and the virtual mass of the ship neglected. Actually it will be found that the writer's result[18] was just twice that Eq. 10 while Russell's statement, as given by him, is in error by a factor $(1/2\ \pi\ g)$.

The authors have rightly pointed to the discrepancies in this field that have come to light in their studies of the literature. Russell's result, they find, for the case when a ship is artificially released from rest at the moment that the water particles at the node of the seiche are also at rest, reduces to precisely 1.5 times that given in Eq. 10. Russell gives no explanation for his derivation of this factor though it must be presumed that it is simply a mass factor, C_M (using the author's terminology). The writer's result, on the other hand, is equivalent to Eq. 10 multiplied by a C_M-value of 2.0, which is probably too high, as will be explained later.

As the authors state, Joosting[8], has recently (1957) pointed up an omission in the writer's original theory in respect of the influence of the wave slope, but has retained the writer's concept of an acceleration force due to the relative acceleration of the water moving past the ship. This, they note, is considered by Russell[6] to be in error.

There is obvious need for clarification on these somewhat divergent views, and as their own contribution towards framing the problem analytically, the authors have advanced Eq. 1, the terms of which are covered by succeeding Eqs. 2 to 6. Eq. 1, however, would seem to be valid only so long as the inertial term, Eq. 2, is taken negative. The writer accepts the statements of Eq. 6 for the excitation force, expressive of net fluid pressure acting on the ship, provided that L is the wave length. It can, in fact, be quite readily proved that the force from the net horizontal standing-wave pressures acting on a circular cylinder floating in water with its axis lying in the free surface along the node is exactly equivalent to the tendency of the cylinder to slide up or down the water slope. In respect of Eq. 2, however, the writer considers the treatment rather too summary and would wish to return to the point, refuted by Russell, that consideration is necessary of the time-rate-of-change of the velocity of the water relative to the ship.

The equation of motion of a cylinder of mass, m, accelerated by a force F in the positive x-direction through an inviscid fluid initially at rest has been shown

---

18 "Ship Response to Range Action in Harbor Basins," by B. W. Wilson, Transactions, ASCE, Vol. 116, 1951, Eqs. 25 and 34a.

by Lamb[19] to be

$$m\ddot{x} = F - m'' \ddot{x} \quad \ldots\ldots\ldots\ldots\ldots\ldots (11)$$

in which m'' is the so-called added mass and the term $m'' \ddot{x}$ represents the resistance offered by the fluid pressures in the resulting potential flow, in which, relatively, the fluid accelerates backward past the cylinder at the rate $\ddot{x}$. If now the cylinder is drawn through a fluid which is flowing with varying velocity, $u(t)$, in the same direction of pull, the relative velocity backward of the water past the cylinder is $(\dot{x} - u)$, and the resistance from its acceleration is in $m''\, d/dt\, (\dot{x} - u)$. The equation of motion thus becomes $m\ddot{x} = F_1 - m''\, d/dt\, (\dot{x} - u)$ or

$$m' \ddot{x} = F_1 + m'' \dot{u} \quad \ldots\ldots\ldots\ldots\ldots\ldots (12)$$

in which $m' = m + m''$ and is the virtual mass of the cylinder. Obviously, if the water accelerates equally with the cylinder, there can be no fluid pressures on the cylinder opposing the motion and the only force required to pull the body is that required to overcome the inertia of the body, namely, $m\ddot{x} = F_2$.

In the case of a floating cylinder such as a ship subject to wave action, the force F_1 propelling the ship, is provided by the net pressures in the direction of motion (deriving from the acceleration of the fluid) evaluated over the boundary of the cylinder, as if the cylinder were not present. In other words, the force on any imaginary boundary already exists in an accelerating fluid regardless of the presence of any such real boundary. This is the excitation force referred to by the authors as the integrated components of the wave-induced pressure over the wetted surface of the ship.

Accordingly, the equation of motion of a ship moving across the node of a standing wave under the stimulus of the accelerative flow is given by Eq. 12 by suitably replacing F_1 in terms of the author's Eq. 6b and by introducing the appropriate value of $\dot{u}$. If, in addition, the damping effect of the friction and form drag of the relative flow be considered and the restraints of mooring ropes be introduced, Eq. 12 becomes

$$m'\ddot{x} = mg\,(KA) \sin \sigma t + m'' \dot{u} - \frac{1}{2} C_d \rho A_S (\dot{x} - u)^2 - \sum_{i=1}^{N/2} k_i x^{ni} \quad \ldots\ldots (13)$$

in which $K = 2\pi/L$, $\sigma = 2\pi/T$ and A_S refers to the projected (or wetted) area of the ship. On the assumption that the mass of the ship is entirely concentrated at the node of the seiche or standing wave, $\eta = A \cos Kx' \sin \sigma t$, where x' is taken with reference to some origin for the standing wave system at still water level, the values of u and $\dot{u}$ at $x' = L/4$ (the node point) are given by

$$(i)\ u = -A\sqrt{\frac{g}{d}} \cos \sigma t \quad \ldots\ldots\ldots\ldots (14a)$$

and

$$(ii)\ \dot{u} = A\sigma\sqrt{\frac{g}{d}} \sin \sigma t \quad \ldots\ldots\ldots\ldots (14b)$$

The friction term, which is small (as shown by the authors), may be linearized to the form $G(\dot{x} - u)$ with G a constant and Eq. 13 can then be rewritten

[19] "Hydrodynamics," by H. Lamb, Cambridge Univ. Press, England, 1932.

with the aid of Eq. 14:

$$m' \ddot{x} + G\dot{x} + \sum_{i=1}^{N/2} k_i x^{n_i} = mg\, K\, A \sin \sigma t + m''\, A\, \sigma \sqrt{\frac{g}{d}} \sin \sigma t - GA \sqrt{\frac{g}{d}} \cos \sigma t \quad \ldots\ldots\ldots (15)$$

Noting that m' is equivalent to the author's C_M m, Eq. 15 is in accord with the author's concept but contains two additional terms in the forcing function on the right hand side. On dividing through by C_M m and gathering terms, Eq. 15 reduces to

$$\ddot{x} + \frac{G}{C_M m}\dot{x} + \frac{1}{C_M m} \sum_{i=1}^{N/2} k_i x^{n_i} = \frac{A}{C_M}\left[g\, K + C_m\, \sigma \sqrt{\frac{g}{d}}\right] \sin \sigma t - \frac{GA}{C_M m} \sqrt{\frac{g}{d}} \cos \sigma t \quad \ldots\ldots\ldots (16)$$

If it be assumed that the various ropes i can collectively be considered to impose a restraint Cx^n, Eq. 16 may be expressed, after further simplification, as

$$\ddot{x} + \left(\frac{G}{C_M m}\right)\dot{x} + \left(\frac{C}{C_M m}\right) x^n = \sigma\, A \sqrt{\frac{g}{d}} \left(\frac{1 + C_m}{C_M}\right) \sin \sigma t - \frac{GA}{C_M m} \sqrt{\frac{g}{d}} \cos \sigma t \quad \ldots\ldots\ldots (17)$$

This, substantially, is the equation given by Joosting[8] for a C_M value of 2. The writer's original differential equation[20] was of this form (with $C_M = 2$) but had reversed (incorrect) signs to the forcing function on the right hand side and underestimated the first term of the latter by $1/C_M$. At that time, the writer was unable to find a formal solution to the equation but managed to evade the obstacle by recourse to dimensional analysis involving the quantities $(G/C_M m)$, $(C/C_M m)$, σ and $(A\sqrt{g/d})$, with $C_M = 2$.

It will be pertinent here to review the solution obtained by this method but for an unspecified value of C_M. To simplify matters

for (i) $$G/C_M m = 2\beta\omega \quad \ldots\ldots\ldots (18a)$$

for (ii) $$C/C_M m = \omega 2 \quad \ldots\ldots\ldots (18b)$$

and

for (iii) $$A\sqrt{g/d} = V \quad \ldots\ldots\ldots (18c)$$

so that Eq. 17 becomes, with $C_M = 1 + C_m$,

$$\ddot{x} + 2\beta\omega\dot{x} + \omega^2 x^n = V(\sigma \sin \sigma t - 2\beta\omega \cos \sigma t) \quad \ldots\ldots\ldots (19a)$$

---

20 "Ship Response to Range Action in Harbor Basins," by B. W. Wilson, Transactions, ASCE, Vol. 116, 1951, Eq. 20.

The formal solution of Eq. 19a for n = 1 is easily obtained and yields

$$x = e^{-\beta\omega t}(a \sin \gamma t + b \cos \gamma t) + f(t) \quad \ldots\ldots\ldots \quad (19b)$$

in which a and b are constants, f(t) is the forced oscillation and $\gamma = \omega\left(1 - \beta^2\right)^{1/2}$. The natural period of the free oscillation, T_1, is given by $T_1 = 2\pi/\gamma$ or

$$T_1 = \frac{2\pi}{\omega}\left[1 - \beta^2\right]^{-1/2} \quad \ldots\ldots\ldots\ldots\ldots \quad (20)$$

By dimensional analysis it can be shown that the corresponding natural period in the general case will be

$$T_n = \left(\omega^2\right)^{-i\,Vj}\,\phi\left[(2\beta\omega)\left(\omega^2\right)^{-i\,Vj}\right] \quad \ldots\ldots\ldots\ldots \quad (21)$$

in which

for (i) and $$i = \frac{1}{1+n} \quad \ldots\ldots\ldots\ldots\ldots\ldots (22a)$$

for (ii) $$j = \frac{1-n}{1+n} \quad \ldots\ldots\ldots\ldots\ldots\ldots (22b)$$

For the case of n = 1, Eq. 21 gives $T_1 = \frac{1}{\omega}\phi(\beta)$ which agrees identically with Eq. 20 if

$$\phi(\beta) = 2\pi\left[1 - \beta^2\right]^{-1/2} \quad \ldots\ldots\ldots\ldots\ldots (23)$$

The writer assumed[18] that the function ϕ in Eq. 21 could simply be approximated by 2π, thus yielding the result

$$T_n = 2\pi\left(C/C_M m\right)^{-i}\left(A\sqrt{g/d}\right)^{j} \quad \ldots\ldots\ldots\ldots \quad (24)$$

This is identical to Eqs. 7 or 8 if

for (i) $$k = DN/2C_M \quad \ldots\ldots\ldots\ldots\ldots (25a)$$

and

for (ii) $$k' = \frac{ND}{2C_M}\cdot\left(\frac{NDd}{2C_M mgA^2}\right)^{j} \quad \ldots\ldots\ldots (25b)$$

It thus transpires that the writer's[18] results, despite the error in the forcing function of the differential equation, are quite valid for the case of $C_M = 2$ within the limits of the assumption regarding $\phi = 2\pi$.

Abramson and the writer[21] finally gave the mathematical solution of the writer's original differential equation. The error in the forcing function was unfortunately inherited but the method remains unaffected and the results are correct in all but their quantitative aspects. It was there shown that the writer's[22] result for the case of resonance for which $T_n = T$ (the wave period), could be expressed in the form

$$\left(\frac{\sigma}{\omega}\right)^2 = X^{n-1} \quad \ldots\ldots\ldots\ldots\ldots\ldots (26)$$

---

21 "A Further Analysis of the Longitudinal Response of Moored Vessels to Sea Oscillations," by H. N. Abramson and B. W. Wilson, Proceedings, Joint Mid-West Conf. Solid and Fluid Mechanics, Purdue Univ., September, 1955, pp. 236-251.

22 "Ship Response to Range Action in Harbor Basins," by B. W. Wilson, Transactions, ASCE, Vol. 116, 1951, Eq. 24.

in which X represents the maximum amplitude of the ship movement. The mathematical solution, however, yielded for the free, undamped oscillation

$$\left(\frac{\sigma}{\omega}\right)^2 = X^{n-1}\,\psi\,(n) \quad \ldots\ldots\ldots\ldots\ldots \quad (27)$$

in which $\psi\,(n)$ is a numerical function of n only, from which it was concluded that a selection of $\phi = 5/2\pi$ in Eq. 21, rather than $\phi = 2\pi$, would have been a closer approximation to the truth.

For the forced oscillation without damping the solution was

$$X^n\,\psi\,(n) - \left(\frac{\sigma}{\omega}\right)^2 X = -\frac{V}{\omega} \quad \ldots\ldots\ldots\ldots \quad (28)$$

and the maximum restoring force therefore

$$R_{max} = C X^n \quad \ldots\ldots\ldots\ldots\ldots\ldots \quad (29)$$

Joosting[8] has independently solved the nonlinear Eq. 19. His equation[23] corresponds identically with $1/\psi(n)$, previously mentioned. Apart from the retention of a C_M value of 2, Joosting's results can be considered as fairly representative of the surging motion of a moored ship and of the restraint forces developing in the mooring lines.

The authors have indicated from their findings that C_M varied from about 1.0 to 1.2 for the *USS Norton Sound* in surge motion. Such a value can be confirmed from the formulas given by Wendel.[24] An approximate value of the hydrodynamic mass, m'', in terms of the fluid density ρ, the bean, B, and draft, D, of the ship is

$$m'' = 0.26\,\pi\,\rho\,B^2\,D \quad \ldots\ldots\ldots\ldots\ldots\ldots \quad (30)$$

which for the quoted dimensions of the ship, yields $C_M = 1.20$. It would thus seem that the value of 2 used by the writer and by Joosting is much too high. If allowance be made for this in the writer's original equation for the maximum total force in the moorings, its expression in the form of Eq. 10 would be

$$R_{max} = \frac{2\pi\,C_M WA}{T_n\sqrt{gd}} \quad \ldots\ldots\ldots\ldots\ldots \quad (31)$$

which would be akin to Russell's result (for $C_M = 1.5$). However, Eq. 31 must now be considered superseded by Eqs. 28 and 29.

The condition of the mooring lines of the *Norton Sound*, as remarked by the authors, accords with the linear case of n = 1, for which according to both Eqs. 26 and 27, resonance would only obtain with $\sigma = \omega$, the forced period of the wave agreeing with the free period of ship oscillation. The free period was found to be of the order of 30 sec but no equivalent period surge-waves could be detected. The authors thus rightly concluded that the ship motion was nonresonant, as, indeed, may be inferred also from the fact that the motion was in phase with the excitation, for which σ/ω would have to be less than 1.0.

---

23 "Investigation into Long Period Waves in Ports," by W. C. Q. Joosting, Communication 1, Section 2, 19th International Navigation Congress, London, July, 1957, Eq. 10.

24 "Hydrodynamic Masses and Hydrodynamic Moments of Inertia," by K. Wendel, Translation 260, David Taylor Model Basin, U. S. Dept. of the Navy, 1956.

In Fig. 6 the authors detect only the presence of 0.98 and 2.50 min waves but between the period 1104 and 1110 there seems to be clear evidence of a 0.76 min oscillation. The rope tensions at the corresponding interval[25] suggest an excitation of this order. With a degree more of slackness in the mooring ropes it would seem that resonance could easily be excited by this wave.

As the authors have demonstrated convincingly, the damping factor $2\beta\omega$ of Eq. 19 is very small and for most practical purposes is negligible. This was stressed, too, by Abramson and the writer[21] and has been remarked upon by Russell[6] and by Joosting.[8] Eq. 19 for n = 1 thus reduces to

$$\ddot{x} + \omega^2 x = V\sigma \sin \sigma t \quad \ldots\ldots\ldots\ldots \quad (32)$$

and would define the nonresonant, in-phase simple harmonic motion directly correlated with the surface slope as found by the authors.

Eq. 32 can also be written

$$m\ddot{x} + \frac{R}{C_M} = m g KA \sin \sigma t \quad \ldots\ldots\ldots\ldots \quad (33)$$

in which R is the restoring force. Because the quantity representing the excitation on the right hand side of Eq. 33 was computed by the authors as - mgs, in which s is the water surface slope, and the restoring force computed as $(-mgs - m\ddot{x})$, it follows from Eq. 33 that this computed force, R_c, is really

$$R_c = \frac{R}{C_M} \quad \ldots\ldots\ldots\ldots\ldots\ldots \quad (34)$$

and that therefore the true or measured restoring force should be $R = C_M R_c$. This implies that the measured forces should have been approximately 20% larger than those calculated (for C_M from 1.0 to 1.2), whereas the authors have found almost the contrary in Fig. 9. The writer is unable to account for this rather considerable discrepancy other than to suggest that the estimation of the ship movement from the forces in the moorings may have been unreliable owing to the inevitable hysteresis effect that is characteristic of mooring line loading. The possibility that a sign error in the sum $(-mgs - m\ddot{x})$ may have led to the discrepancy is ruled out since, for in-phase response, the excitation (-mgs) and the ship acceleration $(\ddot{x})$ are always of opposite sign, leading to a simple arithmetical sum of the two terms, as taken by the authors. The authors' results are otherwise a good demonstration of the expected linear dependence of the ship movement and restoring force upon the water surface slope.

J. T. O'BRIEN,[26] F. ASCE, AND D. I. KUCHENREUTHER,[27] A. M. ASCE.—With regard to Eq. 10 of Mr. Wilson's discussion the writers had quoted a previously published work by Mr. Wilson.[28] However, the writers are informed

---

25 "Forces Induced on a Large Vessel by Surge," by J. T. O'Brien and D. I. Kuchenreuther, Proceedings Paper 1571, ASCE, March, 1958, Fig. 9, p. 1571-16.

26 Dir., Harbor Div., U. S. Naval Civ. Engrg. Research and Evaluation Lab., Bureau of Yards and Docks, Dept. of the Navy, Port Hueneme, Calif.

27 Hydr. Engr., U. S. Naval Civ. Engrg. Research and Evaluation Lab., Bureau of Yards and Docks, Dept. of the Navy, Port Hueneme, Calif.

28 "Ship Response to Range Action in Harbor Basins," by B. W. Wilson, Transactions, ASCE, Vol. 116, 1951, p. 1144, Eq. 41.

by letter from Wilson that this equation is in error, due to a misprint, and that it should read:

$$R_{max} = \frac{4\,W\,A}{T_n\,(g\,d)^{\frac{1}{2}}} \quad \ldots\ldots\ldots\ldots\ldots \quad (35)$$

which result can be derived from two equations in Mr. Wilson's paper.[29]

It seems necessary to present Deacon, Russell and Palmer's[6] statement referred to by Wilson and the writers before it can be discussed further. As published it reads

"* * * the expression for the maximum total force in all the cables together emerges finally as

$$(R_{max} =) \frac{(\text{mass of the ship})\quad(\text{height of the standing wave})}{\text{wave period}\qquad(g\ \text{X water depth})^{1/2}} * * *"$$

which, when stated symbolically in terms of this discussion and assuming that by "mass of ship" Deacon, et al., perhaps more as a physicist than engineer, meant what is usually termed, in the United States, as "weight," can be written as

$$R_{max} = 2\,W\,A/T_n\,(g\,d)^{\frac{1}{2}} \quad \ldots\ldots\ldots\ldots \quad (36)$$

From a comparison of Eqs. 35 and 36 it can be concluded that Deacon, et al. misquoted Wilson by a factor of $1/2\pi$ and not $g/2\pi$ as stated by Wilson in his discussion.

As to the important controversy, that which engages Wilson beginning just prior to Eq. 11, concerning the hydrodynamic behavior of a moored ship driven by a standing wave acting at its node, the writers, at least in the paper under discussion, seem to subscribe to the position taken by Deacon, et al. rather than Wilson, where Deacon, et al.[6] assumes that:

> ". . . the inertia force is the product of (acceleration of the water particles) and (the mass of the ship and its virtual mass). Accordingly the acceleration of the ship is that of the water particles. . ."

The writer's position may be pointed up by considering first that the expression from Horace Lamb as given by Wilson, $m\,\ddot{x} = F - m''\,\ddot{x}$ can, by substitution of terms as given by Wilson and the writers ($m'' = m' - m = C_M\,m - m$) be written as

$$m\,C_M\,\ddot{x} = F \quad \ldots\ldots\ldots\ldots\ldots\ldots \quad (37)$$

Now, by combining Eqs. 2, 3, 5 and 6b we have

$$m\,C_M\,\ddot{x} + C_d\,A\,\rho\,(\dot{x})^2/2 + \sum k_i\,x^{n_i} = (mg2\pi\,A/L)\,\sin\,2\pi\,t/T \quad \ldots \quad (38)$$

If damping is considered negligible and there is no restraint to the motion and the term on the right hand side of Eq. 38, the excitation, is denoted by the symbol F, then $m\,C_M\,\ddot{x} = F$ which is obviously the same as Eq. 37.

Thus, it would seem that the writers, and perhaps Deacon, et al. consider the oscillation of the unmoored and undamped ship to be analogous to that given

---

[29] "Ship Response to Range Action in Harbor Basins," by B. W. Wilson, Transactions, ASCE, Vol. 116, 1951, pp. 1140, 1142, Eqs. 25, 34(a).

by Lamb[30] for the motion of a cylinder accelerated by a force through an ideal frictionless fluid, initially at rest.

After this somewhat summary scientific pronouncement, a comparison is made of the writers equation of motion with that given by Wilson, (Eq. 19). To simplify and make the symbolism of the writers consistent with Wilson the following substitutions are made in Eq. 38: $C_d A \rho (\dot{x})^2/2 = 0$, $\sum k_i x^{n_i} = C x^n$ and $L = T c = T (g d)^{\frac{1}{2}}$ in which C is an empirically derived constant expressing the elongation behavior of the mooring lines. Eq. 38 can now be written as

$$m C_M \ddot{x} + 0 + C x^n = \left(m 2\pi g A/T (g d)^{\frac{1}{2}}\right) \sin 2\pi t/T$$

$$= (m A 2\pi/T) (g/d)^{\frac{1}{2}} \sin 2\pi t/T \quad \ldots\ldots\ldots (39)$$

Multiplying Eq. 39 by $1/m C_M$ and substituting $V = A (g/d)^{\frac{1}{2}}$, $\sigma = 2\pi/T$ and $\omega^2 = C/m C_M$ Eq. 40 is obtained.

$$\ddot{x} + \omega^2 x^n = \left(\frac{1}{C_M}\right) V \sigma \sin \sigma t \quad \ldots\ldots\ldots (40)$$

This is compared with Eq. 19 with damping zero.

$$\ddot{x} + \omega^2 x^n = V \sigma \sin \sigma t \quad \ldots\ldots\ldots\ldots (41)$$

Thus it is apparent that when damping is considered negligible, the writers' expression and that of Wilson differ only in that the writers' expression for the excitation is less than that of Wilson by factor of $1/C_M$ where, of course, the two become equal when C_M is equal to 1. Therefore, generally any restoring force $(\omega^2 x^n)$ computed from the Eq. 40 would be less than that computed by use of Wilson's Eq. 41. In this regard, the writers are unable to add anything significant to Wilson's explanation as to why the computed values of the restoring force in Fig. 9, are greater than those measured (a mass which is too large may have been used) but would suggest that apparently experimental and theoretical deficiencies in explaining nature are still rampant.

Further, either Eq. 40 or 41 appear to be identical in principal with those obtained for the approximate mechanical behavior of a mass forced to vibrate without damping against the restrain of a nonlinear spring as outlined, for example, by Den Hartog.[31] In the solution of such an equation it is assumed that the motion is sinusoidal and has the "forced" frequency where Den Hartog states with regard to this assumption,

> "this is obviously not true, and the degree of approximation can be estimated only by the seriousness of the deviation from this assumption . . ."

If sinusoidal motion is assumed $x = x_o \sin \sigma t$ where x_o = maximum amplitude of oscillation then following Den Hartog, the inertia term in Eq. 40 can be written as $\ddot{x} = -\sigma^2 x_o \sin \sigma t$ so that Eq. 40 with $C_M = 1$ can be written as

$$-\sigma^2 x_o \sin \sigma t + \omega^2 x_o^n = V \sigma \sin \sigma t \quad \ldots\ldots\ldots (42a)$$

---

30 "Hydrodynamics," by H. Lamb, Dover Publications, New York, 1945, Article 68, pp. 77, Eq. 6.

31 "Mechanical Vibrations," by Den Hartog, McGraw-Hill Co., Inc., 1947, 3d Ed., pp. 431–435.

or

$$\omega^2 x_o^n = V \sigma \sin \sigma t + \sigma^2 x_o \sin \sigma t \quad \ldots\ldots\ldots (42b)$$

Eq. 42b can be solved graphically, following Den Hartog, by rectangularly plotting $\omega^2 x_o^n$ vertically and amplitude (x_o) horizontally, then noting that the left side of Eq. 42 is the nonlinear spring characteristic, while the right side expresses a straight line with the ordinate intercept, $V \sigma \sin \sigma t$, and the slope $\tan^{-1} (\sigma^2 x_o \sin \sigma t)$. Thus, values of x_o for various values of $V \sigma \sin \sigma t$ can be obtained by graphical means. Depending on the value of σ there can be from 1 to 3 values of x_o for a particular value of $V \sigma$.

Toward an interesting example based on material contained elsewhere[32] the lines of the *USS Norton Sound* have been loosened over those used in the paper and are considered to constitute a symmetrical even though nonlinear spring such that the combined restoring force term, $\omega^2 x_o^n$ with C_M taken as 1, m as 835,000 slugs, C as 5000 pounds per (foot)^n and n as 2.01 can be expressed as:

$$\omega^2 x_o^n = (5000/835{,}000\ (1)) x_o^{2.01} = .00598\ x_o^{2.01} \quad \ldots\ (43)$$

If Eq. 43 is substituted in Eq. 42b along with the value for V corresponding

TABLE 3.—VALUES OF X_o.

Point	T, in seconds	A, in feet	x_o, in feet		
1	25	0	10.5		-10.5
2	25	0.3	11.6	-1.4	- 9.2
3	25	0.7	12.9		
4	30	0	7.5		- 7.5
5	30	0.3	8.6	-1.9	- 5.4
6	30	0.7	9.9		

to a depth (d) of 32 ft with g conveniently rounded to 32 fps per sec and maximum amplitudes of oscillation only considered, $\sin \sigma t = 1$, Eq. 44 is obtained

$$.00598\ x_o^{2.01} = A \sigma + \sigma^2 x_o \quad \ldots\ldots\ldots\ldots\ (44)$$

in which A, the wave amplitude, must be in feet. Now, by application of the graphical technique as presented by Den Hartog[31] toward solution of Eq. 44 values are obtained for the amplitude of the ships undamped oscillation (x_o) as excited by standing waves of particular amplitude (A) and frequency $(\sigma = 2\pi/T)$ as shown in Table 3. When the wave excitation $A \sigma$ and movement (x_o) have the same sign they are considered to be in-phase (ship apparently moving downhill). A difference in sign denotes an out-of-phase relationship (ship apparently moving uphill). Note that in some cases that the same excitation can produce both in-phase and out-of-phase ship movement. Point No. 2, for example shows one of the former and two of the latter is possible. When the excitation is zero (still water) there exists a case of free vibration as shown, for example, in point No. 1.

32 "Forces Induced by Waves on the Moored U. S. S. Norton Sound (A. V. M.-1)," Technical Memorandum M-129, U. S. Naval Civ. Engrg. Lab., Port Hueneme, Calif., April, 1958.

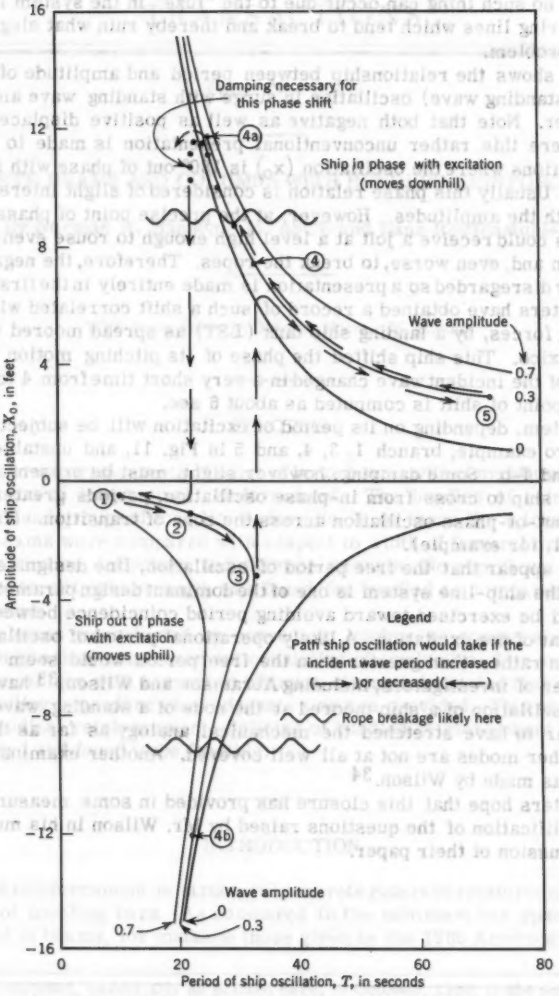


FIG. 11.—RELATIONSHIP BETWEEN PERIOD AND AMPLITUDE OF SHIP OSCILLATION

When the solutions to Eq. 44 are extended over those presented in Table 3 and the results plotted, curves of the type given in Fig. 11 are obtained which show strikingly the tendency of the ship movement and restoring force to become infinite when the natural period of vibration (when $A\sigma = 0$) is approached. Of course, no such thing can occur due to the "fuze" in the system in the form of the mooring lines which tend to break and thereby ruin what elegance there is in this problem.

Fig. 11 shows the relationship between period and amplitude of a moored ship (and standing wave) oscillation in surge with standing wave amplitude as a parameter. Note that both negative as well as positive displacements are plotted where this rather unconventional presentation is made to emphasize those situations where the oscillation (x_o) is 180° out of phase with the excitation ($A\sigma$). Usually this phase relation is considered of slight interest in comparison with the amplitudes. However, at the precise point of phase switching many ships could receive a jolt at a level high enough to rouse even the sleepiest seaman and, even worse, to break the ropes. Therefore, the negative signs are usually disregarded so a presentation is made entirely in the first quadrant.

The writers have obtained a record of such a shift correlated with changes in mooring forces, by a landing ship tank (LST) as spread moored in the open Gulf of Mexico. This ship shifted the phase of its pitching motion by 180° as the period of the incident wave changed in a very short time from 4 to 7 1/2 sec where the point of shift is computed as about 6 sec.

The system, depending on its period of excitation will be subject to stable-motions, fro example, branch 1, 3, 4, and 5 in Fig. 11, and unstable-motions, branch 3 and 4-b. Some damping, however slight, must be present in order to permit the ship to cross from in-phase oscillation, periods greater than free period, to out-of-phase oscillation across the zone of transition. (from 4-a to 2 in Fig. 11, for example).

It would appear that the free period of oscillation, line designated $A = 0$ in Fig. 11, of the ship-line system is one of the dominant design parameters where care should be exercised toward avoiding period coincidence between this period and that of the excitation. A likely operational period of oscillation which is less than rather than greater than the free period would seem desirable.

A number of investigators, including Abramson and Wilson,[33] have discussed surge oscillation of a ship moored at the node of a standing wave, although none appear to have stretched the mechanical analogy as far as the writers herein. Other modes are not at all well covered. Another examination of the problem was made by Wilson.[34]

The writers hope that this closure has provided in some measure answers to and amplification of the questions raised by Mr. Wilson in his much appreciated discussion of their paper.

---

33 "A Further Analysis of the Longitudinal Response of Moored Vessels to Sea Oscillation," by H. N. Abramson, and B. W. Wilson, Proceedings, Joint Mid-West Conf., Solid and Fluid Mechanics, Purdue Univ., September, 1955.

34 "The Energy Problem in the Mooring of Ships Exposed to Waves," by B. W. Wilson, Proc. of Princeton Conference on Berthing and Cargo Handling in Exposed Locations, October, 1958, pp. 1–67.

AMERICAN SOCIETY OF CIVIL ENGINEERS

Founded November 5, 1852

TRANSACTIONS

Paper No. 3047

CONCRETE BEAMS AND COLUMNS WITH BUNDLED REINFORCEMENT

By Norman W. Hanson,[1] M. ASCE and Hans Reiffenstuhl[2]

With Discussion by Messr. Homer M. Hadley

SYNOPSIS

This paper reports on tests of pairs of large beams with conventionally spaced and with bundled longitudinal reinforcement. The bundles of reinforcement used comprised groups of four No. 6, four No. 8, or three No. 9 touching bars. Pairs of beams were compared with respect to width of flexural cracks, steel stress distribution, deflection, and ultimate strength. No significant difference in behavior or ultimate strength was found for bundled as compared to spaced reinforcement.

Tied columns were tested by concentric loading to compare spaced and bundled longitudinal reinforcement consisting of twelve No. 6 or twelve No. 8 bars. Comparison with respect to ultimate strength indicated that bundling is a safe detailing procedure when adequate ties are provided. This true even for 6.6% longitudinal reinforcement. Splicing of bundled reinforcement in columns was explored and found to be feasible.

INTRODUCTION

Bundled reinforcement in structural concrete refers to reinforcement placed in groups of touching bars. As compared to the minimum bar spacings commonly used in beams, for instance those given by the 1965 American Concrete

Note.—Published, essentially as printed here, in October, 1958, in the Journal of the Structural Division, as Proceedings Paper 1818. Positions and titles given are those in effect when the paper or discussion was approved for publication in Transactions.

[1] Assoc. Development Engr., Research and Development Div., Portland Cement Assn., Chicago, Ill.

[2] Visiting Engr., Research and Development Div., Portland Cement Assn., Chicago, Ill.

Institute (ACI) Building Code Requirements for Reinforced Concrete (ACI 318-56 Section 505(a)), bundling permits the necessary bars to be placed in much narrower sections. As a result, bundling permits construction of lighter, more graceful and more economical beams of box, channel or T-B6, section. In beams of normal width, the clear distance between bundles will be considerably greater than the distance between individual evenly spaced bars. Bundling greatly facilitates concrete placement and insertion of spud vibrators, particularly when heavy negative moment reinforcement must be embedded in the top of beams. In columns, bundled reinforcement permits a reduced concrete cross section, which may be an important advantage in the lower stories of tall buildings. Bundling also permits interior ties to be omitted, so that concrete placement is facilitated. Finally, bundled bars in beams and columns may be a satisfactory alternate to large sizes of specially rolled reinforcing bars that are occasionally used in very large structures.

Practical use of bundled reinforcement in beams has been pioneered, and several structures with bundled reinforcement have been built,[2,3,4,5,6] for which good service records have been reported.

Laboratory tests that have been reported[7,8] concern principally bundles of four $\frac{1}{2}$-in. square bars in beams, and there may be some question regarding the performance of bundles of larger bar sizes. No tests of bundled reinforcement in columns have been reported. An experimental investigation was therefore carried out in the Research and Development Laboratories of the Portland Cement Association during 1955-57 to investigate the performance of large deformed bars placed in bundles as longitudinal beam and column reinforcement.

Notation.—The letter symbols adapted for use in this paper are defined where they first appear, in the text or in the illustrations, and are arranged alphabetically, for convenience of reference, in the Appendix.

TEST BEAM ARRANGEMENT

As compared to spaced bars, bundling may be questioned primarily with respect to the bond integrity of beams. The most serious conditions may then be expected for bars placed as negative reinforcement near the top of deep and short beams. Previous tests[9] have clearly indicated that, due to adverse effects of settlement, the bond resistance of top bars is less than that of bottom bars. They have also indicated that a short beam span leads to high bond stress

2 "Unusual Concrete Roof of Hollow Girders and Precast Slabs," by H. M. Hadley, Journal, A.C.I., Proceedings Vol. 37, February, 1941, pp. 453-460.

3 "Brazil's Wonder Hotel and Casino," by A. J. Boase, Engineering News-Record, Vol. 136, January, 1946, pp. 112-116.

4 "Bundle Reinforcing Saves Materials," Engineering News-Record, Vol. 140, April, 1948, pp. 509-510.

5 "Bridge with 'Bundled' Reinforcement," by H. M. Hadley, Western Construction, Vol. 26, June, 1951, pp. 89-90.

6 "'Bundled' Reinforcement," by H. M. Hadley, Journal, A.C.I., Proceedings Vol. 49, October, 1952, pp. 157-159.

7 "Precast Box Beams for High Strength," by H. M. Hadley, Engineering News-Record, Vol. 125, Dec., 1940, pp. 383-839.

8 "Tests of Beams Reinforced with 'Bundle Bars'," by H. M. Hadley, Civil Engineering, Vol. 11, February, 1941, pp. 90-93.

9 "An Investigation of Bond, Anchorage and Related Factors in Reinforced Concrete Beams," by C. A. Menzel and W. M. Woods, Bulletin 42, Research Dept., Portland Cement Assn., November, 1952, p. 114.

before the flexural ultimate strength is developed. Therefore, the test specimens for this investigation were short, deep beams, with the tension steel at the top as cast.

In the beam designations to follow, the first number shows the number of bars and the second number their size; the letter S indicates spaced bars and B indicates bundled bars; H indicates high-strength steel.

The test beams 8-6S, 8-6SH, 8-8SH and 6-9S, with spaced reinforcement, shown in Fig. 1, were designed by first determining the minimum beam width for a chosen group of bars. By the ACI code previously mentioned, this width is governed by a minimum protective cover of 1-½ in. and, for 1-½ in. maximum size aggregate, a clear distance of 2 in. between parallel bars. The beam depth was chosen so that the ratio of reinforcement was 1.5%. Finally, the distance from the face of a centrally located column stub to the beam support was chosen as twice the effective beam depth. Thus, the test span L is 85 in. for the beams with No. 6 bars, 134.5 in. for the beams with No. 8 bars, and 151.8 in. for those with No. 9 bars. The beams and all bars were extended 6 in. beyond the supports. The gross concrete dimensions of beams 8-6S, 8-8S and 6-9S, excluding the column stubs, were 13 in. by 21 in. by 97 in., 14.5 in by 33.5 in. by 146.5 in., and 11.5 in. by 38.8 in. by 163.8 in., respectively.

The beams with bundled reinforcement, beams 8-6B, 8-8B and 6-9B were identical to the corresponding beams with spaced bars except for the bar arrangement. The effect of decreasing the beam width for bundled reinforcement was investigated through beams 8-6BH and 8-8 BH. For these two beams, and their companions with spaced reinforcement, high-strength reinforcement was used to delay flexural failure and develop very high bond stress.

The column stubs of all beams were reinforced with four bars of the same size as the longitudinal beam reinforcement, and these bars were extended through the beam. Vertical stirrup reinforcement was provided to prevent diagonal tension and shear failures. The stirrups also served the function of preventing horizontal splitting that might otherwise have been caused by high bond stress. Beams 8-6SH and 8-6BH had two No. 6 bars placed as compression reinforcement to prevent flexural compression failure. Beams 8-8SH and 8-8BH had two No. 8 bars placed as compression reinforcement.

Properties of Bundles.—The external perimeter for a bundle of four bars as shown for beam 8-6B and 8-8B in Fig. 1 is $3\pi D$, that is, 25% less than for the same bars spaced in the usual manner. On the other hand, a single large bar with the same cross-section area as a bundle of four bars with diameter D would have a diameter of 2D and a perimeter of $2\pi D$. Accordingly, the bundle of four bars has an exposed perimeter 50% greater than that of the single large bar. The bundle of three bars used for beam 6-9B similarly has an exposed perimeter 16.7% less than that for the same spaced bars, and 55% greater than that of a larger bar of the same area.

These geometric properties indicate that bundling leads to only a moderate increase in bond stress as compared to spaced bars. Replacing a single large bar by a bundle with the same area, leads to a reduced bond stress. It should be noted, however, that the deformation of lug height, as defined by ASTM A-305-53T, would be greater for a single large bar than for a bundle of bars, and bond resistance for top bars is known[9] to increase with increasing lug height.

Materials.—A laboratory blend of Type I cements was used. Sand and gravel aggregates were combined to gradations within the limits given by ASTM C-33-55T for 1-½ in. maximum size. The concretes were mixed in 6 cu ft

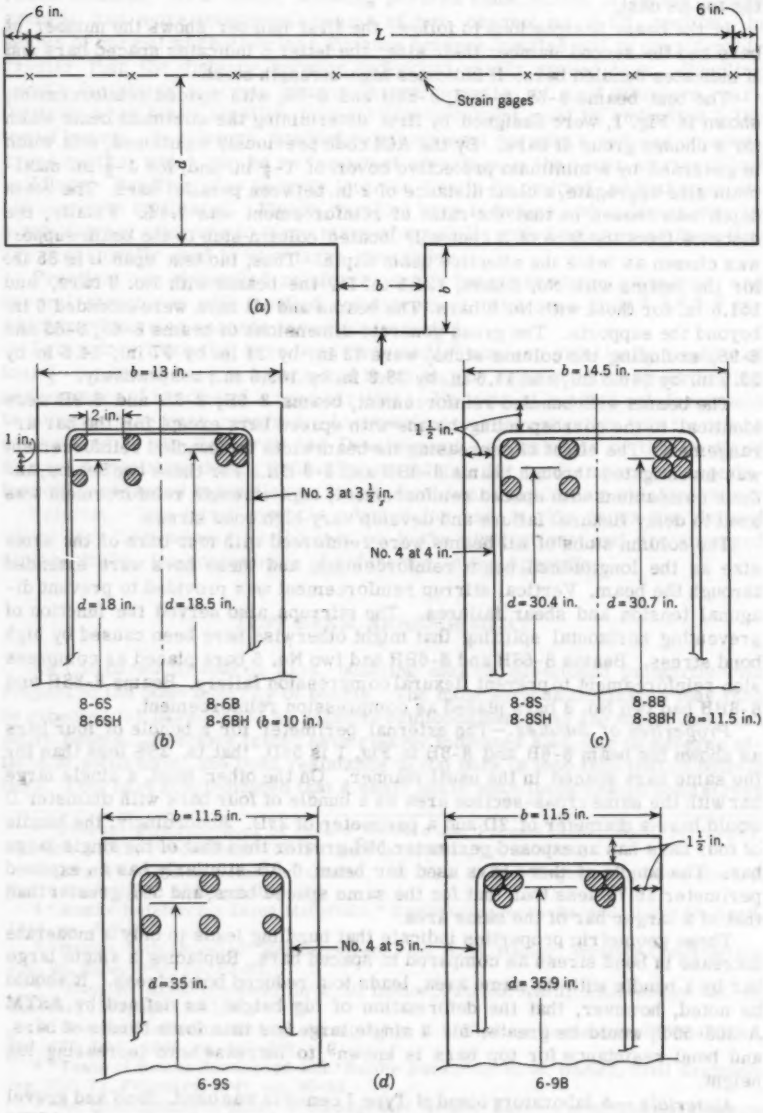


FIG. 1.—TEST BEAMS

batches, and had a slump of 2-$\frac{1}{2}$ to 3 in. The cement content was 4.0 to 4.2 bags per cu yd, and the water-to-cement ratio, by weight, was 0.62 to 0.70. The compressive strengths reported with the beam test data in Table 1 are averages of twelve to sixteen 6-in.-by-12-in. cylinders made, cured, and tested with each beam.

All reinforcing steel used conformed to ASTM A-305-53T for deformations and had the yield points given in Table 1. For No. 6, 8, and 9 bars, respectively, lug height was 0.048, 0.055, 0.067 in. and lug spacing was 0.35, 0.48, 0.50 in. The steel was purchased in such lengths that each bar yielded two beam lengths and a 3 ft length for tension test. By using one of these lengths in each beam of a pair, variation in steel properties between pairs was minimized. The No. 3 stirrups used in beams with eight No. 6 longitudinal bars had a yield point of 52,100 psi, whereas the No. 4 stirrups used in the remaining beams

TABLE 1.—BEAM STRENGTH

Beam Designation	Main Steel (f_y), in pounds per square inch	Cylinder Strength f'_c, in pounds per square inch	Test Age, in Days	Yield Load P_{yield}, in kips	Ultimate Load P_{test}, in kips	Calculated Flexural Ultimate Load P_{calc}, in kips	$\frac{P_{test}}{P_{calc}}$	Calculated Bond Stress at Ultimate Load, in pounds per square inch
(1)	(2)	(3)	(4)	(5)	(6)	(7)	(8)	(9)
8-6S	47,000	2935	15	137.5	150	142	1.05	252
8-6B	47,000	3080	16	137.5	161	148	1.09	351
8-8S	48,300	4375	26	280	314	281	1.12	235
8-8B	48,300	4240	28	260	349	283	1.23	345
6-9S	46,800	4480	14	240	308.5	255	1.21	238
6-9B	46,800	4600	15	240	281	256	1.10	253
8-6SH	84,200	4960	14	----	310	262	1.18	520
8-6BH	84,200	3805	16	----	235	253	---	513
8-8SH	80,000	4870	14	----	450	462	---	337
8-8BH	80,000	3840	14	----	396	443	---	391

had a yield point of 48,700 psi. All reinforcement for each beam was tied together without welding.

Casting.—All beams were cast in plastic coated plywood forms with the column stub down so that in the same manner as the longitudinal reinforcement was embedded near the top of the beam, because this reinforcement is near the columns in continuous beams. Concrete was placed through the use of spud vibrators in the test beams and their companion test cylinders. It was found that bundling of the bars eased the placing operation substantially. After testing the beams it was found that mortar had penetrated into and filled the cavity between the bars of all bundles. The test beams and their companion cylinders were cured one week under moist burlap. The beams were then turned upside down and stored in the laboratory until they were tested at the ages given in Table 1.

Test Method.—All beam specimens were tested as shown in Fig. 2, supported on a roller at one end and on a rocker at the other, with a 6-in. overhang at each end. The testing machine load was applied in increments to the column

stub through a 2-in. steel plate. The total duration of each beam test was approximately two hours.

Deflection dial gages were mounted directly below the two faces of the column stub and mid-way between these points and the supports. The widths of all cracks were measured by a graduated microscope at the level of the centroid of the longitudinal reinforcement.

To minimize the amount of bar surface area isolated from bond by the waterproofing of the electric strain gages, SR-4 Type A-12 gages were placed in the intermediate grade bars in milled slots 3/32 in. wide, 3/8 in. deep, and approximately 6 in. long. The high-strength bars could not be milled. Thus, the location of the strain gages in Fig. 1(a) does not refer to the beams using high-strength steel rods. A gage was cemented to the side of each slot, lead



FIG. 2.—TESTING ARRANGEMENT FOR BEAMS

wires were attached, and the slot was filled to the bar surface with wax waterproofing. Tension tests indicated that gages so placed yielded measurements in close accord with mechanical strain measurements over the same reduced section. The stress at any bar load was 5% to 9% higher in the slotted section than in the full bar section. Eight strain gages for each beam were located as shown in Fig. 1(a). Two gages were placed on each of four bars symmetrically about mid-span. The measured strain without correction was assumed to represent the average strain in all bars at the location of the gage. Therefore, measured strain is reported herein as stress obtained by multiplying the average strain in the two half spans by the modulus of elasticity for the full section of the various bar sizes as obtained in tension tests.

BEAM TEST RESULTS

All beams with intermediate-grade steel, beams 8-6S through 6-9B in Table 1, failed by yielding of the longitudinal reinforcement, followed by large de-

flections and final crushing of the concrete compression zone at the column face. As shown in Fig. 2, both flexural and diagonal cracks tended to extend upward toward the corner at the column stub so that it was hardly possible to differentiate between flexural and diagonal cracks. No indication of bond failure was found in any of these beams, and no visual difference in behavior was noted for beams with bundled as compared to spaced bars.

Three beams with high strength reinforcement failed in bond as indicated by large amounts of bar slip at the beam ends. For beam 8-6SH the tension steel yielded following bar slip at the beam ends.

Steel Stress and Deflection.—Measured steel stress and deflection at various load levels for the three beam pairs with intermediate grade steel are shown in Figs. 3(a),(b)and(c). Both steel stress and deflection are given as an average of two measurements symmetrical about midspan for each beam.

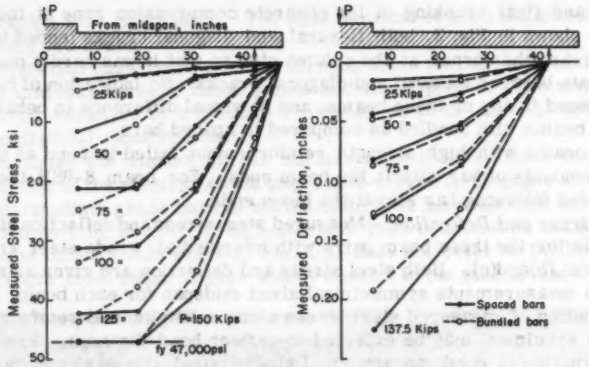
Distribution of measured steel stress along a longitudinal reinforcing bar, in a beam specimen, may be expected to reflect bond distress. Preceding a final destruction of bond, an abnormal rise of steel stress should take place toward the beam ends. Fig. 3 shows that the distribution of steel stress was very similar for the two members of each pair of test beams even at high steel-stress. It may be noted, on the other hand, that the steel-stress for all beams was practically uniform at high loads in the middle third of the span. This was certainly caused by a stress redistribution resulting from the deep-beam type of crack pattern seen in Fig. 2. It is also seen that the overhangs contributed to the bonding action because the steel-stress of all beams is not zero over the supports at high loads. It is felt that this behavior is related to local stress disturbances in the support region where heavy reaction forces entered the abnormally short beams.

The deflection curves are also similar for all beam pairs. Accordingly, both steel stress and deflection measurements indicate that there was no significant difference in behavior between bundled and spaced reinforcement.

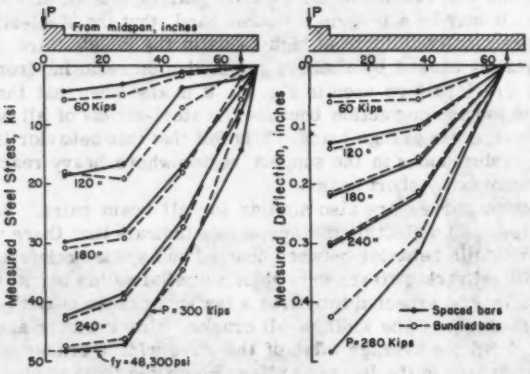
Crack Width.—Crack patterns were closely similar within pairs for all tests. Bond distress may be expected to open up a few wide cracks near the beam ends rather than to increase the width of all cracks. Crack widths are therefore given in Fig. 4, as the average width of the three widest cracks in the beam. Steel stress is given in the figure as values computed from applied moment at the column face section, taking the internal moment arm as 7/8 times the effective depth. It is seen that there is no systematic difference between the crack widths for bundled and for spaced reinforcement. Furthermore, no crack opened suddenly before yielding of the reinforcement was in progress. This indicates that even the high local bond stress, which acts near cracks, resulted only in the normal minor bond slip for bundled as well as for spaced reinforcement.

For the four beams with high strength reinforcement, a similar lack of systematic difference was observed between crack widths for bundled and spaced reinforcement. However, for beams 8-6BH, 8-8SH, and 8-8BH, as the ultimate load was reached, a few cracks near the beam ends became very wide shortly before final bond failure took place.

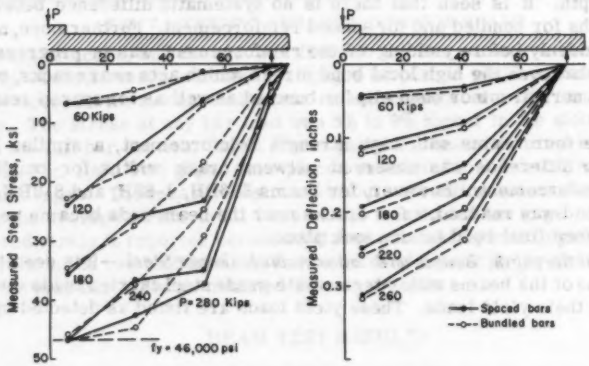
Flexural Strength, Beams with Intermediate Grade Steel.—It is seen in Table 1 that some of the beams with intermediate grade steel carried loads considerably above their yield loads. These yield loads are listed as detected by strain



(a) BEAMS 8-6S and 8-6B



(b) BEAMS 6-8S and 6-8B



(c) BEAMS 6-9S and 6-9B

FIG. 3.—MEASURED STEEL STRESS AND DEFLECTIONS

and crack width measurements. Considering the external moment at the face of the column the computed flexural ultimate loads, P_{calc}, were obtained by the equation for ultimate internal moment

$$M_u = b\, d^2\, f'_c\, q(1-0.59\, q) \quad \ldots\ldots\ldots\ldots\ldots \quad (1)$$

in which f'_c is the concrete cylinder strength, and q is the factor pf_y / f'_c, in which p equals A_s (the effective cross-sectional area of reinforcement) divided by bd, and f_y is the yield point of reinforcement. This equation is given in ACI 318-56, A605(b). The ratio of measured to computed ultimate load exceeds one (1) for all beams. The average ratio for the three beams with spaced bars is 1.13, and the average ratio for the beams with bundled bars is also 1.13. This indicates that there was no systematic difference in ultimate flexural strength developed by spaced and by bundled bars except that the beams with bundled bars were slightly stronger by virtue of the slight increase in effective beam depth.

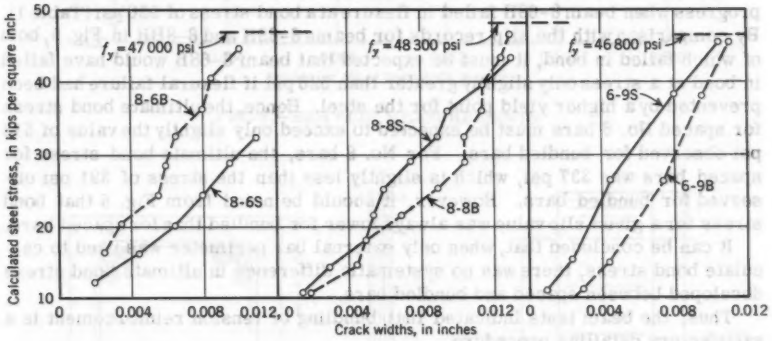


FIG. 4.—CRACK WIDTH MEASUREMENTS

The average ratio of 1.13 also confirms previous findings that the equation for ultimate moment, which was developed essentially by tests of small beams, is also applicable to the large beams of this investigation. It is believed that the excess of measured ultimate loads over the computed load resulted principally from strain hardening of the reinforcement. A biaxial state of stress at the column stub appeared to delay crushing of the compression zone so that large steel strains were developed locally at the major flexural cracks.

Bond stresses are given in Table 1 as computed at ultimate load, by dividing the shearing force by the external perimeter of the bars times 7d/8. These bond stresses, for the beams with intermediate grade steel, were sustained without any indication of bond failure. They are in no way to be regarded as ultimate bond stresses. To develop higher bond stresses with intermediate-grade steel it would have been necessary to make special test beams with part of the tension zone removed, or to make the beams so short that they would act as walls rather than beams. Both of these cases were thought not to represent practical conditions under which bundled bars may be used. High-strength steel was therefore used to study ultimate load stress.

Bond Strength, Beams with High-Strength Steel.—Table 1 shows that the beams with high-strength reinforcement failed at ultimate loads close to the flexural strengths computed by ACI 318-56, A606(a),

$$M_u = \left(A_S - A'_S\right) f_y\, d\left[1 - \frac{0.59\,(p - p')\,f_y}{f'_c}\right] + A'_S\, f_y\,(d - d') \quad \ldots . (2)$$

in which A_S is the area of tensile reinforcement, A'_S is ' the area of compressive reinforcement, d equals the distance from the extreme compressive fiber to the centroid of tensile reinforcement, whereas d' is the distance from this fiber to the centroid of compressive reinforcement and p' is the factor A'_S/bd. Beam 8-6SH failed in flexure after bond slip had been observed at the beam ends. The remaining three beams failed at loads below the computed ultimate flexural strength. Failure was in bond, as indicated by large amounts of bar slip observed by dial gages as a relative movement between bar ends and the concrete surface at the beam ends.

Bar slip is plotted as a function of computed bond stress in Fig. 5. Bond stresses at ultimate strength, calculated by dividing shearing force by external-bar-perimeter times 7d/8, are also shown. It is seen that bond slip was in progress when beam 8-6SH failed in flexure at a bond stress of 520 psi (Table 1). By comparison with the slip records for beams 8-8SH and 8-8BH in Fig. 5, both of which failed in bond, it must be expected that beam 8-6SH would have failed in bond at a stress only slightly greater than 520 psi if flexural failure had been prevented by a higher yield point for the steel. Hence, the ultimate bond stress for spaced No. 6 bars must be expected to exceed only slightly the value of 513 psi observed for bundled bars. For No. 8 bars, the ultimate bond stress for spaced bars was 337 psi, which is slightly less than the stress of 391 psi observed for bundled bars. However, it should be noted from Fig. 5 that bond stress for a given slip value was always lower for bundled than for spaced bars.

It can be concluded that, when only external bar perimeter was used to calculate bond stress, there was no systematic difference in ultimate bond stress developed between spaced and bundled bars.

Thus, the beam tests indicated that bundling of tension reinforcement is a satisfactory detailing procedure.

TEST COLUMN ARRANGEMENT

A series of ten tied columns was designed to study bundled compression reinforcement. Concentric loading was chosen. An outline of the test program is shown in Fig. 6. All columns were 12-in.-by-12-in. with a height of 6 ft. Two amounts of longitudinal reinforcement were used. These were 6.58% and 3.67%, made up of 12 No. 8 and 12 No. 6 bars, respectively. The 1/4-in. tie-diameter used is the minimum permitted by ACI 318-56, 1104(c). The corresponding maximum tie spacing of forty-eight tie diameters in 12 in., which is also the maximum spacing as governed by the 12-in. column size and by sixteen times the diameter of the No. 6 bars.

Five columns with 12 No. 8 bars were tested. Column 12-8S contained bars spaced in the normal manner and surrounded by a square tie. The interior bars were held firmly by two interior rectangular ties. All ties of this column were spaced at 12 in. Column 12-8B-1 contained bars bundled at the corners. Interior ties were omitted, and the exterior tie spacing was maintained at 12 in. For column 12-8B-2, the exterior tie spacing was decreased to 6 in. A splice was provided at mid-height of column 12-8B-3 as shown in Fig. 6. The spliced bars were cut by a saw, and each bar was touching its longitudinal extension. The tie spacing in both columns 12-8 B3 and 12-8 B4 was 6 ins. The

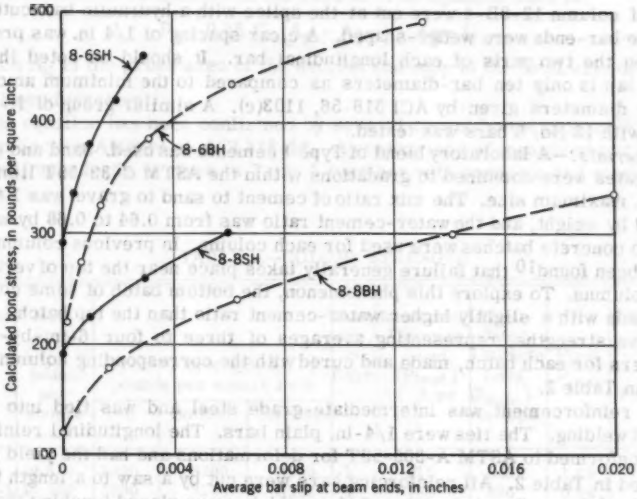


FIG. 5.—BAR SLIP MEASUREMENTS

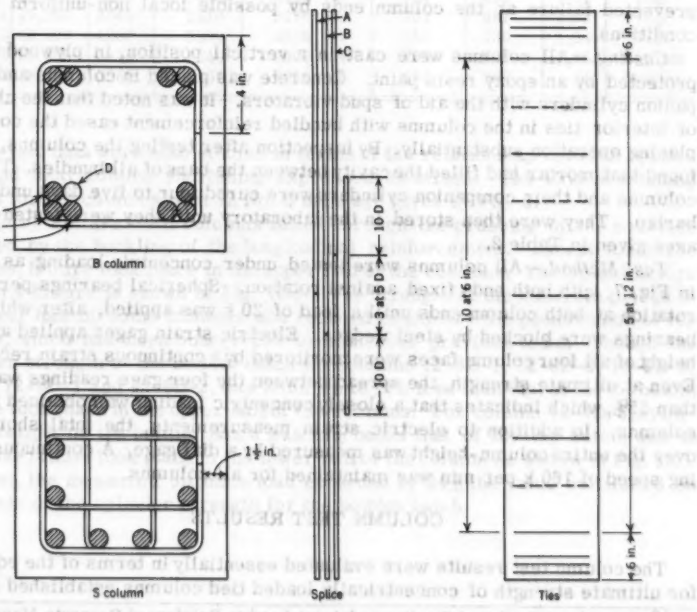


FIG. 6.—TEST COLUMNS

bars of column 12-8B-4 were cut at the splice with a hydraulic bar cutter so that the bar-ends were wedge-shaped. A clear spacing of 1/4 in. was provided between the two parts of each longitudinal bar. It should be noted that the splice lap is only ten bar-diameters as compared to the minimum amount of twenty diameters given by ACI 318-56, 1103(c). A similar group of five columns with 12 No. 6 bars was tested.

Materials.—A laboratory blend of Type I cements was used. Sand and gravel aggregates were combined to gradations within the ASTM C-33-55T limits for 3/4-in. maximum size. The mix ratio of cement to sand to gravel was 1 to 3.58 to 2.38 by weight, and the water-cement ratio was from 0.64 to 0.68 by weight.

Two concrete batches were used for each column. In previous column tests it has been found[10] that failure generally takes place near the top of vertically cast columns. To explore this phenomenon, the bottom batch of some columns was made with a slightly higher water-cement ratio than the top batch. Compressive strengths, representing averages of three to four 6-in.-by-12-in. cylinders for each batch, made and cured with the corresponding columns, are given in Table 2.

All reinforcement was intermediate-grade steel and was tied into cages without welding. The ties were 1/4-in. plain bars. The longitudinal reinforcement conformed to ASTM A-305-53T for deformations and had the yield points reported in Table 2. All reinforcing bars were cut by a saw to a length tolerance of 1/32-in. Bearing plates, 3/4-in. thick, were placed touching the bars at the top and bottom of the columns. The lower plate was placed in the form before casting, the upper plate was set in a thin layer of high-strength plaster after the concrete was cured. The heavy tie reinforcement shown in Fig. 6 prevented failure at the column ends by possible local non-uniform stress conditions.

Casting.—All columns were cast in a vertical position, in plywood forms protected by an epoxy resin paint. Concrete was placed in columns and companion cylinders with the aid of spud vibrators. It was noted that the absence of interior ties in the columns with bundled reinforcement eased the concrete placing operation substantially. By inspection after testing the columns, it was found that mortar had filled the cavity between the bars of all bundles. The test columns and their companion cylinders were cured four to five days under wet burlap. They were then stored in the laboratory until they were tested at the ages given in Table 2.

Test Method.—All columns were tested under concentric loading as shown in Fig. 7, with both ends fixed against rotation. Spherical bearings permitted rotation at both column ends until a load of 20 k was applied, after which the bearings were blocked by steel wedges. Electric strain gages applied at mid-height of all four column faces were monitored by a continuous strain recorder. Even at ultimate strength, the spread between the four gage readings was less than 15%, which indicates that a closely concentric loading was obtained for all columns. In addition to electric strain measurements, the total shortening over the entire column-height was measured by a dial gage. A continuous loading speed of 160 k per min was maintained for all columns.

COLUMN TEST RESULTS

The column test results were evaluated essentially in terms of the equation for ultimate strength of concentrically loaded tied columns established during

[10] "A Study of Combined Bending and Axial Load in Reinforced Concrete Members," by E. Hognestad, Bulletin No. 399, Engrg. Experiment Sta., Univ. of Illinois, 1951.

the ACI column investigations in the 1930's. The equation used is

$$P_o = 0.85\, f'_c \left(A_g - A_{ST}\right) + A_{ST}\, f_y \quad \ldots\ldots\ldots\ldots \quad (3)$$

in which A_g is the gross area of the section and A_{ST} is the total area of longitudinal reinforcement.

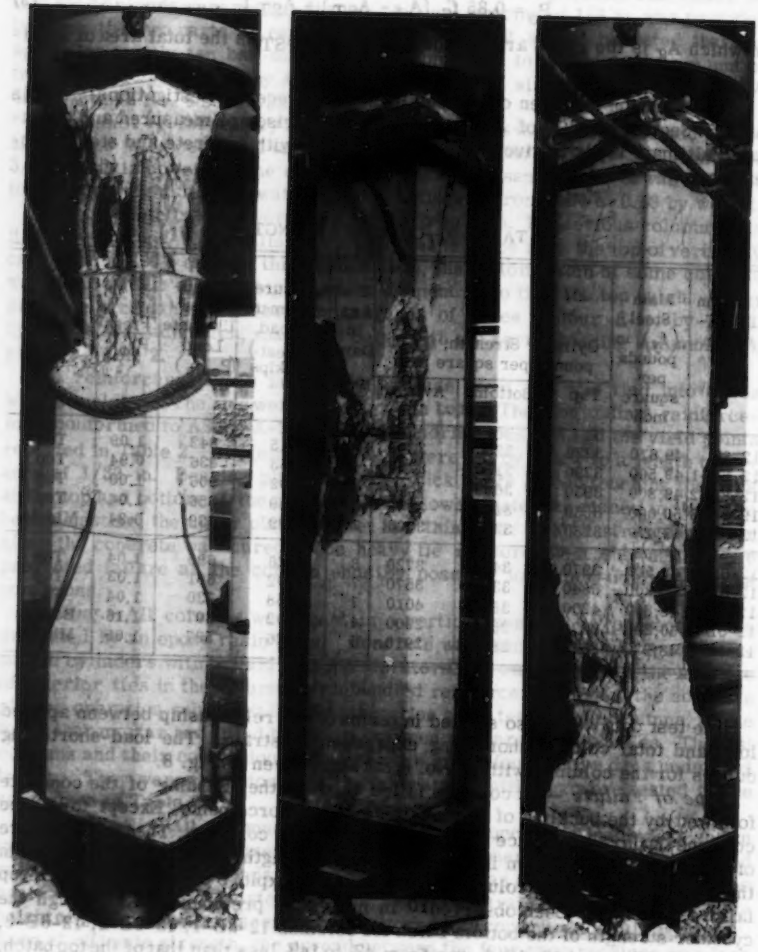
This equation has been confirmed by several recent investigations[10] and is used in Section A608(b) of ACI 318-56. A comparison of measured and calculated ultimate loads is given in Table 2 together with concrete and steel properties.

TABLE 2.—COLUMN STRENGTH

Column Designation	Main Steel, (f_y), in pounds per square inch	Cylinder Strength, f'_c, in pounds per square inch			Test Age, in Days	Measured Ultimate Load, (P_{test}), in kips	Calculated Ultimate Load (P_{calc}) in kips	$\frac{P_{test}}{P_{calc}}$	Location of Failure
		Top	Bottom	Average					
12-8S	49,610	3220	3290	3250	5	915	842	1.09	Top
12-8B-1	49,500	3290	3150	3220	8	783	836	0.94	Top
12-8B-2	49,800	3930	3680	3800	6	909	906	1.00	Top
12-8B-3	50,000	3550	3150	3350	6	889	856	1.04	Top
12-8B-4	48,470	3280	3360	3320	7	789	839	0.94	Middle
12-6S	48,510	3970	3470	3720	8	726	695	1.04	Top
12-6B-1	49,300	3840	3310	3570	7	702	681	1.03	Top
12-6B-2	48,800	4200	3820	4010	7	758	730	1.04	Top
12-6B-3	50,200	3270	2540	2900	4	702	607	1.16	Bottom
12-6B-4	48,230	2960	2860	2910	6	626	597	1.05	Middle

The test data were also studied in terms of the relationship between applied load and total column shortening expressed as strain. The load-shortening durves for the columns with 12 No. 8 bars are given in Fig. 8.

Type of Failure.—All columns failed through the crushing of the concrete followed by the buckling of the longitudinal reinforcement. Except for three columns, failure took place in the upper half of the columns. The typical nature of such a failure is shown in Fig. 7(a). The strength of the concrete placed in the lower half of some columns was reduced to explore the phenomenon of top failure, which had been observed[10] in numerous previous tests. Though the cylinder strength of the bottom batch for columns 12-8B-1, 12-8B-2, 12-8B-3, 12-6S, 12-6B-1 and 12-6B-2, was from 4% to 14% less than that of the top batch, failure took place in the upper half of the columns. For column 12-6B-3, cylinder strength of the bottom batch was 22% below that of the top batch, and in this case failure took place in the lower half of the column as shown in Fig. 9(c). Even so, the measured ultimate load exceeded by 24% the value calculated on the basis of the cylinder strength for the bottom batch.



No. 12-8B-1 (a) No. 12-8B-4 (b) No. 12-6B-3 (c)

FIG. 7.—TYPICAL COLUMN FAILURES

These findings confirm the previously reported observation that the column strength of the concrete placed in the lower half of columns is increased, probably by the improved compaction afforded when the upper half is cast. Similarly, the column strength of the concrete placed in the upper half may decrease somewhat by water gain from below. To evaluate effects of bundling, therefore, measured ultimate loads were compared to calculated values based on the average cylinder strength for the top and bottom batches for each column.

The two spliced columns 12-8B-4 and 12-6B-4, which had 1/4 in. clear between bars at the splice, failed in the splice region at mid-height as shown in Fig. 7(b).

Effect of Bundling.—The ratios between measured and calculated ultimate load given in Table 2 exceed one (1) for all except two columns. This confirms previous findings that led to the ACI column investigation equation.

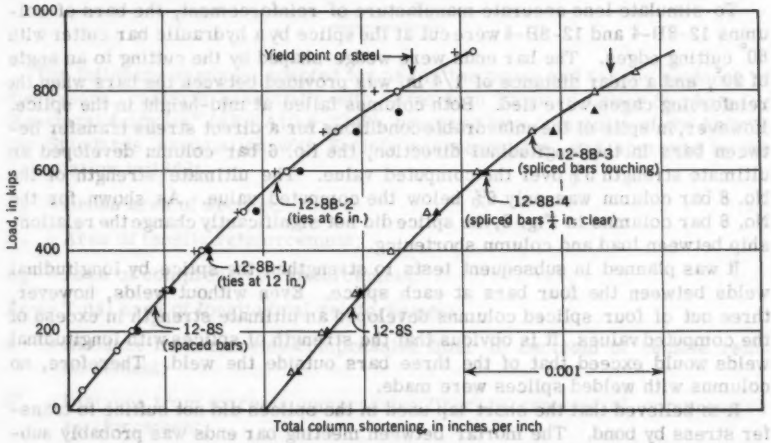


FIG. 8.—LOAD-SHORTENING CURVES FOR COLUMNS

The load ratios of columns 12-6B-1 and 12-6B-2 were 1.03 and 1.04 respectively as compared to a value of 1.04 for column 12-6S that had conventionally spaced bars. For 3.67% longitudinal reinforcement, therefore, no detrimental effect of bundling was found regardless of tie spacing.

For the columns with 6.58% reinforcement, which exceeds the maximum value of 4% given by ACI 318-56, 1104(a), the 12-in. tie spacing of column 12-8B-1 led to a load ratio of 0.94 as compared to 1.09 for column 12-8S with spaced bars. By reducing the tie spacing to 6 in. for column 12-8B-2, the load ratio increased to 1.00. Furthermore, column 12-8B-3, which had a 6-in. tie-spacing and failed above the splice, had a load ratio of 1.04. Therefore, even for 6.58% reinforcement, no detrimental effect of bundling was found when the tie spacing for bundled bars was reduced to 6 in., which is equal to 24 tie-diameters, or one-half of the least dimension of the column.

Bundling did not significantly affect the relationship between applied load and column shortening. This is shown for the columns with No. 8 bars in Fig. 8.

The results for the columns with No. 6 bars indicated a similar lack of effect of bundling.

Splicing.—Bundled reinforcement placed in the corners of a column section may be spliced in the same manner as single corner bars. The bars from below may be offset to a position inside the bars above the splice, and a proper amount of lap may then be provided. The bars may also be butted and welded.

In these tests, a splice particularly suitable for bundled bars was explored. As shown in Fig. 6 the splices of the three bundled corner bars were staggered a distance of five bar-diameters, and a fourth splice-bar, 35 bar-diameters long, was added at each corner. For columns 12-8B-3 the bars were cut by a saw, and each bar was touching its longitudinal extension. The contact was not perfect and after testing, a mortar layer 1/32 in. to 1/16 in. thick was found between the bars. Both of these columns failed outside the splice, and the measured ultimate loads exceeded the computed values by 4% and 16%, respectively.

To simulate less accurate manufacture of reinforcement, the bars of columns 12-8B-4 and 12-6B-4 were cut at the splice by a hydraulic bar cutter with 60° cutting edges. The bar ends were wedge-shaped by the cutting to an angle of 90°, and a clear distance of 1/4 in. was provided between the bars when the reinforcing cages were tied. Both columns failed at mid-height in the splice. However, in spite of the unfavorable conditions for a direct stress transfer between bars in the longitudinal direction, the No. 6 bar column developed an ultimate strength 5% over the computed value. The ultimate strength of the No. 8 bar column was only 6% below the computed value. As shown for the No. 8 bar columns in Fig. 8, the splice did not significantly change the relationship between load and column shortening.

It was planned in subsequent tests to strengthen the splice by longitudinal welds between the four bars at each splice. Even without welds, however, three out of four spliced columns developed an ultimate strength in excess of the computed values. It is obvious that the strength of splices with longitudinal welds would exceed that of the three bars outside the weld. Therefore, no columns with welded splices were made.

It is believed that the short lap used in the splices did not suffice to transfer stress by bond. The mortar between meeting bar ends was probably subjected to a triaxial state of stress so that a compressive strength far in excess of the cylinder strength could be developed. To assure that the longitudinal bars do not buckle in the splice, the reduced tie-spacing used in the tests, twenty-four tie-diameters or one-half the column dimension, may be necessary. If a splice of the type studied is used in eccentrically loaded columns so that tensile stress may be developed in the longitudinal bars, the mortar between bars cannot be expected to transfer stress and welds, or a longer lap, are obviously necessary.

CONCLUDING REMARKS

The test results reported confirm the previous findings that the use of bundled reinforcement is a sound detailing procedure. It can be expected that bundling of tension reinforcement in beams will not lead to detrimental consequences as compared to spaced bars, for the following conditions: 1. There are not more than four touching bars in each bundle, 2. Bond stress computed on the basis of external bar perimeter is limited to the values now permitted

for spaced bars, 3. Each bar in a bundle is a deformed bar and is individually well anchored, and 4. Stirrup reinforcement is provided in regions of high bond stress.

Bundling of compression reinforcement in tied columns can also be used even for high ratios of longitudinal reinforcement, if the provisions of ACI 318-56 regarding other details are strictly complied with. For large amounts of longitudinal bundled reinforcement, it is advisable to reduce the maximum tie-spacing to about one half of that given by the ACI Building Code.

Because bundling of reinforcement was found to be safe in tests involving the extreme cases of bending alone and compression alone, bundling should also be satisfactory for members subject to combined bending and axial load.

APPENDIX.—NOTATION

The following symbols, adapted for use in the paper and for the guidance of discussers, conform essentially with "American Standard Letter Symbols for Structural Analysis" (ASA A10.8-1949), prepared by a committee of the American Standards Association with Society representation, and approved by the Association in 1949:

A_g = Gross area of section;

A_S = Area of tensile reinforcement;

A'_S = Area of compressive reinforcement;

A_{ST} = Total area of longitudinal reinforcement;

d = Distance from extreme compressive fiber to centroid of tensile reinforcement;

d' = Distance from extreme compressive fiber to centroid of compressive reinforcement;

f_y = Yield point of reinforcement not to exceed 60,000 psi;

f'_c = Concrete cylinder strength of test specimen;

p = A_S/bd;

p' = A'_S/bd; and

q = $(pf_y)/f'_c$.

DISCUSSION

HOMER M. HADLEY,[11] **F. ASCE.**—The writer was pleased to read this paper on the testing of bundled reinforcement in both beams and columns. On

[11] Cons. Engr., Seattle, Wash.

numerous occasions, he has found bundling highly advantageous in beams particularly in precast channel-shaped concrete sections for short-span bridge decks, for which A. C. I. or AASHO bar spacing is peculiarly ill-adapted. There are probably several hundred of such short spans - 16-ft-to-30-ft long and ten or fewer years old - installed and in service in various parts of the state of Washington. These have been made with four bundled bars in each leg of the channel. The bar size depends on the span length, with single-bar stirrups looped around the bundle at the bottom. The stems of the channel webs are usually given a 6-in. bottom thickness with a 7-in. top thickness at the underside of the slab. These over-all web thicknesses, except in the case of the outer curb units, are initially reduced to approximately 4 in. by notching with a 2-in. plank on their outer faces. The notch starts approximately 6 in. above the bottom of the stem. When the units are placed side by side, these notched spaces, and any additional spaces are filled with concrete and thereafter there is full cover of the bundle everywhere.

There have been a few such small bridges on Federal Aid projects. After quite a number of small county bridges had been successfully installed, permission was granted on a project having twenty-eight ft trestly spans to use the precast units with four bar bundled reinforcement in each web. This project was likewise successfully installed and to the best of the writer's knowledge has proven entirely satisfactory. Unfortunately, an engineer from Washington, D. C. visited the project during construction and voiced some misgivings about bundling. This brought on a local reaction of rejection to the practice and permission to bundle reinforcement was withdrawn for several years. It is the writer's understanding that currently three bars may be bundled on local Federal Aid projects but not four bars. He is unable to explain the rationale of this ruling. The California Highway Department has bundled four bars on Federal Aid projects since 1949 and continues to do so.

Not mentioned by the authors among the named advantages of bundling is the fact that it affords opportunity for having the quantity of beam reinforcement conform roughly with the moment diagram, by stopping unneeded steel areas somewhere near the points at which they become unneeded. In these days of high-priced reinforcement, such savings can total a considerable sum. The original use of 1/2 in. square bars in contrast with 1-in. square bars was in demonstration of this fact. In the beam with the single 1-in.-square bar, that bar had to run through from end to end of the beam, whereas with the bundled four 1/2-in. square bars only two of them carried through from end to end, and slightly offset longitudinally in the beam, provided as much effective bond area as the 1-in.-square bar offered.

The authors state in their conclusion that "bundling of tension reinforcement in beams will not lead to deterimental consequences as compared to spaced bars for the following conditions: 1. There must not be more than four touching bars in each bundle; 2. Bond stress computed on the basis of external bar perimeter must be limited to the values now permitted for spaced bars . . . "

Strictly limited to their test findings these statements are correct. However, attention should be drawn to the fact that they did not test five or six bars in a bundle and that there is nothing to be found in these tests to indicate or imply that a larger number of bars should not be bundled if that is desirable. The writer has used six No. 10 bars in a bundle, stacked 1-2-3 from top down in one bridge in beams of 9 in. width, and 2-2-2 from top down in a second bridge in beams of the same 9 in. width. No ill-effects have been observed. In the

latter case the two vertical tiers were not in contact with one another but there was considerably less than orthodox spacing between the tiers.

In the writer's mind it has been the long-held and continued concept that if the bars in a large bundle are successively well anchored in the concrete at their ends, so that they can develop their designed stress at these ends, it then matters little how much or how little bond they have between these terminal zones. It is at these end zones that anchorage is indeed vital. The intermediate concrete is simply fireproofing or weatherproofing. With a dozen bars in a bundle, with good plastic concrete and with vibration, the fines of the mortar will penetrate and fill the interstitial spaces of the bundle and afford all needed protection. But the dozen bars must be well anchored at their several ends. About that necessity there must be no misunderstanding.

The writer is particularly pleased to see bundling applied to columns, where it will unquestionably effect marked improvement in economy and quality. The contrasting column cross-sections in Fig. 6 convincingly show this. The authors and whoever else participated in this development are to be congratulated upon its excellence.

AMERICAN SOCIETY OF CIVIL ENGINEERS

Founded November 5, 1852

TRANSACTIONS

Paper No. 3048

ARCH DAMS

A SYMPOSIUM

PAGE

FOREWORD 910

DESIGN AND OBSERVATION IN PORTUGAL
By M. Rocha, F. ASCE; J. Laginha Serafim, F. ASCE; and A. F. da Silveira 911

DEVELOPMENT IN ITALY
By Carlo Semenza, F. ASCE 954

OBSERVED BEHAVIOR IN ITALY
By Dino Tonini, F. ASCE 974

FOREWORD

This symposium presents data concerning the development of arch dams in Portugal and Italy. Model testing and field observations of six Portuguese arch dams have made it possible to obtain fundamental data on the most suitable shapes. A review of the analysis and construction of Italian arch dams is given. The results obtained from the analysis of deflection, strain, temperature, and other measurements on several Italian dams is also offered.

DESIGN AND OBSERVATION IN PORTUGAL

By Manuel Rocha,[1] F. ASCE, J. Laginha Serafim,[2] F. ASCE, and Antonio F. da Silveira[3]

Discussion by Messrs. Robert E. Glover; Fred A. Houck; Manuel Rocha, J. Laginha Serafim, and Antonio F. da Silveira

---

SYNOPSIS

Data are presented on design model testing and field observations of six arch dams ranging in height from 60 m to 135 m. These data have enabled later designs to be modified to gain increased economy with safety. Model studies determined stress conditions at irregularities in foundation and around special structures in the arch.

INTRODUCTION

Notation.—All dimensions are given in the metric system. To convert into the English system, the following should be used: 1 m = 3.2808 ft, 1 cm = 0.3937 in., and 1 mm = 0.03937 in.

The lack of mineral fuel in Portugal has led to a large program of hydroelectric developments beginning in 1946. Many of the rivers that were considered for these developments were characterized by large flows in the winter and very small flows in the summer. Therefore, it was necessary to create large reservoirs by constructing high dams.

Arch dams were constructed where the rivers flow through narrow valleys in which the ratio between the length and the height is less than four. The majority of these sites had rocks of a suitable quality. The undoubted safety and economy of this type of dam contributed largely to its adoption even in the cases in which the site had not appeared too favorable.

The designs of all the dams were based on model studies and detailed observations of their behavior. This factor has made it possible to evaluate the methods for analyzing arch dams and to obtain fundamental data on the most suitable shapes. Thus, whereas the first two arch dams built are of the arch-

---

Note.—Published, essentially as printed here, in June, 1956, in the Journal of the Power Division, as Proceedings Paper 997. Positions and titles given are those in effect when the paper or discussion was approved for publication in Transactions.

[1] Director, Laboratorio Nacional de Engenharia Civil, Lisbon, Portugal.

[2] Head, Dams Studies Section, Laboratorio Nacional de Engenharia Civil, Lisbon, Portugal.

[3] Asst. Research Engr., Laboratorio Nacional de Engenharia Civil, Lisbon, Portugal.

gravity type with a cylindrical upstream face, the latter ones are of the cupola type—that is, with a vertical curvature and varying radius arches.

CHARACTERISTICS AND FOUNDATIONS

This paper describes important studies conducted on the major Portuguese arch dams built since 1946 (Fig. 1). Table 1 lists the principal characteristics of these dams.

In the construction of the dams, use was made of Portuguese cements, similar to Type II of the American Society for Testing Materials (ASTM) standards, and concretes having an aggregate with a maximum dimension of 15 cm.

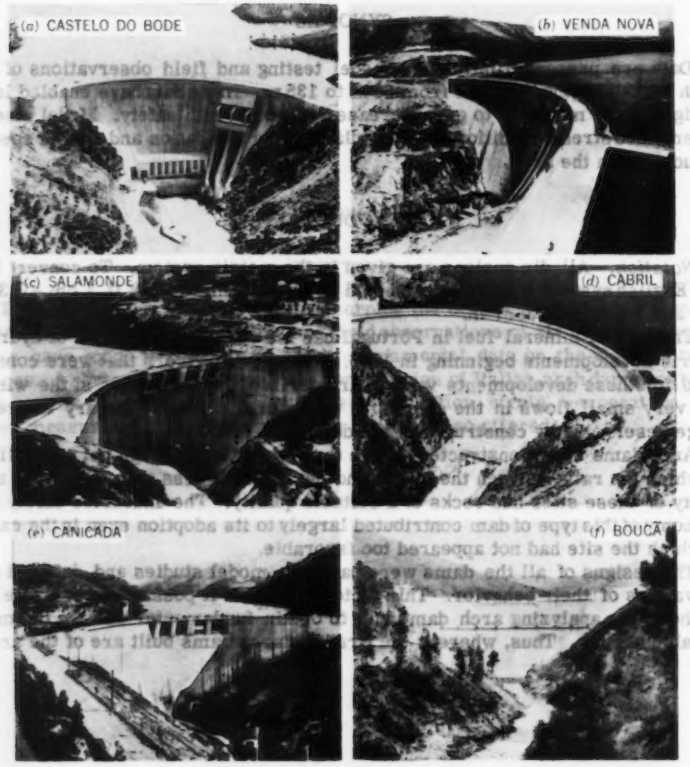


FIG. 1.—MAIN PORTUGUESE ARCH DAMS

The dams were built in separate blocks with a maximum distance between the radial joints of 15 m. Lifts of 1.5 m to 2 m were laid, with an interval between each lift of from 4 days to 5 days. High frequency vibrators were used for compaction. Only in the Castelo do Bode Dam, on the Zêzere River, near Tomar, and in the Cabril Dam, on the Zêzere River, near Coimbra, was cold water and ice used in mixing the concrete. No artificial cooling of the concrete in place was done.

The foundation characteristics were surveyed geologically by borings and galleries. However, in view of the importance of the deformability of the foundation on the behavior of arch dams, the need was recognized for determining these characteristics both by laboratory tests and site tests. The laboratory tests consisted of the determination of the modulus of elasticity of the cores obtained from the various borings and of the prisms from the galleries. The tests on site were carried out on all dam foundations mentioned herein, except for Venda Nova, on the Rabagão River, near Braga. One test method[4] consisted of loading a section of a circular gallery with water under pressure and measuring the diameter variations. The other consisted of loading simultaneously two opposite walls of a section of a gallery by means of jacks and metallic cushions filled with oil to distribute the load on the rock uniformly. These tests were, in many cases, made before and after grouting the rock around the galleries.

TABLE 1.—MAIN PORTUGUESE ARCH DAMS

Name of Dam	Type[a]	Height, in meters	Thickness at the base, in meters	Upstream radius at the crest, in meters	Angle at centre, in degrees	Volume of concrete, in cubic meters	Date of Construction	
							Commencement of laying concrete	Conclusion
(1)	(2)	(3)	(4)	(5)	(6)	(7)	(8)	(9)
Castelo do Bode	AG, c.r.	115	34	150	112°	450,000	Jun. 1948	Aug. 1950
Venda Nova	AG, c.r.	97	33	754.5	95°	220,000	Oct. 1949	May 1951
Salamonde	A, v.r.	75	8	115	100°	93,000	Apr. 1952	Apr. 1953
Cabril	A, v.r.	135	19	155	110°	360,000	Jun. 1952	Dec. 1953
Caniçada	A, v.r.	76	8	105	107°	80,000	Jul. 1953	Aug. 1954
Bouçã	A, v.r.	60	7.5	95	102°50'	35,000	Nov. 1954	Aug. 1955

[a] AG represents arch-gravity; A denotes arch; c.r. represents constant radius; and v.r. denotes variable radius.

Table 2 shows the foundation characteristics of the dams and the values of the moduli of elasticity, E_r, of the rock along the valley, deduced from all the tests performed. It shows also the type and number of tests made.

MODEL TESTS

Present-day designs are based on the values of the stresses produced by the loadings. It therefore becomes necessary, particularly for structures involving great responsibility and cost, to seek methods that produce the value of these stresses with reasonable accuracy.

In 1946, when construction of the large arch dams was begun in Portugal, there was already some experience of model studies obtained from model tests

[4] "Deformability of Foundation Rocks," by M. Rocha, J. L. Serafim, A. F. da Silveira, and J. M. R. Neto, Report 75, 5th International Cong. on Large Dams, Paris, 1955.

TABLE 2.—FOUNDATION

Dam	(a) Location of Samples[a]					
	Right bank				Bottom of the Valey	
	Upper part		Lower part			
	Rock	E_r	Rock	E_r	Rock	E_r
(1)	(2)	(3)	(4)	(5)	(6)	(7)
Castelo do Bode	altered schist	40,000	cristal schist	110,000	cristal schist	110,000
Venda Nova	schist (on top)	40,000	granite	100,000	hard granite	200,000
Salamonde	granite	80,000	hard granite	200,000	hard granite	200,000
Cabril	granite	150,000	hard granite	200,000	hard granite	220,000
Caniçada	granite	100,000	hard granite	200,000	hard granite	200,000
Bouçã	altered schist	20,000	schist	60,000	schist granite	100,000

[a] E_r, in Kg per sq cm.

of the Santa Luzia Dam, on the Pampilhosa River near Coimbra.[5] One criticism that was presented of the then current analytical methods for dam design was that they were either insufficient or very complex. It was concluded that among the existing methods the trial load method was the one that would supply the most reliable results, although its full application—that is, with radial, tangential, and twist adjustments—was laborious and lengthy. In principle, this method takes into consideration the true foundation deformability and can be applied to concrete dams of any shape. However, when the valley is considerably asymmetric or the foundation profile irregular, or the dam has important gravity abutments or large openings such as spillway openings, or when the foundations are heterogeneous, then the number of arches and cantilevers that have to be considered, as well as the number of trials, entail excessive work and time.

In addition, whenever the hypotheses of strength of materials are inadequate, as happens in the fields of stress existing for very irregular shapes, the trial load method by its very nature cannot give satisfactory results.

In any case, this method in its abridged form was applied to all the dams mentioned herein. In the abridged form, only radial adjustment was made of the arch and cantilever displacements. The comparisons that were made between the results obtained by this abridged method and the results from models and observations[6] led to the conclusion that the abridged method can be used

[5] "Model Tests of Santa Luzia Dam," by M. Rocha and J. L. Serafim, 3d International Cong. on Large Dams, Communication 5, Stockholm, 1948.

[6] "Model Tests, Analysis, and Observations of an Arch Dam," by M. Rocha, J. L. Serafim, A. F. da Silveira, and J. M. R. Neto, Transactions, ASCE, Vol. 122, 1957, pp. 903-949.

CHARACTERISTICS

Left bank				(b) Location of Test		
Lower part		Upper part		Laboratory		
Rock	E_r	Rock	E_r	Number of cores	Number of prisms	Site
(8)	(9)	(10)	(11)	(12)	(13)	(14)
cristal schist	110,000	hard cristal schist	200,000	41	12	1 Shaft with water
hard granite	200,000	altered granite (on top)	50,000	73	10	. . .
granite	80,000	altered granite	20,000	30	11	5 galleries with jacks, 2 with water
hard granite	200,000	granite	70,000 and 150,000 (upper)	78	16	5 galleries with jacks
hard granite	150,000	altered granite	50,000	55	6	2 galleries with jacks
granite	100,000	altered granite	20,000	78	34	2 galleries with jacks

only for an estimate of the stresses in a preliminary design. As a rule, in the case of regular shapes, the stresses determined in the arches by this method are from 10% to 20% greater than those obtained from the models, whereas at the base cantilevers the stresses determined by the abridged method are much greater than those obtained from the models. It should also be noted that the maximum arch compressive stresses given by computation and by the models, when of the same magnitude, are not found at the same points. The computed radial displacements are also from 10% to 20% greater than those determined from the models.

These results led to the use of model tests as the basis for the design of the Portuguese dams. The improvement in testing techniques not only made it possible to be confident of the experimental results but also to reduce the time of testing, which is now less than that needed for the use of the abridged trial load method. Thus, for the majority of the dams, the final design was based on successive studies of models in which the shapes were progressively improved. These studies were begun as soon as the preliminary design of the structure had been made. The test techniques used at present have been described elsewhere.[6,7] Table 3 shows the number and characteristics of the models, the duration of the tests, and the cost of the model tests. As indicated in Table 2, it is the practice to test at least two equal models simultaneously for each shape of dam analyzed. By this method, the reliability of the results is increased and the accuracy is improved by taking the mean values of the two models.

7 "Analysis of Concrete Dams by Model Tests," by M. Rocha and J. L. Serafim, 5th International Cong. on Large Dams, Communication 36, Paris, 1955.

In model studies, as in computations, it is assumed that the dam is a homogeneous, isotropic, elastic, and continuous solid supported on an elastic foundation.

The models were usually analyzed for hydrostatic pressure only, but in some cases the stresses due to the weight of some parts of the structure itself were also determined. Usually, the stresses due to this loading were computed by assuming that the dam was built in separate blocks. The effects of the remaining loadings, such as temperature, earthquakes, and uplift, were computed analytically and added to the stresses due to hydrostatic pressure. It should be noted that the stresses due to hydrostatic pressure were ordinarily much greater than the stresses due to a combination of the other loadings.

TABLE 3.—ARCH DAM MODELS

Dam	Studies carried out	Number of models tested	Scale of the models	Material of the model and loading system[b]	Duration of the tests, in months	Cost of the tests, in dollars
(1)	(2)	(3)	(4)	(5)	(6)	(7)
Castelo do Bode	Study I	1	1/ 75	Pd M	8	4,800
	Study II	4	1/500	Pd J	4	
Venda Nova	Study I	1	1/100	Pd M	8	6,000
	Study II	2	1/300	Pd J	4	
	Study III	2	1/ 30	Pd J	3	
Salamonde	Study I	2	1/200	Pd M	6	7,200
	Study II	2	1/200	Pd M	4	
	Study III	2	1/200	Pd M	4	
	Study IV	2[a]	1/200	Pd M	4	
Cabril	Study I	2	1/300	Pd M	6	7,800
	Study II	2	1/300	Pd M	4	
	Study III	2	1/300	Pd M	4	
	Study IV	1	1/400	A M	6	
	Study V	1	1/400	A M	3	
Caniçada	Study I	2	1/200	Pd M	6	4,200
	Study II	2	1/200	Pd M		
Bouçã	Study I	3	1/200	Pd M	6	3,000

[a] A Marco model was also built (scale 1/250). [b] Pd represents the mixture of plaster of Paris and diatomite; A denotes Alkathene; M represents mercury contained in a rubber bag; and J denotes the use of a set of jacks.

The stresses in the models were determined by electrical strain gages, the SR-4 Baldwin types A-7 and A-8 being most often used. Before obtaining the stresses, however, the isostatics of the two faces were determined with brittle lacquers. Radial, tangential, and vertical displacements were also measured.

The measurements were determined for various water levels in the reservoir, which was particularly important for comparing them with the prototype observations. This shows another advantage of the models in comparison to the computation methods.

Recently, a supplementary experimental method was investigated in the search for the best shapes for arch dams. It consisted of determining the

shapes taken by a rubber membrane fixed across a valley and loaded from downstream with water and with upward forces proportional to the weight of the concrete.[8]

OBSERVATIONS

The observation of dams both during and after construction has two objectives, the control of safety and the investigation of its behavior. Observation yields a check of the methods used in design, whether analytical or experimental, and also provides a basis for judging the building methods that were used.

For observations to be of value, the equipment must be chosen carefully and the work of installing and reading the instruments and computing and interpreting the results must be performed by teams of fully-trained specialists. Supporting these specialists is a laboratory in which the various tests, both of the instruments and of the materials of the dam, can be made.

However, in comparing the results of observations of a structure with the results of model tests, a difficulty arises from the fact that the prototype is subject to many actions that are not easily reproducible in the model. Such actions may be temperature variations, either from external changes or from dissipation of the heat of hydration of the cement, the inelasticity of the concrete and rock, foundation settlements, and movement of the reservoir banks.

The Laboratorio Nacional de Engenharia Civil (L.N.E.C.) conducts[9,10] all of the observation work in which other government departments and the owners of the dams take part. An elaborate plan for observation is drawn up by the L.N.E.C., which also maintains a team on the site for the placing and reading of the apparatus. The readings are sent regularly to the laboratory where they are combined with laboratory test results. This information is then plotted and evaluated.

Observations made of the dams included the absolute displacements of points of the dam and corresponding points on the ground as determined by geodetic and alinement methods.[11] Also included were vertical displacements as found by precision leveling at the crest of the dam and at points on the rock located downstream,[12] the relative displacements determined by pendulums,[13] the rotations measured with clinometers, and the joint movements, found inside by using joint meters and outside with the use of extensometers.[14]

The temperature of the air, concrete and reservoir water was measured by thermo-electric couples, and the strains were determined by means of strain meters.[15] The compressive stresses were measured by stress-meters, the

---

8 "Principios orientadores do projecto de barragens abobada," by J. F. L. Fialho, Publicacao No. 65, Laboratorio Nacional de Engenharia Civil, Lisbon, 1955.

9 "The Observation of the Behaviour of the Portuguese Concrete Dams," by M. Rocha, J. L. Serafim, A. F. da Silveira, and O. V. Rodrigues, 5th International Cong. on Large Dams, Communication 33, Paris, 1955.

10 "Observation of Dams: Methods and Apparatus Used in Portugal," by M. Rocha, J. L. Serafim, and A. F. da Silveira, RILEM Symposium on the Observation of Structures, Lisbon, 1955.

11 "Mesure des déplacements absolus des grands barrages portugais," by O. V. Rodrigues, RILEM Symposium on the Observation of Structures, Lisbon, 1955.

12 "Sur l'emploi de nivellements géometriques de précision dams l'observation d'ouvrages," by A. Ferrer de Lemos, ibid.

13 "Observation of Dam Displacements by Means of Pendulums," by A. F. da Silveira, ibid.

14 "Observation of Joint Movements in Dams," by A. F. da Silveira, ibid.

15 "Measurement of Strains in Portuguese Concrete Dams," by J. L. Serafim, ibid.

TABLE 4.—APPARATUS

Dam	(a) Displacements by geodetic method					(b) Displacements by pendulum method		
	Theodolite stations	Sighting marks	Check points	Alinements	Leveling points	Plumb-wires	Coordinometer bases	Coordinometer-Clinometer bases
(1)	(2)	(3)	(4)	(5)	(6)	(7)	(8)	(9)
Castelo do Bode	4	17	4	4	25	3	...	20
Venda Nova	3	18	5	...	15	3	...	...
Salamonde	4	14	4	6	10	1	...	6
Cabril	4	19	5	3	21	2	...	6
Caniçada	4	14	4	6	10	1	...	6
Bouçã	4	14	5	6	10	...	...	...

[a] Telemac meter. [b] Galileo meter. [c] Carlson meter.

neutral pressures by pore pressure cells, humidity was determined by humidity-measuring instruments, and the pressure tubes equipped with manometers were used to determine the uplift pressures. Table 4 gives the apparatus used in each of the arch dams referred to herein.

THE CASTELO do BODE DAM

The Castelo do Bode Dam (Figs. 1(a), 2, and Table 1) presents some important physical features. The right bank is a deformable promontory which, in the upper part, supports a large artificial abutment. Although it is approximately symmetrical, the dam has two flood spillway openings of 15 m × 12 m. Above these openings the dam was thickened to transmit the forces from one side of the opening to the other more effectively. The design of the dam included radial adjustments between 4 arches and 3 cantilevers.

Model studies were undertaken to determine the general field of stresses, the most suitable dimensions for the thickening of the dam in the neighborhood of the spillway openings and the dimensions of the artificial abutment. The first model was built (Table 3) to a scale of 1 to 75 and contained the various mechanical properties of the foundation. The failure of this model, which occured during the third test load, indicated the advisability of increasing the dimensions of the artificial abutment.

To expedite the construction and drying, four smaller models were later built to a scale of 1 to 500. These models were loaded with a system of 26 hydraulic jacks of different diameters.

PLACED IN DAMS

(b) Other Observations

Clinometer bases	Strain-meters	Stress-meters[c]	Resistance thermometers	Thermo-electric couples	Uplift points	Pressure meters[c]	Joint movements		Moisture content meters	Length of cables, in meters
							Detachable gages	Joint-meters		
(10)	(11)	(12)	(13)	(14)	(15)	(16)	(17)	(18)	(19)	(20)
3	164[a]	...	71	44	...	...	151	...	...	15,000
3	181[a]	...	80	53	...	...	55	...	...	8,000
14	140[b]	...	...	50	...	...	43	21[b]	...	3,000
14	189[c]	...	...	50	12	...	100	55[c]	6	7,000
14	184[c]	6	...	26	...	6	50	21[c]	6	6,000
10	179[c]	9	...	33	...	6	50	49[c]	6	11,500

The results of the tests (Fig. 3) showed that in the spillway area the directions of the principal stresses were diverted by the openings made in the dam. The compressive stresses due to hydrostatic pressure did not exceed 45 kg per sq cm on the upstream face or 28 kg per sq cm on the downstream face. For these regions the computations gave maximum horizontal stresses in the arches, of 42 kg per sq cm and 43 kg per sq cm, respectively. The maximum tensile stresses observed in the heel of the dam for the hydrostatic pressure were 21 kg per sq cm.

For points in the upstream face of the dam base, Fig. 3 also gives the sum of the stresses due to the hydrostatic pressure and those due to the weight of the dam itself, the latter having been computed analytically. The tensile stresses in the upstream face of the dam base, due to hydrostatic pressure are almost completely annuled, as are the tensile stresses in the base of the abutment of the right bank.

It was concluded that the spillway openings, despite their large dimensions, only influence the stresses of the dam locally, the continuity being assured by the arch passing above these openings. The thickness of this arch should have been reduced, because in view of its rigidity, the stresses developed in the neighborhood of the arch were high.

The model tests also made it possible to design the reinforcement, to be placed inside the vertical walls of the openings, needed for the support of the high tensile stresses which are developed there.[7]

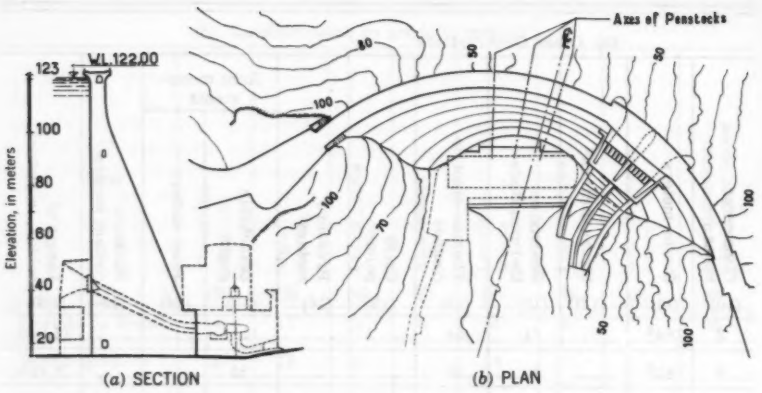


FIG. 2.—CASTELO DO BODE DAM, PLAN AND SECTION

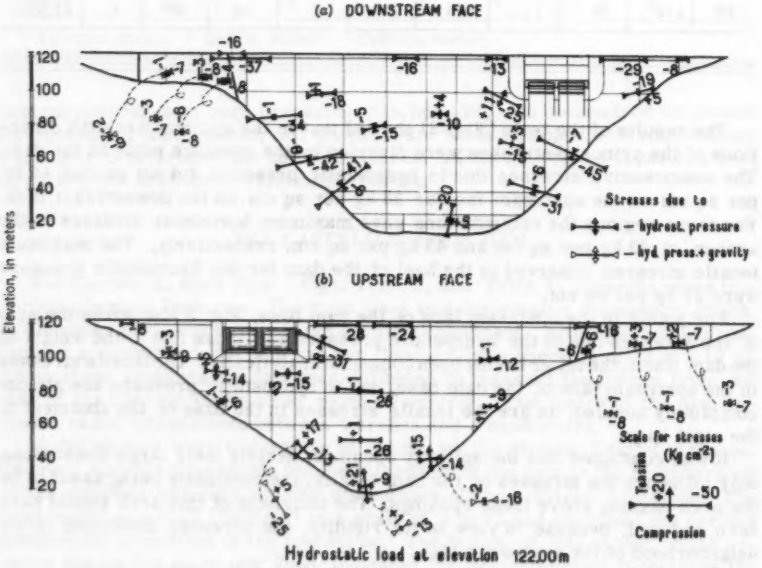


FIG. 3.—CASTELO DO BODE DAM, STRESSES FROM MODEL STUDIES

Geodetic observations of the dam displacements (Fig. 4) show a movement of the whole dam toward the right bank and important movements of the abutment that reached a value of 2 cm. These displacements are a result of hydrostatic pressure on the actual promontory supporting the dam and also of the low modulus of elasticity of the rock in this region (approximately 40,000 kg per sq cm). However, because the displacements are asymptotic with time, it can be concluded that the structure is safe.

It was noted that the displacements observed in the upper part of the dam are greatly influenced by air temperature variations.

Typical results of observations made with strain meters are shown in Fig. 5. The strain meters were arranged in 45° rosettes of four meters each[16] and placed 1 m from the upstream and downstream faces.

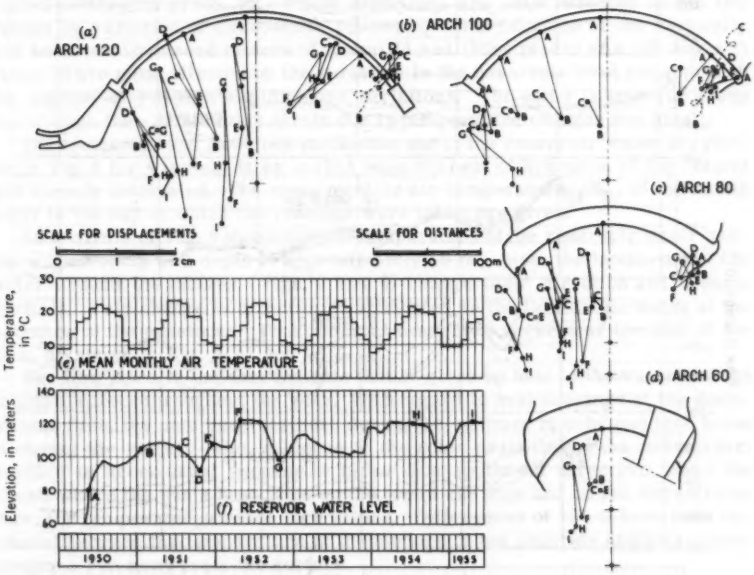


FIG. 4.—CASTELO DO BODE DAM, HORIZONTAL DISPLACEMENTS

The analysis of the curves in Fig. 5 shows a considerable difference in their development. The curves of the downstream groups 2d and 3d (Fig. 5(f) and (h) respectively) accompany the air temperature variations showing compression with a rise in temperature. The curves of groups 1u, 2u, and 3u (Fig. 5 (c), (e), and (g) respectively) placed 1 m from the upstream face, and the group 1d, (Fig. 5(d)) which is protected by the powerhouse, show little influence of temperature variations.

During 1949, group 1u registered a continuous increase of negative strains due to the weight increase occurring during construction. At the end of the

[16] Discussion by J. L. Serafim of "The Development of Stresses in Shasta Dam," by J. M. Raphael, Transactions, ASCE, Vol. 118, 1953, pp. 311-313.

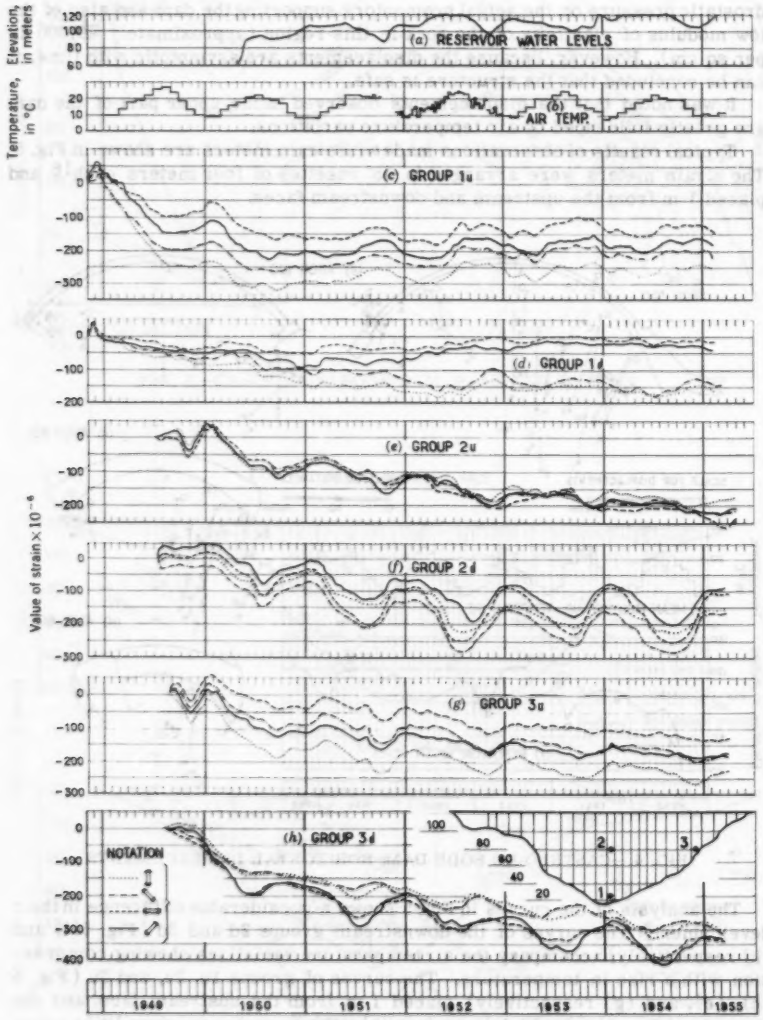


FIG. 5.—CASTELO DO BODE DAM, CORRECTED OBSERVED STRAINS

year there was a reduction of the compression due to the temperature decrease and then a further increase in negative strain due to temperature rise. After the reservoir had been filled, the effect of air temperature variations was no longer apparent in the behavior of the diagrams and the strain meters registered only slight effects due to water level variations and the general cooling of the dam.

Group 1d never registered large strain variations but the effect of the reservoir level variations was noticeable, principally in the results from the vertical meter.

The effect of the annual air temperature cycle is recorded without any appreciable time lag in groups 2d and 3d. The temperature cycle produced a state of hydrostatic stress as shown by the parallel development of the diagrams of the diagonally-placed meters in group 2d and of the vertically and horizontally-placed meters in group 3d. These directions are least affected in the two groups by variation of hydrostatic pressure. The diagrams of the vertically and horizontally placed meters of group 2d and those placed at a 45° angle in group 3d are most affected by the variation in the reservoir level and approach one another and separate with those variations. The same is true for group 3u although the variations in strain due to temperature changes are small.

The isotherms and flowlines in the dam and in the reservoir water are plotted in Fig. 6 for 4 typical dates in 1954 when the heat of hydration of the cement had already dissipated. The mean monthly air temperatures, T_A, of the month prior to the day in which the readings were taken are given.

An analysis of Fig. 6 shows that the temperature of the reservoir water varies considerably to a depth of approximately 50 m. Also, the isotherms of the water around the intakes (Figs. 2 and 6) change their direction and became vertical. This change in direction is attributed to the flow of the water at the entrance to the penstocks. Thus, unusual heat flows occur near the heel of the dam, as shown in Fig. 6(c) and (d).

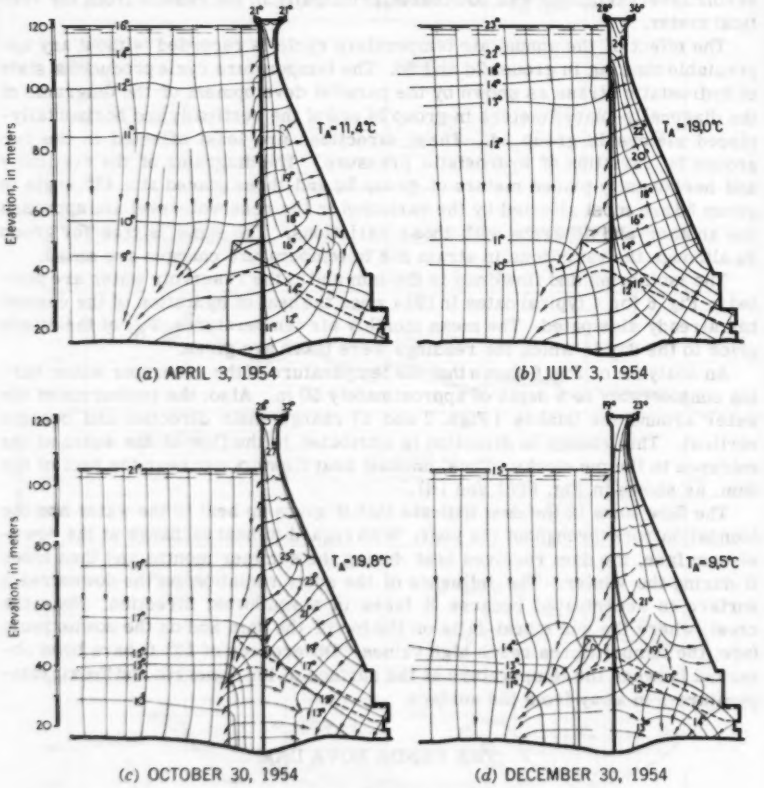
The flow lines in the dam indicate that it gives up heat to the water and the foundation rock throughout the year. With regard to heat exchange at the downstream face, the dam receives heat during the summer months and then loses it during the winter. The influence of the solar radiation on the downstream surface is accentuated because it faces in a southwest direction. Near the crest, where the sun's heat falls on the top of the dam and on the downstream face, the temperatures reach high values. Differences of 12° C have been observed between the temperature at the surface of the concrete and the air temperature 1 m away from the surface.

THE VENDA NOVA DAM

The Venda Nova Dam (Fig. 1(b)) is similar to the Castelo do Bode Dam except that the lower part of the valley is narrower for the Venda Nova Dam. It has a lateral spillway for which it was necessary to leave two 8 m × 6 m openings in the structure. The dam was computed by the abridged trial load method with 4 arches and 3 cantilivers.

The first model (Study I) had a projecting rock in the lower upstream left bank, which is represented by the broken line in Fig. 7(a). A tension of 43 kg per sq cm due to hydrostatic pressure was measured in this region on the model, and after superimposing the weight of the dam, a stress of 32 kg per sq cm still

remained. For this reason, the canyon profile was made more regular by removing the projecting rock and Study II was carried out, in which tensile stresses of 15 kg per sq cm were derived for the combined effect of hydrostatic pressure and weight. The studies on the models were begun after construction was already in progress and therefore it was not possible to make large modifications in the design with the foundation opened up. Therefore, it was decided to make a joint ending in a gallery in the upstream face, as shown in Fig. 7(b).



(a) APRIL 3, 1954 (b) JULY 3, 1954

(c) OCTOBER 30, 1954 (d) DECEMBER 30, 1954

FIG. 6.—CASTELO DO BODE DAM, ISOTHERMS AND FLOW LINES

The purpose of this joint was to prevent the dam from cracking and endangering its watertightness. Once the joint opens, the stresses due to the weight of the dam compensate for the tensile stresses due to the hydrostatic pressure at the inside end of the joint. In models of this solution (Study III) the stresses at the bottom of this joint and at various points on the two faces of the dam were determined. The tensile stresses in the middle region were annuled by the joint but near the ends of the joint there were still tensions with values of 13 kg per sq cm for the combined effect of hydrostatic pressure and the weight.

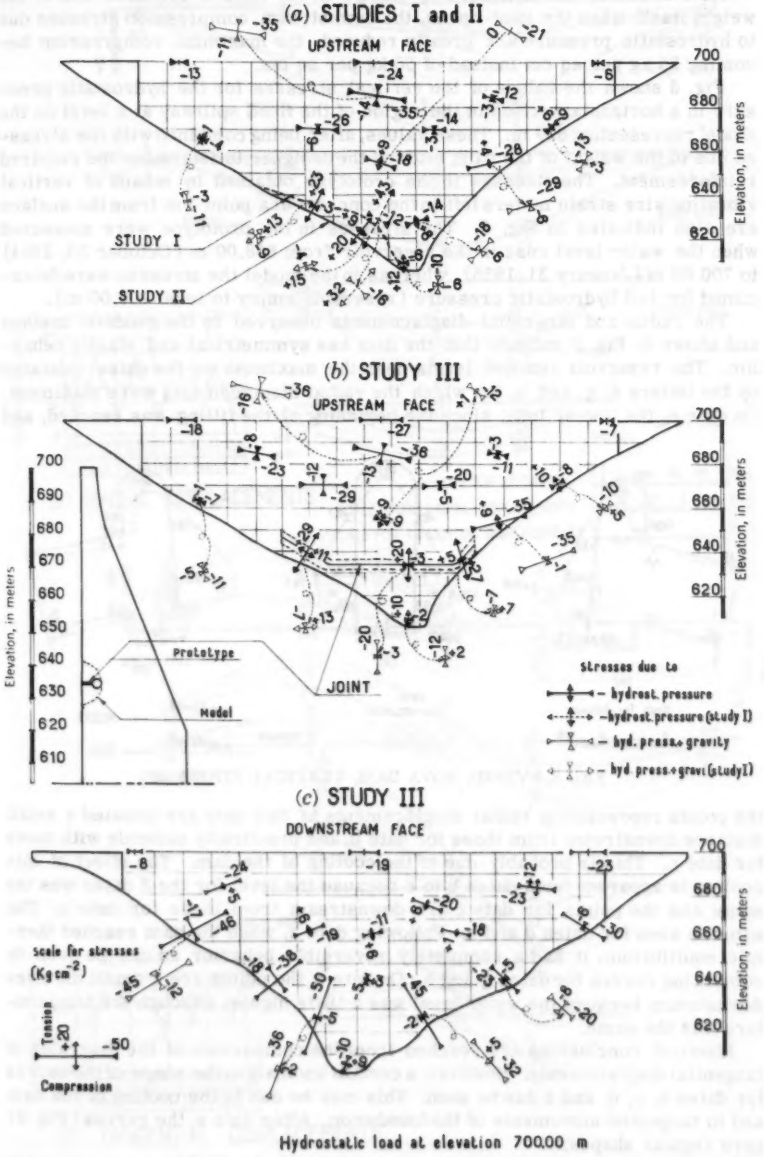


FIG. 7.—VENDA NOVA DAM, STRESSES FROM MODEL STUDIES

As a result of the considerable change in the field of stresses due to the weight itself when the joint opens, the downstream compression stresses due to hydrostatic pressure are greatly reduced, the maximum compression becoming 36 kg per sq cm instead of 50 kg per sq cm.

Fig. 8 shows the values of the vertical stresses for the hydrostatic pressure in a horizontal section in the region of the flood spillway at a level on the model representing 690 m. These values, after being combined with the stresses due to the weight of the dam, enabled the designer to determine the required reinforcement. The stresses in the prototype obtained by means of vertical vibrating wire strain meters left in the concrete at a point 1 m from the surface are also indicated in Fig. 8. The stresses in the prototype were measured when the water level rose in the reservoir from 668.00 m (October 30, 1954) to 700.00 m (January 31, 1955), whereas in the model the stresses were determined for full hydrostatic pressure (reservoir empty to level 700.00 m).

The radial and tangential displacements observed by the geodetic method and shown in Fig. 9 indicate that the dam has symmetrical and elastic behavior. The reservoir reached levels near the maximum on the dates indicated by the letters d, g, and h, for which the radial displacements were maximum. On date e, the lowest level since the beginning of the filling was reached, and

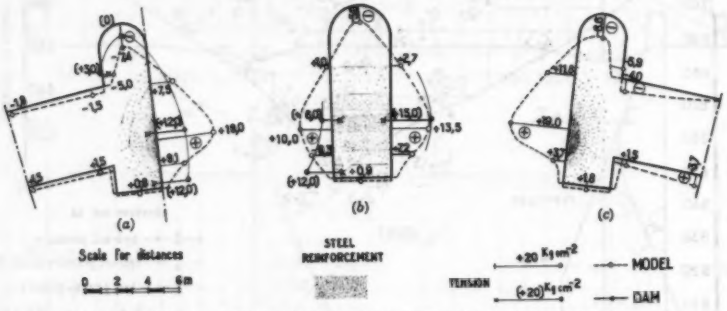


FIG. 8.—VENDA NOVA DAM, VERTICAL STRESSES

the points representing radial displacements at this date are situated a small distance downstream from those for date b, and practically coincide with those for date c. This is probably due to the cooling of the dam. The effect of this cooling is apparent from dates b to c because the level for the 2 dates was the same and the points for date c are downstream from those for date b. The same is seen for dates d and h. Following date e, when the dam reached thermic equilibrium, it had a completely reversible behavior as can be seen by comparing curves for dates g and h. On date h, the points are a small distance downstream because the water level was a little higher, although the temperature was the same.

Identical conclusions are reached from the comparison of the diagrams of tangential displacements. However, a certain anomaly in the shape of the curves for dates b, c, d, and e can be seen. This may be due to the cooling of the dam and to tangential movements of the foundation. After date e, the curves (Fig. 9) have regular shapes.

The radial displacements given by the model (Fig. 9(a)) are considerably smaller than those measured in the prototype. The apparent agreement at levels representing 700 m and 680 m results because the initial measuring date

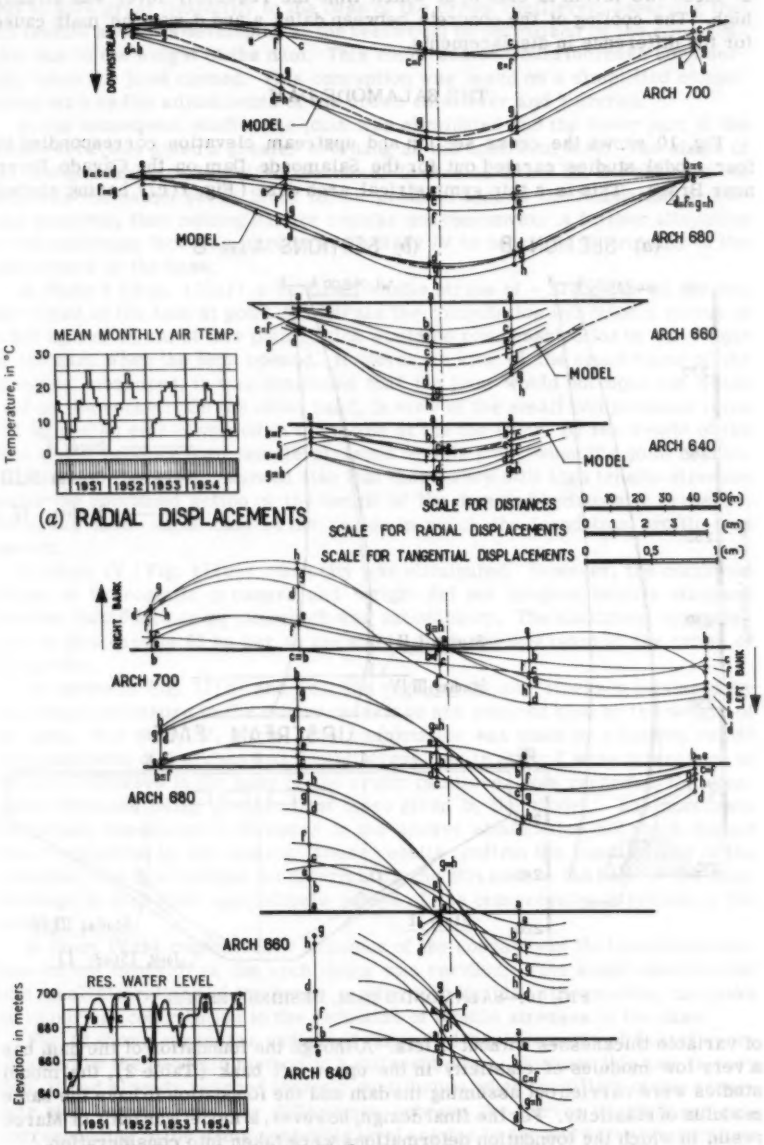


FIG. 9.—VENDA NOVA DAM, HORIZONTAL DISPLACEMENTS OF THE ARCHES

at these two levels is date b, at which time the reservoir level was already high. The cooling of the concrete between dates a and d was the main cause for the difference in displacements.

THE SALAMODE DAM

Fig. 10 shows the cross section and upstream elevation corresponding to four model studies carried out for the Salamonde Dam on the Cávado River near Braga. This is a thin symmetrical arch dam (Fig. 1(c)) having arches

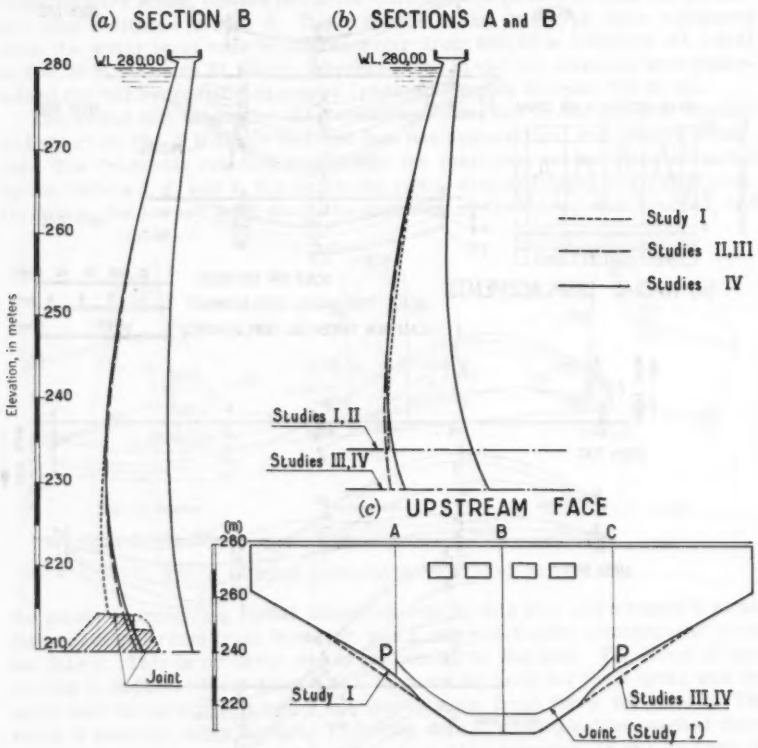


FIG. 10.—SALAMONDE DAM, DESIGNS TESTED

of variable thicknesses without fillets. Although the foundation of the dam has a very low modulus of elasticity in the upper left bank (Table 2), the model studies were carried out assuming the dam and the foundation to have the same modulus of elasticity. For the final design, however, a model was built of Marco resin, in which the foundation deformations were taken into consideration.

In the first preliminary design (Study I), a reduction of the cross section at the heel and the construction of a socket to support the dam was utilized (Fig. 10). The joint between the socket and the dam was closed by copper sheets and a gallery was left inside for the inspection of the joint. The plan

was to give great flexibility to the base of the crown cantilever, assuming that the tensile stresses developing at the heel would be nutralized by the compression due to the weight of the dam. This compression would increase considerably when the joint opened. This conception was based on a simplified computation with radial adjustments of the crown cantilever and 7 arches.

In the subsequent studies the joint was eliminated and the lower part of the cantilevers was given a greater overhang at the upstream face. The shape of the downstream face remained the same. In Studies II and III, the shape of the dam was the same, but in Study III the protuberance of the foundation profile was removed, thus making it more regular and nonconvex. A further alteration to the upstream face was introduced in Study IV to decrease the rigidity of the cantilevers at the base.

In Study I (Fig. 11(a)) a vertical tensile stress of + 32 kg per sq cm was developed in the heel at point A, whereas the computation indicated a stress of + 200 kg per sq cm at this point, which would be compensated for by the weight of the dam when the joint opened. However, in view of the small value of the stresses measured, it was concluded that the joint would not open but would rest on the socket. On the other hand, in view of the small compression value (11 kg per sq cm) observed in the model at the toe (point B) the weight of the dam would produce high tensile stresses at this point when the joint opened.

Study II (Fig. 11(b)) showed also that there were still high tensile stresses under the combined action of the weight of the dam and hydrostatic pressure. This was most significant in the region in which the foundation profile was convex.

In Study IV (Fig. 11(c)) convexity was eliminated. However, the combined action of hydrostatic pressure and weight did not produce tensile stresses greater than 6 kg per sq cm, which was satisfactory. The maximum compression in this case is 61 kg per sq cm and is produced upstream at the crown of the arches.

As shown in Fig. 11(b) and (c), the vertical tensile stresses produced by hydrostatic pressure in the downstream face are reduced also by the weight of the dam. For Study IV, a trial load computation was made by adjusting radial displacements of 5 arches and 7 cantilevers. As in Study I, wide divergence of vertical stresses in the base of the crown cantilever was recorded, the computed stresses being greater than those given by the model. The maximum horizontal compressive stresses in the arches attain value not much higher than those given by the models. These results confirm the insufficiency of the abridged trial load method for determining the stresses in the base of the dam, although it does give approximate values of the compressive stresses in the arches.

In Study IV the considerable influence of the convexity of the foundation surface on the behavior of the arch dams was verified. This study showed also how small alterations of thickness, easily reproducible in the models, can make an important contribution to the reduction of tensile stresses in the base.

Fig. 12 shows curves for radial and tangential displacements of 5 cantilevers obtained by the geodetic method on 5 different dates. Because this dam is very thin, it had already reached thermic equilibrium when the filling of the reservoir was begun. Thus, the differences between the curves of displacements corresponding to the same reservoir level are due to air and water temperature variations.

An analysis of the radial displacement diagrams (Fig. 12(a)) shows that with the first water rise, dates A to B, the dam underwent downstream displacements except for the points in the crest. These points moved upstream

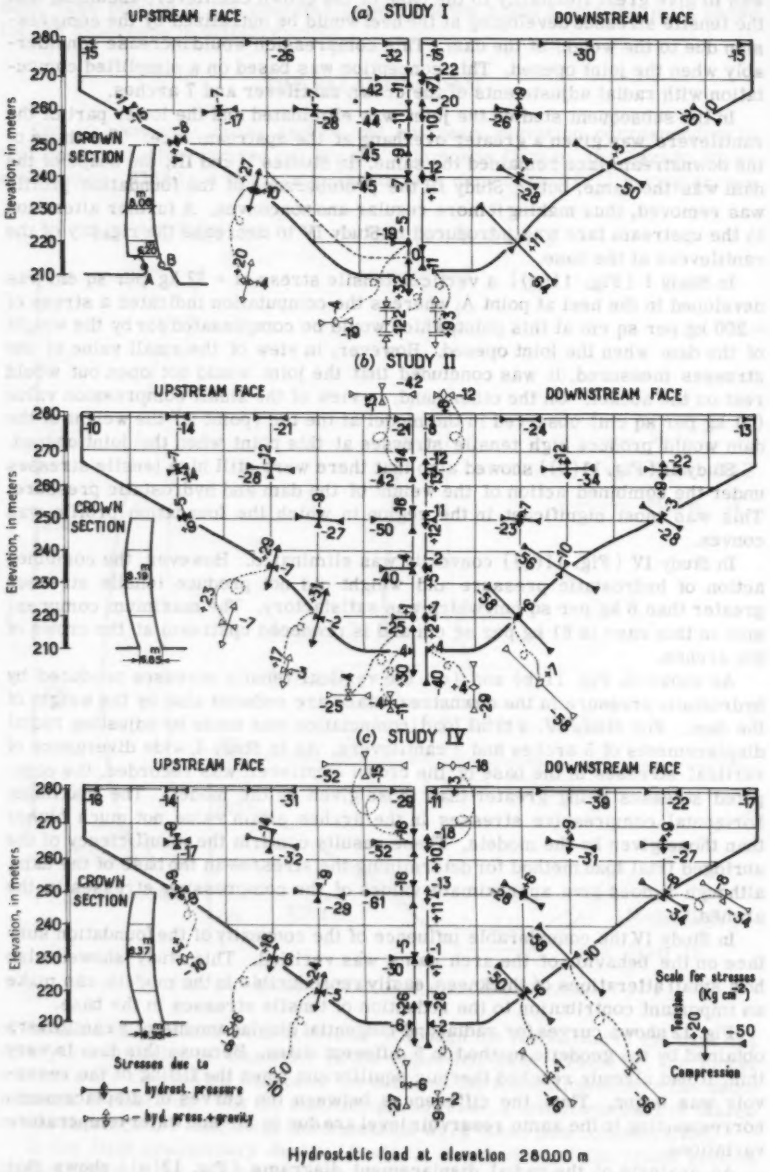


FIG. 11.—SALAMONDE DAM, STRESSES FROM MODEL STUDIES

because of the rise of air temperature. This has an immediate effect, because the crest is only 2 m wide. On dates B and C, with the water practically at the same level, there was a large fall in temperature that caused a considerable downstream displacement. When the water level reached its maximum (dates D and F), the dam experienced its greatest downstream displacements, although the points of date F were slightly below those of date D. Because the concrete

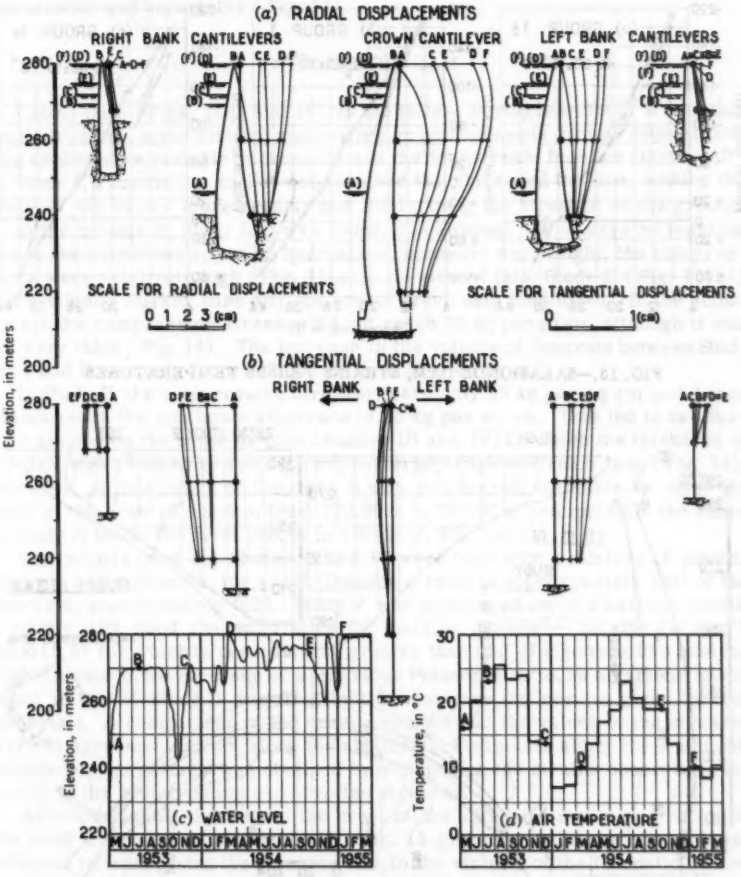


FIG. 12.—SALAMONDE DAM, HORIZONTAL DISPLACEMENTS OF THE CANTILEVERS

temperatures observed on dates D and F are equal, the displacement between these dates is probably due to foundation movement.

Fig. 12(b) shows that during the first loading of the dam, between dates A and B, there was a displacement toward the right bank. This was probably due to the settling of the bank. Subsequently, the behavior of the dam has been almost symmetrical.

In Fig. 13 the curves are plotted of the concrete length changes registered by three no-stress strain meters in the dam as a function of temperature. The three no-stress meters serve three groups of strain meters placed in the base of the crown cantilever, one at 1 m from the upstream face (Fig. 13(c)), another at a point halfway through the dam[4] (Fig. 13(b)), and the third at 1 m from the downstream face (Fig. 1(a)). The concrete in the region where the

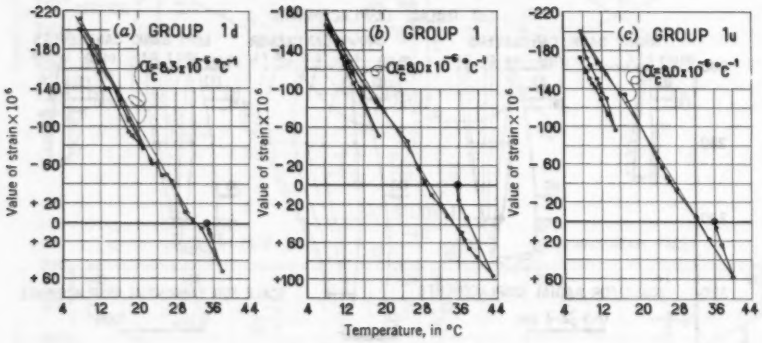


FIG. 13.—SALAMONDE DAM, STRAINS VERSUS TEMPERATURES

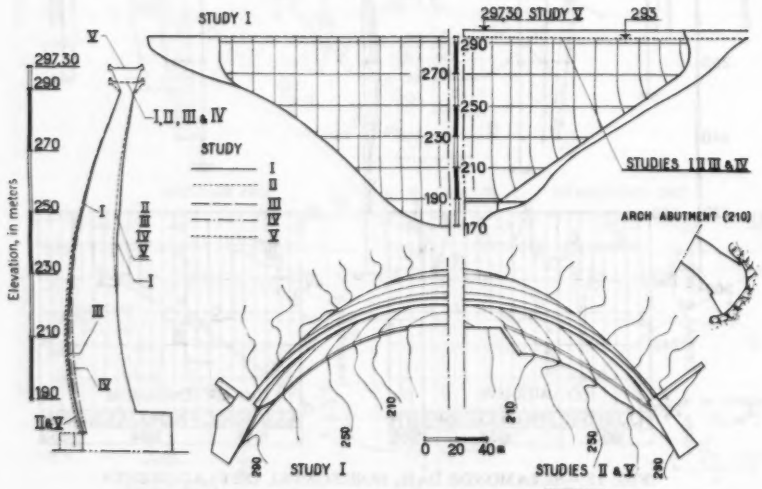


FIG. 14.—CABRIL DAM, STUDIES TESTED

no-stress meters were placed was laid at approximately 20° C and it reached a maximum temperature of 43° C at the center of the block. When the temperature reached 36° C, the measurement of length changes in the concrete began, Once the temperature began to fall, the length decreased at the rate shown in

the longer branch of the curves in Fig. 13(b) and 13(c). This branch has a different angular coefficient from the first one, that corresponds to the temperature rise. The minimum temperature of approximately 8° C and the minimum length were reached. There were two further temperature cycles, which are represented in the two further branches of the curves.

The coefficients of thermal expansion corresponding to the branches representing the greatest temperature falls were computed, and the values obtained are similar and acceptable (Fig. 13).

THE CABRIL DAM

Cabril Dam (Figs. 1(d) and 14), is the tallest Portuguese dam. It is a thin arch structure, symmetrical, and resting on homogeneous granite foundations. The arches have variable thicknesses and the downstream face has fillets. After Study I, a foundation socket was designed that thickened the dam, making the shape of the valley more regular and diminishing the stresses on the ground.

In the models of Study I, it was found that although there were no tensions due to the combined action of hydrostatic pressure and weight, the compressions were relatively high (Fig. 15(a)). In view of this, Study II (Fig. 15(b)) had a slightly thicker base and the socket previously mentioned. In the actual socket the compression stresses did not reach 30 kg per sq cm, although it was not very thick (Fig. 14). The increase in the volume of concrete between Studies I and II was only from 348,000 cu m to 354,000 cu m.

In Study II the compressive stresses were only 53 kg per sq cm and hence did not reach the maximum allowance of 65 kg per sq cm. This led to two further studies on the same models (Studies III and IV) in which the thickness of the dam was reduced by cutting away material at the upstream face (Fig. 14). However, at this stage of the tests it was considered advisable to raise the level of the crest of the dam from 293.00 m to 297.30 m and maintain the shape of Study II below the level 290.00 m (Study V, Fig. 15(c)).

The models used for Studies II and IV were built with a mixture of plaster of paris and diatomite, for which Poisson's ratio is approximately that of the concrete, approximately 0.20. Study V was performed on an alkathene model, a plastic with good characteristics for building models[6,7] but the Poisson's ratio (0.5) for which is considerably greater than that of concrete. To analyze the influence in the stresses of a high value Poisson's ratio, an alkathene model equal to that of Study II was first built to compare the results given by both materials. A comparison of the results showed that the values of the stresses were in agreement except along the abutment. For points along the abutment, satisfactory agreement was obtained by transposing the strains observed in the model to the prototype instead of to the stresses.

After concluding these thest the crest of the alkathene model was raised to the level corresponding to Study V. Fig. 15 gives the values of the stresses obtained by transposing the stresses and, in the vicinity of the foundation, those obtained by transposing the strains and computing the stresses in the prototype by means of its elastic constants E and ν. The maximum compressions did not exceed 65 kg per sq cm and there were practically no tensile stresses from the combined action of hydrostatic pressure and weight, both in the heel of the dam and in the downstream upper part of the crown cantilever. This is due to the upstream overhang in the lower region and downstream overhang in the upper region.

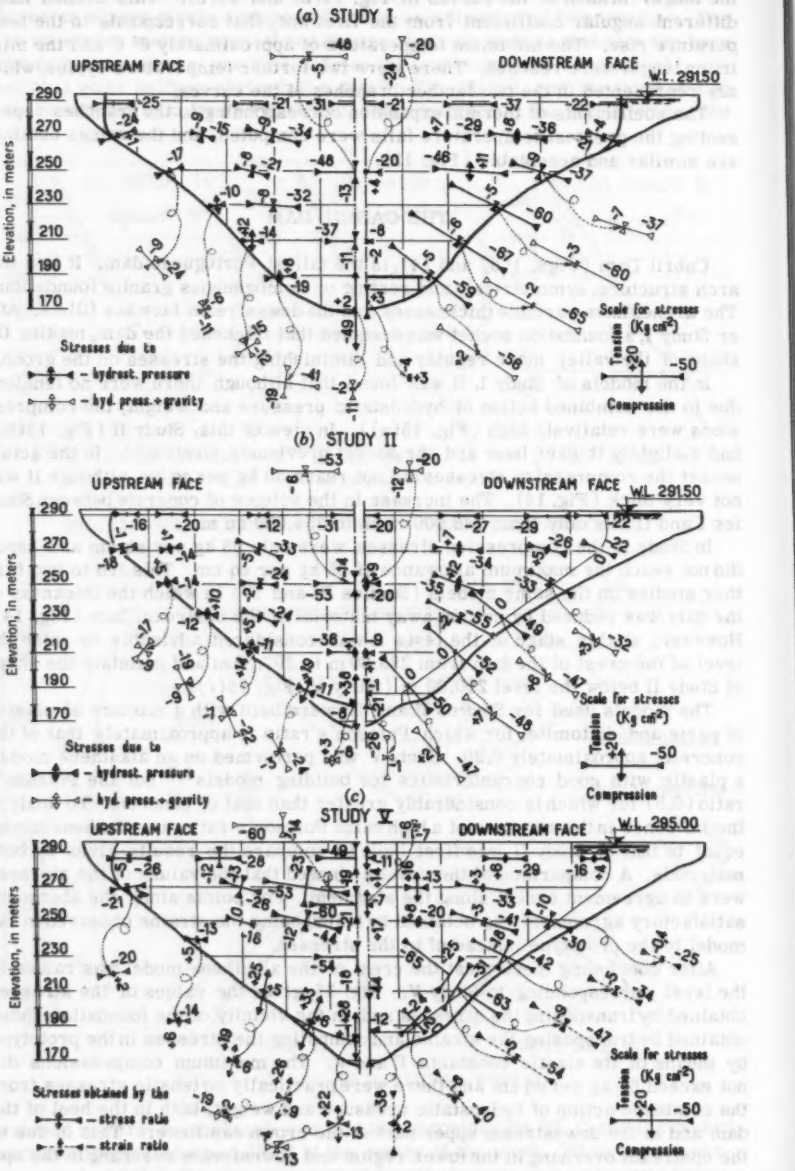


FIG. 15.—CABRIL DAM, STRESSES FROM MODEL STUDIES

The radial and tangential displacements as well as the rotations also were measured in the models. For Study I, in addition to making one computation with only radial adjustments for 6 arches and 9 cantilevers, a complete trial load analysis was made with radial, tangential and twist adjustments for 3 arches and 5 cantilevers. The results of the first computation gave maximum compressions in the arches similar to those given by the model, and stresses in the bases of the cantilevers and radial displacements greater than those given by the model. The complete computation gave tangential displacements and rotations practically equal to those of the model,[7] but the radial displacements and stresses were a little lower than those of the model.

For the final design (Study V) a computation was made simply with radial adjustments of 6 arches and 9 cantilevers. For the hydrostatic pressure the compressive stresses in the crown of the arches for this analysis were 60 kg per sq cm at the 230-m level in which the model gave 54 kg per sq cm, and the tensile stresses at the base of the crown cantilever were 30 kg per sq cm in which the model gave 22 kg per sq cm based on the strain relation.

The Cabril Dam studies showed again that the trial load computation, with only radial adjustments, gives compressions in the arches that approximate those of the models and stresses at the base of the cantilevers, greater than those of the models. This dam does not have any irregularities in shape.

The vertical displacement diagrams in Fig. 16(a) were measured by precision leveling and show that during the first loading the crest rose (dates A to C). This rise is in agreement with the rise found in the model. Between dates A and C the effect of temperature variations was not apparent, because the lower 100 m of the dam had a mean temperature drop of 1° C and the upper 30 m a mean rise of 4° C (Fig. 17(b)). The water level drop between dates C and F did not cause the crest to return to its initial position even when the temperature variations and the rise of the abutments revealed by the end points of the diagrams were considered. The rise of the water level between dates F and K caused a further rise of the crest. However, because there was a mean temperature drop in the dam of 5° C, the curve corresponding to date K should not be far from that corresponding to date F. It is therefore concluded from the observations of the vertical displacements that there must be another cause for the rise of the crest in addition to hydrostatic pressure and temperature.

The analysis of the horizontal displacements (Fig. 16(b) and 17(a)) shows that the dam has an almost reversible and symmetrical behavior. However, from date A to date F, regardless of there having been a large temperature rise above elevation 230 m, the points observed in the crown cantilever did not go upstream of the positions occupied on date A. This is probably due to a displacement of the foundation.

The maximum reservoir water level was attained on the second filling (dates K and L). The greatest displacements were observed on date K at elevations 290 m and 250 m and on date L at elevation 210 m. This was due to the mean temperature of the concrete having risen by 10° C in the arch at elevation 290 m between dates K and L, and having fallen by 1° C in the arch at elevation 250 m, and 2° C at elevation 210 m (Fig. 17(b)).

The lateral points at the crest of the dam (arch 290) underwent displacements that were influenced strongly by temperature variations. Between dates C and D, when the mean temperature of the crest rose by 10° C, these points were displaced upstream by the same amount that occurred between dates A and C. With the fall of the mean temperature at the crest following date D, and until date K (Fig. 17(b)) these points moved continually downstream regardless of important variations in hydrostatic pressure.

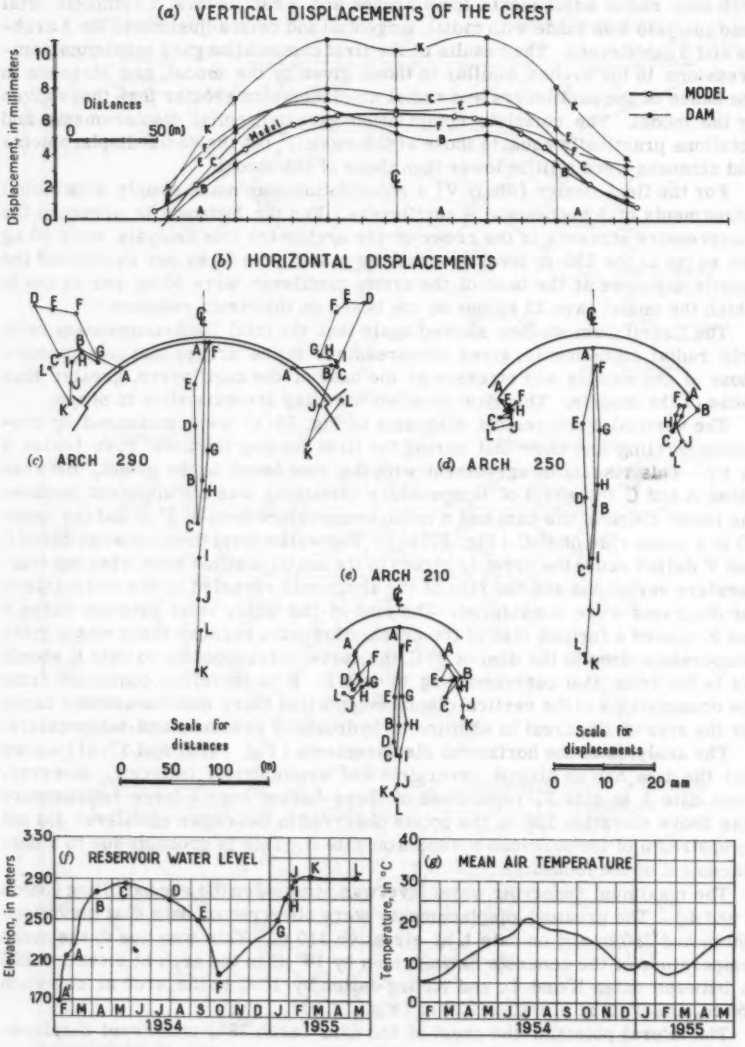


FIG. 16.—CABRIL DAM, DISPLACEMENTS

The lateral points of arches 250 and 210 have paths that are similar to those displacements observed on points of the rock near the dam.[9] These lateral points also show movements similar to those of the crown of the arches at the various levels.

In Fig. 17(a) curves are plotted for the displacements of the crown cantilever observed by the geodetic method versus the reservoir water level. The curves of Fig. 17(b) show the mean temperatures of the concrete and the mean

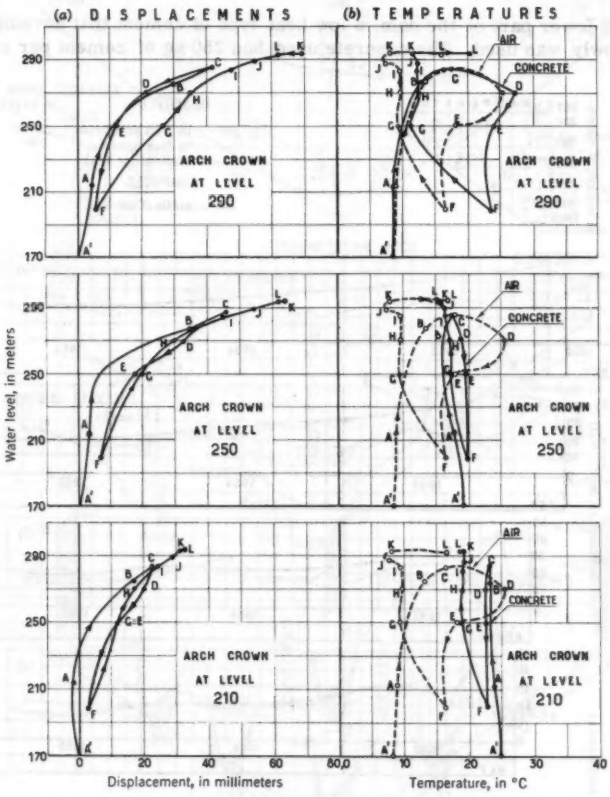


FIG. 17.—CABRIL DAM, OBSERVED RADIAL DISPLACEMENTS AND MEAN CONCRETE TEMPERATURES

monthly air temperature versus the reservoir level. The displacement diagrams, when taking the temperatures into consideration, reveal the general reversibility of the dam. In addition to the irreversibility between dates A and F previously mentioned, these diagrams show also an anomaly in the behavior during the second filling. On date H the points on the crowns of arches 250 and 210 were situated upstream of the positions occuried in date D. This was true,

although for these two dates the reservoir levels were equal and the concrete temperatures were lower on date H than on date D. This is probably due to the final grouting of the joints which was carried out on date F, when they opened in the lower part of the dam.

Fig. 18(a) to (d) shows the temperatures measured in four cross sections of Cabril Dam at 1 m from the two faces and halfway through the dam from 1952 until 1955. Also shown are the computed temperatures for the intermediate points which agree very closely with the temperatures observed at these points.

In the lower part of the dam, a low heat type of cement that developed heat very slowly was used. The concrete used had 250 kg of cement per cu m and

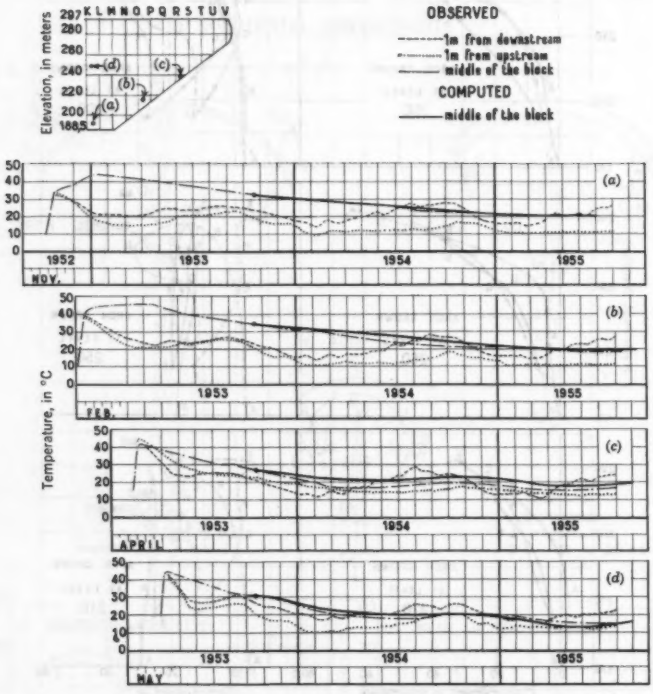
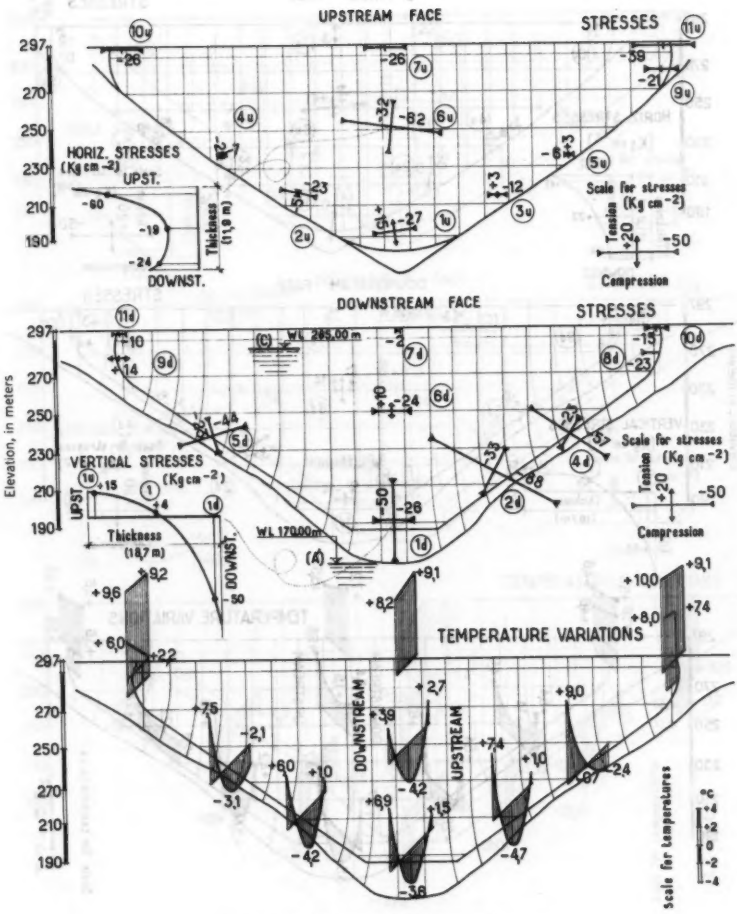


FIG. 18.—CABRIL DAM, OBSERVED AND COMPUTED TEMPERATURES

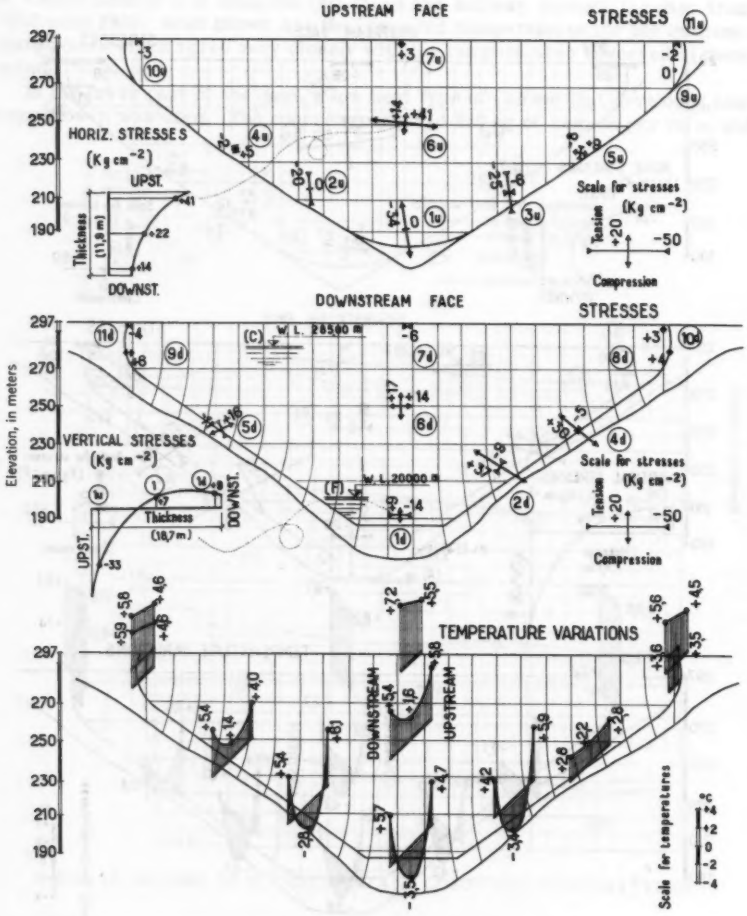
1.5-m lifts were poured at intervals of 4 days. As Fig. 13(a) and (b) indicates, the maximum temperature was reached only 3 months after laying. The upper half of the dam was built with normal portland cement using 250 kg of cement per cu m. The maximum temperature was reached 3 days after pouring and the heat of hydration was dissipated much more rapidly than in the lower part.

Fig. 19(a) to (c) shows the variations of the principal stresses at points 1 m from the faces between various periods. The temperature variations of the concrete at 1 m from the faces and at the mean surface are also plotted. The



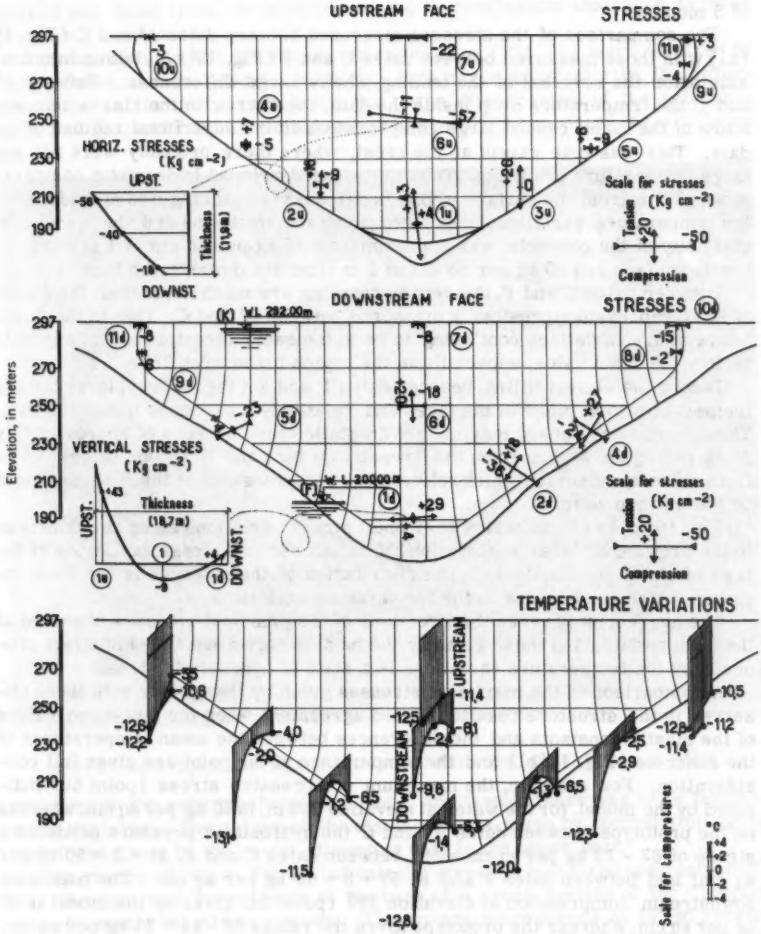
(a) FIRST LOADING (DATES A' TO C)

FIG. 19.—CABRIL DAM, OBSERVED STRESSES AND TEMPERATURES



(b) FIRST UNLOADING (DATES C TO F)

FIG. 19.—CONTINUED



(c) SECOND LOADING (DATES F TO K)

FIG. 19.—CONTINUED

stresses were computed from the strains using values for the modulus of elasticity and Poisson's ratio obtained in rapid tests on specimens of concrete from the structure. In this case, ignoring the creep does not lead to serious errors because the filling of the reservoir began when the greater part of the concrete was more than 1 yr old, and the loading and unloading cycles lasted a maximum of 5 months.

The comparison of the stresses measured between dates A' and C (Fig. 19 (a)) with those measured between dates C and F (Fig. 19(b)), taking into consideration the reversal of the loading, shows large differences. Between A' and C the temperature drop inside the dam, together with the rise in temperature of the faces, caused large compressions in the superficial regions of the dam. This was true except at the crest, where there probably were not any large temperature gradients. This skin effect developed hydrostatic compressions at 1 m from the surface whose maximum value, taking into consideration the temperature variations measured along the thickness and the modulus of elasticity of the concrete, was approximately 15 kg per sq cm at 1 m from the upstream face and 30 kg per sq cm at 1 m from the downstream face.

Between dates C and F, the decompressions are much lower than the values of the compressions previously measured between A' and C. This is due to the temperature variations continuing to be in the same direction and of approximately the same value, especially in the region below arch 260.

During the second filling, between dates F and K (Fig. 19(c)), large falls in temperature took place in the faces and relatively small ones inside the dam. These variations caused maximum hydrostatic tensile stress of approximately 30 kg per sq cm at 1 m from the downstream face and 10 kg per sq cm at 1 m from the upstream face which relieved the compressions at the faces produced by the water pressure.

Fig. 19(a) to (c) indicates horizontal stress variations along the thickness in the crown cantilever at elevation 250 m and vertical stress variations at the base of the same cantilever. The distribution of the stresses is far from the linear, which must be due to the temperature variations.

The argeement between the directions of the principal stresses observed at the various dates and those given by the models shows that the skin effect produced by the temperature variations is a state of hydrostatic stress.

A comparison of the maximum stresses given by the models with those observed in the structure results in good agreement when the measured values of the elastic constants and the differences between the mean temperatures of the concrete (Fig. 17(b)) and the temperature at the point are given full consideration. For example, the maximum compressive stress (point 6u) indicated by the model, for the water at elevation 290 m, is 50 kg per sq cm, whereas on the prototype between dates A' and C the hydrostatic pressure produced a stress of 62 - 12 kg per sq cm = 50; between dates C and F, 41 + 9 = 50 kg per sq cm; and between dates F and K, 57 + 6 = 63 kg per sq cm. The maximum downstream compression at elevation 220 (point 2d) given by the model is 60 kg per sq cm, whereas the prototype gives the values 88 - 24 = 64 kg per sq cm; 37 + 18 = 55 kg per sq cm; and 36 + 27 = 63 kg per sq cm.

THE CANICADA DAM

The Canicada Dam (Fig. 1(e)) on the Cávado River near Braga, has a shape similar to Salamonde Dam and its design was assisted by the studies made on this dam. After the first model studies it was considered advisable to increase

the thickness at the abutments of the lower arches. The final model study led to the conclusion that the shapes tested were satisfactory. Fig. 20 shows the arrangement of the electrical strain gages on the downstream face and the rubber sack in which the mercury rises to reproduce the hydrostatic pressure.

The comparisons between the stresses computed by the abridged trial load method and those from the models led also to conclusions analogous to those previously mentioned.

The curves of radial displacements in the dam (Fig. 21) were obtained by the pendulum and the geodetic methods. Both agree satisfactorily, the difference between the two curves being due to the displacement of the reference point P of the pendulum. The displacements given by the model agree with those

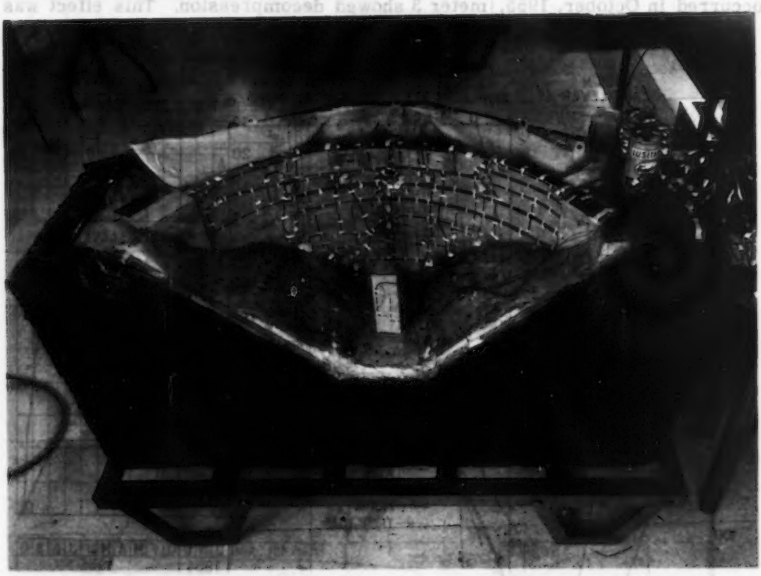


FIG. 20.—CANIÇADA DAM, STRAIN GAUGES ON THE DOWNSTREAM FACE

observed on the prototype between dates C and D when there was little temperature variation. The values of the displacements given by computation agree with those given by the model, diverging only in the upper part.

The curves shown in Fig. 22 indicate the stresses measured upstream, halfway through, and downstream at the base of a cross section of the Canicada Dam by means of stress meters. The meters were placed at 45° to receive the forces normal to the foundation surface. Stress meter 2 shows an initial compression of approximately 13 kg per sq cm, due to the rise in concrete temperature as a result of the development of the heat of hydration, whereas stress meters 1 and 3 registered slight tensile stresses. With the fall in temperature and growth of the block, meter 1 began to register compressive stresses and meter 3 registered tension due to the weight of the concrete as the block leans

upstream. However, the tension in meter 3 is counterbalanced by the compression due to the cooling of the inside of the dam. This cooling tends to cause tension, detected by stress meter 2, which is counterbalanced by the compression from the concrete weight.

When the filling of the reservoir began, meter 1 which was already registering decompression (August, 1954) due to temperature fall on the face of the dam in relation to the inside, showed increased decompression due to the effect of rise in water level. Meter 3 clearly shows compression due to this rise in water level and meter 2 has intermediary values. At the beginning of May, 1955, the temperature of the concrete at the faces began to rise and immediately the compression at meters 1 and 3 did also, whereas meter 2 registered decompression for the same reason. With decrease in water pressure, which occurred in October, 1955, meter 3 showed decompression. This effect was

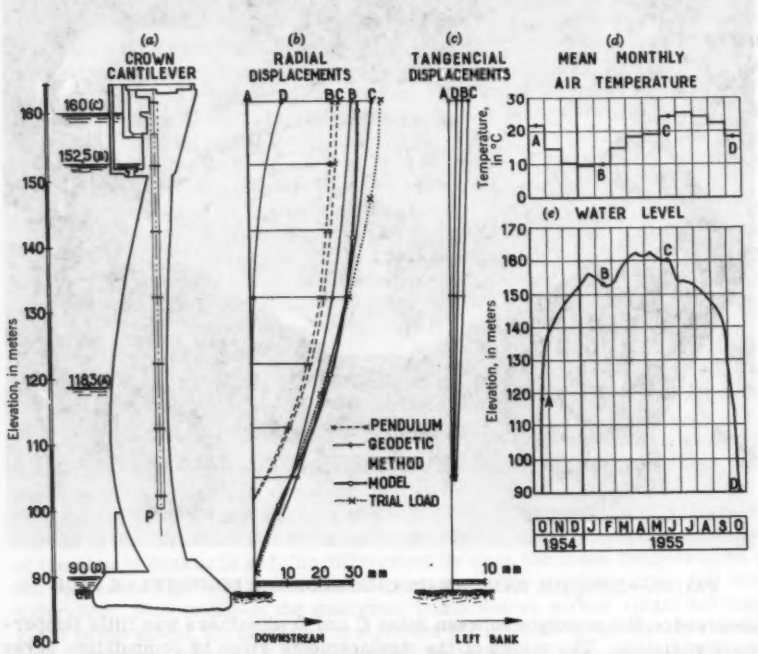


FIG. 21.—CANIÇADA DAM, OBSERVED HORIZONTAL DISPLACEMENTS OF THE CROWN CANTILEVER

accentuated by a fall in temperature of the downstream face, which occurred at the same time. Meter 1 registered an increase in compression due to fall in water level. When the water rose again, meter 3 registered further compression and meter 1, decompression. Meter 2 also registered compression, due mainly to the cooling of the faces rather than to hydrostatic pressure.

The model tests for this dam gave - 50 kg per sq cm and + 18 kg per sq cm for downstream and upstream, respectively, at the same points and direction as the stress meters. These stresses are much greater than those given by

the stress meters, which were - 17 kg per sq cm and + 10 kg per sq cm, between October, 1954, and April, 1955, when the reservoir was filled. The much lower values given by the stress meters can, in part, but not completely, be explained by local thermal effects.

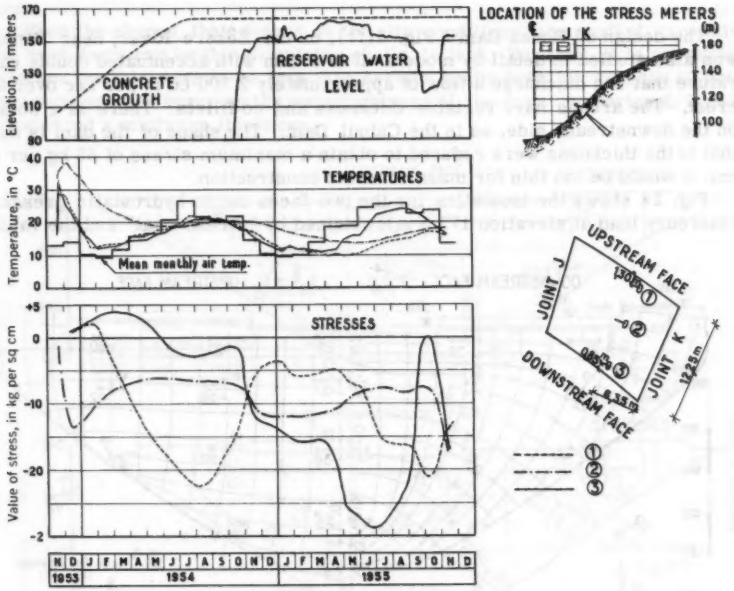


FIG. 22.—CANIÇADA DAM, STRESSES MEASURED BY MEANS OF STRESS METERS

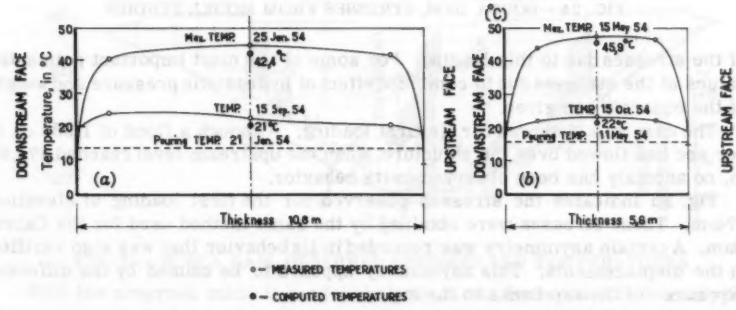


FIG. 23.—CANIÇADA DAM, MEASURED AND COMPUTED TEMPERATURES

Before beginning the construction of the dam, a study was made to estimate temperatures because it was desirable to accelerate the construction by laying 2-m lifts at intervals of 4 days. The proportion of cement used was 250 kg per cu m. At the end of 3 days the cement developed 63 calories per gram, at 7

days, 71 calories per gram, and at 28 days, 84 calories per gram. Fig. 23 shows recorded and computed temperatures for two cross sections of the dam that agree satisfactorily.

BOUCA DAM

The design of Bouca Dam (Fig. 1(f)), on the Zêzere River, near Tomar, was also studied in detail by models. It is a dam with accentuated double curvature that can discharge a flow of approximately 2,300 cu m per sec over the crest. The arches have variable thickness and no fillets. There is a socket on the downstream side, as in the Cabril Dam. The shape of the dam is such that is the thickness were reduced to obtain a maximum stress of 65 kg per sq cm, it would be too thin for mass concrete construction.

Fig. 24 shows the isostatics for the two faces due to hydrostatic pressure (mercury load at elevation 177.5 m), obtained by "Stress-coat" and the values

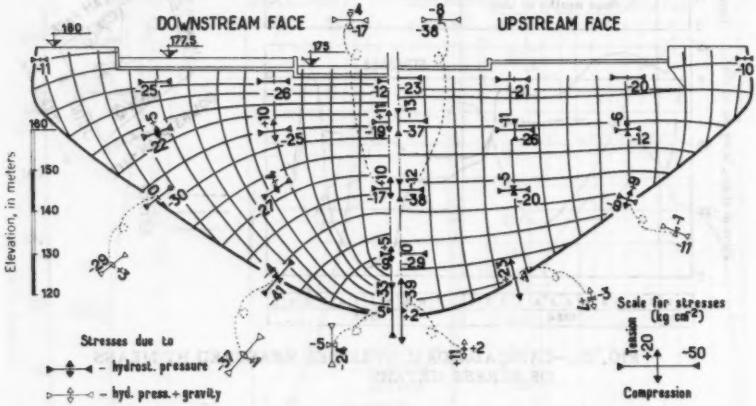


FIG. 24.—BOUÇÃ DAM, STRESSES FROM MODEL STUDIES

of the stresses due to this loading. For some of the most important points, the values of the stresses due to combined effect of hydrostatic pressure and weight of the concrete are given.

The dam was observed for its first loading. Although a flood of 1,500 cu m per sec has flowed over the structure, when the upstream level reached 179.00 m, no anomaly has been observed in its behavior.

Fig. 25 indicates the stresses observed for the first loading at elevation 174 m. These stresses were obtained by the same method used for the Cabril Dam. A certain asymmetry was recorded in its behavior that was also verified in the displacements. This asymmetry appears to be caused by the different exposure of the two banks to the sun.

CONCLUSIONS

The experience obtained leads to the conclusion that the thin arch dams, in relation to all other types, constitute the most economical and safe solution

whenever the foundation characteristics permit and the valley is not excessively wide. This last limitation is not, however, as common as supposed. With regard to the foundations, the requirements are not exacting. In fact, thin arch dams can be built on deformable rocks. Only tests carried out on site over large columns of rock can give information on the deformability of the foundations.

When the shapes, that depend on the site conditions, are studied carefully, the arch dams can be thin—veritable shells, in fact. However, it is not advisable for the thickness to be less than certain limits both for reasons of construction and for ensuring the watertightness of the dam. In Portugal, 2 m is considered a minimum thickness.

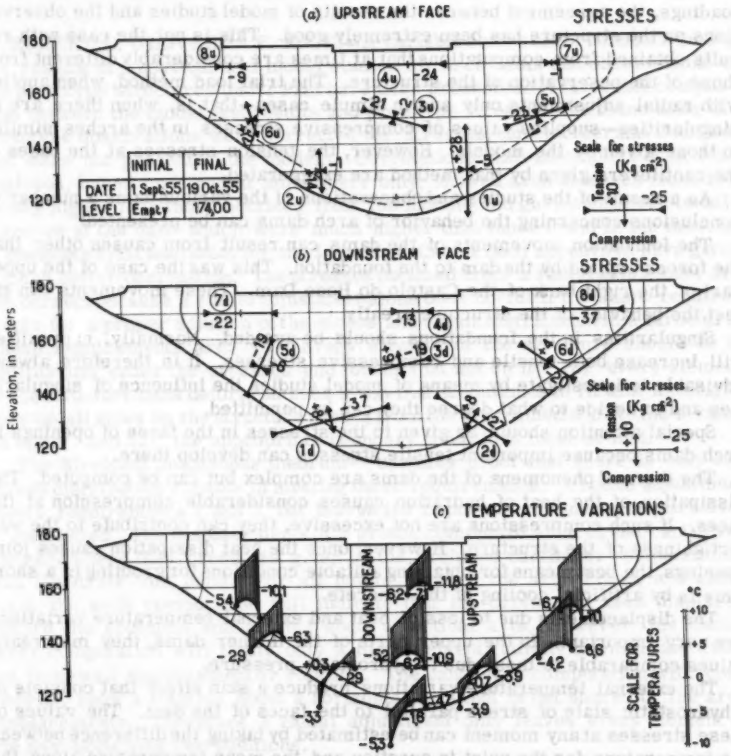


FIG. 25.—BOUÇÃ DAM, OBSERVED STRESSES AND TEMPERATURES

With the progress made in model analysis, it has been possible to study the stresses due to hydrostatic pressure to obtain rapidly, accurately, and economically the most suitable shapes for each case. The materials used in the models should obey conditions of mechanical similarity so that the stresses may be obtained with the necessary accuracy. The influence of foundation deformability, local thickening, possible development of cracks, or any other singularity, can be studied by means of models.

Complete observations of the Portuguese dam behavior has made it possible to control their safety and, above all, to check the value of the analytical and experimental methods used in their design. Furthermore, it is possible to better understand the influence of certain factors such as temperature variations, and to investigate others, such as movements of the banks. A better understanding of the properties of the materials and foundations is also obtainable by observation. It is recognized that a large number of different observations taken regularly is indispensable when interpreting measurements. The most important of these measurements are dam and ground displacements, strains and stresses, temperatures, joint openings, variations in concrete volume, and uplift.

In general, whenever it was possible to separate the effects of the various loadings, the agreement between the results of model studies and the observations on the structure has been extremely good. This is not the case with results obtained from computations that at times are considerably different from those of the observation of the structure. The trial load method, when applied with radial adjustments only and in simple cases—that is, when there are no singularities—supplies values of compressive stresses in the arches similar to those given by the models. However, the tension stresses at the bases of the cantilevers given by that method are exaggerated.

As a result of the studies and observations of the various dams a number of conclusions concerning the behavior of arch dams can be presented:

The foundation movements of the dams can result from causes other than the forces applied by the dam to the foundation. This was the case of the upper part of the right bank of the Castelo do Bode Dam. These movements can effect the behavior of the structure greatly.

Singularities in the foundations should be avoided. Normally, convexities will increase both tensile and compressive stresses. It is therefore always advisable to investigate by means of model studies the influence of singularities and to decide to what degree they can be permitted.

Special attention should be given to the stresses in the faces of openings in arch dams because important tensile stresses can develop there.

The thermal phenomena of the dams are complex but can be computed. The dissipation of the heat of hydration causes considerable compression at the faces. If such compressions are not excessive, they can contribute to the watertightness of the structure. However, once the heat dissipation causes joint openings, the best means for obtaining suitable conditions for grouting in a short time is by artificial cooling of the concrete.

The displacements due to loss of heat and external temperature variations are very important. In the upper parts of the thinner dams, they may reach values comparable to those due to hydrostatic pressure.

The external temperature variations produce a skin effect that consists of a hydrostatic state of stress parallel to the faces of the dam. The values of these stresses at any moment can be estimated by taking the difference between the temperature for the point in question and the mean temperature along the thickness on which the point lies. The agreement between the results of the stresses obtained on models and those on the actual dams, after making this correction for stresses of thermal origin, is very good.

ACKNOWLEDGMENTS

The investigations described herein were possible because of the collaboration of the technical staff of various Portuguese organizations, among which

are "Direcção Geral dos Serviços Hidraulicos," "Commissão de Fiscalização das Obras dos Grandes Aproveitamentos Hidro-Electricos," "Hidro-Eléctrica do Zêzere," and "Hidro-Eléctrica do Cávado." Engineers who contributed to these studies are Orlando V. Rodrigues, Armenio F. de Lemos, J. M. R. Neto, Joao L. Fialho, Fernando P. Rodrigues, Marciano Q. Guerreiro, and Maria Emilia C. e Matos.

DISCUSSION

ROBERT E. GLOVER,[17] F. ASCE.—A valuable series of correlations among the results of analytical and model studies for arch dams and observations of the prototype structures under load have been presented. A favorable comparison between the model test results and prototype stresses was found after the prototype observations were corrected for stresses, due to thermal changes, that were not present in the models. Correlations with incomplete trial load analyses, based on a radial adjustment only, showed arch stresses from 10% to 20% higher than those obtained from the models and gave cantilever tensile stresses at the base which were much higher than those found in the models. A complete trial load study for the important Cabril Dam appears to have given a much better correlation. The stresses obtained from a radial adjustment are not correct because a radial adjustment alone does not fulfil the basic requirements for a proper solution of the stress and strain distribution in a structure. These requirements are: (1) Every element of the structure should be in equilibrium under the stresses and forces that act on it; (2) every element of the structure must deform in such a way that it continues to fit with its neighbors on all sides as the structure passes from the unstrained state to the strained state; and (3) the appropriate boundary conditions must be met.

The Kirchhoff uniqueness theorem[18] contains proof that there is only one stress distribution capable of meeting these requirements. A radial adjustment meets requirements 1 and 3, but leaves the important continuity requirement 2 unsatisfied. The displacements of a prism, common to an arch and cantilever element where they cross, as given by the arch and cantilever computations, will illustrate this point. For all points between the arch crown and abutment, the arch computation will indicate that the prism has been displaced toward the abutment and rotated about a vertical axis. However, the cantilever computation will imply only a displacement radially downstream without tangential displacement or rotation. The cantilever computation will, conversely, show a rotation about a horizontal axis that is not shared by the arch displacements. Therefore, a radial adjustment only leaves every element of the dam occupying two positions.

This situation is unsatisfactory. If this distribution is tested against the Kirchhoff requirements it can only be concluded that it is not the unique stress

17 Research Engr., U. S. Bureau of Reclamation, Denver, Colo.

18 "The Mathematical Theory of Elasticity," by A. E. H. Love, 4th Ed., Cambridge Univ. Press, 1927, paragraph 118.

distribution that must prevail. It should be expected, therefore, that a trial load study, based on a radial adjustment alone, will not agree with the results of a model test. This expectation is confirmed by many such comparisons.

It is the purpose of the tangential and twist adjustments to elimate the tangential and rotational displacement discrepancies left by the radial adjustment. These adjustments bring into evidence the tangential and vertical shear forces that act on the top, bottom, and sides of the element. By so doing, the important elements of strength provided by shearing and twist resistances of the arch and cantilever elements are accounted for.

The effect of adding these two adjustments is generally to decrease the computed deflections and to lower the computed stresses. A trial load analysis including carefully made radial, tangential, and twist adjustments will generally agree closely with the results of model tests. The tangential and twist effects contribute most effectively to the strength of arch dams constructed in wide sites. They may be nearly absent in dams built in very narrow canyons.

A complete agreement between the results of a model test, made within the elastic range, and an analysis satisfying the equilibrium continuity and boundary condition requirements is to be expected. There can be but one solution to the elastic equations, and when a computer has satisfied these three requirements he has this one solution. This solution will be identical with the model distribution, because the conditions it must meet are precisely those enumerated.

It is important to arch dam designers that the analytical and experimental techniques they use for design be brought into complete accord. This can be done if engineers bring their analyses into agreement, by trial load procedures or otherwise, with all three of the requirements previously described.

It may be noted that correlation with test data makes more exacting demands on a computer than does the task of designing a dam to carry to specified loading with a given safety factor. If the design computations neglect certain elements of strength, the net result will generally be a structure that is somewhat overdesigned, but which may, nevertheless, be expected to serve well. In order to correlate with test data, however, the computer must find the unique solution, and this is a more difficult task.

FRED A. HOUCK,[19] F. ASCE.—The writer appreciates the authors' conclusion that the trial load method in its full application is laborious and lengthy. However, aside from this criticism, which will be discussed subsequently as a relative point of view, it has not been demonstrated that the method is inadequate for design. Therefore, the statements made under the heading "Model Tests" may appear misleading to engineers who have not had much experience in evaluating the results of more than one method of analysis. Also, the authors' conclusion that the trial load method, based on a single radial adjustment of the arch and cantilever displacements, can be used only for an estimate of the stresses in a preliminary design, is inconclusive to an engineer who understands the relative effects of tangential shear and twist in the over-all evaluation of an analysis. It may, therefore, be well to examine a number of general tendencies and effects that have been observed from a large number of United States Bureau of Reclamation (USBR) and other dams analyzed by condensed and complete trial load methods. Neglecting those zones of an arch structure

[19] Chief Civ. Engr., Engrg. Consultants, Inc., Denver, Colo., Formerly Superv. Civ. Engr., Concrete Dams Section, Office of Asst. Comm. and Chf. Engr., Bureau of Reclamation, U. S. Dept. of the Interior, Denver, Colo.

in which irregularities of base and profile occur and where localized stresses exist, the following general effects of tangential shear and twist are evident:

1. The maximum stresses in both arch and cantilever elements in most parts of a structure are reduced, except in the top arch elements in which the effects due to thrust sometimes cause a tendency toward tensile stresses in the abutments and at the crown intrados.
2. In the cantilever elements there is a tendency toward increased compression at the upstream face and a corresponding decrease of stresses at the downstream face. This is especially true in the lower elevations of a dam in which the effects of twist are invariably greater.
3. In the central part of a structure, reduction of both radial deflection and stresses is general. The stress changes at and near the crown point of arch elements are generally small in comparison with the greater reductions at the abutments. At the abutments, the tendency is toward an increase in compression at the extrados and a decrease in compression at the intrados, whereas at the crowns of the arches near midheight the opposite effects are usual.
4. In dams in which the abutments have been sharply thickened by the addition of fillets, the stresses in the arch abutments increase considerably due to tangential shear effects. It is impossible to compute these shear effects by means of a radial adjustment of deflections only, but they can be estimated by comparison with the computed effects from other comparable studies.

The USBR has been able to save time, effort, and expense in design costs by the judicious application of the previous generalities to obtain final or nearly final design dimensions. The conjugate points of the arches and cantilever elements representing the structure of a particular design are adjusted into radial deflection agreement by the trial load process. The initial succeeding design dimensions are altered to yield approximate desired stresses in accordance with the previously mentioned characteristics applied to the results of analyses made to account for only the radial adjustment of deflections in the arches and cantilevers. The final analysis is made to complete the stress study and is usually done with a simultaneous adjustment of radial, tangential, and twist effects on representative elements of the structure.

The cost of making the analyses of stresses sometimes amounts to a large share of the total cost of designing an arch dam. The costs of analyses vary with the complexity of the method used, the number, time, and pay scale of the people employed, and to a lesser degree with the cost of materials, equipment, or other services involved. Contrary to the experience of the authors, the USBR has found that design of arch dams by trial load methods yields the most reliable results in less time and cost than by model tests. The question of reliability of results has heretofore been involved in the USBR experience because model testing has not been as conclusive in comparison with computed and observed results as Portuguese and other European experience.

In verifying the fundamental accuracy of new and existing theories, the use of models took an important part in the solution of many hydraulic and structural problems in the designs of Hoover Dam on the Colorado River near Las Vegas, Nevada-ARR; Grand Coulee Dam on the Columbia River near Coulee City, Wash , and other USBR dams. In contrast to the hydraulic models, which provide direct empirical data, the principal function of the structural models of these dams was to furnish a check on analytical methods of design. Although considerable information that could not be readily obtained by analytical methods was derived and used in design from the arch dam model tests, this was

only incidental to their use in determining the adequacy of the trial load method of analysis. From this viewpoint, the method of applying results of structural model tests of dams by the USBR differed somewhat from the use of other types of structural models.

However, the authors have contributed valuable evidence which demonstrates that with careful simulation of all known dimensions, loading conditions, mechanical and physical properties of the dam and foundation, and by the skilful use of testing techniques, model tests may be used as a reliable basis for designing an arch dam. The writer believes that whenever model tests are to be made the basis of determining stresses or movements for design, that they should always be checked by proven analytical methods as much as possible.

With an experienced team of engineers, the USBR expends an effort averaging 120 man-days to analyze one loading condition on an ordinary arch dam design with variable thickness elements by adjusting to account for radial movements only. By ordinary arch design is meant that the layout is considered sufficiently symmetrical and than no unusual loading, structural, or abutment conditions exist that would prohibit the structure from being analyzed by symmetrical conditions. If the analysis is carried to completion, including the total effects of tangential shear and twist, an additional average time of 280 man-days is required for this further effort. It costs approximately 40% more than the aforementioned figures to analyze each additional loading condition for the same layout.

MANUEL ROCHA,[20] F. ASCE, J. LAGINHA SERAFIM,[21] F. ASCE, And ANTONIO F. Da SILVEIRA.[22]—The writers have presented previously their opinion on the advantages and disadvantages of the trial-load method.[23, 24] It is not intended that the reasons already given be repeated. However, the trial load method can supply the same results as a model test when the dam is not complex—that is, when both shape irregularities and heterogeneity in the properties of the materials are absent. Because the designer has to take into account irregularities and heterogeneities chiefly in the foundation rock, he has no tool to preview the behavior of the structure, unless Mr. Glover's suggestion is followed, thus obtaining an overdesigned structure. The advantage of experimental methods is that they can be applied both to simple and complex cases, always with the same accuracy and at a cost lower than the complete trial load computation, provided that adequate techniques are used. At present (1959), with the modern high precision testing techniques using small models, a model test costs less than a computation by the complete trial load method.

A complete adjustment supplies information on one reservoir level only, whereas information on the different reservoir levels can be obtained without any change whatsoever in the arrangement of the measuring apparatus. It is also possible to study various solutions on the same model, if care is taken to begin with the thickest shape. The writers believe that not only were the model

---

[20] Director, Laboratorio Nacional de Engenharia Civil, Lisbon, Portugal.

[21] Head, Dams Studies Section, Laboratorio Nacional de Engenharia Civil, Lisbon, Portugal.

[22] Asst. Research Engr., Laboratorio Nacional de Engenharia Civil, Lisbon, Portugal.

[23] "Arch Dams: Trial Load Studies for Hungry Horse Dam," by R. E. Glover and M. D. Copen, Proceedings Paper 960, ASCE, March-April, 1956.

[24] Closure to "Model Tests, Analysis, and Observation of an Arch Dam," by M. Rocha, J. L. Serafim, A. F. da Silveira, and J. M. R. Neto, Transactions, ASCE, Vol. 122, 1957, pp. 946-949.

tests carried out at the USBR the first of their kind to be made, but also that the measuring techniques were insufficiently developed, which resulted in a great waste of time and money and a lack of reliable results. In Portugal, the preliminary design justified by analytical computations supplies the first dam shapes to be tested on models whereas the final shapes—that is, the design proper—are based exclusively on the model tests.

Mr. Glover is to be congratulated on the interesting synthesis presented regarding the need for making all the adjustments in the computations by the trial load method and the influence of the tangential and twist adjustments on the stress distribution.

DEVELOPMENT IN ITALY

By Carlo Semenza,[1] F. ASCE

SYNOPSIS

The reasons for extensive development of arch dams in Italy are listed, and the historical stages in that development are traced with numerous examples. The methods of analysis are briefly reviewed and special features of construction procedure are explained. A section is devoted to an explanation of the benefits of the perimetral joint, which has been used successfully by the author in several large arch dams.

INTRODUCTION

Notation.—All dimensions are given in the metric system. To convert into the English system the following should be used: 1 m = 3.2808 ft, 1 cm = 0.3937 in., and 1 mm = 0.03937 in.

The development of arch dam construction in Italy is due to several related factors:

1. The primary factor is the geological characteristics of the country. In the Alps, which constitute the principal hydraulic power area, and in part of the Apennines, there is a prevalence of relatively recent geological formations. Narrow gorges are common, for which arch dams are the most natural solution.
2. The cost of skilled and specialized labor in the construction industry is still relatively low and is hence a small factor in the total cost. Materials, on the contrary, particularly cement and steel—hence the volume of the concrete—constitute the major element cost.
3. Given the same degree of safety, the choice of the type of dam should depend only on economic factors. Thus, refined structures are preferred to reduce the volume of the structure to a minimum.
4. The widespread and elastic application of varied structural forms had developed from the engineers' attitude that each dam constitutes a problem in itself, to be solved according to criteria free from any preconceived idea.
5. This tendency has been reinforced to some extent, both by tradition and artistic environment, since the arch, from the time of ancient Rome, has been a common architectural element. Thus it was both logical and natural that it should be used by modern designers of hydraulic structures.
6. The realization of the exceptional resistance of the arch has grown through centuries of experience. Even for structures in housebuilding, small and slender brick arches have been widely used.

Note.—Published, essentially as printed here, in June, 1956, as Proceedings Paper 1017. Positions and titles given are those in effect when the paper was approved for publication in Transactions.

[1] Central Mgr. and Chf. Engr., Hydr. Constr. Dept., Societa Adriatica di Elettricita, Lido Venezia, Italy.

The over-all safety of an arch structure is higher than that of a gravity structure, as proven by models tested to failure. The collapse of a dam takes place at loads that vary between 5 and 11 times the normal, the lower values usually corresponding to failure of abutments and not of the dam itself.

In the dome structure an attempt is made to realize a sail structure following the funicular polygon of the hydraulic loads and working in every direction with simple compressive stresses and with as uniform a value as possible. These ideal limits cannot be reached in practice, but would correspond to maximum rationality and economy.

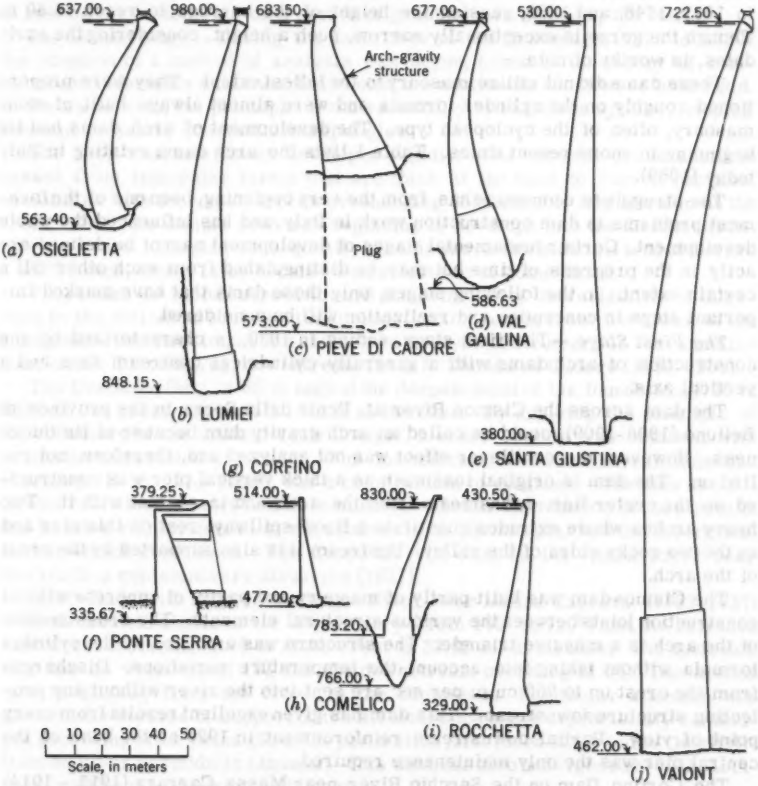


FIG. 1.—TYPICAL ITALIAN ARCH DAMS

The arch-gravity dams are designed in accordance with a more complex conception because the effect to weight must be considered. Here there is a tendency toward structures in which the maximum compressive stresses are of the same order whether the reservoir is empty or full, and are spread as evenly as pos-

ible throughout the whole structure. Fig. 1 shows several typical Italian arch dams.

THE DEVELOPMENT OF ARCH DAMS IN ITALY

The oldest dams are the barrages built by government engineers for flood control purposes, or to stop debris, in the narrow mountainous valleys. Some were also used for irrigation and to drive flour mills. Perhaps the oldest of all is that of Ponte Alto on the Fersina River, in the neighborhood of Trento. The construction of this barrage was begun in 1537 and the arch was heightened in 1611, 1748, and 1883, causing the height of the barrage to reach 46.80 m. Though the gorge is exceptionally narrow, such a height, considering the early dates, is worthy of note.

These dams did not utilize masonry to the fullest extent. They were proportioned roughly on the cylinder formula and were almost always built of stone masonry, often of the cyclopean type. The development of arch dams had its beginning in more recent times. Table 1 lists the arch dams existing in Italy today (1959).

The struggle to economize has, from the very beginning, been one of the foremost problems in dam construction work in Italy, and has influenced the whole development. Certain fundamental stages of development cannot be defined exactly in the progress of time but may be distinguished from each other till a certain extent. In the following stages, only those dams that have marked important steps in conception and realization will be considered.

The First Stage.—The first stage, ending in 1930, is characterized by the construction of arch dams with a generally cylindrical upstream face and a vertical axis.

The dam across the Cismon River at Ponte della Serra in the province of Belluno (1906-1909), could be called an arch gravity dam because of its thickness. However, the cantilever effect was not analyzed and, therefore, not relied on. The dam is original inasmuch as a thick vertical pier was constructed on the center line, downstream from the arch and in contact with it. Two heavy arches whose extrados constitute a flood-spillway, rest on this pier and on the two rocky sides of the valley. Upstream it is also supported by the crest of the arch.

The Cismon dam was built partly of masonry and partly of concrete without construction joints between the various structural elements. The cross section of the arch is a massive triangle. The structure was analyzed by the cylinder formula without taking into account the temperature variations. Discharges from the crest up to 750 cu m per sec are sent into the river without any protecting structure downstream. This dam has given excellent results from every point of view. Partial downstream reinforcement in 1929 at the base of the central pier was the only maintenence required.

The Corfino Dam on the Serchio River near Massa Carrara (1913 - 1914) was the first example in Italy of a thin arch dam. It rises to a height of 35 m, has a radius of 28 m, and a base thickness of 5.50 m. The dam has withstood a violent earthquake without the slightest damage. Other dams of this period are the Muro Lucano, on the Sele River near Potenza Turrite di Gallicano, on the Serchis River near Massa Carrara and the Furlo on the Metaurs near Pesaro (1919 - 1921). The Ritter method was used for the computation of the Furlo Dam.

The planning of the Sottosella Dam on the Isonzo River near Gorizia (1937-1939) in territory now held by Jugoslavia, was done on conservative lines. However,

it did not represent a return to the idea of massive dams with a cylindrical upstream face. The solution chosen was due entirely to the peculiar requisites of the site and construction. The main problem was to construct the foundations in a narrow, rocky river bed subject to heavy and frequent floods. Therefore, the structure of the dam had to be adapted to the foundations. The foundation consisted of a single, large, compressed air caisson, built on the two sides of the gorge, and sunk to the bottom.

In a previous design of this dam[2] a flood crest spillway (up to 2000 cu m per sec) was designed with a 12-m water head and a large flume connected to the dam, but statically independent of it. The structure of the flume did not have to rest on the bottom, but on a series of great arches spanning the banks.

The Second Stage.—During the last 10 yr of the first stage (1920 to 1930) the adoption of a method of analysis was begun, based on the theory of horizontal arch elements with encastrement at the abutments which were held rigid. At the same time, the principle of the variability of radii was applied, keeping constant or nearly constant central angles.

The arch characteristics developed rapidly. The vertical cross sections passed from triangular forms that are thick at the base to curved profiles, sometimes with the upper arches overhanging considerably downstream at the crest. Thus, the simple arch was beginning to develope into the double curvature structure. The plan consequently became more complex and tended toward a shell shape, which later became characteristic of dome dams.

There also developed a trend toward the principle of the variability of thickness in the individual arches with appropriate thickening from the crown to the abutments. The first important example of this type of structure is the Comelico Dam on the Piave River, downstream from S. Stefano di Cadore (1930-1931).

The Comelico Dam is 66 m high at the deepest point of the foundation, 1.20 m thick at the crest, and 8.66 m. thick at the base. By applying the principle of the constancy of the arches' central angle, a cross section was obtained with an upstream face that overhangs 17 m downstream, and a downstream face that overhangs 10 m. The result was a construction of elegance. The dam is built of concrete with light steel reinforcement for a better distribution of the stresses and heavier reinforcement at the abutments, to put into practice the theoretical encastrement conditions. The Ceppo Morelli dam on the Anza River near Novara is a contemporary structure (1931).

In the Rocchetta Dam on the Magra River, near Massa Carrara, (1935-1937) even the central angles of the arches vary (from 100° to 120°) and the extrados radii decrease from 71.90 m at the crest to 33.90 m. at the base. The upstream face has an overhang of 17% and the downstream overhang is 5%. The arches thicken slightly from the crown to the abutments. Particular attention was given to the surface of support of the structure to render it practically continuous according to the principle of the perimetral joint (used later in the Osiglietta Dam on River Bormida in Liquria.) This dam has also undergone several earthquakes without suffering any damage.

The Fortezza Dam on the Isarco River near Bolzano (1938-40) has a steep downstream overhang. Its radii, central angles, and thickness of the arches vary continually throughout the structure. The arch, with overhang lip, has no encastrement and rests both at the abutments and at the base on a continuous cradle, as in the case of Osiglietta Dam.

---

[2] "Un caso caratteristics nella costrusione di grandi dighe," by Carlo Semenza, L'Energia Elettrica, 1940.

TABLE 1.—ITALIAN ARCH DAMS

Number	Name of dam	River basin	Owner	Year constructed	Dam		Reservoir	
					Maximum height, in meters	Volume, in cubic meters x 10^3	Storage capacity, in cubic meters x 10^6	Maximum elevation
(1)	(2)	(3)	(4)	(5)	(6)	(7)	(8)	(9)
			(a) Simple curvature arch dams					
1.	Crosis[a]	Isonzo	Filatura Cascami Set	1901	38,20	. . .	0,150	259,15
2.	Ponte della Serra[a,c]	Brenta	Sade	1907-1909	44,40	19,70	4,00	379,25
3.	Corfino[a]	Serchio	Selt-Valdarno	1913-1914	37,50	2,20	0,87	514,00
4.	Muro Lucano[a]	Sele	Soc. Lucana I. I.	1914-1917	53,25	10,00	5,78	567,00
5.	Turrite di Gallicano[a,c]	Serchio	Selt-Valdarno	1915-1916	42,00	9,05	0,89	298,00
6.	Lago Sucotto[a]	Serio	Az. El. Crespi	1919-1923	15,20	0,43	0,45	1.863,50
7.	Ogna Superiore[a]	Serio-Adda-Po	Villa Carlo e F.lli	1922	35,50	. . .	0,300	709,70
8.	Ogna Inferiore[a]	Serio-Adda-Po	Villa Carlo e F.lli	1922	38,50	. . .	0,295	698,70
9.	Gurzia[a,c]	Dora Baltea	Ovesticino	1922-1925	50,00	8,00	1,25	427,50
10.	Val Molinara[a]	Pioverna-Adda-Po	Soc. An. Orobia	1923	17,00	. . .	0,06	918,30
11.	Valla (L. Scuro)[a,c]	Bormida	A. F. L. Falck	1923-1925	47,00	23,00	2,89	280,00
12.	Lago Campelli[a]	Serio	Az. El. Crespi	1924	20,00	1,24	0,47	2.044,15
13.	Rimasco[a]	Sesia-Po	Soc. Idr. Valsesia	1925	30,50	. . .	0,20	887,50
14.	Tul[a,c]	Tagliamento	Soc. El. del Tul	1925-1928 1947-1949	40,10	1,98	0,80	268,10
15.	Orichella[a,c]	Neto	Meridionale	1926-1928	36,20	9,50	0,20	795,90
16.	San Colombano[a]	Avisio-Adige	Soc. E. Jacob	1928	19,00	. . .	0,60	. . .
17.	Ceppo Morelli[b]	Toce (Ticino)	Montecatini	1929	46,00	10,50	0,47	780,75
18.	Comelico[b]	Piave	Sade	1930-1931	66,50	31,50	2,08	830,00
19.	Moledana[b,c]	Adda Alpina	A. F. L. Falck	1930-1931	42,60	12,80	0,11	909,00
20.	Malciaussia[b,c]	Stura di Viù	Ovesticino	1932-1933	30,50	7,30	1,15	1.805,00
21.	Rocchetta[b]	Magra	A. F. L. Falck	1935-1937	76,00	49,00	5,00	403,50
22.	Sottosella[a,c]	. . .	Sade	1937-1939	57,75	24,35	9,60	153,00
23.	Giaredo[a,c]	Magra	A. F. L. Falck	1940-1941	27,50	1,80	0,12	362,00
24.	Panigai[b,c]	Adda	Orobia	1941	41,50	5,00	0,12	704,00
25.	Provvidenza[b,c]	Vomano	Terni	1941-1943 1946-1947	52,20	70,80	2,00	1.060,00
26.	Novarza[a,c]	Tagliamento	Sade	1946-1947	38,75	1,35	0,15	997,65
27.	Santa Giustina[b]	Adige	Edison	1946-1950	152,50	112,00	182,81	530,00
28.	Ganda[b,c]	Adda Alpina	A. F. L. Falck	1947	30,00	6,00	0,07	913,00
29.	Zoldani[a]	Sturia-Entella	Cons. Idr. Monte Alona	1923	19,00		0,08	382,00
			(b) Double-curvature (dome) dams					
30.	Osiglietta[c]	Bormida	A. F. L. Falck	1937-1939	76,80	75,00	13,00	637,00

26.	Novarza[a,c]	Tagliamento	Sade	1946-1947				
27.	Santa Giustina[b]	Adige	Edison	1946-1947	38,75	1,35	0,15	997,65
28.	Ganda[b,c]	Adda Alpina	A. F. L. Falck	1946-1950	152,50	112,00	182,81	530,00
29.	Zoldani[b]	Sturia-Entella	Cons. Idr. Monte Alona	1947	30,00	6,00	0,07	913,00
				1923	19,00		0,06	352,00

(b) Double-curvature (dome) dams

30.	Osigliettac	Bormida	A. F. L. Falck	1937-1939	76,80	75,00	13,00	637,00
31.	Fortezzac	Isarco (Adige)	Ferrovie Stato	1938-1940	63,50	15,00	3,35	722,50
32.	La Maina di Sauris[c]	Tagliamento	Sade	1942-1947	136,15	100,32	73,00	980,00
33.	Bau Mandara[c]	Alto Flumendosa	Soc. El. Sarda	1942-1948	20,30	1,30	0,31	803,30
34.	Monte Zovo (Avandiga)	Piave	Sade	1946-1949	28,40	1,43	(sub-merged)	(sub-merged)
35.	Ponte Racli[c]	Livenza	Snia Viscosa	1948-1951	75,35	18,00	25,00	313,00
36.	Valle di Cadore[c]	Piave	Sade	1949-1950	61,25	4,607	4,90	706,50
37.	Val Gallina[c]	Piave	Sade	1949-1951	92,37	99,10	6,40	677,00
38.	Pezzè di Moena[c]	Avisio	Trentina di El.	1950	28,30	1,50	0,46	1.197,00
39.	Barrea[c]	Sangro	Com. Sangro-Sme-Terni	1950-1951	62,75	4,50	24,30	973,00
40.	Carboi	Carboi	Ente Rif. Agr. Sic.	1950-1951	47,00	32,00	35,50	179,00
41.	Isolato[c]	Mera	Edison	1951-1952	38,50	6,50	1,76	1.246,80
42.	Senaiga[c]	Senaiga-Cismon-Brenta	S. I. I. A.	1954	68,00	25,00	5,75	404,00
43.	Corlo[c]	Cismon-Brenta	S. I. I. A.	1954	71,00	25,00	42,60	268,00
44.	Barcis[c]	Cellina-Meduna-Livenza	Sade	1954	50,15	9,00	21,99	402,00
45.	Grotta Campanaro[c]	Melfa-Liri-Garigliano	Soc. Alto Liri	1954	49,00	5,40	0,39	783,00
46.	Rio Freddo	Stura di D-Rio Freddo	Edison	1954-1955	41,30	30,00	0,33	1.202,50
47.	Forra dei Cami ni (Stramentizzo)	Avisio	Soc. Ind. Trentina	1954-1956	63,00	24,00	12,00	789,50
48.	Pontesei	Maè-Piave	Sade	1956	93,00	65,00	9,1	800,00
49.	Ambiesta	Ambiesta-Tagliamento	Sade	1956	59,00	29,00	3,6	484,00
50.	Ponte Piè	Mincio-Sarca	S. El. Sarca-Molveno	1956	57,50	9,00	3,63	463,00
51.	Van Noana	Noana-Cismon-Brenta	Selt- Val d'Arno	1956-1958	130,00	166,40	10,82	1.015,00
52.	Speccheri	Leno-Vallarsa Adige	Az.GG.SS.Municip.-Verona	1956-1958	156,65	118,00	10,00	805,00
53.	Monguelfo	Rienza-Adige	Soc. Idroel. Atesina	1958	51,00	15,00	6,1	1.057,00
54.	Vodo	Boite-Piave	Sade	1959	41,40	6,80	1,2	850,00
55.	Vaiont	Vaiont-Piave	Sade	under constr.	261,60	360,00	150,00	722,50
56.	Busa	Leno-Vallarsa Adige	Az.GG.SS.Municip.-Verona	under constr.	30,00	4,00	0,50	588,00
57.	Sessera	Sesia	Soc. Zegna	under constr.	38,00	10,00	1,6	
58.	Talvacchia	Talvacchia-Tronto Castellano	Unes	under constr.	76,00	110,00	14,35	512,50
59.	Montagna Spaccata	Torto-Volturno	Ente Auton. Volturno	under constr.	71,00	7,00	7,00	1.071,00
60.	Punta Gennarta	Canonica	Cons. Bonifica Cuixerri	under constr.	60,00	49,00	12,7	

[a] Constant radius, [b] Constant angle, [c] Overflowing.

TABLE 1.—CONTINUED

Number	Name of dam	River basin	Owner	Year constructed	Dam		Reservoir	
					Maximum height, in meters	Volume, in cubic meters x 10^3	Storage capacity, in cubic meters x 10^6	Maximum elevation
(1)	(2)	(3)	(4)	(5)	(6)	(7)	(8)	(9)
			(c) Arch-gravity dams					
61.	Pontebba	Tagliamento	Friulana di El.	1901-1902	23,50	1,55	0,01	616,00
62.	Fusino	Adda	A. E. M.-Milano	1920-1924	59,00	42,00	0,20	1.153,50
63.	Furlo	Metauro	Unes	1921-1952	62,22	. . .	1,80	174,28
64.	Pieve di Cadore	Piave	Sade	1946-1949	112,00	377,00	68,50	683,50
65.	Cecita	Crati	Meridionale	1949-1951	55,00	60,00	108,22	1.142,25
66.	Val d'Auna	Talvera (Adige)	Trentina di El.	1950-1951	53,00	54,00	0,42	916,00
67.	Prà da Stua	Aviana-Sorne (Adige)	S. A. El. Valeggio sul Mincio	1950-1951	42,87	30,50	1,50	1.041,50
68.	Publino	Adda Alpina	A. F. L. Falck	1950-1951	42,00	34,00	5,00	2.134,40
69.	Forte Buso (Travignolo)	Avisio	Smirrel	1950-1952	110,00	260,00	32,10	1.458,00
70.	Lago di Valsoera	Orco (Po)	A. E. M.-Torino	1950-1953	54,00	37,00	8,40	2.412,00
71.	Beauregard	Dora Baltea	SIP	1951-1957	132,00	547,00	72,00	1.770,00
72.	Fiastra	Fiastrone-Chienti	Unes	1955	87,00	160,00	20,40	640,00
73.	Pian Telessio	Rio Piantonetto-Orco -Po	A. E. M.-Torino	1955	80,00	380,00	24,00	1.917,00
74.	Piaganini	Vomano	Terni	1955	45,50	26,00	0,55	400,00
75.	Monte su Rei	R. Mulargia-Flumendosa	Ente Autonom. Flumendosa	1956-1957	100,00	240,00	310,00	260,00
76.	Bellicai	R. Bellicai-R.Corongiu	Soc. Monteponi	1953	30,00	20,00	1,02	365,50
77.	Cancano II	Adda 1° f. / 2° f.	A. E. M.-Milano	1954-1956 / to be constructed	136,00	525,00	120,00	1.900,00
					172,00	586,00	240,00	1.935,00
78.	Nuraghe Arrubiu (Flumendosa)	Flumendosa	Ente Auton. Flumendosa	1956-1957	119,00	330,00	260,00	270,00
79.	Frera	Belviso-Adda	A. F. L. Falck	1957-1959	138,00	400,00	50,00	1.484,00
80.	Pertusillo	Agri	Ente Transformazione Fondiaria Puglia-Lucania	under constr.	101,00		155,00	533,00
81.	Bosa	Temo	Provveditorato OO.PP. Sardegna	under constr.	62,00	147,00	30,00	77,00
82.	Place Moulin	Buthier-Dora Baltea	Consor. Elettrico Buthier	under constr.	146,00	1576,00	100,7	1.967,00
83.	Valle di Lei	Leno di Lei-Reno sup.	Soc. Kraftwerke Hinterrhein-Edison	under constr.	141,00	850,00	200,00	1.932,00

Note: This table does not claim to be complete, especially with reference to dams under construction.

The Third Stage.—All the dams constructed in the third stage may be considered as transitional structures leading toward the more refined type of dome dam, now widely used in Italy. The first example is that of the Osiglietta Dam in the Apennines of Liguria (1937-1939). Approximately 67 m high with a crest 224 m long and a 75,000 volume cu m., it has many interesting characteristics. The dam consists of horizontal elements of varying thicknesses, with downstream face radii of 21 m at the base to 101 m at the crest, and arch central angles from 79° to 129°. The crown cross section has an upstream overhang of 2.40 m at the base and a downstream overhang of 15.45 m at the crest. Both faces are strongly curved. As seen in Fig. 2 the dam is perfectly symmetrical and its abutments have a practically continuous curvature. Another characteristic is the suppression of the lateral encastrement. The dam rests on a continuous concrete saddle that follows the surface of support. It constitutes the first example of this device.

The Osiglietta Dam was soon followed almost by the Lumiei Dam on the Lumiei, near Udine. This dam was planned in 1939-1940 and completed in 1946-1947. After World War II many dome dams of great height were constructed. These dams were built at sites that were different from each other, and therefore their characteristics vary. Nevertheless they were designed and constructed along similar lines. In the region of the Tre Venezie alone there are approximately 20 structures of this type.

The Lumiei Dam, called also La Maina di Sauris Dam, (1942-1947) in Fig. 3 is the first of this group. It is one of the thinnest structures of its kind, 136.15 m high with a crest length of 138 m, and having a volume of 100,320 cu m. It was for several years the highest arch dam in the world and was the first dam in Italy whose analysis took into account the effect of rock deformation. Another dam built during this period and noted for its abutment-saddle details is the Val Gallina Dam on the Val Gallina River, near Belluns (1949-1951).

Outstanding for its peculiar site conditions, characteristics and height (h = 152.59 m) is the Santa Giustina Dam on the Noce River near Trento. The characteristics of the gorge at Santa Giustina, with practically vertical sides (Fig. 4) required a solution in which the small variation in the central angles and the almost vertical upstream face made it resemble the cylindrical type very closely.

The dam of Rio Freddo in the Western Alps near Cuneo is peculiar because it consists of a thin arch supported by two large concrete shoulders 45 m high that sustain the pressure of the arch. From the two artificial abutments, two short gravity walls keep the water upstream.

The construction of the large Vaiont Dam on the Vaiont River near Belluns, in a narrow limestone gorge in the Dolomites is being completed (1960). With a height of 261,60 m, a chord of 190 m and volume equal to 360,000 cu m, it will be the highest arch dam and among the highest dams of every kind in the world.

The Fourth Stage.—In the past 25 years the problem of arch-gravity dams has been thoroughly explored in Italy. The design of the Pieve di Cadore dam (Fig. 5) considered weight as a determining static element for the first time in an Italian arch dam. The behavior of the dam as a dome in this particular case is of secondary importance due to the features of the site. On the contrary, the other great arch-gravity dams constructed since 1945 tend to use the dome function to fullest extent.

The Pieve di Cadore Dam on the River Piave, near Belluns, is unique both for its dimensional ratios and its arched structure (of constant height on the perimetral joint) rests for the most part on a rocky plateau. The remainder of the structure is supported by a concrete plug that closes a deep narrow gorge lying alongside the plateau. The developed elevation along the middle



FIG. 3.—LUMIEI DAM



FIG. 2.—OSIGLIETTA DAM

fiber of the arches from the downstream side as shown in Fig. 6. The dam has a maximum height (from the base of the plug) of 111.50 m, the average of the arch gravity structure on the general foundation line (elevation 634) is 55 m, the crest length is 410 m, and the total volume is 377,000 cu m. The thickness varies from 6 m at the crest to 26 m at the base of the arch, and 36 m at the base of the lateral foundation plug. The arches, up to elevation 640 m are fundamentally circular with a constant radius for the upstream face, whereas the downstream face is polycentric. Above elevation 640 the axis gradually



FIG. 4.—SANTA GIUSTINA DAM

becomes polycentric with increasing substantial differences between the radii. Hence the cross sections vary continuously from the crown to the abutments, bending downstream at the crown and straightening out at the abutments, as in dome dams.

Following the construction of the Pieve di Cadore Dam (1949) other arch-gravity structures were built. Among these are the Publino Dam on the Adda River near Sondris (Table 1 (c), the Travignolo Dam (Table 1 (c)), on the Avizio River, the Cecita Dam on the Mucone River near Cosenza (h = 55 m, volume = 62,500 cu m) and the Fiastrone Dam on the Chienti River near Macerata (Table 1 (c)). The most recent ones are the Beauregard Dam on the Dora Baltea near

Aosta (h = 132, volume = 440,000 cu m), the Cancano Dam on the Adda River near Sondris (h = 173 m. volume = 1,100,000 cu m), the Mulargia Dam on the Ris Mulargia (h = 99 M, volume = 240,000 cu m) and Flumendosa Dam on the Flumendosa River (h = 119 m volume = 305,000 cu m) in Sardinia, and the Frera Dam on the Belviso near Sondrio (h = 138 m, volume = 420,000 cu m).

Several of the dams constructed during the past 15 yr are interesting because of the peculiar problems solved in connection with construction on unreliable rock. Among those previously mentioned is the Val Gallina Dam, the foundation of which had to be substantially reinforced. In regard to the Beauregard Dam, an enormous pocket of alluvial sand 30 m high was discovered at the foot of the left abutment after the main part of the excavation was performed. A considerable amount of concrete was required to fill this pocket. The previous examples



FIG. 5.—PIEVE DI CADORE DAM

indicate that arch structures can be used even when unfavorable geological conditions are present, provided that appropriate measures are taken. The study of the measures and of the special precautions to be taken in these cases have been widely developed in Italy.

METHODS OF ANALYSIS

The principles underlying the analysis of arch dams in Italy have followed the same evolution as they have in other countries. The basic computation, which gives the first preliminary estimate, is based on the cylinder formula, assuming correlatively low stresses. The Italian Dams Regulation allows the application of the cylinder formula for the lower part of the structure, where the thickness of the arches is too great in relation to the radius to permit the

use of elastic arch analysis. For the remainder of the structure, elastic arch analysis is fundamental. As a rule, Italian regulations sanction its use for arch and dome dams. Elastic arch analysis was studied in Italy in a classic work by Camills Guidi.[3] A new regulation is being issued, which will consider the different types of arch dams.

In structures in which the ratio of the dimensions causes the cantilevers to have an actual static function, but does not make it necessary to consider them as actual arch-gravity structures, an ordinary analytical check of the effect of their weight is considered. In certain cases the study is limited to the central cantilever, following the Ritter[4] and Stucky[5] systems, and in some cases the computation is extended to other cantilevers.

Furthermore, the behavior of the upper parts of the structure is sometimes checked considering the inclined arches (the "arches plongeants" of the French engineers). However, this control sometimes gives unsatisfactory results because the choice of the arches is often difficult to define. At other times, the analysis with the membrane-type computation is adopted—that is, an extension to thin revolution arches of the classic criterion of Schwedler,[6] also reported by Krall.[7]

The foregoing refers to the relatively slender true arch or dome dams, in which the resistance of the cantilevers can be totally or partially ignored. When

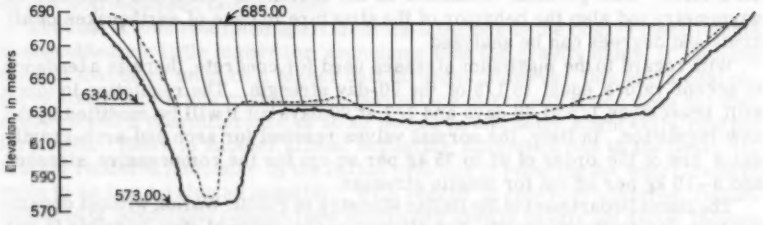


FIG. 6.—PIEVE DI CADORE DAM DEVELOPED ELEVATION ALONG THE MIDDLE FIBER OF THE ARCHES

this concept does not apply, recourse is made to the computation of arch gravity structures according to the methods of Tölke[8] and the Trial Load.

Applications of these methods have been performed by Italian specialists. Arturo Danusso[9] and Guido Oberti[9] used the Tölke method, adding their own original ideas. For the planning of the Piave Dam Filippo Arredi[10] studied special methods that were later generalised, amplified, and applied to the analysis of many other structures. Dino Tonini,[11] F. ASCE used the Trial Load

---

3 "Statica delle dighe per laghi artificiali," by Camillo Guidi, Torino, 1926.

4 "Die Berechnung von bogenförmigen Staumauern," by H. Ritter, 1913.

5 "Contribution à l'étude des barrages-voûtes," by A. Stucky, F. Panchaud et E. Schnitzler, Bullettin Technique de la Suisse Romande, 1950.

6 "Die construction der Kuppeldächer," by Franz Schwedler, Berlin, 1877.

7 "La diga di sbarramento a volta-cupola per laghi artificiali," by Giulio Krall, Roma, 1951.

8 "Talsperren und Staumauern," by Friedrich Tölke, Berlin, 1928.

9 "Studi teorici e sperimentali sulla diga ad arco-gravità del Piave," by A. Danusso, and G. Oberti, L'Energia Elettrica, 1954.

10 "Lo studio morfologico e statico della diga di Pieve di Cadore," by Arredi Filippo, L'Energia Elettrica, 1955.

11 "Calcolo di verifica della diga di Pieve di Cadore con il metodo della ripartizione dei carichi tra archi e mensole," by Dino Tonini, L'Energia Elettrica, 1955.

Method repeatedly and introduced simplifications and additions of practical interest, substituting research by systems of equations in place of trials.

As a consequence of the improved knowledge of the distribution of stresses in arches, due to theoretical studies and model tests, the monocircular arch form and the constant thickness have now been completely abandoned. The present (1960) normal form for the arch has increasing thickness and increasing curvature toward the abutments (the fillet) arches, sometimes with local points of variation as in the case of polycentric curves, and sometimes with gradual points of variation as in the case of special curves.

The hypotheses of foundation deformability was applied for the first time in Italy by Oberti[12] in 1938 according to widely known principles and formulas also found in European[13] American technical literature.[14]

Important studies of the stresses due to temperature variations were made by Guidi[15] Puppini,[16] Ippolito,[17] and Arredi.[18]

A typical Italian contribution to dam analysis and construction is the model technique. Large model tests are considered genuine tools for three-dimensional computation of structures. Their use is widespread and has been a great help in the study of every kind of dams and especially of arch dams in Italy. The scale of these models is often around 1:35, as in the case of Vaiont Dam model whose height exceeds 7.5 m. In particular, model tests permit the analysis of special circumstances of great interest for the study and adoption of arch structures. Such peculiar conditions as the abutments' rock, the influence of asymmetry and also the behavior of the structure in case of earthquakes of all kinds and degrees can be analyzed.

With regard to the maximum stresses used for concrete, there is a tendency to accept values equal to 1/5 of the 90-day strength. The regulation in force still prescribes 1/5 at 28 days and 1/7 at 90 days but it will be modified by the new regulation. In Italy, the normal values reached for arch and arch-gravity dams are of the order of 65 to 75 kg per sq cm for the compressive stresses and 8—10 kg per sq cm for tensile stresses.

The Dams Department of the Italian Ministry of Public Works, without departing from its safety standards, has allowed every rational step possible in our field

CONSTRUCTION METHODS

The principles of construction used in Italy do not differ substantially from those practised in other countries. The time required for the construction of an arch-dam is not considered a more serious problem than that for any other

12 "Criteri di progetto e studi sperimentali per la diga del Lumiei," by Guido Oberti, L'Energia Elettrica, 1948.

13 "Die Berechnung der Fundament deformation," by F. Vogt, Oslo, 1925.

14 "Engineering for dams," by W. P. Creager, J. D. Justin and J. Hinds, Vol. II, New York, 1945.

15 Camillo Guidi, op. citata.

16 "Variazioni di temperatura entro le dighe a volta," by Umberto Puppini, Il Monitore Tecnico, 1922, n. 32; and "Temperatura nelle dighe di muratura. Interpretazione di esperienza," l'Elettro tecnica, 1934, n. 1.

17 "Calcolo delle dighe ad arco," by Girolamo Ippolito, Hoepli Editore, Milano, 1923.

18 "Le sollecitazioni indotte da variazioni di temperatura nelle dighe a gravità," by Filippo Arredi, Giornale del Genio Civile, 1945, n. 1, and 1947, n. 2. Also: "Dighe ad arco-Nuovo contributo al problema delle sollecitazioni indotte dalle variazioni di temperatura," L'Energia Elettrica, 1955, n. 10.

type of concrete dam. A dam, simply because it has to be built as an arch dam instead of as a straight dam does not take longer to construct.

Actually, construction difficulties might arise exclusively from climatic conditions, which in many Alpine districts are peculiarly severe. The arch solution with its lower volume may with suitable organization involve less time. A monthly concrete pouring of 44,150 cu m for many consecutive months was obtained for the Piave Dam in 1948 and 1949. The figure of 54,700 cu m was reached in 1955 for the Cancano Dam in the Upper Valtelline. These figures were almost reached on the Pian Telessio dam on Rio Piantonetto near Torino and Beauregard Dam.

For arch-gravity dams of great thickness, in the case of necessity, the daily pouring could be increased to quantities comparable with those of a gravity dam, at least in proportion to their respective thicknesses. The arrangement of radial blocks, normally 10 m to 15 m thick in Italy, corresponds approximately to the pouring for blocks in gravity dams. The difficulties of longer concrete pourings do not lie so much in the lesser thickness as in the height of the layer that can be poured daily, and this is true in general for any type of dam. There may be further limitations to the height of the layer in the case of arch dams with considerable overhang.

To assist in the placement of concrete and to maintain its constant good quality, preliminary studies of mix design are generally performed in specialized and well-equipped laboratories.

The cost of concrete itself apart from the influence of the cost of installations is undoubtedly a little higher for arch dams than for gravity dams, if only for the fact that there must be a higher unit strength. However, this extra cost reduces itself in practice to the higher percentage of cement, which does not normally exceed a plus difference of 50 kg per cu m and some slight extra cost for formwork. There is another almost negligible difference due to the heavy vibration rendered inevitable by the Italian practice of reducing the water-cement ratio to as low a value as possible. With regard to concrete mixtures, Italian mixtures of pozzolanic cement (now commonly used in nearly all dams) include also the pozzolana computed in the weight as cement, so that the values involved are not comparable with analogous American values. For example, the mass concrete used in the construction of the Hungry Horse Dam on the South Fork of the Flathead River near Columbia Falls, Mont., was made up in the proportion of 111 kg of cement and 56 of fly ash, for a total of 167 kg, as against 200 kg of the ferrico-pozzolanic cement used in the Pieve di Cadore Dam.

In Italy, dams are often built in high mountain areas or in cold regions in which the problem of freezing is of first importance. The consequence of this is that even for a gravity dam there is need for special mixtures of concrete and special care in pouring, at least in the neighborhood of the faces.

Difficulties encountered in the construction of arch dams may be due to the formwork made necessary by the curvature of the surfaces. Also, the curve of the axis in certain cases renders some forms of transport and concrete-laying inappropriate. This last difficulty, however, can be easily overcome by widening the operating range of the cable-way equipment or, as was done in the Piave Dam and others, with the use of movable distribution towers on curved rails that follow the ground plan of the structure. On the contrary, gravity dams often require longitudinal joints and artificial cooling of the concrete, both of which are seldom necessary for arch dams and rarely needed for arch-gravity dams. Furthermore, a curve showing the pouring as a function of height is often more favorable to good utilization of the installations in the case of curved

dams than in that of gravity dams. This is due to the fact that in arch dams the maximum surface area is exposed in the middle of the construction period.

When comparing the cost of recently-built Italian arch and dome dams with gravity structures, the difference in cost is, in practice, nonexistent for arch-gravity dams. Actually, it is reduced to the influence of the lower concrete volume in the incidence of the building installation. The fundamental factor in the unit cost is the volume of concrete, which has already been explained by others.[19] The unit cost rises, for thin arch and dome dams, but even for these not in an inverse ratio to the volume.

In Italy, the total cost for the arch solution opposed to the gravity solution cannot, generally speaking, be higher, because the percentage saving in volume is usually higher than the percentage increase in the unit cost. Therefore, the total cost always shows an actual and substantial saving.

PARTICULAR CONSIDERATIONS

The ideas previously explained are applied to single cases encountered in practice, with some variations according to the ideas of the designers and builders. Whereas in a certain sense there is a uniformity of treads in the field of analysis, it cannot be said that any such uniformity exists in particular applications, although a certain tendency toward standardization is discernible.

The following is an explanation of the principles on which many Italian designers and builders have worked. These principles do not constitute normal practice or Italian compulsory regulations, but merely reflect the ideas and practical experience of some designers:

1. The arch and dome, even if computed as if they were composed of a series of independent elements, must always be considered as continuously curved three-dimensional plates, which they actually are. In this light also the problem of asymmetrical solutions for arch dams should be considered.

Asymmetry causes a less uniform distribution of stresses with higher maximum values than exist in a symmetrical structure having the same mean stresses with the maximum values (usually high) proper to arch dams. Therefore, an asymmetrical solution although having a smaller surface development than a symmetrical one, might involve greater volume. This occurs if the stresses are kept within the same limits as in a symmetrical solution, which results in the thicknesses being substantially increased in certain parts of the dam.

Moreover, the analysis of an asymmetrical structure is more difficult and delicate in concept and therefore the design must depend to a great extent on model tests, unless more conservative stresses are adopted.

In summary, it is not a question of taking an absolute position in favor of symmetry, but of choosing between solutions that may be technically sound but differ in cost. The choice must be based on economic criteria.

At any rate, geometrical symmetry can be deceptive from a functional point of view, because the characteristics of the rock and the termal conditions are usually not equal on both sides of the location. Therefore, the symmetry attained in the shape would not be reflected in the static performance.

2. If the concept of symmetry has a relative importance, a greater importance is given to the geometrical continuity of the structure. The idea of geo-

19 "Considerations sur la comparison entre des éléments du prix de revient de quelques barrages italiens en béton," by N. A. Biadene, I. C. O. L. D., Fifth Congress, Paris, 1955.

metrical continuity must be applied not only to the arch itself (whose horizontal and vertical sections must vary gradually, as must all the geometrical parameters of the structure) but to the supporting surfaces to some extent.

Every abrupt variation in the perimeter of the curved plate gives rise to considerable concentrations in the stresses, with static repercussions on part of the adjacent areas, resulting in marked static differences in the behavior of the structure.

This principle of a relative continuity of the abutments' surface may cause serious increases in the excavations as well as in the volume of the arch when there are abrupt local variations of the natural profile. For example, should a completely continuous perimeter be sought, a deep recess in the abutment would made considerable increases of volume in the adjoining zones necessary. In such cases, the discontinuity must be eliminated by means of a type of plug that fills in the recess. The plug is separated from the curved plate by a construction joint, as are all the parts that, owing to the irregularity of the rock surface, do not follow a reasonably continuous line for the surface of the supports.

On the basis of continuity of the abutment surface, many Italian designers have eliminated stepping of the rock in arch dam abutments. Thus they are achieving excavation lines that are as continuous as possible without abrupt changes of relief.

3. The perfect encastrement on which the analysis of arches is often based on only a hypotheses that rarely corresponds to reality. For a perfect encastrement, the perimetral part of the plate should be locked in a trench of solid rock whose side walls encase the structure to a sufficient depth. Furthermore, the part to be encased and the adjacent part should be strongly reinforced. The need to realize the perfect encastrement would arise only if the curve of pressure came out of the middle third of the abutment. In general, the abutment of the structure tends to be a simple support, and it is certainly so when the plate rests on a plug.

The adoption of the simple support permits greater freedom and ease in constructing the abutments, and in many cases results in a saving of cost. Besides, the concept of the continuity of the surface of support, as underlined above, has already led the designers to separate in certain points where the surface was irregular, the concrete part against the rock from the arch proper, by means of a joint. Combining the two ideas, it was logical to extend the joint itself to the whole perimeter;—that is to place the arch or dome structure designed with a continuous perimetral line, on a type of distribution saddle or cradle running all along the surface of support. This saddle is separated from the structure by a construction joint, termed the perimetral joint. Fig. 7 shows the profile of a perimetral joint.

Thus, the curved plate rests on the rock by means of this distribution structure, on a saddle called through architectural analogy, the pulvino, or cushion. The pulvino makes a clear break between the dam and the rock, to which it becomes to all intents and purposes a transitional part.

4. The following are the advantages of this arrangement:

a. From the static point of view, there is a reduction of the tensile stresses that under certain conditions (thermal variations, shrinkage, earthquakes) may be present near the abutments in the upstream face of the arches. This is especially true in the lower, thicker abutments, and at the foot of the central cantilevers. In the neighborhood of the joint the tensile stresses can be considered completely suppressed.

b. In this way the danger of cracking on the upstream face near the abutments becomes more remote. Actually, the engineer predetermines the zone in which he prefers eventual cracks to appear, and in which he can adequately protect them from infiltrations that might cause abnormal stresses in the body of the dam and prove detrimental to its conservation.

c. Similarly, any tendency toward separation of the plate from the rock in the upstream part, subject to tensile stresses, is limited.

d. The construction of a joint at the abutment at the point of contact with the rock would not be easy. It would require the unreliable construction of a small concrete block adhering to the rock to realize the joint between two concrete surfaces. The perimetral joint is instead planned and rationally constructed at a short distance from the rock.

e. The construction of the perimetral joint allows the surface between the plate and the supporting structure (pulvino) to be given a transverse shape that is naturally appropriate to the elastic functioning of the plate. A cradle-shaped surface is generally preferred or a broken surface following approximately a flattened cradle surface and crossing perpendicular to the upstream

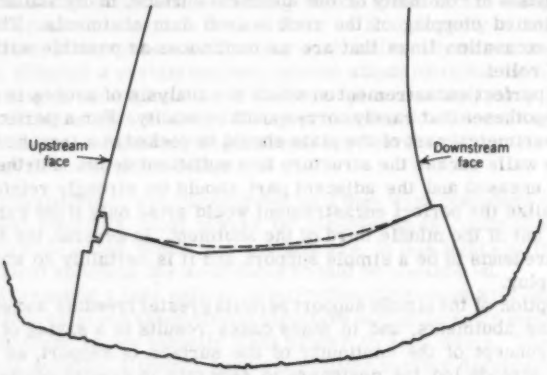


FIG. 7.—PROFILE OF A PERIMENTRAL JOINT

and downstream faces. It might be considered similar to a continuous hinge along the whole perimetral joint. Details of the perimetral joint are shown in Fig. 8.

f. It appears evident from the prior consideration that the pulvino facilitates a good transition between the arch proper itself and the surface of abutment. It also facilitates a good geometric definition of the curved plate since the first design stage. Hence it permits early starting of model tests and excavations. Otherwise the final geometric characteristics of the plate could only be fixed at completion of excavations.

g. From the construction viewpoint the pulvino can be cast in stages, days or weeks, or even months in advance of the dam blocks next to it. This seems to be a rational and practical system. Furthermore, it can simplify the performing of the grouting. In particular, the presence of the pulvino facilitates the operations of joining through grouting to the rock.

6. Due to the reasons explained previously the perimetral joints have been adopted in several Italian dams.

After its initial use in the Osiglietta Dam, the joint was applied to many other Italian dams, principally those of the Vemeto area. To check the practical results of the perimetral joint, it would be necessary to build the same dam both with and without the joint to be able to compare the behavior of the two. This is obviously impossible. Therefore, the engineers have to confine themselves to comparing the dam models constructed on the two principles.

A comparison of the Lumiei Dam models as reported by Guido Oberti[20] proved that the joint provided good, if not decisive, advantages. The stresses in the structure were lower and better distributed. This result has been verified by the excellent static behavior of the actual structure. All the other dams with perimetral joints have given good results. This does not mean that without the joint the results would not have been good. The conclusion is clearly positive without excluding other possibilities.

7. Another question frequently encountered is whether there is the possibility of a slipping movement of the dam in a downstream direction on the surface of the joint. There should be no such possibility because the joint is designed

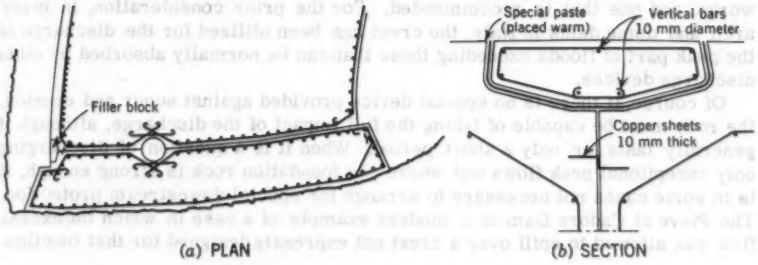


FIG. 8.—DETAILS OF THE PERIMENTRAL JOINT

spatially to obviate any chance of movement in the downstream direction. It is roughly normal to the line of pressures and could not allow sliding movements. The joint could exercise its function only on the surfaces tangential to the dam faces, thus facilitating the structure's respiration—that is, the tiny rotations of the curved plate in respect to the pulvino.

In the case of the Val Gallina Dam, in which an early model built without taking into account the structure weight, had indicated the possibility of sliding downstream, the joint in the base zone of the dam was limited to only the upstream third of the section.

8. From the functional point of view, the pulvino could be built of concrete having elastic characteristics that render it able to act as an intermediary between the concrete of the arch and the rock. This will further increase its capacity of work as a transition structure between the arch and the rock, a function already implicit in its conception from the structural and position points of view. One of the functions of the pulvino is that of distributing and reducing

20 "Criteri di progetto e studi sperimentali per la diga del Lumiei," by Guido Oberti, L'Energia Elettzica, 1948.

the stresses in the rock. Its form and its dimensions can be adapted, with appropriate widening and reinforcement, to the characteristics of the rock. Inversely, the pulvino is capable of reducing the repercussion on the curved plate of the discontinuities and irregularities in those elastic characteristics along the surface of support.

In particular, the pulvino can be thickened, widened, and, if necessary strengthened by adequate steel reinforcements, so that it may work as a sort of bridge over the weaker areas of the abutment surface. This bridge function can also be performed by the adjacent areas of the curved plate itself, but the presence of the pulvino facilitates this function. The pulvino plays a more defined part, which can be easily adjusted and analyzed so that the plate confines itself to absorbing a limited proportion of the abnormal and additional stresses.

9. Another device frequently used in Italian arch dams is that of the discharge of floods over the crest. It is assumed that for actual safety, it is necessary that at least one of the various discharge provisions be an open spillway followed by an open conduit. Indeed, the consequence of only closed conduit, would be a sudden and uncontrollable raising of the water level whenever the peak-flood exceeded the computed maximum. A crest-spillway probably constitutes in many cases the most economical solution for the open discharge works, and one that is recommended. For the prior consideration, in many arch and dome dams in Italy, the crest has been utilized for the discharge of the peak part of floods exceeding those than can be normally absorbed by other discharge devices.

Of course, if there is no special device provided against scour and erosion, the rock must be capable of taking the full impact of the discharge, although it generally lasts for only a short period. When it is a question of discharging only exceptional peak flows and where the foundation rock is strong enough, it is in some cases not necessary to arrange for special downstream protection. The Pieve di Cadore Dam is a modern example of a case in which the excess flow was allowed to spill over a crest not expressly designed for that function.

CONCLUSIONS

Construction of arch dams in Italy is widely developed. It is due to numerous factors, and essentially to the geologic and topographic characteristics of the valleys and cost of materials which is still comparatively high.

The development of arch dams can be divided into three main stages: Dams with nearly cylindrical upstream face and vertical axis; dams with variable radii and constant or almost constant center angles; and dome dams. The arch-gravity type too was largely used in the past twenty years.

Design methods are based as a rule on elastic arch analysis. In the case of thin and very curved structures, methods that assimilate the structures to membranes or revolution surfaces are also used. Systems which also take into account the weight of cantilevers are used for arch-gravity structures, including the trial-load method with special modifications studied in our country.

Particular attention is given to model tests which are always considered an indispensable completion of analysis and, in some cases, a substitute for it. The characteristics of the surface of support and the stability of foundations are also studied with great care.

Among particular problems, the choice between asymmetric and symmetric structures is solely based on economic criteria, each case being judged on its own merits. Great importance is attached to geometric continuity both in the

structure and in the surfaces of support. This particular consideration led many Italian engineers to the conception of the pulvino-perimetral joint system. The dam proper is thus supported by a continuous concrete cradle along the whole abutment surface which acts as a transition element between the dam and the rock.

The problem of flood discharges is also given serious consideration in Italy. It is the belief of the writer that at least one free discharge is necessary to ensure the safety of a dam.

ACKNOWLEDGMENTS

The author wishes to express his appreciation to Messrs. Guido Oberti, Filippo Arredi, Francesco Sensidoni, and Mario Scalabrini, and to his staff, whose important additions and suggestions have been invaluable in the writing of this paper.

OBSERVED BEHAVIOR IN ITALY

By Dino Tonini,[1] F. ASCE

SYNOPSIS

A summary of the results obtained from the analysis of deflection, strain, temperature, and other measurements on several Italian arch dams is presented. The influence of temperature changes on arch dam behavior is shown. The results of testing for foundation moduli by seismic methods before, during, and after construction of arch dams are described.

INTRODUCTION

Notation.—All dimensions are given in the metric system. To convert into the English system the following should be used: 1 m = 3.2808 ft, 1 cm = 0.3937 in, and 1 mm = 0.03937 in.

Each of the dams considered herein was provided with a system of control that normally included the following measurements: (a) temperature and humidity in the interior of the structure; (b) deflections of characteristic points of the structure and profiles of the basin upstream and downstream of the dam, by means of large range collimators, pendulums, inclinometers, and high-precision triangulations and leveling surveys; (c) strains and stresses in characteristic points of the structure by means of rosettes of strain and stress meters; and (d) various phenomena, such as the variations of uplift pressures, and elastic properties of the rock and the structure.

A meteorological station was established near each dam, and a seismographic station was also set up near the Pieve di Cadore (Piave River) and Ambiesta Dams (Tagliamento River).

The measurements, as far as possible, were recorded in a single station situated in the central control room of the intakes of the dam. This solution requires a greater length of cable than would be necessary if more measurement stations were used, but was preferred because of the local conditions in which the dam's staff lived. The system of control is studied jointly by the departments charged with the planning and construction of the dam and those in charge of its operation.

In general, a single phenomenon was studied by means of different methods of measurement. This was done to achieve, from the possible differences that cannot be imputed to the precision of the measurement, information on the complementary phenomena that accompany that which at the first approximation was considered to be the main phenomenon.

The observations were begun during the construction stage and continued without interruption after the dam was in service. They were taken more or less frequently, according to the sensitivity of reaction of the structure to the

Note.—Published, essentially as printed here, in December, 1956, in the Journal of the Power Division, as Proceedings Paper 1134. Positions and titles given are those in effect when the paper was approved for publication in Transactions.

[1] Dir., Studies Office, Societa Adriatica di Elettricita, Venice, Italy.

various actions to which it is subjected. A special office superintends the various measurements, collects them, and interprets them to make the transition from the numerical measurements of the observations of measurements that may have a physical significance in relation to corresponding phenomena.

Actually, not all measurements can be easily and immediately interpreted, because they are generally the result of many factors that are not readily distinguishable. However, from the numerous series of observations available, some of the most typical have been selected concerning the functioning of dams as arch structures. The aim of this paper is, therefore, to provide some information on the subject.

In general, to obtain observations of some significance, averages have been taken at intervals of from 3 days to 30 days. The correlation between instantaneous cause and effect cannot, in most cases, be easily determined. This is due to the multiplicity of causes that do not always produce the same effects and to determine the most probable value of the several elements in question would involve many readings for every measurement.

Thus, given the type of phenomena under examination, the features of the instruments and the possibilities of the observers, it has been held that, in the first stage of research, an average of 10 measurements read successively on 10 different days and so corresponding to the average conditions of the structure in that period of time, is more significant than an average of 10 values corresponding to a particular moment. The latter is an average that can give a more accurate measurement of the state of the phenomena in that single moment, but does not allow a more general interpretation.

For a geodetic survey the usual procedure of compensation is adopted but duly reduced. Excluding the first measurement the concern is not with the absolute measurements of the various sizes, but only with the differential ones. However, the geodetic surveys also refer to an average condition of the structure corresponding to the interval of time included between the beginning and the end of the measurements. This interval, for fairly extensive triangulation nets, is always several days.

For some investigations, mobile averages taken over a period of 1 yr have been adopted. In fact, some of the most important actions affecting the structures (air and water temperature, load variations, and so forth) show seasonal periodical variations during the year. The average values of these variations may be considered in many cases to be practically constant, also taking into account the attenuation in reflected phenomena. If this constancy is not found in the annual mobile averages of the supposed effects (temperatures, deflections, and strains of the structure) it can be deduced that other nonperiodical phenomena have been added to the former (development of setting heat, creep of the concrete and of the rocks, and imbition of the rocks themselves,). Thus, in many cases there is a simple method of evaluating these nonperiodical phenomena and their progress.

MEASUREMENTS OF TEMPERATURE

The measurements of temperature of concrete structures are known to be among the simplest and quickest. There is also a good agreement between experimental results and those deduced from the application of Fourier's theory, when the range of external temperatures (air and water), the heat and specific weight of the concrete together with the coefficient of thermal diffusion are known.

In a given structure the number of instruments may therefore be reduced to a minimum for reference and control. They are concentrated mainly near the faces and the middle where, because of the possible interference of thermal waves coming from upstream and downstream, experimental measurements are obtained that are not in close agreement with the theoretical results. An example of the correspondence between theoretical and experimental results is shown for the Lumiei Dam (Tagliamento River) in Fig. 1.

The method of mobile averages has been adopted to determine the end of the period of dissipation of the setting heat of the concrete, assuming that the average annual range for the temperature of air and water do not very greatly

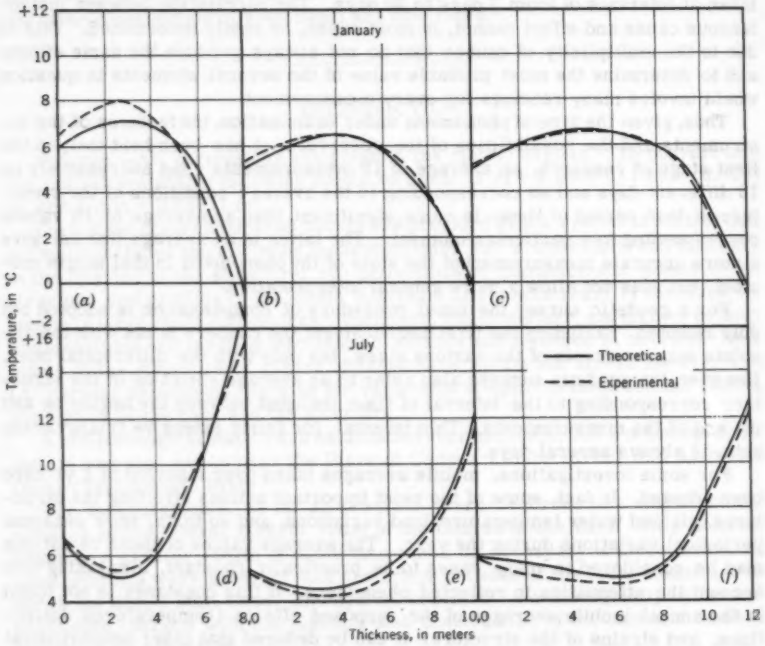


FIG. 1.—DISTRIBUTION OF TEMPERATURES

from one year to the next. When these mobile averages of temperatures in the interior of a dam have an asymptotic trend, it is correct to assume that the setting heat is practically exhausted. Fig. 2 shows how the asymptotic trend is reached at the middle of a section of 18.6 m thickness after approximately 40 months for the Pieve di Cadore Dam.

The annual ranges of temperature in the interior of the concrete dams are shown in Fig. 3. For some of the structures in question the measurements checked at the middle of various sections are recorded. These results are not necessarily the lowest for the section under examination because at the middle there are often interferences of thermal waves from upstream and downstream.

Fig. 3 shows clearly that similar graphs are obtained for the Pieve di Cadore and Val Gallina Dams (Piave River), which have the same technological qualities (cement and aggregates). The Lumiei Dam (Tagliamento River), on the other hand, differs in its behavior because of different technological and climatic features.

Lower measurements are found for the Valle di Cadore Dam (Piave River), which has practically the same technological and climatic features as the Pieve di Cadore Dam. However, the Valle di Cadore Dam is protected upstream and downstream by concrete facing blocks of 0.30 m thickness, which clearly reduces the range of thermal variations. On this matter it must be noted that the protection mentioned was not built to reduce the thermal variations, but against the effects of frost. It is believed that satisfactory protection against thermal

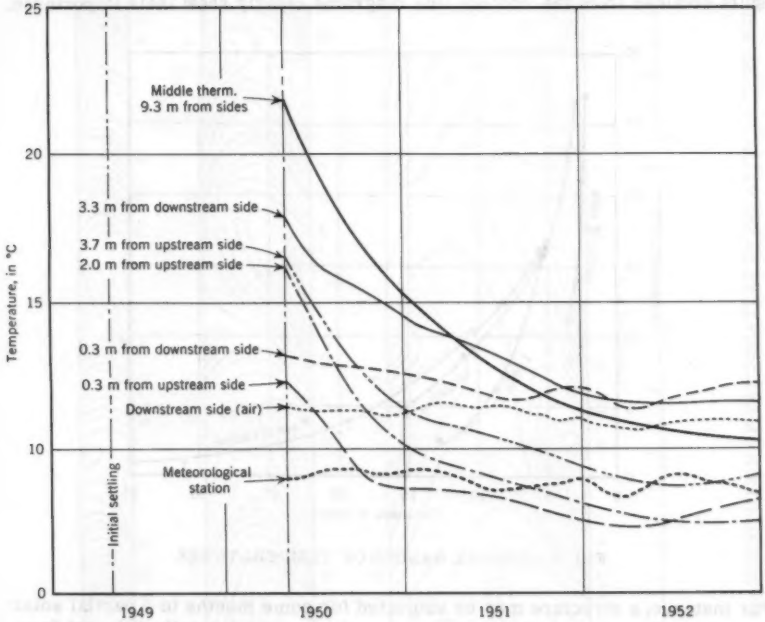


FIG. 2.—MOBILE ANNUAL AVERAGES OF TEMPERATURES

variations could be achieved economically by the use of antiradiation varnish on the downstream face.

A demonstration of the temperature trend along a section of the structure as a function of the time for the Pieve di Cadore Dam is obtained with contour line diagrams in Fig. 4. These diagrams can easily be used for typical stereometric drawings. Fig. 5 shows the stereometric representation of the distribution of temperature in relation to time and thickness at different elevations for the Pieve di Cadore Dam.

From the combined investigation of these diagrams relative to the greatest possible number of sections of the dam, the average temperature of the dam,

or average thermal regime, can be determined. The thermal regime cannot be expressed, as is sometimes done, only by means of the variations of air and water temperatures. These variations, to which should be added those of the setting and rock temperatures, lead, because of successive interferences and displacements, to a more complex thermal regime of the structure. As its complexity increases, it falls behind time in relation to the determining waves. The waves coming from the downstream face have a sufficiently regular and periodic trend. This is not true for the waves coming from the upstream face because of the succession of filling and emptying of the reservoir.

Still other factors interfere in the formation of the thermal regime of the structure, particularly solar radiation and the action of the wind. Although the reciprocal influences of these factors cannot easily be distinguished, depending on the thermal regime pre-existent in the structure, and other factors, the results obtained from the contour line diagrams clearly show their importance.

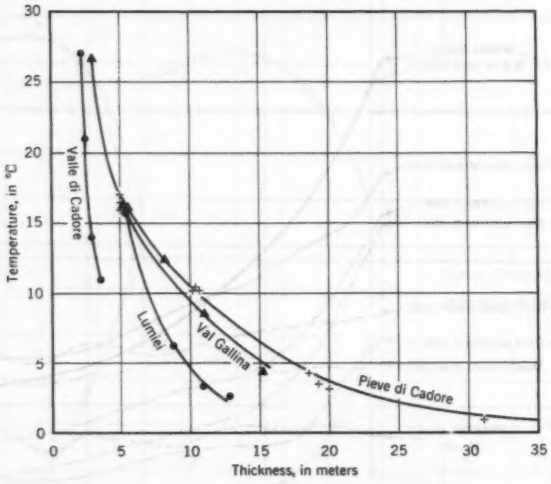


FIG. 3.—ANNUAL RANGES OF TEMPERATURES

For instance, a structure may be subjected for some months to a partial solar radiation. This causes a thermal regime on the sunny side totally different from that of the shadowed side, as found by experiments for the Valle di Cadore and Pieve di Cadore Dams. For this reason a skew thermal load is established in contrast to the hypotheses of symmetry usually assumed by the designer.

The finding of the thermal regime by means of the actual average temperature of the dam is certainly not immediate. It requires the drawing of fairly close isotherms on parallel and perpendicular planes and their graphic integration. In practice, after some years of observation, it is possible to refer to a number of thermometers, the average observations of which can reliably represent the average temperature of the whole structure. As an example, in Fig. 6 the average temperatures of the Pieve di Cadore, Valle, Val Gallina, and Lumiei Dams are shown compared with the average temperatures of the air, at intervals of 10 days. These diagrams show the previously mentioned differences.

FIG. 4.—DISTRIBUTION OF TEMPERATURE IN RELATION TO TIME AND THICKNESS

Knowledge of the dam's thermal regime is not enough to compute the thermal load, which is a function of the distribution of the regime itself in the interior of the structure. Good results are obtained by expressing the thermal load as a function of the difference between the average temperatures of the crest and foundation arches and the difference between the average temperatures of the downstream and the upstream faces. Even if these differences are confined to the temperatures of a given section (the crown one), reliable results can be obtained quickly when the dam is subjected to a uniform solar radiation and ventilation.

MEASUREMENTS OF DEFLECTIONS

The correlations between the variations in the thermal load and deflections in the structure are not immediate. This is due to the previously mentioned

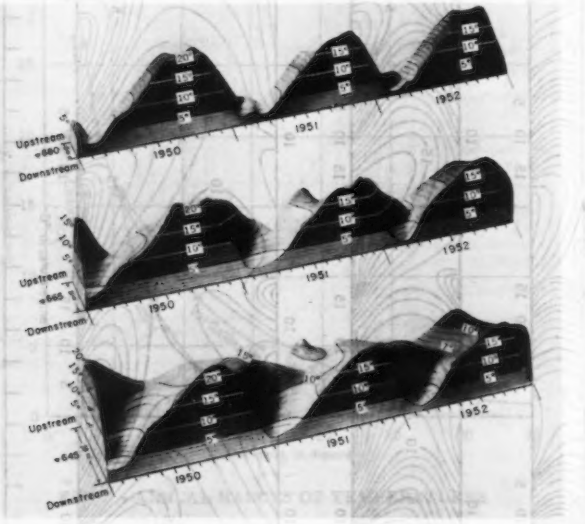


FIG. 5.—STERIOMETRIC REPRESENTATIONS OF TEMPERATURE

difficulties of defining the thermal load, the continuous interferences by the actions caused by the hydrostatic load, the evolution with time of other factors (creep and plasticity of the concrete and rock), and the frequent occurrence of nonperiodic events such as microseisms, seiches, and waves.

Research with inclinographs has clearly shown a rotation of the structure due to the action of the daily thermal wave that is known to penetrate the mass of the concrete for 0.40 m to 0.60 m. This rotation, which in the Pieve di Cadore Dam a maximum at 10" to 15" occurs on days of high solar radiation, and is therefore at its minimum on cloudy or rainy days, even if the range of temperature is large. Fig. 7 shows this phenomenon for the Pieve di Cadore Dam for a block at elevation 624. The greater the difference of temperature between the upstream and downstream faces, a difference that may be considered

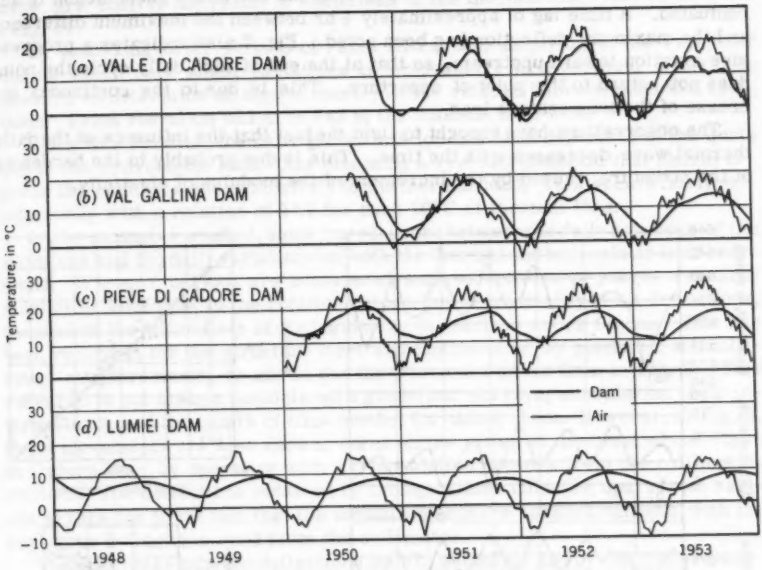


FIG. 6.—AVERAGE DAM TEMPERATURES

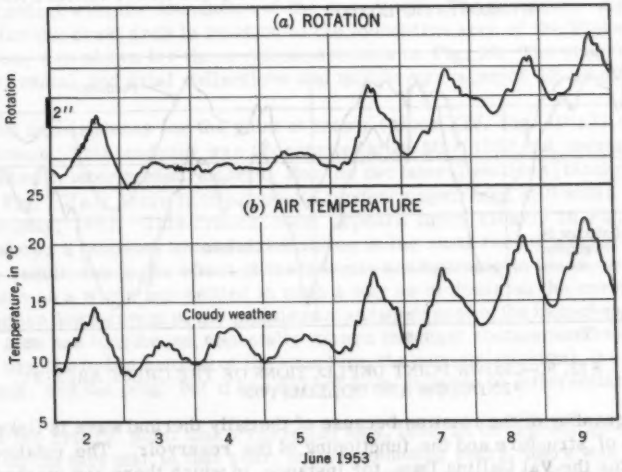


FIG. 7.—DAILY VARIATIONS OF TEMPERATURE AND CORRELATIVE ROTATIONS

typical of the thermal load of the structure, the more this phenomenon is accentuated. A time lag of approximately 4 hr between the maximum difference and the maximum deflection has been noted. Fig. 7 also indicates a progressive rotation toward upstream, so that at the end of each daily cycle the point does not return to the point of departure. This is due to the continuous increase of the temperature load.

The observations have brought to light the fact that the influence of the daily thermal wave decreases with the time. This is due probably to the hardening of the structure, caused by the increment of the modulus of elasticity.

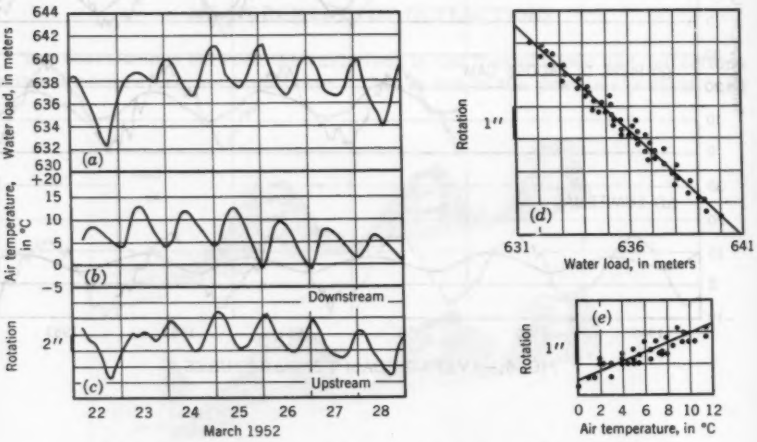


FIG. 8.—CORRELATIONS BETWEEN ROTATIONS AND THERMAL AND HYDROSTATIC LOADS

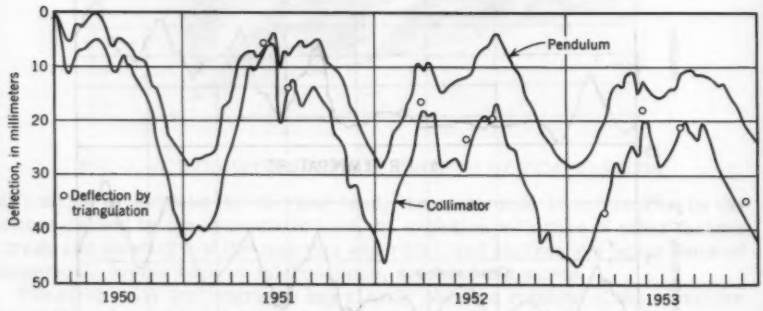


FIG. 9.—CROWN POINT DEFLECTIONS OF THE CREST ARCH BY PENDULUM AND COLLIMATOR

The quantity of the rotation because of the daily thermal wave is linked with the type of structure and the functioning of the reservoir. The rotations recorded for the Val Gallina Dam, for instance, in which there are marked daily variations of load due to the requirements of the nearby power station of Sover-

zene, are clearly the result of variations in the thermal and hydrostatic loads (Fig. 8).

By analyzing brief periods of rapid filling and emptying of the reservoir during which only slight variations in temperature are verified, it has been possible to determine an approximately linear relation between loads and rotations. From elevation 632 m to 642 m the rotation is of 6".6.

Using this relation, the daily global rotation has been depurated of the quote due to the hydrostatic load, thus obtaining a residual diagram that should express the rotations due exclusively to the thermal load. This occurs fairly satisfactorily with a rotation of 1".7 for each 10° C of thermal load.

In the examples studied, some correlations between the daily rotations of the structure and the daily variations of both the thermal and hydrostatic load were found. If longer periods are considered, such as seasons or years, research must be extended not to the rotations alone, but to the totality of all deflections, because of the difficulties of distinguishing the various acting forces. This has been recorded, for the structure itself and continuously, by pendulum and collimator measurements, as shown for the Pieve di Cadore Dam in Fig. 9. This research is not always possible with geodetical surveys, considering their intermittency and the length of time needed for taking them. However, in Fig. 9, these movements are also shown, taken on the crown at the crest of the Pieve di Cadore Dam, by operating with a triangulation network from the collimation stations. The deflections obtained by triangulations coincide, apart from various errors due to the fact that the measurements are nonsimultaneous, with the analogous deflections read from the collimator.

The difference between deflections done by pendulum and by collimator measurements is due to the reciprocal movements of the dam and foundation rock. Further information on these reciprocal movements may be obtained by measuring the deflections of metal tubes inserted in the rock itself. Because practical necessities limit the length of these tubes, the data that can be noted are restricted to the corresponding deflections of the dam and the strata of rock in direct contact with the foundation of the dam itself. The pendulum measurements, for the crest arch in relation to the foundation arch of the Pieve di Cadore Dam, are shown for three typical sections in Fig. 10. The observations refer to radial and axial deflections and mobile averages of 12 months were used.

There is a tendency for the point at crown (block XIV, Fig. 10(a)) to move downstream. This tendency was accentuated after May, 1952, but seems to have diminished in later measurements. For the two lateral sections (blocks IV and XXIX, Fig. 10(a)) there is the opposite tendency upstream, still with a critical point in May, 1952. This critical point appears more clearly in Fig. 10(b)) which shows a tendency toward stabilization in the most recent measurements.

The result, due to the effect of the thermal and hydrostatic loads, is that the structure as a whole has settled in such a way as to diminish the curvature by a deflection downstream of the middle part and upstream of the haunches, whereas the axis has lengthened, especially toward the right abutment. These alterations are due to the settling of the structure, the pulvino (cushion), the foundation rock, and the plug, but it has not yet been possible to differentiate among them.

For the critical point that occurred in May, 1952, an interpretation might be based on the fact that, in that year, unlike preceding years, there was no complete emptying of the reservoir to elevation 630 m, but only to elevation 644 m.

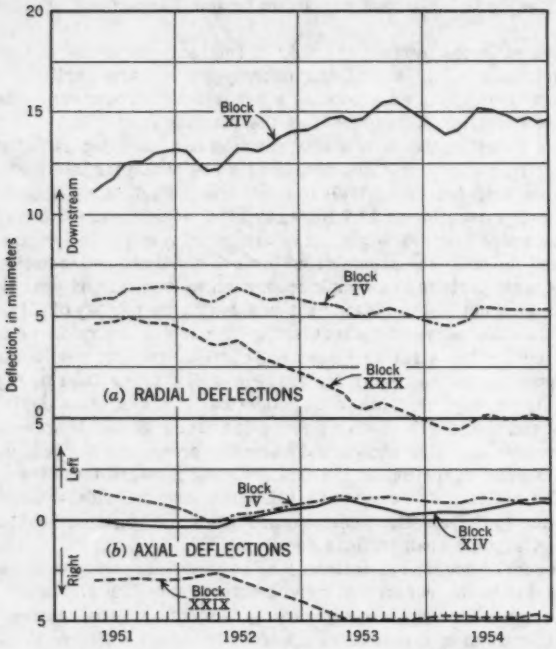


FIG. 10.—MOBILE ANNUAL AVERAGES OF RADIAL AND AXIAL DEFLECTIONS

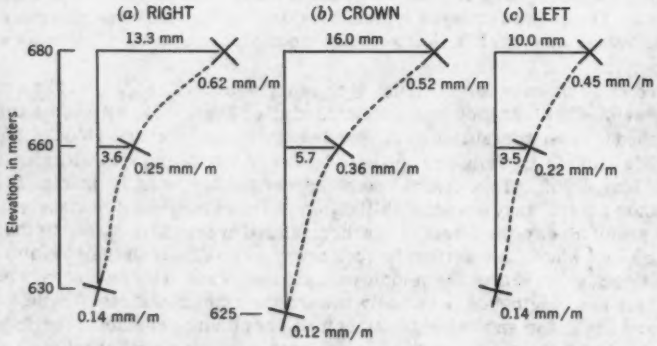


FIG. 11.—AVERAGE ANNUAL RANGE OF DEFLECTIONS AND ROTATIONS FOR THREE CANTILEVERS

The structure, while still at the settling stage, was subjected to a prolonged load that influenced the phenomena of creep and plasticity of the structure and of the rock. This hypothesis is partly confirmed by the fact that the measurements of the modulus of elasticity of the rock showed a diminution of the modulus from 1949, prior to the first complete filling, until 1952, whereas the modulus has remained practically constant since this period.

On completion of the research for the Pieve di Cadore Dam, the results obtained with inclinometers were compared with those given by pendulums. The comparisons were made for the three sections, one approximately central (blocks XXIX and IV), at elevations 680 m, 660 m, and 625 m for section XIV. These comparisons refer to average monthly figures to prevent any possible inaccuracy in the measurements.

Most of the rotations expressed by these two methods correspond closely, but always with higher figures for the inclinometers. This indicates that the rigidity of the structure varies according to the height. The section with the greatest increase of rotation and consequently the least rigidity is from elevation 660 m to 680 m. As an example, Fig. 11 shows the average yearly range between May, 1952, and December, 1955, for the Pieve di Cadore Dam.

Thus, as could be foreseen, the widest deflections marked by the pendulums are on the crown, the lateral ones being smaller and practically symmetrical. For the rotations, on the other hand, those at the base are practically equal. At elevation 660 m there is a maximum on the crown, and lower, fairly symmetrical figures at the abutments. At elevation 680 m there is a maximum at the right side, decreasing as it moves toward the crown and the left side. This is probably due to the fact that on the right side, although the rock has a greater elasticity than that of the left side, there is a lesser resistance to the action of the arch, because of its morphology.

The deflections of the crest arch of the Pieve di Cadore Dam have been the subject of studies performed between May, 1950, and April, 1954. Use was made of numerous experimental data available, such as averages of the measurements taken over 3-day periods, introducing them as coefficients in a system of equations in which the unknown quantities should represent the laws of variation of the deflections as a function of the acting causes. This has been done by the method of the least squares to compute the most likely values of the parameters.

The deflections expressed in millimeters and referring to the foundation line have been considered a function of (1) the difference between the average temperatures (θ_a expressed in degrees centigrade) of the crest arch at elevation 680/m and of the foundation arch at elevation 624/m; (2) the difference between the average temperatures of the downstream and upstream faces considered in their whole extent (θ_p expressed in degrees centigrade); (3) the hydrostatic load, h, expressed in meters starting from elevation 630 m; and (4) an asymptotic function of time, t, expressed in months beginning with May, 1950, in correlation with the creep and plasticity of the concrete and the rock.

The expression resulting of the type

$$1 = \alpha_1 \theta_a + \alpha_2 \theta^2_a + \alpha_3 \theta^3_a + \beta_1 \theta_p + \beta_2 \theta^2_p + \beta_3 \theta^3_p + \gamma_1 k + \gamma_2 k^2 + \gamma_3 k^3 + \delta_1 e^{-\delta_2 t} + h \quad \ldots\ldots\ldots\ldots \quad (1)$$

has been resolved. The values of the unknown parameters for practical applications proved to be the following: $\alpha_1 = +1.18$ mm per degree centigrade; $\alpha_2 = +0.0073$ mm per degree centigrade; $\alpha_3 = -0.002983$ mm per degree centi-

grade; $\beta_1 = +0.43$ mm per centigrade; $\beta_2 = +0.0232$ mm per degree centigrade; $\beta_3 = 0.001479$ mm per degree centigrade; $\gamma_1 = -0.04$ mm per meter; $\gamma_2 = -0.0012$ mm per meter; $\gamma_3 = -0.000029$ mm per meter; $\delta_1 = +7.16$ mm per month; $\delta_2 = 0.109$ mm per month; $k = +9.88$.

The features of this research are summarized in Fig. 12, in which

$$l_\alpha = 1.18\ \theta_a + 0.0073\ \theta_a^2 - 0.002983\ \theta_a^3 \quad \ldots\ldots (2)$$

for Fig. 12 (a), (b), and (e)

$$l_\beta = 0.43\ \theta_p + 0.0232\ \theta_p^2 - 0.001479\ \theta_p^3 \quad \ldots\ldots (3)$$

for Fig. 12 (c), (d), and (f)

$$l_\gamma = -0.04h - 0.0012h^2 - 0.000029\ h^3 \quad \ldots\ldots (4)$$

for Fig. 12 (g), (h), and (k)

$$l_\delta = 7.16\ e^{-0.109t} - 7.16 \quad \ldots\ldots (5)$$

for Fig. 12 (i), (j), and (l).

Using the same results, for the deflections under examination, classification has been sought for the several effects according to their single causes, as they have been postulated. That is to say, the persistence of the loads has been verified by means of the results of single deflections for the time of their duration. In this elaboration no account has been taken of the phenomena connected with time, such as creep, and plasticity, because it is to be supposed that the external causes would every time affect a settled dam.

The following classification of the deflections results:

Quota due to the thermal load:

(1) Difference of temperature between the crest and foundation arches (α)	32%
(2) Difference of temperature between downstream and upstream faces (β)	13%
	45%
Quota due to the hydrostatic load (γ)	45%
Quota due to various unspecified causes and to errors (δ)	10%
	100%

The same research has been performed for the Val Gallina Dam, with satisfactory results of the same type as those seen for the Pieve di Cadore Dam. Geodetical surveys have also been adopted to check the movement of the upstream shores of the reservoir caused by successive fillings and emptyings. There are fourteen measurements for the Pieve di Cadore Dam, for the first eight of which there is a satisfactory correlation between the filling of the reservoir and the approach of the shores. This correlation, however, is not maintained in measurements taken after May, 1952.

For the Val Gallina and Lumiei Dams, the measurements taken are not sufficient in number to define the phenomenon with precision. This is confirmed only for the first 2 yr that the Pieve di Cadore Dam was in operation.

Apart from the errors affecting these measurements, which do not always mutually eliminate themselves, it is considered that the thermal conditions of the rock (all the dams mentioned are built on limestone) and the thermal regime

of the structure itself cannot but influence the movements of the shores. In addition, the fixed stations of the triangulation network, however carefully constructed, are still anchored in the surface stratum of rock particularly subject to thermal variations.

The results observed for the Pieve di Cadore Dam would lead to the conclusion that the rock, as the structure, is subject to movements of a certain significance, especially in the first cycle of the working of the reservoir. Subsequently a settling takes place which, in this specific case, corresponds to some degree to the uniform imbibition of the rocks. But the problems is too closely connected with geological and morphological characteristics and those of the cycle of the reservoir to make any generalization for it.

The great importance of research on the actions and reactions of the rock is made evident, which had perhaps been subordinated to that on the structure itself.

MEASUREMENT OF DEFORMATIONS

Numerous data relating to deformations are recorded for the structures under examination by acoustical and resistance strain-meters placed either singly or in rosettes. The strain-meters are generally laid in the interior of the dam at 0.60 m to 1.00 m from sides to eliminate the troubled external zone. But the elaboration from the elastic deformations to stresses is not immediate because of the lack of information on the accuracy of the values of variations of the modulus of elasticity. This modulus increases with time, but the increase generally is opposed and overcome by the phenomena of plasticity and creep due to the action of the loads.

For a structure subjected to continuous or periodical loads it is convenient to adopt a *conventional modulus* based on the behavior of the structure itself to the various actions of elasticity, plasticity, and creep. Various methods have been suggested for finding this modulus for the structure as a whole, such as the use of jacks or residual tensions, because results from tests in the laboratory have no application in this field of research.

In addition to the seismic method, which will be mentioned subsequently, research on tests loaded according to the method of Guido Oberti,[2] F. ASCE, has been chosen, with some variants. These are primsmatic tests of approximately 2 by 0.2 by 0.2 m supported merely at the ends and loaded, including their own weight to obtain a stress of 15 and 25 kg per sq cm. The load is applied 28 days from the setting and the deformations are recorded periodically on the upper and lower faces by means of removable strain-meters.

Fig. 13 shows the variation of the deformation for elasticity, plasticity, and creep due mainly to the load (half the difference of the upper and lower side deformations) and the variation of the deformation due principally to actions of shrinkage, thermal expansion, and other causes (half the sum of the upper and lower side deformations) for the Val Gallina Dam. From the study of these deformations, it appears that the initial modulus of 260,000 kg per sq cm is reduced, after approximately 40 months of load, to a conventional modulus of 145,000 kg per sq cm for the tests loaded at 25 kg per sq cm and to 165,000 kg per sq cm for those loaded at 15 kg per sq cm.

---

[2] "Deformazioni anelastiche del calcestruzzo della diga di Osiglietta," by G. Oberti, Giornale del genio civile, Vol. 83, 1945, p. 536.

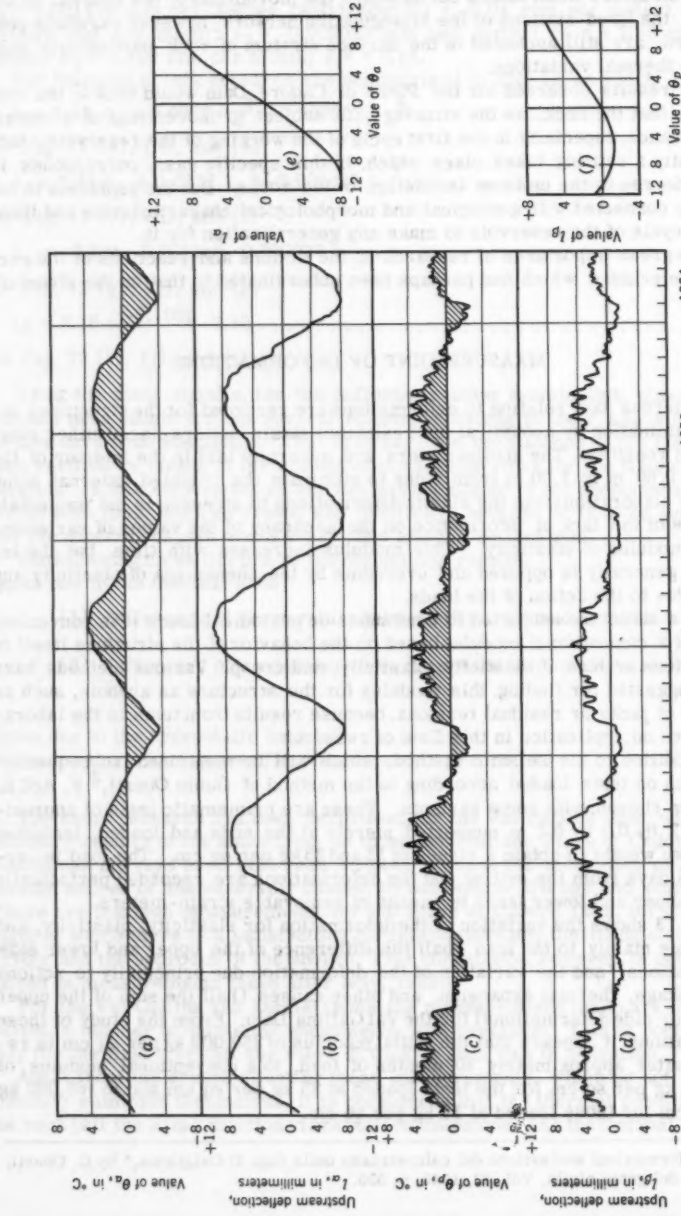


FIG. 12.—ANALYSIS OF THE CREST ARCH DEFLECTIONS

FIG. 12.—ANALYSIS OF THE CREST ARCH DEFLECTIONS

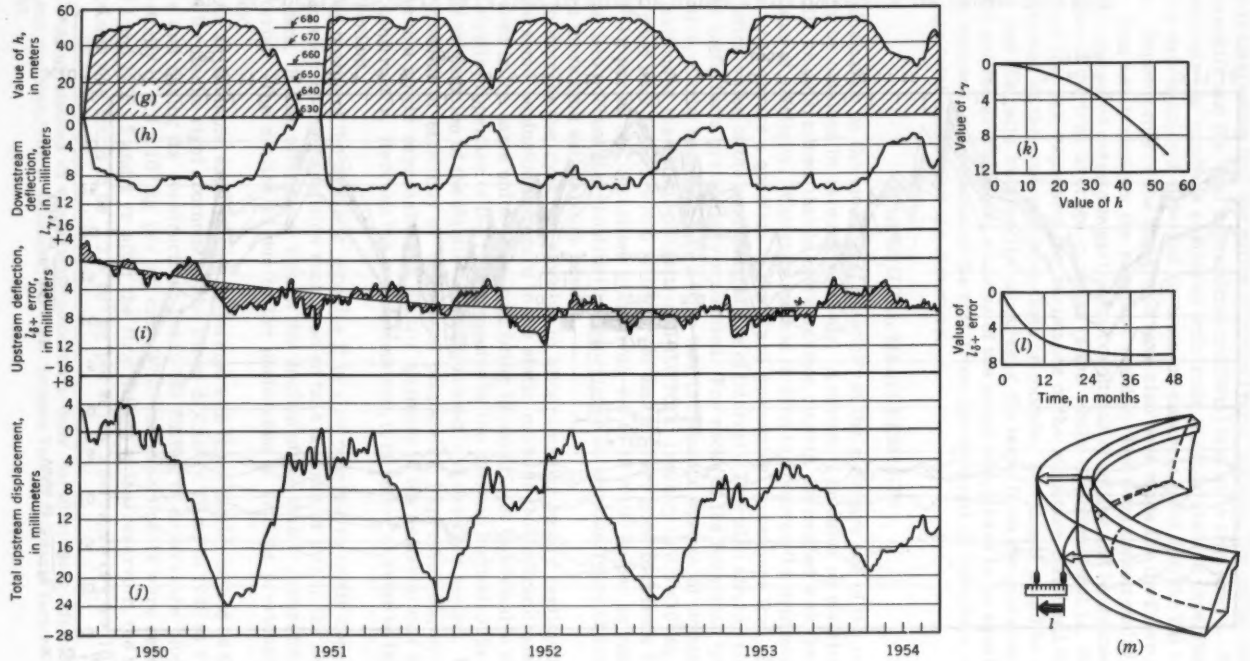


FIG. 12.—CONTINUED

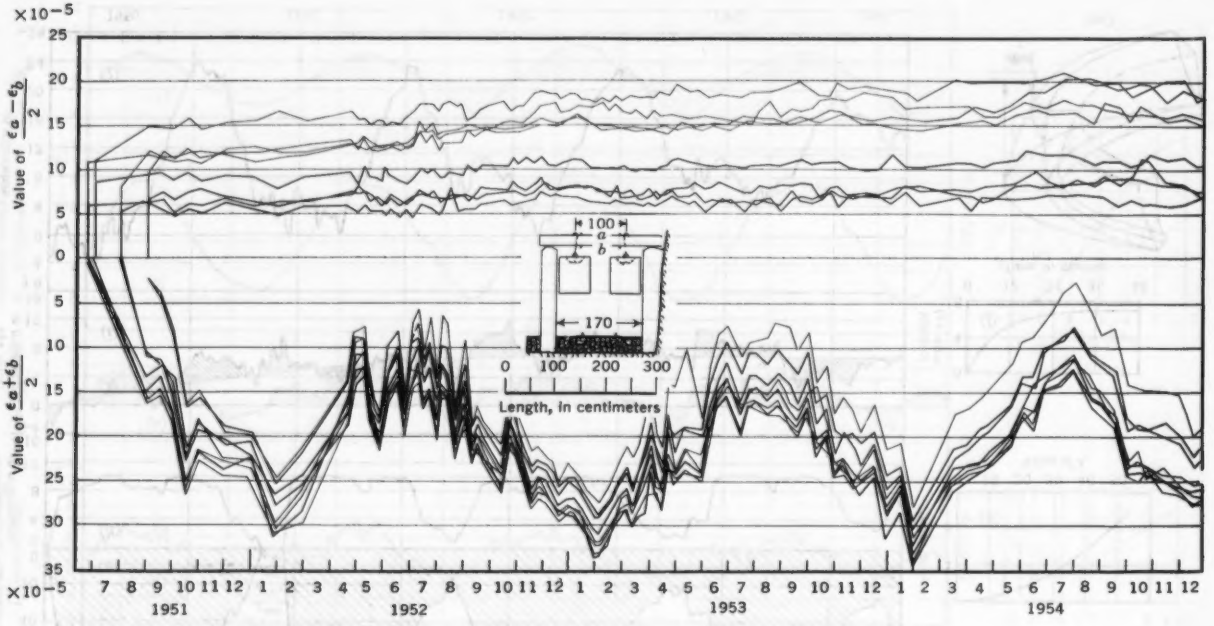


FIG. 13.—DEFLECTIONS IN RELATION TO TIME OF UPPER AND LOWER SIDE OF PRISMATIC TESTS

It is interesting that the ratios of creep (ratio between the initial modulus of elasticity and the final conventional modulus) is a little less than 2. This is a relatively low numbers compared with those in other similar experiments.

The data examined referred to tests of concrete used for the Val Gallina Dam. Experiments of the same type have also been made for the Pieve di Cadore Dam which confirm the previous results. But even these results of the moduli computed on tests in particular conditions of setting and load cannot give an idea of the true average modulus of the whole structure—that is, the only element that can represent the resistance of the structure itself and that can be obtained on the contrary from tests on models. For this it would be necessary that the ratio between the modulus of the tests from the material of the model and the average total modulus of the model would have to be equal to the ratio between the modulus of the test from the material of structure and the average total modulus of the structure.

GEOPHYSICAL MEASUREMENTS

Information on the modulus of elasticity of the structure and of the rock can easily be obtained by seismic methods. A dynamic modulus of elasticity can readily be determined that is more or less closely correlated with the static modulus of elasticity. Whatever method is used to discover the dynamic modulus, it is always a question of rapid and economical processes that afford a statistical value of the modulus that are of interest. This also affords comparisons useful for a preliminary evaluation. For rocks of the limestone type, for example, Carlo Semenza,[3] F. ASCE, has proposed a system of comparative evaluations of the elastic properties of the rock; (rock up to 2.5×10^5 kg per sq cm; good rock from 2.5 to 5×10^5 kg per sq cm; very good rock from 5 to 7.5 $\times 10^5$ kg per sq cm; excellent rock from 7.5 to 10×10^5 kg per sq cm) that, taking into account the construction experience on various types of rock, has given more than satisfactory results.

To express the dynamic modulus in kilograms per square centimeter may cause some confusion in regard to the static modulus that is traditionally expressed in the same units. Far from being impossible, it is advisable to refer the elastic properties of the rock computed by the seismic method to the velocity of propagation of the elastic waves expressed in meters per second. In fact, the modulus of elasticity or velocity of propagation represent conventions to state in a single expression the elastic qualities of the material that interest the constructor. Between the two conventions, it is better to refer to the more convenient.

By means of the dynamic modulus it is also possible to easily observe the anisotropy of the foundation rock, and so take account of this in the design of the dam. It also affords an idea of the decline of the elastic properties of the material. The decline is due to the phenomena of settling previously mentioned.

As an example, experiments performed with the dynamic method on the rock that forms the right abutment of the Pieve di Cadore Dam, in 1948 to 1949 before and during its construction, led to the finding of an average modulus of elasticity of 4.8×10^5 kg per sq cm. When the experiments were repeated in 1952 and 1953, 3 and 4 yr after the first filling of the reservoir, the average modulus was found to be 3.3×10^5 kg per sq cm, a decrease of 1.5×10^5 kg per

[3] "Su un sistema di valutazioni comparative delle caratteristiche elastiche delle masse rocciose," by C. Semenza, Atti dell 'Istituto Veneto di Scienze Lettere ed Arti, 1955.

sq cm compared with the original measurement. In 1953 other experiments of the same kind were repeated at the Lumiei Dam, built in 1947. Whereas, downstream from the dam the modulus was approximately 1.0×10^5 kg per sq cm, the measurement upstream was approximately 8.0×10^5 kg per sq cm. There was a decline on elastic properties in the area affected by the waters, although somewhat less than that observed at Pieve di Cadore Dam. The decline of the modulus may be caused by an increase in the porosity of the rock, determined by the stress due to the increased pressures and their variations.

Seismographic observations led to the conclusion that a continuous settling has been in progress in the rock that forms the bed of a reservoir, especially near the foundations. The settling that occurred at the beginning of the work continued through its completion and the first filling of the reservoir, and to a lesser degree in subsequent fillings. It was determined by the disruption of the equilibrium previously existing between the forces in the medium. The upsetting of this equilibrium may manifest itself in actual small earthquakes, or at least in myriads of small shocks affecting the rock surrounding the dam.

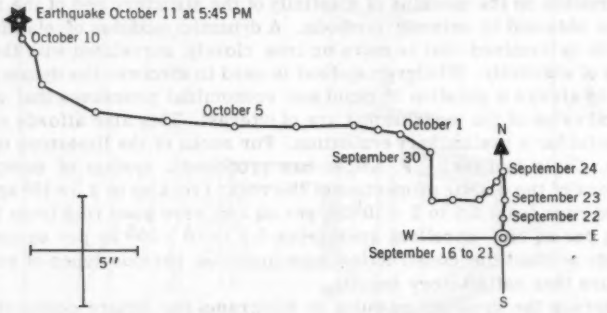


FIG. 14.—INCLINOGRAPHIC ACTIVITY OBSERVED NEAR THE FOUNDATION ROCK

This shock action, if continued for years, causes minute fractures in the rock and innumerable small lesions that tend to increase its porosity. This minute wearing action is manifested particularly in the rocks supporting the dam, especially in arch dams. This interpretation might be used to explain the diversity of elastic properties found in rocks of the same geological period and the same chemical composition. The diversity would be due to the different stresses that the various rocks have undergone during the ages. By geophysical means, such as inclinographs, seismographs, and vibrometers, aspects of the behavior of the structure and foundations that would escape other kinds of investigations may be examined.

Thus, with the combined use of seismographs and inclinographs it has been possible to establish the fact that the Pieve di Cadore Dam belongs to a single geodetic block. Geophysicists have concluded that the surface stratum of the earth crust is made up of relatively small blocks—horizontal dimensions of the order of 7 to 14 km with analogous thicknesses—bounded by recent faults or by surfaces of fractures liable as a mass to mutual sliding without perceptible deformations. This is especially true in areas subjected to earthquakes. It is important for a dam, especially an arch dam, to be based on a single geodetic block. Research is therefore necessary above all in the preliminary stage of study and planning.

An important correlation exists between a preliminary abnormal clinographic activity and a subsequent abnormal macro and microseismic activity. This would indicate an intimate dependence between the gradual movements of strata of the rocks, under the influence of tensions acting in them, and the sudden destructions of equilibrium (earthquakes) that these tensions may ultimately provoke.

As an example, Fig. 14 shows the variations of rotation according to their components, that since September 22, 1954, have gradually started in the foundation rock of the Ambiesta Dam. The rotation is first in a northerly, then in a westerly direction. The rotation in this direction was shown to be particularly active from October 3 to October 8, 1954. During this period the first slight instrumental shocks occurred, gradually increasing in frequency, confirming the tension present in the areas in slow movement. Subsequently the rotations again took a northerly direction. On October 11, 1954, a seismic shock of the intensity of 10^{18} erg occurred, corresponding to this change of rotation. This was followed by an almost uninterrupted series of small instrumental shocks with the task of exhausting the residual tensions in the stratifications affected by the earthquake.

CONCLUSIONS

The observations and results presented are intended to show the difficulty of arriving quickly at conclusions of general interest from the control measurements of dams. What can be ascertained for one structure can hardly, even qualitatively, be applied to another, even though both are apparently of the same type, built and situated in analogous conditions. The fact is that, although there may be dams of the same type, technological features, means, and time taken for construction, the elastic properties of the rock interfere in such a variety of ways as to give every dam its own individuality. This can only be discovered after years of accurate and continuous observations. However, the structure and rock form a single whole, influencing each other. Thus, investigations on their behavior must be extended to both these elements, which react together to the effect of the various acting forces. There is a need for appropriate geophysical research that is given the scope and importance of structural research.

Interpretation of measurements can be greatly assisted by experiments on models: A significant example is the deflection of the crest arch of the Val Gallina Dam. This could not entirely be interpreted, on first examination, according to the normal behavior of a structure of that type. A model reproducing the elastic properties of the various types of rocks affected by the foundation of the dam was constructed. The deformations recorded in the model proved to be in exact agreement with the experimental ones. The experimental deformations were thus clearly understood.

The control measurements of dams, not confined to simple safety measurements, are intended to perform the task of investigating the actual behavior of a structure that is particularly complex, not only in itself, but because of the not always easily definable surrounding conditions.

Therefore, only through a succession of numerous and uninterrupted observations may some light be shed on this subject, by differentiating the elementary causes of variation from the corresponding effects. For each structure and every period, the combination of the greatest possible number of elementary causes should be considered to attempt to achieve an interpretation of the final resulting whole.

AMERICAN SOCIETY OF CIVIL ENGINEERS

Founded November 5, 1852

TRANSACTIONS

Paper No. 3049

GEOTECHNICAL PROPERTIES OF GLACIAL LAKE CLAYS

By Tien H. Wu,[1] M. ASCE

With Discussion by Messrs. T. Cameron Kenney; and Tien H. Wu

SYNOPSIS

A study of the properties of glacial lake clays is reported. Data collected from a number of sites in the Great Lakes area of the United States are presented. Despite local variations in subsoil conditions and the large distances between the sites, the clay deposits investigated have much in common and it is possible to study them as a related family. An analysis was made of the principal factors that control the strength characteristics of the clays. The shearing resistance and sensitivity were found to be intimately related to the structure of the clay as well as the stress history.

INTRODUCTION

In North America the activities of continental glaciers led to the formation of glacial lakes during Pleistocene times. Many of these lakes have since disappeared or now exist in diminished sizes. A number of soft clay deposits extending to great depths are known to exist in areas formerly occupied by glacial lakes. Among the most notable deposits are the clays in the Great Lakes region. These deposits consist primarily of a heterogeneous and unstratified silty clay with some sand and gravel. The texture of these soils closely resembles that of glacial tills. Also present is the laminated clay and silt known as varved clay, generally considered as representative of lacutrine sediments.

Note.—Published, essentially as printed here, in August, 1958, in the Journal of the Soil Mechanics and Foundations Division, as Proceedings Paper 1732. Positions and titles given are those in effect when the paper or discussion was approved for publication in Transactions.

[1] Assoc. Prof. of Civ. Engrg., Michigan State Univ., East Lansing, Mich.

Because the majority of the glacial lake clays exhibit low strength accompanied by high compressibility, their properties have long been subjects of interest. This paper contains information of the physical properties and strength characteristics of several clay deposits in the Great Lakes region. These deposits were selected for detailed study because of their uniformity and extensive depth. The fundamental factors that govern the important characteristics of sensitivity and strength-consolidation relationship were analyzed. Also included are supplementary data from a number of sites which, although lacking in completeness, provide considerable information that support the main thesis.

DESCRIPTION OF CLAY DEPOSITS

During the last great ice invasion (the Wisconsin) the continental glacier moved into the area from the north and east. The glacier covered all of Michigan and extended deep into Indiana and Ohio. Subsequent recession of the



FIG. 1.—LOCATION OF SOIL DEPOSITS

glacier followed the same general directions. The numerous retreats and readvances of the glacier resulted in the formation of large ice-front lakes. The shorelines[2,3] of these lakes are shown in Fig. 1.

As indicated in Fig. 1 the four soil deposits investigated are all in the Great Lakes area near the cities of Fremont, Detroit, Saginaw and Sault Ste. Marie. Fig. 2(a) is a profile showing the subsoil conditions north of Fremont, Ohio.

[2] "Glacial Formations and Drainage Features of the Erie and Ohio Basins," by F. Leverett, Monograph 41, U. S. Geological Survey, 1902.

[3] "The Pleistocene of Indiana and Michigan," by F. Leverett and F. B. Taylor, Monograph 53, U. S. Geological Survey, 1915.

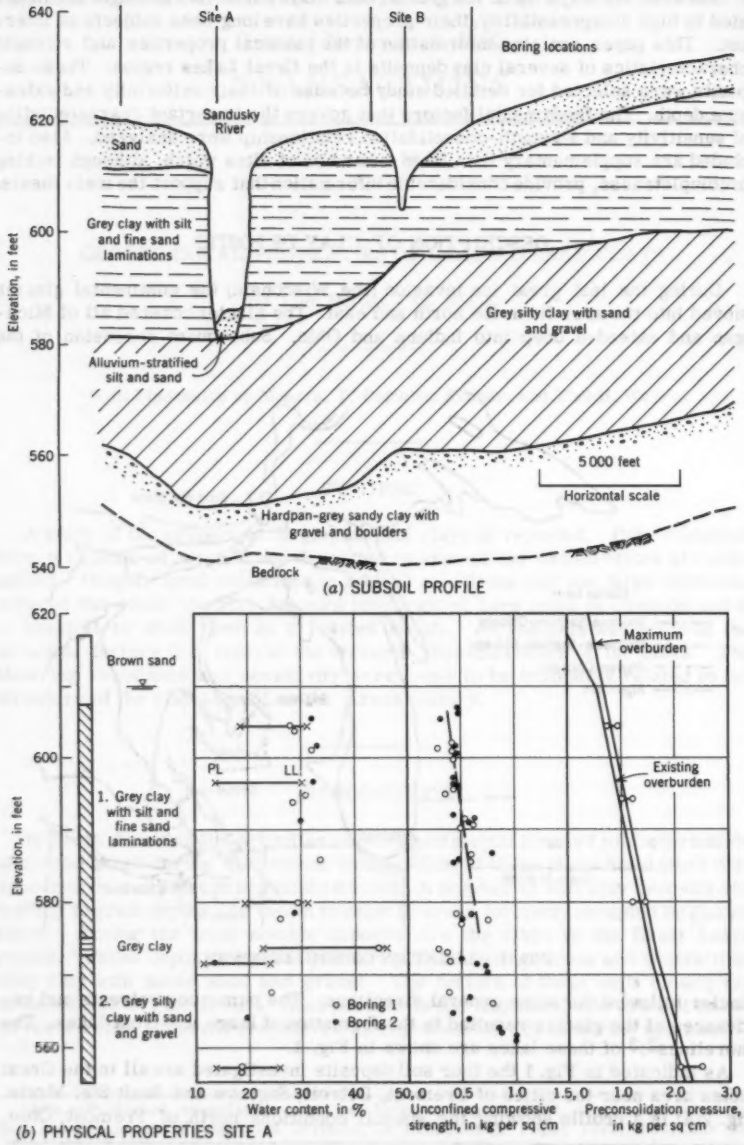
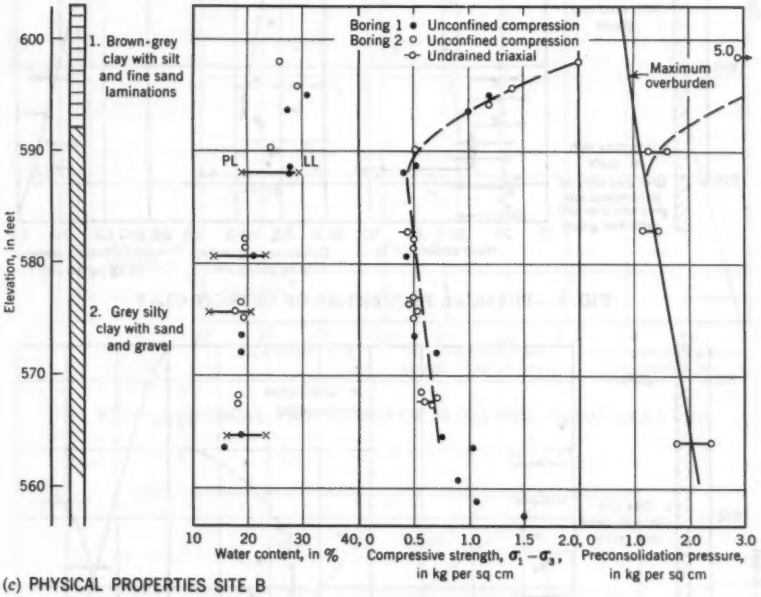


FIG. 2.—SUBSOIL PROFILE AND PHYSICAL PROPERTIES OF FREMONT CLAY

The major units in the subsoil consist of a layer of stratified clay and silt overlying a deposit of unstratified silty clay with sand and gravel. Both are soft to medium in consistency. Beneath these layers are found one or more old till sheets of very stiff clay with gravel and some boulders. Bedrock is encountered at El. 540 representative boring logs describing the physical properties of the stratified and unstratified clays at the Fremont site are shown in Fig. 2(b) and 2(c).

Similar subsoil conditions are found in the Detroit area. Fig. 3 contains a detailed log and summary of the test results obtained from a site near the Industrial Expressway and River Rouge. The data are representative of the subsoil conditions in this area. The uppermost unit is a layer of stratified clay



(c) PHYSICAL PROPERTIES SITE B

FIG. 2.—CONTINUED

and silt and it lies over a fairly thick deposit of unstratified clay with sand and gravel. In the transition a thin stratum of clay containing many irregular layers and lenses of sand is revealed in some borings. The thickness of this stratum where encountered, does not exceed 2 ft. At a depth of 75 ft, the unstratified clay with sand and gravel changes gradually into a layer of soft clay with occasional silt laminations. Remnants of old till sheets and heavily precompressed lacustrine clay are found between the soft clay and bedrock, which is located at approximately El. 480.

At the site near Saginaw, the unstratified silty clay extends down to depth of 51 ft and 65 ft and beneath this are layers of sand and stiff clay till. Data obtained from a representative boring are shown in Fig. 4.

An extensive deposit of soft stratified clay and silt up to 60 ft thick is located between Mackinac Straits and Sault Ste. Marie, in Northern Michigan.

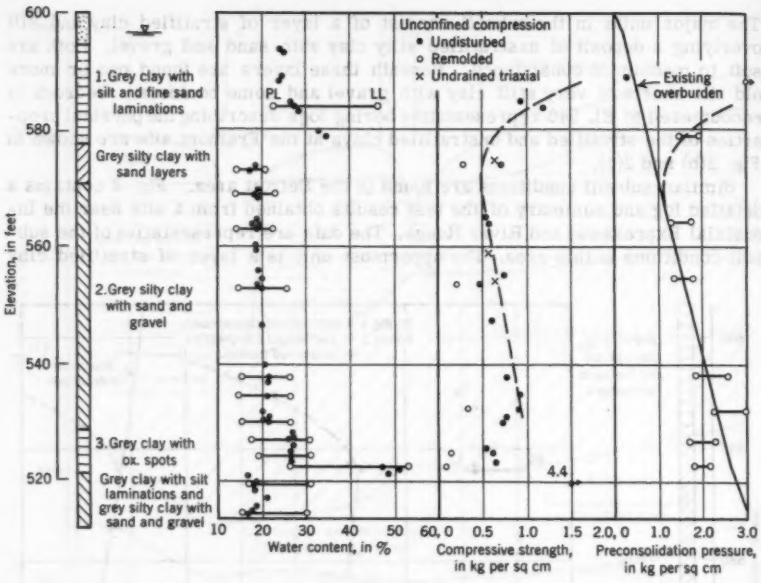


FIG. 3.—PHYSICAL PROPERTIES OF DETROIT CLAY

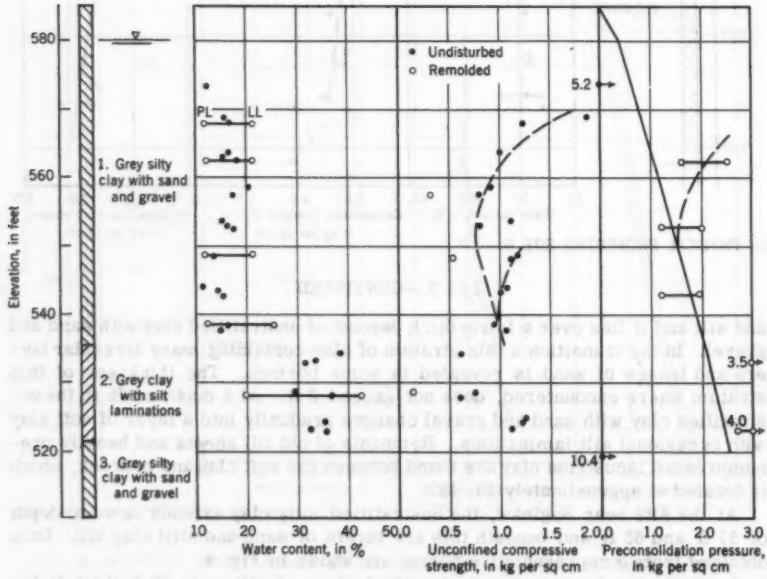


FIG. 4.—PHYSICAL PROPERTIES OF SAGINAW CLAY

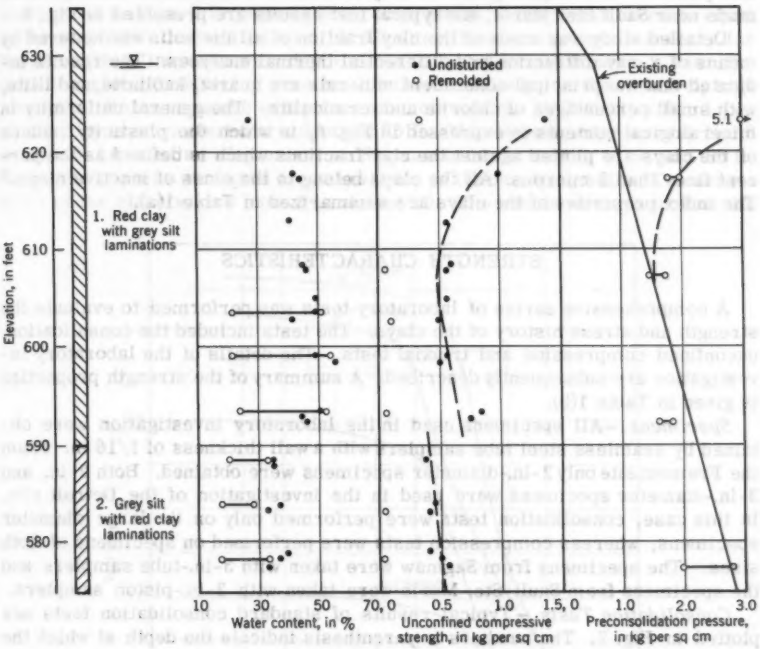


FIG. 5.—PHYSICAL PROPERTIES OF SAULT STE. MARIE CLAY

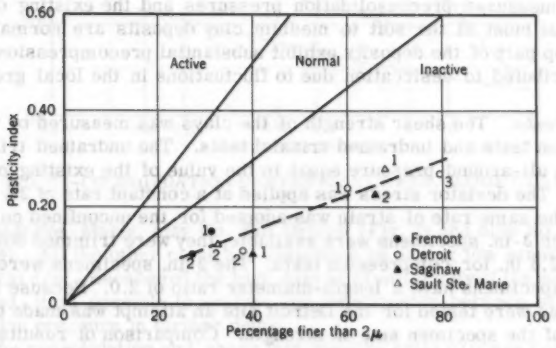


FIG. 6.—ACTIVITY OF CLAYS

The presence of hematite gives the clay a distinctive red color. Borings were made near Sault Ste. Marie, and typical test results are presented in Fig. 5.

Detailed study was made of the clay fraction of all the soils encountered by means of x-ray diffraction and differential thermal analyses. The results indicated that the principal constituent minerals are quartz, kaolinite, and illite, with small percentages of chlorite and vermiculite. The general uniformity in mineralogical contents is expressed in Fig. 6, in which the plasticity indices of the clays are plotted against the clay fractions which is defined as the percent finer than 2 microns. All the clays belong to the class of inactive clays.[4] The index properties of the clays are summarized in Table 1(a).

STRENGTH CHARACTERISTICS

A comprehensive series of laboratory tests was performed to evaluate the strength and stress history of the clays. The tests included the consolidation, unconfined compression and triaxial tests. The details of the laboratory investigation are subsequently described. A summary of the strength properties is given in Table 1(b).

Specimens.—All specimens used in the laboratory investigation were obtained by seamless steel tube samplers with a wall thickness of 1/16 in. From the Fremont site only 2-in.-diameter specimens were obtained. Both 2-in. and 3-in.-diameter specimens were used in the investigation of the Detroit site. In this case, consolidation tests were performed only on the large diameter specimens, whereas compression tests were performed on specimens of both sizes. The specimens from Saginaw were taken with 3-in.-tube samplers and the specimens from Sault Ste. Marie were taken with 3-in.-piston samplers.

Consolidation Tests.—Typical results of standard consolidation tests are plotted in Fig. 7. The numbers in parenthesis indicate the depth at which the specimens were taken. From these pressure versus void-ratio curves the preconsolidation pressures were determined by Casagrande's graphical method. Figs. 2 through 5 show the measured preconsolidation pressures as well as the existing overburden pressures at the various sites. The good agreement between the measured preconsolidation pressures and the existing overburden indicate that most of the soft to medium clay deposits are normally loaded. Only the top part of the deposits exhibit substantial precompression and these can be attributed to desiccation due to fluctuations in the local ground water table.

Shear Tests: The shear strength of the clays was measured by unconfined compression tests and undrained triaxial tests. The undrained triaxial tests utilized an all-around pressure equal to the value of the existing overburden pressure. The deviator stress was applied at a constant rate of 2% strain per minute. The same rate of strain was adopted for the unconfined compression tests. When 3-in. specimens were available, they were trimmed down to a diameter of 2.8 in. for compression tests. The 2-in. specimens were not trimmed. All specimens have a length-diameter ratio of 2.0. Because specimens of both sizes were tested for the Detroit site an attempt was made to evaluate the effect of the specimen size on strength. Comparison of results from five borings revealed no noticable difference in strength between the two types of specimens.

---

4 "The Colloidal Activity of Clays," by A. W. Skempton, Proceedings, 3d Internatl. Conf. on Soil Mechanics and Foundations Engrg. VI, 1953, p. 57.

The values of compressive strengths as determined by the laboratory tests are plotted in Figs. 2 through 5. The compressive strength was taken as equal to the maximum deviator stress. At all sites there is a general tendency for the strength to increase with depth within each individual stratum. Near the ground surface, the effect of preconsolidation is reflected in the relatively high strengths. However, some exceptions are noteworthy. At Detroit, a thin layer of soft clay is encountered at a depth of 75 ft. This is designated as clay No. 3 in Fig. 3. A similar clay exists at Saginaw between depths of 51 and 65 ft. Both units possess strengths far below those of the overlying soils. The sensitivity of the clays varied from 2 to almost 10. The sensitive clays include the

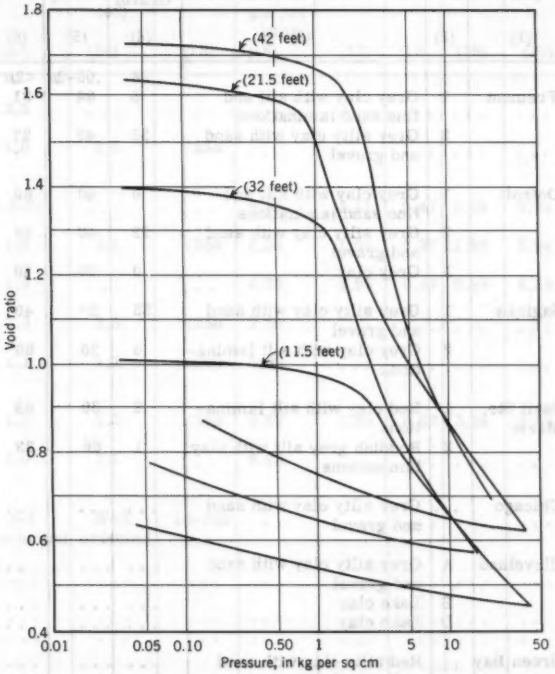


FIG. 7.—CONSOLIDATION CURVES—SAULT STE. MARIE CLAY

clays at Sault Ste. Marie, clay No. 3 at Detroit (Fig. 3) and clay No. 2 at Saginaw (Fig. 4). All the other clays are classified as having low sensitivity.

The Ratio c/p: Because of the high degree of uniformity of the soil deposits investigated, it is possible to analyze the relationship between strength and consolidation pressure in further detail.

From the consolidation and shear test data the ratio c/p was computed. In this ratio c denotes the shear strength or one-half the compressive strength and p the preconsolidation pressure. For normally loaded clays, the existing overburden pressures were used in the computations. A few clay layers are preconsolidated. For these clays it was assumed that the swelling that accompanied the unloading was negligible. The ratio c/p was computed with p equal to

TABLE 1.—PROPERTIES

Location	Unit	Description	(a) Index Properties						(b) Stren... character...	
			Particle Size Distribution			Atterberg Limits		p, in Kg per sq cm	c/p	S_t
			Sand and Gravel	Silt	Clay	PI	LI			
(1)	(2)	(3)	(4)	(5)	(6)	(7)	(8)	(9)	(10)	(1...
			.06	.06-2μ	<2μ					
Fremont	1	Grey clay with silt and fine sand laminations	5	64	31	.15	.63	1.00	0.20	3...
	2	Grey silty clay with sand and gravel	33	40	27	.10	.50	1.60	0.16	2...
Detroit	1	Grey clay with silt and fine sand laminations	0	40	60	.24	.20	9.00	0.22	3...
	2	Grey silty clay with sand and gravel	22	40	38	.11	.53	1.70	0.20	2...
	3	Grey clay	0	20	80	.27	.85	2.65	0.12	8...
Saginaw	1	Grey silty clay with sand and gravel	33	27	40	.10	.43	1.50	...	2...
	2	Grey clay with silt laminations	4	30	66	.23	.74	2.25	0.15	5...
Sault Ste. Marie	1	Red clay with silt laminations	2	30	68	.28	1.14	1.90	0.13	8...
	2	Reddish grey silt with clay laminations	1	66	33	.13	1.28	2.40	0.09	10...
Chicago	...	Grey silty clay with sand and gravel	...	...	...	.16	.56	1.20	0.23	2...
Cleveland	A	Grey silty clay with sand and gravel	...	...	...	.15	.45	2.40	0.19	...
	B	Lake clay	...	...	...	.15	.27	12.00	0.17	3...
	D	Lake clay	...	...	...	.13	.46	14.00	0.18	3...
Green Bay	...	Red silty clay with sand and gravel	...	...	...	.22	.63	2.40	0.19	...

[a] Orientation around silt and sand particles at Fremont, Detroit and Saginaw.

OF CLAY DEPOSITS

(b) Strength characteristics			(c) Particle Orientation			(d) Salt Concentration and Exchangeable Cations				
			Orientation factor[a]			Salt concentration in water, in gm per liter	Exchangeable cation-molecular equivalent per 100 gm of soil			
c/p	S_t	E_p	Over large area (>5mm)	Over small area (estimated)	Size of small oriented area		Na	K	Ca	Mg
(10)	(11)	(12)	(13)	(14)	(15)	(16)	(17)	(18)	(19)	(20)
0.20	3.0	0.12	2.5	...	...	...	...	...	...	...
0.16	2.5	0.35	1.0	2.5	<25μ	...	...	...	...	...
0.22	3.0	0.10	2.5–3.0	...	...	0.85	1.41	0.47	6.66	3.94
0.20	2.9	0.35	1.0	2.5	<25μ	2.98	1.04	0.27	11.98	3.94
0.12	8.6	0.02	1.3	...	...	0.76	1.96	0.47	9.98	6.58
...	2.3	0.30+	1.0	2.5	<25μ	2.59	...	...	...	...
0.15	5.8	0.07	1.1	1.2	<10μ	0.89	...	...	...	...
0.13	8.0	0.03	1.1	1.2	<10μ	0.62	1.39	0.62	15.96	4.68
0.09	10.0	0.02	1.0	1.1	...	0.93	...	...	...	...
0.23	2.6	7.20	Not oriented	Well oriented	10–20μ	...	...	...	...	...
0.19	...	...	...	...	...	...	...	...	...	...
0.17	3.0	7.20	...	...	...	...	...	...	...	...
0.18	3.0	...	...	...	...	...	...	...	...	...
0.19	...	...	...	...	...	...	...	...	...	...

the measured preconsolidation pressure. The computed values are listed in Table 1(b), in which S_t represents the sensitivity.

In addition to these clay deposits considerable data are also available from other sites in this area, especially Chicago. The Chicago clay[5] is an unstratified silty clay with variable percentages of sand and gravel. It extends to a depth of about 60 ft. After a thorough analysis of numerous boring data, it was concluded that the Chicago clay consists of a succession of till sheets deposited under water.[6] Consolidation test results indicate that the range of measured preconsolidation pressure agrees well with the existing overburden between elevations of -5 and -22, Chicago Datum.[7] The most probable preconsolidation pressure is slightly greater than the existing overburden. These results are in good agreement with those from another site in East Chicago shown in Fig. 8. When the most probable consolidation pressure is used, the computed c/p ratio for the Chicago clay is about 0.20.

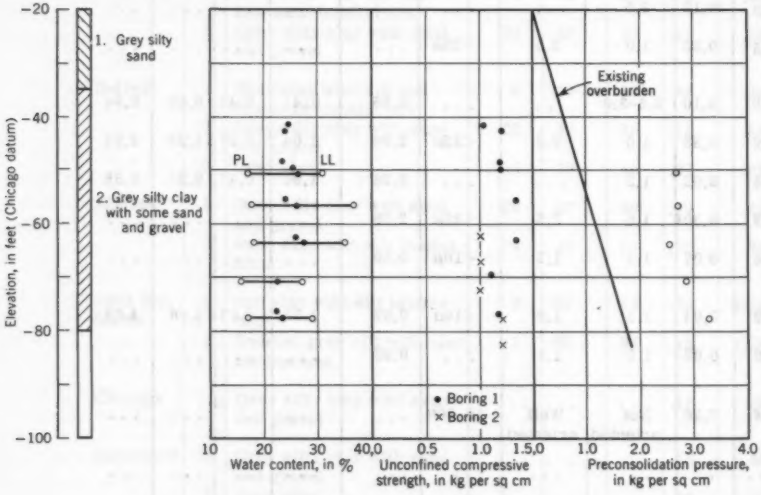


FIG. 8.—SUBSOIL PROPERTIES—EAST CHICAGO

In the Cleveland area the repeated advances and retreats of the glacier ice alternated with the formation of ice front lakes. This has resulted in a complex series of lacustrine clays with or without silt laminations and unstratified clays with sand and gravel classified as tills. The Cleveland clay is heavily preloaded and no particularly soft materials are found in the area.[8] It is possible to estimate the value of the c/p ratio as somewhere between 0.17 and 0.18

5 "Engineering Properties of Chicago Subsoils," by R. B. Peck and W. C. Reed, Bulletin 423, Engrg. Experiment Sta., Univ. of Illinois, 1954.

6 "An Interpretation of the Glacial Stratigraphy of the City of Chicago," by G. H. Otto, thesis presented to the Univ. of Chicago, in 1942, in partial fulfilment of the requirements for the degree of Doctor of Philosophy.

7 Discussion by J. D. Parsons and R. B. Peck of "The Action of Soft Clay Along Friction Piles," by H. B. Seed and L. C. Reese, Proceedings Paper 842, in Proceedings Paper 1028, July, 1956.

8 "Foundation Conditions in the Cuyahoga River Valley," by R. B. Peck, Proceedings Paper 513, ASCE, October, 1954.

for units B and D (Table 1(b) column 10). Fig. 9 shows laboratory test results on clay unit A at a site in the same area. The c/p ratio is about 0.19.

At Green Bay, Wisconsin, a thick deposit of reddish clay exists to a depth of over 100 ft. The deposit consists of a succession of reddish silty clay till and some stratified material of lacustrine origin. Data from one boring are shown in Fig. 10. Between elevations 530 and 550, the clay is uniform. Preconsolidation pressures were determined only at elevations 539 and 540. From this, the computed c/p ratio is 0.19.

In Fig. 11 the c/p ratios are plotted against the plasticity indices. The numerals designate the clays stratum. The straight line in the figure is the relationship obtained[9,10] for estuarine and marine clays. The overall trend is one of increasing c/p ratio with increasing plasticity index. However, the data obtained in this investigation appear to fall into two distant alignments. The

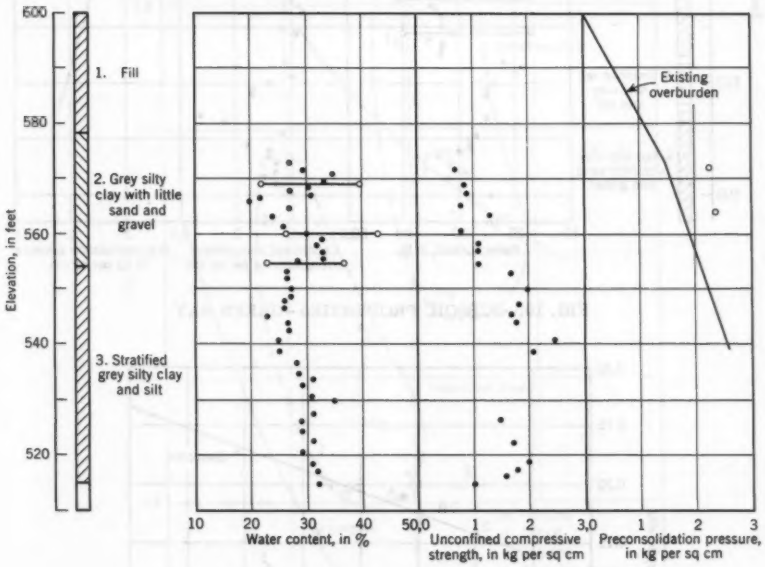


FIG. 9.—SUBSOIL PROPERTIES—CLEVELAND

first one, consisting of clays with low sensitivity, is slightly above but very close to Skempton's line. The second group falls far below the first one, and is composed entirely of sensitive clays.

The liquidity indices of the clays are plotted against their preconsolidation pressures in Fig. 12. The numerals designate the clay stratum. Also shown

9 "The Post Glacial Clays of the Thames Estuary at Tilbury and Shellhaven," by A. W. Skempton and D. J. Henkel, Proceedings, 3d Internatl. Congress on Soil Mechanics and Foundation Engrg., VI, 1953, p. 302.

10 "Geotechnical Properties of Norwegian Quick Clays," by L. Bjerrun, Geotechnique V4, 1954, p. 49.

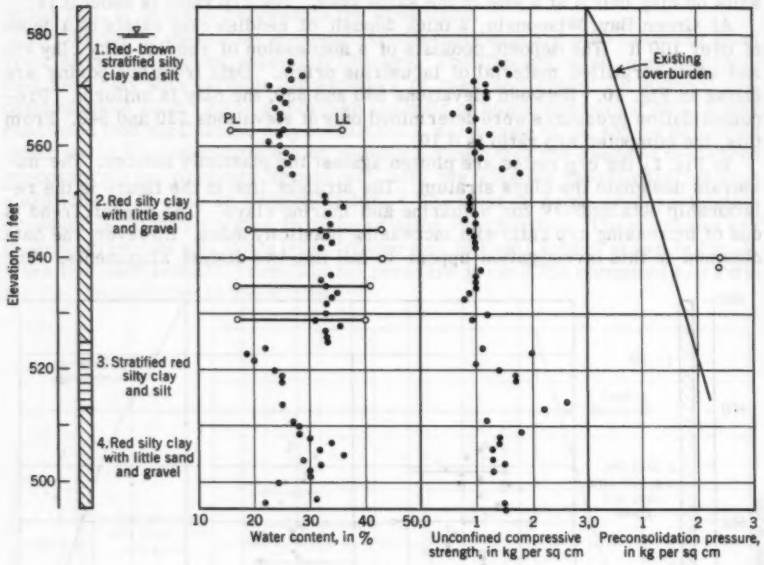


FIG. 10.—SUBSOIL PROPERTIES—GREEN BAY

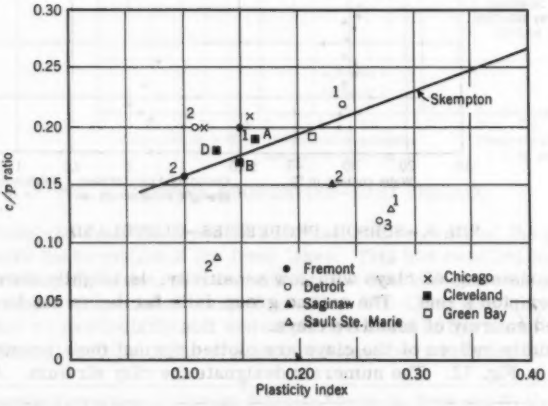


FIG. 11.—RELATIONSHIP BETWEEN c/p AND PLASTICITY INDEX

are curves for the Horten clay[11] with a sensitivity of 17 and the Gosport clay[12] with a sensitivity of 2.4. For a given clay, consolidation under increasing pressures always progressively reduces the liquidity index. However, as is obvious in Fig. 12, different clays may possess very different liquidity indices at same preconsolidation pressures. As explained[13] this relationship depends primarily on the microstructure of the clay particles. Because the data in Fig. 9 show that low c/p ratio and high sensitivity are limited to clays with a

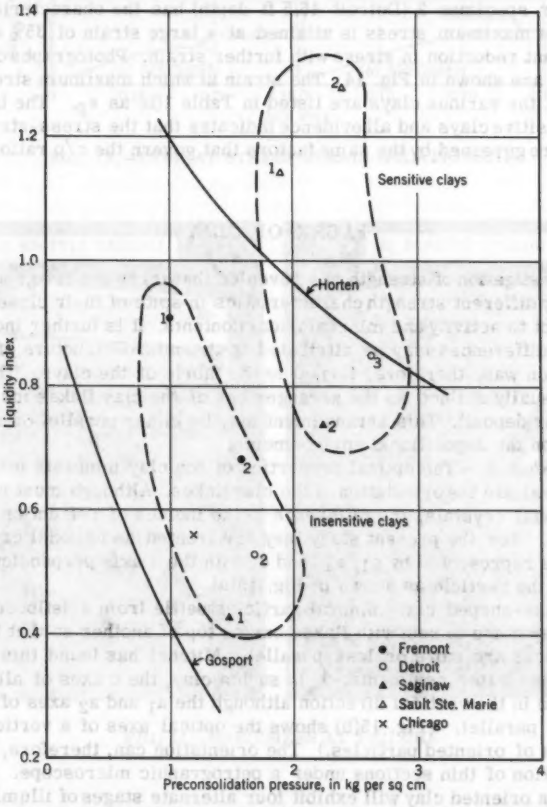


FIG. 12.—RELATIONSHIP BETWEEN PRECONSOLIDATION PRESSURE AND LIQUIDITY INDEX

11 "Vane Tests in a Norwegian Quick Clay," by J. B. Hansen, Geotechnique V2, 1950, p. 58.

12 "The Geotechnical Properties of a Deep Stratum of Post-Glacial Clay at Gosport," by A. W. Skempton, Proceedings, 2d Conf. on Soil Mechanics and Foundation Engrg. VI, 1948, p. 145.

13 "The Sensitivity of Clays," by A. W. Skempton and R. D. Northey, Geotechnique V3, 1953, p. 30.

high liquidity index, it follows that these properties must be determined by the micro structure of the clay.

Stress-strain Relationship.—The larger number of unconfined compression tests also yielded considerable information on the stress-strain characteristics of the clays. This relationship may be classified into two distinctive types as illustrated in Fig. 13. The plot for specimen 1 (Detroit 77.5 ft depth) exhibits a brittle material with a rather high value of initial modulus. The stress rapidly decreases after attaining a peak value at low strain. In contrast to this, the plot for specimen 2 (Detroit 46.5 ft depth) has the characteristic plastic nature. Its maximum stress is attained at a large strain of 35% and there is no significant reduction in stress with further strain. Photographs of the failed specimens are shown in Fig. 14. The strain at which maximum strength is attained with the various clays are listed in Table 1(b) as ϵ_p. The brittle soils are all sensitive clays and all evidence indicates that the stress-strain characteristics are governed by the same factors that govern the c/p ratio and sensitivity.

FABRIC OF CLAYS

The investigation of strength has revealed that there are two groups of clays having very different strength characteristics in spite of their close similarity with respect to activity and mineralogical contents. It is further indicated that the major differences may be attributed to the micro-structure of the clays. The attention was, therefore, turned to the fabric of the clays. The fabric of a clay is usually defined as the arrangement of the clay flakes inside a given specimen or deposit. This arrangement may be either parallel or random depending upon the depositional environments.

Optical Studies.—The optical properties of the clay minerals provide some means to evaluate the orientation of the clay flakes. Although most clay minerals are biaxial crystals, the difference in the indices of refraction are known to be small. For the present study they are treated as uniaxial crystals with optical axes represented by a_1, a_2, and c, with the c axis perpendicular to the flat face of the particle as shown in Fig. 15(a).

When flake-shaped clay-mineral particles settle from a deflocculated suspension, they come to rest with flakes one on top of another so that their basal plane surfaces are more or less parallel. Mitchel has found this to be true also for fresh water sediments.[14] In such a clay, the c axes of all the flakes are oriented in the vertical direction although the a_1 and a_2 axes of the flakes may not be parallel. (Fig. 15(b) shows the optical axes of a vertical section thru a mass of oriented particles.) The orientation can, therefore, be studied by examination of thin sections under a petrographic microscope. A vertical section of an oriented clay will exhibit four alternate stages of illumination and extinction when placed between crossed nicols of the microscope since light passing through such a section is polarized to vibrate in two perpendicular planes. A horizontal section will show no extinction or illumination as the a_1 and a_2 axes of the individual flakes lie in all directions. (Fig. 15(c) shows the optical axes of a horizontal section through a mass of oriented particles.) On

14 "The Fabric of Natural Clays and Its Relation to Engineering Properties," by J. K. Mitchell, Proceedings, Highway Research Bd., Vol. 35, 1956, p. 693.

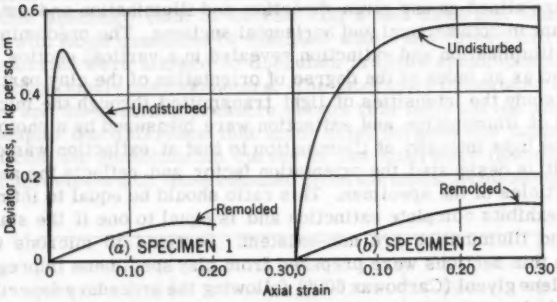


FIG. 13.—TYPICAL STRESS-STRAIN RELATIONSHIP

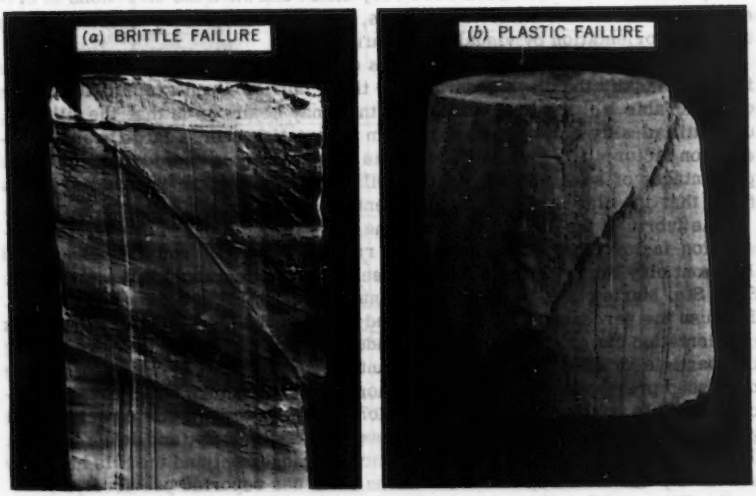


FIG. 14.—SPECIMENS AT FAILURE

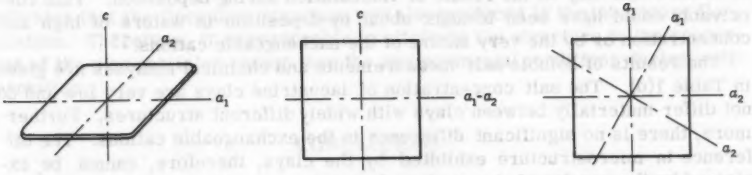


FIG. 15.—OPTICAL AXES OF CLAYS

the other hand, in a group of randomly oriented particles, none of the optical axes are alined in any given direction and illumination and extinction are non-existant in both vertical and horizontal sections. The predominance of the stages of illumination and extinction revealed in a vertical section, therefore, can be used as an index of the degree of orientation of the clay particles.

In this study the intensities of light transmitted through the microscope at the stages of illumination and extinction were measured by a phototube. The ratio of the light intensity at illumination to that at extinction was determined readily. It is designated the orientation factor and reflects the arrangement of clay particles of the specimen. This ratio should be equal to infinity when a specimen exhibits complete extinction and is equal to one if the stages of extinction and illumination are non-existent. Sections 30 microns thick were used. The thin sections were prepared from clay specimens impregnated with a polyethylene glycol (Carbowax 6000) following the procedure described previously.[14] At least two thin sections were made from each clay and light readings were taken through the microscope with a 10x eyepiece and objectives of 1.0x, 10x and 45x. The values of the readings are listed in Table 1(c). However, when the oriented areas were very small and when the directions of orientation were not the same in all areas, it was possible only to estimate the degree of orientation by visual examination.

Significance of Fabric.—On the basis of the optical studies it is possible to further classify the clays according to their fabric. Upon examination of the data in Table 1(c) the first conclusion that may be drawn is that the till-like, unstratified silty clays all show random orientation over a large area. (Orientation factor = 1.) This, of course, is understandable considering the large percentages of sand and silt in the soil. When magnified 450 times, it was found that the clay is actually well oriented around the silt and clay particles.

The fabric of the stratified lacustrine clays varied from well oriented (orientation factor from 2 to 3) to almost random. Both Detroit clay No. 1 and Fremont clay No. 1 exhibit a high degree of parallel arrangement whereas the Sault Ste. Marie clays 1 and 2 and Saginaw clay No. 2 show little orientation. Because the percentages of silt and sand are very low in these clays, this lack of orientation can only result from a random structure. The findings regarding the particle orientation further substantiate the concept of micro-structure discussed previously. A flocculent or honeycomb structure is necessarily accompanied by random particle orientation. Therefore, it is this structure that gives the clays their high liquidity index, high sensitivity, and low c/p ratio. The clays with pronounced parallel particle arrangement and the tills have low sensitivity and their c/p ratios are close to values reported previously.[9,10]

Conditions of Deposition.—To further check the microstructure of the clays, the concentration of soluble salts in the porewater and the exchangeable cations were determined for the clays. It was reasoned that the flocculent structure of some clays may be the result of flocculation during deposition. This conceivably could have been brought about by deposition in waters of high salt concentration or by the very nature of the exchangeable cations.[15]

The results of soluble salt measurements and chemical analyses are given in Table 1(d). The salt concentration of lacustrine clays are very low and do not differ materially between clays with widely different structures. Furthermore, there is no significant difference in the exchangeable cations. The difference in microstructure exhibited by the clays, therefore, cannot be explained by the results of chemical analyses.

[15] "Investigations in the Clay-Electrolyte-Water System," by I. Th. Rosenquist, Publication No. 9, Norwegian Geotechnical Inst., 1955.

As a check, consolidation tests were performed on laboratory flocculated samples. One specimen each of Detroit clay 3 and Sault Ste. Marie clay 1, were mixed with large quantities of distilled water and turned into thin slurries. The slurries were allowed to flocculate in lucite standpipes attached to the top of conventional consolidometers. The laboratory flocculated clays were consolidated and the resulting pressure versus void ratio curves are shown in Fig. 16. Despite the difference that must exist between the laboratory and field conditions, the consolidation curves of the laboratory flocculated clays are in good agreement with those obtained from the undisturbed samples. This

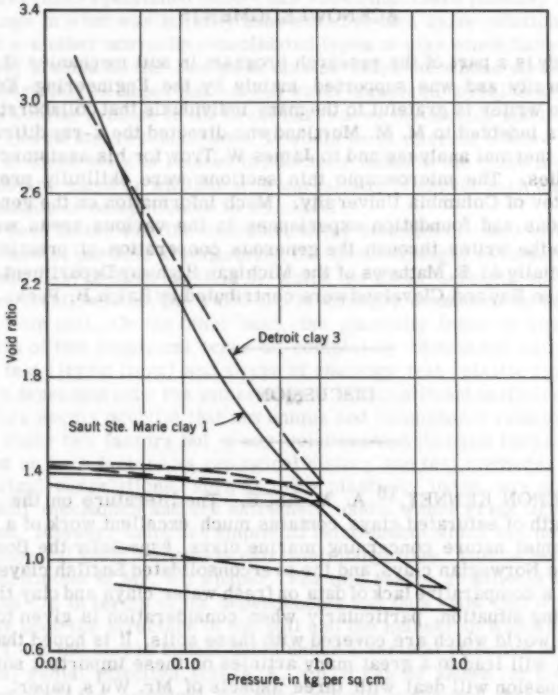


FIG. 16.—CONSOLIDATION CURVES

indicates that the flocculent structure was also produced in the laboratory flocculation. Therefore, it is reasonable to attribute the structure to the properties of the clay particles rather than the environmental conditions during sedimentation.

CONCLUSIONS

The soft clays investigated are either lacustrine clays or tills deposited by glaciers under water. Consolidation of these soils is accomplished largely by

the weight of the overburden and most of the clays can be considered as normally loaded. Despite the overall similarity, with respect to move of deposition and mineralogical, content and micro-structure of the clays were found to vary widely. In the case of lacustrine clays, the structure may be honeycombed and flocculent or the arrangement of the flake-shaped clay particles may be more or less parallel. The structure is accurately reflected by the relationship between the liquidity index and preconsolidation pressure. Important strength characteristics as sensitivity and the c/p ratio were found to be dependent upon the micro-structure of the clays.

ACKNOWLEDGMENTS

This study is a part of the research program in soil mechanics at Michigan State University and was supported mainly by the Engineering Experiment Station. The writer is grateful to the many individuals that collaborated in this effort. He is indebted to M. M. Mortland who directed the x-ray diffraction and differential thermal analyses and to James W. Trow for his assistance with the optical studies. The microscopic thin sections were skillfully prepared by George S. Rev of Columbia University. Much information on the general subsoil conditions and foundation experiences in the various areas were made available to the writer through the generous cooperation of practicing engineers, especially Al. E. Mathews of the Michigan Highway Department. The data from Green Bay and Cleveland were contributed by Ralph B. Peck, F. ASCE.

DISCUSSION

T. CAMERON KENNEY,[16] A. M. ASCE.—The literature on the subject of shear strength of saturated clays contains much excellent work of a practical and fundamental nature concerning marine clays, especially the Boston clay, the sensitive Norwegian clays, and the overconsolidated English clays. There, is, however, a comparative lack of data on fresh water clays and clay tills. This is a disturbing situation, particularly when consideration is given to the vast areas of the world which are covered with these soils. It is hoped that the author's paper will lead to a great many articles on these important soils.

This discussion will deal with three aspects of Mr. Wu's paper: (1) The apparent relationship between c/p and plasticity index; (2) the shear strength of varied clays and its measurement; and (3) the origin of the unstratified, till-like soils in the Great Lakes region.

Relationship Between c/p and Plasticity Index.—Much data concerning the undrained shear strength of natural clays has been obtained since the vane came into general use as a piece of field testing equipment. One of the most important facts is that the shear strength of a homogeneous deposit of normally consolidated clay increased linearly with depth, or more specifically, the ratio of the undrained shear strength of a clay and the vertical effective stress under which the soil was consolidated in the field was a constant. This ratio has since

[16] H. G. Acres & Co., Ltd., Cons. Engrs., Niagara Falls, Ontario, Canada.

been denoted by c/p. As more data concerning the ratio, c/p, became available, attempts were made to correlate this factor with more fundamental properties of the soil, such as the liquid limit[17] and the plasticity index. It was found that some correlation seemed to exist between this latter parameter and c/p in the case of normally consolidated marine clays.[18]. This has proved to be convenient correlation because it has been confirmed by sufficient field evidence to allow natural shear strengths of marine deposits to be estimated for preliminary design purposes on the basis of the results of simple laboratory tests. However, it must be borne in mind that this correlation between c/p and plasticity index has only been shown to be applicable in the special case of marine clays and even here published data[19] has shown that there possibly is an appreciable range in what was initially considered to be a close relationship.

There are other normally consolidated types of clay which have not been as extensively studied as the European marine clays but whose strength properties are certainly as important: fresh water lacustrine and alluvial clays, glacial clays similar to those in the Great Lakes area in America and in some Scandanavian fjords, and residual clays. It would be of interest to know if the shear strength of these soils is related to plasticity index in the same manner as for natural marine clays or whether it is unrealistic to expect such a general type of relationship to be applicable to all clays.

It has been shown that the undrained shear strength of clays is dependent on the structure or particle arrangement, the shear strength parameters, the history of the clay, and the method by which the shear strength is determined. Therefore it follows that the ratio c/p is strongly dependent on the geological history of the soil. On the other hand, the plasticity index is dependent upon the results of two empirical tests on completely remoulded soil: a dynamic strength test (liquid limit) and a type of rheology test (plastic limit), both of which are dependent upon the mineralogy of the constituent particles of the soil. It therefore seems doubtful that any unique and independent relationship exists between these two factors but if any relationships do exist they are probably dependent on such factors as geological history and test methods.

Empirical correlations, such as c/p - plasticity index, are common in the field of soil mechanics and are extremely useful where great accuracy is not warranted. However using any empirical relationship which has not been shown to have physical justifications is extremely dangerous. This is not meant to be a direct criticism of Mr. Wu's paper. For this reason an attempt will be made to express c/p in terms of its dependencies and thus show that it is dependent primarily upon the structure of the soil and the manner in which it is tested.

Case I.—If the clay is consolidated under a vertical effective stress, p, and horizontal radial effective stress, $K_c \times p$, it can be shown for the case where the direction of the principal stresses remain unchanged that the undrained

---

17 "Vanetests in the Alluvial Plain of the River Forth, Near Grangemouth," by A. W. Skempton, Geotechnique, Vol. I, 1948, p. 111.

18 "Discussion on the Planning and Design of the New Hong Kong Airport," by A. W. Skempton, Proceedings, Inst. of Civ. Engrs., Vol. 7, 1957, p. 305.

19 "Micropaleontology Applied to Soil Mechanics in Norway," by R. W. Feyling - Hanssen, Norwegian Geotechnical Inst., 1957, Publication No. 20.

shear strength can be expressed in the following form:

$$\frac{c}{p} = \frac{1}{2}\frac{(\sigma_1 - \sigma_3)_f}{p}$$

$$= \frac{\frac{c' \cdot \cos\phi'}{p} + K_c + A_f\{1 - K_c\}\sin\phi'}{1 + (2A_f - 1)\sin\phi'} \quad \ldots\ldots (1)$$

in which c denotes the undrained shear strength, A_f represents the value at failure of the pore water pressure parameter relating changes in pore water pressure and deviator stress,[20] c' and ϕ' are the shear strength parameters of the clay, and $(\sigma_1 - \sigma_3)_f$ denotes the deviator stress at failure. Failure is considered to occur when the deviator stress reaches its maximum value.

For normally consolidated soils c' = 0 and Eq 1 can be simplified to the following form:[21]

$$\frac{c}{p} = \frac{(K_c + A_f\{1 - K_c\})\sin\phi'}{1 + (2A_f - 1)\sin\phi'} \quad \ldots\ldots (2)$$

Case II.—In a similar fashion it can be shown that if a sample is consolidated under the same stress conditions as in Case I but the major and minor principal stresses at failure act in a horizontal direction while the vertical stress remains unchanged, the resulting shear strength can be expressed as:

$$\frac{c}{p} = \frac{K_c \cdot \sin\phi'}{1 + (2A_f - 1)\sin\phi'} \quad \ldots\ldots (3)$$

In nature, normally consolidated clays generally consolidate under the imposed condition of no lateral yield and for this condition the ratio of the principal stresses is denoted by K_o. Values of K_o have been determined[22,23] for a limited number of soils ranging in plasticity index from 0 to 45%. For these soils K_o is related to ϕ' as shown in Fig. 17 and in the following manner.

$$K_o = 1 - \sin\phi \quad \ldots\ldots (4)$$

Substituting this expression into Eqs. 2 and 3, the following relationships are obtained:

Case I:

$$\frac{c}{p} = \frac{(1 - \sin\phi' + A_f \cdot \sin\phi')\sin\phi'}{1 + (2A_f - 1)\sin\phi'} \quad \ldots\ldots (5)$$

Case II:

$$\frac{c}{p} = \frac{(1 - \sin\phi')\sin\phi'}{1 + (2A_f - 1)\sin\phi'} \quad \ldots\ldots (6)$$

---

20 "The Pore-Pressure Coefficients A and B," by A. W. Skempton, Geotechnique, Vol. 4, 1954, p. 143.

21 "Building Materials Their Elasticity and Inelasticity," by A. W. Skempton, and A. W. Bishop, Soils, Chapter X, North-Holland Publishing Co., Amsterdam, 1954.

22 "Test Requirements for Measuring the Coefficient of Earth Pressure at Rest," by A. W. Bishop, Brussels Conference on Earth Pressure Problems, Vol. 1, 1958, p. 2.

23 "The Measurement of Soil Properties in the Triaxial Test," by A. W. Bishop and D. J. Henkel, Edward Arnold, London, 1957.

Eq. 5 represents the strength which would be measured in the laboratory if a sample were consolidated under an axial stress of p for the condition of no lateral yield and was failed in compression by increasing the axial load. It also represents the strength which would be measured in a laboratory compression test on a sample which had been consolidated in situ under a vertical effective stress p and had been sampled without causing any disturbance to the soil structure. Eq. 6 represents the strength which would be mobilized in a vane test if the shear strength mobilized along the end surfaces was equal to the shear strength mobilized along the vertical cylindrical surface. This assumption introduces a small error since the shear strength mobilized along the end surfaces is higher.

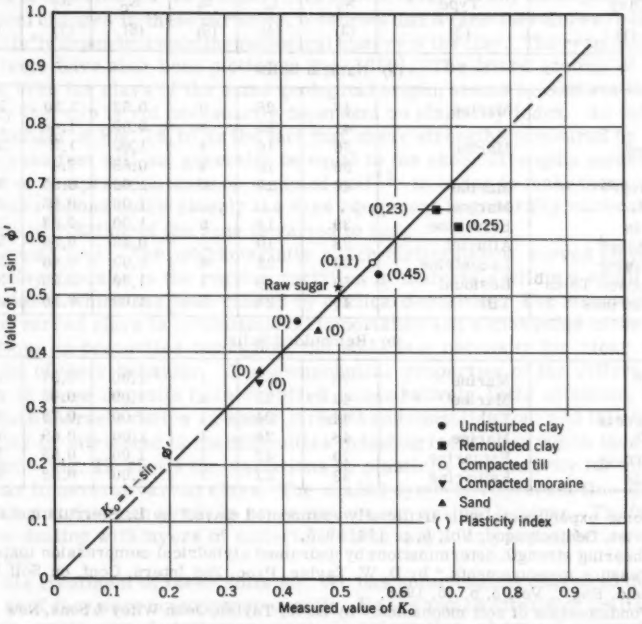


FIG. 17.—RELATIONSHIP BETWEEN K_o AND ϕ'

It is thus seen that the value of c/p measured by means of compression tests and vane tests is dependent on two parameters, the pore water pressure parameter A_f and the shear strength parameter ϕ'. The value of A_f for any soil is dependent upon the rigidity and resiliency of the clay structure and upon the type of test used to cause sample failure. In Table 2, where the liquid limit is represented by w_L, I_p represents the plasticity index, and S_t is the sensitivity, values of A_f are listed for various natural and remoulded soils. These values were all measured in triaxial compression tests and the writer knows of no reference where values of A_f have been published for tests other than axial compression tests. Unfortunately, the unstable structure of sensitive clays partially collapses during reconsolidation in the laboratory and thus it is likely

that the values of A_f for the natural sensitive soils noted in Table 2 are smaller than the values for these clays in their natural state.[24] The following conclusions can be drawn from the results listed in Table 2:

(1) - the value of A_f varies at least from 0.26 to 2.4;

(2) - the more sensitive the soil the higher the values of A_f; and

(3) - A_f is independent of plasticity index.

TABLE 2.—VALUES OF A_f FOR NORMALLY CONSOLIDATED SOILS

Clay (1)	Type (2)	w_L (3)	I_p (4)	S_t (5)	K_c (6)	A_f (7)	ϕ' (8)
		(a) Natural Soils					
Toyen[a]	Marine	47	25	8	0.52	1.50	28.5
		47	25	8	0.60	1.48	...
Drammen	Marine	36	16	4	1.00	1.2	35.0
		36	16	4	0.68	2.4	...
Saco River[b]	Marine	46	17	10	1.00	0.95	32.5
Boston[c]	Marine	...	...	...	1.00	0.85	34.6
Bersimis	Estuarine	39	18	6	1.00	0.63	38.7
Chew Stoke[d]	Alluvial	28	10	...	0.43	0.59	33.0
Kapuskasing	Lacustrine	39	23	4	1.00	0.46	30.0
Decomposed Talus[b]	Residual	50	18	1	1.00	0.29	34.6
St. Catharines	Till	49	28	3	1.00	0.26	25.6
		(b) Remoulded Soils					
London[e]	Marine	78	52	1	1.00	0.97	19.0
Weald	Marine	43	25	1	1.00	0.95	23.0
Beauharnois	Till	44	24	1	1.00	0.73	30.5
Boston[b]	Marine	48	24	1	1.00	0.69	30.7
Beauharnois	Estuarine	70	42	1	1.00	0.65	32.8
Bersimis	Estuarine	33	13	1	1.00	0.38	39.0

[a] "Some experiments with artificially sedimented clays," by L. Bjerrum and I. Th. Rosenqvist, Géotechnique, Vol. 6, p. 124, 1956.

[b] "Shearing strength determinations by undrained clyindrical compression tests with pore pressure measurements," by D. W. Taylor, Proc. 2nd Intern. Conf. on Soil Mech. and Found. Engr., Vol. 5, p. 45, 1948.

[c] "Fundamentals of soil mechanics," by D. W. Taylor, John Wiley & Sons, New York, 1948.

[d] "Pore pressure changes during shear in two undisturbed clays," by A. W. Bishop and D. J. Henkel, Proc. 3rd Intern. Conf. on Soil Mech. and Found. Engr., Vol. 1, p. 94, 1953.

[e] "The effect of overconsolidation on the behaviour of clays during shear," D. J. Henkel, Géotechnique, Vol. 6, p. 139, 1956.

In order that the possible ranges of c/p for various values of plasticity index could be shown graphically, a correlation between sin ϕ' and plasticity is used for convenience (Fig. 18(a)). This correlation is independent of soil structure. It has been found that the angle of shearing resistance, ϕ', for normally consolidated soils is essentially the same for both undisturbed and fully remoulded samples. There is an obvious scatter of points in Fig. 18(a) and it is seen

24 "Some Experiments with Artificially Sedimented Clays," by L. Bjerrum and I. Th. Rosenqvist, Geotechnique, Vol. 6, 1956, p. 124.

that the less active soils exhibit higher values of ϕ'. The test data are results of drained tests and undrained tests with pore water pressure measurements on normally consolidated natural and remoulded marine, fresh water and residual clays. Possible values of c/p for conditions of failure implicit in Eqs. 5 and 6 have been computed for several values of A_f by using the relationship between sin ϕ' and plasticity index indicated by the dashed line in Fig. 18(a). These values are plotted in Fig. 18(b). It is seen that theoretically c/p is essentially independent of ϕ' and therefore independent of plasticity index and is primarily dependent upon the type of test and the magnitude of A_f. Because the magnitude of A_f for a certain type of test reflects the rigidity and the resiliency of the soil structure, and because these properties are dependent upon the method of deposition of the soil particles and the nature of any subsequent physiochemical changes in these particles, it follows that A_f and therefore c/p is probably chiefly dependent upon the geological history of the clay. The results of field vane tests have also been plotted in Fig. 18(b). The board scatter of these points, even for clays of the same geological origin, seems to confirm the possibility that c/p is not necessarily dependent on plasticity index. An interesting sidelight of Fig. 18(b) is the fact that shear strengths measured by means of the vane test will not generally be equal to the shear strengths measured by means of compression tests on sampled soil[25]. In order to make these two results correspond more closely the vane equipment is generally calibrated and the rate of rotation of the vane is varied to suit.

Varved Clays.—The characteristic which distinguishes varved clays from other clay deposits is the regular variation in materials within a small vertical distance which has been caused by cyclical deposition. The structural feature of varved clays is of fundamental importance and a knowledge of the in situ variations in properties throughout the soils is a necessity for clear understanding of their behavior. The geotechnical properties of the different soil layers in these deposits have received comparatively little attention, especially such characteristics as shear strength and consolidation, and this fact can probably be attributed to the difficulties in testing techniques which these soils present. Fig. 19 shows the variations in plasticity and activity for different laminae in several varved clays. The shaded symbols represent fine-grained, laminae and the open symbols represent coarse-grained laminae. The fact that we are dealing with layers of materials which vary widely in properties is quite apparent.

In his treatment of these soils Mr. Wu has unfortunately chosen to deal with them as if they were homongeneous soils. He has quoted Atterberg limits, water content, grain size distribution, particle orientation, chemical properties and associated properties without making reference to the particular lamina of the varve to which the properties correspond or without stating whether these properties were obtained from tests on mixed samples of several laminae. It is realized that in some cases the varves are too thin to separate out and in this case it seems only practicable to used mixed samples. The results in Mr. Wu's paper would be of more value if he would specify the type of lamina (coarse-grained or fine-grained) to which the test results correspond.

The shear strength of varved clays is a subject which warrants a great deal of study and research. The subject is complicated by the fact that the soil consists of layers with different shear strength, stress-strain, and consolidation

25 "Opptagning av uforstyrrede jordprver," by R. Chr. Vold, Publication No. 17, Norwegian Geotechnical Inst., 1956.

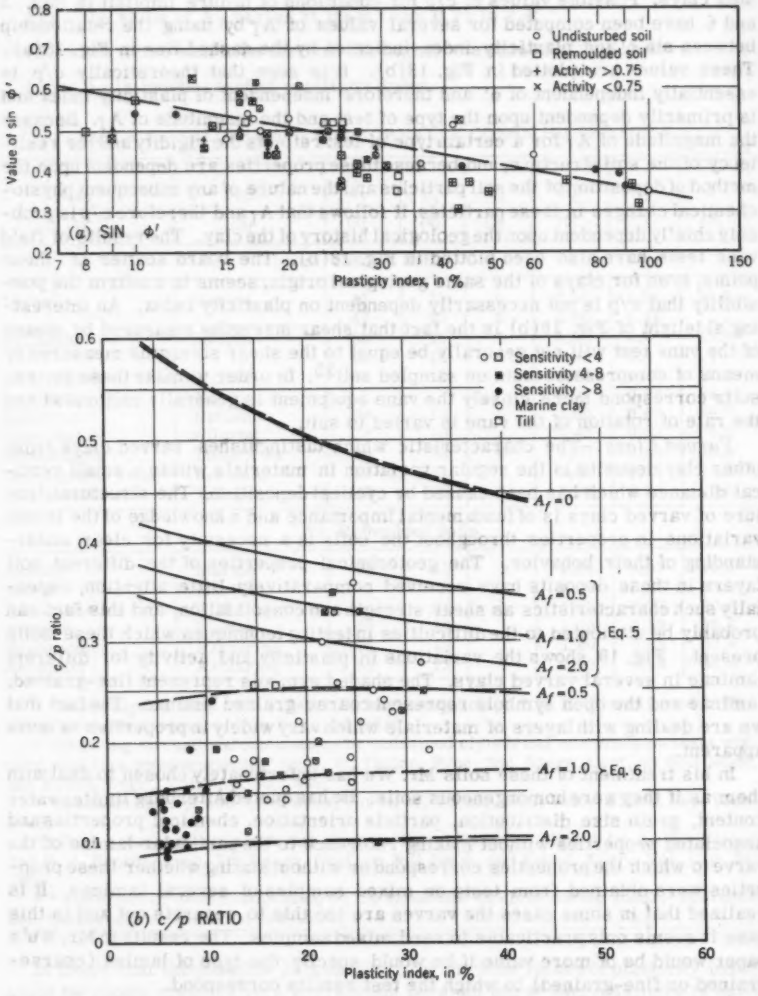


FIG. 18.—RELATIONSHIP BETWEEN c/p, SIN ϕ, AND PLASTICITY INDEX

properties. Thus far it has been found difficult to establish the correct laboratory testing procedure which will reproduce conditions and give strengths that are in agreement with those existing in the field. Failure in the field usually takes place along a smooth surface rather than a broken or irregular surface. The soil everywhere along this smooth surface fails in shear, except for that portion near the ground surface where a tension crack may form. To produce this type of failure in the laboratory or in a field test, the failure surface must be made planar. In homogeneous soils a planar type of failure should always occur if the pore water pressures are positive or only slightly negative, but in varved clays where the soil properties may change appreciably within short distances the sample might fail along an irregular surface in the process of seeking out the surface of least resistance. It has been shown[26] that this can occur in the unconfined compression test where samples have failed partly in tension and partly in shear. This type of failure is kinematically impossible in the field and the refore the value of any test in which failure takes place in this manner is questionable. It has also been shown[27] that in some compression tests on varved clays the material of the weaker laminae has squeezed out from between two of the stronger laminae. The results of such tests would be

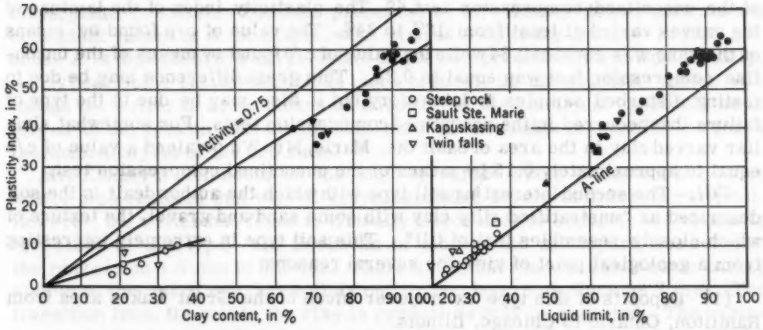


FIG. 19.—VARIATION IN PLASTICITY AND ACTIVITY OF LAMINAE IN VARVED CLAYS

a measure of the shear strength of the weaker lamina, but if analyzed as a standard compression test the resulting value for shear strength would represent neither the actual shear strength of the weaker layer nor that of the varved sample.

If the shearing surface was planar the shear strength of the soil would still be dependent on the orientation of the shear surface relative to the varves. If failure takes place wholly within one lamina, the shear strength mobilized along the failure surface would be expected to equal the shear strength of the soil making up that lamina. If, however, failure takes place across the varves, it can be shown that, for differing values of the shear strength, strain at failure, and thickness of the different laminae, the mobilized shear strength may vary

26 "A Laboratory Study of Varved Clay from Steep Rock Lake, Ontario," by W. J. Eden, American Journal of Science, Vol. 253, 1955, p. 659.

27 "The Determination of the Shearing Strength of Varved Clays and Their Sensitivity to Remoulding," by G. P. Tschebotarioff and J. R. Bayliss, Proceedings, 2d Internatl. Conf. on Soil Mechanics and Foundation Engrg., Vol. 1, 1948, p. 203.

from a value less than the shear strength of the weaker layer to a value greater than the shear strength of the weaker layer. However, the mobilized shear strength is always less than the shear strength of the stronger layer.

Therefore, the simple compression test is probably an unsatisfactory method of measuring the undrained shear strength of varved clays. The type of laboratory test that appears to satisfy the requirements best is the shear box test in which the sample fails in direct shear and the orientation of the failure plane can be controlled. Some difficulties might be encountered in controlling the drainage conditions satisfactorily in this test. The field vane test is another test in which the failure plane is controlled but this test would measure only the composite strength of several laminae.

In his treatment of the subject of undrained shear strength of varved clays the author has used the unconfined compression test to determine shear strength. It would be appreciated if Mr. Wu would comment upon the type of failure observed in his test work on varved clays in view of the effect that the type of failure might have upon the test results if the tests were analyzed in the standard manner.

It may be noted that the shear strength of the varved clay at Sault Ste. Marie was measured in the field by means of the vane and in the laboratory by means of the unconfined compression test.[28] The plasticity index of the laminae of the varves varied at least from 16% to 34%. The value of c/p found by means of the vane was equal to 0.34 while the value of c/p found by means of the unconfine compression test was equal to 0.24. This great difference may be due to testing disturbed samples in laboratory but it also may be due to the type of failure that occurred in the unconfined compression tests. For somewhat similar varved clay in the area of Sault Ste. Marie, Mr. Wu obtained a value of c/p equal to approximately 0.15 by means of the unconfined compression test.

Till.—The second interesting soil type with which the author dealt is the soil described as "unstratified silty clay with some sand and gravel, the texture of which closely resembles that of till". This soil type is extremely interesting from a geological point of view for several reasons:

(1) Deposits of this type extend over much of the Great Lakes area from Hamilton, Ontario to Chicago, Illinois.
(2) Some of these deposits are extremely homogeneous over depths of 100 ft.
(3) These soils are generally normally consolidated.
(4) These soils have sensitivity values equal to approximately 3.
(5) The fabric or structure of the clay portion of these soils is similar to the structure of a soil sedimented in a deflocculated state and is also similar to the structure of a remoulded soil.[29]

If it is assumed that this material is till, it would be of interest to know why the soil is so homogeneous in texture, and how it was deposited in a normally consolidated state. If it is assumed that this soil is a lacustrine deposit, why is the material so homogeneous with respect to particle size gradation and why does it contain a wide range of particle sizes from clay to gravel? It would be appreciated if Mr. Wu would comment on the geological history of these soils.

---

28 "Performance of a Steel Sheet Piling Bulkhead," by N. D. Lea, Proceedings, 3d Internatl. Conf. on Soil Mechanics and Foundation Engrg., Vol. 2, 1953, p. 180.

29 "Sub-Polar Quick Clays," by I. Th. Rosenqvist, Lecture given to the Toronto Soil Mechanics Group, 1958.

It may be noted that a similar material was found in a Norwegian fjord to a depth of at least 20 ft and possibly as great as 80 ft, and its formation is thought to have been due to ice rafting.[30]

TIEN H. WU,[31] M. ASCE.—The writer appreciates Mr. Kenney's interesting contribution to the subject to lake clays.

The relationship between the c/p and the plasticity index is empirical. The writer, however, cannot agree completely with Mr. Kenney's views regarding the value of c/p. In the first place, the magnitude of the pore-water pressure at failure in the unconfined compression test is always very small and its value is usually negative. Furthermore, the material fails at normal stresses much smaller than its preconsolidation pressure. Therefore, Eq. 5, based on the assumption that $c' = 0$, is not valid for the stress conditions existing in the unconfined compression test.

The writer accepts Mr. Kenney's equation for the vane test, but he is not certain that Mr. Kenney's conclusion regarding the relationship between the c/p and the plasticity index is justified. It is true that the value of c/p depends more on the value of A than on that of ϕ'. However, it is difficult to predict A. In addition to the knowledge that high values of A have been measured in quick clays, little is known. The data presented by Mr. Kenney do not indicate any consistent values of A for clays in the various sensitivity groups. In fact, because A is dependent to a large extent on the compressibility and expansibility, it may bear some relationship to an index property as the plasticity index. Although the writer is by no means an advocate of the empirical approach, he is forced to the opinion that the present state of knowledge is insufficient for a thorough analysis of the c/p ratio.

Mr. Kenney's comments on the topic of varved clays is instructive. The writer also realizes that varved clays consist of layers of different material. However, the writer has found it virtually impossible to separate the elements in a study of this type. The thickness of most of the silt layers lies between the range from 1.0 mm to 3.0 mm. There are thinner laminations, some barely visible to the naked eye, as well as one or two layers as thick as 7 mm. The transition from the silt to the clay is gradual as may be expected. The variation in the thickness of the clay layers is even greater. In general, layers with a thickness of less than 10 mm are very uncommon. In all the unconfined compression tests, there is no indication of the composite type of failure.

Lastly, Mr. Kenney asked some interesting questions about the geological origin of the till-like clay deposits. On this topic, the writer regrets that he is unable to offer any comments because very little factual information is available. It may be noted, however, that George H. Otto,[6] in his thesis, stated that the soft clays in the Chicago area form continuous strata with till sheets of stiff clay in the surrounding areas. His hypothesis is that the soft clays consist of till deposited under water.

---

[30] "Geotechnical Investigations for a Quay Structure in Horten," by L. Bjerrum, J. B. Hansen, and R. Sevaldson, Publication No. 28, Norwegian Geotechnical Inst., 1958.

[31] Assoc. Prof., Civ. Engrg., Michigan State Univ., East Lansing, Mich.

AMERICAN SOCIETY OF CIVIL ENGINEERS

Founded November 5, 1852

TRANSACTIONS

Paper No. 3050

DESIGN FEATURES OF THE GEORGE WASHINGTON BRIDGE LOWER DECK

By Irvine P. Gould,[1] F. ASCE

SYNOPSIS

The George Washington Bridge was completed and opened to traffic on October 31, 1931. The original design for this 3,500-ft suspension bridge included provisions for a second or lower deck to be constructed when traffic conditions warranted such a modification. Whereas the original concept contemplated four tracks of rapid transit on this lower deck, the present design will incorporate 6 lanes of vehicular traffic, with provisions for converting the 2 center lanes to 2 rapid transit tracks, if that should become necessary.

This paper examines the design features incorporated in the present structure and the modifications that will be necessary not only to the bridge, but to the New York and New Jersey approaches.

INTRODUCTION

The culmination of more than 4 yr of study and the realization of the ultimate concept of its design as visualized nearly 30 yr ago was reached on July 11, 1957, when the Commissioners of The Port of New York Authority authorized vast improvements to the George Washington Bridge. The expected cost is $182,000,000, exclusive of possible Federal Aid on the New York approaches. Fig. 1 shows the 6-lane lower deck as it will appear beneath the present 8-lane roadway of the George Washington Bridge.

Scope of Project.—In addition to the construction of the 6-lane lower deck, the New York approaches (Fig. 2) will be improved to provide a 12-lane expressway that will cross upper Manhattan between West 178th Street and West 179th Street. Astride the below street-level expressway and just east of the bridge plaza will be built a new 2-story bus passenger facility and an elevated bus turnaround. This will enable interstate commuter buses to drive off the

Note.—Published, essentially as printed here, in May, 1958, in the Journal of the Structural Division, as Proceedings Paper 1632. Positions and titles given are those in effect when the paper was approved for publication in Transactions.

[1] Engr. of Design, The Port of New York Authority, New York, N. Y.



FIG. 1.—GEORGE WASHINGTON BRIDGE



FIG. 2.—PROPOSED NEW YORK APPROACHES

bridge's upper deck directly into the passenger depot to unload patrons. Finally, in New York, substantial improvements will be made in the approach connections to Riverside Drive and the Henry Hudson Parkway more than 115 ft below the bridge ramps.

In New Jersey, the approach improvements (Fig. 3) will include 2 new depressed toll plazas, 2 tunnels to carry vehicles on and off the lower deck, connections to the new Bergen Expressway, and the major arteries, New Jersey

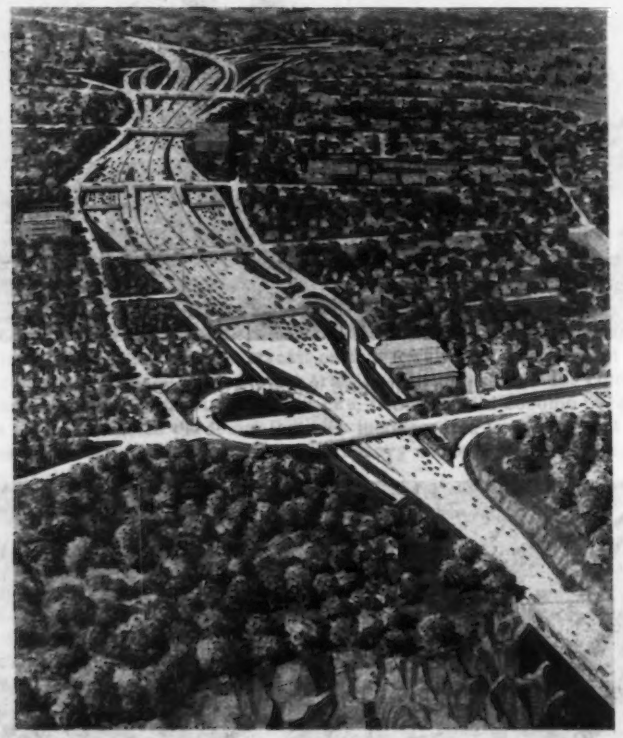


FIG. 3.—PROPOSED NEW JERSEY APPROACHES

Route 4 and U. S. Route 46. The Port Authority will also build a new administration building and will finance and construct a 500 car municipal parking lot, which will be conveyed to the Borough of Fort Lee after recovery of debt service charges.

INITIAL DESIGN CONCEPT

The George Washington Bridge was opened to traffic on October 31, 1931. With a main span of 3,500 ft, it was then the longest suspension bridge in the

world, but was soon to be surpassed by the 4,200 ft mainspan of the Golden Gate Bridge in San Francisco. The bridging of the Hudson River at New York was one of those civic and engineering undertakings that for generations had attracted the ambition, talents, and efforts of many engineers, but its actual development took some 50 yr to consummate. Early designs centered on various types of suspension bridges, but a 2,850 ft arch and a 2,100 ft cantilever received serious consideration. In its final conception, the selection of the specific suspension system and its proportions were governed by maximum economy consistent with the required degree of rigidity and aesthetic considerations.

The original design of the late 1920's contemplated 7 lanes of vehicular traffic on the upper deck, as shown in Fig. 4. By narrowing the side lanes and rearranging the center dividing curbs, an eighth lane could be obtained. Beneath the upper deck and connected to it by rigid frames, a lower deck designed to carry 4 tracks of heavy rapid transit trains was to be erected at a later data; or, as recognized even 30 yr ago by the designers, "utilized for additional vehicular lanes in case that should ever become necessary and desirable." This decision was reached after computations, supplemented by observations on a model, proved that the omission of the trusses and lower deck in the initial stage could still secure an ample degree of rigidity for the structure.

Upon its completion in 1931, the bridge and approaches cost $54,860,000, including the cost of engineering, administration, real estate, and financial expenses. It was estimated, at that time, that a bridge designed and built with only 1 deck for 6 lanes of traffic and 2 sidewalks, and without provisions for a second deck, would have cost approximately $40,000,000. Of the $15,000,000 difference, approximately 95% was expended for provisions for the increase in capacity of the bridge proper, and only 5% for provisions in the bridge approaches. In retrospect, this additional outlay was more than well spent.

Today (1960) this major arterial facility carries nearly 36,000,000 vehicles and is about to undergo what may be its final alteration, almost as conceived some 30 yr ago. The modifications necessary to provide additional capacity for the bridge structure proper will follow closely the original plan; the approaches on both sides of the river will undergo radical changes.

DESIGN FEATURES OF LOWER DECK

As previously noted, the lower deck was initially designed for 4 rapid transit tracks. The present design, as shown in Fig. 5(a), provides for 6 lanes of vehicular traffic with provisions to permit conversion of the 2 center lanes to double track rapid transit use should such be necessary at a future time (Fig. 5(b)). In order to provide for the future construction of this second deck, it was necessary to design initially the stiffening trusses, floor system, and bracing in considerable detail, as well as to determine the intensity of the live load. Based on these computations, the assumed dead plus live loads for the completed structure was 47,000 lb per lin ft. This included approximately 3,100 lb per lin ft for a future wearing surface on the upper deck.

The present design anticipates a total dead plus live load of 45,500 lb per lin ft when the lower deck carries 6 lanes of vehicular traffic, and 46,300 lb per lin ft when the lower deck carries 4 vehicular lanes and 2 rapid transit tracks.

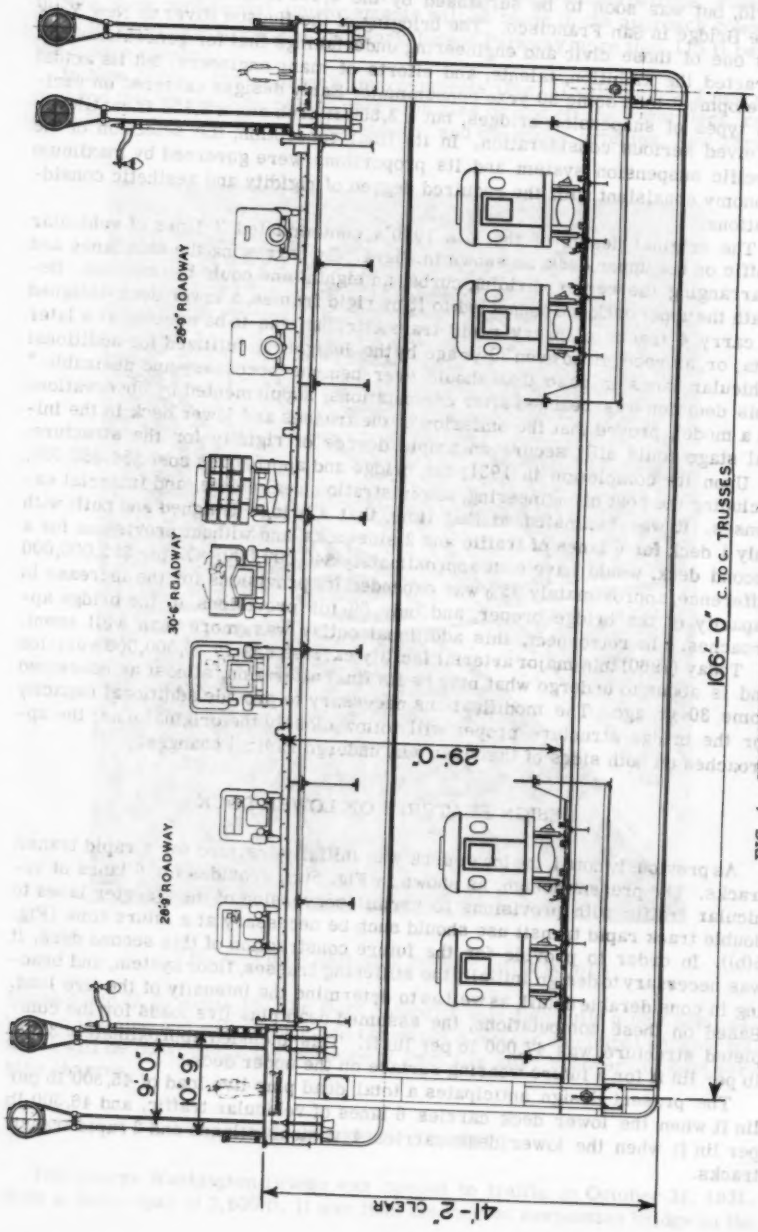
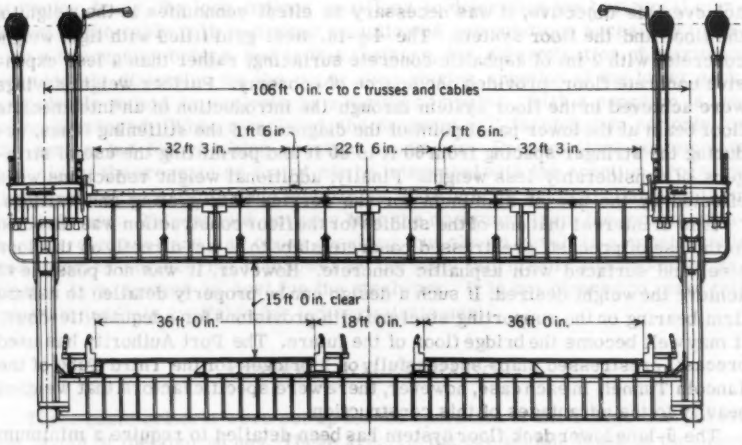
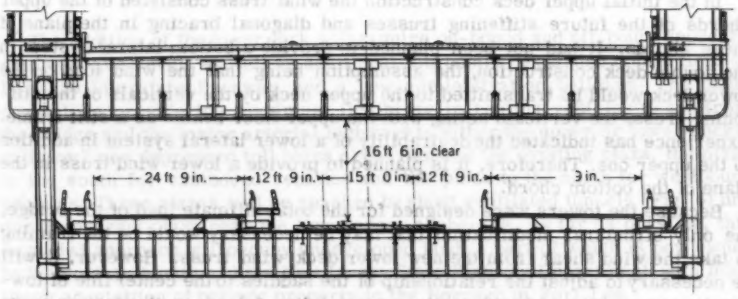


FIG. 4.—CROSS SECTION AS ORIGINALLY CONTEMPLATED



(*a*) SIX LANES OF VEHICULAR TRAFFIC ON LOWER DECK



(*b*) FOUR LANES OF VEHICULAR TRAFFIC AND TWO RAPID TRANSIT TRACKS ON LOWER DECK

FIG. 5.—CROSS SECTION OF BRIDGE

In recent years the Port Authority has been investigating various types of skin coat installations for resurfacing the concrete decks of its bridge facilities. One of the most promising found to date is a 1/2 in. surfacing of silica sand asphalt, which if placed on the upper deck, would add only 500 lb per lin ft to the dead load. Thus, it would be possible to resurface the upper deck and still not exceed the total design dead plus live load of the bridge. In order to achieve this objective, it was necessary to effect economies in the weight of the floor and the floor system. The 4 $\frac{1}{4}$-in. steel grid filled with light weight concrete, with 2 in. of asphaltic concrete surfacing, rather than a less expensive concrete floor, provides one source of economy. Further weight savings were achieved in the floor system through the introduction of an intermediate floor beam at the lower panel point of the diagonals of the stiffening truss, reducing the stringer spacing from 60 ft to 30 ft and permitting the use of stringers of considerably less weight. Finally, additional weight reductions were effected by the use of aluminum for the service walk grating and railings.

It is of interest that one of the studies for the floor construction was directed to the use of precast, prestressed concrete slabs to be set directly on the floor steel and surfaced with asphaltic concrete. However, it was not possible to achieve the weight desired. If such a design can be properly detailed to assure firm bearing on the supporting steel and with provisions for adequate tie-down, it may well become the bridge floor of the future. The Port Authority has used precast, prestressed slabs successfully on 2 bridges for the Third Tube of the Lincoln Tunnel. In each case, however, there were specific factors that weighed heavily to the advantages of this construction.

The 6-lane lower deck floor system has been detailed to require a minimum of modification for conversion of the 2 center lanes to 2 rapid transit tracks (Fig. 5(b)). This can be done at a later date, if necessary, by removing the floor deck in these lanes and rearranging the stringers.

In detailing the top chord of the stiffening truss, the original designers provided rivet holes, temporarily filled with bolts, for connection of the verticals to the present floor beams. In turn, gusset plates were also provided for connection of the diagonal web members. These, however, were left blank and are to be drilled in the field.

In the initial upper deck construction the wind truss consisted of the upper chords of the future stiffening trusses and diagonal bracing in the plane of these chords. It had not been planned to provide a bottom lateral system in the double deck construction, the assumption being that the wind load on the lower deck would be transmitted to the upper deck by the verticals of the stiffening truss, the verticals acting with the upper floor beams as a stiff frame. Experience has indicated the desirability of a lower lateral system in addition to the upper one. Therefore, it is planned to provide a lower wind truss in the plane of the bottom chord.

Because the towers were designed for the total ultimate load of the bridge, the only structural modification that may be necessary would be the framing to take the wind shear from the new lower deck wind truss. However, it will be necessary to adjust the relationship of the saddles to the center line of towers to compensate and reduce the eccentricity of load as the towers move riverward under the added load of the second deck. This will be done by jacking between the saddles and the towers to roll the towers shoreward approximately 13 in. In their final position, the saddles will be approximately 5 in. shoreward of the center line of towers.

As noted previously, the stiffening trusses were designed in some detail during the original design period so that proper provisions could be made for the ultimate condition. These computations were carefully stored and are now available for review and checking by the present designers. However, some modifications must be made for the new dead loads.

The laborious "cut and try" methods for the deflection of the cable and the stiffening truss, the long tedious equations to determine the horizontal component of the cable pull, and other complicated computations necessary to design a suspension bridge, and in this instance, the determination of maximum permissible distortion on the upper deck during erection of the lower deck, are ideally suited to analysis by a digital computer. Such a program is now being developed. When completed, the program will furnish data not only for the design, but for checking erection conditions. Present plans contemplate organizing the program so that it can be integrated with the erection programs developed by the major bridge companies, and would be made available to them for their use. This should not only free the designers from the tedium of laborious computations and cross checking, but should result in a considerable reduction in engineering manpower by the steel fabricator, and should be reflected in a savings in cost for the steelwork. It is not planned to make this program publicly available for indiscriminate use.

CRITERIA FOR OPERATION

Three basic criteria were set up for the operation of the bridge that govern the layout of the approaches. These are: 1. the two middle lanes of the upper deck would continue to be reversible so that a total of 8 lanes of the 2-level 14-lane structure would be available for traffic in the preponderant direction; 2. approaches in New York and New Jersey would be designed so that the motorist could reach his desired route from either the upper or lower deck; and 3. the design would permit all traffic to be routed to the upper deck should this be desirable at any time, such as during periods of low traffic volume.

NEW JERSEY APPROACH MODIFICATIONS

The addition of the lower deck will require on-bound and off-bound approach roads to this level, as well as additional toll booths, expanded connections to Palisade Interstate Parkway, and a new administration building. The basic concept, to provide for maximum flexibility in routing vehicles to and from the bridge and the major arterial highways to either the upper or lower decks, calls for 2 new depressed toll plaza areas flanking the existing plaza, the plaza to the south for eastbound vehicles and the plaza to the north for westbound vehicles. These plazas will be reached by short ventilated tunnels (Fig. 6) under the present plaza near the New Jersey anchorage. As far as possible, this expanded approach will occupy undeveloped land, a part of which is now owned by the Port Authority and the New Jersey State Highway Department, with minimum acquisition of private property in the Borough of Fort Lee.

In determining the number and type of toll booths for the depressed plaza, reference was made to an operations research study of traffic delays at toll booths.[2] This study, made in 1952-53, clearly demonstrated that, capacity-wise, left-hand collection booths are far superior to a combination of right and

[2] "Traffic Delays at Toll Booths," by Leslie C. Edie, Journal, Operations Research Society of America, Vol. 2, No. 2, May, 1954.

left-hand booths during peak operating conditions and under all combinations of traffic composition (percentage of passenger vehicles, buses, and trucks). A standard handling time per vehicle has been fixed at eleven seconds and varies, of course, about this mean to some extent due to human factors. During recent reconstruction of the toll plaza at the Lincoln Tunnel to accommodate traffic for the third tube, it had originally been planned to install a combination of 22 right and left-hand toll booths. As a result of the research effort, it was found necessary to construct only 18 left-hand booths, which resulted in a substantial saving in construction costs.

This study also developed superior scheduling techniques so that the service standard of 11 sec could be maintained with a minimum number of toll booths in operation, at an estimated operational savings of $50,000 per year for the present plaza booths.

NEW YORK APPROACH MODIFICATIONS

The New York approaches to the lower deck will provide interchange with the Henry Hudson Parkway and Riverside Drive as well as to the local Washington Heights area by means of an extensive modification of the existing approaches. Such connections will be constructed of elevated ramps or roadways

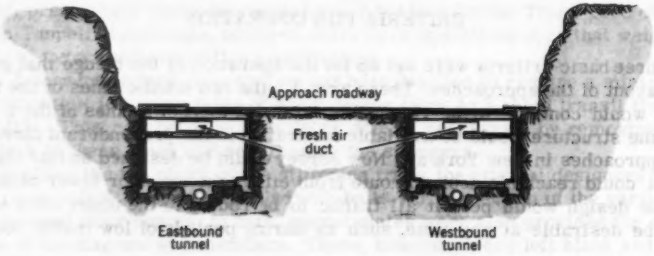


FIG. 6.—SECTION THROUGH NEW JERSEY APPROACH TUNNELS

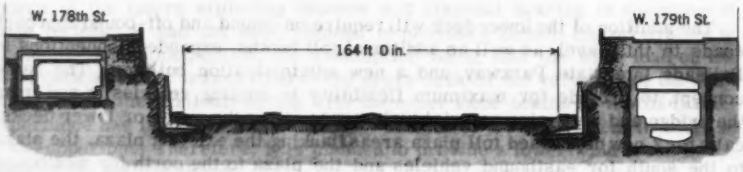
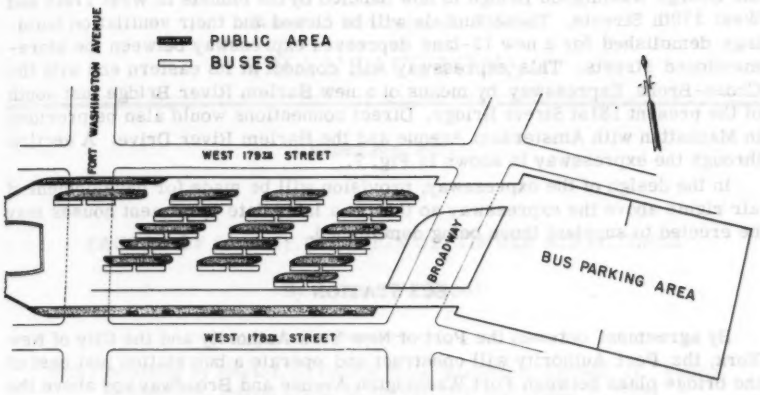


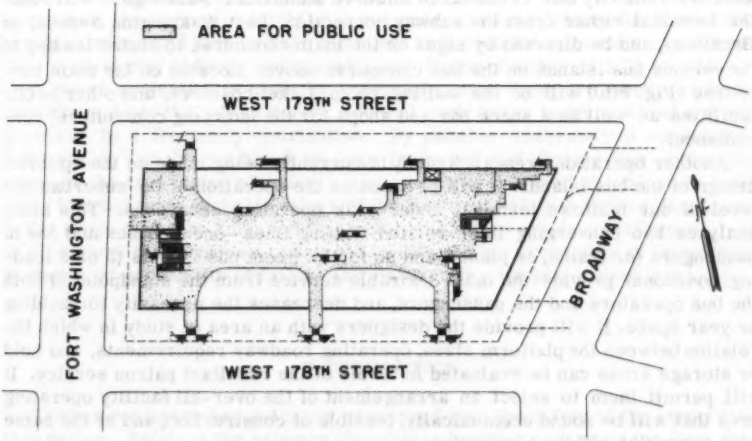
FIG. 7.—SECTION THROUGH TRANS-MANHATTAN EXPRESSWAY

on fill. Engineering of these approaches will tax the ingenuity of the designers to accomplish the construction with an absolute minimum of interference to the high density traffic traversing the present approach connections.

So complex is the problem of scheduling the construction and visualizing the relationship between traffic and completed areas, and the work to be done and clearances in the many levels of the approaches, that it has been necessary to construct a special model for staging the construction. This model will not only supplement the scheduling of the contracts, but will give the operating staff a clearer picture of traffic flow and thus facilitate vehicle movement



(*a*) PLAN AT SUBURBAN BUS LEVEL



(*b*) PLAN AT CONCOURSE LEVEL

FIG. 8.—BUS PASSENGER STATION

through the construction area. Express traffic across Manhattan to and from the George Washington Bridge is now handled by the tunnels in West 178th and West 179th Streets. These tunnels will be closed and their ventilation buildings demolished for a new 12-lane depressed expressway between the aforementioned streets. This expressway will connect at its eastern end with the Cross-Bronx Expressway by means of a new Harlem River Bridge just south of the present 181st Street Bridge. Direct connections would also be provided in Manhattan with Amsterdam Avenue and the Harlem River Drive. A section through the expressway is shown in Fig. 7.

In the design of the expressway, provision will be made for development of air rights above the expressway so that at a later date apartment houses may be erected to supplant those being demolished.

BUS STATION

By agreement between the Port of New York Authority and the City of New York, the Port Authority will construct and operate a bus station just east of the bridge plaza between Fort Washington Avenue and Broadway and above the expressway. This structure will serve the New Jersey buses that now traverse the city streets by circuitous routes to reach the local subways. Direct ramps from the upper deck to the bus level (Fig. 8(a)) and an elevated storage and turnaround east of Broadway will relieve the Washington Heights streets of this heavy interstate suburban bus traffic. For convenience of the bus patrons, direct underground passage will connect with the Eighth Avenue Subway.

The layout of the terminal is based on experience gained from operation of the Port Authority Bus Terminal in midtown Manhattan. Passengers will enter the terminal either from the subway connection, Fort Washington Avenue, or Broadway, and be directed by signs on the main concourse to stairs leading to the various bus islands on the bus concourse above. Located on the main concourse (Fig. 8(b)) will be the waiting room, ticket counters, and other public facilities as well as a snack bar and shops for the hurrying commuters' convenience.

Another operations research study is currently being made on the optimum design of the bus islands. It will be based on the operation of the suburban bus level of our midtown terminal under peak operating conditions. This study analyzes two converging inter-related waiting lines—one of buses and one of passengers (or trains, or planes, and so forth). Short bus islands (2 or 3 loading positions) provide the most desirable service from the standpoint of both the bus operators and the passengers, and decreases the necessity for holding or year space. It will provide the designers with an area of study in which the relation between the platform sizes, operating roadway requirements, and hold or storage areas can be evaluated in terms of the resultant patron service. It will permit them to select an arrangement of the over-all facility operating area that will be sound economically, feasible of construction, and at the same time permit an efficient operation.

The present program, as outlined, is estimated to cost $182,000,000, or three times the cost of the original bridge when it was opened in 1931. If it had not been for the foresight of the earlier engineers and planners, in all likelihood it would now be impractical or too costly to consider.

AMERICAN SOCIETY OF CIVIL ENGINEERS

Founded November 5, 1852

TRANSACTIONS

Paper No. 3051

FACTOR OF SAFETY IN DESIGN OF TIMBER STRUCTURES

By Lyman W. Wood[1]

With Discussion by Messrs. E. George Stern; Richard G. Kimbell, Jr.; Emilio Rosenblueth; Ludvik Cizek; Milos Vorlicek; and Lyman W. Wood

SYNOPSIS

Much of the reduction in the average strength of clear wood, that is made to obtain a design stress, is made necessary by its conditions of structural use. Such a reduction does not in itself produce a margin for safety. A simple way to estimate the degree of safety is to use near-minimum values for these conversion factors and then to make a further reduction for unforeseen conditions. This method may indicate a near-minimum factor of safety of 1.25 to 1.50.

A better evaluation is made by recognizing that there are many factors in strength and use that affect safety, and that each factor is multivalued and expressible by a frequency distribution. By suitable mathematical operations, these values can be combined into one frequency distribution that shows the range of the true factor of safety. An example of this kind of evaluation indicates that the most probable values of the factor of safety in timber design are in the range of 2.0 to 2.50, and that nearly all values are in the range of 1 to 4. The same distribution can be used to indicate the probability of failure and to show that probability of failure is related to the working stress level.

INTRODUCTION

Timber engineers are naturally concerned with the safety of the structures they design. Safety is the primary objective of building codes and the first duty of the building official. Much thought has been given to the factor of safety in design with steel, concrete, and other structural materials. This paper deals

Note.—Published, essentially as printed here, in November, 1958, in the Journal of the Structural Division, as Proceedings Paper 1838. Positions and titles given are those in effect when the paper or discussion was approved for publication in Transactions.

[1] Engr., Forest Products Lab., Forest Service, U. S. Dept. of Agri., Madison, Wis.

with the work of the Forest Products Laboratory of the Forest Service, U. S. Department of Agriculture, on the establishment of factors of safety for timber construction.

What is a factor of safety? A material may have an average strength value of 10,000 psi, and may be used with a design stress of 2,000 psi. Superficially, it might be said that there is a factor of safety of 5, yet this is not generally true. A reduction to the design-stress level may be necessary to convert from the conditions of laboratory test to those of structural use. It seems more reasonable to think of the factor of safety as a provision for something beyond the foreseeable conditions of structural use. The factor of safety is almost a "factor of ignorance."

This is not a new idea. It was[2] reported in 1927 that "The average timber has a factor of safety of about 2.25 for long-time loading, and for a few minutes will show a factor of safety of 4." A 1940 observation[3] on recommended working stresses reads, "No actual failure would be expected with loads 50% in excess of those computed from the tabulated stress values or with decrease in strength of the timber through decay or other deterioration to two-thirds its original value, but numerous failures are to be expected if such loads are doubled or if the strength of the timber decreases to one-half its original strength."

AN APPROACH TO THE FACTOR OF SAFETY

A simple way to estimate the factor of safety, based on near-minimum values, has been widely used. The strength of clear wood, the duration of load, and the presence of "defects" (natural strength-reducing characteristics) are major factors affecting the safety of structural timbers.

The strength of clear wood has a normal variability among trees or among pieces of lumber from the same tree. Fig. 1 shows the range of bending strength values in standard tests[4] of green, clear Douglas fir from all heights of the merchantable tree. This range closely approximates a normal frequency distribution. More than 95% of the values are higher than 5,435 psi, which is three-quarters of the average. 5,435 psi is acceptable as a near-minimum value, whereas the average value is 7,247 psi.

Fig. 2 is working stress chart that shows the relation of the strength of wood to the duration of load. That relation has been verified in many tests[5] and is approximately the same in all kinds of wood and in all strength properties. Fig. 2 shows that the long-time loading strength of wood is only approximately nine-sixteenths of the strength in short-time loading, as in a standard test. The long-time level of strength as 100% is shown and can thus be used to indicate possible increases of working stresses for conditions where the full design loading is of less than permanent duration.

All structural grades of lumber contain knots or other natural strength-reducing characteristics. These defects are limited in size and number, and

---

2 "Unit Stresses in Timber," by J. A. Newlin, Transactions, ASCE, Vol. 91, 1927, p. 387.

3 "Wood Handbook," U. S. Forest Products Laboratory, U. S. Dept. of Agriculture, 1940.

4 "Standard Methods of Testing Small Clear Specimens of Timber," Designation D143-52, ASTM, 1952.

5 "Relation of Strength of Wood to Duration of Load," by L. W. Wood, Report No. R1916, Forest Products Laboratory, 1951.

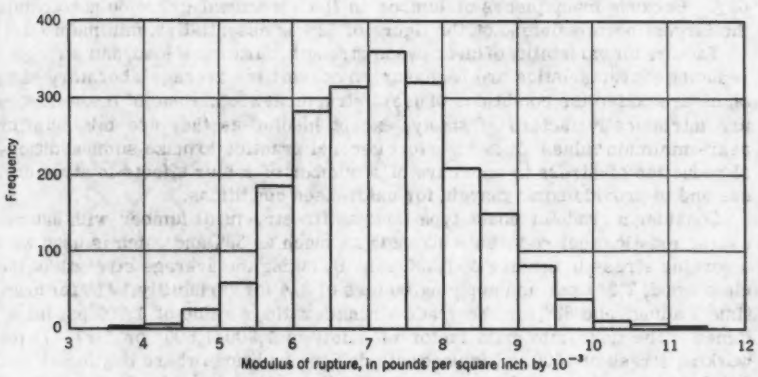


FIG. 1.—FREQUENCY DISTRIBUTION OF BENDING STRENGTH

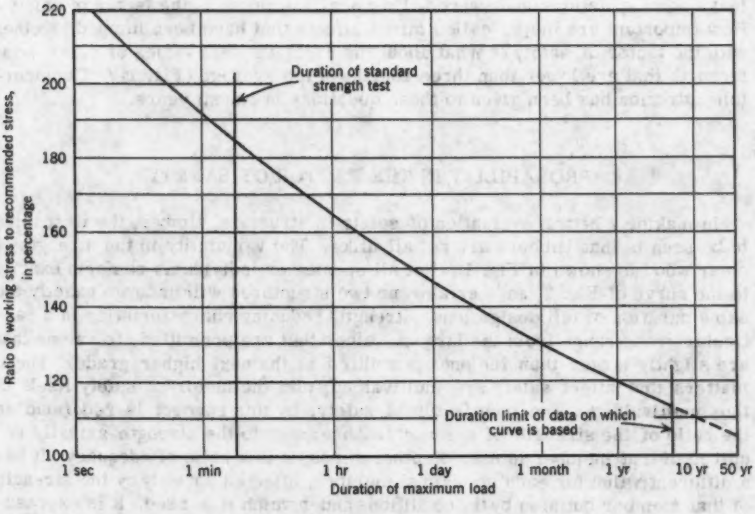


FIG. 2.—RELATION OF WORKING STRESS TO DURATION OF LOAD

their effect on strength is recognized in a "strength ratio." Thus, if the largest knot or greatest slope of grain permitted in a structural grade reduces the strength of clear wood by 38%, the strength ratio for that grade is said to be 62%. Because many pieces of lumber in the structural grade do not contain the largest permissible knot, the figure of 62% is essentially a minimum value.

Factors for variability of clear-wood strength, duration of load, and strength-reducing characteristics are necessary to convert the average laboratory value on clear wood to the conditions of use of structural wood. None of these factors are intrinsically factors of safety, except insofar as they are minimum or near-minimum values. It is therefore general practice to make some additional reduction of stress to take care of a number of minor affects in structural use and to provide some margin for unforeseen conditions.

Consider a grade of coast-type Douglas fir structural lumber with natural characteristics that reduce its strength as much as 38% and which is used with a working stress in bending of 1,500 psi. By taking the average strength of the clear wood, 7,247 psi, and applying factors of 3/4 for variability, 9/16 for long-time loading, and 62% for the grade strength ratio, a value of 1,900 psi is obtained. The near-minimum factor of safety is 1,900/1,500, or 1.27. If the working stress of 1500 psi is used with design conditions where the duration of full load is not expected to exceed 10 yr throughout the life of a permanent structure, the duration factor might be taken as 5/8 (Fig. 2) and the near-minimum factor of safety would be 2,110/1,500, or 1.43.

This is a simple approach to the factor of safety in timer design that has been widely used and is satisfactory for many purposes. It does, however, leave some questions unanswered. How near minimum is the factor of safety? How important are the so-called minor effects that have been lumped together with the factor of safety? What about the 5% of the test values of clear-wood strength that are lower than three-fourths of the average (Fig. 1)? Considerible attention has been given to these questions in recent years.

PROBABILITY IN THE FACTOR OF SAFETY

In making a better evaluation of safety in structural timber, the first thing to be seen is that timbers are not all alike. The variability in the strength of clear wood is shown in Fig. 1. Not all species or individuals conform exactly to the curve of Fig. 2, and certainly no two structures will undergo exactly the same duration of full design load. Strength-reducing characteristics in a particular grade range from the largest values that are permitted, to values that are slightly larger than the ones permitted in the next higher grade. These matters that affect safety are multivalued, and the factor of safety itself is thus multivalued. The true factor of safety, by this concept is redefined as the ratio of the strength of a structural member to the strength actually required of that member in use. In other words, it is a ratio of adequacy. It has a different value for each structural member, affected not only by the strength of that member but also by the conditions under which it is used. It is expressible, not as a single value, but as a frequency distribution of values. It can be thought of in terms of probability.

Engineers working with other structural materials have dealt with similar ideas. It has been pointed out that strength can be affected by combinations of

probabilities of strength values in the elementary units that compose a structural member.[6] More recently, it was recognized that factors of load and strength affect the adequacy of structural members and that each factor may have a different value for each individual instance.[7]

To estimate the distributed ratio of adequacy, it is necessary to consider the distributed values of the factors that affect it. By expressing each factor as a frequency distribution, the resulting mathematical expressions can be combined to show the frequency distribution of the factor of safety.

FACTORS AFFECTING SAFETY

Table 1 is a list of the factors involved in strength and use that may be considered to affect the safety of structural members, such as beams or joists, that carry flexural loads. Columns or other nonflexural members have similar

TABLE 1.—FACTORS AFFECTING SAFETY IN TIMBERS

Factor	Type of distribution[a]	Average value	Standard deviation	Limiting values	
				Lower	Upper
Variability of clear wood	N	1.00	0.160	-	-
Indeterminacy of stress analysis	N	1.00	0.030	-	-
Use of standard sizes	U	1.12	-	0.96	1.28
Depth factor	U	0.91	-	0.87	0.95
Efficiency of grading rules	N	1.12	0.200	-	-
Efficiency of inspection	N	1.00	0.011	-	-
Range of defects within grade	U	0.67	-	.60	.74
Off size	N	0.97	0.018	-	-
Imperfection of fabrication	N	0.95	0.020	-	-
Duration of load	N	0.62	0.030	-	-
Temperature	N	0.95	0.095	-	-
Expected versus actual load	N	1.10	0.080	-	-
Other conditions of service	N	0.95	0.070	-	-

[a] N = Normal distribution; U = uniform distribution.

factors. The values listed in Table 1 are expressed in terms of either normal or uniform frequency distributions. The normal frequency distribution would have a probability-curve shape, whereas the uniform frequency distribution would have a rectangular shape. Although the assumed values are believed to be representative, it is recognized that some are based almost entirely on judgment or a consensus of engineering opinion. Other factors or additional factors may apply in other instances.

Variability of Clear Wood.—To express the typical variability chart (Fig. 1) as a frequency distribution, the average value is represented by 1.0. The frequency distribution is nearly normal and has a computed standard deviation that is 15.4% of the average value. Studies of this and other species show that

[6] "Statistical Theory of Effect of Dimensions and of Loading Upon the Modulus of Rupture of Beams," by John Tucker, Jr., Proceedings, A.S.T.M. 41, 1941.

[7] "Variation of Strength Properties in Woods Used for Structural Purposes," by L. W. Wood, Report No. R1780, Forest Products Lab., 1950.

a general representative value of standard deviation is approximately 16%. The mean value of 1.0 and the standard deviation value of 0.16 define the normal frequency distribution. As defined, 6% of the values are below the level of three-quarters of the average value. The distribution is in approximate agreement with Fig. 1.

Indeterminacy of Stress Analysis.—This factor recognizes indeterminacy in the method and approximations in the computation of the stress analysis. No margin for error is included. A perfect stress analysis is represented by a factor of 1.0. Inaccuracies may cause the actual load or stress to vary from the expected and the adequacy of the timber to vary accordingly. From an appraisal of engineering experience and judgment, a normal distribution and a standard deviation of 0.03 are chosen. This implies that 1 timber in 22 is more than 5% over or under its expected adequacy from this cause, or that one in eight hundred is more than 9% over or under.

Use of Standard Sizes.—Ordinarily, designers specify only standard sizes of structural members. If the stress analysis calls for a section modulus greater than that provided by a standard size, the next larger standard size is used. If the requirements are only somewhat over, by an amount called the design tolerance, the smaller size is taken. A questionnaire to a number of prominent timber design engineers indicated that the design tolerance ranged from 0% to 10% with an average of 4%. Standard sizes of timber are generally such that a particular size has one-third more bending strength than the next smaller size. When this was considered in relation to design tolerance, it was computed that the timbers of standard size range from 1.00/1.04 to 1.33/1.04, or 0.96 to 1.28 times their required size in terms of strength. In other words, most timbers are more than adequately strong for this reason. A uniform distribution of this factor is assumed, because required sizes are a continuous and uniform progression of values.

Depth Factor.—Wood beams have a lower unit strength value in the large structural sizes than in the small sizes used in the standard strength tests. The depth factor is such that if the strength of the standard specimen is represented by 1.0, the strength of sawn structural beams, in common sizes, ranges uniformly from approximately 0.87 to 0.95. Glued, laminated beams of greater depth are not considered here.

Efficiency of Grading Rules.—Rules for strength grading of timber are based on principles[8] accepted by the American Society for Testing Materials (A.S.T.M.). Comparisons of actual strength values and values estimated according to the accepted principles show good general agreement even though there are many individual variations. An investigation of 239 timber beams and 69 joists showed that the average piece was 1.12 times as strong as it was estimated to be, and that an approximately normal distribution of individual values around that average value had a standard deviation of 0.20. This implies that three of four bending timbers will develop more strength than would be estimated from the grading rules.

Efficiency of Inspection.—The grading of structural lumber is done visually, and there is usually no time for actural measurement of characteristics. A questionnaire to lumber inspection bureaus indicated that estimates of knot sizes may be as much as 10% too low in 4% of the timbers inspected. A 10% error in knot size corresponds to approximately a 2% error in strength. Knot

---

[8] "Tentative Methods for Establishing Structural Grades of Lumber," Designation D245-57T, A.S.T.M., 1957.

sizes are presumed to be overestimated and underestimated with equal probability. The ratio of adequacy from this cause is considered to have a normal distribution with a mean of 1.0 and a standard deviation of 0.011, which corresponds to a 2% deficiency in strength in 4% of the pieces.

Range of Defects Within Grades.—A typical structural grade may permit natural characteristics that reduce the strength of the clear wood by 40%. Its working stress is therefore computed from a strength ratio of 60%. The next higher grade may have a minimum strength ratio of 75%. Within the lower grade, therefore, are pieces with strength ratios ranging uniformly from 60% to 74% of the strength of clear wood. This range defines the frequency distribution.

Off Size.—Either rough or dressed structural lumber may vary slightly from its expected or standard size. Extensive research on this factor in the width of boards is applicable also to structural lumber. The effective width of boards averaged approximately the same as the standard width and varied normally around it, with a standard deviation of 12%. Timbers are commonly sized at the saw and then lightly dressed, so their average dimensions are reduced to approximately 98% of standard. Strength in bending is proportional to the dimension in width and to the square of the dimension in depth. Since off size may occur with equal probability in width or depth, the assumed ranges of dimension are increased to their three-halves power. Thus, in comparison to the expected or standard size, the effect of off size is expressed by a normal frequency distribution with an average value of 0.97 and a standard deviation of 0.18.

Imperfection of Fabrication.—The factor of imperfect fabrication cannot be made large enough to cover the effects of poor fabrication, but it recognizes the difference between good fabrication by field standards and the precise cutting and fitting of laboratory test specimens. The ratio of adequacy from this cause is taken to be normally distributed with an average of 0.95 and a standard deviation of 0.02. This implies that practically all timbers are in the range of 90% to 100% of the laboratory strength values in this respect.

Duration of Load.—The range of values for duration of load can vary from the permanent load imposed on a structure by its own weight to the few seconds duration of earthquake loading. To reduce this spread, industrial buildings were assumed in Table 1. The most probable duration of dead plus full design live load was taken to be 5 yr during the life of a permanent structure. The corresponding strength was taken to be 62% of the standard laboratory test strength. This factor is thus expressed by a normal frequency distribution with an average value of 0.62. A standard deviation of 0.03 is assumed, this implying that full design dead and live loads are permanently present on approximately 2 1/2% of the timbers so used.

Temperature.—Wood is stronger when cold than when warm. Standard strength tests are made at an average temperature of 70° F. The service temperature of timbers in industrial buildings is assumed to have an average value of 80° F, and a normal distribution with a standard deviation of 19° F is taken to be representative. This means that 98 of 100 building timbers are in service at the range of 35° to 125° F. Each change of 1° F in temperature results in a change in strength of 0.5%. This change in terms of strength gives a normal frequency distribution, with an average of 0.95 and a standard deviation of 0.095.

Expected Versus Actual Load.—Because an overloaded timber may be thought of as less than adequate and an underloaded timber as more than adequate in strength, the variations of load can be put into a frequency distribution along

with those that represent strength factors. The most probable value for the ratio of actual to expected load is 90%, so that the average timber is approximately 10% more than adequate in this respect. A normal distribution is assumed, with an average value of 1.10 and a standard deviation of 0.08. This implies a possibility of overload on 1 in 10 timbers. This is a generalized value, and other values could be assumed for more specific uses.

Other Conditions of Service.—Timbers in interior service may gain more than enough strength as they dry to offset the checking or splitting that occurs. On the other hand, many timbers are exposed in various degrees to such hazards as decay, insect attack, fire damage, or chemical deterioration. Where such conditions are expected, the working stress may be adjusted for them, with only the unexpected conditions taken into account in the factor of safety. Largely from judgment it is estimated that the ratio of adequacy of timber beams in this respect is normally distributed, with an average of 0.95 and a standard deviation of 0.07. This implies that the strength of 58 in 60 timbers will range from 0.80 to 1.10 from this cause.

COMBINATION OF FACTORS

Because of the mathematical terms in which these factors that affect safety have been described, their combined effect may be shown by multiplying all of them together. This is possible because all are mutually independent and all operate simultaneously. The product of this multiplication is the over all ratio of adequacy of bending timbers in relation to the average laboratory strength.

The mathematical problem of computing the product of a number of distributed values is difficult, and no exact solution has been found. Three methods have been developed[9] to give an approximate result. These are the method of random products, the use of a Gram-Charlier series, and the method of Pearson distributions. The first method is the easiest to understand and can be readily used with modern computing equipment. Therefore, it is the only one examined in this paper.

The method of random products consists of taking a random value from the frequency distribution that represents each factor and multiplying these random values together to obtain a random product. Five hundred or more of such random products serve adequately to define the product distribution. Random multipliers can be obtained by use of a table of random numbers. A table of random numbers consists of numbers in a selected range, often from 0000 to 9999, picked at random so that each number has an equal chance of being used. A table for the selected range may be of any length, with any number in the selected range able to appear more than once, depending on the length of the table. If an electronic computer is used, it can generate its own random numbers. By this method, the random numbers are first divided into classes, and a multiplier is computed in each factor distribution to correspond to the midpoint of each random-number class. That multiplier is then used with every random number in the class.

The method of random products is best explained with an example. Such an example has been worked with all the values in Table 1. For simplicity, however, a shorter series of factors is used. It includes the variability of clear wood, range of defects within grade, duration of load, and expected versus actual load. Other factors in Table 1 that affect strength are combined into a

[9] "Evaluation of the Factor of Safety in Structural Timbers," by L. W. Wood and M. Tasker, Report No. 2068, Forest Products Lab., 1957.

single normal distribution assumed to have an average of 1.00 and a standard deviation of 0.200.

Random numbers from 0000 to 9999 are divided into 39 classes, as shown in Table 2. Class intervals are equal for dealing with the uniform distribution (column 7, Table 2), because in such a distribution each value has an equal chance to appear. With the normal frequency distributions, class intervals are varied to represent the varying frequencies in the normal distribution throughout its range (column 1, Table 2). In the widest intervals near the middle of the distribution, the corresponding normally-distributed multipliers occur with the greatest frequency.

A multiplier is computed that will correspond to the midpoint of each of the 39 classes of random numbers. These multipliers appear in columns 3, 4, 5, and 6 of Table 2 for the normal distributions, and in column 9 for the uniform distribution. To illustrate, in the fourth class of random numbers with normal intervals, the center of that class interval is at the average value minus 3.2 times the standard deviation. In the frequency distribution representing variability of clear wood, the average value is 1,000, and the standard deviation is 0.160 (Table 1). Then $1{,}000 - (0.160 \times 3.2) = 0.488$, the value that appears in column 3 of Table 2. In like manner, in the fourth class of random numbers with uniform intervals, the average of 0.67 and the range of 0.14 from Table 1 are used. Then $0.670 - [(16/38) \times 0.14)] = 0.611$, the value that appears in column 9 of Table 2.

In computing one random product, the first random number drawn might be 8,522, and its corresponding multiplier from column 3 of Table 2 is 1,160. This means that the hypothetical timber to be represented by the product has clear wood 16% stronger than the species average. The second random number may be 5,265 and the corresponding multiplier from column 4 is 1.000, meaning that other factors affecting strength will combine in a way that is just average. The third random number may be 2,349, and the corresponding multiplier from column 5 is 0.596, implying that the duration of load on the timber is somewhat more than the designer anticipated. The fourth random number may be 2,728, and the corresponding multiplier from column 6 is 1.052; this means that the maximum load sustained is approximately 95% of the assumed design load. The fifth random number may be 4,217, and the corresponding multiplier from column 9 is 0.659, meaning that the actual strength ratio of the hypothetical timber is 66%. The product of these five multipliers is 0.479. If the working stress on this hypothetical timber is one-sixth of the average strength-test value for the species, the ratio of adequacy of the timber is 0.479/0.167, or 2.9.

A magnetic data-processing machine was used to compute 500 random products from the data of Table 2. The programming was coded on 100 punch cards and included the generation of random numbers. After the cards had been fed into the machine, the process of computing and classifying these random products took 15 min in the computer, with an additional 10 min in a tabulator to decode and print the results. This type of operation is well adopted to such a computer, and 1,000 or more products could have been computed without difficulty.

DISTRIBUTION OF THE RATIO OF ADEQUACY

Fig. 3 is the frequency distribution of the 500 random products of the five factors in the preceding illustrative example. It shows graphically the range of the adequacy of structural timbers in relation to the average strength of

TABLE 2.—COMPUTATION OF MULTIPLIERS IN THE METHOD OF RANDOM PRODUCTS

Normal frequency distributions						Uniform frequency distribution (Range of defects within grade)		
Intervals in table of random numbers	Multiples of standard deviation corresponding to centers of intervals	Multipliers corresponding to centers of intervals				Intervals in table of random numbers	Unit multipliers corresponding to centers of intervals	Multipliers corresponding to center of intervals
		Variability of clear wood	Other factors affecting strength	Duration of load	Expected versus actual load			
(1)	(2)	(3)	(4)	(5)	(6)	(7)	(8)	(9)
0000 –	-3.8	0.392	0.240	0.506	0.796	0000 - 0256	-19	0.600
0001 –	-3.6	.424	.280	.512	.812	0257 - 0513	-18	.604
0002 - 0004	3.4	.456	.320	.518	.828	0514 - 0769	-17	.607
0005 - 0009	-3.2	.488	.360	.524	.844	0770 - 1,026	-16	.611
0010 - 0018	-3.0	.520	.400	.530	.860	1,027 - 1,282	-15	.615
0019 - 0034	-2.8	.552	.440	.536	.876	1,283 - 1,538	-14	.618
0035 - 0061	-2.6	.584	.480	.542	.892	1,539 - 1,795	-13	.622
0062 - 0106	-2.4	.616	.520	.548	.908	1,796 - 2,051	-12	.626
0107 - 0178	-2.2	.648	.560	.554	.924	2,052 - 2,307	-11	.629
0179 - 0286	-2.0	.680	.600	.560	.940	2,308 - 2,564	-10	.633
0287 - 0445	-1.8	.712	.640	.566	.956	2,565 - 2,820	- 9	.637
0446 - 0667	-1.6	.744	.680	.572	.972	2,821 - 3,077	- 8	.640
0668 - 0967	-1.4	.776	.720	.578	.988	3,078 - 3,333	- 7	.644
0968 - 1,356	-1.2	.808	.760	.584	1.004	3,334 - 3,589	- 6	.648
1,357 - 1,840	-1.0	.840	.800	.590	1.020	3,590 - 3,846	- 5	.652
1,841 - 2,419	- .8	.872	.840	.596	1.036	3,847 - 4,102	- 4	.655
2,420 - 3,084	- .6	.904	.880	.602	1.052	4,103 - 4,359	- 3	.659
3,085 - 3,820	- .4	.936	.920	.608	1.068	4,360 - 4,615	- 2	.662
3,821 - 4,601	- .2	.968	.960	.614	1.084	4,616 - 4,871	- 1	.666
4,602 - 5,397	0	1.000	1.000	.620	1.100	4,872 - 5,128	0	.670
5,398 - 6,178	.2	1.032	1.040	.626	1.116	5,129 - 5,384	1	.674
6,179 - 6,914	.4	1.064	1.080	.632	1.132	5,385 - 5,640	2	.678
6,915 - 7,579	.6	1.096	1.120	.638	1.148	5,641 - 5,897	3	.682
7,580 - 8,158	.8	1.128	1.160	.644	1.164	5,898 - 6,153	4	.686
8,159 - 8,642	1.0	1.160	1.200	.650	1.180	6,154 - 6,410	5	.689
8,643 - 9,031	1.2	1.192	1.240	.656	1.196	6,411 - 6,666	6	.693
9,032 - 9,331	1.4	1.224	1.280	.662	1.212	6,667 - 6,922	7	.697
9,332 - 9,553	1.6	1.256	1.320	.668	1.228	6,923 - 7,179	8	.701
9,554 - 9,712	1.8	1.288	1.360	.674	1.244	7,180 - 7,435	9	.704
9,713 - 9,820	2.0	1.320	1.400	.680	1.260	7,436 - 7,692	10	.708
9,821 - 9,892	2.2	1.352	1.440	.686	1.276	7,693 - 7,948	11	.712
9,893 - 9,937	2.4	1.384	1.480	.692	1.292	7,949 - 8,204	12	.715
9,938 - 9,964	2.6	1.416	1.520	.698	1.308	8,205 - 8,461	13	.719
9,965 - 9,980	2.8	1.448	1.560	.704	1.324	8,462 - 8,717	14	.723
9,981 - 9,989	3.0	1.480	1.600	.710	1.340	8,718 - 8,973	15	.726
9,990 - 9,994	3.2	1.512	1.640	.716	1.356	8,974 - 9,230	16	.730
9,995 - 9,997	3.4	1.544	1.680	.722	1.372	9,231 - 9,486	17	.734
9,998	3.6	1.576	1.720	.728	1.388	9,487 - 9,743	18	.737
9,999	3.8	1.608	1.760	.734	1.404	9,744 - 9,999	19	.740

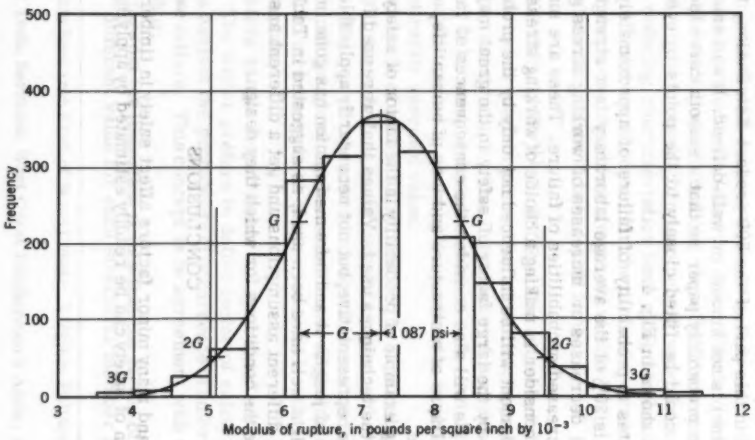


FIG. 3.—FREQUENCY DISTRIBUTION OF THE RATIO OF ADEQUACY

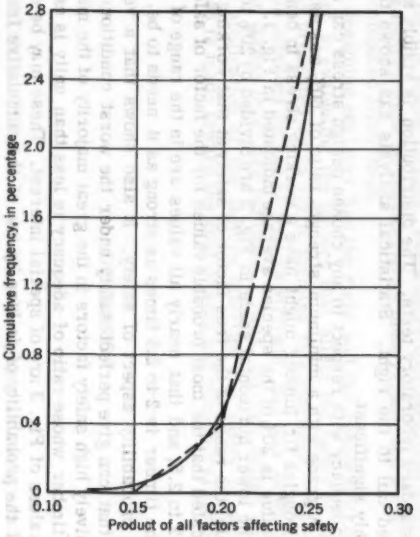


FIG. 4.—PORTION OF THE CUMULATIVE FREQUENCY DISTRIBUTION OF FIG. 3

clear wood in standard laboratory tests. The distribution is visibly skewed, with an elongated tail to the right. Statistical analysis has shown that the skewness is highly significant.

The ratio of adequacy with respect to any chosen design stress can also be seen in Fig. 3. A grade with a minimum strength ratio of 60% was assumed. Such a grade in Douglas fir lumber might have a working stress in bending of 1,450 psi. That value is 20% of the species average indicated in Fig. 1. Therefore, values on the lower horizontal scale in Fig. 3 are divided by 20% to show, in the upper scale, the range of the true factor of safety at that working stress level. It is indicated that the most probable values for the factor of safety are in the range of 2 to 2.5, and that nearly all values are in the range of 1 to 4. Most probably the timber is 2 to 2.5 times as strong as it needs to be. Fig. 3 emphasizes the probability aspect of safety. It also shows that a very low working stress that can give perfect safety under the worst conditions would result in excessively high safety factors in the great majority of the material.

Because any timber whose ratio of adequacy is less than unity is expected to fail, the low values of Fig. 3 are of special interest. These may be considered in terms of the probability of failure by use of the cumulative frequency distribution. The cumulative distribution is the continuous summation of area under the frequency polygon. Fig. 4 shows, on a magnified scale, the left-hand part of the frequency distribution of Fig. 3 in cumulative form. Because so few values occurred in this part of the 500 product distribution, the actual distribution (dashed line) is not smooth or well-defined. It was smoothed by plotting it on logarithmic probability paper so that a smooth curve (solid line), almost a straight line, could be fitted closely to the points by eye. A part of that smooth curve is shown in Fig. 4.

Fig. 4 indicates a probability of failure of approximately 0.5% where the working stress is 20% of the average laboratory test strength of clear wood. Relatively small decreases or increases of working stress give considerably decreased or increased probabilities of failure. These are matters for the design engineer to consider in making a choice of working stresses for structural lumber. His judgment will be influenced not only by the probability of failure (Fig. 4) but also by the large factor of safety in the great majority of the material (Fig. 3). He will also consider the consequences of failure, whether it may result in collapse of a structure and loss of human life, or only in limited property damage.

The preceding example of probability in the factor of safety has been worked through to show the techniques used. Values that were used for the factors affecting safety are representative, but not necessarily applicable in all instances. A large element of judgment and informed opinion has gone into some of them. More factors might well have been used, as suggested in Table 1. Other engineers may make different assumptions and get a different answer that is more acceptable under the conditions for which they design.

CONCLUSIONS

A few major and many minor factors affect safety in timber design. A near-minimum margin of safety can be readily estimated by applying near-minimum

values for the major factors. For a more thorough consideration, however, the various factors must be considered as multivalued, and a multivalued factor of safety computed from them.

The designing engineer has the right and the responsibility to use his own judgment in evaluating the factors that affect the safety of his design. This paper is presented as an aid in forming this judgment. The manner in which safety is affected by use as well as strength, and how safety is related to the working stress level are indicated. Thus, through better understanding and logical application of the factors affecting the safety of structural lumber, progress is made toward the goal of safe and economical timber design.

DISCUSSION

E. GEORGE STERN,[10] F. ASCE.—The paper on safety factors is of great value, because it promotes the proper use of wood as a result of a better understanding of the material.

During testing in the 1950's of full-size structural components, the effectiveness of grading rules with respect to boxed-pith lumber aroused concern. Members that looked perfectly satisfactory were found to incorporate overgrown knots and pin knots, which reduced the effective cross section of the members excessively and resulted in unexpected wood failures. Had these natural strength-reducing characteristics been along the lumber surface, the members would not have been accepted for the particular grade involved. However, as large as they were, these knots were not visible. It is perhaps desirable to give special consideration to boxed-pith lumber.

RICHARD G. KIMBELL, JR.,[11] F. ASCE.—The author is to be complimented on the contribution he has made in presenting a realistic approach to the factor of safety for timber construction. The importance of a realistic evaluation of the factor of safety to be used in design cannot be underestimated. It is gratifying to see more attention being given by the profession to what in the past has often been an arbitrarily assumed value.

Although this concept of safety as related to the probability of occurrence of factors tending to cause failure is not new, this paper is the first application to timber design. The use of this procedure should result in a better balanced and more economical design of timber structures. This same philosophy can be applied as well to structures built of other materials using factors applicable to these materials.

The author refers to the term "factor of ignorance" as synonomous with factor of safety. The writer prefers to define factor of safety as an insurance factor that guards against the probability of occurrence of unforeseen phenomena tending to cause failure. This concept is in agreement with the concept presented by the author.

The author brings out the important points that the factor of safety is multivalued, having a "different value for each structural member affected not only

10 Earle B. Norris Research Prof. of Wood Constr., Virginia Polytechnic Inst., Blacksburg, Va.

11 Asst. Dir. of Tech. Services, West Coast Lumbermen's Assn., Portland, Ore.

by the strength of that member but also by the conditions under which it is used," and that there is always a probability of occurrence of failure, even with a large factor of safety.

This premise is supported by a statement,[12] "The difference between the 'safe' and the 'unsafe' design is in the degree of risk considered acceptable, not in the delusion that such risk can be completely eliminated."

With the continuing progress in the development of electronic computers and an increasing awareness of the usefulness of statistics as a tool, it becomes practical to express the factor of safety in terms of its most probable value, and, more important, to indicate to the designing engineer the probability of failure. The author's presentation is devoted principally to the factor of safety of individual members. Where structural systems utilize repetitive members spaced at close intervals, such as joists, rafters, and laminated decks, the failure of an individual member would not necessarily result in the failure of the entire structure because there would be a redistribution of loads to adjacent members. Because there is a range of growth characteristics within a lumber grade, the improbability of occurrence of a consecutive number of low line pieces should also be considered. For this type of framing system the most probable factor of safety of the individual member is of less importance that the most probable factor of safety of the framing system.

EMILIO ROSENBLUETH[13] M. ASCE.—The author's clear presentation of such a basic subject should point the way for workers in structures built of other materials to attempt similar applications in their fields. The methods expounded can supply a basis for fixing safety factors in building codes in a more rational and acceptable manner than has been possible.

However, certain aspects of the problem seriously demand further research. The writer ventures the opinion that as a result of that research revisions of importance will be in order. The following points require further scrutiny.

1. In statically determinate structures, such as most timber trusses, failure of one member may cause total collapse. Many of the variables considered by the author are likely to affect all the members in the same manner and to the same degree, but others are not. The actual probability of failure may thus be appreciably larger than computed and, in some measure, the problem becomes one of obtaining the distribution of the smallest sample in a group. Under the assumption that the method of random products, or some equivalent procedure, will eventually find place in the study of steel and reinforced concrete structures, it is well to point out that the problem of the weakest link will become critical in multistory buildings.

2. Live loads to be used in design should not be specified in an almost arbitrary manner but should be based on extensive surveys followed by careful statistical studies. It is well established that most types of live loads are such that the design unit-load decreases with increasing loaded area.[14,15,16] But the rate of decrease is a function of the permissible probability of failure.

12 "Safety and Probability of Failure," by A. M. Freudenthal, Transactions, ASCE, Vol. 121, 1956.

13 Director and Research Prof., Inst. of Engrg., Univ. of Mexico, Mexico City, Mexico.

14 "Design Live Loads in Buildings," by J. W. Dunham, Transactions, ASCE, Vol. 112, 1947, pp. 725–739.

15 "The Steel Skeleton," by J. F. Baker, M. R. Horne, and J. Heyman, Vol. 2, Cambridge Univ. Press, Cambridge, 1956, p. 346.

16 "Teoria de la Carga Viva en Edificios," by E. Rosenblueth, Rev. Ingenieria, 1959.

Hence, the live load and its distribution that are considered in computing the factor of safety are not independent of the permissible probability of failure.

3. The permissible probability of failure is affected by the cost of a potential failure. This cost is influenced by such matters as loss of prestige, loss of human lives, and other near-imponderables. It is true that estimating the allowable probability of failure is less objectionable than a direct estimate of the factor of safety. But unless the near-imponderables are evaluated quantitatively and the permissible probability of failure established on rational bases, little further progress may be expected in the field of load factors.

The method of random products is attractive when individual distribution functions are known with a high degree of precision. Otherwise a simpler though less accurate method is preferable. One simple method can be derived from relations between distribution functions of individual variables and the distribution function for their combination. These relations have been published repeatedly in connection with structural design.[17,18,19]

When stability is governed by the additive association of normally distributed variables, the relation is simple. Assume, for example, that a structural element of strength S is called upon to resist the sum of live load L and dead load D. Variables D, L, and S may be said to be additively associated in determining the stability of the member, for failure will be impending when $S - D - L = 0$. If each of the variables possesses normal distribution, the factor of safety, C, required will be

$$C = 1 + \sqrt{(C_D - 1)^2 + (C_L - 1)^2 + (C_S - 1)^2}$$

in which each of the C's represents the factor by which the corresponding load would have to be multiplied (or the strength divided) in order that the probability that the load be exceeded (or the strength not reached) be equal to a given value. In other words, C_D, C_L, or C_S is the factor of safety required to give a certain probability of failure if the dead load, the live load, or the strength is the only random variable, the other two being determinable. Use of the global factor of safety C in conjunction with the expected value of each variable leads to the same probability of failure when all the variables are random. In general, for normally distributed variables associated additively,

$$C = 1 + \sqrt{\sum_i (C_i - 1)^2} \quad \ldots\ldots\ldots\ldots\ldots\ldots \quad (1)$$

Similarly, for variables with log-normal distributions associated multiplicatively, such as the ones considered by the author,

$$C = \exp \sqrt{\sum_i \log^2 C_i} \quad \ldots\ldots\ldots\ldots\ldots\ldots \quad (2)$$

except that here each factor of safety is taken with respect to the exponential of the expected logarithm of the variable.

Factors of safety computed from Eq. 2 are always slightly smaller than those from Eq. 1. Moreover, the distributions of most variables of interest in structural design lie either between the log-normal and the normal distributions or quite close to one of them. This is also true of the product of several

17 "Safety and the Probability of Structural Failure," by A. M. Freudenthal, Transactions, ASCE, Vol. 121, 1956, pp. 1337-1375.

18 "Strength, Safety and Economical Dimensions of Structures," by A. I. Johnson, Bulletin, Div. of Bldg. Statics and Struct. Engrg., Royal Inst. of Technology, Stockholm, Sweden, 1953.

19 "La Securite dans les Constructions," by R. Levi, Travaux, Vol. 40, August, 1956, pp. 435-440.

variables, each of which has normal distributions. Indeed, the log-normal distribution is the limit for the product of an infinite number of well-behaved random variables. Because strength and load may each be regarded as such products or sums of variables, and stability is governed by their difference, one may expect Eq. 1 to give reasonable accurate results, almost always on the safe side.

In the case of timber structures, the author has shown that only three of the thirteen variables affecting safety have uniform distribution, and the corresponding ranges are quite narrow compared with variations of the other variables. Hence, Eq. 1 would be expected to yield satisfactory results.

Assuming a permissible probability of failure of 0.5% the terms C_i for each of the ten variables with normal distributions is obtained from

$$C_i = \frac{E(X_i)}{E(X_i) - 2.58_{\sigma}(X_i)}$$

in which E denotes expectation and σ is the standard deviation. (The factor 2.58 is that required for an 0.5% chance of failure; for 0.05% it would be 3.29.) For the three variables with uniform distribution,

$$C_i = \frac{E(X_i)}{\min(X_i) + 0.005\left[\max(X_i) - \min(X_i)\right]}$$

in which min (X_i) and max (X_i) define the range of X_i. Thus,

$$C_1 = \frac{1.00}{1.00 - 2.58 \times 0.160} = 1.704$$

$$C_2 = \frac{1.00}{1.00 - 2.58 \times 0.030} = 1.083$$

and

$$C_3 = \frac{1.12}{0.96 + 0.005 \times 0.32} = 1.164$$

A safety factor of 2.2368 is obtained in this manner from Eq. 1. This is with respect to the product of expected values, $1.00 \times 1.00 \times 1.12 \times \ldots = 0.4338$. To find the factor of safety with respect to nominal load and strength, it must be divided by this product, so that $C = \frac{2.2368}{0.4348} = 5.156$.

As compared with the factor of safety of 5.0 computed by the author, the error is 3% on the safe side.

The present method was carried out in a few minutes on a desk computer. If many such computations have to be performed the procedure is amenable to programming for electronic computation.

LUDVIK CIZEK.[20]—The writer has prepared the frequency distribution (Fig. 5) by means of the theoretical curve of Gauss with the maximum ordinate

(max y) equal to 0.399, Δ/δ (n) = 0.399, and 500/1,087 (2,038) = 374.

The standard deviation equals 1,087 psi and the theoretical minimum strength (min k) equals m - 3 δ = 7,247 - (3 × 1,087) = 3,986 psi correspond closely to the real minimum strength. The long-time loading strength (min k) equals 9/16 (3,986) = 2,245 psi and the working stress (k) equals 0.62 (2,245) = 1,400 psi, in which 0.62 is the factor for largest permissible knots. This method is based on the real minimum strength in which min k = M - 3 δ and not from the near-minimum strength where min k = M - 1.66 δ.

---

20 Czechoslovak Academy of Sciences, Praque, Czechoslovakia.

This statistical method was also used for the determination of working load of joints with two split-ring, 10 cm round connectors. The arithmetical mean from these tests of 30 specimens was M = 8.50 tons, the standard deviation δ = 0.649 tons. Then the real minimum (min S) equals 8.50 - (3 × 0.649) = 6.55 tons. The strength under the long-time loading (min S) equals 0.625 × 6.44 tons = 4.10 tons. With the coefficient of safety 1.25, the working load for one split-ring connector is $K = \frac{4.10}{2\ (1.25)} = 1.64$ tons. The standard that was used gives, for this case, the value of K = 1.60 tons.

The same method was applied for tests of thirty specimens with two bulldog-connectors 10 cm square. The arithmetical mean for M was 5.97 tons, the standard deviation δ was 0.499 tons. Then the real minimum (min S) is M - 3 δ = 5.97 - (3 × 0.499) = 4.77 tons. The strength under the long-time loading

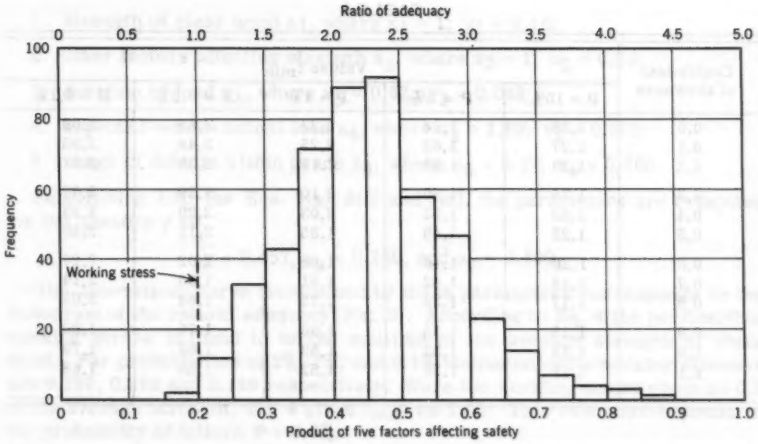


FIG. 5.—THEORETICAL FREQUENCY DISTRIBUTION OF BENDING STRENGTH

(min S) is 0.625 (4.77) = 2.98 tons. With the coefficient of safety 1.25, the working load for one bulldog-connector is $B = \frac{2.98}{(2.1)25} = 1.19$ ton.

The same method was used to determine the working load of nails. The working load of any connection is given by the statistical minimum, min S = M - 3 δ, from long-time loading strength (min S') = 0.625 (min S) and from the minimum safety factor of 1.25. The value min S = M - 3 δ is closer to reality than the "near-minimum" value min S = M - 1.66 δ.

MILOS VORLICEK.[21]—The factors affecting the safety of timber structures must be considered as random variable quantities. Mr. Wood has shown the method of random products to be a very interesting method of establishing

[21] Cand. Tech. Sc., Czechoslovak Academy of Sciences, Prague, Czechoslovakia.

safety of construction. But it would be rather tiresome to use this method in practical numerical cases, especially without an electronic computer.

The factors affecting safety shall be indicated $x_1, x_2, \ldots, x_n$. It is possible to establish the distribution of the product y of these mutually independent random variables, in which $y = x_1, x_2, \ldots x_n$. From logarithms this equation becomes $\log y = \sum_{i=1}^{n} \log x_i$. The variable y should have log-normal distribution in the case in which either n would be very great or the transformed variables ($\log x_i$) would be normally distributed. Since neither of these conditions are normally fulfilled, it is necessary to use another procedure.

Taking the quantities x_i for random variables which can have a skewed frequency distribution, every variable x_i is therefore defined by the mean $\bar{x}_i$, by the coefficient of variation v_i and by the coefficient of skewness a_i.

TABLE 3

Coefficient of skewness	Values t_{min}				
	P = 10%	P = 5%	P = 1%	P = 0.5%	P = 0.1%
0.0	1.28	1.64	2.33	2.58	3.09
0.1	1.27	1.62	2.25	2.48	2.95
0.2	1.26	1.59	2.18	2.39	2.81
0.3	1.25	1.56	2.10	2.29	2.67
0.4	1.23	1.52	2.03	2.20	2.53
0.5	1.22	1.49	1.95	2.11	2.40
0.6	1.20	1.46	1.88	2.02	2.27
0.7	1.18	1.42	1.81	1.93	2.14
0.8	1.17	1.39	1.73	1.84	2.02
0.9	1.15	1.35	1.66	1.75	1.90
1.0	1.13	1.32	1.59	1.66	1.79
1.1	1.11	1.28	1.52	1.58	1.68

The equation for y is developed through the Taylor series. Putting this series in the formulas for the mean $\bar{y}$, for the coefficient of variation v_y and for the coefficient of skewness a_y of the variable y, the following relations are obtained:

$$\bar{y} = \bar{x}_1 . \bar{x}_2 . \ldots, \bar{x}_n \quad \ldots\ldots\ldots\ldots\ldots\ldots \quad (3a)$$

$$v_y = \left(v_1^2 + v_2^2 + \ldots + v_n^2 + v_1^2 v_2^2 + v_1^2 v_3^2 + \ldots + v_{n-1}{}^2 v_n{}^2\right)^{\frac{1}{2}} \quad \ldots \quad (3b)$$

$$a_y = \frac{6\left(v_1^2 v_2^2 + v_1^2 v_3^2 + \ldots + v_{n-1}^2 v_n^2 + a_1 v_1^3 + a_2 v_2^3 + \ldots + a_n v_n^3\right)}{\left(v_1^2 + v_2^2 + \ldots + v_n^2 + v_1^2 v_2^2 + v_1^2 v_3^2 + \ldots + v_{n-1}^2 v_n^2\right)^{\frac{3}{2}}} \quad \ldots \quad (3c)$$

These three parameters y, v_y and a_y define the frequency distribution of the quantity y (the product of factors affecting safety).

The most suitable mathematical expression for this distribution is the so-called Pearson's curve of type III. The minimal value, y_{min} is established, using a small probability, P, of occurrence of a lower value than y_{min} according to the equation

$$y_{min} + \bar{y} \left[1 = \left(t_{min} v_y\right)\right] \quad \ldots\ldots\ldots\ldots \quad (4)$$

in which the value of t_{min} would be taken from Pearson's curve of type III. Table 3 shows the values t_{min} computed for various probabilities and for coefficients of skewness from 0.0 to 1.1. It is evident that the last quantity which is of interest to us, namely working stress, must not be greater than y_{min}. If a value of working stress is given and the probability, P, of failure of the construction is desired the value t_{min} is computed from the Eq. 4 and the quantity P is determined from Table 3.

To show this, an example given by Mr. Wood is computed by this method. The quantity y depends on five variables:

1. strength of clear wood x_1, where $x_1 = 1$; $v_1 = 0.16$;
2. other factors affecting strength x_2, where $x_2 = 1$; $v_2 = 0.20$;
3. duration of load x_3, where $x_3 = 0.62$; $v_3 = 0.048$;
4. expected versus actual load x_4, where $x_4 = 1.10$; $v_4 = 0.073$;
5. range of defects within grade x_5, where $x_5 = 0.67$; $v_5 = 0.060$.

Substituting into the Eqs. 3(a), 3(b) and 3(c), the parameters are computed for the quantity y as

$$\bar{y} = 0.457, v_y = 0.280, \text{ and } a_y = 0.490.$$

The theoretical curve determined by these parameters corresponds to the histogram of the ratio of adequacy (Fig. 3). According to Eq. 4 the permissible working stress is found to be the multiple of the average strength of clear wood. For probabilities of 2%, 1%, and 0.1% the permissible working stresses are 0.299, 0.206 and 0.149 respectively. Were the working stress given as 0.2 of the average strength, Eq. 4 gives t_{min} as 2.00. This value corresponds to the probability of failure P = 0.8%.

Some of the factors affecting safety of the construction (Table 3) can be asymmetrically distributed. It would be better to consider some quantities x_i as divisors and not as multipliers (for example actual value of the load). The equation for y is therefore expressed more generally as

$$y = \frac{x_1 \cdot x_2 \cdots x_k}{x_{k+1} \cdot x_{k+2} \cdots x_n}$$

In this case we could easily deduce the formulas, similar to Eqs. 3.

LYMAN W. WOOD.[22]—In reply to Mr. Stern's discussion, it should be noted that the grading of lumber for strength is not perfect, either in principle or in practice. At the same time, rules for the structural grades of lumber are carefully considered and do a generally good job in assuring the expected strength values.

22 Engr., Forest Products Lab., Forest Service, U. S. Dept. of Agri., Madison, Wis.

In reply to Mr. Kimbell's discussion the writer would like to state that repetitive structural members, such as joists or rafters, are subject to an analysis similar to that shown in the paper, but with different values for one or more of the factors affecting safety. The range of growth characteristics within a grade of lumber was recognized as a specific factor in Table 1 and also in the illustrative example of the product frequency distribution.

Mr. Rosenblueth discusses several factors that can be considered one at a time. It would seem that key members whose failure might cause total collapse should have an analysis of safety separate from that of other members in the same structure whose failure has less disastrous consequences. Such key members might well be designed with a lower working stress for a smaller probability of failure.

Load assumptions used in the paper were based on rather limited surveys of actual loadings in service. More complete studies, carefully analyzed, would permit a better evaluation of this factor in the safety of structural members. As Mr. Rosenblueth points out, the variation of live load may be a function of the loaded area. It does not necessarily follow from this that live-load distribution is dependent on the permissible probability of failure.

Establishment of the permissible probability of failure on a rational basis is a desirable objective, but beyond the scope of the present paper. Mr. Rosenblueth's analysis, based on probabilities of individual variables, is interesting and useful. Probability analysis was considered by the author, but was given up in favor of the method used in the paper, which appeared to give a more complete picture of safety. The author prefers to think of the factor of 5.0 (or 5.156) between the nominal and the safe strength, not as a factor of safety, but as a reduction factor whose purpose is to convert laboratory test values to the conditons of structural use as well as to provide safety.

Mr. Cizek's analysis based on minimum test values with appropriate reduction for long-time loading and for grade is a simple and direct approach that gives a good working stress when other factors affecting are equally balanced between plus and minus. However, this balance between plus and minus does not occur in all strength properties and all structural uses. The more comprehensive method in the writer's paper is believed to have more general application even though it involves a substantial amount of work.

The method outlined by Mr. Vorlicek is interesting. In the early work leading to this paper, it was thought that at least two, and possibly more (normal, uniform, and so forth), types of frequency functions were needed to define the variates, and that definition by the mean, the coefficient of variation, and the coefficient of skewness was not enough. The random products method has the advantage of being usable with any or all types of mathematically defined frequency functions, or even with an observed frequency function that has no mathematical expression. However, some recent work has indicated a likelihood that all of the variates can be approximated reasonably well by normal frequency functions that can be defined as Mr. Vorlicek has suggested. If this is true, Mr. Vorlicek's solution is preferable, especially where an electronic computer is not available.

The writer wishes to express his thanks to all of those who have taken time to study his paper and to prepare their thoughtful comments on it. Their discussions have contributed significantly to the study of the important subject of safety in timber structures.

AMERICAN SOCIETY OF CIVIL ENGINEERS

Founded November 5, 1852

TRANSACTIONS

Paper No. 3052

SLEUTHING THE BEHAVIOR OF A RIVER

BY EDWARD J. CLEARY,[1] F. ASCE

With Discussion by Messrs. Bernd H. Dieterich; George E. Walker; and Edward J. Cleary

SYNOPSIS

In 1951 the Ohio River Valley Water Sanitation Commission instituted a program for systematic surveillance and appraisal of quality conditions and flow variations. Purpose of this program, which includes the operation of a network of forty-five monitor stations, is threefold: To provide a continuing record of vital information to aid in the diagnosis of stream conditions; to be alerted on pollution potentials; and to provide the facts for the formulation of control measures. A description is provided of the genesis of the project, of how the work is done in collaboration with volunteer monitors and the Geological Survey, of the manner in which data are prepared for evaluation, and of the cost of the operation.

INTRODUCTION

The title "Sleuthing the Behavior of a River" suggests some obvious and even exciting possibilities for perfecting the art of pollution-control practice. It should at least appeal to those who feel that, too often, they have known too little too late about the varying moods of the streams with which they deal.

It was on this premise that the staff of the Ohio River Valley Water Sanitation Commission (ORSANCO) inaugurated a program of sleuthing river behavior.

Note.—Published, essentially as printed here, in November, 1958, in the Journal of the Sanitary Engineering Division, as Proceedings Paper 1847. Positions and titles given are those in effect when the paper or discussion was approved for publication in Transactions.

[1] Exec. Dir. and Chf. Engr., Ohio River Valley Water Sanitation Comm., Cincinnati, Ohio.

In more prosaic terms this means a systematic surveillance and appraisal of quality conditions and flow variations. Because of the interest in establishing a national network of river-quality monitor stations, it might be useful to outline experiences with the Ohio Valley project. In so doing the following aspects will be described: Genesis of the ORSANCO project, how the job is being done, interpretation of information, and what it costs.

As a matter of orientation, it should be mentioned that ORSANCO is an interstate agency. It was established in 1948 by a compact among the states of Illinois, Indiana, Ohio, Pennsylvania, New York, Virginia, West Virginia, and Kentucky. These eight states pledged a pooling of their resources and their police powers in a regional crusade for clean waters. To carry out this purpose a commission was created, consisting of three representatives from each state appointed by the Governor of the state and three representatives of the Federal Government appointed by the President of the United States. The role of the commission is to promulgate interstate pollution-control regulations and to assert such powers as may be necessary for the enforcement of obligations outlined by the compact.

GENESIS OF MONITOR PROJECT

The ORSANCO stream surveillance project had its genesis in the fall of 1951. At that time the executive director requested Commission authorization to initiate a program for securing river quality and flow information on a continuous and systematic basis. It was emphasized that in dealing with a dynamic river system like the Ohio—that includes 1,000 miles of main-stem streams and nineteen major tributaries—something better than sporadic stream surveys was required for diagnosis of river conditions and the formulation of control measures. Because there are hundreds of industries and municipalities discharging wastes into the river system at various points, the question of checking compliance with control requirements foreshadowed the necessity of a monitor program. Through routine observation of quality variations at selected points on the river, it would be possible to institute a system for alerting downstream water users of abnormal conditions as well as to fix the responsibility for their origin. From these considerations emerged the concept of establishing a network of monitor stations whose activities would be coordinated to produce a comprehensive array of facts about the river. How to realize this ideal concept within the limitations of a small budget presented problems.

Possessing more enthusiasm than funds, the Commission invited the interest of eleven managers of public and private waterworks plants that were situated at various points along the Ohio River. These men had more than an academic concern with river water quality, and they responded to an appeal to serve as volunteer monitors. This resulted in the organization, on January 7, 1952, of the Water Users Committee of the Commission, and the formal inauguration of quality data assembly. Each member of the committee agreed to furnish a twice-weekly analysis of Ohio River water. Incidentally, operating expenses of the committee, which meets every three months with the ORSANCO staff for an exchange of experiences, have not exceeded (as of 1960) the $1,000 allotted annually in the Commission budget.

In 1954, the Commission budget permitted the next step in the program. This was the establishment, under a contract arrangement with the Geological Survey, United States Department of the Interior (USGS), of six additional monitor stations. These stations are located near state lines and at other strategic points at which quality information was desired. The $5,000 made available

by ORSANCO was matched with an equal sum by the USGS, a typical arrangement under the cooperative basic data program ably conducted by the USGS for many years.

In 1955, the USGS contract was amplified to include analyses during low-flow months for certain trace constituents, notably those in the heavy metals group. Three locations on the Ohio River were chosen for these observations. Beginning in October, 1956, the contract with the USGS was expanded further to secure quality data from twenty-nine stations, mainly on tributaries to the Ohio River. Fifteen of these are cooperatively financed by the Commission and the remainder by the individual states of Kentucky, Ohio, and Pennsylvania. The present (1960) ORSANCO monitor network includes stations at forty-five locations. Sixteen of these are serviced by an enlarged Water Users Committee on a volunteer basis, and the remainder under contract with the USGS.

OBTAINING THE INFORMATION

Activities of the volunteer monitor stations are coordinated through the Water Users Committee. The members, each of whom operates one station, meet every three months with the staff and representatives of the USGS for examination of analytical techniques, review of observations, and the exchange of experiences. In addition, this meeting offers a unique opportunity for the ORSANCO staff to become intimately acquainted with conditions at municipal and industrial water-treatment plants, as revealed by practical experts in processing of river water. This is important in terms of providing the staff with essential background to aid in the evaluation of analytical data. When abnormal situations occur in the river—as evidenced by a spill, detection of a slug of waste, or fish-kill—members of the committee alert ORSANCO headquarters by telephone. Headquarters, in turn, keeps the monitor stations informed regarding unusual conditions revealed by incoming data. In this fashion a patrol system of great usefulness has been established. It serves two important purposes: It provides a ready means to alert all downstream water plants of potential difficulties so that steps can be taken to cope with a situation, and it facilitates the task of determining where the trouble originated so that action can be taken by the appropriate state control agencies to prevent a recurrence.

There have been several occasions in which the Water Users Committee monitor stations made it possible to quickly bracket a stretch of river and locate responsibility for troublesome situations. One of these situations involved a thoughtless industrial-plant manager who ordered the by-passing of a recovery unit in order to make some repairs, with the resultant discharge of several thousand pounds of phenolic wastes and the temporary ruination of a water supply. Prompt notification to downstream users of this slug of waste helped to minimize the trouble. Another incident concerned a shift-foreman at an industrial plant who shut down his operations for the week-end on a Friday night but forgot to stop a pump that was filling storage tanks with oil. The tank overflowed into a creek leading to the Ohio River. When a boat club gave notification of the condition of the river, it was possible to bracket the discharge between two upstream monitor stations. This information, relayed to the appropriate state agency, made it possible for field inspectors to spot the location and halt the pumping, which had continued unobserved by the plant watchman.

Nine USGS stations are located at navigation locks and dams where an arrangement has been made with the Corps of Engineers, United States Department of the Army, for collection of samples. At the remaining six stations samples

are collected through a contract arrangement with a local resident. A truck, operating from the USGS Columbus, Ohio laboratory, picks up samples on a semi-monthly schedule. At a few remote stations at which the extension of this routine pick-up service would be costly, the samples are shipped. In the laboratory, a measurement of specific conductance is first made on each of the daily samples to provide a quick check on the daily variation in quality. The daily samples are then combined into ten-day composites for analysis. However, this routine applies only to samples used for mineral analysis. Samples for constituents that have a fade-away characteristic, such as cyanides and phenols, are individually collected and analyzed. The samples are chemically fixed at the time of collection and then sent by mail to the laboratory.

INTERPRETATION OF THE INFORMATION

Operation of the monitor network constitutes only one phase of the river-sleuthing project. Equally painstaking efforts are applied to recording and compiling the data. The conscientious review and appraisal of data promptly upon their arrival in the office is of paramount importance. To do less than provide for immediate scrutiny of the nature and meaning of the information received and to relate this to prior observations, would be to deny a fundamental purpose of the surveillance program. Dedication to this task of prompt evaluation stems from the recognition that the quality variation data are not to be regarded simply as historical events, but are matters of vital intelligence.

Sleuthing the river is a dynamic activity. For example, the records reveal, almost to the day, when a certain industry placed into operation its new dephenolyzer unit, and give an interesting picture of the times when difficulties were experienced in operating the unit at desired efficiencies. Again, the record shows when and where an abnormal slug chloride started down the river, as well as the time of arrival and magnitude of its effect at various points. Among other things, there are indications that there is a build-up of fluoride in a certain stretch of the river, and that manganese and iron are occuring more frequently in unusual amounts. These and other facts are not only alerting the staff on present and potential water quality problems, but provide a reliable basis for shaping judgment regarding appropriate means for coping with them. For example, if 95% of a certain constituent in the river is traceable to natural sources, one would hardly display good engineering judgment by suggesting that control of 5% originating from industrial wastes would have much effect on quality conditions.

The manner in which the USGS analytical and flow data are consolidated on a tabulation sheet for each monitor station is shown in Table 1(a). With slight variations, the same tabulation sheet was adapted for compilation of the Water Users Committee data (Table 1 (b)), and for the special analyses on heavy metals, cyanides, and phenols (Table 1(c)). In addition, there is noted on the sheet the sampling point, drainage area, record period, and flow data. From this array of basic data as recorded for each station, each month and for each year, a pattern emerges from which it becomes possible to compare, to probe, and even to forecast conditions with some assurance. A study related to chloride concentrations in the Ohio River is a case in point. The availability of 4 yr of data made possible a revealing diagnosis, one example of which is typified in Fig. 1. Similar comprehensive studies are made with regard to other constituents preparatory to making recommendations for control measures based on the evidence of adequate facts.

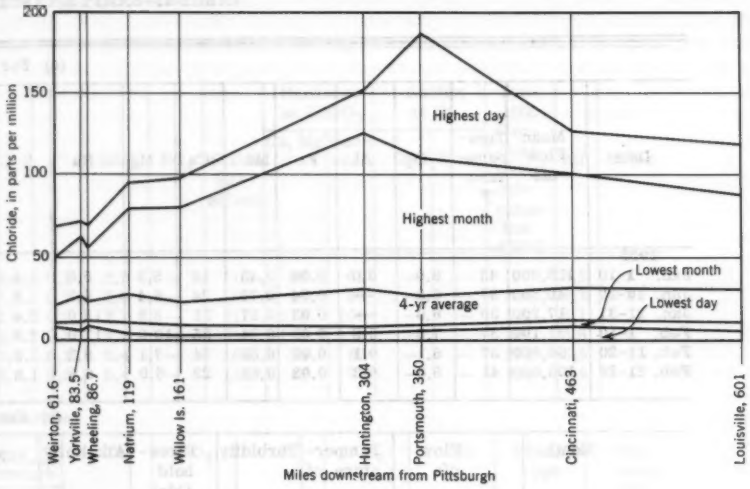


FIG. 1.—CHLORIDE CONCENTRATIONS ALONG THE OHIO RIVER

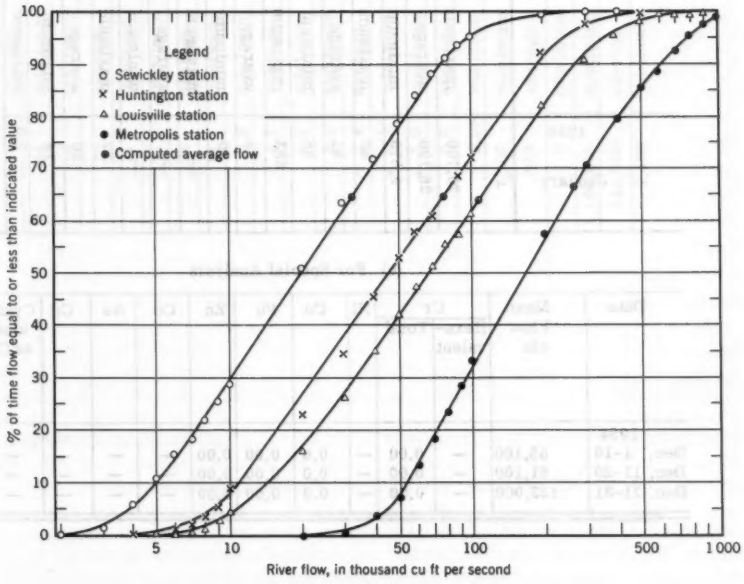


FIG. 2.—DAILY FLOW DURATION CURVES

TABLE 1.—SAMPLE TABULATIONS

(a) For Monitor

Date	Mean Flow cfs	Temperature °F	S_1O_2	Al	Fe	Mn	Ca	Mg	Na	K	HCO_3
1955											
Jan. 1-10	113,000	43	6.0	0.0	0.08	0.43	18	5.3	5.6	1.4	7
Jan. 10-20	40,500	37	6.3	—	0.04	0.70	24	6.4	9.2	1.8	8
Jan. 21-31	17,200	36	6.6	—	0.03	0.87	31	8.8	15.0	2.4	7
Feb. 1-10	51,100	37	7.0	0.3	0.01	0.84	35	10.0	17.0	2.5	5
Feb. 11-20	66,800	37	6.1	0.1	0.00	0.56	24	7.1	8.2	1.5	4
Feb. 21-28	106,000	41	5.6	0.3	0.03	0.62	22	6.9	6.9	1.8	7

(b) For Water

Month	Flow cfs			Temperature of			Turbidity			Threshold Odor			Alkalinity			pH			
	maximum	average	minimum	maximum	average	minimum	maximum	average	minimum	maximum	average	minimum	maximum	average	minimum	maximum	average	minimum	maximum
1954																			
January	76,700	28,190	8,570	46	41	38	283	79	20	—	—	—	27	20	14	7.0	—	6.5	118

(c) For Special Analysis

Date	Mean Flow cfs	Cr		Ni	Cu	Pb	Zn	Co	As	Cd	Cyanides as CN	Phenols as C_6H_5OH ppb
		Hexavalent	Total									
1954												
Dec. 1-10	55,100	—	0.00	—	0.0	0.00	0.00	—	—	—	—	—
Dec. 11-20	81,100	—	0.00	—	0.0	0.00	0.00	—	—	—	—	—
Dec. 21-31	123,000	—	0.00	—	0.0	0.00	0.00	—	—	—	—	—

FOR ANALYTICAL AND FLOW DATA

Stations

SO_4	Cl	F	NO_3	PO_4	Solids (dissolved	Hardness as $CaCO_3$ Ca, Mg	Hardness as $CaCO_3$ Noncorb	Acidity as Ht Hot	Acidity as Ht Cold	Specific Conductivity micromhos at 25°C	pH	Color
63	6.4	0.1	2.2	—	113	66	61	—	—	187	6.2	1
86	7.0	0.2	2.0	—	151	87	80	—	—	255	6.3	3
118	12.0	0.2	2.1	—	211	115	108	—	—	332	6.1	3
141	18.0	0.3	2.1	—	242	129	124	—	—	381	5.6	5
91	10.0	0.1	2.4	—	164	89	86	—	—	254	5.5	3
79	8.2	0.1	5.4	—	148	85	78	—	—	230	5.9	4

Users Committee

Hardness Total	Hardness Noncorb		Cl		SO_4		F		Fe		Mn		Phenols ppb		Coliform per 100 milliliter	
average	minimum	maximum	average	minimum	maximum	average	minimum	maximum	average	minimum	maximum	average	minimum	maximum	average	minimum	maximum	average	minimum
84	74	104	64	54	36	28	21	177	126	91	0.3	0.1	0.0	3.5	1.4	0.2	1.0	0.6	0.05	7,200	755	3	1,100,000	140,000	2,400

Not the least important information derived from the monitor program is an accurate portrayal of the ranges of water quality. The information for the Ohio River as revealed from the first 4 yr of record is shown in Table 2. With such a compilation, documented evidence is provided on water-quality variations as revealed by minimum and maximum monthly averages, as well as in terms of highest observed values.

TABLE 2.—RANGES IN QUALITY OF WATER IN THE OHIO RIVER

Constituent	Ranges in Terms of Monthly Averages		Highest Observed Value
	Minimum	Maximum	
(1)	(2)	(3)	(4)
Alkalinity, as $CaCO_3$	2.0	108.0	142.0
Aluminum	0.0	0.3	0.6[a]
Calcium	20.0	58.0	70.0[a]
Chloride	6.7	126.0	188.0
Color	1.0	29.0	55.0[a]
Fluoride	0.0	0.8	1.0
Total Hardness as $CaCO_3$	61.0	271.0	353.0
Noncorb Hardness, as $CaCO_3$	37.0	244.0	342.0
Iron	0.0	2.4	5.0
Magnesium	6.0	17.0	19.0[a]
Manganese	0.0	1.2	2.0
Nitrate	1.1	7.5	9.6[a]
Odor, threshold number	1.0	71.0	200.0
Phenols; as C_6H_5OH -ppb	1.0	84.0	200.0
Potassium	1.4	4.6	5.8[a]
Silica	3.0	11.0	19.0[a]
Sodium	5.0	40.0	45.0[a]
Solids, dissolved	137.0	390.0	440.0[a]
Specific Conductance; in micromhos	220.0	600.0	652.0[a]
Sulfate	37.0	362	451.0
Turbidity	20	576	1500.0

[a] 10 day composite results.

HYDROGRAPHIC DATA AND EVALUATION

Chemical and bacteriological data alone cannot be considered adequate, of course, for the engineering evaluation of stream conditions. Rational design of a pollution-control program requires knowledge of the availability of dilution water. These reasons support the necessity of incorporating flow data as

an essential element of monitor records. Fortunately, information on stream discharges has been meticulously gathered by the USGS over a long period of time. From these data it is possible to make studies for the establishment of the flow variability pattern of many streams, particularly with regard to minimum flows.

Such studies form part of the river monitor project of ORSANCO. One of these studies deals with the statistical distribution of all recorded flows, for the development of so-called duration curves. With the stream-flow pattern depicted in this form, it becomes possible to make accurate and rapid estimates of the availability of dilution water. A typical set of curves developed from daily flow records is shown in Fig. 2. This reveals the frequency of occurrence for flows of various magnitudes at each of four USGS gaging stations on the Ohio River. The duration curve's limitation is that it reveals only the pattern of availability of water based on all flows of record. In pollution-control practice a primary concern is with minimum stream flow and its probability of occurrence. Hence, the ORSANCO hydrographic studies are designed to include an analysis of drought-flow probabilities. Specifically, a determination of the minimum daily, weekly, two-week, and monthly flows is made.

Results from a typical drought-flow analysis tabulation are shown in Table 3. Table 3 (a) lists the observed minimum daily flow and with it the computed value for various time intervals. Table 3 (b) shows the flows augmented by the appropriate increment of flow resulting from discharge of water from upstream, multiple-purpose reservoirs. Table 3 (c) shows the flows computed for various drought severity classifications, based on augmented flow. The drought-flow probabilities are based on the statistical theory of extreme values developed by E. J. Gumbel.[2]

A schematic representation, called the "Empire State Building chart" (Fig. 3) shows the minimum flows along the Ohio River. The location and magnitude of successive increases, for an entire stretch of the river, are shown. On this chart are shown the once in 5 yr and the once in 10 yr minimum monthly averages. Also shown in Fig. 3 are the names and mile-point locations of major tributaries to the Ohio River. The last feature adds considerably to the reference value of the chart. All of the chemical, bacteriological and flow data for the first 4 yr of record are available.[3]

WHAT DOES IT COST?

Collection and analysis of stream samples is generally conceded to be one of the more costly elements of a water-pollution-control program. It is not unusual for single stream surveys of only a few months duration and of limited scope to range in cost from $10,000 to more than $75,000. What, then, is the cost of conducting a monitor program to provide a continuous and systematic record of stream quality?

A summary covering the first 4 yr of record from the ORSANCO monitor program is shown in Table 4. Because the number of stations, as well as the number of months they were in operation, has varied from year to year, the comparisons are made on a station-month basis. There are several things

2 "Probability Interpretation of Observed Return Periods of Floods," by E. J. Gumbel, Transactions, Am. Geophysical Union, 1941, p. 836, pt. III.

3 "Water Quality and Flow Variations in the Ohio River 1951-55," Ohio River Valley Water Sanitation Commission, Cincinnati, Ohio.

TABLE 3.—DROUGHT FLOW ANALYSIS TABULATIONS—ALL FLOWS IN cfs

(a) Minimum Flows

Year	1934	1936	1938	1940	1942	1944	1946	1948	1950
Day	4,900	6,150	4,600	7,200	15,200	9,120	5,500	5,780	18,000
Week	8,890	8,000	9,040	10,100	19,940	9,580	7,910	11,460	25,576
Two Weeks	10,090	8,376	10,260	10,950	27,590	10,020	9,970	12,760	29,710
Month	16,200	15,010	12,270	12,930	33,720	13,440	11,050	17,650	37,000
Month Minimum Occurred	July	Sept.	Oct.	Oct.	Sept.	Aug.	Sept.	Sept.	Aug.

(b) Augmented Minimum Flows

Year	1934	1936	1938	1940	1942	1944	1946	1948	1950
Day	6,310	7,560	5,670	8,270	16,270	9,820	6,200	5,980	18,200
Week	10,300	9,410	10,110	11,170	21,010	10,280	8,610	11,660	25,770
Two Weeks	11,500	9,780	11,330	12,020	28,660	10,720	10,670	12,960	29,910
Month	17,610	16,420	13,340	14,000	34,790	14,140	11,750	17,850	37,200

(c) Expected Drought Severities

Drought Severity	Minimum Daily Average	Minimum Weekly Average	Minimum Two-week Average	Minimum Monthly Average
Most Probable Drought	7,720	11,030	12,160	17,040
Once in Five Years	6,100	8,830	9,220	11,970
Once in Seven Years	5,700	7,660	8,490	10,730
Once in Ten Years	5,290	6,980	7,740	9,440
Once in Fifteen Years	4,840	6,220	6,910	8,010
Once in Twenty Years	4,520	5,690	6,340	7,020

TABLE 4.—SUMMARY OF MONITOR STATION COSTS—ALL COSTS IN DOLLARS

Year	1952	1953	1954	1955	Total
Station-Months	116	141	164	240	—
Direct Costs	3,000	3,000	4,300	10,000	20,300
Volunteer and Contract Services	20,000	25,000	28,000	38,000	111,000
Total Cost	23,000	28,000	32,300	48,000	131,300
Average Cost per Station per Month	200	200	200	200	—

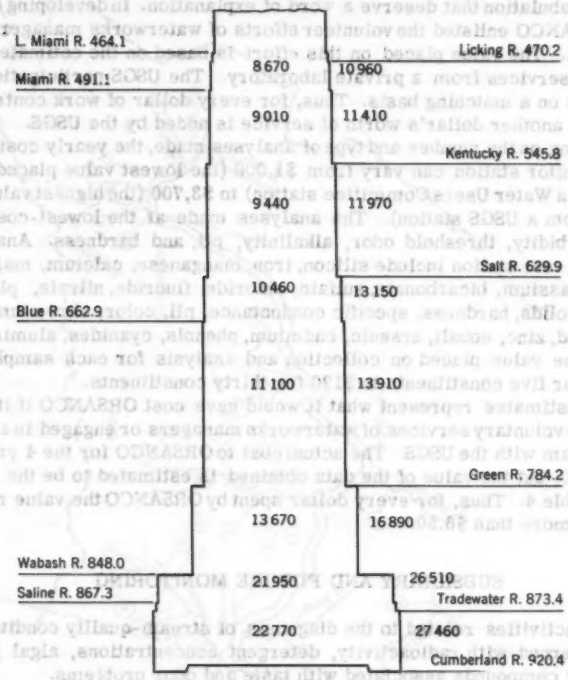


FIG. 3.—MINIMUM MONTHLY AVERAGE FLOWS

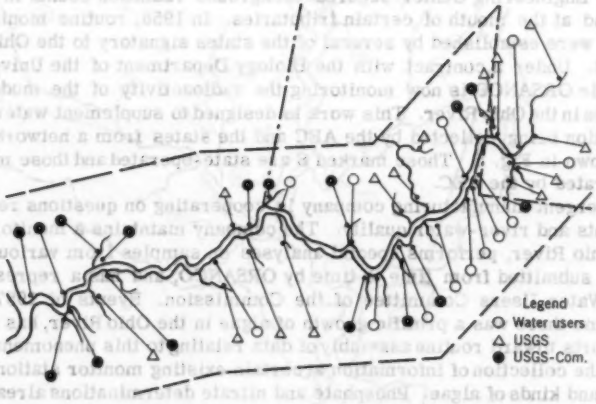


FIG. 4.—NETWORK OF WATER QUALITY MONITORING STATIONS

about this tabulation that deserve a word of explanation. In developing this program, ORSANCO enlisted the volunteer efforts of waterworks managers for securing data. The value placed on this effort is based on the estimated cost of equivalent services from a private laboratory. The USGS participation in the program is on a matching basis. Thus, for every dollar of work contracted by ORSANCO, another dollar's worth of service is added by the USGS.

Depending on the number and type of analyses made, the yearly cost of operating a monitor station can vary from $1,000 (the lowest value placed on data supplied by a Water Users Committee station) to $3,700 (the highest value placed on data from a USGS station). The analyses made at the lowest-cost station include turbidity, threshold odor, alkalinity, pH, and hardness. Analyses at the highest cost station include silicon, iron, manganese, calcium, magnesium, sodium, potassium, bicarbonate, sulfate, chloride, fluoride, nitrate, phosphate, dissolved solids, hardness, specific conductance, pH, color, chromium, nickel, copper, lead, zinc, cobalt, arsenic, cadmium, phenols, cyanides, aluminum, and acidity. The value placed on collection and analysis for each sample varies from $10 for five constituents to $120 for thirty constituents.

These estimates represent what it would have cost ORSANCO if it had not enlisted the voluntary services of waterworks managers or engaged in a cooperative program with the USGS. The actual cost to ORSANCO for the 4 yr of work was $20,000, but the value of the data obtained is estimated to be the $131,000 listed in Table 4. Thus, for every dollar spent by ORSANCO the value received, in data, is more than $6.50.

SUBSIDIARY AND FUTURE MONITORING

Among activities related to the diagnosis of stream-quality conditions are those concerned with radioactivity, detergent concentrations, algal growths, and organic compounds associated with taste and odor problems.

The monitoring of radioactivity has been conducted for several years in the Ohio Valley by the Atomic Energy Commission (AEC). In 1956, at the request of ORSANCO, the United States Public Health Service (USPHS) through its Taft Sanitary Engineering Center secured background radiation counts in the Ohio River and at the mouth of certain tributaries. In 1958, routine monitor procedures were established by several of the states signatory to the Ohio Valley Compact. Under a contract with the Biology Department of the University of Louisville ORSANCO is now monitoring the radioactivity of the muds, biota, and fishes in the Ohio River. This work is designed to supplement water-quality information being collected by the AEC and the states from a network of stations shown in Fig. 5. Those marked S are state-operated and those marked A are operated by the AEC.

A detergent manufacturing company is cooperating on questions relating to detergents and river-water quality. The company maintains a monitor station in the Ohio River, performs special analyses on samples from various places that are submitted from time to time by ORSANCO, and has a representative on the Water Users Committee of the Commission. Events of 1957, during which time there was a prolific growth of algae in the Ohio River, has directed staff efforts toward routine assembly of data relating to this phenomena. Plans include the collection of information at certain existing monitor stations on the number and kinds of algae. Phosphate and nitrate determinations already form part of the established program.

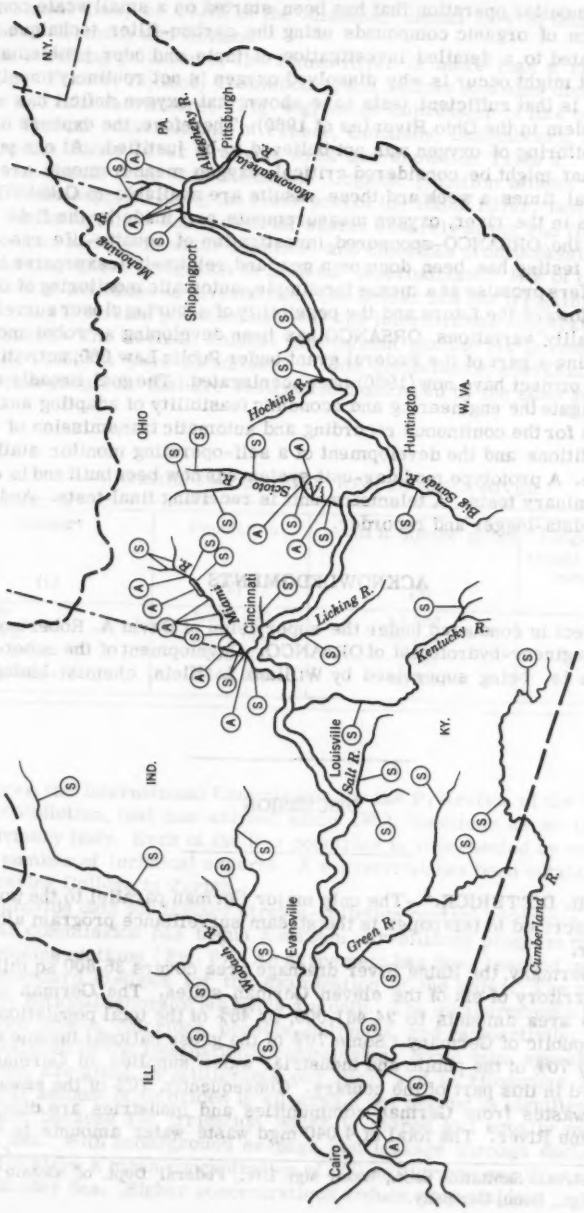


FIG. 5.—NETWORK OF RADIOACTIVITY MONITORING STATIONS

Another monitor operation that has been started on a small scale concerns the extraction of organic compounds using the carbon-filter technique. This work is related to a detailed investigation of taste and odor problems. One question that might occur is why dissolved oxygen is not routinely monitored. The answer is that sufficient tests have shown that oxygen deficit has not become a problem in the Ohio River (as of 1960). Therefore, the expense of continuous monitoring of oxygen was not believed to be justified. At one point in the river that might be considered critical, oxygen measurements are being made several times a week and these results are available to ORSANCO. At other points in the river, oxygen measurements are made by the field crews engaged on the ORSANCO-sponsored investigation of aquatic-life resources. Meanwhile, testing has been done on a new and relatively inexpensive instrument that offers promise as a means for simple, automatic monitoring of oxygen.

Looking toward the future and the possibility of securing closer surveillance of river-quality variations, ORSANCO has been developing a "robot monitor" system. Using a part of the Federal grant under Public Law 660, activities related to this project have now (1960) been accelerated. The goal, broadly stated, is to investigate the engineering and economic feasibility of adapting analytical instruments for the continuous recording and automatic transmission of river-quality conditions and the development of a self-operating monitor station for this purpose. A prototype modular-unit system has now been built and is undergoing preliminary tests. A telemetry unit is receiving final tests. And under design is a data-logger and recorder.

ACKNOWLEDGMENTS

The project is conducted under the supervision of David A. Robertson, Jr., M. ASCE, engineer-hydrologist of ORSANCO. Development of the robot-monitor stations is being supervised by William L. Klein, chemist-biologist of ORSANCO.

DISCUSSION

BERND H. DIETERICH.[4]—The only major German parallel to the work that has been described in this paper is the stream surveillance program along the Rhine River.

Within Germany, the Rhine River drainage area covers 36,800 sq miles. It cuts into territory of six of the eleven German states. The German population of this area amounts to 24,461,000, or 46% of the total population of the Federal Republic of Germany. Some 70% of the gross national income and approximately 70% of the public and industrial water supplies of Germany are concentrated in this part of the country. Consequently, 70% of the sewage and industrial wastes from German communities and industries are discharged into the Rhine River. The total of 4,040 mgd waste water amounts to 8.0% of

[4] Chief, Stream Sanitation Sect., Water Mgt. Div., Federal Dept. of Atomic Energy and Water Mgt., Bonn, Germany.

mean annual flow, or 19.5% of the minimum annual flow of this river at the border of Germany and Holland.

The resulting pollution of the Rhine River is more than a mere national problem. France, Holland, Luxembourg, and Switzerland also discharge waste water into this watercourse. Fig. 6 gives an impression of this complex situation. Typical contributions of France, Germany, Luxembourg, and Switzerland to the Rhine River drainage area are shown in Table 5. Three major problems result from this situation: Organic pollution affects German and Dutch water supplies along the lower part of the Rhine River; tastes and odors from oil (navigation) and industrial wastes severely affect and frequently upset German and Dutch water supplies; and chlorides from potassium and hard coal mining affect irrigation in Holland. Approximately 10% of the mean annual flow of the Rhine is diverted into the Zuider Sea for irrigation purposes.

To control stream pollution national and international cooperation has been established. The German federal government and the six German states are forming (1960) a joint commission. This commission coordinates stream-sanitation programs that are designed and enforced by the state governments.

TABLE 5.—CONTRIBUTIONS TO RHINE RIVER

Country (1)	Population (2)	Area in square miles (3)	Long-range mean annual flow in cubic feet per second (4)
France	2,935,000	10,300	11,800
Germany	24,641,000	36,800	39,400
Luxembourg	299,000	1,000	1,100
Switzerland	3,641,000	9,000	22,800

Moreover, the International Commission for the Protection of the Rhine River against Pollution, that has existed since 1952, functions as an investigating and advisory body. Each of the five countries is represented by two delegates and a number of technical experts. A secretariat has been established at the Engineering College in Zurich.

To provide data for further stream-pollution control programs, the international commission has begun a stream surveillance program that includes ten sampling stations (Fig. 6). An agreement has been reached on the applicable standard methods for the examination of the water. The samples are taken by national laboratories twice a month. The measurements include pH, dissolved oxygen, chlorides, phenols, hardness, and radioactivity. All results are published by the international commission. Some data, especially that on chlorides, are given in milligrams per liter, and in kilograms per second. The total amount of chlorides in kilograms per second is significant to Dutch engineers because the irrigation water is stored and equally mixed in the Zuider Sea. With underground seepage and leakage through docks included, the Dutch allow a mean concentration of 300 milligrams per liter of chlorides in the Zuider Sea. Higher concentrations reduce crop yields.

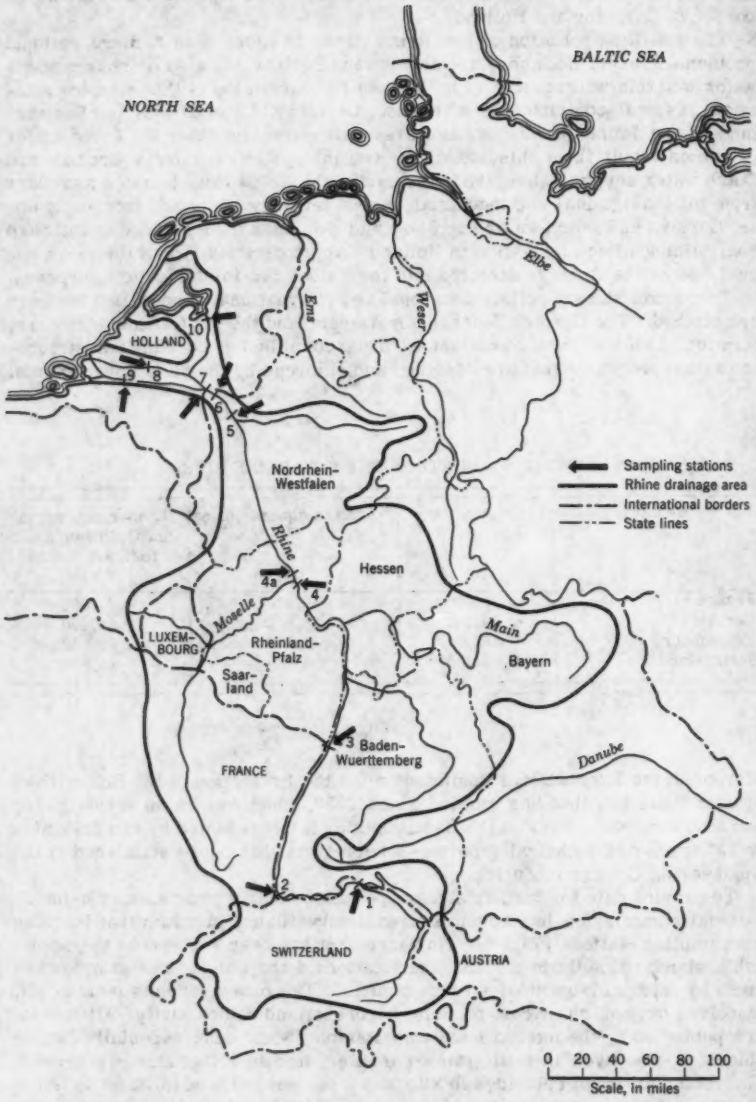


FIG. 6.—STREAM SURVEILLANCE OF THE RHINE RIVER

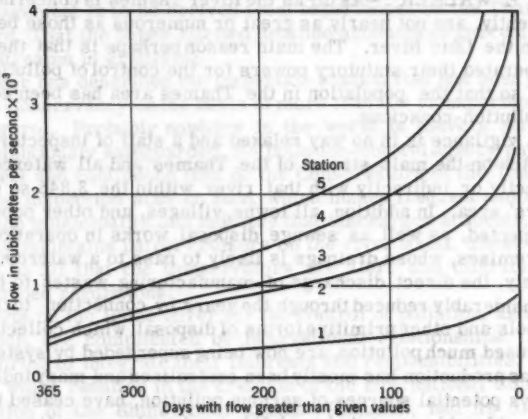


FIG. 7.—DURATION CURVES FOR RHINE RIVER STATIONS

TABLE 6.—CHLORIDE INCREASE

Sampling station or part of river (1)	Correlation coefficient (2)	Correlation (3)	Annual increase in Cl^- pollution, or Cl^- discharge, in kilograms per second (4)
between Stat. 2 and 3	0.94	significant	12.3
between Stat. 3 and 4	0.16	insignificant	(1.2)
between Stat. 4 and 4a	0.88	significant	1.7
between Stat. 4a and 6	-0.41	insignificant	(- 2.1)
at Stat. 6	0.81	significant	12.6

Typical results at or near the Dutch-German border are (mean values 1955-1956): a flow of 72,300 cfs; dissolved oxygen content of 7.23 mg per 1; 66% oxygen saturation; chlorides at 138.1 mg per 1; 242.2 kg per sec of chlorides; and phenols at 0.0441 mg per 1. In the reports, the international commission has chosen several different schemes of graphical representation. Long-range data, collected on flow values, are used to predict the flow behavior of the river. Five duration curves are given in Fig. 7.

Of great importance is the development of chloride pollution. In the period from 1955 to 1960, the annual mean values of chloride pollution have been analyzed statistically. The correlation coefficients and the annual increase in chlorides are shown in Table 6.

GEORGE E. WALKER[5].—As far as the River Thames is concerned, the problems, apparently, are not nearly as great or numerous as those being met and dealt with on the Ohio River. The main reason perhaps is that the Conservators have operated their statutory powers for the control of pollution for more than 100 yr, so that the population in the Thames area has been educated into becoming pollution-conscious.

However, vigilance is in no way relaxed and a staff of inspectors maintains constant watch on the main stream of the Thames and all watercourses connecting directly or indirectly with that river within the 3,845 sq miles of the Conservators' area. In addition, all towns, villages, and other population centers are inspected, as well as sewage disposal works in operation, factories and other premises, whose drainage is likely to pass to a watercourse.

Fortunately, the direct discharge of manufacturing wastes to the streams has been considerably reduced through the years by connection to the soil sewers. Cesspools and other primitive forms of disposal, which collectively in the past have caused much pollution, are now being superseded by systems of main drainage. Gas production has mostly been centralized and many individual gasworks, always potential sources of serious pollution, have ceased to operate.

A very considerable amount of work is being done in connection with the provision of new sewage disposal works and the improvement of existing works. It is the effluents from the many sewage works within the Conservators' area that are the main concern. Samples of these effluents are taken regularly and submitted to the Conservators' analyst. In each case in which an adverse report on a smaple is received, the matter is taken up at once with the local authority or person responsible. The Conservators' policy is to endeavor, as far as possible, to obtain cessation of pollution by persuasion. In this matter they have been very successful. Failing this, statutory notices may be served on the offenders requiring discontinuance of the pollution within 3 months. For noncompliance with a notice and in the more serious cases, usually willful pollution, proceedings may be taken. In addition to sampling the sewage effluents, river water samples are taken periodically and, at the last point of the river within the Conservators' jurisdiction, the water is sampled weekly. In all, more than 2,000 samples of effluents and waters are examined annually.

Occasional fish mortalities do occur. Anything of a serious nature is usually caused by some toxic materials being disposed of illegally into surface-water systems. More frequently, fish are killed in the tributaries during conditions of low flow and hot weather when the oxygen content of the water is seriously depleted. Whatever the cause, however, samples of river water are taken above and below the area in which the dead fish are found, as well as samples of any discharges in the vicinity. In addition, specimens of the fish are submitted to a biologist for examination.

The effect of these endeavors for the control of pollution is that, on chemical analysis, the River Thames water continues to be generally satisfactory. The importance of this work cannot be too strongly stressed when it is realized that approximately two thirds of the total quantity of water supplied daily to London is taken from the River Thames within the Conservators' area.

[5] Secy., Solicitor, Parliamentary Officer, Thames Conservancy, London, England.

EDWARD J. CLEARY,[6] F. ASCE.—Much valuable information in river-quality management is to be derived from experiences on the Thames, and the Rhine Rivers. That the paper elicited detailed accounts of current practice on both these streams is gratifying.

Mr. Walker has described the inspection system that has been perfected by the Thames Conservancy on the basis of more than 100 yr experience in water-pollution control. Probably nowhere in the world is there a stream that is more conscientiously safeguarded. No pollution-control agency enjoys greater public respect and confidence than do the Conservators of the Thames. In addition to the inspection staff on land, which makes frequent and regular contact with each municipality and industry that discharges effluents, the Thames Conservancy maintains patrol cruisers on the river itself. These patrol boats give notice to all that the Conservators are alert and tolerate no deviation from prescribed regulations.

The efforts on the Rhine River for the control of pollution, as described by Mr. Dieterich, are complicated by international relationships. Five nations are endeavoring to integrate their interests and responsibilities. This laudable effort, which resulted in the creation of the International Commission for the Protection of the Rhine River against Pollution, had its origin in 1952. When one considers the years of discussion and negotiations that have surrounded efforts in the United States to promote interstate cooperation on pollution control (more than half a century for federal legislation and at least twenty years in the case of one interstate compact), the accomplishments on the Rhine compel admiration.

---

[6] Exec. Dir. and Chief. Engr., Ohio River Valley Water Sanitation Comm., Cincinnati, Ohio.

AMERICAN SOCIETY OF CIVIL ENGINEERS

Founded November 5, 1852

TRANSACTIONS

Paper No. 3053

FREEWAYS IN URBAN PLANNING

By Harold M. Lewis,[1] F. ASCE

With Discussion by Messrs. Richard A. Haber and William J. Miller, Jr.; George H. Herrold; and Harold M. Lewis

SYNOPSIS

The history and development of freeways as elements in urban and metropolitan plans will be reviewed in this paper. A concept that originated in 1930 has now spread to encompass state and federal plans. The impact of these highways, that have no direct access from abutting property, to the various elements of urban planning as embodied in master plans, urban renewal programs, and municipal zoning will be described. Coordinated transportation plans and the prevention of continuous strips of urban development through zoning are suggested as urgent problems for the immediate future.

INTRODUCTION

The term freeway[2] was first coined by Edward M. Bassett, who then headed the Legal Division of the Regional Plan of New York and Its Environs. He defined a freeway as, "a strip of public land, dedicated to movement, over which

Note.—Published, essentially as printed here, in June, 1959, in the Journal of the City Planning Division, as Proceedings Paper 2055. Positions and titles given are those in effect when the paper or discussion was approved for publication in Transactions.

1 Cons. Engr. and City Planner, New York, N. Y.

2 "The Freeway—A New Kind of Thorofare," by E. M. Bassett, The American City, February, 1930.

the abutting owners have no right of light, air or access," and described the need for such a facility as:

> "the need of a new kind of thoroughfare—one which will be like a highway for both pleasure and business vehicles, but which will be like a parkway in preventing the cluttering-up of its edges. We have no name for such a thoroughfare. No law in this country provides for such a novel trafficway. I suggest the name freeway. A freeway denotes freedom from grade intersections and from private entrance ways, stores and factories. It will have no sidewalks and will be free from pedestrians. In general, it will allow a free flow of vehicular traffic. It can be adapted to the intensive parts of great cities for the uninterrupted passage of vast numbers of vehicles."

Mr. Bassett thought of the freeway as a solution for urban traffic and did not foresee its extension to interregional and transstate routes. During the 1950's this concept has taken root and spread, even to transcontinental routes.

At the time of the freeway's conception (1930) the total automobile registration in the United States was 26,532,000. The normal running speed on major highways was approximately 25 mph and 40 mph was considered a top speed. Many of our state highways had lanes 9 ft in width whereas the newer ones were being built with what was then thought to be a generous width of 10 ft. In urban centers traffic congestion was a matter of great public concern. This is one phase of the problem that has not changed very much. The then modern system of traffic control was a system of stop-and-go lights that was just starting to replace either hand signals by a traffic policeman or a free-for-all contest when no policeman was available.

The legal provision for freeways required state legislation. This took time and has developed different terminologies among states, but in each case they have embodied Mr. Bassett's concept. The first freeway bill was introduced in California in 1933 but action was slow and it was not enacted until 1939. New York came first with the adoption of a Limited Access Highway Act on April 19, 1937, followed on April 27, 1937 by the Rhode Island Freeways Act. During the next five years Connecticut, California, West Virginia, Colorado, Maryland, Michigan, and Ohio followed. Under the Congressional action of 1956 all states will obtain freeways.

EARLY STUDIES FOR EXPRESSWAY SYSTEMS

The Regional Plan of New York and Its Environs included in its 1929 Comprehensive Plan a proposed system of express highways for the metropolitan area.[3] Whereas its report pointed out the advantage of uninterrupted movement on such routes, its mention of "an approximately uninterrupted traffic flow," indicated that it expected that there would be some compromise in such a program.

In 1936, the Regional Plan Association published a bulletin describing the application of the freeway in the solution of regional traffic problems in metropolitan areas.[4] At the same time it proposed a comprehensive system of such routes for the New York-New Jersey-Connecticut metropolitan area. This sys-

3 "The Graphic Regional Plan," prepared by the staff of the Regional Plan, Vol. 1, Regional Plan of New York and Its Environs, 1929, pp. 264–269.

4 "The Freeway, a Modern Highway for General Traffic in Metropolitan Areas," prepared by the staff of the Regional Plan, Information Bulletin No. 33, Regional Plan Assn., December, 1936.

tem was to provide for all types of traffic, the type of express movement that the modern parkways, then under construction in Westchester County, N. Y., provided for passenger vehicles only. As a precedent, the proposal referred to the national system of Reichautobahnen which had begun in Germany in 1933, following the Autostrada built as toll roads a few years earlier in Italy by private corporations.

The Regional Plan Bulletin presented plans and cross sections for the typical treatment of freeways under varying conditions. The ultimate capacity of such routes was shown as six lanes, carried on two 37-ft roadways with a median strip 26 ft wide. Grade separations to permit completely uninterrupted movement were proposed, with interchanges only at important highways. A minimum right-of-way width under normal circumstances was shown as 160 ft with control of at least 35 ft additional on each side of the right-of-way through "state zoning, purchase of easement, contractual agreements with abutting owners or special border control legislation." Through urban centers, a minimum right-of-way of 90 ft was suggested by reducing the median strip to 8 ft, and substituting retaining walls for side slopes. More than 22 years later (1959), these standards are still fairly sound.

As an application of these new principles to the Graphic Regional Plan of 1929, this bulletin included a proposal for an expanded system of freeways for general traffic, and parkways for passenger traffic, that would serve the entire regional area. Nine of the radial routes were proposed to extend beyond the area and become inter-regional highways.[5] During the succeeding years, the freeway concept has spread rapidly throughout the country and has been discussed fully in many papers before the American Society of Civil Engineers.

The most extensive development of parkways without direct access has occurred in the New York metropolitan area, with the Bronx River Parkway in Westchester County being the pioneer route. This is not completely express as a few traffic lights are found at minor intersections. The newer parkways are completely express routes, except for an occasional grade crossing with a minor roadway in rural areas. The latest of these parkways in the New York-New Jersey metropolitan area is the Garden State Parkway that runs the full length of New Jersey.

Systems of freeways in metropolitan areas have been developed intensively in Los Angeles County, California, and in the New York-New Jersey-Connecticut metropolitan area. Others are being rapidly developed in other metropolitan centers such as Chicago, Ill., Philadelphia, Pa., Boston, Mass., and the District of Columbia, to mention only a few. During the 1950's the individual states have gone in for state-wide systems of inter-urban freeways, spearheaded by the Pennsylvania Turnpike. A continuous route is provided (1959) free of traffic lights, between New York, New York, and Chicago, Illinois. A similar system of freeways also exists along the eastern seaboard from Maine to Delaware. Upon completion of gaps in Delaware and Maryland this route will continue to Washington, D.C. This work is already planned and is partly under construction. The purpose of these state routes was primarily to connect main urban centers within their respective states. Such roads are designated as turnpikes, freeways, or thruways.

With the initiation of the federal-aid interstate highway system in 1956, it is expected that by 1970 motor vehicles will be able to cross the country in almost

5 Discussion by Harold M. Lewis of "The Modern Express Highway," by Charles M. Noble, Transactions, ASCE, Vol. 102, 1937, p. 1123.

any direction by a continuous system of freeways with convenient connecting routes into all major urban centers. This is being undertaken as a crash program under the direction of a newly created Office of Federal Highway Administrator in the United States Bureau of Public Roads, Dept. of the Interior (USBPR). The procedure worked out to guaranted a sound plan generally includes the following steps:

1. Inclusion of the route by the USBPR, with a general description, as a part of the interstate system authorized by Congress under the federal-aid highway act of 1956.

2. Preparation of a preliminary study by a private engineering firm, under contract with the state highway department and working in close collaboration with that department.

3. Public hearings by the state highway department, with representatives of the USBPR present, at which alternative routes are presented and discussed on the basis of analyses made by the state's consultants.

4. Recommendation to the USBPR by the state highway department of a specific location.

5. Reaching of an agreement between the state highway department and the municipalities along the route.

6. Publication by the state highway department of the report of its consultants showing preliminary designs and estimates of the right-of-way costs and construction costs for the route recommended.

7. Approval by the USBPR.

8. Preparation of the route's contract designs and specifications by sections, with each section allotted to a different engineering firm so as to make the best use of available engineering manpower.

9. Advertising for bids, leading to letting of contracts and actual construction.

IMPACT OF FREEWAYS ON URBAN PLANNING

To use a medical analogy, where Freeways have been built within cities which have been suffering, in common with other cities, from a bad case of traffic congestion, the freeways have improved the circulation of the patient. Strangulation of its main arteries has been replaced by freer flow of traffic on the new routes. However, serious congestion within its principal organs (such as downtown shopping, wholesale, and office centers) still remains. In general, the life of the patient seems to have been saved, but he still needs corrective treatment if he is going to survive. There are several phases of urban planning on which freeways have had great impact.

Increased Scope of Planning.—City planning commissions, in studying their highway problems, as well as in other phases of planning, must give consideration to regional planning. This is particularly true in metropolitan areas where a balanced economy in the region must be established if each of its individual political units is to find its proper function in a regional development. This is particularly true in the planning of those elements of the federal interstate system which pass through metropolitan areas.

The procedure involved for the federal interstate system does not specifically provide a responsibility for the city planner or the official planning commission in the areas involved. Nevertheless, there is general agreement that the expressway should not unduly disrupt any existing city or regional plans and should give consideration to planning principles.

Under the United States Housing Act of 1949, the Housing and Home Finance Agency established procedures for its approval of urban projects calling for clearance and rebuilding of blighted areas. These made reference to an approval by the local city planning commission a prerequisite of federal approval for any loan and grant contracts. Could such a requirement have been written into the 1956 highway act? There is a lack of active planning agencies throughout much of the area traversed by the routes, and where there are active agencies, they generally are not well-enough financed to promptly undertake the necessary studies. Thus, the author believes that such a requirement would have resulted in delays that would have seriously upset the program.

Existing city plans can be effectively applied to the problem only if there is effective cooperation between the local planning agencies and the state highway departments that handle the design contracts. This is not likely to happen unless the planning commissions take the initiative and unless they are broad-minded enough to examine the problem from a regional as well as a local point of view. The attitude of "put the highway somewhere else as long as you don't come through our community" is no solution to the problem and leaves the state in a difficult position, particularly where adjoining communities take this same attitude.

In designing a system of urban expressways, it should be remembered that they work in two directions. They encourage the decentralization of certain types of industries and certain types of residence and, by making it easier to reach urban centers, they stabilize and encourage downtown business, entertainment centers, wholesale uses, expanded port development, and homes for the many people who prefer urban living.

Land Use Plan.—Any freeway, with its wide right-of-way and the difficulty and cost of continuing local streets across it without grade crossings, is bound to create a barrier between adjacent portions of the city. This effect can be minimized by careful design and is least noticeable when the freeways are depressed. Their location and design should be worked out in close relationship with the city's master plan. If this is done, the separation of the city into segments may be a means of stabilizing the plan rather than a process of disrupting it.

Any urban area will group itself into a pattern of residential neighborhoods. In areas where urban land use plans have been adopted, the boundaries of these neighborhoods are usually incorporated in such a plan. It is highly desirable that any freeway crossing a municipality should not cut across these neighborhoods but should, where possible, follow along their boundaries. In some cases, these boundaries will follow railroad rights-of-way, watercourses, bridges, or other features, natural or man-made, which dictate their locations. In other cases, boundaries may follow the line of demarcation between an apartment-house district and a one-family home district or between a residential district and an industrial district. Sometimes topography may dictate the location of the freeway, and some adjustment in neighborhood boundaries, by revision of the local land use plan, may prove to be desirable.

Thoroughfare Plan.—A system of freeways will establish the principal elements of a street-thoroughfare plan for any metropolitan area. It is obvious that the entire system of main highways, that includes major routes of a non-expressway type, secondary thoroughfares and important connecting routes, together with any parkway system that may be existing or proposed, should form a coordinated regional plan for highway movement. The importance of fitting the federal interstate system of expressways into municipal thoroughfare plans has been shown clearly in those metropolitan areas in which these routes are now being laid out. In a few cases, thoroughfare plans adopted as parts of master plans have indicated the logical location for such routes. Often local plans have not provided for the type of expressway contemplated in the interstate system. In many communities no thoroughfare plans or land use plans have been officially adopted. Where existing planning commissions did not take the initiative in presenting proposed routes to the state highway departments, or where there were no such commissions, the state departments and their consultants have had to go ahead without the benefit of any comprehensive planning for the areas with which they were dealing.

In most communities planning moves so slowly that agreements on and adoption of master plans is often delayed through inadequate financing and local controversies. In spite of these handicaps, the state highway departments and the USBPR are making a serious effort to see that the interstate expressways are located in conformance with sound planning principles.

Local Traffic Problems.—Whether the interstate expressways completely bypass the smaller municipalities or go through the edges of the larger ones, they will create local traffic problems in each. These problems concern highway connections with the urban centers and the parking problems created by traffic using such connections.

Interchanges of freeways with existing street systems, that require left turns on the expressways and, generally, no such turns on local streets, will occur at a limited number of points. Selection of these points will determine the downtown approach routes that, in many cases, may not be able to handle resulting traffic without widenings or other improvements. Because the expressways will carry both trucks and passenger vehicles, interchanges in residential areas create local problems of diverting truck traffic on to routes where such traffic will not adversely affect residential neighborhoods.

In some cases there will be obvious approach routes to which connections can be made, but this may prove to be the exception rather than the rule. In any event, where a city already has adopted a street-thoroughfare plan, some adjustments to it are sure to be required. In order to reach a satisfactory solution, a progressive city planning commission must study these adjustments while the highway planning is still in its preliminary stages. Frequently it may prove desirable to have an interchange connected with a pair of streets, each of which can be operated for one-way traffic, to avoid overloading a single street. Here again, cooperation between the city and the designer of the expressway, through the state's highway department, can prove helpful.

Wherever freeways may be located, there will be a need for improved arterial routes to connect them with the downtown areas. This will result in a concentration of parking requirements where these routes enter the downtown area. Adjustments in any earlier plan for off-street parking facilities are sure to be needed as the interstate expressways take shape and their interchanges with local street systems are determined. Where the resulting concentration of

traffic entering downtown is great enough, it may prove desirable to substitute multilevel garages for either existing or proposed parking lots.

Recreation Plan.—Generally, consulting firms retained by the state highway departments have made their preliminary locations for the interstate routes on air maps of the area. These maps show clearly where the built-up areas are and what areas are still free from development. They do not show the use of these open areas. Serious conflicts with the park and recreation systems of municipalities have resulted from this.

Some preliminary locations have taken the most direct routes with little regard to their effect upon the local community. In other cases, they appear to have utilized any open spaces that appeared on the maps without any detailed study as to their present use or that for which they are most suitable. In the case of direct routing, local municipalities have objected strenuously to the cutting up of their community and have requested locations either along their boundaries or in adjoining municipalities. In the case of routing through open areas, it has sometimes developed that the proposed locations have cut directly across parks and playgrounds, threatening irreparable damage to the recreation system of the municipality. In such situations the local park commissions have registered strong objections. It has been pointed out that parks as well as improvements have great value and are often less replaceable than other properties.

An example of this occurred in Wilmington, Del., during the preliminary planning for an interstate route which is proposed to pass through the residential areas in the western portion of that city. The route first recommended by the Delaware State Highway Department was objected to by the president of the Board of Park Commissioners on the grounds that it would destroy 51 acres of the city's 311 acres of park land and would run for 2.1 miles through park property. He claimed that the highway planners had selected their location because the highway could be built more cheaply on park property. After the preliminary series of hearings the state highway department recommended, and the city and the USBPR approved, a different alignment a few blocks nearer downtown which not only avoided the elimination of the small parks and playgrounds along the earlier route but included in the design the provision for some park and recreation facilities along the borders of the proposed new highway. It was still necessary to cross Brandywine Park, the city's main public park, but this is proposed to be done by way of a viaduct that is designed to insure minimum injury to that park.

Through the cooperation of park commissions and city planning commissions it should be possible, through comprehensive planning, to expand recreation facilities of a municipality in conjunction with the construction of freeways. Such recreation facilities can be used as partial buffers between the expressway and adjoining residential areas.

Urban Renewal.—The coordination of freeway location with the clearance and rehabilitation of blighted areas as part of a city's urban renewal program can be very advantageous. Where the private reuse of a slum clearance project can be combined with a section of the interstate system, the municipality will have a direct saving in its contribution to the net loss between the costs of clearance and redevelopment. Under the United States Housing Act of 1949, including amendments through 1959, the municipality must pay one-third of this loss, the balance being assumed by the federal government. If a joint condemnation procedure can acquire part of a blighted area as a right-of-way for a federal interstate route, the municipality will not have to pay anything for that

portion of the area, because the federal government assumes 90% of the cost of the freeway and the state contributes the remaining 10%.

The present urban renewal programs are not concerned solely with slum clearance and rebuilding. They also envisage stabilizing and rehabilitating areas that are uneconomic and show serious signs of becoming blighted unless remedial action is taken through code enforcement, supplemented by some partial clearance. The major objective is to improve the economy of the city by increasing values through promoting new and stable improvements.

Freeways, with their wide rights-of-way, necessarily require substantial demolition of existing structures where they pass through built-up urban areas. Many municipalities, when discussing such routes, hear claims from property owners that taxes will be increased, not only through the loss of taxable structures but also through depreciation of values of developed property bordering such highways. There is, however, substantial evidence to show that the construction of freeways, particularly where they are depressed beneath existing streets and the rights-of-way are wide enough to establish landscaped borders, has had little deleterious effect on abutting improvements and has often increased land values.

Municipalities should make a fair appraisal of potential increases in value of land abutting proposed freeways. Such increases may much more than compensate for the loss in taxable values as a result of the property acquired for a public use.

Zoning.—Whereas the land use plan as discussed previously should be effective in guiding the general pattern of land use of the community, the only binding and legal control of such use is through the process of zoning. As the establishment of freeways inevitably raises some questions as to their effect on the use of adjoining property, changes in the zoning map are naturally considered. Because almost all our urban areas are zoned today, the invasion of urban residential districts along freeways by the spotty development of business and commercial development has generally been guarded against. This is not the case in large stretches of the interstate expressway system where the highway passes through suburban or rural areas which are without zoning protection. Prompt zoning of such areas is essential if these areas are going to grow in accordance with a plan. That problem is outside the scope of this paper.

As a freeway is without any direct access from abutting property, its borders cannot become cluttered with roadside industries or commercial uses that have ruined the traffic usefulness of many main highways in suburban areas. There will, however, be pressures to rezone, for commercial uses, areas around the interchanges between freeways and major arterial streets. This should be done only after careful study has demonstrated the need for additional business sites in that portion of the city. Indiscriminate rezoning of such areas is bound to increase the degree of turning of traffic in the vicinity of these interchanges and create serious bottle-necks on the arterial routes.

Whereas urban freeways may result in the establishment of some new industrial or business sites within the areas they traverse, residential use can be stabilized along much of their borders and the general zoning pattern of the municipality need not be seriously upset. In any event, the zoning map should be restudied to make sure that any needed adjustments are taken care of. In

some cases new apartment districts may be justified, particularly in those neighborhoods lying between a freeway and the downtown area.

CONCLUSIONS

A city's highway system has always been the framework and skeleton on which it has been built. A system of freeways in an urban area has much more effect, because it has a definite impact on many other elements of a city's master plan as well as on the plans of its suburbs. In metropolitan areas the influence of the freeway extends throughout the complex structure of such areas.

The mileage of freeways within the United States will be tremendously increased upon the completion, of the 41,000 miles of the federal-aid interstate expressway system. Through the example they will provide, more freeways will be built by state agencies, probably financed through the collection of tolls.

If freeways are to become a useful and integral part of urban areas, it is essential that, starting with the preliminary planning of such routes, the highway engineers and the city planners cooperate closely. This is particularly urgent in the development of the federal-aid interstate expressways. City planning commissions must broaden their horizons and review such plans from a regional, and not just a local, outlook. Where municipalities have already adopted master plans, whether they be for highways, land use, recreation facilities, urban renewal, or in the form of zoning maps, they should take a fresh look at them in relation to any freeway proposals.

The complexity of the impact of freeways emphasizes the need for designing them as part of coordinated transit and transportation plans for handling both passengers and freight. There is a danger that people may conclude that all our transportation problems will be solved by new highways. The only sound solution is one that retains a consideration of mass transportation. Otherwise, our urban areas are likely to become choked with vehicles which can find no place to stop or park.

Railroads throughout our country have serious problems many of which they blame on their losses in carrying commuter traffic. Recent (1958) statements in the New York City newspapers have prophesied that within another decade railroad commuter traffic into New York City will be abandoned. This seems to be fatalistic thinking and its effect would border on the disastrous. This type of outlook comes about from looking at only part of the problem. In addition it emphasizes the need for broader thinking. In the case of New York City there are three states involved. Instead of planning only highway rights-of-way, we should think more of "communications corridors," a term used in the New York Regional Plan, as a means of providing "for all major types of land communication facilities."[6]

The late Daniel L. Turner was working toward such a solution in his report as consulting engineer to the Detroit Rapid Transit Commission, Detroit, Michigan, submitted on April 10, 1924. He recommended a system of 204-ft-wide super-highways, plans for which were later adopted in the Detroit Master Plan. Such a super-highway was designed to combine four tracks of rapid transit with both local and express highways. The plan has been only partly carried out.

John I. Snyder, Jr., an industrial executive, has made a strong plea for retaining railroads in the transportation picture.[7]

---

6 "The Graphic Regional Plan," prepared by the staff of the Regional Plan, Vol. 1, 1929, p. 222.

7 "Unsnarling Traffic on the Roads, Rails, and Airways," by John I. Snyder, Jr., Harper's Magazine, November, 1958, pp. 31–36.

"Our national transportation system is in one hell of a mess. That is a flat statement of fact, and it is true whether you look up at our great airliners in the sky, or down at our more prosaic vehicles on the ground. It is true of every pathway we travel, and something has to be done about it soon."

He describes the advantages of railroads in the transportation picture:

"Even today they can carry traffic between many of our cities, during peak hours, faster than most of us can drive the same runs in our private cars. The explanation is that the railroads already possess the physical characteristics of any sensible rapid ground-transport system—the rights of way directly connecting our metropolitan centers. Their terminals are far better than any airport can be. Moreover, excellent studies have shown that a railroad right of way can accommodate twenty times more people than an express highway lane, and that it costs only one-fifth as much to transport people by rail as by road."

He claims a new kind of railroad must be developed through research:

"All we need is a vehicle that can carry us faster along the ground. from the center of Boston to the center of Washington, say, than a 500 mph aircraft can carry us—and this can be done by a safe land carriage moving at only 100 mph!"

Suggestions have been made that the future city should assume the form of multilevel strips built along and around expressways, with offices, dwellings, and all services combined in the same structures. Thus, vertical transportation could be substituted for much of the horizontal movement along a city's streets. The author does not consider this a happy solution, and much prefers the Garden City concept of Ebenezer Howard.[8]

Our interregional expressways should not become strip cities, but should rather do what their name implies—connect regions and, within those regions, connect urban centers, with plenty of greenbelts between such centers.

DISCUSSION

RICHARD A. HABER,[9] M. ASCE, AND WILLIAM J. MILLER, JR.[10] F. ASCE.—Mr. Lewis developed his paper after a review of the initial conception of the use of the word freeway, which he traces back several years. It is thought that it would be appropriate for him to include the presently accepted definition of freeway as it has been advanced by the American Association of State Highway Officials, and in addition, to perhaps include the freeway definition as presently accepted with the definition of parkways and expressways.

8 "Garden Cities of Tomorrow," by Ebenezer Howard, Faber and Faber, London, 1946, a republication, with introduction by F. J. Osborn, of original book published by S. Sonnenschein and Co., London, 1902.

9 Chf. Engr., Delaware State Highway Dept., Dover, Del.

10 Deputy Chf. Engr., Delaware State Highway Dept., Dover, Del.

A review defines "freeway" as follows:[11]

> "A freeway is an expressway with full control of access. A freeway is distinguished from all other expressways by the degree of separation of crossroads and the manner of providing access. A freeway has no cross traffic at grade. Other expressways may have crossings at grade where separations are not justified by the volume of cross traffic. With "full" control of access, as distinct from "partial," a freeway has no private driveway connections and access connections are suitably spaced, made only at crossroads which are separated in grade or connected by right turns only and generally located and designed to provide safe and efficient access and through operation appropriate for the traffic. Under "Partial" control, there may be access connections at existing streets and at some private driveways, and they are more closely spaced. Other expressways may have full control of access for some sections, but a freeway has full control of access throughout."

Throughout the procedure worked out to guarantee a sound . . . interstate highway . . . plan, Mr. Lewis assumes that consulting engineers are automatically used by state highway departments in the engineering work necessary for the Interstate System. It should be pointed out that much of the work may be done by consulting engineers, but that this is a choice to be made by the various states. In addition, the state highway departments do not necessarily need to publish a report of its preliminary design, nor is approval by the USBPR necessary.

The author mentions the need to fit freeways into street thoroughfare plans for a metropolitan area. It seems important to mention, that it is hardly adequate for a local planning commission or similar agency to use the attitude, "we were not contacted" during the course of a location study. Actually, much grief can be spared the local agencies and the state agency, if a large degree of inquisitiveness on the local level is pursued. It is granted that the sponsoring agency (in this case, the state) should fit their plans to local conditions. The local agencies can certainly make it their business to inquire into the state or regional agency plans.

Comments are presented by the author about local traffic problems in interchange areas. It would be advantageous to the interested parties if some form of public hearings could be scheduled and held as the design details were completed for interchanges within the urban area. Specific problems could then be worked out before construction, and I am sure that the local residents and businessmen would feel better about the proposed work. Perhaps this could be advanced in civic meetings, at service club meetings, and at local Chamber of Commerce meetings.

The author mentions in regard to the section on zoning, that under federal legislation, commercial establishments are prohibited from Interstate System highways. It follows, therefore, that such commercial activity can be expected to flourish in interchange areas, and in turn, that zoning requests for such activity can be expected to increase.

In the conclusions, some reference could be made to the Sagamore Conference at which the role of the planning officials and the highway engineer was fully developed in addition to the seminars sponsored by the Institute of Traffic Engineers concerning freeway operations. These seminars have been conducted throughout the United States during 1959 and additional ones are scheduled.

---

[11] "A Policy on Arterial Highways in Urban Areas," AASHO.

The author refers to a super-highway master plan set up in 1924 by Daniel L. Turner. A similar master plan for a super-highway in Delaware was envisioned by the late T. Coleman duPont, which included not only the divided roadways, but also areas for pedestrians, railroads, and bridle paths. This perhaps would be of some interest in connection with these remarks about Mr. Turner. The records of the Delaware State Highway Dept. indicate that this plan was envisioned in approximately 1911.

GEORGE H. HERROLD,[12] F. ASCE.—Mr. Lewis presents the original concept of freeways; their use in the regional plan of New York and environs, the development of parkways for passenger cars only, servicing the home-to-work crowd, shoppers and office building patrons of New York City, and the general evolution of freeway concept in the Highway Act of 1956.

The author reviews the impact of freeways on urban planning and the master plan, including the barrier created between adjacent parts on the city because of the wide right-of-way required for a freeway. It is noted that where freeways have been built, although they have improved traffic circulation, they have not eliminated serious congestion in the downtown shopping and wholesale districts.

In reviewing the literature on the value of freeways, it appears that there are some misconceptions, much confusion, and some serious doubts as to their value in intracity travel. Some freeways are located directly through residential districts. This displaces many families, and removes much valuable property from the tax roll on the expectancy that the new roads will relieve congestion in central districts. Where freeways adjoin public and institutional buildings they may also bring heavy traffic objectionably close. For example, in one capital city of the United States, there is a freeway that cuts the city in two, skirts the capital grounds, and has an interchange immediately in front of the capital plaza. This interchange extends in a southerly direction between the two largest hospitals that would be reached by overpasses across the interchange.

Highway departments are versed in the economics of locations across country, in the economy of moving earth, building bridges, constructing pavements, designing devices for drainage, braided highways, interchanges, and landscaping, but they appear to have no fundamental knowledge of a city, per se. There are practicing city planners of many professions—architects, civil engineers, economists, lawyers, landscape architects, sociologists, urban geographers, and so forth. City planning has thus developed in an idealogical manner from these various disciplines. It is natural for each profession to push forward its own major skill, and if the members of the profession have no technical training in highway location, they may not wish to become involved with a highway commission. Those who might be called conversational city planners but who do not speak the same language as businessmen or highway people have to choose between agreeing with the highway departments decisions or being ignored.

A comprehensive city plan requires a knowledge of the functions of a city (economically, politically, physically, and performance-wise), a concept of land use and land abuse, and the competition that exists for land for certain uses. The value of land is based on anticipated income. Income, in turn, depends on location with a superior location being one that is most convenient and attractive

[12] Planning and Zoning Consultant, 1952-53, Formerly Director of City Planning, 1920-1951, City of St. Paul, Minn.

for a given use in relation to other activities. The highest land values in a city are in the central business district. The permanency of these values is dependent on creating and maintaining districts of high purchasing power, and on methods of getting people with money to spend from these districts to the central business district by easy, attractive, and pleasant routes such as the parkways, exclusively for passenger cars, leading into New York City.

Mr. Lewis mentions the Autobahns of Germany. These do not run through cities. They were made continuous by skirting cities, using undeveloped lands, and disturbing few people.

Because of the fine work of state highway departments people have been slow in believing that a freeway through their city might act as a moat or a chinese wall and an economic menace. These controlled access and controlled exit freeways in cities have been "sold" to urban residents as a means of lessening congestion on city streets and in central business districts. Because they do not or will not serve this function, why should they run through the city? It is believed that urban dwellers are beginning to take a long hard look at these monolithic structures that they must live with for years.

The freeway idea for a city has been oversold. It requires the moving of thousands of people and the loss of much taxpaying property. These people must give up their homes, churches, schools, neighbors, and their valued social contacts. They lose the institutions they have built for themselves, paid for in taxes and by priviate subscriptions. There is the loss of the money that they have spent on maintaining and operating these institutions for years. They have lost everything worth living for except, of course, that they are to receive some money in exchange for their home.

Where freeways are to run through cities they disturb all the utility facilities, sewers, water mains, gas mains, electric power, light cables, telephone and telegraph lines, and conduits. Where the freeway is depressed 18 ft to 20 ft below street grades, all these utilities must be dug up, lowered below the freeway, and raised again at tremendous expense. There is also the unaccountable expense of detours, disruptions of business, and annoyance.

A city is made up of blocks and streets. Each block is a traffic generator of from 5 to 30 cars. Every morning many of these cars leave for work in the central business district, manufacturing district, or other points. If a car is driven several miles to the freeway and several miles in the freeway and several miles after getting out of the freeway to it's destination, it has doubled its mileage and lost time. So why should one use the freeway?

The use of the Edens Expressway, entering Chicago, Ill. from the north shore traffic corridor, has been analyzed.[13] In this corridor, that is approximately 5 miles wide, there are two railroads and four highways which are not expressways. When the intent is to use the expressway for its entire length (13.5 miles), approximately 70% of the vehicle traffic in the corridor does so. But, for local trips, the use drops to approximately 20% because of the loss of time in entering and leaving the expressway.

The freeway is a fine idea for travel between cities, but for intracity travel it is a great misconception of the needs of an urban community.

With respect to the thoroughfare plan and local traffic problems, it should be noted that in many cities these are federal and state trunk highways that are located to serve the metropolitan area in harmony with the urban plan. In such

[13] Traffic Quarterly, July, 1956.

cities, if the freeway followed the edge of the city of paralleled railroad rights-of-way in the city, it could be reached in a few minutes from these trunk routes. Such a plan would (a) result in savings in the cost of the rights of way, (b) reduce the cost of utility relocations, (c) reduce the loss of taxes to the community, and (d) improve public relations.

Freeways in a city will result in much moving of business and obsolescence and blight in the new areas. The highway specialist for the United States Chamber of Commerce, J. E. Johnson states[14] "There will be a rush by many businessmen to relocate near the freeway." This is, of course, the natural thing to happen. The city streets that lead to the access points or exit points of the freeway and interchanges will be rezoned for commercial use and businessmen will move, at great expense, to these new locations. Old congested spots will disappear, and obsolescence and blight will set in. New congested spots will be created but there will be no decrease in congestion. These great changes are likely to offset the increase in values along the freeway. It is a well-known municipal fact that the cost of policing, fire protection, and welfare in a blighted district will run to more than five times the sum collected in taxes from such an area.

A freeway in a city is an enclosure between entrance and exit. It must be a self-contained unit for all emergencies that occur in it. In the northern states, snow will blockade it at times. A 3-in. rain on its wide right-of-way will produce a river over the pavement. It must be policed 24 hours a day. When cars catch fire, how will fire apparatus reach the burning car, and what about panic? When people in cars become sick, or accidents occur, will an ambulance be able to reach them? How will a car that runs out of gas be pulled out of the line of moving traffic? There will be many new problems within the freeway. It is said that the government will pay 90% of the cost of the right-of-way and construction, but several states have stopped letting contracts because the government has failed to collect this 90% from taxed motorists.

To resolve this problem, the writer suggests, first, that each city decide whether it wants a freeway or not. It if does, then it should employ a firm of consulting city planners of established reputation to work with the state highway department on the freeway location, and the city council should refuse to approve the freeway location until these two agencies come to an agreement. Freeways, if needed in an urban community, are too important to be left to a highway department.

HAROLD M. LEWIS,[15] F. ASCE.—The discussions have shown the differences in terminology when one talks or writes about various types of expressways, and the variations in procedures in different states in designing the federal-aid interstate highway system. They have also elaborated on the problems that occur in urban areas when freeways cross through them.

Messrs. Haber and Miller quoted the definition of a freeway advanced by the American Association of State Highway Officials (AASHO) and suggested that the writer should tie in Edward M. Bassett's 1930 definition with this later "presently accepted definition." Since Mr. Bassett made his proposal, a variety of terms have been applied to modern express routes designed to serve both passenger and commercial vehicles, including freeways, expressways, controlled-access highways, limited-access highways, superhighways, and (in the 1956 High-

14 Traffic Quarterly, April, 1957.

15 Cons. Engr. and City Planner, New York, N. Y.

way Act) "national system of interstate and defense highways." Highway engineers and city planners need a standard terminology.

The writer believes that the term expressways should cover all types of highways where the design aims at uninterrupted movement and the elimination of the right of direct access from abutting property, whether or not such routes are limited to certain types of vehicles and whether the control of access is full or partial as those terms are used in the AASHO definition.

A freeway should serve both passenger and commercial vehicles, have full control over access, and be free of crossings at grade and lefthand turns. A parkway should be an expressway limited to passenger vehicles, with control of access through the fact that its roadway lies within a strip of park land, the strip being a part of the parkway. The writer does not believe that Mr. Bassett pictured a parkway as being completely free of grade crossings, as the modern parkway is, with some occasional exception in rural areas where traffic did not justify the cost of a grade separation. As traffic increases such grade crossings should be eliminated. There appears to be no basic conflict with the aforementioned definitions and those of either Mr. Bassett or the AASHO.

The procedure described in the paper for developing the interstate freeways was not presented as prescribed or universal, but only as a typical procedure, having in mind particularly that which has been followed in Delaware. It is recognized that some of the larger states handle more of the detail with the State Highway Department staffs. The Delaware State Highway Department suggested in the fall of 1959, that because of delays resulting from cutbacks on federal spending for the interstate system, the state complete as a toll road (financed by revenue bonds) the one route under construction, so that future available federal funds could be allotted to the other two Delaware routes.

The writer fully agrees with Messrs. Haber and Miller on the need for closer cooperation between state highway departments and local planning and zoning agencies as well as local civic and business groups.

The superhighway proposal advanced by the late T. Coleman duPont is of historical interest. This proposal had no provision for grade separations at intersections nor for access to abutting property, although the inclusion of trolley tracks implies that considerable development was expected to follow the superhighway construction. The total right-of-way width is comparable to the 204 ft in Mr. Turner's proposal of 1924, mentioned in the paper, but the latter was much more realistic in the allocation of space and width of roadways. The duPont Parkway and duPont Boulevard, that grew out of Mr. duPont's proposal, is now a dual highway with a wide central mall.

The writer described in his paper those features of a city plan which have been most seriously affected by freeways that cross through their areas. In discussing these, Mr. Herrold mentioned the different points of view from which highway departments and city planners approach their problems. He would like to keep freeways out of cities where possible, and suggests that the first step in a location study should be "that each city decide whether it wants a freeway or not." This would seem an attempt to solve a regional and interstate problem from a local point of view, which as pointed out in the paper, may simply move the freeway location to a bordering community where opposition may be equally vocal.

Even though a municipality may not want a freeway to pass through it, it does want convenient access to the interstate system. The provision of such access

may involve serious dislocations of population and business through street widenings and other needed improvements.

There are examples of close cooperation between public works officials of local and state governments, such as was carried out in Contra Costa County in California.[16] What Mr. Herrold stressed is the necessity of bringing the city planners into the picture in the preliminary stages of discussion. Similarly, Messrs. Haber and Miller urged that local planning commissions should "make it their business to inquire into the state or regional agency plans." Some state highway departments have recently appointed city planners to their staffs. This is helpful, but still leaves it desirable to obtain the combined benefits of local, meltropolitan, and state planning in determining the best location of the interstate freeways and the location and design of their connections with urban areas. It is within these urban areas that most of the freeway traffic originates and is destined.

Mr. Herrold refers to a case in a capital city where he feels a downtown location has violated sound planning principles. There are other cases, however, where planning commissions have urged downtown locations and they have worked out advantageously. Two such cases have occurred along that part of the Connecticut Turnpike which has since been incorporated in the interstate system of federal freeways.

The Bridgeport section of the Connecticut Turnpike was originally planned as a freeway relocation of part of U.S. Route No. 1. Original plans of the Connecticut State Highway Department favored a location passing some distance north of the central business district. After much examination of alternative routes, the state highway Commissioner announced on May 28, 1952, a southerly location as recommended by the Bridgeport City Planning Commission. This passed through the edge of the central business district, eliminated a substantial area of blight in accordance with plans of the Bridgeport Housing Authority, acting as the city's redevelopment agency, and provided convenient connections for downtown shoppers and the city's main industrial areas. The need for costly feeder routes was eliminated.

The other example is in New Haven, Conn., where the turnpike location has resulted from outstanding cooperation between the state and federal highway agencies, the city's planning commission, redevelopment agency and traffic department, private commercial interests, and institutions. The resulting location skirted the central business area, passing through industrial areas and crossing part of the harbor so as to create new land by reclamation, and included an Oak Street Connector to the core of the city and tied in with a Church Street redevelopment project. Along this connector the city's oldest slum area was cleared and the combined redevelopment plans include modern apartments, retail shops, offstreet parking, a hotel, and a new telephone company building.

It is evident, therefore, that the answer as to where freeways should go varies with the city and its region and their peculiar conditions, but, if there are both city and regional master plans that have been coordinated and the planning commissions' viewpoints are given full consideration, the location decided on should be a sound one.

---

16 "A Plan for a County Motor Vehicle Transportation System," by Victor W. Sauer, Proceedings Paper 2144, ASCE, September, 1959.

AMERICAN SOCIETY OF CIVIL ENGINEERS

Founded November 5, 1852

TRANSACTIONS

Paper No. 3054

STRUCTURAL DYNAMICS IN EARTHQUAKE-RESISTANT DESIGN

By John A. Blume,[1] F. ASCE

With Discussion by Messrs. Lydik S. Jacobsen; A. A. Eremin; Emilio Rosenblueth; Michael J. Murphy, R. Ivan Skinner, and Keith M. Adams; Reuben W. Binder; and John A. Blume

SYNOPSIS

Research efforts utilizing high-speed digital computers and electric analogs have indicated vast differences between earthquake shear values arrived at by design and adherence to codes and for structures' actual earthquake behavior. This paper attempts to reconcile these differences, with the aid of comprehensive structural and dynamic analyses and research efforts on a traditional filler-wall type office building and a modern glass-wall structure. Included are values for strengths, rigidities, and inelastic energy-absorption for the traditional building under various distortions up to failure. The results of a comprehensive series of analog tests for the modern 20-story structure, using four complete earthquake records with sixteen various systems of damping and rigidity values are also included. Certain inconsistencies and pitfalls in present-day design practice are demonstrated and new considerations are suggested for resisting the occasional but extreme energy releases of nature that are involved in earthquakes.

INTRODUCTION

There have been several investigative efforts wherein given vibrating systems were subjected to the actual and complete motion of destructive earthquakes as recorded (1)[2] by the Seismological Division of the Coast and Geo-

Note.—Published, essentially as printed here, in July, 1958, in the Journal of the Structural Division, as Proceedings Paper 1695. Positions and titles given are those in effect when the paper or discussion was approved for publication in Transactions.

[1] Pres., John A. Blume & Associates, Engineers, San Francisco, Calif.

[2] Numerals in parentheses—thus, (1)—refer to corresponding references in the Bibliography.

detic Survey United States Dept. of Commerce (USC&GS). In most of this analysis, which has been made economically feasible with high-speed computing equipment and electric analogs, a single-mass system has been assumed (2) (3)(4) and in some cases multi-mass systems dynamically representing buildings of several stories have been used (5)(6)(7)(8). This research has led to further information about the dynamic response of hypothetical and existing structures to actual earthquake motion. It has also confirmed the importance in the seismological design problem of damping, period, velocity, energy and other dynamic considerations.

Engineering seismology has come a long way since the "force-equals-mass-times-acceleration," the "dominant-period," and the "simple-sinusoidal-motion" concepts were the only approaches to design. However, the accelerations and shears obtained with modern computing techniques and also the accelerations recorded on the ground and in structures during strong-motion earthquakes are so much greater than those called for by modern codes and normal engineering procedures that the inquisitive engineer and the research worker are perhaps more bewildered than before. The confusion is heightened when customary analysis procedures yield a value of less than 1% of gravity for a building that withstood one of the worst earthquakes in the recorded history of the world (9) with no major structural damage. The problem was made more critical when buildings in the Los Angeles, Calif. area suffered "non-structural" damage from the 1952 Kern County (California) earthquake, approximately 75 miles away (10).

There are still so many paradoxes and so many anomalies in the subject of earthquake resistance that it must be concluded that there is a whole world of missing links that is either avoided or not fully recognized. It is proposed, herein, to examine this situation and to attempt to reconcile some of these apparent paradoxes and to investigate in detail reasons why two similar structures may have entirely different degrees and types of resistance to moderate and to severe earthquakes.

The writer has delayed writing on this subject because of the feeling that some concepts might lack rigorous proof. However, there is a pressing need for more information about the way our structures react structurally and dynamically to earthquakes. The concern about lack of rigorous proof is also reduced in part by the fact that many efforts in this complex field do not have general application, as may be assumed from the mathematical treatment. Often the assumptions necessary to support the mathematics, have lacked depth but have had a considerable effect on the results and conclusions. As additional knowledge from future earthquakes and research is awaited, billions of dollars of new structures are being created. The basic and sound philosophy under engineering procedure is to gather all pertinent facts and to consider and evaluate these completely before arriving at conclusions. This procedure has not always been followed in the earthquake field because of the extreme complexity of the problem, the lack of availability of all the facts, the lack of recognition of the facts, which is largely because of traditional procedures and empirical results, and the fact that generalizations have sometimes been made without a realization that certain data or conditions observed may not apply to all structures.

SEISMIC CODES AND DESIGN PRACTICE

General Considerations.— Structural designers generally think in terms of weight and strength of materials but their concept of strength is still largely

confined to "safe" or "basic" unit stresses, prescribed by building codes or other design criteria. The codes generally permit a 33-1/3% increase in basic unit stresses for occasional lateral "forces" of wind or earthquake and designers eagerly take advantage of these higher unit stresses to meet established design criteria. Modern seismic codes attempt to provide minimum, legal, static, lateral forces that vary with the height or period of the building under consideration so as to approach a lateral loading, similar, but not necessarily equal, to that which may be expected in response to earthquake motion. Fig. 1 illustrates shear values of two such codes for two different buildings. It also shows shear values obtained by other means including analysis and actual response. The traditional type of building (Fig. 1(a)) was erected long before either seismic code was in effect and yet its noncomputed materials provide shear value as indicated. The modern structure (Fig. 1(b)) is lighter and more flexible, yet its dynamic shears are considerable in a major earthquake. Values are electric analog results for stiffness system A as per Table 4, and 5% damping.

The great differences between code design requirements and recorded or computed accelerations and shears from major earthquakes do not necessarily mean that the codes are inadequate nor can these differences be accounted for merely with the reserve of unit stress value from 1-1/3 times the basic value to the failure point of materials. It would seem, however, that codes and design procedures are not always in tune with nature and that the building resistances could be extremely inconsistent. This follows from the philosophy that if there is not an awareness of all the important factors in a situation, variations in those factors cannot properly be provided for.

Factors that have not been generally recognized.—A great deal of the apparent conflict between design practice, research, computation, and observation in aseismic design (aseismic is used herein in the sense of resisting seismic reactions) may be attributed to inadequate recognition of one or more of the following factors:

1. The earthquake problem is one of dynamics involving mass, movement, velocity, acceleration, energy, and work. The forces, shears, and moments are a result of resistance to motion. Deflection is necessary but it must be controlled.

2. All materials that are subject to strain by the structure's movement participate, not only as mass, but in energy absorption up to their point of failure. Even after rupture, some of these materials absorb more energy under continued earth movement by grinding and hammering together and in finally being dislodged.

3. Because materials in both old and new structures vary in amount, character, and disposition over a wide range, observed results cannot be logically or safely applied in general to all structures.

4. Materials have many properties in addition to strength and elasticity. These various properties and their variations should be considered up to the point of rupture.

5. Severe earthquake accelerations can be many times code values. The resulting forces are not necessarily equal to mass times acceleration because of yielding and dynamic phenomena. However, that approach to the problem has some uses in design.

6. Earthquakes have vertical movement as well as horizontal. The vertical motion may have considerable potency because the structure may be quite rigid

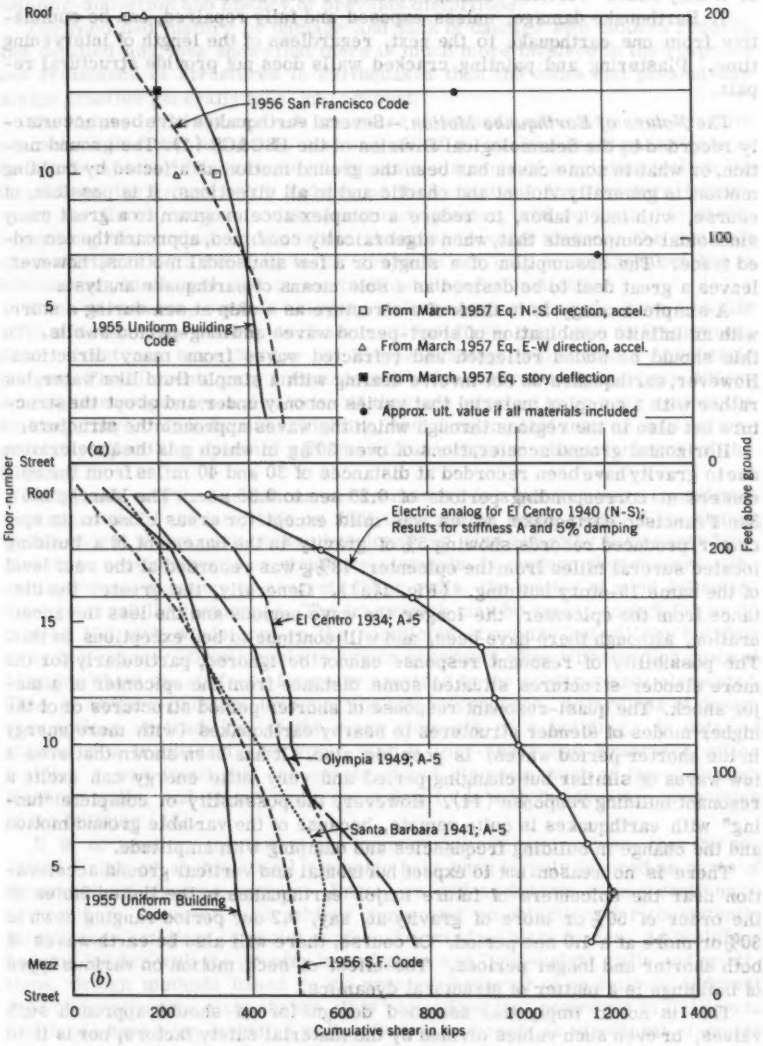


FIG. 1.—COMPARATIVE SHEARS FOR TWO BUILDINGS

vertically. Moreover, this vertical component may reduce the weight of some element whose weight has been relied upon in design to decrease tensile effects, or it may cause "vertical" damage leading to lateral failure.

7. Earthquake damage, unless exposed and fully repaired, can be cumulative from one earthquake to the next, regardless of the length of intervening time. Plastering and painting cracked walls does not provide structural repair.

The Nature of Earthquake Motion.—Several earthquakes have been accurately recorded by the Seismological Division of the USC&GS (1). The ground motion, or what in some cases has been the ground motion as affected by building motion, is generally violent and chaotic and in all directions. It is possible, of course, with much labor, to reduce a complex accelerogram to a great many sinusoidal components that, when algebraically combined, approach the recorded trace. The assumption of a single or a few sinusoidal motions, however, leaves a great deal to be desired as a sole means of earthquake analysis.

A simple analogy is to think of a structure as a ship at sea during a storm with an infinite combination of short-period waves and long-period swells. To this should be added reflected and refracted waves from many directions. However, earthquakes do not involve dealing with a simple fluid like water, but rather with a complex material that varies not only under and about the structure but also in the regions through which the waves approach the structure.

Horizontal ground accelerations of over 30%g in which g is the acceleration due to gravity have been recorded at distances of 30 and 40 miles from the epicenters at corresponding periods of 0.20 sec to 0.35 sec. The March, 1957, San Francisco earthquake, which was mild except for areas close to its epicenter, produced records showing 5% of gravity in the basement of a building located several miles from the epicenter. 13%g was recorded at the roof level of the same 15-story building. (Fig. 1(a)). Generally, the greater the distance from the epicenter, the longer the wave periods and the less the acceleration, although there have been, and will continue to be, exceptions to this. The possibility of resonant response cannot be ignored, particularly for the more slender structures situated some distance from the epicenter of a major shock. The quasi-resonant response of shorter period structures or of the higher modes of slender structures to nearby earthquakes (with more energy in the shorter period waves) is possible also. It has been shown that even a few waves of similar but changing period and very little energy can excite a resonant building response (11). However, the possibility of complete "tuning" with earthquakes is quite remote, because of the variable ground motion and the change in building frequencies and damping with amplitude.

There is no reason not to expect horizontal and vertical ground acceleration near the epicenters of future major earthquakes in the United States on the order of 50% or more of gravity at, say, 0.2 sec period ranging down to 30% or more at a 1.0 sec period. Of course, there will also be earth waves of both shorter and longer periods. The effect of such motion on various types of buildings is a matter of structural dynamics.

This is not to imply that assumed design forces should approach such values, or even such values divided by the material safety factors, nor is it to imply that acceleration is the only measure of destructability. It should indicate, however, that the static approach based only upon mass times acceleration and using only so-called structural materials at code stresses can neither economically nor consistently cope with the situation. Nor can the matter be

dismissed on the basis of assumed damping values, which no doubt vary greatly from one type of building to another, and will also vary depending upon the building-distortion and history of previous distortions.

The recorded history of damage and lack of damage with modern records and detailed analyses shows that there is much more involved in the response and resistance of structures to earthquakes than the codes and present-day design practice generally take into account.

The Nature of Structures.—A structure possesses structural and dynamic characteristics determined by the way all of its various parts participate in the whole system. The structural-dynamic elements of a building include its foundations, the ground below and around the foundations, the structural framework, the floors, stairs, walls, partitions, plaster, and so forth. In short, everything that makes up the whole changes, to some degree, the over all characteristics of a building in its response not only to earthquakes but to windstorms, blast, and even minor traffic-induced vibrations.

Some structures, such as bridges, tank towers, or wharves, have no walls or partitions, while others, such as small buildings, may have no framework. Some structures have X-type or K-type bracing, while others have rigid frames. The elements vary tremendously between structures and have different relative properties and values. If they are attached to or bear against the building, they contirbute mass, rigidity, and damping that may or may not appreciably affect the dynamic and structural response characteristics of the building.

In the past, only the foundations and framework in a building were considered as "structural." In fact, this is still the case in many parts of the United States except where earthquake, hurricane, or wind sidesway have caused engineers to consider walls as structural elements. In modern skyscrapers without traditional masonry or concrete filler walls, the matter of wind deflection must be carefully considered. The framework may be strong enough for an 80 mph or 100 mph windstorm on the completed structure but will the building sway in a manner objectionable to human occupants when withstanding gusts of 50 mph without the stiffness formerly provided by the nonstructural elements? This is another problem involving the interdependence, regardless of design assumptions or tradition, of the many elements of a building. In detailed studies of a traditional pre-World War II (pre-1939) San Francisco office building it was found that the nonstructural elements such as fire-proofing, masonry walls, and stairs had a great deal to do with the dynamic properties of the building (12).

It is no wonder, in view of the many complications involved, that the so-called finish or architectural elements have been largely ignored as parts of the structural-dynamic system. Engineers and architects cannot continue to ignore them, however, and achieve agreement on objectives for consistently satisfactory buildings to resist earthquake, wind or blast forces. As buildings become lighter with the greater use of glass and light-weight walls and partitions, design methods based on the previous behavior of an entirely different type of construction must change. It is recognized that engineers in California and Japan have been including walls, floors, and roofs as structural elements in earthquake resistance for over two decades. Progress has been made, but factors and elements are still being ignored that might explain the great variations between design shears and those obtained by structural-dynamic analyses using actual earthquake records. Any part of a structure which will be strained as the structure responds to these natural forces should be considered not on-

ly as a potential hazard to life and investment, but also as a possible element of resistance if effectively utilized.

The Nature of Building Materials.—In order to cope economically and consistently with actual (dynamic) earthquake forces, engineers should employ all available materials under all possible degrees of stress and strain up to complete failure. Building materials have different properties, not only of strength and density, but also of toughness, ductility, energy absorption, damping, fatigue resistance, and so forth.

For a structure or a member to withstand violent abuse such as the impact and motion of a major earthquake it must be tough, and well tied together in order to act as and to remain a unit. Toughness implies the ability to absorb punishment and still retain integrity and resistance against additional punishment. If the toughness of a material is measured by the amount of work required to cause a unit volume of the material to fail, it is found that the work done or strain energy for ductile materials in the elastic range is very small as compared to that in the plastic range. Fig. 2 indicates, in the shaded area,

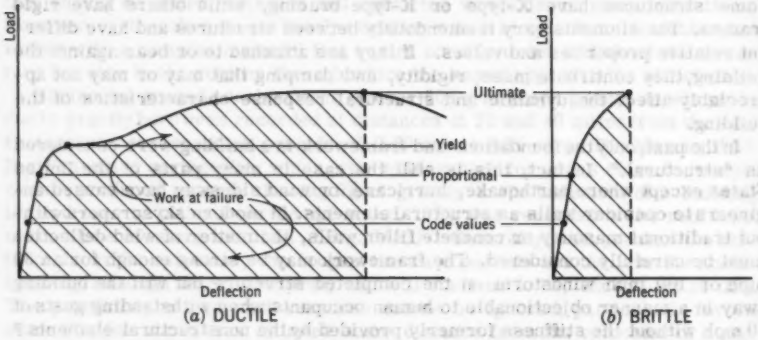


FIG. 2.—BUILDING MATERIAL CHARACTERISTICS

the work capacity of ductile (Fig. 2(a)) and brittle (Fig. 2(b)) materials. For brittle materials, failure occurs abruptly without the plastic strain that not only absorbs energy but also distributes the load in an indeterminate structure to other parts. Structural steel frames, particularly when of a rigid-frame type or construction, have generally had an excellent seismic record (9), largely because of toughness. However, a building with a structural steel frame that cannot exert its toughness until the costly brittle materials have first failed may still be a poor risk economically. This design problem is recognized by modern seismic codes in requiring relative-rigidity computations. These codes do not generally reflect the value of tough materials and indeterminate construction in preventing severe damage or collapse in the range of force and distortion which can apparently be expected in a major catastrophe. The 1956 San Francisco code, based on the report of a joint committee of the San Francisco Section of the American Society of Civil Engineers (ASCE) and the Structural Engineers Association of Northern California (13) does allow in small degree for the value of toughness in an emergency.

The use of steel or other ductile and tough materials to impart such desirable properties in various degrees to less ductile materials is, of course, basic in seismic resistance. It is not necessary to discard a material that has low ductility, providing it can be combined with ductile materials to create a composite material which will absorb energy and hold together. It is common practice, for example, to use steel reinforcement in concrete and in masonry (14) for aseismic construction and thus provide a composite material with strength and toughness.

A material such as plate glass may have great strength but will lack the ability to withstand much unit strain without sudden rupture. It would seem obvious that such glass should not be obliged to share in the resistance to distortion between the floors of a building. If the structural elements of a building must deflect a certain amount to function, either elastically under code stresses or in the plastic range which absorbs much more energy under severe conditions, the glass should be so mounted as to be secure and weathertight but not be strained under the necessary seismic movement. This is not always done. The March, 1957, San Francisco earthquake, that was by no means a severe shock, caused glass breakage in various types of buildings including concrete buildings constructed under aseismic code requirements (15).

Much has been written about damping in reference to the earthquake problem. All materials have some viscous damping value which is proportional to velocity and varies with strain. The term damping as used in relation to earthquake response in modern technical literature implies not just the viscous damping but the over-all effect including rubbing friction (16)(17), breakage, grinding, and so forth. It is as yet difficult to assign composite damping values to buildings although such have been obtained in a few cases by consideration of the response to forced vibration in the range of resonant periods (12)(11b)(18).

MULTI-STORY BUILDING REACTION TO EARTHQUAKE MOTION

The results of two research efforts will be presented to provide specific data on the many items considered in the general terms previously presented. The first work extends previous comprehensive studies of the dynamic properties of an actual traditional type of building under low amplitude vibration into a hypothetical range of progressive failure under extreme conditions. The second study considers the shears developed in a proposed 20-story modern building with sixteen various systems of assumed stiffness and damping values under the complete actual motion recorded for four different earthquakes.

A Traditional Office Building.—A 15-story San Francisco office building has been subjected to a great deal of research since approximately 1935 with particular reference to its dynamic characteristics. A complete summary of the work to date with references and a description of the building, which has been termed the seismological "guinea pig," has been published (12). In addition to detailed analyses of the factors contributing toward the various natural periods of vibration of the building, records have been made of the actual response to windstorm, earthquake motion and to a vibrating machine.

The Alexander Building is typical of a great many tall office buildings constructed in the United States before 1940 in that it has a riveted steel frame, exterior unreinforced brick filler walls, tile partitions, concrete floors and stairs, and interior concrete fireproofing. It is rectangular in plan and in ele-

vation, is practically free of adjoining structures, and is founded on firm alluvial materials. Although no seismic code was in force at the time of its design and construction, the provision for wind forces provides an equivalent-code seismic value of approximately 2% in the exterior steel frame with its deep spandrel connections. Following the prevailing practice the wall materials were not used structurally.(12).

From previous exhaustive research in the first four modes of vibration in each plan direction of the building, the relative contributions to the various natural periods of shear, flexure, and ground yielding were determined as were the shear spring factors for each story and the elements contributing to these factors (12). Estimates of the composite damping capacities were also made. However, for all of this work the measured amplitudes of building motion were quite small. They never exceeded approximately 0.10 in. in the fundamental mode, 0.06 in. in the second mode, and 0.03 in. in higher modes. The steel frame, the concrete fireproofing, and the concrete stairs contribute to the building stiffness in proportion to their relative rigidities as do the exterior brick filler walls and brick exterior fireproofing. However, for the small amplitudes involved, it was found that the masonry was only partly effective as

TABLE 1.—EARTHQUAKE RESPONSE IN 15-STORY BUILDING

	North-South Direction			East-West Direction		
Level	Acceleration, in percent of g	Amplitude, in inches	Period, in seconds	Acceleration, in percent of g	Amplitude, in inches	Period, in seconds
(1)	(2)	(3)	(4)	(5)	(6)	(7)
Roof	8.2	0.063	0.28	13.2	0.087	0.26
10th Floor	6.7	0.055	0.29	4.9	0.038	0.28
Basement	4.9	0.025	0.23	5.5	0.033	0.25

shown by the very low value, 60,000 psi, obtained for the "effective" modulus of elasticity of the masonry working in conjunction with the steel and concrete. This participation, however, greatly affects the dynamic properties of the building. The tile partitions were found to be essentially noncontributing to stiffness for the small amplitudes recorded.

Accelerograms due to earthquake motion were obtained simultaneously on March 22, 1957, at the roof level, the 10th floor, and at the basement level with the USC and GS instruments. These undoubtedly represent the greatest accelerations to which this structure has been subjected. The absolute maximum (but not simultaneous maximum) values of acceleration and the corresponding periods and single amplitudes were determined by the writer as shown in Table 1.

During a considerable portion of the record, the building was vibrating in or close to its third mode frequency in each direction, although some second mode waves appear, and there is some minor beating effect with the fundamental mode in the north-south direction. The simultaneously recorded motion (third mode) that indicated the greatest shear distortion between floors is shown in Fig. 3. The gross recorded single amplitude has been reduced to

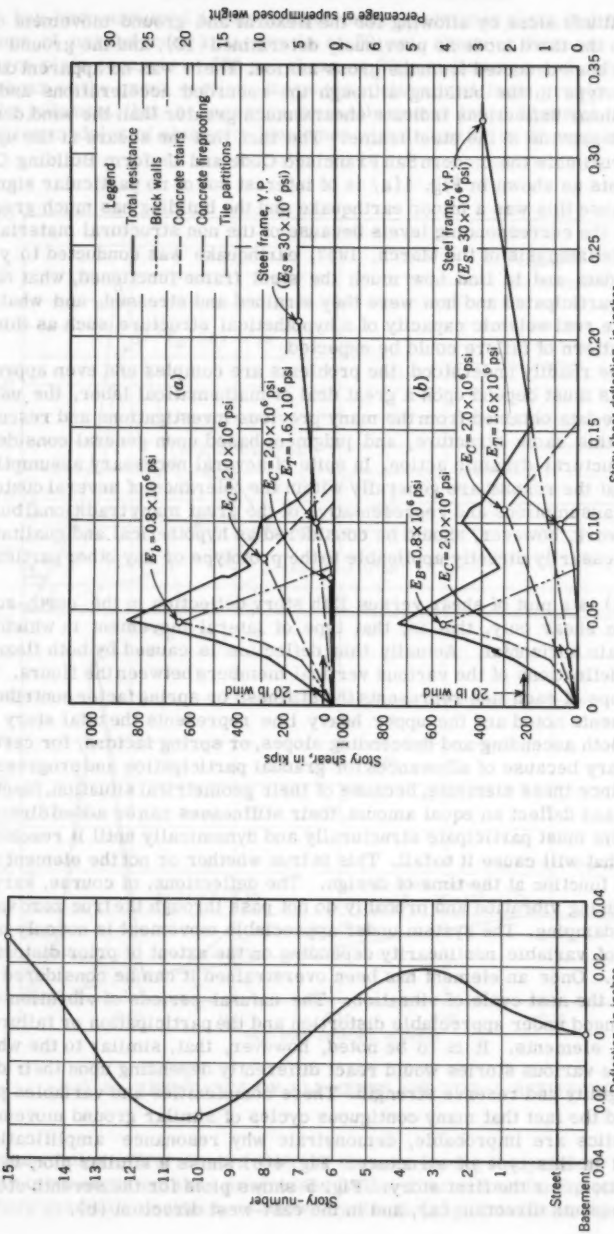


FIG. 3.—EARTHQUAKE RESPONSE

FIG. 4.—RESISTANCE OF ELEMENTS AND TOTAL RESISTANCE

shear amplitude alone by allowing for the flexural and ground movement contribution to the third mode as previously determined (12), and the ground amplitude has been deducted from the gross motion. There was no apparent damage of any type in the building although the recorded accelerations and the computed shear deflections indicate shears much greater than the wind design basis would provide in the steel frame. The fact that the shears at the upper levels approximate the modern San Francisco Code and Uniform Building Code requirements as shown in Fig. 1(a) is of interest but of no particular significance, because this was a minor earthquake and the building has much greater strength at the corresponding levels because of the non structural materials.

A detailed analysis of the March, 1957, earthquake was conducted to yield additional data and to find how much the steel frame functioned, what other materials participated and how were they strained and stressed, and what the approximate real seismic capacity of a hypothetical structure such as this is and what pattern of failure could be expected.

As can be readily understood, the problems are complex and even approximate results must depend upon a great deal of mathematical labor, the use of all available data obtained from the many previous investigations and research efforts on this same structure, and judgment based upon general considerations of structural-dynamic action. In spite of several necessary assumptions it is felt that the results are generally within the tolerance of several customary design assumptions and representative of the great many traditional buildings. The work, however, should be considered as hypothetical and qualitative and not necessarily directly applicable to the prototype or any other particular building.

Fig. 4(a) is a plot of shear versus 13th story deflection in the north-south direction in shear only, that is, that type of lateral movement in which the floors remain horizontal. Actually this deflection is caused by both flexural and shear deflections of the various vertical members between the floors. The positive slope of each line represents the stiffness or spring factor contributed by the elements noted and the upper heavy line represents the total story resistance. Both ascending and descending slopes, or spring factors, for certain elements vary because of allowances for gradual participation and progressive failures. Since these elements, because of their geometrical situation, function in parallel and deflect an equal amount, their stiffnesses can be added directly. Each element must participate structurally and dynamically until it reaches a distortion that will cause it to fail. This is true whether or not the element was assumed to function at the time of design. The deflections, of course, vary in direction during vibration and probably do not pass through the true zero value because of damping. The system under appreciable movement is not only nonlinear but of variable nonlinearity depending on the extent of prior distortion and damage. Once an element has been overstrained it can be considered out of action on the next cycle of vibration. The natural periods of vibration will thus be changed under appreciable distortion and the participation or failure of the various elements. It is to be noted, however, that, similar to the whole building, the various stories would react differently depending upon their distortions, rigidity and reserve strength. These complexities and variables plus damping and the fact that many contiguous cycles of similar ground movement characteristics are improbable, demonstrate why resonance amplifications are limited in this type of structure. Fig. 4(b) shows a similar plot, in the same direction, for the first story. Fig. 5 shows plots for the seventh story, in the north-south direction (a), and in the east-west direction (b).

It has been assumed in developing these resistance plots that the point of rupture of unreinforced masonry is at 80 psi, shear or flexure, whichever governs plain concrete at 200 psi shear or 200 psi flexure; and clay tile at 40 psi shear on the gross section. It was also determined, from previous research and by judgment, that the masonry gradually comes into full action, that is, its effective modulus of elasticity increases with distortion to its maximum value.

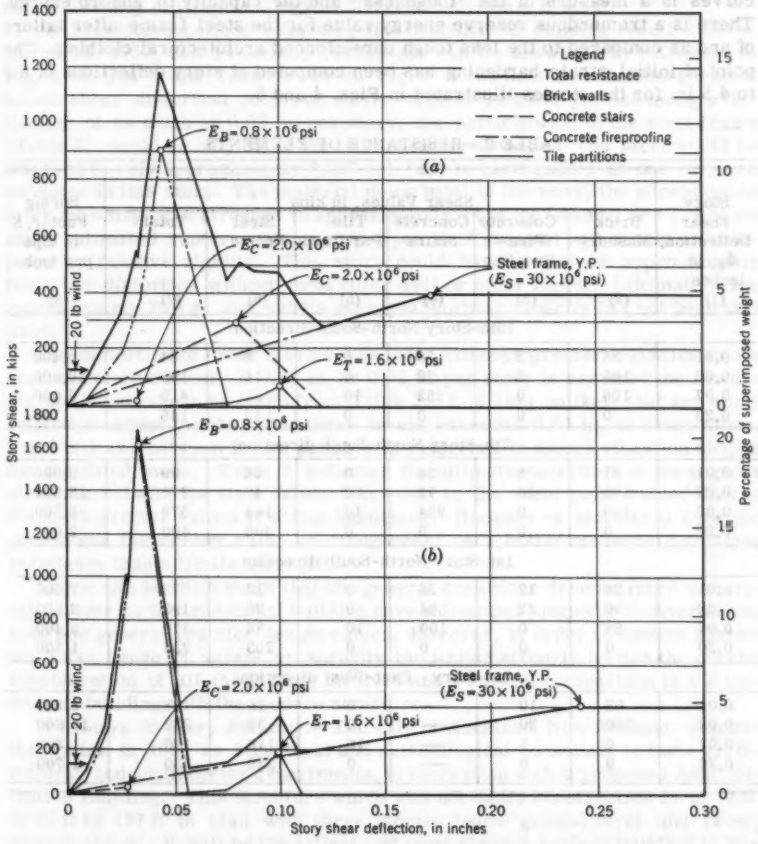


FIG. 5.—RESISTANCE OF ELEMENTS AND TOTAL RESISTANCE

Because failure first occurs with the element having the greatest ratio of rigidity to strength and then progresses to the other elements, the resistance as a whole gradually declines, as shown by the sloping lines, beyond peak resist-

ance. The tile partitions also come into action to an increasing degree, but no participation is assumed until the story deflection is appreciable.

The plots can be used not only to estimate the total shear and stiffness for any distortion, but also to estimate how much is carried by each of the various elements and to visualize when each will participate and when they will fail. The building periods at any stage of failure can be estimated with revised spring factors determined by the slope of the total resistance line projected back to the origin from any point of deflection. The area under the various curves is a measure of the "toughness" and the capacity to absorb energy. There is a tremendous reserve energy value for the steel frame after failure of and as compared to the less tough unreinforced architectural clothing. The point of initial strain hardening has been computed at story deflections of 2.5 to 4.5 in. for the stories illustrated in Figs. 4 and 5.

TABLE 2.—RESISTANCE OF ELEMENTS

Story Shear Deflection, Δ_s, in inches	Shear Values, in kips						Spring Factor, K in kips per inch
	Brick Masonry	Concrete Fire-Proofing	Concrete Stairs	Tile Partitions	Steel Frame	Total	
(1)	(2)	(3)	(4)	(5)	(6)	(7)	(8)
13th-Story North-South direction							
0.01	38	2	36	0	8	84	8,400
0.02	106	5	72	0	16	199	10,000
0.07	106	0	252	10	51	419	6,000
0.20	0	0	0	0	145	145	700
7th-Story North-South direction							
0.01	31	8	36	0	24	99	9,900
0.02	135	16	72	0	47	270	13,500
0.07	150	0	254	10	164	578	8,300
0.20	0	0	0	0	400	400	2,000
1st-Story North-South direction							
0.01	24	12	26	0	13	75	7,500
0.02	90	22	54	0	26	192	9,600
0.07	88	0	190	10	88	376	5,400
0.20	0	0	0	0	253	253	1,300
7th-Story East-West direction							
0.01	62	10	—	0	16	88	8,800
0.02	280	20	—	0	32	332	16,600
0.07	0	0	—	10	116	126	1,800
0.20	0	0	—	0	330	330	1,700

Table 2 indicates approximate shear values for different stories and story distortions. It is assumed for this tabulation that none of the elements at any deflection value had been damaged by prior excessive deflections.

It is apparent for this traditional type of building that the nonstructural items such as masonry filler walls do most of the work at low amplitudes due to earthquake or wind in both the structural and the dynamic sense. It is to be noted that the window area of the hypothetical building averages 33% of the

north-south wall areas and over 22% of the east-west wall areas. The steel frame, which has tremendous reserve capacity for both shear and the absorption of dynamic energy does not take much of the stress until the unreinforced masonry fails. Such wall failure, particularly under sustained ground motion, could occur in severe earthquakes with little or no danger of building collapse but with a large percentage of economic loss. This is an example of the fact that no material should be condemned for its earthquake history unless credit is given for any abnormal work load thrust upon it and until its potential has been rationally utilized in a logical structural-dynamic system.

The previous questions regarding the hypothetical building reaction to the March 22, 1957, San Francisco earthquake can be answered by reference to Fig. 3, 4, and 5 and Table 2. From Fig. 3 it can be shown that the greatest known shear distortion occurred in the 13th or 14th story. Assuming a deflection of as much as 0.02 in. per story, the participation of the steel frame (Table 2) would be only 8% of the total shear resistance. The steel would be stressed to only approximately 3,000 psi (due to earthquake) at one or more locations in this story. The material doing most of the work, the unreinforced brick masonry, was stressed to approximately 7% of its flexural and 17% of its shear estimated rupture values at the points of greatest unit stress as computed by relative rigidity. This story could have withstood approximately twice the distortion without local filler wall or other rupture (ultimate value approximately 25% g) and yet its energy-absorbing capacity had not been utilized.

The distortion of lower stories was less, although greater rigidities invite greater relative shear. If 0.01 in. or 0.02 in. per story is assumed the resulting participation can be taken from Table 2. It is very unlikely that any story deflection except for the upper three levels exceeded 0.01 in. in shear alone. Fig. 3 is drawn between known points with reference to forced vibration shapes for the third mode. Table 3 indicates the ultimate capacities of the various elements, but with the steel values taken only to the yield point rather than to the much greater values at strain hardening. Because of structural-dynamic phenomena the energy value or "toughness" is a better measure of collapse resistance than ultimate strength.

There can be little doubt that the general conditions demonstrated numerically above for the traditional building have influenced judgment in determining code and general practice design values. However, in order to caution against any false sense of values or security the writer strongly invites the careful consideration of all the factors involved and a careful comparison of the traditional building with the modern structure.

A Modern 20 Story Building.—The City of Auckland, New Zealand, engaged the writer in 1956 as structural and seismological consultant to their architectural and engineering departments, in connection with a proposed Administration Building. This structure which was not under construction as of 1958, is 45 ft by 127 ft in plan with three stories below ground level and twenty stories above. It will be the tallest and most slender modern building in New Zealand and one of the most slender in any active seismic region of the world. The assignment was made particularly interesting by the fact that traditional items such as massive masonry or concrete filler walls, concrete fireproofing, and heavy partitions would be almost entirely nonexistent. The greater height-to-width ratio of the proposed building is 5 to 1 above street level. The problem was soon determined to be that of providing sufficient strength, flexibility, and energy absorption for earthquake emergencies and yet to have enough

rigidity to withstand windstorms without human discomfort. These two factors are basically opposed to each other for a structure of the given dimensions and modern construction.

After the development of preliminary designs of a structural steel rigid frame without rigid bracing or shear walls, an investigation was made of the analog response of several hypothetical 20-mass dynamic systems to recorded earthquakes. The Dominion Physical Laboratory of New Zealand had previously developed an electric analog and had already conducted certain experiments with a 10-mass system (5). Because no New Zealand earthquake recordings were available several complete "shadow" graphs of California earthquakes were carefully prepared from CGS records in such a manner as to be

TABLE 3.—ESTIMATED ULTIMATE CAPACITY

Element (1)	Approximate Capacity		Energy Valve	
	Percentage of g (2)	Percentage of Total (3)	Foot-Pounds (4)	Percentage of Total (5)
13th-Story North-South direction				
Brick Masonry	20.7	54	745	23
Concrete Fire-proofing	0.5	1	58	2
Concrete Stairs	9.5	25	1000	31
Tile Partitions	2.6	7	109	3
Steel Frame	4.9	13	1340	41
7th-Story North-South direction				
Brick Masonry	11.0	53	937	19
Concrete Fire-proofing	0.3	1	39	1
Concrete Stairs	3.6	17	1000	20
Tile Partitions	1.0	5	107	2
Steel Frame	4.9	24	2830	58
1st-Story North-South direction				
Brick Masonry	4.0	41	633	9
Concrete Fire-proofing	0.2	2	41	1
Concrete Stairs	2.1	21	1320	18
Tile Partitions	0.6	6	110	1
Steel Frames	2.9	30	5370	72
7th-Story North-South direction				
Brick Masonry	19.9	73	1220	22
Concrete Fire-proofing	0.3	1	37	1
Tile Partitions	2.3	8	214	4
Steel Frame	4.9	18	4033	73

suitable for use with the existing Dominion Laboratory equipment. These were provided the laboratory along with sixteen systems of dynamic characteristics each with ten masses and ten spring factors designed to be a dynamic equivalent of the proposed 20-story structure. In addition to the use of four actual earthquake records, four assumed damping factors were assigned and various spring factors were computed to represent the rigidity of the building frame both alone and with the possible additional participation of partitions and wall panels. Altogether sixty-four experimental runs were made, each for a complete United States earthquake record. The results of this work were not only

valuable as an aid to judgment in the specific assignment, but provide very enlightening basic research information.

Table 4 indicates the mass and spring factor systems that were furnished the Dominion Laboratory. The total mass was 14,650 kips. The spring factor for each composite story or mass number representing two coupled prototype stories was made equal to the product divided by the sum of the corresponding prototype spring factors. For example, the spring factor KV for the 5th analog mass, which is the dynamic equivalent of the 9th and 10th building stories, is

$$K_V \text{ (analog)} = \frac{K_q \times K_{10}}{K_q + K_{10}} \text{ (building)}$$

The above relationship can be derived from the facts that the sum of the deflections of the two coupled stories equals the deflection of the coupled story, while the shear is constant through each coupled story and equal to the analog shear. The prototype stiffnesses were developed from trial designs. The mass of an analog-story was made equal to the sum of the two corresponding prototype story masses. Periods and damping are the same for the analog as for the proposed building. Table 5 gives all available values of periods and corresponding damping factors in percentage of critical damping for the actual analog systems as used in the test series. Four complete records of actual earthquakes were used to excite motion and determine shears for each of the sixteen dynamic systems. These earthquakes are described in Table 6.

TABLE 4.—ALTERNATE DYNAMIC SYSTEMS FOR ANALOG TESTS

Mass Number	Mass, in Kips	Spring Factor or Stiffness System,[a] in kips per inch				Equivalent Building Stories (Coupled)
		A	B	C	D	
1	1680	630	540	1530	810	1-2
2	1520	1320	970	3300	1460	3-4
3	1500	1010	880	2520	1310	5-6
4	1550	940	830	2370	1240	7-8
5	1440	580	610	1450	920	9-10
6	1440	580	540	1450	810	11-12
7	1400	570	440	1430	670	13-14
8	1380	480	340	1200	510	15-16
9	1590	420	260	1050	390	17-18
10 (top)	1150	230	150	580	220	19-20
Average:		676	556	1688	834	

[a] With each of the four stiffness systems above, damping coefficients of 2%, 5%, 10% and 20% of critical damping were to be employed in the tests.

The average of the maximum base shears for all four nominal damping values for each earthquake is plotted on Fig. 6 against the fundamental period for each analog model. These are averages of the "envelope" maxima for

TABLE 5.—ANALOG CHARACTERISTICS

Stiffness System	Nominal Damping C/C_0 percentage	Fundamental Mode		Second Mode		Third Mode		Fourth Mode	
		T, in seconds	percentage Damping	T, in seconds	percentage Damping	T, in seconds	percentage Damping	T, in seconds	percentage Damping
A	2	2.68	2.2	1.14	2.15	-	2.2	0.518	3.3
	5	2.78	5.9	1.17	3.2	0.686	5.2	0.532	6
	10	2.76	11.0	1.15	8.1	-	9.5	0.518	13.8
	20	2.79	18.6	1.17	15.5	-	-	-	-
B	2	3.28	3.3	1.35	2.4	0.845	2.7	0.642	3.2
	5	3.26	5.1	1.35	4.4	0.836	5.5	0.640	8.4
	10	3.25	10.2	1.35	10	0.820	11.3	-	-
	20	3.27	21	1.29	18	-	-	-	-
C	2	1.94	3	0.77	2.2	0.494	3.2	0.372	2.5
	5	1.92	5	0.765	4.3	0.490	5.6	0.366	5.6
	10	1.94	11	0.765	8.2	0.480	10	-	-
	20	1.96	21	0.765	16.5	-	-	-	-
D	2	2.64	3.1	1.12	2.1	0.703	2.4	0.533	3.1
	5	2.64	5.1	1.11	4	0.695	5.7	0.526	4.3
	10	2.63	10.1	1.11	9	0.680	9.3	-	-
	20	2.68	19.2	1.11	17	-	-	-	-

TABLE 6.—EARTHQUAKE RECORDS

Location	Component	Date	Distance to epicenter in miles	Maximum Acceleration in percent of g	Modified Mercalli rating	Richter magnitude	Relative Intensity	
							C/Co = 0%	C/Co = 20%
(1)	(2)	(3)	(4)	(5)	(6)	(7)	(8)	(9)
Olympia, Washington	S 80° W	April 13, 1949	40	0.31	8	7.1	6.05	2.74
El Centro, California	N-S	May 18, 1940	30	0.33	7.5	6.7	8.94	3.36
El Centro California	N-S	Dec. 30, 1934	40	0.26	6	6.5	5.93	2.55
Santa Barbara, California	N 45° E	June 30, 1941	15	0.23	7	5.9	3.15	1.75

each damping system representing the entire response to the entire earthquake exposures. These average values are used for simplicity in illustrating the results. The absolute maximum base shears for all runs are shown by the upper dash line on Fig. 6. It can be seen that although El Centro 1940 produces the greatest base shears at all periods (that is, for all stiffness systems), at the shortest fundamental period the base shears from El Centro 1934 and Olympia 1949 are approaching those of El Centro 1940. El Centro 1934 is consistently greater in base shear than Olympia 1949 for this structure although, on the basis of the various earthquake ratings shown in Table 6, Olympia is rated somewhat greater than El Centro 1934. The reader should keep in mind that all of the data shown in Fig. 6 (and elsewhere for these tests) include the response of all natural frequencies of the analog model. The fundamental

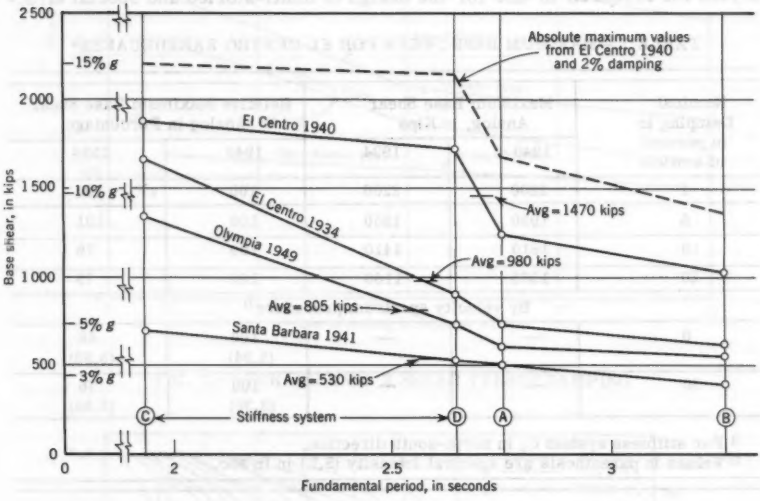


FIG. 6.—AVERAGE BASE SHEAR VERSUS FUNDAMENTAL PERIOD

mode is shown here only for identification simplicity. The periods of the highest four modes are given in Table 5. The shears developed by stiffness system D are relatively greater for the 1940 El Centro record than for the other three records.

Another interesting finding was that for stiffness system C the 1940 and 1934 El Centro earthquake produced the same absolute maximum base shears for the low damping values. Table 7 shows these shears, the relative shears for these two earthquakes, and the available relative earthquake intensities from a velocity spectrum procedure. The agreement in relative intensity between the multi-mass model response to these two earthquakes and the velocity spectrum rating is fair at the 20% damping value (70% versus 76%). How-

ever, at the low damping values there is poor agreement (101% versus approximately 70% at 5% damping). For El Centro 1940 considered alone, the base shear obtained with the multi-mass tests at 2% damping is 1.40 times that at 20% damping. This compares with the spectrum ratings for the same conditions of 1.7 at 2% damping to 1.0 at 20% damping (20). The variations are more pronounced in consideration of shear distribution over the height of the structure, Fig. 1(b). System C has no natural period longer than 2 sec and nine natural periods below this value. The spectrum ratings are for the encompassing period ranges of 0.1 sec to 2.5 sec. There is obviously some mechanical error in each procedure but this should be of insignificant magnitude compared to the nature of the problem and also to the differences noted above. Although the average-velocity spectrum basis is not intended to be precise it would seem that the differences indicated are sufficient in the probable critical range of 5% to 10% damping to indicate the desirability of special dynamic analyses for research in and for the design of multi-storied and special structures. Modern buildings without the reserve strength of non-computed elements and materials need particular attention if optimum resistance is to be developed at lowest first cost and with lowest non-structural repair costs.

TABLE 7.—MAXIMUM BASE SHEAR FOR EL CENTRO EARTHQUAKES[a]

Nominal Damping in in percent of critical	Maximum Base Shear Analog, in Kips		Relative Maximum Base Shear Analog in Percentage	
	1940	1934	1940	1934
2	2200	2200	100	100
5	1930	1950	100	101
10	1810	1410	100	78
20	1575	1100	100	70
By velocity spectrum procedure[b]				
0	—	—	100 (8.94)	66 (5.93)
20	—	—	100 (3.36)	76 (2.55)

[a] For stiffness system C; in north-south direction.
[b] Values in parenthesis are spectral intensity (S.I.) in ft/sec.

The variations in base shear for each earthquake and for the four nominal coefficients of the test series are shown in Fig. 7 as are the absolute maximum base shears that are obtained. Although an increase in damping reduces the base shear values the rate of increase is greatly reduced above 10% of critical for this building. It might be assumed that the 20% values would hold for any greater damping values. It is to be noted that the Santa Barbara record produced practically constant (maximum) base shears at all damping values and also that the 20% value shears are not a great deal less than for 10% damping under any earthquake. The effectiveness of damping might be somewhat greater, however, for more rigid structures with shorter periods where the fundamental (and most responsive) mode would be closer to ground waves of greater energy. However, the greater stiffness would invite greater shear (Fig. 6).

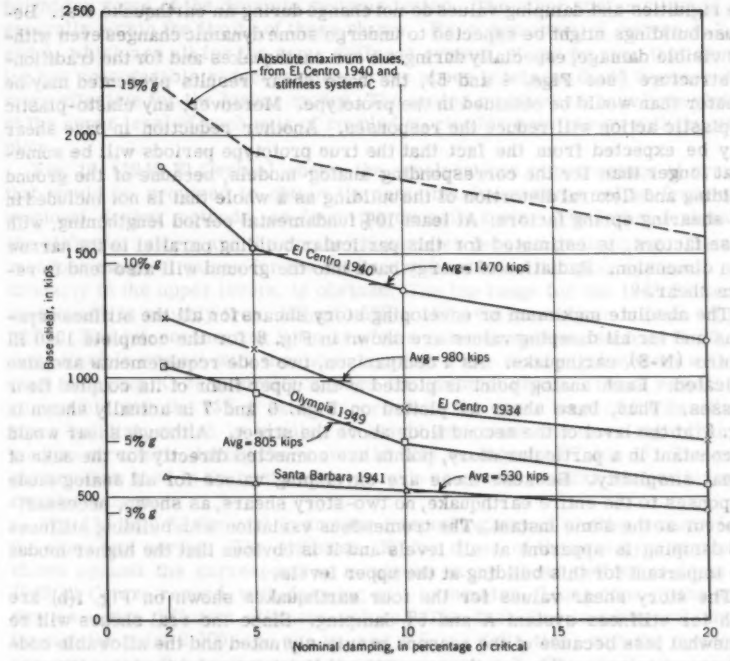


FIG. 7.—AVERAGE BASE X SHEAR VERSUS DAMPING

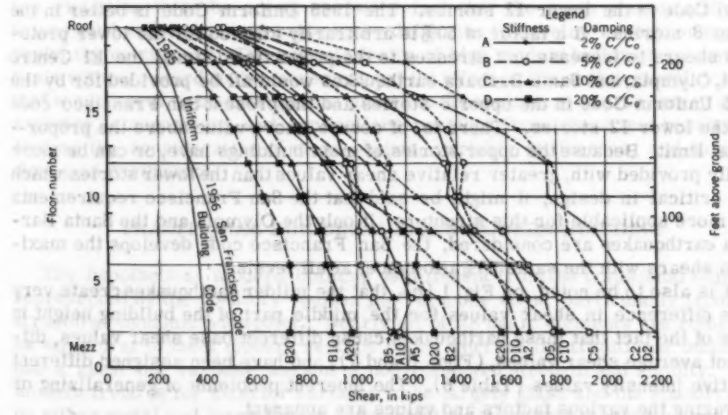


FIG. 8.—ELECTRIC ANALOG SHEARS FOR 20-STORY BUILDING

These analog results are for constant dynamic or elastic systems wherein the rigidities and damping values do not change during an earthquake test. Because buildings might be expected to undergo some dynamic changes even without visible damage, especially during severe earthquakes and for the traditional structure (see Figs. 4 and 5), the base shear results presented may be greater than would be obtained in the prototype. Moreover, any elasto-plastic or plastic action will reduce the responses. Another reduction in base shear may be expected from the fact that the true prototype periods will be somewhat longer than for the corresponding analog models, because of the ground yielding and flexural distortion of the building as a whole that is not included in the shearing spring factors. At least 10% fundamental period lengthening, with these factors, is estimated for this particular building parallel to its narrow plan dimension. Radiation of energy back into the ground will also tend to reduce shear.

The absolute maximum or enveloping story shears for all the stiffness systems and for all damping values are shown in Fig. 8 for the complete 1940 El Centro (N-S) earthquake. As a comparison, two code requirements are also indicated. Each analog point is plotted at the upper floor of its coupled floor masses. Thus, base shear as plotted on Figs. 6 and 7 is actually shown in Fig. 8 at the level of the second floor above the street. Although shear would be constant in a particular story, points are connected directly for the sake of visual simplicity. Because these are enveloping values for all analog mode responses to the entire earthquake, no two-story shears, as shown, necessarily occur at the same instant. The tremendous variation with building stiffness and damping is apparent at all levels and it is obvious that the higher modes are important for this building at the upper levels.

The story shear values for the four earthquakes shown on Fig. 1(b) are each for stiffness system A and 5% damping. Since the real shears will be somewhat less because of the reasons previously noted and the allowable code unit stresses are well below the proportional limit, it can be seen that the prevailing codes generally provide for the three milder earthquakes without structural failure. For this structure, with rigidity system A and 5% damping, the 1956 San Francisco Code adheres better to natural factors than the Uniform Code in the lower 12 stories. The 1955 Uniform Code is better in the upper 8 stories. If a factor of 50% is arbitrarily allowed for the lower prototype shears to increase unit stresses to the proportional limit, the El Centro 1934, Olympia, and Santa Barbara earthquakes would all be provided for by the 1955 Uniform Code in the upper 8 stories and the present San Francisco code for the lower 12 stories. There is, of course, more value above the proportional limit. Because the upper stories of most buildings have, or can be more easily provided with, greater relative shear values than the lower stories which are critical in design, it might be said that the San Francisco requirements are more applicable for this structure. If only the Olympia and the Santa Barbara earthquakes are considered, the San Francisco code develops the maximum shears with the same 50% allowance, at all levels.

It is also to be noted, on Fig. 1 (b), that the milder earthquakes create very little difference in shear values for the middle part of the building height in spite of the fact that these earthquakes cause different base shear values, different average shear values, (Figs. 6 and 7), and have been assigned different relative intensity values (Table 6). The inherent problems of generalizing or averaging the various factors and values are apparent.

Fig. 9 (1940, El Centro) shows the relative shear distribution with story height for some of the dynamic systems tested. The other systems tested are generally within the limits of those shown. By comparison of curves 1, 2, 3, and 4, which are all for the same stiffness system, it can be seen that damping has considerable reducing effect at the upper levels, no doubt because it is more effective for the higher modes. The analog mass points have been plotted at the upper level of each pair of coupled stories for consistency with the other plots.

Fig. 10 (1940 El Centro) shows the accelerations in percentage of gravity that would be required to obtain the same maximum shear values from conventional design methods, as from the dynamic tests. The letter designates the stiffness system and the number designates percentage damping. The tremendous range of values for the various stiffness and damping systems, particularly in the upper levels, is obvious. The top range for the 1940 El Centro earthquake is roughly from 12%g to 55%g while the base shear is from 5%g to 15%g. The interconnecting lines are for a common system, such as B-20, the most flexible system with the most damping. The most rigid system with the least damping, C 2, naturally suffers the greatest shear. These results are compatible with the 13% g value recorded at the upper level of the San Francisco building, which is similar in height and mass but more rigid than the modern structure, during the very mild 1957 earthquake (Table 1). The other earthquakes used in the test series provide somewhat similar shapes but with smaller values.

Fig. 11 (1940 El Centro) is another interesting way of plotting results from the same test series. The stiffness, K, for three of the prototype stories is shown against the corresponding maximum story shear deflection from the 1940 El Centro record, with damping as a parameter. Lines connect the same stories under different stiffness values. The dash line is arbitrarily drawn through the point 2,000 kips per in. and 1.0 in. deflection, with the deflection proportional to the reciprocal of the square root of K. The similarity in slope is generally apparent except at the lower damping values where this "averaged" relationship fails. All plotted points represent the results of the 1940 El Centro earthquake on the proposed building. The great amount of story deflection at low rigidities is to be noted, as is the fact that the much greater stiffness values still require considerable story deflection to develop enough energy to resist the earthquake. The seismic design of high modern buildings on a static basis without regard to the movement and its effect on the architectural "clothing" would seem to be a dangerous practice. There are, of course, many other analyses, comparisons and applications possible from these test results including the consideration of mode-shapes, variable stiffnesses, and damping during an earthquake.

TRADITIONAL BUILDING VERSUS MODERN BUILDING

The hypothetical modern building is different from the traditional building represented by the 15-story "guinea pig" in many ways, particularly from the structural-dynamic viewpoint. Nearly all of its basic elements are computed as structural to meet modern seismic codes whereas the traditional buildings had a great but variable amount of non-computed strength and rigidity. The modern trend is for exterior surfaces to be largely glass and the spandrels to be either metal and insulation or lightweight masonry or concrete units. The

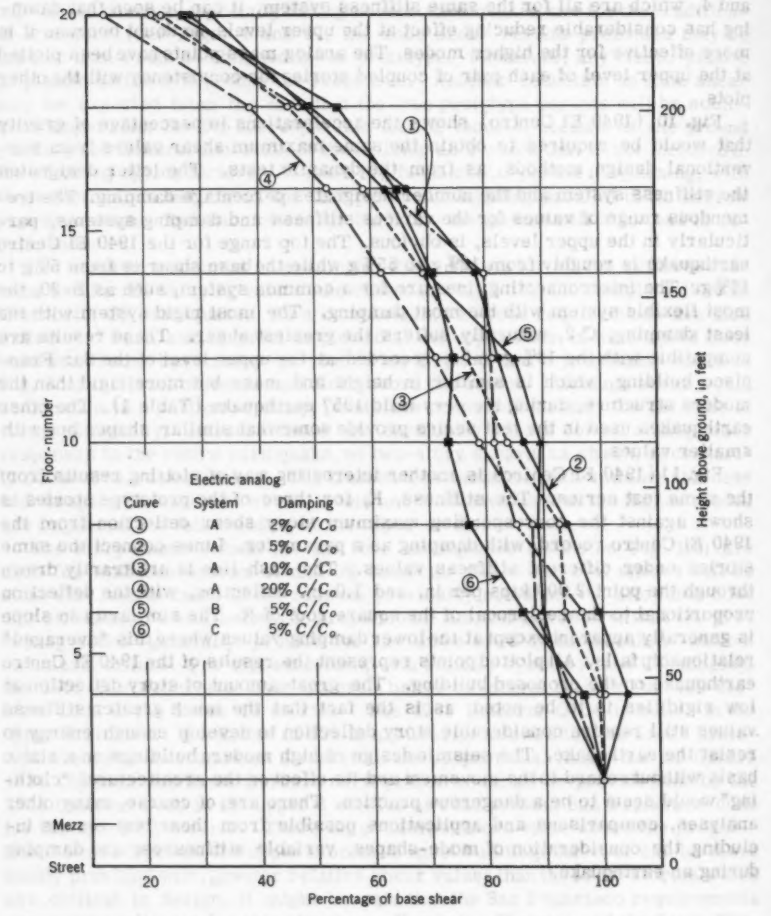


FIG. 9.—SHEAR DISTRIBUTION FOR MODERN BUILDING—1940 EL CENTRO

partitions are often of lightweight materials of little rigidity. The stairs must be allowed to yield or be considered expendable. The fireproofing is of lightweight material offering little rigidity as compared to the frame. The framework, regardless of its design basis, must be somewhat heavier and stiffer than for the traditional building for which no earthquake provision, per se, was made. The frame is "on its own" as to the structural-dynamic value of the building. The comparisons shown in Table 8 are average values for the two types of buildings.

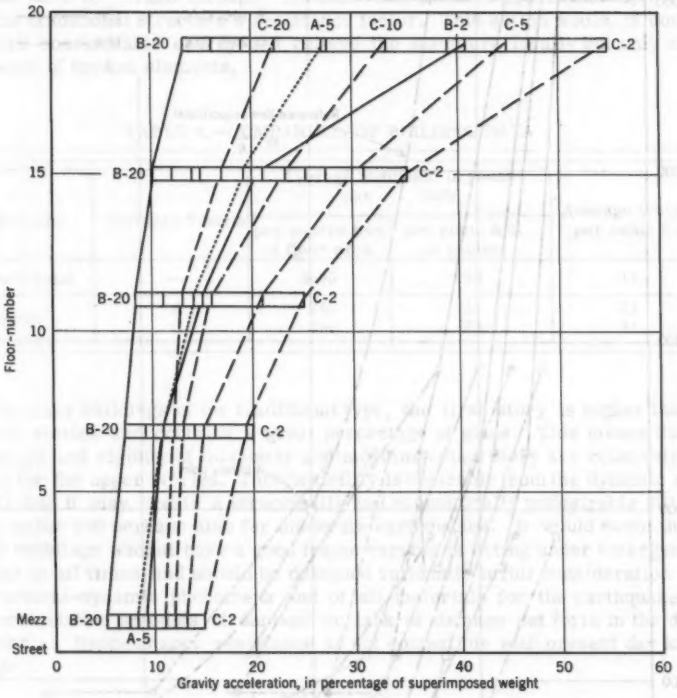


FIG. 10.—EQUIVALENT ANALOG ACCELERATIONS—1940 EL CENTRO

If it were postulated that seismic shears would be proportional to the square root of the product of unit weight and unit stiffness, the traditional building shears would be twice to four times greater (in the undamaged condition) than those in the modern building. Because shears for the latter are considerable (Figs. 1(b) and 8) in relation to code requirements, it is obvious that either cracking of the traditional walls must occur under such disturbing forces or the older buildings are much stronger than the modern ones at low distortion values. Actually, both conditions are realized.

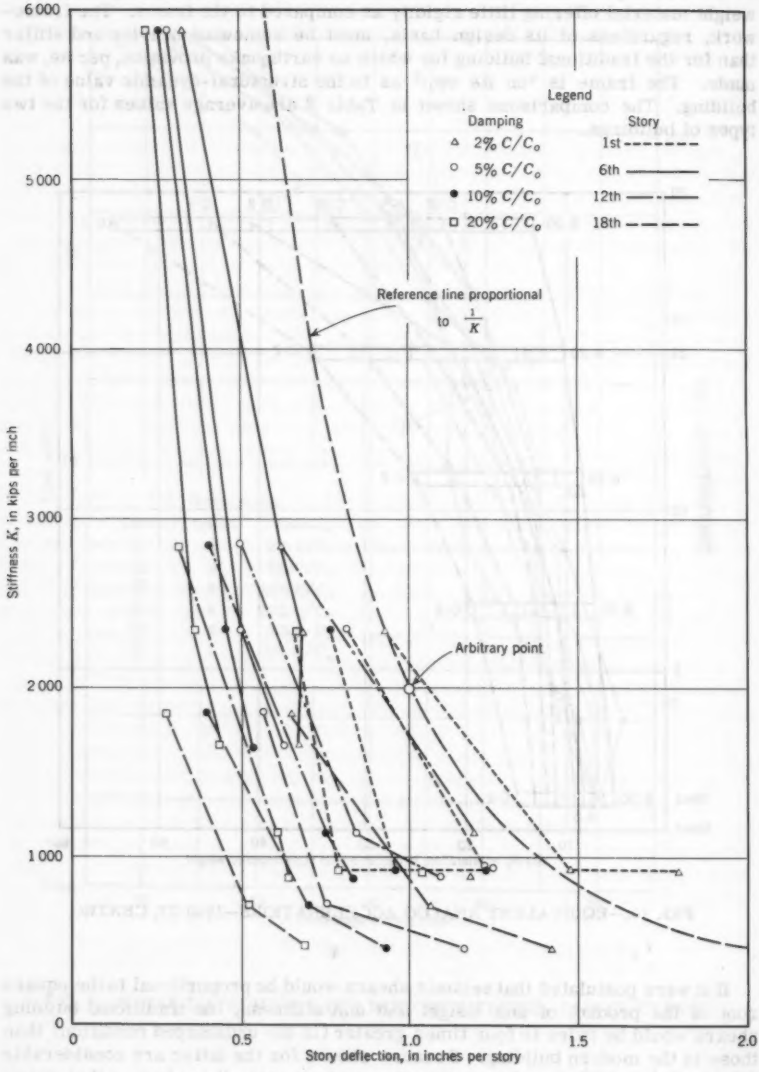


FIG. 11.—STORY DISTORTION IN MODERN BUILDING—1940 EL CENTRO

Fig. 12(a) indicates the comparative strengths and stiffnesses for the third story down, from the top, of both the traditional and the modern buildings and Fig. 12(b) is the same for the ninth story, from the top, of each building. The Traditional building, being more rigid and stronger but more brittle, and the Modern building, being stronger and tougher for greater deflections, a great difference is shown for the two buildings. If the graphs were extended to the ultimate strength for the steel, or even to greater deflections, the reserve energy value would be much greater for the modern building with its heavier framework. In consideration of Fig. 11, it is apparent that a major shock would have to "crash through" the deflection peaks of approximately 0.05 in. on the traditional structure's resistance factor. This action would, of course, absorb considerable energy and relieve the structure locally but only at the expense of broken elements.

TABLE 8.—COMPARISON OF BUILDING DATA

Building	Stiffness System	Average Stiffness, in pounds per inch		Average Weight, per cubic foot
		per square foot of floor area	per cubic foot of volume	
Traditional	—	2400	190	17
Modern	A	240	21	11
	C	590	53	11

In many buildings of the traditional type, the first story is higher than the other stories and contains a great percentage of glass. This means that the strength and rigidity of this lower and most important story are relatively less than for the upper stories. This flexibility is desirable from the dynamic sense (31) but it may create a structurally and economically undesirable situation for major and perhaps also for moderate earthquakes. It would seem that all tall buildings should have a good frame capable of acting under emergencies, if not at all times, and should be designed rationally in full consideration of all structural-dynamic phenomena and of all materials for the earthquakes and corresponding amounts of damage or lack of damage set forth in the design criteria. Happenstance resistance is not compatible with present day knowledge.

THE DESIGN PROBLEM

The valuable data obtained from the analog tests for the modern building indicate the shears that can be expected in the prototype for various earthquakes. These data do not indicate, however, that the maximum shears should be used in design at code unit stresses. Not only would the cost of construction be prohibitive, but the computed risk would not justify this procedure, and, lastly, the basic question of allowable unit stresses and building deflection must be honestly faced with the full realization that a 1940 El Centro-type earthquake does not happen very often within 30 miles of the structure under consideration. Moreover, the record of multi-story buildings in major earthquakes has certainly not always been catastrophic and in some cases has been fairly good, even though many such buildings were designed to be only wind-resistant. Here

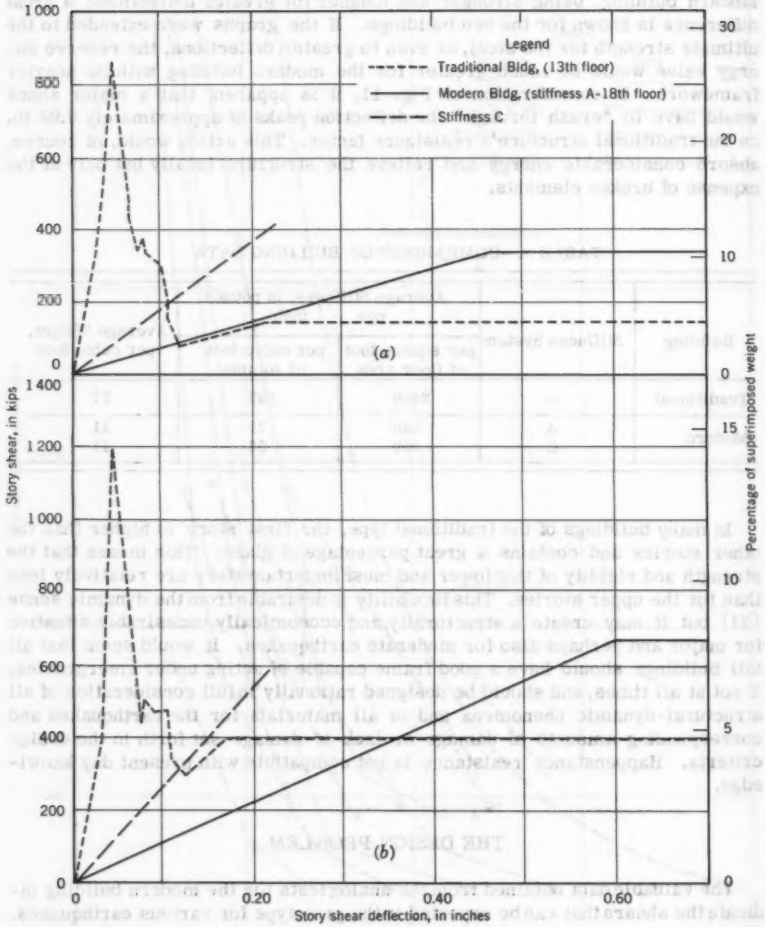


FIG. 12.—LATERAL LOAD RESISTANCE FOR TWO BUILDING TYPES

is the point where the engineer has to include economics, risk, probability, public welfare, and so forth, in his thinking.

For cases where adequate dynamic analyses for special or unusual structures indicate shears considerably greater than the code-shear values, the following general steps (not necessarily in order) are indicated to convert the dynamic analyses into a final design:

1. Compare the earthquake or earthquakes used in the analysis to the probable earthquake risk of the locality in question. After careful consideration of available local earthquake history, intensity, duration, frequency, damage, geology, possible dominant site periods, soil conditions, probability factors, and so forth, make any indicated adjustments to the shear values obtained.

2. Correct the shears in consideration of any effects of flexure and ground movement on the building periods and response.

3. Compare the proposed structure to those of a similar type or size that have been subjected to severe earthquakes. In so comparing, however, fully consider all noncomputed elements and materials. Fully utilize all possible elements and materials in resistance but with consideration of relative rigidity and strength at various distortions.

4. Determine the maximum deflection for human comfort and occupancy in probable windstorms. In spite of the technical literature on building sway there is little information available on the actual wind performance of modern skyscrapers that do not utilize massive curtain walls, partitions, and stair systems. It is hoped that discussion of this paper will produce more data on this matter which would be most useful to the profession. By analogy to the 15-story "guinea pig" building (Figs. 4 and 5) and other references, it is obvious for traditional buildings, that may have been designed with a wind deflection limit of 0.002 H to 0.003 H, (H is the height of building or story) that the steel frame can not function because of its "clothing," and the "clothing" provides most of the rigidity (21, 22, 23, 24, 25, 26). Thus for modern lightweight building design, there are few applicable empirical data or criteria. This problem is one in dynamics and it also involves human perception which is apparently more sensitive to acceleration from gust effects than amplitude (21, 26, 27, 28, 29). This subject is inserted here because it is part of structural dynamics and because there is little value in conducting a complete seismic design until the affect on the structure of wind design is first determined.

5. The question of allowable seismic motion should be considered with reference to possible damage to the nonstructural elements. Because a major earthquake is a relatively rare occurrence that is a frightening experience to most people, it does not seem necessary to stiffen a building because of human reaction to earthquake motion. Panic precautions would be more logical. The architectural "clothing," which may constitute an appreciable part of the total cost, must either be fully detailed and inspected during construction to allow for the structural deflection under earthquake stimulus, or its materials will fail as they try to do the work. It is basic, of course, that all materials must be tied to a building, but there are ways of doing this tying that can prevent or minimize costly damage.

6. Make a trial design based on applicable-code wind and seismic forces and the deflection considerations previously mentioned. Compare the lateral shear value of this structure at the code unit stresses to the dynamically determined seismic shears. The better the code applies to the particular building, the more constant the ratio of the two will be. In any event, the difference may still be appreciable and has to be accounted for.

7. Consistent with the various psychological, legal, and economic considerations outlined, the goal is to provide the most flexibility, damping and energy absorbtion in order to keep the true shears to a minimum. The addition of bracing, shear walls, or other rigid elements is not desirable for a multi-story, naturally flexible building or structure except as expendable items or as a last resort, because such items not only have a poor seismic history but also inject abrupt transitions of rigidity into the system and increase over all rigidity and thus dynamic shear (Fig. 6). If the design contemplates such items as expendable elements that would stiffen the structure for wind and mild earthquakes, there should be another ductile system in reserve for major earthquakes. With ductile materials or ductile combinations of materials there is a double opportunity—first, to stress to the yield point, and, second, to provide for severe but rare emergencies by absorbing energy in the elasto-plastic or inelastic range as long as secondary buckling does not govern. The latter procedure can be of tremendous value in preventing catastrophes and saving money for the owner.

8. After developing a trial design, the rigidity of the system should be checked and, if necessary, the system should be re-analyzed and the structure revised to meet the specific earthquake criteria.

9. A step-by-step or "plateau" design procedure using two or more earthquakes of different probabilities and energy values is logical and desirable. For example, the El Centro-1934 dynamic shears or the applicable code might be met at code stresses and the El Centro-1940 dynamic shears could be provided for (with or without permissible failures) under high stress, and in the inelastic range, for energy absorption.

10. In the final analysis, sound engineering judgment based on structural-dynamic phenomena must prevail to design consistent, reliable, and economical structures.

Although this entire procedure as outlined is not necessary for all structures, it can well be used as a basis for the design of special structures, for research, and for an approach to code problems. In many cases, the combination of dynamic analyses, consideration of deflections and of all the materials, and the use of limit-design techniques for emergency loading can create a consistently good structure at nominal design coefficients referred to code procedures and unit stresses. The excellent behavior of the high Tower Latino-Americana, in Mexico City, Mexico, which was dynamically designed with a base shear of approximately 4% g (30), in the Mexico City earthquake of 1957 is an example of the value of the structural-dynamic approach and attention to detail in design and construction.

OTHER TYPES OF STRUCTURES

There is another type of building that may be termed intermediate between the two types already mentioned. This is the multi-story type which is designed under modern seismic codes and which has an appreciable amount of concrete or masonry wall area. The difference between this and its traditional predecessor is that these walls are used structurally and are well anchored to the building. The buildings thus produced are more rigid and may be subjected to a far greater dynamic shear than the codes prescribe. This may be estimated by analogy or extrapolation of the various results previously pre-

sented. With allowance for the nature of the problem and the use of high unit stresses and the consideration of distortion and energy absorption, a good, balanced design may be achieved for any intensity of earthquake which may be desired. For structures important enough to allow the extra expense, a reserve ductile framework is most desirable in withstanding severe earthquakes. This type of building may be expected to "hold together" much better and longer than its unreinforced and untied predecessor the traditional or pre-seismic-code type, even though its rigid elements might crack. In cracking they will absorb energy and provide more damping value under continued motion. This building's spring factor curves would thus be more extended after the peak values than shown in Figs. 4 and 5 for plain masonry. If the building is of short period, as compared to the earthquake waves, and very strong, it may not even suffer a crack under a severe shock.

Structures such as tank towers have generally had a poor seismic history. They involve heavy masses generally supported by X-bracing high above their foundations. This is a vulnerable form of construction, because it is rigid and determinate, and its axial-loaded bracing members have relatively little reserve material volume to absorb energy in the high stress and plastic range required under the severe loading of major earthquakes. Moreover, these structures, as well as many other types of structures other than buildings, do not enjoy the benefit of noncomputed filler walls, partitions, stairs, and so forth. The stretched and failed rods, the pulled anchor bolts, and the fallen tanks constitute ample recorded evidence of the energy in earthquakes and the fact that many an old building has remained vertical only because its structure was protected by coincidental nonstructural elements.

The engineer responsible for framed structures without "clothing" would do well to think not only in terms of relatively high possible forces, but also in terms of high unit stresses and energy dissipation under dynamic phenomena for safety, economy, and consistency of results.

Other violent natural releases of energy such as windstorms, hurricanes, and large ocean swells, and also man's blast forces and the impact of ships on wharves, all involve the factors of probability, computed risk, energy-absorption, and so forth. They should therefore also be dealt with in terms of realistic forces, high unit stresses for rare emergency occurrences, and as problems in structural-dynamics and energy rather than statics alone.

CONCLUSIONS

The following general conclusions have been reached largely from the research efforts reported in this paper, but they are necessarily also dependent in some degree on prior research, and observation and design experience.

1. Moderate to severe earthquakes produce deflections and lateral reactions the amount of which depends to a considerable degree on the structural-dynamic characteristics of each specific structure. In general, the dynamic shears developed by major earthquakes are greater than those required by the earthquake provisions of building codes, particularly for rigid buildings and buildings with low damping values.

2. The strength and rigidity of traditional buildings with non-computed filler walls, partitions, and stairs are many times those of the frames intended to provide the entire structural resistance. Although this value varies

widely between buildings and between various stories of the same building, it generally accounts for the relatively good seismic and windstorm history of multi-story steel frame buildings of this type. However, these frames cannot function effectively in lateral resistance under severe shocks until the surrounding rigid materials have failed, with perhaps considerable economic loss. This fact plus the random character of the noncomputed wall resistance justifies the more advanced design techniques of today.

3. The modern building without any appreciable lateral resistance except in the frame proper will be subject to large story distortions in major and, to an appreciable degree, in moderate earthquakes in spite of meeting present-day seismic codes. Engineers and architects should revise the customary procedures of injecting rigid but brittle elements into otherwise flexible structures without provision for story distortion because the nonstructural damage may constitute not only a severe financial loss but also a physical danger to persons in and about such buildings. All items should either be permitted to move with the structure or be expected to fail and should be so classified.

4. Rigid bracing members or shear walls in a modern glass-walled multistory building stiffen the structure against mild earthquakes and wind but also invite greater seismic shears. Unless designed for more shear than code values generally prescribe, such rigid elements should be considered expendable and other provisions made for severe emergencies. Where a ductile moment-resisting frame cannot be provided for all the design lateral forces, the design can be accomplished on a "plateau" basis. This involves providing for a moderate shock of approximately a 15-yr frequency wherein rigid elements carry the code or other shear and also provide rigidity for the normal wind force and drift considerations, or providing for a severe but possible earthquake of 40-yr or 50 yr frequency during which the rigid elements would fail and allow a reserve ductile frame to then provide controlled flexibility, absorb energy, and prevent building collapse.

5. The allowable flexibility of a tall building may be determined by human perception of motion under frequent wind conditions, or it may be determined by the manner in which the architectural materials are employed.

6. Present-day seismic codes are reasonably adequate for moderate earthquakes but because of the oversimplification of a very complex subject they cannot produce consistent results. The real earthquake values of various types of buildings and structures are not necessarily proportionate to the lateral-force factors used in design. Stated another way, code requirements are not producing constant safety factors because of too much reliance on coefficients without adequate regard to the structural-dynamic phenomena and ultimate resistances involved in various types and rigidities of construction. Codes can and will be improved, but no designer or owner should assume that any code can replace sound conscientious engineering and the detailed knowledge needed to provide resistance against the tremendous energy and mathematical complexity of a severe earthquake.

7. The fundamental period of vibration is a logical index of relative base shear for general code purposes. However, the height and width of the building considered either individually or together are not adequate indicators of the period of modern, flexible structures without walls. These periods should be specifically computed or improved approximate methods should be utilized.

8. Building codes should encourage structural-dynamic analyses, realsitic forces and shears, inelastic design procedures, ductility, and moment-resisting frames for severe emergencies.

9. Competent supervision and inspection of construction are essential for obtaining the results desired from code requirements and design procedures.

10. Damage, if not found and completely repaired after each earthquake, is cumulative except for ductile and tough materials for which minor yielding may be of no consequence. Thus, a building may not fare as well in future shocks if only plaster and paint are employed in its repair operations.

It is hoped that many important reasons for apparent paradoxes between design practice, observed behavior, and research have been demonstrated and that a better understanding of seismic shears and building resistances has been provided herein. It is also hoped that such procedures as designing a frame for forces it cannot be loaded with because of accidental design features and highly variable surrounding materials, and designing a glass or skin-walled building without regard to the results of necessary lateral movement in earthquakes, can be replaced in time with balanced structural-dynamic designs that consider all the many factors, deal in terms of energy, and have a realistic approach to distortions and unit stresses. The results can be much more satisfactory, predictible and consistent, and cost of construction need be no more. It would certainly be less for the same calculated risk.

ACKNOWLEDGMENTS

The electric analog responses for the proposed 20-story building were obtained in the Dominion Physical Laboratory, Department of Scientific and Industrial Research, Lower Hutt, New Zealand, M. J. Murphy was in charge of this work for the Director. The proposed building is for the City of Auckland, New Zealand, with A. J. Dickson Director of Works and City Engineer, A. T. Simmons, Assistant to the City Engineer, T. K. Donner, Chief Architect and V. G. Coleman, Senior Structural Engineer. The writer extends his gratitude to these men and to Mr. Murphy and the Laboratory personnel for their splendid efforts and cooperation in this work and also for permission to use the experimental data for more general purposes of research.

The records for the analog experiments were prepared in the writer's office from United States Coast and Geodetic Survey accelerograms. The original work for the proposed New Zealand building was extended to more general application and the resistance studies of the traditional building were conducted as part of the voluntary research program of John A. Blume and Associates, Engineers. Eric Elsesser of the firm's Research Division took an active part in the mathematical studies reported herein.

APPENDIX. BIBLIOGRAPHY

1. "United States Earthquakes," U. S. Coast and Geodetic Survey, U. S. Govt. Printing Office, Washington, D. C.

2. "A Mechanical Analyzer for the Prediction of Earthquake Stresses," by M. A. Biot, Bulletin, Seismological Soc. of America, Vol. 31, No. 2, April, 1941.

3. "Computations on the Response of One-mass Undamped Structures to the El Centro Accelerograph Record," by Edward G. Robison, Watson Scientific Computing Lab., Columbia Univ., New York, N. Y.

4. "Spectrum Analyses of Strong-Motion Earthquakes," by J. L. Alford, G. W. Housner, and R. R. Martel, Contract N 6 ONR-244, Office of Naval Research, August, 1951.

5. "Electrical Analogy for Earthquake Stresses in a Multi-Story Building," by M. F. Murphy, G. N. Bycroft, and L. W. Harrison, Proceedings, World Conf. on Earthquake Engrg., June, 1956, Chapter 9.

6. "Shears in a Tall Building Subjected to Strong Motion Earthquakes," by T. P. Tung and N. M. Newmark, ibid., Chapter 10.

7. "On the Importance of Higher Modes of Vibration in the Earthquake Response of a Tall Building," by Ray W. Clough, Bulletin, Seismological Soc. of America, Vol. 45, October, 1955, p. 289.

8. "Earthquake Forces in a Tall Building," by Ray W. Clough, Civil Engineering, Vol. 26, January, 1956, p. 54.

9. "Lateral Forces of Earthquake and Wind," by Anderson, et al., Transactions, ASCE, Vol. 117, 1952, p. 716.

10. "An Engineering Study of the Southern California Earthquake of July 21, 1952, and Its Aftershocks," by K. V. Steinbrugge and D. F. Moran, Bulletin, Seismological Soc. of America, Vol. 44, April, 1954, pp. 39-429, Second Part.

11. "A Machine for Setting Structures and Ground into Forced Vibration," by John A. Blume, Bulletin, Seismological Soc. of America, Vol. 25, October, 1935, (a) p. 366. (b) 368-369.

12. "Period Determinations and Other Earthquake Studies of a Fifteen-Story Building," by John A. Blume, Proceedings, World Conf. on Earthquake Engineering, June, 1956, Chapter 11.

13. "Lateral Forces of Earthquake and Wind," by Anderson, et al, Transactions, ASCE, Vol. 117, 1952, p. 749.

14. "Reinforced Brick Masonry and Lateral Force Design," by H. C. Plummer and John A. Blume, Structural Clay Products Inst., Washington, D. C., 1953.

15. "Mineral Information Service," Calif. State Div. of Mines, May 1, 1957, pp. 1-5.

16. "Steady Forced Vibration as Influenced by Damping," by L. S. Jacobsen, Transactions, ASME, Vol. 52, 1930, p. 69.

17. "Friction in Buildings: Its Magnitude and its Importance in Limiting Earthquake Stresses," by M. P. White, Bulletin, Seismological Soc. of America, Vol. 31, April, 1941, pp. 93-99.

18. "A Dynamic Test of a Four-Story Reinforced Concrete Building," by J. L. Alford and G. W. Housner, Bulletin, Seismological Soc. of America, Vol. 43, January, 1953, pp. 14-16.

19. "Intensity of Ground Motion During Strong Earthquakes," by G. W. Housner, Contract N60NR-244, Office of Naval Research, August, 1952, p. 25.

20. Ibid., p. 14.

21. "Wind Forces on a Tall Building," by J. C. Rathbun, Transactions, ASCE, Vol. 105, 1940, pp. 1-82.

22. "Wind Bracing in Steel Buildings," Final Report of Sub-Committee No. 31, Committee on Steel, of the Structural Division, Transactions, ASCE, Vol. 105, 1940, pp. 1713-1739.

23. "Ground Vibration Due to Blasting and its Effect Upon Structures," by F. J. Crandell, Journal, Boston Soc. of Civil Engrs., April, 1949.

24. "Stiffness of Skyscrapers," by D. C. Coyle, Transactions, 1st Cong., International Assoc. of Bridge and Structural Engrs., Paris, 1932, pp. 535-539.

25. "Trussed Framing Stiffens Tall, Slender Buildings," by R. H. Bryan, Civil Engineering, August, 1956, pp. 54-55.

26. "Wind Pressure on a Model of the Empire State Building," by H. L. Dryden and G. C. Hall, Research Paper No. 545, Natl. Bureau of Standards, Journal of Research, Vol. 10, April, 1933.

27. "Human Engineering Guide for Equipment Designers," by W. E. Woodson, Univ. of California Press, 1954.

28. "Human Susceptibility to Vibration," by F. Postlethwaite, Engineering, Vol. 157, 1944, pp. 61-63.

29. "Relation Between Motion and Sensation," by D. C. Coyle, Civil Engineering, May, 1931, p. 200.

30. "Aseismic Design of Latino Americana Tower In Mexico City," by L. Zeevaert and N. M. Newmark, Proceedings, World Conf. on Earthquake Engineering, June, 1956, Chapter 35.

31. "Experimentally Determined Dynamic Shears in a Sixteen-Story Model," by L. S. Jacobsen and R. S. Ayre, Bulletin, Seismological Soc. of America, Vol. 28, October, 1938, p. 269.

32. "Intensity of Ground Motion During Strong Earthquakes," by G. W. Housner, Contract N60NR-244, Office of Naval Research, August, 1952, pp. 56-59.

33. "Report of the Committee for Seismic Tests on Structures," Publication No. 1, Building Research Inst., Ministry of Construction, Tokyo, September, 1947, to August, 1950.

34. "Report on Behavior of Structural Elements Under Impulsive Loads, I and II," by J. B. Wilbur and R. J. Hansen, Contract No. W-19-016-eng-3215, Massachusetts Inst. of Technology, April, 1950, and November, 1950.

35. "Tests to Determine the Behaviour of Riveted Joints of Steel Structures under Alternate Bending Moments," by Rio Tanabashi, Memoir, Vol. VIII,

No. 4, College of Engineering, Kyoto Imperial Univ., 1935, pp. 164-190 (in English).

36. "Static Tests on Welded Joints of Steel Structures subjected to Bending Moments," by Rio Tanabashi, Journal, Japanese Soc. of Welding, Vol. 9, 1939, pp. 587-598 (in Japanese).

37. "A Basis for Aseismic Design of Firmly Founded Structures," by L. E. Goodman, E. Rosenblueth, and N. M. Newmark, Transactions, ASCE, Vol. 120, 1955, pp. 782-802.

38. "Some applications of probability theory in aseismic design," by E. Rosenblueth, Proceedings, World Conf. on Earthquake Engrg., June, 1956, Chapter 8.

39. "Reglamento de las Construcciones y de los Servicios Urbanos en el Distrito Federal," Gaceta Oficial del Departamento del D. F., Federal District Dept., Mexico, D. F., September, 1957.

40. "The Behavior of One-Story Brick Shear Walls," by J. R. Benjamin and H. A. Williams, Proceedings Paper 1723, ASCE, July, 1958.

41. "Mexico Earthquake,—July, 1957," by R. W. Binder, Proceedings, AISC Annual Convention.

42. "Earthquake Design Criteria For Stack-like Structures," by John R. Rinne, Proceedings Paper 1696, ASCE, July, 1958.

DISCUSSION

LYDIK S. JACOBSEN[3].—The author should be complimented on having produced an excellent and timely research paper in which he has combined theory, numerical analysis, experience, and good judgment to clarify ideas of how the traditional as well as the modern glass-wall structure can be assumed to resist earthquake loadings. Mr. Blume brings into the open the undeniable fact that vast differences exist between dynamic design values and legal code values for earthquake-induced shears. He shows that several factors, difficult to deal with in a quantitative manner, can explain, if not actually account for, all of these differences.

It is the writer's opinion that Figs. 4 and 5 constitute an important contribution toward enlightening the viewpoint of the structural engineer on this subject. An idea of the nonlinear character of a composite structure as well as its inherent energy-absorption capacity or hysteresis, has not been represented before with such clarity and simplicity. In spite of the fact that the author's work is hypothetical in some respects, it is undeniably based on sound common sense and on judgment educated by long experience.

Referring specifically to Fig. 4(b), it can be said that, due to variable clearances in the joints, a gradual coming into action of the composite structural ele-

[3] Prof. of Mechl. Engr., Chairman of Dept., Stanford Univ., Stanford, Calif.

ments will occur, and the positive slopes of each component curve might therefore have to be changed slightly. The peaks of these curves will certainly become rounded. As the author readily admits, considerable uncertainty exists about the parts of the curves with negative slopes. This means that the "two humped" character of the total resistance of the first story in the N-S direction might be either more or less distinct than represented. These details of a possibly changed curve appearance do not detract at all from the salient fact that a great deal must have happened to the first story by the time its shear deflection becomes mainly dependent on the resistance of the steel frame.

The amount of energy lost by the time the shear deflection reaches the value of 0.15 ins is 40 ft-lbs, 1,300 ft-lbs, 130 ft-lbs, and 1,800 ft-lbs, for the fireproofing, brick walls, tile partitions, and concrete stairs respectively, or a total of approximately 3,300 ft-lbs as compared to approximately 1,100 ft-lbs of elastic potential energy in the frame itself. Accordingly, for a shear deflection of 0.15 in. the story's specific damping capacity, defined as the ratio of lost energy to total energy, is 3,300/4,400, or 3/4, which is a relatively large ratio.

The question may now be raised as to what will happen if at this point, 0.15 in., the loading is reversed. Admittedly we cannot embark on pure speculation. An opinion should be substantiated, preferably by experiments on several full-scale composite structures. If such experiments are lacking or very few in number, a tentative opinion, obtained from carefully conducted experiments on composite structural elements of respectable size, may still be warranted as an heuristic answer to the question.

Based on references 1 to 6 the writer ventures to hazard the tenative opinion that a reversed loading on the first story of the building studied by the author will result in a mirror image of Fig. 4(b), beginning at a shear deflection located somewhere between 0.15 in. and 0.10 in. and reproducing, with softened features, the "two humped" characteristic of the building's original earthquake response. It will be expected that the loads at the two humps will reach values of 90 % of the direct loads, and that in so doing an amount of energy comparable to the 3,300 ft-lbs will be lost.

For a second reversal of shearing load the softening of the building's performance features may be so great that the two "humps" will merge to one, and the maximum load may be expected to decrease further. Consequently for many load reversals a progressive deterioration of the composite structure is inevitable. Just how additional reversals of load between the deformation limits of $\pm$ 0.15 in. will affect the successive maximum load values must remain an unanswered question for the present.

The writer's intention has been to point out, even more strongly than was done by the author, that joint friction and crack friction of structural composite elements can be responsible for the absorption, without return, of a great deal of vibrational energy. Moreover, for this to occur, the cracks need not be very large and extensive. Thus, if the total shear distortion of the first story ranges between $\pm$ 0.05 in., one-third of the previously assumed range, the specific damping capacity of the story, as obtained from Fig. 4(b), is approximately 0.7. Consequently, its equivalent viscous damping value, C/C_O, will be slightly more than 10 %. It is clear that the cracks in fireproofing and brickwork, corresponding to shear distortations of less than 1/16 in. per story, that is, 4×10^{-5} radians, will not be critical.

During 1957-1958 the writer had an opportunity to study damping in buildings on a research project sponsored by the California State Department of

Architecture at Stanford University, Stanford, Calif. A thorough survey of the literature, combined with tests on very simple types of joints have convinced the writer about the presence of surprisingly large amounts of damping in composite structural joints.

A. A. EREMIN,[4] A.M. ASCE.—The author has shown various limitations in the methods of analysis of seismic stresses in frame rigid structures. Furthermore, the author has shown that the seismic forces can not (as yet) be accurately determined. The seismic forces are diffcult to determine even at an assumed distance from the epicenter of an earthquake. Nevertheless, design of rigid frame structures, when performed in accordance with the recommended building codes, results in relatively safe structures. Obviously, further research is needed to determine the effect of dynamic forces on structural deformations, periods, accelerations and the effect of various rigid frame details on these factors. In rigid frame buildings the present trend is to place several floors below the ground surface. Therefore, the analysis of stresses should be extended by investigating the effect of various ground formations and the ability of the ground to absorb the seismic stresses.

It is gratifying to note that the author has graphically shown the effect of composite parts of wall panels in the multi-story rigid frame structures on distribution of the seismic forces. However, the effect of "grinding and hammering" of the broken parts of walls was not included in the graphs. After the composite parts of panel walls in building frames are cracked, the structure may behave in an entirely different manner than that assumed in the original analysis. It is difficult to assume that the seismic stresses in the cracked walls are accumulating.

The seismic research on rigid frames should also include consideration of the prestressed bracings recently introduced in construction of rigid multistory frames.

The author has made a valuable contribution to a study of the seismic stresses and deserves sincere appreciation.

EMILIO ROSENBLUETH,[5] M. ASCE.—The author's contribution marks a milestone in engineering seismology. It gives valuable quantitative information about the influence of characteristics such as stiffness and damping on the seismic response of tall buildings. More important, it shows the feasibility of accurate dynamic analyses of these structures. It gives qualitative pictures of shear distributions in diverse types of buildings, and points out most of the important variables in aseismic design.

Much more research is necessary in this field. It is true that reliable designs can be obtained by subjecting an idealized structure to one or several records of actual earthquakes. The method is, however, more expensive and time-consuming than a dynamic analysis to compute the first few natural modes of vibration, followed by a combination of the stresses in these natural modes. If the procedure for combining the natural modes is based on a study that extrapolates to small probabilities of failure under the action of the universe of possible earthquakes, it will be more reliable than the analysis based on responses to a small number of earthquakes. Nevertheless the writer hesitates to recommend

---

4 Assoc. Bridge Engr., Bridge Dept., Calif. State Highways, Sacramento, Calif.

5 Director and Research Prof., Inst. of Engrg., Univ. of Mexico, Mexico City, Mex.

the available probabilistic methods, such as the assumption that, for small probabilities of failure, design stresses should equal the square root of the sum of squared responses in the natural modes (38) (39) there is yet insufficient substantiation of the theory. Some indications (40) are that it may be satisfactory, whereas others (41) cast doubts on its adequacy.

Efforts intended to improve probabilistic theories of aseismic design seem, therefore, to be worthwhile. This is particularly true because for more refined assumptions, say including ground coupling or considering explicitly more than one component of earthquakes, analyses will become much more complex, and some simplicity is achieved by computing natural modes rather than seismic responses.

In the question of inelastic behavior, the writer agrees fully with Blume's advocation of elastic analysis to predict structural behavior under minor to moderate shocks, plus allowance for inelastic energy absorption under severe motions. Since there is, at present, no reliable method to make that allowance, the best that can be done is to design for stresses which are smaller than, and proportional to, those which would develop under a major earthquake if the structure even then behaved elastically. There is good reason in a multi-story building for taking the design shear distribution to be proportional to one based on the assumption of elastic behavior, for if a few stories were underdesigned, or the rest overdesigned, those few stories would be overly taxed in energy absorption. But there is no reason to assume that the underdesign of some frames, if the rest are sufficiently ductile, would not result in a better structural performance, under a wide range of earthquake intensities, than an elastic distribution, besides resulting in greater economy.

Inelastic magnification of dynamic torsion is one phenomenon about which, as far as the writer is aware, nothing is known except that it may be important.

These considerations point out the immediate need for research of inelastic behavior of multi-story buildings. Differences in energy absorption capacity of various systems (unaided frames versus X-braced frames versus shear walls, and so on) are at present either ignored or taken into consideration through crude, almost intuitive, variations in seismic coefficients. It is not going too far to say that a stage will likely be reached where explicit consideration of energy absorption capacity, coupled with a design based on drift limitations, will supplant stress computations. But a great deal more research is due before the time becomes ripe for such procedures.

The author recommends high working stresses associated with the admittance of high seismic forces. This tendency was followed in the 1957 revision of Mexico's Federal District Building Code (42), although it is now generally felt that coefficients specified are too high for typical framed buildings. Doubtless the practice leads to a more uniform factor of safety and a better balanced design than the usual one-third increase in working stresses and the assumption of less than moderate earthquake intensities. This practice should be advocated, but not without a word of caution concerning reductions in overturning moment. The fact that many structures have resisted apparently irresistible overturning moments is surely due in some measure to the reserve of their columns to resist high compressive forces, and this reserve comes largely from the use of low working stresses in static load and small increases for combined loading. In the use of high coefficients and stresses, reductions of overturning moments should be more conservative than in conventional practice. Indeed, allowable reductions in overturning moment were purposely left unspecified in the revision of Mexico's Federal District Code, for it was felt that the matter deserved

considerable study, especially because working stresses were being increased at the same time that local soil conditions led to a proportionally greater response in the fundamental modes than in higher natural modes.

The problem of overturning moment reduction is more acute when results of dynamic analyses are preferred to static methods. In the latter the shear envelope, if correct for certain stories, is almost surely conservative for the rest, and the computed overturning moment is also conservative (aside from the fact that all maximum shears are unlikely to occur simultaneously). In a design based on dynamic analysis, all the shears may be essentially correct (again ignoring the unlikelihood of simultaneous occurrence), and the computed overturning moment not quite so conservative. It would be interesting to learn the author's recommendations on overturning moment reduction when analysis and design follow his other recommendations.

The author's assumed load-deformation curves for brick walls and tile partitions contradict some available data, which indicate a fairly flat portion after reaching the ultimate load.(43) Admittedly this part of load-deflection curves for walls must be very sensitive to the manner in which the wall is connected to the frame but this fact merely points out the need for considerable research. The energy absorbing capacity of walls and partitions with a flat portion in the load-deflection diagram is especially interesting in the plateau scheme proposed by the author.

In brief, without detracting from the paper's exceptional value, the writer believes probabilistic methods more promising than analyses based on responses to a short number of earthquakes. The writer also maintains that a practice more conservative than is usually accepted must be followed with respect to overturning moments when using the author's proposed criteria of design.

Agreeing with the author's belief in the necessity of considering energy absorption beyond the elastic limit, the writer feels there is no rational way to make that allowance. Research is urgently needed in this connection.

The author's load-deflection curves for walls and partitions may be correct under some conditions. But sometimes they may grossly underestimate the energy absorbing capacity of these elements. This is one of the many pressing problems of aseismic design meriting intensive research. It would be valuable for the profession to learn the author's views on these questions as well as on other important matters which he either omits or barely touches upon. Such as, accidental torsion, ground coupling, and the combined effects of the six earthquake components (three displacements and three rotations).

MICHAEL J. MURPHY,[6] R. IVAN SKINNER,[7] and KEITH M. ADAMS.[8]—The analysis of the 15-story Alexander building does much to explain the difference in actual performance of a real traditional structure, and the performance that elastic dynamic theory predicts for a structure whose "cladding" strength and energy-absorption characteristics have been ignored. This difference has been a stumbling block for some time and has led many engineers to take a cautious view of dynamic theory in general. If one accepts the author's explanation for

[6] Chief Mechanical Engineer, Dominion Physical Laboratory, Department of Scientific and Industrial Research, Lower Hutt, New Zealand.

[7] Senior Scientific Officer, Dominion Physical Laboratory, Department of Scientific and Industrial Research, Lower Hutt, New Zealand.

[8] Scientific Officer, Dominion Physical Laboratory, Department of Scientific and Industrial Research, Lower Hutt, New Zealand.

the real source of seismic strength in a traditional building (and the evidence seems to us to be incontrovertible) it becomes necessary to take a closer look at the modern building in which crushable masonry walls are dispensed with and pains are taken to prevent architectural damage.

If the structural engineer can state the floor masses and inter-story stiffnesses correctly, dynamic analysis can provide the inter-story shears dependent on only one variable—the damping. It has been customary to assume 10% to 20% viscous damping as a realistic figure. But where in nature does viscous damping come from? Air damping would seem to be the only thing which is truly viscous, but unfortunately negligible. The internal viscous damping of materials which has been postulated is very small indeed. There are many possible sources of energy loss which may fairly be described as not resulting in architectural damage.

Foundation Damping.—Actual loss of energy, through movement of the soil, is possible but it seems unlikely to be large. Where a building is supported on long piles, however, the upper ends of these piles must move through the soil. This could well provide significant damping but just how much remains to be assessed. Foundations on rock, of course, would not have this form of damping.

Foundation Yield.—The static bearing qualities of soils have been thoroughly examined but as yet there are no dynamic data available. Even if soils showed a readiness to yield under dynamic loads, few engineers would care to appeal to this source of energy absorption, postulating as it does the possibility of unequal settlement.

Loss of Energy by Radiation into the Ground.—Normally there is a large discontinuity in the impedance to shear-wave propagation at the base of a building. Hence, whenever the base of the building is small compared to the wavelength in the surrounding material, little radiation of energy will occur.

Hysteretic Damping of Materials.—Below yield point, steel has practically no hysteretic damping properties. Concrete has some, but nothing as large as the 10% damping figure.

Frame Yield.—This represents a major possibility for energy absorption whether the frame is of steel or reinforced concrete and the Dominion Physical Laboratory has recently submitted to publishers an initial enquiry into the amounts of yield to be expected with different building periods and different levels of yield force. If, as the author and the writers think, yield represents a major source of seismic strength, it is as well to note at this stage that prestressed concrete, at the present stage of development, has virtually no yield at all, and its indiscriminate use in seismic areas is, to say the least, suspect. The subject of yield has only been touched on so far and there are certainly not sufficient data available to provide a basis for a design procedure.

Friction Damping.—The possibility of providing quite large amounts of friction damping in a modern building has been brought to the writers' attention by Bruce H. Falconer, consulting engineer, of Wellington, New Zealand. Interior walls and weather cladding, which modern practice requires should be free of the frame, could well be attached by means of friction clamps arranged to slip at a value below that which would cause architectural damage. It would also be possible to provide adequate damping at the bottom of the building with a specially constructed friction device.

The traditional building owes its good seismic reputation to the strength and energy absorption characteristics at failure of the masonry panels and archi-

tectural features. The modern structure is either eliminating these features or attaching them to the frame in such a manner that architectural damage is not sustained. In short, the design has become so clean that the basic assumptions of dynamic analysis are justified and the answers (showing very high shears even at 20% damping) are valid. It becomes a matter of some urgency then to examine (1) the amount of damping that can be expected from foundations, on piles; (2) the amount of damping that can be built in with friction panels; (3) the amount of yield that can be allowed between stories and still leave Euler stability in the columns and services unimpaired, and (4) to make a dynamic analysis of the design features from the preceeding matters and see that the designed building, within the limits of its known properties, is capable of surviving an earthquake.

The author makes short reference to bearing-wall structures which deflect not in shear but in bending. This is a point that worries the writers as we are not yet able to analyze them and there are many quite tall buildings of this sort in New Zealand (up to 10-stories). They are inherently stronger than frame structures but unfortunately it is not possible to postulate yield damping.

REUBEN W. BINDER,[9] F. ASCE.—A review of earthquake-resistant design procedures will show that some 30 years ago, (about 1928), although the earthquake problem was understood to be one of dynamics, the approach was nevertheless primarily one of statics with special details incorporated to obtain a reasonable earthquake-resistant structure. In other words, it might be said that earthquake-resistant design at that time was in most instances more of an art than it was a science.

In the early 1940's considerable research studies brought about a change in thinking, and a pseudo-dynamic design approach came into being.[44] The practical application of design from about 1940 until 1952 stimulated further important research on the dynamic aspects of the earthquake problem. Thus, today those who are familiar with the research work may consider earthquake-resistant design as much a science as an art.

This paper not only contributes to the theory, but in a most enlightening manner also develops important factors of the art of earthquake-resistant design. The manner in which this subject matter is developed makes it a most important paper and one that should be studied very carefully by those who desire to have a better insight into the subject of earthquake-resistant design.

The area in which an earthquake occurs will still continue to be a huge laboratory for the investigation of the effects of earthquake shock. From a study of the author's paper an observer can readily avoid the pitfall of drawing intuitive conclusions and being influenced by repeated statements which have become cloaked with authority.

About the time that Mr. Blume was presenting his paper, the writer was also presenting a paper[41] on the Mexico earthquake of July, 1957. Blume states, under the heading "The Nature of Building Materials,"

> "For a structure or a member to withstand violent abuse such as the impact and motion of a major earthquake it must be tough, and well tied together, in order to act as and to remain a unit. Toughness implies

[9] Chf. Engr., Fabricated Steel Construction, Bethlehem Steel Co., Pacific Coast Div., Torrance, Calif.

the ability to absorb punishment and still retain integrity and resistance against additional punishment."

The writer in his paper wrote,

"This type of construction is similar in one respect to the reactions of football players. The All-American player, when tackled hard, is almost always relaxed, and thus will suffer no injury; however, the player who stiffens up stands a good chance of being cracked up."

It would seem that a good structure, like a good athlete, should, as necessary, be capable of rolling with the punch and be tough enough to absorb a maximum of punishment.

Figs. 4 and 5 and the companion tables represent an important compilation and cover some aspects of the science and the art of earthquake-resistant design, pointing up the fact that the designer should have in mind not one design but rather two designs in order to achieve an economical and sound structure. The energy absorption of still or rigid elements at low strains may involve other problems in considering the over-all design. Variable stiffness resulting from construction differences, temperature changes, and so on, may result in torsional effects. The complete lateral-force-resisting structural frame in this case is of extreme value, as it represents many stress paths to take up torsional effects and the vibrations resulting from a strong shock.

JOHN A. BLUME,[10] F. ASCE.—The discussion indicates a keen interest in inelastic response and energy absorption as basic factors in the reconciliation of seismic damage history with research data and design procedures. The writer appreciates and wishes to thank the discussers for their thought, contributions, suggestions, and complementary statements. It is regretted that more practicing design engineers did not participate in the discussion, because many have expressed considerable interest in the subject matter of the paper in connection with design techniques and building code provisions.

Mr. Jacobsen has contributed valuable considerations of damping equivalents and of the effect of reversals and additional cycles on the nonlinear force-deflection diagram of the composite traditional-type building. The writer concurs that variable clearances in the joints between building elements would tend to cause variations in the positive slopes of the daigrams and also that there be a tendency for rounding of the peaks even on the initial performance. In the research effort it was necessary to utilize certain simplifying assumptions in order to reduce the already significant amount of mathematical labor and to provide for consistency. The assumptions were carefully considered, however, usually with the aid of numerical or empirical treatment, and they are not such as to affect the overall results to any significant degree.

It is the writer's opinion that, on the first reversal, the mirror image humps would not be greatly softened in the prototype because of the characteristics and the geometry of the unreinforced wall materials. These are expected to fail in flexural tension as well as in shear even though the story distortion considered is of the "shear" type with the floors remaining level. In other words, the hysteresis loop would be expected to be initially quite distorted because of the great variation between the tensile and compressive strength of unreinforced "brittle" materials. It is hoped that the discussion illustrates the value

[10] Pres., John A. Blume & Assoc., Engineers, San Francisco, Calif.

of reinforcement of such materials and of typing them adequately to the main structural framing. With such construction, these elements can retain integrity even though cracked, and would have a much slower deterioration rate with repeated cycles, greater residual energy value, and more symmetry of resistance about the origin. The ductility of steel reinforcement greatly prolongs the hump values to provide more toughness and energy value. It is not to be overlooked, however, that even without reinforcement (and this is not recommended for new construction) there is a considerable degree of non-computed value in most traditional buildings.

Mr. Jacobsen computed the total energy and the lost energy to a deflection of 0.15 in. on Fig. 4(b) and also obtained the specific damping capacity and equivalent viscous damping ratio at 0.05 in. deflection. The writer has extended these considerations and added other data for the first story of the traditional building, north-south direction, as shown on Fig. 13. The increase in energy

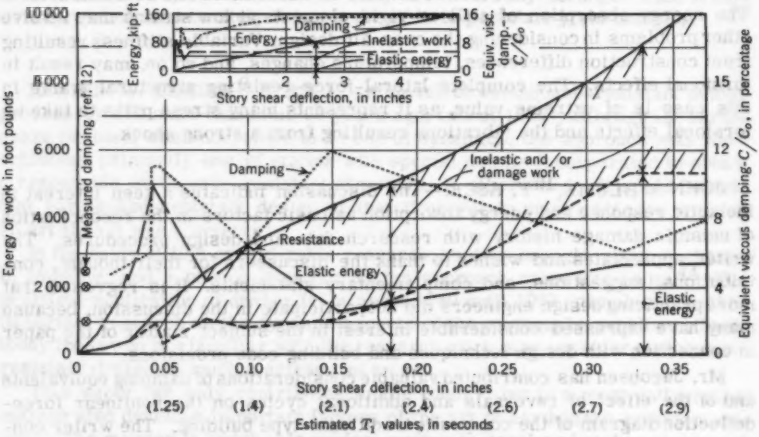


FIG. 13.—ENERGY, DAMPING AND PERIOD ON FIRST HALF CYCLE

value with deflection is notable, as is the fact that the equivalent viscous damping, as defined by Mr. Jacobsen, averages 8% of critical from the point of wall cracking to the yield point of the steel frame and rapidly attains the 12% to 15% range beyond the yield point. These considerations are approximate in this range but they are presented as an aid to judgment and a possible guide to further research.

It would be expected that the period would initially shorten due to the hardening characteristics of the structure and then lengthen after passing the peaks and lengthen further on repeat cycles. However, even where the brittle materials have cracked, there is still residual strength, stiffness and energy value. Mr. Jacobsen states this in another way by referring to the "softening" characteristics on the second and subsequent reversals of loading. It would thus be expected that the fundamental period, even after one complete cycle, would not be a function of the stiffness of the steel frame alone, but a function of a characteristic somewhere between the original and that of the steel frame. The

values of period shown in Fig. 13 are estimated on the assumptions that no mass is lost, similar damage occurs throughout the building, and the effective average spring factor at the first attainment of each deflection is based on an elastic resistance having a triangular area equal to the gross energy area minus half the area of the "inelastic" portion.

The fact that the characteristics of the composite structure depend not only on deflection but on the prior history of both deflection and the number of cycles indicates the extreme difficulty of substantial resonant magnification in such buildings. Conversely it also indicates that buildings which have very little to participate beside the frame may be subject to much more resonant magnification than has been indicated thus far by seismic history.

It is somewhat disappointing that the equivalent viscous damping ratios are not even greater and more effective. Fig. 7 indicates that there would be relatively small decrease in base shear for greater value of damping. The reconciliation with damage and lack of damage has to include more forms of energy absorption than viscous damping for assumed linear systems of vibration. Research work in nonlinearity such as Mr. Jacobsen is conducting for the California State Division of Architecture should be of great interest.

Mr. Eremin points out the need for further research as do other discussers, in which the writer heartily concurs. He also mentions the need for further consideration of the ground, as do others. There is no doubt that the ground is an important part of the structural-dynamic system and it must not only deliver energy to the structure but it must receive a portion back. Mr. Eremin also states that the design of rigid frame structures, when performed in accordance with the recommended building codes, results in relatively safe structures. The writer concurs, in general, with this statement but with the reservation that all parameters of the problem should be considered, in view of our relatively brief and infrequent seismic history and also in view of the changing character of buildings. There was no intention to imply in the original presentation that the structure would continue to act in the same manner as its original structural-dynamic characteristics after walls or other elements crack or fail. On the other hand, neither should it be implied that mere cracking would completely eliminate all of the participation of even the brittle elements. This is apparently not the case. Instead, a progressive deterioration would be expected with repeated cycles. Allowance for the grinding and hammering of the broken parts is included at least in part, in the graphs, and in Mr. Jacobsen's discussion, by not reducing the amount of the "humps" more than a nominal amount for each repeating cycle. It might thus be said that the grinding and hammering converts the kinetic energy of movement into heat and, exclusive of possible local distress from impact, can have a valuable, though costly, beneficial effect in resisting the earthquake. The writer inspected buildings in Arequipa, Peru, shortly after the severe January, 1958 earthquake and found some plain masonry walls completely shattered into pieces no larger than a few square feet and yet all pieces were in place. Obviously the frictional energy and work energy were the significant factors of resistance to the earthquake centered essentially below the city.

Mr. Rosenblueth offers many suggestions for future research including the probabilistic approach to the earthquake problem. This technique offers interesting avenues of research but, as he states, available methods are probably not at the stage where they could be reliably or conveniently used as a sole method of design. Probability is basic in the earthquake field. Most designers fail to realize that there is a probability of not only combinations of various

mode distortions in one direction but also combinations of mode distortions in both translational directions and also in torsion, all combined with vertical movement. The probability of these modes combining in their worst degree is, of course, extremely remote, but the possibility of reasonable combinations by the root mean square or other procedures should not be ignored in research and should be given much more consideration in design for special structures.

Mr. Rosenblueth concurs with the writer's "plateau"-type design for certain flexible structures where moderate shocks are provided for on an elastic basis and severe emergencies result in motion in the inelastic range, but he indicates that there is no reliable method for such design. There is a simple

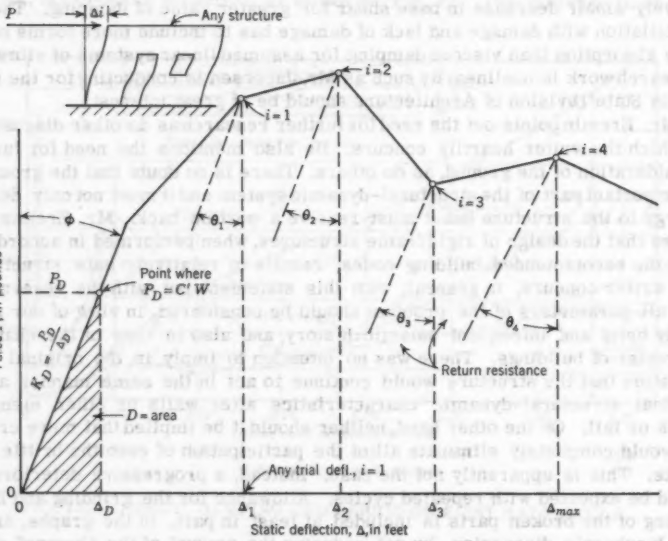


FIG. 14.—FORCE-DEFLECTION DIAGRAM FOR RESERVE ENERGY TECHNIQUE

method which, based on carefully studied assumptions, has sufficient accuracy, if used not to supplant but to confirm or refine designs made under accepted elastic code requirements. This "reserve energy technique" is offered as a means of considering energy and inelastic behavior and for providing a numerical evaluation of "plateaus" or ductility in any combination of materials.

Fig. 14 indicates a plot of static deflection versus force. The heavy line is the total initial resistance, attained by rigidity, of all elements and materials. Terms to be used in this technique are Δ Max, the point beyond which the curve never becomes level or slopes upwards; or, the point of collapse from local buckling; U_i, the total area under curve up to trial point Δ i = 1, 2,...n ft lbs; Hi, the hump area above a straight line from origin to any point, i = 1, 2,...n

ft lbs; αi, the spectral or analog acceleration, ratio to gravity, at period Ti and 5% damping; C', the static elastic value a structure may have, as a ratio of gravity; C = C' if code requirement C is just met; W, the total weight of the structure and fixed contents at and above the level under consideration; T, the fundamental natural period of the whole structure before the earthquake, in seconds; Ti, the assumed structure period at Δi, which is equal to $T\sqrt{Kd/Ki}$. If angle θi of Fig. 14 is between $0.9\,\phi$ and $1.1\,\phi$, the system is assumed elastic-plastic Ki = Kd, otherwise, let $Ki = \frac{2\,Ui - Hi}{\Delta i^2}$. Ri, is the reserve energy reduction coefficient.

$$R_i = \rho \frac{Ti}{T}\sqrt{\frac{D}{Ui - 0.5\,Hi}} \quad \ldots\ldots\ldots\ldots\ldots (1)$$

The numerical value of ρ in Eq. 1 is 1 for a linear single-mass system or a non linear system for which $T = 2\pi\sqrt{\frac{W}{2\,K_D}} = 2\pi\sqrt{\frac{A_D}{g\,C}}$. If this does not apply, then $\rho = 0.9\,T\sqrt{\frac{C'}{A_D}}$.

The procedure for single mass structures is as follows: (1) Design or analyze structure as per elastic seismic code in effect; (2) plot the total resistance diagram as indicated; (3) for trial Δi, compute Ui, Hi, Ki, and Ti; let i = 1; (4) obtain αi for period Ti and compute Ri αi; use selected earthquake; (5) if Ri αi is equal to design coefficient, C, the structure (or portion of same under consideration) is adequate (no safety factor) at deflection Δi and with damage or yield indicated by Hi. If Ri αi exceeds C, the structure is inadequate and the corrective choices are; (a) assume a greater deflection or deflections and repeat, or (b) add material to the structure or modify the design or (c) reduce αi on the basis of any reliable data for energy loss to the ground, or for greater (non-destructive) damping than 5% (in no case reduce αi more than 20% total) or (d) combinations of the preceeding; (6) if Ri αi is equal to or less than C but the damage or deformation at Δi as indicated by Hi is not acceptable, the procedure would be as in (5) except that lesser deflections would be tried, probably with a modified design.

An earthquake spectrum or spectra, or analog accelerations such as in Fig. 10, are used to determine αi for 5% of critical damping. If only velocity spectra are available such values can be converted by $\alpha i = \frac{2\,\pi\,V}{T_i\,g}$. It is assumed that the area under the static resistance curve, less half the "hump" area (for deterioration), equals in inelastic work or strain energy the kinetic energy due to the earthquake. Period adjustments are also provided for yield or cracking. The assumptions tend to balance each other with a slight tendency toward the safe side, especially if all materials are reinforced. It is suggested however, that the safety factor for the selected earthquake be considered the ratio of $R_i\alpha_i$ for Δ_{max}. This method is general and may be applied to any type of structure to estimate its resistance to, deflection under, and damage from a specified earthquake. Table 9 gives useful values from the El Centro 1940 N-S earthquake spectrum, single = mass elastic system, with a damping of 5% of critical. In the 10-mass analog runs for the New Zealand building under the same earth-

quake and for the same damping, the α^1 = values for base shear are 0.13, 0.12, and 0.08 for 2.0 sec, 2.5 sec, and 3.0 sec periods respectively. The difference (from the one-mass systems of the same periods) may result from energy utilization in higher mode motion.

TABLE 9.—1940 EL CENTRO SPECTRUM VALUES

Factor	Values of T_i, in Seconds										
T_i :	0.25	.30	.40	.50	.60	.75	1.00	1.50	2.0	2.5	3.0
α_i : use	0.88	.80	.70	.60	.55	.46	.37	.26	.21	.18	.16
Velocity in feet per second	1.13	1.30	1.44	1.54	1.70	1.80	1.90	2.00	2.16	2.31	2.47

Fig. 14 is for equivalent single-mass systems with a direct structural connection to the ground. Where multi-story or multi-panels of resistance transmit shear in series, it would be unreasonable and unsafe to assume that all such units participate simultaneously to their full capacity of energy absorption. (This consideration is distinct from that of higher modes.) On the other hand, work done anywhere in the structure normally assists other parts because input energy is drained. The following modifications to the single-mass system procedures are suggested for multi-unit systems. Let Z be the number of stories, panels, or other units acting in series above and including the one under consideration. For tall slender units without floors or other discontinuities, arbitratily assume Z the number of 30-ft units of height. Then for each unit, z starting at the top with z = 1, a modified R_i value, R_{iz}, is ontained in which

$$R_{iz} = \rho \frac{Ti}{T} \sqrt{\frac{D_z \sqrt{Z}}{\sum_1^z (U_i - 0.5\, H_i)}} \quad \ldots\ldots\ldots\ldots\ldots\ldots (2)$$

In determining the $(U_i - 0.5\, H_i)$-values for each unit or story, the absolute positions of all units should be proportional to the first mode shape of the structure. However, only the net story deflection is used, to obtain U_i and H_i. Thus, Δ_i could vary between different stories under the same trial, i, unless a straight line mode deflection is assumed and the stones are of equal height. $R_{iz}\, \alpha_i$ is compared to the coefficient for each story, C, as in the single-mass system. The lower story need be the only one considered as affecting T_i in many cases, perhaps with an arbitrary additional decrease in K_i to allow for upper story yield. C is the coefficient used to determine shear, not force, at any level.

For multi-mode systems, an additional reduction, up to 10% of maximum, may be made in α_i (from one-mass system spectra) to allow for energy of motion in higher modes. The entire α_i reduction from the spectral value shall still not exceed 20% without special analysis. However, if the α_i-values are taken from multi-mass analogs as presented herein, no further reduction is indicated or needed.

Table 10 presents a related but independent earthquake rating system for structures. It is intended to provide a yardstick for behavior comparison under a reference (standard) earthquake spectrum and thus to facilitate communication about behavior in the inelastic range. This device is also based on energy capacity, and the force-deflection diagram.

The procedure is to determine the ratings for Table 10 from a total resistance curve for the structure as in Fig. 14. h is the height of the structure or story. The energy index is the ratio of provided energy resistance to 90% of the energy demand for a "standard" envelope of earthquake spectra. 10% of

TABLE 10.—RATING FORMULAS

Symbol (1)	Valve of i (2)	Rating Name (3)	Deflection Position (4)	Index Considerations		
				Energy (5)	Drift (6)	Damage (7)
BN	n	No damage	Δ_n, @ first peak; or Δ_n where $H_n < 0.1U_n$	$\frac{\Sigma(U_n - 0.5H_n)}{0.108\ W\sqrt{T_h}\ Z}$	$\frac{\Delta_n \times 10^3}{h}$	$\frac{H_n}{2U_n}$
BD	d	Drift (slope)	Δ_d @ 0.004h	$\frac{\Sigma(U_d - 0.5Hd)}{0.108\ W\sqrt{T_d}\ Z}$	$\frac{\Delta_d \times 10^3}{h} = 4$	$\frac{H_d}{2U_d}$
BE	e	Energy	Δ_e such that BEI = 1.0	$\frac{\Sigma(U_e - 0.5\ H_e)}{0.108\ W\sqrt{T_e}\ Z} = 1$	$\frac{\Delta_e \times 10^3}{h}$	$\frac{H_e}{2U_e}$
BF	f	Failure	$\Delta f = \Delta_{max}$	$\frac{\Sigma(U_f - 0.5\ H_f)}{0.108\ W\sqrt{T_e}\ Z}$	$\frac{\Delta_f \times 10^3}{h}$	$\frac{H_f}{2U_f}$

the energy is deducted for ground "feedback". This standard envelope, or "spectragraph," might be considered similar to an absolute zero temperature. Although the values may never be attained, they are a basis for comparison of structures of all periods and types. The formula for the estimated 5% damping velocity response to the spectragraph is V 2.77 1/4 Ti FPS. From this and the expression for kinetic energy, $(W/2\ g)\ v^2$, the general energy index formula is

$$\frac{\Sigma(U_i - 0.5\ H_i)}{0.108\ W\sqrt{Ti}\ Z}$$

$$\text{The drift index} = \frac{\Delta_i \times 10^3}{h}$$

$$\text{The damage index} = \frac{Hi}{2\ U_i}$$

These numerical ratings provide a great deal of information about a structure of any type and how it would be expected to react to the standard earthquake envelope as compared to other structures. The El Centro 1940 = energy index would be roughly 2.3 times greater than for the "standard" earthquake envelope. In the many cases that the BD-values and BE-values may not be attainable that fact is noted. High BN and BF energy values with low damage indexes are desirable. The optimum combinations of values will vary with the type of risk desired. The system provides a means of evaluation and communication in the

several considerations of aseismic structural dynamics that are not brought to light in customary design procedures. For multi-story buildings the lowest story and one typical upper story should be reported. Reports consist merely of the tabulated ratios.

The writer agrees with Rosenblueth that one or even several actual earthquake records do not create an adequate history of seismic disturbance. However, for complex structures and with electric analog techniques, it seems quite appropriate and simple to use available complete earthquake records in both research and design. Judgment must provide for the nonrecorded probabilities.

Mr. Rosenblueth is concerned with a weak story in a multi-story building being overtaxed in energy absorption, because the energy absorption of the adjacent stronger stories would be much less and possibly create a dangerous condition. There is no doubt that an "underdesigned" element could be dangerous. A sacrificial "fuse" is not practical if the stability of a structure depends on the fuse not failing or yielding too far. Stability must always be considered. This points out the great advantage of indeterminate or continuous construction with two or more stress paths that nature will seek out under emergency conditions. The writer is convinced that indeterminate multiple-path design, even though complex, is a most desirable earthquake-resistant construction and a type that would do a great deal to reduce the danger Rosenblueth describes. Consistant safety factors are desirable, of course, to prevent weak links, but they should be consistent with structural dynamic conditions rather than building codes alone. The reserve energy procedure lends itself well to complex multi-path structures.

The variations in energy absorption capacity that Rosenblueth mentions between various types of elements such as X-braces, shear walls, frames, and so forth, can be considered, with, at least, more than crude intuition by means of the reserve energy technique previously described. A structure does not necessarily have to be ductile if it has adequate capacity, but with greater stiffness much greater capacity is indicated except for very low, rigid buildings. The design challenge that is unfolding is almost limitless.

The question of overturning moment is, of course, deeply involved with column stability is involved with the type, the amount, and the capacity of restraining elements and their connections to the columns. The overturning moment design of tall slender structures is often governed by wind rather than seismic considerations. There is more recent thinking available on the subject of seismic overturning moment. No new developments, however, should lead anyone to believe that overturning from wind should be reduced or that buckling of compression members under lateral deflection of either wind or earthquake should not be a prime consideration. It would seem in our present state of knowledge that using full overturning from accepted wind forces or overturning moment from static seismic forces reduced by dynamics, whichever governs, would produce adequate and economic results. Unusual problems, of course, need special analysis.

Mr. Rosenblueth questions the sharp peaks on the masonry force-deflection curves since the Benjamin-Williams[11] tests indicate flat portions after obtaining ultimate load. These excellent tests, which were not available to the writer at the time of preparing the diagrams, are for high quality workmanship under

11 "Behavior of Reinforced Concrete Shear Walls," by J. R. Benjamin and H. A. Williams, Transactions, ASCE, Vol. 124, 1959, p. 669.

laboratory conditions. It would be expected that the fit of the masonry to the boundary framing and other factors, would be far better than for normal field workmanship. Benjamin-Williams specimens 3b2-1 and 3b2-1a, which had no boundary frames, failed abruptly and at low values. Some of the other specimens such as 3b2-2 and 3b2-3 had fairly sharp peaks. It might be considered that the walls of the prototype building, in conjunction with its steel frame, would perform in a manner intermediate to that of the steel framed walls and the unbounded test walls until the frame would become the principal resisting element. The shape of the total resistance curve of Fig. 4b resembles that of their specimen SF1 which is actually a test of a steel frame and brick window-wall combination. The peaks of force-deflection curves could well be rounded and extended in various cases depending on several factors. However, the curves shown herein are on the conservative side and any greater area of energy capacity would only reinforce the conclusions. Another source of additional energy capacity lies in the fact that the curves based on static test results do not show the entire resistance that would be obtained for ductile material under dynamic or rapid loading conditions.

Because Mr. Rosenblueth asked for comments on "accidental torsion" the writer's opinion is that some provision should be made in static-type codes to protect against a "hunting" or beating type of motion developing between the translational modes and the torsional modes. Particular warning is expressed against buildings of the so-called "core" type where, for architectural reasons and convenience, the lateral strength is limited to a small central area, usually around the stairs and elevator shafts. The lack of adequate polar moment of inertia in such designs can lead to considerable torsional movement. For best results the designer should be required to provide some resistance in the exterior wall planes, where it belongs. For the engineer who obtains a coincidental center of mass and center of rotation under elastic (code) design conditions and ignores torsion, the writer asks what happens to the paper symmetry when inelastic action develops, as it will, on one side of the structure before the other side. The writer also concurs in principle with the Mexico City, Mexico, building code requirement which is directed against sudden transitions in torsional value between adjacent stories because abrupt transitions are dangerous in any structure or member.

Messrs. Murphy, Skinner, and Adams make an important point in that many engineers have had a cautious view of dynamic theory because it has not always seemed to reconcile the behavior of actual structures. There is nothing wrong with theory, providing all of the factors of a situation are considered. To ignore the most important elements in response has been, of course, untenable with progress. There is no doubt that various forms of ground energy loss including foundation damping, foundation yield, and loss of energy by radiation play a part in saving some structures. Obviously, the solution depends to a great extent upon many factors, principally the structural-dynamic characteristics of the structure, the ground, and of the coupled ground and structure. In our present state of knowledge it would not seem wise in reserve energy design to assume more than a nominal percentage, say 5% to 10%, of the total building energy as fed back to the ground. In the writer's opinion there have been cases where soft or granular ground has been blamed for deleterious earthquake affects on a structure where there actually has been a net attenuation effect.

Messrs. Murphy, Skinner, and Adams also discuss hysteresis damping, friction damping, and frame yield. The hysteretic damping of materials in the elastic range is admittedly fairly small. Certainly any general assumption of greater

than 5% damping in this regard would be on the unsafe side. That is why 5% is used in the writer's reserve energy technique. A few damping measurements have been made in actual buildings. The values obtained may be said to range from roughly 5% to 15% (12), (19). Obviously such values include friction in the joints between various materials and building elements as has been discussed by Mr. Jacobsen. Assumed high damping values of 20% to 30% of critical do not seem to reconcile either probable values or seismic history with the spectral results for assumed elastic systems. It seems that the principal remaining element to be considered, in reconciliation, is the work done in frame yielding, cracking, grinding, hammering, and so on, of damaging motion that has occurred in the traditional structures. The reserved energy technique is offered as a procedure until more data are available.

Messrs. Murphy, Skinner and Adams refer to bearing-wall structures that deflect not in shear but in bending. The so-called cantilever-type of deformation of the structure as a whole can become quite significant with increasing slenderness ratios or with walls containing few openings. In such cases, and this would include high bearing-wall structures such as described, cantilever-type deformation due to shortening of compression elements and lengthening of tension elements, may well amount to more than the shear deformation. The flexural distortion should increase shears in the upper levels but not otherwise affect the over all dynamic results. The lack of a complete structural frame, however, would seem to create a structure that would be extremely vulnerable upon any severe cracking of the bearing walls. Stating this another way, there would be no reserve elastic or elasto-plastic frame to yield, to do work, to absorb energy, and to retain the wall pieces, if and when the wall should be severely damaged. In the writer's opinion, there would be a typical initial damping value but, unless a very strong structure is provided, the reserve energy, that would be recommended would not be present.

Mr. Binder briefly mentions the general history of earthquake design procedure in California, a subject in which he has long been active and is most familiar. There should be no doubt that earthquake-resistance design is both a science and an art. The latter phase is still extremely important and will probably remain so for a very long time. The reserve energy technique and the rating system of Table 10, for example, are not intended to replace judgement, but to sharpen it. Unfortunately, many designers and research workers are not familiar with the great amount of work done in the early 1930's as well as in the 1940's that Mr. Binder mentions. As in all new technical developments, it takes time or stimuli for the utilization of research efforts.

Mr. Binder correctly states that the designer should have in mind not one design but two. To this the writer would add that the designer should have in mind not one dimension but three, and also the fourth dimension of time, as well as reverse loading, possible deterioration, and torsional effects. Assumptions in engineering are necessary and serve a very useful function in providing practical design tools. There are many common assumptions in nonseismic design regarding stress distribution, stress-strain relationships, equivalent static wind or impact loadings, and so on. There is no reason why similar tools cannot be utilized in the earthquake design field as is recommended in modern seismic codes. However, the responsibilities involved together with the possibly great energy releases of nature are such that the engineer should constantly bear in mind the true nature of the problem regardless of its complexity. It would seem that there is a professional obligation to clients and to the public

on important or unusual structures, if not all structures, to not only comply with the most modern seismic code but also to consider the structural-dynamic phenomena which involve too much science and art to either belong in or to be capable of being included in any code.

AMERICAN SOCIETY OF CIVIL ENGINEERS

Founded November 5, 1852

TRANSACTIONS

Paper No. 3055

RESISTANCE PROPERTIES OF SEDIMENT-LADEN STREAMS

By Vito A. Vanoni,[1] F. ASCE, and George N. Nomicos[2]

With Discussion by Messrs. Emmett M. Laursen; Tsung-Lienchow; and Vito A. Vanoni and George N. Nomicos

SYNOPSIS

Experiments were made to determine the relative effects on the friction factor of a flow of the suspended sediment load and the configurations which form on sand beds of streams. Results showed that the friction factor of a stream carrying suspended sediment is less than a comparable one without sediment. They also showed that the reduction of friction factor due to changes in bed configuration is much larger than that due to suspended sediment.

INTRODUCTION

The resistance to flow of clear water in a channel with fixed boundaries has been studied extensively and can be predicted with a satisfactory degree of certainty. Values of friction factors to be used in the flow equations, such as the Manning or Darcy-Weisbach formulas, have been determined and are given in reference works on hydraulics as a function of the texture or roughness of the channel walls and the Reynolds number.

However, when a stream has a movable bed, and sediment is being transported, the problem of determining the resistance is much more complicated than in the simple case of clear water flowing in a channel with fixed walls. Observations have shown that the friction factors for such sediment-bearing or alluvial streams vary over appreciable ranges. However, the problem has not

Note.—Published, essentially as printed here, in May, 1959, in the Journal of the Hydraulics Division, as Proceedings Paper 2020. Positions and titles given are those in effect when the paper or discussion was approved for publication in Transactions.

[1] Prof. of Hydr., California Inst. of Technology, Pasadena, Calif.

[2] Specialist-Scientific Research Engr., Republic Aviation Corp., Farmingdale, N. Y.

been studied sufficiently to enable hydraulic engineers to predict a friction factor for given conditions.

The fact that the friction factors for alluvial streams vary has been known for a long time. Despite this, the problem is not considered at any length in the literature, and textbooks are particularly silent on this point. This leaves all but the expert in this field with the erroneous impression that the friction factor of streams is constant and can be determined once for all time. The lack of examination in the literature of the resistance of alluvial streams may be explained by the fact that the problem is not well understood, and information on it is often conflicting. For instance, some evidence presented shows that the friction factor of a stream increases as the sediment load increases, whereas other evidence supports the opposite conclusion.

The variation of roughness of sediment-laden streams is caused by two distinct processes: (1) appearance of dunes and bars on the bed, which may increase the roughness several fold because of the additional form resistance; and (2) the damping effect of the suspended sediment on the turbulence in the stream tending to reduce the hydraulic roughness. Because of these two opposing processes, there has often been confusion about the effect of sediment load on roughness. Indeed, it is very difficult to separate the two effects because, for streams in which a significant amount of bed material is carried in suspension, the two processes are always acting together, but with differing relative effects. For example, in a sediment-laden stream flowing at high velocity over a flat bed of sand, the friction factor, or roughness coefficient, will probably be lower than that for a clear flow over a fixed bed of comparable grain roughness because of the damping effect of the suspended load. On the other hand, at a lower velocity with light suspended load, dunes may form, and the net result will be an increase in the friction factor over that for a fixed flat bed of the same sand roughness.

This paper presents results of experiments in which an effort was made to separate the two processes in order to determine qualitatively their relative order of magnitude. To accomplish this, runs were made with suspended load and a movable bed, and then with clear water but with no change in the bed configuration. This necessitated the development of a procedure for solidifying a natural bed configuration in place so that the clear water could be made to flow over exactly the same bed as the sediment-laden flow. A comparison of friction factors then showed directly the damping effect of the sediment separately from the effect of changing bed configuration. A brief review of available information on the problem is given, and then the experiments are described and the results and conclusions derived from them are given.

RESISTANCE OF SEDIMENT-LADEN STREAMS

Early Studies of the Resistance Problem.— One serious obstacle to the understanding of the resistance of alluvial streams by the hydraulician of the latter part of the last century was the theory developed to explain the phenomenon. The reasoning back of the theory began with the logical idea that the loss in energy head between any two stations on a stream is merely the difference in elevation between the stations. It was then argued that this drop, or head loss, was used up in two ways: (1) in overcoming the hydraulic friction of the flow, and (2) in transporting sediment. According to this concept, the more energy used in transporting sediment, the less was available to overcome friction, and

vice versa. According to the Chezy formula, the velocity of a stream is proportional to the square root of the energy slope where the energy slope is merely the loss of energy to overcome friction per unit length of stream. If a turbid stream uses part of the total available energy to transport sediment, it will have a smaller energy slope and hence a smaller velocity than it would have if it carried no sediment. Thus, it was concluded that a clear stream would have a larger energy slope and hence, according to the Chezy formula, would flow faster than a comparable one carrying sediment.

In view of present knowledge of flow problems, it is clear that some of the ideas on which this conclusion was based were incorrect. To begin with, much of the energy to transport sediment comes from the turbulence which itself results from the expenditure of energy in overcoming the friction. Therefore, this energy of turbulence is no longer available to overcome friction, and the fact that some of it is used to transport sediment should not necessarily affect the dissipation of the main energy head. Also, apparently it was not recognized that the friction, or roughness factor, of sediment-bearing streams varies widely with load and flow rate, and that because of this the mean velocity can vary even without a change in energy gradient or depth.

The energy concept held by the hydraulicians of the last century, and the deductions resulting from it, were so firmly established that they influenced the thinking of many workers of that era, and some vestiges of the ideas are to be found even in relatively recent literature. It appears from early publications[3,4] that Grove K. Gilbert adhered firmly to this concept.

In 1886, it was reported[5] that observations of a storm sewer 4 ft in diameter in Croydon, England, over a period of years showed that the mean velocity for a given water depth was always greater when the water was clear than when it was turbid. He concluded that the retardation of the turbid water was due to the load of sediment it was carrying. Elon H. Hooker,[4] in commenting on Latham's conclusions, noted that Gilbert also reached the same conclusion. Hooker also went on to state, "The law of conservation of energy will not admit any other decision in this matter, though the statement has sometimes been made that such a retardation of velocity does not exist." One statement contradicting the belief that a stream at a given stage would flow faster when clear than when turbid, was made by R. E. McMath, and was included in the paper by Hooker,[4] McMath[6] was apparently citing some observations of the Mississippi River which contradicted the accepted views of the time.

In his classical flume experiments in sediment transportation, Grove K. Gilbert[7] expected to confirm the idea that a clear stream flows with less resistance than a comparable loaded one. He selected pairs of runs from his experiments which had the same depth and slope except that one of them carried sediment and the other did not. The bed in both cases was composed of a pavement of sand grains which did not move. According to the then prevalent theory, the mean velocity of the clear flow should exceed that of the loaded flow. However,

---

[3] "The Colorado Plateau Province as a Field for Geological Study," by G. K. Gilbert, American Journal of Science, July-August, 1876.

[4] "The Suspension of Solids in Flowing Water," by E. H. Hooker, Transactions, ASCE, Vol. 36, 1896, pp. 239, 288, 289.

[5] Minutes of Proceedings, Inst. of C. E., by Baldwin Latham, Vol. 71, London, 1886, p. 46.

[6] "Silt Movement by the Mississippi," by R. E. McMath, Van Nostrand's Engineering Magazine, 1883, p. 36.

[7] "The Transportation of Debris by Running Water," by G. K. Gilbert, Professional Paper 86, U. S. Geological Survey, 1914.

the opposite result was found in eleven of the sixteen pairs of runs selected for the comparison. The depth measurements in these runs were apparently not as reliable as desired, and it was thought that this may have introduced a systematic error into the result. Therefore, Gilbert selected thirteen more sets of comparable runs, eleven of which showed higher velocity for the clear flows than for the loaded flows. However, it was also noted that the reduction in mean velocity due to sediment transport was greater for small load than for large, for gentle slopes than for steep, for low velocity than for high, and for large depths than for small. As a result of these data, Gilbert was forced to admit that the theory was not supported and there was probably some physical law which escaped his analysis.

A valuable contribution to the resistance problem was made by Arthur B. Buckley[8] in his work on the Nile. He made elaborate continuous observations of slope, mean velocity, and cross-sectional area at several stations on the river which showed an appreciable fluctuation of the coefficient of roughness.

TABLE 1.—MEASUREMENTS AT THE KHANNAQ NILE DISCHARGE STATION

Date	River elevation, in meters	Condition of flood	Flow rate, in cubic meters per second	Sediment concentration, in per cubic meter (parts per million)	Mean velocity, in meters per second
(1)	(2)	(3)	(4)	(5)	(6)
Aug. 16, 1920	87.54	rising	7200	1900	1.48
Sept. 16, 1920	87.54	falling	6400	1000	1.32

Typical values of these observations are shown in Table 1 and data applying to this station for both dates are

Cross-sectional area . . . . 4850 square meters

Slope 0.000072

Hydraulic radius . . . . . 8.6 meters

These data show clearly that at the given stage the mean velocity of the river is larger on the rising than on the falling stage, while other channel characteristics remain unchanged. The reduction in mean velocity represents an increase in the Manning friction factor of 11%. A further pertinent point to be noted is that the sediment concentration, like the velocity, is higher on the rising than on the falling flood.

Fig. 1 shows the measurements made by Arthur B. Buckley[8] in 1921 at Beleida Station on the Nile. The station is 28 miles upstream from Cairo and 40 miles upstream from the Delta Barrage, or dam, which diverts water to the canals of the delta system. The variation in slope shown is due to the change in level of the water at the Delta Barrage required to feed the canals. The value of Kutter's roughness coefficient is seen to decrease appreciably as the

8 "The Influence of Silt on the Velocity of Water Flowing in Open Channels," by A. B. Buckley, Minutes of Proceedings, Inst. of C. E., Vol. 226, Pt. II, London, 1922-1923, p. 183.

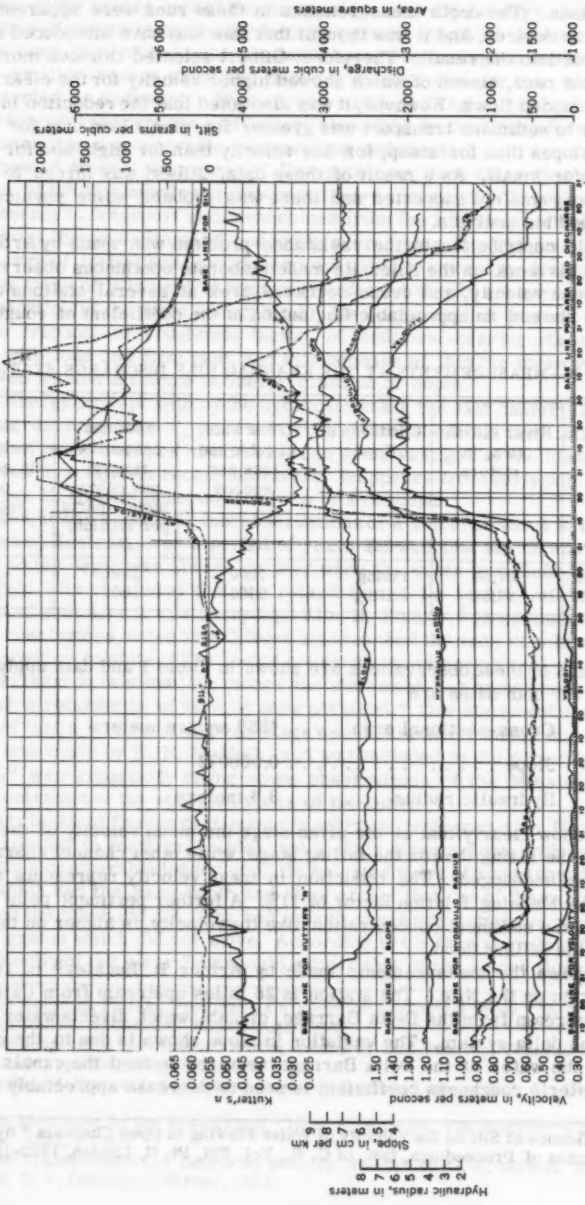


FIG. 1.—MEASUREMENTS ON THE NILE RIVER AT BELEIDA

discharge and mean velocity increase. For example, the following extreme values are obtained from Fig. 1:

	April 12, 1921	Sept. 8, 1921
Discharge, in cubic meters per second	500	6200
Kutter n	.063	.027
Hydraulic radius, in meters	3.1	7.8

Such great reduction in channel roughness during the flood must have been due primarily to smoothing out of dunes and bars on the river bed, with the damping effect of the suspended sediment being secondary. This will be seen from the laboratory experiments described subsequently.

In examining Buckley's,[8] Gerald Lacey showed that in the report of the Indus River Commission covering the period 1906 to 1910, it was stated that the velocity and discharge for a rising river were higher than for a falling river for the same stage, and the reverse was true for the water cross section of the stream.

F. E. Kantlack[6] cited evidence which disagreed with that obtained by Buckley. He called attention to the result of research on rivers by Swiss and French engineers which showed that the stream velocity was decreased in every case as the sediment concentration increased. According to Kantlack, this had been demonstrated prior to 1870. Kantlack also stated that in his experience in the Punjab Canal system of India there was never an excess of flow during the time of high sediment load, as would be expected from Buckley's findings on the Nile and as was reported by other workers in India. Buckley[8] also called attention to some laboratory work by Duponchel which showed that a sediment load tended to increase the mean velocity of flow.

Recent Studies of the Resistance Problem.—Interest in the resistance problem in the past two or three decades has been stimulated by both laboratory and field studies of the sediment problem. One of the main objectives of research in sedimentation is to develop a theory which will enable one to predict the sediment load of a stream as a function of the water discharge and the stream channel characteristics. Once the discharge is given it is necessary to compute the flow velocity and depth, which requires that the roughness coefficient of the channel be known. Thus the need for knowledge of resistance of streams arises naturally in dealing with sedimentation problems.

Experiments by Vito A. Vanoni,[9,10] using a flume with fixed, artificially roughened bed, showed that a flow with suspended load had a smaller friction factor than a clear water flow of the same depth in the same channel. These experiments were made first with clear water and then with varying small amounts of sand, so that the sediment load was controlled. Experiments by Hassan M. Ismail,[11] using a rectangular pipe, showed a decrease in friction factor with increase in load in some cases, but the opposite trend in others, thus duplicating the conflicting results reported by field observers. The apparent paradox was probably due to the fact that in some runs the bed became

---

9 "Transportation of Suspended Sediment by Water," by Vito A. Vanoni, Transactions, ASCE, Vol. 111, 1946, pp. 67-133.

10 "Some Effects of Suspended Sediment on Flow Characteristics," by Vito A. Vanoni, Bulletin 34, Proceedings, 5th Hydr. Conf., State Univ. of Iowa, Iowa City, Studies in Engineering, 1953.

11 "Turbulent Transfer Mechanism and Suspended Sediment in Closed Channels," by Hassan M. Ismail, Transactions, ASCE, Vol. 117, p. 409, 1952.

roughened with small dunes, making the roughness increase instead of decrease when sediment was added to the system.

Fig. 2 shows velocity profiles measured at the center of a flume 0.295 ft deep and 33.5 in. wide for two flows of the same slope and depth. One of the flows is with clear water and the other is with a mean sediment concentration of 15.8 grams per liter of 0.1 mm sediment. It is clear that the sediment-laden flow that has the higher velocity has the lower friction factor. In Fig. 2(b) the relative distance up from the bed is plotted on a logarithmic scale and shows that the velocity profile follows the von Karman logarithmic law. For two-dimensional flow, profiles can be expressed by

$$u = \bar{u} + \frac{1}{k}\sqrt{\frac{\tau_0}{\rho}} + \frac{2.3}{k}\sqrt{\frac{\tau_0}{\rho}}\log_{10}\frac{y}{d} \quad \ldots\ldots\ldots (1)$$

in which u is the point velocity at a distance y up from the bed, $\bar{u}$ represents the mean velocity at the profile, τ_0 denotes the shear stress at the bed, ρ is equal to the mass density of the fluid, d represents the flow depth, and k is the von Karman constant. From Eq. 1

$$u_2 - u_1 = \frac{2.3}{k}\sqrt{\frac{\tau_0}{\rho}}\log_{10}\frac{y_2}{y_1} \quad \ldots\ldots\ldots\ldots (2)$$

in which u_1 and u_2 are the velocities at levels y_1 and y_2, respectively. Since τ_0 can be computed from the measured slope and depth, k can be computed from a pair of points on the velocity profile by Eq. 2. The effect of the suspended sediment in reducing k, as indicated by Fig. 2, is a general one occuring at all times[10] in the laboratory as well as in the field.

Experiments[12] demonstrated clearly how the friction factor is affected by the dunes that develop on the sand bed of a stream. He obtained friction factors for dune-covered beds that were as much as seven times as large as those for flat sand beds of the same material. Other studies also showed[13,14] clearly the importance of dunes on the channel roughness.

Recent studies of rivers have contributed appreciably to the understanding of the resistance problems. One such study[15] presented detailed observations of streams which show that at a given discharge high sediment loads are associated with high mean velocities and low water depths. This means that high loads are also accompanied by low friction factors, as was found on the Indus River system by Gerald Lacey[8] over 35 years ago.

A study of Manning's roughness coefficient n as a function of river stage for the lower Mississippi River showed that n varied from about 0.040 at low stages

---

12 "Mechanics of Streams with Movable Beds of Fine Sands," by Norman H. Brooks, Proceedings Separate No. 668, ASCE, April, 1955.

13 "Some Aspects of Roughness in Alluvial Channels," by Said M. Ali and Maurice L. Albertson, Dept. of Civil Engrg., Colorado A. and M. College, Fort Collins, Colorado, August, 1953, revised August, 1956.

14 "A Study of Sediment Transport in Alluvial Channels," by James R. Barton and Pin-Nam Lin, Report No. 55 J.R.B. 2, Civil Engrg. Dept., Colorado A. and M. College, Ft. Collins, Colorado, March, 1955.

15 "Relation of Suspended Sediment Concentration to Channel Scour and Fill," by Luna B. Leopold and Thomas Maddock Jr., Bulletin 34, Proceedings, 5th Hydr. Conf., State Univ. of Iowa, Studies in Engrg., 1953.

to about 0.030 or less at flood stages.[16] A recent investigation of the bed configuration of the lower Mississippi River by means of a sonic fathometer found that sand waves were present at all times and that the largest waves were formed at the highest flow rates.[17] It was concluded that these waves must be a major factor in determining the friction coefficient of the river, although it could not be measured during the investigations. The loop in the rating curve of the River could be explained, at least partially, by a lag in the adjustment of the sand waves to the flow, that is, during the rising flood the waves are growing and hence have a smaller resistance than they do at the same flow rate during the receding flood when the sand waves are diminishing.

Data were presented on the Missouri River near Fort Randall showing that the Manning roughness coefficient diminished with increase in discharge.[18] The minimum roughness coefficient obtained was approximately equal to that which would be expected by a sand roughness equal to the grain size of the bed material. Therefore it seemed reasonable to conclude that dunes existed on the bed at lower discharges.

APPARATUS AND PROCEDURE

The equipment and techniques used in the experiments are essentially those described by Norman H. Brooks[12] ASCE, and therefore are mentioned only briefly herein. The experiments were performed by George N. Nomicos and are described elsewhere.[19,20]

Flume.—The flume used in these studies is 40 ft long, 10 1/2 in. wide, and 10 in. deep. It is equipped with an axial-flow pump with a variable speed drive, venturi meter, transparent section in the return pipe, and electric immersion heaters to control the temperature of the water. The open flume section is made of hot rolled steel, and its interior is painted with a smooth bitumastic paint. Along the top of the channel are mounted steel rails and a movable instrument carriage which can measure vertical elevations relative to the flume to the nearest 0.001 ft. The entire flume is mounted on a truss, the slope of which can be easily adjusted even during the course of a run. Although the channel itself is 10 in. deep, experiments were made with depths of flow less than 4 in. to avoid excessive wall effects on the velocity and shear distribution of the flow.

Depth and Slope.—The elevation of the water surface and sand bed relative to the rails on the flume was read with the point gage. To determine the bed

16 "A Study of Bed Movement and Hydraulic Roughness Changes in the Lower Mississippi River," by Edwin W. Eden, thesis presented to the State University of Iowa, at Iowa City, in 1938, in partial fulfilment of the requirements for the degree of Master of Science.

17 "Systematic Changes in the Beds of Alluvial Rivers," by Walter C. Carey, and M. Dean Keller, Proceedings Paper 1331, ASCE, August, 1957.

18 "Study of Effects of Channel Stabilization and Navigation Project on Missouri River Levels: - Memo. No. 18, Sediment Characteristics of the Missouri River, Sioux City to the Mouth," by Omaha District Corps of Engrs., U. S. Army, January, 1954.

19 "Effects of Sediment Load on the Velocity Field and Friction Factor of Turbulent Flow in an Open Channel," by George N. Nomicos, thesis presented to California Inst. of Tech., at Pasadena, in 1956, in partial fulfilment of the requirements for the degree of Doctor of Philosophy.

20 "Laboratory Studies of the Roughness and Suspended Load of Alluvial Streams," by Vito A. Vanoni and Norman H. Brooks, Report No. E-68, Sedimentation Lab., California Inst. of Tech., December, 1957.

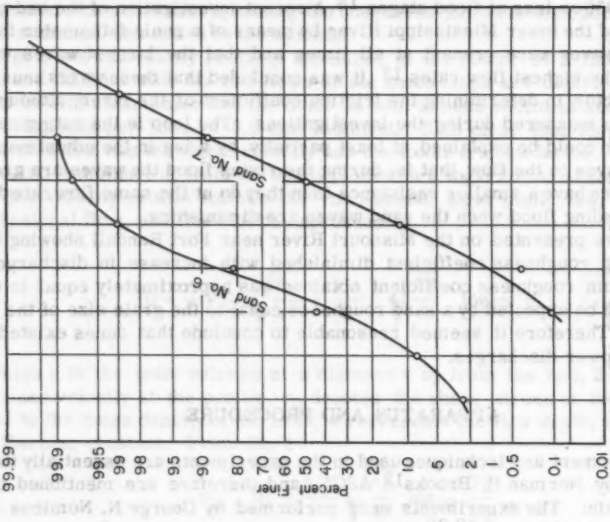


FIG. 3.—CUMULATIVE SIZE FREQUENCY CURVES

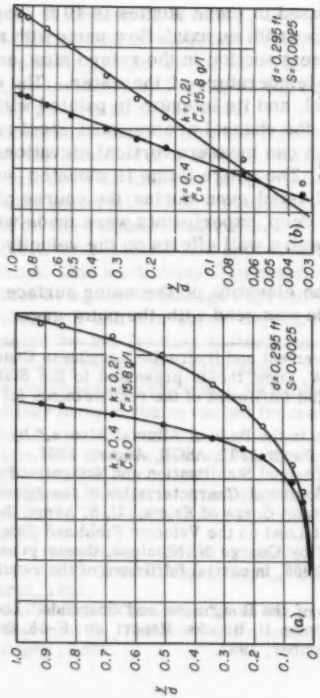


FIG. 2.—VELOCITY PROFILES

elevation once the water surface had been measured, the flow was stopped and the water drained out. The bed was then leveled in reaches of 3 ft or 4 ft with a scraper carried on the instrument carriage rails. The elevation of this leveled surface was taken as the mean elevation of the bed. The water depth at any point was taken as the difference between water surface and bed elevations and the local elevation of the energy grade line was computed by adding the velocity head based on mean depth to the water surface elevation.

Profiles along the flume of the water surface, bed, mean depth, and energy grade line were plotted for each run to determine if uniform flow was obtained. Usually several trail runs were required before uniform conditions were established. The water surface and energy grade line were not always parallel to the flume itself, even with uniform flow. Therefore, the actual slopes were obtained by adding the slope of the flume and the slope of the water surface or energy grade line relative to the flume.

Velocity.—The discharge was measured with a venturi meter having a throat diameter of 3.00 in. placed in a 4-in. diam standard pipe return line. The mean velocity was computed as the discharge divided by the mean depth times the flume width. Point velocities were measured with a 3/16 diam Prandtl pitot-static tube and a water manometer reading to .001 ft.

Sediment Concentration.—The mean sediment discharge concentration, $\overline{C}$, was determined by sampling the flow in the suction well of the pump at the downstream end of the flume. The sampler was a brass tube 0.302 in. in inside diameter with a half-loop at the end so that when the tube was held vertically during sampling the inlet faced upward into the flow which was downward.

Point concentrations, c, in the flume were determined from samples taken with a 3/16 in. outside diameter brass tube flattened at the end so the tip opening was 0.040 in. high by 0.217 in. wide. The tube was bent in a right angle similar to the common pitot tube, and was mounted on the instrument carriage with the tip pointing upstream.

The velocity at the inlets to both samplers was kept the same as the local flow velocity by controlling the sampling rate. Each sample consisted of at least three one-liter bottles of the sediment-water mixture. The concentrations were determined by filtering, drying, and weighing the sediment collected in each bottle.

Temperature.—The water temperature in all runs was maintained at 25° ± 1°C. This was accomplished with immersion heaters in the return pipe which could be regulated manually to give power input ranging up to 4,000 w in convenient steps.

Side-Wall Corrections.—Because the width-to-depth ratio of the flows used in the experiments were small compared with natural streams, the effects of side-wall friction are relatively more important. A correction is made to reduce the laboratory results to correspond to those that would be obtained for much wider streams. This follows a method presented by Joe W. Johnson[21] using a procedure developed by Brooks.[20,22] This yielded an hydraulic radius r_b, shear velocity U_{*_b}, and Darcy-Weisbach friction factor f_b applying to the bed itself relatively free of side-wall influence. The friction factor f_b is de-

---

21 "The Importance of Side-Wall Friction in Bed-Load Investigations," by J. W. Johnson, Civil Engineering, Vol. 12, June, 1942, pp. 329-331.

22 "Laboratory Studies of the Mechanics of Streams Flowing Over a Movable Bed of Fine Sand," by Norman H. Brooks, thesis presented to Calif. Inst. of Tech., at Pasadena, in 1954, in partial fulfilment of the requirements for the degree of Doctor of Philosophy.

fined by the Darcy-Weisbach equation,

$$S = f_b \frac{1}{4r_b} \frac{V^2}{2g} \quad \ldots\ldots\ldots\ldots\ldots\ldots (3)$$

in which S is the slope of the energy grade line, V represents the mean flow velocity in the cross section, and g denotes the acceleration of gravity. To compute the mean value, f, of the friction factor, the hydraulic radius r of the section is substituted into Eq. 3 in place of r_b.

Sand Characteristics.—Cumulative size frequency curves for the two sands used in these experiments are shown in Fig. 3, and the size characteristics are summarized in Table 2. These sands were prepared from white foundry

TABLE 2.—CHARACTERISTICS OF SAND USED IN EXPERIMENTS

Sand No. (1)	Experiments used in, set No. (2)	Geometric mean diameter, D_g, in millimeters (3)	Geometric standard deviation, σ_g (4)	Mean sediment diameter, D_s, in millimeters (5)	Mean fall velocity at 25° C, in feet per second (6)
6	I, II, II	0.091	1.16	0.105	0.031
7	IV	0.148	1.16	0.161	0.062

sands with well-rounded grains. The material was almost entirely silica, so that the mean specific gravity of the grains was 2.65. The mean settling velocity, w, of the various sands used was determined from sedimentation diameters of sieve fractions measured by Vanoni[23] where the fractions were obtained with a nest of sieves with openings of adjacent sieves in the ratio $\sqrt[4]{2}$. These sedimentation diameters are shown in Table 3.

TABLE 3.—RELATION BETWEEN SEDIMENTATION DIAMETER AND SIEVE DIAMETER FOR NEVADA WHITE SAND

Tyler Sieve No. retained on (1)	Sieve opening next above, in millimeters (2)	Sieve opening retained on, in millimeters (3)	Mean sieve diameter, in millimeters (4)	Mean sedimentation diameter, D_{si}, in millimeters (5)	Fall velocity, w_i, in feet per second	
					at 20°C (6)	at 25°C (7)
80	0.208	0.175	0.191	0.198	0.078	0.083
100	0.175	0.147	0.161	0.168	0.061	0.066
115	0.147	0.124	0.135	0.153	0.053	0.058
150	0.124	0.104	0.114	0.128	0.038	0.042
170	0.104	0.088	0.096	0.107	0.029	0.032
200	0.088	0.074	0.081	0.096	0.024	0.027
250	0.074	0.061	0.0675	0.086	0.020	0.022

[23] "Experiments on the Transportation of Suspended Sediment by Water," by Vito A. Vanoni, thesis presented to California Inst. of Tech., at Pasadena, in 1940, in partial fulfilment of the requirements for the degree of Doctor of Philosophy.

Procedure for Experiments.—A run with uniform flow was first established by the usual techniques with determinations of depth, water discharge, sediment discharge, and slope. After the final determination of the bed profile by the leveling process, the flow was again started in order to regenerate the bed configuration which was destroyed when the bed profile was taken. When the bed was re-established, the flow was stopped and the water carefully drained off. The bed was then solidified by spraying with chemicals, as explained in detail subsequently. After the chemicals had set, experiments with the stable bed were made, first using clear water and then with varying small amounts of sediment added to the system.

Stabilization of Sand Bed.—The method of stabilizing the sand bed was developed by tests of samples in trays and in actual flume tests. The most satisfactory method involved the use of sodium aluminate and sodium silicate as stabilizing chemicals. The steps followed in the stabilizing process are:

a. Drain the water from the flume and allow the sand to dry for 24 hr to 48 hr so that the moisture content is approximately 10% by weight.

b. Spray the sand with a mixture of the following three materials: 68% by volume of a 2% solution of sodium aluminate; 22% by volume of a solution of sodium silicate of specific gravity 1.2; and 10% by volume of pure water. This mixture was applied to the bed with a paint sprayer until the sand showed signs of saturation. This required an amount of the mixture almost equal to 10% by weight of the sand being treated.

c. After drying for approximate 12 hr, the sand was sprayed with a light application of a calcium chloride solution with specific gravity 1.2.

d. Finally, a thin coat of synthetic varnish was sprayed on the sand to form a waterproof surface.

One of the most difficult problems in the stabilization process was the preservation of the proper grain roughness of the surface of the bed. To disturb the surface characteristics as little as possible, care was taken not to apply an excess of chemicals which would flood the surface, and the solutions were applied gently with a paint sprayer aimed parallel to the bed instead of at the bed. Although the results appeared satisfactory visually, there was, unfortunately, no method of testing whether the grain roughness of the finished surface was exactly the same as that of the loose sand itself.

RESULTS

Outline of Experiments.—The general plan of the experiments and some of the principal quantities measured are presented in Table 4. The experiments are divided into sets and individual experiments. The flow depth, discharge, and mean velocity are kept the same in each set of experiments, but the slope is varied. In Sets III and IV the depth, discharge, and velocity are kept constant throughout. Sets I, II, and III were made with a .091 mm sand and a .148 mm sand was used in Set IV.

Each set contains runs with movable bed, stabilized bed and clear water, and stabilized bed with varying amounts of loose sand added to the system where the material added is the same as that in the bed. In Runs 2, 4, 6, and 8, the bed was stabilized and no sediment was being transported by the flow, that is, the flow consisted only of clear water.

Table 4 shows the important measured and computed quantities obtained in the experiments. Where blank spaces occur in the table, the items were either

not measured or not computed. Measured values of the exponent z in the suspended load equation (Eq. 7) are listed subsequently in Fig. 8 for Runs 1, 3, 5, and 7, which were those with a movable bed.

Bed Configuration.—Observations of the bed configuration and the movement of the configuration were made visually and by means of systematic photographs during the experiments. Fig. 4(a) shows a side view of the bed for Run 1 and Fig. 4(b) shows a plan view for Run 2, where the bed configuration for Run 2 is the same as that for Run 1 except that it has been stabilized by the method previously described. Fig. 5 shows similar pictures for Run 3 and 4. Fig. 6(a) shows the side view and Fig. 6(b) the plan view of the bed in Run 5, which has been described as flat in Table 4. It will be seen that the bed is actually not entirely flat but that there are small ripples near the wall. Figs. 4, 5, and 6 show the meaning of the terms used to describe the bed condition in column 15 of Table 4.

Velocity profiles.—Velocity profile measurements were made at the centerline of the flume at Station 24, that is, 24 ft downstream from the inlet to the flume. These measurements fitted the logarithmic law (Eq. 1) very well, as may be seen in Fig. 7, which shows the profiles for Runs 1, 3, 5, and 6. The quantity m noted is the slope of the lines fitted to the points in fps per cycle. Eq. 2 can be transposed to give

$$m = \frac{u_2 - u_1}{\log \frac{y_2}{y_1}} = \frac{2.3}{k} \sqrt{\frac{\tau_o}{\rho}} = \frac{2.3}{k} u_* \quad \ldots\ldots\ldots\ldots (4)$$

from which

$$k = \frac{2.3}{m} u_* \quad \ldots\ldots\ldots\ldots\ldots\ldots\ldots (5)$$

The von Karman constant k_{cl} for the centerline profile was determined from

$$k_{cl} = \frac{2.3}{m} u_{*cl} \quad \ldots\ldots\ldots\ldots\ldots\ldots (6)$$

in which the center line shear velocity u_{*cl} is given by

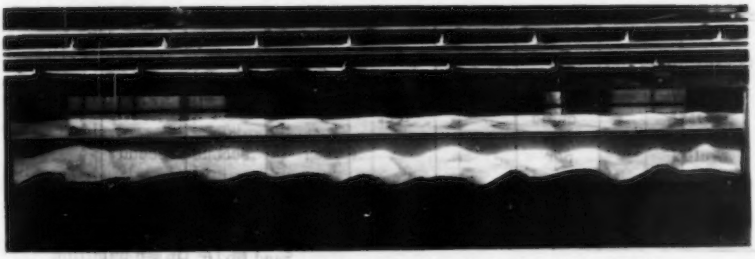
$$u_{*cl} = \sqrt{\frac{f}{8}}\ \bar{u}_{cl} \quad \ldots\ldots\ldots\ldots\ldots\ldots (7)$$

and $\bar{u}_{cl}$ is the mean velocity computed from the measured profile at the centerline and f is the friction factor for the channel obtained from Eq. (3) using the hydraulic radius of the section r instead of r_b. The values of k_{cl}, that are listed in Table 4, consistently decrease as the concentration $\overline{C}$ increases.

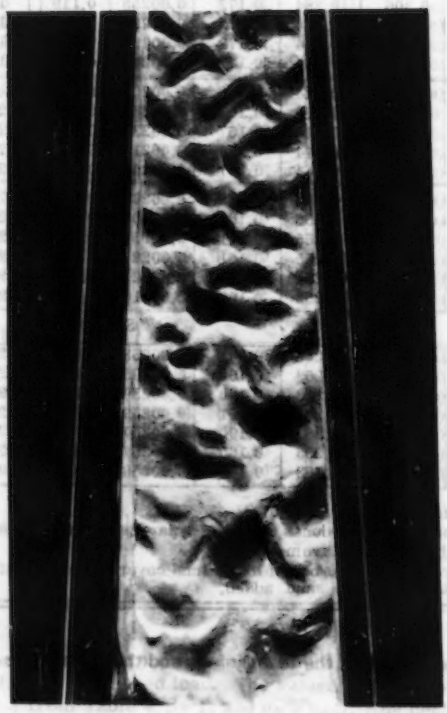
Sediment Concentration Profiles.—The suspended load equation for distribution of concentration c of particles with settling velocity w over a vertical is

$$\frac{c}{c_a} = \left(\frac{d - y}{y}\ \frac{a}{d-a}\right)^z \quad \ldots\ldots\ldots\ldots\ldots\ldots (8)$$

in which y is the distance up from the bottom, d represents the flow depth, c_a



(*a*) RUN NO. 1, SIDE VIEW, LOOSE SAND, DURING FLOW



(*b*) RUN NO. 2, PLAN VIEW, STABILIZED BED, LOOKING UPSTREAM, WITHOUT FLOW

FIG. 4.—BED CONFIGURATION, SET I, U = 1.23 FEET PER SECOND, d = .284 FEET

TABLE 4.—SUMMARY OF

Set No.	Run No.	Discharge Q, in cubic feet per second	Depth, d, in feet	Hydraulic radius, r, in feet	Slope, S	Shear velocity U_*, in feet per second	Average velocity U, in feet per second	Friction factor, f
(1)	(2)	(3)	(4)	(5)	(6)	(7)	(8)	(9)
					Sand No. 6, D_g = 0.091			
I	1	0.306	0.284	0.172	0.0025	0.118	1.23	0.074
	1A	0.306	0.284	0.172	0.00245	0.117	1.23	0.073
	2	0.306	0.284	0.172	0.0026	0.121	1.23	0.077
	2a	0.306	0.284	0.172	0.00255	0.119	1.23	0.076
	2b	0.306	0.284	0.172	0.00255	0.119	1.23	0.074
	2c	0.306	0.284	0.172	0.0025	0.118	1.23	0.073
	2d	0.306	0.284	0.172	0.00245	0.117	1.23	0.073
II	3	0.433	0.244	0.157	0.0020	0.101	2.02	0.0198
	4	0.433	0.244	0.157	0.0025	0.112	2.02	0.0246
	4a	0.433	0.244	0.157	0.0023	0.108	2.02	0.0226
	4b	0.433	0.244	0.157	0.0021	0.103	2.02	0.0207
	4c	0.433	0.244	0.157	0.0020	0.101	2.02	0.0198
III	5	0.509	0.257	0.162	0.00206	0.104	2.26	0.0169
	5A	0.509	0.255	0.161	0.00206	0.104	2.28	0.0165
	6	0.509	0.255	0.161	0.00251	0.114	2.28	0.0208
	6a	0.509	0.255	0.161	0.00227	0.108	2.28	0.0182
	6b	0.509	0.254	0.161	0.00227	0.108	2.28	0.0180
	6c	0.509	0.252	0.160	0.00210	0.104	2.30	0.0163
					Sand No. 7, D_g = 0.148			
IV	7	0.509	0.255	0.161	0.00258	0.116	2.28	0.0207
	8	0.509	0.253	0.160	0.00293	0.123	2.29	0.0230
	8B	0.509	0.253	0.160	0.00259	0.116	2.29	0.0203
	8a	0.509	0.254	0.161	0.00259	0.116	2.28	0.0206
	8b	0.509	0.253	0.160	0.00257	0.116	2.29	0.0202
	8c	0.509	0.253	0.160	0.00257	0.116	2.29	0.0202
	8d	0.509	0.253	0.160	0.00259	0.116	2.29	0.0203

[a] Temperature for all runs was 25.0° C.
[b] Key for bed condition: (1) dunes, (2) dunes, larges at walls tapering down to near-ripples extending about 2 in. out from walls.
[c] Key for bed treatment: (a) bed of loose sand covering bottom of flume, (b) sand natural configuration with loose sand added.

denotes the concentration at the level y = a, and the exponent z is given by

$$z = \frac{w}{\beta k u_*} \quad \ldots\ldots\ldots\ldots\ldots\ldots\ldots\ldots (9)$$

in which β is the ratio of the diffusion coefficients for sediment and momentum. Fig. 8 shows logarithmic graphs of (d-y)/y versus c for measurements made on the longitudinal centerline of the flume of Station 24 for runs 1, 3, 5 and 7.

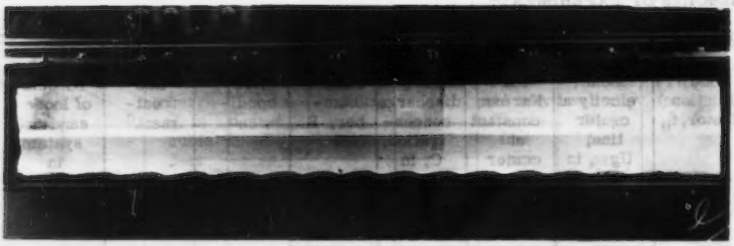
RESULTS OF EXPERIMENT[a]

Bed friction factor, f_b	Shear velocity at center line, $U_{*_{cl}}$, in feet per second	von Karman constant at center line, k_{cl}	Sediment discharge concentration, $\bar{C}$, in grams per liter	Froude number, F	Bed condition[b]	Bed treatment[c]	Amount of loose sand in system, in kilograms
(10)	(11)	(12)	(13)	(14)	(15)	(16)	(17)
millimeters, σ_g = 1.16							
0.106	0.151	0.369	3.64	0.41	(1)	(a)	90
0.104	0.150	0.367	3.38	0.41	(1)	(a)	90
0.112	0.155	...	0.00	0.41	(1)	(b)	0
0.109	0.153	...	0.31	0.41	(1)	(c)	...
0.107	0.152	...	0.47	0.41	(1)	(c)	...
0.105	0.151	...	0.60	0.41	(1)	(c)	...
0.104	0.150	...	0.83	0.41	(1)	(c)	...
0.0211	0.110	0.265	4.60	0.72	(2)	(a)	85
0.0283	...	...	0.00	0.72	(2)	(b)	0
0.0253	...	...	1.71	0.72	(2)	(c)	...
0.0225	...	...	3.44	0.72	(2)	(c)	...
0.0211	...	...	3.63	0.72	(2)	(c)	...
0.0170	0.111	0.223	6.92	0.78	(4)	(a)	55
0.0165	0.109	0.219	8.08	0.79	(4)	(a)	55
0.0229	0.136	0.384	0.00	0.79	(4)	(b)	0
0.0189	0.116	0.255	3.99	0.79	(4)	(c)	3.00
0.0187	0.116	0.236	5.71	0.80	(4)	(c)	6.00
0.0164	0.114	0.209	6.82	0.81	(4)	(c)	9.00
millimeters, σ_g = 1.16							
0.0227	0.135	0.299	3.61	0.79	(4)	(a)	55
0.0262	0.150	0.364	0.00	0.80	(4)	(b)	0
0.0222	0.134	0.355	0.00	0.80	(4)	(b)	0
0.0225	0.135	0.345	0.51	0.80	(4)	(c)	0.50
0.0219	0.133	0.330	1.41	0.80	(4)	(c)	1.50
0.0219	0.133	0.319	2.43	0.80	(4)	(c)	3.00
0.0222	0.134	0.310	3.27	0.80	(4)	(c)	6.00

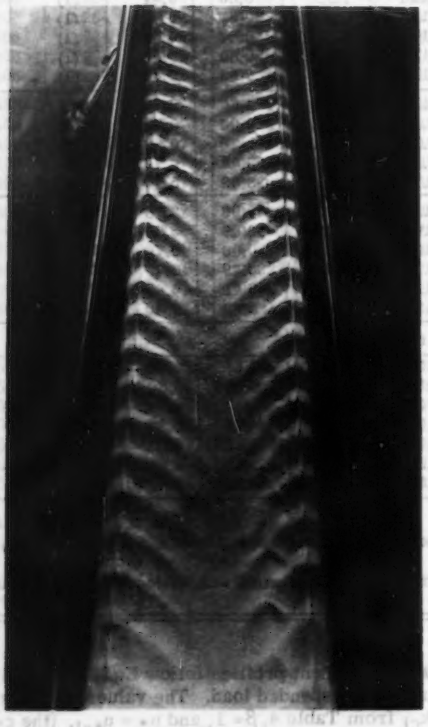
ly flat in center of flume, (3) ripples near walls, flat in center, (4) flat except for slight

bed stabilized in natural configuration with no loose sand, (c) sand bed stabilized in

It is seen that these sediment profiles follow Eq. 8, the well-established equation for distribution of suspended load. The values of the exponent z computed by Eq. 8 using k_{cl} from Table 4, $\beta = 1$, and $u_* = u_{*_{cl}}$, (the centerline value defined by Eq. 7 are close to those appearing in Fig. 8 which are determined from the slope of the lines in the figure. It is of interest to note that the profile for Run 1 agrees with the theory as well as the other runs in spite of the fact that it is the only one of the four for which the bed was covered with dunes.

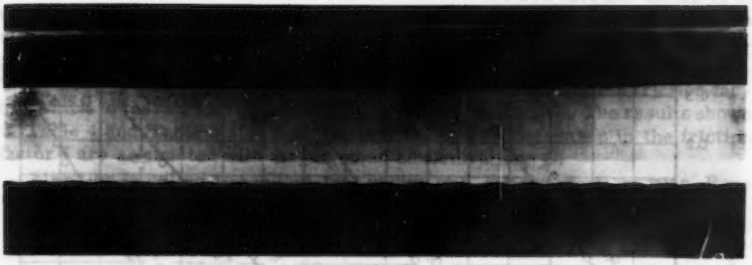


(*a*) RUN NO. 3, SIDE VIEW, LOOSE SAND, DURING FLOW

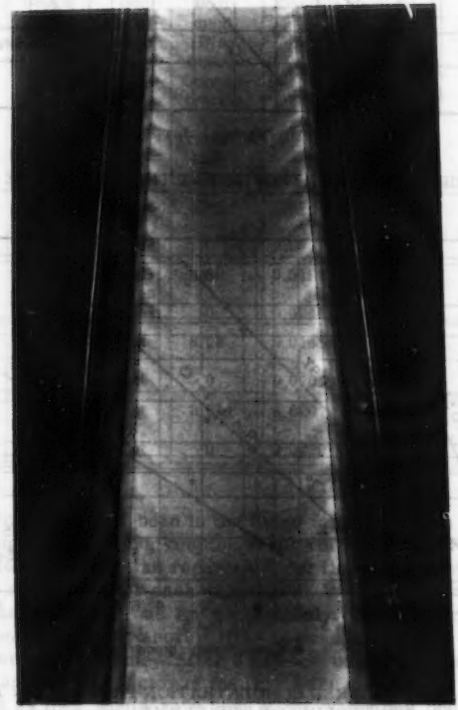


(*b*) RUN NO. 4, PLAN VIEW, STABILIZED BED, LOOKING UPSTREAM, WITHOUT FLOW

FIG. 5.—BED CONFIGURATION, SET II, U = 2.02 FEET PER SECOND, d = .244 FEET



(*a*) RUN NO. 5, SIDE VIEW, LOOSE SAND, WITHOUT FLOW



(*b*) RUN NO. 5, PLAN VIEW, LOOKING UPSTREAM, LOOSE SAND

FIG. 6.—BED CONFIGURATION, SET III, U = 2.28 FEET PER SECOND, d = .255 FEET

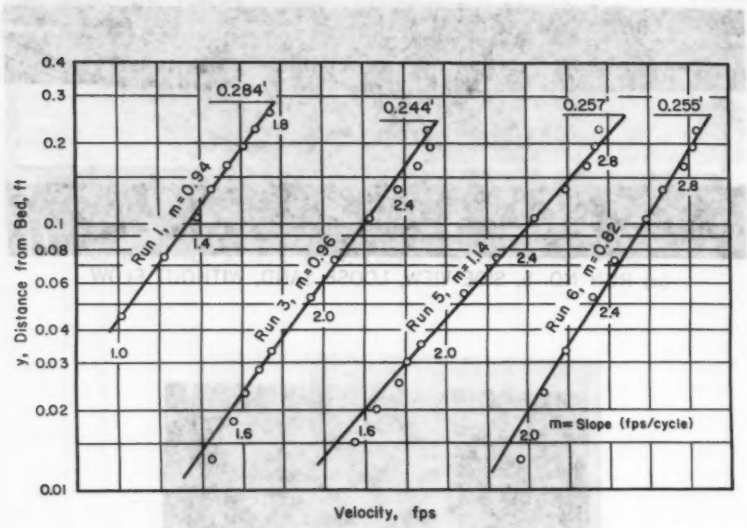


FIG. 7.—MEASURED VELOCITY PROFILES AT THE CENTERLINE OF THE FLUME

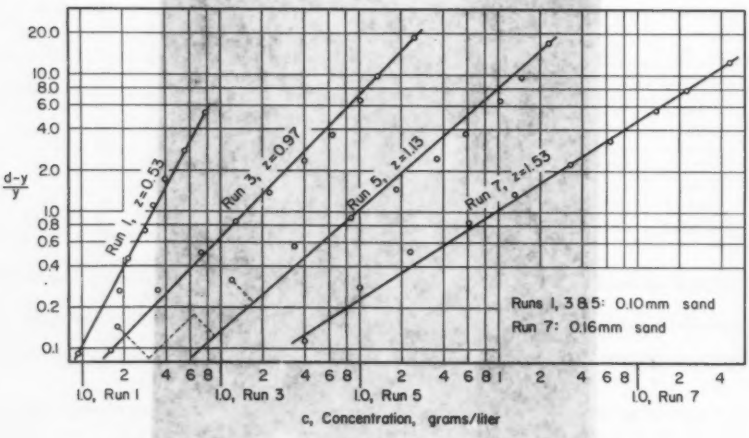


FIG. 8.—MEASURED CONCENTRATION PROFILES ON THE CENTERLINE OF THE FLUME

Friction Factor.—From Table 4 it is seen that the bed friction factor f_b is smaller for sediment-laden flow over loose sand beds than for comparable clear flow over fixed beds of the same configuration. The values of f_b for comparable sediment-laden and clear-water flows are summarized in Table 5. This shows clearly the effect of moving sediment in reducing the friction factor, which in these experiments amounted to from 5% to 28%. The results shown in Table 4 and Table 5 also indicate that the larger decreases in the friction factor f are associated with larger mean concentrations $\overline{C}$.

Attention is called to the fact that values of f_b for the identical runs, Runs 8 and 8B, with clear water and stabilized bed, are not the same. Run 8 was made once and then repeated on the following day, and the results agreed closely.

TABLE 5.—COMPARISON OF FRICTION FACTORS FOR SEDIMENT-LADEN FLOWS WITH THOSE FOR CLEAR WATER FLOWS OVER STABILIZED SAND BEDS OF THE SAME CONFIGURATION.

Set No.	Run No.	Depth, in feet	Bed Condition	Sediment Discharge Concentration, $\overline{C}$, in grams per liter	Friction Factors		Decrease	
					Mean f	For Bed f_b	Δf_b	%
(1)	(2)	(3)	(4)	(5)	(6)	(7)	(8)	(9)
I	1	0.284	Dunes	3.64	0.074	0.106	.006	5
	2	0.284	Dunes	0	0.077	0.112		
II	3	0.244	Small dunes	4.60	0.0198	0.0211	.0072	25
	4	0.244	dunes	0	0.0246	0.0283		
III	5A	0.255	Flat	8.08	0.0165	0.0165	.0064	28
	6	0.255	Flat	0	0.0203	0.0229		
IV	7	0.255	Flat	3.61	0.0207	0.0227	.0035	13.5
	8	0.253	Flat	0	0.0230	0.0262		

However, when the water had been in the flume for longer than a total time of 10 hr, some changes occurred, giving the results of Run 8B. To further investigate this problem, Run 8B was repeated three times, once on each of three days, drying the sand bed after each experiment.

On the first day the water was run continuously. On the second day the experiment was completed in as short a time as possible and the pump stopped, leaving the water in the flume. After 3 hr the run was repeated. The flow characteristics and friction factor of the flow were changed by approximately the same amount as they would have been if the water had been running continuously. The run for the third day was a repetition of that for the first, with approximately the same results. From this it was concluded that the water was in some way affecting the varnish coat applied to the sand when the water

remained in the flume for long periods. Run 8 is considered to give the valid results, with Run 8B being affected by swelling of the varnish between grains.

RESULTS

Effect of Sediment Load on the Friction Factor.—The effect of the sediment load on the friction factor may be seen in Table 5 by comparing the results of clear and sediment-laden water for each set of runs. Sets I, II, and III were made with the same sediment, so the results are directly comparable. Set IV was made with a coarser material. It is clear that by adding a sediment load to a flow the friction factor is decreased, since in all four sets of experiments the sediment-laden flows had smaller friction factors than the comparable clear flows. The relative magnitude of the reduction in friction factor seems to vary with concentration, the values with highest concentration producing the largest change. Referring again to Table 5, it is seen that in Set I the friction factor f_b for a flow with a concentration of 3.64 grams per liter was 5% lower than in the comparable clear flow. In Series II and III the reductions in f_b were 25% and 28% with concentrations of 4.60 and 8.08 grams per liter, respectively. From these figures it appears that rate of change in f_b with concentration decreases at high values of the concentration.

The reduction in f_b may be attributed to alterations of the turbulent structure of the flow by the suspended load. The mechanism of this process will be examined in more detail.

Effect of Bed Configuration on the Friction Factor.—The effect of dunes and ripples on the friction factor agrees with the data obtained by others.[12,13,14] For example, the large dunes in Set I cause f_b to attain the high value of 0.106 in Run 1, compared with the values for all other runs which were less than 0.030 because of predominantly flat beds. From these data it can be concluded that in flume experiments changes in friction factor due to dunes can greatly exceed changes due directly to the moving sediment.

In a study of the Mississippi River, it was observed that at Vicksburg the largest dunes occurred at the highest stage.[16] Whereas at Memphis, bed irregularities were observed only on the rising part of the highest stage. The largest of these had heights as much as 34 ft. In another study, bed configurations of the Mississippi River near Baton Rouge were observed by means of a sonic fathometer,[17] and it was found that the largest dunes occurred at the highest stages. There were several systems of dunes of varying wavelengths, the largest of which had lengths of as much as two miles and heights of the order of 30 ft. The shorter dunes were superposed on the larger ones. A study of these profiles showed that at low stage some of the longer waves disappeared but that short waves of the order of 20 ft to 50 ft in length and 1 ft to 5 ft in height remained. Fig. 9, reproduced from one of the studies,[17] shows profiles at Donaldsonville gage for two stages. For the high stage which occurred on April 10, 1956, it is seen that there are waves of considerable length. For the lower stage which occurred in July, some of the longer waves are no longer present. Despite the increase in dune height with stage, it was found that the Manning coefficient n decreased as the stage increased.[16] The sediment load also increases with stage, and can account for some reduction in the roughness factor but not necessarily for all of it. It is possible that the long waves actually do not contribute much of the bed roughness and that the shorter, steeper ones, which seem to predominate at the low stages, may actually result

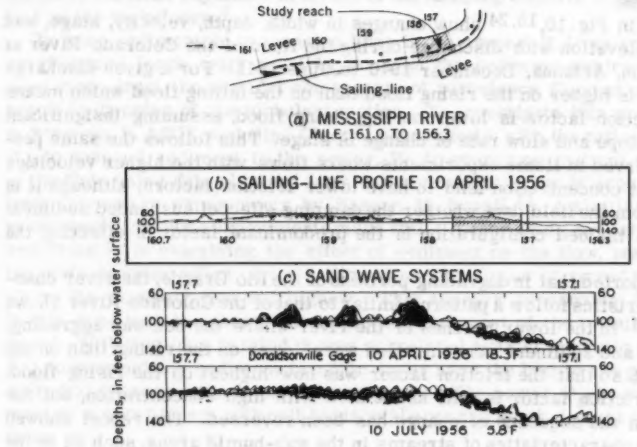


FIG. 9.—BED PROFILES FOR THE LOWER MISSISSIPPI RIVER

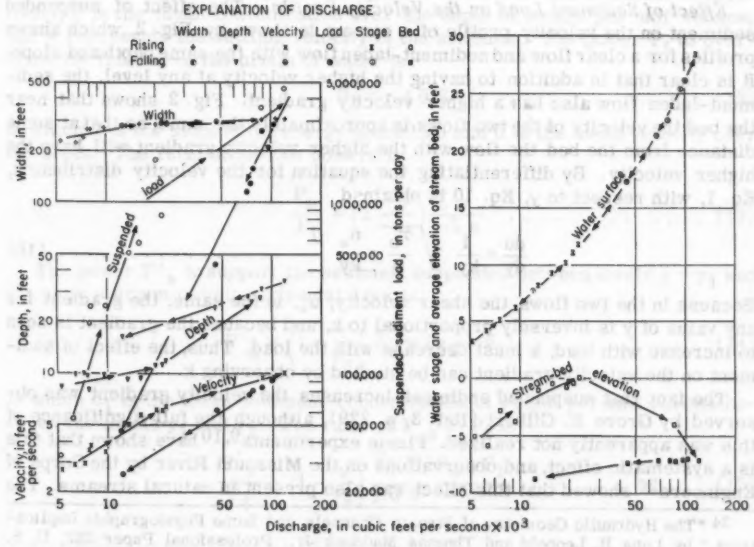


FIG. 10.—COLORADO RIVER FLOOD DATA

in a higher roughness than the larger ones which have been observed at the highest stages.

The data in Fig. 10,[15,24] show changes in width, depth, velocity, stage, and streambed elevation with discharge during the flood of the Colorado River at Grand Canyon, Arizona, December 1940 to June 1941. For a given discharge the velocity is higher on the rising flood than on the falling flood which means that the friction factor is lower on the rising flood, assuming insignificant changes in slope and slow rate of change of stage. This follows the same pattern as observed in flume experiments where flows with the higher velocities and sediment concentration tend to have lower friction factors, although it is not clear from the field data whether the damping effect of suspended sediment or change in the bed configuration is the predominant factor in effecting the change.

It was reported that in degrading portions of the Rio Grande, the river channel characteristics follow a pattern similar to that of the Colorado River shown in Fig. 10.[25] In the lower reaches of the river where the bed was aggrading, the velocity and sediment concentration were lower on the rising than on the falling flood, so that the friction factor was now highest on the rising flood. The lower friction factor is still associated with high concentration, but for some reason the sequence of change has been reversed. The report showed also that the characteristics of streams in the sub-humid areas, such as in the eastern United States, are much more stable than those of the arid western part.[25] In these streams the sediment loads are much lower and the beds apparently much more stable, so that the changes in the bed are probably much smaller than in streams whose beds are easily eroded.

Effect of Sediment Load on the Velocity Profile.—The effect of suspended sediment on the velocity profile of a stream is shown by Fig. 2, which shows profiles for a clear flow and sediment-laden flow with the same depth and slope. It is clear that in addition to having the higher velocity at any level, the sediment-laden flow also has a higher velocity gradient. Fig. 2 shows that near the bed the velocity of the two flows is approximately the same, so that at some distance from the bed the flow with the higher velocity gradient will have the higher velocity. By differentiating the equation for the velocity distribution, Eq. 1, with respect to y, Eq. 10 is obtained

$$\frac{du}{dy} = \frac{1}{ky}\sqrt{\frac{\tau_0}{\rho}} = \frac{u_*}{ky} \qquad \ldots\ldots\ldots\ldots\ldots (10)$$

Because in the two flows the shear velocity, u_*, is the same, the gradient for any value of y is inversely proportional to k, and because the gradient is seen to increase with load, k must decrease with the load. Thus, the effect of sediment on the velocity gradient can be studied by observing k.

The fact that suspended sediment increases the velocity gradient was observed by Grove K. Gilbert (Ref. 3, p. 229), although the full significance of this was apparently not realized. Flume experiments[9,10] have shown that this is a systematic effect, and observations on the Missouri River by the Corps of Engineers[26] showed that this effect was also present in natural streams. The

[24] "The Hydraulic Geometry of Stream Channels and Some Physiographic Implications," by Luna B. Leopold and Thomas Maddock Jr., Professional Paper 252, U. S. Geol. Survey, 1953.

[25] "Floods in Relation to the River Channel," by Luna B. Leopold and M. Gordon Wolman, Publication No. 42, Internatl. Assn. of Hydrology, Dijon, France, 1956.

[26] "Sediment Characteristics Study of Missouri River at Omaha, Nebraska," U. S. Engr. Office, Omaha, Nebr., 1951.

mechanism by which the sediment increases the gradient, and hence the mean velocity, has been explained in terms of the damping effect of suspended material on the turbulence.[9]

To keep sediment in suspension, that is, to prevent it from settling due to gravitational force, work must be done on the sediment grains. This work must come from the vertical components of turbulence fluctuations and must result in damping of the turbulent motion. To investigate this problem, Hans A. Einstein, F. ASCE, and Ning Chien[27] correlated k with the ratio of the power, P_s, to suspend sediment to the power, P_f, to overcome hydraulic resistance to the flow, using data obtained from measurements on the Missouri River and from laboratory experiments by Hassan M. Ismail.[11] A similar graph was presented[10] for flume experiments made with 0.1 mm sand. Arthur B. Buckley[8] and Chien,[28] in examining the effect of sediment on the flow, postulated that the main damping effect of the sediment on turbulence occurred near the bed where the concentration was highest. This appears reasonable, because it is in this zone that the shear rate is highest and most of the turbulence is produced. With this idea in mind, k was correlated against the ratio of the power P'_s to suspend the sediment in a thin layer near the bed to the power P_f required to overcome the frictional resistance. The power, P_s, to support sediment in a water prism with unit horizontal area and depth d equal to the stream depth is

$$P_s = \frac{\gamma_s - \gamma}{\gamma_s} \bar{c}\, w\, d \quad \ldots\ldots\ldots\ldots\ldots (11)$$

in which γ and γ_s are the specific weights of the water and sediment respectively, $\bar{c}$ is the mean concentration over the depth in weight per unit volume, and w represents the settling velocity of the sediment. The power P_f to overcome the friction of the prism of water is

$$P_f = \gamma\, d\, \bar{u}\, S \quad \ldots\ldots\ldots\ldots\ldots (12)$$

in which S is the slope of the energy grade line and $\bar{u}$ is the mean velocity over the depth. The ratio of the two powers is

$$\frac{P_s}{P_f} = \left(1 - \frac{\gamma}{\gamma_s}\right) \frac{\bar{c}\, w}{\gamma\, \bar{u}\, s} \quad \ldots\ldots\ldots\ldots\ldots (13)$$

The power P'_s to support the sediment suspended between levels $y = y_1$ and $y = y_2$ in a prism of unit horizontal area is,

$$P'_s = \left(1 - \frac{\gamma}{\gamma_s}\right) \bar{c}_1\, w \left(y_2 - y_1\right) \quad \ldots\ldots\ldots\ldots\ldots (14)$$

in which $\bar{c}_1$ is the mean sediment concentration in weight per unit volume between the levels y_1 and y_2. The ratio of P'_s to P_f is

$$\frac{P'_s}{P_f} = \left(1 - \frac{\gamma}{\gamma_s}\right) \frac{\bar{c}_1\, w}{\gamma\, \bar{u}\, S} \frac{y_2 - y_1}{d} \quad \ldots\ldots\ldots\ldots\ldots (15)$$

---

27 "Second Approximation of the Suspended Load Theory," by H. A. Einstein and Ning Chien, Series 47, Issue No. 2, Univ. of California, Berkeley, Calif., January, 1952.

28 "The Present Status of Research on Sediment Transport," by Ning Chien, Transactions, ASCE, Vol. 121, 1956, p. 833.

Fig. 11(a) shows a graph P'_s/P_f plotted against k for flume data obtained with uniform sand of 0.1 mm size, where y_1 and y_2 have been taken as .001 and .01 times the flow depth, respectively. Fig. 11(b) shows a graph of the same data[10] plotted according to the method of Einstein and Chien,[27] that is, k is plotted against P_s/P_f. It is seen that the correlation of the data in Fig. 11(a) is better than in Fig 11(b). This tends to support the ideas of Buckley and Chien and may also explain why the velocity remains logarithmic in a sediment-laden flow, as seen in Fig. 2, even though the turbulence has been modified considerably. If significant damping of the turbulence occurred over the entire depth, a distortion would be expected in the distribution of the turbulence, and

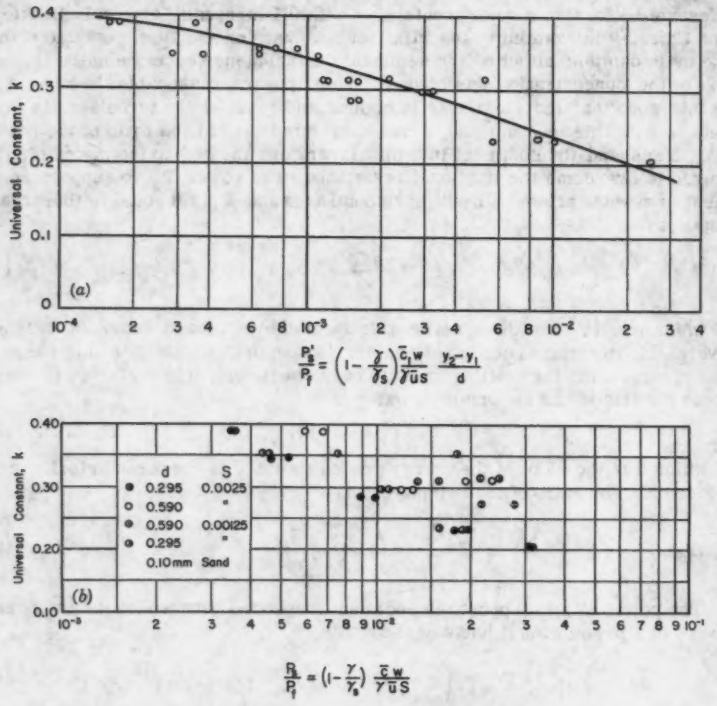


FIG. 11.—REDUCTION OF THE VON KARMAN CONSTANT IN SEDIMENT LADEN FLOW

hence in the shape of the velocity profile. However, if the principal interference with the turbulence occurs near the bed, the turbulence energy will be reduced, but it may still follow the same laws in diffusing through the section, and the same shape of velocity distribution might be expected.

Referring again to Fig. 2, it is seen that the two flows have the same depth and hence, hydraulic radius, and the same slope. The one with the higher mean velocity, that is, the sediment-laden flow, will have the lower friction factor. The decrease in f, shown in Table 4, for the sediment-laden flows, results

from the damping phenomenon examined previously. A comparison of the k-values listed in Table 3 will show that the turbid flows have much the lower values, thus indicating that damping has occurred.

General Examination.—The present experiments have shown that a sediment-laden stream acts in two ways to change its roughness coefficient: (1) a smoothing-out of the bed configurations tends to reduce the coefficient as the velocity increases; and (2) damping of the turbulence by suspended sediment tends to increase the velocity gradients so that the difference between the velocity near the bed and near the surface increases along with the mean velocity. In the present laboratory experiments with 0.091 mm sand, the change in the bed friction factor, f_b, resulting from change in bed configuration alone was as much as five-fold in going from a dune-covered bed to a flat bed. On the other hand, the maximum reduction in f_b due to the sediment load was only 28% (Run 5A). Because the Manning roughness coefficient n is approximately proportional to $\sqrt{f_b}$, the corresponding changes in n are about twofold and 13%, respectively. It is significant that the run which showed the maximum reduction in friction factor (Run 5A) also had the lowest value of k as determined from the centerline velocity profile. From these few data, it appears that the change in bed configuration has a much larger influence on the roughness coefficient than the damping effect. From this it can be judged that the large reductions in roughness coefficients reported by Buckley for the Nile, Eden for the Mississippi, and Lindley for the Indus River, could not be the result only of damping, but must have been also affected by significant changes in dunes on the bed. Judging from the flume experiments it can be expected that the dunes will diminish as the velocity increased, while at the same time, the load increased. Because both of these effects tend to reduce the roughness coefficient, the field observations are in agreement with flume studies and the process can be explained at least qualitatively by the combination of the two effects.

The explanation of the observations that for the same discharge the roughness coefficient of a stream on a rising flood is smaller than on a falling flood presents some difficulties. Buckley and Lindley noted that for a given flow the concentration was higher during the rising flood than during the falling flood, and explained the reduction in roughness by the effect of the higher load. Judging from the results of the present experiments as shown by Table 5, the changes in roughness factor observed in the field are too large to be accounted for by damping effect alone, and some readjustment of the bed must be involved in order to achieve the changes observed. During the rising stage the stream bed probably becomes smoother because the transportation of a high sediment load requires a lower depth and higher velocity compared with the falling-stage flow for which the transport rate is usually less. However, because the damping effect also reduces the roughness, it is not possible to determine the relative magnitude of the two effects from the field data alone. Bottom configuration data of the kind obtained by Carey and Keller, along with stage, slope, discharge and load data, would do much to clarify this problem.

The field data of Buckley, Lindley, and Leopold and Maddock on the variation of stream characteristics, report only total sediment concentration and do not give size distribution of the load or division between wash load and bed-material load. As seen from Fig. 11, the effect of concentration on k, and hence upon friction factor, depends on the settling velocity w as well as the concentration, so that for the same $\overline{C}$, coarse material with high settling velocity has a greater effect on k and on the reduction in friction factor. By the same token, fine materials such as silt and clay have low settling velocities, and hence

small damping effects even for large concentrations. The loads in streams such as the Indus, Colorado, and Rio Grande, which show a correlation between mean concentration and velocity (or friction factor)[8,15] are predominantly fine sediments which should have small damping effects, yet changes in load are accompanied by substantial changes in friction factor for the same discharge. According to laboratory results it is unlikely that all of this is caused by damping effects and changes in bed configuration are probably involved.

Thus far the paper has dealt with those observations that show a reduction in friction coefficients as the load increases. However, it will be recalled that it was reported[8] that Swiss engineers found that the velocity was reduced by an increase in the load, and that a similar behavior was reported[5] in a storm sewer. The latter might be explained by postulating that dunes were formed when sediment was being transported, thus causing a high friction factor, and that during clear flows sediment was cleaned out of the sewer, leaving the water in contact with the smooth walls, which resulted in low friction at low flow. The explanation of the behavior of the Swiss rivers may be associated with a phenomenon observed in a flume study at low transportation rates.[29] It was observed that there was a tendency at low velocities (low transportation rates) for the friction factor to increase with the velocity to a maximum, and then to decrease as the velocity increased further. The experiments which showed these results were made in a flume 33.5 in. wide. Two similar sets of experiments made by Brooks in the 10.5-in. flume used in the present experiments did not yield a maximum for f_b but showed f_b decreasing as the velocity increased for all values of the velocity. Therefore, the explanation previously offered, based on this one set of experiments, must be considered as speculative.

CONCLUSIONS

Four sets of runs were made in a flume 10.5 in. wide in an effort to separate the direct effect of suspended sediment on the friction factor from that of the bed configuration. First, a natural run was established over a loose bed of fine sand, and then, after draining the water, the bed was chemically solidified in its naturally formed configuration. Loose sand was removed from the system then and a flow of clear water was run over the stabilized bed, with the usual measurements being taken. Small increments of sand were then added, noting the change in the friction factor which resulted. The principal conclusions from these experiments are as follows:

1. Suspended sediment reduces the friction factor of a flow. In a limited series of laboratory experiments, the amount of this reduction varied from 5% to 28%.

2. The changes in the friction factor due to variation in bed configuration are much larger than those due to the suspended load itself. A friction factor may change by a factor of 3 to 6 in the laboratory flume between runs of differing velocity at constant depths.

3. Evidence indicates that the suspended load reduces the friction factor by damping the turbulence or interfering with its production near the bed where the sediment concentration is the highest and the rate of turbulence production is the greatest.

---

[29] Closure to "Mechanics of Streams with Movable Beds of Fine Sand," by Norman H. Brooks, Transactions, ASCE, Vol. 123, 1958, p. 572.

4. As observed by previous investigators, the von Karman constant, k, is also substantially reduced by the suspended sediment.

5. In the field it is impossible to distinguish between the two previously mentioned factors affecting alluvial channel roughness. However, it has been established that the reduction due to the suspended sediment is of importance only for streams carrying a high suspended load over a flat bed, and is of minor importance when there are dunes on the bed.

ACKNOWLEDGMENTS

The research work on which this paper is based was sponsored by the Missouri River Division, Corps of Engineers, U. S. Army.

DISCUSSION

EMMETT M. LAURSEN,[30] M. ASCE.—The authors clearly demonstrate the truth of their statement that "when a stream has a movable bed, and sediment is being transported, the problem of determining the resistance is much more complicated than in the simple case of clear water flowing in a channel with fixed walls." On the basis of their observations and measurements they conclude that the interaction of the sediment and the water as if effects the resistance to flow can be considered in two distinct ways. The larger effect is due to the bed configuration (whether ripples, dunes, or flat)—the conditions of flow, and the properties of the fluid and the sediment in some still unknown manner creating a certain bed configuration, and the roughness of this bed configuration affecting the resistance to flow. The observed qualitative relationship between roughness and resistance is entirely in accord with experience with fixed walls, and the magnitude of the effect is not surprising because the dune is much greater in size than the sediment particle.

The other and smaller effect observed by the authors is a decrease in the resistance to flow with an increase in sediment transport, all other conditions being presumably unchanged. This effect they ascribe to the damping of the turbulence by the presence of suspended sediment. Certainly, the presence of the suspended sediment must effect the flow and it may well have the effect on resistance suggested by the authors. However, the writer would like to suggest that this is not yet proved beyond a reasonable doubt because the sediment load could conceivably effect the resistance in another way. Considering a flat bed for simplicity, there is cited a decrease in the friction factor of approximately 25% when a normal sediment load is added to the flow over the fixed granular bed (returning to the conditions of the unfixed bed). In the case of the flow of clear water over the fixed granular bed there is a force transmitted to the flow through the pressure and shear forces on the individual fixed grains. When a sediment load is now added, there will be bed load movement as well as suspended load movement. The resisting force of the fixed grains is now transmitted to the flow at least partly in a different manner. The particles rolling and sliding along the boundary as bed load will be

[30] Assoc. Prof. of Civ. Engrg., Michigan State Univ., East Lansing, Mich.

moving at a velocity less than that of the fluid around them in order to receive a propelling force from the fluid. This propelling force will be transmitted to the fixed particles by solid contact. Thus conditions at the boundary and the interaction between the flowing water and the fixed boundary should be somewhat different depending on whether or not the water is transporting a sediment load.

Whether or not the rolling and sliding particles of the bed load movement could account for the observed difference in resistance could be checked by a pair of runs such as those reported but with a coarser sand so that the sediment would be transported entirely as bed load.

TSUNG-LIEN CHOU,[31] F. ASCE.—In Table 4, it is shown that in each set of observations, all important hydraulic characteristics are identical except the slope S and the sediment discharge concentration, $\overline{C}$. With these two, the authors attribute a direct cause-effect correlation of friction factor f_b and $\overline{C}$. As repeated in Table 5, the figures are consistent and impressive, though not quite proportional. What this amounts to is that the structure of this part of the problem depends on the accuracy and reliability of the measurement of S, which is always delicate and complicated. At this junction, it may be mentioned that in empirical formulas such as that of Darcy - Weisbach $H_f = f\frac{L}{4r}\frac{u}{2g}$ or of Chezy $u = c\sqrt{rs}$, the coefficients f and c are used to fit in the observed values and they are supposed to take care of all losses. In modern hydrodynamical terminology, these losses will include losses due to skin friction, form resistance and turbulence in the pure fluid side, and losses in knocking out solid particles from embedment, bringing them into suspension, and accelerating them to the same velocity as the dispersion medium, and other unknown losses. The velocity u varies with space and time, even in a uniform conduit under steady flow. With the empirical relation of u and S as indicated previously, synchronously together with u varies the slope S, which may include many ups and downs, even negative values in backflow pockets. In natural streams, only mean values are taken for both. Therefore, in a real sense, both u and S are statistical in nature and nothing more than mathematical fictions. Similar are the friction factors, Darcy-Weisbach f, or Manning n. Furthermore, these factors are not universal constants as shown in Table 6. Thus, each friction factor has its own structure and the relations among them are not homogeneous. The fact that they can be used to compute flow in their special forms does not necessarily mean they can represent certain factors of modern hydrodynamics. In Table 4, f is held to count for the variation of minute vortices and others. This is apparently outside the function assigned to it in the original design.

In applying the empirical formula in a flume like this, S should cover only that portion with established normal flow, and with the entrance and tailwater regions deducted and the cross-section of observation would be set at the geometrical center of the portion. Any average value from tilting of flume bed or the differences of water levels at the ends of the flume may bring in drop-down or back water effect, which would not represent the true value of S.

By solidifying the flume bed after running with sediment, the authors tried to eliminate all factors due to bed configuration in order to emphasize the influence of sediment of hydraulic resistance. It may be worthwhile to recall that the turbulence produced on a movable bed is not the same as on similar bed which is

[31] Hydr. Engr., Clinton Bogert, Con. Engrg., New York, N. Y.

fixed, even though the configurations are the same. On a movable bed, turbulence is evened out by picking up solid particles at points of strong intensity and dumping some of its load at points of weak intensity, or the distribution of turbulence contours is more or less conformal to the bed topography. Contrarily, on fixed bed, irregular configuration tends to amplify the turbulence at points of strong intensity, and therefore greater turbulence is expected on a fixed bed. Thus, some part of the computed value might be offset by this cause.

The velocity profile shown in Fig. 2 is apparently not taken from the experiments of this flume ($10\frac{1}{2}$ in. wide). As the depth, the slope, and the width are identical for the two profiles, the one with higher velocities will give higher mean velocity and thereby bigger discharge. In that case, more power is required by the flow and there is hardly any strict comparison of the two.

The authors maintain that the suspended sediment reduces hydraulic roughness by its damping effect on turbulence by the following reasoning: "To keep

TABLE 6.—EMPIRICAL FORMULAS

Empirical Formulas (1)	Chezy (2)	Darcy-Weisbach (3)	Hazen-Williams (4)	Manning (5)
Original Forms	$v = c\sqrt{rs}$	$H_f = f\frac{L}{4r}\frac{v^2}{2g}$	$v = 1.318c_1 r^{0.63}s^{0.54}$	$v = \frac{1.486}{n} r^{2/3} s^{1/2}$
Friction Factors	c	f	c_1	n
Energy Slope	$s = \frac{v^2}{c^2 r}$	$s = \frac{v^2}{r}\left(\frac{f}{8g}\right)$	$s = \frac{v^{1.85}}{1.667\, c^{1.85} r^{1.167}}$	$s = \frac{v^2 n^2}{2.208\, r^{4/3}}$
For equal S, Ratios of Factors	$c = \sqrt{\frac{8g}{f}}$	$f = \frac{8g}{c}$	$c_1 = \frac{c^{1.08} v^{0.081}}{1.117\, r^{0.093}}$	$n = \frac{1.486}{c} r^{1/6}$
	$= 1.11 c_1^{0.925}\left(\frac{0.083}{0.075}\right)$	$= \frac{154.5}{c_1^{1.85} r^{0.165} v^{0.15}}$	$= \frac{15.25}{f^{0.54} r^{0.089} v^{0.081}}$	$= 1.486 r^{1/6}\left(\frac{f}{8g}\right)^{1/2}$
	$= \frac{1.486}{n} r^{1/6}$	$= \frac{3.63\, n^2}{r^{1/3}}$	$= \frac{1.372 r^{0.091} v^{0.081}}{n^{1.08}}$	$= \frac{1.151 r^{0.084}}{c^{0.925} v^{0.075}}$

sediment in suspension, i.e., to prevent it from settling due to gravitational force, work must come from the vertical component of turbulence fluctuations and must result in damping of turbulent motion" and "this means that the momentum transfer coefficient is also decreased, thus allowing the velocity and velocity gradient to increase."

It should be remembered that turbulence is created at the expense of energy stock of the flow. That is to say, as soon as the turbulence is generated, a certain amount of energy is lost from the flowing stream, no matter whether energy is used in keeping sediment in suspension or in supplying vortex motion of minute masses and finally dissipated into heat. To keep sediment continuously in suspension, an uninterrupted supply of the necessary energy through turbulence is required. However, this damping action may have the effect of preventing the eddies from spreading out into the entire stream by localizing them to the lower strata. Finally, in a stream where the saturated suspension tends to dump its load, there is a chance of releasing some energy for accelerating the flow. These conditions are limited to certain parts or certain periods of flood where suspended load is dumped.

Furthermore, the transportation processes of solid particles are different for different effective sizes and distributions. Only fine particles less than 0.2 mm can be thrown up into suspension by and move with turbulence generated purely by hydraulic resistance. On the other hand, bigger particles create extra turbulence by their projections into flowing stream and produce suction effect helping them into sliding, rolling, and saltation. This demands more energy consumption and thereby increases the hydraulic resistance. These conditions are observed in pumping sands in suspension and suspension tests.

In addition to the direct experimentation in the laboratory, the authors collected some interesting information of field data from natural streams. Here the direct cause-effect correlation of f and $\bar{C}$ is further overshadowed by the additional factors of a source of solid supply, varying with the topographical and geological conditions of the river valley, and the hydraulic properties of the stream, aggrading or degrading. The mutual action and reaction of these factors can easily produce contradictory effects.

In general, a rising stage has higher average velocities for two reasons. First, in the rising stage the energy slope is a drop-down curve with increasing velocities toward each downstream section. Thus, the velocity is accelerated. Second, the potential head is converted into kinetic head with smaller loss.

In most cases, the amount and the intensity of sediment load vary with the stage. If a freshet is originated from an upstream watershed and gains strength in flowing downstream, it will pick up silt to its optimum capacity. This happens often in the rising stage. After passing over the peak flow, the river tends to dump its suspended load. However, there may be exceptions to this rule in dealing with difference sources of solid supply. For instance, on the Yellow River at Tung-Kuang, the intensity of suspended sediment varies with the source of flood. If it comes from the north bank tributaries (Shansi Province) where steeper grades of river beds with thicker eolian deposits of loess, the river has a tendency to dump its load even in a rising period. The contrary is true, if the flood is started from the south side. Similar situation is observed at Chingling Chi on the Yangtze River where the discharge from the south is clarified by passing the Tung-Ting Lake which acts as settling basin.

The prior examples show the complicated relations of various factors in natural streams and the cause-effect correlations can easily be reversed, unless comprehensive assessments are made for some period.

On the theoretical side, the sediment can reduce hydraulic resistance in the following ways: (1) smoothing up the surface roughness by scouring off the mound and filling up the depressing; (2) evening off the aquatic growths; (3) exposing fresh surfaces which are more pliable; (4) compacting particles by selective deposition and distribution; and (5) keeping down the vertical component of turbulence (as the authors' main item). Again, every factor must be properly appraised.

The problem of suspended load hydraulic resistance is complicated but interesting. The authors have opened up a new vista for both practical and theoretical investigation. Perhaps another way of attack may be the direct measurements of the turbulence itself for the similar condition of turbid and clear flows.

DARYL B. SIMONS,[32] M. ASCE., and EVERETT V. RICHARDSON,[33] A. M., ASCE.—One of the problems associated with a study of this type is the difficulty of evaluating the effect of flume size on data and observed flow phenomenon.

[32] Hydr. Engr., U. S. Geological Survey, Ft. Collins, Colo.
[33] Hydr. Engr., U. S. Geological Survey, Ft. Collins, Colo.

The writers found that the results obtained with a given bed material using a large recirculating flume 150 ft long, 8 ft wide, and 2 ft deep could not be reproduced in a smaller recirculating flume 60 ft long, 2 ft wide and 3 ft deep. For example, the forms of bed roughness observed in the order of increasing shear in the small flume were: (1) plane bed before beginning of motion; (2) plane bed after beginning of motion; (3) dunes; (4) transition from dunes to plane bed and standing waves; (5) standing sinusoidal sand and water waves which were in phase; and (6) antidunes.

Using the same bed material in the large flume the forms of bed roughness in order of increasing shear were: (1) plane bed before beginning of motion; (2) ripples; (3) ripples superposed on dunes; (4) dune; (5) transition from dunes to plane bed and standing waves; (6) standing sinusoidal sand and water waves which were in phase; and (7) antidunes.

The large flume produced the forms of bed roughness observed in the field, whereas the small flume did not. It was also noted that the height of dunes is

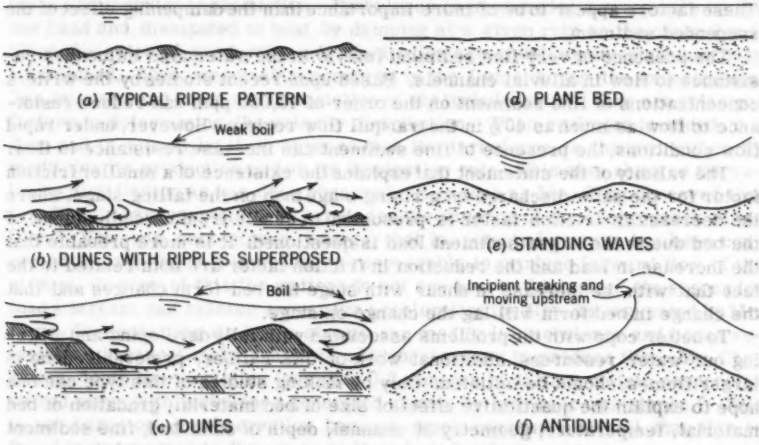


FIG. 12.—FORMS OF BED ROUGHNESS OBSERVED IN ALLUVIAL CHANNELS

related to the depth of sand bed. As depth of bed material is decreased the amplitude of the dunes is decreased. These differences in results, over and above those which can be compensated for by correcting for side wall effect, present a serious problem to those who are trying to utilize data collected by the various investigators, particularly that data gathered in very small flumes.

No mention is made by the authors of the fact that the form of bed roughness is related to size and gradation of bed material. This may be due to the limited range of conditions which they investigated. To show using sand sizes ranging from $d = 0.2$ mm to $d = 0.5$ mm, the writers have observed that the amplitude of the dunes is independent of size of bed material but the spacing and shape of the dunes are related to size of bed material. The spacing of the dunes increases with decreasing size and the angle the fore plane of the dune makes with the horizontal decreases with decreasing size of bed material. The net result is that resistance to flow is smaller with the fine sand than with the coarser sand by as much as 20%. This discussion perhaps raises the question

of bed form terminology. To avoid confusion, the major forms of bed roughness which have been observed in alluvial channels by the writers are shown in Fig. 12. From this figure, it is apparent that the form of bed roughness described by the authors, according to this classification, is ripples.

Referring to the difference in the bed friction factor for sediment-laden flow over a loose sand bed and clear water flow over a fixed sand bed, of the same configuration, it is doubtful that the total difference can be explained by the presence of the suspended sediment. The writers have observed that the scale and intensity of turbulence is entirely different on a rigid bed with no bed material transport than on a loose sand bed having on the order of 10 ppm of bed material transport, none of it in suspension, and other flow factors the same.

The effect of sediment load on resistance to flow is significant, as shown. However, the authors conclusion that all of the computed decrease in resistance to flow can be attributed to the damping effect of the suspended sediment on the turbulence is not concurred in. The presence of fine sediment causes effects on fluid properties which change the entire fluid bed material interrelationship. These factors appear to be of more importance than the dampening effect of the suspended sediment.

The presence of very fine sediment (clays) in the water also influences resistance to flow in alluvial channels. Based upon recent studies by the writers concentrations of fine sediment on the order of 40,000 ppm can reduce resistance to flow as much as 40% in the tranquil flow regime. However, under rapid flow conditions, the presence of fine sediment can increase resistance to flow.

The validity of the statement that explains the existence of a smaller friction factor for the same discharge on a rising stage than on the falling stage, where the decrease in friction factor is presumed to result from a readjustment of the bed due to the larger sediment load is questioned. It is more probable that the increase in load and the reduction in friction factor are both related to the fact that with the increase in shear with stage the bed form changes and that the change in bed form will lag the change on stage.

To better cope with the problems associated with fully developing and utilizing our water resources, additional work of this caliber, preferably done in larger flumes, should be initiated. Only by making studies of this type can one hope to explain the quantitative effect of size of bed material, gradation of bed material, temperature, geometry of channel, depth of sand bed, fine sediment load, and rate of change discharge with time on total bed material transport, the forms of bed roughness which develop, and the related resistance to flow.

VITO A. VANONI,[34] M. ASCE, and GEORGE N. NOMICOS[35].—Messrs. Laursen and Chou have advanced the idea that the resistance to flow offered by grains in the stream bed is different when they are moving than when they are fixed. They suggest that this may account for the lowering of the resistance observed for sediment laden flows. Although such an effect may exist it cannot account for all of the observed change in flow resistance. The fact that the Von Karman k is observed to decrease even for small amounts of suspended load means that there is a substantial internal effect which modifies the turbulence. This effect is always in the direction of reducing the friction factor or the flow resistance.

Mr. Laursen's suggestion that it is possible to study experimentally the effect of moving grains on resistance represents an interesting extension of the

[34] Prof. of Hydr., California Inst. of Technology, Pasadena, Calif.
[35] Specialist-Scientific Research Engr., Republic Aviation Corp., Farmingdale, N. Y.

present work. This raises the whole question of the effect of sediment on flow during cases where the transport rate of sediment is low and most of the material is being carried as bed load. An investigation of this problem would shed further light on the validity of the idea that the principal action of the sediment on the turbulence occurs near the bed where the concentrations are high and where most of the turbulence is generated.

Mr. Chou was correct in inferring that the slope is difficult to measure. As a matter of fact, this is one of the most difficult measurements to make both in the field and laboratory and the one which probably has the greatest error in it. In performing the experiment great care was taken to avoid end effects which would involve either backwater or drop down curves. When a sample as small as one liter was taken from the flume to determine sediment concentration a change in depth of water could be observed immediately. This was corrected by replacing clear water as the samples were being withdrawn from the flume.

The writers are in agreement with Mr. Chou's general description of turbulence and turbulence production. Turbulence is produced at a given rate on the one hand and dissipated to heat by damping at a given rate on the other hand. When the rates of production and dissipation are equal steady state has been established. This presumably occurred in the flume during the experiments. The intensity and other characteristics of the turbulence in a flow are principal factors in determining the velocity distribution. When sediment is added to a flow and is moved by it, it appears that the turbulence is changed either by modifying its production and or its dissipation rate. This also changes the velocity distribution as has been observed. It is true as Mr. Chou observed that in a flow "turbulence has been created at the expense of the energy stock of the flow." However, once stream energy, that is, potential energy, has been converted to turbulence it is no longer recoverable to produce forward flow of the stream. In view of this the writers do not see how by "dumping" its suspended load a stream can release energy for accelerating the flow as suggested by Mr. Chou. By depositing its load a stream can modify its turbulence and hence velocity but it cannot make available additional energy to produce flow. Mr. Chou states, "only fine particles less than 0.2 mm can be thrown up into suspension by and move with turbulence generated purely by hydraulic resistance." This is not borne out by observation because much coarser material than this is found in suspension in flumes as well as in natural streams.

Mr. Chou states that velocities are higher on rising than on falling stages of a stream, because the slope is higher during the rising stages and less energy loss is involved. This seems like a reasonable statement, but in large rivers the rates of rise and hence the above effects are extremely small and one must look for other explanations for the observed phenomena. As an example it has been reported[17] that the duration of the rising part of the hydrograph in the lower Mississippi was approximately 3 months. In this case it seems reasonable to assume that the effect of the rate of rise is very small and that one can consider the flow as being essentially uniform.

Mr. Chou's suggestion that one way to attack and clarify this problem is through direct measurements of turbulence is certainly a pertinent one. It points up the dire need for instruments for making such measurements which at the present time are only in the very initial phases of development.

Messrs. Simons and Richardson bring up the interesting and important problem of the effect of the scale of the system on sediment transportation phenomena. This is a problem that workers in sedimentation have hardly touched and

is one which must be faced if results of laboratory work are to be applied to field conditions. Certainly one of the ways to study the problem is actually to work in larger and larger streams. However, it appears to the writers that considerable understanding of transport problems can also be gained by continuing to study the phenomena involved. Much of this can be done in small flumes which are cheaper to operate and more convenient to work with than large ones. In this way laboratories that do not have large facilities can continue to make significant contributions to this field.

The writers welcome the discussions of bed forms. The terminology used by the writers is that outlined by the subcommittee on sediment terminology of the American Geophysical Union.[36] This committee did not recommend a term to describe a bed without dunes or other forms. The writers used the term "flat" and Simons and Richardson use "plane" to describe such a bed. The writers prefer the term flat over the absolute term plane because according to definition it allows for slight irregularities in surface which in fact do occur and hence is a more precise term. It is apparent that some additional forms have been found by Simons and Richardson and that the problem is not as simple as it first appeared. To the list of bed forms should be added the "sand wave" observed by Brooks[12] to occur between the condition of "dunes" and "flat bed" shown respectively in Fig. 12(c) and (d). The information reported on the effect of size and grading of the bed material on the form of the bed roughness is most interesting. In experiments reported in the paper the gradation of the two materials used was about the same, however there was a change in the mean size as shown in Table 2. Experimental results reported previously[20] (Ref. 12, Table 7) indicate that for flows of the same depth and velocity in a 10 1/2-in. flume which form dunes, the grading of sand does not greatly affect the observed friction factor. Detailed measurements of the dunes were not made in these experiments but photographs show only modest differences in size and shape of dunes.

Simons and Richardson question the validity of ascribing all of the change in friction factor between sediment laden flows and comparable clear flows to the damping effect of the sediment. They would ascribe some of the effect to the change in the intensity of turbulence in the two cases. The writers have used the idea that the significant difference between the two cases, that is, the one with the loose bed and sediment in motion and the other with the fixed bed and clear water, is the sediment load and that therefore the cause of the observed change in roughness must in some way be due to this sediment load. If the turbulence intensity is greater in one case than in the other then the argument would be that this is caused by the sediment in the flow or the lack of it whichever the case may be.

Simons and Richardson also refer to their very interesting findings that extremely high concentrations of fine material such as silt and clay have a very important effect on the behavior of a stream. The explanation of these effects must involve one or both of the mechanisms for changing the roughness factor of a stream, that is, modification of the turbulence and of the bed forms.

They question the contention of the writers that the smaller friction factor of the rising flood can be explained by a difference in bed configurations between the river on rising and falling stages. They are more inclined to explain this difference by a time lag in the change of the bed forms. The writers feel that because during floods the stream actually has a tremendous capacity for

[36] Report of the Subcommittee on Sediment Terminology, Transactions, Amer. Geophysical Union, Vol. 28, December, 1946, p. 936.

transporting sediment and hence changing the bed configuration there would not be a very large lag. This is especially true in the case of the Mississippi River where the times involved are measured in days and weeks and are not only a matter of a few hours. A further reason for not accepting the idea of "time lag" is that the writers are not willing to discard the idea advanced by Brooks that in order to get a single-valued relation for stream characteristics one must consider the sediment load as an independent or imposed variable. According to this concept, a stream would adjust its bed forms, friction factor, mean velocity, and stage to enable it to transport the sediment load delivered to it. The bed forms and other hydraulic quantities can be thought of as resulting from the sediment load instead of vice versa. This idea can now be applied to explain the rating curver with a loop in it.[17] It can be first observe that the sediment load is higher during the rising than during the falling stage. Then according to the previously mentioned concept the stream will adjust itself to carry the load. To carry the heavier load delivered to it on the rising stage the stream will reduce the friction factor of the bed by modifying the bed form which will result in reducing the stage as observed. The validity of this concept and the results deduced from it as well as the idea of "time lag" in changing bed configurations need further evidence to determine their validity.

AMERICAN SOCIETY OF CIVIL ENGINEERS

Founded November 5, 1852

TRANSACTIONS

Paper No. 3056

ELASTI-PLASTIC ANALYSIS OF CONTINUOUS FRAMES AND BEAMS

By Lawrence P. Johnson, Jr.,[1] M. ASCE, and Herbert A. Sawyer, Jr.,[2] F. ASCE

With Discussion by Messrs. Giuliano Augusti; Tullio Renzulli; Emilio Rosenblueth; A. A. Eremin; and Lawrence P. Johnson, Jr., and Herbert A. Sawyer, Jr.

SYNOPSIS

A practical analytical solution which considers both elastic and plastic flexural deformations is presented for continuous beams and frames. This method has limitations characteristic of limit design methods except that it determines strength as defined by the moment-curvature relationship as well as an ultimate moment, and it allows ready determination of deflections.

INTRODUCTION

As stated in previous papers,[3,4] for many loading conditions the strength of a flexural structure can best be evaluated by an analysis which considers the entire moment-curvature (M-ϕ) relationship of its members. A practical solution of this type for single-span beams and frames has been previously

Note.—Published, essentially as printed here, in December, 1958, in the Journal of the Structural Division, as Proceedings Paper 1879. Positions and titles given are those in effect when the paper or discussion was approved for publication in Transactions.

1 Special Design Engr., Water Bureau, Metro. Dist. Comm., Hartford, Ct.

2 Prof. of Civ. Engrg., Univ. of Connecticut, Storrs, Conn.

3 "Theory of Inelastic Bending with Reference to Limit Design," by A. Hrennikoff, Transactions, ASCE, Vol. 113, 1948, pp. 213-268.

4 "Elasti-plastic Design of Single-span Beams and Frames," by H. A. Sawyer, Jr., Proceedings Paper 851, ASCE, December, 1955.

presented.[4] For steel WF-section frames, a method has been devised for determining[5] the concentrated forces required to produce given inelastic deflections. This method is a valuable research tool for experimental work with impulsive lateral loadings. A method has been presented for reinforced concrete design[6,7] which consists of satisfying sets of simultaneous equations. A different set of equations is usually written for each loading condition.

The purpose of this paper is to present a method for the usual design problem for which loads rather than deflections are given and for which loads are often distributed. The solution is numerical rather than algebraic, using many of the techniques[8] originated by Hardy Cross, and the same elastic coefficients are used for all loadings. The method is applicable to continuous beams and frames made of any structural material and with any number of plastic regions, provided that the moment-curvature relationships of all the structure's members are known.

For this method, a previously used[4] division of the flexural deformation or curvature into two parts was found convenient, one part being elastic and the other plastic (Fig. 1). Then the total flexural deformation of a structure may be obtained by superimposing the plastic deformations, that are usually localized, and the elastic deformations. With total flexural deformations obtainable by this means, a solution of a structure is attained by satisfying the usual basic conditions: (a) the force system must satisfy statics; (b) deformations must be consistent with the force system; and (c) deformations must be consistent with the geometry of the structure and its restraints.

As is common for complex problems, a solution by successive approximations will be used, in each step of which a statically permissible set of moments is assumed, the corresponding plastic deformations are computed, and, finally, the actual moments induced in the loaded structure from these plastic deformations are computed and compared with the assumed moments. The solution will consist of the following steps:

1. Determine the elastic-solution moments.
2. Assume a statically permissible elasti-plastic-solution moment-diagram.
3. Compute the angle changes from the assumed moments caused by the plastic portion of the moment-curvature (M-ϕ) curve, assuming the maximum diagram-moment to be the ultimate moment (M_u).
4. Apply these angle changes to the loaded structure, assumed to be otherwise elastic, and determine the resulting moments. (That is, add the elastic-solution moments of Step 1 to the elastic moments caused by the plastic angles.)
5. Compare these moments with the assumed moments. If they are practically equal, the structure is solved; if not, select intermediate values as the assumed moments for the next trial.

---

5 "A Method for the Analysis of Frames Subjected to Inelastic Deformation into the Range of Strain-hardening," by A. Ang and J. M. Massard, Univ. of Illinois, Report of Project 1080, Contract AF33 (616)-170, Air Force Special Weapons Center, Kirtland Air Force Base, New Mexico, November, 1956.

6 "Ultimate Load Theory Applied to the Design of Reinforced and Prestressed Concrete Frames," by A. L. L. Baker, Concrete Publications Ltd., London, 1956.

7 "The Ultimate Strength and Deformation of Plastic Hinges in Reinforced Concrete Frameworks," by W. W. L. Chan, Magazine of Concrete Research, Vol. 7, November, 1955, pp. 121-132.

8 "Analysis of Continuous Frames by Distributing Fixed End Moments," by H. Cross, Transactions, ASCE, Vol. 96, 1932, pp. 1-156.

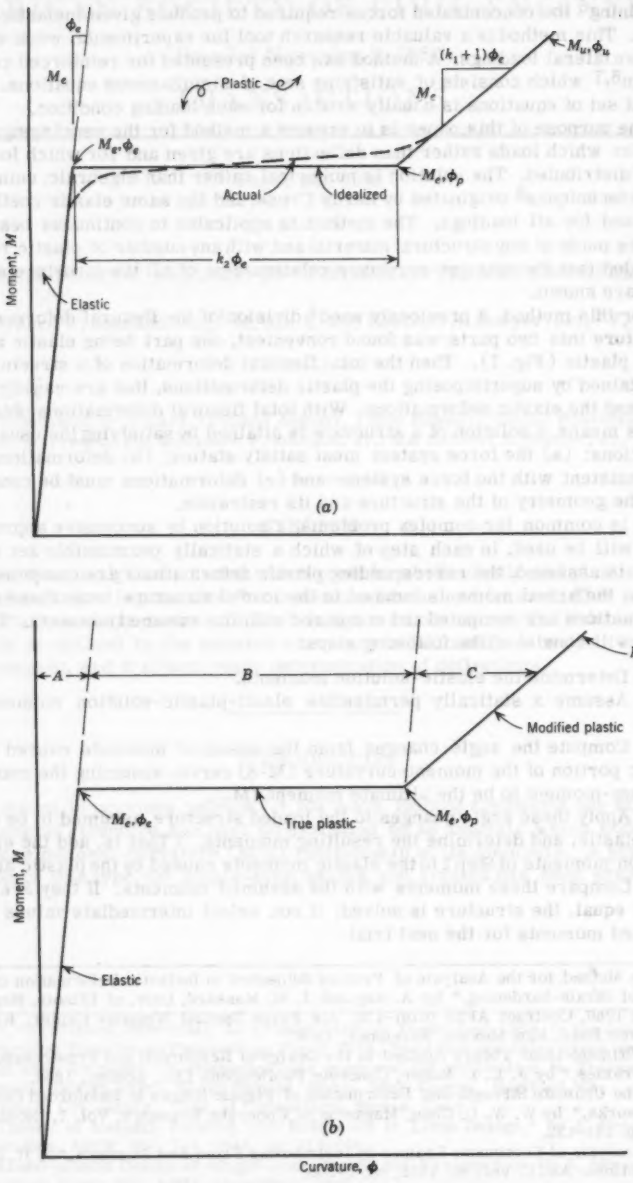


FIG. 1.—MOMENT-CURVATURE RELATIONSHIP

The important problem of the determination either theoretically or experimentally, of the M-ϕ relationship is beyond the scope of this paper. There are recent papers available that include information on M-ϕ relationships for steel members,[9,10,11] and other papers that include such information for reinforced concrete members.[12,13]

ULTIMATE LOAD VERSUS ULTIMATE MOMENT

It should be noted that an important assumption of this paper, is that the ultimate value of a slowly increasing proportional load system for a structure is attained when the ultimate moment (M_u) is first attained at any section of a structure. Actually, if the load on the structure were to exceed this value, two phenomena would occur which would have opposite effects on the resistance of the structure to the load. First, a load increase would increase the plastic angle for the initial-M_u region, thereby allowing the moments of the remainder of the structure to continue approaching their plastic mechanism-collapse values, thus tending to increase structural resistance. Second, the increase in curvature at the section of initial-M_u will cause the moment at this section to decrease. This decrease, in itself, would tend to decrease structural resistance; and it would cause a reduction of moment for the whole region, if the statically-determined moment-gradients or shears are not to be violated. The reduction of moment would tend to reduce the beneficial increase of bending angles of the region and thus oppose the approach of the remaining moments to their mechanism-collapse values.

Therefore, the change in structural resistance caused by these opposing phenomena could be positive or negative. Not only is computation of this change difficult and tedious but, if it were computed, the accuracy would be so poor, because of many uncertain factors, as to make the result insignificant. Also, any error resulting from neglect of this change is always conservative. Therefore, the assumption of simultaneous attainment of ultimate moment and ultimate load is generally believed to be justified.

EVALUATION OF ANGLE CHANGES FROM PLASTIC CURVATURES

An M-ϕ curve is shown in Fig. 1(a) which can be closely approximated by three linear relationships. Note that, knowing M_e elastic limit moment and ϕ_e

---

9 "A Study of the Resistance of Model Frames to Dynamic Lateral Load," by R. J. Mayerjak, Structural Research Series No. 108, Univ. of Illinois, August, 1955.

10 "Shear Deflection of Wide Flange Steel Beams in the Plastic Range," by W. J. Hall and N. M. Newmark, ASCE, Vol. 81, October, 1955.

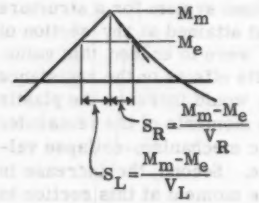
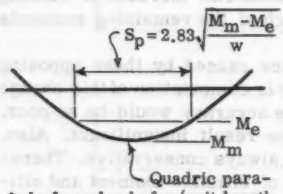
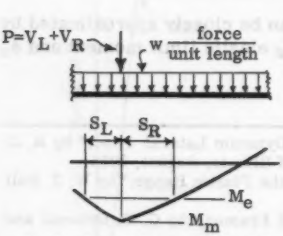
11 "The Plastic Behavior of Structural Members and Frames," by G. C. Driscoll and L. S. Beedle, Vol. 36, June, 1957, pp. 275s-286s.

12 "An Investigation of the Load-Deformation Characteristics of Reinforced Concrete Beams up to the Point of Failure," by J. R. Gaston, C. P. Siess, and N. M. Newmark, Structural Research Series No. 40, Univ. of Illinois, December, 1952.

13 "Load-Deformation Characteristics of Simulated Beam Column Connections in Reinforced Concrete," by H. M. McCollister, C. P. Siess, N. M. Newmark, Structural Research Series No. 76, Univ. of Illinois, June, 1954.

elastic limit curvature, the idealized curve is defined by the three quantities, k_1, k_2, and the ratio M_u/M_e. It should also be noted from Fig. 1(a) that, for

TABLE 1

MOMENT DIAGRAM	VALUE OF PLASTIC ANGLE
	$\theta_p=\frac{\phi_e}{M_e}\left\{k_2M_e\,(M_m-M_e)+\frac{k_1}{2}(M_m-M_e)^2\right\}\left(\frac{1}{V_L}+\frac{1}{V_R}\right)$ If $k_2=0$; $\theta_p\frac{M_e}{\phi_e}=\theta'_p=\frac{k_1}{2}(M_m-M_e)^2\left(\frac{1}{V_L}+\frac{1}{V_R}\right)$ If $k_1=0$; $\theta_p\frac{M_e}{\phi_e}=\theta'_p=k_2M_e\,(M_m-M_e)\left(\frac{1}{V_L}+\frac{1}{V_R}\right)$
	$\theta_p=\frac{\phi_e}{M_e}\sqrt{\frac{M_m-M_e}{w}}\left\{2.83k_2M_e+1.89k_1\,(M_m-M_e)\right\}$ If $k_2=0$; $\theta_p\frac{M_e}{\phi_e}=\theta'_p=\frac{1.89k_1}{\sqrt{w}}(M_m-M_e)^{\frac{3}{2}}$ If $k_1=0$; $\theta_p\frac{M_e}{\phi_e}=\theta'_p=2.83k_2M_e\sqrt{\frac{M_m-M_e}{w}}$
	$S_L=\sqrt{\left(\frac{V_L}{w}\right)^2+\frac{2(M_m-M_e)}{w}}-\frac{V_L}{w}$ For S_R, replace subscripts L with R $\theta_p=\theta_{pL}+\theta_{pR}=\frac{\phi_e}{M_e}\left(\theta'_{pL}+\theta'_{pR}\right)$, where $\theta'_{pL}=S_L\left\{k_2M_e+\frac{k_1}{2}\left(M_m-M_e+\frac{wS_L^2}{6}\right)\right\}$ For θ'_{pR}, replace subscripts L with R

the best approximation, M_e and ϕ_e usually exceed the true elastic-limit moment and curvature. This idealized curve is useful for many steel WF and I

sections, and, for relatively large values of k_2, the value of k_1 may be set at zero with little error. For most other types of members M-ϕ curves may be best and most simply approximated by appropriate values of k_1 and M_u/M_e, with k_2 equal to zero.

For any given moment, M, between M_e and M_u, as shown in Fig. 1(b), the total curvature is made up of the parts A, loosely termed the elastic portion, and B and C, the plastic portions. The angle change in a certain plastic region of length S_p in a member caused by the plastic portions (B and C) will then be:

$$\theta_p = \int_{S_p} \left(\phi - \frac{M}{M_e}\,\phi_e\right) ds = k_2\,\phi_e\,S_p + \int_{S_p} \left(M - M_e\right) k_1 \frac{\phi_e}{M_e}\,ds \quad \ldots\ldots (1)$$

The integral of this expression involving k_1 has been evaluated[4] for certain common moment diagrams. These formulas (with k_2 equal to zero) are repeated for ease of reference in Table 1. The component of the plastic angle θ_p caused by the existence of k_2, which is $k_2\phi_e S_p$, is also shown in Table 1. If the term M_e/ϕ_e (or EI) is constant throughout a structure, it may be omitted

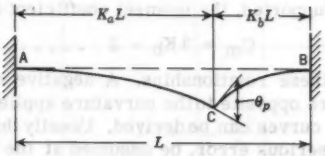


FIG. 2.—BEAM SUBJECTED TO CONCENTRATED ANGLE CHANGE

from the computations for both the plastic angle (the resulting relative angle is denoted as θ'_p, as shown in Table 1) and the moments caused by it.

MOMENTS CAUSED BY A PLASTIC ANGLE

If a single-span beam of length L, having a fixed end, is subjected to any angle change,

$$\theta_p = \frac{\phi_e}{M_e}\,\theta'_p \quad \ldots\ldots\ldots\ldots\ldots\ldots (2)$$

the location of whose centroid is known, the resulting change in the elastic fixed-end moments (FEM) can be defined as

$$\Delta\text{FEM} = C_m \frac{\theta'_p}{L} \quad \ldots\ldots\ldots\ldots\ldots\ldots (3)$$

Considering the beam with a fixed end and constant-EI shown in Fig. 2, with an angle change θ_p either concentrated at C or with centroid at C, the moment

M_o and the vertical force Y_o necessary at the elastic center to satisfy the restraint conditions are

$$M_o = -\frac{\theta_p}{\int \frac{ds}{EI}} = -\frac{\theta_p EI}{L} \quad \ldots\ldots\ldots\ldots\ldots (4a)$$

$$Y_o = -\frac{\theta_p\left(L/2 - K_b L\right)}{\int \bar{x}^2\, ds/EI} = -\frac{\theta_p\, L\left(\frac{1}{2} - K_b\right)}{L^3/12EI}$$

$$= -\frac{12\,\theta_p\, EI\left(\frac{1}{2} - K_b\right)}{L^2} \quad \ldots\ldots\ldots\ldots\ldots\ldots (4b)$$

The moment at B caused by M_o and Y_o is then:

$$M_B = M_o + \frac{L}{2} Y_o = \left(6K_b - 4\right)\frac{\theta'_p}{L} \quad \ldots\ldots\ldots (4c)$$

and the moment coefficient for B is:

$$C_m = 6K_b - 4 \quad \ldots\ldots\ldots\ldots\ldots\ldots (5)$$

If end A were simply supported, the moment coefficient for B becomes:

$$C_m = 3K_b - 3 \quad \ldots\ldots\ldots\ldots\ldots\ldots (6)$$

Fig. 3 is a plot of these relationships. A negative coefficient indicates a ΔFEM causing curvature opposite to the curvature applied at C. For members of variable EI, similar curves can be derived. Usually the centroid of the plastic angle can, without serious error, be assumed at the point of the maximum moment. For extremely asymmetrical curvature diagrams, the actual location of the centroid can be computed.

For ease of computation and clarity, a geometric sign convention is presented and used in this paper. This convention indicates the sense of a bending moment by a picture-symbol of the corresponding curvature, Fig. 4(a). The sense of a plastic angle in a member is indicated by a similar picture-symbol of the member's axis at the angle. An algebraic sign convention of the slope-deflection type is unsatisfactory for elasti-plastic computations because of its ambiguity for intra-span moments. If preferred, an algebraic sign convention of the mechanics-of-materials type could be used by a designer. However, this convention is believed to be inferior to the geometric convention because it tends to obscure the action of the structure and it becomes ambiguous for inclined members.

In members subjected to uniform loading, the location and magnitude of the maximum intra-span moment is not obvious. Fig. 4(a) shows such a member. Note, in Fig. 4(b), that the maximum intra-span moment occurs at the point at which the slopes of the simple-beam parabolic diagram and the net moment diagram are equal, and its magnitude is the ordinate from datum to the parallel tangent. Fig. 5 is a plot of these solutions in terms of the ratio of end and maximum intra-span moments to (WL) 8, and K, the ratio of the distance to the maximum intra-span moment to the span length. If it is given, from Fig. 4, that $M_L/M_s = -0.2$ and $M_R/M_s = -0.4$ then by following the arrows of Fig. 5, $M_m = 0.7\ M_s$ and $K = 0.525$.

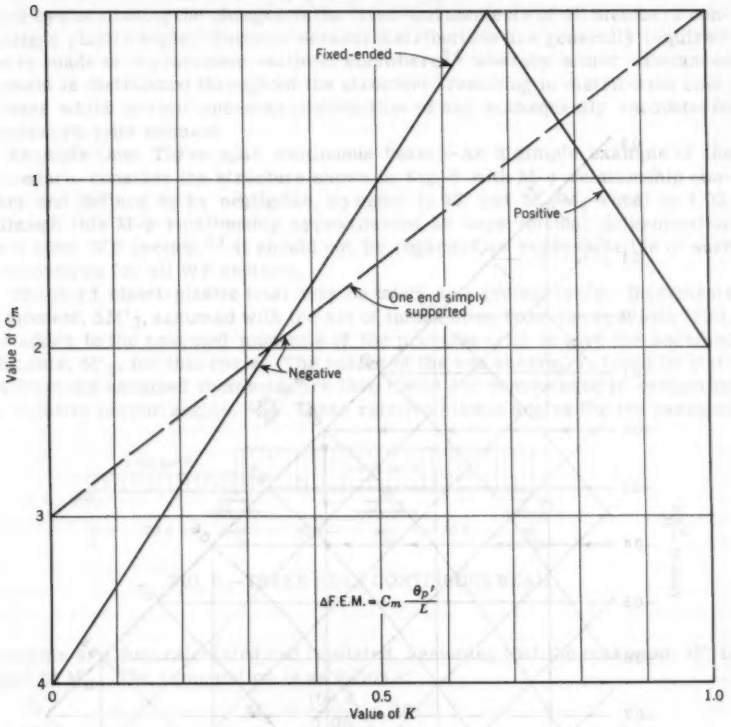


FIG. 3.—MOMENT COEFFICIENTS

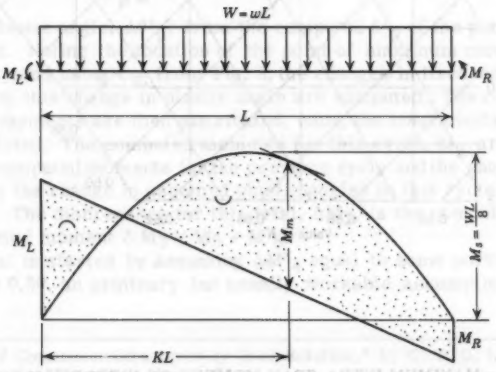


FIG. 4.—EXAMPLE FOR UNIFORMLY LOADED BEAM

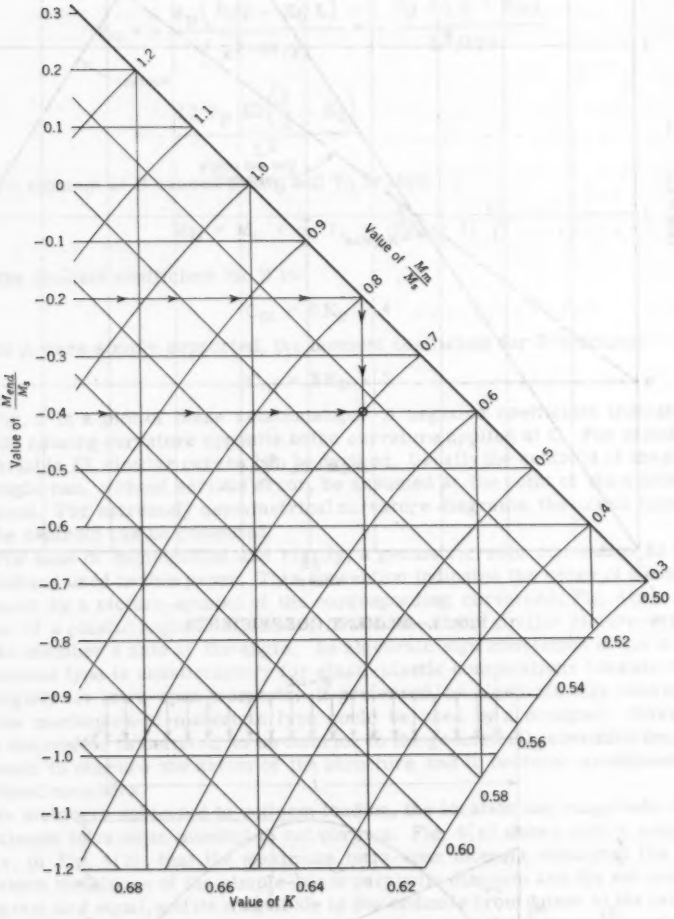


FIG. 5.—MAXIMUM INTRA-SPAN MOMENT ON UNIFORMLY LOADED BEAM

The moment effects caused by plastic bending in a continuous structure are found by distributing the changes in the fixed-end moments of all members containing a plastic angle. Because several distributions are generally required, use is made of a procedure outlined elsewhere[14] whereby a unit unbalanced moment is distributed throughout the structure, resulting in distribution coefficients which permit one-step distribution of any subsequently encountered unbalanced-joint moment.

Example One; Three-span continuous beam.—As a simple example of the procedure, consider the structure shown in Fig. 6 with M-ϕ relationship constant and defined by k_1 negligible, k_2 equal to 12, and M_u/M_e equal to 1.05. Although this M-ϕ relationship approximates an experimental determination for a steel WF section,[11] it should not be regarded as representative of such relationships for all WF sections.

The third elasti-plastic trial may be taken as a typical cycle. Increments in moment, $\Delta M'_3$, assumed with the aid of information from the previous trial, are added to the assumed moments of the previous trial to give the assumed moments, M'_3, for this cycle. The values of the end shears, V, found by statics from the assumed moments, are then listed for convenience in computing the relative plastic angles, θ'_p. These relative plastic angles for the assumed

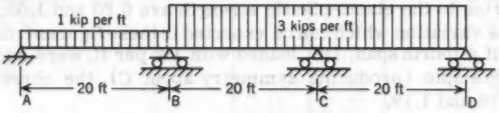


FIG. 6.—THREE-SPAN CONTINUOUS BEAM

moments are then calculated and tabulated, assuming that the maximum M' is equal to M_u. The computation is as follows:

$$M_e = \frac{106.4}{1.05} = 101.3$$

$$\theta'_p @\ C = \frac{12 \times 101.3 \times 5.1}{V}$$

The change in plastic angle, $\Delta\theta'_p$, from the computed θ'_p of the previous trial is then tabulated. Noting the location of the point of maximum moment in the zone of plasticity and using C_m from Fig. 3, the changes in fixed-end moment, ΔFEM, caused by this change in plastic angle are computed. The corresponding unbalanced moments are then distributed, using the coefficients that were previously tabulated. The computed moments for this cycle, M_3, are the summations of the computed moments for the previous cycle and the change in moments caused by the change in assumed plastic angles in this cycle ($M_3 = MD + \Delta FEM + M_2$). The discrepancy for this trial, δM_3, is the computed moment minus the assumed moment $\delta M_3 = M_3 - M'_3$.

The next trial is started by assuming $\Delta M'_4$ equal to some portion of δM_3. In this example 0.50, an arbitrary but usually workable assumption, is taken

14 "Analysis of Continuous Structures by Joint Rotation," by C. T. G. Looney, Proceedings Separate No. 679, ASCE, May, 1955.

as the portion of the discrepancy of the previous trial to be used. If δM is opposite to and greater than $\Delta M'$ for that cycle, the cycle should be crossed out and repeated with a new $\Delta M'$ being assumed at some lesser value.

The first elasti-plastic trial is of course somewhat modified because no previous plastic angle has, at that point, been incorporated into the computation. The assumed moments can safely be taken as the elastic solution, or, a designer who wishes to exercise his judgment to save computation may assume an initial set of reasonable increments of moment to modify the elastic solution.

An exact elasti-plastic solution is accomplished when all $\delta M'$s are zero. However, observation of $\Delta M'$ in seccessive trials soon makes the final moments, within the desired accuracy, obvious so that a complete convergence is not necessary.

The divergence evidenced by δM_4 in Trial No. 4 is caused by a θ_p' pf (2.83) (12) (100.2) $\sqrt{5/3}$ forming on CD.

A check on the computations of all preceding elasti-plastic incremental trials may be made at any point by comparing the sum of the elastic solution moments and moment changes caused by all plastic angles, to the assumed moments for that cycle.

For this example the ratios of the strengths predicted by the elastic and rigid-plastic theories to the elasti-plastic strength are 0.80 and 1.03, respectively. To show the variation which can be expected in these figures from structure, to structure if a fourth span, DE, loaded with 1 k per ft, were added to the structure of this example (producing symmetry about C), the corresponding ratios would be 0.78 and 1.19.

Example Two; Three-span continuous frame.—As a further example of the procedure, consider the reinforced concrete frame shown in Fig. 7, for which the width of all members is constant and for which the column depth is equal to two-thirds of the beam depth. The M-ϕ relationship for the beam is defined by k_1 equal to 7.55, k_2 negligible and M_u/M_e equal to 1.23. (These are experimentally-indicated[15] for 2.2% steel at plastic regions, a concrete strength of 4 ksi. a steel yield strength of 40 ksi. and a loading time of 4 hrs.)

For the same materials and percentage of tensile steel, the values of k_1, k_2 and M_u/M_e are assumed to remain constant with variation in depth of beams. Although the introduction of an axial load would probably affect the values of these factors, this effect will be assumed negligible for example, and the values previously listed for the beams will also be used for the columns. Conversely, M_u varies with the square of the depth, and the elastic stiffness, M_e/ϕ_e or EI, varies as the cube of the depth, other factors remaining equal. Hence, if column depth equals two-thirds of beam depth, the combined ultimate strength of the two columns at each joint will be 8/9 of the strength of a beam, and the elastic stiffness of two columns will be 16/27, or approximately 0.6 that of a beam. That is $M_{u\,c} = \frac{8}{9}(M_u)_b$ and $\left(\frac{M_e}{\phi_e}\right)_c = 0.6\left(\frac{M_e}{\phi_e}\right)_b$ in which subscripts c and b refer to column and beam, respectively. For convenience, in the analysis of the frame shown in Fig. 6 the stiffnesses of the two columns at each joint

15 "The Behavior of Under-Reinforced Concrete Beams under Long-Term Loads," by H. A. Sawyer, J. E. Stephens, and E. S. Alling, No. 12, September, 1956.

TABLE 2.—DESIGN OF THREE-SPAN CONTINUOUS BEAM[a]

Operation[b]	Span AB	Joint B BA	Joint B BC	Span BC	Joint C CB	Joint C CD	Span CD
1) Elastic Solution							
Shear V, Simply Supported		10.0	30.0		30.0	30.0	
Moments Simply Supported	⌣ 50			⌣ 150.			⌣ 150
Distribution Coefficient,							
Unit moment; ⊕ Joint B		⌒ 0.467	⌣ 0.533		⌒ 0.134	⌒ 0.134	
⊕ Joint C		⌣ 0.134	⌣ 0.134		⌒ 0.533	⌣ 0.467	
Fixed End Moment, FEM		⌒ 50.0	⌒ 100.0		⌒ 100.0	⌒ 150.0	
Moment Distribution, MD, ⊕ B		⌒ 23.3	⌣ 26.7		⌒ 6.7	⌒ 6.7	
Moment Distribution, MD, ⊕ C		⌣ 6.7	⌣ 6.7		⌒ 26.7	⌣ 23.3	
Solution	⌣ 23.0	⌒ 66.6	⌒ 66.6	⌣ 59.0	⌒ 133.4	⌒ 133.4	⌣ 91.0
2) Elasti-Plastic Trial No. 1							
Shear V					33.3	36.7	
Relative Plastic Angle[c] θ_p'					∧ 291.0	∧ 264.0	
Change in Fixed End Moment:							
ΔFEM (θ_p' ⊕ C)			⌒ 29.1		⌣ 58.2	⌣ 39.6	
MD ⊕ B		⌒ 13.6	⌣ 15.5		⌒ 3.9	⌒ 3.9	
MD ⊕ C		⌣ 2.5	⌣ 2.5		⌒ 10.0	⌣ 8.8	
Moment, M_1:							
M_1 = (MD + ΔFEM + elastic solution)		⌒ 77.7	⌒ 77.7		⌒ 89.1	⌒ 89.1	
Change in Moment δM_1							
δM_1 = M_1 - elastic solution		⌒ 11.1			⌣ 44.3		
3) Elasti-Plastic Trial No. 2							
Increment of Moment, $\Delta M_2'$		⌒ 5.6			⌣ 22.2		
(assumed as 0.5 δM_1)							
Assumed Moment, M_2'		⌒ 72.2	⌒ 72.2		⌒ 111.2	⌒ 111.2	
V'					32.0	35.6	
θ_p'					∧ 210	∧ 189	
Increment of Relative							
Plastic Angle, $\Delta\theta_p'$					∨ 81.0	∨ 75.0	
ΔFEM			⌣ 8.1		⌒ 16.2	⌒ 11.3	
MD ⊕ B		⌣ 3.8	⌒ 4.3		⌣ 1.1	⌣ 1.1	
MD ⊕ C		⌒ 0.7	⌒ 0.7		⌣ 2.6	⌒ 2.3	
M_2		⌒ 74.6	⌒ 74.6		⌒ 101.6	⌒ 101.6	
δM_2		⌒ 2.4			⌣ 9.6		
4) Elasti-Plastic Trial No. 3							
$\Delta M_3'$		⌒ 1.2			⌣ 4.8		
M_3'		⌒ 73.4	⌒ 73.4		⌒ 106.4	⌒ 106.4	⌣ 101.1
V'					31.7	35.3	
θ_p'					∧ 194	∧ 174	
$\Delta\theta_p'$					∨ 16	∨ 15	
Δ FEM			⌣ 1.6		⌒ 3.2	⌒ 2.2	
MD ⊕ B		⌣ 0.7	⌒ 0.9		⌣ 0.2	⌣ 0.2	
MD ⊕ C		⌒ 0.1	⌒ 0.1		⌣ 0.5	⌒ 0.5	
M_3		⌒ 74.0	⌒ 74.0		⌒ 104.1	⌒ 104.1	
δM_3		⌒ 0.6			⌣ 2.3		
5) Elasti-Plastic Trial No. 4							
$\Delta M_4'$		⌒ 0.3			⌣ 1.2		
M_4'		⌒ 73.7	⌒ 73.7		⌒ 105.2	⌒ 105.2	⌣ 101.7
V					31.6	35.3	
θ_p'					∧ 191	∧ 171	∨ 4400
$\Delta\theta_p'$					∨ 3.0	∨ 3.0	∨ 4400
ΔFEM ($\Delta\theta_p'$ ⊕ C)			⌣ 0.3		⌒ 0.6	⌒ 0.4	
ΔFEM ($\Delta\theta_p'$ on CD)						⌒ 273.	
MD ⊕ B		⌣ 0.1	⌒ 0.2				
MD ⊕ C		⌣ 36.6	⌣ 36.6		⌒ 145.4	⌣ 127.4	
M_4		⌒ 37.3	⌒ 37.3		⌒ 250.1	⌒ 250.1	
δM_4		⌣ 36.4			⌒ 144.9		
Elasti-Plastic Solution	⌣ 21.0	⌒ 74.0	⌒ 74.0	⌣ 60.0	⌒ 106.0	⌒ 106.0	⌣ 101.0

[a] See Fig. 6. [b] All units in kips and feet. [c] θ_p' is in k-ft^2.

have been combined, as well as the moments. It follows that the relative plastic angles formed in the beams and columns respectively will be

$$(\theta'_p)_b = \frac{7.55\,(M_m - M_{eb})^2}{2V}$$

$$(\theta'_p)_c = \frac{7.55\,(M_m - M_{ec})^2}{(0.6)\ 2V}$$

The computations for each trial of this example parallel the computations for each trial of example one. For this example the ratios of strengths pre-

TABLE 3.—INITIAL COMPUTATIONS FOR ELASTI-

Operation		Member CA			Member	
		Joint A	Span AC	Joint C	Joint C	Span CD
Elastic Solution						
Distribution	@ C	) 0.363		(0.726	⌣ 0.274	
Coefficient, Unit	@ D	(0.041		) 0.082	⌣ 0.082	
Clockwise Moment	@ F	) 0.006		(0.012	⌢ 0.012	
Moments, CF →1, sway		(2.36		) 1.12	⌣ 1.21	
Fixed End Moment		(6.0		(6.0	45.0	
MD @ C, 39.0		) 14.1		(28.3	10.7	
MD @ F, 45.0		(0.3		) 0.5	0.5	
Sub-total		) 7.8		(33.8		
Sway Force on CF				→5.47	→ 4.00	
Moment, CF → 5.50		(13.0		) 6.7	⌣ 6.7	
Elastic Solution		(5.2	(4.1	(27.1	⌢ 27.1	⌣ 26
Elasti-Plastic Trial No. 1						
Assumed Moment, M_1'		(5.0		(30.0	⌢ 30.0	
Shear, V						
Relative Plastic Angle, θ_p'						
Increment of Fixed End Moment: ΔFEM					⌢ 14.1	
MD @ C, 14.1		) 5.1		(10.2	⌣ 3.9	
MD @ D, 32.0		(1.3		) 2.6	⌣ 2.6	
MD @ F, 20.4		(0.1		) 0.2	⌣ 0.2	
Sub-total		) 3.7		(7.4		
Increment Force on CF				→0.93		
Δ Moment, CF →4.65		(11.0		) 5.6	⌣ 5.6	
Computed Moment, M_1		(12.5		(28.9	⌢ 28.9	
$\delta M_1 = M_1 - M_1'$		(7.5		) 1.1	⌣ 1.1	

[a] See Fig. 8. Units used are kips and feet.

dicted by the elastic method and the rigid-plastic method to elasti-plastic-computed strength are 0.95 and 1.22, respectively.

Example Three; Frame with sway.—With a slight extension, the aforementioned method may be used for the elasti-plastic solution of continuous frames whose joints are free to translate or sway with one or more degrees of freedom.

As a preliminary step, moments in the elastic structure produced by unit force acting in the direction of a freedom and on the joints which are free must be determined by conventional moment distribution or an equivalent method. The effect of sway may then be included in an elasti-plastic solution by introducing into each step of the solution the increments of these sway forces needed for equilibrium of the swaying joints along with the elastic moment-increments resulting from these sway forces.

Table 3 shows the initial computations of a solution involving sway, using a purely arbitrary M-ϕ relationship defined by $k_1 = 0$, $k_2 = 12$, and $M_u/M_e = 1.10$. The structure shown in Fig. 8 has one degree of sway freedom in that member

PLASTIC DESIGN OF FRAME FREE TO SWAY[a]

CD	Member DE		Member DF			Member FG	
Joint D	Joint D	Joint E	Joint D	Span DF	Joint F	Joint F	Joint G
⌢ 0.112	) 0.081	(0.040	⌢ 0.031		⌣ 0.012	(0.012	) 0.006
⌢ 0.213	(0.574	) 0.287	⌣ 0.213		⌢ 0.082	) 0.082	(0.041
⌣ 0.031	) 0.081	(0.040	⌣ 0.112		⌢ 0.274	(0.726	) 0.363
⌢ 1.04	) 2.07	(2.79	⌣ 1.04		⌢ 1.21	) 1.21	(2.36
⌢ 45.0			⌢ 45.0		45.0		
⌢ 4.4	) 3.2	(1.6	⌢ 1.2		0.5	(0.5	) 0.2
⌢ 1.4	(3.6	) 1.8	⌢ 5.0		12.3	) 32.7	(16.3
	(0.4	) 0.2				) 32.2	(16.1
	→0.05					← 4.02	
⌢ 5.7	) 11.4	(15.3	⌣ 5.7		⌢ 6.7	) 6.7	(13.0
∧ 56.5	) 11.0	(15.1	⌢ 45.5	⌣ 26	⌢ 38.9	) 38.9	(29.1
⌢ 45.0	) 5.0	(12.0	⌢ 40.0		⌢ 42.0	) 42.0	(34.0
9.50					9.07	6.33	
∧212					∧ 59	> 85	
⌣ 28.2			⌢ 3.9		⌣ 7.9	(28.3	) 14.2
⌢ 1.6	) 1.1	(0.6	⌢ 0.4		⌣ 0.2	(0.2	) 0.1
⌢ 6.8	(18.4	) 9.2	⌣ 6.8		⌢ 2.6	) 2.6	(1.3
⌢ 0.6	(1.7	) 0.8	⌢ 2.3		⌣ 5.6	) 14.8	(7.4
	(19.0	) 9.4				(11.1	) 5.6
	→2.37					→1.35	
⌢ 4.8	) 9.6	(13.0	⌣ 4.8		⌢ 5.6	) 5.6	(11.0
⌢ 42.1	) 1.6	(18.7	⌢ 40.5		⌢ 33.4	) 33.4	(34.5
⌣ 2.9	(3.4	(6.7	⌢ 0.5		⌣ 8.6	(8.6	(0.5

CF may translate laterally. Therefore, as a preliminary, the elastic moments in the structure from a unit lateral load acting on CF are found by any conventional method and entered following the other distribution coefficients. For the elastic solution, after the distribution of moments with sway prevented, the resulting horizontal forces on CF are computed (in this case the three column shears and the 4_k external force). The resultant of these forces (5.50_k) is

applied as a sway force to produce equilibrium, and the moments caused by this resultant are added to the non-sway moments.

For the elasti-plastic solution, similar sway corrections are merely introduced into each trial so that no unbalanced sway forces are associated with the final computed moments of that trial. For example, for the first trial of example three, additional increments of moment resulting from occurrence of the assumed plastic angles in the non-swaying structure are calculated as in previous examples. Then, because the sway forces had been balanced for all previously calculated moments (in this case the elastic solution moments), it is only necessary to balance the resultant sway forces accompanying these new moment increments.

Example three also shows the assumption of arbitrary trial moments at the beginning of the first trial in an effort to hasten convergence. It is usually not difficult to assume initial moments for the first trial that are closer to the elasti-plastic solution than the elastic solution moments, thus hastening convergence. Of course, the sway forces accompanying these arbitrary moments do not necessarily have to be balanced.

For those structures with members for which $k_1 = 0$, such as example three, it soon becomes apparent to the designer that, in establishing those trial moments exceeding M_e for each step, the relationship between the plastic angle and the quantity $(M - M_e)$ is more nearly linear than the relationship between

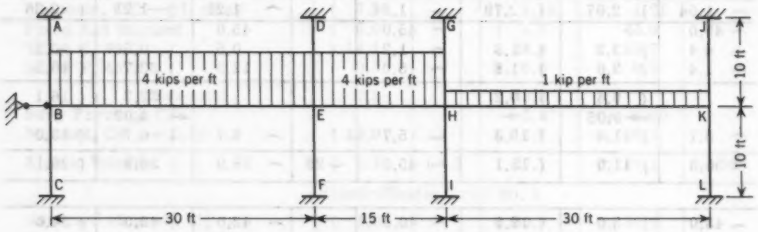


FIG. 7.—THREE-SPAN CONTINUOUS FRAME

the plastic angle and M. Corresponding adjustments may be made in trial moment increments, thereby hastening convergence. It is evident that with experience in elasti-plastic computations the designer can expect to both improve his judgment and discover other techniques for improving the trial moments and thus reduce the number of trials necessary.

For example three, the ratios of strength predicted by the elastic and rigid-plastic theories to the elasti-plastic strength are 0.74 and 1.24, respectively. It is obvious that these ratios, which have been given for all three examples, are not only functions of the geometry of the structure and the type of loading, but of k_1, k_2, and M_u/M_e. Therefore, these ratios can be expected to vary over a considerable range depending on the variables involved.

DESIGN

The method demonstrated in the previous three examples has the limitation with respect to design of the traditional elastic analytical methods, that is the

structure being designed must be known prior to the analysis. However, the method is more adaptable to design needs than shown in the examples in that the plastic portion of any moment-curvature relationships may be changed at the discretion of the designer from trial to trial of a solution. This flexibility is valuable to the designer of a constant-section steel frame who finds from the results of the first trial that he must use a section with an M-ϕ relationship appreciably different from that initially assumed. This flexibility is even more valuable to the designer of a reinforced concrete frame who, by changing placement of reinforcement from trial to trial, can change M-ϕ relationships and hence the distribution of moments and even the location of plastic regions at his discretion. C. W. Yu[16] and A. U. Baker[6] have investigated some design potentialities of such planned redistributions of moments.

Deflections.—Elasti-plastic deflections of continuous beams and frames may be calculated by the same techniques used to compute elastic deflections of such structures. That is, after moments and plastic angles have been determined by an elasti-plastic solution, deflections may be computed by any usual

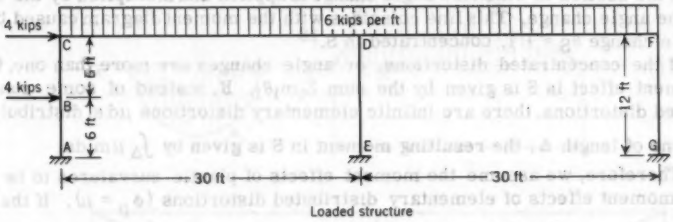


FIG. 8.—FRAME FREE TO SWAY

method provided these plastic angles are included. For the moment area method, localized areas equal to each plastic angle, θ_p (or θ'_p/EI), should be added to the M/(EI) diagram. For the conjugate beam method, concentrated loads equal to each plastic angle are added to the conjugate beam, following which deflections may be computed by the usual techniques of the respective method.

CONCLUSIONS

The method of this paper is valuable in that, unlike the rigid-plastic methods, it allows determination of ultimate strength as limited by an ultimate deformation as well as ultimate moment. That is, by mere adjustment of coefficients which express the magnitude and strain-hardening characteristics of the plastic deformation, it may be used for ultimate load determination for structures of any material ranging from the most brittle to the most ductile and with any number of plastic regions. Also, it provides data from which elasti-plastic deflections may be readily computed. However, all other limitations characteristic of limit design methods apply to this method.

16 "An Analystical Investigation of the Ultimate Load Design of Reinforced Concrete Framed Structures," by C. W. Yu, thesis presented to the University of London, at London, in 1954, in partial fulfilment of the requirements for the degree of Doctor of Philosophy.

DISCUSSION

GIULIANO AUGUSTI.[17]—In this paper, the moment effects caused by the plastic portion of the curvature are computed assuming that these curvatures are angle changes concentrated at the point of maximum moment. The author has, in some numerical examples, realized that this shortcoming sometimes causes significant errors.

Therefore, it would be better to remove these shortcomings, and to compute the moment effect of the plastic curvatures considering them as distributed, as they actually are. This computation can easily be made by means of the moment influence lines for traveling distortions.

The moment influence line in a section S for a traveling distortion is a diagram that gives the bending moment in S caused by a concentrated angle change, θ_i. The ordinate m_i of the moment influence line is read in correspondence with the section in which the angle change is applied and multiplied by the value of the angle change. This line coincides with the moment diagram caused by an angle change $\theta_S = +1$, concentrated in S.[18]

If the concentrated distortions, or angle changes are more than one, their moment effect is S is given by the sum $\Sigma_i m_i \theta_i$. If, instead of some concentrated distortions, there are infinite elementary distortions μds, distributed in a zone of length Δ, the resulting moment in S is given by $\int_\Delta \mu m \, ds$.

Therefore, we assume the moment effects of plastic curvatures to be like the moment effects of elementary distributed distortions ($\phi_p = \mu$). If the moment influence line for that section is known, then from $\int \Delta \phi_p m \, ds$. The moment at any section is known. (Angle changes are assumed positive if positive bending moments make positive work for them. Thus, plastic angle changes are always opposite in signs to moments causing them.)[19]

To get the whole moment diagram caused by plastic curvatures in a rectilinear span frame or in a continuous beam, it is sufficient to compute the values at the moment diagram at the joint sections. Thus, it is only necessary to draw the influence lines for these sections.

The reason for the difference in evaluation of moment effects caused by concentrated or distributed plastic curvatures is shown in Fig. 9. The actual moment diagram for a given load, which doesn't attain its ultimate value, is given in Fig. 9 (b); the plastic curvature diagram is given in Fig. 9 (c), assuming the moment-curvature relationship of Fig. 10; the moment influence line at B for a travelling angle change is given in Fig. 9 (d).

In evaluating moment effects, when the plastic curvatures ϕ'_p and ϕ''_p are considered as two angle changes concentrated at points of maximum moment (that is D and B), areas $\int \Delta_1 \phi'_p \, ds$ and $\int \Delta_2 \phi''_p \, ds$ (3) are computed and then

---

[17] Dr. Civ. Engrg., Asst. of Bridge Constr., Univ. of Naples, Naples, Italy.

[18] "Scienza delle Costruzioni," by V. Franciosi, Vol. 2, Cap. 20, Pellerano-del Gaudio Ed., Naples, 1959.

[19] "Le linee d'influenza per distorsioni, etc.," by G. Augusti, Rend. Accad. Sc. Fis. e Mat., Serie 4, Vol. 26, Naples, 1959.

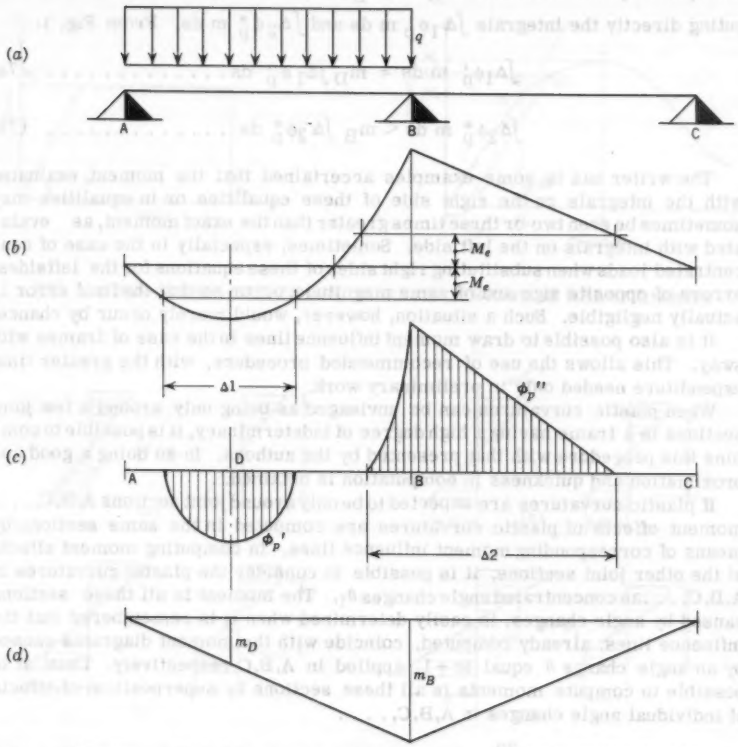


FIG. 9.—RELATIONSHIPS FOR LOADED BEAM

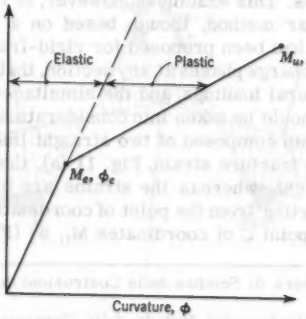


FIG. 10.—MOMENT-CURVATURE RELATIONSHIPS

multiplied by the ordinates m_D and m_B of the influence line, instead of computing directly the integrals $\int \Delta_1 \phi'_p \, m \, ds$ and $\int \Delta_2 \phi''_p \, m \, ds$. From Fig. 1:

$$\int \Delta_1 \phi'_p \, m \, ds = m_D \int \Delta_1 \phi'_p \, ds \ldots\ldots\ldots\ldots \quad (7a)$$

$$\int \Delta_2 \phi''_p \, m \, ds < m_B \int \Delta_2 \phi''_p \, ds \ldots\ldots\ldots\ldots \quad (7b)$$

The writer has in some examples accertained that the moment evaluated with the integrals on the right side of these equalities or in equalities may sometimes be even two or three times greater than the exact moment, as evaluated with integrals on the left side. Sometimes, especially in the case of concentrated loads when substituting right sides of these equations for the leftsides, errors of opposite sign and of same magnitude, occur so that the final error is actually negligible. Such a situation, however, would merely occur by chance.

It is also possible to draw moment influence lines in the case of frames with sway. This allows the use of recommended procedure, with the greater time expenditure needed only in preliminary work.

When plastic curvatures can be envisaged as being only around a few joint sections in a frame having a high degree of indeterminacy, it is possible to combine this procedure with that presented by the authors. In so doing a good approximation and quickness in computation is obtained.

If plastic curvatures are expected to be only around joint sections A,B,C,. . ., moment effects of plastic curvatures are computed in the same sections by means of corresponding moment influence lines. In computing moment effects at the other joint sections, it is possible to consider the plastic curvatures in A,B,C,. . .as concentrated angle changes θ_i. The moment in all these sections caused by angle changes, is easily determined when it is remembered that the influence lines, already computed, coincide with the moment diagrams caused by an angle change θ equal to +1, applied in A,B,C respectively. Thus, it is possible to compute moments in all these sections by superposition of effects of individual angle changes in A,B,C,. . . .

TULLIO RENZULLI.[20]—The procedure proposed for the computation of a frame is without doubt more exact than those which are based on a limited stress-strain diagram, or those which take no account of the elastic strains in comparison with plastic ones. This exactness, however, is linked to more extended computations. A similar method, though based on a less general moment-curvature relationship, has been proposed for rigid-frame computations.[21,22]

The possibility of discharge phases at any section, that is, moment decreasing during a phase of structural loadings, and the simultaneous presence of normal and shearing stresses should be taken into consideration. Starting with an ideal stress-strain relationship composed of two straight lines, the second of which stops at the value of the fracture strain, Fig. 11 (a), the moment-curvature ($M - \phi 1/r$) diagram is straight, whereas the strains are in the elastic range and becomes curvilinear starting from the point of coordinates M_e, ϕ_e, and reaches its highest value at the point C of coordinates M_i, ϕ_i (Fig. 11 (b)).

---

[20] Assistente alla cattedra di Scienza delle Costruzioni della Facoltà di Ingegneria di Napoli-Libero Docente.

[21] "Contributo alla Evoluzione del Metodo delle Cerniere Plastiche-Giornale del Genio Civile Roma," by A. Galli and T. Renzulli, Nos. 11-12, 1954.

[22] "Sul Calcolo delle Strutture Monodimensionali in Regime Elasticoplastico-Rend," by T. Renzulli, Napoli Serie 4, Accad. di Scienze Fis. e Mat., 1954.

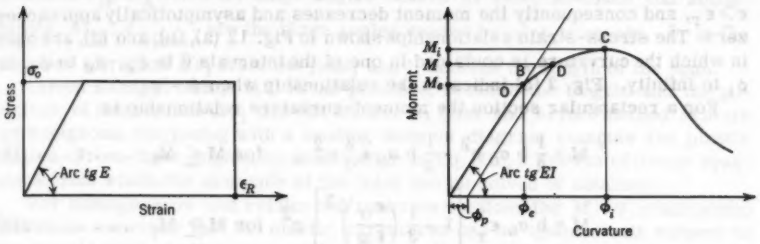


FIG. 11(a,b).—STRESS-STRAIN AND MOMENT-CURVATURE RELATIONSHIPS

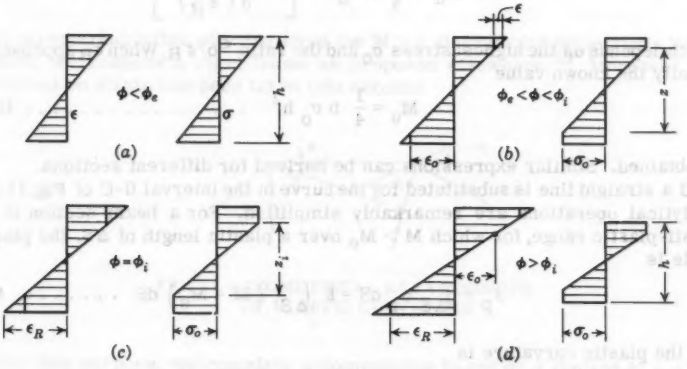


FIG. 12.—STRESS-STRAIN RELATIONSHIPS FOR VARIOUS CURVATURE RANGES

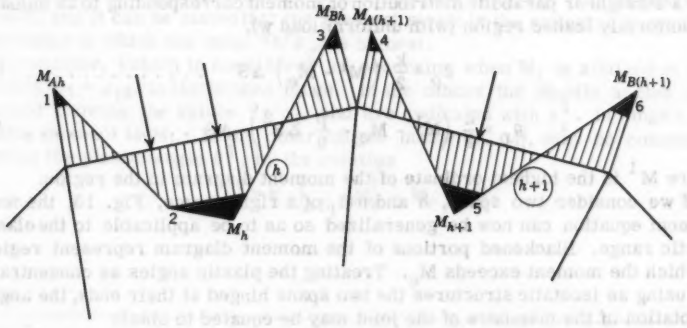


FIG. 13.—MOMENT DIAGRAM APPLIED TO TWO SPANS OF A RIGID FRAME

With increasing curvature there is a fracture of elements of the section where $\epsilon \geq \epsilon_r$, and consequently the moment decreases and asymptotically approaches zero. The stress-strain relationships shown in Fig. 12 (a), (b), and (d), are ones in which the curvature is contained in one of the intervals 0 to ϕ_e, ϕ_c to ϕ_i, or ϕ_i to infinity. Fig. 3 (c) indicates the relationship when $\phi = \phi_i$.

For a rectangular section the moment-curvature relationship is

$$M = \frac{1}{4} b \sigma_o h^2 - \frac{1}{3} b \sigma_o \epsilon_o^2 r^2 \qquad \text{for } M \leq M_i \quad \ldots\ldots\ldots (8)$$

$$M = b \sigma_o \epsilon_r^2 \left[1 - \frac{1}{3}\left(\frac{\epsilon_o}{\epsilon_R}\right)^2\right] r^2 \qquad \text{for } M \geq M_i \quad \ldots\ldots\ldots (9)$$

The highest value of the moment, M_u, is

$$M_u = \frac{1}{4} b \sigma_o h^2 \left[1 - \frac{1}{3}\left(\frac{\epsilon_o}{\epsilon_R}\right)^2\right] \quad \ldots\ldots\ldots (10a)$$

which depends on the highest stress σ_o and the ratio ϵ_o/ϵ_R. When ϵ_R approaches infinity the known value

$$M_u = \frac{1}{4} b \sigma_o h^2 \quad \ldots\ldots\ldots\ldots\ldots (10b)$$

is obtained. Similar expressions can be derived for different sections.

If a straight line is substituted for the curve in the interval 0-C of Fig. 11 (b), analytical operations are remarkably simplified. For a beam section in the elasti-plastic range, for which $M > M_e$ over a plastic length of ΔS, the plastic angle is

$$\theta_p = \int_{\Delta S} \phi_p \, dS = k \int_{\Delta S} (M - M_e) \, dS \quad \ldots\ldots\ldots (11)$$

and the plastic curvature is

$$\phi_p = k (M - M_e) \quad \ldots\ldots\ldots\ldots\ldots (12)$$

in which k is a constant whose value can be obtained from Eq. (12) with $M = M_i$. For a straight or parabolic distribution of moment corresponding to an unloaded or uniformly loaded region (with uniform load w),

$$\theta_p = \frac{k}{2} (M^1 - M_e) \Delta S \quad \ldots\ldots\ldots\ldots (13)$$

$$\theta_p = \frac{k}{2} \left(M^1 - M_e - \frac{p}{6} \Delta S^2\right) \Delta S \quad \ldots\ldots\ldots\ldots (14)$$

where M^1 is the highest ordinate of the moment diagram in the region.

If we consider two spans, h and h+1, of a rigid frame, Fig. 13, the four-moment equation can now be generalized so as to be applicable to the elasti-plastic range. Blackened portions of the moment diagram represent regions in which the moment exceeds M_e. Treating the plastic angles as concentrated and using as isostatic structures the two spans hinged at their ends, the angles of rotation of the members of the joint may be equated to obtain

$$\theta_B^h + \theta_A^{h+1} = \theta_{Bh} + \theta_{A\,(h+1)} + \sum_i^{3,4} \int_{\Delta S_i} \phi_p \, dS - \sum_i^{2,5} \int_{\Delta S_i} \frac{l_i \, \xi_i}{l_i} \phi_p \, dS \quad \ldots (15)$$

in which θ_B^h, θ_A^{h+1} are the hinge angles caused by external loads and settlements; θ_{Bh}, $\theta_{A(h+1)}$ are the hinge angles caused by joint moments, ξ is the distance of region Δs_i from the joint; and l_i denotes the length of the span.

Direct solution of Eq. (15) is not possible, because the lengths and the positions of the regions ΔS_i are not known. A trial and error method is more advantageous. Beginning with a bending moment diagram compute the plastic angles. From these angles, by substitution in Eq. (15), a system of linear equations from which the moments at the joint can be solved is obtained.

For homogeneous and reinforced concrete sections the M - θ relationship indicates sometime that the elastic curvatures can be ignored with respect to the plastic ones. In this case, with increased external loads, only plastic curvatures are considered. Then Eq. (15) reduces to the geometric relationship shown in Fig. 14.

$$\theta_2 = \theta_1 + \theta_3 \quad \ldots\ldots\ldots\ldots\ldots\ldots \quad (16)$$

It is remarkable that, starting from the M - θ diagram and neglecting elastic strains, we compute a rigid frame as proposed elsewhere.[23] Moreover the limitation on strain has been taken into account.

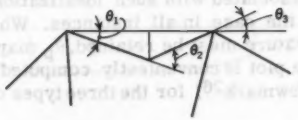


FIG. 14.—GEOMETRICAL RELATIONSHIPS OF PLASTIC CURVATURE

For this purpose, we complete a computation based on a limited M - ϕ relationship and obtain, for an n-degree hyperstatic frame, the positions of the n+1 hinges necessary for rigid collapse. The angle between any two sections linked by a plastic hinge i is α_i. These angles are known through a proportionality constant. The plastic angles θ pi are obtained using Eq. (11) or Eqs. (13) and (14), and it can be stated that the greatest strain in the material is reached at section t in which the value α_t/θ_{pt} is highest.

At collapse, (which is considered as occurring when M_i is attained at any section), $\alpha_t = \theta_{pt}$, in the broken hinge. In the others the plastic angles are obtained knowing the values α_i/α_t, and are indicated with θ_i^1. In hinge t the bending moment is M_i. In the other hinges moments, M_i^1, may be computed, knowing the plastic angle θ_i^1, by the relation

$$\theta_i^1 = k \int_{\Delta S_i} \left(M_i^1 - M_e \right) dS \quad \ldots\ldots\ldots\ldots \quad (17)$$

---

23 "Limit Design of Beams and Frames," by H. Y. Greenberg and W. Prager, Proceedings, Separate No. 59, ASCE, February, 1951.

and in particular cases of an unloaded or uniformly loaded region by the relations

$$\theta_i^1 = \frac{k}{2}\left(M_i^1 - M_e\right)\Delta S_i \quad \ldots\ldots\ldots\ldots (18)$$

$$\theta_i^1 = \frac{k}{2}\left(M_i^1 - M_e - \frac{p}{6}\Delta S_i^2\right)\Delta S_i \quad \ldots\ldots\ldots\ldots (19)$$

In Eqs. (18) and (19) the lengths ΔS_i are obtained by trial moment diagrams, then, considering the moments M_i^1 so obtained, these lengths are recomputed and the new values substituted.

EMILIO ROSENBLUETH,[24] M. ASCE.—The authors have presented a neat and useful method of analysis applicable to continuous beams and frames constituted by members having any moment-curvature diagrams. This method leads to curved relations between bending moment and angle change at inelastic hinges. Due to its generality the method might well have been termed inelastic analysis. As shown by one of the authors in an earlier paper[25] (of which the present one may be regarded as a generalization) the advantage of idealizing a moment-curvature diagram, as formed by two or three straight lines, lies in the feasibility of resorting to the relatively simple tabulated formulas for the plastic angle change θ_p in terms of the bending moment diagram.

Usually the error associated with such idealizations in quite tolerable, but this is not necessarily the case in all instances. When curved ralations between moment and curvature must be retained, θ_p may be obtained from a plot as a function of M. The plot is conveniently computed by a numerical procedure (such as that of Newmark[26]) for the three types of moment diagram considered in Table 1.

For structures with a large number of joints it is possible to develop a method that often involves less computational work than is involved in the authors' method. It requires knowledge of the distribution constants for prismatic members having elastic hinges. Consider the member in Fig. 15. It is a prismatic beam of span L, having hinges connected by springs. These are located at distances $\xi_1 L, \xi_2 L, \ldots$ from the left support, and at $\eta_1 L, \eta_2 L, \ldots$ from the right-hand support. It is easily shown that the carry-over factor from left to right is

$$t_{ab} = \frac{0.5 + \Sigma \alpha_i \eta_i}{1 + \Sigma \alpha_i \xi_i} \quad \ldots\ldots\ldots\ldots\ldots\ldots (20)$$

and the left-hand stiffness, when the right-hand support is fixed against rotation, is

$$K_a = \frac{3EI/L}{(1 + \Sigma\, \beta_i \eta_i)\,(1 - t_{ab} t_{ba})} \quad \ldots\ldots\ldots\ldots (21)$$

---

24 Director and Research Engr., Prof. Inst. of Engr., Univ. of Mexico, Mexico City, Mexico.

25 "Elasti-Plastic Design of Single-span Beams and Frames," by H. A. Sawyer, Jr., Proceedings Paper 85, ASCE, Vol. 81, December, 1955.

26 "Numerical Procedure for Computing Deflections, Moments, and Buckling Loads," by N. M. Newmark, Transactions, ASCE, Vol. 108, 1943, pp. 1161–1234.

in which $\alpha_i = \frac{3EI\xi_i}{k_iL}$, and $\beta_i = \frac{3EI\eta_i}{k_iL}$, and k_i is the stiffness (moment divided by angle change) of the ith spring.

If the right-hand end is simply supported, Eq. 20 becomes

$$K'_a = \frac{3EI/L}{1 + \Sigma\, \beta_i\eta_i} \quad \ldots\ldots\ldots\ldots\ldots\ldots \quad (21b)$$

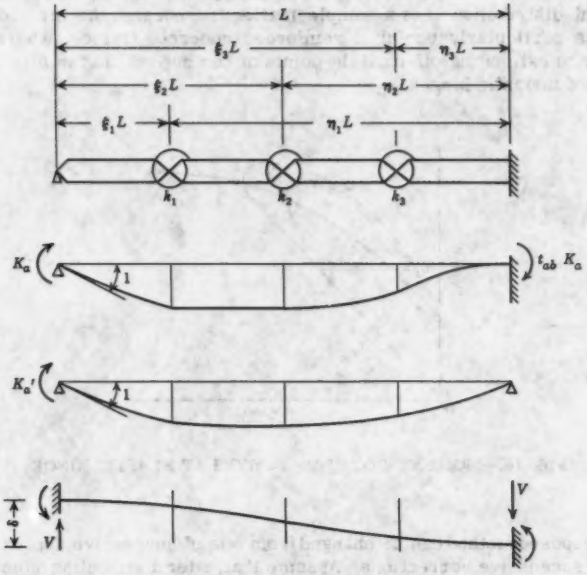


FIG. 15.—BEAM WITH ELASTIC HINGES

The stiffness of the beam, when its supports are displaced laterally without rotation, is found to be

$$\frac{V}{\delta} = \frac{1 + \Sigma\, \frac{EI}{k_iL}}{1 + \Sigma\, \frac{EI}{k_iL}\left(1 - 3\xi_i + 3\xi_i^2\right)}\, \frac{12EI}{L^3} \quad \ldots\ldots\ldots\ldots \quad (22)$$

in which V denotes the shear corresponding to a displacement δ.

Eqs. 20 to 22 permit a straightforward moment distribution in frames with elastic hinges or semi-rigid connections. The method proposed begins by estimating the redundances so as to obtain a preliminary moment diagram.

The structure is then dimensioned and, at every region where the bending moment exceeds the elastic-limit moment, an inelastic hinge is placed. A moment-rotation diagram can be drawn for every inelastic hinge, such as the solid curve in Fig. 16. From the preliminary moment diagram, the bending moment at the hinge has in effect been estimated and a secant (OA in Fig. 16) can be drawn through the origin. The slope of the secant defines a preliminary stiffness of the hinge and one can carry out a first moment distribution using Eqs. 20 to 22.

Results of the moment distribution provide a new moment diagram, which in general will differ from the original. The final moment diagram will usually be intermediate between the original and that found from moment distribution. Hence, one can assume a new diagram, closer to the solution of the frame, and repeat the process in a series of successive approximations. At any stage after a moment distribution it is a simple matter to redesign the structure. This feature is particularly useful in reinforced-concrete frames, where there is difficulty in estimating off-hand the points of bar cut-off, that in turn affect the location of inelastic hinges.

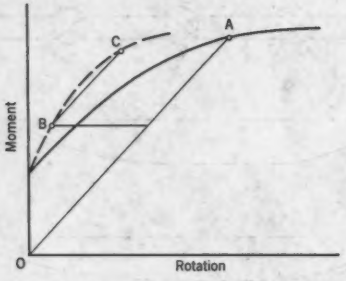


FIG. 16.—MOMENT-ROTATION CURVES AT ELASTIC HINGE

The proposed method can be changed from one of successive approximations to one of successive corrections. Assume that, after distributing moments, the moment at one hinge is equal to the ordinate of point B in Fig. 16 while the originally assumed moment equalled the ordinate of A. In the figure, point B has been placed on a revised moment-rotation curve (dashed line), that corresponds to the new estimated moment diagram. If in the new diagram the moment at the hinge in question is equal to the ordinate of point C on the same dashed line, a correction to the originally estimated diagram is obtained by distributing the difference between the ordinates of A and B, and similar differences in the rest of the hinges, with an assumed hinge stiffness equal to the slope of BC.

This process has been successfully applied to analysis of frames having inelastic semi-rigid connections without need of applying Eqs. 20 to 22. The connection is merely replaced by a "phantom member"[27], with stiffness equal

---

[27] Discussion by W. Sholtz of "Elastic Properties of Riveted Connections," by J. Rathbun, Transactions, ASCE, Vol. 101, 1936, pp. 568-569.

to the slope of its moment-rotation curve and a carry-over factor of -1 (in the static-moment sign convention). It is equally successful when the positions of most hinges are correctly estimated from the start and redesign at "mid-analysis" is not contemplated. Otherwise the successive-approximations version is preferable.

In essence, the operations carried out in the proposed method are the same as those in the authors' but are performed in a manner that seems more efficient when the number of joints is large. Conversely, in frames with a small number of joints the labor involved in distributing a unit moment applied successively at each of the joints is not excessive, and the authors' method offers greater advantages.

Based on the work of A.L.L. Baker,[28] it would seem that moment-angle change diagrams for reinforced concrete members might be adequately approximated for design purposes by two straight lines, the first through the origin, coinciding with perfectly elastic behavior, and the second horizontal, with limited rotation. This proposal is attractive in view of the many uncertainties involved when failure is impending. This type of moment-rotation diagram lends itself to analysis according to the following steps:

1. Invent a solution satisfying statics. In this step, four considerations usually govern selection of the solution: a) Economy is achieved by keeping the maximum moment down in rectangular sections to obviate the need for compression reinforcement of increase in concrete section beyond that which is required to take shear economically, and also by making minor adjustments to utilize the reinforcement as close to its working stress as possible. b) Ease in placing concrete. c) Minimum deflections and crack formation. To this end the solution should be close to the elastic solution (although the latter need not be computed accurately). Test results and application of Baker's proposed load factors indicate that as much as 33% reduction in design bending moments may be tolerated with respect to the elastic solution without special provisions, as long as statics are satisfied. d) Uniformity in bar lengths. For instance, the design moment over the first interior support of a continuous beam or girder having several equal spans can often be made equal to that over other interior support so that all except end spans require the same distribution of reinforcement.

2. Assuming elastic behavior, compute "dislocations" (finite angle changes) required at plastic hinges to satisfy continuity elsewhere in the frame. Tables of end slopes of simple beams are helpful in this step.

3. Compare with allowable dislocations (ultimate hinge rotations). If computed angle changes are smaller than these, the frame has been solved. Otherwise apply end moments to close the gaps sufficiently to keep them within allowable limits, or else add stirrups, ties, or spirals to increase allowable angle changes.

For routine analysis of reinforced concrete frames this method seems preferable to most others. However, even though it could easily be extended to more general moment-rotation curves, it would loose its simplicity and conceivably no longer be more advantageous than the authors' method or than the one described earlier in this discussion.

Whatever method is chosen for analysis in connection with design, it is important that it be adapted to permit changes in the structure at intermediate

---

28 "Ultimate Load Theory Applied to the Design of Reinforced and Prestressed Frames," by A. L. L. Baker, London, 1956.

stages of the analysis. Fortunately the authors' method as well as the two procedures described herein apparently lend themselves to such adaptation. The writer hopes that in their closing discussion the authors will more fully describe this aspect of their proposed method.

A. A. EREMIN,[29] M. ASCE.—The authors have shown the method of distribution of bending moments in rigid frames by considering the elasti-plastic deformations. It is interesting to note that the operations involved in distributing the plastic moments is similar to those involved in distributing elastic

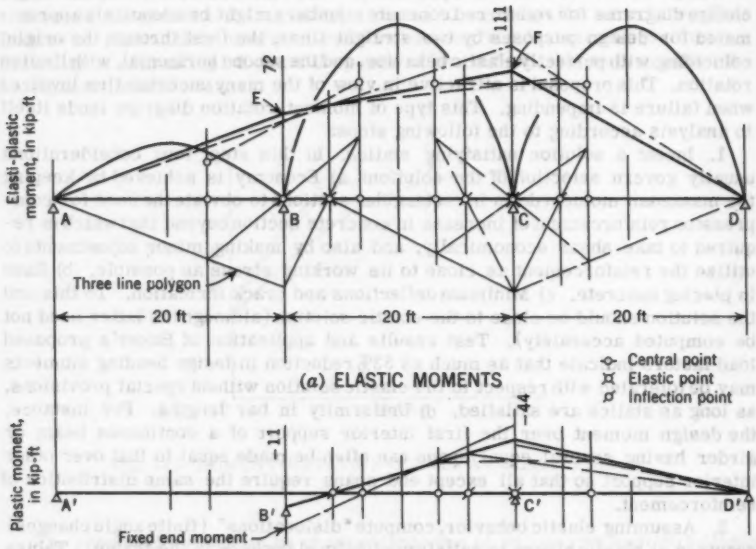


FIG. 17.—ELASTIC AND PLASTIC MOMENTS

moments. The same elastic properties of rigid frame members were considered in both cases. For checking purposes and also for visual presentation of the elastic properties of the continuous beam in the illustrative example shown by the authors in Table 2, the moments were determined by graphical distribution.

[29] Assoc. Bridge Engr., California State Highways, Sacramento, Calif.

Distribution of elastic bending moments from the given loading is shown in Fig. 17(a) and the graphical distribution of the plastic bending moments is shown in Fig. 17(b). The final resulting bending moments for the elasti-plastic condition of the continuous beam are determined by summation of the elastic bending moments in Fig. 17(a) and one-half of the value of plastic bending moments from Fig. 17(b). The final bending moment closing line is shown in Fig. 17(a) by line AEFD.

It may be noted that the final bending moments determined with the graphical constructions vary from the moments computed by the authors by less than 6%. By means of graphical construction the effect of the elastic properties of the members of the continuous beams may easily be revealed.

The characteristic points in the beam, Fig. 17(a), are determined by the graphical construction termed "three line polygon."[30,31]

LAWRENCE P. JOHNSON, JR.,[32] M. ASCE and HERBERT A. SAWYER, JR.,[33] F. ASCE.—Mr. Augusti used influence lines and integration to show the error of the approximation in assuming that a distributed plastic curvature is concentrated at the point of maximum moment. Actually, as stated by the authors, for any given span, including non-prismatic and curved spans, the location of this concentration for exact results is at the centroid of the distributed curvature. This principle is based on the linear relationship between the location of any angle change and the end-moment or force caused by the angle change. This linearity is expressed for the general case by the first terms of Eqs. 4(a) and 4(b) (Y_0 being a linear function of K_b), and it is also expressed by Mr. Augusti's influence lines, which must always be linear. Therefore, the error discussed by Mr. Augusti is simply the error in assuming the centroid of curvature at the point of maximum moment, and it can usually be dismissed by inspection. As stated, to eliminate this error "for extremely asymmetrical curvature diagrams, the actual location of the centroid can be computed." Although this error was insignificant and thus tolerated for the illustrative examples, the authors would certainly agree with Mr. Augusti that this error may occasionally be significant.

Because Mr. Renzulli's analytical determination of the M-ϕ relationship for a rectangular section of an ideal material is outside the scope of the paper, it will not be commented on herein. References were listed in the paper for work in this area for steel and reinforced concrete. Mr. Renzulli's expressions for plastic angles, Eqs. 13 and 14, are identical to those in Table 1 for $k_2 = 0$. Eq. 15, the general equation for joint continuity, is interesting as a mathematical expression of the problem to be solved. To be completely general, terms expressing the joint angles from sway should be added to this equation. As the discusser stated, direct solution of the system of nonlinear simultaneous equations obtained by writing this equation for all joints is practically impossible. He therefore recommends that the nonlinear terms be estimated using an assumed set of moments, and that the resulting linear system of equations then be solved for the moments and sways. Generally, the moments and sways so obtained will not agree with the assumed moments and

---

30 "Simplified Graphical Distribution of Bending Moments," by A. A. Eremin, 1948.

31 Discussion by A. A. Eremin of "Continuous Arches and Bents Analyzed by Column Analogy," by T. M. Yu, Transactions, ASCE, Vol. 115, 1950, p. 630.

32 Special Design Engr., Water Bureau, Metro. Dist. Comm., Hartford, Conn.

33 Prof. of Civil Engrg., Univ. of Conn., Storrs, Conn.

sways, and new trials based on new sets of assumed moments will be necessary. Actually, this algebraic procedure is equivalent to the authors' numerical procedure, with the only important difference being that in the latter the moments of each trial are obtained by a moment distribution rather than by solution of simultaneous equations. The superiority of moment distribution over an algebraic method is well known (although with electronic computers this superiority is reduced). For example, for the algebraic solution of example two, each trial would involve the solution of twenty-two equations for twenty-two unknowns, whereas the corresponding solution by moment distribution occupies four or five horizontal lines of computations.

On the other hand, the interesting alternative approach to the problem suggested by Mr. Rosenblueth, involving the assumption of elastic hinges at the plastic regions, is like the method of the paper in that it uses moment distribution for each trial. To the authors, however, an important point of difference is that the spring constants of the elastic springs change with each trial, necessitating a recomputation of the fixed-end moments, relative stiffnesses, and carry-over factors of all hinged spans for each trial. These elastic quantities remain constant in the method presented by the authors.

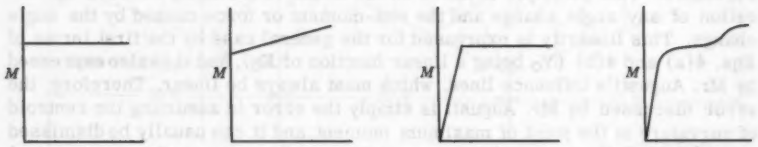


FIG. 18.—COMPARISON OF MOMENT CURVATURE DIAGRAMS

The design of a structure usually involves analyses for several loading conditions, and several moment-distributions are required for each elasti-plastic analysis. Because of this repetition, the authors recommended and showed use of unit-moment distribution factors as the most efficient method of moment distribution. The authors agree with Mr. Rosenblueth that the advantages of this method diminish as the number of joints increase. However, this method is optional, and the usual method of moment distribution may be reverted to at any time in the design process without affecting the over-all operation of the method.

Both Mr. Renzulli and Mr. Rosenblueth present interesting simplifications of the general method of the paper, the former a method in which the elastic deformations are neglected, Fig. 18(b), and the latter a method in which there is a sudden and complete transition from elasticity to plasticity without strain-hardening, Fig. 18(c). Both of these methods are compromises between the general elasti-plastic method based on Fig. 18(d), and the well-known, simple rigid-plastic theory, based on Fig. 18(a). The potential value of these compromises is that they may, unlike simple plastic theory, account for deformations, and that this accounting may be accurate enough for design purposes without resorting to the more complex elasti-plastic methods.

The authors cannot agree that Mr. Renzulli's approximation involving neglect of elastic strains is generally good for "homogeneous and reinforced concrete sections". The ratio of total elastic to total plastic angle change for any member with a linear moment diagram is equal to the ratio of the elastic to plastic areas below the level of M of the M-ϕ diagram, Fig. 1(a). For the M-ϕ diagram derived and presented by Mr. Renzulli in Eqs. 8 and 9 and Fig. 11(b), using his "ideal" stress-strain relationship with $\epsilon_R = 3\epsilon_0$, this ratio has been computed to be approximately five for $M = M_u$, and it approaches infinity as M approaches M_e. Elastic strains seem to be equally important for reinforced concrete. As an example, for the M-ϕ relationship used example two, based on tests of reinforced concrete, the minimum ratio of elastic angle to plastic angle for a linear moment diagram is 3.8. Certainly the major source of strain cannot be neglected in a strain analysis. Therefore, the approximation of Fig. 18(b) should not be used for reinforced concrete.

As for steel, tests recently conducted by one of the authors at the University of Connecticut for rolled steel sections with linear moment diagrams, yielded minimum ratios of elastic angle to plastic angle of from 0.06 to 0.70. Because sections with rather slender elements were used for many of these tests, the lower of these ratios is probably more representative of the usually-used sections than the higher. Although these ratios are much lower than those for reinforced concrete, other considerations cause the authors to question the use of the neglect-of-elastic-strain approximation for steel. First, an important purpose of a strain analysis is presumably to detect those structures for which a limiting strain may prevent attainment of the ultimate load indicated by the rigid-plastic theory. Unfortunately, those members with the smallest limiting strain are also the members with the highest ratios of elastic to plastic angles. Hence, the error of this approximation is greatest (and on the unsafe side) for the very members or structures for which a strain analysis may be important. A second, and secondary, consideration is that the post-elastic portion of the moment-curvature diagram for rolled steel sections, consisting as it does of an essentially horizontal, "true plastic" line and an inclined strain-hardening or "modified plastic" line, as shown in Fig. 1(b), cannot be accurately represented by any single line.

The two other possible purposes of a strain analysis of a steel structure in the plastic range should also be mentioned. One is the determination of the amount that strain-hardening will allow the load on a structure to exceed the fully-plastic ultimate load, and the second is the determination of deflections. For both of these purposes, the previously mentioned errors would make the use of the neglect-of-elastic-strain approximation for steel very questionable.

The Baker-Rosenblueth approximation avoids the aforementioned errors by accounting for elastic strains, and thus the authors would agree that this approximation is of potential value for reinforced concrete design. Because one of the authors has recenlty discussed the relationship between this approximation and the elasti-plastic methods,[34] further discussion will be limited to two observations. One is that the strain-hardening portion of the M-ϕ relationship, neglected in this approximation, is essential for any rational determination of the plastic-region curvatures at the time the limiting strain is attained, and therefore essential for rational determination of ultimate hinge-rotation capacities.[4] Second, the authors believe that this advantage and the

[34] Discussion by H. A. Sawyer, Jr., of "Review of Limit Design for Structural Concrete," by C. W. Yu and E. Hognestad, Proceedings Paper 1878, ASCE, in Proceedings Paper 2152, September, 1959.

other advantages of elasti-plastic methods which result from use of the full M-ϕ relationship do not seem to be outweighed by any increase in computational difficulty. It is primarily a lack of definitive information on M-ϕ relationships which presently discourages use of elasti-plastic methods for reinforced concrete design.

The authors appreciate Mr. Rosenblueth's elaboration on the possibilities, valuable in design, of making structural changes at intermediate stages of a limit analysis. As Mr. Ermin mentioned, the elastic properties used with an elasti-plastic method are independent of the magnitude, location, or quantity of the plastic regions, so the designer can make adjustments in reinforcing steel without redoing previous computations and without change of procedure for the next trial. Mr. Eremin's presentation of an alternative graphical method of moment distribution, with its attendent advantage of pictorial clarity, is appreciated.

The elasti-plastic method of a preceding paper[4] is analogous to the column analogy or elastic center methods used for elastic solutions, and it should be used for an elasti-plastic solution in any situation for which the column analogy is suitable for an elastic solution. The method of the present paper is analogous to the Hardy Cross moment distribution method used for elastic solutions, and it is suitable for elasti-plastic solutions in situations for which moment distribution is suitable for elastic solutions.

The authors thank the discussers for their imaginative and valuable contributions to our knowledge of the elasti-plastic behavior, analysis, and design of structures.

AMERICAN SOCIETY OF CIVIL ENGINEERS

Founded November 5, 1852

TRANSACTIONS

Paper No. 3057

AMBUKLAO ROCK-FILL DAM, DESIGN AND CONSTRUCTION

By E. Montford Fucik,[1] F. ASCE, and Robert F. Edbrooke,[2] M. ASCE

With Discussion by Messrs. Frederic L. Lawton; Jose O. Lahoz; and E. Montford Fucik and Robert F. Edbrooke

SYNOPSIS

The problems of designing and constructing a 430 ft high, vertical core rock fill dam are described herein. As nearly as can be determined, this is the highest dam of this type in the world now operating at maximum reservoir level. In addition to the dam, the Ambuklao project consists of a chute spillway, an underground powerhouse, and a low level outlet works. The river was diverted through three tunnels in the right abutment of the canyon, two of the tunnels being converted for use as a power tunnel and a low level outlet tunnel after diversion.

Field exploration and sampling, coordinated with laboratory and field testing, provided a sound basis for the selection and design of the dam.

Records of settlement and seepage after operation at maximum reservoir bear out the adequacy of design and construction procedures.

GENERAL DESCRIPTION

The Ambuklao Rock Fill Dam is part of the Ambuklao Hydroelectric Project, located on the Agno River, Island of Luzon, Republic of the Philippines. The Project is owned and operated by the National Power Corporation, a Philippine government-owned corporation whose function it is to develop hydroelectric power projects throughout the Republic. The total cost of the project was approximately 132,000,000 pesos ($66,000,000), of which approximately $20,000,000 was loaned by the Export-Import Bank of the United States. The

Note.—Published, essentially as printed here, in December, 1958, in the Journal of the Soil Mechanics and Foundations Division, as Proceedings Paper 1864. Positions and titles given are those in effect when the paper or discussion was approved for publication in Transactions.

[1] Exec. Vice Pres., Harza Engineering Co., Chicago, Ill.

[2] Proj. Mgr., Harza Engineering Co., Chicago, Ill.

remaining funds, 92,000.000 pesos ($46,000,000) were provided by the Philippine government. The construction of the Project was started in 1952, and the first generating unit was put in operation in December, 1956. The Project is located 135 miles North West of where the bulk of the power generated at Ambuklao is used.

The Agno River has a drainage area of almost 265 sq miles above the damsite. The flow regimen of the river has a distinct dry season and a wet season. As can be seen in the river hydrographs in Fig. 1, the dry season extends from December to April, and the wet season from May to November. This well-defined runoff pattern, typical of most areas in the tropics, was influential in determining the pattern of the construction procedures on the dam.

The maximum flood of record at the damsite was estimated to have had a peak daily flow of 210,000 cfs, which is equivalent to a runoff of 800 cfs per

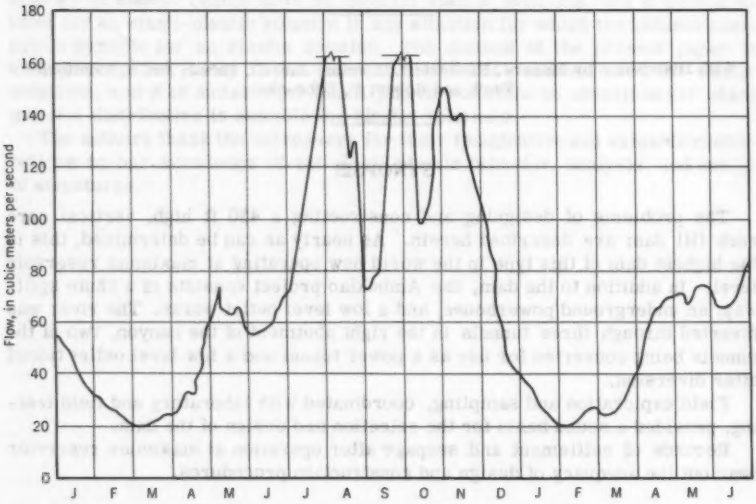


FIG. 1.—TYPICAL HYDROGRAPH

sq mile of drainage area. This high runoff is not surprising when it is realized that a rainfall of 48 in. in 24 hr has been recorded at Baguio City approximately 12 miles from the site. The spillway design flood for the project is 390,000 cfs.

Fig. 2 is a plan of the major structure of the project. The rock fill dam is placed at a narrow point in the river valley, and the spillway is located at the left end of the dam. This spillway location takes advantage of the return loop made by the river downstream of the dam, and thus the discharge from the spillway enters the river a mile downstream from the toe of the dam, riverwise, but only 500 ft away measured in a straight line.

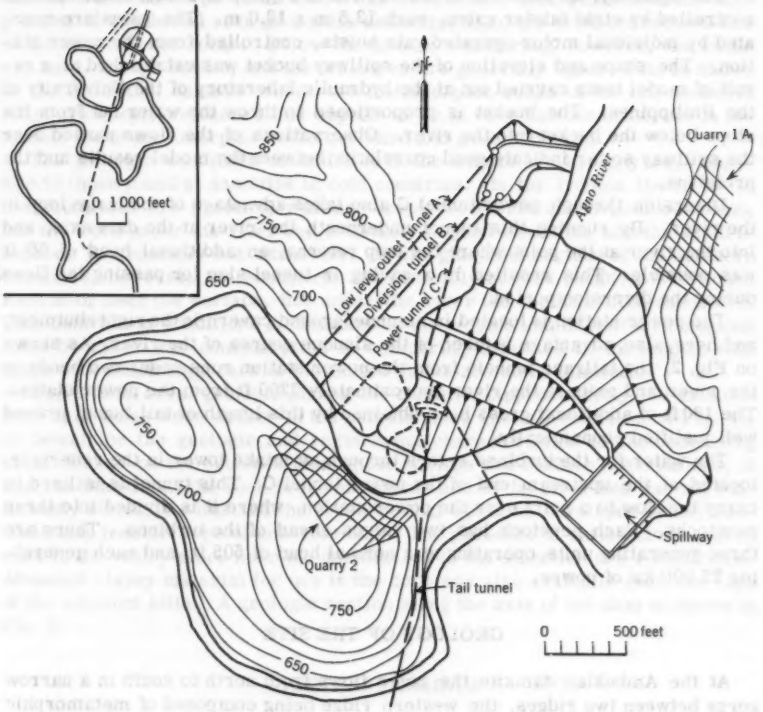


FIG. 2.—AMBUKLAO POWER PROJECT

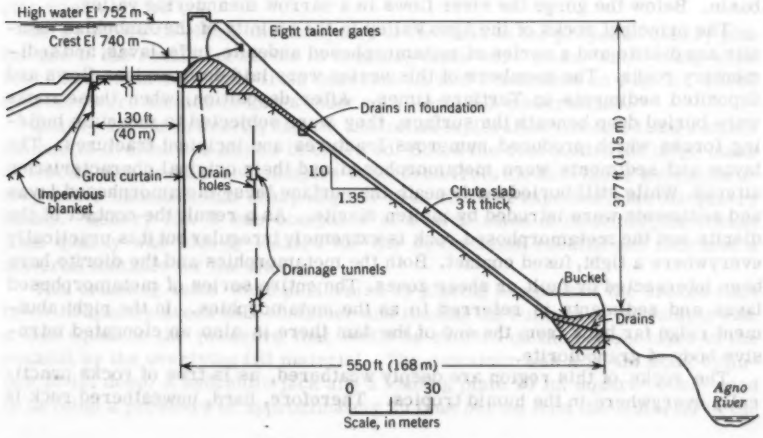


FIG. 3.—SPILLWAY SECTION

The spillway, as shown in cross section in Fig. 3, is a high chute section, controlled by eight tainter gates, each 12.5 m x 12.0 m. The gates are operated by individual motor operated gate hoists, controlled from the power station. The shape and elevation of the spillway bucket was established as a result of model tests carried out at the hydraulic laboratory of the University of the Philippines. The bucket is proportioned to throw the water out from the slope below the bucket into the river. Observations of the flows passed over the spillway so far indicate good correlation between the model results and the prototype.

Diversion through power tunnel C also takes advantage of the large loop in the river. By running this tunnel underneath the river at the dam axis, and into the river at the point where the loop returns, an additional head of 60 ft was possible. This resulted in a saving in tunnel size for passing the flows during the diversion period.

The power station is located in an underground cavern in the right abutment, and here, also, advantage is taken of the sinuous course of the river. As shown on Fig. 2, the tailrace tunnels from the power station runs under two bends in the river and exits to the river approximately 7200 ft from the power station. The 180 ft of additional gross head obtained by this length of tail tunnel proved well justified economically.

The water for the turbines enters through an intake tower in the reservoir, located at the upstream end of the power tunnel C. This tunnel is utilized to carry the flow to a point over the power station, where it is divided into three penstocks. Each penstock has two valves ahead of the turbines. There are three generating units, operating at a normal head of 505 ft, and each generating 25,000 kw of power.

GEOLOGY OF THE SITE

At the Ambuklao damsite the river flows from north to south in a narrow gorge between two ridges, the western ridge being composed of metamorphic rocks and the eastern ridge of both metamorphic rocks and diorite. Above the gorge the river is in a relatively wide valley which will form the reservoir basin. Below the gorge the river flows in a narrow meandering valley.

The principal rocks of the Agno Valley in the vicinity of the Ambuklao damsite are diorite and a series of metamorphosed andesite, tuffs, lavas, and sedimentary rocks. The members of this series were laid down as lava flows and deposited sediments in Tertiary times. After deposition, when those rocks were buried deep beneath the surface, they were subjected to mountain building forces which produced numerous fractures and incipient fractures. The lavas and sediments were metamorphosed and their original characteristics altered. While still buried far beneath the surface these metamorphosed lavas and sediments were intruded by molten diorite. As a result the contact of the diorite and the metamorphosed rock is extremely irregular but it is practically everywhere a tight, fused contact. Both the metamorphics and the diorite have been intersected by fault or shear zones. The entire series of metamorphosed lavas and sediments is referred to as the metamorphics. In the right abutment ridge far back from the end of the dam there is also an elongated intrusive body of granodiorite.

The rocks of this region are deeply weathered, as is true of rocks practically everywhere in the humid tropics. Therefore, hard, unweathered rock is

seldom exposed except where there has been recent geological erosion. Exposures of weathered rock give little indication as to the true characteristics of the unweathered rocks. Below the zone of weathering, however, the rocks are hard, though brittle, and the fractures are generally tight. This is shown at the Ambuklao damsite where the metamorphic rocks of the left abutment ridge are deeply weathered and appear to be in very bad condition, but in the tunnels these metamorphic rocks are hard and generally tight.

The geologic conditions at damsites in the tropics are in many ways opposite to those found at damsites in cold countries. In the tropics the rocks in the abutments are practically always deeply weathered and in poor condition, but the rock under the river bed is usually in good condition, and the depth to bedrock is generally not excessive. In the glaciated regions of the northern countries, however, the abutments are generally in good condition with sound rock at or near the surface, but under the river the depth is often excessive. This contrast of conditions at damsites in the tropics and in northern regions must be taken into consideration in comparing damsites in the tropics with those with which engineers of the United States are more familiar.

Fig. 4 is an areal geologic map of the damsite. Approximately 150 diamond core drill holes were drilled in the damsite area (not all indicated on Fig. 4), to determine the geologic and engineering characteristics of the underlying rock. Based on the evidence from these borings and surface observations, it was concluded that the rock in the abutments and in the river bed was not sufficiently strong to withstand the pressure that would be developed by any economically feasible type of concrete dam. The presence of satisfactory quarry rock in the valley sides near the damsite led to the selection of a rockfill dam. Abundant clayey material for use in the core was also available near the tops of the adjacent hills. A geologic section along the axis of the dam is shown in Fig. 5.

TESTING PROGRAM

To determine the suitability of the rock and clay material for use in the shells and core of the dam an extensive series of exploratory drifts and test pits were carried out.

In an effort to check the adequacy of the rock in the proposed quarry pits for use in the rockfill, a series of crushing tests were made. These tests were concentrated on materials from quarries 1A and 2 indicated on Fig. 2. These quarries were located in areas most convenient for construction.

Quarry 1A was primarily diorite and initial exploration indicated that a small amount of overburden should be expected. Below the overburden the large mass of diorite was present and samples recovered from the drill holes and exploratory drifts indicated that sharp angular rock could be expected from the quarry blasts. Quarry No. 2 was composed of a large mass of metamorphic rocks. This quarry was ideally located for the downstream rockfill and indicated a material suitable for the shell.

The crushing tests were performed by placing samples of the broken rock from the quarry areas in a container and loading the surface of the sample with a load equal to the pressure that would be exerted on the bottom layer of the rockfill by the overlying fill material. The container was a 30 in. diam cylinder 20 in. deep. A hydraulic jack and a loading plate 20 in. square were used to develop a pressure of approximately 25 tons per sq ft on the material in the

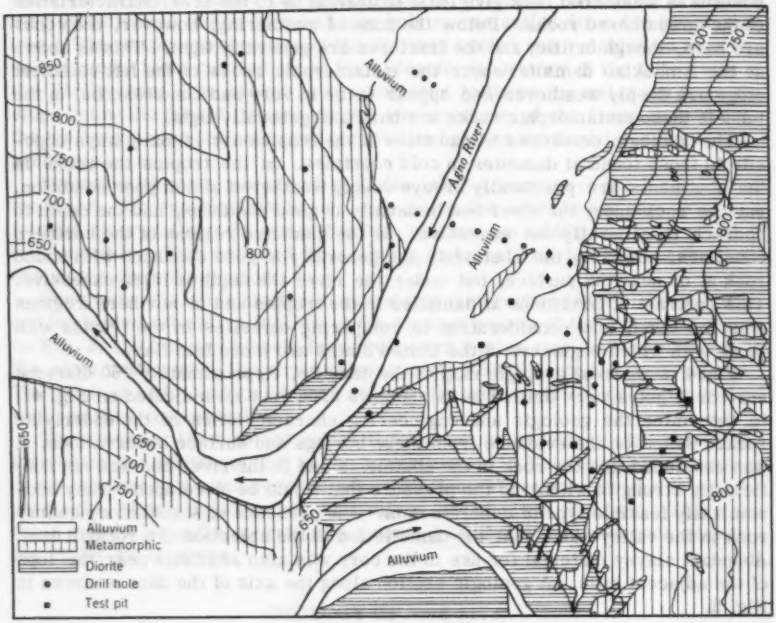


FIG. 4.—GEOLOGICAL MAP OF THE DAMSITE

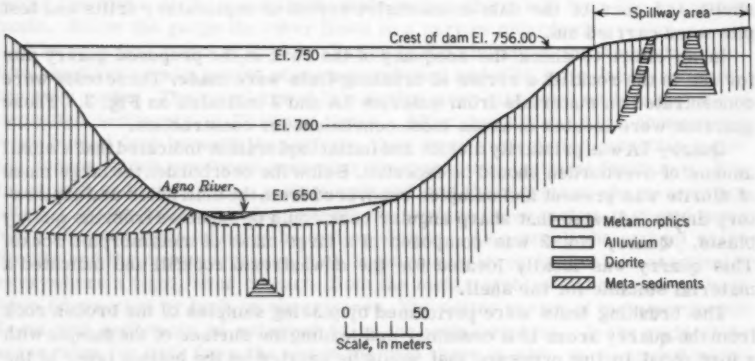


FIG. 5.—GEOLOGICAL SECTION

box. The settlement under the load shown in Fig. 6 and the gradation curves of the rock before and after the test indicated how much the rock might break down under the pressures to be expected in the dam. Prior to this test the general expectations were that the diorite would prove to be much stronger than the metamorphic rock. The results were so contrary to what had been expected by visual inspection of the two rock types that at first it was suspected that the results had been reversed. However, the breakdown of the diorite during blasting, handling, and placing in the dam was much greater than the metamorphics, indicating the value of such tests as an indicator of the relative values of different rocks for use in rockfill.

In addition to the rock crushing tests, the more usual compaction, grading, triaxial, and consolidation tests were made on the core material from the borrow pit areas. Examination of the borrow pits disclosed that high moisture contents could be expected throughout the year. The natural moisture contents ranged from 5% to 10% more than the optimum moisture content. The long rainy season and high humidity, even in the dry parts of the year, were the prime factors causing this condition.

Three field test fills using the impervious borrow materials were made under conditions simulating those expected during construction of the dam. Samples of the test fill were tested to determine compaction, shear strength, and permeability. Additional samples were sent to the United States for confirmation tests and triaxial shear tests because access to a triaxial machine was not possible.

Approximately ten quick triaxial series were made in the United States at varying moisture contents. The triaxial tests were run at 1, 3, and 5 kg per sq cm. This was considered sufficient to establish the trend of the materials' characteristics when coordinated with consolidation and permeability tests. The tests indicated that high pore pressures could be expected at moisture contests above the optimum. With this information the field testing program was extended to determine if there was a possibility of reducing the moisture content by additional scarifying of the borrow material. The scarification proved to be a long and expensive procedure of dubious effect, in fact, a reduction of the moisture content 5% required two or three days of scarifying. Therefore, the design was predicated on having high pore pressures in the core.

DESIGN

Preliminary layouts, stability studies, and quantity take-offs were made of three types of dams: large earth fill core with rock shells; sloping core rock fill; and narrow center core rock fill.

These design studies indicated that a dam with a large center core of earth would require flatter slopes for stability than either of the rock fill types. Also the earthen fill presented a difficult construction problem because of the high humidity and rainfall at the site. The choice then narrowed down to a sloping core or vertical core rock fill.

The design studies indicated that a rockfill dam with a vertical core could be built with less quantities of material than a sloping core rockfill. Referring to Fig. 2, it can be seen that the downstream shell of the dam is at a much narrower section of the canyon than the upstream section. A sloping core dam permits a steeper downstream slope than for a vertical core, but requires some flattening of the upstream slope because the core is located in an area

of high shear stress, and thus requires more rock shell for stability. Flattening the upstream slope increased the quantities more than the saving made by steepening the downstream slopes. This was a major factor in the deciding to use a central core type dam. In addition, the increased contact area between the vertical core and the rock foundation gives a longer seepage path under the core than could be obtained with a sloping core. This is greatly to be desired under the 400 ft of head to which Ambuklao is subjected. Fig. 7 shows a section through the dam.

Another feature of the vertical core design that led to its selection was the fact that the full weight of the dam is applied to the contact area between the core and the foundation, thus giving the maximum protection against possibility of leakage along the contact. The pressure along the contact surface of the sloping core, at the foundation level, is considerably less.

The stability of the dam was analyzed by two basic theories of design, the sliding-wedge and slip circle. The sliding-wedge theory was considered the most applicable to the analysis of a structure where the most critical plane of stability is located predominantly in a frictional, noncohesive material. Conversely, when the most critical plane of stability passes through a cohesive material of little or no frictional strength, the slip-circle is the most applicable.

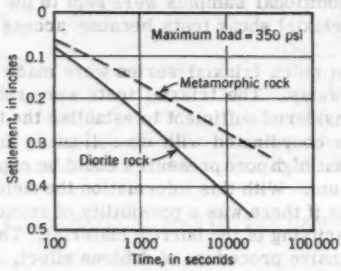


FIG. 6.—SETTLEMENT CURVES

The vertical core type of rockfill dam is best analyzed by the sliding-wedge method. Fig. 8 shows an example of this analysis for the construction condition with maximum pore pressure development (pool empty). The driving forces are P = 1440 kips and U = 421 kips, Tan ϕ_1 = 0.268 and Tan ϕ_2 = 0.58. The resisting forces

$$R_1 = (N_1 - U) \text{ Tan } \phi_1 = 189 \text{ kips}$$

and

$$R_2 = N_2 \text{ Tan } \phi_2 = 1832 \text{ kips}$$

The factor of safety

$$\text{F.S.} = \frac{R_1 + R_2}{P} = 1.40$$

and the minimum (earthquake) F.S. = 1.21.

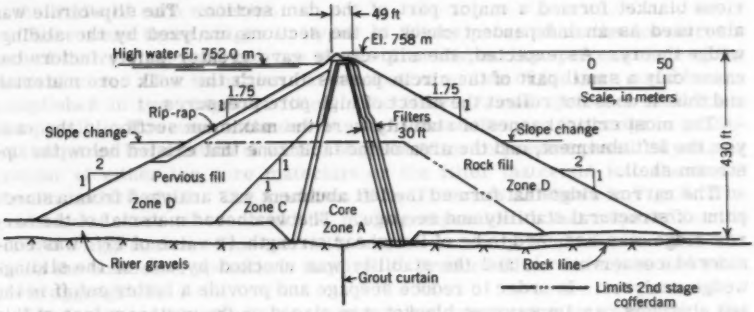


FIG. 7.—SECTION THROUGH THE DAM

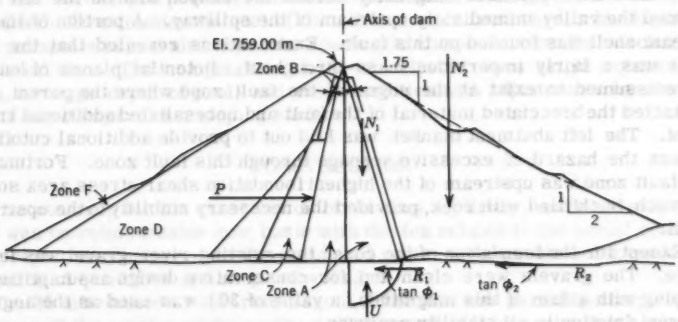


FIG. 8.—SLIDING-WEDGE ANALYSIS

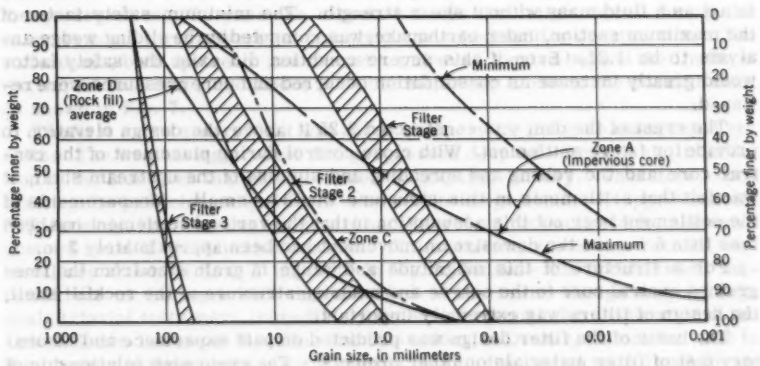


FIG. 9.—GRAIN SIZE CURVES

The slip-circle analysis was applied to the left abutment where the impervious blanket formed a major part of the dam section. The slip-circle was also used as an independent check of the sections analyzed by the sliding-wedge theory. As expected, the slip-circle gave greater safety factors because only a small part of the circle passes through the weak core material, and thus it does not reflect the effect of high pore pressures.

The most critical zones of stability were the maximum section in the canyon, the left abutment, and the area of the fault zone that existed below the upstream shell.

The narrow ridge that formed the left abutment was analyzed from a standpoint of structural stability and seepage. The weathered material of the narrow ridge was assumed to be of low shear strength (a value of 17° was considered conservative), and the stability was checked by use of the sliding-wedge analyses. In order to reduce seepage and provide a better cutoff in the left abutment, an impervious blanket was placed on the upstream face of this narrow ridge and was continuous with the main core of the rockfill dam as partially shown on Fig. 3.

A fault zone extended diagonally across the canyon and on the left bank formed the valley immediately upstream of the spillway. A portion of the upstream shell was founded on this fault. Examinations revealed that the fault zone was a fairly impervious mass throughout. Potential planes of leakage were assumed to exist at the edges of the fault zone where the parent rock contacted the brecciated material of the fault and necessitated additional treatment. The left abutment blanket was laid out to provide additional cutoff and reduce the hazard of excessive seepage through this fault zone. Fortunately the fault zone was upstream of the highest foundation shear stress area so that a trench, backfilled with rock, provided the necessary stability to the upstream shell.

Except for the foundation of the core, the existing river gravel was left in place. The gravels were clean and for conservative design assumptions, in keeping with a dam of this magnitude, a value of 30° was used as the angle of internal friction in all stability analyses.

To check the stability under the most severe conditions of pore pressure rise and the corresponding loss of strength of the core material the core is assumed to act as a fluid mass without shear strength. The minimum safety factor of the maximum section, under earthquake, was computed by the sliding wedge analysis to be 1.21. Even if this severe condition did exist the safety factor would greatly increase as consolidation occurred and pore pressures were relieved.

The crest of the dam was constructed 3.25 ft above the design elevation to provide for future settlement. With close control during placement of the central core and the rolling and spreading and sluicing of the upstream shell, it was felt that settlements in this structure would be small. Measurements of the settlement bear out this assumption in that the vertical settlement has been less than 6 in. and the downstream movement has been approximately 3 in.

For a structure of this magnitude and range in grain size from the fine-grained central core to the coarse and massive structure of the rockfill shell, the design of filters was extremely important.

The basis of the filter design was predicted on past experience and laboratory test of filter materials on other projects. The grain size relationship of the 15% size of the coarser material to the 85% size of the finer material was specified to be less than a factor of five. Also the gradation of each material

should be sufficiently uniform to prevent piping or migration of particles within the limits of each material.

There were three stages or types of filters provided on the downstream face of the vertical core and two stages provided on the upstream face of the vertical core. The transition on the upstream side of the core could be accomplished in two stages of filter. The finer grained upstream shell made this possible. However, on the downstream side of the core the range in gradation required the addition of a third stage of filter to prevent possibility of migration of either the core materials or the filter materials into the downstream rockfill shell. The gradation of the filters is as shown in Fig. 9. The gradation of these filters could be made comparable to that required for the concrete aggregates. This permitted some economy of production and reduced the number of operations required to produce filter materials and concrete aggregates.

The freeboard provided to protect against overtopping by wave action under typhoon winds was about 13 ft. Although the freeboard is approximately 19.5 ft at normal operating pool elevations the design freeboard is measured from the surcharged pool elevation that would occur during the event of a design flood. To minimize the cost of the allowance for freeboard, a hand-placed rock parapet was provided above the roadway to compensate for the surcharged pool condition. The computation of the anticipated wave height equated the fetch, average depth of pool, and wind velocities with adjustments for the effect of wave impact on a sloping surface.

CONSTRUCTION

The contract for the construction of the dam, spillway, and diversion tunnels was on reimbursable cost basis with the fee related to the actual costs of the project as compared to the estimated costs, adjustments being made for variation of quantities and scope of work.

The 25 mile access road from Baguio to the site was partially completed at the time of the signing of the contract. The owner and the contractor completed the road to the site. After completion of the access road to the site the contractor initiated work on the diversion tunnels, cofferdams, and preparation of the quarry sites. To pass the expected floods that might occur during the rainy season, three diversion tunnels were scheduled for construction. The cofferdams, both upstream and downstream, were located beyond the limits of the impervious core, and where possible within the limits of the rockfill shell as shown in Fig. 7.

The first large quarry blast was made at quarry 1A and gave unexpected results. The weathering process had progressed deep into the hillside, in addition to the fractures that had developed in geologic history. Therefore, upon blasting the particles ranged from sand size to large boulders, approximately 60% were smaller than coarse gravel and, therefore, not suitable for the usual dumped rockfill construction methods. Grain-size curves of this rockfill material are shown as Zone D material in Fig. 9. Because this rockfill shell material was at variance with that assumed in the initial design stages, large scale triaxial tests were immediately scheduled through the cooperation of the United States Bureau of Reclamation Laboratory in Denver, Colorado. Due to the urgency of these tests, approximately 500 lb of material were flown by air express from the Philippines to Chicago and then transported to Denver for the testing program. The triaxial tests were run on representative samples of the

material from quarry 1A. Lateral pressures as high as 75 psi used to simulate leading conditions anticipated to the prototype. Basically, the results of this program indicated that the outside dimensions of the dam would not require a revision. The frictional strength of this finer-grained quarry material was equal to or better than that assumed in the design stages. Frictional shear strength in the order of 40° to 45° was obtained in these triaxial tests. In order to reduce the amount of waste within the upstream shell, Zone C shown in Fig. 7, was the finest grained material and had the least structural strength, friction angles being 35° for design purposes. Placed in this area just upstream of the core and below El 710, it has little effect on the ultimate strength of the rockfill dam.

On the upstream side of the dam, cofferdamming was done in two stages. The first stage was a low cofferdam, built during the dry season, to turn the river into the 13 ft diam circular diversion tunnel A (Fig. 2). This was necessary to permit a full clean-up of the fault zone that was located under the upstream shell. By the advent of the second rainy season of the construction period a diversion capacity of 74,000 cfs was required to assure reasonable safety from overtopping. The higher second stage cofferdam was incorporated within the limits of the rockfill shell. The core was also raised during this period and the downstream shell was built to lines that would afford temporary stability to the core. In this way the maximum amount of equipment could be utilized in construction of the upstream shell.

A late season typhoon caused flows that overtopped the first stage cofferdam late in November, 1953, of the first year of construction. Repairs were made quickly and only slight damage was done to the existing construction and little time was lost. For the remainder of the construction program there was no difficulty in diverting the river.

Tunnels B and C (Fig. 2) were designed for passing flood flows. Both tunnel B and tunnel C were concrete lined horseshoe tunnels, 25 ft and 23 ft in diameter, respectively. After diversion tunnel C was converted into the power tunnel the previously mentioned 13-ft tunnel A became the low level outlet tunnel. Tunnel B was plugged after the diversion period, having served its function for the construction of the project.

The preparation of the foundation for the core and the shell was started at the abutments prior to closure of the river. After closure the preparation of the central portion was completed. Both hydraulic and mechanical methods of excavation were used. Portions of the area under the core where deep depression existed were backfilled with concrete. In general, the use of hand tamped impervious fill was all that was necessary to bring the foundation to a level surface where the mechanical equipment could function.

The grout curtain for the dam is shown in Fig. 10. The deep cutoff grout curtain was designed to reduce uplift and increase the seepage path so that gradient would be low and thereby reduce the danger of blow outs, excessive seepage volume, or both.

The full depth of the grout curtain was developed by the stage grouting method, with a thorough washing and pressure testing prior to grouting. As each zone was grouted the permissible pressure was increased for next lower zone. Table 1 shows the pressure used.

The split spacing method was specified for all areas exhibiting large grout take and was to be a field adjustment. Packers were used to extend the grout curtain for each successive zone. Split spacing is the procedure whereby a primary set of holes is drilled and grouted throughout a section for a depth

zone at a prescribed maximum spacing, and succeeding sets of holes are drilled and grouted located so as to split the interval between previously completed sets. This process is continued until the spacing is such that no appreciable amount of grout can be injected into the hole. The maximum spacing prescribed is shown in Table 1, Column 5.

The holes in Zone 5 served as check holes to determine if any deep seated seepage channels existed, and the pressure tests at 200 ft and 100 ft to the bottom of the holes confirmed the general tightness of the area and the effectiveness of the grout curtain.

The grouting operations in the lower portions of the canyon were done by drilling and grouting through the core material because of the pressure of time. The portion of the hole through the core was cased and the casing set in the

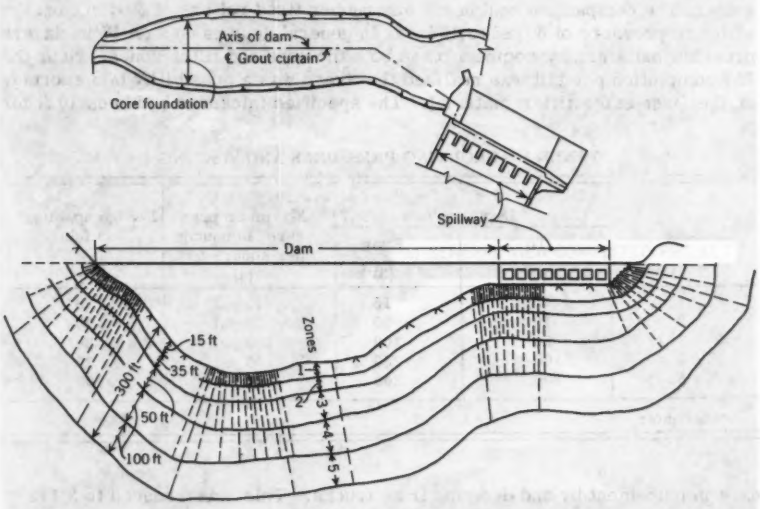


FIG. 10.—DEVELOPED SECTION

rock. The abutments were drilled and grouted from the excavation line, prior to placing of the core material. The grouting in both cases was carried out by the stage grouting method, using packers. The holes were thoroughly washed and pressure tested before injecting the grout, and after grouting, deep check holes were drilled and pressure tested to establish the effectiveness of the grouting accomplished. A total of 72,500 lineal feet of grout holes was drilled and grouted with an average take of 0.3 bags of cement per lineal foot of hole. The split spacing for zones 2, 3, and 4 started at 20 ft on centers. The closest spacing was 5 ft for zone 2, 10 ft for zone 3, and 20 ft for zone 4. The zone 5 check holes were pressure tested at each zone to indicate the adequacy of the completed grout curtain and finally grouted. In general, the holes were very tight. The highest take was encountered in the spillway area and the lowest in the canyon floor. This was in keeping with the general geologic analogy previously mentioned, that is, the best rock could be anticipated below river level.

Placement of the rockfill shell, filters, and impervious core was a continuous operation except for short periods when the rains made core placement impossible. The maximum rate of placement was approximately 500,000 cu m (650,000 cu yd) per month including all zones.

The upstream shell zones C and D were placed in 24 in. layers and compacted by rubber tired rolers and sluicing. The materials from the upstream quarries broke down quite fine and were not suitable for the more usual rockfill placement by end dumping and sluicing. Sluicing operations, however, were effective in creating a compact mass. The 50-ton rubber tired rollers were valuable in locating areas of below optimum compaction. In two passes, soft spots would be quite evident and remedial measures could be taken immediately.

The impervious core and filter materials were placed and compacted together. The compaction equipment was rubber tired rollers of 50-ton capacity with tire pressure of 80 psi to 100 psi. In general, four passes on 18 in. layers provided satisfactory compaction in both the core and filter zones. Near the 75% completion point, it was realized that there was a possibility of a shortage of the first stage filter material. The specified thickness had been 10 ft for

TABLE 1.—GROUTING PRESSURES AND SPACING

Zone	Depth, in feet		Maximum pressure, in pounds per square foot	Design spacing,[a] in feet
	To	From		
(1)	(2)	(3)	(4)	(5)
1	0	15	15 psi	5
2	15	50	50 psi	20
3	50	100	100 psi	20
4	100	200	200 psi	20
5	200	300	300 psi	200

[a] On center.

ease in placement by end dumping from trucks. This was reduced to 3 1/2 ft and placement was done by dumping into a sliding form with some hand tamping of the faces prior to placing additional core or stage 2 filter material.

The downstream shell zone D material was composed of large boulders grading down to smaller sizes. This material was suitable for placing by end dumping and sluicing. The hydraulic monitors were directed so that they forced the fines down into the fill, reducing the voids and thus keeping future settlement to a minimum. The lifts for end dumping varied from 30 ft to 90 ft, generally in the lower ranges.

The riprap on the upstream face extended from below minimum drawdown level to the crest. A parapet of hand placed rockfill was provided above the roadway for protection from wave action and also service as a guard rail.

CONCLUSIONS

The filling of the Ambuklao reservoir was started in the wet season 1955, and the reservoir was filled to spillway crest elevation 740, by early 1956. Fig. 11 shows the project completed. Observations of the completed structure

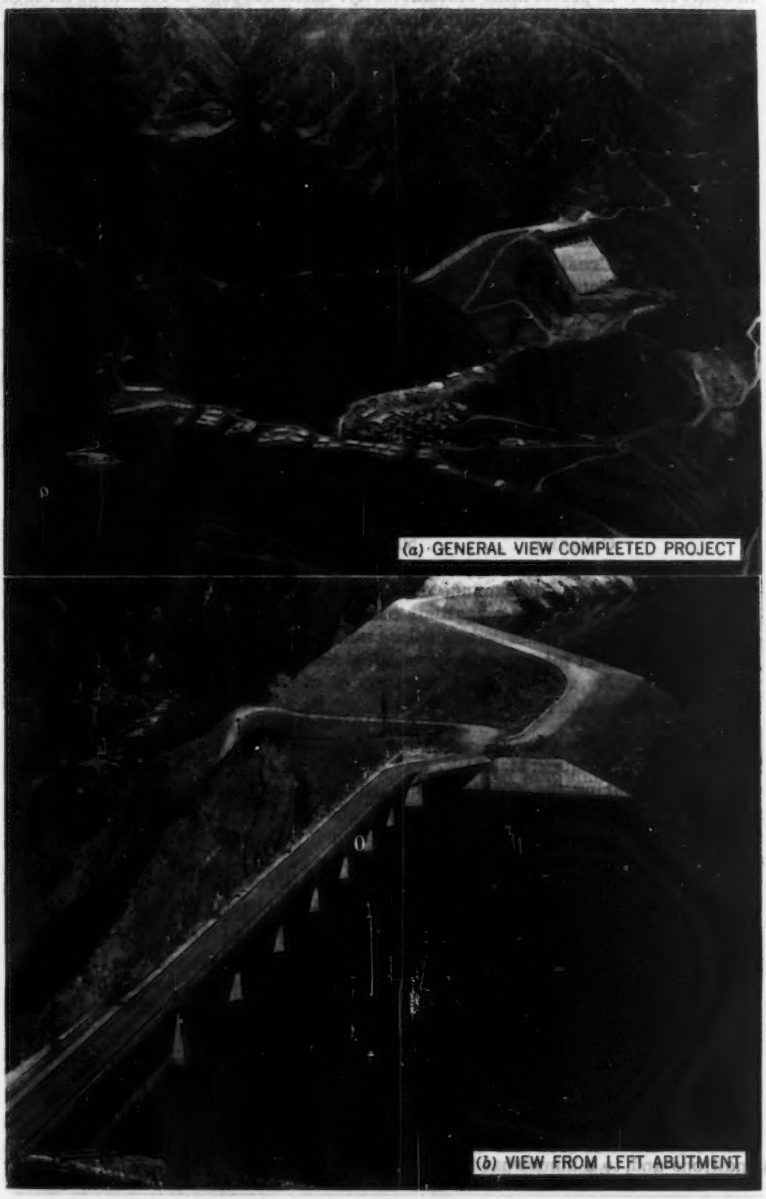


FIG. 11.—AMBUKLAO DAM COMPLETED

indicate that it is performing satisfactorily. Little seepage is evidenced through the left abutment ridge, indicating that the blanket on the upstream face of this ridge is performing well. Some seepage is still in evidence into the access tunnel and power station cavern in the right abutment and grouting is being done to seal this off. It appears probable that the grout curtain in the right abutment will have to be extended to provide additional cutoff.

Significant data for the Ambuklao dam is as follows:

Drainage Area	265 square miles
Length of Reservoir	7.5 miles
Maximum Height of Dam	430 feet
Width at Base	1455 feet
Crest Length	1480 feet
Total Volume of Fill	10,050,000 cubic yards

Material Characteristics

	Value of ϕ
Zone A	15°
Zone B	35°
Zone C	35°
Zone D	40°
River Gravels	30°

Cohesion . . . . . 500 pounds per square foot

The satisfactory performance of this high rockfill dam provides additional evidence that dams of this magnitude can be constructed economically and safely where a concrete dam would not be suitable, thus opening up for development damsites that might otherwise not be developed.

ACKNOWLEDGMENTS

Fileman Rodgriquez, M. ASCE, was General Manager of the National Power Corporation during the construction. His assistant was Fileman M. Zablan. Resident Engineer was Crispin Ubaldo, and the Chief Construction Engineer was Ramon Ravanzo. Guy F. Atkinson Company of San Francisco constructed the dam and spillway.

The geologic studies were made by Irving B. Crosby, Consulting Geologist for the National Power Corporation. The liaison between the field and the design office of the Harza Engineering Company was provided by Erik Rettig, F. ASCE.

DISCUSSION

FREDERIC L. LAWTON,[3] F. ASCE.—The significance of the topographic conditions and, to a somewhat lesser degree, the geologic features is apparent

[3] Chf. Engr., Power Dept., Aluminium Labs. Ltd., Montreal, Canada.

to the writer, who visited the site during the period of initial investigations. Thus, the authors' observations on the site geology are welcomed as a penetrating statement of the distinctive differences between the geologic conditions commonly found at damsites in the tropics and in temperate regions. Justification for the paragraph "The geologic conditions at damsites in the tropics *** are more familiar" is afforded by Ambuklao geologic features as well as those at many other tropical sites.

The authors have taken full advantage of the topographic situation in utilizing the additional head of 60 ft in connection with diversion through tunnel C, and perhaps more significantly in utilizing 180 ft additional gross head (with respect to the normal 505 ft) made possible by the 7,200-ft tail tunnel. It would be of interest to know if this head could have been developed any other way at anything similar to the cost achieved.

It is interesting to note that "Based on the evidence from these borings and surface observations, it was concluded that the rock in the abutments and in the river bed was not sufficiently strong to withstand the pressure that would be developed by any economically feasible type of concrete dam." Foundation conditions and availability of economically-utilizable core and shell materials are the two principal reasons rock and earthfill dams are likely to be more and more widely used in relatively undeveloped tropical countries as well as elsewhere.

The authors observe that "Except for the foundation of the core, the existing river gravel was left in place." The approximate maximum thickness would be of interest.

The authors' crushing tests on the samples of broken rock from the quarry areas are particularly interesting, having demonstrated that the diorite was subject to greater breakdown than the metamorphics during blasting, handling, and placing in position, contrary to expectation from visual inspection. This demonstrates the value of adequate tests on all components of a rock-fill dam.

Although no reference thereto is apparent from the text, the writer would be interested in knowing if any attempt was made to determine the pore pressures in the three field test fills.

The design studies that led to the use of a rock fill with vertical core rather than a sloping one demonstrate clearly conditions that may sometimes be overlooked, that is, length of seepage path due to increased contact area between the core and the foundation, and increased loading on the contact area with probable minimization of leakage at the contact. The relative weight given these two factors as compared with the saving in fill materials would be of interest.

The vertical settlement and downstream deflection have been most moderate, at less that 6 in. and at approximately 3 in., respectively. A comparison of the vertical settlement with that predicted from tests such as shown by Fig. 6 would be of interest to the writer.

It is hoped that continuing observations on the performance of the Ambuklao rock-fill dam and particularly on the vertical settlement and downstream deflection will be made available.

JOSE O. LAHOZ.[4]—To further increase the usefulness of Ambuklao in the development of future rockfill dams the writer presents detailed settlement data for the first four years of service of the dam. The help of J. Barry Cooke, M. ASCE, in preparation of the data is greatfully acknowledged.

---

[4] Asst. General Mgr., Philippine National Power Corp., Manila, Philippines.

The thin central core dam represented the most economical type and the safest with respect to the special foundation conditions. It is 430 ft high and has a crest length of 1400 ft. The only settlement points are monuments at 50-m (164 ft) centers along the crest on the centerline of the core, the axis of the dam. Measurements are of vertical movement and up-downstream movement. Cross-canyon movements, that is, lateral movement of the dam from it's abutments were not taken. It is considered that these measurements should be for future large rockfill dams.

Observations and measurements were taken at irregular intervals varying from several days to two months during the first year of operation in 1956. Only one measurement in 1957 is on record. Measurements were resumed in July, 1959, and have continued to date.

Fig. 12 presents the complete vertical and horizontal settlement data for the crest of Ambuklao Dam, together with the related data of reservoir operation and foundation profile. The tabulation presents all the readings for the 4-yr, 0.6-month period of record and also the height of dam at each settlement point, and the 4-yr settlement in terms of precentage of height. The vertical settlement in terms of percentage of height is seen to vary from 0.37% to 1.73% and for the maximum control section at Station 6 + 20 to be 0.77% with a vertical movement of 3.14 ft.

The plotting of "CREST SETTLEMENT - VERTICAL AND HORIZONTAL" profiles the movement of each point. The upstream movement of all points between December 1, 1957, and July 19, 1959, is a measure of the elastic nature of the dam. The water level on December 1, 1957, was 389 ft, and on July 19, 1959, was 232 ft. At station 6 + 20 the horizontal movement increased 0.29 ft as the reservoir filled between July 19, 1959, and January 8, 1960, while the downward vertical movement was only 0.05 ft. The high vertical settlements at Stations 9 + 48 and 11 + 12, on the steep abutment are of special interest.

The diagram, "RESERVOIR OPERATION," shows the reservoir operation for the full period of service to January, 1960. It is plotted to the same vertical scale and datum as the "VERTICAL PROFILE AT AXIS." The time scale of "RESERVOIR OPERATION" is the same as that for "SETTLEMENT - STA. 6 + 20" in order to show the relation between reservoir operation, time, and settlement for the maximum section STA. 6 + 20. Any movement that might have occurred between completion of the fill in June, 1955, and December 22, 1966, the date of initial permanent monument reading, is not recorded. The maximum rate of settlement was in October and November, 1956, as the top 30 ft of the reservoir was filled for the first time. The settlement during the long intervals of time from November 21, 1956, to December 1, 1957, and from December 1, 1957 to July 19, 1959 are shown dotted because the shape of the curve is not known.

At the beginning of this discussion the writer mentioned, "special foundation conditions." The paper covers the geology of the site, but some additional comment may emphasize the consideration given to adapting the dam to the site. In its 1951 report[5] the owner of the Ambuklao Dam, states in part that ". . . by numerous borings and test pits, it is known definitely that no fault crosses the dam site under the river; that the depth to bed rock under the river is moderate, averaging approximately 7 meters; and that the condition of the rock under the river is good. The left abutment ridge is composed of

[5] "Report on the Development of Power in the Agno River in Luzon, at the Ambuklao Site," National Power Corp., 1951.

DATE	TIME	RES LEVEL	POINT A V	POINT A H	POINT B Vert	POINT B Horiz	POINT C V	POINT C H	POINT D V	POINT D H	POINT E V	POINT E H	POINT F V	POINT F H	POINT G V	POINT G H	POINT H V	POINT H H	POINT I V	POINT I H	DATE
12 22 55	INITIAL	309	0	0	0	0	0	0	0	0	0	0	0	0	0	0	0	0	0	0	12 22 55
1 21 56	90DAYS	311	0	02	05	02	05	02	00	01	04	02	07	02	07	02	06	02	06	02	1 21 56
3-7	75 -	313	05	05 05	05	05	07	05	08	07	10	11	11	12	12	14	15	11	13	08	3-7
5 7	136 -	344	11	0	14	09	17	09	18	09	22	11	26	15	26	16	29	15	21	12	6-7
7-13	202 -	349	12	01	17	07	21	12	24	07	34	16	41	23	45	27	46	26	41	17	7-13
9 3	254	347	17	02	18	08	24	16	31	26	46	42	62	54	72	59	75	55	67	37	9 3
10-7	288	350	17	08	20	12	29	23	39	35	61	55	88	71	97	79	100	71	91	46	10 7
10 12	293	353	17	04	20	16	29	28	39	39	62	64	91	80	107	89	112	81	102	53	10-12
10-15	296	357	17	03	20	15	31	29	43	43	69	70	97	88	115	93	117	88	111	56	10 15
10 22	303	359	18	03	21	15	32	30	47	48	71	76	104	98	123	102	127	96	120	61	10-22
11-11	323	394	18	04	23	17	39	38	53	69	88	105	142	130	180	136	167	124	161	76	11-11
11-21	333	393	18	06	23	17	41	38	53	69	90	118	155	135	173	139	178	128	172	79	11-21
12-1-57	YR 11.8 MO	389	28	00	41	22	76	51	101	88	161	139	248	181	238	186	249	152	254	90	12 1 57
7-19-59	3 - 6.9 -	232	40	365 12	67	17	112	67	141	79	212	133	309	177	286	178	323	147	292	86	7-19 59
9-7	3 - 8.5 -	331	43	335 16	69	18	114	63	145	86	213	138	309	182	288	182	326	148	296	88	9-7
10 10	3 - 9.6 -	357	48	365 13	69	12	116	62	146	85	216	146	312	185	291	189	331	152	300	91	10 10
1-8-60	4 YR 0.6 MO	390	44	00	69	17	116	48	147	99	218	156	314	206	291	199	333	162	300	97	1-8-60
HEIGHT AT AXIS - FT		72			171		312		396		400		410		410		368		174		97 FT
100 x V ÷ H - HEIGHT = %			0.61	--	0.39	0.10	0.87	0.15	0.37	0.23	0.95	0.39	0.77	0.80	0.71	0.49	0.86	0.42	1.73	0.56	% HT
			0+00		1+64		2+28		3+92		4+56		6+20		7+84		9+48		11+12		12+76

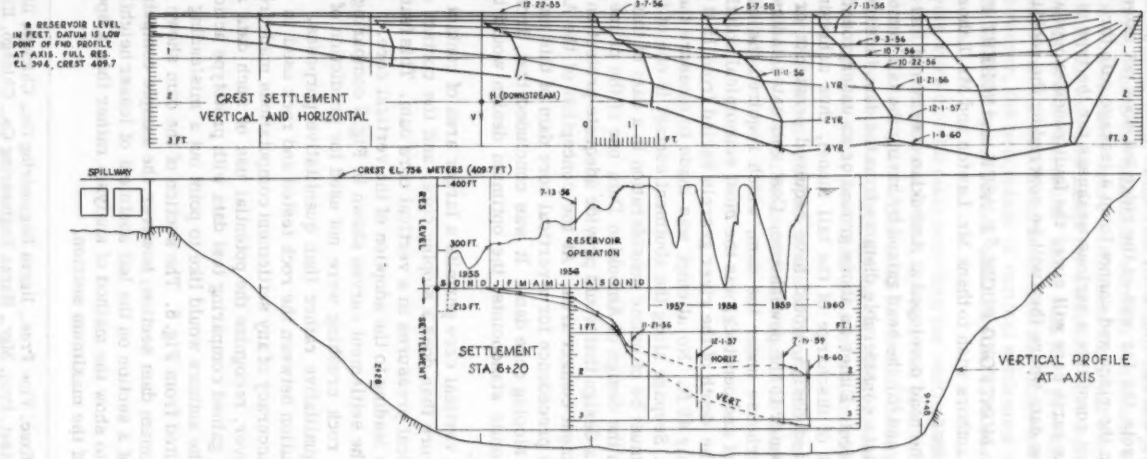


FIG. 12.—CREST SETTLEMENT, PROFILE AT AXIS, AND RESERVOIR OPERATION AMBUKLAO DAM

diorite and metamorphic rock with very complex relations. One of the fault zones underlies the gully on the upstream side of the ridge, and the other intersects the far end of the ridge but does not extend to the river downstream from the ridge and cannot form a leakage path thru the ridge. The fault zones do not constitute a serious weakness for the type of dam planned. The impervious earth core will cover the fault zones except at the extreme upstream toe of the dam where they will be covered by the rockfill."

E. MONTFORD FUCIK,[6] F. ASCE, and ROBERT F. EDBROOKE,[7] M. ASCE.—The authors wish to thank Mr. Lawton and Mr. Lahoz for their informative discussions.

The head developed at Ambuklao consists of (a) the head developed by the dam, and (b) the head gained by having the tail tunnel discharge to the river at a point a considerable distance from the dam, thus taking advantage of the river gradient. Either an above ground or an underground powerhouse located at the point of discharge of the tail tunnel, thus achieving the same head as in the adopted design, would have required penstocks or pressure tunnels to carry the water to the powerhouse. Cost estimates indicated that the location of the powerhouse under the dam, which required the minimum length of pressure tunnel and penstock, was the most economical solution.

The depth of the river gravels varied from 15 ft to a maximum of approximately 45 ft. No attempt was made to measure the pore pressure in the test fills. Seepage along the abutment contact is one of the critical areas of design and must be of prime consideration in a dam of this magnitude.

In the design of Ambuklao Dam one of the prime considerations was to obtain a design that would provide adequate protection against seepage along the abutment contact area. At the conception of the Ambuklao project there was little precedence for a vertical core dam of this magnitude and no precedence as a sloping core dam. It was concluded that, from both the engineering and economic standpoints, the optimum design would be provided by the vertical core.

A vertical core permits a larger area of contact between the foundation and the core than does a sloping core, and the contact area is also under greater vertical pressures in a vertical core dam. This feature was a major consideration leading to the adoption of the vertical core.

The settlement curves shown in Fig. 6 comparing the diorite and metamorphic rock crushing were not used for prediction of settlement. The test was for qualitative rather than quantitative purposes. Further, the variation in gradation between the rock tested and rock used in the fill made questionable the accuracy of any settlement computations made from this data. The authors, however, recognize the potential use of such data after more experience has been gained comparing test data with prototype action.

The authors would like to point out a misleading impression that may have resulted from Fig. 8. The section of the dam shown in Fig. 8 appears to be the maximum dam section; however, the sample computations represent an analysis of a section on the left abutment of lesser height. The purpose of the figure was to show the method of analysis rather than a specific mathematical analysis of the maximum section.

---

[6] Exec. Vice Pres., Harza Engineering Co., Chicago, Ill.
[7] Asst. Proj. Mgr., Harza Engineering Co., Chicago, Ill.

Mr. Lahoz has presented a valuable record of the horizontal and vertical movements of the crest of Ambuklao Dam. This record, which was not previously available to the writers, shows the maximum vertical settlement to be 3.33 ft at Sta. 9+48. This is considerably more settlement than that cited by the writers, but is well within the expected range for a vertical core rockfill dam. The crest of Ambuklao Dam was "overbuilt" about 3.25 ft to provide for future settlement, so it appears that the maximum settlement has exceeded this by about 1 in. In general, however, the percentage of vertical settlement is of the same order of magnitude as that experienced at other central core rockfill dams.

The horizontal movements were considerably less than the vertical movements. The largest horizontal movement was 2.06 ft downstream at Sta. 6+20 midway between the abutments. At least half of the total horizontal movement recorded in the 4-year period of record took place during the initial raising of the reservoir. There is some indication that horizontal rebound occurred when the reservoir level was lowered.

The writers agree with Mr. Lahoz that measurements of lateral movements could provide useful information, and such measurements should be taken on future vertical core rockfill dams.

AMERICAN SOCIETY OF CIVIL ENGINEERS

Founded November 5, 1852

TRANSACTIONS

Paper No. 3058

STABILITY OF COASTAL INLETS

By Per Bruun,[1] F. ASCE, and Frans Gerritsen[2]

With Discussion by Messrs. Robert E. Hickson; and Per Bruun and Frans Gerritsen

SYNOPSIS

Existing theories of the relationship between tidal range, tidal prism, and inlet cross section are reviewed and compared. Existing data on inlets are introduced, as well as the effect of the quantity and type of littoral material on the inlet action.

INTRODUCTION

The birthplace of navigation was probably in some river or intracoastal waterway. Soon man extended his interest in navigation to the oceans. The ocean activity was based in rivers and other estuaries which were the first harbors in existence. The ancient Egyptian, Phoenician, Greek, Roman, and Viking naval fleets had their bases in estuaries, fjords, and lagoons. Now, as was true 3,000 years ago, the tidal estuary, river, or inlet is a factor of extreme importance.

A tidal inlet is the waterway connection between the sea and a bay, lagoon, or river entrance. Tidal and other currents flow through the tidal inlet. Earl I. Brown, in examining[3] the origin of tidal inlets, concluded that most inlets have been cut by nature through a barrier which nature herself had built by wave action.

Note.—Published, essentially as printed here, in May, 1958, in the Journal of the Waterways and Harbors Division, as Proceedings Paper 1644. Positions and titles given are those in effect when the paper or discussion was approved for publication in Transactions.

[1] Head, Coastal Engrg. Lab., Univ. of Florida, Gainesville, Fla.

[2] Research Engr., Coastal Engrg. Lab., Univ. of Florida, Gainesville, Fla.

[3] "Inlets on Sandy Coasts," by Earl I. Brown, Proceedings, ASCE, Vol. LIV, Pt. II, February, 1928.

It is possible to distinguish between three main groups of inlets: Inlets that have a geological background, inlets with a hydrological background, and inlets with a littoral-drift background. Examples of inlets with a geological background are the Golden Gate, the entrance to San Francisco Bay, and the Alaskan and Norwegian fjords. Such inlets may have rocky gorges and do not follow the physical laws of normal tidal inlets. The Thames estuary in England and the Loire estuary in France are examples of inlets with a predominantly hydrological origin. In both cases large rivers, combined with heavy tidal action, are responsible for the funnel-shaped entrances that gradually decrease in area upstream, in proportion to the actual quantity of flow through the cross section.

Fig. 1 shows some examples of such inlets. In some cases it has been difficult to indicate one particular reason for their creation. Some of the barriers, perhaps the major part of them, are the result of wave action on the sea bottom

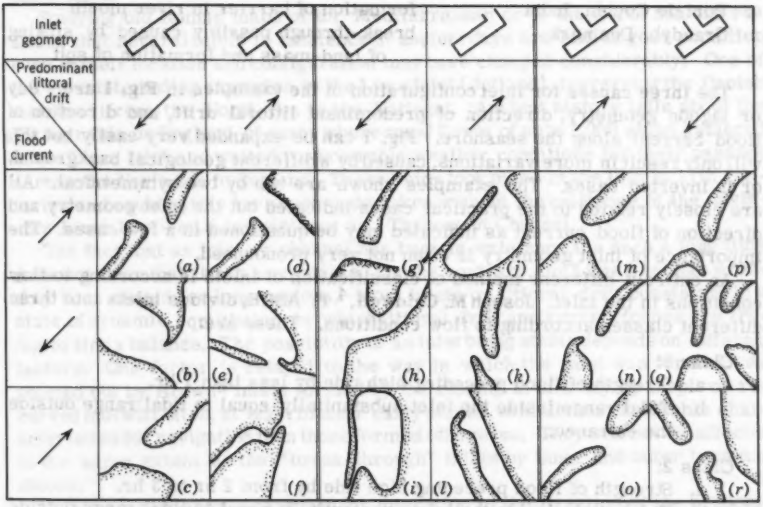


FIG. 1.—INLET CHARACTERISTICS

in shallow water by which a barrier was created. Most inlets are break-throughs, but not all inlets created in this way will exist for long because they are choked by littoral-drift deposits. The following indicates the reasons for the formations in Fig. 1:

a.	Ocracoke, N.C.	break-through
b.	Spurn Head, England	formation of barrier at bay-river mouth
c.	Absecon Inlet, N.J.	break-through
d.	Exmouth, England	formation of barrier across bay
e.	Katama Bay, Mass.	formation of barrier across bay
f.	Wells Harbor, England	formation of barrier across river mouth
g.	Puerto-Samoza, Nicaragua	formation of barrier at river mouth
h.	Sarasota Pass, Fla.	break-through, possibly caused by sinking of land-mass or rise of sea level and formation of spit

i.	Nymindegab, Denmark (now closed)	formation of barrier across bay
j.	Kurisches Haff, Poland	formation of barrier across bay
k.	Big Pass, Fla.	break-through, possibly caused by sinking of land-mass or rise of sea level and formation of spit
l.	East Rockaway, N.Y.	formation of barrier
m.	Den Helder, Holland	break-through probably caused by consolidation of soil and rise of sea level
n.	Longboat Pass, Fla.	break-through, possibly caused by sinking of land-mass or rise of sea level
o.	Vliestroom, Holland	probably an old river mouth now enlarged because of rise in sea level
p.	Thyborøn, Denmark	break-through
q.	Port de Cochin, India	formation of barrier in river mouth
r.	Graadyb, Denmark	break-through possibly caused by sinking of land-mass and formation of spit

The three causes for inlet configuration in the examples in Fig. 1 are: Bay or lagoon geometry, direction of predominant littoral drift, and direction of flood current along the seashore. Fig. 1 can be expanded very easily but this will only result in more variations, caused by a different geological background, or in inverted cases. The examples shown are two by two symmetrical. All are closely related to the practical cases indicated but the inlet geometry and direction of flood current as indicated may be questioned in a few cases. The importance of inlet geometry is often not very pronounced.

An entirely different method of classification of inlets is according to flow conditions in the inlet. Joseph M. Caldwell,[4] F. ASCE, divides inlets into three different classes according to flow conditions. These are:

Class 1:
- a. Strength of flood preceding high tide by less than 1 hr.
- b. Tidal range inside the inlet substantially equal to tidal range outside the entrance.

Class 2:
- a. Strength of flood preceding high tide by from 2 hr to 3 hr.
- b. Tidal range inside the inlet substantially equal to tidal range outside the inlet.

Class 3:
- a. Strength of flood preceding high tide by less than 1 hr.
- b. Tidal range inside the inlet only a small fraction of the range outside.

Class 1 entrances are backed by long estuaries and the tidal flow moves freely past the entrance. Examples of such entrances are the river estuaries such as the Thames, the Loire, the Hudson, and Chesapeake Bay. Class 2 entrances include those backed by short estuaries and with tidal flow moving freely past the entrance. Examples of such entrances are Big Pass, Fla. (Fig. 1(k)), East Rockaway Inlet, N.J. (Fig. 1(l)), and Graadyb Inlet, Denmark (Fig. 1(r)). Class 3 entrances include those sufficiently constricted to prevent free movement of

[4] "Tidal Currents at Inlets in the United States," by J. Caldwell, Proceedings-Separate 716, ASCE, 1955.

tidal flow past entrances. Examples of such entrances are Ocracoke Inlet, N.C., (Fig. 1(a)) and Nymindegab, Denmark (Fig. 1(i)).

Notation.—The letter symbols adapted for use in this paper are defined where they first appear, in the illustrations or in the text, and are arranged alphabetically for convenience of reference in the Appendix.

NATURAL INLET REGIMEN

General.—It is customary to talk about the delicate balance of nature that man cannot touch without bringing about an adverse effect, the fact is that everything in nature is in a process of development. Man, by interfering with this development, can influence the process in one way or another. The accompanying effects will, as a matter of course, be adverse in certain ways, but advantageous in other ways.

Studying old Roman maps of the Mediterranean or of the North Sea one realizes that several inlets in existence in ancient days are still in good condition even if their location and configuration may have changed considerably. One of the most interesting examples is the Lime Inlet (Jutland), traversing the Danish mainland from the North Sea to the Kattegat. Ancient history tells about the Viking raids on England, of cases where naval fleets of up to 1,000 ships gathered in the Lime Inlet and waited for favorable weather conditions for their passage across the North Sea to England. These raids took place in the 10th to 11th centuries and could hardly have been undertaken without the existence of the navigable Lime Inlet—still in existence as "Thyboroen Channel."

The fact that an inlet or channel has been in existence for such a long time does not mean that it has been stable. On the contrary, the Lime Inlet has probably been closed for long periods. Most inlets on littoral-drift coasts are in a state of dynamic equilibrium by which littoral drift and current forces are trying to find a balance. The possibility of an inlet being stable depends on different factors. One factor is related to the way in which the inlet was formed. As pointed out by Brown[3] inlets formed by the closing in of a bay by a spit or recurved spit will often, at least in their early stages, exhibit more favorable characteristics for navigation than those formed otherwise. They will not be affected to the same extent as the "break-through" inlets by inner and outer bars and shoals.

Inlets usually show a tendency for migration in the direction of the predominant littoral drift if the migration is not prohibited because of rock formation. Meanwhile, if migration of such inlet stops, as when the inlet is stabilized by jetties, then the inlets will often be plagued with shoaling on sea and/or bay shoals. It is an interesting phenomenon that coastal inlets will often try to place themselves where offshore conditions are most favorable for maintenance of an inlet, as at San Diego, California and Coos River, Oregon.

Before entering into an examination of the stability of an inlet on a physical basis, it may be worthwhile to see how inlets shoal. Most inlets are plagued with shoals on the sea side, or on the bay side, or both sides. Continued shoaling will choke the inlet if the flow around it does not increase at the same rate as the shoaling effect, or if the inlet channel is not dredged or protected from sudden shoaling by jetties.

Due to the fact that the sea-shoals or offshore bars are much more exposed to wave and current action than bay-shoals, the sea-shoals are commonly stunted in their growth and margined by contours of simple curvature. Bay-shoals are apt to become large and acquire the lobate form of an ordinary delta.

A typical example of this is the Ocracoke Inlet, North Carolina (Fig. 1(a)). The dimensions of the delta formation outside a tidal inlet are a function of the flow capacity of an inlet (its tidal prism). Large inlets have extensive bar formations outside their entrances. Sea-shoals as well as bar-shoals are usually penetrated by a number of channels of which the configuration and number is a function of the mechanics of sand transport and flow conditions in the inlet.

During flood-tide, littoral-drift material is transported in the land-ward direction by the flood currents and deposited in shoals inside the inlet. Depending on the inlet and shoal configuration, and the depth of the bay, part of this material is returned in a seaward direction by the ebb currents. Other parts of the material, especially the finer grain sizes, remain inside. This finer material is deposited at the landward end of flood channels, thus building up the inner shoal. Coarser material returned to sea will build up the outer bar or shoal. This shoal differs from the inner shoal in that the material is not as permanent here as it is on the inner shoal. The outer bar or shoal may establish a natural "by-passing sand plant" upon which material will pass across the inlet. After having been deposited momentarily in the inlet channel, material is pushed out by the ebb current, to be used for building up the outer shoal or for delivery back to the normal littoral drift, or both.

For hydraulic reasons the tidal currents will generally be more concentrated on the discharge side of the inlet channel. This means that flood current will be more concentrated on the bay side and less concentrated on the sea side than the ebb current. One can distinguish between flood channels and ebb channels, in that flood channels are predominant on the bay side while ebb channels are predominant on the sea side. Certain channels may carry both flows equally and can be classified as neutral. The inlet gorge if cleary defined in nature is an example of such a neutral channel. A description[5] of the mechanism of flood and ebb channels has been given by Johan Van Veen.

Because of this situation, bay shoals will tend to develop predominantly along the flood channel while the sea shoal will develop in a less pronounced manner along the ebb channel. For both cases, it is valid to say that a continuous extension of the channel will increase the resistance against flow. When this resistance has reached a certain point new channels may break through, thereby creating the half-moon shaped shoal which, because of the wave action, is more stunted on its sea side. This channel development is most predominant on the bay shoal. The location of the sea-shoal channel, as pointed out by Van Veen[6], depends on the direction of propagation of the tidal wave. Other pertinent factors are the longshore current velocity, the phase difference between tidal currents in the inlet and in the ocean, and the direction and magnitude of the littoral drift.

Most inlets on littoral-drift coasts migrate in the direction of the prevailing littoral drift. A very few inlets move in the opposite direction. The latter is the case with the closed Indian River in Delaware and the stablized Thorsminde Inlet on the Danish North Sea coast. In both cases the predominant littoral drift is southward but the inlets tended to migrate northward. Both exceptions can be explained by special combinations of tide, flow, and wave action.

---

5 "Ebb and Flood Channels in the Dutch Coastal Waters," by John van Veen, Tydschrift, Koninklyk Nederlandsch Aardrykskundig Genootschap, Tweede Reeks, Deel LXVII, No. 3, May, 1950, Amsterdam.

6 "The 'Waterweg,' a Tidal River," by Johanvan Veen, De Ingenieur, No. 28, Den Haag, Netherlands, 1952.

The rate of migrating inlets on sandy coasts depends on the magnitude of littoral drift and the velocity of tidal and other currents. As a result of the unequalness of sand deposits on the two sides, the inlet channel is forced against the downdrift side and consequently causes excessive erosion (Fig. 1(a), (c), (h)). By such a process the spit of the updrift side barrier may extend outward and in front of the downdrift side barrier or land area so as to overlap it (Fig. 1(f), (i)). Such a situation will usually be shortlived. Most likely the inlet will be closed and a new break-through will result, in some cases because of overflooding of the barrier from storage water on the bay side and in others as a result of wave and current action. Examples of such developments are the Little Egg Inlet, N.J., and the Aransas Pass, Tex. On the other hand, some of the big inlets in the Baltic, such as Stettiner Haff, Frisisches Haff, and Kurisches Haff have developed satisfactory and stable conditions for navigation in this way (Fig. 1(j)).

In some cases the whole inlet migrates, whereas in other cases the gorge of the inlet keeps its place, and only the tidal channels through the outer bar migrate. Such is the case at Grays Harbor, Wash., where the migration of the channels furthermore takes place in a direction opposite to the littoral drift.

Reasons Why Inlets Shoal.—It is clear that there are different reasons why inlets in littoral-drift coasts shoal. In most cases the reason is of hydraulic nature, that is, that the tidal prism decreases because of increasing resistance against the tidal flow. Reasons in general are prolongation of the inlet channel or channels, overwhelming supply of littoral-drift material during serious storms, the dividing of the main inlet channel into several channels, a change in the bay area from which water flows to the inlet, and other special reasons or combinations of reasons.

Most inlets shoal as a result of continuous prolongation of the inlet channel. This prolongation takes place in the sea (Fig. 1(k), (n)), in the bay (Fig. 1(a), (p)), or parallel to the shore line (Fig. 1(f), (i)). Other inlets shoal very quickly as a result of violent storms during which excessive amounts of deposited sand encroach on the inlet channel, decreasing the tidal prism.

As a result of storms, new channels may develop quickly, due to an increase in the migration process of the tidal channels. With respect to navigation, this situation is unfortunate, because the old and new channels together will have about the same tidal prism as the original one. This means less cross section and less depth for each of them if compared with the original single channel.

With respect to change in bay area, the problem of bay-fills as it takes place along Florida's east and west coasts should be considered. A decrease in the bay area by fills always causes a decrease in flow and tidal prism of the connected inlets. In the case of very long bays, the cutting-off of part of the bay may cause an increase in the tidal prism of the inlet, because of reflection and phase displacement of the tide. An example of this is the closing-in of the Zuider Zee in the Netherlands.

It seems worthwhile mentioning the shoaling effect, often of great magnitude, that occurs where fresh water flows to the sea through an inlet. Because of the difference in specific density between debris-laden salt water and fresh water, there is a tendency for the salt water to scoop itself in the bay below the fresh water which in turn will often cause severe silting. Examples among river in-

lets are the Delaware estuary and Charleston Harbor[7] in the United States, and the Ostende and Zeebrugge harbors[8] in Belgium.

PREVIOUS STUDIES OF THE STABILITY OF RIVERS AND INLETS

Empirical River Studies.—Much work has been done with respect to the stability of channels in alluvium, the results of which were to be used in irrigation design. Although the factors governing the stability of alluvial channels and tidal inlets differ in several ways, the results of the alluvial channel studies show certain similarities to the results of the study of tidal inlets.

The historical development of the alluvial channel studies is described by Emory W. Lane, F. ASCE.[9] In 1930, Gerald Lacey developed[10] the formula

$$P = 2.668\, Q^{0.5} \quad \ldots\ldots\ldots\ldots\ldots\ldots \quad (1)$$

in which Q is the flow, or rate of discharge, and P equals the wetted perimeter (not including water surface.) He also developed the formula

$$Q f^2 = 3.8\, V_0^6 \quad \ldots\ldots\ldots\ldots\ldots\ldots \quad (2)$$

in which f is the silt factor, which is $8\sqrt{D}$ when D is diameter is particles, in inches, and V_0 is the critical velocity from the standpoint of silting. Replacing V_0 by Q/A_1 when A_1 equals the cross-section area, gives

$$A_1 = \sqrt[6]{\frac{3.8}{f^2}}\, Q^{5/6} \quad \ldots\ldots\ldots\ldots\ldots\ldots \quad (3a)$$

Charles R. Pettis from data on the Miami River, Fla., developed the relationship

$$A_1 = 1.25\, Q^{0.8} \quad \ldots\ldots\ldots\ldots\ldots\ldots \quad (3b)$$

Thomas A. Blench, F. ASCE, has developed the relationships

$$W = \sqrt{\frac{F_b}{F_s}}\, Q^{1/2} \quad \ldots\ldots\ldots\ldots\ldots\ldots \quad (4a)$$

$$d = \sqrt[3]{\frac{F_s}{F_b^2}}\, Q^{1/3} \quad \ldots\ldots\ldots\ldots\ldots\ldots \quad (4b)$$

$$S = \frac{F_b^{5/6} F_s^{1/12} Q^{-1/6}}{(3.63\, g/v)^{1/4}} \quad \ldots\ldots\ldots\ldots \quad (4c)$$

---

7 "Fresh Water-Salt Water Density Currents, a Major Cause of Siltation in Estuaries," by E. A. Schultz and H. B. Simmons, 19th International Navigation Cong., Sect. II, Comm. 3, London, 1957.

8 "Etude des Ports Belges de la Mer du Nord," by J. Lamoen, Annales des Travaux Publics de Belgique, Bruxelles, 1948.

9 "Progress Report on Results of Studies on Design of Stable Channels," by E. W. Lane, Hyd. Lab. Report, No. Hyd-352, Bureau of Reclamation, U.S. Dept. of the Interior, Washington, D. C., 1952.

10 "Stable Channels in Alluvium," by Gerald Lacey, Minutes of Proceedings, Inst., C. E., Vol. 229, London, 1930.

in which W is the mean width in terms of depth d, so that Wd equals the cross-sectional area of flow, in feet. V is the mean speed of flow in feet per second, S is the slope; F_b, the "bed-factor", equals V^2/d, and F_s, the "side factor", equals V^3/W. Combining Eq. 4(a) with Eq. 4(b) the cross-sectional area equals $Q^{5/6} \cdot \sqrt[6]{1/F_bF_s}$

Theoretical River Studies.—The best known works on this subject are by Emory W. Lane[11] and Ning Chien[12] based mostly on investigations of bed-load transport carried out by Einstein[13] and Chien. Also well known are the investigations[14] of Lorenz Straub, F. ASCE, on the effect of channel-contraction works.

Lane's theory is based on securing a distribution of the tractive force along the sides and bottom of the channels such that the magnitude of this force at all points will be sufficiently large to prevent sediment deposits in objectionable quantities and at the same time will be small enough to prevent objectionable scour. It is possible for a given discharge to build a stable channel which has the property of impeding motion over the entire periphery. Computations on these effects are based on certain limiting values for the tractive force. A considerable amount of work has been done on the same question in the USSR's Bureau of the Methodology of the Hydro-Energo Plan and in Germany's Nuernberg Kulturamt.

Ning Chien explains how to determine channel depth and slope to conduct a specified unit discharge and sediment load. Lorenz Straub's formula for the effect of channel contraction works upon regimen of movable-bed streams is

$$d_2 = \frac{d_1}{(1 - \alpha)^{9/4}} \quad \ldots\ldots\ldots\ldots\ldots\ldots (5)$$

in which d_1 is the water depth at the uncontracted section; d_2 is the depth in the contracted section; and α is the amount of contraction. It is possible to carry the same discharge and sediment load in a smaller cross-sectional area by merely deepening the channel.

The work done by A. E. Bretting (Denmark) will be dealt with in a forthcoming publication.

Empirical Inlet Studies.—In 1884, Thomas Stevenson published a table of ratios of low water sectional areas of rivers at their confluence with the sea and the tidal capacity of their estuaries and discharge of fresh water. Since then the relationship between the cross-sectional area of inlets and estuaries and the flow capacity has been the subject of many investigations.

If the cross section below mean tide A_1 is expressed in square feet and the tidal prism Ω in acre feet, the following results are known from previous studies: La Conte found the quantity Ω/A_1 to be equal to 0.695 with the tidal prism at spring tide. In 1931, Morrough P. O'Brien, F. ASCE, published the results of

---

11 "Design of Stable Channels," by E. W. Lane, Transactions, ASCE, Vol. 120, 1955, p. 1253.

12 "Graphic Design of Alluvial Channels," by Ning Chien, Transactions, ASCE, Vol. 121, 1956, pp. 1267-1287.

13 "The Bed-Load Function for Sediment Transportation in Open Channel Flows," by H. A. Einstein, Technical Bulletin No. 10260, U. S. Dept. of Agriculture, Washington, D.C., September, 1950.

14 "Effects of Channel Contraction Works upon Regimen of Movable-Bed Streams," by Lorenz G. Straub, Transactions, ASCE, Vol. 81, 1934, pp. 454-463.

a study[15] of the relation between tidal prism and channel area, based on the data of a great number of inlets. He found

$$A_1 = 1{,}000 \left(\frac{Q}{640}\right)^{0.85} \quad \ldots\ldots\ldots\ldots\ldots\ldots \quad (6)$$

when the tidal prism is taken between mean higher high water and mean lower low water, typical characteristics of the west coast of the United States. From a study of the Sacramento, San Joaquin, and Kern Rivers, in California, in 1931, the following results were obtained. The quantity Q/A_1 was found to be equal to 0.93 for unrestricted areas and equal to 1.22 for restricted estuaries, in which Q is the tidal prism at mean tide.

In the studies made by O'Brien and others it was taken as axiomatic that inlet geometry was primarily a result of littoral drift constantly encroaching on each inlet to force its closure, and tidal ebb and flood flow on the other hand flushing these deposits and preventing the inlet from closing. Although it is known that the inlet morphology is an important factor, it is realized that there are other elements involved, such as those related to characteristics of tides and currents.

A semitheoretical approach to estuarine geometry is described[16] by Herbert Chatley. He derived the formula

$$\kappa = \frac{W^2 h}{Q} \quad \ldots\ldots\ldots\ldots\ldots\ldots \quad (7)$$

in which κ is the rate of converging and h is the tidal amplitude. G. B. Pillsbury gives[17] an equation for the ideal form of an inlet estuary and shows that this equation fits for the Delaware Bay.

Tidal Hydraulic Considerations.—Tides are seldom of purely gravitational origin. They are often affected by meteorological conditions, sometimes to a considerable degree. Tidal hydraulics deal with storm-tides as well as normal, undisturbed, astronomical tides. Tidal motion can be described as a tidal wave of great length, and a certain velocity of propagation. On the other hand, tidal currents and the differences in water levels are governed by the same laws as regular currents of permanent nature. Formerly, these two viewpoints on tidal hydraulics were considered to be basically different, but modern analysis has shown that both methods of analysis are based on the same differential equations.

Mathematically, tidal motion can be described by two differential equations, the one expressing the conservation of mass (equation of continuity), and the other expressing the equilibrium of forces and momentum in the length of the channel (dynamic equation). The dynamic equation is

$$\frac{\delta v}{\delta t} + v \frac{\delta v}{\delta x} = - g \frac{\delta H}{\delta x} - g \frac{v|v|}{C^3 R} \quad \ldots\ldots\ldots\ldots \quad (8)$$

and the equation of continuity is

$$\frac{\delta d}{\delta t} = - \frac{1}{W} \frac{\delta Q}{\delta x} \quad \ldots\ldots\ldots\ldots\ldots\ldots \quad (9)$$

---

15 "Estuary Tidal Prisms Related to Entrance Areas," by M. P. O'Brien, Civil Engineering, Vol. 2, May, 1931.

16 "Problems in the Theory of River Engineering," by Herbert Chatley, Proceedings, Inst. of C. E., London, 1929.

17 "Tidal Hydraulics," by G. B. Pillsbury, Professional Paper of the Corps of Engineers No. 34, U. S. Govt. Printing Office, 1940.

In these equations, v is the mean velocity in the direction of the channel, x equals the distance along the channel, H is the elevation of water level, d denotes water depth, g refers to the acceleration of gravity, and R is the hydraulic radius.

As expressed[18] by Hans A. Einstein, F. ASCE, and Robert A. Fuchs, those equations are so general and all inclusive that knowledge of them in itself is not a great help. Only a solution of these equations that satisfies the boundary conditions of the particular channel and of the given tide cycle and hydrographs, actually gives the water surface lines and flow velocities that the engineer needs for the design of the canals and its works. To find the explicit solution of the equation for a given set of boundary conditions involves time-consuming computation work, in which iterative or numerical step-methods have great advantage.

The other method of approach is to introduce simplifying assumptions into the basic equations. The most commonly used assumptions are average elevation of water surface is constant along horizontal channel; simple harmonic tide exists; the friction term is linearized; constant rectangular channel cross section exists; and nonlinear terms in differential equations are neglected.

William B. Parson's harmonic theory is based on the introduction of all five approximations mentioned previously. It was one of the first solutions of the tidal flow equations and was used for the solution of the tidal flow problems of the Cape Cod Canal, Mass. It has much similarity with the Hendrik A. Lorentz method, used in the Netherlands for the tidal computations made for the study of the closing in of the Zuider Zee. Because of the linear character of the equations a solution is possible in a closed form. The linear character also permits the superimposition of solutions of different harmonic components of the tide.

In Earl I. Brown's reflected wave theory[19] linear differential equations are used and the effect of abrupt changes in cross section is taken into consideration. G. B. Pillsbury's theory is based[17] on a method of excessive approximations, in which the corrections are based on the so-called "primary currents."

Brown develops[3] a method, in which the basic equations are simplified further. This method consists of omitting the terms $\frac{\delta v}{dt}$ and $(v)\frac{\delta v}{\delta x}$ from the dynamic equation and the equation of continuity, is used in the integrated form. The resulting dynamic equation is

$$-\frac{\delta H}{\delta x} = \frac{v|v|}{C^2 R} \quad \ldots\ldots\ldots\ldots\ldots\ldots \quad (10a)$$

$$v = C\sqrt{R\,S}\ \text{(Chezy formula)} \quad \ldots\ldots\ldots\ldots \quad (10b)$$

and the equation of continuity

$$\int^{t/2} Q\,dt = 2h\,\Delta \quad \ldots\ldots\ldots\ldots \quad (11)$$

when °2h represents the tidal range in the bay.

The above simplifications of the two basic equations involve the elimination of the wave characteristics of the solution.

Further assumptions in Brown's derivations are:

a. The propagation of the tidal wave in the bay is neglected, so that high water and low water occur at the same time in all locations of the bay;

---

18 "Computation of Tides and Tidal Currents—United States Practice," by H. A. Einstein and R. A. Fuchs, Proceedings-Separate 715, ASCE, 1955.

19 "Flow of Water in Tidal Canals," by Earl I. Brown, Transactions, ASCE, Vol. 96, 1932, pp. 747-834.

b. The inlet has a uniform cross section and depth;

c. The tidal curves in the sea and in the interior basin are sinusoidal;

d. The basin is nearly circular, so that at any given instant the tidal plane is the same in the entire basin;

e. The length of the inlet channel is well defined;

f. The inlet channel under consideration is the only connection between the basin and the sea; and

g. The fresh water draining into the basin from the upland area is inconsequential, so that the volumes of inflow and outflow during a mean tidal cycle may be assumed to be equal.

Brown derives formulas for the determination of the mean range of tide in the basin, maximum current velocities, and mean tidal prism.

In the course of its inlet studies, the Philadelphia District of the Corps of Engineers, U.S. Department of the Army, simplified the application of Brown's theory. The value of the tidal prism is computed from the relationship $Q = 17{,}040$. $A\,v_{max}$ when A is the cross section of the gorge of the inlet and v_{max} is the maximum-average current velocity.

Garbis H. Keulegan gives[20] a more precise approach to the problem. He omits $\frac{\delta v}{\delta t}$ from the dynamic equation and uses $Q = \Delta \frac{dH_1}{dt}$ as continuity equation. It is an improvement over Brown's method, because the term $V \frac{\delta v}{\delta x}$ is taken into consideration and the continuity equation is applied in a more correct form. With respect to schematization, his assumptions are more or less the same as Brown's. By omitting the term with δt, from the dynamic equation the wave characteristics of the phenomenon are eliminated also.

In combining the two fundamental equations, Keulegan arrives at

$$\frac{\delta H}{\delta \theta} = K\sqrt{h}\sqrt{H_2 - H_1} \quad \ldots\ldots\ldots\ldots\ldots \quad (12)$$

for flood flow, and

$$\frac{dH_1}{\delta \theta} = -K\sqrt{h}\sqrt{H_1 - H_2} \quad \ldots\ldots\ldots\ldots\ldots \quad (13)$$

for ebb flow.

These are the differential equations of the surface fluctuation in the basin, if H_2 and H_1 represent the water level elevations in the sea and in the bay, 2h is tidal range in the ocean (sinus-curve), θ the phase angle, $\frac{t}{T}$ and K the coefficient of filling or repletion.

In the results obtained, the coefficient of repletion plays a decisive role. It summarizes the effects of the channels and the basin dimensions, the roughness of the channel walls, and the period and range of the tidal fluctuations on the limits of the water level changes in the basin. It is felt by the writers that Keulegan's approach is quite rational for bay areas of relatively short length that can be considered as filling basins, because the propagation of the tidal wave in the bay is to be neglected.

---

20 "Third Progress Report on Tidal Flow in Entrances," by G. Keulegan, Report National Bureau of Standards, No. 1146, September 10, 1951.

The Lorentz Method[21] belongs to the harmonic methods because of the manner in which the basic equations are simplified.

a. the term $v\,\delta v/\delta x$ is omitted in the dynamic equation.
b. the friction term $-g(v1v1)(C^2R)$ of the dynamic equation is linearized.
c. the bay area and cross section are introduced as constant values.
d. in the storage equation $\frac{1\delta Q}{W\delta x}$ is replaced by $d\frac{\delta v}{\delta x}$, in which term d is considered constant.

The preceding assumptions result in the following equations:

$$\frac{\delta v}{\delta t} = -g\frac{\delta t}{\delta x} - k\,v \quad \ldots\ldots\ldots\ldots\ldots\ldots \quad (14)$$

$$\frac{\delta d}{\delta t} = -d\frac{\delta v}{\delta x} \quad \ldots\ldots\ldots\ldots\ldots\ldots \quad (15)$$

By means of energy considerations the linearization coefficient k is found to equal $\left(\frac{8}{3\pi}\right)\left(\frac{g}{C^2}\right)\left(\frac{v_m}{d}\right)$

where v_m is the average maximum velocity along the considered channel section.

Writing $k = \frac{2\pi}{T}\,t\,g^2\,\delta$ in which δ is the friction angle, expressions are found for the amplitude and phase of the tide and also for the flow conditions. Both tide and flow curves are harmonic functions because of the linearized assumptions.

The velocity of propagation of the tidal wave is

$$C = \sqrt{g\,d(1-t\,g^2\,\delta)}$$

Tidal characteristics are introduced as complex function; the tidal motion must be analyzed into its principle harmonic components. The linear method has been worked out by Jan P. Mazure[22] for cases of important fresh water discharge.

In the prediction of tidal currents in operations such as closing-in of tidal gaps of estuaries, there is a need for a method by which all terms in the dynamic and storage equations are considered without any simplification. In Joop J. Dronker's method[23] these requirements have been fulfilled. It belongs to the "direct method" group in which the equations are subjected to a numerical integration process. Writing the basic equations in the form

$$\frac{\delta Q}{\delta x} = -(b)\frac{\delta H}{\delta t} + (2b)\,(UQ)\,\delta Q/\delta t \quad \ldots\ldots\ldots \quad (16)$$

and

$$\delta H/\delta x = -(m)\frac{\delta Q}{\delta +} \mp w\,Q^2 + (2b)(U\,Q)\,\delta H/\delta t \quad \ldots\ldots\ldots (17)$$

---

21 "Report of the State Commission Zuiderzee, 1918-1926," by H. A. Lorentz, (Dutch text).

22 "The Computation of Tides and Storm Surges on Maritime Rivers," by J. P. Mazure, Dissertation, Dr. Sc., Technological University, Delft, Holland, 1947 (Dutch text).

23 "Tidal Computations in Shallow Water," by J. J. Dronkers and J. C. Schonfeld, Proceedings-Separate 714, ASCE, June, 1955.

in which b is the width, w equals $1/C^2 A^2 h$), U Q^2 is the velocity head $v^2/2g$, and m equals $1/g A$.

The approximation $Q = Q_0$ (t) and $H = H_0$ (t) can then be substituted in the right-hand members and be integrated from 0 to x. This yields the first subsequent approximations

$$Q_I = Q_o - b \frac{\delta H_o}{\delta t} x + 2 b U Q_o \frac{\delta Q_o}{\delta t}$$

and

$$H_I = H_o - m \frac{\delta Q_o}{\delta t} x + w Q_o^2 x + 2 b U Q_o \frac{\delta H_o}{\delta t} x$$

The second subsequent approximations are found by substituting the latter two equations in the right-hand members of the basic equations and integrating once more. Continuation of the process yields Q_{III} and H_{III}. However, as a rule, the approximation Q_{II} and H_{II} are sufficient for practical computing.

In the Netherlands, numerous tidal computations have been carried out based on Dronkers' method. The method was intensively used in predicting the tidal currents in the tidal gaps formed during the flood disaster of 1953.

The above mentioned methods of tidal computations are based on a schematization of the inlet, the bay geometry, and of the flow patterns. More detailed investigations are desirable such as, in order to find the relationship between gorge and bar channels under different flow and littoral drift conditions. Model studies will be very helpful in this respect. John C. French[24,25] made a theoretical approach to similar problems.

PERTINENT FACTORS INVOLVED IN INLET STABILITY

In order to obtain a stable tidal inlet channel in alluvial material, it appears to be an inevitable assumption that littoral-drift material must be supplied to the inlet. This material is deposited on the inlet bottom where tidal currents will move material, as a kind of "rolling carpet," including bed as well as suspended load over the bottom. In order to obtain a stable situation this carpet must not move back and forth too rapidly because it thus runs the risk of being lost or "worn out" at both ends (the sea and the bay). Nor can it be allowed to move too irregularly, changing its velocity and travel time continuously, since it may soon pile up at one or at both ends in the form of excessive deposits. If no material is available for building up this carpet the inlet will be constantly "shaved" and will gradually develop open-bay or perhaps estuary characteristics rather than tidal inlet characteristics.

To analyze the stability problem the cross-section area, A, is considered explicit as a function of different factors:

$$A = F (\Omega, \beta, \tau, B, \bar{c}, W_a, Q_o, t)$$

The factors Ω (tidal prism) and β (form factor) are interrelated, and shear stress τ, bottom composition B, and the littoral drift M, also have a certain direct influence on β. The factors τ, β, $\bar{c}$ (sediment concentration), W_a (wave

24 "First Progress Report on Tidal Flow in Entrances: The Velocity Distribution at the Entrance," by John L. French, Report, National Bureau of Standards, No. 1052.

25 "Second Progress Report on Tidal Flow in Entrances: The Velocity Distribution in the Jet Issuing from a Channel into an Ocean or Lagoon," by John L. French, Report, National Bureau of Standards No. 1141.

action), and M are also interrelated. The fresh-water discharge Q_o (head water) is independent of all other factors but may have a certain influence on τ and, indirectly, on β. The time factor, t, represents "the time history" which is important because of the time lag between action of forces and the large-scale reaction of the elements acted upon by the forces.

The Influence of the Tidal Prism.—Consider $A = F(\Omega, \ldots\ldots)\Omega$, represents the tidal prism through the inlet. The relationship between A and Ω can be expected to be fairly linear because, if one inlet is stable with cross-sectional area A, and tidal prism Ω "by accident" joins with a neighbor-inlet that also has cross-section A and tidal prism Ω (both from their own separare bay areas), the result most likely will be a combined inlet with cross-sectional area of the order 2A and tidal prism 2Ω. This must at least be true for inlets of considerable size. For smaller inlets the result of the alliance may be a new cross section with area somewhat different from 2A for 2Ω. The actual size will depend upon the utilization of the cross section for flow and the distribution and actual size of shear stresses between flow and bottom.

Tidal prism Ω according to Keulegans theory[20] is related to the maximum discharge Q_m by the expression:

$$\Omega = \frac{Q_m \; T}{\tau \; C_2} \qquad \ldots\ldots\ldots\ldots\ldots\ldots \quad (18)$$

The Influence of the Shape Factor "β".—Consider $A = F(\Omega, \ldots\ldots)$ A study of the configuration of inlet gorges demonstrates a certain similitude between the cross section of different gorges. Meanwhile, a considerable number of inlets are provided with gorges that do not have a simple, univalent defined cross section, but that, in the main, consist of two or more parts—one with comparatively shallow water and one with deeper water (the "real gorge"). The "coefficients of utilization" of the different parts of the cross section are not equal. The shallow parts have a comparatively small utilization factor for flow activity, but they sometimes count considerably in the cross section. Even if such inlets are fairly old, the question exists as to whether they can be considered stable because they often demonstrate a considerable amount of instability in the form of shifting shoals and shallows and changing cross-sectional area.

The velocity of flow in any cross section is given by an expression of the following shape:

$$v = k \; R^x \; S^y$$

in which k is a ratio factor.

The corresponding discharge is:

$$Q = k \frac{A^{(1+x)}}{p^x} \; S^y$$

$$A = \left(\frac{Q}{k \cdot S^y}\right)^{\left(\frac{1}{1+x}\right)} p^{\left(\frac{x}{1+x}\right)}$$

It can be seen that the velocity for a given S is at its maximum when $R = \frac{A}{p}$ is at its maximum. The circular pipe is, therefore, the most advantageous for closed conduits and the half-circle for open conduits.

For a trapezoidal cross section, it can be shown that the most advantageous (minimum) cross section for maximum flow is one-half part of a hexagon.

The cross section of natural inlets in loose material can never develop such an ideal cross-section because this would require very steep side slopes.

The tidal flow computations by Keulegan[20] mentioned above, include a factor $C_2 = \frac{T Q_m}{\tau \Omega}$ that depends on the "coefficient of repletion" K. The larger K is, the faster the tide water will pass through the inlet (Q_m increases).

$$K = \frac{T\sqrt{2g}}{2\pi} \sqrt{\frac{R}{\lambda L + R}} \frac{A}{\sqrt{H}} \frac{1}{\Delta}$$

where the relation between λ and Manning's n is given by:

$$\sqrt{\lambda} = \frac{n\sqrt{2g}}{1.486 \quad R^{1/6}}$$

in which T is the tidal period, R refers to the hydraulic radius, L is the channel length, A denotes cross-sectional area, and Δ is the tidal area of bay.

As it comes forth from the K-expression, variation of λ with the hydraulic radius or mean depth of the inlet channel and the hydraulic roughness is taken into consideration but the shape of the cross section is not. Keulegan, to some extent, converts this by introducing a "prismatic equivalence of irregular channels and multiplicity of channels" to be used for "practical inlet channels" that are irregular.

Such irregular cross section can be split into parts. If the hydraulic radius for these parts is $R_1, R_2, \ldots R_n$ the average hydraulic radius is:

$$R = \frac{R_1 + R_2 + R_n}{n}$$

By computing the flow based on the single cross sections, different velocites will result because the depth and relative roughness is not the same for each separate cross section. In nature this unequal distribution of velocity is demonstrated not only by different velocities in the different parts of the cross-section but by eddies and transversal currents, all causing a certain amount of energy loss. This, again, means that the cross-sections do not utilize a given flow in an economical way, which increases the $\frac{A}{\Omega}$ ratio. Littoral drift, particularly with coarser material, will often tend to develop a more economic cross-section with steeper side slopes. Increased fresh-water flow in certain periods may work similarly. Compare the situation in a river.

With jetty-protected "improved inlets" the cross section is improved for flow. Generally there is only one channel with greater depth (greater hydraulic radius) and with less "large-scale" friction and energy loss from banks and shoals. Flow conditions are, in other words, better "organized." For this reason it can be expected that a comparatively smaller area is sufficient for a given value of the maximum tidal flow.

It is interesting to note some results by Van Bendegom[26]. Based on the assumption that for a given value of water discharge and sand discharge the number of possible river cross sections is restricted. Van Bendegom's conclusion is that for a given water discharge and sand discharge, only one stable cross section is possible, with the shape of the cross section depending on the ratio between the sand and water discharges. Fig. 2 shows the results of Van Bendegom's investigations of the Dutch Wadden Sea. A correlation appears to exist between the width and the depth of the different tidal channels in this area. Van Bendegom developed a theory, based on an equilibrium between the slope of the profile and the exchange of sand in a direction perpendicular to the current caused by the variation of shear stress in this direction $\left(\frac{\delta \tau x}{\delta y}\right)$.

The Influence of the Shear Stress, "τ".—Consider $A = F(\Omega, \tau, \ldots\ldots)$

τ is the shear stress (force per unit bottom area acting between the flow and the bottom). For a cross section with horizontal bottom and unlimited width a linear relation between A and Ω involving a certain shear stress τ can be expected under otherwide equal and well-defined conditions.

With hydraulic radius R and slope of water surface S one has for a vertical section of unit width and length (assuming steady or slowly varying conditions):

$$\tau = \rho g R S$$

whereby τ is the average shear stress along the wetted perimeter.

By introducing the well-known Chezy relationship;

$$v = C\sqrt{RS}$$

and

$$Q = Av = A C\sqrt{R S}$$

we find $A = A C\sqrt{\frac{\tau}{\rho g}}$ or in terms of tidal prism: $\frac{\Omega}{A} = \frac{C T}{C_2 \pi}\sqrt{\frac{\tau}{\rho g}}$

It is obvious that for a bottom consisting of loose sand material the requirement of stability must be that the shear stress either stays below the critical shear stress for material movement or that the flow conditions are such that the total transport of material from a section equals the transport to this section.

The conditions of stability can be mathematically described as follows: Consider a section dx of the gorge (Fig. 3) and let Q_s dt be the total rate of sand flow passing through section a within a time interval dt, and $\left(Q_s + \frac{\delta Q_s}{\delta x} dx\right)dt$ is the amount of sand transport that passes through section x + dx. The erosion of the section during that time is equal to the difference between sand inflow and outflow. Erosion is equal to $\left(Q_s + \frac{\delta Q_s}{\delta x} dx\right)dt - Q_s dt$ or $\frac{\delta Q_s}{\delta x} dx\, dt$. Erosion per linear foot of channel length is equal to $\frac{\delta Q_s}{\delta x} dt$.

26 "Considerations About the Principle of Coastal Protection," by L. van Bendegom, Report, Rykswaterstaat, Netherlands, December, 1949 (in Dutch).

The condition of stability involves that neither erosion nor depositing of material occur in the section under consideration; in mathematical form,

$$\int_0^t \frac{\delta Q_s}{\delta x}\, dt = 0 \quad \ldots\ldots\ldots\ldots\ldots \quad (19)$$

The integral is taken over a certain length of time. In the case of subsequent equal tidal cycles, for the upper boundary, t, the tidal period T, can be chosen.

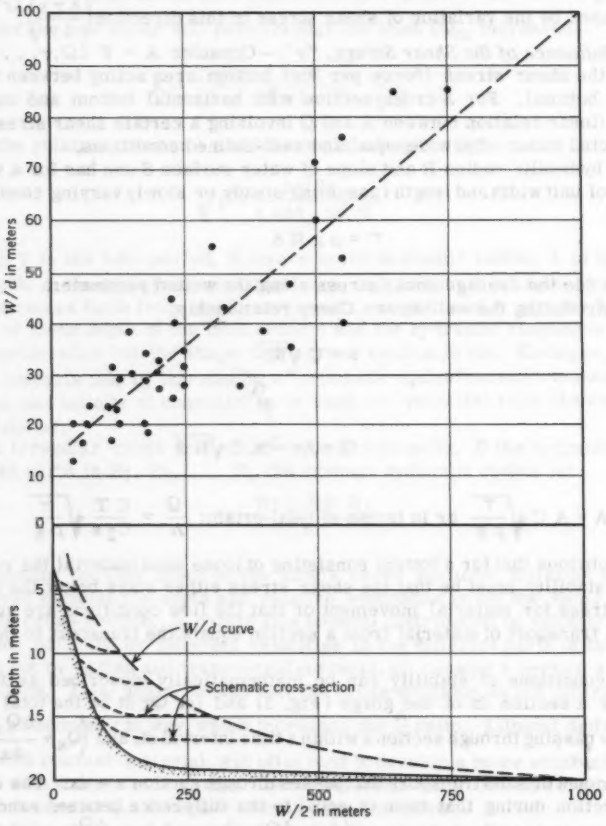


FIG. 2.—WIDTH TO DEPTH RELATIONSHIPS OF TIDAL CHANNELS IN THE DUTCH "WADDENSEA"

It is assumed that "stability" is related to a certain value of the average shear stress. For analysis of field data there is a definite advantage in using the average value of τ because of the difficulty in defining the shear stress distributions.

Let us call the average shear stress along the bottom, by which an inlet cross-section is stable, under maximum flow conditions "the determining shear stress" or "stability shear stress" τ_s. We then have for stable conditions:

$$\frac{\Omega}{A} = \frac{C\,T}{C_{2\pi}} \sqrt{\frac{\tau_s}{\rho\, g}} \quad \ldots\ldots\ldots\ldots\ldots\ldots \quad (20)$$

whereby Ω is the tidal prism under springtide conditions.

The problem of inlet stability has, in fact, then been reduced to the determination of the stability shear stress τ_s.

In regard to the influence of channel friction, the channel roughness parameter (Manning "n" or relative roughness $\frac{k}{R}$, reference is made to the comprehensive literature file dealing with flow in rivers, streams and channels.

Factors influencing τ_s are mentioned in the following sections. It is indicated that coarse bottom material will usually give higher τ_s than finer material for the velocities in question. Sediment load from river or from littoral drift (fine material) will increase τ_s. An increase in C (decrease in Manning n) is usually associated with an increase in τ_s. Wave action will decrease τ_s.

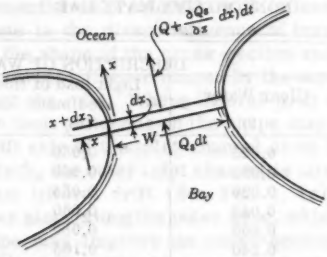


FIG. 3.—CONDITIONS OF STABILITY

Increase of littoral drift will raise τ_s relatively. Fresh water flow may also increase τ_s, particularly if it is of a seasonal nature and causes "at a station changes" of a temporary nature, as observed in rivers.

The Influence of Soil Condition of the Bottom or Bed, "B"—Consider $A = F(\Omega, \tau_s, B, \ldots\ldots)$

$$\tau_s = f\,(B, \ldots\ldots)$$

The "limiting values of τ" (usually called τ_c) for different grain sizes of noncohesive materials, according to Russian standards that refer to rivers and canals, are given in Table 1.

For cohesive materials less information is available. Reference is made to Russian data mentioned in Lane's publication.[11] It must be remembered, however, that tidal inlets almost always run through noncohesive materials and that if they do not, the bottom may soon be covered with such material carried to the inlet by the littoral drift.

Fig. 6 in Lane's publication,[11] indicates different critical tractive forces observed in rivers and recommended for canals as a function of the mean diameter of the bed material and the amount of suspended load. Although in tidal

inlets the flow is continuously reversing its direction, which will have a certain influence upon the roughness characteristics of the bottom, it seems reasonable to assume that the trend in the figures from the river technology may be similar to those at tidal inlets.

The Influence of Suspended Sediment Load, "$\bar{c}$"—Consider $A = F\ (\Omega, \tau_s, \bar{c}, \ldots\ldots)$

$$\tau_s = f\ (\bar{c}, \ldots\ldots)$$

Sediment load in the inlet flow has its origin in three basically different sources:

(1) Suspened load in the tidal flow, caused by the stirring up of material from the bed under turbulent flow conditions.
(2) Silt load from rivers carrying material from upland sources into the estuary or inlet.
(3) Suspended material stirred up by wave action and being transported as littoral drift into the inlet channels.

TABLE 1.—LIMITING VALUES OF TRACTIVE FORCES, RIVER AND CANAL FLOW NONCOHESIVE MATERIAL

Median size of material, in millimeters (1)	DESCRIPTION OF WATER		
	Clear Water (2)	Light load of fine sediment (3)	Heavy load of fine sediment (4)
0.1	0.025	0.050	0.075
0.2	0.026	0.052	0.078
0.5	0.030	0.055	0.083
1.0	0.040	0.060	0.090
2.0	0.060	0.080	0.110
5.0	0.140	0.165	0.185

According to Table 1, sediment load increases the limiting shear stress. It seems reasonable to assume that in this respect conditions at inlets on littoral-drift coasts are comparable to those of rivers and canals with high content of fine sediment in water, as represented by one line in Fig. 6 of Lane's publication.[11] Considering this line, the critical tractive force varies from 360 to 900 grams per sq m (about 0.08 to 0.2 psf), when the mean diameter varies from 0.1 mm to 5 mm. It should be noticed, however, that for the lower values of the mean diameter (below 1 mm) the increase of limiting shear stress is small. It should also be mentioned that the ability of a stream to transport fine sediments in suspension may be greatly increased with decreased water temperature, since sedimentation rates of alluvial bed materials are lower in water of low temperature than in water of higher temperature. The result is a tendency toward channel degradation in the cold season. It is possible that a similar situation exists on seashores (but temperatures may vary less than in rivers).

The Influence of Wave Action, "W_a"—Consider $A = F\ (\Omega, \tau_s, W_a, \ldots\ldots)$

$$\tau_s = f\ (W_a, \ldots\ldots)$$

The influence of wave action is twofold. Wave action makes the actual τ value vary and increases material transport as suspended as well as at bedload by stirring up material from the bottom to be carried away by currents. Such currents may within themselves be too weak to erode the bottom. Because of the great variation in wave action and combinations with current activity nothing specific can be said about the influence of wave action at the present stage of our knowledge of tidal inlets. However, it is apparent that τ_s decreases relatively where the bottom is under direct influence of wave action. In the entrance area the flow will be more or less saturated by material stirred up by wave action and this will result in a decrease in turbulence and friction and therefore in an increase of the stability shear stress τ_s for bottom stability for the parts of the inlets further inland where wave action is of little importance. An adjustment of the channel cross-section to this situation may result in a smaller cross-section. The waves may also cause a certain (minor) increase of transportation as bed-load by mass transport of water. This extra bed-load transport, which will decrease with decreasing wave action, may have a decreasing effect on cross-sectional area. Normally the maximum cross-section of the inlet channel is to be found at the point where the combined effect of current and wave action has its maximum and where suspension load may also have its maximum capacity. This is usually the case at the entrance.

The Influence of Littoral Drift, "M"—Consider $A = F(\Omega, M, \ldots\ldots)$ The littoral drift, as mentioned previously, will influence the development of inlets in two ways; one is the direct influence of transported and deposited bed-load material on the shape of the cross-section and on the channel length, and the other is the indirect influence caused by the supply of suspended material on the flow through the inlet. Where littoral-drift deposits encroach upon an inlet cross-section their influence on the shape may be noticeable either at the updrift or downdrift side of the inlet channel or on both sides. Due to the effect of the littoral drift, the outer inlet channel is often curved in the direction of the predominant littoral drift (See Fig. 1, (c), (g), (h)). A curved channel has its steeper slope along the outer bend, which is usually the updrift side. Such steep slope may improve the cross-sectional shape factor β and in turn may increase Ω and Q_m without increase in A, as mentioned previously.

If the littoral drift material is rather coarse, a relatively steep slope may develop at the updrift side. If the material is fine, the updrift side of the inlet may develop a comparatively gentle slope, while the downdrift side may still develop a steep slope. By misconfiguration of the cross-section, one or more deep channels may develop which will carry the main flow with higher velocities while the shallow and gently sloping sections carry only little flow at lower velocities. This means less efficiency of the combined water currents and, thereby, "surplus" cross-sectional area. In some cases when the littoral drift is supplied to the channel almost equally from both sides the result may be a more economical cross-section, with steeper slopes on both sides eliminating the less effective shallow or gently sloping bank parts and improving the shape factor β.

Deposits in the outer inlet region may wholly or partly be washed away by the ebb-currents. This is provided equally distributed deposits m over the width W of the cross-section A, m is proportioned to A.

The total amount of material which will be eroded from the deposit area during a half-tidal cycle is:

$m = \int_0^{T/2} q_s \, dt$ when q_s is the amount of sediment transport as bed load in

cubic feet per linear foot. Using the extended Kalinske bed-load formula[27] according to which $q_s \sim \tau^{2.5} \sim v^5$ and Keulegans[20] expression for $v = v_m (\sin \omega t)^{1/2}$ (first approximation) and Keulegans[20] relationship between v_m Ω and A: $v_m = \frac{C_2 \pi \Omega}{T A}$ one has: $A \sim \Omega^{5/6}$ which is the same A/Ω relation as found for rivers. (See Eq. 3(a)).

The Influence of River Discharge, "Q_0"—Consider $A = F(\Omega, Q_0 \ldots\ldots)$ In the estuary type inlet a river discharges through the tidal inlet. This may change the relation between Ω and A, particularly if the river carries ample silt load[28]. Density differences may create a more complex current distribution and siltation problems.[29]

In cases of a more simple nature, such as, when density currents have difficulty entering the inlet because of shoals in the other part, the normal all-tide approach may be useful for description of the average stability condition but a consequence of the fresh-water discharge most usually is that flood and ebb flow have a different current distribution in the vertical plane.

The Time History of the Inlet, "t"—Consider $A = F(\Omega, \ldots\ldots)$ The section on Natural Inlet Regimen, mentions briefly the development of inlets and explains that it is common for inlets to have breached through barriers. In some cases the inlet closed very soon while in other it remained open for a long period. Some inlets migrated; others remained in one place for a long time passing through various stages of development.

In earlier paragraphs the relationship between cross-sectional area and length of inlet channel and the influence of splitting up of one main channel into several was explained. Apparently whole sets of solutions exist, but their degree of stability varies. The single solution depends not only upon the actual value of number of factors including Ω, Q_m, β, τ_s, B, $\bar{c}$, W_a, M, and Q_0 but also upon the way these factors are put together, as well as of the relative magnitude.

In river technology we are able to distinguish between "at a station characteristics" and "downstream characteristics." The latter is comparable to normal inlet stability but under extreme tide conditions we may also experience "at a station" changes in inlets comparable to changes caused by variations in river stages. This interesting problem will be dealt with in a forthcoming paper by the authors.

RESULTS OF STUDY OF EXISTING DATA

Brief Review of Results of Earlier Date.—In the preceding paragraphs, several formulas for the relationship between Ω and A have been mentioned.

The similarity between those formulas is notable although the ways these formulas have been derived are different. The question of whether the similarity between river and actual tidal flow is a matter of coincidence must remain unanswered at the present moment. A comparison between Lacey's formulas $(A \sim Q^{5/6}\ (Q \sim \Omega))$, Pettis' results from Miami River $(A \sim Q^{0.8}$,

27 "Engineering Hydraulics," by Hunter Rouse (Chapter XII), John Wiley and Sons, New York-London, 1950.

28 "The Behavior and Control of Rivers and Canals," by Claude Inglis, Yerardo Jail Press, Poona, India, 1949.

29 "The Role of Density Currents in Estuaries," by H. Stommel, Proceedings, Minnesota International Hydr. Convention, 1953.

Blench's formula $\left(A \sim Q^{5/6}\right)$, and O'Brien's inlet formula $\left(A = 1000\left(\frac{\Omega}{640}\right)^{5/6}\right)$, is striking. The gorge formula (Eq. 20) is in agreement with stability considerations (Eq. 19) and gives good agreement for the number of inlets to which it has been applied. If mean values for the different factors are introduced, the gorge formula gives $\Omega/A = 1.26$ for heavy sediment load; $\Omega/A = 1.17$ for average condition; and $\Omega/A = 1.06$ for light sediment load. These values are for conditions at springtide, with Ω expressed in acre feet, and A expressed in square feet.

LaConte found $\Omega/A = 0.695$ (Ω at springtide). From a study of the Sacramento-San Joaquin and Kern Rivers (1931), $\Omega/A = 0.93$ for unrestricted areas (Ω at meantide) and $\Omega/A = 1.22$ for restricted areas (Ω at meantide). LaConte's results apparently were related to a situation for which a lower value of the stability shear stress was valid. Finer grain size is an example of such a situation.

Studies by the Coastal Engineering Laboratory of the University of Florida— After careful investigation of the material available, a number of inlets were selected for further analysis. Basis of selection was the availability of different data to determine the cross section of the inlet, the tidal prism, and the velocities in the gorge with adequate accuracy. Besides a number of inlets in the United States, two inlets from Denmark and six inlets from Holland were incorporated in the study.

Most inlets which have been chosen present comparatively simple inlet geometry. They are inlets with one simply-defined gorge with comparatively regular shape with not more than one channel, no shoals, and with a simple configuration, that is, mainly straight-lined. The reason for this is the desire to eliminate shape and configuration factors involved in the problem by obtaining well-defined flow conditions and thereby a simple distribution of shear stresses over the cross section. At the same time, typical tidal inlets without any appreciable fresh water and silt, flow have been sought. The results therefore are mainly valid for inlets with such simple natural conditions.

The reason for this approach is for comparison with Lane's theory for stable channels that is based on shear stress analysis. Lane used[11] the limiting tractive force, but considered canals with movable bed material as well. The approach here is to replace Lane's limiting with the determining tractive force.

Use of any theory based on removal of deposits would involve difficulties in determining the inlet characteristics where these deposits take place, because this is not very well known and is changing all the time. The study of a number of inlets, of simpler geometrical nature on littoral-drift coasts in the United States as well as in Holland and Denmark, has shown that a maximum average springtide velocity of 1.1 m per sec and a Chezy coefficient value of 50 $m^{1/2}$ sec^{-1} often go together, resulting in a stability shear stress factor:

$$\left(\frac{V}{C}\right) = \frac{\tau_s}{\rho g} \text{ of } 2.2 \times 10^{-2}\ m^{1/2} \quad \ldots\ldots\ldots\ldots (21)$$

Under normal tide conditions, this is approximately 10% less, or, 2.0×10^{-2} $m^{1/2}$, which gives a computed value of τ_s of 411 g per sq m.

In Fig. 4(a) and 4(b) the computed values of Ω and A are plotted in a diagram. Fig. 4(a) represents only small inlets, whereas Fig. 4(b) covers inlets with cross sections up to 900,000 sq ft. The nonscouring channels of Fig. 4 are indicated with an asterisk. In order to compare the plotted values with

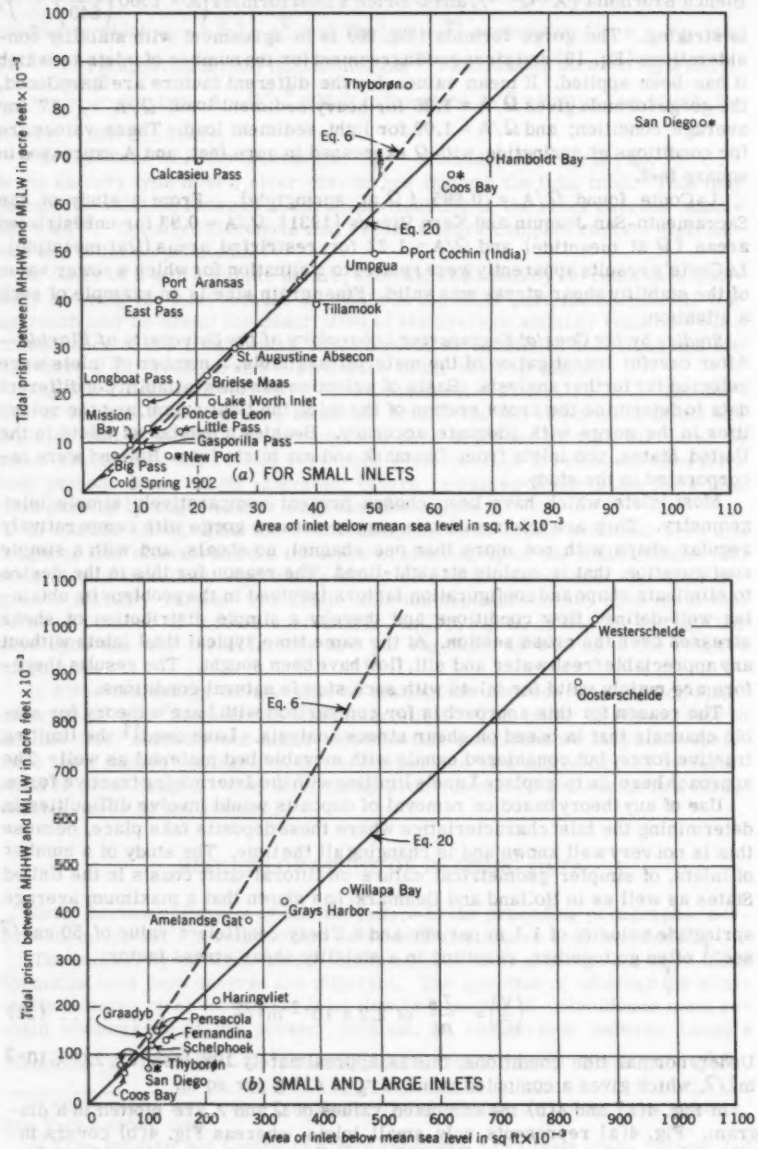


FIG. 4.—STATISTICAL RELATIONSHIP BETWEEN TIDAL PRISM AND CROSS-SECTION

some semitheoretical relationships, two dotted lines have been drawn in each of the diagrams. The relationships plotted are O'Brien's exponential curves (Eq. 6) and the linear relationship between Ω and A, as based on gorge stability consideration (Eq. 20). If in Eq. 20 the following values are introduced: $C = 90$ ft$^{\frac{1}{2}}$ sec^{-1} $= 50$ m$^{\frac{1}{2}}$ sec^{-1}; $V = 3.6$ fps $= 1.1$ m per sec; $C_2 = 1.0$; and $t = 44{,}600$ sec. The linear relationships are $\Omega/A = 1.56 \times 10^4$ m, or $\Omega/A = 1.17$ acre-ft. This is the value plotted for Eq. 20 on Fig. 4.

The following conclusions can be arrived at:

1. The linear relationship is in fair agreement with observed values for both small and large inlets, although some remarkable deviations exist.
2. The exponential formula (Eq. 6) gives sufficient agreement for smaller inlets (cross sections below 50,000 sq ft) but deviates from the observed data for the bigger inlets. The rocklined gorge of the Golden Gate has less than half the area, relative to volume of tidal prism, of inlet gorges with sand bed and banks. It seems less reasonable to let this condition at this inlet carry the same weight as conditions at inlets developed freely in granular material. Yet it is still possible that further studies of the very large inlets will give the result that such inlets need comparatively smaller cross sections. Density currents and special boundary-wave phenomena between water layers may play a role.

The inlets with values of Ω that are too high are all located on the Gulf Coast, which has a pronounced diurnal tide, for which the tidal period is 86,400 sec instead of 44,600 sec. Considering the linear relationships these inlets should be compared with the lines $\Omega/A = 3.02 \times 10^{-4}$ m or $\Omega/A = 2.27$ acre-ft that would produce a much more satisfactory agreement.

San Diego, Calif., and New Port, Calif. belong to the group of nonscouring channels, in which a larger cross section is created artificially by dredging. In these inlets no natural stable conditions exist and it is therefore not surprising that their plottings deviate in the diagram. Even though the greater deviations have been explained, the remaining differences between the average line and the individual plottings need further analysis.

In the linear relationship between Ω and A, different values of C, C_2, B, and τ_s have to be taken into consideration. The values of C, and C_2 can be computed from inlet geometry, and the value of τ is known also. The remaining unknown factor is τ_s.

When substituting the average value $\tau'_s/\rho g = 2.2 \times 10^{-2}$ m$^{\frac{1}{2}}$ for τ_s, the variations in τ_s can be found by comparing the plotted data and the computed line with $\tau_s = \tau'_s$. The results of this analysis are shown in Fig. 5, in which the ratio

$$\frac{\Omega}{\frac{CT}{C_2\pi}\sqrt{\frac{\tau'_s}{\rho' g}}}$$

indicated by G in Fig. 5, is plotted against the cross section A. A dimensionless diagram has been obtained by dividing both variables by Δ, the area of the bay. The plot of $G = 1.08A$ is for heavy sediment load while that of $G = 0.91A$ is for light sediment load.

Because A is proportional to Ω, the ratio A/Δ is proportional to the tidal range in restricted bay areas and a grouping of data has been obtained according to tidal characteristics in the bay. From this diagram it can be seen that

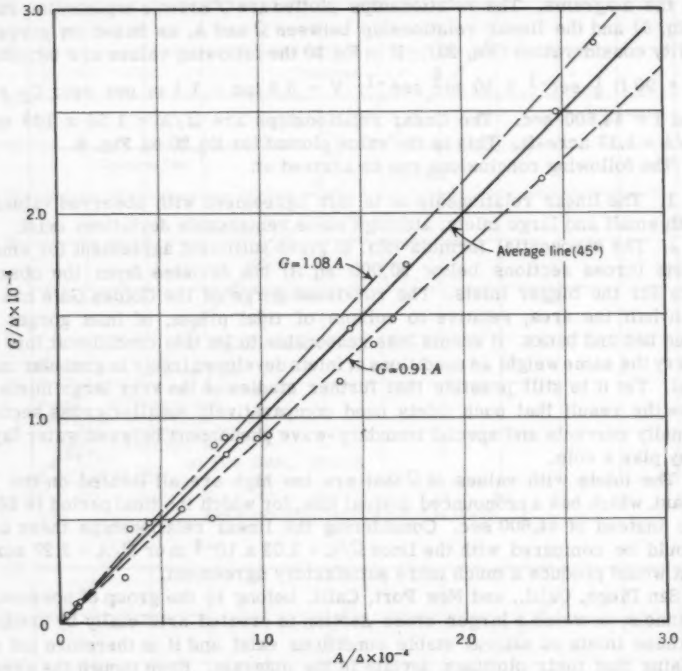


FIG. 5.—RELATIONSHIP BETWEEN TIDAL PRISM AND CROSS SECTION IN A DIMENSIONLESS FORM

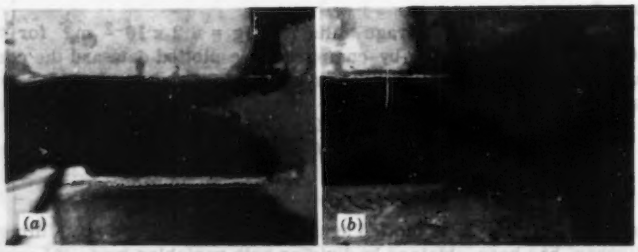


FIG. 6.—(a) FLOOD FLOW (b) EBB FLOW MODEL STUDIES OF LAKE WORTH INLET

inlets with a comparatively higher value of Ω than indicated by the average line generally have a higher sediment load or littoral drift and for the points with lower values of Ω, the sediment load or littoral drift is generally lower.

In considering the influence of the littoral drift, it has to be realized, that the resulting littoral drift should not be taken as a value of comparison, but rather the total "numerical" amount of littoral drift, that encroaches from both sides upon the inlet.

Two lines have been drawn in the figure, one on each side of the line for average τ'_s indicating the relationships between Ω and A, for high and low values of τ_s. The differences from the average, + 8% and -9%, respectively, are proportional to the square root of the stability shear stresses for the different inlet. That means that with respect to the average, the shear stresses vary approximately ± 17% under the simpler conditions on which the study is based.

The combination of phenomena, as presented previously, is responsible for the deviations. It is not yet possible to determine the influence of the different factors involved separately. For inlets of more complex configuration, the shape factor and configuration factor must be expected to be rather important. Most of the inlets under consideration have maximum velocities between 3.1 and 3.9 fps. Most likely the littoral drift is an important agent indirectly or directly. A part of the difference may also be caused by differences in bottom material (grain size) and particularly by varying exposure to wave action.

MAN'S EFFORTS IN IMPROVING THE STABILITY OF COASTAL INLETS

The development of navigation made it necessary to provide harbors for an increasing number of vessels of increasing size. It became necessary to fix the position of inlets and estuaries, to dredge wider and deeper navigation channels and protect these channels against unpredictable wave and current action, and against shoaling.[30]

It is outside the scope of this paper to examine technical details of such regulatory steps but it is self-explanatory that definite knowledge of the relationship between flow and inlet geometry is of vast importance as is a thorough understanding of other pertinent physical factors involved. Methods for inlet improvements are dredging operations, protection of the inlet against littoral-drift deposits by jetties, and contraction of the inlet channel by dams, groins, spurs or baffles. By-passing sand plants with the double effect of limiting the erosion on the downdrift side of the inlet and decreasing the amount of deposits in the inlet channel have been built in recent years. Theories have also been developed for determination of the ideal shape of an inlet estuary, but the over-all result is still that no integrated method exists that can be applied with confidence to the solution of tidal inlet problems.

With a limited amount of funds, much knowledge and experience has already been gained, but the problem is one that involves ten to twenty variables, if not more. These variables can be combined in more than a hundred different ways and even if most of these combinations are considered unrealistic, there are still so many combinations remaining that it is all but impossible to give a definite answer to any particular problem based on our present experience.

What can be accomplished is that for a given desirable cross section the size of the tidal flow necessary to keep this cross section fairly stable, can be

30 "The Improvement of Tidal Entrances," by Martin A. Mason, Report No. 1, Corps of Engrs., U. S. Army (Evaluation of present state of knowledge of factors affecting tidal hydraulics and related phenomena), Committee on Tidal Hydraulics, 1950.

computed and vice versa, taking the actual situation of tides, bottom material, material-load and different friction elements into consideration. As described previously, a certain amount of data are already available for such purposes.

A choice can be made for the value of the stability shear stress, taking the different inlet characteristics into consideration, in which Lane's data[11] are very helpful. The friction factor can be computed based on known flow and material characteristics. The coefficient C_2 is a function of Keulegan's coefficient of repletion.

Although the necessary data for a preliminary estimated design are available, such a design would be based on average conditions, and nature does not always respect the statistical mean. Heavy storms pour littoral-drift deposits in the inlet channel regardless of how ideal its cross section is, compared to the average flow. The technical answer is jetties as protection against such events. Jetties will result in a different and special type of cross-section development, but this forced cross section is still able to be handled by tidal computations. The shape factor of the cross section is now out of consideration because the shape is given as approximately rectangular or trapezoidol. The influence of littoral drift is incorporated in the choice of τ_s and the computations of flow conditions are much simplified. Yet such a simplified case is in fact not yet adequately investigated. The result of such consideration would most likely be a more economical and improved relationship between Ω and A. If a by-passing sand plant is installed, everything seems to be in proper order. Much has been accomplished but there is not, as yet, enough data to insure a continuous stability of an inlet. Most likely the inlet will still have deposits in the channel. These deposits often appear suddenly and restrict the size of the cross section.

At the Coastal Engineering Laboratory of the University of Florida, Gainesville, Fla., model experiments with fixed beds have been made to study the influence of a deepening of Lake Worth Inlet, Fla., on the behavior of the water table in the Lake Worth bay. The Lake Worth Inlet is protected by two parallel jetties, perpendicular to the shoreline.

It is outside the scope of this paper to examine this study in detail, but the flow conditions in the inlet channel have considerable interest for this paper. During flood, the flow at the entrance is subject to contraction, as shown in Fig. 8(a) of the improved inlet. Littoral-drift deposits have actually accumulated on the updrift side of the northern jetty. South of the inlet, erosion has taken place, resulting in a greater effective length of the southern jetty. Because of this difference in actual length between the two jetties, the flow pattern at the entrance is asymmetrical.

Fig. 6(b) depicts the ebb-flow pattern that shows agreement with the jet-flow theory because no natural tidal channels outside the inlet are present. French's progress reports[24,25] dealing with the velocity distribution in tidal entrances, are of interest in this respect.

In order to investigate the influence of the contracted flood flow in the case of parallel jetties for a group of inlets the cross sections at different locations in the inlet have been plotted against the distance from the seaward end. The diagram (Fig. 7) has been made dimensionless by plotting A/A_0 against x/L, in which A_0 is the cross section at the end of the jetties, L is the length of the inlet, x is the distance from the entrance, and A is the cross section at location x. Except in the case of Fernandina Harbor, Fla., the entrance cross sections are greater than in the rest of the channel. At Fernandina material is deposited in the inlet entrance channel by the contracted flood currents, and the ebb currents are not strong enough to clean the channel satisfactorily.

Another example of an improved inlet is Grays Harbor, Wash., on the Pacific coast (Fig. 8(a) and 8(b)). To protect the entrance from shoaling (predominant littoral drift is to the south) a south jetty was built during the period from 1898 to 1902 and north jetty was added during the years from 1907 to 1916. These are convergent in the direction of the entrance, and have improved the situation considerably with respect to navigation. Although a new bar has developed in front of the new entrance and outside of the jetties, a stable navigation channel has been obtained by annual dredging of the bar. No dredging in the outer bar has been required since 1942. Unfortunately, the improvement of the harbor has created a serious erosion problem at Point Chehalis, near the east end of the southern jetty. This problem has not yet been solved.

In the case of the Thyboroen Inlet in Denmark a great number of groins were built as inlet protection. Dredging work on the outer bar was unsatisfactory. When major dredging operations were undertaken on the bay shoals the situation improved and a jetty constructed out over the outer bar on the updrift side of the inlet further improved the situation.

The problem of avoiding difficulties from sand deposits apparently can be solved, partly or wholly, in two different ways:

1. By dredging a nonscouring channel, the tidal prism of which is too small to maintain the cross-sectional area, so that only low-current velocity occurs

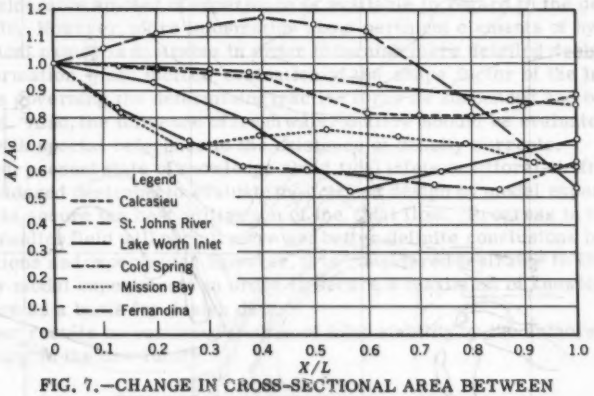


FIG. 7.—CHANGE IN CROSS-SECTIONAL AREA BETWEEN TWO PARALLEL JETTIES

in the inlet channel. Part of the cross section in this way functions as a sand trap for littoral-drift deposits. An example of this is San Diego Harbor, Calif. The nonscouring channel must be characterized as a good, but also expensive solution. However, high initial costs may be justified by more stability and less maintenance. But a nonscouring channel cannot be used in all cases. Special conditions such as a comparatively small tidal prism must be available. Needless to say, the more important the inlet from an economic point of view, the more justified the development of a nonscouring channel.

2. By model studies. Numerous model studies of harbor and inlet problems have been made. The purpose of these studies has always been to examine or check the design more closely. The importance of such studies is to assure the highest possible benefit from the tidal flow through the inlet by giving the inlet and bay channel and the protective jetties the best configuration and cross sections for the purpose. Such studies can be carried out with fixed as well as movable beds. In the latter case littoral-drift experiments are normally included so that the influence of the jetties on the longshore drift can be investigated at the same time and the jetties designed accordingly.

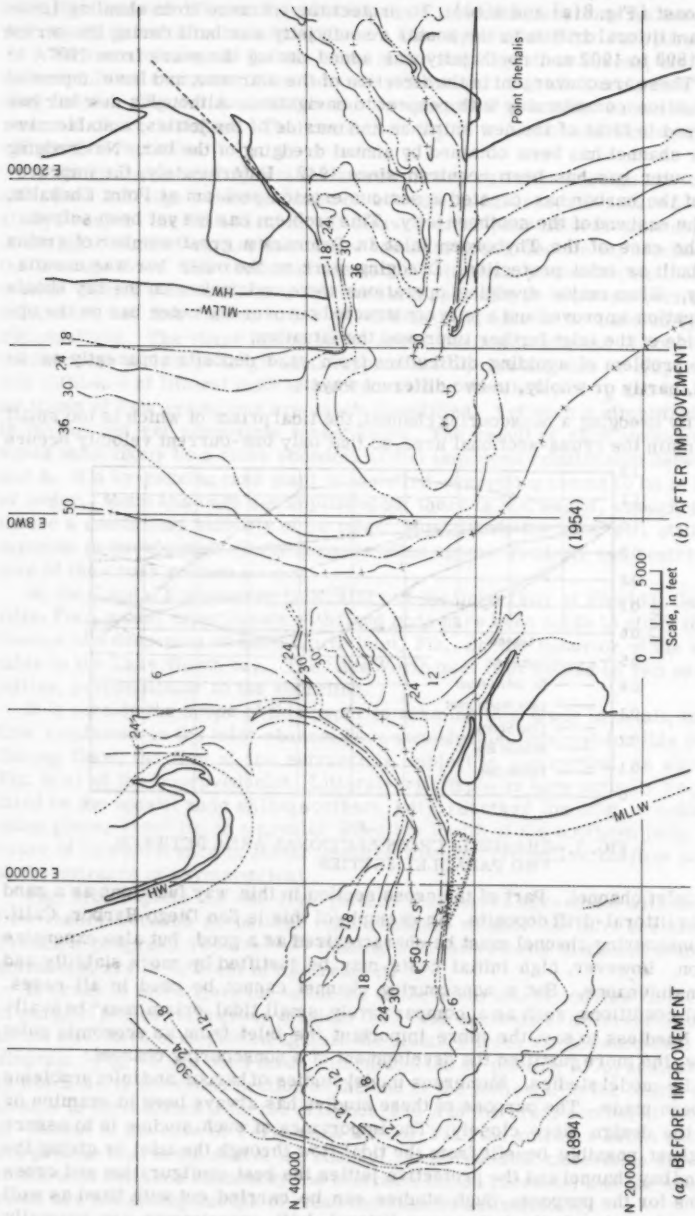


FIG. 8.—IMPROVEMENT OF GRAYS HARBOR

A considerable amount of experience is available and in some cases model experiments function primarily as a check on the design. Meanwhile, the experienced coastal engineer knows that one can never be certain of the behavior of tidal inlets on littoral-drift coasts. For this reason, they often prefer to let field surveys and model studies provide a maximum amount of information. The cost of such experiments is usually so low that there is little or no economic justification for omitting them. The time factor involved in a model study should not be of any great importance when high costs are involved.

Examples of such studies are not as numerous in the United States where less opportunity has been given for such experiments as elsewhere. The Absecon Inlet study by the Corps of Engineers, U.S. Dept. of the Army, Philadelphia District, provided a number of interesting results. The best-known model experiments of this nature have been the Dutch experiments with the harbors of Abidjan, Lagos, and Ada on the west coast of Africa. Similar experiments are presently in progress in England, Holland, France, India, Denmark, and at several other places in the world. It is believed that any cost involved in these studies will eventually pay highly satisfactory dividends.

CONCLUSIONS

A considerable amount of experience is available in regard to the design of tidal inlets. However, more information about pertinent elements of hydraulic and physical nature is desirable in order to furnish more detailed design data. Such information must include evaluation of the shape factor of the inlet and of factors governing the determining tractive force as suspended and bed-load materials. Also, the influence of freshwater outflow should be evaluated more closely with special reference to the existence of density currents.

With our present state of knowledge about tidal inlets on littoral-drift coasts, it is considered desirable to evaluate the detailed design by model experiments in order to secure the best utilization of the tidal flow. Progress in the tidal inlet hydraulics field will permit more and better definite conclusions based on computations and experience. However, it is considered desirable to check the design by model experiments in order to secure a maximum of knowledge and experience as a basis for design data.

Further results on continued studies of inlet stability by the authors will be forthcoming in the new future.

ACKNOWLEDGMENTS

The greatest part of the work mentioned herein was made on a contract between the Tidal Hydraulics Committee, Corps of Engineers (Beach Erosion Board), U.S. Dept. of the Army, and the Coastal Engineering Laboratory of the University of Florida.

Valuable information on existing data on tidal inlets has been furnished by Richard O. Eaton, F. ASCE, Chief Engineer, Beach Erosion Board; Clarence F. Wicker, F. ASCE, Chief Engineer, Corps of Engineers, Joseph W. Johnson, F. ASCE, University of California, and by several districts of the Corps of Engineers on the behalf of the Tidal Hydraulics Committee of the Corps of Engineers. Data from abroad have been furnished by the Royal Dutch Board of Maritime Works (Rijkswaterstaat), Chief Engineer Jon Schijf; Under-State Secretary Carlos C. Abecasis, Ministerio Do Ultramar, Portugal; and District Engineer Johannes Beck, the Royal Danish Board of Maritime Works.

APPENDIX. NOTATION

A = cross-sectional area;

B = bottom composition or soil condition of bed;

b = breadth or width;

C = Chezy coefficient;

D = diameter of particles;

d = depth of water;

d_2 = 50% diameter of sediment particle;

f = silt factor;

H = elevation of water level;

2h = tidal range;

K = coefficient of filling or repletion;

k = linearization coefficient; ratio factor;

M = average amount of littoral drift / amount of time;

m = a littoral drift deposit in a specific area.

P = wetted perimeter (not including wetted surface);

Q = flow;

Q_m = maximum discharge of flow;

Q_s = transport of sand

Qu = fresh water discharge;

q_s = volume of sediment transported as bed-load;

R = hydraulic radius;

S = slope of water surface;

T = tidal period;

F_b = bed-factor

F_s = side-factor

t = time;

v = mean speed of flow;

v_m = maximum velocity;

v_o = critical velocity from standpoint of silting;

W = width of channel;

W_a = nondefined factor describing the influence of wave action;

x = distance along channel;

a = amount of contraction;

β = shape factor of gorge;

γ = specific weight;

κ = rate of converging

Δ = area of the bay;

ϵ = factor in ratio of tractive force required to start motion on the sloping sides to that force required to start motion on a level surface;

θ = phase angle $\frac{t}{T} \cdot 2\pi$;

θ_1 = angle of repose of material;

ρ = specific density;

ν = kinematic viscosity;

τ = mean value of shear stress on channel bottom;

ϕ = angle of side slope; and

Ω = tidal prism.

DISCUSSION

ROBERT E. HICKSON,[31] F. ASCE.—The subject the authors have presented in their paper is a most interesting one. The problems are in many cases not susceptible to solution with the certainty and accuracy that other hydraulic problems may be solved. As stated, there are involved "ten to twenty or more variables" plus many combinations of these.

The authors examine inlets at the mouths of rivers and others that are openings through barrier bars or spits built generally be littoral currents, wave action, or combinations of these factors. The controlling influences in the two general cases are very different, especially where the river flow is relatively large.

This discussion and data submitted will be related principally to the cases affected by river flow, with which the writer has had more experience.

In the case of upland freshwater flow and a substantial tidal range, the discharge of the river flow to the sea is stopped entirely during a major part of the flood-tide phase. Then, during the succeeding ebb, the outflow of fresh water has to be nearly double the headwater flow of the river to make up for the time lost during the flood-tide phase. Where the river flow constitutes a considerable part of the prism to be discharged, the ebb flow and velocities accordingly exceed those of the flood flow by substantial amounts. Another consideration is that in cases of the mixed type of tide with large diurnal inequality the maximum outflow and tidal prism discharged is on the great ebb

[31] U.S. Army Engr. Retired, Portland, Ore.; formerly member of Committee on Tidal Hydraulics.

running down to the lower low, following the higher high tide. This is characteristic of the North Pacific coast tides, and others.

The density current prevailing in the inlet for an hour or two at low-water turn of the tide also introduces a complication making mathematical solution more difficult.

Observations were made during a comprehensive current survey[32] at the mouth of the Columbia River near the "gorge" section in 1932, at three different stages of the river (low, intermediate, and high). Velocity measurements

TABLE 2.—MEAN VELOCITIES IN SECTION OF COLUMBIA RIVER AT CLATSOP SPIT.

River Stage (1)	Month (2)	Number of Tides (3)	Velocities in feet per second	
			Range (4)	Average (5)
Low;	September			
Ebbs		7	4.35 to 5.39	4.85
Floods		7	4.09 to 4.96	4.51
Intermediate;	April			
Ebbs		8	4.48 to 5.65	5.06
Floods		8	3.38 to 4.12	3.85
High;	May-June			
Ebbs		17	4.57 to 7.20	5.58
Floods		16	1.95 to 4.32	3.36

TABLE 3.—PREVALENCE OF VARIOUS BOTTOM[a] VELOCITIES DURING RIVER STAGES.

River Stage (1)	Percentages of Times in Excess of Various Velocities			
	+ 1 fps (2)	+ 2 fps (3)	+ 3 fps (4)	+ 4 fps (5)
Low;				
Ebbs	37.6	19.8	3.3	0.0
Floods	40.2	22.0	4.5	0.4
Intermediate;				
Ebbs	36.8	18.2	2.3	0.2
Floods	34.0	16.3	2.3	1.0
High;				
Ebbs	44.6	25.5	9.0	3.5
Floods	31.2	14.5	2.5	0.0

[a] Velocities measured at 9/10 depth.

were made at five points in the verticles, at five boat stations in the section, every 20 min, for periods of several days for each river stage.

The following tables are taken from this report. Table 2 covers maximum, minimum, and mean velocities at the three river stages on ebb and flood tides, and Table 3 shows percentages of tine various bottom velocities prevailed during the three river stages. Fig. 9 shows graphically how the flood and ebb bottom velocities were affected by the variations in headwater flow for 5%, 10%, and 40% of the total time of observations. The mean tidal range at 120,000

[32] "Columbia River Current Survey 1932-33," report made by U. S. Dist. Engr. to Chief of Engrs.

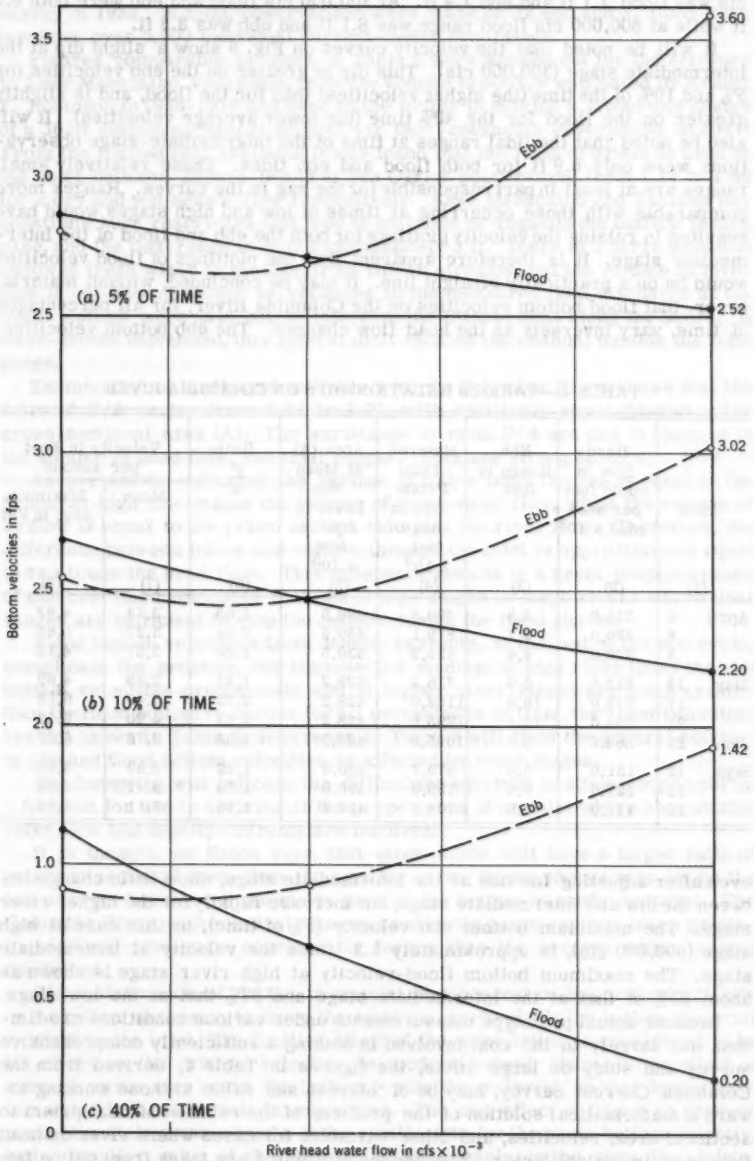


FIG. 9.—RELATIONSHIPS AT MOUTH OF COLUMBIA RIVER

cfs was flood 7.1 ft and ebb 7.4 ft. At 300,000 cfs flood and ebb were both 6.9 ft while at 600,000 cfs flood range was 8.1 ft and ebb was 8.5 ft.

It will be noted that the velocity curves on Fig. 9 show a slight dip at the intermediate stage (300,000 cfs). This dip is greater on the ebb velocities for 5% and 10% of the time (the higher velocities) than for the flood, and is slightly greater on the flood for the 40% time (the lower average velocities). It will also be noted that the tidal ranges at time of the intermediate-stage observations were only 6.9 ft for both flood and ebb tides. These relatively small ranges are at least in part responsible for the sag in the curves. Ranges more comparable with those occurring at times of low and high stages would have resulted in raising the velocity plottings for both the ebb and flood of the intermediate stage. It is therefore apparent that the plottings of flood velocities would be on a practically straight line. It may be concluded, without material error, that flood bottom velocities on the Columbia River, for all percentages of time, vary inversely as the head flow changes. The ebb bottom velocities,

TABLE 4.—VARIOUS RELATIONSHIPS ON COLUMBIA RIVER

Date 1932		Head flow in cubic feet per second x 10^3	Ebb Range in feet	Metered Tidal Prism (P) in Acre feet x 10^3	Area (A) at Mean Sea Level in square feet x 10^3	Ratio $\frac{P}{A}$	Velocity in Feet per second	
							Mean	Maximum Avg. in Vert.
(1)		(2)	(3)	(4)	(5)	(6)	(7)	(8)
April	6	316.0	5.8	709.8	430.5	1.65	3.14	4.92
	8	320.0	8.7	879.1	430.5	2.04	3.27	5.65
	8	320.0	4.4	535.2	430.5	1.24	2.57	4.12
May	14	512.0	5.0	776.3	428.2	1.83	2.89	4.62
	17	579.0	10.0	1152.0	428.2	2.70	3.49	6.12
	21	554.0	12.1	1295.8	428.2	3.03	4.20	6.52
June	22	564.0	9.2	1095.9	428.2	2.55	3.75	6.27
Sept.	12	131.0	5.3	579.7	450.0	1.29	2.80	4.35
	13	127.0	8.8	789.0	450.0	1.75	3.41	4.99
	15	121.0	7.9	704.5	450.0	1.56	3.11	4.74

even after adjusting for tide at the intermediate stage, show little change between the low and intermediate stage, but increase rapidly for the higher river stage. The maximum bottom ebb velocity (5% of time), in this case at high stage (600,000 cfs), is approximately 1.3 times the velocity at intermediate stage. The maximum bottom flood-velocity at high river stage is shown as about 92% of that at the intermediate stage and 87% that at the low stage.

Because actual prototype measurements under various conditions are limited, due largely to the cost involved in making a sufficiently comprehensive survey and study on large inlets, the figures in Table 4, derived from the Columbia Current Survey, may be of interest and value to those working toward a mathematical solution of the problem of the relation of tidal prism to sectional area, velocities, and other variables for cases where river or head flow is an important factor. The figures of Table 4 are taken from only a few

of the observations made in April, May, June, and September in the current-survey of 1932. In total, observations were made on 32 ebb and 31 flood tides involving over 5,600 individual current-meter recordings.

Figures comparable to those in Table 4 were worked out for the entrance to Lake Maracaibo, Venezuela, from the volume of outflow estimated by Ernest F. Robinson in 1938-1939 and used by the writer in making a layout and design of a 36-ft entrance-channel project for the Venezuelan government in 1947. From the limited data available it was found that the ratio of prism to area in the inlet between Zapara Island at San Carlos point ranged from 1.23 to 1.86 for a dry and wet season flow respectively. Lake Maracaibo and Tablazo Bay constitute huge reservoirs that tend to stabilize or regulate the outflow in this case, and the tidal range is only approximately 3 ft. There is a large seasonal inflow of fresh water to the lake, from fifteen streams, but the volume of river flow is not known, except as reflected in the measured tidal discharge at the inlet. Jetties were laid out to intercept the littoral drift along the shore. A wave-driven movement, this littoral drift shoaled the channel outside the inlet gorge.

Examination of the figures in Table 4 for the Columbia River shows that the ratio of P/A varies from 1.24 to 3.03, with relatively small changes in the cross-sectional area (A). The variations in ratio P/A are due to changes in the volume of head flow, and tidal ranges. Both are strong factors.

As previously indicated, the volume of inflow from the sea is equal to the prism at high tide minus the volume of river head flow, while the volume of outflow is equal to the prism at high tide plus the river flow. Therefore, the difference between inflow and outflow through the inlet is approximately equal to two times the head flow. This difference results in a great preponderance of ebb over flood velocities at times of high stages in large rivers where tidal ranges are sufficient to stop the outflow during the flood phase.

Flood bottom velocities from density currents, at the last of the ebb cycle, complicate the problem, but because for medium to high river flows the ebb bottom velocities predominate and at higher river stages are much greater than the flood bottom velocities for all percentages of time, the flood velocities are not shown in Table 4. Reference to Table 3 will show the general relation of ebb and flood bottom velocities as affected by river stages.

The foregoing will indicate the difficulties involved in attempting to set up a formula for use in arriving at the proper area of an inlet where appreciable river flow and density currents are involved.

It is thought, as Eaton says, that large inlets will have a larger ratio of prism to sectional area, than the smaller ones. Rocky shores may not be the full answer, however, if the major part of the bottom is sandy material. The Columbia River, with relatively coarse sand in the gorge section, has a prism-to-sectional-area ratio considerably larger than the average under normal conditions.

The maintenance of depths in an inlet is dependent on the critical velocity on the bottom necessary to move the material, particularly the bottom material existent in the inlet. The limiting effect of the wave action is considered to be its effect on the critical velocity. In moderate-depth channels the effect of average waves may reach the bottom to stir the material, so that lesser bottom velocities will result in movement. The end effect of this is to produce proportionately greater depths in the small inlets for the same bottom velocity, and a smaller value of the ratio P/A. Conversely, in the very deep inlets, normal wave action may not reach the bottom to stir the materials, thus re-

quiring a higher bottom velocity and a smaller section for stability. This agrees with the authors' thoughts on this subject. If in large deep channels, the ratio of bottom velocity to the mean velocity (V_o/V_m) is less than for smaller, shallower channels, a condition of equilibrium requires that P/A be greater for the larger deeper inlets, or that the sectional area be relatively smaller.

Reference to Table 4 shows the effects of high head flow in the Columbia River as well as large tidal ranges on the ratio of P/A. It also shows the effect of these on mean velocities in the gorge section and the maximum average in any vertical (6.52 fps). The maximum (at peak of ebb) measured discharge on other tides was 3,065,000 cfs with a maximum average in a vertical of 7.2 fps. Peak measured velocity near the surface was 12.25 fps.

Using the O'Brien formula with prism measured on September 13, 1932 gives a cross section in fair agreement with the prototype. The ratio P/A under these conditions was 1.75. Under other conditions of river flow and tidal ranges the ratio varied widely as previously stated and shown.

The curves of Fig. 7 show graphically that the fundamental equation $Q = AV$ holds for inlet channels as well as for rivers. Contrary to this, it is known that in earlier times many engineers laid down the controlling jetties with a convergence toward the sea end. Such a layout often leads to trouble if the convergence is great, as the inner channel is then largely uncontrolled. It meanders out of the desired alinement, and shoals as a result of excessive width, or develops deep water at a location not satisfactory to navigation, with a shoal where the channel should be.

This subject of inlet size and maintenance is a most interesting one and much has been gained from studies of the somewhat limited prototype data presently available. Existing channels developed by natural flow over a long period of years, in which time the effects of all the contending forces have been integrated by nature as shown by surveys extending over many years, furnish compelling evidence as to what may be expected under the circumstances and conditions in any case. This evidence should be fully recognized and evaluated.

Every waterway is a problem in itself, differing from others in some respects. While these differences are not always apparent, some of them may be vital to the problem at hand. The engineer must, therefore, take into consideration indicated answers nature may have provided.

The authors are to be commended for the comprehensive analysis and presentation made of this complex subject, and it is hoped that the foregoing discussion and data submitted may add something toward the solutions desired.

PER BRUNN,[33] F. ASCE, and FRANS GERRITSEN.[34]—The problem of stability of tidal inlets includes, as stated by the writers, many factors that may be permitted in different ways. In regard to the two problems named by Mr. Hickson, the Columbia River and the channel that connects Lake Maracaibo with the Gulf of Venezuela, it is obvious that such conditions cannot easily be included in a "formula." What is being attempted in studying these problems, therefore, is to analyze and try to understand the simple problems first. Before this has given results, no chance exists for an understanding of the more difficult problems.

---

[33] Director, Coastal Engrg. Lab., Univ. of Florida, Gainesville, Fla.
[34] Research Engr., Coastal Engrg. Lab., Univ. of Florida, Gainesville, Fla.

In his commentary Mr. Hickson illustrates the variation in ratio factor between the tidal prism and the cross section for the Columbia River under various river discharge conditions (head flow). It is interesting to note that a similar variation in the value of the ratio factor exists for tidal inlets without head flow, but with a variation in tidal conditions in the sea. Examples of such inlets can be found on the Florida gulf coast where the tide is a mixture of diurnal and semi-diurnal. In all such cases the analysis should be based on the time history of the shear stress along the wetted perimeter of the gorge. The following definition of τ_s may be practical:

$$\tau_s = \frac{1}{t_2 - t_1} \int_{t_1}^{t_2} |\tau| \, dt \quad \ldots\ldots\ldots\ldots (22)$$

The time interval $t_2 - t_1$ should be long enough for profile adjustment. In determining τ_s from the preceding equation it should be remembered that the shear stress at the bottom is proportional to the square of the bottom velocity, that has to be known.

For practical reasons the writers, in line with O'Brien's approach of 1931, assumed the mean spring tide conditions to give a close approximation to the determining values.

Even in the complex cases it is considered proper to the problem of stability in terms of the forces exerted by the flow on the bottom. Otherwise a rational understanding cannot possibly be achieved.

In case of rivers the difference between bottom velocities during ebb and during flood may necessitate special treatment of the case, but bottom shear stresses, being the direct cause for transport of bottom material, will still determine the stability of the bottom whether or not they are caused by salt, brackish, or fresh water.

In regard to the channel at Venezuela, the water-body between the bar at the Gulf of Venezuela and the Strait of Maracaibo which is the entrance to the main body of the lake, is called Tablazo Bay. Tidal and current observations have demonstrated that practically all of the water that causes the tide to rise and fall in Tablazo Bay may come from the Strait of Maracaibo, rather than from the Gulf of Venezuela which, in turn, means that a nodal point for the tidal current exists someplace in Tablazo Bay. Perhaps this nodal point can be considered as a node for a seiche in Lake Maracaibo. The existence of density currents is also clearly demonstrated in the Strait of Maracaibo where salt water inflow is predominant at greater depths and fresh water outflow in the upper layers. In the dry season the flow is mainly lakeward, while in the rainy season it is mainly seaward. The average flow is seaward for nine months and lakeward for three months. In a case such as this, the stability is still determined by shear stresses, but they have to be measured under the actual current conditions depending on a variety of factors that have no simple relation to the actual tidal prism and must count on the existence of density currents also.

The most important result of the writers' recent studies is the determination that the tidal prism Ω should be replaced by the maximum flow Q_m. Again, in determining the value of Q_m, the time history of the flow should be considered during a period long enough to allow adjustment of the profile to the actual flow conditions. Proper values for τ_s should be determined with different sediment load, waves, bottom material characteristics, and so forth.

AMERICAN SOCIETY OF CIVIL ENGINEERS

Founded November 5, 1852

TRANSACTIONS

Paper No. 3059

DELTA PROJECT

A SYMPOSIUM

PAGE

GENERALITIES ON COASTAL PROCESSES AND PROTECTION
By Johannes B. Schijf 1267
Discussion:
By Richard Silvester 1278
Johannes B. Schijf 1279

TIDAL COMPUTATIONS IN COASTAL AREAS
By J. J. Dronkers 1281

HYDRAULIC INVESTIGATIONS FOR THE DELTA PROJECT
By H. A. Ferguson 1290

DELTA PROJECT

GENERALITIES ON COASTAL PROCESSES AND PROTECTION

By Johannes B. Schijf[1]

With Discussion by Messrs. Richard Silvester; and Johannes B. Schijf

SYNOPSIS

The engineering basis of coastal protection is examined in general with some emphasis on experience on the seacoast of the Netherlands. The paper supports a shift in the old philosophy of protection by groins and seawalls to a new philosophy of protection by sand fill.

INTRODUCTION

Never before in history has the engineer had such a widespread interest in coastlines, both as research worker and as construction worker.

Everywhere, around the oceans of the world, problems of deterioration of beaches and other forms of erosion are encountered. One would think that a world-wide peak of coastal erosion has set in. There is no reason to believe that the sea and the wind have grown so much more agressive. The cause is not to be found there, but in the activities of mankind itself.

Until recently nobody had much interest in the major part of the world's coasts. There was interest only in the coasts of a few European countries, in particular those around the North Sea, that have been relatively densely populated for a long time already. However, in the United States and elsewhere the potential of the beaches for recreation has been utilized on a large scale, involving huge capital investment in the immediate vicinity of the sea. Also, more harbors are being established and extended on behalf of industry and trade, highways and railroads and other materializations of human activity in the shape of site-bound investments appear in an increasing rate along and close behind the shore.

Perhaps the most characteristic element of a sandy coast is its mobility. Even if a coast is in equilibrium (the meaning of this term will be examined further on), this does not imply immobility. Nature applies her variable forces to maintain an equilibrium in the sense of a more or less regular fluctuation between certain boundaries, that are usually not very clearly defined.

Note.—Published, essentially as printed here, in March, 1959, in the Journal of the Waterways and Harbors Division, as Proceedings Paper 1976. Positions and titles given are those in effect when the paper or discussion was approved for publication in Transactions.

[1] Chief Engr., Dir., Water Resources and Hydraulic Research, the Rijkswaterstaat, s-Gravenhage, the Netherlands.

A section of beach may accrete temporarily and thereafter begin to degrade again. Meanwhile in the next section the reverse may take place. River mouths and lagoon outlets wander some distance and return or begin a new cycle. Spits appear, grow, and disappear again. Islets are eroded away at one end and grow at the other end, and, by this process, travel along the coast.

As long as no one lives and works in the zone in which these processes develop, the problem of erosion does not arise. Even if a native population gains its living by fishing, dwelling in huts of single construction, easy to remove or to replace, nothing of an alarming nature is happening. The situation becomes quite different, however, as soon as the area is developed and capital is invested in site-bound establishments. When highways and railroads are constructed, bridges and other expensive works erected, and solid buildings for a multitude of purposes appear, every infringement, even if temporary, endangering these investments is a menace and a fresh erosion problem has arisen. Coastal erosion is an accompaniment of civilization.

That is not all. We cannot afford to let our property get lost without taking action. The coast has to be protected against erosion. Unfortunately, in all too many cases the protective measures have done more harm than good.

It is quite easy to be aware of errors made in the design and construction of coastal protection works. It is much more difficult, however, to indicate the right course. The reason is that as yet our knowledge of the physical processes in action on the coast is very incomplete. Even in a qualitative sense, in some aspects, our ideas on the manner in which currents and waves, separately and combined, set the shore material in motion and transport it are rather vague, while in the quantitative sense the adequate methods are still in their infancy. In many cases it is not easy to even determine if a stretch of coast can be said to be in equilibrium or not.

During the past quarter of a century the understanding of coastal processes has advanced considerably. It need not be surprising that the activity in this sphere, apart from those areas where coastal protection has been practiced for a long time already, is particularly abundant in a few countries where the maintenance of the coast has grown to be imperative recently and where experience is young. The United States is one of these countries.

The Notion of Equilibrium.—Is it possible to apply the term equilibrium on a sandy shore of which the loose elements are constantly in motion under the action of currents and waves? It cannot be done in the strict sense, but it becomes feasible if we think in terms of a dynamic equilibrium, a quasi-equilibrium. In order to probe this point further, it is necessary first of all to distinguish between the movement of sand perpendicular to and along the coast. Many of the difficulties and mishaps experienced in coastal defense work are attributable to a lack of appreciation of this distinction.

GENERALITIES TO BE CONSIDERED

Coasts without Littoral Drift.—The first consideration is the necessity to distinguish between the movement of sand perpendicular to and along the coast. Many of the difficulties and mishaps experienced in coastal defense work are attributable to a lack of appreciation of this distinction. First, consider the behavior of straight beaches and shores under the impact of regular waves approaching at a 90° angle and in the absence of other agents that could produce

a lateral drift. Very valuable studies have been made on the equilibrium profiles associated with this mechanism. Of course, the conception of equilibrium in this connection has a relative significance, because at no time is the profile actually at rest. The materials from which it is built are not in a stable position, but they are continuously or intermittently in motion. The term "equilibrium" should be understood in this sense to mean that during regular intervals the profile repeats approximately the same sequence of identical shapes, and as long as the waves are absolutely regular, these shapes do not diverge greatly. However, outside of the laboratory such a regular wave action does not exist. In nature, at best, the wave-field has a constant spectrum. In that case, engineers may employ the term "equilibrium profile," because there is still a certain sequence that will be regularly repeated. But the deviations between the extremes will be greater and will cover longer periods, associated with the character of the wave spectrum. Such a state of relative equilibrium will always remain a temporary affair, that might last for an appreciable period on a tideless coast under the sway of a regular ocean-swell, but on other coasts, where the water-level rises and falls and wind-waves of less venerable age are dominant, it will never really materialize.

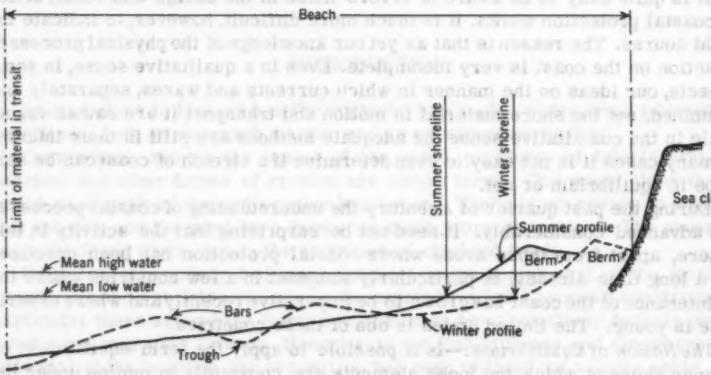


FIG. 1.—SEASONAL VARIATIONS OF A BEACH PROFILE

The limits of the conception of equilibrium may be further extended to cover a succession of tidal cycles, and even a succession of recurring cycles of identical of at least greatly identical sea-conditions. One type of a recurring cycle of sea-conditions brings the seasonal variations that on certain coasts show a fairly ture "repeatability" (Fig. 1). Of course the longer the period of the cycle and the greater the variations in sea-conditions, the larger also are the deviations between the extreme profiles of the equilibrium cycle. In the seasonal case, this difference is between the summer and winter profiles.[2]

On other coasts, particularly those of the North Sea and similar seas, there are even important variations from one year to another. The effect of an individual winter season on these coasts is fairly well characterized by the number and severity of the gales occurring during that winter.

The effect of the gales not only depends on the intensity of the wave-action they engender, but perhaps mainly on the rise in sea level that accompanies

[2] "Characteristics of Natural Beaches," by W. N. Bascom, Proceedings, 4th Conference on Coastal Engrg., Council on Wave Research, Engrg. Foundation, 1954, Ch. 1.

them. Thereby they not only erode the beach, but often even erode the front slope of the dunes. In this way during a single gale, such as that of February 1, 1953, in the North Sea, a section of the dune of some 20 mi to 30 mi (33 ft to 66 ft) can be swept away and it may take a series of years with relatively quiet winters to build it up again (Fig. 2). Still, in the absence of lateral drift and provided no material gets lost, this may eventually happen. Therefore, even in conditions such as these, it is still possible to employ the conception of equilibrium although the deviations between the extreme profiles may be considerable and a more or less periodic cycle may not be in evidence. There is still an equilibrium in the sense that no lasting erosion takes place and that more-or-less identical profiles appear again and again, although they are by no means stable.

For the maintenance of such an equilibrium the natural forces require space, and a stock of sand. The space required is limited by the two extreme positions of the beach and dune front, and the stock of sand is being shifted to and fro continuously within this zone (Fig. 3). The only thing to guard against is hindering the play of the natural forces. Construction should be kept out of this zone and the buffer stock of sand should be left alone.

It is clear that in the absence of a resulting lateral transport, groins or other structures designed for or having the effect of impeding such transport have no meaning. On the other hand they are also rather harmless.

Constructions that aim at the prevention of the shifting of sand seaward are also useless and they can easily do much harm. It may, for instance, be hard to withstand the urge of (and perhaps the clamoring for) protecting the foot of the dunes from further recession after a heavy gale, but, nevertheless, it is much better left undone. At best such a protection will not hinder the natural forces of recuperation, which means that the structure will soon be covered with sand and cannot be proudly pointed at by the designer. In many cases, however, they will hinder the natural process of rebuilding of the beach and the dunes with the result that further erosion will follow. Of course a policy of letting nature take its course cannot always be pursued. There are cases where only a dangerously narrow ridge of dune is left and the possibility of a further attack before a new phase of building-up has set in, has to be guarded against or where very valuable property is directly endangered. The protective works in such cases, however, should be designed with extreme care. They must be sloping and, in general, should be shaped so as to avoid reflection or excessive turbulence.

An alternative to protective works in these cases is the artificial supply of sand to the endangered spot. The sand may be placed either in front of or, as is preferable, behind the ridge of dune that needs reinforcing. This procedure is preferable to a protective structure because it does not involve the same risks in regard to worsening the erosive action of the waves. No harm can be done by this method whereas harm may be done by building fixed structures.

It might also be tempting to try to consolidate the dune-foot in a forward position after a period of advance. This would not actually be coastal defense, but would rather come under the heading of land reclamation. Such a temptation should also be disregarded, however, because no real advantage can be gained from it and the structures for such a purpose will do more harm than good. The possible harmful effect of such a structure will be felt particularly on the adjoining stretches. It has to be borne in mind that, along the coast, gain in one place practically always means loss in another place.

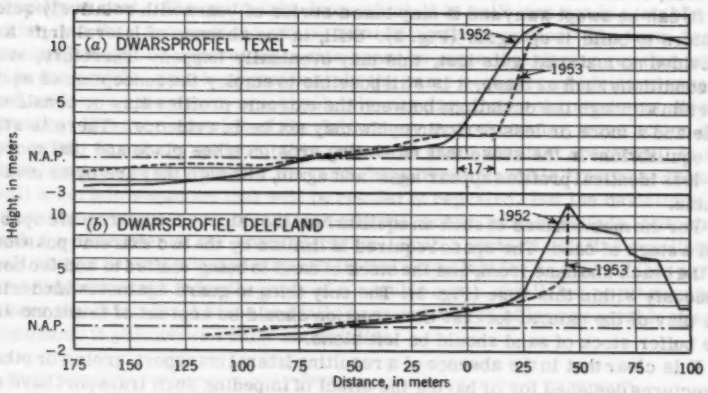


FIG. 2.—DUNE EROSION AFTER 1953 GALE

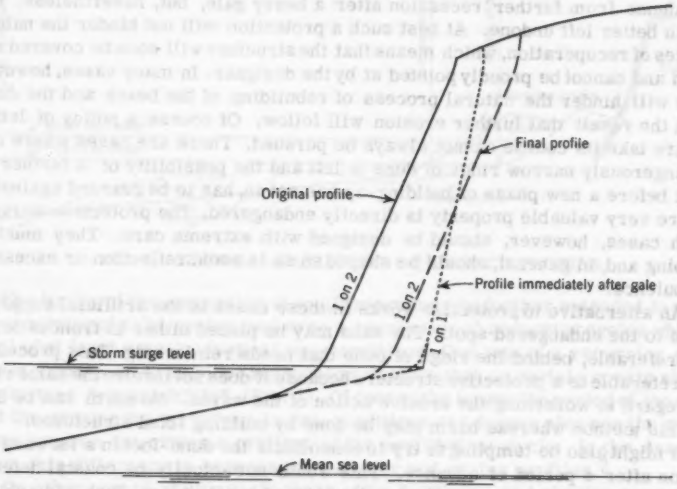


FIG. 3.—RELATIONSHIP BETWEEN STORM SURGE LEVEL AND DUNE EROSION

Another conclusion is that within this buffer zone structures or buildings for other purposes should not be allowed. In spite of this, many otherwise clear-headed people with an enthusiasm and a tenacity worthy of a far better cause, strive to encumber the beach and the front and crest of the dunes with promenades, hotels, and other buildings, or with gun emplacements and pillboxes. In too many cases the results are not only disastrous to the owners (Fig. 4) but also dangerous for the coast. When opposing such projects, one is confronted with the difficulty of defining the width of the buffer zone to be kept clear. This is particularly true on a coast where the fluctuations extend over a number of years and are fairly large and irregular.

From recent studies in the Netherlands it appears that the erosion caused by a heavy gale is closely related to the mean sea level accompanying the gale.



FIG. 4.—REMNANTS OF THE ATLANTIC WALL AFTER EROSION

The dune-foot will recede approximately to the point of intersection of this level with the line continuing the slope of the higher part of the beach. Afterwards, the crest line of the dune will recede still further, because--in the conditions prevailing in the Netherlands--the dune front will initially assume a slope of 1-on-1, but will thereafter gradually adjust itself to an equilibrium slope of 1-on-2 (Fig. 3) through the choosing of a design-gale or succession of several gales, to arrive at the fixation of a limiting line for buildings, and other structures.

Gain or Loss of Sand.—Thus far it has been assumed herein that no material is lost from or supplied to the coast. Even on a stretch of coast without any littoral drift this assumption is not necessarily valid. In particular, when there is deep water fairly close inshore, sand may be lost by dispersion. That is to

say it is lost by being carried seaward, during a phase of erosion, to a depth at which it is out of reach of the waves during the following phase of restoration. On the other hand, when shallows are found offshore, sand may be carried to the coast. In either of these cases a slow but sure general retreat or advance of the entire zone, in which the coastal processes are enacted, will be superimposed on the fluctuations of the profile. A similar effect will be produced by a slow rise or fall of the mean sea level.

When it becomes necessary to counteract a slow but steady erosion of this nature, it is again obvious that the building of groins will be futile. In this case a protection of the dune-foot can, at best, temporarily slow down the process, but in the long run it will aggravate the situation. Short of protecting the entire stretch of shore in question by a continuous breakwater or a series of breakwaters—a very unattractive proposition,—the only effective remedy is an artificial supply of sand to the beach, that in this case would have to be more or less uniformly distributed along its length.

Coast with Littoral Drift.—Thus far, a stretch of coast without any littoral drift has been considered. Of course this is rather an academic proposition, because such stretches are very rare and even if the net drift were zero, it would be the result of alternating periods of drift in one direction or the other. On a coast with a littoral drift, however, the considerations set forth still hold good. The only difference is that if the littoral drift is not in equilibrium, just as in the case of a permanent supply from or loss to offshore regions, a general advance or retreat will be superimposed on the fluctuations of the profile.

Permanent displacement of the coast, either through advance or recession, is generally the result of a decrease or increase in the rate of littoral drift in the sense of its propagation. Barring the consideration that the advance of a coastline may be gained at the cost of depletion somewhere nearby, the engineer is, as a rule, interested in a receding coastline. Therefore, we will limit ourselves to the case of an increasing rate of drift. On a coast where the littoral drift is mainly brought about by wave action, this increasing rate of drift means that the three elements (wave energy, effective angle of incidence of the waves, and supply of sand) are not in harmony. This is necessarily a state of incomplete adjustment, because if the same conditions remain in control long enough, an equilibrium will always be established. It follows that either an equilibrium has not yet been obtained or that, by some agency, an existing state of equilibrium has been disturbed. Thus, it is implied that at least one of the three elements mentioned has been modified. It also follows that, in general, such a stretch of coast cannot be straight, but will present a convex curve.

Several empirical formulas have been proposed more or less tentatively for linking the rate of transport to the wave-energy and the angle of incidence. By imposing appropriate sets of boundary conditions and with the application of some simplifying assumption it is possible to derive[3,4] mathematically certain forms of coastline. It will be observed in passing that the notion of equilibrium has been used by Per Bruun, F. ASCE, in a different sense than in this paper.

In dealing with an eroding coast, the engineer must first ascertain whether the coast is permanently eroding. In many cases the littoral drift has an undulating character,[5] that is to say, the material moves in humps. In that case,

---

[3] "Essai de theorie de l'evolution de formes de rivage en plage de sable et de galets," by R. Pelnard-Considere, IVe Journee de l'Hydraulique, Paris, 1956.

[4] "Coast Stability. Forms of Equilibrium of Coasts with a Littoral Drift," by Per Bruun, Doctoral thesis, Copenhagen, 1954.

[5] "Migrating Sand Waves or Sandlumps, etc.," by Per Bruun, 5th Conference on Coastal Engrg., Council on Wave Research, The Engrg. Foundation, 1955, Ch. 21.

periods of advance will alternate with periods of recession, so that even generally eroding stretches will show a retreat. Such a temporary retreat should not be mistaken as a symptom of a permanent erosion. It may be just another element to be included in a still wider conception of equilibrium, that is, contributing to the magnitude of the fluctuations. Again, as long as it is not absolutely necessary because of threatening danger to the sea-defense, the wise course is not to take measures against it.

If interference should become unavoidable, it should be done by way of an artificial supply of sand or as a direct protection of the dune-foot and certainly not by groins or other structures impeding the littoral drift. Such structures would cause the supply of sand to the downdrift stretch to be decreased with consequences that are possibly far worse than the danger to be averted.

Causes of Erosion.—As has been said, a permanent erosion is a result of a relative lack of supply of sand at the updrift end of the stretch of coast in question. In some cases this can be brought about by natural causes as, for instance, from a decreasing discharge of bed load by a river as a result of modified conditions in its watershed, or because in a deltaic region the distribution of the bed load over different branches has undergone a modification. The cause may have nothing to do with the supply of sand itself, but, due to a gradual climatic change, the wave-energy or the effective angle of incidence may be varying in such a way that the capacity of the drift mechanism has outgrown the supply. Also, tectonic upheavals may be at the origin.

However, in the great majority of erosion problems the world has to cope with today, it is not nature, but mankind that bears the responsibility. Mankind harnesses rivers and bottles up their bed load, thereby depriving the coast of its lawful tribute. Mankind builds breakwaters and harbor moles, and regulates river mouths and inlets, thereby barring the littoral drift; mankind dredges huge quantities of sand and dumps them in the sea or uses them for reclamation and so robs the coast; mankind inflicts unnecessary or badly-designed works of protection along the coasts, thereby in many cases creating excessive turbulence and increasing the eroding action of the waves. And while, on the whole, it is not possible to control the forces of nature working on a coast, the engineer should at least try to control the human forces.

The first thing of course is to refrain from all activity that is not strictly necessary. On former occasions reference has been made to a certain moronic ingenuity that is sometimes let loose on coasts. These things of course should not happen and part of the engineer's task is to see that they do not happen. There remain many other manifestations of human activity that are necessary in this regard. Rivers sometimes have to be regulated, harbor moles have to be constructed and the depths in fairways for navigation have to be maintained. But each time the engineer should realize what the repercussions of this work on the coast will be and try, to the best of existing knowledge, to minimize the effects as far as they are harmful (as they generally are).

Measures Against Erosion.—Even then, the results of much of the engineering activities will be erosion of downdrift stretches of coast for which countermeasures must be taken. Of course, the first step in every case will be to examine the cause of the erosion, and to determine if its effects can be mitigated. In some cases, that will be found possible, as for instance if the littoral drift is cut off by harbor moles or jetties, there is the possibility of bypassing the drift. Or if the natural supply is impoverished by dredging, the spoils can be re-fed to the coast. Generally speaking, the balance between the capacity of

drift mechanism and supply can always be restored by bringing the supply up to the required amount.

A second possibility is reducing the drift mechanism in the established manner of constructing groins. Just how groins should be arranged and constructed has been, and apparently will continue to be a subject of much study and examination. Up till now it has largely been a matter of tradition and experience, in which, apart from the function of the groins as drift-reducing elements, the construction technique and the maintenance problem have played an important part. The engineer will be able to approach the subject more scientifically when a better understanding of the drift mechanism itself has been acquired. This understanding will, no doubt, show that there is no such thing as a universal solution to the problem, but that the shape and arrangement of groins have to be varied according to the local conditions. In any case, they should be groins and not disguised jetties or breakwaters and they should be as low as is compatible with their reducing effect on the drift. Groins that emerge to an imposing height above the beach cut off the windblown drift and so prevent the formation, development, and restoration of dunes. Also, they should, like structures protecting a dune-foot, not give rise to reflection of waves or excessive turbulence. Groins may improve the situation along the stretch of coast in which they are situated and the updrift coast. Along the downdrift coast they necessarily aggravate the deficiency in the supply of drift material.

A great deal of thought and energy has been devoted to the arrangement of the downdrift termination of a group of groins so as to avoid or reduce the harmful effect on the downdrift stretch. It is an illusion that these endeavors should ever be successful, because an accelerated erosion downdrift of a groin system is inevitable if the system serves its purpose well. At best some local effects, such as undercutting or outflanking of the end groin, may be prevented, but the over all result on the downdrift stretch of coast will remain. It will therefore be found that after groins have been introduced on a particular stretch of coast, it will become necessary to extend the system downdrift until the end of the physiographic unit has been reached, unless of course a recession can be tolerated.

Choice Between Artificial Supply and Groins.—A number of factors may enter in the decision if an artificial supply of sand or the construction of groins should be chosen to combat an erosion of this nature. The economic point of view must be considered. Generally speaking, on short stretches the economic factor will favor groins, on long stretches artificial supply will be the cheapest solution. Along the coast of the Netherlands the balance will be at a length of the order of 1 km for every 100,000 cu mi (1/2 mile per 100,000 cu yd) annual supply required, provided that suitable sand can be found in the vicinity. The type and manner of construction of groins to be chosen, the availability and price of materials, and the availability and cost of transport and conveying of suitable sand are among the factors that have their influence on this balance.

A really exhaustive comparative evaluation of costs is possible only if one is concerned with a really limited physiographic unit. If the downdrift boundary is not well-defined, the influence of the groins may be felt even beyond it and may be difficult to assess. On the other hand, provisioning the coast with an adequate supply of sand continues its benefit along the entire coast downdrift from the location of the supply as far as the drift mechanism extends its influence.

An important point in favor of artificial supply is the fact that it does not entail a permanent commitment. Certainly it can do no harm. It can be experi-

mentally adjusted to the requirements of the coast and can even be abandoned and be replaced by a groin system if later considerations should make this appear preferable. Groins, on the other hand, once constructed, are there to stay and to be maintained. If they are badly constructed, they constitute a menace. Although it is possible to modify, lengthen, or shorten them, should the original dimensions not work out satisfactorily, this would involve a difficult and costly undertaking. Therefore, other considerations being equal or perhaps even slightly unequal, it would appear that artificial sand supply is the more natural and more attractive solution.

Evidently, the choice is not always open. On many coasts, especially in Europe, the heritage of past works must be dealt with. Bypassing, or any system of artificial supply, was first suggested at the Navigation Congress in Brussels in 1935. Prior to that time, the universal remedy was the building of groins. It has been left to the United States as a younger country, neither blessed nor handicapped by an ancient tradition in coastal engineering, to introduce artificial supply as a recognized remedy for coastal ailments and to explore its possibilities and its requirements. It appears most probable that artificial supply will become the general procedure in coastal protection, to be replaced by groins or other methods in a dwindling number of special cases.

Channel Erosion.—As a special class of coastal defense problems, in cases in which currents other than wave-induced longshore currents play an important part, an additional factor has to be considered. This is, in general, the case in the vicinity of estuaries and inlets. In these regions continually shifting tidal channels that have a major influence on the shore formations are found. Therefore, a second distinction has to be made that is just as important as the distinction between cases with or without a resulting littoral drift.

When a stretch of shore is endangered because a shifting channel approaches, none of the measures previously cited can be efficacious. As the transporting capacity of a tidal channel easily exceeds many times the capacity of a drift mechanism due to waves, artificial supply can hardly be considered an economic proposition. Groins might have a slight effect, but only if the channel is a very minor one.

A structure designed as an impediment to wave-induced drift cannot serve to control the flow in a tidal channel that may have depths of 20 mi or even more. What is needed in this case is either a longitudinal jetty or a system of transverse jetties, so constructed that they are safe against undercutting and outflanking. When, because of the nearness of the channel to the shore, the beach has become too narrow and the dunes have not sufficient width to be safe, it may become necessary, in addition, to protect the foot of the dunes directly.

As soon as the lateral progress of the channel begins to be checked by the jetties, the channel will deepen and scour around the base of the jetties. Eventually the channel may become considerably deeper than it was as a free channel and thereby necessitate a strengthening of the base of the structures. If transverse jetties are used, they should have well-rounded heads and should not be spaced too far apart in order to limit the scour. Even then they will require constant attention and frequent maintenance.

As long as they are left to themselves, the channels leading to and from tidal inlets usually shift about in a more or less well-ordered and roughly periodic pattern. An individual channel may swing out over quite a distance and then swing back, or, as is more usual, it may gradually shoal and be replaced by a newly-formed channel. The period may in some cases, be fifty years or more. The engineer should always be very watchful before starting any construction

interfering with these movements and take good care not to obstruct a channel when it is near the end of its swing, unless it becomes absolutely necessary to safeguard really valuable interests. It should be given the chance of wandering back again or dying down, because once an obstruction to this natural swing has been constructed and the channel has bitten into it, the natural rhythm will be disturbed and the channel will dig itself in. In some cases it will be possible to help or accelerate a natural development, tending to bring relief to the threatened spot, by a carefully-planned dredging campaign. Dredging against the natural development will always prove an expensive disappointment.

Perhaps, in these cases of channel erosion even more than along a wave-controlled shore, once a fixed structure has been established, it will have to remain functioning. It will, quite probably, have to be extended later on and certainly will have to be looked after continuously.

CONCLUSIONS

It goes without saying that there are any number of intermediate situations, where combinations of the conditions examined previously are in evidence. As this paper deals with general principles only, the possible combinations will not be enlarged upon herein.

The moral of this paper is that in coastal defense one should do as little as possible, in particular as regards construction of fixed structures, and, if one cannot avoid them, design them to do as little harm as possible.

1. If an erosion problem has to be dealt with, first make very sure that it is real, that is to say permanent, erosion and not just a passing eroding phase, which may be expected to be followed by a phase of restoration.
2. Inquire very thoroughly into the first cause of the erosion and see if this can be remedied or mitigated. In cases where human activities are responsible for the erosion, this can often be done. When planning new developments try to design them so as to limit their erosive effects to the utmost. Prevention is better than healing.
3. Study the mechanism of the coast and try to distinguish between the effects of sand displacement perpendicular to the coast, longitudinal drift, and the action of currents.
4. Whenever technically possible and economically feasible, accomplish the remedy by artificial supply rather than by fixed structures.
5. If fixed structures must be made, design them very carefully so that they just fulfill their purpose and have no additional effects, which may make them more harmful than beneficial.

DISCUSSION

RICHARD SILVESTER.[6]—The author is to be commended for drawing attention to the ineffectiveness of groins. The writer has recently come to the same

[6] Senior Lecturer in Civ. Engrg. (Hydraulics), University of Western Australia, Nedlands, Australia.

conclusion[7] although he would not wholeheartedly support the alternative of artificial nourishment that was submitted. The writer would prefer to see the offshore breakwater used more widely. These, floated into position and sunk in echelon fashion, could impede sediment movement over a wide area of the ocean bed. They could even be removable should changing conditions demand. Of course, the same problems of down-coast erosion would arise, but this can be removed to an undeveloped section of coast or the end of a physiographic unit.

The author states, "that in the absence of a resulting lateral transport, groins or other structures designed for or having the effect of impeding such transport have no meaning. On the other hand they are also rather harmless." Although the situation is rather academic, the writer would disagree with the latter sentence because storm conditions could sponsor rip currents more readily in the moon-shaped beaches between the groins than on a plane beach. These currents throw the sand out of reach of the waves or help it to by-pass the groin system.

The author mentions some permanent erosive conditions. Perhaps another condition, in general not fully appreciated, is that occurring at the updrift end of a physiographic unit. Such a situation is a sharp change of direction in a coastline where sediment is being removed from a "cape." The littoral drift diminishes with time as the sand nearest the cape is removed and the waves find it harder to remove the remainder. Downdrift of the cape, where there once was a substantial littoral drift, the coast becomes undernourished. The effect of this may not be exhibited on the foreshore for many years.

The author states, under the heading "Choice Between Artificial Supply and Groins," "An important point in favor of artificial supply is the fact that it does not entail a permanent commitment. It certainly can do no harm." It might be said that groins also may not be a permanent commitment. They can be allowed to silt up or to be undermined like any natural rock outcrop. Certainly reducing them in size is an uneconomical proposition. Artificial nourishment, on the other hand, may do harm by silting up a harbor entrance downdrift of the area. The author would presume that such mismanagement could not occur.

The author states, under the heading "Channel Erosion," "A structure designed as an impediment to wave-induced drift cannot serve to control the flow in a tidal channel that may have depths of 20 mi or more." This seems to imply that sand cannot be transported in these depths unless currents exist which are not associated with wave action. Evidence is available from nature and scaled models to show that sand can be moved in such depths solely by wave action. The mass-transport current and other phenomena associated with the oscillatory motion of the water particles at the ocean bed effect a considerable movement. This all points to the fact that groins have little influence on the total width of ocean bed over which coastal sediment movement takes place.

JOHANNES B. SCHIJF.[8]—The writer wishes to thank Mr. Silvester for his interest. The writer's purpose has been to emphasize the need for a clear understanding of the physical processes active on the coast as a basis for the design of coastal protection works, and in particular the necessity of distinguishing between the effects of transverse and lengthwise displacements of coastal material by waves and the effects of currents.

---

[7] "Engineering Aspects of Coastal Sediment Movement," by R. Silvester, Proceedings Paper 2168, ASCE, September, 1959.

[8] Chief Engr., Dir., Water Resources and Hydraulic Research, the Rijkswaterstaat, 's-Gravenhage.

Mr. Silvester's comments indicate an agreement with the general term of the paper, in the light of which a slightly different emphasis on some matters of detail does not seem to warrant a lengthy discussion on the writer's part.

If the impression has been created that the writer considers groins as ineffective, he wants to correct this. Perhaps it is to be attributed to the numerous instances of indiscriminate use of groins seen. Some of those were probably placed on the assumption that what is useful in one place should be so in another. The writer knows cases where groins are ineffective, where they are effective enough and where they are too effective. The point is not so much if groins are effective or not, but if they are the most effective (and least harmful) means in the given conditions. May we agree in considering them a more permanent commitment than artificial supply?

In spite of the fact that material can be transported by waves and wave-induced currents in depths of 10 or 20 mi, the writer maintains that groins are not the proper type of structure to control the flow in a tidal channel, at least as long as we understand by a groin a rather shallow structure on a gently sloping shore. There is a very marked difference in the scouring action on the tip of a construction of waves and of the eddying flow in a steep-sided tidal channel encroaching on a stretch of coast. This is one of the points the writer has sought to underline in his paper.

TIDAL COMPUTATIONS IN COASTAL AREAS

By J. J. Dronkers[1]

SYNOPSIS

The purpose of this paper is the computation of the tidal motion in shallow coastal waters by means of the so-called harmonic method. This method is relatively simple in application. As an example the propagation of the tide in Tampa Bay on the coast of Florida is examined.

INTRODUCTION

The field of hydraulic engineering in coastal waters, estuaries, and inlets is confronted with the tidal motion and possibly with the propagation of storm surges. The extent of the engineer's interest in the tides is dependent on the size of the structures to be planned.

In order that there be no serious interference with the tidal motion as a whole, it will be sufficient to collect observational data on the existing tide in the design of local structures. The influence of the structure on the local flow pattern can then best be investigated by a model of the local situation.

If, however, a substantial interference with the movement of the tides is contemplated, it will be necessary to thoroughly investigate the mechanism of the tidal motion, in order to correctly predict the effect of the intended interference. For this purpose recourse may be had to computations, to research on a model of the entire estuary, or to an electric analogue.

In the Netherlands all three of these methods are used. As each of the methods have their typical merits and limitations, there are purposes for which one or the other may be more suitable, or in some cases they may complement each other when used in conjunction. No attempt will be made to enter upon a comparative examination of the three methods.

As long as river sections and more or less clearly defined tidal channels are being dealt with (that is to say as long as the path of the flow is determined by the topography) the flow can be regarded as unidimensional for the mathematical treatment. This means that the flow can be described by a set of equations in the x-direction and transverse flow and Coriolis effects can be disregarded.

In the simplest form the continuity equation is

$$\frac{\partial Q}{\partial x} + b \frac{\partial H}{\partial t} = 0 \quad \ldots\ldots\ldots\ldots\ldots\ldots (1)$$

Note.—Published, essentially as printed here, in March, 1959, in the Journal of the Waterways and Harbors Division, as Proceedings Paper 1977. Positions and titles given are those in effect when the paper was approved for publication in Transactions.

[1] Chf. Mathematician of the Rijkswaterstaat, The Hague, The Netherlands.

and the dynamic equation

$$\frac{\partial H}{\partial x} + \frac{1}{A\,g}\frac{\partial Q}{\partial t} + \frac{|Q|\,Q}{C^2\,A^2\,a} = 0 \quad \ldots\ldots\ldots\ldots\ldots (2)$$

in which x is distance along the river, positive upstream; t is time; Q is discharge (with flood positive); H indicates water level above datum; b refers to storing width of water surface; A is the cross-sectional area of the streambed; a is depth below water surface; C is the Chézy coefficient; and g refers to the gradient of gravity. The appropriate boundary and initial conditions have to be added to these equations.

Several methods are available[2] for solving these equations: Direct methods involving numerical integration by finite differences; iteration process; the characteristic method involving integration along characteristics; and harmonic methods involving a Fourier development.

THE HARMONIC METHOD

Determination of the Equations.—In this paper only the harmonic method will be considered. From the practical viewpoint the consideration of two components is sufficient. Then, putting

$$H(x,t) = h_0(x) + h_1(x)\cos\left(w\,t + \phi_1(x)\right) + h_2(x)\cos\left(2\,w\,t + \phi_2(x)\right) \quad .. (3)$$

$$Q(x,t) = q_0 + q_1(x)\cos\left(w\,t + \psi_1(x)\right) + 2\,q_2(x)\cos\left(2\,w\,t + \psi_2(x)\right) \quad .. (4)$$

in which $h_0(x)$ is the mean head above datum; $h_1(x)$ refers to the amplitude of the fundamental tide, namely the diurnal moon tide with period T equals 24 h 50 m or the semi-diurnal moon tide with period 12 h 25 m; $h_2(x)$ indicates the amplitude of the second harmonic tide (in case h_1 is the amplitude of the diurnal tide, h_2 is the amplitude of the semi-diurnal tide; in the other case h_2 is the amplitude of the quart-diurnal tide with period 6 h 12,5 m); q_0 is upland discharge; $q_1(x)$ indicates the amplitude of the discharge curve belonging to the fundamental tide; $q_2(x)$ the amplitude of the discharge curve of the second harmonic tide; $\phi_1(x)$, $\phi_2(x)$, $\psi_1(x)$, and $\psi_2(x)$ refer to the phase angles of the harmonic components; w is the angular frequency of the fundamental tide; $2\,w = 2\pi/T = 0{,}702 \cdot 10^{-4}$ (in seconds) in case of a diurnal tide; $w = 1{,}405 \cdot 10^{-4}$ for a semi-diurnal tide.

This is an approximate method, sufficiently accurate for many cases (in particular when the observational data are incomplete) and relatively easy to carry out.

In regions with a fairly regular tidal motion it is usually unnecessary to consider more than two components. It is not very difficult to compute the propagation of the components separately.

However, the computations become considerably more complicated if the mutual interference of the two components has to be taken into account. This interference arises from the fact that the hydraulic resistance is not linear but quadratic. If, however, the upper-water discharge may be neglected and the amplitudes of the successive components (h_1, h_2) decrease in a sufficiently rapid manner and, moreover, if the range $2\,h_1$ is small with respect to the

[2] "Tidal Computations in Shallow Water," by J. J. Dronkers and J. C. Schönfeld, Proceedings-Separate 714, ASCE, June, 1955.

depth of the river, in the first approximation this interference can be studied in a rather simple way.

The quadratic resistance may be written as

$$|Q|Q = \pm\left[{q_1}^2\cos^2\left(w\,t+\psi_1\right)+{q_2}^2\cos^2\left(2\,w\,t+\psi_2\right)+2\,q_1\,q_2\cos\left(w\,t+\psi_1\right)\cos\left(2\,w\,t+\psi_2\right)\right]$$

$$=\pm\left[\frac{1}{2}{q_1}^2\left\{1+\cos\left(2\,w\,t+2\,\psi_1\right)\right\}+\frac{1}{2}{q_2}^2\left\{1+\cos\left(4\,w\,t+2\,\psi_2\right)\right\}+q_1\,q_2\left\{\cos\left(w\,t+\psi_2-\psi_1\right)+\cos\left(3\,w\,t+\psi_1+\psi_2\right)\right\}\right] \quad \ldots\ldots (5)$$

The term q_o is disregarded, assuming the upper-water discharge of the river is negligible.

In case the tide h_2 is small with respect to the tide h_1 and, therefore, q_2 small as compared to q_1, the term with ${q_2}^2$ may be neglected. It is then possible to assume that the moments of slack-water are mainly determined by the h_1 tide so that the moments for which $Q = 0$ may be approximated by $q_1 \cos\left(w\,t+\psi_1\right) = 0$. In addition a Fourier expansion for the step function ± 1 may be determined that is $+1$ if $Q > 0$ and -1 if $Q < 0$. Then it follows that

$$T(t) = \pm 1 = \frac{4}{\pi}\cos\left(w\,t+\psi_1\right)-\frac{4}{3\pi}\cos\left(3\,w\,t+3\,\psi_1\right)+(-1)^{p+1}\frac{1}{(2p-1)}\left(\frac{4}{\pi}\right)\cos\left[(2\,p-1)\left(w\,t+\psi_1\right)\right],\ p>2 \quad \ldots\ldots (6)$$

Thus, the product of $T(t)$ has been determined considering the first three terms and the development of Q^2 between the brackets of Eq. 5. From a mathematical point of view this method may only be applied if a few harmonics are considered.

Following computation that leaves out of consideration the higher harmonics with 3wt and so on, it is deduced that

$$|Q|Q = \frac{4}{3\pi}q_1q_2\cos\left(2\psi_1-\psi_2\right)+\frac{8}{3\pi}{q_1}^2\cos\left(w\,t+\psi_1\right)+\frac{4}{\pi}q_1q_2\cos\left(2\,w\,t+\psi_2\right)-\frac{4}{15\pi}q_1q_2\cos\left(2\,w\,t+4\psi_1-\psi_2\right) \quad \ldots\ldots\ldots (7)$$

Then the underlined terms determine the influence of the interference of the h_1 and h_2 tides as a consequence of the quadratic resistance.

In virtue of the fact that the number value of $\frac{4}{15\pi}$ is $\frac{1}{15}$ of that of $\frac{4}{\pi}$ and, because q_2 is considerably smaller than q_1, the last term in Eq. 7 may be neglected. From the foregoing, the linear equations that determine the propagation of the h_1 and h_2 tide can be derived.

For the presentation of the equations there is some advantage in the introduction of complex quantities. Then it may be stated that

$$h_1(x)\cos\left(w\,t+\phi_1(x)\right)=\frac{1}{2}h_1(x)\left\{e^{i\left(wt+\phi_1(x)\right)}+e^{-iwt+\phi_1(x)}\right\}$$

$$=H_1(x)\,e^{iwt}+H_{-1}(x)\,e^{-iwt} \quad \left(i^2=-1\right),\ H_1(x)=\frac{1}{2}h_1(x)\,e^{i\phi_1(x)},$$

$$H_{-1}(x)=\frac{1}{2}h_1(x)\,e^{-i\phi_1(x)},\ h_1(x)=2\,|H_1(x)|, \quad \ldots\ldots (8)$$

and analogous expressions for the rest of the gonimetric functions in Eqs. 3 and 4. Thus, after computation of the complex functions $H_1(x)$, $Q_1(x)$, $H_2(x)$ and $Q_2(x)$, will be known.

The function $|Q|Q$ may be written

$$|Q|Q = \frac{16}{3\pi}|Q_1(x)|Q_1(x)e^{iwt} + \frac{8}{\pi}|Q_1(x)|Q_2(x)e^{2iwt} + \text{c.c.} \quad \ldots\ldots (9)$$

in which c.c. indicates conjugated complex functions. Further the terms, which do not depend on t, have been left out of consideration. The equations determining $H_1(x)$ and $Q_1(x)$, are obtained by substituting $H_1(x)\,e^{iwt}$ and $Q_1(x)\,e^{iwt}$ in Eqs. 1 and 2, provided Eq. 9 has been substituted for $|Q|Q$. From this computation

$$\frac{dQ_1}{dx} + i\,b\,w\,H_1 = 0;\ \frac{dH_1}{dx} + \frac{i\,w}{A\,g}Q_1 + \frac{16}{3\pi}\frac{|Q_1|\,Q_1}{C^2A^2\,a} = 0 \quad \ldots\ldots (10)$$

and for $H_2(x)$, $Q_2(x)$

$$\frac{dQ_2}{dx} + 2\,i\,b\,w\,H_2 = 0;\ \frac{dH_2}{dx} + \frac{2\,i\,w}{A\,g}Q_2 + \frac{8}{\pi}\frac{|Q_1|\,Q_2}{C^2\,A^2\,a} = 0 \quad \ldots\ldots (11)$$

The Solution of the Equations.—Eqs. 10 and 11 are two linear homogeneous equations, provided $|Q_1|$ is known. Let a channel be divided into a number of sections, so that for each section the quantities b, A, and a may be considered independent on the length x. For the j-section the quantities are designated b_j, A_j, a_j and C_j for C. Furthermore, for $|Q_1|$ the mean value in the j-section is considered. This value is estimated provisionally.

After the elimination of H_1, the equation for Q_1 is found to be

$$\frac{d^2Q_1}{dx^2} + \frac{b\,w^2}{A\,g}Q_1 - i\,\frac{16}{3\pi}\frac{b\,w}{C^2\,A^2_a}|Q_1|\,Q_1 = 0 \quad \ldots\ldots (12)$$

The solutions have the form $Q_1(x) = |Q_1|\,e^{ux}$, $H_1(x) = |H_1|\,e^{ux}$ with u complex. After substitution in Eq. 12 it appears that the term u has to satisfy the quadratic equation

$$u^2 + \left(\frac{b\,w^2}{A\,g} = -\,i\,\frac{16}{3\,\pi}\frac{b\,w}{C^2\,A^2_a}\,|\,Q1|\right) = 0 \quad \ldots\ldots\ldots (13)$$

Its roots are termed u and -u. Then the general solution for H_1 and Q_1 of the section considered is

$$Q_1 = |Q_1|_1\,e^{ux} + |Q_1|_2\,e^{-ux}, \quad \ldots\ldots\ldots\ldots (14)$$

and, therefore,

$$H_1 = \frac{i\,u}{b\,w}|Q_1|_1\,e^{ux} - \frac{i\,u}{b\,w}|Q_1|_2\,e^{-ux} \quad \ldots\ldots\ldots\ldots (15)$$

in which $|Q_1|_1$ and $|Q_1|_2$ are integration parameters.

With the aid of these relationships it is possible to determine the relation between the values Q_{1a} and H_{1a} at the beginning of a section and the quantities Q_{1b} and H_{1b} at the end of this section. Then $|Q_1|_1$ and $|Q_1|_2$ are eliminated.

Similar relations hold good for each section. Furthermore, after the elimination of the values of Q_1 and H_1 on the borders of the intermediate sections, Q_1 and H_1 at the beginning of the first section can be expressed in terms of the values of Q_1 and H_1 at the end of the p-th section.

As an example assume that the beginning of the first section H_1 is given and let the channel be closed at the end of the p-th section. Then Q_1 can be computed at the beginning of the first section, as well as H_{1b} at the end of the channel. Therefore, the whole computation is based on the elimination of quantities in a system of linear equations. After the values T at the extreme sections are known the values of H and Q for all sections can be computed.

At the dividing point of channels the water level H_1 must be the same for the various channels, while the algebraic sum of the currents Q_1 at this point must be zero, because the total discharge is equal to the total supply. Then the estimations $|Q_1|$ for each section must be checked. In case the differences are too great, the computations must be repeated with a better estimate for the values of $|Q_1|$. The computation must be repeated until there is sufficient concurrence.

The solutions of Eq. 11 for the determinations of H_2 and Q_2 take place in an analogous way. As the values for $|Q_1|$ for the different sections are known, these computations need not be repeated after the first solution. This is also the case with the coefficient of the resistance term in Eq. 11. The computation of the propagation of the second harmonic is, therefore, much easier than that of the first one. After the computation of the tide, the change in the mean level along the river, according to Eq. 2 and Eq. 7, can be computed by

$$h_{o,b} - h_{o,a} = - \left[\frac{4}{3\pi} q_1 q_2 \cos \left(2\psi_1 - \psi_2 \right) \right] l ,$$

in which $h_{o,b}$ and $h_{o,a}$ are the mean levels at the end and the beginning of the section, with length l; q_1, q_2 and $2\psi_1 - \psi_2$ refer to the mean values of these quantities in the section.

SOLUTION OF EXAMPLE

As an example, the propagation of the tide in Tampa Bay on the Gulf Coast of Florida has been considered. The bay penetrates inland over a distance of approximately 35 miles. At approximately 20 miles from the mouth, the main channel divides into two branches, the western one 15 miles long the eastern one 11 miles long. The width of the bay below the dividing point is 7 miles and the width of the branches are, respectively 5.5 miles, and 5 miles. The mean depth of the main channel is 25 ft to 30 ft, while that of the branches is 13 ft to 17 ft (Fig. 1). The mouth of this inlet is partly obstructed by islands.

The vertical tide at the sea shows considerable variations. In the course of a year nearly pure diurnal tides as well as nearly pure semi-diurnal tides occur and every conceivable intermediate pattern. Data for the computation were available from Topographic Chart 1257, United States Coast and Geodetic Survey, Dept. of Commerce (USC & GS), 1932. Heights and times of high water, (HW) and low water (LW) are known at St. Petersburg, Fla. from "Tide Tables, East Coast North and South America, United States Coast and Geodetic Survey, Dept. of Commerce (USC & GS), 1955." Ranges of mean and spring tides and time lag with respect to Tampa Bay at six stations are shown in Table 1.

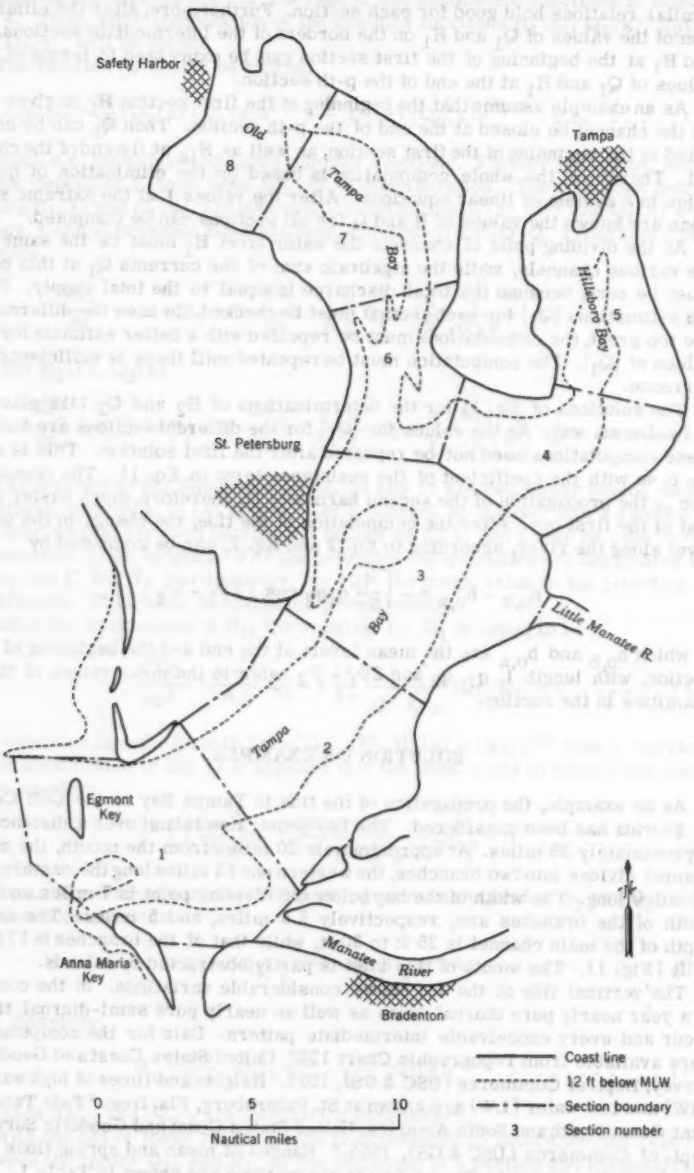


FIG. 1.—TOPOGRAPHY OF TAMPA BAY ESTUARY

In the computations two cases were dealt with. These were mainly semi-diurnal tide and mainly diurnal tide, with both at spring tide. Observed tidal curves were not available, so the curves at St. Petersburg had to be evaluated from the predicted HW and LW levels and times. Making use of time curves with diurnal, semi-diurnal and quarter-diurnal periods, tidal curves were constructed. As an example for the diurnal tidal curve at St. Petersburg was put $h = 1{,}7 \cos wt + 0{,}3 \cos 2\,wt$, and for the semi-diurnal tidal curve was $h = 0{,}8 \cos 2\,wt + 0{,}1 \cos 4\,wt$, with $w = 0{,}702\ 10^{-4}$. The propagation of the tides was then computed both inland to Tampa and Safety Harbor, and seaward to Egmont Key.

In spite of the great width of the bay (7 miles) it proved possible to determine a simple schematization with a number of channels. In order to carry out any tidal computation, a region has to be schematized into a network of sections each having constant hydraulic parameters, such as width, depth of the channels, and the storing width of the water surface.

With a view to reducing the computations as much as possible, large sections were considered. Three sections nearly 7 miles in length downstream of the point of division, two sections 5.5 miles long for the eastern branch, and

TABLE 1.—DATA FOR TAMPA BAY

Station	Range in feet		Time lag, in hours and minutes
	Mean Tide	Spring Tide	
Egmont Key	1.3	1.7	-2.25
Anna Maria	1.4	1.9	-2.20
Bradenton	1.4	1.9	-0.45
St. Petersburg	1.4	1.6	0
Tampa-Hillsboro Bay	1.8	2.4	+0.15
Safety Harbor	1.9	2.5	+1.45

three sections for the western branch, with lengths of 6 miles, 6 miles, and 3.5 miles respectively, were assumed for the computations.

The value of C (Eq. 2) was put at 110 for the downstream sections. For the three sections around the division point the value of C = 100 was kept and for the sections at the closed ends of the branches C = 90 was used. The surface width of the stream bed was put at approximately one-half or two-thirds of the storing width. This is based on the existing banks and shallow coast areas.

For a sufficiently accurate computation of the quart-diurnal M_4 tide, being considered together with the semi-diurnal M_2 tide, the number of sections had to be taken twice as large as for the computation of the M_2 tide. The transverse gradients of the water level in the bay are small, because the maximum velocities are small (2 fps maximum). Therefore, the maximum difference in head as a result of Coriolis forces is approximately 2 in.

Results of Computations for the Tide Curves.—A summary of the results of the several computations are presented and, as far as possible, compared with the available tide data in Table 2. The first case considered is one of a semi-diurnal tide (M_2) and a quarter-diurnal tide (M_4) in which a spring tide is assumed.

In the computed amplitudes there are important differences between the results of the computations and those of the predictions (according to Tide

TABLE 2.—COMPUTED TIDE DATA, TAMPA BAY

	Egmont Key	St. Petersburg[a]	Tampa	Safety Harbor	date
a) Time of Propogation from St. Petersburg, in minutes					
M_2 Tide	-175	—	+15	+ 90	3/4 Sept. 1955
M_4 Tide	-120	—	+40	+125	
Composed Tide	-150	—	+25	+100	
Predicted Tide	-145	—	+15	+105	
M_1 Tide	-185	—	+15	+ 70	19/20 June 1955
M_2 Tide	-175	—	+20	+115	
Composed Tide	-165	—	+20	+110	
b) Computed Amplitudes, in feet					
M_2 Tide	1.20	0.80	1.00	1.05	3/4 Sept. 1955
M_4 Tide	0.25	0.10	0.15	0.05	
Composed Tide	1.25	0.80	1.00	1.05	
Predicted	0.95	0.80	1.20	1.25	
Percentage Increase[b]	20	—	50	55	
M_2 Tide	0.5	0.5	0.6	0.7	approximately mean tide
M_4 Tide	0.2	0.1	0.2	0.1	
Composed Tide	0.6	0.5	0.65	0.75	
Percentage Increase[b]	20	—	30	50	
M_1 Tide	1.75	1.65	1.70	1.75	19/20 June 1955
M_2 Tide	0.70	0.35	0.40	0.35	
Composed Tide	2.10	1.75	1.85	1.90	
	Section a	Section b	Section c	Section d	
c) Computed Velocities, in feet per second					
1) Semi-diurnal tide; Spring tide					
M_2 Tide	1.75	1.30	0.70	1.45	3/4 Sept. 1955
M_4 Tide	0.25	0.20	0.20	0.15	
Composed:					
ebb tide	1.75	1.35	0.80	1.55	
flood tide	1.90	1.35	0.70	1.40	
2) Diurnal tide; Spring tide					
M_1 Tide	1.95	1.30	0.65	1.35	19/20 June 1955
M_2 Tide	0.70	0.50	0.30	0.50	
Composed:					
ebb tide	2.60	1.75	0.95	1.85	
flood tide	1.70	1.05	0.60	1.00	
d) Maximum T velocities,[c] in feet per second					
ebb	2.5	1.6	0.8	1.8	
flood	1.6	1.3	0.7	1.3	

[a] Assumed Values.
[b] With respect to St. Petersburg.
[c] Based on "Tidal Current Charts of Tampa Bay.

Tables East Coast, North and South America; United States Coast and Geodetic Survey, Dept. of Commerce (USC & GS) 1955. However, it must be noted that these predictions relate to an average tide and do not show the exact tidal conditions that correspond with these computations, and the relation of diurnal and semi-diurnal tides. A complete comparison is therefore difficult to obtain.

For the previously mentioned semi-diurnal tide the situation for the computed tides was considered on September 3 and 4, 1955, and the diurnal tide on June 19 and 20, 1955. The tides considered belong to the strongest ones of their type.

The difference between the computed compound tides and the predicted tide can be reduced by considering a smaller amplitude of the M_2 tide (Table 2), by which, presumably, the average tide is more closely approximated. This appears from the results of the tidal computation, which has been executed in case the amplitude at St. Petersburg for the M_2 and M_4 tides are respectively 0.5 ft and 0.1 ft.

RESULTS OF COMPUTATIONS FOR THE VELOCITIES

The computed mean maximum velocities for ebb and flood in the various sections of the bay are given in Table 2. In the atlas "Tidal Current Charts of Tampa Bay" serial no f43, 1951 United States Coast and Geodetic Survey, Dept. of Commerce (USC & GS) the hourly "tropic" velocities during the tide are noted at many places in the bay. It is not clear from these charts which type of vertical tide they correspond with. The average maximum values which may be derived from the data of this atlas are also presented in Table 2.

It appears that there is a fair agreement with the results of the computed maximum velocities for ebb and flood in the case of the diurnal tide previously mentioned. As has already been indicated, in view of the restricted nature of the available data, the results obtained are valid in broad outline only.

CONCLUSIONS

Generally the relative decrease or increase along the bay is larger for the M_4 tidal range than for the M_2 tidal ranges. The latter tidal range changes more than the M_1 ranges. The propagation time of the M_1 and M_2 tides are practically equal whatever the character of the tide (neap, spring, diurnal, or semi-diurnal), it depends mainly on the depth.

It is gratifying to note that with a simple method of computation that can be mastered with relatively little effort by the hydraulic engineer, and with a rather crude schematization of the system and with scant observational data, the mechanism of the tidal motion could be explained to a sufficient degree for many practical purposes. This is true provided the data concerning the tides are extended beyond those now available.

HYDRAULIC INVESTIGATION

By H. A. Ferguson

PREVIOUS HISTORY AND DESCRIPTION OF THE PROJECT

For many centuries the Dutch have struggled to force from the sea a boundary that would be as favorable to them as possible. In the northern part of their country they succeeded in crowning this struggle by damming the dangerous Zuiderzee. This project resulted in a better protection of that area as well as in a considerable land reclamation. In the distant future the sea will possibly be driven back even farther northward by means of closing the gaps in the north coastline, which consists of a girdle of islands (Frisian Islands). The plans relating to such a closure have not nearly matured as yet (1960).

For the time being the field of operations lies chiefly in the southern part of the coastal area, where the realization of the Delta project is being undertaken. It provides for the enclosure of the three large sea arms situated between Westerschelde and Waterweg, one of which connects Rotterdam with the sea.

The project represents a set of radical changes to be brought about in a system of sea arms, estuaries, and lower rivers, in which the tidal movement is considerable and the sandy bottom very unstable. In the area concerned the sea has had free play, comparatively speaking, and the struggle for the reclamation and preservation of newland has always been a difficult one.

The changes which have occurred in this area in the course of centuries bear plain testimony to its eventful history. About the year 1300, there lay a rather straggling group of islands surrounded by creeks of irregular shapes, that did not show a definite system (Fig. 1). Several of those islands were already inhabited and partly provided with dikes. However, these dikes were far from strong, so that they did not protect the shores effectively. Several islands disappeared owing to storm surges, others grew together and new ones came into existence. Gradually, as he began to build sea-walls, man influenced this natural process. These defenses, built as they were by primitive means, did not endure long. But, little by little, more success was achieved, thanks to improved materials and methods. Eventually the situation resolved itself into what it is now (1960 - Fig. 1), representing more or less a state of balance. Although uncommonly heavy losses of land are no longer suffered, neither are there spectacular accretions any more. Certain changes do take place, but they are in the main confined to the present channels and come about very gradually. Roughly speaking, the two northern sea arms, Haringvliet and Brouwershavense Gat, tend to be filled, whereas the Oosterschelde gets deeper.

The dikes that had to protect the low-lying islands against floods were repeatedly strengthened and heightened. However, the greater security thus effected was partly neutralized by a settling of the soil, a general sinking of the surface of the islands, and a general rise of the sea level. As a result many

Note.—Published, essentially as printed here, in March, 1959, in the Journal of the Waterways and Harbors Division, as Proceedings Paper 1978. Positions and titles given are those in effect when the paper was approved for publication in Transactions.

[1] Chf. Engr., Rijkswaterstaat, Deltadienst, The Hague, The Netherlands.

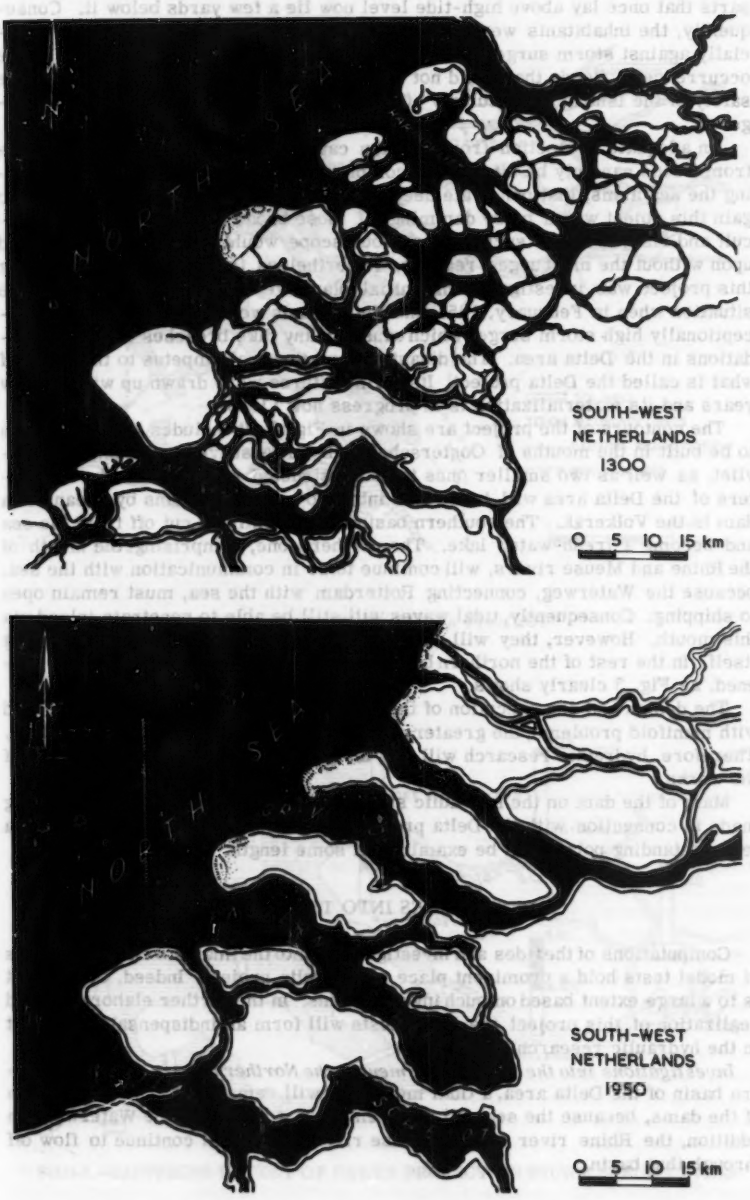


FIG. 1.—HISTORIC CHANGES IN RHINE-MEUSE-SCHELDT DELTA

parts that once lay above high-tide level now lie a few yards below it. Consequently, the inhabitants were as yet insufficiently safe against the sea, especially against storm surges. There was a chance, although a slight one, of the occurrence of floods that could not be resisted by the dikes, in which case the safety of the islands, particularly of the very low-lying parts, would be endangered.

An adequate protection from erosion caused by tidal currents as well as from floods can only be effected by completely preventing the sea from entering the sea arms, that penetrate deep into the land. The only way, however, to gain this object would be by damming off those broad and deep waters. Difficult and risky work of such an enormous scope would not readily be decided upon without the most urgent reasons. Nevertheless, the feasibility of realizing this project was investigated and initial plans were drawn up. This was the situation when in February, 1953, the Netherlands were suddenly hit by an exceptionally high storm surge, which caused many dike breaches and vast inundations in the Delta area. The disaster gave the final impetus to the birth of what is called the Delta project. Its main features were drawn up within a few years and its materialization is in progress now (1958).

The contours of the project are shown in Fig. 2. It includes three big dams to be built in the mouths of Oosterschelde, Brouwershavense Gat and Haringvliet, as well as two smaller ones to be constructed farther inward. The waters of the Delta area will be divided into two separate basins by means of a dam in the Volkerak. The southern basin will be entirely cut off from the sea and become a fresh-water lake. The northern one, comprising the mouth of the Rhine and Meuse rivers, will continue to be in communication with the sea, because the Waterweg, connecting Rotterdam with the sea, must remain open to shipping. Consequently, tidal waves will still be able to penetrate inland via this mouth. However, they will cause high water levels only in the Waterweg itself. In the rest of the northern basin their effect will be considerably weakened, as Fig. 3 clearly shows.

The design and the execution of the plans confront the engineers concerned with manifold problems, the greater part of which lie in the field of hydraulics. Therefore, hydraulic research will play an important part in the realization of the works.

Many of the data on the hydraulic studies and investigations which are being made in connection with the Delta project are presented in this paper. Only a few outstanding points will be examined at some length.

RESEARCHES INTO THE TIDES

Computations of the tides and investigations into the tidal movement by means of model tests hold a prominent place in the Delta project. Indeed, the project is to a large extent based on such investigations. In the further elaboration and realization of this project the model tests will form an indispensable element in the hydraulic researches.

Investigations into the Water Movement in the Northern Basin.—In the northern basin of the Delta area, a tidal movement will remain after the completion of the dams, because the sea will go on entering it by way of the Waterweg. In addition, the Rhine river and the Meuse river water will continue to flow off through that basin.

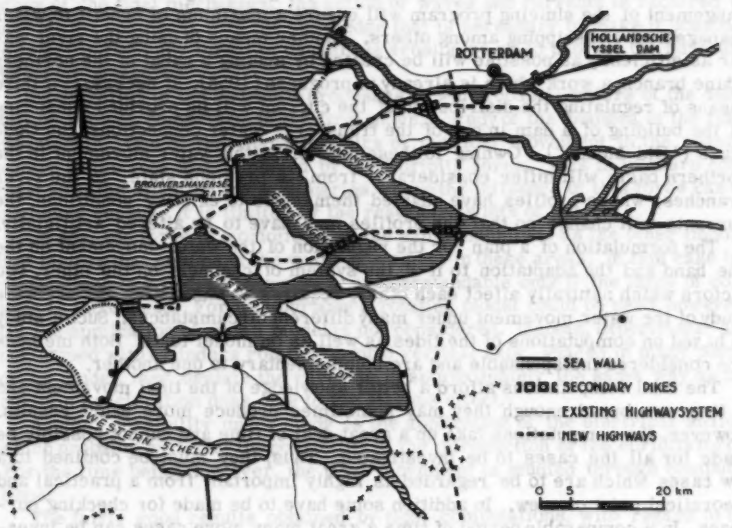


FIG. 2.—LAYOUT OF DELTA PROJECT

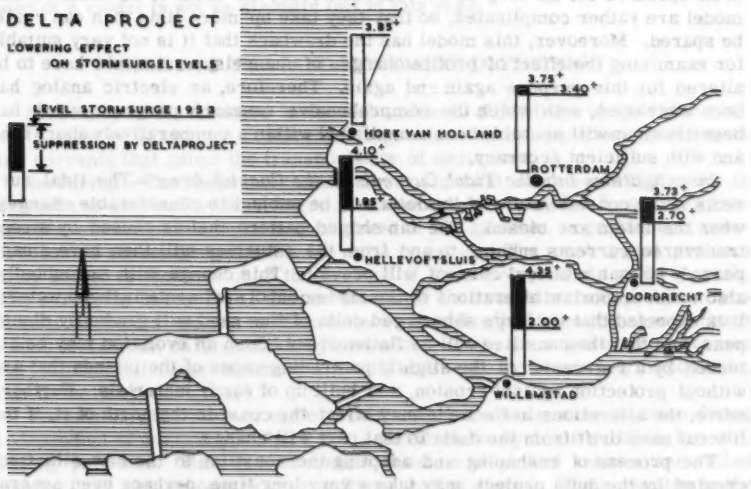


FIG. 3.—LOWERING EFFECT OF DELTA PROJECT ON STORM SURGE LEVELS

However, the big sluices that will be built in the Haringvliet will provide a means of controlling this water movement to a great degree. A sensible arrangement of the sluicing program will ensure a maximum of benefit to water management and shipping among others. Another means of using the river water as efficiently as possible will be created by making a canal of the northern Rhine branch, a work which is already in progress (1958). If necessary a third means of regulating the distribution of the current will be provided consisting of the building of a dam in one of the transverse water connections, the Oude Maas ("Old Meuse"). Owning to these provisions the water movement in the northern basin will differ considerably from its previous state. In the river branches, whose profiles have adapted themselves to existing conditions, the currents will change so that the profiles may have to be altered artificially.

The formulation of a plan for the regulation of the water movement on the one hand and the adaptation to it of the system of channels on the other, two factors which naturally affect each other, requires an exhaustive and accurate study of the water movement under many different circumstances. Such a study is based on computations of the tides as well as on model tests. Both methods are considered indispensable and are complementary to one another.

The tidal computations afford a better knowledge of the tidal movement and if they are broad enough they may sometimes produce more exact results. However, the computations take up a great deal of time and cannot possibly be made for all the cases to be investigated. Thus, they must be confined to a few cases which are to be regarded as highly important from a practical and theoretical point of view. In addition some have to be made for checking purposes. In a comparable period of time a great many more cases can be investigated by model tests than by tidal computations. Therefore, model tests are expecially fit for examining whole series of situations.

Model tests are carried out for the main part in a hydraulic model that has been operated for as long as 10 yrs. However, the tests to be made in this model are rather complicated, so that they take up more time than can really be spared. Moreover, this model has the drawback that it is not very suitable for examining the effect of profile changes of channels, as it would have to be altered for this purpose again and again. Therefore, an electric analog has been developed, with which the comprehensive research program which has been drawn up will probably be accomplished within a comparatively short time and with sufficient accuracy.

Investigations Into the Tidal Currents in the Coastal Area.—The tidal currents in the coastal waters of the delta will be subject to considerable changes, when the inlets are closed. The fan shaped pattern that is caused by strong transverse currents running to and from the estuaries will then have disappeared, so that a lateral current will prevail. This change will, undoubtedly, also cause important alterations of the movement of sediments in these waters. It is expected that the large submerged delta of fine sand will gradually disappear, and that the coastline will be flattened out. Such an evolution may be attended by a regression of the slightly protruding capes of the islands that are without protection against erosion, and built up of sandy materials. Furthermore, the alterations in the delta may affect the coast to the north of it, if the littoral sand drift from the delta to that part will change.

The process of reshaping and adapting the coastline to the new situation, created by the delta project, may take a very long time, perhaps even several hundreds of years. This development, although slow, may cause in its first stage the previously mentioned dangerous effects of erosion. It is extremely

difficult to forecast what will happen and at what rate of time. A comprehensive study of the tidal mechanism, the action of waves and currents is required to provide the engineers with the knowledge that is necessary to make it possible to detect in time any threat of dangerous erosion so as to provide the adequate defensive measures.

Investigation of the hydraulic processes to which coastal waters of the delta will be subject, comprises, in the first place, a study of the changes in the tidal movements. One of the characteristics of the tidal movement in the coastal waters is the role that is played by the Coriolis force. This is in sharp contrast with the situation in the estuaries where the influence of this force can be neglected because it is limited by the restricted width of the bed.

On sea, the force of coriolis is of the same magnitude as the other important factors that command the water movement in these areas. In this case investigations in a hydraulic model are understandable only if the force of coriolis is introduced. For this purpose a rotating model could be used, however, but the application of such a model is not considered. Instead, experiments are performed with cylinders rotating around vertical axis. Placed in many points of the model, they deviate the currents in approximately the same way as the coriolis acceleration does, due to the Magnus effect.

Another possibility under study is the application of the electrical analog, which probably will offer the possibility of the introduction of the coriolis force. For the time being, however, the tidal movement is studied through computations.

The fairly good results obtained by tidal computations, with regard to the present situation, give confidence that in this way a reliable forecast can be made of the future tidal movement when the estuaries are closed. Because only a few different situations have to be considered, the fact that these computations are rather toilsome is not a strong inconvenience. Therefore, the need of a model is not as strongly felt in this case.

STUDY OF THE SAND MOVEMENT IN THE DELTA

Forecasts of the changes in the delta, due to alterations of the tidal currents, must be based on a comprehensive study of the combined action of waves and currents that cause the transportation of sediments.

Surveying.—The basic information about the sand movements that occur in the delta is obtained by soundings. Because a methodical and frequent hydrographic survey of the delta is considered of the greatest importance, a comprehensive survey program for the delta is set up. The most urgent problem to be solved is the location of the position of the survey vessels while at work. The surveying has to cover a broad stretch of the coastal waters, and positions have to be fixed at distances of up to more than 6 miles from the shore. Exact visual orientation on landmarks, by means of sextants or rangefinders, becomes very difficult at these distances and will most usually be entirely impossible, due to the poor visibility.

Fortunately, the modern radio-location systems have made position-fixing independent of visibility. There are several radio systems suitable for surveying purposes. This chosen system consists of a chief transmitter called master, and two secondary transmitters, called slaves. Their position in the delta is indicated on Fig. 4(a). Location with the aid of this system is based on the measuring of phase differences between radio-waves, emitted from the

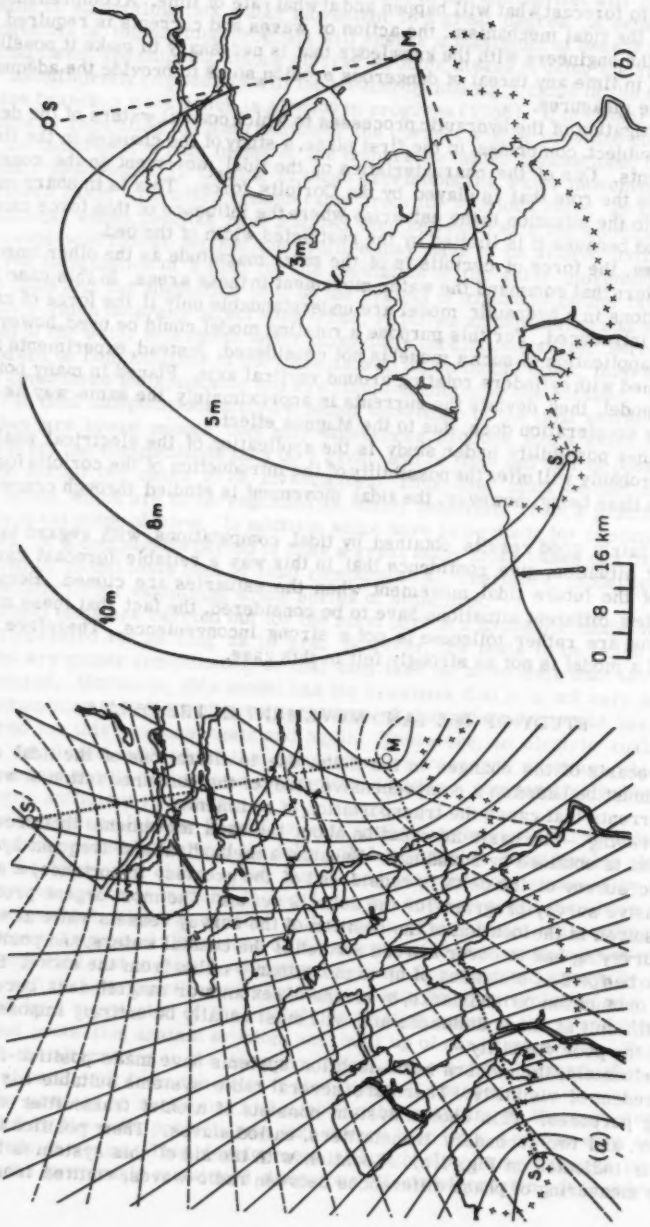


FIG. 4.—RADIO-LOCATION SYSTEM SURVEY CHAIN

three stations, with the receiver placed on board the survey vessel. All locations with the same phase differences lie on a hyperbole so that a pair of stations produces a pattern of hyperboles, each of which corresponds with a certain phase difference between the waves emitted from the stations. Thus the ship can fix its position within two nets of these hyperboles, each net based on a master and a slave as focuses. The hyperbole patterns are shown on Fig. 4(a). The accuracy of fixing within this pattern is fairly high, as is shown on Fig. 4(b), which gives the accuracy contours for the Delta survey.

Besides the possibility of a fairly accurate fix at long distances from the shore, this system offers the advantage of a far more efficient surveying than was possible in the orthodox way. In the first place, it offers the possibility of repeatedly running exactly the same section lines without having to mark these on shore. By making the section lines coincide with hyperboles of the radio, the location is simple and very exact. The transmission stations are situated in such a way that the hyperbole pattern offers the best opportunity in this respect. Another advantage of the system is that it makes it quite easy to mark at every turn the same spots along the section lines. Thus, an easy and fairly accurate tabular comparison is made possible between successive soundings of the same area.

A special problem is the determination of the water level from point to point while the surveying is in progress. Considering that the tidal range in the coastal area of the delta amounts to more than 10 ft, and that there are important phase differences from place to place due to the comparatively slow propagation of the tidal wave in these shallow waters, important mistakes in the estimation of the height of the water level are easily made if the tide is not registered at many points. It is necessary to have registrations of the tide not only at stations along the shore, but also on full sea, at distances many miles from the shore. Poles shall have to be erected for this purpose, equipped with instruments for radiographic transmission of the water level to the shore.

Measurement of Sand Movement by Radioactive Tracers.—By the program for hydrographic survey previously described, an account will be obtained of the displacements of sand that occur in general in the delta. Without doubt the soundings will provide data that will enable one to draw rough conclusions with respect to the mechanism of wave and current action that cause this sand transportation. This information will not give direct and immediate evidence of the process of the sand movement, but will only show where sediments have settled or have been eroded. For direct measurements of the sand transport use should be made of bed-load meters or suspended-load meters. However, in the present case measurements with such devices would surely not be successful, because the use of these instruments is not practicable during rough weather, and it is especially the sand transport during such periods that is of interest.

More success is expected from the use of radioactive tracers, to produce a more detailed view of the sand movements. Application of radioactive tracers in the field has been prepared by model tests that gave rather promising results. The tracer that will be used is the so-called greensand (Ionac C 50), which has a specific weight nearly that of the sand in the delta. The detector used is a scintillation counter, mounted on a sledge on which it can be moved along the seabottom. The greatest difficulty of the trace method seems to lie in the fact that part of the inserted tracer may temporally be covered by other sand, especially when there are moving sand ripples of some size. In such a case the vertical distribution of the tracer in the soil must also be determined,

which will be done by borings. For this purpose a boring device is developed that can procure samples of sand up to a length of 7 ft.

BOTTOM EROSION DURING THE ENCLOSURE OPERATIONS

Fig. 5 shows how the enclosure of the big estuaries will be executed. The The shallow sections and the smaller channels will be bridged first and the main channels afterwards. In this way the operation will proceed gradually, the main current not being disturbed until the end of the work, when the remaining deep channels shall be closed by caissons. The current through the remaining gaps will increase considerably in strength as the dam on the shoals makes headway. Moreover, alongside the contracted current a complex of vortex trails and eddies will come into being, as is shown in Fig. 5. These irregularities in the current pattern may cause dangerous erosion of the mobile sandbottom, in which case special measures would be taken to keep this in check.

The boundaries of the gap shall first be carefully designed, especially the shape of the sill foundation for the caissons and the adjoining bottom of the channel. In addition, part of the sand bottom will have to be protected by defensive layers. As this bottom protection is very expensive, the area to be covered by it should not be exaggerated. On the other hand, no great risks should be taken. It follows from these considerations that careful studies have to be made of the current and its pattern that is to be expected in and around the gap and of the erosion that it will effect.

To answer these questions model tests are indispensable, but they have their limitations. A model may give a farily exact imitation of a flow pattern, but the prediction of the erosion that it will effect in nature is much less reliable. Therefore the relation between current, current pattern and the erosion caused thereby has to be studied in nature. When the connection between current and erosion has been detected in the field, it is time to draw conclusions from currents in a model with regard to erosion that has to be expected in nature. Field studies of erosion caused by complex current patterns play an important role in the program of hydraulic investigations for the delta project. An example of these investigations is illustrated in Fig. 6. This represents the situation in the Haringvliet, created by building the construction pit for the big sluices, that is the first phase in the enclosure operations. It was evident that such an obstacle, taking approximately one-third of the cross section of the estuary, would lead to an important change of the flow pattern, and that these changes in their turn will cause considerable erosion in the neighborhood of the pit. The flow patterns of the maximum flood and ebb current before and after the construction pit was built, are shown in Figs. 8(a), (b), (c), and (d). In Figs. 8(e) and (f), the cross sections are given in the axis of the pit, before, and some months after its construction, with corresponding current diagrams. The current near the northern boundary of the pit is rather turbulent and from Fig. 8(f) it may follow that at this boundary the spot of strongest erosion does not coincide with the place where the current is greatest.

For a closer study of these phenomena, not only the average current has to be measured, but also the degree of turbulence, with special emphasis on its vertical component. For this purpose, two types of turbulence meters are under development. One of these is based on the principle of pressure measurements and is able to measure not only the horizontal but also the vertical fluctuations of the current, while the other uses a propeller to measure only the horizontal fluctuations.

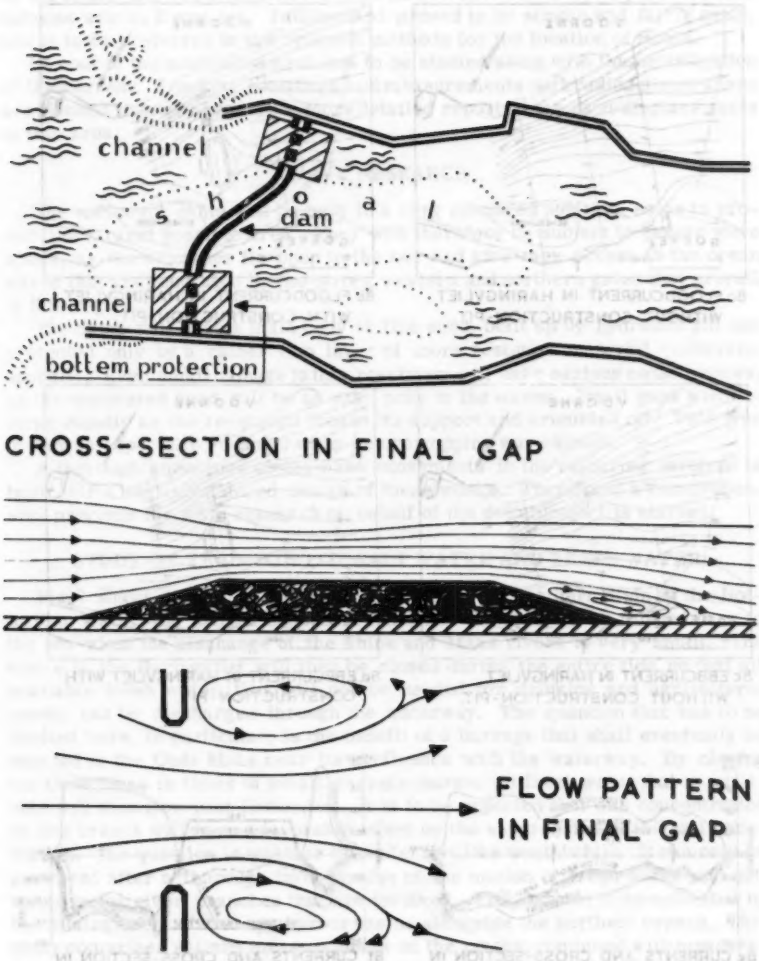
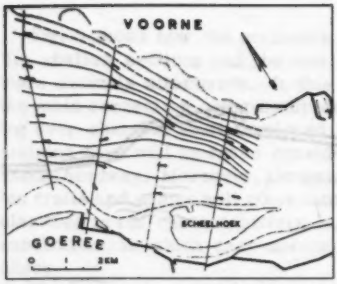
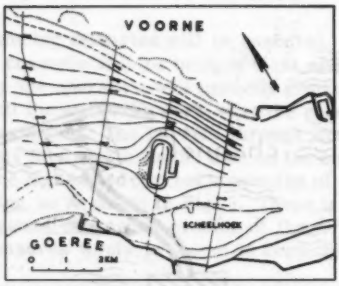


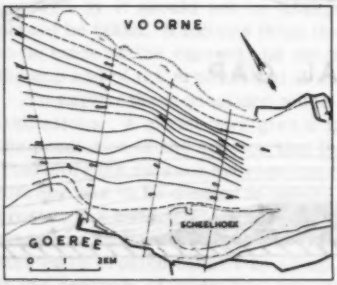
FIG. 5.—SCHEME OF CLOSING AN ESTUARY



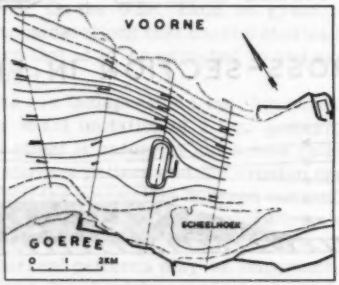
8a. FLOODCURRENT IN HARINGVLIET WITHOUT CONSTRUCTION-PIT.



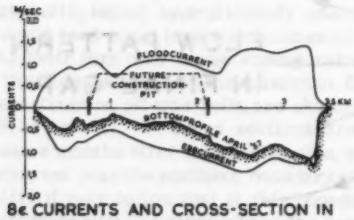
8b. FLOODCURRENT IN HARINGVLIET WITH CONSTRUCTION-PIT.



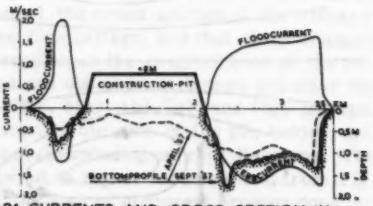
8c. EBBCURRENT IN HARINGVLIET WITHOUT CONSTRUCTION-PIT.



8d. EBBCURRENT IN HARINGVLIET WITH CONSTRUCTION-PIT.



8e. CURRENTS AND CROSS-SECTION IN AXIS OF PIT BEFORE ITS CONSTRUCTION.



8f. CURRENTS AND CROSS-SECTION IN AXIS OF PIT AFTER ITS CONSTRUCTION.

FIG. 6.—FLOW PATTERN IN THE HARINGVLIET

For measuring the flow pattern at the water surface by floats, use is made of radar. By equipping the floats with radar deflectors, they can easily be detected on the radar screen. By photographing the screen at intervals, the tracks of the floats can be reconstructed in an easy way. The radar applied for this purpose was an 8 mm set. This method proved to be simple and fairly exact, and is to be preferred to the orthodox methods for the location of floats.

Of course the sand movement has to be studied along with the investigation of the current. Frequent soundings and measurements with radioactive tracers are planned that will procure a more detailed report of the sand displacements in this area.

WAVE RESEARCH

The enclosure dams will be built in a very advanced position, so as to protect the largest possible area. They will therefore be subject to severe wave attack, as the estuaries lie open to the sea and give easy access to the ocean waves that are generated by the strong western and northern gales that prevail in this region.

The dams will have a main body of fine sand, built up by hydraulic fill and protected only by a rather thin layer of more resistant material (concrete, asphalt). Even small damage to this revetment will have serious consequences, as the uncovered sand will be an easy prey to the waves. Small gaps will enlarge rapidly as the revetment looses its support and crumbles off. This type of dam is especially endangered by an overtopping wave attack.

A thorough knowledge of the wave movements in the estuaries involved is basic for a well-considered design of these works. Therefore, a comprehensive program for wave research on behalf of the delta project is started.

STUDY OF THE MIXING OF SALT WATER AND FRESH WATER

Fig. 7 shows roughly how salt penetration into the northern basin by the Rotterdam Waterway, will be suppressed and how the salt will be flushed back to the sea when the discharge of the Rhine and Maas rivers is very small. The sluice in the Haringvliet will then be closed during the entire tide so that all available fresh water, that will not be needed for drinking and agricultural needs, can be discharged through the waterway. The question that has to be studied here, in particular, is the benefit of a barrage that shall eventually be erected in the Oude Maas near its confluence with the waterway. By closing the Oude Maas in times of small river discharges all fresh water that is available will then flow past Rotterdam. It is to be expected that this concentration on one branch will have a favorable effect on the suppression of the salt penetration. The question is whether this effect will be worth while. It can only be answered after a thorough investigation of the motion of fresh water and salt water in the river branches that are involved. This motion is complicated by the mixing effect of the huge harbor basins alongside the northern branch. This study comprises salinity measurements on the rivers, combined with measurements of the turbulence in the mixing zones, next to which fundamental model tests are foreseen where the principles of the movement of the salt wedge, its turbulent diffusion and the effects of the storing basins will be studied.

STUDY OF THE MOVEMENT OF DRIFT ICE

Fig. 8 shows roughly the situation of the movement of drift ice in the northern basin during severe winters. On the average, such a situation has to be

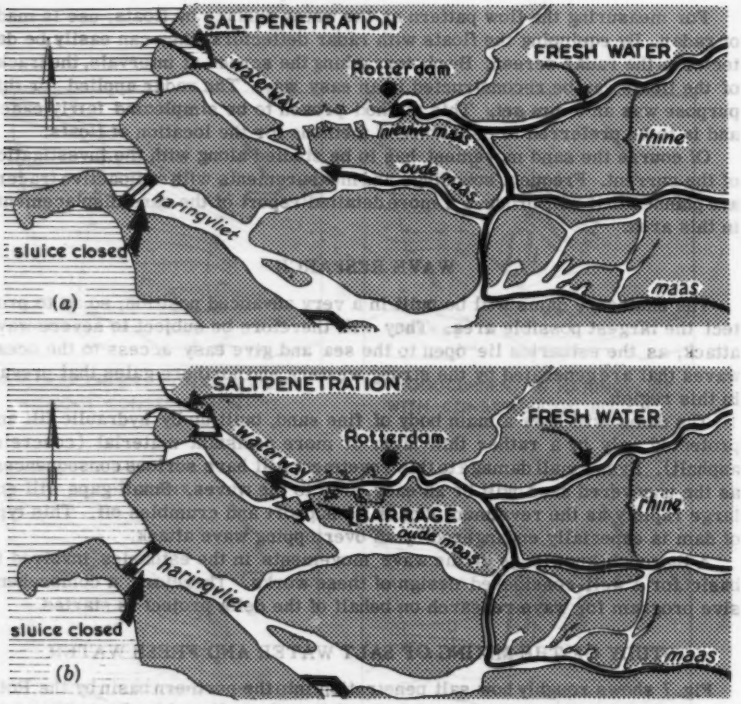


FIG. 7.—SUPPRESSION OF SALT PENETRATION IN NORTHERN DELTA AREA

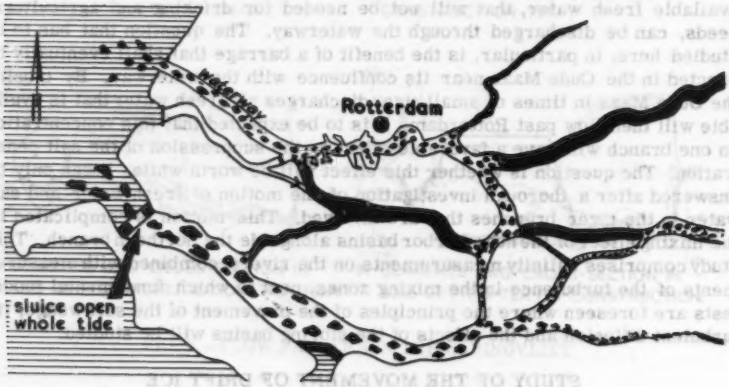


FIG. 8.—MOVEMENT OF DRIFT ICE IN NORTHERN DELTA AREA

expected once in 5 yrs, because the winters are mostly rather mild in the Netherlands.

The aim is to keep the ice on the main branch of the Rhine floating, in order to prevent the formation of ice barriers that would endanger the dikes when thaw has set in and the discharge of the rivers is rapidly increased. The ice has to be discharged mainly through the Haringvliet sluices.

In addition to the ice that comes from the Rhine, the Haringvliet basin itself is an important producer of ice. It is considered to keep the Haringvliet sluice in these ice periods open during the entire tide. By doing this, the tidal currents in the basin are enlarged, so that they may keep the ice adrift. Moreover, the penetration of salt water from the North Sea, that has a higher temperature than the Rhine water, may suppress the formation of ice fields in the basin, especially near the sluices.

However, regardless of the open sluice, the tidal currents on Haringvliet and adjoining river branches will be considerably decreased compared with the existing situation. It has to be expected, therefore, that the discharge of drift ice will meet with much more obstructions when the delta project has come into being. The measures that are necessary to meet this difficulty must be known, so that no dangerous situation will occur in the future. The study of this question includes temperature measurements during ice periods in the existing situation, reconnaissances (mainly from the air of the movements of drift ice and especially of colored ice flows), measurements of the relative velocity of the ice flows with respect to the surrounding water. Special investigations will be made into the effect of wind on the movement of the drift ice.

CONCLUSIONS

The Delta-project leads to considerable changes of the hydraulic regime of a wide-spread area. In general, near the works under construction, local disturbances may occur.

The alluvial formations of the estuaries and the bordering islands are liable to erosion, while the important agricultural and industrial areas of the Delta are very sensitive to changes of the water-management in the region effected. Miscalculations as to the hydraulic effects of the Deltaplan may, therefore, have very unpleasant consequences. Thus, comprehensive hydraulic investigations are needed to answer urgent questions in many fields.

Most important, and equally difficult, are the researches into the tides, and the study of sandmovements and the wave-research connected with the project.

Thanks to extensive amount of modern equipment, fair progress in all these fields is being made, but there remains much to be done in the many years before the project will be realised.

AMERICAN SOCIETY OF CIVIL ENGINEERS

Founded November 5, 1852

TRANSACTIONS

Paper No. 3060

METEORIC VERSUS NONMETEORIC GROUND WATER

By Harold E. Thomas[1] and Donald E. White[2]

SYNOPSIS

As the demand has increased for surface water and ground water that is replenished by the hydrologic cycle, speculation has developed concerning the possibilities of developing potable, nonmeteoric water supplies. However, recent research indicates that practically all juvenile water is too highly mineralized for most uses.

Nearly all scientific reports on ground water are concerned exclusively with meteoric water, that is, water of the hydrologic cycle that involves evaporation, atmospheric circulation, precipitation as rain or snow, and surface and subsurface movement toward the oceans. But what of water that is not of meteoric origin? Many geologists have described several types of water that have originated by recrystallization, dehydration, compression, cooling, and other processes that are active in the earth's crust. Perhaps we have missed an opportunity by neglecting such possible sources. This is particularly pressing in areas where there is an insufficient supply of meteoric water and in which such water may be involved in controversies concerning water rights. The imagination is excited by the idea of discovering a source of proven juvenile water that, by being outside the realm of the hydrologic cycle, might also be deemed to be beyond the realm of established water law.

It is not easy to differentiate juvenile water (water that has never appeared at the earth's surface) from rejuvenated water. However, the distinction is not important because both originate in processes related to rock development. A logical classification of nonmeteoric waters might, therefore, correspond to the broad classification of rock types of igneous, sedimentary, and metamorphic.

Note.—Published essentially as printed here, in June, 1959, in the Journal of the Irrigation and Drainage Division, as Proceedings Paper 2060. Positions and titles given are those in effect when the paper was approved for publication in Transactions.

[1] Geologist, Ground Water Branch, Water Resources Div., U. S. Geol. Survey, Menlo Park, Calif.

[2] Geologist, Mineral Deposits Branch, Geologic Div., U.S. Geol. Survey, Menlo Park, Calif.

Magmatic water has been described[3] as being in, or derived from magma. Such water may be called[4] plutonic water if it originates at a considerable depth, and volcanic water if it comes from magma at the surface of the earth or at a shallow depth. Metamorphic water is, or has been, associated with rocks during their metamorphism, and is probably derived largely from hydrous minerals during recrystallization to anhydrous minerals at depths of many thousands of feet, where temperatures probably exceed 400°F. Connate water is the interstitial water in unmetamorphased sediments. It is largely, or entirely, of meteoric origin but has been out of contact with the atmosphere for perhaps millions of years and, during that time, it is likely to have been changed drastically from the original meteoric water. Presumably there are gradations among these three major types of nonmeteoric waters, just as there are gradations among the major types of rocks.

A basic distinction between meteoric and nonmeteoric waters is suggested by the fact that the hydrologic cycle includes a distillation process of vaporization and precipitation that has no counterpart in the development of nonmeteoric waters, except for volcanic steam. Thus meteoric water is more likely to be fresh—and fresh water is much more likely to be meteoric—than nonmeteoric water. There are of course numerous exceptions to this rule, notably of meteoric water that has passed through soluble rocks and become highly mineralized. There is little possibility that nonmeteoric waters will not be highly mineralized. The consumer's demand for fresh water explains why groundwater hydrologists have been concerned especially with meteoric waters. Many economic geologists have been interested[5] in the nonmeteoric waters because of their relation to ore deposits.

Meteoric waters are understandably dominant at land surface and at the level of the streams that provide the drainage of water to the ocean. Meteoric waters may also go to far greater depths, depending upon the rock permeabilities and opportunities for circulation of water. In some sediments fresh water has been found at depths exceeding a half-mile below sea level. There is a greater chance, however, that deep waters may be of nonmeteoric origin. Much of our present information about deep waters comes from thermal springs, some of which are associated with volcanism, and some of which rise in nonvolcanic areas, presumably from great depths.

Some major types of water of deep origin are believed[3] to be recognizable from their chemical composition. Oil-field brines dominated by sodium and calcium chlorides differ markedly from average ocean water. In general, the brines are believed to be connate in origin ("fossil" sea water) and may have a proportion of modern meteoric water ranging from negligible to high. Brines whose salinity approximates that of sea water are generally higher, relative to sea water, in bicarbonate, iodine, boron, lithium, silica, ammonium, and water-soluble organic compounds, and lower in sulfate, potassium, and magnesium. Many brines are much higher in salinity than sea water and are enriched in calcium chloride as well as sodium chloride.

Volcanic waters, although similar in some respects to connate waters, are believed to be, distinguishable. They may be distinguished by much higher tem-

---

3 "Magmatic, Connate, and Metamorphic Waters," by D. E. White, Geological Society of American Bulletin, Vol. 68, 1957, pp. 1659-1682.

4 "Thermal Waters of Volcanic Origin," by D. E. White, Geological Society of America Bulletin, Vol. 68, pp. 1637-1658.

5 "Thermal Springs and Epithermal Ore Deposits," by D. E. White, Economic Geology, 50th Ann. Vol., 1955, pp. 99-154.

perature and associated heat flow, by relatively high contents of lithium, fluorine, silica, boron, sulfur, carbon dioxide, arsenic, and antimony, by relatively low calcium and magnesium, and by lack of hydrocarbons, water-soluble organic compounds, and perhaps ammonia and nitrate. Relatively high boron and combined CO_2 alone are not reliable indicators of a volcanic origin.

During the compaction that accompanies deep burial of sedimentary rocks, the rocks lose most of their interstitial, high-chloride water. Additional water may be lost during progressive metamorphism, and the water content changes from approximately 5% in shale to, perhaps, 1% in the highly metamorphased rock, gneiss. The expelled water is termed "metamorphic." Because, normally, pressure increases downward and permeability of deeply buried rocks increases upward, the water must escape upward and mix with connate and meteoric water. Even though large quantities of such water must exist, no example of metamorphic water has been positively identified.

Recent studies of the hydrogen, isotopes, tritium (T or H^3), deuterium (D or H^2), and of oxygen (O^{18}) provided important new tools for determining the origin of ground water. The appearance of tritium in a water sample provides conclusive evidence that the water is meteoric, at least in part, because the tritium originates chiefly by action of cosmic rays upon the nitrogen atoms of the atmosphere and, recently, as a by-product of the hydrogen bombs, has been distributed throughout the world by atmospheric circulation. However, because tritium has a half-life of only 12.4 yr, the tritium content of meteoric water becomes too low to be measurable after the water has been isolated from the atmosphere for over approximately 50 years. Thus, absence of tritium is not proof of nonmeteoric origin of water because meteoric ground waters are commonly more than 50 yr old. On the other hand, neither is its presence proof that the sample is entirely of meteoric origin.

The relative concentrations of deuterium and O^{18} may also be of value in identifying the origin of water. Evidence from analyses of these constituents indicates that the water from most thermal springs is predominantly, if not exclusively, meteoric. The average ocean water is constituted of approximately 99.77% H_2O^{16}, 0.03% HDO^{16}, 0.20% H_2O^{18}, and a minute percentage of molecules containing tritium. Since H_2O^{16} has the highest volatility of the three most common water molecules, ocean waters should have high concentrations of the heavy isotopes, and terrestrial, fresh waters should be relatively depleted of these isotopes. This pattern is confirmed experimentally. Craig, Boato, and White report[6] that, in several hundred samples of water from snow, rain, rivers, and lakes, the deuterium concentration varies approximately 30% from 3% higher to 27% lower than that in average ocean water. The O^{18} concentration is reported to vary 4%, from 0.6% higher to 3.4% lower than that in average ocean water. The depletions in both isotopes show a general correlation with distance from the ocean, and there is a general decrease in heavy-isotope concentration with increasing latitude, reflecting the continuous loss of vapor from the poleward-moving air masses. In a few highly evaporated waters, generally in lakes having little or no external discharge, the water is "heavier" than that in the ocean. In any given area the average meteoric water is likely to be isotopically different from the meteoric waters of other areas. Any deep water of nonmete-

[6] "Isotopic Geochemistry of Thermal Waters," by Harmon Craig, Giovanni Boato, and Donald E. White, Proceedings, 2nd Conf. on Nuclear Processes in Geol. Settings, Acad. Sci. Nat. Res. Council Publ. 400, 1956, pp. 29-38.

oric origin, that is, rising to the surface, is especially likely to differ isotopically from the meteoric water that happens to characterize the area into which it rises.

As Craig, Boato, and White point[6] out

> ". . . Thermal waters show a strict dependence on the isotopic composition of the local surface water. They display a knowledge of the local climatic conditions on the earth's surface, knowledge of which magmatic waters should surely be ignorant . . . We have no positive isotopic evidence for any juvenile or magmatic water in any of the hot spring systems we have studied."

White has reported[4] that magma is required as a source of the observed temperatures and calculated heat flow in the thermal springs of many volcanic areas, and he concludes that even in these volcanic areas the thermal waters have a volcanic component that probably does not exceed 5% to 10% of the total. He concludes that meteoric water circulates to great depths and in some places mixes with a small proportion of magmatic water. Thus, the thermal waters of certain well-known volcanic areas, such as Yellowstone Park, are predominantly of meteoric rather than magmatic origin.

In contrast, the highly mineralized connate water of oil fields and the water of certain saline springs are different[3] isotopically from the meteoric waters at and near the surface of the same areas. These mineral waters cannot have mixed appreciably with "modern" meteoric water.

During a recent conference on nuclear process, Harmon Craig summarized[6] the present status of isotopic geochemistry:

> ". . . With our present knowledge we could not distinguish magmatic water of original oceanic origin from truly juvenile water. Furthermore, a low tritium content is not, of course, unequivocal, since one cannot thus distinguish between dead rain water and juvenile water mixing in. The most important thing is to combine stable and radioactive isotope studies on problems of this kind, and use as many isotopes in conjunction as you can. Then you really begin to hit hard at questions such as sources, rates, and so forth, and you have a really powerful tool."

White has also shown[3,4] that any large supply of water, actively flowing to the surface from great depth, must be anomalously high in temperature. In general, temperature rises 1°F per 100 ft below the surface. A small quantity of water could rise slowly from some depth and lose most of its heat by conduction, but water with a large rate of flow should arrive at the surface with most of its original heat content.

CONCLUSIONS

Fresh water of low temperature is virtually certain to be of meteoric origin in whole or in part. Future study of isotopes may be expected to substantiate this interpretation.

Water of nonmeteoric origin, including that formed in volcanic and metamorphic processes, is characteristically highly mineralized. Thus, although they have been the source of mineral waters, mineral baths, and various chemicals of economic value, and will continue to do so, "juvenile" waters are likely to be of negligible value in meeting the national demand for fresh water.

AMERICAN SOCIETY OF CIVIL ENGINEERS

Founded November 5, 1852

TRANSACTIONS

Paper No. 3061

HYDROLOGY OF URBAN RUNOFF

By A. L. Tholin,[1] M. ASCE, and Clint J. Keifer,[2] A. M. ASCE

With Discussion by Messrs. Peter O. Wolf; M. B. McPherson and M. Joseph Willis; Paul Bock; Carl F. Izzard and Charles L. Armentrout; A. L. Tholin; and Clint J. Keifer

SYNOPSIS

Presented in this paper is a detailed study of rainfall runoff relationships in urban areas based on a "Design Storm" of three hours duration. The "Chicago Hydrograph Method" of sewer design evaluates, in detail, the rainfall abstractions and flow detentions which intervene between the hyetograph of rainfall and the hydrographs of sewer supply and sewer outflow. Several types of uniform land use with various values of ground slope and depression pondage have been studied.

Based on the sewer hydrographs, thus derived, a series of easy-to-use design charts are presented, that can later be expanded to cover other combinations of the interdependent variables. The use of electronic computers has made such computations feasible.

For economical trunk sewer design in drainage areas, of a square mile or more, the authors present a further study of the hydrographs of sewer flow to delineate the surface profiles of instantaneous backwater-drawdown curves. An evaluation of the effect of nonuniform areal distribution of rainfall on the sewer flow hydrographs in large drainage areas is also presented. A sewer gauging station, coupled with a recording rain gauge, is being established in a fully developed, ten acre, residential area. The Chicago sewer pattern includes approximately ten thousand such "unit" areas, with various types of land use.

INTRODUCTION

Immediately following World War II, the city of Chicago, Ill. embarked on the largest sewer construction program in its history. An engineering report

Note.—Published, essentially as printed here, in March, 1959, in the Journal of the Sanitary Engineering Division, as Proceedings Paper 1984. Positions and titles given are those in effect when the paper or discussion was approved for publication in Transactions.

[1] Admin. Engr. of Pub. Wks., Dept. of Pub. Wks., Chicago, Ill.
[2] Engr. of Sewer Hydr., Bureau of Engrg., Chicago, Ill.

prepared in 1944 by the Bureau of Sewers had indicated the urgent need for $86,000,000 worth of new sewer construction. Further studies and the continued growth of the city have raised that figure for the total program to $165,000,000. A new sewer planning division was organized to prepare plans and specifications. Bond issues totalling $96,000,000 have been approved by the voters, and additional bond issues are planned.

The "rational method" for determination of quantities of stormwater runoff had been used by the city for several decades. This method which first appeared around the year 1900 is still the most widely accepted method in the United States. With a program of sewer construction involving more than $100,000,000 in expenditures, it seemed proper to re-examine the validity of the rational method, as it was applied to the problems or urban runoff, and to explore the possibilities of a new approach to the understanding and solution of such problems.

Many books have been published dealing with the hydrology of stream flow in mixed urban and rural areas. In large drainage areas involving river systems, the concept of hydrographs has become the basic approach. Some studies of the application of hydrographs to the problems of urban drainage have been made but none of these have been sufficiently developed to produce a simple, yet comprehensive method for sewer design.

Sewers with widths as great as 20 ft, as in Chicago, draining thousands of acres of highly developed urban area are essentially underground rivers and the concepts of the river hydrologists seem applicable. In Chicago, therefore, it became desirable to attempt an understanding of the time of occurrence versus rate-of-flow relationship at principal points in the trunk lines during actual or hypothetical rainstorms. If these relationships could be established in the form of sewer flow hydrographs, instantaneous backwater or drawdown curves could be computed from them and the performance of the trunk sewer more adequately understood.

The use of the rational method without modification is, without doubt, the simplest means of obtaining an answer to the rainfall runoff relationship. The rational formula is usually expressed as $Q = Ci_{ave} A$, in which A is defined as the area, in acres, tributary to the point of design; and i_{ave} is the average intensity of precipitation for a duration equal to the time of flow from the most remote portion of the drainage area to the point of design. This average intensity must be selected from rainfall statistics related to the probable frequency of occurrence of storms of such intensities. Q is the rate of runoff expressed in cubic feet per second.

The remaining component of the equation, C, is a complex variable having concealed within it numerous interdependent variables such as the character of land use, the extent of land coverage by impervious surface, the slope of ground surface, the infiltration capacity of the pervious area, the cumulative volume of minor or major puddles and pools, the length of overland flow, and the roughness coefficient of all overland flow surfaces and channels. Where drainage areas are now only partly developed, a future stage of development must be assumed. The compositing of all of these interdependent variables in their proper proportion to develop the value of C cannot be methodically conceived by any form of mental exercise. Consequently, the determination of C must come out of years of experience in a particular locality and cannot be adequately nor easily conveyed to a novice. Too often, due to economic necessity, the value of C, being the only adjustable value in the formula, is, therefore, adjusted to match the available dollars.

In the following presentation, various types of uniform land use, ranging from suburban residential to industrial and commercial, have been analyzed and the end results determined. The principal influences which have been evaluated for each type of land use are infiltration capacity of pervious areas; depression storage; overland flow detention; detention in gutters; and detention in lateral sewer systems.

Having developed a methodology and derived or assumed the numerical values of these peak-reducing factors, each of these factors can be subject to examination and review by other investigators, and such efforts will clarify the concepts of rainfall-runoff relationships in urban areas.

The unit of 10 acres is typical of the Chicago street pattern and may be typical of some other cities. There are more than 10,000 such lateral sewers in the city of Chicago. At any rate, the computed outflow hydrographs from a 10-acre drainage area, with the rate of runoff expressed in inches per hour, would be directly comparable with similar hydrographs for areas of approximately the same size and land use in other cities having similar rainfall.

A condensed description of the hydrograph type of analysis as used by the city of Chicago is outlined in this paper. The Chicago methodology will be described step by step.

The intricacy and volume of computations required for the derivation of the final series of charts would have been too formidable without the introduction of the electronic computer. The basic concepts have been adjusted slightly and the graphical relationships have been translated into mathematical formulas in order to utilize the time-saving value of the electronic computer. Such adjustments have been checked as to their effect by comparison at critical points with results obtained by the manual computations.

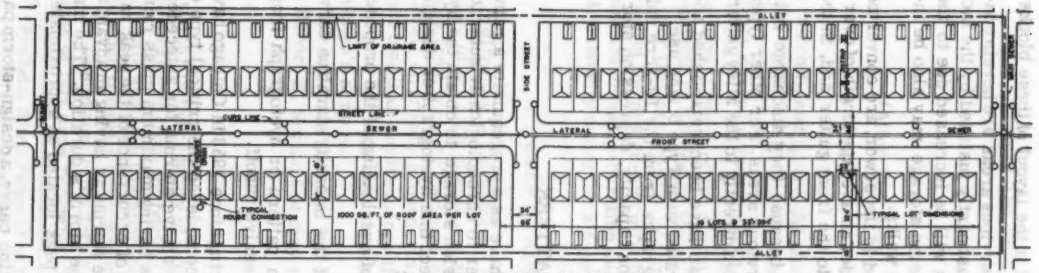
Notation.—The letter symbols adapted for use in this paper are defined where they first appear, in the illustrations or in the text, and are arranged alphabetically, for convenience of reference, in the Appendix.

STEP 1. STREET LAYOUT AND LAND USE

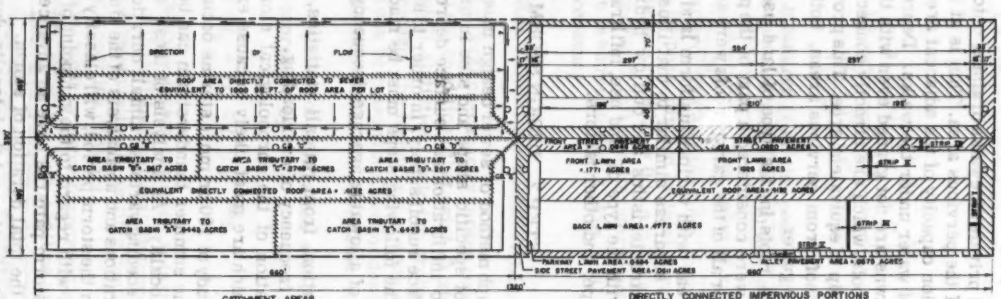
A determination must be made of the layout of the basic drainage area. The path that the water must take to reach the underground sewer system, the length and slope of overland flow strips, the location of gutter summits, the length and slope of gutters, the building arrangement, a determination of whether the roofs are directly connected to the underground sewers or whether they discharge through the downspouts on to lawn areas, the roughness factor to be used on all surfaces, and other physical measurements must be determined before computation can proceed.

For the city of Chicago, in general, a system of parallel main sewers are laid out at half-mile intervals. Each of these mains has a set of lateral sewers extending for a quarter-mile on each side of the main sewer. It was decided to use the 10-acre catchment area of the laterals as the unit area to be studied. This area consists of two standard 5-acre blocks, with each block being 330 ft wide by 660 ft in length.

Fig. 1 shows the drainage plan of a typical 10-acre unit area using Type 5 land use as an example. The upper plan shows the lot dimensions and arrangement, the street lines, curb lines, and the location of catch basins and manholes. For the lower plan, the left-hand side gives the tributary areas of each catch basin, and the arrows show the direction of flow. On the right-hand side, the



PLAN SHOWING LAND USE AND SEWERAGE



CATCHMENT AREAS — DIRECTLY CONNECTED IMPERVIOUS PORTIONS

PLAN SHOWING DRAINAGE AREA AND DIRECTION OF FLOW

STRIP	DESCRIPTION	LENGTH IN FT.	SLOPE	IZZARD'S ROUGHNESS FACTOR "r"
I	DENSE BLUE GRASS TURF, PERVIOUS	16	.01	.06
II	DENSE BLUE GRASS TURF, PERVIOUS	40	.01	.09
III	DENSE BLUE GRASS TURF, PERVIOUS	70	.01	.20
IV	STREET PAVEMENT, IMPERVIOUS	17	.02	.015
V	ALLEY PAVEMENT, IMPERVIOUS	8	.0375	.012
VI	COMMON COMPOSITION ROOFING, IMPERVIOUS	12	.667	.020

○ CATCH BASINS
○ MANHOLES

TOTAL IMPERVIOUSNESS

PERVIOUS AREAS	5.37 ACRES	53.7 %
IMPERVIOUS AREAS		
DIRECTLY CONNECTED	3.00 ACRES	30.0 %
DISCHARGING ONTO PERVIOUS AREAS *	1.63 ACRES	16.3 %
UNIT AREA	10.00 ACRES	100.0 %

* INCLUDES GARAGE ROOFS, PUBLIC WALKS AND PRIVATE WALKS

FIG. 1.—DRAINAGE PLAN OF A TYPICAL TWO-BLOCK UNIT AREA

catchment areas are broken down into pervious and impervious portions, with the impervious areas cross-hatched. The areas in acres are given for each of these subareas. Also shown are the elemental strips for which overland flows are computed, and a table below for description, length, slope, and Izzard's factor C for each of these strips.

Several simplifying assumptions are introduced in the layout of these blocks.

1. Public and private sidewalks draining onto pervious areas are herein considered a part of the pervious area. This is at least partly justified by the fact that the infiltration capacity of the adjacent areas will be increased due to the lateral spread of water under the walks. Depression storage may also be increased if the lawns are not graded even with the walks.
2. Building roofs, which are directly connected to the sewer, are converted into a uniform strip of equivalent area. This provides an average length of overland flow, for runoff from pervious areas, both to the front gutter and, in the rear, to the alley gutter.
3. The garage roofs in this type of land use, because they discharge onto backyard lawns, were considered a part of the pervious areas. For other types of land use, part or all of the garage roofs were added directly to the alley gutter.

Other unit areas with various uniform land use have been established and were divided into subareas similar to that illustrated with Type 5 land use.

The runoff characteristics and outflow hydrographs from the 10-acre unit area will vary with the type of land use, infiltration capacity, depression storage, surface slope, and other factors.

STEP 2. DESIGN STORM PATTERN

The hydrograph method of sewer design must have as a prerequisite a rainfall hyetograph of specific shape and size in order to chronologically subtract the losses due to infiltration and surface depression storage to obtain the hydrograph of surface runoff supply. In order to select this hyetograph or design-storm pattern, the following steps must be made:

1. Selection of allowable average frequency of overloading of the proposed sewer.
2. Determination, from rainfall statistics, of the intensity-duration curve for the selected frequency of overloading.
3. Determination of the chronological storm pattern or hyetograph from those storms which are most likely to cause excessive runoff.

A detailed study of 100 or more storms occurring since 1933 in Chicago have indicated that the summer thunderstorm can be considered the critical type of storm for that locality. An analysis of these excessive storms for antecedent precipitation preceding various rainfall durations having maximum mass rainfall for such durations and an analysis of the time of occurrence of the peak rate of rainfall within the storm period, will classify the storms as having an advanced or delayed peak with regard to the midpoint of the storm's duration. The majority of these storm patterns have an advanced peak located at approximately three-eighths of the total duration of storm.

Using the peak location and the intensity-duration curve, a design-storm pattern or hyetograph can be computed so as to conform at all points to the intensity-duration curve. The 3-hr duration of the design rainstorm was selected to

cover the time of travel from headwater to outlet in the largest individual sewer systems within Chicago.

The equation[3] for the design-storm pattern is

$$\text{(Before The Peak)} \quad i = \frac{a\left[(1-b)\left(\frac{t_b}{r}\right)^b + C\right]}{\left[\left(\frac{t_b}{r}\right)^b + C\right]^2} \quad \ldots\ldots\ldots (1a)$$

$$\text{(After The Peak)} \quad i = \frac{a\left[(1-b)\left(\frac{t_a}{1-r}\right)^b + C\right]}{\left[\left(\frac{t_a}{1-r}\right)^b + C\right]^2} \quad \ldots\ldots\ldots (1b)$$

in which t_b and t_a are the time measured from the peak to the left and to the right respectively, and a, b, and c are constants found in the rate-duration-frequency curve formula such as $i_{ave} = \frac{a}{t_d^b + C}$. The value of r is a measure of the advancement of the storm pattern, (the elapsed time, in minutes from the beginning of the design storm to its peak, divided by total duration of storm).

For this example the constants are a = 90, b = 0.9, c = 11, and r = 3/8. The graph of the design-storm pattern (Fig. 2 (b)), and its interrelation with the concomitant intensity-duration curve is shown in Fig. 2. Fig. 2 (a) shows the rainfall-intensity curve for a 5-yr frequency.

STEP 3. ABSTRACTIONS FROM RAINFALL

Infiltration.—The selection of infiltration-capacity curves requires an examination of the type of soil and surface conditions that exist. A study needs to be made from local or regional rainfall statistics, as to the probability of heavy rainfall on frozen ground. In Chicago, the frequency of such occurrences is much less than any frequency that can be reasonably used for design of the sewer systems. Such an occurrence is, therefore, not applicable to the design of Chicago's sewers.

The accepted formula for the capacity of infiltration was first suggested[4] by Robert E. Horton and may be expressed by

$$f = f_c + (f_o - f_c)\, e^{-kt_f} \quad \ldots\ldots\ldots\ldots (2a)$$

in which f is the capacity of infiltration in inches per hour, t_f is the time in minutes measured from the beginning of the infiltration capacity curve, f_c is the constant rate at which f is approached asymptotically as time continues, f_o is the rate when t_f equals zero, and k is a positive constant.

For this example, the infiltration-capacity curve for normal antecedent conditions of turf area recommended[5] by Stifel W. Jens, shall be used to evaluate

---

[3] "Synthetic Storm Pattern For Drainage Design," by Clint J. Keifer and Henry Hsien Chu, Proceedings Paper 1332, ASCE, August, 1957.

[4] "An Approach Toward a Physical Interpretation of Infiltration Capacity," by R. E. Horton, Proceedings, Soil Science Society of America, Vol. 5, 1940, pp. 399–417.

[5] "Drainage of Airport Surfaces—Some Basic Design Considerations," by S. W. Jens, Transactions, ASCE, Vol. 113, 1948, p. 785.

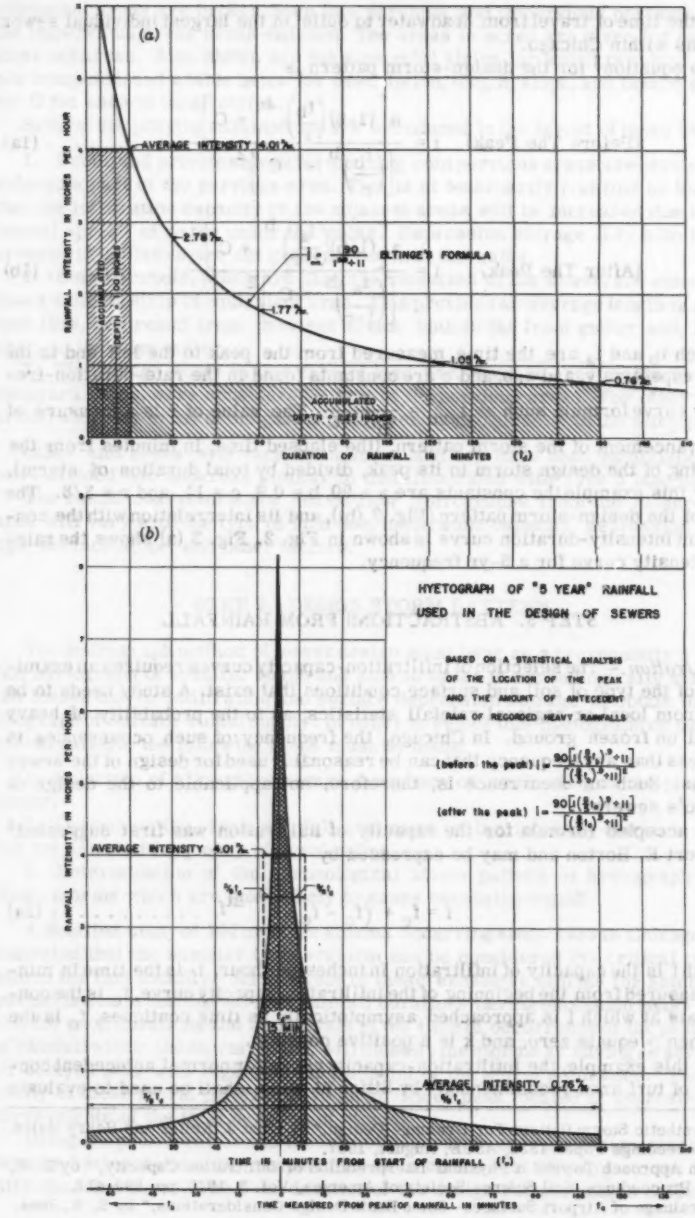


FIG. 2.—INTENSITY DURATION CURVE AND CONCOMITANT STORM PATTERN

the constants in Eq. 2a. Thus, Eq. 2a becomes

$$f = 0.53 + 2.47\, e^{-0.07\, t_f} \quad \ldots\ldots\ldots\ldots \quad (2b)$$

and its graph is plotted in Fig. 3. The area under this curve represents the accumulated mass infiltrated, which can be expressed as

$$F = \int_0^{t_f} \frac{f}{60}\, dt_f = 0.00883\, t_f + 0.59\left(1 - e^{-0.07\, t_f}\right) \quad \ldots\ldots (3)$$

in which F is the mass infiltrated in inches until the time t_f. The graph of this equation is also shown in Fig. 3. In cases where the rainfall at the beginning is less than the infiltration capacity curve, the actual amount absorbed by the soil is, of course, limited by the mass rainfall.

Assuming,[6] that "overland flow and depression storage supply" commences when the antecedent mass of rainfall equals the antecedent mass of infiltration, the time of the beginning of any excess is found, as in Fig. 4a, by shifting the infiltration mass curve on its time scale until it is tangent to the rainfall mass curve. The amount of shift required to bring the two curves into tangency shall be termed the offset. The offset in Fig. 4 (a) was found, by scaling, to be 48.5. At the point of tangency where t_o equals approximately 60 min, the masses are the same, because the ordinates are of equal heights and the rates are also the same, because the slopes are equal. Fig. 4 (b) shows the rate curves of the design-storm pattern, infiltration capacity, and the actual infiltration. The actual infiltration curve follows the design rainfall curve until it intercepts the offsetted infiltration-capacity curve, following which it proceeds along the latter. It will be noted, starting at approximately 60 min after the beginning of the rainfall, that the rainfall exceeds the infiltration, thus producing excess water which will begin to fill small depressions on the ground surface. Subtracting the ordinates of the actual infiltration curve from the rainfall rate and plotting against the same time scale, a new curve will be obtained which shall be termed the overland flow and depression storage supply. This curve is plotted in Fig. 5, together with its accumulated mass, which may be obtained by subtracting the actual mass infiltrated from the accumulated mass of the design-storm pattern, in Fig. 4 (a).

Surface Depression Storage.—Even with carefully-graded lawns there are still many small depressions that must be filled before surface runoff begins. Where blocks contain vacant lots, some, or all, of the lots may be depressed below the sidewalks, thus creating large pools of depression storage. For storm-sewer design, however, it will generally be assumed that these larger areas will be filled and graded at some later date. To evaluate the effect of depression storage an estimate must be made of the mass or average depth of rainfall which is retained in surface depressions where its dissipation can only be accomplished either by evaporation or post-storm infiltration. An assumption must also be made of the relationship between the mean depths of depressions and the proportionate areas covered by such depressions.

Because the mean depth of each depression in a drainage area is different from that of all other depressions, the runoff supply will be affected by the manner of variations of the depth of the individual depressions from the average

[6] "Surface Runoff Determination From Rainfall Without Using Coefficients," by W. W. Horner and S. W. Jens, Transactions, ASCE, Vol. 107, 1942, p. 1039.

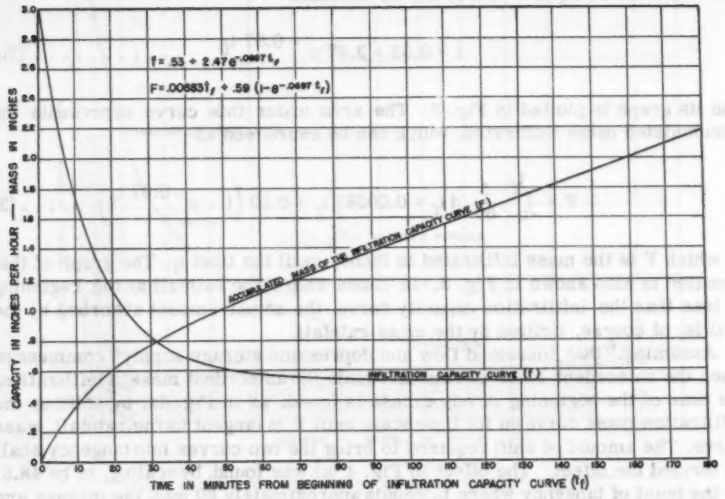


FIG. 3.—INFILTRATION CAPACITY AND MASS CURVES

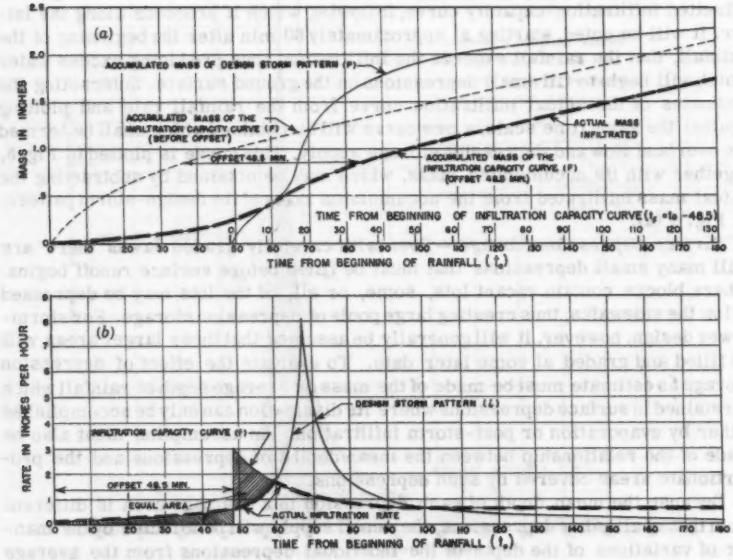


FIG. 4.—DETERMINATION OF INFILTRATION OFFSET

depth of all depressions. The shallowest depressions will overflow immediately, and the deeper ones will follow in the order of their depth.

Some investigators have assumed that all depressions must be filled before overland flow supply begins (Fig. 6). This relationship would occur only if the larger depressions were grouped near the downstream end of all overland flow strips. The smaller depressions would fill and overflow into the larger ones, finally filling all depressions before overflowing into the gutter.

Other investigators have used[7] an exponential relationship such as

$$V_d = s_d \left(1 - e^{-K_d (P-F)}\right) \quad \ldots\ldots\ldots\ldots\ldots \quad (4)$$

in which V_d equals the volume of water in surface depressions, s_d is the overall volume of depression storage available, P-F is the mass overland flow and

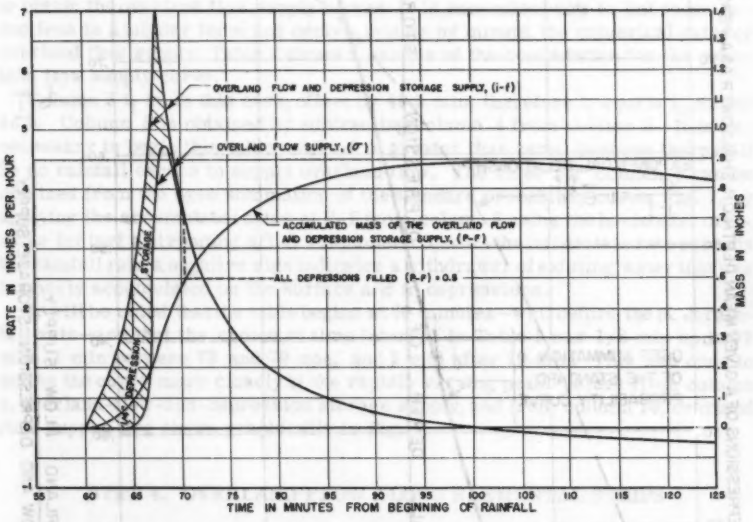


FIG. 5.—DERIVATION OF OVERLAND FLOW SUPPLY CURVE

depression storage supply, and K_d is a storage constant. This equation can be transferred into the rate relationship of overland flow supply to overland flow and depression storage supply,

$$\frac{\sigma}{i-f} = 1 - e^{-\frac{P-F}{S_d}} \quad \ldots\ldots\ldots\ldots\ldots \quad (5)$$

and is plotted for comparison in Fig. 6.

[7] "Applied Hydrology," by R. K. Linsley, Jr., M. A. Kohler and J. L. H. Paulhus, McGraw-Hill Book Company, Inc., New York, 1949.

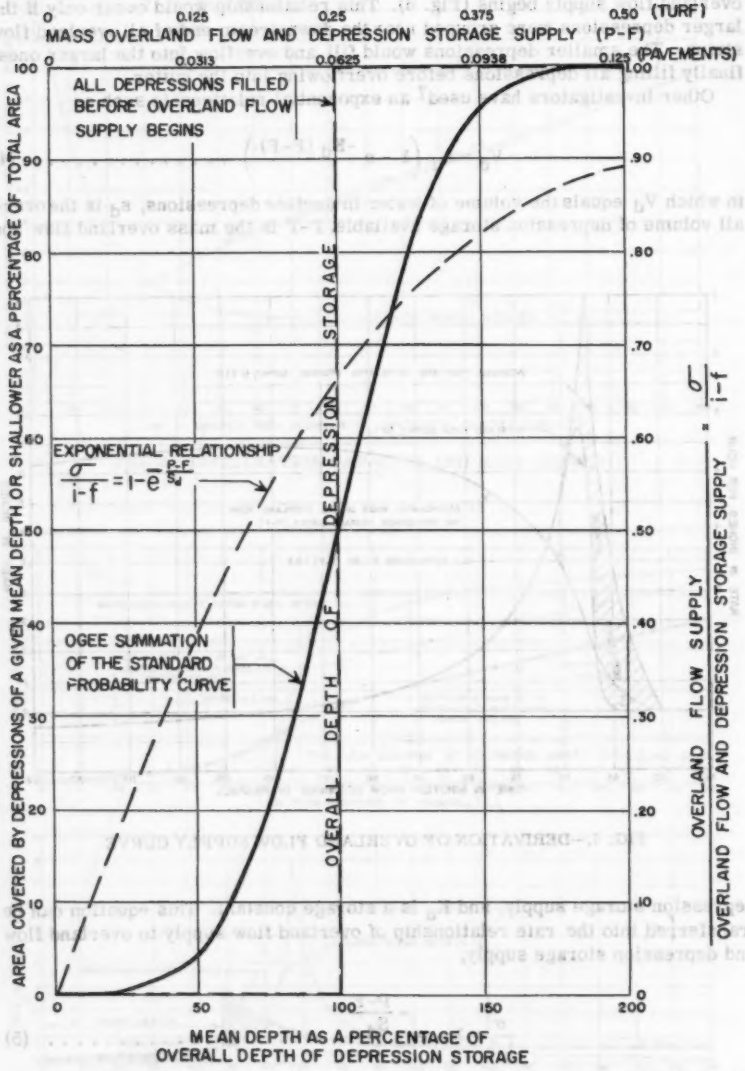


FIG. 6.—DEPTH DISTRIBUTION CURVE OF DEPRESSION STORAGE

It is believed, however, that some curve lying between these relationships as plotted in Fig. 6 would better represent the probable depth-distribution relationship for fully-developed urban areas in which depressions of a given mean depth may be found at any random location. A not too rigorous analysis of the problem has indicated the curve may be of ogee shape. The ogee summation of the standard probability curve was thereupon adopted for the depth-distribution curve of depression storage, as shown in Fig. 6.

For the following computations of overland flow supply the over-all volume of depression storage is assumed equal to 1/4 in. on pervious areas, and individual depressions range in depths from 0 in. to 1/2 in. The over-all depression storage on pavement areas is set at 1/16 in., with the depth of depressions ranging from 0 in. to 1/8 in. These assumptions seem reasonable, from observations made during heavy rainfalls.

Overland Flow Supply.—The procedure has been outlined herein for evaluating the deductions of infiltration and depression storage from the rainfall hyetograph to obtain the overland flow supply curves. It is convenient now to list these deductions in a tabular form and derive, minute by minute, the numerical rates of overland flow supply. Table I shows a sample of the computation for the overland flow supply curve.

Column 3 t_f is, in this case, offset by 48.5 min, therefore t_f equals t_o minus 48.5. Column 5 is obtained by subtracting column 4 from column 2. It is unnecessary to begin this table until i-f is greater than zero, because there will be no rainfall excess to supply overland flow. The value for column 9 can be obtained from the ogee summation of the standard probability curve, Fig. 7, by applying the accumulated mass of P-F from column 8 using the horizontal ordinates for turf and reading σ/i-f. For column 5, when the infiltration rate exceeds the rainfall rate a negative sign indicates a withdrawal of existing water that was formerly accumulated on the surface and in depressions.

It will be noted that the table begins at 60 minutes—well before the peak rainfall rate—and that the choice of time interval in Table I was 1/2 min up to 72 min, 1 min between 72 and 79 min, and 2 min after 79 min. This was done to define the curve more closely at the rapidly varying peak. Values from column 5, overland-flow-and-depression storage supply, and from column 10, overland flow supply, are shown graphically in Fig. 5.

STEP 4. OVERLAND FLOW ALONG ELEMENTAL STRIPS

The overland flow supply of rainfall-excess curves have been developed by the deduction of retention and infiltration from the design-storm pattern. As this supply increases, it builds up a sheet of water over the surface, and the water begins to flow toward the collecting gutter. This movement of the water is designated overland flow and the volume of transient water on the surface is termed surface detention.

Carl F. Izzard, in experimental work done by the Public Roads Administration, U.S. Dept. of the Interior (PRA) and the Soil Conservation Service, U.S. Dept. of Agriculture, found[8] that under steady flow conditions, the average depth

[8] "Hydraulics of Runoff From Developed Surfaces," by C. F. Izzard, Proceedings, Highway Research Board, National Research Council, December, 1946, pp. 129-150.

TABLE 1.—OVERLAND FLOW SUPPLY FOR PERVIOUS AREAS

Time, from beginning of rainfall, t_o, in minutes	Rate of rainfall, i in inches per hour	Time from beginning of infiltration capacity curve, t_f, in minutes	Infiltration rule, f, in inches per hour	Overland flow and depression storage supply, in inches per hour, i-f	Accumulated mass, in inches			$\frac{\sigma}{i-f}$	Overland flow supply rate, σ, in inches per hour
					design storm P	actual infiltration F	P-F		
(1)	(2)	(3)	(4)	(5)	(6)	(7)	(8)	(9)	(10)
60.0	1.72	11.5	1.64	0.08	0.426	0.426	0	—	0
60.5	1.81	12.0	1.60	0.21	0.439	0.439	—	—	—
61.0	1.92	12.5	1.56	0.36	0.452	0.452	—	—	—
61.5	2.04	13.0	1.53	0.51	0.466	0.464	0.002	—	—
62.0	2.18	13.5	1.49	0.69	0.482	0.478	0.004	—	—
62.5	2.36	14.0	1.46	0.90	0.500	0.490	0.010	—	—
63.0	2.58	14.5	1.43	1.15	0.520	0.502	0.018	—	—
63.5	2.82	15.0	1.40	1.42	0.540	0.515	0.025	—	—
64.0	3.11	15.5	1.37	1.74	0.565	0.526	0.039	—	—
64.5	3.43	16.0	1.34	2.09	0.594	0.538	0.056	—	—
65.0	3.81	16.5	1.31	2.50	0.630	0.550	0.080	0.012	0.03
65.5	4.27	17.0	1.28	2.99	0.66	0.56	0.10	0.023	0.07
66.0	4.87	17.5	1.25	3.62	0.70	0.57	0.13	0.053	0.19
66.5	5.60	18.0	1.23	4.37	0.75	0.58	0.17	0.121	0.53
67.0	6.62	18.5	1.21	5.41	0.80	0.59	0.21	0.316	1.71
67.5	8.18	19.0	1.18	7.00	0.86	0.60	0.26	0.526	3.68
68.0	7.17	19.5	1.16	6.01	0.92	0.61	0.31	0.777	4.67
68.5	6.47	20.0	1.14	5.33	0.97	0.62	0.35	0.887	4.72
69.0	5.83	20.5	1.12	4.71	1.02	0.63	0.39	0.959	4.51
69.5	5.33	21.0	1.10	4.23	1.07	0.64	0.43	0.99	4.19
70.0	4.87	21.5	1.08	3.79	1.11	0.65	0.46	0.99	3.78
70.5	4.48	22.0	1.06	3.42	1.16	0.66	0.50[a]	1.0	3.42
71.0	4.14	22.5	1.05	3.09	—	—	—	↑	3.09
71.5	3.86	23.0	1.03	2.83	—	—	—	↑	2.83
72	3.65	23.5	1.01	2.64	—	—	—	↑	2.64
73	3.21	24.5	0.98	2.23	—	—	—	↑	2.23
74	2.85	25.5	0.95	1.90	—	—	—	↑	1.90
75	2.58	26.5	0.92	1.66	—	—	—	↑	1.66
76	2.34	27.5	0.89	1.45	—	—	—	↑	1.45
77	2.15	28.5	0.87	1.28	—	—	—	↑	1.28
78	1.97	29.5	0.84	1.13	—	—	—	↑	1.13
79	1.82	30.5	0.82	1.00	—	—	—	↑	1.00
81	1.57	32.5	0.79	0.78	—	—	—	↓	0.78
83	1.38	34.5	0.76	0.62	—	—	—	1.0	0.62

[a] All depressions filled and overflowing.

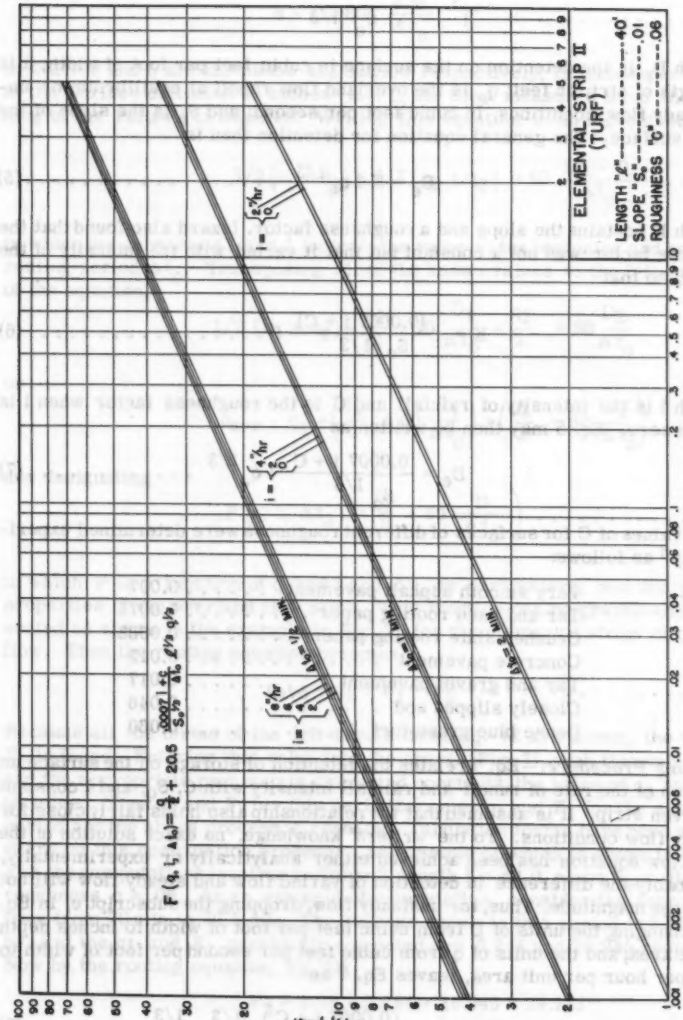


FIG. 7.—ROUTING CHART FOR ELEMENTAL STRIP

of flow is proportional to the cubic root of the discharge at the end of the strip, and inversely proportional to the cubic root of the slope of the surface. Thus,

$$\frac{D_e}{l} \propto \frac{q_e^{1/3}}{S_o^{1/3}}$$

in which D_e is the detention on the surface in cubic feet per foot of width; l is the length of strip in feet; q_e is the overland flow runoff at equilibrium or under steady flow conditions, in cubic feet per second; and S_o is the slope of the ground surface. The general equation for detention then is

$$D_e = K\, l\, q_e^{1/3} \quad \ldots\ldots\ldots\ldots\ldots\ldots (5)$$

in which K contains the slope and a roughness factor. Izzard also found that the roughness factor was not a constant but that it varied with the intensity of the rainfall, so that

$$K = \frac{(0.0007\, i + C)}{S_o^{1/3}} \quad \ldots\ldots\ldots\ldots\ldots\ldots (6)$$

in which i is the intensity of rainfall and C is the roughness factor when i is equal to zero. Eq. 5 may then be written as

$$D_e = \frac{0.0007\, i + C}{S_o^{1/3}}\, l\, q_e^{1/3} \quad \ldots\ldots\ldots\ldots\ldots\ldots (7)$$

The values of C for surfaces of different roughness were determined experimentally[8] as follows:

Very smooth asphalt pavement	0.007
Tar and sand roofing paper	0.0075
Crushed slate roofing paper	0.0082
Concrete pavement	0.012
Tar and gravel pavement	0.017
Closely slipped sod	0.046
Dense blue grass turf	0.060

Routing Procedure.—Eq. 7 relates the detention or storage on the surface as a function of the rate of runoff and rainfall intensity with C, S_o, and l constant for a given strip. It is assumed that the relationship also holds fairly close for unsteady flow conditions. To the writers' knowledge, no exact solution of the varied flow equation has been achieved either analytically or experimentally, but probably the difference in detention of varied flow and steady flow will not be of large magnitude. Thus, for unsteady flow, dropping the subscript e, in Eq. 7, and changing the units of D from cubic feet per foot of width to inches depth per unit area, and the units of q from cubic feet per second per foot of width to inches per hour per unit area, leaves Eq. 7 as

$$D = 0.342\left(\frac{0.0007\, i + C}{S_o^{1/3}}\right) l^{1/3}\, q^{1/3} \quad \ldots\ldots\ldots (8)$$

To determine the overland flow runoff hydrograph from the overland flow supply curve, a storage routing procedure is used similar to that used to route floods in river hydrology. The equation of continuity or storage equation takes the following form:

$$\sigma - q = 60 \frac{d D}{d t_o} \quad \ldots\ldots\ldots\ldots\ldots\ldots (9)$$

in which σ and q are the inflow and outflow respectively, in inches per hour; D is the surface detention in inches; and t_o the time measured from the beginning of the rainfall in minutes. Writing this equation in an incremental form

$$1/2(\sigma_1 + \sigma_2) - 1/2(q_1 + q_2) = 60 \frac{D_2 - D_1}{\Delta t_o} \quad \ldots\ldots (10)$$

in which the subscripts 1 and 2 indicate the value at the beginning and end of the routing period Δt_o. Transposing all of the known values to the left-hand side of the equation,

$$1/2(\sigma_1 + \sigma_2) - \frac{q_1}{2} + 60 \frac{D_1}{\Delta t_o} = \frac{q_2}{2} + 60 \frac{D_2}{\Delta t_o}$$

or

$$\sigma_{ave} - q_1 + \left(\frac{q_1}{2} + 60 \frac{D_1}{\Delta t_o}\right) = \left(\frac{q_2}{2} + 60 \frac{D_2}{\Delta t_o}\right)$$

and designating

$$F(q, i, \Delta t_o) = \left(\frac{q}{2} + 60 \frac{D}{\Delta t_o}\right) \quad \ldots\ldots\ldots\ldots (11)$$

in which F is a function of q and i and Δt_o as parameters, and the physical properties of the overland flow strip. This function can be graphically represented as shown in the example in Fig. 7, for the elemental strips of overland flow. Then the routing equation becomes

$$\sigma_{ave} - q_1 + F_1 = F_2 \quad \ldots\ldots\ldots\ldots\ldots (12)$$

Because all the terms of the left-hand side of Eq. 12 are known, the value of F_2 is found. Entering this value into the chart, (Fig. 7), with this value of F_2, and the appropriate parametric curve and constants, the value of q_2 can be determined. Then q_2 and F_2 for this period becomes q_1 and F_1 for the subsequent period and the above process is repeated. Tabulation forms have been set up to carry on this computation procedure, an example of which is shown in Table 2. For the computations involved in Table 2, length l = 40 ft, slope S_o = .01, and the roughness c = .06. As an example of computation, consider the increment of time from 70 min to 70.5 min. The average supply in this period is 3.58 in. per hr, and the q_1 and F_1 previously computed are 0.244 and 25.945 respectively. Now by the routing equation, Eq. 12,

$$F_2 = 3.58 - 0.244 + 25.945 = 29.281$$

Entering this number into the chart, Fig. 7, the parametric curve, for i = 4.47 in per hr and Δt_o = 1/2 min gives q_2 = 0.353 in per hr. This procedure may then be repeated for the next time increment, and so on.

In Table 1 the values of overland flow supply were computed at time intervals so chosen as to define the rapidly varying peak and to eliminate unnecessary computations in the flatter portions. These same intervals have been carried on to overland flow as the routing periods. It will be noted in Table 2 that each time the increment, Δt_o, is changed, two spaces are allotted for the time of the change. Because F is a function of q, i, and Δt_o, its value reflects the change in any of its parameters, but for a given instance the values of q and i are unique, so F reflects only the change in Δt_o. Thus, when a change of time

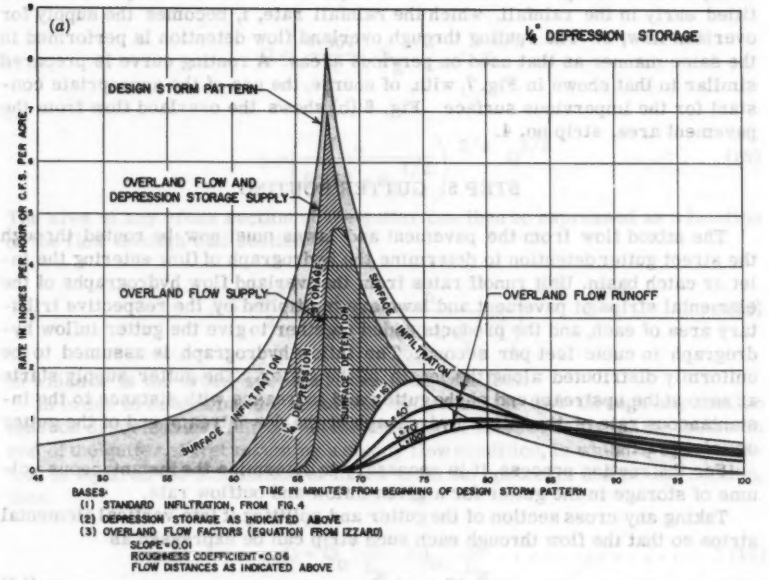
TABLE 2.—COMPUTATION SHEET FOR ROUTING OVERLAND FLOWS

Time interval, t_o, in minutes (1)	Time, t_o in minutes (2)	Average Supply, σ, in inches per hour (3)	Runoff, q, in inches per hour (4)	F (q, i, Δt_o) in inches per hour (5)	Rainfall intensity, i, in inches per hour (6)
	64.0	—	—	—	3.09
	64.5	0.000	—	—	3.42
	65.0	0.015	—	0.015	3.70
	65.5	0.05	—	0.065	4.25
	66.0	0.13	—	0.195	4.82
	66.5	0.36	—	0.555	5.58
	67.0	1.12	—	1.675	6.57
	67.5	2.69	0.001	4.365	8.18
0.5	68.0	4.17	0.008	8.534	7.18
	68.5	4.69	0.032	13.216	6.44
	69.0	4.62	0.070	17.804	5.32
	69.5	4.39	0.149	22.124	5.30
	70.0	3.97	0.244	25.945	4.86
	70.5	3.58	0.353	29.281	4.47
	71.0	3.25	0.476	32.178	4.14
	71.5	2.96	0.596	34.662	3.88
	72.0	2.71	0.715	36.776	3.62
	72.0	—	0.715	18.551	3.62
	73.0	2.41	0.925	20.246	3.21
	74.0	2.08	1.10	21.401	2.87
	75.0	1.79	1.22	22.091	2.58
1.0	76.0	1.56	1.28	22.431	2.35
	77.0	1.36	1.30	22.511	2.14
	78.0	1.20	1.29	22.411	1.09
	79.0	1.06	1.27	22.181	1.82
		—			

increment occurs, the new F = values can be obtained from that set of curves corresponding to the new time interval in Fig. 7, while holding q and i unchanged. This operation must be done at every change of time interval.

The overland flow supply and runoff hydrographs for the various elemental strips are shown in Fig. 8 (a). These were plotted from computations similar to those in Table 2. In this graphical form it is easy to visualize the relative reduction and delaying effects on the peak of the supply hydrographs when routed through the overland flow storage.

The computation procedure for impervious surfaces is the same as that outlined for the pervious surfaces, with the exception that the rainfall is not reduced by surface infiltration. Therefore, for impervious surfaces, columns 3,



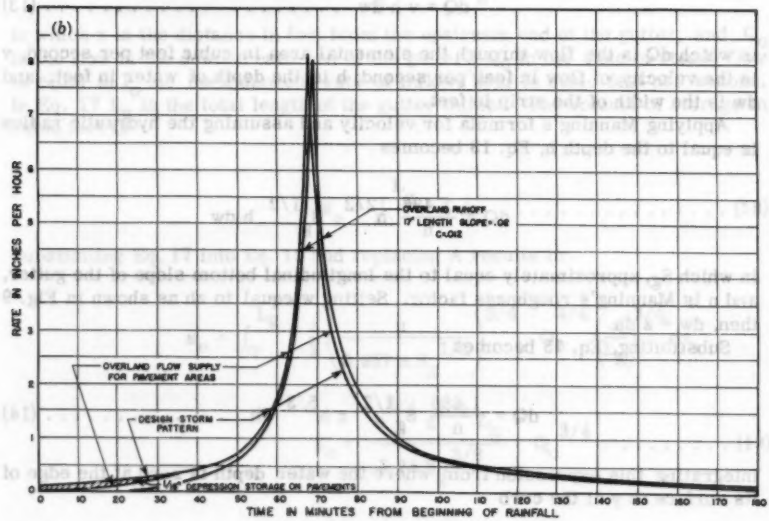


FIG. 8.—OVERLAND FLOW

4, 5, and 7 in Table 1, need not be filled in. Because usually only a small amount of depression storage is assumed on the impervious areas, the depressions are filled early in the rainfall, which the rainfall rate, i, becomes the supply for overland flow, σ. The routing through overland flow detention is performed in the same manner as that used on pervious areas. A routing curve is prepared similar to that shown in Fig. 7, with, of course, the use of the appropriate constant for the impervious surface. Fig. 8 (b) shows the overland flow from the pavement area, strip no. 4.

STEP 5. GUTTER ROUTING

The mixed flow from the pavement and lawns must now be routed through the street gutter detention to determine the hydrograph of flow entering the inlet or catch basin. Unit runoff rates from the overland flow hydrographs of the elemental strips of pavement and lawn are multiplied by the respective tributary area of each, and the products added together to give the gutter inflow hydrograph in cubic feet per second. The inflow hydrograph is assumed to be uniformly distributed along the length of the gutter. The gutter supply starts at zero at the upstream end of the gutter and increases with distance to the instantaneous rate of the inflow hydrograph at the downstream end of the gutter or inlet grating.

For the routing process, it is necessary to determine the instantaneous volume of storage in the gutter for a given inflow and outflow rate.

Taking any cross section of the gutter and splitting it into vertical elemental strips so that the flow through each such strip can be expressed as

$$dQ = v\,h\,dw \quad \ldots\ldots\ldots\ldots\ldots\ldots\ldots (13)$$

in which dQ is the flow through the elemental area in cubic feet per second; v is the velocity of flow in feet per second; h is the depth of water in feet; and dw is the width of the strip in feet.

Applying Manning's formula for velocity and assuming the hydraulic radius is equal to the depth h, Eq. 13 becomes

$$dQ = \frac{1.486}{n}\, h^{2/3}\, S_g^{1/2}\, h\,dw$$

in which S_g, approximately equal to the longitudinal bottom slope of the gutter, and n is Manning's roughness factor. Setting w equal to zh as shown in Fig. 9 then, dw = z dh.

Substituting, Eq. 13 becomes

$$dQ = \frac{1.486}{n}\, S_g^{1/2}\, z\, h^{5/3}\, dh \quad \ldots\ldots\ldots\ldots (14)$$

Integrating this expression from where the water depth is zero at the edge of its surface to y at the curb

$$Q = \int_0^y \frac{1.486}{n} S_g^{1/2} z h^{5/3} dh$$

$$Q = \frac{0.557}{n} S_g^{1/2} z y^{8/3}$$

or

$$y = \left(\frac{n}{0.557 z S_g^{1/2}} \right)^{3/8} Q^{3/8} \quad \ldots\ldots\ldots (15)$$

The area of any cross section of the gutter can then be expressed as a function of the flow through that section by

$$A = \frac{zy^2}{2} = \frac{z}{2} \left(\frac{n}{0.557 z S_g^{1/2}} \right)^{3/4} Q^{3/4} \quad \ldots\ldots (16)$$

in which A is the cross-sectional area in square feet.

In order to determine the volume in the gutter, the flow through any section must be described as a function of the distance of that section from the upstream end of the gutter. First assuming a steady flow condition, in which Q at any section is equal to the summation of inflow from the upstream end to that section, then

$$Q = Q_o \frac{x}{L_g} = I_o \frac{x}{L_g} \quad \ldots\ldots\ldots\ldots\ldots (17)$$

in which x is the distance in feet from the upstream end of the gutter, and Q_o is the flow at the downstream end of the gutter. Q_o in the case of steady flow is equal to I_o the instantaneous rate of inflow, both in cubic feet per second. In Eq. 17 L_g is the total length of the gutter in feet. The volume of storage in cubic feet is

$$s_e = \int_0^{L_g} A \, dx \quad \ldots\ldots\ldots\ldots\ldots (18)$$

Substituting Eq. 17 into Eq. 15 and replacing A results in

$$s_e = \int_0^{L_g} \frac{z}{2} \left(\frac{n}{0.557 z S_g^{1/2}} \right)^{3/4} Q_o^{3/4} \left(\frac{x}{L_g} \right)^{3/4} dx$$

$$s_e = \frac{n^{3/4} z^{1/4} L_g}{2.26 S_g^{3/8}} Q_o^{3/4} \quad \ldots\ldots\ldots (19)$$

Eq. 19 relates the storage s_e in the gutter to the outflow Q_o when the flow in the gutter is under equilibrium condition.

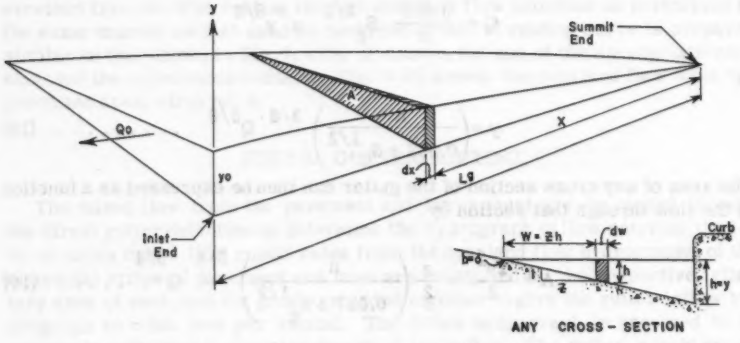


FIG. 9.—GUTTER CONFIGURATION

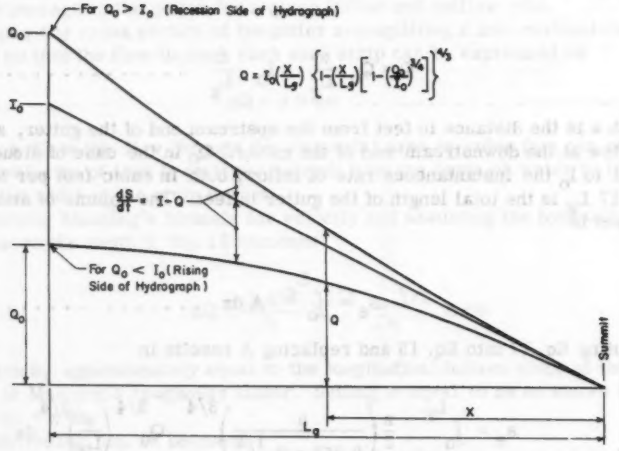


FIG. 10.—INSTANTANEOUS DISTRIBUTION ALONG GUTTER

For the case of varied flow, it will be assumed that the volume of storage in the gutter is a function of both the inflow and the outflow. The flow Q at the downstream end of the gutter must be equal to Q_o; moving upstream Q must approach the rate of inflow, because I-Q equals the rate of change of the volume of storage upstream of the section. Near the upstream end of the gutter, the storage is very small and the rate of change of storage approaches zero, thus I-Q approaches zero, as shown in Fig. 10. Setting the boundary conditions as $Q = Q_o$ when $x = L_g$ and $\frac{dQ}{dx} = \frac{I_o}{L_g}$ when $x = o$ the equation $Q = \frac{x}{L_g}\left[I_o - \frac{x}{L_g}(I_o - Q_o)\right]$ would fit these boundary conditions, but would be difficult to integrate when raised to the 3/4th power. A slight modification in the expression can both fit the given boundary conditions and make it simple to integrate.

$$Q = I_o\left(\frac{x}{L_g}\right)\left\{1 - \frac{x}{L_g}\left[1 - \left(\frac{Q_o}{I_o}\right)^{3/4}\right]\right\}^{4/3}$$

$$Q^{3/4} = I_o^{3/4}\left(\frac{x}{L_g}\right)^{3/4} - I_o^{3/4}\left(\frac{x}{L_g}\right)^{7/4}\left[1 - \left(\frac{Q_o}{I_o}\right)^{3/4}\right] \quad \ldots\ldots (20)$$

Combining with Eqs. 16 and 18

$$s = \frac{z}{2}\left(\frac{n}{0.557\, z\, S_g^{1/2}}\right)^{3/4} I_o^{3/4} \int_o^{L_g}\left\{\left(\frac{x}{L_g}\right)^{3/4} - \left(\frac{x}{L_g}\right)^{7/4}\left[1 - \left(\frac{Q_o}{I_o}\right)^{3/4}\right]\right\} dx$$

Integrating and substituting Eq. 19

$$s = s_e \frac{4\left(\frac{I}{Q_o}\right)^{3/4} + 7}{11}$$

$$s = \frac{n^{3/4} z^{1/4} L_g}{2.26\, S_g^{3/8}}\left(\frac{4}{11} I_o^{3/4} + \frac{7}{11} Q_o^{3/4}\right) \ldots (21)$$

Eq. 21 will be used to evaluate the volume of storage as a function of inflow and outflow.

Routing through the gutter will be performed similar to the routing of overland flow. The equation of continuity can be expressed as $I_o - Q_o = \frac{1}{60}\frac{ds}{dt_o}$. Writing it in incremental form, dropping the subscript in Q_o and I_o, and transposing all the known values, at the beginning of the period Δt_o, to the left-hand side of the equation, gives

$$\frac{1}{2}(I_1 + I_2) - \frac{1}{2} Q_1 + \frac{s_1}{60\,\Delta t_o} = \frac{1}{2} Q_2 + \frac{s_2}{60\,\Delta t_o} \quad \ldots\ldots (22)$$

Designating

$$F_g\,(Q,I) = \frac{1}{2}\,Q + \frac{s}{60\,\Delta t_o} \quad \ldots\ldots\ldots (23)$$

in which s is described by Eq. 21, and F_g, is a function of inflow and outflow having the parameters of the physical shape and roughness of the gutter and

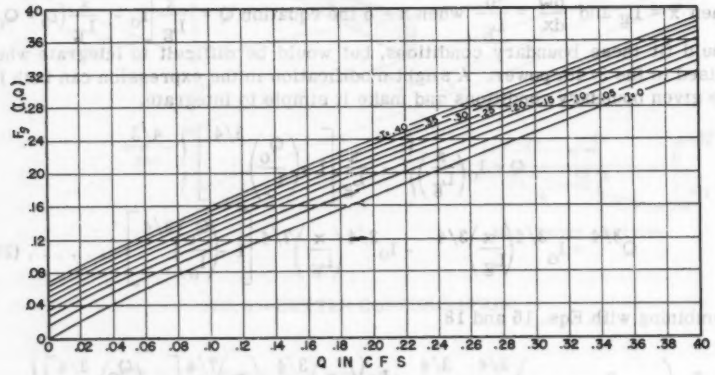


FIG. 11.—STORAGE ROUTING CURVE

TABLE 3.—ROUTING OF GUTTER FLOW

Time, t_o in minutes	Inflow in cubic feet per second		Outflow, Q, in cubic feet per second	Storage, F, in cubic feet per second
	I	I ave		
(1)	(2)	(3)	(4)	(5)
20.5	0.0001	—	—	—
		0.0002		
22.5	0.0003		0.0001	0.0002
		0.0006		
24.5	0.0010		0.0004	0.0007
		0.0018		
26.5	0.0026		0.0008	0.0021
		0.0038		
28.5	0.005		0.0018	0.0051
		0.0063		
30.5	0.0077		0.0042	0.0096
		0.0089		
32.5	0.0101		0.0076	0.0143
		0.0110		
34.5	0.0119		0.0102	0.0177
		0.0126		
36.5	0.134		0.0121	0.0202
		0.0141		
38.5	0.0147		0.0136	0.0222
		0.0154		
40.5	0.0161		0.0150	0.0240
		0.0169		
42.5	0.0177		0.0165	0.0259
		0.0186		
44.5	0.0195		0.0181	0.0281
		0.0206		
46.5	0.0216		0.0200	0.0305
		0.0229		

the time increment used in the routing. A graph of the function, F_g, is shown in Fig. 11 and will be used for routing the flow through the gutter storage. For the graph of Fig. 11 n = 0.02, z = 28.2, L_g 105 ft, Δt = 2 min, and S_g = 0.004.

By the substitution of Eq. 23 into Eq. 22 the routing formula becomes

$$I_{ave} - Q_1 + F_1 = F_2 \quad \ldots\ldots\ldots\ldots\ldots\ldots (24)$$

Table 3 indicates a sample of the gutter routing using the graph in Fig. 11 and Eq. 24.

STEP 6. ROUTING THROUGH LATERAL SEWER

Several methods of routing through the lateral sewer were examined. Storage routing procedures similar to that used to compute overland flow and gutter flow were explored and compared with the time-offset methods that will be described.

TABLE 4.—ROUTING THROUGH LATERAL SEWER

Time, t_o in minutes	Gutter hydrograph in cubic feet per second		Roof hydrograph in cubic feet per second	Inflow, I, in cubic feet per second	Mass, I, in cfs times minutes		Change in Mass Δ Mass I	Quantity, Q, in cubic feet per second $\frac{\Delta \text{ Mass I}}{7\frac{1}{3}}$
	24x - Type B-C-D	8x - Type A-E			at t_o	at $t_o - 7\frac{1}{3}$		
(1)	(2)	(3)	(4)	(5)	(6)	(7)	(8)	(9)
0.5	—	—	0.2032	0.2032	0.0508	—	0.0508	0.0069
2.5	—	—	0.2171	0.2171	0.4711	—	0.4711	0.0642
4.5	—	—	0.2251	0.2251	0.9133	—	0.9133	0.1245
6.5	—	—	0.2337	0.2337	1.3721	—	1.3721	0.1871
8.5	—	—	0.2429	0.2429	1.8487	0.1226	1.7261	0.23539
10.5	—	—	0.2529	0.2529	2.3435	0.5434	1.8001	0.24548
12.5	—	—	0.2637	0.2637	2.8611	0.9893	1.8718	0.25525
14.5	—	—	0.2754	0.2754	3.4002	1.4511	1.9491	0.26579
16.5	—	—	0.2881	0.2881	3.9637	1.9310	2.0327	0.27720
18.5	—	—	0.3020	0.3020	4.5537	2.4300	2.1237	0.28959
20.5	—	—	0.3172	0.3172	5.1729	2.9499	2.223	0.30307
22.5	—	—	0.3339	0.3339	5.8240	3.4940	2.330	0.31779
24.5	—	—	0.3524	0.3524	6.5103	4.0613	2.449	0.3339
26.5	—	—	0.3728	0.3728	7.2355	4.6564	2.5791	0.3517
28.5	0.0152	—	0.3908	0.4060	8.0143	5.2863	2.728	0.3720
30.5	0.1006	0.0090	0.4147	0.5243	8.9446	5.9486	2.996	0.4085
32.5	0.1814	0.0558	0.4434	0.6806	10.1495	6.6435	3.506	0.4781
34.5	0.2434	0.1193	0.4758	0.8385	11.6686	7.3746	4.294	0.5856
36.5	0.2895	0.1817	0.5130	0.9842	13.4913	8.1643	5.327	0.7265
38.5	0.3213	0.2252	0.5455	1.0920	15.5675	9.0295	6.538	0.8915
40.5	0.3550	0.2692	0.5951	1.2193	17.8788	10.2858	7.593	1.0354

Due to its simplicity, the method of routing through the lateral sewer by time-offset was adopted. Every particle of water is assumed to travel at a constant velocity along the distance from where it enters the underground sewer system, to the outlet end of the lateral sewer. Each hydrograph is shifted or offset by the time taken to traverse this distance. Referring to Fig. 1, it can be seen that there are many points of entry of flow into the lateral sewer. Because each of these inflow points has a different time of travel to the outlet, the

peaks of the hydrographs are offset by different amounts, causing the summation of these offset hydrographs to be less than the summation of all the inflow hydrographs. The handling of up to 36 pairs of house drain hydrographs draining from the roofs of the houses and 10 pairs of gutter hydrographs would be laborious. A simplified time-offset method will be outlined that is much easier to use and will produce almost the same results.

All of the inflow hydrographs from the gutter and roofs are added together, forming the total inflow hydrograph to the lateral sewer system. The tabular values are listed in columns 2, 3, 4, and 5 of Table 4. The roof hydrograph is obtained from in. per hr times 1.65 acres. The total inflow hydrograph is then divided equally into a number of smaller hydrographs which are assumed to enter the lateral sewer at uniformly spaced points along the length of the lateral. Each of these local inflow hydrographs are then offset by the time of flow from its point of entry to the lateral outlet. To illustrate the principle, Fig. 12 (a) shows the procedure when there are only five points of entry. The total time of travel from upstream end of the lateral to its outlet is shown as t_r. The summation of the vertical ordinates of all the local offset hydrographs at any time t_o is equal to the vertical ordinate of the outflow hydrograph at t_o. Another way of obtaining the same sum without drawing the local hydrographs is shown in Fig. 12 (b). The outflow Q at any time t_o can be computed by summing the instantaneous inflow I at time t_o, $(t_o - 1/4\ t_r)$ $(t_o - 3/4\ t_r)$ and $(t_o - t_r)$ and dividing by five. Expressing this mathematically.

$$Q(t_o) = \frac{1}{n} \sum_{i=o}^{i=(n-1)} I\left(t_o - \frac{i}{n-1}\ t_r\right) \quad \ldots\ldots\ldots (25)$$

Multiplying and dividing the equation by $\Delta t_r = \frac{t_r}{n}$ gives

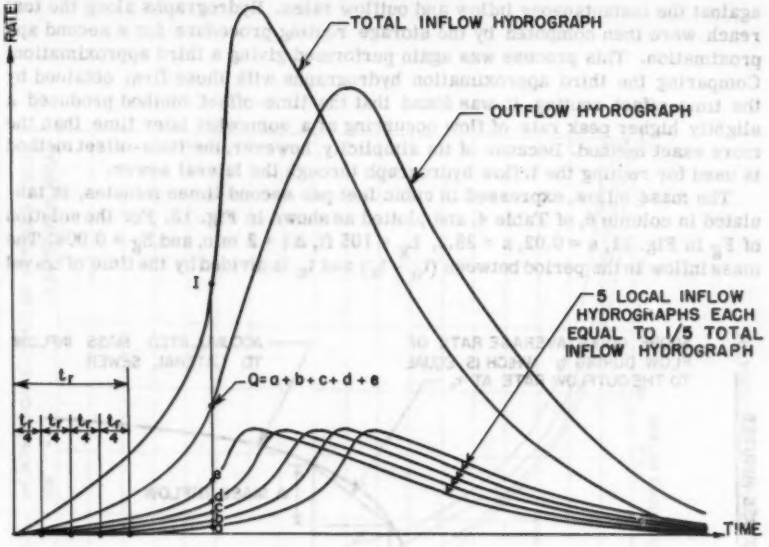
$$Q(t_o) = \frac{\sum_{i=o}^{i=(n-1)} I\left(t_o - \frac{i}{n-1}\ t_r\right) \Delta t_r}{n\,\Delta t_r} \quad \ldots\ldots\ldots (26)$$

If the number of points of entry into the lateral sewer are increased to a large number and Δt_r becomes small, the limit of the sum approaches the integral

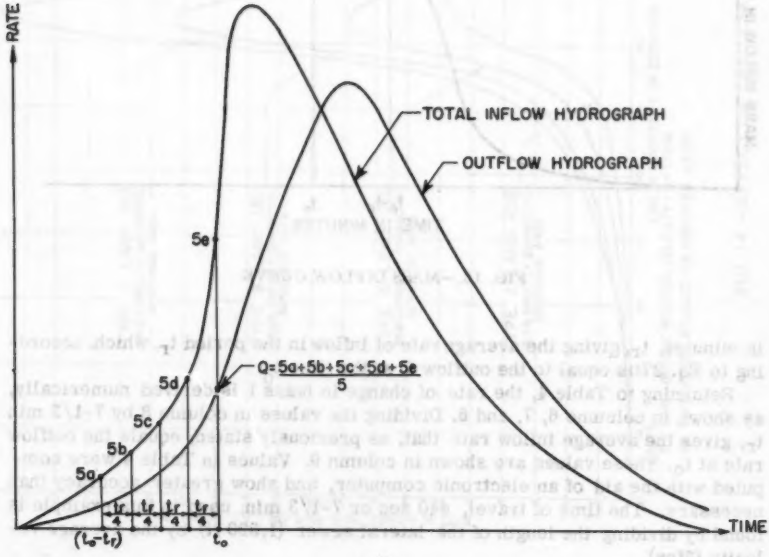
$$Q(t_o) = \frac{\int_{t_o - t_r}^{t_o} I(t_o)\, d\, t_r}{t_r} \quad \ldots\ldots\ldots\ldots (27)$$

This is the expression for the average inflow rate for the period $(t_o - t_r)$ and t_o. Thus, it appears that the value of Q at t_o is equal to the average inflow rate during the period t_r preceding the time t_o, if the number of inflow entry points along the sewer is large.

The time-offset routing method as described herein, gives a fair approximation of the actual outflow hydrograph. As a test of the accuracy of the time-offset method, a series of computations were performed. Hydrographs along a test length of sewer were obtained by the time-offset method and instantaneous rates of flow were taken from these hydrographs and backwater curves computed. Storage values under the backwater curves were determined and plotted



(a)



(b)

FIG. 12.—ROUTING THROUGH LATERAL SEWER

against the instantaneous inflow and outflow rates. Hydrographs along the test reach were then computed by the storage routing procedure for a second approximation. This process was again performed giving a third approximation. Comparing the third approximation hydrographs with those first obtained by the time-offset routing, it was found that the time-offset method produced a slightly higher peak rate of flow occurring at a somewhat later time than the more exact method. Because of its simplicity, however, the time-offset method is used for routing the inflow hydrograph through the lateral sewer.

The mass inflow, expressed in cubic feet per second times minutes, is tabulated in column 6, of Table 4, and plotted as shown in Fig. 13. For the solution of F_g in Fig. 11, n = 0.02, z = 28.2, L_g = 105 ft, Δt = 2 min, and S_g = 0.004. The mass inflow in the period between $(t_o - t_r)$ and t_o is divided by the time of travel

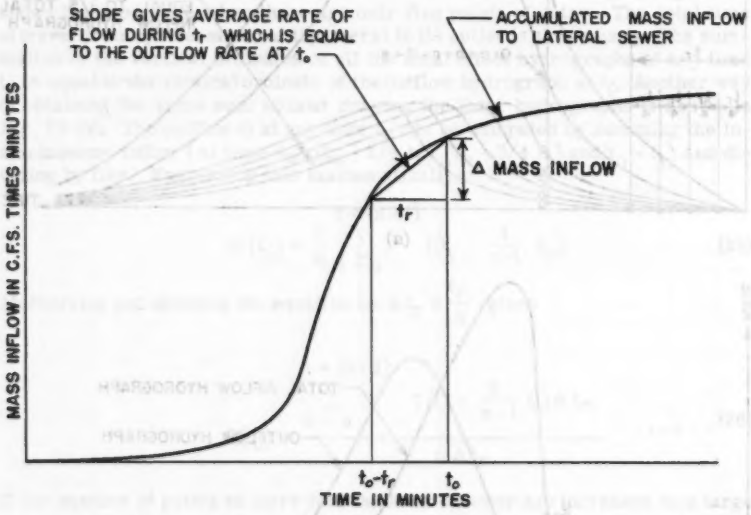


FIG. 13.—MASS INFLOW CURVE

in minutes, t_r, giving the average rate of inflow in the period t_r, which, according to Eq. 27 is equal to the outflow Q at the time t_o.

Returning to Table 4, the rate of change in mass I is derived numerically, as shown in columns 6, 7, and 8. Dividing the values in column 8 by 7-1/3 min t_r, gives the average inflow rate that, as previously stated, equals the outflow rate at t_o. These values are shown in column 9. Values in Table 4 were computed with the aid of an electronic computer, and show greater accuracy than necessary. The time of travel, 440 sec or 7-1/3 min, used in this example is found by dividing the length of the lateral sewer (1,320 ft) by the average velocity (3fps).

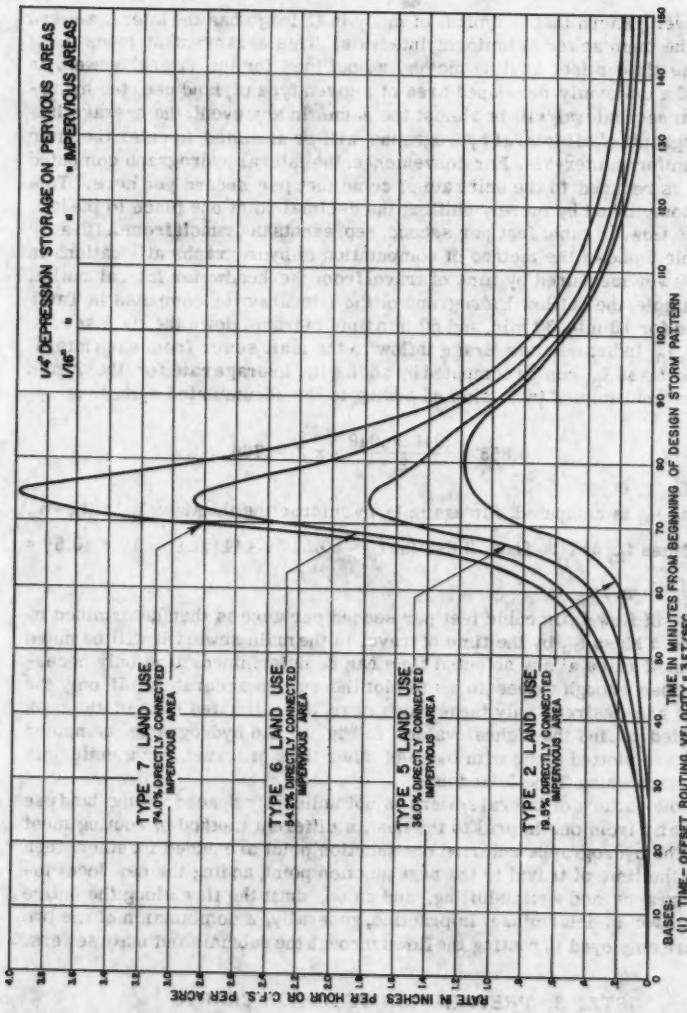


FIG. 14.—EFFECT OF LAND USE ON OUTFLOW HYDROGRAPH

The hydrographs of the outflow from the lateral sewer draining a 10-acre unit area having this and other types of land use is shown in Fig. 14.

STEP 7. ROUTING THROUGH MAIN SEWER

The sewer pattern that is typical of many in Chicago has the lateral sewers entering the main sewer at uniform intervals. This arrangement lends itself to the same time-offset routing method as outlined for the lateral sewer. In the case of a uniformly developed area of a given type of land use, the hydrograph from each lateral will be almost the same. In any event, the average lateral hydrograph of all lateral hydrographs will be assumed to enter the main sewer at uniform intervals. For convenience, the lateral hydrograph computed in Table 4 is reduced to the unit rate of cubic feet per second per acre. This can be accomplished by merely shifting the decimal point one place to the left, because the flow, in cubic feet per second, represents the runoff from a 10-acre area. Table 5 shows the method of computation of hydrographs at locations in the main sewer measured by time of travel from the headwater lateral outlet. In this example, the outflow hydrograph of the lateral sewer computed in Table 4, is routed for 10 min, 30 min, and 60 min time of travel down the main sewer. In Table 5, I_m indicates the average inflow to the main sewer from each lateral sewer. The Mass I_m can be computed by adding the average rate for the 2 min interval and multiplying by 2 min and adding to the accumulated sum, thus

$$0.855 = \frac{.041 + .048}{2} \times 2 + .766$$

The Δ Mass I_m is computed, for example, by subtracting the Mass I_m at $(t_o - t_r)$ from the Mass I_m at t_o. Thus, 2.848 $(\text{at } t_o = 50.5)$ - 1.444 $(\text{at } t_o - 10 = 40.5)$ = 1.404 $(\Delta \text{ Mass } I_m)$.

The rate of flow Q, in cubic feet per second per acre is then determined by dividing the Δ Mass I_m by the time of travel in the main sewer. It will be noted that the runoff rates at any selected time can be determined. It is only necessary to choose enough values so as to plot the curves accurately. If only the peak rates are desired, only these rates near the estimated time of the peak are computed to find the highest value. In Fig. 15 the hydrographs computed in Table 5 are plotted along with those of other time of travel, for a uniformly developed area using Type 5 land use.

Where the pattern of lateral sewers is not uniformly spaced, or the land use varies greatly from one lateral to the next, a different method of routing must be used. The hydrographs entering one junction point are added together, then shifted by the time of travel to the next junction point, adding the new local inflow hydrographs and again shifting, and so on, until the flow along the entire length of sewer is determined. In practice, generally, a combination of the two methods are employed in routing the flows through the submain and main sewers.

STEP 8. PREPARATION OF DESIGN CHARTS

Convenient design charts can be developed after routing the lateral hydrographs through the main sewers and producing sets of hydrographs at various times of travel, like those shown in Fig. 15.

The peaks of each of these hydrographs and other hydrographs that are similarly routed for areas having different imperviousness, are plotted against the time of concentration, used in the rational method, as shown in Fig. 16. The bases used in Fig. 16 are as follows: (1) Hydrograph method using 5-yr design-storm pattern; (2) peak rates derived from Fig. 15 and similar charts for other types of land use; (3) time of concentration assumed to equal 10 min plus the

TABLE 5.—ROUTING THROUGH MAIN SEWER

Time, t_o in minutes	Average Inflow, I_m in cfs per acre	Mass I_m, in cfs per acre times minutes	Charge in Mass I_m, in cfs per acre times, minutes			Quantity, Q in cfs per acre		
			$t_r = 10$	$t_r = 30$	$t_r = 60$	$t_r = 10$	$t_r = 30$	$t_r = 60$
(1)	(2)	(3)	(4)	(5)	(6)	(7)	(8)	(9)
30.5	0.041	0.766	—	—	—	—	—	—
32.5	0.048	0.855	—	—	—	—	—	—
34.5	0.058	0.966	—	—	—	—	—	—
36.5	0.073	1.092	—	—	—	—	—	—
38.5	0.088	1.253	—	—	—	—	—	—
40.5	0.103	1.444	0.678	—	—	0.068	—	—
42.5	0.118	1.665	—	—	—	—	—	—
44.5	0.131	1.914	—	—	—	—	—	—
46.5	0.146	2.191	—	—	—	—	—	—
48.5	0.162	2.499	—	—	—	—	—	—
50.5	0.187	2.848	1.404	—	—	0.140	—	—
52.5	0.217	3.252	—	—	—	—	—	—
54.5	0.240	3.709	—	—	—	—	—	—
56.5	0.277	4.226	—	—	—	—	—	—
58.5	0.322	4.825	—	—	—	—	—	—
60.5	0.381	5.528	2.680	4.762	—	0.268	0.159	—
62.5	0.472	6.381	—	—	—	—	—	—
64.5	0.607	7.460	—	—	—	—	—	—
66.5	0.856	8.923	—	—	—	—	—	—
68.5	1.217	10.996	—	—	—	—	—	—
70.5	1.599	13.811	8.283	12.367	—	0.828	0.412	—
72.5	1.765	17.175	—	—	—	—	—	—
74.5	1.782	20.722	—	—	—	—	—	—
76.5	1.678	24.182	15.259	—	—	1.526	—	—
78.5	1.519	24.379	16.383	—	—	1.638	—	—
80.5	1.439	30.337	16.526	24.489	—	1.653[a]	0.916	—
82.5	1.353	33.129	15.954	—	—	1.595	—	—
84.5	1.254	35.736	15.014	—	—	1.501	—	—

[a] Peak value.

time of travel from the outlet of the extreme headwater lateral. The approximate time of concentration can be obtained by adding 10-min to the time of travel in the main sewer. Curves showing intensity-duration data for a 5-yr frequency rainfall and percentages from such rainfalls are given for comparison.

Another chart can be obtained by taking the peak rates of flow from the hydrographs in Fig. 15 and plotting these rates against the corresponding percentage of directly connected imperviousness for the particular type of land use.

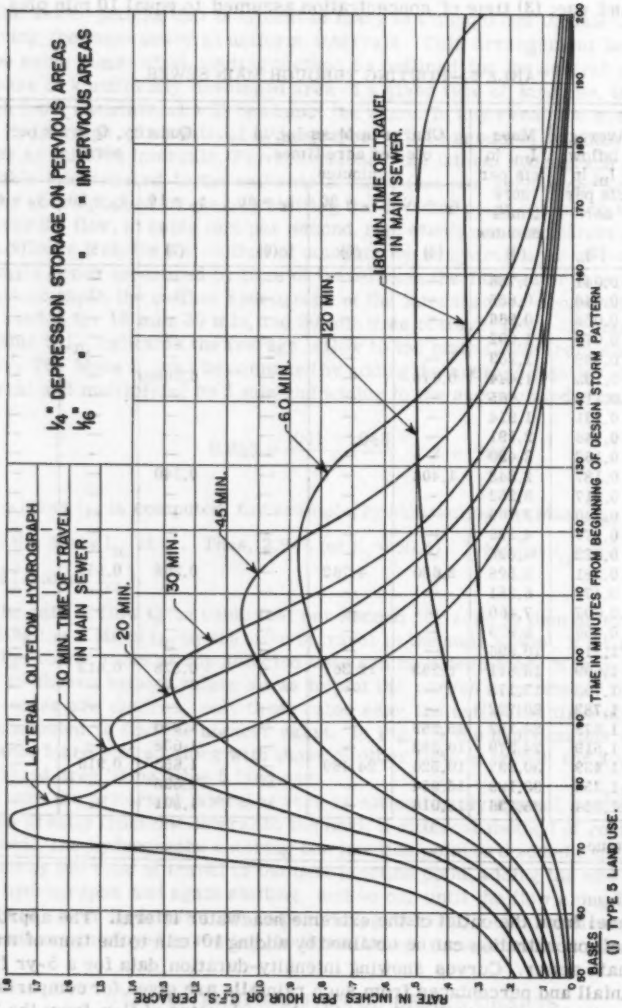


FIG. 15.—ROUTING OF LATERAL HYDROGRAPHS ALONG MAIN SEWER

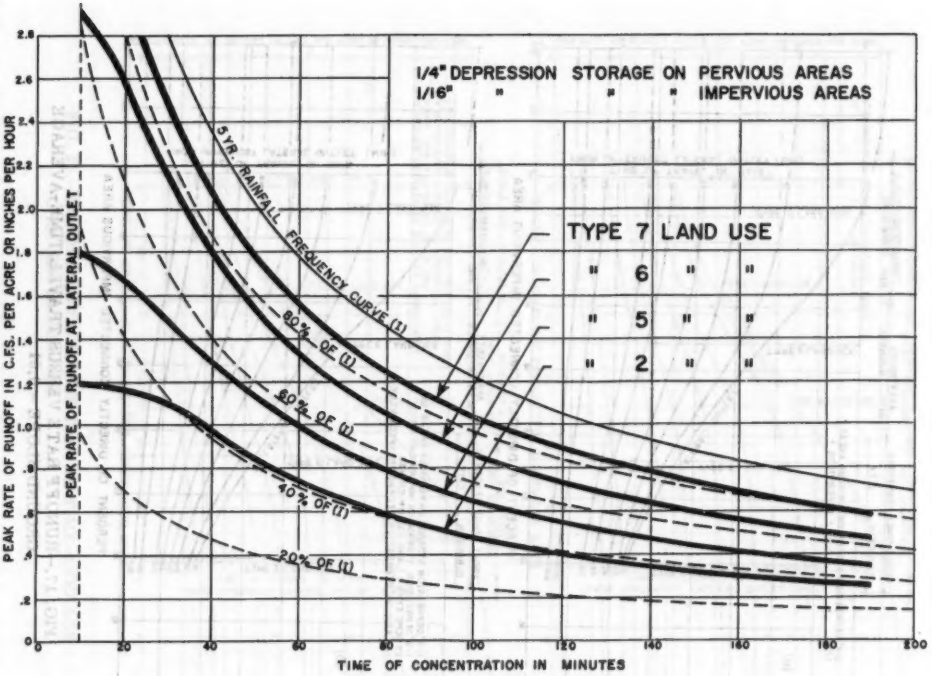


FIG. 16.—EFFECTS OF LAND USE

The time of travel is recorded as a parameter. Similar plottings are made for other types of land use having different percentages of directly connected imperviousness. Continuous lines are drawn through the points of equal time of travel producing the type of chart shown in Figs. 17 and 18. The bases for Fig. 17 are as follows: (1) Hydrograph method using 5-yr design-storm pattern; (2) standard infiltration curve for types 2, 5, and 6 land use, as shown in Fig.

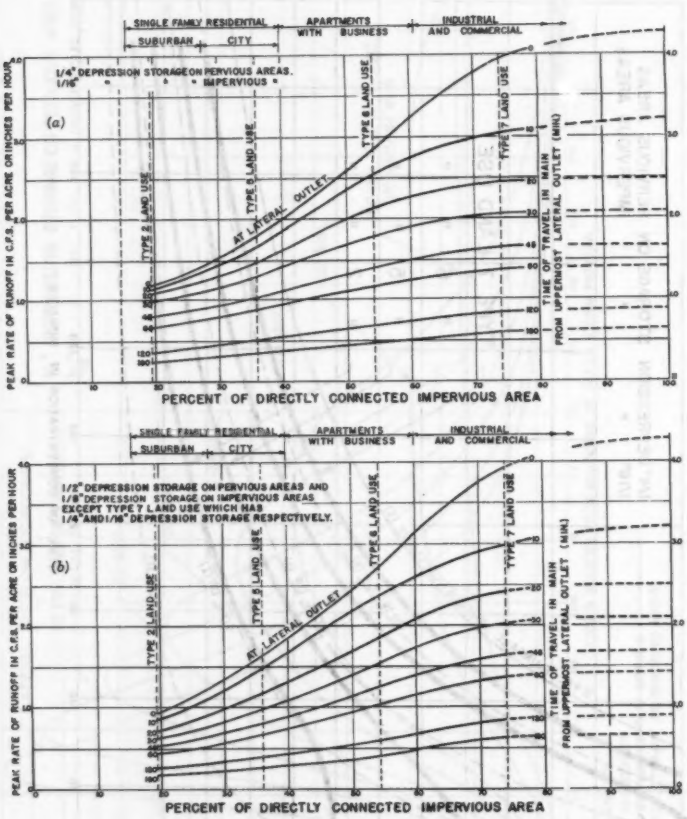


FIG. 17.—RUNOFF RATE VERSUS TRAVEL TIME-AVERAGE GROUND SLOPE = 0.01

3, and reduced infiltration curve for type 7 land use; (3) rates at lateral outlet are taken from hydrographs in Fig. 14; (4) rates at other travel times downstream taken from Fig. 15 and similar charts for other types of land use; (5) depression storage as indicated in the figure; (6) average ground slope = 0.01. The bases for Fig. 18 are the same, except that average ground slope = 0.02.

A comparative examination of Figs. 17 and 18 reveals that doubling the ground slope for overland flow without changing any of the other constants increases the peak runoff from areas with low percentages of imperviousness but the increased ground slope loses its relative impact upon the peak rates as the imperviousness or time of travel increases. Also, when depression storage is

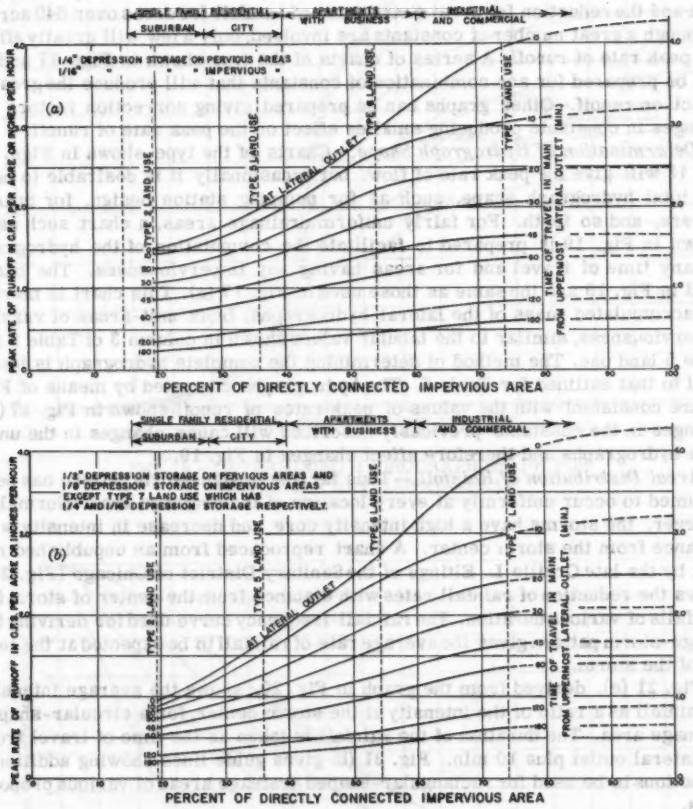


FIG. 18.--RUNOFF RATE VERSUS TRAVEL TIME-AVERAGE GROUND SLOPE = 0.02

large, as indicated in Figs. 17 (b) and 18 (b), ground slope is overshadowed by the effect or larger storage volume in the depressions.

The peak rates of flow given by these charts will change by varying degrees with each change in the constants used in the previous seven steps. A summary of the constants used are as follows: for the design-storm pattern the frequency constants, advanceness ratio, and maximum duration of rainfall is

known, and the infiltration constants are known. For the depression storage, the average depths, for pavement, pervious area and roof area are known. For the overland flow the constants for the pavement, pervious area, and roof area are known. The gutter flow for the 1st and 2nd types of gutter are known. For the lateral routing the types of gutter, area of the roofs, and time of travel in lateral sewer are known and the time of travel in the main sewer is known for routing in the main sewer. It is then necessary to determine the peak runoff rate and the reduction for areal distribution of rainfall for areas over 640 acres. Although a great number of constants are involved, only a few will greatly affect the peak rate of runoff. A series of charts of the type shown in Figs. 17 and 18 can be prepared for any combination of constants that will produce the greater effect on runoff. Other graphs can be prepared giving correction factors for changes in constants producing smaller effect on the peak rate of runoff.

Determination of Hydrograph Shape.—Charts of the type shown in Figs. 17 and 18 will give the peak rate of flow, but occasionally it is desirable to have the total hydrograph shape, such as for pumping station design, for branch sewers, and so forth. For fairly uniform drainage areas, a chart such as is shown in Fig. 19 is prepared to facilitate the computation of the hydrograph for any time of travel and for areas having any imperviousness. The bases used in Fig. 19 are the same as those used in Fig. 17 (a). This chart is merely the accumulated mass of the lateral hydrographs, from unit-areas of varying imperviousness, similar to the tabular values shown in column 3 of Table 5 for Type 5 land use. The method of determining the complete hydrograph is identical to that outlined for Table 5. The hydrographs computed by means of Fig. 19 are consistent with the values of peak rates of runoff shown in Fig. 17 (a). Changes in the constants previously described will cause changes in the unit-area hydrographs and therefore affect changes in Fig. 19.

Areal Distribution of Rainfall.—Thus far, the design-storm pattern has been assumed to occur uniformly at every location of the drainage area. Normally, however, the storms have a high intensity core and decrease in intensity with distance from the storm center. A chart reproduced from an unpublished report by the late Orville L. Eltinge of the Sanitary District of Chicago (Fig. 20), shows the reduction of rainfall rates with distance from the center of storm for rainfalls of various duration. The rainfall-frequency curve used for deriving the design-storm pattern gives the average rate of rainfall to be expected at the center of the storm.

Fig. 21 (c), derived from the graph in Fig. 20, shows the average intensity of rainfall as a ratio of the intensity at the storm center, for a circular-shaped drainage area. The duration of the rainfall is taken as the time of travel from the lateral outlet plus 10 min. Fig. 21 (b) gives guide lines showing additional reductions to be used for rectangular-shaped drainage areas of various proportions.

If the average rainfall over the drainage area is reduced by a factor, how much is the peak rate of runoff reduced? To answer this question, runoff rates were computed using 90% and 80% of the design-storm pattern. The fixed values of infiltration and depression storage effectively reduces the runoff to a greater extent on pervious areas. For 100% impervious areas, it is assumed that the runoff rates will reduce by the same percentage as the reduction in rainfall. Fig. 21 (c) indicates guide lines that will give the reduction factor to be applied to the peak rate of runoff.

The tributary area and the time of travel for any reach in the sewer system is entered into Fig. 21 (c), and the reduction factor is determined for a circular-shaped drainage area. A map of the drainage area is then inspected to determine

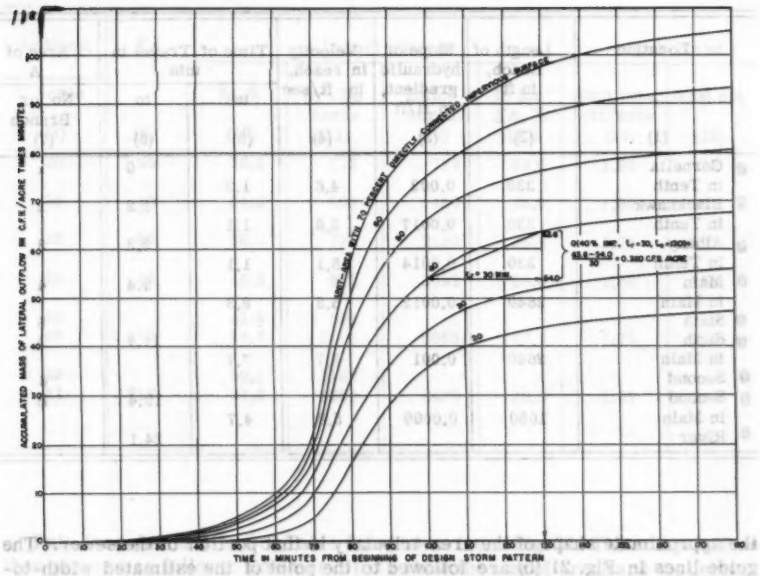


FIG. 19.—DETERMINING HYDROGRAPH SHAPE FOR UNIFORMLY DEVELOPED AREAS

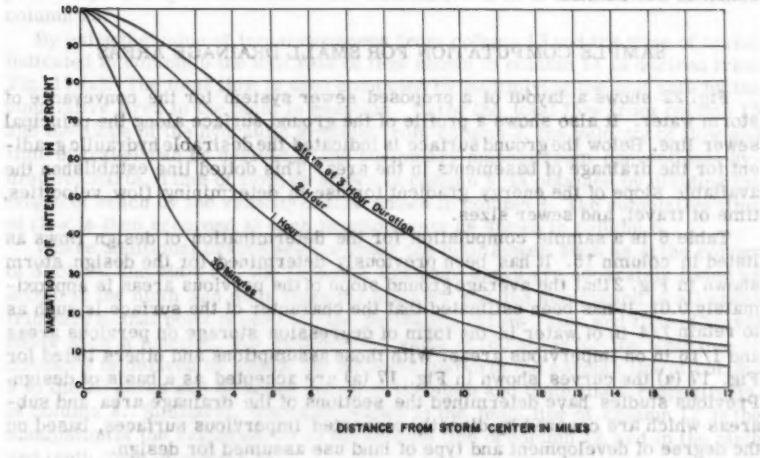


FIG. 20.—VARIATION OF RAINFALL INTENSITY

TABLE 6.—COMPUTATION

Location	Length of Reach, in ft	Slope of hydraulic gradient, in ft/ft	Velocity in reach, in ft/sec	Time of Travel in min		Area of A
				in	to	No. or Branch
(1)	(2)	(3)	(4)	(5)	(6)	(7)
@ Cornelia					0	1
in Tenth	330	0.002	4.6	1.2		
@ Blackhawk					1.2	2
in Tenth	330	0.0017	5.0	1.1		
@ Albany					2.3	3
in Tenth	330	0.0014	5.1	1.1		
@ Main					3.4	4
in Main	2640	0.0012	5.3	8.3		
@ Sixth						5
@ Sixth					11.7	A
in Main	2640	0.001	5.7	7.7		
@ Second						6
@ Second					19.4	B
in Main	1650	0.0009	5.8	4.7		
@ River					24.1	

the approximate shape of the area tributary to that portion of the sewer. The guide lines in Fig. 21 (b) are followed to the point of the estimated width-to-length ratio of the drainage area, and the reduction factor for the average rainfall rate over the tributary drainage area is obtained. Applying this reduction factor to Fig. 21 (a) and following the guide lines to the imperviousness of the tributary drainage area, the reduction factor to be applied to the peak rate of runoff is determined.

SAMPLE COMPUTATION FOR SMALL DRAINAGE AREAS

Fig. 22 shows a layout of a proposed sewer system for the conveyance of storm water. It also shows a profile of the ground surface along the principal sewer line. Below the ground surface is indicated the desirable hydraulic gradient for the drainage of basements in the area. This dotted line establishes the available slope of the energy gradient for use in determining flow velocities, time of travel, and sewer sizes.

Table 6 is a sample computation for the determination of design flows as listed in column 15. It has been previously determined for the design storm shown in Fig. 2 that the average ground slope of the pervious areas is approximately 0.01. It has been estimated that the character of the surface is such as to retain 1/4 in of water in the form of depression storage on pervious areas and 1/16 in on impervious areas. With those assumptions and others listed for Fig. 17 (a) the curves shown in Fig. 17 (a) are accepted as a basis of design. Previous studies have determined the sections of the drainage area and subareas which are covered by directly connected impervious surfaces, based on the degree of development and type of land use assumed for design.

FOR SMALL DRAINAGE AREA

Addition,	ΣA	Imperviousness				Peak Flows	
Acres		Ip, %	(A · Ip) Acres	ΣAIp, Acres	Ip for ΣA, %	Unit rate, cfs/acre	total cfs
(8)	(9)	(10)	(11)	(12)	(13)	(14)	(15)
20	20	38.6	772	772	38.6	1.93	39
20	40	34.5	690	1462	36.5	1.80	72
20	60	36.0	720	2182	36.4	1.78	107
20	80	45.5	910	3092	38.6	1.88	150
20		42.8	856				
60	160	35.2	2112	6060	37.9	1.75	280
23		50.1	1152				
34	217	37.2	1268	8480	39.0	1.59	345
							345

Data for columns 1 to 3 of Table 6 are taken from Fig. 22. The computations then proceed as follows: Columns 7 to 13 show the size of areas and the derivations of the percentage of imperviousness for such areas tributary to the street intersections indicated in column 1. By multiplying the acreage of each subdrainage area by the percentage of imperviousness of that subarea, adding the products and then dividing the cumulative products by the cumulative area, the percentage of imperviousness of the cumulative area is derived and listed in column 13.

By using the value of imperviousness from column 13 and the time of travel indicated in column 6 the unit rate of flow shown in column 14 is derived from Fig. 17 (a). The total flow is then computed by multiplying the unit rate by the cumulative area to the point in question. Using the total flow from column 15 and the slope of the hydraulic gradient from column 3, the velocity of flow and time of travel can be derived in the customary manner from conventional hydraulic charts. Time of flow, as shown in column 5, is obtained by dividing the length of reach by the velocity of flow shown in column 4. The cumulative time of flow is then recorded at each junction point as shown in column 6.

Where additional branch sewers enter the main sewer, such as at the corner of Sixth St. and Main St., the separate drainage areas are separately listed as shown in the ninth and tenth lines for Sixth St. and the summation of all areas tributary to that point is used for the derivation of flow rates and time of travel below such a junction. For example, the value of 160 acres for the tenth line of column 9 is derived by adding the 80 acres shown in the seventh line of column 9 to the 20 acres and 60 acres shown in the ninth and tenth lines, respectively, of column 8. Similarly, the value shown in the tenth line of column 12 is the summation of the values shown in the seventh line of column 12, and in the ninth and tenth lines of column 11.

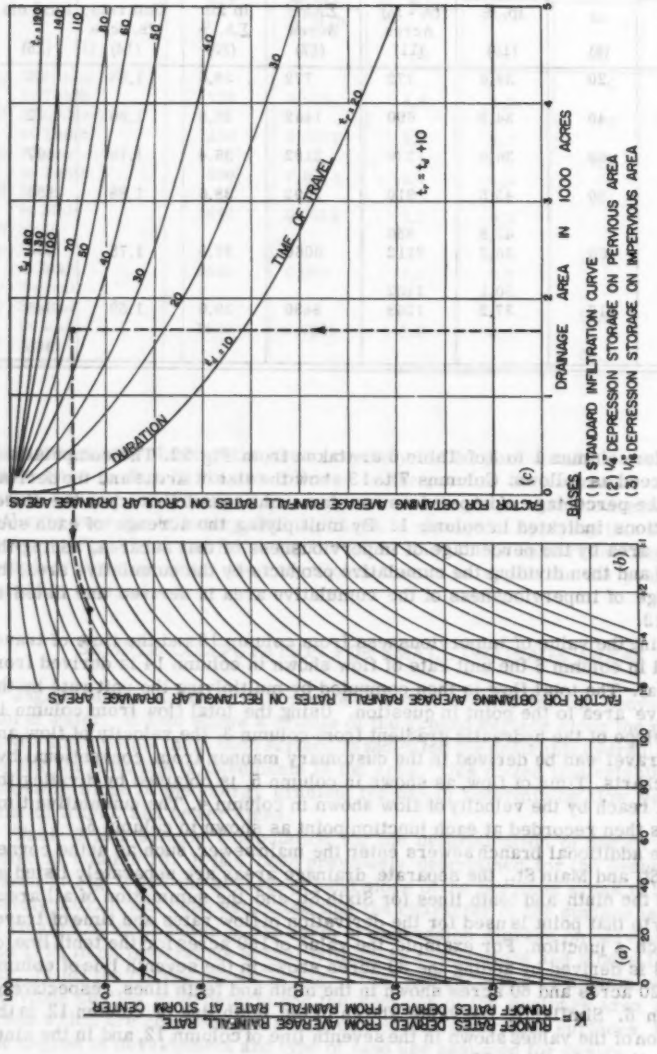


FIG. 21.—RUNOFF REDUCTION FACTORS

These computations indicate the simplicity of design for small or moderately-sized sewer systems by the use of the hydrograph method.

SAMPLE COMPUTATION FOR LARGE DRAINAGE AREAS

Applying the hydrograph method to a large drainage area will illustrate the use of the charts developed in the eighth step. Rainfall-reduction factors and instantaneous backwaters are applied for the determination of required sewer sizes and gradients.

A typical layout of the drainage area to be studied is shown in Fig. 23. An examination is made of the various subareas to determine the size of the area

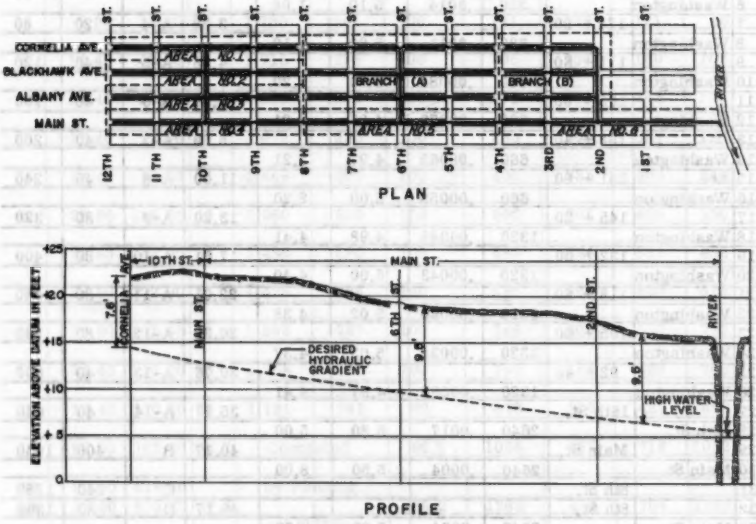


FIG. 22.—LAYOUT OF PROPOSED SEWER SYSTEM

and its imperviousness. Routes along which the main sewer and branch lines are to be built are selected so as to take advantage of the natural ground slopes. Profiles are drawn along the selected routes and, as illustrated in Fig. 22, the maximum permissible hydraulic gradient lines are established to adequately drain basements in the area. Computation forms such as those shown in Tables 6 and 7 are then prepared. For the branch sewers or for drainage areas nearly uniformly developed, charts like those shown in Figs. 17 and 18 can be used to determine the peak rate of flow, and, with the aid of Fig. 19, the entire hydrograph at any location can be determined.

The computation procedure for area A, illustrated in Table 7, columns 1 to 16 and lines 1 to 27, is similar to that outlined for Table 6 for the small drainage areas. Because the total drainage area substantially exceeds the 640-acre

TABLE 7.—COMPUTATION FORM

Line	Location		Length of Reach	Slope of Hyd. Grad.	Velocity in Reach	Time of Travel Tr		Area of Addition		ΣA
						in Reach	To	No.	Acres	
	In	At	ft	ft/ft	ft/sec	Min	Min			Acres
	(1)	(2)	(3)	(4)	(5)	(6)	(7)	(8)	(9)	(10)
1		184 + 80					0	A-1	20	20
2	Washington		330	.0028	5.05	1.09				
3		181 + 50					1.09	A-2	20	40
4	Washington		330	.0017	4.95	1.11				
5		178 + 20					2.20	A-3	20	60
6	Washington		330	.0014	5.10	1.08				
7		174 + 90					3.28	A-4	20	80
8	Washington		330	.0011	5.00	1.10				
9		171 + 60					4.38	A-5	40	120
10	Washington		660	.00084	5.00	2.20				
11		165 + 00					6.58	A-6	40	160
12	Washington		660	.00073	4.97	2.21				
13		158 + 40					8.79	A-7	40	200
14	Washington		660	.00063	4.97	2.21				
15		151 + 80					11.00	A-8	40	240
16	Washington		660	.00058	5.00	2.20				
17		145 + 20					13.20	A-9	80	320
18	Washington		1320	.00048	4.98	4.41				
19		132 + 00					17.61	A-10	80	400
20	Washington		1320	.00043	5.00	4.40				
21		118 + 80					22.01	A-11	80	480
22	Washington		1320	.00040	5.02	4.38				
23		105 + 60					26.39	A-12	80	560
24	Washington		1320	.00038	5.03	4.37				
25		92 + 40					30.76	A-13	40	600
26	Washington		1320	.00035	4.97	4.41				
27		16th St.					35.17	A-14	40	640
28	16th St.		2640	.0017	8.80	5.00				
29		Main St.					40.17	B	400	1040
30	Main St.		2640	.0004	5.50	8.00				
31		8th St.						C	240	1280
32		8th St.					48.17	D	80	1360
33	Main St.		2640	.0004	5.80	7.60				
34		River Rd.						E	240	1600
35		River Rd.					55.77	F	80	1680
36	Main St.		660	.00035	5.80	1.90				
37		Outfall					57.67			

limit for use of uniform areal distribution of rainfall, columns 17 and 18 are added to Table 6 to enable the application of the areal-distribution reduction factor K as presented in Fig. 21. The factor of unity is used for any area less than 640 acres. Columns 19, 20, and 21 are used to record the instantaneous discharge rates taken from a set of hydrographs like those shown in Fig. 15. For example, in line 25 the time of travel is 30.76 min, the area is 600 acres, and the imperviousness is 36%. From the hydrograph in Fig. 15, with time of travel slightly longer than 30 min, the rate of rainfall at 80 min after its begin-

FOR A LARGE DRAINAGE AREA

Imperviousness				Peak Flows				Instantaneous Flows		
Ip	Ip x A	Σ Ip x A	Ip for ΣA	q	Q = qA	K	Qp = KQ	KQ75	KQ80	KQ95
%	Acres	Acres	%	cfs/Acres	cfs	%	cfs	cfs	cfs	cfs
(11)	(12)	(13)	(14)	(15)	(16)	(17)	(18)	(19)	(20)	(21)
36	7.20	7.20	36	1.792	36	100	36	36	29	15
36	7.20	14.40	36	1.782	71	100	71	71	59	32
36	7.20	21.60	36	1.772	106	100	106	106	90	49
36	7.20	28.80	36	1.760	141	100	141	140	121	66
36	14.40	43.20	36	1.715	205	100	205	200	180	102
36	14.40	57.60	36	1.690	270	100	270	255	245	145
36	14.40	72.00	36	1.672	335	100	335	300	320	190
36	14.40	86.40	36	1.668	400	100	400	335	400	244
36	28.80	115.20	36	1.560	500	100	500	365	480	350
36	28.80	144.00	36	1.450	580	100	580	384	522	455
36	28.80	172.80	36	1.425	685	100	685	396	540	612
36	28.80	201.61	36	1.335	748	100	748	406	550	736
36	14.40	216.00	36	1.268	760	100	760	384	520	760
36	14.40	230.40	36	1.191	761	89	678	310	427	660
38	152.00	382.40	36.7	Computed		86.5	1058	467	710	1052
40	96.00	478.40		by Plotting						
40	32.00	510.40	37.5			86.2	1268	484	706	1230
				and Shifting						
45	108.00	618.40								
50	40.00	658.40	38.1	Hydrographs		86.2	1445	698	924	1332
							1445	698	924	1332

ning is 0.87 cfs per acre. Multiplying 0.87 cfs per acre by 600 acres with K equal to 1.0 gives 520 cfs. This is recorded in column 20. Similar computations, as shown in Table 7, lines 1 to 27, are performed for every branch sewer.

The table in Fig. 23 shows the tributary area, the average imperviousness, and the time of travel for each of the branch sewers. With the values given in this table and with the use of the mass curves in Fig. 19, the hydrographs of flow into the main sewer can be computed. The branch and local inflow hydrographs at each of the junction points are shown in Fig. 23.

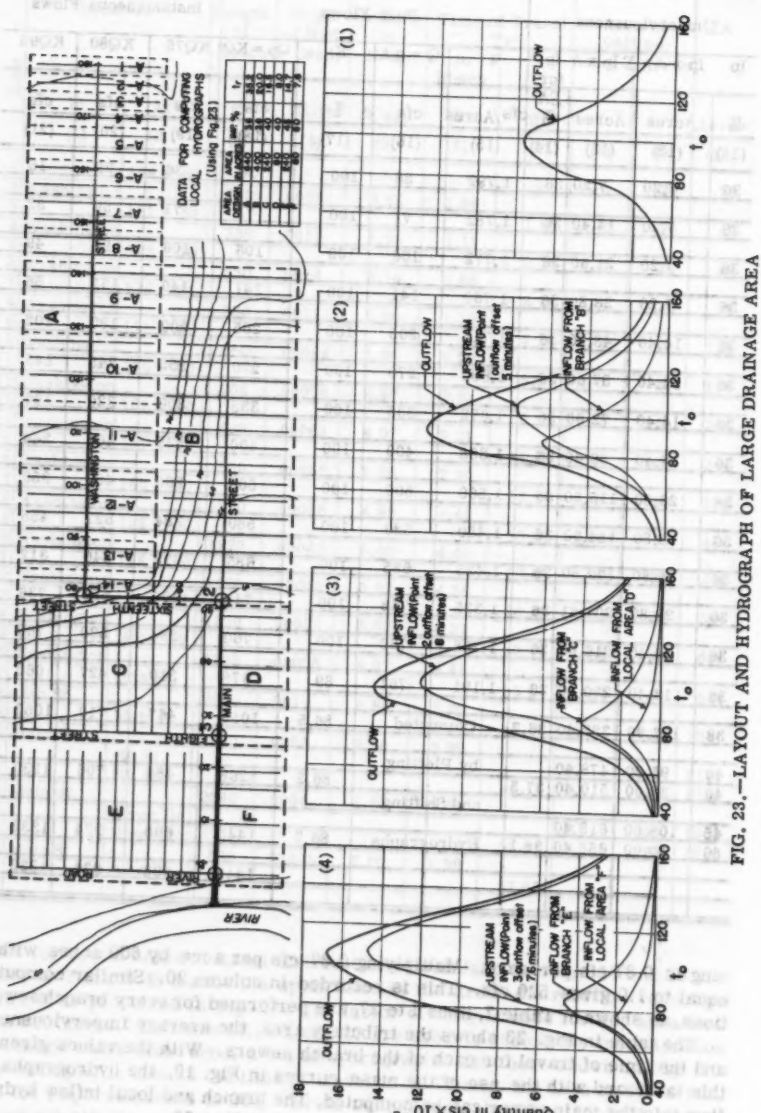


FIG. 23.—LAYOUT AND HYDROGRAPH OF LARGE DRAINAGE AREA

The branch and local area hydrographs are routed through the main sewer by offsetting the hydrographs by the time of travel between junction points. The hydrograph at junction point 1 is offset by 5.0 min and added to the branch B hydrograph giving the outflow hydrograph at junction point 2. The outflow hydrograph at point 2 is then shifted by 8.0 min and added to the branch C and local area D hydrographs, producing the outflow hydrograph at junction point 3. The outflow hydrograph at junction point 3 is shifted by 7.6 min to point 4 and added to the branch E and local area F hydrographs producing the outflow hydrograph at junction point 4.

Simultaneous with the development of the main sewer hydrographs, entries are made in Table 7, for the time of travel in the reach downstream of the junction point, the tributary area, average imperviousness, and the K factor. The peak rates and the rates at instantaneous times are taken from the main sewer hydrographs and are multiplied by the K factor and entered into columns 18 to 21. Preliminary size and profile of the main sewer is based on the peak flow data taken from column 18.

A profile along the main line and branch A is shown in Fig. 24 (b). In Fig. 24 (a), the instantaneous rates and the envelope of all the peak rates are plotted graphically. Shown for comparison are the capacities of the sewers flowing full with the friction loss being equal to invert slope. Instantaneous backwater curves were computed and are shown on the profile along with a backwater curve using the envelope of all the peak discharges. The envelope backwater was computed although there was an awareness of its not being a true relationship at any one time, because the loss of energy at the time of occurrence of the downstream peak cannot be added directly to the losses obtained for the upstream peaks occurring at an earlier time. Before beginning the backwater curves, the downstream control must be determined. If the flow enters a river having variable water surface, the stage of the river must be estimated for the time of the instantaneous backwater curve.

An examination of the instantaneous backwater curves will indicate the travel of the flood wave along the sewer. Often, after examination of the instantaneous backwater profiles, the preliminary sizing of sewer can be reduced, resulting in savings in sewer costs.

CONCLUSIONS

After a series of charts, such as Figs. 17 and 18 are prepared, the ease of determining the peak runoff rate is equal to that of using the rational method. With the advent of the electronic computing machine, it becomes feasible to prepare many charts of this type covering the complete range of those parameters which principally affect the peak rates of runoff and to prepare correction charts for parameters causing minor changes in the peak rates of runoff. In selecting the proper chart, the engineer must consider the physical aspects of the drainage area such as type of soil (so as to determine the proper infiltration curve); the amount of depression storage; the slope, length and roughness coefficients of the average overland flow strips; and other measurable quantities. An estimation of the value to be assigned to a number of individual parameters should produce more logical results than the selection of a single all-embracing coefficient such as that used in the rational method.

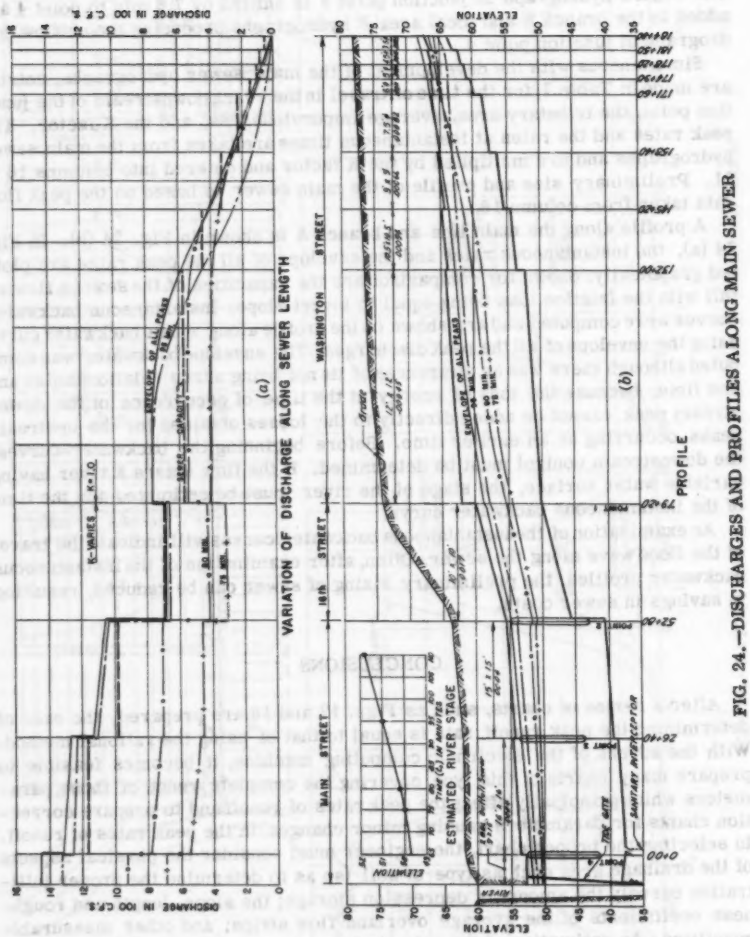


FIG. 24.—DISCHARGES AND PROFILES ALONG MAIN SEWER

Although a great deal of time has been spent in the development of the methods outlined herein, it is believed that each step can and should be improved. Further studies are being made on more exact storage routing procedures to be used in the lateral and main sewers.

An examination of Fig. 8 (a) reveals the large effect of depression storage on the runoff rates from elemental strips of pervious area. Knowledge of depression storage, therefore, is very important in sewer design for open residential or suburban areas. More research is desirable to determine the amounts of depression storage to be used for design.

Ground slope has little effect on sewer design for densely-populated urban drainage areas, because, in such areas, the delaying effect of overland flow causes the runoff from these surfaces to reach the sewer well after the peak runoff from the roofs and pavements. Roof slopes are not related to ground slopes, and pavement slopes are interrelated with spacing of street inlets so as to produce compensating storage volumes in the gutter channels. In suburban areas, on the other hand, the proportion of directly-connected impervious areas is less and runoff from ground surfaces may be the principal influence upon peak flows. Ground slope, therefore, becomes a more important factor. Other abstractions and reducing factors that should be considered are evaporation, interception by trees and shrubs, wetting of surfaces, and leakage into and out of house drains.

This paper does not purport to be a final diagnosis of the intricate relationships between rainfall and runoff in an urban area. It is hoped however, that it may, in some measure, guide the thinking of the sewer designer to a clearer visualization of what happens, hydrologically, when rain falls on the heterogeneous catchment surfaces of a city. From such an improved visualization should emerge more logical sewer design and more efficient and economical sewer systems.

ACKNOWLEDGMENTS

The writers wish to express their gratitude to Mr. Henry Hsien Chu, who has helped in much of the development of the "Chicago Hydrograph Method," and to Mr. Nello DiGiusto and Mr. Ganji G. Tanaka, who, before the introduction of the electronic computing machine did much of the laborious computation. The programming for the computing machine was prepared by Mr. Aizad N. Khan.

APPENDIX. NOTATION

The following symbols, adapted for use in the paper, conform essentially with "American Standard Letter Symbols for Hydraulics" (ASA Z10.2--1942), prepared by a committee of the American Standards Association, with Society representation, and approved by the Association in 1942:

A_D = drainage area, in acres;

A_g = cross-section area of gutter, in square feet;

a = constant used in rainfall rate-duration-frequency curve;

b = constant used in rainfall rate-duration-frequency curve;

C = coefficient used in rational method;

c = constant used in rainfall rate-duration-frequency curve;

D, D_e = detention on ground surface in inches depth, or cubic feet per foot width;

F = accumulated mass infiltration in inches;

$F(q,i,t) = F$ = functional relationship of q with i and t as parameters used in overland flow routing;

$F(Q,I) = F_g$ = functional relationship of Q and I, used in gutter routing;

f = capacity of surface infiltration in inches per hour;

f_o, f_c = constants used in infiltration capacity curve;

h = depth of gutter flow, in feet;

I = total instantaneous inflow into lateral sewer in cubic feet per second;

I_m = total instantaneous inflow into main sewer in cubic feet per second per acre;

I_o = total instantaneous inflow into gutter in cubic feet per second;

i = rate of rainfall in inches per hour;

i_{ave} = average rate of rainfall for a given duration, in inches per hour;

K = coefficient of overland flow containing Izzard's C;

k = constant used in infiltration capacity curve;

L_g = length of gutter, in feet;

l = length of overland flow strips, in feet;

n = Manning's coefficient of roughness;

p = accumulated mass of rainfall, in inches;

Q = rate of runoff in cubic feet per second, or cubic feet per second per acre;

q, q_e = overland flow runoff in inches per hour;

R = rainfall, in inches;

r = ratio of advanceness of storm pattern;

S_g = longitudinal slope of gutter;

S_o = slope of overland flow strips;

s, s_e = volume of storage in gutter, in cubic feet;

s_d = over-all average depression storage, in inches;

t_f = time measured from beginning of the infiltration capacity curve, in minutes;

t_o = time measured from beginning of rainfall, in minutes;

t_r = time of travel in sewers, in minutes;

V_d = volume of water in surface depressions;

v = velocity of flow, in feet per second;

w = variable width of gutter, in feet;

y = water depth at gutter curb, in feet;

Z = ratio of total width of water surface to the depth at the flow line; and

δ = overland flow supply in inches per hour.

DISCUSSION

PETER O. WOLF,[9] F. ASCE.—The authors base their runoff computations on a study of the effect of infiltration, retention and detention on a design rainstorm of three hours in duration. The variation of rainfall intensity within the period of the storm is based on the empirical rainfall formula of Eltinge and Towne, which, for a 5-yr frequency, is given as

$$i_{av} = \frac{90}{t_d^{0.9} + 11} \quad \ldots\ldots\ldots\ldots\ldots\ldots (28)$$

in which i_{av} is the average rainfall intensity, in inches per hour, over the period t_d in minutes.

In 1957 the writer put forward a rainfall formula[10] for the same purpose. This formula is

$$i_{av} = \frac{R}{\sqrt{T_1}} \cdot \frac{1}{\sqrt{T_d}} \quad \ldots\ldots\ldots\ldots\ldots\ldots (29)$$

in which R represents a rainfall in inches, associated with a unit duration T_1 in hours, and T_d is the actual duration of the storm in hours (which in the authors' case would be 3 hours.)

If the origin of the scale of time, T, in hours is taken at the peak intensity, the instantaneous intensities of the rising and falling limbs, corresponding respectively to Eqs. 1a and 1b are with r = 1/3

$$i = \frac{R}{\sqrt{\pm 12 T_1 \cdot T}} \quad \ldots\ldots\ldots\ldots\ldots\ldots (30)$$

---

[9] Reader in Hydrology at the Univ. of London, England, and Visiting Prof. of Civ. Engrg., Stanford Univ., Stanford, Calif.

[10] "Synthetic Storm Pattern for Drainage Design," by C. J. Keifer and H. H. Chu, Proceedings Paper 1332, ASCE, August, 1957.

and

$$i = \frac{R}{\sqrt{6\,T_1 \cdot T}} \quad \ldots\ldots\ldots\ldots\ldots\ldots \quad (31)$$

Eq. 28 has been plotted to logarithmic scales on Fig. 25 on which has been drawn a straight line with a slope of -1/2 representing

$$i_{av} = \frac{1.85}{\sqrt{T_d}} \quad \ldots\ldots\ldots\ldots\ldots\ldots \quad (32a)$$

or

$$i_{av} = \frac{14.3}{\sqrt{t_d}} \quad \ldots\ldots\ldots\ldots\ldots\ldots \quad (32b)$$

Over a range of $5 < t_d < 180$ minutes, Eqs. 28 and 32 are seen to be in fair agreement. This means that no great numerical change would result in the au-

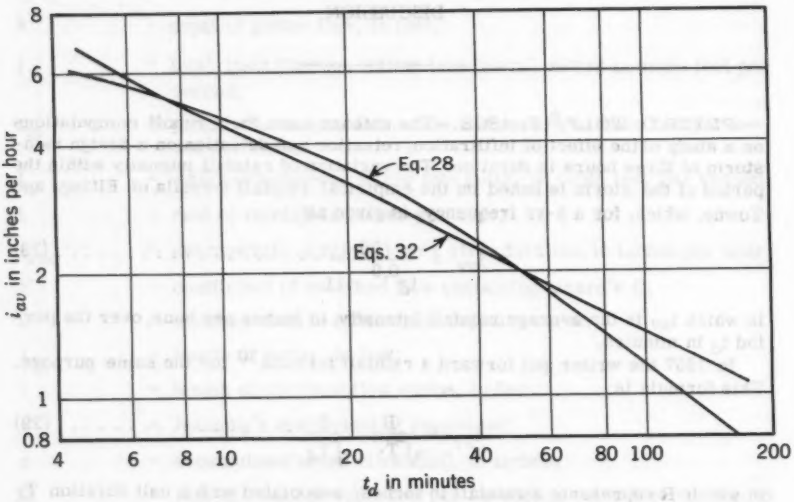


FIG. 25.—GRAPH OF EQUATIONS

thors' conclusions on the flood runoff in the sewers of Chicago, from the substitution of Eqs. 32 a or b for Eq. 28. However, the writer suggests that Eqs. 32 a or b is preferable because it is dimensionally consistent and it is physically more likely to be correct than Eq. 28.

The justification for the statement that it is more likely to be correct may be found in considering the values of total rainfall over periods in excess of the 180 min that represent the authors' upper limit. As t_d becomes large, the value of c becomes negligible compared with $t_d^{0.9}$ and the total precipitation, in inches, tends to become $P = (i_{av}) \cdot (t_d / 60) - 1.5\, t_d^{0.1}$ which clearly represents too small a rate of increase of total precipitation with duration of storms of a given frequency.

According to Eqs. 29 and 32 a or b the intensity i_{av} or the instantaneous intensity i would increase to infinity as T_d or T approach zero. As the variations of rainfall within the peak have no practical effect on runoff if a short enough interval is chosen, the writer has suggested[11] that the time interval considered should be greater than 45 secs. With the five-year frequency adopted by the authors, the peak average intensity would, accordingly, become

$$i_{av,\,max} = \frac{14.3}{\sqrt{0.75}} = 16.5 \text{ in. per hr}$$

for a duration of 45 secs.. Although this is twice the authors' maximum rate, this peak average is quickly reduced with increasing duration. In fact, the instantaneous value i = 8 in. per hr would occur at the beginning and end of a high-intensity rainfall burst lasting only a few seconds more than the suggested peak period of 45 secs.

M. B. McPHERSON,[12] and M. JOSEPH WILLIS,[13] MEMBERS, ASCE.—Some of the most modern theory has been ingeniously incorporated into the authors' analyses in a clear and elegant manner, taking full advantage of modern computing equipment. Nearly all of the assumptions and limitations characterizing the several elements of the analyses have been well-defined. It must be noted that the numerical results presented by the authors represent combinations of synthetic and hypothetical arguments applied to specific complexes of urban development without benefit of a broad experimental base or verification by means of field measurement. Despite the large number of hypothetical conditions and assumptions which cannot be avoided in this type of analysis, the assemblage of the several constituents into a hydrological whole gives the reader a better comprehension and appreciation of the separate factors that contribute to an urban runoff hydrograph.

The many procedural steps of the paper can be consolidated into four principal parts for the purpose of discussion. These are (1) synthetic hyetograph; (2) conveyance of rainfall to outlet of laterals; (3) routing of flows in main sewers; and (4) attenuation of rainfall with distance from the storm center. One of the writers has commented on the[14] synthetic hyetograph in an earlier discussion. In connection with the item 2 it should be noted that the overland flow computations were based on experimental tests on sprinkled plats that had a homogeneous cover and embodied uniform rates of rainfall supply. As a consequence, any application of these laboratory tests to a continuously varying rainfall supply on a heterogeneous cover must be regarded as a possible gross over-extension of the limits of the original experiments. According to the techniques employed, the routing of flows in the main sewers appears to be the section of the analysis subjected to the least number of assumptions. The section on areal distribution of rainfall and the accompanying Fig. 20 do not include sufficient documentation and explanation.

---

11 "The Influence on Flood Peak Discharges of Some Meteorological, Topographical and Hydraulic Factors," by Peter O. Wolf, International Union of Geodesy and Geophysics, I. A. Hydrology, Gen. Assembly, Toronto, 1957, Vol. III, pp. 26-39.

12 Prof. of Hydr. Engrg., C. E. Dept. Univ. of Illinois, Urbana, Ill.

13 Assoc. Prof. of Civ. Engrg., Swarthmore College, Swarthmore, Pa.

14 Discussion of "Synthetic Storm Pattern for Drainage Design," by C. J. Keifer and H. H. Chu, Proceedings Paper 1332, ASCE, August, 1957, by M. B. McPherson, Proceedings Paper No. 1558, ASCE, pp. 49-57, February, 1958.

The Johns Hopkins University has conducted field[15] measurements since 1948 of urban storm water runoff in Baltimore, Md. Peak flows at a large number of inlets and in several main sewers draining areas of as much as 153 acres in size have been recorded simultaneously with concomitant storm rainfall. This project represents the most extensive measurement program attempted in the United States. Unfortunately a direct comparison of the field measurements with the authors' computations for smaller areas cannot be made because all gaged-area roofs drain directly into the gutters as opposed to the direct connections to sewers that exist in Chicago. The results of the Johns Hopkins study have indicated a strong relation between peak runoff and (1) the percentage of total imperviousness of the drainage area; (2) the maximum five-minute intensity of the storm; and (3) the duration of the intense part of the storm. There is, unfortunately, no direct mathematical correlation between the last two items. Although the directly connected imperviousness of Type 5 land use is 36% (Fig. 8(a)), the total imperviousness appears to be 46.3%. The writers have applied their own interpretation and abbreviation of the Johns Hopkins method of analysis to the case of 46.3% total imperviousness, and have found that the peak flow at the outlet of the lateral would be approximately 140 to 160% of the 1.8 cfs per acre shown in Fig. 17(a). The following values were utilized: Maximum five-minute average intensity of 5.9 in. per hr from the upper curve of Fig. 2; a duration of the intense part of the storm of 20 mins (determined by the writers to be reasonably consistent with the theoretical 5-yr recurrence interval sewer discharge rate for both Baltimore and Philadelphia. Referring to the mass curve of rainfall in Fig. 4(a), 20 min appears to be a reasonable estimate for the synthetic hyetograph; a simplified generalization of the time-distance attentuation procedure employed at Johns Hopkins; and a "lateral outlet" drainage area of 10 acres, with a time of travel in the lateral of seven and one-third min. Other combinations were used to establish a range of estimated peak flow values, but the results were not significantly different. It would be improper to conclude that the divergence in answers is due solely to different types of roof connections. There is presently no real basis for comparison. If the authors could rerun the computations for Type 5 land use for Fig. 17(a), restrictions for the case of roof drains connected to gutters, a more sound basis for comparison with field measurements might then be available. [Fig. 17(a) and Type 5 land use are suggested because there are more details for these combinations presented in the paper]. This request is an obvious imposition, but the great potential value of this information should be adequate justification. Both an inlet and a lateral outflow hydrograph would be quite useful, together with the inlet hydrograph that is not shown in Fig. 15 (it appears that column 5 of Table 4 is for the Type 5 inlet hydrograph). It would also be interesting to know the total imperviousness of the other three land-use types.

The "rational" method implies that the attenuation of peak flow in a sewer system is related directly to the declination of an intensity-duration curve. Because intensity-duration curves represent a statistical manipulation of individual intensities for each duration arbitrarily separated from the sum total of the selected point-rainfall data, there is no logical way to "rationalize" any basic principles for the "rational" method. The designer who has been obliged

---

15 "Progress Report on the Storm Drainage Research Project, July 1, 1956 to June 30, 1958," by Paul Bock and Warren Viessman, Jr., Dept. of Sanitary Engrg. and Water Resources, The Johns Hopkins Univ., Baltimore, Md., July, 1958.

to use the completely empirical "rational" method for lack of anything better should derive some comfort from Fig. 16. The routing computations show that there is a similar trend in the time-distance attenuation of the curves for the two different methods. However, the rates of change of the curves and the absolute ordinate values offered by the authors must be regarded as pure estimates pending generalized substantiation via carefully controlled field measurements.

From Fig. 17, it is apparent that each curve is a trace through the four peak runoff values determined from the computations for each of the four land use types. The authors appear to have extrapolated the curves to an imperviousness of 100%. What bases or additional assumptions were used for this purpose?

Perhaps the most influential factor from a cost-design standpoint is the "areal distribution of rainfall" given in Fig. 20. The authors have failed to explicitly define the ambiguous term "duration". Because a large share of the pertinence and value of their paper must be based on the acceptance of Fig. 20, and because the source of information is "an unpublished report" not available to the public, it is hoped that the authors will enlarge considerably on their coverage of this subject in their closing comments. It is evident that Fig. 21 was obtained through an interpretation of Fig. 20, but the methodology used has been implied and not demonstrated. Under the heading "Sample Computation Method for Large Drainage Areas", they cite a "640-acre limit for use of uniform areal distribution of rainfall," that is not mentioned or explained in any prior section. From this and a succeeding remark it appears that the curves on the right side of Fig. 21 are not considered applicable to areas less than one square mile, or were possibly so treated. Inasmuch as neither Fig. 20 nor Fig. 21 are mentioned in connection with the developments leading to Fig. 17, the question arises as to exactly what allowance, if any, was provided for areal distribution in the computations leading to Figs. 15, 16, and 17. If no allowance for areal distribution was made for the analysis curves in Fig. 16, has a fair comparison with the rational method been given in this figure?

Over a year ago the authors kindly supplied one of the writers with data on the times of occurrence of peak flows from their computation files for all four land use types, to supplement the data of Figs. 14 and 15. These data have been plotted in Fig. 26, and represent the computation conditions applied to Fig. 17. The time-displacement of peaks is seen to be approximately 0.7 of the time of travel. A value of 2/3 was used by[16] Hicks in an earlier hydrograph analysis. In the analytical procedure[14] employed at Johns Hopkins a value of 0.8 is used. A recent review of the Johns Hopkins field data files[17] by Warren Viessman, Jr. has indicated that the peak flow in Baltimore inlets has generally occurred approximately 1 min after the most intense burst of rainfall. The arbitrary extrapolation of data in Fig. 26 for the three most impervious land use types indicates a peak flow time at the inlet $1\frac{1}{2}$ min after the peak intensity of the synthetic hyetograph. (In Table 4, the peak lateral inflow occurs at 68.5 min). If the authors compute the Type 5 land use values for the situation with all house roof drains connected to gutters, it is hoped that a comparison with the characteristics of Fig. 26 will be made, using those results,

---

16 "A Method of Computing Urban Runoff," by W. I. Hicks, Transactions, ASCE, Vol. 109, 1944, Paper No. 2230, pp. 1244–1245.

17 "Progress Report on the Storm Drainage Research Project," July 1, 1958 to June 30, 1959, by Warren Viessman, Jr., Dept. of Sanitary Engrg. and Water Resources, The Johns Hopkins Univ., Baltimore, Md., June, 1959.

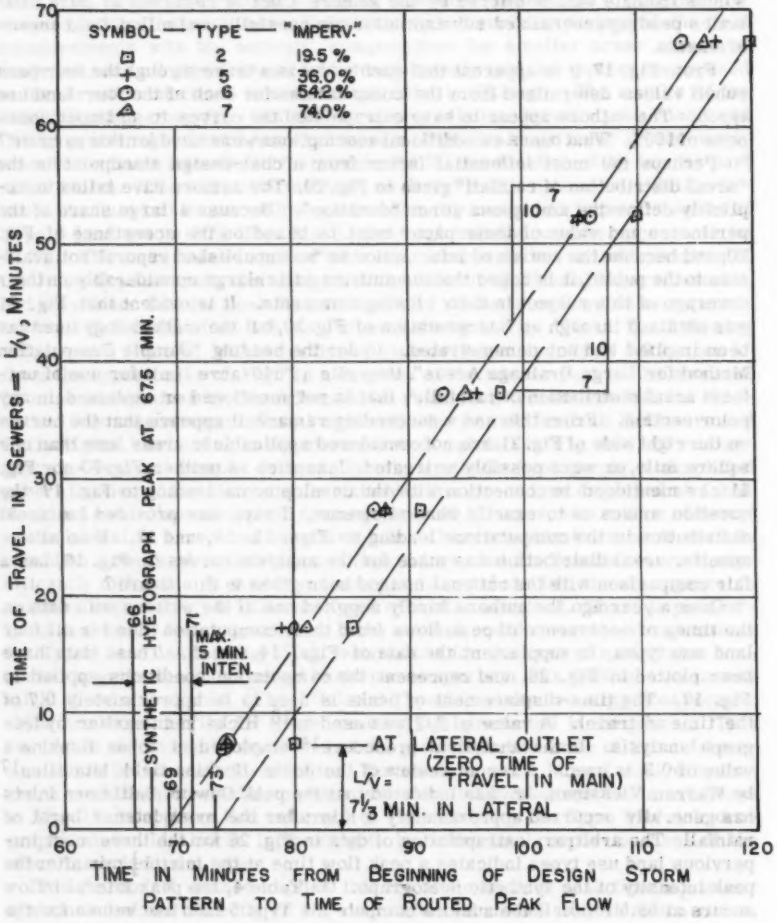


FIG. 26.—TIME-ATTENUATION CURVES

to further extend the value of the computations. Referring again to Fig. 25, it would appear that the authors' statement under the heading, "Step 8, Preparation of Design Charts," "The approximate time of concentration can be obtained by adding 10 min to the time of travel in the main sewer" is quite reasonable except for the case of Type 2 land use.

The paper gives an excellent qualitative picture of the urban rainfall-runoff process. However, the writers are concerned with the quantitative difficulties of the problem which may possibly render the authors' qualitative approach unusable for design or analytical purposes. The quantitative assumptions the authors must perforce make and that appear to be reasonable in terms of present knowledge regarding the synthetic hyetograph, infiltration capacity, depression storage, overland flow, routing, and rainfall attenuation are all subject to considerable individual errors. Furthermore, because the magnitudes used are chosen by the engineer, the errors may on occasion tend to be cumulative rather than having any compensating tendencies. When it is considered that the representative infiltration curve chosen by the authors may, under certain conditions, be 50% or more in error, and bearing in mind the possibility of errors of similar magnitude in the manipulation of data for the hyetograph, depression storage, overland flow, and rainfall attenuation, it is quite conceivable that a final computed value of runoff might be more unrealistic than the runoff computed by the rational method through the selection of a single all-embracing coefficient. The writers believe that the value of the paper would be enhanced by a discussion of the magnitude of the errors likely to occur in each step of the authors' method at the present state of its development.

The authors have succeeded in their avowed aim: To "guide the thinking of the sewer designer to a clearer visualization of what happens, hydrologically, when rain falls on the heterogeneous catchment surfaces of a city." However, the extensive computations contained in the paper may lead many readers to expect that the approach used by the authors for qualitative clarification of the rainfall-runoff process may soon come of age quantitatively. The writers question whether this is possible for some time to come, considering how much remains to be learned about the mechanics of infiltration, detention, overland flow, and so forth. It is suggested that a simpler approach based on actual measurements of rainfall-runoff relationships from urban drainage areas might prove much more fruitful until such time as sufficient knowledge is gained of all components of the urban runoff process. By then it may be possible to develop a computing procedure approaching the qualitative model. On the other hand, because of the many factors inherent in evaluation using the quantitative model, it would seem that a simpler method of computation backed by extensive field measurements holds more promise for the future. The 1959 field program of the Water Dept. of the City of Philadelphia, under the supervision of the writers, includes seven urban gaging stations for drainage areas from 8 to 260 acres in size.

PAUL BOCK.[18]—The Chicago hydrograph method is an example of the "microscopic approach" to urban storm drainage design. In general, the microscopic approach attempts to define a chronological design-storm pattern and then quantify all pertinent physical phenomena from the input (rainfall) to output (runoff). To evaluate the individual phenomenon the drainage area is divided into different types of surfaces. The flow from each surface is then computed and the individual flows synthesized by routing techniques to obtain the

[18] Assoc. Prof., Dept. of Civ. Engrg., Univ. of Delaware, Newark, Del.

outflow hydrograph. The main advantages of the authors' method are its generally sound physical approach, its susceptibility to systematic improvement as knowledge increases, and, as stated under the heading "conclusions," its "* * * clearer visualization of what happens, hydrologically, when rain falls on the heterogeneous catchment surfaces of a city." Its principal disadvantage for practical engineering applications is that it requires the use of numerous assumptions, simplifications, untested individual coefficients, and other data not generally available.

On the other hand, the rational method[19,20,21,22,23] is an example of the "macroscopic approach" which considers a drainage area as being homogeneous through use of an over-all weighted runoff coefficient, flow from a drainage area considered only at its outflow point, and rainfall assumed to be acting uniformly in time and space. The essence of the rational method is the judicious selection of the runoff coefficient which, as the authors state, "must come out of years of experience in a particular locality and cannot be adequately nor easily conveyed to a novice." The advantages of the rational method are its simplicity of application and, apparently, its popular faith in it efficacy. Its disadvantages are that its concepts are physically unsound, ambiguous, and untested (for example, the writer is unaware of any measurements of "time of concentration" on urban areas as defined by the authors); it is inherently not susceptible to improvement; and its predictions of peak flows have been found to be unreliable as based upon measurements of rainfall-runoff.

Both the authors' method and the rational method assume a design storm as a first step. Although not generally stated, the design-storm of the rational method is assumed to be of uniform intensity, i, lasting for the time of concentration. Because i is computed as the total amount of rainfall (in inches) divided by the duration (in hours), it represents an average rainfall rate that is constant throughout the duration. Again a uniform rainfall rate is implied because of the preclusion of values of runoff coefficient greater than 1. Thus, if the rational method's design storm were considered nonuniform, then rates greater than i_{ave} must be present. These higher intensities could cause a runoff rate greater than that computed by using a runoff coefficient equal to or less than unity. Emil Kuichling, originator of the rational method in 1889, assumed[23] that the rainfall rates were steady. Without benefit of recording rain gages he concluded he could "form tolerably accurate estimates of the rate of precipitation from both the sound of the rain upon the roof of the building and the appearance of the street gutters." Modern rain gagings indicate that rainfall seldom, if ever, is steady.

---

19 "Report on Drainage Verification at Military Establishments, Freeman Field and St. Anne Auxiliary Field, Indiana, Godman Field, Kentucky, Lockbourne Army Air Base and Wright Field, Ohio," Corps of Engrs., U.S. Dept. of the Army, Louisville, Ky., July, 1947, p. 311.

20 "Principles of Storm Water Runoff Derived from A Study of Sewer Gagings," by Clifford Seaver, The Municipal Engineers Journal, 3d Quarterly Issue, Vol. 35, 1949, p. 76.

21 "Surface Runoff from Agricultural Watersheds," by W. H. Potter, Research Report No. 11-B, Highway Research Board, National Research Council, December, 1950, pp. 23-24.

22 "A New Method of Urban Drainage Design," by Ian R. Wood, Canberra, Australia, 1957. (unpublished)

23 "A Study of Urban Rainfall-Runoff Relationships," by Paul Bock, thesis presented to the Johns Hopkins University at Baltimore, Md., in May, 1958, in partial fulfilment of the requirements for the degree of Doctor of Engineering.

The design storm used in the Chicago hydrograph method is a chronological storm pattern derived from two sources: (1) rainfalls at eighty-three station (considered excessive) for durations of 15, 30, 60, and 120 min for obtaining the relative time position r of the peak rainfall rate, and (2) the local rainfall intensity-duration-frequency curve for obtaining the 5-yr intensities. Although the actual hyetalgraphs were not shown, the data tabulated indicate[3] the ordinal position of the peak 5-min rainfall for 15, 30, 60, and 120 minute durations. For example, the ordinal positions for the 120-min duration are 20, 19, 6, 6, 16, 9, 6, 3, 15, 6, 12, 5, 13, 21, 3, 3, 15, 10, 10, 15, 4, 10, 18, 4, 2, 2, 6, 9, 7, 4, 24, 5, 4, 15, 3, and 5. The mean ordinal position is 9.30 which yields a mean location of the peak within rainfall duration, r of 0.366. The large value of the standard deviation of the ordinal positions, $\sigma = 6.1$, indicates that the design value, $r = 3/8$ is highly questionable. Because the Chicago design storm is based on a 180-min duration, it appears appropriate that r should also be computed for this duration.

The authors have quite correctly not attached a frequency to the Chicago design-storm pattern although Fig. 2 might suggest that it is, as the authors state, a "hyetalgraph of 5 year rainfall" with an average frequency of occurrence of once in 5 yr. The chronological pattern itself would have a frequency considerably rarer than 5 yr, although the intensities for durations from 5 to 180 min correspond to a 5-yr frequency. Because the design-storm pattern has no assigned frequency (in the usual statistical sense), it would be revealing for the authors to discuss their "engineering reasons" for selecting the 5-yr rainfall-intensity-duration frequency curve shown in Fig. 2.

In a previous study, the writer examined[24] the time distribution of excessive precipitation rates for Baltimore from 1894 to 1935. During this period, the U. S. Weather Bureau data were published as "accumulated depths for consecutive periods of time." This convenient tabulation makes it possible to determine whether the rainfall rates were uniform or variable over durations of excessive rates. The 21 storms containing the greatest rainfall depths for 15, 30, and 60-min durations in Baltimore for the 42-yr period from 1894 - 1935 are plotted in dimensionless form in Fig. 27. The scatter appears to be so wide that no meaningful typical chronological pattern can be detected for these storms of design intensity.

The authors have explicitly noted assumptions and simplifications made throughout the development of their method. Many of these, of course, are hidden in the rational method's runoff coefficient. It is revealing to list some of the authors' assumptions:

Sidewalks and garage roofs considered as pervious areas; roofs considered as uniform strips of equivalent area; evaluation of design storm's chronological pattern and magnitudes (implicit assumption); selection of infiltration capacity curve (implicit assumption); time of commencement of overland flow and depression storage supply; over-all volume of depression storage; ogee distribution curve of depression storage; Eq. 7 holds for unsteady flow conditions; distributions of inflow hydrograph to gutter; Eq. 15 obtained by integration is not mathematically rigorous[25] (8), because the choice of a differential element of integration affects the computed flow. The conventional form of the

---

24 "The Relation Between the Rainfall and the Discharge of Sewers in Populous Districts," by Emil Kuichling, Transactions, ASCE, Vol. 20, January-June 1889, p. 28.

25 "Progress Report of the Storm Drainage Research Project," by Paul Bock, The Johns Hopkins Univ., July 1, 1955-June 30, 1956, Baltimore, Md.

equation Q = AV is more valid and gives a 19% lower value of Q for a given value of n. Published values of n have been derived from the equation Q = AV. Steady flow conditions in gutter; Eq. 19 states equilibrium conditions for flow in gutter; Uniform velocity distribution in lateral sewer; Spatial distribution of gutter and roof hydrographs to form total in-flow hydrograph; Spatial distribution of lateral hydrograph into main sewer; Time of concentration.

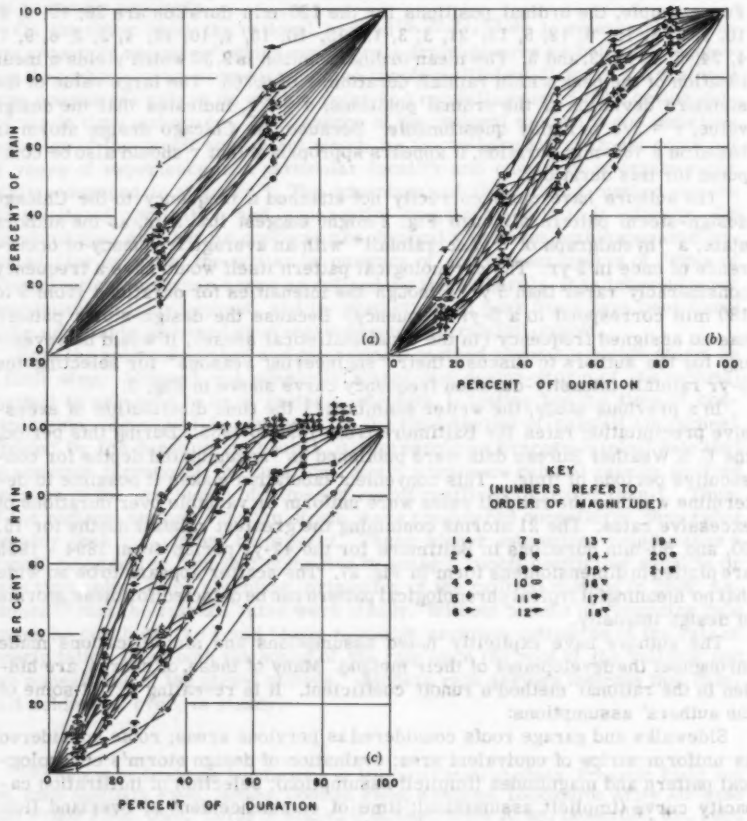


FIG. 27.—STORMS IN BALTIMORE, MARYLAND (1894-1935)

The final answer desired, peak runoff rate, is affected by the accuracy of the determination of all losses and hydraulic phenomena, and the validity of the simplifying assumptions. If the errors are small and noncumulative, the prediction of the runoff is valid. Otherwise, this detailed approach may give no better practical answers than use of a single gross runoff coefficient that "cannot be methodically conceived by any form of mental exercise."

The improvement and verification of any method for urban storm drainage design rests ultimately on measurements of rainfall-runoff on urban areas. At present, the Chicago hydrograph method suffers from lack of experimental verification. Ideally, to check this method, there should be sufficient independent data of rainfall-runoff on actual urban areas and elemental units of urban areas to check each of the authors' steps, particularly, steps 3 to 7 inclusive. For example, there should be measurements of infiltration, volume of depression storage, and flows in the gutter, lateral sewers and main sewer outlet.

Unfortunately, there exists a paucity of gagings of rainfall-runoff on urban areas. The dates of the authors' references indicate the serious inadequacy of research on urban drainage. Except for the analytical study of Chicago storm patterns,[3] the specific references are from 11 to 19 yr old. Only one applies particularly to urban drainage and none is adequately supported by actual field gagings on urban areas. Where urban gagings have been made, the gagers (almost without exception) have introduced methods of their own based on the experimental data. Likewise, the writer plans to publish the "Inlet Method," a "Quasi-Microscopic Method," based upon nearly 10 yr of rainfall-runoff gagings in Baltimore.

The authors should be commended for stimulating interest and suggesting desirable research in urban drainage design. Undoubtedly, ideas presented in their paper will have a beneficial influence on future research and thinking on hydrology of urban areas.

CARL F. IZZARD,[27] M. ASCE, and CHARLES L. ARMENTROUT.[28]—The authors present a comprehensive study of a multitude of factors that may affect the rainfall runoff relationship. While this work is a definite contribution to the field of urban drainage, it must be examined for verification and simplification of the procedure. An effort has been made by the writer to simplify the gutter hydrograph computations and to compare the results with actual runoff hydrographs measured at inlets in residential areas.

While the Chicago hydrograph method provides a means of reproducing the runoff hydrograph from a given rainfall pattern, complications would arise in its application to a suburban development having drainage areas with varying shapes and slopes. Separate overland flow routing curves such as Fig. 7 would be required for variations of length or slope encountered in the design. The same would be true of gutter-storage curves such as Fig. 11. By use of a few simplifying assumptions, the storage curves shown in Figs. 7 and 11 can be combined into one set of curves that can be used for any drainage area or gutter, regardless of grade, cross-slope, or roughness.

The first step involves the detention constant, K, which is defined by Eq. 6. The use of a constant value of rainfall intensity for the determination of K simplifies the computations and introduces little discrepancy in the results. Thus, for a given storm, K would be computed for an average intensity and this value of K would be used to compute the equilibrium detention for a strip of unit width from Eq. 7.

---

26 "Wetted Perimeter and Hydraulic Radius as Parameters in Flow Equations," by Paul Bock, 40th Meeting, Am. Geophysical Union, 1959.

27 Chief, Div. of Hydraulic Research, Bureau of Public Roads.

28 Formerly Hydr. Engr. (Research), Bureau of Public Roads.

The storage in the gutter at equilibrium is expressed by Eq. 19. Substituting the value for the cross-sectional area of flow in the gutter from Eq. 16, the gutter storage equation becomes

$$s_e = \frac{4}{7} A_e L_g \quad \ldots\ldots\ldots\ldots\ldots\ldots \quad (33)$$

in which A_e denotes area at equilibrium. The gutter storage equation (Eq. 21) can be expressed identically as

$$s = \frac{s_e}{Q_e{}^{3/4}} \left[\frac{4}{11} I_o{}^{3/4} + \frac{7}{11} Q_o{}^{3/4} \right] \quad \ldots\ldots\ldots\ldots \quad (34a)$$

From analytical studies using the step method of routing steadily varying flow through a gutter, it was found that combining the overland flow detention and gutter storage in the storage equation would give a close approximation of the outflow hydrograph. The storage equation would become

$$s = \frac{s_e + D_e L_g}{Q_e{}^{3/4}} \left[\frac{4}{11} I^{3/4} + \frac{7}{11} Q^{3/4} \right] \quad \ldots\ldots\ldots\ldots \quad (34b)$$

Using this storage value in Eq. 23 a graph similar to Fig. 11 would serve for routing both overland detention and gutter storage. In this form, however, the graph would serve for only one particular drainage area and road section. A change of slope, roughness, or length would require preparation of a new graph.

An expansion of Eq. 23 leads to a simplification

$$F(Q) = \frac{1}{2} Q + \frac{s_e + D_e L_g}{Q_e{}^{3/4}} \left[\frac{\frac{4}{11} I^{3/4} + \frac{7}{11} Q^{3/4}}{60\ \Delta t} \right] \quad \ldots\ldots\ldots \quad (35a)$$

The independent variables are all contained in s_e, D_e, and $Q_e{}^{3/4}$. By transposing,

$$\frac{F(Q) - \frac{Q}{2}}{\frac{s_e + D_e L_g}{Q_e{}^{3/4}}} = \frac{\left(\frac{4}{11} I^{3/4} + \frac{7}{11} Q^{3/4} \right)}{60\ \Delta t} \quad \ldots\ldots\ldots\ldots \quad (35b)$$

The result is a mathematical relationship of inflow and outflow that pertains to all sections. Standard storage curves can be prepared (Fig. 28) with the left side of Eq. 35b as ordinate versus the outflow as abscissa for different values of inflow. In order to shorten terminology, $(s_e + D_e L_g)$ will be referred to as s_{DE} and $\frac{s_{DE}}{Q_e{}^{3/4}}$ will be referred to as E. Technically, it would be necessary to compute a value of E for each rainfall intensity encountered. However, this value does not vary greatly with differing rainfall intensities. The procedure is greatly simplified by using the same constant value of i as used in computing

K and D_e. This resulting constant value of E will cause only a small percentage of error in the shape and peak of the hydrograph.

The routing equation, (Eq. 24) would not be changed by these adjustments but two columns would be added to the computations shown in Table 3. After F(Q) is computed by Eq. 24, the next column would be for F(Q) - Q/2 and another column for $\frac{F(Q) - Q/2}{E}$, that is the ordinate on the storage routing curves.

The methods presented in the authors' paper and in this discussion can be evaluated by application. Actual rainfall patterns have been routed through overland detention and gutter storage, using the standard storage curves. The computed hydrograph has been compared with measured runoff at one inlet.

The field data used were obtained from the Storm Drainage Research Project conducted by The Johns Hopkins University, Baltimore, Md., and sponsored

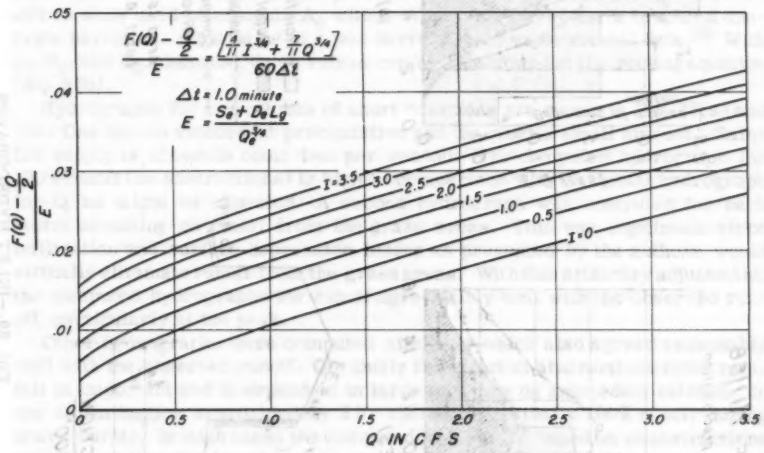


FIG. 28.—STANDARD STORAGE CURVES

by the city of Baltimore, Baltimore County, and the United States Bureau of Public Roads. Runoff is measured with weir installations in the inlets. Rainfall is measured by a tipping bucket rain gage. Runoff at each inlet and rainfall at the centrally-located gage are recorded on a single chart by means of a multi-pen recorder. The particular inlet area used was a group housing residential development in the Midwood area of Baltimore. The steep roofs drain to downspouts that discharge onto lawns and thence to the street gutter. The drainage area, which is fairly well defined, is 400 ft long and 70 ft wide. The typical cross section is shown in Fig. 29(c).

The overland flow detention in the gaged area was computed for four surfaces; roof, grass, walks, and street. The flow from the roof discharged onto the lawn. Sample computations indicated that routing the roof discharge uniformly across the lawn by overland flow caused the computed hydrograph to

delay behind the measured runoff. Actually, it would be expected that flow from the downspouts would be somewhat concentrated and possibly flow down the walks leading to the houses. There was some erosion of the grass area adjacent to the sidewalk caused by flow which had been concentrated on the sidewalk. Consequently, it was assumed that the runoff from the roofs was added directly to the walks and the combined flow routed to the gutter. This was the only assumption used in an otherwise straightforward application of the combined routing procedure.

Eq. 7 was used to compute detention on each surface. Values of C used were 0.007 for roofs, 0.045 for grass, 0.012 for walks and street. A constant value of 3 in. per hr was used for i in computing the storms shown on Figs. 28(a) and (b).

The gutter storage was computed by Eq. 33. The value of A_e pertains to the area of the flow at the lower end of the gutter at equilibrium. The same constant value of i was used to compute the equilibrium discharge, Q_e. Eqs. 15 and 16 were used to compute A_e with a value of n = 0.012 for a broomed concrete pavement. This value of n was derived from experimental data.[29] With s_e, D_e, and Q_e computed, these values can be substituted in the routing equation (Eq. 35b).

Hydrographs for two storms of short durations are shown in Fig. 29(a) and (b). One has no antecedent precipitation and the other a small amount. Rainfall supply is shown in cubic feet per second. The computed hydrograph for 100% runoff (no abstractions) is high in comparison with the actual hydrograph for Q, as might be expected. A second hydrograph was computed for each storm assuming no runoff from the grass areas. This was legitimate since infiltration and surface depression losses as presented by the authors would virtually eliminate runoff from the grass areas. With this arbitrary adjustment, the computed hydrographs for runoff agree fairly well with the observed runoff, particularly at the peak.

Other hydrographs were computed similarly which also agreed reasonably well with the observed runoff. Obviously the effect of abstractions from rainfall is important and is dependent in large measure on antecedent rainfall. In one storm lasting approximately 2 hr there was virtually 100% runoff during heavy bursts. In such cases the computed hydrograph based on no abstractions reproduced that portion of the observed hydrograph.

While these tests of the method are made for only one small watershed, they do indicate that the simplified method does reproduce observed hydrographs fairly well, provided the proper assumption is made regarding abstractions. In other words, it is possible by this method to route a known rainfall, or rainfall minus abstractions, through a simple drainage system to a storm drain inlet with confidence that the entire hydrograph will be substantially correct. The more precise procedure proposed by the authors would probably give a little more accuracy, but in view of the uncertainties regarding probable rainfall and abstractions, the simplified method is accurate enough.

The authors assume that each inlet will intercept all the water coming to it. This assumption is adequate for the drainage plan in Fig. 1 when all inlets are in low points along the gutter. More commonly, some inlets will be on continuous grades where some bypass flow probably occurs at the higher rates of

[29] "Airfield Drainage Structure Investigation," Corps of Engineers, St. Paul District Sub-office, Hydraulic Laboratory, Iowa City, Iowa, Hydraulic Laboratory Bulletin No. 54, April, 1949.

FIG. 29.—INLET HYDROGRAPHS

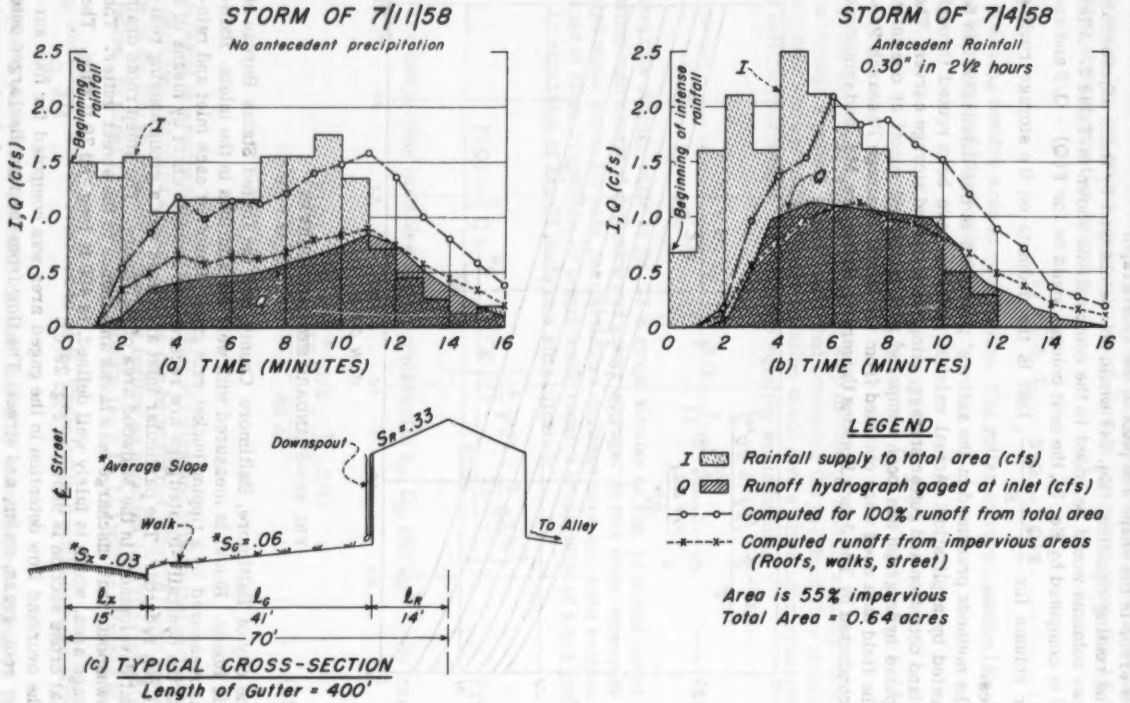


FIG. 29.—INLET HYDROGRAPHS

flow in the gutter. The writers have taken this factor into consideration in studies of flood routing along an express highway. The bypass flow was assumed to move down the gutter at a wave velocity one-third greater than the mean velocity in the reach. Flow in the storm drain was routed by the offset method used by the authors. The whole procedure can be programmed easily for electronic computation, thus making it feasible to route any given rainfall pattern through a system of storm drains along a highway. There is some doubt that the effort would be worthwhile because of recognized deficiencies in the knowledge of the hydraulics of the inlets. In addition, more needs to be known about the translation of flood waves in the main storm sewer, especially at junctions on steep slopes.

While the authors went to considerable pains to derive the equations for a design storm pattern having duration and intensities suitable to the Chicago area, the simplified method herein presented can be used for any desired storm pattern and abstractions.

The earlier methods of overland flow routing[8] by Izzard, which were somewhat laborious, have been improved by the authors' introduction of the storage equation. While some approximations are involved, these are insignificant as demonstrated by the fact that earlier laboratory measurements of the overland flow hydrographs have been reproduced quite faithfully using a routing chart similar to Fig. 7. The writers then combined overland flow with gutter routing to further simplify the process. The results demonstrated in Fig. 29 indicate that down to the inlet, at least, the simplified method gives reasonable results.

The writers do not suggest that a design engineer should use the storage routing procedures presented herein for storm drain design. Abstractions from rainfall cannot be accounted for by such a simple procedure as eliminating runoff from the pervious area. This simplified method is a handy research tool which can be used to provide a better understanding of the relationship between rainfall and runoff. It can be used in conjunction with gaged rainfall and runoff records to study empirically the abstractions from rainfall. The computations can be performed easily and quickly with a slide rule and are also readily adaptable to programming for electronic computation.

An understanding of the rainfall runoff relationship is important to the drainage engineer. Nevertheless the solution to urban runoff on a frequency basis may lie in a statistical analysis of runoff records over a sufficient period of years rather than computing runoff from a storm having a given frequency. Unfortunately, little data are available other than The Johns Hopkins project. This situation could be remedied if progressive engineering organizations in various sections of the country should initiate accurate gaging programs in urban areas and gather sufficient date for analysis.

A. L. THOLIN,[30] M. ASCE.—Since the preparation of this paper, the writer has assumed administrative duties in the general field of public works and, as a consequence, has been less intimately associated with the design of sewers, although such work is still within the writer's administrative assignments. The co-author, however, has continued some basic studies of the rainfall-runoff relationship and the application of the electronic computer to the "Chicago Hydrograph Method," as outlined in the authors' paper.

In view of the partial separation of their present daily duties, the authors have decided to write separate closing discussions. The writer will limit his

[30] Admin. Engr. of Public Works, Chicago, Ill.

discussion to general concepts. Mr. Keifer will cite some specific results obtained from a gaging station established since the original presentation of the paper and indicate the results of additional computations programmed for and performed with the aid of an electronic computer, also made available to the Sewer Planning Division since that time. He will also discuss other specific matters raised by the discussions.

The writer appreciates the high degree of competence represented by those who have contributed to the discussion. It is hoped that other competent writers may be stimulated to present independent papers on the subject in the near future.

Since the height and shape of the intensity-duration-frequency curve of anticipated rainfall is basic to the development of the Chicago hydrograph method, the comments on this subject by Mr. Wolf are very pertinent and will, I believe, stimulate the Chicago Sewer Planning Division to reappraise the correctness of the Eltinge-Towne formula. This formula was statistically derived from data collected over a 42-yr period, prior to 1942. A study of other storms of more recent record may indicate, as Mr. Wolf suggests, that our values of rainfall intensity are too low for the storms of longer duration. An upward adjustment of these values for the longer rainfall periods would affect computed runoff rates for the larger drainage areas. In Chicago, there are, at present, four such areas delivering runoff to storm-water pumping stations. Another such area and pumping station is contemplated. A current reappraisal, prior to the design of the latter, is in order.

The writer wishes to point out, however, that as shown in Fig. 24 the values obtained from the Eltinge-Towne formula are in close agreement with his suggested revision for all precipitation periods less than 60 min. Most of the drainage areas in Chicago have "time of concentration" values of less than 60 min, and sewers designed for these shorter periods of rainfall will not be overloaded by the attenuation of the rainfall hyetograph at rates susceptibly higher than those now assumed.

With regard to rainfall rates used in the design-storm pattern, Mr. McPherson and Mr. Willis correctly point out that in the illustrative problems, the authors disregard the reducing effect of less than "point rainfall" as an average rate for drainage areas of less than 640 acres. This is purely arbitrary, for the sake of simplification of computations for the larger number of smaller areas. The application of the reduction factor K in Table 7 makes a sudden downward adjustment of 11% in the estimated peak flows when the cumulative drainage area reaches 640 acres. Perhaps this adjustment should take place at a smaller cumulative area. McPherson and Willis also inquire about the mean of "duration" in Fig. 19. The terminology on this chart should have been "Storm of 3 Hr duration or maximum 3 hrs of longer storm" and so forth. The curves were derived from records of 22 major rainstorms occurring over a 12-yr period.

Mr. Bock raises a question with regard to the validity of the value of r as being equal to 3/8, for the establishment of the chronological location of the peak rate of rainfall with regard to the total duration of the design storm. The derivation of this value was more thoroughly discussed in a previous paper[3] by Messrs. Keifer and Chu. The value derived agrees closely with the value suggested for summer thunderstorms in St. Louis in the paper[6] by Messrs. Horner and Jens. No assumed design storm is ever reproduced in nature, but the authors still believe that the assumed location of the peak rate is a reasonable assumption for design purposes in Chicago.

Mr. Bock correctly states that "the improvement and verification of any method for urban storm drainage design rests ultimately on measurements of rainfall-runoff on urban areas." His work in Baltimore, Md. is a notable contribution of factual data in this regard. For proper application of such factual data, however, to drainage areas other than the one gaged, it is necessary to know not only what the rates of runoff were but why they were what they were. No two drainage areas have identical physical characteristics. If one or more of the variable characteristics of an ungaged area are different from those in the gaged area, how should one adjust the data? Such a question leads back to the analytical methods dealt with in the authors' paper.

The writer believes that gagings by themselves, as a basis for design, must be far more voluminous than presently available and all the physical features of the drainage area must be considered in the appraisal and use of gaging data. Gagings, on the other hand, performed for verification or modification of rigid methods of analysis and synthesis of ascertainable physical characteristics and their effect on runoff, can establish the validity of the analytical methods so that in the future, such gagings are no longer necessary. Because they are expensive and have limited direct applicability to nonidentical areas gagings for verification of basic analytical methods are, in the long run, more economical than gagings for direct use in design.

Messrs. Izzard and Armentrout state, in their discussion of this paper, that "while this work is a definite contribution to the field of urban drainage, it must be examined for verification and simplification of the procedure." To this I am sure both authors agree. The rainfall-runoff gaging station established in 1959 has been discontinued for the winter months but will be returned to service in early spring of 1960. Some mechanical difficulties were experienced this year, so that few rainstorms produced reliable records. Mr. Keifer will present some data in his discussion. More accurate measurements of the physical characteristics of the test area will be made. The writer hopes also that some on-the-site infiltration capacity tests may be initiated and a means found to determine the actual value of depression storage.

With regard to simplification of office design procedures, it has been the writer's hope that, with the aid of the electronic computer, now intermittently available, a large number of charts of the types shown in Figs. 14, 15, and 17 can be produced, embracing the maximum expected ranges of each of the important variables in the rainfall-runoff relationship, and all combinations thereof. It would be assumed that such simplified charts would be directly usable by the designer for areas up to at least 320 acres, or, as assumed in the authors' paper, up to 640 acres.

With such a series of charts in hand, the designer, in selecting the proper chart would ask questions of himself such as; 1. What intensity-duration-frequency shall I use? 2. What shall I assume with regard to chronological location of peak rainfall to the total rainstorm? 3. What are the shape and numerical values of the infiltration capacity curve? 4. What is the value, in inches, of depression storage? 5. What are the factors affecting overland flow to the street gutter? (a) The ground slope. (b) The surface frictional coefficient. 6. What percentage of the drainage area is "directly-connected impervious area?" 7. What percentage of the drainage area is "indirectly-connected impervious area?" (a) Connected by way of street gutter? (b) Connected by way of turfed areas to street gutter and then to sewer?

Question 7 is not pertinent to the Chicago problem because all roofs, parking lots, and so forth are required by ordinance to be directly connected to the

sewer system, but the question may be pertinent in other cities. Question 7(b) would often apply to suburban areas.

Such an extensive series of charts would not be feasible but for the advent of the electronic computer. Unfortunately for this program in Chicago, the electronic computer purchased by our Bureau of Engineering has been put to use in numerous other fields and the production of an extensive series of runoff charts has been delayed.

The charts would be arranged in groups and cross-indexed for ease of reference, so that the designer could pick whatever combination of values of the principal variables that would fit the rainfall, physical characteristics, and land use of the particular drainage area. Future research would be directed at verification of the component values and the hydraulics of overland and channel flow. For larger areas, areal distribution of rainfall must be considered and hydrographs of the smaller tributary areas synchronized to determine downstream hydrographs.

In conclusion, the writer wishes to state again that to obtain a fuller understanding and eventually a simplified method for evaluation of the rainfall-runoff relationship in urban areas, we must not only know what happens but why. A sufficient number of gagings could answer the "what," but the "why" must be dealt with by the methods of microscopic analysis, followed by a synthesis of the component parts. The final synthesis must then be verified by gagings at carefully selected locations. Only then can we proceed with any high degree of certainty to design an initial system of sewers in an ungaged area. Otherwise, as we approach a new sewer problem, we are confronted with the dilemma of two opposing questions. "How can we design this sewer system without a gaging?" and, "How can we gage the runoff without a sewer system?"

The coefficient in the rational method is, on the other hand, too easily "rationalized" downward to meet available dollars, while still purporting to give protection from a storm of a given frequency. The frequency of occurrence affects only the I in the Rational Method. The C is flexible and mysterious.

CLINT J. KEIFER,[31] M. ASCE.—The writer is grateful to those who have taken part in the discussion of the subject paper. Their constructive comments are well appreciated and should enhance the value of these studies.

Mr. Wolf's discussion pertains mostly to the design storm pattern that is covered thoroughly in the work of Clint Keifer and Henry Chu.[3]

The Eltinge-Towne formula Eq. 28 currently used in Chicago, compares closely to Yarnell's curves, and to the more recently published curves by the U.S. Weather Bureau.[32]

In the latter publication, rainfall-frequency-duration curves for over 200 localities in the United States have been plotted and very few take the straight line shape as suggested by Mr. Wolf.

Mr. Wolf states that no great numerical change would result if Eq. 32 were to be substituted for Eq. 28. This is probably true for most durations of storms including the very short durations. The high intensity rainfall at the peak for the short duration would not greatly affect the peak runoff because routing through overland flow and gutter storage would immediately attenuate such peak.

---

[31] Engr. of Sewer Hydraulics, Bur. of Engrg., Chicago, Ill.
[31] U. S. Dept. of Agriculture, Misc. Pub. #204, August, 1935.
[32] Technical Paper No. 25, 1955.

However, for the duration of 180 min, Eq. 32 would produce an average rainfall intensity one-third greater than obtained from Eq. 28. Due to the constancy of the volume of abstractions of infiltration and depression storage, the resulting runoff rates would be considerably more than one-third greater than the runoff obtained from Eq. 28.

Messrs. McPherson and Willis point out that the overland flow relationships are based on experimental tests on sprinkled plots and are possibly a "gross" over-extension of the original experiments. It is true that the variation of cover, slope, length, and so forth, on city lots are unlike the homogeneous conditions used in the tests. However, the writer believes that the average conditions on hundreds of lots can be closely represented so as to produce the correct detention-runoff relationship with the equations derived[8] by Izzard.

As requested by Messrs. McPherson and Willis, a re-run was made of Type 5 land use under Fig. 17(a) restrictions for the case of roof drains connected to the gutters. The results were not significantly different than that shown for

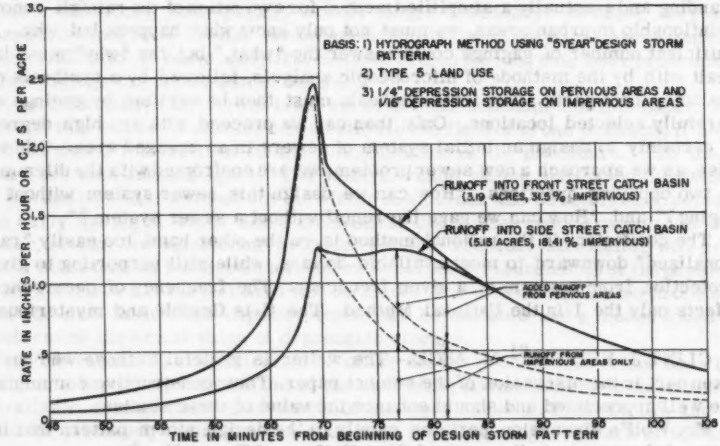


FIG. 30.—INLET HYDROGRAPHS AT FRONT AND SIDE STREET CATCH BASINS

Type 5 land use in Fig. 14. To obtain a peak runoff rate 160% greater than the 1.8 cfs per acre shown in Fig. 14 as determined by the John Hopkins Method, all private walks and driveways would need to be treater as directly-connected impervious surface and the infiltration on pervious areas would have to be greatly reduced.

McPherson and Willis request that inlet hydrographs would be helpful in comparing methods. Shown in Fig. 30 are the inlet hydrographs at the front and side street catch basins. These inlet hydrographs are multiplied by their total tributary areas and added to the roof hydrograph to form the inflow into the lateral sewer system. After routing this lateral inflow hydrographs 7 1/3 minutes by time offset, the lateral outflow hydrograph shown in Fig. 15 is obtained.

In Figs. 17 and 18, the dotted portion of the curves were extrapolated by arbitrarily assuming that for completely impervious surfaces, the runoff would be 90% of the average rainfall rate. For the average rainfall rate the maximum period of rainfall is taken 10 min greater than the indicated time of travel.

McPherson and Willis would like to have more coverage given to the part on areal distribution of rainfall. For the derivation of the curves shown in Fig. 20, Mr. Eltinge took 22 storms having volumes "arbitrarily limited to those exceeding 1.0 in at 30 min, 1.25 in at 1 hr, 1.50 in at 2 hr and 1.7 at 3 hr." For each rainfall he took the gage giving the maximum reading for an hour period as the storm center. He then plotted the intensities of the other 16 gages for the same hour period against their distances from the storm center. Similar graphs were plotted for 30 min, 2 hr and 3 hr periods. From these graphs he derived the curves shown in Fig. 19. Mr. Eltinge then compared his results with data[33] given by Frank A. Marston.

The derivation of Fig. 21 from the curves shown in Fig. 20 was as follows: Each of the curves in Fig. 20, limited to a given distance from the storm center, were rotated about the vertical axis forming a volume of revolution. This volume was then divided by its base area giving the average rainfall factor for circular areas.

No allowance for areal distribution of rainfall was used in deriving the curves shown in Fig. 14 thru 18. As can be seen in the computation form, Table 7, column 17, the factor K is applied to the runoff after determining the quantities of runoff based on the intensities at the storm center.

It is true that in comparing the hydrograph method with the rational method in Fig. 16 the values of C inherently include an areal distribution factor if they were derived by dividing the peak runoff gaged by the average rainfall from a number of rainfall gages evenly distributed over the drainage area. However, if a single gage was used the C = values would not necessarily reflect an areal distribution factor.

With reference to Fig. 25, McPherson and Willis show that the authors' method produces a time-displacement of the peaks of 0.7 of the time of travel in the sewers, while Hicks used 2/3 and the Johns Hopkins data produce 0.8. The writer believes the shape of the lateral hydrographs will influence the slope of the lines in Fig. 25. In Fig. 31 two triangular-shaped lateral hydrographs, one having a delayed peak, and the other having an advanced peak, are routed for 15 min and 60 min times of travel, by the method set up in Eq. 27. It can be seen in Fig. 31 that for the delayed-shape lateral hydrographs, the time of travel of the peak is very short, thus indicating a high velocity flood-wave. For the advance-shape lateral hydrographs, the time of travel of the peak is much longer, thus the velocity of the flood-wave approaches the velocity of the water particals. By this procedure, it can be shown that the time-displacement of the peaks to the time of travel in the sewer will vary from 1.0 for the completely advanced-shape lateral hydrograph to 0.0 for the completely delayed-shape lateral hydrographs. For the latter case, the peak discharge for each section would occur simultaneously all along the main sewer.

McPherson and Willis are understandably concerned with the quantitative difficulties of the rainfall-runoff process as computed by the Hydrograph Method. In Chicago, a slow transitionary process of converting from the rational method to the hydrograph method was used over a number of years. Results computed by the hydrograph method were checked for reasonableness with the previously accepted rational method. On the other hand, of the many factors used in the hydrograph method, most have been tested by field or laboratory experiments.

---

33 "The Distribution of Intense Rainfall and Some Other Factors in the Design of Storm-Water Drains," by Frank A. Marston, Transactions, ASCE, 1924, p. 535.

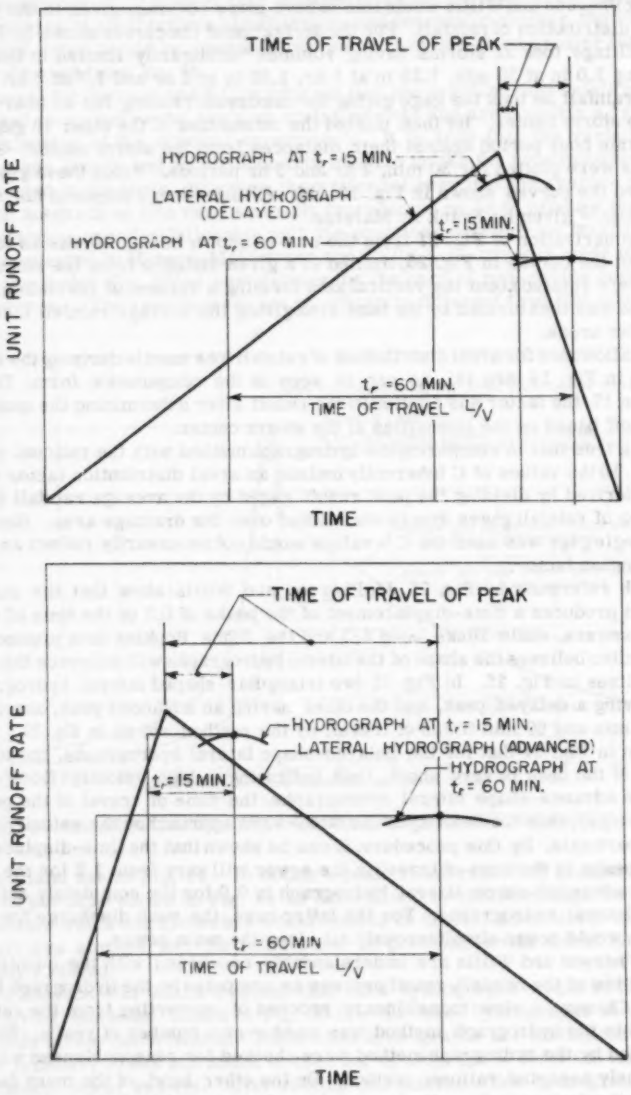


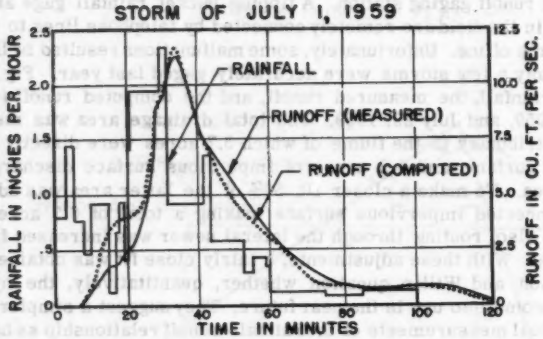
FIG. 31.—EFFECT OF SHAPE OF LATERAL HYDROGRAPH ON TIME OF TRAVEL OF PEAK

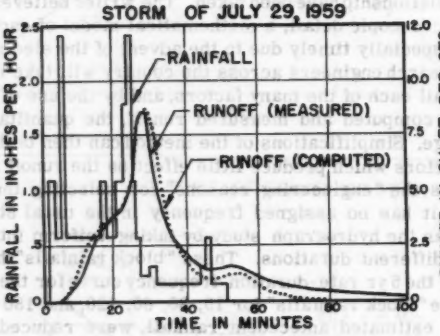
There is a need however, for the comparison of the runoff computed from actual rainfalls with field gagings of runoff. To this end, Chicago has set up a rainfall and runoff gaging station. A tipping bucket rainfall gage and a parabolic flume in the field are remotely connected by telephone lines to recorders in the writer's office. Unfortunately, some malfunctions resulted in this equipment, and only a few storms were accurately gaged last year. Fig. 32 shows the gaged rainfall, the measured runoff, and the computed runoff for storms of July 1, 1959, and July 29, 1959. The total drainage area was measured at 13.9 acres tributary to the flume of which 5.7 acres were directly connected impervious surface, and 1.2 acres of impervious surface discharging on to pervious area. To make a closer fit, 50% of the latter area was added to the directly connected impervious surface making a total of 6.3 acres directly connected. Also, routing through the lateral sewer was increased from 7 1/3 min to 8 min. With these adjustments, a fairly close fit was obtained.

McPherson and Willis question whether, quantitatively, the hydrograph method will come into use in the near future. They suggest a simpler approach based on actual measurements of the rainfall-runoff relationship as being more fruitful in the near future. Over the last hundred years, many gagings of the rainfall-runoff relationship have been taken. The writer believes it is time now to develop, in microscopic detail, a methematical model of each of the factors involved. It is especially timely due to the advent of the electronic computing machines. If research engineers across the country will take up the challenge to analyze in detail each of the many factors, and by the use of computing machines, compare computed and measured runoff, the quantitative model can soon become of age. Simplifications of the method can then be developed by the elimination of factors which produce little effect on the runoff hydrographs.

Mr. Bock asks the "engineering reasons" for selecting the design-storm pattern because it has no assigned frequency in the usual statistical sense. The authors began the hydrograph study by taking uniform intensity rainfalls for a number of different durations. These "block rainfalls" had the uniform intensity equal to the 5 yr rate-duration-frequency curve for the selected durations. Each of the "block rainfalls" for 15, 30, 60, 120, and 180 min. durations, after adding the estimated antecedent rainfall, were reduced by rainfall abstractions and routed through overland flow, gutter flow, lateral sewer, and main sewers to obtain the peak runoff rates of the flood wave as it traveled down through the sewer system. The envelope curve of the peaks from the separate block rainfalls was then to be used for design. This procedure had to be performed over again for each type of land use. The tremendous amount of labor required to perform the above procedure, led the writer to probe for a better method. If a single storm pattern—perhaps not occurring in nature—could be found that, after being reduced for abstractions and routed, would produce peak runoff rates equal to the envelope curve, described above, that storm pattern could then be used for design of a sewer system and would reduce the computation by 80%. This single storm pattern and the resulting envelope of the peak discharges would not have an assigned frequency of recurrence such as the block rainfalls, but would result in the same design. The synthetic storm pattern shown in Fig. 2 will produce a flood wave with peaks that are only slightly higher than the envelope of the peak flows derived from a number of separate block rainfalls of different durations, each of which has the correct antecedent precipitation.

It is true as Mr. Bock states that "the scatter of actual rainfalls is so wide that no meaningful typical chronological pattern can be detected." However,





BASIS: TOTAL AREA DRAINED ..... 13.9 ACRES
DIRECTLY CONNECTED IMPERVIOUS AREA..... 5.7 "
IMPERVIOUS SURFACES DISCHARGING INTO PERVIOUS AREAS..... 1.2 "
RAINFALL GAUGED 1/2 BLOCK FROM CENTER OF DRAINAGE AREA
RUNOFF MEASURED AT LATERAL OUTLET BY PARABOLIC FLUME
STANDARD INFILTRATION CURVE
1/4" DEPRESSION STORAGE ON PERVIOUS AREAS
1/16" " " " IMPERVIOUS AREAS
ROOF HYDROGRAPHS DIRECTLY CONNECTED TO LATERAL
TIME-OFFSET ROUTING THROUGH LATERAL SEWER OF 8 MINUTES.

FIG. 32.—COMPARISON OF MEASURED AND COMPUTED RUNOFF

the engineer is faced with the problem that he must have a storm pattern. The writer therefore believes that the storm pattern should embody the major factors that affect the runoff hydrograph. These factors are the average rainfall, the correct antecedent rainfall, and the location of the peak as determined from statistics for each duration.

Messrs. Izzard and Armentrout have combined routing through overland flow detention and gutter storage into a single routing procedure. This greatly simplifies that part of the problem. Also, by their method, storage curves need not be redrawn for each change in constants, such as length, slope, roughness, and so forth.

In Eq. 34(b), storage on the overland flow surface plus that in the gutter is assumed to be a function of rainfall minus abstrations, I, and the discharge at the inlet, Q. The routing procedure, Eq. 35(b), can be used where the flow from one surface enters a gutter, however, when the flow from two surfaces, such as pavement and lawns, enter a single gutter, the net supply cannot be represented by a single value, I, since the rainfall minus abstractions is different for each surface.

Messrs. Izzard and Armentrout have applied the hydrograph method using their simplified routing procedure to compare computed runoff with inlet gagings at Baltimore. This study resulted in a fairly close agreement between computed and measured runoff.

In making these studies Izzard and Armentrout came to the conclusion that "the effect of abstrations from rainfall is important and is dependent in large measure on antecedent rainfall." The authors have had the same findings in their studies using the hydrograph method. If these findings are correct, that abstractions and antecedent rainfall play such an important part in the rate of runoff, should not an attempt be made to study these factors in greater detail?

AMERICAN SOCIETY OF CIVIL ENGINEERS

Founded November 5, 1852

TRANSACTIONS

Paper No. 3062

PROGRESS IN ASCE

ANNUAL ADDRESS AT THE CONVENTION
RENO, NEVADA, JUNE 22, 1960

By Frank A. Marston,[1] President, ASCE

INTRODUCTION

Progress is defined as "the action of moving forward or onward." The word became commonly known to the English public in 1678 through the publication of John Bunyan's "Pilgrim's Progress." It is a familiar word to Americans, and is used in slogans such as "Progress is Our Most Important Product." It is a most essential characteristic of American life and activities today, whether it be in business, or education, or science, or engineering in general, or in the American Society of Civil Engineers in particular.

Progress in ASCE has been noteworthy in many ways, among which some may be reviewed briefly at this time. The Society now is approximately two-thirds of the way through this fiscal year, and at a point where one is justified in examining the progress.

MEMBERSHIP IN ASCE CONTINUES TO GROW

The total enrollment of ASCE for the past 5 yr has been as follows:

September 30, 1956	38,786
September 30, 1957	40,023
September 30, 1958	41,500
September 30, 1959	43,291
May 9, 1960	45,198

Thus there has been a steady increase each year in the enrollment. Of this membership approximately 40% have been younger members, now designated Associate Members.

[1] Partner, Metcalf & Eddy, Boston, Mass.

Looking further back into past records, the total member enrollment has grown from

November, 1852	14	(Beginning)
May, 1902	2,603	(50th Anniversary)
September, 1942	18,000	
September, 1952	34,979	(Centennial)

Such growth is highiy encouraging, but it incurs an obligation to make the Society even more attractive and of greater value to the individual members.

The requirements for membership in the Society have been strengthened, particularly for the grade of "Fellow." Professional registration has been given status by the requirement that in order to transfer from the grade of "Member" to that of "Fellow," the applicant must have been registered or licensed, to practice as a "Professional Engineer" in one of the states or in the District of Columbia, or the equivalent.

Governmental employees, while not required by law to be registered, are being urged, more and more, to become registered, particularly where they hold responsible supervisory engineering positions.

Members of the Army Corps of Engineers and engineers in the United States Air Force are being enthusiastically encouraged, if eligible, to become registered as professional engineers.

Some corporations are requiring registration as one qualification for holding supervisory engineering positions, and thus justify the title of "Engineer."

This legal status with the initials "P.E." after a name is a worthy addition to the distinction of being a "Fellow" or "Member" in the American Society of Civil Engineers.

DEVELOPMENT OF ENGINEERING TECHNIQUE

A multitude of activities is conducted through the organization of the Society to develop engineering technique. The obligation to improve constantly the practice of engineering is thus recognized. Such activities of the Society are carried on through 14 Technical Divisions under the over-all leadership of the Committee on Division Activities, a committee of the Board of Direction. At present, under the guidance of these Technical Divisions, there are some 268 committees and approximately 1,300 members working on many important subjects of technical interest to civil engineers.

These efforts produce many of the papers on technical subjects which are presented at sessions of the Technical Divisions held during the national conventions and speciality conferences.

Each member of the Society has the privilege of registering to receive the publications of two of the Technical Divisions. Such Registrations have increased rapidly in number from 23,000 in 1955 to a total now of over 60,000.

RESEARCH ACTIVITIES ARE VITAL TO TECHNICAL GROWTH

ASCE has undertaken recently a greater responsibility for research, particularly basic research, in the broad field of civil engineering. The Society

is now furnishing the administrative and fiscal services for two research councils:

Reinforced Concrete Research Council
Research Council on Pipeline Crossings of Railroads and Highways

All 14 Technical Divisions now have research committees studying ways by which research can improve engineering techniques, operating under the general administration of the Society's Committee on Research. That Committee has been active in organizing conferences to aid in developing more effective and stronger research programs in civil engineering.

It has become the practice of ASCE to make five research awards each year at a convention of the Society to recognize meritorious achievements by engineers in the field of basic research.

The ASCE Research Fellowship was established in 1958 by the Board of Direction, "for the purpose of aiding in the creation of new knowledge for the benefit and advancement of the science and profession of civil engineering." A grant in the amount of $5,000 is made annually, the first being awarded in 1959. This fellowship award advances ASCE one step further toward the leading position that ASCE should take in the field of civil engineering research.

In September, 1959, the Society's Committee on Research conducted a successful Second Conference on Research in Civil Engineering at Northwestern University. The report of the Committee to the Board of Direction contained a summary of the results of the Conference. One recommendation, of particular interest, is that a Research Director be appointed "to promote, supervise and solicit support for the research activities of the Society". . . The report concluded with a statement in part as follows:

> "Finally, it may be stated in conclusion that the participants in the Second Research Conference share the view that present research activities of the Society are inadequate, that this lack is detrimental to the professional standing of the civil engineer. . ."

To progress in ASCE, basic research in civil engineering is an important phase. We have made progress already. There is much more that can be accomplished through planned effort and dedicated service.

LOCAL SECTIONS ARE THE GRASS ROOTS OF ASCE

Through the 78 Local Sections, their 65 Branches, 8 Younger Member Forums, and 11 Wives' Groups (a total of 162 organized units) and a total membership of 41,000 and over, one of the principal fields of activity of the Society is maintained.

In 1956, Past-President Mason G. Lockwood conducted a survey of the Society by asking the local regional leaders what the principal weaknesses of the Society are and what remedial measures would be suggested.

One of the weaknesses stated was the "personal and individual apathy and lack of enthusiasm" of some members. That this is still true is indicated by various measures of member interest.

Lockwood reported that: "A staff study made some time ago would indicate that only about 15 percent of our membership really is active." Under present conditions it is probable that the percentage of activity is more nearly double that figure, or 30%.

One measure of the active interest of the assigned members to the Local Sections is the extent to which local dues are collected. During the 1958 fiscal year, for 69 Local Sections in the United States, local dues were collected from 59% of the assigned members. During the present fiscal year, for 61 Sections, the average percentage of members paying local dues is about 63%. The Texas and Florida Sections were particularly successful in this respect. What a man pays for is likely to be of more interest to him. Local Section officers are urged to increase their efforts to get new members and a greater percentage of paying members. It is good business financially and for membership interest. More Branch Sections are needed to serve Society members in areas not now reached by existing Sections and Branches.

More Local Section conferences have been recommended by the Committee on Local Sections.

Another measure of active interest is the extent to which members have contributed to the United Engineering Center building fund. Recent figures indicate this to be about 31% for ASCE as a whole, which is a disappointingly low participation. In certain Local Sections the percentages have been much higher as a result of unusual efforts to personally contact the individual members.

Another measure of member interest may be found in the fact that some 23,000 copies of the 1958 Directory were distributed to members of the Society in response to self-mailing order forms distributed in June, 1958. This may indicate active interest on the part of 56% of the membership.

According to the 1959 ASCE Annual Report, the 1958 edition of Transactions was mailed to 16,404 members of the Society who had placed orders for the volume. Corresponding figures for the 1959 Transactions show that about 18,000 were sent to members. According to this measure, 40% of the members of ASCE are sufficiently interested in Transactions to increase, on a regular basis, their annual payment to the Society.

While all members of the Society receive the monthly issues of Civil Engineering and many get copies of Journals of the Technical Divisions, it would be of great benefit if more of the members could be brought into active participation in ASCE affairs through the Local Section activities, and through Branch Sections.

Past-President Francis S. Friel, in his Annual Address of 1959, in commenting on the disclosures developed by the UEC campaign, stated:

> ". . .more needs to be done to give the individual engineer in the local section a sense of professional indentification and pride not only with his local unit but with all that goes on nationally."

STUDENT CHAPTERS TRAIN FUTURE LEADERS OF ASCE

From the 140 Student Chapters will come future members and leaders of the Society. As one meets these fine young men, representatives of 11,000 and more civil engineering Student Chapter members, the future of civil engineering in this country and of the American Society of Civil Engineers seems well assured of continued success. A tribute is due the Faculty Advisers and Contact Members who are serving these Student Chapters and the Society so well.

Not only through the Student Chapters are these student engineers being brought into direct contact with the aims and activities of the American Society

of Civil Engineers, but they are introduced to the professional phase of engineering and its importance in their careers.

PUBLICATIONS OF ASCE MAKE A VALUABLE LIBRARY

In the field of publications, the Society has maintained its world-wide reputation and wide-spread coverage over the fourteen specialized phases of civil engineering defined by its fourteen Technical Divisions. In the field of Professional Practice the Society supplements articles in Civil Engineering by issuing a Journal of Professional Practice. Since 1953, the Society has continually explored the possibility of using photolithography for its Technical Publications, and whereas the initial step in 1953 visualized the dissemination of the greatest amount of technical material consistent with available resources, succeeding years have clearly indicated that the membership was not content with quantity alone. Revisions in the original proposal of 1953 have been steadily toward improving the appearance and quality standards of the Technical Journals in response to a well-defined demand by the membership.

Authorization has been given by the Board of Direction to the compilation and printing of combined annual indexes to Proceedings, Transactions, and Civil Engineering; also for a complete cumulative index volume, containing separate indexes for each of these three publications. Such index volumes will be of inestimable value to members of the Society and to the profession in general.

There was a time in the Society's history when one printed page of original paper would produce one to two pages of discussion material. In the immediate past decade that ratio diminished until the flow of discussion into Technical Publications was almost negligible. That discouraging trend now begins to show an encouraging upturn so that an average of 10 pages of technical material in the Journals can be counted upon to generate approximately 4 pages of discussion.

The dissemination of personal news and Society news has been an ever-present problem. Such news of a general character and interest across the Society is presented as generously as possible in the monthly magazine Civil Engineering, which goes to every member. However, there is need for specialized news items in the Technical Divisions and these are being met by an increasing emphasis on the Division Newsletter.

It is essential that the century-long series of annual Transactions be continued. The volume for 1959 contained 48 papers of varied interest and of high value to civil engineers. Competition for space in this volume has been acute. It is a question whether all papers which might have justified inclusion were so included, and thus the Committee on Publications is looking forward to the issuance of four volumes of Transactions in one year.

Some limitations have been placed by the Board of Direction on the writing and publishing of Manuals of Engineering Practice. From the viewpoint of the Society as a whole, the writing of such Manuals, although prepared in draft form by individual committees, should be reviewed and discussed by many qualified members before being published as the opinion of the civil engineering pro-

fession or sponsored by the Society. The importance of discussion and the use of the Technical Journals for this purpose is essential.

CIVIL ENGINEERING, THE ASCE MAGAZINE

In October, 1930, a new publication greeted civil engineers - the 14,366 members of ASCE received their first issue of Civil Engineering. Because of the advice of some that this was not the time for a new venture, the plan was studied and discussed for nearly a decade before the first issue appeared. The late Harrison P. Eddy, Past-President of ASCE, was a leading figure in getting it underway.

The total run for the first 68-page issue was 16,000. Leading off for this issue was a story of the great project of the day - - Hoover Dam.

In 1960, more than 45,000 members plus 5,000 libraries and construction subscribers receive issues that are approximately 2-1/2 times as big as Volume 1, Number 1, with a 10-fold increase in advertising.

Over the past 30 yr Civil Engineering has maintained its position as a leader in the field of engineering publications. Reader surveys indicate that our members spend much time reading Civil Engineering. Twice in recent years Civil Engineering has been awarded plaques for editorial excellence by the publication, Industrial Marketing.

As an extra service to Society members, Civil Engineering sent out nearly 100,000 pieces of literature last year through its Catalog Digest.

Prior to 1956, Civil Engineering did not produce sufficient revenue to cover the cost of its operation. In that year, however, revenues exceeded costs, and every year since then there has been a surplus which has been used for other Society activities.

During the past year Civil Engineering has put greater emphasis on professional activities within ASCE. More space and a more attractive layout of ASCE News is being used to attract the attention of readers and to develop greater interest in the Society. Some of the ASCE News pages have been interspersed with the feature articles to attract the attention of those whose primary interest lies in the feature articles. Considerable space in Civil Engineering has been devoted to promoting the United Engineering Center. A new feature, the Younger Viewpoint page, has gained in status and is attracting increasingly more interest from younger members of ASCE.

INTERNAL COMMUNICATIONS ARE ESSENTIAL

Advances have been made in inter-society communications, the lack of which has been a source of criticism in the past, aside from the benefits of civil engineering.

All technical divisions now have newsletters going to those members registered in the divisions of their choice. While it probably can be said that these newsletters have not yet been utilized to their fullest advantage, they will become more valuable as a means of communication.

The Society's Annual Report is deserving of special mention here. The content, appearance, and handling of the Annual Report has improved considerably

in the past few years, and it will continue to be an effective instrument in reaching the members of the Society, and in attracting new members.

PUBLIC RELATIONS CAN ADD TO THE ENGINEER'S PRESTIGE

The Department of Public Relations of ASCE, now in its third year of operation, has through increased efforts brought to public notice more of the work of the civil engineer.

One important development has been the award for the "Outstanding Civil Engineering Achievement of the Year."

A plaque is awarded for permanent display for "an engineering project that demonstrates the greatest engineering skills, and represents the greatest contribution to engineering progress and mankind," and which was completed during the year. The project selected through annual competition is thus given fitting recognition at a public ceremony, thereby bringing to public notice ASCE and the accomplishments of the engineering profession.

The first award, that for the year 1959, was made on May 19, 1960, at Messena, N. Y. by the presentation of four plaques; two to the agencies in Canada and two in the United States responsible for the St. Lawrence Power and Seaway Development. This award is most significant, in these times of dissention between nations, in that it illustrates that projects of great magnitude and complexity can be conceived, designed, managed, and built by two nations working together in harmony, and except for certain necessary legislation, with only the time-honored method of a Gentlemen's Agreement.

Looking back on the colorful ceremony of awards held in the beautiful new Robert Moses Power House at Massena, attended by a distinguished audience of leading engineers, administrators, and ladies, one cannot but have the conviction that this "Outstanding Civil Engineering Achievement of the Year" award in the years to come will add much prestige to, and greater public appreciation of the American Society of Civil Engineers.

The Local Sections of ASCE have been aided and encouraged in public-relations activities through improved and more regular Section newsletters, through television programs devoted to civil engineering, and through better publicity for Section activities. One project being adopted by Local Sections is naming the "Civil Engineer of the Year," which at the same time focuses attention on the work of all civil engineers. All of this is desirable in bringing ASCE closer to the individual members as well as making the public generally aware of the importance of the civil engineer in the American way of life.

UNITED ENGINEERING CENTER, A GREAT ENGINEERING PROJECT

In March, 1960, the Board of Direction set June 20, 1960, as the target date for the completion of the ASCE quota of $800,000 in the building fund campaign.

The ground-breaking ceremony for the building was held in New York on October 1, 1959. The cornerstone was laid on June 16, 1960, with an appropriate program in which ASCE was represented. On that date steel erection reached above the 11th floor.

Past-President Friel, in his address of May 5, 1959, summed up the benefits to be derived from the United Engineering Center in the following words:[2]

2 "Current Challenges in Civil Engineering," by Francis S. Friel, Transactions, ASCE, Vol. 124, 1959, p. 1045.

"A powerful symbol of unity in the engineering profession is available to us in the new Engineering Center which will stand on the United Nations Plaza. This spectacular building will focus the attention of the peoples of the nation and of the world on the position that engineers hold in the affairs of the American people. This is not just office space for the people who are employed by our societies or meeting facilities for those members who serve our profession. It is much more -- a spectacular and lasting symbol to the public of the importance of engineering and the engineer in our way of life -- for the benefit of mankind."

Returns from the campaign, as of June 22, 1960, show against the ASCE quota of $800,000 that less than $30,000 remains to be raised. The campaign will continue until the full amount is pledged. Personally, I am confident that the job will be completed long before the end of this fiscal year so that my successor, as President, can devote his energies to other important matters.

Forty-one Local Sections have equaled or exceeded their quota. To those officers and solicitors who have accomplished so much we owe a dept of gratitude.

Over 14,000 contributions have been made which represents 31% of the ASCE membership.

Contributions from many Student Chapters indicate the interest taken by these young engineers in this great project.

Any civil engineer who considers himself to be a professional engineer and an integral part of the American Society of Civil Engineers should not fail to have a part in this most important project. In this way he will have no regrets when he derives the benefits that will accrue from the UEC.

As professional engineers we have an obligation to our profession and to our Society to give this United Engineering Center our full support. Do not put it off. Let's get the job done!

IMPROVEMENT OF PROFESSIONAL PRACTICE

Much has been said and written during the last few years relating to unity of the engineering profession, an accomplishment earnestly desired by almost all engineers.

On August 7, 1959, the Executive Committee of the Board of Direction, ASCE, issued a statement with regard to "The ASCE philosophy of engineering unity." The reaction of the members of ASCE to this statement has been overwhelmingly favorable, coming from the oral and written statements of individuals as well as from Local Sections and Regional Councils:[3]

"In ASCE unity means cooperative effort in the common interest. The Society welcomes the opportunity to work with other organizations in the attack on and solution of common problems. At the same time, ASCE will continue to apply itself to the same activities and problems to advance the special interests of the civil engineer."

In October, 1958, the Board of Direction of ASCE, expressly stated the desire of ASCE to collaborate with the National Society of Professional Engineers in the advancement of the profession of engineering. The hope was expressed,

[3] "The ASCE Philosophy of Engineering Unity," Civil Engineering, September, 1959, p. 33.

also, that the Board might have the opportunity to approve and welcome the affiliation of NSPE with both EJC and ECPD on an equivalent status with that of each of the five Founder Societies:[3]

> ". . .ASCE encourages its 78 Local Sections to join in State and local activities with local units of other societies. This has been done effectively in State and local councils. The principle of cooperative effort in the common interest is applicable at any level."

A good example of such effective cooperation is the "Engineering Societies of New England," an organization made up of 35 affiliate and allied engineering societies, working together on area problems of mutual interest.

While the desired full unity of the engineering profession has not yet been realized, an optimistic view can be had in believing that progress has been made and that ultimately it will be accomplished by consolidation of effort rather than by division of functions of societies.

The Department of Conditions of Practice has grown in effectiveness during the few years it has been in existence. It is active in various phases of the professional side of civil engineering as well as in other nontechnical matters.

PROFESSIONAL OBLIGATIONS MUST BE RECOGNIZED

Today there appears to be a growing disregard for honesty and fair dealing in business relations, in television shows, in some labor union managements, in competition for engineering projects, and in other phases of everyday life. This is to be regretted greatly if it applies to a member of the engineering profession.

The civil engineer, who in his vocation would be truly professional, must be not only competent in his technique, but his behavior must conform to the general requirements for professional behavior which have been developed over the years by the learned professions. For members of the American Society of Civil Engineers, there is the Code of Ethics consisting of ten Articles, all of which may be summed up, as a general statement, in the following:

> "It shall be considered unprofessional and inconsistent with honorable and dignified bearing for any member of the American Society of Civil Engineers: To act in any manner or engage in any practice which will tend to bring discredit on the honor or dignity of the engineering profession."

Considerable study has been given by the ASCE Committee on Professional Practice to the Code of Ethics with a view toward revision or expansion of its principles, and to prepare a single manual that would combine the interpretation, amplification, and application of the Code, and include other matters related to the ethics of engineering practice.

The Committee, in an interim report to the Board of Direction, has stated that it

> ". . .is keenly aware of the importance, both to the profession and to the public, of maintaining high standards of professional conduct and service. In all of the areas covered by the Code of Ethics, there is need for clarification of the intended and proper application to many borderline circumstances which are fairly frequently encountered in engineering practice."

The Society in January, 1950, by Board action, adopted the Canons of Ethics which were formulated by the Engineers' Council for Professional Development, consisting of twenty-eight Sections. The Foreword to these Canons begins with this statement:

"Honesty, justice, and courtesy form a moral philosophy which, associated with mutual interest among men, constitutes the foundation of ethics."

The Bible states this principle, the Golden Rule, in modern language as:[4]

"And as you wish that men would do to you, do so to them"

The Engineering Institute of Canada is sponsor of the only professional indoctrination to my knowledge in the engineering field. It is "The Calling of the Engineer" or the "Iron Ring" ceremony that is conducted by trained teams in each of the leading Canadian engineering schools.

The impressive ritual was written by Rudyard Kipling, and it is profoundly effective in its introduction of the young engineer to his profession. The ceremony is available to all graduates of accredited engineering schools in Canada and to other qualified engineers. Many engineers in the United States have been privileged to experience this ritual.

ECPD is presently studying the possibility that "The Calling of the Engineer" ceremony or a similar indoctrination might be initiated in the United States. This is a most commendable objective.

The American Institute of Architects has adopted "Standards of Professional Practice" consisting of 15 Articles, with interpretations. The following quotation is taken from the introductory statement relating to "Obligations of Good Practice":

"The profession of architecture calls for men of the highest integrity, judgment, business capacity, and artistic and technical ability. An Architect's honesty of purpose must be above suspicion; he acts as professional adviser to his client and his advice must be unprejudiced; he is charged with the exercise of judicial functions as between client and contractors and must act with entire impartiality; he has moral responsibilities to his professional associates and subordinates; he is engaged in a profession which carries with it grave responsibility to the public. These duties and responsibilities cannot be properly discharged unless his motives, conduct, and ability are such to command respect and confidence."

According to the issue of "Life" for June 6, 1960, the United States Congress has printed and distributed a "Code of Ethics for Government Service" consisting of ten articles which "any person in Government service should 'uphold,' . . . ever conscious that public office is a public trust."

It is of interest in this consideration of professional ethics to compare the requirements of the professions of law, medicine and the ministry.

An attorney upon being admitted to the Bar in Massachusetts:[5]

"shall in open court take and subscribe the oaths to support the constitution of the United States and of the Commonwealth; and the following oath of office shall be administered to and subscribed by him:

"I, (repeat the name), solemnly swear that I will do no falsehood, nor consent to the doing of any in court: I will not wittingly or willingly promote

[4] Luke 6:31 Rev. St. Ver. 1952.
[5] Mass. G. L. (Ter. Ed.) C. 221, p. 38.

or sue any false, groundless or unlawful suit, nor give aid or consent to the same; I will delay no man for lucre or malice; but I will conduct myself in the office of an attorney within the courts according to the best of my knowledge and discretion, and with all good fidelity as well to the courts as my clients. So help me God."

The oath may vary in form in other States.

The American Bar Association has adopted "Canons of Professional Ethics" consisting of forty-seven canons. As published, each canon is supplemented by references to appropriate state and federal cases, which throw light on the interpretations of them.

With respect to the medical profession, physicians and surgeons must be registered in the State in which they practice, and must conform to the State laws. Upon being admitted as a member of the medical profession a solemn pledge is required. Originally this was the oath of Hippocrates, and was quite long and detailed in its coverage. To add solemnity to the oath it began (as translated) as follows:

"I swear by Apollo, the physician, by Aesculapius, by Hygieia, Panacea, and all the gods and goddesses, that according to my ability and judgment I will keep this oath and stipulation;"

Abridged forms have been used over the years in various places and under varying conditions.

In 1948 the "Declaration of Geneva" was adopted by the General Assembly of the World Medical Association, as follows:

"I solemnly pledge myself to consecrate my life to the service of humanity; I will give to my teachers the respect and gratitude which is their due; I will practice my profession with conscience and dignity; The health of my patient will be my first consideration; I will respect the secrets which are confided in me; I will maintain by all the means in my power, the honor and the noble traditions of the medical profession; My colleagues will be my brothers; I will not permit considerations of religion, nationality, race, party politics or social standing to intervene between my duty and my patient; I will maintain the utmost respect for human life, from the time of conception; even under threat, I will not use my medical knowledge contrary to the laws of humanity. I make these promises solemnly, freely, and upon my honor."

In 1949 an "International Code of Medical Ethics" was adopted consisting of fifteen paragraphs which supplement the "Declaration of Geneva."

Revised "Principles of Medical Ethics" were adopted in 1957 by the American Medical Association, consisting of ten sections. The Preamble is as follows:

"These principles are intended to aid physicians individually and collectively in maintaining a high level of ethical conduct. They are not laws but standards by which a physician may determine the propriety of his conduct in his relationship with patients, with colleagues, with members of allied professions, and with the public."

Those entering the profession of the ministry do so through four or more years of specialized education and practice. Ordination is the result of careful examination as to qualifications and with solemn pledges as to conduct in

accordance with the ritual prescribed by the respective church as developed over many years of experience. The great importance and full solemnity of this is indicated by the following quotation.[6]

> "As a sacrament bestows something spiritual, the power to administer sacraments is sacred. In the Roman Catholic, Orthodox and Anglican Churches, this power is conferred through the sacrament of Ordination, by which bishops or higher prelates make ministers or priests. "As my Father hath sent me," Christ said to His Apostles, "even so send I you" (John 20:21). The Apostles chose others to ordain and the process has continued in what is called Apostolic Succession.
> Ordination's decisive point is the laying on of hands. Even Protestants who deny Apostolic Succession use this gesture as a meaningful way of handing down the ministry, perpetuating both the church and God's word for all time."

Considerable emphasis has been given herein to the practices developed over the years to demonstrate the requirement that being a member of one of the learned professions, whether it be in law, medicine, the ministry, architecture, or engineering, requires the solemn obligation to act honorably and with dignity, and to follow the prescribed rules of practice and code of ethics. The more these established principles can be followed in engineering the greater will be the acknowledged position of engineering as a profession in the world today. The more they are followed by members of the American Society of Civil Engineers, the stronger will be the Society and the greater the impact it will have on national affairs.

---

[6] "The World's Great Religions," Time, Inc., New York, 1957.

MEMOIRS OF DECEASED MEMBERS

Abstracts[a]

Arthur Rich Alling 1395
Clifton Thorne Barker 1395
John Schuyler Bates 1396
John Albert Baumgartner 1397
Tulla Ethan Bliss 1397
Ronald Axel Boesel 1398
William Harris Bosier 1399
Richard Ludwig Brandt 1399
Daniel Joseph Brumley 1400
Pecos Hill Calahan 1401
Welling Hall Craft 1401
Fred Wilbur Crocker 1402
John Wilbur Cunningham 1403
Starks Conrad Dougherty 1404
John Arthur Elliott 1404
Gilbert Dudley Fish 1405
Earl Nesby Floyd 1406
Charles E. Fraser 1406
Robert James Gammie 1407
Charles Goetz 1408
Arthur Selden Hatch 1409
Robert Hawxhurst, Jr. 1409
Randolph Olaf Helland 1410
Charles O. Holman 1411
Robert Charles Hunter 1411
Howard Langdon King 1412
Carl Gustaf Levander 1413
Frank Redmond Lewis 1414
Walter Harrison Lilly 1414
Penn Poore Livingston 1415
Robert Lee Lowry 1416
Raul Jose Felix Lucchetti 1417
Alfred Majendie Lund 1417
Claude Kelsey Mathews 1418
Rossiter Magers McCrone 1419
Robert Emmett McDonnell 1419
Frank Ray McFarland 1420
Tollef Bache Monniche 1421
Phillip Daniel More 1421
Grover Cleveland Morriss 1422

[a] The memoir abstract is intended as a statistical record, leading the searcher to a more complete biographical memoir manuscript catalogued in the Engineering Societies Library.

Lawrence Kenneth Needham 1423
Stewart Smith Neff 1423
Frank Austin Nikirk 1424
Clayton Whitney Paige 1425
Clifford Allen Philo 1425
George William Prichard 1426
Asa Glisson Proctor 1427
Charles Alley Reed 1428
Garfield Hugh Russell 1428
Walter Frederick Schulz 1429
Elwyn E. Seelye 1430
William James Shackelford 1431
Thomas Clark Shedd 1431
Jack William Sheetz 1432
Clarence Osborne Sherrill 1433
Micajah Thomas Singleton 1433
Arthur Alvord Stiles 1434
Abraham Streiff 1435
Melvin Oliver Sylliaasen 1436
Adolphus Gustavus Trost 1436
Leo Vernon Uhrig 1437
Jamison Vawter 1438
Francis K. Wai 1439
Richard Benskin Ward 1439
Levi Romulus Whitted 1440
Jackson Heath Wilkinson 1441
Thomas H. Winchester 1441
Whitby Foster Wise, Jr. 1442
Alfred Henry Witholder 1443
Alexander Ririe Young 1444

ARTHUR RICH ALLING, M. ASCE[1]

Died February 26, 1958

Arthur Rich Alling, the son of Ebenezer B. and Julia (Fitch) Alling, was born in Canon City, Colo., on August 6, 1888. He was graduated from the University of Colorado (Boulder) where he received the degree of Bachelor of Science in civil engineering in 1914.

After graduation Mr. Alling began his professional career with the City of San Antonio, Tex., doing street and bridge construction. He then entered the field of highway location and construction. For two years he was in Washington County, Miss., supervising the construction of an extensive highway program. He was made division engineer on the Arkansas-Louisiana highways in which capacity he supervised 153 miles of highways built by a four and one-half million dollar bond issue. From 1919 to 1923 Mr. Alling was resident engineer in charge of highways in the Little Rock, Ark., area. In 1923 he organized and developed the Alling Blue Print Company.

Mr. Alling held membership in the San Antonio Chamber of Commerce, and the Rotary Club. He attended the Laurel Heights Methodist Church.

Mr. Alling married Blanche Dart in Dallas, Tex., in 1915. He is survived by his widow; and two daughters, Evelyn Randolph, and Marjorie Weeks; and six grandchildren.

Mr. Alling was elected an Associate Member of the Society in 1919, and a Member in 1923. He became a Life Member in 1954.

CLIFTON THORNE BARKER, M. ASCE[2]

Died June 8, 1959

Clifton Thorne Barker, son of Sylvanus E. and Nira (Marsh) Barker, was born in St. Paul, Minn., on May 17, 1898. He was graduated from the University of Minnesota (Minneapolis) in 1922 with the degree of Engineer of Mines.

His early experience included appointments with two construction companies and a steel mill in the upper Ohio Valley region. The remainder of his life was spent in the service of the Federal Government. With the United States Engineer Department, he worked on the Tennessee River Survey at Chattanooga (1924-28), on the Missouri River studies for multipurpose projects at Kansas City (1928-32), and on navigation improvement at Sioux City, Iowa (1932-33).

[1] Abstract of a memoir prepared by Charles P. Reming, F. ASCE.
[2] Abstract of a memoir prepared by Robert Forbes, M. ASCE.

He was transferred to Wilson Dam, Ala., to take charge of navigation and power engineering studies.

Mr. Barker was with the Tennessee Valley Authority from its establishment in 1933. His knowledge of the design and economics of inland waterway navigation led to his appointment as chief of the River Transportation Division in 1938. He was made a staff specialist in transportation in 1946.

Mr. Barker was a member of Tau Beta Pi, Sigma Rho, the American Institute of Mining and Metallurgical Engineers, the Society of American Military Engineers, and The Technical Society of Knoxville. He was active in the Scouting movement, and devoted much of his time to gardening.

Mr. Barker married Bernice E. Ritter in 1930, at Kansas City, Mo. He is survived by his widow.

Mr. Barker was elected an Associate Member of the Society in 1935. He became a Member in 1959.

JOHN SCHUYLER BATES, M. ASCE[1]

Died September 11, 1958

John Schuyler Bates, the son of Henry H. and Fannie (Searles) Bates, was born December 26, 1877, in Monmouth, Ill. He was graduated from the University of Illinois (Urbana) with the degree of Bachelor of Science in civil engineering in 1902.

After graduation, he spent four years with the Chicago, Burlington and Quincy Railroad. He was then appointed city engineer in Monmouth, Ill., and taught at Monmouth College. In 1911 he was retained by cities in the San Joaquin Valley (Calif.) as city engineer. Mr. Bates planned extensive subdivision developments in San Diego, Calif., from 1927 to 1929. Moving to the San Francisco Bay area he was assistant designing engineer for the Chenery Water Filtration Plant of the California Water Service Company. During the Civil Works Administration program he directed 45 field survey parties of the Coast and Geodetic Survey. From 1931 to 1933 he was chief of triangulation and surveys for the San Francisco-Oakland Bay Bridge. Mr. Bates maintained a consulting engineering office in Berkeley, Calif., from 1933 until he retired in 1956.

He was a registered civil engineer in California and Nevada, and a licensed land surveyor in California; a member of the Kiwanis Club and the Commonwealth Club of California; and was affiliated with St. John's Presbyterian Church, Berkeley.

On June 29, 1905, he was married at Monmouth to Mary Elizabeth Brent. He is survived by two sons, Kenton S. and Robert B. Bates; a daughter, Margaret Bates Trotter (Mrs. Roy M.); a brother; sister; and four grandchildren.

Mr. Bates was elected an Associate Member of the Society in 1910, and a Member in 1923. He became a Life Member in 1945.

[1] Abstract of a memoir prepared by Arthur J. Grier, F. ASCE, and Roy M. Trotter, M. ASCE.

JOHN ALBERT BAUMGARTNER, A. M. ASCE[1]

Died February 22, 1959

John Albert Baumgartner, the son of John and Anna (Walder) Baumgartner was born near Portland, Ore., April 6, 1902. He was graduated from Oregon Agricultural College (now Oregon State College, Corvallis) in 1923 with the degree of Bachelor of Science in civil engineering.

After working with the Southern Pacific Railway Company for one year, he began his life-long career with the United States Geological Survey as a junior engineer in the Water Resources Division, Tuscon District. He advanced through the following civil service grades during his twenty-nine years of service: Junior engineer, 1925-1928; assistant engineer, 1929-1934; associate engineer, 1935-1946; engineer, 1946-1950; senior engineer, 1950-1956; and principal engineer, 1956-1959. From 1930 to 1950, he was responsible for most of the Arizona flood-peak estimates and gave leadership to the construction of 110 gaging stations in the Tuscon District. In addition to field work and construction, Mr. Baumgartner was an acknowledged specialist in the preparation of stream-flow records. After 1956, in conjunction with the Point Four Program, he served as technical advisor to the Iranian government on water resources investigations.

Mr. Baumgartner, active in civic affairs, was also a member and officer in Toastmasters International and a former president of the Arizona Section of the Society. He initiated the news-letter published by that Section.

Mr. Baumgartner was married to Margaret Clinton in 1925 in San Bernardino, Calif. He is survived by his widow; two daughters, Jo Anne (Mrs. Donald G. Andrews), and Margaret N.; and two grandchildren.

Mr. Baumgartner was elected an Associate Member of the Society in 1931.

TULLA ETHAN BLISS, M. ASCE[2]

Died April 12, 1959

Tulla Ethan Bliss, the son of Charles P. and Mary E. (VanCleave) Bliss, was born in Oskaloosa, Kans., April 22, 1884. He was graduated from the University of Kansas (Lawrence) with the degree of Bachelor of Science in 1909.

Before graduation he worked with the Atcheson Topeka and Santa Fe Railway Company as chairman, rodman, and draftsman. After graduation he joined the

[1] Abstract of a memoir prepared by Joseph S. Gatewood, F. ASCE.
[2] Abstract of a memoir prepared by John A. Focht, F. ASCE.

Saint Louis and Santa Fe Railway Company and continued in their employ for his entire professional career. He served as rodman, transitman, and draftsman at Springfield, Mo. From 1914 to 1916 he was assistant engineer at Chaffee, Mo. During the next two years he was assistant engineer at Memphis, Tenn., and the following year, served as district engineer at Birmingham, Ala. In 1919 he was transferred to Fort Worth, Tex., where he served as district engineer and division engineer. Mr. Bliss was transferred in 1940 to the River Division with headquarters at Chaffee. He then returned to Fort Worth as division engineer in 1951, and he continued in his position until he retired in May, 1954.

Mr. Bliss was a past-president of the Fort Worth Branch of the Texas Section of the Society, president of the Carter Bible Class and an Elder of the First Christian Church at the time of his death. He was a member of the American Society of Military Engineers and was a registered professional engineer in Texas and Missouri.

He married Elizabeth M. Fitzgerald in 1912. He is survived by his widow; and son, Bryan E.

Mr. Bliss was elected an Associate Member of the Society in 1917. He became a Member in 1931.

RONALD AXEL BOESEL, J. M. ASCE[1]

Died October 28, 1958

Ronald Axel Boesel, the son of Louis Walter and Emilie (Andreasen) Boesel was born January 24, 1931, at Portland, Ore. He was graduated from Oregon State College (Corvallis) in 1957, with the degree of Bachelor of Science in civil engineering.

During the summer vacations of his college years, Mr. Boesel was employed by the Southern Pacific Company as a technical student in the engineering department. He served in the United States Army from the fall of 1954 until the summer of 1956, at which time he returned to the employ of the Southern Pacific Company. At the time of his death he had been promoted to Technical Student Class A.

He was a member of the Methodist Church and engaged in church activities.

On June 8, 1957, Mr. Boesel married Murlene Lavon Thompson at Shedd, Ore. He is survived by his widow; father; two brothers, Wilmer, and Louis; and one sister, Mrs. C. W. Wirfs.

Mr. Boesel became a Junior Member of the Society in 1957.

[1] Abstract of a memoir prepared by Frank A. Bartlett, M. ASCE.

WILLIAM HARRIS BOSIER, M. ASCE[1]

Died December 31, 1958

William Harris Bosier, the son of William M. and Mary Elizabeth (Harris) Bosier was born on June 22, 1871, in New Franklin, Mo. He studied law and was admitted to the Missouri Bar in 1900. He studied bridge engineering and civil engineering with the International Correspondence School.

After preliminary experience with bridge construction projects, Mr. Bosier joined the Kansas City Bridge Construction Company (1905) and was soon thereafter elected its secretary. He was connected with the Missouri Valley Bridge and Iron Works Company from 1907 to 1916. From 1916 to 1918 Mr. Bosier was contracting manager for the Union Bridge and Construction Company of Kansas City, Mo. He served as the Gulf District manager of the United States Shipping Board and Emergency Fleet Corporation. In 1919 he returned to the Union Bridge and Construction Company. In 1930 Mr. Bosier joined the Kansas City Bridge Company. During World War II, he was comptroller of the Gray Iron Works at Galveston, Tex.

Mr. Bosier held life membership in the AF & AM. He was a member of the Christian Church in Kansas City and was a life member of the Missouri Bar.

On October 24, 1894, he married Myrtle Evalina Averitt in Stanberry, Mo. He is survived by two daughters, Aliff Margaret (Mrs. A. G. Bradt) and Helen Dorothy (Mrs. E. B. Slason); five grandchildren; and fourteen great grandchildren.

Mr. Bosier was elected a Member of the Society in 1921.

RICHARD LUDWIG BRANDT, A. M. ASCE[2]

Died October 15, 1957

Richard Ludwig Brandt, the son of Otto and Lina (Trappe) Brandt was born April 14, 1884, at San Diego, Duval County, Tex. He received the degree of Bachelor of Science in civil engineering from Texas Agricultural and Mechanical College (College Station) in 1906.

After graduation he entered the employ of the Lufkin Foundry in Lufkin, Tex. He moved to San Antonio, Tex., and worked for the Southern Steel Company, and later, the Alamo Iron Works. In 1921, he established the Brandt Iron Works,

[1] Abstract of a memoir prepared by Glynn E. Hands, F. ASCE.
[2] Abstract of a memoir prepared by C. P. Reming, F. ASCE.

and remained in active control of its management and development until 1948 when he disposed of his interests and retired.

Mr. Brandt was a member of St. Mark's Episcopal Church.

He married Chester Elder on June 5, 1912, in San Antonio. He is survived by his widow; and two daughters, Beverly (Mrs. Jack C. Young), and Bitsy (Mrs. William S. Shields).

Mr. Brandt was elected an Associate Member of the Society in 1918. He became a Life Member in 1953.

DANIEL JOSEPH BRUMLEY, F. ASCE[1]

Died September 6, 1959

Daniel Joseph Brumley, the son of Joseph and Phillipina (Leffler) Brumley was born March 19, 1865, near Belmore, Ohio. He was graduated from Ohio State University (Columbus) in 1895 with the degree of Civil Engineer. The University, in 1933, conferred upon him the honorary degree of Doctor of Engineering.

Mr. Brumley's 40-year career with the railroad industry began with the Louisville and Nashville Railroad in 1895. In 1904 he transferred to the Illinois Central Railroad, remaining with them until his retirement at the age of seventy. He progressed from principal assistant to chief corporate engineer and chief engineer of the Chicago Terminal improvements. In this period the terminal underwent a program of reconstruction and electrification at a cost of $67,000,000. After his retirement he was employed by the American Railway Engineering Association to revise their Manual, which is used as a guide by all railroads in the construction of new trackage.

Mr. Brumley took an active role in organizing the Chicago suburb of Flossmoor (1925) in addition to aiding in the development of the Rich Park District (1933) and serving as its Justice of the Peace. He was chairman of the Cook County Relief Committee and a leader in the Boy Scout program.

He held membership in the following organizations: The American Railway Engineering Association (past president); Western Society of Engineers (past president); American Railway Guild; Chicago Regional Planning Association; Art Institute of Chicago; and the Ohio State University Association (past president).

He was married to Susanna Lytle in 1908 in Deshler, Ohio. He is survived by his son, David Joseph; and sister, Mrs. A. G. Stewart.

Mr. Brumley was elected a Member of the Society in 1908. He became a Fellow in 1959.

[1] Abstract of a memoir prepared by Robert L. Hall, F. ASCE.

PECOS HILL CALAHAN, M. ASCE[1]

Died June 7, 1959

Pecos Hill Calahan, the son of Alvin W. and Lora (Hill) Calahan, was born in Pecos, Tex., on October 14, 1885.

From 1904 to 1910 he worked as an engineering aid with the United States Reclamation Service and in the Engineering Department of the California Development Company in Mexico. During these years he took special civil engineering correspondence courses. Mr. Calahan entered the employ of the Wichita Falls & Northwestern Railway before going with the Chicago Rock Island Pacific Railway, where he worked on the construction of their Southwest lines. He was employed by the Atchison, Topeka & Santa Fe Railroad from 1920 until 1924. He formed the partnership of McKee & Calahan which handled grading and paving contracting in the Los Angeles area. Mr. Calahan devoted much of his energy to promulgating the passage of an engineers' licensing law. Upon its adoption in 1929, he became the assistant secretary of the State Board of Registration of Civil Engineers. When the law was revised in 1946 to include other branches of engineering, Mr. Calahan was appointed executive secretary of the new State Board of Registration for Civil and Professional Engineers.

Soon after his retirement from the Registration Board (1950), he assumed the position of Executive Secretary of the Consulting Engineers Association of California. Mr. Calahan was instrumental in the formation of the nationwide Consulting Engineers' Council in Washington, D. C.

In 1918 he was married to Nora Delaney in Chickasha, Oklahoma. He is survived by his widow; and son, Lloyd.

Mr. Calahan was elected as an Associate Member of the Society in 1931, and a Member in 1959.

WELLING HALL CRAFT, M. ASCE[2]

Died March 18, 1959

Welling Hall Craft, the son of William and Ella (Hall) Craft, was born April 27, 1899, in Sharron (Pittsburgh), Penn. He attended Oregon State College (Corvallis) and studied civil engineering.

He began his professional career in 1924 as county engineer in Lincoln County, Ore., remaining there through 1927. From 1928 through 1933 he was

[1] Abstract of a memoir prepared by Mark M. Falk, M. ASCE.
[2] Abstract of a memoir prepared by Harold A. Kidby, F. ASCE.

an assistant resident engineer for the bridge section of the California Department of Public Works. He was resident engineer with the San Francisco Bay Bridge from 1933 to 1936. For the next ten years he served as district superintendent of roads and bridges in Pierce County for the Washington Department of Highways and as field engineer with the MacDonald Building Company on the construction of the army depot at Auburn, Wash. Mr. Craft was chief engineer during construction of additional facilities at the Veterans' Hospital at American Lake, Wash. Returning to California in 1946 he spent eight years in private practice as a consultant. Illness forced his retirement for two years. He was then employed on the engineering staff of West Coast Telephone Company at Beaverton, Ore., from 1956 to 1958 when he became totally disabled.

Mr. Craft was a member of the AF & AM in Toledo, Ore., and a licensed engineer in California and Oregon.

He was married in 1923 to Eva Barbara Jankins at Olympia, Wash. He is survived by his widow; a son, Robert Andrew; and two brothers, J. Earl and W. Arthur.

Mr. Craft was elected Associate Member of the Society in 1947. He became a Member in 1959.

FRED WILBUR CROCKER, M. ASCE[1]

Died December 29, 1957

Fred Wilbur Crocker, the son of Joel W. and Abbie Louisa (Clark) Crocker, was born in Portland, Ore., on September 29, 1885. He was graduated from the University of California with the degree of Bachelor of Science in civil engineering in 1904.

Mr. Crocker's early experience included surveying for the Southern Pacific Railroad and serving as resident engineer for the Western Pacific Railroad. In 1911, he became vice-president and chief engineer of the Mercereau Bridge and Construction Company. From 1914 to 1926 he was with the Pacific Bridge Company in Portland, and in 1926, Mr. Crocker was chief structural engineer for the Port of Oakland (Calif.). During 1930-1931 he designed the piers for both sides of the Golden Gate Bridge at San Francisco. From August, 1931, to November, 1932, he was plant engineer for Six Companies on Boulder Dam. He then returned to the Golden Gate Bridge project and was responsible for the Pacific Bridge Company engineering on pier construction. From December, 1934, to July, 1936, he was plant engineer for the Columbia Construction Company on the Bonneville main spillway dam. In 1941 Mr. Crocker became chief engineer of the Todd California Shipbuilding Company.

In 1942, as chief engineer of the Pacific Bridge Company, he received a Navy Certificate of Merit for planning the salvage operations in Pearl Harbor.

[1] Abstract of a memoir prepared by Everett C. Crocker.

Following World War II, Mr. Crocker worked in Korea, Pakistan, Alaska, Hong Kong, and India.

On January 14, 1933, he was married to Bessie Hardy Hoxsie McClure. He is survived by a brother, Everett C.; and a sister, Ruth Emily Norton.

Mr. Crocker was elected a Member of the Society in 1935.

JOHN WILBUR CUNNINGHAM, F. ASCE[1]

Died September 17, 1959

John Wilbur Cunningham, the son of Eugene and Adelia (Smith) Cunningham, was born March 21, 1887, in Watertown, S. Dak. He was graduated from the University of Wisconsin (Madison) in 1908 with the degree of Bachelor of Science in civil engineering.

Mr. Cunningham was first employed in the bridge designing department of the North Coast Railroad. From 1911 until 1912 he was engaged as a design engineer for the Kittitas Reclamation District of Ellensburg, Wash. He spent the following two years as office engineer for the Northwest Steel Company in Portland, Ore. In 1914 he formed the consulting engineering firm of Baar and Cunningham, that specialized in irrigation work and later, water supply and sewer projects. The firm was reorganized in 1937 as John W. Cunningham and Associates with Mr. Felix S. Zeidlhack, and Carl E. Green later joining the firm. Mr. Cunningham was a member of the engineering board that designed a sewage treatment plant for Portland. In addition, his firm designed and supervised construction of sewage treatment plants and industrial and domestic water supply improvements for many northwest cities. Military projects handled by the firm since 1937 include the designs for the Camp Adair military base, and Tillamook Naval Air Station, both in Oregon.

He was a former director of District 12 and vice-president of Zone IV of the Society; a life member of the Professional Engineers of Oregon, the American Water Works Association; and a member of the State Board of Engineering Examiners. He was vice-president of the Federation of Sewage and Industrial Wastes Association.

Mr. Cunningham was married to Mary O. Schousten in 1911 and to LaRue Davenport in 1940. In 1958 he was married to Ethel Fullerton. He is survived by his widow; four daughters, Mrs. Dorothy McKelligon, Mrs. Molly Harrow, Mrs. Suzanne Fisher, Mrs. Carol Shaw; and twelve grandchildren.

Mr. Cunningham was elected a Junior Member of the Society in 1909, an Associate Member in 1914, and a Member in 1925. He became a Fellow in 1959.

---

[1] Abstract of a memoir prepared by Ben S. Morrow, M. ASCE, and Felix S. Zeidlhack.

STARKS CONRAD DOUGHERTY, A. M. ASCE[1]

Died March 4, 1958

Starks Conrad Dougherty, the son of Nathan Starks and Betty Dougherty was born in Anson, Tex., on July 20, 1893. He attended the University of Texas (Austin).

In 1919 he began his highway engineering career as a draftsman and instrument man in Erath Co. Tex. From 1920 to 1925 he was assistant engineer for the Texas counties of Kleberg, Coleman, and Nolan. In 1928 he became resident engineer in Nolan. During 1933-34 he also served as resident engineer in Fisher County, Tex. In 1936 he served as City Engineer of Big Spring, Tex., and in February, 1939 he became Resident Engineer of Midland County where he remained for the rest of his professional career. He was responsible for the planning and construction of the four-lane divided highways with the grade separations to accommodate the increased volume of traffic caused by development of the oil industry in this area.

Mr. Dougherty was a member of the Missionary Baptist Church and the AF & AM. He participated in numerous civic affairs, including the Chamber of Commerce and the Lions Club. He was a member of the Texas Society of Professional Engineers, and a past president of the Permian Basin Chapter.

He was married to Burna Inez Falkner on July 6, 1927 at Sweetwater, Tex. He is survived by his widow; son, Starks Frederick; and daughter, Burna Margaret (Mrs. Milton H. Fortson).

Mr. Dougherty was elected an Associate Member of the Society in 1928.

JOHN ARTHUR ELLIOTT, M. ASCE[2]

Died March 3, 1956

John Arthur Elliott, the son of Thomas Easter and Emeline (Bowden) Elliott was born October 16, 1886 in Columbus, Ohio. In 1907 Mr. Elliott was graduated from Willemette University (Salem, Ore.) with the degree of Bachelor of Arts, and from the University of Washington (Seattle) in 1909 with the degree of Bachelor of Science in civil engineering. He received the degree of Civil Engineer from the University of Washington in 1929.

Mr. Elliott was employed by the Washington State Highway Commission from 1908 to 1911 and for the United States Department of Interior, Bureau of Reclamation in 1914. He then entered the employ of the Oregon State Highway

[1] Abstract of a memoir prepared by John A. Focht, F. ASCE.
[2] Abstract of a memoir prepared by Carl T. Nitteberg, F. ASCE.

Commission, serving as locating engineer and, later, as a district engineer. In 1918 he was appointed highway engineer in the office of Public Roads and Rural Engineering, United States Department of Agriculture. In 1932 Mr. Elliott was promoted to assistant to the district engineer, and the following year, placed in charge of all federal-aid highway activities of the central office of the Bureau of Public Roads in Denver, Colo. In 1936 he was transferred to Fort Worth, Tex., and placed in charge of the administration of federal-aid highway funds for the Bureau Roads in Region Six. He served in this capacity until the time of his death.

Mr. Elliott was married to Bess Emily Cornelius in 1910, in Salem. He is survived by his widow; son, Arthur Leonard; daughter, Marjorie Kay Bevlin; and four grandchildren.

Mr. Elliott was elected an Associate Member of the Society in 1915 and a Member in 1927.

GILBERT DUDLEY FISH, F. ASCE[1]

Died September 7, 1959

Gilbert Dudley Fish, the son of James Horace and Isabel (Coggeshall) Fish, was born October 28, 1893, in New York, N. Y. He received the degree of Bachelor of Science in civil engineering from Columbia University (New York) in 1913.

After graduation Mr. Fish remained at Columbia teaching mechanics of materials and astronomy. In 1917 he was appointed a lieutenant in the Corps of Engineers, served in Europe, and rose to the rank of major.

In 1920 he established an engineering practice, specializing in welded construction. After constructing a 5-story, welded factory for the Westinghouse Electric and Manufacturing Company in 1927, he was retained by them as a consulting structural engineer. Some of the outstanding structures credited to Mr. Fish include the library bookstack, the Sheffield Scientific School administration building and the Calhoun College dormatories, all at Yale University (New Haven); the Jersey City Medical Center, Nurse's Home and Hague Maternity Hospital (1939-1940); the Airlines Terminal at 42nd Street and Park Avenue in New York City (1940); seven public schools for the City of New York; an 11-story addition to the Mt. Sinai Hospital in New York City (1950); the Engineering Laboratory for IBM in Poughkeepsie, N. Y. He researched the structural design of the David Taylor Model Basin for the United States Navy in 1951. The Navy's giant radio telescope, under construction in Sugar Grove, W. Va., incorporated the basic dual wheel design developed by Mr. Fish in 1958. During World War II he helped organize a firm which manufactured heavy-duty cranes. In another field, he and his son, Dr. Gilbert D. Fish, Jr., developed an audio amplifier designed to provide an audible check on a patient undergoing surgery. He published "Arc Welded Steel Frame Structures" in 1933.

[1] Abstract of a memoir prepared by Stanley Rosanoff, M. ASCE.

Mr. Fish was a registered engineer in New York; a member of Tau Beta Pi, the Structural Engineering Advisory Panel of the Building Research Advisory Board, and the American Welding Society.

Mr. Fish was married to Alwarda Casselman in Washington, D. C., in 1919. He is survived by his widow; a son, Dr. Gilbert D., Jr.; a daughter, Mrs. John G. Davis; and six grandchildren.

Mr. Fish was elected a Member of the Society in 1927 and a Fellow in 1959.

EARL NESBY FLOYD, M. ASCE[1]

Died January 16, 1933

Earl Nesby Floyd, son of Henry W. and Celia (Weatherby) Floyd, was born on February 22, 1881, near Columbia, Maury County, Tenn. He was graduated from the University of Tennessee (Knoxville) in 1906 with the degree of Bachelor of Science in civil engineering.

Mr. Floyd began his engineering career with the Louisville and Nashville Railroad Company. From 1909 to 1911, he was engaged on survey work near Muscle Shoals, Ala. and from 1911 to 1913 he worked with the Pittsburgh Testing Laboratories. With the Miami Conservancy District (Dayton, Ohio), 1914-1918, he helped negotiate settlements with three major railroads whose lines were affected by the works of the District. He served as a fire protection and insurance engineer for the Big Four Railroad (Cincinnati, Ohio) from 1919 to 1925. During the next five years Mr. Floyd was a contractor in Florida and Texas. He worked with the corps of engineers at Louisville, Kentucky, from 1930 to 1933.

Mr. Floyd was a member of the Christian (Disciples) Church. He was a 32nd Degree member of the AF & AM.

Mr. Floyd was married in 1911 to Mae Jarret of South Pittsburgh, Tenn. He is survived by his widow; a son; and daughter.

Mr. Floyd was elected an Associate Member of the Society in 1911, and a Member in 1924.

CHARLES E. FRASER, F. ASCE[2]

Died August 23, 1959

Charles E. Fraser, the son of William J. B. and Mary (Fallon) Fraser, was born in Montreal, Quebec, April 7, 1873. He was graduated with the degree of

[1] Abstract of a memoir prepared by Roger B. McWhorter, F. ASCE.
[2] Abstract of a memoir prepared by Leland B. Fraser, F. ASCE.

Bachelor of Science in civil engineering from McGill University (Montreal) in 1899. He was awarded the honorary degree of Doctor of Science by his alma mater in 1954.

He began his career in 1900 working on an extension to the Equitable Life Assurance Society Building (New York, N. Y.). In 1902 he was placed in full charge of the construction work on the I.R.T. Subway section between 14th and 42nd Streets under Park Avenue. In 1904 he was appointed superintendent for Pearson and Son on the construction of the Manhattan ends and access shafts of the four Pennsylvania Railroad tunnels under the East River. In 1908 he established his own construction company, and was joined in partnership by James H. Brace in 1910. George C. Clarke became associated with the firm in 1912. Mr. Fraser remained active for near fifty years as president or chairman of the board. His companies' activities ranged from the construction of ships and the manufacture of TNT during the war years, to metallurgical, paper, chemical, and hydro-electric operations.

He was a registered professional engineer in New York and Quebec and a member of the Moles and the Engineers' Clubs of New York and Montreal.

Mr. Fraser was married to Helen Pettit Sweezy, who passed away in 1935. In 1936 he married Phyllis L. R. Steeves. He is survived by his widow; two sons, Leland B., and Dougall C.; two daughters, Mrs. Muriel Scovil, and Mrs. Maron Beggs; eight grandchildren; and fourteen great grandchildren.

Mr. Fraser was elected a Junior Member of the Society in 1901, an Associate Member in 1903, and a Member in 1908. He became a Fellow in 1959.

ROBERT JAMES GAMMIE, F. ASCE[1]

Died October 19, 1959

Robert James Gammie, the son of James and Lois (Nichols) Gammie, was born on October 12, 1889, at Arkansas City, Kans. He was graduated from the Agricultural and Mechanical College of Oklahoma (Stillwater), with a degree of Bachelor of Science in civil engineering in 1910.

Upon graduation Mr. Gammie began his railway engineering career with the Kansas City Southern Railway as a rodman. This was followed by a brief period in the contracting business, after which he returned to the railroad industry serving with The Texas and Pacific Railway Company until he was called into military service with the Army Corps of Engineers during World War I. While with the army Mr. Gammie was a member of the First Officer's Training Camp and did engineering work on the Muscle Shoals Dam project. After being discharged he resumed his career with The Texas and Pacific Railway. He held assignments as instrumentman, assistant roadmaster, general roadmaster, and engineer maintenance of way. Later, as chief engineer (1941-1957), he supervised the railroad crossing of the Morganza Floodway in Louisiana. He

[1] Abstract of a memoir prepared by William J. Savage, F. ASCE.

was chairman of the Engineering Committee of the Dallas Union Terminal Company during the terminal's remodeling in 1947-1949.

Mr. Gammie was a Life Member of the American Railway Engineering Association, and served on its Board of Direction from 1951 to 1953. He was a member of the National Society of Professional Engineers, the AF & AM, and the Shriners. He was affiliated with the Episcopalian Church.

In 1915, Mr. Gammie married Georgia William Talley. He is survived by his widow; and brother, Colonel Thomas G. Gammie.

Mr. Gammie was elected a Member of the Society in 1942. He became a Fellow in 1959.

CHARLES GOETZ, F. ASCE[1]

Died March 3, 1960

Charles Goetz, the son of Charles and Ida (Geiger) Goetz, was born March 26, 1905, in Baltimore, Md. He graduated from Baltimore Polytechnic Institute in 1923 and received the degree of Bachelor of Science in industrial engineering from Johns Hopkins University (Baltimore) in 1940.

Mr. Goetz began his professional career as an assistant topographic engineer with the City of Baltimore in 1924. Three years later, in 1927, he was employed by the Pennsylvania Water and Power Company as squad chief and worked on field investigations and studies for the design of Safe Harbor Hydroelectric Development on the Susquehanna River. Later, he supervised design and engineering for the relocations necessitated by the project. In 1942 he was promoted to general engineer with duties in the company's Baltimore office. Following company consolidations and the closing of the Baltimore office in 1955, Mr. Goetz entered Government service as a civilian employee of the United States Army Corps of Engineers working on flood control projects in Pennsylvania. Among these projects were the Kettle Creek Reservoir and the Stillwater Reservoir.

Mr. Goetz was a member of the Johns Hopkins Club, the Annapolis Yacht Club, and served as a local officer of the National Federation of Federal Employees. He was affiliated with the Luthern Church.

He was married in 1933 to Pearl Walter in Baltimore. He is survived by his widow; and sister, Catherine (Mrs. William Stange).

Mr. Goetz was elected a Member of the Society in 1958 and a Fellow in 1959.

[1] Abstract of a memoir prepared by Willard J. Prentice, F. ASCE.

ARTHUR SELDEN HATCH, M. ASCE[1]

Died September 26, 1958

Arthur Selden Hatch, the son of Selden Levett and Emma (Fairfield) Hatch, was born February 24, 1892, in Somerville, Mass. He was graduated from Harvard University (Cambridge), with the degree of Bachelor of Arts and a second degree in civil engineering in 1913. He received the degree of Master of Science in mining engineering from the Massachusetts Institute of Technology (Cambridge) in 1914.

After preliminary experience he joined the Firestone Tire and Rubber Company for whom he organized a factory branch in Scranton, Pa., and acted as its service manager. While an officer with the United States Army Ordnance (1917-1919), he served as head of the Metals Section in Washington, D. C. In Texas, after his discharge, Mr. Hatch became an independent oil operator and producer. In 1926 he joined the Pure Oil Company of Houston as engineer in charge of seismograph work and as general field engineer with geological field work. He entered the employ of the Water Department of the City of Houston in 1931. Here, he served as engineer in charge of the city-sponsored Works Progress Administration construction program, the Public Works Administration construction program, and as the engineer in charge of design and cost estimates of distribution systems. He took an active role in the design and construction of the dam across the San Jacinto River.

He held memberships in various civic and professional organizations. He served as secretary of the Houston Branch of the Society for a number of years.

Mr. Hatch is survived by a sister, Mrs. Mabel Hatch Jordan; a niece; and a nephew.

Mr. Hatch was elected a Member of the Society in 1943.

ROBERT HAWXHURST, JR., M. ASCE[2]

Died April 6, 1958

Robert Hawxhurst, Jr., the son of Robert and Kate (Stephens) Hawxhurst, was born in San Francisco on July 19, 1875. He attended the University of California and Stanford University (Calif.).

Mr. Hawxhurst spent his long career as engineer and geologist for many mining and oil companies. His activities from 1895 to 1905 included assignments in Central and South America, Hawaii, the Philippine Islands, China, and

[1] Abstract of a memoir prepared by John A. Focht, F. ASCE.
[2] Abstract of a memoir prepared by Walter L. Huber, F. ASCE.

Malaya. He was consulting engineer for the Truro Syndicate and the Charles Kaufman Mining Interests at London from 1905 to 1909. He was also general manager of the Ponderosa Mining Company of Chile from 1906 to 1909. He was a member of the firm of Hawxhurst, Aisinmann and Wolff, Mining Engineers and Petroleum Geologists, London and Bucharest, from 1906 to 1916, and was general manager of the Eden Mining Company of Nicaragua from 1916 to 1919. Mr. Hawxhurst maintained an office as consulting engineer and geologist in San Francisco from 1919 until his death.

He was a member of the American Institute of Mining and Metallurgical Engineers (past chairman, San Francisco Section); the Societe Geologique de France; the Seismological Society of America; a fellow of the California Academy of Sciences and of the American Association of the Advancement of Science; a member of Le Conte Geological Club and of the Engineers' Club of San Francisco.

Mr. Hawxhurst was elected an Associate Member of the Society in 1904 and a Member in 1907.

RANDOLPH OLAF HELLAND, A. M. ASCE[1]

Died September 7, 1958

Randolph Olaf Helland, the son of Ole and Ragnhild (Kringle) Helland, was born March 17, 1886, in Black Earth, Wis. He was graduated from the University of Wisconsin (Madison) in 1913 with the degree of Bachelor of Arts in Science, and in 1916 the Bachelor of Science in Agriculture. He also studied at George Washington University (Washington, D. C.) to qualify for an appointment with the United States Geological Survey.

Mr. Helland rose through the grades of junior and assistant classifier, assistant scientist, and associate and hydraulic engineer before retiring as regional hydraulic engineer with the Portland, Ore. office of the Geological Survey, in 1955. He entered the Geological Survey in 1917, as a junior land classifier. After a brief absence while abroad, Mr. Helland rejoined the Geological Survey in 1923 in the Hydrographic Section of the Land Classification Branch (now the Water and Power Branch of the Conservation Division). He made numerous surveys of Western streams and prepared reports on the waterpower value of the adjoining lands. In 1943 he became regional hydraulic engineer for the Oregon-Idaho Region. This region includes the State of Oregon, and the Snake River Basin in Washington, Idaho, Nevada, Utah, Wyoming. He was co-author of Water-Supply Papers Numbers 558 and 995. Both papers were entitled "Index to River Surveys made by the U. S. Geological Survey and other Agencies." Mr. Helland was the author of 28 reports on water supply for the Geological Survey.

He was a member of the AF & AM in Washington, D. C.

[1] Abstract of a memoir prepared by Harold A. Kidby, F. ASCE.

In 1928 he was married to Mabel Maynard in Washington, D. C. He is survived by his widow; a son, Bruce M.; and a sister, Marie Eidsmore.

Mr. Helland was elected an Associate Member of the Society in 1939.

CHARLES O. HOLMAN, JR., A. M. ASCE[1]

Died August 19, 1958

Charles O. Holman, Jr., the son of C. Oscar and Lois (Allene) Holman, was born in Vernon, Tex. on March 4, 1924. He was graduated from Texas Technological College (Lubbock) in 1949, with the degrees of Bachelor of Science in civil engineering and Bachelor of Science in petroleum engineering.

After his graduation in 1949, he was associated with the Stimson Contracting Company in Dallas and Waco, Tex. Mr. Holman was president of this company at the time of his death. During World War II, from 1943-1946, he served as a pilot with the Troup Transport Command in the China-Burma-India Theater.

Mr. Holman was a professional engineer of the State of Texas, a member of the American Contractors Association, and the alumni association of his college. He belonged to the Methodist Church.

Mr. Holman was married to Dorothy Jane Riggs on August 27, 1944, at Wellington, Tex. He is survived by his widow; and three daughters, Beverly Jane, Patricia Louise, and Rebecca Anne.

Mr. Holman was elected a Junior Member of the Society in 1949, and became an Associate Member in 1958.

ROBERT CHARLES HUNTER, M. ASCE[2]

Died November 13, 1958

Robert Charles Hunter, the son of Charles March and Julia (Timmons) Hunter, was born in Charlestown, Mass., on February 26, 1888.

In August, 1917, he was appointed 1st Lieutenant, Corps of Engineers, United States Department of the Army, and served with the AEF during World War I. Between 1920 and 1939, he was with the 3rd Engineers in Hawaii, was engaged on the design and construction of the Cape Cod Canal bridges with the Boston Engineer District, and served as corps area engineer and army engineer at posts in Fort Sam Houston and Laredo, Tex., and in Chicago, Ill. From 1939

[1] Abstract of a memoir prepared by J. Dwight Morgan, M. ASCE.
[2] Abstract of a memoir prepared by Henderson E. McGee, F. ASCE.

to 1940 he served as district engineer at San Francisco, Calif. In 1940 he was appointed district engineer at Sacramento, Calif., and there directed a World War II military construction program in Central California, Nevada, and Utah. In 1945 he was assigned to the Pacific Area as district engineer of the General Engineer District at Manila, P. I. In 1945 he became district engineer at Los Angeles, Calif., in which position he served until his retirement from the Army on March 31, 1947. Mr. Hunter was appointed Executive Secretary of the State of California Lands Commission in 1947, and served in that capacity until his retirement in 1949.

Mr. Hunter received the Purple Heart, Legion of Merit, and Victory Medals of World War I and World War II, American Campaign and Defense Service Medals, and the Asiatic-Pacific Campaign Medal. He was a member of the Society of American Military Engineers; held life membership in the Minerals Association of Northern California; and was a registered civil engineer in California.

On September 16, 1912, he was married to Catherine Madden in Boston, Mass. He is survived by his widow; one son, Col. Robert C. Hunter, Jr.; two daughters, Dorothy (Mrs. Palmer Burns), and Mary Jane (Mrs. William B. Smith); and eleven grandchildren.

Mr. Hunter was elected a Member of the Society in 1946.

HOWARD LANGDON KING, M. ASCE[1]

Died September 21, 1958

Howard Langdon King, the son of Lewis Cass and Katharine (Bruen) King, was born in New York City, on April 9, 1889. He was graduated from The City College of New York with the degree of Bachelor of Arts in 1908. He received the degree of Master of Arts from Columbia University in 1912 and in 1915 the degree of Bachelor of Science in civil engineering from Massachusetts Institute of Technology (Cambridge).

After graduation, Mr. King was employed by the New York City Board of Transportation. During World War I he served in France as a 1st Lieutenant with the 27th Engineers, United States Department of the Army. After the war, Mr. King was employed on the construction of industrial plants in Atlanta and Savannah. From 1921 until 1928 he was with the New York and New Jersey Bridge and Tunnel Commission on construction of the Holland Tunnel under the Hudson River. Mr. King became associated with the Mason & Hanger Company in 1928, and remained with them until his death, becoming chief engineer in 1937 and vice president and chief engineer in 1953.

Projects with which Mr. King was associated include the Montague Street Tunnels, Fulton Street Tunnels, and Rutgers Street Tunnels, New York, N. Y., the south and north tubes of the Lincoln Tunnel, New York, N. Y., the Rays

[1] Abstract of a memoir prepared by Robert B. Jewell, F. ASCE.

Hill Tunnel, Pa., the Merriman Dam, the Brooklyn Battery Tunnel, New York, N. Y., the Fort Randall Dam on the Missouri River, and the third tube of the Lincoln Tunnel in New York.

Mr. King was an honorary member of the Engineering Alumni of The City College of New York; a member of Phi Beta Kappa, the Engineer's Club of New York, and the Moles. He was a recipient of the Townsend Harris Medal of The City College of New York in 1950, The Moles Member Award in 1956, and was named "Engineer of the Year" by the Metropolitan Section of the Society in 1957. He was a licensed professional engineer in New York State.

On July 2, 1921, Mr. King married Margretta Struss in New York. He is survived by his daughter, Marion King Schlefer; and three grandchildren.

Howard L. King was elected a Junior Member of the Society in 1917, an Associate Member in 1920, and a Member in 1936.

CARL GUSTAF LEVANDER, M. ASCE[1]

Died October 14, 1958

Carl Gustaf Levander, the son of Charles Richard and Maria Natalia (Johnson) Levander, was born in Norwich, Conn., on December 5, 1898. He was graduated from Valparaiso University (Valparaiso, Ind.) with the degree of Bachelor of Science in civil engineering in 1922.

After graduation Mr. Levander joined the Illinois Highway Department, continuing on with them until 1925 when he became sewer engineer in Lakeland, Fla. In 1928 he became assistant city engineer in Austin, Tex., holding this position until 1949, when he was made director of public works. In this capacity Mr. Levander was primarily responsible for the expansion of the sanitary sewer system, the storm sewer system, a new sewer disposal plant, as well as the extension of water mains, the preparation of plans for a new water filtration plant. In 1955 Mr. Levander and the former city manager of Austin formed a consulting engineering firm specializing in municipal affairs. In 1957 Mr. Levander became a third partner in the firm of Montgomery and Williams which specialized in municipal problems of water, sewer, and city planning.

Mr. Levander served in the United States Army during World War I. He was active in the Boy Scout movement in his community. He was an officer in the Austin Council of Churches, and a member of the Official Board of the Hyde Park Christian Church, the AF & AM, the Austin Scottish Rite Bodies, the American Water Works Association, and the Texas Society of Professional Engineers.

Mr. Levander married Eva Katherine Sheppard in Valparaiso, Ind., in 1922. He is survived by his widow; three sons, Dale N., Ted C., and Charles Richard; and one daughter, Mrs. Mary Elmendorf.

Mr. Levander was elected an Associate Member of the Society in 1931 and a Member in 1943.

[1] Abstract of a memoir prepared by John A. Focht, F. ASCE.

FRANK REDMOND LEWIS, M. ASCE[1]

Died December 3, 1958

Frank Redmond Lewis, the son of James Madison and Leona A. (Dunica) Lewis, was born at Forney, Tex., on September 16, 1873. He was graduated from the Agricultural and Mechanical College of Texas (College Station) with a degree in civil engineering in 1894.

Immediately after graduation he joined the Texas Midland Railroad and was stationed in Terrell, Tex., and in the Territory of Oklahoma until 1912. For several years he was a surveyor of public lands under the United States Geological Survey and a townsite surveyor at Muskogee, Indian Territory. From 1902 to 1903 he was surveyor in charge of allotment surveys, school lands, and all lands set aside by treaties in the Seminole and Cherokee areas. In 1903 he became associated with the United States Commission to the Five Civilized Tribes of Indians, and was later placed in charge of a field party in the allotment of Osage Lands in Indian Territory that is now the State of Oklahoma. From 1908 to 1912 he was city engineer in Tahlequah, Okla. In 1912 he returned to Forney, and opened a practice in general engineering including subdivision work, development of estates, land surveying, highways, and water works. He did extensive levee work in the Texas counties of Dallas, Kaufman, and Ellis.

Mr. Lewis was a member of the Methodist Church and the AF & AM. He was active in many civic affairs.

Mr. Lewis was married to Daisy Calhoun.

Mr. Lewis was elected a Member of the Society in 1921 and became a Life Member in 1943.

WALTER HARRISON LILLY, F. ASCE[2]

Died September 19, 1959

Walter Harrison Lilly, the son of Winship Reed and Eunice (Jenkins) Lilly, was born June 9, 1888, in Woolwich, Me. He was graduated from the University of Maine (Orono) in 1912 with the degree of Bachelor of Science in civil engineering.

[1] Abstract of a memoir prepared by John A. Focht, F. ASCE.
[2] Abstract of a memoir prepared by John A. Focht, F. ASCE.

His first position was as a draftsman with the Wabash Railway Company in St. Louis, Mo. In 1913, he joined the Hanan-Hickey Brothers Construction Company of St. Louis. The following two years were spent as a construction superintendent for the Miller Engineering Company building flood control works on the Mississippi, White, Arkansas, Red, Black, and Ouachita Rivers. From January, 1917, to May, 1917, he was a draftsman for the Texas Company, Houston, Tex., working on plans for a refinery in Tampico, Mexico. In 1917 he graduated from the First Officer's Training Camp with a captain's commission, and he served with the 315th Engineers 90th Division in France and Germany. While in France he was promoted to major. He was associated with Hunt Engineering Company, Kansas City, Mo., before establishing the partnership of Lewis and Lilly in Eldorado, Ark., in 1921. In 1926 he moved to San Antonio, Tex., and opened a general engineering office. Two years later, he formed the partnership of Lilly and Drought, specializing in structural design, which was dissolved in 1936 when he became the first Federal Housing Director of the City of San Antonio. Mr. Lilly returned to active duty during World War II, received the Legion of Merit, and was discharged with a colonel's rank. Returning to San Antonio he became the first director of the San Antonio Planning Board, drawing up a master plan for the city, which was adopted in 1950. He maintained a consulting office until his retirement in 1956.

Mr. Lilly was an alderman in Alamo Heights, and served as chairman of zoning and planning committees. He was a member of the Kiwanis Club, the American Legion, and Tau Beta Pi. He was a vestryman at St. Mark's Episcopal Church.

Mr. Lilly married Marie Seacord in Galesburg, Ill., in 1920. He is survived by his widow; and son, Harrison Seacord.

Mr. Lilly was elected an Associate Member in 1920 and became a Life Member in 1955. He became a Fellow in 1959.

PENN POORE LIVINGSTON, M. ASCE[1]

Died January 17, 1959

Penn Poore Livingston, the son of Mr. and Mrs. V. R. Livingston was born October 14, 1899, in Elk Mound, Wis. He was graduated from the University of Wisconsin (Madison) in 1922 with degree of Bachelor of Science.

Mr. Livingston began his career with the United States Geological Survey, Ground Water Branch, as a junior engineer in Chatanooga, Tenn. He worked in Honolulu, Hawaii (1924), Tusculoosa, Ala. (1928), and Austin, Tex. (1930). In 1934 he was detailed to the Washington, D. C. office of the Geological Survey. After being promoted to a hydraulic engineer in 1939, he was stationed in Texas (1940-1944), Santa Barbara, Calif. (1945), and Austin (1945-1955). From 1952 until the date of his retirement, Mr. Livingston served as engineer-in-charge of the National Observation Well Program. After his retirement

[1] Abstract of a memoir prepared by Raymond W. Sundstrom, F. ASCE.

from the Geological Survey, he was associated with the Ralph M. Parsons Company, working in Delhi, India. He returned to Texas and was employed by William F. Guyton and Associates. In 1958 he accepted the position of Chief of the Ground Water Division of the Texas Board of Water Engineers.

Mr. Livingston was a senior member of the American Association of Engineers, and a member of the American Geophysical Union. In 1948 an honorary degree in civil engineering was conferred upon him by the University of Wisconsin.

He was married to Evelyn Kendall in Chicago, Ill., in 1924. He is survived by his widow; and one son.

Mr. Livingston was elected an Associate Member of the Society in 1927 and a Member in 1935.

ROBERT LEE LOWRY, M. ASCE[1]

Died May 30, 1959

Robert Lee Lowry, the son of Robert Lee and Bessie (Ray) Lowry, was born in Waxahachie, Tex. He was graduated from Trinity University (now in San Antonio, Tex.) in 1922 with the degree of Bachelor of Arts and the University of Texas (Austin) in 1929 with the degree of Bachelor of Science in civil engineering.

His early employment experience included positions with the Morgan Engineering Company (1929), the Texas Board of Water Engineers (1931), the Texas Railroad Commission (1932-1933) and the Texas Reclamation Department. In 1935 he was employed by the Brazos Conservancy District and the Texas Planning Board. He prepared the report on "Flood Control by the Marshall Ford Dam" in 1935 for the Reclamation Bureau at Denver, Colo. Mr. Lowry was a special consultant for the Colorado Water Conservation Board before joining the International Boundary and Water Commission in 1942. He also worked with Mexican engineers on hydrologic studies of the Rio Grande and on a part time basis with the Pecos River Commission. In 1950 Mr. Lowry opened a consulting office. He was appointed a member of the international commission studying a water dispute between Afghanistan and Iran in 1951.

Mr. Lowry was a member of the AF & AM, the American Geophysical Union, Texas Society of Professional Engineers, and a past president of the Texas Section of the Society.

He married Laura Eckels in Temple, Tex., in 1924. He is survived by his widow; and two daughters, Francis Adell (Mrs. E. G. Feuille), and Betty Lee (Mrs. B. O. Greenwade).

Mr. Lowry was elected an Associate Member of the Society in 1934 and a Member in 1940.

[1] Abstract of a memoir prepared by John A. Focht, F. ASCE.

RAÚL JOSE FELIX LUCCHETTI, M. ASCE[1]

Died November 6, 1959

Raúl Jose Felix Lucchetti, the son of Antonio and Amelia (Chevalier) Lucchetti, was born February 11, 1897, at Ponce, P. R. He was graduated from Cornell University (Ithaca, N. Y.) in 1919 with the degree of Bachelor of Science in civil engineering.

After working with the Lackawanna Bridge Company in Buffalo, N. Y., he returned to Puerto Rico in 1921. He held various positions with the Insular Department of Public Works including resident engineer on the construction of the system for the City of Humacao; assistant engineer (1922-1923); and engineer in charge of the Bridge Design Division (1925-1930). Returning to New York in 1930, he held positions with the Electric Bond and Share Company and the Irving Iron Works before joining the Port Authority of the City of New York (1932-1936). He returned to Puerto Rico and was employed by the Puerto Rico Rehabilitation and Reconstruction Administration of the Insular Department of Public Works (1937-1940; 1942-1944) and the Mayaguez Housing Authority. In 1944 he entered the employ of the Puerto Rico Water Resources Authority where he held the following positions: Senior engineer (1944-1947); resident engineer of the San Juan Stream Electric Station (1948-1951); and principal structural design engineer.

He was a registered professional engineer in New York and Puerto Rico, and a member of the American Concrete Institute.

Mr. Lucchetti was married to Providencia Sampayo on January 8, 1925 in San Juan, P. R. He is survived by his widow.

Mr. Lucchetti was elected an Associate Member of the Society in 1927 and a Member in 1959.

ALFRED MAJENDIE LUND, M. ASCE[2]

Died October 31, 1958

Alfred Majendie Lund, the son of Henry Majendie and Sarah Ann (Stephenson) Lund, was born on July 8, 1879, in Louisville, Kentucky. He was graduated from Vanderbilt University (Tenn.) with the degree of Bachelor of Science in civil engineering in 1902.

After graduation he was employed by Ford, Bacon, and Davis, Engineers of New York City. In 1906 Mr. Lund formed a partnership with Phillip B. Hill

[1] Abstract of a memoir prepared by Juan R. Figueroa-Laugier, M. ASCE.
[2] Abstract of a memoir prepared by Roy E. Warden, F. ASCE.

under the firm name of Lund and Hill, Engineers. In 1925 he planned and supervised construction of the first hard-surface highway from Little Rock to Hot Springs National Park, Ark. Mr. Lund was commissioned a major in the Engineering Branch of the Sanitary Corps during World War I and was chief of the Smaller War Plant Corporation during World War II. Mr. Lund retired from active practice in 1955.

Mr. Lund was a past president of the Little Rock Branch, Mid-South Section, and the past president of the Little Rock Engineers' Club. He was an Elder and Trustee in the First Presbyterian Church in Little Rock.

On November 15, 1911, he was married to Arline House. He is survived by his widow.

Mr. Lund was elected an Associate Member of the Society in 1912, a Member in 1917, and became a Life Member in 1947.

CLAUDE KELSEY MATHEWS, F. ASCE[1]

Died August 19, 1959

Claude Kelsey Mathews, the son of Samuel and Mary (Kelsey) Mathews, was born in Lexington, Mo., on November 12, 1896. He was graduated from the University of Kansas (Lawrence) in 1919 with the degree of Bachelor of Science in civil engineering.

After two years' employment with the Burns & McDonnell Engineering Company, he went to the University of Illinois to do graduate work and teach. In 1924, he returned to Burns & McDonnell, where he planned and supervised the construction of 22 sanitary projects, 32 hydraulic projects, and 18 electric and power projects. Mr. Mathews made appraisals and rate studies of 34 utility systems. During World War II, he was chief engineer on design and construction of Camp Crowder, Missouri Contonement. In 1947 he became a partner in the firm, Burns & McDonnell. He was the author of numerous papers on sanitary and water works engineering and on electric, water and gas rates.

Mr. Mathews was a member of the American Institute of Consulting Engineers, the American Water Works Association, and the National Society of Professional Engineers. He was a deacon and moderator at the Garfield Avenue Baptist Church and taught a young men's bible class.

Mr. Mathews was married to Edna Alice Major in 1921, in Sedalia, Mo. He is survived by his widow; three children, William K., Robert M., and Mary Lou Deay; one brother; and seven grandchildren.

Mr. Mathews was elected an Associate Member of the Society in 1924 and a Member in 1931. He became a Fellow and a Life Member in 1959.

[1] Abstract of a memoir prepared by Glenn E. Hands, F. ASCE.

ROSSITER MAGERS McCRONE, M. ASCE[1]

Died December 16, 1958

Rossiter Magers McCrone, the son of James Edgar and Ida (Magers) McCrone was born in Baltimore, Md., on November 29, 1885. He studied civil engineering at Cornell University (Ithaca, N. Y.).

Mr. McCrone began his career in the Philippines as a surveyor with the Bureau of Lands. With the exception of the time spent in military service (1918-1919), he worked as assistant engineer and divisional engineer for the Royal Irrigation Department in Bangkok, Siam (1914-1920). In 1921 he entered private practice and headed the McCrone Company, Inc., of Bangkok. He was later associated with the Standard Oil Company of Venezuela (1925), and the Pantepec Oil Company of Venezuela (1925). In 1928, Mr. McCrone was employed by the United States War Department, Corps of Engineers, at the Montgomery, Alabama, District and later moved to the Gulf of Mexico Division office, New Orleans, La. Transferred to the Mississippi River Commission, he became principal engineer (1943) and special assistant to the president (1948).

Mr. McCrone was a member of the American Society of Testing Materials, and the Permanent International Association of Navigation Congresses. He was a registered professional engineer in the State of Louisiana.

On June 30, 1928, he married Elinor Newitt Spicknell in Baltimore, Md. He is survived by his widow; and one daughter, Elinor Josephine.

Mr. McCrone was elected an Associate Member of the Society in 1915 and a Member in 1921.

ROBERT EMMETT McDONNELL, F. ASCE[2]

Died January 4, 1960

Robert Emmett McDonnell, the son of John and Harriet (Stuff) McDonnell was born November 16, 1874 in Callatin County, Mont.

In 1892 he entered Stanford and became a classmate and close friend of Herbert Hoover. Mr. McDonnell earned his way through college as a newspaper reporter, surveyor, cook on a Smithsonian geological expedition, fourth assistant steward on a cruise to Japan, and as a mule skinner. He was graduated from Stanford in 1897, with the degree of Bachelor of Science in civil engineering.

[1] Abstract of a memoir prepared by Harvill E. Weller, F. ASCE.
[2] Abstract of a memoir prepared by Glenn E. Hands, F. ASCE.

With Clinton S. Burns, he founded the consulting engineering firm of Burns and McDonnell in 1898, specializing in water works design. The firm has served over 1,000 clients under his leadership as senior partner, including the cities of Cincinnati, Ohio; Kansas City, Kans.; Knoxville, Tenn.; Milwaukee, Wis.; Tampa, Fla.; Kansas City, Mo.; Omaha, Neb.; Little Rock, Ark.; Cleveland, Ohio; Springfield, Ill. During World War II his staff, more than 700 persons, worked on the design and supervised construction of 22 war projects, costing more than one hundred million dollars. He retired in 1948.

Mr. McDonnell was a former president of the City Club, the Engineers Club of Kansas City, and the Citizens League. He held membership in Tau Beta Pi and Sigma Xi. Mr. McDonnell was a member of the Roman Catholic Church.

In 1904 Mr. McDonnell married Georgia Hewlett in Kansas City, Mo. He is survived by his widow; a son, Robert M.; and two grandchildren.

Mr. McDonnell was elected a Member of the Society in 1909 and a Life Member in 1943. He became a Fellow in 1959.

FRANK RAY McFARLAND, M. ASCE[1]

Died August 30, 1957

Frank Ray McFarland, the son of Frank and Jessie (Thompson) McFarland was born September 30, 1894, at Hope, Mo. He was graduated from Washington University (St. Louis, Mo.) in 1917 with the degree of Bachelor of Arts in civil engineering.

For the two years following graduation he served in the United States Army with the field artillery. In 1919 he began his association with several construction firms in the St. Louis area. In January, 1923, he went to the Kansas City Bolt and Nut Company (now Sheffield Division, Armco Steel Corporation) as a construction engineer. He designed and set up production for many of the company's products which included bar joists and guard rails. In 1941 and 1942 he was in charge of the construction of the Sheffield plant in Houston, Tex. After this project he became works engineer and in 1947, he was appointed works manager of the Houston plant.

Mr. McFarland was a member of the board of directors at the A. O. Smith Corporation and at the First National Bank of Pasadena, Tex. He was a member of the Houston Club, the Houston Country Club, and Theta Zi.

Mr. McFarland married Lucille Cole in June, 1920, in St. Louis. He is survived by his widow; and three children, Virginia (Mrs. R. L. Wolf), Ruth Elizabeth (Mrs. G. S. Robertson, Jr.), and F. R. McFarland, Jr.

Mr. McFarland was elected a Member of the Society in 1939.

[1] Abstract of a memoir prepared by James R. Sims, F. ASCE.

TOLLEF BACHE MONNICHE, M. ASCE[1]

Died December 14, 1958

Tollef Bache Monniche, the son of Carl Alexander and Sophia Gunrun (Bache) Monniche was born in Surnadalen, Norway, August 27, 1874. He attended the Otto Anderson School, Oslo (1888-93); the Royal Norwegian School of War in Oslo (1893-94); and the Royal Polytechnic University, Dresden, Germany (1894-1901), graduating with the title of "Diplom Ingeniur."

Mr. Monniche came to the United States after graduation and gained experience, from 1901 through 1906, with the American Bridge Company as a draftsman and assistant engineer; the Pennsylvania Railroad as an instrumentman; the Rapid Transit Company of Philadelphia, Pa. as an assistant engineer; and the Virginian Railway Company as an assistant and resident engineer. In 1907 he became assistant engineer with the Isthmian Canal Commission, Division of Locks and Dams, Washington, D. C., working on the design of lock gates for the Panama Canal. In 1908 he was appointed design engineer for the six emergency dams in Culebra, Canal Zone and, later, supervised the erection and final tests on these structures. In 1914 he was made engineer of docks for the Panama Railroad Company, Cristobal, Canal Zone, in charge of the design and construction of the Atlantic Terminal Piers. While working for the Panama Railroad, he designed the bascule bridge at Monte Lirio, the bridge over the old French Canal, and re-designed ten Mayo cranes in use at the dock in Balboa. In 1914 Mr. Monniche was appointed to investigate the collapse of the huge floating crane, the "Ajax." In 1919, in Norway, he was employed by the Royal Norwegian Railway. In 1922, returning to Boquete, he developed his coffee plantation, until he settled in Austin, Tex., in 1957.

Mr. Monniche was a holder of the King Olav Medal of Norway. He was a member of the National Geographic Society.

Mr. Monniche married Julia Trible Huger on August 3, 1909, in Roanoke, Va. He is survived by his widow.

Mr. Monniche was elected an Associate Member of the Society in 1906, and a Member in 1912. He became a Life Member in 1941.

PHILLIP DANIEL MORE, A. M. ASCE[2]

Died April 30, 1959

Phillip Daniel More, the son of Mr. and Mrs. Philip H. More, was born August 1, 1922 in Denver, Colo. He was graduated from Colorado State University (Fort Collins) in 1947 with the degree of Bachelor of Science in civil engineering.

[1] Abstract of a memoir prepared by John A. Focht, F. ASCE.
[2] Abstract of a memoir prepared by Glenn E. Hands, F. ASCE.

Mr. More was inducted in the United States Army in May, 1943, as a corporal and was discharged in October, 1946, as a first lieutenant. From March, 1947, until his death he was employed by Black and Veatch, Kansas City, Mo., as a structural engineer.

He was a High Priest in the Church of Jesus Christ of the Latter Day Saints. He was a registered professional engineer in Missouri, and held membership in Sigma Tau.

In May 1943 Mr. More married Genevieve Bischoff in Fort Collins, Colo. He is survived by his widow and four children, Michael, Patricia, Dana, and Laural.

Mr. More was elected an Associate Member of the Society in 1957.

GROVER CLEVELAND MORRISS, M. ASCE[1]

Died November 2, 1958

Grover Cleveland Morriss, the son of Simon and Mary Lucy (Taylor) Morriss, was born in Atlanta, Tex. on January 8, 1882. He attended Burleson College (Greenville Tex.) and received a diploma in shorthand, typing, bookkeeping, and commercial law.

Mr. Morriss was a committee clerk in the Texas State Senate (1899-1900) and in the State Treasury Department (1901 - 1905). He was employed next by the Kirby Lumber Company and the Allardyce McMahon Piling and Timber Company (1905-1912). In 1912 he began his career with the General Land Office of Texas as a draftsman. He resigned this position when he became assistant state auditor (1929 - 1934). For one year he was surveyor-draftsman and senior engineer for the United States Forest Service. In 1935, Mr. Morriss was appointed chief cadastral engineer of the Brazos River Conservation and Reclamation District, in charge of mapping thirteen reservoir areas from aerial photographs and multiplex projection. In 1940 he returned to the General Land Office as draftsman and engineer, becoming chief of engineering and mapping, retaining this position until his retirement in 1952.

Mr. Morriss was a member of the Chartered Institute of American Inventors, National Society of Porfessional Engineers, American Society of Military Engineers, the Congress on Surveying and Mapping. Mr. Morriss was a registered professional engineer in Texas. He was affiliated with the first Presbyterian Church in Temple, Tex.

Mr. Morriss married Mary Johnson Stoner in 1927. He is survived by his widow.

Mr. Morriss was elected an Associate Member of the Society in 1937, and a Member in 1953.

---

[1] Abstract of a memoir prepared by John A. Focht, F. ASCE.

LAWRENCE KENNETH NEEDHAM, A. M. ASCE[1]

Died April 22, 1959

Lawrence Kenneth Needham, the son of Millard and Elizabeth (Kirkpatrick) Needham, was born in Homer, Ill., on October 7, 1883. He was graduated from the University of Nebraska (Lincoln) with the degree of Bachelor of Science in civil engineering in 1907.

He was employed by the Panama Railroad Company from 1907 until 1912, as a transitman and levelman and later as assistant engineer. He joined the Spokane, Portland and Seattle (SP&S) Railway in 1912 serving as resident engineer in charge of construction in East Portland, Ore. Mr. Needham left railroad work during World War I to become a resident engineer for the Oregon State Highway Commission. In 1915 he returned to the SP&S and remained with them except for the one year spent with the Oregon Trunk Railway (1927-1928) as a construction engineer. Mr. Needham was employed as draftsman and assistant engineer with the SP&S Railway from 1915 to 1918. He served as resident engineer, Portland Division, during the next nine years. From 1928 until 1933 he was in charge of the construction of the Pacific Cooperative Poultry Producers warehouse built with SP&S funds in Portland. He was appointed roadmaster, Portland Division, in charge of maintenance of way in 1933, becoming resident engineer in 1942. From 1944 until his retirement in 1951, he was resident engineer, Portland Division, in charge of all surveys and contract work for approximately 500 mi. of tracks including the Vancouver yards.

Mr. Needham was a member of Sigma Tau and the Portland City Commercial Club. He was a member of Friendship Masonic Lodge #60, AF & AM, Royal Arch Masons.

In 1909, Mr. Needham was married to Jessie Cook in Lexington, Neb. He is survived by his widow; five daughters; Marjorie (R. Quigley), Laurine (C. Kingsley), Elizabeth (G. Bennett), Marian (B. Russell), and Barbara; two sisters; and eight grandchildren.

Mr. Needham was elected an Associate Member of the Society in 1912 and a Life Member in 1947.

STEWART SMITH NEFF, F. ASCE[2]

Died February 14, 1960

Stewart Smith Neff, Jr., the son of Stewart Smith and Anna (Kennedy) Neff, was born on September 18, 1887 in Bryn Mawr, Pa. He received a certificate in railroad engineering from Lowell Technical College (Lowell, Mass.) in 1912.

[1] Abstract of a memoir prepared by Harold A. Kidby, F. ASCE.
[2] Abstract of a memoir prepared by Gustave J. Angele, Sr., F. ASCE.

Mr. Neff was employed on the construction of the Cape Cod Canal from 1914 to 1917 before serving with the United States Marine Corps in Santo Domingo. He was employed by the United Fruit Company from 1920 to 1922 before joining Hugh L. Cooper and Company of New York in connection with the construction of Wilson Dam. Mr. Neff was associated with the United States Bureau of Roads before joining the Portland Cement Association as a field engineer in Buffalo, N. Y. (1928), and Knoxville, Ky. (1939). In 1941 he was associated with the War Production Board and later served as district manager for the Small War Plants Corporation. In succeeding years he worked with the Reconstruction Finance Corporation as a senior engineer (1945), the Knoxville City School Board (1947), and the Public Housing Administration as a project engineer. His last association was with the J. Fruchtbaum Engineering Company of Buffalo.

Mr. Neff was a former secretary - treasurer of the Buffalo Section of the Society, and a former president of the Erie County Chapter of the New York State Society of Professional Engineers. He was a member of the St. Stephan's Episcopal Church (Oak Ridge, Tenn.) and the AF & AM.

He was married to Mary Elizabeth Nixon in Lawrenceburg, Tenn., in 1924. He is survived by his widow; and children, Mrs. William R. Hall, and George Stewart Neff.

He was elected an Associate Member of the Society in 1922 and a Life Member in 1957. He became a Fellow in 1959.

FRANK AUSTIN NIKIRK, M. ASCE[1]

Died January 5, 1950

Frank Austin Nikirk, the son of John Hill and Jane (Stout) Nikirk, was born in Butte County, Calif., on May 9, 1881. He was graduated from Stanford University (Stanford, Calif.) with the degree of Bachelor of Science in civil engineering in 1904.

Mr. Nikirk contributed to technical engineering knowledge in the field of the selection and use of construction equipment. He carried on early investigation to determine the application and use of equipment. He did extensive writing for trade journals and consultation work for equipment companies. In his seventieth year he undertook to introduce the technical and professional aspects of construction into the civil engineering curriculum of the University of California (Berkeley).

He was a member of the American Society for Engineering Education.

Mr. Nikirk was married to Ruby Alice Brooks, in 1909. He is survived by his widow; his daughter, Mrs. Martha N. Konig; and his sister, Minnie E. Rohrback.

Mr. Nikirk was elected a Member of the Society in 1940.

[1] Abstract of a memoir prepared by Paul F. Keim, F. ASCE.

CLAYTON WHITNEY PAIGE, F. ASCE[1]

Died February 14, 1960

Clayton Whitney Paige, the son of Dr. Charles and Ella (Clayton) Paige, was born in Fraser, Iowa, October 12, 1902. He was graduated with the degree of Bachelor of Science from Iowa State University (Ames) in 1922 and studied business administration at Lafayette Institute (Lafayette, Ind.).

Mr. Paige was employed by the City of Milwaukee, Wisc., before joining the Los Angeles County Surveyor in 1925 as field engineer. He served as a field engineer for the R. G. Ferguson Corporation preceding his appointment as assistant engineer with the Alhambra, Calif., water department in 1931. In 1941 he was appointed city engineer in Burbank, Calif., a position he held except for the time of military service until his death. In this position he was responsible for the development of the cut and cover rubbish disposal system, a municipal golf course, three street grade separations, a flood channel, and several storm drain projects. His military duty (1942-46) was spent as a lieutenant commander and commander with the 29th Construction Battalion.

He was a member of numerous civic and professional organizations including the Southern California Chapters of the American Public Works Association (former director and first vice-president), the League of California Cities (past director), and the Institute of Traffic Engineers. He was chairman of the Metropolitan Transportation Engineering Board in Los Angeles and a past director and treasurer of the Los Angeles Section of the Society. He was a member of the AF & AM and Delta Tau Delta.

Mr. Paige was married to Jeanne Tarver in 1946 at Glendale, Calif. He is survived by his widow; a son, William Whitney; and brother William J. Paige.

Mr. Paige was elected an Associate Member of the Society in 1929, and a Member in 1940. He became a Fellow in 1959.

CLIFFORD ALLEN PHILO, F. ASCE[2]

Died August 15, 1959

Clifford Allen Philo, the son of William and Ella (Cameron) Philo, was born June 27, 1891, at Wadena, Minn. He was graduated from the University of Minnesota (Minneapolis) in 1923, with the degree of Bachelor of Science in civil engineering.

[1] Abstract of a memoir prepared by Clarence Shadel, F. ASCE.
[2] Abstract of a memoir prepared by Glenn E. Hands, F. ASCE.

Mr. Philo worked on railroad survey parties from 1909 until after his graduation. He worked for several construction companies as construction engineer and superintendent before joining the United States Forest Service in 1933. He transferred to the Corps of Engineers as resident engineer in 1941, and was placed in charge of numerous projects: the Lake City Arsenal; Sunflower Ordnance Plant; Central Industrial Floodwall; Liberty Bend Bridge; and a prisoner of war camp in Winegarten, Mo. From 1951 to 1953, Mr. Philo took a leave of absence from the Corps to serve as project manager for Patti, Massman and MacDonald, Construction Company, contractors for the air base at Tullahoma, Tenn. At the time of his death, Mr. Philo was resident engineer at Whiteman Air Force Base, Knobnoster, Mo., supervising construction on a jet runway and office building.

He was a member of the Society of American Military Engineers. Mr. Philo, a veteran of World War I, was awarded the Purple Heart.

He was married to Helen Raasch in 1927, in Milwaukee, Wis. He is survived by his widow; two sons, Donald R. and Kenneth W. Philo; and three grandchildren.

Mr. Philo was elected a Member of the Society in 1951 and a Fellow in 1959.

GEORGE WILLIAM PRICHARD, F. ASCE[1]

Died March 28, 1960

George William Prichard, the son of William Marvin and Almede (Lawson) Prichard, was born in Gallatin, Mo. on March 11, 1908. He was graduated from the University of Missouri (Columbia) with the degree of Bachelor of Science in civil engineering in 1947.

Mr. Prichard served as a field engineer with the Missouri Highway Department from 1929 until 1938, and as a civil engineer for Black and Veatch Consulting Engineers in Kansas City, Mo., from 1938 to 1952 except for that time spent in military service (1940-1946). From 1952 until his death, he owned and operated the Prichard Company, Incorporated.

Mr. Prichard's military service began in 1933 as a private in the Missouri National Guard. He entered active service in 1940 and was graduated from the Command and General Staff College (Ft. Leavenworth, Kans.) and the Army Engineers School (Fort Belvoir, Va.). His assignments included that of executive officer and commander with the 40th Engineers Combat Regiment in Africa, Sicily, Italy, France, Germany, Austria, Belgium, and England. He directed the repair of the Port of Naples, the Sisteron Bridge and Bar River Crossing in France. He was the author of Amphibious Assault Landing Procedure. Some of the decorations he received include the Purple Heart, Bronze Star, and the Croix de guerre with star. Returning to the reserves in 1946 with the rank of colonel, he became commanding officer of 455 Engineering Group Army Reserve, Records Center, in Kansas City.

[1] Abstract of a memoir prepared by Glenn H. Kevan, M. ASCE.

Mr. Prichard was active in civic affairs and held membership in the AF & AM, Rotary International, National Society of Professional Engineers, Society of American Military Engineers, and the American Water Works Association.

In 1932 he was married to Mary Elizabeth Love in New Hampton, Mo. He is survived by his widow; two sons, Dr. J. W., and Vincent; his mother; and a brother, Robert V.

Mr. Prichard was elected an Associate Member of the Society in 1938, and Member in 1949. He became a Fellow in 1959.

ASA GLISSON PROCTOR, M. ASCE[1]

Died December 10, 1958

Asa Glisson Proctor, the son of William Edwin and Lenna (Hadley) Proctor, was born on April 15, 1885, in Woodland, Calif. He attended Stanford University (Palo Alto, Calif.).

In 1908 he entered the employ of Yolo County, Calif., as an instrument man. The following year Mr. Proctor opened private practice which he maintained for 50 years. He served as City Engineer of Woodland (1911-1915, 1919-1956), Davis (1920-1940), and Winters (1920-1958). As Yolo County Surveyor and Engineer of Design and Construction (1915 to 1931) he built more than 200 county road bridges and 94 miles of hard-surfaced highways. He was engineer for the Broderick and West Sacramento Sanitary Districts in Yolo County. In other capacities he built sewage systems, treatment plants, street lighting, and water supply systems. He subdivided and prepared improvement plans for tracts in Yolo County involving more than 2,000 residential lots. He served on the State Board of Registration for Civil Engineers for 27 years. He was president of the board from 1938 to 1940 and from 1953 to 1958.

Mr. Proctor was a member of the California Sewage Works Association and of the County Engineers Association of California (past president), Structural Engineers Association of California, Lions Club (past president), Woodland Chamber of Commerce, Yolo Fliers Club (charter member and past president), Woodland Lodge 1299 BPOE, St. Luke's Episcopal Church (vestryman). He was first vice-president of the Sacramento Section of the Society in 1942. In 1958 he was awarded a citation for outstanding service to the engineering profession by the Engineering Council of Sacramento Valley.

He was married to Elamae Lambert in 1912 in Woodland. He is survived by his widow; and son, Edwin.

Mr. Proctor was elected a Junior Member of the Society in 1910, an Associate Member in 1915, and a Member in 1935.

[1] Abstract of a memoir prepared by William A. White, M. ASCE, Clair A. Hill, F. ASCE, and William L. Meikle, M. ASCE.

CHARLES ALLEY REED, M. ASCE[1]

Died March 20, 1959

Charles Alley Reed, the son of Charles Oliver and Lydia (Alley) Reed was born in S. Dak., May 10, 1887. He was graduated from the University of California (Berkeley) with the degree of Bachelor of Science in civil engineering in 1910.

After leaving college, Mr. Reed spent several months in Mexico making a survey of a large hacienda for a land company. In 1913 he was employed as draftsman in the engineering department of the City of Oakland, Calif. Mr. Reed was then engaged in surveying work for an irrigation district in the San Joaquin Valley, after which he returned to the engineering department of Oakland. He held the positions of office engineer, 1st assistant engineer, street improvement engineer, assistant city engineer and superintendent of streets and ex officio city engineer in 1949. He held this last appointment until his retirement July 6, 1953.

Mr. Reed held membership in Ashmes Temple, Oakland; Oakland Consistory, M.R.S.; the AF & AM; Oakland Municipal Civil Service Employees Association; East Bay Engineers Club; and the American Public Works Association. In 1949, he attained national recognition by receiving the Samuel A. Greeley Service Award of the American Public Works Association for service to the City of Oakland.

In 1913, Mr. Reed was married to Cora Huestis in Mound, Minn., who passed away in 1943. He was married to Ruth Beresford Skinner in Oakland, in 1945. He is survived by his widow; and his daughters, Beatrice (Mrs. Ben Culver), Barbara (Mrs. David L. Cook), Beverley (Mrs. Robert Sherrard), and Marilyn (Mrs. William Davis); and eleven grandchildren.

Mr. Reed was elected an Associate Member of the Society in 1918 and a Member in 1936.

GARFIELD HUGH RUSSELL, M. ASCE[2]

Died January 8, 1959

Garfield Hugh Russell, the son of Nathaniel and Mary (Stansberry) Russell, was born on June 5, 1880 in Sandyville, Ohio. He was graduated from Fairmont College (now Wichita University, Kans.). He received the degree of Bachelor of Science in civil engineering from the University of Michigan (Ann Arbor) in 1907.

[1] Abstract of a memoir prepared by James C. Barrett, M. ASCE.
[2] Abstract of a memoir prepared by Sidney Twichell Harding, F. ASCE.

After working on the Detroit River Tunnel for the Michigan Central Railway, Mr. Russell joined the Surface Water Branch of the United States Geological Survey at Denver, Colo. In 1913 he was associated with the Elberta Land and Water Company near Spanish Fork, Utah. From 1919 to 1920 he was engineer-appraiser for the Federal Land Bank at Dallas, Tex., and in 1920, he worked for the State of California on water resources investigations in Tulare County. In 1926 Mr. Russell became the engineer-appraiser for the Federal Land Bank of Berkeley, Calif., a position which he filled until his retirement in 1947. His work with the Land Bank dealt particularly with the evaluation of water supplies and water rights in relation to the appraisal of irrigated lands.

On March 20, 1912 Mr. Russell was married to Hazel May Taylor in Denver, Colo. He is survived by three children and 15 grandchildren.

Mr. Russell was elected a Member of the Society in 1935.

WALTER FREDERICK SCHULZ, M. ASCE[1]

Died July 1, 1955

Walter Frederick Schulz, the son of Werner and Gertrude (Niebert) Schulz was born on August 15, 1876 in Berlin, Germany. He received the degree of Bachelor of Science in civil engineering from Purdue University (Lafayette, Ind.) in 1902.

After graduation he worked with the Northern Pacific and the Louisville and Nashville Railroads. In 1911, the Louisville and Nashville Railroad Company placed him in charge of constructing the Memphis Union Station, Memphis, Tenn., and the terminal yards back of it. In 1916 he opened a private engineering and architectural office in Memphis. Here, he planned and supervised several hospitals, the City Auditorium, the Industrial Building, and several City Fairgrounds buildings. In 1918 he built the first of his 25 river-rail barge terminals on the Mississippi River. He erected shops and terminals for the Belt Line Railroad in New Orleans. Mr. Schulz did consulting work on the Huey Long Bridge at New Orleans, and terminal facilities in Fort Worth, Tex. and Shreveport, La. He supervised seven grade separation projects in Memphis and two in Atlanta, Ga. During War II he planned the Army General Depot in Memphis and the Army Reconstruction Depot in Montgomery, Ala.

He was a charter member of the Memphis Engineers' Club, a member of the Shriners, and a Red Cross committeeman. In 1935 he was chosen by the State Department to represent this country at the 16th International Congress on Navigation in Belgium.

Mr. Schulz married Clara Brown in St. Paul, Minn., in 1902. He is survived by a daughter, Mrs. Walter R. Streuli; a son, Barton; three sisters; and three grandchildren.

Mr. Schulz was elected a Member of the Society in 1910 and became a Life Member in 1945.

[1] Abstract of a memoir prepared by Frank A. Busse, F. ASCE.

ELWYN E. SEELYE, F. ASCE[1]

Died December 28, 1959

Elwyn E. Seelye, the son of Elwyn and Elizabeth G. (Eggleston) Seelye was born on August 20, 1884, in Warren County, N. Y. He was graduated from Cornell University (Ithaca, N. Y.) in 1904 with a degree in civil engineering.

After graduation he was employed by the New York Central Railroad on the design of the structural arrangement of Grand Central Terminal and a grade crossing project in Yonkers, N. Y. In 1912 he established private practice. In 1947 the partnership of Seelye, Stevenson and Value was created, and in 1951 expanded to include A. Wilson Knecht. Projects engineered by Mr. Seelye's firm include: Camp Shanks (Orangeburg, N. Y.), Camp Kilmer (Selton, N. J.), and air bases at Fort Dix (N.J.), France, the Azores, Pakistan, and on the DEW line. The Queensboro Low Cost Housing Development (Long Island City), the Thomas Jefferson Memorial (Washington, D. C.), the addition to the British Museum (London), and the Congressional Library Annex were enterprises of the Seelye firm. Industrial contracts include factories and service stations for the International Motor Company, the Endicott Johnson Corporation, and the International Business Machines Corporation.

Mr. Seelye was a member of the Chaguaramas Joint Commission, and the Pershing Commission to study the erection of the Montfaucon Monument at Verdun in 1919. In 1939 he was cited by Fiorello H. LaGuardia, Mayor of the City of New York, for distinguished and exceptional public service. He was also awarded the Fuertes Medal for Original Research by Cornell University in 1948. He was the author of four textbooks including "Foundations, Design and Practice." Mr. Seelye was designated in 1956 to consider the structural adequacy of the dome of the United States Capitol and to supervise necessary modifications.

Mr. Seelye was a member of the American Institute of Consulting Engineers, the American Concrete Institute, and the Architectural League of New York. He was a registered engineer in 15 states and the District of Columbia.

Mr. Seelye was married to Eleanore Janeway in 1914 in Staten Island, N. Y. He is survived by his widow; two sons, Elwyn, and Edward E.; and two daughters, Eleanore Janeway West, and Elizabeth W. Williams.

Mr. Seelye was elected an Associate Member of the Society in 1912 and a Member in 1915. He became a Life Member in 1947 and a Fellow in 1959.

[1] Abstract of a memoir prepared by Richard E. Dougherty, F. ASCE.

WILLIAM JAMES SHACKELFORD, M. ASCE[1]

Died July 30, 1957

William James Shackelford, the son of Edmond and Nannie (Embry) Shackelford, was born in Madison County, Kentucky, on November 18, 1870. He attended Center College (Danville, Ky.).

After leaving college he worked as an instrument man on railroad location surveys in Kentucky. Sometime later he was retained by the Mississippi River Commission to work on one of their annual surveys of the Mississippi River.

In 1890 he secured a position with the Engineer Corps at Vicksburg, Miss. doing levee work. Later he transferred to the Mississippi Levee Board, at Greenville, becoming chief engineer in July, 1910. From 1913 until 1915 he was engaged in levee contracting. He returned to government service as chief of a large willow revetment placing unit, connected with the corps of Engineers Office at Memphis, Tenn. He resigned this position in 1926, when he and several associates bought a large road gravel pit in Columbus, Miss. Mr. Shackelford retired in 1938 and moved to Rosedale, Miss. where he remained until his death.

He was married to Alice Buckner Alexander in Rosedale, Miss., in 1897. Mr. Shackelford was elected a Member of the Society in 1912.

THOMAS CLARK SHEDD, F. ASCE[2]

Died July 11, 1959

Thomas Clark Shedd, son of Edward Whitten and Jessie (Dexter) Shedd, was born July 2, 1890 in Worcester, Mass. He was graduated from Brown University (Providence, R. I.) with the degree of Bachelor of Science in mechanical engineering in 1913. The degrees of civil engineer and Master of Science in civil engineering were conferred on him by the University of Illinois in 1925 and 1933, respectively.

Thirty-nine of the forty-five years following his graduation were devoted to teaching mechanical and civil engineering. Before joining the civil engineering faculty at the University of Illinois in 1922, he taught at Brown University (1913-1915, and Lehigh University (1918). In the interim he was associated with the

[1] Abstract of a memoir prepared by Robert H. Shackelford.
[2] Abstract of a memoir prepared by Edward E. Bauer, F. ASCE.

Phoenix Bridge Company. From 1934 until his retirement in 1958 he served as professor of structural engineering at the University of Illinois. At the time of his death he was an associate of Clark, Daily and Dietz, consulting engineers, Urbana, Ill.

His two textbooks "Theory of Simple Structures" (with Jamison Vawter), and "Structural Design in Steel," contributed to the understanding of fundamentals of analysis and design.

From 1953 to 1956 Mr. Shedd served as the national director for District VIII of the Society. He was a former chairman of the Illinois Structural Engineers' Examining Committee, and the Illinois Professional Engineers' Examining Committee. He served as president and director of the National Council of State Boards of Engineering Examiners and was president of the Illinois Engineering Council for two terms. He was a member of the Urbana City Planning Commission and of the Urbana Zoning Appeals Board.

Mr. Shedd was married to Mary Margaret Campbell in 1916 in East Providence, R. I. He is survived by his widow; two sons, Thomas Clark, Jr., and Milton Campbell; a daughter, Harriet M. (Mrs. Richard L. Pfister); seven grandchildren; three brothers; and one sister.

He was elected an Associate Member of the Society in 1923, a Member in 1926, and a Life Member in 1958. He became a Fellow in 1959.

JACK WILLIAM SHEETZ, A. M. ASCE[1]

Died September 21, 1958

Jack William Sheetz, the son of William and Dorothy (Flinn) Sheetz, was born in Allen, Kan., on February 18, 1905. He attended Kansas State University (Manhattan).

After graduation, Mr. Sheetz entered the employ of the Illinois and Missouri State Highway departments. In 1944 he was retained by the City of Whittier, (Calif.) as director of public works. He received his registration as a civil engineer in the State of California in 1958 and was appointed city engineer in Whittier. The position placed him in charge of all major construction work in the city.

Mr. Sheetz was a member of the American Public Works Association, the Central Basin Water Association, and the Retired Officers Association, having served as captain in the Anti-Aircraft Coast Artillery.

He was married to Ruth Watkins on June 22, 1931, in Bloomington, Ill. He is survived by his widow; his father; and two sisters, Mrs. Robert Beattie, and Mrs. Theodore Rodger.

Mr. Sheetz was elected an Associate Member of the Society in 1947.

---

[1] Abstract of a memoir prepared by Kenneth R. Warren.

CLARENCE OSBORNE SHERRILL, M. ASCE[1]

Died February 6, 1959

Clarence Osborne Sherrill, the son of Miles Osborne and Sarah Rosanna (Bost) Sherrill, was born in Newton, N. C. on May 24, 1876. He attended Trinity College (now Duke University, N.C.) from 1895 to 1897 and was graduated from West Point (N.Y.) in 1907.

In 1901 Mr. Sherrill, a second lieutenant of engineers, was assigned to duty in the Philippines. He was next appointed an instructor in engineering at the Army Service Schools, Fort Leavenworth, Kans., where he wrote several military manuals on map reading, topographic surveying, and rapid sketching. From 1911 to 1914, Mr. Sherrill, now a major, served as district engineer at New Orleans. During the three succeeding years he commanded the 3rd Battalion of Engineers in the Philippines, and served as assistant to the department engineer. In 1917, having attained the rank of colonel, he commanded the 302nd Engineers in France, and later became the Chief-of-Staff of the 77th Division and the 29th Division.

In 1921, while serving as Chief Military Aid to the President, he was made Director of Public Buildings and Public Parks in the nation's capital. He was in charge of the building of the Lincoln Memorial, and the Arlington Memorial Bridge. In 1925 he became City Manager of Cincinnati, Ohio. He resigned this position in 1930 to accept a vice-presidency with the Kroger Grocery chain and later, the presidency of the American Retail Federation. He was awarded three campaign clasps, the Croix de Guerre, with Palm, and the Distinguished Service Medal for his service in World War I. Mr. Sherrill was a member of numerous professional and civic organizations.

Mr. Sherrill was married to Geraldine Caldwell Taylor in Fort Leavenworth in 1906. He is survived by his son, Clarence; and daughter, Minnie Elizabeth.

Mr. Sherrill was elected a Member of the Society in 1920.

MICAJAH THOMAS SINGLETON, F. ASCE[2]

Died August 19, 1959

Micajah Thomas Singleton, son of Micajah Thomas and Emma (Wood) Singleton was born in Arcadia, Fla., in 1892. He attended the Georgia Institute of Technology (Atlanta), where he studied civil engineering.

[1] Abstract of a memoir prepared by Hunter W. Hanly, F. ASCE, Warren W. Parks, F. ASCE, and Herbert H. Schroth, M. ASCE.

[2] Abstract of a memoir prepared by C. E. Drummond, Jr., F. ASCE.

He was a captain in the First World War and served overseas for 14 months with the 2nd Engineers, 2nd Division. In 1925 he and his partner formed the firm of Wiedeman and Singleton to serve as consulting engineers in the design and construction of municipal improvements, particularly water supply, sewerage and sewage treatment. This work included the first complete sewage treatment plant constructed in the State of Georgia.

For his efforts in obtaining a state licensing law for professional engineers and surveyors, he was appointed the first civil engineering member of the State Board of Registration for Professional Engineers and Surveyors, a position which he filled for about twenty years. He was honored by fellow members by being made the recipient of the first license issued to a professional engineer in Georgia.

During the Second World War, Mr. Singleton was resident partner for his firm on the War Department contracts for Fort McClellan Cantonment, Coosa River Ordnance Plant and for Greenwood, Miss., Basic Flying School.

He was a past-president of the Georgia Section, ASCE, and, for a number of years, was a member of the Sanitary Engineering Committee. Mr. Singleton was a charter member of the Georgia Engineering Society and of the Georgia Society of Professional Engineers. He was also a member of the American Water Works Association.

He was married to Lila Huddleston in Atlanta, in 1927. He is survived by his widow; two sisters, Mrs. H. W. Bass, and Mrs. Hugh Montgomery; and two brothers, A. G. Singleton, and J. L. Singleton.

Mr. Singleton was elected a Member of the Society in 1925, and a Fellow in 1959.

ARTHUR ALVORD STILES, M. ASCE[1]

Died February 20, 1958

Arthur Alvord Stiles, the son of William and Margaret (Lyford) Stiles, was born near Austin, Tex., on August 28, 1871. He attended the University of Texas (Austin) from 1891 to 1894.

In 1894 Mr. Stiles was appointed a topographic field assistant in the United States Geological Survey, and assigned to Colorado. In 1897, he was appointed an assistant topographer in the United States Geological Survey, and continued in civil service work until 1910. In this capacity, he worked on topographic maps of Western United States territory. From 1910 to 1924 he served as state reclamation engineer in Texas, doing levee and drainage work and drawing up many of the Texas laws dealing with reclamation work. In 1921 he became the principal engineering witness for the State of Texas in the Texas-Oklahoma Boundary case, and, in 1924, he was appointed by the United States Supreme Court to determine, locate, and mark this boundary line along the Red River.

[1] Abstract of a memoir prepared by John A. Focht, F. ASCE.

On this project, he originated the gradient boundary principle which was adopted by the Supreme Court of Texas. During this period he was employed also by oil companies as a land surveyor for contested boundaries. In 1928 he was appointed the Official Surveyor for the 53rd District Court of Travis County, Tex., in a suit involving the ownership of the bed of the North Fork of the Red River. In 1929 until his retirement in 1956, Mr. Stiles was associated with the Pure Oil Company as a cadastral engineer.

Mr. Stiles was a member of the First Presbyterian Church of Austin. He was a charter member of the American Society of Military Engineers, a colonel of Engineers Officers Reserve Corps, United States Army, and a registered professional engineer in Texas. Mr. Stiles was the author of several copyrighted publications.

He was married to Susie Mary Aden at Austin, Tex., June 14, 1905. He is survived by one son, Aden Edmund; and two grandsons.

Mr. Stiles was elected a Member of the Society in 1914.

ABRAHAM STREIFF, F. ASCE[1]

Died January 4, 1960

Abraham Streiff, the son of Johann and Marianna (Boesch) Streiff, was born in Java, August 21, 1880. He graduated from the Technologic Institute at Delft, Holland, in 1901 and took graduate studies at Federal Polytechnikum in Zurich, Switzerland, where he also served as an assistant in hydraulic engineering.

Mr. Streiff worked for five years as a hydraulic engineer, and for three years as a hydraulic designer, before joining the Fargo Engineering Company of Jackson, Mich. Here, he was engaged in the design of major hydroelectric plants for periods totaling 30 years. During interim periods, Mr. Streiff was associated with the Consumers Power Company, the Commonwealth and Southern Corporation, and the Ambursen Engineering Company in the capacity of vice-president. He conducted his own consulting business for a time and for the last eight years of his life, he served as a hydraulic consultant to the American Smelting and Refining Company.

Mr. Streiff, a frequent contributor to the technical literature of the Society was well-known for his studies of the correlation between sunspots and rainfall. He was a pioneer in the design of large, tainter gates. Projects with which he was connected as chief engineer and consultant include several important power plants in Texas, the Rasgo Project in Brazil, and the Narrows Dam and power plant in Arkansas.

He was married to Josephine Doerig in 1904, in Paramaribo, Dutch Guiana. He is survived by his widow; three sons, John F., Anton J., and William H.; two sisters; and nineteen grandchildren.

Mr. Streiff was elected an Associate Member of the Society in 1925, and a Member in 1927. He became a Fellow in 1959.

[1] Abstract of a memoir prepared by C. A. Hunt, M. ASCE.

MELVIN OLIVER SYLLIAASEN, M. ASCE[1]

Died July 29, 1956

Melvin Oliver Sylliaasen, the son of Christian T. and Johanne (Pedersen) Sylliaasen was born in Yankton, S. Dak., on November 1, 1890. He received the degree of Bachelor of Science in civil engineering from the University of Washington (Seattle) in 1913.

Mr. Sylliaasen specialized in structural design following graduation and his name became indentified with many of Seattle's major structures, including the Dexter Horton Building, the Exchange Building, the Bon Marche Store, and the Ballard Bridge. He was associated with the late John Graham, Seattle architect, for a number of years and served as City Engineer of Seattle from 1932 to 1934.

During World War II he was responsible for the design of several army installations, including a large shipping terminal. In his latter years, Mr. Sylliaasen maintained his own consulting office. He assisted in the preparation of plans for the Seattle sewage treatment plant situated near the mouth of the Duwamish river.

Mr. Sylliaasen was a member of the University Lutheran Church and of the Norwegian Male Chorus. He was president of the Seattle Section in 1931.

He was married to Bertha Sande on August 19, 1914, in Seattle. He is survived by his widow; a daughter, Mrs. David Will; three brothers; and two grandchildren.

Mr. Sylliaasen was elected a Junior Member of the Society in 1914, an Associate Member in 1919 and a Member in 1931. He became a Life Member in 1954.

ADOLPHUS GUSTAVUS TROST, M. ASCE[2]

Died July 27, 1957

Adolphus Gustavus Trost, the son of Ernest and Wilhelmina Trost, was born June 20, 1876, in Toledo, Ohio.

In 1908, after serving an apprenticeship with architects in Toledo, he joined the firm of Trost and Trost, Architects and Engineers, of El Paso, Tex. He held a partnership in the firm until it was dissolved in 1951, following the death of his uncle, H. C. Trost, and brother, G. A. Trost.

[1] Abstract of a memoir prepared by Samuel DeMoss, F. ASCE.
[2] Abstract of a memoir prepared by H. J. Ponaford, F. ASCE.

The firm of Trost and Trost was responsible for many of the outstanding buildings in El Paso, including the Mills Building, which was, in 1911, the largest reinforced concrete office building in the world. They also constructed the Hilton, Paso del Norte, and Cortez hotels; the State National, El Paso National and First National Bank buildings; The White House and Popular department stores; the El Paso County Court House, the O. T. Bassett Tower, the Y.M.C.A., Masonic Temple, and the El Paso Country Club. They designed the Texas College of Mines, Loretto College, the El Paso High School, and the Austin and Bowie High Schools. Their work includes many of the leading hotels in the southwest. The Franciscan and Fidel Hotels (Albuquerque, N. M.), the Pioneer and Santa Rita Hotels (Tucson, Ariz.), and the Meadows (Las Vegas, Nev.), were designed by Trost and Trost. The Luhr's office building (Phoenix, Ariz.) and the First National Bank Building (Albuquerque, N. M.) are typical of their work.

In 1915, Mr. Trost was married to Carolyn Hayes in El Paso. He is survived by his widow.

He was a member of the AF & AM and the Scottish Rite Bodies of El Paso. He was affiliated with the Lutheran Church.

Mr. Trost was elected an Associate Member of the Society in 1913 and a Member in 1917. He became a Life Member in 1947.

LEO VERNON UHRIG, M. ASCE[1]

Died February 13, 1960

Leo Vernon Uhrig, the son of C. A. and Nettie (Shields) Uhrig, was born in Carrollton, Mo. on May 15, 1903. He graduated from the University of Missouri (Columbia) with the degree of Bachelor of Science in civil engineering in 1925.

Upon graduation Mr. Uhrig started to work for the water department in Detroit, Mich. In 1926, he resigned to become an instructor in civil engineering at Rich Institute (Houston, Tex.), which position he held until 1936. From 1927 to 1931 he worked part time for the water department in Houston. From 1936 until 1960 he was with the Production Research Department of the Humble Oil and Refining Company of Houston, and, at the time of his death, served as senior research specialist. During World War II, as an employee of Humble, he worked on two projects under the supervision of the National Defense Research Council. From April until July of 1942, he worked with the Manhattan Project at the University of Chicago, and from August, 1944 to March, 1945, he worked on the flame-thrower problem at Massachusetts Institute of Technology. He worked on the same problem at the University of Iowa during that year.

[1] Abstract of a memoir prepared by John A. Focht, F. ASCE.

Mr. Uhrig was a member of the South Main Baptist Church, the Houston Philosophical Society, Houston Lodge 1189 AF & AM, and Tau Beta Pi. He was a registered professional engineer in Texas.

He married Susie Jackson in 1930, in Lake Charles, La. He is survived by his widow; and son, Allan Jackson.

Mr. Uhrig was elected a Junior Member of the Society in 1927, and an Associate Member in 1932. He became a Member in 1959.

JAMISON VAWTER, M. ASCE[1]

Died May 23, 1959

Jamison Vawter, the son of Jamison and Sallie (Snyder) Vawter, was born April 21, 1889, in Arkansas City, Kans. He was graduated from the University of Kansas (Lawrence) in 1916 with the degree of Bachelor of Science in civil engineering. In 1923 he received the degree of Civil Engineer from the University of Kansas and in 1934 the Master of Science degree from the University of Illinois.

Following graduation he served for a year as an assistant engineer on the Gulf, Colorado, and Santa Fe Railway. He spent two years with the United States Army Engineers in France, as first lieutenant and captain, before he began his thirty-seven year teaching career. From 1920 to 1922 he taught at the University of Kansas. The remaining thirty-five years he spent in the Civil Engineering Department at the University of Illinois. Here he published, "Theory of Simple Structures" (with Thomas C. Shedd), and "Elementary Design of Flexural Members" (with James G. Clark).

He was a member of the College Policy and Development Committee and served on the Urbana City Council for twenty years (1937-1957). He belonged to many professional organizations including the American Railway Engineering Association, and Theta Tau (Grand Treasurer 1924-1951, and Grand President, 1953-1955). He was president of the Professional Interfraternity Conference, 1931-33, and president of the Central Illinois Section of the Society in 1936.

Mr. Vawter was married to Theresa C. O'Brien, in 1922, at Lawrence, Kans. Surviving him are his widow; two daughters, Frances Jeanne (Mrs. George H. Weatherbe), and Margaret Patricia (Mrs. George H. Klein); and three grandchildren.

Mr. Vawter became an Associate Member of the Society in 1923, and a Member in 1926. He became a Life Member in 1958.

[1] Abstract of a memoir prepared by Edward E. Bauer, F. ASCE.

FRANCIS K. WAI, M. ASCE[1]

Died September 19, 1959

Francis K. Wai, the son of Weikin and Lee Shee Wai, was born on November 7, 1914, in Pahala, Hawaii. He received the degree of Bachelor of Science in civil engineering from the University of Hawaii (Honolulu) in 1936.

Mr. Wai worked with the Territory of Hawaii Highway Department from 1938 to 1939, the Ready-Mix Company as civil engineer from 1939 to 1945. For his last fourteen years he was employed as a civil engineer by the Honolulu Construction and Draying Company.

Mr. Wai served as past president of the Hawaii Section of the Society. He was a past director of the Engineering Association of Hawaii and in other ways worked toward the welfare of the engineering profession. He was active in church and community affairs.

In 1938 he was married to Vera Young. He is survived by his widow; a son, Gary Paul; and daughter, Karen Leslie.

Mr. Wai was elected an Associate Member of the Society in 1950 and a Member in 1959.

RICHARD BENSKIN WARD, M. ASCE[2]

Died April 27, 1959

Richard Benskin Ward, the son of Richard B. and Margaret (Van Natta) Ward, was born in Belleville, Kans., on December 28, 1888. He was graduated from the University of Kansas (Lawrence) in 1913, with the degree of Bachelor of Science in civil engineering.

From 1913 to 1925 he was engaged in railroad construction in Alaska, irrigation projects in Montana and Wyoming for the United States Bureau of Reclamation, and the construction of a number of earthfill dams. He was a design engineer with the County Sanitation Districts of Los Angeles County, Calif., from 1925 to 1931. Mr. Ward served in the United States Army in World War I.

In 1931 Mr. Ward was employed by the Metropolitan Water District of Southern California, and prepared estimates and specifications for the Colorado River Aqueduct. In 1935 he became resident engineer on the construction of the dam and dike and appurtenant works for the Cajalco Reservoir (now Lake Mathews).

[1] Abstract of a memoir prepared by Paul E. S. F. Liu, A. M. ASCE.
[2] Abstract of a memoir prepared by R. A. Skinner, F. ASCE.

In 1938 he accepted a position with the United States Bureau of Reclamation in Denver, Colo. During the next eleven years he served as construction engineer on the Green Mountain Dam, Kremmling, Colo., location engineer on the San Diego Aqueduct, Calif., and construction engineer on four earthfill dams for the Horsetooth Reservoir, Fort Collins, Colo. From 1949 to 1954 he was construction engineer on Falcon Dam and Power Plant on the Rio Grande River, near Laredo, Tex., for the United States International Boundary and Water Commission.

In 1954 Mr. Ward returned to the Bureau of Reclamation as engineer-advisor to Snowy Mountains Hydro-Electric Authority in New South Wales, Australia. After returning to the Metropolitan Water District in 1956 he was in charge of the construction work required to enlarge Lake Mathews, Calif.

Mr. Ward was a member of the AF & AM, the Scottish Rite, and the Al Malaikah Shrine Temple.

On June 7, 1922, he was married to Eleanore Louise Larsh at Cheyenne, Wyo. He is survived by his widow; two daughters, Nancy (Mrs. William Fabian) and Eleanore (Mrs. John Ellis); a sister; two brothers; and five grandchildren.

Mr. Ward was elected an Associate Member of the Society in 1933, and a Member in 1938. He became a Life Member in 1959.

LEVI ROMULUS WHITTED, M. ASCE[1]

Died October 17, 1959

Levi Romulus Whitted, the son of Levi and Emily (Powell) Whitted, was born on October 11, 1874, in Pleasant Grove, N. C. He was graduated with the degree of Bachelor of Civil Engineering from North Carolina State College of Agriculture and Mechanical Arts (Raleigh) in 1896. He received the professional degree of Civil Engineer from North Carolina State College in 1898.

From 1896 to 1898 he was assistant professor of civil and electrical engineering at North Carolina State College, as well as engineer in charge of the college electric generating plant. Mr. Whitted also served as assistant to the city manager of Raleigh during this time. From 1899 to 1903 he was junior and assistant engineer for the United States Engineers, Port Royal, S. C., Naval Station, and the Norfolk, Va., Navy Yard. He was next appointed draftsman in charge of construction of the navy yard at Charleston, S. C. From 1904 to 1925 Mr. Whitted was superintendent of construction for the United States Treasury Department on the erection of public buildings throughout the United States. A construction accident in 1925 forced his retirement.

Mr. Whitted was a member of the Baptist Church and of the AF & AM.

He is survived by two nephews, Banks A. Murray, and Levi R. Whitted; and two nieces, Frances Powell Whitted, and Mrs. Myra Anderson Wyatte.

[1] Abstract of a memoir prepared by Thomas A. Cox, Jr., M. ASCE, and Robert H. Nagel, M. ASCE.

Mr. Whitted was elected a Junior Member of the Society in 1900 and an Associate Member in 1906. He became a Member in 1959.

JACKSON HEATH WILKINSON, M. ASCE[1]

Died November 29, 1958

Jackson Heath Wilkinson, the son of William W. and Maida (Heath) Wilkinson, was born October 29, 1892, at Bethany, Ill. He was graduated from the University of Illinois (Urbana) in 1915 with the degree of Bachelor of Science in civil engineering. He was awarded the degree of Master of Science in civil engineering in 1916. He served with the United States Army during World War I, rising to the rank of captain.

From 1917 to 1928 he gained experience in structural design with the Illinois Division of Highways, Fargo Engineering Company of Jackson, Mich., Cuban Portland Cement Company, Illinois Central Railroad, and in private practice. He was placed in charge of structural design for Morgan Engineering Company on the following assignments: the City and County of Dallas, Tex., Improvement District; Trinity River valley (1928); and the Willacy County, Tex., irrigation project (1929-31). He returned to the Illinois Division of Highways as assistant chief bridge designer (1931-33).

He joined the Tennessee Valley Authority in 1934 and played a major role in the development and perfection of the forecasting procedure necessary for the operation of the multipurpose system of dams and reservoirs. This system was the first, largest, and most complex in the world. He was considered a specialist in his field and for five years before his retirement in 1957 he was special assistant to the branch chief in water dispatching.

Mr. Wilkinson was a member of the American Geophysical Union, The Technical Society of Knoxville, and the American Legion.

He married Mildred Wheeler on August 15, 1922, at Bethany, Ill. He is survived by his widow.

Mr. Wilkinson was elected an Associate Member of the Society in 1929 and a Member in 1942.

THOMAS H. WINCHESTER, M. ASCE[2]

Died December 10, 1958

Thomas Harrison Winchester, the son of Weems Ridout and Sarah (Powell Harrison) Winchester, was born on December 29, 1884, in Macon, Ga. He attended Virginia Military Institute and the University of Georgia.

[1] Abstract of a memoir prepared by Robert Forbes, M. ASCE.
[2] Abstract of a memoir prepared by Richard King, M. ASCE.

From 1906 to 1924 he was associated with various engineering companies, including Stone & Webster of Boston and New York, and Rust Engineering Company of Pittsburgh. In 1924 he returned to Macon and worked with the Georgia Power Company as a civil engineer and land surveyor. He was construction engineer of the Jackson Dam Hydro Electric Plant on the Ocmulgee River and of the Goat Rock Dam on the Chattachoochee River near Columbus. He made a study of the stream flow of the Ocmulgee, Flint, Oconee and Toccoa Rivers in Georgia to determine their feasibility for economical development. He served for several years with the National Park Service as project superintendent at Fairy Stone State Park, Va., and as an engineer-technician, he supervised the design and construction of engineering improvements in the state parks of Georgia and Florida. From 1944 until his retirement in 1954, he was in private practice in Macon.

Mr. Winchester was a member of St. Paul's Episcopal Church in Macon, Ga., the Georgia Society of Professional Engineers, the Kappa Alpha Order, and the American Legion. He was elected to the Macon Board of Water Commissioners in 1953. Mr. Winchester was a veteran of both world wars, and had attained the rank of major with the Corps of Engineers.

In 1919, he was married to Laura Dobson. He is survived by his widow; one son, Thomas H., Jr.; two daughters, Mrs. Laura W. Rahm, and Mrs. Harriotte W. Hurley; a sister; and seven grandchildren.

Mr. Winchester was elected a Junior Member of the Society in 1909, an Associate Member in 1913, and a Member in 1932. He became a Life Member in 1948.

WHITBY FOSTER WISE, Jr., A. M. ASCE[1]

Died January 19, 1959

Whitby Foster Wise, Jr., the son of Whitby and Frances (Blaine) Wise, was born in Jefferson, Tex., on October 9, 1889. He was graduated from Texas A&M College (College Station) in 1909, with the degree of Bachelor of Science in civil engineering.

After graduation Mr. Wise worked for various railroad companies before establishing a rock crushing plant at Stringtown, Okla., in 1919. In 1925 he moved to San Antonio, Tex., to oversee the establishment of a second stone crushing plant at Knippa, Tex. Mr. Wise established the Chico Plant near Dallas, Tex., in 1929. At this time he founded the Southwest Stone Company, served as its president for many years, and was still chairman of the board at the time of his death. Mr. Wise was past-president of the Nation Crushed Stone

[1] Abstract of a memoir prepared by J. Dwight Morgan, M. ASCE.

Association and served in many capacities with the organization including that of an executive committee member. At the time of his death he was a member of the board of directors.

Mr. Wise, a Master Mason, was a member of the Hella Temple Shrine, St. Matthew's Episcopal Parish, Texas A&M Club, Texas Society of Professional Engineers, and the American Society of Military Engineers. He was a licensed Professional Engineer.

In 1914 he was married to Ruth Mackey. Mr. Wise is survived by his widow; three sons, W. Foster, Jr., W. Denman, and Whitby J.; and a daughter, Mrs. W. L. Richardson.

Mr. Wise was elected an Associate Member of the Society in 1928.

ALFRED HENRY WITHOLDER, M. ASCE[1]

Died November 30, 1957

Alfred Henry Witholder, the son of William and Barbara (Korkey) Witholder, was born in El Paso, Tex., on August 22, 1904. He attended the University of Texas (Austin) from 1930 until 1933.

His first working experience as architectural draftsman with Trost and Trost, Architects and Engineers, of El Paso, extended from 1922 to 1932. He then joined R. E. McKee, General Contractor, in 1922 as draftsman and estimator. From 1933 to 1934 Mr. Witholder was employed as draftsman and assistant building inspector by the Engineering Department of the City of El Paso. In 1934 he began work with the United States Section of the International Boundary and Water Commission as an engineering draftsman and, later, as principal engineering draftsman. In 1941 he was promoted to the professional grade of assistant architect. Promotion to civil engineer followed on July 1, 1944. His last assignment was with the Office of Water Control and in this position he played a key role in the determination of the equitable division between Mexico and the United States of waters stored in the Falcon Dam and on the Rio Grande.

Mr. Witholder was affiliated with St. Patrick's Catholic Church. He was a member of the American Geophysical Union, the 20-30 Club, and the Tennis Club of El Paso.

Mr. Witholder was married to Hazel Miller Lockhart on February 18, 1939, in El Paso. He is survived by his widow; two sons, Alfred Henry, Jr., and William Fred; and daughter, Mary Jane.

Mr. Witholder became an Associate Member of the Society in 1947 and a Member in 1953.

[1] Abstract of a memoir prepared by F. P. Brown, F. ASCE.

ALEXANDER RIRIE YOUNG, M. ASCE[1]

Died February 26, 1959

Alexander R. Young, the son of Robert R. and Margaret (Ririe) Young, was born on January 3, 1876, in Chatsworth, Illinois. He was graduated from the University of Kansas (Lawrence) with the degree of Bachelor of Science in civil engineering in 1905.

After graduation Mr. Young was employed by the Atchinson, Topeka and Santa Fe Railway. He was appointed transit man and, later, supervisor of construction of a dam and reservoir at Welda, Kans. In 1907 he became city engineer and superintendent of the water department for Chanute, Kans. As City Engineer of Topeka, Kans., 1911-1917, he developed a new type of fine grade, asphaltic concrete wearing surface, now generally referred to as the "Topeka Mix." In 1917, Mr. Young went to the Texas Company (Texaco) as chief engineer of the Asphalt and Road Oil Sales Department. He was made manager of the western division of that company.

In 1941, Mr. Young retired and spent the remainder of his life managing his Kansas farms, a hobby of his many years prior to his retirement.

Mr. Young was a member of the Kansas Engineering Society, Kansas City Engineers Club, Missouri Society of Professional Engineers, Sigma Xi, Tau Beta Pi, and an honorary member of the Triangle Fraternity.

In 1908, Mr. Young married Lulu May Schmidler at Marysville, Kans. He is survived by his three children, Ferrile S., Alexander R., and Katherine Young Maichel; and seven grandchildren.

Mr. Young was elected an Associate Member of the Society in 1941, and a Member in 1916.

---

[1] Abstract of a memoir prepared by Glenn E. Hands, F. ASCE.

TRANSACTIONS

OF THE

AMERICAN SOCIETY OF CIVIL ENGINEERS

INDEX

VOLUME 125, PART I

1960

SUBJECT INDEX, PAGE 1447

AUTHOR INDEX, PAGE 1466

Titles of papers are in quotation marks when given with the author's name.

TRANSACTIONS

OF THE

AMERICAN SOCIETY OF CIVIL ENGINEERS

INDEX

TO

VOLUME LIX—PAPERS 1049 TO 1217

VOLUME 125, PART I

SUBJECT INDEX

AERATION
See also OXYGENATION
"Self-Aerated Flow in Open Channels," Lorenz G. Straub and Alvin G. Anderson (with discussion), 456.
AIR ENTRAINMENT
See WATER, FLOW OF...
ALLUVIATION
See SEDIMENT AND SEDIMENTATION; SILT AND SILTING...
AMERICAN SOCIETY OF CIVIL ENGINEERS (General)
"Progress in ASCE,": Annual Address at the Convention, Reno, Nevada, June 22, 1960, Frank A. Marston, 1380.
Addresses
1960—Annual Address at the Convention, Reno, Nevada, June 22, 1960, Frank A. Marston, 1380.
Memoirs of Members
See name of member in Author Index. (*See also* p. 1393)
ANALOGS AND ANALOGIES
See under relative subject, e.g., MODELS; STRUCTURES, THEORY OF
ANALYSIS, DESIGN
See under relative subject, e.g., CONCRETE—Design
ARCHES
See also DAMS, ARCH; STRESS AND STRAIN—Arches; STRUCTURES, THEORY OF...
"Arch Dams": A Symposium, Manuel Rocha, J. Laginha Serafim, and Antonio F. da Silveira; Carlo Semenza; and Dino Tonini (with discussion), 909.
"Digital Computation for Stiffness Matrix Analysis," John S. Archer, 1.
ATOMIC BLAST
"Blast Phenomena from a Nuclear Burst," Ferd E. Anderson, Jr., 667.
"Digital Computation for Stiffness Matrix Analysis," John S. Archer, 1.
BARGES
"Construction of the Variable-Angle Launcher," Arthur C. Bravo, 181.
BASIN
"Forces Induced on a Large Vessel by Surge," John T. O'Brien and David I. Kuchenreuther (with discussion), 855.
BEAMS (General)
See also BUCKLING; GIRDERS; STRESS AND STRAIN—Beams; STRUCTURES, THEORY OF—Beams and Girders; *also* under structure or structural part, e.g., BRIDGES; COLUMNS; GIRDERS... *also* under name of material, e.g., CONCRETE.
"Concrete Beams and Columns with Bundled Reinforcement," Norman W. Hanson and Hans Reiffenstuhl (with discussion), 889.
"Inelastic Buckling in Steel," Geerhard Haaijer and Bruno Thurlimann (with discussion), 308.
"Moments in Beams by the Method of Partial Moments," Harry Posner, with discussion, 430. *Discussion:* William S. Walker and Joseph T. Kolibal; Anatol A. Eremin; Lembit Kald; and Harry Posner; 451.
"Numerical Solutions for Beams on Elastic Foundations," Henry Malter, 757. *Discussion:* Norman J. Ryker, Jr.; Alexander Dodge; Lymon C. Reese; Victir R. Bergman; and Henry Malter, 770.
"Numerical Solutions for Interconnected Bridge Girders," Henry Malter (with discussion), 365.
"Strength of Reinforced Concrete Beams," Sidney A. Guralnick, 603. *Discussion:* Henry J. Cowan; Robert F. Warner; Bela Gdschy and George Balazs; Kuang-Han Chu; and Sidney A. Guralnick, 633.
BEAMS, CONTINUOUS
See also STRESS AND STRAIN—Beams, Continuous; STRUCTURES, THEORY OF—Beams and Girders, Continuous; STRUCTURES, THEORY OF—Frames, Continuous.
"Digital Computation for Stiffness Matrix Analysis," John S. Archer, 1.
"Elasti-Plastic Analysis of Continuous Frames and Beams," Lawrence P. Johnson, Jr., and Herbert A. Sawyer, Jr. (with discussion), 1176.
"Torque-Loaded Continuous Beams of Profile Section," Donovan H. Young and John F. Brahtz, 846.
BEARING CAPACITY (foundations, rocks, soils)
For more general interpretation *see* cross references under LOAD.
BED LOAD
See CHANNELS; RIVERS; SILT AND

BED LOAD (continued)
SILTING...; TURBULENCE; WATER, FLOW OF, IN OPEN CHANNELS
BENDING
See under relative structure, structural part, or material, e.g., GIRDERS
BIOGRAPHIES OF DECEASED MEMBERS
See cross reference under MEMOIRS OF DECEASED MEMBERS. *See also* p. 1393)
BLAST, ATOMIC
See ATOMIC BLAST
BLASTING
"Garrison Dam Test Tunnel": A Symposium, Harris H. Burke, and Kenneth S. Lane (with discussion), 228.
BOW GIRDERS
See GIRDERS
BRACING
See WIND BRACING
BRIDGE APPROACHES
"Design Features of the George Washington Bridge Lower Deck," Irvine P. Gould, 1022.
BRIDGE FLOORS AND FLOORING
See STRESS AND STRAIN—Bridge Floors and Flooring
BRIDGES (General)
See also BEAMS...; GIRDERS; STRESS AND STRAIN—Bridges...; STRUCTURES, THEORY OF—Bridges; TRAFFIC, BRIDGE; TRUSSES
"Construction of the Variable-Angle Launcher," Arthur C. Bravo, 181.
"Design Features of the George Washington Bridge Lower Deck," Irvine P. Gould, 1022.
"Numerical Solutions for Interconnected Bridge Girders," Henry Malter (with discussion), 365.
BRIDGES, GIRDER
"Numerical Solutions for Interconnected Bridge Girders," Henry Malter (with discussion), 365.
BRIDGES, SUSPENSION
See also STRESS AND STRAIN—Bridges, Suspension
"Design Features of the George Washington Bridge Lower Deck," Irvine P. Gould, 1022.
BRIDGES, TRUSS
See also STRESS AND STRAIN—Bridges, Truss; TRUSSES
"Construction of the Variable-Angle Launcher," Arthur C. Bravo, 181.
"Design Features of the George Washington Bridge Lower Deck," Irvine P. Gould, 1022.
BRIDGE TRAFFIC
See TRAFFIC, BRIDGE
BUCKLING
"Amplified Stress and Displacement in Guyed Towers," Robert S. Rowe, (with discussion), 199.
"Inelastic Buckling in Steel," Geerhard Haaijer and Bruno Thurlimann, 308. *Discussion:* P. P. Bijlaard; and Geerhard Haaijer and Bruno Thurlimann, 338.
"Lateral Bracing of Columns and Beams," George Winter, 807. *Discussion:* Anthony A. Chibaro; Giles G. Green; Bruce G. Johnston; Marvin A. Larson; William Zuk, 826.
"Torque-Loaded Continuous Beams of Profile Section," Donovan H. Young and John F. Brahtz, 846.
BUILDINGS
See also STRUCTURES...
"Digital Computation for Stiffness Matrix Analysis," John S. Archer, 1.
CANALS (General)
See also CHANNELS; COSTS, CANAL; EROSION; STREAM; IRRIGATION CANALS (cross reference thereunder); SEDIMENT AND SEDIMENTATION; SEEPAGE; SILT AND SILTING, CHANNEL; WATER, FLOW OF IN OPEN CHANNELS; WATERWAYS; WAVES
"Lower-Cost Canal Lining Practice," Richard J. Willson, with discussion, 487.
"Stability of Coastal Inlets," Per Brun and Frans Gerritsen (with discussion), 1228.
CANAL LININGS
"Lower-Cost Canal Lining Practice," Richard J. Willson, 487. *Discussion:* Frederick L. Hotes; and Richard J. Willson, 500.
CHANNEL LININGS
"Resistance Properties of Sediment-Laden Streams," Vito A. Vanoni and George N. Nomicos (with discussion), 1140.
CHANNELS (waterways)
See also EROSION, STREAM; RIVERS; SILT AND SILTING, CHANNEL; WATER, FLOW OF, IN OPEN CHANNELS
"Delta Project" A Symposium, Johannes B. Schijf; J. J. Dronkers; and H. A. Ferguson (with discussion), 1267.
"Resistance Properties of Sediment-Laden Streams," Vito A. Vanoni and George N. Nomicos (with discussion), 1140.
"Self-Aerated Flow in Open Channels," Lorenz G. Straub and Alvin G. Anderson (with discussion), 456.
"Stability of Coastal Inlets," Per Brun and Frans Gerritsen (with discussion), 1228.
CHEMISTRY
See under relative technical subject, e.g., EARTHWORK

CITIES
See also CITY PLANNING; EXPRESSWAYS, (cross reference thereunder); REGIONAL PLANING; SEWAGE . . .; SEWERS (cross reference thereunder); TRAFFIC . . .; ZONING
"Freeways in Urban Planning," Harold M. Lewis (with discussion), 1072.
"Hydrology of Urban Runoff," A. L. Tholin and Clint J. Keifer (with discussion), 1308.
CITY PLANNING (General)
See also HIGHWAYS AND ROADS
"Freeways in Urban Planning," Harold M. Lewis (with discussion), 1072.
CIVIL ENGINEERS AND ENGINEERING
See AMERICAN SOCIETY OF CIVIL ENGINEERS; ENGINEERS AND ENGINEERING (and cross references thereunder)
CLAY
See also SOIL . . .; STRESS AND STRAIN—Clay (cross reference thereunder)
"Compacted Clay": A Symposium, T. William Lambe, 681. *Discussion:* D. Hugh Trollope; B. P. Warkentin and Raymond N. Y. Yong; Gerald A. Leonards; D. P. Krynine; Dean R. Freitag; and T. William Lambe; Alfred C. Scheer; Raymond N. Y. Yong and B. P. Warkentin; J. MacNeil Turnbull; Jose A. Jimenez Salas; D. Hugh Trollope; and T. William Lambe, 706, 741.
"Clay Strength Increase Caused by Repeated Loading," H. Bolton Seed, Robert L. McNeill, and Jacques de Guenin, 141. *Discussion:* Richard G. Ahlvin; D. Hugh Trollope; and H. Bolton Seed, Robert L. McNeill, and Jacques de Guenin, 161.
"Design and Performance of Vermilion Dam," Karl Terzaghi and Thomas M. Leps, (with discussion), 63.
"Garrison Dam Test Tunnel": A Symposium, Harris H. Burke, and Kenneth S. Lane (with discussion), 228.
"Geotechnical Properties of Glacial Lake Clays," Tien H. Wu, 994. *Discussion:* T. Cameron Kenney, 1012.
COFFERDAMS
"Cellular Cofferdams and Docks," Edward M. Cummings, 13. *Discussion:* Samuel Heyman; Cevdet Z. Erzen; and Edward M. Cummings, 34.
First cellular cofferdam was constructed at Black Rock Harbor, near Buffalo, N. Y. in 1908, 13.
COLUMNS
See also BUCKLING; STRUCTURES, THEORY OF—Columns; *also* under name of material, e.g., STEEL
"Concrete Beams and Columns with Bundled Reinforcement," Norman W. Hanson and Hans Reiffenstuhl (with discussion), 889.
"Inelastic Bucling in Steel," Geerhard Haaijer and Bruno Thurlimann (with discussion), 308.
COMPACTION
See BEARING CAPACITY (cross reference thereunder); SOILS
COMPRESSION
See STRESS AND STRAIN
COMPUTATION AND COMPUTERS
See also ELECTRONIC INSTRUMENTS
"Digital Computation for Stiffness Matrix Analysis," John S. Archer, 1.
"Hydraulic Problem Solution on Electronic Computers," Edward A. Lawler and Frank V. Druml, 517.
COMPUTERS, ANALOG
See ELECTRONIC INSTRUMENTS; *also* under relative subject
COMPUTERS, ELECTRONIC
See COMPUTATION AND COMPUTERS; ELECTRONIC INSTRUMENTS; *also* under relative subject
CONCRETE (General)
See also FAILURES, CONCRETE; STRESS AND STRAIN—Concrete; STRUCTURES, THEORY OF—Concrete Reinforced; *also* special structure or structural part, e.g., BEAMS; COLUMNS
"Concrete Beams and Columns with Bundled Reinforcement," Norman W. Hanson and Hans Reiffenstuhl (with discussion), 889.
"Construction of the Variable-Angle Launcher," Arthur C. Bravo, 181.
Construction
See also under specific structure, e.g., TUNNELS
"Construction of the Variable-Angle Launcher," Arthur C. Bravo, 181.
"Garrison Dam Test Tunnel"; A Symposium, Harris H. Burke, and Kenneth S. Lane (with discussion), 228.
Cracks and Cracking
"Concrete Beams and Columns with Bundled Reinforcement," Norman W. Hanson and Hans Reiffenstuhl (with discussion), 889.
"Strength of Reinforced Concrete Beams," Sidney A. Guralnick (with discussion), 603.
Design
"Strength of Reinforced Concrete Beams," Sidney A. Guralnick, (with discussion), 603.
Linings
See under structure, e.g., CANAL LININGS
CONNECTORS AND CONNECTIONS
See also JOINTS . . .; WELDS AND WELDING

CONNECTORS AND CONNECTIONS (continued)
"Welded Pipeline Branch Connections," Everett C. Rodabaugh and Henry H. George, 554.
CONSTRUCTION
See also CONCRETE—Construction; MATERIALS OF CONSTRUCTION; STRESS AND STRAIN . . . ; STRUCTURES, THEORY OF . . . ; *also* under type of construction, e.g., TUNNELS
"Ambuklao Rock-Fill Dam, Design and Construction," E. Montford Fucik and Robert F. Edbrooke (with discussion), 1207.
"Construction of the Variable-Angle Launcher," Arthur C. Bravo, 181.
"Factor of Safety in Design of Timber Structures," Lyman W. Wood (with discussion), 1033.
"Garrison Dam Test Tunnel": A Symposium, Harris H. Burke, and Kenneth S. Lane (with discussion), 228.
"Trends in Pipeline Construction," James W. Hall, 123.
Variable-angle torpedo launcher permits study of water-entry performance p. 181.
CONSTRUCTION OF MATERIALS
See MATERIALS OF CONSTRUCTION
COSTS, CANAL
"Lower-Cost Canal Lining Practice," Richard J. Willson (with discussion), 487.
COSTS, CANAL (IRRIGATION CANALS)
"Lower-Cost Canal Lining Practice," Richard J. Willson (with discussion), 487.
COSTS, PIPE LINE
See under relative subject, e.g., PIPE LINES
COSTS, RESERVOIR
"Distribution of Sediment in Large Reservoirs," Whitney M. Borland and Carl R. Miller, 166.
COSTS, RESERVOIR (MULTI-PURPOSE RESERVOIRS)
"Distribution of Sediment in Large Reservoirs," Whitney M. Borland and Carl R. Miller, 166.
COSTS, SEDIMENT DISPOSAL
"Distribution of Sediment in Large Reservoirs," Whitney M. Borland and Carl R. Miller, 166.
COSTS, WATER CONSERVATION
"Lower-Cost Canal Lining Practice," Richard J. Willson (with discussion) 487.
"Water-A Limiting Resource," Robert O. Thomas (with discussion), 101.
COSTS, WATER POLLUTION CONTROL
"Sleuthing the Behavior of a River," Edward J. Cleary, (with discussion), 1053.
COSTS, WATER POWER
"Water-A Limiting Resource," Robert O. Thomas (with discussion), 101.
CRACKS AND CRACKING
See under relative subject, e.g., CONCRETE—Cracks and Cracking
CURVES (design curves)
See relative subject of design, e.g., GIRDERS; SEDIMENT AND SEDIMENTATION
CURVES (elastic curves)
See STRUCTURES, THEORY OF
CURVES (graphic curves)
See GRAPHICAL CHARTS
CUTOFFS (General)
See DAMS
DAMPING
See STRESS AND STRAIN
DAMS (General)
See also FOUNDATIONS, DAM; GROUND WATER; LOCKS; MODELS, HYDRAULIC; RESERVOIRS . . . ; SPILLWAYS; STRESS AND STRAIN—Dams (General); STRUCTURES, THEORY OF—Dams
"Ambuklao Rock-Fill Dam, Design and Construction," E. Montford Fucik and Robert F. Edbrooke (with discussion), 1207.
"The Columbia River Controlled," Louis H. Foote, (with discussion), 583.
"Distribution of Sediment in Large Reserviors," Whitney M. Borland and Carl R. Miller, 166.
"Underseepage Control at Fort Randall Dam," Stanley T. Thorfinnson, 792.
DAMS, ARCH
See also STRESS AND STRAIN—Dams, Arch
"Arch Dams": A Symposium, Manuel Roccha, J. Laginha Serafim, and Antonio F. da Silveira; Carlo Semenza; and Dino Tonini, 909. *Discussion:* Robert E. Glover, and Fred A. Houck, 949.
Lack of mineral fuel in Portugal led to large hydroelectric development program beginning in 1946, 911.
DAMS, EARTH
See also SEEPAGE
"Design and Performance of Vermilion Dam," Karl Terzaghi and Thomas M. Leps, 63. *Discussion:* Maurice L. Dickinson; John R. Kiely; Ralph W. Spencer; Phillip J. West; Joseph H. Berman; Bruce R. Laverty; and Karl Terzaghi and Thomas M. Leps, 86.
DAMS, ROCK-FILL
"Ambuklao Rock-Fill Dam, Design and Construction," E. Montford Fucik and Robert F. Edbrooke, 1207. *Discussion:* Frederic L. Lawton; Jose O. Lahoz; and E. Montford Fucik and Robert F. Edbrooke, 1222.

DEFLECTIONS
See DEFORMATION (cross reference thereunder); MOMENTS; STRESS AND STRAIN . . .; STRUCTURES, THEORY OF; *also* under relative structure or structural part, e.g., BEAMS, CONTINUOUS; COLUMNS; DAMS, ARCH
DEFORMATION
See STRESS AND STRAIN; *see also* under type of material, e.g., CLAY
DESIGN
See under relative subject, e.g., BRIDGES; CONCRETE . . .; DAMS . . .; DOCKS AND WHARVES; GIRDERS; HIGHWAYS AND ROADS; PIPE LINES; RESERVOIRS; STRUCTURES, TIMBER
DESIGN ANALYSIS
See under relative subject, e.g., STRUCTURES, THEORY OF
DESIGN CURVES
See CURVES (design curves) (cross reference thereunder)
DIGITAL COMPUTERS
See ELECTRONIC INSTRUMENTS
DIKES
See also LEVEES
"The Columbia River Controlled," Louis H. Foote (with discussion), 583.
DISTILLATION
See also EVAPORATION
"Meteoric Versus Nonmeteoric Ground Water," Harold E. Thomas and Donald E. White, 1304.
DOCKS AND WHARVES
See also STRESS AND STRAIN—Docks and Wharves
"Cellular Cofferdams and Docks," Edward M. Cummings (with discussion), 13.
"Forces Induced on a Large Vessel by Surge," John T. O'Brien and David I. Kuchenreuther (with discussion), 855.
DRAINAGE
See also RUNOFF
"Hydrology of Urban Runoff," A. L. Tholin and Clint J. Keifer (with discussion), 1308.
DROP-DOWN
See SPILLWAYS; WATER, FLOW OF, IN OPEN CHANNELS
DURATION CURVES
See also HYDROGRAPHS
"Ambuklao Rock-Fill Dam, Design and Construction," E. Montford Fucik and Robert F. Edbrooke (with discussion), 1207.
"Hydraulic Problem Solution on Electronic Computers," Edward A. Lawler and Frank V. Druml, 517.
EARTH . . .
See also SOIL . . .
EARTH DAMS
See DAMS, EARTH
EARTH PRESSURE
"Compacted Clay": A Symposium, T. William Lambe (with discussion), 681.
"Garrison Dam Test Tunnel": A Symposium, Harris H. Burke, and Kenneth S. Lane (with discussion), 228.
EARTHQUAKE RECORDING INSTRUMENTS
"Earthquake Response of Elevated Tanks and Vessels," Donald F. Moran and James A. Cheney (with discussion), 503.
EARTHQUAKES
See also SEISMOLOGY; STRUCTURES, THEORY OF—Earthquake Problems; VIBRATION
"Earthquake Response of Elevated Tanks and Vessels," Donald F. Moran and James A. Cheney, 503. *Discussion:* A. A. Eremin; and Donald F. Moran and James A. Cheney, 515.
EARTHWORK
See SOILS . . .
ECONOMICS
See COSTS . . .
EDUCATION
"Progress in ASCE,": Annual Address at the Convention, Reno, Nevada, June 22, 1960, Frank A. Marston, 1380.
ELASTIC CURVES
See CURVES (elastic curves) (cross reference thereunder)
ELASTICITY
See also PLASTICITY; STRESS AND STRAIN
"Elasti-Plastic Analysis of Continuous Frames and Beams," Lawrence P. Johnson, Jr., and Herbert A. Sawyer, Jr., (with discussion), 1176.
"Inelastic Buckling in Steel," Geerhard Haaijer and Bruno Thurlimann (with discussion), 308.
"Numerical Solutions for Beams on Elastic Foundations," Henry Malter (with discussion), 757.
ELASTO PLASTIC STRUCTURES
"Elasti-Plastic Analysis of Continuous Frames and Beams," Lawrence P. Johnson, Jr., and Herbert A. Sawyer, Jr., 1176. *Discussion:* Giuliano Augusti; Tullio Renzulli; Emilio Rosenblueth; A. A. Eremin; and Lawrence P. Johnson, Jr., and Herbert A. Sawyer, Jr., 1192.
ELECTRONIC COMPUTERS
See COMPUTATION AND COMPUTERS; ELECTRONIC INSTRUMENTS; *also* under relative subject
ELECTRONIC INSTRUMENTS
See also COMPUTATION AND COMPUTERS

FOUNDATIONS, DAM (continued)
Antonio F. da Silveira; Carlo Semenza; and Dino Tonini (with discussion), 909.
"Design and Performance of Vermilion Dam," Karl Terzaghi and Thomas M. Leps (with discussion), 63.
FOUNDATIONS, UNDERWATER
See also PILES AND PILE DRIVING (cross reference thereunder)
"Water Forces on Accelerated Cylinders," Alan D. K. Laird, Charles A. Johnson, and Robert W. Walker, 652.
FRAMES (General)
See BEAMS . . .
FREEWAYS
See HIGHWAYS AND ROADS (General)—Location
FRICTION
See also TURBULENCE (cross reference thereunder)
"Cellular Cofferdams and Docks," Edward M. Cummings (with discussion), 13.
"Compacted Clay": A Symposium, T. William Lambe (with discussion), 681.
"Resistance Properties of Sediment-Laden Streams," Vito A. Vanoni and George N. Nomicos (with discussion), 1140.
FRICTION COEFFICIENTS, FLUID
"Resistance Properties of Sediment-Laden Streams," Vito A. Vanoni and George N. Nomicos (with discussion), 1140.
GAGES, LIQUID
"Flow Testing by Ammonia Displacement," Jack N. White and Thomas Thawley, 673.
GAGES, PRESSURE
"Design and Performance of Vermilion Dam," Karl Terzaghi and Thomas M. Leps (with discussion), 63.
"Water Forces on Accelerated Cylinders," Alan D. K. Laird, Charles A. Johnson, and Robert W. Walker, 652.
GAGES, RAIN
"Hydrology of Urban Runoff," A. L. Tholin and Clint J. Keifer (with discussion), 1308.
GAGES, STREAM
See also WATER LEVEL RECORDING AND INDICATING INSTRUMENTS
"Sleuthing the Behavior of a River," Edward F. Cleary (with discussion), 1053.
GAS AND GASWORKS
See also PIPE LINES; TUNNELS, GAS
"Flow Testing by Ammonia Displacement," Jack N. White and Thomas Thawley, 673.
GATE VALVES
"Hydraulic Design of Columbia River Navigation Locks," George C. Richardson and Marvin J. Webster, 345.
GEOCHEMISTRY
See CHEMISTRY (cross reference thereunder)
GEOLOGY
"Design and Performance of Vermilion Dam," Karl Terzaghi and Thomas M. Leps (with discussion), 63.
GIRDER BRIDGES
See BRIDGES, GIRDER
GIRDERS (General)
See also BEAMS; BRIDGES; STRESS AND STRAIN—Girders; STRUCTURES, THEORY OF—Beams and Girders
"Analytical and Experimental Study of Helicoidal Girders," Yee F. Young and Alexander C. Scordelis, 46.
"Numerical Solutions for Interconnected Bridge Girders," Henry Malter, 365.
Discussion: Dronnadula V. Reddy; Henry Malter; 383.
GIRDERS, CONTINUOUS
See BRIDGES, GIRDER; STRUCTURES, THEORY OF—Beams and Girders
GRAPHICAL CHARTS
"Selection of Design Wave for Offshore Structures," Charles L. Bretschneider (with discussion), 388.
GRAVEL
See also SAND; SOILS
"Geotechnical Properties of Glacial Lake Clays," Tien H. Wu (with discussion), 994
GROINS
See also RIVER BANKS AND BANK PROTECTION (cross references thereunder); SHORES AND SHORE PROTECTION
"Delta Project" A Symposium, Johannes B. Schijf; J. J. Dronkers; and H. A. Ferguson (with discussion), 1267.
GROUND WATER
See also SEEPAGE; WATER SUPPLY
"Meteoric Versus Nonmeteoric Ground Water," Harold E. Thomas and Donald E. White, 1304.
"Underseepage Control at Fort Randall Dam," Stanley T. Thorfinnson, 792.
"Use of Models to Study Ground-Water Problems," Kenneth B. Wright, 133.
HARBORS (General)
See also SHORES AND SHORE PROTECTION
"Stability of Coastal Inlets," Per Brun and Frans Gerritsen (with discussion), 1228.
HEAD GATES
See INTAKES
HIGHWAYS AND ROADS (General)
See PAVEMENT AND PAVING
Location
"Freeways in Urban Planning," Harold M. Lewis (with discussion), 1072.

ELECTRONIC INSTRUMENTS (continued)
"Digital Computation for Stiffness Matrix Analysis," John S. Archer, 1.
"Hydraulic Problem Solution on Electronic Computers," Edward A. Lawler and Frank V. Druml, 517.
ENERGY
See STRUCTURES, THEORY OF
ENGINEERING HISTORY
See AMERICAN SOCIETY OF CIVIL ENGINEERS
ENGINEERS AND ENGINEERING (General)
See ENGINEERS AND ENGINEERING—History; *also* under relative subject, e.g., DAMS . . .; PIPE LINES
See also AMERICAN SOCIETY OF CIVIL ENGINEERS (For memoirs of deceased members, *see* name of member in Author Index) *(See also* p. 1393); EDUCATION; RESEARCH; SOCIETIES, TECHNICAL
"Progress in ASCE," Annual Address at the Convention, Reno, Nevada, June 22, 1960, Frank A. Marston, 1380.
History
"Arch Dams": A Symposium, Manuel Rocha, J. Laginha Serafim, and Antonio F. da Silveira; Carlo Semenza; and Dino Tonini (with discussion), 909.
"Freeways in Urban Planning," Harold M. Lewis (with discussion), 1072.
ENGINEERING SOCIETIES
See AMERICAN SOCIETY OF CIVIL ENGINEERS; SOCIETIES, TECHNICAL
EROSION, BEACH
"Delta Project" A Symposium, Johannes B. Schijf; J. J. Dronkers; and H. A. Ferguson (with discussion), 1267.
EROSION, STREAM
"Delta Project" A Symposium, Johannes B. Schijf; J. J. Dronkers; and H. A. Ferguson (with discussion), 1267.
ESTUARIES
See RIVERS
EVAPORATION
See also DISTILLATION
"Meteoric Versus Nonmeteoric Ground Water," Harold E. Thomas and Donald E. White, 1304.
EXCAVATION (General)
See also EARTH PRESSURE; *also* under specific substructure, e.g., TUNNELS
"Garrison Dam Test Tunnel": A Symposium, Harris H. Burke, and Kenneth S. Lane (with discussion), 228.
EXPERIMENTS AND EXPERIMENTATION
See under material structure or structural part tested, e.g., GIRDERS
EXPLORATION
See FOUNDATIONS . . .
EXPLOSION, ATOMIC
See ATOMIC BLAST
EXPRESSWAYS
See HIGHWAYS AND ROADS; TRAFFIC, HIGHWAY AND ROAD
FAILURES (General)
See BEARING CAPACITY (cross reference thereunder); STRENGTH OF MATERIALS; STRESS AND STRAIN *also* under relative subject, e.g., HIGHWAYS; PIPE LINES
FAILURES, CONCRETE
"Strength of Reinforced Concrete Beams," Sidney A. Guralnick, (with discussion), 603.
FAILURES, RESERVOIR
"Distribution of Sediment in Large Reservoirs," Whitney M. Borland and Carl R. Miller, 166.
FLANGES
See also STRESS AND STRAIN—Flanges
"Inelastic Buckling in Steel," Geerhard Haaijer and Bruno Thurlimann (with discussion), 308.
FLEXURE
See STRESS AND STRAIN; STRUCTURES, THEORY OF
FLOOD ROUTING
See also WATER DIVERSION
"Hydrology of Urban Runoff," A.L. Tholin and Clint J. Deifer (with discussion), 1308.
FLOODS (General)
See also HYDROGRAPHS, STREAM FLOW; LEVEES
"The Columbia River Controlled," Louis H. Foote (with discussion), 583.
FLOORS AND FLOORING
See STRESS AND STRAIN—Floors and Flooring
FLOW
See GROUND WATER; LIQUIDS, FLOW OF . . .; (cross reference thereunder); SEEPAGE; SEWAGE . . .; SEWERS
FLOW OF FLUIDS
See GAS . . .; LIQUIDS, FLOW OF (cross reference thereunder); PIPES AND PIPING
FLOW OF WATER
See WATER, FLOW OF . . .
FORMULAS
See under relative subject, e.g., BEAMS; LOAD
FOUNDATIONS (General)
See also SEEPAGE; STRESS AND STRAIN—Foundations; STRUCTURES, THEORY OF—Foundations
"Numerical Solutions for Beams on Elastic Foundations," Henry Malter (with discussion), 757.
FOUNDATIONS, DAM
"Ambuklao Rock-Fill Dam, Design and Construction," E. Montford Fucik and Robert F. Edbrooke (with discussion), 1207/.
"Arch Dams": A Symposium, Manuel Rocha, J. Laginha Serafim, and

HIGHWAY TRANSPORTATION
See also HIGHWAYS AND ROADS—Location
"Freeways in Urban Planning," Harold M. Lewis (with discussion), 1072.
HURRICANES
See WIND...
HYDRAULIC LABORATORIES
"Sleuthing the Behavior of a River," Edward J. Cleary (with discussion), 1053.
HYDRAULIC MODELS
See MODELS; HYDRAULIC
HYDRAULICS
See also FLOW... (cross reference thereunder); GROUND WATER; HEAD GATES (cross reference thereunder); LOCK GATES; LOCKS; SEEPAGE: MODELS, HYDRAULIC; SPREADING WATER; STRUCTURES, THEORY OF
"Hydraulic Design of Columbia River Navigation Locks," George C. Richardson and Marvin J. Webster, 345.
HYDROGRAPHS (General)
See also DURATION CURVES
"Ambuklao Rock-Fill Dam, Design and Construction," E. Montford Fucik and Robert F. Edbrooke (with discussion), 1207.
"Hydraulic Problem Solution on Electronic Computers," Edward A. Lawler and Frank V. Druml, 517.
HYDROGRAPHS, RAINFALL
"Hydrology of Urban Runoff," A. L. Tholin and Clint J. Keifer (with discussion), 1308.
HYDROGRAPHS, RUNOFF
"Hydrology of Urban Runoff," A. L. Tholin and Clint J. Keifer (with discussion), 1308.
HYDROGRAPHS, STREAM FLOW
"Hydraulic Problem Solution on Electronic Computers," Edward A. Lawler and Frank V. Druml, 517.
"Sleuthing the Behavior of a River," Edward J. Cleary (with discussion), 1053.
HYDROLOGY
See also DRAINAGE; EVAPORATION; GROUND WATER; RUNOFF; WATER...
"Hydrology of Urban Runoff," A. L. Tholin and Clint J. Keifer (with discussion), 1308.
"Meteoric Versus Nonmeteoric Ground Water," Harold E. Thomas and Donald E. White, 1304.
IMPACT
See also IMPULSE; VIBRATION
"Forces Induced on a Large Vessel by Surge," John T. O'Brien and David I. Kuchenreuther (with discussion), 855.
IMPULSE
See also IMPACT; STRUCTURAL DYNAMICS
"Blast Phenomena From a Nuclear Burst," Ferd E. Anderson, Jr., 667.
INFLUENCE LINES
See MOMENTS
INTAKES
"Hydraulic Design of Columbia River Navigation Locks," George C. Richardson and Marvin J. Webster, 345.
IRRIGATION
"The Columbia River Controlled," Louis H. Foote (with discussion), 583.
IRRIGATION CANALS
See COSTS, CANAL (IRRIGATION CANALS)
JOINTS, WELDED
"Pipeline Field Welding and Quality Control Methods," Armand G. Barkow, 417
"Welded Pipeline Branch Connections," Everett C. Rodabaugh and Henry H. George, 554.
LAKES (General)
See also SILT AND SILTING...
"Geotechnical Properties of Glacial Lake Clays," Tien H. Wu (with discussion), 994.
LEVEES
See also DIKES
"The Columbia River Controlled," Louis H. Foote (with discussion), 583.
LIBRARIES
"Progress in ASCE,": Annual Address at the Convention, Reno, Nevada, June 22, 1960, Frank A. Marston, 1380.
LIMIT DESIGN, THEORY OF
"Elasti-Plastic Analysis of Continuous Frames and Beams," Lawrence P. Johnson, Jr., and Herbert A. Sawyer, Jr. (with discussion), 1176.
LININGS
See under relative type, e.g., CANAL LININGS
LIQUIDS, FLOW OF...
See VISCOSITY
LOAD
See BEARING CAPACITY (cross reference thereunder); BUCKLING; EARTH PRESSURE; STRESS AND STRAIN (cross reference thereunder) *also* under structure, structural member or part, e.g., BEAMS...; TUNNELS
LOCK-GATES
See also STRUCTURES, THEORY OF—Lock-Gates
"Hydraulic Design of Columbia River Navigation Locks," George C. Richardson and Marvin J. Webster, 345.
LOCKS
See also HEAD GATES (cross reference thereunder)

LOCKS (continued)
Highest lift navigation locks on the Columbia River Basin Projects. 345.
"Hydraulic Design of Columbia River Navigation Locks," George C. Richardson and Marvin J. Webster, 345.
MATERIALS OF CONSTRUCTION
See also CLAY; CONCRETE . . .; EARTHQUAKES; PERMEABILITY OF MATERIALS (cross reference thereunder); SAND; SEEPAGE; SILT; SOILS; STEEL; STRENGTH OF MATERIALS; STRUCTURES, THEORY OF; TIMBER AND TIMBERING
"Ambuklao Rock-Fill Dam, Design and Construction," E. Montford Fucik and Robert F. Edbrooke (with discussion), 1207.
"Concrete Beams and Columns with Bundled Reinforcement," Norman W. Hanson and Hans Reiffenstuhl (with discussion), 889.
"Construction of the Variable-Angle Launcher," Arthur C. Bravo, 181.
"Factor of Safety in Design of Timber Structures," Lyman W. Wood (with discussion), 1033.
"Garrison Dam Test Tunnel": A Symposium, Harris H. Burke, and Kenneth S. Lane (with discussion), 228.
"Geotechnical Properties of Glacial Lake Clays," Tien H. Wu (with discussion), 994.
"Structural Dynamics in Earthquake-Resistant Design," John A. Blume (with discussion), 1088.
MATRIX ALGEBRA
See COMPUTATION AND COMPUTERS
MEASURING INSTRUMENTS
See GAGES . . .
MEMBERS (ASCE)
See AMERICAN SOCIETY OF CIVIL ENGINEERS. (For memoirs of deceased members, *see* name of member in Author Index) (*See also* p. 1393)
MEMOIRS OF DECEASED MEMBERS
See name of member in Author Index. (*See also* p. 1393)
METEOROLOGY
See also EVAPORATION; RAINFALL
"Meteoric Versus Nonmeteoric Ground Water," Harold E. Thomas and Donald E. White, 1304.
MODEL ANALYSIS INSTRUMENTS
"Analytical and Experimental Study of Helicoidal Girders," Yee F. Young and Alexander C. Scordelis, 46.
MODELS (General)
"Cellular Cofferdams and Docks," Edward M. Cummings (with discussion), 13.
"Use of Models to Study Ground-Water Problems," Kenneth R. Wright, 133.
MODELS, ELECTRIC
"Use of Models to Study Ground-Water Problems," Kenneth R. Wright, 133.
MODELS, HYDRAULIC
"Arch Dams": A Symposium, Manuel Rocha, J. Laginha Serafim, and Antonio F. da Silveira; Carlo Semenza; and Dino Tonini (with discussion), 909.
"Hydraulic Design of Columbia River Navigation," George C. Richardson and Marvin J. Webster, 345.
"Use of Models to Study Ground-Water Problems," Kenneth R. Wright, 133.
MODELS, STRUCTURAL
"Analytical and Experimental Study of Helicoidal Girders," Yee F. Young and Alexander C. Scordelis, 46.
"Arch Dams": A Symposium, Manuel Rocha, J. Laginha Serafim and Antonio F. da Silveira; Carlo Semenza; and Dino Tonini (with discussion), 909.
MOMENT DISTRIBUTION
See STRUCTURES, THEORY OF
MOMENTS
See also STRESS AND STRAIN; STRUCTURES, THEORY OF; *also* under specific type of stress, e.g., LOAD; SHEAR
"Analytical and Experimental Study of Helicoidal Girders," Yee F. Young and Alexander C. Scordelis, 46.
"Elasti-Plastic Analysis of Continuous Frames and Beams," Lawrence P. Johnson, Jr., and Herbert A. Sawyer, Jr. (with discussion), 1176.
"Numerical Solutions for Beams on Elastic Foundations," Henry Malter (with discussion), 757.
OBITUARIES OF MEMBERS
See name of member in Author Index. (*See also* p. 1393)
OCEAN CURRENTS
See also EROSION, BEACH; TIDES; WAVES
"Delta Project": A Symposium, Johannes B. Schijf; J. J. Dronkers; and H. A. Ferguson (with discussion), 1267.
"Forces Induced on a Large Vessel by Surge," John T. O'Brien and David I. Kuchenreuther (with discussion), 855.
"Water Forces on Accelerated Cylinder," Alan D. K. Laird, Charles A. Johnson, and Robert W. Walker, 652.
OIL, FLOW OF
See PIPE LINES
OIL STORAGE
See TANKS, OIL STORAGE
OXYGENATION
See also AERATION
"Self-Aerated Flow in Open Channels," Lorenz G. Straub and Alvin G. Anderson (with discussion), 456.

PAVEMENT AND PAVING (General)
"Clay Strength and Increase Caused by Repeated Loading," H. Bolton Seed, Robert L. McNeill, and Jacques de Guenin (with discussion), 141.
PENSTOCKS
"Trends in Pipeline Construction," James W. Hall, 123.
PERMEABILITY OF MATERIALS
See SEEPAGE; *also* under type of material, e.g., CLAY
PIERS (waterway structures)
See DOCKS AND WHARVES
PIEZOMETERS
See GAGES, PRESSURE
PILES AND PILE DRIVING
See FOUNDATIONS, UNDERWATER
PIPE LINES
See also COSTS, PIPE LINES; PENSTOCKS; PIPES AND PIPING (fluid conveyance); STRESS AND STRAIN—Pipe Lines
"Electric Pipeline for High-Viscosity Fuel," Albert G. Purdue, 644.
First high pressure, long distance line built in 1891 from Greentown, Ind., to Chicago, Ill. p. 418
"Flow Testing by Ammonia Displacement," Jack N. White and Thomas Thawley, 673.
One-hundreth anniversary of oil and gas industry in America coincides closely with the birth of oil and gas pipelining. p. 123.
"Pipeline Field Welding and Quality Control Methods," Armand G. Barkow, 417.
"Trends in Pipeline Construction," James W. Hall, 123.
"Welded Pipeline Branch Connections," Everett C. Rodabaugh and Henry H. George, 554.
PIPES AND PIPING (fluid conveyance)
See also PIPE LINES
"Electric Pipeline for High-Viscosity Fuel," Albert G. Purdue, 644.
"Flow Testing by Ammonia Displacement," Jack N. White and Thomas Thawley, 673.
"Trends in Pipeline Construction," James W. Hall, 123.
PIPES AND PIPING, COSTS
"Trends in Pipeline Construction," James W. Hall, 123.
PLASTICITY
See also ELASTICITY; STRESS AND STRAIN
"Elasti-Plastic Analysis of Continuous Frames and Beams," Lawrence P. Johnson, Jr., and Herbert A. Sawyer, Jr. (with discussion), 1176.
"Inelastic Buckling in Steel," Geerhard Haaijer and Bruno Thurlimann (with discussion), 308.
PLATES
"Digital Computation for Stiffness Matrix Analysis," John S. Archer, 1.
POWER (General)
See also DAMS; WATER POWER
"Ambuklao Rock-Fill Dam, Design and Construction," E. Montford Fucik and Robert F. Edbrooke (with discussion), 1207.
"The Columbia River Controlled," Louis H. Foote (with discussion), 583.
"Water-A Limiting Resource," Robert O. Thomas (with discussion), 101.
POWER PLANTS (General)
See also STRUCTURES, THEORY OF—Power Plants
"Containment Sphere for Dresden Station," Leonard P. Zick, James T. Dunn, and James B. Maher, 536.
PRESIDENTIAL ADDRESSES (American Society of Civil Engineers)
See AMERICAN SOCIETY OF CIVIL ENGINEERS—Addresses; *see also* under subject of address
PRESSURE
See IMPACT; STRESS AND STRAIN
PUBLIC WORKS
"Water-A Limiting Resource," Robert O. Thomas (with discussion), 101.
RAINFALL (General)
See also DRAINAGE; EVAPORATION; GAGES, RAIN; HYDROGRAPHS, RAINFALL; HYDROLOGY; RUNOFF; SEEPAGE
"Meteoric Versus Nonmeteoric Ground Water," Harold E. Thomas and Donald E. White, 1304.
RECREATIONAL FACILITIES
See RESERVOIRS; RIVERS
REDUNDANCE, STRUCTURAL
See STRUCTURES, THEORY OF
REGIONAL PLANNING
See also CITY PLANNING; HIGHWAYS AND ROADS—Location: ZONING
"Freeways in Urban Planning," Harold M. Lewis (with discussion), 1072.
REINFORCED CONCRETE
See CONCRETE
RESEARCH
See also AMERICAN SOCIETY OF CIVIL ENGINEERS; MODELS . . .; TESTS AND TESTING (cross references thereunder)
"Progress in ASCE,": Annual Address at the Convention, Reno, Nevada, June 22, 1960, Frank A. Marston, 1380.
RESERVOIRS (General)
See also COSTS, RESERVOIR; DAMS; FAILURES, RESERVOIRS; SEDIMENTATION; SILT AND SILTING; RESERVOIR; WATER STORAGE
"Ambuklao Rock-Fill Dam, Design and Construction," E. Montford Fucik and

RESERVOIRS (General) (continued)
Robert F. Edbrooke (with discussion), 1207.
"The Columbia River Controlled," Louis H. Foote (with discussion), 583.
"Distribution of Sediment in Large Reservoirs," Whitney M. Borland and Carl R. Miller, 166.
RESERVOIRS, MULTI-PURPOSE
See COSTS, RESERVOIR (MULTI-PURPOSE RESERVOIRS)
RESERVOIRS, STREAM REGULATION
See RESERVOIRS, WATER STORAGE
RESERVOIRS, WATER STORAGE
"Distribution of Sediment in Large Reservoirs," Whitney M. Borland and Carl R. Miller, 166.
RESONANCE
See VIBRATION; WAVES
RETAINING WALLS
See also SEA WALLS
"Delta Project" A Symposium, Johannes B. Schijf; J. J. Dronkers; and H. A. Ferguson (with discussion), 1267.
RIVER BANKS AND BANK PROTECTION
See EROSION, STREAM; SEDIMENT AND SEDIMENTATION; SILT AND SILTING, CHANNEL
RIVER BASINS
See RESERVOIRS...
RIVER DELTAS
"Delta Project" A Symposium, Johannes B. Schijf; J. J. Dronkers; and H. A. Ferguson, 1267. *Discussion:* Richard Silvester, Johannes B. Schijf, 1278.
"Stability of Coastal Inlets," Per Brun and Frans Gerritsen (with discussion), 1228.
RIVER REGULATIONS
See RIVERS
RIVERS (General)
See also CHANNELS; FLOODS; GAGES, STREAM; HYDRAULIC LABORATORIES; HYDROGRAPHS, STREAM FLOW; LEVEES; RESERVOIRS...; SEDIMENT AND SEDIMENTATION; SILT AND SILTING, CHANNELS; TIDES; TRAFFIC, RIVER; TRAFFIC, WATERWAY; WATER...; WATERWAYS...; WAVES
"The Columbia River Controlled," Louis H. Foote, 583. *Discussion:* Roy F. Bessey; Louis H. Foote, 597.
"Resistance Properties of Sediment-Laden Streams," Vito A. Vanoni and George N. Nomicos (with discussion), 1140.
"Sleuthing the Behavior of a River," Edward J. Cleary (with discussion), 1053.
"Stability of Coastal Inlets," Per Brun and Frans Gerritsen (with discussion), 1228.
RUNOFF (General)
See also HYDROGRAPHS, RUNOFF
"Hydrology of Urban Runoff," A. L. Tholin and Clint J. Keifer (with discussion), 1308. *Discussion:* Peter O. Wolf; M. B. McPherson and M. Joseph Willis; Paul Bock; Carl F. Izzard and Charles L. Armentrout, 1355.
"Water-A Limiting Resource," Robert O. Thomas (with discussion), 101.
SAFETY (General)
"Factor of Safety in Design of Timber Structures," Lyman W. Wood (with discussion), 1033.
SAND
See also GRAVEL; SEDIMENT AND SEDIMENTATION; SILT AND SILTING...; SOILS
"Resistance Properties of Sediment-Laden Streams," Vito A. Vanoni and George N. Nomicos (with discussion), 1140.
SAND DUNES
See also BED LOAD (cross references thereunder)
"Delta Project" A Symposium, Johannes B. Schijf; J. J. Dronkers; and H. A. Ferguson (with discussion), 1267.
SANITATION
See also WATER...
"Sleuthing the Behavior of a River," Edward J. Cleary (with discussion), 1053.
SEA WALLS
See also RETAINING WALLS; SHORES AND SHORE PROTECTION; WAVES
"Delta Project" A Symposium, Johannes B. Schijf; J. J. Dronkers; and H. A. Ferguson (with discussion), 1267.
SEDIMENT AND SEDIMENTATION
See also COSTS, SEDIMENT DISPOSAL; SILT AND SILTING
"Delta Project" A Symposium, Johannes B. Schijf; J. J. Dronkers; and H. A. Ferguson (with discussion), 1267.
"Distribution of Sediment in Large Reservoirs," Whitney M. Borland and Carl R. Miller, 166.
"Geotechnical Properties of Glacial Lake Clays," Tien H. Wu (with discussion), 994.
"Resistance Properties of Sediment-Laden Streams," Vito A. Vanoni and George N. Nomicos, 1140. *Discussion:* Emmett M. Laursen; Tsung-Lienchow; and Vito A. Vanoni and George N. Nomicos, 1167.
"Stability of Coastal Inlets," Per Brun and Frans Gerritsen (with discussion), 1228.
SEEPAGE
See also GROUND WATER

SEEPAGE (continued)
"Design and Performance of Vermilion Dam," Karl Terzaghi and Thomas M. Leps (with discussion), 63.
"Lower-Cost Canal Lining Practice," Richard J. Willson (with discussion), 487.
"Meteoric Versus Nonmeteoric Ground Water," Harold E. Thomas and Donald E. White, 1304.
"Underseepage Control at Fort Randall Dam," Stanley T. Thorfinnson, 792.
"Use of Models to Study Ground-Water Problems," Kenneth R. Wright, 133.
SEISMOLOGY
See also EARTHQUAKES
"Earthquake Response of Elevated Tanks and Vessels," Donald F. Moran and James A. Cheney, 503.
"Structural Dynamics in Earthquake-Resistant Design," John A. Blume (with discussion), 1088.
SETTLEMENT OF FILL
See SOILS—Construction
SETTLING BASINS (water supply)
See also TANKS, SEDIMENTATION (sewage)
"Hydrology of Urban Runoff," A. L. Tholin and Clint J. Keifer (with discussion), 1308.
SEWAGE DISPOSAL (General)
See also TANKS . . .
"Hydrology of Urban Runoff," A. L. Tholin and Clint J. Keifer (with discussion), 1308.
SEWERS (General)
See DRAINAGE; RAINFALL; RUNOFF
SHEAR
"Amplified Stress and Displacement in Guyed Towers," Robert S. Rowe (with discussion), 199.
"Arch Dams": A Symposium, Manuel Rocha, J. Laginha Serafim, and Antonio F. da Silviera; Carlo Semenza; and Dino Tonini (with discussion), 909.
"Cellular Cofferdams and Docks," Edward M. Cummings (with discussion), 13.
"Clay Strength Increase Caused by Repeated Loading," H. Bolton Seed, Robert L. McNeill, and Jacques de Guenin (with discussion), 141.
"Compacted Clay": A Symposium, T. William Lambe (with discussion), 681.
"Concrete Beams and Columns with Bundled Reinforcement," Norman W. Hanson and Hans Reiffenstuhl (with discussion), 889.
"Moments in Beams by the Method of Partial Moments," Harry Posner (with discussion), 430.
"Numerical Solutions for Beams on Elastic Foundations," Henry Malter (with discussion), 757.
"Strength of Reinforced Concrete Beams," Sidney A. Guralnick (with discussion), 603.
SHELL STRUCTURES
See also STRESS AND STRAIN—Shell Structures; STRUCTURES, THEORY OF—Shell Structures
"Containment Sphere for Dresden Station," Leonard P. Zick, James T. Dunn, and James B. Maher, 536.
SHIP . . .
"Forces Induced on a Large Vessel by Surge," John T. O'Brien and David Kuchenreuther (with discussion), 855.
SHIP MOORINGS AND MOORAGES
See DOCKS AND WHARVES
SHOCK
See ATOMIC BLAST; EARTHQUAKES; IMPACT; VIBRATION
SHORES AND SHORE PROTECTION (lands adjacent to lake, ocean, or sea water)
See also EROSION, BEACH; RETAINING WALLS; RIVER BANKS AND BANK PROTECTION (cross reference thereunder); SAND DUNES; WAVES
"Delta Project": A Symposium, Johannes B. Schijf; J. J. Dronkers; and H. A. Ferguson (with discussion), 1267.
"Selection of Design Wave for Offshore Structures," Charles L. Bretschneider (with discussion), 388.
"Stability of Coastal Inlets," Per Brun and Frans Gerritsen, 1228. *Discussion:* Robert E. Hickson, 1259.
SILT AND SILTING (General)
See also SEDIMENT AND SEDIMENTATION
"Design and Performance of Vermilion Dam," Karl Terzaghi and Thomas M. Leps (with discussion), 63.
"Distribution of Sediment in Large Reservoirs," Whitney M. Borland and Carl R. Miller, 166.
"Geotechnical Properties of Glacial Lake Clays," Tien H. Wu (with discussion), 994.
"Resistance Properties of Sediment-Laden Streams," Vito A. Vanoni and George N. Nomicos (with discussion), 1140.
SILT AND SILTING, CHANNELS
See also RIVER DELTAS
"Delta Projects" A Symposium, Johannes B. Schijf; J. J. Dronkers; and H. A. Ferguson (with discussion), 1267.
"Resistance Properties of Sediment-Laden Streams," Vito A. Vanoni and George N. Nomicos (with discussion), 1140.

SILT AND SILTING, CHANNELS (continued)
"Stability of Coastal Inlets," Per Brun and Frans Gerritsen (with discussion), 1228.
SILT AND SILTING, RESERVOIR
"Distribution of Sediment in Large Reservoirs, Whitney M. Borland and Carl R. Miller, 166.
SOCIETIES, TECHNICAL
See also AMERICAN SOCIETY OF CIVIL ENGINEERS; ENGINEERS AND ENGINEERING; *also* under relative subject
"Progress in ASCE," Annual Address at the Convention, Reno, Nevada, June 22, 1960, Frank A. Marston, 1380.
SOIL . . .
See also EARTH . . .
SOIL MECHANICS
See SOIL . . .
SOILS (General)
See also BEARING CAPACITY (cross reference thereunder); CLAY; EARTH PRESSURE; FRICTION . . .; GRAVEL; HIGHWAYS; PAVEMENT AND PAVING; SAND; SEDIMENT AND SEDIMENTATION; SILT AND SILTING . . .; STRESS AND STRAIN
"Compacted Clay": A Symposium, T. William Lambe (with discussion), 681.
"Stability of Coastal Inlets," Per Brun and Frans Gerritsen (with discussion), 1228.
Compaction
See BEARING CAPACITY (cross reference thereunder)
Construction
"Design and Performance of Vermilion Dam," Karl Terzaghi and Thomas M. Leps (with discussion), 63.
"Ambuklao Rock-Fill Dam, Design and Construction," E. Montford Fucik and Robert F. Edbrooke (with discussion), 1207.
Tests and Testing
"Clay Strength Increase Caused by Repeated Loading," H. Bolton Seed, Robert L. McNeill, and Jacques de Guenin (with discussion), 141.
"Compacted Clay": A Symposium, T. William Lambe (with discussion), 681.
"Delta Project" A Symposium, Johannes B. Schijf; J. J. Dronkers; and H. A. Ferguson (with discussion), 1267.
SPILLWAYS (General)
See also DAMS; DROP-DOWN (cross references thereunder)
"Ambuklao Rock-Fill Dam, Design and Construction," E. Montford Fucik and Robert F. Edbrooke (with discussion), 1207.
SPREADING, WATER
"Use of Models to Study Ground-Water Problems," Kenneth R. Wright, 133.
STEAM POWER
See POWER
STEEL (General)
See also BRIDGES; MATERIALS OF CONSTRUCTION; REINFORCED CONCRETE (cross reference thereunder); STRENGTH OF MATERIALS; STRESS AND STRAIN—Steel; *also* under special structure or structural part, e.g., COLUMNS; FLANGES; PLATES; TOWERS
"Amplified Stress and Displacement in Guyed Towers," Robert S. Rowe (with discussion), 199.
"Construction of the Variable-Angle Launcher," Arthur C. Bravo, 181.
"Concrete Beams and Columns with Bundled Reinforcement," Norman W. Hanson and Hans Reiffenstuhl (with discussion), 889.
"Garrison Dam Test Tunnel"; A Symposium, Harris H. Burke, and Kenneth S. Lane (with discussion), 228.
"Inelastic Buckling in Steel," Geerhard Haaijer and Bruno Thurlimann (with discussion), 308.
Tests and Testing
"Inelastic Buckling in Steel," Geerhard Haaijer and Bruno Thurlimann (with discussion), 308.
STIFFNESS
"Analytical and Experimental Study of Helicoidal Girders," Yee F. Young and Alexander C. Scordelis, 46.
"Clay Strength Increase Caused by Repeated Loading," H. Bolton Seed, Robert L. McNeill, and Jacques de Guenin (with discussion), 141.
STORAGE
See OIL STORAGE (cross reference thereunder)
STREAM FLOW
See WATER, FLOW OF, IN OPEN CHANNELS and cross references thereunder
STREAMS
See RIVERS and cross references thereunder
STRENGTH OF MATERIALS
See also FAILURES . . .; STRESS AND STRAIN; *also* under specific material (*See* list of materials under MATERIALS OF CONSTRUCTION)
"Amplified Stress and Displacement in Guyed Towers," Robert S. Rowe (with discussion), 199.
"Compacted Clay": A Symposium, T. William Lambe (with discussion), 681.
"Factor of Safety in Design of Timber Structures," Lyman W. Wood (with discussion), 1033.
"Geotechnical Properties of Glacial Lake Clays," Tien H. Wu (with discussion), 994.

STRENGTH OF MATERIALS (continued)
"Strength of Reinforced Concrete Beams," Sidney A. Guralnick (with discussion), 603.
"Structural Dynamics in Earthquake-Resistant Design," John A. Blume (with discussion), 1088.
STRESS AND STRAIN (General)
See also EARTHQUAKES; ELASTICITY; FAILURES . . . ; IMPACT (cross references thereunder); PLASTICITY; STRENGTH OF MATERIALS; STIFFNESS; STRUCTURES, THEORY OF; VIBRATION; WIND . . . *also* under specific type of stress, e.g., BUCKLING; SHEAR; TORSION
"Amplified Stress and Displacement in Guyed Towers," Robert S. Rowe (with discussion), 199.
"Arch Dams": A Symposium, Manuel Rocha, J. Laginha Serafim, and Antonio F. da Silveira; Carlo Semenza; and Dino Tonini (with discussion), 909.
"Garrison Dam Test Tunnel": A Symposium, Harris H. Burke, and Kenneth S. Lane (with discussion), 228.
"Moments in Beams by the Method of Partial Moments," Harry Posner (with discussion), 430.
"Strength of Reinforced Concrete Beams," Sidney A. Guralnick (with discussion), 603.
"Structural Dynamics in Earthquake-Resistant Design," John A. Blume (with discussion), 1088.
Arches
"Arch Dams": A Symposium, Manuel Rocha, J. Laginha Serafim, and Antonio F. da Silveira; Carlo Semenza; and Dino Tonini (with discussion), 909.
Beams (General)
See also BUCKLING; SHEAR; TORSION
"Concrete Beams and Columns with Bundled Reinforcement," Norman W. Hanson and Hans Reiffenstuhl (with discussion), 889.
"Lateral Bracing of Columns and Beams," George Winter (with discussion), 807.
"Moments in Beams by the Method of Partial Moments," Harry Posner (with discussion), 430.
"Numerical Solutions for Beams on Elastic Foundations," Henry Malter (with discussion), 757.
"Strength of Reinforced Concrete Beams," Sidney A. Guralnick (with discussion), 603.
Beams, Continuous
"Elasti-Plastic Analysis of Continuous Frames and Beams," Lawrence P. Johnson, Jr., and Herbert A. Sawyer, Jr. (with discussion), 1176.
"Moments in Beams by the Method of Partial Moments," Harry Posner (with discussion), 430.
"Torque-Loaded Continuous Beams of Profile Section," Donovan H. Young and John F. Brahtz, 846.
Bridge Floors and Flooring
"Design Features of the George Washington Bridge Lower Deck," Irvine P. Gould, 1022
Bridges (General)
"Design Features of the George Washington Bridge Lower Deck," Irvine P. Gould, 1022.
Bridges, Suspension
"Design Features of the George Washington Bridge Lower Deck," Irvine P. Gould, 1022.
Bridges, Truss
"Design Features of the George Washington Bridge Lower Deck," Irvine P. Gould, 1022.
Clay
See SHEAR
Columns
"Inelastic Buckling in Steel," Geerhard Haaijer and Bruno Thurlimann (with discussion), 308.
Concrete (General)
See also TORSION
"Concrete Beams and Columns with Bundled Reinforcement," Norman W. Hanson and Hans Reiffenstuhl (with discussion), 889.
"Strength of Reinforced Concrete Beams," Sidney A. Guralnick (with discussion), 603.
Dams (General)
"Ambuklao Rock-Fill Dam, Design and Construction," E. Montford Fucik and Robert F. Edbrooke (with discussion), 1207.
Dams, Arch
See also SHEAR
"Arch Dams": A Symposium, Manuel Rocha, J. Laginha Serafim, and Antonio F. da Silveira; Carlo Semenza; and Dino Tonini (with discussion), 909.
Docks and Wharves
"Forces Induced on a Large Vessel by Surge," John T. O'Brien and David Kuchenreuther (with discussion), 855.
Flanges
"Inelastic Buckling in Steel," Geerhard Haaijer and Bruno Thurlimann (with discussion), 308.
Floors and Flooring
"Lateral Bracing of Columns and Beams," George Winter (with discussion), 807.
Foundations
"Numerical Solutions for Beams on Elastic Foundation," Henry Malter (with discussion), 757.

STRESS AND STRAIN (General) (continued)
Frames, Continuous
"Elasti-Plastic Analysis of Continuous Frames and Beams," Lawrence P. Johnson, Jr., and Herbert A. Sawyer, Jr. (with discussion), 1176.
Pipe Lines
"Welded Pipeline Branch Connections," Everett C. Rodabaugh and Henry H. George, 554.
Shell Structures
"Containment Sphere for Dresden Station," Leonard P. Zick, James T. Dunn, and James B. Maher, 536.
Soils
"Clay Strength Increase Caused by Repeated Loading," H. Bolton Seed, Robert L. McNeill, and Jacques de Guenin (with discussion), 141.
Steel
"Amplified Stress and Displacement in Guyed Towers," Robert S. Rose (with discussion), 199.
"Lateral Bracing of Columns and Beams," George Winter (with discussion), 807.
Timber
"Factor of Safety in Design of Timber Structures," Lyman W. Wood (with discussion), 1033.
Towers
"Amplified Stress and Displacement in Guyed Towers," Robert S. Rowe (with discussion), 199.
Tunnel Linings
"Garrison Dam Test Tunnel": A Symposium, Harris H. Burke, and Kenneth S. Lane (with discussion), 228.
Tunnels
"Garrison Dam Test Tunnel": A Symposium, Harris H. Burke, and Kenneth S. Lane (with discussion), 228.
Wood
"Factor of Safety in Design of Timber Structures," Lyman W. Wood (with discussion), 1033.
STRUCTURAL DYNAMICS
See also EARTHQUAKES; STRUCTURES, THEORY OF; VIBRATION
"Blast Phenomena from a Nuclear Blast," Ferd E. Anderson, Jr., 667.
STRUCTURAL MODELS
See MODELS, STRUCTURAL
STRUCTURAL STEEL
See STEEL
STRUCTURES (General)
See also CONSTRUCTION; MATERIALS OF CONSTRUCTION
"Construction of the Variable-Angle Launcher," Arthur C. Bravo, 181.
STRUCTURES, THEORY OF (General)
See also STRESS AND STRAIN; *also* under type of structure or structural part
"Amplified Stress and Displacement in Guyed Towers," Robert S. Rowe (with discussion), 199.
"Analytical and Experimental Study of Helicoidal Girders," Yee F. Young and Alexander C. Scordelis, 46.
"Cellular Cofferdams and Docks," Edward M. Cummings (with discussion), 13.
"Factor of Safety in Design of Timber Structures," Lyman W. Wood (with discussion), 1033.
"Garrison Dam Test Tunnel": A Symposium, Harris H. Burke, and Kenneth S. Lane (with discussion), 228.
"Numerical Solutions for Beams on Elastic Foundations," Henry Malter (with discussion), 757.
"Strength of Reinforced Concrete Beams," Sidney A. Guralnick (with discussion), 603.
"Structural Dynamics in Earthquake-Resistant Design," John A. Blume (with discussion), 1088.
Arches
"Design and Observation in Portugal," Manuel Rocha, J. Laginha Serafim, and Antonio F. da Silveira (with discussion), 911.
Beams and Girders (General)
"Concrete Beams and Columns with Bundled Reinforcement," Norman W. Hanson and Hans Reiffenstuhl (with discussion), 889.
"Lateral Bracing of Columns and Beams," George Winter (with discussion), 807.
"Numerical Solutions for Interconnected Bridge Girders," Henry Malter (with discussion), 365.
"Moments in Beams by the Method of Partial Moments," Harry Posner (with discussion), 430.
"Strength of Reinforced Concrete Beams," Sidney A. Guralnick (with discussion), 603.
Beams and Girders, Continuous
"Digital Computation for Stiffness Matrix Analysis," John S. Archer, 1.
"Elasti-Plastic Analysis of Continuous Frames and Beams," Lawrence P. Johnson, Jr., and Herbert A. Sawyer, Jr. (with discussion), 1176.
"Torque-Loaded Continuous Beams of Profile Section," Donovan H. Young and John F. Brahtz, 846.
Bridges
"Design Features of the George Washington Bridge Lower Deck," Irvine P. Gould, 1022.
Columns
"Lateral Bracing of Columns and Beams," George Winter (with discussion), 807.

STRUCTURES, THEORY OF (continued)
Concrete, Reinforced
"Concrete Beams and Columns with Bundled Reinforcement," Norman W. Hanson and Hans Reiffenstuhl (with discussion), 889.
"Strength of Reinforced Concrete Beams," Sidney A. Guralnick (with discussion), 603.
Dams
"Ambuklao Rock-Fill Dam, Design and Construction," E. Montford Rucik and Robert F. Edbrooke (with discussion), 1207.
"Arch Dams": A Symposium, Manuel Rocha, J. Laginha Serafim, and Antonio F. da Silveira; Carlo Semenza; and Dino Tonini (with discussion), 909.
"Underseepage Control at Fort Randall Dam," Stanley T. Thorfinnson, 792.
Earthquake Problems
"Earthquake Response of Elevated Tanks and Vessels," Donald F. Moran and James A. Cheney (with discussion), 503.
"Structural Dynamics in Earthquake-Resistant Design," John A. Blume (with discussion), 1088.
Foundations, Building
"Numerical Solutions for Beams on Elastic Foundation," Henry Malter (with discussion), 757.
Frames, Continuous
"Elasti-Plastic Analysis of Continuous Frames and Beams," Lawrence P. Johnson, Jr., and Herbert A. Sawyer, Jr. (with discussion), 1176.
Lock Gates
"Hydraulic Design of Columbia River Navigation Locks," George C. Richardson and Marvin J. Webster, 345.
Materials and Tests
"Garrison Dam Test Tunnel": A Symposium, Harris H. Burke, and Kenneth S. Lane (with discussion), 228.
"Inelastic Buckling in Steel," Geerhard Haaijer and Bruno Thurlimann (with discussion), 308.
Power Plants
"Containment Sphere for Dresden Station," Leonard P. Zick, James T. Dunn, and James B. Maher, 536.
Shell Structures
"Containment Sphere for Dresden Station, Leonard P. Zick, James T. Dunn, and James B. Maher, 536.
Wind Stresses
"Amplified Stress and Displacement in Guyed Towers," Robert S. Rowe (with discussion), 199.
STRUCTURES, TIMBER
"Factor of Safety in Design of Timber Structures," Lyman W. Wood, 1033.
Discussion: E. George Stern; Richard G. Kimbell; Emilio Rosenblueth; Ludvik Cizek; Milos Vorlicek; and Lyman W. Wood, 1045.
SURGES (Water Surface)
See WAVES
TANKS, OIL STORAGE
"Electric Pipeline for High-Viscosity Fuel," Albert G. Purdue, 644.
TANKS, SEDIMENTATION (sewage)
See also SETTLING BASINS (water supply)
"Hydrology of Urban Runoff," A. L. Tholin and Clint J. Keifer (with discussion), 1308.
TANKS, WATER
"Earthquake Response of Elevated Tanks and Vessels," Donald F. Moran and James A. Cheney (with discussion), 503.
TESTING STATIONS
See under relative subject, e.g., CONSTRUCTION
TESTS AND TESTING
See also BUCKLING; ELASTICITY; FAILURES . . .; MODELS . . .; SHEAR; STRENGTH OF MATERIALS; STRESS AND STRAIN; STRUCTURES, THEORY OF—Materials and Tests; *also* under material, structure, or structural part tested, e.g., DAMS; PIPELINES; TUNNELS
"Analytical and Experimental Study of Helicoidal Girders," Yee F. Young and Alexander C. Scordelis, 46.
"Pipeline Field Welding and Quality Control Methods," Armand G. Barkow, 417.
THERMAL POWER
See STEAM POWER (cross reference thereunder)
TIDES
See also OCEAN CURRENTS; WAVES
"Delta Project" A Symposium, Johannes B. Schijf; J. J. Dronkers; and H. A. Ferguson (with discussion), 1267.
"Forces Induced on a Large Vessel by Surge," John T. O'Brien and David I. Kuchenreuther (with discussion), 855.
"Stability of Coastal Inlets," Per Brun and Frans Gerritsen, 1228. *Discussion:* Robert E. Hickson, 1259.
"Water Forces on Accelerated Cylinders," Alan D. K. Laird, Charles A. Johnson, and Robert W. Walker, 652.
TIMBER AND TIMBERING
See aslo STRESS AND STRAIN—Timber; WOOD
"Factor of Safety in Design of Timber Structures," Lyman W. Wood (with discussion), 1033.
TIMBER STRUCTURES
See STRUCTURES, TIMBER

TORSION
"Analytical and Experimental Study of Helicoidal Girders," Yee F. Young and Alexander C. Scordelis, 46.
"Concrete Beams and Columns with Bundled Reinforcement," Norman W. Hanson and Hans Reiffenstuhl (with discussion), 889.
"Strength of Reinforced Concrete Beams," Sidney A. Guralnick (with discussion), 603.
"Torque-Loaded Continuous Beams of Profile Section," Donovan H. Young and John F. Brahtz, 846.
TOWERS
See also STRESS AND STRAIN—Towers
"Amplified Stress and Displacement in Guyed Towers," Robert S. Rowe (with discussion), 199.
TRAFFIC, BRIDGES
"Design Features of the George Washington Bridge Lower Deck," Irvine P. Gould, 1022.
TRAFFIC, HIGHWAY AND ROAD
See also HIGHWAYS AND ROADS—Location
"Freeways in Urban Planning," Harold M. Lewis (with discussion), 1072.
TRAFFIC, RIVER
"The Columbia River Controlled," Louis H. Foote, (with discussion), 583.
TRAFFIC, WATERWAY
"The Columbia River Controlled," Louis H. Foote (with discussion), 583.
TRUSSES (General)
See also BRIDGES; BRIDGES, TRUSS
"Construction of the Variable-Angle Launcher," Arthur C. Bravo, 181.
"Design Features of the George Washington Bridge Lower Deck," Irvine G. Gould, 1022.
TUNNEL LININGS
See also STRESS AND STRAIN—Tunnel Linings
"Garrison Dam Test Tunnel": A Symposium, Harris H. Burke, and Kenneth S. Lane (with discussion), 228.
TUNNELS (General)
"Garrison Dam Test Tunnel": A Symposium, Harris H. Burke, and Kenneth S. Lane, 228. *Discussion:* A. A. Eremin, 307.
TUNNELS, GAS
"Flow Testing by Ammonia Displacement," Jack N. White and Thomas Thawley, 673.
TURBULENCE (water agitation)
See FRICTION . . . ; WATER, FLOW OF . . .
UNDERSEEPAGE
See SEEPAGE
URBAN . . .
See CITIES
VALVES
See also VALVES, GATE
"Hydraulic Design of Columbia River Navigation Locks," George C. Richardson and Marvin J. Webster, 345.
VESSELS
See SHIP . . .
VIBRATION
See also EARTHQUAKES; IMPACT
"Blast Phenomena from a Nuclear Blast," Ferd E. Anderson, Jr., 667.
"Digital Computation for Stiffness Matrix Analysis," John S. Archer, 1.
"Forces Induced on a Large Vessel by Surge," John T. O'Brien and David I. Kuchenreuther (with discussion), 855.
"Structural Dynamics in Earthquake-Resistant Design," John A. Blume (with discussion), 1088.
VIBRATION MEASURING INSTRUMENTS
"Forces Induced on a Large Vessel by Surge," John T. O'Brien and David I. Kuchenreuther (with discussion), 855.
VISCOSITY
"Flow Testing by Ammonia Displacement," Jack N. White and Thomas Thawley, 673.
WATER
"Water-A Limiting Resource," Robert O. Thomas, 101. *Discussion:* Douglas R. Woodward; Donald McCord Baker; Alfred R. Golze; and Robert O. Thomas, 112.
WATER . . .
See also GROUND WATER; RAINFALL
WATER ANALYSIS
See also WATER TREATMENT
"Meteoric Versus Nonmeteoric Ground Water," Harold E. Thomas and Donald E. White, 1304.
WATER CONSERVATION
See also COSTS, WATER CONSERVATION; PUBLIC WORKS; RESERVOIRS; WATER STORAGE
"The Columbia River Controlled," Louis H. Foote, (with discussion), 583.
"Lower-Cost Canal Lining Practice," Richard J. Willson, with discussion, 487.
WATER, CONSUMPTION OF (consumer usage)
See WATER, WASTE OF (cross reference thereunder)
WATER, CONSUMPTIVE USE OF (in agriculture)
"Water-A Limiting Resource," Robert O. Thomas (with discussion), 101.
"Meteoric Versus Nonmeteoric Ground Water," Harold E. Thomas and Donald E. White, 1304.
WATER, CONSUMPTIVE USE OF (in industry)
"Water-A Limiting Resource," Robert O. Thomas (with discussion), 101.

WATER, DEMINERALIZATION OF
See WATER TREATMENT
WATER DIVERSION
See also FLOOD ROUTING
"Hydrology of Urban Runoff," A. L. Tholin and Clint J. Keifer (with discussion), 1308.
WATER, DUTY OF
"The Columbia River Controlled," Louis H. Foote (with discussion), 583.
WATER FLOW ANALYSIS
"Use of Models to Study Ground-Water Problems," Kenneth R. Wright, 133.
WATER, FLOW OF (General)
See also FLOODS; GROUND WATER; MODELS, HYDRAULIC; SPILLWAYS; TURBULENCE (cross references thereunder)
"The Columbia River Controlled," Louis H. Foote (with discussion), 583.
"Resistance Properties of Sediment-Laden Streams," Vito A. Vanoni and George N. Nomicos (with discussion) 1140.
"Self-Aerated Flow in Open Channels," Lorenz G. Straub and Alvin G. Anderson (with discussion), 456.
WATER, FLOW OF, IN OPEN CHANNELS
See also DROP-DOWN; SEDIMENT AND SEDIMENTATION; SILT AND SILTING, CHANNEL
"Resistance Properties of Sediment-Laden Streams," Vito A. Vanoni and George N. Nomicos (with discussion) 1140.
"Self-Aerated Flow in Open Channels," Lorenz G. Straub and Alvin G. Anderson, 456. *Discussion:* Michele Viparelli; and Lorenz G. Straub and Alvin G. Anderson, 482.
"Sleuthing the Behavior of a River," Edward J. Cleary, (with discussion), 1053.
"Stability of Coastal Inlets," Per Brun and Frans Gerritsen (with discussion), 1228.
WATER, FLOW OF, OVER DAMS AND WEIRS
"Self-Aerated Flow in Open Channels," Lorenz G. Straub and Alvin G. Anderson (with discussion), 456.
WATER LEVEL RECORDING AND INDICATING INSTRUMENTS
"Sleuthing the Behavior of a River," Edward J. Cleary (with discussion), 1053.
"Water Forces on Accelerated Cylinders," Alan D. K. Laird, Charles A. Johnson, and Robert W. Walker, 652.
WATER POLLUTION (General)
See also COSTS, WATER POLLUTION CONTROL
"Sleuthing the Behavior of a River," Edward J. Cleary (with discussion), 1053.
WATER POWER (General)
See also COSTS, WATER POWER; DAMS; POWER
"Ambuklao Rock-Fill Dam, Design and Construction," E. Montford Fucik and Robert F. Edbrooke (with discussion), 1207.
WATER PRESSURE
See also GAGES, PRESSURE; WAVES
"Forces Induced on a Large Vessel by Surge," John T. O'Brien and David Kuchenreuther (with discussion), 855.
"Water Forces on Accelerated Cylinders," Alan D. K. Laird, Charles A. Johnson, and Robert W. Walker, 652.
WATER SPREADING
See SPREADING, WATER
WATER STORAGE
See also RESERVOIRS . . .; TANKS . . .; WATER CONSERVATION
"The Columbia River Controlled," Louis H. Foote (with discussion), 583.
"Distribution of Sediment in Large Reservoirs," Whitney M. Borland and Carl M. Miller, 166.
"Hydrology of Urban Runoff," A. L. Tholin and Clint J. Keifer (with discussion), 1308.
WATER STORAGE (RESERVOIRS, MULTI-PURPOSE)
See also RESERVOIRS . . .
"Distribution of Sediment in Large Reservoirs," Whitney M. Borland and Carl R. Miller, 166.
WATER SUPPLY (General)
See also DAMS . . .; GROUND WATER; RAINFALL; WELLS
"Meteoric Versus Nonmeteoric Ground Water," Harold E. Thomas and Donald E. White, 1304.
"Underseepage Control at Fort Randall Dam," Stanley T. Thorfinnson, 792.
"Use of Models to Study Ground-Water Problems," Kenneth R. Wright, 133.
WATER TANKS
See TANKS, WATER
WATER TOWERS
See TANKS, WATER
WATER TREATMENT
See also WATER ANALYSIS
"Meteoric Versus Nonmeteoric Ground Water," Harold E. Thomas and Donald E. White, 1304.
WATER, WASTE OF
See WATER, CONSUMPTIVE USE OF
WATERWAYS (General)
See also CHANNELS; HARBORS; RIVERS
"Stability of Coastal Inlets," Per Brun and Frans Gerritsen (with discussion), 1228.
WAVE RECORDING AND RECORDING APPARATUS
"Forces Induced on a Large Vessel by

WAVE RECORDING AND RECORDING APPARATUS (continued)
Surge," John T. O'Brien and David I. Kuchenreuther (with discussion), 855.
"Selection of Design Wave for Offshore Structures," Charles L. Bretschneider (with discussion), 388.
"Water Forces on Accelerated Cylinders," Alan D. K. Laird, Charles A. Johnson, and Robert W. Walker, 652.
WAVES
See also EROSION, BEACH; OCEAN CURRENTS; RETAINING WALLS; SEA WALLS; SHORES AND SHORE PROTECTION; TIDES; WATER PRESSURE
"Delta Project": A Symposium, Johannes B. Schijf; J. J. Dronkers; and H. A. Ferguson (with discussion), 1267.
"Forces Induced on a Large Vessel by Surge," John T. O'Brien and David I. Kuchenreuther, 855. *Discussion:* Basil W. Wilson, 877.
"Selection of Design Wave for Offshore Structures," Charles L. Bretschneider, 388. *Discussion:* J. E. Chappelear; and Charles Bretschneider, 414.
"Stability of Coastal Inlets," Per Brun and Frans Gerritsen (with discussion), 1228.
"Water Forces on Accelerated Cylinders," Alan D. K. Laird, Charles A. Johnson, and Robert W. Walker, 652.
WELDED JOINTS
See JOINTS, WELDED
WELDS AND WELDING
See also JOINTS, WELDED
"Pipeline Field Welding and Quality Control Methods," Armand G. Barkow, 417.
"Welded Pipeline Branch Connections," Everett C. Rodabaugh and Henry H. George, 554.
WELLS
See also GROUND WATER
"Underseepage Control at Fort Randall Dam," Stanley T. Thorfinnson, 792.
WHARVES
"Forces Induced on a Large Vessel by Surge," John T. O'Brien and David I. Kuchenreuther (with discussion), 855.
WIND
See also WAVES
"Selection of Design Wave for Offshore Structures," Charles L. Bretschneider (with discussion), 388.
WIND BRACING
"Lateral Bracing of Columns and Beams," George Winter (with discussion), 807.
WIND PRESSURE
See also STRUCTURES, THEORY OF—Wind Stresses
"Amplified Stress and Displacement in Guyed Towers," Robert S. Rowe (with discussion).
WOOD
See also STRESS AND STRAIN—Wood; TIMBER...
"Factor of Safety in Design of Timber Structures," Lyman W. Wood (with discussion), 1033.
ZONING
See also CITIES; CITY PLANNING; REGIONAL PLANNING
"Freeways in Urban Planning," Harold M. Lewis (with discussion), 1072.

AUTHOR INDEX

(including Memoirs of deceased members)

ADAMS, M.
Earthquake-resistant design, 1126.
AHLVIN, RICHARD G.
Clay strength, 161.
ALLING, ARTHUR RICH
Memoir of, 1395.
ANDERSON, ALVIN G.
"Self-Aerated Flow in Open Channels," 456.
ANDERSON, FERD E.
"Blast Phenomena from a Nuclear Burst," 667.
ARCHER, JOHN S.
"Digital Computation for Stiffness Matrix Analysis," 1.
ARMENTROUT, CHARLES L.
Urban runoff, 1365.
AUGUSTI, GUILIANO
Elasti-plastic analysis, 1192.
BAKER, DONALD McCORD
Water, 114.
BALAZS, GEORGE
Shear strength, 635.
BARKER, CLIFTON THORNE
Memoir of, 1395.
BARKOW, ARMAND G.
"Pipeline Field Welding and Quality Control Methods," 417.
BATES, JOHN SCHUYLER
Memoir of, 1396.
BAUMGARTNER, JOHN ALBERT
Memoir of, 1397.
BERGMAN, VICTOR R.
Numerical methods, 789.
BERRITSEN, FRANS
"Stability of Coastal Inlets," 1228.
BERTERO, VITELMO
Towers, 215.
BESSEY, ROY
Columbia River, 597.
BIJLAARD, P. P.
Buckling, 338.
BINDER, REUBEN W.
Earthquake-resistant design, 1128.
BIRMAN, JOSEPH H.
Vermilion dam, 93.
BLISS, TULLA ETHAN
Memoir of, 1397.
BLUME, JOHN A.
"Structural Dynamics in Earthquake Resistant Design," 1088.
BOCK, PAUL
Urban runoff, 1361.
BOESEL, RONALD AXEL
Memoir of, 1398.
BORLAND, WHITNEY M.
"Distribution of Sediment in Large Reservoirs," 166.
BOSIER, WILLIAM HARRIS
Memoir of, 1399.
BRAHTZ, JOHN F.
"Torque-Loaded Continuous Beams of Profile Section," 846.
BRANDT, RICHARD LUDWIG
Memoir of, 1399.
BRAVO, ARTHUR C.
"Construction of the Variable-Angle Launcher," 181.
BRETSCHNEIDER, CHARLES L.
"Selection of Design Wave for Offshore Structures," 388.
BRUMLEY, DANIEL JOSEPH
Memoir of, 1400.
BRUNN, PER
"Stability of Coastal Inlets," 1228.
BURKE, HARRIS H.
"Garrison Dam Test Tunnel (Symposium): Investigation and Construction," 230.
CALAHAN, PECOS HILL
Memoir of, 1401.
CHAPPELAR, J. E.
Design wave, 414.
CHENEY, JAMES A.
"Earthquake Response of Elevated Tanks and Vessels," 503.
CHIBARO, ANTHONY A.
Lateral bracing, 826.
CHOU, TSUNG-LIEN
Resistance properties, 1168.
CHU, KUANG-HAN
Shear strength, 636.
CIZEK, LUDVIK
Timber structures, 1048.
CLEARY, EDWARD J.
"Sleuthing the Behavior of a River," 1053.
COWAN, HENRY J.
Shear strength, 633.
CRAFT, WELLING HALL
Memoir of, 1401.
CROCKER, FRED WILBUR
Memoir of, 1402.
CUMMINGS, EDWARD M.
"Cellular Cofferdams and Docks," 13.
CUNNINGHAM, JOHN WILBUR
Memoir of, 1403.
da SILVEIRA, ANTONIO F.
"Arch Dams (Symposium): Design and Observation in Portugal," 911.

DE GUENIN, JACQUES
"Clay Strength Increase Caused by Repeated Loading," 141.
DICKINSON, MAURICE L.
Vermilion dam, 86.
DIETERICH, BERNARD H.
River behavior, 1066.
DODGE, ALEXANDER
Numerical methods, 774.
DOUGHERTY, STARKS CONRAD
Memoir of, 1404.
DRONKERS, J. J.
"Tidal Computations in Coastal Areas," 1281.
DRUML, FRANK V.
"Hydraulic Problem Solution on Electronic Computers," 517.
DUNN, JAMES T.
"Containment Sphere for Dresden Station," 536.
EDBROOKE, ROBERT F.
"Ambuklao Rock-Fill Dam, Design and Construction," 1207.
ELLIOTT, JOHN ARTHUR
Memoir of, 1404.
EREMIN, A. A.
Earthquake-resistant design, 1124.
Earthquake response, 515.
Elasti-plastic analysis, 1202.
Garrison Dam, 307.
Partial moments, 452.
ERZEN, CEVDET Z.
Cellular cofferdams, 37.
FERGUSON, H. A.
"Hydraulic Investigations for the Delta Project," 1290.
FISH, GILBERT DUDLEY
Memoir of, 1405.
FLOYD, EARL NESBY
Memoir of, 1406.
FOOTE, LOUIS H.
"The Columbia River Controlled," 583.
FRASER, CHARLES E.
Memoir of, 1406.
FREITAG, DEAN R.
Compacted clay, 714.
FUCIK, E. MONTFORD
"Ambuklao Rock-Fill Dam, Design and Construction," 1207.
GAMMIE, ROBERT JAMES
Memoir of, 1407.
GEORGE, HENRY H.
"Welded Pipeline Branch Connections," 554.
GLOVER, ROBERT E.
Arch dams, 949.
GOETZ, CHARLES
Memoir of, 1408.
GOLZE, ALFRED R.
Water, 117.
GOSCHY, BELA
Shear strength, 635.
GOULD, IRVINE P.
"Design Features of the George Washington Bridge Lower Deck," 1022.
GREEN, GILES G.
Lateral bracing, 827.
GURALNICK, SIDNEY A.
"Strength of Reinforced Concrete Beams," 603.
HAALJER, GEERHARD
"Inelastic Buckling in Steel," 308.
HABER, RICHARD A.
Freeways, 1081.
HADLEY, HOMER M.
Bundling, 905.
HALL, JAMES W.
Trends in Pipeline Construction," 123.
HANSON, NORMAN W.
"Concrete Beams and Columns with Bundled Reinforcement," 889.
HATCH, ARTHUR SELDEN
Memoir of, 1409.
HAWXHURST, ROBERT, JR.
Memoir of, 1409.
HELLAND, RANDOLPH OLAF
Memoir of, 1410.
HERROLD, GEORGE H.
Freeways, 1083.
HEYMAN, SAMUEL
Cellular cofferdams, 34.
HICKSON, ROBERT E.
Coastal inlets, 1259.
HOLMAN, CHARLES O., JR.
Memoir of, 1411.
HOTES, FREDERICK L.
Canal lining, 487.
HOUCK, FRED A.
Arch dams, 950.
HUNTER, ROBERT CHARLES
Memoir of, 1411.
IZZARD, CARL F.
Urban runoff, 1365.
JACOBSEN, LYDIK S.
Earthquake-resistant design, 1122.
JOHNSON, CHARLES A.
"Water Forces on Accelerated Cylinders," 652.
JOHNSON, LAWRENCE P.
"Elasti-Plastic Analysis of Continuous Frames and Beams," 1176.
JOHNSTON, BRUCE G.
Lateral bracing, 830.
KALD, LEMBIT
Partial moments, 453.
KEIFER, CLINT J.
"Hydrology of Urban Runoff," 1308.
KENNEY, T. CAMERON
Glacial lake clays, 1012.
KIELY, JOHN R.
Vermilion dam, 88.
KIMBELL, RICHARD G.
Timber structures, 1045.
KING, HOWARD LANGDON
Memoir of, 1412.

KOLIBAL, JOSEPH T.
Partial moments, 451.
KRYNINE, D. P.
Compacted clay, 712.
KUCHENREUTHER, D. I.
"Forces Induced on a Large Vessel by Surge," 855.
LAHOZ, JOSE O.
Ambuklao dam, 1223.
LAIRD, D. K.
"Water Forces on Accelerated Cylinders," 652.
LAMBE, WILLIAM T.
"Compacted Clay (Symposium): Engineering Behavior," 718.
"Compacted Clay (Symposium): Structure," 682.
LANE, KENNETH S.
"Garrison Dam Test Tunnel (Symposium): Evaluation of Test Results," 268.
LARSON, MARVIN A.
Lateral bracing, 830.
LAURSEN, EMMETT M.
Resistance properties, 1167.
LAVERTY, BRUCE R.
Vermilion dam, 94.
LAWLER, EDWARD A.
"Hydraulic Problem Solution on Electronic Computers," 517.
LAWTON, FREDERIC L.
Ambuklao dam, 1222.
LEONARDS, GERALD A.
Compacted clay, 709.
LEPS, THOMAS M.
"Design and Performance of Vermilion Dam," 63.
LEVANDER, CARL GUSTAF
Memoir of, 1413.
LEWIS, FRANK REDMOND
Memoir of, 1414.
LEWIS, HAROLD M.
"Freeways in Urban Planning," 1072.
LILLY, WALTER HARRISON
Memoir of, 1414.
LIVINGSTON, PENN POORE
Memoir of, 1415.
LOWRY, ROBERT LEE
Memoir of, 1416.
LUCCHETTI, RAUL JOSE FELIX
Memoir of, 1417.
LUND, ALFRED MAJENDIE
Memoir of, 1417.
MAHER, JAMES B.
"Containment Sphere for Dresden Station," 536.
MALTER, HENRY
"Numerical Solutions for Beams on Elastic Foundations," 757.
"Numerical Solutions for Interconnected Bridge Girders," 365.
MARSTON, FRANK A.
"Annual Address at the Convention, Reno, Nevada, June 22, 1960," 1380.
MATHEWS, CLAUDE KELSEY
Memoir of, 1418.
McCRONE, ROSSITER MAGERS
Memoir of, 1419.
McDONNELL, ROBERT EMMETT
Memoir of, 1419.
McFARLAND, FRANK RAY
Memoir of, 1420.
McNEILL, ROBERT L.
"Clay Strength Increase Caused by Repeated Loading," 141.
McPHERSON, M. B.
Urban runoff, 1357.
MILLER, CARL R.
"Distribution of Sediment in Large Reservoirs," 166.
MILLER, WILLIAM J., JR.
Freeways, 1081.
MONNICHE, TOLLEF BACHE
Memoir of, 1421.
MORAN, DONALD F.
"Earthquake Response of Elevated Tanks and Vessels," 503.
MORE, PHILLIP DANIEL
Memoir of, 1421.
MORRISS, GROVER CLEVELAND
Memoir of, 1422
MURPHY, MICHAEL J.
Earthquake-resistant design, 1126.
NEEDHAM, LAWRENCE KENNETH
Memoir of, 1423.
NEFF, STEWART SMITH
Memoir of, 1423.
NIKIRK, FRANK AUSTIN
Memoir of, 1424.
NOMICOS, GEORGE N.
"Resistance Properties of Sediment-Laden Streams," 1167.
O'BRIEN, J. T.
"Forces Induced on a Large Vessel by Surge," 855.
PAIGE, CLAYTON WHITNEY
Memoir of, 1425.
PHILO, CLIFFORD ALLEN
Memoir of, 1425.
POSNER, HARRY
"Moments in Beams by the Method of Partial Moments," 430.
PRICHARD, GEORGE WILLIAM
Memoir of, 1426.
PROCTOR, ASA GLISSON
Memoir of, 1427.
PURDUE, ALBERT G.
"Electric Pipeline for High-Viscosity Fuel," 644.
REDDY, DRONNADULA V.
Bridge girders, 383.
REED, CHARLES ALLEY
Memoir of, 1428.
REESE, LYMON C.
Numerical methods, 786.
REIFFENSTUHL, HANS
"Concrete Beams and Columns with Bundled Reinforcement," 889.

RENZULLI, TULLIO
Elasti-plastic analysis, 1194.
RICHARDSON, EVERETT V.
Resistance properties, 1170.
RICHARDSON, GEORGE C.
"Hydraulic Design of Columbia River Navigation Locks," 345.
ROCHA, MANUEL
"Arch Dams (Symposium): Design and Observation in Portugal," 911.
RODABAUGH, EVERETT C.
"Welded Pipeline Branch Connections," 554.
ROSENBLUETH, EMILIO
Earthquake-resistant design, 1124.
Timber structures, 1046.
ROWE, ROBERT S.
"Amplified Stress and Displacement in Guyed Towers," 199.
RUSSELL, GARFIELD HUGH
Memoir of, 1428.
RYKER, NORMAN J.
Numerical methods, 770.
SALAS, JOSE A. JIMENEZ
Compacted clay, 746.
SAWYER, HERBERT A., JR.
"Elasti-Plastic Analysis of Continuous Frames and Beams," 1176.
SCHEER, ALFRED C.
Compacted clay, 741.
SCHIJF, JOHANNES B.
"Generalities on Coastal Processes and Protection," 1268.
SCHULZ, WALTER FREDERICK
Memoir of, 1429.
SCORDELIS, ALEXANDER C.
"Analytical and Experimental Study of Helicoidal Girders," 46.
SEED, H. BOLTON
"Clay Strength Increase Caused by Repeated Loading," 141.
SEELYE, ELWYN E.
Memoir of, 1430.
SEMENZA, CARLO
"Arch Dams (Symposium): Development in Italy," 954.
SERAFIM, J. LAGINHA
"Arch Dams (Symposium): Design and Observation in Portugal," 911.
SHACKELFORD, WILLIAM JAMES
Memoir of, 1431.
SHEDD, THOMAS CLARK
Memoir of, 1431.
SHEETZ, JACK WILLIAM
Memoir of, 1432.
SHERRILL, CLARENCE OSBORNE
Memoir of, 1433.
SILVESTER, RICHARD
Delta project, 1278.
SIMONS, DARYL B.
Resistance Properties, 1170.
SINGLETON, MICAJAH THOMAS
Memoir of, 1433.
SKINNER, R. IVAN
Earthquake-resistant design, 1126.
SPENCER, RALPH W.
Vermilion dam, 89.
STERN, E. GEORGE
Timber structures, 1045.
STILES, ARTHUR ALVORD
Memoir of, 1434.
STRAUB, LORENZ G.
"Self-Aerated Flow in Open Channels," 456.
STREIFF, ABRAHAM
Memoir of, 1435.
SYLLIAASEN, MELVIN OLIVER
Memoir of, 1436.
TERZAGHI, KARL
"Design and Performance of Vermilion Dam," 63.
THAWLEY, THOMAS
"Flow Testing by Ammonia Displacement," 673.
THOLIN, A. L.
"Hydrology of Urban Runoff," 1308.
THOMAS, HAROLD E.
"Meteoric Versus Nonmeteoric Ground Water," 1304.
THOMAS, ROBERT O.
"Water—A Limiting Resource," 101.
THORFINNSON, STANLEY T.
"Underseepage Control at Fort Randall Dam," 792.
THURLIMANN, BRUNO
"Inelastic Buckling in Steel," 308.
TONINI, DINO
"Arch Dams (Symposium): Observed Behavior in Italy," 974.
TROLLOPE, D. HUGH
Clay strength, 163.
Compacted clay, 706, 753.
TROST, ADOLPHUS GUSTAVUS
Memoir of, 1436.
TURNBULL, J. MacNEIL
Compacted clay, 743.
UHRIG, LEO VERNON
Memoir of, 1437.
VANONI, VITO A.
"Resistance Properties of Sediment-Laden Streams," 1140.
VAWTER, JAMISON
Memoir of, 1438.
VIPARELLI, MICHELE
Self-aerated flow, 482.
VORLICEK, MILOS
Timber structures, 1049.
WAI, FRANCIS K.
Memoir of, 1439.
WALKER, GEORGE E.
River behavior, 1070.
WALKER, ROBERT W.
"Water Forces on Accelerated Cylinders," 652.
WALKER, WILLIAM S.
Partial moments, 451.

WARD, RICHARD BENSKIN
Memoir of, 1439.
WARKENTIN, BENNO
Compacted clay, 707, 742.
WARNER, ROBERT F.
Shear strength, 634.
WEBSTER, MARVIN J.
"Hydraulic Design of Columbia River Navigation Locks," 345.
WEST, PHILLIP J.
Vermilion dam, 90.
WHITE, DONALD E.
"Meteoric Versus Nonmeteoric Ground Water," 1304.
WHITE, JACK N.
"Flow Testing by Ammonia Displacement," 673.
WHITTED, LEVI ROMULUS
Memoir of, 1440.
WILKINSON, JACKSON HEATH
Memoir of, 1441.
WILLIS, JOSEPH
Urban runoff, 1357.
WILLSON, RICHARD J.
"Lower-Cost Canal Lining Practice," 487.
WILSON, BASIL W.
Surge forces, 877
WINCHESTER, THOMAS H.
Memoir of, 1441.
WINTER, GEORGE
"Lateral Bracing of Columns and Beams," 807.
WISE, WHITBY FOSTER
Memoir of, 1442.
WITHOLDER, ALFRED HENRY
Memoir of, 1443.
WOLF, PETER O.
Urban runoff, 1355.
WOOD, LYMAN W.
"Factor of Safety in Design of Timber Structures," 1033.
WOODWARD, DOUGLAS R.
Water, 112.
WRIGHT, KENNETH R.
"Use of Models to Study Ground-Water Problems," 133.
WU, TIEN H.
"Geotechnical Properties of Glacial Lake Clays," 994.
YONG, RAYMOND N. Y.
Compacted clay, 707, 742.
YOUNG, ALEXANDER RIRIE
Memoir of, 1444.
YOUNG, DONOVAN H.
"Torque-Loaded Continuous Beams of Profile Section," 846.
YOUNG, YEE F.
"Analytical and Experimental Study of Helicoidal Girders," 46.
ZICK, LEONARD P.
"Containment Sphere for Dresden Station," 536.

